Sarah Baatout
Editor

Radiobiology Textbook

sck cen

OPEN ACCESS

Springer

Sarah Baatout
Editor

Radiobiology Textbook

Springer

Editor
Sarah Baatout
Institute of Nuclear Medical Applications
Belgian Nuclear Research Centre (SCK CEN)
Mol, Belgium

ISBN 978-3-031-18809-1 ISBN 978-3-031-18810-7 (eBook)
https://doi.org/10.1007/978-3-031-18810-7

Belgian Nuclear Research Centre (SCK CEN)

This Springer imprint is published by the registered company Springer Nature Switzerland AG
The registered company address is: Gewerbestrasse 11, 6330 Cham, Switzerland

Foreword

I feel immensely delighted and consider it an honour to write the foreword for the *Radiobiology Textbook* edited by Prof Sarah Baatout. I went through the textbook with utter curiosity and found it irresistible to stop reading from beginning to end. Indeed, the book will prove a boon and treasure of knowledge for radiobiology researchers, physicians, clinicians, environmentalists, nuclear workers, industry professionals/managers, and radiation technology developers.

New Discoveries and Early Excitements

With the discoveries of X-ray in 1895 and radioactivity in 1898, unusual excitement was witnessed among scientists and researchers all over the world. It was commonly perceived that a new revolution had arrived in science, which might prove a panacea for every enigma. Besides researchers and academicians, the general public was highly enthusiastic and saw the emergence of new discoveries as an auspicious signal to humankind. Interestingly, physicians were quick to show the courage and enthusiasm to apply newly discovered radiation for treating cancer. That was a great medical challenge at that point in time. It was remarkable learning that X-radiation could kill living cells, including cancer cells, and had the potential to provide marked relief to cancer patients. In fact, X-radiation and radiation emitted from radioactive materials like radium became a public curiosity and an object of fun for those who wanted to have new experiences such as visualizing bones in the body and using radium lipsticks. In early years, both the scientists and common people were unaware and unmindful of the harmful effects of radiation. However, over a short span of time, it became known that radiation researchers suffered from harmful effects of radiation such as induction of cancer.

Radiobiology Was Born

It soon became apparent that understanding the mechanisms of biological effects of ionizing radiation like X-ray and gamma ray was important, and the field of radiobiology was born. Scientists also realized that setting safety standards for radiation was most urgent. Since radiation cannot be seen, tasted, or smelled, scientists began studying the interaction of radiation with matter, including radiation effects on living systems. Early studies showed that radiation could kill living cells, including tumour cells. How radiation kills living cells became the main focus of radiobiological researchers. Those who engaged themselves in radiobiology research came from diverse backgrounds, such as physics, chemistry, and biological sciences (life science, zoology, microbiology, etc.). Researchers from specific disciplines started intense investigations on physical effects (radiation physics), chemical effects (radiation chemistry), and biological effects (radiobiology) of radiation. One of the most significant contributions of radiobiological research was the discovery of the oxygen effect, which emphasized free radical production mechanisms in the radiation action on biological and chemical systems. Experiments on cellular colony formation showed that, in the presence of oxygen, more cell death occurred for the same irradiation dose.

Further radiobiological studies then laid the foundations for setting the safety standards and regulations for radiation exposure. The international radiation research community established organizations of experts, and the International Commission on Radiation Protection (ICRP) was formed in 1928 to provide recommendations and guidance about protecting humans against the risks of ionizing radiation. The United Nations Scientific Committee on Effects of Atomic radiation (UNSCEAR) was then formed in 1955 to determine the level and effects of ionizing radiation from atomic bombs and nuclear accident exposures. The same year, the US Academy of Sciences Committee on Biological Effects of Ionizing Radiation (BEIR) was established to determine and guide risks of radiation exposure on living organisms. The International Atomic Energy Agency (IAEA), created in 1957, aimed to guide and advise on safe radiation dose regulations for workers and the public.

With the intensive use of X-rays and gamma rays in medical practice, radiation has now become a household word amongst the public. In fact, medical science has acquired an extraordinary capability to diagnose and treat human diseases by radiation-based devices and protocols. Against this backdrop, the need for a comprehensive textbook was made clear by researchers and clinicians. This *Radiobiology Textbook* is designed to meet the demands of radiation and medical professionals, provides a thorough description of radiobiology, and stimulates young talents to engage in research and accept the challenges of advancing knowledge to serve humankind. More radiobiological research is needed to answer and explain several controversial issues, such as the dose-response curve, the observed differences in individual radiosensitivity, the radiation resistance of cancer cells, and many other questions. The radiation effect on somatic cells can be immediate or delayed, but radiation genetic effects are displayed only years and centuries later, something that needs to be further investigated in the future.

How Radiation Kills Living Cells/Tissues

Fundamentally, radiobiologists aim to understand the effects of radiation on cells, tissues, organs, and organisms, for animals, plants, microbial systems, and eventually humans. In this context, the discovery of DNA structure, as double-stranded helix with nucleotides as the basic units by Watson and Crick in the 1950s, propelled radiobiological studies on the mechanism of radiation-induced cell death. Radiological studies showed that radiation can kill exposed cells by damaging the DNA in the nucleus, which if not repaired prove fatal for cells. Since tumour cells divide faster than normal cells, it was hypothesized that radiation could kill these cells more efficiently. However, due to hypoxia in the tumour core, tumour cells showed resistance to radiation, leading to disappointment amongst radiation therapists. Therefore, research was undertaken to develop sensitizers of tumour cells to radiation, oxygen being the best radiosensitizer. These developments in radiobiological concepts and understanding of radiation cell killing mechanisms sustained the active research excitement in radiobiology. The medical field witnessed revolutions in caring for and treating cancer patients by using newer radiation technologies. Today, more than 40% of cancer patients are treated by radiation for therapeutic and palliative procedures. The technology consists of carefully targeting radiation beams and certain radiopharmaceuticals to destroy cancer cells while minimizing the damage to nearby healthy cells. Radiobiological studies in the 1920s helped design patient treatment protocols in what is popularly called fractionated radiotherapy.

Limitations in Radiotherapy

Radiation acts equally on normal and tumour cells. Therefore, radiation therapy of cancer patients is limited by any toxicity towards normal cells. The next goal of radiobiology was to inflict selective damage on a tumour whilst sparing normal cells. Based on radiobiological

effectiveness of different cell types to the same dose of radiation, particle radiation therapy and ion beam therapies were being developed to improve the radiotherapy for patients. In addition, the rapidly increasing applications of radiation in research, industry, medicine, biotechnology, and the environment required more intensified radiobiological studies. Today, the public's major radiation exposures arise from medical applications such as diagnostic X-rays and CT scans to diagnose diseases, and cancer radiotherapy, including treatment of injuries. Therapeutic drugs with radioactive material attached, known as radiopharmaceuticals, are also routinely used in clinics to diagnose and treat some diseases. These procedures are a valuable tool to help doctors save lives through quick and accurate diagnosis.

The Book Contents

This *Radiobiology Textbook* is a comprehensive, advanced, and up-to-date volume, carefully designed and meticulously compiled by experts and practicing radiobiologists in the field drawn from reputed universities and institutes across the world. Both the experts and contributors to each chapter have remained focused to create an outstanding book useful to young radiation researchers, mid-careerists, accomplished scientists and radiation researchers in biology, biotechnology, medicine, environment, industry, and workers in nuclear power plants. There are 12 chapters written by international specialists, followed by a thorough review from experts in the respective fields. A notable and marked feature of the book is the coverage of a wide range of relevant radiobiology topics and applications. To make learning easy and enjoyable, and to enable the basic principles and core concepts to be grasped, each chapter has been designed to provide rich and up-to-date contents together with the learning objectives, chapter summary, a few exercises, key references, and suggested future readings. It is hoped that learners find the book smooth reading and a gradual building of their knowledge repository, stimulating curiosity for a deeper insight to the subject. The book begins with a brief account of the history of radiobiology, followed by the chapter on basic concepts in radiation biology, which covers basic mechanisms of radiation damage to cellular molecules, direct and indirect effects, and low-dose radiation effects with relevance to health and environment. Chapter 3 on the molecular radiation biology describes molecular details of radiation-induced lesions in DNA, types of DNA damage and mechanisms of DNA damage repair, mis-repair, and consequences to the life of cells. The following chapter on mechanistic, modelling, and dosimetry radiation biology covers the basic principles of radiation dosimetry, micro-dosimetry, dose-response and related issues. The chapter on clinical radiation biology for clinical oncology makes it attractive reading for radiation therapists and nuclear medicine physicians but will also hopefully stimulate interest of basic researchers as well as tumour therapy professionals. The objective of treating cancer patients effectively by radiation involves understanding the radiation damage mechanisms of tumour and normal tissues and the prediction of radiation response. Going over the contents of Chap. 6 provides the required specialized knowledge on clinical radiation oncology modalities such as external and internal (brachytherapy) radiation treatments, high LET therapy, and rationale of dose fractionation. Chapter 7 describes individual radiosensitivity and biomarkers for disease and treatment outcomes in therapies. Radiobiology has a crucial role in situations of nuclear plant accidents and mass exposures expected from terrorist groups. The chapter on radiobiology of accidental, public, and occupational exposures deals with the radiation accident scenario, radiation health effects, radiation risks and bio-dosimetry aspects to provide safety to workers and general public. The chapter on environmental radiobiology is most timely and relevant, describing the mobility and distribution of radionuclides in water, air, and soil with the safety and environmental perspectives. Studies on radiation effects on non-human organisms such as plants and microbial systems to measure, assess, and monitor the impacts of radiation exposures are equally important. A most fascinating chapter in this book describes various aspects of space radiobiology, which is a futuristic and young branch of radiobiology to which bright curious minds are expected to be attracted and to engage in

radiobiological research. The last but one chapter concerns radioprotectors, radiomitigators, and radiosensitization, which are topics of practical importance to ensure human and environmental safety and strategies for protection. The last chapter covers ethical, legal, and social issues of radiation exposure, which re-defines the values of ethics in the radiation research field and addresses legal and social aspects of professional and public concern. The much-publicized negative aspects of radiation technology (radiophobia) are misconceived perceptions that need to be corrected by considering the diagnostic and therapeutic power and future promise of radiobiological research and applications. Without doubt, both radiation research professionals and curiosity-driven general readers will find the book stimulating, interesting, and informative.

Perspectives and Future Scope in Radiobiology

I must re-emphasize that with the ever-increasing applications of radiation technology in health and society, environment, industry, space research, and nuclear power, the radiobiology textbook of this high quality and with the coverage of frontline topics in the field is invaluable and highly warranted. The wide range of topics covered in this book with updated knowledge will prove a boon to researchers, policy makers, academicians, clinicians, and industry professionals. It is hoped that the book will arouse renewed interest among young students and will prove useful to beginners as well as senior researchers in radiobiological research and applications. More importantly, the book will prove a good reference and will help catapult future advances in radiation science and technology especially in the understanding of biological effects of radiation on living cells, tissues, and organs relevant to human health.

Kaushala Prasad Mishra
Radiation Biology and Health Sciences Division
Bhabha Atomic Research Center
Mumbai, India
Nehru Gram Bharti University
Prayagraj, India
Asian Association for Radiation Research
Mumbai, India

Preface

Welcome to the *Radiobiology Textbook*, which was built upon the expertise of 126 international specialists, at the forefront of various aspects of radiobiology, to bring the reader the latest and most comprehensive update in the field.

Radiobiology is the branch of biology concerned with the effect of ionizing radiation on organisms. It is also a field of clinical and basic medical science that involves the study of the health effects of radiation, and the application of biology in radiological techniques and procedures for treatment and diagnostics. Multidisciplinary radiobiological research forms the scientific basis of various disciplines such as radiation protection, radiotherapy, and nuclear medicine. The goal of radiobiological research is to understand better the effects of radiation exposure at the cellular and molecular levels in order to determine the effects on health. Therefore, radiobiology encompasses various disciplines including biology, clinical applications, pharmacy, environmental and space life sciences, which make radiobiology overall a broad and rather complex topic. Throughout this textbook, we tried to organize the information from the multifaceted fields of radiobiology to enable the reader to see the Big Picture. To accomplish this synthesis of the information, unifying themes were necessary. These themes are represented by the various chapters.

This textbook aims to provide a solid foundation to those interested in the basics and practice of radiobiology science, and its relevance to clinical applications, environmental radiation research, and space research. It is intended to be a learning resource to meet the needs of students, researchers or any citizen, with an interest in this rapidly evolving discipline who is eager to learn more about radiobiology, but it is also a teaching tool with accompanying teaching materials to help educators. This book offers a unique perspective to students and professionals, covering not only radiation biology but also radiation physics, radiation oncology, radiotherapy, radiochemistry, radiopharmacy, nuclear medicine, space radiation biology and physics, environmental radiation protection, nuclear emergency planning, radiation protection, molecular biology, bioinformatics, and DNA repair.

The Contributors

The world is a better place thanks to those people who want to help others. What makes it even better are the people who share their expertise to mentor and educate future professionals. We have invited some of the leading writers and thinkers in the field of radiobiology to provide, in this textbook, an overview of the major considerations associated with the topic of radiobiology.

This textbook is an international endeavour, which started during the worldwide COVID pandemic and gathered 126 experts from all over the world. It includes leading radiation biologists, physicists, and clinicians from all over the world. Many contributors to this textbook regularly teach this material at both national and international levels and have many years' experience of explaining, elaborating, and clarifying complex theoretical and practical concepts in their particular field of radiobiology. Each contributor has a unique expertise and set of competences related to radiobiology, always with a critical and open mind. Where needed,

they did not hesitate to address the challenges, the pitfalls, the limitations, and the beauty of the various aspects of radiobiology.

Various Chapters and Themes

The textbook is organized into chapters that can be used to support student/reader preparation in any type of educational arrangement. The chapters are intended to be complete in themselves and as such can be read independently and out of sequence.

This resource is intended to provide readers with a high-level view of the most relevant topics related to radiobiology. It is also intended to include all content a learner would need about a particular subject area within radiobiology. Furthermore, this textbook combines the best attributes of many different educational formats into one single resource that best supports the learning environment of the reader interested in the subject of radiobiology.

The textbook intends to cover all sub-disciplines involved in radiobiology. With its 12 chapters, it provides a comprehensive review of the history of radiation biology, the development of therapeutic evidence, and the basic concepts, an understanding of the molecular mechanisms induced by radiation as well as clinical, environmental, and space radiobiology. It deepens our knowledge of individual radiation sensitivity and biomarkers and gives a complete update on the use of potential radioprotectors, radiomitigators, and radiosensitizers. Finally, it discusses the legal, epistemological, ethical, and social concerns regarding radiation exposure.

A brief description of each chapter is given below:

Chapter 1, entitled "History of Radiation Biology", describes the discovery of X-rays in 1895 by Wilhelm Röntgen and of radioactivity by Pierre and Marie Curie shortly after. It details the early observations of radiation effects that promoted the early development of radiotherapy. It then presents the first evidence of radiation epidemiology and radiation carcinogenesis.

Chapter 2 (Basic Concepts of Radiation Biology) reviews basic radiation biology and associated terminology to impart a better understanding of the importance of the basic concepts of interactions of ionizing radiation with living tissue. The chapter familiarizes the reader with basic and important radiation biology concepts, the use of radioactivity and its applications, the various types of interactions of radiation with living tissue, and possible effects from that exposure. It then focuses on theoretical dose–response curves and how they are used in radiation biology, and discusses stochastic versus non-stochastic effects of radiation exposure, and what these terms mean in relation to both high- and low-dose radiation exposure. Finally, a part dedicated to targeted and non-targeted effects, as well as low-dose radiation effects, ends the chapter.

Chapter 3 concerns molecular radiation biology, which has become a powerful discipline and tool for detailed investigations into biological mechanisms of modern radiobiology. The chapter reviews the types of radiation-induced lesions in DNA, the types of DNA damage repair pathways as well as the importance of chromatin architecture in DNA damage and repair. It also describes the cytogenetic, oxidative stress and clonogenic cell survival methods, as well as the impact of radiation on cell cycle progression, cell death mechanisms, telomere shortening, and on the connectivity between cells. Finally, it highlights omic changes (genetics, lipidomics, proteomics, and metabolomics) as well as the involvement of specific pathways and the epigenetic factors modified by radiation.

In Chapter 4 (Mechanistic, Modeling, and Dosimetric Radiation Biology), the principles of radiation dosimetry are explained and the relationship of track structure to early DNA damage and the importance of microdosimetry are addressed. The chapter establishes the relation between target theory and dose-response models.

Chapters 5 (Clinical Radiobiology for Radiation Oncology) and 6 (Radiobiology of Combining Radiotherapy with Other Cancer Treatment Modalities) are both clinical chapters. Chapter 5 is dedicated to the principles of tumour radiotherapy, the therapeutic window and

therapeutic ratio, tumour growth and tumour control, and the 6Rs concept. The next part of the chapter reviews the principles of dose fractionation, whole body irradiation, and the impact of tumour hypoxia. Tumour resistance and progression, and the role of tumour microenvironments are also considered and discussed. Chapter 5 finishes with sections dedicated to normal tissue damage, response to radiotherapy, the importance of stem cells and the microbiota in radiotherapy, as well as radiomics.

Chapter 6 reviews the various conventional and alternative radiation schemes and analyses the various radiotherapy modalities in combination with other cancer treatment modalities (e.g. chemotherapy, targeted therapy, hormone therapy, and hyperthermia). Specific sections are dedicated to brachytherapy, radionuclide therapy, charged particle therapy, and the use of nanoparticles in cancer therapy.

Chapter 7 addresses individual radiation sensitivity and biomarkers. From general considerations and classification of biomarkers, it then moves on to the collection of samples for radiation studies and the existing predictive assays. It then reviews the variation of radiation sensitivity as a function of age, biological sex, and genetic syndromes. The chapter ends with a perspective on personalized medicine.

Chapter 8 provides in-depth coverage of radiobiology in accidental, public, and occupational exposures, reviewing the various radiation exposure scenarios, the long-term health effects of low-dose radiation in exposed human populations, and the problem posed by radon. A technical part of the chapter is dedicated to triage methods used after a radiation accident and to the available biodosimetry techniques.

Chapter 9 (Environmental Radiobiology) provides an overview of the behaviour and fate of radioelements in the environment. It then reviews the impact of ionizing radiation on non-human biota (plants, invertebrates, vertebrates, microorganisms) and discusses the specific case of NORM (naturally occurring radioactive materials) contamination.

Chapter 10 (Space Radiobiology) starts with a thorough review of the history of space radiation studies, followed by a description of the space radiation environment. It continues with a description of the impact of space travel on human health. It then reviews the various models (animals, plants, small organisms, microorganisms) sent to space and the biological changes induced by space radiation. It then focusses on space radiation resistance and gives a thorough description of the irradiation tests with ground-based facilities similar to the space environment.

The authors of Chapter 11 present a review of radioprotectors, radiomitigators, and radiosensitizers, as well as internal contamination by radionuclides and possible treatment. It provides an exhaustive overview of molecules and the mechanisms able to intervene in the biological effects of ionizing radiation and discusses their potential clinical use in radiotherapy or in the field of radiation protection following accidental exposure to radiation and/or nuclear emergencies.

Finally, Chapter 12 explores the ethical, social, epistemological, and legal considerations relevant to radiobiology. The chapter provides an overview of the basic principles relevant to each aspect whilst discussing contentious topics and potential future developments, along with more in-depth analysis where relevant.

Didactical and Pedagogical Approach

To write such a textbook, a strong didactical and pedagogical approach was crucial. To be effective, a textbook must be readable, challenging, and also exciting to the reader. Special care was taken to make the reader read, the teacher teach, and the student study this textbook, and to motivate and maintain their interest through the textbook. To make complex concepts or material easily understood, we provided the readers with thorough explanations, free of unnecessary terminology.

The general title *Radiobiology Textbook* illustrates the intention to provide detailed information about the entire field of radiobiology for anyone who is studying or is interested in this field. The textbook includes a table of contents in which all topics are listed with page references to enable the reader to locate topics quickly within a chapter. The standard chapter outline begins with an introduction giving a brief overview statement about what the reader can expect from the chapter and how the book can be used to teach a course. The learning objectives are intended to give a clear list of the educational scope and aims of the chapter. Before starting to read or study a chapter, the reader is encouraged to scan the introduction and learning objectives to understand the relationship of the material to be read. A set of keywords at the start of each chapter highlights the most significant words used specifically as an index to the content of the chapter.

The textbook is also enriched with high-resolution images, graphs, figures, and high-quality supporting illustrations, to make it as clear, didactical, and appealing as possible to the reader. In all figures, for which we used a consistent colour code for all chapters, particular attention was paid to aid understanding, summarizing, and visualizing of the concepts detailed in the text. Simplicity was the most important consideration in figures, to help the reader grasp and interpret clearly and quickly. The easy access to the complex ideas presented in the figures and in the text is one of the important hallmarks of this textbook. Many figures in this textbook are true pieces of art meant to teach, but also to astonish with their beauty, the different aspects covered by radiobiology. Various types of graphs (bar charts, pie charts, histograms, plots, line graphs) are also used to display quantitative relationships between variables.

Where needed, the text has been enhanced with tables to help summarize existing literature, present the results of epidemiological studies, or convey specific variables or statistical data on a particular domain. Tables have also been used as an alternative to numerical or listed data in order to make the text more readable, accessible, and understandable. In some cases, published figures, graphs, or tables have been used. Where needed, the necessary copyright permission was obtained.

In each chapter, textboxes have been added to draw the reader's attention to the section highlights, and these will be helpful to remember the most important topics covered within the chapter. These textboxes are embedded within the text narrative and summarize the content of the chapter at a glance, and enable the reader to rapidly scan and preview the content and direction of a chapter at a high concept level before beginning the detailed reading.

Abbreviations have been used with moderate frequency in the textbook. These allow concepts that would otherwise require many words, were they to be written out completely, to be communicated quickly and effectively. Each nonstandard abbreviation is defined clearly when it is first introduced in the chapter and then used consistently throughout the chapter.

The exercises and self-assessment at the end of each chapter allow the reader to evaluate and test their understanding of the chapter's material but also to apply what they have learnt. The exercises are aimed at requiring the reader to use critical thinking skills. The questions are tied directly to the concepts taught in the chapters and are meant to help the reader determine whether they have mastered the important concepts of the chapter. The questions cover important information presented in the chapter. Answers are provided for each exercise.

Recent reviews of publications in radiobiology suggest that the volume of research literature has been on the rise. Therefore, a careful analysis of the literature in the field from major databases (such as Web of Science, PubMed/Medline) was conducted ensuring highly relevant material is cited in this textbook. The list of references provided at the end of each chapter summarizes the main publications in the field addressed within each topic. Supplemental information in the section "further reading" is also included as appropriate at the end of each chapter. This is intended for readers who wish to deepen their knowledge and understanding. The "further reading" sections helps to illustrate, clarify, and apply the concepts encountered in the chapter.

An index at the end of the textbook offers the reader an informative and balanced picture of the textbook's contents, and serves as a concise and useful guide to all pertinent terms used in the textbook. These terms are presented as an alphabetically ordered list of the main entries.

The textbook is open access as a support to worldwide education. It is targeted at an international audience, but in particular at those countries facing challenges in accessing educational material. The creation of this open access resource was also intended to address one of the predominant challenges in education, namely the cost of textbooks. The most commonly required textbooks in undergraduate and graduate education remain traditional and discipline-based. In the absence of an integrated resource, students are requested to purchase and juggle preparation materials from many different discipline-based textbooks. With no fee required for readers to access or download this textbook, we hope to achieve the highest level of accessibility and to contribute to a better and more widespread knowledge of radiobiology as a discipline, as well as to facilitate efficient and focused learning by the reader.

Reviewing

This textbook has been reviewed extensively. As it contains an important amount of information, the editor and authors have taken the utmost care to ensure accuracy and minimize potential errors or omissions. Each chapter has been cross-reviewed by authors of other chapters, after which each chapter was reviewed by more than 20 external experts, all renowned in their field of competence.

We hope that each reader will feel gratified by the knowledge gathered from this textbook and that the textbook will become the radiobiologist's trusted companion.

Prof. Sarah Baatout
Institute of Nuclear Medical Applications
Belgian Nuclear Research Centre, SCK CEN
Mol, Belgium

Gent University (UGent), Ghent, Belgium

Catholic University of Leuven (KULeuven), Leuven, Belgium

United Nations Scientific Committee on the Effects of Atomic Radiation (UNSCEAR)
Vienna, Austria

The European Radiation Research Society, Brussels, Belgium

Acknowledgements

As editor, and on behalf of all the contributors, I am pleased to provide readers the required theoretical and practical tools at a time when all areas of radiobiology are expanding rapidly.

One hundred twenty-six international experts contributed to this textbook, sharing their endless expertise. Each one has contributed in significant ways and *strived to help readers learn. Each one has* provided their extraordinary insights into the complex subject of radiobiology. *They have been an inspiration and foundation for this textbook. Without their expertise, support, and dedication, this book would not exist.*

It took just more than one year to write this textbook from the day of the kick-off meeting at the height of the COVID pandemic. During this period, online meetings dedicated to each chapter were held every 3 weeks to discuss the progress of the writing of each chapter and to review the content of each chapter.

I would therefore like to express my immense gratitude upon the completion of this tremendous collaborative work and would like to thank each contributor warmly for their time, their energy but also the wonderful friendship, kindness, and teamwork that made each meeting and each part of the written text such a wonderful and constructive experience.

The figure below indicates the geographical distribution of the contributors according to their country of employment.

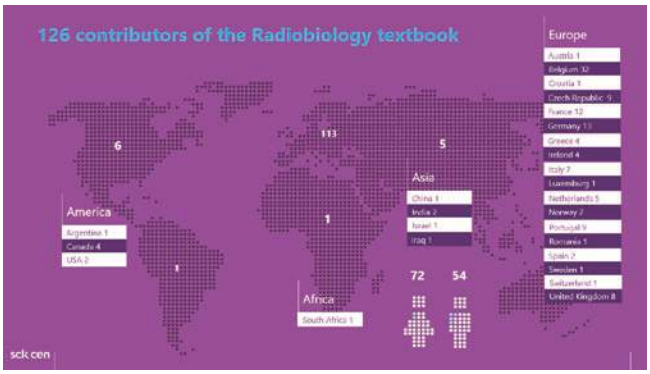

Of all the contributors, I have particularly appreciated the dedication of Dhruti Mistry (for making most of the beautiful figures of this book), Alexandra Dobney (for taking care so patiently of all the copyright permission issues), Kristina Viktorsson and Judith Reindl (for checking all issues related to plagiarism).

The contact points for each chapter (Yehoshua Socol, Ans Baeyens, Judith Reindl, Giuseppe Schettino, Peter Sminia, Vidhula Ahire, Liz Ainsbury, Christine Hellweg, Ruth Wilkins, Joana Lourenço, Alegría Montoro, and Alexandra Dobney) have played a crucial role in the coordination and the finalization of the writing of each chapter.

The list of references per chapter required special support and help from Nathalie Heynickx, Silvana Miranda, Ans Baeyens, Ruth Pereira, Anne-Sophie Wozny, Cristian Fernandez, and Kristina Viktorsson, which I would also particularly like to acknowledge.

Thank you also to Olivier Guipaud, Tom Boterberg, Bjorn Baselet, Nicholas Rajan, Abel Gonzalez, and Hussam Jassim for different aspects related to the reviewing, the coordination of specific written parts, and help with the figures or the guiding of the younger experts of the textbook.

More than 20 external reviewers willingly agreed to carefully review parts of the textbook and we would like to thank them for taking the time and effort needed to review this textbook. Their insightful recommendations and suggestions were very helpful in evaluating the quality of the writing and the relevance of each section of the textbook.

I would also like express my gratitude to SCK CEN general management, legal department, and communication department for their support throughout the process of the preparation of the textbook and for covering all the publishing costs related to this textbook in order to make it open access. A special thanks to the staff of the radiobiology unit who were extremely supportive during this endeavour.

Figures were made thanks to the use of Biorender software.

I would also like to thank the publishers and authors of the published data used in this textbook for having allowed their published figures, tables, and graphs to be used for free.

As editor, I also greatly appreciated the dedication and professionalism of the editorial and publishing staff of Springer for their wonderful support in producing this textbook, in particular that of Antonella Cerri, Saraniya Vairamuthu, Kripa Guruprasad, and Parvathy Devi Gopalakrishnan.

The final words of thanks are for my family. To my brother Akim, my father Sammy, my mother-in-law Brenda, and my father-in-law John who are no longer with us, but who were always wonderful supporters. To my Mum, Elise, teacher with a deep respect for education at all levels, for her generosity, never ending support, and kindness. To my rather wonderful husband, Andrew, a patient and uncommonly discerning critic, for his love, support, and encouragement in this adventure. To our children, Alexandra and William, for their love, kindness, unconditional support, and honesty, and for making it all worthwhile.

Prof. Sarah Baatout
Institute of Nuclear Medical Applications
Belgian Nuclear Research Centre, SCK CEN
Mol, Belgium
Gent University (UGent), Ghent, Belgium
Catholic University of Leuven (KULeuven), Leuven, Belgium
United Nations Scientific Committee on the Effects of Atomic Radiation (UNSCEAR)
Vienna, Austria
The European Radiation Research Society, Brussels, Belgium

Contents

Contributors

Ana Margarida Abrantes Institute of Biophysics, Faculty of Medicine, iCBR-CIMAGO, Center for Innovative Biomedicine and Biotechnology, University of Coimbra, Coimbra, Portugal

ESTESC-Coimbra Health School, Instituto Politécnico de Coimbra, Coimbra, Portugal

Vidhula Ahire Chengdu Anticancer Bioscience, Ltd., Chengdu, China

J. Michael Bishop Institute of Cancer Research, Chengdu, China

Niloefar Ahmadi Bidakhvidi Department of Nuclear Medicine, University Hospitals Leuven, Leuven, Belgium

Elizabeth A. Ainsbury Radiation, Chemical and Environmental Hazards Directorate, UK Health Security Agency, Oxford, UK

Carmen Arena Department of Biology, University of Naples Federico II, Naples, Italy

Omid Azimzadeh Section Radiation Biology, Federal Office for Radiation Protection, Oberschleißheim, Germany

Sarah Baatout Institute of Nuclear Medical Applications, Belgian Nuclear Research Centre, SCK CEN, Mol, Belgium

Ans Baeyens Radiobiology, Department of Human Structure and Repair, Ghent University, Ghent, Belgium

Bjorn Baselet Radiobiology Unit, Belgian Nuclear Research Centre, SCK CEN, Mol, Belgium

Kristina Beblo-Vranesevic Radiation Biology Department, Astrobiology, Institute of Aerospace Medicine, German Aerospace Center, Cologne, Germany

Maria Filomena Botelho Institute of Biophysics, Faculty of Medicine, iCBR-CIMAGO, Center for Innovative Biomedicine and Biotechnology, University of Coimbra, Coimbra, Portugal

Clinical Academic Center of Coimbra, Coimbra, Portugal

Tom Boterberg Department of Radiation Oncology, Ghent University Hospital, Ghent, Belgium

Particle Therapy Interuniversity Center Leuven, Department of Radiation Oncology, University Hospitals Leuven, Leuven, Belgium

Michel Bourguignon University of Paris Saclay (UVSQ), Paris, France

Valentina Bravatà National Research Council (IBFM-CNR), Institute of Bioimaging and Molecular Physiology, Cefalù (PA), Italy

Laboratori Nazionali del Sud, INFN-LNS, National Institute for Nuclear Physics, Catania, Italy

Marco Calvaruso National Research Council (IBFM-CNR), Institute of Bioimaging and Molecular Physiology, Cefalù (PA), Italy

Laboratori Nazionali del Sud, INFN-LNS, National Institute for Nuclear Physics, Catania, Italy

Francesco P. Cammarata National Research Council (IBFM-CNR), Institute of Bioimaging and Molecular Physiology, Cefalù (PA), Italy

Laboratori Nazionali del Sud, INFN-LNS, National Institute for Nuclear Physics, Catania, Italy

Nicol Caplin Human Spaceflight and Robotic Exploration, European Space Agency, Noordwijk, The Netherlands

Francisco Caramelo University of Coimbra, Coimbra, Portugal

Pankaj Chaudhary The Patrick G. Johnston Centre for Cancer Research, Queen's University Belfast, Belfast, United Kingdom

Vinita Chauhan Consumer and Clinical Radiation Protection Bureau, Health Canada, Ottawa, ON, Canada

Francois Chevalier UMR6252 CIMAP, Team Applications in Radiobiology with Accelerated Ions, CEA-CNRS-ENSICAEN-Université de Caen Normandie, Caen, France

Jana Cizkova Department of Radiobiology, Faculty of Military Health Sciences, University of Defence, Hradec Králové, Czech Republic

Richard Coos Laboratory of Analysis by Nuclear Reactions, University of Namur, Namur, Belgium

Noami Daems Radiobiology Unit, Belgian Nuclear Research Centre, SCK CEN, Mol, Belgium

Nicholas Dainiak Department of Therapeutic Radiology, Yale University School of Medicine, New Haven, CT, United States of America

Fabiana Da Pieve Royal Belgian Institute for Space Aeronomy, Brussels, Belgium

European Research Council Executive Agency, European Commission, Brussels, Belgium

Wendy Delbart Nuclear Medicine Department, Hôpital Universitaire de Bruxelles (H.U.B.), Brussels, Belgium

Veronica De Micco Department of Agricultural Sciences, University of Naples Federico II, Naples, Italy

Christophe M. Deroose Department of Nuclear Medicine, University Hospitals Leuven, Leuven, Belgium

Alexandra Dobney Queen Mary University of London, London, United Kingdom

Caitlin Pria Dobney Department of Physics, University of Toronto, Teddington, Canada

Marek Dostál Department of Radiology and Nuclear Medicine, Faculty of Medicine, Masaryk University and University Hospital Brno, Brno, Czech Republic

Department of Biophysics, Faculty of Medicine, Masaryk University, Brno, Czech Republic

Nina Frederike Jeppesen Edin Department of Physics, University of Oslo, Oslo, Norway

Martin Falk Department of Cell Biology and Radiobiology, Institute of Biophysics of the Czech Academy of Sciences, Brno, Czech Republic

Cristian Fernandez-Palomo Institute of Anatomy, University of Bern, Bern, Switzerland

Alžběta Filipová Department of Radiobiology, Faculty of Military Health Sciences, University of Defence, Hradec Kralove, Czech Republic

Nicolas Foray Inserm Unit 1296 "Radiation: Defense, Health, Environment", Centre Léon-Bérard, Lyon, France

Giusi I. Forte National Research Council (IBFM-CNR), Institute of Bioimaging and Molecular Physiology, Cefalù (PA), Italy

Laboratori Nazionali del Sud, INFN-LNS, National Institute for Nuclear Physics, Catania, Italy

Agnès François Radiobiology of Medical Exposure Laboratory, Institute for Radiological Protection and Nuclear Safety (IRSN), Fontenay-aux-Roses, France

Nicolaas A. P. Franken Department of Radiation Oncology, Amsterdam University Medical Centers, Location University of Amsterdam, Amsterdam, The Netherlands

Center for Experimental and Molecular Medicine (CEMM), Laboratory for Experimental Oncology and Radiobiology (LEXOR), Amsterdam, The Netherlands

Cancer Center Amsterdam, Cancer Biology and Immunology, Amsterdam, The Netherlands

Sandrine Frelon Health and Environment Division, Research Laboratory of Radionuclide Effects on Environment, Institute for Radiological Protection and Nuclear Safety (IRSN), Saint-Paul-Lez-Durance, France

Benjamin Frey Translational Radiobiology, Department of Radiation Oncology, Universitätsklinikum Erlangen, Friedrich-Alexander-Universität Erlangen-Nürnberg, Erlangen, Germany

Udo S. Gaipl Translational Radiobiology, Department of Radiation Oncology, Universitätsklinikum Erlangen, Erlangen, Germany

Lorain Geenen Radiobiology Unit, Belgian Nuclear Research Centre, SCK CEN, Mol, Belgium

Department of Radiology and Nuclear Medicine, Erasmus Medical Center, Rotterdam, The Netherlands

Mallia Geiger Radiobiology of Medical Exposure Laboratory, Institute for Radiological Protection and Nuclear Safety, Fontenay-aux-Roses, France

Alexandros G. Georgakilas DNA Damage Laboratory, Physics Department, School of Applied Mathematical and Physical Sciences, National Technical University of Athens (NTUA), Athens, Greece

Abel Julio González Argentine Nuclear Regulatory Authority, Buenos Aires, Argentina

Olivier Guipaud Radiobiology of Medical Exposure Laboratory, Institute for Radiological Protection and Nuclear Safety (IRSN), Fontenay-aux-Roses, France

Michael Hausmann Kirchhoff Institute for Physics, University Heidelberg, Heidelberg, Germany

Christine Elisabeth Hellweg Radiation Biology Department, Institute of Aerospace Medicine, German Aerospace Center, Cologne, Germany

Boris Hespeels Namur Research Institute for Life Sciences, Institute of Life-Earth-Environment, Research Unit in Environmental and Evolutionary Biology, University of Namur (UNamur-LEGE), Namur, Belgium

Anne-Catherine Heuskin Namur Research Institute for Life Sciences, Laboratory of Analysis by Nuclear Reactions, University of Namur, Namur, Belgium

Nathalie Heynickx Radiobiology Unit, Belgian Nuclear Research Centre, SCK CEN, Mol, Belgium

Department of Molecular Biotechnology, Ghent University, Ghent, Belgium

Daniela Hladik Bundesamt für Strahlenschutz, Oberschleißheim, Germany

Alistair Hunter Radiobiology Section, Department of Radiation Oncology, University of Cape Town and Groote Schuur Hospital, Cape Town, South Africa

Hussam Jassim Radiotherapy Department, General Najaf Hospital, Kufa, Najaf, Iraq

Department of Medical Physics, University Al-Hilla College, Babylon, Iraq

Karl Jordan School of Physics, Clinical and Optometric Sciences, Technological University Dublin, Dublin, Ireland

Munira Kadhim Department of Biological and Medical Sciences, Oxford Brookes University, Oxford, United Kingdom

Dimitrios Kardamakis Department of Radiation Oncology, University of Patras Medical School, Patras, Greece

Irena Koniarová Department of Radiation Protection in Radiotherapy, National Radiation Protection Institute, Prague, Czech Republic

Jessica Kronenberg Radiation Biology Department, Institute of Aerospace Medicine, German Aerospace Center, Cologne, Germany

Felicia Kruse Radiation, Chemical and Environmental Hazards Directorate, UK Health Security Agency, Oxford, United Kingdom

Hugo Levillain Medical Physics Department, Hôpital Universitaire de Bruxelles (H.U.B.), Université Libre de Bruxelles, Bruxelles, Belgium

Joana Lourenço CESAM & Department of Biology, University of Aveiro, Aveiro, Portugal

Fiona M. Lyng Center for Radiation and Environmental Science, Technological University Dublin, Dublin, Ireland

Inês Alexandra Marques Institute of Biophysics, Faculty of Medicine, iCBR-CIMAGO, Center for Innovative Biomedicine and Biotechnology, University of Coimbra, Coimbra, Portugal

Clinical Academic Center of Coimbra, Coimbra, Portugal

Aidan D. Meade School of Physics and Clinical and Optometric Sciences, Faculty of Science, Technological University Dublin, Dublin, Ireland

Sónia Mendo CESAM & Department of Biology, University of Aveiro, Aveiro, Portugal

Gaston Meskens Science and Technology Studies Unit, Belgian Nuclear Research Centre, SCK CEN, Mol, Belgium

Centre for Ethics and Value Inquiry, Ghent University, Ghent, Belgium

Anna Jelínek Michaelidesová Nuclear Physics Institute, Czech Academy of Sciences, Czech Technical University, Faculty of Nuclear Sciences and Physical Engineering, Prague, Czech Republic

Czech Academy of Sciences, Rez, Czech Republic

Mirta Milic Mutagenesis Unit, Institute for Medical Research and Occupational Health, Zagreb, Croatia

Fabien Milliat Radiobiology of Medical Exposure Laboratory, Institute for Radiological Protection and Nuclear Safety, Fontenay-aux-Roses, France

Tetyana Milojevic Space Biochemistry Group, Department of Biophysical Chemistry, University of Vienna, Vienna, Austria

Luigi Minafra National Research Council (IBFM-CNR), Institute of Bioimaging and Molecular Physiology, Cefalù (PA), Italy

Laboratori Nazionali del Sud, INFN-LNS, National Institute for Nuclear Physics, Catania, Italy

Silvana Miranda Radiobiology Unit, Belgian Nuclear Research Centre, SCK CEN, Mol, Belgium

Faculty of Bioscience and Engineering, Ghent University, Ghent, Belgium

Kaushala Prasad Mishra Radiobiology Unit, Bhabha Atomic Research Center, Mumbai, Maharashtra, India

Dhruti Mistry Radiobiology Unit, Belgian Nuclear Research Centre, SCK CEN, Mol, Belgium

Simone Moertl Department of Effects and Risks of Ionising and Non-Ionising Radiation, Federal Office for Radiation Protection, Oberschleißheim, Germany

Jade F. Monaghan Center for Radiation and Environmental Science, Technological University Dublin, Dublin, Ireland

Alegría Montoro Radiological Protection Service, University and Polytechnic La Fe Hospital of Valencia, Valencia, Spain

Laboratorio de Dosimetría Biológica, Servicio de Protección Radiológica Hospital Universitario y Politécnico la Fe, Valencia, Spain

Jayne Moquet Radiation, Chemical and Environmental Hazards Directorate, UK Health Security Agency, Oxford, United Kingdom

Victoria Moris Research Unit in Environmental and Evolutionary Biology (URBE), University of Namur (UNamur-LEGE), Namur, Belgium

Laboratory of Molecular Biology and Evolution (MBE), Department of Biology, Université Libre de Bruxelles, Brussels, Belgium

Carmel Mothersill Faculty of Science, McMaster University, Hamilton, Canada

Elena Obrador Department of Physiology, Faculty of Medicine, University of Valencia, Valencia, Spain

Arlene L. Oei Department of Radiotherapy Oncology, Amsterdam UMC, Location University of Amsterdam, Amsterdam, The Netherlands

Center for Experimental and Molecular Medicine (CEMM), Laboratory for Experimental Oncology and Radiobiology (LEXOR), Amsterdam, The Netherlands

Cancer Center Amsterdam, Cancer Biology and Immunology, Amsterdam, The Netherlands

Ursula Oestreicher Bundesamt für Strahlenschutz, Oberschleißheim, Germany

Deborah Oughton Norwegian University of Life Sciences (NMBU), Ås, Norway

Sébastien Penninckx Medical Physics Department, Hôpital Universitaire de Bruxelles (H.U.B.), Université Libre de Bruxelles, Bruxelles, Belgium

Ruth Pereira GreenUPorto—Sustainable Agrifood Production Research Centre/Inov4Agro, Department of Biology, Faculty of Science of the University of Porto, Campus de Vairão, Vila do Conde, Portugal

Tanja Perko Belgian Nuclear Research Centre, SCK CEN, Mol, Belgium

University of Antwerp, Antwerp, Belgium

Yann Perrot Institut de Radioprotection et Sûreté Nucléaire, Fontenay-aux-Roses Cedex, France

Ana Salomé Pires Institute of Biophysics, Faculty of Medicine, iCBR-CIMAGO, Center for Innovative Biomedicine and Biotechnology, University of Coimbra, Coimbra, Portugal

Clinical Academic Center of Coimbra, Coimbra, Portugal

Constantinus Politis Department of Oral and Maxillofacial Surgery, University Hospitals Leuven, Leuven, Belgium

Department of Imaging and Pathology, OMFS IMPATH Research Group, Faculty of Medicine, KU Leuven, Leuven, Belgium

Roel Quintens Radiobiology Unit, Belgian Nuclear Research Centre, SCK CEN, Mol, Belgium

Wilhelmina E. Radstake Radiobiology Unit, Belgian Nuclear Research Centre, SCK CEN, Mol, Belgium

Faculty of Bioscience and Engineering, Ghent University, Ghent, Belgium

Nicholas Rajan Radiobiology Unit, Belgian Nuclear Research Centre, SCK CEN, Mol, Belgium

Raghda Ramadan Radiobiology Unit, Belgian Nuclear Research Centre, SCK CEN, Mol, Belgium

Emil Rehnberg Radiobiology Unit, Belgian Nuclear Research Centre, SCK CEN, Mol, Belgium

Department of Molecular Biotechnology, Ghent University, Ghent, Belgium

Judith Reindl Section Biomedical Radiation Physics, Institute for Applied Physics and Measurement Technology, Department for Aerospace Engineering, Universität der Bundeswehr München, Neubiberg, Germany

Petra Rettberg Radiation Biology Department, Astrobiology, Institute of Aerospace Medicine, German Aerospace Center, Cologne, Germany

Franz Rödel Department of Radiotherapy and Oncology, Goethe University, Frankfurt am Main, Germany

Peter Rogan Departments of Biochemistry and Oncology, Schulich School of Medicine and Dentistry, University of Western Ontario, London, ON, Canada

Frances Romain University of Manchester, Manchester, United Kingdom

Diana Savu Department of Life and Environmental Physics, Horia Hulubei National Institute of Physics and Nuclear Engineering, Magurele, Romania

Giuseppe Schettino National Physical Laboratory, Teddington, United Kingdom

University of Surrey, Guilford, United Kingdom

Vinodh Kumar Selvaraj Department of Radiation Oncology, Thanjavur Medical College, Thanjavur, India

Alexandra Sémont Radiobiology of Medical Exposure Laboratory, Institute for Radiological Protection and Nuclear Safety, Fontenay-aux-Roses, France

Peter Sminia Department of Radiation Oncology, Amsterdam University Medical Centers, Location Vrije Universiteit/Cancer Center Amsterdam, Amsterdam, The Netherlands

Yehoshua Socol Jerusalem College of Technology, Jerusalem, Israel

Kevin Tabury Radiobiology Unit, Belgian Nuclear Research Centre, SCK CEN, Mol, Belgium

Department of Biomedical Engineering, University of South Carolina, Columbia, SC, USA

Georgia I. Terzoudi Health Physics, Radiobiology and Cytogenetics Laboratory, Institute of Nuclear and Radiological Sciences and Technology, Energy and Safety, National Centre for Scientific Research "Demokritos", Athens, Greece

Ales Tichy Department of Radiobiology, Faculty of Military Health Sciences, University of Defence, Hradec Králové, Czech Republic

Sotiria Triantopoulou Health Physics, Radiobiology and Cytogenetics Laboratory, Institute of Nuclear and Radiological Sciences and Technology, Energy and Safety, National Centre for Scientific Research "Demokritos", Athens, Greece

Vlastimil Válek Department of Radiology and Nuclear Medicine, Faculty of Medicine, Masaryk University and University Hospital Brno, Brno, Czech Republic

Karine Van Doninck Research Unit in Environmental and Evolutionary Biology (URBE), University of Namur (UNamur-LEGE), Namur, Belgium

Université Libre de Bruxelles, Molecular Biology and Evolution, Brussels, Belgium

Margot Vanheukelom Biosphere Impact Studies, Belgian Nuclear Research Centre, SCK CEN, Mol, Belgium

Olivier Van Hoey Research in Dosimetric Applications Unit, Belgian Nuclear Research Centre, SCK CEN, Mol, Belgium

Koen Vermeulen Institute of Nuclear Medical Applications, Belgian Nuclear Research Centre, SCK CEN, Mol, Belgium

Kristina Viktorsson Department of Oncology/Pathology, Karolinska Institutet, Solna, Sweden

Carmen Villagrasa Institut de Radioprotection et Sûreté Nucléaire, Fontenay-aux-Roses Cedex, France

Guillaume Vogin Centre Francois Baclesse, University of Luxembourg and Luxembourg Institute of Health, Luxembourg, Luxembourg

Centre François Baclesse, National Radiotherapy Center of Luxembourg, Esch-sur-Alzette, Luxembourg

Anthony Waked Radiobiology Unit, Belgian Nuclear Research Centre, SCK CEN, Mol, Belgium

Laboratory of Nervous System Disorders and Therapy, GIGA Neurosciences, Université de Liège, Liège, Belgium

Ruth Wilkins Environmental and Radiation Health Sciences Directorate, Health Canada, Ottawa, ON, Canada

Tim Wils KU Leuven, Leuven, Belgium

Anne-Sophie Wozny Cellular and Molecular Radiobiology Lab, UMR CNRS 5822, Lyon 1 University, Oullins, France

Department of Biochemistry and Molecular Biology, Lyon-Sud Hospital, Hospices Civils de Lyon, Pierre-Bénite, France

Reviewers

Gersande Alphonse Laboratoire de radiobiologie Cellulaire et Moléculaire, Faculté de médecine Lyon-Sud, IP2I CNRS UMR 5822, Oullins, France

Adayabalam Balajee Oak Ridge Associated Universities, Oak Ridge, TN, United States of America

Marc Benderitter Department of Research in Radiobiology and Regenerative Medicine, Institut de radioprotection et de sûreté nucléaire (IRSN), Fontenay-aux-Roses, France

Virginie Chapon Aix Marseille Université, CEA, CNRS, BIAM, Saint Paul-Lez-Durance, France

Eric Deutsch Radiotherapy Department, Gustave Roussy Institute, Paris, France

Nicolaas A. P. Franken Amsterdam Medical Center, Amsterdam, The Netherlands

Anna Friedl Department of Radiation Oncology, LMU University Hospital Munich, Munich, Germany

Almudena Real Gallego Radiation Protection of the Public and the Environment Unit, CIEMAT, Madrid, Spain

Stephanie Girst Institute of Applied Physics and Metrology, Department of Aerospace Engineering, Universität der Bundeswehr München, Neubiberg, Germany

Eric Grégoire Institut de radioprotection et de sûreté nucléaire (IRSN), Fontenay-aux-Roses, France

Makoto Hosono Department of Radiology, Kindai University Faculty of Medicine, Osaka-Sayama, Osaka, Japan

Nagraj G. Huilgol Nanavati Hospital, Mumbai, India

Marek Janiak Dept. of Radiobiology and Radiation Protection, Military Institute of Hygiene and Epidemiology, Warsaw, Poland

Wook Kang Keon Department of Nuclear Medicine, Seoul National University College of Medicine, Seoul, South Korea

Laure Marignol Radiobiology, Discipline of Radiation Therapy, School of Medicine, Trinity College, Dublin, Ireland

Kaushala Prasad Mishra Radiation Biology and Health Sciences Division, Bhabha Atomic Research Center, Mumbai, India

Nehru Gram Bharti University, Prayagraj, India

Asian Association for Radiation Research, Mumbai, India

Judith Reindl Institute of Applied Physics and Metrology, Department of Aerospace Engineering, Universität der Bundeswehr München, Neubiberg, Germany

Vassiliki Rizomilioti University of Patras, Patras, Greece

Viacheslav Soyfer Tel Aviv Sourasky Medical Center, Ichilov Hospital, Tel Aviv, Israel

Simon Stuttaford Castletown Law, Edinburgh, Scotland, United Kingdom

Walter Tinganelli Clinical Radiobiology Group, Biophysics Department, GSI Helmholtzzentrum für Schwerionenforschung GmbH, Darmstadt, Germany

Nathalie Vanhoudt Unit for Biosphere Impact Studies, SCK CEN, Belgian Nuclear Research Centre, Mol, Belgium

Moshe Yanovskiy Jerusalem College of Technology, Jerusalem, Israel

History of Radiation Biology

1

Dimitrios Kardamakis, Sarah Baatout,
Michel Bourguignon, Nicolas Foray, and Yehoshua Socol

Nothing in life is to be feared, it is only to be understood. Now is the time to understand more, so that we may fear less.

—Marie Curie.

Learning Objectives

- To learn about the lives and scientific achievements of the pioneers in radiation
- To understand the logic behind the applications of ionizing radiation in modern times
- To understand the progression of the scientific knowledge of the physiological and biological effects of ionizing radiation

1.1 Introduction

In November 1895, Wilhelm Conrad Roentgen discovered X-rays; in March 1896, Henri Becquerel discovered natural radioactivity; and in December 1898, Marie and Pierre Curie produced polonium and later radium.

Almost immediately after these discoveries, radiation biology, defined as the study of the effects in biological systems of exposure to radiation, began (Fig. 1.1).

A plethora of clinical observations, initially on the skin, contributed to a better knowledge of the biological effects of ionizing radiation. The first molecular and cellular mechanistic models of the radiation action were proposed in the 1930s and 1940s and then after the discovery of the DNA structure in the 1950s. It is noteworthy that the first theories unifying molecular and cellular features of irradiated human cells emerged in the 1980s during which the first quantitative features of human radiosensitivity were pointed out [1–4].

These great discoveries at the turn of the twentieth century initiated a new era in human history. Especially, medicine has greatly profited from their applications in diagnosis and treatment of various diseases, revolutionizing our understanding of diseases. The discoveries had a vast impact on society in general and on healthcare in particular.

In this chapter, we present the main landmarks in the history of X-rays and, more generally, of ionizing radiation. Brief biographies of the pioneers in this field are presented in a chronological description of the whole field and emphasis is placed on the continuity in the development of the application of ionizing radiation to human life.

D. Kardamakis
Department of Radiation Oncology, University of Patras Medical School, Patras, Greece
e-mail: kardim@upatras.gr

S. Baatout
Institute of Nuclear Medical Applications, Belgian Nuclear Research Centre, SCK CEN, Mol, Belgium
e-mail: sarah.baatout@sckcen.be

M. Bourguignon
University of Paris Saclay (UVSQ), Paris, France

N. Foray
Inserm Unit 1296 "Radiation: Defense, Health, Environment", Centre Léon-Bérard, Lyon, France
e-mail: nicolas.foray@inserm.fr

Y. Socol (✉)
Jerusalem College of Technology, Jerusalem, Israel
e-mail: socol@g.jct.ac.il

S. Baatout (ed.), *Radiobiology Textbook*, https://doi.org/10.1007/978-3-031-18810-7_1

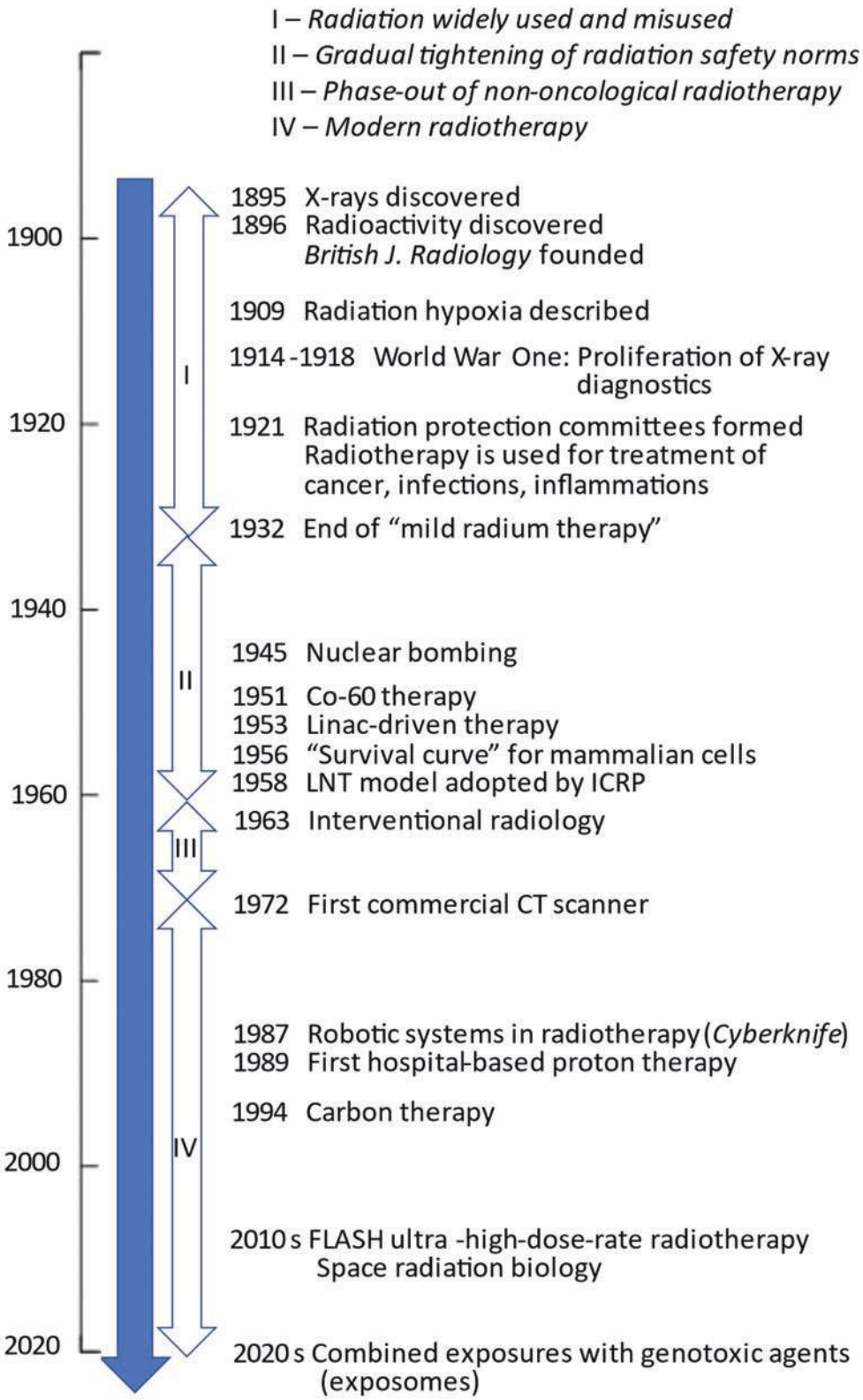

Fig. 1.1 Milestones of radiation biology

1.2 Early Observations of Radiation Effects

1.2.1 The Discovery of X-Rays and Radioactivity

By the end of the nineteenth century, "Newtonian" physics had explained nearly all the phenomena involving mass, speed, electricity, and heat. However, some questions remained unanswered, notably the origin of the luminescence phenomena observed either in glass vacuum tubes subjected to a high voltage (e.g., the Crookes tubes—Fig. 1.2) or on certain ores [4]. In both cases, one of the major questions was their inducibility vis-à-vis the sunlight. The German physicist Wilhelm Conrad Roentgen addressed the first challenge by putting some opaque boxes on the Crookes tube, while the Frenchman Henri Becquerel focused on the second one by studying light emitted by uranium ores in the darkness. The two series of experiments became legendary and led to two Nobel prizes in physics [4].

In November 1895, Wilhelm Conrad Röntgen (Roentgen) (1845–1923) detected electromagnetic radiation of a sub-nanometer wavelength range, today known as X- or Roentgen rays. For this discovery, he was awarded the first Nobel Prize in Physics in 1901. Although he investigated these X-rays and learned much about their interactions with matter, for a long time, he was not entirely convinced that he had made a real discovery [5] (Box 1.1).

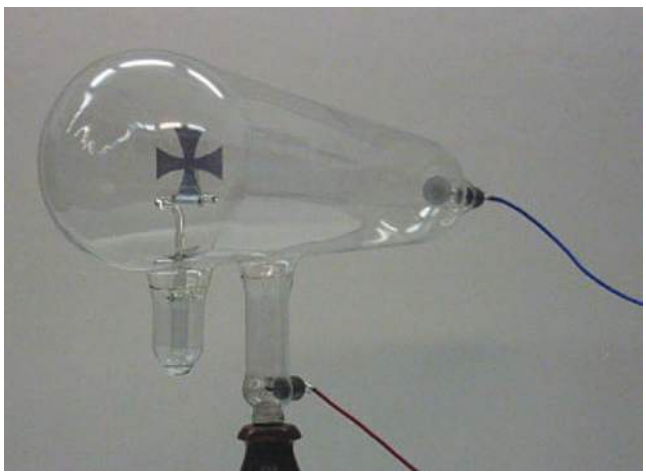

Fig. 1.2 Crookes, or cathode ray, tube. (Source: Wikimedia. Reproduced with permission)

Box 1.1 Wilhelm Conrad Röntgen

- Wilhelm Conrad Röntgen (1845–1923) experimented with Crookes tubes and in November 1895 detected electromagnetic radiation of a sub-nanometer wavelength range (X-rays).
- He earned the first Nobel Prize in Physics in 1901.

Roentgen was born in Lennep, Rhineland, Germany [6]. When he was 3 years old, his family moved to the Netherlands. He was an average student in the primary and secondary school, and in November 1865, he enrolled in the polytechnical school of Zurich, graduating as a mechanical engineer in 1868. After that, Roentgen remained at the University of Zurich as a postgraduate student in mathematics having August Kundt, an expert in the theory of light, as a mentor. Roentgen's first experiments in Zurich concerned the properties of gases and proved to be important for his subsequent discoveries. His doctoral thesis "Studies on Gases" led to his being awarded a PhD degree in 1869 and being appointed as an assistant to Kundt. In 1870, Roentgen, following Kundt, returned to Germany to the University of Wurzburg (Bavaria). In the autumn of 1893, he was elected Rector at the University of Wurzburg, having 44 publications and being highly respected by his colleagues and the larger academic community. Richard I. Frankel gives an excellent description of the life of W. C. Roentgen as a scientist and describes in detail the events leading up to his groundbreaking discovery.

On November 8, 1895, after experimenting with cathode rays produced in tubes developed by Johann Hittorf and William Crookes, Roentgen made his discovery. He repeated and expanded his work and gave the first description of the physical and chemical properties of X-rays. He demonstrated that these rays could penetrate not only glass and air but also other materials, including various metals. However, a thin sheet of lead completely blocked them. Roentgen inferred that the radiation he observed was in fact rays because it traveled in straight lines and created shadows of the type that would be created by rays (Fig. 1.3). While studying the ability of lead to stop the rays, Roentgen held a small piece of this metal between his thumb and index finger and placed it

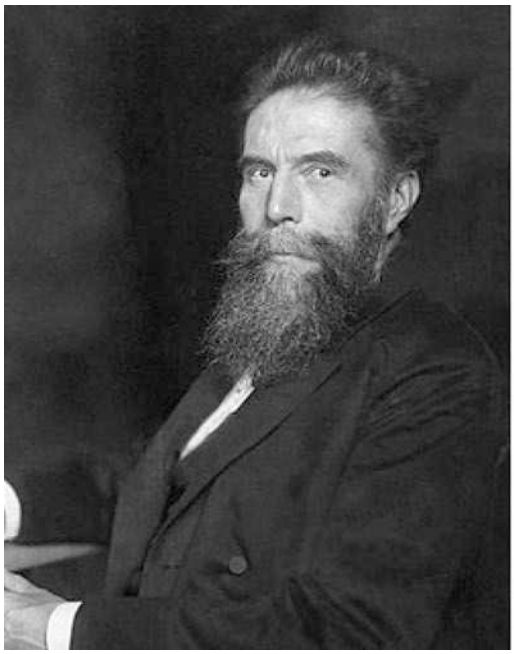

Fig. 1.3 Left: Wilhelm Conrad Röntgen (1845–1923), a portrait by Nicola Perscheid, circa 1915. Right: The first roentgenogram—the hand of Röntgen's wife after its irradiation with X-rays (Dec 22, 1895)

in the path of the rays. He noted that he could distinguish the outline of the two digits on the screen and that the bones appeared as shadows darker than the surrounding soft tissue. Roentgen continued his work over the next weeks, during which he made additional images and showed that the rays darkened a photographic plate. In his manuscript entitled "Uber eine neue Art von Strahlen" ("On a New Kind of Rays") submitted to the Physikalisch-Medizinische Gesellschaft in Wurzburg on December 28, 1895, he used the term "X-rays" for the first time [5].

Roentgen did not leave any autobiography, so all information regarding people and events which had an influence on his work comes from his biographers. Scientists whose work had greatly influenced Roentgen were the physicist August Kundt (1839–1894), the physicist and mathematician Rudolf Clausius (1822–1888), and the physicist and physician Hermann Ludwig Ferdinand von Helmholtz (1821–1894), all three of German origin. Of importance is his lifelong friendship with the physicist Ludwig Zehnder who served as Roentgen's chief assistant and became an occasional co-author.

It is worth mentioning the relationship between Roentgen and his contemporary German experimental physicist Philipp Lenard (1862–1947), director of the Physical Institute at Heidelberg University. Lenard (Fig. 1.4) first published the results of his experiments on cathode rays in 1894 and was awarded for this the Nobel Prize in Physics in 1905. Prior to Roentgen's discovery, the two scientists exchanged several letters regarding the aspects of the cathode ray research, and Roentgen referenced Lenard in his initial publications on

Fig. 1.4 Philipp Eduard Anton von Lenard (1862–1947)

X-rays and used Lenard's modified tube for his experiments (Box 1.2).

Box 1.2 Philipp Lenard

- Philipp Lenard (1862–1947) was awarded the Nobel Prize in Physics in 1905 for "his work on cathode rays."
- However, Lenard became extremely embittered by not winning the Prize in 1901. He became one of Adolf Hitler's most ardent supporters, eventually becoming "Chief of Aryan Physics" under the Nazi regime.
- After World War II, he was not sentenced (for his prominent role in the Nazi regime) only due to his old age.

However, when Roentgen alone was awarded the Nobel Prize in 1901 "in recognition of the extraordinary services he has rendered by the discovery of the remarkable rays subsequently named after him," Lenard became extremely embittered, and for the rest of his life, he insisted that he had shown Roentgen the way to his discovery. Lenard became one of the early adherents of the National Socialism and one of Adolf Hitler's most ardent supporters, eventually becoming "Chief of Aryan Physics" under the Nazi regime. In 1933, he published a book called "Great Men in Science" in which he failed to mention not only Jews, such as Einstein or Bohr, but also non-Aryans like Marie Skłodowska-Curie and even Roentgen. When World War II ended, Lenard's prominent role in the Nazi regime led to his arrest, but due to his old age, instead of being sentenced to prison, he was sent to live in a small German village, where he died at the age of 83 [7, 8].

A few months after the discovery of X-rays, radioactivity was described. Antoine-Henri Becquerel (1852–1908) (Fig. 1.5) was a member of a distinguished family of four generations of physicists, all being members of the French Académie des Sciences. Becquerel's initial research was in phosphorescence, the emission of light of one color following a body's exposure to the light of another color. In early 1896, following Röntgen's discovery, Becquerel "began looking for a connection between the phosphorescence he had already been investigating and the newly discovered X-rays" [9] and initially thought that phosphorescent materials, such as some uranium salts, might emit penetrating X-ray-like radiation, but only when illuminated by bright sunlight. By May 1896, after a series of experiments with non-phosphorescent uranium salts, he correctly concluded that the penetrating radiation came from the uranium itself, even without any external excitation. The intensive study of this phenomenon led Becquerel to publish seven papers in 1896 only. Becquerel's other experiments allowed him to figure out what happened when the "emissions" entered a magnetic field: "When different radioactive substances were put in the magnetic field, they deflected in different directions or not at all, showing that there were three classes of radioactivity: negative, positive, and electrically neutral" [10] (Box 1.3).

Box 1.3 Henri Becquerel

- Henri Becquerel (1852–1908) discovered radioactivity in 1896 while studying phosphorescent uranium salts.
- Later in the same year, upon experimenting with non-phosphorescent uranium salts, he concluded that the penetrating radiation came from the uranium itself.
- He was awarded the Nobel Prize in Physics in 1903.

Interestingly, radioactivity could have been discovered nearly four decades earlier. In 1857, the photographic investor Abel Niépce de Saint-Victor (1805–1870) observed that uranium salts emitted radiation that darkened photographic emulsions. Later in 1861, he realized that uranium salts produced invisible radiation. In 1868, Becquerel's father

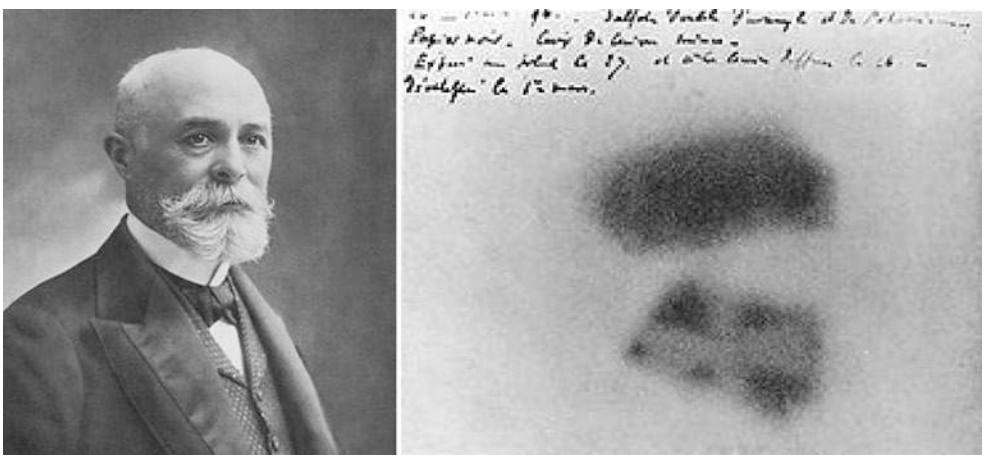

Fig. 1.5 Left: Henri Becquerel (1852–1908), circa 1905. Right: Becquerel's photographic plate exposed to a uranium salt

Edmond published a book entitled "La lumière: ses causes et ses effets (Light: Its causes and its effects)," where he mentioned that Niépce de Saint-Victor had observed that some phosphorescent objects could expose photographic plates even when unexposed to sunlight. It is known that "gamma rays" emitted from radioactive materials were first observed in 1900 by the French chemist and physicist Paul Ulrich Villard (1860–1934). Villard investigated radiation from radium salts impinging onto a photographic plate from a shielded container through a narrow aperture. He used a thin layer of lead that was already known as alpha-absorber [11]. He was able to show that the remaining radiation consisted of a second and third type of rays. The second type was deflected by a magnetic field similar to the known "canal rays" and could be identified with beta rays described by Ernest Rutherford. The third type, however, was very penetrating and had never been identified before [12]. Being a modest man, he did not suggest a specific name for the type of radiation he had discovered, and in 1903, it was Rutherford who proposed that Villard's rays should be called gamma rays [13].

It is of great importance to read the following notes written by Becquerel on 2 March 1896: "I will insist particularly upon the following fact, which seems to me quite important and beyond the phenomena which one could expect to observe: The same crystalline crusts (of potassium uranyl sulfate), arranged the same way with respect to the photographic plates, in the same conditions and through the same screens, but sheltered from the excitation of incident rays and kept in darkness, still produce the same photographic images. Here is how I was led to make this observation: among the preceding experiments, some had been prepared on Wednesday the 26th and Thursday the 27th of February, and since the sun was out only intermittently on these days, I kept the apparatuses prepared and returned the cases to the darkness of a bureau drawer, leaving in place the crusts of the uranium salt. Since the sun did not come out in the following days, I developed the photographic plates on the 1st of March, expecting to find the images very weak. Instead, the silhouettes appeared with great intensity …" Becquerel used an apparatus to show that the radiation he discovered was different from X-rays in the way that the new radiation emitted by radioactive materials was bent by the magnetic field so that the radiation was charged. When different radioactive substances were put in the magnetic field, their radiation was either not deflected or deflected in different directions. Becquerel discovered therefore three classes of radioactivity emitting negative, positive, and electrically neutral particles [14].

A story like that of "Roentgen and Lenard" has developed between "Becquerel and Thompson." In London, Professor of Physics Silvanus Thompson (1851–1916), the founding President of the Roentgen Society, had been experimenting with uranium nitrate and at the end of January 1896 (a few weeks before Becquerel) found that when the uranium salt was exposed to sunlight while placed on a shielded photographic plate, film blackening appeared beneath the uranium. Thompson delayed writing a communication to the Royal Society and so he lost the paternity of radioactivity!

Becquerel was awarded the 1903 Nobel Prize for Physics jointly with Pierre Curie (1859–1906) and Marie Curie (1867–1934) "in recognition of the extraordinary services he has rendered by his discovery of spontaneous radioactivity." He received one-half of the Prize with the Curies receiving the other half [15].

The physicist Ernest Rutherford (1871–1937) is often credited as the father of nuclear physics. In his early work, he developed the concept of radioactive materials' half-life; discovered the radioactive element radon; named the radiation types alpha, beta, and gamma; and classified them by their ability to penetrate different materials. The abovementioned experiments were performed at McGill University in Montreal, Quebec, Canada (Fig. 1.6). In 1903, Rutherford and Frederick Soddy published the "Law of Radioactive Change" to account for all their experiments with radioactive materials.

Though the Curies had already suggested that radioactivity was an intra-atomic phenomenon, the idea of the atoms of radioactive substances breaking up was principally new. Until then, atoms had even been assumed to be indivisible (Greek: a-tom), and it was Rutherford and Soddy who demonstrated that radioactivity involved spontaneous disintegration of "radioactive" atoms into other elements. The results of this work provided the basis for the Nobel Prize in Chemistry awarded to Rutherford in 1908 "for his investigations into the disintegration of the elements, and the chemistry of radioactive substances" [16] (Box 1.4).

Box 1.4 Ernest Rutherford

- Ernest Rutherford (1871–1937) is known as the father of nuclear physics. He was the first to suggest the existence of nuclei.
- He developed the idea that radioactivity involved spontaneous disintegration of atoms.
- In 1908, he was awarded the Nobel Prize in Chemistry "for his investigations into the disintegration of the elements, and the chemistry of radioactive substances."

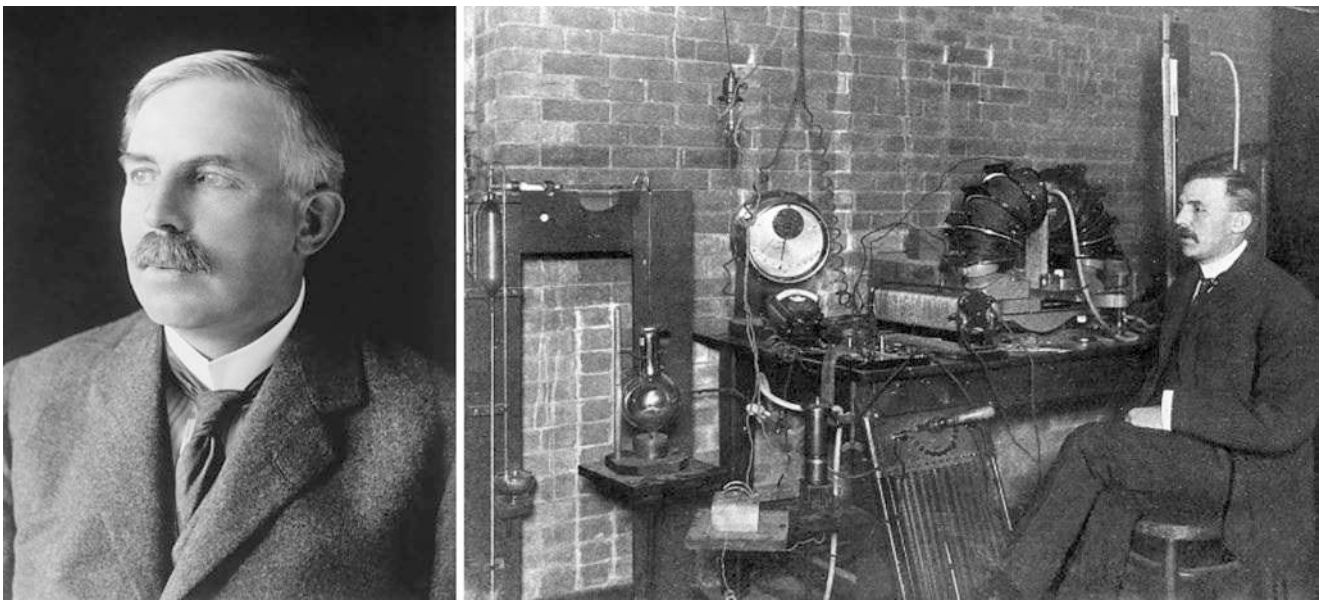

Fig. 1.6 Left: Ernest Rutherford (1871–1937). Right: Rutherford in his laboratory at McGill University (Canada), 1905. (Reproduced with permission)

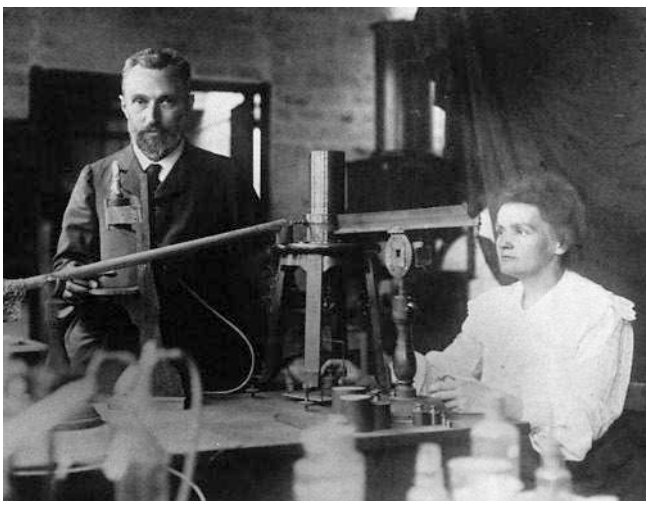

Fig. 1.7 Marie and Pierre Curie in their Laboratory, circa 1904

Pierre Curie (1859–1906) was a French physicist and a pioneer in crystallography and radioactivity. In 1900, he became Professor at the Faculty of Sciences, University of Paris, and in 1903, he received the Nobel Prize in Physics together with his wife Marie (Fig. 1.7), which they shared with Henri Becquerel. Notably, Marie had been Pierre's assistant at the City of Paris Industrial Physics and Chemistry Higher Educational Institution (ESPCI Paris).

The term "radioactivity" was coined by Marie Curie, who together with her husband Pierre extracted uranium from pitchblende (uraninite). To their surprise, the left-over ore was more radioactive than pure uranium, and they assumed that other radioactive elements were present in the ore, a hypothesis which resulted in the discovery of the new elements, polonium and radium. However, 4 years of processing tons of the uranium ore had to pass before they isolated enough polonium and radium to determine their chemical properties. It should be noted that one ton of pitchblende contains only about 0.15 g of radium.

Pierre Curie and his student Albert Laborde discovered nuclear energy by identifying the continuous emission of heat from radium particles. Incidentally, as early as 1913, H. G. Wells coined the term "atomic bomb"—a bomb of unprecedented power based on the use of nuclear energy—appearing in his novel "The World Set Free." It should be mentioned, however, that "his" atomic bomb had nearly nothing in common with the actual atomic bomb created three decades later.

The *curie* (Ci) became the unit of radioactivity, originally named as such by the Radiology Congress in 1910, clearly in honor of Pierre Curie. Corresponding to the activity of about 1 g of radium, the Ci is not a SI unit, and in 1964, it was formally replaced by the *becquerel* (Bq, this time to honor

Henri Becquerel), a SI unit which corresponds to one disintegration per second (Box 1.5).

Box 1.5 Pierre and Marie Curie

- Pierre Curie (1859–1906) and his wife Marie Salomea Skłodowska-Curie (1867–1934) discovered the elements radium and polonium.
- The term "radioactivity" was coined by Marie Curie.
- Pierre Curie discovered nuclear energy by identifying the continuous emission of heat from radium particles.
- In 1903, Pierre and Marie Curie were awarded the Nobel Prize in Physics (together with H. Becquerel) for the discovery of radioactivity.
- In 1913, H. G. Wells coined the term "atomic bomb" mentioned in his novel "The World Set Free."

Marie Salomea Skłodowska-Curie, also known as Madame Curie (1867–1934), was a Polish physicist and chemist. She was the first woman to win the Nobel Prize (1903) and the first person to win it twice (1911) in two different scientific fields (physics and chemistry).

In July 1898, Pierre and Marie Curie published a joint paper announcing the existence of a new element they named "polonium," and in December of the same year, they proclaimed the existence of another element, "radium." Between 1898 and 1902, the Curies published a total of 32 scientific papers including one on the radiobiological effects of "radium rays" on normal and tumor cells [17]. Noteworthy, Mr. and Mrs. Curie did not patent their discoveries and benefited little from the increasingly profitable application of radium for the therapy of various ailments.

During World War I, the radiologist Antoine Béclère persuaded Marie Curie to use X-rays for the diagnosis of wounded soldiers on the front lines. She gave her full support to this project and, using her authority as a Nobel Prize winner, organized the Mobile Radiology Units (Fig. 1.8), 20 of which were installed in the first year of the war. She also designed needles containing "radium emanation" to be used for sterilizing infected tissues.

The half-life of radium 226 is 1600 years, which is very much shorter than that of uranium (4.5×10^9 years), so radiation of the former is much more intense. Hence, for the study of radioactivity, radium was much more convenient than the very weakly radioactive uranium. The rays emitted by radium proved also to be an excellent tool for exploring the microscopic structure of matter; radium became to be used for this purpose already at the end of 1901 (Box 1.6).

Fig. 1.8 Marie Curie in a mobile military X-ray unit during the Great War (WWI), circa 1915

Box 1.6 Maria Salomea Skłodowska-Curie

- Marie Salomea Skłodowska-Curie (1867–1934) was the first woman to win a Nobel Prize (1903 in physics) and the first person to win the Nobel Prize twice (1911 in chemistry).
- During the Great War (WWI), she focused on the use of radiation to diagnose wounded soldiers. She developed and organized mobile X-ray units, 20 of which she installed in the first year of the war.

While uranium was the first radioactive element to be discovered, radium was much more popular, as it was a spontaneously luminous material that emitted an incredible quantity of radiation. The popularity of radium is shown in a novel by Maurice Leblanc, "The Island of Thirty Coffins," published in 1919 where a central role is played by a stone "shivering with radium, from where goes steadily a bombardment of invigorating and miraculous atoms."

The research that led to the discovery of radium in 1898 was performed despite considerable difficulties, including inadequate lab and lack of funding. However, Pierre Curie managed to get uranium ore from Bohemia, which at the time belonged to Austria. The help of the Austrian Government, which gave one ton of pitchblende, as well as the help of the chairman of the Austrian Academy of Sciences, was gratefully acknowledged in a letter by Marie Curie, who wrote: "The preparation of radium has been very expensive. We thank the Académie des sciences [...]." After 2 years, however, the Curies became famous, and the situation had improved considerably.

The collaboration between Pierre and Marie Curie is exemplary in many ways. These two people really complemented each other, as Pierre was dreamy and imaginative, ready to undertake various difficult projects, and Marie was full of energy pursuing her goals. Sadly, Marie Curie died at the Sancellemoz Sanatorium in Passy (Haute-Savoie), France, of aplastic anemia, presumably from exposure to radiation during her scientific research, compounded by her exposure to X-rays in the field radiology units during World War I.

Immediately after the discovery of radium and polonium by Marie and Pierre Curie, the latter examined the possibility to use radium as a powerful therapeutic tool [18, 19]. First successful results were obtained in patients with lupus vulgaris, a form of tuberculosis of the skin. For patients with lesions situated in deeper organs, radium salts were used. In 1904, John MacLeod at Charing Cross Hospital designed one of the first glass radium applicators to treat throat cancer [20], and in 1917, Benjamin Barringer used needles containing radium salts for treating prostate cancer [21]. After World War I, a number of technological devices were proposed to treat a wide spectrum of tumors. This therapeutic approach was initially called curietherapy in Europe and brachytherapy in the USA [22].

Along with the first medical applications of X-rays or radium, the first radiation-induced tissue reactions were also observed. In the first decade of the nineteenth century, three major applications of X-rays were developed, namely radiography and radiotherapy, mainly against skin diseases such as lupus rather than cancers, as well as radiation-induced hair removal. From a number of these applications, numerous adverse tissue reactions directly due to radiation have been described. In this period, the term "radiodermatitis" was proposed [2]. In 1906, the participants of a Congress of Radiologists organized in Lyon (France) concluded that some patients may show some unexpected skin reactions probably due to radiation [23]. In 1911, the radiologist Léon Bouchacourt, based on the results of the application of radiation treatment for hypertrichosis to a couple of young people, published a paper with a premonitory title: "About the sensitivity to Roentgen Rays of the skin of different individuals and, for a given individual, of the different part of the body" [24, 25]. In this paper, Bouchacourt suggested not only that each individual may show a specific sensitivity to radiation but also that some tissues/organs may be characterized by a specific response to radiation [2]. It is clear that the radiation-induced adverse tissue reactions were documented very early and that the notion of individual radiosensitivity is an old concept [25].

1.2.2 Recognition of the Acute Injury

The toxicity of X-rays became apparent soon after their discovery by Roentgen (Fig. 1.9). Hair loss has been recognized by May 1896, and skin toxicity was noted a few months later. Early X-ray images required exposures of as long as 80 min, and thus early X-ray workers were among the most severely affected. Dr. Hall-Edwards, the British physician responsible for the first clinical X-ray "photograph" in England in early 1896, developed cancer of the hands from radiation exposure incurred while holding patients' extremities on photographic plates. In 1896, a commercial demonstrator at Bloomingdale Brothers store in New York, whose X-ray machine ran con-

Fig. 1.9 Radiation injury. (Sources: left—Finzi [26], right) https://wellcomecollection.org/works/g94c5mtb

tinuously for 2–3 h a day, reported the development of dry skin, followed by changes like a strong sunburn and later scaliness of the skin. He also noted the cessation of fingernail growth and loss of hair from the involved portions of the skin (Box 1.7).

Box 1.7 Radiation Poisoning

- Acute radiation effects (radiodermatitis. etc.) were observed almost immediately after the discovery of ionizing radiation.
- In spite of this, the so-called mild radium therapy was extensively misused.

By chance, Roentgen had conducted virtually all his experiments in a zinc box, which gave better definition of the X-ray beam. He had also added a lead plate to the zinc and thus, fortuitously, protected himself from the radiation that he discovered [5]. In 1902, Guido Holzknecht (1872–1931) devised a color dosimeter ("chromoradiometer") based on the discoloration of crystals after exposing them to X-rays. Holzknecht, like a number of other physicians in the early days of radiology, died from the consequences of radiation "poisoning," and his name is displayed on the Monument in honor of the X-ray and Radium Martyrs of All Nations erected in Hamburg, Germany [27].

However, these injuries were not initially attributed to X-ray exposures. Nevertheless, formal action to protect from the harmful effects of radiation was required, and in March 1898, a Committee of Inquiry was established by the British Roentgen Society to "investigate the alleged injurious effects of Roentgen rays" [28]. The Committee mentioned explicitly the known adverse effects: skin inflammation, loss of hair, and more it urged collecting information on various effects of X-rays.

Right from the first days of the use of radiation, the press reported on the death of "radiological" personnel from cancer, and so European countries and the USA established radiation protection Committees [29]. In 1925, the "First International Congress of Radiology" was organized in London, and it was decided to establish the "International X-ray Unit Committee." Hence, the ancestor of the "International Commission on Radiation Units and Measurements (ICRU)" was born [30, 31].

Exposure to radium also caused acute injuries. Two incidents are worth mentioning. The first cases of radium "poisoning" were recorded among girls painting the luminous watch dials in the Radium Luminous Materials Company, New Jersey, USA ("the radium girls"). The luminous paint was a mixture of radium salts with zinc sulfide. The workers swallowed and inhaled the paint, and this resulted in the death of 18 out of 800 employed workers between 1917 and 1924 [32]. The causes of death were either cancer (probably osteosarcoma of the jaw) or aplastic anemia, necrosis of the jaw, and spontaneous fractures [33, 34]. But it was the death of the wealthy American iron and steel industrialist Eben Byers in 1932 which put an end to the so-called mild radium therapy. His death was attributed to the enormous quantities of *Radithor* (Fig. 1.10) that he had consumed. *Radithor*, produced in the Bailey Radium Laboratories in New Jersey and advertised in the newspapers as "Science to cure all the living dead," was commercially available in the USA. Each bottle contained 1 μCi of ^{226}Ra and 1 μCi of ^{228}Ra in 16.5 mL of liquid. Byers started drinking Radithor in 1927 and stopped by 1930 when his teeth started to fall out (it was estimated that he had emptied between 1000 and 1500 bottles). Eventually, he died from sarcoma of the upper and lower jaws [35]. This event was probably the reason why the era of the "mild radium therapy" came to an end [36] (Box 1.8).

Fig. 1.10 A bottle of *Radithor*—one of the most famous varieties of radium-infused water commercially available in the USA in the 1920s

Box 1.8 Radium Misuse

- Radium was extensively misused before World War II via consumption of various radium-containing products.
- The first cases of radium "poisoning" were recorded among the "radium girls" painting the luminous watch dials.
- The death of the American millionaire Eben Byers in 1932 seems to be the event that ultimately led to cessation of radium misuse.

1.2.3 The Law of Bergonié and Tribondeau

The so-called fundamental Law of Bergonié and Tribondeau put forward in 1906 postulated that normal tissues appear to be more radiosensitive if their cells are less differentiated, have a greater proliferative capacity, and divide more rapidly. Various data suggest that this law applies to tumors as well.

Heinrich Ernst Albers-Schönberg, Jean Alban Bergonié, Claudius Regaud, and Louis Tribondeau made significant contributions to our knowledge of the biological effects of ionizing radiation. Between 1895 and 1908, they studied histological features of irradiated gonads in numerous animal models. Although the law of Bergonié and Tribondeau that links radiosensitivity with proliferation is not generally applicable, the enormous efforts these scientists made to fight cancer by using ionizing radiation should be acknowledged (Box 1.9).

Box 1.9 The Law of Bergonié and Tribondeau

- The "law of Bergonié and Tribondeau" was formulated in 1906 and postulated that normal tissues appear to be more radiosensitive if their cells are less differentiated, have a greater proliferative capacity, and divide more rapidly.
- The law of Bergonié and Tribondeau has not been verified. However, it has facilitated the advances in radiation biology and understanding of the relationship between cell proliferation and tissue radiosensitivity.

In 1906, Jean Bergonié and Louis Tribondeau published a communication to the French Academy of Sciences about the link between cellular proliferation and response to radiation. According to Bergonié and Tribondeau [37], "X rays act on cells inasmuch efficiently as cells have a greater reproductive activity, their karyokinetic fate is longer, their morphology and function are at least definitively fixed." While they never used the term "radiosensitivity," this article has with time been read as "cells are inasmuch radiosensitive as they grow fastly" and is still considered as a founding law of radiation oncology. Today, however, there is evidence that this "law" can be contradicted by numerous counterexamples. An epistemological analysis of the archives of Claudius Regaud, another pioneer of radiation biology and a contemporary of Bergonié and Tribondeau, sheds new light on this law [38]. Let us now briefly review some important facts about the life and work of these three French scientists.

Jean Alban Bergonié (1857–1925) (Fig. 1.11) was a physicist and a medical doctor. His expertise in the two areas allowed him to use electrical currents in medical therapy and to develop many new devices based on the discovery of X-rays and radium. In 1911, because of his hitherto intense use of X-rays in the therapy of patients, he developed dermatitis on the right index, and in 1922, his hand (and thereafter his arm) was amputated. Ultimately, he died from lung cancer in 1925 [39]. Of note, Bergonié funded the Journal *Archives d'Électricité Médicale* where he wrote that X-rays were discovered "simply thanks to the invention of the Crookes tube some 15 years earlier" [39]. In 1906, he expressed the opinion that "there are two

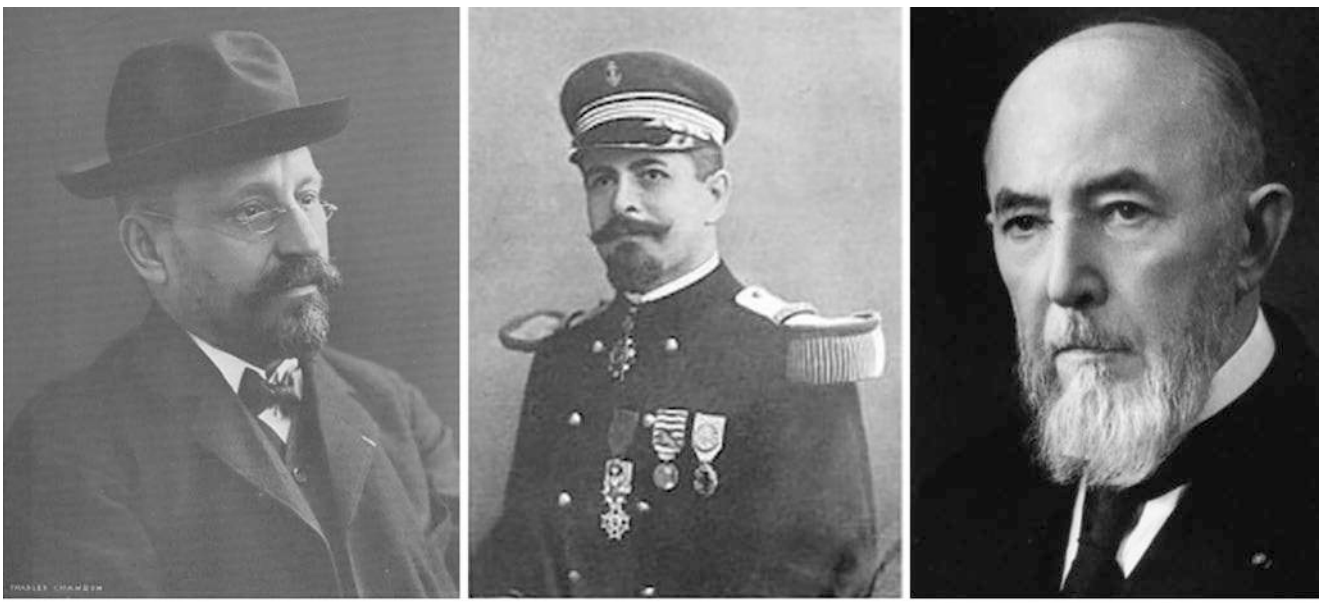

Fig. 1.11 Bergonié, Tribondeau, and Regaud

error types that may affect the medical application of X-rays: (1) the uncertainties in the assessment of radiation dose, … and (2) the differences in the sensitivity of the patients" [23].

Louis Tribondeau (1872–1918) (Fig. 1.11) was born in Sète in Southern France and in 1890 joined the Health Corps of the French Navy. Tribondeau was one of the first histologists who described the microscopic features of tuberculous epididymitis. But he became famous thanks to his staining techniques for bacteriology. In 1918, he died from the Spanish flu [39].

Born in Lyon, France, Claudius Regaud (1870–1940) (Fig. 1.11) studied medicine in Lyon and attended the microbiology lectures at the Pasteur Institute [40]. In 1893, he worked in Lyon in the laboratory of Joseph Renaut, an eminent histologist, known for his staining technique based on mercury. In Renaut's laboratory, Regaud improved the staining technique of Ehrlich (methylene blue) and developed his own staining method based on ferric hematoxylin, which reveals mitochondria and cytoplasm [40–42]. In 1912, Regaud became head of the Biology Section of the new Radium Institute of Paris, where Marie Curie headed the Physics Section. During World War I, he served as head of an Army Hospital. Not only did he organize the emergency services very effectively, but he also managed multidisciplinary meetings between surgeons, radiologists, hygienists, nurses, and other staff. From 1918 until 1939, he treated thousands of cancer patients and developed a method of fractionated radiotherapy. He died of pneumonia in December 1940 [40].

On August 5, 1895, Regaud presented the new improvements on his staining technique at the Congress of Neurology in Bordeaux [41]. Tribondeau and Bergoni also attended the sessions and had probably read the papers by Regaud in which the histology of the rodent reproductive system was described in detail based on his new staining technique.

After the discovery of X-rays by Roentgen in December 1895, two German scientists, H. E. Albers-Schönberg and H. Frieben, began to study the effects of this type of radiation on spermatogenesis by irradiating testicles of rabbits and guinea pigs [39, 43, 44]. In Bordeaux, Bergonié undertook to reproduce the experiments of the two Germans. As a physicist, he was able to build irradiation devices but, owing to his limited knowledge of histology, he asked Tribondeau for his technical savoir faire [39]. Between 1904 and 1905, Bergonié and Tribondeau published their first observations about irradiated testicles of rats having used Regaud's staining technique [45]. They emphasized the role of spermatogonia as pluripotent cells and as the most radiosensitive cells of the reproductive system. However, since the experiments involved irradiation with X-rays, interpretation of the data remained ambiguous.

Regaud realized that there might be misinterpretations of his own technique. Unlike Bergonié, Regaud was a histologist and not a physicist and was helped by Thomas Nogier, a specialist in medical physics. Regaud and Nogier replicated the experiments of Bergonié and Tribondeau using rat models, single exposures, and Regaud's staining technique [46]. In 1908, Regaud claimed that in young rats, spermatogonia are less radiosensitive than in the adult animals although proliferation rates of these cells are similar in the two groups of rats [47]. However, according to Regaud and Lacassagne [48], Bergonié and Tribondeau generalizations were "imprudently" based on the studies of rat testes. In 1925, Regaud did not hesitate to write about the law of Bergonié and the Tribondeau-Bergonié's eulogy that "Actual law as so many people believe it? No. But nice formula of the first approximation" [49].

These days, several oncology lectures still cite Bergonié and Tribondeau's law as a founding principle of radiotherapy according to which tumors are more radiosensitive than healthy tissues due to the higher proliferation rate of the former. In this erroneous claim, three kinds of errors were made:

1. Tumors are not necessarily more radiosensitive than normal tissues.
2. Proliferation rate is not necessarily correlated with the cellular death rate after irradiation.
3. Radiosensitivity and cancer susceptibility to irradiation are two different notions [50].

The link between proliferation rate and radiosensitivity is far from obvious, and the law of Bergonié and Tribondeau should have been modified as follows: "the faster cells proliferate, the faster cell death will appear." Besides, reviews about the *T*pot (the potential doubling time parameter) have shown that the yield of cell death clearly does not correlate with proliferation rate [51, 52]. For example, fibroblasts from ataxia telangiectasia are hyper-radiosensitive, while their proliferation rate is lower than that of fibroblasts from healthy patients [53]. When fibroblasts are transformed by the Simian Virus 40 (SV40), the cells become unstable and their proliferation rate increases while they are less radiosensitive than their non-transformed counterparts [54]. Other counterexamples of the law of Bergonié and Tribondeau are as follows: the Li-Fraumeni syndrome (caused by the p53+/− mutations) confers radioresistance associated, however, with impaired cell cycle arrests, instability, and cancer proneness. Similarly, some highly proliferating tumors may be very radioresistant [55].

To conclude, despite its popularity, the law of Bergonié and Tribondeau has not been fully validated. Yet, it has made a significant contribution to the advances in radiation biology and the relationship between proliferation and radiosensitivity.

1.2.4 Early Optimism and Pessimism

The report of the discovery of "mysterious rays" (X meaning unknown) created a great sensation and spread rapidly in many countries: The first report in the press of Roentgen's feat appeared in Vienna on January 5, 1896, and days later in Germany, England, and the USA [56]. Of all the properties of X-rays, their ability to make the "invisible visible" was the most fascinating and remained for several years the principal topic for their use in the imaging of anatomical and technical objects (Fig. 1.12).

The first X-ray machines were large, loud, sparkling, and smelly devices, prone to causing accidents and injury. Such bizarre and sometimes mind-boggling presentations solidified the current public perception of X-rays as a fantastically powerful and yet controversially useful tool. As one of the symbols of the new scientific medicine, X-rays have largely lived up to the public's expectations of a technological panacea, which was reinforced by the spectacle of their generation and their undeniable effects on the body. This "domestication" of X-ray machines highlighted their failure as modern heroic medicine, while reinforcing at the same time the emerging understanding of radiation as a "subtle, cumulative, and insidious threat" [57, 58] (Box 1.10).

Box 1.10 X-rays Sensation

- The report of the discovery of "mysterious rays" created a great sensation and spread rapidly in many countries.
- As one of the icons of the new scientific medicine, X-rays bore much of the public's expectations for a technological panacea.

In addition to the discovery of X-rays, the year 1895 also saw the death of Louis Pasteur. After a plethora of controversies, the "microbial" theory developed by Pasteur triumphed at the end of the nineteenth century to such an extent that nearly all the diseases were believed to originate from a microbial etiology [59]. This was also the case with cancer, a disease that was already well known, but much less frequent than tuberculosis or diphtheria. The so-called parasitic theory of cancer suggested that tumors arise as a result of infection of tissues by microorganisms. This theory opposed the

Fig. 1.12 Cartoon from "Life," February 1896. The New Roentgen Photography. "Look pleasant, please"

"cellular" theory, which explained carcinogenesis as due to the transformation of one or more cells. Hence, early after the discovery of X-rays, the first experiments involving both X-rays and microbes revealed the biocidal properties of X-rays [60].

In this historical context, Victor Despeignes, a hygienist and physician in a village of Savoy, Les Echelles, France, in February 1896 was visited by a man of 52, who suffered from pain in his abdomen [3, 60] and had been diagnosed with stomach cancer. Convinced by the works of his former colleagues of the Medical Faculty of Lyon, who in March 1896 demonstrated the curative effects of X-rays in patients with tuberculosis [61], in July 1896, Despeignes performed the first anticancer radiotherapeutic trial by irradiating his patient's tumor with X-rays in two daily sessions. However, although the therapy led to a significant decrease of the tumor volume, the patient died 22 days after the beginning of the treatment. Despeignes described all these observations in two articles in the Lyon Medical Journal [3, 60, 62–64]. The reconstitution of the radiotherapy of Despeignes suggested that his patient did not suffer from a stomach cancer, a rather radioresistant neoplasm, but from gastric lymphoma, possibly the mucosa-associated lymphoid tissue (MALT) lymphoma of a high-grade Burkitt type, which is very radiosensitive. Unfortunately, following the opposition or reservations of his colleagues vis-à-vis the therapeutic properties of X-rays, Despeignes discontinued further trials with X-rays [3, 60].

Emil Grubbe (1875–1960), who received his medical degree in 1898, was allegedly the first American to use X-rays as a treatment for cancer. According to his own report, on January 26, 1896, he treated in Chicago a woman with breast cancer and, the following day, a man suffering from ulcerating lupus [65]. However, the validity of these statements remains questionable for many reasons. Firstly, no death certificates or medical records of Grubbe's patients have been found. Secondly, these treatments were not described in any peer-reviewed publications. Grubbe did not describe any clinical features potentially resulting from these treatments [65].

In August 1896, Leonhard Voigt irradiated in Germany a cancer of the nasopharynx, but, as in Grubbe's case, the records of this treatment cannot be validated [65]. The first radiation treatment considered to be successful was given in 1897 in Germany by Eduard L. Schiff to a patient suffering from erythematous lupus [66, 67]. While the X-rays generated by the Crookes tubes manufactured in the first two decades of the twentieth century were too "soft" to fully permeate the tumorous tissue, the later technological advances permitted Claudius Regaud and Antoine Lacassagne to perform in the 1930s the first series of anticancer radiotherapy at the Curie Institute in Paris, France [2] (Box 1.11).

Box 1.11 Radiology

- Counterintuitively for the modern reader, ionizing radiation was initially used mostly for treatment rather than for diagnosis.
- Development of diagnostic radiology remained slow till the outbreak of the Great War (WWI) in 1914.

The development of diagnostic radiology remained slow until about 1914, when two incidents precipitated its growth: the invention in 1913 of a new type of the cathode tube by the American physicist W. D. Coolidge (1873–1975) and the beginning of the Great War (World War I) associated with the need for medical assistance to the wounded soldiers.

Beginning from the 1920s, X-rays were used regularly for the detection of pulmonary tuberculosis. Before that, the "radiologists" were almost no more than "photographers." "Thanks to" tuberculosis, the "photographers" became skilled diagnosticians and thus the medical specialty of radiology emerged. Noteworthy, the Roentgen Society founded in London in November 1897 was in 1927 renamed the British Institute of Radiology; in 1931, the section of Radiology was established at the Royal Society of Medicine; and in 1934, the British Association of Radiologists was founded (5 years later, it was renamed the Faculty of Radiologists).

At that period, radiology was faced with two problems: First, physicians regarded radiology as an intruder in their territory and contrasted the "dead photograph" with the "living sound" of auscultation, and second, the images obtained were of poor quality because all the anatomical structures were superimposed. To overcome this latter problem, B. G. Ziedses des Plantes (1902–1933) built the first machine for planigraphy, in which the X-ray tube and the film moved together around the plane of interest allowing to reconstruct an arbitrary number of planes from a set of projections. He also designed the subtraction method to improve images after the injection of contrast agents [68].

The history of radiation therapy (radiotherapy) can be traced back to experiments made just after the discovery of X-rays, when it was shown that exposure to ionizing radiation may lead to cutaneous burns. In 1902, several physicians began the systematic use of radiation for the treatment of malignant tumors. The increased use of electrotherapy and escharotics (the medical application of caustic substances) inspired doctors to use radiation for the treatment

of nearly any disease—lupus, basal cell carcinoma, epithelioma, tuberculosis, arthritis, pneumonia, and chronic ear infections (https://www.cdc.gov/nceh/radiation/nri/patientinfo.htm; [4, 69, 70]). Active use of ionizing radiation for treatment of various diseases continued until the early 1960s. Since then, radiation therapy has been used nearly exclusively in cancer therapy. Two factors contributed to phasing out of radiotherapy for non-oncological purposes: the growing awareness of the radiation-induced carcinogenesis and the development of efficient drugs, primarily, antibiotics (Box 1.12).

Box 1.12 Radiation Therapy

- Ionizing radiation was successfully used for the treatment of numerous diseases until the early 1960s.
- Since then, radiation therapy has been used almost exclusively in cancer therapy.
- Two factors contributed to phasing out of radiotherapy for non-oncological purposes: the growing awareness of the radiation-associated carcinogenesis and the development of efficient drugs.

Until 1920, patients with cancer were treated mainly by surgeons who assumed that the mechanism of radioactivity involved a "caustic effect." At that time, when the sources of X-rays produced "weak" radiation, capable of only superficial penetration, it was logical that it was dermatologists who strived to use X-rays in therapy. The crucial experiments performed by Robert Kienböck (1871–1953) entailed the proof that an X-ray dose, rather than electric phenomena, was the active agent causing biological effects when "illuminating the skin using Roentgen tubes" [71].

In the 1910s and 1920s, radiobiology was at its infancy, based mainly on empirical observations of the effects of radiation on the skin. The technical progress made with the Coolidge tubes and the higher voltage that these tubes could be operated with introduced the techniques of the "deep X-ray treatment." The first radiotherapy textbook titled "Treatment of Cancer by Radium" was authored by surgeon Sir Stanford Cade and appeared in 1928 [72].

At the same time, the Scottish radiotherapist Ralston Paterson (1897–1981) who used X-rays for the treatment of lung cancer wrote, "In cases of true primary carcinoma of the lung, surgery as yet offers little hope of relief … A group of nineteen patients treated by high-voltage roentgen rays is reported. All died within ten months, all but three within four months. This brief period of survival is the same as that in a group of cases in which there was no treatment. Although life is not prolonged, roentgen-ray treatment in all, but advanced cases give marked temporary palliation" [73].

In 1929, the pioneer Swedish radiotherapist Gösta Forssell (1876–1950) delivered the tenth Mackenzie Davidson Memorial Lecture and summarized the current state of radiotherapy [74, 75]. Figure 1.13 shows a table from Forssell's summary.

In 1896, less than a year after the discovery of X-rays, Walter Levitt wrote on modern developments in X-ray therapeutic techniques and stressed that it is Leopold Freund from Vienna to whom "belongs the credit of having carried out the first X-ray treatment." Freund had noticed that epilation was one of the most constant effects of the exposure to X-rays, and when a patient with a hairy mole on the face came to him for advice, he conceived the idea of treating it with X-rays [76].

At about the same time, Robert McWhirter from Edinburgh wrote on the radiosensitivity in relation to radiation intensity. Frank Ellis from the Sheffield National Radium Centre during his long life (1905–2006) also contributed to the development of radiotherap; in June 1939, he reported on the radiosensitivity of malignant melanoma [77, 78]. Other publications of this period on the use of radium include illustrations of masks holding the radium needles applied to the skin (Fig. 1.14) and tubes containing radium for the internal use in cervical cancer [79].

Concurrently, the late effects of radiation on the skin were studied and reported in detail, and plastic surgery was applied to the treatment of radiodermatitis and radionecrosis [26, 80].

At this gestational period, the pioneers of radiotherapy did not really know (a) what doses to use and how to measure them and (b) what are the advantages and disadvantages of using single or fractionated doses of X-rays. The concept of fractionation of the X-ray treatment was introduced by Claudius Regaud from the Foundation Curie in Paris and his brilliant collaborator Henri Coutard at the first International Congress of Radiology held in 1925 in London. Still, well into the 1930s, most radiotherapists were not convinced that fractionated therapy was superior to the single-dose schedule. With the establishment of the fractionation as standard treatment, radiotherapy ceased to rely solely on clinical observation, without rigid, preconceived planning, and began to be based on detailed physical modeling and dosimetry, to avoid as much as possible the irradiation of healthy tissues. This required a very close cooperation between radiotherapist and radiophysicists and led to the birth of two new disciplines, radiobiology and medical physics [81].

Only Radiotherapy. (Results obtained at Radiumhemmet.)				
Cases treated between		Total No. of cases.	Cases cured.	
			Number.	Percentage.
1910–1915	*Carcinoma cutis*			
	Total No. of cases treated	207	142	69%
	Operable cases *without* glandular metastases	182	142	78%
1910–1917	*Carcinoma labii*			
	Total No. of cases treated	66	45	68%
	Operable cases *without* glandular metastases	52	45	**86%**
1916–1921	*Carcinoma oris*			
	(Ca. linguae; ca. subling.; ca. mandib.; ca buccae)			
	Total No. of cases treated	113	21	18%
	Cases *without* glandular metastases	68	21	31%
	Operable prim. tumours	29	16	**55%**
	Local recurrences	19	4	21%
	Inoperable prim. tumours	20	1	5%
	Ca. linguae without apparent metastases	11	6	60%
1914–1923	*Carcinoma cervicis uteri*			
	Total No. of cases examined	790	163	20·6%
	Total No. of cases treated	737	163	21·1%
	Operable and border-line cases	188	76	**40·4%**
1913–1921	*Carcinoma corporis uteri*			
	Total No.of cases examined (all treated)	46	20	43·5%
	Operable and border-line cases	25	15	**60%**
1910–1922	*Sarcomata*			
	Primary tumours	238	58	24%
	Recurrences after operation	154	28	18%

Fig. 1.13 Summary of the effects of radiotherapy of cancer performed in Sweden between 1910 and 1923 [75]

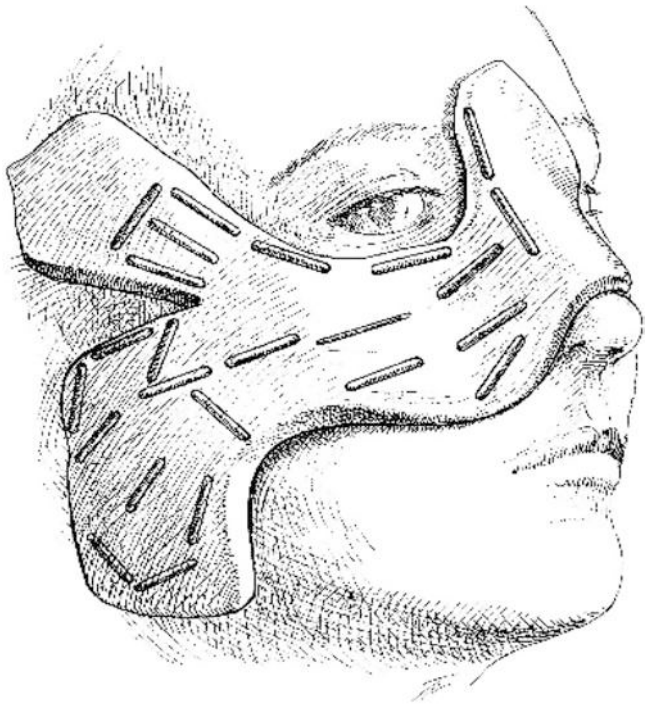

Fig. 1.14 Mask to hold the radium needles for treatment of skin cancer [79]

1.3 Development of Fractionation in Radiotherapy

1.3.1 Early Fractionation

As mentioned above, Victor Despeignes in his historical attempts applied a bi-fractionated radiotherapy based on the hypothesis that the dose should not be too high to spare healthy tissues. Fractionated treatments can be traced back to the first trials performed by Leopold Freund in 1896 in Vienna, Austria. Today, Freund is considered the founder of medical radiology and radiotherapy [3, 82]. During the first decade of the twentieth century, many different anticancer strategies involving ionizing radiation were applied to treat various tumors. However, the energy of X-rays provided by the available tubes was limited to some tens of kilovolts, and therefore the radiation penetration into the body was very limited. Between the 1920s and 1930s, pioneers from the "French school" at the *Institut Curie* in Paris led by Henri Coutard, Claudius Regaud, and Juan A. del Regato showed that hypofractionation might lead to severe tissue reactions and promoted the hyperfractionated regimen by spreading the delivery of the dose over a longer period of time. In 1911, Claudius Regaud showed that a ram's testes could be sterilized without causing major burns to the scrotal skin if three irradiations were delivered 15 days apart. This practice was opposed to the "German school" led by Holzknecht and Wintz who preferred to apply high doses in a short period of time (intensive radiotherapy) [4]. Particularly, Henri Coutard suggested that high doses per fraction should be avoided due to the damage they caused to the connective tissues [83]. Coutard applied the concept of fractionated radiotherapy with treatment courses protracted over several weeks. With this strategy, Coutard managed to cure patients with various head and neck malignancies that are difficult to treat even today. It should be noted that the French radiotherapist was among the first to recognize that tumors of different histologies vary in their sensitivity to radiation.

These observations led to the conclusion that radiation oncologists should protract the treatment duration to spare healthy tissues while increasing the dose per fraction to kill a tumor. Obviously, the current standard fractionation scheme of 1.8–2 Gy per fraction five times per week originated from individual observations of patients and empirical experience rather than from a purely scientific basis [84].

1.3.2 Cure with Fractionated Treatment

The technological race to produce the highest X-ray energies permitted the cure of the deepest tumors and helped in extending the application of hyperfractionated treatments to various cancers. For instance, the first electrostatic generator, developed by Robert van de Graaff in 1929, permitted the installation at the Huntington Memorial Hospital Boston, MA, USA, of a 2 MV irradiator dedicated to radiotherapy, and the first treatments with ^{60}Co source began there in 1951. Two years later, the first 4 MV double-gantry linear accelerator (linac) was installed at the Newcastle Hospital in the UK [4] (Box 1.13).

Box 1.13 Evolution of Radiation Therapy

- The first fractionated radiation treatment was performed in 1896.
- Accelerator-based therapy has been performed since 1929 (with 2 MV electrostatic accelerator).
- Treatments with the ^{60}Co source emerged in 1951.

With these technological advances, the early and late post-radiotherapy tissue reactions were more and more accurately documented and standard current hyperfractionated treatments were progressively defined for all types of tumors. In 1967, Frank Ellis developed the so-called Strandqvist's concept and suggested a formula defining the nominal standard dose (NSD) [85, 86]. Many variant formulas derived from the original one have since been devised [87]. Unfortunately, while the NSD formula has had a significant influence on clinical practice and was successful in predict-

ing isoeffective regimens for the early effects, it dramatically failed in the prediction of severe late effects after the large-dose fractions. Progressively, the use of the parameters of the linear quadratic (LQ) model permitted a better approach to guide clinicians in their choice of the dose fractionation regimen [88].

Today, the generally accepted model explaining both early and late effects consists of four independent processes that are thought to occur between fractions and favor the survival of normal tissues over cancers: (a) repair of sublethal cellular damage, (b) redistribution of tumor cells from radioresistant (late S phase) into radiosensitive (G2-M) portions of the cell cycle, (c) reoxygenation of the hypoxic (and hence radioresistant) portions of tumors, and (d) migration of normal cells into the irradiated healthy tissues close to the tumor to repopulate them with new functional cells.

Recently, the debate about dose hypofractionation has been relaunched with the advent of stereotactic technologies that permit targeting the tumor with great precision, limiting therefore the exposure of healthy tissues surrounding the tumor. Particularly, anticancer treatments with stereotactic radiosurgery (SRS) and stereotactic body radiation therapy (SBRT) are based on the combination of a high-precision tumor targeting with hypofractionation [89]. *Cyberknife* (Accuray Incorporated, Sunnyvale, CA, USA) is one of the most recent and innovative techniques developed for the SBRT. It is a robotic system delivering many (usually a hundred) independent and noncoplanar beams converging onto the tumor with sub-millimetric accuracy under continuous X-ray image guidance [90]. Studies have shown the efficiency and safety of the SRS and SBRT techniques in many instances, including some involving the *Cyberknife*. Still, however, owing to the lack of a clear radiobiological mechanistic model that will define objective criteria, no consensus about the total dose, dose per fraction, and treatment duration has been achieved [89].

1.4 Development of the Therapeutic Ratio

In 1936, the German radiologist Hermann Holthusen (1886–1971) considered the effect of a radiation dose on the probability of controlling tumor and the development of normal tissue complications [91]. By 1975, this concept was formalized and further developed. Nowadays, the ultimate objective of radiation therapy is to control tumors without causing excessive normal tissue toxicity. The term "therapeutic ratio" defines the relationship between the tumor control probability (TCP) and the likelihood of normal tissue damage—normal tissue complication probability (NTCP). The difference between TCP and NTCP is called a "therapeutic ratio" or "therapeutic window" (Fig. 1.15) (Box 1.14).

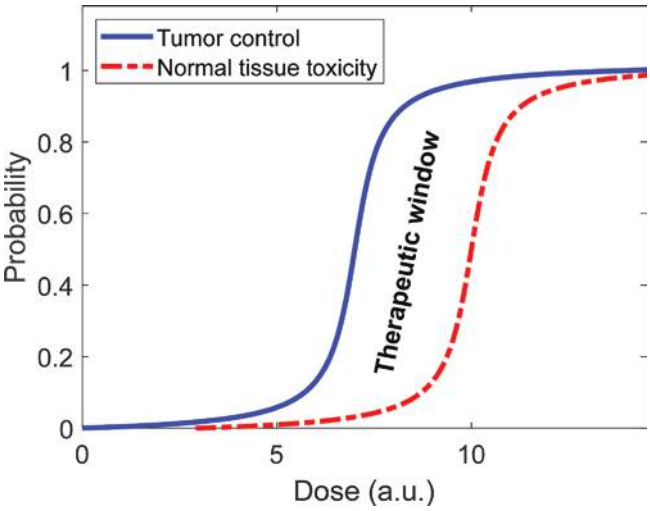

Fig. 1.15 Therapeutic window

Box 1.14 Therapeutic Window

- The ultimate objective of radiation therapy is to control tumor growth without causing excessive damage to normal tissues.
- Tumor control probability (TCP) and normal tissue complication probability (NTCP) depend differently on the radiation dose.
- The difference between TCP and NTCP is called "therapeutic ratio" or "therapeutic window.

Clinical studies have validated the benefit of contemporary irradiation techniques for improving the therapeutic ratio. Large meta-analyses have shown that concurrent radio- and chemotherapy improves local control in many types of cancer. Clinical trials using molecularly targeted therapies have not yielded satisfactory results yet. The notable exception is head and neck squamous cell carcinoma treated with combined radiotherapy and cetuximab. Noticeably, irradiation of normal tissue should not be viewed only as a source of toxicity, because both the abscopal and bystander effects (discussed in Chap. 2) suggest that such irradiation may also result in therapeutic outcomes [92–95].

Today, clinical strategies enhancing the efficacy and decreasing the toxicity of radiotherapy, i.e., increasing the overall therapeutic window, are of paramount importance and there is demand for novel radiation sensitizers that are expected to scale up the window. This is especially important for tumors characterized by high probability of recurrence, such as locally advanced lung carcinoma, and head

and neck and gastrointestinal tumors. Molecular target therapies with identified mechanisms of action should be given top priority. Examples include targeting cell survival and proliferation signaling such as the EGFR and PI3K/AKT/mTOR pathways, DNA repair genes including PARP and ATM/ATR, angiogenic growth factors, epigenetic regulators, and immune checkpoint proteins. By manipulating various mechanisms of tumor resistance to ionizing radiation, targeted therapies hold significant value to increase the therapeutic window of radiotherapy. Furthermore, the use of novel nanoparticle-based therapies, such as nanoparticle delivery of chemotherapies, metallic (high-Z) nanoparticles, and nanoparticle delivery of targeted therapies, may improve the therapeutic window by enhancing the tumor response to ionizing radiation and/or reducing normal tissue toxicity [96].

1.5 Radiation Epidemiology and Radiation Carcinogenesis

Radiation effects can be divided into early and late outcomes. Another classification is into deterministic and stochastic effects.

The most common radiation-induced deterministic injuries include skin burns and cataracts. Since these effects occur after absorption of high doses of radiation, they can be easily avoided by adherence to the rules of radiological protection. The most important stochastic effect of significant irradiation is malignancy. Data suggest an elevated risk from medical radiation [97], especially with the highest exposures [98].

As mentioned earlier, biological effects caused by X-rays and radium were noted very soon after the discoveries of Roentgen, Becquerel, and the Curies. Early pathologies, such as radiation dermatitis and hair loss (epilation, alopecia), led to the birth of radiobiology and prompted scientists to follow up patients for long periods of time to study late effects of irradiation as well.

While radiosensitivity reactions require rather high doses, exposure to ionizing radiation may also induce cancer [50]. The first radiation-induced cancer was reported by Frieben in 1902 on his own hand [99]. Cancers, but also leukemia, were mainly diagnosed in the pioneers of radiation. Hence, the incidence of radiation-induced cancers among clinicians manipulating X-ray tubes increased drastically [13]. Before the Second World War, a cohort of hundreds of female workers ("the radium girls"—see Sect. 1.2.2) in watch factories in New Jersey, Illinois, and Connecticut between 1917 and 1924 contracted some radiation-induced tumors probably due to self-luminous paintings containing radium [32]. This episode had a major societal, ethical, and legal impact in the USA and in the world. This period was contemporary with the organization of the first world congresses of radiology from which the International X-ray and Radium Protection Committee (IXRPC) arose and the first radiation protection recommendations were proposed [13].

Regarding epidemiology, radio-induced cancers were observed historically in pioneers of ionizing radiation, later in patients from various medical cohorts [97], and then in the atomic bomb survivors [100].

In the 1920s, the American geneticist, Hermann Joseph Muller, who irradiated fruit flies (*Drosophila melanogaster*) with large doses of X-rays, discovered radiation-induced mutations [101]. At that time, geneticists were convinced that no mechanism for gene repair existed and therefore that mutagenic damage was cumulative. From their point of view, no tolerant dose could ever be set, and the safety level should only be weighed against the cost of achieving it [102]. In 1946, Muller was awarded the Nobel Prize for his discovery, and in his Nobel Prize Lecture, he argued that the dose-response for radiation-induced mutations was linear and that there was "no escape from the conclusion that there is no threshold dose" [103]. This statement may be ethically questionable since Muller was already aware of counterevidence when he delivered his lecture [104].

After the Hiroshima and Nagasaki bombings, geneticists were concerned that exposure to radiation from the nuclear fallout would likely have devastating consequences on the gene pool of the human population. Later (at the end of the 1950s), after no radiation mutagenesis was found in the A-bomb survivors' descendants [105], carcinogenesis became the main concern.

During the next decades, there was considerable controversy and both logical and circular arguments were exchanged. It has been said that among scientists, "the data to support the linearity at low dose perspective were generally viewed as lacking, but the fear that they may be true was a motivating factor" [102].

- The linear no-threshold (LNT) model for radiation risk assessment gradually gained ground after Muller's Nobel lecture. In 1956, the ICRP officially abandoned the tolerance level concept (that was in use since 1931) and substituted LNT for it. The latter model suggests that any radiation exposure presents carcinogenic risk and that the risk is proportional to the absorbed dose of radiation. Formally, LNT has been introduced and remains a practical operational model only for radiation protection. Alas, contrary to the plethora of the existing evidence [106], this hypothesis has acquired de facto the status of a scientific theory and remains the driving

force of the prevailing radiophobia in the society (Box 1.15).

Box 1.15 LNT

- The linear no-threshold (LNT) model for radiation risk assessment was introduced following Muller's discovery of radiation-induced mutations in 1927.
- Evidence supporting LNT is inconclusive at very low doses.

Over the last decades, the attitude to risk associated with ionizing radiation has become more sensible. We now know that exposures to low doses of radiation initiate cellular and intercellular changes leading to stress-induced adaptive responses and metabolic alterations. Furthermore, repair mechanisms preventing the accumulation of damage—also of non-radiogenic origin—were also discovered [107]. Consequently, it became obvious that while high doses of ionizing radiation certainly cause harm, low doses can be beneficial for human health; such an effect is called hormesis [108], but the circumstances in which hormesis might occur in humans are not known.

Recently, the so-called secondary neoplasms which appear in patients treated with radiotherapy for a primary tumor have become the focus of interest in the studies of radiation-induced cancer [109]. It is still not clear whether secondary cancers are triggered by radiation or other factors. Characteristic features of these cancers are as follows:

- As a rule, they appear near the high-dose treatment volume, which supports their radiation origin [110].
- Cancer patients are at a high risk in general for developing secondary malignancies [111]. It has been estimated that radiotherapy is responsible for only about 8% of the secondary cancers [112].
- The usual confounding factors of carcinogenesis (genetic, lifestyle, environmental, etc.) increase the risk of the secondary and radiation-induced cancer. Individual radiosensitivity may play a major role [3].
- The relative risk of radio-induced cancer is organ dependent, the thyroid being by far the most radiosusceptible organ [113]; however, the recently acknowledged problem of thyroid cancer overdiagnosis [114] demands re-evaluation of the entire field of thyroid cancer epidemiology [115] (Box 1.16).

Box 1.16 Secondary Cancers

- As a rule, secondary cancers appear near the high-dose treatment volume; this is a major argument supporting their radiation origin.
- Cancer patients in general are at a high risk for developing secondary neoplasms. Radiotherapy is probably responsible for only 8% of the secondary cancers.
- The primary carcinogenic factors—genetic, lifestyle, and environmental—increase the risk of the radiation-induced and secondary cancer. Individual radiosensitivity may play a crucial role.
- The relative risk of radio-induced cancer is organ dependent. It has been assumed that the thyroid is by far the most radiosusceptible organ; however, the recently acknowledged problem of thyroid cancer overdiagnosis requires re-evaluation of the entire field of thyroid cancer epidemiology.

Various epidemiological studies indicate an association between cancer and previous exposure to ionizing radiation even at rather low doses. Most studies do not consider the potential medical exposures of people, as in the case of the A-bomb survivor studies. Although these studies do not establish a link between exposure to ionizing radiation and cancer, the existence of a dose-effect relationship, when it can be established, is in favor of a possible link. The risk evaluation thus requires that dosimetry should be precisely and accurately monitored. These epidemiological observations give consistency to the linear no-threshold (LNT) relationship, which has been used for regulatory purposes in radiological protection, although, as mentioned above, it has no indisputable scientific basis [116].

Radiation-induced carcinogenicity stems from the fact that ionizing radiation is one of the causes of the DNA lesions. Each DNA insult when unrepaired, particularly in persons with an abnormal DNA damage response (DDR), contributes to the overall DNA dysfunction and paves the way to oncogenesis [117]. Abnormal DDR has been reported following low-dose exposures to X-rays [118]. However, multiple repair and defense mechanisms operating at the

molecular, cellular, tissue, and organismal levels may assure the effective elimination of potentially carcinogenic cells and may make the LNT model irrelevant to the biological reality [107].

To conclude, the responsibility of high-dose ionizing radiation in the stochastic appearance of cancers is certain. However, it is very likely that there are no radio-induced cancers at low doses and low dose rates in the sense that they would be due to the sole ionizing radiation. However, low doses of ionizing radiation and of other genotoxic stressors (exposomes) should not be examined independently from each other (Box 1.17).

Box 1.17 Radio-Induced Cancers

- High-dose ionizing radiation can be associated with the stochastic appearance of cancers.
- It is likely that exposures to low doses of ionizing radiation are not alone responsible for radio-induced cancers.
- Low doses of ionizing radiation and other genotoxic stressors should not be examined independently from each other.

1.6 Exercises and Self-Assessment

Q1. Who made and when were made the major discoveries in the field of ionizing radiation?
Q2. What is the basis for conclusion about the carcinogenic effects of ionizing radiation?
Q3. (Open question) How was ionizing radiation misused in the first third of the twentieth century? What were the main events that led to cessation of the misuse?
Q4. (Open question) What were the main stages in the development of radiation therapy?

1.7 Exercise Answers

QA1. Wilhelm Roentgen, Henry Becquerel, Pierre and Marie Curie, and Ernest Rutherford laid the foundations of understanding the ionizing radiation from 1895 until the beginning of the Great War (1914).
QA2. (a) Historical observations
(b) Epidemiologic studies, especially with the cohort of atomic bomb survivors of Hiroshima and Nagasaki
(c) Basic understanding of the cellular mechanism regarding DNA insults and DNA damage response

References

1. Brecher R, Brecher EM. The rays: a history of radiology in the United States and Canada. Baltimore: Williams and Wilkins Company; 1969.
2. Foray N. Claudius Regaud (1870–1940): a pioneer of radiobiology and radiotherapy. Cancer Radiother. 2012;16(4):315–21.
3. Foray N. Victor Despeignes, the forgotten pioneer of radiation oncology. Int J Radiat Oncol Biol Phys. 2016;96(4):717–21. https://doi.org/10.1016/j.ijrobp.2016.07.019.
4. Mould RF. A century of X-rays and radioactivity in medicine: with emphasis on photographic records of the early years. New York: CRC Press; 1993.
5. Frankel RI. Centennial of Röntgen's discovery of X-rays. West J Med. 1996;164(6):497–501.
6. Glasser O. Wilhelm Conrad Röntgen and the early history of roentgen rays. Berlin: Springer; 1931.
7. Patton DD. Insights on the radiologic centennial—a historical perspective. Roentgen and the "new light". I. Roentgen and Lenard. Investig Radiol. 1992;27(6):408–14. https://doi.org/10.1097/00004424-199206000-00002.
8. Patton DD. Roentgen and the "new light"-Roentgen's moment of discovery. Part 2: the first glimmer of the "new light". Investig Radiol. 1993;28(1):51–8. https://doi.org/10.1097/00004424-199301000-00016.
9. Tretkoff E. Henri Becquerel discovers radioactivity. 2008. https://www.aps.org/publications/apsnews/200803/physicshistory.cfm. Accessed 25 Apr 2022.
10. Radvanyi P, Villain J. The discovery of radioactivity. CR Phys. 2017;18:544–50.
11. Villard P. Sur les rayons cathodiques. J Phys Theor Appl. 1899;8:148–61.
12. Villard P. Sur la réflexion et la refraction des rayons cathodiques et des rayons déviables du radium. C R Acad Sci Paris. 1900;130:1010–2.
13. Clarke RH, Valentin J. The history of ICRP and the evolution of its policies: invited by the commission in October 2008. Ann ICRP. 2009;39(1):75–110. https://doi.org/10.1016/j.icrp.2009.07.009.
14. Becquerel H. Sur les radiations émises par phosphorescence. Comptes Rendus de l'Acad Sci. 1896a;122:420–1.
15. The Nobel Prize in Physics 1903. NobelPrize.org. Nobel Prize Outreach AB 2022. https://www.nobelprize.org/prizes/physics/1903/summary. Accessed 25 Apr 2022.
16. The Nobel Prize in Chemistry 1908. NobelPrize.org. Nobel Prize Outreach AB 2022. https://www.nobelprize.org/prizes/chemistry/1908/summary. Accessed 25 Apr 2022.
17. Gale Research Inc. Encyclopedia of world biography, vol. 4. 2nd ed. Detroit: Gale; 2004. p. 339–41.
18. Curie P. Oeuvres de Pierre Curie [Diaries of Pierre Curie]. Paris: Editions des Archives Contemporaines; 1984.
19. Curie P, Becquerel H. Action physiologique des rayons du radium. C R Acad Sci. 1901;82:1289.
20. MacLeod JM. Further observations on the therapeutic value of radium and thorium. Br Med J. 1904;1:1366–9.
21. Barringer BS. Radium in the treatment of prostatic carcinoma. JAMA. 1917;68:1227–30.
22. Kemikler G. History of brachytherapy. Turk J Oncol. 2019;34:1–10.
23. Bordier H, Gallimard P. Une nouvelle unité de quantité de rayons X: l' unité I. Discussions. Comptes-Rendus du 35ème Congrès de l ' Association Française pour l ' Avancement des Sciences. Lyon: Masson; 1906.
24. Bouchacourt L. Sur la différence de sensibilité aux rayons de Roentgen de la peau des différents sujets, et, sur le même sujet

des différents régions du corps. In: Comptes-Rendus des Sessions de l'Association Française pour l'Avancement des Sciences 40ème Congrès. Dijon: French Association for the Advancement of Science; 1911. p. 942–7.
25. Foray N, Colin C, Bourguignon M. 100 years of individual radiosensitivity: how we have forgotten the evidence. Radiology. 2012;264(3):627–31. https://doi.org/10.1148/radiol.12112560.
26. Finzi NS. Late X-ray, and radium effects. Incidence, etiology and medical treatment. Br J Radiol. 1933;6(63):148–61.
27. Anonymous. Memorial to X-ray Martyrs. Br J Radiol. 1936;9(102):351–3.
28. Oliver R. Seventy-five years of radiation protection. Br J Radiol. 1973;46:854–60. https://doi.org/10.1259/0007-1285-46-550-854.
29. BXRPC (British X-ray and Radium Protection Committee). X-ray and radium protection. J Roentgen Soc. 1921;17:100.
30. Kaye GWC. X-ray protective measures. Br J Radiol Röntgen Soc Sect. 1927;23(91):155–63.
31. Quimby EH. The history of dosimetry in roentgen therapy. Am J Roentgenol Radium Ther. 1945;54:688–703.
32. Gunderman RB, Gonda AS. Radium girls. Radiology. 2015;274(2):314–8. https://doi.org/10.1148/radiol.14141352.
33. Clark C. Radium girls: women and industrial health reform, 1910–1935. Chapel Hill: University of North Carolina Press; 1997.
34. Hunter D. The diseases of occupation. 6th ed. London: Hodder and Stoughton; 1978. p. 892–5.
35. Macklis RM. The great radium scandal. Sci Am. 1993;269(2):94–9. https://doi.org/10.1038/scientificamerican0893-94.
36. Blaufox MD. Radioactive artifacts: historical sources of modern radium contamination [Erratum in: J Med Imaging Radiat Sci. 2021 Mar;52(1):152–153]. J Med Imaging Radiat Sci. 2019;50(4S1):S3–S17. https://doi.org/10.1016/j.jmir.2019.11.004.
37. Bergonié J, Tribondeau L. Interprétation de quelques résultats de la radiothérapie et essai de fixation d'une technique rationnelle. Comptes Rendus de l'Acad Sci. 1906;143:983–4.
38. Vogin G, Foray N. The law of Bergonié and Tribondeau: a nice formula for a first approximation. Int J Radiat Biol. 2013;89(1):2–8. https://doi.org/10.3109/09553002.2012.717732.
39. Hoerni B. Jean Bergonié. Paris: Glyphe; 2007.
40. Regaud J. Claudius Regaud. Paris: Maloine; 1982.
41. Regaud C. Sur la technique de la coloration des cellules nerveuves par le bleu de méthylène. In: Gounouilhou G, editor. Congrès des médecins aliénistes et neurologistes. Bordeaux: Elsevier; 1895. p. 1–18.
42. Regaud C. Etudes sur la structure des tubes séminifères et sur la spermatogenèse chez les mammifères. Arch d'anatomie microscopique. 1901;4:101–55.
43. Albers-Schönberg H, Frieben A. Hodenveranderungen bei Tieren nach Rontgenbestrahlungen. Munchen Med Wschr. 1903;50:2295.
44. Heilmann HP. Radiation oncology: historical development in Germany. Int J Radiat Oncol Biol Phys. 1996;35(2):207–17.
45. Bergonié J, Tribondeau L. Actions des rayons X sur le testicule du rat blanc. C R Soc Biol (Paris). 1904;57:400–2.
46. Regaud C, Blanc J. Action des rayons X sur les diverses générations de la lignée spermatique. Extrême sensibilité des spermatogonies à ces rayons. Comptes-Rendus de la Société de Biologie. 1906;61:163–5.
47. Regaud C, Nogier T. Recherches sur les rayons X et la radiothérapie. In: Fonds Claudius Regaud (1905–1940). Paris: Institut Curie CR1B; 1908.
48. Regaud C, Lacassagne A. Effets histophysiologiques des rayons de Roentgen et de Becquerel-Curie sur les tissus adultes normaux des animaux supérieurs. Fascicule I. Volume I. In: Regaud C, editor. Radiophysiologie et Radiothérapie. Paris: Presses Universitaires de France; 1927.
49. Regaud C. Notice nécrologique sur M. Bergonié. Bulletin de l'Académie de Médecine. 1925;93:88–92.
50. Foray N, Bourguignon M, Hamada N. Individual response to ionizing radiation. Mutat Res Rev Mutat Res. 2016;770(Pt B):369–86. https://doi.org/10.1016/j.mrrev.2016.09.001.
51. Antognoni P, Terry NHA, Richetti A, Luraghi R, Tordiglione M, Danova M. The predictive role of flow cytometry-derived tumor potential doubling time (Tpot) in radiotherapy: open questions and future perspectives. Int J Oncol. 1998;12(2):245–56.
52. Begg AC. The clinical status of Tpot as a predictor? Or why no tempest in the Tpot! Int J Radiat Oncol Biol Phys. 1995;32:1539–41.
53. Foray N, Priestley A, Alsbeih G, Badie C, Capulas EP, Arlett CF, Malaise EP. Hypersensitivity of ataxia telangiectasia fibroblasts to ionizing radiation is associated with a repair deficiency of DNA double-strand breaks. Int J Radiat Biol. 1997;72(3):271–83. https://doi.org/10.1080/095530097143266.
54. Arlett CF, Green MH, Priestley A, Harcourt SA, Mayne LV. Comparative human cellular radiosensitivity: I. The effect of SV40 transformation and immortalisation on the gamma-irradiation survival of skin derived fibroblasts from normal individuals and from ataxia-telangiectasia patients and heterozygotes. Int J Radiat Biol. 1988;54(6):911–28.
55. Chavaudra N, Bourhis J, Foray N. Quantified relationship between cellular radiosensitivity, DNA repair defects and chromatin relaxation: a study of 19 human tumour cell lines from different origin. Radiother Oncol. 2004;73(3):373–82.
56. Kraft E, Finby N. Beginning of radiology in 1896; first newspaper report of discovery of X-ray. N Y State J Med. 1981;81(5):805–6.
57. Lavine M. The early clinical X-ray in the United States: patients experiences and public perceptions. J Hist Med Allied Sci. 2012;67(4):587–625.
58. Willis K. The origins of British nuclear culture. J Br Stud. 1995;34(1):59–89.
59. Plimmer HG. The parasitic theory of cancer. Br Med J. 1903;2241(2):1511–5.
60. Foray N. Victor Despeignes (1866–1937): how a hygienist became the first radiation oncologist. Cancer Radiother. 2013;17(3):244–54.
61. Lortet L, Genoud P. Tuberculose expérimentale atténuée par les rayons de Roentgen. Comptes Rendus de l'Acad Sci. 1896;122:1511.
62. Despeignes V. Observation concernant un cas de cancer de l'estomac traité par les rayons Roentgen. Lyon Med. 1896a;82(26):428–30.
63. Despeignes V. Observation concernant un cas de cancer de l'estomac traité par les rayons Roentgen. Lyon Med. 1896b;82(9):503–6.
64. Despeignes V. Nouvelle observation de cancer traité par les rayons de Roentgen. Lyon Med. 1896c;83(20):550–1.
65. Mould RF. X-rays in 1896–1897. Nowotwory J Oncol. 2011;61(6):100–9.
66. Schiff E, Freund L. Contribution à l'étude de la radiothérapie. Ann d'Electrobiol. 1898;1:468–82.
67. Serwer DP. The rise of radiation protection: science, medicine and technology in society, 1896–1935. Princeton: Princeton University; 1976.
68. van Gijn J, Gijselhart JP. Ziedses des Plantes: uitvinder van planigrafie en subtractie [Ziedses des Plantes: inventor of planigraphy and subtraction—Dutch]. Ned Tijdschr Geneeskd. 2011;155:A2164.
69. Calabrese EJ, Dhawan G. How radiotherapy was historically used to treat pneumonia: could it be useful today? Yale J Biol Med. 2013;86(4):555–70.

70. Calabrese EJ, Dhawan G, Kapoor R. Radiotherapy for pertussis: an historical assessment. Dose Response. 2017;15(2):1559325817704760.
71. Wagner JP, Chung KC. A historical report on Robert Kienböck (1871–1953) and Kienböck's disease. J Hand Surg Am. 2005;30(6):1117–21. https://doi.org/10.1016/j.jhsa.2005.08.002.
72. Westbury G, Ellis H. Sir Stanford Cade KBE CB FRCS (1895–1973): a pioneer in the modern treatment of cancer. J Med Biogr. 2009;17(1):14–7. https://doi.org/10.1258/jmb.2008.008030.
73. Paterson R. Roentgen-ray treatment of primary carcinoma of the lung. Br J Radiol. 1928;1(3):90–6.
74. del Regato JA. Gösta Forssell. Int J Radiat Oncol Biol Phys. 1977;2(7–8):783–90. https://doi.org/10.1016/0360-3016(77)90064-5.
75. Forssell G. Radiotherapy of malignant tumors in Sweden. Br J Radiol. 1930;3(29):198–234.
76. Levitt W. Some modern developments in X-ray therapeutic technique. Br J Radiol. 1930;3(31):304–15.
77. Ellis F. The radiosensitivity of malignant melanoma. Br J Radiol. 1939;12(138):327–52.
78. McWhirter R. Radiosensitivity in relation to the time intensity factor. Br J Radiol. 1936;9(101):287–99.
79. Murdoch J. Dosage in radium therapy. Br J Radiol. 1931;4(42):256–84.
80. Gillies HD, McIndoe AH. Plastic surgery in chronic radiodermatitis and radionecrosis. Br J Radiol. 1933;6(63):132–47.
81. Kardamakis D, Gustavson-Kadaka E, Spiliopoulou E, Nilsson S. The history of Radiumhemmet in Stockholm in the period 1895–1950. The transformation of an outpatient clinic to an academic department. Vesalius. 2010;16(2):95–9.
82. Kogelnik HD. The history and evolution of radiotherapy and radiation oncology in Austria. Int J Radiat Oncol Biol Phys. 1996;35(2):219–26.
83. Webster JH. The protracted-fractional X-ray method (Coutard) in the treatment of cancer of the larynx: (section of radiology). Proc R Soc Med. 1934;27(7):901–24.
84. Willers H, Heilmann HP, Beck-Bornholdt HP. Ein Jahrhundert Strahlentherapie. Geschichtliche Ursprünge und Entwicklung der fraktionierten Bestrahlung im deutschsprachigen Raum [One hundred years of radiotherapy. Historical origins and development of fractionated irradiation in German speaking countries]. Strahlenther Onkol. 1998;174(2):53–63. https://doi.org/10.1007/BF03038475.
85. Ellis F. Fractionation in radiotherapy. In: Wood DA, editor. Modern trends in radiotherapy, vol. 1. London: Buttersworth; 1967. p. 34.
86. Moulder JE, Seymour C. Radiation fractionation: the search for isoeffect relationships and mechanisms. Int J Radiat Biol. 2018;94(8):743–51.
87. Dixon RL. General equation for the calculation of the nominal standard dose. Acta Radiol Ther Phys Biol. 1972;11:305–11.
88. van Leeuwen FE, Oei AL, Creeze J, Bel A, Franken NAP, Stalpers LJA, Kok HP. The alpha and beta of tumours: a review of parameters of the linear-quadratic model, derived from clinical radiotherapy studies. Radiat Oncol. 2018;13:96.
89. Trifiletti DM, Chao ST, Sahgal A, Sheehan JP. Stereotactic radiosurgery and stereotactic body radiation therapy. Cham: Springer Nature Switzerland AG; 2019.
90. Kilby W, Dooley JR, Kuduvalli G, Sayeh S, Maurer CR Jr. The CyberKnife robotic radiosurgery system in 2010. Technol Cancer Res Treat. 2010;9(5):433–52. https://doi.org/10.1177/153303461000900502.
91. Chargari C, Magne N, Guy JB, Rancoule C, Levy A, Goodman KA, Deutsch E. Optimize and refine therapeutic index in radiation therapy: overview of a century. Cancer Treat Rev. 2016;45:58–67. https://doi.org/10.1016/j.ctrv.2016.03.001.
92. Bernier J, Hall EJ, Giaccia A. Radiation oncology: a century of achievements. Nat Rev Cancer. 2004;4(9):737–47. https://doi.org/10.1038/nrc1451.
93. Bloomer WD, Hellman S. Normal tissue responses to radiation therapy. N Engl J Med. 1975;293(2):80–3. https://doi.org/10.1056/NEJM197507102930206.
94. Holthusen H. Erfahrungen über die Verträglichkeitsgrenze für Röntgenstrahlen und deren Nutzanwendung zur Verhütung von Schäden. Strahlentherapie. 1936;57:254–68.
95. Zindler JD, Thomas CR Jr, Hahn SM, Hoffmann AL, Troost EGC, Lambin P. Increasing the therapeutic ratio of stereotactic ablative radiotherapy by individualized isotoxic dose prescription. JNCI J Natl Cancer Inst. 2016;108(2):djv305. https://doi.org/10.1093/jnci/djv305.
96. Reda M, Bagley AF, Zaidan HY, Yantasee W. Augmenting the therapeutic window of radiotherapy: a perspective on molecularly targeted therapies and nanomaterials. Radiother Oncol. 2020;150:225–35. https://doi.org/10.1016/j.radonc.2020.06.041.
97. Wakeford R. The cancer epidemiology of radiation. Oncogene. 2004;23:6404–28. https://doi.org/10.1038/sj.onc.1207896.
98. Suárez Fernández JP. The downfall of the linear non-threshold model. Rev Esp Med Nucl Imagen Mol (Engl Ed). 2020;39(5):303–15. https://doi.org/10.1016/j.remn.2020.05.006.
99. Frieben A. Cancroid des rechten Handrückens. Deutsche Medicinische Wochenschrift. 1902;28:335.
100. Ozasa K. Epidemiological research on radiation-induced cancer in atomic bomb survivors. J Radiat Res. 2016;57(Suppl 1):i112–7. https://doi.org/10.1093/jrr/rrw005.
101. Muller HJ. Artificial transmutation of the gene. Science. 1927;66:84–7.
102. Calabrese EJ. The road to linearity: why linearity at low doses became the basis for carcinogen risk assessment. Arch Toxicol. 2009;83:203–25.
103. Muller HJ. Nobel Lecture: The Production of Mutations. 1946. http://www.nobelprize.org/nobel_prizes/medicine/laureates/1946/muller-lecture.html. Accessed 15 Jan 2022.
104. Calabrese EJ. Muller's Nobel prize lecture: when ideology prevailed over science. Toxicol Sci. 2012;126(1):1–4.
105. Satoh C, Takahashi N, Asakawa J, Kodaira M, Kuick R, Hanash SM, Neel JV. Genetic analysis of children of atomic bomb survivors. Environ Health Perspect. 1996;104(Suppl 3):511–9. https://doi.org/10.1289/ehp.96104s3511.
106. Taylor LS. Some nonscientific influences on radiation protection standards and practice. The 1980 Sievert lecture. Health Phys. 1980;39(6):851–74.
107. Feinendegen LE. Conference summary. Health Phys. 2020;118(3):322–6. https://doi.org/10.1097/HP.0000000000001207.
108. Rattan SIS, Kyriazi M, editors. The science of hormesis in health and longevity. Amsterdam: Academic Press; 2018.
109. Cosset JM, Hetnal M, Chargari C. Second cancers after radiotherapy: update and recommendations. Radioprotection. 2018;53(2):101–5.
110. Hall EJ. Intensity-modulated radiation therapy, protons, and the risk of second cancers. Int J Radiat Oncol Biol Phys. 2006;65(1):1–7. https://doi.org/10.1016/j.ijrobp.2006.01.027.
111. Suit H, Goldberg S, Niemierko A, Ancukiewicz M, Hall E, Goitein M, Wong W, Paganetti H. Secondary carcinogenesis in patients treated with radiation: a review of data on radiation-induced cancers in human, non-human primate, canine and rodent subjects [Erratum in: Radiat Res. 2007;167(6):748]. Radiat Res. 2007;167(1):12–42.
112. Berrington de Gonzalez A, Curtis RE, Kry SF, Gilbert E, Lamart S, Berg CD, Stovall M, Ron E. Proportion of second cancers attributable to radiotherapy treatment in

adults: a cohort study in the US SEER cancer registries. Lancet Oncol. 2011;12(4):353–60. https://doi.org/10.1016/S1470-2045(11)70061-4.
113. Cosset JM, Chargari C, Demoor C, Giraud P, Helfre S, Mornex F, Mazal A. Prévention des cancers radio-induits [prevention of radio-induced cancers]. Cancer Radiother. 2016;20:S61–8. https://doi.org/10.1016/j.canrad.2016.07.030.
114. Vaccarella S, Franceschi S, Bray F, Wild CP, Plummer M, Dal Maso L. Worldwide thyroid-cancer epidemic? The increasing impact of overdiagnosis. N Engl J Med. 2016;375(7):614–7. https://doi.org/10.1056/NEJMp1604412.
115. Socol Y, Shaki YY, Vaiserman A. Thyroid cancer overdiagnosis: implications for understanding radiation carcinogenesis and for medical imaging. Chem Biol Interact. 2019;305:1–2. https://doi.org/10.1016/j.cbi.2019.03.020.
116. ICRP (International Commission on Radiological Protection). The 2007 recommendations of the international commission on radiological protection. ICRP publication 103, vol. 37. Ottawa: ICRP; 2007. p. 2–4. https://doi.org/10.1016/j.icrp.2007.10.003.
117. Hanahan D, Weinberg RA. Hallmarks of cancer: the next generation. Cell. 2011;144(5):646–74. https://doi.org/10.1016/j.cell.2011.02.013.
118. Colin C, Devic C, Noël A, Rabilloud M, Zabot MT, Pinet-Isaac S, Giraud S, Riche B, Valette PJ, Rodriguez-Lafrasse C, Foray N. DNA double-strand breaks induced by mammographic screening procedures in human mammary epithelial cell. Int J Radiat Biol. 2011;87(11):1103–12. https://doi.org/10.3109/09553002.2011.608410.

Further Reading

Berger H. The mystery of a new kind of rays. Scotts Valley: CreateSpace; 2012.
Bernier J, editor. 1895–1995: Radiation oncology: a century of progress and achievement. ESTRO: Lambert; 1995.
Mould FM. Radium history mosaic. Warsaw: Nowotwory Journal of Oncology; 2007.
Thomas AMK, Isherwood I, Wells PNT. The invisible light—100 years of medical radiology. Oxford: Blackwell Science; 1995.
Weinberg RA. The biology of cancer. New York: Garland Science; 2014.

Basic Concepts of Radiation Biology

2

Ans Baeyens, Ana Margarida Abrantes, Vidhula Ahire, Elizabeth A. Ainsbury, Sarah Baatout, Bjorn Baselet, Maria Filomena Botelho, Tom Boterberg, Francois Chevalier, Fabiana Da Pieve, Wendy Delbart, Nina Frederike Jeppesen Edin, Cristian Fernandez-Palomo, Lorain Geenen, Alexandros G. Georgakilas, Nathalie Heynickx, Aidan D. Meade, Anna Jelinek Michaelidesova, Dhruti Mistry, Alegría Montoro, Carmel Mothersill, Ana Salomé Pires, Judith Reindl, Giuseppe Schettino, Yehoshua Socol, Vinodh Kumar Selvaraj, Peter Sminia, Koen Vermeulen, Guillaume Vogin, Anthony Waked, and Anne-Sophie Wozny

A. Baeyens (✉)
Radiobiology, Ghent University, Ghent, Belgium
e-mail: Ans.Baeyens@Ugent.be

A. M. Abrantes
Institute of Biophysics, Faculty of Medicine, iCBR-CIMAGO, Center for Innovative Biomedicine and Biotechnology, University of Coimbra, Coimbra, Portugal

ESTESC-Coimbra Health School, Instituto Politécnico de Coimbra, Coimbra, Portugal
e-mail: mabrantes@fmed.uc.pt

V. Ahire
Chengdu Anticancer Bioscience, Ltd., and J. Michael Bishop Institute of Cancer Research, Chengdu, China

E. A. Ainsbury
Radiation, Chemical and Environmental Hazards Directorate, UK Health Security Agency, Oxford, UK
e-mail: Liz.ainsbury@ukhsa.gov.uk

S. Baatout · D. Mistry · K. Vermeulen
Institute of Nuclear Medical Applications, Belgian Nuclear Research Centre, SCK CEN, Mol, Belgium
e-mail: sarah.baatout@sckcen.be; koen.vermeulen@sckcen.be

B. Baselet
Radiobiology Unit, Belgian Nuclear Research Centre, SCK CEN, Mol, Belgium
e-mail: bjorn.baselet@sckcen.be

M. F. Botelho · A. S. Pires
Institute of Biophysics, Faculty of Medicine, iCBR-CIMAGO, Center for Innovative Biomedicine and Biotechnology, University of Coimbra, Coimbra, Portugal

Clinical Academic Center of Coimbra, Coimbra, Portugal
e-mail: mfbotelho@fmed.uc.pt; pireslourenco@uc.pt

T. Boterberg
Department of Radiation Oncology, Ghent University Hospital, Ghent, Belgium

Particle Therapy Interuniversity Center Leuven, Department of Radiation Oncology, University Hospitals Leuven, Leuven, Belgium
e-mail: Tom.Boterberg@UGent.be

F. Chevalier
UMR6252 CIMAP, Team Applications in Radiobiology with Accelerated Ions, CEA-CNRS-ENSICAEN-Université de Caen Normandie, Caen, France
e-mail: chevalier@ganil.fr

F. Da Pieve
Royal Belgian Institute for Space Aeronomy, Brussels, Belgium

European Research Council Executive Agency, European Commission, Brussels, Belgium

W. Delbart
Nuclear Medicine Department, Hôpital Universitaire de Bruxelles (H.U.B.), Brussels, Belgium
e-mail: wendy.delbart@hubruxelles.be

N. F. J. Edin
Department of Physics, University of Oslo, Oslo, Norway
e-mail: nina@fys.uio.no

C. Fernandez-Palomo
Institute of Anatomy, University of Bern, Bern, Switzerland
e-mail: cristian.fernandez@unibe.ch

L. Geenen
Radiobiology Unit, Belgian Nuclear Research Centre, SCK CEN, Mol, Belgium

Department of Radiology and Nuclear Medicine, Erasmus Medical Center, Rotterdam, The Netherlands

S. Baatout (ed.), *Radiobiology Textbook*, https://doi.org/10.1007/978-3-031-18810-7_2

A. G. Georgakilas
DNA Damage Laboratory, Physics Department, School of Applied Mathematical and Physical Sciences, National Technical University of Athens (NTUA), Athens, Greece
e-mail: Alexg@mail.ntua.gr

N. Heynickx
Radiobiology Unit, Belgian Nuclear Research Centre, SCK CEN, Mol, Belgium

Department of Molecular Biotechnology, Ghent University, Ghent, Belgium
e-mail: nathalie.heynickx@sckcen.be

A. D. Meade
School of Physics, Clinical and Optometric Sciences, Faculty of Science, Technological University Dublin, Dublin, Ireland
e-mail: aidan.meade@tudublin.ie

A. J. Michaelidesova
Nuclear Physics Institute of the Czech Academy of Sciences, Rez, Czech Republic

Czech Technical University, Faculty of Nuclear Sciences and Physical Engineering, Prague, Czech Republic
e-mail: michaelidesova@ujf.cas.cz

A. Montoro
Radiological Protection Service, University and Polytechnic La Fe Hospital of Valencia, Valencia, Spain
e-mail: montoro_ale@gva.es

C. Mothersill
Faculty of Science, McMaster University, Hamilton, Canada
e-mail: mothers@mcmaster.ca

J. Reindl
Section Biomedical Radiation Physics, Institute for Applied Physics and Measurement Technology, Universität der Bundeswehr München, Neubiberg, Germany
e-mail: judith.reindl@unibw.de

G. Schettino
National Physical Laboratory, Teddington, UK
e-mail: Giuseppe.schettino@npl.co.uk

Y. Socol
Jerusalem College of Technology, Jerusalem, Israel
e-mail: socol@jct.ac.il

V. K. Selvaraj
Department of Radiation Oncology, Thanjavur Medical College, Thanjavur, India

P. Sminia
Department of Radiation Oncology, Amsterdam University Medical Centers, Location Vrije Universiteit/Cancer Center Amsterdam, Amsterdam, The Netherlands
e-mail: p.sminia@amsterdamumc.nl

G. Vogin
Centre Francois Baclesse, University of Luxembourg and Luxembourg Institute of Health, Luxembourg, Luxembourg
e-mail: guillaume.vogin@baclesse.lu

A. Waked
Radiobiology Unit, Belgian Nuclear Research Centre, SCK CEN, Mol, Belgium

Laboratory of Nervous System Disorders and Therapy, GIGA Neurosciences, Université de Liège, Liège, Belgium
e-mail: anthony.waked@sckcen.be

A.-S. Wozny
Cellular and Molecular Radiobiology Lab, UMR CNRS 5822, Lyon 1 University, Oullins, France

Department of Biochemistry and Molecular Biology, Lyon-Sud Hospital, Hospices Civils de Lyon, Pierre-Bénite, France
e-mail: anne-sophie.wozny@univ-lyon1.fr

Learning Objectives

- To understand what radiation is, how the different types of radiation differ, and how the energy is transferred to matter
- To describe the natural and artificial sources of ionizing radiation to which we are exposed
- To understand the principles of radioactive decay, the production of artificial radioactive isotopes, and some important aspects of their environmental and clinical applications
- To describe the different dose quantities and units used to describe radiation
- To understand the concept of linear energy transfer (LET) and ionization clustering and how these are used to describe the relative biological effectiveness (RBE)
- To understand how ionizing radiation induces biological effects following energy deposition within biological tissues
- To understand the different types of health effects following different ionizing radiation doses and exposure scenarios
- To explain the factors influencing the results of low doses and introduction of the concept of targeted and non-targeted radiation effects

2.1 Physical and Chemical Aspects of Radiation Interactions with the Matter

2.1.1 Matter and Energy

There exists a wide variety of different types of particles in nature. These vary across those more commonly known, such as the constituents of atoms like electrons spinning around nuclei and protons and neutrons inside the nuclei. Particles generated through other particles' decay and those which are the carriers of the fundamental electromagnetic, strong and weak nuclear, and gravitational force are also incredibly important in nature.

In physical science, a particle is characterized either as a localized entity which can be described by its own physical characteristics such as volume, density, and mass or as a wave, the latter being a less intuitive concept. Such dual nature of particles is named the wave-particle duality. The de Broglie wavelength associated with a particle is inversely proportional to its momentum, p, through the Planck constant, h:

$$\lambda = \frac{h}{p} = \frac{h}{E/c}(\text{photons}) = \frac{h}{m \cdot v}(\text{particles with mass}). \quad (2.1)$$

When particles interact with objects much larger than the wavelength of the particles themselves, they show negligible interference effects. To get easily observable interference effects in the interaction of particles with matter, the longest wavelength of the particles and hence the smallest mass possible are needed. The wavelengths of high-speed electrons are comparable to the spacings between atomic layers in crystals. Therefore, this effect was first observed with electrons as diffraction, a characteristic wave phenomenon, in 1927 by C.J. Davisson and L.H. Germer [1] and independently by G.P. Thomson [2]. Such experiments established the wavelike nature of electron beams, providing support to the underlying principle of quantum mechanics. Thomson's experiment of a beam of electrons that can be diffracted just like a beam of light or a water wave is a well-known case taught in basic courses of quantum mechanics [3].

For electromagnetic radiation for energies $E = hc/\lambda$ of a few keV, the wavelength λ becomes comparable with the atomic size. At this energy range, photons can be practically considered as particles with zero mass and momentum $p = E/c$. Indeed, despite photons having no mass, there has long been evidence that electromagnetic radiation carries momentum. The photon momentum is, however, very small, since $p = h/\lambda$ and h is very small [$6.62606957 \times 10^{-34}$ (m^2 kg/s)], and thus it is generally not observed. Nevertheless, at higher energies, starting from hard X-rays (which have a small wavelength and a relatively large momentum), the effects of photon momentum can eventually be observed. They were observed by Compton, who was studying hard X-rays interacting with the lightest of particles, the electron. On a larger scale, photon momentum can have an effect if the photon flux is considerable and if there is nothing to prevent the slow recoil of matter due to the impinging and conservation of the total momentum. This may occur in deep space (a quasi-vacuum condition), and "solar" sails with low mass mirrors that would gradually recoil because of the impinging electromagnetic radiation are actually being investigated and tested to actually take spacecraft from place to place in the solar system [4–6].

While for photons the concept of wavelength is more intuitively directly related to the phenomena and excitations they can trigger in matter, for particles with mass (massive particles), the wavelength is usually too small to have a practical impact on our observation of interaction phenomena. Nevertheless, depending on the phenomenon or on the specific aspect one is looking at, it may be more convenient to consider the particles either as localized entities or in terms of waves.

Understanding the phenomenon of the passage of charged particles, in particular protons and other hadrons, heavy ions, electrons, and neutral particles, such as neutrons and photons, in matter has been a tempting and fascinating topic since the early development of quantum mechanics. The study of the passage of a particle through matter requires knowledge of the many interactions that govern the response of the target to the incoming (strong or weak) particle in the target itself. The number of these interactions is daunting, especially for the case of high-energy particles. In principle, to understand the types of possible particle-matter interactions and thus the response of the matter to radiation, it is more appropriate to consider the speed of the particle rather than the energy. The energy is less meaningful as the high energy of a heavy ion may be associated mostly to its mass, rather than purely to its speed. It is nevertheless common also to refer to the kinetic energy of the particle when looking at the induced interactions a particle can have when traveling through matter, distinguishing the particles with different mass. The interaction of a massive particle with matter can be understood by looking at Fig. 2.1, where the particle's kinetic energy is plotted against the de Broglie wavelength, and the relevant dimensions of a nucleon, nucleus, electron orbitals, and water molecule (O–H distance) are reported. At high-projectile kinetic energies in the region of 1–10 GeV (reported are the cases of a proton, a neutron, and a ^{12}C ion), the wavelength of the projectile is similar to the size of the nucleon, and hence the projectile is able to interact directly with the components of the single nucleons (quarks, gluons) in the nucleus of the target atom. At slightly lower kinetic energies (~1 MeV–1 GeV), the

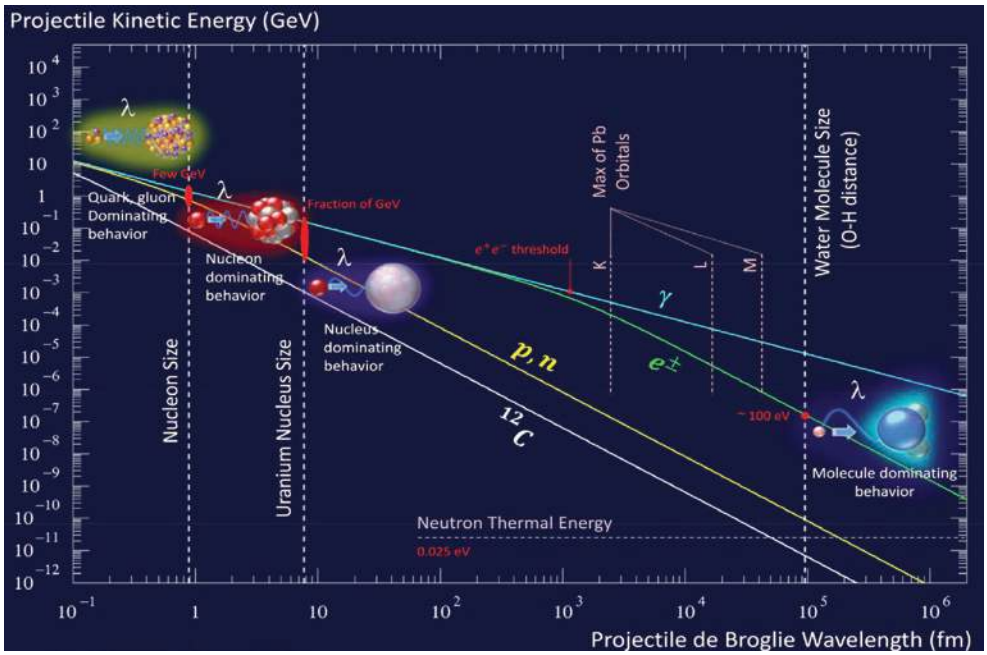

Fig. 2.1 Plot of the projectile kinetic energy vs. the de Broglie wavelength. The sizes of a nucleon, uranium nucleus, lead orbitals and water molecule are also reported. (Courtesy of Dr. Marc Verderi, Laboratoire Leprince-Ringuet, CNRS/IN2P3, Ecole Polytechnique, Institut Polytechnique de Paris, France)

wavelength of the projectile becomes comparable to that of the nucleus of uranium, and thus the projectile can interact with the nucleons, but not with the constituents of the nucleons. This can cause fragmentation of the nucleus and generation of secondary species and decay particles that are emitted in the de-excitation of the nucleus, which is brought in an excited state by the impacting particle. Descending in kinetic energy, the wavelength of the incoming radiation on the order of the entire nucleus means that the impacting particle can interact with the entire nucleus but not with the nucleons. Further lower in energy and at increased wavelength, the incoming radiation has a wavelength of similar size to the electronic orbitals (reported here are lead orbitals), and still further of similar size to a water molecule, thus entering the regime of molecule-dominating behavior. It is thus clear that when spanning large energy windows, many different physical interactions take place with the target, which probe the different units of matter which are considered as elemental for different sub-disciplines of physics.

It has to be stressed that in its path through matter, the primary particle can generate several secondary particles, such as electrons, by ionization and/or decay particles of excited nuclei in nuclear inelastic collisions. In the latter case, "daughter nuclei" are generated, which also act as projectiles interacting within the system. In the case of biological targets, primary radiation can generate ions, electrons, excited molecules, and molecular fragments (free radicals) that have lifetimes longer than approximately 10^{-10} s. The new species in turn travel and diffuse and start chemical reactions, the evolution of which is a main contributor to the effects at biological level.

Nowadays, apart from the well-known fields of the high-energy physics and nuclear science, radiation science is important in numerous sub-disciplines, such as ion beam therapy [7, 8], radiation protection in medicine [9] and nuclear facilities [10], development of risk assessment models for nuclear accidents [11], or radiation protection in deep space manned missions [12–14]. Apart from the effects on humans, parallel streams of research exist for the studies on radiation effects induced in plants, seeds, and animals, for the survival and adaptation around the Chernobyl site and even for the effects on small biological molecules of interest in studies on the search of life on other planets or their moons [15–19] (Box 2.1).

Box 2.1 Description of Particle Interactions

- The appropriateness of a description of particles as localized entities or as waves depends on the wavelength of the particle, the characteristics of the probed dimension of the target system, and the resulting phenomenon (change in the state of the target) which we are interested in.
- There exists a wide range of interactions that particles can induce in matter, from the interactions with quarks and gluons in high-energy collisions to excitations of electrons and vibrations in molecules which dominate at lower energies.

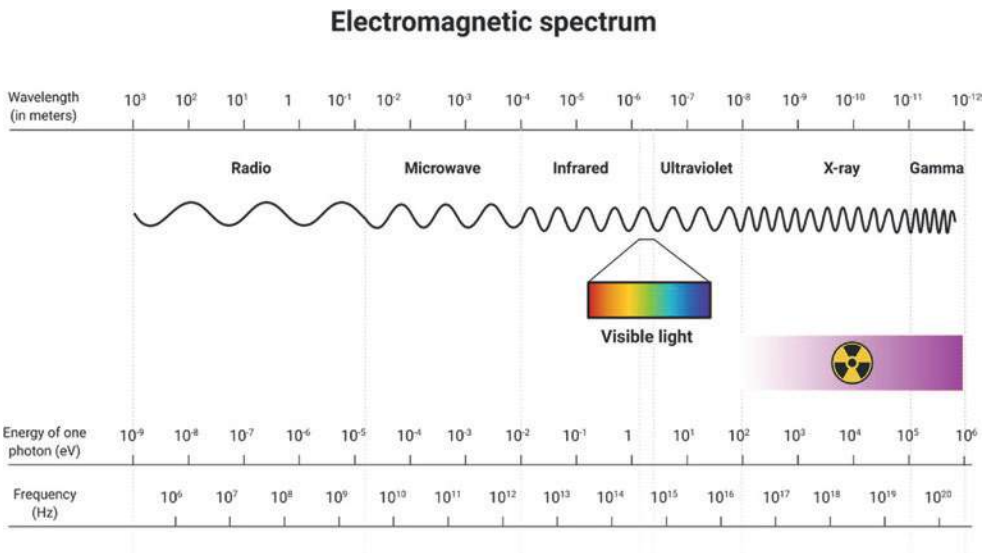

Fig. 2.2 The electromagnetic spectrum (Created with BioRender)

2.1.2 Electromagnetic Radiation

Electromagnetic radiation transfers energy without any atomic or molecular transport medium. According to the wave-particle duality of quantum physics, electromagnetic radiation can be described either as a wave or as a beam of energy quanta called photons.

To understand how electromagnetic radiation interacts with matter, we need to think of electromagnetic radiation as photons, and it is the energy of each photon, which determines how it interacts with matter. Figure 2.2 shows the spectrum of electromagnetic radiation. It is divided into radio waves, microwaves, infrared, (visible) light, ultraviolet (UV), and X- and γ-rays depending on the frequency and energy of the individual photons. Depending on the photon energy, the photon interaction with an atom can result in ionization, where an electron gets enough energy to leave the molecule/atom; excitations, where the electron gets the exact energy needed to move from an inner electron shell to an outer shell; or changes in the rotational, vibrational, or electronic valence configurations (Box 2.2).

Box 2.2 Ionizing Radiation

- It is not the total energy but the energy per photon which determines how the radiation interacts with matter.
- Ionizing radiation is the radiation with enough energy per photon to kick out one atomic electron.

Radiation can be divided into ionizing and nonionizing radiation. Ionizing radiation carries more than 10 eV, which is enough energy to break chemical bonds. Unlike ionizing radiation, nonionizing radiation does not have enough energy to remove electrons from atoms and molecules.

2.1.2.1 Nonionizing Electromagnetic Radiation

The UV spectrum is in the range of 3.1–124 eV. Even though the high-energy UV (UVC) can be ionizing, this is absorbed in the atmosphere and does not reach the Earth. Only UVA (3.10–3.94 eV) and UVB (3.94–4.43 eV) are transmitted through the atmosphere. UVB radiation has the energy to excite DNA molecules in skin cells. This can result in aberrant covalent bonds forming between adjacent pyrimidine bases, producing pyrimidine dimers. Most UV-induced pyrimidine dimers in DNA are removed by the process known as nucleotide excision repair, but unrepaired pyrimidine dimers have the potential to lead to mutations and cancer. UVA can induce production of reactive oxygen and reactive nitrogen species (ROS, RNS), which happens through interaction with chromophores such as nucleic acid bases, aromatic amino acids, NADH, NADPH, heme, quinones, flavins, porphyrins, carotenoids, 7-dehydrocholesterol, eumelanin, and urocanic acid [20]. ROS can induce ionizations in DNA. In summary, the UV light that reaches the Earth (UVA and UVB) has too low photon energies to induce direct ionization but can cause DNA instability through excitation (Box 2.3).

Box 2.3 Characteristics of UV—Radiation

- Ionizing UV radiation (UVC) is absorbed in the atmosphere.
- UVB can induce pyrimidine dimers in DNA.
- Both UVA and UVB can induce ROS, which in turn can induce DNA damage.

2.1.2.2 Ionizing Electromagnetic Radiation

An X-ray photon is emitted from an electron that is either slowed down or moves from one stationary state to another in an atom; a γ-photon is sent out by disintegration of an atomic nucleus. Except for the origin, from the physical perspective, there is no difference between X-ray and γ-photon radiation.

A photon can interact with matter by three different processes depending on its energy and the atomic number of the elements of the matter.

In the *photoelectric effect*, an atomic electron absorbs all the energy of the incoming photon and is emitted from the atom. Note that the photoelectric effect cannot occur with an electron that does not belong to an atom. This is because both energy and momentum need to be conserved, which cannot be achieved without an atom carrying the rest momentum.

The *Compton effect* implies, just like the photoelectric effect, that an electron is knocked out from an atom by transfer of energy from the photon. However, for the Compton effect, a secondary photon is also emitted, which preserves the momentum (Fig. 2.3). Therefore, the process may also apply to a nonatomic, or free, electron. The amount of energy transferred from the incident wave to the electron depends on the scatter angle as follows:

$$\lambda' - \lambda = \lambda_c \left(1 - \cos\theta\right), \tag{2.2}$$

where $\lambda_c = \dfrac{h}{m_e c}$ is a constant denoted "*the Compton wavelength for electrons*" which equals the wavelength of a photon having the same energy as the rest-mass energy of the electron. Notice that maximum energy transfer to the electron is obtained with a scatter angle of 180° (backscatter), but it is not possible to transfer all the energy of the incoming photon to the electron (conservation of momentum).

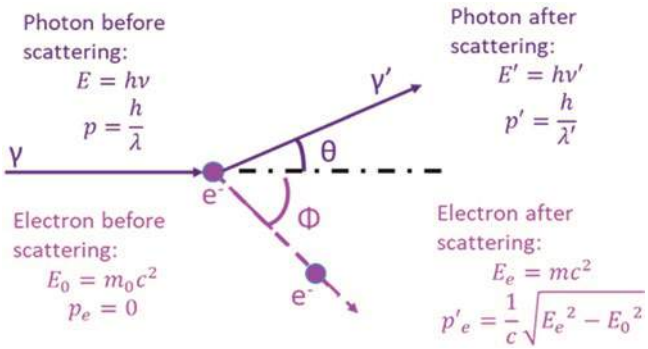

Fig. 2.3 The Compton process. The incident photon (γ-ray) interacts with an electron initially at rest resulting in a scattered photon (at angle θ) and electron (at angle Φ). The energy (E) and momentum (p) of the photon and electron before and after (marked with ′) scattering are given in the figure (Created with BioRender)

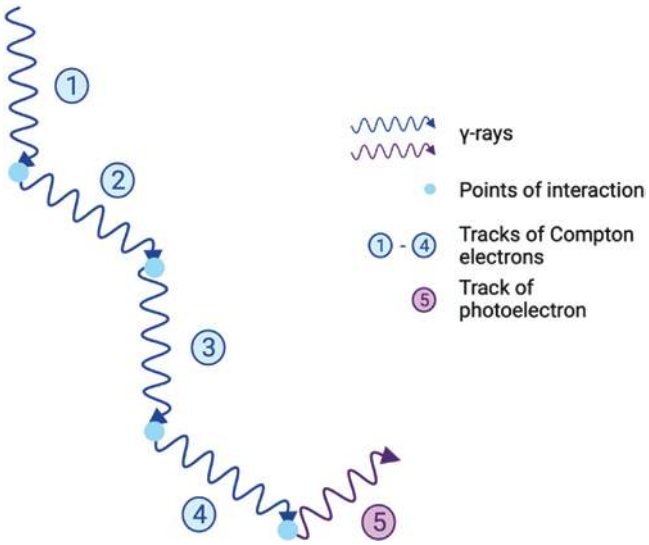

Fig. 2.4 A typical example of a sequence of energy deposits. The energy of an original 1.25 MeV photon is deposited in five subsequent Compton processes with a final energy deposition in the form of a photoelectric process. The figure shows the mean range in water (dotted arrows) for the incoming photon and the reduced-energy photons emitted for each Compton process. The scale shown in the bottom left only applies to photons. The electron mean range is much shorter starting at about 2 mm going down to about 36 μm in the last Compton scattering (which is still larger than a typical cell diameter) (Created with BioRender)

As seen in Fig. 2.4, depending on the incoming photon energy, there will be a series of Compton processes, each with emission of an electron, followed by a photoelectric process in the end. The result of such a Compton track is an energy distribution of secondary electrons with many low-energy electrons but also a few with high energy. The high-energy electrons are important for the dose distribution in the irradiated material, because they transport energy away from the place of the primary photon interaction and deposit their energy further into the irradiated material.

Pair production occurs by the incoming photon interacting with the nuclear forces in the irradiated material resulting in an electron-positron pair. The rest energy of the two newly formed particles is 1.022 MeV, so the incoming photon must have higher energy than this for the process to occur. In body tissues and cells, more than 20 MeV in photon energy is required for pair production to dominate over the Compton processes.

The Compton process dominates in biological material for energies relevant for medical use of photons. However, the cross section (an expression of the probability of interaction) for each process also depends on the atomic number Z. The cross section is proportional to Z^4 for photoelectric effect, Z for Compton effect, and Z^2 for pair production.

Thus, the higher the effective atomic number, the lesser the importance of the Compton effect (Box 2.4).

Box 2.4 Interaction of Photon with Matter

- Electromagnetic radiation can ionize atoms/molecules through three different processes (photoelectric effect, Compton process, and pair production) depending on the photon energy and atomic number of the elements involved.
- The Compton process dominates in biological material for energies relevant for medical use of photons, but a Compton track ends with the photoelectric effect.

2.1.3 Particle Radiation

As described above, in physics, a particle is considered to be an object, which can be described through its properties including volume, density, and mass. In the context of particle radiation, two types of particles are defined: charged particles, such as electrons, protons, α-particles, or other ions and uncharged particles such as neutrons. In general, particle radiation can interact with matter through a number of different processes, where the frequency of occurrence depends on the particles' mass, velocity, and charge. In the first type of the process called electronic interaction, the particle interacts with electrons in the atomic shell, and in the second, called nuclear interaction, the particle interacts with the atomic nuclei. All interactions can be considered as collisions between two masses, which can be either elastic or inelastic.

There are three types of electronic or Coulomb interactions, which can occur with or without energy loss from the incident particle. Elastic scattering of the particle in the atomic shell occurs with only neglectable energy transfer, as only the energy which needs to be transferred is that which is necessary to fulfill energy and momentum conservation. In this case, the incident particle is scattered and changes its direction. The two inelastic electronic processes are shown in Fig. 2.5 (left). The particle described through its atomic number z, its mass m, and its energy E is interacting with an atom of the matter characterized by the atomic number Z, the mass number A, and the density of the matter ρ. In the inelastic collision, the particle transfers energy to the hit electron. If sufficient energy is transferred, the electron will leave the atom, thus ionizing it. When the transferred energy is higher, the electron gets additional kinetic energy and can then itself act as particle radiation. If the energy is lower and fits the energy difference between two electron shells (the defined energies at which electrons "orbit"), the electron is excited, which means lifted to the higher shell. After a certain time, the electron falls back while emitting a photon with the energy corresponding to the energy difference between the shells.

In nuclear interactions, again three types can be defined. Firstly, elastic nuclear scattering, also called nuclear coulomb scattering, describes the elastic collision of a particle with the atomic nucleus. Here, the particle does not lose energy and only a deflection occurs (Fig. 2.5). In inelastic nuclear scattering, the particle is deflected and emits light, the so-called bremsstrahlung. Lastly, an interaction with the target nuclei itself is possible inducing nuclear reactions.

2.1.3.1 Charged Particle Radiation

Charged particle radiation describes high-energy massive particles such as electrons, protons , and other ions. These particles interact with matter through the described electronic or nuclear interactions. In each interaction, only a small amount of the total energy is transferred, and although the whole process of interaction is statistical in its nature, one can say that the particles stop more or less uniformly at a certain distance called the range. Furthermore, in each interaction, a certain angular deflection happens, which causes the particle to travel in a crooked path, and which effectively causes the incident particle beam to widen, while traversing a medium. The types of interactions can be described through the occurring energy loss and deflection of particle radiation in matter.

Ionizations and excitations, which occur in the electronic interactions, can be differentiated into soft and hard collisions. Interactions of the charged particle with the electrons in the outer atomic shell are called soft collisions, as the energy transfer is low (a few eV). The electrons, which are ionized, have a low energy and therefore emit all the energy in close proximity to the point of interaction. These soft collisions are responsible for approximately 50% of the total

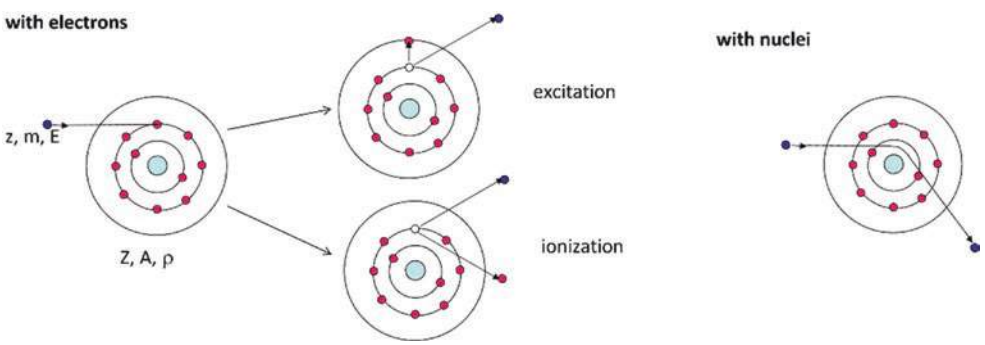

Fig. 2.5 Visualization of the electronic interactions (left) and the nuclear interaction (right) of a particle with atomic number z, mass m, and energy E with matter with atomic number Z, mass number A, and density ρ (Created with BioRender)

energy transfer of a particle. As the energy transfer of a single collision is very low, the particle velocity decrease is also low. But as a lot of these interactions occur, the slowing is, although of statistical nature, on average happening continuously. For particles which have a very high energy and thus velocity, the Cherenkov effect can occur. This effect describes the emittance of light, when a particle flies through matter with a velocity larger than the speed of light in this corresponding matter. This light is called Cherenkov radiation and can be seen as blue in the cooling water of nuclear reactors. The Cherenkov effect does not play a role in the effects of particle radiation on biological matter.

Coulomb interactions with the electrons of the inner shells are called hard collisions. Here, the electrons produced in ionizations have a higher energy and larger deflection angles compared to the ones from soft collisions. These electrons are called δ-rays, and they transfer their energy via soft collisions to the matter, thus spreading the energy distribution of an incident particle up to several μm distance to the incident particle track. This effect plays a major role in the microdosimetry.

Electronic interactions are the main contributors to the energy loss for high ion energies (see Fig. 2.6) but have a negligible deflection per collision.

Energy loss through elastic nuclear scattering as described above is only an important contribution to the total energy loss for ion energies below approximately 0.01 MeV/u. Here, the ions are already close to stopping and have a remaining range in the order of nanometers. For high ion energies

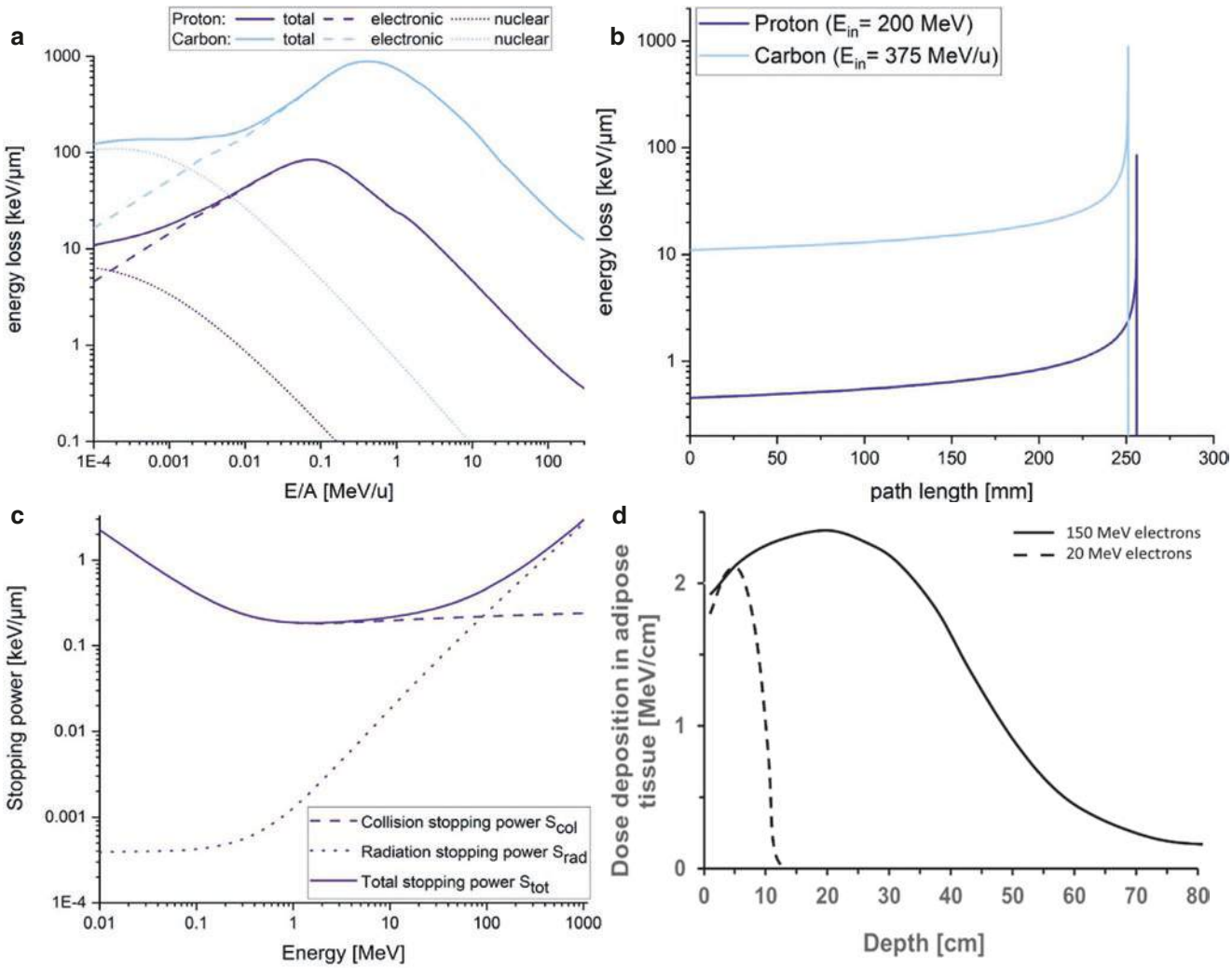

Fig. 2.6 (**a**) Energy loss for protons (purple) and carbon (blue) ions depends on ion type and ion energy. For lower energies, the nuclear energy loss (dotted lines) starts to get an influence. At energies above ~0.0005 MeV/u for protons and ~0.005 MeV/u for carbon ions, the electronic energy loss is dominant (dashed lines) and the nuclear energy loss can be even neglected for higher energies. *E/A* is the energy divided by mass number. (**b**) Energy loss for a proton with initial energy of E_{in} = 200 MeV with a range in water of 256 mm on the left and for a carbon ion with initial energy of E_{in} = 375 MeV/u with a range in water of 251 mm on the right: at the end of range at a path length, the energy loss is increasing and rapidly goes to zero when the ion stops. The curve shape for the carbon ion is the same as for the proton but with a higher energy loss at all times. Energy losses are calculated via SRIM (SRIM—The Stopping and Range of Ions in Matter, J. Ziegler, http://www.srim.org/). (**c**) Stopping power of electrons depending on electron energy simulated using estar (https://physics.nist.gov/PhysRefData/Star/Text/ESTAR.html). (**d**) Energy loss of electrons in adipose tissue with penetration depth (inspired by Hazra et al. 2019) (licensed under CC-BY-4.0) [26]

($E >$ several 100 MeV/u), elastic and inelastic nuclear scattering are again mainly responsible for deflection but also for energy loss through emission of bremsstrahlung. There are also other mechanisms possible, happening quite rarely at the energies used in society, but which should be mentioned here [21, 22]. These are direct interactions with the nuclei, namely transfer reactions like stripping or pickup, where nucleons are transferred from or to the incident particle. Also charge exchange can happen, which is a combination of stripping and pickup, where a neutron of the particle is exchanged with a proton of the atom or vice versa. Also, fragmentation can occur, where the incident particle and/or the atomic nucleus break up into (more than two) fragments. And finally, fusion reactions can occur, where the incident particle is fused into the atomic nucleus and both together form a new nucleus.

Energy Loss and Range

The exact energy loss during an interaction is described through the so-called stopping power S and is made up of the collision S_{col} and the radiation S_{rad} stopping power [23]:

$$S = \frac{\mathrm{d}E}{\mathrm{d}x} = S_{\text{col}} + S_{\text{rad}}. \tag{2.3}$$

The collision stopping power is the energy loss through collisions along the track in matter. For high energies of the impacting particles, the collisional stopping power can be described by the known Bethe–Bloch formula, which is based on perturbation theory and can also incorporate relativistic corrections.

For protons or heavier ions, the collision power is

$$S_{\text{col}} = \left(\frac{\mathrm{d}E}{\mathrm{d}x}\right)_{\text{col}} = \rho \cdot 4\pi \cdot r_e^2 \cdot m_o c^2 \cdot \frac{Z}{u \cdot A} \cdot z^2 \cdot \frac{1}{\beta^2} \cdot R_{\text{col}}(\beta). \tag{2.4}$$

For electrons or positrons, this is

$$S_{\text{col}} = \left(\frac{\mathrm{d}E}{\mathrm{d}x}\right)_{\text{col}} = \rho \cdot 2\pi \cdot r_e^2 \cdot m_o c^2 \cdot \frac{Z}{u \cdot A} \cdot z^2 \cdot \frac{1}{\beta^2} \cdot R^*_{\text{col}}(\beta). \tag{2.5}$$

This formula includes the properties of the particle energy, charge number, and velocity characterized by $m_o c^2$, z^2, and β^2 and the properties of the matter density ρ, charge number Z, and mass number A. r_e is the classical electron radius and u the atomic mass unit. The terms $R_{\text{col}}(\beta)$ and $R^*_{\text{col}}(\beta)$ are called rest function for heavier particles or electrons and positrons, respectively. These are dimensionless quantities, which contain the complex energy and matter-dependent cross sections for collision stopping.

In practical use, especially in radiobiology, it is just important to know some proportionalities:

$$S_{\text{col}} \propto \rho \cdot \frac{Z}{A} \cdot z^2 \cdot \frac{1}{v^2}. \tag{2.6}$$

The radiation stopping power does not play a role for protons and heavier particles, due to their heavy masses, but for electrons, which are more than three orders of magnitudes lighter.

The radiation stopping power for electrons is

$$S_{\text{rad}} = \left(\frac{\mathrm{d}E}{\mathrm{d}x}\right)_{\text{rad}} = \rho \cdot \frac{1}{u} \cdot r_e^2 \cdot \alpha \cdot \frac{Z^2}{A} \cdot E_{\text{tot}} \cdot \left(R_{\text{rad},n} + \frac{1}{Z} R_{\text{rad},e}\right). \tag{2.7}$$

With E_{tot} the total energy of the electron and α the fine-structure constant. Again, dimensionless rest functions occur describing the cross sections for interactions with nuclei $R_{\text{rad},n}$ and electrons in the atomic shell $R_{\text{rad},e}$.

For quantification in radiobiology, the detailed description of the stopping power is not used, as it would be too complicated, and the perturbation parts only contain a small correction. Conventionally, the linear energy transfer $\text{LET} = \frac{\mathrm{d}E}{\mathrm{d}x}$ is used instead. The LET only takes electronic interactions into account. The difference between LET and electronic stopping lies in their origin. The electronic stopping is focused on the energy loss of the impacting particle, and it has a negative sign as it acts as a friction force. The LET has a positive sign, and it is the energy that the target sees deposited in itself; this "positive amount of energy" creates the nonequilibrium dynamics, which are the first radiation-induced effects. The LET and the electronic stopping are equal for big samples, which is the case in radiobiology. Therefore, the LET is the same as the electronic stopping, which can be looked up in programs such as pstar, astar, or SRIM [24, 25].

For protons and heavier ions at energies larger than ~0.01 MeV/u, the electronic energy loss is the dominant process, as can be seen in Fig. 2.6, whereas for low ion energies, the nuclear energy loss becomes dominant, validating the use of LET as the most appropriate measurement quantity for radiobiologically relevant energies of >1 MeV. The energy loss has a peak at

$$v \approx z^{\frac{2}{3}} \cdot \frac{c}{137} \approx z^{\frac{2}{3}} \cdot 25 \frac{\text{keV}}{u}. \tag{2.8}$$

For even higher ion energies, the energy loss decreases again.

For a single collision, considering a maximum energy ΔE_{max} which can be transferred through electronic interactions is

$$\Delta E_{\text{max}} \approx 4 \frac{m_e}{m} E. \tag{2.9}$$

With m_e being the electron mass, m the ion mass, and E the ion energy. For protons, this maximum energy transfer

per collision is $\Delta E_{\mathrm{max},p} \approx 0.2\ \%\ E_p$. For carbon ions, it is even lower at $\Delta E_{\mathrm{max,C}} \approx 0.02\ \%\ E_{\mathrm{C}}$. Therefore, thousands of collisions are necessary before an ion stops, and the more energy it has lost, the slower it gets and therefore the interactions get closer together.

If one looks at the energy loss of an ion depending on the path length traveled in a target medium, a unique distribution is visible (Fig. 2.6b). The energy loss at the entrance is low and only slightly increasing with depth. Just in the last millimeters or even below, the energy loss sharply increases. After the peak, an even sharper decrease is visible until the ion stops only shortly after reaching the peak energy loss. This distribution is called the Bragg curve. Due to this distribution, a range of the particle can be defined, which is the average distance the ion travels before it stops. Due to the statistical nature of the interactions, the range can only be given as an average quantity. The ion range can be calculated as [23]:

$$R\left(E_{\mathrm{kin}}\right) = \int_0^{E_{\mathrm{kin}}} \left(-\frac{\mathrm{d}E}{\mathrm{d}x}\right)^{-1} \mathrm{d}E. \tag{2.10}$$

For example, for protons with therapy-relevant energies between approx. 10 MeV and 200 MeV, the range can be approximated to

$$R_p \cong 19\,\mu\mathrm{m}\left(\frac{E}{\mathrm{MeV}}\right)^{1.8} \text{ with } E = \frac{mc^2}{\sqrt{1-\beta^2}}. \tag{2.11}$$

The unique energy loss distribution, with a peak energy loss just at the end of range, gives particles a great advantage in tumor therapy compared to photons, as the tissue behind the tumor will not get irradiated at all, as explained in Chap. 6.

For low-energy electrons, the collision stopping power is the dominant process, whereas for higher energies, the radiation stopping power gets dominant (Fig. 2.6c). The energy loss distribution with penetration depth is due to the contribution of the radiation stopping power different to protons and heavier ions (Fig. 2.6d). There is no clear range visible, but after a small buildup, the maximum is reached, followed by a decrease, and with higher depth the energy loss will be zero; this is when the electron has stopped. The possible penetration depth and especially the maximum of energy loss are dependent on energy. This is relevant for therapy, where low-energy electrons are used to irradiate skin tumors, whereas for deeper lying tumors, higher energies are necessary (Box 2.5).

Box 2.5 Characteristics of Charged Particles

- Charged particles transfer their energy mainly through coulomb interactions with electrons and nuclei of the atoms of the matter.
- The energy loss of the particle can be described by the Bethe–Bloch formula of the stopping power.
- For ions, only collision stopping power plays a role, and for electrons also radiation stopping power.
- Ions have a defined range, where energy loss follows the Bragg curve.

Scattering and Deflection

The interaction of particles with matter is not only responsible for energy loss but also for a deflection of the incident particle. For the coulomb interactions with electrons, only negligible deflection occurs. The nuclear Coulomb interactions also give small deflections per collision. Furthermore, Rutherford scattering with the atomic nucleus can occur. Taking all the interactions into account, significant deflection of particles is common. This process is called multiple small-angle scattering. Additionally, the Rutherford scattering can lead to single large-angle scattering events, but this effect is very rare. The scattering of single ions leads to widening of the incident beam of particles with penetration depth. Due to the dominance of the multiple small-angle scattering, the lateral profile of the beam can be approximated by a Gaussian distribution. It is important to know that for larger lateral distances, the Gaussian distribution no longer holds, as the large-angle scattered ions are deflected in this region. But as already mentioned, this is a rare process and does not have an influence on the beam size. The lateral spread defined as the σ of the Gaussian distribution is $\sigma \propto \frac{z}{E_{\mathrm{kin}}} x^{\frac{3}{2}}$, with E_{kin} the kinetic energy of the particle, z the charge, and x the distance traveled (Box 2.6).

Box 2.6 Scattering of Particles

- Coulomb interactions are responsible for scattering of the particle.
- Multiple coulomb scattering leads to a deflection of the particle.
- Single Rutherford scattering with the atomic nuclei leads to large deflections, but these are very rare.
- An incident particle beam will have a Gaussian energy distribution profile in the lateral direction due to the statistical nature of scattering.

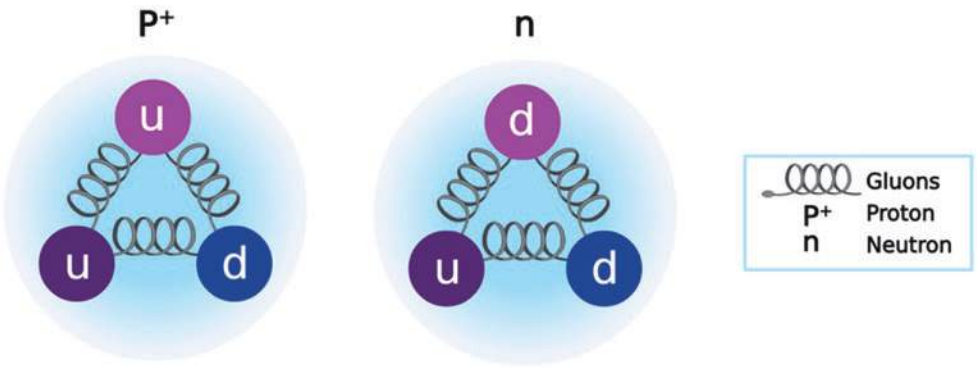

Fig. 2.7 Quark structure of proton and neutron, with binding gluons shown (Created with BioRender)

2.1.3.2 Neutron Radiation

The existence of the neutron as a component of the atom was first proposed by Rutherford in 1911, though it was Chadwick who in 1932 detected the particle as a result of experiments involving gamma irradiation of paraffin [27]. Advances in particle physics have led to our current understanding of hadronic matter which includes neutrons, such that the quark model of the neutron envisages the particle as consisting of two down quarks and an up quark (*udd*), as shown in Fig. 2.7.

The neutron differs from the proton (*uud*) by a single quark such that it has almost identical mass (m_n = 939.6 MeV/c^2, m_p = 938 MeV/c^2) though the neutron has zero charge. It also differs further in that, while the proton is thought to be stable (current $T_{1/2}$ of ~10^{38} years), the free neutron is unstable with a mean lifetime of approximately 879.6 s. While electrically neutral, the neutron does have a magnetic moment of approximately −1.93 $\lceil N$, where that for the proton is approximately 2.79 $\lceil N$ (and where $\lceil N$ is the nuclear magneton). As the neutron is a fermion, it has a spin of ½ [28].

Early experiments with neutrons relied upon their production in prototype nuclear reactors. Here, neutrons were classified according to their energies as thermal (E ~ 0.038 eV, on average associated with a Maxwell–Boltzmann distribution of particles at room temperature), slow (E < 0.1 MeV), fast (E > 10 MeV), or relativistic (with energies producing velocities of 0.1 c or above) [29].

Exploration of neutron interactions with matter has revealed that they have very complex energy cross sections, which vary substantially with the target material. However, the interactions may be broadly classified as elastic or inelastic interactions, with elastic collisions having a greater cross section at high neutron energies [29].

In elastic interactions, the neutron collides, typically, with a target nucleus, transferring some of its kinetic energy to the nucleus, which then recoils. It may be demonstrated that the maximum energy Q that a neutron of energy E_n and mass M may transfer to a recoil nucleus of mass m is given by [29].

$$Q = \frac{4mME_n}{(M+m)^2}. \tag{2.12}$$

In general, one may observe a cosine-squared spatial distribution of recoil energies for nuclei, Q, from which the original energy of the neutron beam may be estimated [29]:

$$Q = E_n \cos^2\theta. \tag{2.13}$$

In inelastic scattering events, either the neutron can promote the nucleus of element X to an excited state, from which the nucleus itself decays by re-emitting the neutron with different energy and momentum [(n,n') reactions], or, for neutrons with energy below 0.5 MeV, the nucleus absorbs ("captures") the incident neutron, causing it to transmute to a new elementary state, Y, generally with the emission of some product projectile, b, such as a proton, alpha particle, or gamma ray. The latter nuclear reactions are written as

$$X(n,b)Y, \tag{2.14}$$

where examples include ^{9}Be(n,γ)^{10}Be and ^{75}As(n,γ)^{76}As (radiative capture reactions).

The development of sources of neutrons for industrial purposes has been a highly complex undertaking. Spallation sources of neutrons, where a material is bombarded with a projectile particle and then emits a beam of neutrons, have existed for some time. However, these systems require acceleration of a projectile beam, which renders them costly from an energy-input perspective, though they produce highly intense beams which are useful in the imaging of materials, as well as for both breeding and burning of nuclear fuel. Most neutron beams are produced via collimation and focusing of neutron beams from nuclear reactors, for similar applications to those already highlighted, and importantly for therapeutic applications in medicine. The development of Wolter mirrors and lenses has provided the means to direct and focus beams of neutrons in a highly precise manner allowing for controlled therapeutic applications.

2.2 Sources and Types of Ionizing Radiation

Humans are continuously exposed to low levels of ionizing radiation from the surroundings as they carry out their normal daily activities; this is known as background radiation,

which is present on Earth at all times [30]. In addition, we are exposed to ionizing radiation from artificial sources during medical examinations and treatments, during processing and using radioactive materials, and during operation of nuclear power plants or accelerators (Figs. 2.8 and 2.9). Below we provide a summary of the possible scenarios of exposure to natural and artificial radiation.

2.2.1 Natural Background Radiation

Natural radiation is all around us, and we receive it from the atmosphere, rocks, water, plants, as well as the food we eat (Fig. 2.8). Naturally occurring radioactive materials are present in the Earth's crust; the floors and walls of our homes, schools, or offices; and food. Radioactive gasses are also present in the air we breathe. Our muscles, bones, and other tissues contain naturally occurring radionuclides [31]. Hence, our lives have evolved, and our bodies have adapted to the world containing considerable amounts of ionizing radiation. As per the United Nations Scientific Committee on the Effects of Atomic Radiation (UNSCEAR), terrestrial radiation, inhalation, ingestion, and cosmic radiation are the four foremost sources of public exposure to natural radiation.

1. **Terrestrial Radiation:** One of the major sources of natural radiation is the Earth's crust, where the key contributors are the innate deposits of thorium, uranium, and

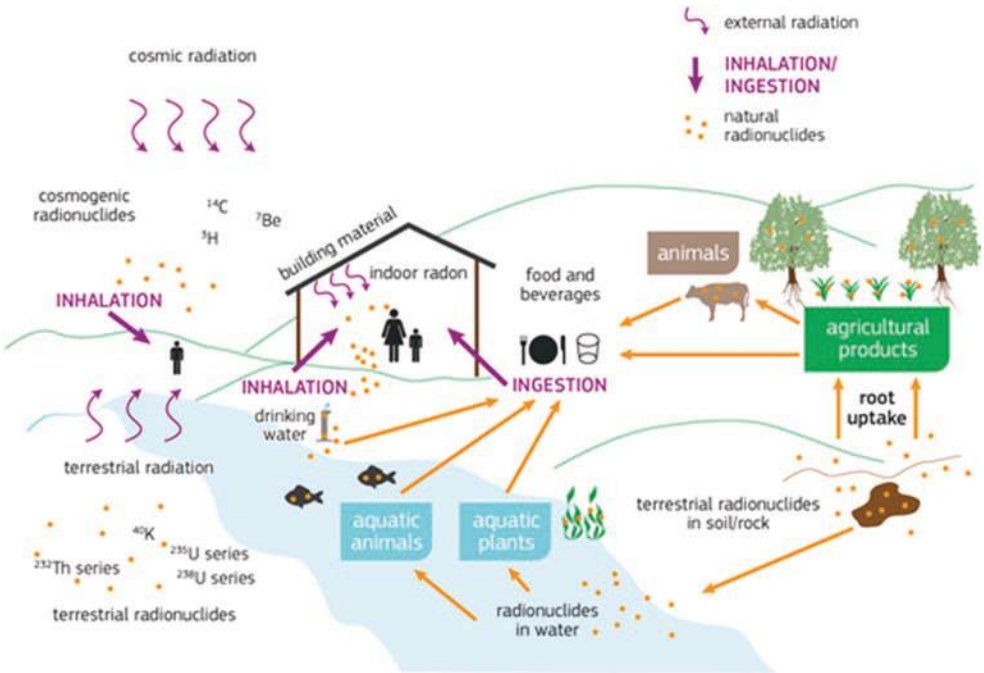

Fig. 2.8 Natural sources of ionizing radiation and their pathways (Figure from European Commission, Joint Research Centre—Cinelli, G., De Cort, M. & Tollefsen, T., *European Atlas of Natural Radiation*, Publication Office of the European Union [41]) (licensed under CC-BY-4.0)

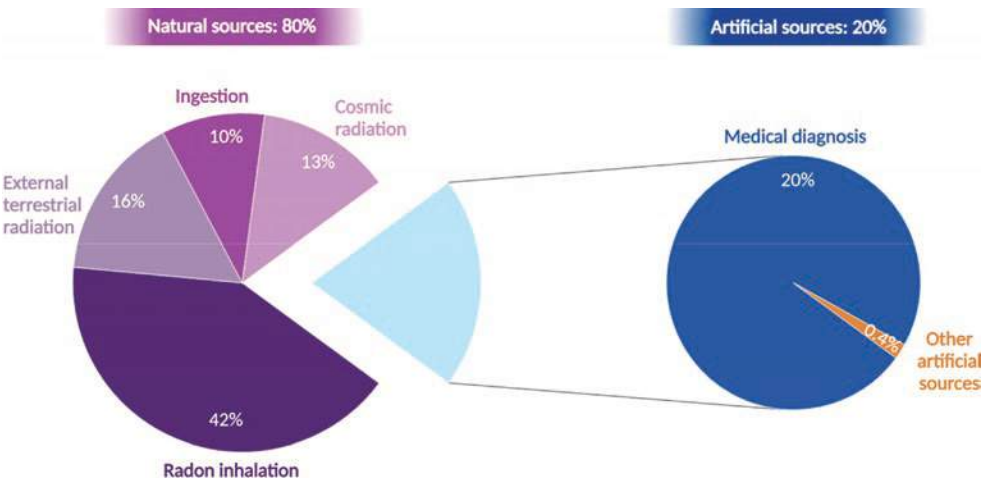

Fig. 2.9 Worldwide average annual human exposure to ionizing radiation (from UNSCEAR (2008) Sources and effects of ionizing radiation) (Created with BioRender)

potassium. These minerals are called primordial radionuclides and are the source of terrestrial radiation. These deposits discharge small quantities of ionizing radiation during the process of natural decay, and these minerals are found in building materials. Therefore, humans can get exposed to natural radiation both outdoors and indoors. These radiation levels can fluctuate substantially depending on the location. Traces of radioactive materials can be found in the body where nonradioactive and radioactive forms of potassium and other elements are metabolized in the same way [32].

2. **Inhalation:** Humans are exposed to inhalation of radioactive gasses that are formed by radioactive minerals found in soil and bedrock. For example, uranium-238, during its decay, produces radon (^{222}Rn) which is an inert gas and thorium produces thoron (^{220}Rn). These gasses get diluted to harmless levels when they traverse the Earth's atmosphere. However, at times, these gasses escape through cracks in the building foundations, are trapped, and accumulate inside buildings where they are inhaled by the occupants (indoor living) [30].
3. **Ingestion:** Vegetables and fruits are grown in the soil and groundwater, which usually contain radioactive minerals. We ingest these minerals and subsequently are exposed to internal natural radiation. Carbon-14 and potassium-40 are naturally occurring radioactive isotopes which possess similar biological characteristics as their nonradioactive isotopes. These radioactive and nonradioactive elements are used not only in building our bodies but also in maintaining them. Therefore, such natural radioisotopes recurrently expose us to radiation [30].
4. **Cosmic Radiation:** Space is permeated by radiation, not only of electromagnetic type but also constituted by ionizing particles with mass. The electromagnetic radiation in space spans all wavelengths, from infrared to visible, from X-ray to gamma rays. In general, however, "space radiation" mostly refers to corpuscular radiation, which has three main sources:
   (a) Galactic Cosmic Rays (GCRs): The GCRs constitute the slowly varying, low-intensity, and highly energetic radiation flux background in the universe, mostly associated with explosions of distant supernovae. The GCR spectrum consists of approximately 87% hydrogen ions (protons) and 12% helium ions (α-particles), with the remaining 1–2% of particles being HZE (high charge Z and energy) nuclei. The energies are between several tenths and 10×10 GeV/nucleon and more. GCRs directly hit the top of the Earth's atmosphere, generating secondary particle showers. However, some direct GCRs and generated secondary particles infiltrate the Earth's atmosphere reaching the ground. Such radiation gets absorbed by humans, and it thus constitutes a source of natural radiation exposure. Since at higher altitude the amount of atmosphere shielding us from incoming radiation is less, the higher we go in altitude, the higher dose we receive. For example, those living in Denver, Colorado (altitude of 5280 ft = about 1610 m), receive a higher annual radiation dose from cosmic radiation than someone living at sea level (altitude of 0 ft) [32]. GCR ions are a major health threat to astronauts for missions beyond the near-Earth environment and for interplanetary travel [33]. For Mars, the thin atmosphere combined with the absence of a planetary magnetic field essentially offers very little shielding from the incoming GCRs [34, 35]. Also, GCRs directly reach the surface of airless bodies such as the Moon [36].
   (b) Radiation from the Sun: This consists of both low-energy particles flowing constantly from the Sun (the solar wind) and of solar energetic particles (SEPs), originating from transient intense eruptions on the Sun [37]. The solar wind is stopped by the higher layers of the atmosphere of our planet (and other celestial bodies with an atmosphere). SEPs come as huge injections and are composed predominantly of protons and electrons. Typical proton energies range from 10 to 100 of MeV. They are generally quite efficiently stopped in the Earth's atmosphere, but some direct SEPs and their high flux of secondaries could eventually be dangerous for high-altitude/latitude flights and their crew [38] and for astronauts of the International Space Station (ISS) in extravehicular activities. Finally, SEPs can be a strong concern also for astronauts during interplanetary travel, such as a trip to Mars, even inside the spacecraft [39], or for humans on the surface of the Moon.
   (c) Trapped Radiation: This consists of GCRs and SEPs and their secondaries trapped by the Earth's magnetic field into the Van Allen radiation belts. Such belts comprise a stable inner belt of trapped protons and electrons (energies are between keV and 100 MeV) and a less stable outer electron belt. The inner Van Allen belt comes closest to the Earth's surface, down to an altitude of 200 km, in a region just above Brazil. This area is named the South Atlantic Anomaly [40]. An increased flux of energetic particles exists in this region and exposes

orbiting human missions to higher-than-usual levels of radiation (Box 2.7).

Box 2.7 Sources of Natural Radiation

The natural radiation to which we are continually exposed has its sources in:

- Cosmic radiation (the portion of it reaching the ground)
- Radiation from radioactive elements in rocks
- Radioactive gasses, generally at harmless concentration in the air but that can potentially also get trapped in building walls
- Food, grown in soil and groundwater, which can contain radioactive minerals

2.2.2 Artificial Radiation Sources

Nuclear power stations/plants use uranium to drive a fission reaction that heats water to produce steam. The latter drives turbines to produce electricity. During their normal activities, nuclear power plants release small amounts of radioactive elements, which can expose people to low doses of radiation. The water that passes through a reactor is processed and filtered to remove these radioactive impurities before being returned to the environment. Nonetheless, minute quantities of radioactive gasses and liquids are ultimately released to the environment. Such releases must be continuously monitored and are under the legislative framework of international organizations dealing with nuclear energy, such as the European Atomic Energy Community (EURATOM), established by one of the Treaties of Rome in 1958. Similarly, uranium mines and fuel fabrication plants release some radioactivity that contributes to the dose of the public [42]. The eventual release of radioactive materials should also be monitored and kept under established levels during the decommissioning of a nuclear power plant, from the shutdown of the reactor to the operation of radioactive waste facilities, and also including the short- and intermediate-term storage of spent nuclear waste to the transport to and storage in long-term geological disposal areas.

Technologically enhanced naturally occurring radioactive materials (TENORM): All minerals and raw materials contain radionuclides, commonly denoted as naturally occurring radioactive materials (NORM). When concentrations of radionuclides are increased by technological processes, the term technologically enhanced NORM (TENORM) is applicable. Coal-fired power stations, for example, emit an amount of radioactivity compared to or even higher (especially in the past) than nuclear power plants. Just for example, US coal-fired electricity generation in 2013 gave rise to 1100 tonnes of uranium and 2700 tonnes of thorium in coal ash. Other TENORM industries include oil and gas production, metallurgy, fertilizer (phosphate) manufacturing, building industry, and recycling [43].

Accelerators: The operation of accelerators, such as the Large Hadron Collider (LHC) at CERN for fundamental high-energy physics experiments, results in the production of radiation, in particular protons, because of the nuclear interactions between high-energy beams and accelerator components. Thus, the radiation levels around accelerators must be monitored continuously to ensure the protection and safety of the workers and of the public [44].

Radionuclide production facilities: Radionuclides are used worldwide in (a) medical imaging, fundamental to make correct diagnoses and provide treatments, in which radionuclides are injected into patients at low doses for functional imaging to detect diseases, and (b) therapy, in which radionuclides bound to other molecules or antibodies can be guided to a target tissue, for a local treatment of cancer. Facilities that produce radionuclides and facilities in which radionuclides are processed are reactors and particle accelerators. Radionuclides used in imaging and therapy are often beta or alpha emitters, or both. Thus, the facilities, reactors, and particle accelerators can present radiation hazards to workers and must be properly controlled and monitored, as is the case with the subsequent processing of radioactive material. Among the 238 research reactors in operation in 2017, approximately 83 were considered useful for regular radioisotope production [45]. Approximately 1200 cyclotrons worldwide were used to some extent for radioisotope production in 2015 [46]. The facilities must ensure the application of the requirements of the IAEA [47] (2014) intended to provide for the best possible protection and safety measures.

Hospitals: Daily, healthcare workers and patients are exposed to various diagnostic and therapeutic radiation sources [48, 49]. The radiation environment in different hospital departments (nuclear medicine, diagnostic radiology, radiotherapy, …) can be generated by different sources. Hospitals providing radionuclide-based treatments need to protect the staff involved and keep their dose within the acceptable levels. Similarly, the discharged patient must be monitored and measurements for protection purposes must be taken to keep dose to the public within acceptable levels. This may require hospitalization with isolation during the first hours or days of treatment [50, 51]. Waste should be minimized and segregated, and packages labeled and stored for decaying. Measures should also be in place for patients' household waste related to, for example, urine. In a radiology department, the radiation emitted during fluoroscopic procedures is responsible for the greatest radiation dose to the medical staff. Radiation from diagnostic imaging modalities, such as mammography, computed tomography, and nuclear medical imaging, is a minor contributor to the cumula-

tive dose incurred by healthcare personnel [52]. In radiotherapy departments, photons and electrons are mainly produced by linear accelerators. Rarely, cobalt sources are used to produce radiation. With the current safety regulations, radiotherapy staff will get almost no dose during normal operation. The same is true for modern brachytherapy machines, which are almost all after loading machines avoiding direct contact between the radioactive source and the operator.

Ion radiotherapy facilities: Most currently existing ion radiotherapy facilities use protons, with new facilities now being built for the acceleration of other ions, such as carbon. They are mostly cyclotrons or synchrotrons. For such facilities, the major issue is the massive production of neutrons. Ionizing radiation results from the passage of such neutrons through matter and from the radioactivity induced in exposed materials. In accelerator facilities, radioactivity is produced in the very material components, such as their beam delivery/shaping components, as well as in all the structural components and other materials in the facility. Induced radioactivity in treated patients could also reach considerable levels.

Nuclear bombs: Nuclear weapons have an explosive power deriving from the uncontrolled fission reaction of plutonium and uranium. This yields a large number of radioactive substances (isotopes) that are blown into the atmosphere. These radioactive isotopes gradually fall back to Earth. If a weapon is exploded near the Earth surface, radioactive fallout is formed in the vicinity of the burst point in a matter of tens of minutes to a couple of days (depending on the burst yield and the distance to the burst point); if a weapon is detonated aboveground (e.g., in Hiroshima and Nagasaki, the bombs exploded about 500 m above the ground level), local fallout is not formed but the radionuclides fall worldwide over a period of many years. Gamma-ray and neutron exposures leading to increased cancer incidence have been studied in the survivors of the atomic bombings in Japan since 1950 (the so-called Life Span Study, LSS, cohort), and currently all potentially suitable risk estimates are built on the excess risk from the LLS study [53]. Interestingly, the numerous tests of nuclear weapons performed by many countries since after World War II and the ensuing fallout have contributed minimally to the overall background radiation exposure (Box 2.8).

Box 2.8 Sources of Artificial Radiation

Artificial radiation sources are:

- Medical and radionuclide production facilities, accelerators for ion beam cancer therapy
- Technologically enhanced naturally occurring radioactive materials (TENORM)
- Nuclear power plants
- Accelerators for purely fundamental research in physics

2.3 Direct and Indirect Effects of Radiation

The interaction of ionizing radiation (IR) with matter leads to biological damage that can impair cell viability. Biological damage induced by IR arises from either direct or indirect action of radiation. Direct effects occur when IR interacts with critical target molecules such as DNA, lipids, and proteins, leading to ionization or excitation, which causes a chain of events that ultimately leads to the alteration of biomolecules. Indirect effects occur when IR interacts with water molecules, the major constituent of the cell. This reaction, called water radiolysis, generates high-energy species known as reactive oxygen species (ROS) that are highly reactive toward critical targets (cell macromolecules) and, when associated with reactive nitrogen species (RNS), lead to damage to the cell structure. Mechanism and critical targets for ionizing radiation to produce biological damage through direct and indirect effects are shown in Fig. 2.10. Damages to cell macromolecules may be multiple and are detailed in Chap. 3.

2.3.1 Direct Effects of Radiation

Direct effects occur when the ionization takes place within a critical target with relevance to cell functions, such as DNA, lipids, and proteins. These effects are produced by both high and low linear energy transfer (LET) radiation. However, it is the predominant mode of action of high LET radiation such as alpha particles and neutrons, comprising about two-thirds of the radiation effects.

When critical molecules in the cell are directly hit by radiation, their molecular structure may be altered resulting in their functional impairment. While molecules from all cell organelles (including mitochondria, endoplasmic reticulum, or Golgi apparatus) may be hit, the nuclear DNA molecule has always been seen as the most critical target (because, unlike proteins, lipids, and carbohydrates, only a single copy of DNA is present in a cell) and was, therefore, the most thoroughly studied. The DNA damage produced by radiation includes base alterations, DNA–DNA cross-links, single- or double-strand breaks (SSB or DSB), or complex damages (described in Chap. 3).

2.3.2 Indirect Effects of Radiation

Indirect damages produced by IR in the cell macromolecules are mediated by ROS (resulting from water radiolysis) and by RNS (formed following the reaction of O_2 with endogenous nitric oxide). The indirect effects contribute to about two-thirds of the damages induced by low LET radiation (X-rays, gamma-rays, beta particles), which is explained by

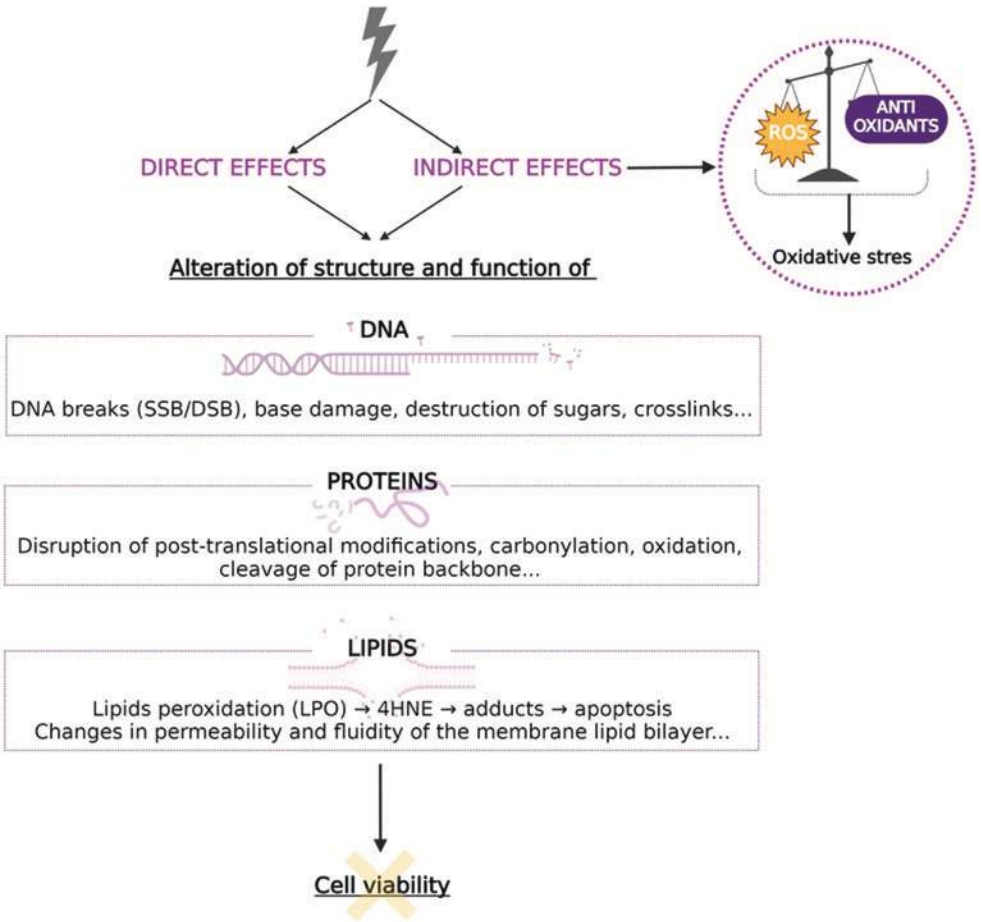

Fig. 2.10 Mechanism and critical targets for ionizing radiation to produce biological damage through direct and indirect effects (Created with BioRender)

the fact that they are more sparsely ionizing compared to high LET radiation.

When radiation deposits energy in a biological tissue, it takes time until perceiving that an effect has occurred. The succession of the generation of events determines the four sequential stages that translate into the biological effects. These stages, with very different duration, are physical, physicochemical, chemical, and biological [54–56].

The physical stage is very transient, lasting less than 10^{-16}–10^{-15} s, during which energy (kinetic if particles, or electromagnetic if waves) is transferred to the electrons of atoms or molecules, determining the occurrence of ionization and/or excitation. It is at this stage that ions are formed, which will initiate a sequence of chemical reactions that end up in a biological effect. In the case of water radiolysis (decomposition of water molecules due to IR), the ions H_2O^+ and e^- are formed, as well as the excited water molecule (H_2O^*) [54–56].

Very soon (10^{-12} s) after the formation of these ions, the physicochemical stage begins, with their diffusion in the medium and consequent intermediate formation of oxygen and nitrogen radical species, i.e., atoms, molecules, or ions that have at least one unrepaired valence electron and hence are very reactive chemically. Following the example of water radiolysis, it is at this stage that $H^{\cdot} + HO^{\cdot}$, $H_2 + 2HO$, $HO^{\cdot} + H_3O^+$, $HO^{\cdot} + H_2 + OH^-$, and e^-_{aq} are formed [55, 56], but also superoxide anion ($O_2^{\cdot -}$) and hydrogen peroxide (H_2O_2). Peroxynitrite anion ($ONOO^-$) is also formed following the reaction of $O_2^{\cdot -}$ with endogenous nitric oxide (NO). Together with peroxynitrous acid (ONOOH), nitrogen dioxide ($NO_2^{\cdot}$), dinitrogen trioxide (N_2O_3), and others, they are referred to as RNS. The activation of the nicotinamide adenine dinucleotide phosphate (NADPH) oxidase, the mitochondrial electron transport chain (ETC), or the nitric oxide synthase by IR can also contribute to ROS/RNS generation.

In the next chemical stage, the formed radicals and ions recombine and interact with critical cellular organic molecules (DNA, lipids, proteins), inducing structural damages that will translate into disruption of the function of these molecules. Within the DNA molecule, possible chemical reactions with nitrogenous bases, deoxyribose, or phosphate group may result in breaks and recombinations with the consequent formation of abnormal molecules. Among ROS, OH, which has a strong oxidative potential, is a main contributor to cell damages. The chemical stage can last from 10^{-12} s to a few seconds [55, 56]. ROS and RNS have also been largely implicated in

the so-called non-targeted effects of IR (further discussed in Sect. 2.8.2).

Finally, the biological phase occurs, as a consequence of the spreading of chemical reactions involving various biological processes. The existence of more or less effective cellular damage repair mechanisms is responsible for the more or less belated appearance of biological effects and explains the possible long duration of this stage: from a few minutes to decades, depending on the type of radiation, the dose and dose rate, and the radiosensitivity of the irradiated tissue.

Differences in tissue radiosensitivity can be partially explained by the cellular antioxidant capacity, which may vary between cell types. Indeed, to counteract oxidative insults, cells have evolved several defense mechanisms that consist of enzymatic and nonenzymatic systems. When the amount of ROS/RNS exceeds the antioxidant capacity of the cells, a state of oxidative stress arises, characterized by a decreased pool of antioxidants and modifications in nucleic acids, lipids, and proteins. Oxidative stress can persist for much longer and extend far beyond the primary targets as well as can be transmitted to progeny of the inflicted cells. Responsible for this seems to be the continuous production of ROS and RNS, which can last for months.

2.3.3 Biological Damages Induced by Direct and Indirect Effects of Radiation on Cell Organelles

Virtually all cell molecules and organelles may be damaged by IR, with consequences for the cell function depending on the impact of the damage inflicted.

According to the radiobiology paradigm, a nucleus is regarded as the main target of IR due to the genetic information contained in the DNA. Therefore, damages to this molecule are considered the most critical ones for cell survival. While efficient repair mechanisms exist to preserve the genome integrity, IR may break bonds in purine and pyrimidine nitrogenous bases in the DNA (which may lead to mutations), SSBs or DSBs, cross-linking, and complex damages. Among these lesions, DSBs and complex damages are the most serious due to the difficulty of their repair. A thorough description of DNA lesions is provided in Chap. 3.

Mitochondria can also be subject to radiation damage, both directly and indirectly. These organelles may represent more than 30% of the total cell volume, and the mitochondrial circular DNA can suffer strand breaks, base mismatches, or even deletions of variable length. In this context, mitochondria constitute a major target of IR [57]. Besides the DNA, changes in mitochondrial morphology have also been observed [58]. Absorption of IR may lead to the enlargement of mitochondria and the increase in length and number of branches of the cristae [58, 59], rupture of the outer and inner membranes, as well as vacuolization and loss of the matrix. These alterations are accompanied by the decreased activity of the respiratory chain, with special emphasis on complexes I, II, and III, which are systematically referred to as especially sensitive to the direct effects of IR. Additionally, there is a decrease in the respiratory capacity driven by succinate and the ATP synthase, with a consequent impact on oxidative phosphorylation. The radiation-induced decrease in the rate of oxidative phosphorylation can recover over time, depending on the cell type [60, 61]. The electrons in the respiratory chain can leak during their transport and reduce oxygen molecules leading to the formation of superoxide anions, which are precursors of most ROS. Upon irradiation, the level of ROS produced in the mitochondria greatly increases, although under physiological conditions, it is already high.

Irradiation may also cause morpho-functional changes in the endoplasmic reticulum (ER). After exposure to IR, ER dilates, vesicles appear, and its cisternae break into fragments. In the case of rough endoplasmic reticulum, irradiation induces degranulation accompanied by transformation of the membrane-bound ribosomes into free organelles [59, 62].

Likewise, irradiation may also disorganize the structure of the Golgi apparatus due to the induced fragmentation and rearrangement of its cisterns. In view of the effects of IR on the endoplasmic reticulum-Golgi apparatus complex, the ensuing alterations in the synthesis and maturation of proteins in the irradiated cells come as no surprise. Lysosomes may also increase in number and volume in the irradiated cells, which is accompanied by upregulation of the enzymatic activity in these organelles [58, 59] (Box 2.9).

Box 2.9 Direct and Indirect Effects of Radiation

- Direct effects predominate after exposure to high LET radiation (e.g., alpha particles, neutrons).
- Exposure to low LET radiation (e.g., X-rays, gamma rays, beta particles) induces mostly indirect effects.
- Indirect effects are mediated by ROS/RNS produced during and after the radiolysis of water.
- Apart from nuclear DNA, other cellular molecules and organelles may be altered by IR, including mitochondrial DNA, plasma membrane lipids, endoplasmic reticulum, Golgi apparatus, and lysosomes.

2.4 Radioactivity and Its Applications

Radiation and radioactivity have been existing ever since the Earth was formed and long before life started to evolve. All living organisms on Earth are continuously exposed to both natural and artificial radioactivity, and without it, life in the present form would have not evolved. Since the first experiments with radioactivity, our understanding of this phenomenon has increased, and consequently, today radioactivity has numerous applications important to human life and health.

2.4.1 Radioactive Decay

2.4.1.1 Natural Radioactivity

The rate of decay of a radioactive source is proportional to the amount of the substance that is present at any given instant. Therefore, if the number of radioactive nuclei in a sample is N, then we may say the following:

$$\begin{aligned} &-\frac{\mathrm{d}N}{\mathrm{d}t} \propto N \\ &\Rightarrow -\mathrm{d}N \propto N \cdot \mathrm{d}t, \\ &\therefore -\mathrm{d}N = \lambda \cdot N\mathrm{d}t \end{aligned} \tag{2.15}$$

where λ is the decay constant, which describes the rate of decay for a particular radioactive isotope.

If we integrate both sides of Eq. (2.15), we get the following more familiar equation:

$$N = N_0 e^{-\lambda t}. \tag{2.16}$$

If we let the variable $T_{1/2}$ be the "half-life of the substance," i.e., the time taken for the activity of the substance to reduce from its initial value to half of its initial value, then we may modify Eq. (2.16) as

$$\begin{aligned} &\frac{N_0}{2} = N_0 e^{-\lambda T_{1/2}} \\ &\therefore T_{\frac{1}{2}} = \frac{\ln 2}{\lambda} = \frac{0.693}{\lambda} \end{aligned} \tag{2.17}$$

The activity, A, of a given sample of a radioactive substance, i.e., the number of decays per second (in Bq), is given by the following equation:

$$A(t) = \lambda \cdot N(t), \tag{2.18}$$

where calculations based on activities may be performed using Eqs. (2.2) and (2.3) above with the values of A inserted instead of N. The radioactivity of a sample is quoted in terms of the units of Curies, Ci (the radioactivity of a gram of ^{226}Ra), where 1 Ci =3.7 × 10^{10} decays per second. This is more commonly quoted in terms of the S.I. unit the Becquerel, Bq, where 1 Bq = 1 decay per second. Therefore, 1 Ci = 3.7 × 10^{10} Bq (Box 2.10).

Box 2.10 The Activity of a Radioactive Substance

- The activity (A) of a radioactive substance is given in becquerel (1 Bq is the number of decays per second).
- The radioactivity of a sample can also be expressed in curies (Ci), where 1 Ci = 3.7 × 10^{10} Bq.

2.4.1.2 Radioactive Equilibrium

In nature, the abundance of the isotopes of certain radioactive nuclei depends on the abundance of their precursors, and the rate at which these precursors decay. Hence, the rate of production of each daughter nuclide of a certain radioactive isotope depends upon the rate at which its parent nuclide decays. All naturally occurring radioactive nuclides that are located below plutonium, ^{239}Pu, in the periodic table are produced from the decay of just four parent (progenitor) isotopes: thorium (4n series), neptunium (4n + 1 series), uranium/radium (4n + 2), and actinium (4n + 3). Each of these nuclides then has a decay series or chain (see example in Fig. 2.11) with associated rates of decay at each step that determine the abundance of all other radionuclides in the universe.

The neptunium series is not observed in nature at the present time as ^{237}Np, and all of its daughter nuclides have decayed since the birth of the universe, although the product of the series, bismuth ^{209}Bi, is observed as a stable isotope in nature, pointing to the existence of the series at one time in the past. Each decay series begins with a radioactive isotope and ends with a stable daughter product. The parent isotopes of the isotopes at the beginning of the thorium, neptunium, and actinium series are produced as follows:

Th series: ^{252}Cf → ^{248}Cm → ® ^{244}Pu → ® ^{240}U → ® ^{240}Np → ® ^{240}Pu → ® ^{236}U

Np series: ^{249}Cf → ® ^{245}Cm → ® ^{241}Pu → ® ^{241}Am → ® ^{237}Np

Ac series: ^{239}Pu → ® ^{235}U

If we consider a hypothetical decay series as in Fig. 2.12, the three daughter isotopes of isotope A (namely isotopes B, C, D) are produced at different rates, each dependent on the decay constants of the isotope that is their parent. Say only N_0 atoms of A exist at time $t = 0$; then

$$N_A = N_0 e^{-\lambda_A t} \tag{2.19}$$

$$\frac{\mathrm{d}N_B}{\mathrm{d}t} = \lambda_A N_A - \lambda_B N_B \tag{2.20}$$

$$\frac{\mathrm{d}N_C}{\mathrm{d}t} = \lambda_B N_B - \lambda_C N_C. \tag{2.21}$$

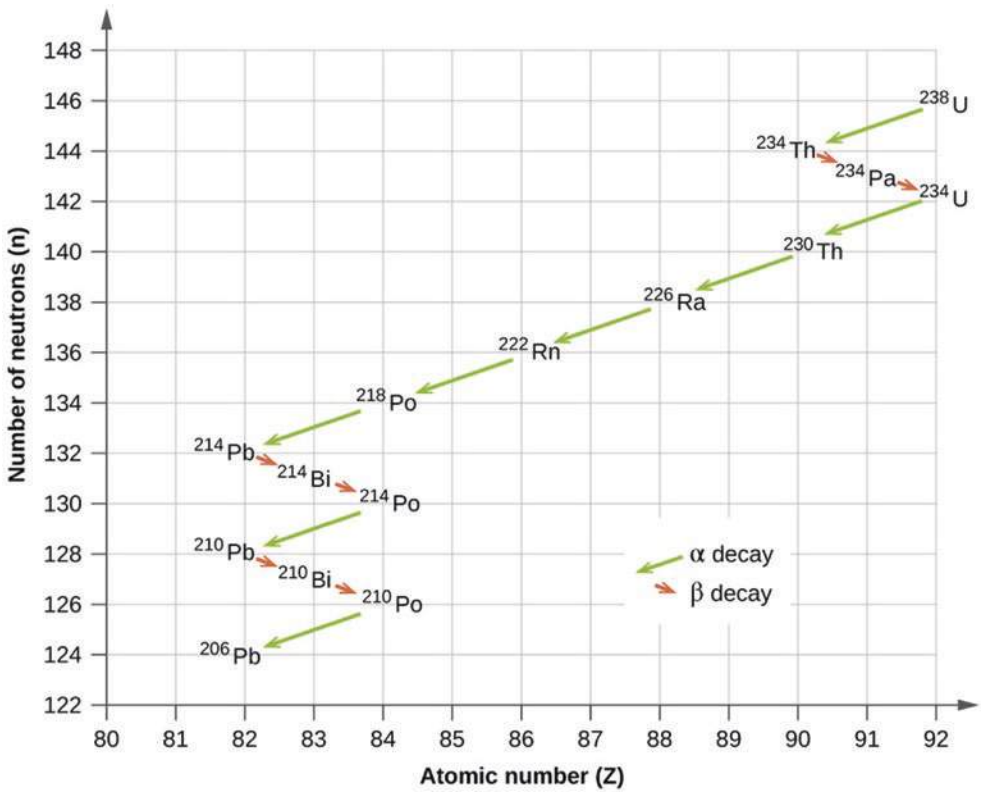

Fig. 2.11 Uranium, ^{238}U/radium, ^{226}R (4n + 2) decay series. Radioactive decay series. (2020, September 8). [Retrieved August 16, 2021, from https://chem.libretexts.org/@go/page/86256 (open-source CC-BY textbook)]

From Eqs. (2.19) and (2.20):

$$\frac{dN_B}{dt} + \lambda_B N_B = \lambda_A N_0 e^{-\lambda_A t}. \tag{2.22}$$

Multiplying across by $e^{\lambda_B t}$

$$e^{\lambda_B t}.\frac{dN_B}{dt} + \lambda_B N_B e^{\lambda_B t} = N_0 \lambda_A e^{(\lambda_B - \lambda_A)t}$$

$$\Rightarrow \frac{d\left(N_B e^{\lambda_B t}\right)}{dt} = N_0 \lambda_A e^{(\lambda_B - \lambda_A)t}.$$

Integrating both sides then gives

$$N_B e^{\lambda_B t} = N_0 \frac{\lambda_A}{\lambda_B - \lambda_A}\left[e^{(\lambda_B - \lambda_A)t} - 1\right]$$

And multiplying across by $e^{-\lambda_B t}$ gives

$$N_B = N_0 \frac{\lambda_A}{\lambda_B - \lambda_A}\left(e^{-\lambda_A t} - e^{-\lambda_B t}\right). \tag{2.23}$$

If the parent is very much shorter lived than the daughter, i.e., if $\lambda_A > \lambda_B$, we then have *radioactive equilibrium* (Fig. 2.12a). If the parent is longer lived than the daughter, then $\lambda_A < \lambda_B$ and a particular case called *transient equilibrium* arises (Fig. 2.12b). In Fig. 2.12b, the daughter product *C* is stable and so no further decrease in activity occurs. Finally, *secular equilibrium* occurs when the parent is much longer lived than its daughter $\lambda_A << \lambda_B$. In this case, Eq. (2.23) reduces to the following (also see Box 2.11)

$$N_B = N_0 \frac{\lambda_A}{\lambda_B}\left(e^{-\lambda_A t}\right)$$

$$\therefore N_B = N_0 \frac{\lambda_A}{\lambda_B}. \tag{2.24}$$

Box 2.11 Natural Radioactivity

- The natural abundance of radionuclides is largely determined by the nuclear decay series of four parent nuclides, thorium, neptunium, uranium/radium, and actinium.
- Each decay series starts from an unstable radioactive parent isotope and ends with a stable daughter product.
- Various states of equilibrium can be reached depending on the relationship between the lifetime of the parent and daughter isotopes.

2.4.1.3 Artificial Radioactivity

Experiments demonstrating the production of radioactive nuclei in the laboratory were performed by Irène and Frédéric Joliot-Curie in 1934 through the bombardment of aluminum and boron atoms with alpha particles. Those scientists observed that positrons were produced long after the bom-

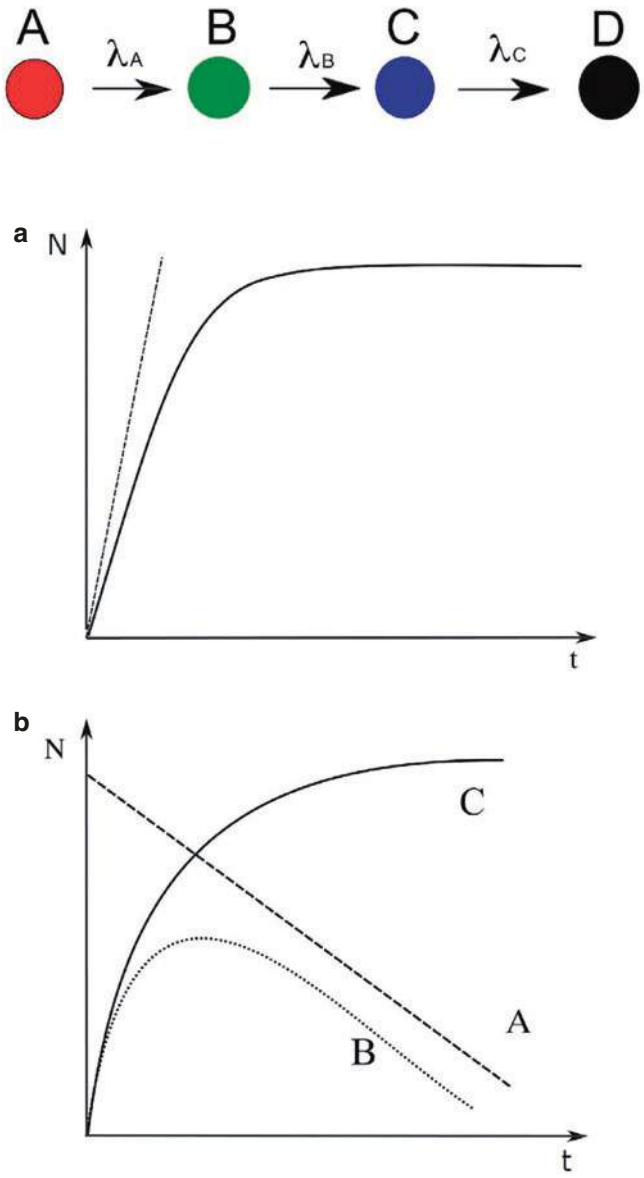

Fig. 2.12 Hypothetical decay series involving four nuclides A, B, C, and D, with various different decay constants λ_A, λ_B, etc. (**a**) Radioactive equilibrium. (**b**) Transient equilibrium

bardment and neutron production had ceased. They postulated that radioactive isotopes of phosphorus and nitrogen had been produced, which decayed to silicon and carbon in the following reactions:

$$\begin{aligned} &{}_{13}\mathrm{Al}^{27} + {}_{2}\mathrm{He}^{4} \rightarrow {}_{15}\mathrm{P}^{30} + \mathrm{n}_{0}^{1} && T_{1/2} = 150 \\ &{}_{15}\mathrm{P}^{30} \rightarrow \beta_{-1}^{0+} + {}_{14}\mathrm{Si}^{30} && \text{seconds} \\ &{}_{5}\mathrm{B}^{10} + {}_{2}\mathrm{He}^{4} \rightarrow {}_{7}\mathrm{N}^{13} + \mathrm{n}_{0}^{1} && T_{1/2} = 600 \\ &{}_{7}\mathrm{N}^{13} \rightarrow \beta_{-1}^{0+} + {}_{6}\mathrm{C}^{13} && \text{seconds} \end{aligned}$$

Neither of the two radioactive isotopes of phosphorus and nitrogen produced in these reactions occurs in nature. The majority of the artificially produced isotopes are produced via the same bombardment as illustrated here, and most of them decay by the production of $\beta^+/\beta b^-$, the ratio of n/p in the nucleus determining which of the two reactions occurs.

Consider a situation where a nuclear reaction occurs by bombardment of nucleus X with particle a, producing a nucleus Y and another projectile particle b:

$$X(a,b)Y. \tag{2.25}$$

Assuming that the rate of production, R, of Y is constant and its decay is also constant, then the infinitesimal change, dN, in the numbers of product atoms of Y over infinitesimal time, dt, is

$$\mathrm{d}N = R\mathrm{d}t - \lambda N\mathrm{d}t, \tag{2.26}$$

where Rdt provides the number of nuclides of Y produced per unit time and λNdt the number decaying over this time period. We can then rearrange to obtain a differential equation for the system:

$$\frac{\mathrm{d}N}{\mathrm{d}t} = R - \lambda N, \tag{2.27}$$

for which we can obtain a general solution for the number of nuclides of Y at any time $t > 0$:

$$N(t) = \frac{R}{\lambda}\left(1 - e^{-\lambda t}\right). \tag{2.28}$$

And since activity $A = \lambda N$, we may obtain a relationship for the variation in activity with time as

$$A(t) = R\left(1 - e^{-\lambda t}\right). \tag{2.29}$$

We may use a Taylor expansion in $e^{-\lambda t}$ to then obtain

$$A(t) = R\left(1 - \left[1 - \lambda t + \cdots\right]\right) \tag{2.30}$$

which allows a solution to be obtained for the special case where $t << T_{1/2}$ for the nuclide Y such that the following is true: (also see Box 2.12)

$$A(t) \approx R\lambda t. \tag{2.31}$$

Box 2.12 Artificial Radioactivity

- In 1934, Irène and Frédéric Joliot-Curie demonstrated for the first time that artificial, i.e., not occurring in nature, radioactive nuclei can be produced.
- Artificial nuclides are produced by bombarding a nucleus (X) with a particle (a) resulting in the production of a new nucleus (Y) and a projectile particle (b).

Table 2.1 Summary of the different types of nuclear decay

Mode of radioactive decay	Released particles	General reaction	Example
α-Decay	Helium nucleus	$ZAP \rightarrow Z-2A-4P+24He$	$92238U \rightarrow 90234Th + 24He$
β-Decay **β–** **β+**	Electron Positron	$ZAP \rightarrow Z+1AD+e^- + \bar{\nu}^a$ $ZAP \rightarrow Z-1AD+e^+ + \nu^b$	$90234Th \rightarrow 91234Th + e^- + \bar{\nu}^a$ $611C \rightarrow 511B + e^+ + \nu^b$
γ-Decay			
γ-Emission	Gamma ray	$ZAP \rightarrow ZAD + 00\gamma$	$92238U \rightarrow 24He + 90234Th + 200\gamma$
Internal conversion	Internal conversion electron	$ZAP \rightarrow ZAD + IC\ e^-$	
Electron capture (EC)	Atomic X-ray	$ZAP + e^- \rightarrow Z-1AD + \nu^b$	$47Be + e^- \rightarrow 37Li + \nu^b$
Spontaneous fission (SF)	2 fragment nuclei	$ZAP \rightarrow Z_1A_1D_1 + Z_2A_2D_2$	$100256Fm \rightarrow 54140Xe + 46112Pd$
Proton emission (PE)	Proton	$ZAP \rightarrow Z-1A-1D+11p$	$711N \rightarrow 610C + 11p$
Neutron emission (NE)	Neutron	$ZAP \rightarrow ZA-1D+n^{0c}$	$413Be \rightarrow 412Be + n^{0c}$

[a]∇ Antineutrino
[b]Neutrino
[c]n^0 Neutron

2.4.1.4 Modes of Radioactive Decay

Unstable nuclei will transform spontaneously or artificially into an energetically more stable configuration by the emission of certain particles or electromagnetic radiation. This process, termed nuclear decay, is characterized by a parent nuclide (P) transforming into a daughter nuclide (D), which differs from the former in atomic number (Z), neutron number (N), and/or atomic mass number (A) [63]. The different types of nuclear decay are summarized in Table 2.1 (Box 2.13).

Box 2.13 Nuclear Decay

- During nuclear decay, unstable nuclei transform into an energetically more stable configuration by emission of certain particles or energy.
- Different modes of nuclear decay exist, each with their own mode of reaching this energetically stable configuration (Table 2.1).

2.4.2 The Chart of Nuclides

The term nuclide refers to an atom characterized by the number of protons and neutrons present in the nucleus. Nuclides can be sorted according to their number of protons and neutrons in a chart of nuclides. In contrast to the well-known periodic table, a chart of nuclides organizes the currently known radionuclides according to the number of protons and neutrons in their nucleus. Furthermore, it summarizes basic properties of these nuclides, such as atomic weights, decay modes, half-lives, and energies of the emitted radiations [64, 65].

In 2018, the tenth version of the Karlsruhe chart of radionuclides was published, containing nuclear data on 4040 experimentally observed nuclide ground states and isomers [66]. As mentioned earlier, this chart organizes data of currently known radionuclides according to the number of protons and neutrons present in their nucleus (Fig. 2.13a). Stable nuclides are shown in black, while the colored boxes indicate the decay mode of each nuclide (Fig. 2.13c). Data on individual nuclides can be found in the individual nuclide boxes (Fig. 2.13b). When a single nuclide has different decay modes, it is represented by different sizes of triangles, representing the branching ratios for each decay mode (Fig. 2.13b, ^{226}Ac). A nuclide box can also be subdivided into different sections with a vertical line (Fig. 2.13b, ^{135}Cs). An undivided box refers to the ground state of a nuclide, while when subdivided, the right section corresponds to the ground state and the subsections on the left represent the nuclear isomers (nuclides with the same number of protons and neutrons in the nucleus, but a different energy). Nuclides with a black upper section in the nuclide box represent primordial nuclides, formed during the formation of terrestrial matter and still present on Earth due to their extremely long half-lives. For such nuclides, the upper section provides information on the isotopic abundance, while the lower section indicates decay modes and half-lives (Fig. 2.13b, ^{232}Th) [66]. Radionuclide charts are available in printed or online versions.

A chart of nuclides can be used to investigate decay chains and nuclear reactions of different radionuclides. By following the specific decay rules of each type of nuclear decay, complete decay chains can be obtained manually. In a similar way, the chart can be used to obtain different activation and reaction products of nuclear reactions [66]. In this way, this chart can be of great assistance to obtain information on

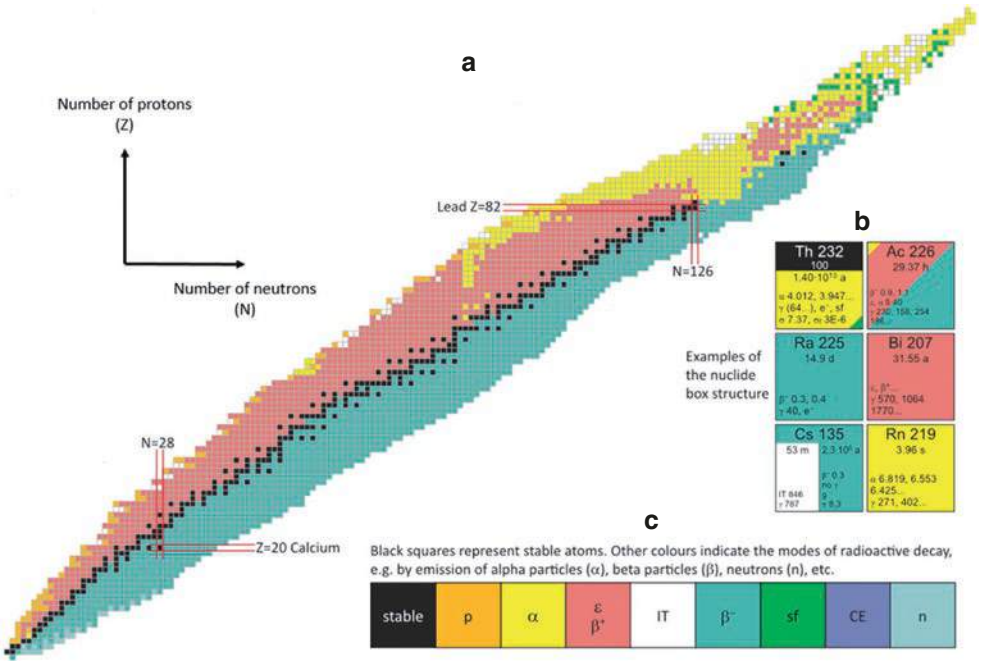

Fig. 2.13 (**a**) Schematic representation of the complete Karlsruhe radionuclide chart. (**b**) Detailed representation of different radionuclide boxes. (**c**) Different colors of boxes representing the different decay modes, from left to right: stable isotope, proton emission (p), alpha decay (α), electron capture or beta-plus decay (ε or β+), isomeric transition (IT), beta-minus decay (β−), spontaneous fission (SF), cluster decay (CE), and neutron decay (n). [(Figure adapted from Soti et al., 2019) (licensed under CC-BY-4.0)]

nuclear decay chains and isotope stability. It can help with both planning of experiments and interpretation of results [64, 65] (Box 2.14).

Box 2.14 Definition of a Nuclide

- A "nuclide" refers to an atom with a certain number of protons and neutrons in the nucleus.
- Nuclides can be sorted based on their characteristics in a nuclide chart.
- A nuclide chart can be used to investigate nuclear decay chains of different radionuclides.

2.4.3 Applications of Radioisotopes

The pioneering experiments performed by Wilhelm Conrad Roentgen (1895), Henri Becquerel (1896), and Marie and Pierre Curie (1898 and 1911) showed the potential of different radioactive elements. Over the decades to follow, radioisotopes have been applied in various fields, including medicine and food industry. In this section, some of the most common applications of radioisotopes will be discussed.

2.4.3.1 Radiometric Dating

Radiometric dating is a technique used to date materials such as rocks or fossils, in which trace radioactive impurities were selectively incorporated when these materials were formed. The method compares the abundance of a naturally occurring "parent" radioactive isotope within the material to the abundance of its decay products ("daughter isotopes"), arriving at a known constant rate of the decay process.

Today, there are more than 40 different radiometric dating techniques based on different parent-daughter isotope pairs (each with a different half-life) that are useful for dating various geological materials and samples of biological origins. The relative amounts of the parent and daughter isotopes can be measured by different chemical and mass spectrometric techniques. Table 2.2 lists some of the most commonly used isotope pairs in radiometric dating.

One of the most well-known examples is the dating using radioactive ^{14}C (half-life of 5730 years) formed by nuclear

Table 2.2 Naturally occurring radioactive isotopes commonly used in radiometric dating [67]

Radioactive isotope (parent)	Decay product (daughter)	Half-life (years)
Samarium-147	Neodymium-143	106 billion
Rubidium-87	Strontium-87	48.8 billion
Rhenium-187	Osmium-187	42 billion
Lutetium-176	Hafnium-176	38 billion
Thorium-232	Lead-208	14 billion
Uranium-238	Lead+-206	4.5 billion
Potassium-40	Argon-40	1.26 billion
Uranium-235	Lead-207	0.7 billion
Beryllium-10	Boron-10	1.52 million
Chlorine-36	Argon-36	300,000
Carbon-14	Nitrogen-14	5715
Uranium-234	Thorium-230	248,000
Thorium-230	Radium-226	75,400

reactions in the atmosphere. The constantly produced ^{14}C reacts with oxygen, leading to the formation of $^{14}CO_2$. This radioactive form of carbon dioxide is absorbed by plants via photosynthesis and will eventually become incorporated into all living organisms through the food chain. Once an organism dies, its metabolism stops, halting the incorporation of ^{14}C. Therefore, by knowing the characteristic half-life and the ratio of ^{14}C to the total carbon content, the age of the sample can be determined. The same principle applies to dating with the potassium-argon pair, which is commonly used to estimate the age of rocks, volcanic layers around fossils, and artifacts [68].

2.4.3.2 Sterilization by Gamma Irradiation

Sterilization is the complete killing or removal of all living organisms from a particular location or material. Several methods can be used to achieve sterilization, each with their own benefits and limitations. Irradiation with gamma rays (from a cobalt-60 or cesium-137 source, with a dose of around 15–25 kGy) is often used for the sterilization of medical products and pharmaceuticals, including implants, artificial joints, blood bags, and ointments. Sterilization by radiation has several benefits, the most important of which is that it can be used on heat-sensitive items that cannot be sterilized by other common methods such as autoclaving. It is also safer and cheaper because it can be done after the item is packaged. The sterile shelf life of the item is then practically indefinite provided that the seal is not broken. Indeed, it is estimated that irradiation technologies are used to sterilize almost half of the global supply of single-use medical products.

The use of gamma rays is, however, not strictly limited to the medical world. By irradiating food, we can significantly reduce their microbial burden, depending on the dose delivered. This prolongs the shelf life of the food in cases where microbial spoilage is the limiting factor. Some foods, e.g., herbs and spices, are irradiated at sufficient doses (5 kGy) to reduce the microbial counts by several orders of magnitude; such ingredients do not carry over spoilage or pathogenic microorganisms into the final product. It has also been shown that irradiation can delay the ripening of fruits or the sprouting of vegetables. Insect pests can be sterilized (be made incapable of proliferation) using irradiation at relatively low doses. The use of low-level irradiation can also be used as an alternative treatment to pesticides for fruits and vegetables that are considered hosts to a number of insect pests, including fruit flies and seed weevils. Food irradiation is currently permitted by over 50 countries, and the volume of food treated is estimated to exceed 500,000 metric tons annually worldwide [69].

2.4.3.3 Radioimmunoassays

Radioimmunoassays were first developed in the 1960s by Solomon Berson and Rosalyn Sussman Yalow for which they received the Nobel Prize in 1977. It was the first technique being able to determine hormone levels in blood. This type of in vitro assay can be used to measure the concentration of any antigen with very high sensitivity. To date, radioimmunoassays are among the most sensitive and specific laboratory tests employed by immunologists and other specialists. The general principle of an immunoassay is competition for binding to an antibody (Fig. 2.14). More specifically, the

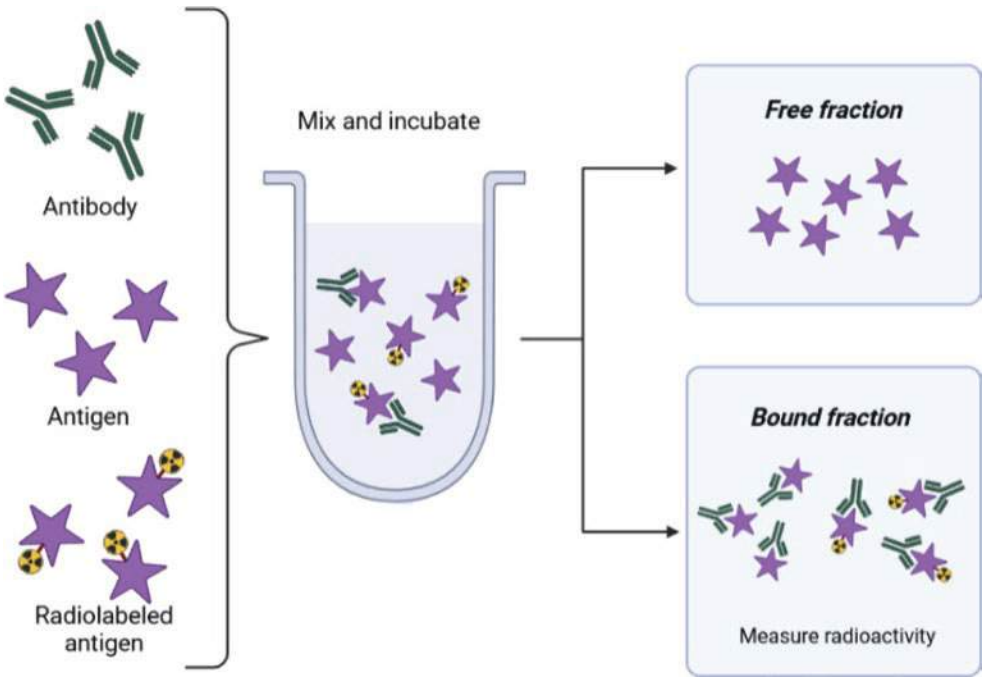

Fig. 2.14 General principle of the radioimmunoassay (Created with BioRender)

unlabeled antigen (sample) is incubated together with a fixed amount of the radiolabeled antigen and the antibody, resulting in competition between the unlabeled and labeled antigens for binding to the antibody. With increasing amounts of an unknown sample (unlabeled antigen), decreasing amounts of labeled antigen (tracer) will bind to the antigen [70]. The antibody–antigen complexes are separated from the free antigen by precipitation using a secondary antibody or chemical solutions. The antibody–antigen complexes are then measured in a scintillation counter. By running a set of standards, a standard curve is generated from which the concentration of the unknown sample can be calculated. The most commonly used radioisotopes for radioimmunoassays are iodine-125, iodine-131, and tritium (^{3}H) [71] (Box 2.15).

Box 2.15 The Use of Radioisotopes

- Radioactive decay can be used as a natural clock to determine the age of different materials.
- The strong ionizing ability of gamma rays, along with their high penetration range, can be used for the killing or reduction of microorganisms in different items, ranging from medical to food products.
- The use of radioisotopes in immunoassays provides a very high level of sensitivity allowing the measurement of antigens in pictogram quantities.

2.4.3.4 Radionuclide Therapy

In radionuclide therapy (RNT), radioisotopes are administered to patients with cancer or other medical conditions. Particles emitted from the isotopes will deliver cytotoxic levels of radiation to target sites within the human body, resulting in destruction of the targeted tissue (Fig. 2.15).

Three types of ionizing radiation can be used for radionuclide therapy (RTN), namely alpha and beta particles and Auger electrons (their most important characteristics are summarized in Fig. 2.16). The linear energy transfer (LET) and tissue particle range are the most important parameters to be considered for this type of therapy. Ideal therapeutic radionuclides have a short particle range so it only damages targeted tissue and a high LET so it deposits as much radiation as possible on its short path length. All of the above-listed particles fulfill these criteria to ensure lesion-specific damage.

The major breakthrough for RNT was in 1946, when iodine-131 was first used for the treatment of thyroid cancer. In the following years, a large variety of other radionuclides were introduced for the treatment of different cancer types, palliation of bone pain due to metastases, and treatment of inflammatory processes such as rheumatoid arthritis [72]. This was followed by the development of the peptide receptor radionuclide therapy (PRRNT), utilizing low-molecular-weight radiolabeled peptides targeted at specific cell surface receptors which are very often upregulated on cancer cells. Lutathera® (^{177}Lu-DOTA-TATE) was the first-in-class PRRNT drug to be formally approved (by the EMA in 2017 and the FDA in 2018) for the treatment of gastroenteropancreatic neuroendocrine tumors (GEP-NETs). The initial success of Lutathera® led to the development of new radiopharmaceutical-based strategies for treating other can-

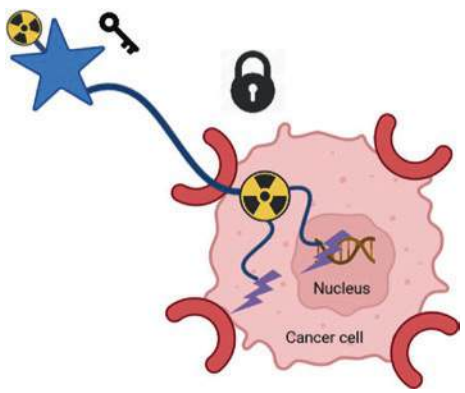

Fig. 2.15 Schematic representation of the mechanism of action of radionuclide therapy. The blue line represents the path of ionizing radiation (Created with BioRender)

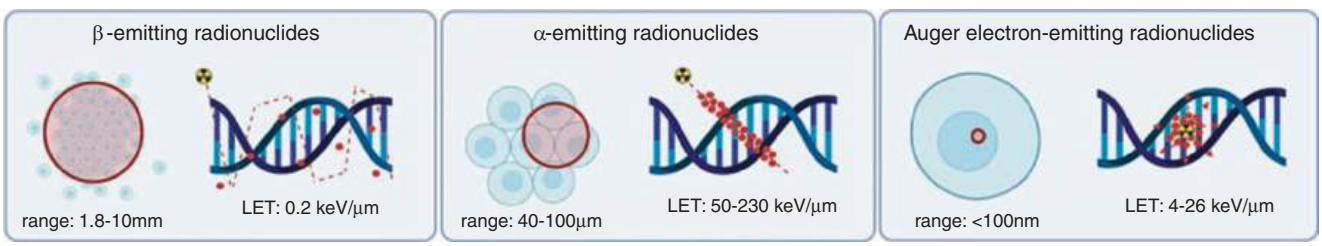

Fig. 2.16 Schematic representation of the energy deposition of the ionizing radiation and tissue range of the different emission types used for targeted radionuclide therapy, being β^-, α, and Auger electron emitters (Created with BioRender)

cer types. These include the PSMA-targeted radionuclide therapy for prostate cancer and radioimmunotherapy with nanobodies for glioblastoma (Table 2.3) (Box 2.16).

Table 2.3 Examples of radionuclides used for therapy (World Nuclear Association)

Radioisotope	Half-life	Therapeutic applications
Actinium-225	10 days	Targeted alpha therapy (TAT) Prostate cancer
Bismuth-213	46 min	TAT Leukemia, cystic glioma, and melanoma
Erbium-169	9.4 days	Arthritis pain relief in synovial joints
Holmium-166	26 h	Diagnosis and treatment of liver tumors
Iodine-131	8 days	Thyroid cancer treatment Nonmalignant thyroid disorders
Iridium-192	74 days	High-dose-rate brachytherapy Prostate, head, and breast cancer
Lead-212	10.6 h	TAT, alpha radioimmunotherapy, or PRRT Melanoma, breast, pancreatic, and ovarian cancer
Lutetium-177	6.7 days	Imaging and therapy of multiple tumor types (e.g., endocrine, prostate)
Phosphorus-32	14 days	Polycythemia vera treatment (excess red blood cells)
Radium-223	11.4 days	TAT brachytherapy in the bone
Samarium-153	47 h	Pain relief of bone metastases from, e.g., prostate and breast cancer

Box 2.16 Radionuclide Therapy

- In radionuclide therapy (RNT), radioisotopes are used to treat cancer or other medical conditions by administration of radiation sources to patients.
- Three types of radioisotopes can be used for RNT, namely alpha and beta particles and Auger electrons.
- The most important applications to date of RNT are iodine-131 for thyroid cancer, Lutathera® for neuroendocrine tumors, and PSMA-targeted RNT for prostate cancer.

2.4.3.5 Clinical Diagnostics

Nuclear imaging techniques such as positron-emission tomography (PET) and single photon emission tomography (SPECT) are noninvasive procedures, which make use of radiolabeled probes to examine biological processes on the cellular or molecular levels in vivo. These techniques enable 3D visualization, quantification, and characterization of the target (enzyme, receptor, transporter, protein aggregates, etc.) under investigation [73]. For these purposes, the compounds are labeled with a radioisotope, with a fairly short half-life ($T_{1/2}$, min to days). Both PET and SPECT allow visualization and quantification of targets expressed in very low quantities (nano-to-femtomoles per milligram tissue) or detection of molecular aberrancies before phenotypical or morphological changes have occurred [74] (Fig. 2.17).

Single Photon Emission Tomography (SPECT)

SPECT makes use of the inherent decay properties of specific radionuclides, which decay with the emission of a photon (X-ray) (Hutton 2014).

The nuclides of choice are those which emit electromagnetic rays in the energy range of 100–200 keV. This is determined based on the absorption of the electromagnetic rays by the subject and the designated detector and is a trade-off between sensitivity and resolution. Low-energy rays are more easily absorbed by surrounding tissue (tissue not under investigation), leading to higher patient doses and less efficient detection. However, higher energy levels are not opti-

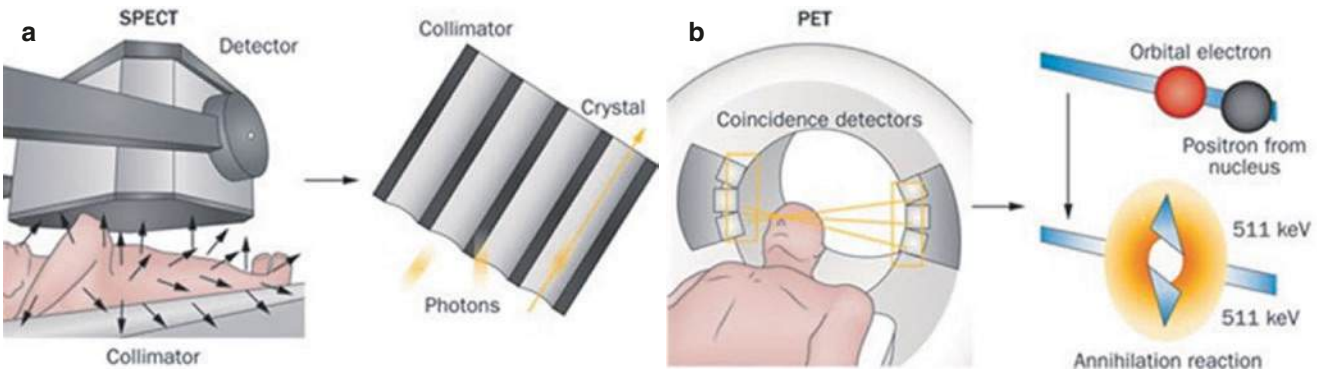

Fig. 2.17 Comparison of the SPECT (**a**) and PET (**b**) imaging techniques used for clinical diagnostic (adapted with permission of Hicks and Hofman, 2012) [75]

mally detected (stopped) by the scintillation NaI crystals. Additionally, the half-life ($T_{1/2}$) of the radionuclide should be tailored to the conducted experiment.

A SPECT apparatus typically contains two cameras which rotate around the body of the patient and are focused on an area under investigation. The cameras contain a lead collimator to directionalize the incoming radiation. As such, only rays parallel to the holes of the collimator will reach the detector, and radiation coming from scatter or other tissues not under investigation will be absorbed less by the scintillation detector, leading to less interference in image reconstruction and in turn increase in the contrast and hence the resolution but decrease in the sensitivity significantly.

Compared to planar (2D) X-ray imaging, where the electromagnetic rays are projected on an imaging detector leading to reduced contrast of the tissue under investigation compared to the background, SPECT imaging provides a noninvasive 3D method to determine the accumulation of administered diagnostic radiopharmaceuticals [73]. The term tomography indicates the use of a combination of individual "slices" to generate a 3D image.

The most widely used SPECT radioisotope, ^{99m}Tc, is metastable and decays via isomeric transition with emission of γ-rays of approximately 140 keV with a $T_{1/2} = 6$ h. Further, ^{99m}Tc is a radiometal that can be complexed by various chelators and can be incorporated into different ligands used in different investigations of a plethora of diseases (bone, heart, cancer, brain, liver). Another benefit of ^{99m}Tc is the cost and the ease of acquirement via a ^{99}Mo/^{99m}Tc generator.

Frequently clinically used radionuclides are depicted in Table 2.4.

Table 2.4 SPECT radionuclides [73, 76]

Radionuclide	$T_{1/2}$	Nuclear reaction	Mode of decay	Energy (keV)
^{67}Ga	3.26 days	^{67}Zn(p,n)^{67}Ga ^{68}Zn(p, 2n)^{67}Ga	EC (100%)	93
^{67}Cu	3 days	^{68}Zn(γ,p)^{67}Cu	β⁻ (100%) γ (52%)	185
^{299m}Tc	6.06 h	^{99}Mo/^{99m}Tc-generator	IT (89%)	140
^{111}In	2.83 days	^{111}Cd(p,n)^{111}In ^{112}Cd(p,2n)^{111}In	EC (100%)	245
^{123}I	13.2 h	^{123}Xe/^{123}I generator ^{124}Xe(p,pn)^{123}I	EC (100%)	159
^{201}Ti	73 h	^{203}Ti (p,3n) ^{201}Ti	EC (100%)	69–80 (Hg X-rays) 135 (9%) 167 (27%)

EC electron capture, *IT* internal transition, thermal neutron bombardment

Positron-Emission Tomography (PET)

PET probes generally consist of a pharmaceutical vector molecule, which carries a coupled radionuclide to the target. Because of the radioactive decay, only a low mass amount of the tracer needs to be administered to the subject. As such, pharmaceutical or toxicological effects are avoided. The radioactive decay further enables highly sensitive detection of emitted γ-rays by a dedicated ring of detectors. PET allows to detect early molecular changes and follow-up of disease progression [74]. Typically, low atomic mass radioisotopes (C, N, O, F), with a rather short $T_{1/2}$ of minutes to hours, are coupled to the pharmaceutical vector. Additionally, these radioisotopes are commonly found in different small molecules and biomolecules, so they can be incorporated without changing the chemical structure of the compounds. Advances in radiolabeling techniques are continuously increasing the radiochemical and -pharmaceutical space, which allows for a more robust and quicker radiolabeling [77]. PET is increasingly used in the drug development stream, as it enables examination of pharmacodynamics, drug-target interaction, and dose occupancy [78].

Radionuclides with an excess of protons in their core will decay by conversion of a proton to a neutron with emission of a positron (β^+, a positively charged electron) and a neutrino (ν, a quasi-massless particle) over which the decay energy is distributed to fulfill the quantum mechanical rule of conservation of energy and angular momentum. Based on the kinetic energy obtained from the decay, the β^+ particle will travel a short distance (positron range, up to 0.5 cm for ^{18}F, 1–2 cm for ^{11}C) and collides with an electron in the environment after which the masses of both are converted into energy in an annihilation event. Two γ-ray photons of 511 keV are emitted back-to-back over an angle of approximately 180°. These two γ-rays travel through the body and can be coincidentally detected by a ring of detectors (within a time interval of 10 ns), allowing to localize the imaginary "line of response" along which the annihilation event occurred. Many response lines can then be combined to determine the position of the PET radionuclide of which tissue concentrations can be derived. Compared to SPECT, thicker scintillation crystals are necessary to detect the higher γ-ray energy of 511 keV. These detectors typically consist of bismuth germanate (BGO) or lutetium oxyorthosilicate (LSO) and are more expensive compared to NaI crystals used in conventional SPECT and gamma counting. Hybrid imaging techniques such as PET/MRI and PET/CT allow a combination of morphological and functional imaging, where molecular and anatomical changes can be detected simultaneously with high accuracy. State-of-the-art PET technology research is investigating total-body PET with

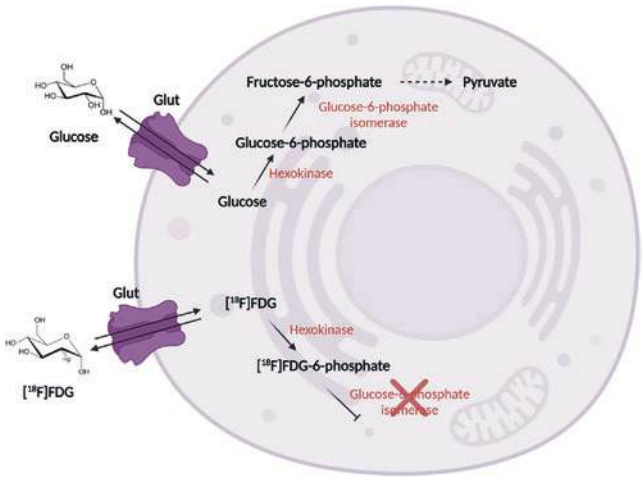

Fig. 2.18 Metabolization of glucose and its radioactive analogue [^{18}F]FDG (Created with BioRender)

increased sensitivity (up to 40-fold) compared to normal PET scanners [79]. The worldwide workhorse of PET imaging is a radiolabeled glucose derivative, 2-[^{18}F]fluoro-2-deoxy-D-glucose ([^{18}F]FDG), which visualizes the glucose metabolism and is hence taken up and trapped in organs with extensive glucose metabolism such as brain and heart and aberrant growth. Because of this, [^{18}F]FDG can be applied in the diagnostic imaging of cancer, inflammation, cardiology, and neurology [80]. [^{18}F]FDG differs from glucose by the replacement of the hydroxyl moiety by ^{18}F at C-2. This has consequences for the metabolization process of [^{18}F]FDG and is depicted in Fig. 2.18. Both glucose and [^{18}F]FDG are taken up by glucose transporters (Glut) and processed by glycolysis. Hexokinase will phosphorylate the C-6 OH-moiety of both molecules. As this brings a negative charge to the molecules, they will remain trapped inside the cell. Glucose is then further processed to fructose-6-phosphate by glucose-6-phosphate isomerase on the C-2 OH-moiety, and further metabolization will yield pyruvate. As [^{18}F]FDG lacks the C-2 OH-moiety, further metabolization will not take place and the molecule will remain trapped in the cell until decay ($T_{1/2}$ = 109.7 min) of ^{18}F to ^{18}O, after which metabolization can resume.

PET radiopharmaceutical development has been favored over investigation into SPECT tracers over the last years. PET omits the use of mechanical collimation, replacing it with electronic collimation, increasing detector efficiency 100-fold compared to SPECT. The spatial resolution of PET is also higher with less influence of scattered photons. Attenuation correction is more efficient, and the imaging contrast is also better compared to SPECT [81]. A disadvantage of PET is the cost and the availability of PET radioisotopes, which need to be generated in a cyclotron (except for ^{68}Ga, which is generator based). Furthermore, the short $T_{1/2}$ of routinely used PET isotopes (carbon-11, fluorine-18, nitrogen-13, oxygen-15) requires production by an in-house cyclotron [82, 83].

Typical radionuclides, used for PET imaging, are listed in Table 2.5 (Box 2.17).

Table 2.5 PET radionuclides (Vermeulen et al. 2019)

Radionuclide	$T_{1/2}$	Nuclear reaction	Mode of decay	Energy (MeV)
^{11}C	20.4 min	^{14}N(p,α)^{11}C	β$^+$ (100%)	0.960 (β$^+$ E_{max})
^{13}N	10.0 min	^{16}O(p,α)^{13}N	β$^+$ (100%)	1.199 (β$^+$ E_{max})
^{15}O	2.0 min	^{14}N(d,n)^{15}O	β$^+$ (100%)	1.732 (β$^+$ E_{max})
^{18}F	109.7 min	^{18}O(p,n)^{18}F ^{20}Ne(d,α)^{18}F	β$^+$ (97%) EC (3%)	0.634 (β$^+$ E_{max})
^{64}Cu	12.7 h	^{64}Ni(p,n)^{64}Cu	β$^+$ (18%) EC (24%) β$^-$ (37%)	0.653 (β$^+$ E_{max}) 0.3293–1.675 0.5794
^{68}Ga	67.6 min	^{68}Ge/^{68}Ga-generator	β$^+$ (89%) EC (11%)	1.899 (β$^+$ E_{max}) 0.227–2.821
^{76}Br	16.0 h	^{76}Se(p,n)^{76}Br	β$^+$ (55%) EC (45%)	3.382 (β$^+$ E_{max}) 0.599
^{82}Rb	1.3 min	^{82}Sr/^{82}Rb-generator	β$^+$ (100%)	3.378 (β$^+$ E_{max})
^{86}Y	14.7	^{86}Sr(p,n)^{86}Y	β$^+$ (32%) IT (68%)	1.221, 1.545, 1.988 (β$^+_{1,2,3}$ E_{max}) 0.433–1.920
^{89}Zr	78.4 h	^{89}Y(p,n)^{89}Zr	β$^+$ (23%) EC (77%)	0.902 (β$^+$ E_{max}) 0.909
^{124}I	4.2 days	^{124}Te(p,n)^{124}I	β$^+$ (26%) EC (74%)	2.138, 1.535 (β$^+_{1,2}$ E_{max}) 602

EC electron capture, *IT* isomeric transition

Box 2.17 SPECT and PET

- SPECT and PET are noninvasive imaging techniques that allow to functionally diagnose different pathologies, including cancer, neurodegenerative diseases, and cardiovascular aberrations.
- SPECT and PET make use of radiolabeled drugs to specifically target aberrantly expressed receptors, enzymes, etc.

- SPECT makes use of the inherent γ- or X-ray decay of the used radioisotope, whereas the PET principle is based on the coincidental detection of the emission of 511 keV γ-rays, resulting from the annihilation of a β^+ and an electron.
- The most frequently used SPECT radioisotope is ^{99m}Tc, which can be incorporated in a plethora of vector molecules.
- The most widely used PET radiotracer is [^{18}F]FDG, a radioactive glucose analogue.

2.5 Doses, Dose Rates, and Units in Radiation Protection

2.5.1 Dose and Absorbed Dose

Dose or absorbed dose is the mean energy imparted by ionizing radiation to a material.

Absorbed dose = d*E*/d*m*

where d*E* is the mean energy imparted by ionizing radiation and d*m* is the mass of the material.

The SI unit of dose is *gray* (Gy) and is defined as absorbed energy per unit of mass of tissue, given by one joule per kg. The old unit is *rad*, and the conversion is defined as 1 Gy = 100 rad [84].

2.5.2 Dose Rate

Dose rate is defined as the dose of ionizing radiation absorbed or delivered per unit time. It is measured in *gray per hour*.

The biological effect of a certain dose is dependent on its dose rate, known as the dose rate effect. The biologic effect of a given dose is reduced if the exposure time is extended, and so if the dose rate is lowered. This is due to repair of sublethal damage that occurs during long radiation exposure. It is also due to redistribution of cells in cell cycle and cell proliferation (see Chap. 5 for details).

On the contrary, inverse dose rate effect is observed when increased biologic effects of a given dose at lowering the dose rate occur. This only happens at a limited range of dose rates. This is attributed to progression of cells through the cell cycle and accumulation in the G2 cell cycle phase, which is a radiosensitive phase. Further lowering of the dose rate below this critical level leads to lowering of biologic effects as cells cross the G2 block and divide, leading to cell proliferation.

Importantly, dose rate reduction has a differential effect between most tumors or early-responding normal tissues and late-responding normal tissues. Late-responding normal tissues are more sensitive to dose rate changes, like changes in fraction size in external beam radiotherapy [85].

The dose rate of environmental exposure is low (around 0.1 μGy/min). Clinically, the concept of dose rate is utilized in brachytherapy. Accordingly, there are different categories such as

1. Ultralow dose rate (ULDR)—less than 0.4 Gy/h
2. Low dose rate (LDR)—0.4–2Gy/h
3. Medium dose rate (MDR)—2–12 Gy/h
4. High dose rate (HDR)—more than 12 Gy/h

Low-dose-rate irradiation can be considered as an extreme form of fractionation.

There is another entity called pulsed dose rate (PDR), which is used in brachytherapy. Dose and treatment time are prescribed for LDR, but radiation is delivered in a pulsed manner every 1–4 h in many small fractions. Contrastingly, in FLASH radiotherapy, an ultrahigh dose rate of more than 1,44,000 Gy/h is administered [86].

The biological effect will be explained in Chaps. 5 and 6 (Box 2.18).

Box 2.18 Definition of Dose and Dose Rate

- Dose or absorbed dose is the mean energy imparted by ionizing radiation to a material. The SI unit of dose is *gray* (Gy).
- Dose rate is defined as a dose of ionizing radiation absorbed or delivered per unit time. The SI unit of dose rate is *gray*/hour.

2.5.3 Units of Radiation Protection

2.5.3.1 Equivalent Dose

The interaction of radiation with matter or tissue is also influenced by the type of radiation. Some types of radiation produce different effects than others for the same amount of energy. This is because the pattern of dose distribution and the density of ionization events will be different. To account for these variations when describing human biological harm from radiation exposure, the "equivalent dose" is used. For example, for equal absorbed doses, neutrons may be 20 times as damaging as X-rays. The equivalent dose is the product of the absorbed dose averaged over the tissue or organ and the radiation weighting factor W_R particular for the type and energy of radiation involved. It is based on the absorbed dose to an organ, adjusted to account for the effectiveness of the type of radiation [85, 87]:

$$H_T = w_R D_T. \quad (2.32)$$

The SI unit of equivalent dose is *sievert* (Sv). The unit "rem" (roentgen equivalent in man) is also still used. One rem is equivalent to 0.01 Sv.

The radiation weighting factors recommended by the ICRP are shown in Table 2.6.

If a mixture of radiation types is used, the equivalent dose is the sum of the individual doses of the various types of radiation, each multiplied by the corresponding weighting factor:

$$H_T = \sum w_R D_T. \quad (2.33)$$

2.5.3.2 Effective Dose

The effective dose is the addition of equivalent doses to all organs, each adjusted to account for the sensitivity of the organ to radiation. If a body is uniformly exposed to radiation, the probability of biological effects is assumed to be proportional to the equivalent dose. However, various tissues react to ionizing radiation in different ways and have different sensitivity to radiation. The ICRP has introduced the tissue weighting factor (W_T), which represents the relative contribution of each tissue or organ to the total damage or "effect" resulting from uniform irradiation of the whole body [85, 87, 88] (Table 2.7).

Table 2.6 Radiation weighting factors (ICRP 103)

	W_R
X-γ-rays	1
β^+–β^-	1
Protons and charged particles	2
Neutrons	5–20
α-Particles	20

Table 2.7 Tissue weighting factors (ICRP 103)

Tissue/organ	2007 W_T
Bone marrow	0.12
Breast	0.12
Colon	0.12
Lung	0.12
Stomach	0.12
Bladder	0.04
Esophagus	0.04
Gonads	0.08
Liver	0.04
Thyroid	0.04
Bone surface	0.01
Brain	0.01
Salivary glands	0.01
Skin	0.01
Remainder tissues	0.12

The effective dose is the product of the equivalent dose and the tissue weighting factor:

$$E = \sum w_T H_T. \quad (2.34)$$

The SI unit of effective dose is *sievert* (Sv).

Despite differences in the sensitivity of tissue due to age and sex of the person, for the purpose of radiation protection, the values for tissue weighting factors are taken as constants and are applicable to the average population. The effective dose is a calculated quantity and not a physical, measurable quantity.

The effective dose is used to compare radiation exposure and risks between different radiation types and exposure modes and a total body exposure. According to the ICRP Publication 103, effective dose is to be used for "prospective dose assessment for planning and optimization in radiological protection, and retrospective demonstration of compliance for regulatory purposes."

Annual dose limits for occupational and public exposure are given in terms of the annual effective dose.

2.5.3.3 Committed Equivalent Dose

In case of external irradiation, the absorbed dose is delivered at the time of exposure. In the case of internal irradiation, when radionuclides are taken into the body, the total absorbed dose is distributed over time as well as to different tissues in the body. The dose rate falls depending on the half-lives of the radionuclides. The committed equivalent dose considers the varying time distributions of dose delivery. The committed equivalent dose is calculated as the integral over 50 years of the equivalent dose in each tissue after intake of a radionuclide [85, 87].

2.5.3.4 Committed Effective Dose

This is the sum of the committed equivalent dose to the individual tissues or organs multiplied by their respective W_T.

2.5.3.5 Collective Equivalent Dose

The radiation doses discussed above relate to exposures of individuals. The collective equivalent dose is used to measure the total impact of a radiation exposure to a group or population. The collective equivalent dose is the product of the average equivalent dose to a population and the number of persons exposed. It is measured in man-sievert (man-Sv).

2.5.3.6 Collective Effective Dose

The collective effective dose allows a rough estimation of the potential health risks to a population after exposure to radiation. It is the product of the average effective dose to a population and the number of persons exposed. It is measured in man-sievert (man-Sv).

2.5.3.7 Collective Committed Effective Dose

If a population is exposed to internal exposure by radionuclides, the integral of the effective dose over 50 years is called the collective committed effective dose. It is measured in man-sievert (man-Sv) (Box 2.19).

Box 2.19 Definition of Units in Radiation Protection

- The effective dose is the product of the equivalent dose and the tissue weighting factor. The SI unit of effective dose is *sievert* (Sv).
- The equivalent dose is the product of the absorbed dose averaged over the tissue or organ and the radiation weighting factor W_R. The SI unit of equivalent dose is *sievert* (Sv).

2.6 Linear Energy Transfer and Relative Biological Effectiveness

2.6.1 Linear Energy Transfer

Ionizing radiation causes significant physical and chemical modifications, which eventually lead to biological effects in the exposed tissue. The amount of energy absorbed by the tissue (absorbed dose) and the rate at which such energy is deposited (dose rate and fractionation for clinical applications) play a critical role in determining the type and extent of the effects. However, other physical parameters can also affect the biological response. It is therefore necessary to introduce a radiation quality term to discriminate between different radiation types. Radiobiological data and models clearly point to the spatial distribution of energy deposition as a key radiation quality parameter. However, the stochastic nature of the interaction of radiation with matter prevents a comprehensive and unique description and measurements of the ionization patterns produced by the pathway of charged particles in matter. The alternative is, therefore, to define a suitable but inevitably incomplete characterization of radiation quality that will enable radiobiological predictions with sufficient accuracy.

The concept of linear energy transfer (LET), the amount of energy transferred per unit length, was introduced by Zirkle et al. [89] to account for the density of energy transfer occurring along the track of charged particles, including excitations and ionizations, until the particles reach the end of their range. LET values are generally reported in keV/μm. The symbol LET∞ (unrestricted LET) is used when all possible energy transfers are included, and also the energy deposition by particles that in principle exit the volume of interest. The LET∞ is numerically equivalent to electronic stopping power, i.e., the energy loss by the incoming particle (which may be a primary or a secondary particle) without any restrictions in energy and range. The formula for the electronic stopping power contains a negative sign as it is seen as the slowing force acting on charged particles, due to interaction with matter, resulting in loss of particle energy:

$$S(E) = -(\mathrm{d}E / \mathrm{d}l) = -\mathrm{LET}\infty, \qquad (2.35)$$

where $S(E)$ is the stopping power, $\mathrm{d}l$ is the distance traversed by the particle, and $\mathrm{d}E$ is the mean energy loss due to collisions with energy transfers.

There is however a conceptual difference: the stopping power deals with the energy loss of the particle, while the LET∞ focuses on the energy deposition in the medium, and thus, the LET generally has an opposite sign. For large volumes, the electronic stopping and the LET∞ coincide (same absolute value), as for large volumes all the energy loss by the impacting particles is well likely deposited in the sample.

In radiobiology, the concept of "restricted LET" is mostly used. This is the locally transferred energy per unit length, with "locally" restricting to only the energy fraction, which leads to ionizations and/or excitations within the considered site. The remaining kinetic energy of particles leaving the site is excluded. This is particularly relevant for electrons since they may possess considerably long ranges. For example, for ions with $E > 1000$ MeV/μ, these electrons can have energies higher than 1 MeV. The lateral spread of the track is usually 100 s of nm, but for higher energies of the ions such as 1000 MeV/μ, this lateral spread can even be 1 cm.

According to the ICRU 1970, the linear energy transfer of charged particles in a medium is the quotient of $\mathrm{d}E$ by $\mathrm{d}l$. Here, $\mathrm{d}E$ is less than some specified value Δ. The definition includes an energy cutoff rather than a range cutoff as this is of more practical use:

$$\mathrm{LET}_{\Delta} = (\mathrm{d}E / \mathrm{d}l)_{\Delta}. \qquad (2.36)$$

It has become customary to specify a limit of energy deposition below which the deposition is considered to be local (energy restriction); 100 eV has been widely accepted, which corresponds to an electron range of about 5 nm. Electrons of longer ranges are called "δ electrons" or "δ rays."

X-rays and gamma rays are considered low LET (sparsely ionizing) radiation types, while high-energetic protons, neutrons, and heavy charged particles are considered as high LET (densely ionizing) radiation. A proton can have high or low LET, depending on its energy. Although commonly high-energy protons have been considered low LET radiation, recently this has been questioned, starting a new "paradigm in radiation biology" [90]. For indirectly ionizing neutrons, LET refers to that of the secondary charged particles they produce. The value which is generally considered to mark the distinction between low and high LET is about 10 keV/μm.

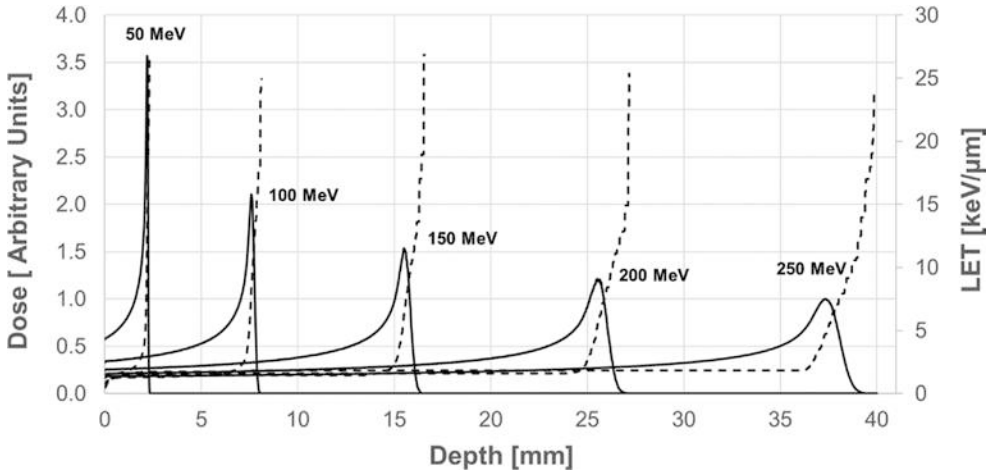

Fig. 2.19 Dose and LET distribution for proton beams of various energy in water (simulated using TOPAS MC)

As ionizing particles decelerate along their track, the LET decreases, leading to a LET distribution, and consequently two different LET average concepts can be defined. The "track average LET" is calculated by performing a weighted average considering the proportion of the total track length that is within specified LET intervals and assigning equal statistical weight to each unit of the track length. On the other hand, the "dose average LET" is a weighted average of the LET values taking into account the proportion of the energy that is deposited for each LET interval so equal statistical weight is assigned to each unit of the energy deposition. In the first approximation, the dose-averaged LET is more suitable as the radiation quality factors are based on such quantity.

Apart from ionizations and excitations, among which ionizations bring the highest contribution to electronic stopping over a wide range of energies [91], other mechanisms cause energy loss of the impinging particle and thus induce deposited energy. At energies below some few keV/µm of the traveling ion, also nuclear collisions can occur. Such elastic nuclear collisions (described by the concept of nuclear stopping), which cause displacement of atoms, can induce alteration and breaking of bonds, and thus also contribute to biological damage. For particles with high energy, inelastic nuclear collisions, where the impacting particle causes fragmentation of the nuclei generating daughter nuclei with emission of several secondary particles, can also occur. These loss mechanisms are not described by the concept of stopping. A significant loss of primary beam fluence is caused by such nuclear reactions. The inelastic nuclear cross section determines the number of particles left at a certain depth. For instance, for protons hitting a water target with an energy of 160 MeV, at the Bragg peak position, approximately 20% of the incident protons will be lost [92].

The Bragg curve represents the energy loss, in this case electronic stopping or LET, as a function of the distance through a stopping medium. The energy loss is characterized primarily by the square of the nuclear charge, Z, and the inverse square of the projectile velocity, β. This gives the Bragg curve its familiar shape, peaking at very low energies (Bragg peak), just before the projectile stops (Fig. 2.19). The stopping of charged particles increases with decreasing ion energy; in particular, around the Bragg peak, the stopping (or the LET) is maximum, near the very end of the particle's range. Ions of the same specific energy (energy per nucleon) have a similar range, typically on the order of 10 µm at ~1 MeV/µ up to 1 mm at ~100 MeV/µ [25].

Sparse energy deposition events along the track of a particle per unit of energy deposited appear to be less biologically damaging than "dense" deposition. The value of the LET that seems "optimal" for cell killing is in the range of 100 keV/µm. This is linked to the fact that the average separation of ionization events at this LET is about the same as the diameter (2 nm) of the DNA double helix, implying a higher probability of DSB, from the passage of a single particle. Clusters of lesions in the DNA molecule play a key role in biological damage [93] (Box 2.20).

Box 2.20 Definition of LET

- LET is a parameter that quantifies the amount of transferred energy per unit length.
- LET is reported in units of keV/µm.
- LET increases with the ion mass and with decreasing ion energy.

2.6.2 From Microdosimetry to Nanodosimetry: Spatial Pattern of Ionization Events

There is an intrinsic relationship between the quantities in dosimetry, e.g., absorbed dose (see Sect. 2.5), linked to the electronic stopping power, and quantities at the microscale and down to the nanoscale.

The study of the pattern of energy deposition at micrometer length scale is called microdosimetry [94]. In particular, microdosimetry studies the fluctuations and pattern of energy deposition in a micrometer-sized target, providing a comprehensive view of the energy deposition more detailed than the one given just by the LET alone. The measured spectra are distributions of energy depositions in the microscopic volume, which are a combination of several stochastic processes including the LET distribution, the track length distribution, the energy loss straggling (statistical fluctuation of energy loss along the particle track) of the primary particles, and the transport of energy by δ-rays [95]. Microdosimetric quantities are stochastic and therefore given in terms of particle interaction probabilities [95, 96]. The relevant quantities in microdosimetry are as follows:

- y: the lineal energy, which is defined as the energy imparted to matter in the microscopic volume by a single event divided by the mean chord length in that volume and the mean length of randomly oriented chords in a given convex volume
- $f(y)$: the probability distribution of linear energy
- $\underline{y_F} = \int_0^\infty y f(y)\,\mathrm{d}y$: the first moment of $f(y)$, also called the frequency mean lineal energy
- $\mathrm{d}y = y f(y)/\underline{y_F}$: the dose distribution, which is important for obtaining the dose components of the microdosimetric spectrum
- • $\underline{y_D} = \int_0^\infty y \mathrm{d}(y)\,\mathrm{d}y$: the first moment of d (y), also called the dose mean lineal energy

2.6.3 Induced Biological Effects Depend on LET

2.6.3.1 Definition of RBE

Relative biological effectiveness (RBE) is a method to quantify and compare the biological damage of different types of radiation [97]. The RBE is a dimensionless quantity and can be described as a radiation quality index with regard to biological damage. Quantitatively, RBE is the ratio between the absorbed dose of a reference radiation type and the absorbed dose of the radiation type of interest, such that both the absorbed doses compared produce the same amount of a biological effect, known as isoeffect. The reference radiation is defined as a low LET radiation. Previously, the standard radiation used was 250 keV of X-ray; however, nowadays, it is more common to use as standard 1 MeV photons (from a cobalt-60 source). This means that RBE is 1, when cobalt-60 biological effect is compared with itself.

RBE guides in the selection of the weighting factors, which are required to define the effective dose (E) (Sect. 2.5). RBE varies with several factors described in detail later, namely LET, radiation dose, fractionation, dose rate, biological system, endpoint measured, and radiation quality.

$$\mathrm{RBE} = \frac{\text{Absorbed dose of the standard radiation needed for an isoeffect}}{\text{Absorbed dose of the test radiation needed for an isoeffect}}. \tag{2.37}$$

2.6.3.2 Efforts to Develop Radiation Quality Factors and RBE Models Based on Nanodosimetry

Over the past decades, radiobiology and nanodosimetry studies have pointed out that the characteristic spatial distribution of energy deposition at the subcellular scale induced by different particles at different speed is a key aspect at the origin of the RBE of different radiation qualities [91]. Localized clusters of energy deposition within the DNA molecule play a critical role. The frequency and topological distribution of clustered lesions determine the effectiveness of the DNA repair mechanisms. Isolated lesions are more efficiently repaired, while for complex lesions, errors are more likely to occur in the repair, often leading to permanent damage [98]. One of the main aims of the radiation community is to develop models for the radiation quality factors, the RBE and cell survival, which are consistent with nanodosimetry. Several efforts have been done recently to (a) develop biologically relevant quantities based on nanodosimetry [99], in order to overcome the simplistic description of the quality factor as a (continuous) function of the sole LET; (b) develop new quality factors incorporating a formula that relates to densely and sparsely ionizing components of the radiation tracks and core track contributions and penumbra contributions [13]; (c) develop an RBE based on a radiation quality descriptor depending on energy deposition clustering [100]; (d) develop a cell damage/survival model based on the interactions between lesions at both the nanometer and micrometer scale [101]; and (e) perform a detailed analysis of the radial distribution of ionization cluster size distribution [102].

2.6.3.3 Colony Survival Assay and α/β Ratio

Prediction of radiobiological response is a major challenge in radiotherapy. Survival curves allow to determine the radiosensitivity of a cell line to different types of radiation, as well as to compare the response of one different cell type to one

type of radiation. The linear-quadratic (LQ) model has been best validated by experimental and clinical data and describes the surviving fraction (SF) of cells as a function of radiation dose D: SF (D) = $e^{-\alpha.D - \beta D2}$. It allows determining important biological parameters such as the survival fraction or the ratio α/β, which represents the intrinsic radiosensitivity. Cells with a higher α and β are more sensitive to radiation. The shape of the curves depends on the LET. Indeed, cells irradiated with the same dose of different LET induce different biological effects translated into different cell survivals. As the LET increases, the slope of the curve becomes steeper and straighter with less shoulder. This indicates a higher ratio of lethal to potentially lethal lesions or a less efficient repair of the high LET radiation damage. For the LQ representation, this is shown by a higher α/β ratio for high LET radiation. However, the lower the α/β ratio is (high β relative to α), the more curved the clonogenic curve is.

2.6.3.4 Limitations of the LET Concept

Although the LET is a common and useful parameter to quantify the distribution of absorbed radiation energy, there are considerable limitations, which need to be considered. The limitations in terms of using the LET for predicting biological effects are strongly related to the RBE models and have been discussed in previous sections. There are also caveats of more physical nature. In particular, LET measurements are complex, difficult to relate to clinical or radiobiological setups, and affected by several constraints particularly if LET distributions are to be reported rather than single LET values. Direct measurements of dE/dl can be attempted with very thin particle detectors (such that multiple interactions within the active volume rarely occur) with high-energy resolution and able to discriminate between secondary particles and photons. In this case, the energy loss (ΔE) by a particle passing through is related to the thickness of the detector (Δl). Ideally, detectors with different thickness would be employed and the energy detected plotted against the detector thickness from which the slope at the origin is extrapolated. The density of the sensitive material of the detector should also be considered to convert the measurements into water. This provides an estimation of the stopping power and therefore the LET∞. The development of several Monte Carlo-based codes has offered the possibility to quickly calculate LET values taking also into consideration the specific experimental settings.

The definition of the LET concept also implies that an average LET value may not always be adequate to describe the radiation quality to which biological samples are exposed. As mentioned, the LET changes significantly along the path of an individual charged particle and it is affected by the specific irradiation setup including any scattering conditions. Single LET values are suitable for "track segment" experiments where thin biological samples are exposed to monoenergetic charged particle beams. Even under such conditions, however, the energy loss by a charged particle over a cellular distance fluctuates and it can occasionally reach extreme high or low values, which are not well accounted for in an averaging process. Also, the angular deflection and the lateral extension of the particle tracks due to the finite range of δ-rays are in principle not taken into account in the LET concept. The restricted LET, which only includes energy transfer below a specified cutoff, can actually partially take into account the second point. However, a set of LET distributions that belong to different cutoff values would be needed, but still little information about the actual structure of particle tracks would be gained [103]. A quantitative evaluation has shown that the LET concept is quite inadequate for electrons; there are no sites sufficiently small to disregard the finite range of the electrons and simultaneously sufficiently large to disregard the lateral escape of δ-rays and the energy loss straggling [103].

Contrarily, for heavy ions, there are site sizes and particle energies for which the LET predicts adequately the energy deposition. LET increases approximately as the square of the ion charge, Z, and the inverse square of its velocity, v. On the other hand, the maximum range of the δ-ray electrons depends on the velocity of the particle but not its charge. Thus, the consideration of the sole LET of a particle is not sufficient for a description of the particle's track structure, as two particles of identical LET but very different velocity and charge will have very different track structures [104].

2.6.4 Relative Biological Effectiveness Depends on Many Factors

2.6.4.1 LET

RBE increases as LET increases, up to a maximum LET value of about 100 keV/μm, and then decreases as LET increases (Fig. 2.20—RBE and LET) [97]. In general, high LET radiations allow the deposition of a given amount of energy over a shorter distance, being more efficient in producing biological effects than low LET radiations. In other

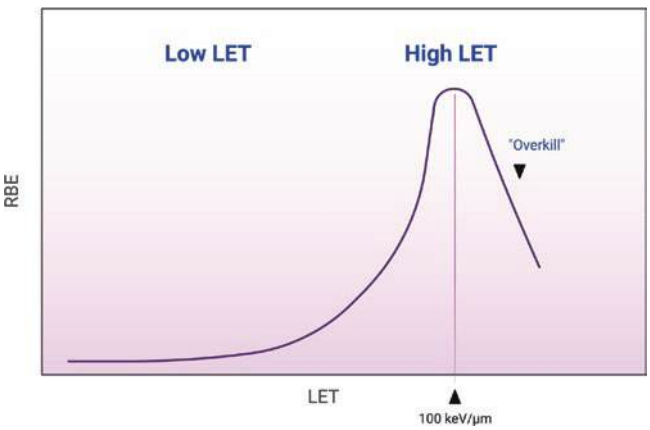

Fig. 2.20 RBE variation with LET. RBE increases as LET increases, up to a maximum LET value of about 100 keV/μm. An "overkilling" effect is observed for higher LET values (Created with BioRender)

words, low LET radiation creates sparse ionization, requiring more than one radiation track to pass through the cell and induce lethal biological damage, while high LET radiation is more effective, since one radiation track through the cell is enough to induce lethal biological damage. However, over 100 keV/μm, there are many "wasted" ionizations due to the very high ionization densities (number of ions per unit of path length). This phenomenon is the so-called overkilling and reflects the RBE declining for further increases in LET, for which biological effect is reduced since most of the energy is wasted.

2.6.4.2 Radiation Dose

When determining RBE, it is important to understand that RBE values also depend on the radiation dose and, consequently, on the isoeffect level chosen for the comparison between radiation types [97]. For small radiation doses, RBE is particularly variable tending to increase. This is explained by the fact that at low doses, the difference in the biological damage induced by low and high LET radiation is huge; that is, high LET radiation is very effective in killing cells, while low LET radiation is ineffective in doing so. For high radiation doses, the difference between the effects induced by low and high LET radiation becomes smaller, considering that low LET radiation becomes more lethal. At very high doses, the RBE no longer depends on the dose.

2.6.4.3 Fractionation and LET

The shape of the cell survival curve determines the presence or absence of a fractionation effect. With repeated daily low-dose X-ray fractions, the shoulder curvature is repeated, and cell survival is increased relative to a single high-dose radiation fraction at equal total dose. As mentioned previously, the bending of the cell survival curve is described by the α/β ratio parameter of the LQ model equation. The principle of fractionation is the repeat of the shoulder of the cell survival curve. The broader the shoulder, the lower the α/β ratio and the higher the cell survival in fractionated irradiation, i.e., the higher the sparing effect. In other words, the straighter the curve is, the less the fractionation effect is. The cell survival curve of high LET irradiation such as alpha particles is a straight line (e.g., Fig. 2.22); hence, the effect of fractionation is lost. Fractionation of carbon ions does not influence its biological effectiveness.

The same effect is seen when the dose per fraction is reduced in vivo. While low LET X-ray irradiation shows—related to the α/β ratio of the LQ model—sparing effect with multiple low dose fractions, high LET irradiation does not show such typical fractionation sparing effect, as illustrated in Fig. 2.21 [105]. Figure 2.21 (left) shows large sparing, and thus an increased tolerance to low LET irradiation, for late-responding normal tissues (with a low α/β ratio such as the spinal cord and kidney) with decreasing dose per fraction, while early-responding normal tissues (e.g., jejunum) and tumors (e.g., fibrosarcoma), both characterized with a high α/β ratio in the LQ model, are marginally spared. With high LET neutron irradiation, very little normal tissue sparing of fractionation has been demonstrated (Fig. 2.21, right), neither for early-responding normal tissues and tumors nor for late-responding normal tissues. The current view is to use at least two high LET fractions to obtain some sparing and ben-

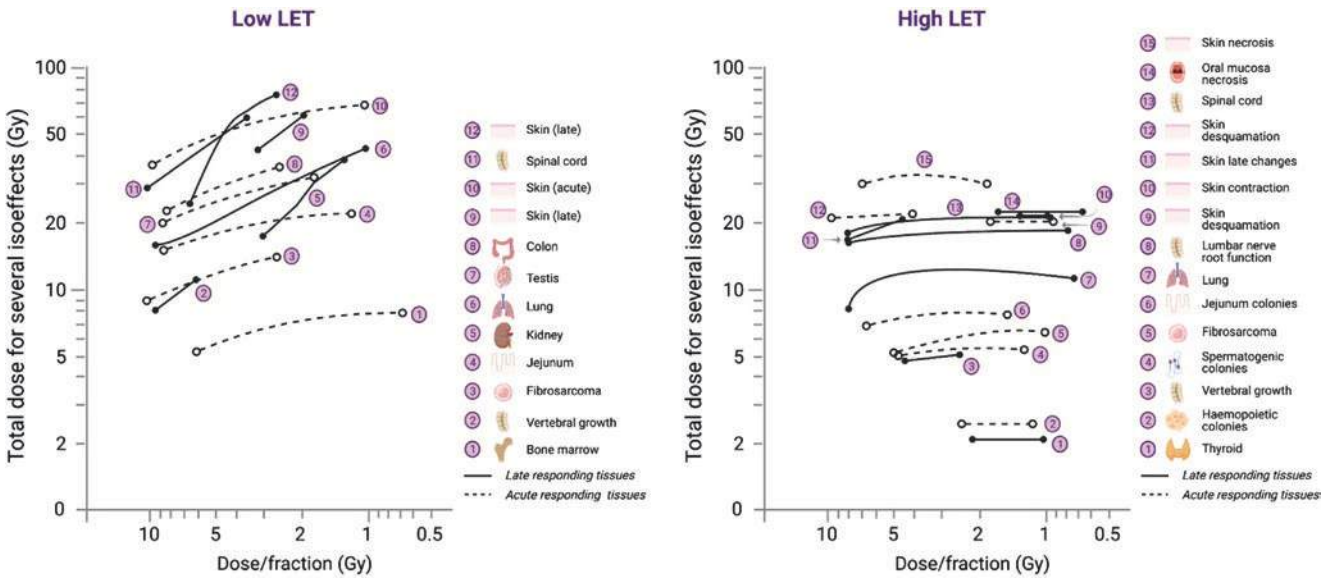

Fig. 2.21 Isoeffect curves as a function of total dose and the number of fractions for low LET X-rays or gamma rays (left) and high LET neutrons (right). See insert for explanation of symbols and curves. [Redrawn from Withers et al. [105] with permission]

efit from reoxygenation, but multiple fractions would not be further beneficial [106] (Box 2.21).

Box 2.21 Fractionation and LET

- The higher the LET, the straighter the radiation–cell survival relationship, and the lower the sensitivity to dose fractionation.
- The RBE of high LET irradiation decreases with increasing dose or dose per fraction for both cells and tissues.
- Little normal tissue sparing after fractionated high LET irradiation: Few fractions are sufficient.

2.6.4.4 The Dose Rate

The dose rate is defined as the ratio of the radiation dose [Gy] to the duration of the radiation exposure [hour]. The spectrum of dose rates used in radiation oncology is broad: from low dose rate (LDR < 2 Gy/h) to ultrahigh dose rate (FLASH, >144.000 Gy/h). The dose rate of radiation exposure largely determines its RBE. Lowering the dose rate reduces the effectiveness of radiation in many ways. In terms of the 6 Rs of radiobiology, the dose rate affects the induction and repair of DNA damage and related clonogenic cell survival, cell cycle (re-)distribution and activation of cell cycle checkpoints, and cell repopulation and reoxygenation and likely influences the immune response as well. For a particular equal biological effect, a biological endpoint, lowering the dose rate relative to a reference radiation quality (usually high-dose-rate 250 keV X-rays), the RBE decreases (Fig. 2.22). The dose rate effect could also be defined with the dose reduction factor (DRF), also termed the dose recovery factor. The DRF indicates the ratio of the radiation dose to achieve an equal biological effect at specified dose rate and the dose at high dose rate. The term DRF is used by analogy with the dose enhancement factor or sensitizer enhancement ratio, to quantify a change toward steeper cell survival curves. With increasing dose rate, the DRF value is >1.

The increase in biological effectiveness with increasing dose rate applies to all tissues and organs and, importantly, discriminates between early-responding tumors and normal tissues and late-responding normal tissues. In late-responding normal tissues, characterized by a low α/β ratio of the LQ model, the increase of dose rate is more detrimental than for tumors and early-responding normal tissues with a high α/β ratio. Literature data show that, at ultrahigh dose rate in FLASH radiotherapy, this differential effect could be inverted [108]. This inverse effect could be explained by the oxygen depletion hypothesis, the DNA damage hypothesis, and the immune response hypothesis.

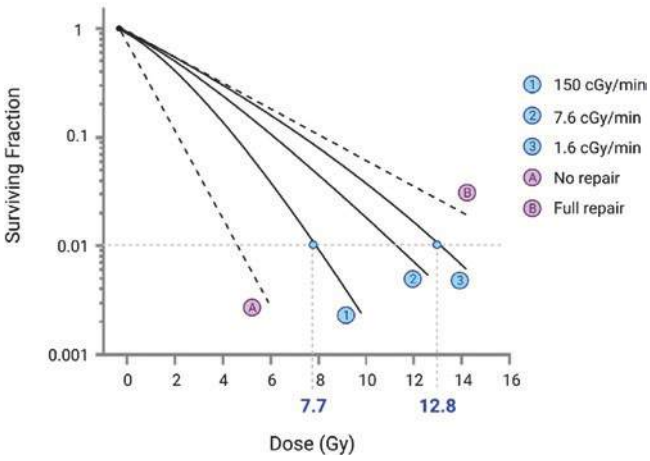

Fig. 2.22 Effects of the dose rate on clonogenic cell survival for a human melanoma cell line irradiated at dose rates of 1.6, 7.6, and 150 cGy/min. At equal biological effectiveness, e.g., 0.01 cell survival (broken line), high-dose-rate irradiation has larger relative biological effect than low-dose irradiation, resulting in a dose reduction of approximately 5 Gy, i.e., a DRF of 1.6 (12.8/7.7). Dotted lines: (**A**) no repair; (**B**) condition of full repair at infinitely low dose rate. (Figure adapted from Steel [107], with permission)

Box 2.22 Definition of Dose Rate and Dose Rate Effect

- Dose rate: radiation dose delivery per unit time (e.g., Gy/hour)
- Dose rate effect: decrease in biological effectiveness with decreasing dose rate

2.6.4.5 Biological System and Endpoints Measured

During the last decades, many tissues and cells were characterized by survival curves in response to different types of radiation, especially X-rays. They underlined a great variation of the RBE for all the biological systems studied. Indeed, large variable shoulder regions were observed in response to X-rays, whereas less variation was observed with neutrons, explaining that the RBE is different for each cell line. In response to heavy ions, the depth of the irradiation has also to be considered and explains in part the different RBE calculated for one cell line compared with X-rays.

While the physical and dosimetric aspects of radiobiology are well understood, the biological aspects such as the complex biological endpoints induced need further attention. The current estimates of RBE listed above depend on the biological system, but also depend on the detection methods used as it has been demonstrated that DNA damage and the resulting apoptotic responses vary greatly depending on the radiation quality in a tissue- and dose-dependent manner. Experimental data emerging from recent studies suggest that, for several endpoints of clinical relevance, the biological response is differentially modulated by particles compared to photons. However, up to date, only few studies have been performed to understand the differential response on the molecular and cellular levels between different radiation qualities.

2.6.4.6 Radiation Quality (Type of Radiation): Relation to Space

The biological effects of ionizing radiation relate strongly to the dose, dose rate, and quality of the radiation. To distinguish the different types of radiation, from low LET to high LET particle radiation, the quality factor Q (L) has been introduced. This factor reflects all cumulative knowledge on the dependence of the detrimental effects of radiation on physical characteristics and mainly LET (ionization density). Therefore, this factor can be used to multiply the absorbed dose (rad or gray) to obtain a quantity that expresses, on a common scale for all ionizing radiations, the biological damage (rem or sievert) to the exposed tissue. Although Q (L) has been superseded by the radiation weighting factor W_R in the definition of equivalent dose, it is still being used in calculating the operational dose equivalent quantities used for example in monitoring [109].

In order to encompass the dependence of biological effects to LET, many studies have been performed in order to measure RBE for a specific biological endpoint (usually reproductive cell death) for radiations of different LET [110]. In most cases, survival curves are evaluated assuming a linear-quadratic dose dependence of the induction of reproductive death of cells. The linear term accounts for damage from single particle tracks and the quadratic term for damage due to interaction of lesions from independent tracks. Although for many years 250 kVp X-ray was considered the standard reference radiation for the determination of RBE, the International Commission on Radiation Protection (ICRP) recommended in their 92nd report to use gamma rays of ^{60}Co as the reference radiation [111]. In both cases of low LET radiation, RBE is assumed to be equal to 1.0. When specific biological effects of high LET radiation (such as fast neutrons) on human cells are measured, the RBE ranges from about 3 to greater than 100 for various biological effects.

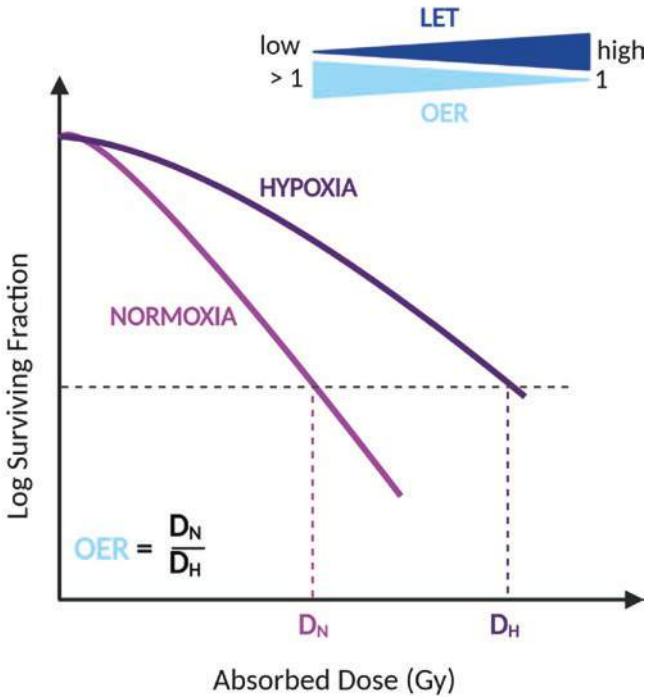

Fig. 2.23 OER as a function of LET (Created with BioRender)

2.6.5 Oxygen Enhancement Ratio and LET

The oxygen effect is an important parameter in radiation therapy. Its influence on the tissue's biological response (typically survival curves) will differ according to the radiation type used. This concept is represented by the oxygen enhancement ratio (OER).

The OER is a measure of the influence of the oxygen effect. It is defined as the ratio of radiation doses that produce the same biological effect in hypoxic compared to aerobic (well-oxygenated) conditions:

$$\text{OER} = \frac{\text{dose that produces a given biological response under hypoxic conditions}}{\text{dose that produces the same biological response under aerobic conditions}}$$

The OER varies with the LET (ionization density) (Fig. 2.23). The OER decreases as the LET increases and approaches OER = 1 at LET ≈ 150 keV/μm, meaning that the level of oxygenation has little or no influence on the cell survival in case of high LET radiation (α particles, neutrons, and heavily charged particles). This is explained by the fact that high LET radiation mostly induces direct damage, which is not oxygen dependent. Therefore, high LET radiation is

expected to lead to a better tumor control of hypoxic tumors compared to low LET radiation.

It should be noted that these OER values were originally derived from in vitro experiments. Recently, the oxygen effect during carbon ion therapy was questioned due to low LET values in the spread-out Bragg peak, giving rise to a possible impact of oxygen on carbon ion treatment outcome [112]. In case of low LET radiation (X- and γ-rays, electrons), the OER increases and is in the range of 2.5–3.5, meaning that a 2.5–3.5 times higher dose is needed to achieve the same killing effect in hypoxic cells compared to normoxic cells. Indirect effects, relying on reactive oxygen species (ROS) production, are the dominant process associated with low LET radiation and explain the importance of oxygen for low LET radiation. Hypoxic regions within a tumor may therefore show radioresistance to low LET radiation. The OER has an intermediate value for neutrons. Based on this concept, a massive work on oxygen-based radiosensitization is being done and is discussed in Chap. 5.

2.7 Deterministic and Stochastic Effects

2.7.1 Introduction

The damage caused by ionizing radiation in the body can become clinically apparent as a number of different health effects. The type and severity of the effect are strongly dependent on dose and exposure conditions, but also on the health status of the exposed individual. For radiation protection purposes, and to ensure the safe use of radiation in society, the health effects of ionizing radiation exposure are classified into two types [113]:

Deterministic effects, which are also called tissue reactions, are those for which there is a defined threshold below which the effect is not expected to occur. In addition, the severity of the effect increases with dose. The acute radiation syndromes are examples of early effects following high doses. However, deterministic effects are not a synonym for acute effects, as some, e.g., fibrosis, can occur much later.

Stochastic effects have no threshold, and the occurrence of the effect is probabilistic, such that any exposure to ionizing radiation increases the risk of these effects. The severity of the effect is not related to the dose. Stochastic effects tend to manifest many years postexposure and include cancer and heritable effects.

2.7.2 Deterministic Effects or Tissue Reactions

2.7.2.1 Mechanisms of High-Dose Effects

High-dose penetrating radiation causes damage both to functional tissues and to stem cell compartments. In general, maintenance of health depends on a balance between loss and replacement of cells in many, but not all, organs and tissues of the body, reflecting physiological "wear and tear."

Cellular damage is known to occur after exposing tissues to ionizing radiation. If the number of cells damaged is small relative to the total number of stem cells in the tissue, then the remaining stem cells can repopulate adequate numbers of functional cells. Consequently, there will be no obvious loss of tissue function. Conversely, if the stem cell population is reduced below a critical size, the tissue will cease to function efficiently, either transiently or permanently.

Organs and tissues differ in their sensitivity to radiation (Chap. 7), and the damage from radiation particularly affects the more radiosensitive cells, for example the lymphocytes in the lymphatic tissue, red bone marrow precursor cells, and crypt cells in the mucosal lining of the gastrointestinal tract.

Whether or not recovery will be possible will strongly depend upon the rate at which viable stem cells (that is, those cells undamaged or repaired) can repopulate the depleted stem cell population by self-renewal. The whole process of recovery is dependent upon feedback mechanisms stimulated by the body's recognition of depleted functional cell numbers. Following exposure of a large proportion of or all of the body, the normal steady state of cellular regeneration for tissues throughout the body is interrupted: cells and tissues break down and cannot be replaced. This is the basis for the observed threshold for such deterministic effects or tissue reactions.

It is, however, very important to note that there is a variation in sensitivity among individuals in an exposed population with any particular dose and exposure scenario. This variation reflects differences in the ability of individuals to cope with radiation-induced cellular damage, which is influenced by the age and state of health of the individual at the time of irradiation [85].

2.7.2.2 Radiation Syndromes

When individuals are exposed to sufficiently high doses of acute, penetrating ionizing radiation, the acute radiation syndrome begins with the prodromal phase [114, 115]. Following this, there will be a latent period, which represents the time period between initial exposure and manifestation of full acute radiation syndrome (ARS) due to a lack of cell renewal, as described above. The severity of the initial prodromal effects, the time for their development, the timing and any symptoms experienced during the latent period, and the type and severity of the full manifestation of ARS are all dependent on the dose and exposure scenario. This is described in more detail in Fig. 2.24 (Box 2.23).

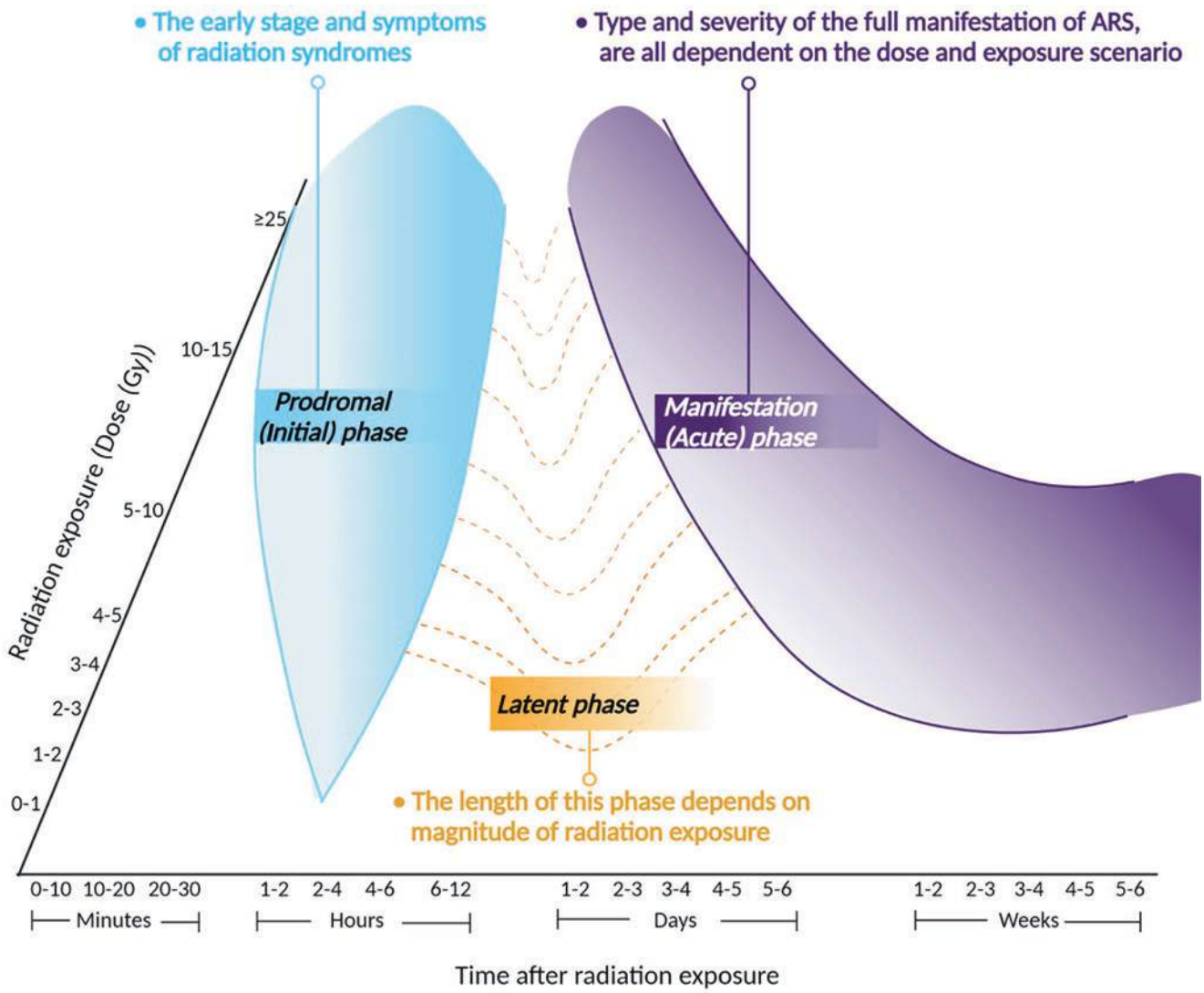

Fig. 2.24 Radiation syndrome phases (Created with BioRender)

Box 2.23 Symptoms of Exposure to Radiation

- The clinical signs and symptoms of high-dose radiation exposure are observed up to ~6 days after exposure (with a high degree of uncertainty). These come as soon as a few minutes after a very high dose.
- The symptoms of deterministic effects are dependent on dose (deterministic), with increased symptoms associated with higher doses.
- In general, individuals exhibit flu-like symptoms, vomiting, diarrhea, and headache. For doses in the region of:
  - 1–2 Gy, these are classified as "mild," and we would expect 10–50% people vomiting, and others experiencing fatigue and weakness.
  - 2–4 Gy, these are classified as "moderate," following which 70–90% people would be constantly vomiting, 2–6 h after exposure; 50% people would have a headache; 10–80% people would have a slight increase in body temperature.
  - 4–8 Gy, these are "severe," following which ~100% of people would be vomiting <1 h after exposure; 50–80% people would have a headache; most others would have a constant fever <1 h after exposure; some people might lose consciousness or feel confused; 10% of individuals would have diarrhea 1–8 h after exposure.
  - 8 Gy, these are "very severe/lethal" (depending on the medical resources available); most people lose consciousness fairly quickly; temperature peak at about 41 °C is usually observed, and many patients would present with skin burns at these doses.

Following these initial signs and symptoms, for doses less than approximately 6 Gy, the latency period is generally fairly asymptomatic, and individuals usually start to feel a little better. Then, unless radiation has been identified as the cause of the observed prodromal symptoms, often nothing is done, because the symptoms can be mistaken for those of many other non-radiation-related illnesses. However, if ionizing radiation has been identified as a potential cause, differential white blood cell counts should be taken as a marker of the potential severity of the effects. A summary of the different types of ARS is given in Fig. 2.25.

Hematopoietic Effects

Following exposures greater than around 2 Gy, and with this syndrome dominating up to around 10 Gy, the fall in blood cell counts may result in death from septicemia or hemorrhage, due to bone marrow failure, unless the symptoms can be treated. When the bone marrow is acutely exposed to radiation, this causes hypoplasia, aplasia, and/or hemolysis of cells. This leads to a sudden and dose-dependent reduction in the stem cell population, and ultimately atrophy of the lymph nodes and spleen. Differentiating and maturing cells may initially be only marginally affected. Depletion of cellular components of blood leads to infection and hemorrhage.

The stem cell population may attempt to recover and, if successful, increasing numbers of granulocytes will appear in the blood about 3 weeks after exposure. Loss and recovery of blood platelet cell numbers follow a similar dose- and time-related pattern.

The severity of the radiation effect can be estimated based on differential white blood cell counts (neutrophils and lymphocytes). If neutrophil and lymphocyte levels are measured repeatedly following initial exposure (the half-life of circulating neutrophils is only about 6–8 h), this can give an indication of the likely severity of the ARS or other tissue effects: A large initial peak of neutrophils and a rapid drop-off could indicate a dose ~>5 Gy.

Gastrointestinal Effects

The mucosal crypt stem cells provide the protective mucosal cell lining of the intestinal tract wall. Due to the high turnover of these cells, particularly in the small intestine, damage to these cells results in a denudation of the gut surface as the epithelial cells are not replenished, within 5–10 days after exposure of the gastrointestinal tract to doses of radiation >1 Gy. Leakage of blood from damaged blood vessels into the gut then occurs, and blood appears in the feces. Simultaneously, translocation of normally harmless intestinal bacteria from the gut through the damaged blood vessels occurs, leading to infection. Once in the blood, these bacteria become pathogenic. Symptoms include severe bloody diarrhea, anemia, severe electrolyte disturbances, malnutrition, and sepsis.

This gastrointestinal syndrome is seen in individuals who have received acute doses to the gastrointestinal tract in excess of about 8–10 Gy.

Cerebrovascular Effects

With the traditional paradigm of the dependence of severity of response on cell turnover, it was thought for a long time that the effects in the brain, beyond direct cell killing, were minimal. However, we now know that ionizing radiation can otherwise affect the way the brain functions, e.g., through changes in mediation of substance release.

For doses to the brain >~15 Gy, swelling (edema) of the brain, cerebral death (breakdown of the nerve impulse path-

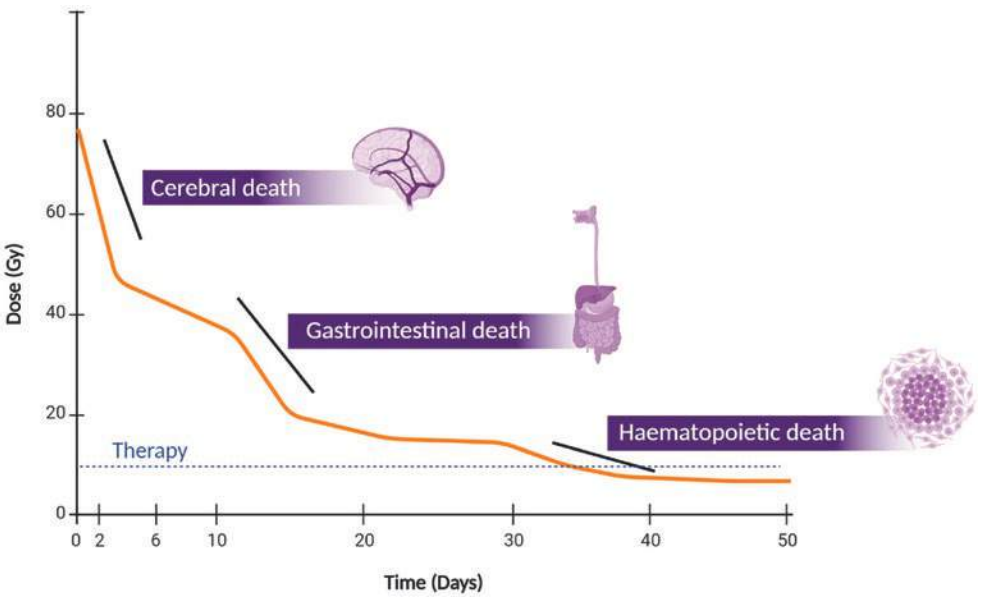

Fig. 2.25 The dominant syndromes leading to death vary with dose and time postexposure. Therapy is possible for doses lower than approximately 8–10 Gy (depending on medical resources) (Created with BioRender)

ways), and generalized shock lead to coma and death. At such high doses, this happens very quickly, with loss of consciousness followed by death within a few hours or days at most, before the wider systemic prodromal reaction can start.

At lower doses, the regulatory functions of the central nervous system (CNS) within the body are affected—either through vascular injury or through changes in how various neurotransmitters are released or by affecting the functioning of the brain itself. After whole-body exposure, the prodromal symptoms in the case of brain effects can also be detected as abnormalities on an electroencephalogram (EEG). This "neurovascular syndrome" tends to manifest around 10 Gy, and the vascular changes lead to hypertension, dizziness, confusion, impaired cognitive function, and neurological deficit later on. For cerebrovascular (and cardiovascular) effects, the assumed threshold is approximately 0.5 Gy.

It should be noted that multiple-organ dysfunction syndrome (MODS) can also occur—this is a clinical syndrome with the development of progressive and potentially reversible physiological dysfunction in two or more organs or organ systems induced by a variety of acute insults, like ionizing radiation.

2.7.2.3 Systemic and Late Effects

Pulmonary Effects

Cell proliferation is generally slower in the lung than in the hematopoietic or gastrointestinal systems; however, in the weeks and months following initial exposure, pulmonary effects may lead to death due to massive respiratory failure. Damage to the cells lining the alveoli may result in acute inflammation of the lungs (pneumonitis) at doses in the range of 5–15 Gy. This leads to pulmonary edema, which can result in adult respiratory distress syndrome and secondary bacterial and viral pneumonia. Pulmonary failure then occurs due to fibrosis as a direct result of the radiation itself or as a result of infection, between around 6 months and 2 years or more postexposure.

Local Radiation Injury

Local radiation injury (LRI) may be defined as a setting of signs and symptoms following local overexposure to ionizing radiation of the skin. Although sometimes called cutaneous radiation syndrome, this term applies better to skin manifestations in the context of ARS.

Skin injuries caused by the high initial dose occur initially as burning, itching, and acute pain coupled with very painful primary erythema (reddening of the skin). This is usually followed by edema, accumulation of fluid in the skin as a result of tissue damage. Cutaneous syndrome is usually characterized by a fairly short latency phase, but if edema occurs within a few hours, this will usually result in very severe ARS. After a few days, hair loss occurs and the skin starts to break down leading to ulceration and necrosis—tissue death occurs. Bacteria may use this as an entrance to the body ultimately followed by sepsis. Skin transplantation or amputation may be needed. As a late effect, telangiectasia and secondary erythema (and associated pain) can be very long lasting.

Fetal Effects

Evidence of the deterministic effects of radiation on the embryo and fetus is derived almost entirely from animal experiments. Extrapolation of the results of these studies can be used to predict the consequences of radiation exposure in humans.

The effects on the embryo depend on the time of exposure relative to its development. When the number of cells in the embryo is small (i.e., in the first 6 days of pregnancy) and the cells are not yet specialized, damage is frequently seen in animals as failure of the embryo to implant in the wall of the uterus. In humans, the only manifestation of this would be a late or missed menstrual period. However, evidence from in vitro human embryo research has shown that the survival of even one cell in the early embryo before implantation can allow normal development, since all the necessary genetic components are present in each cell of the embryo at this stage of development. The consequences of any of these cells carrying a point mutation are unknown, but the possibility of stochastic (genetic, heritable) effects occurring cannot be excluded.

Because of the lack of direct human evidence, it is useful to look in brief at the animal data. The data taken from animal experiments suggest that threshold doses in humans for radiological protection purposes are in the order of 0.05 Gy for reabsorption of preimplantation embryos; 0.05 Gy for minor skeletal abnormalities; 0.20 Gy for impaired fertility in the female; 0.2 Gy for functional disorders of the central nervous system; and between 0.20 and 0.50 Gy for serious skeletal abnormalities and growth retardation. Such information provides a basis for guidelines to ensure that pregnant women are adequately protected.

Brain development has been particularly well studied in animals. It is when neurons (the information-conducting cells in the brain) are developing and when they are migrating to their predetermined sites in the cerebral cortex that irradiation is most damaging. In humans, this corresponds to between 8 and 25 weeks postconception. Only a very small amount of human data exists. For example, data were published in 1984 from a relatively small study on intellectual disability in children exposed in utero following the atomic bombs dropped on Hiroshima and Nagasaki in 1945.

Intellectual disability is associated particularly with irradiation between the 8th and 15th weeks following conception. From these data, it has been estimated that the excess probability is about 40% per Gy; that is, at a dose of 1 Gy, 40 out of every 100 children exposed would be expected to

experience severe intellectual disability. This compares with a background frequency of 0.8%. It is less marked between the 16th and 25th weeks, and no effect has been seen at other times of pregnancy.

The uncertainties at each measured dose point are extremely wide, because of the small numbers. Thus, the presence or absence of a threshold for developmental effects remains highly uncertain. However, school performance and IQ scores have been measured for children irradiated in utero, with a decrease of approximately 30 points at 1 Gy for children irradiated in the 8th to 15th week of pregnancy (but not before or after) [116].

Other Effects

A variety of additional effects can occur, but of particular note, ionizing radiation can also cause nephropathy, which is reduced renal function, leading to progressive scarring kidneys and ultimately failure months to years following exposure.

Other tissue effects may be seen many years postradiation exposure, for example cataract, which has an assumed threshold of approximately 0.5 Gy but which for low dose likely has a very long latency period. This topic is further considered in Chap. 8.

2.7.2.4 Dose-Response

The probability of detecting tissue reactions, characterized by loss of tissue function, in healthy individuals following exposure to radiation is non-existing in some tissues at doses of up to a few hundred mGy. In other tissues, the threshold of detection is above a few thousands of mGy. Above the threshold, the probability of a tissue reaction increases steeply in a sigmoid manner, with the severity of effect increasing linearly with dose. It is important to note that protracting the dose will result in a lower frequency of effects and less severe symptoms at a given dose compared with acute exposure [113, 117].

The range of doses associated with death from these syndromes after acute exposure to low linear energy transfer (LET) radiations is given in Table 2.8.

Table 2.8 Range of doses associated with death after exposure to low LET radiations

Whole-body absorbed dose	Principal effect contributing to illness or death	Time of death after exposure
1–6 Gy	Damage to bone marrow[a]	30–60 days
5–15 Gy	Damage to gastrointestinal tract and lungs[b]	10–20 days
>15 Gy	Damage to nervous system and shock to cardiovascular system	1–5 days

[a]Dose range considered to result in 50% of an exposed population dying (LD_{50}) without medical treatment is LD_{50} = 3–4 Gy

[b]Damage to vasculature and cell membranes, especially at high doses, is an important factor in causing death

In an exposed population, there is a chance of death of approximately 5% of the population (5 persons dying in a population of 100) exposed to about 2 Gy or of about 50% without medical treatment (lethal dose, LD_{50}) within the dose range of 3–4 Gy. Most individuals would be expected to die at doses between about 6 Gy and 10 Gy, unless they receive treatment to prevent infection and bleeding. Above about 10 Gy, death is very likely, even after attempts to stimulate the bone marrow or bone marrow transfusion from a suitable donor. The risk of death thus also depends on the number of exposed individuals, and the available expertise and facilities for appropriate treatment, as discussed further in Chap. 7.

2.7.2.5 Mortality or Morbidity

High exposures do not always prove fatal, especially if the irradiation is nonuniform so that sufficient vital bone marrow stem cells are spared. Recent advances in immunology and in the administration of growth factors or cytokines to accidentally irradiated persons may rescue the bone marrow so that the hematopoietic syndrome might no longer be the limiting lethal condition. Matched stem cell transplantation is an alternative, provided that such stem cells are available at short notice. Death would then depend on whether damage to the lungs or intestine was sufficient to cause fatal pneumonitis or breakdown of the gut wall.

Table 2.9 shows proposed values of the LD_{50} and/or ED_{50} and 1% thresholds for a selection of the most important conditions of ARS (Table 2.10).

Table 2.9 Parameters for acute mortality (various sources including ICRP, 2007)

Threshold (Gy)	LD_{50} (Gy)	1%
Bone marrow syndrome		
First aid only	3.0	1.5
Supportive treatment	4.5	2.2
Pneumonitis	10.0	5.5
Gut syndrome	15.0	10.0

Table 2.10 Parameters for acute morbidity (various sources including ICRP, 2007)

Threshold (Gy)	ED_{50} (Gy)	1%
Prodromal		
Vomiting	2	0.5
Diarrhea	3	0.5
Lung fibrosis	5	2.7
Skin burns	20	8.6
Hypothyroidism	60	2.3
Cataract	3	1.3
Temporary sterility		
Males	0.7	0.5
Females	3.5	0.8

2.7.3 Stochastic Effects

2.7.3.1 Cancer

Cancer develops in tissues through the accumulation of various mutations over several conceptual stages [118]. Initiation of the process can occur following exposure to various environmental agents including radiation, but further changes in neoplastic development require a complex interaction between various factors in the host and environment. For this reason, it is not possible to attribute causal relationships between a particular environmental agent (in this case, radiation exposure) and cancer in individuals [119]. Instead, attribution is made for increased cancer incidence in an exposed population over a known baseline rate either pre-exposure or in a nonexposed population. This attribution is expressed through risk estimates.

Present risk estimates for cancer following radiation exposure are based on a number of epidemiological studies, most notably the Life Span Study (LSS) of the Japanese atomic bomb survivors. The study is a gold standard against which the results of other studies on long-term radiation effect on humans are evaluated. In the latest analysis of mortality patterns between 1950 and 2003 [120] of the 50,234 deceased cohort members with dosimetric measurement data, there were 10,929 deaths from solid cancers and 695 deaths from hematological malignancies. Of these, 527 (4.8%) solid cancer deaths can be attributed to radiation exposure from the bomb in 1945. A dose-dependent increase in the rate of solid cancer deaths can be observed (Table 2.11).

In the analysis of solid cancer incidence among the LSS population between 1958 and 2009 [53], the latest follow-up data of a cohort of 105,444 people who were alive without known history of cancer was presented. For a person exposed at age 30, the excess relative risk (ERR) for any cancer by the age of 70 was estimated to be 0.50 per Gy without adjusting for smoking. The dose-response was linear with an estimated ERR of 0.64 per Gy for females, but for males, a linear quadratic fit was observed instead, with ERR of 0.20 per Gy at 1 Gy and 0.010 per Gy at 0.1 Gy (Fig. 2.26).

Table 2.11 Observed and excess death from solid cancer and non-cancer diseases (adapted from Ozasa et al. 2012)

Colon dose (Gy)	Number of subjects	Number of deaths	Number of excess cases	Attributable fraction (%)
<0.005	38,509	4621	2	0
0.005–	29,961	3653	49	1.3
0.1–	5974	789	46	5.8
0.2–	6536	870	109	12.5
0.5–	3424	519	128	24.7
1–	1763	353	123	34.8
2+	624	124	70	56.5
Total	86,611	10,929	527	4.8

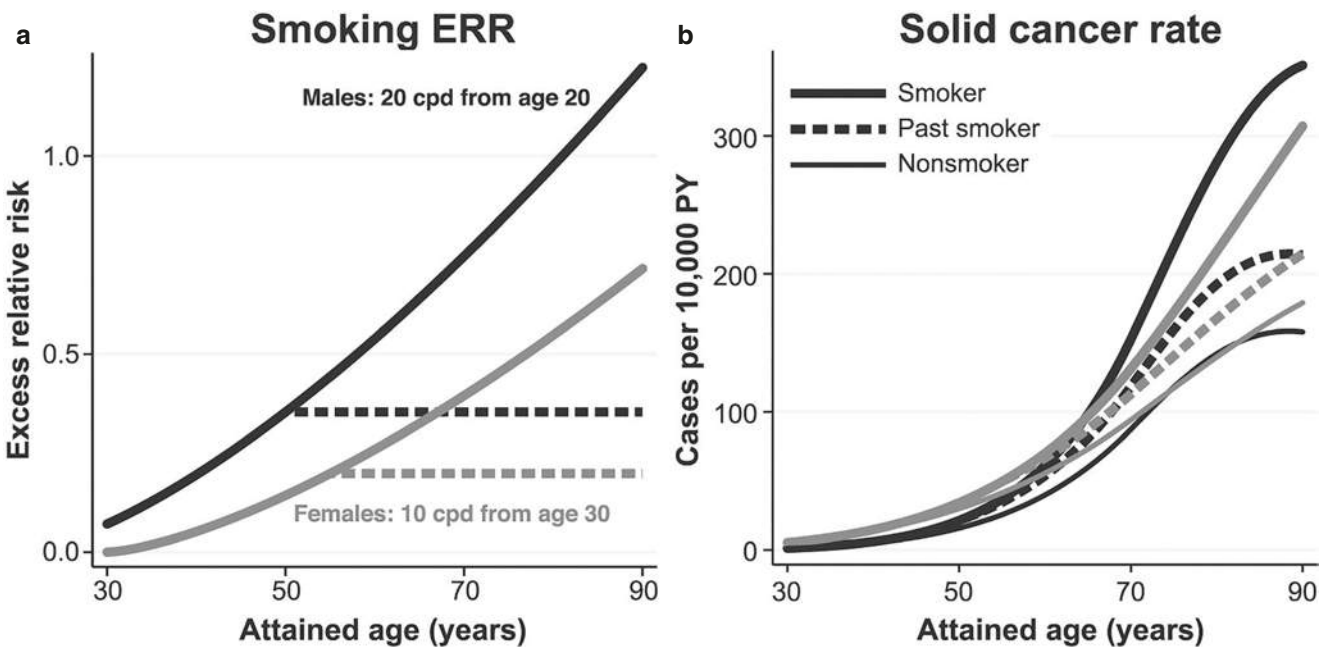

Fig. 2.26 Smoking effects on solid cancer baseline rates. (**a**) Smoking ERR as a function of attained age for males (black curves) and females (gray curves). The solid curves represent lifelong smokers, while the dashed curves represent past smokers from the age at which they quit (shown are male past smokers quitting at age 50 years and female past smokers quitting at age 55 years). (**b**) Total smoking risk for current smokers, past smokers, and those who never smoked (thin solid curves) for males and females. The curves represent typical smoking histories. Male smokers started at age 20 years and smoked 20 cigarettes per day, while female smokers started at 30 years and smoked 10 cigarettes per day (reproduced with permission from Grant et al. © 2017 Radiation Research Society) [53]

At the moment, 0.1 Gy is the lowest dose for which the overall cancer risk from radiation exposure can be reliably estimated. Uncertainties from various factors such as limited statistical power, dosimetric uncertainties, and confounders begin to grow increasingly large and mask any possible effects in lower dose ranges or site-specific risk estimation. Unless properly addressed, these uncertainties distort the results and lead to erroneous estimation of risk [119].

2.7.3.2 Heritable Effects

Together with radiation-induced cancers, the hereditary effects of radiation are stochastic effects. By comparison with cancer, induced hereditary diseases are considered to be a minor component of the total stochastic disease risk due to radiation exposure of an individual or of the population generally.

There is little direct human evidence of hereditary effects; however, it is clear that ionizing radiation can cause mutations of the types seen in hereditary effects.

Multifactorial diseases are an additional class of effect, which combine heritable aspects in addition to influence from environmental factors. These include congenital abnormalities present at birth or chronic conditions, which appear later in life (Box 2.24).

Box 2.24 Classes of Mendelian Type Gene Mutations

There are three classes of Mendelian-type gene mutations, where genes are inherited from each parent:

(a) *Dominant conditions*, where even in the heterozygote (a person inheriting one mutant and one normal gene), the abnormality is seen in the individual. Their effects in the homozygote (double dose of the mutant gene) are usually more severe, if not lethal. An example of a dominant gene condition is Huntington's chorea (HC), which is characterized by nerve cell damage and changes in physical, emotional, and mental state. HC is caused by a faulty gene on chromosome 4.

(b) *Recessive conditions*, which have an effect only when present in the homozygote (two genes with the same, disease-linked, mutation). Recessive disorders are usually rare, as the mutation would need to be inherited from both parents. However, some recessive genes even when present in a single dose, i.e., heterozygote accompanied by a dominant normal gene, do still confer slight deleterious effects. An example of a recessive gene disorder is cystic fibrosis, which is caused by mutations on a gene located on chromosome 7.

(c) *Sex-linked conditions,* which involve genes located on the X chromosome. A large proportion of mutations that are inherited are related to the X chromosome. Since there is only one X chromosome in males, mutant genes here act as dominant genes in males who suffer, whereas they are masked in the female with two X chromosomes who act as carriers. Mutations in these genes will exert their effect in females only when present in homozygotes and therefore appear as a recessive condition. Half the male offspring of a carrier mother will suffer and half her female offspring will be carriers. Examples of sex-linked conditions are color-blindness and hemophilia.

2.8 Low-Dose Radiation Effects

2.8.1 What Is a "Low Dose"?

A low dose of irradiation can be defined as acute and chronic. An acute low dose is defined as less than 0.1 Gy (100 mGy), while a chronic low dose is defined as less than 6 mGy/h (or Sv equivalent). In this low-dose range, there are a variety of phenomena that dominate the dose-response relationship and lead to nonlinear and unpredictable outcomes.

2.8.1.1 What Are the Effects of a "Low Dose"?

A key finding in low-dose radiobiology is that the effects seen are not directly proportional to the dose received. Rather, there are a number of factors such as genetic background, age, gender, and lifestyle, which can modify the outcome. After higher doses, DNA strand breaks are the predominant cause of radiation effects, and these are more directly related to dose deposited in the tissue or cells. Figure 2.27 depicts the usual dose-response relationship with the low-dose region shown as of uncertain outcome. The expanded section shows the variety of factors and outcomes which can be expected.

2.8.1.2 What Are the Mechanisms Involved?

Mechanisms involved in non-targeted effects are described in Sect. 2.8.2, and low-dose hypersensitivity, hormesis, and adaptive response mechanisms are described in Chap. 3. Global mechanisms underlying LDR are mentioned here and include production of oxidative stress, mitochondrial and membrane channel changes, signaling to neighboring cells, release of exosomes carrying modified cargos, and changes in the proteome. It is important to recognize that these changes may be proactive damage responses and not harmful per se. Change does not necessarily equate with harm.

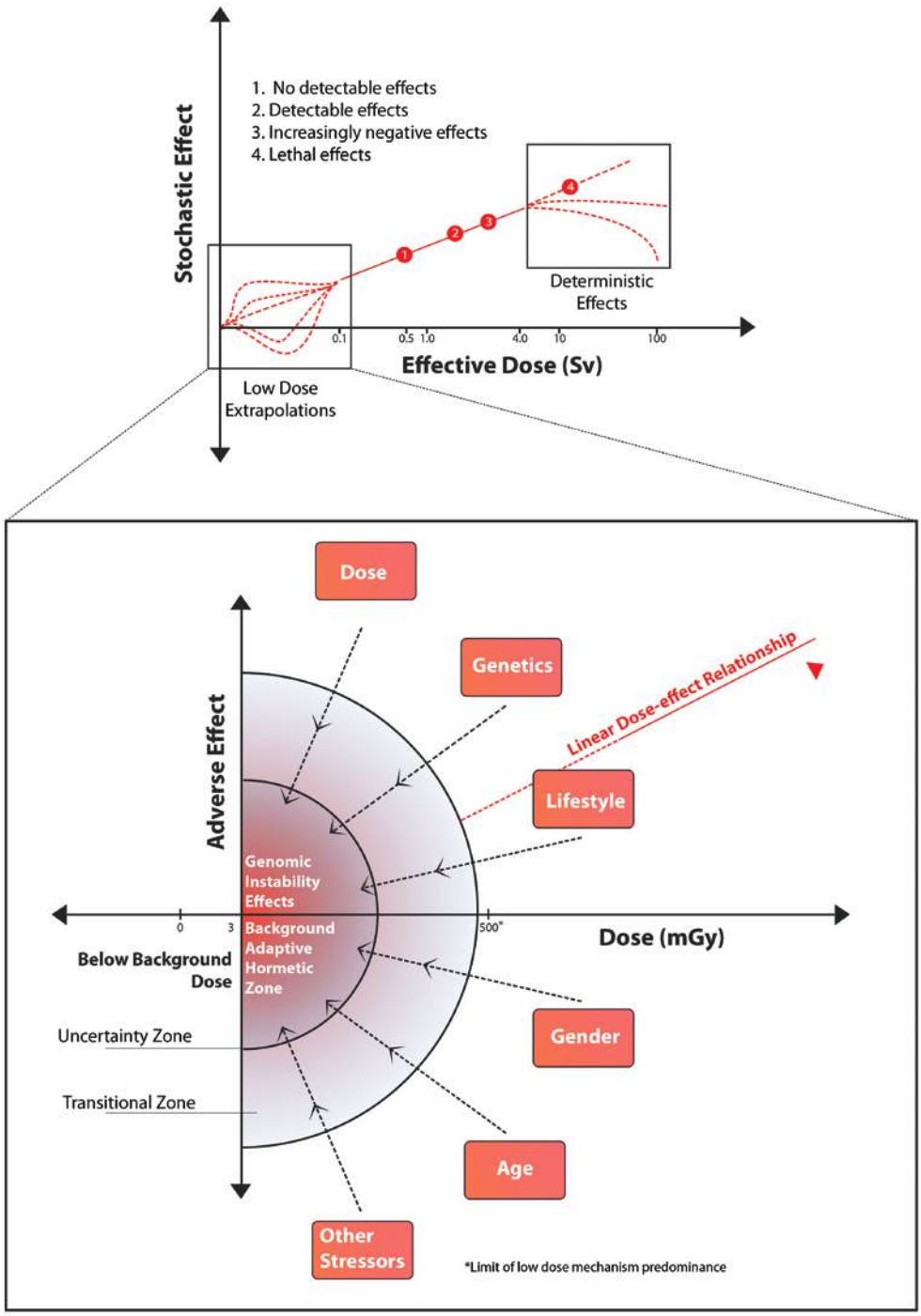

Fig. 2.27 Usual dose-response relationship with the low-dose region shown as of uncertain outcome. (Figure from Kugathasan and Mothersill, 2022 [121])

2.8.2 Targeted Effects

It is quite common that while a high dose/amount/rate of some medication or procedure is detrimental, a low dose is beneficial. Classical well-known examples include physical exercise (as opposed to forced labor), immunization (as opposed to virulent infection), and—directly related to biologically active radiation—controlled sun tanning (as opposed to sunburns and skin cancer caused by overexposure). Therefore, low-dose radiation effects may well be different from the effects of high doses. Actually, people have been using ionizing radiation for centuries: already, Herodotus and Hippocrates described healing properties of what we now know as radon springs. Radon treatment is considered to be a legitimate tool by mainstream medicine in Europe, especially for treating arthritis and other inflammatory diseases [122]. During the past four decades approximately, there has been a growing body of biological evidence regarding low-dose radiation effects. This evidence is concurrent with the shift in radiobiology from a DNA-centric view on radiation damage to a more systemic view that incorporates multi-level protection and nonlinear systems—adaptive response [123].

2.8.2.1 Adaptive Response

There is emerging evidence that low doses induce cellular and intercellular changes, which can lead to adaptive metabolic alterations. Adaptive responses against accumulation of damage—also of non-radiogenic origin—were also discovered [124]. Many studies demonstrated that radiation effects are far from linear [125]. Moreover, experimental, epidemiological, and ecological studies have shown that low doses of ionizing radiation can be beneficial to health [126, 127].

2.8.2.2 Hormesis

Beneficial low-dose effects of an agent that is harmful in high doses are called *hormesis*. Back in 1884, Hugo Schulz observed that low doses of many toxic agents, mercury and formaldehyde for example, enhanced the vitality of yeast cells. The term "hormesis" was introduced by John Ehrlich (also in the context of chemical toxicity) in 1942 [128]. The term "hormesis" is applied now to any kind of biphasic dose-response, i.e., when low doses of some agent are beneficial while higher doses are detrimental [128]. Physical exercise (as opposed to hard labor) is a typical example of hormetic response. According to the present knowledge, "hormetins"—agents inducing hormesis—include but are not limited to heat and oxidative stress, various food components, micronutrients, intermittent fasting, calorie restriction, etc. [129]. Radiation hormesis is the most thoroughly investigated among all hormesis-like phenomena.

Speaking about radiation hormesis, we should point out two somewhat different uses of the terms "hormesis" and "low dose." Since radiation carcinogenesis is often considered as the single most important health hazard of ionizing radiation, radiation hormesis is usually understood in the narrow sense that low radiation doses may suppress cancer. In this narrow sense, curing arthritis or pneumonia is not viewed as a hormetic effect. Accordingly, there are two quite different meanings of the term "low dose." In the context of radiation protection and many fields of radiobiology, "low dose" is understood to be 100 mGy or less as defined above. However, in the field of radiation therapy, the daily dose fraction is typically 2000 mGy and 6 weeks of therapy amounts to a total dose of 60,000 mGy—hence a single 1000 mGy dose to treat pneumonia may be regarded as a low dose [130].

2.8.2.3 HRS/IRR

Low-dose hyper-radiosensitivity (HRS) and induced radioresistance (IRR) describe a type of survival curve which has a dose range usually below 500 mGy acute dose, where the dose-response is significantly more radiosensitive than the overall fit to the higher dose points would suggest (see Fig. 2.28). The phenomenon is seen in a large variety of both tumor and normal cell lines and has been detected in human skin from patients [131]. It is seen following acute and fractionated irradiation meaning that it is likely to be relevant for radiotherapy and diagnostic radiology/medical imaging. It was first described by Lambin et al. (1993) and Marples and Joiner (1993) [132, 133]. The HRS phenomenon results in a significant reduction of clonogenic cell survival, increase in chromosome breaks, micronuclei, unrepaired DSB, or gene mutations after a single low dose in the range of 100–800 mGy. The maximal HRS effect is generally obtained at 200 mGy and corresponds to a biological effect equivalent to a dose 5–10 times higher. The mechanism of HRS/IRR is discussed in Chap. 3 (Box 2.25).

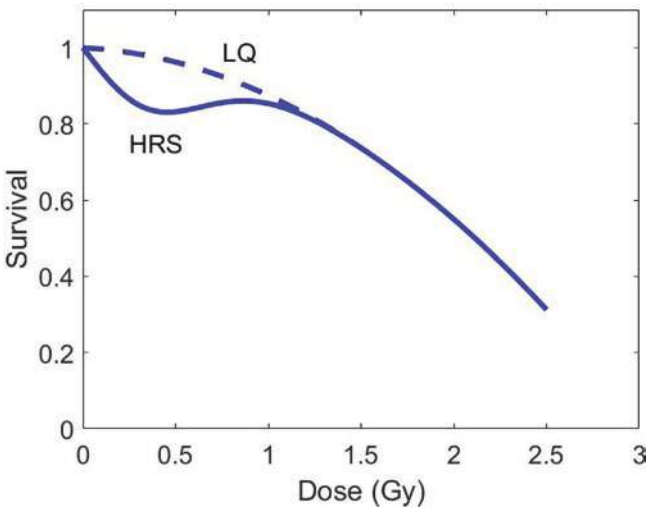

Fig. 2.28 Low-dose hyper-radiosensitivity (HRS) can be observed in a typical survival curve. The dashed line represents the linear-quadratic (LQ) model, while the solid line shows the induced repair (IR) model

Box 2.25 Low Dose Effects of Radiation

Dominant mechanisms below 100 mGy

Direct effects:

Low-dose hypersensitivity: Increased sensitivity to low-dose radiation which is not apparent at doses above 0.5 Gy.

Adaptive response: The ability of a low first dose of radiation to "protect" against the effects of a subsequent high dose.

Hormesis: Beneficial effects seen after low-dose exposure compared to unirradiated controls.

Non-targeted effects:

Bystander effects: One of the non-targeted effects defined as radiation-like effects seen in cells which did not get any energy deposition but which received signals from irradiated cells.

Genomic instability: Detection of non-clonal chromosomal damage or other DNA changes in distant progeny of cells which are genetically normal in the first postirradiation mitosis.

Lethal mutations: A form of genomic instability, detected as a permanently reduced plating efficiency of progeny cells which survived irradiation.

2.8.3 Non-targeted Effects

*N*on-DNA-targeted effects (NTE) refer to effects in cells, tissues, organs, or individuals which have not themselves received any radiation energy deposition but are in receipt of signals from irradiated entities. They include bystander effects, abscopal effects, clastogenic effects, genomic instability, and lethal mutations. Sometimes, adaptive responses and low-dose hypersensitivity are included as NTE, but although they can be induced by signaling in bystander cells, they are not strictly speaking NTE as they occur in directly exposed cells. Box 2.25 defines the terms. Box 2.25 shows the different effects observed in bystander cells and progeny cells compared to those seen in directly irradiated cells. The lists are the same showing that signaling can induce in bystanders most of the effects associated with low-dose direct radiation exposure. An NTE dose-response saturates in the low-dose region (Fig. 2.28). In general, increasing the dose beyond 0.5 Gy produces no additional NTE.

2.8.3.1 Bystander Effects

The United Nations Scientific Committee on the Effects of Atomic Radiation (UNSCEAR) defines bystander effect as a radiobiological effect that is transmitted from irradiated cells to neighboring unirradiated cells, generating biological alterations in the receiver cells that can influence the radiation-associated cancer risk [134]. As a communicative effect, bystander effects occur mainly at the primary site over a few millimeters or cellular diameters. This effect is mediated by the secretion of soluble factors or by signaling through gap junctions as well as through networks involving inflammatory cells of the microenvironment [135].

The term radiation-induced bystander effect (RIBE) is described as the ability of irradiated cells to transport manifestations of damage to other cells which were not directly targeted by irradiation. An irradiated cell sends out signals and induces response in nonirradiated neighboring cells. The intensity of the bystander response in nonirradiated cells is not necessarily proportional to the dose delivered to the irradiated cells and can occur even at low doses. The RIBE is highly dependent on the cell tissues concerned and the irradiation sources (such as radiation doses, LET, dose rates) and can influence the nature of the bystander factors secreted by irradiated cells, the intensity of the bystander response in nonirradiated cells, and the timing of the events in the bystander signaling [136]. This amplification can cause similar radiation-induced effects in cells not directly exposed to radiation and exhibit the heritable changes that include cellular damage, DNA damage, mutations, chromosomal aberrations, chromosomal instability, senescence, apoptosis, genomic instability, micronucleation, oncogenic transformations, etc. [137–139].

Some RIBEs can have deleterious effects, which involve the type of cell inducing the bystander signal after irradiation and the type of cells receiving these signals. Such effects can be determined by intercellular communication and level of amplification of original consequences of the event. Knowledge of the mechanism(s) by which non-targeted bystander effects are activated is still in its infancy and not well understood; however, it is believed that multiple pathways are involved in this phenomenon and also different cell types respond differently to bystander signaling.

RIBE is believed to be an incredibly complex phenomenon considering the involvement of sheer number of proteins, inorganic molecules, and cofactors. This effect encompasses a number of distinct signal-mediated effects (Figs. 2.29 and 2.30). Lately, communication of bystander signals between adjacent cells connected by gap junctions has been studied extensively. Signaling molecules are propagated through direct intercellular communication via gap junctions or through diffusible secretion in the surrounding environment of irradiated and bystander cells. Exosomes and signaling mRNAs also play a potential role in mediating bystander effect [140]. Exosomes can be released by bystander cells exposed to radiation-induced UV biophoton signals [141, 142], while miRNAs have a pivotal role in intercellular signaling between irradiated and bystander cells [143]. ROS and secondary messengers (such as nitric oxide), protein kinase, as well as cytokines (such as TGF-β and TNF-α) are also considered to be involved in RIBE. Additionally, irradiated dying cells (predominantly from apoptotic rather than necrotic cells) release cell-free chromatin (cfCh) particles, which can integrate into genomes of surrounding healthy cells to induce extensive genomic instability (DNA damage) and inflammation [144]. In the absence of macrophages, cfCh shows direct involvement in the activation of H2AX by bystander cells. The bystander effect can be observed in different cell types with different endpoints.

2.8.3.2 Abscopal Effects on Normal Tissues

The term abscopal or out-of-field effect is an in vivo phenomenon in normal tissue that describes the occurrence of radiation-like damage in organs that have never been irritated. In other words, abscopal effects are bystander effects in vivo. Abscopal effects are known to occur after exposure to high or low doses of ionizing radiation in vivo and are often observed after high doses of targeted partial-body radiotherapy [145, 146]. The mediation of the effect is attributed to systemic factors such as the blood or the endocrine system [136, 147–149]. The immune system is also thought to play an important role. Experiments show that high levels of macrophage activation and neutrophil infil-

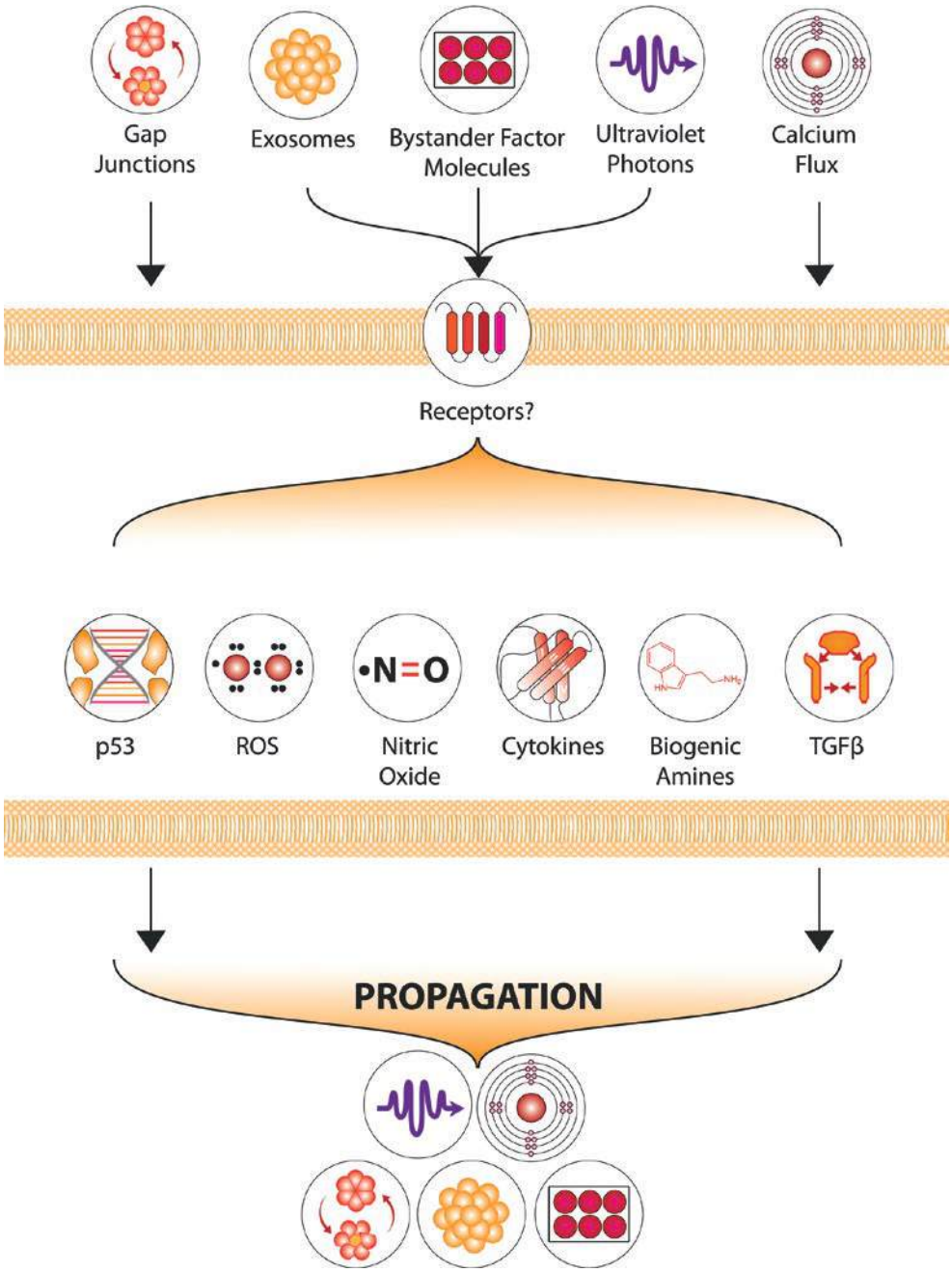

Fig. 2.29 Probable players driving the non-targeted effects of radiation

tration in mice are a consequence of radiation-triggered recognition and elimination of apoptotic cells [150]. The abscopal effect on normal tissue differs conceptually from the abscopal effect on tumors, which is often described in radiation oncology. The abscopal effect on tumors refers exclusively to systemic antitumor immune responses induced by radiotherapy alone or in combination with immunotherapy to only part of the tumor load. These antitumor immune responses are capable of completely eliminating primary tumors and unirradiated metastases in patients. For more information about the abscopal effect on tumors, see Chap. 5.

2.8.3.3 Clastogenic Factors

Clastogenic factors (CFs), *potential biomarkers of a prooxidant state*, are composed of endogenous lipid peroxidation products, cytokines such as necrosis factor alpha, unusual nucleotides, and other oxidants with chromosome-damaging properties. They are frequently noticed in the plasma of patients exposed to radiation [151]. Subsequently, it has been shown that CFs are not specific for irradiated subjects (Table 2.12), but are found in a variety of pathological conditions accompanied by oxidative stress. In both conditions, they can be considered as biomarkers of oxidative stress [152] as well as risk factors for carcinogenesis.

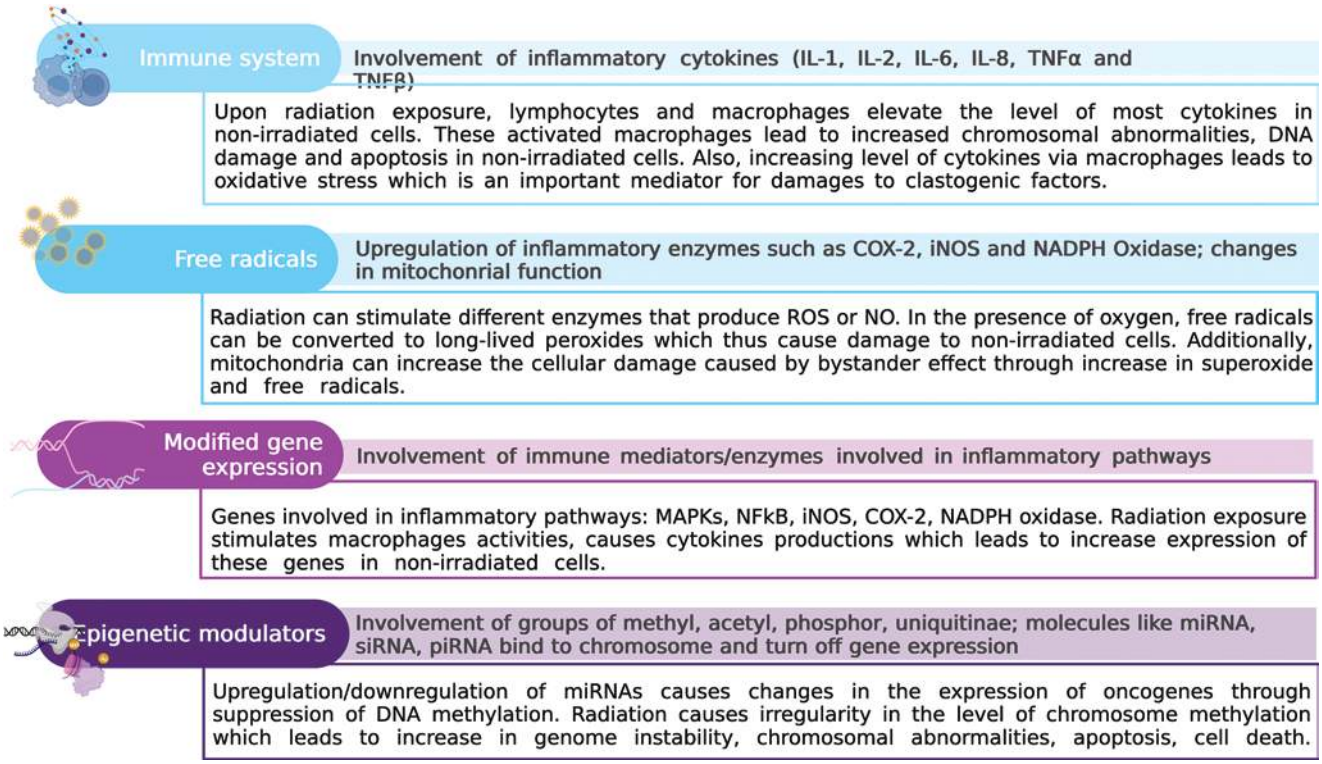

Fig. 2.30 Factors involved in RIBE (created with BioRender)

Table 2.12 Clastogenic factors (irradiation)

Clastogenic factors (irradiation)	
Therapeutic and accidental exposure	(Goh and Summer, 1968; Hollowell and Littlefield, 1968)
Exposure at Chernobyl	(Emerit et al., 1994; Emerit et al., 1997)
A-bomb survivors	(Pant and Kamada, 1977)
PUVA treatment for psoriasis	(Alaoui-Youssefi et al., 1994; Emerit et al., 2011)

Occurrence and Formation of CF

The non-targeted effect is a dynamic complex response of epigenetic dysfunctions, DNA damage, and cell death in nonirradiated tissues as consequences of secretion of clastogenic factors—"chromosome breakage factors" from irradiated cells. The formation of these breakage factors (CF) with their chromosome-damaging actions is mediated by the superoxide anion radicals, which are regularly inhibited by exogenous superoxide dismutase (SOD). These free radicals are an initiator of a series of events leading to formation of clastogenic materials. In vitro experiments provide strong evidence for the role of O_2 in those cells exposed to superoxide-generating systems, such as the xanthine–xanthine oxidase reaction, a phorbol 12-myristate-13 acetate (PMA)-stimulated photodynamic reaction. The supernatant of these cells contains CF, while cell-free systems do not lead to CF formation. Studies of CFs originating from observations on the plasma from irradiated persons were shown to induce chromosomal aberrations when co-cultured with cells from unexposed persons (Fig. 2.31). However, this phenomenon is common in a large number of health defects as well [153].

Possible Mechanisms of Action of CF

TNF-α and inosine triphosphate (ITP) stimulate the production of superoxide by monocytes and neutrophils. The lipid peroxidation product, 4-hydroxynonenal, inhibits superoxide production; however, it has the capacity to decrease the activity of DNA polymerases by inactivating their sulfhydryl groups leading to genotoxic effects. Formation of CF often damages/changes the chromatid structure; which indicates that they are not immediate and occur late in the S phase or in the G2 phase of cell cycle where they have duplicated their chromatids. These chromosome-damaging effects can be detected by classical cytogenetic techniques.

Ionizing irradiation is known to have mutagenic and carcinogenic potential for the exposed host as it induces chromosomal aberrations in directly exposed cells.

2.8.3.4 Genomic Instability

Genomic instability (GI) is a hallmark of cancer cells, which includes variations of increased frequencies of base pair mutation, microsatellite instability (MSI), and chromosome instability (CIN) [154]. GI is a complex multiple-

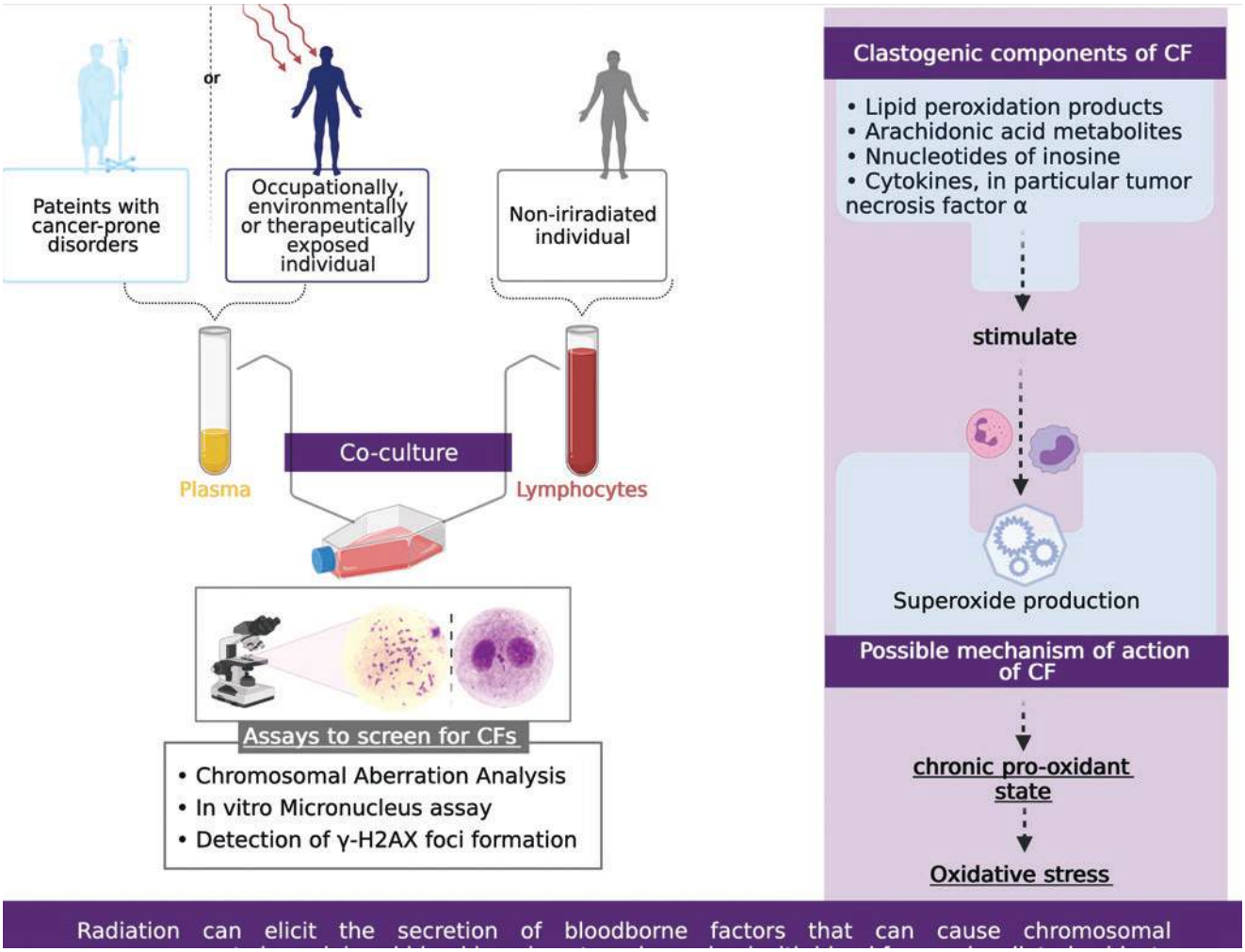

Fig. 2.31 Clastogenic factors (created with BioRender)

gene event marked during the development of some but not all cancers and also induced effectively by ionizing radiation. Radiation can provoke cellular communications eliciting a cascade of cellular events, which results in the destabilized genome in irradiated as well as unirradiated (bystander) cells. Radiation-induced genomic instability (RIGI) is observed in the progeny of irradiated cells as a delayed and elevated stochastic appearance of de novo chromosomal aberrations, gene mutations, and reproductive cell death [137, 155]. The effects of instability occur at a stable rate and are persistent in the postirradiation survivors for many generations.

Radiation-induced bystander effects are also involved in RIGI [156] due to contribution of indirect (by stimulating the reactive intermediates over many generations) and delayed effects (delayed DNA breakage, delayed reactivation of p53, delayed induction of various phenotypes) to cellular outcomes after radiation exposure. More detailed molecular studies on RIGI can provide deep insights into radiation-induced carcinogenesis (Box 2.26).

Box 2.26 Genomic Instability

- Genomic instability (GI), a characteristic of most cancers, is a complex multigene event and is often expressed by the appearance of chromosome aberrations many generations later.
- Microsatellite instability or chromosomal instability due to mutations in DNA repair genes or mitotic checkpoint genes is the underlying basis for GI in hereditary cancers.
- In sporadic (non-hereditary) cancers, GI occurs at least at the early stages of cancer development.

Potential Causes of RIGI

Biological effects of IR-induced GI are transmitted over several generations after irradiation via the progeny of surviving cells with delayed phenotypic expression, but not uniformly. Delayed manifestations of induced GI include delayed cell death, chromosomal instability, and mutagenesis.

The incidence of GI is significantly higher than that of conventional gene mutation, which eventually induces delayed reproductive death or delayed lethal mutations and increases the frequency of giant cells, micronuclei, senescence-like growth arrest, apoptosis, or necrosis in the progeny of surviving cells [157], suggesting that one of the potential initiators of RIGI is *delayed cell death*.

Exposure to sparse LET or dense LET radiation produces non-clonal chromosome aberrations (NCCAs), a highly significant feature for *delayed chromosomal instability*, genome heterogeneity, and complexity, in clonal descendants or stem cells that result in transmission of chromosome-type and chromatid-type aberrations to their progeny after irradiation [158].

Radiation may induce a type of GI in cells which results in an increased rate of spontaneous mutation that persists for many generations of cells. Clonal populations of cells surviving radiation exposure indicate such instability in a fraction of irradiated cells, which can persist longer over generations. Subpopulation of genetically unstable cells may arise from irradiated cells with a high frequency of even featureless minisatellite mutations [159], signifying the *delayed* appearance of certain *mutational events* in the progeny of irradiated cells.

Mechanism of RIGI

The mechanism of perpetuation in progeny populations is thought not only to be epigenetic but also to involve an excess generation of ROS over the course of time, cell-to-cell gap junction communication, dead and dying cells in the unstable population, and/or secreted factors from unstable cells (Fig. 2.32).

Initiation of RIGI

DNA-damaging agents (such as X-rays, IR, restriction endonuclease HinfI), radiomimetic drugs (bleomycin and neocarzinostatin), DNA DSBs, and DNA damage at the site of their decay are considered as effective initiators of RIGI. In some cases, sufficiently small or powerful environmental cues can directly exert their impact upon a cell's DNA, which is a critical target for RIGI. DNA strand breaks, the most lethal lesions induced by IR, activate a number of cellular DDR signaling cascades such as the activation of DNA damage-sensing and early transduction pathways, cell cycle arrest, and DNA repair. To a certain degree, it could convert the initial sites of DNA DSBs to unforeseen structures and

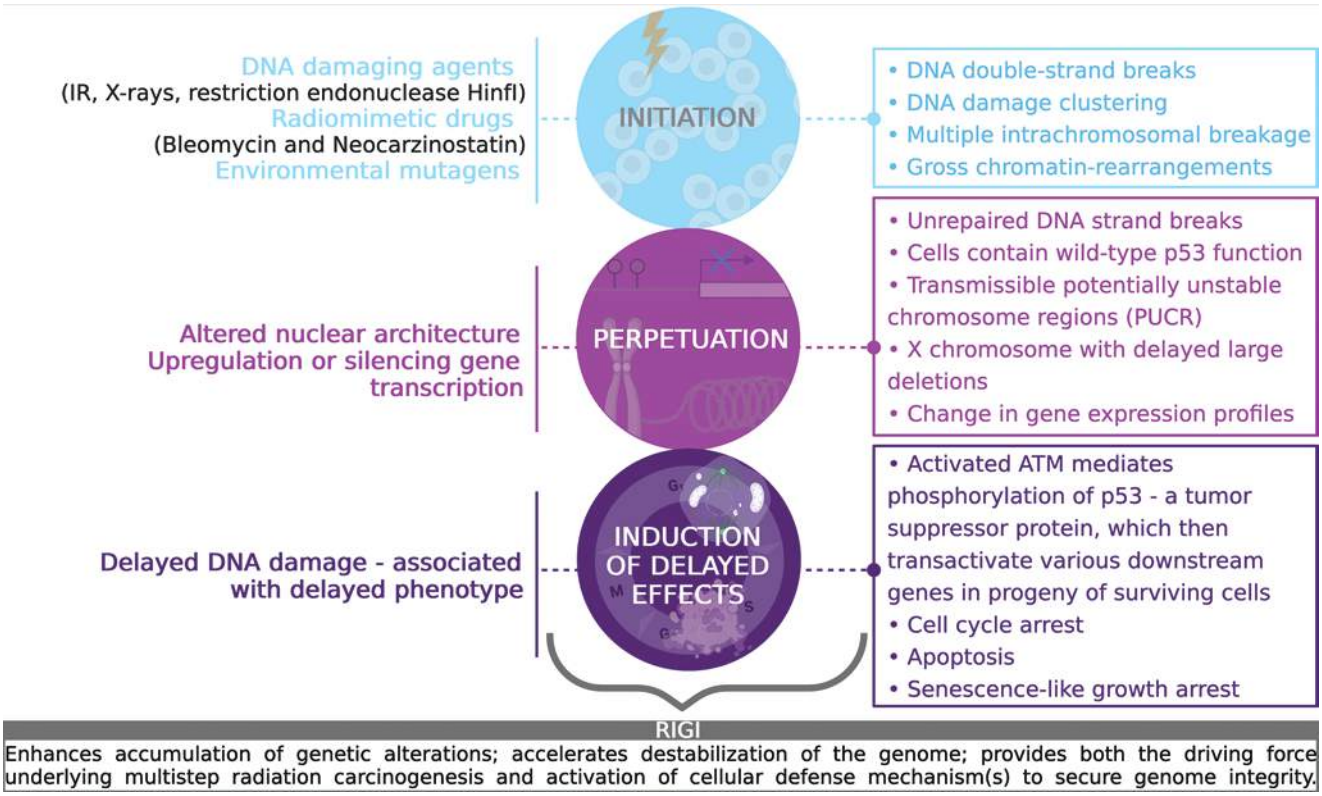

Fig. 2.32 Mechanisms involved in radiation-induced genomic instability (Created with BioRender)

results in reorganized chromatin domains and a disrupted genome structure, evident as a mutation induction. Generation of gross chromosomal rearrangements, or multiple intrachromosomal aberrations, or DNA damage signatures is accountable for the initiation of GI.

Perpetuation

RIGI is transmitted through many generations after irradiation, suggesting that the memory of unrepaired DNA damage can be perpetuated over time by a number of processes involving ROS, communication through cell-to-cell gap junction, unstable dying cell population, and/or secreted factors from unbalanced cells. RIGI appears to be independent of the p53 status of the irradiated cells, but a number of genetic factors influence the expression of the unstable phenotype.

Radiation-induced DNA DSBs could cause nonlethal, "potentially unstable chromosome regions (PUCR)" and altered chromatin architecture within the nucleus through DNA repair, which are transmissible through the progeny of surviving cells for many generations after irradiation [160]. Indeed, though PUCRs are potentially unstable, they are capable of persisting for prolonged periods through bridge-breakage-fusion (BBF) cycle [161] and thus could be the regions susceptible for causing delayed DNA breakages [162], inducing telomere instability and delayed cell death.

PUCRs can possibly be reactivated by large deletions or abnormal positioning of telomeres, loss of nuclear matrix-attachment regions (MARs), translocations of the chromosomes, distorted nucleosome, and altered nuclear architecture, leading to upregulating or silencing gene transcription, delayed p53 reactivation, and delayed manifestation of GI in the progeny of surviving cells (Table 2.13).

Induction of Delayed Effects

IR-induced DSB repair defects predominantly persuade various delayed phenotypes, indicating that delayed DNA damage is associated with delayed phenotypes. It is expected that delayed DNA damage arising in the progeny of surviving cells activates the uniquely sensitive tumor suppressor p53 protein, a multifunctional, highly regulated, and promoter-specific transcription factor. It is known to depend on the kinase ATM, which acts via the downstream kinases Chk2/hCds1 and mediates phosphorylation of various nuclear proteins, including p53. Stabilized and activated p53 protein transactivates a variety of downstream gene products, which direct either a prolonged cell cycle arrest in G1, senescence-like growth arrest or an apoptotic pathway.

RIGI enhances the accumulation of genomic alterations, resultant of delayed unscheduled DNA breakage, which triggers deferred activation of p53 in the progeny of irradiated cells; however, RIGI can be induced in all cell types regardless of the presence and status of a p53 function. Reactivated PUCRs and delayed DNA breakage are directly or indirectly involved in the delayed expression of instability phenotypes (Box 2.27).

Table 2.13 PUCR effects

PUCRs near the telomeres	PUCRs in the interstitial regions
Could cause telomere instability, chromosomal aberrations involving telomeric sequences	Interstitial telomeric sequences are potentially more unstable than non-telomeric sequences
Less detrimental to the cell, as it would result in loss of less genetic material	More destructive as it may lose chromosome fragments or large deletions
Lead to genomic instability across many generations	Lead to different consequences in the long-term progeny

Box 2.27 Radiation-Induced Genomic Instability

- Radiation-induced genomic instability (RIGI) is characterized by an elevated and persistent rate in the accumulation of de novo genetic alterations in the progeny of irradiated cells after the initial insult.
- Delayed manifestations, e.g., chromosomal instability, mutational events, and cell death, are the potential initiators of RIGI for multiple generations following irradiation or exposure to DNA-damaging agents.
- Unirradiated progeny cells display phenotypic changes due to RIGI at delayed times after radiation of the parental cells.
- Along with changes in DNA, epigenetic aberrations may be involved in RIGI, suggesting that epigenetics may also be the link to understand the initiation and perpetuation of GI.

2.9 Exercises and Self-Assessment

Q1. As seen in the figure below, the difference between the attenuated radiation, i.e., the radiation lost from the beam, and the absorbed dose is much larger for the energies where the Compton process dominates. Can you explain this?

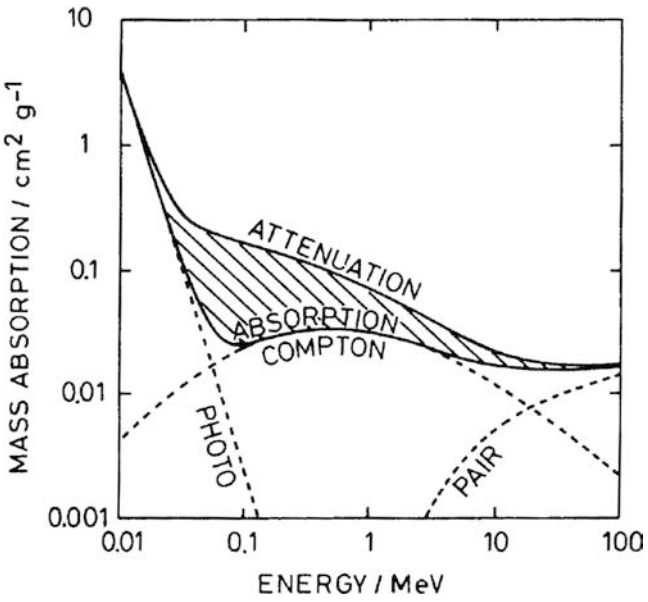

Absorption and attenuation in water for photons with different energies [Figure from Kiefer, J. (1990). Biological radiation effects. Germany: Springer.]

Q2. Can you tell why people living at high altitudes are more exposed to cosmic radiation? Can you tell which is the treatment at hospitals which is of most concern for radiation exposure?

Q3. Which of the following is the most harmful to cells?
(a) H_2O_2
(b) H·
(c) OH·
(d) e^-_{aq}

Q4. Name the four stages of indirect effects of ionizing radiation.

Q5. Low LET radiation mostly induces direct effects: true or false?

Q6. Fill in the missing items in the table (modes of radioactive decay).

Q7. Describe the difference between the well-known periodic table and a chart of nuclides (chart of nuclides).

Q8. The unit of effective dose is:
(a) Gy
(b) Sv
(c) Bq
(d) J

Q9. The dose that takes into account both the quality of the radiation and the radiosensitivity of the tissue, and is thus a direct measure of the likelihood of developing cancer, is called:
(a) Absorbed dose
(b) Equivalent dose
(c) Effective dose
(d) Dose rate

Q10. X-rays and beta particles have been given a radiation weighting factor of 1 because they produce:
(a) Virtually the same biological effect in tissue for equal absorbed doses
(b) No biological effect in tissues for equal absorbed doses
(c) Varying degrees of biological effect in body tissue for equal absorbed doses
(d) None of the answers above

Q11. During flash radiotherapy, an ultralow dose rate is used. True or false?

Q12. Arrange the following radiations in order of increasing LET in water:
(a) 5 MeV alpha particle
(b) 100 MeV carbon ion
(c) 10 MeV proton
(d) Cobalt-60 γ-rays
(e) 200 MeV iron ion

Q13. Explain why high LET irradiation exerts a relatively larger RBE in the low-dose range.

Q14. With decreasing dose rate, a discriminative biological effect can be obtained between late-responding normal tissues and tumors. Please explain.

Mode of radioactive decay	Released particles	General reaction	Example
α-Decay			92238U → 90234Th + 24He
	Two fragment nuclei		100256Fm → 54140Xe + 46112Pd
		ZAP → ZA − 1D + n^{0***}	413Be → 412Be + n^{0***}

Q15. The consequences for human exposure to ionizing radiation can be classified into two categories—stochastic or deterministic effects/tissue reactions. Explain the reasoning behind this classification and describe the main features of these effects, giving examples.

2.10 Exercise Answers

SQ1. The Compton process results in a secondary photon, which has its own track, and an electron, which may also have enough energy to move away from where the primary ionization took place. In both cases, some of the dose is deposited in a different position than where the energy was lost from the beam.

SQ2. When going higher in altitude, the amount of atmosphere shielding us from incoming radiation is smaller than at the Earth's surface. Thus, at higher altitudes, the "shielding" provided by the atmosphere against the incoming radiation from space is less efficient. Radionuclide-based treatments are the main concern in terms of radiation exposure at hospitals. There is the need to protect healthcare staff and to keep dose to caregivers and the public within the acceptable levels.

SQ3. OH•.

SQ4. Physical, physicochemical, chemical, biological.

SQ5. False.

Mode of radioactive decay	Released particles	General reaction	Example
α-Decay	Helium nucleus	$ZAP \rightarrow Z-2A-4P+24He$	$92238U \rightarrow 90234Th + 24He$
Spontaneous fission (SF)	Two fragment nuclei	$ZAP \rightarrow Z_1A_1D_1 + Z_2A_2D_2$	$100256Fm \rightarrow 54140Xe + 46112Pd$
Neutron emission (NE)	Neutron	$ZAP \rightarrow ZA-1D+n^{0***}$	$413Be \rightarrow 412Be + n^{0***}$

SQ6. The periodic table organizes chemical elements by their respective atomic number, while a chart of nuclides organizes nuclides according to the number of protons (*Y*-axis) and neutrons (*X*-axis) present in the nucleus.

SQ7. B.

SQ8. C.

SQ9. A.

SQ10. False.

SQ11. Cobalt-60 γ-rays (0.2 keV/μm) < 10 MeV proton (~5 keV/μm) < 5 MeV alpha particle (~100 keV/μm) < 100 MeV carbon ion (~200 keV/μm) < 200 MeV iron ion (>300 keV/μm).

SQ12. The RBE is defined as the ratio of the high LET dose and the low LET reference dose (generally 250 kV X-rays) at isoeffect. The high LET dose-effect cell survival relation is a straight line over the full dose range. The low LET cell survival curve is however characterized by a broad shoulder in the low-dose range, followed by a straight, parallel steep downward curve in the higher dose range. Hence, the RBE in the low-dose range is higher than in the high-dose range.

SQ13. Late-responding normal tissues (low alpha/beta ratio) are better spared than tumors and early-responding normal tissues (high alpha/beta ratio) by decreasing the dose rate. Lowering the dose rate can be considered as decreasing the "fraction size," with larger sparing of late-responding normal tissues than of tumors, hence a therapeutic beneficial effect.

SQ14. Deterministic effects or tissue reactions are those for which there is a threshold (varying between different effects), below which the effect is not seen. Above the threshold, the severity of the effect increases with dose. The syndromes of ARS are examples of deterministic effects.

Stochastic effects are the probabilistic ones, for which there is no threshold—any increase in dose slightly increases the risk of the effect, and severity does not increase with increasing dose. Radiation cancers and genetic/hereditary effects are classified as stochastic effects.

References

1. Davisson C, Germer LH. The scattering of electrons by a single crystal of nickel. Nature. 1927;119(2998):558–60.
2. Thomson GP. The diffraction of cathode rays by thin films of platinum. Nature. 1927;120(3031):802.
3. Thomson GP, Thomson JJ. Experiments on the diffraction of cathode rays. Proc R Soc Lond Ser A Contain Pap Math Phys Charact. 1928;117(778):600–9.
4. Mori O, Matsumoto J, Chujo T, Matsushita M, Kato H, Saiki T, et al. Solar power sail mission of OKEANOS. Astrodynamics. 2020;4(3):233–48.
5. Mori O, Sawada H, Funase R, Morimoto M, Endo T, Yamamoto T, et al. First solar power sail demonstration by IKAROS. Trans Jpn Soc Aeronaut Space Sci Aerosp Technol Jpn. 2010;8(ists27):To_4_25–31.
6. Spencer DA, Betts B, Bellardo JM, Diaz A, Plante B, Mansell JR. The LightSail 2 solar sailing technology demonstration. Adv Space Res. 2021;67(9):2878–89.
7. Tommasino F, Durante M. Proton radiobiology. Cancers. 2015;7(1):353–81.

8. Tinganelli W, Durante M. Carbon ion radiobiology. Cancers (Basel). 2020;12(10):3022.
9. Bentzen SM, Heeren G, Cottier B, Slotman B, Glimelius B, Lievens Y, et al. Towards evidence-based guidelines for radiotherapy infrastructure and staffing needs in Europe: the ESTRO QUARTS project. Radiother Oncol. 2005;75(3):355–65.
10. Wu Y, Chen Z, Wang Z, Chen S, Ge D, Chen C, et al. Nuclear safety in the unexpected second nuclear era. Proc Natl Acad Sci U S A. 2019;116(36):17673–82.
11. Piguet F, Eckert P, Knüsli C, Deriaz B, Wildi W, Giuliani G. Modeling of a major accident in five nuclear power plants from 365 meteorological situations in western Europe and analysis of the potential impacts on populations, soils and affected countries. Genève: Sortir du Nucléaire, Suisse Romande; 2019.
12. Walsh L, Schneider U, Fogtman A, Kausch C, McKenna-Lawlor S, Narici L, et al. Research plans in Europe for radiation health hazard assessment in exploratory space missions. Life Sci Space Res (Amst). 2019;21:73–82.
13. Cucinotta FA. Review of NASA approach to space radiation risk assessments for Mars exploration. Health Phys. 2015;108(2):131–42.
14. Cucinotta FA, Alp M, Rowedder B, Kim MH. Safe days in space with acceptable uncertainty from space radiation exposure. Life Sci Space Res (Amst). 2015;5:31–8.
15. Dartnell LR. Ionizing radiation and life. Astrobiology. 2011;11(6):551–82.
16. Moller AP, Barnier F, Mousseau TA. Ecosystems effects 25 years after Chernobyl: pollinators, fruit set and recruitment. Oecologia. 2012;170(4):1155–65.
17. Boratynski Z, Arias JM, Garcia C, Mappes T, Mousseau TA, Moller AP, et al. Ionizing radiation from Chernobyl affects development of wild carrot plants. Sci Rep. 2016;6:39282.
18. Rashydov NM, Hajduch M, Chernobyl seed project. Advances in the identification of differentially abundant proteins in a radiocontaminated environment. Front Plant Sci. 2015;6:493.
19. Pavlov A, Cheptsov V, Tsurkov D, Lomasov V, Frolov D, Vasiliev G. Survival of radioresistant bacteria on Europa's surface after pulse ejection of subsurface ocean water. Geosciences. 2019;9(1):9.
20. Svobodova A, Vostalova J. Solar radiation induced skin damage: review of protective and preventive options. Int J Radiat Biol. 2010;86(12):999–1030.
21. Battistoni G, Toppi M, Patera V, The FOOT Collaboration. Measuring the impact of nuclear interaction in particle therapy and in radio protection in space: the FOOT experiment. Front Phys. 2021;8:568242.
22. Kraan AC. Range verification methods in particle therapy: underlying physics and Monte Carlo modeling. Front Oncol. 2015;5:150.
23. Attix FH. Quantities for describing the interaction of ionizing radiation with matter. In: Introduction to radiological physics and radiation dosimetry; 1986. p. 20–37.
24. Berger MJ. ESTAR, PSTAR, ASTAR A PC package for calculating stopping powers and ranges of electrons, protons and helium ions, version 2. Vienna: International Atomic Energy Agency (IAEA); 1993.
25. Ziegler JF, Ziegler MD, Biersack JP. SRIM—the stopping and range of ions in matter (2010). Nucl Instrum Methods B. 2010;268(11–12):1818–23.
26. Hazra D, Mishra S, Moorti A, Chakera JA. Electron radiography with different beam parameters using laser plasma accelerator. Phys Rev Acceler Beams. 2019;22(7):074701.
27. Chadwick J. The existence of a neutron. Proc R Soc Lond Ser A Contain Pap Math Phys Charact. 1932;136(830):692–708.
28. Martin B. Basic concepts. Nuclear and particle physics. New York: Wiley; 2006. p. 1–31.
29. Turner JE. About atomic physics and radiation. Atoms, radiation, and radiation protection. New York: Wiley; 2007. p. 1–13.
30. Commission CNS. Types and sources of radiation. http://nuclearsafety.gc.ca/eng/resources/radiation/introduction-to-radiation/types-and-sources-of-radiation.cfm#natural-background-radiation.
31. IAEA. Radiation in everyday life. https://www.iaea.org/Publications/Factsheets/English/radlife.
32. EPA. Radiation sources and doses. https://www.epa.gov/radiation/radiation-sources-and-doses.
33. Durante M, Cucinotta FA. Heavy ion carcinogenesis and human space exploration. Nat Rev Cancer. 2008;8(6):465–72.
34. Guo J, Zeitlin C, Wimmer-Schweingruber RF, Hassler DM, Ehresmann B, Kohler J, et al. MSL-RAD radiation environment measurements. Radiat Prot Dosim. 2015;166(1–4):290–4.
35. Da Pieve F, Gronoff G, Guo J, Mertens CJ, Neary L, Gu B, et al. Radiation environment and doses on mars at oxia planum and mawrth vallis: support for exploration at sites with high biosignature preservation potential. J Geophys Res Planet. 2021;126(1):e2020JE006488.
36. Schwadron NA, Baker T, Blake B, Case AW, Cooper JF, Golightly M, et al. Lunar radiation environment and space weathering from the cosmic ray telescope for the effects of radiation (CRaTER). J Geophys Res Planet. 2012;117:2011JE003978.
37. Papaioannou A, Sandberg I, Anastasiadis A, Kouloumvakos A, Georgoulis MK, Tziotziou K, et al. Solar flares, coronal mass ejections and solar energetic particle event characteristics. J Space Weather Space Clim. 2016;6:A42.
38. Zheng Y, Ganushkina NY, Jiggens P, Jun I, Meier M, Minow JI, et al. Space radiation and plasma effects on satellites and aviation: quantities and metrics for tracking performance of space weather environment models. Space Weather. 2019;17(10):1384–403.
39. Baiocco G, Giraudo M, Bocchini L, Barbieri S, Locantore I, Brussolo E, et al. A water-filled garment to protect astronauts during interplanetary missions tested on board the ISS. Life Sci Space Res (Amst). 2018;18:1–11.
40. Amit H, Terra-Nova F, Lezin M, Trindade RI. Non-monotonic growth and motion of the South Atlantic Anomaly. Earth Planets Space. 2021;73(1):38.
41. Commission E, Centre JR. In: Cinelli G, De Cort M, Tollefsen T, editors. European atlas of natural radiation. Publications Office; 2020.
42. NRC. Uses of radiation. https://www.nrc.gov/about-nrc/radiation/around-us/uses-radiation.html#npp.
43. Association WWN. Naturally-occurring radioactive materials (NORM). https://world-nuclear.org/information-library/safety-and-security/radiation-and-health/naturally-occurring-radioactive-materials-norm.aspx.
44. Scibile L, Perrin D, Millan GS, Widorski M, Menzel HG, Vojtyla P, et al. The LHC radiation monitoring system for the environment and safety: from design to operation. Dordrecht: Springer; 2008.
45. IAEA. Research reactor database (RRDB). 2017. https://nucleus.iaea.org/RRDB/RR/ReactorSearch.aspx.
46. Goethals PE, Zimmermann RG. Cyclotrons used in nuclear medicine: world market report and directory. Louvain-la-Neuve: MEDraysintell; 2015.
47. IAEA. Radiation protection and safety of radiation sources: international basic safety standards. Vienna: International Atomic Energy Agency; 2014.
48. Ilyas F, Burbridge B, Babyn P. Health care-associated infections and the radiology department. J Med Imaging Radiat. 2019;50(4):596.
49. Parikh JR, Geise RA, Bluth EI, Bender CE, Sze G, Jones AK, et al. Potential radiation-related effects on radiologists. Am J Roentgenol. 2017;208(3):595–602.
50. Kurth J, Krause BJ, Schwarzenbock SM, Stegger L, Schafers M, Rahbar K. External radiation exposure, excretion, and effective half-life in (177)Lu-PSMA-targeted therapies. EJNMMI Res. 2018;8(1):32.

51. Levart D, Kalogianni E, Corcoran B, Mulholland N, Vivian G. Radiation precautions for inpatient and outpatient (177) Lu-DOTATATE peptide receptor radionuclide therapy of neuroendocrine tumours. EJNMMI Phys. 2019;6(1):7.
52. A. FNB. Radiation safety and protection. Treasure Island (FL): StatPearls Publishing; 2021.
53. Grant EJ, Brenner A, Sugiyama H, Sakata R, Sadakane A, Utada M, et al. Solid cancer incidence among the life span study of atomic bomb survivors: 1958–2009. Radiat Res. 2017;187(5):513–37.
54. ICRP. Chemical and biological effects of radiation. In: Atoms, radiation, and radiation protection. New York: Wiley; 2007. p. 399–447.
55. Mondelaers W, Lahorte P. Radiation-induced bioradicals. In: De Cuyper M, Bulte JWM, editors. Physics and chemistry basis of biotechnology. Dordrecht: Springer; 2000. p. 249–76.
56. Sureka CSA, C. Radiation biology for medical physicists. Boca Raton: CRC Press; 2017.
57. Kam WW, Banati RB. Effects of ionizing radiation on mitochondria. Free Radic Biol Med. 2013;65:607–19.
58. Betzold JM, Saeger W, Ludecke DK. Ultrastructural-morphometric effects of radiotherapy on pituitary adenomas in acromegaly. Exp Clin Endocrinol. 1992;100(3):106–11.
59. Somosy Z. Radiation response of cell organelles. Micron. 2000;31(2):165–81.
60. Hall JC, Goldstein AL, Sonnenblick BP. Recovery of oxidative phosphorylation in rat liver mitochondria after whole body irradiation. J Biol Chem. 1963;238:1137–40.
61. Hwang JJ, Lin GL, Sheu SC, Lin FJ. Effect of ionizing radiation on liver mitochondrial respiratory functions in mice. Chin Med J. 1999;112(4):340–4.
62. Dong C, Tu W, He M, Fu J, Kobayashi A, Konishi T, et al. Role of endoplasmic reticulum and mitochondrion in proton microbeam radiation-induced bystander effect. Radiat Res. 2020;193(1):63–72.
63. Podgorsak EB. Compendium to radiation physics for medical physicists: 300 problems and solutions. Dordrecht: Springer; 2016.
64. Golashvili T, Badikov S, Chechev V, Huang XL, Ge ZG, Wu ZD. Nuclide guide and international chart of nuclides-2006. In: International conference on nuclear data for science and technology, vol 1, proceedings. Les Ulis: EDP Sciences; 2008. p. 85.
65. Bleam W. Chapter 1: Element abundance. In: Bleam W, editor. Soil and environmental chemistry. 2nd ed. Cambridge: Academic Press; 2017. p. 1–38.
66. Sóti Z, Magill J, Dreher R. Karlsruhe Nuclide Chart—new 10th edition 2018. EPJ Nucl Sci Technol. 2019;5:6.
67. Gopalan K. Principles of radiometric dating. Cambridge: Cambridge University Press; 2017.
68. Das NR. Radiometric dating. Sci Cult. 2017;83(7–8):225–34.
69. Farkas J, Mohacsi-Farkas C. History and future of food irradiation. Trends Food Sci Technol. 2011;22(2–3):121–6.
70. Sharma A, Pillai MRA, Gautam S, Hajare SN. MYCOTOXINS | immunological techniques for detection and analysis. In: Batt CA, Tortorello ML, editors. Encyclopedia of food microbiology. 2nd ed. Oxford: Academic Press; 2014. p. 869–79.
71. Kricka LJ, Park JY. Assay principles in clinical pathology. Pathobiology of human disease: a dynamic encyclopedia of disease mechanisms. Amsterdam: Elsevier Inc.; 2014. p. 3207–21.
72. Knapp FF, Dash A. Introduction: radiopharmaceuticals play an important role in both diagnostic and therapeutic nuclear medicine. In: Knapp FF, Dash A, editors. Radiopharmaceuticals for therapy. New Delhi: Springer India; 2016. p. 3–23.
73. Konik A, O'Donoghue JA, Wahl RL, Graham MM, Van den Abbeele AD. Theranostics: the role of quantitative nuclear medicine imaging. Semin Radiat Oncol. 2021;31(1):28–36.
74. Ametamey SM, Honer M, Schubiger PA. Molecular imaging with PET. Chem Rev. 2008;108(5):1501–16.
75. Hicks RJ, Hofman MS. Is there still a role for SPECT-CT in oncology in the PET-CT era? Nat Rev Clin Oncol. 2012;9(12):712–20.
76. Pimlott SL, Sutherland A. Molecular tracers for the PET and SPECT imaging of disease. Chem Soc Rev. 2011;40(1):149–62.
77. Lewis JS, Windhorst AD, Zeglis BM, editors. Radiopharmaceutical chemistry. Cham: Springer International Publishing; 2019.
78. Passchier J, Gee A, Willemsen A, Vaalburg W, van Waarde A. Measuring drug-related receptor occupancy with positron emission tomography. Methods. 2002;27(3):278–86.
79. Cherry SR, Jones T, Karp JS, Qi JY, Moses WW, Badawi RD. Total-body PET: maximizing sensitivity to create new opportunities for clinical research and patient care. J Nucl Med. 2018;59(1):3–12.
80. Kitson LS, Cuccurullo V, Ciarmiello A, Salvo D, Mansi L. Clinical applications of positron emission tomography (PET) imaging in medicine: oncology, brain diseases and cardiology. Curr Radiopharm. 2009;2(4):224–53.
81. Bateman TM. Advantages and disadvantages of PET and SPECT in a busy clinical practice. J Nucl Cardiol. 2012;19(Suppl 1):S3–11.
82. Challapalli A, Aboagye EO. Positron emission tomography imaging of tumor cell metabolism and application to therapy response monitoring. Front Oncol. 2016;6:44.
83. Vermeulen K, Vandamme M, Bormans G, Cleeren F. Design and challenges of radiopharmaceuticals. Semin Nucl Med. 2019;49(5):339–56.
84. Khan FM, Gibbons JP. Khan's the physics of radiation therapy. Philadelphia: Wolters Kluwer; 2016.
85. Hall EJ, Giaccia AJ. Radiobiology for the radiologist. Philadelphia: Wolters Kluwer; 2019.
86. Favaudon V, Caplier L, Monceau V, Pouzoulet F, Sayarath M, Fouillade C, et al. Ultrahigh dose-rate FLASH irradiation increases the differential response between normal and tumor tissue in mice. Sci Transl Med. 2014;6(245):245ra93.
87. International Atomic Energy Agency V. Radiation oncology physics: a handbook for teachers and students. Vienna: IAEA; 2005.
88. Fisher DR, Fahey FH. Appropriate use of effective dose in radiation protection and risk assessment. Health Phys. 2017;113(2):102–9.
89. Zirkle RE, Tobias CA. Effects of ploidy and linear energy transfer on radiobiological survival curves. Arch Biochem Biophys. 1953;47(2):282–306.
90. Girdhani S, Sachs R, Hlatky L. Biological effects of proton radiation: what we know and don't know. Radiat Res. 2013;179(3):257–72.
91. Brenner DJ, Ward JF. Constraints on energy deposition and target size of multiply damaged sites associated with DNA double-strand breaks. Int J Radiat Biol. 1992;61(6):737–48.
92. Gottschalk B. Physics of proton interactions in matter. Proton therapy physics. Boca Raton: CRC Press; 2018.
93. Nikjoo H, Uehara S, Wilson WE, Hoshi M, Goodhead DT. Track structure in radiation biology: theory and applications. Int J Radiat Biol. 1998;73(4):355–64.
94. Rossi HH, Zaider M. Introduction. In: Rossi HH, Zaider M, editors. Microdosimetry and its applications. Berlin: Springer; 1996. p. 1–16.
95. Palmans H, Rabus H, Belchior AL, Bug MU, Galer S, Giesen U, et al. Future development of biologically relevant dosimetry. Br J Radiol. 2015;88(1045):20140392.
96. Rossi HH, Zaider M. Microdosimetric quantities and their moments. In: Rossi HH, Zaider M, editors. Microdosimetry and its applications. Berlin: Springer; 1996. p. 17–27.
97. Kelsey CA, Heintz PH, Chambers GD, Sandoval DJ, Adolphi NL, Paffett KS. Radiation biology of medical imaging. New York: Wiley; 2013.
98. Sutherland BM, Bennett PV, Sutherland JC, Laval J. Clustered DNA damages induced by X-rays in human cells. Radiat Res. 2002;157(6):611–6.
99. Rabus H, Palmans H, Hilgers G, Sharpe P, Pinto M, Villagrasa C, et al. Biologically weighted quantities in radiotherapy: an EMRP joint research project. EPJ Web Conf. 2014;77:00021.

100. Villegas F, Bäckström G, Tilly N, Ahnesjö A. Energy deposition clustering as a functional radiation quality descriptor for modeling relative biological effectiveness. Med Phys. 2016;43(12):6322.
101. Cunha M, Monini C, Testa E, Beuve M. NanOx, a new model to predict cell survival in the context of particle therapy. Phys Med Biol. 2017;62(4):1248–68.
102. Braunroth T, Nettelbeck H, Ngcezu SA, Rabus H. Three-dimensional nanodosimetric characterisation of proton track structure. Radiat Phys Chem. 2020;176:109066.
103. Kase KR, Bjarngard BE, Attix FH. The dosimetry of ionizing radiation. Volume 1. Orlando: Academic Press Inc.; 1985. p. 411.
104. Curtis SB. Introduction to track structure and Z*2/β2. 2016. https://three.jsc.nasa.gov/articles/Track-Structure-SCurtis.pdf.
105. Withers HR, Thames HD Jr, Peters LJ. Biological bases for high RBE values for late effects of neutron irradiation. Int J Radiat Oncol Biol Phys. 1982;8(12):2071–6.
106. Williams J. Basic clinical radiobiology. Milton Park: Taylor & Francis; 2019.
107. Steel GG, Deacon JM, Duchesne GM, Horwich A, Kelland LR, Peacock JH. The dose-rate effect in human tumour cells. Radiother Oncol. 1987;9(4):299–310. https://doi.org/10.1016/s0167-8140(87)80151-2. PMID: 3317524.
108. Vozenin MC, Hendry JH, Limoli CL. Biological benefits of ultra-high dose rate FLASH radiotherapy: sleeping beauty awoken. Clin Oncol (R Coll Radiol). 2019;31(7):407–15.
109. International Commission on Radiological Protection. The recommendations of the international commission on radiological protection. Oxford: Elsevier; 2007. p. 2007.
110. Barendsen GW. The relationships between RBE and LET for different types of lethal damage in mammalian cells: biophysical and molecular mechanisms. Radiat Res. 1994;139(3):257–70.
111. Valentin J. Relative biological effectiveness (RBE), quality factor (Q), and radiation weighting factor (w(R)). A report of the international commission on radiological protection. Ann ICRP. 2003;33(4):1–117.
112. Antonovic L, Lindblom E, Dasu A, Bassler N, Furusawa Y, Toma-Dasu I. Clinical oxygen enhancement ratio of tumors in carbon ion radiotherapy: the influence of local oxygenation changes. J Radiat Res. 2014;55(5):902–11.
113. Stewart FA, Akleyev AV, Hauer-Jensen M, Hendry JH, Kleiman NJ, Macvittie TJ, et al. ICRP publication 118: ICRP statement on tissue reactions and early and late effects of radiation in normal tissues and organs—threshold doses for tissue reactions in a radiation protection context. Ann ICRP. 2012;41(1–2):1–322.
114. Ricks RC, Berger ME, O'Hara FM. The medical basis for radiation-accident preparedness, III. New York: Appleton & Lange; 2001.
115. Fliedner T. Medical management of radiation accidents—manual on the acute radiation syndrome. London: British Institute of Radiology; 2001.
116. Streffer C, Shore R, Konermann G, Meadows A, Uma Devi P, Preston Withers J, et al. Biological effects after prenatal irradiation (embryo and fetus). A report of the international commission on radiological protection. Ann ICRP. 2003;33(1–2):5–206.
117. Martin AD. An introduction to radiation protection. Boca Raton: CRC Press; 2019.
118. Fearon ER, Vogelstein B. A genetic model for colorectal tumorigenesis. Cell. 1990;61(5):759–67.
119. UNSCEAR. Sources, effects and risks of ionizing radiation. Report to the General Assembly, with Scientific Annexes A and B 2015. Vienna: UNSCEAR; 2012.
120. Ozasa K, Shimizu Y, Suyama A, Kasagi F, Soda M, Grant EJ, et al. Studies of the mortality of atomic bomb survivors, report 14, 1950–2003: an overview of cancer and noncancer diseases. Radiat Res. 2012;177(3):229–43.
121. Kugathasan T, Mothersill C. Radiobiological and social considerations following a radiological terrorist attack; mechanisms, detection and mitigation: review of new research developments. Int J Radiat Biol. 2022;98(5):855–64.
122. Franke A, Franke T. Long-term benefits of radon spa therapy in rheumatic diseases: results of the randomised, multi-centre IMuRa trial. Rheumatol Int. 2013;33(11):2839–50.
123. Brooks AL. A commentary on: "A history of the United States Department of Energy (DOE) low dose radiation research program: 1998–2008". Radiat Res. 2015;183(4):375–81.
124. Feinendegen LE. Conference summary. Health Phys. 2020;118(3):322–6.
125. Rockwell T. Human lung cancer risks from radon: influence from bystander and adaptive response non-linear dose response effects. Radiat Prot Dosim. 2013;154(2):262–3.
126. Brooks AL. Paradigm shifts in radiation biology: their impact on intervention for radiation-induced disease. Radiat Res. 2005;164(4 Pt 2):454–61.
127. MotherSill C, Seymour C. Changing paradigms in radiobiology. Mutat Res. 2012;750(2):85–95.
128. Calabrese EJ. Chapter 1: The dose–response revolution: how hormesis became significant: an historical and personal reflection. In: Rattan SIS, Kyriazis M, editors. The science of hormesis in health and longevity. Cambridge: Academic Press; 2019. p. 3–24.
129. Rattan SIS, Kyriazi M. The science of hormesis in health and longevity. Cambridge: Academic Press; 2019.
130. Soyfer V, Socol Y, Bragilovski D, Corn BW. The theoretical value of whole-lung irradiation for COVID-19 pneumonia: a reasonable and safe solution until targeted treatments are developed. Radiat Res. 2021;195(5):474–9.
131. Martin LM, Marples B, Lynch TH, Hollywood D, Marignol L. Exposure to low dose ionising radiation: molecular and clinical consequences. Cancer Lett. 2013;338(2):209–18.
132. Lambin P, Marples B, Fertil B, Malaise EP, Joiner MC. Hypersensitivity of a human tumour cell line to very low radiation doses. Int J Radiat Biol. 1993;63(5):639–50.
133. Marples B, Joiner MC. The response of Chinese hamster V79 cells to low radiation doses: evidence of enhanced sensitivity of the whole cell population. Radiat Res. 1993;133(1):41–51.
134. United Nations. Sources and effects of ionizing radiation. In: UNSCEAR 2008 report to the general assembly with scientific annexes. Volume 1. New York: United Nations; 2010.
135. Daguenet E, Louati S, Wozny AS, Vial N, Gras M, Guy JB, et al. Radiation-induced bystander and abscopal effects: important lessons from preclinical models. Br J Cancer. 2020;123(3):339–48.
136. Blyth BJ, Sykes PJ. Radiation-induced bystander effects: what are they, and how relevant are they to human radiation exposures? Radiat Res. 2011;176(2):139–57.
137. Morgan WF. Non-targeted and delayed effects of exposure to ionizing radiation: I. Radiation-induced genomic instability and bystander effects in vitro. Radiat Res. 2003;159(5):567–80.
138. Morgan WF. Non-targeted and delayed effects of exposure to ionizing radiation: II. Radiation-induced genomic instability and bystander effects in vivo, clastogenic factors and transgenerational effects. Radiat Res. 2003;159(5):581–96.
139. Widel M. Radiation induced bystander effect: from in vitro studies to clinical application. Int J Med Phys Clin Eng Radiat Oncol. 2016;5:1–17.
140. Al-Mayah AH, Irons SL, Pink RC, Carter DR, Kadhim MA. Possible role of exosomes containing RNA in mediating nontargeted effect of ionizing radiation. Radiat Res. 2012;177(5):539–45.
141. Le M, McNeill FE, Seymour C, Rainbow AJ, Mothersill CE. An observed effect of ultraviolet radiation emitted from beta-irradiated HaCaT cells upon non-beta-irradiated bystander cells. Radiat Res. 2015;183(3):279–90.
142. Le M, Fernandez-Palomo C, McNeill FE, Seymour CB, Rainbow AJ, Mothersill CE. Exosomes are released by bystander cells exposed to radiation-induced biophoton signals: reconciling the mechanisms mediating the bystander effect. PLoS One. 2017;12(3):e0173685.

143. Dickey JS, Zemp FJ, Martin OA, Kovalchuk O. The role of miRNA in the direct and indirect effects of ionizing radiation. Radiat Environ Biophys. 2011;50(4):491–9.
144. Kirolikar S, Prasannan P, Raghuram GV, Pancholi N, Saha T, Tidke P, et al. Prevention of radiation-induced bystander effects by agents that inactivate cell-free chromatin released from irradiated dying cells. Cell Death Dis. 2018;9(12):1142.
145. Kaminski JM, Shinohara E, Summers JB, Niermann KJ, Morimoto A, Brousal J. The controversial abscopal effect. Cancer Treat Rev. 2005;31(3):159–72.
146. Zeng J, Harris TJ, Lim M, Drake CG, Tran PT. Immune modulation and stereotactic radiation: improving local and abscopal responses. Biomed Res Int. 2013;2013:658126.
147. Mancuso M, Pasquali E, Giardullo P, Leonardi S, Tanori M, Di Majo V, et al. The radiation bystander effect and its potential implications for human health. Curr Mol Med. 2012;12(5):613–24.
148. Munro AJ. Bystander effects and their implications for clinical radiotherapy. J Radiol Prot. 2009;29(2a):A133–42.
149. Tomita M, Maeda M. Mechanisms and biological importance of photon-induced bystander responses: do they have an impact on low-dose radiation responses. J Radiat Res. 2015;56(2):205–19.
150. Lorimore SA, Coates PJ, Scobie GE, Milne G, Wright EG. Inflammatory-type responses after exposure to ionizing radiation in vivo: a mechanism for radiation-induced bystander effects? Oncogene. 2001;20(48):7085–95.
151. Faguet GB, Reichard SM, Welter DA. Radiation-induced clastogenic plasma factors. Cancer Genet Cytogenet. 1984;12(1):73–83.
152. Emerit I. Reactive oxygen species, chromosome mutation, and cancer: possible role of clastogenic factors in carcinogenesis. Free Radic Biol Med. 1994;16(1):99–109.
153. Emerit I. Clastogenic factors as potential biomarkers of increased superoxide production. Biomark Insights. 2007;2:429–38.
154. Roschke AV, Kirsch IR. Targeting karyotypic complexity and chromosomal instability of cancer cells. Curr Drug Targets. 2010;11(10):1341–50.
155. Kadhim MA, Moore SR, Goodwin EH. Interrelationships amongst radiation-induced genomic instability, bystander effects, and the adaptive response. Mutat Res. 2004;568(1):21–32.
156. Mothersill C, Seymour C. Radiation-induced bystander effects: past history and future directions. Radiat Res. 2001;155(6):759–67.
157. Trott KR, Teibe A. Lack of specificity of chromosome breaks resulting from radiation-induced genomic instability in Chinese hamster cells. Radiat Environ Biophys. 1998;37(3):173–6.
158. Kadhim MA, Macdonald DA, Goodhead DT, Lorimore SA, Marsden SJ, Wright EG. Transmission of chromosomal instability after plutonium alpha-particle irradiation. Nature. 1992;355(6362):738–40.
159. Little JB, Nagasawa H, Pfenning T, Vetrovs H. Radiation-induced genomic instability: delayed mutagenic and cytogenetic effects of X-rays and alpha particles. Radiat Res. 1997;148(4):299–307.
160. Suzuki K, Ojima M, Kodama S, Watanabe M. Radiation-induced DNA damage and delayed induced genomic instability. Oncogene. 2003;22(45):6988–93.
161. Marder BA, Morgan WF. Delayed chromosomal instability induced by DNA damage. Mol Cell Biol. 1993;13(11):6667–77.
162. Suzuki K. Multistep nature of X-ray-induced neoplastic transformation in mammalian cells: genetic alterations and instability. J Radiat Res. 1997;38(1):55–63.

Further Reading

Albandar H. Basic modes of radioactive decay. In: Almayahi B, editor. Use of gamma radiation techniques in peaceful applications. London: IntechOpen; 2019.
Alpen EL. Radiation biophysics. San Diego: Academic Press Inc; 1998.
Antoni R, Bourgis L. Applied physics of external radiation exposure. New York: Springer; 2017.
Dale RG, Jones B, Cárabe-Fernández A. Why more needs to be known about RBE effects in modern radiotherapy. Appl Radiat Isot. 2009;67(3):387–92.
Fliedner TM, Friesecke I, Beyrer K. Medical management of radiation accidents: manual on the acute radiation syndrome. Oxford: Alden Group; 2001.
Hall EJ, Giaccia AJ. Radiobiology for the radiologist. 8th ed. Baltimore: Wolters Kluwer; 2019.
Jadiyappa S. Radioisotope: applications, effects, and occupational protection. In: Rahman RA, Saleh HE, editors. Principles and applications in nuclear engineering—radiation effects, thermal hydraulics, radionuclide migration in the environment. London: IntechOpen; 2018. https://doi.org/10.5772/intechopen.79161. https://www.intechopen.com/chapters/62736.
Karotki AV, Baverstock K. What mechanisms/processes underlie radiation-induced genomic instability? Cell Mol Life Sci. 2012;69(20):3351–60.
Lehnert S. Biomolecular action of ionizing radiation: medical physics and biomedical engineering. San Diego: Taylor & Francis Group, LLC; 2008.
Martin A, Harbison S, Beach K, Cole P. An introduction to radiation protection. 7th ed. San Diego: Taylor & Francis Group, LLC; 2019.
Murshed H. Fundamentals of radiation oncology physical, biological, and clinical aspects. 3rd ed. Amsterdam: Elsevier Inc; 2019.
Murshed H. Fundamentals of radiation oncology: physical, biological, and clinical aspects. 3rd ed. San Diego: Academic Press; 2019.
Parodi K. The biological treatment planning evolution of clinical fractionated radiotherapy using high LET. Int J Radiat Biol. 2018;94(8):752–5.
Podgoršak EB. Modes of radioactive decay. In: Podgorsak EB, editor. Compendium to radiation physics for medical physicists: 300 problems and solutions. Berlin, Springer; 2014. p. 693–786.
Ricks RC, Berger ME, O'Hara FM Jr. The medical basis for radiation accident preparedness the clinical care of victims. Lancaster: Parthenon Publishing Group; 2002.
Sureka CS, Armpilia C. Radiation biology for medical physicists. San Diego: Taylor & Francis Group, LLC; 2017.
Tepper J, Foote R, Gunderson MJ. Tepper's clinical radiation oncology. 5th ed. Amsterdam: Elsevier; 2020.
Thames HD, Bentzen SM, Turesson I, Overgaard M, Van den Bogaert W. Time-dose factors in radiotherapy: a review of the human data. Radiother Oncol. 1990;19(3):219–35.

Molecular Radiation Biology

3

Judith Reindl, Ana Margarida Abrantes, Vidhula Ahire, Omid Azimzadeh, Sarah Baatout, Ans Baeyens, Bjorn Baselet, Vinita Chauhan, Fabiana Da Pieve, Wendy Delbart, Caitlin Pria Dobney, Nina Frederike Jeppesen Edin, Martin Falk, Nicolas Foray, Agnès François, Sandrine Frelon, Udo S. Gaipl, Alexandros G. Georgakilas, Olivier Guipaud, Michael Hausmann, Anna Jelinek Michaelidesova, Munira Kadhim, Inês Alexandra Marques, Mirta Milic, Dhruti Mistry, Simone Moertl, Alegría Montoro, Elena Obrador, Ana Salomé Pires, Roel Quintens, Nicholas Rajan, Franz Rödel, Peter Rogan, Diana Savu, Giuseppe Schettino, Kevin Tabury, Georgia I. Terzoudi, Sotiria Triantopoulou, Kristina Viktorsson, and Anne-Sophie Wozny

J. Reindl (✉)
Section Biomedical Radiation Physics, Institute for Applied Physics and Measurement Technology, Department for Aerospace Engineering, Universität der Bundeswehr München, Neubiberg, Germany
e-mail: Judith.reindl@unibw.de

A. M. Abrantes
Institute of Biophysics, Faculty of Medicine, iCBR-CIMAGO, Center for Innovative Biomedicine and Biotechnology, University of Coimbra, Coimbra, Portugal

ESTESC-Coimbra Health School, Instituto Politécnico de Coimbra, Coimbra, Portugal
e-mail: mabrantes@fmed.uc.pt

V. Ahire
Chengdu Anticancer Bioscience, Ltd., and Michael Bishop Institute of Cancer Research and Anticancer Biosciences Ltd., Chengdu, China

O. Azimzadeh
Section Radiation Biology, Federal Office for Radiation Protection, Oberschleißheim, Germany
e-mail: oazimzadeh@bfs.de

S. Baatout
Radiobiology Unit, Belgian Nuclear Research Centre (SCK CEN), Mol, Belgium

Institute of Nuclear Medical Applications, Belgian Nuclear Research Center (SCK CEN), Mol, Belgium
e-mail: sarah.baatout@sckcen.be

B. Baselet · D. Mistry · R. Quintens · N. Rajan
Radiobiology Unit, Belgian Nuclear Research Centre (SCK CEN), Mol, Belgium
e-mail: bjorn.baselet@sckcen.be; roel.quintens@sckcen.be; nicholas.rajan@sckcen.be

A. Baeyens
Radiobiology, Department of Human Structure and Repair, Ghent University, Ghent, Belgium
e-mail: Ans.Baeyens@UGent.be

V. Chauhan
Consumer and Clinical Radiation Protection Bureau, Health Canada, Ottawa, ON, Canada
e-mail: vinita.chauhan@hc-sc.gc.ca

F. Da Pieve
Royal Belgian Institute for Space Aeronomy, Brussels, Belgium

European Research Council Executive Agency, European Commission, Brussels, Belgium
e-mail: fabiana.dapieve@aeronomie.be

W. Delbart
Nuclear Medicine Department, Hôpital Universitaire de Bruxelles (H.U.B.), Brussels, Belgium
e-mail: wendy.delbart@bordet.be

C. P. Dobney
Department of Physics, University of Toronto, Toronto, Canada

N. F. J. Edin
Department of Physics, University of Oslo, Oslo, Norway
e-mail: nina@fys.uio.no

M. Falk
Department of Cell Biology and Radiobiology, Institute of Biophysics of the Czech Academy of Sciences, Brno, Czech Republic
e-mail: falk@ibp.cz

N. Foray
INSERM Unit U1296 “Radiation: Defense, Health and Environment”, Centre Léon-Bérard, Lyon, France
e-mail: nicolas.foray@inserm.fr

S. Baatout (ed.), *Radiobiology Textbook*, https://doi.org/10.1007/978-3-031-18810-7_3

A. François · O. Guipaud
Radiobiology of Medical Exposure Laboratory, Institute for Radiological Protection and Nuclear Safety (IRSN), Fontenay-aux-Roses, France
e-mail: agnes.francois@irsn.fr; olivier.guipaud@irsn.fr

S. Frelon
Health and Environment Division, Research Laboratory of Radionuclide Effects on Environment, Institute for Radiological Protection and Nuclear Safety (IRSN), Saint-Paul-Lez-Durance, France
e-mail: sandrine.frelon@irsn.fr

U. S. Gaipl
Translational Radiobiology, Department of Radiation Oncology, Universitätsklinikum Erlangen, Erlangen, Germany
e-mail: udo.gaipl@uk-erlangen.de

A. G. Georgakilas
Physics Department, School of Applied Mathematical and Physical Sciences, National Technical University of Athens (NTUA), Athens, Greece
e-mail: Alexg@mail.ntua.gr

M. Hausmann
Kirchhoff Institute for Physics, University Heidelberg, Heidelberg, Germany
e-mail: hausmann@kip.uni-heidelberg.de

A. J. Michaelidesova
Nuclear Physics Institute, Czech Academy of Sciences, Czech Technical University, Faculty of Nuclear Sciences and Physical Engineering, Prague, Czech Republic
e-mail: michaelidesova@ujf.cas.cz

M. Kadhim
Deparment of Biological and Medical Sciences, Oxford Brookes University, Oxford, United Kingdom
e-mail: mkadhim@brookes.ac.uk

I. A. Marques
Institute of Biophysics, Faculty of Medicine, iCBR-CIMAGO, Center for Innovative Biomedicine and Biotechnology, University of Coimbra, Coimbra, Portugal
e-mail: ines.marques@student.uc.pt

M. Milic
Mutagenesis Unit, Institute for Medical Research and Occupational Health, Zagreb, Croatia
e-mail: mmilic@imi.hr

S. Moertl
Department of Effects and Risks of Ionising and Non-Ionising Radiation, Federal Office for Radiation Protection, Oberschleißheim, Germany
e-mail: smoertl@bfs.de

A. Montoro
Radiological Protection Service, University and Polytechnic La Fe Hospital of Valencia, Valencia, Spain
e-mail: montoro_ale@gva.es

E. Obrador
Department of Physiology, Faculty of Medicine, University of Valencia, Valencia, Spain
e-mail: elena.obrador@uv.es

A. S. Pires
Institute of Biophysics, Faculty of Medicine, iCBR-CIMAGO, Center for Innovative Biomedicine and Biotechnology, University of Coimbra, Coimbra, Portugal

Clinical Academic Center of Coimbra, Coimbra, Portugal
e-mail: pireslourenco@uc.pt

F. Rödel
Department of Radiotherapy and Oncology, Goethe University, Frankfurt am Main, Germany
e-mail: Franz.Roedel@kgu.de

P. Rogan
Departments of Biochemistry and Oncology, Schulich School of Medicine and Dentistry, University of Western Ontario, London, ON, Canada
e-mail: progan@uwo.ca

D. Savu
Department of Life and Environmental Physics, Horia Hulubei National Institute of Physics and Nuclear Engineering, Magurele, Romania
e-mail: dsavu@nipne.ro

G. Schettino
National Physical Laboratory, Teddington, United Kingdom
e-mail: giuseppe.schettino@surrey.ac.uk

K. Tabury
Belgian Nuclear Research Centre (SCK CEN), Mol, Belgium

Department of Biomedical Engineering, University of South Carolina, Columbia, SC, United States of America
e-mail: kevin.tabury@sckcen.be

G. I. Terzoudi · S. Triantopoulou
Health Physics, Radiobiology and Cytogenetics Laboratory, Institute of Nuclear and Radiological Sciences and Technology, Energy and Safety, National Centre for Scientific Research "Demokritos", Athens, Greece
e-mail: gterzoudi@rrp.demokritos.gr; iro@rrp.demokritos.gr

K. Viktorsson
Department of Oncology/Pathology, Karolinska Institutet, Solna, Sweden
e-mail: Kristina.viktorsson@ki.se

A.-S. Wozny
Cellular and Molecular Radiobiology Lab, UMR CNRS 5822, Lyon 1 University, Oullins, France

Department of Biochemistry and Molecular Biology, Lyon-Sud Hospital, Hospices Civils de Lyon, Pierre-Bénite, France
e-mail: anne-sophie.wozny@univ-lyon1.fr

Learning Objectives

- To gain familiarity with biomolecules that undergo radiolysis after ionizing radiation (IR) and to learn about some of the damaged products and the expected biological consequences
- To understand how IR influences various DNA repair mechanisms, cell cycle phases, and cell death mechanisms as well as associated signaling cascades that are involved
- To get knowledge on higher order chromatin organization and its connection to DNA damage repair
- To be able to distinguish between cell survival and cell viability and understand different *in vitro* and *in vivo* assays used to evaluate clonogenic capacity

- To understand chromosomal aberrations including chromosomal translocations in different cell cycle phases, formation of micronuclei, radiation-induced foci, and their dependence on the type of the incidental radiation as well as to acknowledge the health risks of such cellular damages
- To get familiar with mechanisms of oxidative stress, telomeres/senescence, and immunity in the context of cancer biology and/or radiation response
- To get acquainted with the types and underlying mechanisms of cellular hyper-radiosensitivity
- To describe how radiation resistance can be induced by external factors such as hypoxia and previous low-dose exposure or as part of the tumor cell evolution
- To get knowledge on the role of epigenetic factors, e.g., various types of RNAs, extracellular vesicles, as well as DNA methylation; histone modification; and gene expression in the cellular radiation response
- To define signatures of radiation response comprised of changes at gene transcription level and their biological consequences
- To become acquainted with CRISPR-CAS9 genome editing system and its application in molecular biology science as well as in DNA DSB repair analyses

3.1 Radiolysis Products with Carbohydrates, Proteins, and Lipids

As described in Chap. 2, ionizing radiation (IR) can interact with matter directly, via molecule ionization, or indirectly, via the radiolysis of water. The result of this interaction is highly reactive ionized molecules that undergo a rapid cascade of chemical reactions, which leads to the breaking of chemical bonds. The radiolytic damage of biomolecules, such as carbohydrates, lipids, and proteins, is described as an indirect effect following water radiolysis and depends on biomolecule concentration in the irradiated medium. The products of water radiolysis—radicals—are often found in clusters and react with the biomolecules present within cells before they have a chance to diffuse and form a homogeneous distribution of products. To date, the studies on radiation-induced damage of these biomolecules are mainly based on the radical analysis of model molecules or on the molecular analysis of cellular mixtures after irradiation. Figure 3.1 shows an overview of the radiolysis products described in this chapter. The description of radiolysis products of the different biomolecules clearly demonstrates possible interactions and reactions between radicals and subcellular targets [1].

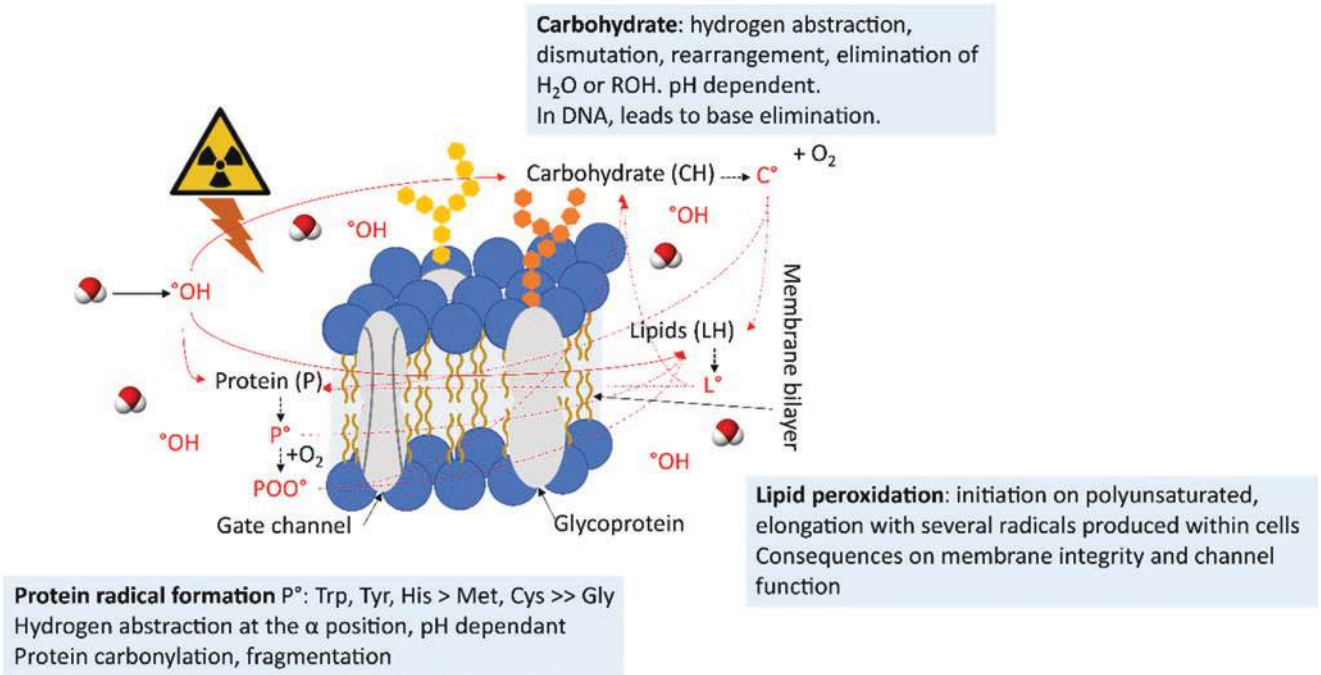

Fig. 3.1 Summary of the radicals produced with proteins, lipids, and carbohydrates following external IR exposure. Cellular exposure to IR leads to dissociation of biological macromolecules. Radiolysis of carbohydrates, proteins, and lipids is explained in their respective blue boxes. *PO* protein radicals, *CO* carbohydrate radicals, *LO* lipid radicals, *OOH* hydroxyl radicals, *POOO* protein peroxyl radicals, *Trp* tryptophan, *Tyr* tyrosine, *His* histidine, *Met* methionine, *Cys* cysteine, *Gly* glycine, *ROH* alcohol—an analog of water where R is alkyl group, O is oxygen atom, and H is hydrogen atom

3.1.1 Carbohydrates

Carbohydrates are hydrated organic molecules consisting of carbon (C), hydrogen (H), and oxygen (O), characterized by the formula $C_x(H_2O)_y$, where x and y denote the numbers of carbon or water in the molecule. Chemically, most carbohydrates are polyhydroxy aldehydes, ketones, alcohols, and acids, which can polymerize, form connected chains of molecules, and, therefore, become more complex [2]. In biological media, such as cells, some carbohydrates are a major energy source for all non-photosynthetic organisms (e.g., glycogen), and others have vital structural functions (e.g., chitin, cellulose) or are essential components of RNA, DNA, and biochemical cofactor synthesis (e.g., adenosine mono/di/triphosphate).

Investigations of ionization damage to carbohydrates were done mainly in the fields of food and DNA [3]. Food irradiation can be used to extend shelf life (0.5–3.0 kGy), to inhibit sprouting (0.03–0.12 kGy), for insect disinfestation (0.2–0.8 kGy) and parasite disinfestation (0.1–3.0 kGy), and to eliminate pathogenic bacteria that do not form spores (1.5–7.0 kGy). In this context, it is important to know the chemical transformations occurring at a molecular level, including carbohydrates, that might have an adverse impact on the nutritional, sensory, or functional state of food [4]. In DNA, the sugar moiety plays an important role in the radiation-induced strand breaking process, even if not all the carbohydrate alterations are implied [3].

Model molecules of carbohydrates, such as ethylene glycol, glycerol, and glucose, were used to understand radiation products yielded from carbohydrates. Furthermore, they were used to study the formation of radicals via electron spin resonance (ESR) and electron paramagnetic resonance (EPR) or molecular products via high-performance liquid chromatography-mass spectrometry (HPLC-MS_2) [4].

The radiolysis of carbohydrates in aqueous system is pH dependent and occurs mainly by an indirect interaction of hydroxyl radical (°OH) with C–H bonds producing carbohydrate radicals. In contrast, carbohydrates react slowly with superoxide radicals (coming from solvated electrons) and scarcely with °H radicals [3, 4]. The carbohydrate radicals readily react with molecular oxygen or experience dismutation, dimerization, and elimination of alcohol or water (the most ubiquitous). Thus, radiolysis of carbohydrate inside the DNA molecule can lead to a degradation of the sugar structure and a loss of the base.

3.1.2 Lipids

Lipids are small organic molecules, representing 21% of the eukaryotic cell content. Biochemically, they originate entirely or in part from carbanion-based condensations of thioesters, forming fatty acids, which are components of triacylglycerols (TAGs), phospholipids, and sphingolipids, or by carbocation-based condensation of isoprene units, forming isoprenol derivatives including sterols [2]. Lipids perform many essential functions in the cell including signaling and energy storage (due to their highly reduced state) and are the hydrophobic units of bilayers that form cellular and organellar membranes, which contribute to their function and topology.

In aqueous biological media, during IR, lipids (mostly polyunsaturated acids) are likely to undergo lipid peroxidation. This is initiated by some water radiolysis species and presence of endogenous transition metals [5] and propagates the chain reaction and produces several other organic reactive radicals. These primary and secondary radicals, being able to penetrate the membrane interior, may react either with the lipid matrix or with integral membrane proteins.

This radio-induced lipid peroxidation can thus contribute to the loss of cellular function through the inactivation of membrane enzymes and even of cytoplasmic (i.e., water soluble) proteins. Moreover, consequences include also perturbation of membrane function itself (thinning, change of structure or charge distribution, polarity) and consequently some carrier ion complexes and ion channels: efficiency can increase due to accumulation of polar oxidation products, but also be inhibited due to depolarization following conductance leakage [6].

3.1.3 Proteins

Proteins are biomolecules made of many linear chains of amino acid residues arranged in a three-dimensional structure, with various binding types (covalent or weak electrostatic bonds). Proteins constitute about 74% of the eukaryotic cell organic content. Amino acids, peptides, and proteins undergo a variety of reactions with radio-induced radicals which in most cases are pH dependent. These reactions involve mostly hydrogen abstraction at the α position of the amino acid, electron transfer, addition, fragmentation and rearrangement, dimerization, disproportionation, and substitution [7]. Many studies showed that the most reactive amino acids are the aromatic (Trp, Tyr, His) and sulfur-containing (Met, Cys) amino acids, whereas the least reactive is glycine (Gly) [7, 8]. Once generated, the formed protein radicals can interact with oxygen, yielding a peroxyl radical, and with other biological components for instance yielding other reactive radicals or initiating lipid peroxidation.

Some of the most commonly measured oxidative protein modifications are protein carbonyl groups originating from the oxidation of the amino acid residues or their side chains [9]. This leads to the formation of carbonyl derivatives, protein backbone cleavage, or beta scission of side-chain alk-

oxyl radicals of aliphatic residues (e.g., Ala, Val). In addition, oxidation of the sulfur of cysteine residues can lead to disulfur bond rearrangement.

Studies performed in biological media, e.g., cells, tend to show that in case of hydroxyl radicals coming from external irradiation, damage to DNA and lipids is a secondary process and proteins are more likely the initial targets, due to their relative amount and reactivity [7, 8] (Box 3.1).

Box 3.1 In a Nutshell: Radiolysis Products with Carbohydrates, Proteins and Lipids

- Radiolysis of carbohydrates and proteins occurs mostly via OH, begins with an abstraction of one hydrogen atom, and is pH dependent.
- Radiolysis of the carbohydrates within DNA may result in the loss of the base and thus DNA damage.
- Lipids are likely to undergo peroxidation following IR processes, initiating a chain reaction leading to the production of organic reactive radicals.
- Lipid peroxidation may lead to the loss of cellular functions including those associated with membranes.
- In proteins, the most reactive amino acids are the aromatic (Trp, Tyr, His) and sulfur-containing (Met, Cys) ones, whereas the least reactive is glycine (Gly).
- Protein radicals may react with oxygen-yielding peroxyl radicals or with other biological compounds such as lipids, leading to lipid peroxidation or formation of other reactive radicals.
- Some of the most measured oxidative protein modifications are protein carbonyl groups.
- In cells, proteins are the initial targets, due to their relative amount and reactivity.

3.2 Types of Radiation-Induced Lesions in DNA

In contrast to the above-described effects of IR in carbohydrates, lipids, and proteins, DNA radiolytic lesions occur both directly and indirectly, with the proportion being dependent on radiation type (α, β, γ, heavier ions). Deoxyribonucleic acid (DNA) molecules are, unlike other biomolecules within a cell, unique, and if they get damaged and stay unrepaired, this may lead to serious and often lethal consequences.

Due to the importance of DNA, cells have a complex DNA damage response system, consisting of several interrelated signaling pathways, which can recognize the damage and initiate its repair. DNA can be damaged by different mutagens, such as oxidizing agents and alkylating agents, as well as by IR or UV light. However, the type of DNA damage depends on the type of mutagen, as well as the type, dose, and energy of radiation.

3.2.1 DNA Structure

DNA is a large molecule composed of two polynucleotide chains that coil around each other to constitute a double-stranded helix structure. DNA molecules carry the genetic information for most biological processes. The two antiparallel DNA strands are connected by hydrogen bonds, and the backbone of each strand is composed of nucleotides. Each nucleotide consists of an alternating sugar (2-deoxyribose), a phosphate group, and one of the four nitrogen-containing nucleobases [adenine (A), cytosine (C), guanine (G), or thymine (T)]. The structure of the bases is shown in Fig. 3.2. Two of the bases, thymine and cytosine, are single-ring groups (pyrimidines), whereas two other bases, adenine and guanine, are double-ring groups (purines).

On one strand, nucleotides are joined to another by covalent bonds between the sugar of one nucleotide and the phosphate group of the next one (phosphodiester bond). The

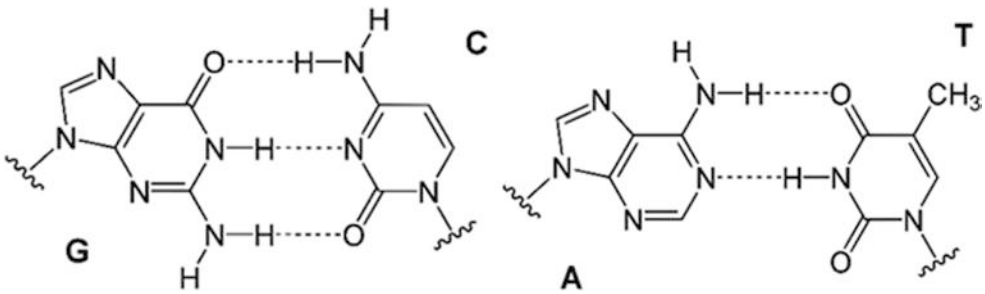

Fig. 3.2 The four DNA bases with respective hydrogen bonds (dashed lines). *G* guanine, *C* cytosine, *A* adenine, *T* thymine

bases on the opposite strands are complementary, adenine pairs with thymine and guanine pairs with cytosine through hydrogen bonds [10].

3.2.2 Damage of Sugar and Bases

A base lesion is defined as a modification (oxidation, alkylation, and deamination) of the chemical structure of one of the four DNA bases. Modification can occur through the loss of an electron, called oxidation, the transfer of an alkyl group, called alkylation, or the removal of an amino group, called deamination. After the break of the N-glycosidic bond between the DNA base and the 2-deoxyribose, a base can get lost and an abasic site can be created [11]. A representation of base lesion and abasic site is shown in Fig. 3.3. Sugar and base damages are quite easy for the cell to repair, as will be shown in Sect. 3.4.

Most of the sugar and base modifications are due to the hydroxyl radical (OH°). This radical reacts with the bases by addition to double bonds and by abstraction of hydrogen from the methyl group of thymine or from any C–H bond, but more likely from the C4 and C5 positions of the deoxyribose [12]. Pyrimidine base modifications are more readily formed after radiation compared with purines. The main radiation-induced base degradation products can be found in the work of Cadet and Wagner [13].

3.2.3 DNA Cross-Links

A DNA–DNA intrastrand cross-link (intra CL) is formed when chemical bonds are created between two DNA bases of the same DNA strand, while a DNA–DNA interstrand cross-link (inter CL) is created when the chemical bonds are between bases of opposing strands. A chemical cross-link can also be generated with another endo- or exogenous molecule such as surrounding proteins to produce a DNA-protein cross-link (DPC). A DPC is formed as a covalent linkage between the protein and DNA after radiation-induced generation of DNA base radicals and amino acid radicals, mostly via hydroxyl radicals, which interact with each other [12]. A representation of the cross-links is given in Fig. 3.4.

They are problematic since replication and transcription mechanisms require a separation of the DNA strands. The most frequent cross-links observed are between tyrosine and thymine, tyrosine and cytosine, or lysine and thymine.

3.2.4 Single-Strand Breaks

Single-strand breaks (SSBs) result from endogenous processes and exposure to exogenous agents such as radiation and chemicals. A representation of this process is given in Fig. 3.5. More frequently, IR creates free highly reactive radicals, especially hydroxyl radicals (OH°), which may react with nearby DNA and produce an SSB. The repair of SSB is rather simple, as it will be discussed in Sect. 3.4, and thus most of the time, an SSB does not cause any serious problems to the cell. The quantity of SSBs increases linearly with the IR dose applied, and their formation decreases when the linear energy transfer (LET) increases [14].

3.2.5 Double-Strand Breaks

Double-strand breaks (DSBs) are produced when two SSBs on the two opposite DNA strands appear in close vicinity (one or two helix turns, thus about 15–20 DNA base pairs apart) [11]. Since DSBs are considered as the most important

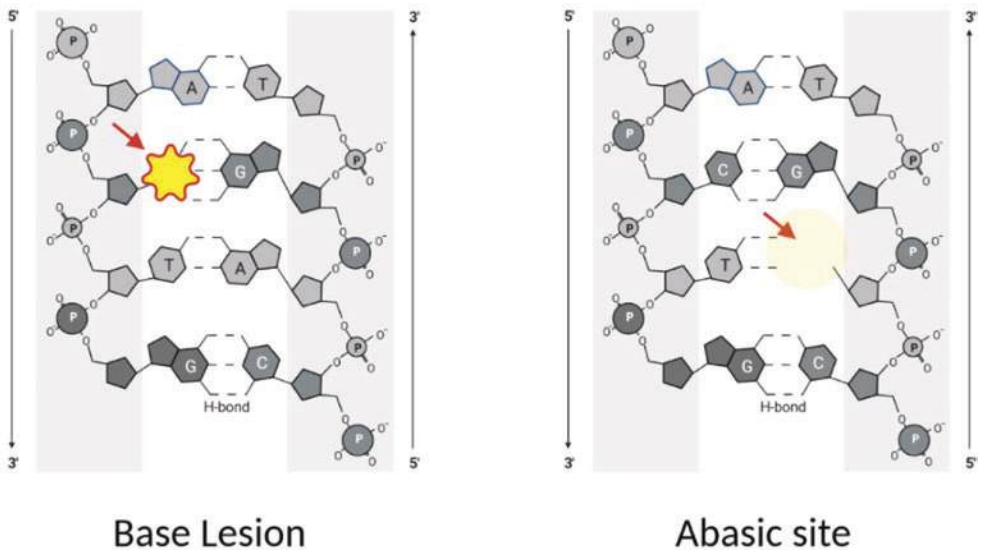

Fig. 3.3 Examples of DNA base damages. In base lesions, the chemical structure of any DNA base is modified (highlighted with yellow and red), whereas in abasic sites, the N-glycosidic bond between the DNA base and the 2-deoxyribose is broken (as shown with red arrow). *G* guanine, *C* cytosine, *A* adenine, *T* thymine, *H-bond* hydrogen bond, *P* phosphate

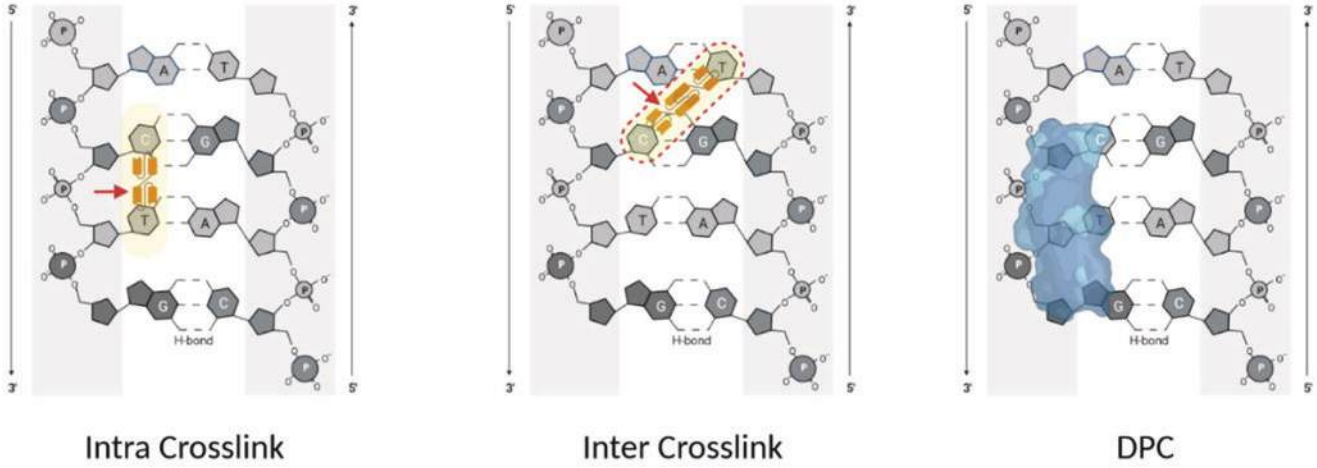

Fig. 3.4 Examples of DNA cross-links. Chemical bonds (yellow) are created between two DNA bases within the same DNA strand (intra cross-link) or opposite strands of double-stranded DNA (inter cross-link). Proteins (blue) can become cross-linked to DNA to form DNA-protein cross-link (DPC). *G* guanine, *C* cytosine, *A* adenine, *T* thymine, *H-bond* hydrogen bond, *P* phosphate

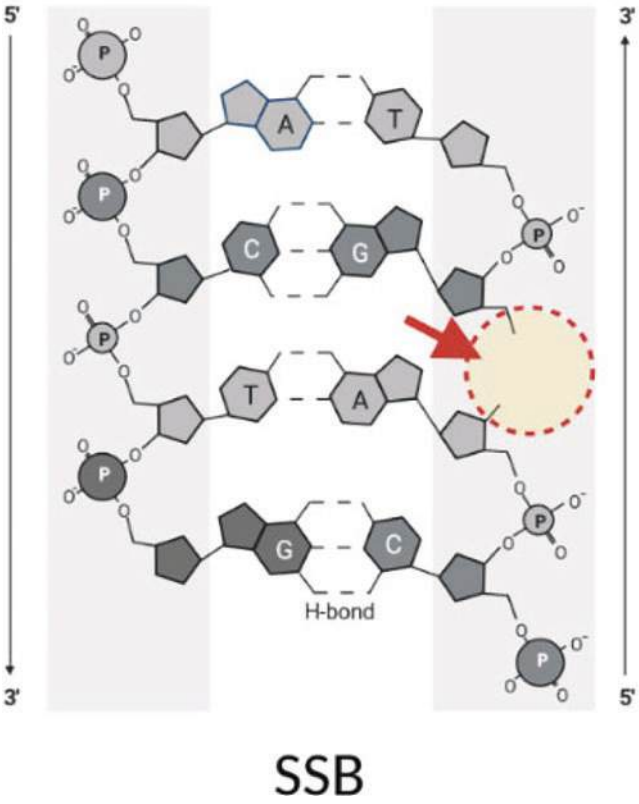

Fig. 3.5 Single-strand breaks (SSB): an illustration of a single-strand break in DNA. *G* guanine, *C* cytosine, *A* adenine, *T* thymine, *H-bond* hydrogen bond, *P* phosphate

cause of cell death after IR, understanding their mechanisms of formation is essential. Radiation-induced DSBs increase linearly with radiation doses up to several hundred Gray (Gy) and have been detected at as low as 1 mGy [15]. As explained in Chap. 2, low linear energy transfer (LET) IR consists of electrons and photons that liberate secondary electrons and produce reactive oxygen species (ROS). However, even if they can create closely spaced lesions, the collision between particles and atoms in tissues is infrequent, thus leading to less, randomly distributed DSBs. On the contrary, the damages induced by high-LET particles are distributed along the particle tracks, which exhibit higher rates of collision and lead to nonrandom DSB distributions. Furthermore, there is a complexity of the nature of the DSBs formed according to the dose and the type of radiations, which influence the DNA damage response (DDR) and its efficacy. One can talk about "clean DSBs," produced by hydrolysis of the phosphodiester bonds, which are easier to repair compared to "dirty DSBs," which contain residual modified sugar residues produced by reaction of the 2-deoxyribose with hydroxyl radicals [11] (see Fig. 3.6). "Dirty" DSBs are more frequently created by high-LET heavy ions or α particles.

Induction of DSB lesions by radiation is reviewed by Sage and Shikazono [16]. The ROS produced by the water radiolysis mediated by irradiation induces oxidized bases and loss of bases. Both lesions are repaired by base excision repair (BER, see Sect. 3.4), which can lead to DSB formation. Usually, DNA gaps of 1 or 2 nucleotides are filled by DNA polymerase and sealed by DNA ligase IIIα. During this process, SSBs can be generated in both DNA strands, and when they are close enough lead to a DSB. Moreover, the repair of a cluster lesion, e.g., an SSB opposite to an oxidative DNA lesion, could also result in the formation of a DSB as a result of irradiation. Additionally, through replication, if a damage is complex, e.g., effect on DNA secondary structures, formation of abasic sites, cross-links, and effect on DNA-binding proteins, the replication fork can stall and a DSB might occur. Moreover, conformational variables of the chromatin, which is a dynamic entity, and nuclear factors might affect DSB formation caused by radiation-induced

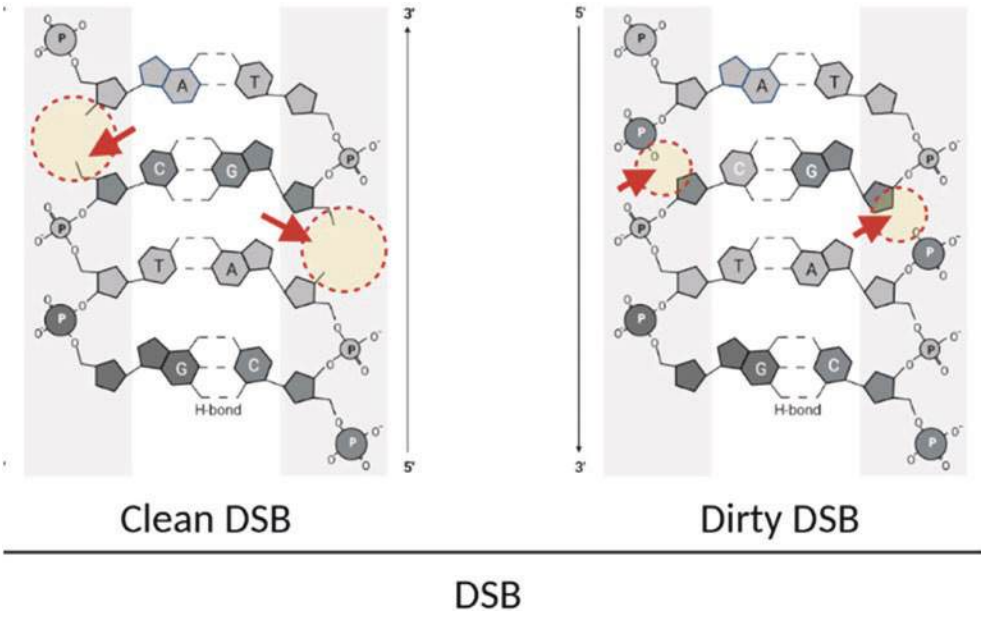

Fig. 3.6 Double-strand breaks (DSB): an illustration depicting different types of double-strand breaks in DNA. *G* guanine, *C* cytosine, *A* adenine, *T* thymine, *H-bond* hydrogen bond, *P* phosphate

radicals across the genome and according to the different points of the cell cycle.

3.2.6 Complex DNA Damage

Complex DNA damages, described as clustered DNA damages, are also named "locally multiple damaged sites" (LMDSs). LMDSs consist of closely spaced DNA lesions within a short DNA segment and are responsible for an increased cellular lethality since they are more difficult to repair. Two or more DNA lesions of the same or different type may be induced by IR within one or two helical turns of the DNA molecule, on the opposite strand. This clustered bistranded damage can be SSBs, DSBs, oxidized bases, and abasic sites. For example, at a dose of 1 Gy of IR, all this damage can be generated isolated or up to 10 bp apart [17]. Furthermore, the number of lesions per cluster depends on the radiation type and dose [18]. Experimental and theoretical studies have evidenced an increased complexity of the DNA damage induced by high-LET IR due to clustered ionizations, making complex DNA damage the signature of high-LET IR. Indeed, such lesions are considered the most important ones in terms of biological effects since they are the most challenging for the DNA repair machinery.

3.2.7 Overview of Ionizing Radiation-Induced DNA Damage

Not all cellular DNA damage is caused by exogenous factors; it can also be the result of cell metabolism as well as other normal cell processes. An overview of the average yield of DNA damage by endogenous factors per day and by low- and high-LET IR by 1 Gy is given in Table 3.1. One can see that even though the number of particles in the nucleus for high-LET radiation is much lower compared to low-LET radiation, the number of ionizations is the same. The dose deposition profile of high-LET IR induces more localized, complex, and clustered damages, which are more difficult to repair.

Table 3.1 Comparison of DNA damage for endogenous factors and low- or high-LET radiations

	Endogenous/cell/day	Low-LET IR/Gy	High-LET IR/Gy
Tracks in nucleus	–	1000	A few <1
Ionizations in nucleus	–	100,000	100,000
Ionizations in DNA	–	1500	1500
Base damage	16,000	10,000	10,000
DNA single-strand breaks	10,000–55,000	700–1000	300–600
DNA double-strand breaks	8	40	>40
Cross-link DNA/DNA	8	30	–
Cross-link DNA/protein	A few	150	–
Locally multiple damaged sites	A few	Increased with LET	

The number of tracks in the cell nucleus as well as the number of induced damages for high-LET IR depends on the particle type and energy; therefore, the given values represent only an estimate

3.2.8 UV Radiation-Induced DNA Damage

Ultraviolet (UV) light (100–400 nm) is a natural genotoxic agent able to induce deleterious effects affecting biological processes and structures, but also DNA structure, leading to a genomic instability [19]. DNA damage induced by UV is

mainly pyrimidine dimers, oxidized bases, as well as SSBs and DSBs. Nucleotides absorb UV radiations, which raise the DNA base to a highly reactive singlet or triplet state, leading therefore to photochemical reactions. The chemical nature and the amount of DNA damage strongly depend on the wavelength of the incident photons. Three main types of DNA lesions are formed involving two successive pyrimidine bases (CC, TT, TC, and CT) and leading to a DNA double-helix distortion: cyclobutane pyrimidine dimers (CPDs), pyrimidine 6-4 pyrimidone photoproducts (6-4PPs), and their Dewar isomers. The most energetic part of the solar spectrum corresponding to UVB (290–320 nm) leads to the formation of CPDs and 6-4PPs, whereas less energetic but 20 times more intense UVA (320–400 nm) also induces the formation of CPDs associated with a wide variety of lesions such as single-strand breaks and oxidized bases. Furthermore, in addition of the direct photolesions induced, some indirect DNA damage can occur through the production of ROS, especially hydroxyl radicals (OH°) and RNS. ROS can induce the oxidation of pyrimidine and purine bases, and also the deoxyribose backbone of DNA, such as the induction of the most frequent, i.e., the 8-hydroxyguanine (8-oxo-G) and in a smaller extent SSBs and DSBs. Moreover, the ROS induced by UV can lead to the alkylation of bases and to cross-linking of DNA–DNA or DNA-protein. CPDs and 6-4PPs are mostly formed between TT and TC, and in less proportion for CT and CC sequences. Additionally, the chromatin structure, as well as the composition of the neighboring nucleotide sequence of pyrimidine dimers, also influences the formation of UV-induced DNA damage. More recently, some studies discussed the influence of the epigenetic markers (DNA methylation, histone posttranslational modifications) in the induction of UV-induced lesions at a particular locus. Indeed, the methylation of DNA at C5 of cytosine (5-mC) was associated with an increase by 80% of the CPD yield and a decrease by 3 of the 6-4PP [20] (Box 3.2).

Box 3.2 In a Nutshell: Types of Radiation-Induced Lesions in DNA

- Deoxyribonucleic acid (DNA) is a large molecule composed of two polynucleotide chains that coil around each other to constitute a double-stranded helix structure.
- IR can cause DNA base or sugar damage, single- or double-strand breaks, DNA interstrand, intrastrand, or protein cross-links.
- DSBs are considered to be one of the most serious DNA lesions.
- High-LET IR induces more localized, complex, as well as clustered damage, which has the most serious potential biological consequences.

3.3 Types of DNA Repair Pathways

As described above, various types of DNA lesions occur through endogenous and exogeneous factors frequently in a human cell. Depending on the complexity, these lesions challenge cellular genomic integrity. At the time of cell division, many cellular processes are coordinated to ensure the maintenance of the stable genome and ascertain the preservation of the nuclear material [21]. These processes are known as the DNA damage response (DDR). The types of DNA damage and their primary repair pathway are listed in Table 3.2. The DDR signaling capacity can, if not sufficient, cause problems for the cell to maintain genome stable, which may result in a mutation. This may, as a last consequence, trigger transformation into a tumor or cancer cell. As DNA damage occurs physically, it can be repaired; however, when the mutation is established, the alterations that took place in the base sequence cannot be repaired. Accordingly, it is essential for normal cells to maintain DDR function to avoid such process.

3.3.1 Base Excision Repair

Base excision repair (BER) is the most common and important DNA repair process involved in removing minor DNA base defects. Many BER genes are extremely maintained from bacteria to humans demonstrating that BER is a fundamental repair process [22]. BER is a well-studied pathway for damage repair caused by respiration, spontaneous hydrolysis, and alkylation events, such as single-nucleotide bases (small, non-helix-distorting base lesions), that occur hundreds of times every day in each cell [23]. Thus, the BER system is critical to eliminate damaged bases that could otherwise produce mispair mutations or DNA replication breakdowns. In BER, SSBs are formed and repaired in an organized chain of events involving multiple proteins. Within BER, two pathways are simultaneously active: short patch repair (SP-BER), which is used to eliminate a broken base which has a non-bulky character, and long patch repair (LP-BER), which can replace the area in which the damaged DNA base is found. A schematical view of SP- and LP-BER can be found in Fig. 3.7.

In BER, specialized proteins called glycosylases recognize and remove the majority of the damaged DNA bases. There are multiple glycosylases, each of which is unique to a certain form of base damage. All these enzymes have, as their primary function, to cut out the base which got damaged yet without impacting the DNA backbone, causing further damage in an abasic place in the DNA (either apurinic or apyrimidinic site) [25]. Although each DNA glycosylase is specialized to a certain substrate and works in a distinct manner, they all have a single principal way of action: first, tak-

Table 3.2 DNA damage repair mechanisms

DNA repair mechanism	DNA damaging/genotoxic agents	DNA lesion feature	DNA damage example	DNA repair features
Base excision repair (BER)	Reactive oxygen species, X-rays, alkylating agents	Oxidative lesion	Oxidation (8-oxo-G) uracil, single-strand break	Removal of base by N-glycosylase abasic sugar removal, replacement
Nucleotide excision repair (NER)	UV lights and polycyclic aromatic hydrocarbons	Helix-distortion lesion	Bulky adducts, intrastrand cross-link	Removal of DNA fragment and replacement
Mismatch repair (MMR)	Replication	Replication error	A–G mismatch, T–C mismatch, insertion, deletion	Removal of strand by exonuclease, digestion, and replacement
Double-strand break repair (DSBR)	X-rays, ionizing radiations, reactive oxygen species, anti-tumor agents	Double-strand DNA breaks	Double-strand break, interstrand cross-link	Unwinding, alignment, ligation

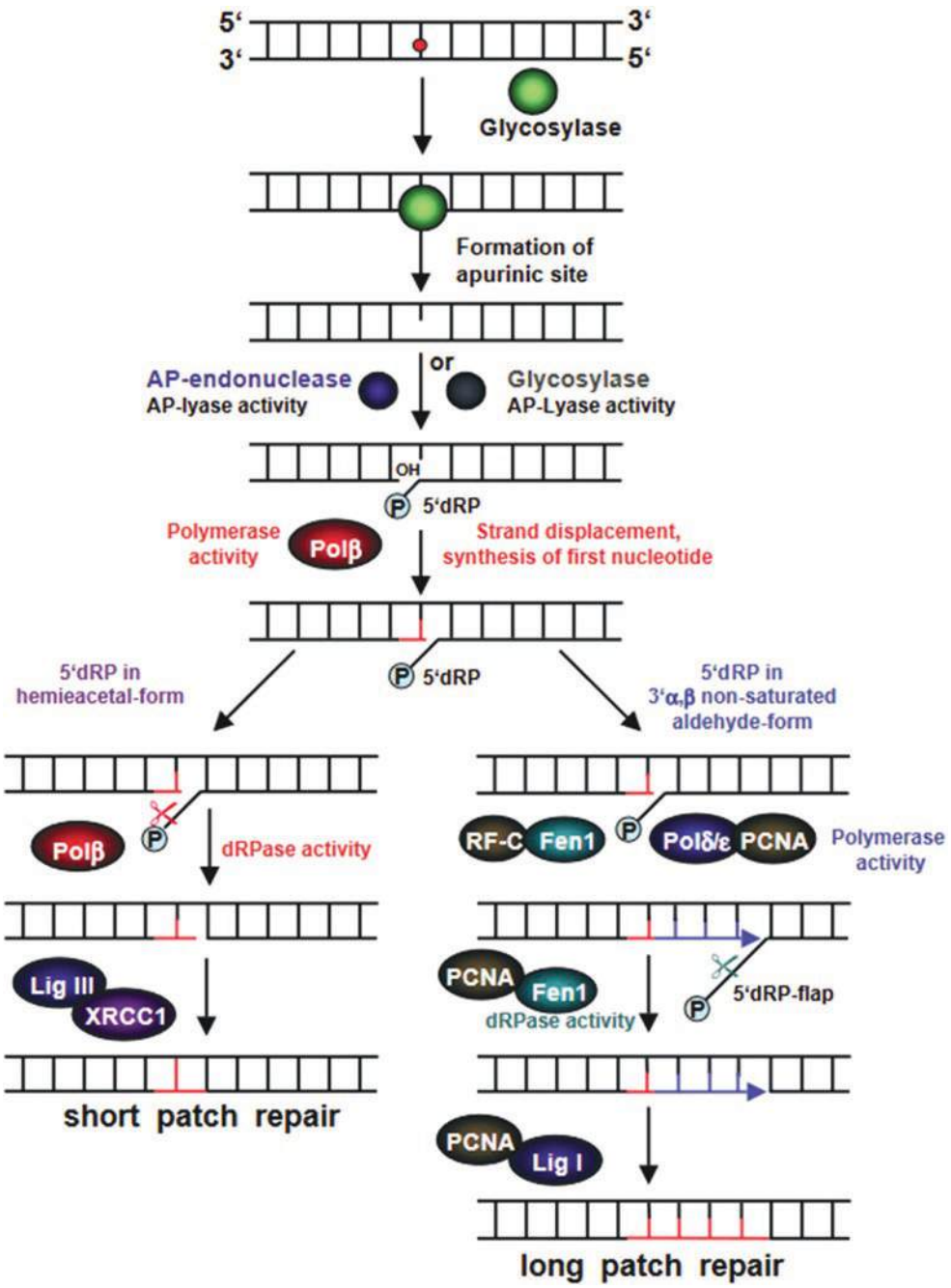

Fig. 3.7 Short and long patch base excision repair: recognition of the DNA lesion occurs by a specific DNA glycosylase which removes the damaged base by hydrolyzing the N-glycosidic bond. The remaining AP site is processed by APE. Depending on the cleavability of the resulting 5′dRP by Polβ, repair is performed via the short or long patch BER pathway. Reproduced with permission from [24]. *AP-endonuclease* apurinic/apyrimidinic endonuclease, *AP-lyase* apurinic/apyrimidinic lyase, *OH* hydroxide, *P* phosphate, *5’dRP* 5′ deoxyribose phosphate, *Lig III* ligase III, *XRCC1* X-ray repair cross-complementing 1, *RF-C* replication factor C, *Fen1* flap structure-specific endonuclease 1, *PCNA* proliferating cell nuclear antigen, *Lig I* ligase I

ing the damaged base outside the DNA helix, thus assisting the detection of bases with minute alterations, and, second, triggering the cutting of an N-glycosidic bond, which in turn enables the formation of an abasic site [22]. Humans have 11 DNA glycosylases, which are classified as monofunctional (removing a base which results in formation of an AP site), bifunctional (removing a base and cutting the DNA backbone close to the damaged base), or Nei-like (which removes the base but also cuts each side of it).

Once the monofunctional DNA glycosylase has created the AP site, another repair enzyme, AP endonuclease 1 (APE1), incises and hydrolyzes the AP site, removing the base followed by the sugar residue, cutting the DNA backbone, and as a result an SSB is formed. APE1 also operates on bifunctional glycosylase products, creating a one-nucleotide gap product after hydrolysis. Polynucleotide kinase phosphatase (PNKP), whose product is suitable for DNA polymerase action, is required for the repair of oxidized DNA bases. When there is a gap or SSB is formed, poly(ADP-ribose) polymerase 1 is activated (PARP1) [23]. In this way, the integrity of the break can be maintained. PARP1 also orchestrates, via its poly(ADP-ribosyl)ation activity, a cascade of proteins binding to the SSBs with the main aim to detect and promote its further repair.

The most common polymerase used in BER is DNA polymerase (Pol), which fills the gap with the proper nucleotide and catalyzes a lyase reaction. SP-BER is linked by the DNA ligase III-XRCC1-mediated mechanism to complete the process [25]. In contrast to SP-BER, LP-BER occurs when a lesion is resistant to Pol cleavage, and polymerases such as PCNA, flap endonuclease 1 (FEN1), and PARP are recruited. While displacing the broken strand, the polymerase synthesizes DNA and inserts a repair patch consisting of 2–12 of the correct nucleotides into the gap. The repair synthesis is carried out by the T complex of the replication factor C (RFC)/proliferating cell nuclear antigen (PCNA)/DNA polymerase δ/ε. Here, the lap endonuclease 1 (FEN1) acts by taking out the flap structure that is overhanging the damaged base site, and the nick that is formed is ligated by DNA ligase I [14]. SP-BER and LP-BER primarily differ in how many of the DNA bases are cut out during the repair (see Fig. 3.8). SP-BER only replaces the bases which are damaged, whereas LP-BER cuts out and replaces up to ten nucleotides.

IR-induced base damage is effectively repaired by BER. BER deficiencies can result in a higher mutation rate but seldom cause cellular radiosensitivity [26]. The X-ray cross-complementing factor 1 (XRCC1) gene mutation, which causes a 1.7-fold increase in radiation sensitivity, is an exception. The radiation sensitivity of XRCC1-deficient cells, on the other hand, could be due to XRCC1's involvement in other repair processes, such as SSB repair. Reduced repair and radiosensitization can be caused by mutations, deletions, or inhibition of either of these genes.

In both BER and SSB repair, DNA polymerase beta (pol) is a key enzyme. Under some situations, cells lacking pol or expressing a dominant negative construct to pol, which inhibits its function, have been demonstrated to be more vulnerable to ionizing radiation in vitro [27]. Small-molecule medicines that block PARP1 have also been produced. The PARP inhibitors are a medication that targets BER and SSB repair and are now being tested in clinical trials for cancer treatment, as described in Chap. 6 (Box 3.3).

Box 3.3 In a Nutshell: Base Excision Repair

- BER is a specific repair mechanism that is used to handle DNA base damage.
- BER removes single-nucleotide base lesions (small, non-helix-distorting base lesions) from the genome.
- SP-BER and LP-BER are two complementary BER systems essential for removing base damage and fixing SSB in DNA, minimizing mutagenesis but differing in what base damages they can handle.
- BER inhibitors have showed potential as radio/chemosensitizers in a variety of malignancies, or they can create synthetic deadly alliances with common cancer mutations.

3.3.2 Nucleotide Excision Repair

From unicellular bacteria to complex humans and plants, nucleotide excision repair (NER) works in a similar way. In humans, NER is known for its one-of-a-kind repair process to remove photolesions caused by UV radiation. However, there is one circumstance in which NER genes can influence the IR response. More DNA cross-links are formed when cells are irradiated under hypoxia than when irradiated under normoxic circumstances. Excision activity of two NER genes, DNA excision repair protein (ERCC1) and DNA repair endonuclease (XPF), is required for such cross-links, among other things. Defects in either of these genes may cause hypoxic cells to become more radiosensitive. As a result, the status of the NER pathway is relevant to radiotherapy in combination with specific chemotherapeutic drugs, as well as hypoxic tumors treated only with radiotherapy [28].

The principle of NER is shown in Fig. 3.8. The lesion-recognizing NER factors look for unpaired single-stranded DNA on the other side of the damaged strand [22]. The oligonucleotide that contains the lesion is eliminated, and to restore the DNA to its original form, a repair patch is created using

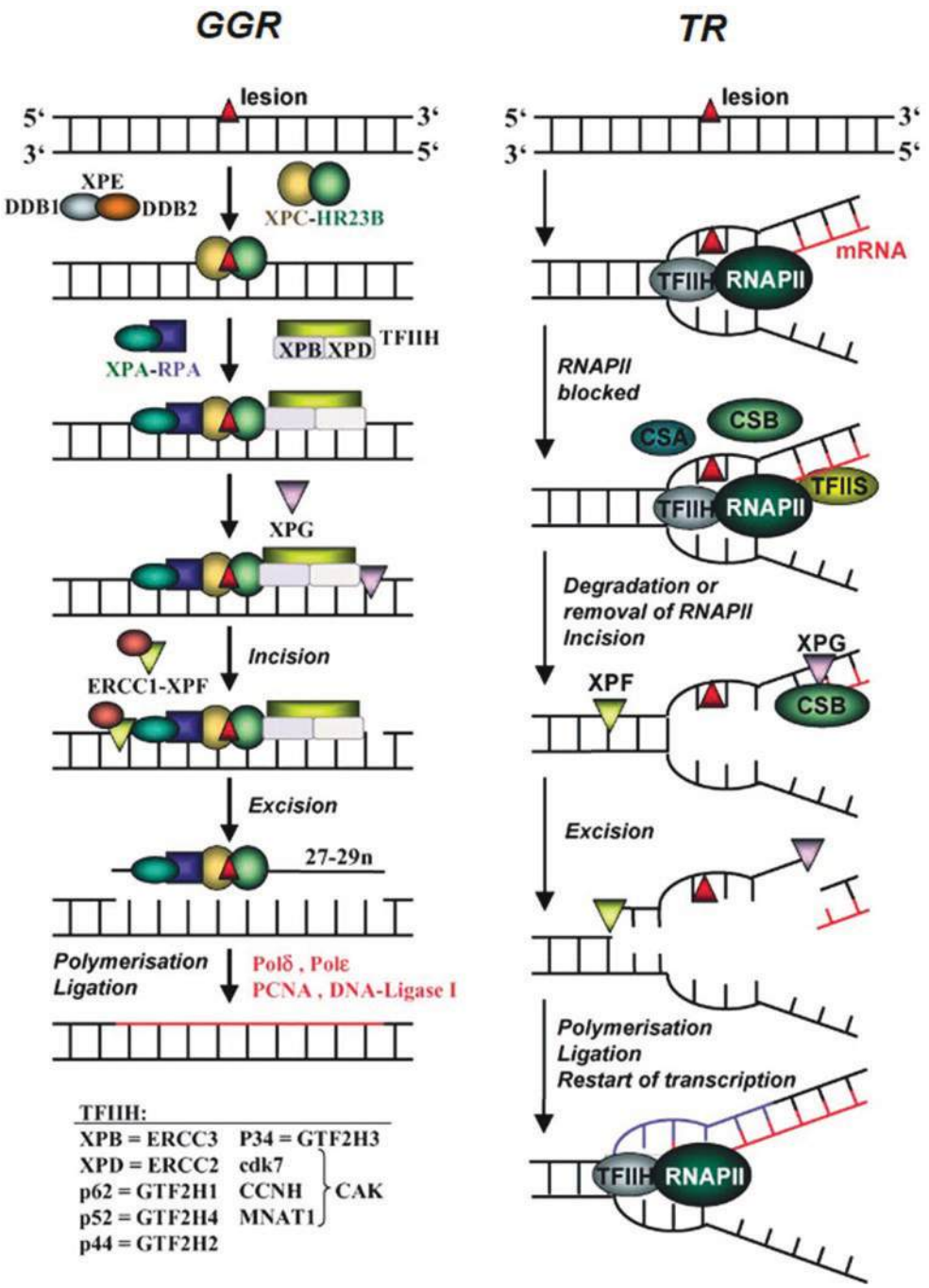

Fig. 3.8 Nucleotide excision repair (NER) pathway: during global genomic repair (GGR), recognition of the DNA lesion occurs by XPC–HR23B, RPA–XPA, or DDB1–DDB2. DNA unwinding is performed by the transcription factor TFIIH and excision of the lesion by XPG and XPF–ERCC1. Finally, resynthesis occurs by Polδ or Polε and ligation by DNA ligase I. During transcription-coupled repair (TCR), the induction of the lesion results in blockage of RNAPII. This leads to assembly of CSA, CSB, and/or TFIIS at the site of the lesion, by which RNAPII is removed from the DNA or displaced from the lesion, making it accessible to the exonucleases XPF–Ercc1 and XPG cleaving the lesion-containing DNA strand. Resynthesis again occurs by Polδ or Polε and ligation by DNA ligase I. 23B: Reproduced with permission from Christmann et al. [24]. *DDB1* DNA damage-binding protein 1, *DDB2* DNA damage-binding protein 2, *RPA* replication protein A, *TFIIH* transcription factor IIH, *ERCC1* excision repair cross-complementing group 1 protein, *Polyδ/ε* DNA polymerase delta/epsilon, *PCNA* proliferating cell nuclear antigen, *Lig1* DNA ligase 1, *RNAPII* RNA polymerase II, *CSA and CSB* Cockayne syndrome factors A and B, *TFIIS* transcription initiation factor IIS, *HR23B* homologous recombinational repair group 23B

the opposite undamaged complementary strand as a template. With varied degrees of success, NER eliminates lesions from the entire genome and can be separated into two paths [24]:

1. Global Genome Repair (GGR or GG-NER): GG-NER is a genome-wide process, i.e., lesions can be eliminated from DNA that encodes, or not, for genes.
2. Transcription-Coupled Repair (TCR or TC-NER): TC-NER exclusively eliminates lesions in the DNA strands of genes that are actively transcribed. If a DNA strand that is actively transcribed is broken, the RNA polymerase could inhibit DNA repair by blocking access to damage sites. TC-NER has evolved to overcome RNA polymerase's barrier by essentially eliminating it from the damage site, allowing repair proteins access.

In the early damage recognition phase, the two NER sub-pathways vary. In GGR, the NER proteins are recruited by the stalled RNA polymerase in collaboration with Cockayne syndrome protein B and A (CSB and CSA). In TCR, the NER proteins are engaged by the stalled RNA polymerase in collaboration with CSB and CSA [14].

Mutations in the NER genes do not cause IR sensitivity. However, defective NER increases sensitivity to UV-induced DNA damage and anticancer drugs that create bulky adducts, such as alkylating agents. Human DNA repair deficiency such as xeroderma pigmentosum, in which individuals are hypersensitive to UV radiation, is caused by germline mutations in the NER genes [14] (Box 3.4).

Box 3.4 In a Nutshell: Nucleotide Excision Repair

- Nucleotide excision repair (NER) is a technique for removing bulky adducts from DNA, chiefly those caused by UV.
- Defects in certain NER proteins may result in enhanced radiosensitivity of hypoxic cells.
- Large DNA lesions like thymine dimers and cisplatin adducts are repaired using a DNA repair pathway.
- The two types of NER pathways are global genome repair (GGR or GG-NER) and transcription-coupled repair (TCR) (TCR or TC-NER).

3.3.3 Mismatch Repair

The mismatch repair (MMR) system has a role after the cellul replication process, where sometimes incorrect bases pair with each other (which is called a mismatch). Therefore, MMR aids in keeping DNA homeostasis and plays a major role in evolutionary genomic stability [29]. Its basic purpose is to rectify the small insertion-deletion loops (indels) and the base-base mispairs that are spontaneously generated at the time of DNA replication. These mis-incorporated bases have escaped the proofreading action of replication polymerase. Usually, the polymerase that carries out the DNA synthesis process is not completely error-free. The DNA polymerase on average makes one mistake for every 10^5 nucleotides [29], which implies that ~100,000 errors arise through each S phase of the cell. Even though the DNA polymerase is there to ascertain that such mistakes do not occur, a few mutations can go unnoticed by it and hence the MMR-associated genes act as the second line of defense. However, if the cell is deficient in the MMR process, these errors remain uncorrected. Therefore, the mutational rate and sequence length modification in the microsatellites, which is a known trait of tumor cells, increase. The relevance of MMR in radiation-induced damage and cellular radiosensitivity is a matter of controversy. The mismatch repair (MMR) pathway was first discovered in *E. coli* cells [30]. Researchers have explored and understood that the MMR pathways and its associated proteins are evolutionarily conserved in almost all organisms including humans [31]. MMR works by inserting or deleting the mispaired bases by recognizing the mispaired lesion; excision, i.e., removal of the erroneous strand; and DNA resynthesis and gap repair by filling it with the correct resynthesized DNA.

The parent strand, which includes a palindrome DNA sequence "GATC" and adenine, is methylated by the enzyme deoxy-adenine-methylase. However, after replication when there are two new incorrect strands, methylation in the newly formed daughter strand is not seen [32] (Fig. 3.9). Such alterations are recognized and repaired by the methyl mismatch repair. The specific region of mispairing is recognized by the Mut S protein, which is coupled by the MutL. The activity of MutS is stimulated by the heterodimer MSH2–MSH6, along with MutSα. The MutSα recognizes small IDLS comprising 1–2 nucleotides, whereas the MSH2–MSH6 identifies longer insertion-deletion loop-type mismatches. After the binding of MutS to the DNA, it is followed by the ATP-dependent prerequisite of MutL homolog (MSH) complex. The parent strand is recognized by the MutL, which brings the misrepaired region nearer and leads to a loop formation around the area. Another protein, MutH, an endonuclease enzyme, performs the activity of cleaving. Next, UVr-D, a helicase, releases the cut strand leading to the formation of a gap where the new error-free or accurate nucleotide sequence is included by the polymerase 1 and joined by ligase. Cells that are deficient in the MMR proteins exhibit a high frequency of mutations and also irreversible microsatellite instability. Accordingly, individuals with germline mutations in MMR genes are more susceptible to various types of cancers [33] (Box 3.5).

Box 3.5 In a Nutshell: Mismatch Repair

- MMR targets DNA mismatches that arise mainly during replication, as well as repairing mismatches that occur in DNA following treatment with alkylating agents.
- The MMR pathway detects and repairs erroneous insertions, deletions, and base substitutions that have not been detected by the proofreading function of DNA polymerase during DNA replication, thus maintaining the genome stability.
- It works by recognition of mispair, excision of the affected strand, and filling of the gap.

3.3.4 Double-Strand Break Repair

Double-strand breaks (DSBs) are the most lethal kind of DNA damage because even one uncorrected DSB can result in loss of genetic information and finally lead to cell death. Moreover, such unrepaired or misrepaired DSBs can lead to

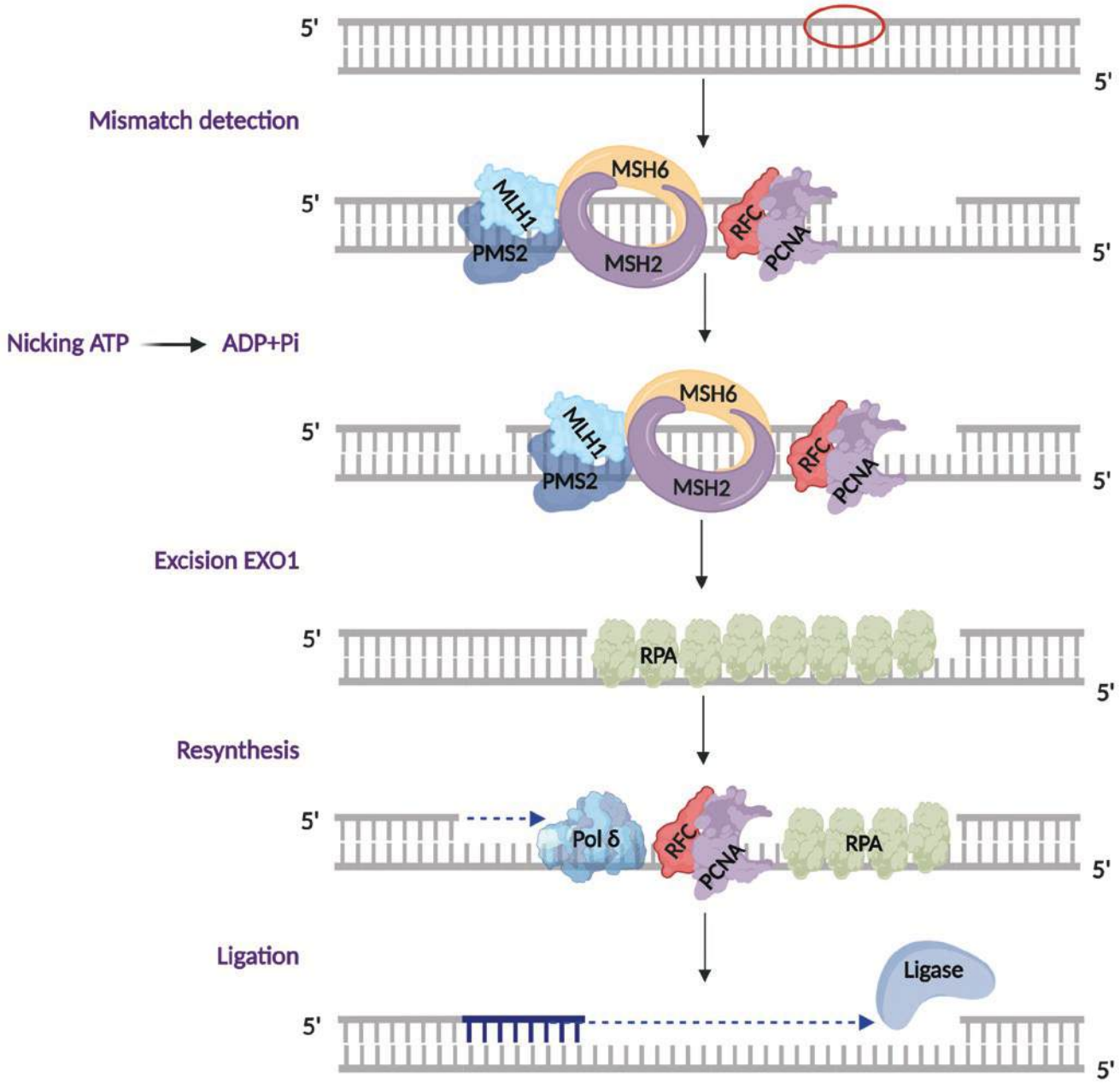

Fig. 3.9 Overview of eukaryotic mismatch repair system. In the human cell, the predominantly found MutSα (MSH2–MSH6) or the MutSβ recognizes the DNA mismatch repair and initiates its repair. Some of the crucial molecules which participate in the repair are the MutLα (MLH1-PMS2), the proliferating cell nuclear antigen (PCNA), and the replication factor (RCF). EXO1 catalyzes the repair, and ligase finally ligates the repaired DNA

augmented genomic instability and eventually tumorigenesis [21]. Accordingly, for a cell to pursue its genetic information, a functional DSB repair system is of major importance. As a result, cells have evolved a dedicated response to identify and mend DSBs. For repair of DNA DSBs, two principal pathways are used, namely homologous recombination (HR) and Non-homologous end joining (NHEJ).

These pathways differ with respect to the use of homologous template DNA as well as in DNA repair fidelity. HR utilizes undamaged sister chromatid as its template to repair the damage, and therefore it is error-free. However, NHEJ works by eliminating the damaged DNA followed by direct ligation and hence is error-prone. As HR needs an undamaged template, it only operates in late S and G2, in contrast to NHEJ, which has the capacity for DSB repair regardless of the cell's position in the cell cycle phase [33].

3.3.4.1 Homologous Recombination (HR)

The homologous recombination (HR) molecular pathway is associated with a large number of cellular processes, from

imparting genetic diversity to DNA repair or replication. HR is evolutionarily conserved from bacteria to mammalian cells. This pathway is essential for fixing DNA damages with high accuracy by using the genomic code of the chromosomal copy which was not damaged [34]. HR works by precisely repairing the DSB, shielding cells from any chromosomal abnormalities such as those observed in many cancers. Throughout the process of DNA replication, HR-associated proteins endorse the faithfulness and restoring of distressed DNA replication forks. This adds sturdiness, serving the replication machinery to circumvent under replication and succeeding segregation tribulations of the chromosome. Inherent HR insufficiency in cells can persuade instability in the genome and further lead to cancer. Conversely, discrepancy in the HR pathway also sensitizes tumors not only to DNA damage treatment but also to other potential DNA repair inhibitors for remedial repair pathways.

For the commencement of the HR pathway, the break site 5′–3′ end resection is a requirement, which not only exposes the single-stranded DNA (ssDNA) overhangs but also averts the NHEJ pathway to repair the DNA breaks (Fig. 3.10) [36]. The repair proteins MRE11 (meiotic recombination 11), RAD50 (RAD50 double-strand break repair protein), and NBS1 (nibrin) form the MRN complex, and together with the ataxia-telangiectasia mutated (ATM) kinase, they are the first to recognize the DNA damage. By attaching to the DNA ends, the MRN complex instigates the process of DNA end resection. Next C-terminal binding protein 1 interacting protein (CtIP) is employed so as to produce the overhangs at the 3′ end of the single-stranded DNA [36]. The preference of the choice of repair pathway is governed by the p53-binding protein 1 (53BP1) and breast cancer-associated protein 1 (BRCA1) contrasting activity in addition to the MRE11 resection activity. Whenever a DNA break is identified, both BRCA1 and 53BP1 compete to govern the commitment of the cell to undergo NHEJ or HR, respectively. By hindering the DNA end resection and concurrently securing two double-stranded DNA (dsDNA) ends, facilitating their successive ligation, 53BP1 supports the NHEJ pathway [37]. The mechanism by which BRCA1 suppresses 53BP1 still remains uncertain. Ubiquitination of CtIP occurs when BRCA1 interacts with BRCA1-associated RING domain protein 1 (BARD1). This subsequently enhances the affinity of CtIP for DNA and as a consequence promotes resection [37]. At this time, the DNA ends are protected and prevented from resection by replication timing regulatory factor 1 (RIF1), which is a 53BP1-interacting partner and a Shieldin complex. The increased HR activity can be attributed to either the loss of 53BP1 or the Shieldin complex that weakens the NHEJ pathway. Blocking wide-ranging end resection is central, meant for preventing the hyper-recombination by HR and stopping the loss of genetic material. Some other lethal repairing pathways like break-induced replication (BIR) or single-strand annealing (SSA) can lead to wide-ranging resection whose outcome is loss of heterozygosity [35].

A full functional HR pathway can be utilized after the DNA end resection. A detailed review of this process can be found in the work of Ranjha et al. [38]. The canonical HR pathway not only restores a direct DSB, but also repairs damage created by stalled or collapsed replication forks [21]. As soon as an extensive resection is executed by the action of several nucleases, cells are obligated to follow a homology-governed mode of repair. The DSB goes through a nuclease-driven progression known as DNA end resection in order to produce 3′-end ssDNA segments all through HR. This is crucial for the searching and strand invasion that occurs later during the recombination process. Along with the CtIP nuclease, DNA end resection is instigated by the MRE11 nuclease within the MRN complex. MRN/CtIP in combination with Bloom syndrome protein (BLM) or exonuclease 1 (EXO1) and DNA replication helicase/nuclease (DNA2) arbitrates the short- as well as long-term resections. During this resection, the 3′ ends of ssDNA get exposed that are rapidly covered by replication protein A (RPA) complex. The ssDNA region covered by RPA further recruits and stimulates the ataxia-telangiectasia and Rad3-related (ATR) kinase. This in turn triggers the checkpoint kinase 1 (Chk1) kinase. The RPA coating not only ascertains the nondegradation of ssDNA overhangs but also avoids the formation of secondary structures. To form the presynaptic filament, RAD51 dislocates RPA, which is then involved in the action of several RAD51 mediator proteins. To construct a displacement loop (D-loop), the RAD51 nucleoprotein filament explores a homologous sequence to occupy and dislocate one strand of the homologous template. This structure aids in the formation of a heteroduplex by pairing the broken strand with the displaced strand, and DNA synthesis at the break site repairs for any missing nucleotides. The outcome of the second end capture leads to the configuration of a double-Holliday junction (dHJ). The resolution of such an intermediate occurs either by a resolution mechanism or by a dissolution, which makes it susceptible to crossover (CO) or noncrossover (NCO). On the other hand, at the time of synthesis-dependent strand annealing (SDSA), no more than one-end invasion takes place, therefore leading to the formation of a single-Holliday junction. This transitional structure is suspended into an NCO. The HR repair pathway is known to also involve chromatin modifiers, remodelers, and even integration of histone variant so as to deal with the obstructions that the nucleosomes produce to the resection machinery. HR is active during the late S phase and the G2 phase and therefore is able to utilize the sister chromatid as a guiding template to repair the DSBs. Hence, this pathway is error-free [38].

3.3.4.2 Non-homologous End Joining

The Nonhomologous end joining pathway (NHEJ) pathway (Fig. 3.11) has long been demonstrated to be central in

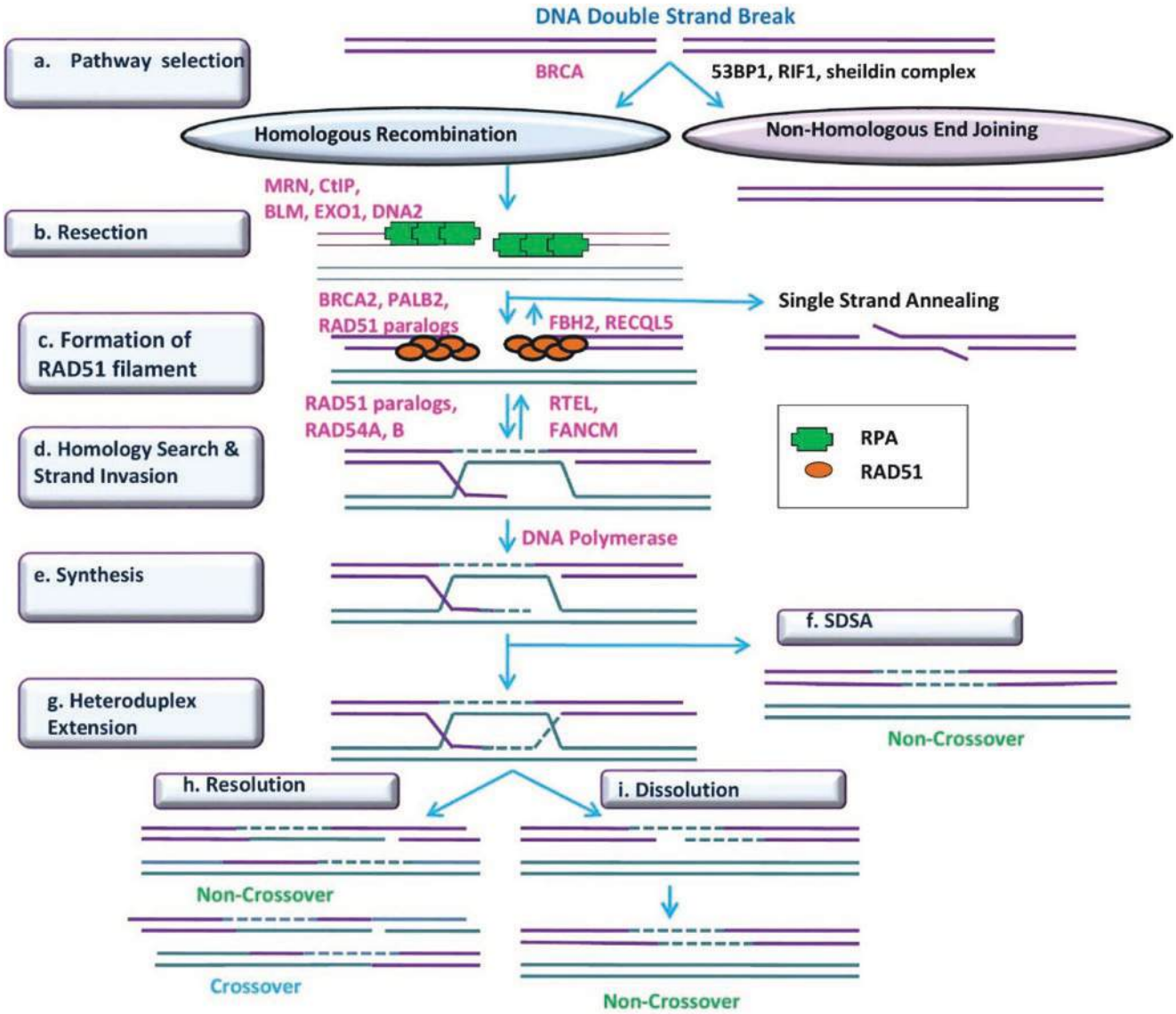

Fig. 3.10 Overview of homologous recombination (HR) pathways in double-strand break repair. When cells suffer a DSB (purple lines), they can repair them either by HR, with the help of a template that is homologous (turquoise lines), or by the NHEJ pathway. (**a**) BRCA1 promotes the HR pathways, whereas the Shieldin complex, RIF1, and 53BP1 promote the NHEJ pathway. (**b**) The resection process is performed by the MRN complex along with CtIP, EXO1, BLM, and DNA2 that form the 3′ ssDNA overhangs. These overhangs are then coated with the RPA (green boxes), which is later shifted by the RAD51 (brown circles). On the other hand, single-strand annealing occurs in case of the RAD-independent repair process, where annealing of the complementary DNA sequences takes place followed by overhangs cleaved by the flap endonuclease and finally the ends of the DNA are ligated. (**c**) Positive regulators of RAD51 such as RAD51 paralogs, BRCA2, and PALB2 aid in the formation of the RAD51 filament, whereas RECQL5 and FBH2 negatively regulate RAD51. (**d**) The RAD51 paralogs and RAD54A-B support the RAD51-mediated homology searching and strand invasion. At the same time, FANCM and RTEL negatively govern the RAD51-mediated D loops. (**e**) The homologous template in the form of sister chromatid or a homologous chromosome is used by the DNA polymerases to copy the missing sequence. (**f**) The DNA is resolved into a noncrossover product when SDSA dislodges the D loop. (**g**) In case there is an extension of the heteroduplex and development of Holliday junction created by the second-end capture, the intermediate states can be resolved by either resolution or dissolution. (**h**) The outcome of resolution is both the crossover and noncrossover products. (**i**) The outcome of dissolution is a noncrossover product. Adapted with permission (CCBY) from Sullivan and Bernstein [35]. Abbreviations: *DSB* double-strand DNA break, *HR* homologous recombination, *NHEJ* Non-homologous end joining, *BRCA1* breast cancer gene 1, *RIF1* Rap1-interacting factor 1, *53BP1* p53-binding protein 1, *MRN* MRE11–RAD51–NBS1 complex, *CtIP* CtBP-interacting protein, *EXO1* exonuclease 1, *BLM* Bloom's syndrome helicase, *RecQ* helicase-like gene, *DNA2* DNA replication helicase/nuclease 2, *ssDNA* single-stranded DNA, *RPA* replication protein A, *RAD51* RAD51 recombinase, *PALB2* partner and localizer of BRCA2, *RECQL5* RecQ-like helicase 5, *FBH2* also GNA11, G protein subunit alpha 11, *FANCM* FA complementation group M, *RTEL* regulator of telomere elongation helicase 1, *SDSA* synthesis-dependent strand annealing

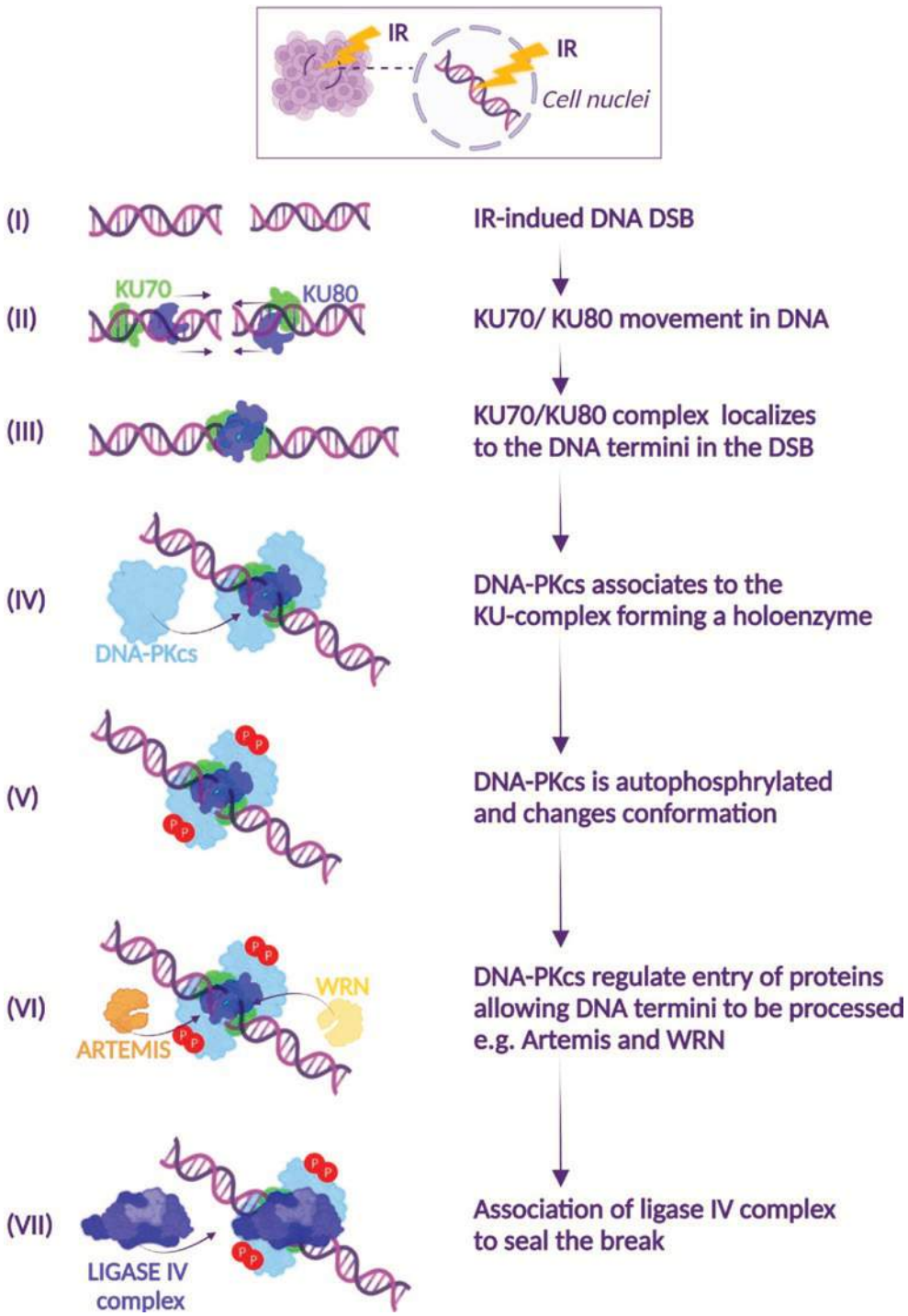

Fig. 3.11 Schematic of the principal steps of NHEJ. (I) IR triggers the formation of DNA DSB in the cell nucleus. (II) To act on these, the NHEJ pathway commences with the movement of Ku (Ku70/Ku80) proteins towards the loose ends in the DNA DSB. (III) Ku70/Ku80 forms a complex embracing the ends protecting DNA integrity. DNA DSBs with noncomplex termini can be ligated directly after this step as end processing is not required. (IV) When the ends in the DSB require end trimming, the DNA-PKcs is recruited onto DNA via association to the Ku70/Ku80 complex forming a platform for subsequent steps. (V) Once associated to Ku proteins and DNA, DNA-PKcs undergoes autophosphorylation which changes its conformation. (VI) In this way, DNA-PKcs is active as a kinase and regulates the association of multiple DNA end-trimming proteins (e.g., Artemis, WRN, Polμ/λ, PNK), which restores the nucleotides at the termini allowing ligation to take place. (VII) The ligation step is controlled by the DNA ligase IV complexes, which apart from ligase IV also include XRCC4, XLF, and PAXX. At the end of the trimming and ligation step, some bases may be lost causing loss of genomic information which may cause mutations. Abbreviations: *DNA DSB* DNA double-strand break, *NHEJ* Nonhomologous end joining, *Ku* dimeric Ku70/Ku80 protein complex, *DNA-PKcs* DNA-dependent protein kinase catalytic subunit, *WRN* protein deleted in Werner syndrome, *Polμ/λ* DNA polymerase μ/λ, *PNK* polynucleotide kinase, *XRCC4* X-ray repair cross-complementing protein 4, *XLF* XRCC4-like factor, *PAXX* paralog of XRCC4 and XLF

repairing DNA DSBs, and cells deficient in some of these signaling components are known to be very IR sensitive [39]. Moreover, NHEJ has a critical role in V(D)J-recombination when B and T lymphocytes are developed in the immune system. This is also illustrated by severe combined immunodeficiency (SCID) patients who, due to lack or alteration in some of the NHEJ components including the catalytical subunit of DNA-PK (DNA-PKcs) as well as others, have T and B lymphocytes that do not have proper function [39]. Importantly, cells from such patients also display high IR sensitivity.

The NHEJ process starts at the DNA end termini, also known as the break synapsis, where a heteromeric complex of the Ku proteins, Ku70/Ku80, forms a ringlike structure around the DNA. The Ku70/Ku80 complex then moves towards the break to bring the free DNA ends together and protect them from nuclease digestion (Fig. 3.11). This is critical for NHEJ function and for IR sensitivity as cells deficient in either Ku subunits have impaired NHEJ and also are IR sensitive [41].

The end structures within the DNA DSB which are sensed and protected by the Ku protein complexes are 3′ or 5′ overhangs, blunt ends, closed hairpin, and complex structures including those found in IR-induced DSBs [41]. The current understanding is that the Ku complex heterodimer slides along the DNA strand and multiple subunits align onto DNA to form a protein scaffold. The end structure in the DSB, i.e., the blunt ends, 3′ or 5′ overhangs, thereafter dictates what route the NHEJ takes as some proteins are required for certain end termini to be processed prior to ligation while others are not [41, 42]. For example, when the end termini have some regions with certain nucleotides that overlap, the ends are ligated by the DNA ligase IV and X-ray repair cross-complementing 4 (XRCC4) complex alone. However, in the majority of the cases, the DNA protein kinase catalytic subunit (DNA-PKcs) orchestrates the reactions forming a holocomplex with the Ku proteins on the DNA [42] (Fig. 3.11).

DNA-PKcs is a kinase with the capacity to phosphorylate proteins on serine or threonine resides. It belongs to a protein family also named the PIK kinases to which also ATM and ATR belong. DNA-PKcs requires DNA binding for its kinase activity to control the end-processing activity within NHEJ as well as inactivation of its own function [42]. Thus, when the Ku complex binds DNA-PKcs, it causes autophosphorylation of multiple residues in the kinase domain and thereafter DNA-PKcs can phosphorylate its downstream substrates.

Multiple studies in rodent and human cells using various genetic approaches have shown that a defective DNA-PKcs activity impairs the repair of some but not all IR-induced DNA DSBs, but nevertheless causes increased radiation sensitivity [39]. To further study the function of DNA-PKcs for repair of IR or chemotherapy-induced DNA damage, inhibitors towards the kinase pocket have been developed, some of which have also been demonstrated to function as IR sensitizers of tumor cells and in tumor-bearing mice (reviewed in the work of Myers et al. [43]). All in all, it is clear that DNA-PKcs orchestrates the NHEJ pathway, but despite decades of research, the understanding of the entire molecular mechanisms is still not complete.

The end processing of the nucleotides is required as a DNA DSB seldom has the 3′OH and 5′P termini that are required for ligation. Therefore, the ends in the DNA DSB need to be processed by exonucleases such as Artemis, which has intrinsic 5′ exonuclease function and 5′ exonuclease acquired once in complex with DNA-PKcs [44]. The critical role for Artemis in the NHEJ processing has been shown as cells deficient in Artemis are sensitive to IR. However, Artemis is only required for repair of a subset of ~10–20% of the DNA DSBs, while the others are rejoined efficiently in the absence of Artemis. Therefore, it has been suggested that Artemis is responsible for repair of DNA DSBs that display slow repair kinetics. Apart from Artemis, there are also other proteins involved in the end-processing activity including Werner syndrome ATP-dependent helicase (WRN). It exhibits helicase and exonuclease function and suppresses 5′ end resection as well as HR by blocking MRE11 and CtIP association. Other examples are the polynucleotide phosphatase/kinase (PNKP) and tyrosyl-DNA phosphodiesterase 1 (TDP1) that modify the phosphorylation of the nucleotides and trim the ends to a state allowing ligation to take place. As some nucleotides may be lost in the end termini, the DNA polymerase μ and DNA polymerase λ are also part of the end-trimming activity in NHEJ.

Ligation of broken ends by NHEJ is carried out in a protein complex, which bridges around the DNA end in the DSB. The complex contains, among other proteins, XRCC4, DNA ligase IV, and XRCC4-like factor (*XLF*). Out of all the proteins involved in NHEJ, DNA ligase IV stands out when it comes to repair of DNA DSBs because mice, in which this gene is disrupted, experience lethality as embryos and dissection of such embryos have revealed extensive apoptosis, in particular in the nervous system [45]. Both ligase IV and XLF mutations, that impair their function, are reported in humans in different tumor types, e.g., leukemias and lymphomas, with the patients showing various degrees of deficiency in B and T lymphocyte function [46] (Box 3.6).

Box 3.6 In a Nutshell: Non-homologous End-Joining

- The NHEJ pathway plays a crucial role in the repair of DNA DSBs generated endogenously and by IR.
- NHEJ has less fidelity in repair than HR and may therefore in certain circumstances cause mutations.
- NHEJ deficiency results in increased radiation sensitivity.
- Some of the NHEJ pathway components, e.g., DNA ligase IV, are essential for NHEJ repair, while others are required for efficient repair of certain subsets of DNA DSBs.
- NHEJ components, e.g., DNA-PKcs, offer a target that can be used for radiation sensitization purposes in various tumor types.

3.3.4.3 Alternative DSB Repair Pathways

Cells fundamentally utilize two conventional mechanisms to repair their DSBs, i.e., the HR and the NHEJ pathways. However, in recent times, a third pathway is discovered which is known as the alternative NHEJ (alt-NHEJ or aNHEJ), microhomology-mediated end joining (MMEJ), and B (backup)-NHEJ. This is an extremely error-prone pathway that operates in NHEJ-proficient as well as -deficient cells. Unlike HR, this pathway does not require any long homologous DNA templates and is therefore called as "alternative end-joining" pathways. This mechanism typically but not always depends on the microhomologies that exist at or near the DNA DSB ends, which implicates that it might not be completely divergent from the mechanism of HR. The junctions of this repair pathway demonstrated overlapping microhomologies of 3–16 nucleotides as well as nucleotide deletions. Earlier, it was known that the NHEJ pathway could recover short microhomologous region of up to five nucleotides in mammalian cells. However, the alt-NHEJ can operate even in the NHEJ-deficient cells [47]. It is a unique pathway that is seen to be ongoing throughout the cell cycle but found to be augmented in the G2 phase when compared to the G1 phase. Although it is arguable if there are other alt-NHEJ overlapping pathways, there is evidence of a microhomology-mediated end joining (MMEJ) that involves the arrangement of microhomologous series on the inner side of the broken ends prior to fusion and is linked with deletion adjoining the original DSB. This is also an error-prone pathway leading to chromosomal translocations.

One of the characteristics of alt-NHEJ is the excessive deletions and frequent microhomologies at the junction, while such microhomologies are not always present. The exclusivity of alt-NHEJ products implicates the usage of end resection-promoting enzymes, their association of proteins that get benefitted from the microhomologies that can support the intermediates to stabilize, nucleases competent of eliminating the noncompatible 5′ and 3′ overhangs, and finally ligation. The MRE11 complex and CtIP in end resection are known to facilitate the alt-NHEJ, and DNA ligase III emerges to uphold the ligation step.

It is observed that the microhomology-mediated DNA repair proceedings take place via RAD52-dependent single-strand annealing (SSA)-type machinery where the minimum SSA-dependent DSB repair lies between 5 and 29 base pairs of homology. In this mechanism, it is mandatory to have direct repeats on both the sides of the DNA break. Since SSA does not involve any strand invasion events, it is independent of RAD51. As MMEJ depends on the already existing microhomologies around the break, its probable mode of action is associated with SSA. Finally, for the sealing event, MMEJ depends on ligase III [47].

3.4 Importance of Chromatin Architecture (at Nano- and Microscale) in DNA Damage and Repair

3.4.1 Multifaceted Importance of Chromatin Architecture in DNA Damage Induction and Repair

Although repair processes have been intensively investigated for decades, many principal questions concerning the mechanisms of radiation DNA damage induction and repair remain open [reviewed in the work of Falk and Hausmann [48]]. Chromatin in the cell nucleus is arranged into numerous hierarchical levels (Fig. 3.12) from micrometer to nanometer, which leads to the formation of a three-dimensional (3D) architectural chromatin network.

This network is dynamic and influenced by the cellular status and ongoing processes in the cell nucleus. Chromatin architecture is precisely regulated by physical and biochemical regulation systems and, in turn, regulates global and local genome functions. Local chromatin arrangement thus both reflects and determines the functions of the particular genetic locus, such as its transcriptional activity. Importantly in the context of radiobiology, nonrandom chromatin architecture seems to co-determine the response of cells to irradiation in numerous ways: First, in a tight interplay with physical characteristics of the radiation, functional chromatin structure states increase or decrease DNA susceptibility to DNA damage induction. Second, the chromatin architecture acts as an additional level of DSB repair regulation, cooperating with "standard" biochemical genetic and epigenetic regulation systems. Chromatin architecture may regulate DSB repair at individual DSB sites and also globally, via tuning the transcription intensity of genes involved in DNA repair and other processes related to the complex response of cells to radiation DNA damage (e.g., cell cycle progression or apoptosis). Theoretically, chromatin architecture might collect and unify

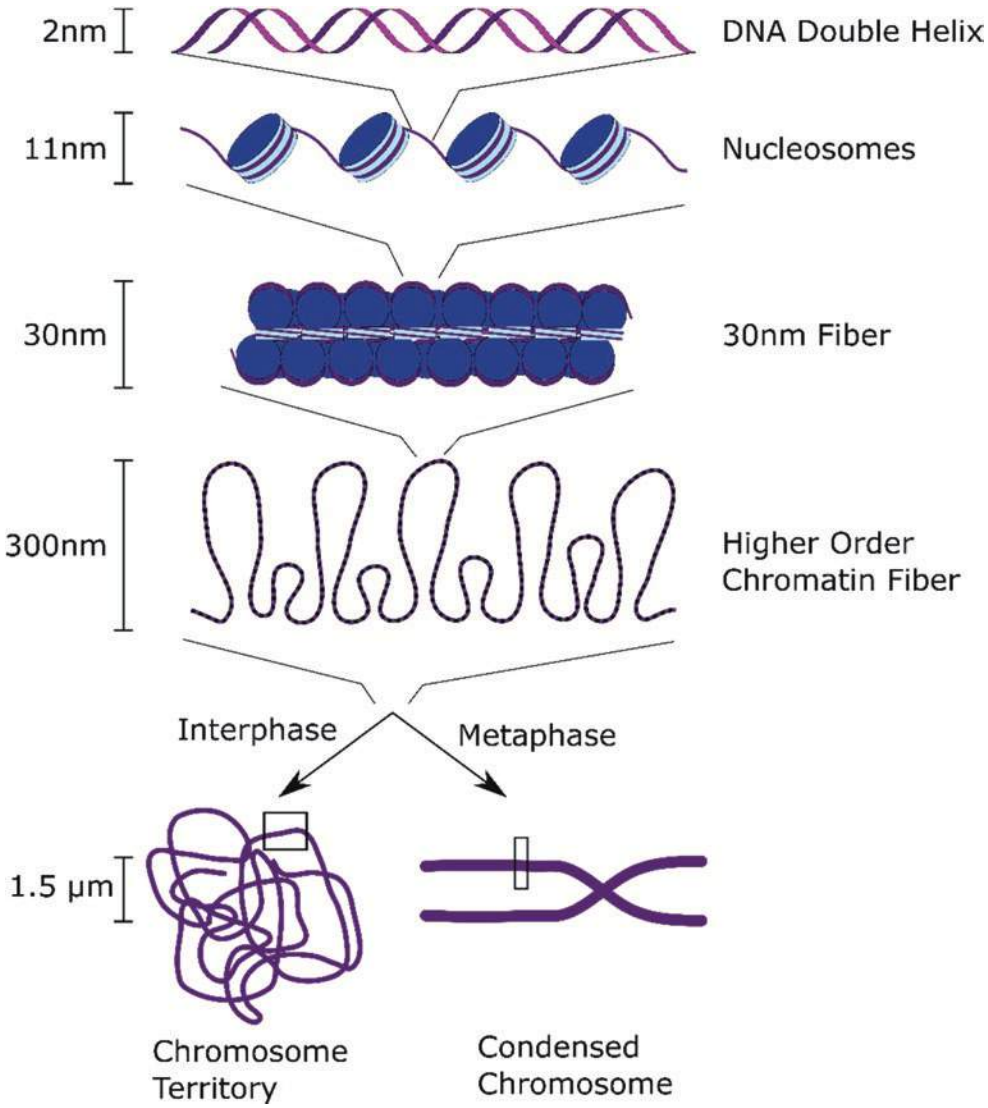

Fig. 3.12 Structure of DNA organization. The DNA forms a double-helix structure, which is wrapped around histones forming so-called nucleosomes. The nucleosomes form complex fibers of 30 nm size, which themselves form the higher order chromatin fibers, which are in the range of 300 nm. In the interphase, these fibers build the chromatin territories, where territories from different chromosomes can overlap, forming so-called networks. In the metaphase, the higher order chromatin fibers are condensed to form chromosomes. (Adapted with permission (CCBY) from Liu et al. [40])

signals of other different signaling networks (biochemical, epigenetic) and transfer these heterogeneous signals into single integrated output signal represented by a specific architectural status of the chromatin network that can be easily interpreted by the cell. Chromatin architecture might thus impersonate a "roofing" regulatory system based on simple physical laws, which allows for a sufficiently fast decision-making process for the optimal repair mechanism at each individual DNA damage site.

Different types (low LET vs. high LET) of IR interact with chromatin in specific ways. Therefore, the relationship between the radiation quality, architecture of structurally and functionally distinct chromatin domains, and DSB induction, repair, and misrepair play a role in the cellular radiation response. Genetically active, decondensed euchromatin and mostly inactive, condensed heterochromatin are the two traditionally recognized structurally and functionally distinct chromatin domains, which affect radiation response. However, it should be noted that radiation response differences may be even more prominent for other chromatin architectural and functional counterparts [49], such as RIDGE (regions of increased gene expression) and anti-RIDGE domains [50], which have even more precisely defined function and more homogenous architecture as compared to euchromatin and heterochromatin (Box 3.7).

Box 3.7 In a Nutshell: Importance of Chromatin Architecture

- DNA is organized in structural units ranging from micrometers to nanometers, forming 3D chromatin architecture.
- Chromatin architecture is a key factor determining local damage induction by radiation.
- Chromatin architecture operates with genetic and epigenetic regulatory factors orchestrating DNA damage response.

3.4.2 DNA Damage and Repair in the Context of Chromatin Architecture at the Microscale

DNA damage and repair processes can be related to specific cell states and chromatin architectures. The spatiotemporal sequence of repair protein binding to DSB and surrounding phosphorylated and thus activated H2AX histone (called γH2AX) sites can be analyzed using microscopy (Fig. 3.13). The analysis of the formation and subsequent dissociation of repair complexes, and the structure of these complexes, brought deep insights into the mechanisms of the two main DSB repair pathways in human cells, nonhomologous end-joining (NHEJ) and homologous recombination (HR)—as discussed above.

The most obvious architectonical chromatin types are condensed (hetero)chromatin with only a low number of active genes and decondensed (eu)chromatin, which is generally considered as genetically (transcriptionally) active. It has been shown that condensed chromatin protects DNA from free radicals generated by ionizing radiation [51], but, at the same time, it is this condensed architecture and a high content of repetitive sequences that complicate and slow down the repair of DSBs located in heterochromatic domains. The protective function against free radicals of the heterochromatic status does not seem to simply result from high condensation of heterochromatin domains but rather from a high amount of proteins that specifically bind to heterochromatin and interact with radiation-induced free radicals before they can damage DNA [51]. However, if a DSB occurs in heterochromatin, its condensed architecture must decondense first in order to allow the formation of huge repair complexes and continuation of repair processes [52]. Moreover, numerous studies indicate that the slower repair of heterochromatic DSBs not only reflects this necessity for the decondensation of a damaged chromatin domain but also points to a slower repair mechanism, specifically homologous recombination (HR) [48]. HR in heterochromatin could be superior over NHEJ for numerous structural reasons and therefore preferred by the architecture of heterochromatin domain; however, at the same time, repetitive sequences present in heterochromatin are a clear contraindication for this repair mechanism. This paradox can be again explained and overcome by the already described heterochromatin decondensation at the beginning of repair. The RAD51 recombinase, which is responsible for complementary DNA strand search and exchange, can bind to heterochromatic DSB sites only upon heterochromatin decondensation and protrusion of a DSB to the domain surface, which ensures spatial separation of the damaged DNA ends from repeats remaining embedded within the heterochromatin domain. HR is thus evidently regulated by chromatin architecture changes, which also ensure the fidelity of this repair mechanism [48]. It remains unknown whether NHEJ or other repair pathways are also associated with some specific chromatin architecture requirements and rearrangements, similar to HR. However, some recent studies suggest that epigenetic and structural regulations are involved in repair pathway selection at individual DSB sites, as it is discussed later. The key properties of hetero- and euchromatin as mentioned here are summarized in Table 3.3.

A serious consequence of irradiation is the formation of chromosomal aberrations, and the chromatin architecture significantly participates in this process. The severity and complexity of the genetic damage are related to the complexity of the underlying DNA damage. The connection between dam-

Table 3.3 Properties of hetero- and euchromatin

Heterochromatin	Euchromatin
Condensed DNA	Decondensed DNA
Low amount of active genes	Transcriptionally active
Protection of DNA from radicals through condensed structure and high amount of radical catching proteins clustering around DNA	No radical protection
	No decondensation necessary and therefore fast repair
Slow repair due to necessary decondensation	No preference of repair mechanisms defined by chromatin architecture
Homologous recombination superior to nonhomologous end joining	

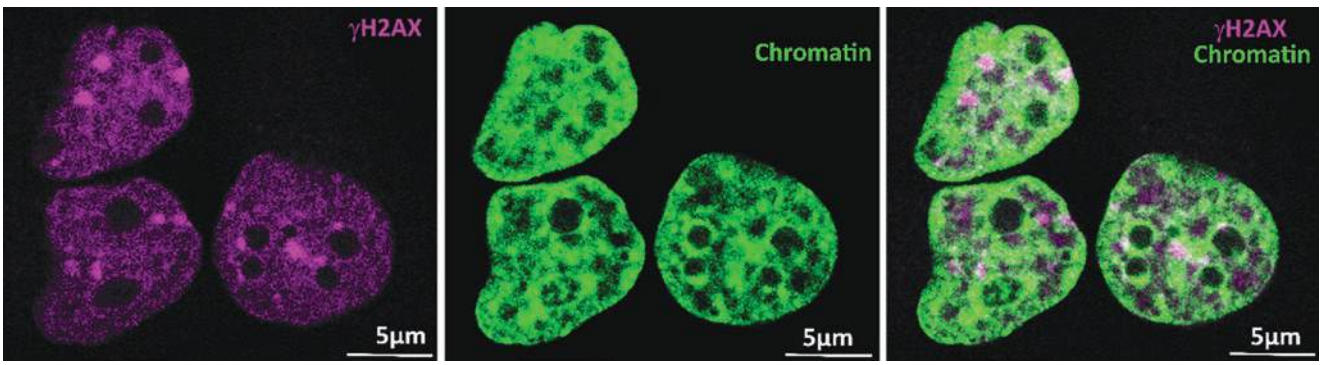

Fig. 3.13 Localization of DNA damage on chromatin: radiation damage induced by high-LET alpha particle radiation microscopically visualized by γH2AX as a biomarker for double-strand breaks (left, magenta), chromatin labeling (middle, green), and merge of the two (right)

age complexity and radiation type was discussed in Sect. 3.2. An additional factor defining the complexity is the chromatin state, and radiation interacts with this. These interactions can be illustrated on the example of chromosomal translocation formation upon irradiation of euchromatin and heterochromatin with low-LET and high-LET radiation, respectively. The type of radiation, chromatin architecture, and consequently initiated DSB repair processes participate in a specific way in free DNA-end misrejoining (review [53, 54]).

The probability of a chromosomal translocation formation between two specific genetic loci, i.e., the linking of the ends of different chromosomes after induction of DSB in both chromosomes at the same time, depends on spatial (3D) separation of these loci in the cell nucleus. Chromatin is non-randomly organized in the cell nucleus, though on the probabilistic basis, this means that chromosomal translocations between some genetic locus pairs appear more frequently than translocations between other pairs. This expectation was confirmed by experiments with interphase cells exposed to neutrons or high-LET particles where translocations appeared most frequently between the neighboring chromosomal territories or even genetic loci statistically located in close proximity [55]. Overall, there are two hypotheses used to explain the processes related to repair of DSB in the context of chromatin organization:

1. Position-first hypothesis: It considers DSBs as immobile structures and emphasizes the role of (preset) chromatin architecture in determining the probability of a chromatin exchange between two specific genetic loci.
2. Breakage-first hypothesis: It considers DSBs as mobile and gives the chromatin architecture a subsidiary role.

Both hypotheses explain different phenomena occurring. While the position-first hypothesis works well in explaining the enhanced probability of translocations to be formed by neighboring chromosomes, it does not allow chromatin exchanges between spatially more distant genetic loci, though such translocations were experimentally observed. Furthermore, although complex chromosomal translocations are only occasional events upon cell exposure to photonic (low-LET) radiation, they do occur. As DSBs are dispersed through the cell nucleus and thus spatially separated in cells irradiated with low-LET radiation, formation of complex translocation between three or more DSBs can hardly be explained without involving DSB movement. Both observations can be explained by the breakage-first hypothesis. However, the idea of highly mobile chromatin at DSB sites in cells exposed to low-LET radiation, where chromatin is not locally fragmented as in cells exposed to high-LET particle radiation, has not been generally confirmed. The explanation of this paradox came with the spatiotemporal tracking of individual radiation-induced protein accumulations (foci) [52], showing the majority of "immobile" DSBs accompanied with a small proportion of highly mobile DSB lesions or by subdiffusive nature of DSB loci [56]. The increased mobility correlated with DSB localization in heterochromatin and can thus be attributed to chromatin decondensation at the beginning of heterochromatin repair process, leading to the protrusion of DSBs onto the surface of heterochromatin domains. Numerous DSBs thus accumulate in nuclear subcompartments of a limited volume, which increases the probability of their mutual interactions and consequently chromatin exchanges even among multiple DSBs.

After irradiation with high-LET particles, on the other hand, locally concentrated energy deposition causes serious chromatin fragmentation and mobilization within cell nucleus micro-volumes along the particle tracks. This situation allows mutual contacts of many short chromatin fragments from one or several neighboring chromosomes and thus easy formation of complex chromatin translocations, irrespectively of the original chromatin architecture and chromatin architecture changes during repair. Chromosomal translocations in cells exposed to high-LET radiation thus occur due to physical rather than biological (repair) processes. We have already mentioned that heterochromatin architecture protects DNA from low-LET radiation as heterochromatin-binding proteins prevent DNA interaction with free radicals, mostly mediating harmful effects of low-LET radiation. With high-LET radiation, however, most damage to DNA is caused by the direct effect of radiation particles or emitted secondary electrons. In this case, heterochromatin represents a more dangerous chromatin architecture, as particles cannot be stopped by any chromatin architecture and heterochromatin provides more DNA targets per a volume unit compared to euchromatin. Hence, in cells exposed to high-LET radiation, translocations in heterochromatin tend to be more complex than in euchromatin (Box 3.8).

Box 3.8 In a Nutshell: DNA Damage and Repair in the Context of Chromatin Architecture

- Hetero- and euchromatin form different chromatin architectural regions within a cell nucleus resulting in different consequences of radiation damage induction.
- Chromosomal aberrations after low-LET radiation can be explained through the "position-first hypothesis" in combination with chromatin decondensation in heterochromatic regions.
- Chromosomal aberrations after high-LET radiation occur due to physical fragmentation of DNA rather due to biological processes.
- Heterochromatin protects DNA from indirect damage (mainly induced by low-LET radiation) but is more sensitive to direct damage (mainly induced by high-LET radiation).

3.4.3 DNA Damage and Repair Processes at the Nanoscale

Using a variety of tools of super-resolution microscopy and image data computing has revealed that γH2AX foci in cell nuclei exposed to low-LET X-rays are subdivided into several equally sized, functionally relevant clusters. The number of clusters increased with the radiation dose according to the well-known linear-quadratic dependence and decreased at later time periods postirradiation. Calculations of the persistence of homology revealed a highly similar topology of γH2AX and other repair protein clusters, especially when these clusters were closely associated with heterochromatin regions. During the repair period, size and topology of these clusters seem to be maintained as long as they are attached to chromatin at actively repairing DSB sites. These findings suggest a functional relevance of the focus/cluster topology [57].

For instance, while the γH2AX clusters had a typical diameter of about 400 nm–600 m, the MRE11 clusters were smaller (about 200 nm) and usually completely embedded within γH2AX clusters [58]. The sizes of clusters were independent of repair time and cell type. On the other hand, the topological similarity of clusters followed the dynamics of the repair protein interaction with chromatin; that is, binding to damage sites was accompanied by ordering while detachments caused the relaxation of topological arrangements. In contrast, γH2AX and MRE11 clusters spontaneously occurring in the nonirradiated cells (e.g., due to replication defects) did not show this topological similarity.

Recent studies discovered spatial distribution changes of tri-methylated H3K9 histone (H3K9me3), ALU repeat sequences (ALU), or long interspersed nuclear element (LINE)-like L1 sequences, indicating chromatin reorganization or movement and DNA strand relaxation after radiation exposure, followed by recovery during repair [59]. Altogether, described results suggest a functional relevance of chromatin and repair focus nano-architecture in DSB repair process and their regulation (Box 3.9).

Box 3.9 In a Nutshell: DNA Damage and Repair Processes on the Nanoscale

- DNA repair locations marked by γH2AX and 53BP1 are subdivided into functional clusters at the nanoscale, in a manner which is cell type and radiation type specific.
- Other repair protein clusters are smaller and are embedded in the γH2AX and 53BP1 clusters.
- After damage induction, chromatin is reorganized accompanied by DNA movement.
- Chromatin reorganization is recovered during DNA repair.

3.5 Consequences of DNA Damage Misrepair or Unrepair

Lack of repair (unrepair) and misrepair of DNA damage can lead to increased chromosome breaks or rearrangements and mutations usually referred to as a status of genomic or genetic instability (GI). GI is usually associated with loss of cell cycle control, senescence, and cell death and in humans with pathological disorders including premature aging and predisposition to various types of cancer and inherited diseases [60]. On the other hand, GI is also fundamental for evolution and induction of genetic diversity. It is known that genomic integrity is carefully supervised by specific surveillance mechanisms like DNA damage checkpoint, DNA repair, or mitotic checkpoint. A deficiency in the regulation of any of these mechanisms often leads to GI, which can predispose a cell to malignant transformation [61].

3.5.1 DNA Lesions and Repair

In huge DNA molecules in the cell, nucleus genes are present. These genes are responsible for the development and function of the cell and the whole organism, because they code proteins. Due to this fact, unrepaired or misrepaired DNA lesions, which can lead to gene mutations, can promote changes in the structure of the encoded protein or lead to the decrease or complete loss of its expression. The types of DNA lesions occurring were already discussed in Sect. 3.3. Based on the current experimental and theoretical evidence, the most repair-resistant lesions are not the single ones but a combination of them in a short DNA segment of 10–20 bp called clustered damage. Clustered DNA lesions are considered the signature of ionizing radiations especially for particle radiation [45]. Various studies suggest that the probability for a break or other DNA lesion to be incorrectly processed and amended is fairly low when damage is spatially separated but increases drastically when multiple breaks and/or non-break lesions coincide. For an analytical description of DNA repair pathways, the reader can refer to Sect. 3.4. As was already mentioned in Sect. 3.3, the DNA molecule consists of nucleotides (deoxyribose + phosphate group + base), which can be for simplicity named based on the four bases [adenine (A), cytosine (C), guanine (G), thymine (T)]. Thus, the DNA alphabet is a very easy one; it only consists of four letters. These four letters are then combined to give rise to groups of three, which define the amino acids that are then the new alphabet for the translation to proteins. For more details on DNA-to-RNA transcription and RNA-to-protein translation, see for example [62]. Even if the cells have a very sophisticated DNA damage response and repair system, it may happen that not all the damage is removed. A mutation is when a permanent change in the DNA sequence occurs.

Mutations can be divided into somatic or germline mutation in terms of what kind of cell is affected. A germline mutation occurs in a sperm or in an egg and can be passed to offspring. Somatic mutations occur in cells of the body and cannot be passed to next generations. Mutations can also be grouped as point or chromosomal mutations. Point mutations are when a single nucleotide is replaced with another single nucleotide, or deleted, or inserted in a place that it should not be. Point mutations do not always have significant consequences on the encoded protein. For example, as is shown in Table 3.4, the mutation can be silent. This means that even if there is a change in the original DNA sequence, the final product of the transcription will be the same, because there are several combinations of the DNA alphabet that lead to the same amino acid. In other cases, the mutation can lead to the change of the final amino acid (missense mutation) or to the creation of a stop codon (nonsense mutation), which then affects the final protein.

Table 3.4 Point mutations and their consequences

		Point mutations		
	No mutation	Silent	Missense	Nonsense
DNA	TTC	TTT	TCC	ATC
mRNA	AAG	AAA	AGG	UAG
Amino acid	Lysine (Lys)	Lysine (Lys)	Arginine (Arg)	Stop

3.5.2 Mitotic Cell Death, Senescence, Cytoplasmic DNA

Mitotic cell death, also called mitotic catastrophe (MC), is the process when a cell dies during or right after mitosis [63]. It can be triggered by DNA damage and its mis- and unrepair and therefore through radiation. MC can be both a caspase-dependent, regulated and caspase-independent, unregulated pathway of cell death. Some characteristic morphologies can be found in Fig. 3.14a.

Senescence in biology refers to a process by which a cell ages and permanently and irreversibly stops dividing but does not die [63]. The number of senescent cells increases with age, but senescence also plays an important role during development as well as during wound healing and can be triggered by radiation. In culture, senescent cells exhibit a different morphology compared to non-senescent cells, called "fried egg" appearance (see Fig. 3.14b). It was shown that among other features, the radiation dose plays a major role in the induction of either senescence or apoptosis and necrosis. In some cell lines, senescence is the major response to low doses of radiation, whereas higher doses lead to apoptosis or necrosis. In IR-treated tissue, enhanced senescence may lead to pathogenic onsets, such as loss of organ function.

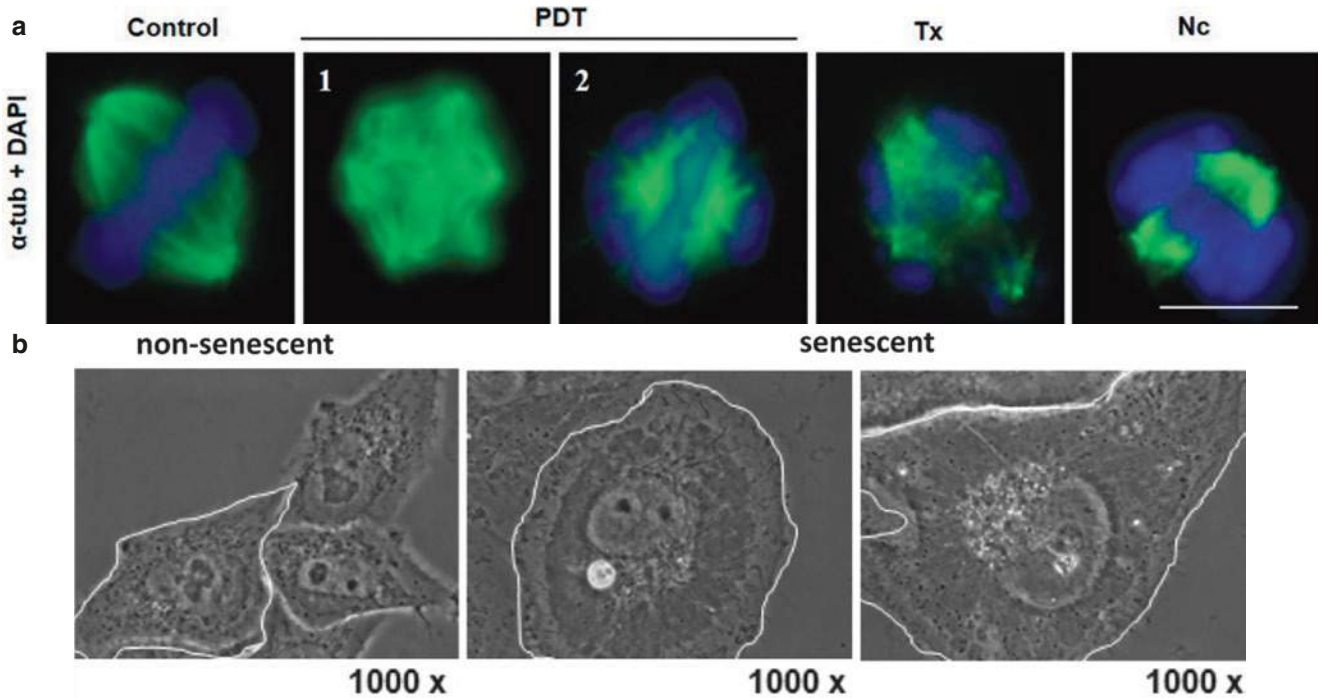

Fig. 3.14 Morphologies of mitotic catastrophe (**a**) and senescence (**b**). (**a**) Fluorescence image of cancer cells undergoing mitosis. The DNA is labeled with DAPI and mitotic spindles using α-tubulin staining. The cells exhibiting mitotic catastrophe are treated with photodynamic therapy (PDT), Taxol (Tx), or nocodazole (Nc). The control shows normal mitotic spindles. The treated cells show various types of altered spindles and mitosis. Scale bar: 10 μm. Reproduced with permission (CCBY) from Mascaraque et al. [64]. (**b**) Phase-contrast images of Chang cells. Senescence was induced using 1 mM of deferoxamine. (Reproduced with permission (CCBY) from Kwon et al. [65])

Recent advances in the field indicate that a further consequence of DNA damage misrepair or unrepair can be the release of cytoplasmic DNA that can also trigger immune responses. In general, it is widely accepted that immune signaling can be activated by the presence of DNA in unusual locations, such as the cytoplasm or the endosomes, as DNA is normally located in the nucleus of eukaryotic cells. Emerging evidence indicates a cross talk between DNA repair machinery and the immune system, and more specifically it has been discovered that DDR factors like DNA repair proteins can enhance innate immune signaling [66]. Defects in DDR and proper processing of DNA damage can therefore trigger a multitude of cellular phenotypes, including autoinflammatory disease, cellular senescence, and cancer. Genotoxic agents such as radiations or high oxidative stress can act as the primary instigators for immune signaling activation through the release of a wide range of biological and chemical factors often referred to as "danger signals" or damage-associated molecular patterns (DAMPs) [67] (Box 3.10).

Box 3.10 In a Nutshell: Consequences of DNA Damage Misrepair and Unrepair

- Genomic instability (GI) collectively refers to a status of increased DNA changes, chromosomal rearrangements, and enhanced tendency for genetic alterations occurring during cell division.
- Unrepaired or misrepaired DNA lesions can lead to chromosomal mutations, which can lead to cell death or loss of genetic material, thus promoting GI.
- Mitotic cell death is the process of a cell dying in relation to mitosis and can be triggered by radiation-induced damages.
- Senescence is the status of irreversible cell cycle arrest, which occurs naturally during aging but can be triggered by radiation, which can lead to pathological onsets.
- Cytoplasmic DNA and DNA repair defects can trigger immune response.

3.6 Cytogenetics and DNA Damage Measurements for Assessment of Radiation Effects

Cytogenetic techniques can be used to analyze chromosomal aberrations in metaphase and morphological abnormalities of DNA content in interphase nuclei. The applicability of these aberrations in the fields of biological dosimetry, clinical cytogenetics, and environmental monitoring is based on a large number of radiobiological and DNA-repair theories.

3.6.1 Micronuclei and Other Nuclear Anomalies

As described before, when cells are exposed to a variety of genotoxic agents (chemical/physical/radiation/DNA-damaging agents), they cause defects in DNA, chromosomes, and other cellular components. Radiation induces extensive DNA damage such as DSBs that, if misrepaired or unrepaired, ordinarily result in asymmetrical chromosome rearrangements and exchanges, which may lead to formation of small chromatinic bodies also known as micronuclei (MN) (see Fig. 3.15). MN are tiny extranuclear bodies that contain damaged chromosome fragments and/or whole chromosomes that were not incorporated into the nucleus after cell division and are surrounded by a membrane. As a variety of genotoxic agents may damage DNA and the mitotic machinery by multiple mechanisms, leading to MN formation, MN are not IR specific.

It is now well established that MN are formed from acentric chromatid fragments caused by misrepaired or unrepaired DNA breaks or lagging acentric chromosomes due to mitotic spindle failure at an anaphase. Additionally, the formation of DNA DSBs and MN is sometimes the result of simultaneous excision repair of damages (e.g., 8-oxo-deoxyguanosine) and inappropriate bases' (e.g., uracil) incorporation in proximity on opposite complementary DNA strands.

A whole chromosome lagging behind (chromosome mal-segregation) during anaphase also results in MN formation. Mal-segregation usually happens due to absence or inappropriate attachment of spindle microtubules to chromosome kinetochore. However, the potential mechanisms behind the formation of MN are hypomethylation repeat sequences in centromeric and pericentromeric DNA, defects in kinetochore proteins or assembly, dysfunctional spindle, defective anaphase checkpoint genes, and malfunctioning in cell cycle control system. Sometimes, mis-segregation events occur when the centromeres of the dicentric chromosomes are pulled towards opposite poles of cells with sufficient forces to detach the chromosome from spindle during anaphase, thus resulting in micronucleus formation from whole chromosome loss.

Furthermore, multiple extrachromosomal acentric double minutes (DMs), cytogenetic hallmarks of genomic amplification, can aggregate after DNA damage and generate cytoplasmic MN that are subsequently eliminated from the cell.

Other nuclear anomalies such as nucleoplasmic bridges (NPBs) and nuclear buds (NBUDs) (see Fig. 3.15) are sensi-

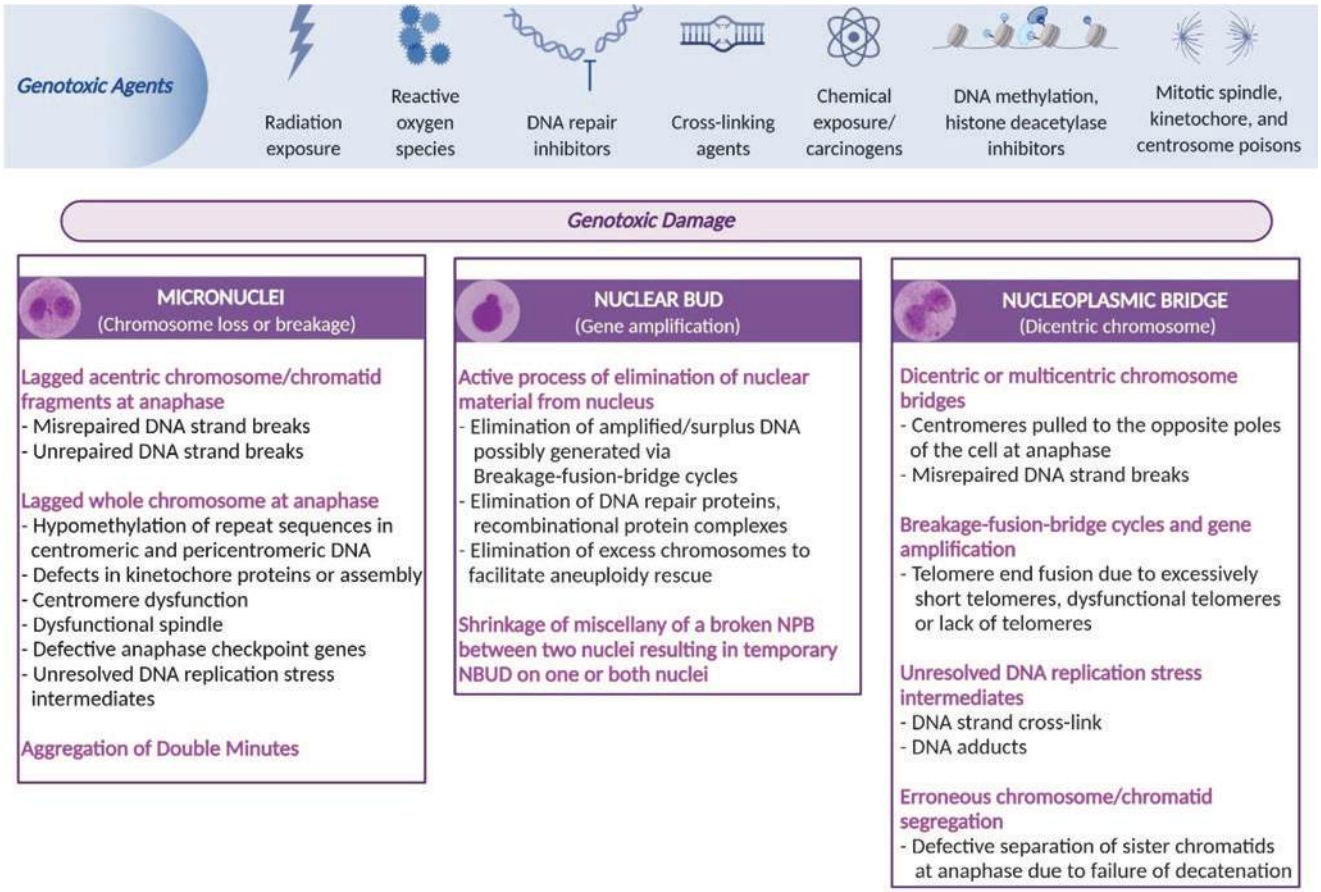

Fig. 3.15 Mechanisms by which genotoxic agents cause micronuclei and other nuclear anomalies. Micronuclei (MN) can originate from lagging acentric chromosomes or chromatid fragments or whole chromosomes at anaphase in mitosis. Nuclear bud (NBUD) formation represents the process of extrusion of the amplified/surplus DNA, DNA repair-recombinational protein complexes, and possibly excess chromosomes from aneuploidic cells. Nucleoplasmic bridges (NPBs) originate from dicentric chromosomes. This arises because the centromeres of dicentric chromosomes are often pulled in opposite directions and defective separation of sister chromatids occurs during anaphase leading to bridge formation, which can be observed as an NPB in telophase

tive and reliable biomarkers for early genotoxic instability and chromosomal breakages and rearrangements. NPBs originate as an aftereffect of misrepair of DNA strand breaks or failure of complete chromatid separation to opposite poles of the cell during anaphase. It can also originate from telomere end-to-end fusion mechanism, a fundamental indication of and a marker for loss of telomere function, which is caused by (a) excessively short telomeres, (b) dysfunctional telomeres due to loss of telomere-binding proteins without telomere erosion, (c) inappropriate assembly of telomere-capping protein structure, (d) defects in recombinational repair proteins, or (e) lack of telomeres. Another distinctive nuclear anomaly, NBUDs, is one of the precursors of MN and is associated with chromosomal instability events. Most NBUDs originate from interstitial or terminal acentric fragments and represent the expulsion of undesirable amplified extrachromosomal DNA content, which localizes to specific sites at the periphery of the nucleus and is eventually eliminated via nuclear budding during the S phase of cell cycle. It is also plausible that NBUDs might occur after elimination of DNA repair-protein complexes in the cytoplasm (Box 3.11).

Box 3.11 In a Nutshell: Micronuclei and Other Nuclear Anomalies

- Micronuclei are small extranuclear bodies surrounded by a membrane that contain damaged chromosome fragments or even whole chromosomes. The genetic information encoded in the MN DNA will get lost and lead to large genomic consequences.
- Chromosome segregation errors and/or fragment loss at anaphase ("inter-cell bridges") and exclusion of acentric fragments from daughter nuclei lead to formation of MN in the cytoplasm.

- Micronuclei occur outside the main cellular nucleus and are prone to rupturing, which leads to changes in DNA that can drive cancer development.
- Extensive DNA damage may cause dicentric/concatenated ring chromosomes and acentric chromatid/chromosome fragments, which can result in the formation of a nucleoplasmic bridge (NPB) at anaphase and micronuclei, respectively.
- Nuclear buds (NBUDs) are the result of elimination of amplified extrachromosomal DNA, which adheres to the nucleus by a thin nucleoplasmic connection, and are observed as double minute-type micronucleus bodies.

Micronucleus assays are frequently used to assess genotoxicity and cytotoxicity of different chemical and physical factors, including IR-induced DNA damage. The cytokinesis-block micronucleus assay can measure MN, NPBs, and NBUDs. A diverse range of reliable micronucleus tests (Fig. 3.16) are executed with different cell types, eventually reflecting chromosomal aberrations, ongoing DNA injury, initial stage in the development of genomic instability, and tumorigenesis. In the widely used cytokinesis-blocked MN assay, MN are scored in once-divided binucleated cells, where cytokinesis is blocked with addition of cytochalasin B, an inhibitor of microfilament ring assembly necessary for the completion of cytokinesis. In order to get statistically solid results, a huge amount of cells need to be scored. Therefore, automatic analysis of MN boosts the reliability of

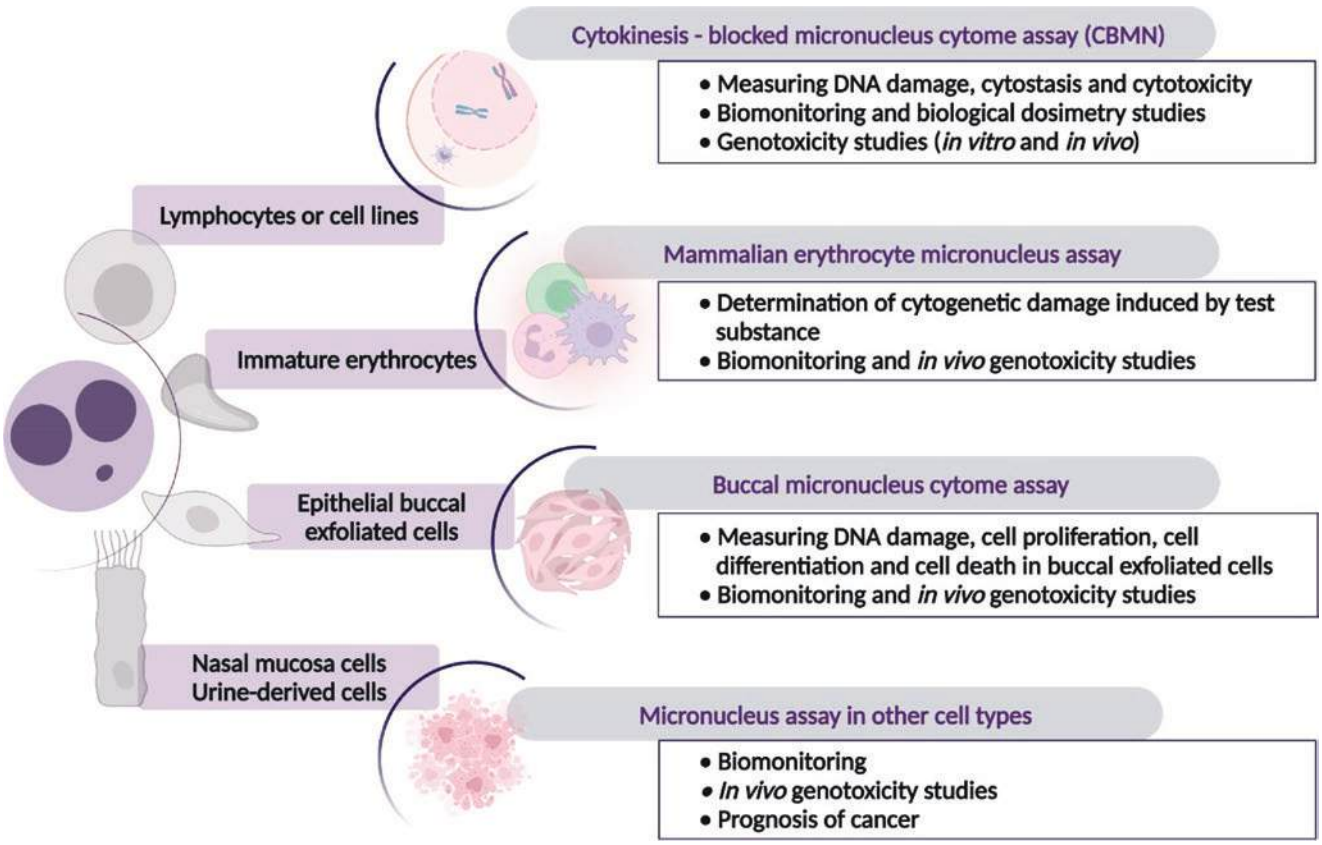

Fig. 3.16 Depending on the cell type, different micronucleus assays can be employed to assess and determine the genotoxicity and cytotoxicity of different chemical and physical factors. Applications of each assay are outlined in their respective boxes. The most popular CBMN assay can be applied to cultured human lymphocytes or cell lines to measure MN and other chromosomal instability biomarkers such as NPBs and NBUD. The mammalian erythrocyte micronucleus assay is performed on immature erythrocytes from bone marrow to determine cytogenetic damage after radiation exposure. The buccal micronucleus cytome assay is done in rapidly dividing buccal epithelial exfoliated cells (oral cavity) to analyze MN and other cytogenetic biomarkers (source of DNA damage, cytotoxicity, etc.). Occasionally, MN assay is performed on nasal mucosa cells or urine-derived cells for detection of chromosomal damage caused by environmental and lifestyle factors, occupational exposures, prognosis of cancer, and certain diseases. Although the objective and method of performance are similar to CBMN or bone marrow MN assays, these tests have not gained much popularity so far

the assays. Concomitantly, it increases the statistical validity after analyzing a large number of cells in one go. Additionally, the existing automatic/semiautomatic micronucleus scoring by microscopic systems, by flow cytometry and imaging flow cytometry, gives high accuracy and sensitivity and leads to rapid analysis (Box 3.12).

Box 3.12 In a Nutshell: The Use of Micronucleus Assay

- Micronucleus assays are used to assess genotoxicity and cytotoxicity of radiation.
- Depending on cell type, different MN assays are used.
- Automated analysis of MN boosts the reliability and statistical validity.

3.6.2 Chromosomal Aberrations

Chromosomal mutations, also called chromosomal aberrations (CA), are observed at the first mitosis after irradiation and are those that incorporate chromosomal changes, such as deletions, inversions, insertions, substitutions, duplications, or translocations of parts of chromosomes. For better understanding, some types of mutations are shown in Fig. 3.17.

The mutations shown can also lead to other aberrations. Three which should be mentioned are dicentric and ring chromosomes as well as acentric fragments as shown in Fig. 3.18. A dicentric chromosome is created when two chromosomes with two centromeres are fused. In metaphase, they are visible as one chromosome with two centromeres. This aberration will most likely die during mitosis. Acentric fragments are either fragments of a single chromosome or fused parts of different chromosomes containing no centromere. A ring chromosome is a chromosome which has two breaks on the opposing ends and is fused to form a ring. Both aberrations cannot be pulled into a daughter cell and most likely will, together with the encoded genetic information, be lost during mitosis [68]. According to the severity of the chromosomal aberration, the cell will more likely die; in some cases, it can get transformed to a cancer cell or, in case of germ line cell or a cell in early embryogenesis, several genetic disorders can occur [69]. For a more detailed view on this, refer to Chaps. 2 and 7.

The frequency of radiation-induced CAs rises with increasing radiation dose to the cells. Different types of CAs depend on the phase of cell cycle at which the nucleus is exposed to irradiation. Chromosome-type aberrations (Table 3.5) occur when pre-synthetic phase (G_1) is exposed to irradiation, while chromatid-type aberrations (Table 3.6) appear if irradiation occurs during post-synthetic phase (G_2). In chromosome-type aberrations, more than one break is unable to rejoin at the correct ends that often results in abnormal chromosomes. There is much hidden damage present, some of which is transmitted to future cell generations. In

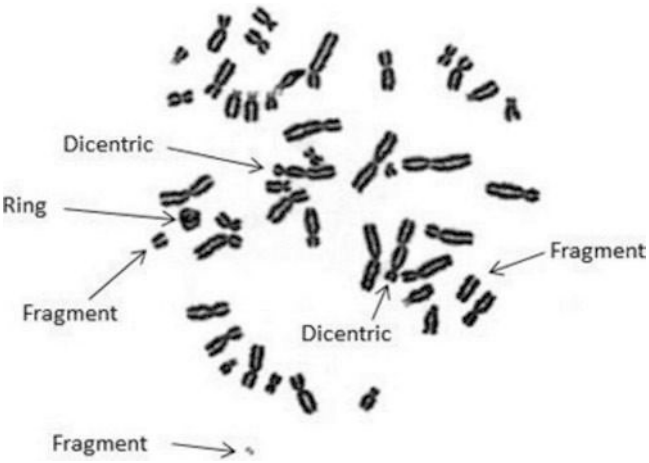

Fig. 3.18 Human metaphase cell irradiated with 5 Gy gamma rays. Two dicentric chromosomes, three acentric fragments, and a ring chromosome could be found. From https://www.qst.go.jp/site/nirs-english/1369.html (accessed 05/2022)

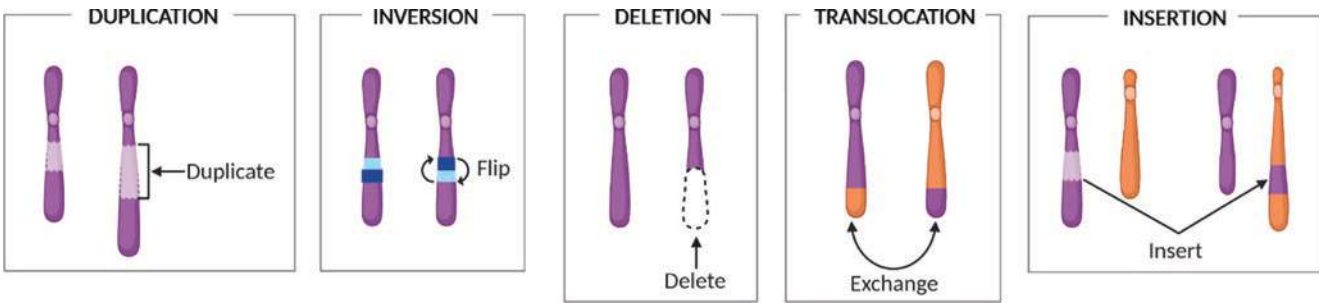

Fig. 3.17 Types of chromosomal mutations. Nonlethal aberrations are observed at the first mitosis after irradiation. Duplication: one or more copies of a DNA segment/a region of a chromosome are formed. Inversion: A segment of a chromosome breaks off and reinserts in reverse orientation within the same chromosome. Deletion: A part of a chromosome/one or more nucleotides from a segment of DNA are missing or deleted. Translocation: It involves two chromosomes in which a piece of one chromosome breaks off and rejoins to another chromosome. Insertion: A segment of one chromosome is removed and inserted to another chromosome or the same chromosome

Table 3.5 Chromosome-type aberrations

Dicentrics	When G1 phase is exposed to irradiation, it causes chromatid breaks in two different chromosomes, which rejoin during S phase and can be seen as dicentric at M phase. Two centromeres in one chromosome appear in dicentrics via breakage-fusion-bridge cycle. These are relatively easy to detect and the main aberration used for biodosimetry
Chromosomal gap	Random achromatic lesions can occur at both the chromatids of a metaphase chromosome, which can be visible as non-stained/lightly stained thinner region. The width of this region is less than the width of chromatid arm
Acentric chromosomal fragments	When single or double breaks occur in the same chromosome arm, either at the end of a chromosome or between centromere and telomere region, it will produce terminal or interstitial acentric fragments, respectively. These acentric chromosomal fragments (without centromere) are lost during anaphase. These are generally associated with dicentric chromosomes
Ring chromosome (centric ring/ acentric ring)	Usually, they result from two terminal breaks in both chromosome arms (chromatids), followed by fusion of the broken ends together to form a circular (centric ring) chromosome, leading to the loss of genetic material. Alternatively, the subtelomeric sequences or telomere-telomere fusion with no deletion also results in complete acentric ring chromosomes
Terminal and interstitial deletion (excess acentrics)	A terminal deletion is the loss of the end of a chromosome (telomere), leaving longer acentric fragment than the width of the chromatid. Interstitial deletion occurs when two breaks are induced in interstitial region and the terminal part rejoins the main body of the chromosome, generating double minutes as acentric fragments
Reciprocal translocation	Reciprocal (complete or two-way) translocations involve non-acrocentric chromosomes, and it occurs when two different (nonhomologous) chromosomes have exchanged segments with each other
Marker chromosome	Marker chromosomes are often referred to as mysterious supernumerary piece of chromosomal material. In addition to normal chromosomes, these are small additional structurally abnormal metacentric/centric chromosome fragments whose genetic origin is unknown; however, it can be determined by FISH analysis using specific probes

Table 3.6 Chromatid-type aberrations

Chromatid gaps (achromatic lesions)	Chromatid gap is a non-staining or very lightly stained region (achromatic lesion) of a single chromatid in which there is a minimal misalignment of the chromatid. The width of this region is less than the width of chromatid arm
Isochromatid deletions	The double breaks (often called isochromatid breaks) at the same position on both chromatids are an apparent exception to the definition of chromatid aberrations. They may be induced upon irradiation in the S and G_2 phases of the cell cycle *Isochromatid deletions with complete and incomplete sister union (SU)*: The side-by-side ends of isochromatid breaks usually undergo a cross union to produce U-shaped fragments *Isochromatid deletion without unions (NU: nonunions)*: Occasionally, the sister union does not occur and such sister nonunions may be in either the proximal (centric) or the distal (acentric) fragments. They are cited as NUp (nonunion proximal) and NUd (nonunion distal), respectively
Terminal and interstitial deletion	Loss of terminal end of one of the chromatids of a chromosome
Symmetric interchanges	Symmetrical chromatid exchanges are equivalents of chromosome-type reciprocal translocation. Exchanges that yield a balanced interchange of genetic material between two identical sister chromatids (i.e., SCE) with no loss of genetic material and no mechanical problems at mitosis
Asymmetric interchanges	Inter-arm interchanges and asymmetrical chromatid exchanges are equivalents of chromosome-type dicentrics. The segments of chromatids are differently joined up, yielding an acentric and dicentric chromatid
Intra-chromatid exchanges/ intra-arm interchanges	Chromatid exchanges may occur between non-sister chromatids of paired homologous chromosomes or between sister chromatids of a homologous chromosome. These exchanges may result in symmetrical or asymmetrical interchanged forms such as intra-chromatid exchange with centric ring, inter-chromatid exchange with dicentric, pericentric inversion, and duplication/deletion
Triradials	A three-armed configuration occurs when there is an interaction between one chromosome with an isochromatid deletion and a second having a chromatid deletion

contrast, radiation can induce chromatid aberrations during late S and G2 phases, when sister chromatids are being duplicated and the DNA DSBs may result in chromatid breaks (deletions), interchanges, or triradials. Mostly, sister chromatids or non-sister chromatids of homologous chromosomes are affected by all the breaks and rejoins. The chromosomal aberrations serve as a biological dosimeter—an indicator of radiation exposure. Furthermore, radiation-induced CAs delineate an early marker of late effects, including cell killing and transformation.

A series of methods and techniques (Fig. 3.19) have been developing to assess stable or unstable type of CAs in order to evaluate the potential of a test compound (chemical/mutagen/radiation exposure). Human peripheral blood lymphocytes offer unique possibilities to study somatic cell division (in vitro) and thus have been utilized for detection of CAs (Box 3.13).

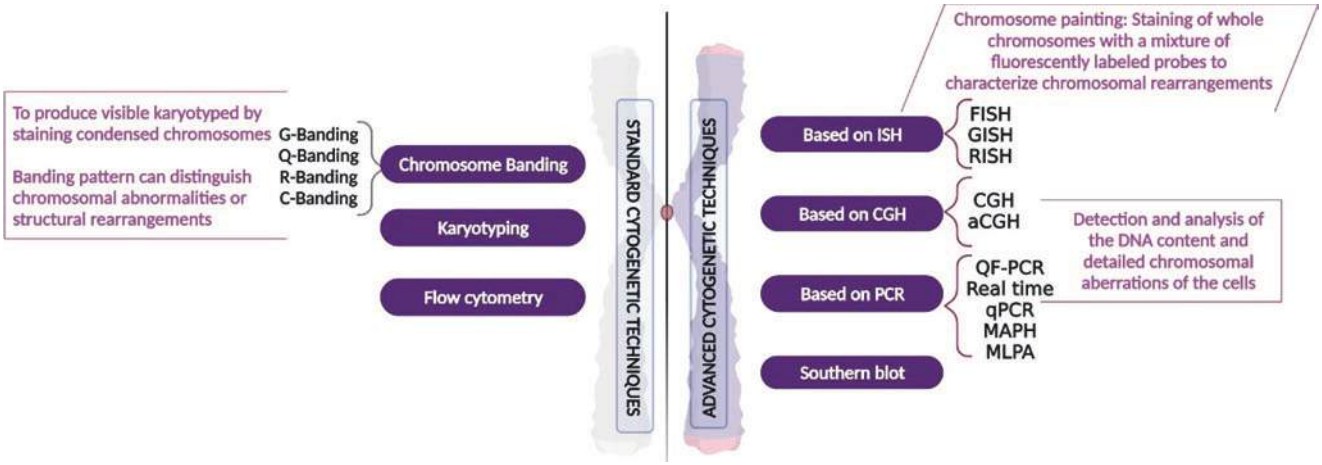

Fig. 3.19 Techniques to assess constitutional or acquired chromosomal abnormalities using standard banding techniques (left) or advanced molecular cytogenetic techniques (right). Standard cytogenetic techniques are traditionally performed by karyotyping of stained metaphase chromosomes or by flow cytometry. Chromosome banding is used to produce alternating light and dark regions, also referred to as "cytogenetic bands," along a chromosome with the use of special stains (abbreviations are listed below). Chromosome banding patterns are essential in pairing and ordering all the chromosomes, known as karyotyping. Flow cytometry-based procedures have been developed to assess numerical (ploidy) and structural (telomere length) chromosomal aberrations in mitotic cells largely based on DNA content. To overcome the limitations of the banding analysis, advanced cytogenetic techniques are introduced. In techniques based on ISH, fluorescently labeled "painting" probes are used to localize nucleic acid sequences. FISH identifies chromosomal rearrangements and mapping-specific genes on individual mitotic chromosomes. GISH determines the origin of genomes or chromatins in hybrids. RISH reveals cellular patterns of mRNA expression in cells. CGH-based techniques provide an overview of chromosome ploidy level (gain and loss) throughout the whole genome. CGH with the use of microarrays—aCGH—detects aneuploidies, deletions, duplications, and amplifications based on DNA content. Southern blotting and PCR-based molecular cytogenetic techniques have good potential to detect chromosomal abnormalities from trace amounts of specific regions of DNA/RNA. *G-banding* Giemsa banding, *Q-banding* quinacrine fluorescence banding, *R-banding* reverse banding, *C-banding* centromere banding, *ISH* in situ hybridization, *FISH* fluorescence in situ hybridization, *GISH* genomic in situ hybridization, *RISH* RNA in situ hybridization, *CGH* comparative genomic hybridization, *aCGH* array comparative genomic hybridization, *QF-PCR* quantitative fluorescence polymerase chain reaction, *qPCR* quantitative polymerase chain reaction, *MAPH* multiplex amplifiable probe hybridization, *MLPA* multiplex ligation-dependent probe amplification

Box 3.13 In a Nutshell: Chromosome-Type and Chromatid-Type Abberations

- Radiation-induced breakage and improper rejoining in pre-replication (G_1) chromosomes may lead to *chromosome-type* aberrations.
- Radiation-induced breakage and inappropriate rejoining in post-replication (late S or G_2) chromosomes may lead to *chromatid-type* aberrations.
- Since the radiation-induced aberrations in G_0 lymphocytes are of the chromosome type, all paired acentric fragments are to be classified as chromosome-type terminal deletions and not isochromatid deletions.
- Unstable aberrations like dicentrics, rings, and anaphase bridges are lethal to cells and not passed on to the progeny. Small deletions and stable symmetric translocations are nonlethal and are passed on to the progeny; thus, they may have genetic consequences.

From the mentioned chromosomal mutations, the translocations are especially dangerous as, in contrast to many other types of chromosomal aberrations, they can be tolerated by the cells. They usually neither cause loss of genetic material nor mitotic cell death and are thus transmitted to the next cell generations. At the same time, translocations are highly oncogenic or affect cell physiology in other ways. Translocations may be simple; reciprocal; i.e., if chromatin fragments are exchanged between two chromosomes; or even complex [70]. Translocations mostly arise due to erroneous DNA end joining by classical NHEJ or mutagenic alternative repair pathways. Although homologous recombination is generally considered a highly precise repair mechanism, recombination between repetitive sequences especially in heterochromatin may also lead to chromatin exchanges [48]. In addition, HR can trigger chromosomal translocations when its intermediates are resolved by crossover between allelic or nonhomologous chromosomes [70]. Although translocations are not associated with extensive losses of the genetic material, they can generate fusion genes (and proteins) with aberrant, often oncogenic, functions. An

example could be the reciprocal translocation t(9;22)(q34;q11) between genes BCR and ABL [71], which is responsible for the development of the well-known chronic myeloid leukemia (for terminology and categorization of translocation types, the reader is referred to specialized books on medical genetics or cytogenetics, e.g., Griffiths et al. [70]). In addition to formation of fusion genes, translocations may activate proto-oncogenes by repositioning them along or between the DNA molecules into a close proximity of a strong promoter of some other gene. If the reading frame of the translocated gene is shifted, its function may be lost. However, the gene activity can be changed also epigenetically, if a gene is moved into an incorrect chromatin environment. This is often a cause of the tumor suppressor silencing, after a tumor suppressor is translocated close to a genetically inactive heterochromatin domain. In the context of radiobiology, it is important to emphasize that cell exposures to different radiation types lead to different types of translocations. Cells irradiated with photonic radiation with low LET mostly contain interchromosomal translocations where one chromatin fragment is translocated to another chromosome or two fragments are reciprocally exchanged between two chromosomes. These lesions are usually simple, but the proportion of complex translocations increases with the radiation dose. Cells exposed to a particle high-LET radiation, on the other hand, mostly suffer from complex chromosomal translocations arising as the consequence of extensive chromatin fragmentation by highly localized energy deposition along the particle tracks [72]. For the same reason, high-LET radiation preferential generates intrachromosomal translocations affecting a single chromosome at multiple sites. To explain this phenomenon, it should be emphasized that chromosomes in the interphase cells occur in the form of chromosomal territories with only a limited extent of mutual intermingling along their borders, as explained in Sect. 3.5. Hence, the areas of chromosome territory borders where translocations between the neighboring chromosomes can be formed represent only a small proportion of the nuclear volume along the radiation particle track [53, 54]. With increasing doses and more particles transversing a single nucleus, however, extensive rearrangements of the genome affecting high numbers of chromosomes can be detected (Box 3.14).

Box 3.14 In a Nutshell: Chromosomal Translocations

- Chromosomal translocations are the consequence of illegitimate rejoining of DNA double-strand breaks generated by radiation.
- Chromosomal translocations pose a risk of formation of a fusion gene/protein with oncogenic functions; even single translocation may be a sufficient genetic defect to initiate leukemia.
- While low-LET radiation generates mostly simple translocations, exposure to high-LET radiation leads to complex genotype rearrangements.
- Due to the character of energy deposition, low-LET radiation produces predominantly interchromosomal translocations; higher occurrence of intrachromosomal translocations is then a sign of a high-LET exposure.

3.6.3 Premature Chromosome Condensation

Chromosome condensation, the landmark event at the onset of prophase, is the dramatic reorganization of the isolated patches of long thin chromatin strands at the nuclear periphery into compact short chromosomes that can be visualized at metaphase during mitosis or meiosis in eukaryotic cells. Maturation-promoting factor (also called mitosis-promoting factor or M phase-promoting factor, abbreviated MPF), the $p34^{cdc2}$/cyclin B complex, serves as a master cell cycle regulator for the M-phase transition and chromatin condensation by phosphorylated condensins (Fig. 3.20). MPF activity mainly depends on the cellular concentration of cyclin B, which usually oscillates through cell cycle. During cell division, chromatin condenses and individualizes to discrete chromosomes, which are further segregated by mitotic spindle fibers. Once divided, chromatin decondenses to re-establish its interphase structure component facilitating DNA replication and protein-making processes.

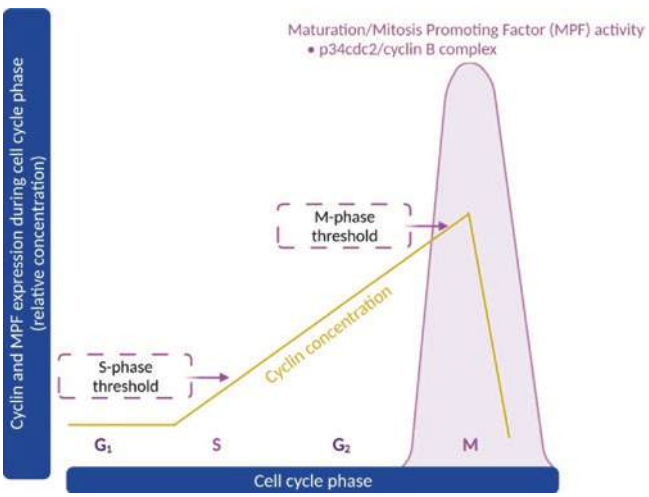

Fig. 3.20 The presence and action of MPF protein in the cell control premature chromosome condensation induction. Cyclin B oscillates through the cell cycle being undetectable during interphase, very low in G1, gradually increasing from S, reaching maximum in G2, and decreasing abruptly at G2/M transition. This corresponds to the MPF activity during cell cycle. *MPF* maturation/mitosis-promoting factor

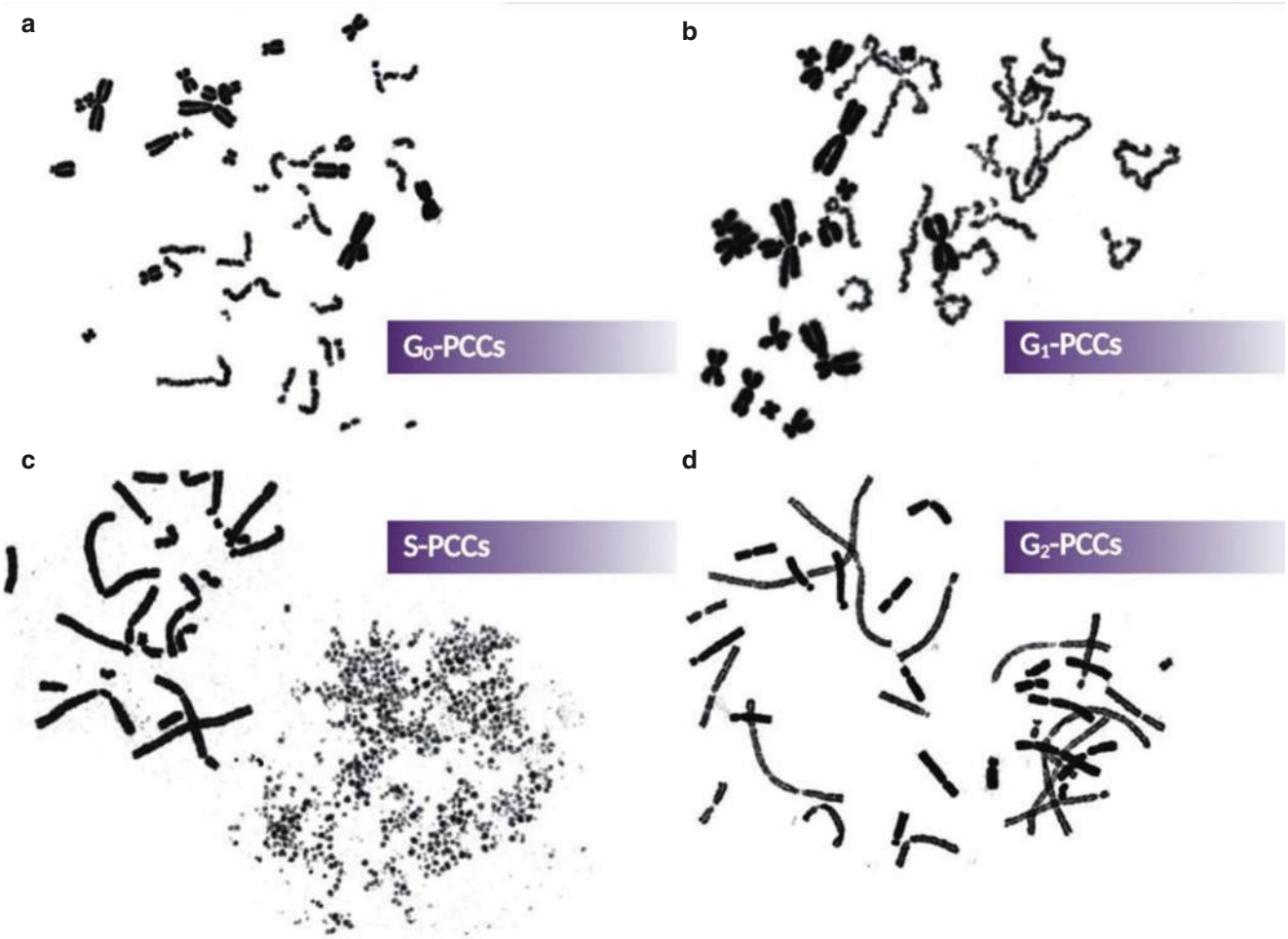

Fig. 3.21 Premature chromosome condensations (PCCs) at various stages of the cell cycle: darkly stained metaphase chromosomes belong to mitotic CHO cells, whereas the lighter stained to the interphase CHO cells. (**a**) G0-PCCs, (**b**) G1-PCCs, (**c**) S-PCCs (reproduced with permission (CCBY) from Pantelias et al. [73]), (**d**) G2-PCCs. *CHO* Chinese hamster ovary

Chromosome condensation may also occur prematurely in interphase test cells when they are fused to mitotic cells or chemically using specific phosphatase inhibitors. The most common approach is the use of Chinese hamster ovary (CHO) cells as mitotic inducer cells. Following cell fusion, the MPF present in a mitotic cell interacts with the interphase nucleus causing dissolution of its nuclear membrane and premature chromosome condensation of interphase chromosomes. This phenomenon is known as *premature chromosome condensation (PCC)*. The morphology of prematurely condensed chromosomes (PCCs) depends on the stage of the interphase cell in the cell cycle (i.e., G_0, G_1, S, and G_2) (Fig. 3.21). PCCs in G_0-phase cells exhibit single chromatids, highly condensed and distinct. During the G_1 phase, G_1-PCCs are despiralized single chromatid chromosomes, while chromosomes condensed during the S phase (S-PCCs) have a "pulverized" appearance because of less condensed chromatin at the sites of replication [73]. Condensation during the G_2 phase (G_2-PCCs) yields distinct elongated double-chromatid chromosomes. Consequently, cell fusion-mediated or chemical induction of PCCs has been proven a powerful cytogenetic tool in radiobiology to study the conversion of radiation-induced DNA lesions into chromosomal aberrations at various cell cycle stages since it enables visualization and quantification of radiation-induced numerical and structural chromosomal alterations directly in interphase cells.

PCC can be induced either by fusion of human lymphocytes with mitotic cells (fusion-mediated PCC) or with the use of specific chemicals (chemical-induced PCC).

In the case of fusion-mediated PCC, the condensation was at first achieved with the use of fusogenic viruses (such as Sendai virus or its equivalent). However, an important disadvantage of this method is that the fusion efficiency depends on various notable factors [74]. These difficulties were overcome by using cell-fusing chemical agents (e.g., polyethylene glycol—PEG). PEG overcomes these difficulties and can be widely used for radiation cytogenetic studies.

Chemical-induced PCC exploits specific inhibitors for serine/threonine protein phosphatase, which can activate endogenous intracellular MPF, which is much simpler and easier than fusion-induced PCC. Chemicals that can be used for the achievement of drug-induced PCC are okadaic acid, calyculin A, 2-aminopurine, staurosporine, wortmannin, and sodium vanadate. A limitation of this method is that no PCC can be induced in G_0 resting-phase cells (Box 3.15).

Box 3.15 In a Nutshell: Premature Chromosome Condensation

- The appearance of a prematurely condensed interphase chromosome depends on the stage of cell cycle.
- PCC can be done in two main ways either by the fusion of human lymphocytes with mitotic cells (fusion-mediated PCC) or by the use of chemicals (chemical-induced PCC).
- G1-PCC displays very long single chromatids; PCC in an early, middle, and late S-phase cell shows crushed and pulverized appearance of both single and sister chromatids; G2-PCC demonstrates still long separated sister chromatids with no clearly visible centromere.
- The dephosphorylated active form of MPF, a p34cdc2/cyclin B complex, promotes chromosome condensation in meiotic and mitotic cells.
- Upon inhibition of protein phosphatase enzymes, cdc25 and cyclin B/cdc2 complex is activated which promotes condensation of chromosomes prematurely.

Because of its unique properties, PCC is used for visualizing and scoring chromosomal damage induced by radiation or other clastogenic agents, measuring the induction yield and repair kinetics of chromosome damage in cells at various cell cycle stages immediately after irradiation. It can also be used for the study of condensation dynamics and conformational changes that occur during the cell cycle. The data obtained using the PCC assay can correlate radiation-induced DNA damage and CAs observable at metaphase [75].

Mitotic cell fusion-induced PCC in human lymphocytes (G_0-PCC) allows early detection of cytogenetic damage in interphase, the stage of human lymphocytes in peripheral blood, and is the most suitable technique especially for biodosimetry applications in radiation emergency accidents as well as for triage biodosimetry [76]. A later ring PCC (rPCC) assay is an alternative biodosimetry method to the "gold standard" cytogenetic approach (dicentric analysis in metaphase) for high-dose exposure to radiation and can be applied in a simulated mass casualty accident either after chemical induction of PCC [77] or by means of cell fusion providing a much faster assessment of dose [78].

3.6.4 Chromothripsis-Like Alterations

During the last decade, it has been reported that high-LET radiation induces chromothripsis-like complex chromosomal alterations, resembling the phenomenon of chromothripsis appearing in tumors [79]. The term chromothripsis arises from the Greek dialect (chromo for chromosome and thripsis for shattering into pieces), and it was initially described in 2011 by Stephens et al. [80]. Rather than a progressive accumulation of sequential alterations induced in the genome, chromothripsis is a process where chromosome segments undergo tremendous but localized shattering and random rearrangements in a single catastrophic event. Inaccurate rejoining of the induced chromosome fragments results in a new genomic arrangement and the formation of complex chromosomal aberrations that may trigger carcinogenesis (Fig. 3.22).

The mechanisms responsible for chromothripsis are still under debate. However, studies have shown several situations that could be catastrophic for the cell and result in chromothripsis. One possible mechanism proposed is that DNA damage such as DSBs and chromosomal aberrations may cause aberrant mitosis and formation of MN including one or more chromosomes that may undergo localized shattering and chromothripsis. Chromosome shuttering and chromothripsis may emerge in MN when the main nucleus enters mitosis while DNA is still being replicated within micronuclei. Additionally, PCC induces a mechanical stress in the asynchronous micronucleated cells leading to chromosome shattering [73]. Random genomic rearrangements in micronuclei can then be integrated into the cell's genome, triggering amplification of oncogenes and cancer development [81]. Other additional mechanisms have also been proposed, such as dicentric chromosome formation, telomere erosion, and abortive apoptosis [82].

Regarding radiation-induced chromothripsis-like chromosomal alterations, it was tested recently whether clustered DNA lesions and chromatin decompaction induced by high-LET irradiation can subsequently evolve in localized chromosome shattering in chromosome domains along the particle tracks. This is a critical risk for chromothripsis to occur, and the results obtained provided experimental evidence that high-LET particle radiation is effective in inducing chromothripsis-like aberrations, which can be used as a fingerprint of high-LET exposure [83]. These discoveries are valuable in the fields of radiation oncology and space radiation protection, since chromothripsis-like aberrations can be responsible for adverse effects and increase the hazard for secondary induced cancer.

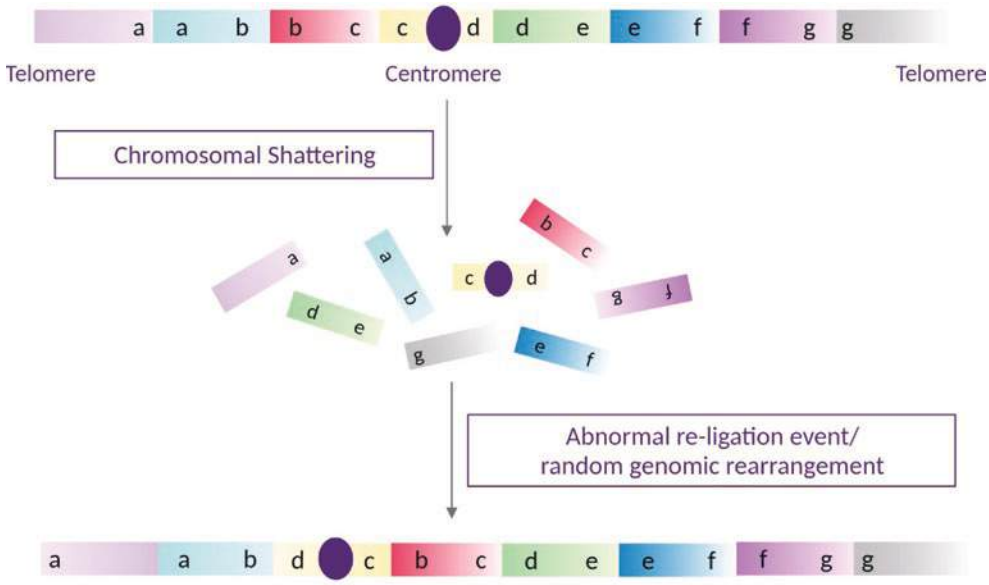

Fig. 3.22 Schematic illustration of chromothripsis. It is a phenomenon where one single catastrophic event leads to a massive and localized shattering of one or few chromosomes. Shattered chromosome fragments are not properly rejoined resulting in a new genome configuration and a large number of complicated chromosomal aberrations

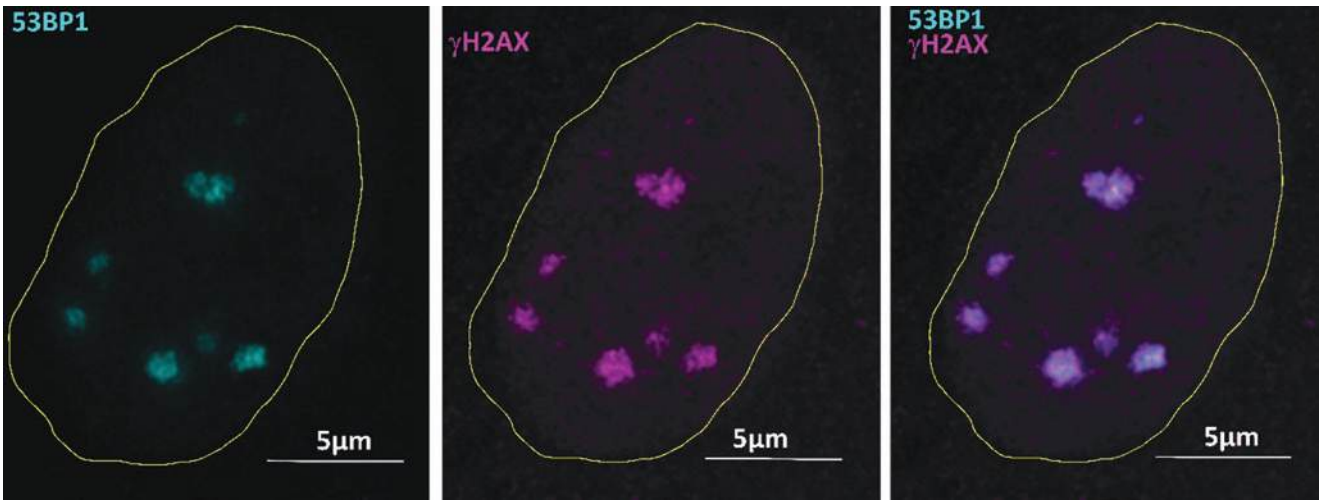

Fig. 3.23 Radiation-induced DNA damage foci. 53BP1 (left, cyan) and γH2AX (middle, magenta) foci in HeLa cells irradiated with 1.2 Gy alpha particles and spatially fixed at 60 min postirradiation. Colocalization of γH2AX and 53BP1 foci is shown (right). Yellow line indicates the cell nucleus

3.6.5 Ionizing Radiation-Induced Foci (IRIF)

This chapter is dedicated to the importance of ionizing radiation-induced foci (IRIF) (Fig. 3.23) in DNA damage measurements. Traditional biomarkers of radiation exposures are chromosomal aberrations and micronuclei. In contrast to quantification of these biomarkers, which emerge due to repair errors in some cells only, IRIF of certain proteins and posttranslational modifications are formed in all cells on all DSB damages, almost immediately after irradiation. Hence, these IRIF can be considered specific biomarkers of DSB lesions [84]. This allows easier and faster victim triage. Moreover, naturally occurring amplification of the DSB damage signal, associated with extensive focal accumulation of γH2AX and numerous repair proteins at DSB sites (for detailed description on DNA repair, see Sect. 3.4), offers the unprecedented sensitivity of radiation dose estimation via the pure counting of IRIF on immunofluorescence microscopy images [84]. The radiation dose absorbed by the cells can be estimated by simple counting of such IRIF or, more automatically, by measuring the integrated intensity of the IRIF signal for high numbers of individual cells by flow cytometry [85]. Under the optimal conditions, especially the time range around 30 min after irradiation, the reported minimal detectable values lie in the range of mGy [86].

Furthermore, DNA damage induction and repair processes can be studied in individual cells using the IRIF assay. In practice, this is important in situations where individual

cells can be differentially affected by irradiation, such as in the cases of a partial-body exposure. The ability to study individual cells is critically important also for radiobiological research as individual cells, even if irradiated homogeneously, appear in different phases of the cell cycle, belong to specific (cancer) cell clones, may be to a various extent affected by the bystander effect, etc.

On the other hand, the biochemical nature of IRIF means that their formation potentially depends on various factors, which may introduce some variability to DSB quantification. It remains a subject of discussion whether all DSBs necessarily require IRIF formation for successful repair. Additionally, some foci may persist at DSB sites even after the break rejoining. A real obstacle could follow from the fact that IRIF occur, to some extent, in nonirradiated cells. However, recent results have proved that the spontaneously forming foci differ in size and topology from the radiation-induced ones. So, staining patterns corresponding, for instance, to replication-stressed or apoptotic cells can be distinguished from IRIF related to DNA repair [87]. Importantly, this phenomenon is more prominent only in cancer cells, which are not relevant for biodosimetry. In any case, "the second γH2AX assay intercomparison exercise" carried out in the framework of the European biodosimetry network (RENEB) confirmed a high fidelity of irradiated victims' triage (dose categorization, rather than dosimetry) based on IRIF detection of the postradiation modification of histone variant H2AX, called γH2AX [84].

γH2AX is formed by the phosphorylation of histone H2AX at ser139 [57]. This process is mediated by ATM, ATR, and DNA-PK kinases, appears in minutes after DNA breakage, and spreads over ~2 Mbps of DSB-surrounding chromatin. Due to this extent of chromatin modification, γH2AX can be microscopically visualized as compact IRIF at DSB sites of 400–600 nm size as described in Sect. 3.5.

The number of γH2AX foci at a particular time postirradiation corresponds to a dynamic equilibrium between the IRIF formation and disassembly as shown in Fig. 3.24. This is the reason why the maximum γH2AX numbers per cell are detected with a short delay after irradiation and the numbers of counted γH2AX are slightly lower compared to physically detected DNA breaks (PFGE, comet assay) [49].

For most cell types, the peak number of γH2AX is detected in the time window between 30 min and 1 h postirradiation on average, and some shift to later postirradiation times may appear in cancer cells as they often suffer from DSB repair defects. If the integrated γH2AX signal is measured by flow cytometry, the maximal values are measured later than with focus counting, at about 1 h postirradiation, as the size of γH2AX foci grows longer than their number [49]. After reaching the peak value, the number of γH2AX foci rapidly reduces (Fig. 3.24) and, at 24 h postirradiation, only few DSBs that are repaired only with difficulty persist in cells irradiated with medium doses (in order of Gy) of low-LET radiation. However, a substantial proportion of DSBs may still be detected at this late period of time or even after several days postirradiation in

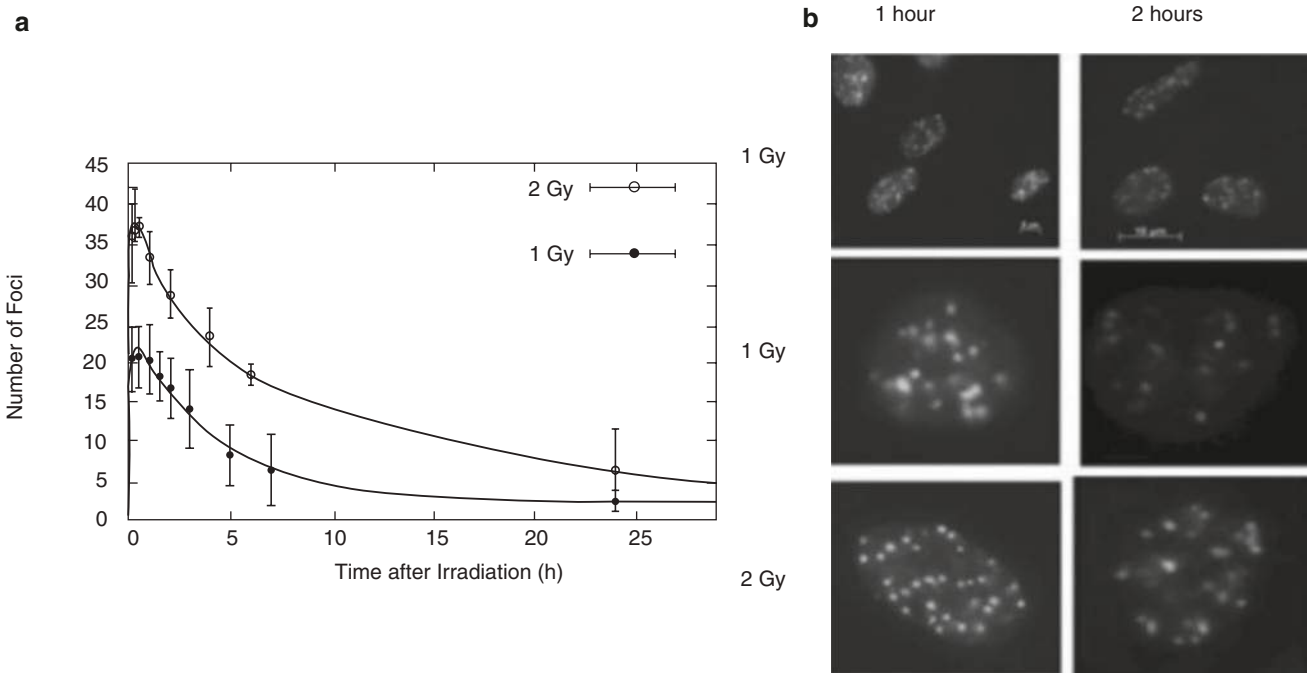

Fig. 3.24 DNA repair kinetics. (**a**) Formation and disassembly of γH2AX foci in human cancer cells irradiated with 1 Gy or 2 Gy X-rays. (**b**) Representative microscopic images for γH2AX foci 1 h and 2 h after X-ray irradiation. (Reproduced with permission (CCBY) from Mariotti et al. [88])

cells exposed to high-LET radiation or high doses of low-LET radiation. From the perspective of biodosimetry, this means that the highest precision of the absorbed dose estimation can be achieved in a few-hour window immediately after irradiation. This requirement can be fulfilled during planned medical care, where, in addition, the monitoring of γH2AX foci formation and disassembly (DSB repair kinetics) may be used to identify patients hypersensitive to radiotherapy or radioresistant tumors. However, in the case of unpredicted accidents with mass screening, IRIF-based biodosimetry must rely on the persistent foci due to the necessary reaction time. This requires suitable mathematical models for the absorbed dose estimation and restricts the method applicability to the acute photon dose range of ~0.5 to ~8.5 Gy and days after exposure (i.e., 1 day after 1 Gy and 14 days after 8.5 Gy) [89]. For military countermeasures, it should also be kept in mind that some chemical warfare agents, such as mustard gas, also generate γH2AX foci. Furthermore, background levels may vary due to non-irradiation-induced IRIF, which are also counted and vary individually, so this assay is best suited for triage rather for accurate dosimetry.

In addition to the analysis of γH2AX IRIF numbers, the spatial distribution of γH2AX foci can be determined by microscopy. This is an important advantage of microscopy over flow cytometry as low-LET and high-LET exposures can be distinguished according to nuclear topology of γH2AX foci [90] as described in Sect. 3.5. On the other hand, flow cytometry offers more room for automation than microscopy and can analyze much higher cell numbers, making it the more suitable method for routine biodosimetry in most circumstances (Box 3.16).

Box 3.16 In a Nutshell: γH2AX as Radiation Damage Marker

- γH2AX IRIF form as the histone H2AX is phosphorylated after DSB induction.
- γH2AX IRIF formation starts a few minutes after irradiation and peaks at 30 min–1 h postirradiation.
- Especially after high-dose irradiation or irradiation with high-LET particles, persistent γH2AX IRIF are left after repair.
- γH2AX IRIF can be used for triage-level biodosimetry by counting foci either in the first hours or persistent foci in microscopic images.

γH2AX attracts numerous proteins with specific signaling and/or repair functions to DSB sites. These proteins, in turn, form IRIF with protein-specific time occurrence and extent of colocalization with γH2AX. Hence, IRIF formed by numerous repair proteins can be used to quantify DSBs and estimate the absorbed dose in the same way as it was described above for γH2AX. Alternatively, repair protein and γH2AX foci can be detected simultaneously to enhance the fidelity of DSB evaluation. Furthermore, the protein composition and structure of IRIF protein complexes (e.g., their specific persistent homology at the nanoscale), and differences of these parameters in specific chromatin domains and after exposure to different types of ionizing radiation, help to understand the mechanisms of DNA repair.

Some proteins like 53BP1 form IRIF morphologically comparable to γH2AX foci. Others, which are required in only a few copies (Ku70 and Ku80), are too tiny and can be visualized only with electron microscopy or super-resolution optical microscopy [91]. Other proteins [such as MRE11, NBS1, or ATM (Fig. 3.25)] create small, but large enough, IRIF to be recognized by standard immunofluorescence microscopy. However, these proteins are, in addition to their IRIF location, also dispersed over the cell nucleus. As IRIF and free aggregates of these proteins may be similar in size, and cannot be discriminated by antibody staining, it is often difficult to reliably distinguish these IRIF from the background [52]. Depending on the function of a particular protein in the repair process, IRIF appear immediately (e.g., MRE11, NBS1, 53BP1) or only later after irradiation (BRCA1, BRCA2, RAD51, etc.). This timing may correspond with repair pathway specificity of a given protein. Some proteins, such as 53BP1 [57], are involved in the regulation of both major DSB repair pathways (NHEJ and HR), while other proteins are selective either for NHEJ or for HR (BRCA1, BRCA2, RAD51).

IRIF of repair pathway nonselective proteins, such as 53BP1, occur in all cells and colocalize with most γH2AX foci [57]. 53BP1 is thus a good DSB marker for biodosimetry, in addition to γH2AX. Moreover, 53BP1 foci have similar size and shape as γH2AX foci so that 53BP1 and γH2AX foci extensively colocalize (Fig. 3.23). This fact improves DSB detection in cells where both types of foci are labeled simultaneously. Co-labeling of γH2AX and 53BP1 foci may be especially useful when cells were exposed to low radiation doses generating only few DSBs or if cancer cells with a strong background signal are analyzed. A significant improvement of DSB number estimation due to γH2AX and 53BP1 co-detection is experienced also in cells exposed to high-LET radiation, where DSBs are extensively clustered and can be thus discriminated only with limitation. However, super-resolution microscopy methods, such as single-molecule localization microscopy (SMLM) or STED microscopy, are necessary for more precise analysis of IRIF foci or even their internal composition and arrangement [48, 57].

It should be noted that not all γH2AX foci necessarily colocalize with 53BP1 (or other repair proteins) at early time periods postirradiation. This includes also the period of 30 min postirradiation when the maximum γH2AX focus

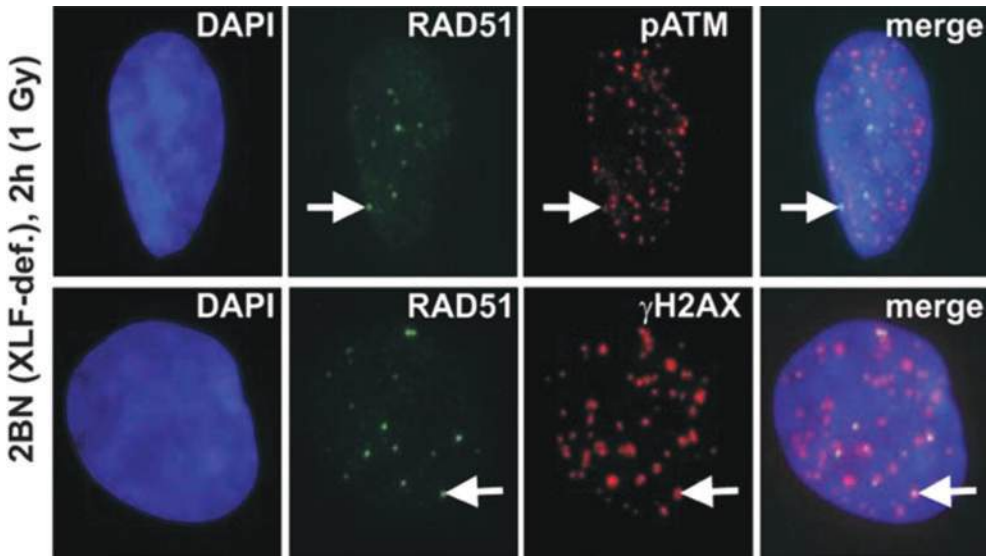

Fig. 3.25 DNA repair protein markers forming small foci. 2BN hTert (XLF-deficient) human fibroblasts were analyzed 2 h post-IR with 1 Gy. Cells were stained against DAPI, pATM, and RAD51, or DAPI, γH2AX, and RAD51. RAD51 is present in a subset of pATM and γH2AX foci. Reproduced with permission (CCBY) from Geuting et al. [92]. *DAPI* 4′,6-diamidino-2-phenylindole used for staining nuclei, *XLF* XRCC4-like factor

Table 3.7 DNA repair proteins and occurrence

Protein/IRIF	Occurrence
γH2AX	All DSB
53BP1	All DSB
NBS1	Part of MRN complex
MRE11	Part of MRN complex
Ku70/80	All DSB
RAD51	Predominantly HR
Brca1	Transition between NHEJ and HR
Brca2	Predominantly HR

numbers are detected. On the other hand, at late time periods after irradiation, 53BP1 foci may persist in cells without being accompanied by γH2AX. These non-colocalizing 53BP1 foci probably label and protect incompletely repaired chromatin [93].

Moreover, as IRIF form also at sites of single-stranded DNA breaks (SSB) or oxidative base damages, co-labeling of γH2AX with suitable markers of these lesions (e.g., XRCC1 or OGG1) [94] can provide information on the complexity of individual DNA damage sites. This information may be correlated to various factors, such as the LET of the incidental radiation or chromatin density and genetic activity at DSB sites [16]. Table 3.7 shows a summary of the IRIF markers mentioned in this section and their occurrence (Box 3.17).

Box 3.17 In a Nutshell: Ionizing Radiation Induced Foci

- Repair protein IRIF, depending on the protein's role throughout repair, can also be used for biodosimetry.
- Repair protein IRIF can be used to understand repair mechanisms and pathways of individual DSB sites.
- IRIF can be used to understand the effect of radiation of different LET.

3.7 Oxidative Stress: Redox Control and Mitochondrial DNA Damage

3.7.1 Oxidative Stress and Consequences for Cell Macromolecules

Exposure to IR induces oxidative damage to cellular molecules such as proteins, lipids, and DNA as a result of oxidative stress (OS), a consequence of the indirect effects of IR (see Chap. 2 and Sect. 3.2), as shown in Fig. 3.26. OS refers to a state of imbalance between oxidants and antioxidants, in favor of oxidants, due to either antioxidant depletion or oxidant accumulation. Oxidants include reactive oxygen (ROS) and nitrogen (RNS) species that comprise free radicals, which are characterized by oneself or more unpaired electrons in the outer shell, and non-radical reactive species. A list of radicals and non-radicals can be found in Table 3.8. Some of these species, e.g., superoxide and hydroxyl radical, are short-lived due to their high reactivity towards other molecules, while others, like hydrogen peroxide, are more stable. Among the ROS, the hydroxyl radical is particularly toxic and involved in the mediation of IR-induced lesions to cell biomolecules. By analogy to OS, nitrosative stress is mentioned when referring to RNS.

Oxidants are produced from exogenous, such as air pollutants, xenobiotics, and IR, and endogenous sources as normal cellular metabolism by-products. Examples are the mitochondrial electron transport chain (ETC), nicotinamide adenine dinucleotide phosphate (NADPH) oxidase, xanthine oxidase, and peroxidases. Low to moderate ROS levels are crucial in physiological function of cell to avoid oxidative stress involved in aging and several neurodegenerative diseases, diabetes, cancer, atherosclerosis, etc. ROS are also signaling molecules involved in the IR non-targeted effects (see Chap. 2).

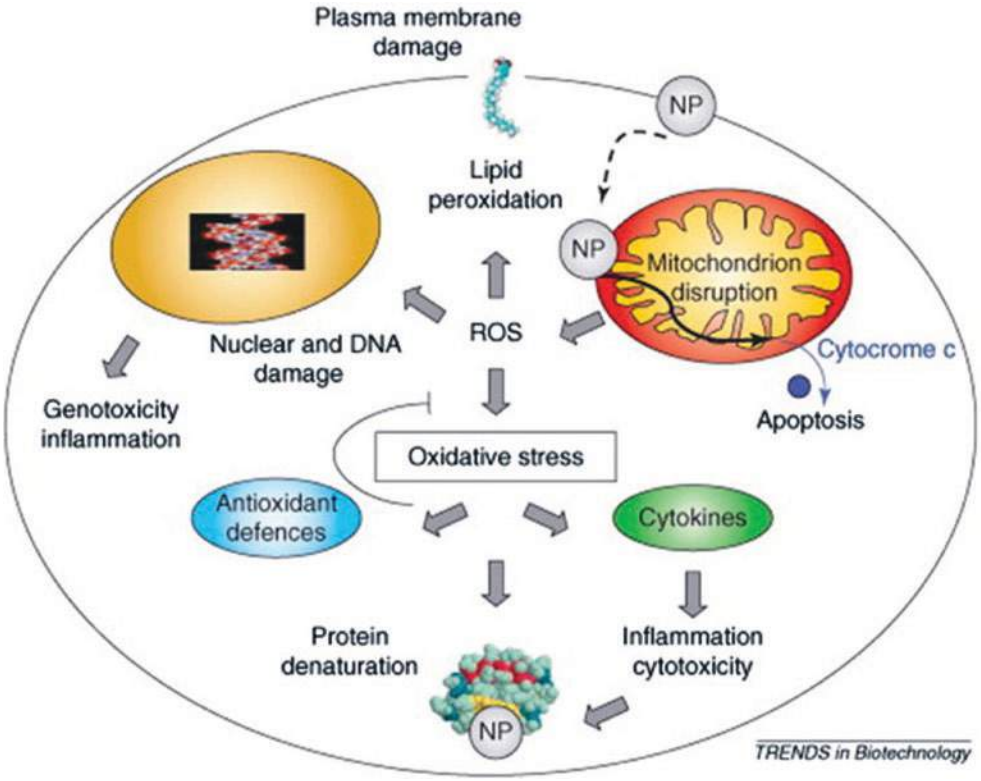

Fig. 3.26 Possible ROS-mediated oxidative stress. Upon exposure to IR, oxidative stress can induce collateral damage, such as lipid peroxidation, protein denaturation, nuclear and DNA damage, mitochondrial damage, and apoptotic death by releasing cytochrome c. Oxidative stress owing to excess ROS generation induces overexpression of antioxidant enzymes in an attempt to control ROS levels. At high levels of oxidative stress, antioxidant defenses are overwhelmed, which leads to inflammatory and cytotoxic responses. (Reproduced with permission from Sanvicens and Marco [95]). *NP* nanoparticles, *ROS* reactive oxygen species

Table 3.8 List of free radicals and non-radicals

Free radicals	Non-radicals
Reactive oxygen species (ROS)	
Superoxide $^{\circ}O_2^-$	Hydrogen peroxide H_2O_2
Hydroxyl °OH	Singlet oxygen $^1O_2$
Peroxyl °ROO	Ozone O_3
Lipid peroxyl LO°O	Hypochlorous acid HOCl
	Lipid peroxide LOOH
Reactive nitrogen species (RNS)	
Nitric oxide °NO	Nitrous acid HNO_2
Nitrogen dioxide $^{\circ}NO_2$	Peroxynitrite $ONOO^-$
	Dinitrogen trioxide N_2O_3

OS occurs in pathologic conditions, when the cellular antioxidant defenses are overwhelmed by free radicals and oxidants. Their great oxidative ability leads to oxidative damages to cellular biomolecules (DNA, proteins, and lipids) resulting in multiple damage affecting cell membrane, cellular signaling, and genome integrity. The accepted radiation biology paradigm considered DNA for a long time as the critical IR target and the primary cause for the harmful effects of IR, due to its content of genetic information, with nucleic acid damage being extensively characterized, without consideration that damaged lipids and proteins may also have detrimental effects on cellular function.

Further targets of radiation-generated ROS are lipids, major constituents of the cell membrane, because of their molecular structure containing abundant reactive double bonds [96]. Upon ROS reaction with polyunsaturated fatty acids (PUFA), chain reactions occur, leading to lipid peroxidation (LP) and generation of toxic decomposition products such as malondialdehyde (MDA), 4-hydroxy-2-nonenal (4-HNE), and isoprostanes (IsoPs), which are quantifiable markers of LP reactions. Biological LP consequences include changes in the permeability and fluidity of the membrane lipid bilayer, ion gradient disruption across membrane, and alterations in membrane-associated protein activity [96].

Potential oxidative damage to proteins is multiple, cysteine, methionine, and tyrosine residues. Chemical modifications include oxidation, carbonylation, and nitration and lead to posttranslational modifications inducing conformational changes affecting protein structure and function, i.e., loss of enzyme activity.

While the physical and chemical reactions initiated by radiation occur in less than a millisecond, the resulting biological effects may take hours, days, months, or years to be expressed and may differ among individuals due to varying intrinsic radiosensitivity. In particular, since the oxidative damage extent depends on the antioxidant availability, increased expression of antioxidant defense systems has been linked to decreased radiosensitivity [97].

OS also has a central role within the inflammatory process. ROS such as superoxide can rapidly combine with NO to form other RNS, such as peroxynitrite, and is 3–4 times faster than the dismutation of superoxide by the SOD. The RNS, in turn, induces nitrosative stress, which

adds to the pro-inflammatory burden of ROS. Injured cells release chemoattractant molecules, and NO increases vascular permeability and vasodilation that trigger local inflammation. Neutrophils are the first inflammatory cells to arrive at the site of injury, and the increased expression of intercellular adhesion molecule 1 (ICAM-1) and platelet endothelial cell adhesion molecule 1 (PECAM-1) on disrupted endothelial surfaces contributes to neutrophil extravasation. When leukocytes come into contact with collagen fragments and fibronectin, they release pro-inflammatory cytokines like tumor necrosis factor alpha (TNF-α), IL-1, and IL-6 that increase ROS production and lead to even greater local inflammation that can perpetuate inducing chronic radiation injury, which in some cases develop into fibrosis [98] (Box 3.18).

Box 3.18 In a Nutshell: Oxidative Stress

- Oxidative stress is characterized by an imbalance between prooxidant molecules and antioxidants.
- Oxidative stress participates in the oxidative damage of cellular components.
- Antioxidants play a key role in stopping the oxidative chain reactions by scavenging the free radical intermediates.
- Excessive generation of ROS, that provokes mitochondrial DNA mutations, impairs the mitochondrial respiratory chain and modifies membrane permeability and mitochondria-associated defense systems.
- Several biomarkers of oxidative stress exist and comprise direct ROS measurement, indirect measure of oxidative stress by quantifying oxidation products, and measure of antioxidant defenses.

3.7.2 Redox Control: Antioxidant Defenses

In order to cope with ROS and RNS, living organisms have evolved essential antioxidant defense mechanisms (Fig. 3.27). These are classified as enzymatic and nonenzymatic systems or as high-molecular-weight and low-molecular-weight compounds. The first line of antioxidant defenses includes the highly abundant glutathione (GSH), catalase, glutathione peroxidase (GPx), and superoxide dismutase (SOD). GSH acts directly as an oxidant scavenger or indirectly as a cofactor of several enzymes such as the GPx. SOD exists in three isoforms using different metals as cofactors: SOD1, which is predominantly cytoplasmic; SOD2, which is mitochondrial; and SOD3, which is extracellular. SOD1 and SOD3 contain copper (Cu) and zinc (Zn), whereas SOD2 has manganese (Mn) in its active site. They catalyze the dismutation of $^{\circ}O_2^-$ to H_2O_2 afterwards converted to water by catalase, GPx, or peroxiredoxin (Prx). GPx transforms reduced GSH to its oxidized form (GSSG). GSH pool regenerates by de novo synthesis and glutathione reductase using NADPH as a reducing equivalent. GPx is also involved in hydroperoxide detoxification. Prx is involved in hydroperoxides and peroxynitrite detoxification, using thioredoxin (Trx) as a source of reducing equivalents. The most reactive and highly toxic $^{\circ}OH$ is produced from H_2O_2 in the presence of reduced transition metal, a reaction known as the Fenton reaction. Apart from GSH, nonenzymatic antioxidants include endogenous compounds which are produced in organism (uric acid, lipoic acid, L-arginine …) and exogenous compounds which are supplemented through the diet, i.e., carotenoids, ascorbic acid (vitamin C), vitamin E and derivatives (tocopherols and tocotrienols), polyphenols (curcumin, resveratrol, quercetin …), and others.

Glutathione is the major low-molecular-weight thiol in mammals. It plays a key role in cell resistance against oxidative and nitrosative damage by providing reducing equivalents to enzymes involved in the metabolism of ROS, by eliminating potentially toxic oxidation products, and by reducing oxidized or nitrosated protein thiols. In its reduced form (GSH), glutathione is the principal intracellular antioxidant. The conversion of the oxidized form (GSSG) into GSH is done by glutathione reductase (GR) in the presence of NADPH, which is generated by glucose-6-phosphate dehydrogenase in the pentose phosphate pathway (Fig. 3.27). Hence, any damages to these enzymes can compromise GSH functions. The processes of glutathione synthesis, transport, utilization, and metabolism are tightly controlled to maintain intracellular glutathione homeostasis and redox balance. Glutathione is exclusively synthesized in the cytosol and about 85% of it remains there, mainly in the reduced form. The ratio of GSH:GSSG in the cytosol is conservatively estimated at about 10,000:1–50,000:1, and the concentration of the cytosolic GSH is as high as 10 mM, while GSSG in the cytosol is as low as nanomolar concentration [99]. Directly and indirectly, GSH effectively scavenges free radicals and other reactive species (e.g., hydroxyl radical, lipid peroxyl radical, peroxynitrite, and H_2O_2) through enzymatic reactions, such as those catalyzed by GPxs, glutathione-S-transferases (GST), formaldehyde dehydrogenase, maleylacetoacetate isomerase, and glyoxalase I (Fig. 3.27). GSH also helps to recover other important antioxidants as vitamin C.

OS was shown to promote the activation of redox-sensitive transcription factors such as the nuclear factor erythroid 2-related factor 2 (NRF2) and the nuclear factor kappa B (NF-κB). The NRF2 transcription factor plays a central role in the maintenance of cellular redox homeostasis via the coordinated transcriptional upregulation of numerous antioxidant proteins (Fig. 3.28). These include more than 500

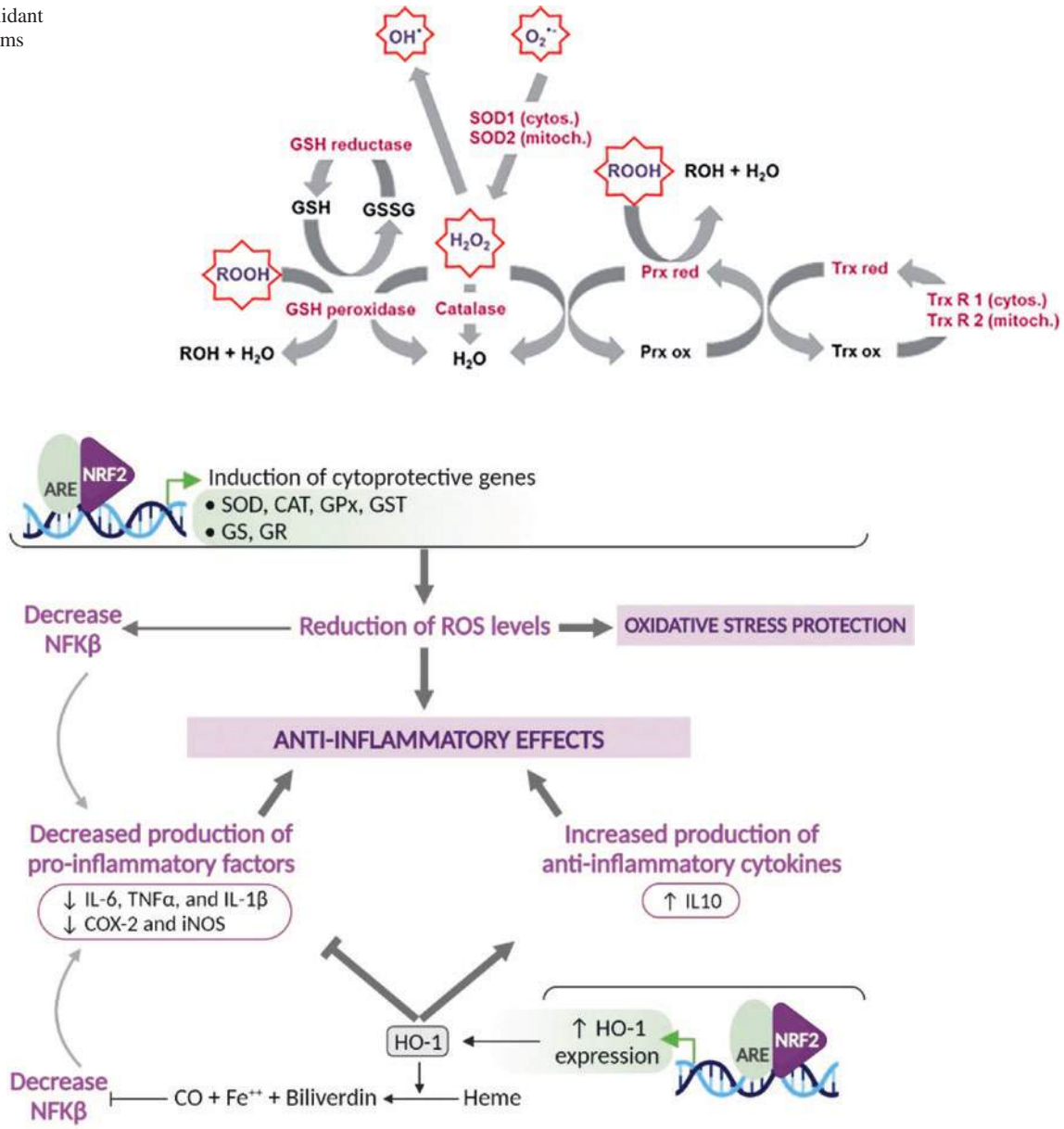

Fig. 3.27 Antioxidant defense mechanisms

Fig. 3.28 NRF2 protection against oxidative stress and excessive inflammatory responses involved in IR injury. NRF2 induces antioxidant response genes, like SOD, CAT, GPX, and GST that enhance ROS elimination. In addition, expression of enzymes such as GR and GS increases GSH cellular content and antioxidant capacity of the cell. Reduction in ROS levels decreases the expression of NFKβ, the main contributor to the inflammatory response. Moreover, NRF2 enhances the expression of HO-1 and its activity in the production of CO that reduces NFKβ activity, pro-inflammatory cytokine secretion (IL-6, TNFα, and IL-1β), and pro-inflammatory enzyme activity (COX-2 and iNOS). *ARE* antioxidant-responsive element, *NRF2* NF-E2-related factor 2, *SOD* superoxide dismutase, *CAT* catalase, *GPx* glutathione peroxidase, *GST* glutathione S-transferase, *GS* glutathione synthetase, *GR* glutathione reductase, *GSH* glutathione, *ROS* reactive oxygen species, *NFKβ* nuclear factor kappa β, *IL-6 and 10* interleukin 6 and 10, *IL-1β* interleukin 1 beta, *TNFα* tumor necrosis factor alpha, *COX-2* cyclooxygenase 2, *iNOS* inducible nitric oxide synthase, *HO-1* heme oxygenase 1

genes that are crucial to metabolize electrophilic attack and protect against OS and inflammatory damage. Kelch-like ECH-associated protein 1 (KEAP1) is a key cytoplasmic repressor of NRF2. KEAP1 interaction with NRF2 leads to NRF2 proteasomal degradation. In the presence of OS or inducers, key "sensor" cysteine thiol groups on KEAP1 are modified, disrupting the degradation process and allowing NRF2 to directly translocate into the nucleus. NRF2 then upregulates the expression of enzymes involved in the synthesis and recycling of GSH, such as the catalytic and modulator subunits of glutamate–cysteine ligase (GCLC and GCLM), GR, GPx, SOD, and several GST. Moreover, several proteins within the redoxin family, such as Trx, TrxRs, Prxs, and sulfiredoxins, are also upregulated by NRF2 [100]

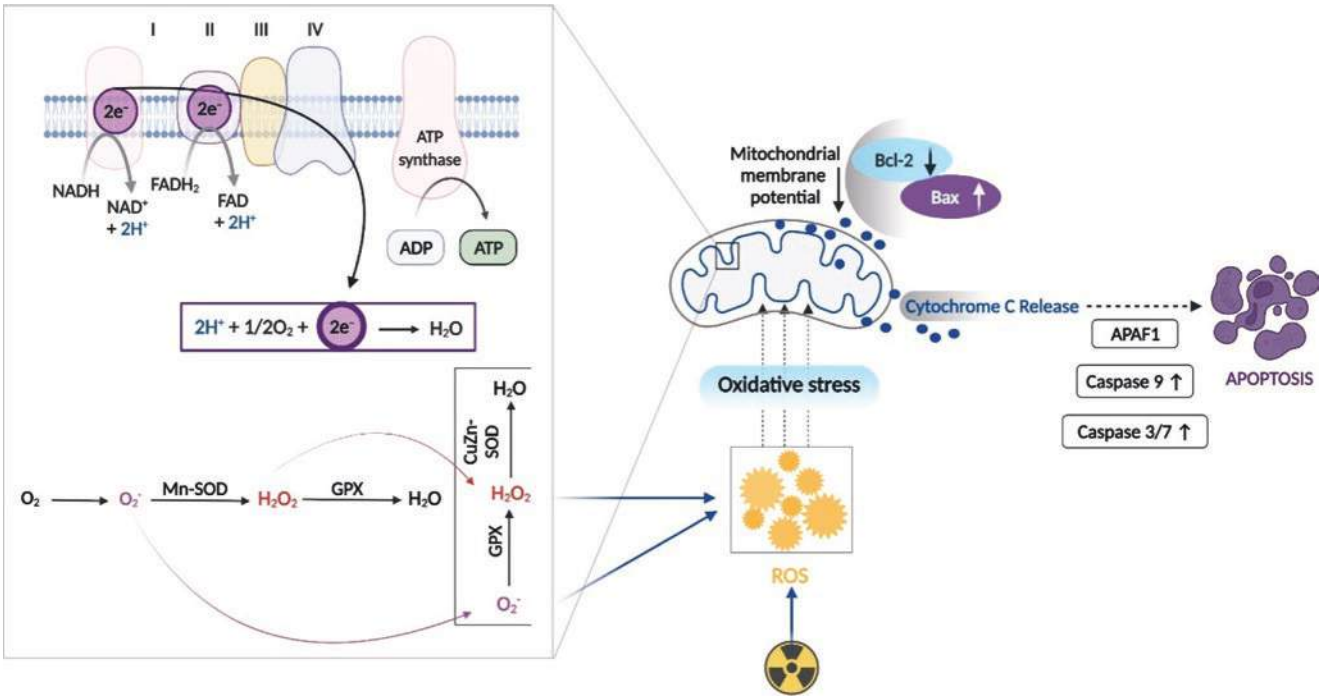

Fig. 3.29 Mitochondria as the key player in radiation-induced oxidative stress-mediated apoptosis. Various stimuli like radiation or improper functioning of the oxidative phosphorylation induce oxidative stress via ROS production. This causes the mitochondria to dysfunction and subsequently leads to cell death by apoptosis. *NAD+* nicotinamide adenine dinucleotide, *NADH* nicotinamide adenine dinucleotide hydrogen, *H+* hydrogen, *FAD* flavin adenine dinucleotide, *FADH2* flavin adenine dinucleotide hydrogen, *ATP* adenosine triphosphate, *ADP* adenosine diphosphate, *Mn-SOD* manganese superoxide dismutase, *GPx* glutathione peroxidase, *H2O2* hydrogen peroxide, *CuZn-SOD* copper zinc superoxide dismutase, *ROS* reactive oxygen species, *Bcl-2* B-cell lymphoma 2, *Bax* Bcl2-associated X, *APAF1* apoptotic protease-activating factor 1

as shown in Fig. 3.29. NRF2 stimulates the mitochondrial biogenesis program through activation of nuclear respiratory factor 1 and indirectly prevents/attenuates inflammation, because NRF2 activation results in the expression of previously mentioned antioxidant enzymes, which detoxify ROS, and in turn this reduces the expression of NLRP3 inflammasome and NFKβ (the main regulator of pro-inflammatory response). Moreover, NRF2 upregulates heme oxygenase activity (HO-1) and increases CO production, which in turn reduces NFKβ activity. In response to this, pro-inflammatory cytokine (IL6 and TNFa) production is reduced, and at the same time the production of anti-inflammatory cytokines (such as IL10) increases. As a consequence of these changes, NRF2 facilitates cells to survive oxidative stress and the inflammatory response that aggravates their cytotoxic effects (Fig. 3.29).

3.7.3 The Role of Mitochondria in Oxidative Stress

Mts are double-membrane multifunctional organelles associated with biosynthesis, metabolism, cell survival, signaling of ROS, etc. In the late 1960s, it was found that radiation could significantly modify the structural form of mts and also the mitochondrial DNA. Human mtDNA is a 16,569 base pair (bp) double-strand circular DNA molecule containing 37 genes, encoding 13 polypeptides for the mt electron transport chain, 2 ribosomal RNA, and 22 transfer RNA for mt protein synthesis. Somatic cells have an average of 100–500 mts with 1–15 mtDNA molecules per mitochondrion.

Although nuclear DNA (nDNA) is the main IR target, mts are constantly removing excess ROS created during energy production and mtDNA is much more vulnerable to IR effects than nDNA. mtDNA is generally repaired less efficiently than nDNA [101], although it uses the same repair mechanisms such as BER, MMR, and HR but not NER and classical NHEJ. Furthermore, the histones for better exposure protection are lacking. Together, this leads to a mutation rate which is 10–1000 times higher than nDNA [102]. Both direct IR exposure and irradiated cell-conditioned medium induce mtDNA damage and alter directed protein synthesis. As a consequence, IR exposure can cause the loss of mt membrane potential, leading to mt undergoing either fission, division of one mitochondrion, or fusion, combination of several mitochondria, autophagy (mitophagy), apoptosis,

modification in the mtDNA copy number per cell (mtDNAcn), and cause DNA damage and mutations, like point mutations or deletions. A common deletion mutation of 4977 base pair deletion in mtDNA genes coding for subunits of the mitochondrial ATPase, NADH dehydrogenase complex I, and cytochrome c oxidase is known as a marker for oxidative damage [101].

Changes in mtDNAcn or mutations in mtDNA both caused by high intra-mtROS control mt-dependent methylation potential of nDNA by decreasing methyltransferase activity and thus causing global DNA hypomethylation or changes in the expression of specific genes [103]. Global DNA methylation levels depend on human mtDNA variants and are also tissue specific and, therefore, may be connected with the differences in susceptibility to the pathogenic processes resulting from IR exposure and OS in different tissues [103].

OS also appears to target the mitochondrial DNA polymerase-γ activity required for replication and repair of mtDNA, thereby reducing the overall repair capacity. Therefore, subsequent to radiation exposure, mtDNA might be damaged, with an ensuing decrease in respiratory chain activity and decrease of mitochondrial function, giving rise to an increased ROS production. Moreover, mutations in mtDNA could lead to an increase in accessibility of reduced components of the ETCs to O_2, which may result in an increase in prooxidant formation. The functional disablement can be weighed by the limitations of the complexes I and III of the mitochondria, reduction of succinate-induced respiratory competence, augmented ROS levels, and increased mitochondrial protein oxidation. The net consequence is persistent metabolic OS that continues to cause de novo oxidative damage to critical biological structures. Such mitochondrial dysfunction can lead to stress signals, which lead to reduced electron transport chain (ETC), and oxidative phosphorylation can cause imbalance in the mitochondrial ROS production, decrease in the mitochondrial membrane potential, and lesser cellular ATP or energy. Although mts are the main producer of ROS, mts themselves can be susceptible to the pathological outcomes once targeted by ROS. By triggering the mitochondrial stress and downstream signaling, the increased levels of free radicals linked to the mtDNA oxidative damage lead to apoptosis.

One of the crucial steps in the process of apoptosis is the permeability transition pore opening (mPTP), followed by drop in the mitochondrial membrane potential. Opening of the pore increases the permeability of the mitochondrial membrane to molecules, leading to mitochondrial swelling and necrosis. NO produced at the basal level (e.g., 5 μM) could S-nitrosylate cyclophilin D (CypD), a critical mPTP regulatory component. This prevents the association of CypD with mPTP that is required for opening the pore and confers a protection to the cell under a stress. On the other hand, NO produced at a high concentration (e.g., 500 μM) could produce peroxynitrite in the presence of large amounts of ROS. Peroxynitrite could oxidize mPTP leading to its opening, which would lead to the opening of mPTP, loss of ATP production, and necrosis. The damaged mitochondria generated excessive ROS like hydrogen peroxide and superoxide anion, which provokes the mitochondrion-driven ROS propagation. ROS themselves accelerate the production of mitochondrial ROS. This process is also called as ROS-instigated ROS release (RIRR) by initiating as inter-mitochondria signaling network [104] (Fig. 3.28). Oxidative insult by radiation to the mt alters the mitochondrial membrane potential and causes the leakage of cytochrome c from the inner membrane compartment, which elicits a sequence of signal transduction progression, the outcome of which is apoptotic cell death. Once the mitochondria are severely stressed, the pro-apoptotic factors like Bax create pores on the mitochondrial membrane, which lets the release of cytochrome c in the cell cytoplasm. It interacts with Apaf-1 to form a complex called apoptosome (Apaf-1, cytochrome c, and ATP). Caspase-9 then gets activated and commences the action of other caspases like caspase-3, -6, and -7. These lead to DNA fragmentation and cell degradation, thereby pushing the cells towards apoptosis. This kind of cell death is known as mitochondrial mediated cell death or intrinsic pathway of apoptosis (Fig. 3.29). However, in this case, apoptosis plays a role in abashing cells that induce excessive ROS.

3.7.4 Oxidative Stress Biomarkers

Biomarkers of OS can be classified as molecules that are modified by interactions with ROS or molecules of the antioxidant system that change in response to increased OS. ROS levels can also be monitored using fluorescent probes of commercial kits, which specifically detect intracellular ROS such as H_2O_2, NO, or $^{\circ}O_2^-$. However, assays that monitor ROS levels are unlikely to be useful for biomonitoring purposes due to the short half-life of ROS and the fact that the response is not specific to radiation exposure.

3.7.4.1 Antioxidant Defenses

S-Glutathionylation is the posttranslational modification of protein cysteine residues by the addition of glutathione. This modification can prevent proteolysis caused by the excessive oxidation of protein cysteine residues under oxidative or nitrosative stress conditions. Measuring S-glutathionylation of the proteins as biomarkers (Fig. 3.30) is hampered by difficulty in accessing the tissue in which these modifications occur. Nevertheless, S-glutathionylation of hemoglobin has been proposed as a biomarker of OS strengthened by finding that it occurs in the circulating erythrocytes in parallel with S-glutathionylation of molecules in the vasculature or myocardium [105].

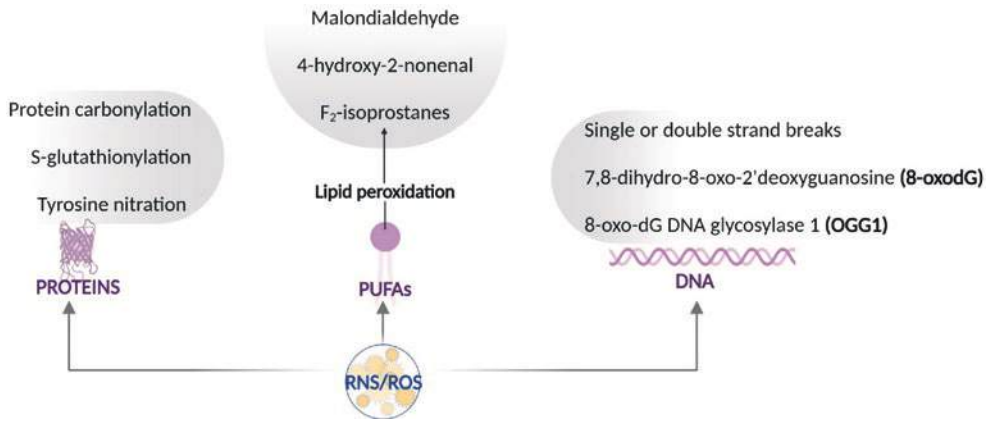

Fig. 3.30 Main oxidative products of DNA, lipids, and proteins. Oxidative products (listed in gray boxes) are formed depending on the free radicals (RNS/ROS) and the biomolecule target (amino acids, proteins, phospholipids, nucleic acids). These products can be used as oxidative stress biomarkers. *RNS* reactive nitrogen species, *ROS* reactive oxygen species

The participation of GSH in antioxidant reactions, either chemically or enzymatically via GPx, results in its own oxidation to GSSG. Decrease in intracellular GSH/GSSG ratio is one of the most used biomarkers of OS. In these conditions, GSSG is preferentially secreted out of the cell, and therefore, blood levels of GSH and GSSG may reflect changes in glutathione status in other less accessible tissues. 6 h after a single dose of irradiation (equivalent to 5 Gy), GSH/GSSG ratio decreases in blood. The decrease in GSH/GSSG is mainly due to an increase in the concentration of GSSG, because GSH levels do not change significantly [106].

3.7.4.2 Total Antioxidant Capacity (TAC) and Other Antioxidant Biomarkers

Antioxidants protect the body from the harmful effects of free radical damage. Thus, measurement of antioxidant levels in target tissues or biofluids has been widely used to assess the extent of oxidant exposure and, in turn, OS. TAC is the measure of the free radical amount scavenged by a test solution, being used to evaluate the antioxidant capacity of biological samples (tissues or biofluids). The TAC system involves enzymes (SOD, CAT, GPxs, and other enzymes), endogenous antioxidants, and dietary antioxidants (mentioned before), which are generally decreased when OS increases. TAC can be easily measured in cells, tissue lysates, and biological fluids by commercial colorimetric kits and represents a global approach (integrated parameter considered as the cumulative effect of all antioxidants of the biological sample) if no specific antioxidant molecule is to be investigated. One of the critical points is that the results obtained with different methods are not always comparable, depending on the different technologies used for their assessment. Moreover, as mentioned by Dr. Sies (who coined the concept of oxidative stress): "neither the term 'total' nor the term 'capacity' are applicable to the in vivo assays using an arbitrarily selected oxidant generator assaying a sample removed from its biological context, which is characterized by enzymatic maintenance of steady state" [107]. For that reason, we agree with him "that investigators should measure individually parameters associated with oxidative stress (GSH, urate, ascorbate, tocopherol, etc.) and antioxidant enzymes activities (in tissues samples and lymphocytes (in the case of blood samples) if their want to have an idea of the exposure of the entire organism to oxidative stress" [108].

3.7.4.3 Oxidation Products of DNA, Lipids, and Proteins

The "comet assay" and newer techniques [e.g., gas chromatography, high-pressure liquid chromatography (HPLC), immunoassays] can distinguish gross DNA damage produced by IR and damage from oxidation (for a detailed description, see Chap. 7). For low doses of radiation, the total number of induced DNA alterations is probably small when compared with the total number of equivalent alterations from endogenous sources. At DNA level, guanine is the most susceptible base to OS, and its oxidation at the C8 of the imidazole ring of deoxyguanosine generates 7,8-dihydro-8-oxo-2′deoxyguanosine (8-oxodG), which is the most predominant and stable DNA oxidative lesion in the genome (Fig. 3.30). A failure to repair oxidized bases creates a risk of mutation during DNA replication. For example, 8-oxodG mispairs with deoxyadenosine (dA) rather than deoxycytosine (dC) resulting in a C-A point mutation, thus increasing the risk of carcinogenesis. Besides the impact of confounding factors like age, sex, and smoking habits, with the help of correction factors, 8-oxodG levels are good and sensitive biological indicators of OS, which can be quantified in serum or urine samples, using HPLC coupled with mass spectrometry [109]. 8-OxodG can be removed by NER or BER with the action of 8-oxodG DNA glycosylase 1 (OGG1), a base excision DNA repair enzyme that cleaves the N-glycosidic bond between the base and the deoxyribose, generating an apurinic/apyrimidinic site (AP) and triggering the BER mechanism. DNA strand breaks and AP sites are effective substrates to activate DNA damage sensor PARP1. Overactivation of PARP1 is associated with apoptosis-inducing factor (AIF)-mediated and caspase-independent cell death. OGG1 seems to guard genome integrity

through lesion repair or cell death depending on the magnitude of guanine oxidation. OGG1 may also be measured as an OS marker.

As previously mentioned, lipid peroxidation products include MDA, 4-HNE, or IsoPs and can be used as oxidative stress biomarkers (Fig. 3.30). The latter are prostaglandin-like molecules formed by the nonenzymatic peroxidation of arachidonic acid (AA). MDA may be formed as a result of enzymatic and free radical peroxidation of PUFAs containing at least three double bonds and is also formed during prostaglandin synthesis. MDA can also react with DNA bases to form deoxyguanosine, deoxyadenosine, and deoxycytidine adducts, and these DNA-MDA adducts have mutagenic effects. Phospholipids containing linoleic acid and AA are considered the main source for 4-HNE production. Many different analytical methods are available for the measurement of MDA, 4-HNE, or IsoPs in biological samples and are reviewed by Tsikas [96].

It has been estimated that proteins scavenge a majority (50–75%) of generated reactive species. To function as biomarkers, protein oxidation products must be stable, accumulate in detectable concentrations, and correlate with OS exposition. Protein carbonylation is an irreversible protein modification, associated with alterations in functional and structural integrity of proteins, contributing to cellular dysfunction and tissue damages. Due to relatively early formation during OS, higher stability in comparison to other oxidation products, and simple analysis methods, protein carbonyls are one of the most OS biomarkers. Protein carbonyls can be easily quantified in plasma, serum, tissue samples, and also saliva by enzyme-linked immunosorbent assay (ELISA) [110].

The reaction between °NO and $^{\circ}O_2^-$ forms peroxynitrite, which can nitrate tyrosine residues in proteins. This process is in competition with the enzymatic dismutation of $^{\circ}O_2^-$ and the diffusion of °NO across cells and tissues. Peroxynitrite-mediated damage has been implicated in a wide range of disease pathologies, and 3-nitrotyrosine (3-NT) and nitrated proteins have been established as a footprint of nitro/oxidative biomarker of progression and severity in conditions. The measurement of 3-NT can be performed in plasma, serum, as well as tissue samples by special mass spectrometry. Commercially available ELISAs are usually used in clinical studies due to standardization and easy sample preparation. In turn, several limitations have been highlighted in the literature, such as low sensitivity and minor specificity. This and other protein oxidation biomarkers in human diseases are extensively reviewed by Kehm et al. [110]. The advancement of proteomics will allow us to assess changes in proteins (including the assessment of carbonylated, S-glutathionylation, S-nitrated, and/or N-nitrated derivatives) that serve as biomarkers of exposure to IR. An overview of the oxidation products of DNA, lipids, and proteins formed can be found in Fig. 3.30.

3.8 Cell Cycle Effects

The cell cycle is a fundamental process through which the cell grows and accurately duplicates the genetic material before it divides to give rise to two daughter cells. The cell cycle is divided into two phases: interphase in which the cell spends most of its time, followed by mitosis during which the cell divides into two daughter cells. The interphase has three distinct phases. The first phase is the G1 phase in which the cell grows and prepares itself for DNA synthesis. Second is the S phase, when the cell actually duplicate its DNA. The third phase is the G2 phase, where it prepares itself for mitosis. The duration of G1 varies considerably from cell to cell, while S, G2, and mitosis show less variation. Quiescence is a reversible state of a cell in which it does not divide but retains the ability to reenter cell cycle. This state is also called G0 phase.

The transition from one cell cycle phase to another is controlled by a variety of proteins, cyclins, and cyclin-dependent kinases. If the system identifies any inaccuracies, the transition from one phase to the next will be delayed and the cells arrested in the so-called cell cycle checkpoints [111]. Cells, which enter mitosis with unrepaired DNA damage, will most likely fail to divide properly resulting in cell death. In order to provide time for DNA damage repair or, if repair is not the best solution for inducing cell death, e.g. apoptosis, before DNA synthesis (S phase) and in particular mitosis is initiated, radiation induces arrest in checkpoints at the end of the G1 and G2 phases. Since the process that kills the cells after radiation damage is related to cell division, cells in G0 or cells which are differentiated or in senescence and have lost the ability to proliferate are very resistant to radiation [112].

3.8.1 Cycle-Dependent Kinases and Cyclins

Cell division is a highly regulated progression allowing cells to divide and to generate daughter cells. The regulation is necessary for the recognition and restoration of genetic injury along with the prevention of uninhibited cell division. It is regulated by cyclins and cyclin-dependent kinases (CDKs). CDKs are serine or threonine kinases, which unite with a separate subunit of functional cyclins, which presents domains essential for enzymatic activity. CDKs are known to have a crucial function not only in cell division but also in amending the transcription responses. Hence, the deregulation of CDKs is a characteristic of cancers and utilized for anticancer therapy purposes. On the other hand, cyclins establish the activity of CDKs as their levels keep changing during the cell cycle. Depending on their participation and function during the cell cycle, cyclins are divided into four

categories: G1 cyclins, i.e., D cyclins; G1/S cyclin, i.e., cyclin E; S-phase cyclins, i.e., cyclins E and A; and M-phase cyclins, i.e., B cyclins. Researchers have discovered around 20 CDK-associated proteins, which makes the cell cycle a complex process that involves the combination of CDKs (Cdk1, Cdk2, Cdk3, Cdk5, Cdk4, Cdk6, Cdk7, Cdk8, etc.) and cyclins (A1, A2, B1, B2, B3, C, D1, D2, D3, E1, E2, F, etc.) in distinct phases of the cell cycle endowing extra governance to the cell cycle apparatus (Table 3.9 and Fig. 3.31). Cyclins impart the specificity for substrates and normal cell cycle regulation, which includes the subunit binding, localization, activation/deactivation, etc. to the Cdk/cyclin complexes [113].

Table 3.9 Cyclins, CDKs, and their function throughout cell cycle

Cell cycle phase	Cyclins	CDKs	Functions
G1	Cyclin D	CDK 4, CDK6	Can act in response to external cues, e.g., growth factors and/or mitogens
G1/S	Cyclins E	CDK2	Control the centrosome duplication
S	Cyclins A and E	CDK2	The main targets are helicases and polymerases
M	Cyclins B	CDK1	Control G2/M checkpoint. The cyclins are produced in S phase but are inactive until the synthesis is entirely completed. Phosphorylate several downstream targets

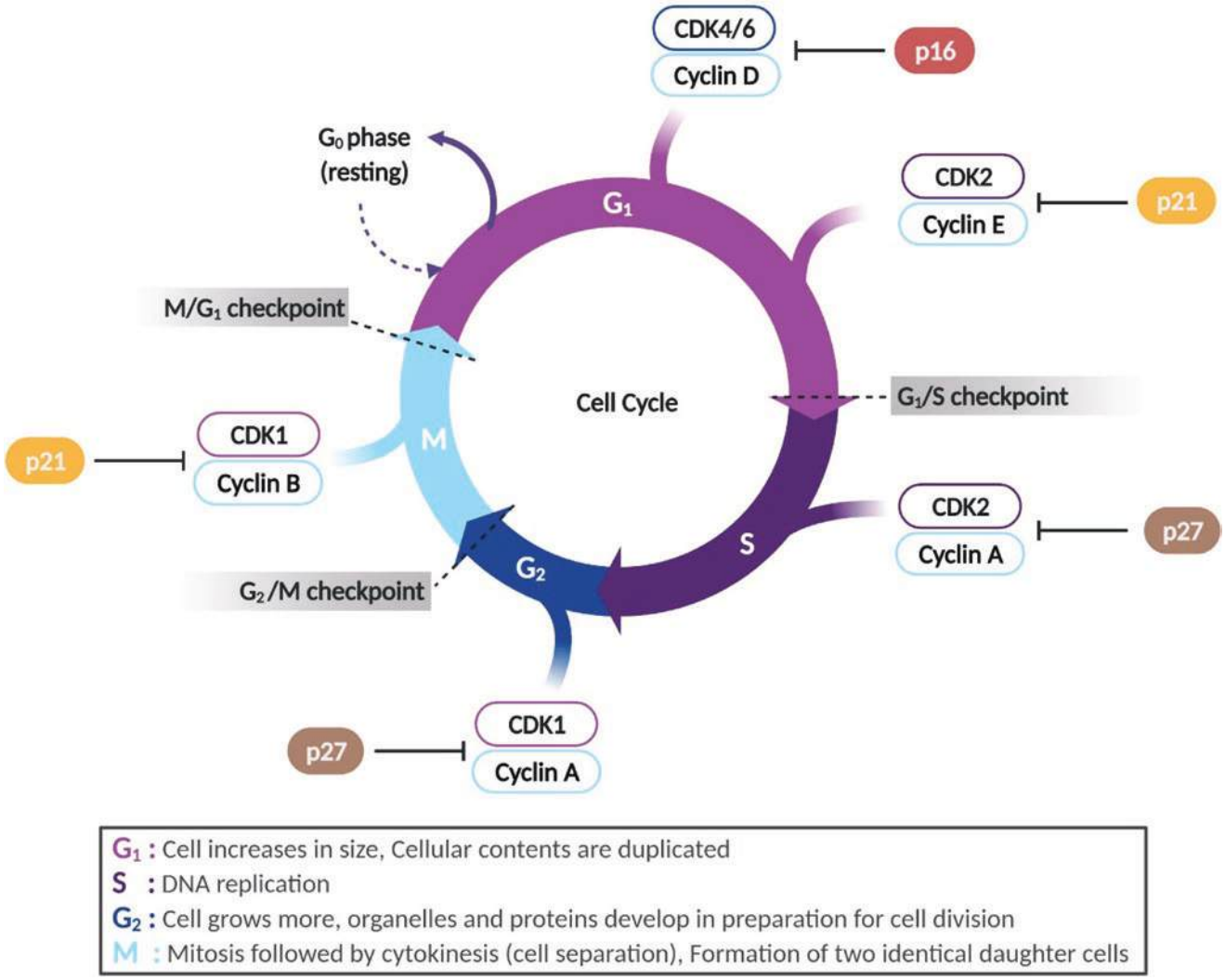

Fig. 3.31 Overview of cell cycle: functions of different phases, cyclins and CDKS, and CDIs

3.8.2 Activation of CDKs by Binding to Cyclins

CDKs have a very limited activity without the presence of a cyclin. To be an active kinase, it should be bound to its cyclin partner and its activity can be further altered by phosphorylation and association of additional proteins like p27. Every CDK/cyclin complex possesses a distinct function that is restricted to a specific cell cycle phase (Table 3.9). Cdk4 and/or Cdk6 are activated by D-type cyclins in the beginning of the G1 phase, and it commences phosphorylation of the retinoblastoma protein (Rb) family (Rb, p107, and p130). This releases the E2F transcription factor and causes the activation and transcription of the E2F-responsive genes that are necessary for the cell cycle progression. The cyclin A and E types are the early E2F-responsive genes. During the later G1 phase, cyclin E binds to Cdk2 to activate it and executes the phosphorylation of Rb (pocket proteins), provoking the further activation of the E2F intervened transcription. This assists in the crossing over of the cell cycle checkpoints at the periphery of the G_1/S phase, and to S-phase commencement. Cdk2 unites with cyclin A and aids the progression of the S phase. During the inception of the S phase, A-type cyclins are synthesized, which phosphorylates proteins associated with DNA replication. Going further, at the time of G_2/M transition, the activity of Cdk1/cyclin A is necessary for the induction of the prophase. Lastly, Cdk1/cyclin B complexes dynamically contribute to the completion of the mitosis process. Cdk1 activity fluctuates throughout cell cycle succession and is proficient of governing varied cell cycle adaptations (G_1/S, S, and G_2/M phases) by connecting with diverse cell cycle phase-associated specific cyclins, and several processes like action of CDK-activating kinase (CAK) and inhibitory phosphorylation on CDK. Regulating the cyclin levels and action of CDK inhibitors during the cell cycle assures that CDKs are active in the precise stage of the cell cycle. Cells exploit many processes such as transcriptional control of cyclin genes and breakdown of cyclins; the transcriptional control of the cyclin subunits is one way that ensures appropriate temporal expression of the cyclins and degradation of cyclins, to confine cyclins to the proper cell cycle phase and to keep them at the accurate concentration [114]. Ubiquitin-mediated protein degradation is one of the most crucial regulatory controls that confine the cyclins to the proper cell cycle phase. However, SCF (Skp1, Cullin, and F-box proteins) and APC/C (anaphase-promoting complex or cydosome) are two ubiquitin proteins involved in the degradation of cyclins. During the G1-S-phase transition, SCF controls degrading G1 cyclins (cyclin D), while APC/C degrades the cyclins of the S phase and mitosis, thus advancing the exit from mitosis. To control the CDK activity, the regulation of cyclin levels is not the only mechanism. Other mechanisms like activation and inhibition of phosphorylation actions on the CDK subunit and existence of inhibitors are critical in controlling cyclin-CDK activity [114].

3.8.3 Inhibitors of Cyclin-Dependent Kinases

CDK inhibitors are a family of proteins that can bind directly to the cyclin-CDK complex and hinder its activity. In the transition of the G1-S phases, these proteins play a very crucial role. CKIs implicated in controlling the S phase and mitotic CKIs are indispensable to avoid early commencement of the S- and M-phase CDKs. However, in human cancers, genes coding these CKIs are often mutated leading to aberrant cell cycle regulation. During normal or extreme conditions (DNA damage, telomere dysfunction, and stress), the functions and activities of the CDK/cyclin complexes are governed and controlled by two families of CKIs. The INK4 family comprises the p16INK4a, p15INK4b, p18INK4c, and p19INK4d which can specifically bind to Cdk4 and Cdk6 and hinder the activity of the D-type cyclin. The other Cip/Kip family (p21Cip1/Waf1/Sdi1, p27Kip1, p57Kip2) obstructs Cdk2/cyclin E, Cdk2/cyclin A, Cdk1/cyclin A, as well as Cdk1/cyclin B activity. The p21 protein hinders the formation of cyclin/CDK protein complexes that are required for the progression from the G1 phase to the S phase of the cell cycle (Box 3.19).

Box 3.19 In a Nutshell: Cell Cycle and Radiation Response

- Irradiated cells display a complex set of responses that can include either progression or arrest of the cell cycle.
- Every phase of the cell cycle has a very specific set of cyclins and cyclin-dependent kinases to perform functions associated with that particular cell cycle phase.

3.8.4 Cell Cycle Phase and Radiosensitivity

To study the variation of radiosensitivity with position in the cell cycle, it is necessary to synchronize the cells to get a population of cells that are all in the same cell cycle phase.

For cells in culture, there are three main techniques.

1. In fluorescence-activated cell sorting (FACS), a flow cytometer is used to sort cells based on fluorescence from a DNA-binding dye, such as Hoechst 33342, which can be used for live cells.
2. Chemically induced cell cycle arrest collects over time all the cells at a cell cycle checkpoint. When the drug is

removed, the cells will go through the cell cycle synchronously for some time before they become more and more asynchronous. The most used drug is hydroxyl urea, which arrests cells at the border between G1 and S. The advantage of this method is that it can also be used in vivo.

3. Mitotic selection was introduced by Terasima and Tolmach [115] and is the most used synchronization method in cell culture in vitro. As cells enter mitosis, they round up and become less attached to the flask bottom. By then shaking the flask, the mitotic cells will detach and can be collected with the medium. The cells can then be irradiated at different time points as they go through cell cycle.

The first age-response curve by Terasima and Tolmach [115] using 3 Gy irradiation of HeLa cells is shown in Fig. 3.32, left panel, together with a curve showing the fraction of labeled cells after pulsed incorporation of [3H]-thymidine during S phase. Cell survival was measured as the ability to form a macroscopic colony. The data indicate four times higher survival if the dose is delivered during early G1 compared to at the start of S phase. Furthermore, there is an increase in cell survival with age during S phase; that is, the radioresistance increases as more and more of the DNA is synthesized. HeLa cells are HPV infected and do not have functional p53, which normally would give the cells time for repair before entering S phase. The cells irradiated early in G1 will have time for repair, which is reflected in a high survival, while the cells in late G1 are more sensitive, because they may enter S phase with unrepaired DNA damages. Cell lines with short G1 are sensitive throughout G1. Terasima and Tolmach also irradiated the synchronized cells with various radiation doses and thereby recorded complete dose-response curves for HeLa cells irradiated in different phases of the cell cycle (see Fig. 3.32, right panel). These curves confirmed the variation in radiosensitivity through the cell cycle, as was demonstrated by the age-response curves. In addition, they also showed that cells irradiated while in mitosis are far more radiosensitive than cells irradiated in any part of interphase.

Measurements of the radiosensitivity of cells in G2 are technically difficult, and it has become customary to suppose that cells are radiosensitive if irradiated in G2. However, the radiosensitivity of cells in G2 has been shown to be dose dependent to a quite different degree than in any other phase of the cell cycle. Cells are hyper-radiosensitive for small radiation doses because the mechanism for early radiation-induced G2 arrest by ATM is not activated by radiation doses in the range below about 0.3–0.5 Gy (Box 3.20).

Box 3.20 In a Nutshell: Radioresistance and Radiosensitivity and Cell Cycle

- Cells increase radioresistance throughout S phase.
- Cell radiosensitivity is highest during mitosis.

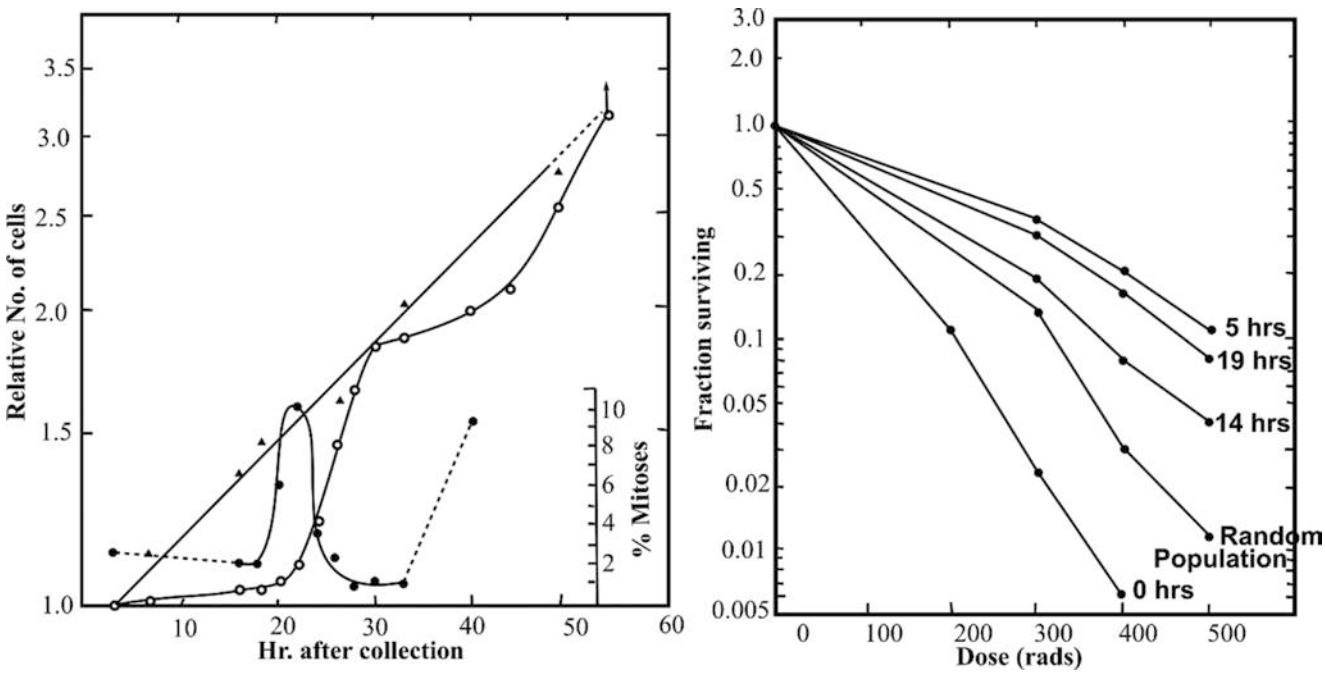

Fig. 3.32 Age-response of cells after radiation. Left: Age-response curves for HeLa-S3 cells (open circles: synchronized cells, triangles: asynchronous cells) irradiated with 3 Gy X-rays (= 300 rad) at different time points after selection in mitosis and the fraction of cells with incorporated [3H]-thymidine in DNA after a 20-min pulse (black circles, right *y*-axis). Right: Dose-response curves for HeLa-S3 cells synchronized by mitotic selection and X-irradiated at different times after selection. 0 h: mitosis, 5 h: early G1 phase, 14 h: S phase, 19 h: late S/G2 phase. [Reproduced with permission from Terasima and Tolmach [115]]

3.9 Telomeres and Senescence

3.9.1 Telomeres and Their Role

Telomeres are nucleoprotein structures located at the end of each linear chromosome in the cell nucleus. They are composed by tandem repeats of the G-rich hexanucleotide TTAGGG and are typically 10–15 kb long [116]. These structures are organized into heterochromatin domains, and they play a significant role in maintaining genome stability. There are at least two very important functions of telomeres in eukaryotes. The first one is the protection of the linear DNA molecules from the DNA repair mechanisms, which may recognize these sites as double-strand breaks. Secondly, they define the maximum number of cell cycles that a cell may undergo [116]. At each cell cycle division, telomeres shorten by 50–200 bp due to the DNA end-replication problem [117]. This problem results from the inefficient copying of the last base pairs of the linear DNA molecule by DNA polymerase. After several cell divisions, the length of telomeres reaches a critical threshold, which means that the cell can no longer divide. The cell has then reached its Hayflick limit, and it proceeds to senescence. Telomere shortening is thus a very-well-known hallmark of cellular senescence and aging. A good example of the telomere shortening is the deficiency of the adaptive immune system in older individuals caused by T cells reaching their Hayflick limit [118].

The telomere attrition can be opposed by an RNA-dependent DNA polymerase known as telomerase. This enzyme can elongate the telomeres by adding 5′-TTAGGG-3′ repeats to the chromosomes 3′ terminal ends. Telomerase is connected with cells' immortality; thus, it is present in germline and malignant cells. There is only little or no telomerase in most somatic cells [118]. This information is summarized in Fig. 3.33. An inverse correlation between the telomere length and the radiation-induced cytogenetic damage was found for lymphocytes, fibroblasts, epithelial cells, and many cancer cell lines. It was shown that telomere shortening leads to chromosome fusion, chromosome bridges, or higher frequencies of micronuclei. Thus, telomere shortening is closely linked to the cell radiosensitivity. Therefore, targeting the telomeres could be a very good radiosensitizing method in our fight with cancer during radiotherapy [116].

3.9.2 Senescence and Its Role

As described in Sect. 3.7, cellular senescence is a cell state triggered by extrinsic (cellular stressors) and intrinsic (physiological processes) factors. It is characterized by a prolonged and generally irreversible cell cycle arrest, associated with secretory features, macromolecular damage, and altered metabolism, with its function to remove potentially harmful cells from the proliferative pool [120]. Senescent cells are

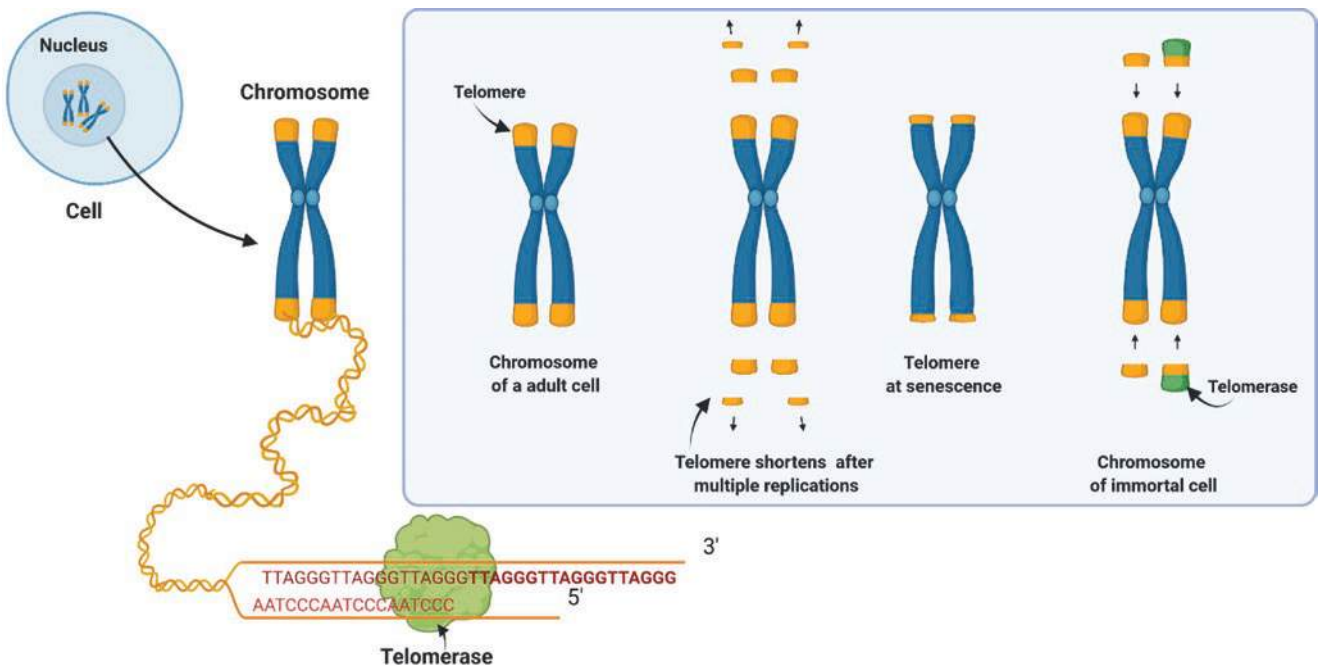

Fig. 3.33 Telomeres, their shortening, the senescence state, and immortal cells. An adult cell chromosome with telomeres and the enzyme telomerase, which plays a crucial role in telomere end lengthening (left). Telomere characteristics in an adult cell's chromosome, after multiple replications, at cell senescence, and when the cell is immortal (left to right, blue box). (Adapted with permission from Aunan et al. [119])

detected at any life stage from embryogenesis (contributes to tissue development) to adulthood (to prevent the proliferation of damaged cells). Yet, senescent cells can also potentiate various aspects of tumorigenesis, including proliferation, metastasis, and immunosuppression by secreting a collection of pro-inflammatory factors collectively termed as senescence-associated secretory phenotype (SASP) [121]. It is important to clarify that senescence is a distinct form of cell cycle arrest and distinct from quiescence, where cells can reenter the cell cycle when favorable growth conditions are restored; terminal differentiation, where cells exhibit functional and morphological changes resulting in loss of original cellular identity; and cell death, where cells are being eliminated and are thus nonfunctional. The existence of multiple senescence programs and the nonspecificity of current senescence markers make it difficult to fully unveil the complex mechanism behind senescence (current understanding presented in Fig. 3.34). It is therefore recommended to apply a multi-marker approach when investigating cellular senescence [120]. Yet, it is currently accepted that two main signaling pathways initiate and maintain the cell cycle arrest: p53–p21–retinoblastoma protein (RB) and p16INK4A–RB. As a consequence, depending on the senescence program, senescent cells express a multitude of hallmarks such as morphological alterations, senescence-associated beta-galactosidase (SA-β-gal), and SASP among others [122].

- Senescence in developmental processes, i.e., in embryogenesis and organogenesis, is induced by paracrine signaling and is mediated by the expression of the cell cycle inhibitor p21. Although SA-β-gal is highly expressed, developmental senescence is not associated with DNA damage, does not secrete the typical range of SASP cytokines, and is independent of p53 and p16INK4a. Senescence in wound healing prevents excessive fibrosis by secreting PDGFA-enriched SASP to stimulate appropriate skin repair. Senescence causes, or at least contributes to, organismal aging through the shortening of telomeres followed by the induction of p16INK4a and resulting in an accumulation of senescent cells over time. Studies by Baker et al. [123], first in BubR1-mutant mice (Cdkn2ap16 knockout mice) and then later in naturally aged mice, demonstrated that in the absence of p16INK4a, it is possible to inhibit the production of senescent cells and improve health span [123]. Also, SASP triggers multiple intercellular communication paths that also promote aging. Finally, the elimination of senescent cells improved several age-associated conditions. Senescence in cancer has shown a dual role as tumor suppressor and tumor promoter. Senescence is a key mechanism of tumor suppression via the inhibition of proliferation of cancer cells or by stimulating immune surveillance. Yet, cells induced to senescence by oncogenes or chemotherapy exhibit stem-

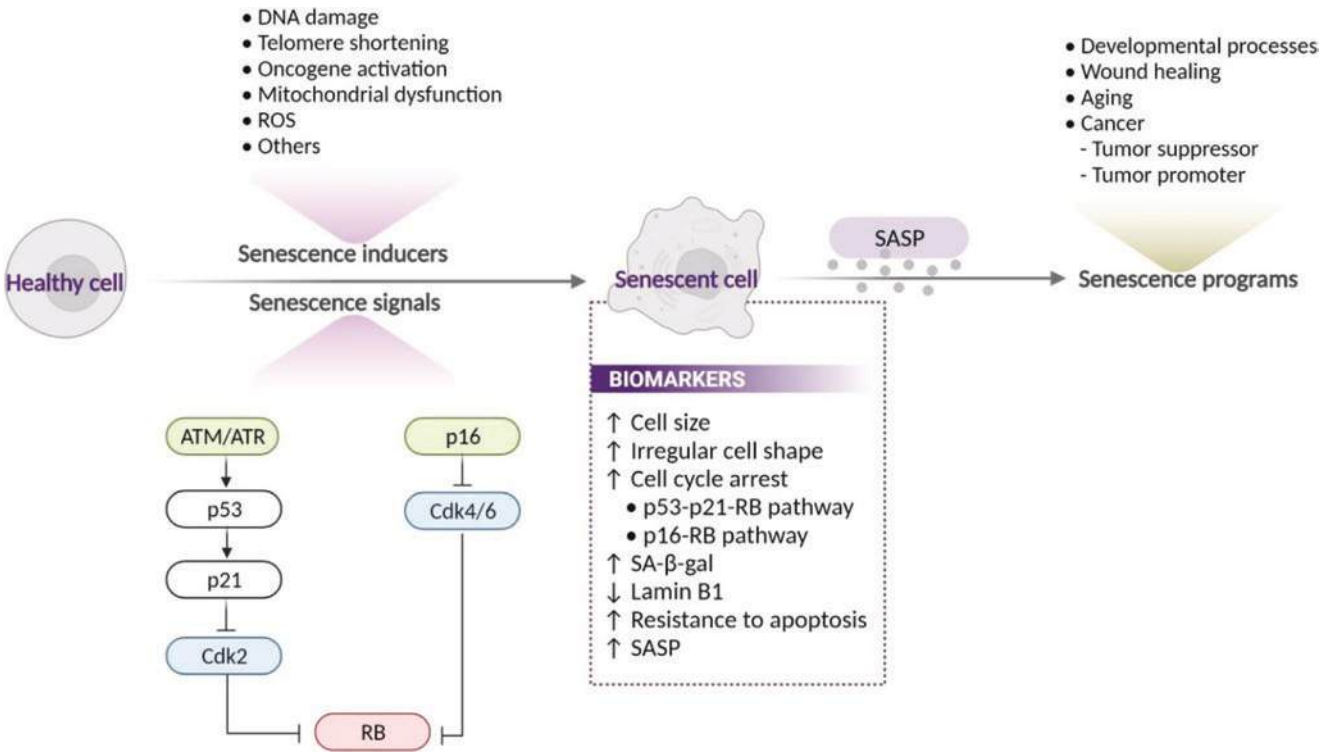

Fig. 3.34 Overview of cellular senescence processes. *ROS* reactive oxygen species, *ATM* ataxia-telangiectasia mutated, *ATR* ATM and Rad3-related protein, *Cdk2/4/6* cyclin-dependent kinase 2/4/6, *RB* retinoblastoma tumor suppressor gene, *SASP* senescence-associated secretory phenotype, *SA-β-gal* senescence-associated beta-galactosidase

like properties that promote cancer. Several stressors can induce cellular senescence and radiation in one of them. Thus, IR may cause cell cycle arrest resulting in a prematurely induced senescence phenotype (including SA-β-gal, p16INK4a, p21, and SASP), which is p53 dependent [121]. Unfortunately, the accumulation of these senescent cells can have a negative impact by promoting tumorigenesis. Thus, eliminating senescent cells from tumors and surrounding healthy tissues may be a successful and beneficial adjuvant strategy (Box 3.21).

Box 3.21 In a Nutshell: Telomeres and Senescence

- Telomeres are part the ending parts of chromosomes, which protect the genome integrity
- Telomeres shorten in each cell division by 50–200 bp due to the DNA end-replication problem.
- Telomere shortening is closely linked to cellular radiosensitivity.
- After several cell divisions, the length of telomeres reaches a critical threshold, the Hayflick limit, and the cell proceeds to senescence.
- Senescence is sometimes addressed as a type of cell death. A cell in senescence cannot proliferate anymore, it lives only metabolically.
- Cellular senescence is characterized by a prolonged and generally irreversible cell cycle arrest, and it functions as a process to remove potentially harmful cells from the proliferative cell pool.
- Senescence is a key mechanism of tumor suppression via the inhibition of proliferation of cancer cells or by stimulating immune surveillance in cancers treated with radiotherapy.

3.10 Cell Death Mechanisms

In response to IR, multiple, molecularly distinct forms of cell death may be initiated. Although the decision points of their initiation are not completely clear, it is known that the level of the DNA damage but also the individual signaling status of different cell death pathways in different cell types, e.g., hematological vs. epithelial cells, influence the decision regarding the cell death route.

The cellular factors that influence include cell type, position in cell cycle when irradiated, DNA repair capacity, as well as functionality of TP53 and similar DNA-damaging sensors [124]. The dose and radiation quality also contribute to the cellular IR response to cell death, and in the tissue, the oxygen levels may impact the cell death route taken [124]. In this section, an overview of four cell death mechanisms are given: (I) mitotic cell death/mitotic catastrophe, (II) apoptosis, (III) necrosis, and (IV) autophagy (Fig. 3.35), some of which are also interconnected in the cell. Furthermore, the underlying molecular mechanisms and importance of these forms of cell death following IR are also described alongside methods of assessment.

3.10.1 Mitotic Cell Death/Mitotic Catastrophe

Mitotic catastrophe (MC) is an important type of IR-induced cell death mechanism, which is triggered when cells enter into the mitotic phase without appropriately completing the S and G2 cell cycle phases [125]. Hence, MC controls cells that are often incapable of successfully completing mitosis. MC works by activating mitotic arrest, and later it may lead to a controlled or a regulated cell death mechanism or senescence. Therefore, MC is a controled cell death that usually follows the intrinsic apoptotic pathway route [124] (Fig. 3.37). MC is also promoted when the proteins that regulate the G2 phase like the $p21^{CDKN1A}$, checkpoint kinases 1 and 2 (CHK1/2), ataxia-telangiectasia mutated (ATM) and ataxia-telangiectasia, and Rad3-related protein (ATR) are inhibited. MC basically commences with the irregular condensation of the chromatin around the nucleoli, which looks similar to early chromosome condensation. Cells may die in the same cell cycle or in the successive cell cycle progression or division after IR. The anomalous mitosis in such cases leads to unusual segregation of the chromosomes and cell division. As a consequence, this causes formation of giant cells which exhibit the uncharacteristic nuclear morphology and numerous micronuclei and nuclei. Also, it is noteworthy that MC induced by IR is accompanied with excess duplication of chromosomes and hyper-amplification, which results in a mitosis that is multipolar and later development of micronuclei. DNA damage and flaws in the DNA repair processes lead to centrosome hyper-amplification. Cyclin-dependent kinase 2 (CDK2) and cyclin A or E initiate the amplification of the centrosomes at the boundary of G1/S phase. This is often observed in cells that lack a functional TP53; however, in cells with a functional TP53 and $p21^{CDKN1A}$, which is known as an inhibitor of CDK2, cellular senescence is promoted.

The outcome of MC in the form of cell death can be elicited in the mitotic phase or in the successive interphase. Some cells activate apoptotic pathways in the metaphase that results in delayed apoptosis, i.e., it can take up to 6 days after IR. Cells that get away with the mitotic arrest of the mitotic

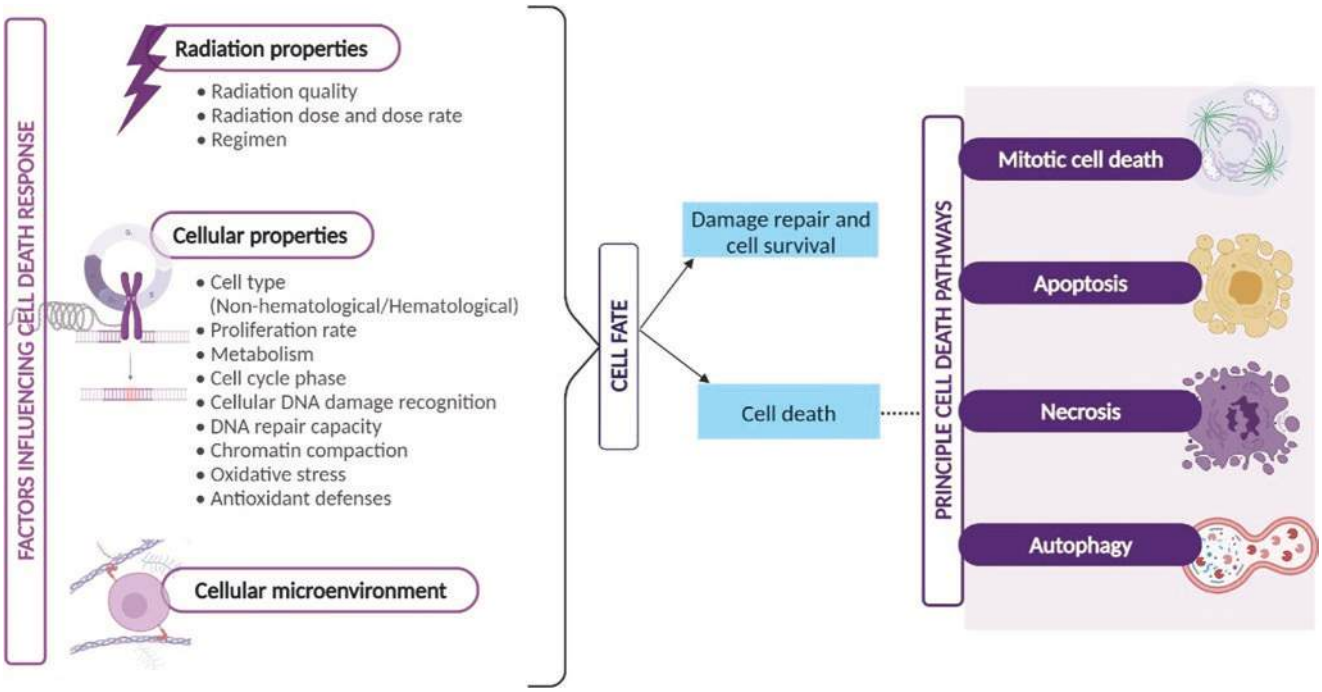

Fig. 3.35 Overview of cell death and cell death-protective mechanisms in response to radiation. Radiation-induced cell death is influenced by different factors, such as radiation factors, cell intrinsic factors, and cellular microenvironment factors (left). Cell death pathways are listed to the right. The mechanisms and importance of these principal cell death forms are described in detail in the text

cell death are frequently observed to have an unsuccessful cytokinesis consequentially exhibiting tetraploid anomalous nuclei developing into giant cells. Giant cells that possess a functional TP53 will eventually undergo apoptosis following the mitochondrial pathway of apoptosis in the subsequent G1 phase. However, cells with mutant TP53 or deficient TP53 function go on with a few number of cell cycles and attain a growing amount of chromosomal anomalies before they finally succumb to either delayed apoptosis or necrotic form of cell death [125]. As the cells that undergo MC are usually the ones who have lost the potential to carry out any further replication, MC is frequently referred to as a genuine type of cell death. One of the most common properties exhibited by cancer cells is that of defects in cell cycle checkpoints. This lets the cells enduring IR-induced damage to hastily inscribe in the mitotic process even with the misrepaired DNA that eventually leads to MC. More than a few cell division attempts can take place before adequate genetic injuries mount up to activate mitotic death, emphasizing why solid tumors frequently display deferred reactions to IR [124]. MC is triggered after IR exhibits diverse mechanisms of action (Table 3.10) [126].

Table 3.10 Examples of IR-induced MC in different tumor cell lines

Inducer of MC	Cell line	Features/signaling components of MC
Ionizing radiation	HeLa (cervical adenocarcinoma)	Increased levels of cyclin B
	U2OS (osteosarcoma)	Checkpoint adaptation
	HT0180 (fibrosarcoma)	Micronucleation
	MOLT4 (leukemia)	Checkpoint adaptation

3.10.1.1 Mode of Action of Mitotic Catastrophe

During MC, the mitotic damage is recognized and guides the cell into one of the three potential antiproliferative fates (Fig. 3.36). In one of them, when cyclin B levels are elevated, the malfunctioning mitotic cells recruit the cell death machinery and die during mitosis. Another cell death pathway that cells can take is by mitotic slippage. Here, cells go out from mitosis and cell death is triggered in the next G1 cell cycle transition. Lastly, cells with a MC character can also undergo senescence after exiting mitosis.

MC may not at all time be accompanied by mitotic arrest. Nevertheless, the mechanism of action that dictates cell fate of subsequent MC continues to remain unclear [127]. When

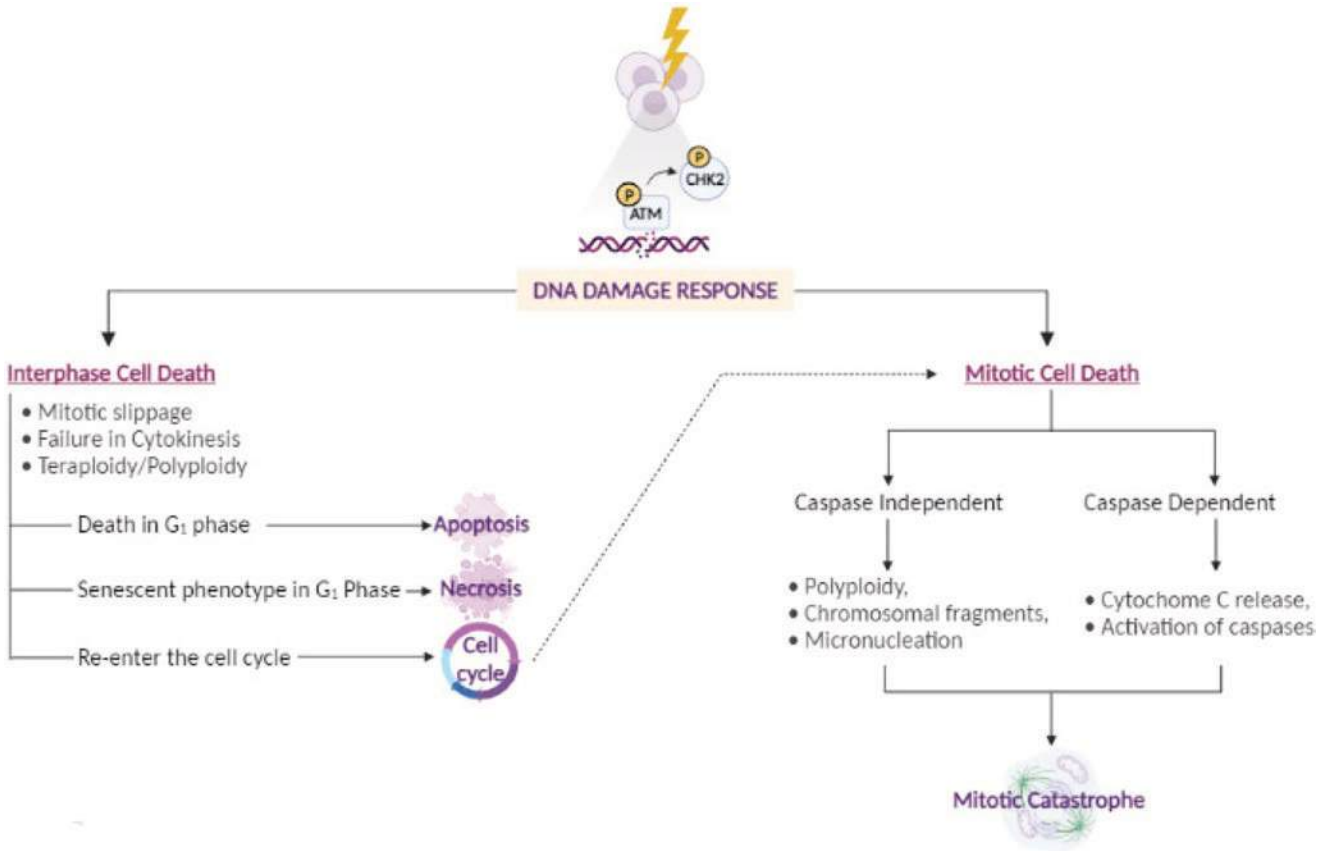

Fig. 3.36 Cell death pathways operative in mitotic catastrophe. Different signaling events triggered in response to a nonfunctional mitosis are shown. Upon DNA damage, cells which lack functional p53 can go out from mitosis without commencing cytokines or initiate cell death even in mitosis. Apoptosis and necrosis signaling in the context of mitotic catastrophe are depicted

mitotic arrest is extended, the amount of cyclin B is decreased albeit the spindle assembly checkpoint (SAC) is functional. As a result, if cyclin B levels drop below the verge that determines mitotic exit, slippage occurs (Box 3.22).

Box 3.22 In a Nutshell: Ionizing Radiation Induced Cell Death

- IR-induced cell death depends on radiation quality, dose as well as cell type, cell cycle position, and functionality in DNA damage signaling.
- Mitotic catastrophe is one of the principal forms of IR-induced cell death that results from early/untimely entry into mitosis, even before the fulfillment of S and G2 phases of the cell cycle.
- The characteristic features of IR-induced mitotic catastrophe are altered nuclear morphology, micronucleation, and formation of multinucleated cells.

3.10.2 Apoptosis

Apoptosis (originally from Greek language translated "falling off") is also known as "cellular suicide." It is a cell death process which may be executed under normal physiology, e.g., organism development, but also in the context of disease. Apoptosis is a highly controlled pathway with distinct molecular features. Thus, some of the rapidly proliferating cells undergo apoptosis, which is an essential part of neurogenesis and tissue development in humans as well as in other mammalians. During apoptosis, cells are disposed in a complex but well-ordered fashion which involves energy-requiring molecularly defined effector mechanisms [128]. To simplify, apoptosis allows the cells to self-destruct with limited tissue damage when they are exposed to different triggers/signals which can be endogenous, e.g., formed DNA damages, telomere shortening, or encountered from the outside of the cell, e.g., cytotoxic or DNA-damaging agents, IR exposure, loss of growth factors, cytokine or glucocorticoid hormone level alterations, or hypoxia [128].

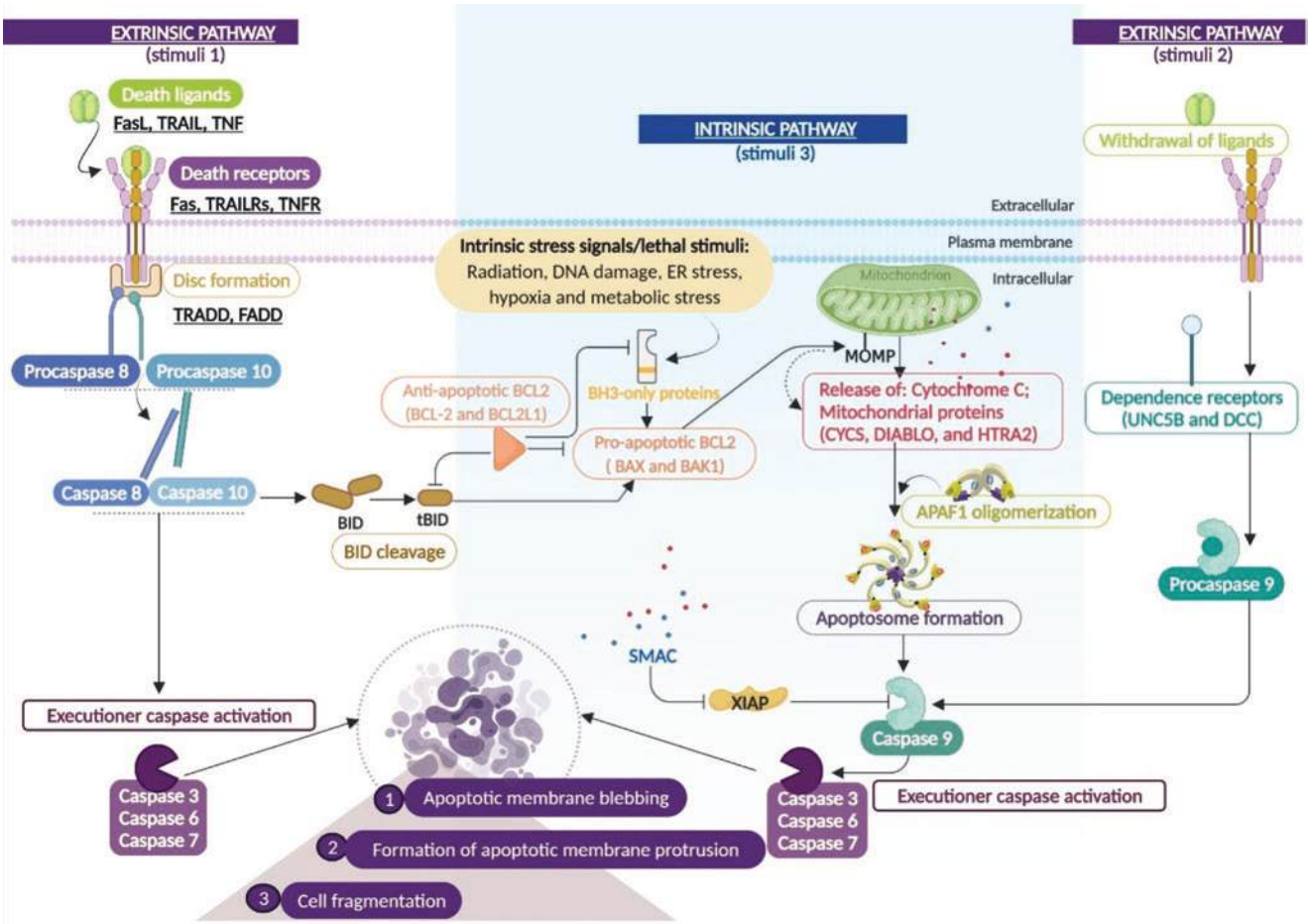

Fig. 3.37 The intrinsic and extrinsic route to apoptosis. Intrinsic stress signals (e.g., DNA damage, hypoxia, metabolic stress) or lethal stimuli (e.g., IR exposure) can induce intrinsic mitochondrial apoptosis (middle). Cleaved or truncated Bid (tBid) can also connect the extrinsic pathway to the intrinsic route. In the extrinsic pathway, ligands for death receptors (left) can trigger caspase activation, but the pathway can also be activated when some dependence receptors are inactivated (right). Abbreviations: *FasL* Fas ligand, *TRAIL* TNF-related apoptosis-inducing ligand, *TNF* tumor necrosis factor, *Fas* Fas cell surface death receptor, *TRAILR* TNF-related apoptosis-inducing ligand receptor, *TNFR* tumor necrosis factor receptor, *TRADD* TNFR1-associated death domain protein, *FADD* Fas-associated protein with death domain, *caspase* cysteine-aspartic proteases, *BID* BH3-interacting domain death agonist, *tBID* truncated BID, *Bcl-2* B-cell lymphoma 2 (an apoptotic inhibitor), *BCL2L1* Bcl-2-like 1, *MOMP* mitochondrial outer membrane permeabilization, *BH3* Bcl-2 homology 3, *DIABLO* direct inhibitor of apoptosis-binding protein with low pI, *APAF-1* apoptotic peptidase-activating factor 1, *Bax* Bcl2-associated X (an apoptotic regulator), *Bak* Bcl-2 homologous antagonist/killer, *XIAP* X-linked inhibitor of apoptosis protein, *SMAC* second mitochondria-derived activator of caspase, *UNC5B* Unc-5 netrin receptor B

Apoptosis results in the production of apoptotic bodies, which are cell fragments, e.g., collapsed cytoskeleton, disassembled nuclear envelope, and fragments of nuclear DNA. An apoptotic cell is also marked by certain "find-me" and "eat-me" signals at the cell surface, which allow the dying cell to be recognized and rapidly engulfed by different macrophage subtypes in the near or distant tissue, thereby avoiding inflammation. A well-recognized potential "eat-me" signal is the expression of phosphatidylserine (PS) on the outer side of plasma membrane, which in turn is being used for assessing early apoptotic cells [129].

In the 1990s, studies which resulted in authors being awarded a Nobel Prize revealed that core machinery components of some apoptotic pathways are highly conserved from nematodes to humans [130]. Subsequently, research on the molecular mechanisms regulating apoptosis has established two major routes of this cell death type, namely intrinsic and extrinsic apoptosis, respectively (Fig. 3.37).

3.10.2.1 Intrinsic Pathway to Apoptotic Execution

Multiple perturbations may trigger intrinsic apoptotic cell death, e.g., growth factor withdrawal, cytokine alterations, endoplasmic reticulum stress, replication stress, formation of reactive oxygen species (ROS), microtubular alterations or mitotic defects, and IR-induced DNA damage. In the context

of DNA damage, mitochondrial release of apoptogenic proteins is central. This commences in part via mitochondrial outer membrane permeabilization (MOMP) that allows cytochrome C and other proteins to be released to cytosol. Once there, cytochrome forms the apoptosome complex together with apoptotic peptidase-activating factor 1 (APAF-1), where pro-caspase-9 is cleaved to active caspase-9 (CASP9). Subsequently, CASP9 cleaves the effector caspases (e.g., caspase-3, caspase-6, and caspase-7), which then causes degradation of cell signaling and structural proteins resulting in an apoptotic morphology. The BCL-2 proteins are regulators of MOMP. These can either promote, e.g., BCL-2-associated X apoptosis regulator (BAX) or BCL-2 antagonist/killer (BAK) or block MOMP, e.g., BCL-2 or BCL-XL members [131]. Another set of BCL-2 members, which only have a BH3 domain, can also promote MOMP, but they act via alleviation of BCL-2 or BCL-XL function or via promotion of BAX/BAK activity. Examples thereof are BCL2-associated agonist of cell death (BAD), BH3-interacting domain death agonist (BID), BCL2-interacting mediator of cell death (BIM), NOXA, and TP53-upregulated modulator of apoptosis (PUMA).

In DNA damage-induced apoptosis, TP53 and BAX/BAK proteins are important. The BCL-2 family members also sense other cellular clues to elicit intrinsic apoptosis including alterations in growth factor receptor/PI3K signaling or microtubule disruption, both of which may have impact in the context of IR-induced cell death. In addition, the mitogen-activated protein kinases 8 and 9 (MAPK8 and MAPK9), more commonly referred to as c-jun N-terminal kinase 1/2 (JNK1/JNK2), are known to regulate the BCL-2 rheostat by phosphorylation of BCL-2 and BAD, via induction of NOXA and PUMA by TP53 transcriptional regulation as well as by association of BIM to microtubuli [132].

3.10.2.2 Extrinsic Pathway to Apoptotic Execution

The extrinsic pathway starts by the activation of membrane receptors, so-called death receptors (DRs), e.g., FAS/CD95 cell surface death receptor and TNF receptor superfamily member 1A (TNFRSF1A)/TNFR1, and is driven by initiator caspases, e.g., caspase-8 (CASP8) and caspase-10 (CASP10). The extrinsic pathway is also used by various immune cells to trigger apoptotic cell death in tumor cells including TRAIL [133]. In addition, the inflammatory cytokine TNF-α produced by activated macrophages, which binds to the TNFR1 and TNFR2 receptors in most human cells, can elicit apoptotic response. Moreover, cytotoxic lymphocytes carry the FasL, which binds and activates the FAS receptor on the surface of the target cell that is followed by death-inducing signaling complex (DISC) formation. Subsequently, adapter proteins bind to the intracellular region of aggregated DISC complex, causing the accumulation of procaspase-8 molecules, which via proteolytic cleavage initiate a proteolytic cascade leading to effector caspase activation. There is also an amplification step where further release of mitochondria-localized pro-apoptotic factors takes place to amplify the initial CASP-3 activation (Box 3.23).

Box 3.23 In a Nutshell: Apoptosis

- Apoptosis is a distinctive and highly controlled form of *programmed cell death*, which requires energy to hit the *self-destruct* button of an affected cell.
- Apoptosis which can be triggered in response to endogenous or exogenous signals is a chain of sequential morphological events during which the early apoptotic cell shrinks and chromatin is irreversibly condensed and cleaved culminating into formation of apoptotic bodies.
- In the mitochondria-mediated or intrinsic route to caspase activation, induction of mitochondrial outer membrane permeabilization (MOMP) is a central event that sets free pro-apoptotic factors such as cytochrome c.
- The BCL-2 proteins can positively and negatively control MOMP.
- The extrinsic pathway is mediated by a death ligand/signal binding to a membrane death receptor and downstream activation of CASP8.

3.10.2.3 Activation of Apoptosis by Ionizing Radiation

IR-induced DNA damages, e.g., unrepaired DNA SSBs or DSBs, primarily trigger apoptosis via the intrinsic pathway [134]; however, at certain IR doses and in certain cell types, the extrinsic apoptotic pathway may also be executed. IR can also initiate mitochondria-mediated signaling in response to ceramide production/formation at the plasma membrane. Moreover, IR can trigger the production of O_2^- and ROS (like H_2O_2 or OH^- radicals), which via release of Ca^{2+} and cytochrome c from mitochondria can cause apoptosis [135].

One important signaling regulator of apoptosis in response to IR is TP53 [136] (Fig. 3.38). Thus, TP53 is phosphorylated in response to DDR signaling, accumulates in the nucleus, and binds to promoters of target genes, e.g., BAX, PUMA, NOXA, p53AIP1, and APAF-1. This results in an alteration in their transcription and hence expression levels, which is followed by mitochondria-mediated apoptosis.

The extrinsic pathway may also play a role in IR-induced apoptosis in which TP53 may upregulate the expression of the FAS receptor and its ligands, which subsequently causes downstream transactivation of initiator CASP8 and apoptosis.

IR may moreover activate the ceramide pathway at the plasma membrane, wherein formation of ROS inflicts lipid

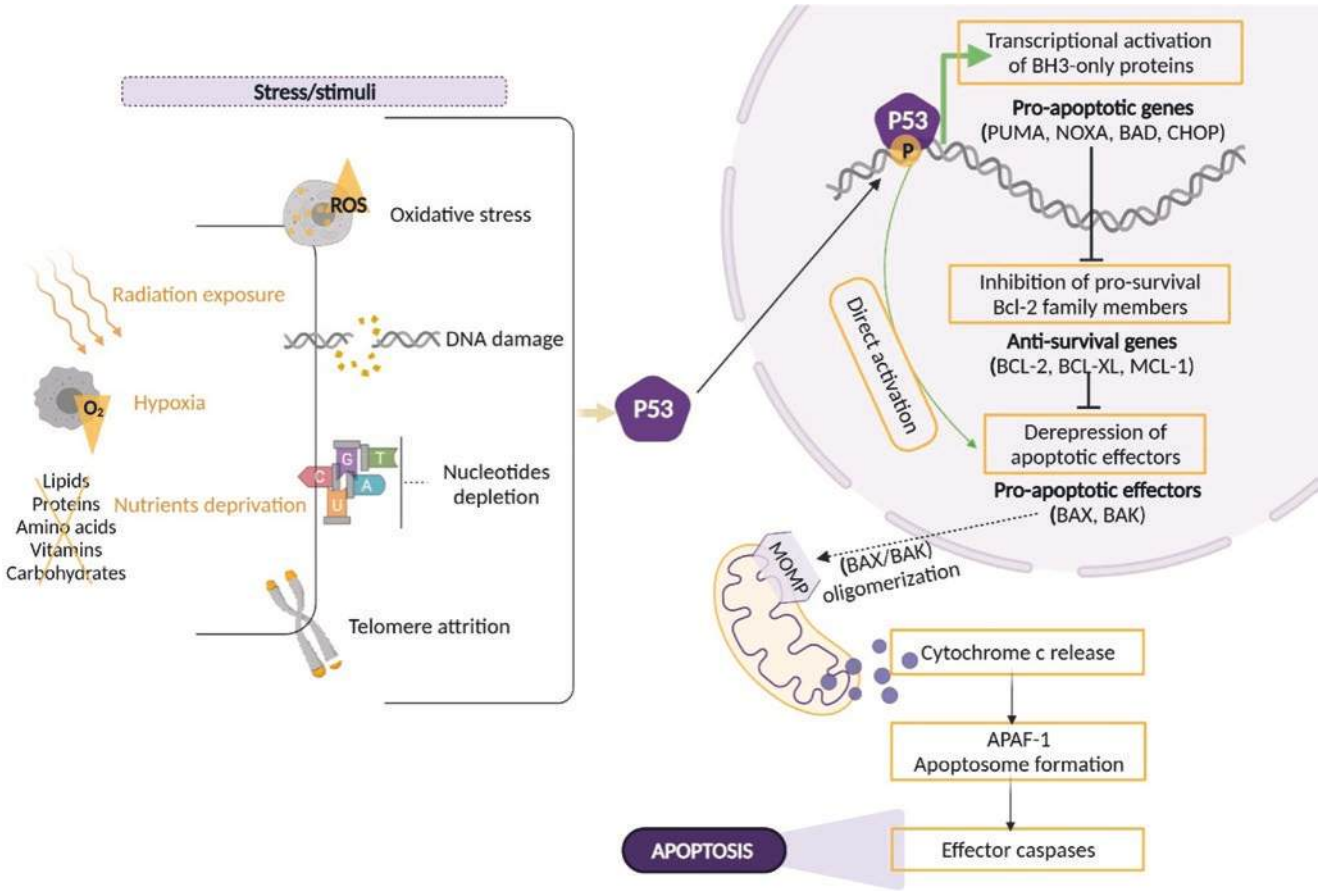

Fig. 3.38 TP53-mediated intrinsic route to apoptosis. The mechanisms of TP53-induced apoptosis through the Bcl-2-regulated pathways in cells undergoing stress are shown. DNA damage triggers stress signaling, which in turn causes stabilization of the TP53 protein in the nucleus. Subsequently, TP53 as a nuclear transcription factor increases the expression of BH3-only proteins such as PUMA and NOXA and downregulation of BCL-2 or BCL-XL expression. The BH3-only proteins bind and inhibit the anti-apoptotic or pro-survival BCL-2 family proteins, so as to unleash the cell death effectors (BAX/BAK) which are often held as hallmarks of apoptosis in affected cells. Oligomerization of BAX/BAK causes MOMP, with subsequent release of cytochrome c, formation of the apoptosome complex, and activation of CASP9 and subsequently effector caspases, which causes apoptotic features of the dying cells. Abbreviations: *ROS* reactive oxygen species, *MOMP* mitochondrial outer membrane permeabilization, *BH3* Bcl-2 homology 3, *PUMA* p53 upregulated modulator of apoptosis, *BAD* Bcl-2-associated agonist of cell death, *CHOP* CCAAT/enhancer-binding protein homologous protein, *Bcl-2* B-cell lymphoma 2 (an apoptotic inhibitor), *Bcl-xL* B-cell lymphoma-extra-large, *Bax* Bcl2-associated X (an apoptotic regulator), *Bak* Bcl2 antagonist killer 1, *APAF-1* apoptotic peptidase-activating factor 1, *caspase* cascade of aspartate-specific cysteine proteases

oxidative damage in the membrane (Fig. 3.39). Subsequently, acid sphingomyelinase is activated, and second messenger ceramide is released as a result of sphingomyelin hydrolysis. IR-induced DNA damage may also trigger mitochondrial ceramide synthase resulting in the accumulation of ceramide which subsequently can induce apoptosis [137].

Ceramide may also activate the RAC1/mitogen-activated protein kinase kinase kinase-1 (MAP3K1) pathway by which MAPK8 and the effector CASP-1, -3, and -6 are induced and which also stimulate the DR pathway. MAPK8/JNK1 is known to be triggered in response to IR as well as other apoptotic stimuli, and depending on the duration of activity, it may induce apoptotic signaling. In summary, the rate of apoptotic events after IR may be executed via different routes and is influenced by cell type, cell cycle phase, dosage number, as well as radiation quality (Box 3.24).

Box 3.24 In a Nutshell: Ionizing Radiation Induced Apoptosis

- IR-induced apoptosis can be executed through intrinsic, extrinsic, or membrane stress (ceramide) pathways.
- IR may trigger apoptosis via mitochondria where TP53 regulation of the BCL-2 family proteins is of major importance.

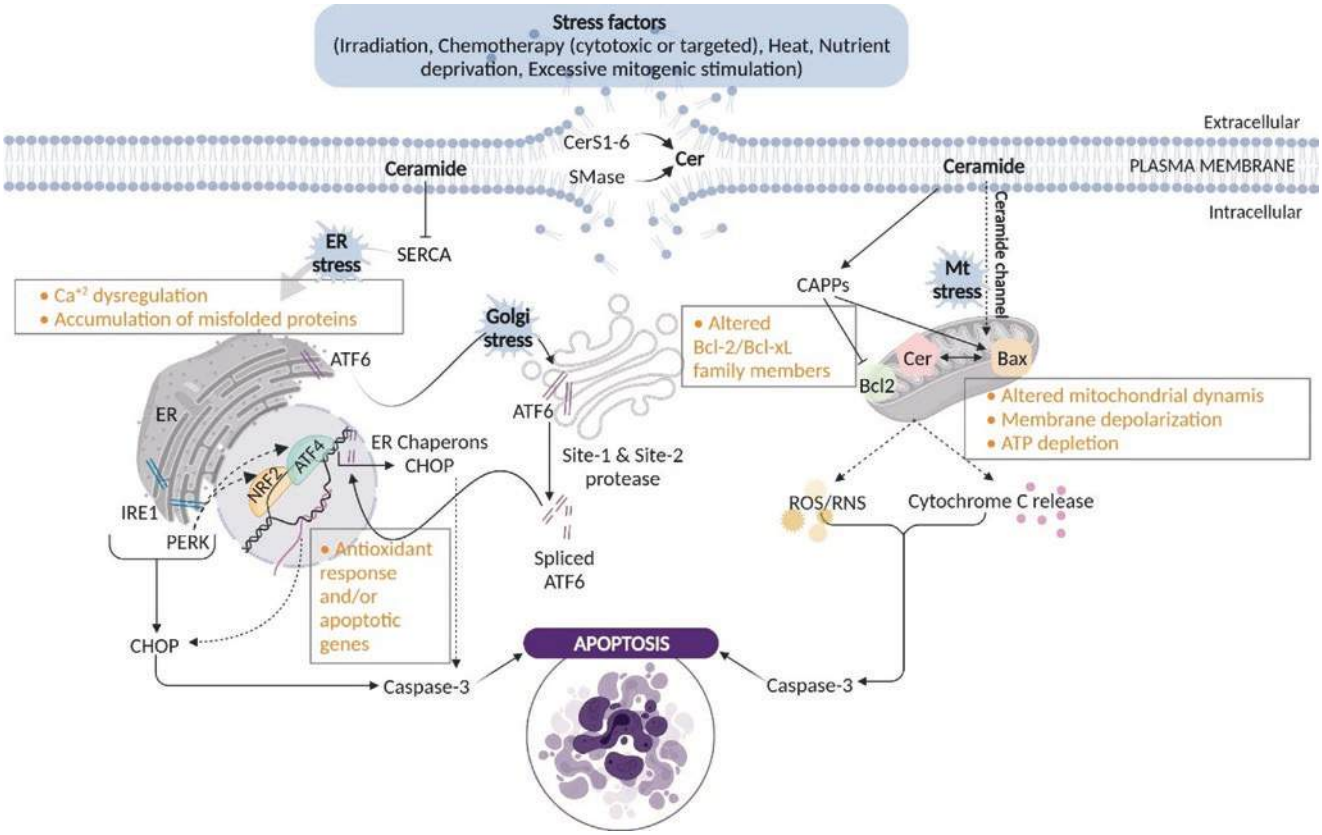

Fig. 3.39 Overview of ceramide signaling and connection to the apoptotic machinery. IR-induced lipid oxidative damage causes sphingomyelinase activation at the plasma membrane, followed by hydrolysis of sphingomyelin and release of ceramide. High dose of IR-induced DNA DSBs can also trigger the mitochondrial ceramide synthase for *de novo* synthesis of ceramide. Inhibition of SERCA and calcium depletion in ER promote ER stress. Expression of downstream pro-apoptotic factor, e.g., CHOP, increases. The UPR activator proteins, ATF6, IRE1, and PERK, alter ER stress. The PERK pathway via ATF4-dependent NRF2 expression triggers the CHOP-mediated apoptotic pathway. CHOP can also be induced by spliced ATF-6 (in Golgi), which regulates the Bcl-2 protein family. CAPPs can alter the BCL-2 protein family, which determines the commitment of cells to apoptosis. Abbreviations: *Cer* ceramide, *CerS1–6* a family of six ceramide synthases, *SMase* sphingomyelinase, *SERCA* sarco-endoplasmic reticulum calcium transport ATPase, *ER* endoplasmic reticulum, *ATF6* activating transcription factor 6, *IRE1* inositol-requiring enzyme 1, *PERK* protein kinase R-like ER kinase, *NRF2* nuclear factor erythroid 2-related factor-2, *ATF4* activating transcription factor 4, *CHOP* CCAAT/enhancer-binding protein homologous protein, *Mt* mitochondria, *CAPPs* ceramide-activated protein phosphatase, *Bcl-2* B-cell lymphoma 2 (an apoptotic inhibitor), *Bcl-xL* B-cell lymphoma-extra-large, *Bax* Bcl-2-associated X (an apoptotic regulator), *RNS* reactive nitrogen species, *ATP* adenosine triphosphate

3.10.2.4 Methods to Detect Apoptotic Cell Death

The apoptotic cell features, i.e., cell morphology, and the activation of different apoptotic signaling routes giving rise to distinguishable phenotypes have been extensively studied with multiple methods at hand. The detection of apoptosis includes methods (Fig. 3.40) related to membrane alterations, e.g., PS exposure monitored by annexin V association [129]; DNA fragmentation assessment; cytotoxicity and cell proliferation assays; analyses of mitochondrial effects, i.e., cell permeabilization; loss of mitochondrial potential; BCL-2 family protein complex formation; association of the apoptosome or DISC complex in cytosol; and pro-caspase cleavage later via different antibody-based, enzymatic assays or by flow cytometry [138]. Moreover, less frequently used technologies such as light-scattering flow cytometry and time-lapse microscopy perfusion platform can be performed to avoid underestimating the extent and timing of apoptosis, temporal aspects of death, cell surface area assessment, cellular adhesion analysis, and genotoxicity-specific chromatin changes.

3.10.3 Necrosis

Necrosis (from the Greek "nekros" designating "to kill") has for long been seen upon as an uncontrolled, irreversible mode of cell death, while recent work suggests that necrosis is a tightly genetically regulated pathway yet triggering inflammatory and/or reparative reactions in the tissue [139]. Necrotic cell death can be classified into accidental cell death

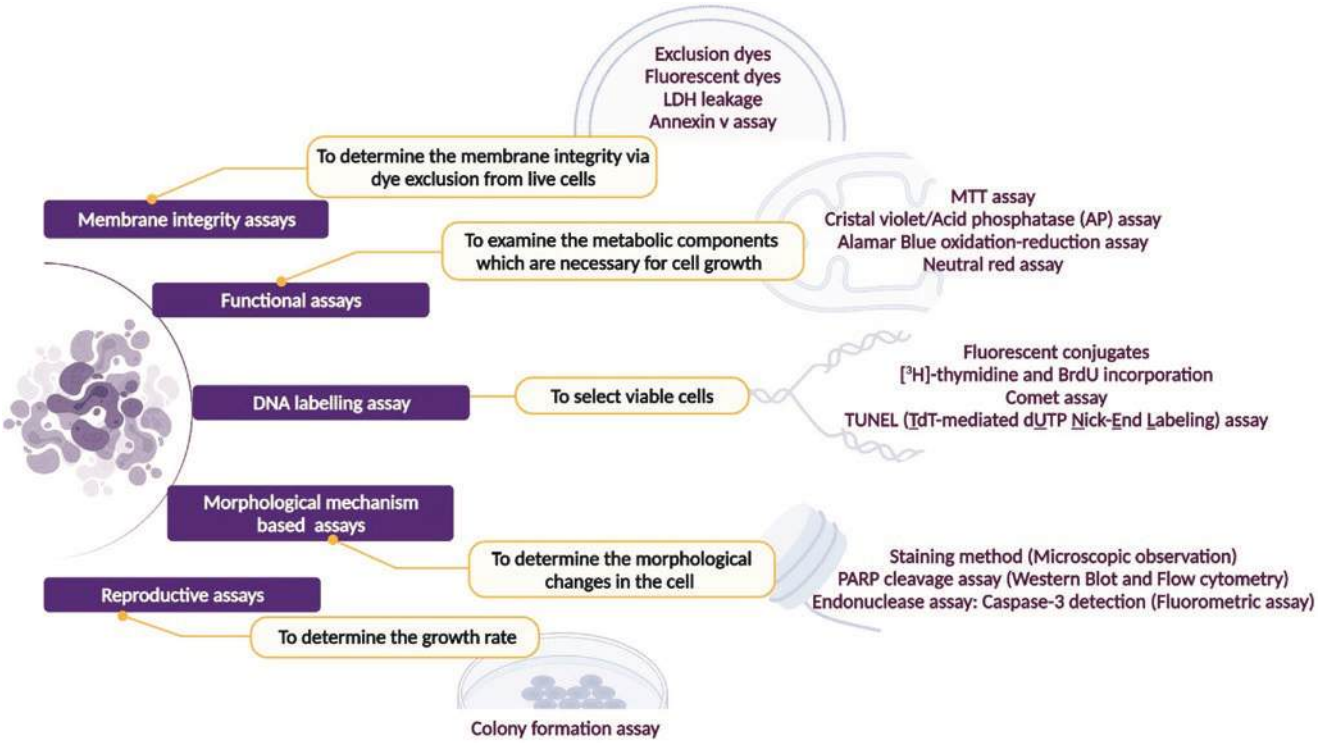

Fig. 3.40 Methods to detect cell death, in particular apoptotic cell death. The schematic diagram outlines various biological assays used to determine apoptotic cell death. Some of these assays can also be used to assess other types of cell death. These assays are based on the morphological criteria and distinguishing features of apoptotic pathways, e.g., staining for PS exposure on the outer plasma membrane (by annexin V assay) and caspase-3 activation or PARP cleavage (by, e.g., western blotting). Cell viability assays such as membrane integrity assays and reproductive assays are performed to monitor live cells in culture and measure an enzymatic activity as a marker of viable cells by using different classes of colorimetric reagents and substrates generating a fluorescent signal. Results from these assays do not always indicate apoptosis, but more about cell death in general. DNA labeling assay, functional assays, and morphological mechanism-based assays detect and quantify the cellular events, some of which are specifically associated with apoptotic cell death, such as formation of apoptotic antibodies, expression of apoptotic inhibitors, caspase activation in either intrinsic or extrinsic pathways, and DNA fragmentation. The principles for each assay are given in the respective yellow boxes. Abbreviations: *MTT* (3-(4, 5-dimethylthiazolyl-2)-2, 5-diphenyltetrazolium bromide), *LDH* lactate dehydrogenase, *BrdU* bromodeoxyuridine, *PARP* polyadenosine diphosphate-ribose polymerase, *PS* phosphatidylserine

Table 3.11 Accidental and regulated necrosis, key features, and methods of detection

Type of cell death	Morphology	Detection methods
Accidental necrosis	Membrane disruption, mitochondria swelling (loss of organelle), cell swelling	LDH quantification, cell-impermeable DNA-binding dye, membrane integrity loss
Necroptosis	Membrane disruption, moderate chromatin condensation, cell swelling	Flow cytometry, western blot, immunohistochemistry—levels of biomarker proteins, mitochondrial depolarization detection, fluorescence microscopy for membrane loss, electron microscopy for morphology
Pyroptosis	Membrane disruption, bubbling, moderate chromatin condensation	LDH quantification, fluorescence microscopy for membrane integrity loss, western blot for GSDM D, IL-1β
Ferroptosis	Membrane disruption, iron accumulation, lipid peroxidation, diminutive mitochondria	Lipid peroxide quantification—flow cytometry and BODIPY-C11 probe
Methuosis	Membrane disruption, accumulation of large fluid-filled vacuoles, cell swelling	Electron microscopy, time-lapse fluorescence microscopy for morphology, metabolic flux analysis
NETosis	Membrane disruption, chromatin condensation	Fluorescence microscopy for morphology, flow cytometry, ELISA, western blot

(ACD) and regulated necrotic cell death (RNCD). RNCD can be further classified into necroptosis, pyroptosis, ferroptosis, NETosis, and methuosis given their molecular routes [139] (Table 3.11).

3.10.3.1 The Role of Necrosis in IR Cellular Responses

Necroptosis, pyroptosis, methuosis, and ferroptosis are all triggered in response to IR [124, 140]. In the context of RT

of cancer, necrosis can be induced either directly following DNA damage or indirectly by ROS formation that reacts with lipids generating lipid peroxides. IR has also been linked to lipid peroxidation and ferroptosis, and necroptosis together with ferroptosis was postulated to occur via ATM signaling.

Both ACD and RNCD trigger immunogenic cell death (ICD). In turn, ICD can stimulate an adaptive immune response after antigen is exposed by cells after RT or chemotherapeutics [141]. In case of immunogenic cell death, damage-associated molecular patterns (DAMPs) are delivered and identified by pathogen recognition receptors (PRRs) exhibited by intrinsic components of the immune system, conducting to the stimulation of an immune response [141]. ACD is an uncontrolled type of cell death which is activated by, e.g., physical damage, hypoxia, inflammatory toxins, and high doses of IR. The cells respond by morphological alterations, such as cytoplasmic swelling of the cell organelles, i.e., oncosis [142], which is a result of disturbance of ionic pumps causing Ca^+ influx, plasma membrane disruption followed by the leakage of intracellular organelles with accidental deteriorated DNA, and absence of clear chromatin condensation [142]. RNCD comprises upregulation of diverse pro-inflammatory proteins and molecules such as nuclear factor-κB, leading to the rupture of the cell membrane causing leakage of the cellular debris, e.g., ATP, DNA, nuclear proteins, heat-shock proteins, and uric acid, into surrounding zones, provoking a cascade of inflammation and tissue injury. Thus, the release of proteins/molecules promotes inflammasome activation and production of pro-inflammatory cytokine interleukin-1 beta (IL1). The methods used to detect necrosis are lactate dehydrogenase (LDH) activity measurement and cell-impermeable DNA-binding dye. These techniques are based on the morphological characteristics proving the cellular release and membrane porosity (Table 3.12).

Table 3.12 Examples of some oncogenes in cancer from Weinberg [143] and Gillies et al. [144]

Oncogene	General function	Major tumor type with deregulation
K-ras	Guanine nucleotide-binding protein	Lung, ovarian, colorectal, bladder carcinomas
N-ras	Guanine nucleotide-binding protein	Head and neck cancers
H-ras	Guanine nucleotide-binding protein	Colorectal carcinomas
c-myc	Transcription factor	Various leukemias, carcinomas
L-myc	Transcription factor	Lung carcinomas
EGFR/HER2	Receptor tyrosine kinase	Glioblastomas, lung cancer, breast cancer
Src	Cytoplasmic tyrosine kinase	Colon cancer, head and neck cancers, chronic myelogenous leukemia
Sis/PDGF	Growth factor	Simian sarcoma

3.10.3.2 Necroptosis/Regulated Necrosis

Necroptosis, also known as a regulated necrosis, which works in a caspase-independent fashion, exhibits a necrotic morphology with membrane disruption and leakage of organelles (reviewed by Weinlich et al. (2017)). Different stimuli can elicit necroptosis: DRs, e.g., members of the TNFR superfamily, pattern recognition receptors (PRRs), Toll-like receptors (TLRs), T-cell receptors (TCRs), multiple chemotherapeutic drugs, and hypoxia. The process of necroptosis commences by the stimulation of receptor-interacting protein kinases (RIPKs) (Fig. 3.41).

RIPKs are stimulated to go into macromolecular complexes from the membrane receptors with the necrosome with RIPK1 and RIPK3 being the main components. RIPK3 subsequently stimulates mixed-lineage kinase domain-like protein (MLKL) through phosphorylation causing its oligomerization and relocalization, resulting in cell membrane permeabilization and subsequent cell death.

Different techniques can be used to identify necroptosis, e.g., flow cytometry, western blotting, and immunohistochemistry. Through these techniques, the expression levels of MLKL, RIPK3, and RIPK1 are evaluated as well as cell by electron microscopy (Table 3.11).

3.10.3.3 Pyroptosis and Ferroptosis: Triggers and Molecular Mechanisms

Pyroptosis, which is stimulated by IR as well as intracellular pathogenic factors in immune cells, follows a series of caspase-dependent events and is pro-inflammatory (reviewed by Yu et al. [146]). Thus, the NOD-like receptors (NLRs) of irradiated/infected macrophages/monocytes recognize cytoplasmic pathogen-associated molecular patterns (PAMPs) as well as DAMPs and trigger inflammasome complex production, which activates CASP1. CASP1 in turn activates gasdermin D, which mediates the plasma membrane rupture (Fig. 3.42) as well as the inflammatory cytokines interleukin 1β (IL-1β) and IL-18, which further regulate inflammation. Pyroptosis also involves cell swelling followed by disintegration of the plasma membrane and leakage of the pro-inflammatory contents, e.g., DAMPs, IL-1β, and IL-18, contributing to elimination of the immunologic challenges locally or systemically. Pyroptosis can be detected by LDH assay, fluorescence microscopy, western blot analysis (for identification of gasdermin D, IL-1β), and measurement of the cell intake of propidium iodide (Table 3.11).

Ferroptosis is a form of caspase-independent regulated necrosis and is distinguished by excessive iron-dependent lipid peroxidation. It presents a necrotic morphology with altered mitochondria, i.e., small mitochondria, fewer cristae, rupture of outer membrane, and an electron-dense ultrastructure. Execution of ferroptosis is decided by the equilibrium between ROS production due to iron increase and antioxidant protection mechanisms that impede lipid peroxidation.

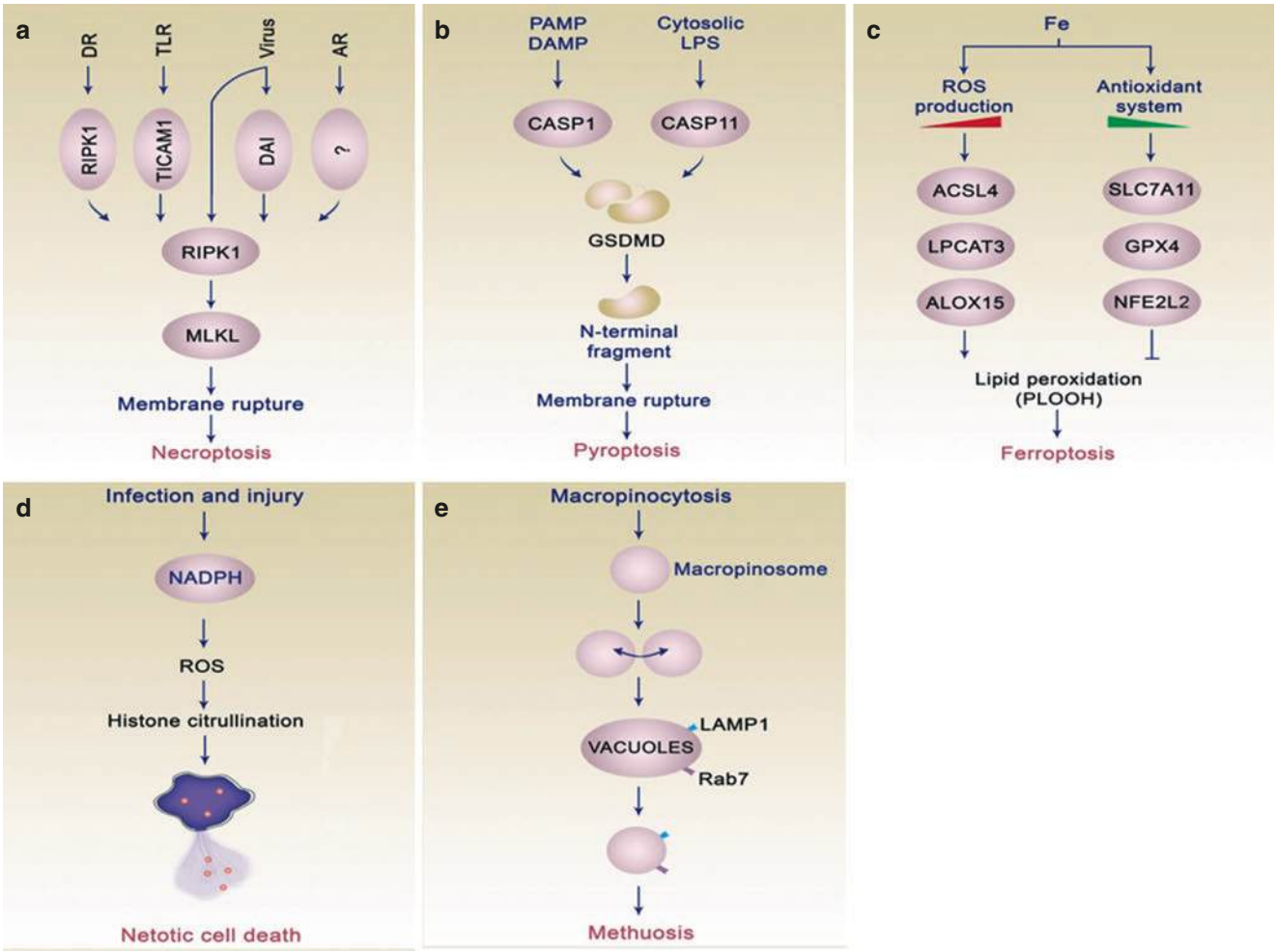

Fig. 3.41 Summary of regulated necrotic cell death. (**a**) Necroptosis elicited by DR, TLR, and viruses stimulates RIPK3 and then MLKL, which is required for membrane disruption. (**b**) Pyroptosis induced by GSDMD following its cleavage by CASP1 and CASP11. The main elicitors: PAMPs and DAMPs, or cytosolic LPS. (**c**) Ferroptosis is dependent on the balance between ROS production due to iron accumulation and antioxidant defense mechanisms that inhibit lipid peroxidation. The ACSL4–LPCAT3–ALOX15 pathway mediates lipid peroxidation, while system xc- (comprising SLC7A11, GPX4, and NFE2L2) impeded this process. (**d**) NETosis is triggered by NET leakage, which is mediated by ROS generation and histone citrullination. (**e**) Methuosis is associated with macropinocytosis. Nascent micropinosomes fused forming large vacuoles that contain late endosomal markers (LAMP1 and Rab7). These do not recycle or unify with lysosomes causing cell death. Reproduced with permission (CCBY) from Tang et al. [145]. *DR* death receptor, *TLR* Toll-like receptor, *RIPK3* receptor-interacting protein kinases 3, *MLKL* mixed-lineage kinase domain-like protein, *GSDMD* gasdermin D, *CASP1* caspase 1, *CASP11* caspase 11, *PAMPs* pathogen-associated molecular patterns, *DAMPs* damage-associated molecular patterns, or cytosolic, *LPS* lipopolysaccharide, *ACSL4* acyl-CoA synthetase long-chain family member 4, *LPCAT3* lysophosphatidylcholine acyltransferase 3, *ALOX15* arachidonate lipoxygenases (ALOXs, specifically ALOX15), *SLC7A11* the catalytic subunit solute carrier family 7 member 11, *GPX4* glutathione peroxidase 4, *NFE2L2* nuclear factor erythroid 2-like 2, *NET* NETosis extracellular trap, *ROS* reactive oxygen species, *LAMP1* lysosomal associated membrane protein 1, *Rab7* lysosomal Rab protein 7. (Adapted from Tang et al. [145])

Thus, ferroptosis is activated after lipid peroxidation in a process catalyzed by iron, either in a Fenton-like manner or through lipoxygenases (Fig. 3.41). Accordingly, the oxidation of polyunsaturated fatty acids (PUFAs), like arachidonic acid (AA), is necessary for lipotoxicity in ferroptosis, which takes place via a catalytic pathway comprising acyl-CoA synthetase long-chain family member 4 (ACSL4), lysophosphatidylcholine acyltransferase 3 (LPCAT3), and arachidonate lipoxygenases (ALOXs, specifically ALOX15) [147]. In addition, lipid peroxidation can be hindered by the various antioxidant systems such as the cystine/glutamate antiporter system, which consists of the catalytic subunit solute carrier family 7 member 11 (SLC7A11), glutathione peroxidase 4 (GPX4), and pro-survival proteins, like nuclear factor erythroid 2-like 2 (NFE2L2). System xc- facilitates the exchange of cystine and glutamate in and out of the cell. The cystine which is taken up is reduced to cysteine in cells, which is needed for the synthesis of glutathione GSH. GSH is used by

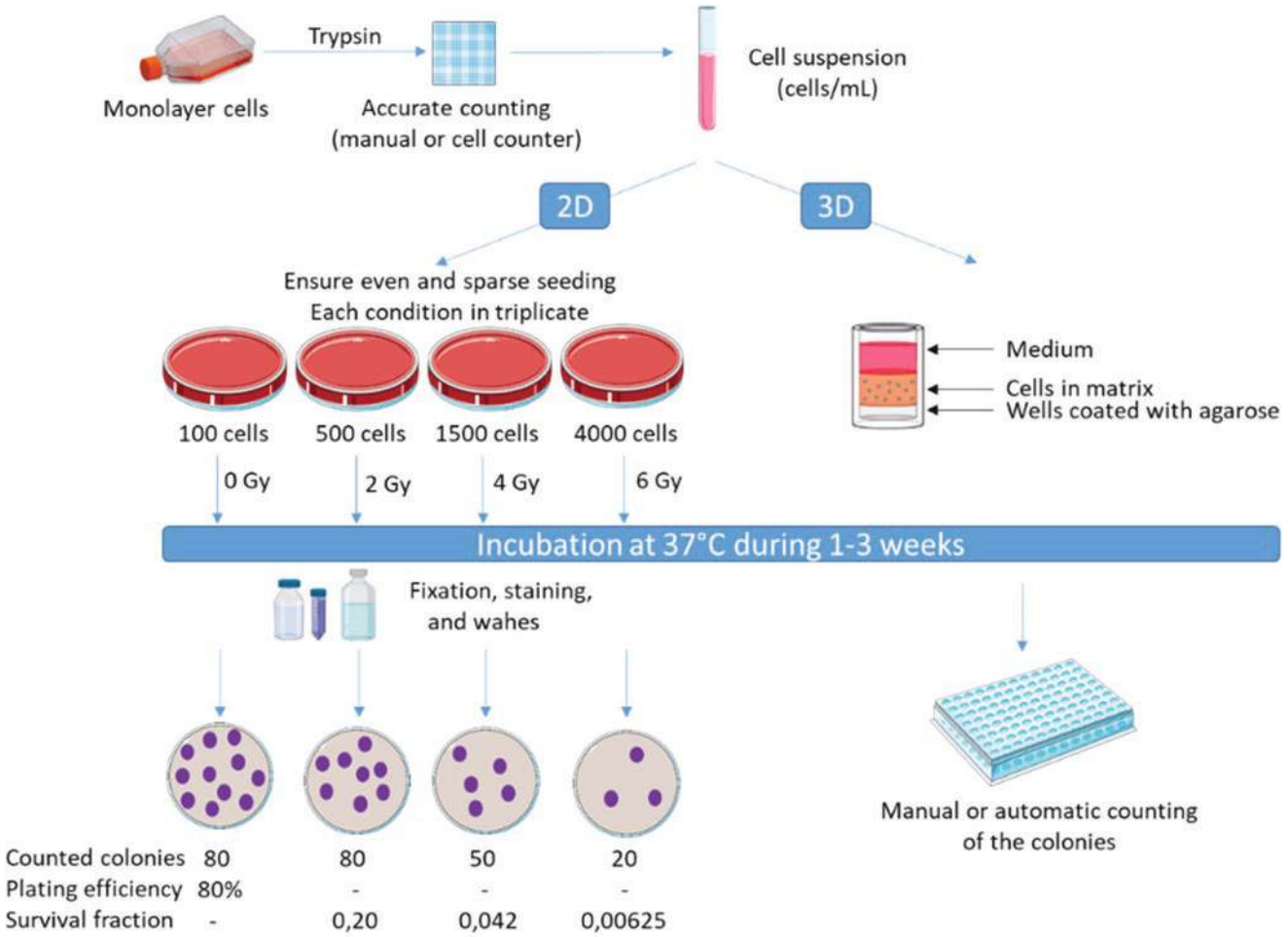

Fig. 3.42 Methodology for 2D (Puck) and 3D clonogenic curves. The clonogenic assay measures the ability of single cells to form colonies. A cancer cell that is not able to form a colony can be regarded as inactivated. Cellular monolayers are dissociated into single cells and counted and diluted to the required concentration, depending on the dose. The cells are then seeded in cell flasks/dishes for colony formation or in a 3D matrix for spheroid formation. After irradiation, the cells are incubated for 1–3 weeks depending on the cell doubling time of that particular cell line, before they are fixed, stained, and counted. The surviving fraction is calculated as the number of colonies in irradiated samples relative to the plating efficiency of unirradiated control dishes

GPX4 to stop the generation of phospholipid hydroperoxides (PLOOH), the key mediator of chain reactions in lipoxygenases. The induction of ferroptosis can be determined by measuring lipid peroxides coupled with flow cytometry (Table 3.11).

3.10.3.4 Neutrophil Extracellular Trap-Associated Cell Death (NETosis) and Methuosis

NETosis is stimulated by various pathogens or other stimuli, which release neutrophil extracellular traps of mainly DNA-protein structures [148] in a process dependent on NADPH oxidase 4 (NOX4), the principal source of ROS (Fig. 3.41). NETosis also comes along with important increase of ROS conducting to the stimulation of protein-arginine deiminase 4 (PAD4). Then, PAD4 citrullinates (converts arginine to citrulline via deamination) the histones, promoting the nuclear chromatin decondensation. Further, the NET is released into the cytosol leading to the disruption of the neutrophil membrane. Then, neutrophil breaks up and the NETs are released into the environment. NETs can be generated by other forms of immune cells, e.g., eosinophils, mast cells, basophils, macrophages, and also epithelial cells and cancer cells as a response to various injuries [145]. NETosis can be studied using various techniques: immunofluorescence, transmission electron microscopy, scanning electron microscopy, ELISA tests, flow cytometry, as well as western blot analyses of NETosis markers (Table 3.11).

Methuosis (from Greek methuo—"drink to intoxification") is another type of caspase-independent regulated necrotic cell death that is induced by exposure to heat, trauma, and infection and which lead to cell swelling, lysis

of plasma membrane, as well as inflammation. Methuosis is correlated to macropinocytosis (referred to as "cell drinking") and is associated with the extensive accumulation of fluid-filled cytoplasmic vacuoles stemmed from macropinosomes, which for example is observed in cancer cells driven by the oncoprotein Ras [149] (Fig. 3.41). Methuosis can be detected by electron microscopy, time-lapse fluorescence microscopy, visualization of vacuoles using fluorescent dyes, and metabolic flux analyses (Table 3.11) (Box 3.25).

Box 3.25 In a Nutshell: Necrosis

- Necrotic cell death is classified into accidental cell death and regulated necrotic cell death with different subtypes: necroptosis, pyroptosis, ferroptosis, NETosis, methuosis, etc.
- IR may stimulate necrosis via direct DNA damage response and via radical oxygen species.
- All types of necrosis are immunogenic cell death types.

3.10.4 Autophagy

Autophagy is an adaptive and catabolic process induced by various forms of cellular stress, intended to mitigate the impact of cell damage to avoid cell death, by recycling biomolecules and damaged organelles. This mechanism occurs via a self-digestion process involving the formation of double-membrane vesicles, called autophagosomes, that merge with lysosomes. Autophagy can be induced by nutrient deprivation (amino acids, in particular leucine and glutamine, and glucose) and cytotoxic insults such as IR or chemotherapy. The main function of autophagy is to provide nutrients and building blocks for vital cellular functions during different forms of stress. Therefore, this pathway is generally considered as a cytoprotective mechanism [150]. Autophagy is a complex mechanism involving several steps. First, the recruitment of autophagy-related proteins (ATG) to a specific subcellular location called the phagophore assembly site (PAS) allows phagophore nucleation (initiation and phagophore nucleation). During phagophore elongation, a portion of the cytoplasm is engulfed (cargo sequestration) and the autophagosome, a double-membrane vesicle, is being formed (autophagosome maturation). Fusion of the autophagosome with lysosome allows the degradation of the autophagic cargo.

A key regulator of autophagy is the mammalian target of rapamycin (mTOR) that exists in two distinct protein complexes, mTORC1 and mTORC2. In its active conformation, mTORC1 prevents autophagy by inhibiting the UNC51-like kinase 1 (ULK1) complex, composed of ULK1, the autophagy-related gene 13 (ATG13), ATG101, and the FAK family-interacting protein of 200 kDa (FIP200). Upon autophagic stimuli, mTORC1 is inhibited, leading to the activation of ULK1. Active ULK1 phosphorylates ATG13 and FIP200, which leads to the activation of the class III phosphoinositide 3-kinase (PI3K) complex, allowing phagophore nucleation. This triggers the production of phosphatidylinositol-3-phosphate (PIP3) at a characteristic ER structure called omegasome. PIP3 recruits WD repeat domain phosphoinositide-interacting proteins (WIPI2) and zinc finger FYVE domain-containing protein 1 (DFCP1) to the omegasome. By binding ATG16L1, WIPI2 recruits the ATG12-ATG5-ATG16L1 complex that allows the conjugation of ATG8 family proteins (including microtubule-associated protein light-chain 3 (LC3) and γ-aminobutyric acid receptor-associated proteins (GABARAPs)) to membrane-resident phosphatidylethanolamine (PE). By this process, LC3-I (diffuse form) is converted into LC3-II (membrane-anchored, lipidated form), a marker of autophagic membranes. The recruitment of ATG9-containing vesicles (coming from the plasma membrane, mitochondria, recycling endosomes, and Golgi complex), delivering additional lipids and proteins, further contributes to autophagosomal membrane expansion. Once the membrane is sealed, the autophagosome is formed and undergoes maturation. Then it can merge with the lysosome, where the autophagic cargo will be degraded by acidic hydrolases. For the molecular details, see Dikic et al. [151].

3.10.4.1 Role of Autophagy in IR Responses

Beyond apoptosis, the commonly studied IR-induced cell death mechanism, autophagy was shown to be frequently induced in response to IR. For example, autophagy can be triggered following DNA damage inflicted by IR or other agents. Indeed, DNA damage repair (DDR) is an energy-demanding process that consumes ATP but also NAD+ via the action of polyADP-ribose polymerase 1 (PARP1). Autophagy induction allows the recycling of metabolic precursors for ATP and provides energy for the DDR. ROS was also shown to trigger and regulate autophagy [152]. The function of IR-induced autophagy is still being debated. Results of in vitro and in vivo studies provided conflicting notions whether autophagy acts as a cytoprotective mechanism, promoting cell survival responsible for radioresistance. In that respect, radiosensitization strategies based on genetic or pharmacological autophagy inhibition led to different outcomes. Several studies also pointed out the non-cytoprotective function of IR-induced autophagy where autophagy inhibition failed to alter radiosensitivity. Although autophagic functions may vary depending on both cell type and treatment regimen applied, specific characteristics able to distinguish cytotoxic, cytoprotective, or non-cytoprotective forms of IR-induced autophagy have not yet been identified. There

are assumptions that autophagy duration may play a role in radiosensitivity, with radioresistance occurring in case of prolonged autophagy, while a transient form of autophagy will ultimately lead to apoptosis [150].

Outcomes of clinical trials conducted with approved autophagy inhibitors (e.g., chloroquine and hydroxychloroquine) were mitigated due to toxicity issues and unsatisfactory autophagy inhibition. Concerns were raised regarding the most probable non-tumor selectivity of autophagy inhibitors, off-target effects, effects on immune response, and difficulty to monitor autophagy inhibition in patients' tumors [153]. Further studies on the molecular mechanisms governing IR-induced autophagy may bring additional evidence on how to optimally modulate autophagy to produce favorable outcomes (Box 3.26).

Box 3.26 In a Nutshell: Autophagy

- Autophagy is triggered by IR and often considered as a cytoprotective mechanism.
- Autophagy inhibition as a radiosensitization strategy led to inconsistent results, suggesting an intricate role of autophagy, being regulated by many factors.

3.11 Clonogenic Cell Survival

As described in the sections before, cells damaged by radiation might suffer from genetic instability and/or die through, e.g., apoptosis or other types of cell death. These consequences of radiation exposure can be used to qualify and quantify the damage and draw conclusions on its severity. In this context, it is possible to look at not only the fatal outcome of radiation damage but also the capability of cells to survive IR. It is important to distinguish between cell survival and cell viability. In radiobiology, the term cell death is used also for cells that are inactivated, i.e., have lost their proliferation ability. Cancer cells and stem cells are characterized by their capacity for sustained proliferation. A cancer cell that has lost the ability to divide is by definition dead as a cancer cell even though it may still have an intact cell membrane and retained metabolic function. While non-proliferating cells retain their function even after radiation doses as high as 50–100 Gy, cancer cells may lose the capacity for uncontrolled cell division after doses in the order of 2 Gy.

There are several assays available to measure cell viability. Some use dye exclusion, such as trypan blue, to measure the proportion of cells with intact cell membrane. Others measure metabolic function through the activity of mitochondrial enzymes, such as the MTT (3-(4,5-dimethylthiazol-2-yl)-2,5-diphenyltetrazolium) assay, cellular reducing conditions such as the Alamar Blue assay, or ATP production. Even though viability measurements over time can give an indication of cell proliferation, the only direct measurement of clonogenic function is the clonogenic assay, the gold standard for cell survival measurements. These assays can be performed in vitro with cultured cells or in vivo from biopsies.

3.11.1 *In Vitro* Dose-Response Assays

The first survival curve, i.e., the relation between survival and delivered doses, was established with HeLa cells cultivated in vitro and irradiated with X-rays by Puck and Marcus in 1956 [154]. A surviving cell is defined as a cell able to divide and form a colony composed of at least 50 cells. To find the surviving fraction, the capacity of nonirradiated and irradiated cells to form colonies is compared. Typically, in vitro cell survival is measured in adherent cells in monolayer culture. The day before the experiment, cells are trypsinized. Viable cells are counted with a hematocytometer or a cell counter. A determined number of cells in suspension is seeded in Petri dishes (or flasks) destined to be a control or irradiated before their first doubling time. Depending on the design of the experiments, the medium can be changed after irradiation. Then cells are incubated at 37 °C for 1–3 weeks according to the cell types (≥8 divisions). When the colonies grow to exceed 50 cells, observable by microscopy or visually detectable, they are fixated with methanol or ethanol and then stained with Giemsa, methylene blue, or crystal violet before several washes with water and drying [155]. After that, the clones formed are counted manually or with an automatic counter (Fig. 3.42).

All cells comprising each colony are the progeny of a single initial cell seeded, which survived irradiation. If we consider 100 untreated cells, the ideal number of colonies formed should be 100. However, this is never the case, depending on diverse factors (medium change, errors and uncertainties in counting the cell suspension, trauma of the detachment …), and in fact 50–90 colonies might be expected. Considering the outcome of the control conditions (nonirradiated), the term plating efficiency (PE) can be defined. This corresponds to the percentage of cells seeded, which grew into colonies. If 75 colonies are counted after seeding 100 cells, we talk about a PE of 75%. It must be noted that the PE may differ according to the number of cells seeded: this is the "feeder effect." This effect is attributed to the need of some cell types to be able to cooperate with neighboring cells [156]. If this communication is missing, the cells are not able to start proliferation. Therefore, the cell density seeded might play a role in the fraction of cells able

to form colonies. This might limit the robustness of the classical analysis of the colony-forming assay. In future, a different way of performing and analyzing this assay might be necessary [156].

In classical colony-forming assay parallel to the control samples, cells are irradiated, then incubated, fixed, and stained at the same time point as control cells. Different cases can therefore be observed: (1) some of the seeded cells being still single and not divided; (2) cells that managed one or two divisions to form a tiny abortive clone; and (3) cells able to form large colonies of at least 50 cells, corresponding to 5–6 cell divisions, but which can look like a little bit different from the untreated cells in terms of aspect and size. These latter cells, able to form colonies, are qualified of "survivors" and counted since they have retained their reproductive integrity. For example, if we seed 3000 cells followed by irradiation of 5 Gy, and if the PE previously determined is 0.75, then we can expect the attachment of 2250 cells (0.75 × 3000). If at 5 Gy 42 colonies grew up after incubation, the surviving fraction can be calculated at 1.9%: 42/(3000 × 0.75) = 0.019. In general, the plating efficiency (PE) and the surviving fraction (SF) are given by

$$\mathrm{PE} = \frac{\text{colonies counted}}{\text{cells seeded}} \times 100 \quad (2)\mathrm{SF} = \frac{\mathrm{PE}(\text{condition})}{\mathrm{PE}(\text{control})} \times 100. \tag{3.1}$$

Survival curves for mammalian cells are usually presented in a form with dose plotted on a linear scale and surviving fraction on a logarithmic scale and can be fitted by several models, as for example the linear-quadratic model (see Chap. 1). The form of the curves, as seen in Chap. 1, depends on the linear energy transfer and allows determining important biological parameters such as the surviving fraction, the ratio α/β, or the relative biological efficiency (RBE) for example (see Chap. 1 for details). The surviving fraction at 2 Gy (SF2) is often used to approximate cell radiosensitivity.

To obtain a survival curve, several doses of irradiation have to be applied. The number of cells seeded per dish needs to be accurate and often adjusted after preliminary experiments to count a significant number of colonies since these parameters are dependent on doses, cell lines, and type of radiation. At least a triplicate of different dilutions is realized for each condition tested (here each dose delivered). If colonies are few, the statistical significance is reduced. On the opposite, if the colonies are too many, some colonies can be merged with another one, and the counting is inaccurate. In some cases, cells could be irradiated first (one flask for one dose) and then detached to be seeded at different dilutions [157]. However, precautions need to be considered since some cells are sensitive to detachment after irradiation, which affects cell survival. In addition, colony-forming assays require very accurate cell counting, since the controls come from a separate trypsinization. Clonogenic curves cannot discriminate the type of cell death, but they give information about the radiosensitivity of the cells.

More recently, the literature showed that survival curves obtained with three-dimensional (3D) cell models more reliably reflect the cell response in vivo than the results obtained with 2D cell monolayer culture [158]. 3D cell models for cell survival can be obtained by embedding single cells in an extracellular matrix, put in 96-well plates pre-coated with agarose, covered with medium, and then exposed to radiations. Cells are grown for a few days until cell clusters reach 50 cells, and the number of colonies is microscopically counted (Fig. 3.42).

3.11.2 *In Vivo* Dose-Response Assays

An in vivo clonogenic assay allows measuring cell survival in an animal model, allowing the study of radiosensitivity of normal or tumor cells treated in vivo. These systems depend on the reproductive integrity of individual cells and allow the observation of a clone of cells regenerated in the irradiated tissue. There are assays developed for early-responding tissues, which divide rapidly and respond early to the effects of radiation, like bone marrow cells, skin, and intestinal epithelium, and assays for late-responding tissues, like lung, kidney, and spinal cord (Fig. 3.43).

The **spleen colony assay**, also called bone marrow stem cell assay, was first described by Till and McCulloch [159]. The basis of this assay relies on the use of one donor mouse and a group of recipient mice. Recipient mice are previously exposed to whole-body irradiation (9 Gy) to sterilize the spleen and suppress endogenous hematopoiesis. Then, from a donor mouse irradiated with a test dose, a cell suspension of bone marrow cells is taken and injected intravenously into the recipient donors. Some of these cells will lodge in the spleen, and after 10–11 days, single cell-derived clones will appear in the surface of the spleen. These colonies are usually called colony-forming units (CFUs). At this point of the experiment, the spleen of the recipient mouse is removed and the CFUs are counted. The surviving fraction is given by Eq. (3.2), similar to the one used for the in vitro assay. The experiment is then repeated for different radiation doses, enabling to trace a survival curve:

$$\text{Surviving fraction} = \text{colonies counted} / \left(\text{cells inoculated} \times \frac{\mathrm{PE}}{100} \right). \tag{3.2}$$

The **skin clone assay** is based on the formation of nodules of mouse skin regrowing from a single surviving cell. In a practical way, after shaving a small area on the back of one mouse, a ring of skin is irradiated with a massive dose of

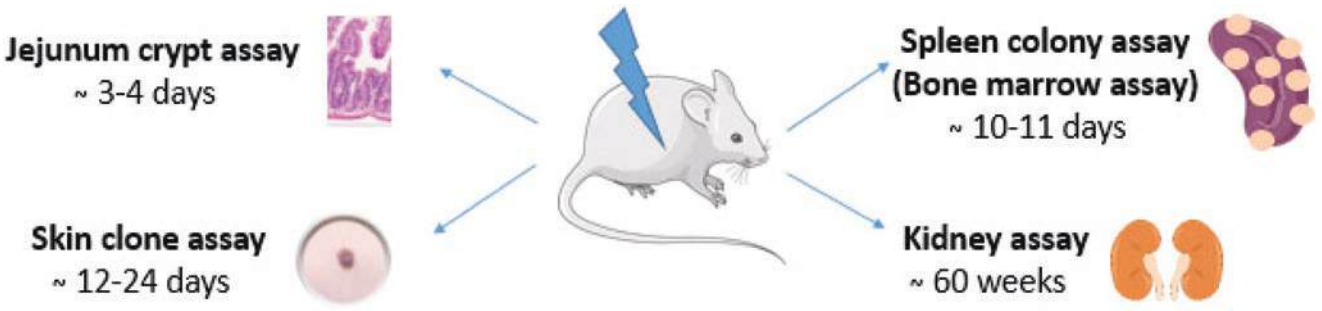

Fig. 3.43 In vivo assays. Four in vivo animal assays to assess clonogenic capacity after irradiation have been important for radiobiology. (1) The jejunum crypt assay measures the regenerative ability of jejunal crypts after high doses of irradiation. The animals are sacrificed 3.5 days after irradiation, and the numbers of regenerating crypts per circumference are measured. One regenerating crypt corresponds to one surviving clonogenic cell. (2) The skin clone assay used pre-irradiation with a high dose in a ring (moat) around the test skin area to avoid migration of neighboring cells into the test area. The test area is then irradiated, and the number of regrowing skin nodules per cm^2 is counted. (3) The spleen colony assay uses transplants of bone marrow cells from an irradiated donor animal. These cells are transferred to recipient animals who have previously been irradiated with a high dose to kill all their own bone marrow cells. After 10–11 days, the recipient animals are sacrificed and their spleens are analyzed for colony-forming units arising from the implanted single cells. (4) The kidney assay uses the same animal for irradiation and control. One kidney of each animal is irradiated, and 60 weeks later, the animals are sacrificed. The number of intact kidney tubules is then counted in both kidneys, and the irradiated kidney can be compared to the unirradiated one

30 Gy to create a "moat" of dead cells. A small metal sphere is put in the central area to protect it from the radiation and create an isolated island of intact skin. This skin island is then irradiated with a test dose. Some days later, nodules of regrowing skin will be observed. The survival curve is obtained after repeating the experiment in different skin areas and by plotting the number of surviving cells per cm^2 of skin as a function of the radiation dose (Gy).

The **jejunal crypt stem cell assay** is based on the self-renewal system of the jejunum. Within this system, the stem cells in the crypts divide rapidly and move up to the villi where they undergo differentiation in functioning cells. For the assay, groups of animals are subjected to increasing doses of whole-body irradiation. The jejunal crypts will begin to regenerate after 3.5 days, time at each animal is sacrificed, and sections of the jejunum are imaged. One regenerating crypt corresponds to one surviving clonogenic cell. The survival curve is obtained by plotting the number of regenerating crypts per circumference of the sectioned jejunum as a function of the radiation dose (Gy).

The **kidney tubule assay** includes the irradiation of one kidney per mouse with a small field. As the kidney is a late-responding tissue, the assay is finished 60 weeks later, when unirradiated and irradiated kidneys are removed, and histologic sections are imaged. The number of intact kidney tubules is compared between the unirradiated and irradiated sides. The survival curve is obtained by plotting the number of tubule-regenerating cells in a defined number of tubule cross sections counted as a function of the radiation dose (Gy).

In addition, the tumor control dose assays (TCD_{50}) relate with tumor survival. During these assays, small parts of tumors (xenografts), which can be derived from tumor cell lines or from patient tumors, are implanted to nude mice. After they reach a desirable size, the tumors are irradiated by several doses and then the local control or recurrence is observed. A plot between the percentage of the controlled tumors versus the dose is made. TCD50 is then the dose to control 50% of the tumors [160] (Box 3.27).

Box 3.27 In a Nutshell: Cell Survival and Clonogenic Assays

- A surviving cell corresponds to a cell able to divide and form a colony.
- Clonogenic assay is based on the ability of a single cell to grow into a colony.
- The only direct measurement of clonogenic function is the clonogenic assay, the gold standard for cell survival measurements.
- Cell survival measurements allow to trace a cell dose-response curve, usually presented with dose plotted on a linear scale and surviving fraction on a logarithmic scale, and can be fitted by several models.
- An in vivo clonogenic assay allows measuring cell survival in an animal model, allowing the study of radiosensitivity of normal or tumor cells treated in vivo.

3.12 Oncogenes and Tumor Suppressor Genes

Transformation of a normal cell into a cancer cell is a multistep process where mutations or other genomic alterations, e.g., copy number alterations, deletions, and gene fusions, alter the normal gene coding sequence. These alterations can occur due to mis- or unrepaired IR damage. Not all alterations lead to the transformation of a normal cell to a cancer cell, called oncogenesis, as it is associated with alterations of specific places on DNA [143]. Cell transformation is mostly related to the activation of proto-oncogenes, which are then named oncogenes and the deactivation of tumor suppressor genes [143]. Proto-oncogenes are genes associated with the activation of cell proliferation and differentiation. When they mutate or are somehow pressed to overexpression, cells proliferate out of control [143]. On the other hand, tumor suppressor genes are genes that control cell proliferation, play significant roles during DNA repair, or activate cell death pathways, when it is needed. Mutations of tumor suppressor genes cause loss of control upon important pathways, which may again lead to unregulated cell proliferation [143]. Oncogenes and tumor suppressor genes can be affected genetically by mutations on the DNA or also switched on or off epigenetically. An overview is given in Fig. 3.44.

3.12.1 Proto-Oncogenes and Oncogenes

The discovery of proto-oncogenes came with investigation of the Rous sarcoma virus (RSV). This virus is able to transform normal chicken cells to cancer cells, and in its structure, the *src* gene was found, which as it was shown later was responsible for this transformation. The *src* gene was later also found in the normal chicken genome, but it was inactivated. These findings meant that the genomes of normal cells carry genes (proto-oncogenes) that have, under certain circumstances, the potential to induce cell transformation when activated [143]. For some time, biologists were convinced that cancer is caused by viruses which present into cells' genes (oncogenes) that activate uncontrolled cell proliferation. It was thus strange that people around these "infected" people do not suffer from the same cancer type as well, due to the fact that viruses are infectious. Indeed, viruses can include oncogenes into a cell's DNA, but viruses are not the main cancer cause. Viruses are responsible only for a minority of all cancers [143]. All this information led to new questions about proto-oncogenes and oncogenes. To find out if oncogenes exist in chemically or physically transformed cells, DNA from cancer cells was introduced to normal cells to see if they will be transformed. This gene transfer procedure is named transfection. Indeed, many other oncogenes were revealed using this method [143]. Another very important issue is that it is sufficient to activate only one of the alleles of a proto-oncogene to get oncogene upregulation [161]. Some of the most common oncogenes in human cancer are given in Table 3.12.

3.12.2 Tumor Suppressor Genes

In general, when a system has an activation "button," there has to be somewhere a deactivation "button" as well. Oncogenes are the genes activating uncontrolled cell proliferation, and on the other hand the deactivation/control of cell proliferation is associated with tumor suppressor genes.

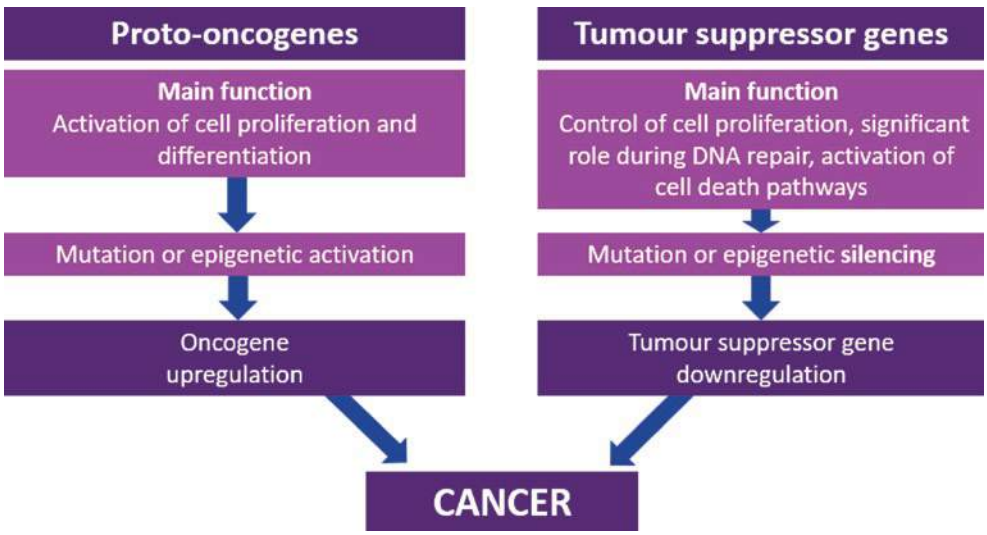

Fig. 3.44 Overview of oncogenes and tumor suppressor genes' function and regulation

Table 3.13 Examples of some tumor suppressor genes and familial cancer syndromes from Macleod [162] and Weinberg [143]

Tumor suppressor gene	General function	Types of cancer	Familial syndrome
TP53	Chromosome stability, transcriptional regulator, growth arrest, apoptosis	Many	Li–Fraumeni syndrome
p16	Cyclin-dependent kinase inhibitor	Many	Familial melanoma
BRCA1	Transcriptional regulator, DNA repair	Many, mostly breast and ovarian cancer	Familial breast cancer
BRCA2	Transcriptional regulator, DNA repair	Many, mostly breast and ovarian cancer	Familial breast cancer
RB1	Transcriptional regulator of cell cycle	Retinoblastoma, osteosarcoma	Familial retinoblastoma
E-cadherin	Cell adhesion regulator	Breast, colon, lung, skin carcinoma	Familial gastric cancer
APC	β-Catenin degradation	Colorectal, pancreatic, stomach, prostate cancer	Familial adenomatous polyposis coli
NF2	Cytoskeleton-membrane linkage	Schwannoma, meningioma, ependymoma	Neurofibroma-predisposition syndrome

Tumor suppressor genes were discovered much later than proto-oncogenes and oncogenes. Some of the tumor suppressor genes are listed in Table 3.13. One of the most important and known tumor suppressor genes is the TP53. A mutation of TP53 is associated with various tumor types. This gene codes the p53 protein, which is also sometimes called the "Master Guardian." p53 is responsible for activation of DNA repair as well as activation of cell cycle arrest, to enable DNA repair.

To deactivate a tumor suppressor gene, both alleles have to be damaged or switched off, because only one allele is enough for the production of a specific protein. Anyhow, if one allele of a tumor suppressor gene of a germ line cell is defective, then there is much higher probability of the born individual to suffer from cancer. This is because for this person, it becomes much more probable that the second allele will be damaged during life as well [143, 161, 162]. Since the defective allele in this case is genetically transferred to offspring, many familial syndromes were identified (Box 3.28).

Box 3.28 In a Nutshell: Oncogenes and Tumor Suppressor Genes

- DNA alterations in genomic or epigenetic level may cause proto-oncogenes to become oncogenes, disrupting normal cell division and causing cancers to form.
- Cell transformation is mostly related to the activation of proto-oncogenes, which are then named oncogenes, and deactivation of tumor suppressor genes.
- Proto-oncogenes are genes associated with the activation of cell proliferation and differentiation.
- Tumor suppressor genes are genes that control cell proliferation, play significant roles during DNA repair, or activate cell death pathways.
- Mutations of tumor suppressor genes cause loss of control upon important pathways, which may again lead to unregulated cell proliferation.
- Oncogenes and tumor suppressor genes can be affected genetically by mutations on the DNA or also switched on or off epigenetically.
- TP53 is one of the most important tumor suppressor genes.

3.13 Interconnectivity Between Cells

Cells are organized in complex cellular systems such as tissues or organs; therefore, it is crucial that they are able to communicate with each other. The most rapid way of communication is directly through cell-to-cell contact. There are various ways of direct interconnectivity of cells as shown in Table 3.14.

3.13.1 Gap Junctions

The most famous type of cell-to-cell connection is gap junction, which is the most direct manner of cell interconnectivity and forms the fastest communication channel. Gap junctions have a pore diameter of 2–3 nm and a length of 2–4 nm and are involved in the exchange of nutrients, ions, second messengers, and small metabolites up to ~1 kDa, allowing ionic and biochemical coupling between neighboring cells. These specialized structure membranes have a

short half-life of a few hours (~1–4 h), and their biosynthesis and assembly are firmly regulated [163]. These transmembrane structures are composed of connexons (Fig. 3.45) constituted of six connexin (Cx) subunits around a central pore, which allow communication between adjacent cells. These connexons could be made up of six similar Cx isoforms (homomeric) or a combination of six different Cx isoforms (heteromeric). To date, 21 Cx isoforms have been identified in human proteosome, each named according to its approximate molecular weight (in kDa), with Cx43 being the most studied till now [163]. According to electron microscopy analyses, all Cx share a common topology composed of four transmembrane proteins, with a cytoplasmatic C- and N-terminal domains, two extracellular loops, and an intracellular loop. In contrast to the transmembrane proteins and the extracellular loop which are highly conserved among the Cx family members, the intracellular loop and the C- and N-terminal showed high variability in terms of the length and amino acid sequence of each Cx. Thus, these regions play an important role in the modulation of the gap junction channel gating and in the intracellular trafficking of connexins, and consequently a variety in their biological roles and interactions [163].

Table 3.14 Summary of the size properties of the three main direct cell connections

Type of connection	Diameter	Length
Gap junctions	2–3 nm	2–4 nm
Tunneling nanotubes	50–1500 nm	Few to >100 μm
Epithelial bridges	1–20 μm	25–1000 μm

The spatial arrangements of Cx43 in breast cancer cells, fibroblasts, and internal mammary artery endothelial cells were studied by CLSM and super-resolution localization microscopy [164]. After radiation treatment (50 min postirradiation with a dose of 4 Gy), these cells behaved differently concerning the trafficking and response of Cx43. In breast cancer cells, high accumulations of Cx43 were found in the cytosol and along the membrane. The results did not significantly differ between non-treated and irradiated cells. In contrast to that, normal fibroblasts and endothelial cells revealed differences at the membrane and in the perinuclear cytosol after radiation exposure. In endothelial cells, a significant Cx43 accumulation and condensation were observed in the perinuclear region, whereas at the membrane, a signal reduction was found. In fibroblasts, Cx43 accumulations were found in the perinuclear region but also at the membrane.

Furthermore, as the Cx are phosphoproteins, they also play an important role in modulating the physiological properties and regulation responses of the channels, such as differentiation process, neuronal activity, development, cell synchronization, and immune response. Therefore, the pres-

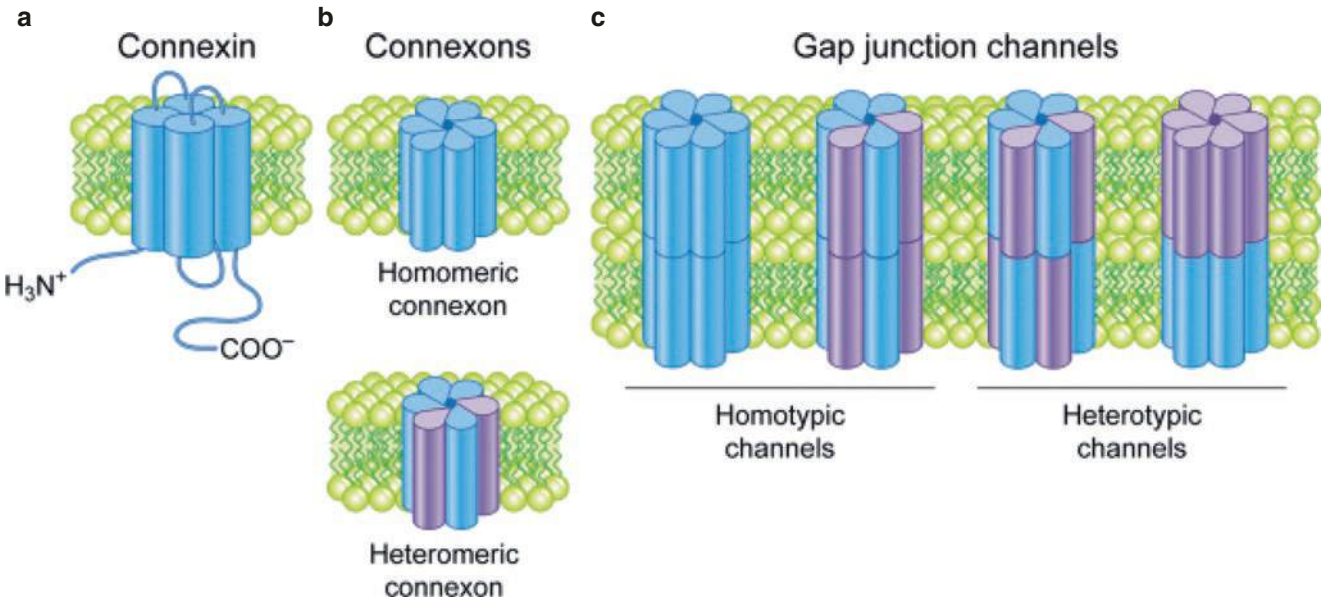

Fig. 3.45 Connexins and gap junctions. Each connexin (**a**) consists of four transmembrane domains. Six connexins form a hexameric torus called connexon (**b**). Depending on the composition, connexons are called homomeric (six equal connexins) or heteromeric (up to six different connexins). (**c**) When the cells form direct contact, the connexons stick together forming gap junctions. Here, the differentiation is made between homotypic channels (both connexons are the same) and heterotypic channels (different connexons). (Reproduced with permission (CCBY) from Totland et al. [163])

ence of mutation in these structures is associated with several human diseases, such as neurodegenerative and skin diseases, deafness, and developmental abnormalities [165]. Also, gap junctions have been described as having a selective permeability, dependent on the combination of Cx isoforms that are made, conferring a single gating, conductance, and permeability to specific molecules, which could allow the association of each channel to a specific disease.

3.14 Membrane Connections

Another type of intercellular communication is via membrane connections such as tunneling nanotubes (TNTs) and epithelial (EP) bridges, which can be distinguished through their structural composition. These connections serve as direct signaling path when cells are separated by greater distances, than necessary for gap junctions. A microscopic image of both connection types can be found in Fig. 3.47.

3.14.1 Tunneling Nanotubes (TNTs)

TNTs are thin cytoplasmic membrane bridges, which appear in straight lines in vitro but also with a curved shape in tissue or in vitro cultures in a three-dimensional extracellular matrix found in various mammalian cells [166]. Their diameter ranges from 50 nm up to 1.5 µm, and they can contact cells over long distances up to several cell diameter length. Even if an obstacle blocks the direct distance between two cells, TNTs, due to their flexible structure, can form a connection. The length of the TNTs dynamically varies when cells migrate up to a certain distance of several 100 µm, which is too large to keep the structure, and the tube disappears. The detailed structure of TNTs is very complex and not yet known in detail. Most TNTs consist of F-actin, and the thicker ones additionally contain microtubules and cytokeratin filaments. Further compounds are sequentially identified as more and more information about the responsibility of TNTs is gathered. TNTs are proven to serve as a highway for exchange of cellular compounds such as mitochondria, vesicles, and many more. Larger compounds are mainly transported along TNTs in so-called gondolas (see Fig. 3.46). Furthermore, TNTs play a key role in direct and active signal transduction including calcium and electric signals, which are known to occur in cells due to radiation stress. Overall, it can be said that the frequency of occurrence and also the complexity of TNT networks within a cell composite are connected to the stress this composite is exposed to. Under stress conditions, the networks are intensified, so that signal and compound exchange is enhanced and fastened. Furthermore, the TNT networks were identified to play a role in the bystander and also the rescue effect and other effects related to radiotherapy [166].

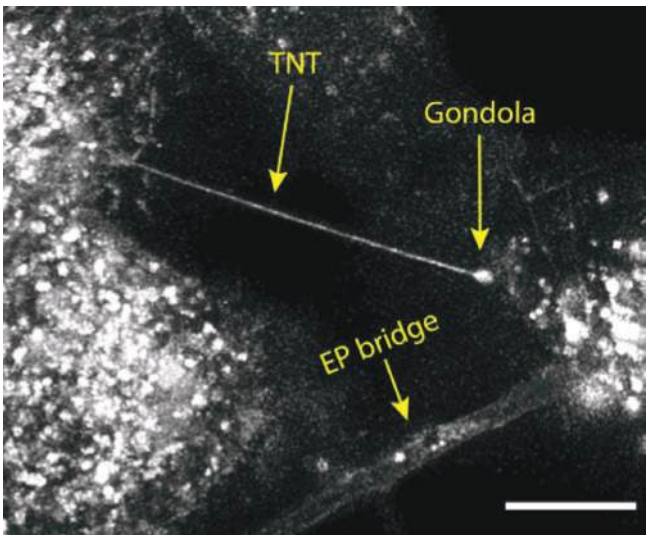

Fig. 3.46 Membrane connections. Microscopic image of membrane label of cells connected by a tunneling nanotube transporting a gondola and an epithelial bridge containing vesicles and cytoplasmic material. Scale bar: 10 µm. *EP* epithelial, *TNT* tunneling nanotube

3.14.2 Epithelial (EP) Bridges

In contrast to TNTs, EP bridges could, as also the name suggests, only be found in normal as well as cancerous human epithelial cells. They also differ from TNTs structurally, as they show a larger diameter of 1–20 µm and also a larger range from 25 µm to over a millimeter [166]. EP bridges consist of F-actin as well as microtubules, which promotes the structural stability allowing these connections to bridge such large distances. As TNTs, the EP bridges play a major role in cellular compound and signal transduction (Box 3.29).

Box 3.29 In a Nutshell: Interconnectivity Between Cells and Communication

- Cells communicate through direct cell-to-cell contact and for interconnectivity networks.
- Gap junctions, constituted by connexins, allow short-range ionic and biochemical coupling.
- TNTs and EP bridges are responsible for long-range signal and molecule transduction.
- Direct cellular communication plays a role in various diseases, spreading of pathogen and health signals, as well as stress and radiation response of cell composites.

3.15 Inflammation and Immunity

3.15.1 Basic Mechanisms of Inflammation

Since inflammation that can be induced by microbial infections and tissue damage is an essential mechanism of innate immune response, the terms "inflammation and immunity" are intrinsically linked [167]. The process of inflammation includes several biochemical events and multi-level cellular interrelationships. In a concerted action, inflammation is initiated, propagated, matured (effector phase), and finally resolved. This implies that radiation exposure under inflamed conditions affects several cell types including many immune cell (sub)types. Macroscopically, vasodilatation and extravasation of immune cells into the inflamed tissue occur that in sum results in the key characteristics of inflammation, namely swelling, redness, pain, loss of function, and increased temperature. The major immune cells involved in the inflammatory process are polymorphonuclear neutrophils (PMNs), which are the most abundant leukocytes in peripheral blood and are very quickly recruited to sites of inflammation, mononuclear monocytes that can differentiate into dendritic cells (DCs) and macrophages, and different subtypes of B and T lymphocytes mediating an antigen-specific adaptive immune response.

3.15.2 Radiation-Induced Modulation of Inflammation

The response of the key immune cells involved in inflammation is strongly dependent on the basal inflammatory status of these cells and the systemic inflammatory (micro)-environment. Further, the monocytic cells are central in all phases of the inflammatory process from initiation to termination and are characterized by an initial high plasticity that is weakened by prolonged tissue residency. Their phenotype is strongly influenced by the microenvironment, and radiation responses are therefore manifold and dose dependent [168]. Regarding inflammatory cytokine expression by macrophages, particularly TNF-alpha and IL1-beta, secretion is reduced following a single radiation exposure of 0.3–0.7 Gy without affecting the immune cell's viability. Further, decreased expression of the inducible nitric oxide synthase (iNOS) protein and, as a consequence, nitric oxide (NO) production in inflammatory macrophages after radiation exposure are observed in inflamed joints. Radiation exposure causes stress in cells via the production of reactive oxygen species (ROS), and a dose of 0.5 Gy, being routinely applied for low-dose radiotherapy of benign chronic inflammatory and destructive diseases, resulted in the strongest reduction of ROS by activated endothelial cells. Besides affecting immune cells and endothelial cells, low/intermediate-dose radiation exposure has osteoimmunological modes of action by reducing the activation of bone-resorbing osteoclasts and by fostering bone construction by osteoblasts [169]. Epidemiological, clinical, and experimental data regarding the effects of low-dose radiation on the homeostasis and functional integrity of immune cells was just recently comprehensively summarized [170]. Finally, particularly in the interactions of radiation with immune cells and cells of the inflammatory process, nonlinear dose relationships are prominent and may reflect a nonlinearity and complexity of immune responses. Figure 3.47 summarizes the key immune cells that are involved in inflammation and are modulated together with the endothelium by radiation in a dose range of 0.1–1.0 Gy. Finally, in polymorphonuclear leukocytes (PMN), irradiation with doses between 0.5 and 1.0 Gy resulted in a discontinuous reduction of chemokine CCL20 secretion that parallels a hampered PMN adhesion to endothelial cells [171].

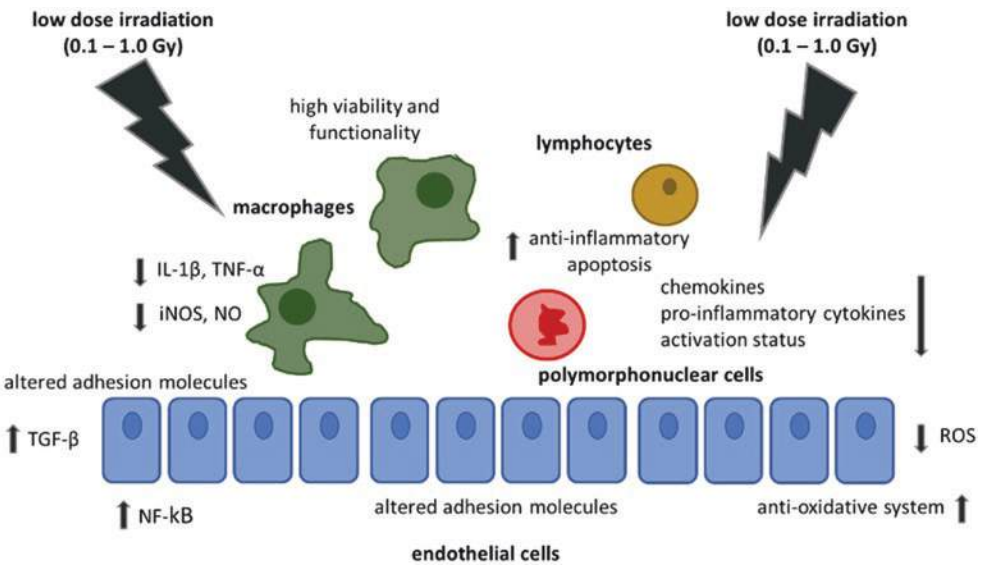

Fig. 3.47 Radiation affects key cells involved in initiation and maintenance of inflammation

3.15.3 Radiation and the Endothelium

Ionizing radiation causes phenotypic changes in endothelial cells, resulting in endothelial activation and ultimately endothelial dysfunction [172]. In vitro, this activation triggers an increase in the expression of the adhesion molecules vascular cell adhesion molecule 1 (VCAM-1), intercellular adhesion molecule 1 (ICAM-1), platelet endothelial cell adhesion molecule (PECAM-1), and E- and P-selectins involved in the recruitment of circulating lymphocytes. In vivo, increased expression of endothelial ICAM-1 and VCAM-1 was demonstrated in a model of radiation-induced intestinal inflammation. ICAM-1 knockout mice showed less severe pulmonary and intestinal inflammation than wild-type mice, suggesting that cellular infiltration may be deleterious in this situation. In humans, the endothelium may be activated by RT via the transcription factor nuclear factor kappa B (NF-kB) pathway, which is likely critical in the development of RT-induced cardiovascular diseases [173]. Overall, these studies demonstrated that radiation-induced increase in adhesion molecule expression by endothelial cells plays a crucial role in circulating cell recruitment and radiation-induced inflammation of the tissue and/or tumor, with a potential deleterious effect on normal tissues. Therefore, the vascular endothelium can be considered as a main control point of radiation-induced inflammatory and immune processes in normal tissues and tumors and may thus cover an ideal target to improve the therapeutic efficacy of radiotherapy of malign diseases. Furthermore, low-dose irradiation was demonstrated to result in a nonlinear expression and activity of major compounds of the antioxidative system in endothelial cells. This might contribute to anti-inflammatory effects in these stimulated cells and be beneficial in low-dose radiotherapy for benign diseases [174]. The effects of higher doses on the immune system in healthy tissue and tumors differ from those of low and intermediate doses and are covered in Chap. 4 (Box 3.30).

Box 3.30 In a Nutshell: Inflammation and Immunity

- Inflammation is intrinsincally linked to the immune response.
- Monocytes/macrophages are key immune cells in the initiation and resolution of inflammation.
- Radiation in a dose range of 0.1–1.0 Gy ameliorates inflammation by mainly affecting macrophages, PMN, lymphocytes, and endothelial cells.
- Ionizing radiation causes several phenotypic changes in endothelial cells
- Vascular endothelium can be considered as a main control point of radiation-induced inflammatory and immune processes.

3.16 CRISPR-CAS9

3.16.1 Definition

Clustered regularly interspaced palindromic repeats (CRISPR)-CAS (CRISPR-associated protein) system is a defense mechanism that has been identified in prokaryotes that effectively acts to fight viruses. The five homologous sequences of 29 nucleotides separated by spacers of 32 nucleotides were observed initially in 1987 by a Japanese research group. The group identified a gene responsible for the conversion of alkaline phosphatase isozyme in *Escherichia coli* [175]. In 2002, another grouping of genes adjacent to the CRISPR locus was revealed which was termed CRISPR-associated system, or Cas. The system has been found in diverse species of bacteria and archaea, however with slightly different composition and mechanism of action. Since this time, new forms of CRISPR systems have been discovered that can be classified into six types and grouped into two classes [176]. Types I–III are well studied, while other types IV–VI, which have more recently been discovered, need further research to fully understand their mechanism of action. These systems have now been realized to be important breakthroughs for modern genetic engineering and are revolutionizing science.

3.16.2 Mode of Action

CRISPR are fragments of RNA that are cloned from the DNA of viruses that have infected a bacterium. Together with other sequences, it forms an adaptive immune system that stores memory of viral DNA within the bacterial host chromosomes. It is comprised of three main components: an RNA sequence made from the relevant CRISPR gene (crRNA) that contains within it a 20-base pair-long sequence complementary to the target DNA sequence; a DNA endonuclease that can edit genes and is referred to as Cas9; and a tracrRNA that acts to help bind the crRNA and Cas9 together. All three components are well studied [177]. In concert, the CRISPR-Cas9 system works to fight virus invasion in prokaryotes. When a bacterium comes across a virus that it was previously exposed to, it produces an RNA copy of the CRISPR that contains that virus' genetic information. The crRNA then binds with the tracrRNA to form a single-guide RNA (sgRNA) that leads the enzyme Cas9 to the correct DNA sequence. The sgRNA binds to the target site in the genome that matches the viral sequence on the crRNA and directs the Cas9 protein to create a double-stranded break. Next to the viral sequence is a protospacer adjacent motif (PAM), which also helps to align the enzyme. Once broken, the strand will experience a change in the viral DNA sequence through the activation of a DNA repair method, either non-

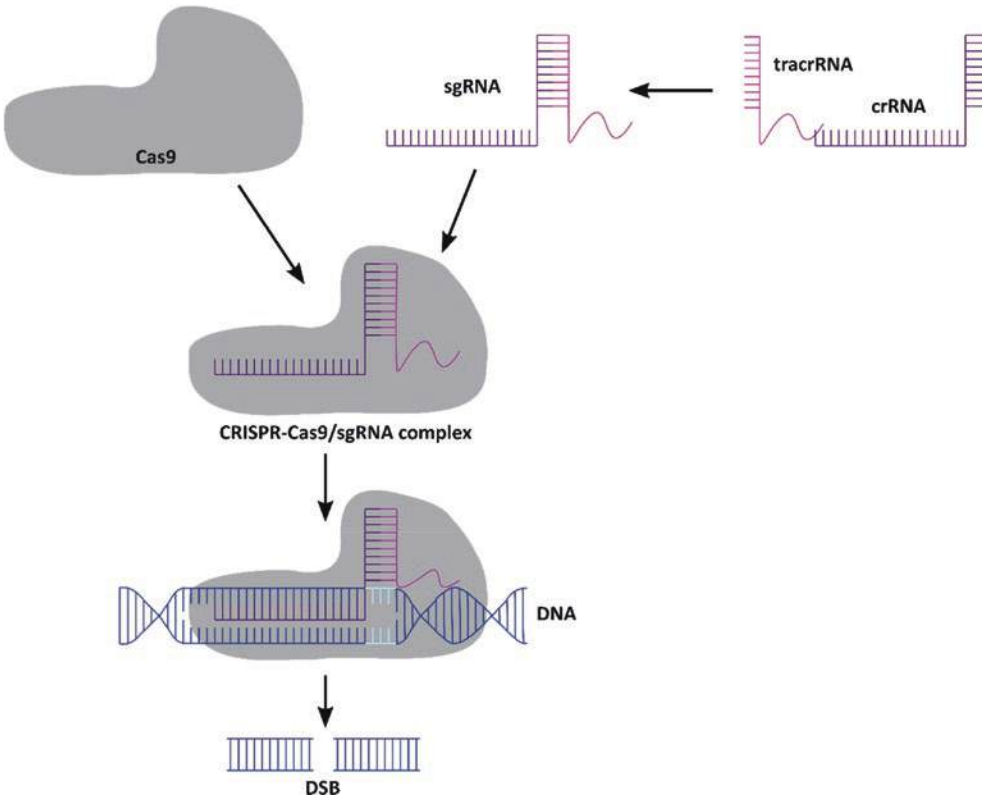

Fig. 3.48 Mechanism of CRISPR-Cas9 to produce a DNA double-strand break. The CRISPR-Cas9/single-guide RNA (sgRNA) complex consists of the Cas9 protein, which is coupled to the sgRNA, consisting of the transactivating crRNA (tracrRNA), responsible for binding of the RNA complex to Cas9 and the CRISPR RNA (crRNA) which encodes the target sequence. The CRISPR-Cas9/sgRNA complex binds to the specifically targeted DNA sequence and induces a DSB. (Adapted with permission (CCBY) from Zhao et al. [178])

homologous end joining or homology-directed repair [177, 178]. The process shown in Fig. 3.48 is very efficient and effective and shown to be a valuable tool for researchers to study gene function and uncover biological mechanisms.

3.16.3 Application

The CRISPR-Cas9 system is unique due to its ability to induce double-strand breaks in almost any type of organism or cell type. The system is more accurate, providing an alternative to previous genome editing tools, such as zinc finger nucleases (ZFNs) and transcriptional activator-like effector nucleases (TALENs) [178]. The technology is an efficient genome editing system that can detect, manipulate, and annotate from diverse species-specific DNA sequences. The system is mainly used for studying DNA because manipulating RNA is difficult due to the lack of a PAM sequence, requiring efficient RNA targeting tools. The most widespread application of the CRISPR-CAS system has been in the context of genome editing of DNA, achieved through three mechanisms: (1) nonhomologous end joining, (2) single-base editing enzymes, and (3) homology-directed repair for DNA repair. The system can be delivered virally (adenovirus or lentivirus) or through nonviral mechanisms (hydrodynamic injection, electroporation, nanoparticles, and transposon carriers) and combined [178].

The technology can be applied to develop a better understanding of a specific gene function or the manipulation of genetic material, as genetic sequences can be removed or edited. For example, a select tissue type can undergo multiplex mutagenesis for high-throughput analysis to identify cancer drivers or correction of a loss-of-function mutation; likewise, gene knockout could be used to enhance a specific cell type. Beyond gene editing, researchers have also used the Cas9 unit for targeting purposes instead of catalytically, known as the dead Cas9 (dCas9) [179]. For instance, epigenetic editing involves the alteration of the chromatin structure without modifying the individual's genomic sequence. The dCas9 is fused to a functional DNA methylation or demethylation enzymes or DNA modifiers [179]. The same idea follows CRISPRi and CRISPRa, which repress and inhibit gene expression. The CRISPRi uses the dCas9 to bind to the DNA-blocking RNA polymerase and transcription factor binding, while CRISPRa combines the dCas9 unit and selects transcription factors targeting activating sequences.

Overall, these advancements provide new avenues to study genetic mechanisms and demonstrate the applicational value of CRISPR-Cas-based tools. It is being used with success in the field of agriculture, therapeutics, food industries, and more. The success of CRISPR has inspired efforts to discover new systems for targeting nucleic acids, including those from Cas9, Cas12, and Cas13 orthologues. The approach is gaining traction for use across multiple fields of research.

3.16.4 Challenges

As the field of CRISPR-Cas rapidly evolves, challenges have emerged which have also been the focus of much research. This is particularly in the context of development of treatment modalities for cancer. Some hurdles that have been identified are in relation to methods for effectively delivering the technology into the host that ensures suppression of the innate immune responses. Injection methods are traditionally used to deliver CRISPR-Cas9 components to cells via delivery vectors; however, the efficiencies of these injection methods are dependent on the target cells and tissues. Traditional delivery methods targeting cancer cells are not yet efficient enough to be applied clinically. For CRISPR-Cas9 to be applied as a therapeutic tool in cancer treatment, delivery must be more efficient and accurate which may require novel delivery methods [180].

Apart from limitations with delivery methods, the delivery vehicle itself also prevents a challenge, as delivery vectors hold a limited amount of genomic material. The most used delivery vehicle is adeno-associated virus (AAV) as it is relatively safe and effective; however, this method has a limited packaging capacity due to its size, which restricts the amount of genetic information that can be transferred to the target cell or tissue. AAVs can contain roughly 5 kB of information, while information for the Cas9 protein and the sgRNA which must be included on the plasmid is roughly 4.2 kB in size. To offset this, current research is being done to find smaller Cas9 orthologues, which in the future may allow for more helpful elements to be added such as reporter genes or fluorescent tags to support more successful gene editing [179].

Immune responses to the Cas9 protein have also been well documented in animal models, which presents an added challenge to the clinical application of the CRISPR-Cas system. A high prevalence of the human population has been exposed to the bacteria from which the Cas9 protein originates, meaning that there is likely a large population with preexisting immunity. While the implications of this are not yet entirely clear, testing of Cas9 orthologues may be required before CRISPR-Cas technology can be applied as a therapeutic to prevent T-cell responses. Alternatively, immunosuppressant drugs could potentially be used during treatment [179]. Off-target effects of the CRISPR-Cas system, such as mutations at undesired sites, also present a challenge. Extensive research has been done to minimize these effects; however, further investigation on increasing precision is required to improve safety [181]. As these hurdles become addressed, CRISPR-Cas9 will play a crucial role in medical treatments, including the treatment of cancers, and will effectively support gene therapy modalities (Box 3.31).

Box 3.31 In a Nutshell: CRISPR-Cas

- CRISPR-Cas system is a defense mechanism that has been identified in prokaryotes that effectively acts to fight viruses.
- CRISPR are fragments of RNA that are cloned from the DNA of viruses that have infected a bacteria.
- Cas9 is a DNA endonuclease that can edit genes.
- Together, CRISPR-Cas9 is an efficient genome editing system that can detect, manipulate, and annotate from diverse species-specific DNA sequences.
- It can be applied to develop a better understanding of a specific gene function or the manipulation of genetic material, as genetic sequences can be removed or edited.

3.17 Epigenetic Factors

DNA methylation, histone modifications, and incorporation of histone variants are chemical alterations of the cellular DNA. Such changes are not necessarily permanent and can be influenced by endogenous and exogenous stressors. One of these stressors is radiation. Radiation induces various alterations in these epigenetic modifications, mainly affecting gene expression and DNA repair.

MicroRNAs are small, highly conserved noncoding RNA molecules that regulate gene expression. They are single-stranded RNA transcripts with a length of 21–25 nucleotides that are derived from hairpin loop precursors. miRNAs affect the cellular radiation response via regulation of vital genes involved in DNA damage repair, cell cycle checkpoints, autophagy, and apoptosis.

Long noncoding RNAs (lncRNAs) are defined as RNA transcripts with a length of more than 200 nucleotides missing a distinct protein-coding region. lncRNAs regulate gene expression on multiple levels, including transcription, RNA stability, and translation. Radiation exposure deregulates lncRNA expression, which affects radiosensitivity by interfering with canonical radiation response pathways, such as cell cycle control, DNA repair, and cell death induction.

Circular RNAs (circRNAs) are a recently described class of RNA molecules that are derived from precursor mRNA (pre-mRNA) in a process called backsplicing. Despite increasing attention, the number of studies investigating the direct effect of ionizing radiation on circRNA expression is still very limited. However, it is now evident that circRNAs are affected by irradiation and that they are important players in the cellular radiation response and sensitivity.

Extracellular vesicles (EVs) are generated by all cells within our body and are important communicators in normal and cancer cells. EVs have different sizes ranging from 40 nm up to several μm and are produced via different biogenesis routes. EVs' cargo contains various RNA species, DNA fragments, proteins, and lipids partly reflecting their cell of origin. EVs may influence neighboring cells via their cargo but also act in distant tissue as illustrated in cancer, where they play a role in both carcinogenesis and metastasis. Exosomes are a particular type of EVs formed by viable cells via the endosomal system, and there are specific cellular mechanisms that determine their cargo. Upon radiation, EVs are generated by both normal and cancer cells and transmit effects in irradiated and nonirradiated cells (e.g., bystander or non-targeted effects). EVs may constitute a source of biomarkers for diseases and stress conditions, including radiation.

3.17.1 DNA and Histone Modifications

Modifications of DNA bases and histone proteins, including the incorporation of histone variants, have important functions in the epigenetic control of gene expression. Both types of alterations add further information to the DNA molecule in addition to the genetic code, which contribute to phenotypic changes without altering the DNA sequence. Importantly, such changes are not necessarily permanent and can be influenced by endogenous and exogenous stressors. Enzymes that add, recognize, and dislodge DNA and histone modifications are called writers, erasers, and readers. The generation of modifications is facilitated by writers. Erasers modify and/or remove labels. Readers recognize and associate to modifications [182].

The methylation of DNA is a heritable epigenetic label in dividing cells. Methylation of DNA segments typically induces its silencing, while demethylation is characteristic for actively transcribed regions. Possible mechanisms for these effects are the binding of methyl-DNA-binding proteins, which affect gene activity or alterations of the chromatin structure. In mammals, DNA methylation patterns are retained or established by DNA methyltransferases (DNMTs) that catalyze the addition of methyl groups to nucleotides. S-Adenyl methionine (SAM) acts as a methyl group donor. DNMT1 function is the maintenance of methylation, and DNMT3a/b is responsible for de novo methylation. On the other hand, DNA demethylases can catalyze active demethylation. Most of DNA methylation takes place at cytosines, which are succeeded by a guanine nucleotide (CpG sites). Regions (>200 nucleotides and CG content >50%) with a high frequency of CpG sites are called CpG islands. Promotor sequences are often located within such CpG islands. Methylation of CpG islands silences gene expression, for example by impeding the binding of transcription factors or by recruitment of repressive methyl-binding proteins. The most common modification of DNA bases is the methylation of cytosine on carbon position 5, leading to 5-methylcytosine (5-mC). This modification accounts for approximately 1% of all bases and is therefore sometimes designated as the fifth base of the DNA. Further less abundant modifications are for example 5-hydroxymethylcytosine, 5-carboxycytosine, and 6-methyladenine.

Histone modifications are covalent modifications joined to histone proteins. These modifications impair DNA-histone interactions, thereby changing chromatin architecture and gene expression. Some reduce DNA-histone interactions leading to nucleosome unwinding, chromatin opening, and increased accessibility for the transcription machinery leading to the activation of gene expression (euchromatin). Others increase DNA-histone interactions, leading to tightly packed chromatin followed by reduced access of the transcription machinery and thus gene silencing (heterochromatin). Currently, acetylation, methylation, phosphorylation, and ubiquitination are the most well understood, while others, like GlcNAcylation, citrullination, crotonylation, and isomerization, are more recent discoveries. All of these modifications are highly dynamic and added to or removed from histone amino acid residues by specific sets of enzymes. A well-described posttranslational histone modification is the trimethylation of histone H3 on the lysine located at position 4 of the protruding N-terminal tail (H3K4me3), which is correlated with promoters of actively transcribed genes. In contrast, the trimethylation of lysine on positions 9 (H3K9me3) and 27 (H3K27me3) is a heterochromatin mark, associated with repressed genes.

In addition to posttranslational modifications, the histone structure of the chromatin can also be influenced by the incorporation of histone variants. Histone variants are low abundant and differ only in one or a few amino acids with their canonical counterparts. They are produced throughout the cell cycle and can be deposited into chromatin independent of replication by rapid exchange processes. Histone variants seem to be especially important for protecting genome integrity by the regulation of damaged chromatin accessibility and restoration.

3.17.1.1 DNA and Histone Modifications in the Context of Radiation

Both DNA methylation and histone modifications are essential components in the cellular stress response. Therefore, it is not surprising that various alterations are reported after radiation exposure. On a molecular level, radiation-induced alterations in histone and DNA modifications either are required for the efficient detection and repair of DNA damage to avoid chromosomal instability or lead to changes in transcriptional activity and thereby alter a variety of cellular

processes, including cell cycle regulation, DNA repair, and cell death induction. At organism level, epigenomic alterations were reported in various radiation-induced cancer and non-cancer diseases. As epigenomic alterations can be transferred to the offspring also, the contribution to radiation-induced transgenerational effects was recently suggested [183, 184].

Altered DNA methylation patterns were found in in vitro and in vivo studies in response to irradiation. The majority of studies showed global hypomethylation, which was often linked with a reduced expression of enzymes involved in DNA methylation. As global hypomethylation is connected to malignant transformations, radiation-impaired DNA methylation may contribute to cancer development. However, hypomethylation is not always evenly dispersed across the genome and also radiation-induced hypermethylation was reported for specific loci. Interestingly, new studies imply that low- and high-LET radiations affect methylation differentially.

A variety of radiation-induced histone modifications affecting transcriptional regulation and particularly DNA repair are described. In regard to DNA repair, an intensively studied histone modification is the phosphorylation of the histone H2A variant H2AX at serin-139 (phosphorylated H2AX is designated as γ-H2AX) at sites of DNA double-strand breaks (DSBs). Formation of γ-H2AX is an initial response after exposure and facilitates a cascade of further histone modifications, including ubiquitination of H2A/H2B as well as changes in the acetylation of H3 and H4. Together, these posttranslational histone modifications contribute to chromatin relaxation that enables the accession of DNA repair factors and influences the repair pathway choice. Moreover, the γ-H2AX modification is widely used as a biomarker for DSBs, and a lot of methods were developed to use γ-H2AX counting for DSB quantification.

With the knowledge about DNA methylation and histone modification in radiation response, the targeted modulation of these features is investigated as a novel strategy to radiosensitize tumor cells during radiotherapy. For example, radiosensitizing activity was shown for DNA demethylation agents, like cytidine analogs. In addition, small-molecule inhibitors of histone deacetylases changing histone acetylation showed the potential to alter radiosensitivity.

The first studies in this field also demonstrated an exchange of histone variants in response to radiation exposure. For example, it was shown that the histone variant H2A-Z.2 is incorporated into chromatin immediately after DSB induction, where it contributes to recombinational repair by assisting RAD51 foci formation. In line, H2A-Z.2 U2OS tumor cells were shown to be more radiosensitive than controls. H2A.J, another histone variant, accumulates during radiation-triggered senescence processes in the vicinity of 53BP1 foci and affects the expression of inflammatory genes (Box 3.32).

Box 3.32 In a Nutshell: DNA and Histone Modifications as Epigenetic Factors

- DNA methylation, histone modifications, and incorporation of histone variants are chemical alterations of the cellular DNA.
- Radiation induces various alterations in these epigenetic modifications, mainly affecting gene expression and DNA repair.
- Phosphorylation of histone H2AX (γ-H2AX) is the most prominent radiation-induced epigenetic alteration with significant impact on DNA repair.

3.17.2 MicroRNAs

MicroRNAs are small, highly conserved noncoding RNA molecules that regulate gene expression. They are single-stranded RNA transcripts with a length of 21–25 nucleotides that are derived from hairpin loop precursors. The basic mode of action of miRNAs is competitive partial binding with the 3′ UTR of the target mRNA, which inhibits translation and/or leads to mRNA destruction. MiRNAs have also been shown to interact with the 5′ UTR, coding regions, and gene promoters via binding complementary sequences [185]. Because each miRNA can act on multiple different target genes, and one target gene can be regulated by many different miRNAs, the miRNA-mediated regulation of cellular phenotype is highly complex. miRNA-mediated regulation is thought to affect roughly 60% of all protein-coding genes, according to estimations. To regulate miRNA abundance at the levels of transcription, maturation, and stability, cells have evolved various sophisticated methods to govern such extensive miRNA-mediated functions. miRNA actions have been linked to the regulation of a variety of cellular processes, including cellular homeostasis and stress responses. Furthermore, they have been linked to a variety of diseases. miRNAs, in addition to their intracellular roles, are also found in the extracellular environment. miRNAs can be identified in physiological fluids such as plasma, saliva, and urine. This extracellular miRNA population is varied and heterogeneous. Although the activities of extracellular miRNAs are not completely understood, it has been demonstrated that extracellular microvesicle-embedded miRNAs can be transferred and incorporated into destination cells [186].

3.17.2.1 Radiation Damage and miRNAs

Ionizing radiation (IR) disturbs cellular equilibrium in a variety of ways. Cellular stress pathways shield cells from the harmful consequences of genotoxic assault. Cells respond to ionizing radiation-induced stress by activating several pathways ranging from DNA damage processing, signal transmission, altered gene expression, cell cycle arrest, genomic

instability, and cell death. The available evidence implies that radiation exposure causes cellular responses that are influenced in part by gene expression networks. miRNAs govern several intracellular processes involved in the response to cellular stress and have been demonstrated to regulate gene expression [187].

Radiation exposure, whether accidental or intentional, is a serious public health issue that demands immediate attention for correct diagnosis and clinical planning. Exposure to large doses of ionizing radiation in a short time causes acute radiation syndrome (ARS), often known as radiation sickness or radiation poisoning. ARS involves a total dose of over 0.7 Gy (70 rad) from an external source, administered in a few minutes. Radiation sources might be accidental or deliberate. Several animal species were used to study the effects of radiation on miRNA expression. For ARS, miRNA analysis has been done in murine and nonhuman primate (NHP) models. Several studies employing different mouse strains (CD2F1, C57BL/6J, C57BL/6, and CBA/J) have identified miRNAs as biomarkers for radiation injury and countermeasure efficacy.

While several miRNAs have been proven to be modulated by radiation, not all studies have showed the same miRNAs. However, most studies have shown downregulation of miR-150 and overexpression of miR-30 and miR-126. Exposure to ^{60}Co γ-radiation, high LET, and high-energy particles reduced miR-150 expression (^{56}Fe, iron-56) [188]. In addition to total-body irradiation, miR-150 downregulation was observed in the lung and blood of female WAG/RijCmcr rats irradiated (15 Gy at 1.43 Gy/min), indicating the potential of employing miRNAs for partial-body exposure and the impact on miRNA expression in organs and biofluids [189]. A profile of seven significantly changed miRNAs (miR-150-5p, miR-215-5p, miR-30a-5p, miR-126-5p, miR-133a-3p, miR-133b-3p, and miR-375-3p) was discovered in rhesus macaques 24 h after exposure to ionizing radiation. Differences in the expression of three miRNAs (miR-133b, miR-215, and miR-375) were used to accurately discriminate between irradiated and nonirradiated NHPs. Two miRNAs (miR-30a and miR-126) were able to predict radiation-induced mortality in NHPs in this study. Another study utilizing rhesus macaques found miR-126-3p upregulated and miR-150-5p downregulated. Unlike rhesus macaques, miR-342-3p was shown to be most affected (tenfold persistent downregulation) at 24 and 48 h postirradiation in baboons [190].

miRNAs strongly affect the cellular radiation response via regulation of vital genes involved in DNA damage repair [187], cell cycle checkpoints [191], and apoptosis [187]. Several important miRNAs, as well as their mRNA targets and signaling pathways implicated in radioresistance and radiosensitivity, are depicted in Fig. 3.49a, b, respectively.

The expression of RAD51 and the subsequent formation of RAD51 foci in response to IR are a critical stage in HR. Following IR, RAD51 was revealed to be a direct target of miR-34a, miR-107, miR-155, and miR-222. Overexpression of miR-34a in lung cancer cells prevented the formation of radiation-induced RAD51 foci. Greater miR-155 levels were associated with lower RAD51 expression and better overall survival in a large dataset of triple-negative breast cancer patients. IR-induced damaged DNA is sensed by ataxia-telangiectasia mutated (ATM), which can initiate the signaling pathway, leading to checkpoint activation and DNA repair. ATM was shown to be downregulated by miR-18a in breast cancer, miR-26a in glioma, and miR-421 in squamous cell carcinoma (SCC), making the cells more sensitive to radiation.

Additionally, in response to IR, two miRNAs, miR-24 and miR-138, have been discovered to directly control H2AX. miR-182 suppressed BRCA1, another important protein in HR, in breast cancer cells. miR-875 also hampered the HR pathway by directly targeting the epidermal growth factor receptor (EGFR) and disrupting the EGFR-ZEB1-CHK1 axis.

PI3K/AKT is one of the key downstream targets of EGFR. The PI3-K/AKT pathway is crucial for establishing radiation resistance and intrinsic radiosensitivity of the cell. It is a critical regulator of normal and malignant development and cell fate decisions via activities such as proliferation, invasion, apoptosis, and activation of hypoxia-related proteins in cell signaling cascades. Several miRNAs are known to target and regulate key components of this pathway and help elicit the cellular response to radiation. AKT, an immediate downstream effector of the PI3K cascade, has been found to be directly targeted by miR-150 in natural killer (NK) and T-cell lymphoma cells. In a xenograft mouse model, miR-150 overexpression increased IR-induced apoptosis by decreasing PI3K/AKT signaling and sensitized NK/T-cell lymphoma cells to radiation. Furthermore, through blocking the AKT/GSK3/Snail signaling pathway, miR-203a-mediated ATM downregulation promoted apoptosis and cell cycle arrest in G1 phase in ovarian cancer cells. The tumor suppressor protein phosphatase and TENsin homolog (PTEN) is the central negative regulator of the PI3K/AKT pathway by dephosphorylation of PIP3 at the plasma membrane.

Several miRNAs generate pro-survival signals in response to IR by targeting PTEN. Activation of the PI3K/AKT pathway, suppression of apoptosis, and improved radioresistance were seen when miR-17, miR-20a, miR-106b, miR-205, miR-221, miR-222, and miR-498 were overexpressed. Regulation of PTEN expression is crucial for cell cycle maintenance. In colorectal cancer cells, miR-106b is known to target the CDK inhibitor p21 as well as

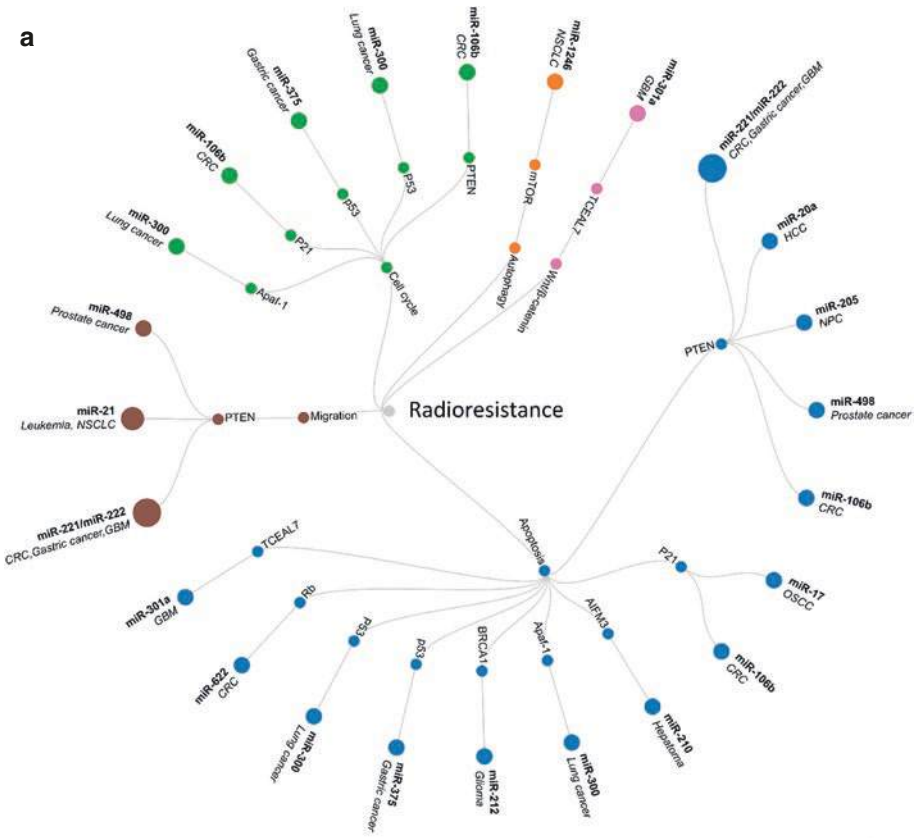

Fig. 3.49 (**a**) miRNAs and cellular radioresistance: a summary representation of miRNAs in different cancers (outer circle) that regulate various mRNA targets (middle circle). These mRNA targets in turn influence various crucial biological pathways (inner circle) responsible for cellular radioresistance. Data for the figure acquired and modified from Ebahimzadeh et al. [192] (data taken with permission); [193] (CCBY). Gene names: *P21* cyclin-dependent kinase inhibitor 1, *AIFM3* apoptosis-inducing factor mitochondria-associated 3, *APAF1* apoptotic peptidase-activating factor 1, *BRCA1* breast cancer gene 1, *p53* TP53 gene and tumor protein p53 gene, *RB* retinoblastoma protein, *TCEAL7* transcription elongation factor A-like 7, *PTEN* phosphatase and tensin homolog, *APAF1* apoptotic peptidase-activating factor 1, *MTOR* mechanistic target of rapamycin kinase. *miR* microRNA, *NSCLC* non-small cell lung cancer, *GBM* glioblastoma, *CRC* colorectal cancer, *HCC* hepatocellular carcinoma, *NPC* nasopharyngeal carcinoma, *OSCC* oral squamous cell carcinoma. (**b**) miRNAs and cellular radiosensitivity. A summary representation of miRNAs in different cancers (outer circle) that regulate various mRNA targets (middle circle). These mRNA targets in turn influence various crucial biological pathways (inner circle) responsible for cellular radiosensitivity. Data for the figure acquired and modified from Ebahimzadeh et al. [192] (data taken with permission); [193] (CCBY). Gene names: *STAT3* signal transducer and activator of transcription 3, *CDK4* cyclin-dependent kinase 4, *MCL1* MCL1 apoptosis regulator, *BCL2* family member, *SIRT1* sirtuin 1, *E2F1* E2F transcription factor 1, *P21* cyclin-dependent kinase inhibitor 1, *EGFR* epidermal growth factor receptor, *BCL2* BCL2 apoptosis regulator, *LDHA* lactate dehydrogenase A, *ATM* ataxia-telangiectasia mutated, *AKT* AKT serine/threonine kinase 1, *H2AX* H2A histone family, member X, *Beclin-1* coiled-coil, moesin-like BCL2-interacting protein, *ATG12* autophagy-related protein 12, *TP53INP1* tumor protein p53 inducible nuclear protein 1, *DRAM1* DNA damage-regulated autophagy modulator 1, *UBQLN1* ubiquilin 1, *DUSP10* dual-specificity phosphatase 10, *STMN1*, stathmin 1, *c-MYC* Myc-related translation/localization regulatory factor, *WNT2B* wingless-type MMTV integration site family, member 2B, *WNT* wingless-type MMTV integration site family, member, *PKM2* pyruvate kinase isozymes M1/M2, *LDHA* lactate dehydrogenase A, *MTOR* mechanistic target of rapamycin kinase. *miR* microRNA, *NSCLC* non-small cell lung cancer, *NK/T-cell lymphoma* natural killer/T-cell lymphoma, *SCC* squamous cell carcinoma, *ESCC* esophageal cancer, *GBM* glioblastoma; *CRC* colorectal cancer, *HCC* hepatocellular carcinoma, *NPC* nasopharyngeal carcinoma, *OSCC* oral squamous cell carcinoma, *DSB* double-strand breaks

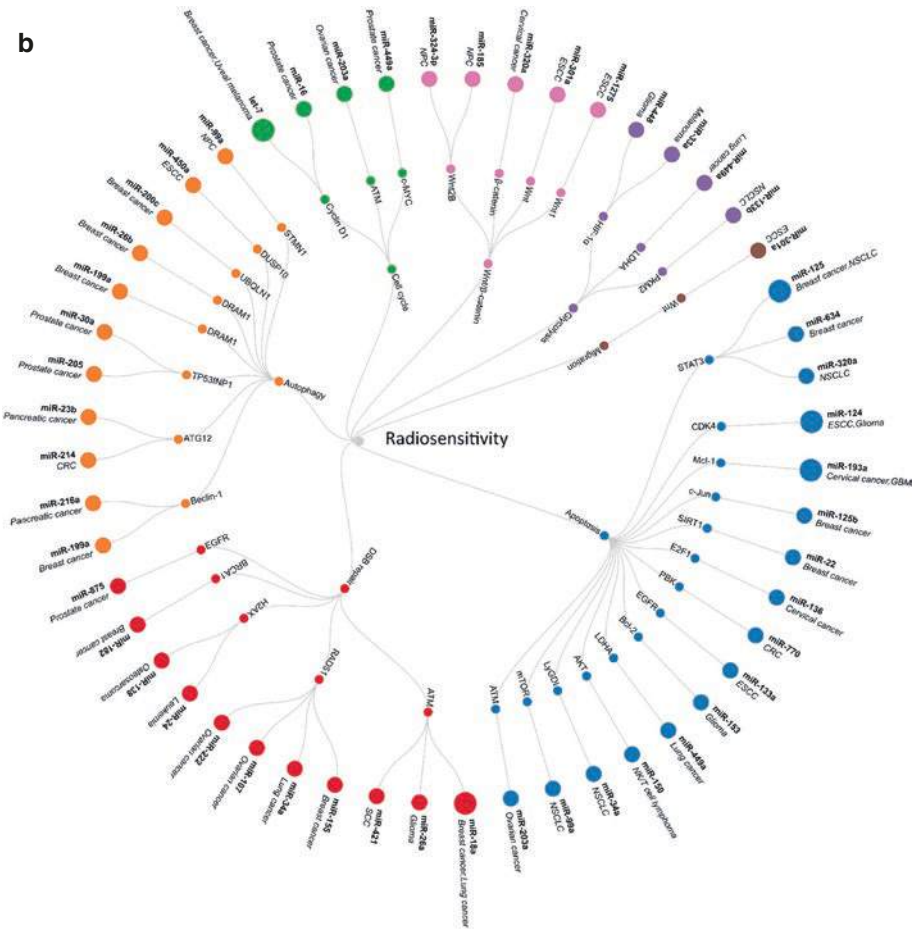

Fig. 3.49 (continued)

PTEN. Overexpression of miR-106b promoted the G1-to-S transition in CRC cells, which was blocked by overexpression of either PTEN or p21. miR-17-mediated PTEN inhibition, like miR-106b, boosted G2-to-M progression and increased NPC cell proliferation through its effects on AKT signaling.

After IR exposure, apoptotic regulatory pathways are activated to remove cells with a high burden of DNA damage. Several miRNAs, including miR-133a, miR-125b, miR-124, miR-320a, and miR-634, are known to exert their effects on IR response via targeting components of crucial survival pathways, i.e., extracellular signal-regulated kinase (ERK), Janus kinase/signal transducer, and activator of transcription (JAK/STAT) as well as PI3K/AKT pathway. These pathways are initiated in response to IR-dependent activation of EGFR. In the JAK/STAT pathway, STAT3 is a direct target of miR-124, 320a, and 634, and the regulatory effect of these miRNAs on STAT3 upon IR is known to promote radiosensitivity. p53 is a critical tumor suppressor that is activated in response to IR to cause cell cycle arrest or apoptosis. Apoptosis mediated by p53 was abolished in IR-treated gastric cancer cells when miR-375 was overexpressed. In lung cancer cells, miR-300 directly regulates Apaf-1, the structural core of the apoptosome. Ectopic miR-300 expression caused radioresistance via reduced Apaf-1-induced apoptosis. P21 (Waf1/Cip1) is a p53 transcription target implicated in both major functions of the tumor suppressor, apoptosis, as well as cell cycle arrest. In oral squamous cell carcinoma (OSCC) cells, miR-17 has been shown to inhibit p21. In xenograft tumors, suppressing miR-17 boosted p21 expression, apoptotic rate, and radiosensitivity. miR-210 improved radioresistance in hypoxic hepatoma cells by targeting AIFM3. The retinoblastoma (Rb) tumor suppressor protein is an important component in the protection of cells from apoptosis. miR-622 was shown to prevent apoptosis by inhibiting the Rb gene in colorectal cancer cells. Another miRNA that reduced IR-induced apoptosis was miR-212, which directly targeted BRCA1 in glioma cells.

IR-induced autophagy is important in defining cell fate and determining whether cells survive or die, and it also impacts radiosensitivity. A multitude of proteins, including Beclin-1, LC3B-II, mTOR, and other autophagy-related proteins, are crucial for the regulation of this multistep process. Beclin-1 is an autophagy central regulator that regulates autophagosome nucleation and maturation. Beclin-1 is known to be directly regulated by miR-216a and miR-199a, which inhibit autophagy and promote radiosensitivity in response to radiation. mir-199 has also been shown to regulate the DNA damage-regulated autophagy modulator protein 1 (DRAM1) in response to IR. In breast cancer cells, miR-26b also targets DRAM1. miR-23b reduced IR-induced autophagy by targeting ATG12, a ubiquitin-like protein involved in the production of autophagy vesicles. miR-214 also targets ATG12, which enhances radiosensitivity while blocking IR-induced autophagy in CRC both in vitro and in vivo. Several additional miRNAs that target autophagy activators have been demonstrated to suppress IR-induced autophagy. These include miR-200c, which targets ubiquilin-1 (UBQLN1), an autophagosome formation promoter; miR-101, which targets autophagy activator stathmin 1 (STMN1) in NPC cells; miR-30a and miR-205 in prostate cancer cells; and miR-450, which targets DUSP10. miR-1246 was one of the miRNAs that enhanced autophagy in NSCLC cells. In vitro and in vivo, ectopic expression of miR-1246 reduced mTOR activity and radiosensitivity in lung cancer cells.

miRNAs have been proven to be valuable diagnostic and prognostic biomarkers in the clinic for over three decades. miRNAs are found in plasma, serum, blood, and urine and even retrieved from formalin-fixed tissues. These benefits make it a biomarker that is persistent after IR exposure and allow for less invasive testing. Two miRNAs (miR-30a and miR-126) were found as predictors of radiation-induced death in nonhuman primates. Another study suggested that serum miRNAs could be utilized as functional dosimeters to detect early hematopoietic radiation harm. After 2 Gy total-body irradiation, miR-130a-3p expression increased, but miR-150-5p, -142-5p, -706, and -342-3p expression dropped. Determining the sublethal dose of 6.5 Gy required five miRNAs (miR-136-5p, -173p, -126-3p, -322-3p, and -34b-3p), while miR-30a-3p/30c-5p discriminated the lethal (8 Gy) and sublethal (6.5 Gy) groups. miRNAs can be used as clinical biomarkers to predict prognostic irradiation effects, in addition to radiation harm biomarkers. Some miRNAs show sensitivity or resistance to IR in cancer patients who have already received radiotherapy (Fig. 3.47). These miRNAs may be utilized as radiosensitivity or radioresistance biomarkers. miRNAs may soon be acknowledged as biomarkers at the level of proteins, which will be utilized to promptly classify harm from radiation exposure, as well as treatment responses, adverse reactions, and personalized radiotherapies.

Research conducted thus far shows a relevant role for miRNAs in the future of radiation oncology, which may offer the basis for predicting patient response to radiotherapy and aid in developing miRNA-based individualized treatments to improve radiosensitivity. Early research indicated that the use of miRNAs as a biomarker for therapeutic monitoring and prognosis, and hence for more precise and individualized patient treatment, is feasible. Applications of miRNA for treatment as radiosensitizers are currently limited to cell culture or xenograft model systems and will need to be expanded into in vivo applications in the future. The role of extracellular miRNAs is still unknown. A thorough examination of radiation-induced mechanisms for secretion, transfer, and activity in recipient cells may aid in the understanding of major RT issues such as abscopal effects and radiation-induced secondary cancers (Box 3.33).

Box 3.33 In a Nutshell: MicroRNAs as Epigenetic Factor

- miRNAs are small, highly conserved noncoding RNA molecules that regulate gene expression.
- miRNAs can be identified in physiological fluids such as plasma, saliva, and urine.
- miRNAs have been identified as biomarkers for radiation injury and countermeasure efficacy.
- miRNAs affect the cellular radiation response via regulation of vital genes involved in DNA damage repair, cell cycle checkpoints, autophagy, and apoptosis.

3.17.3 Long Noncoding RNAs

3.17.3.1 lncRNA basics

Long noncoding RNAs (lncRNAs) are defined as RNA transcripts with a length of more than 200 nucleotides missing a distinct protein-coding region. In the genome, they are located in intergenic, intronic, and exonic regions as well as sense, antisense, and bidirectional with transcripts overlapping sometimes genes [194]. In humans, 30,000–60,000 long noncoding transcripts are estimated compared to 20,000–25,000 protein-coding mRNA transcripts. Details about the biogenesis and functions of lncRNAs are very well summarized by Statello and colleagues [195]. In principle, the biogenesis of most lncRNAs corresponds to the production of mRNAs with transcription by RNA polymerase II and subsequent 5′-end capping and 3′ poly-A-tailing. In comparison to mRNAs, lncRNAs are less efficiently processed and often remain in the nucleus. As mechanisms for nuclear retention, tethering, or degradation on chromatin, weak splicing signals and *cis*- and *trans*-acting motifs are suggested. However, a substantial proportion of lncRNAs is distributed to the cytoplasm, where they can be sorted to specific

organelles (e.g., mitochondria and exosomes) or they associate with diverse RNA-binding proteins. A considerable amount of lncRNAs assembles with ribosomes.

Initially, lncRNAs were considered as transcription by-products, but meanwhile important cellular functions are described for an accumulating number of lncRNAs. In general, lncRNAs are regulators of gene expression, which interact with DNA, RNA, and proteins on various levels. There are examples for both lncRNAs acting locally at the site of transcription (*cis*-acting) and lncRNAs leaving the site of transcription (*trans*-acting). To activate or suppress gene transcription, lncRNAs can regulate chromatin structure to change their accessibility or sequester chromatin-modifying proteins from or to the promoters of target genes. In addition to their roles in transcription regulation and nuclear organization, lncRNAs are involved in posttranscriptional regulation. This can occur by the association between lncRNAs and RNA processing proteins, resulting in altered mRNA splicing and turnover. Other lncRNAs can directly base pair with RNAs and subsequently recruit proteins involved in mRNA degradation or they support translation by promoting polysome association. Also, the binding between lncRNAs and microRNAs can regulate gene expression as miRNAs are sequestered from their target mRNAs by binding to an lncRNA [=sponge or competitive endogenous (ce) RNA] and thus abolish the inhibitory effect of miRNAs on mRNAs.

Through their manifold impacts on the regulation of gene expression, lncRNAs affect widespread aspects of physiology, including differentiation, growth, and responses to diverse stimuli and stresses.

3.17.3.2 lncRNAs in Radiation Response

lncRNAs are involved in many aspects of cellular response to radiation. For a detailed overview, see May et al. [196] and Podralska et al. [193]. Firstly, radiation affects the expression levels of a plethora of lncRNAs in cancer and non-cancer tissues and both up- and downregulation are reported. Radiation-triggered changes are also reported for a wide dose range including low doses (below 100 mGy) as well as therapeutically relevant doses and for single and chronic treatments. The functional relevance in radiation response was shown for a considerable number of lncRNAs, where some enhance radiosensitivity and others increase radioresistance. The affected pathways cover crucial pathways of cellular radiation response, such as cell cycle control, DNA damage repair, and apoptosis. As the mechanism during radiation response of action, frequently, the sponging of microRNAs by lncRNAs and thereby promoting of the expression of target genes are described.

The broad effects of irradiation on lncRNAs suggest valuable applications of this class of RNAs. Applications of biomarkers for radiation exposure may be important for biodosimetry or markers for normal tissue effects and radiotherapy response. Moreover, in vitro and in vivo studies demonstrated that modulation of the levels of lncRNAs can significantly enhance radiosensitivity of tumor cells. This suggests that lncRNAs may be used as targets to improve the outcome of radiotherapy in the future.

Prominent examples for lncRNAs with multiple roles in radiation response are HOTAIR, PVT1, and MALAT1. In breast cancer models, HOTAIR has been shown to increase radioresistance through interfering with DNA damage repair by targeting miR-218 and miR-449b-5p. In pancreatic ductal adenocarcinoma (PDAC), HOTAIR was induced by radiation, while a knockdown increased radiosensitivity. The knockdown increased the expression of Wnt inhibitory factor 1 (WIF-1), which was shown to enhance radiosensitivity. HOTAIR also promoted radiosensitivity of PDAC by increasing autophagosome formation through increasing LC3-II and ATG7A proteins. In cervical cancer, knockdown of HOTAIR increased radiosensitivity by the induction of a G1 cell cycle-phase arrest.

PVT1 contributes to NF90 transcription and HIF-1α stabilization in nasopharyngeal cancer, resulting in enhanced radioresistance. On the other hand, the knockdown of PVT1 resulted in reduced phosphorylation of ATM, p53, and CHk2 leading to increased radiosensitivity by decreased DNA damage signaling and increased apoptosis. In non-small cell lung cancer, PVT knockdown increases radiosensitivity by sponging miR-195.

lncRNA MALAT1 was downregulated after radiation in esophageal squamous cell carcinoma, and its overexpression enhanced radioresistance. It was shown that MALAT1 inhibited the downregulation of cyclin-dependent kinase subunit (Cks1), which resulted in a decrease in irradiation-induced apoptosis. MALAT1 also affected IR-induced apoptosis by interacting with miRNAs. In nasopharyngeal cancer cells, MALAT1 associated to miR-1, which led to increased levels of the anti-apoptotic protein SLUG. In cervical cancer cells, MALAT1 directly interacted with miR-145 to affect radiation-induced apoptosis (Box 3.34).

Box 3.34 In a Nutshell: Long Non-coding RNAs as Epigenetic Factor

- Long noncoding RNAs (lncRNAs) are transcripts >200 bp, which are not translated into proteins.
- lncRNAs regulate gene expression on multiple levels, including transcription, RNA stability, and translation.
- lncRNA expression is deregulated after radiation exposure, and they affect radiosensitivity by interfering with canonical radiation response pathways, such as cell cycle control, DNA repair, and cell death induction.

3.17.4 Circular RNAs

Circular RNAs (circRNAs) are a recently described class of RNA molecules that are derived from precursor mRNA (pre-mRNA) in a process called backsplicing. During this process, which is regulated by the spliceosome, a splice donor is joined to an upstream splice acceptor. This generates a covalently closed RNA molecule, which is typically resistant to degradation by exonucleases, and therefore circRNAs are in general biologically more stable compared to their linear counterparts. Although most circRNAs are expressed in relatively low levels, their increased stability can result in accumulation to levels far exceeding those of their cognate linear mRNAs [197]. This is for instance observed during aging, which led to the hypothesis that certain circRNAs may represent biomarkers for aging tissues (such as the brain) and aging-associated diseases. Recent studies even implicate circRNAs as causative factors in aging and cellular senescence [198]. Since irradiation and excessive DNA damage are often proposed as inducers of senescence and accelerated aging, radiation-responsive circRNAs may contribute to these longer term effects of radiation exposure.

3.17.4.1 Biogenesis and Functions

A detailed description of the biogenesis and function of circRNAs is beyond the scope of this chapter; we therefore refer the readers to some excellent reviews about these subjects [198] and will only briefly discuss matters that may directly relate to DNA damage and radiation.

Unlike original views that circRNAs are no more than aberrant by-products of normal splicing, it has become increasingly clear that they are often generated and function independently from their linear cognates. One important mechanism of circRNA biogenesis acts via the RNA-binding protein quaking (QKI). QKI is an alternative splicing factor that belongs to the STAR family of KH domain containing RNA-binding proteins and binds to specific sequences (QKI-binding motifs) in pre-mRNA [199]. The proposed mechanism for the role of QKI in circRNA biogenesis is that it binds motifs in introns adjacent to the circle-forming exons and subsequently forms a dimer to bring these exons into close proximity for further processing by the splicing machinery [200]. Importantly, QKI is expressed at low levels in epithelial cells but is increased during epithelial-to-mesenchymal transition (EMT), when cells reprogram their gene expression profiles resulting in the loss of intracellular junctions, polarity, and cytoskeletal organization, ultimately leading to a more migratory and invasive mesenchymal phenotype. The increase of QKI during EMT triggers the expression of hundreds of circRNAs [200]. EMT is a process which can be induced by irradiation, and very often the mesenchymal cells display a more radiation-resistant phenotype, highlighting the relevance of EMT, and therefore QKI-regulated circRNAs, for radiation and cancer biology.

Different functions for circRNAs have been identified, including (1) binding and transportation of RNA-binding proteins; (2) generation of protein isoforms; and (3) regulators of transcription and alternative splicing (e.g., Xiao et al. [198]). However, the most established and investigated function of circRNAs is the regulation of microRNA expression and subcellular localization via a sponging mechanism (competing endogenous RNA, ceRNA). However, since most circRNAs are expressed at only low levels, and they usually contain only a limited number of microRNA-binding sites, it is now clear that the function of microRNA sponges or ceRNAs to regulate the expression of microRNA targets cannot be generalized for many circRNAs [198].

An important consideration here is that studies often perform gene ontology enrichment analyses based on the functions of the host genes of differentially expressed circRNAs. However, since there is currently little evidence that circRNAs in general function in the same pathways as their hosts, such analyses should be critically interpreted.

3.17.4.2 circRNAs, Radiation Exposure, and Radiosensitivity

Despite increasing attention, the number of studies investigating the direct effect of ionizing radiation on circRNA expression is still very limited. On the other hand, there have been quite some studies in which the differential expression of circRNAs between radiation-sensitive and radiation-resistant cancer cell lines and patients was compared.

In HEK293-T cells, gamma irradiation (8 Gy, single dose) resulted in very big differences in the expression of circRNAs between control and irradiated cells. Here, the authors focused only on circRNAs detected under both experimental conditions and identified a total of 158 differentially expressed circRNAs. However, among 5592 detected circRNAs in total, 2205 were detected uniquely in control cells while 1026 circRNAs were uniquely found in irradiated cells. This indicates that the differences were actually larger than was reflected by the 158 that were considered to be differentially expressed.

A study by O'Leary and co-workers investigated differential circRNA expression at 4 h and 24 h after exposure of endothelial HUVECs to a medium (0.25 Gy) and high dose (2.5 Gy) of g-rays [202]. Radiation-responsive circRNAs were predominantly produced from genes involved in the p53 pathway, as is in general the case for the early transcriptional response to radiation. The authors furthermore focused on two circRNAs derived from the *WWOX* gene, showing that they are differently regulated by QKI in response to radiation depending on the cell type and that they are enriched in exosomes [202].

Another study focused on specific p53-dependent genes and their circRNA abundance in the embryonic mouse brain and primary neurons [203]. This study showed that the temporal induction of circRNA expression follows that of their linear mRNA hosts and that they remained more abundant for a longer time after irradiation compared to mRNA. This may have important implications for the use of circRNAs as long-term biomarkers of radiation exposure [203]. Indeed, gene expression changes at the level of mRNA are usually short-lived. Therefore, the increased stability of circRNAs may result in prolonged radiation-induced expression as was shown by Mfossa and co-workers [203].

3.17.4.3 Examples of Important circRNAs for Radiation Biology

circPVT1

One of the most extensively studied circRNA host genes related to radiation and cellular radiosensitivity is *PVT1*, a long noncoding RNA (lncRNA) gene from which different circRNAs can be generated. One of these, termed circPVT1 (CircBase ID: hsa_circ_0001821, consisting of the exon 2 of the PVT1 mRNA), is downregulated during both multiplicative and radiation-induced senescence in human diploid WI-38 fibroblasts. This leads to reduced sponging of the hsa-let-7 microRNA and a subsequent reduction of proliferative proteins encoded by let-7 targets (e.g., IGF2BP1, KRAS, and HMGA2) that prevent senescence. Thus, circPVT1 is a suppressor of (radiation-induced) senescence by acting as a decoy for let-7. Interestingly, linear PVT1 lncRNA was not decreased in senescent cells, indicating that the observed effects were exclusively regulated by circPVT1 [204].

Pvt1 was one of the p53 target genes investigated in the aforementioned study of Mfossa et al. [203]. Also, in human head and neck squamous cell carcinoma cells, circPVT1 expression was found to be dependent on p53 as it was enriched in tumors with p53 mutations and silencing of p53 resulted in a downregulation of circPVT1, but not linear PVT1 [205]. Several other studies have implicated circPVT1 as an oncogene in different cancers, and it enhances to chemotherapy resistance in gastric cancer cells and lung adenocarcinoma by acting as a ceRNA for miR-124-3p and miR-145-5p, respectively [201, 205]. In non-small cell lung cancer, circPVT1 expression is induced after irradiation, while it enhances radiosensitivity via inhibition of the PI3K/AKT/mTOR pathway through sponging of miR-1208 [206].

circ-AKT3

The PI3K/AKT/mTOR pathway plays a central role in cancer cell radioresistance in part via activation of EMT [207]. Inhibitors are currently being investigated as therapeutics to improve radiotherapy outcome. AKT is a serine-threonine kinase that exists in three isoforms, AK1, AKT2, and AKT3. The AKT3 gene hosts different circRNAs. Of these, circ-AKT3 (hsa_circ_0017250) is a protein-coding circRNA that competes with AKT phosphorylation, thereby reducing radiation resistance of different GBM cell lines. In contrast, another circ-AKT3 transcript (hsa_circ_0000199) increases chemoresistance of gastric cancer to cisplatin by upregulation of PIK3R1 (Huang et al. 2019). This suggests that different circRNAs originating from the same host gene can have opposite biological functions, as is sometimes also observed with linear splice variants. This furthermore highlights the importance of functional characterization of individual circRNAs. Several other circRNAs have been demonstrated to affect PI3K/AKT/mTOR signaling. Some of these have been described in the review papers by Cui et al. [201] and Jeyaraman et al. [208].

3.18 Future Perspectives

Altogether, it is now evident that circRNAs are affected by irradiation and that they are important players in the cellular radiation response and sensitivity. However, their exact functions in these processes, which furthermore may be cell type dependent, need to be investigated in a case-by-case manner. Novel methods for the genome-wide identification and functional characterization of circRNAs may prove to be useful tools for these future investigations [209].

3.18.1 Extracellular Vesicles

Extracellular vesicles (EVs) are particles generated by all cells in our body by different routes and differ in diameter from <50 nm up to several μm [210]. EVs can based on their physical and molecular characteristics be divided into exosomes, ectosomes, microvesicles, microparticles, oncosomes, and apoptotic bodies. Size and expression of certain proteins reflecting their biogenesis and cellular origin are used for their classification (Table 3.15) [211]. Physical properties, e.g., size, density, and solubility of EVs, are often used for the isolation by differential high-speed centrifugation, size-exclusion chromatography, and precipitation. However, due to overlapping characteristics, pure preparations of individual EV species are challenging.

EVs are enclosed by a lipid-bilayer membrane, and their cargo includes coding and noncoding RNAs, genomic and mitochondrial DNA fragments, proteins, metabolites, and lipids. Initially, EVs were discovered as "garbage bins" to remove unwanted materials. Now, it is clear that most of the cells in our bodies utilize EV secretion into its close or distant microenvironment as a way of communication [212]. Thus, EVs can transfer functional biological molecules to recipient cells either by direct fusion with the

Table 3.15 Characteristics of different extracellular vesicles (EVs)

Type of vesicle [size (nm)]	Description of characteristics
Microvesicles 100–1000 nm	A subgroup of EVs generated at the cell membrane. Found in both body fluids and tissues
Apoptotic bodies 500–2000 nm	A subgroup of EVs composed of cellular organelles and cytoplasm. Formed during apoptotic cell death by budding after the plasma membrane has undergone blebbing
Ectosomes 100–1000 nm	Membrane microvesicles produced by neutrophils or monocytes formed by direct budding from cell membrane. Vesicles larger than 350–400 nm are not always considered as true ectosomes
Oncosomes 100–500 nm Large oncosomes 1–10 µm	EVs of different sizes generated by tumor cells which function as transmitters of oncogenic signals (RNA, protein complexes) between cells
Exosomes 40–150 nm	Membrane-bound EVs formed by the endocytic pathway. These EVs are first formed at the plasma membrane and subsequently transformed into early endosomes. These subsequently mature into late endosomes where they bud off to the ER intracytoplasmic lumen. The formed multivesicular bodies thereafter are unified with the cell membrane, and exosomes are released to the extracellular surroundings of the cell. Exosomal markers include CD63, CD9, CD81, and TSG101 among others

plasma membrane or by internalization but also via interaction with cell surface receptors triggering downstream signaling (Box 3.35).

Box 3.35 In a Nutshell: Extracellular Vesicles

- Extracellular vesicles (EVs) can be of different sizes and are generated via different biogenesis routes from all cells within our body.
- EVs cargo RNA, DNA fragments, lipids, and proteins partly reflecting their cell of origin.
- EVs are important communicators in health and disease.
- EVs regulate carcinogenesis and metastasis.
- Exosomes are generated via the endosomal system and are released from viable cells.

EVs are found to be an integrated part of cell-to-cell communication, thereby contributing to regulation of the immune as well as the nervous system but also to tissue regeneration after damage [213]. Also, in the carcinogenesis and cancer metastasis fields, EVs have been demonstrated to be important communicators. Thus, EVs regulate the tumor and the tumor microenvironment signaling including angiogenic promotion, conversion of fibroblast into cancer-associated fibroblasts, and interplay with the immune system, thereby providing a good milieu for disseminated tumor cells to grow as well as establish themselves as metastases.

Given that EVs can influence a multitude of cell and tissue processes, it is not surprising that EVs today are considered an important source of biomarkers of different diseases including cancer. Thus, analyses of EVs and their cargo have been able to gain the US Food and Drug Administration (FDA) and international approvals to some extent [214]. With such diverse and varied roles of EVs in assisting cancer progression, it is essential that one can understand how IR, given its essential place in cancer therapy, can alter EVs cargo and/or function.

3.18.1.1 Exosomes

Exosomes are generated in the endosomal system of almost all cells (Fig. 3.50). These vesicles of nano size have membranes with parts from their cell of origin but also cargo membrane and cytosolic lipids, proteins, as well as various RNA species and DNA fragments [215].

When exosomes were identified in the 1980s, they were seen upon as "garbage bins," but later it was reported that exosomes generated from B lymphocytes could trigger a T-cell response. From that time, exosomes have been shown to participate in a multitude of cell–cell communication routes by carrying cargoes which are taken up by recipient cells close by or in a multicellular organism, in another tissue as exemplified in the cancer metastasis process [216]. The scientific community have gathered data on the exosome cargo, e.g., protein, lipid, and mRNA or miRNAs, into large databases, e.g., ExoCarta (http://www.exocarta.org/) and Vesiclepedia (http://www.microvesicles.org/), which are growing as more exosomes from cells of different origin and in different contexts are being deciphered and reported (Box 3.36).

Box 3.36 In a Nutshell: Exosomes

- Exosomes are EVs of endosomal origin, which contain nucleic acids, membrane and cytosolic proteins, metabolites, and lipids.
- Once released, exosomes may act on cells in close vicinity or in a distant tissue.
- Exosomes are involved in a multitude of human diseases including cancer where they regulate carcinogenesis, tumor-immune cell interplay, angiogenesis, and metastasis.

It is still to some extent difficult to sort out plasma membrane-derived EVs from exosomes as their sizes are similar and given that there is a cell heterogeneity in the expression of the protein markers that define exosomes

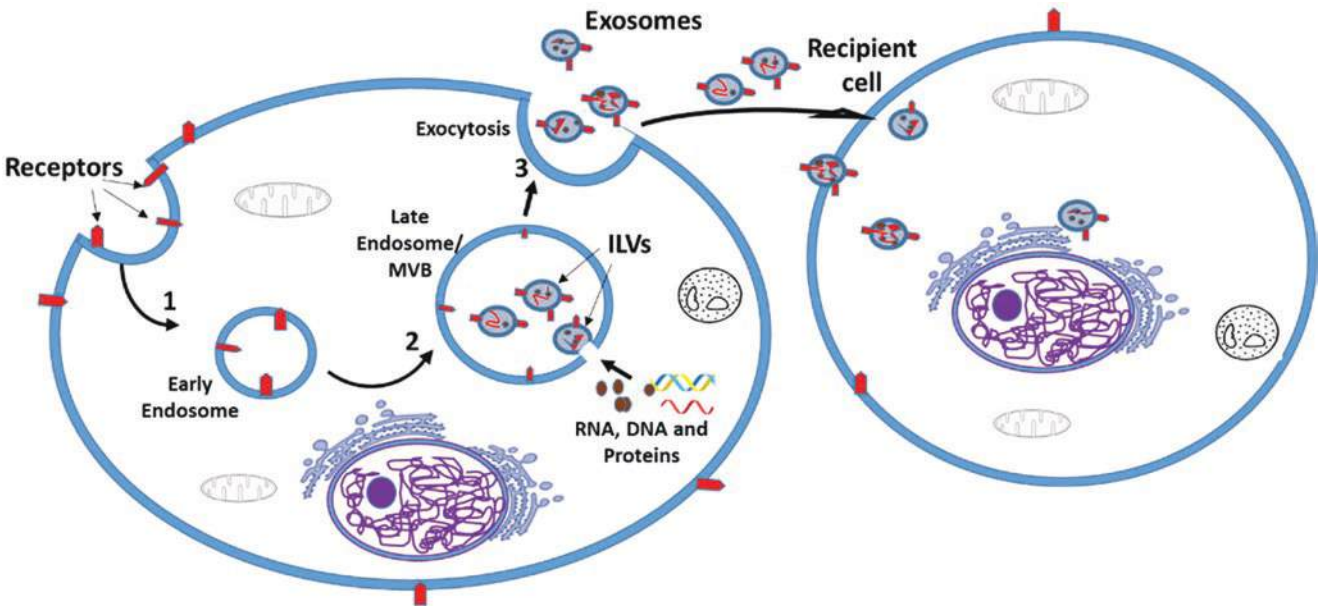

Fig. 3.50 Principal steps in exosome biogenesis. The early endosomes, which are generated at the plasma membrane (1), later undergo maturation, called late endosomes or multivesicular bodies (MVBs) (2). The MVBs' membrane invagination results in the formation of intraluminal vesicles (ILVs). During the invaginating process, particular proteins are incorporated into the invaginating membrane. Other cytosolic biomolecules, i.e., nucleic acids and proteins, are engulfed and enclosed within ILVs. The release of exosomes into the extracellular environment happens after fusion of the MVB with plasma membrane (3)

[210]. However, there are certain proteins that characterize exosomes including Rab GTPases, flotillin, heat-shock proteins (HSP70 and -90), tetraspanins (CD63, CD9, CD81, and CD82), Alix, flotillin, and TSG101. These markers are also suggested by the International Society for Extracellular Vesicles (ISEV) to be used to define exosomes [210].

The lipid membrane of EVs has a different composition relative to plasma membranes. Thus, EV membrane has higher level of sphingomyelin, cholesterol, ceramide, and phosphatidylserine while less expression of phosphatidylcholine. These lipids have been shown to have a profound effect on carcinogenesis and cancer progression including enhancing invasiveness, angiogenesis, and chemoresistance via transport of oncogenic elements.

There is clear evidence that cancer cells may have another rate of exosome release than non-transformed cells [217] while it is still a controversy as to what extent that is reflected in human liquid biopsies, e.g., plasma, and if it can be linked to therapy response. Also, it has been recognized that cancer and normal cells differ with respect to exosome cargo, e.g., miRNA, mRNA protein, and lipids. Exosomes have been found in plasma, serum, lymph fluid, bronchial fluid, cerebral spinal fluid (CSF), urine, saliva, tears, bile and gastric acid, amniotic fluid, breast milk, semen, and synovial fluid [218]. This has spurred an interest in their role as a source of biomarkers.

As indicated above, in human tissues, exosome can act near its cell of release or be transported in the blood to a distant tissue, e.g., site of metastasis in the context of cancer. It has been demonstrated in a large number of publications that once the exosome cargo reaches its target cell, several mechanisms cooperate for uptake as well as for altering signaling in the recipient cells [219]. Similar to EVs, exosomes participate in different processes of the immune system as well as in neurological signaling processes. Exosomes also have a clear function in cancer signaling. Exosomes are described to regulate tumor internal signaling but also tumor–tumor microenvironment interplay. For example, exosomes may promote angiogenesis as well as metastatic spread, and they are important communicators between tumor and different infiltrating immune cells.

Exosomes may exert these events by modulating paracrine, autocrine, and endocrine pathways in different cell types via their cargo. The exosome surface proteins are reported to resemble those of plasma membrane and endosome of a given cell yet with minor contribution of proteins from nucleus or Golgi. It has also been reported that EV membrane composition differs from plasma membrane concerning their lipids. Thus, EV membrane has higher level of sphingomyelin, cholesterol, ceramide, and phosphatidylserine while less expression of phosphatidylcholine.

3.18.1.2 Exosome RNA Loading

Exosomes carry a wide range of cargoes, and it is currently thought that such cargoes, e.g., RNA species, are selectively loaded into exosomes and that loading is not a random pro-

cess. This is supported by observed differences in miRNA abundances in cells compared to exosomes, which have been linked to 3′ uridylation in miRNAs of exosomes, while 3′ adenylated miRNAs are enriched in cellular fractions [220]. Moreover, certain sequence motifs are recognized by the nuclear ribonucleoprotein A2B1 (hnRNPA2B1), which then dictates the miRNA loading process into exosomes, possibly via interaction with cytoskeletal components. The protein AGO2 has also been shown to selectively package exosomes with miRNAs specifically miR-451. In addition, overexpression of the protein neutral sphingomyelinase 2 has been associated with an increase in exosome-associated miRNA. It has also been demonstrated that 3′ mRNA fragments are enriched in exosomes. The conserved 25-nucleotide sequence (also known as a zip code-like 25 nucleotide) is usually incorporated into mRNA's 3′-untranslated region and expressed in many types of cells, leading to mRNA enrichment in the MVs/exosomes. It has been suggested that miR-1289 plays a crucial role in MV enrichment of the mRNA via binding to zip code sequence directly.

3.18.1.3 Exosome Release and Functional Effects

The release of exosomes requires the movement of late endosomes/multivesicular bodies (MVBs) to the cell surface, where they fuse with the cell membrane (Fig. 3.50). The actin cytoskeleton and microtubule network have been shown to be important in facilitating MVB movement towards the cell surface, while Rab GTPases facilitate the release of exosomes into the extracellular space. Interestingly, certain Rabs have been demonstrated to preferentially export exosomes with certain phenotypes; for example, Rab27A/B have been shown to release exosomes positive for CD63-, TSG101-, and Alix expression [221].

Exosomes may, via their cargo, induce both pro-survival and pro-death signaling in recipient cells. Thus, exosomes may promote tumor growth as well as induce inflammation through activation of mesenchymal stem cells (MSCs) and the subsequent secretion of IL-6 as well as IL-8. There is also evidence that exosomes carry inhibitors of apoptosis proteins (IAPs), e.g., survivin, XIAP, cIAP1, and cIAP2, the delivery of which is postulated to offer protection from a continually changing microenvironment, thereby helping tumor progression.

In the context of tumor and immune cell interplay, there is growing substantiation that tumor cells of different origin can via their exosome cargo impair infiltrating T-cell function as illustrated by PD-L1-expressing exosomes [222]. Similarly, CD73, an ecto-5′-nucleotidase and a master regulator in the tumor-immune microenvironment, has been reported in exosomes and also to have functional activity in this context, e.g., impairing T-cell function [222]. The effect exosomes have on tissue poses a number of interesting questions when it comes to radiation biology as radiation has tumor growth-inhibiting effects yet may negatively influence certain normal tissue in the radiation therapy field. Exosomes are also thought to offer some beneficial properties against different tissue damages. Thus, exosomes from MSCs have been reported to offer protection against diabetic nephropathy in the renal system by blocking apoptosis as well as promote vascular regeneration. Moreover, acute kidney injury caused by the DNA-damaging agent cisplatin was found to be blocked by microvesicles as a result of inhibition of apoptosis. Exosomes have moreover been shown to enhance recovery from ischemic brain injury through promoting angiogenesis and providing an extracellular milieu for appropriate brain remodeling.

3.18.1.4 Extracellular Vesicles in Radiation Responses

As EVs are important regulators of multiple cellular signaling events, it is not surprising that EVs are also important communicators in the context of IR [223]. EVs are affected by IR on multiple levels, including alterations in subtype/size, release, cargo, uptake, and function. These changes facilitate the dissemination of IR signals to neighboring cells and to distant sites, which contributes to systemic effects in irradiated and nonirradiated areas. Therefore, EVs are potential mediators of IR-targeted and non-targeted effects, e.g., bystander and abscopal effects.

Several studies suggest increased EV release after irradiation in *in vitro* and *in vivo* models. As an example, it has been shown that IR may increase EV release in different tumor models including head and neck cancer and glioblastoma. Moreover, also in normal tissue after partial-body irradiation of mice, it has been reported that the EV content is altered in different tissues including the liver, brain, and heart. As the potential mechanism for the IR-increased EV release, p53-mediated induction of genes involved in the EV biogenesis and altered MAPK signaling were suggested. It was also shown that the cellular uptake of EVs is affected by radiation exposure. In mesenchymal stem cells, irradiation induced changes in the formation of cell surface CD29/CD81 complexes, which increased the cellular uptake of EVs [224].

IR also induces changes in the composition of EVs released from cancer and non-cancer cells. Alterations seem to be highly related to cell type, radiation dose, and also time postradiation exposure where both microRNA and protein changes have been described. Additionally, changes in lipids and metabolites in EVs from irradiated donor cells are reported. EV cargo changes were also shown for EVs isolated from blood during or after tumor RT. For example, differential expression of serum EV miR-

NAs was monitored in prostate cancer or glioma patients after RT. In the serum of HNC patients, it was shown that tumor-derived exosome (TDE) amount relative to total exosomes increased in patients that were refractory to a combination of radio-, targeted, and immune therapy while the opposite was found in the patients that responded. Moreover, in the same study, results demonstrated an increase in regulatory T-cell (Treg)-derived exosomes as well as in CD3(−)PD-L1+ exosomes in serum after treatment if the patients were refractory. Such alterations in EV cargo open up for potential applications of EVs/exosomes as a source of biomarkers for radiation exposure as well as for prognostic or predictive biomarkers of RT response in the context of cancer.

A substantial amount of studies suggest that EVs play a role in the progression, RT resistance, and metastasis of cancer cells. In glioblastoma, Mrowczynski et al. demonstrated a pro-survival function of EVs derived after IR, which may be triggered by elevated cargo levels of oncogenic miRNAs and mRNAs, while tumor-suppressive RNAs were reduced [225]. In the same cancer type, a pro-migratory role of radiation-related EVs was reported. Likewise, EVs from irradiated HNC and neuroblastoma cells were shown to stimulate survival, migration, and invasiveness. However, there are also studies reporting on an induction of harmful effects of EVs from irradiated cancer cells into recipient cells, like chromosomal damage and increased ROS levels.

EVs are also involved in the communication of radiation signals among normal cells. Early work by Jella et al. showed the transmission of cytotoxic effects between irradiated and nonirradiated keratinocytes in an *in vitro* model system. Thus, EVs from irradiated mice were able to increase DNA damage and reduce viability in co-cultivated mouse embryonic fibroblasts. On the other hand, several reports found beneficial effects of EVs released from irradiated human PBMCs. For example, EVs from irradiated blood cells were shown to reduce radiation-induced apoptosis in endothelial cells [226]. Accordingly, pro-angiogenic and tissue-regenerative capacities were attributed to EVs from irradiated PBMC. In this regard, it was shown that EVs (especially from mesenchymal cells) could be used for the treatment of radiation injury [227].

In summary, current knowledge indicates a vital role of EVs in the IR response of cancer and non-cancer cells. IR not only affects the production and the composition of EVs, but also alters the phenotypes of recipient cells. Therefore, these mechanisms can contribute to the communication between irradiated cells as well as to the systemic distribution of local radiation effects throughout an organism. Moreover, EVs may offer a source of biomarkers for monitoring RT responses in cancer patients (Box 3.37).

Box 3.37 In a Nutshell: Extracellular Vesicles as Epigenetic Factor

- EVs, including exosomes, act as intercellular signaling components in response to IR.
- IR may influence the EV release/uptake as well as cargo in normal as well as tumor cells contributing to both direct and bystander effects of IR.
- EVs/exosomes may contribute to the distribution of systemic IR effects and offer a source of IR response biomarkers.

3.19 Omics

3.19.1 Proteomics

The term proteome was created to describe the set of proteins expressed by the genome [228]. Proteomics analyzes the proteome at a specific time and in a specific state. Proteome profiling provides information not only about the protein expression, but also about the function, structure, and interactions of proteins.

In the well-established paradigm of proteomics, protein mixture will be separated before digestion either by gel electrophoresis (gel-based approaches) or using liquid chromatography (gel-free approaches) to resolve the complexity of the protein mixture [228]. In the next step, proteins were fragmented into smaller units called peptides during digestion. The generated peptides were further separated and sorted in the mass spectrometry system based on the mass and charge, where the abundance of each peptide is translated into numerical values called intensity. To identify a protein, a certain number of good-quality peptides must be detected. Quantitative proteomics compares the peptide intensities for each protein between treated (e.g., irradiated) and non-treated (e.g., nonirradiated) samples. The alterations in peptide intensities represent the changes in the expression level of corresponding protein.

Protein quantification can be performed in two ways: either label based or label free. In label-free methods, protein expression in several samples is compared by measuring the intensity of the corresponding peptides or counting the number of correlated spectra for each protein. Label-based quantification is performed by labeling peptides or proteins with fluorescent dyes, chemical isotopes, radioisotopes, or affinity tags before mass spectrometry. Label-based proteomic approaches are classified into chemical labeling (ICPL, iTRAQ, and iCAT) and metabolic labeling techniques (SILAC).

Advanced proteomics approaches also offer an accurate platform to identify and quantify the posttranslational modifications (PTMs) such as phosphorylation, acetylation, methylation, or ubiquitination [229]. These modifications are crucial for the stability, localization, and conformation and functions of proteins. The analysis of phosphoproteome, acetylome, or ubiquitinome has revealed the regulatory role of these PTMs in cellular function and homeostasis [229].

A comprehensive combination of proteomics and advanced bioinformatics makes the complex biological processes in cells understandable. The bioinformatics tools provide a broad spectrum of information on protein functions, protein-protein interactions, protein interactions with other biomolecules (genes and metabolites), contribution to the signaling pathways, and predictions of diseases [230].

3.19.1.1 Proteomics in Radiation Research

Different proteomics approaches were applied to investigate the biological effects of radiation exposure on normal and tumor tissues, cancer radiotherapy outcome, individual sensitivity, risk assessment, biodosimetry, and biomarker discovery; an extensive review can be found in the work of Azimzadeh et al. [231].

One of the main goals of cancer proteome profiling in radiation research has been to identify biomarkers that predict the tumor's response to radiation exposure. The proteomes of different cancer cell lines such as nasopharyngeal carcinoma, head and neck cancer, oral squamous cell carcinoma, laryngeal cancer, breast cancer, and lung cancer have been analyzed in radiobiological studies to identify signatures of cancer radioresistance and potential prognostic markers for radiotherapy. Although the results of these studies are not uniform, the proteins identified and quantified belong mainly to the family of antioxidant proteins, heat shocks, and structural proteins.

The most challenging aspect of radiotherapy for cancer is to select the radiation dose so that the tumor is killed but the surrounding normal tissue is harmed as little as possible. The effect of radiation on normal tissue has also been analyzed by proteomics approaches. A number of studies have been carried out on in vitro and in vivo models to simulate the effects of radiation on normal tissue such as the heart, brain, and liver. These studies underlined the adverse effects of irradiation on tissue structure and function. The mitochondrial proteins, the metabolic enzymes, and the oxidative stress response proteins are the main groups of proteins affected in the irradiated heart. The structural proteins, proteins involved in cognition and learning function, and inflammatory response were impaired in the irradiated brain.

Biofluids such as serum, plasma, and urine are optimal biomaterials for biomarker discovery, mainly because of the relatively noninvasive collection methods. However, proteomic profiling in biofluids is still an analytical challenge due to the complexity and variable spectrum of protein abundance. Several studies have compared the biofluid proteome before and after radiation exposure. These studies provide a panel of proteins that serve as biomarkers of radiation exposure, radiation damage, cancer radiosensitivity and radiotherapy outcome, and biodosimetry.

Since cellular responses to irradiation are tightly regulated by PTMs, the analysis of these changes is becoming increasingly important in radiation research. PTM profiling is still a young field in radiation research, and only a few studies have analyzed the change in protein phosphorylation, acetylation, and ubiquitination in the context of cancer and normal tissue response to irradiation.

Archival formalin-fixed, paraffin-embedded (FFPE) tissues are the invaluable alternative of fresh frozen biomaterial in radiation research. Proteomic analysis of these samples is challenging, mainly due to the harsh conditions of tissue fixation and, in particular, biomolecule extraction method. The proteomics studies conducted on FFPE tissues from radiobiology archives have mainly investigated the predictive marker for radiotherapy resistance of cancer or adverse effect on normal tissue. They demonstrated the compatibility and applicability of FFPE tissues for proteomics studies [231].

3.19.2 Lipidomics

The study of cellular lipid pathways and networks in biological systems is known as lipidomics [232]. Lipids are a necessary component of biological membranes and play essential roles in biological systems, such as the plasma membrane bilayer structure that separates the cell cytoplasm from the extracellular microenvironment, the provision of a hydrophobic medium for the functional performance and interactions of membrane proteins, and the generation of second messengers through enzyme reactions [233]. Lipidomics refers to the analysis of all lipids present in a sample using liquid chromatography (LC) and mass spectrometry (MS) techniques.

Glycerolipids, saccharolipids, sphingolipids, glycerophospholipids, sterols, polyketides, fatty acyls, and prenols are the eight types of lipids that can be classified based on their chemical structures and hydrophobic and hydrophilic aspects [233]. The most prevalent phospholipids (PLs) are glycerophospholipids, found in biological membranes and essential for numerous cellular activities. PCs and other related phospholipid derivatives like lysophosphatidylcholines (LPCs) are signaling molecules that play a role in regulating cellular death and proliferation. Triacylglycerides (TGs), sphingomyelins (SMs), phosphatidylinositols (PIs), diacylglycerides (DGs), and cholesteryl esters are also among lipids with key roles in cell physiology [234].

Reactive oxygen/nitrogen species (ROS/RNS) react extensively with lipid molecules following irradiation, causing lipid breakdown and eliciting both direct and indirect inflammatory responses. Lipid peroxidation and pro-inflammatory lipid intermediates can have immediate impacts on physiology and can lead to long-term consequences like CVD, lung damages, and even carcinogenesis. Apoptosis can also be triggered by the direct action of radiation or by lipid intermediates, such as the activation of sphingomyelinase, which produces ceramide from the hydrolysis of sphingomyelin. Ceramide is a direct apoptotic cell death [234]. Post-ionizing irradiation (IR) changes affecting lipids have been proven in preclinical investigations and may have biological consequences such as the acute radiation sickness (ARS) or lead to delayed effects of acute radiation exposure (DEARE).

When comparing sham or pre- and post-IR specimens, lipids examined in blood, such as PCs, LPCs, TGs, SMs, and CEs, exhibit modifications.

The link between lipid levels in serum/plasma and radiation has been studied in animal models in several publications. Phosphatidylethanolamine (PE) and phosphatidylserine (PS) levels in rat plasma following gamma irradiation exposure increased dramatically, thus indicating that IR may disrupt phospholipid metabolism [233]. Fatty acids, such as linoleic acid and palmitic acid, were found to be present at reduced levels in the blood following 137Cs exposure in mice, while phosphatidylcholines were among the most disturbed molecules in 137Cs-exposed mouse serum. A total of 67 biomarkers were discovered in some tissues and biofluids of mice exposed to radiation (6 Gy) (serum and urine). Among these, 3-methylglutarylcarnitine was found to be a unique metabolite seen in the liver, serum, and urine that might be employed as a marker of early radiation response.

Changes in lipid metabolism, including key lipid species such as free fatty acids, glycerolipids, glycerophospholipids, and esterified sterols, have also been observed in nonhuman primates exposed to IR. The results show that diacylglycerides decreased 1 day after IR, but triacylglycerides and lysophosphatidylcholines increased from 2 to 7 days after IR. At 7 days, after 10 Gy irradiation, the amount of polyunsaturated fatty acids, such as arachidonic acid and docosahexaenoic acid, increased significantly in the nonhuman primate model. Between 2 and 3 days after irradiation, an increase in LysoPCs and a decrease in SMs could be regarded as viable indicators (6.5 Gy). Compared to nonirradiated controls, recent research in nonhuman primates has discovered plasma-derived exosomal indicators of IR exposure related to the enrichment of N-acyl-amino acids, fatty acid esters of hydroxyl fatty acids, glycolipids, and triglycerides.

Radiation therapy caused blood lipidome disturbances, which were corrected within 1–2 months after IR treatment, according to lipid species quantification in individuals receiving radiation therapy. As a result, radiation-induced lipidome modifications could indicate changes in early time points and, perhaps, alternative damage pathways. Patients undergoing a complete body irradiation at the MSK Cancer Center (NYC), before hematopoietic stem cell transplantation, showed seven urine indicators with changes between pre- and postexposure at 4–6 h (1.25 Gy) and 24 h (three fractions of 1.25 Gy each) postirradiation, which involved trimethyl-*l*-lysine, acetylcarnitine, decanoylcarnitine, and octanoylcarnitine (carnitine conjugates involved in fatty acid transport), as well as hypoxanthine, xanthine, and uric acid (purine catabolism pathway end products).

During the period 2015–2019, the National Cancer Institute's Radiation Research Program, in partnership with the Small Business Innovation Research Development Center, financed four small firms. This led to the development of a metabolomic/lipidomic assay for predicting late effects that have a negative impact on the quality of life in prostate cancer patients treated with radiation. Shuttle Pharmaceuticals (Rockville, MD) intended to move forward by developing and validating a metabolomic/lipidomic biomarker panel that could predict radiation toxicity. In a phase I experiment, metabolites in plasma from 100 patients were examined in order to develop a kit that could support metabolomic analysis and act as a biomarker panel to predict sensitivity to radiation late effects. A phase II SBIR project was set up for the multi-site analytic validation of the metabolite panel kit created in the phase I SBIR project [235].

Lipidomics has then emerged as a reliable technique for lipid identification and quantification and the search for biomarkers that can be used in radiation-related incidents such as nuclear and radiological hazardous occurrences. In this sense, easily available biofluids are critical, especially in the case of irradiated victims, as well as the use of biodosimetry techniques that are both quick and accurate. Huang et al. [233] discovered seven radiation-responsive lipids in the serum of mice and showed their utility in dose calculation. Lipid changes after whole-body exposures have been thoroughly documented in a variety of animals, including atomic bomb survivors [234]. Indeed, estimating the radiation dose has always been a priority in the medical treatment of these events.

Because of the combined effects of neutrons and photons, shielding from structures, and closeness to the epicenter, among other factors, radiation exposures from an IND can be complicated. Using lipidomics, Laiakis et al. [234] evaluated serum samples from mice exposed to varying percentages of neutrons and X-rays to a total dosage of 3 Gy. Several lipids including triacylglycerides, phosphatidylserines, lysophosphatidylethanolamines, lysophosphatidylcholines, sphingolipids, and cholesteryl esters exhibited a delayed increase in mixed exposures, while diacylglycerides declined and phosphatidylcholines (PCs) remained virtually unaltered.

The mammalian lipidome's structural variety is so great that it necessitates a systematic nomenclature for precise categorization (identifying lipid subclasses, or the total number of carbons in the fatty acid chain and the number of double bonds). Because numerous lipid classes showed differences when comparing sham or pre- to post-IR samples, the variable sums and ratios within each metabolite class can increase and must be carefully considered.

3.19.3 Metabolomics: Metabolites

Radiation exposure can cause a complex molecular and cellular response having an impact in metabolic processes and consequently change metabolite levels [236]. This approach aims to detect small molecules (<1000 Da) in biological samples, which occur downstream of genomic, transcriptomic, and proteomic processes, constituting a more complete picture of the system's response to insult even prior to the onset of clinical symptoms [237]. The first use of metabolomics concerning radiation exposure studies was reported in the 1960s according to the experiences developed in human and animal samples; however, the understanding of cellular and molecular effects of ionizing radiation and the identification of radiation exposure biomarkers remain a challenge [236]. To obtain metabolic information, different methodologies can be used as nuclear magnetic resonance (NMR) or mass spectrometry (MS), including gas chromatography (GC) and liquid chromatography (LC). After sample collection, processing, and data acquisition, data analysis is the second step using principal component analysis (PCA) to have an initial perception about patterns and outliers, and if there are any easily discernible biomarkers. After, complex statistical data analysis should be employed in order to at the end perform biomarkers data interpretation and validation [236]. However, it is important to consider that there exist multiple analytical and clinical challenges that constitute an impediment for the successful translation of these biomarkers for clinical use [237].

Despite the few existing studies, some metabolite changes in small-molecule metabolites remain underexplored and underexploited concerning ionizing radiation effects [236]. The role of polyamine metabolism has been studied related to ionizing radiation effects. Present in all cells, polyamines, as putrescine, spermidine, and spermine, are aliphatic polycations with multiple functions related to cell metabolism, cell proliferation, and cell differentiation. These molecules have pleiotropic effects that allow their linkage to DNA, RNA, and proteins, identifying a regulatory role in cell metabolism [236]. Besides this, increased levels of these molecules are reported as healthy cell protectors against oxidative stress. Different studies using animal and patient samples have been performed reporting altered metabolites in response to ionizing radiation, namely creatine, creatinine, carnitine, hypoxanthine, citric acid, taurine, xanthine, threonine, uric acid, and citrulline. Besides these metabolites with high alterations, 2′-deoxyuridine, arginine, glycine, glutamine, hippuric acid, inositol, palmitic acid, uridine, lactic acid, leucine, linoleic acid, methionine, tyrosine, and sebacic acid are described as metabolites with moderate alterations in consequence of ionizing radiation. Therefore, and considering experimental data, among them exist strong candidates for diagnostic biomarkers being considered time- and dose-dependent measures [232]. Data obtained using T cells demonstrated that different metabolic pathways related to amino acid, nucleotide, fatty acid, and glutathione metabolism can be affected by in vivo radiation. Related with cancer and ionizing radiation response, metabolic profiling may help identify metabolites responsible for response to therapy, being the alteration of metabolite production, a feature that can influence tumor microenvironment and consequently cancer progression [237]. The complete characterization of the metabolome can be an opportunity to influence prognostic, predictive, and even pharmacodynamic biomarkers contributing to an individualized and targeted treatment [232]. Notwithstanding the capacity of metabolomics to detect alterations, it is necessary to be aware of the tumor-related responses, namely to the therapy, as inflammation and altered energy metabolism. Besides that, and considering cancer as a syndrome, there are also other cancer-associated conditions such as weight loss that can influence metabolism [238]. Having in consideration that ionizing radiation triggers a complex response influencing molecular and cellular processes and alteration of the metabolic processes and metabolite levels, more research work is necessary to identify biomarkers related to specific type and dose of radiation, genotypic differences, pathological conditions, and specific organs or tissues (Box 3.38).

Box 3.38 In a Nutshell: Omics

- Omics might provide biomarkers of high sensitivity and specificity for radiation research.
- Omics can provide a qualitative and quantitative overview of the global perturbations induced by IR in cells and biological fluids.
- Proteomics provides a comprehensive analytical platform to study the molecular mechanisms of the biological effects of radiation on normal tissues and tumours.
- Proteomic profiling is used to identify biomarkers of radiation exposure, radiation-induced damage, individual sensitivity, and biodosimetry.
- Proteome analyses of cancers deliver information on the outcomes of cancer radiotherapy.

- Metabolomics is used to detect small molecules (<1000 Da) in biological samples.
- To obtain metabolic information, different methodologies can be used as nuclear magnetic resonance (NMR) or mass spectrometry (MS).
- Ionizing radiation triggers a complex response influencing molecular and cellular processes that can be characterized using metabolomics.

3.19.4 Transcriptomics

Molecular signatures provide a composite inventory of radiation-specific responses as changes in the composition of these molecules and their abundance. Transcript levels of signature genes in various tissues, notably blood, saliva, skin, and tumor samples, can discriminate and, in some instances, quantify irradiated from unexposed samples [239]. Expression of coding genes and noncoding miRNAs, and lncRNAs, has been implicated in radiation responses, in some cases, which can be precisely calibrated to dose. For individual genes, e.g., FDXR, alternative splice isoforms have also been demonstrated to arise in a radiation-specific manner.

Transcriptomic approaches to classify radiation response can be based on the evaluation of many known genes, which minimizes technical bias in the selection of optimal combinations of gene subsets. Detection and quantification of ionizing radiation have been based on changes in the expression of a set of genes, primarily in blood from multiple individuals. Generally, signatures selected genes with largest average differences and combined changes in gene expression levels, to predict ionizing radiation exposure in humans and mice [240]. Genes previously implicated or established from genetic evidence and biochemical pathways that are altered in response to these exposures can be used to predict radiation exposure by supervised machine learning (ML) [241] (Fig. 3.51). Termed biochemically inspired ML, diagnostic gene signatures for radiation and chemotherapy have been proven accurate on clinical samples. However, typical sample sizes of typical datasets have limited the effective ML methods for deriving gene signatures.

To establish the reproducibility of these signatures, radiation exposures are predicted with data from independently exposed individuals. Consistent performance on independent dataset depends on the composition of the genes, how genes are ranked, how they validate the response, and how they account for the amplitude of the radiation response. Other important variables include how well signatures differentiate irradiated from unirradiated samples, or even different levels of absorbed radiation from each, or different radiation qualities (energy levels and source, particle types). Transcriptomics can integrate different genes/transcripts in the induced and repressed biochemical pathways that constitute these responses. There is an enormous range of accurate gene signatures that can be derived in many independently derived datasets. Interestingly, there are some core sets of genes and pathways that are present from different studies.

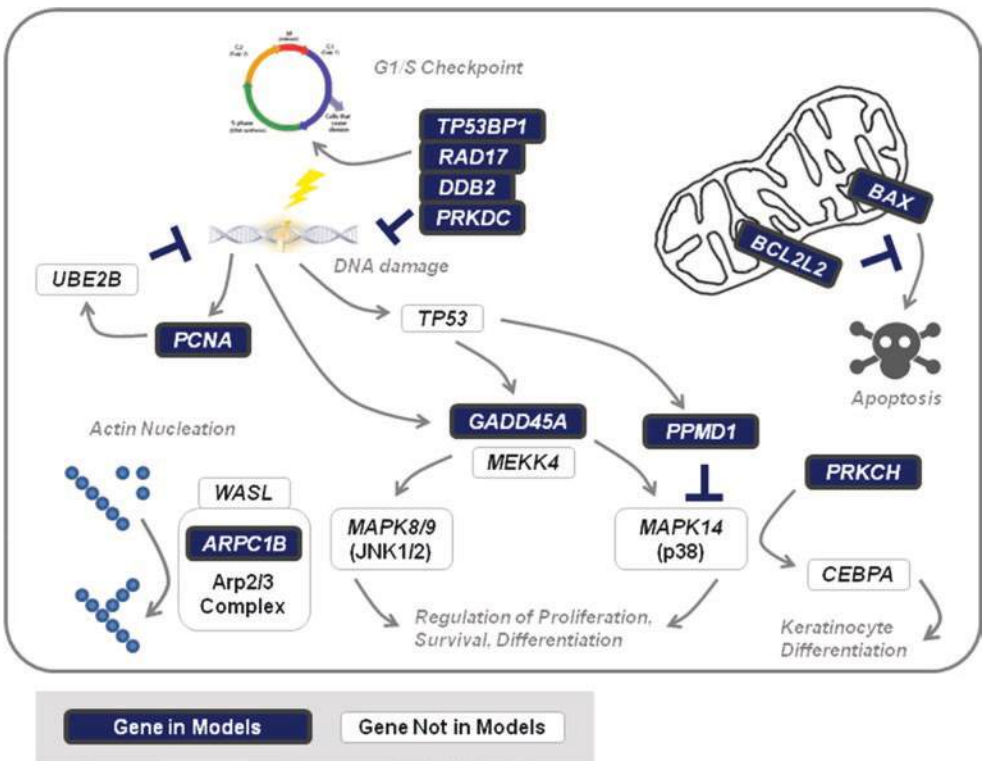

Fig. 3.51 Graphical depiction of major cellular functions containing the most frequently appearing genes of the highest performing human signatures adapted with permission (CCBY) from Zhao et al. [241]. Genes common among these signatures (white lettering) are indicated in pathways which contain products that these genes interact with (black lettering)

Many radiation response genes were frequently selected for multiple blood signatures, which include genes with roles in DNA damage response (*CDKN1A*, *DDB2*, *GADD45A*, *LIG1*, *PCNA*), apoptosis (*AEN*, CCNG1, *LY9*, *PPM1D*, *TNFRSF10B*), metabolism (*FDXR*), cell proliferation (*PTP4A1*), and immune system (*LY9* and *TRIM22*). While biochemical pathways comprising the best performing radiation gene signatures are often shared between human and other species, there are some distinctive differences, notably genes associated with immune cell communication (mice) and redox response (humans).

Expression of gene combinations that detect radiation exposure can also exhibit similar expression patterns in infectious diseases and other blood disorders [242]. Underlying pathways activated by radiation effects, for example DNA damage response and apoptosis, appear to be activated in some individuals affected with other conditions The genes involved are commonly present in multiple published radiation gene signatures and assays. For example, a 74-gene radiation signature comprised of 16 genes present in the human signatures was developed as reported in Zhao et al. [241], including *CDKN1A*, *DDB2*, and *PCNA*. Misclassification of radiation exposures in unexposed individuals with other blood disorders might be mitigated by reevaluating false-positive predictions with signatures containing radiation-responsive genes explicitly derived from other unrelated biochemical pathways, including those encoding secreted proteins.

3.20 Cellular Hyper-radiosensitivity

An important factor in the cellular response to radiation is the ability to repair DNA damage. In some individuals, hereditary mutations in genes involved in DNA repair result in a high sensitivity to irradiation [243]. The A-T syndrome is an example of one such mutation and is described in detail below. However, even with intact DNA repair pathways, it turns out that for small doses, cells refrain from the cell cycle arrest that would give time for repair. This results in a much higher cell kill per unit dose for small doses than higher doses, a phenomenon called low-dose hyper-radiosensitivity (HRS). An explanation to the presence of HRS could be that sacrificing a few cells may be advantageous to the risk of misrepair.

3.20.1 Repair-Deficient Cells (AT)

Ataxia-telangiectasia mutated (ATM) is a serine/threonine protein kinase with a key role in repairing double-strand DNA breaks (DSBs) and is also involved in the regulation of oxidative stress, metabolic syndrome, and neurodegeneration, among others reported [244].

The human ATM gene is located at 11q22-23, contains 66 exons, covers 160 kb of genomic DNA, and encodes the 370 kDa ATM protein. Germline mutation in ATM gene, either loss or inactivation of both copies, leads to the autosomal recessive ataxia-telangiectasia (A-T) syndrome, a devastating childhood condition characterized by chromosomal instability, neurological degeneration, immune dysfunction, premature aging, and high cancer risk. In fact, ATM has a critical role in the activation of the cell cycle progression and checkpoint activation in response to DSBs, as well as in the repair of these lesions through homologous recombination (HR) and nonhomologous end joining (NHEJ) pathway [245]. Thus, these mechanisms need to be active during DNA replication to maintain genome integrity in cells. When disruptions occur in these mechanisms, the cells are more susceptible to damage induced by the exposure to endogenous or exogenous agents, such as radiation exposure. Considering the well-known fact that exposure to IR activates ATM kinases to mediate the cellular response, individuals with these defective mechanisms, like A-T patients, will be more sensitive to the same IR exposure than non-A-T patients. Several published studies have corroborated these hypotheses, showing that failures in cell cycle checkpoints lead to a failure in the arrest in G1/S, S, or G2/M allowing the cells to escape from the proper DSB repair, among other signaling pathways including apoptosis and chromatin remodeling process [243]. Therefore, these non-repaired or misrepaired DBSs are responsible for chromosomal instability also in daughter cells, increasing the radiation sensitivity in these individuals as well as the carcinogenesis risk. It is important to elucidate that this cellular radiosensitivity is not unique for A-T syndrome being also observed in other individuals carrying mutations in other genes related to DNA damage repair and response pathways, namely in FANC, BRCA 1/2, MRE11, and DNA Lig4 genes, among others (Box 3.39).

Box 3.39 In a Nutshell: Cellular Hypersensitivity in AT Repair Deficient Cells

- Individuals carrying mutations in genes related to DNA damage repair are hypersensitive to radiation.
- A-T syndrome is connected to mutations in ATM, which has a critical role in checkpoint activation and DNA damage recognition and repair.
- HRS/IRR has been attributed to the early G2 checkpoint, which is only activated at a certain level of phosphorylated ATM.

3.20.2 Low-Dose Hyper-radiosensitivity

As described in Sect. 3.19.1, cells with defects in DNA DSB repair pathways are very sensitive to radiation. However,

even repair-competent cell lines can be hypersensitive to radiation within a certain low-dose range. This is called low-dose hyper-radiosensitivity (HRS) and is characterized by a high sensitivity to radiation doses below about 0.5 Gy (depending on the cell line and radiation quality) [246], which is followed by a more radioresistant response per unit dose in the dose range of ~0.5–1 Gy. This transition towards radioresistance is described by the term *induced radioresistance* (IRR) (Fig. 3.52) and occurs at doses corresponding to about ten double-strand breaks.

HRS [247] was first identified in vitro in 1993 after having been observed in mouse skin in 1986 and in mouse kidney in 1988. HRS has been observed in cells given acute proton and pi-meson irradiation as well as in cells given high-LET neutrons at a low dose rate and appears to be the default response for all radiation qualities in both tumor and normal cell lines. IRR, on the other hand, is only observed after low-LET irradiation and only in repair-competent cell lines [247].

In 2003, a mechanism explaining the basis for the HRS effect was proposed [248]. A second radiation-induced G2 checkpoint was discovered to be associated with HRS/IRR [249]. The radiation-induced G2 checkpoint that was known earlier, often denoted the Sinclair checkpoint, does not arrest cells irradiated while in G2, because it takes some time for the checkpoint to be activated. Only cells irradiated while in G1 or S phase are accumulated in G2 by the Sinclair mechanism. The newly discovered G2 checkpoint, also called the early G2 checkpoint, is induced immediately after irradiation and therefore arrests cells that were irradiated while in G2.

Contrary to the dose-dependent mechanisms by which cells irradiated in G1 or S phase accumulate in the Sinclair checkpoint, the "early" G2 checkpoint is ATM dependent [249] and independent of dose over the range of 1–10 Gy. Activation of the critical damage sensor molecule ATM by an autophosphorylation event at serine 1981 is detectable at doses of 0.1 Gy with a gradual increase until phosphorylation of more than 50% of the ATM molecules in the cell after

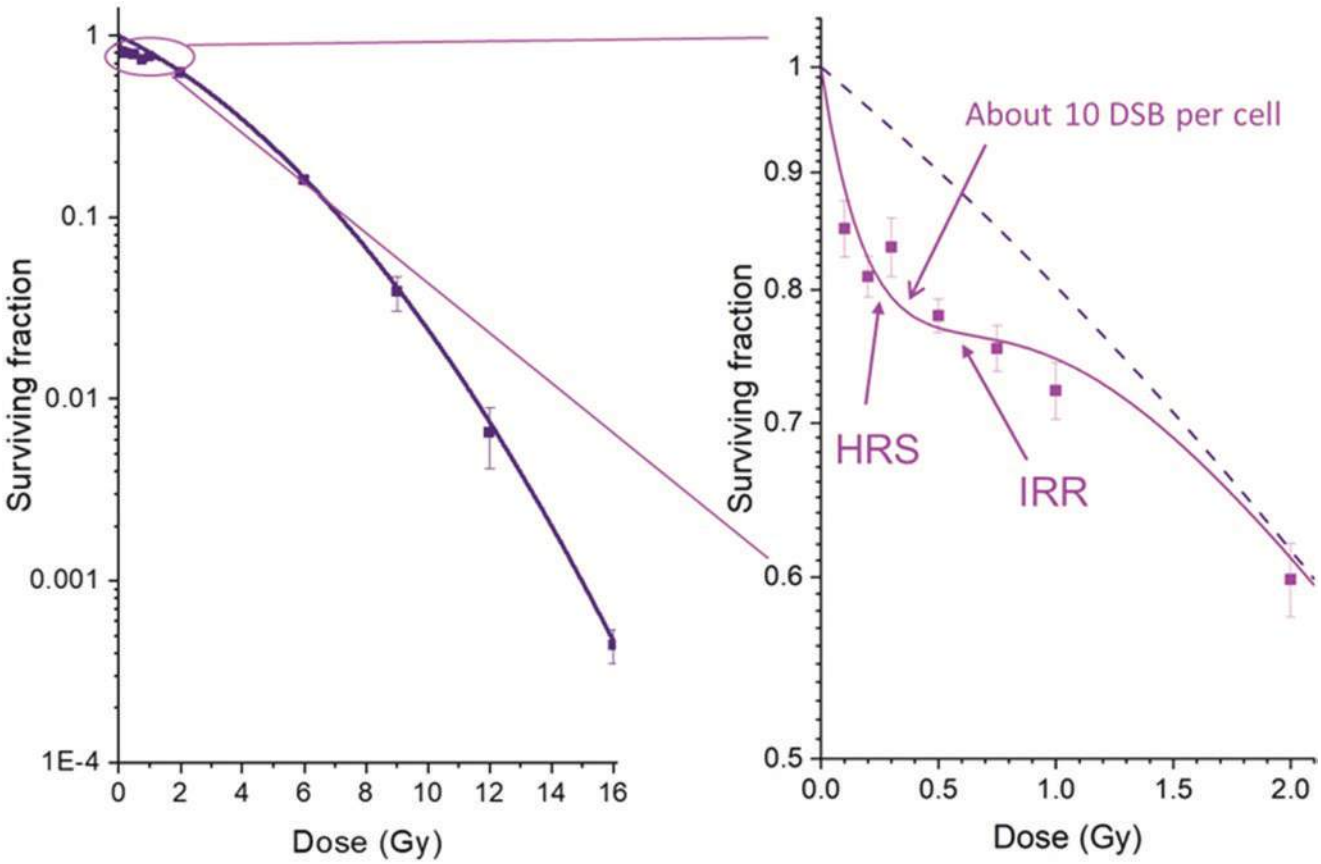

Fig. 3.52 Low-dose hyper-radiosensitivity (HRS) and increased radioresistance (IRR) in T-47D breast cancer cells. The left panel shows a full dose-response curve. The right panel shows the low-dose region. Below about 0.3 Gy, the cells appear to proceed from G2 to mitosis without repair of DNA damage, leading to a steep decrease in survival with dose. For doses above a threshold around 0.3 Gy, the damage is repaired increasingly with dose until the surviving fraction follows the linear-quadratic response curve. The transition dose corresponds to approximately 8–10 double-strand breaks. The dashed line shows a curve fit by the linear-quadratic model, and the solid line by the induced repair model (see Chap. 4)

Fig. 3.53 Path to "increased radioresistance" or "hyper-radiosensitivity." Cells irradiated with doses below about 0.3 Gy while in G2 will not have enough ATM activated by serine 1981-phosphorylation to reach the threshold level for activation of the early G2 checkpoint. They therefore follow the alternative in the left column, which does not give extra time for repair before mitosis resulting in "hyper-radiosensitivity" (HRS). Cells irradiated with doses above 0.3 Gy while in G2 follow the alternative in the right column and thereby are given more time for repair before mitosis resulting in "increased radioresistance" (IRR)

a dose of about 0.5 Gy and saturated expression at larger doses. Thus, the HRS/IRR transition appears to be coincident with both the induction of the early G2-phase checkpoint and activation of ATM.

The hyper-radiosensitivity is thus a result of the progress into mitosis with repairable but unrepaired DNA damages for cells that were irradiated while in G2 but received doses below the threshold for checkpoint activation (see Fig. 3.53).

It has been demonstrated that HRS-negative cell lines have the same ATM activation pattern as cells with HRS, whereas they show an early G2 arrest even after low radiation doses that produce insufficient damage to induce full ATM activation. It has therefore been suggested that the dose-dependent ATM regulatory control is evaded by aberrant early G2-checkpoint response in HRS-negative cell lines caused by dissociation between ATM activity and early G2-checkpoint function [250].

The existence of HRS appears in some cell lines to be associated with an elevated level of caspase-3-mediated apoptosis after low-dose exposures [250], suggesting that the radiation-damaged G2-phase cells that evade the early G2 checkpoint are disposed of by this mechanism when entering mitosis. However, also cell lines deficient in TP53 induction after irradiation or with mutated TP53 have been shown to display HRS/IRR, and no increase in apoptosis in response to HRS-inducing doses was observed in BMG-1 cells with wild-type TP53. In addition, no connection between HRS and apoptosis in the six HRS-competent cell lines investigated measured by DNA-PKcs as early apoptosis marker was found. This corroborates the hypothesis that the transition from HRS to IRR primarily is related to induction of the "early" G2 checkpoint and that the death process of the cells entering mitosis with damages is cell line dependent.

Early G2-checkpoint activation as the underlying mechanism for HRS/IRR is supported by priming experiments where a dose of 0.2–0.5 Gy removes the HRS response to subsequent irradiation given within 6–8 h after the priming. This timing corresponds to the duration of the early G2-checkpoint activation. Surprisingly, the HRS/IRR response can be permanently eliminated by priming irradiation if it is given with a low dose rate of 0.1–0.3 Gy/h for 1 h (shown in T98G glioblastoma and T-47D breast cancer cells). The low dose rate primed cells activated the early G2 checkpoint for all doses. The response was shown to involve transforming growth factor beta 3 (TGF-β3) and inducible nitric oxide synthase (iNOS) activation. The HRS phenotype could be reinstated by inhibition of iNOS [251].

It has been suggested that HRS is a protective mechanism and that it is advantageous to sacrifice a small fraction of cells rather than risking the development of genomic instability and mutations. While cells without the IRR are deficient in DNA repair or checkpoint activation, cells without HRS may have been "turned off" by mechanisms similar to the ones induced by low dose rate priming (Box 3.40).

Box 3.40 In a Nutshell: Low Dose Hyper-Radiosensitivity

- Cells with HRS are very sensitive to doses below about 0.5 Gy.
- Above 0.5 Gy, the survival per dose increases until it reaches the LQ curve.
- HRS/IRR has been attributed to the early G2 checkpoint, which is only activated at a certain level of phosphorylated ATM.

3.20.3 HRS and Bystander Signaling (Cytotoxic or Adaptive)

As described in Chap. 2, irradiated (donor) cells can secrete signals which, when transferred to unirradiated (reporter) cells, make these respond as if they had been irradiated themselves. This is called the bystander effect. For a while, it was believed that HRS and cell kill by the bystander effect were mutually exclusive, but when doses in the HRS dose range were tested on HRS-proficient cells, these were able to induce strong bystander signals. However, when doses reached the level where IRR was dominating, there was no bystander signaling.

Bystander signals may also be protective. Transfer of medium from HRS-deficient HaCaT normal human epithelial cells to HRS-proficient T98G glioblastoma cells increased the survival above the normal plating efficiency for these cells [252]. In addition to the effect on cell survival, bystander signals can also moderate the HRS/IRR response to subsequent irradiation. Medium transferred from cells, in which the HRS/IRR response was permanently eliminated by priming with 0.1–0.3 Gy for 1 h, has been seen to remove the HRS response in recipient cells for 8–12 h [251] (Box 3.41).

Box 3.41 In a Nutshell: Hyper-Radiosensitivity and Bystander Signaling

- HRS-proficient cells irradiated with doses in the HRS range produce bystander signals that reduce the survival of reporter cells.
- HRS-proficient cells, in which the HRS response has been removed by low dose rate priming, produce bystander signals that remove the HRS response to subsequent irradiation in recipient cells.

3.20.4 HRS and Clinical Relevance

The presence of HRS may have implications for cancer radiotherapy in which the aim is to control the eradication of tumor tissue while minimizing the damage to normal tissue. The introduction of intensity-modulated radiation therapy (IMRT) in cancer treatment results in irradiation of a larger proportion of normal tissue but at lower doses when compared to conventional treatment. In some situations, one could fear that HRS will tend to increase the effect of low doses in normal tissue and thus negate the benefits of using IMRT, in particular in tissues with a pronounced volume effect [253].

Since HRS is related to the fraction of cells in G2 phase, it may be of more consequence for early-responding proliferating tissues, such as skin, than for slowly proliferating normal tissues with a small fraction of cells in G2. In support, evidence of HRS has been demonstrated in studies with human skin using basal cell density or skin erythema as endpoint. On the other hand, with the HRS effect being more pronounced in fast-dividing tumor cells than slowly or nondividing normal tissues, it may be possible to exploit HRS clinically using dose fractions within the HRS dose range. However, to obtain the same cell kill as with 2 Gy fractions, more fractions are needed. Increasing treatment time would give the tumor more time to grow; therefore, the time between fractions has to be decreased, but that could be a problem: Experiments with ultrafractionation of 0.4 Gy per fraction, three fractions per day in murine DDL1 lymphoma or in human A7 glioblastoma xenografts, did not show evidence of HRS. This could be because with three fractions per day, the timing between fractions would have been too short for the cell to be released from the early G2-checkpoint arrest induced by the previous dose. Since HRS affects cells in G2, another approach is to synchronize the cells to improve the therapeutic potential of ultrafractionation. A protocol using a taxane (paclitaxel), which synchronizes cells in G2 phase, in combination with carboplatin and low-dose fractionated radiation, was extremely well tolerated by the patients and showed a synergistic effect in patients with squamous cell cancer of the head and neck [254] (Box 3.42).

Box 3.42 In a Nutshell: Hyper-Radiosensitivity and Clinical Relevance

- Attempts to exploit HRS in the clinic using hyperfractionation have not been successful.
- Combination of low radiation doses with chemotherapeutics synchronizing cells in G2 phase has shown promise.

3.21 Induced Radiation Resistance

3.21.1 Basic Mechanisms Leading to Radiation Resistance

By the term radiation resistance, we refer to the inherent ability of specific types of cells and tissues (usually of malignant origin) to show a differential response to ionizing radiation overcoming its damaging effects like cell killing or inactivation. The amount of energy (for example level of dose in Gy) and consecutive damage that each organism can withstand is a characteristic of the organism's ability to respond to radiation by a variety of mechanisms often called as DNA damage response (DDR) mechanisms. At the organism level, usually humans are more sensitive compared to other primates or mammals. In nature, there is a great variety of resistance to radiation with the extreme case of certain extremophiles, such as the bacteria *Deinococcus radiodurans* and the tardigrades, to be able to withstand large doses of ionizing radiation on the order of 5000 Gy. Although none of the strategies discussed in various studies on extreme radioresistance appear to be universal against ionizing radiation, a general trend was found. There are two cellular mechanisms by which radioresistance is accomplished: (a) protection of the proteome and DNA from damage by scavenging and regeneration strategies and (b) recruitment of advanced and highly sophisticated DNA repair mechanisms, in order to reconstruct a fully functional genome [255].

While normal (nonmalignant) mammalian cells compared to tumor ones are usually less radioresistant, one cannot exclude the opposite possibility. Elucidation of the molecular mechanisms and pathways related to radioresistance of tumor cells is of major importance in order to develop strategies maximizing tumor control during chemo- or radiation therapies. Many studies using a wide range of *in vitro*, *ex vivo*, and *in vivo* models as well as bioinformatics have fingerprinted the main pathways leading to cellular radioresistance, and these are primarily implicated in DNA damage repair, oxidative stress, cell pro-survival, hypoxia, cell cycle control, and apoptotic pathways [231].

Another important factor contributing to resistance of tumors is the existence of cancer stem cells (CSCs) as a distinct subpopulation within a tumor. CSCs are able to self-renew and differentiate while showing a high proficiency to repair DNA damage, reveal low levels of reactive oxygen species (ROS), and proliferate at a slower rate compared to other tumor cell populations. These features render CSCs resistant to various therapies, including radiation therapy (RT) [256]. The results of such studies can serve as potential diagnostic/prognostic markers of cancer cell resistance to radiation treatment, as well as for therapy outcome and increase of cancer patient survival.

3.21.2 Adaptive Response

The radiation-induced adaptive response was first described by Olivieri et al. in 1984 [257] as the reduced sensitivity to a challenge irradiation induced by a previous small priming dose. Radio-adaptive responses have been observed in vitro and in vivo using various endpoints, such as cell lethality, chromosomal aberrations, mutation induction, radiosensitivity, and DNA repair [258]. Adaptation is most efficiently induced by doses of 0.01–0.5 Gy at dose rates from 0.01 to 1.0 Gy/min (Tapio und Jacob 2007) with challenge doses in the range of 0.5–2 Gy. The protective effect has been reported to last for about three generations following the priming irradiation. The molecular mechanisms underlying the adaptive response are not well understood, but data indicate involvement of DNA damage repair, antioxidant production (NRF2 pathway), NF-κB inflammatory pathway, MAPK pathway, autophagy, cell cycle regulation, apoptosis, and bystander signaling [258] (Box 3.43).

Box 3.43 In a Nutshell: Induced Radiation Resistance

- Cellular radioresistance can be modulated either through protection against DNA damage or through DNA repair.
- Pre-exposure to a low dose can induce protection against a subsequent high dose.

3.21.3 Cancer Stem Cells

The continuous advances and improvements in anticancer therapies using IR has significantly increased the treatment efficacy and quality. However, radioresistance is still one of the major problems of radiation oncology, since it leads to tumor locoregional recurrence and disease progression. One plausible cause of tumor radioresistance is the failure of the current treatments in eradicating a subpopulation of cells intrinsically more resistant to multiples therapies, the cancer stem cells (CSCs). The biological characteristics and radioresistance mechanisms of CSCs are shown in Table 3.16. Targeting CSCs and controlling their behavior is an approach to overcome radioresistance and to improve on the efficacy of cancer treatments (Box 3.44).

Box 3.44 In a Nutshell: Cancer Stem Cells

- Cancer stem cells are a radioresistant tumor subpopulation due to high DNA repair proficiency, low ROS generation and high ROS scavenging, and slow proliferation (giving time for repair).

Table 3.16 Biological characteristics and radioresistance mechanisms of cancer stem cells

Biological characteristics	Radioresistance mechanisms
Are long-lived and have tumorigenic abilities	To activate pro-survival pathways
Are able to proliferate, maintain their growth indefinitely	To improve DNA repair ability through the activation of DNA damage checkpoint proteins, such as ATM, Chk1, Chk2, SMC1, and TP53
Differentiate, generating different cell populations inside the tumor	To defend against oxidative stress, since CSCs present lower levels of ROS and overexpress ROS scavengers that protect them from ROS produced in response to radiation
Have long-term repopulation potential	To indefinitely self-renew, through the activation of cell signaling pathways, such as Wnt/β-catenin, notch, TGF-β, and PI3K/AKT/mTOR
Have a flexible phenotype (plasticity), since a conversion of a CSC into a non-CSC phenotype can be reversed, a process highly dependent on the epithelial-mesenchymal transition (EMT)	To overcome the cell cycle control by the abnormal expression of cell cycle-related proteins
Can adapt to the tumor microenvironment	To inhibit cell death pathways after radiation exposure, through the upregulation of anti-apoptotic proteins (like BCL-2 and survivin) and the inhibition of autophagy-related proteins (like Beclin-1 and ATG-5)

3.21.4 Hypoxia

Hypoxia refers to conditions with low oxygen. Hypoxia induces radiation resistance by preventing the sensitizing effect of the presence of oxygen during or within microseconds of radiation exposure. Oxygen has high affinity for electrons. It may therefore react with radiation-damaged biomolecules as well as with radiation-induced water radicals (see Chap. 1).

3.21.4.1 The Direct Effect of Oxygen

Radiation creates radicals either directly in a biomolecule (e.g., DNA) or indirectly through water radicals: MH + radiation → M° + H°, where MH is an intact biomolecule while M° is the radical after loss of one hydrogen atom. Oxygen can sensitize by a direct interference with the primary radiation process. This can take place because deposit of radiation energy not always completes the dissociation. Often, the large biomolecule is just polarized as follows: MH + radiation → $^{+}MH^{-}$

This process is however reversible. Thus, a **spontaneous restitution** can take place by the electron falling back to its normal position in the molecule and losing the excitation energy. Due to its great affinity for electrons, oxygen may however "steal" the excited electron before it gives away the excitation energy:

$^{+}MH^{-} + O_2 \rightarrow MH^{+} + O_2^{-}$

By this process, oxygen creates a biomolecule radical after the following dissociation:

$MH^{+} \rightarrow M^{\circ} + H^{+}$

In this way, oxygen increases the gain of biomolecule radicals.

3.21.4.2 The Indirect Effect of Oxygen

Due to its great affinity for electrons, oxygen will easily react with both radiation-damaged biomolecules and radiation-induced water radicals. When oxygen reacts with the biomolecule radical, it forms a stable bond as follows:

$M^{\circ} + O_2 \rightarrow MO_2^{\circ}$

Thereby, oxygen fixates the damage and prevents restitution by hydrogen donors (antioxidants), which is a natural protective means of the cells:

$M^{\circ} + RSH \rightarrow MH + RS^{\circ}$

where RSH represents hydrogen donors, of which glutathione is one example.

In cells, the concentration of SH compounds is normally high, and they represent a fundamental protective means against harmful radicals if not outcompeted by oxygen. Hypoxia thus protects against radiation damage through restitution by hydrogen donors because oxygen is not present to outcompete restitution and fixate the damage (Box 3.45).

Box 3.45 In a Nutshell: Hypoxia and Radiation Resistance

- Hypoxia induces radioresistance by preventing the radiosensitizing effect of oxygen.
- Oxygen radiosensitizes by fixating DNA damage and thus preventing restitution by hydrogen donors.
- Oxygen can also increase the amount of radicals through the direct effect.

3.22 Exercises and Self-Assessment

Q1. Which of the following effects of IR produce free radicals within the cell, which can damage the cellular macromolecules?
(a) Double ionization
(b) Direct action
(c) Indirect action
(d) Single ionization

Q2. What are the most significant differences between the two repair patterns of the base excision repair (BER) repair mechanism?

Q3. Which repair pathway provides a "backup" to the replicative proofreading carried out by most (but not all) DNA polymerases during DNA replication?
(a) Base excision repair
(b) Nucleotide excision repair
(c) Nonhomologous end joining
(d) Mismatch repair

Q4. Compare the two principal DNA DSB pathways. What is similar and what is different in these?

Q5. Complex translocation to some extent depends on the radiation quality. Please indicate when they most often occur. Complex translocation types are characteristic especially for cellular exposure to:
(a) Low-LET radiation
(b) High-LET radiation
(c) Photonic radiation
(d) LET of radiation has no effect on the character of chromosomal translocation

Q6. Pick one incorrect statement for completing the sentence "The superoxide anion is …"
(a) Produced by mitochondria
(b) A free radical reactive oxygen species
(c) Converted to water by superoxide dismutase
(d) Able to react with hydrogen peroxide producing hydroxyl radicals
(e) Less lipid soluble than hydrogen peroxide

Q7. For cell transition in the cell cycle, in which phase do the CDK1/cyclin B complex plays a significant role?
(a) G2 into M
(b) G1 into S
(c) S into G2
(d) G0 into G1
(e) M into G1

Q8. What will the cycling cells do when They get a "go-ahead" indication at the checkpoint?
(a) Directly progress into the telophase
(b) Finish the cell cycle and finally divide
(c) Leave the cell cycle and modify to a nondividing state
(d) Demonstrate a fall in M phase-promoting factor
(e) Finish cytokinesis and generate new cell membranes

Q9. Which is the most radiosensitive cell cycle phase, and which is the most resistant one?

Q10. Why is immortalization so important for cancer cells?

Q11. Cells may execute cell death in different ways in response to IR. Please discuss the factors that may influence the pathway elicited.

Q12. What is the main reason for activation of cell death in response to IR in solid tumor cells?
(a) DNA damage-induced apoptosis
(b) Initiation of senescence as a result of DNA damage
(c) Mitotic catastrophe following improper segregation of genetic material
(d) Oxidation-triggered damage to proteins
(e) Generation of ceramide at the plasma membrane via sphingomyelinase

Q13. Which of the following pathways has been implicated in cellular response to IR:
(a) Autophagy
(b) Apoptosis
(c) Necrosis
(d) Mitotic catastrophe
(e) All of a–d

Q14. Apoptosis can proceed by two main routes, intrinsic and extrinsic signaling. Describe the initial triggers for these two pathways and how they lead to apoptosis.

Q15. Cite the different steps of the autophagy process.

Q16. Considering that 800 colonies have grown at 0 Gy for 1200 cells seeded, and that 126 colonies are counted at 2 Gy for 2000 cells seeded, which of the following statements are correct?
(a) The plating efficiency at 0 Gy is 66.6%.
(b) The plating efficiency at 2 Gy is 6.4%.
(c) The plating efficiency at 2 Gy is 9.5%.
(d) The surviving fraction at 2 Gy is 9.5%.
(e) The surviving fraction at 1 Gy is 100%.

Q17. Which alteration is more likely to lead to the death of an embryo? Alteration of the function of an oncogene or a tumor suppressor gene?

Q18. Which cells are mainly involved in inflammation and modulated by low to medium doses of IR?

Q19. Are the following statements regarding epigenetic DNA alterations true or false?
(a) 5-Methylcytosine is a common DNA modification.
(b) DNA methylation is equally common in all four nucleotides.
(c) Histone variants are only synthesized during S phase.
(d) The amino acid lysine in a histone protein is a target for acetylation.

Q20. Is this statement true?
(a) One miRNA regulates only one mRNA target.

Q21. Is the following statement true or false: ARS involves a total dose of over 0.7 Gy (70 rad) from an external source, administered in a few minutes.

Q22. Is the following statement true or false: PTEN is a central positive regulator of the PI3-K/AKT pathway.

Q23. Which of the following statements are correct about lncRNAs?
(a) lncRNAs are translated into regulatory proteins.
(b) lncRNAs are short RNA transcripts of around 20 nucleotides.
(c) lncRNAs can interact with other RNA subtypes to regulate gene expression.

Q24. Which of the following statements are correct about extracellular vesicles?
(a) Extracellular vesicles have a size range of 40 nm to several μm.
(b) Extracellular vesicles cargo only proteins.
(c) Extracellular vesicles can indicate cell death.
(d) Extracellular vesicles are only formed by cells and tissue undergoing cell death.
(e) Radiation effects on cells and tissue only generate extracellular vesicles to protect against radiation-induced cell death.

Q25. In the field of lipidomics or metabolomics, what is the accurate method to achieve the comprehensive metabolite of a sample using LC-MS/MS?
(a) MRM method
(b) PCR methods
(c) Elisa methos
(d) Dicentric assay

Q26. What happens to cells irradiated while in G2 with (a) 0.1 Gy and (b) 1Gy?

Q27. What is the challenge when exploiting HRS in radiotherapy?

Q28. What is the radiation adaptive response?

Q29. Please refer two mechanisms responsible for the increased radioresistance of cancer stem cells.
Q30. Explain why hypoxic cells are more radioresistant than oxygenated cells.

3.23 Exercise Answers

SQ1. Alternative (c). Free radicals are formed after IR by indirect action.
SQ2. The two BER mechanisms are SP-BER and LP-BER. SP-BER involves replacing the damaged base only. It requires DNA synthesis to replace the missing bases by DNA polymerase β, and to finalize the process, it uses ligase 3. In LP-BER, up to ten nucleotides are cut out and replaced, and the polymerases used are DNA polymerases δ and ε and ligase 1 to finalize the process.
SQ3. Alternative (d). Mismatch repair.
SQ4. Common: End termini protection is used to avoid extensive exonuclease activity, but different proteins are important for HR and NHEJ for this purpose. Differences: HR is operative only when there is an undamaged chromosome to work with, i.e., in late S or G2, while NHEJ can operate on DNA DSBs in all cell cycle phases. The fidelity in repair is higher in HR, while NHEJ may cause alterations in DNA sequence as a consequence of the repair which can result in mutations/chromosomal aberrations and which may cause oncogenic transformation of cells.
SQ5. Alternative (b). High-LET radiation.
SQ6. Alternative (c). Superoxide dismutase converts superoxide anions to hydrogen peroxide.
SQ7. Alternative (a). It works in the G2 into M transition.
SQ8. Alternative (b). Complete the cycle and divide.
SQ9. The mitosis is most sensitive, and early G1 and late S are most resistant.
SQ10. Because otherwise they would reach their Hayflick limit and proceed to senescence, and thus they would not be able to divide continuously to form large tumors.
SQ11. The type of radiation quality, dose, and dose rate as well as the cellular threshold for DNA damage and repair largely influence the cell death route. The position in the cell cycle when the damage is inflicted as well as functionality of DNA damage sensors, e.g., TP53, influence the decision.
SQ12. Alternative (c). Mitotic catastrophe.
SQ13. Alternative (e). Cell death after IR can take place via several routes, including mitotic catastrophe, autophagy, apoptosis, and necrosis.
SQ14. The triggers and execution of the two pathways, intrinsic and extrinsic, are depicted in Fig. 3.38. The answer can be found in the legend of the figure.
SQ15. Initiation and phagophore nucleation-phagophore elongation-cargo sequestration-autophagosome maturation-fusion of the autophagosome with the lysosome.
SQ16. Alternatives (a, b, d, and e). The plating efficiency at 0 Gy is 66.6%, the plating efficiency at 2 Gy is 6.4%, the surviving fraction at 2 Gy is 9.5%, and the surviving fraction at 1 Gy is 100%.
SQ17. The alteration of an oncogene because it then affects the normal embryonic development and causes embryonic lethality. The alteration of a tumor suppressor gene does not affect the embryogenesis; it increases the probability of cancer during life.
SQ18. From the table, it can be seen that the radiosensitivity is correlated to the existence of TNTs and their density and the complexity of networks formed. If all other properties are the same, the hypothesis which can be formulated is the following: The ability of cells to avoid death after irradiation is connected to the ability of the cells to communicate in a direct and fast manner through TNTs. This might be linked to the rescue effect, where less damaged cells are able to send components needed for the damaged cells to survive.
SQ19. Macrophages, endothelial cells, lymphocytes, and PMN.
SQ20. Answers:
(a) True, 5-mC accounts for about 1% of all bases within DNA.
(b) False, guanine is the predominantly modified base.
(c) False, histone variants are synthesized throughout the cell cycle.
(d) True, lysine and arginine are the most frequently acetylated amino acids.
SQ21. No, each miRNA can act on multiple different target genes, and one target gene can be regulated by many different miRNAs.
SQ22. True.
SQ23. False: PTEN is a central negative regulator of the PI3K/AKT pathway.
SQ24. a. Wrong, lncRNAs lack protein-coding sequences and they are not translated.
b. Wrong, lncRNAs are defined as transcripts longer than 200 bp; microRNAs around 20 nucleotides in size.
c. Correct, for example lncRNAs can interact with mRNAs and microRNAs for regulatory purposes.
SQ25. a. correct. The different sizes of extracellular vesicles are given in Table 3.14.

b. Wrong. Extracellular vesicles cargo in addition to proteins also mRNA/miRNA, long noncoding RNAs, DNA fragments, and lipids.
c. Correct. In particular apoptotic bodies; see Table 3.14.
d. Wrong. Exosomes are generated by viable cells (Fig. 3.52) albeit they may act as communicators in cell death.
e. Wrong. Extracellular vesicles may via their cargo participate in both cell pro-survival and pro-death signals.

SQ26. (a) MRM method.

SQ27. (a) The low dose will not phosphorylate enough ATM to activate the early G2 checkpoint, and the cells will proceed to mitosis with unrepaired damage and die. (b) The cells will be arrested in G2, and the DNA damage that is repairable will be repaired before the cells enter mitosis.

SQ28. The timing between doses may coincide with the duration of early G2 arrest.

SQ29. A protection against high radiation doses induced by a low "priming" dose.

SQ30. For example, to activate pro-survival pathways and to improve DNA repair ability through the activation of DNA damage checkpoint proteins.

SQ31. Oxygen fixates DNA damage and sensitizes the cells to radiation.

References

1. Fedorova M, Bollineni RC, Hoffmann R. Protein carbonylation as a major hallmark of oxidative damage: update of analytical strategies. Mass Spectrom Rev. 2014;33(2):79–97. https://doi.org/10.1002/mas.21381.
2. Watts JL, Ristow M. Lipid and carbohydrate metabolism in *Caenorhabditis elegans*. Genetics. 2017;207(2):413–46. https://doi.org/10.1534/genetics.117.300106.
3. von Sonntag C. Carbohydrate radicals: from ethylene glycol to DNA strand breakage. Int J Radiat Biol. 2014;90(6):416–22. https://doi.org/10.3109/09553002.2014.908040.
4. Ramírez-Cahero HF, Valdivia-López MA. Effect of gamma radiation on sugars and vitamin C: radiolytic pathways. Food Chem. 2018;245:1131–40. https://doi.org/10.1016/j.foodchem.2017.11.057.
5. Stark G. The effect of ionizing radiation on lipid membranes. Biochim Biophys Acta. 1991;1071(2):103–22. https://doi.org/10.1016/0304-4157(91)90020-w.
6. Stark G. Functional consequences of oxidative membrane damage. J Membr Biol. 2005;205(1):1–16. https://doi.org/10.1007/s00232-005-0753-8.
7. Houée-Levin C, Bobrowski K. The use of the methods of radiolysis to explore the mechanisms of free radical modifications in proteins. J Proteome. 2013;92:51–62. https://doi.org/10.1016/j.jprot.2013.02.014.
8. Gebicki JM. Oxidative stress, free radicals and protein peroxides. Arch Biochem Biophys. 2016;595:33–9. https://doi.org/10.1016/j.abb.2015.10.021.
9. Hawkins CL, Davies MJ. Detection, identification, and quantification of oxidative protein modifications. J Biol Chem. 2019;294(51):19683–708. https://doi.org/10.1074/jbc.REV119.006217.
10. Alberts B, Bray D, Hopkin K, Johnson AD, Lewis J, Raff M, et al. Essential cell biology. New York: Garland Science; 2015.
11. Ravanat J-L. Endogenous natural and radiation-induced DNA lesions: differences and similarities and possible implications for human health and radiological protection. Radioprotection. 2018;53(4):241–8. https://doi.org/10.1051/radiopro/2018039.
12. Dizdaroglu M. Oxidatively induced DNA damage and its repair in cancer. Mutat Res Rev Mutat Res. 2015;763:212–45. https://doi.org/10.1016/j.mrrev.2014.11.002.
13. Cadet J, Wagner JR. DNA base damage by reactive oxygen species, oxidizing agents, and UV radiation. Cold Spring Harb Perspect Biol. 2013;5:012559. https://doi.org/10.1101/cshperspect.a012559.
14. Hall EJ. Radiobiology for the radiologist. 7th ed. Philadelphia: Lippincott Williams & Wilkins; 2012.
15. Nikitaki Z, Hellweg CE, Georgakilas AG, Ravanat J-L. Stress-induced DNA damage biomarkers: applications and limitations. Front Chem. 2015;3:35. https://doi.org/10.3389/fchem.2015.00035.
16. Sage E, Shikazono N. Radiation-induced clustered DNA lesions: repair and mutagenesis. Free Radic Biol Med. 2017;107:125–35. https://doi.org/10.1016/j.freeradbiomed.2016.12.008.
17. Sutherland BM, Bennett PV, Sidorkina O, Laval J. Clustered DNA damages induced in isolated DNA and in human cells by low doses of ionizing radiation. Proc Natl Acad Sci U S A. 2000;97(1):103–8. https://doi.org/10.1073/pnas.97.1.103.
18. Semenenko VA, Stewart RD. A fast Monte Carlo algorithm to simulate the spectrum of DNA damages formed by ionizing radiation. Radiat Res. 2004;161(4):451–7. https://doi.org/10.1667/RR3140.
19. Johann To Berens P, Molinier J. Formation and recognition of UV-induced DNA damage within genome complexity. Int J Mol Sci. 2020;21(18):6689. https://doi.org/10.3390/ijms21186689.
20. Banyasz A, Esposito L, Douki T, Perron M, Lepori C, Improta R, Markovitsi D. Effect of C5-methylation of cytosine on the UV-induced reactivity of duplex DNA: conformational and electronic factors. J Phys Chem B. 2016;120(18):4232–42. https://doi.org/10.1021/acs.jpcb.6b03340.
21. Shibata A, Jeggo PA. DNA double-strand break repair in a cellular context. Clin Oncol (R Coll Radiol). 2014;26(5):243–9. https://doi.org/10.1016/j.clon.2014.02.004.
22. Lee T-H, Kang T-H. DNA oxidation and excision repair pathways. Int J Mol Sci. 2019;20:6092. https://doi.org/10.3390/ijms20236092.
23. Sureka CS, Armpilia C. Radiation biology for medical physicists. Boca Raton: CRC Press; 2017.
24. Christmann M, Tomicic MT, Roos WP, Kaina B. Mechanisms of human DNA repair: an update. Toxicology. 2003;193(1–2):3–34. https://doi.org/10.1016/S0300-483X(03)00287-7.
25. Gunderson LL, Tepper JE. Clinical radiation oncology. Amsterdam: Elsevier Health Sciences; 2015.
26. Grundy GJ, Parsons JL. Base excision repair and its implications to cancer therapy. Essays Biochem. 2020;64(5):831–43. https://doi.org/10.1042/EBC20200013.

27. Vermeulen C, Bertocci B, Begg AC, Vens C. Ionizing radiation sensitivity of DNA polymerase lambda-deficient cells. Radiat Res. 2007;168(6):683–8. https://doi.org/10.1667/RR1057R.1.
28. Joiner M, van der Kogel AJ, editors. Basic clinical radiobiology. 4th ed. London: Hodder Arnold; 2009.
29. Kunkel TA. Evolving views of DNA replication (in)fidelity. Cold Spring Harb Symp Quant Biol. 2009;74:91–101. https://doi.org/10.1101/sqb.2009.74.027.
30. Modrich P. Mechanisms in *E. coli* and human mismatch repair (Nobel lecture). Angew Chem Int Ed. 2016;55(30):8490–501. https://doi.org/10.1002/anie.201601412.
31. Jiricny J. Postreplicative mismatch repair. Cold Spring Harb Perspect Biol. 2013;5(4):a012633. https://doi.org/10.1101/cshperspect.a012633.
32. Marteijn JA, Lans H, Vermeulen W, Hoeijmakers JHJ. Understanding nucleotide excision repair and its roles in cancer and ageing. Nat Rev Mol Cell Biol. 2014;15(7):465–81. https://doi.org/10.1038/nrm3822.
33. Sudhir AS. DNA: damage and repair mechanisms in humans. Glob J Pharm Sci. 2017;3(2):555613. https://doi.org/10.19080/gjpps.2017.03.555613.
34. Thacker J. Homologous recombination repair. In: Schwab M, editor. Encyclopedia of cancer. Berlin: Springer; 2011. p. 1725–9. https://doi.org/10.1007/978-3-642-16483-5_2801.
35. Sullivan MR, Bernstein KA. RAD-ical new insights into RAD51 regulation. Genes (Basel). 2018;9:629. https://doi.org/10.3390/genes9120629.
36. Symington LS, Gautier J. Double-strand break end resection and repair pathway choice. Annu Rev Genet. 2011;45:247–71. https://doi.org/10.1146/annurev-genet-110410-132435.
37. Chapman JR, Taylor MRG, Boulton SJ. Playing the end game: DNA double-strand break repair pathway choice. Mol Cell. 2012;47(4):497–510. https://doi.org/10.1016/j.molcel.2012.07.029.
38. Ranjha L, Howard SM, Cejka P. Main steps in DNA double-strand break repair: an introduction to homologous recombination and related processes. Chromosoma. 2018;127(2):187–214. https://doi.org/10.1007/s00412-017-0658-1.
39. Zhao B, Rothenberg E, Ramsden DA, Lieber MR. The molecular basis and disease relevance of non-homologous DNA end joining. Nat Rev Mol Cell Biol. 2020;21(12):765–81. https://doi.org/10.1038/s41580-020-00297-8.
40. Liu H, Ma W, Xie J, Li H, Luo K, Luo D, et al. Nucleosome positioning and its role in gene regulation in yeast. In: Abdulkhair WMH, editor. The yeast role in medical applications. London: InTech; 2018. https://doi.org/10.5772/intechopen.70935.
41. Downs JA, Jackson SP. A means to a DNA end: the many roles of Ku. Nat Rev Mol Cell Biol. 2004;5(5):367–78. https://doi.org/10.1038/nrm1367.
42. Goodarzi AA, Jeggo PA. The repair and signaling responses to DNA double-strand breaks. Adv Genet. 2013;82:1–45. https://doi.org/10.1016/B978-0-12-407676-1.00001-9.
43. Myers SH, Ortega JA, Cavalli A. Synthetic lethality through the lens of medicinal chemistry. J Med Chem. 2020;63(23):14151–83. https://doi.org/10.1021/acs.jmedchem.0c00766.
44. Goodarzi AA, Yu Y, Riballo E, Douglas P, Walker SA, Ye R, et al. DNA-PK autophosphorylation facilitates Artemis endonuclease activity. EMBO J. 2006;25(16):3880–9. https://doi.org/10.1038/sj.emboj.7601255.
45. Barnes DE, Stamp G, Rosewell I, Denzel A, Lindahl T. Targeted disruption of the gene encoding DNA ligase IV leads to lethality in embryonic mice. Curr Biol. 1998;8(25):1395–8. https://doi.org/10.1016/s0960-9822(98)00021-9.
46. Woodbine L, Gennery AR, Jeggo PA. The clinical impact of deficiency in DNA non-homologous end-joining. DNA Repair. 2014;16:84–96. https://doi.org/10.1016/j.dnarep.2014.02.011.
47. Decottignies A. Alternative end-joining mechanisms: a historical perspective. Front Genet. 2013;4:48. https://doi.org/10.3389/fgene.2013.00048.
48. Falk M, Hausmann M. A paradigm revolution or just better resolution-will newly emerging superresolution techniques identify chromatin architecture as a key factor in radiation-induced DNA damage and repair regulation? Cancers (Basel). 2020;13:10018. https://doi.org/10.3390/cancers13010018.
49. Falk M, Lukasova E, Kozubek S. Higher-order chromatin structure in DSB induction, repair and misrepair. Mut Res Fundam Mol Mech Mutagenesis. 2010;704(1–3):88–100. https://doi.org/10.1016/j.mrrev.2010.01.013.
50. Caron H, van Schaik B, van der Mee M, Baas F, Riggins G, van Sluis P, et al. The human transcriptome map: clustering of highly expressed genes in chromosomal domains. Science. 2001;291(5507):1289–92. https://doi.org/10.1126/science.1056794.
51. Falk M, et al. Chromatin structure influences the sensitivity of DNA to γ-radiation. BBA MCR. 2008;1783(12):2398–414.
52. Falk M, Lukasova E, Gabrielova B, Ondrej V, Kozubek S. Chromatin dynamics during DSB repair. Biochim Biophys Acta. 2007;1773(10):1534–45. https://doi.org/10.1016/j.bbamcr.2007.07.002.
53. Falk M, Hausmann M, Lukášová E, Biswas A, Hildenbrand G, Davídková M, et al. Determining Omics spatiotemporal dimensions using exciting new nanoscopy techniques to assess complex cell responses to DNA damage: part A—radiomics. Crit Rev Eukaryot Gene Expr. 2014a;24(3):205–23. https://doi.org/10.1615/critreveukaryotgeneexpr.2014010313.
54. Falk M, Hausmann M, Lukášová E, Biswas A, Hildenbrand G, Davídková M, et al. Determining Omics spatiotemporal dimensions using exciting new nanoscopy techniques to assess complex cell responses to DNA damage: part B—structuromics. Crit Rev Eukaryot Gene Expr. 2014b;24(3):225–47. https://doi.org/10.1615/critreveukaryotgeneexpr.v24.i3.40.
55. Lukásová E, Kozubek S, Kozubek M, Kroha V, Marecková A, Skalníková M, et al. Chromosomes participating in translocations typical of malignant hemoblastoses are also involved in exchange aberrations induced by fast neutrons. Radiat Res. 1999;151(4):375–84.
56. Girst S, Hable V, Drexler GA, Greubel C, Siebenwirth C, Haum M, et al. Subdiffusion supports joining of correct ends during repair of DNA double-strand breaks. Sci Rep. 2013;3:2511. https://doi.org/10.1038/srep02511.
57. Reindl J, Girst S, Walsh DWM, Greubel C, Schwarz B, Siebenwirth C, et al. Chromatin organization revealed by nanostructure of irradiation induced γH2AX, 53BP1 and Rad51 foci. Sci Rep. 2017;7:40616. https://doi.org/10.1038/srep40616.
58. Hahn H, Neitzel C, Kopečná O, Heermann DW, Falk M, Hausmann M. Topological analysis of γH2AX and MRE11 clusters detected by localization microscopy during X-ray-induced DNA double-strand break repair. Cancers (Basel). 2021;13(21):5561. https://doi.org/10.3390/cancers13215561.
59. Lee J-H, Laure Djikimi Tchetgna F, Krufczik M, Schmitt E, Cremer C, Bestvater FB, Hausmann M. COMBO-FISH: a versatile tool beyond standard FISH to study chromatin organization by fluorescence light microscopy. OBM Genet. 2018;3:1064. https://doi.org/10.21926/obm.genet.1901064.
60. Prasanna PG, Citrin DE, Hildesheim J, Ahmed MM, Venkatachalam S, Riscuta G, et al. Therapy-induced senescence:

opportunities to improve anticancer therapy. J Natl Cancer Inst. 2021;113(10):1285–98. https://doi.org/10.1093/jnci/djab064.
61. Hanahan D, Weinberg RA. Hallmarks of cancer: the next generation. Cell. 2011;144(5):646–74. https://doi.org/10.1016/j.cell.2011.02.013.
62. Alberts B, et al. Molecular biology of the cell. 4th ed. New York: Garland Science; 2002.
63. Adjemian S, Oltean T, Martens S, Wiernicki B, Goossens V, Vanden Berghe T, et al. Ionizing radiation results in a mixture of cellular outcomes including mitotic catastrophe, senescence, methuosis, and iron-dependent cell death. Cell Death Dis. 2020;11(11):1003. https://doi.org/10.1038/s41419-020-03209-y.
64. Mascaraque M, Delgado-Wicke P, Damian A, Lucena SR, Carrasco E, Juarranz Á. Mitotic catastrophe induced in HeLa tumor cells by photodynamic therapy with methyl-aminolevulinate. Int J Mol Sci. 2019;20:1229. https://doi.org/10.3390/ijms20051229.
65. Kwon SM, Hong SM, Lee Y-K, Min S, Yoon G. Metabolic features and regulation in cell senescence. BMB Rep. 2019;52(1):5–12. https://doi.org/10.5483/BMBRep.2019.52.1.291.
66. Mukherjee S, Abdisalaam S, Bhattacharya S, Srinivasan K, Sinha D, Asaithamby A. Mechanistic link between DNA damage sensing, repairing and signaling factors and immune signaling. Adv Protein Chem Struct Biol. 2019;115:297–324. https://doi.org/10.1016/bs.apcsb.2018.11.004.
67. Heil M, Land WG. Danger signals—damaged-self recognition across the tree of life. Front Plant Sci. 2014;5:578. https://doi.org/10.3389/fpls.2014.00578.
68. Tello Cajiao JJ, Carante MP, Bernal Rodriguez MA, Ballarini F. Proximity effects in chromosome aberration induction by low-LET ionizing radiation. DNA Repair. 2017;58:38–46. https://doi.org/10.1016/j.dnarep.2017.08.007.
69. Venkatesan S, Natarajan AT, Hande MP. Chromosomal instability—mechanisms and consequences. Mutat Res Genet Toxicol Environ Mutagen. 2015;793:176–84. https://doi.org/10.1016/j.mrgentox.2015.08.008.
70. Griffiths AJF, Doebley JF, Peichel C, Wassarman DA. Introduction to genetic analysis. New York: Macmillan International Higher Education; 2020.
71. Kang Z-J, Liu Y-F, Xu L-Z, Long Z-J, Huang D, Yang Y, et al. The Philadelphia chromosome in leukemogenesis. Chin J Cancer. 2016;35:48. https://doi.org/10.1186/s40880-016-0108-0.
72. Cornforth MN, Durante M. Radiation quality and intrachromosomal aberrations: size matters. Mutat Res Genet Toxicol Environ Mutagen. 2018;836(Pt A):28–35. https://doi.org/10.1016/j.mrgentox.2018.05.002.
73. Pantelias A, Karachristou I, Georgakilas AG, Terzoudi GI. Interphase cytogenetic analysis of micronucleated and multinucleated cells supports the premature chromosome condensation hypothesis as the mechanistic origin of chromothripsis. Cancers (Basel). 2019;11:1123. https://doi.org/10.3390/cancers11081123.
74. Gotoh E, Durante M. Chromosome condensation outside of mitosis: mechanisms and new tools. J Cell Physiol. 2006;209(2):297–304. https://doi.org/10.1002/jcp.20720.
75. Okayasu R, Liu C. G1 premature chromosome condensation (PCC) assay. In: Radiation cytogenetics. New York: Humana Press; 2019. p. 31–8. https://doi.org/10.1007/978-1-4939-9432-8_4.
76. Terzoudi GI, Pantelias G, Darroudi F, Barszczewska K, Buraczewska I, Depuydt J, et al. Dose assessment intercomparisons within the RENEB network using G0-lymphocyte prematurely condensed chromosomes (PCC assay). Int J Radiat Biol. 2017;93(1):48–57. https://doi.org/10.1080/09553002.2016.1234725.
77. Lindholm C, Stricklin D, Jaworska A, Koivistoinen A, Paile W, Arvidsson E, et al. Premature chromosome condensation (PCC) assay for dose assessment in mass casualty accidents. Radiat Res. 2010;173(1):71–8. https://doi.org/10.1667/RR1843.1.
78. Lamadrid Boada AI, Romero Aguilera I, Terzoudi GI, González Mesa JE, Pantelias G, García O. Rapid assessment of high-dose radiation exposures through scoring of cell-fusion-induced premature chromosome condensation and ring chromosomes. Mutat Res Fundam Mol Mech Mutagenesis. 2013;757(1):45–51. https://doi.org/10.1016/j.mrgentox.2013.06.021.
79. Rose Li Y, Halliwill KD, Adams CJ, Iyer V, Riva L, Mamunur R, et al. Mutational signatures in tumours induced by high and low energy radiation in Trp53 deficient mice. Nat Commun. 2020;11:394. https://doi.org/10.1038/s41467-019-14261-4.
80. Stephens PJ, Greenman CD, Fu B, Yang F, Bignell GR, Mudie LJ, et al. Massive genomic rearrangement acquired in a single catastrophic event during cancer development. Cell. 2011;144(1):27–40. https://doi.org/10.1016/j.cell.2010.11.055.
81. Crasta K, Ganem NJ, Dagher R, Lantermann AB, Ivanova EV, Pan Y, et al. DNA breaks and chromosome pulverization from errors in mitosis. Nature. 2012;482(7383):53–8. https://doi.org/10.1038/nature10802.
82. Storchová Z, Kloosterman WP. The genomic characteristics and cellular origin of chromothripsis. Curr Opin Cell Biol. 2016;40:106–13. https://doi.org/10.1016/j.ceb.2016.03.003.
83. Pantelias A, Zafiropoulos D, Cherubini R, Sarchiapone L, de Nadal V, Pantelias GE, et al. Interphase cytogenetic analysis of G0 lymphocytes exposed to α-particles, C-ions, and protons reveals their enhanced effectiveness for localized chromosome shattering—a critical risk for chromothripsis. Cancers (Basel). 2020;12:2336. https://doi.org/10.3390/cancers12092336.
84. Moquet J, Barnard S, Staynova A, Lindholm C, Monteiro Gil O, Martins V, et al. The second gamma-H2AX assay inter-comparison exercise carried out in the framework of the European biodosimetry network (RENEB). Int J Radiat Biol. 2017;93(1):58–64. https://doi.org/10.1080/09553002.2016.1207822.
85. Lee Y, Wang Q, Shuryak I, Brenner DJ, Turner HC. Development of a high-throughput γ-H2AX assay based on imaging flow cytometry. Radiat Oncol. 2019;14(1):150. https://doi.org/10.1186/s13014-019-1344-7.
86. Rothkamm K, Löbrich M. Evidence for a lack of DNA double-strand break repair in human cells exposed to very low X-ray doses. Proc Natl Acad Sci U S A. 2003;100(9):5057–62. https://doi.org/10.1073/pnas.0830918100.
87. Falk M, Falková I, Kopečná O, Bačíková A, Pagáčová E, Šimek D, et al. Chromatin architecture changes and DNA replication fork collapse are critical features in cryopreserved cells that are differentially controlled by cryoprotectants. Sci Rep. 2018;8(1):14694. https://doi.org/10.1038/s41598-018-32939-5.
88. Mariotti LG, Pirovano G, Savage KI, Ghita M, Ottolenghi A, Prise KM, Schettino G. Use of the γ-H2AX assay to investigate DNA repair dynamics following multiple radiation exposures. PLoS One. 2013;8(11):e79541. https://doi.org/10.1371/journal.pone.0079541.
89. Blakely WF, Port M, Abend M. Early-response multiple-parameter biodosimetry and dosimetry: risk predictions. J Radiol Prot. 2021;41:R152. https://doi.org/10.1088/1361-6498/ac15df.
90. Hausmann M, Falk M, Neitzel C, Hofmann A, Biswas A, Gier T, et al. Elucidation of the clustered nano-architecture of radiation-induced DNA damage sites and surrounding chromatin in cancer cells: a single molecule localization microscopy approach. Int J Mol Sci. 2021;22:3636. https://doi.org/10.3390/ijms22073636.
91. Lorat Y, Reindl J, Isermann A, Rübe C, Friedl AA, Rübe CE. Focused ion microbeam irradiation induces clustering of DNA double-strand breaks in heterochromatin visualized by nanoscale-resolution electron microscopy. Int J Mol Sci. 2021;22:7638. https://doi.org/10.3390/ijms22147638.
92. Geuting V, Reul C, Löbrich M. ATM release at resected double-strand breaks provides heterochromatin reconstitution to facilitate

homologous recombination. PLoS Genet. 2013;9(8):e1003667. https://doi.org/10.1371/journal.pgen.1003667.
93. Spies J, Lukas C, Somyajit K, Rask M-B, Lukas J, Neelsen KJ. 53BP1 nuclear bodies enforce replication timing at under-replicated DNA to limit heritable DNA damage. Nat Cell Biol. 2019;21(4):487–97. https://doi.org/10.1038/s41556-019-0293-6.
94. Campalans A, Kortulewski T, Amouroux R, Menoni H, Vermeulen W, Radicella JP. Distinct spatiotemporal patterns and PARP dependence of XRCC1 recruitment to single-strand break and base excision repair. Nucleic Acids Res. 2013;41(5):3115–29. https://doi.org/10.1093/nar/gkt025.
95. Sanvicens N, Marco MP. Multifunctional nanoparticles—properties and prospects for their use in human medicine. Trends Biotechnol. 2008;26(8):425–33. https://doi.org/10.1016/j.tibtech.2008.04.005.
96. Tsikas D. Assessment of lipid peroxidation by measuring malondialdehyde (MDA) and relatives in biological samples: analytical and biological challenges. Anal Biochem. 2017;524:13–30. https://doi.org/10.1016/j.ab.2016.10.021.
97. Delbart W, Ghanem GE, Karfis I, Flamen P, Wimana Z. Investigating intrinsic radiosensitivity biomarkers to peptide receptor radionuclide therapy with 177LuLu-DOTATATE in a panel of cancer cell lines. Nucl Med Biol. 2021;96–97:68–79. https://doi.org/10.1016/j.nucmedbio.2021.03.006.
98. Straub JM, New J, Hamilton CD, Lominska C, Shnayder Y, Thomas SM. Radiation-induced fibrosis: mechanisms and implications for therapy. J Cancer Res Clin Oncol. 2015;141(11):1985–94. https://doi.org/10.1007/s00432-015-1974-6.
99. Lv H, Zhen C, Liu J, Yang P, Hu L, Shang P. Unraveling the potential role of glutathione in multiple forms of cell death in cancer therapy. Oxidative Med Cell Longev. 2019;2019:3150145. https://doi.org/10.1155/2019/3150145.
100. He F, Ru X, Wen T. NRF2, a transcription factor for stress response and beyond. Int J Mol Sci. 2020;21:4777. https://doi.org/10.3390/ijms21134777.
101. Wang L, Kuwahara Y, Li L, Baba T, Shin R-W, Ohkubo Y, et al. Analysis of common deletion (CD) and a novel deletion of mitochondrial DNA induced by ionizing radiation. Int J Radiat Biol. 2007;83(7):433–42. https://doi.org/10.1080/09553000701370878.
102. Dahal S, Raghavan SC. Mitochondrial genome stability in human: understanding the role of DNA repair pathways. Biochem J. 2021;478(6):1179–97. https://doi.org/10.1042/BCJ20200920.
103. Szumiel I. Ionizing radiation-induced oxidative stress, epigenetic changes and genomic instability: the pivotal role of mitochondria. Int J Radiat Biol. 2015;91(1):1–12. https://doi.org/10.3109/09553002.2014.934929.
104. Park J, Lee J, Choi C. Mitochondrial network determines intracellular ROS dynamics and sensitivity to oxidative stress through switching inter-mitochondrial messengers. PLoS One. 2011;6(8):e23211. https://doi.org/10.1371/journal.pone.0023211.
105. Ho E, Karimi Galougahi K, Liu C-C, Bhindi R, Figtree GA. Biological markers of oxidative stress: applications to cardiovascular research and practice. Redox Biol. 2013;1:483–91. https://doi.org/10.1016/j.redox.2013.07.006.
106. Navarro J, Obrador E, Pellicer JA, Asensi M, Viña J, Estrela JM. Blood glutathione as an index of radiation-induced oxidative stress in mice and humans. Free Radic Biol Med. 1997;22(7):1203–9. https://doi.org/10.1016/S0891-5849(96)00554-0.
107. Sies H. Total antioxidant capacity: appraisal of a concept. J Nutr. 2007;137(6):1493–5. https://doi.org/10.1093/jn/137.6.1493.
108. Haida Z, Hakiman M. A comprehensive review on the determination of enzymatic assay and nonenzymatic antioxidant activities. Food Sci Nutr. 2019;7(5):1555–63. https://doi.org/10.1002/fsn3.1012.
109. Mello LD. Potential contribution of ELISA and LFI assays to assessment of the oxidative stress condition based on 8-oxodG biomarker. Anal Biochem. 2021;628:114215. https://doi.org/10.1016/j.ab.2021.114215.
110. Kehm R, Baldensperger T, Raupbach J, Höhn A. Protein oxidation—formation mechanisms, detection and relevance as biomarkers in human diseases. Redox Biol. 2021;42:101901. https://doi.org/10.1016/j.redox.2021.101901.
111. Pawlik TM, Keyomarsi K. Role of cell cycle in mediating sensitivity to radiotherapy. Int J Radiat Oncol Biol Phys. 2004;59(4):928–42. https://doi.org/10.1016/j.ijrobp.2004.03.005.
112. Lonati L, Barbieri S, Guardamagna I, Ottolenghi A, Baiocco G. Radiation-induced cell cycle perturbations: a computational tool validated with flow-cytometry data. Sci Rep. 2021;11(1):925. https://doi.org/10.1038/s41598-020-79934-3.
113. Satyanarayana A, Kaldis P. Mammalian cell-cycle regulation: several Cdks, numerous cyclins and diverse compensatory mechanisms. Oncogene. 2009;28(33):2925–39. https://doi.org/10.1038/onc.2009.170.
114. TieLabs. Cell cycle regulation: cyclins and CDKs. 2022.. https://blog.praxilabs.com/2021/07/06/cell-cycle-regulation-en/.
115. Terasima T, Tolmach LJ. Changes in X-ray sensitivity of HeLa cells during the division cycle. Nature. 1961;190:1210–1. https://doi.org/10.1038/1901210a0.
116. Berardinelli F, Coluzzi E, Sgura A, Antoccia A. Targeting telomerase and telomeres to enhance ionizing radiation effects in in vitro and in vivo cancer models. Mutat Res Rev Mutat Res. 2017;773:204–19. https://doi.org/10.1016/J.MRREV.2017.02.004.
117. Vaiserman A, Krasnienkov D. Telomere length as a marker of biological age: state-of-the-art, open issues, and future perspectives. Front Genet. 2020;11:630186. https://doi.org/10.3389/FGENE.2020.630186.
118. Gill Z, Nieuwoudt M, Ndifon W. The Hayflick limit and age-related adaptive immune deficiency. Gerontology. 2018;64(2):135–9. https://doi.org/10.1159/000478091.
119. Aunan JR, Watson MM, Hagland HR, Søreide K. Molecular and biological hallmarks of ageing. Br J Surg. 2016;103(2):e29–46. https://doi.org/10.1002/BJS.10053.
120. Gorgoulis V, Adams PD, Alimonti A, Bennett DC, Bischof O, Bishop C, et al. Cellular senescence: defining a path forward. Cell. 2019;179(4):813–27. https://doi.org/10.1016/J.CELL.2019.10.005.
121. Wang B, Kohli J, Demaria M. Senescent cells in cancer therapy: friends or foes? Trends Cancer. 2020;6(10):838–57. https://doi.org/10.1016/J.TRECAN.2020.05.004.
122. Hernandez-Segura A, Nehme J, Demaria M. Hallmarks of cellular senescence. Trends Cell Biol. 2018;28(6):436–53. https://doi.org/10.1016/J.TCB.2018.02.001.
123. Baker DJ, Childs BG, Durik M, Wijers ME, Sieben CJ, Zhong J, et al. Naturally occurring p16(Ink4a)-positive cells shorten healthy lifespan. Nature. 2016;530(7589):184–9. https://doi.org/10.1038/nature16932.
124. Sia J, Szmyd R, Hau E, Gee HE. Molecular mechanisms of radiation-induced cancer cell death: a primer. Front Cell Dev Biol. 2020;8:41. https://doi.org/10.3389/fcell.2020.00041.
125. Fizazi K, Shore N, Tammela TL, Ulys A, Vjaters E, Polyakov S, et al. Nonmetastatic, castration-resistant prostate cancer and survival with Darolutamide. N Engl J Med. 2020;383(11):1040–9. https://doi.org/10.1056/NEJMOA2001342.
126. Swift LH, Golsteyn RM. The relationship between checkpoint adaptation and mitotic catastrophe in genomic changes in cancer cells. In: Genome stability. Amsterdam: Elsevier; 2016. p. 373–89. https://doi.org/10.1016/B978-0-12-803309-8.00022-7.
127. Vitale I, Galluzzi L, Castedo M, Kroemer G. Mitotic catastrophe: a mechanism for avoiding genomic instability. Nat Rev Mol Cell Biol. 2011;12(6):385–92. https://doi.org/10.1038/nrm3115.
128. Bender T, Martinou J-C. Where killers meet—permeabilization of the outer mitochondrial membrane during apoptosis. Cold Spring Harb Perspect Biol. 2013;5(1):a011106. https://doi.org/10.1101/cshperspect.a011106.

129. Shlomovitz I, Speir M, Gerlic M. Flipping the dogma—phosphatidylserine in non-apoptotic cell death. Cell Commun Signal. 2019;17(1):139. https://doi.org/10.1186/s12964-019-0437-0.
130. Yuan J, Horvitz HR. The Caenorhabditis elegans cell death gene ced-4 encodes a novel protein and is expressed during the period of extensive programmed cell death. Development. 1992;116(2):309–20.
131. Chota A, George BP, Abrahamse H. Interactions of multidomain pro-apoptotic and anti-apoptotic proteins in cancer cell death. Oncotarget. 2021;12(16):1615–26. https://doi.org/10.18632/oncotarget.28031.
132. Dhanasekaran DN, Reddy EP. JNK-signaling: a multiplexing hub in programmed cell death. Genes Cancer. 2017;8(9–10):682–94. https://doi.org/10.18632/genesandcancer.155.
133. Ashkenazi A. Targeting the extrinsic apoptotic pathway in cancer: lessons learned and future directions. J Clin Invest. 2015;125(2):487–9. https://doi.org/10.1172/JCI80420.
134. Wang JYJ. Cell death response to DNA damage. Yale J Biol Med. 2019;92(4):771–9.
135. Orrenius S, Gogvadze V, Zhivotovsky B. Calcium and mitochondria in the regulation of cell death. Biochem Biophys Res Commun. 2015;460(1):72–81. https://doi.org/10.1016/j.bbrc.2015.01.137.
136. Boutelle AM, Attardi LD. p53 and tumor suppression: it takes a network. Trends Cell Biol. 2021;31(4):298–310. https://doi.org/10.1016/j.tcb.2020.12.011.
137. Kolesnick R, Fuks Z. Radiation and ceramide-induced apoptosis. Oncogene. 2003;22(37):5897–906. https://doi.org/10.1038/sj.onc.1206702.
138. Banfalvi G. Methods to detect apoptotic cell death. Apoptosis. 2017;22(2):306–23. https://doi.org/10.1007/s10495-016-1333-3.
139. Yan G, Elbadawi M, Efferth T. Multiple cell death modalities and their key features (review). World Acad Sci J. 2020;2(2):39–48. https://doi.org/10.3892/wasj.2020.40.
140. Tan Y, Chen Q, Li X, Zeng Z, Xiong W, Li G, et al. Pyroptosis: a new paradigm of cell death for fighting against cancer. J Exp Clin Cancer Res. 2021;40(1):153. https://doi.org/10.1186/s13046-021-01959-x.
141. Galluzzi L, Bravo-San Pedro JM, Demaria S, Formenti SC, Kroemer G. Activating autophagy to potentiate immunogenic chemotherapy and radiation therapy. Nat Rev Clin Oncol. 2017;14(4):247–58. https://doi.org/10.1038/nrclinonc.2016.183.
142. Weerasinghe P, Buja LM. Oncosis: an important non-apoptotic mode of cell death. Exp Mol Pathol. 2012;93(3):302–8. https://doi.org/10.1016/j.yexmp.2012.09.018.
143. Weinberg RA. The biology of cancer. 2nd ed. New York: Garland Science; 2014.
144. Gillies RJ, Robey I, Gatenby RA. Causes and consequences of increased glucose metabolism of cancers. J Nucl Med. 2008;49(Suppl 2):24S–42S. https://doi.org/10.2967/jnumed.107.047258.
145. Tang D, Kang R, Berghe TV, Vandenabeele P, Kroemer G. The molecular machinery of regulated cell death. Cell Res. 2019;29(5):347–64. https://doi.org/10.1038/s41422-019-0164-5.
146. Yu P, Zhang X, Liu N, Tang L, Peng C, Chen X. Pyroptosis: mechanisms and diseases. Signal Transduct Target Ther. 2021;6(1):128. https://doi.org/10.1038/s41392-021-00507-5.
147. Jiang X, Stockwell BR, Conrad M. Ferroptosis: mechanisms, biology and role in disease. Nat Rev Mol Cell Biol. 2021;22(4):266–82. https://doi.org/10.1038/s41580-020-00324-8.
148. Yipp BG, Kubes P. NETosis: how vital is it? Blood. 2013;122(16):2784–94. https://doi.org/10.1182/blood-2013-04-457671.
149. Maltese WA, Overmeyer JH. Methuosis: nonapoptotic cell death associated with vacuolization of macropinosome and endosome compartments. Am J Pathol. 2014;184(6):1630–42. https://doi.org/10.1016/j.ajpath.2014.02.028.
150. Patel NH, Sohal SS, Manjili MH, Harrell JC, Gewirtz DA. The roles of autophagy and senescence in the tumor cell response to radiation. Radiat Res. 2020;194(2):103–15. https://doi.org/10.1667/RADE-20-00009.
151. Dikic I, Elazar Z. Mechanism and medical implications of mammalian autophagy. Nat Rev Mol Cell Biol. 2018;19(6):349–64. https://doi.org/10.1038/s41580-018-0003-4.
152. Filomeni G, de Zio D, Cecconi F. Oxidative stress and autophagy: the clash between damage and metabolic needs. Cell Death Differ. 2015;22(3):377–88. https://doi.org/10.1038/cdd.2014.150.
153. Xu J, Patel NH, Saleh T, Cudjoe EK, Alotaibi M, Wu Y, et al. Differential radiation sensitivity in p53 wild-type and p53-deficient tumor cells associated with senescence but not apoptosis or (nonprotective) autophagy. Radiat Res. 2018;190(5):538–57. https://doi.org/10.1667/RR15099.1.
154. Puck TT, Marcus PI. Action of X-rays on mammalian cells. J Exp Med. 1956;103(5):653–66. https://doi.org/10.1084/jem.103.5.653.
155. Rafehi H, Orlowski C, Georgiadis GT, Ververis K, El-Osta A, Karagiannis TC. Clonogenic assay: adherent cells. J Vis Exp. 2011;49:2573. https://doi.org/10.3791/2573.
156. Brix N, Samaga D, Hennel R, Gehr K, Zitzelsberger H, Lauber K. The clonogenic assay: robustness of plating efficiency-based analysis is strongly compromised by cellular cooperation. Radiat Oncol. 2020;15(1):248. https://doi.org/10.1186/s13014-020-01697-y.
157. Munshi A, Hobbs M, Meyn RE. Clonogenic cell survival assay. Methods Mol Med. 2005;110:21–8. https://doi.org/10.1385/1-59259-869-2:021.
158. Eke I, Hehlgans S, Sandfort V, Cordes N. 3D matrix-based cell cultures: automated analysis of tumor cell survival and proliferation. Int J Oncol. 2016;48(1):313–21. https://doi.org/10.3892/ijo.2015.3230.
159. Till JE, McCulloch EA. A direct measurement of the radiation sensitivity of normal mouse bone marrow cells. Radiat Res. 1961;14:213–22.
160. Willers H, Eke I. Introduction to molecular targeted radiosensitizers: opportunities and challenges. In: Willers H, Eke I, editors. Molecular targeted Radiosensitizers. Cham: Springer International Publishing; 2020. p. 1–16. https://doi.org/10.1007/978-3-030-49701-9_1.
161. Hooper ML. Tumor suppressor genes. New York: Wiley; 2006. https://doi.org/10.1038/npg.els.0006005.
162. Macleod K. Tumor suppressor genes. Curr Opin Genet Dev. 2000;10(1):81–93. https://doi.org/10.1016/s0959-437x(99)00041-6.
163. Totland MZ, Rasmussen NL, Knudsen LM, Leithe E. Regulation of gap junction intercellular communication by connexin ubiquitination: physiological and pathophysiological implications. Cell Mol Life Sci. 2020;77(4):573–91. https://doi.org/10.1007/s00018-019-03285-0.
164. Pilarczyk G, Papenfuß F, Bestvater F, Hausmann M. Spatial arrangements of Connexin43 in cancer related cells and rearrangements under treatment conditions: investigations on the nano-scale by super-resolution localization light microscopy. Cancers (Basel). 2019;11:301. https://doi.org/10.3390/cancers11030301.
165. Villanelo F, Escalona Y, Pareja-Barrueto C, Garate JA, Skerrett IM, Perez-Acle T. Accessing gap-junction channel structure–function relationships through molecular modeling and simulations.

BMC Cell Biol. 2017;18(Suppl 1):5. https://doi.org/10.1186/s12860-016-0121-9.
166. Matejka N, Reindl J. Perspectives of cellular communication through tunneling nanotubes in cancer cells and the connection to radiation effects. Radiat Oncol. 2019;14(1):218. https://doi.org/10.1186/s13014-019-1416-8.
167. Xiao TS. Innate immunity and inflammation. Cell Mol Immunol. 2017;14(1):1–3. https://doi.org/10.1038/cmi.2016.45.
168. Deloch L, Fuchs J, Rückert M, Fietkau R, Frey B, Gaipl US. Low-dose irradiation differentially impacts macrophage phenotype in dependence of fibroblast-like synoviocytes and radiation dose. J Immunol Res. 2019;2019:3161750. https://doi.org/10.1155/2019/3161750.
169. Donaubauer A-J, Deloch L, Becker I, Fietkau R, Frey B, Gaipl US. The influence of radiation on bone and bone cells—differential effects on osteoclasts and osteoblasts. Int J Mol Sci. 2020;21:377. https://doi.org/10.3390/ijms21176377.
170. Lumniczky K, Impens N, Armengol G, Candéias S, Georgakilas AG, Hornhardt S, et al. Low dose ionizing radiation effects on the immune system. Environ Int. 2021;149:106212. https://doi.org/10.1016/j.envint.2020.106212.
171. Rödel F, Hofmann D, Auer J, Keilholz L, Röllinghoff M, Sauer R, Beuscher HU. The anti-inflammatory effect of low-dose radiation therapy involves a diminished CCL20 chemokine expression and granulocyte/endothelial cell adhesion. Strahlenther Onkol. 2008;184(1):41–7. https://doi.org/10.1007/s00066-008-1776-8.
172. Gaugler M-H, Vereycken-Holler V, Squiban C, Aigueperse J. PECAM-1 (CD31) is required for interactions of platelets with endothelial cells after irradiation. J Thromb Haemost. 2004;2(11):2020–6. https://doi.org/10.1111/j.1538-7836.2004.00951.x.
173. Halle M, Hall P, Tornvall P. Cardiovascular disease associated with radiotherapy: activation of nuclear factor kappa-B. J Intern Med. 2011;269(5):469–77. https://doi.org/10.1111/j.1365-2796.2011.02353.x.
174. Large M, Hehlgans S, Reichert S, Gaipl US, Fournier C, Rödel C, et al. Study of the anti-inflammatory effects of low-dose radiation: the contribution of biphasic regulation of the antioxidative system in endothelial cells. Strahlenther Onkol. 2015;191(9):742–9. https://doi.org/10.1007/s00066-015-0848-9.
175. Ishino Y, Shinagawa H, Makino K, Amemura M, Nakata A. Nucleotide sequence of the iap gene, responsible for alkaline phosphatase isozyme conversion in *Escherichia coli*, and identification of the gene product. J Bacteriol. 1987;169(12):5429–33. https://doi.org/10.1128/jb.169.12.5429-5433.1987.
176. Wright JB, Sanjana NE. CRISPR screens to discover functional noncoding elements. Trends Genet. 2016;32(9):526–9. https://doi.org/10.1016/j.tig.2016.06.004.
177. Doudna JA, Charpentier E. Genome editing. The new frontier of genome engineering with CRISPR-Cas9. Science. 2014;346(6213):1258096. https://doi.org/10.1126/science.1258096.
178. Zhao Z, Li C, Tong F, Deng J, Huang G, Sang Y. Review of applications of CRISPR-Cas9 gene-editing technology in cancer research. Biol Proced Online. 2021;23(1):14. https://doi.org/10.1186/s12575-021-00151-x.
179. Pickar-Oliver A, Gersbach CA. The next generation of CRISPR-Cas technologies and applications. Nat Rev Mol Cell Biol. 2019;20(8):490–507. https://doi.org/10.1038/s41580-019-0131-5.
180. Liu B, Saber A, Haisma HJ. CRISPR/Cas9: a powerful tool for identification of new targets for cancer treatment. Drug Discov Today. 2019;24(4):955–70. https://doi.org/10.1016/j.drudis.2019.02.011.
181. Lino CA, Harper JC, Carney JP, Timlin JA. Delivering CRISPR: a review of the challenges and approaches. Drug Deliv. 2018;25(1):1234–57. https://doi.org/10.1080/10717544.2018.1474964.
182. Allis CD, Jenuwein T. The molecular hallmarks of epigenetic control. Nat Rev Genet. 2016;17(8):487–500. https://doi.org/10.1038/nrg.2016.59.
183. Belli M, Tabocchini MA. Ionizing radiation-induced epigenetic modifications and their relevance to radiation protection. Int J Mol Sci. 2020;21:5993. https://doi.org/10.3390/ijms21175993.
184. Smits KM, Melotte V, Niessen HEC, Dubois L, Oberije C, Troost EGC, et al. Epigenetics in radiotherapy: where are we heading? Radiother Oncol. 2014;111(2):168–77. https://doi.org/10.1016/j.radonc.2014.05.001.
185. Macfarlane L-A, Murphy PR. MicroRNA: biogenesis, function and role in cancer. Curr Genomics. 2010;11(7):537–61. https://doi.org/10.2174/138920210793175895.
186. O'Brien J, Hayder H, Zayed Y, Peng C. Overview of MicroRNA biogenesis, mechanisms of actions, and circulation. Front Endocrinol (Lausanne). 2018;9:402. https://doi.org/10.3389/fendo.2018.00402.
187. Chen Y, Cui J, Gong Y, Wei S, Wei Y, Yi L. MicroRNA: a novel implication for damage and protection against ionizing radiation. Environ Sci Pollut Res Int. 2021;28(13):15584–96. https://doi.org/10.1007/s11356-021-12509-5.
188. Templin T, Amundson SA, Brenner DJ, Smilenov LB. Whole mouse blood microRNA as biomarkers for exposure to γ-rays and (56)Fe ion. Int J Radiat Biol. 2011;87(7):653–62. https://doi.org/10.3109/09553002.2010.549537.
189. Gao F, Liu P, Narayanan J, Yang M, Fish BL, Liu Y, et al. Changes in miRNA in the lung and whole blood after whole thorax irradiation in rats. Sci Rep. 2017;7:44132. https://doi.org/10.1038/srep44132.
190. Fendler W, Malachowska B, Meghani K, Konstantinopoulos PA, Guha C, Singh VK, Chowdhury D. Evolutionarily conserved serum microRNAs predict radiation-induced fatality in nonhuman primates. Sci Transl Med. 2017;9:2408. https://doi.org/10.1126/scitranslmed.aal2408.
191. Rascio F, Spadaccino F, Rocchetti MT, Castellano G, Stallone G, Netti GS, Ranieri E. The pathogenic role of PI3K/AKT pathway in cancer onset and drug resistance: an updated review. Cancers (Basel). 2021;13:3949. https://doi.org/10.3390/cancers13163949.
192. Ebahimzadeh K, Shoorei H, Mousavinejad SA, Anamag FT, Dinger ME, Taheri M, Ghafouri-Fard S. Emerging role of non-coding RNAs in response of cancer cells to radiotherapy. Pathol Res Pract. 2021;218:153327. https://doi.org/10.1016/j.prp.2020.153327.
193. Podralska M, Ciesielska S, Kluiver J, van den Berg A, Dzikiewicz-Krawczyk A, Slezak-Prochazka I. Non-coding RNAs in cancer radiosensitivity: microRNAs and lncRNAs as regulators of radiation-induced signaling pathways. Cancers (Basel). 2020;12:1662. https://doi.org/10.3390/cancers12061662.
194. Uszczynska-Ratajczak B, Lagarde J, Frankish A, Guigó R, Johnson R. Towards a complete map of the human long non-coding RNA transcriptome. Nat Rev Genet. 2018;19(9):535–48. https://doi.org/10.1038/s41576-018-0017-y.
195. Statello L, Guo C-J, Chen L-L, Huarte M. Gene regulation by long non-coding RNAs and its biological functions. Nat Rev Mol Cell Biol. 2021;22(2):96–118. https://doi.org/10.1038/s41580-020-00315-9.
196. May JM, Bylicky M, Chopra S, Coleman CN, Aryankalayil MJ. Long and short non-coding RNA and radiation response: a review. Transl Res. 2021;233:162–79. https://doi.org/10.1016/j.trsl.2021.02.005.
197. Salzman J, Gawad C, Wang PL, Lacayo N, Brown PO. Circular RNAs are the predominant transcript isoform from hundreds of human genes in diverse cell types. PLoS One. 2012;7(2):e30733. https://doi.org/10.1371/journal.pone.0030733.

198. Xiao M-S, Ai Y, Wilusz JE. Biogenesis and functions of circular RNAs come into focus. Trends Cell Biol. 2020;30(3):226–40. https://doi.org/10.1016/j.tcb.2019.12.004.
199. Hall MP, Nagel RJ, Fagg WS, Shiue L, Cline MS, Perriman RJ, et al. Quaking and PTB control overlapping splicing regulatory networks during muscle cell differentiation. RNA. 2013;19(5):627–38. https://doi.org/10.1261/rna.038422.113.
200. Conn SJ, Pillman KA, Toubia J, Conn VM, Salmanidis M, Phillips CA, et al. The RNA binding protein quaking regulates formation of circRNAs. Cell. 2015;160(6):1125–34. https://doi.org/10.1016/j.cell.2015.02.014.
201. Cui C, Yang J, Li X, Liu D, Fu L, Wang X. Functions and mechanisms of circular RNAs in cancer radiotherapy and chemotherapy resistance. Mol Cancer. 2020;19(1):58. https://doi.org/10.1186/s12943-020-01180-y.
202. O'Leary VB, Smida J, Matjanovski M, Brockhaus C, Winkler K, Moertl S, et al. The circRNA interactome-innovative hallmarks of the intra- and extracellular radiation response. Oncotarget. 2017;8(45):78397–409. https://doi.org/10.18632/oncotarget.19228.
203. Mfossa ACM, Thekkekara Puthenparampil H, Inalegwu A, Coolkens A, Baatout S, Benotmane MA, et al. Exposure to ionizing radiation triggers prolonged changes in circular RNA abundance in the embryonic mouse brain and primary neurons. Cell. 2019;8:778. https://doi.org/10.3390/cells8080778.
204. Panda AC, Grammatikakis I, Kim KM, De S, Martindale JL, Munk R, et al. Identification of senescence-associated circular RNAs (SAC-RNAs) reveals senescence suppressor CircPVT1. Nucleic Acids Res. 2017;45(7):4021–35. https://doi.org/10.1093/nar/gkw1201.
205. Verduci L, Ferraiuolo M, Sacconi A, Ganci F, Vitale J, Colombo T, et al. The oncogenic role of circPVT1 in head and neck squamous cell carcinoma is mediated through the mutant p53/YAP/TEAD transcription-competent complex. Genome Biol. 2017;18(1):237. https://doi.org/10.1186/s13059-017-1368-y.
206. Huang M, Li T, Wang Q, Li C, Zhou H, Deng S, et al. Silencing circPVT1 enhances radiosensitivity in non-small cell lung cancer by sponging microRNA-1208. Cancer Biomark. 2021;31(3):263–79. https://doi.org/10.3233/CBM-203252.
207. Chang L, Graham PH, Hao J, Ni J, Bucci J, Cozzi PJ, et al. Acquisition of epithelial–mesenchymal transition and cancer stem cell phenotypes is associated with activation of the PI3K/Akt/mTOR pathway in prostate cancer radioresistance. Cell Death Dis. 2013;4:e875. https://doi.org/10.1038/cddis.2013.407.
208. Jeyaraman S, Hanif EAM, Ab Mutalib NS, Jamal R, Abu N. Circular RNAs: potential regulators of treatment resistance in human cancers. Front Genet. 2019;10:1369. https://doi.org/10.3389/fgene.2019.01369.
209. Zhang Y, Yang L, Chen L-L. Characterization of circular RNAs. Methods Mol Biol. 2021;2372:179–92. https://doi.org/10.1007/978-1-0716-1697-0_16.
210. Théry C, Witwer KW, Aikawa E, Alcaraz MJ, Anderson JD, Andriantsitohaina R, et al. Minimal information for studies of extracellular vesicles 2018 (MISEV2018): a position statement of the International Society for Extracellular Vesicles and update of the MISEV2014 guidelines. J Extracell Vesicles. 2018;7(1):1535750. https://doi.org/10.1080/20013078.2018.1535750.
211. Veziroglu EM, Mias GI. Characterizing extracellular vesicles and their diverse RNA contents. Front Genet. 2020;11:700. https://doi.org/10.3389/fgene.2020.00700.
212. Mosquera-Heredia MI, Morales LC, Vidal OM, Barceló E, Silvera-Redondo C, Vélez JI, Garavito-Galofre P. Exosomes: potential disease biomarkers and new therapeutic targets. Biomedicine. 2021;9:1061. https://doi.org/10.3390/biomedicines9081061.
213. Gutiérrez-Fernández M, La Cuesta F, de Tallón A, Cuesta I, Fernández-Fournier M, Laso-García F, et al. Potential roles of extracellular vesicles as biomarkers and a novel treatment approach in multiple sclerosis. Int J Mol Sci. 2021;22:9011. https://doi.org/10.3390/ijms22169011.
214. Ayers L, Pink R, Carter DRF, Nieuwland R. Clinical requirements for extracellular vesicle assays. J Extracell Vesicles. 2019. https://doi.org/10.1080/20013078.2019.1593755.
215. Mathieu M, Martin-Jaular L, Lavieu G, Théry C. Specificities of secretion and uptake of exosomes and other extracellular vesicles for cell-to-cell communication. Nat Cell Biol. 2019;21(1):9–17. https://doi.org/10.1038/s41556-018-0250-9.
216. Kalluri R, LeBleu VS. The biology, function, and biomedical applications of exosomes. Science. 2020;367(6478):eaau6977. https://doi.org/10.1126/science.aau6977.
217. Ferguson S, Weissleder R. Modeling EV kinetics for use in early cancer detection. Adv Biosyst. 2020;4(12):e1900305. https://doi.org/10.1002/adbi.201900305.
218. Doyle LM, Wang MZ. Overview of extracellular vesicles, their origin, composition, purpose, and methods for exosome isolation and analysis. Cell. 2019;8:727. https://doi.org/10.3390/cells8070727.
219. Ratajczak MZ, Ratajczak J. Extracellular microvesicles/exosomes: discovery, disbelief, acceptance, and the future? Leukemia. 2020;34(12):3126–35. https://doi.org/10.1038/s41375-020-01041-z.
220. Villarroya-Beltri C, Baixauli F, Gutiérrez-Vázquez C, Sánchez-Madrid F, Mittelbrunn M. Sorting it out: regulation of exosome loading. Semin Cancer Biol. 2014;28:3–13. https://doi.org/10.1016/j.semcancer.2014.04.009.
221. Willms E, Johansson HJ, Mäger I, Lee Y, Blomberg KEM, Sadik M, et al. Cells release subpopulations of exosomes with distinct molecular and biological properties. Sci Rep. 2016;6:22519. https://doi.org/10.1038/srep22519.
222. Vautrot V, Bentayeb H, Causse S, Garrido C, Gobbo J. Tumor-derived exosomes: hidden players in PD-1/PD-L1 resistance. Cancers (Basel). 2021;13:4537. https://doi.org/10.3390/cancers13184537.
223. Yin T, Xin H, Yu J, Teng F. The role of exosomes in tumour immunity under radiotherapy: eliciting abscopal effects? Biomark Res. 2021;9(1):22. https://doi.org/10.1186/s40364-021-00277-w.
224. He C, Li L, Wang L, Meng W, Hao Y, Zhu G. Exosome-mediated cellular crosstalk within the tumor microenvironment upon irradiation. Cancer Biol Med. 2021;18(1):21–33. https://doi.org/10.20892/j.issn.2095-3941.2020.0150.
225. Mrowczynski OD, Madhankumar AB, Sundstrom JM, Zhao Y, Kawasawa YI, Slagle-Webb B, et al. Exosomes impact survival to radiation exposure in cell line models of nervous system cancer. Oncotarget. 2018;9(90):36083–101. https://doi.org/10.18632/oncotarget.26300.
226. Moertl S, Buschmann D, Azimzadeh O, Schneider M, Kell R, Winkler K, et al. Radiation exposure of peripheral mononuclear blood cells alters the composition and function of secreted extracellular vesicles. Int J Mol Sci. 2020;21:2336. https://doi.org/10.3390/ijms21072336.
227. Li S, Shao L, Xu T, Jiang X, Yang G, Dong L. An indispensable tool: exosomes play a role in therapy for radiation damage. Biomed Pharmacother. 2021;137:111401. https://doi.org/10.1016/j.biopha.2021.111401.
228. Abdallah C, Dumas-Gaudot E, Renaut J, Sergeant K. Gel-based and gel-free quantitative proteomics approaches at a

glance. Int J Plant Genomics. 2012;2012:494572. https://doi.org/10.1155/2012/494572.
229. Ramazi S, Zahiri J. Posttranslational modifications in proteins: resources, tools and prediction methods. Database (Oxford). 2021;2021:baab012. https://doi.org/10.1093/database/baab012.
230. Schmidt A, Forne I, Imhof A. Bioinformatic analysis of proteomics data. BMC Syst Biol. 2014;8(Suppl 2):S3. https://doi.org/10.1186/1752-0509-8-S2-S3.
231. Azimzadeh O, Gomolka M, Birschwilks M, Saigusa S, Grosche B, Moertl S. Advanced omics and radiobiological tissue archives: the future in the past. Appl Sci. 2021;11(23):11108. https://doi.org/10.3390/app112311108.
232. Vicente E, Vujaskovic Z, Jackson IL. A systematic review of metabolomic and lipidomic candidates for biomarkers in radiation injury. Metabolites. 2020;10(6):259. https://doi.org/10.3390/metabo10060259.
233. Huang J, Wang Q, Qi Z, Zhou S, Zhou M, Wang Z. Lipidomic profiling for serum biomarkers in mice exposed to ionizing radiation. Dose Response. 2020;18(2):1559325820914209. https://doi.org/10.1177/1559325820914209.
234. Laiakis EC, Canadell MP, Grilj V, Harken AD, Garty GY, Astarita G, et al. Serum lipidomic analysis from mixed neutron/X-ray radiation fields reveals a hyperlipidemic and pro-inflammatory phenotype. Sci Rep. 2019;9(1):4539. https://doi.org/10.1038/s41598-019-41083-7.
235. Prasanna PGS, Narayanan D, Zhang K, Rahbar A, Coleman CN, Vikram B. Radiation biomarkers: can small businesses drive accurate radiation precision medicine? Radiat Res. 2020;193(3):199–208. https://doi.org/10.1667/RR15553.1.
236. Roh C. Metabolomics in radiation-induced biological dosimetry: a mini-review and a polyamine study. Biomol Ther. 2018;8:34. https://doi.org/10.3390/biom8020034.
237. Singh VK, Seed TM, Cheema AK. Metabolomics-based predictive biomarkers of radiation injury and countermeasure efficacy: current status and future perspectives. Expert Rev Mol Diagn. 2021;21(7):641–54. https://doi.org/10.1080/14737159.2021.1933448.
238. Boguszewicz Ł, Bieleń A, Ciszek M, Wendykier J, Szczepanik K, Skorupa A, et al. NMR-based metabolomics in investigation of the radiation induced changes in blood serum of head and neck cancer patients and its correlation with the tissue volumes exposed to the particulate doses. Int J Mol Sci. 2021;22:6310. https://doi.org/10.3390/ijms22126310.
239. Amundson SA. Transcriptomics for radiation biodosimetry: progress and challenges. Int J Radiat Biol. 2021;2021:8784. https://doi.org/10.1080/09553002.2021.1928784.
240. Cruz-Garcia L, O'Brien G, Sipos B, Mayes S, Love MI, Turner DJ, Badie C. Generation of a transcriptional radiation exposure signature in human blood using long-read nanopore sequencing. Radiat Res. 2019;193(2):143–54. https://doi.org/10.1667/RR15476.1.
241. Zhao JZL, Mucaki EJ, Rogan PK. Predicting ionizing radiation exposure using biochemically-inspired genomic machine learning. F1000Res. 2018;7:233. https://doi.org/10.12688/f1000research.14048.2.
242. Mucaki EJ, Shirley BC, Rogan PK. Improved radiation expression profiling in blood by sequential application of sensitive and specific gene signatures. Int J Radiat Biol. 2021;98:924–41. https://doi.org/10.1080/09553002.2021.1998709.
243. Choi M, Kipps T, Kurzrock R. ATM mutations in cancer: therapeutic implications. Mol Cancer Ther. 2016;15(8):1781–91. https://doi.org/10.1158/1535-7163.MCT-15-0945.
244. Wang C, Jette N, Moussienko D, Bebb DG, Lees-Miller SP. ATM-deficient colorectal cancer cells are sensitive to the PARP inhibitor Olaparib. Transl Oncol. 2017;10(2):190–6. https://doi.org/10.1016/j.tranon.2017.01.007.
245. Huang R-X, Zhou P-K. DNA damage response signaling pathways and targets for radiotherapy sensitization in cancer. Signal Transduct Target Ther. 2020;5(1):60. https://doi.org/10.1038/s41392-020-0150-x.
246. Edin NJ, Olsen DR, Sandvik JA, Malinen E, Pettersen EO. Low dose hyper-radiosensitivity is eliminated during exposure to cycling hypoxia but returns after reoxygenation. Int J Radiat Biol. 2012;88(4):311–9. https://doi.org/10.3109/09553002.2012.646046.
247. Marples B, Collis SJ. Low-dose hyper-radiosensitivity: past, present, and future. Int J Radiat Oncol Biol Phys. 2008;70(5):1310–8. https://doi.org/10.1016/j.ijrobp.2007.11.071.
248. Marples B, Wouters BG, Joiner MC. An association between the radiation-induced arrest of G2-phase cells and low-dose hyper-radiosensitivity: a plausible underlying mechanism? Radiat Res. 2003;160(1):38–45. https://doi.org/10.1667/rr3013.
249. Xu B, Kim S-T, Lim D-S, Kastan MB. Two molecularly distinct G(2)/M checkpoints are induced by ionizing irradiation. Mol Cell Biol. 2002;22(4):1049–59. https://doi.org/10.1128/MCB.22.4.1049-1059.2002.
250. Krueger SA, Collis SJ, Joiner MC, Wilson GD, Marples B. Transition in survival from low-dose hyper-radiosensitivity to increased radioresistance is independent of activation of ATM Ser1981 activity. Int J Radiat Oncol Biol Phys. 2007;69(4):1262–71. https://doi.org/10.1016/j.ijrobp.2007.08.012.
251. Edin NJ, Sandvik JA, Cheng C, Bergersen L, Pettersen EO. The roles of TGF-β3 and peroxynitrite in removal of hyper-radiosensitivity by priming irradiation. Int J Radiat Biol. 2014;90(7):527–37. https://doi.org/10.3109/09553002.2014.906767.
252. Fernandez-Palomo C, Seymour C, Mothersill C. Inter-relationship between low-dose hyper-radiosensitivity and radiation-induced bystander effects in the human T98G glioma and the epithelial HaCaT cell line. Radiat Res. 2016;185(2):124–33. https://doi.org/10.1667/RR14208.1.
253. Honoré HB, Bentzen SM. A modelling study of the potential influence of low dose hypersensitivity on radiation treatment planning. Radiother Oncol. 2006;79(1):115–21. https://doi.org/10.1016/j.radonc.2006.01.003.
254. Arnold SM, Regine WF, Ahmed MM, Valentino J, Spring P, Kudrimoti M, et al. Low-dose fractionated radiation as a chemopotentiator of neoadjuvant paclitaxel and carboplatin for locally advanced squamous cell carcinoma of the head and neck: results of a new treatment paradigm. Int J Radiat Oncol Biol Phys. 2004;58(5):1411–7. https://doi.org/10.1016/j.ijrobp.2003.09.019.
255. Coker JA. Recent advances in understanding extremophiles. F1000Res. 2019;8:20765. https://doi.org/10.12688/f1000research.20765.1.
256. Arnold CR, Mangesius J, Skvortsova I-I, Ganswindt U. The role of cancer stem cells in radiation resistance. Front Oncol. 2020;10:164. https://doi.org/10.3389/fonc.2020.00164.
257. Olivieri G, Bodycote J, Wolff S. Adaptive response of human lymphocytes to low concentrations of radioactive thymidine. Science. 1984;223(4636):594–7. https://doi.org/10.1126/science.6695170.
258. Guéguen Y, Bontemps A, Ebrahimian TG. Adaptive responses to low doses of radiation or chemicals: their cellular and molecular mechanisms. Cell Mol Life Sci. 2019;76(7):1255–73. https://doi.org/10.1007/s00018-018-2987-5.

Further Reading

Alberts J et al., Molecular biology of the cell. 6th ed. Garland Press New York 2015

Belyaev IY. Radiation-induced DNA repair foci: spatio-temporal aspects of formation, application for assessment of radiosensitivity and biological dosimetry. Mutat Res. 2010;704(1–3):132–41. https://doi.org/10.1016/j.mrrev.2010.01.011.

Cabrera-Licona A, Pérez-Añorve IX, Flores-Fortis M, del Moral-Hernández O, Claudia H, de la Rosa G, Suárez-Sánchez R, Chávez-Saldaña M, Aréchaga-Ocampo E. Deciphering the epigenetic network in cancer radioresistance. Radiother Oncol. 2021;159:48–59. https://doi.org/10.1016/j.radonc.2021.03.012.

Chakraborty N, Gautam A, Holmes-Hampton GP, Kumar VP, Biswas S, Kumar R, Hamad D, et al. MicroRNA and metabolite signatures linked to early consequences of lethal radiation. Sci Rep. 2020;10(1):1–13. https://doi.org/10.1038/s41598-020-62255-w.

Chen Y, Cui J, Gong Y, Wei S, Wei Y, Yi L. MicroRNA: a novel implication for damage and protection against ionizing radiation. Environ Sci Pollut Res. 2021;28(13):15584–96. https://doi.org/10.1007/s11356-021-12509-5.

Chota A, George BP, Abrahamse H. Interactions of multidomain pro-apoptotic and anti-apoptotic proteins in cancer cell death. Oncotarget. 2021;12(16):1615–26. https://doi.org/10.18632/oncotarget.28031.

Czochor JR, Glazer PM. MicroRNAs in cancer cell response to ionizing radiation. Antioxidants Redox Signal. 21(2):293–312. https://doi.org/10.1089/ars.2013.5718.

Dikic I, Elazar Z. Mechanism and medical implications of mammalian autophagy. Nat Rev Mol Cell Biol. 2018;19(6):349–64. https://doi.org/10.1038/s41580-018-0003-4.

Falk M, Lukasova E, Kozubek S. Higher-order chromatin structure in DSB induction, repair and misrepair. Mutat Res. 2010;704(1–3):88–100. https://doi.org/10.1016/j.mrrev.2010.01.013.

Falk M, Hausmann M, Lukášová E, Biswas A, Hildenbrand G, Davídková M, et al. Determining Omics spatiotemporal dimensions using exciting new nanoscopy techniques to assess complex cell responses to DNA damage: part B—structuromics. Crit Rev Eukaryot Gene Expr. 2014;24(3):225–47. https://doi.org/10.1615/critreveukaryotgeneexpr.v24.i3.40.

Falk M, Hausmann M. A paradigm revolution or just better resolution—will newly emerging superresolution techniques identify chromatin architecture as a key factor in radiation-induced DNA damage and repair regulation? Cancers. 2021;13(1):18. https://doi.org/10.3390/cancers13010018.

Hu H, Gatti RA. MicroRNAs: new players in the DNA damage response. J Mol Cell Biol. 2011;3(3):151–8. https://doi.org/10.1093/jmcb/mjq042.

https://link.springer.com/referenceworkentry/10.1007%2F978-3-642-30018-9_2.

https://www.ncbi.nlm.nih.gov/pmc/articles/PMC4060780/#s005.

https://www.ncbi.nlm.nih.gov/pmc/articles/PMC3980444/.

https://www.sciencedirect.com/science/article/pii/S221323171931064X.

Kawale AS, Sung P. Mechanism and significance of chromosome damage repair by homologous recombination. Essays Biochem. 2020;64(5):779–90. https://doi.org/10.1042/EBC20190093.

Knasmüller S, Fenech M. Micronucleus assay in toxicology. Issues in toxicology, vol. 39. London: Royal Society of Chemistry; 2019. https://doi.org/10.1039/9781788013604.

Kwon M, Leibowitz ML, Lee JH. Small but mighty: the causes and consequences of micronucleus rupture. Exp Mol Med. 2020;52:1777–86.

Liu YG, Chen JK, Zhang ZT, Ma XJ, Chen YC, Du XM, et al. NLRP3 inflammasome activation mediates radiation-induced pyroptosis in bone marrow-derived macrophages. Cell Death Dis. 2017;8(2):e2579. https://doi.org/10.1038/cddis.2016.460.

Lumniczky K, Impens N, Armengol G, et al. Low dose ionizing radiation effects on the immune system. Environ Int. 2021;149:106212.

Obe G, Natarajan AT, editors. Chromosomal alterations, origin and significance. Berlin: Springer; 1994. https://doi.org/10.1007/978-3-642-78887-1.

Obe G, Natarajan AT, editors. Chromosome aberrations. Berlin: Springer; 2004. https://doi.org/10.1159/isbn.978-3-318-01100-5.

Patel NH, Sohal SS, Manjili MH, Harrell JC, Gewirtz DA. The roles of autophagy and senescence in the tumor cell response to radiation. Radiat Res. 2020;194(2):103–15. https://doi.org/10.1667/RADE-20-00009.

Pawlik TM, Keyomarsi K. Role of cell cycle in mediating sensitivity to radiotherapy. Int J Radiat Oncol. 2004;59(4):928–42.

Podralska M, Ciesielska S, Kluiver J, van den Berg A, Dzikiewicz-Krawczyk A, Slezak-Prochazka I. Non-coding RNAs in cancer radiosensitivity: microRNAs and Lncrnas as regulators of radiation-induced signaling pathways. Cancers. 2020;12(6):1–27. https://doi.org/10.3390/cancers12061662.

Prokhorova EA, Egorshina AY, Zhivotovsky B, Kopeina GS. The DNA-damage response and nuclear events as regulators of nonapoptotic forms of cell death. Oncogene. 2020;39(1):1–16. https://doi.org/10.1038/s41388-019-0980-6.

Rascio F, Spadaccino F, Rocchetti MT, Castellano G, Stallone G, Netti GS, Ranieri E. The pathogenic role of PI3K/AKT pathway in cancer onset and drug resistance: an updated review. Cancers. 2021;13(16):949. https://doi.org/10.3390/cancers13163949.

Rödel F, Frey B, Manda K, et al. Immunomodulatory properties and molecular effects in inflammatory diseases of low-dose x-irradiation. Front Oncol. 2012;2:120.

Song M, Xie D, Gao S, Bai CJ, Zhu MX, Guan H, Zhou PK. A biomarker panel of radiation-upregulated miRNA as signature for ionizing radiation exposure. Life. 2020;10(12):1–15. https://doi.org/10.3390/life10120361.

Sia J, Szmyd R, Hau E, Gee HE. Molecular mechanisms of radiation-induced cancer cell death: a primer. Front Cell Dev Biol. 2020;8:41. https://doi.org/10.3389/fcell.2020.00041.

Sun Y, McCorvie TJ, Yates LA, et al. Structural basis of homologous recombination. Cell Mol Life Sci. 2020;**77**:3–18. https://doi.org/10.1007/s00018-019-03365-1.

Tessitore A, Cicciarelli G, Del Vecchio F, Gaggiano A, Verzella D, Fischietti M, Vecchiotti D, Capece D, Zazzeroni F, Alesse E. MicroRNAs in the DNA damage/repair network and cancer. Int J Genomics. 2014;2014:820248. https://doi.org/10.1155/2014/820248.

Wagener-Ryczek S, Merkelbach-Bruse S, Siemanowski J. Biomarkers for homologous recombination deficiency in cancer. J Pers Med. 2021;11:612. https://doi.org/10.3390/jpm11070612.

Isolation, Characterization and Definition of Different Extra Cellular from the International Society for Extracellular Vesicles

Théry C, Witwer KW, Aikawa E, Alcaraz MJ, et al. Minimal information for studies of extracellular vesicles 2018 (MISEV2018): a position statement of the International Society for Extracellular Vesicles and update of the MISEV2014 guidelines. J Extracell Vesicles. 2018;7(1):1535750. https://doi.org/10.1080/20013078.2018.1535750.

Databases for Exosome RNA and Protein Cargo

ExoCarta (http://www.exocarta.org/).
Vesiclepedia (http://www.microvesicles.org/).

The Role of Exosomes in Cancer and Metastasis

McAndrews KM, Kalluri R. Mechanisms associated with biogenesis of exosomes in cancer. Mol Cancer. 2019;18(1):52. https://doi.org/10.1186/s12943-019-0963-9.
Wortzel I, Dror S, Kenific C, Lyden D. Exosome-mediated metastasis: communication from a distance. Dev Cell. 2019;49(3):347–60.

The Role of Exosomes in the Tumor- and Immune Cell Interplay

https://link.springer.com/referenceworkentry/10.1007%2F978-3-642-30018-9_2.
https://www.ncbi.nlm.nih.gov/pmc/articles/PMC4060780/#s005.
https://www.ncbi.nlm.nih.gov/pmc/articles/PMC3980444/.
https://www.sciencedirect.com/science/article/pii/S221323171931064X.
Martin LM, Marples B, Lynch TH, Hollywood D, Marignol L. Exposure to low dose ionising radiation: molecular and clinical consequences. Cancer Lett. 2014;349(1):98–106. https://doi.org/10.1016/j.canlet.2013.12.015.
Whiteside TL, Diergaarde B, Hong CS. Tumor-derived exosomes (TEX) and their role in immuno-oncology. Int J Mol Sci. 2021;22(12):6234. https://doi.org/10.3390/ijms22126234.

Mechanistic, Modeling, and Dosimetric Radiation Biology

4

Giuseppe Schettino, Sarah Baatout, Francisco Caramelo, Fabiana Da Pieve, Cristian Fernandez-Palomo, Nina Frederike Jeppesen Edin, Aidan D. Meade, Yann Perrot, Judith Reindl, and Carmen Villagrasa

Learning Objectives

- To understand the concept of dose and the notion of energy deposition and energy transfer.
- To learn the working principles of the main types of detectors used for radiation dosimetry.
- To understand how the dose is measured in micrometric volumes and what the importance of microdosimetry is in radiobiology.
- To understand how early DNA damage is generated by ionizing radiation.
- And how this can be simulated using Monte Carlo (MC) track structure codes.
- To get an overview of the state of the art of the mechanistic simulation and the DNA damage scoring methods.
- To get to know micro-beams and mini-beams, their production and use, and why they are important for radiobiological research.
- To understand the underlying assumptions and derivation of target theory, which is the basis for all stochastic dose-response models at molecular and cellular level.
- To learn about the linear quadratic model, the strengths and limitations of the model as well as the different interpretations of the model with respect to the underlying biology.
- To understand the difficulties in modeling stochastic effects for whole organisms and for different dose rates.

Fabiana Da Pieve is currently employed by the European Research Council Executive Agency, European Commission, BE-1049 Brussels, Belgium. The views expressed are purely those of the authors and may not in any circumstances be regarded as stating an official position of the European Commission

G. Schettino (✉)
National Physical Laboratory, Teddington, United Kingdom

University of Surrey, Guilford, United Kingdom
e-mail: Giuseppe.schettino@npl.co.uk

S. Baatout
Institute of Nuclear Medical Applications, Belgian Nuclear Research Centre, SCK CEN, Mol, Belgium
e-mail: sarah.baatout@sckcen.be

F. Caramelo
University of Coimbra, Coimbra, Portugal
e-mail: fcaramelo@fmed.uc.pt

F. Da Pieve
Royal Belgian Institute for Space Aeronomy, Brussels, Belgium

European Research Council Executive Agency, European Commission, Brussels, Belgium

C. Fernandez-Palomo
Institute of Anatomy, University of Bern, Bern, Switzerland
e-mail: cristian.fernandez@unibe.ch

N. F. J. Edin
University of Oslo, Oslo, Norway
e-mail: nina@fys.uio.no

A. D. Meade
Technological University Dublin, Dublin, Ireland
e-mail: aidan.meade@tudublin.ie

Y. Perrot · C. Villagrasa
Institut de Radioprotection et Sûreté Nucléaire, Fontenay-aux-Roses Cedex, France
e-mail: yann.perrot@irsn.fr; carmen.villagrasa@irsn.fr

J. Reindl
Universität der Bundeswehr München, Neubiberg, Germany
e-mail: judith.reindl@unibw.de

S. Baatout (ed.), *Radiobiology Textbook*, https://doi.org/10.1007/978-3-031-18810-7_4

4.1 Principles of Radiation Dosimetry

4.1.1 Energy Deposition and Transfer

4.1.1.1 Fluence

Particle fluence, or *planar fluence*, Φ, is defined as the number of ionizing particles which traverse a finite plane in space some distance from the source. If dN particles are incident on a planar surface of area, dA, then the fluence is $\Phi = \mathrm{d}N/\mathrm{d}A$ [1, 2].

We may also define the *energy fluence*, Ψ, which is the radiant energy, dR, which crosses a plane of area, dA, as $\Psi = \mathrm{d}R/\mathrm{d}A$. The radiant energy, R, of a radiation field is defined as the total energy of the particles that cross the plane, excluding their rest mass energy. The *fluence rate* may be defined in terms of energy fluence or planar fluence and is simply the rate at which either energy fluence or planar fluence cross unit area. In the context of the amount of radiant energy absorbed in matter, these concepts provide the basis from which all the remaining dosimetric quantities are defined [1, 2].

4.1.1.2 Exposure

Exposure, X, is defined as the total charge which is liberated per unit mass in air by ionizing radiation [1, 2]. Its unit is the Roentgen, R, where one Roentgen is 2.58×10^{-4} C kg^{-1}. Exposure is related to energy fluence, Ψ, by the following equation:

$$X = \Psi \cdot \left(\frac{\mu_{\mathrm{en}}}{\rho}\right)_{\mathrm{air}} \cdot \frac{e}{W_{\mathrm{air}}}, \tag{4.1}$$

where $(\mu_{\mathrm{en}}/\rho)_{\mathrm{air}}$ is the mass energy absorption coefficient of air which defines the fraction of the energy of a beam of particles which is absorbed per unit mass of air at a particular beam energy. $W_{\mathrm{air}} = 33.97$ eV is the energy required to produce an ion pair in air and e is the charge of the electron.

4.1.1.3 Kerma

Kerma, K, is defined as the kinetic energy released per unit mass of material by a specific combination of an incident radiation field and an absorbing material. Kerma is related to energy fluence, Ψ, by the following equation:

$$K = \Psi \cdot \frac{\mu_{\mathrm{tr}}}{\rho}, \tag{4.2}$$

where μ_{tr}/ρ is the mass energy transfer coefficient, which defines the fraction of the incident radiant energy which is released as kinetic energy in charged particles in a given volume of material. More strictly, the Kerma is the amount of energy liberated through ionization in the volume encompassed by a unit mass of an absorbing material [1, 2]. This energy is transferred through ionization of the material at the atomic level and is ultimately manifested in the kinetic energy of ionization electrons in the material. As may be seen from Fig. 4.1, kinetically charged particles or photons, created in collisions between incident ionizing particles and the material, may not deposit their energy in the mass volume. Therefore, Kerma is a measure of the amount of ionizing energy offered for absorption in the material, which in this case is the initial kinetic energy of the primary electron.

4.1.1.4 Energy Imparted

The energy imparted, ϵ, by ionizing radiation to the matter in a volume is given by the following equation [3]:

$$\varepsilon = \sum R - \sum R_{\mathrm{out}} + \sum Q, \tag{4.3}$$

where the first and second terms in the equation, respectively, describe the sums of all the radiant energies of all ionizing radiations entering and leaving a particular volume. The third term denotes the sum of all the mass energies of all the particles produced during the interactions of the ionizing radiations with the matter to which it is imparting energy. In diagnostic radiology, the photon energy is not sufficient to instigate pair production (production of positrons and electrons in the vicinity of a strongly positive nucleus), and therefore particle production does not occur. Thus, for diagnostic energies, the third term on the right-hand side of Eq. (4.3) is zero [1, 4]. Energy Imparted is quoted in the units of energy, the Joule, J.

A distinction must be made between the term "Energy Imparted" and the term "Imparted Energy." Energy Imparted is the term for a gross quantity or concept, where the energy is imparted to matter that has a macroscopic size. Imparted Energy is the energy that is imparted in a single interaction between any particle and the matter in a given volume. The Imparted Energy, dϵ, in an interaction is a stochastic quantity, and is difficult to measure, and impossible to infer with any great accuracy [3, 5]. Thus, the Energy Imparted is also

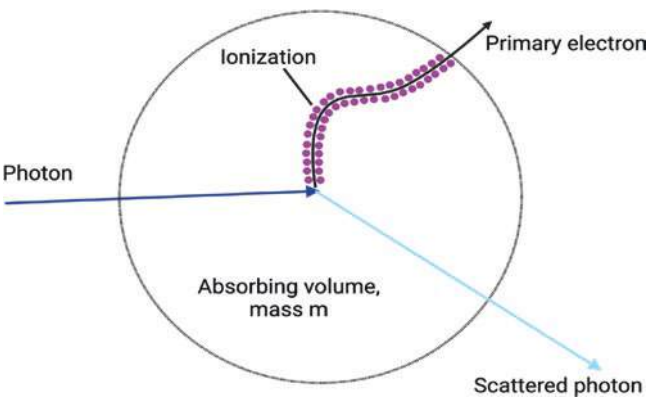

Fig. 4.1 Kerma in relation to interactions between ionizing photons and matter in a unit mass volume

a stochastic quantity. However, repeated measurements can establish mean energy imparted, $\bar{\varepsilon}$, which is a non-stochastic quantity (Box 4.1).

Box 4.1 Dosimetry Quantities: Kerma and Exposure

- Kerma, K, is defined as the kinetic energy released per unit mass of material by a specific radiation field and it is related to energy fluence, ψ
- Exposure, X, is defined as the total charge which is liberated per unit mass in air by ionizing radiation. Its unit is the Roentgen, R.

4.1.2 Absorbed Dose

The absorbed dose (sometimes referred to simply as "dose") is the radiant ionizing energy absorbed per unit mass of absorbing material. It is therefore defined as:

$$D = \frac{\bar{\varepsilon}}{m}. \tag{4.4}$$

The quantity ε/m is sometimes referred to as the specific energy. It is stochastic in the same way that the imparted energy in a given interaction is stochastic, but with repeated measurements, and on macroscopic scales involving many single particle interactions, it becomes a measurable quantity ([1], p. 86; [2, 4]). The unit of Absorbed dose is the Gray, Gy, which is equal to J kg^{-1}.

The Kerma in Eq. (4.2) may be split into two parts depending on the ways in which the energy of the photon is lost through interactions with the material [1]. Photons may either release their energy through collision interactions in which excitation and ionization of the stopping material occur or through radiative processes in which their energy is radiated through the release of photons. Thus, the Kerma can be expressed as:

$$K = K_c + K_r, \tag{4.5}$$

where K_c is the portion transferred through collisions, and K_r is the portion transferred through radiative interactions [1]. Radiative interactions generally occur in situations in which charged particles are incident on a material [1]. In the case of diagnostic radiology, Kerma is released through collision interactions, with Collision Kerma therefore given by:

$$K = \Psi \cdot \frac{\mu_{en}}{\rho}. \tag{4.6}$$

In diagnostic radiology, a simple relationship between Kerma and Absorbed dose may be derived. When charged particle equilibrium (CPE) exists in a medium, the number of charged particles leaving a unit mass volume is replaced by an equal number entering from other mass volumes. In such a situation, which occurs at the photon energies in diagnostic radiology, all Kerma is absorbed in the unit mass volume. It has been shown by Attix, that for a medium of uniform density and atomic composition, such a situation does indeed exist for a field of X-ray photons and a uniformly irradiated medium [1, 2]. In this case the Absorbed dose, D, and Collision Kerma, K_c, are equal, such that

$$D = K_c = \Psi \cdot \frac{\mu_{tr}}{\rho}. \tag{4.7}$$

Box 4.2 Dosimetry Quantities: Absorbed Dose

- The Absorbed Dose is the energy absorbed per unit mass of material. The unit of Absorbed Dose is the Gray, Gy, which is equal to J kg^{-1}

4.1.3 Radiation Detectors

In general, radiation detectors operate by providing the means to measure the energy deposited over time in the detector absorbing material from exposure to a source of ionizing radiation. This is typically measured as the quantity of charge, Q, over time elicited from an absorbing medium forming the main component of the detecting element. An ideal radiation detector is one that gives spatial resolution, temporal resolution, information regarding the energy of the particle, and information regarding the identity of the radiation. In reality, single detectors of this type are difficult to construct such that practical detectors that are used in the field have a focused range of capabilities which should be taken into consideration when a detector is chosen for a particular application [6, 7].

4.1.3.1 Ionization Chambers

Ionization chambers are designed to measure the number and/or total energy deposited as a result of the ionizations produced when a charged particle or ionizing photon traverses the detector medium. Therefore, they are not suitable for the detection or analysis of neutral particles. Ionization detectors consist of an isolated detection medium, generally a gas such as air that can be easily ionized (i.e., has a low ionization potential), which is placed between two oppositely charged electrodes (Fig. 4.2). The medium should be chosen such that it does not respond adversely to ionization such that its characteristics will not change with use.

The charged particle will ionize the detector medium along its path and these ions will then be accelerated towards the detector electrodes. In general, a high electric field is

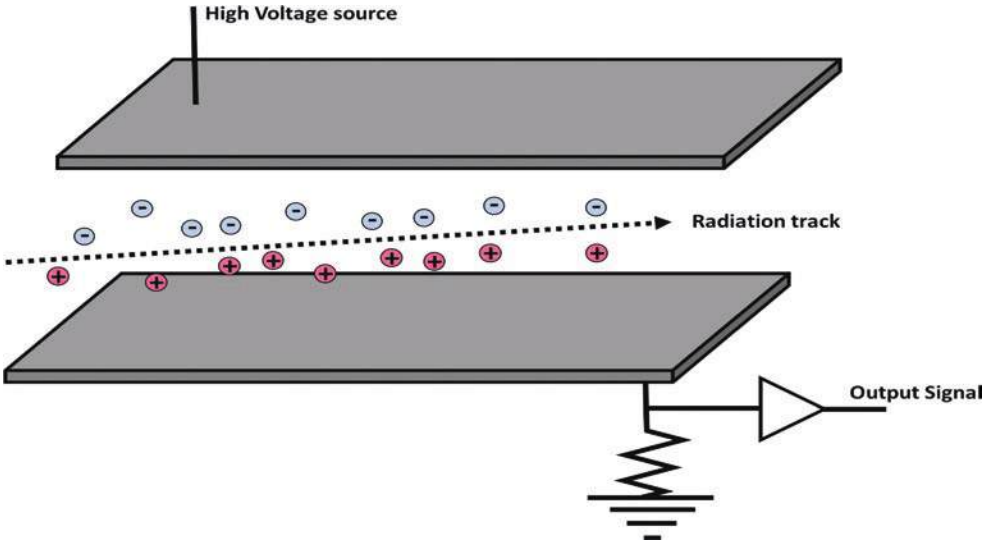

Fig. 4.2 Schematic of the basic elements of an ionization detector

applied between the electrodes to prevent the recombination of ions produced by the traversal of the charged particle. As the charged particle traverses the sensitive region of the detector (i.e., the gas) it produces multiple electron-ion pairs, which begin to drift along the electric field lines and reach the plates of the detector. These ions may produce further ionization of the neutral gas atoms via further collision, ultimately producing a small current that induces a voltage drop across the resistor. These chambers typically generate very low measurement currents per ionizing particle, and therefore require low noise amplifiers to improve their operating performance.

The amplified output signal from the detector may be used to trigger a counting mechanism to measure the number of incident charged particles or ionizing photons (i.e., exposure) or its pulse height may be analyzed to determine the total energy within the beam (i.e., dose). The amount of ionization that is detected is dependent on the nature of the gas used in the detector, the level of the applied electrical field, and the characteristics of the plates used in the detector. How the chambers operate, i.e., as a device for the measurement of absolute energy deposition or number of charged particle incident on the detector, depends on the HV level applied to the detector, as depicted in Fig. 4.3 [7].

When the applied voltage is small, the electrons and ions can recombine soon after they are produced and only a small fraction of the ions reach their respective plates in the detector (Fig. 4.3). As the applied voltage between the plates is increased, a region is reached where the output pulse reflects the amount of ionization seen in the chamber (Ionization region). When the voltage is increased still further, the electrons and positive ions released by the initial ionization can themselves cause further ionizations in the medium and thus amplify the ionization pulse (Proportional region). Increasing the applied field still further (Geiger region) creates an avalanche effect and a highly amplified output signal. Any further increases in the applied voltage lead to a continuous discharge of the detector [6].

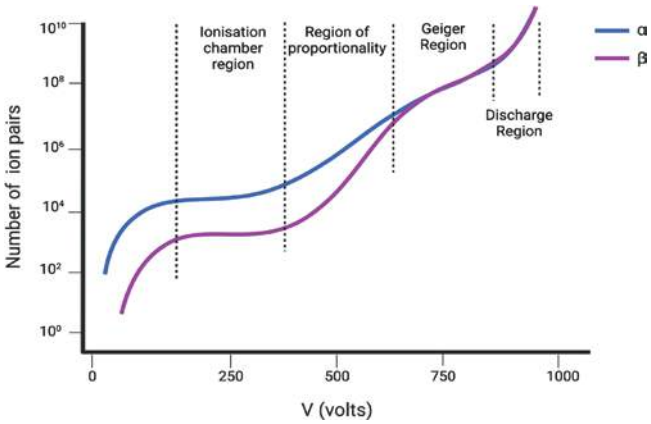

Fig. 4.3 Signal response to ionization as a function of the applied voltage for heavily ionizing (top curve) and weakly ionizing particles (lower curve). In the Geiger region, the output does neither depend on the voltage nor on the amount of deposited energy or initial ionization. [Adapted from Fig. 4.12 Martin and Shaw (2006). Copyright (2006), Wiley Publishers]

It is possible to determine the typical output current that will be generated by an ionization chamber in the presence of a source of known activity. Consider the case of an in-air ionization chamber (where air has an ionization potential of 30 eV) which is exposed to alpha particles ($E_\alpha = 5.486$ MeV) from a 10 MBq Am-241 source. The total number of ionizations produced by a single Am-241 α-particle will be the ratio of the energy of the alpha particle to the ionization potential of air:

$$n = \frac{5.486 \times 10^6}{30} = 1.829 \times 10^5.$$

In this case, the total number of ionizations produced will be the product of the activity of the source and the number of ionizations produced by a single alpha particle, or $N = 1.829 \times 10^{12}$ ionizations, which are observed in a single second (as the unit of activity, the Bq is s^{-1} in SI units). The final step is then to compute the product of the total number of ionizations with the charge on the electron such that the total current observed will be:

$$I = N \cdot e = \left(1.829 \times 10^{12}\right)\left(1.602 \times 10^{-19}\right)$$

$$2.93 \times 10^{-7} A = 29.3 \mu A.$$

Frequently, ionization chambers are open to the air to allow for changes in ambient pressure which could collapse or expand a sealed chamber, damaging the thin chamber walls. As a consequence, chamber outputs must be adjusted for changes in ambient temperature, T, and pressure, P, from those at which the chamber was calibrated, T_n and P_n, respectively. In practice, we can multiply the chamber output by the following correction factor to adjust for ambient conditions (where all temperatures are expressed in Kelvin and pressures in Pascals [6]):

$$k_{T,P} = \frac{T}{T_n} \cdot \frac{P_n}{P}. \tag{4.8}$$

4.1.3.2 Proportional Counters

While the ionization chamber provides a device for the measurement of absolute energy deposition, it does not provide information on directionality. Proportional counters are ionization chambers that may be used for both measuring absolute energy deposition (through a measurement of the pulse height) in addition to giving directional information on the path of charged particle (through the output of a given anode wire, each of which is independently amplified).

Multi-wire proportional chambers (MWPCs) such as those shown in Fig. 4.4 are used in high-energy particle physics experiments as a means of tracking the path of charged particles. Anode wires (typically with a ~2 mm separation) are positioned between the cathode plates of the chamber (which have a typical separation of 1 mm) and the construct is sandwiched between thin mylar windows or some other superstructure, with an operating gas infused into the region between the plates. In practice, several individual chambers may then be joined together to provide fine detail on the direction of passage of individual charged particle, where pulses will be produced on the anode electrodes closest to the path of the charged particle through the detector as a result of ionization of the gas in the region closest to each anode. MWPCs can be used to infer further information on the momentum of beams of charged particles via the degree of their deflection in a magnetic field (which is typically how they have been used in collider experiments such as the LHC at CERN [6]).

4.1.3.3 Scintillators and Photomultiplier Tubes

Scintillators are materials that react to the passage of a charged particle by the emission of a very small flux of photons of light. Charged particles may excite electrons within atoms of the scintillating material to a higher energy state; these atoms then emit photons as they de-excite to their ground state. Scintillators can be developed from organic (e.g., naphthalene or anthracene) or inorganic (including sodium iodide or cesium iodide) materials and have applications as the first detection element with gamma cameras used in nuclear medicine.

Scintillating materials typically need to be chosen to detect photons of a specific wavelength and may often be doped to achieve specific wavelength sensitivity. They are generally coupled to photomultiplier tubes (PMT) to amplify the intensity of the weak photon signal output from the scintillator, either for photon counting or imaging applications.

In Fig. 4.5, a schematic of a photomultiplier tube is shown. An incoming charged particle or ionizing photon impacts the scintillator, which emits a photon flux towards a photocathode material (constructed typically with a negatively charged plate covered by a photosensitive material such as gallium–arsenide or indium–gallium–arsenide).

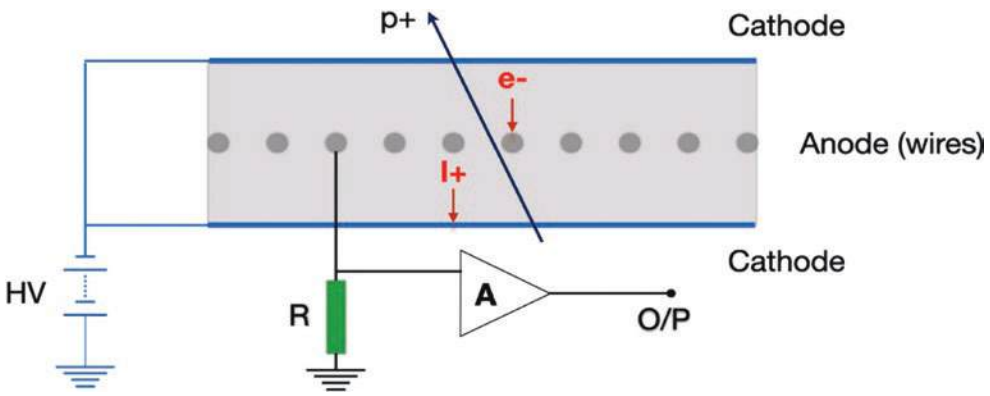

Fig. 4.4 Schematic of a multi-wire proportional chamber [6, 7]

Here, the photon flux is converted to an electron flux as they enter the inner (evacuated) environment of the PMT tube. These electrons are accelerated towards the first of several dynodes by the high-voltage field between the photocathode and the anode. When each electron collides with a dynode, it causes the emission of several electrons (typically 5–10), which are then accelerated towards subsequent dynode and amplify the electron flux through collision and reemission. At the detector anode, a significant and measurable electric current is then generated as a result of the acquisition of a single photon. Apart from a small degree of signal fluctuation, the current seen at the anode is linearly proportional to the photon flux seen at the photocathode [6, 7].

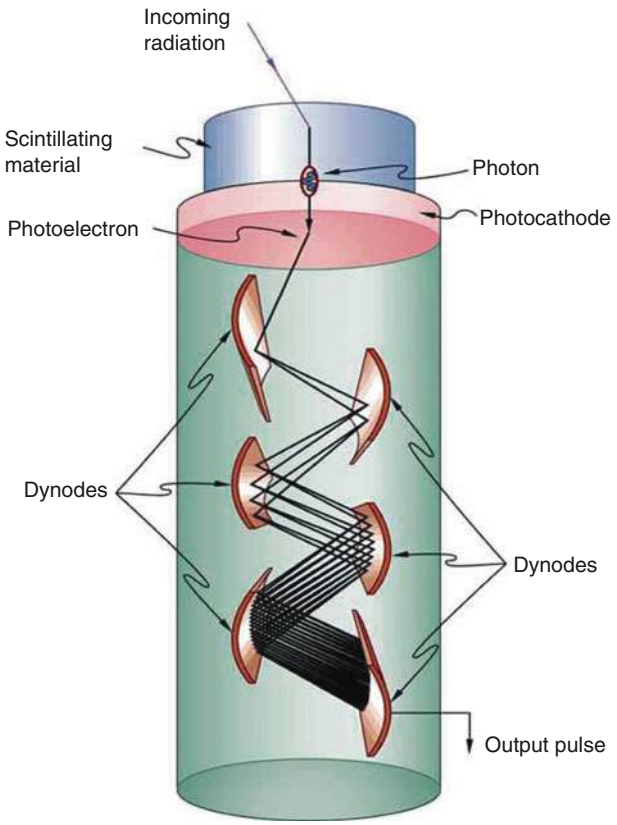

Fig. 4.5 Schematic diagram of a photomultiplier tube (PMT) (courtesy of Physics Libretexts, Fig. 31.2.3)

4.1.3.4 Semiconductor Detectors

Semiconductor detectors based upon p–n junction diodes offer a practical and robust option for detector construction, operating in a similar manner to an ionization chamber [6, 7]. Here a p–n junction is constructed through the joining together of a piece of p-type semiconductor (such as silicon or germanium) to a piece of n-type silicon. P-type material is doped with atoms of a material with one vacant outer-electron state, such as boron, B, while N-type material is doped with atoms of a material with an extra "free" electron in its outermost energy level, such as antimony, Sb. At the junction between the two materials a "depletion layer" is formed where electrons from the N-type material migrate to the P-type material to fill vacant energy states or "holes" leaving behind holes in the N-type material surrounding the junction. This creates a region where electrons and holes are depleted around the junction and creates a barrier to conduction. For the purposes of photon or particle detection, the depletion region is the sensitive portion of the electronic detector. When operated in reverse bias (Fig. 4.6a, b), this depletion region is larger and these detectors are typically operated in reverse bias with a voltage of 100 V to increase the depletion layer and therefore the sensitive region of the detector [6, 7].

When the sensitive element of the detector is exposed to a charged particle or ionizing photon, this causes electrons within the depletion layer to be promoted from the valence band to the conduction band (Fig. 4.7), and their conduction through the junction towards the positive terminal of the

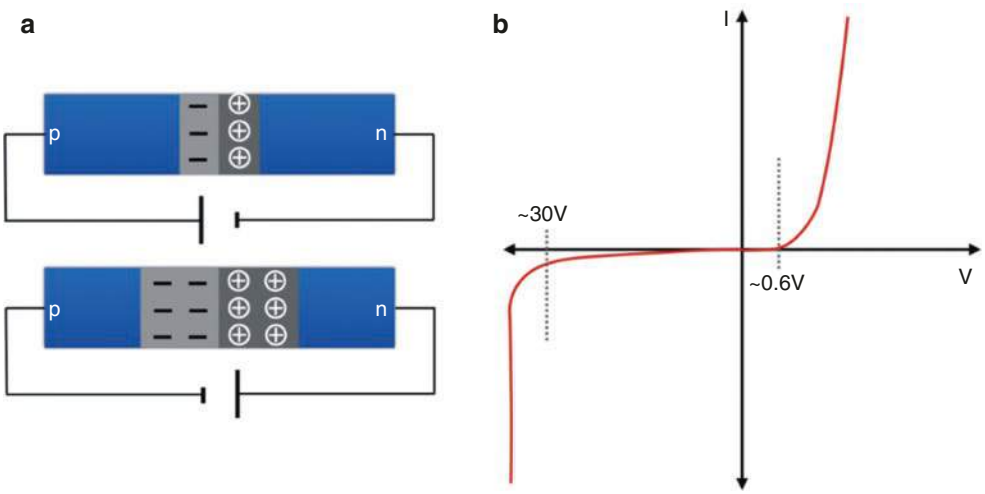

Fig. 4.6 (**a**) Schematic of a p–n junction diode operated in forward and reverse bias. (**b**) Operating characteristics of the diode in forward and reverse bias

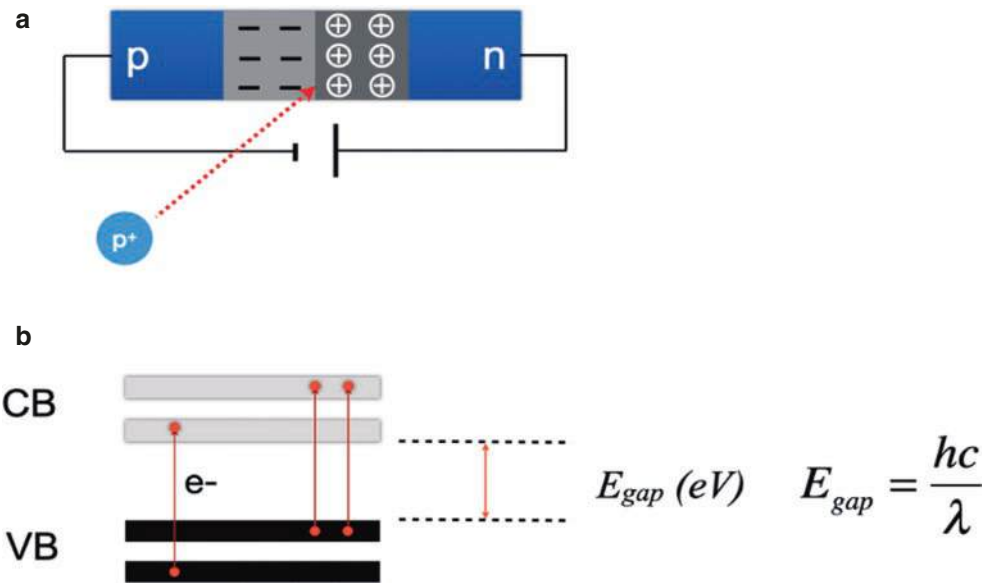

Fig. 4.7 Operation of a semiconductor particle detector (**a**) where an incident proton causes the promotion of one or more electrons from the valence to the conduction band within the detector (**b**)

detector. Here, the valence band is equivalent to the energy level of the outermost electron, while the conduction band is the energy level of the next vacant energy state above the valence band. A current is produced which is proportional to the energy loss by the charged particle or photon within the depletion layer [6, 7]

The creation of an electron–hole pair in a silicon or germanium semiconductor requires as little as ~3 eV in comparison to the 30 eV required for in-air ionization chambers. Detectors can be constructed and tuned to radiation of a specific wavelength, λ, by altering the energy difference between the valence and conduction bands, or the band gap, E_{gap}, as shown in Fig. 4.7 and Table 4.1.

Semiconducting materials, when incorporated in radiation detectors can therefore produce a large signal in response to irradiation with a small photon flux. The detectors can be constructed very thinly (as little as 200–300 μm) for the detection of ionized particles, or larger for stopping of photons. Their performance is approximately linear if an electric field is applied that prevents the recombination of the electrons and holes formed by the radiation [6, 7].

Table 4.1 Typical semiconducting materials used for radiation detection, including bandgaps, wavelength, and electro magnetic (EM) band sensitivity

Material	E_{gap} (eV)	λ (nm)	Band
C (diamond)	5.65	220	UV
GaN	3.45	360	UV
AlGaN	3.45–5.64	360–260	UV
CdZnTe	1.4–2.12	870–580	Visible
Si	1.12	1100	Visible
GaAs	1.42	875	Visible
Ge	0.66	1800	NIR
PtSi	0.41–0.25	3000–5000	IR
HgCdTe	0.41–0.25 or 0.16–0.10	3000–5000 or 8000–12,000	IR
HgCd	0.7–0.1	1700–12,500	NIR-FIR

4.1.3.5 Cerenkov Detectors

The phenomenon of Cerenkov radiation was first observed and described by Pavel Cerenkov in 1934 and characterized by Franck and Tamm in 1937. This work resulted in all three being given the Nobel Prize in physics in 1958.

To understand the operation of Cerenkov detectors we must first describe the effect itself. Suppose that we have a charged particle traveling at a relatively low velocity though a static medium. As the particle travels slowly relative to the speed at which the ions/molecules of the material can orient and reorient themselves as it passes, the ions/molecules will orient themselves such that the part of the ion/molecule that is charged opposite to the charge of the ionizing projectile would be in the direction of the particle (Fig. 4.8a). The molecules are displaced in an isotropic conformation relative to the position and direction of movement of the charged particle, and therefore there is no overall change in the energy of the medium locally [6, 7].

However, in instances where the velocity of the particle, $v \sim c/n$ or $v > c/n$, the molecules of the medium that are displaced by the passage of the charged particle are generally anisotropic relative to the position and diNurUhr (Fig. 4.8b). By Huygens principle of wavelets, each of the reoriented molecules of the medium can reradiate the energy delivered to them and do so as point wavelet sources. These sources will be coherent along a direction as shown in Fig. 4.8c. If ϑ is the angle at which the point sources reradiate, then it may be shown that

$$\cos\theta = \frac{1}{\beta n}, \tag{4.9}$$

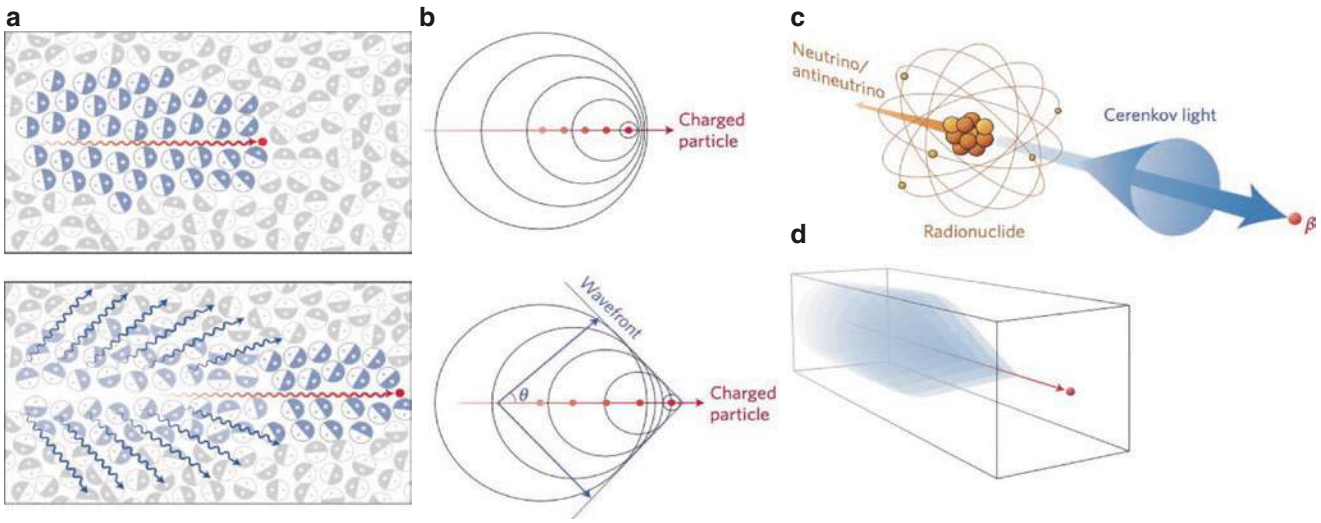

Fig. 4.8 (**a**) Passage of a charged particle through a medium of refractive index n at velocities that polarize the medium. (**b**) The generation of coherent light waves via the Cerenkov effect. (**c**) The formation of a cone of Cerenkov light along the path of the charged particle through a medium with positive and (**d**) negative refractive index. [Taken from Shaffer et al., Nature Nanotechnology, 12, 106–117 (2017). Copyright Springer Nature]

where n is the refractive index of the medium and $\beta = v/c$, where v is the velocity of the particle and c is the speed of light.

It is therefore possible to discriminate the identity of high energy charged particles purely based on the angle of Cerenkov emission or the threshold value of n at which Cerenkov emission is observed [6, 7]. In particle physics, experiments materials of various refractive indices are typically used to provide several potential Cerenkov thresholds for the detection of a variety of radiation types. The weak Cerenkov photons can be detected using PMTs or electronic photodetectors. Cerenkov photons are also observable as a result of the passage of charged particles through human tissue and Cerenkov imaging has seen a recent application for in vivo dosimetry in radiotherapy [8].

4.1.3.6 Calorimeters

Calorimeters allow the estimation of the total energy of a high-energy charged particle or ionizing photon through absorption of its total energy, via successive ionization of the material in the detector in a process that is termed a particle shower (Fig. 4.9), in a detector that is capable of absorbing all of the particles incident radiation. These devices may be ionization chambers as described earlier or semiconductor detectors, or a combination of the two. Depending on the nature and identity of the incident particle, it can create ionizing photons through bremsstrahlung or can produce further "hard" ionizing particles that may not be stopped easily in detectors with unsuitable absorbing characteristics, and therefore a single detector type will not achieve the experimental objectives (Box 4.3).

Box 4.3 Radiation Detectors

- Radiation detectors measure the energy deposited over time in the detector-absorbing material
- An ideal radiation detector provides spatial resolution, temporal resolution, information regarding the energy of the particle, and information regarding the identity of the radiation. No single detector can offer these simultaneously
- Ionization chambers are common dosimeters that measure the ionizations produced when a charged particle or ionizing photon traverses the detector medium (generally a gas, requiring temperature and pressure corrections). An electric field is applied between the electrodes to prevent the recombination of ions produced.
- Proportional counters are ionization chambers that also provide directional information on the path of charged particles
- Scintillator materials are also used as dosimeters by relating the flux of photons emitted to the energy deposited. They are generally coupled to photomultiplier tubes (PMT) to amplify the intensity of the photon signal
- Semiconductor detectors measure the number of charge carriers produced by the radiation in the detector material. Semiconductor materials are used due to the small energy required to produce electron-hole pairs

- Cerenkov detectors record light produced by charged particles traveling through materials at a velocity greater than that at which light can travel through the material
- Calorimeters quantify the absolute dose absorbed by measuring the increase in temperature produced by radiation

4.1.4 Monte Carlo Methods

The Monte Carlo (MC) method is a numerical calculation method based on random draws. A succession of draws is carried out in order to sample the random variables of the treated problem to deduce a value of interest. Repeated several times, this procedure allows to obtain a distribution of the values of interest and thus an estimation of their mean and their associated confidence interval. However, the number of samples must be sufficiently large for the empirical mean of the results to be an unbiased estimator of the expectation of the quantity of interest and its distribution as predicted by the central-limit theorem. In this process, the quality of the random number generator is essential. However, only pseudo-random numbers (having a period) can be generated and each Monte Carlo calculation code uses a different mathematical algorithm for that purpose.

The Monte Carlo method is currently used in many fields of physics to model the interactions of particles in a medium. In particular, it is used in dosimetry to estimate the energy loss of the particles in the medium and thus the absorbed dose.

To simulate the course of the particles, MC codes use the notion of cross-sections expressed in barn (b) (1 barn = 10^{-22} cm^2). This cross-section is a physical quantity representing the probability of collision between an incident particle and a target, as it is proportional to the ratio between the interaction rate (T) and the incoming particle fluence (φ):

$$T = \sigma\phi N_{\text{target}} = \sigma\phi s_{\text{target}} S, \tag{4.10}$$

with N_{target} the number of target particles in the target volume, corresponding to the surface S of the beam intercepting the target and s_{target} the number of target particles per surface unit.

Therefore, we can calculate the probability p for a particle to interact with the target in the following way:

$$p = \frac{T}{\phi S} = \sigma s_{\text{target}} = \sigma N_A \left(\rho \cdot d\right) / A. \tag{4.11}$$

With N_A the Avogadro's constant, ρ the target medium density, d the target thickness, and A the atomic mass of the target medium. Sigma?

We see that the probability of interaction depends directly on the quantity $(\rho \cdot d)$, which has the unit of g cm^{-2}. Moreover, we see the unit of σ: p appear without dimension, σ has the dimensions of a surface. One can imagine σ as a geometrical surface: a particle striking the target in this area would interact, while outside this area it would cross the target without diffusion (Fig. 4.10).

From this concept of interaction cross-section, it is possible to define the mean free path (λ) of a particle by means of the equation:

$$\lambda = \frac{1}{\sigma N_{\text{target}}}. \tag{4.12}$$

This mean free path corresponds to the average value of a random variable representing the path traveled by a particle between two interactions (l). The probability density of this

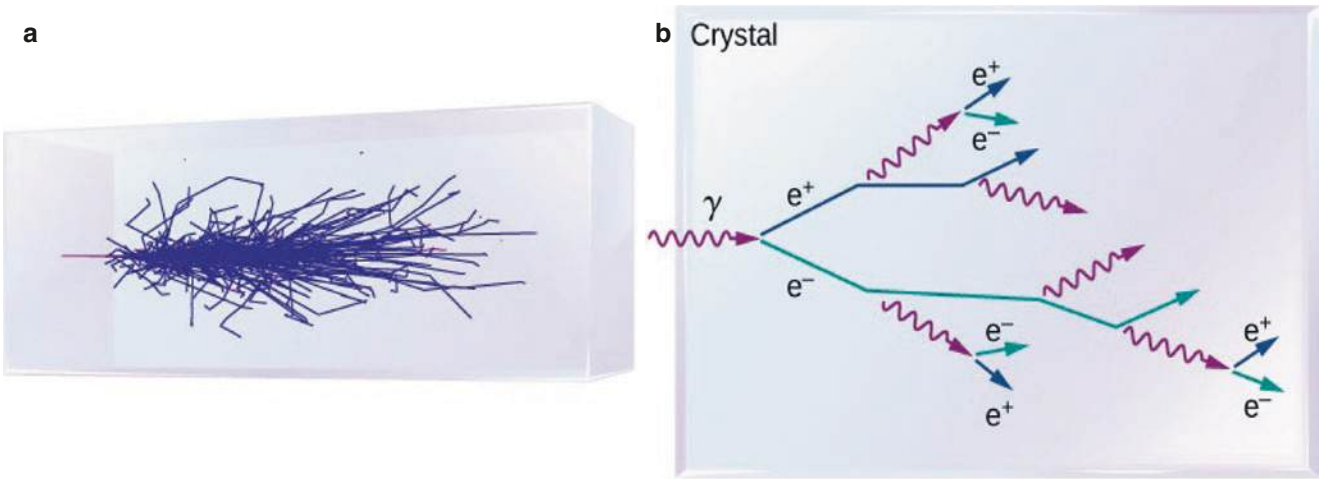

Fig. 4.9 (**a**) A particle shower within a calorimeter; (**b**) a particle shower caused by the incidence of a photon on a calorimeter

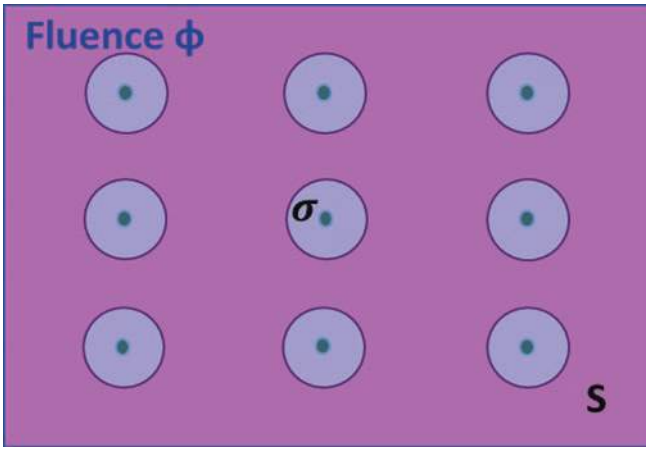

Fig. 4.10 Schematic representation of the cross-section for a target with $N_{target} = 9$ and an irradiated surface S

random variable is given by: $p(l) = \frac{1}{\lambda} e^{-l/\lambda}$. This probability density allows to sample the distance traveled by a particle between two interactions using a random variable ξ_0 uniformly distributed between 0 and 1 as follows $l = -\lambda \ln \xi_0$.

Cross-sections used in the MC codes are obtained either experimentally or are calculated from theoretical diffusion models and then used to determine the probability distributions of the random variables related to a trajectory as mean free path but also the type of interaction or the energy loss.

A key point of these MC calculations is related to the simulation of the electron (and positron) interactions. Indeed, these particles lose a very small part of their energy at each interaction they undergo. Thus, they generate a very large number of events before being finally absorbed into the medium. The detailed simulation of this cascade of interactions and of these weak energy deposits is particularly slow. Thus, most Monte Carlo codes apply simplifying theories called "condensed histories" or "multiple scattering" that summarize a certain number of interactions in a single step, allowing to reduce the simulation time. The compromise between the detail of the simulation and the speed of the calculation conditions the performance of the calculation code. Among the most used MC codes in dosimetry, we can highlight PENELOPE « Penetration and ENErgy LOss of Positrons and Electrons, EGSnrc « Electron Gamma Shower », MCNP6 and MCNPX « Monte-Carlo N-Particle eXtended », or Geant4 « GEometry And Tracking » [9–13].

Thanks to their capacity to include a large part of the physical processes involved in radiation–matter interactions and the possibility of taking into account all the different components of the experimental geometry of the problems, MC codes have clear advantages since they can provide information on the values of certain quantities that cannot be determined experimentally.

In radiotherapy, it is required to deliver a dose to the tumor with an uncertainty equal to or less than 5% [14]. Prescribed dose metrology involves the determination of quantities characterizing the transfer and absorption of energy in the irradiated media. In principle, Monte Carlo simulations allow the dose calculation with the required accuracy using phantoms or even patient's voxelized images and thus provide information on dose distribution in the organ volume. However, to do this it is necessary to have quite exact knowledge of the beam characteristics, which means the need for detailed consideration of each accelerator including head shielding and structural components, which is very time-consuming and often submitted to industrial secret. Therefore, up to now, Monte Carlo codes have been mainly used to calculate the correction factors, often close to unity, to be applied to the experimental values obtained at the hospital during this metrological control.

Nevertheless, The Monte Carlo technique is increasingly used for clinical treatment planning by implementing MC-based algorithms that are used in situations where conventional analytical methods used by the Treatment Planning Systems (TPS) of the machines are not enough. To decrease the computation time, most implementations for radiotherapy divide the calculation into two steps. The first one consists in simulating the head of the treatment machine. This part being fixed and independent of the ballistics associated with the treatment of patients, a phase space can be recorded at the output of the treatment head and be reused. The second step consists in tracking the particles previously recorded in the phase space in the specific geometry of a patient for a specific treatment. Both parts must be, of course, experimentally verified by comparisons with percentage depth dose curves (PDD) and absorbed dose profiles at various depths in water or with measurements in situations where electronic equilibrium is not respected, for example, at the interfaces of materials of different densities (Box 4.4).

Box 4.4 Monte Carlo Simulation Method

- The Monte Carlo (MC) method is a numerical calculation method used to estimate the dose deposited through simulation of the stochastic events through which radiation deposits energy

4.2 Radiation Microdosimetry

Microdosimetry was first introduced by H.H. Rossi in 1955 and is a fundamental and evolving research field in experimental radiation science [15, 16]. It studies the interaction

between radiation and matter in micrometric volumes of cell-like dimensions taking into account the stochastic nature of the energy deposition process.

4.2.1 Definition, Concepts, and Units

The interaction between radiation and matter is a stochastic process that manifests itself as energy deposition, δ-electron production, or nuclear reactions. The latter produce charged particles, called secondaries, which in turn interact with surrounding matter, releasing energy, as δ-electrons do. The fundamental quantity in microdosimetry is the lineal energy, y, which aims to quantify the individual energy deposition events. Energy deposition is a stochastic quantity defined as the energy deposited at the point of interaction:

$$\varepsilon_i = T_{\text{in}} - T_{\text{out}} + Q_{\Delta m}, \tag{4.13}$$

where T_{in} is the energy of the incident ionizing particle (exclusive of rest mass), T_{out} is the sum of the energies of all ionizing particles leaving the interaction site (exclusive of rest mass), and $Q_{\Delta\text{m}}$ is the change of rest mass energy of the atom and all particles involved in the interaction. ε_{i} is usually expressed in eV. The lineal energy, y, is therefore defined by the ICRU report 36 ([17], p. 36) as the quotient of ε_{tot} by l, where ε_{tot} is the total energy imparted to a volume of matter by a single energy deposition event and l is the mean chord length in that volume:

$$y = \varepsilon_{\text{tot}} / l. \tag{4.14}$$

The lineal energy is usually expressed in keV/μm. A single energy deposition event denotes the energy imparted by correlated charged particles. Due to the stochastic nature of radiation interaction, each particle traversal gives rise to a different lineal energy value thus producing a probability distribution function. Such probability distribution functions fully characterize the irradiation at a given point. The individual energy deposition events (opportunely corrected for the detector charge collection efficiency and converted into energy to tissue equivalent material) are collected in a form of spectrum [$f(\varepsilon)$ vs ε] where $f(\varepsilon)$ is the probability of an energy deposition event ε. From these energy spectra, the lineal energy spectra [$f(y)$ vs y; with y = lineal energy] can be calculated by dividing the energy events by the average chord length of the detector, which is the average distance that the particle will traverse in the detector. In the case of a spherical detector, this can be demonstrated to be 2/3 of the diameter, while for thin plate detectors in a unidirectional particle beam, this can be approximated to the detector thickness [18]. The probability density function $f(y)$, also called lineal energy frequency distribution, is independent of the absorbed dose or dose rate. Its expectation value $\bar{y}_F$ is called frequency mean lineal energy and, being a mean value, is no longer a stochastic quantity.

$$\bar{y}_F = \int_0^\infty y^* f(y)\,\mathrm{d}y. \tag{4.15}$$

As the radiation biological damage is proportional to the dose delivered, it is useful to consider also the lineal energy dose distribution d (y), as it provides the fraction of the total absorbed dose in the interval [y, $y + \delta y$]. The dose-weighted lineal energy distribution $d(y)$ is therefore given by:

$$\mathrm{d}(y) = \frac{y^* f(y)}{\int_0^\infty y^* f(y)\,\mathrm{d}y}. \tag{4.16}$$

By definition, this distribution is normalized and is generally plotted as d (y) vs log (y) to make it easier to appreciate the relative contribution of various energy deposition events (see Fig. 4.11).

Similar to the frequency mean lineal energy $\bar{y}_F$, the dose-weighted mean lineal energy $\bar{y}_D$ can be defined as

$$\overline{y_D} = \int_0^\infty y^* \mathrm{d}(y)\,\mathrm{d}y, \tag{4.17}$$

This quantity provides the average lineal energy value when each energy deposition event is weighted based on its contribution to the total dose.

A crucial parameter for the calculation of the lineal energy is the mean cord length ($\bar{l}$), as the energy lost by a charged particle traversing a finite volume is proportional to the path traveled (track length) in that volume. The cord length however is itself a random quantity and for microdosimetric calculations, its mean can be estimated through Monte Carlo simulations or, for convex volumes, using the Cauchy formula $\bar{l} = 4\,V/S$ where V is the body volume and S is its surface area.

4.2.2 Technologies and Detectors

The first microdosimeter detector was designed and developed by Rossi in 1955 [16]. It was a spherical proportional counter made of tissue-equivalent plastic walls and filled with low-pressure tissue-equivalent gas (TEPC—Tissue Equivalent Proportional Counter). The low pressure allows to simulate micrometer volumes using a millimeter-size chamber (10–150 mm diameter), which is easier to handle and manufacture. Methane or propane-based gases are typically used at a pressure of ~0.9 kPa to simulate volumes of a few micrometer in diameter. The electrons produced by the traversal of the radiation through the chamber are amplified and collected by an electric field. Every radiation traversal

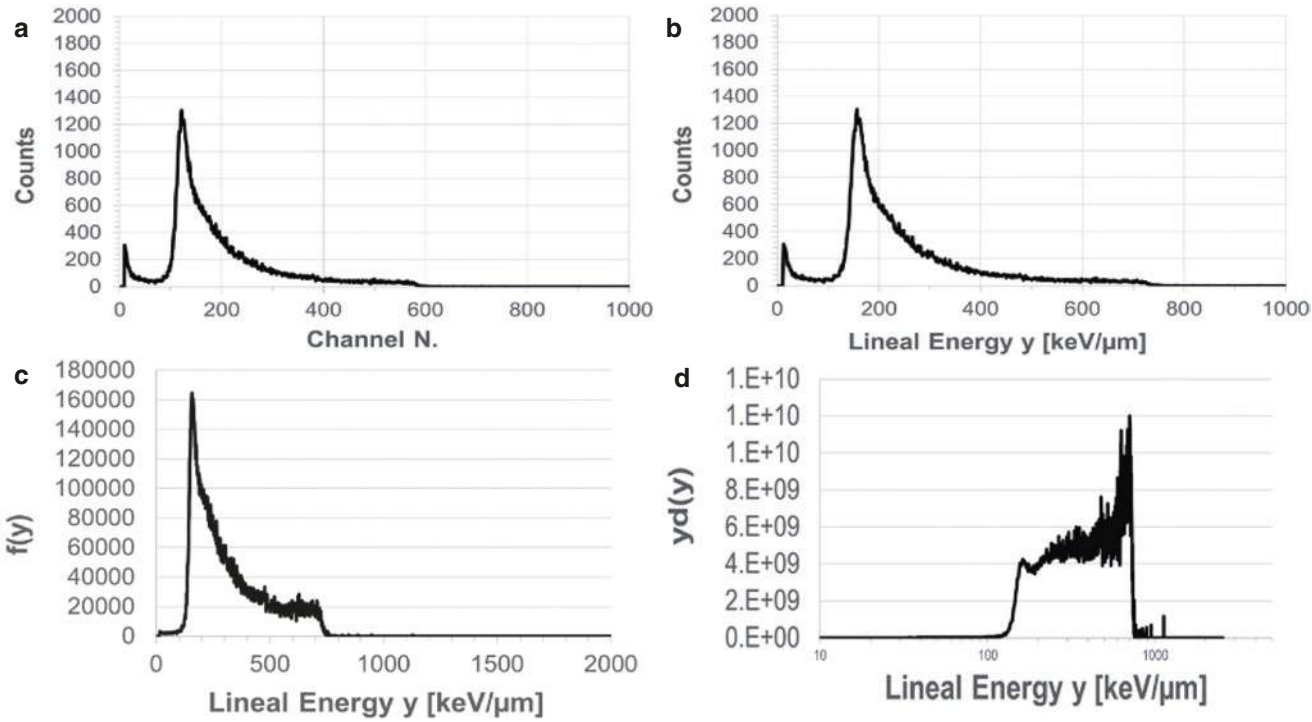

Fig. 4.11 The same microdosimetric spectrum represented through the raw counts per channel acquired (**a**), counts as a function of the lineal energy (y) after a channel calibration (**b**), converted into lineal energy frequency (**c**) and dose (**d**) distributions

generates therefore a small current that gives rise to a pulse later processed by the acquisition electronics. This allows the quantification of the energy deposited in micrometer volumes by individual radiation events. TEPCs are still the most common detector for microdosimetry measurements. Their main limitation is related to the wall-effects, which are events generated by the interaction of the incoming radiation with the walls of the device, and to controlling the electron avalanche process caused by high electric fields, which are required to simulate very small volumes. New devices are addressing these limitations with wall-less TEPC where specially designed electrodes are aligned to generate an electric field within a confined volume and reduce electron avalanches (avalanche confinement TEPCs). The new devices are also less cumbersome than the first TEPC designed by Rossi and can be operated in clinically relevant radiation beams.

More recently, solid-state detectors have been employed as microdosimeters taking advantage of their unique characteristics including compact size, economic development, and low sensitivity to vibrations, which makes them particularly suitable for clinical environment. The working principle is based on the electron-hole pairs produced by the radiation as it crosses the sensitive volume of the semiconductor crystal. The number of electron-hole pairs is proportional to the total energy deposition (ΔE) and the crystal ionization energy (W; average energy required to produce an electron-hole pair) by

$$N_{e-h\_\text{pair}} = \Delta E / W. \tag{4.18}$$

The ionization energy is specific for each crystal and in the order of a few eV for typical semiconductor materials, which is an order of magnitude lower than that required for gas detectors. Furthermore, it is largely independent of the energy of the incoming radiation. Similar to TEPCs, the current generated by the collection of the produced electrons is used to quantify the energy deposition events. As the sensitive volume of the detector can be of a few micrometers, the pulses generated provide a microdosimetric spectrum of the incident radiation. In order to serve as a microdosimeter, solid-state detectors need to have well-defined and micrometer-sized sensitive volumes coupled to an efficient charge collection mechanism, as the electrical signal generated can be very small. A potential drawback of solid-state microdosimeters is their non-tissue equivalence, which generally requires additional conversion calculations provided by Monte Carlo simulations.

Silicon and diamond microdosimeters have been realized with sensitive volumes as low as 1 μm in thickness and a few hundred μm^2 area and collection charges approaching 100%. Their small geometry provides also high-spatial resolution and the possibility to measure full therapeutic beam intensities, as the electronic chain is not saturated by the large number of particles required for clinical use. A main limitation of semiconductor microdosimeters is the electronic noise, as the devices work with little or no electronic gain due to the

small voltage that can be applied to the small-volume semiconductor. This limits the lowest energy events that can be detected. The fixed size of the crystal also implies that different detectors may need to be used to obtain microdosimetric information for different sensitive volumes while gas-based detectors can achieve this by varying the gas-pressure. The advantages and disadvantages of both detector types are confronted in Table 4.2.

4.2.3 Biological Relationship Response

In the framework of radiation biology, either the linear energy transfer LET or the lineal energy can be used to specify the radiation quality. While the LET is frequently used, at least for broad classifications of different radiation qualities (high vs low LET, i.e., densely vs sparsely ionizing radiation), the use of the lineal energy is less common due to the limited experimental data and the complexity in analyzing the microdosimetric spectra. However, the use of LET to determine radiation quality is affected by some intrinsic limitations such as different particles of different mass and energy having the same LET being still characterized by a different energy distribution of the secondary electrons. In general, the microdosimetric spectra provide information that is not captured in the LET and it may be very beneficial for fundamental radiobiological studies aimed at linking biological response to energy deposition events, as well as for radiation protection and clinical work, e.g., predicting treatment efficacy.

Several LET-based RBE models have been developed over the years. The Microdosimetric Kinetic Model (MKM) is a model based on the dual radiation action theory and specifically developed to link microdosimetric measurements to radiobiological effects [19]. The central hypothesis of the dual radiation action theory is that the number of lethal lesions is, through a linear quadratic relationship, proportional to the specific energy deposited in a microscopic site. The specific energy (z) is defined as the ratio between the energy imparted (ε) and the mass of the microscopic volume (m) [17]:

$$z = \varepsilon / m. \tag{4.19}$$

As both the specific energy (z) and the lineal energy (y) measured by microdosimetry are related to a microscopic volume, the two quantities are linked through the microscopic volume mass (m) and mean chord length (l):

$$\overline{z} = l / m \cdot \overline{y}_D = \overline{y}_D / \left(\rho \cdot \pi \cdot r_2^d \right). \tag{4.20}$$

with l, m, ρ, and r_d the mean chord length, the mass, the density, and the radius of the microscopic volume, respectively.

Kase et al. [20] formalized the link between cell survival fraction SF and the microdosimetric measurements:

$$\mathrm{SF} = \exp\left(-\alpha D - \beta D^2\right) = \exp\left(-\left(\alpha_0 + \frac{\beta_0}{\rho \pi r_d^2} y^* \right) D - \beta_0 D^2 \right). \tag{4.21}$$

with

$$y = y_0^2 \int, \tag{4.22}$$

where α_0 and β_0 are the linear quadratic parameters specific for each cell line (usually taken from X-ray measurements), D is the macroscopic dose absorbed by the cell and ρ is the cell density. y_0 and r_d are fixed parameters accounting for the overkill effect observed at high lineal energy values (usually set at y_0 = 150 keV/μm) and for the sensitive critical volume of the specific cell line, respectively. The parameter y^* includes the measured microdosimetric spectrum (f (y)) providing therefore a direct link between radiobiological response and physical measurements. The use of the MKM and microdosimetry is the only approach providing a link between physical and biological measurements, considering that LET values cannot be experimentally determined. Supported by the fast development of technologies that will facilitate microdosimetric measurements, there is renewed interest in this approach. However, the precise estimation of the y_0 and r_d parameters requires further investigation (Box 4.5).

Table 4.2 Comparison of tissue equivalent proportional counters (TEPC) and solid-state microdosimeters

	TEPC	Solid-state microdosimeter
Advantages	Tissue equivalence Easy handling and manufacturing Operation for clinically relevant beams	High-spatial resolution Compact size Economic development Low sensitivity to vibrations Suitable for clinical environment
Disadvantages	Wall-effects High electric fields	No tissue equivalence

Box 4.5 Microdosimetry

- Microdosimetry quantifies individual energy deposition events through the lineal energy
- Microdosimetry is performed through tissue equivalent proportional counters (TEPC) or solid state microdosimeters
- Microdosimetry is able to directly link radiobiological response to physical measurements

4.3 From Track Structure to Early DNA Damage

4.3.1 Introduction

When ionizing radiation (IR) interacts with a biological sample (which is composed of ~70% water in weight and the rest biological molecules), it can either directly hit the biological molecules or the water molecules. In both cases, these interactions can lead to an energy deposition at the interaction point (inelastic scattering) and the production of secondary particles, mostly electrons that can, in turn, also interact with the target. The ionized or excited molecules, particularly those of water, generate radicals (water radiolysis) that also can attack the biological unit molecules or aggregates, leading to subsequent structural damage of these molecules, which could ultimately have consequences on the functioning of the cell and its outcome.

In this section, we will review the current state of knowledge concerning the different stages that lead from the physical interactions between ionizing radiation and biological matter (known as the physical stage) to the formation of damage to biomolecules as schematically depicted in Fig. 4.12. As indicated above, this includes the description of the production of radicals and their chemical interactions with molecules (chemical stage) but also the consideration of the geometrical and chemical structure of the target molecules. In particular, we will look at the effect of these interactions on the DNA contained in the cell nuclei, because it is well established that the DNA is a privileged target with regard to the effects of radiation on cells [21]. This continuous description will reveal differences at each stage level between the various types of radiation that will enable us to categorize them according to their capacity to produce these damages in terms of number and complexity.

Different experimental techniques have been developed and used in recent years to measure this damage, as we will see in Sect. 4.3.3. However, in most cases, these techniques do not allow to have access to the total number of strand breaks or double strand breaks as well as to the base damage or to the complexity of the damage cluster. Thus, the Monte Carlo simulation method has become the "gold standard" for the prediction of these damages. This means however that it is necessary to know, with the least possible uncertainty, all the data allowing the description of these stages to feed the codes. In Sect. 4.3.4, we will detail what these data or parameters are, their current uncertainties, and therefore the current simulation capabilities with the different codes.

4.3.2 Physical Stage (Direct Damage)

Ionizing radiation interacts with the exposed target through a cascade of random interactions with the atoms of the medium. The result concerns as much the interactions of the primary radiations as the slowing down of the secondary radiations emerging from them. During these interactions, radiation can be scattered or absorbed by gradually losing energy. If these absorption processes lead to sufficiently high energy transfers (typically >10 eV in radiobiology), they can lead to the ejection of electrons and modify the electronic layer of atoms and molecules and their chemical properties, which gives them the power to induce effects. Indeed, IR can be categorized as directly and indirectly ionizing depending on whether it is composed of charged or uncharged particles, respectively, but in all cases with enough energy to produce ions in matter.

While ionization is considered the most important physical phenomenon to explain radiation-induced effects, excitation, a phenomenon in which electrons are transferred to higher atomic or molecular levels, is also considered among the possible events to be precursors of the radiation-induced effect. It is assumed that the ratio of energy loss by ionization and excitation is stable between radiations of different natures and energies, and, therefore, that the measurement of ionizations alone is sufficient. This approximation is important for the validity of reference dosimetric and microdosimetric measurement techniques using gas detectors. These

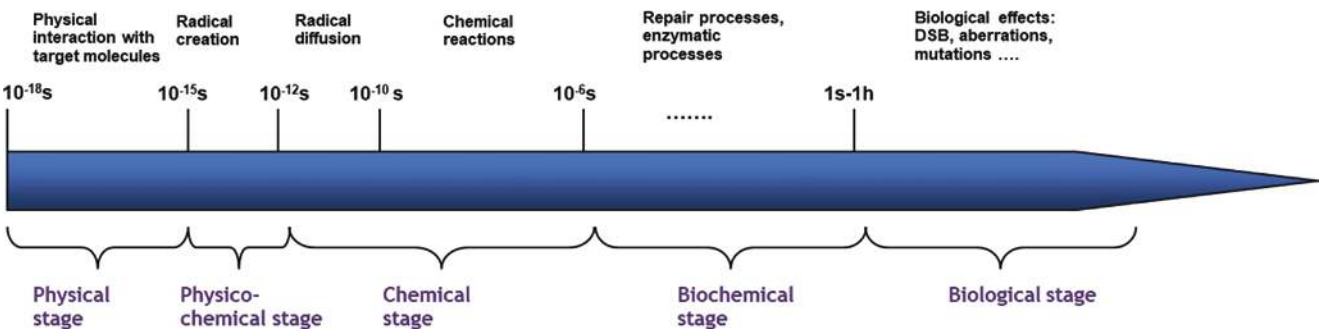

Fig. 4.12 Schematic representation of the different processes leading to the damage produced by irradiation in the cells and their characteristic times

techniques only "see" the ionizations but apply global physical data such as the average ionization energy (W) that accounts for both phenomena. It is generally recognized that the distinction between ionization and excitation is more blurred in condensed states, which are ultimately the ones targeted in dosimetry using other measurement methods than gas meters, and in radiobiology.

From a mechanistic perspective, if one wants to identify which energy deposition will result in damage to the structure of the target biomolecules, this proportionality between the number of ionizations in a volume (however small it may be) and the deposited energy is therefore not detailed enough. Indeed, in this context, it is necessary to "zoom in" on the scale of the target's constituents at the nanometric scale to look at all the energy deposits (or energy transfers) produced by the initial radiation, as well as the secondary particles, notably the electrons. This is the study of the so-called **track structure** of radiation. At this scale, the differences between the spatial distribution of energy deposits defined by the tracks produced by different types of radiation (photons, electrons, energetic ions of different energies, etc.) lead to variations in early damage sufficient to produce a great diversity of later effects at both the cellular and tissue levels.

Thus, for example, in the case of irradiation by high energy ions, we can look at the track they produce as being formed by a "**core**" and a "penumbra" region. The core is formed by the energy deposits of the projectile itself and is almost straight as elastic scattering does not have an important influence on the ion direction at energies under 10 MeV. The **penumbra** region is formed by the energy deposits of secondary electrons produced during ionizations with energies of ~1–100 MeV, interacting with many molecules in the target [22, 23].

However, when the primary particle ionizes water molecules, the main component of biological matter, many of the electrons are produced with low energy [24, 25]. Indeed, the energy of the emitted electrons for a given material is mainly determined by the oscillator-strength distribution of its valence electronic structure. The long-range of Coulomb interactions and the cross section that peaks at ~20–30 eV and decreases to very low values at 100 eV leads to the formation of electrons with energies, in general, less than 100 eV [26]. These low energy electrons (more extensively defined as those ≤10 keV) have a small penetration range (<1 μm) and inelastic mean free path (IMFP) (<10 nm) in typical condensed media [27] like water or DNA components. Therefore, most of the direct damage is produced around the track and, more specifically, at the track ends, where they are produced in high quantity.

In fact, the electrons below ~20 eV seem to be particularly effective because, in addition to participating in the production of direct damage by ionizations or excitations of the constituents of the DNA, they can undergo resonant scattering with molecules, generating reactive radicals and molecular species, which can themselves contribute to DNA breaks [28] and oxidative damage. Experiments have indicated that electrons (or photons) with energies as low as ~10 eV can still induce double strand breaks, possibly through a resonance mechanism [29, 30].

4.3.3 Physicochemical and Chemical Stages (Indirect Effect)

In the previous section, we were interested in the interactions between IR and the target molecule (DNA) and how some of these interactions can cause damage in a direct way. However, IR interacts in the same way with the surrounding water medium and induces local electronic instability. The **physicochemical stage** corresponds to the set of rapid electronic and atomic modifications resulting from the readjustments of the medium in order to return to thermal equilibrium. Thus, water molecules that are in an excited or ionized state can dissociate into new chemical species (radiolysis):

$$H_2O + \text{radiation} \rightarrow H^\circ, OH^\circ, e_{aq}, H_2, H_2O_2, HO^\circ_2, H_3O^+.$$

Among these species, the OH° (hydroxyl) radical is particularly interesting in radiobiology, because it can be the origin of DNA damages that are difficult to repair by the cell. This radical is mainly produced from the radiolysis of pure water following different mechanisms (dissociation directly after an ionization or an excitation of the water molecule).

Moreover, under-excitation electrons (with an energy lower than the last excitation shell of the water molecule, 8.22 eV) will undergo elastic scattering and will continue to lose energy by vibrational and rotational interactions until reaching the energy of the medium, the so-called thermalization energy. This thermalization process is in competition with two processes of electron capture, either by a neutral water molecule ("dissociative attachment") or by an ionized water molecule ("geminal recombination") and is supposed to be completed within a picosecond after the irradiation.

Beyond the picosecond, the newly created radiolytic species are free to diffuse randomly in the medium and to interact with each other, which is the **chemical stage**. Initially localized around the energy deposits of the track, they propagate and distribute more homogeneously in the medium as time evolves. The initial distribution of species depends strongly on the LET of the incident particle. In the case of high-energy electron projectiles (low LET), the initial distribution in the form of clusters will be more strongly marked than in the case of ions, where the LET is more important, and thus the energy depositions are more homogenously located all over the track. It is generally accepted that beyond

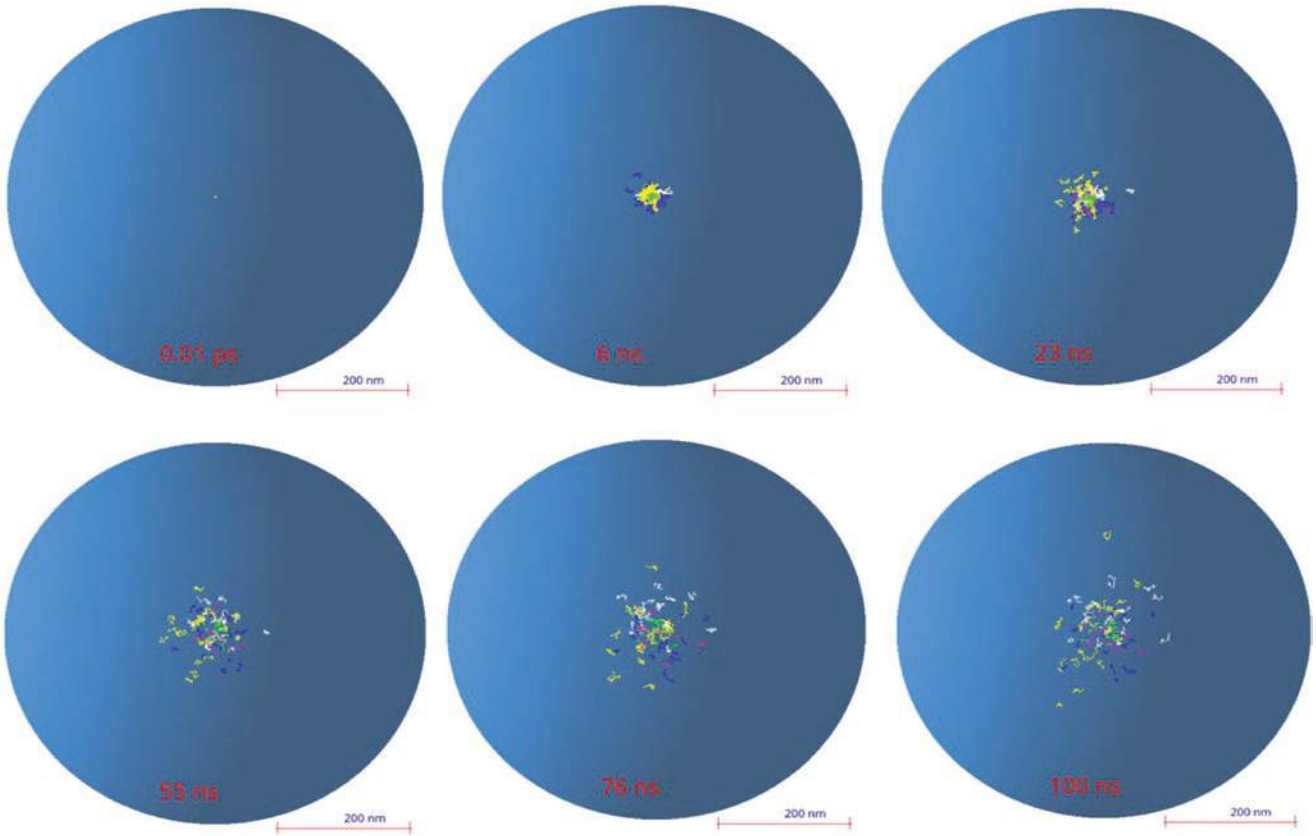

Fig. 4.13 Spatial and temporal evolution of the radiolysis products of a 1 keV electron in liquid water computed by Monte Carlo simulation (Geant4-DNA)

the microsecond, most of the reactions between different clusters are completed and the chemical stage can be considered as finished for a given track.

As indicated, all the simultaneous reactions are thus in competition and the temporal evolution of the chemical species, as shown in the example in Fig. 4.13, can strongly depend on the initial parameters. These reactions are very numerous in a liquid water medium [31] and increase even more in complex biological media. Thus, even in rigorous radiation chemistry experiments studying the kinetics of elementary chemical reactions, it can be difficult to measure the impact of secondary and competing reactions. In this context, simulation becomes a powerful tool to predict the complex dynamics of macroscopic observables, starting from elementary mechanisms [32].

To do so, one category of numerical simulations consists in dividing the modeling into two phases with different levels of granularity and acceptable simplifying assumptions. In the first one, each radical species is considered individually, and we are interested in the calculation of the reaction rate, the diffusion coefficient, or the branching ratios. This first phase can be simulated using molecular dynamics (like Born–Oppenheimer or Car–Parrinello) and/or quantum mechanical calculations like TD-DFT. However, this approach is unfortunately prohibitive in terms of computation time for a high number of molecules, which limits their application to systems such as a cell. In the second phase, approximations can be made to significantly reduce the computation time. For example, molecules of the same species can be grouped in order to describe their evolution by a unique variable (concentrations) and two types of methods are often applied: either probabilistic (Gillespie algorithms) or based on the solution of differential equations.

A second category of numerical simulations consists of describing the medium as a solvent or continuum and only calculating the diffusion and the chemical reactions of particular interesting species. This method is well adapted when the number of molecules is relatively small and, more particularly, when their distribution is inhomogeneous like in this case. Therefore, most of the track structure codes including the simulation of the chemical stage use this approach (Sect. 3.3.4) and include other simplifications as considering each molecule spherical and diffusing independently of the other molecules. In this frame of a diffusion-reaction model, their diffusion in the medium can be solved with the Green Function of the Diffusion equation (GFDE). The eventual reaction of two particles is considered when the interparticle

distance is smaller than their reaction radius. The reactions can be either fully or partially diffusion-controlled and involve neutral or charged particles. This gives four classes of reactions that were introduced by Green et al. [33]. For totally diffusion-controlled reactions (type I), the rate constant is assumed to be infinite, meaning that the particles react whenever they collide. In this case, the GFDE solution can be calculated using the Smoluchowsky boundary conditions in three dimensions [34]. This reaction mechanism is the one most often triggered when radiolytic species diffuse and encounter a reactive site that is either representing other radicals or a DNA constituent (sugar-phosphate backbone or bases with high rate constants). For other reaction types, including those representing the scavenger effects, please refer to the literature [35, 36].

Within this frame (GFDE), different stochastic simulation techniques have been proposed in order to calculate the probability of reactions to happen depending on the position of each molecule at a given time [33, 37, 38] as the step by step method or the IRT for Independent Reaction Time method.

Indirect damages are the consequence of these reactions for the DNA molecule and can represent between 30 and 90% of the total DNA damage depending on the LET of the irradiation. Among them, of importance are the strand breaks produced by the hydroxyl radical capturing the hydrogen of the deoxyribose at the C4 position or the addition of hydroxyl radical to a nitrogenous base, resulting in base alterations. These altered bases are often unstable and can either decompose or react with environmental molecules and radiolytic species. The underlying reactions are therefore multiple and complex [39]. DNA-protein or DNA–DNA bridging can also occur under the effect of radical species produced by radiation [40].

It should be noted that the description of the chemical stage process as explained above becomes much more complex if we take into account a more realistic chemistry of the cellular environment adding factors such as the pH, the oxygen concentration, or the presence of more complex molecules around the DNA, commonly called "scavengers" because of their action on the radical species. In particular, the concentration of oxygen has been shown to have a significant impact on radiation resistance: indeed, carcinogenic cells, which are hypoxic, are 2–3 times more resistant to radiation than healthy, normoxic cells. This "oxygen effect" is also believed to be one of the possible explanations for the protective effect on healthy tissue in the case of FLASH radiotherapy as the depletion of oxygen during irradiation could create a temporary hypoxic environment for both healthy and cancer cells. Nevertheless, this hypothesis is still not completely proven and the mechanism behind this FLASH effect however remains unknown [41].

4.3.4 Biological Stage (Early DNA Damage Scoring)

Radiation-induced damage is multiple and depends on numerous factors such as the type of radiation, the DNA configuration, or the irradiated medium condition. They are the result of the physical, physicochemical, and chemical processes explained in the previous sections and thus generated either by direct or indirect effects. The main DNA damages are strand breaks (simple, double, or clustered), base alterations, protein-DNA, and DNA–DNA bridges. Of these, the radiobiology and simulation communities have historically been most interested in double strand breaks (DSB) or clustered damage including at least one DSB. Indeed, in most repair models this type of DNA damage is called "lethal" or "semi-lethal," as they are considered to lead to misrepair and cell death [42–44]. In all cases, and even if they can sometimes be correctly repaired by cellular repair mechanisms, it is established that these complex damages can have important consequences on the cellular survival or its functioning. Moreover, DSB can be detected experimentally and compared to the results of predictions from simulations. Several detection techniques exist, which are adapted according to the irradiation configuration, the dose used, or the cell type. Historically, comet assay or pulsed field electrophoresis (PFE) has been used with high-dose irradiation in order to generate DNA fragments that can be separated and measured leading to a given number of DSB detected. Data obtained in this way, for example, in the case of proton irradiations at different energies or gamma rays [40, 45], have been used extensively to validate codes such as PARTRAC [46], KURBUC [47], or, more recently, Geant4-DNA [48].

Other techniques, used at low dose, consist in using immunofluorescent probes to localize the radio-induced DSB within the genome. For example, in the case of H2AX immunofluorescence; the histone closest to a double strand break that contains the H2AX variant of histone H2A (approximately present at 25% of H2A histones and evenly distributed in the DNA) allows the detection of DNA double strand breaks through its phosphorylation. This phosphorylation is visible using specific antibodies, containing a fluorochrome substance, making the double strand breaks appear as luminous points called "foci" or IRIF (ionizing radiation-induced foci) [49].

An important quantity of experimental data has been obtained recently using this technique or with other fluorescent biomarkers such as the 53BP1 protein, which allows to quantify the DSB produced by different types of radiation and to compare them with the simulation results. However, an important bias of this technique is that, in general, one detectable focus does not correspond to a single DSB formed in the DNA [50], and therefore the irradiation conditions and

the geometry of the target must be explicitly considered in the simulation for such validations [51, 52] .

4.3.5 Track Structure Monte Carlo Codes

As we described earlier in this chapter, particle transport through matter using MC codes is generally handled via a "condensed history" (CH) approach [53], currently used for dosimetry and the majority of microdosimetry applications for very energetic particles. In such a CH approach, many scattering events are grouped into fewer artificial steps, much longer than the mean free path of the particle, using multiple-scattering theories and a continuous energy loss along those steps. However, in order to simulate the physics at the nanoscale and to possibly link it to the biological effects of radiation with track structure properties in the nm regime [54], an event-by-event tracking of the different physical events is necessary to allow for better spatial resolution. Therefore, so-called track structure codes have been developed for applications in micro- and mostly nanodosimetry. In Table 1 taken from [55], we present the list of the main track structure codes that have been developed since the 80 s of the last century. In this table, it is indicated if the code includes the possibility of simulating the chemical stage and the materials available for the simulation of the physical stage.

Indeed, in order to model all the physical interactions taking place in the physical stage, these codes need to include cross sections for simulating ionization, electronic excitations below the ionization threshold, and, ideally, vibrational or rotational excitations of the medium, in principle for all the interacting particles but particularly for secondary electrons, for the reasons explained in Sect. 4.3.2. Therefore, track structure codes either rely on pre-parameterized or tabulated sets of total and differential elastic and inelastic cross sections in order to calculate the energy deposition in condensed matter. An important point to consider is that at these low energies, the interaction cross sections depend on the composition of the material but also on its state. That is to say that the cross sections are not the same for a medium in a gaseous or a solid state. This leads to a particular difficulty because it is very difficult (not to say, almost impossible) to obtain experimental cross sections for biological media in their condensed state [24]. Only a few data obtained under very specific conditions exist for liquid water [56, 57] and these data are the basis for the set of models utilized to calculate the cross sections used by most track structure codes.

However, still, some track structure codes use atomic ionization/electronic excitation cross sections [58] obtained in the gas phase even if, in principle, they are not suitable for low energy excitations of valence electrons in water, since such excitations are sensitive to the electronic structure of the target [54, 59–61].

Nevertheless, most of the theoretical models for the calculation of the cross sections used in these codes are based on the first Born approximation that uses the dielectric formalism. Here, the properties of a given material in terms of characterizing the inelastic interactions with charged particles are given in what is called the Energy Loss Function (ELF). This function allows calculating the mean free path and thus the inelastic cross sections. However, this function depends on the energy and momentum of the charged particles. As the existing experimental data have been obtained in the optical limit (i.e., for a zero momentum transfer), it is necessary to extend the calculation of this function for non-zero momentum transfers. Different dispersion algorithms based on the electron gas theory [53] are then used to redistribute the imaginary part of the function between the different ionization and excitation levels while preserving the agreement of their sum with the initial experimental data.

However, differences in results of inelastic scattering obtained with different dispersion algorithms to extrapolate optical data to finite momentum transfer reach about a factor 2 in the range 50–200 eV (and even further at still lower energies) [62] and consequently, these differences impact the obtained results. Recent studies have reported a potentially relevant effect of ionization clustering [63] or DNA damage induction [64].

The description of the dielectric function of water also continues to be studied. Thus, only recently have works been published that address exchange and correlation effects based on the electron gas model or that improve the description of effects beyond the first Born approximation [27, 65]. The objective is to improve previous dispersion algorithms [66], to develop new TS codes [67, 68], and to clarify differences in inelastic scattering between different condensation phases [69]. Besides, other authors still work on measuring or adapting the theoretical model, using, for example, pre-parametrized models [70], to obtain cross-sections for targets other than water to be included in TS codes.

Concerning the elastic scattering models for low-energy electrons, different theoretical approaches are also developed and included in TS codes. Some use screening parameters derived from experiments to enlarge the applicability of the first Born approximation [71] and others use the Dirac partial wave analysis [72, 73].

Overall, the accuracy of the results for water at energies below 100 eV remains questionable, and it would be desirable to have results for the dielectric function, the electron energy loss and the inelastic mean free path from ab initio TD-DFT approaches, i.e., with no free parameters and which, as a consequence, are prone to have predictive power and to be extended to a variety of targets (Table 4.3).

Table 4.3 MC track structure codes used in various radiation effects studies in biological cells

Code	Particles	Energy range	Target materials	Chemical stage
CPA100	e^-	Thermalization −256 keV e^-	Water (*l*), DNA	Yes
DELTA	e^-	≥10 eV–10 keV e^-	Water (*v*)	Yes
EPOTRAN	e^-, e^+	≥7.4 eV–10 keV	Water (*l*, *v*)	No
ETRACK	e^-, p, α	≥10 eV–10 keV e^-	Water (*v*)	Yes
ETS	e^-	≥10 eV–10 keV	Water (*l*, *v*)	Yes
Geant4-DNA	e^-, p, H, α, ions	Thermalization −1 MeV e^-, 100 eV–100 MeV p, H 1 keV–400 MeV α 0.5–10^6 MeV/u ions	Water (*l*), DNA, gold, N_2, and C_3H_8 (in progress)	Yes
IONLYS/IONLYS-IRT	e^-, p, ions	0.2 eV–150 keV e^-, p 0.1–300 MeV ions	Water (*l*)	Yes
KAPLAN	e^-	≥1–10 keV e^-	Water (*l*, *v*)	Yes
KITrack	e^-, ions	≥10 eV–100 keV	Water (*l*)	No
KURBUC (KURBUC/LEAHIST/LEPHIST/CHEM-KURBUC)	e^-, p, α, C	10 eV–10 MeV (10 keV, liq.) e^-, 1 keV–300 MeV, p, 1 keV/u–2 MeV/u α, 1 keV/u–10 MeV/u carbon ≥0.3 MeV/u	Water (*l*, *v*)	Yes
LEEPS	e^-, e^+	0.1–100 keV	All materials	Yes
LEPTS	e^-, e^+, p	Thermalization −10 keV e^-, Thermalization −10 MeV p	Water (*v*), CH_4, C_2H_4, C_4H_8O, SF_6, $C_4H_4N_2$	No
Lion track	e^-, p, ions	>50 eV e^-, 0.5–300 MeV/u p, ions	Water (*l*)	No
MC4	e^-, ions	≥10 eV e^-, ≥0.3 MeV/u ions	Water (*l*, *v*)	No
MOCA8B	e^-	10 eV–100 keV e^-	Water (*v*)	Yes
NASIC	e^-	Thermalization −1 MeV e^-	Water (*l*)	Yes
NOTRE DAME	e^-, ions	≥10 eV e^-, ≥0.3 MeV/u ions	Water (*l*, *v*)	Yes
OREC/NOREC	e^-	7.4 eV–1 MeV e^-	Water (*l*)	No
PARTRAC	e^-, e^+, p, H, α, ions	1 eV–10 MeV e^- 1 keV–1 GeV p, H, α 1 MeV/u–1 GeV/u ions	Water (*l*), DNA	Yes
PITS04	e^-, ions	≥10 eV e^-, ≥0.3 MeV/u ions	Water (*l*)	No
PITS99	e^-, ions	≥10 eV e^-, ≥0.3 MeV/u ions	Water (*v*)	Yes
PTra	e^-, p, α	1 eV–10 keV e^-, 1–10 MeV α, 300 keV–10 MeV p	Water (*l*, *v*), DNA, N_2, C_3H_8	No
RITRACKS/RETRACKS	e^-, ions	0.1 eV–100 MeV e^-, ions 10^{-1}–10^4 MeV/u	Water (*l*, *v*)	Yes
SHERBROOKE	e^-, ions	≥10 eV e^-, ≥0.3 MeV/u ions	Water (*l*, *v*)	Yes
STBRGEN	e^-, ions	≥10 eV e^-, ≥0.3 MeV/u ions	Water (*l*, *v*)	Yes
TILDA-V	e^-, p, H, ions	≥7.4 eV e^-, 10 keV/u–100 MeV/u ions	Water (*l*, *v*), DNA	No
TRAX	e^-, p, ions	1 eV—few MeV e^- 10 eV—few hundred MeV/u ions	Water (*v*)	Yes
RADAMOL (TRIOL/STOCHECO)	e^-, ions	≥7.4 eV–2 MeV e^-, ≥0.3–200 MeV/u ions	Water (*l*)	Yes
TRION	e^-, ions	≥10 eV e^-, ≥0.3 MeV/u ions	Water (*l*, *v*)	No
TRACEL/RADYIE/RADIFF	e^-, ions	≥10 eV e^-, ≥0.3 MeV/u ions	Water (*l*, *v*)	Yes

Associated particles, energy ranges, and target media (e.g., whether vapor or/and liquid phase cross sections are used) are indicated. (Taken from [55])

4.3.6 Simulation of DNA Damage

DNA damage is calculated from the energy depositions at nanometric scale in liquid water simulated with track structure codes and overlaid onto DNA models. DNA geometrical description can be as simple as cylindrical models of the DNA [74, 75] or as complex as a full atomistic description of human chromosomal DNA [76]. Nowadays, some of these models are directly included in the physical stage simulation (see Fig. 4.14) [48, 78], in order to facilitate the use of DNA material cross-sections instead of liquid water if they are available in the MC TS code. Besides, some subcellular structures are implemented in some TS codes [79] for the calculation of energy deposited in mitochondria or cellular membranes, for instance.

From the resulting energy deposition values or interactions registered in the DNA volumes, direct damages are calculated using different approaches depending on the TS code. For instance, in some cases, an energy threshold value (often of 17.5 eV) in the nucleotide backbone is used to define a direct strand break [30, 80]. Others, as in the case of the PARTRAC code, use a uniform probability linear function from 5 to 37.5 eV [81] in order to calculate the resulting direct strand breaks, taking into account that very small energy depositions from vibrational excitations can also lead to this kind of DNA damage.

After the simulation of the physical stage, the geometrical model of the DNA target (essentially the position of all its constituents) as well as the position of the surrounding ionized or excited liquid water molecules are "translated" in terms of chemical species and injected in the code for the simulation of the chemical stage as described in Sect. 4.3.3. Here also, different codes use different parameters for the definition or the calculation of the indirect strand breaks depending on the DNA geometrical model; the number of included reactions or the duration of the chemical stage simulation [32].

Finally, in order to quantify the results, an important issue is the definition of double strand breaks and, above all, of clustered damage. Indeed, these notions are fundamental if we want to be able to compare the results of the simulation predictions with the experimental data, representing either the fragments produced (PFE, comet assay) or the signaling of a repair process set in motion by the cell (foci). The way of quantifying the damage predicted by the modeling of the physical, physicochemical, and chemical stages must thus be adapted each time to the characteristics of the experimental observable used for the validation. Nevertheless, for a relative comparison of different radiations, other types of classification can be used. Finally, in order to extend the modeling to later stages and include the repair mechanisms, the scoring method must also be adapted to the initial damage defini-

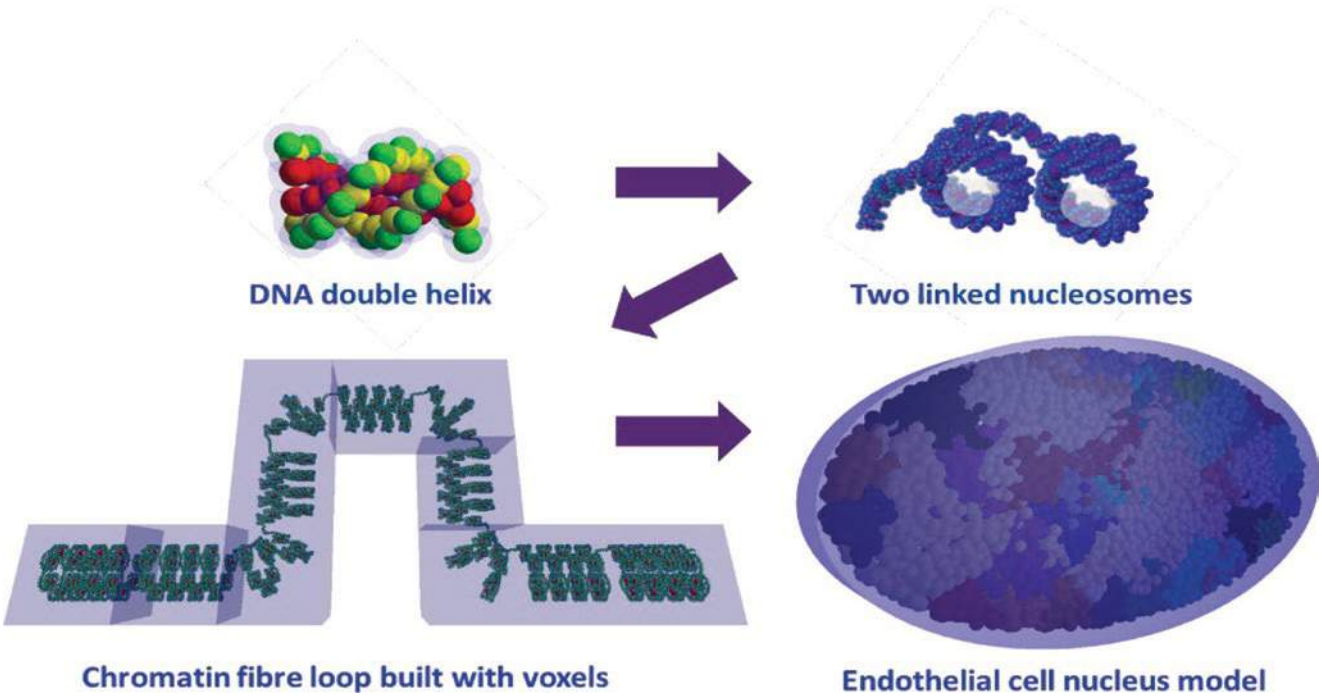

Fig. 4.14 Example of DNA target geometrical model used in the mechanistic simulation of DNA radiation-induced damage with the Geant4-DNA code [48]. The generation of this geometrical model was done with the DNAFabric software [77] from the nucleotide description to the complete genome of an eukaryotic cell nucleus in the G0/G1 phase

tions of each repair model. Thus, the definition of a double stranded break is relatively well established as two breaks in the sugar-phosphate group on opposite strands separated by less than 10 base pairs (bp). More complex breaks or clustered damages are very author-dependent: DSBs accompanied by altered bases or single breaks at less than 10 bp, two double breaks separated by less than 25 bp, for instance [82], or more complete definitions as the classification proposed by Nikjoo et al. [83].

Recently, a standardized format for the simulation output results [84] has been proposed by different researches of this community, in order to preserve a maximum of information on the DNA damage simulated by the different codes and their location in the genome. This standard output amounts to a mapping of the individual damages produced (and the information of their direct or indirect origin) so that it can then be adapted to the scoring required for each use of the code, validation with experimental data, or use as input to repair models (Box 4.6).

Box 4.6 Radiation Track Structures

- MC Track structure developed over the years allow the simulation of energy deposition at nanometric scale
- From these results and a DNA geometrical target model, direct DNA damages can be calculated
- Chemical reactions between radiation-induced chemical species in the cell nucleus and the DNA target generate the so-called indirect effects that account for up to 70–90% of the total strand breaks
- The way of considering damage and its complexity must be adapted to the different experimental methods

4.4 Micro-Beams and Minibeams

4.4.1 Micro-Beams and Minibeams

Conventional radiobiological studies are using broad (in the range of cm) irradiation fields for irradiating a whole cell population with a homogeneous dose in order to be able to screen an average reaction of this population to radiation. Already in the 1950s, the reaction of single cells to homogeneous irradiation or even to irradiation of subcellular parts became of interest [85].

Furthermore, in the 1990s the question arose whether there is a reaction of non-irradiated cells when they are located close to an irradiate one—the so-called bystander effect. To address these and other related topics, it is necessary to be able to apply a single, subcellular-sized radiation beam (in the range of sub-micron to a few micron) with an accuracy in the range of 1/*a* few μm. This is the field of microbeam research, where the term microbeam is used for beam sizes at full width at half maximum in the range of ~1 to ~10 μm for photon as well as particle beams. Additionally, the development of micro-beams makes it possible to not only apply single beams but also arrays of beams, which can then be used to directly study the kinetics of DNA repair, the movement of damage sites, the connection to chromatin organization, and their relation to radiation quality and outcome.

Table 4.4 Definition of micro- and minibeam pattern and corresponding beam size and their application

Type	Single beam size (fwhm)	Application
Single microbeam	~1–~10 μm	– Radiosensitivity of subcellular Structures – Bystander effect – Adaptive effect
Array microbeam	~1–~10 μm	– DNA repair kinetics – Effects of high-LET particles
Single minibeam	~100 μm–~1 mm	– Dose-volume effect
Array minibeam	~100 μm–~1 mm	– Modern therapy approaches

When beam sizes get larger (~100 μm–~1 mm), the beam or beam array is then termed minibeam or minibeam array. Here, the beam sizes become large compared to cell size and the difference in the effects switch from single cell differences to differences in cell population. An effect in this size range was described in the 1980s as the so-called dose-volume effect [86].

This effect is exploited in modern radiotherapy approaches such as Microbeam radiation therapy (MRT) using photon beams with a beam size around 100 μm and particle minibeam radiotherapy (MBRT) using submillimeter-sized beams of protons or heavier ions (Table 4.4).

4.4.1.1 Micro-Beams

A new wave of interest worldwide in the use of microbeams in radiation biology in the 1990s has led to the development of a number of tools that eventually evolved into facilities with potential clinical utility [87, 88]. Single cell micro-beams provide a unique opportunity to control precisely the dose to individual cells in vitro and the localization of dose within the cell. This makes it possible to study a number of important radiobiological processes in ways that cannot be achieved by other methods. Figure 4.15 shows such micro-beams as single or array application visualized on fluorescent nuclear track detectors and also via the foci of 53BP1 repair protein in human HeLa cells.

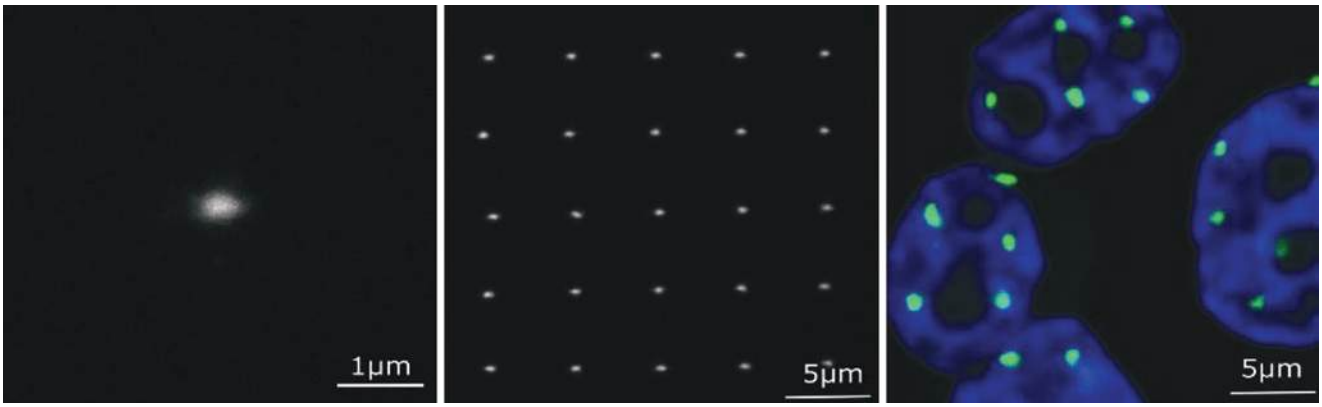

Fig. 4.15 Proton microbeam with a size of 0.8 μm (fwhm) visualized by a fluorescent nuclear track detector. Array of proton micro-beams with a point distance of 5 μm in both directions. 53BP1 accumulation in HeLa cells after microbeam array irradiation with a single carbon ion per point [beam size 0.8 μm (fwhm) and point distance 5 μm]

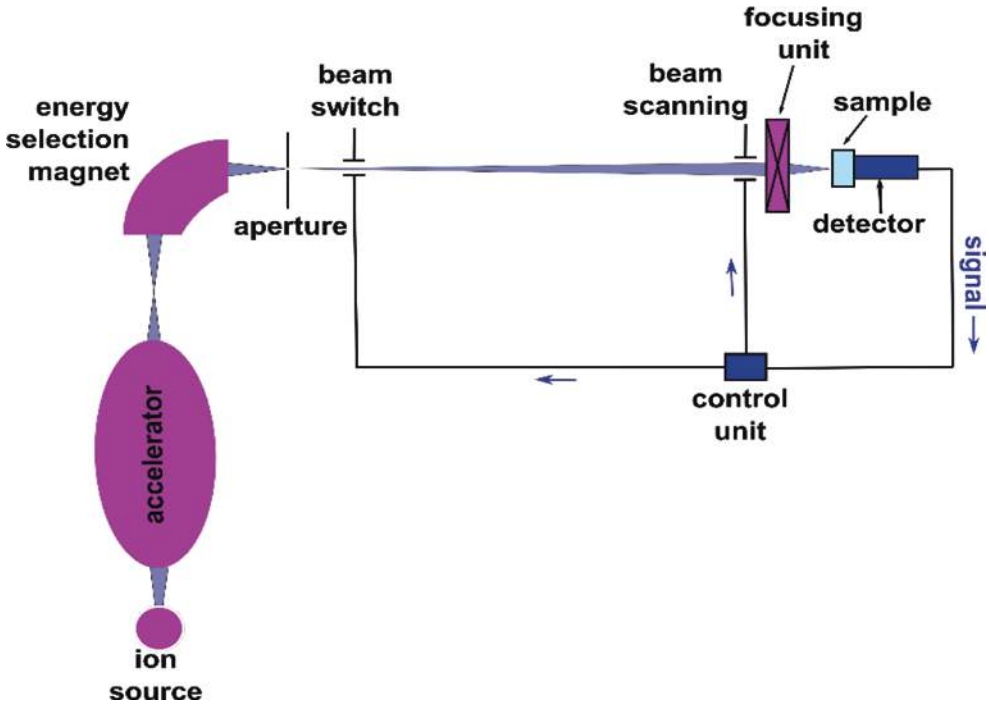

Fig. 4.16 Schematic view of a single cell microbeam for radiobiological research using ions. The ions are produced in the ion source and accelerated. Energy selection is carried out with a 90° magnet. Into the focus of this magnet, the aperture needs to be placed, which defines the object that is focused by the focusing unit. The biological sample is placed in its focus. Either in front or behind (shown here) the sample, the ion detector counts the ions and gives the signal to the control unit. Here the signal is processed and the beam switch and scanning unit can be regulated

Specifically, using charged particle micro-beams, it is possible to deliver exactly one particle per cell providing an ideal method for reproducing in vitro situations relevant to environmental exposure to naturally occurring radioactive radon gas, where virtually no cell receives more than one alpha particle traversal in its lifetime [89]. The high-spatial accuracy offered by micro-beams provides also a useful method to investigate subcellular spatial sensitivity such as the radiosensitivity of DNA close to the nuclear membrane [90] or of specific cellular organelles ([91, 92], p. 2019). Finally, single cell micro-beams have played a crucial role in the understanding of the bystander effect elucidating some of the mechanisms responsible for the transmission of the radiation effects from irradiated to non-irradiated cells [93]. Microbeam facilities can be used to selectively irradiate individual cells that can subsequently be revisited to ascertain what changes have occurred to that cell, and to its unirradiated neighbors.

There are four key aspects for the development of a single cell radiobiological microbeam: the radiation source, the radiation collimation or focusing, the radiation detection, and the cell alignment. A schematic view of a single cell microbeam can be found in Fig. 4.16.

As the main aim of single cell micro-beams is to be able to irradiate individual cells with high-spatial accuracy, the majority of micro-beams utilize low-energy radiation sources as penetration is not a requirement and higher radiation energies have stronger focusing or collimating requirements.

Linear particle accelerators [94–96] or lab bench X-ray sources have been mainly used [93], although synchrotron sources have also been employed [97]. Energy resolution and stability are key parameters in order to achieve small radiation probes. The collimation or focusing system is a crucial element, as it provides a method for reducing the radiation beam to a micron or sub-micron size beam with which to probe the cells. Collimation systems (such as devices with high length-aperture ratio) are generally easier to implement and the final opening can be placed close to the cells in their wet environment, although it is very difficult to achieve beams smaller than a few microns [98]. The focusing approach offers the possibility to achieve sub-micron spot sizes while keeping cells in their physiological environment ([99], p. 2019; [100], p. 2017; [101]). The next important element is the particle detection, as a key aspect of the cellular micro-beams is being able to count single ions so one can deliver an exact number of particles (or dose) to a single cell. Charged particle micro-beams achieve this through individual particle counting systems placed either after the biological samples (in which case the radiation energy has to be high enough to traverse the samples) or between the collimation/focusing system and the cells (which may degrade the radiation spot size). Detector systems using a combination of plastic scintillators and photomultiplier tubes have been successfully employed achieving basically 100% detection efficiencies [87, 88]. The final element consists of imaging and micropositioning devices required to identify the biological targets of interest and align them with the radiation probe. Speed is essential because many assays of biological radiation effect require several hundreds, or even thousands of cells to be micro-irradiated individually. The performance of the various single cell micro-beams varies according to the methods adopted and particularly the radiation used. However, state-of-the-art systems can achieve targeting accuracies in the range of a μm and detection efficiency approaching 100% [91]. These systems can also irradiate 10,000 s of cells per hour.

One of the first key studies to make use of micro-beams was completed using the RARAF facility in New York. Miller et al. [102] demonstrated that the transformation frequency of a single alpha particle traversal is not statistically different that of no traversals. The finding has strong implications for radiation protection, and it supports the threshold hypothesis for radiation risks. Many radiobiological studies using micro-beams have been aimed at investigating the bystander effect. In particular, experiments with co-cultured glioma and fibroblast cells showed that micronuclei formation can be induced through bystander signaling across genotypes [103]. These studies also provided information about the signaling processes involved in the bystander response suggesting nitric oxide (NO) and reactive oxygen species (ROS) play a critical role [103]. Another important radiobiological contribution from micro-beams comes from adaptive response studies [104]. The adaptive response manifests itself as a reduction in the effect of a high dose of radiation when a small (<0.2 Gy) priming dose is given first, typically a few hours ahead of the high dose. This observation undermines traditional thinking with regard to radiation effects and has been linked to radiation hormesis; the concept that radiation at low doses may actually be beneficial. Also, the investigation of the radiosensitivity of subcellular structures is a key application for ion micro-beams [91, 92, 105]. For example, it could be shown that radiation-induced localized damage with high-LET particles only triggered localized inhibition of rRNA transcription in nucleoli rather than pan-nucleolar reaction, as it was seen in drug treatment or under UV irradiation [91].

Micro-beams cannot only be used in single beam mode but also with an array of micro-beams. Arrays of particle micro-beams are used especially for two applications. First for understanding the kinetics of DNA repair. The major advantage of micro-beams arrays here is that the damage is induced within a known pattern with defined distances at a defined time. With this method, repair kinetics of various proteins such as 53BP1, Rad52, Mdc1 [106], and PARP1 [107] could be measured. Furthermore, it was found that the sites of DSBs induced by micro-beams show a non-directed, sub-diffusion movement within the cell nucleus [108].

Furthermore, by focusing low-LET protons to ~1 μm beam size the RBE can be increased. With this information, it was possible to further understand the enhanced RBE of high-LET particles [99, 109–111], which is an effect on several scales. An enhancement of LET is possible when focusing the ions to ~1 μm beam size but this enhancement does not reach the RBE of a single high-LET particle, where most of the damage is caused in the core region of a few 100 nm diameter. The explanation of this is that when ions are focused to ~1 μm sizes, the DSB get closer together and therefore complex damages occur. If the damage is caused on even smaller scales, single strand breaks will get so close together that they cause further DSB, which enhances the biological effect [110] (Box 4.7).

Box 4.7 Microbeams

- Micro-beams are beams of photon or particle radiation and have a size of ~1–~10 μm
- Micro-beams can be applied as a single beam or array of beams
- Collimation is easy to implement but beamsize only a few μm
- Focusing is more complex but beamsizes <1 μm are possible
- Micro-beams can be used to study bystander effect, radiosensitivity of subcellular structures, and the enhanced RBE of high-LET particles

4.4.1.2 Minibeams

A minibeam is a narrow radiation beam, whose width is in the range from ~100 μm to approximately 1 mm. The minibeams play a key role in the development of new therapy approaches, which aim to lower the side effects of external radiotherapy by spatially sparing the healthy tissue, especially in front of the tumor. Using photons, this method is called microbeam radiation therapy (MRT) in order to be able to separate from the particle minibeam therapy (MBRT) using protons and ions. MRT uses beam sizes in the order of 100 μm, whereas in pMBRT the beam sizes are a bit larger up to ~1 mm. There are different approaches of how to irradiate the tumor with minibeams; with photons or heavy ions the minibeam pattern with peaks and valleys is typically maintained, while with protons or light ions homogeneous irradiation of the tumor is feasible.

Nevertheless, both methods rely on the same effect, that the smaller the volume which is irradiated, the more dose is tolerated by tissue, the so-called dose-volume effect [86]. This is attributed to undamaged migratory cells surrounding the damaged tissue, which are able to infiltrate and thus reduce tissue necrosis. A further effect that plays a role in the tissue response to submillimeter beams is the microscopic prompt tissue repair effect. For such small irradiation fields, the capillary blood vessels can be repaired within days or even hours. The intact blood vessels are then able to support the repair of surrounding tissue. The detailed underlying radiobiological effects are yet not completely understood and topic of investigation worldwide. Nevertheless, the use of minibeams in radiation therapy is already used in spatially fractionated radiation therapy such as GRID therapy or is on the way to clinical studies (Box 4.8).

Box 4.8 Minibeams

- Minibeams are beams of photon or particle radiation and have a size of ~100 μm–~1 mm
- Minibeams can be applied as a single beam or an array of beams
- Collimation is easy to implement but can give secondary radiation and limits flexibility
- Focusing is more complex to implement but has no secondary radiation and full flexibility
- Minibeams are used to study the dose-volume effect and the microscopic prompt tissue repair
- Minibeams are transferred into clinical application in microbeam radiation therapy (MRT) for photons and minibeam radiation therapy (MBRT) for particles

4.5 Target Theory and Dose-Response Models

4.5.1 Cell Survival Modeling Using Hit and Target Theory

Suppose an object (say a macromolecule) is irradiated. Assume that the radiation deposits one or more primary ionizations (i.e., ion clusters) within the molecule. Assume that the molecule has a particular function within our cells and that this function is destroyed only if the ion cluster destroys one particular part of the molecule and that the molecule still works equally well if the ion cluster damages any other part. The sensitive area inside the molecule is then called the target (Fig. 4.17) (Box 4.9).

Box 4.9 Target Theory

- Target theory postulate: only energy deposits in the target can destroy the function of the object

4.5.1.1 An Approach to the Concept of Dose

For the sake of simplicity, assume that one hit represents one primary ionization. This can in some cases be an oversimplification since a primary ionization can give rise to many ion pairs however the probability is largest for a primary ionization to give rise to only one ion pair [112].

We can now introduce the dose as the number of hits per cm^3. In an elegant experiment, Rauth and Simpson [113] found that the energy deposition per primary ionization is about 60 eV on average. Although this is not the exact average energy per hit, it can be used as an approximate value. Since the dose gives the energy deposition per cm^3 (it indi-

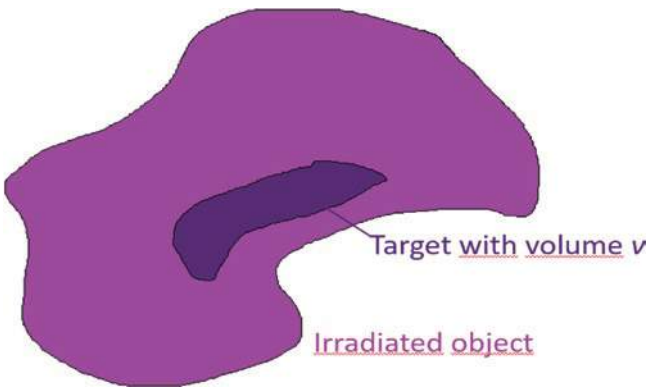

Fig. 4.17 One assumes that the target only consists of a small area of the object being irradiated. The object may be a macromolecule or an organism

cates the energy per g or kg, but when we know the density of the irradiated substance we easily convert it to cm^3), we can use Rauth's and Simpson's measurement to convert the dose to the number of primary ionizations per cm^3 and as a first approach use this as an indication of the number of hits per cm^3.

4.5.1.2 Single-Target Single-Hit Model of Radiation Survival

This theory relies on certain key assumptions

1. Ionizing radiation deposits the energy into discrete energy packages that we call hits.
2. The response of a molecule (or cell) occurs only if a number of n hits is deposited in the target.
3. The number of hits deposited in the target in the irradiated material must be Poisson distributed.

Assumption number 3 can generally only be considered satisfied when the dose is high. Note that the average number of hits in a volume equal to the target volume is $\mu = vD$ where the dose is given in hits/cm^3 and the target volume, v, is given in cm^3. If n is the actual number of hits in the target in a particular irradiated object, the probability of this number of hits being seen is Poisson distributed as:

$$p(n) = \frac{(vD)^n}{n!} e^{-vD}. \tag{4.23}$$

If the irradiated object is a macromolecule in a cell, and if this macromolecule is inactivated (i.e., loses its biological function) if it receives n hits in the target, then the molecule retains its function if the number of hits in the target is $n-1$ or less. We can therefore calculate the probability, p_f, for the molecule to retain its function. It must be the sum of the probabilities that it will receive one, two, three, etc., up to $n-1$ hits in the target [112]:

$$p_f = \frac{(vD)^0}{0!} e^{-vD} + \frac{(vD)^1}{1!} e^{-vD} + \cdots + \frac{(vD)^{n-1}}{(n-1)!} e^{-vD}, \tag{4.24}$$

or

$$p_f = e^{-vD} \sum_{k=0}^{n-1} \frac{(vD)^k}{k!}. \tag{4.25}$$

Here, p_f represents the probability that a target molecule will not be inactivated by the dose D. However, this can also be viewed as p_f representing the fraction of the irradiated molecules that do not become inactivated by the radiation [112]. If one irradiates N_0 molecules and the number that is not inactivated is N, Eq. (4.25) can be rewritten as:

$$\frac{N}{N_0} = e^{-vD} \sum_{k=0}^{n-1} \frac{(vD)^k}{k!}. \tag{4.26}$$

If the molecule becomes inactivated by only one hit in its target, $n = 1$ and Eq. (4.26) becomes:

$$\frac{N}{N_0} = e^{-vD}. \tag{4.27}$$

This is the Single-Hit Single-Target model of radiation survival. While simple, it is a very powerful equation that can provide insights into the characteristics of cellular response to radiation exposure (Fig. 4.18).

One key insight is that the equation allows us to determine the molecular weight of the target. From the previous derivation, we know that if we express dose in the unit hits/cm^3, we can determine the target volume. If we also know the density of the irradiated molecules we can, based on the target theory, determine the molecular mass of the target. The dose is normally given in Gy so the calculation must be based on this unit:

$$1\text{Gy} = 1\frac{\text{J}}{\text{kg}} = \frac{6.242 \cdot 10^{18}\,\text{eV}}{1000\text{g}} = 6.242 \cdot 10^{15}, \tag{4.28}$$

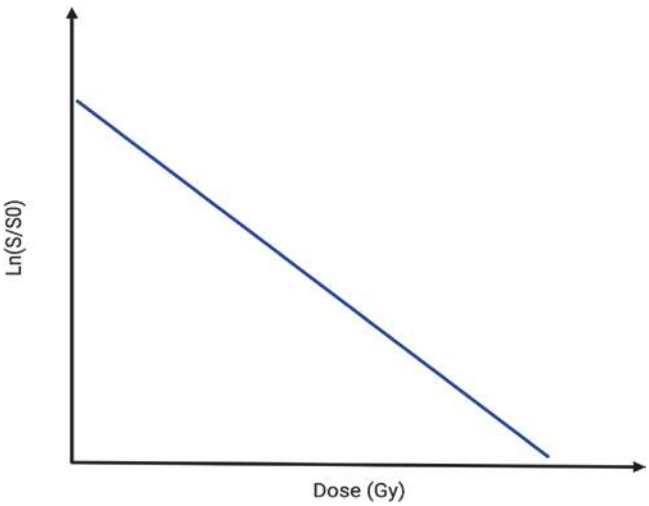

Fig. 4.18 The relationship between the predictions of the single-hit single-target model on cellular survival versus radiation dose [here N/N_0 from Eq. (4.27) is replaced by S/S_0 or the ratio of cell survival at any dose D to that at 0 Gy]

using that 1 J = 6.242 × 10^{18} eV. From the experiments by Rauth and Simpson, we know that it takes an average 60 eV to give a primary ionization in an organic material. This value is not necessarily the correct amount of energy needed for a hit, but as an example it can be used. Then we can convert [*Gy*] into [*hits per gram*]:

$$1\text{Gy} = \frac{6.242 \cdot 10^{15} \left[\frac{\text{eV}}{\text{g}}\right]}{60}. \tag{4.29}$$

D_{37} is the dose that gives on average one hit per target, i.e., $v \cdot D_{37} = 1$. The surviving fraction at this dose is $e^{-vD} = e^{-1} \approx 0.37 = 37\%$, which gives rise to the name of the quantity. If we assume that we irradiate the molecules with different doses and find the $D_{37,}$ we have on average one hit per target at this dose ($v \cdot D_{37} = 1$). Suppose the D_{37} is given in the unit *hits/g*. We can then calculate the mass of the target in the unit gas:

$$M_T = \frac{1}{D_{37}}. \tag{4.30}$$

In practice however the dose is in *Gy* and we must use Eq. (4.29) to convert from *hits/g* to *Gy*:

$$M_T = \frac{1}{1.04 \cdot 10^{14} \cdot D_{37}} = \frac{0.96 \cdot 10^{-14}}{D_{37}}. \tag{4.31}$$

If the density of the target is $\rho = M_T/v$ we can then calculate the target volume:

$$v = \frac{M_T}{\rho} = \frac{0.96 \cdot 10^{-14}}{\rho \cdot D_{37}} \text{cm}^3, \tag{4.32}$$

(where ρ is in units of g/cm^3).

In Eq. (4.32) the dose is in *Gy*. The final calculation of the target volume is left to the reader.

4.5.1.3 Multiple-Target and Multiple-Hit Models

Complicated molecules or cellular organisms may well have more targets and it also may take more than one hit per target to inactivate the molecule or cell.

Recall Eq. (4.25), which calculates the probability that a molecule will *not* be inactivated if it has one target and that this is deactivated by n hits. The probability of one target being deactivated is then:

$$\frac{N^{ii}}{N_0} = 1 - e^{-vD} \sum_{k=0}^{n-1} \frac{(vD)^k}{k!}, \tag{4.33}$$

where N^{ii} means the number of molecules that were inactivated. If we now assume that the molecule has a number of *m* targets that all must be inactivated for the molecule to be inactivated, the probability of inactivation becomes:

$$\frac{N^{ii}}{N_0} = \left(1 - e^{-vD} \sum_{k=0}^{n-1} \frac{(vD)^k}{k!}\right)^m, \tag{4.34}$$

and the probability that the molecule will *not* be inactivated is then:

$$\frac{N}{N_0} = 1 - \left(1 - e^{-vD} \sum_{k=0}^{n-1} \frac{(vD)^k}{k!}\right)^m. \tag{4.35}$$

In the most likely case, it only takes one hit per target for the molecule to be inactivated, that is, $n = 1$. This gives the following special case:

$$\frac{N}{N_0} = 1 - \left(1 - e^{-vD}\right)^m. \tag{4.36}$$

This is the famous multi-target single-hit equation. For many decades, this was the model radiobiologists fitted to their dose-response curves when they tested the effect of ionizing radiation on human cells. Much of the formalism of this equation and parameter values are still in use when dose-response curves are discussed and described. Therefore, it is important that we perform an analysis of this function:

- The equation has a shape with an initial shoulder at small doses followed by, a straight line for large doses. This is seen if the equation is expanded by a power series:

$$\frac{N}{N_0} = 1 - \left(1 - me^{-vD} + \frac{m}{2}(m-1)e^{-2vD} - \frac{m}{6}(m-1)(m-2)e^{-3vD} + \cdots\right). \tag{4.37}$$

Focusing on high-dose regions, all terms with $(e^{-vD})^2$ and higher power can be ignored. We then end up with the following expression, which only is valid for high doses:

$$\frac{N}{N_0} = me^{-vD} \text{ or } \ln\frac{N}{N_0} = -vD + \ln m. \qquad (4.38)$$

This is a straight line in a semi-logarithmic plot, and the line intersects the ordinal at point m as shown in Fig. 4.19.

4.5.1.4 Some Interpretations of the Hit and Target Theory

Note that in Fig. 4.19, the actual dose-response curve has an initial shoulder followed by a straight line at higher doses. Thus, only the straight line at higher doses is described in Eq. (4.38). The dose-response curve itself is described in Eq. (4.36).

Figure 4.19 illustrates a dilemma with regard to the common definition of radiation sensitivity. It is common to say that the target volume is an expression of radiation sensitivity. For a single-hit, single-targeted model, one obtains a value $v = 1/D_{37}$. For a single-hit, multi-target model like the one shown in Fig. 4.19, we can say that $v = 1/D_0$ expresses radiation sensitivity. D_0 is the dose, which reduces the surviving fraction by 63% in the linear part of the curve (Box 4.10).

Box 4.10 Radiosensitivity for Hit and Target Theory

$v = \frac{1}{D_{37}} \vee v = \frac{1}{D_0}$ is an expression of the radiosensitivity

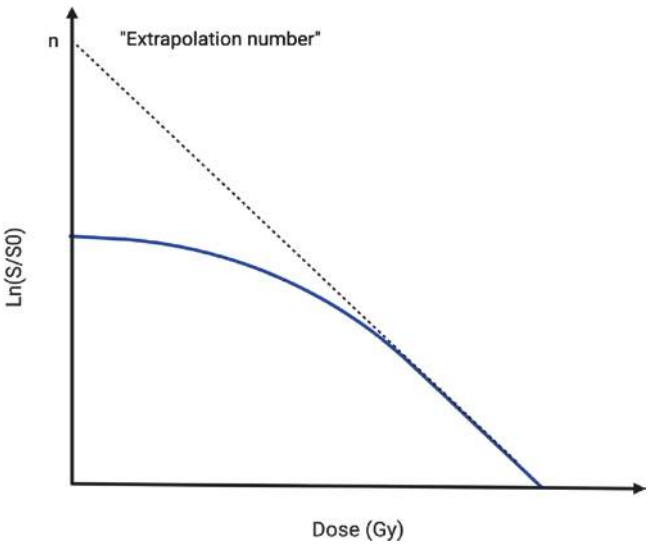

Fig. 4.19 The relationship between the predictions of the multi-hit single-target model on cellular survival S and radiation dose. $S0$ is the plating efficiency of the unirradiated controls

This may seem a bit odd: If we have two types of molecules, one with one single target and one with m targets, but where the target volumes are the same, such that $D_{37} = D_0$, as is the case in Fig. 4.19, then the radiation sensitivity is the same in the two cases and is only given by the slope of the dose-response curves at high doses. Nevertheless, one can immediately see that the curve that has a shoulder shows a higher survival value for a particular dose than the one that does not have a shoulder. This is because it is an advantage for a molecule that the radiation must destroy two or more targets rather than just one to inactivate the molecule. Still, many authors have chosen to use the target size as a mathematical expression of the radiation sensitivity.

One term is important to get into at this stage, namely sublethal damages. So far, we have most talked about irradiating molecules and not cells. However, we can talk about cells in the same way that we have discussed molecules in the hit and target theory. The radiation damage then inactivates some function that the cells usually have. Very often, the effect is referred to as cell death or lethality. This term suggests that radiation should produce some form of death. Often, this will give incorrect associations to the chemical or biological responses we measure. However, the terms lethal, sublethal, and potentially lethal damages have been so incorporated that it is completely impossible to avoid their use.

Note that, based on the formalism of the target theory, sublethal damage is damage to the target. A hit outside the target is no damage according to this theory. When damage in the target does not produce any effect, it is because we have a multi-hit system or a multi-target system (Box 4.11).

Box 4.11 Sublethal Damage in Hit and Target Theory

- Sublethal damage refers to damage, or really ion pairs, which is the cell or molecular target, but does not cause any effect in itself

Later in this chapter, we will talk about dose rate effects. These state that there usually is a stronger effect of a dose when given in a short time than when given over a long period of time. The reason for this is, according to the target theory's formalism, that the first hit is not enough to inactivate, but that it can interact with the next so that the two or more together can inactivate. However, if the cells or molecules are able to repair the first hit before the next, we will not get such interactions. The fact that this effect decreases with decreasing dose rate is therefore a sign that the radiation damage is repaired.

Note also, that the shoulder of the multi-target curve in Fig. 4.19 has nothing to do with repair in the target theory's

formalism. It is just because the cells or molecules can either tolerate one or more hits in their one target or that they have more than one target.

4.5.2 The Linear Quadratic Model

While target models are useful to generate an initial understanding of the relationship between radiation dose, cell survival, and the process of energy deposition, these models have not been generally adopted because of their use of multiple terms, and also because the "targets" which the models predict have never been identified. Several models have been developed based on target theory, among which the linear quadratic model (LQ) has emerged for application clinically and preclinically [114]. The expression for cell survival according to the LQ model is:

$$S = e^{-\alpha D - \beta D^2}, \tag{4.39}$$

where S represents the probability of cell survival when subjected to dose D and the α and β parameters determine the linear and quadratic components of cell damage, respectively. The dose-squared dependence implies that the survival plot on a logarithmic scale has the characteristic appearance of a quadratic curve (Fig. 4.20). A linear relationship dominated by the α-parameter is observed at very low doses, while for higher doses the quadratic relationship governed by the β parameter becomes dominant. This characteristic feature of the survival curve is commonly referred to as the shoulder.

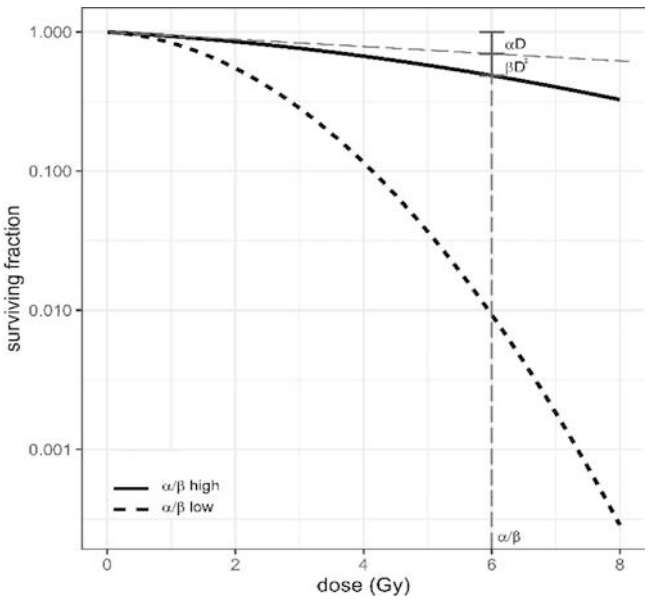

Fig. 4.20 Illustration of LQ curves for high and low α/β ratios. For the low α/β, the shoulder of the curve is more pronounced. The α/β-ratio can be found by drawing a line with the initial slope (α) of the curve and finding the dose where the contribution from the linear and the quadratic terms are equal

4.5.3 Interpretations of the LQ Model

The linear quadratic model needs only two parameters and shows a good fit for experimental observations. As for its biological interpretation, different approaches have been presented, such as those of Kellerer and Rossi, Chadwick and Leenhouts, and Bodgi and Foray.

4.5.3.1 LET-RBE (Kellerer and Rossi)

Kellerer and Rossi sought to analyze the relationship between dose and effect in a way that was invariant to the quality of radiation, as they considered that the biological effect, in addition to its dependence on the deposited energy, also depended on its microscopic distribution [115]. Having observed the simplicity of the relationship between the doses of two different types of radiation with different LET (see Sect. 1.6) that lead to the same effect (relative biological effectiveness—RBE, see Sect 1.6) they proposed a theoretical model that arrives at a linear and quadratic relationship with the dose. The model assumes three possible states for the biological entity: non-damage, pre-damage, and effect. The probability of transition between states (without allowing for reversion) depends on the dose and a careful choice of these values results in different models [115]. According to the model, the biological effect can be achieved by a direct transition from the non-damage state to the biological effect or by two consecutive transitions between non-damage to pre-damage and pre-damage to biological effect. The first case represents the situation of reaching the biological effect with one hit (single-hit event), which is dominant for high-LET radiation, and for the second case, two hits (double-hit event) are required.

4.5.4 DSB-SSB, Asymmetric Chromosome Aberrations

Chadwick and Leenhouts started from the hypothesis that cell death resulted from a double strand break in DNA (DSB) and that the probability of these events was related in a linear quadratic manner with dose. The model assumes:

- that DNA is a critical molecule that determines the cell's ability to reproduce and a DSB is considered critical damage;
- radiation produces DNA breaks that can be repaired, and the radiobiological effect reflects the degree of repair [116].

- that the rate of critical breaks relative to dose (dN/dD) is proportional to the number of critical bonds (N) and that a critical event (DSB) can occur in two ways: either as a single radiation event that results in a DSB or as two events each inducing a single strand break (SSB), which is close enough in time and space interact to form a DSB.

Therefore, the combination of these assumptions leads to an exponential model with a linear term and a quadratic term, similar to the one developed by Kellerer and Rossi, producing the linear quadratic model of cell survival.

There are various ways of interpreting this model. In one, two DSBs can interact and lead to chromosomal aberrations that impair cell division. In particular, asymmetric aberrations, such as the dicentric, the ring, and the anaphase bridge, make cell division impossible. In another interpretation by Hall, the linear and quadratic terms can be interpreted as asymmetric chromosome aberrations produced in one or two radiation events.

In both the interpretations by Chadwick and Leenhouts and Hall, the shoulder of the LQ-curve is a result of sublethal damage, i.e., damage that is not lethal in itself but can interact with other sublethal damage to become lethal. The difference lies in what is regarded as sublethal damage. Hall assumes that one DSB in itself is not lethal such that lethal damage is created only when two DSBs create an asymmetric chromosome aberration. Chadwick and Leenhouts also acknowledge that asymmetric chromosome aberrations are lethal DNA damage, but they adjust for this by multiplying by a factor, which represents a linear relationship between the number of DSB and the number of asymmetric chromosome aberrations. In their interpretation, sublethal damage is a single strand break (SSB), which needs to interact with another SSB close in time and space to form a DSB.

If the dose is fractionated (i.e., split up into several parts separated in time) or the dose rate is decreased, a linear survival curve will emerge. This is a reflection of the sublethal damage being repaired before it can interact with other sublethal damage to become lethal. With the repair time for DSB and SSB in mind (see Sect. 2.4), this supports Chadwick's and Leenhouts' interpretation.

4.5.4.1 ATM Shuttling

In 2016, Bodgi and Foray proposed a new model for radiation-induced cell death whose mathematical derivation results in the linear quadratic model. In this model, DSB recognition mechanisms are mediated by ataxia telangiectasia mutated monomers (ATM) that are induced in the cytoplasm by radiation and diffuse to the nucleus (nucleo-shuttling of IR-induced ATM monomers). Once in the nucleus, these monomers participate in the DSB recognition mechanism that allows its repair [117]. The rates of DSB production by radiation and monomerization are assumed to have a linear relationship to dose. The same model also includes the notion of cell tolerance, taking into account that not all DSB lead to cell death, which in this case is assumed to be due to unrepaired DSB in cells entering mitosis. Among unrepaired DSB, those that are not recognized and therefore not repaired are distinguished from those that are recognized but not repaired within a suitable time window. The number of unrecognized DSBs in the model has a quadratic relationship to dose, whereas the number of recognized but unrepaired DSBs has a linear relationship to dose. Finally, unrepaired DSBs are assumed to follow a Poisson distribution, which leads to cell survival being modeled by a linear quadratic exponential. In addition to presenting a biological mechanism of cell death by radiation, this model provides an explanation for cellular hypersensitivity at low doses, since it assumes that radiation does not produce enough ATM monomers to cross the membrane and enter the nucleus. Therefore, there is no recognition of DSB and they remain unrepaired, which leads to cell death.

4.5.5 Low-Dose Modifications and High-Dose Limitations

The linear quadratic model is arguably the most used tool in radiation biology and physics, as it provides a simple relationship between the dose absorbed and the number of surviving cells (or the probability that a single cell will survive). In its basic format ($SF = \exp(-\alpha \times D - \beta \times D^2)$), it has been used to analyze and explain both in vivo and in vitro experiments and after some modest simplifying assumptions, it can be related to a number of mechanistic models such as multihit and potentially lethal lesion models. However, despite its widespread usage, questions remain about its applicability, particularly at the very low and very high-dose regions where significant discrepancies have been observed between the model predictions and the experimental data. Such questions spring from the complexity of the underlying biology and modern radiotherapy, where the response of cells and tissues can be modulated by both intrinsic genetic factors as well as the cellular environment and the radiation delivery modality. The linear quadratic model has therefore been the subject of extensive investigations and suggestions for modification to better fit the experimental data and therefore to explain a wide range of radiation conditions.

In the low-dose region, high-resolution in vitro measurements demonstrated increased X-ray effectiveness below 0.6 Gy [118]. The measured survival levels were significantly lower than those predicted by extrapolating the high dose points using the linear quadratic models. The phenomenon, named *hypersensitivity,* was reported with a range of cell lines and radiation qualities and data suggest that the observed response was unlikely to be due to a subpopulation

of radiosensitive cells. In order to account for the increased effectiveness per unit dose at doses lower than 1 Gy and in line with the hypothesis that repair mechanisms are only triggered when sufficient damage has been accumulated, modification to the linear quadratic models has been suggested. Joiner and Johns [119] proposed a simple modification in which the alpha parameter decreases with increasing radiation dose, representing an increased induced radio resistance. The modification only concerns the alpha parameter, as the contribution of the beta parameter is negligible at low doses due to its quadratic influence. The modified linear quadratic models for low doses can therefore be expressed as

$$\begin{aligned} &\mathrm{SF} = \exp\left(-\alpha \times D - \beta \times D^2\right) \\ &\text{with } \alpha = \alpha_{\mathrm{Res}}\left(1 + g\exp\left(-D / d_c\right)\right), \end{aligned} \tag{4.40}$$

where d_c is the dose at which 63% of the induction has occurred and g is the amount by which the alpha parameter changes at low doses (Fig. 4.21).

The interest in radiotherapy treatments delivered with a smaller number of high-dose fractions (hypofractionation) and stereotactic radiosurgery (SRS) has also instigated investigation into the validity of the linear quadratic model at high doses. A number of investigations have shown that the linear quadratic model in its basic form is not suitable in the high-dose region where it underestimates the surviving fraction and does not reproduce the straightening of the curve observed experimentally [120, 121]. To cope with this drawback, modifications of the linear quadratic model have also been suggested at high doses [122]. The starting point is an early modification of the linear quadratic expression to account for repair during a protracted radiation exposure:

$$\begin{aligned} &\mathrm{SF} = \exp\left(-\alpha \times D - G\left(\lambda T\right) \times \beta \times D^2\right) \\ &\text{where} G\left(\lambda T\right) = 2\left(\lambda \times T + \exp\left(-\lambda \times T\right) - 1\right) \\ &/\left(\lambda \times T^2\right), \end{aligned} \tag{4.41}$$

with λ as the repair rate parameter, T is the delivery time for the dose D, alpha and beta as previously described for the basic linear quadratic model. This version of the LQ model is able to predict survival curves taking into consideration scenarios where significant repair occurs during the dose delivery and is in accordance with other mechanistic models (i.e., Lethal, Potentially Lethal model). In order to reproduce the behavior of acute high doses however an additional term needs to be added to the G parameter:

$$G\left(\lambda T\right) \to G\left(\lambda T + \delta D\right).$$

The new parameter (δ) is introduced to match the final slope of the survival curve and can be interpreted as a reduction in survival due to interaction between lesions. Using Eq. (4.41), it can be shown that at high acute doses $G\ (\lambda T + \delta D) = 1/2\ \delta D$ and therefore the modified LQ model assumes the form: $\mathrm{SF} = \exp\ (-(\alpha + \beta/2\delta) \times D)$, which has a linear behavior. Therefore, this model is referred to as a linear quadratic linear or LQL model (Fig. 4.22).

Although both modifications of the linear quadratic model are able to accurately describe experimental data at low and high doses, they introduce new parameters, which need to be experimentally determined.

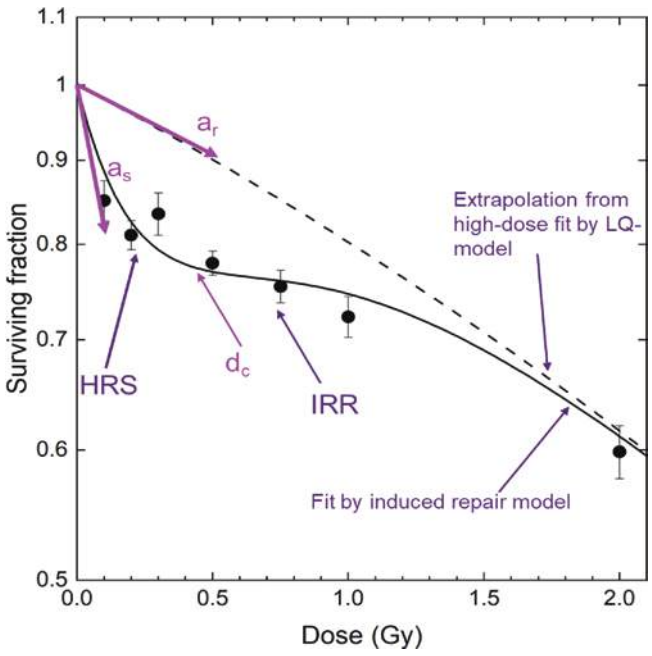

Fig. 4.21 Low dose hypersensitivity showing a clear downward bend on the survival curve for doses below 1 Gy, followed by an "increased radio resistance" at doses above 2 Gy. The image also shows the key parameters for the linear quadratic modification

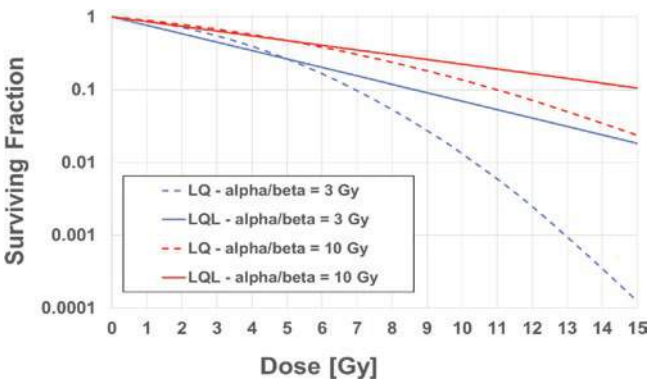

Fig. 4.22 Difference in the surviving fraction predicted by the LQ and the LQL model for cell lines with different radiosensitivity (alpha/beta ratio)

4.5.6 The Dose Rate Effect

The reaction of cells and tissues to radiation damage involves the repair of DNA and a complex interplay between repair and cell survival. The ability of a cell to repair the damage it experiences depends on the part of the dose it receives, the part of the cell cycle in which it is irradiated, and the rate at which the dose is delivered. Therefore, we must give attention not just to the molecular mechanisms of damage and repair but also to cell cycle regulation of repair and ultimately their biological consequences.

Here we return to using the terms sublethal, lethal, and potentially lethal damage. By sublethal damage, we simply mean damage which will not be lethal to the cell even if the damage is not repaired. We will later see that it is still of great importance whether or not these damages are given time for repair hence the temporal aspect.

Lethal damage is fixed in such a way that they cannot be repaired. Potentially lethal damage may well be repaired but will be lethal if not repaired in time, where the notion of "*in time*" relates to cell cycle regulation.

4.5.6.1 Repair of Potentially Lethal Radiation Damage

If the cell passes through *S* phase with DSBs, the formation of dicentric chromosomes or rings may take place, which is potentially lethal to the cell [123]. If the cell thereafter enters mitosis with such asymmetric chromosomal aberrations, it may not be able to give each of the daughter cells a complete set of genes. If such asymmetric chromosomal aberrations are formed, they are therefore usually lethal for proliferating cells. However, if cells are given time to repair DSB before they can develop into asymmetric chromosomal aberrations, i.e., before the cell enters into *S* phase, damage such as DSB are only potentially lethal.

These concepts were supported by early experiments by Stapleton [124] and Phillips [125], where, respectively, culture of cells under suboptimal conditions for growth, or in the presence of inhibitors of the cell cycle produced an increased level of cell survival Seminal experimental findings which support this view include work in vivo by Shipley [126], where rat adenocarcinoma cells were irradiated in situ with gamma rays or neutrons, after which explants of the tumor were grown in vitro either immediately after, or from 4 to 24 h after irradiation, whereupon the survival of these cells was assessed in terms of their clonogenic capacity. While situated in functioning tissue within the animal, these cells had limited access to nutrients and growth factors, which set a natural limit on cell density thereby limiting cell growth and proliferation. Within tissues, such cells may well be cycling though they could take several days to do so, and as such have time to repair their DNA. When cultured as explants in vitro post-irradiation they have greater access to nutrients and as such proliferate strongly, with surviving cells able to produce colonies. Cells which were cultured immediately after irradiation exhibited lower survival rates than those which remained in situ for a period of time after irradiation. Clearly, cells that could not proliferate in tissue have an increased opportunity to repair their damage owing to them being prevented from progressing within the cell cycle. Further experimental evidence demonstrated that this repair process could continue up to 24 h after irradiation, indicating the complexity of this repair process [127].

The experiments by Shipley et al. also showed that there is no increase in cell survival for the cells explanted up to 24 h after high-LET-neutron irradiation. The implication of this is, that the damage induced by high-*LET*-neutron radiation must be too complex to allow for successful repair, which would increase the survival. This finding suggests that complex DSB are not reparable, even with non-homologous end joining (NHEJ), which has been reinforced by observations that not all DSB from high-LET irradiation initiate NHEJ-repair [128].

4.5.6.2 Repair of Sublethal Damage

Following the pioneering development of the clonogenic assay by Puck and Marcus [129], experiments by Elkind and Sutton [130] demonstrated that fractionated irradiation could allow cells to repair their sublethal damage (Fig. 4.23).

In this work, V79 cells of the Chinese hamster were irradiated with one single dose or with two dose fractions where the time between the fractions was varied. The results shown in Fig. 4.23 are from an experiment where they kept the time between the dose fractions constant at 18 h.

These results aligned with the target theory of the time, whereby the combined effects of several sublethal damage events in DNA may result in lethal damage, such that damage created by hits which are not lethal by themselves may be repaired, but cells will not have time to do such repair if a large dose is given acutely, i.e., at a high dose rate. With a large enough acute dose, the degree of sublethal damage for each cell is so high that it combines to form lethal damage.

It is well worth reflecting on both the differences and the similarities regarding sublethal damages between the traditional multi-target/single-hit model and the newer LQ model. On the one hand, in the multi-target/single-hit model, one does not make any assumption regarding the nature of the molecular damage induced. Still, it introduces the concept of sublethal damage and shows that such damage inevitably leads to an initial shoulder on the survival curve. Thus, Elkind's and Sutton's data show that if cells are given time for repair, DNA damage can be repaired.

On the other hand, in the LQ model, one assumes two specific types of molecular damages as being sublethal, namely single strand breaks in DNA (SSB) (which are all sublethal separately) and the repairable double strand breaks

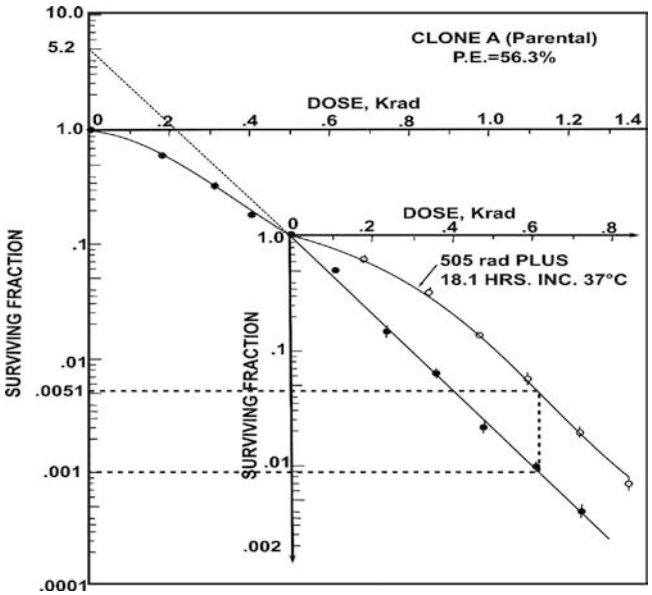

Fig. 4.23 The surviving fraction of V-79 Chinese hamster cells irradiated either with a single dose or with two dose fractions separated by 18.1 h. The first dose fraction of 5.05 Gy was given at time 0 and then the cells were incubated for 18.1 h at 37 °C before the second dose fraction (varied between 2 and 8 Gy) was given. As seen, the incubation time between the two dose fractions has led to a complete reconstitution of the curve shape. The explanation was that through repair of the sublethal damage induced by the first dose fraction, the cells had regained their sublethal damage potential. Unrepaired, these damages would have added to the new sublethal damages and become lethal [130]. (Adapted with permission from Springer Nature: Elkind and Sutton, X-ray damage and recovery in mammalian cells in culture. Nature, 1959)

in DNA (DSB). In reality, no distinction is made between SSB and DSB concerning repair of sublethal damage observed by dose fractionation in the LQ model. According to the LQ model, the dose-response curve has a downward bending, because two sublethal SSB may give rise to a DSB. The DSB may develop into lethal damage and therefore is potentially lethal but probably may also in some cases be sublethal.

The question then arises as to the timeframe required for the repair of sublethal damage events. While Elkind and Sutton did go some way towards measuring the value of this variable (suggesting that it was as much as 12 h), it was not until experiments by Terasima and Tolmach and further experiments by Elkind that refined this estimate and gave an explanation for its value.

As indicated by Fig. 4.26, the repair curves are different if cells are incubated at room temperature (24 °C) between dose fractions compared to at 37 °C, where this difference has to do with differences in cell cycle progression. The cell cycle is halted almost completely at room temperature but continues almost uninhibited between dose fractions at 37 °C. Thus, the explanation is that the first dose fraction primarily kills more V79-cells in mitosis, G1, and early *S* than in late *S* phase where they are resistant (be mindful that V79 cells have a cell cycle duration of approximately 10 h and almost no G1 phase).

At 24 °C, surviving cells stay in the stage of the cell cycle where they are resistant between the dose fractions and therefore their radiosensitivity is constant with time. At 37 °C, they continue through the cell cycle after the first fraction and at some time later will have reached a cell cycle stage where they have maximum radiosensitivity, whereupon the second dose fraction is given. Consequently, survival as a function of the time between fractions will decrease with increasing time.

The customary notion for cell cycle progression between dose fractions is redistribution (also denoted as "reassortment"). So, this notion is used to state that cells, which have not been lethally damaged by a preceding dose fraction, will move to a different cell cycle phase before the next dose fraction (Fig. 4.24).

From Fig. 4.26, one can see that the surviving fraction increases considerably with about 8–10 h repair time at the temperature of 37 °C. This increase is not due to repair. It has to do with the fact that some V79 cells reach completion of

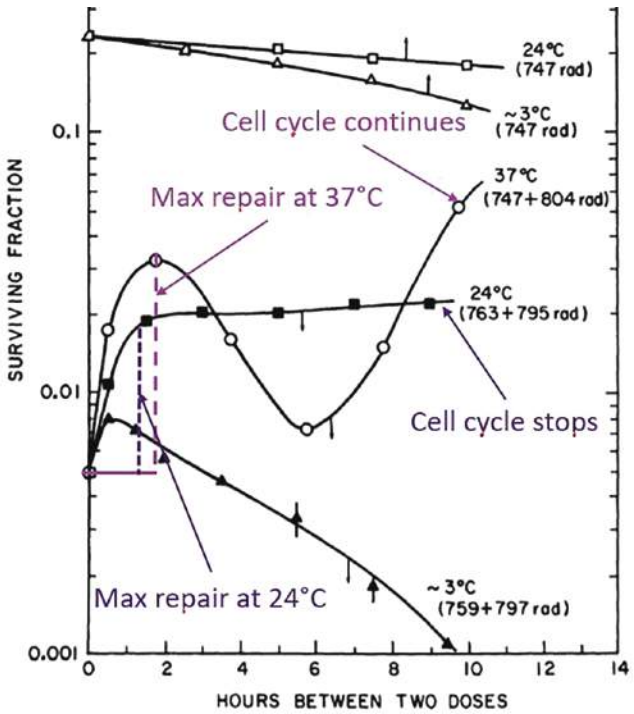

Fig. 4.24 Chinese hamster V79-cells were irradiated with two dose fractions separated by different time spans (lower abscissa) and with different temperatures in the incubator between dose fractions; respectively 3, 24, and 37 °C. In particular, the curves representing 37 and 24 °C are of interest since the first one represents cells that cycle between the dose fractions while the other one represents cells, which do not cycle between the dose fractions. (Adapted from [131] with permission, © 2022 Radiation Research Society [131])

cell division before the next dose fraction is given (notice that these cells have a median cell cycle duration of just about 10 h). The consequence of this is that some colony-forming units consist of two daughter cells instead of just one at the time when the second dose fraction is given.

A simple calculation illustrates the importance of this phenomenon. If the probability to kill a cell is p, the probability for this cell to survive is $S = 1-p$. However, the probability to kill both cells in a doublet or all four cells in a quartet is p^2 and p^4, respectively. The probability for a doublet or a quartet to form a colony is therefore $S = 1-p^2$ and $S = 1-p^4$, respectively.

If we suppose that the number of V79 cells has doubled during a 12 h period at 37 °C following the first dose fraction in Fig. 4.26, we can understand the increased surviving fraction between 10 and 12 h. It is indicated that the surviving fraction after two dose fractions 2 h apart with full repair is 0.035. The surviving fraction after the first dose fraction alone is about 0.23. This means that normalized survival after the second dose fraction alone, assuming full repair of the sublethal damage induced by the first fraction, is 0.035/0.23 = 0.152. The probability that this dose fraction alone would kill a cell is therefore 1–0.152 = 0.848. However, if the cell reaches cell division between the two dose fractions, the probability for the doublet to become unable to form a colony is $0.848^2 = 0.719$. The probability for survival therefore increases from 0.152 for the single cell up to 1–0.719 = 0.28 for the doublet. The surviving fraction after both doses and full repair then should be 0.28 × 0.23 = 0.065. Thus, the surviving fraction has increased from 0.035 to 0.065 because of a doubling of the cell number per colony-forming unit. From Fig. 4.26 one can see that this corresponds well with the survival observed by Elkind et al. with 12 h repair time between the dose fractions, quite in agreement with the cell cycle kinetics for V79 cells (cell cycle duration ~10 h).

In radiotherapy, the notion used for cell proliferation between dose fractions is *repopulation*. By repopulation, we mean that cells which survive a preceding dose fraction get enough time before the next dose fraction to complete the cell cycle and divide. This is an important concept in connection with fractionated radiotherapy. Although cell cycle times in tissues are usually much longer than for V79 cells in culture, 24 h between the dose fractions is sufficient for at least some proliferation of both cancer cells and normal cells between the fractions.

From Fig. 4.26, one can furthermore see that the survival increases almost by the same factor over the first 2 h repair time irrespective of the temperature being 24 or 37 °C. As seen, the surviving fraction increases from the single-dose level of 0.005 and up to 0.02 at 24 °C and 0.03 at 37 °C at 2 h repair time. Thus, the data indicate that the repair itself is less influenced than the cell cycle progression by the temperature (in fact some DNA repair persists at temperatures as low as 3 °C) (Fig. 4.25).

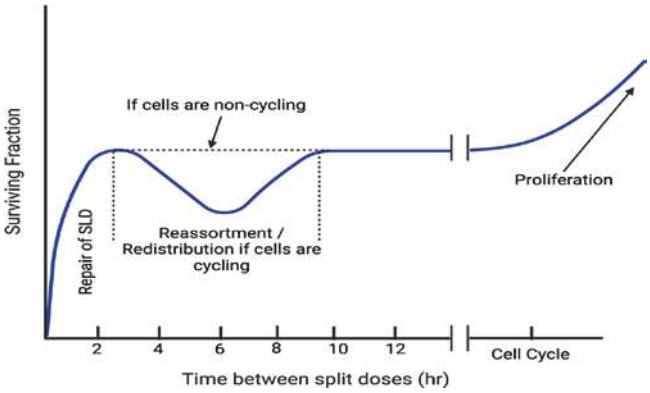

Fig. 4.25 The increased cell survival with increasing time between two dose fractions (up to 2 h) is due to increased time for repair of the sublethal damages induced by the first dose fraction. After about 2 h, all sublethal damage has been repaired. Most surviving cells after the first dose fraction would however be in late *S* or mid G1, the phases where cells are most radio resistant. If cells are offered optimal growth conditions between the dose fractions (37 °C), these surviving cells will continue cell cycle progression and may after 6 h reach a phase where they are more radiosensitive. If the second dose fraction is given at that instant, the survival will be reduced. Therefore, the curve bends downwards between 4 and 6 h, before an upwards turn between 6 and 8 h, when the cells have proceeded to a phase of higher resistance. After a long time, which depends on cell doubling time (typically >12 h), cell division results in an increased multiplicity of the colony-forming units and we see an increased survival that is caused by repopulation. Curve extracted and generalized from Fig. 4.24

In Fig. 4.25, three concepts are listed that are all related to fractionated radiotherapy: *repair* (meaning in this connection repair of sublethal damage) *redistribution* (or reassortment), and *repopulation* (or proliferation). These concepts cover three of the phenomena usually referred to as the 6 Rs of radiotherapy (see Sect. 5.5). All these mechanisms are interesting from a radiotherapeutic point of view because they can all be manipulated by variations in the fractionation regime chosen.

4.5.7 Fractionated Irradiation and Dose Rate Effects

Elkind and Sutton demonstrated that cells irradiated with several dose fractions separated by enough time for full repair would repeat the repair of sublethal damage over and over again [132]. Steele also demonstrated that an increase in cell survival is observed when a given dose is delivered at a low dose rate [133]. Some consistent features in the cell survival curves for cells irradiated with fractionated or low-dose radiation were also observed:

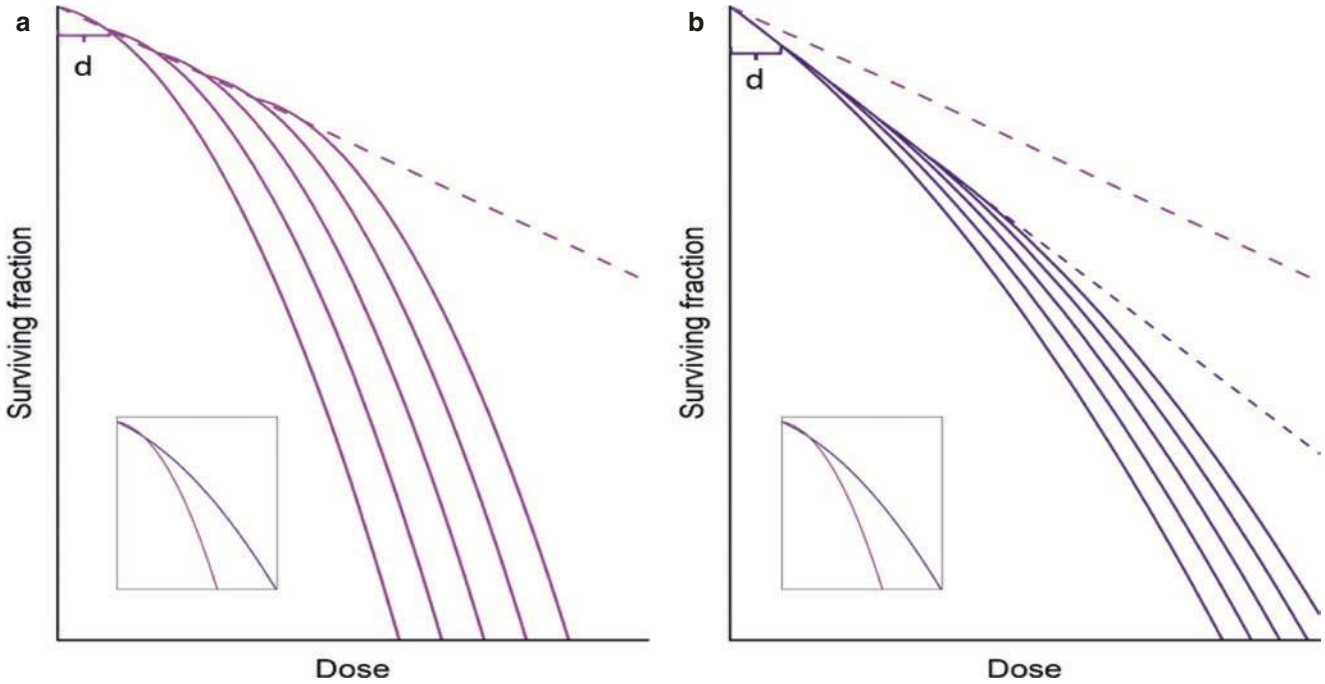

Fig. 4.26 A cartoon to illustrate the difference in sparing effect of fractionated irradiation versus acute irradiation for two cell types having dose-response curves with a broad (late-responding tissues, panel (**a**) compared to a small (early-responding tissues, panel (**b**) shoulder region. The small insert shows the curve shapes after acute irradiation to compare. In conclusion, even if cells characterized by a broad-shouldered dose-response curve are the most sensitive ones to high acute doses, these cells are the most resistant ones to fractionated or low dose rate irradiation

- While the initial slopes of each cell survival curve differed, the final slopes were consistent. Using the LQ model to describe the cell survival curve would indicate that for a given cell line under fractionated or low dose irradiation, the α-values would change, while the β-values would remain consistent.
- The differences between the response of cells of different types (with varying radiosensitivity) were more pronounced with low dose rate irradiation than with acute irradiation. This is a first indication of a more general principle, which is of utmost importance for radiotherapy. The sparing effect of fractionated or low dose rate radiation is most pronounced for cells having a dose-response curve with a broad shoulder (or a shallow initial slope).

This latter feature is illustrated by the cartoon in Fig. 4.26, showing an example of a fractionation regime (with dose fractions of *d*) for two different cell types having dose-response curves characterized by different shoulder regions (curves shown together in the small insert), one with a broad shoulder (small α) and one with a small shoulder (large α). The two dashed lines shown in panel (b) indicate the difference in response for the two cell types. If radiation is given continuously at a dose rate low enough for the cells to complete repair of all sublethal damage at the same rate as they were induced, the β-term of the LQ model will not contribute (all sublethal damage would be repaired before they could cowork to produce potentially lethal damages). This would be equivalent to very many very small doses and the response curve would be a tangent to the initial part of the dose-response curve for acute irradiation. Continuous irradiation at such a low dose rate results in the largest difference obtained for the two cell types.

One should notice that the final slopes of the single-dose curves indicate that the cells having the broadest shoulder are in fact *more* radiosensitive than those having the smallest shoulder at high single doses. Still, with fractionated or low dose rate irradiation it is the other way around. This phenomenon is an important principle, which is the basis for radiotherapeutic practice.

In radiotherapy, it is customary to express this principle in some other words as based on the LQ model. The sparing effect of fractionated or low dose rate irradiation as compared to acute irradiation is most pronounced for cells having a dose-response curve with a small α-parameter.

4.5.8 The Inverse Dose Rate Effect Illustrating the Importance of Cell Cycle Progression

Cellular radiosensitivity varies with cell cycle stage. At the same time, ongoing low dose rate irradiation may activate cell cycle arrest in the various restriction points in the cell

cycle as has been explained by the activation of regulatory cascades related to p53 (at G1k) and the ATM-kinase activated by DNA-DSB. This gives rise to an *inverse dose-rate effect* (Fig. 4.27), where at very low dose rates cells may see an increase in cellular killing.

The standard approach to the explanation of this effect is that cells progress to G2 and undergo a "block" in the G2 phase during ongoing very low-dose irradiation. As cells are radiosensitive during G2, much of the radiation is delivered during a radiosensitive phase of the cell cycle. While the mechanism has some clarity, work by Furre et al. in 1999 [134] and 2003 [135] on the effects of lowering dose rates on the survival of a cervical cancer cell line, NHIK 3025, and a breast cancer line, T47-D, has added a further degree of molecular evidence as to the origin of the effect. Of the two cell lines, only the NHIK3025 had an inverse dose rate effect. Both the NHIK 3025 cells and the T-47D cells lack p53-function, but unlike NHIK 3025 cells, T-47D cells have normal pRB-function. They found that T47-D cells accumulated in G2 during low dose rate irradiation in the same manner as the NHIK 3025 cells, but the T-47D cells still remained resistant during the arrest. The effect of pRB-function here appears to be key. Although pRB is normally not bound to the cell nucleus in G2 (only in G1), the nuclear-bound pRB increased in the arrested cells during radiation-induced prolonged G2 arrest. Although the mechanism for this seeming protection is not clear, there are indications that pRB may have a special protective function under severe cellular stress and that this is not limited to any special cell cycle phase.

4.5.9 The Importance of the Initial Slope and the α/β-Dose in Radiotherapy

Over time, and as radiobiological experience increased regarding the radiation response of cells of different types and from different organs, etc., it was gradually realized how the initial slope of the dose-response curve is of fundamental importance in radiotherapy. This has to do with the observation demonstrated in Fig. 4.28 above, showing the importance of the initial slope of the dose-response curve regarding cellular sensitivity to a fractionated radiation with time for sub-lethal damage (SLD)-repair between dose fractions. Of equal importance are the two following general observations:

- Cells that are mainly proliferating such as cancer cells or some normal stem cells, all seem to have dose-response curves with a large initial slope (i.e., a large α). Such cells are denoted as "early responders" since radiation damage induces cell loss early under ongoing irradiation. Most of these cells enter mitosis within a few days after the start of the radiation treatment. Thus, the cells express a response to the radiation early after the onset of treatment.

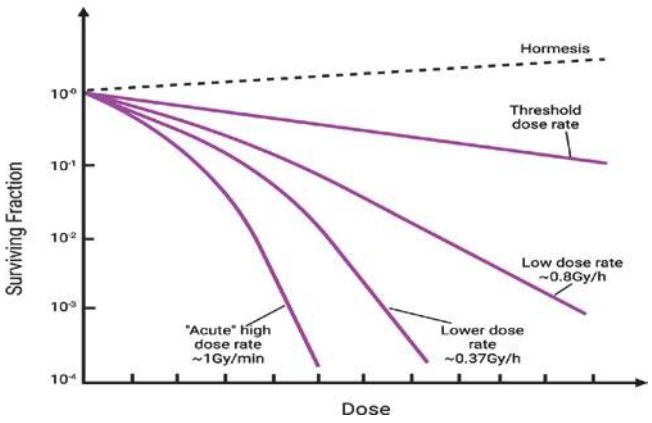

Fig. 4.27 The effect of dose rate on the cell survival curve. Repair processes are the primary mechanism that adjusts survival curves as the dose rate decreases from an acute level (~1 Gy/min) to a low level (~0.8 Gy/h). An increase in the slope of the cell survival curve (indicating an increase in radiosensitivity, the "inverse dose rate effect") occurs due to the redistribution of cells throughout the cell cycle when the dose rate further decreases from ~0.8 Gy/h to 0.37 Gy/h. Finally, increased proliferation of cells occurs as the dose rate decreases further towards a threshold or critical dose rate, which varies by cell type. Notice that this cartoon presents a very special case of a cell type having an inverse dose rate effect, which is probably associated with a simultaneous lack of both p53- and pRB-function. The dose rate that can produce a hormetic effect is unclear and not indicated, but is several orders of magnitude lower than the lowest one depicted here (0.37 Gy/h)

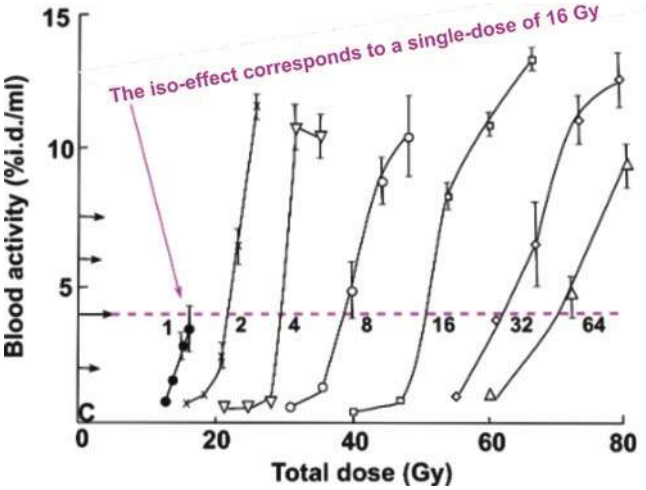

Fig. 4.28 Mice of age 9–11 weeks were given fractionated irradiation with 240 kV X-rays to the dorsal trunk over a period of 3 weeks (i.e., more than one fraction per day for regimes with 32 and 64 fractions). Chromium-51-ethylene-diamine-tetra-acetate ($[^{51}Cr]$-EDTA) was injected intraperitoneally (i.p) 26 weeks after completed irradiation and the blood level of radioactivity was measured in blood samples taken 60 min after injection. Increasing blood levels indicate reduced kidney filtration capability and the red line indicates an isoeffect level of reduced kidney function. [Modified from [136] with permission [136], © 2022 Radiation Research Society]

- Cells which are more prone to stay in the resting phase, like differentiated cells or cells in tissues where growth factor or mitogen stimulation is low, largely seem to have dose-response curves with a small initial slope (i.e., a small α). Such cells are denoted as "late responders" since radiation damage induces cell loss at a late stage after the onset of the treatment. Most of these cells enter mitoses weeks or even months after the start of the treatment. Thus, tissues of such cells express a response to the radiation late; not only late after the onset of the treatment but in many cases long after the end of the treatment.

This difference is central to the whole concept of radiotherapy. Without this difference, radiotherapy of cancer would probably have had little curative success. The reason is that proliferation is an activity that is typical for almost all cancer tumors but only for a few organs of normal tissues. Resting cells, on the other hand, are largely characteristic of most normal tissues and not of cancer tissues.

Thus, while cancer cells largely proliferate and have a large α-parameter, highly differentiated normal cells largely rest and have a small α-parameter. The result of this is that if radiation is given over a prolonged time, (either by repeated dose fractions separated by time for repair or by continuous low dose rate irradiation) there is a much more sparing effect on late-responding normal tissues than on most cancer tissues.

The interesting question is then, How did we obtain the knowledge that late-responding tissues have cells with a small initial slope on their dose-response curves? These cells are largely not proliferating. They are furthermore seated in tissues and do not grow in culture. So, how is it possible to measure the ability of these cells to form a colony after irradiation? The answer is that we cannot do such measurements directly. Still, as mentioned above, we know that these cells have dose-response curves characterized by a small α-parameter. This knowledge stems from the use of the LQ model to measure not α, but the α/β-ratio. The α/β-ratio is actually the dose (D_1) where the contribution to cell inactivation by single event killing matches that from multiple event killing, i.e.,

$$\alpha \cdot D_1 = \beta \cdot D_1^2 \tag{4.42}$$

or

$$D_1 = \alpha / \beta. \tag{4.43}$$

These measurements are based on the following idea: The function of a tissue depends on the functionality of the tissue cells. If the radiation inactivates a certain fraction of the cells, the tissue may lose some of its function and the loss of function can be measured. Such measurements as a result of irradiation are usually denoted as measurements of "Functional endpoints." Two examples of such functional endpoints representing late and early-responding tissues, respectively, are: (a) Kidneys, the clearance of a very small amount of an injected substance from the blood can be measured and (b) Skin, the severity of damage to an irradiated area of skin can be observed and graded (from mild reddening to irreparable wounds and necrosis).

In Fig. 4.28, an example of kidney function damage is shown. As a measure of kidney function, the clearance from blood of the compound ethylene diamine tetra acetate (EDTA) as a function of the total dose given by various fractionation regimes to mice was detected [136]. EDTA was labeled with [^{51}Cr] so that minute amounts in blood could be accurately detected by blood samples taken 1 h after EDTA injection. The red line indicates an isoeffect level and the numbers 1–64 indicate the number of dose fractions given to the animals over a period of 3 weeks. Kidneys are late-responding tissues (the filtration units of kidneys consist of highly differentiated cells) and therefore the clearance was measured late (26 weeks) after the end of irradiation.

Since all fractionation regimes gave the same functional effect along the red line in Fig. 4.30, we assume that cell survival is the same along this red line. For one such fractionation regime with n dose fractions of size d the LQ model predicts the following cell survival as long as time is given for the full repair of SLD between dose fractions:

$$S(D) = \left[S(d)\right]^n = \left[e^{-\alpha d - \beta d^2}\right]^n = e^{-\alpha D - \beta d D}. \tag{4.44}$$

where the total dose is $D = nd$.

We now rearrange to get the following expressions (and we write S_D for $S(D)$ and S_d for $S(d)$:

$$-\frac{\ln S_D}{D} = \frac{-n \ln S_d}{D} = \alpha + \beta d \tag{4.45}$$

or

$$-\frac{1}{D} = \frac{\alpha}{n \ln S_d} + \frac{\beta}{n \ln S_d} d. \tag{4.46}$$

If we now remember that $D = nd$ this formula can also be rewritten as follows:

$$-\ln S_d = \alpha d + \beta d^2. \tag{4.47}$$

The data from Fig. 4.28 can be plotted according to Eqs. (4.45) (left panel) and Eq. (4.46) (right panel) as shown in Fig. 4.29 [137].

From Fig. 4.29a, one can see that the data points are well-fitted by a straight line as predicted by the LQ formula (Eq. 4.45). Furthermore, according to Eq. (4.45) we have for $1/D = 0$ that $\frac{\alpha}{\ln S} = -\frac{\beta}{\ln S} d_{(1/D)=0}$ and thus that $d_{(1/D=0)} = -\alpha/\beta$.Therefore, since the line crosses the abscissa

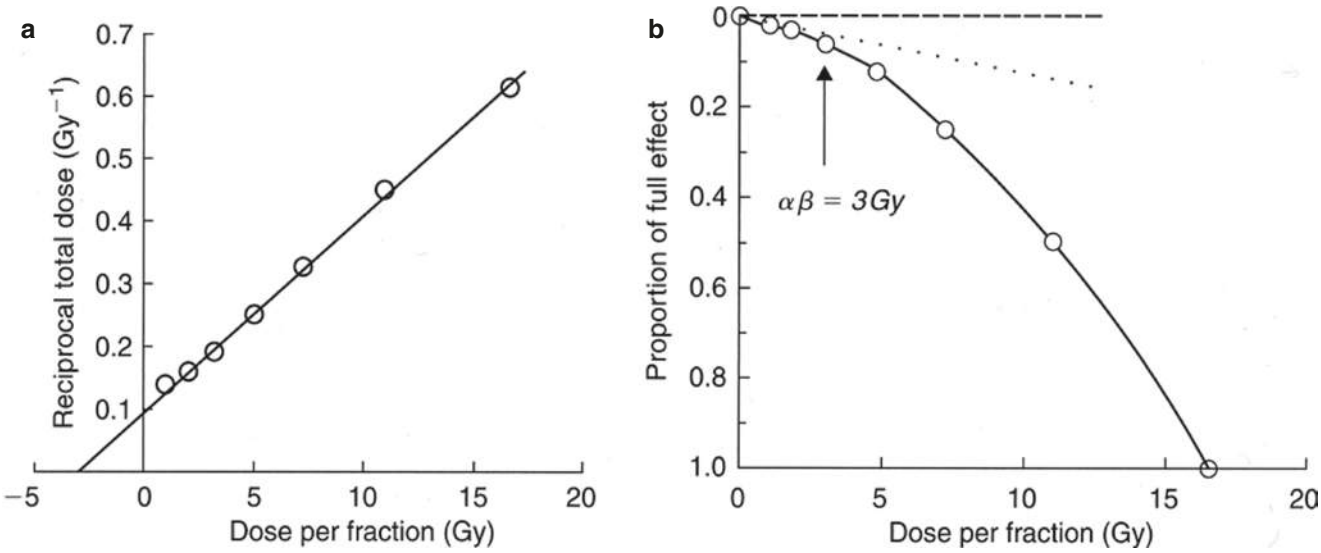

Fig. 4.29 The isoeffect data defined by the red line in Fig. 4.30 are replotted after the two transformations described by Eqs. (4.45) (plotted in panel **a**) and (4.46) (plotted in panel **b**). Reprinted with permission from [137]

at $d = -3$ Gy, the nominal value of the α/β-dose must be 3 Gy.

In Fig. 4.29b, one can see that Eq. (4.46) actually reconstructs the shape of the dose-response curve, but in this case with the survival axis plotted as the fractional effect of a single dose fraction relative to the effect induced by the single-dose acute irradiation of 16 Gy. As indicated in the figure, also this plot results in the α/β-dose being 3 Gy since the contributions at 3 Gy by single and multiple event killing as defined in the LQ model are equal. The importance of the value of the α/β-dose in relation to fractionated radiotherapy is clearly illustrated by the isoeffect tolerance curves plotted in Fig. 4.30 [137].

These isoeffect curves show which total dose is necessary in order to obtain a certain effect as a function of the dose per fraction (or number of fractions) for two different tissues. Notice that both axes are logarithmic. In (a), the mouse kidney data of Stewart et al. are plotted as an example of a late-responding tissue with $\alpha/\beta = 3$ Gy and in (b), data on mouse skin are plotted as an example of an early-responding tissue with $\alpha/\beta \approx 12$ Gy. Thus, while the upper curve represents a dose-limiting normal tissue, the lower curve represents an early-responding tissue such as cancer or some highly proliferative normal tissues. A list of typical values for α/β can be found in Table 4.5.

The arrows in Fig. 4.30 show that four large dose fractions of 10 Gy each will represent an advantage to the early-responding tissue (like the tumor), while 64 small dose fractions of 1 Gy each represent an advantage to the late-responding tissue (normal tissue). If tissues are irradiated

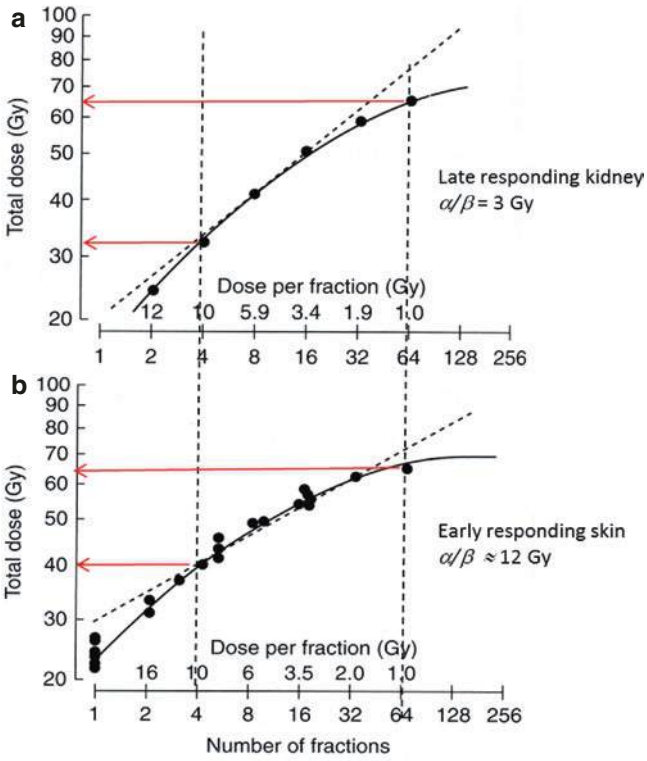

Fig. 4.30 In (**a**), the data of Fig. 4.28 on late-responding mouse kidney are replotted as isoeffect tolerance curves with total tolerated dose in a fractionation scheme as a function of the dose per fraction (both axes logarithmic). In (**b**), similar data are shown for an early-responding normal tissue, namely mouse skin. Notice that the α/β-dose is 3 Gy for the late-responding tissue and 12 Gy for the early-responding tissue. (Reprinted with permission from [137])

Table 4.5 Ratios of α/β for early and late radiation reactions in normal tissues, determined from laboratory animal and clinical data (Fowler, copyright © 2005 Acta Oncologica Foundation, reprinted by permission of Taylor & Francis Ltd) [138]

Early reactions	$\frac{\alpha}{\beta}$ (Gy)	Late reactions	$\frac{\alpha}{\beta}$ (Gy)
Skin	9–12	Kidney	2–2.4
Jejunum	6–10	Rectum	2.5–5
Colon	9–11	Lung	2.7–4
Testis	12–13	Bladder	3–7
Mucosa	9–10	CNS: Brain, spinal cord	1.8–2.2

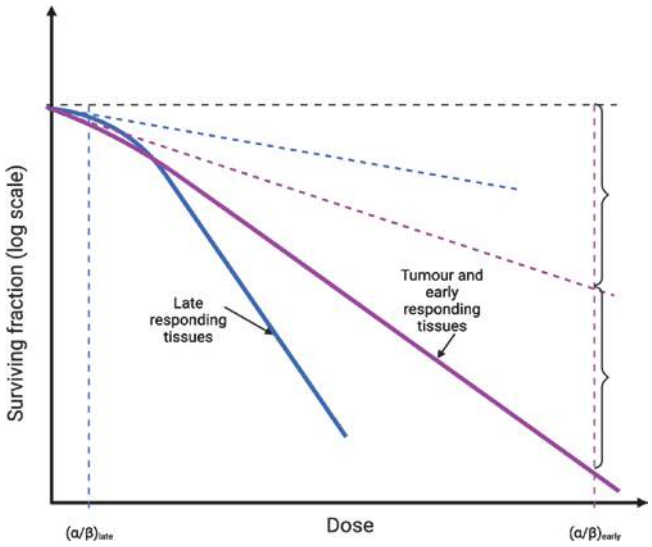

Fig. 4.31 These cell survival curves illustrate typical differences in the dose-response curves of **early**- (purple: α/β-ratio of ≈3 Gy) and **late**- (blue: α/β-ratio of ≈12 Gy) responding tissues. Note that the α/β-dose is the dose where the contributions to the cell kill from the αD-term is the same as for the βD^2-term, as indicated with brackets for the late-responding tissues

continuously with a low dose rate, the cells may repair sublethal damage during irradiation and the lower the dose rate, the smaller the probability will be for two or more sublethal damages to combine to create a potentially lethal damage. For the LQ model, this means that reducing the dose rate results in reduced influence by the β-term and more and more dominance by the α-term. The connection between the shape of the dose-response curve and the isoeffect tolerance curves (dashed lines) by continuous irradiation is illustrated in Fig. 4.31. The blue curves represent late-responding tissues (i.e., small α/β-ratio of ≈3 Gy) while the purple curves represent early-responding tissues (i.e., large α/β-ratio of ≈12 Gy). The steep isoeffect tolerance curve at high doses for late-responding tissues indicates good sparing for these tissues by reduced fraction doses and prolonged treatment time. Early-responding tissues will experience much less sparing by prolonged treatment times (Box 4.12).

Box 4.12 The Linear Quadratic Model

- The linear quadratic model is a mathematical model, which is a good fit for cellular survival data in a median dose range. For low and high dose, the model needs modifications
- There have been several biological interpretations of the model
- To compare different clinical fractionations regimens, the biologically effective dose can be calculated from the $\frac{\alpha}{\beta}$-value

4.5.10 Recruitment: Limitations Caused by Compensatory Cell Proliferation in Early- and Late-Responding Tissues

From the discussion so far, one might get the impression that most problems with radiotherapy can be resolved by just a further increase of the treatment time, using, for example, larger numbers of smaller dose fractions over a longer time period, or by reducing the dose rate in case of continuous low dose rate irradiation. However, such changes are met with other limitations such as recruitment and proliferation (repopulation). The problem is that if the tissue is given a small dose each day, the induced cell loss will after a while induce increased proliferation (and probably recruitment) in the surviving cells to compensate for the cell loss. The point is that this activity favors the malignant tissue more than most normal tissues. The reason has to do with the very difference between early- and late-responding tissues, which was the basis for the notion of early and late. While early-responding tissues start compensatory proliferation early after the onset of the radiation treatment, late-responding tissues start compensatory proliferation much later, and in humans, long after completed treatment. This is illustrated in Fig. 4.32, which is based on experimental data from rodents using mouse skin as a model for early-responding tissue (cancer included) and rat spinal cord as a model for late-responding tissue. One should keep in mind here that a complete fractionation scheme for radical radiotherapy of a solid tumor with external radiation is typically 6 weeks, i.e., 42 days.

As indicated, the compensatory proliferation starts after the end of the treatment for nerve tissues, while it starts after just 2 weeks of treatment for the cancer-modeling skin tissues. The compensatory proliferation (repopulation) initiated by fractionated irradiation is thus more favorable for early-responding tissues (including cancer) than for late-responding normal tissues. Therefore, one must be careful not to increase the overall treatment time too much. The 6 weeks that are typical for the duration of conventionally frac-

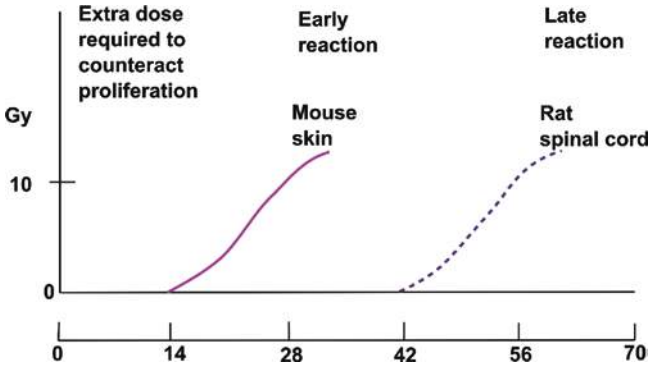

Fig. 4.32 The curves indicate what extra radiation dose is required to counteract only proliferation during treatment with one daily dose fraction in two different rodent tissues. Human tissues react more slowly than rodent tissues. Thus, the time for increased proliferation therefore would probably start at a later time than indicated in the figure for corresponding human tissues. (Adapted with permission from [139])

tionated radiation treatment thus is a compromise taking into consideration several different aspects to obtain the maximal probability for a positive effect on the cancer tumor with a minimum of side effects.

4.5.11 BED and Clinical Use

We can rewrite Eq. (4.45) to:

$$\mathrm{BED} = \frac{-n \ln S_d}{\alpha} = D\left(1 + \frac{d}{\frac{\alpha}{\beta}}\right) \tag{4.48}$$

$\frac{-n \ln S_d}{\alpha}$ is called the Biologically Effective Dose (BED) and describes the dose needed to induce the same effect as if the number of dose fractions was infinitely large and the single dose fractions d approaching zero. This is the equivalent of continuous irradiation with a dose rate sufficiently small for cells to repair sublethal damage at the same rate as they are induced preventing them to cooperate to create lethal damage. BED is a useful parameter to calculate and compare fractionation regimes.

Standard treatment for many cancers is 2 Gy daily fractions (for example, over 7 weeks with five treatment days per week). It is therefore often relevant to compare other fractionation regimes to 2 Gy fractions.

The equivalent total dose D for 2 Gy fractions is called

$$\mathrm{EQD2} = \frac{\mathrm{BED}}{\left(1 + \frac{2}{\frac{\alpha}{\beta}}\right)}. \tag{4.49}$$

$$D_d = \frac{\mathrm{BED}}{\left(1 + \frac{d}{\frac{\alpha}{\beta}}\right)}$$

For the fractionation regime we want to compare with .

We then get $\mathrm{EQD2} = D_d \frac{\left(d + \frac{\alpha}{\beta}\right)}{\left(2 + \frac{\alpha}{\beta}\right)}$, which can be used to calculate fraction dose d and number of fractions $n = D_d/d$ to get the same BED as 2 Gy fractions to a total dose of EQD2.

4.5.12 Dose-Response Models for Radiation Carcinogenesis

While it is relatively straightforward to develop a model relating dose to survival at the cellular level, modeling of dose response at the organ and organism (human) level is far more complex. There remains considerable debate regarding the most appropriate model for use in describing the variation in response to dose in humans [140]. However, each of the models has its basis in radiobiology, and the interaction of ionizing radiation with human tissue at the cellular level [140, 141]. The previous section on target theory provides a basis to begin to define models of human radiation survival. The effects of ionizing radiation on cells may be divided into two types: deterministic and stochastic effects [141]. Deterministic effects result from the substantial injury of cells in affected tissues, and the severity of the effect is a function of the absorbed dose. Stochastic effects are those for which the probability of occurrence of an effect, and not its severity, is a function of dose [141]. Deterministic effects have a well-defined dose threshold in mammalian cells of a particular organ and type, while it is assumed that no threshold exists for stochastic effects [142]. Deterministic effects occur at relatively high doses (0.5 Gy and above depending on the organ system involved), while stochastic effects generally occur at relatively low doses (below 0.5 Gy) [141]. Both sets of effect are modified by the rate at which the dose is administered as well as by the biological damage responses such as DNA repair and immune responses [141]. Stochastic effects usually constitute the mechanisms by which the hereditary (mutagenic) and somatic (carcinogenic) effects of ionizing radiation occur [140]. Carcinogenesis is a multistage process in which radiation may induce one or more of the changes necessary to cause DNA damage, while mutagenesis is usually thought to be the result of single biological changes in germ cells. [140]

From Eq. (4.26), we may simplify and introduce a variable change to obtain a single-hit model of radiation survival in cells where the frequency, f, of cells with one or more hits in a given population of cells is:

$$f = 1 - e^{-n} = 1 - e^{-\lambda D}. \tag{4.50}$$

where n is the number of critical hits per cell at dose D, and λ is the mean number of critical hits per cell at dose D. For low frequency hits (low doses), the number of critical hits, n, per cell is small and thus Eq. (4.49) reduces to:

$$f \approx \lambda \cdot D. \tag{4.51}$$

Thus, the dose-response is approximately linear with no threshold. At high hit frequencies, where hit saturation occurs, the equation takes the form of Eq. (4.49), since after the first critical hit in a cell, further hits in it cannot lead to additional effects [140].

Multi-track models may be utilized to describe the effect of the interaction between multiple tracks in a cell. The interaction may either be positive or negative and may result in visible curvature to the dose response [140]. A mathematical description of such a model may be achieved by inserting a general polynomial into Eq. (1.50) as follows [140]:

$$f = 1 - e^{-\left(\alpha_1 D + \alpha_2 D^2 + \cdots\right)} \tag{4.52}$$

which, for low frequency effects (low doses) reduces to:

$$f \approx \alpha_1 D + \alpha_2 D^2. \tag{4.53}$$

In practice, many models have been found to fit the dose response of various bodily organs, depending on the organ in question [143]. The two most common models used are the linear no threshold, LNT (Eq. 4.50), and the linear quadratic (Eq. 4.52) models [143]. At low doses, in a homogeneous cell population, Eq. 4.50 would be the most appropriate dose-response model theoretically, since it is assumed that every cellular hit may be biologically critical and that a single cell is unlikely to be hit more than once [143]. However, for low doses, other mechanisms come into play, such as low dose hypersensitivity, hormesis, and adaptive response mechanisms, as described in Sect. 2.9 and non-targeted effects as described in Sect. 2.10, which will modify the radiation response. In an inhomogeneous cell population, where groups of cells have differing radiosensitivity, the response for single-track events in each subpopulation should follow the form of Eq. (4.52), the overall response should show a decreasing sensitivity with increasing dose, consistent with the LQ model [140].

Historically, the LNT model for radiation risk assessment was introduced after Muller's discovery of radiation-induced mutations in 1927. After the atomic bombing of Japan in 1945 and the start of the nuclear arms race, ionizing radiation became connected in public mind with nuclear apocalypse. In 1945–1956, there was great controversy and extensive arguments pro and contra LNT. In general, it can be said that among scientists "*the data to support the linearity at low dose perspective was generally viewed as lacking but the fear that it may be true was a motivating factor*" [144]. In 1956, ICRP officially abandoned the tolerance level concept (that was in use since 1931) and substituted LNT for it. Formally, LNT has been introduced and remains a practical operational model for radiation protection only. De facto however LNT acquired the status of a scientific theory, though supporting evidence is at least inconclusive. Moreover, about 40 years ago, low dose-induced changes in cell signaling with delayed responses were discovered. There is emerging evidence that low doses induce cellular and intercellular changes, which can lead to stress response (adaptive response) metabolic alterations. Adaptive responses against the accumulation of damage—also of non-radiogenic origin—were also discovered [145]. The above evidence suggests that while high-dose ionizing radiation is certainly harmful, low doses may be beneficial for human health; such an effect is called *hormesis* [146]. At the joint US ANS/HPS conference "Applicability of Radiation-Response Models to Low Dose Protection Standards" in 2018, neither of the three viewpoints—supporting LNT, tolerance level, or hormesis—was marginal [145].

4.6 Exercises and Self-Assessment

Q1. **Principles of radiation dosimetry?**

Q2. **Radiation microdosimetry**

(a) What is lineal energy?

(b) How is it related to the LET?

Q3. **From track structure to early DNA damage**

(a) What are the main differences between a general MC code and a track structure (TS) MC code?

(b) What are the main sources of uncertainty in the calculation of DNA damage with MCTS code?

Q4. **Micro-beams and minibeams**

(a) Please allocate the research questions mentioned in the following figure to the irradiation pattern, which is best used for investigation, as it is done in the example.

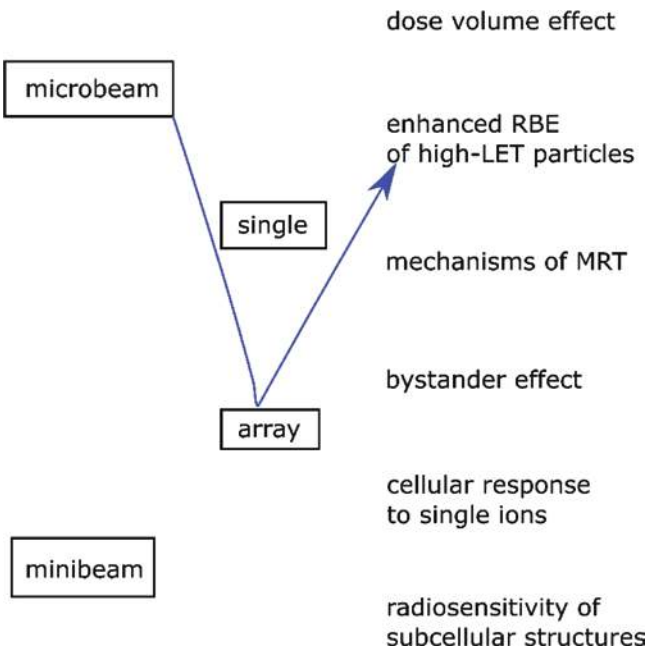

Q5. **Target theory and dose-response models**

Use the data in the table below (A549 lung cancer cells irradiated with 220 kV X-rays) to:

(a) Find the α/β-value both from a LQ-fitting and by drawing the initial slope and comparing the contributions from each term (see figure provided in Sect. 4.5 above).

(b) Calculate the surviving fraction using α and β from your LQ-fitting for 5 fractions of 2 Gy (24 h apart) and compare to a single dose of 10 Gy.

(c) How many fractions of 2 Gy should we give to get the same biological effect as for 1 fraction of 10 Gy?

Dose [Gy]	Surviving fraction	Standard error
0	1	
0.5	0.88	0.07
1	0.64	0.06
2	0.41	0.04
5	0.07	0.02
10	0.0008	0.0003

4.7 Exercise Solutions

SQ1. **Principles of radiation dosimetry**

SQ2. **Radiation microdosimetry**

(a) The lineal energy is the quotient of the total energy imparted to a volume of matter by a single energy deposition event and the mean chord length in that volume.

(b) In large-size targets, the number of interactions is large and the distribution of lineal energy converge to an expected value, which is the LET.

SQ3. **From track structure to early DNA damage**

1. Two main characteristics differentiate these two types of MC calculation:
   (a) TS MC codes do not use the condensed history approach for electron transport and they discretely simulate all electron interactions (elastic and inelastic)
   (b) TS MC codes include electron interaction cross sections to explicitly transport the electrons down to very low energies (of the order of 10 eV), which allows to calculate the energy depositions in micrometric and nanometric volumes.
2. Cross sections, mainly for liquid water, used by MCTS codes have uncertainties due to the lack of experimental data that could validate them. All the complexity of radiolysis and reactions of radiolytic species with biomolecules is not taken into account. DNA geometrical models require approximations. The conversion of particle interactions or reactions of radiolytic species into damage is a source of interpretation.

SQ4. **Micro-beams and Minibeams**

(a)

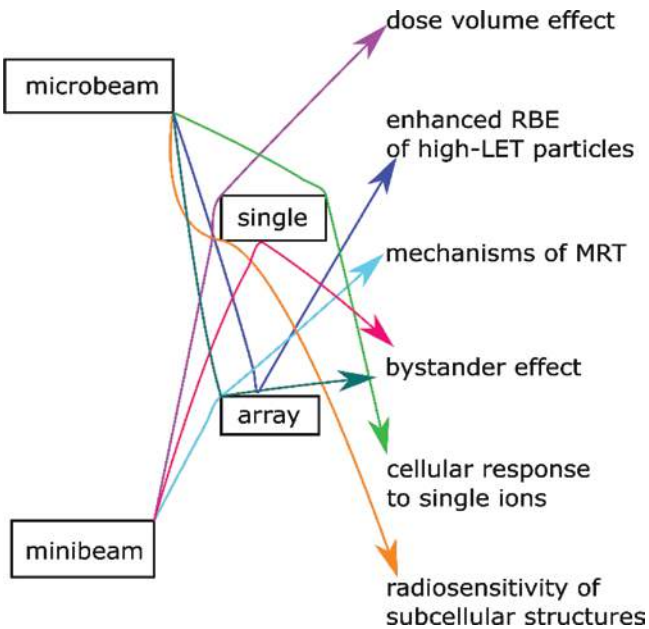

SQ5. **Target theory and dose-response models**

(a) $\alpha/\beta = 12$

(b) and 0.001

(c) 8

References

1. Attix FH. Introduction to radiological physics and radiation dosimetry. New York: Wiley; 1986.
2. Pawlicki T, Scanderbeg DJ, Starkschall G, Hendee WR. Hendee's radiation therapy physics. 4th ed. Hoboken: Wiley; 2016.
3. Attix FH. Energy imparted, energy transferred and net energy transferred. Phys Med Biol. 1983;28:1385–90.
4. Carlsson CA, Carlsson GA. Chapter 2: Dosimetry in diagnostic radiology and computerized tomography. In: Kase KR, Bjärngard BE, Attix FH, editors. The dosimetry of ionizing radiation. San Diego: Academic Press; 1990. p. 163–257. https://doi.org/10.1016/B978-0-12-400403-0.50006-3.
5. Gustafsson M. Energy imparted in roentgen diagnostic procedures. Results of two surveys during the periods 1958–1960 and 1974–1976 related to technical modifications. Acta Radiol Diagn (Stockh). 1979;20:123–44.
6. Das A. Introduction to nuclear and particle physics. Singapore: World Scientific; 2003.
7. Martin BR, Shaw G. Nuclear and particle physics: an introduction. 3rd ed. Hoboken: Wiley; 2019.
8. Hachadorian RL, Bruza P, Jermyn M, Gladstone DJ, Pogue BW, Jarvis LA. Imaging radiation dose in breast radiotherapy by X-ray CT calibration of Cherenkov light. Nat Commun. 2020;11:2298. https://doi.org/10.1038/s41467-020-16031-z.
9. Allison J, Amako K, Apostolakis JEA, Araujo H, Dubois PA, Asai M, et al. Geant4 developments and applications. IEEE Trans Nucl Sci. 2006;53:270–8.
10. Goorley T, James M, Booth T, Brown F, Bull J, Cox LJ, et al. Initial MCNP6 release overview. Nucl Technol. 2012;180:298–315. https://doi.org/10.13182/NT11-135.
11. Kawrakow I, Rogers DWO. The EGSnrc code system: Monte Carlo simulation of electron and photon transport. 2010
12. Pelowitz DB. MCNPX user's manual version 2.5.0. Los Alamos Natl Lab. 2005;76:473.
13. PENELOPE 2008 (2008: Barcelona), Francesc SG, Fernández Varea JM, Sempau Roma J. Organització de Cooperació i Desenvolupament Econòmic. PENELOPE-2008 workshop proceedings Barcelona, Spain 30 June–3 July, 2008. Paris: OECD; 2009.
14. ICRU. REPORT 35—Radiation dosimetry: electron beams with energies between 1 and 50 MeV | Engineering 360. ICRU; 1984.
15. Rossi HH, Biavati MH, Gross W. Local energy density in irradiated tissues: I. Radiobiological significance. Radiat Res. 1961;15:431. https://doi.org/10.2307/3571286.
16. Rossi HH, Rosenzweig W. A device for the measurement of dose as a function of specific ionization. Radiology. 1955;64:404–11. https://doi.org/10.1148/64.3.404.
17. Booz J, Braby L, Coyne J, Kliauga P, Lindborg L, Menzel H-G, et al. Microdosimetry. J Int Comm Radiat Units Meas. 1983;os19:36. https://doi.org/10.1093/jicru/os19.1.Report36.
18. Magrin G. A method to convert spectra from slab microdosimeters in therapeutic ion-beams to the spectra referring to microdosimeters of different shapes and material. Phys Med Biol. 2018;63:215021. https://doi.org/10.1088/1361-6560/aae655.
19. Hawkins RB. A statistical theory of cell killing by radiation of varying linear energy transfer. Radiat Res. 1994;140:366. https://doi.org/10.2307/3579114.
20. Kase Y, Kanai T, Matsumoto Y, Furusawa Y, Okamoto H, Asaba T, et al. Microdosimetric measurements and estimation of human cell survival for heavy-ion beams. Radiat Res. 2006;166:629–38.
21. Jorgensen TJ. Enhancing radiosensitivity: targeting the DNA repair pathways. Cancer Biol Ther. 2009;8:665–70. https://doi.org/10.4161/cbt.8.8.8304.
22. Dingfelder M, Jorjishvili IG, Gersh JA, Toburen LH. Heavy ion track structure simulations in liquid water at relativistic energies. Radiat Prot Dosimetry. 2006;122:26–7. https://doi.org/10.1093/rpd/ncl415.
23. Muroya Y, Plante I, Azzam EI, Meesungnoen J, Katsumura Y, Jay-Gerin J-P. High-LET ion radiolysis of water: visualization of the formation and evolution of ion tracks and relevance to the radiation-induced bystander effect. Radiat Res. 2006;165:485–91. https://doi.org/10.1667/RR3540.1.
24. Pimblott SM, LaVerne JA. Production of low-energy electrons by ionizing radiation. Radiat Phys Chem. 2007;76:1244–7.
25. Plante I, Cucinotta FA. Ionization and excitation cross sections for the interaction of HZE particles in liquid water and application to Monte Carlo simulation of radiation tracks. New J Phys. 2008;10:125020.
26. Michaud M, Wen A, Sanche L. Cross sections for low-energy (1–100 eV) electron elastic and inelastic scattering in amorphous ice. Radiat Res. 2003;159:3–22.
27. Emfietzoglou D, Kyriakou I, Garcia-Molina R, Abril I. Inelastic mean free path of low-energy electrons in condensed media: beyond the standard models. Surf Interface Anal. 2017a;49:4–10.
28. Boudaıffa B, Cloutier P, Hunting D, Huels MA, Sanche L. Resonant formation of DNA strand breaks by low-energy (3–20 eV) electrons. Science. 2000;287:1658–60.
29. Huels MA, Boudaïffa B, Cloutier P, Hunting D, Sanche L. Single, double, and multiple double strand breaks induced in DNA by 3–100 eV electrons. J Am Chem Soc. 2003;125:4467–77.
30. Prise KM. Critical energies for SSB and DSB induction in plasmid DNA by low-energy photons: action spectra for strand-break induction in plasmid DNA irradiated in vacuum. Int J Radiat Biol. 2000;76:881–90.
31. Buxton GV, Greenstock CL, Helman WP, Ross AB. Critical review of rate constants for reactions of hydrated electrons, hydrogen atoms and hydroxyl radicals (·OH/·O⁻) in aqueous solution. J Phys Chem Ref Data. 1988;17:513–886. https://doi.org/10.1063/1.555805.
32. Plante I. A review of simulation codes and approaches for radiation chemistry. Phys Med Biol. 2021;66:03TR02.
33. Green NJB, Pilling MJ, Pimblott SM, Clifford P. Stochastic modeling of fast kinetics in a radiation track. J Phys Chem. 1990;94:251–8.
34. Berg HC. Random walks in biology. Princeton: Princeton University Press; 1993.
35. Frongillo Y, Goulet T, Fraser MJ, Cobut V, Patau JP, Jay-Gerin JP. Monte Carlo simulation of fast electron and proton tracks in liquid water-II. Nonhomogeneous chemistry. Radiat Phys Chem. 1998;51:245–54.
36. Tomita H, Kai M, Kusama T, Ito A. Monte Carlo simulation of physicochemical processes of liquid water radiolysis. Radiat Environ Biophys. 1997;36:105–16.
37. Karamitros M, Luan S, Bernal MA, Allison J, Baldacchino G, Davidkova M, et al. Diffusion-controlled reactions modeling in Geant4-DNA. J Comput Phys. 2014;274:841–82. https://doi.org/10.1016/j.jcp.2014.06.011.
38. Uehara S, Nikjoo H. Monte Carlo simulation of water radiolysis for low-energy charged particles. J Radiat Res (Tokyo). 2006;47:69–81. https://doi.org/10.1269/jrr.47.69.
39. Cadet J, Douki T, Gasparutto D, Ravanat J-L. Oxidative damage to DNA: formation, measurement and biochemical features. Mutat Res Mol Mech Mutagen. 2003;531:5–23.
40. Frankenberg-Schwager M. Induction, repair and biological relevance of radiation-induced DNA lesions in eukaryotic cells. Radiat Environ Biophys. 1990;29:273–92.

41. Boscolo D, Scifoni E, Durante M, Krämer M, Fuss MC. May oxygen depletion explain the FLASH effect? A chemical track structure analysis. Radiother Oncol. 2021;162:68–75.
42. Curtis SB. Lethal and potentially lethal lesions induced by radiation—a unified repair model. Radiat Res. 1986;106:252–70.
43. Goodhead DT. Saturable repair models of radiation action in mammalian cells. Radiat Res. 1985;104:S58–67.
44. Tobias CA. The repair–misrepair model in radiobiology: comparison to other models. Radiat Res. 1985;104:S77–95.
45. Campa A, Ballarini F, Belli M, Cherubini R, Dini V, Esposito G, et al. DNA DSB induced in human cells by charged particles and gamma rays: experimental results and theoretical approaches. Int J Radiat Biol. 2005;81:841–54.
46. Friedland W, Jacob P, Bernhardt P, Paretzke HG, Dingfelder M. Simulation of DNA damage after proton irradiation. Radiat Res. 2003;159:401–10.
47. Nikjoo H, O'Neill P, Wilson WE, Goodhead DT. Computational approach for determining the spectrum of DNA damage induced by ionizing radiation. Radiat Res. 2001;156:577–83.
48. Meylan S, Incerti S, Karamitros M, Tang N, Bueno M, Clairand I, et al. Simulation of early DNA damage after the irradiation of a fibroblast cell nucleus using Geant4-DNA. Sci Rep. 2017;7:1–15.
49. Rogakou EP, Pilch DR, Orr AH, Ivanova VS, Bonner WM. DNA double-stranded breaks induce histone H2AX phosphorylation on serine 139. J Biol Chem. 1998;273:5858–68.
50. Lorat Y, Brunner CU, Schanz S, Jakob B, Taucher-Scholz G, Rübe CE. Nanoscale analysis of clustered DNA damage after high-LET irradiation by quantitative electron microscopy—the heavy burden to repair. DNA Repair. 2015;28:93–106.
51. Barbieri S, Babini G, Morini J, Friedland W, Buonanno M, Grilj V, et al. Predicting DNA damage foci and their experimental readout with 2D microscopy: a unified approach applied to photon and neutron exposures. Sci Rep. 2019;9:1–17.
52. Gonon G, Villagrasa C, Voisin P, Meylan S, Bueno M, Benadjaoud MA, et al. From energy deposition of ionizing radiation to cell damage signaling: benchmarking simulations by measured yields of initial DNA damage after ion microbeam irradiation. Radiat Res. 2019;191:566–84.
53. Nikjoo H, Uehara S, Emfietzoglou D, Cucinotta FA. Track-structure codes in radiation research. Radiat Meas. 2006;41:1052–74.
54. Dingfelder M. Track structure: time evolution from physics to chemistry. Radiat Prot Dosimetry. 2006;122:16–21.
55. Kyriakou I, Sakata D, Tran HN, Perrot Y, Shin W-G, Lampe N, et al. Review of the geant4-dna simulation toolkit for radiobiological applications at the cellular and DNA level. Cancers. 2022;14:35.
56. Hayashi H, Watanabe N, Udagawa Y, Kao C-C. The complete optical spectrum of liquid water measured by inelastic X-ray scattering. Proc Natl Acad Sci. 2000;97:6264–6.
57. Heller JM Jr, Hamm RN, Birkhoff RD, Painter LR. Collective oscillation in liquid water. J Chem Phys. 1974;60:3483–6.
58. Villagrasa C, Francis Z, Incerti S. Physical models implemented in the GEANT4-DNA extension of the GEANT-4 toolkit for calculating initial radiation damage at the molecular level. Radiat Prot Dosimetry. 2011;143:214–8.
59. Champion C. Theoretical cross sections for electron collisions in water: structure of electron tracks. Phys Med Biol. 2003;48:2147.
60. Emfietzoglou D, Papamichael G, Nikjoo H. Monte Carlo electron track structure calculations in liquid water using a new model dielectric response function. Radiat Res. 2017b;188:355–68.
61. Garcia-Molina R, Abril I, Kyriakou I, Emfietzoglou D. Inelastic scattering and energy loss of swift electron beams in biologically relevant materials. Surf Interface Anal. 2017;49:11–7.
62. Emfietzoglou D, Kyriakou I, Abril I, Garcia-Molina R, Nikjoo H. Inelastic scattering of low-energy electrons in liquid water computed from optical-data models of the Bethe surface. Int J Radiat Biol. 2012;88:22–8.
63. Villagrasa C, Bordage M-C, Bueno M, Bug M, Chiriotti S, Gargioni E, et al. Assessing the contribution of cross-sections to the uncertainty of Monte Carlo calculations in micro-and nanodosimetry. Radiat Prot Dosimetry. 2019;183:11–6.
64. Lampe N, Karamitros M, Breton V, Brown JM, Kyriakou I, Sakata D, et al. Mechanistic DNA damage simulations in Geant4-DNA part 1: a parameter study in a simplified geometry. Phys Med. 2018;48:135–45.
65. de Vera P, Abril I, Garcia-Molina R. Excitation and ionisation cross-sections in condensed-phase biomaterials by electrons down to very low energy: application to liquid water and genetic building blocks. Phys Chem Chem Phys. 2021;23:5079–95.
66. Nguyen-Truong HT. Low-energy electron inelastic mean free paths for liquid water. J Phys Condens Matter. 2018;30:155101.
67. Quinto MA, Monti JM, Week PF, Fojón OA, Hanssen J, Rivarola RD, et al. TILDA-V: a full-differential code for proton tracking in biological matter. J Phys Conf Ser. 2015;635:032063.
68. Verkhovtsev A, Traore A, Muñoz A, Blanco F, García G. Modeling secondary particle tracks generated by intermediate-and low-energy protons in water with the low-energy particle track simulation code. Radiat Phys Chem. 2017;130:371–8.
69. Signorell R. Electron scattering in liquid water and amorphous ice: a striking resemblance. Phys Rev Lett. 2020;124:205501.
70. Zein SA, Bordage M-C, Francis Z, Macetti G, Genoni A, Dal Cappello C, et al. Electron transport in DNA bases: an extension of the Geant4-DNA Monte Carlo toolkit. Nucl Instrum Methods Phys Res Sect B Beam Interact Mater At. 2021;488:70–82.
71. Uehara S, Nikjoo H, Goodhead DT. Cross-sections for water vapour for the Monte Carlo electron track structure code from 10 eV to the MeV region. Phys Med Biol. 1993;38:1841.
72. Sempau J, Fernández-Varea JM, Acosta E, Salvat F. Experimental benchmarks of the Monte Carlo code PENELOPE. Nucl Instrum Methods Phys Res Sect B Beam Interact Mater At. 2003;207:107–23.
73. Shin W, Bordage M, Emfietzoglou D, Kyriakou I, Sakata D, Min C, et al. Development of a new Geant4-DNA electron elastic scattering model for liquid-phase water using the ELSEPA code. J Appl Phys. 2018;124:224901.
74. Charlton DE, Nikjoo H, Humm JL. Calculation of initial yields of single-and double-strand breaks in cell nuclei from electrons, protons and alpha particles. Int J Radiat Biol. 1989;56:1–19.
75. Nikjoo H, Goodhead DT, Charlton DE, Paretzke HG. Energy deposition in small cylindrical targets by ultrasoft X-rays. Phys Med Biol. 1989;34:691.
76. Pomplun E. A new DNA target model for track structure calculations and its first application to I-125 Auger electrons. Int J Radiat Biol. 1991;59:625–42.
77. Meylan S, Vimont U, Incerti S, Clairand I, Villagrasa C. Geant4-DNA simulations using complex DNA geometries generated by the DnaFabric tool. Comput Phys Commun. 2016;204:159–69.
78. Tang N, Bueno M, Meylan S, Incerti S, Tran HN, Vaurijoux A, et al. Influence of chromatin compaction on simulated early radiation-induced DNA damage using Geant4-DNA. Med Phys. 2019;46:1501–11.
79. Friedland W, Dingfelder M, Kundrát P, Jacob P. Track structures, DNA targets and radiation effects in the biophysical Monte Carlo simulation code PARTRAC. Mutat Res Mol Mech Mutagen. 2011a;711:28–40.
80. Lobachevsky PN, Martin RF. DNA strand breakage by 125I-decay in a synthetic oligodeoxynucleotide: quantitative analysis of fragment distribution. Acta Oncol. 1996;35:809–15.
81. Friedland W, Jacob P, Kundrat P. Mechanistic simulation of radiation damage to DNA and its repair: on the track towards

systems radiation biology modelling. Radiat Prot Dosimetry. 2011b;143:542–8.
82. Friedland W, Schmitt E, Kundrát P, Dingfelder M, Baiocco G, Barbieri S, et al. Comprehensive track-structure based evaluation of DNA damage by light ions from radiotherapy-relevant energies down to stopping. Sci Rep. 2017;7:1–15.
83. Nikjoo H, Martin RF, Charlton DE, Terrissol M, Kandaiya S, Lobachevsky P. Modelling of Auger-induced DNA damage by incorporated125I. Acta Oncol. 1996;35:849–56.
84. Schuemann J, McNamara AL, Warmenhoven JW, Henthorn NT, Kirkby KJ, Merchant MJ, et al. A new standard DNA damage (SDD) data format. Radiat Res. 2019;191:76–92.
85. Zirkle RE, Bloom W. Irradiation of parts of individual cells. Science. 1953;117:487–93.
86. Withers HR, Thames HD. Dose fractionation and volume effects in normal tissues and tumors. Am J Clin Oncol. 1988;11:313–29.
87. Folkard B, Vojnovic KJ, Hollis M. A charged-particle microbeam: II. A single-particle micro-collimation and detection system. Int J Radiat Biol. 1997a;72:387–95. https://doi.org/10.1080/095530097143167.
88. Randers-Pehrson G, Geard CR, Johnson G, Elliston CD, Brenner DJ. The Columbia University single-ion microbeam. Radiat Res. 2001;156:210–4.
89. Brenner DJ, Miller RC, Huang Y, Hall EJ. The biological effectiveness of radon-progeny alpha particles. III. Quality factors. Radiat Res. 1995;142:61–9.
90. Cole A. Mechanisms of cell injury. In: Radiation biology in cancer research. New York: Raven Press; 1980. p. 33–58.
91. Siebenwirth C, Greubel C, Drexler GA, Reindl J, Walsh DWM, Schwarz B, et al. Local inhibition of rRNA transcription without nucleolar segregation after targeted ion irradiation of the nucleolus. J Cell Sci. 2019;132:jcs.232181. https://doi.org/10.1242/jcs.232181.
92. Walsh DW, Siebenwirth C, Greubel C, Ilicic K, Reindl J, Girst S, et al. Live cell imaging of mitochondria following targeted irradiation in situ reveals rapid and highly localized loss of membrane potential. Sci Rep. 2017;7:1–11.
93. Deshpande A, Goodwin EH, Bailey SM, Marrone BL, Lehnert BT. Alpha-particle-induced sister chromatid exchange in normal human lung fibroblasts: evidence for an extranuclear target. Radiat Res. 1996;145:260–7.
94. Dollinger G. Life cell micro-irradiation. Nucl Phys News. 2010;20:27–32. https://doi.org/10.1080/10619127.2010.506125.
95. Hauptner A, Cremer T, Deutsch M, Dietzel S, Drexler GA, Greubel C, et al. Irradiation of living cells with single ions at the ion microprobe SNAKE. ACTA Phys Pol Ser A. 2006;109:273.
96. Voss KO, Fournier C, Taucher-Scholz G, Voss KO, Fournier C, Taucher-Scholz G. Heavy ion microprobes: a unique tool for bystander research and other radiobiological applications. New J Phys. 2008;10:075011. https://doi.org/10.1088/1367-2630/10/7/075011.
97. Kobayashi K, Usami N, Maezawa H, Hayashi T, Hieda K, Takakura K. Synchrotron X-ray microbeam irradiation system for radiobiology. J Biomed Nanotechnol. 2006;2:116–9.
98. Folkard M, Vojnovic B, Schettino G, Forsberg M, Bowey G, Prise KM, et al. Two approaches for irradiating cells individually: a charged-particle microbeam and a soft X-ray microprobe. Nucl Instrum Methods Phys Res Sect B Beam Interact Mater At. 1997b;130:270–4.
99. Greubel C, Ilicic K, Rösch T, Reindl J, Siebenwirth C, Moser M, et al. Low LET proton microbeam to understand high-LET RBE by shaping spatial dose distribution. Nucl Instrum Methods Phys Res Sect B Beam Interact Mater At. 2017;404:155–61. https://doi.org/10.1016/j.nimb.2016.11.032.
100. Schmid TE, Greubel C, Hable V, Zlobinskaya O, Michalski D, Girst S, et al. Low LET protons focused to submicrometer shows enhanced radiobiological effectiveness. Phys Med Biol. 2012;57:5889–907. https://doi.org/10.1088/0031-9155/57/19/5889.
101. Tao Y, Tan HQ, Mi Z, Chen C-B, Lam VYM, Osipowicz T, et al. The radiobiology beam line facility at the Centre for Ion Beam Applications, National University of Singapore. Nucl Instrum Methods Phys Res Sect B Beam Interact Matter At. 2019;456:26–31. https://doi.org/10.1016/j.nimb.2019.06.038.
102. Miller RC, Randers-Pehrson G, Geard CR, Hall EJ, Brenner DJ. The oncogenic transforming potential of the passage of single α particles through mammalian cell nuclei. Proc Natl Acad Sci. 1999;96:19–22.
103. Shao C, Folkard M, Michael BD, Prise KM. Bystander signaling between glioma cells and fibroblasts targeted with counted particles. Int J Cancer. 2005;116:45–51.
104. Sawant SG, Randers-Pehrson G, Metting NF, Hall EJ. Adaptive response and the bystander effect induced by radiation in C3H 10 $T_{1/2}$ cells in culture. Radiat Res. 2001;156:177–80.
105. Yokoya A, Usami N. Targeting specific sites in biological systems with synchrotron X-ray micro-beams for radiobiological studies at the photon factory. Quantum Beam Sci. 2020;4:2. https://doi.org/10.3390/qubs4010002.
106. Hable V, Drexler GA, Brüning T, Burgdorf C, Greubel C, Derer A, et al. Recruitment kinetics of DNA repair proteins Mdc1 and Rad52 but not 53BP1 depend on damage complexity. PLoS One. 2012;7:e41943. https://doi.org/10.1371/journal.pone.0041943.
107. Buchfellner A, Yurlova L, Nüske S, Scholz AM, Bogner J, Ruf B, et al. A new nanobody-based biosensor to study endogenous PARP1 in vitro and in live human cells. PLoS One. 2016;11:e0151041. https://doi.org/10.1371/journal.pone.0151041.
108. Girst S, Hable V, Drexler GA, Greubel C, Siebenwirth C, Haum M, et al. Subdiffusion supports joining of correct ends during repair of DNA double-strand breaks. Sci Rep. 2013;3:1–6.
109. Friedland W, Kundrát P, Schmitt E, Becker J, Ilicic K, Greubel C, et al. Modeling studies on dicentrics induction after submicrometer focused ion beam grid irradiation. Radiat Prot Dosimetry. 2019;183:40–4.
110. Friedrich T, Ilicic K, Greubel C, Girst S, Reindl J, Sammer M, et al. DNA damage interactions on both nanometer and micrometer scale determine overall cellular damage. Sci Rep. 2018;8:1–10.
111. Schmid TE, Friedland W, Greubel C, Girst S, Reindl J, Siebenwirth C, et al. Sub-micrometer 20 MeV protons or 45 MeV lithium spot irradiation enhances yields of dicentric chromosomes due to clustering of DNA double-strand breaks. Mutat Res Toxicol Environ Mutagen. 2015;793:30–40.
112. Dertinger H, Jung H. Molecular radiation biology: the action of ionizing radiation on elementary biological objects. New York: Springer; 1970.
113. Rauth AM, Simpson JA. The energy loss of electrons in solids. Radiat Res. 1964;22:643–61. https://doi.org/10.2307/3571545.
114. McMahon SJ. The linear quadratic model: usage, interpretation and challenges. Phys Med Biol. 2018;64:01TR01. https://doi.org/10.1088/1361-6560/aaf26a.
115. Kellerer AM, Rossi HH. RBE and the primary mechanism of radiation action. Radiat Res. 1971;47:15. https://doi.org/10.2307/3573285.
116. Chadwick KH, Leenhouts HP. A molecular theory of cell survival. Phys Med Biol. 1973;18:78–87. https://doi.org/10.1088/0031-9155/18/1/007.
117. Bodgi L, Foray N. The nucleo-shuttling of the ATM protein as a basis for a novel theory of radiation response: resolution of the linear-quadratic model. Int J Radiat Biol. 2016;92:117–31. https://doi.org/10.3109/09553002.2016.1135260.
118. Marples B, Joiner MC. The response of Chinese hamster V79 cells to low radiation doses: evidence of enhanced sensitivity of the whole cell population. Radiat Res. 1993;133:41–51.

119. Joiner MC, Johns H. Renal damage in the mouse: the response to very small doses per fraction. Radiat Res. 1988;114:385–98.
120. Garcia LM, Leblanc J, Wilkins D, Raaphorst GP. Fitting the linear–quadratic model to detailed data sets for different dose ranges. Phys Med Biol. 2006;51:2813.
121. Kirkpatrick JP, Meyer JJ, Marks LB. The linear-quadratic model is inappropriate to model high dose per fraction effects in radiosurgery. Semin Radiat Oncol. 2008;18:240–3. https://doi.org/10.1016/j.semradonc.2008.04.005.
122. Guerrero M, Li XA. Extending the linear–quadratic model for large fraction doses pertinent to stereotactic radiotherapy. Phys Med Biol. 2004;49:4825.
123. Hall EJ, Giaccia AJ. Radiobiology for the radiologist. Philadelphia: Lippincott Williams & Wilkins; 2012.
124. Stapleton GE, Billen D, Hollaender A. Recovery of X-irradiated bacteria at suboptimal incubation temperatures. J Cell Comp Physiol. 1953;41:345–57.
125. Phillips RA, Tolmach LJ. Repair of potentially lethal damage in X-irradiated HeLa cells. Radiat Res. 1966;29:413–32.
126. Shipley WU, Stanley JA, Courtenay VD, Field SB. Repair of radiation damage in Lewis lung carcinoma cells following in situ treatment with fast neutrons and gamma-rays. Cancer Res. 1975;35:932–8.
127. Weichselbaum RR, Little JB. Repair of potentially lethal X-ray damage and possible applications to clinical radiotherapy. Int J Radiat Oncol Biol Phys. 1983;9:91–6.
128. Lorat Y, Timm S, Jakob B, Taucher-Scholz G, Rübe CE. Clustered double-strand breaks in heterochromatin perturb DNA repair after high linear energy transfer irradiation. Radiother Oncol. 2016;121:154–61.
129. Puck TT, Marcus PI. Action of X-rays on mammalian cells. J Exp Med. 1956;103:653–66.
130. Elkind MM, Sutton H. X-ray damage and recovery in mammalian cells in culture. Nature. 1959;184:1293–5.
131. Elkind MM, Sutton-Gilbert H, Moses WB, Alescio T, Swain R. Radiation response of mammalian cells grown in culture: V. Temperature dependence of the repair of X-ray damage in surviving cells (aerobic and hypoxic). Radiat Res. 1965;25:359–76.
132. Elkind MM, Sutton H. Radiation response of mammalian cells grown in culture: I. Repair of X-ray damage in surviving Chinese hamster cells. Radiat Res. 1960;13:556–93.
133. Steel GG. The ESTRO Breur lecture cellular sensitivity to low dose rate irradiation focuses the problem of tumour radioresistance. Radiother Oncol. 1991;20:71–83.
134. Furre T. Inverse dose rate effect due to pre-mitotic accumulation during continuous low dose rate irradiation of cervix carcinoma cells. Int J Radiat Biol. 1999;75:699–707.
135. Furre T, Eggen Furre I, Koritzinsky M, Åmellem Ø, Pettersen EO. Lack of inverse dose rate effect and binding of the retinoblastoma gene product in the nucleus of human cancer T-47D cells arrested in G2 by ionizing radiation. Int J Radiat Biol. 2003;79:413–22.
136. Stewart FA, Soranson JA, Alpen EL, Williams MV, Denekamp J. Radiation-induced renal damage: the effects of hyperfractionation. Radiat Res. 1984;98:407–20.
137. Joiner MC, Bentzen SM. Fractionation: the linear-quadratic approach. In: Basic clinical radiobiology. 4th ed. Boca Raton: CRC Press; 2009.
138. Fowler JF. The radiobiology of prostate cancer including new aspects of fractionated radiotherapy. Acta Oncol Stockh Swed. 2005;44:265–76. https://doi.org/10.1080/02841860410002824.
139. Fowler JF. La Ronde—radiation sciences and medical radiology. Radiother Oncol. 1983;1:1–22.
140. United Nations Scientific Committee on the Effects of Atomic Radiation. Sources and effects of ionizing radiation, United Nations scientific committee on the effects of atomic radiation (UNSCEAR) 1993 report: report to the general assembly, with scientific annexes. New York: United Nations; 1993.
141. Nias AHW. An introduction to radiobiology. New York: Wiley; 1998.
142. ICRP. ICRP Publication 60: 1990 Recommendations of the International Commission on Radiological Protection. Amsterdam: Elsevier; 1991.
143. National Research Council (U.S.). Health effects of exposure to low levels of ionizing radiation: BEIR V. Washington, DC: National Academy Press; 1990.
144. Calabrese EJ. The road to linearity: why linearity at low doses became the basis for carcinogen risk assessment. Arch Toxicol. 2009;83:203–25.
145. Feinendegen LE. Conference summary. Health Phys. 2020;118:322–6. https://doi.org/10.1097/HP.0000000000001207.
146. Rattan SIS, Kyriazis M, editors. The science of hormesis in health and longevity. London: Academic Press; 2019.

Further Reading

Principles of Radiation Dosimetry

Radiation Microdosimetry

Lindborg L, Waker A. Microdosimetry: experimental methods and applications. Boca Raton: CRC Press; 2017.

From Track Structure to Early DNA Damage

Computational Approaches in Molecular Radiation Biology | SpringerLink

Micro-beams and Minibeams

Radiation Protection Dosimetry, Section: Micro-beams and biological applications. https://academic.oup.com/rpd/search-results?f_TocHeadingTitle=Micro-beams+and+biological+applications.

Target Theory and Dose Response Models

Chapman JD, Nahum AE. Radiotherapy treatment planning—linear-quadratic radiobiology. Boca Raton: CRC Press Inc; 2015.

Clinical Radiobiology for Radiation Oncology

5

Peter Sminia, Olivier Guipaud, Kristina Viktorsson, Vidhula Ahire, Sarah Baatout, Tom Boterberg, Jana Cizkova, Marek Dostál, Cristian Fernandez-Palomo, Alzbeta Filipova, Agnès François, Mallia Geiger, Alistair] Hunter, Hussam Jassim, Nina Frederike Jeppesen Edin, Karl Jordan, Irena Koniarová, Vinodh Kumar Selvaraj, Aidan D. Meade, Fabien Milliat, Alegría Montoro, Constantinus Politis, Diana Savu, Alexandra Sémont, Ales Tichy, Vlastimil Válek, and Guillaume Vogin

P. Sminia (✉)
Department of Radiation Oncology, Amsterdam University Medical Centers, Locatie Vrije Universiteit/Cancer Center Amsterdam, Amsterdam, The Netherlands
e-mail: p.sminia@amsterdamumc.nl

O. Guipaud · A. François · M. Geiger · F. Milliat · A. Sémont
Radiobiology of Medical Exposure Laboratory, Institute for Radiological Protection and Nuclear Safety, Fontenay-aux-Roses, France
e-mail: olivier.guipaud@irsn.fr; agnes.francois@irsn.fr; Mallia.geiger@irsn.fr; fabien.milliat@irsn.fr; Alexandra.semont@irsn.fr

K. Viktorsson
Department of Oncology/Pathology, Karolinska Institutet, Stockholm, Sweden
e-mail: Kristina.viktorsson@ki.se

V. Ahire
Chengdu Anticancer Bioscience, Ltd., Chengdu, China

J. Michael Bishop Institute of Cancer Research, Chengdu, China

S. Baatout
Institute of Nuclear Medical Applications, Belgian Nuclear Reseach Center (SCK CEN), Mol, Belgium
e-mail: sarah.baatout@sckcen.be

T. Boterberg
Department of Radiation Oncology, Ghent University Hospital, Ghent, Belgium

Particle Therapy Interuniversity Center Leuven, Department of Radiation Oncology, University Hospitals Leuven, Leuven, Belgium
e-mail: Tom.Boterberg@ugent.be

J. Cizkova · A. Filipova · A. Tichy
Department of Radiobiology, Faculty of Military Health Sciences, University of Defence, Hradec Králové, Czech Republic
e-mail: jana.cizkova@unob.cz; alzbeta.filipova@unob.cz; ales.tichy@unob.cz

M. Dostál
Department of Radiology and Nuclear Medicine, Faculty of Medicine, Masaryk University and University Hospital Brno, Brno, Czech Republic

Department of Biophysics, Faculty of Medicine, Masaryk University, Brno, Czech Republic
e-mail: dostal.marek@fnbrno.cz

C. Fernandez-Palomo
Institute of Anatomy, University of Bern, Bern, Switzerland
e-mail: cristian.fernandez@unibe.ch

A. Hunter
Radiobiology Section, Department of Radiation Oncology, University of Cape Town and Groote Schuur Hospital, Cape Town, South Africa
e-mail: Alistair.Hunter@uct.ac.za

H. Jassim
Radiotherapy Department, General Najaf Hospital, Kufa, Najaf, Iraq

Department of Medical Physics, University Al-Hilla College, Babylon, Iraq

N. F. J. Edin
Department of Physics, University of Oslo, Oslo, Norway
e-mail: nina@fys.uio.no

K. Jordan · A. D. Meade
School of Physics and Clinical and Optometric Sciences, Faculty of Science, Technological University Dublin, Dublin, Ireland
e-mail: k.jordan@svph.ie; aidan.meade@tudublin.ie

I. Koniarová
Department of Radiation Protection in Radiotherapy, National Radiation Protection Institute, Prague, Czech Republic
e-mail: irena.koniarova@suro.cz

V. K. Selvaraj
Department of Radiation Oncology, Thanjavur Medical College, Thanjavur, India

S. Baatout (ed.), *Radiobiology Textbook*, https://doi.org/10.1007/978-3-031-18810-7_5

A. Montoro
Radiological Protection Service, La Fe University Hospital, Valencia, Spain
e-mail: montoro_ale@gva.es

C. Politis
Department of Oral and Maxillofacial Surgery, University Hospitals Leuven, Leuven, Belgium

Department of Imaging and Pathology, OMFS IMPATH Research Group, Faculty of Medicine, KU Leuven, Leuven, Belgium
e-mail: Constantinus.Politis@uzleuven.be

D. Savu
Department of Life and Environmental Physics, Horia Hulubei National Institute of Physics and Nuclear Engineering, Magurele, Romania
e-mail: dsavu@nipne.ro

V. Válek
Department of Radiology and Nuclear Medicine, Faculty of Medicine, Masaryk University and University Hospital Brno, Brno, Czech Republic
e-mail: valek.vlastimil@fnbrno.cz

G. Vogin
Centre Francois Baclesse, University of Luxembourg and Luxembourg Institute of Health, Luxembourg, Luxembourg
e-mail: guillaume.vogin@baclesse.lu

Learning Objectives

- To understand that tumor targeting includes a proportion of healthy tissues.
- To recognize that the radiobiology of tumors and healthy tissues is different.
- To acknowledge that healthy tissues limit the possibilities of tumor control and are responsible for radiotherapy-associated toxicity.
- To be able to recognize and make estimates about tumor growth as well as tumor control, both important factors for determining the response to radiotherapy.
- To obtain knowledge about biological factors which determine the outcome of radiotherapy in cancer treatment.
- To familiarize with the principles of dose fractionation and how different tissues respond to changes in fraction sizes, number of fractions and frequency.
- To learn about the radiobiological effects of the dose rate and its clinical application.
- To understand tumor hypoxia, its methods of evaluation, oxygen effect, and oxygen enhancement ratio (OER) as well as to familiarize with different therapeutic approaches to tumor hypoxia.
- To understand the role of different factors in tumor radiation resistance and progression including those coming from the tumor microenvironment and as a result of cells with a stem cell phenotype.
- To be able to define the role of the human microbiota in healthy or pathologic gut and to use radiotherapy effects as an example for the microbiota implication in disease.
- To acknowledge the goals of palliative radiotherapy in contrast to radical radiotherapy; become aware of the applications of palliative radiotherapy and potential biological targets.
- To become aware of the abscopal effect; the type of biological damage caused by ionizing radiation leading to abscopal effects; the main biological damages caused by radiation that are recognized by the immune system; how irradiated tumors can show an immune response; how systemic antitumor immune responses occur.
- To be able to define and describe the acute/early adverse effects as well as late adverse effects of radiotherapy.
- To recognize that if tissues are part of a heavily irradiated volume, late toxicity will occur.
- To explain Normal Tissue Complication Probability (NTCP) and the advantages and drawbacks of using radiobiology modeling for NTCP as well as to give an overview of different NTCP models.

5.1 Principles of Tumor Radiotherapy

Box 5.1 Radiation Therapy in Cancer Treatment

- RT is one of the cornerstones in cancer treatment.
- The objective of RT resides in finding an optimal balance between chances of cure and risk of associated toxicity.
- Differential effect of RT between tumors and normal tissues depends on multiple factors related to both malignant and healthy tissue radiobiology, but also on beam characteristics and treatment schedule.
- Technical advances and sophistication of RT devices improve ballistic accuracy and allows unprecedented changes in treatment schedules, probably changing both malignant and healthy tissue radiobiology.

Radiation therapy (RT) is a locoregional treatment modality for cancer. Using radiation for therapeutic purposes began only a few months after the discovery of X-rays by Wilhelm Röntgen in 1895. The first "true" RT succeeded in managing a case of lupus erythematosus in 1897 by Eduard Schiff (1899). More than 120 years later, RT is still one of the cornerstones of tumor treatment, with more than half of all cancer patients treated by radiation in the course of their therapeutic management [1] (Box 5.1).

The interesting (but also dangerous) properties of ionizing radiation (IR) reside in its ability to penetrate more or less deeply in biological tissues, depending on its energy, and to react with the environment. These reactions consist in direct energy deposition and the generation of free radicals near and within living cells. The consequence of energy deposition is damage to the DNA structure leading to cell death if unrepairable [2]. Of course, all cells are concerned, tumor cells as well as cells in the healthy tissues, and within the irradiated volume, no difference is made between tumor and healthy cells. Treating a tumor would be easily achievable by the administration of a very high dose if it was not surrounded by the patient. Therefore, several strategies have been developed to ensure both the best tumor control and the least consequences ensuing from healthy tissues exposure, taking advantage of differences between tumor and healthy cells, known as the benefit/risk balance (Fig. 5.1).

Some biological processes favor the benefit/risk ratio in RT and the differential effect between tumor and healthy cells. Except for some very radiosensitive or radioresistant tumors, healthy and tumor cells demonstrate quite similar radiation sensitivities. However, DNA damage is less efficiently repaired by tumors than by healthy cells. This is the basis for the dose fractionation principle, demonstrated by Claudius Regaud and applied in the clinic by Henri Coutard in 1934, and which still is used today in modern RT. The total dose necessary to control the tumor is generally delivered in a series of small daily doses. The time lapse between each fraction allows DNA damage to be repaired by healthy cells whereas tumor cells do not repair or do so to a lesser extent. The biological effectiveness (the chances of tumor control but also the risk of damage to normal tissues) is reduced when using fractionated doses due to DNA repair and cell repopulation in both tumors and healthy tissues [3].

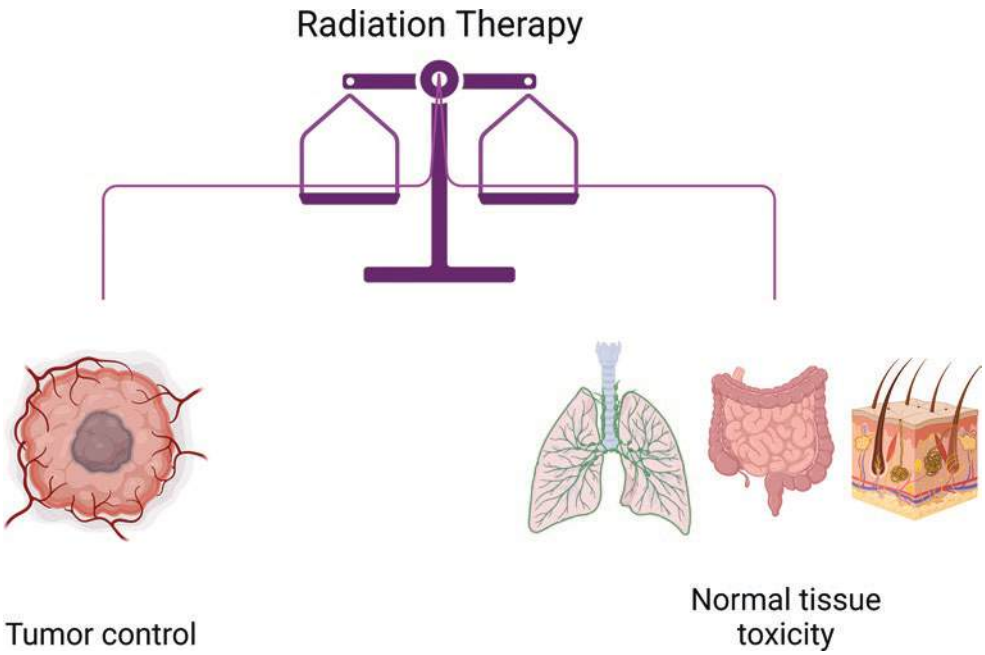

Fig. 5.1 The benefit/risk balance. The objective of RT is to control the tumor while sparing normal tissues, to ensure the patient's cure without unacceptable side effects

Numerous parameters associated with fractionation regimens, such as the total dose, the dose per fraction, and the time between fractions and the total treatment time, will influence both tumor response and normal tissue damage and will be described in more detail below [4]. Another biological factor participating in the differential effect is radiation-induced cell death. In a majority of cases, the initial radiation exposure is not what kills cells but rather unrepaired DNA damage, which condemns them to death as soon as they re-enter in the cell cycle. Rapidly proliferating tumor tissues will suffer significant cell death under these conditions compared to slowly proliferating healthy tissues. However, some healthy tissues such as oral and intestinal mucosa or hematopoietic cells proliferate rapidly and may be susceptible to early mitotic cell deaths if present in the irradiated volume. Finally, tumor control will also depend on other factors such as tumor heterogeneity (the tumor cannot be simply considered as a cluster of tumor cells), oxygenation status before RT and variations during treatment, tumor vascularization, resident and recruited immune cells, and so forth. Considering all these biological factors, the objective of treatment planning in RT is to find the best compromise between chances of cure and risk of associated toxicity [5].

In an ideal world, RT may target only the tumor volume; however, in real life, this is never the case. For healthy tissues, besides dose and fractionation, the volume exposed is of paramount importance in determining the risk of developing toxicity. Technical advances in dose delivery, planning systems and associated imaging devices have helped to achieve ever increasing ballistic accuracy. Advanced technologies, such as volumetric modulated arc therapy (VMAT), image-guided radiotherapy (IGRT), stereotactic body radiotherapy (SBRT), heavy ions [6], or proton therapy have all contributed to progress [7]. Consequently, the use of highly focused beams reduces the volume of normal tissues present within the irradiated volume and can spare very sensitive organs, thus minimizing the risk of toxicity. Reducing the volume also permits changes in fractionation schedules. For example, SBRT uses hypofractionation, delivering ablative doses per fraction between 8 and 20 Gy instead of the conventional 2 Gy/fraction. The gain in biological effectiveness strongly increases tumor control as illustrated in early-stage primary lung cancer. These changes in fractionation schemes may also induce a "new" radiobiology of tumors and healthy tissues in response to very high doses of IR, an area that remains to be explored [8]. Finally, ultra-high dose rate FLASH RT demonstrates a very sharp differential effect between tumor and healthy tissues and is the subject of intense research for future clinical applications [9].

Technical advances have strongly contributed to the chances of cure for numerous cancers and increased patients' survival. This increased life expectancy following cancer treatment, however, favors the emergence of side effects, especially long-term sequelae. Normal tissues can be divided into "early" and "late" responding tissues. Early-responding tissues (intestinal mucosa, hematopoietic system, skin, gonads) are characterized by the presence of cell proliferation compartments and are mostly implicated in acute radiation-induced toxicity. Late-responding tissues demonstrate no distinct cell proliferation compartment and are mostly implicated in late toxicity. For each normal tissue, dose constraints, which vary depending on the RT technique used, may be applied. These constraints help to minimize the risk of developing severe treatment-associated toxicity [10].

RT still plays a significant role in cancer cures. Its efficiency depends on numerous parameters related to both tumor and normal tissue radiobiology. The objective of cancer therapy, using modern RT often concurrently with other therapeutic strategies (surgery, chemotherapy, immunotherapy, etc.) is for the patients to survive without debilitating sequelae. This goal may be achieved using technological advances in RT, combined with strategic knowledge of both tumor and healthy tissue radiobiology.

5.2 Therapeutic Window and Therapeutic Ratio (Box 5.2)

Box 5.2 The Therapeutic Window and Therapeutic Ratio

- Therapeutic window: The difference between tumor control probability (TCP) and normal tissue complication probability (NTCP) at identical irradiation dose.
- Therapeutic ratio: The relation between TCP and NTCP or efficacy to toxicity ratio.

5.2.1 The Therapeutic Window

RT is one of the most effective treatment modalities in cancer therapy. However, despite modern precision RT, it is generally unavoidable to deposit IR to the tumor volume without risk of radiation injury to the surrounding healthy normal tissues or organs. Hence, the therapeutic effectiveness of radiation is dependent on the balance between tumor control and normal tissue adverse effects. In fact, the tolerance dose of the normal tissues or organs at risk determines the dose which can be safely applied to the tumor volume. For almost all normal tissues and organs, dose-volume constraints are well documented in the literature, for example, the QUANTEC (QUantitative Analysis of Normal Tissue Effects in the Clinic) data, as guidance in the clinical practice (see Sect. 5.13.6) [11]. The so-called therapeutic window is a conceptual window of opportunity between the tumor con-

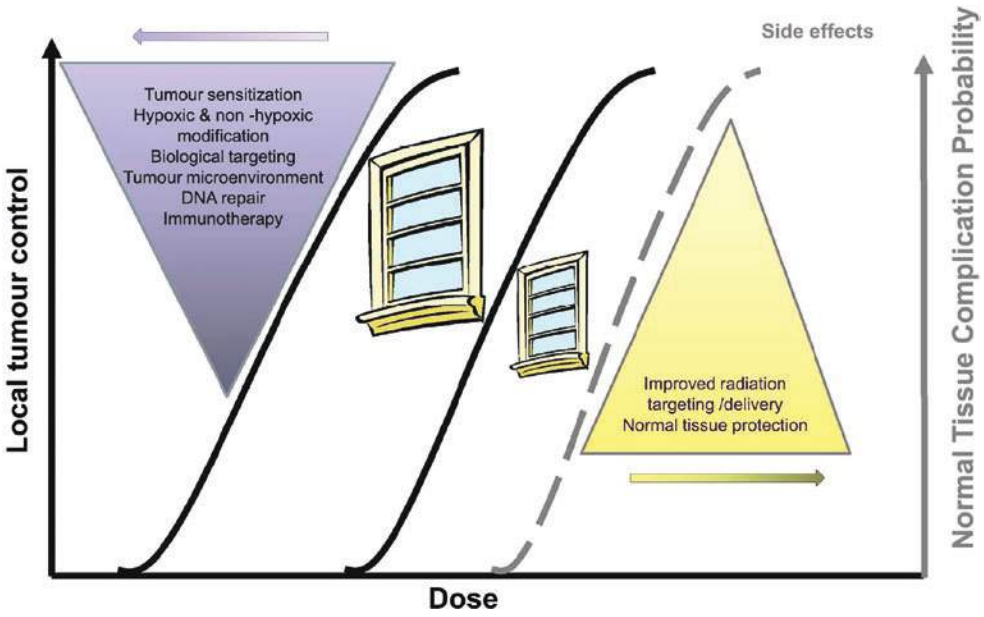

Fig. 5.2 Illustration of the therapeutic window. For an identical delivered dose, the curves show the difference between tumor control probability and normal tissue complication probability and methods to widen the window. (Reprinted from Drug radiotherapy combinations: review of previous failures and reasons for future optimism; Figure from Higgins et al. [12], with permission)

trol probability (TCP) and normal tissue complication probability (NTCP) (Fig. 5.2).

The ultimate aim of RT in the clinic is accomplished when the therapeutic window is large, with an optimized balance between benefits and risks, hence a treatment that is highly likely to be effective and safe. The shape and position of the dose–response curves for tumor control and toxicity to the normal tissues (Fig. 5.2) determines the probability that enough radiation is delivered to destroy the tumor cells without serious complications. The position of the curves determines the feasibility of the application of RT to the patient. The therapeutic window is large in radiosensitive tumor types like lymphoma, but small for other tumor types such as brain and pancreatic cancer. If the dose–response curve for normal-tissue toxicity is positioned at the left side of the tumor control curve or in case the curves are close together, the aimed tumor response could only be achieved at the cost of a high complication risk. The standard RT treatment is that one with tumor control probability (TCP) ≥0.5 and normal tissue complication probability (NTCP) ≤0.05 [13].

It is worth noting that Fig. 5.2 illustrates an ideal situation. The TCP curve might in particular however deviate for two main reasons. First, tumors are more heterogeneous compared with normal tissue; subsequently, the expression of the TCP curve becomes shallower than that of the NTCP curve. Secondly, not only the region of interest does contain the malignant cells, but there might be metastatic extensions outside the irradiation treatment volume. Hence, it is unlikely that the TCP curve for local control of specific tumors scores 100% [14, 15].

Several treatment parameters influence the therapeutic window. For example, when the overall treatment time is prolonged, the therapeutic window is narrowed (Fig. 5.3) [15, 16]. It is however difficult to practice this strategy because each complication translates the effect of a treatment parameter on the therapeutic window differently.

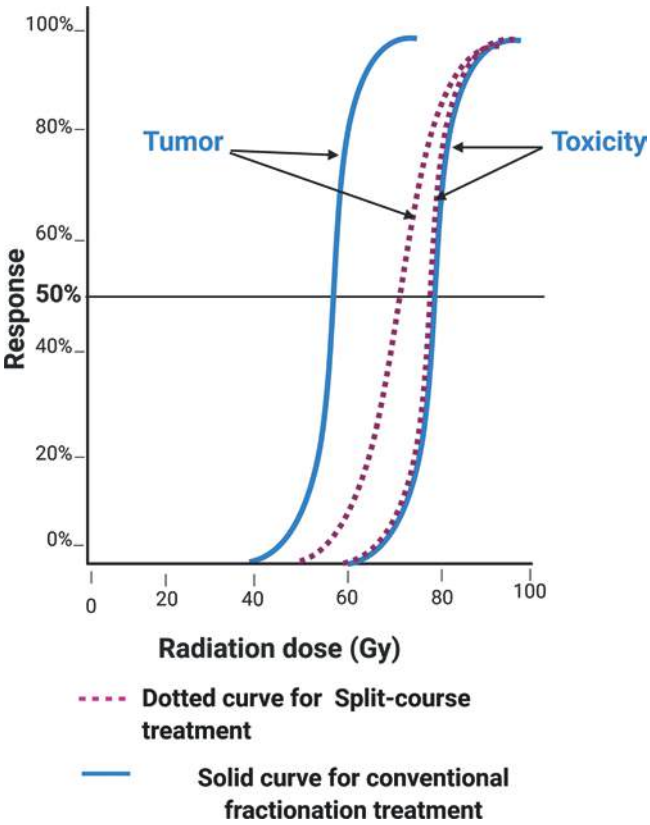

Fig. 5.3 Prolongation of the overall treatment time narrows the therapeutic window. Conventional irradiation course in 6 weeks versus a split-course course in 10 weeks. (Adopted from [16])

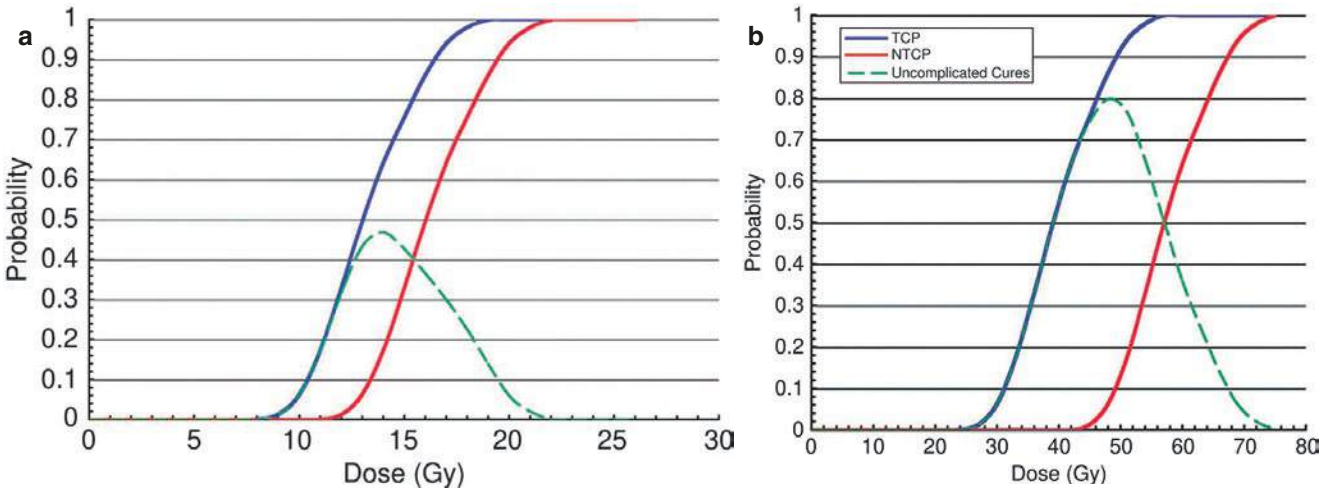

Fig. 5.4 Fractionation as an effective method to widen the therapeutic window. Curves schematically represent the probability of normal tissue side effects (NTCP, red curve), the probability of tumor control (TCP, blue curve) as well as the complication free tumor control curve (green) following single-dose radiation (**a**) and dose fractionation (**b**). (Figure from Shrieve and Loeffler [17], with permission from Wolters Kluwer Health, Inc.)

Several methods can be used to widen the therapeutic window, to increase the probability of complication-free tumor control:

- Fractionated RT. See Fig. 5.4. Decrease of the organ or tissue at risk volume using precision RT techniques allowing optimal dose distribution (e.g., stereotactic irradiation/particle irradiation).
- Combination therapy with molecular targeting or immune-modulating drugs. Optimally, drugs should be carefully chosen to selectively sensitize tumor and not normal tissue cells, taking the 6R's or Hallmarks of Radiobiology into account (see Sect. 5.4).

5.2.2 The Therapeutic Ratio

The therapeutic ratio or therapeutic index is an imperative measure used in the treatment planning to ensure that the RT course achieves its goals [18]. The ratio represents the difference between the TCP and NTCP curves for the same delivered dose at a fixed endpoint of NTCP [14]. Therefore, it represents the quantity used in the tumor treatment planning for the purpose of disease cure without complications. The ratio is defined as the relationship between TCP and NTCP, i.e., efficacy/toxicity ratio. Chang et al. stated that a common method used to calculate the therapeutic ratio which is the probability of cure without complications [19] and given by:

$$\text{Therapeutic ratio } (\text{TR}) = (\text{TCP}) \times (1 - \text{NTCP}) \text{ as defined by } (\text{cure probability}) \times (1 - \text{complication probability}).$$

As the difference between TCP and NTCP becomes large it means that TR approaches 1 and treatment is fairly effective for tumor control than for causing normal tissue morbidity, but the pattern is reversed when the difference between TCP and NTCP becomes small. That is, TR approaches 0 and the treatment may fail and be relatively more toxic [14]. As explained above, there are many treatment parameters and methods that affect the therapeutic ratio, for example, combination therapy with a radiosensitizing agent or drug. This effect is revealed in practice as increasing tumor cure rate with improved quality of life as a result of a therapeutic gain [13, 16]. In this circumstance, the therapeutic ratio is the ratio of dose-modifying factors (DMFs) of tumor over that for normal tissues.

$$\text{Therapeutic ratio} = \frac{\text{Dose Modifying Factor Tumor}}{\text{Dose Modifying Factor Normal Tissue}}.$$

Finally, the therapeutic ratio differentiates between early and late responding normal tissues in terms of their response to concomitant RT and chemotherapeutics or targeted agents. While the therapeutic ratio of early responding tissue is usually <1, the therapeutic ratio of late responding tissues is >1 which reflects the advantageous consequence of concomitant RT and chemotherapy. This may lead to a high level of early injury, but a neutral level of late damage to late responding tissues. Fortunately, early side effects can be relieved by using either extensive supportive care or adaptation of the

standard treatment. The combination of RT and chemotherapy may prove effective if selective radiosensitization of malignancy is obtained and the probability of late-responding normal tissue damage is not increased. However, early toxicities might also be a concern.

5.3 Tumor Growth and Tumor Control (Box 5.3)

Box 5.3 Tumor Response Following Radiotherapy

- Tumor control probability (TCP) is guided by dose, tumor characteristics, and normal tissue radiation sensitivity.
- Killing of clonogenic cells within a tumor partly explain TCP during RT, but the effect is also influenced by host factors, for example, immune cell attack.

5.3.1 Tumor Control

The main objective of curative RT is to successfully achieve local tumor control [16]. The relationship between TCP and radiation dose is shown in Fig. 5.5 which illustrates that there is poor tumor control with low dose, but high tumor control with high dose [20]. The steepness of the curve depends on differences in tumor size, tumor cell radiation sensitivity and repopulation as well as other factors. These factors give rise to variation in TCP of different tumors but also inter-patient variation in clinical practice. Subsequently, this improvement in tumor control is reflected in an increase in the life expectancy of cancer patients. To this end, it is preferable to evaluate RT success based on tumor control.

Complete tumor control requires that every clonogenic cell is destroyed. Unfortunately, cell killing is randomly distributed within a population of tumor cells, and there are about 10^9 cells in each gram of tumor. A small fraction of these cells (about 1%), in reality, contains cells with clonogenic-forming ability; so, a human tumor could have billions of clonogenic cells; therefore, eliminating every such cell is a great challenge. The likelihood of obtaining tumor control is related to radiation dose, features of control probability of the tumor and the number of surviving clonogenic tumor cells (Fig. 5.6.).

5.3.2 Tumor Growth

The tumor growth rate can be used to determine how a cancer will respond to RT treatment by predicting or understanding the key features of the tumor tissue response to radiation. The tumor growth rate was developed for examining the capacity of clonogenic-forming cells of a tumor and assumes that the regrowth component is a function of repopulation by the surviving of cells with colony-forming ability [20, 21].

There are considerable differences in growth rate between different tumors due to differences in size and biology. Therefore, the tumor growth curve has exponential and non-

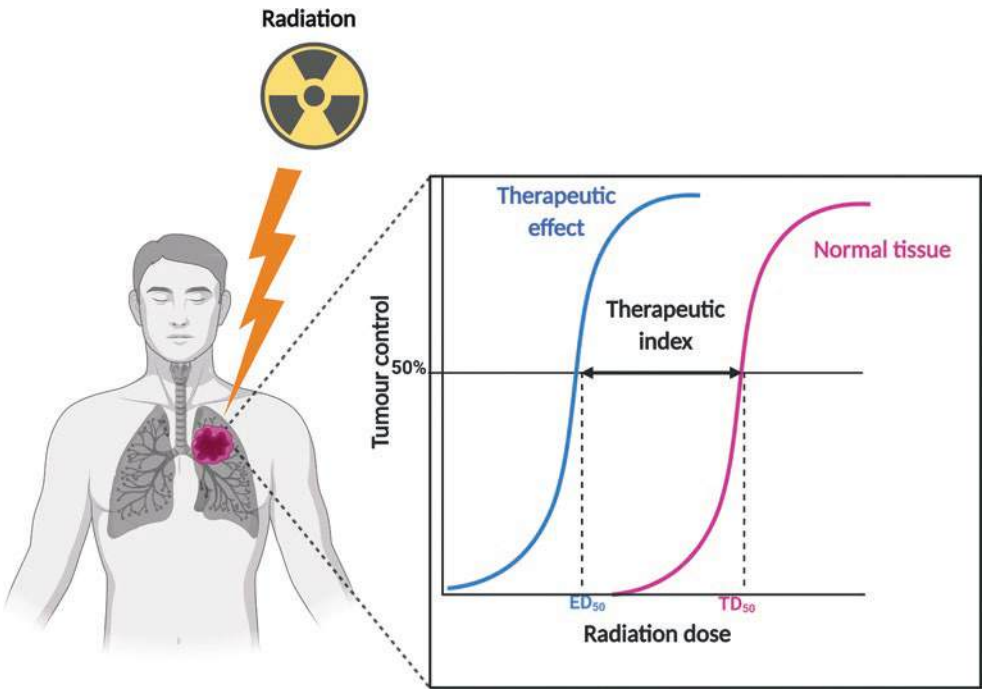

Fig. 5.5 Tumor Control Probability (TCP) and radiation dose relationship. The scheme demonstrates the sigmoid relationship of probability of tumor control and normal tissue damage to radiation dose

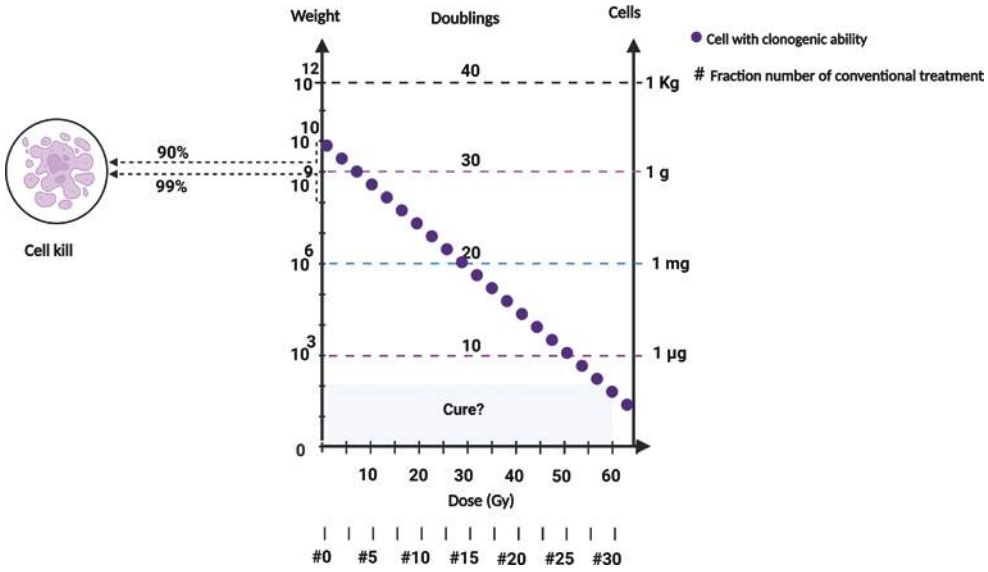

Fig. 5.6 The response of clonogenic tumor cells at 2 Gy/fraction as a function of the total dose. Assuming that each 2 Gy fraction reduces the clonogenic cell population with 50%, 30 fractions of 2 Gy will reduce 10^{10} clonogenic tumor cells to ten surviving cells. In order to eliminate each clonogenic tumor cell, additional fractions of 2 Gy are required to reach tumor control

exponential parts when plotted on a logarithmic scale. That is, the tumor volume doubling time (VDT), the duration of time required for the tumor to double in size, increases for small tumors because there is a sufficiency in nutrient and oxygen supply resulting in a reduction of cell cycle, a higher proportion of cycling cells or and a lower cell death rate. As a result, the slope of the growth curve, which reflects the doubling time of the cells, has an exponential pattern for small tumors. Conversely, VDT decreases for large tumors because of the limitation of nutrient and oxygen supply. This leads to a prolongation of cell-cycle progression but also a high rate of cell death. As a result, the slope of the growth curve has no exponential patterns for large tumors. The Gompertz equation describes such progressively slowing tumor growth:

$$V = V_0 \exp \qquad (5.1)$$

where V_0 is the volume at arbitrary zero time while A and B are parameters that determine the speed of growth [16]. VDTs are remarkably variable in human tumors, both between primary and metastatic lesions and among tumors with different histology (Table 5.1). Please also note that even within one tumor entity (localization, histology, and primary or metastasis similar) there is a range in VDT illustrating the problem of tumor heterogeneity.

5.3.2.1 Cell-Cycle Kinetics and Growth Fraction in Tumors

The growth fraction (GF) refers to the proportion of cycling cells that has highly colony-forming ability and is in the active process of cell cycling (omitting cells in G0 phase), with capacity of DNA duplication and cell division [22].

Table 5.1 Volume Doubling Times (VDTs) for different human tumors (adapted from [16])

Tumor site, histology	Primary vs metastasis	Number of tumors measured	Mean VDT (days) (confidence limits)
Colon-rectum	Primary	19	632 [426–938]
Colon-rectum, adenocarcinoma	Metastasis	55	95 [84–107]
Lung, squamous cell carcinoma	Primary	85	85 [75–95]
Lung, adenocarcinoma	Primary	64	148 [121–181]
Lung, undifferentiated	Primary	55	79 [67–93]
Breast	Primary	17	96 [68–134]
Breast carcinoma	Superficial metastasis	66	19 [16–24]
Breast, adenocarcinoma	Metastasis	44	74 [56–98]
Head and neck, squamous cell carcinoma	Metastasis	27	57 [43–75]
Head and neck, teratoma	Metastasis	80	30 [24–38]
Head and neck, osteosarcoma	Metastasis	34	65 [46–93]
Head and neck, fibrosarcoma	Metastasis	28	69.5 [46–93]
Kidney, adenocarcinoma	Metastasis	14	60 [37–98]
Thyroid, adenocarcinoma	Metastasis	16	67 [44–103]
Uterus, adenocarcinoma	Metastasis	15	78 [55–111]

Similarly, as in normal tissue, some tumor cells are not involved in active proliferation for different reasons, for instance as a result of hypoxia, differentiation, and catabolic insufficiency. Moreover, it is estimated that about 50% of cells in a tumor are not neoplastic cells but are cells making up the tumor stroma. Therefore, it is clear that the cell population in tumors contains quiescent (Q) cells, and since GF is defined as the proportion of cycling cells, it can be calculated as stated by [13, 22]:

$$\mathrm{GF} = \frac{p}{p+Q} \tag{5.2}$$

where p is proliferating cells.

For estimation of the cell-cycle kinetics (T_C), three principal methods are used: (1) bromodeoxyuridine (BrdUrd) or thymidine analogues iododeoxyuridine (IdUrd), (2) ^{3}H-thymidine for the synthesis of DNA and (3) positron emission tomography (PET) imaging of the tumors in vivo by radiolabeled ^{18}F-fluoro-3′-deoxy-3′-L-fluorothymidine (*FLT)* [13, 16].

The first method includes labeling of the cells with BrdUrd or IdUrd. When cells pass through the S-phase, these labels are incorporated into the newly created DNA strand. An antibody against BrdUrd or IdUrd as well as a DNA-specific dye are used to stain a single-cell suspension prepared from a cell culture in vitro or a tumor biopsy, and the duration of the S phase (T_S) and fraction of cells in S phase are assessed using flow cytometry.

In the second method, cell-cycle kinetics (T_C) is estimated from labeled cells by measuring the duration of the cell cycle by either pulse or continuous labeling with ^{3}H-thymidine. The labeling agent is incorporated into the DNA as cells progress through S-phase and the cell-cycle kinetics (T_C) is estimated from the labeled cells [16].

The third principal method applies PET tracers to detect and evaluate tumor proliferation in vivo. In this method, radiolabeled ^{18}F-fluoro-3′-deoxy-3′-L-fluorothymidine (FLT) is used. FLT is phosphorylated by thymidine kinases (TK) and since regulation of TK activity occurs in the S-phase, it means that metabolites of FLT (mono-, di-, and tri-phosphates) are reflecting the number of cells in S-phase and hence replication status. The FLT tracer activity in a tumor is subsequently evaluated by a PET scanner from which the cell-cycle kinetics can be estimated [16].

For estimation of the GF, according to literature the GF is obtained by assessment of two distinct cell subpopulations, one that does not grow and another which grows with a uniform cell-cycle distribution [13, 21]. This method includes the exposure of a growing culture of cells with ^{3}H-thymidine for the synthesis of DNA, and then after the period of at least one complete cell cycle to ensure all cells producing DNA pass through the S-phase and are labeled, an autoradiography of tumor section is taken, and GF is calculated by:

$$\mathrm{GF} = \frac{\text{Fraction of cells labeled}}{\text{Fraction of mitoses labeled}}$$

There is also a possibility to take proliferation into account by immunohistochemistry assessment of tumor tissue sections by staining of the nuclear antigen Ki-67, which in tumors has different levels depending on the tumor proliferation. The method includes staining of tumor cell cultures or a tumor biopsy with a Ki-67 specific antibody followed by counting the number of positive tumor cells. The GF growth fraction is estimated from labeled cells by measuring the proportion of proliferating cells using continuous labeling. Although the method is frequently used to assess S-phase cells, recent results have indicated that Ki-67 also has different functions in other cell-cycle phases which may in fact influence proliferation estimations [23].

5.3.2.2 The Potential Doubling Time (T_{pot})

"The potential doubling time (T_{pot}) of a tumor is defined as the cell doubling time without any cell loss." There are two methods used to estimate T_{pot}. In the first method, DNA is labeled with thymidine analogues and then the cells fraction in S phase (LI) and the duration of the S phase (T_S) are estimated by using flow cytometry to calculate T_{pot} by:

$$T_{pot} = \frac{\lambda T_S}{\mathrm{LI}} \tag{5.3}$$

where λ is a correction parameter for the non-rectangular age distribution of growing cell populations, in the order of 0.7–1.

Different tumor tissues have different values of LI, but they have similar T_S, in the range of 12 h. As a result, T_{pot} has a spectrum of values ranging from 4 to 34 days, as shown in Table 5.2. Of note, it has been demonstrated that in a clinical RT context, the pre-treatment T_{pot} does not predict outcome as one also needs to consider the repopulation rate of colony-forming cells [13].

5.3.2.3 Cell Loss in Tumors

Slow tumor growth is not only explained by the fact that not all cells within a tumor are proliferating but also due to considerable cell loss where multiple parameters regulate these two factors. If there was no cell loss and if every tumor cell was actively proliferating, the tumor doubling time would imitate the cell-cycle kinetics (T_C). Therefore, when there is

Table 5.2 Cell kinetic parameters of human tumors derived from in vivo labeling with iodo-deoxyuridine (IdUrd) or bromo-deoxyuridine (BrdUrd) and monitored by flow cytometry (adapted from [16])

Tumor site	Tumor type	Patients number	Average T_{pot} (days)	Average LI (%)	Average T_S (h)
Skin	Melanoma	24	7.2	4.2	10.7
Hematological	–	106	9.6	13.3	14.6
Head and neck region	–	712	4.5	9.6	11.9
CNS	–	193	34.3	2.6	10.1
Breast	–	159	10.4	3.7	10.4
GIT (upper intestine)	–	183	5.8	10.5	13.5
GIT (colorectal)	–	345	4	13.1	15.3
Kidney	Renal cell carcinoma	2	11.3	4.3	9.5
Bladder	–	19	17.1	2.5	6.2
Prostate	–	5	28	1.4	11.7
Ovarian	–	55	12.5	6.7	14.7
Cervix	–	159	4.8	9.8	12.8

cell loss the T_D is long and when there is reduced GF the T_{pot} of the tumor is longer than the time of cell cycle [14].

The net growth rate, or the VDT, of tumors results from the balance of cell production and cell loss. In clinical settings, the GF and knowledge of the cycle time of the individual cells does not reflect the speed of tumor growth; namely, the cycle time of the individual cells is much faster than the speed of tumor growth. Such discrepancy is attributed to cell loss which can be considered by calculating cell loss factor (CLF). The cell-loss factor refers the ratio of the cell loss rate to the production of new cells, and it can be calculated by:

$$\mathrm{CLF} = 1 - \frac{T_{pot}}{\mathrm{VDT}} \tag{5.4}$$

where T_{pot} is the potential tumor doubling, and VDT is the tumor volume doubling time that is calculated by the essential time for the tumor to double its volume (V) by using:

$$\mathrm{Td} = \frac{\mathrm{time} \times \in 2}{(V)} \tag{5.5}$$

When the cell loss factor is high, it means that there is loss of newly produced cells from the GF; thus, tumor growth is slow. Cell loss has been attributed to different parameters [16, 24]: (1) Cells are in the inactive phase of cell cycling (in G0 phase) which is a non-proliferative compartment, (2) There is inadequate nutrition and oxygen levels due to the tumor outgrowth that gives rise to pushing cells into areas at a distance from blood supply, (3) Metastasis, (4) Immune cell killing of the tumor, and (5) Exfoliation (the complete removal of a single epithelial cell or group of cells from a layer of epithelium by spontaneous or induced means). In animal models of tumors, this would not apply but could be a mechanism by which cells lose their integrity in carcinomas of the gastrointestinal tract, for example, where the epithelium is renewed rapidly (Box 5.4).

Box 5.4 Tumor Growth Kinetics

- Tumor volume doubling time (VDT) is influenced by tumor localization site, primary or metastatic status as well as histology but also by intra-tumor heterogeneity factors.
- There are differences in growth rates between different tumor types and metastatic lesions tend to grow faster than primary lesions.
- A logarithmic scale can be used to judge treatment effectiveness. An estimate of tumor growth rate is determined by cell-cycle kinetics, the growth fraction, the cell loss rate (CL), and the potential doubling time (T_{pot}). Even among tumors of the same histological type, these parameters differ greatly. Cell kinetics cycle of cells and growth fraction in tumors can be monitored ex vivo using various DNA-labeling strategies and in vivo using PET tracers.
- Ki67 immunohistochemistry staining of tumor biopsies is a method for assessing S-phase cell proportion.
- The potential doubling time (T_{pot}) refers to the time it would take for volume to double without loss of cells. Consequently, the potential doubling time and the observed volume doubling time are different because tumors show a high amount of cell loss.
- Tumor cell loss also contributes to VDT and may be attributed to limited nutrition and oxygen supply, metastatic propensity, immune cell killing, and tumor cell exfolia.

5.4 6R's Concept

Box 5.5 The Hallmarks of Radiobiology

- The Hallmarks of Radiobiology or 6R's are six typical molecular, cellular, or tissue processes which determine the effects of radiation on both malignant and healthy tissues.
- The 6R's are: Radiosensitivity, Repair, Redistribution, Repopulation, Reoxygenation, Reactivation of the immune response.

The so-called 6R's are six biological features which determine the outcome of RT in the clinic: the balance between the complication rate (side effects due to normal tissue injury) and the tumor control rate (palliation or curation due to tumor cell sterilization) (Fig. 5.7). These basic principles or Hallmarks of Radiobiology have been evolved from Withers' 4R's—"Recovery/repair, Redistribution, Repopulation and Reoxygenation"—[25] via Steels' 5R's—the addition of "intrinsic cellular Radiosensitivity" [26] to 6R's by including "Reactivation of the immune response" [27] (Box 5.5).

The six Hallmarks of Radiobiology (Fig. 5.7) in brief:

- Radiosensitivity: Intrinsic and acquired radioresistance of normal tissue cells and tumor cells to radiation, in particular cancer (stem) cells among the heterogenic tumor cell population.
- Repair capacity, efficiency, and mechanisms of sublethal DNA damage repair, and related sensitivity to fractionated irradiation—which is high for most healthy tissues and low for most tumors.
- Redistribution of cells in the cell-cycle affects their radioresistance. Cells in mitosis are most sensitive to radiation, while cells in the S-phase are radioresistant. Redistribution following irradiation will push radioresistant S-phase cells towards a radiosensitive cell-cycle phase.
- Repopulation: Cell repopulation of—not by radiation eradicated cancer cells—involved in the (accelerated) repopulation of the tumor—which is detrimental—and beneficial repopulation of normal tissue cells recovering from acute injury.
- Reoxygenation: Cells in hypoxic niches within the tumor are radioresistant. Reoxygenation between multiple radiation fractions given in a radiation course is an important phenomenon by which originally hypoxic tumor cells will be reoxygenated and hence radiosensitized.
- Reactivation of the immune response: Local irradiation induces a systemic immune activation to attack distant tumor cell niches which can be located outside the irradiated volume (abscopal effect).

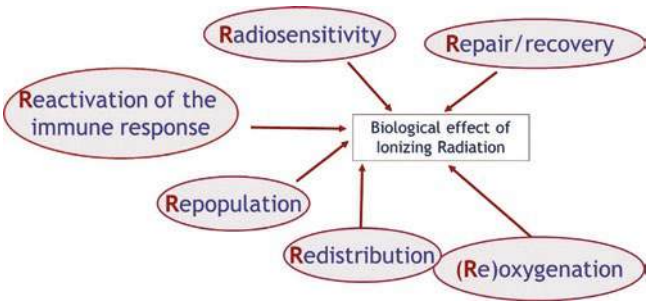

Fig. 5.7 The Hallmarks of Radiobiology, the 6R's

5.4.1 The 6R's in Detail

5.4.1.1 Radiosensitivity

Many authors refer to the radiosensitivity as the degree of tumor and normal tissue regression following irradiation. There are many factors that determine the radiosensitivity which are the proportion of cells with clonogenic capacity, growth rate and reproduction rate, mitosis activity, metabolic rate, tissue type, radiation dose, inherent radiosensitivity, and hypoxia. For example, cells with fast growth or high metabolic rate are highly radiosensitive. Essentially, since the reproductive capacity of cancer cells is higher than the reproductive capacity of late responding normal tissue cells, cancer cells are more sensitive to radiation, but this depends on the cancer tissue type.

5.4.1.2 Repair

Tumor and normal cells differ in terms of repair after radiation-induced damage. Unlike normal cells, the repair process and mechanism of tumor cells are defective. While normal tissue cells do repair their radiation-induced DNA damage efficiently, malignant cells often cannot.

There are three types of radiation damage to mammalian cells:

1. Potentially lethal damage (PLD): Cell death depends on the environmental conditions. In a normal situation, damaged cells will not repair and die, but in case of reformed environmental conditions, cells can repair their DNA damage.
2. Sublethal damage (SLD): The death of a cell depends on the sublethal damage condition. DNA damage can be repaired if no extra injury is taking place. The recovery kinetics, the repair time, lies in the range of a few hours following DNA double strand break (DNA DSB) induction.
3. Lethal damage (LD): Irreparable and irreversible damage leading to cell death.

The main reason for cell death is the production of the asystematic generation of chromosomal aberrations, includ-

ing rings and di-centric aberrations that result from an interaction between more than one DNA DSB [28]. Details regarding the DNA Damage Response and repair pathways are given in Chap. 3.

5.4.1.3 Redistribution (Re-assortment)

Figure 5.8, panel a shows the distribution of eukaryotic cells over the four cell-cycle phases, which include the G1 phase, S-phase (synthesis phase), G2 phase (interphase phase), and M phase (mitosis and cytokinesis). Cells in the different phases of the cell cycle vary in radiation sensitivity. Cells in the S-phase are resistant to radiation (Fig. 5.8, panel a) while cells in the M and G2 phase are sensitive to radiation [14].

When cells experience radiation-induced insult, three effects occur:

1. Recruitment: Stem cells of some tumors are in the G0 phase, which is a radioresistant phase; therefore, they may repair their damage and survive. In order to kill these cells efficiently, these cells are recruited into the cell cycle so as to arrive in a radiosensitive phase.
2. Cells are blocked in the radiosensitive phase (G2). Cells in G2 are highly likely to be sterilized by the first radiation dose.
3. Cells are allowed to re-assort and progress to the radiosensitive phase. Cells in radio-resistant phases survive, yet since they continue to cycle, there is a likelihood that they will arrive at a sensitive phase and be sterilized by a second or later fraction.

5.4.1.4 Repopulation

The renewal capability of tissue clonogenic cells that follows the reduction of tissue cells, with clonogenic-forming capacity, is referred to as repopulation (regeneration). Following radiation-induced tissue injury, the tissues will react by repopulation of surviving clonogenic cells, i.e., compensation for the lost cells occurs relatively quickly, with decreasing clonogenic doubling times from 9.8 to 3.4 days. This will result in a larger number of tumor cells which is detrimental. For normal tissue injury, repopulation from the stem cell compartment will regenerate the damaged tissue, there with reducing early radiation toxicity [16].

Biologically, there are three reasons for accelerated repopulation. Firstly, when tissue is exposed to radiation, cell kinetics, which may be reminiscent of a normal epithelium is stimulated; thus, this response causes regenerative reaction of clonogenic cells to initiate repopulation by activating growth factors, such as keratinocyte growth factor (KGF). Secondly, reoxygenation will occur during the course of fractionated RT, facilitating tissue regeneration. Finally, signaling such as that via the epithelial growth factor receptor (EGFR) is activated after irradiation; hence, this signal works as the regulated regenerative response [22].

The onset of repopulation in many cases is thought to be about 3 weeks after the start of fractionated RT. Its mechanism and kinetics depend on tissue types and might be dose dependent [29] (see also Chap. 6). From the clinical point of view, the total dose should be delivered over a controlled period of time. Any reduction in overall time is limited by the

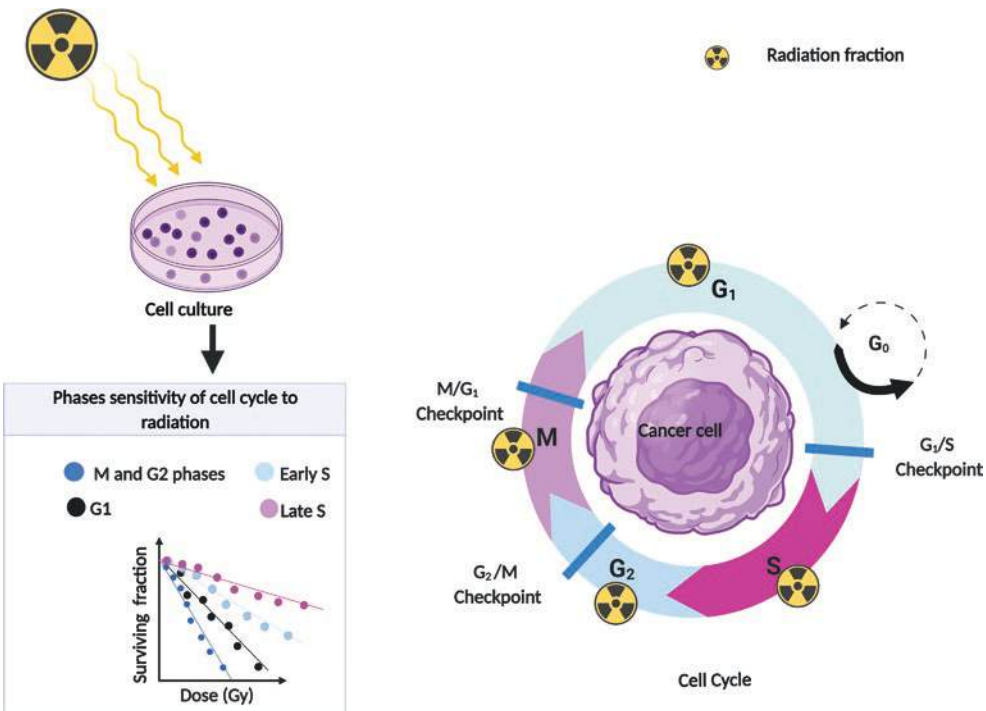

Fig. 5.8 The cell-cycle phase and radiation sensitivity. Cell survival curves of V79 Chinese hamster cells irradiated at different phases of the cell cycle on the left side

radiation tolerance of acutely responding normal tissues, but an extended overall treatment time might lead to diminished tumor response due to the increase of cells as a result of repopulation.

5.4.1.5 Reoxygenation

The empirical observation that oxygen levels in tumors may be enhanced in the period after irradiation is known as reoxygenation. Reoxygenation of originally hypoxic tumor cells, besides exploiting differences in DNA repair between normal tissue cells and tumor cells, is an important mechanism and reason for fractionated RT. During the fractionation course, lethally damaged cells are removed, and the blood supply increases. Thereby, initially radioresistant hypoxic cells are gradually reoxygenated and become sensitive to radiation (Fig. 5.9).

The oxygen enhancement ratio and the role of oxygen in the radiation response has been explained in Chap. 2. If reoxygenation is efficient between dose fractions, the presence of hypoxic cells does not have a significant effect on the outcome of a multi-fractionation scheme. In a hypofractionation regimen, the time period to obtain full reoxygenation of hypoxic tumor cells might however be too short (discussed in Chap. 6).

5.4.1.6 Reactivation of the Immune System

When irradiating a tumor, the tumor microenvironment (TME) will also be exposed. Such exposure of the TME might affect the immune system, both locally and systemically. Activation of an anti-tumor response depends on the treatment regimen, i.e., the fractionation schedule, dose, and timing because these factors disturb the balance between immunosuppressive and immune-stimulatory effects. As a result, a specific radiation treatment protocol can induce an anti-tumor immune reaction. When cells of tissues are exposed to radiation, the immune response to attack tumor cells is generated in a few steps (Fig. 5.10).

Different radiation treatment schemes with respect to the total dose and fraction size have been shown to have diverse effects on the immune response, and therewith also on target expression with consequences for combination treatments like with immunotherapy. To obtain optimal modulation of the radiation response, specific immunomodulating or targeted drugs can be selected. The radiation-induced TME effects modulating the immune response requires further research to find the ideal immunotherapy and RT regimen [30].

The 6R's offer options for modulation of the radiation response. Modulation strategies, such as via combination therapy with immunomodulating agents, should be aimed to widen

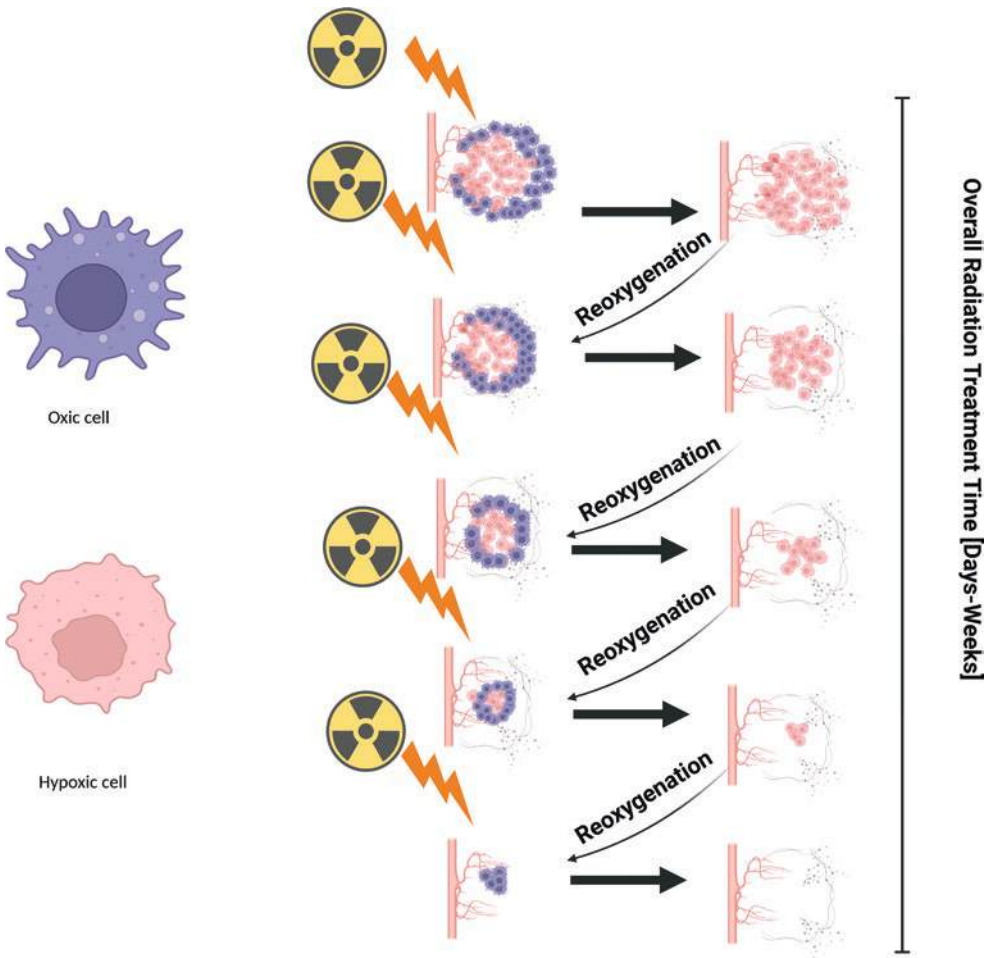

Fig. 5.9 Simplified illustration of the reoxygenation process. Tumor cell compartments include anoxic, hypoxic, and aerated cells. Most tumors show a heterogeneous pattern of hypoxia with gradients of oxygen pressure decreasing with increasing distance from blood vessels. The oxygen status of the tumor cells is not constant; it is a dynamic, constantly changing phenomenon. Following exposure to irradiation, well-oxygenated cells will be sterilized, but many hypoxic cells will not. During the course of fractionated RT hypoxic cells can be reoxygenated, and therefore become sensitive to radiation and can be sterilized. (Figure was adapted from [13])

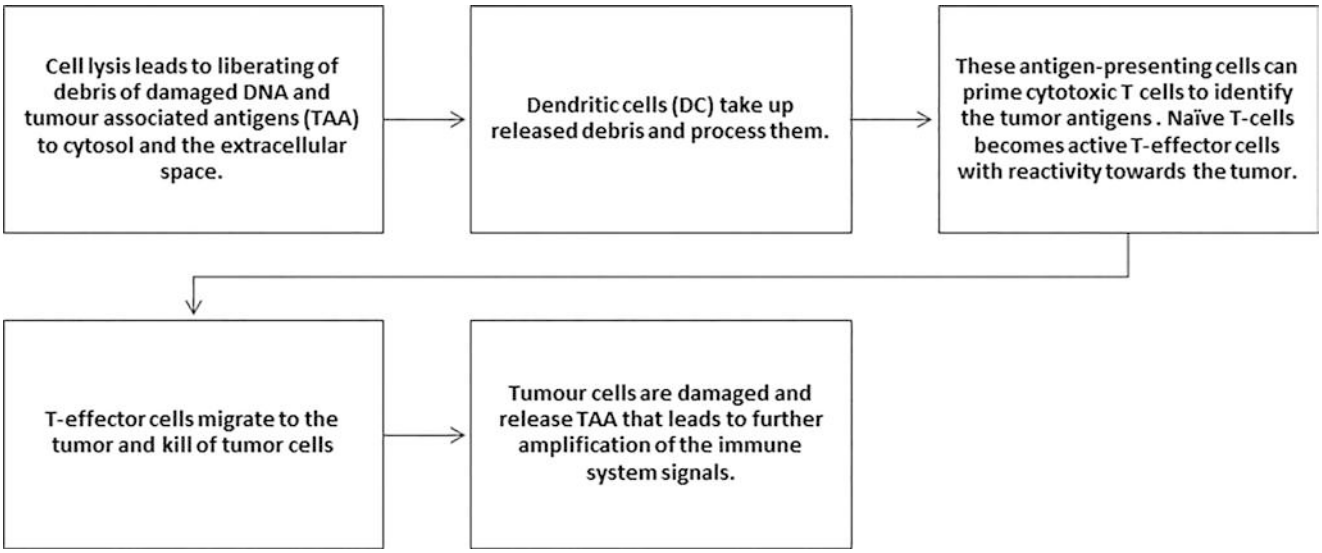

Fig. 5.10 Illustration of the steps of radiation-induced systemic immune activation contributing to attack on distant/metastatic tumor cells

the therapeutic window (Sect. 5.12) using approaches such as via radioprotection of the normal tissues thus decreasing the NTCP or by tumor radiosensitization by increasing TCP. Options for clinical application of such strategies are highly dependent on the tumor and normal tissue type included in the radiation treatment volume. Finally, to be noted is the close link between the Hallmarks of Radiobiology and the Hallmarks of Cancer [31] and therewith related therapeutic options, which have been discussed in detail elsewhere [32, 33].

5.5 Dose Fractionation (Box 5.6)

Box 5.6 Fractionation and the Dose Rate

- Clinically used fractionation schemes are aimed at eradicating malignant tissue while sparing late responding healthy tissue.
- The biological rationale of fractionated irradiation is based on the typical radiation response of the dynamic and heterogeneous exposed tissue and cell population.
- Dose rates used in clinical RT vary from low dose rate with exposure times in hours-days to ultra-high dose rates with radiation dose delivery in the millisecond range.
- The biological effect of radiation decreases with decreasing dose rate to a larger extent for normal tissue with low α/β ratio than for tumors with high α/β ratio.
- Experimental data demonstrate that ultra-high dose rate irradiation might better spare late responding normal tissue.
- The 6R's of radiobiology are the biological processes involved in the dose rate effect.

5.5.1 Evolution of Fractionation

In the early years of RT, radiation oncologists soon realized that a radiation treatment course delivered in multiple fractions over several weeks resulted in better tumor control than a treatment course delivered in a single fraction and also reduced normal tissue toxicity [21]. The history of RT and fractionation is described in detail in Chap. 2. Generally spoken, a treatment course consisting of 30 daily 2 Gy fractions (total dose 60 Gy) is, at isoeffective normal tissue late response level, more effective in eradication of the tumor than a treatment course consisting of a few high dose fractions. Hence, if the total prescribed dose is divided into multiple small radiation fractions with a time interval between the fractions, tumor control could be enhanced at an acceptable level of associated morbidity, relative to a single large dose fraction [13]. However, modern RT techniques allow to give higher dose per fraction while sparing more efficiently the surrounding normal tissue. This may affect this fractionation concept further in future.

The irradiated cell population comprises the malignant tissue as well as acute and late responding healthy ("normal") tissues. When an RT dose is delivered in several fractions, there are advantages and disadvantages in terms of tumor cell kill and normal tissue cell sparing, which are discussed in detail in Sect. 5.14.

5.5.2 Fractionation Parameters and Their Significance

Acute normal tissue effects of RT depend on both fraction size and the overall treatment time. The intensity of acute reactions depends on weekly applied total dose, i.e., the dose per fraction and number of fractions in a week. After an acute reaction has peaked, further stem cell killing cannot increase the intensity of acute reactions but can prolong the

healing time. A persistent early response from severe depletion of regenerating cells is termed a consequential late injury [13]. In contrast, non-consequential late normal tissue effects depend predominantly on fraction size, while the overall treatment time has little influence. Therefore, during hypofractionation, late effects are severe while early effects are matched by appropriate dose adjustment, as discussed in detail in Chap. 6 (Sects. 6.2 and 6.3).

Another important parameter is the inter-fraction interval. Due to the slow repair kinetics of sublethal damage (SLD) in late responding tissues, a minimum of 8 h of inter-fraction interval is recommended for most tissues. The overall treatment time affects both acute effects and tumor control. Prolongation of the overall treatment time (within normal RT range) has a large sparing effect on early responding normal tissues but little sparing effect on late responding normal tissues. However, excessive prolongation of overall treatment time causes the surviving tumor cells to proliferate during treatment. For any prolongation in treatment time, extra dose is required to counteract tumor cell proliferation, due to the phenomenon of accelerated repopulation. For example, in head and neck cancer, after a lag period of 4 weeks during a course of RT, the tumor doubling rate could increase due to triggering of surviving clonogens to divide more rapidly as tumor shrinks after initiation of treatment. A dose of up to 0.6 Gy of each daily dose would be "wasted" due to increased tumor cell load [34]. When the overall treatment time is prolonged, for each extra day, local control would decrease by 1.4% (0.4–2.5%) due to accelerated repopulation.

5.5.3 Clinical Fractionation and the Dose Rate Effect

5.5.3.1 Clinical Fractionation

Differential responses of normal and cancerous tissues when fractionating RT doses can be explained by biological factors that are known as the 6R's (see Sect. 5.4). During fractionation, tumor cells are redistributed and reoxygenated, causing further tumor damage. Moreover, the fractionation process will spare normal tissues by allowing repair of SLD between dose fractions and by allowing repopulation with new cells to occur over the overall treatment time. Therefore, a prolonged radiation treatment given over several weeks results in a greater therapeutic ratio than one or few short duration sessions because of tumor reoxygenation and early reacting normal tissue regeneration.

Radiation fractionation can lead to biologically optimal RT when the equi-effective total dose is related to the dose per fraction for tumors, early responding tissue, and late responding tissue. This relationship is determined by dose per fraction number, fraction number, tumor type, treatment site, and treatment plan. Using different normal tissues as models, it was found that with decreasing dose per fraction, the isoeffective total dose increases more rapidly than for acute effects or tumor response. This relationship can be described by the linear-quadratic (LQ) model. According to the LQ model, with appropriately chosen α/β values to represent isoeffect dose relationships at least at the 1–6 Gy dose range, a standard fractionation scheme with five small sized fractions per week over a few weeks would be beneficial regarding the tumor cure-normal tissue complication balance. Hence, deviation from standard fractionation affects the Biological Effective Dose (BED), which includes schedules with different fraction size and inter-fraction time as well as overall treatment duration. The BED is the total dose required to produce a particular effect in small dose fractions, used as the quantity to compare different fractionation regimens, see Table 5.3 for models that are used to deal with a deviation from standard fractionation.

Table 5.3 Models of biological effective dose (BED) for isoeffect calculations for modified fractionation regiment (adopted from [16])

Model	Formula	Statement
Equivalence dose 2 Gy (EQD_2)	$EQD_2 = D\dfrac{d+\left(\dfrac{\alpha}{\beta}\right)}{2+\left(\dfrac{\alpha}{\beta}\right)}$ D is total dose and d is dose per fraction.	• EQD_2 is the 2 Gy dose that carries the same biological effect as a total dose D with a fraction size d Gy. • The purpose of this model is to compare the effectiveness of schedules containing doses per fraction and different total doses. This is equivalent to converting each schedule into a 2-Gy fraction that has the identical biological effect.
Total effect (TE)	$E/\beta = D[(\alpha/\beta) + d] = TE$ E = isoeffect	• It is used for schedules with different doses per fraction. • TE and BED are conceptually similar and have been cited in literature, but E is divided by β instead of α.
Extrapolated tolerance dose (ETD)	$(\dfrac{E}{\alpha}) = D((1 + d(\alpha/\beta)) = BED$	• The ETD refers to levels of effectiveness that imply full tolerance. It is used for schedules with different doses per fraction.
Basic EQD_2 formula with incomplete repair factors (H_m).	$EQD_2 = D\dfrac{\left(1+H_m+\alpha/\beta\right)}{2+\left(\alpha/\beta\right)}$	• Used for tolerance calculations, taking into account the increase in the overall damage caused by interaction of subsequent fractions.
Basic EQD_2 formula with Incomplete repair factors (g factors).	$EQD_2 = D\dfrac{\left(dg+\alpha/\beta\right)}{2+\left(\alpha/\beta\right)}$	• Used for low dose rate exposures.

5.5.3.2 The Dose Rate Effect

The dose rate is defined as the ratio of the radiation dose to the duration of the radiation exposure. The term should be used only in the context of short periods of time, for example, dose per second or dose per hour, the SI dose rate unit is Gy/h. Acute exposure refers to a high radiation dose delivered in seconds or minutes, and chronic exposure means that the radiation dose is delivered over a longer period of continuous exposure over hours to days to even months and years. The spectrum of dose rates used in radiation oncology is presented in Table 5.4.

Physical aspects of the dose rate are presented in Chap. 2. The application of low dose rate irradiation in brachytherapy in the clinic, is discussed in Chap. 6. FLASH is a novel RT treatment technique using ultra-high dose rates. Using FLASH, multiple studies indicate sparing of healthy tissue acute and late toxicities while maintaining tumor control, hence widening the therapeutic window (Sect. 5.2). FLASH is discussed in detail in Chap. 6. The radiation dose rate has a large biological impact on exposed cells and tissues. Both in vitro and in vivo experimental data revealed that, for a defined biological endpoint, for example, cell survival or a certain late normal tissue reaction like myelitis of the spinal cord, the biological effect decreases with decreasing dose rate. With decreasing dose rate, the total dose to obtain a certain *isoeffective* biological endpoint—for example, a probability of 50% loss of kidney function or reduction of the cell survival with a fraction of 0.4, is increased. Dose rate sparing is almost absent for acute responding normal tissues and tumors.

In terms of fractionation, the decrease in dose rate can be considered as lowering the fraction size of the total radiation dose to be delivered in external beam HDR radiotherapy (Fig. 5.11). Referring to the LQ model (Sect. 5.5) for comparison of biological effectiveness of different radiation treatment schemes, low dose rate irradiation could be considered as super-fractionation (Fig. 5.11 and Box 5.7).

Table 5.4 Dose delivery conditions used in the clinic, for internal radiation therapy (brachytherapy) and external beam irradiation, and related dose rates (ICRU 38 definitions and FLASH)

Dose delivery condition	Dose rate (Gy/h)[a]
Low dose rate (LDR)	<2
Medium dose rate (MDR)	2–12
High dose rate (HDR)	>12
Pulsed dose rate (PDR)	±75% HDR, ±25% MDR and LDR
Ultra-high dose rate (FLASH)	≥144.000

[a]The International System of Units (SI) defined dimension for the dose rate is "Gy/h"

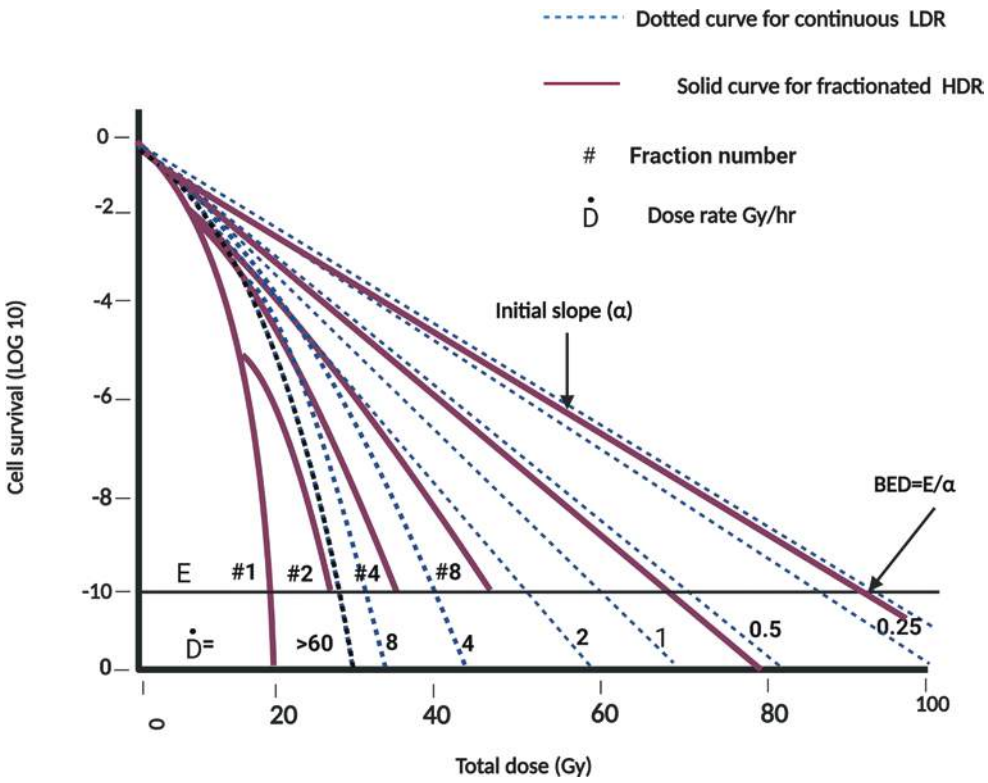

Fig. 5.11 The dose rate effect seen as an extreme form of fractionation. Cell survival following fractionated HDR irradiation with increasing number of fractions (solid curves). With an infinite number of tiny fractions, and complete sublethal damage repair, the dose-squared β parameter of the LQ tends to zero, and only the dose-linear β parameter plays a role. Then, the Biologically Effective Dose (BED) is reached for a certain endpoint effect E. Similar sparing phenomenon with decreasing dose rate in continuous LDR exposure (dotted curves)

Box 5.7 The Dose Rate and the Biological Effective Dose

- At extremely low dose rate, i.e., irradiation with an infinitely large number of infinitesimally small dose fractions, the theoretical total dose required to produce an isoeffect is the Biological Effective Dose (BED) of the LQ model.

Thus, as exposure is elongated, the shoulder of the cell survival curve tends to become shallower, this is because the α parameter of the linear-quadratic model does not change significantly, while the β parameter tends towards 0.

This situation also implies, dependent on the fractionation sensitivities of irradiated tumor and normal tissues involved (i.e., their repair capacity characteristics expressed in their α/β values) as well as of their DNA repair kinetics (the half time for sublethal damage repair $T_{1/2}$), an optimal therapeutic ratio situation. For the LQ model adaptation to correct for the dose rate effect and incomplete repair, additional parameters are introduced (e.g., Joiner and van der Kogel [16]). The dose rate effect of continuous low dose irradiation is discussed in view of the 6R's of radiobiology in Sect. 5.4 below.

The repair process of radiation-induced DNA lesions has been explained in depth in Chap. 3. DNA DSB, if not repaired, are lethal to the cell. A DNA DSB can either be induced by single-track action or double-track action. A single-track X-ray lesion is independent of dose rate and linearly proportional to dose (the contribution of α in the LQ model). In double-track action, the two interactive single strand DNA lesions are produced by different tracks of X-ray photons, and the formation of double strand lesions is therefore dependent on the dose rate and is proportional to the radiation dose squared (the contribution of β in the LQ model). In fact, the protracted delivery of a given radiation dose reduces the effect of double-track action because time offered between lesions is long enough for repair to occur [28] (Fig. 5.12).

5.5.3.3 Repair and the LQ Model Parameters

Figure 5.13 shows that lowering the dose rate has greater effect on cells or a tissue with a low α/β ratio, for example, 3 Gy than with a high α/β ratio of, for example, 10 Gy. At a low α/β ratio, the curves are spread out more, implying that late responding normal tissues are particularly spared relative to tumors when decreasing the dose rate.

Also, for a tissue having an equivalent α/β ratio, larger sparing is obtained with decreasing tissue-specific half time ($T_{1/2}$) for sublethal damage repair. Similarly, as with fractionated radiation, this can be attributed to incomplete repair between the "fractions" or during continuous exposure. Hence, at longer repair half time, low dose rate irradiation is causing more damage, and less discriminative between tissues with different α/β ratio.

It is well recognized that cells in the G2 or M phase of the cell cycle are more sensitive to radiation than cells in the G1, G0, or S cell-cycle phases (Sect. 5.4, Fig. 5.8). During continuous low dose rate irradiation, the process of redistribution would push initially relative radioresistant cells into a radiosensitive cell-cycle phase. This process is dependent on numerous cellular and tissue factors, and therefore difficult to predict.

Another phenomenon that might occur is the inverse dose rate effect, which represents a reversal of the typical pattern of the conventional sparing with decreasing dose rate. For

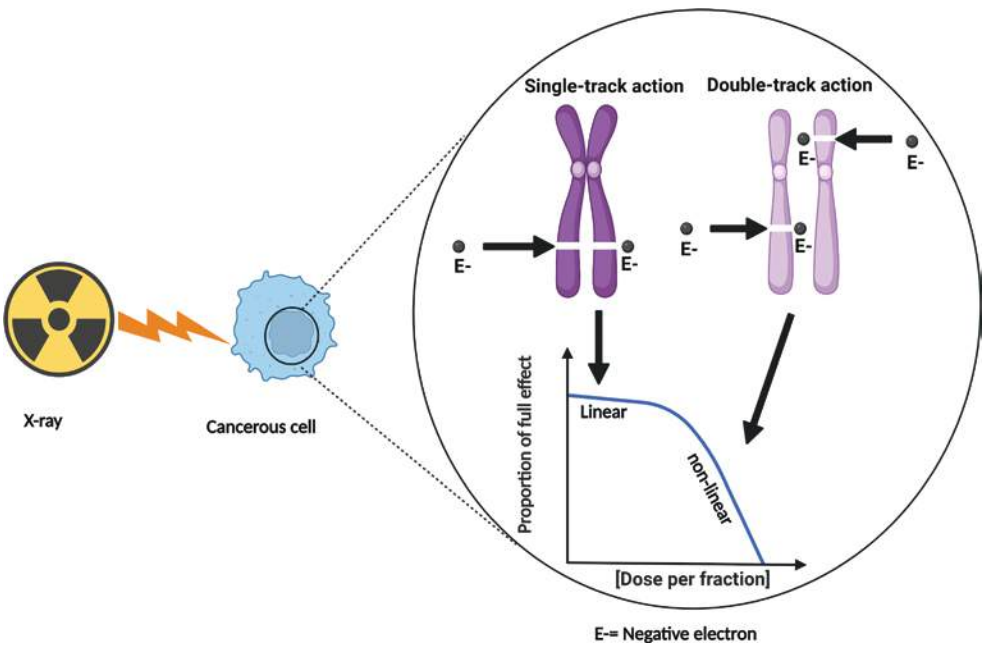

Fig. 5.12 Illustration single-track action and double-track action. In single-track action, the two interactive lesions are produced by a single track of ionization induced by an X-ray photon that subsequently produces a dose which is independent of dose rate and linearly proportional to dose. In double-track action, the two interactive lesions are produced by a different track of ionization induced by X-rays which subsequently produces a dose which is dependent on the dose rate (decreasing the dose rate reduces double-track action) and non-linearly proportional to the radiation dose squared

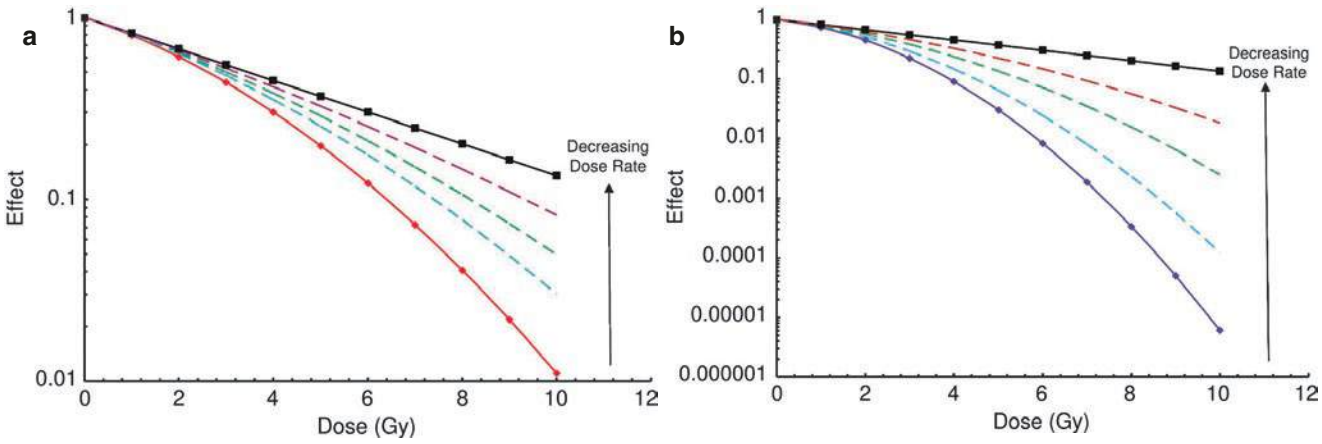

Fig. 5.13 The effect of lowering the dose rate on the survival of cells. (**a**) Cells characterized with an α/β ratio of 10 Gy (typical for a tumor or early responding normal tissue). (**b**) Cells with an α/β ratio of 3 Gy (typical for a late responding normal tissue). See text for details. (Figure from Shrieve and Loeffler [17], with copyright permission from Wolters Kluwer Health, Inc.)

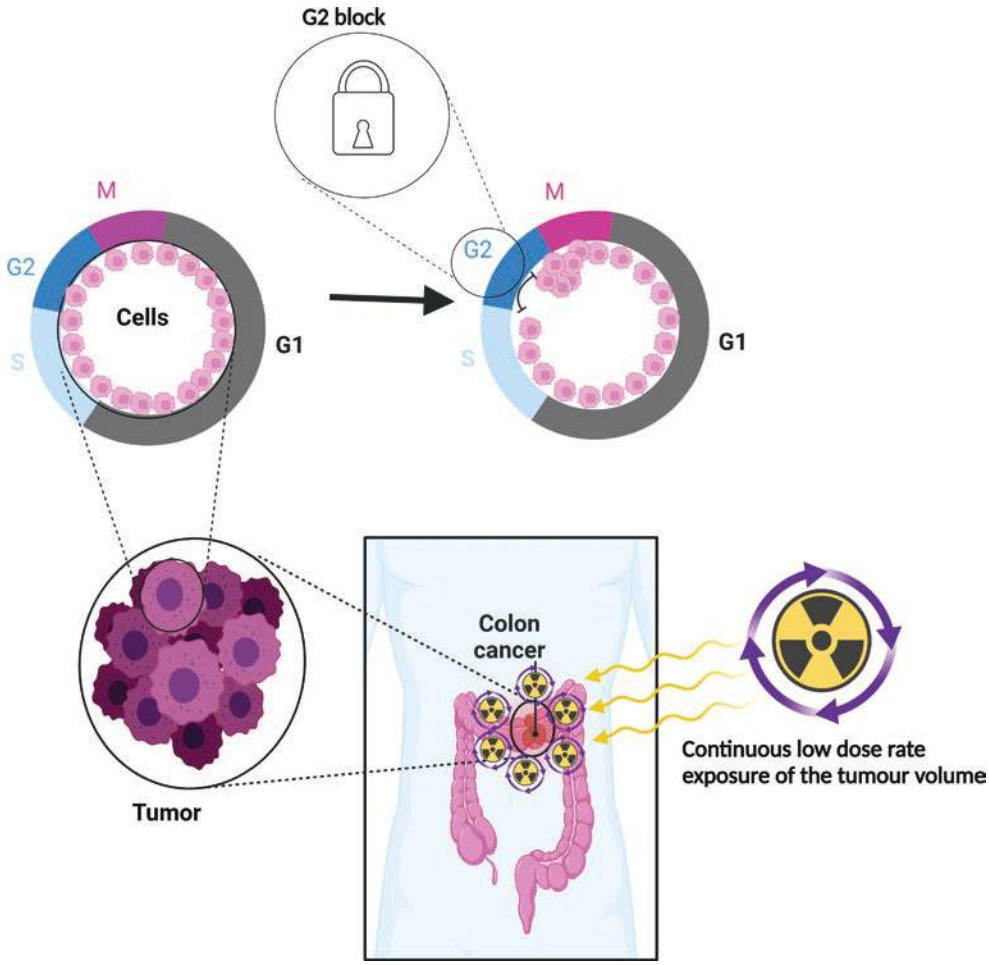

Fig. 5.14 The inverse dose rate effect. When the dose rate delivered to HeLa cells is decreased from 1.54 to 0.37 Gy/h, the efficiency of cell killing increases, with damage generated similar to that from an acute exposure [35]. When cells are exposed to higher dose rates, they are kept in the phase of the cycle in which they are at the beginning of irradiation. However, use of lower dose rates may allow cells to continue cycling during irradiation. When cells are exposed to 0.37 Gy/h, cells tend to progress from other phases of the cell cycle and arrest in G2, which is a radiosensitive phase of the cycle. As a result, an enriched population of G2 cells is responsible for increasing the radiosensitivity of cells

the same radiation dose, radiation delivered at a certain specific lower dose rate *increases* the radiosensitivity of cells in comparison to radiation delivered at a higher dose rate. This is illustrated in Fig. 5.14.

Tumor cell repopulation during continuous low dose rate (LDR) exposure might negatively influence treatment outcome since a larger number of cells have to be sterilized if the repopulation rate outflows the duration of exposure,

which might occur with fast repopulating tumor cells (e.g., cell doubling time of 24 h).

The impact of irradiation on the immune response has been shown to be dependent on the radiation dose (see Chap. 6), and the dose rate of exposure is likely to play a role [36]. The effect of low dose rate irradiation regarding reactivation of the immune response is however not well described.

Chronic low dose rate exposure will not cause oxygen depletion in initially well-oxygenated tumor cells. Initially, hypoxic cells might benefit from reoxygenation during long-term radiation exposure. However, as pointed out in Sect. 5.4, the kinetics of reoxygenation is very much dependent on the tumor type.

5.6 Whole-Body Irradiation

5.6.1 Introduction

Whole-body irradiation (WBI) or total body irradiation (TBI) refers to the therapeutic protocol in which a patient's total body is irradiated with γ/X-rays. WBI is used as part of the conditioning regimen for transplantation of bone marrow or hematopoietic stem cells for lymphoma, leukemia, or multiple myeloma and as a palliative regimen in selected cases of lymphoma and leukemia [37]. WBI implicates irradiation of the total body, with reduction of the dose to the lungs, to lessen the hazard of radiation-induced lung toxicity [38, 39]. Historically, in the fifth and sixth decade of the last century scientists trying to reverse early responding tissue effects of radiation, demonstrated experimentally that bone marrow engrafted with hematopoietic stem cells from a donor animal "could recapitulate the blood system" and thus showed that previously irradiated bone marrow could be rescued. This contributed to the development of therapeutic techniques involving bone marrow ablation followed by bone marrow engraftment with hematopoietic stem cells for the treatment of some marrow cancers, for example, leukemia or multiple myeloma [37]. This procedure is mainly used to eliminate residual cancer cells in the transplant recipient, and to further suppress or destroy the immune system; subsequently, it serves to prevent immunologic rejection of blood stem cells or transplanted donor bone marrow. Thus, the chances of engraftment are increased, and the bone marrow stromal cells of the patient are spared [38, 39].

5.6.2 Details of Radiobiological Mechanisms of Whole-Body Irradiation

5.6.2.1 Leukemia

Since a characteristic of WBI is that it can sterilize small numbers of widely spread cells that are sensitive to radiation, this makes it a treatment option for (residual) marrow disease. Biologically, leukemia is associated with a spectrum of intrinsic cellular radiosensitivity that ranges from notable radiosensitivity to significant radioresistance, which determine the extent of leukemic cell killing. The molecular biology responsible for the variety in radiosensitivity of leukemia is not entirely known, but increased apoptosis seems to require functional *p53*, *c-myc*, and *Bcl2* genes. Therefore, it seems that radiosensitivity results from the apoptosis retention after activating *p53*, *c-myc*, and *Bcl2* genes by radiation [40]. RT in conjunction with a wide range of treatment modalities such as (myeloablative) chemotherapy and the subsequent graft-versus-tumor effect are therefore required to obtain significant eradication of malignant clones [22, Chap. 16].

5.6.2.2 The Normal Hematopoietic System

Bone marrow stem cells typically have D_0 values ranging from 0.5 to 1.4 Gy. These cells are therefore intrinsically radiosensitive. Even though hematopoietic rescue (i.e., stem cells) could allow the delivery of high doses that eliminate the recipient's marrow cells which in turn prepares the stem cell microenvironment for repopulation to occur, this procedure is associated with long-term or life-threatening consequences. Critical organs of concern in WBI are those described as late responding tissues. Fortunately, as effect on these tissues is dependent on total dose, dose rate and fractionation, appropriate scheduling of the treatment allows some protection. While a modest number of cancer cells being radiosensitive will be killed, complete cancer cell killing may not always be possible with radiation alone. Therefore, TBI often needs to be given together with chemotherapy. Moreover, incomplete bone marrow ablation may result in mixed chimerism of bone marrow after transplant [22, 40].

As a result of immunological mismatch between recipient and donor, rejection of donor stem cells may occur. In order to avoid this, TBI is used to prevent the recipient from rejecting donor stem cells.

Bone marrow transplantation results are influenced by the treatment schedule. Lymphoid cells repair a large amount of radiation-induced DNA damage during the time interval between fractions. Hence, the effectiveness of fractionated TBI is reduced significantly in comparison with single-dose TBI and results in more graft rejections. However, the fractionation effect is reversed for bone marrow stromal cells ("colony-forming unit fibroblasts"). The success of engraftment is based on the likelihood of sparing bone marrow stromal cells, and when treatment is delivered as single-dose TBI, the likelihood of damaging both bone marrow stromal cells and their progenitors increases. Importantly, the effectiveness of single-dose TBI is increased significantly in comparison with fractionated TBI, but at the cost of increased long-term toxicity [22].

5.6.2.3 Palliation

Unlike curative RT, palliative RT is used to control the symptoms of advanced, incurable cancer (the primary tumor or metastatic deposits) by slowing down tumor growth, controlling symptoms and causing cancer to regress [41]. WBI may be effective for palliation, especially for advanced leukemia or lymphoma, using rather low doses in the order of 0.1 Gy/fraction. In experiments with solid tumors, tumor cells with colony-forming abilities in both experiments of formation of artificial metastases and naturally developing metastases, these tumors could be suppressed with specific low doses [42]. It is assumed that either chronic TBI or low dose total body irradiation may stimulate the immune system to eliminate metastatic cancer cells. However, nowadays, TBI is only very rarely used for this indication. For further information, see tumor microenvironment changes and abscopal effect discussed in Sect. 5.15.

5.6.3 Fractionation Dose Effect in Whole-Body Irradiation

In WBI, the doses delivered for transplantation of bone marrow or stem cells are in the range of 10–12 Gy [43]. To reduce long-term complications in the recipient, this dose is typically divided into 2 Gy fractions [14, 44]. In the so-called reduced conditioning regimens, single fractions of 2 Gy or two fractions of 2 Gy are given. When WBI is split into multiple small fractions and spread over a period of time, outcomes are generally improved, and toxicity is diminished. While the former is due to the fact that the dose is still adequate to eradicate both any cells of residual malignant tissue and the recipient's bone marrow, the latter is explained in Sect. 5.2 [45].

5.6.4 Dose Rate Effect in Whole-Body Irradiation

The dose rate in RT influences the effectiveness of the radiation exposure. An explanation of how a survival curve may become shallower at low dose rates was discussed in Sect. 5.5. In WBI, the pattern is different from localized RT because the effect of radiation dose depends on the tissue type. When low dose rate is used, the incidence of normal tissue toxicity is decreased in comparison with high dose rates [46–48]. However, changing the radiation dose rate from the low dose rate to high does not affect the probability of engraftment success [49, 50].

5.7 Prediction of Radiation Response of Tumors (Box 5.8)

Box 5.8 Tumor Response Prediction

- Functional parameters including reoxygenation, redistribution, repopulation, repair, and radiosensitivity are traditionally used to define radio-responsiveness.
- The role of repopulation also proved to be a robust predictive marker as illustrated in head and neck cancer where increased tumor expression of EGFR indicates efficacy of accelerated radiation.
- DNA, RNA, and proteins have recently been identified to define tumor RT responsiveness yet few of them have attained clinical validation and/or application.

5.7.1 Principles of Prediction of Radiation Response of Tumors

Radiation treatment has been improved greatly over the last two decades by integrating 3-D anatomy into planning systems, and developing of image-guided (IGRT), intensity-modulated (IMRT) and intensity modulated arc radiation therapy (IMAT) techniques, resulting in individualization of treatment. Radiation treatment portals and arcs are much more tailored to the anatomy of each patient's tumor and normal tissue. Today medical professionals prescribe RT taking into account the type of primary tumor, its grade, stage, location, size, biological characteristics, and concomitant treatments. However, these clinical parameters do not give an accurate prediction of the effect of RT since wide variations in response occur between patients given the same treatment and having similar tumors [51–53]. Furthermore, diverse treatment options are now available. Moreover, several tumor RT sensitizing strategies using different drugs which can enhance the effects of RT, especially those that target the molecular pathways, are becoming available now. Treatments frequently employ combined approaches. One such avenue currently underway involves trials that combine chemotherapy/RT with immunotherapy.

RT can differentially affect tumor responses due to a variety of radiobiological factors, which are referred to as the 6R's. Among them, hypoxia, proliferation, and radiosensitivity have proved to be fairly good predictive markers [51–34]. Beyond these well-known classical biomarkers (BMs), there are also a number of promising candidate molecular bio-

markers currently being tested in preclinical and clinical studies such as genetic and epigenetic factors as discussed in Sect. 5.10. In this section, classical and modern BMs as well as their role in predictive assays will be discussed in addition to the available methods used to detect them.

5.7.2 Classical Factors

RT constitutes approximately 60% of cancer treatment. If a clinical assay could successfully predict the RT response, it would have wide-ranging clinical implications. A broad group of old-fashioned radiobiological variables that affect RT outcome including tumor oxygen status, the degree of repopulation or proliferation rate, intrinsic radiosensitivity, and both individual and tumor radiosensitivity is shown in Fig. 5.15.

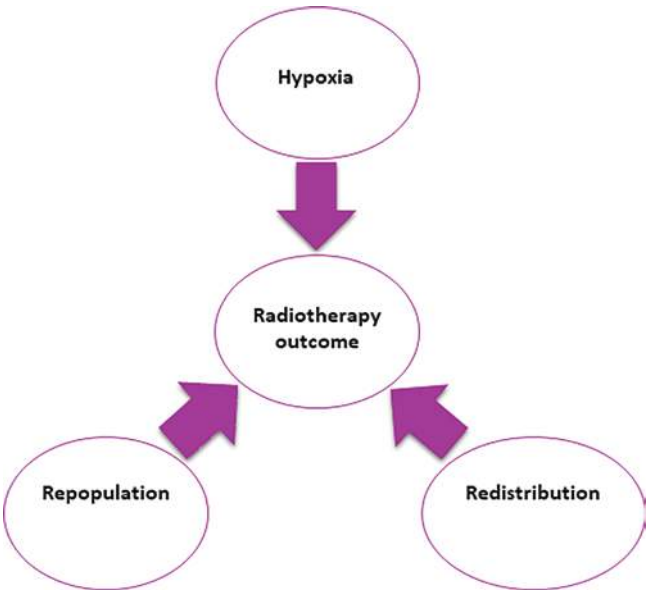

Fig. 5.15 Review of classical biomarkers used to obtain information on relevant features of radiobiology

Predictive factors in therapy may relate more directly to primary tumors and their local control. Metastatic disease may need to be considered separately even though it clearly plays a significant role in survival of the patient. Research to develop predictive assays for tumor RT response should generally measure local control and normal tissue effects [16, 51, 52].

5.7.2.1 Tumor Oxygen Status

Tumor vascular beds differ significantly from those in normal tissues in their structure and physiological characteristics. Tumor-related blood vessels are composed of single-layered endothelium, commonly containing gaps between the endothelium taken up by tumor cells, resulting in immature capillaries. A dysfunctional blood supply through the tumor reduces oxygen delivery, resulting in areas of tumor hypoxia, acidic intra-TME nutritional deprivation, and therewith the tumor response to IR For more information about predictive tests to assess Oxygen Effect to Tumor Hypoxia see Sect. 5.8.

5.7.2.2 Repopulation

Tumor repopulation is a key factor contributing to treatment failure after RT. Alternative fractionation schemes have been proposed as methods for modulating interfraction tumor repopulation. A phase III randomized trial in over 1000 patients with head and neck cancer showed significant improvement in regional control following accelerated and hyperfractionated RT as compared to conventional fractionated RT. Additional evidence, which has shown the importance of proliferation, demonstrated that higher doses are needed to control a tumor when overall time of treatment is prolonged. Clinical evidence that tumor repopulation is an important mechanism for treatment failure is notably apparent in a subset of patients. Therefore, evaluation of tumor repopulation has been a priority for developing predictive tests [52]. Table 5.5 shows several tests that can be performed in vitro and in vivo to measure tumor repopulation.

Table 5.5 Description of biomarkers and laboratory assays for assessing repopulation

Test	Procedure	Method	Statements
The mitotic index	Using tissue sections to calculate mitosis ratios	Biopsy staining	A correlation exists between outcome results and the labeling index, but it is weak
DNA flow cytometry	Calculating the percentage of cells that are in the S phase of the cell cycle	Flow cytometry	
The tumor potential doubling time, T_{pot}	Using bromodeoxyuridine as a stain in a tumor biopsy	Flow cytometry	T_{pot} is not a significant predictor for RT response
Endogenous markers (Ki67)	Proliferation-associated proteins can be detected using antibodies	Gene signature, biopsy studies, or plasma/serum	
Molecular marker profiles (p-53, Bcl-2, Ki-67, or EGFR expression)	Measuring the level of these markers		Continuous hyperfractionated accelerated radiotherapy (CHART) is recommended in head and neck cancer patients who have high expression of EGFR in tumor or low organized patterns of Ki-67 and is negative for Bcl-2 or p53 expression

5.7.2.3 Intrinsic Radiosensitivity

Various types of cell death, such as apoptosis and autophagy, which also result in a loss of colony-forming ability, contribute to tissue reactions caused by IR. Many publications proposed that cellular radiosensitivity could be measured by the clonogenic assay. A technical challenge of dispersing tumor cells ex vivo has interfered with its clinical application, however [52].

For more information about predictive tests to assess radiosensitivity, see Chap. 7.

5.7.3 Modern Factors

Radiation responsiveness was traditionally defined using the 6R's (see Sect. 5.4) but only three factors proved reliable as prognostic markers: hypoxia, repopulation, and radiosensitivity, and hence RT regimens have been modified according to fraction size, dose per fraction, and overall treatment time as depicted in Fig. 5.16. Individual assessments of these parameters could have predictive value since each of these parameters has a substantial effect on the outcome of the RT. Assays based on measurements of these parameters, however, had mixed success in developing predictive assays for many reasons. Firstly, the lack of success may be explained by the fact that few quantitative differences exist between human tumors and normal tissues, and their heterogeneity

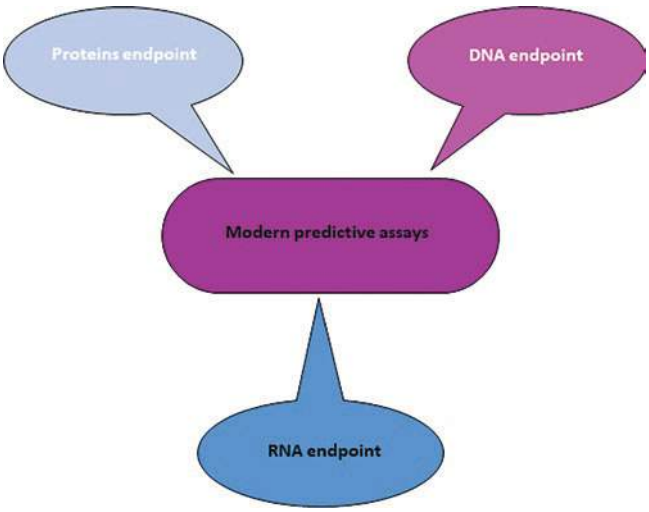

Fig. 5.16 Review of modern biomarkers used to obtain information on relevant features of radiobiology

overlaps in many ways. Secondly, it was intended that the 6R's can be used to understand emerging phenomena in radiation biology rather than predicting its outcomes.

The first molecular techniques were applied to radiobiology about two decades ago and soon revealed the existence of proteins and genes that respond to and influence the cellular outcome of IR [53]. Radiation response of tumors is associated with a complex series of gene and protein alterations some which also are influenced by the underlying genomic alterations, for example, mutations. When cells experience IR-induced damage, it was early on observed that key proteins are induced [57, 58]. An example is the p53 protein which upon exposing cells to a photon beam is induced and control multiple pathways. For instance, a single fraction of 20 Gy X-rays was observed to induce key proteins such as MDM2 and CDKN1A in some cell lines, both which is regulated by p53 [58]. Furthermore, the response to radiation is influenced by polymorphisms in genes encoding proteins that participate in DNA damage repair, as well as by mutations affecting these genes. When cells experience radiation insult, multiple genes undergo a series of up and down regulations interacting through many pathways including p53-regulated genes such as p21 (CIP1/WAF1) and GADD45A. Also, the response to radiation is influenced by methylation, acetylation, ubiquitylation, phosphorylation, and sumoylation of genes and proteins which control the DNA damage repair. For instance, the presence of hyper-methylated promoters means that a gene is becoming actively transcribed; hyper-methylation of promoters attracts proteins that inhibit transcription and turn it off. Non-coding RNAs also contribute to radiation response. There are complementary forms of RNA, namely microRNA (miRNA) that are not translated into protein and play an important role in the initiation and progression, repopulation and programmed cell death (see Chap. 3). Therefore, this mechanism is reflected in terms of sensitivity or resistance to IR [16, 59]. Overall, gene and protein expression are altered in the tumor itself and by radiation which affects cellular outcomes and causes a heterogeneity of RT response in tumors. Accordingly, protein, DNA and RNA analysis can be used to obtain information on relevant features of radiobiology using several types of measurements such as genomics, transcriptomics, epigenomics, or proteomics, which analyze DNA, RNA, DNA–chromatin interactions and proteins, respectively, as described in Fig. 5.17 and Table 5.6.

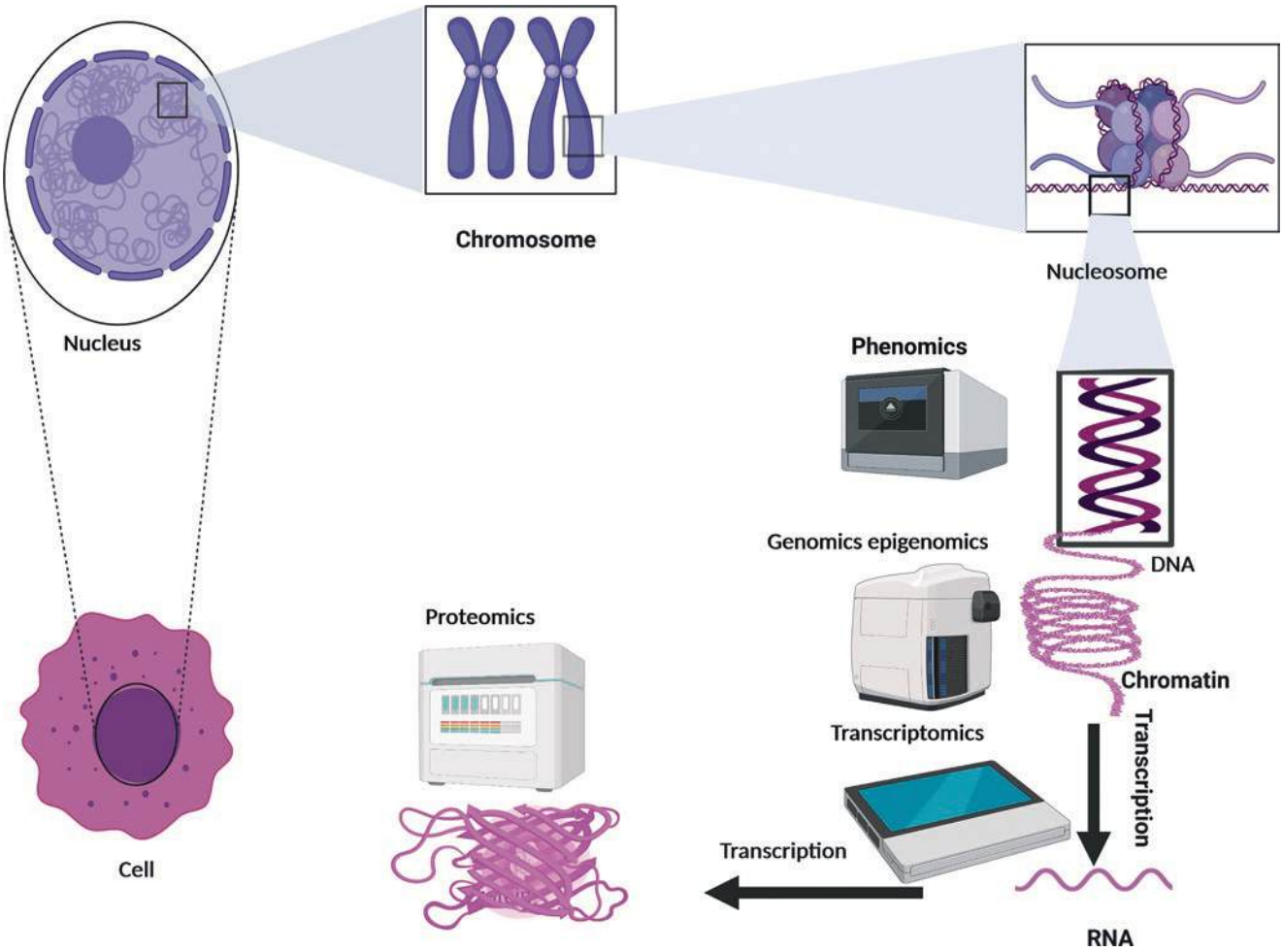

Fig. 5.17 Schematic view of biomarkers. Proteins, DNA chromatin, DNA, or RNA that are analyzed by proteomics, genomics epigenomics, genomics, or transcriptomics, respectively

Table 5.6 Description of modern biomarkers and assays for analyses of RT response

Marker	Advantage	Assay
Protein	Expression profiling at the protein level can be a good candidate marker as proteins are responsible for the actual cellular functions.	Tissue microarrays for high-throughput immuno-histochemistry, luminex technology for multi-analyte immunobead-based profiling, mass spectrometry methods and antibody chip.
DNA	The DNA level can be a good candidate marker because everyone is genetically unique, cancer is caused by genetic changes, and is characterized by genomic instability. Variation in individual genes influences risk for cancer development. Variations in a patient's response to treatment are ascribed to the heterogeneity of genetic changes in cancer.	In situ hybridization (ISH) for identifying a DNA sequence in tumor tissue, genetic variation sequence for analyses of duplications and deletions of large region DNA (copy number variation (CNV) and Single Nucleotide Polymorphisms (SNPs), epigenetic variation sequence for chromatin modification and DNA acetylation, ubiquitylation, phosphorylation, sumoylation, and methylation.
RNA		Low-density Taqman arrays for detecting small signatures after whole genome profiling, ISH and FISH for detecting RNA in sample in situ. Quantitative polymerase or real-time chain reaction for quantify and amplify a targeted DNA molecule. Gene expression array for deriving profiles, classifiers or signatures associated with prediction of treatment results or prognosis. Next-generation sequencing technologies for the study of gene expression profiles of different species of mRNA.

5.8 Tumor Hypoxia and Therapeutic Approaches

Hypoxia refers to conditions with low oxygen. The oxygen concentration of most normal tissue in the human body is around 5–7% and tissues with less than 3% oxygen are regarded as hypoxic. Hypoxic cells are known to be more resistant to radiation and chemotherapy. Hypoxia is also a potent microenvironmental factor promoting metastatic progression of cancer [60].

Hypoxia in tumor cells can be of two types—acute hypoxia or chronic hypoxia. Acute hypoxia is a transient perfusion-limited hypoxia due to transiently occluded blood vessels [61]. Chronic hypoxia is a diffusion-limited hypoxia and can lead to necrosis [62].

Oxygen can generally diffuse approximately 150 μm at the arterial end of the capillary and less at the venous end (Fig. 5.18). Therefore, when the radius of the tumor is less than 160 μm, there is no central necrotic region. Between 160 and 200 μm, there may or may not be a hypoxic center. When the radius is more than 200 μm, the central portion consists of anoxic necrotic cells while the next layers consist of cells with different degrees of hypoxia and aerobic actively dividing cells at the outer layer [62]. The central portion becomes necrotic because the cells are deprived of both oxygen and nutrients.

As hypoxic cells are more radioresistant than oxygenated cells (Chap. 3), irradiation of a tumor will predominantly kill the outer layer of cells leaving the hypoxic cells. One way to reduce this problem is to divide the radiation dose into many daily fractions, which will allow the hypoxic cells nearest to the oxygenated cells to be reoxygenated after the oxygenated cells have been killed [63]. In this section, we will give an overview of the most important mechanisms and pathways induced by hypoxia since these are potential targets in connection with treatments.

5.8.1 Oxygen Effect

As described in Chap. 3, oxygen modifies the biological effects of low LET IR. For such radiation, DNA damage predominantly occurs through the indirect effect of radiation-induced water radicals. In the absence of oxygen, DNA radicals can become chemically restituted through donation of hydrogen atoms by SH-compounds (such as glutathione). However, if molecular oxygen is present, $RO_2\cdot$ is produced which cannot be restored. Oxygen thus "fixes" the damage produced by free radicals (i.e., makes the radiation damage permanent). Therefore, cells are more sensitive to radiation in the presence of oxygen than in its absence.

The relative radiosensitivity of cells increases dramatically when the oxygen tension increases from 3 mmHg (0.4% O_2) to about 30 mmHg (4% O_2), which corresponds to the oxygen concentration in venous blood [64]. Beyond this, it reaches a plateau with no further effect of increasing the oxygen tension. In order to compete with restitution, molecular oxygen must be present during or within microseconds after the radiation exposure because the lifetime of the free radicals generated by the radiation is less than about 10^{-5} s.

The oxygen enhancement ratio (OER) is the ratio of doses under hypoxic to aerated conditions that produce the same biologic effect. In vitro studies have shown OER of X-rays to be around 3.5 for high doses and around 2.5 in low dose regions of the cell survival curves [65].

High LET radiations like alpha particles cause direct and complex damage to DNA with little possibility for restitution. Therefore, there is no enhanced effect with presence of oxygen (i.e., OER is 1). It is intermediate for neutrons and comparatively high for low LET radiations such as X-rays and gamma rays [66, 67]. OER decreases as LET increases. The OER falls slowly until about 60 keV/μm of LET, then falls rapidly and reaches 1, i.e., no oxygen effect, when LET

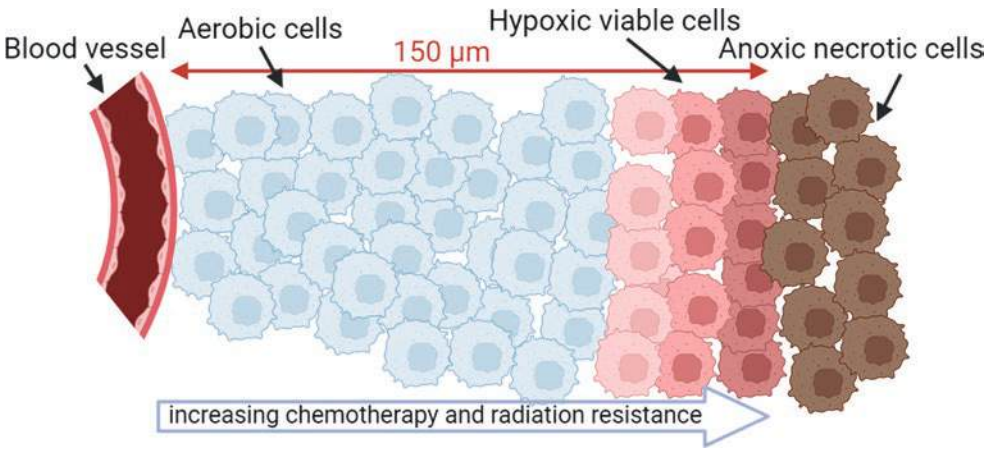

Fig. 5.18 Diffusion of oxygen through tumor. As the distance from the blood supply increases, the oxygen levels available for the cells decreases. As the cells grow more hypoxic, they become more radioresistant

reaches about 200 keV/μm [66]. Thus, one way to target hypoxia is to use high LET radiation (Box 5.9).

Box 5.9 The Oxygen Enhancement Ratio
The oxygen enhancement ratio varies with:
- Cell cycle phase
- Type/quality of radiation
- Radiation dose and dose rate

5.8.2 Hypoxia Response Pathways

When a tumor grows, the existing vasculature will not be able to provide oxygen and nutrients to the more distant cells resulting in regions of hypoxia. During hypoxic conditions, the cells that survive are those that undergo adaptive responses, which are not only critical to survival but also promote malignancy and metastasis. The main purposes of the adaptive responses are to uphold ATP production and save energy as well as nutrients. ATP production is maintained by the formation of new blood vessels (angiogenesis), increased production of red blood cells (erythropoiesis), switch to anaerobic metabolism, and migration to a more favorable environment (metastasis). The processes to save energy include reduction of protein synthesis and recirculation of nutrients (autophagy). The signaling pathways regulating these processes are induced by upregulation of hypoxia-inducible factors (HIFs) and activation of the unfolded protein response (UPR).

5.8.2.1 Hypoxia-Inducible Factor (HIF)

HIF-1 was discovered in 1995. Its importance is emphasized by the award of the Nobel prize in Physiology or Medicine 2019 to William Kaelin Jr., Peter J. Ratcliffe and Gregg L. Semenza for their work in elucidating how HIF senses and adapts cellular response to oxygen availability. The HIF protein family consists of three different alpha subunits (HIF-1α, HIF-2α, HIF-3α), which bind to the same type of β-subunit. In this section, we will only discuss HIF-1, which is the only one which is ubiquitously expressed and the most well studied. In the presence of molecular oxygen, proline-hydroxylase enzymes (PHD) hydroxylate HIF-1α, i.e., PHDs add two OH-groups to proline residues on HIF-1α using oxygen as a cofactor. Hydroxylated HIF-1α is recognized by von-Hippel-Lindau (VHL)-ubiquitin ligase complexes, which then adds ubiquitin-groups that target HIF-1α for degradation. Without oxygen, HIF-1α is stabilized allowing it to bind to the β-subunit and activate gene transcription.

HIF-1 is known to induce transcription of more than 60 genes by binding to a common promoter called hypoxia response element (HRE). Some of these genes are involved in increasing oxygen supply, such as VEGF (which induces angiogenesis), erythropoietin (which stimulate red blood cell production), and iron transport to erythroid tissue. HRE-regulated genes are also involved in cell proliferation, such as insulin-like growth factor-2 (IGF-2) and transforming growth factor-α (TGF-α). HIF-1 also induces transcription of genes involved in switching of metabolic pathways to use glycolysis as a primary mechanism of ATP production. HIF thus regulate transcription of genes involved in glucose transport into the cell (i.e., GLUT1 and GLUT3), and in maintaining intracellular pH during increased lactate production such as carbonic anhydrase 9 (CAIX) and monocarboxylate transporter 4 (MCT4).

In addition to promoting hypoxia tolerance, HIF-1 also upregulates transcription of genes involved in several steps of metastasis: angiogenesis, epithelial-mesenchymal transition (EMT), cell motility, intra/extravasation, and the formation of a premetastatic niche facilitating colonization of metastatic tumor cells.

Stabilization of HIF and activation of its downstream pathways occur at relatively moderate levels of hypoxia (<about 2% O_2) as compared to radiation resistance, which occurs below about 0.1% O_2 [68].

5.8.2.2 The Unfolded Protein Response (UPR)

Similar to IR resistance, activation of the unfolded protein response (UPR) occurs below about 0.2% O_2 and contributes to hypoxia tolerance by reducing protein synthesis and inducing autophagy. UPR is activated by accumulation of unfolded and misfolded proteins in the endoplasmic reticulum (ER). Such accumulation takes place under hypoxia because post-translational disulfide bond formation, which is necessary for correct protein folding, have been shown to be oxygen dependent [69]. There are three ER stress sensors in the ER membrane, PERK (protein kinase RNA-like endoplasmic reticulum kinase), IRE1a (inositol requiring kinase 1a), and ATF6 (activating transcription factor 6). All three are activated by the release of BiP (Binding immunoglobin Protein) from the ER membrane. Activated PERK phosphorylates eIF2α (Eukaryotic translation initiation factor 2 subunit α), which inhibits translation of protein except for some key proteins, which remain translated [70]. One of these is ATF4 (activating transcription factor 4), which induces transcription of genes required for autophagy, amino acid synthesis and import, redox balance, and angiogenesis [71]. However, if the stress becomes excessive, ATF4 can switch from pro-survival to pro-death and induce apoptosis [72]. Active IRE1α (Inositol-requiring transmembrane kinase/endoribonuclease 1α) reduces protein synthesis through the degradation of selected mRNAs. It also activates an inflammatory response and promotes autophagy as well as apoptosis. BIP release allows ATF6 translocation to Golgi, where cleavage of this protein results in release of transcriptionally

active ATF6 (DNA-binding cytoplasmic domain of ATF6), which contributes to restoring ER homeostasis [70].

5.8.3 Measurement of Tumor Hypoxia

Hypoxia in tumor cells can be measured using oxygen probes or protein markers for hypoxia. Polarographic electrodes, in particular Eppendorf electrodes, have long been regarded as the gold standard for measuring tumor hypoxia. The limitations of these are that they must be inserted into the tumor damaging the tissue and that they consume oxygen resulting in a high signal-to-noise ratio for low oxygen levels [73]. Fiber-optic probes have also been developed [74], but the disadvantage of both is that this is an invasive method, which can only be used in accessible tumors. Another method is injection of pimonidazole to patients before biopsies or total resection of the tumor. Pimonidazole is a 2-nitroimidazole compound, which binds to thiol-containing proteins specifically in hypoxic cells, and it can be used in immunohistochemical analyses to quantitative assessment of tumor hypoxia [75].

A noninvasive alternative method is hypoxia PET imaging. 2-Nitroimidazoles have been developed as radiosensitizers due to their ability to undergo up to six electron reductions. However, they can also be used as radiotracers carrying a positron emitter. The reduction requires the activity of reductases that are only present in viable hypoxic cells resulting in the radiolabeled molecules being accumulated in hypoxic regions visible to PET imaging. Examples of nitroimidazole or nitroimidazole-derivative tracers are ^{18}F-Fluoromisonidazole (^{18}F-FMISO), ^{18}F-Fluoroazomycin-Arabinofuranoside (^{18}F-FAZA), ^{18}F-labeled fluoroerythronitroimidazole (^{18}F-FETNIM), ^{18}F-fluoroetanidazole (^{18}F-HX4), and ^{18}F-2-(2-Nitro-1H-imidazol-1-yl)-*N*-(2,2,3,3,3-pentafluoropropyl) acetamide (^{18}F-EF5) [73, 76]. Other redox-sensitive compounds include Copper(II) diacetyl-bis (N4-methylthiosemicarbazone) (^{60}Cu-ATSM) and ^{123}I-iodoazomycinarabinoside (^{123}I-IAZA) [77]. Of these, ^{18}F-MISO is the most extensively used in both preclinical and clinical studies. F-MISO is highly lipophilic, which means it can easily diffuse across cell membranes but also that the clearance of the tracer from normoxic tissue is very slow. This results in a low tumor to blood ratio and the need to wait for typically 2 h between tracer injection and imaging. A general problem in PET imaging is the low spatial resolution.

Magnetic resonance imaging (MRI) is non-ionizing and has a better spatial resolution than PET. Different MRI techniques have been evaluated for quantification of the blood oxygenation level in tissue. Blood oxygen level-dependent MRI (BOLD-MRI) uses the paramagnetic quality of deoxyhemoglobin in contrast to oxygenated hemoglobin. This can be measured as an increase in T2*-relaxation rate. A similar technique, tissue oxygen level-dependent MRI (TOLD-MRI) uses an increase in T1 relaxation caused by the presence of dissolved oxygen. A third technique is dynamic contrast-enhanced MRI (DCE-MRI) in which a paramagnetic contrast agent such as gadolinium is used and imaged over time [78].

HIF and its target proteins such as CA9 and GLUT1 are upregulated under hypoxia (see above). Accordingly, they have been studied as endogenous markers for hypoxia and seem to co-localize with 2-nitroimidazoles. However, their expression can also be regulated by other factors than oxygen, which reduces their reliability in quantifying tumor hypoxia.

5.8.4 Therapeutic Approaches to Tumor Hypoxia

Tumor hypoxia is a major barrier for effectively treating cancer patients. Various approaches have been investigated both in vitro *a*nd in vivo to overcome hypoxia in tumor cells. The main clinical strategies to mitigate treatment resistance due to tumor hypoxia are either to improve oxygenation, mimic the effect of oxygen, use drugs that are cytotoxic only in hypoxic cells, apply dose escalation to hypoxic areas, or inhibit pathways that are important for cell survival under hypoxia (Table 5.7).

Table 5.7 A summary of different approaches to improve treatment of hypoxic tumors

Approaches	Rationale
High LET radiotherapy	Direct damage to DNA, less dependent on oxygen levels
Hyperbaric oxygen	Improve tumor oxygenation
Blood transfusion	Improve oxygen supply
Perfluorocarbons	Artificial blood substances to improve oxygen supply
Nicotinamide	Vitamin B3 analogue to overcome acute hypoxia
Carbogen	95% oxygen + 5% carbon dioxide to overcome chronic hypoxia
Hypoxic cell radiosensitizers	Compounds that mimic oxygen and can radio-sensitize tumors
Bioreductive drugs	Reduces to cytotoxic form during hypoxic conditions
Hypoxia-targeted radiotherapy	Dose escalation/adaptation in hypoxic sub-volumes of tumor
Dichloroacetate	Inhibits pyruvate dehydrogenase kinase 1, alter tumor metabolism, enhances efficacy of hypoxic cytotoxins
Electron transport chain inhibitors	Decreased oxygen consumption in mitochondria and increased radiosensitivity

5.8.4.1 Improving Oxygenation to Tumors

The simplest approach to reduce tumor hypoxia is to let the patient breathe hyperbaric oxygen (HBO) (2–4 atmosphere 100% oxygen). However, this may cause vasoconstriction. To avoid this, a mixture of 5% carbon dioxide and 95% oxygen called carbogen was introduced. Carbogen breathing reduces chronic diffusion limited hypoxia. For acute hypoxia, nicotinamide can be used to mitigate transient fluctuations in tumor blood flow [79]. In the ARCON strategy, a combination of carbogen and nicotinamide was used in association with accelerated hyperfractionated RT to reduce tumor proliferation during treatment and spare normal tissues [80].

5.8.4.2 Hypoxic Cell Radiosensitizers

Hypoxic cell radiosensitizers are chemical or pharmacologic agents that can increase the radiosensitivity of cells, which are deficient in oxygen. These agents are oxygen substitutes that diffuse into poorly vascularized areas of tumors and penetrate to reach hypoxic cells within the tissue. Therefore, when administered with radiation these agents cause fixation of the free radical damage caused by IR and thereby increases its lethal effect. A radiosensitizer should have an increased effect on tumors relative to normal cells to achieve a therapeutic window/gain. An ideal hypoxic cell radiosensitizer should be chemically stable; have low metabolic breakdown; be highly soluble in water and lipids; act at all phases of cell cycle; be active at low doses of radiation; and cause low toxicity to normal cells [81].

The commonly used hypoxic cell radiosensitizers belong to the nitroimidazole group of drugs. In the nitroimidazole ring structure, a nitro group can be present in any of positions 2–5. Based on the position of the nitro group, drugs are named 2-nitroimidazole to 5-nitroimidazole. The presence of the nitro group in position 2 increases electron affinity and IR sensitization capacity [82]. Therefore, 2-nitroimidazole is a more efficient hypoxic cell radiosensitizer. Three widely used nitroimidazole compounds in clinical trials and their characteristics are summarized in Table 5.8.

Table 5.8 Nitroimidazole group hypoxic cell radiosensitizers (adapted from [13])

Compound name	Position of nitro group	Properties	Toxicity
Misonidazole	2-Nitroimidazole	Lipophilic, crosses blood–brain barrier	Neurotoxic—dose limiting
Etanidazole	2-Nitroimidazole	Hydrophilic, shorter half-life, does not cross blood–brain barrier	Less neurotoxic
Nimorazole	5-Nitroimidazole	Less active	Less toxic

The enhancement ratio is the ratio of X-ray doses needed to control 50% of the tumors in the absence and presence of the drug. It was found to be around 1.82 for misonidazole in a mouse mammary tumor model for a single-dose treatment but for multifraction regimens, it is usually less [83].

The Danish Head and Neck Cancer 5 (DAHANCA 5) study which comprised 422 patients with pharyngeal and supraglottic carcinomas found a clear benefit of using nimorazole as a radiosensitizer. Thus, no increase in late radiation toxicity and a highly significant benefit in 5-year local control rates and disease-free survival rates. The use of nimorazole as a radiosensitizer in head and neck cancer is standard practice in Denmark [55].

5.8.4.3 Bioreductive Drugs

Bioreductive drugs are drugs that are reduced by cells to form active cytotoxic agents only under hypoxic conditions while being non-reduced in an oxic cell. Thus, the differential action on hypoxic cells (i.e., tumor cells) compared to oxic cells, i.e., normal cells) gives a therapeutic window/gain. Unlike the direct action of hypoxic cell radiosensitizers, which increases the radiosensitivity of cells, bioreductive drugs act synergistic with radiation to improve tumor cell kill [84].

The hypoxic cell cytotoxicity ratio (HCR) is the dose of a drug required to kill a certain fraction of oxic cells compared to the dose of drug required to kill an equal fraction of hypoxic cells. HCR varies for different classes of bioreductive drugs [85]. The main classes of bioreductive compounds are fused ring benzoquinones (e.g., mitomycin C), organic N-oxides (e.g., tirapazamine), and nitroheterocyclic compounds (e.g., RSU-1089), among which tirapazamine is the widely investigated drug.

5.8.4.4 Hypoxia-Targeted Radiotherapy

As described above, imaging techniques such as PET and MRI can be used to identify hypoxic regions within the tumor. They are used in RT treatment planning to define radioresistant sub-volumes that can be targeted with boost dose or dose escalation. Targeting hypoxic sub-volumes in tumors by adaptive RT/dose painting can lead to improved tumor control. There is early clinical evidence from a phase 2 randomized trial that dose escalation to hypoxic volumes using ^{18}F-FMISO PET is feasible without increased normal tissue toxicity in head and neck cancers [86]. The utility of hypoxia-directed RT dose painting is being studied in other cancer subsites such as lung, pancreas, and cervix cancer [87–89].

5.8.4.5 Molecular Targeted Drugs

Drugs that target specific molecules to improve radiosensitivity in hypoxic tumors are being investigated in preclinical and clinical studies. Examples are dichloroacetate, electron transport chain inhibitors, and other pathway inhibitors.

Dichloroacetate (DCA) is a specific inhibitor of the pyruvate dehydrogenase kinase (PDK), which has been shown to increase ROS production in hypoxic cancer cells but not in aerobic cells leading to radiosensitization of hypoxic tumor cells [90]. Electron transport chain inhibitors have been developed to reduce oxygen consumption and thereby improve tumor oxygenation. One such is an anti-diabetic drug, Metformin, which has been shown to reduce oxygen consumption through inhibition of mitochondrial complex I and thus improve tumor oxygenation and response to RT [91]. Other approaches include inhibition of pathways that are important for cell survival under hypoxia (e.g., HIF-1α, CAIX, MCT4, VEGF, and lactate dehydrogenase-A (LDHA) [92].

Box 5.10 Tumor Hypoxia in Radiotherapy

- Tumor hypoxia can be acute (perfusion-limited) or chronic (diffusion-limited).
- Tumor hypoxia leads to resistance to RT and chemotherapy.
- Hypoxic tumor cells undergo adaptive responses that are critical to survival but also promote malignancy and metastasis.
- Strategies to either increase oxygenation or interfere with the hypoxic response pathways can improve the outcome of RT.
- Drugs that either mimic the effect of oxygen or are toxic under hypoxic conditions can be used to increase the effect of RT.

5.9 Tumor Resistance and Progression

- RT is an effective cancer treatment, but a large portion of patients subsequently experience radioresistance and recurrence of their cancers.
- Mechanisms of radioresistance in cancer treatment are related to several factors: Increased DNA damage repair capacity, cell-cycle redistribution, cancer stem cell resilience, signaling pathways, epithelial-mesenchymal transition (EMT), and tumor metabolism.

5.9.1 Introduction

RT is one of the most efficient therapeutic regimens for various tumors. The main factor in determining the therapeutic effect is the tumor radiation response that is correlated to intrinsic or acquired radioresistance after the treatment [93]. Intrinsic radioresistance relies on inherent characteristics of the tumor (for instance, the presence of cancer stem cells (CSCs). The acquired radioresistance is a process of tumor adaptation to the RT-induced changes and develop resistance to the IR. This complex process involves multiple genes, factors, and mechanisms [94, 95]. Radioresistance leads to poor prognosis in cancer patients, and it represents the main reason for RT failure, which can ultimately lead to tumor recurrence and/or progression/metastases [95]. Radioresistance of tumors is influenced by several factors, including increased DNA damage repair capacity, cell-cycle redistribution, CSCs resilience, signaling pathways, epithelial-mesenchymal transition (EMT), and tumor metabolism (Fig. 5.19).

5.9.2 DNA Damage Repair Ability

RT kills cancer cells mostly by inducing DNA damage. Radiation-induced DNA lesions are multiple including base and sugar modifications, cross-links, single-stranded breaks (SSBs), and double-stranded breaks (DSBs) [96] (see also Chap. 3). DNA DSBs are responsible for most of IR-induced cell killing [97]. To respond to DNA damage, cells initiate signaling pathways named DNA damage response (DDR) signaling. The capacity of tumor cells to trigger a DDR following radiation, through initiation of DNA repair and cell-cycle checkpoints, promotes radiation resistance and tumor cell survival. In radiobiology, it is considered that cells with a high capacity to trigger DSBs repair will be radioresistant, while cells with frail repair ability will be more sensitive in response to radiation [93].

Activation of DDR and proper repair of DNA lesions are of paramount importance for cellular integrity, survival, and genomic stability [98]. There are four main DNA repair pathways in tumor cells: DNA DSB repair, base excision repair (BER), nucleotide excision repair (NER), and mismatch repair (MMR) [99]. BER and SSB repair (SSBR) are important for repairing altered bases and SSBs. Besides DSBs caused directly by IR unrepaired damaged bases and SSBs, can generate DNA DSBs when they face a replication fork. Non-homologous end joining (NHEJ) and homologous recombination (HR) two principal cellular DSB repair pathways (see Chap. 3).

5.9.2.1 Dysfunctional DNA Repair in Cancer

Defects in DNA repair factors are a characteristic of many cancers which promote genomic instability and mutation in cells [98, 100–102]. Deficiency of DDR and DNA repair genes caused diseases such as Xeroderma pigmentosum, Ataxia Telangiectasia (ataxia telangiectasia mutated (ATM)), Nijmegen breakage Syndrome (Nibrin (NBS1)), Werner syndrome (WRN), Fanconi anemia (FA), associated breast cancer syndrome (BRCA1 and BRCA2), lead to cancer susceptible disease syndromes (reviewed in [98, 102] and in Chap. 7). Cancers present germ line mutations, somatic

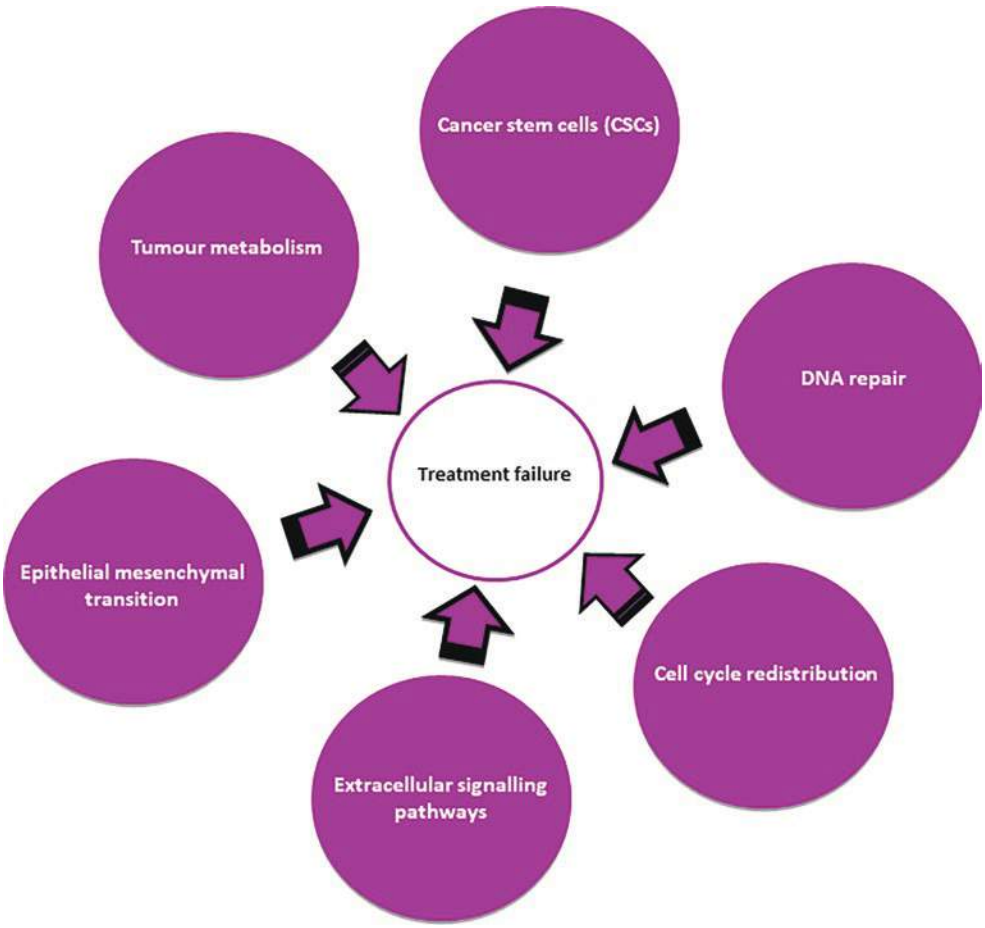

Fig. 5.19 Description of the tumor biological responses to radiation and the mechanisms for its resistance

mutations or distinctive expression of DDR components that lead to the impairment of DDR and altered checkpoints. In addition, DNA replication stress due to oncogene stimulation also causes initiation of DDR and tumor progression.

The same DNA repair deregulation that commenced carcinogenesis is associated with cancer progression, aggressiveness [102]. There are situations in which the tumor is preserved after the therapy, becoming even more aggressive. It is known that IR can activate stress and adaptive response to DNA lesions causing cancer progression, metastatic behavior [103]. Several dysfunctional DDR signaling genes are found in cancer and correlated with radioresistance (Table 5.9).

5.9.3 Cell-Cycle Redistribution

Activation of cell-cycle checkpoints is important downstream IR-induced DDR signaling. Several molecules in the cell-cycle checkpoints regulate and block cell-cycle progression to allow for DNA repair and prohibit premature entering into mitosis with unrepaired DNA lesions. The same machinery responsible for DNA damage recognition, ATM and ATR, activates the cell-cycle checkpoints kinases CHK1 and CHK2 to regulate the checkpoints and repair DNA damage. Two distinct signaling cascades, the ATM-Chk2 and ATR-Chk1 axes respond to DSBs damages, respectively, to ssDNA. Activated Chk1 and Chk2 inactivate CDC25C by phosphorylation. In the absence of CDC25C phosphatase activity, WEE1 kinase impedes cyclin-dependent kinase 1 and 2 (CDK1/2) activity triggering cell-cycle arrest in the G2/M phase and promoting DNA damage repair (reviewed in [93, 95, 111]). Molecules in the cell-cycle checkpoints were also found to be linked with the development of radioresistance (e.g., ATM, p53, p21, Chk2, Cdc2).

5.9.4 Modification of Extracellular Signaling Pathways and Tumor Suppressors

A considerable amount of research has been done on the modulation of cellular signaling pathways in response to IR and many of them are involved in radioresistance, including extracellular and intracellular signaling cascades. This subsection focuses specifically on the major oncogenic signaling pathways such as Ras and phosphatidylinositol-3′-kinase pathways (PI3K)/AKT that contribute to radioresistance (Fig. 5.20).

Table 5.9 Examples of dysfunctional DNA damage response signaling genes found in cancer and linked with cancer radioresistance and progression

Molecule	Function(s)	Type of defects	Reference
ATM	DDR—DSBs Cell-cycle redistribution	Mutations; increased copy number and autophosphorylation, overexpression	Squatrito et al. [104], Zhang et al. [105]
DNA PKcs	NHEJ	Overexpression	Kotula et al. [106]
Ligase IV/XRCC complex	NHEJ	Polymorphism in LIG4 gene	Srivastava et al. [107]
RAD51	HRR	Overexpression	Chen and Kuo [96] Bhattacharya and Asaithamby [98]
RPA	HRR	Overexpression	Liu et al. [93]
BRCA1 and BRCA2	HRR transcriptional regulation of many DNA repair genes	Loss-of-function mutation; BRCA1 overexpression	Kan and Zhang [108]
HSP90	Regulates HRR Regulates protein related to DDR signaling (ATM, NBS1, ATR)	Overexpression	Kinzel et al. [109]
APE1 (apyrimidinic endonuclease 1)	BER	Overexpression	Kiwerska and Szyfter [102], Madhusudan [110]
DNA polymerase β (pol β)	BER	Overexpression; missense mutations in pol β gene coding for variant proteins	Bhattacharya and Asaithamby [98]
PARP	PARP 1 and PARP 2-SSB, BER	Overexpression	Li et al. [111]
Ku 70/80	NHEJ	Overexpression	Baptistella et al. [112]
MSH6/MSH2	MMR	Reduced expression	Uraki et al. [113]
ERCC1	NER	Overexpression Polymorphism	Kiwerska and Szyfter [102], Peng et al. [114]
XRCC1	Excision repair	Polymorphism	Li et al. [115], Liu et al. [93]

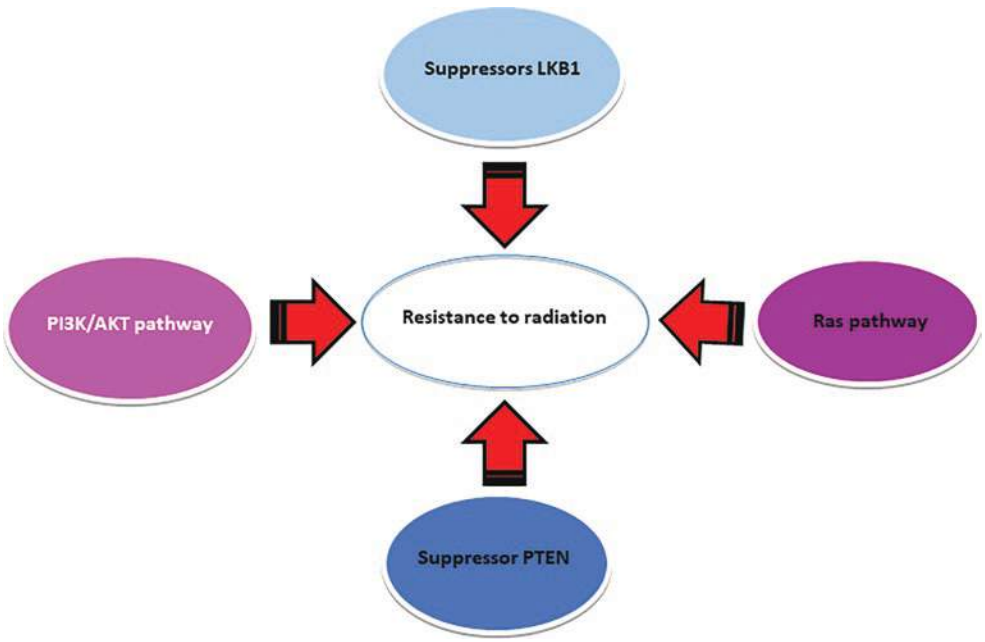

Fig. 5.20 Review of tumor suppressors and the molecular signal pathways that contribute to radioresistance

Radiation causes many behavioral changes in the extracellular domain of EGFR as well as to its kinase domain, including truncations and common mutations of an extracellular domain of EGFR [16, 116, 117]. Photon radiation can cause EGFR aberrations that over-activate downstream pro-oncogenic signaling pathways, including the RAS-RAF-MEK-ERK MAPK and AKT-PI3K-mTOR pathways that modulate cell processes, including cell resistance to RT, angiogenesis, migration, invasion, and apoptosis [118–120].

When EGFR is activated by photon radiation, this activation, triggers the RAS-RAF-MEK-ERK MAPK pathways. Radiation resistance is associated with this pathway targets due to its pro-survival nature, and mutated *RAS* has been associated with resistance to photon-irradiation in cancer cells [121–124].

Also, when EGFR is activated by photon radiation, this triggers the AKT-PI3K-mTOR pathways and activated EGFR induces the phosphorylation of PI3K and downstream AKT phosphorylation [124]. Radiation resistance is also linked to activation of this target with tumor cells being protected by decreased autophagy and apoptosis, as well as increased DNA repair capacity [125].

Overall resistance to photon irradiation appears to be modulated by the transmembrane protein EGFR but also repression of tumor suppressors. In this circumstance, the tumor suppressors LKB1 and PTEN has been reported to correlate to resistance.

5.9.5 Activation of Epithelial-to-Mesenchymal Transition (EMT)

EMT is a series of changes involving epithelial cells that phenotypically transform into mesenchymal cells [126]. To acquire local invasiveness, the first step involves a profound phenotypic shift within the primary tumor of cancer cells. The progression of cancer is dependent on tumor cells undergoing the EMT and invading blood vessels [127, 128]. This results in invasion and distant metastasis, the main cause of cancer-related death. Normal epithelial cell layers cannot accommodate the motility and invasiveness of malignant carcinoma cells, yet this epithelial organization plan continues to be recognized in many primary carcinomas. Despite their overall topology differing quite a bit from that of comparable normal epithelia, these tumors contain well-organized sheets of epithelial cells. Although it's not confirmed, cancer cells require a partial or complete EMT to become invasive as in the following steps [129]:

1. Factors, including growth factor (GF), initiate EMT by promoting E-cadherin replacement by N-cadherin.
2. Due to its ability to allow these tumor cells to form homotypic interactions with a variety of types of mesenchymal cells, N-cadherin increases the affinity of cancer cells for stromal cells composed of fibroblasts, which support tumor cell invasion.
3. N-cadherin forms a weaker intermolecular band than E-cadherin, so molecules whose intermolecular bands are weaker favor motility.

When normal cells transform into cancerous cells, E-cadherin turns into N-cadherin and such cancer cells can escape their keratinocyte neighbors. Thus, the switch from E- to N-cadherin expression promotes invasion of the stroma. N-cadherin allows cancer cells to form homotypic interactions with mesenchymal cells, including endothelium, fibroblasts, and others in the stroma of the organ (Fig. 5.21).

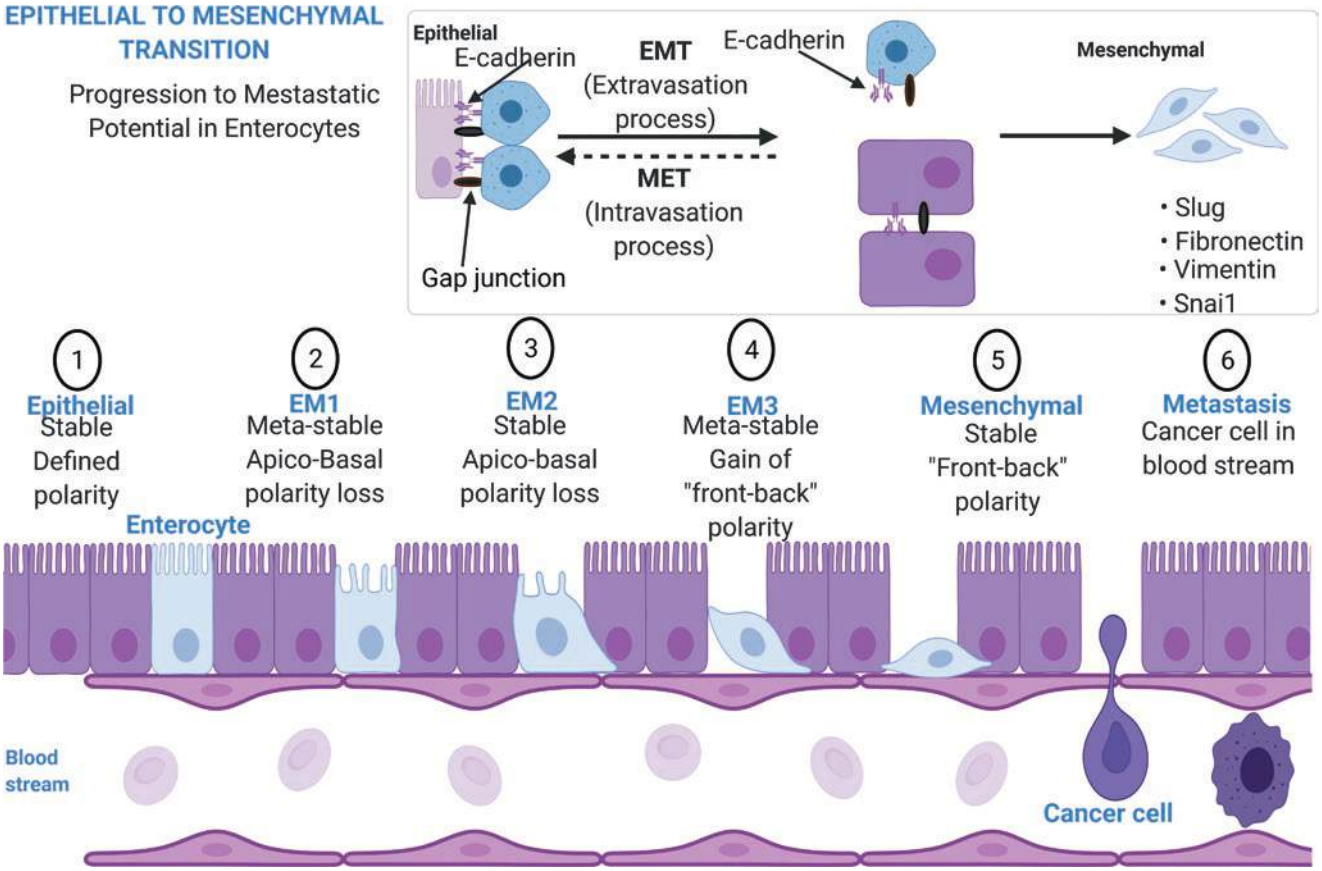

Fig. 5.21 An overview of a typical EMT program that causes cadherin shifts in the cell and invasion of cancers

In vitro and in vivo, EMT is induced by a variety of factors, including radiation, ROS, hypoxia, and transforming growth factor [130–132]. Radiation causes many changes in a cell, which are directly affiliated with epithelial cancer. These include aberrant multicellular organization, genomic instability, dysregulation of differentiation, and phenotypic transition, i.e., EMT. Multiple evidence suggests that Notch1 signaling is essential for EMT [133]. Unlike normal tissue, when cancerous tissues experience radiation insult, the irradiated cells show overexpression of an active Notch-1 protein in both cytoplasm and nucleus. This results in decreased expression of E-cadherin and increased expression of vimentin and fibronectin, which consequently alleviate radiation-induced EMT as reported both in in vitro and in vivo models [134, 135]. Furthermore, low dose IR promotes NF-κB p65 signaling in cervical cancer cells. The transcription factor NF-κB regulates tumorigenesis as well as apoptosis and is essential for the initiation and maintenance of EMT. This signaling subsequently induces EMT that downregulates of expression of the epithelial markers E-cadherin and Cytokeratin 18 (CK-18), which is a hepatocyte-secreted protein that is released into the blood during apoptosis and necrosis while it upregulates vimentin and the mesenchymal markers N-cadherin. Therefore, this leads to improving the progression of cancer cells [136]. Additionally, a variety of evidence indicates that Granulocyte Colony-Stimulating Factor (G-CSF) (formerly believed to promote granulocytes) is strongly associated with lung cancer progression [137]. Moreover, it has been reported that IR activates Granulocyte Colony-Stimulating Factor Receptor (G-CSFR)/JAK/STAT3 signaling pathways via secreted G-CSF, resulting in EMT in non-small cell lung cancer cells (NSCLCs) [137]. The matrix metalloproteinase (MMP) family proteins are essential for EMT, as well. The γ-IR treatment of nodular NSCLC cells was associated with increased invasion via EMT induction, which is characterized by a highly active MMPs system [138]. Following irradiation, an EMT program is induced, causing breast cancer cells to develop a resistance and progression behavior. The proto-oncogene tyrosine-protein kinase (SRC), being a non-receptor kinase, integrates diverse signal transduction pathways that contribute to a variety of cellular processes including survival, proliferation, angiogenesis, differentiation, migration, and angiogenesis. Upon irradiation, SRC is activated, which promotes EMT through AKT, p38, and PI3K activation. Similarly, fractionated IR inhibits PTEN-related expression, which is associated with activation of the Drosophila embryonic protein SNAI1 (Snail) protein accumulation and Akt/GSK-3β signaling and provoking EMT [139]. As a result of radiation, GSK-3β is phosphorylated at serine 9 residue, and silencing the tank-binding kinase-1 (TBK1) tones down the phosphorylation, indicating that TBK1 inhibition is associated with activating GSK-3β. Indeed, GSK-3β functions in several key signaling pathways that can contribute to EMT, such as the Wnt, TGF-β, Hedgehog, Notch, and PI3K pathways. Upon phosphorylation at its N-terminus, GSK-3β can be inactivated and Snail is stabilized and succumbs to EMT. In this way, it is suggested that TBK1 inhibition has the potential to reduce radiation-induced Zinc Finger E-Box Binding Homeobox 1 (ZEB1) expression via activation of GSK-3β. This hypothesis is supported by the observation that pre-treatment of cells with the GSK-3β inhibitor SB216763 increases TBK1 inhibition, increases E-cadherin expression, and reduces ZEB1. In conclusion, it was seen that TBK1 signaling is influenced by GSK-3β in radiation-induced EMT [140]. RT can cause both lessening of tumor cells and killing of them as it can also lead to damage to normal tissues, radioresistance, invasion, and distant metastases. Several studies have suggested that EMT generates malignant characteristics such as a propensity to recurrence, resistance to treatment, and dissemination of metastatic cells. Radiation is generally considered a key initiating factor for EMT, as it activates signal pathways that initiate the process.

5.9.6 Changing Tumor Metabolism

Radiation resistance has in multiple studies been linked to tumor metabolism alterations as a result of radiation-induced changes in mitochondrial metabolism or glycolysis [141, 142]. The development of radioresistance is closely related to glucose- as well as mitochondrial metabolism. The radiosensitivity of the tumors can be explained by radiation-induced metabolic changes in glucose and mitochondrial functions or by tumor-induced metabolic changes (Table 5.10).

After the tumor cells have been exposed to radiation for an extended period of time, these cells experience alteration in the glucose metabolic pathway. As an important kinase, AKT regulates multiple biological processes, including cellular metabolism. As described in the previous section AKT is phosphorylated in cells after IR exposure to radiation which results in radioresistance of tumor cells through the AKT-mediated alteration of cellular glucose metabolism. A disruption in glucose metabolism also occurs after radiation exposure of tumor cells, resulting in an accumulation of lactic acid. This is the primary product of glycolysis and contributes to the development of malignant tumors. Moreover, glycolysis may cause tumor metastasis, recurrences, and resistance to RT.

Table 5.10 Glucose and mitochondrial metabolism induced by the tumor itself that contribute to tumor resistance and progression

Entity	Type	Cause	Effect	Outcome
Nicotinamide adenine dinucleotide phosphate (NADPH)	Glucose metabolism	The decrease in OxPhoslevels in mitochondria and the pentose phosphate pathway (PPP)	Increasing tumor dependence on glycolysis and reducing intracellular ROS levels	Tumor proliferation
An organic compound (dinitrophenol)	Glucose metabolism	Mitochondrial respiratory modulators	Increase in the glycolytic index	Rejoining of DNA strand breaks that leads to reducing the probability of cancer cells damage by radiation
Proteins (GLUT1)	Glucose metabolism	GLUT family in cell membrane	Upregulated under hypoxic circumstances	Poor prognosis, radioresistance, oncogene activation and inhibition of tumor suppressors, stimulation of hypoxia, and the regulation of different signaling pathways, including PI3K/AKT and MAPK
Lactic acid	Glucose metabolism	Products of glycolysis	Accumulation in tumor tissues	Promoting recurrence, tumor metastasis and radioresistance
			Fibroblasts in tumors release hyaluronic acid in response to lactic acid	Neovascularization, cell clustering, migration, and VEGF secretion
Lactate dehydrogenase (LDHA)	Glucose metabolism	Distribute in human tissues	Enzyme helps make lactic acid from pyruvate	Overexpression indicates hypoxic conditions, which can be associated with radioresistance, lower survival rate, local recurrence, and distant metastases
Soluble adenylate cyclase (sAC)	Glucose metabolism	Activation of BRAF/ERK1/2 signaling	Release of LDHA	The anti-irradiation effects and cell proliferation.
HIF-1β	Glucose metabolism	Activated in hypoxic environments	The adaptive cellular responses to hypoxia, important mediator of the conversion of OxPhos to glycolysis in the metabolism of carbohydrates convert ADP and phosphoenolpyruvate into ATP and pyruvate	Radioresistance by removing ROS from the cells and activating cell autophagy
Pyruvate kinase (PK)	Glucose metabolism	Enzyme involved in glycolysis	Convert ADP and phosphoenolpyruvate into ATP and pyruvate	PK expression correlates with radioresistance
Hexokinase 2 (HK2)	Glucose metabolism	A critical role in glucose metabolism	Upregulation of this enzyme can induce glycolysis	HK induces glycolysis, making it essential for the progression and maintenance of tumors
Antigen 2 (NG2)	Mitochondrial metabolism	A glial cell antigen	By interacting with serine protease OMI/HtrA2 of mitochondria, protect oligodendrocyte precursor cells from oxidative stress	Development of radioresistance
Protein 3A (ATAD3A)	Mitochondrial metabolism	Cancer patients	Activating ATAD3A leads to the expressions of histone H3, H2AX and ATM increase	Inhibit the IR-induced apoptosis in glioblastoma cells
Matrix metalloproteinase	Mitochondrial metabolism	The extracellular protein	Radiation resistance is induced by molecules or signaling pathways that increase MMP or inhibit its decrease	Radiation resistance

Radiation exposure of tumor cells likewise disrupts mitochondrial metabolism. In the post-RT setting, manganese superoxide dismutase (MnSOD) activity increases significantly in pancreatic cancer cells irradiation. MnSOD is the enzyme which catalyzes the formation of superoxide anion radicals, fighting the effects of oxidative stress ROS-induced damage. As a consequence, G2 checkpoint block is activated and cells are protected against mitochondrial oxidative stress by mitochondrial antioxidant systems, promoting radioresistance development. Radiation exposure to Burkitt lymphoma similarly disrupts mitochondrial metabolism by inducing the proteins (mitochondrial proteomes) that prompt radioresistance. Radiation of tumor cells targets Mitochondrial MAPK phosphatase (MKP1). Radiation increases MKP1 expression in breast cancer cells, where it translocates into the mitochondria and inhibits apoptosis by phosphorylating the c-Jun N-terminal kinase (JNK).

5.10 Palliative Radiotherapy

Box 5.11 Palliative Radiotherapy

- Palliative RT may be used to slow down tumor growth, prevent or treat symptoms, and improve quality of life.
- Common applications include prevention of bleeding and pain and treatment of metastases.
- Brain and spinal cord metastases are often treated to relieve neurological symptoms.
- Palliative RT is often hypofractionated with potentially unique radiobiology.
- The radiobiological mechanisms of palliative RT are currently not well understood.

While radical RT aims to eliminate cancer cells with the intention of cure, palliative RT is used to slow down tumor growth, to prevent or treat symptoms and improve quality of life. It is estimated that more than 50% of RT patients receive palliative RT. This is particularly relevant in populations in less well-resourced countries where the burden of advanced disease is high, and palliation is commonplace (Box 5.11).

Typically, palliative RT is used to treat or prevent bleeding [143–146] or obstruction [147]. In addition, palliative RT is commonly used to treat pain, particularly bone pain, as well as brain and spinal cord metastases to address neurological symptoms [148]. Sites frequently treated palliatively include bone, brain, pelvis, and lung.

Despite the widespread use of RT with palliative intent, the radiobiology of palliative RT is not well understood. Radiation can reduce tumor burden by targeting proliferating tumor cells, and thus reduce tumor growth and result in relief of obstructions and pressure. However, mechanistic effects of how RT can stop bleeding and pain are still somewhat obscure. It has been speculated that cytokine modulation may alter pain levels and targeting of vascular components may prevent bleeding [149]. Palliative regimens are also typically shorter and frequently involve hypofractionated approaches or single (7–8 Gy) fraction schedules, which may induce differential biological effects to those induced by typical conventionally fractionated radical treatments. Enhanced vascular targeting and immune modulation have been implicated [150].

5.11 Tumor Microenvironment Changes Tumor Sensitivity

Box 5.12 The Tumor Microenvironment and Radiotherapy

- Tumor microenvironments (TME) can recourse the tumor origination, expansion, invasion, metastasis, and its response to therapies like RT and chemotherapy.
- RT immunomodulates the TME to induce a local anti-tumor immune response leading to tumor regression.

The tumor microenvironment (TME) is an "ecological niche" to facilitate the promotion and the succession of cancer cells. TME intricacy is coupled with tumor expansion, metastasis, and reaction to therapy. Potent alteration stirring in the TME is the basis of tumor cell variant selection, which may endorse genomic instability [31]. Cancer is an exceptionally assorted disease as the cells within the tumor have diverse mutations at different locations within the primary tumor and the metastatic site. Tumor growth and development are not only by actions relating tumor cells, but also by the milieu they inhabit, the TME. In 1889, Stephen Paget introduced "seed and soil" proposition which recommended that metastasis does not occur due to accidental events, but some tumor cells (the "seeds") nurture ideally in particular organs (the "soil") and metastases only emerges when the appropriate seed and soil combination takes place [151] (Box 5.12).

5.11.1 Components of the TME

Tumors are normally greatly heterogeneous and intricate in genetics. Different cell types, such as adipocytes, fibroblasts, immune cells, endothelial cells, and neuroendocrine (NE) cells, possess unique purpose in TME (Table 5.11). Acellular constituents of the TME like the extracellular matrix (ECM), extracellular vesicles (EVs), and cytokines remain adjacent to these cells. Physical and chemical uniqueness of the TME that are considered as vital the microenvironmental components comprise of the high interstitial pressure, hypoxia, fibrosis, and low pH. Further, communications involving

Table 5.11 Functions of various components of the tumor microenvironment (adapted from [152])

TME components	Function
Neutrophils	Augmentation of angiogenesis and metastasis; associated with poor diagnosis.
Tumor-associated macrophages (TAMs)	Promote deterioration of the extracellular matrix; support the increase of inflammatory cytokines (TNF-β); augment of angiogenesis and remodeling.
CD8+ cytotoxic T cells (CTL)	Provoke apoptosis, necrosis, and growth arrest by secreting INF-γ and other cytotoxic cytokines; set up an anti-tumor environment.
Regulatory T cells (Tregs)	Exude cytokines such as IL-10, TGF-β; set up an immunosuppressive environment; associated with poor diagnosis.
Myeloid-derived suppressor cells (MDSCs)	Linked with tumor development and neoangiogenesis; repress T cells and NK cells; differentiating into TAMs in a hypoxic environment.
Mesenchymal stem cells (MSCs)	Differentiating into mesenchymal tissues such as bone, cartilage, and fat tissues, vasculogenic mimicry; form the premetastatic niche; promoting cancer initiation and malignancy.
Endothelial cells	Constitutes of tumor blood vessels; secreting angiocrine factors such as adhesion molecules; intercommunicating with tumor cells via secreting EVs including CD106, CD49a.
Adipocytes	Regulating the balance of systematic energy and metabolism; secreting exosomes, cytokines, chemokines, and hormones; promoting cancer progression.
Neuroendocrine cells (NE cells)	Promoting proliferative signaling; secreting neurotransmitters, including CgA, chromophilic, and vasoactive polypeptide; regulating NK cell migration and toxicity ability.
Vascular network	Providing oxygen, clearing carbon dioxide, and metabolizing wastes; providing nutrition support for cancer cells; promoting angiogenesis and metastasis.
Lymph vessels	Helping immune cells to avoid immunity and dissemination; providing a physical link between lymph nodes and tumor.
Extracellular matrix (ECM)	Forming the complex macromolecular network; controlling cancer invasion and metastasis, angiogenesis; contribution to growth and proliferation signaling, inhibiting cancer cell apoptosis.
Extracellular vesicles (EVs)	Carrying biologically active molecules such as proteins, miRNAs, and lncRNAs from donor cell to recipient cell; regulating key signaling pathways, proliferation, drug resistance, and stemness; reprogramming stromal cells to create a niche for survival.
Cancer-associated fibroblasts (CAFs)	Sustaining proliferative signaling; activating angiogenesis and metastasis; tumor-promoting inflammation; evading immune destruction; reprogramming cellular metabolism; promoting genome instability and mutation.

cells and stromal elements also play an important role in cancer evolution and development [152].

5.11.2 Effect of Radiation on TME

IR can modify exchanges among tumor cells and their microenvironment. The TME does not only persuade tumor cell proliferation, invasion and metastasis of cancer cells, angiogenesis, modulation of immune cell infiltration and the immune response, but also has a brunt on the therapeutic response [151]. The effects of radiation on the TME diverge with dose and fractionation plan. Radiation stimulates the cellular and DNA damage that can lead to both production as well as release of tumor-associated neo-antigens and secretion of cytokines from tumor and the stromal cells. These proceedings can budge the equilibrium towards an immunoreactive microenvironment, as contrasting to immunosuppressive microenvironment, causing the recruitment and activation of cytotoxic T cells. Figure 5.22 gives an overview as to how radiation affects the TME.

The damage induced by IR affects many cells in the TME. The sensitivity of tumor cells is higher to radiation and their death commences the inflammatory signaling cascade. Also, the levels of intercellular adhesion molecule 1 (ICAM) and vascular cell adhesion molecule 1 (VCAM) expression go high as that of the cells of the innate immune system. Interestingly, the upregulation of the integrins present on the endothelial cells is associated with better survival as it acts as a system for radioresistance. Vascular diminution heightened the effect of hypoxia inducing the HIF-1α signaling. It also leads to the pro-angiogenic and pro-vasculogenic stimuli through VEGF and chemokine (C-X-C motif) ligand 12 (CXCL12). Following radiation cancer-associated fibroblast (CAF) activation stimulated the altered growth factor secretion and secret several ECM and cytokine modulators. Also, the transforming growth factor-β (TGF-B) signaling pathway is not only complex but also pleiotropic. It directly affects the tumor cells and CAFs, driving the HIF-1 signaling and reducing the activation of T cells and the dendritic cells (DC). In the immune compartment, due to high levels of mTOR there is not only an increase in the accessibility of tumor cell antigen but also a boost in the processing of the antigen in combination with damage-associated molecular pattern (DAMP) related Toll-like receptor (TLR) responses. Also, there is an increased pro-inflammatory cytokine signaling to activate the DCs and as a consequence T cells. The activated DCs move to the proximal

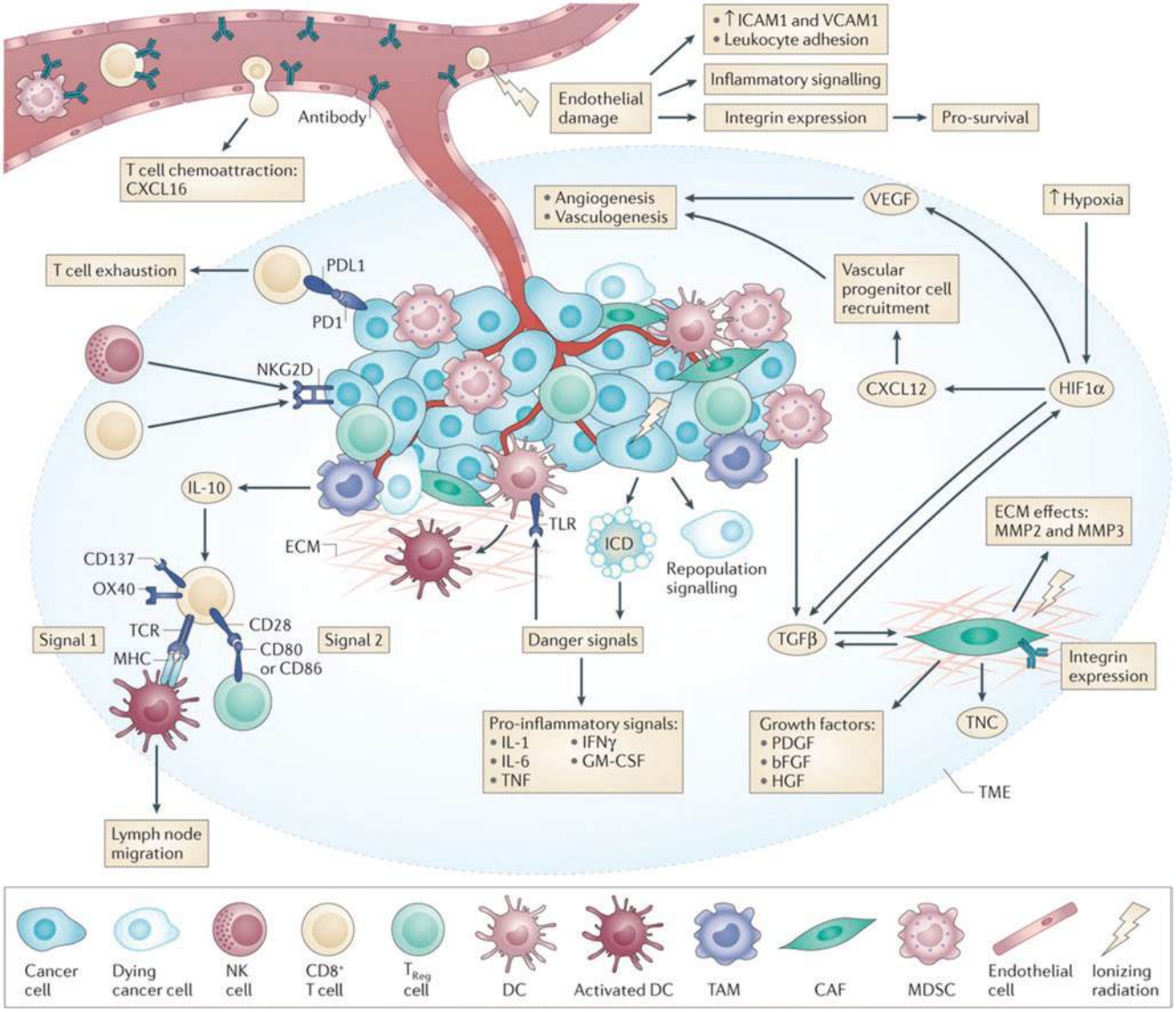

Fig. 5.22 Overview of effects of radiation on the tumor microenvironment. (Figure adapted from Barker et al. [153], with permission)

lymph nodes. In the TME, such signaling is frequently obstructed by high Treg cytotoxic T lymphocyte antigen 4 (CTLA-4) suppression of co-stimulation. Radiation upregulates the NKG2D signals on the tumor cells that enforce direct cytotoxic effects by the CD8+ T cells and NK cells. However, there are other tumor cells which getaway with the PD-L1 signaling but the MDSC derived IL-10 immunosuppression remains intact.

Hence, depending on the organ, there are organ-specific interstitial cells such as the presence of astrocytes in the central nervous system or the osteoblasts in bone tissues. Such cells are collectively called as the stroma of the tumor and along with other essential factors like the surrounding pH, oxygen levels, extracellular matrix make up the microenvironment of the tumor [139].

5.11.2.1 Effect on Stroma and Cancer-Associated Fibroblasts (CAFs)

The tumor cells are known to interact with the stroma or the adjacent milieu. The tumor stroma comprises of a range of diverse cells, and extracellular matrix (ECM), that are known to advocate in limiting the host immune reaction against tumor cells. The tumor stroma puts forward a versatile complex network that maintains the tumor propagation by secreting immunosuppressive cytokine, diverse cellular processes and metabolic alterations [154]. Stromal cells involving the endothelial cells and adipocytes can modify the radiosensitivity by their roles in angiogenesis and vasculogenesis, and their secreted adipokines, respectively. The extracellular matrix can control radiation sensitivity by manipulating the oxygen proximity and managing the equilibrium and bio-

availability of growth factors and cytokines [155]. Even though several RT-mediated stromal transformations like the renewal of or polarization towards tumor-suppressing immunity are valuable, RT can operate as a double-edged sword in tumors.

Chronic inflammation is one of the radiation effects on the stroma which acts as a chief driver of fibrosis during which there is occurrence of persistent immune responses in addition to tissue remodeling and repair processes. Some of the radiation-induced alteration on the TME is by altering the way CAFs manage their collagen assembly. In addition, CAFs that receive RT-undergo variation and modification in terms of their variety, secretome, and phenotype. Moreover, RT augments the stimulation of the proliferating machinery linking the RAS and mitogen-activated protein kinase (MAPK) signaling pathway; the invasion pathway that is associated with tumor evolution, resistance, and metastasis. When the stroma receives RT, there is augmentation in the invasiveness of the tumor because of the augmented hepatocyte growth factor (HGF)/c-Met (HGF receptor) signaling and MAPK activity. This aids the improvement in the tumor movability which can prove to be fatal. RT can also stimulate the stromal traits that can potentially impart resistance to therapy. Studies are still ongoing in understanding as to how fractionated RT alters the TMEs stromal machinery and how all the modifications can affect after the cancer cells response to RT [155].

5.11.2.2 Effect on Vasculature

An important feature of solid tumors is the vascular network that develops from the vasculogenesis, angiogenesis, and fibroblasts. A characteristic of these vessels is that they lack their supporting pericytes or basement membrane, which makes them vulnerable to radiation [156–158]. When tumor tissue is exposed to radiation, blood vessels at the level of the microvessel network are firstly destructed and the degree of this destruction depends on the radiation dose. The vessel's thickness increases, which raises the risk of atherosclerotic changes and intimal proliferation, since the destructed microvessel network reduces distance between functional vessels and vascular density, resulting in hypoperfusion. Irradiation not only modulates the vessel structure, but it also has long-term effects, including medial necrosis and fibrosis, but these effects are affected by radiation dose. When a radiation dose is high, for instance, blood flow is permanently reduced; necrosis and fibrosis are produced, and the tumor is revascularized by vasculogenesis, which is a disorganized process of vessel growth in comparison to angiogenesis. Secondly, radiation to tumor tissue induces the chemokine receptor CXCR4 which induces bone marrow of matrix metalloprotease 9 that is responsible for radiation vasculogenesis and subsequent post irradiation [159, 160].

5.11.2.3 Effect on Immune System

IR kills cancer cells directly (atomic ionization) and indirectly (radiolysis of water) [16, 20, 158]. IR also induces a host immune response to tumor cells and facilitates tumor recognition and healing. These effects occur in a variety of ways, including immune response signaling. When cells are dying, they translocate calreticulin (ERp57) and their endoplasmic reticulum (ER) protein complex to the cell membrane which functions as a "eat me" signal. Secondly, upon IR of a tumor, inflammatory molecules, such as ATP and high mobility group protein B1 (HMGB1), are released, promoting a T cell and DC response. Signaling of this type uses three types of signals in anti-tumor immune responses, which are:

1. DCs take captive of released danger signals and process them.
2. Danger signals are presented into T cells by MHC molecules. As a result, naïve tumor-specific T cells are activated and become effector T cells.
3. Finally, macrophages and DCs may be recognized by cytotoxic T cells, and they destroy remaining cells of tumor tissues through their circulation through the bloodstream [161–165].

However, not all irradiated cells sustain damage, and some survive. These IR surviving cells may expose surface molecules like antigen-presenting molecules of major histocompatibility complex class I (MHCI), death receptor Fas, and ICAMs which lead to an improvement in the recognition and killing of tumors by immune cells that are reactivated by tumor antigens.

To cure tumors, radiation needs to cause cell death. There are five different types of cell death depending on the pathways in the response system of DNA damage, namely, apoptosis, senescence, autophagy, mitotic catastrophe, and necrosis [13, 157, 158]. Via apoptosis pathways macrophages may be triggered to clean out these dying cells which causes polarized M1 macrophages thereby driving an anti-tumor immune response and indirectly killing of tumors. However, this process may also contribute to carcinogenesis and inflammation [163].

5.11.3 Tumor Radiosensitivity and Underlying Mechanisms

The most well-known tumors in declining order of radiosensitivity as follows: (1) lymphoma, (2) embryonal tumors, (3) cellular anaplastic tumors, (4) basal cell carcinoma, (5) adenoma and adenocarcinoma, (6) desmoplastic tumors, such as squamous carcinoma, (7) fibroblastic sarcoma; osteosarcoma; neurosarcoma. Tumors composed of fast-growing

cells like the embryonal tumors are sensitive to radiotherapy.

Lymphoid cells are predominantly vulnerable to radiation. On the other hand, the radioresistant category comprises of the neurosarcomas, gliomas, and melanomas. Tumor sensitivity to radiation is affected by the variation on the radiosensitivity exhibited by the subgroups of major cancer forms. There are numerous factors affecting the cancer radiosensitivity and at times they are even obscure. The most important factor that plays the most vital role in influencing the tumor behavior under RT is the general condition of the patient. Also, there is an explicit association between radiosensitivity and the grade of malignancy which might not be uniform always. Hence, all these factors should be carefully evaluated before imparting radiotherapy and predicting its outcomes.

5.11.3.1 Factors Affecting Tumor Radiosensitivity

One of the most prominent factors imparting the tumor radiosensitivity and which was recognized very early on was the high metabolism of the tumor cells. This is similar to the fast growth and also understood as the tumor growth rate imparting radiosensitivity. Augmented or uneven vascularity also goes with fast growth. These factors combined provide the rapidly growing tumor cells with sensitivity to radiation. Especially when tumors are bulky hypersensitivity can be encountered in the treatment of such tumors. Therefore, to avoid accidents like bulky necrosis or interstitial hemorrhage appropriate precaution should be taken. Other factors like the large quantity of autolytic cell ferments and susceptibility of mitotic nuclei are also crucial in imparting tumor sensitivity to rapidly growing tumor cells. It is seen that the tumors exhibiting the embryonic trait in the origin cells provide the complete group of embryonal tumors a very high radiosensitivity. Hence, their response to radiation treatment is probably quicker and complete compared to other tumors. Therefore, such tumors should be identified as especially favorable.

5.12 Systemic Anti-tumor Immune Responses and Abscopal Effects

5.12.1 Introduction

While radiation effects classically result from direct damage to cells and tissues within the target, effects outside the field also known as abscopal effects have been observed in both tumors and normal tissue. For example, irradiation often leads to systemic fatigue [166], and bilateral pneumonitis sometimes occurs after unilateral lung irradiation [167]. Occasionally, metastatic tumors have been observed to regress dramatically outside the primary irradiation field, which is a manifestation of the systemic anti-tumor effect [168].

An illustrative example is the case of a man diagnosed with ulcerated malignant melanoma in his left arm [169]. The arm was resected, and no further treatment was indicated. Twenty months later, the patient had a painful skin lesion on the head and an asymptomatic metastatic lesion in the lung. The skin lesion was irradiated with 3 Gy in 10 sessions, after which the lesion and pain disappeared. Unexpectedly, the lung lesion also disappeared although it had never been treated. Reports of cases of abscopal effects in melanoma are relatively common. Another example is the case of a woman with squamous carcinoma of the anal canal with metastases to pelvic lymph nodes, liver, and bone. After palliative RT limited to the pelvis with sensitizing chemotherapy, complete regressions were observed 4 months after treatment not only in the primary tumor but also in the bone and liver metastases, an effect that persisted 4 years later [170]. Figure 5.23 gives an overview as to how radiation induces Abscopal Effects.

The previous clinical cases showing unexpected regression of tumors outside the irradiated field are examples of a phenomenon first described by Mole as the “abscopal effect” [171]. The word abscopal comes from the Latin ab (position away from) and Scopus (target). However, there is now clear evidence that the abscopal effects associated with RT are due to systemic anti-tumor immune responses triggered by the RT. However, despite millions of patients receiving RT, abscopal effects are too unpredictable to be a therapeutic target, as only a limited number of cases have been identified. In a recent study, only 46 cases were identified between 1969 and 2014 [172]. With the advent of immune checkpoint blockade therapy, clinical interest has soared. Since the introduction of the anti-CTLA-4 antibody ipilimumab into clinical practice in 2011, abscopal effects have been observed in several patients who received RT while taking ipilimumab [173, 174]. Other immune checkpoint therapies have also shown promise. There are reports of abscopal effects following treatment with RT and anti-PD1 therapies such as pembrolizumab or nivolumab [175]. In this section, we will cover the biological events in cancer cells that precede the occurrence of radiation-induced abscopal effects.

5.12.2 Radiation-Induced Immunogenicity

Radiation can alter the immunogenicity of tumors by promoting tumor antigens, neoantigens, and danger signals.

5.12.2.1 Tumor Antigens

Tumor antigens result from protein degradation due to damage to cellular proteins caused by radiation-induced

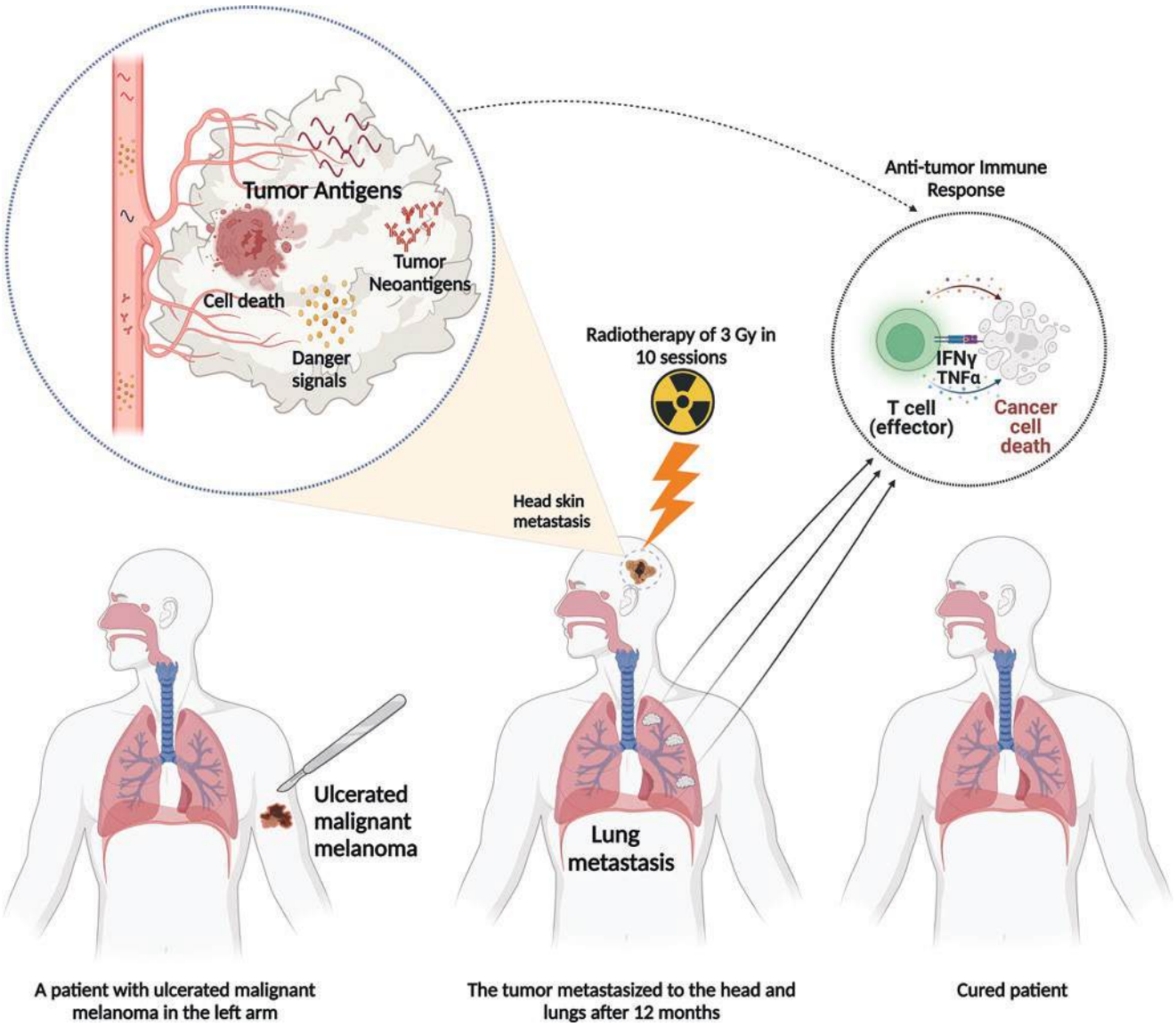

Fig. 5.23 The abscopal effect of RT. On the left side of this schematic case, the patient suffers from a tumor in the shoulder (e.g., a melanoma) that has metastasized to the lung. The treatment protocol consisted of surgery of the primary tumor and the metastatic nodules were treated with a combination of RT and immune checkpoint blockade, which promotes abscopal anti-tumor immunity. On the right side of this schematic case, RT triggers the release of tumor antigens, neoantigens, and DAMPs, which are recognized and processed by macrophages and DCs. Subsequently, these antigen-presenting cells present these tumor antigens to T cells in a draining lymph node of the tumor. The antigen-presenting cells are then taken up by cytotoxic T cells, which subsequently destroy the remaining cells of the cancerous tissue

free radicals. Radicals such ROS are generated during radiation-induced radiolysis of water. RT then causes cellular damage that is independent of DNA and leads to an increase in the pool of peptides, i.e., tumor antigens that bind to the major histocompatibility complex (MHC) [176].

Tumor neoantigens are tumor-specific antigens resulting from the expression of a large number of mutations which may be a result of tumor genetic instability but also due to severe DNA damage. The degrees of DNA damage can strongly influence the immunogenicity of the tumor. In this context, RT leads to DNA SSBs or DSBs or other DNA alterations (see Chap. 3) [177]. DSBs are the most lethal DNA lesions if not repaired. Repair depends on the type of radiation causing the damage. Low LET radiation causes simple DSBs, which are repaired by NHEJ pathway. High LET radiation causes clustered DNA lesions (or multiple damaged sites) that are usually repaired by HR. Non-DSB lesions at clustered DNA damage sites are corrected with Base Excision Repair. If the DNA repair mechanisms are not sufficient to repair the damage, or if the RT itself causes defects in the DNA repair mechanisms, mutations occur that can lead to the

expression of tumor neoantigens. These neoantigens are then processed by tumor cells and presented by MHCs [178].

5.12.2.2 Damage-Associated Molecular Pattern (DAMP)

Damage signals properly known as Damage-Associated Molecular Patterns (DAMPs) are endogenous molecular signals released by irradiated cells after damage or when dying [176]. These signals enable enhanced recognition and killing of the tumor by macrophages and DCs resulting in antigen presentation to T cells [161, 164]. Some of the most frequently found radiation-induced DAMPs in tumor cells are:

- *Fragmented double-stranded DNA and micronuclei.* These self-DNA fragments and micronuclei appear as cytosolic DNA in tumor cells, which are later recognized by immune cells.
- *High mobility group box 1 (HMGB1)* is a nuclear protein associated with chromatin that is released extracellularly by dying tumor cells, normally necrotic cells [179]. HMGB1 binds to Toll-like receptor 4 (TLR4) expressed by DCs and activates them.
- *Nucleotide release* by apoptotic cells function as a chemotactic signal for phagocytic myeloid cells including DCs by stimulating the Purinergic receptor 2 (P2RY2) [180].
- *Extracellular ATP* can also function through the activation of Purinergic receptor 7 (P2RX7) to initiate inflammasome activation and subsequent Interleukin 1β production. This mechanism was shown to be required for the induction of tumor antigen-specific CD8+ T cells following challenge with dying tumor cells [181].
- *Calreticulin* is an ER protein that gets translocated to the cellular membrane after RT. Calreticulin is essential for efficient uptake of dying tumor cells by antigen-presenting cells [182].
- Chemokines are a frequent part of DAMPs. Chemokines, such as C-X-C motif (CXC) ligand 16, 10, and 19 (CXCL16, CXCL10, and CXCL9), are known for being released after radiation exposure; they trigger differentiation of immune cells, and stimulate immune modulators such as Interferons, Tumor necrosis factor α, and Interleukin 1β [162, 183–185].

In summary, radiation increases the immunogenicity of tumors by simultaneously promoting the release of tumor antigens, neoantigens, and DAMPs. This radiation-induced immunogenicity may counteract the progression of tumors that have escaped immune surveillance, especially if an abscopal effect can be triggered.

5.12.2.3 Anti-tumor Immune Responses: Abscopal Effects

To reproduce the radiation-induced abscopal effect has been challenging as its underlying biological mechanisms are not fully understood. However, some crucial cellular signaling pathways have been identified alongside the IR doses that appear to be fundamental for their occurrence.

- The *accumulation of cytosolic double-stranded DNA fragments (dsDNA)* is usually a sign of microbial infection and alerts the host's innate immune system to initiate a defense response. Interestingly, the accumulation of dsDNA after RT has been shown to be an essential step in the abscopal response. Mitochondrial DNA and dsDNA are recognized by cyclic GMP-AMP synthase (cGAS), which produces messengers that bind and activate the transmembrane protein Stimulator of interferon genes (STING), triggering a robust innate immune response [186]. In particular, activation of the type I interferon signaling pathway (IFN-1) and production of Interferon β cytokines by cancer cells trigger the accumulation of basic leucine zipper ATF-like transcription factor 3 (Batf3)-dependent DCs, which are required for the maturation of anti-tumor CD8+ T cells.
- The *irradiation dose* and *fractionation schemes* are crucial for the induction of abscopal effects. With increasing radiation dose, more dsDNA fragments accumulate in the cytoplasm of cancer cells. However, the increased radiation dose of over 12 Gy also triggers the activation of three prime repair exonuclease 1 (Trex1), which degrades dsDNA and prevents an immune response. Interestingly, Interferon β production can be enhanced with repeated radiation doses that do not trigger Trex1 [186]. Radiation regimens that have been shown to be effective in preclinical and clinical studies are 3 × 8 and 5 × 6 Gy.
- *Transforming growth factor beta (TGF-β)* is a potent immunosuppressive cytokine in established tumors that impairs the antigen presentation function of DCs, prevents T cell priming and thus inhibit the abscopal effect [164].
- *TGF-β expression* increases in irradiated tissues. However, the abscopal effect can be restored if TGF-β neutralizing antibodies are administered during RT. Current research is investigating if the use of dual-function drugs that simultaneously target TGF-β and PD -L1 in combination with RT can be a good strategy to overcome tumor immune escape [187].

5.13 Normal Tissue Damage and Response to Radiotherapy

5.13.1 Introduction

The tolerance of normal tissues to RT is the limiting factor in delivering a radiation dose high enough to eradicate tumor cells [188, 189]. The dose delivered to the target structure is

limited by the dose constraints to the organs at risk (OAR), which are in close proximity to the tumor. In the case of external RT, standard recommendations for OAR doses have been issued based on the volumes irradiated and are regularly updated to reflect new practices.

Despite ongoing technical and technological advances, the planning target volume (PTV) necessarily contains a volume of normal tissue for several reasons. First, the target volume, which receives the prescribed dose, is always larger than the actual tumor volume. Indeed, this volume must take into account the visible tumor volume (gross tumor volume, GTV), the possible microscopic extension of the tumor (clinical target volume, CTV), the movements of the different volumes (internal target volume, ITV), small errors in patient set-up and technical precision, all together making up the PTV. Secondly, the tumor contains normal tissues such as soft tissues and blood vessels, which receive the entire prescribed dose. Finally, especially for external beam RT, the radiation beam inevitably passes through normal tissue, depositing doses that may be clinically relevant. Effective RT is therefore necessarily associated with a risk of adverse effects. Side effects may occur during RT or a few weeks after treatment (acute effects). In the long term, late effects, which may occur months or years after RT, are the most critical because they are chronic, disabling, painful, and most often irreversible.

Limiting adverse events to reduce morbidity and optimize the therapeutic index of RT remains a priority in the fight against cancer. To this end, NTCP modeling is widely used in treatment planning as a tool to differentiate treatment plans [11]. In future, cellular and animal models of radiotoxicity aimed at understanding the sequence of molecular and cellular events that drive the pathogenesis of early and late normal tissue radiation injury should enable the development of tools to reduce the impact of RT on normal tissues [190].

5.13.2 Acute Tissue Response

Box 5.13 Radiation-Induced Acute Normal Tissue Response

- Acute effects of radiation are observed in days to weeks after exposure.
- The time scale of clinical manifestation of most acute responses is independent of the radiation dose and related to the proliferative rate of injured cells.
- Acute effects are transient and reversible.
- Typical acute responding normal tissues are: intestine, mucosa, skin, hair follicles, bone marrow.

Acute responses are primarily observed in tissues with rapid cell renewal where cell division is required to maintain the function of the organ. In these renewing tissues, physiological cell loss occurs constantly from the post-mitotic tissue compartments while actively cycling cell populations in the germinal parts of the tissue proliferate to replenish them. The radiation response is related to death of critical cell populations such as the stem cells in the crypts of the small intestines, in the bone marrow, or in the basal layer of the skin. When sufficiently large numbers of critical cell populations are affected, cell production capacity is no longer able to compensate for the physiologically occurring cell loss, leading to hypoplasia and cell depletion. For this reason, the time scale of clinical manifestation of most acute responses is independent of dose and instead reflects the rate of loss of functional cells and the demand of proliferation of the supporting stem cells of the different tissues (Box 5.13).

In general, acute responses are transient, but sensitive to the overall radiation treatment time. Recovery may occur by rapid repopulation from the surviving stem cell compartment or by recruitment of stem cells from neighboring sites (non-irradiated/damaged areas). Hence, the latent period of manifestation of tissue reactions is specific, depending on the cell type and its proliferation rate (Table 5.12) as well as on its intrinsic sensitivity to radiation and capacity to repair damaged DNA.

Apart from the number of sterilized cells, several other non-lethal mechanisms like proliferative impairment and disturbances in molecular cell signaling play a role in the acute tissue reaction to radiation. For example, the release of 5-hydroxytryptamine by mast cells have been shown to be responsible for several early clinical reactions such as erythema following irradiation of the skin and nausea/vomiting following irradiation of the intestines. Immunological reactions associated with local and systemic release of cytokines have also been demonstrated. In the hematopoietic system, apoptosis plays an important role in acute normal tissue response. Apoptotic death directly following irradiation, particularly of the lymphoid lineage, causes additional cell loss on top of the physiological cellular loss rate of circulating cells and explains earlier onset particularly for the lymphoid lineage. Furthermore, the typical tissue or organ architecture has a principal role in the response to irradiation. Threshold irradiation doses (Table 5.13) are often dependent on the irradiated normal tissue volume.

Table 5.12 Tissue and target cell-specific latency times

Tissue	Target cells	Latency times (after single exposure)
Epidermis	Basal cells	3–4 weeks
GI-tract	Crypt cells	<1 week
Bone marrow	Hematological stem cells and precursor cells	0.5–2 weeks
Testes	Spermatogonial stem cells	2–4 weeks

Table 5.13 Threshold radiation doses for a selected group of tissues. Estimate of threshold doses for an approximate 1% incidence of morbidity for early and late tissue reacting human tissues and organs following acute exposure to radiation (modified after Table 4.4 from [191])

Organ/ tissue	Threshold dose (Gy)	Biological effect	Latency period
Testis	~0.10	Temporary sterility	3–9 weeks
Testis	~6	Permanent sterility	3 weeks
Ovaries	~3	Permanent sterility	<1 week
Bone marrow	~0.5	Depression of hematopoiesis	3–7 days
Skin (large areas)	<3–6	Main phase of skin reddening	1–4 weeks
Skin (large areas)	5–10	Skin burns	2–3 weeks
Skin	~4	Temporary hair loss	2–3 weeks
Skin (large areas)	10	Late atrophy	>1 year
Skin (large areas)	10	Telangiectasia at 5 years	>1 year
Eye	~0.1 per 5 years[a]	Cataract (visual impairment)	>20 years
Brain	0.1–0.2	Cognitive defects infants <18 months	Several years
Carotid artery	~0.5	Cardiovascular disease	>10 years
Kidney	~7–8	Renal failure	>1 year

[a] An equivalent dose limit for the lens of the eye of 20 mGy/year is recommended for workers. The dose should be spread over defined 5 years periods, with no single year exceeding 50 mGy [192]

The tissue architecture is generally organized in the so-called functional subunits (FSUs). Some tissues are built of anatomically demarcated FSUs, like nephrons in the kidney, liver- and lung lobules. These types of organs—with a parallel arrangement of FSUs show large reserve capacity. Non-radiation exposed volumes of the organ can take over the function of the damaged tissue. Other tissue types like the spinal cord and mucosa do not show clear anatomical demarcation in FSUs. In such serial arranged FSUs tissues, radiation injury to a small tissue volume can result in function loss of a larger volume or even the whole organ. The threshold radiation dose can be defined as the safe, tolerated, dose below which no tissue-specific reaction occurs. This particular dose is difficult to determine [191]. In general, it is the estimated dose that is required to cause a typical tissue reaction in 1% of the exposed individuals (ED1) relative to non-irradiated controls. To be noticed is that radiation doses <ED1 could also induce biological effects above baseline levels in non-irradiated, age-matched individuals, i.e., above natural incidence. Table 5.13 lists threshold doses and latency times for tissue reactions to a single radiation exposure for a selected number of healthy tissues and organs.

5.13.3 Late Tissue Response

Box 5.14 Radiation-Induced Late Normal Tissue Response

- Late effects of radiation occur months, years, or decades after radiation therapy.
- Late effects are progressive and irreversible.
- The latent phase of chronic reactions is inversely proportional to the radiation dose.
- The late effects are based on an interactive response of parenchymal cells, vascular endothelium and fibroblasts, with a contribution from immune cells, especially macrophages, as well as other cells.
- Tissues and organs are affected by atrophy, fibrosis, and/or necrosis, which can severely impair their functions and lead to a loss of function.

The classification that distinguishes between early and late effects is based exclusively on the time of first diagnosis of pathological changes, with a threshold arbitrarily set at 3 months after the start of RT [5, 193]. Unfortunately, there is no general biological rationale for this threshold, whereas a classification of early and late effects is clinically relevant and essential for comparing studies. Nevertheless, there are specific biological characteristics of early and late effects that distinguish them (Tables 5.13 and 5.14). As discussed in Sect. 5.13.2, the early symptoms most often appear in highly proliferative tissues, such as the intestinal mucosa, epidermis, and bone marrow. In these tissues, irradiation causes a progressive but potentially reversible depletion of cells by preventing their physiological renewal, associated with a direct or indirect radiation-induced inflammatory reaction. In contrast, late side effects can affect all tissues. The pathogenesis leads to fibrosis, atrophy, vascular damage as well as other detrimental side effects on normal tissues such as hormonal deficiencies, infertility, and second malignancies (discussed in Chap. 7). Late side effects are chronic, progressive, in most cases irreversible and their severity tends to increase over time (Fig. 5.24 and Box 5.14).

The mechanisms that lead to these effects are more complex than for acute effects. They involve organ-specific changes in parenchymal cells, including cell death and alterations in cellular metabolism. Consequential late effects from severe acute reactions may contribute to chronic damage due to unresolved regeneration of rapidly proliferating tissues which contributes additional damage to connective tissue and endothelium [194].

Table 5.14 Typical characteristics of acute and late responding normal tissues and organs. Please note that early as well as late effects could occur in the same tissue or organ

	Early reactions	Late reactions
Cell turnover of target cells	High	Low
Latency	<90 days	>90 days
Time factor	Shorter time	No influence of time
	>Damage	
Clinical course	Transient	Irreversible
Fractionation sensitivity	Low	High
α/β ratio	~10 Gy	~3 Gy
Examples:	Mucositis dermatitis bone marrow depletion (tumor response)	Myelopathy
		Intestinal fibrosis
		Telangiectasia

The pathogenesis leading to radiation-induced fibrosis is a result of fibroblast differentiation into myofibroblasts, proliferation of surviving fibroblasts and extracellular matrix and collagen deposition. Seen as wound healing that goes wrong, this pathological process plays a key role in the development and expression of most late effects. Atrophy is caused by the loss of fibroblasts and collagen reabsorption. Examples of fibrotic-atrophic response include hardening and shrinkage of an irradiated breast, or strictures and malabsorption of irradiated small intestine. Vascular damage is caused by either small vessel dilation or constriction as well as losses of the vascular endothelial cells from small blood vessels and capillaries. Vascular damage results, for instance, in skin telangiectasias, bleeding, ischemia with intestinal perforation and fistula formation. The immune system also contributes significantly to the tissue response through the involvement of macrophages and mast cells, which interact with other cells in the irradiated tissue and other organs through the release of cytokines and growth factors [195–198]. More generally, the response of a tissue is mediated by different types of cells such as inflammatory, stromal, endothelial, and parenchymal cells that actively communicate through the release of cytokines, chemokines and growth factors, and/or the activation of molecular pathways downstream of these messengers. Altogether, these effects lead progressively to parenchymal damage and potentially to loss of organ function in the irradiated volume.

The tissues of cancer survivors treated with RT still bear the traces of RT to varying degrees. Although patients are usually asymptomatic, all irradiated patients, especially those with late effects, have a common histological feature of radiation-induced fibrosis and atrophy. Fibrosis predominates in the breast, skin, small intestine, lungs, kidneys, and liver, while atrophy and necrosis predominate in the later stages after RT alone or in combination with surgery and local trauma to bone (osteoradionecrosis of the mandible, ORN), nerve, or brain. The clinical severity correlates with

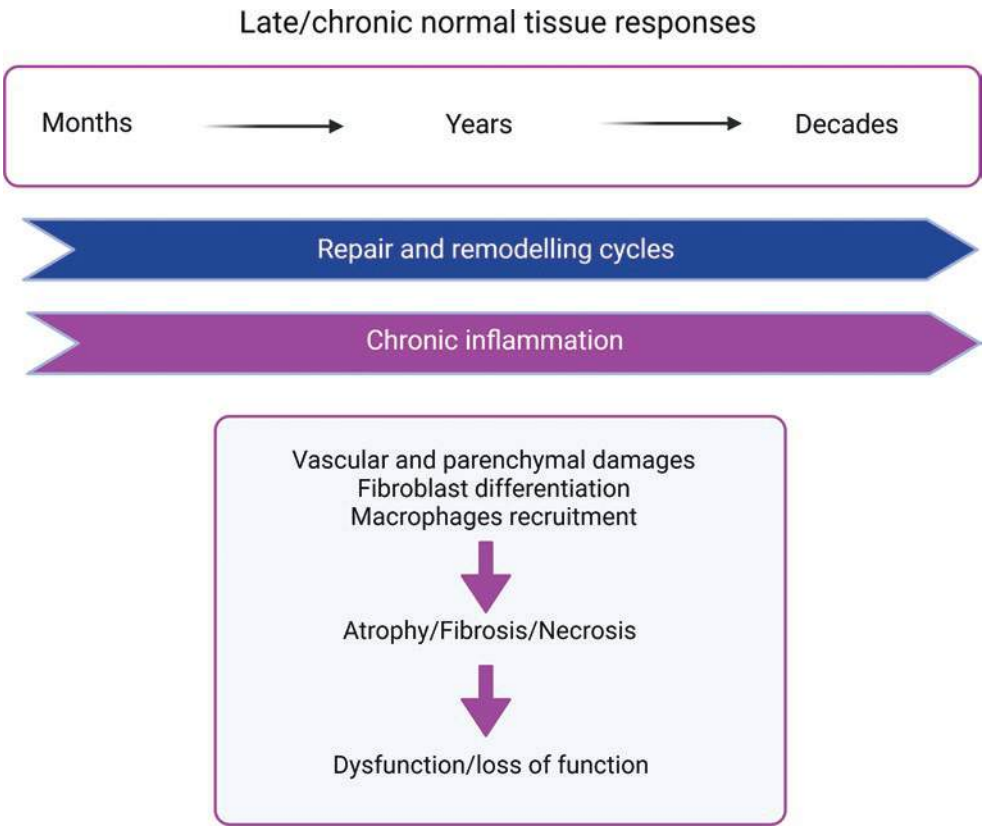

Fig. 5.24 Radiation-induced chronic damage to healthy tissues. Late damage develops within months to decades post RT and may concern all normal tissues. Successive cycles of tissue remodeling and repair, together with chronic inflammation induce vascular and parenchymal damage leading to tissue atrophy/fibrosis/necrosis compromising organ function

the extent of the underlying pathophysiological process, which is usually invisible and often depends on the level of parenchymal cell loss.

It is often mentioned that 5–10% of patients, and sometimes up to 20% for the treatment of pelvic malignancies, including prostate, rectal and cervical cancer, develop late side effects. However, some authors believe that the rates of patients with late side effects may be greatly underestimated [193]. For example, in the case of abdominal or pelvic cancers, more than half of patients would suffer from some form of chronic bowel dysfunction [199]. Most of the effects observed today were caused several years ago by RT techniques that are less used today (2D- and 3D-CRT), and which are progressively being replaced by more precise and more efficient techniques and technologies (IMRT, SBRT and their derivatives, hadrontherapy, and maybe FLASH RT in the future). It is therefore likely that the landscape of side effects will be completely different in a few years.

As cancer detection and management continue to improve, there is an increase in the number of long-term cancer survivors in the more economically developed countries. For example, in the USA, the 5-year survival rate has increased from 49% in the period 1975–1977 to 67% in the period 2010–2016 (American Cancer Society, Cancer Facts and Figures, Atlanta, Georgia, 2021). On the other hand, given that about half of patients are treated with RT, it can be estimated that several tens of thousands of patients will develop side effects each year in this country. Worldwide, with more than 19 million new cancer cases in 2020 (and about 30 million expected in 2040), and an estimated 5-year prevalence of more than 50 million [200], the number of patients developing side effects affecting their quality of life is expected to be in the millions each year. Beyond the fact that the late side effects of RT still limit the effectiveness of this treatment, these figures reveal a real public health concern facing the public authorities and the medical profession.

5.13.4 Radionecrosis

Box 5.15 Radiation-Induced Fibrosis and Necrosis

- 10% survivors of RT will suffer from fibrosis/radionecrosis.

Radionecrosis is a late toxicity phenomenon with the occurrence depending on radiation dose, the tissue affected and a number of site-specific risk factors; as treatment options are scant, preventive measures should be facilitated by providing the treatment team with the forecasted 3D RT isodose curves (Box 5.15).

Radiation accidents and therapy have shown that, in principle, all human tissues can suffer from necrosis as a late toxicity as result of progressive ischemia of irradiated tissues in the context of chronic inflammation. Pathologic samples show necrosis with fibrinous exudates and dystrophic changes of the vessels in the exposed tissues. In daily practice, radionecrosis most commonly involves bone (head and neck (jaws-mastoïd-temporal bone-larynx-cartilage)/femoral head), breast, CNS, bowel, skin and rarely ribs or sclera (Sect. 5.14.3). Even when standard dosage schedules are followed, serious radiation complications would occur in 5–10% of long-term survivors. Yet, general incidence rates on most tissues are difficult to present as most studies have specific settings and constraints resulting in large heterogeneity of data. In the following section, osteonecrosis of the jaws and brain radionecrosis will be discussed in greater detail.

5.13.4.1 Osteoradionecrosis (ORN) of the Jaw

Osteoradionecrosis (ORN) of the jaw is a late complication of RT in the treatment of head and neck cancer. It is defined as exposed irradiated bone that fails to heal over a period of 3 months without any evidence of persisting, recurrent tumor or metastatic disease. ORN occurs in bone that was exposed to a radiation total dose exceeding 60 Gy. However, in the presence of concomitant risk factors, lesions can develop in bone exposed to a lower dose, usually above 50 Gy. The overall susceptibility ratio between mandible and maxilla is for the development of ORN 24/1, with the posterior areas of the mandible most at risk and the upper jaw rarely affected.

The overall incidence of ORN in IMRT patients is reported to vary between 5.1% and 12.4% [201] with excess figures (up to 25.5%) [202] in the presence of risk factors and higher figures with longer follow-up. ORN usually develops during the first 3 to 24 months after RT; however, the real risk for ORN lasts a lifetime and can occur at any time following RT.

The pathophysiology of ORN is still uncovered. In essence, the viability of the irradiated bone is lost due to ischemic necrosis in the irradiated atrophic tissue without sufficient capability of repair, leading to secondary soft tissue breakdown and exposure of bone. Pathological fractures following ORN typically form no callus formation [203], illustrating the absence of periosteal healing. The presence of *Actinomyces* in necrotic bone is best detected with a PCR-based method and its role needs further investigation.

ORN may remain asymptomatic for a prolonged period but signs and symptoms may also occur before the development of bony exposure. Presenting clinical features include pain, tooth mobility, mucosal swelling, erythema, ulceration, malocclusion, dysphagia, trismus, paresthesia, or even anesthesia of the associated branch of the trigeminal nerve.

Different classifications of ORN exist, usually based on following criteria: extent of the lesion [204], symptoms [204, 205] and response to hyperbaric oxygen therapy. The extent of lesions can vary and range from a non-healing extraction site to exposure and necrosis of large sections of the jaw. Late stage ORN often present with fistula from the oral mucosa or skin, complete devitalization of bone, pathological fractures, and even life-threatening complications.

Panoramic radiographs are mostly used for diagnosis, follow-up, and monitoring patients who are at risk of osteonecrosis. However, only at a loss of 30–50% in bone density injury will be visible on X-ray. CBCT, CT, and MRI allow to analyze the jaws more extensively and to better assess the extent of injuries and are also very helpful in differentiating osteonecrosis from other causes of osteolysis.

Although ORN may occur spontaneously [206], most ORN develop after dental surgery (extractions of teeth, dento-alveolar surgery, dental implant placement).

The most important risk factors for ORN are dose >50–60 Gy and post-RT dento-alveolar surgery in the high-risk zone. Other factors are tumor size, proximity of the tumor to bone, age >60 years, diabetes mellitus, poor oral hygiene, concomitant chemotherapy, active smoking, excessive alcohol consumption, and chronic use of corticosteroids [207]. Many of these published risk factors still need confirmation with robust data and study designs.

Pre-treatment dental screening aims to reduce the risk of developing ORN after RT by eliminating all teeth with an elevated risk in an area of bone that will get exposed to a high dose of IR. It is therefore mandatory to provide the dentist and/or oral surgical team with the forecasted 3D RT isodose curves (Fig. 5.25) to allow a differential approach for teeth within and outside the high ORN risk perimeter [208].

In the areas with a high risk of developing ORN (>50 Gy), an extraction is done whenever teeth represent a risk for future need for extraction of a risk for future infection. Teeth which will be extracted as part of the surgical resection approach can be left in situ. In other areas of the jaws, the extraction therapy will depend on regular extraction guidelines, the clinical experience of the supervising surgeon considering the level of oral hygiene of the patient and the expected future limitation of mouth opening. In the upper jaw, due to the far lower incidence of ORN, most clinicians opt for regular extraction guidelines.

Depending on the extent of the affected area (both soft tissues and bone), the symptoms, the existence of a pathological fracture the treatment will vary from a conservative to a surgical approach. In early stages, conservative measures such as antibiotics, debridement, and irrigation will be preferred while surgical resection and reconstruction (reconstruction plates, free vascularized osteomyocutaneous flaps) are reserved for more advanced cases. Whenever resection of ORN is needed, 3D RT isodose curves should be allowed to be included in the virtual planning of the procedure.

HBO as adjunctive therapy to conventional treatment has not been proven to yield consistently significantly favorable results compared to conventional treatment alone. Therapeutic regimens composed of Pentoxifylline and Tocopherol combined have been shown to have a synergistic effect in treating small areas of ORN with visual and symptomatic resolution of the condition. Clonodrate, a first-generation non-aminobisphosphonate, has been described as effective when combined with pentoxifylline and tocopherol for refractory ORN (PENTOCLO-protocol).

Lifestyle changes should accompany both conservative and surgical procedures: proper oral hygiene, smoking and alcohol cessation, healthy and adequate nutrition intake, well-fitting dentures [209]. Dento-alveolar surgical procedures in a highly radiated mandible should be avoided if possible and whenever needed following principles should be kept in mind: minimal periosteal degloving, antibiotic coverage, local anesthesia without epinephrine.

5.13.4.2 Brain Radionecrosis

Brain radionecrosis (RN) is an irreversible late radiation-induced tissue complication that can occur after irradiation of brain parenchyma inducing a vascular lesion of the white matter, developing in the irradiation field, secondary to chronic inflammation of the brain parenchyma, with a tendency for spontaneous extension [210]. Its

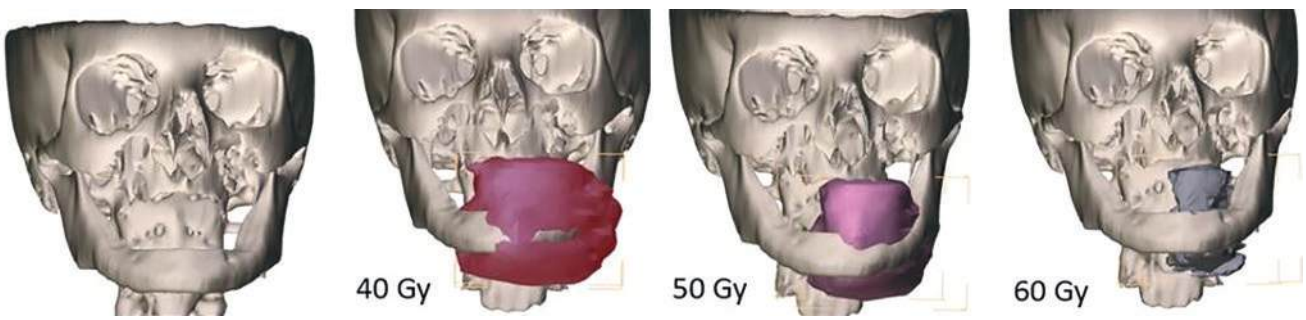

Fig. 5.25 3D RT isodose curves

pathophysiology is not yet clear. Brain RN induces hypocellular zones of necrosis and fibrinous exudates with degenerative or dystrophic changes in the vasculature, with telangiectasia, hyaline thickening of vessels, and fibrinoid necrosis including intravascular thrombosis responsible for an increase of vascular permeability. The occurrence and severity are correlated with dose-volume parameters [211]. An actuarial incidence of brain RN up to 34% two years after stereotactic radiotherapy (SRT) was recently reported—symptomatic and sometimes lethal or severely debilitating in 10–17% of the patients [212]. Approximately 80% of cases occur within 3 years from the completion of RT.

The symptoms of RN are those of a non-specific intracerebral expansive process. A seizure is inaugural in half of the cases, signs of intracranial hypertension and a progressive deficit syndrome (sensory, motor, or aphasia) are frequently present. The semiology often reproduces the initial signs of the primary tumor. In pituitary tumors, lesions preferentially affect the chiasma and the optic nerves causing severe visual disturbances; damage to the temporal, frontal, and hypothalamus lobes is often associated, causing cognitive impairment.

The main differential diagnosis is tumor progression due to very similar clinical and radiological characteristics.

The gold standard for the diagnosis with certainty is the pathological analysis. On histological analysis, 50% of lesions are pure RN, the remaining 50% associated with radionecrosis and tumor cells without predicting their viability.

There is not yet a validated imaging technique that distinguishes the two entities though advanced imaging techniques such as DTI (ADC and fractional anisotropy ratios), perfusion MR imaging (CBV, rPH, and relative PSR), MR spectroscopy, and amino acid PET hold promise [213]. The MRI shows a persistent central hypointense and an enlargement of a pre-existing enhancement in T1 gadolinium associated with a hypersignal in T2 with an appearance of "Swiss cheese" or "soap bubble." Perfusion MRI, spectro-MRI and PET amino acid imaging may provide additional arguments. Other avenues are showing interest in the differential diagnostic strategy—notably radiomics.

When this documentation is not possible, the decision-making process is guided by clinical and imaging criteria collected over a significant period of follow-up. Such criteria were proposed by the Association of Neuro-Oncologists of French Expression (ANOCEF) [214]. The treatment options of brain RN include steroids, bevacizumab, surgical resection, and hyperbaric oxygen.

5.13.5 Pathogenesis of Early and Late Normal Tissue Radiation Injury

Box 5.16 Normal Tissue Radiation Pathology

- Cellular depletion by radiation-induced death is not the only one responsible for initiation and progression of lesions.
- Radiation-induced effects on the vascular endothelium drive the propagation of the inflammatory response and chronic effects.
- Molecular and cellular damage after exposure to IR impacts cellular homeostasis and potentially leads to chronic organ dysfunction.
- The notion of a continuum of effects, orchestrated by all the compartments and chronic cytokine cascades, opens up fields of therapeutic approaches.

Improving the quality of life of patients by reducing sequelae of cancer treatment is one of the main future challenges. Beyond the dose itself to the organs at risk, the probability of occurrence of side effects is related to a multitude of factors: the nature of the radiation (photons, electrons, charged particles), the volume irradiated, the fractionation, the spread, the dose rate, but also the nature of the exposed tissue (hierarchical versus flexible tissue, in parallel or in series organization) or the individual susceptibility of the patient. Furthermore, in a simplified manner, acute toxicity is mainly observed in rapidly proliferating tissues (skin, gastrointestinal tract, and hematopoietic system) and late effects are observed in slower proliferating tissues (central nervous system, kidney, heart) [215]. Historically, tissue response to radiation has long been explained by the target cell concept which suggests that the severity of tissue effects is mainly due to the depletion of cells in a target compartment by radiation-induced death resulting in a functional impairment of the organ. This hypothesis can be considered for early effects but is more questionable for late effects. Cellular depletion by radiation-induced death is an important element of the tissue response, but it is not the only one responsible for the initiation and progression of lesions. Molecular and cellular damage after exposure to IR will disrupt cellular homeostasis and potentially lead to chronic organ dysfunction. It is now agreed that the tissue response to IR is the result of the activation and integrated involvement of all the compartments that make up the tissue (Fig. 5.26 and Box 5.16).

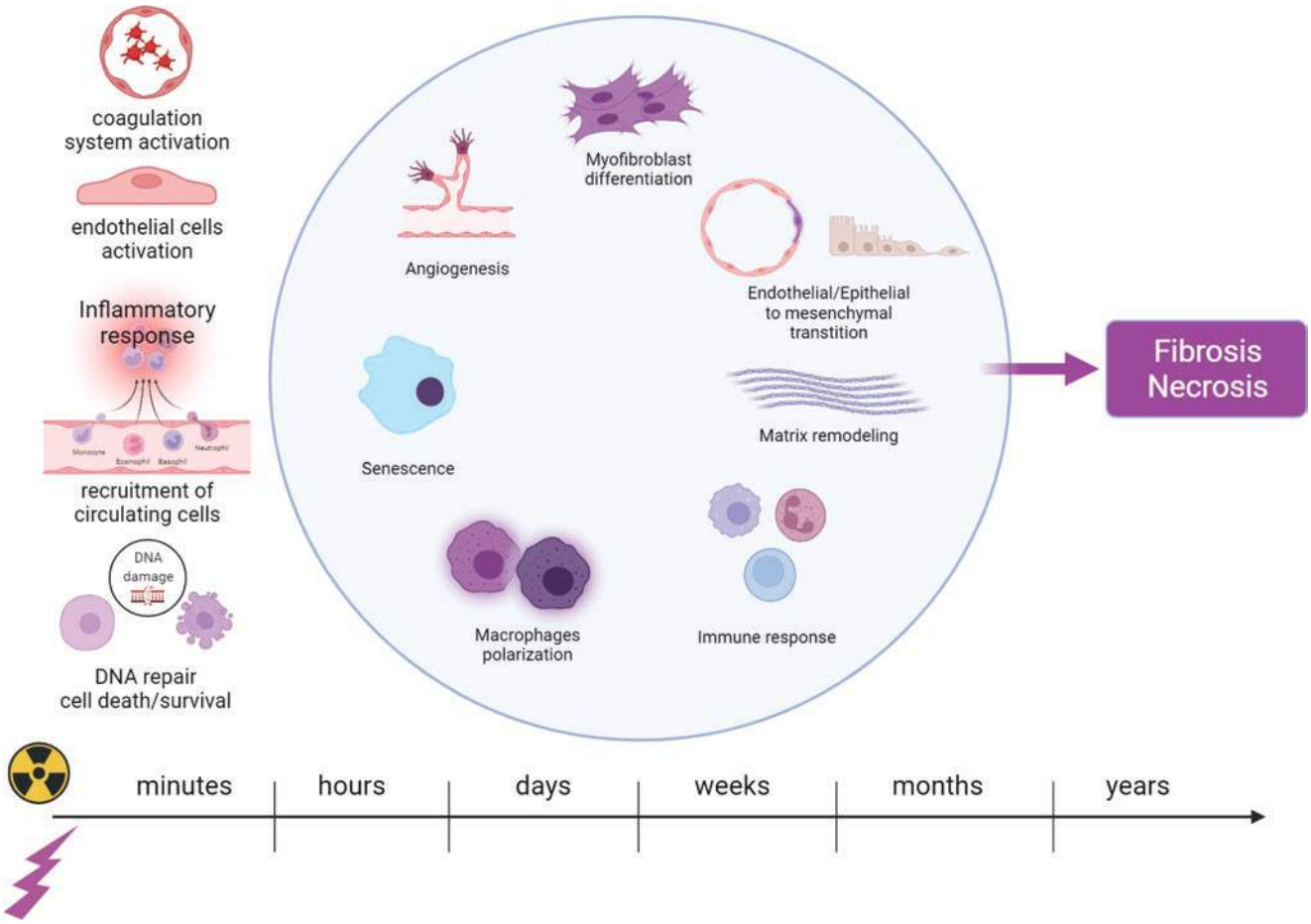

Fig. 5.26 Irradiation and progression of radiation-induced normal tissues damage. Tissue damage results from several acute events such as cell loss and endothelial cells activation. Damage progression includes a continuum of effects orchestrated in time and space leading to tissue fibrosis/necrosis and organ dysfunction

The notion of a continuum of effects, orchestrated by all the compartments and chronic cytokine cascades, opens up fields of investigation into various therapeutic approaches [190]. The contemporary view involves several cell types and molecular mechanisms, which together form an orchestrated response, and contribute to the initiation, progression, and chronicity of radiation-induced injury. A better understanding of these event kinetics should allow the identification of molecular and cellular targets, associated functions, and relevant times for therapeutic action. Radiation-induced effects on the vascular endothelium and epithelial barriers are important for the propagation of the inflammatory response and the recruitment of immune cells. The concept that the microvasculature plays a central role in the radiation toxicity of many tissues is emerging and demonstrated now. Irradiation leads to endothelial cell apoptosis, increased vascular permeability, and acquisition of a pro-inflammatory and pro-coagulant phenotype. Moreover, tissue-specific deletion in the endothelium of key molecular actors impacts the severity of acute and normal tissue injury [216].

Rapidly after exposure to IR, damage to the endothelium and epithelial cells leads to the release of damager signals (such as DAMPS) and the activation of adhesion molecules. This reaction allows the recruitment of a large panel of immune cells to the damaged site, which are able to repair the tissue but which, in the case of chronic inflammation, can strongly also participate in the installation of fibrosis [196]. For example, macrophages are rapidly recruited after irradiation and are a heterogeneous immune cell population with multiple pro- or anti-inflammatory as well as pro- or anti-fibrosis functions. The recruitment dynamics of macrophages, as well as their phenotypic orientation impacted by their microenvironment over time, are increasingly shown to play an essential role in the evolution of radiation-induced injury [195]. Radiation-induced immune effects are propagated by a large panel of cytokines including interferon-γ (IFNγ), Interleukin-1β (IL-1β), Interleukin-6 (IL-6), CC-chemokine ligand 2 (CCL2), tumor necrosis factor (TNF), and transforming growth factor-β (TGFβ). Interestingly, beyond their roles in the inflammatory

response, some of these cytokines also play essential roles in several other processes contributing to the evolution of radiation-induced lesions. TGFβ induces the differentiation of fibroblasts into myo-fibroblasts with a consequent increase in the extracellular matrix. In addition, in association with other cytokines such as IL-1β, TGFβ promotes endothelial-mesenchymal (endoMT) [217] and EMT, two key processes also demonstrated in radiation-induced lesions to healthy tissues [218]. Finally, it has recently been shown in several studies that senescence also contributes to the pathogenesis of radiation-induced injury to healthy tissue. Senescence is a durable cell-cycle arrest with a persistent pro-inflammatory Senescence-Associated Secretory Phenotype (SASP) characterized by the secretion of multiple growth factors and cytokines, the senescence-messaging secretome (SMS) [219]. Premature senescence can be produced by a large panel of DNA-damaging agents and genotoxic stress including IR. In several preclinical models of radiation-induced lung injury, it has been shown that many types of cells bear senescence marks such as pneumocytes, macrophages, and endothelial cells [220, 221]. Interestingly, senolytic agents that selectively can kill senescent cells limit radiation-induced lung injury provided the evidence that senescence participates to the pathogenesis and that senolytic drugs could be a good strategy to reduced late normal tissue damages [222].

Recent research clearly shows that normal tissue injury is a dynamic and progressive process. The main challenge in the future will be to perfectly decipher this dynamic of events for each organ and its own characteristics. This will allow to propose new molecular and functional tools to predict, prevent, and treat damage to healthy tissues after irradiation.

5.13.6 Dose-Volume Effects and Constraints (QUANTEC, PENTEC, and HyTEC)

The evaluation of treatment plans in the treatment planning system is based on dose-volume histogram analysis for PTV and critical organs. Final plan quality evaluation should be based on plan complexity, plan robustness, and dose distribution analysis including dose-volume control. Constraints for any dose-volume relationship should be connected to the radiobiological outcome.

In 2010, a series of articles were published in the International Journal of Radiation Oncology Biology Physics as a meta-analysis of published dose–response observations for different critical organs. The project called Quantitative Analyses of Normal Tissue Effects in the Clinic (QUANTEC) aimed to review meaningful data published in the previous 18 years for common critical organs in terms of dose/volume values connected to radiobiological effects [223]. This endeavor was a challenge because it involved the amalgamation of different analytic methodologies, calculation methods, endpoints, and grading schemes, which were used in different studies to address the relationship between dosimetric parameters and the clinical outcomes of normal tissues.

QUANTEC consists of two introductory papers about the overview and history with some scientific issues related to the QUANTEC effort and about the suggestions on how to rationally incorporate the QUANTEC metrics/models into clinical practice. The core of the QUANTEC project is described in 16 articles for different organs at risk or complications:

- Bladder
- Brain
- Brainstem
- Esophagus
- Hearing loss
- Heart
- Kidney
- Larynx and pharynx
- Liver
- Lung
- Optic nerves and chiasm
- Penile bulb
- Rectum
- Salivary gland
- Spinal cord
- Stomach and small bowel

For each organ, there are associated sections describing: clinical significance, endpoints, challenges in defining volumes, review of dose/volume data, factors affecting risk, mathematical/biological models, special situations, recommended dose/volume limits, future toxicity studies, and toxicity scoring.

The QUANTEC reviews provide focused summaries of the dose/volume/outcome information for many organs, but these were usually obtained for 3D conformal RT or other techniques that have in many cases already been replaced by more modern techniques, such as VMAT or SRT. It should be emphasized that dose/volume constraints and other information in QUANTEC are expected to be updated in the future for relevant techniques. The data is not intended to be extrapolated to pediatric patients. Pediatric Normal Tissue Effects in the Clinic (PENTEC) is a recent initiative to review tolerance constraints for children, who may have different tolerance to that of adults [224].

For hypofractionated RT such as SRS or SBRT, relatively small target volumes receive hypofractionated RT schedules, typically in 1–5 fractions. As an extension to QUANTEC and other previous guides to tissue tolerance, high dose per fraction, Hypofractionated Treatment Effects in the Clinic

(HyTEC) was published as a series of articles [225]. This project served to provide guidance on dose/volume constraints for hypofractionated regimens for 7 normal tissues as well as 9 disease sites (TCP). Interestingly, the possibility of so-called "new radiobiology" of hypofractionation is also alluded to—the possibility that large fractions may induce enhanced radiobiological effects in tumors by additional vascular targeting and anti-tumor immune responses [150]. Radiobiological aspects of hypofractionation are discussed in detail in Chap. 5.

Overall, the recommendations of QUANTEC, PENTEC, HyTEC, and other constraint guidelines should be used judiciously as a guide and should not replace clinical judgment.

5.13.7 Radiobiology Models for Normal Tissue Toxicity

Box 5.17 Normal Tissue Toxicity Modeling

- Normal tissue complication probability (NTCP) describes the probability of organ/structure complication related to radiation treatment specified by physical and clinical factors in radiation oncology.
- There are various approaches to NTCP modeling which usually are based on different statistical distributions.
- The predictive power of the NTCP model is dependent on the parameters of models, which can include dosimetry as well as other clinical and treatment conditions.

The normal tissue complication probability (NTCP) is the probability that for a given dose distribution organ or structure complication can be expected. These complications can be multiple for one organ or structure and usually are called as endpoints in the models. NTCP is aimed at quantification of dependence of tolerance dose for a certain radiation effect on the size of treated volume. The NTCP models are supposed to be predictive and to be used to estimate the complication risk for organs at risk (OARs) after RT. OARs can be used to individualize the tumor dose for a given acceptable NTCP (Box 5.17).

NCTP models are used to describe dose–response curve shape for particular endpoint for an organ at risk, which is usually sigmoidal. These models are usually connected to Dose-Volume Histogram (DVH) of the applied treatment plan; therefore the models are sometimes called DVH-reduction models. More complex approach [226] moves towards spatial dose distribution in the patient and not dose-volume reduction only. When voxel-based evidence on organ radiosensitivity was acknowledged and attempts were made to develop a probabilistic atlas for NTCP in radiation oncology. However, there are other clinical factors that influence complications, such as chemotherapy, fraction size, pre-existing medical conditions, and comorbidities. The predictive strength for models can be enhanced with considering other important clinical and medical features for the patient. This information is expected to provide a boost for further deployment of biological models in the clinical treatment planning process.

Common NTCP models as described by [227] are:

1. Lyman-Kutcher-Burman (LKB) model (Gaussian)
2. Parallel architecture model (Logit)
3. Weibull model (Weibull)
4. Critical element model (Poisson)
5. Relative seriality model (Poisson)
6. Critical volume model (Binomial)
7. Inverse tumor model (Poisson)

Models are based on different statistical distributions (in parentheses). The first four models are using cell-survival-based response, while others are phenomenological. However, each model may be expressed in terms of the parameters D_{50} (dose that is associated with the 50% response probability) and γ_{50} (gradient of the dose-response curve at the level of the 50% response probability). The steepness of the NTCP curve can be expressed in the models by parameter m. It is inversely proportional to the steepness of the dose response.

Commonly used model is the Lyman-Kutcher-Burman (LKB) model. This model assumes that the tolerance dose increases inversely as power of n of the partial volume irradiated. Examples of NTCP curves obtained for the LKB model are presented in Fig. 5.27.

Serial (critical element models) and parallel (critical volume models) are also common models. These mechanistic models are based on tissue architecture. It is assumed that organs consist of functional subunits, which can be organized in chains for serial organs or independently for parallel organs. Damage of one functional subunit impairs the function of the whole organ, while the function of a parallel organ is more dependent on the irradiated volume.

NTCP models are usually incorporated into in-house developed software in RT centers. Currently, they are also available in commercial treatment planning systems. Parameters for different NTCP models adopted from literature must be used with caution when the probability estimation is applied as a decision criterion for the treatment plan. NTCP can be used also for comparisons between different treatment plans or RT modalities. In these cases, NTCP is used as a relative value in the plan evaluation process and this approach is safer. However, the software should always

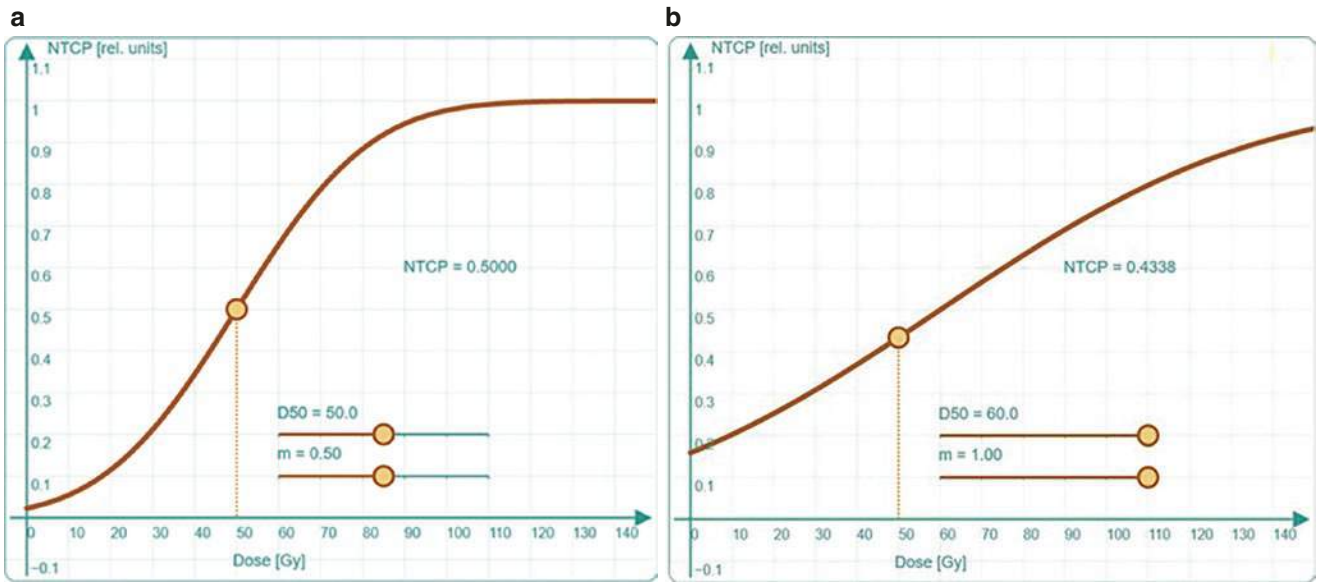

Fig. 5.27 NTCP curves calculated from Lyman-Kutcher-Burman model for two parameters combinations. Parameter m is inversely proportional to the steepness of the curve. (**a**) NTCP curve calculated by LKB model for D_{50} = 50 Gy and m = 0.50. For a dose of 50 Gy, the value of NTCP is 0.50. (**b**) NTCP curve calculated by LKB model for D_{50} = 60 Gy and m = 1. For a dose of 50 Gy, the value of NTCP is 0.43

allow the user to update model parameters. There should be detailed documentation for the models available. It is obvious that the value of NTCP is strongly dependent on the parameters of the model, and therefore should be used with caution.

5.14 Stem Cells in Radiotherapy

5.14.1 Introduction

Stem cells have been described as undifferentiated cells which are found in most adult mammalian tissues. Stem cells are divided into two principal groups: embryonic and adult stem cells. Embryonic cells, which have a pluripotency phenotype have the blastocyst inner cell mass as their origin. It means that they can be differentiated into all cells from the three main germ layers (endo-, meso-, and ectoderm). On the other hand, adult stem cells can be differentiated into cell types according to their origin tissue, thus they are multipotent. Under physiological conditions, adult stem cells are slow growing with a long G0 cell-cycle phase. The main function of such stem cells is to maintain tissue homeostasis including continuous regeneration and associated constant number of cells. The way they are divided is as follows: from the origin stem cell arises one daughter cell with stem cell properties and one progenitor cell with a higher proliferative capacity [228]. Below the normal stem cells in different tissues are described alongside cancer stem cells and their IR response or resistance together underlying molecular mechanisms.

5.14.2 Normal Stem Cells in Different Tissues

In the healthy human tissue, there are multiple cell populations with different stem cell phenotypic characteristics and radiation sensitivity. These different stem cell niches are discussed below based on the tissue localization.

5.14.2.1 Bone Marrow Stem Cells

Stem cells of the bone marrow are divided into two groups: hematopoietic and mesenchymal stem cells. From the hematopoietic stem cells arise leukocytes, erythrocytes, and thrombocytes and from the mesenchymal stem cells adipocytes, chondrocytes, myocytes, and osteocytes are generated [229]. One function of mesenchymal stem cells is to establish the hematopoietic stem cell niche [230]. When it comes to IR toxicity, the progenitors from the hematopoietic stem cells are more sensitive than the origin, more primitive, stem cells. Such a difference is linearly dose dependent in the progenitor cells and is one of the factors causing the development of one of the early radiation effects, the hematopoietic syndrome [231]. Importantly, both of these stem cell populations are responsible for the repopulating of the damaged bone-marrow homeostasis after IR exposure.

5.14.2.2 Neural Stem Cells

The neural stem cell pool can be divided according to the localization. Hence, we recognize the subventricular and the subgranular group [232]. Even within these two subtypes are heterogenous. Thus, one can distinguish four main types of cells from the subventricular niche: activated neural stem cells, dormant neural stem cells, progenitor cells, and quies-

cent neural stem cells [233]. Generally, neural stem cells can differentiate into multiple neuronal- and glial cell types. The most IR sensitive populations are activated neural stem cells and progenitor cells because IR induces their cell death, for example, apoptosis. Such effects lead to a reduced population of new neurons. To prevent the negative effects of IR on the neural stem cells different protective strategies have been tested, for example, administration of lithium [234, 235] or the natural polyphenol resveratrol [236]. It has been shown that lithium pre-treatment can reduce DNA damage and increase microglial activation [234, 235]. Resveratrol, on the other hand, has a neuroprotective effect, because it can reduce oxidative stress [236].

5.14.2.3 Skin Stem Cells

Several types of the stem cells exist in the skin which can differentiate into more than two dozen cell types, including epidermal-, keratinocyte-, and melanocyte stem cells [237]. The keratinocytes progenitors are the most IR sensitive ones, if damaged they are eliminated thereby contributing to the high epidermal sensitivity to IR. In contrast, more primitive keratinocyte stem cells possess active repair mechanisms and increased cell survival, but their rapid and faultier repair contribute to the genomic instability. Interestingly, while the keratinocyte stem cells favor repair of DNA damage, the melanocyte stem cells are not involved in tissue regeneration after IR damage [231].

5.14.2.4 Intestinal Stem Cells

Gastrointestinal syndrome, a known acute toxicity response to IR, promoted the first exploration of intestinal stem cells in radiation biology studies, which included the exposure of mice to doses greater than 14 Gy, inducing death after 7 to 12 days due to small intestine damage. This high sensitivity has been attributed to the fast cell turnover in the intestinal mucosa which, in mice, completely renews the epithelium every 5 days [231]. These studies allowed the characterization of intestinal regeneration, revealing the presence of a stem cell population near the bottom of the intestinal crypt. These actively cycling cells are highly sensitive to IR, undergoing apoptosis in response to doses as low as 1 Gy although this sensitivity seems to be dependent upon their position within the crypt [238]. Another stem cell subpopulation, known as crypt base columnar cells and characterized by the expression of Lgr5 (Leucine-Rich Repeat Containing G Protein-Coupled Receptor 5), are less radiosensitive than the previously described cells yet more sensitive than small intestine progenitor cells. Radiation toxicity can occur at low doses; however, crypt loss is only observed after exposure to higher radiation doses. This may be because crypts only disappear after total loss of the stem cell population, which only happens at doses greater than 8 Gy. This radiosensitivity could be caused by the accumulation of DNA damage or pro-apoptotic proteins after genotoxic stress, i.e., p53, ATM, and PUMA. The difference in radiosensitivity between the small intestine and the colon could be due to a more efficient p53 signaling, DNA repair and G2-phase checkpoint delay in the latter. The high expression level of the anti-apoptotic protein Bcl-2 in colon progenitors could be another reason. Paradoxically, the risk of developing cancer after exposure to IR is lower in the small intestine, suggesting the interplay between cell resistance and lower genomic stability. It should be noted that most of this knowledge is based on studies in mice; therefore, human models are still required in order to understand the intestinal stem cell radiation biology [231] (Box 5.18).

Box 5.18 Normal Tissue Stem Cells and Radiosensitivity

- Stem cells are divided into two principal groups, embryonic and adult stem cells, respectively. Some examples are bone marrow-, neural, skin, and intestinal stem cells.
- The main function of stem cells is to maintain the tissue homeostasis.
- In the normal human tissue, there are multiple cell populations with different stem cell phenotypic characteristics and different IR sensitivity.

5.14.3 Cancer Stem Cells: Their Role in Radiation Therapy Sensitivity and Resistance

Tumor heterogeneity is found among patients with the same histological diagnosis as well as within each patient's tumor as a result of genetic or phenotypic variations [31]. Further, the tissue of origin also influences the inter-tumoral heterogeneity because some of the driving signaling networks (e.g., those that maintain genomic integrity) may vary. Moreover, tumor progression, treatment sensitivity including towards RT and tumour aggressiveness are largely influenced by the origin of the carcinogenic transformation as well as the TME. Tumor heterogeneity plays a significant role in cancer cell survival, thus setting a significant challenge in the development of effective cancer treatment, or in the prevention of tumor progression and metastasis [239].

Recent studies describe two models, i.e., clonal evolution and cancer stem cells (CSCs) which in part can explain tumor heterogeneity as well as alterations during progression of malignancy. The clonal evolution model shares the idea that all cells can accumulate genetic mutations; therefore, any cell has tumorigenic potential [240, 241]. On the other hand, the CSCs' model describes a hierarchy system in which tumor growth and progression can be maintained with a small proportion of cancer cells displaying stem-like characteristics, such as self-renewal. These stem-like cancer cells can drive tumorigenesis and differentiation, which

Table 5.15 Example of cancer stem cells (CSCs) Markers

Type of tumor	CSC markers	References
Breast cancer	$CD44^+/CD24$, $CD44^-/CD24^{-/low}$ ALDH1	Coppes and Dubrovska [247], Filipova et al. [243]
Esophageal cancer	CD44 CD133 CD90	Smit et al. [252], Yang et al. [253]
Glioma	CD133	Bao et al. [245]
Head and neck cancer	CD98	Coppes and Dubrovska [247], Digomann et al. [254] Martens-de Kemp et al. [255]
Larynx	CD44 CD133	Yang et al. [253]
Small cell lung cancer	CD133	Sarvi et al. [256]
Non-small cell lung cancer	CD133	Bertolini et al. [246], Lundholm et al. [250], Moro et al. [251], Shien et al. [257]

can to some extent explain tumor cell heterogeneity [240, 242, 243]. It is believed that CSCs originate from the malignant transformation of normal stem cells or progenitor cells. Thus, CSCs possess key properties such as self-renewing and differentiation capacity, thereby being able to produce a phenotypically variable progeny [244]. Due to these characteristics, CSCs are thought to be important for tumor formation, recurrence, and resistance. Indeed, experimental data from xenograft studies in mice where different tumor cells with diverse CSCs characteristics have been engrafted and formed tumors, have demonstrated that CSCs are involved in tumor growth and metastasis and that they are resistant to a multitude of cancer treatments including RT [245–251]. It has been noted that only a few surviving CSCs in a heterogeneous tumor are enough to cause local tumor relapse after RT but also to promote metastasis [243, 247]. It is difficult to calculate the frequency of CSCs within a tumor as it is dependent on the type of malignancy. Further, the identification of CSCs is challenging as specific markers are not entirely clear. This is in part due to the high intra- and inter-tumor heterogeneity as well as by tumor plasticity, and variable genotypes and phenotypes. Regardless, a few markers, i.e., CD44, CD98, CD90, $CD44^+/CD24^-$, and CD133, are robust enough to be used in the identification of CSCs (Table 5.15) in breast cancer, small-cell lung cancer (SCLC), esophageal cancer, larynx, head and neck cancer, non-small cell lung cancer (NSCLC), etc. Interestingly, these markers are also associated with response to RT as illustrated in NSCLC and glioblastoma [245, 246, 248–251].

The variable phenotype of CSCs has a strong association with cells of origin thus making the comparison between different tumors complicated. In addition, the number of CSCs within a tumor is relatively small; therefore, the use of CSC markers is a poor predictor for treatment response [258]. Regardless, the characterization of CSCs remains important, as it may provide essential information in the development of more efficient treatment strategies and the prevention of tumor relapse as well as metastasis [240, 247–249, 251, 259].

A successful RT treatment largely depends on the elimination of cells with tumorigenic capacity, i.e., the number of clonogenic cells, which in part are CSCs, seeking to inactivate these permanently and to take control of tumor growth. Should a single CSC survive, the possibility of tumor relapse is tangible, with the consequent concern that this new tumor may now be RT resistant. In part RT resistance of tumors depends on the number of CSCs within the tumor mass, with greater numbers often being responsible for the failure of therapy [240, 260]. Some of the signaling networks involved are shown in Fig. 5.28.

CSCSs are also reported to have activated DDR signaling and increased DNA repair capacity, for example, ATM, Chk1/2, and NHEJ [245, 250], increased cell death resistance as well as upregulation of the signaling pathways involved in cell survival and proliferation, such as HIF-1α, WNT (Wingless-related integration site), NOTCH, or Hedgehog [247]. Moreover, it was recently shown that tumors with a higher count of CSCs had an impaired local control of the tumor and lower effect of RT than tumors with less CSCs [240, 261]. Several studies have suggested that RT sensitization is linked to the same signaling pathways involved in the preservation of CSCs cells, for example, WNT, NOTCH, or Hedgehog signaling pathways; therefore, these pathways have been indicated as possible targets for CSC-targeted therapies [247, 253]. Other strategies propose the inhibition of the DNA damage response (ATM, Chk1/2), the promotion of apoptosis, and the inhibition of epigenetic-related proteins, for example, histone deacetylase (HDAC), Enhancer of zeste homolog (EZH2). [247]. However, at present very few of these strategies have been clinically tested, due to complex cellular characteristics of CSCs. Nevertheless, further CSCs exploration and their signaling networks could reveal new potential therapeutic targets (Box 5.19).

Box 5.19 Cancer Stem Cells and Radiosensitivity

- Tumor heterogeneity is explained by theory of clonal evolution and/or existence of CSCs.
- Clonal evolution presumes accumulation of genetic mutation(s) while CSCs model describes a hierarchy system of tumor growth and progression maintained with only by a small subpopulation of CSCs.
- Few specific markers are at hand for characterization of CSCs due to high inter- and intra-tumor heterogeneity, tumor plasticity, and variable genotypes and phenotypes.
- Tumors with a higher count of CSCs show lower efficacy of RT and impaired local tumor control.
- Multiple signaling cascades controlling DDR signaling, cell death, EMT, and hypoxia are reported to be altered in CSCs of tumors offering a putative way for RT sensitization for the future.

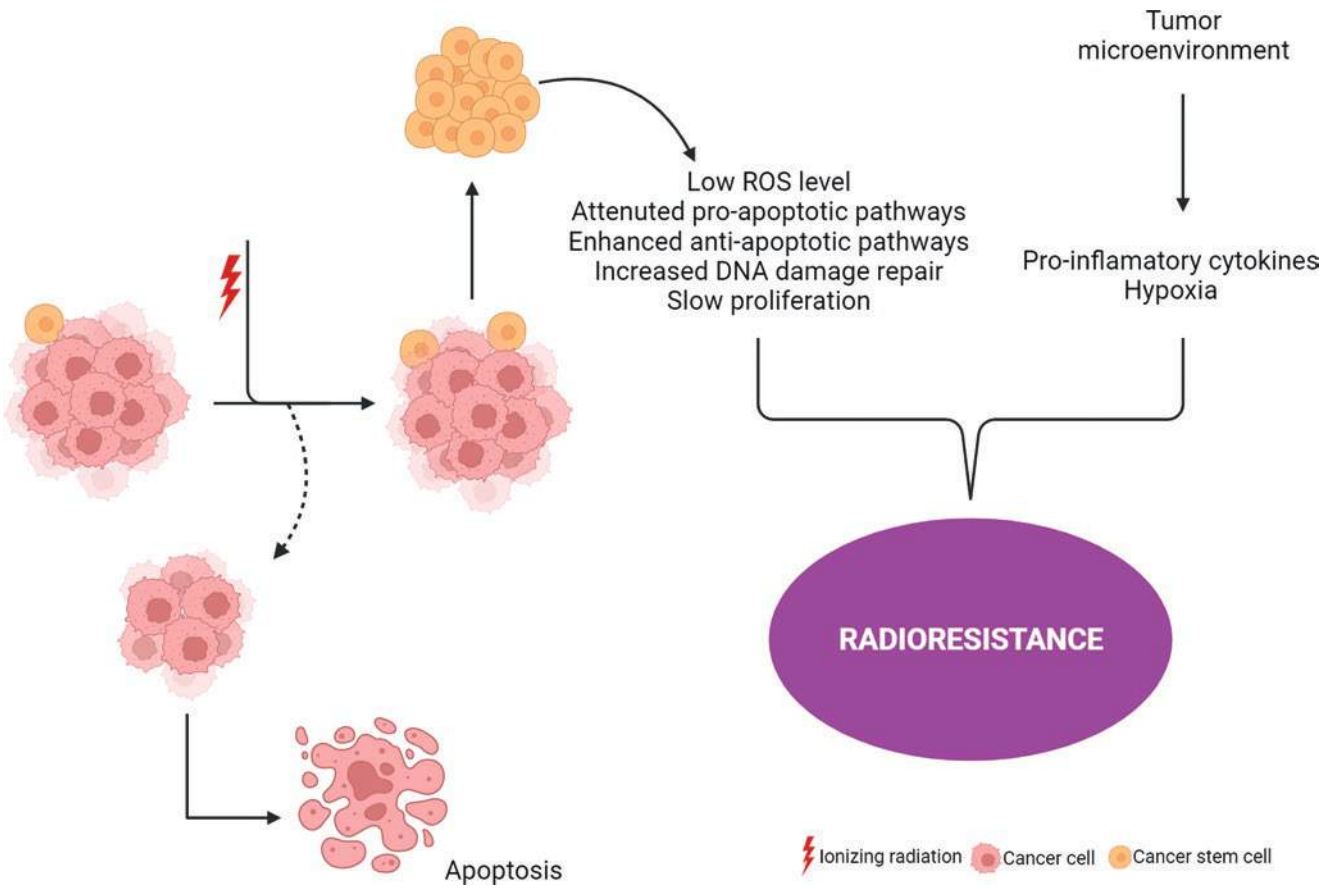

Fig. 5.28 Ionizing radiation and factors associated with cancer stem cells and tumor microenvironment contribute to tumor resistance to IR. (Adapted from [240, 260])

5.15 Radiotherapy and the Human Microbiota (Box 5.20)

Box 5.20 The Human Microbiota and Radiotherapy

- The microbiota is composed of many microorganisms such as bacteria (most represented and studied), viruses, fungi, and archaea.
- The microbiota plays a key physiological role in maintaining the gut health and well-being of the host.
- Composition and abundance of the microbiota can be modified by various stresses and a stable alternative state of the microbiota can lead to pathologies.
- Reduction of the fecal microbiota diversity and composition after RT are consistently associated with intestinal toxicity.
- The microbiota can modify the tumor response effectiveness of RT.
- The microbiota can be a therapeutic target for personalized medicine that might be used to increase patient's quality of life during or after RT.

5.15.1 What Is the Human Microbiota?

The human body has around 500 billion cells including microorganisms such as bacteria, viruses, fungi, and archaea, on the surface of organs in contact with the outside. All of these microorganisms, hosted by the body, represent the human microbiota. Several microbiotas exist in an organism: in the digestive tract system (from mouth to anus), in the respiratory system, in the urogenital tract, and on the skin. Nevertheless, the larger community of microorganisms resides in the digestive system. The intestinal microbiota can be considered as an organ, given that it has specific functions of its own. Indeed, the intestinal microbiota makes it possible to maintain intestinal homeostasis by transforming nutrients that cannot be digested by the intestine into essential metabolites, by maintaining an effective epithelial barrier avoiding intestinal colonization by pathogens and also by participating to the development as well as the function of the immune system.

Among microorganisms, the most prevalent and studied ones are bacteria. The human GI tract is colonized by more than 2000 different individual bacteria species. Proportional representation and genus level

distribution are dependent on the organ localization and vary with diet, age, and geographical localization of the host. As other microorganisms within the microbiota, bacteria have an important role in maintaining the health and well-being of the host. In the healthy gastrointestinal tract, *Firmicutes* and *Bacteroidetes* represent the predominant phylum in the microbiota (up to 80%). Other phylums which are less represented in the microbiota are *Actinobacteria* (3%), *Proteobacteria* (1%), *Verrucomicrobia*, and *Fusobacteria* (less than 1%).

In a physiological environment, the microbiota is in a state considered stable and healthy, also called eubiosis, where very little modifications take place in its composition. The relationship between host and microbiota is therefore beneficial for both entities. However, multifactorial events can cause transitory disturbances in the microbiota state and therefore population reorganization. Because of the resilience ability of the microbiota, such modifications are often transient. The microbiota then has the capability to return to its basic stable healthy state. However, the microbiota can also tend towards another stable state, called alternated state or dysbiosis, which becomes deleterious for the host [262]. Dysbiosis is defined as a condition where there is an excessive presence of pathogenic microorganisms, a defect in the communities of beneficial microorganisms and a loss of ecosystem structure, i.e., decrease in richness and diversity of microorganism species and increase of the low-grade inflammation, the intestinal permeability, and the oxidative stress. The dysbiotic state of the microbiota questions the scientific and medical community about its involvement in the development of certain pathologies like inflammatory bowel disease (IBD), metabolic disease (obesity or diabetes), neurological pathology (Alzheimer, autism, or Parkinson) but also cancers. Recently, dysbiosis was also reported in patients treated by RT (Fig. 5.29).

5.15.2 Pelvic Radiotherapy and the Human Fecal Dysbiosis: Prospective Clinical Trials

Currently, at least eight prospective clinical studies assessed the effect of RT combined [263–266] or not [267–270] with other anti-tumors treatments, like chemotherapy, on the gut microbiota dysbiosis. The results of these studies have recently been presented in Byeongsang Oh's review in 2021 [271]. Fecal microbiota changes by pelvic cancers (gynecological, colorectal/rectal, prostate, lymph node, and anal cancers) and/or after RT are briefly summarized below. Prior to RT, patients suffering from pelvic cancers have a loss of their fecal microbial diversity [266, 269]. The clinical studies also performed taxonomic analyses at the phyla level in feces from cancer patients. Results highlight variations of the relative bacteria abundance with an increase of the *Firmicutes* [269] and the *Actinobacteria* [266] and decrease of the *Bacteroidetes* [269] and the *Fusobacteria* [266]. Low fecal bacterial diversity has also been described in patients during and after pelvic RT [266, 267, 269]. Pelvic RT gradually reshapes microbiota bacterial composition in such cancer patients. Indeed, the prospective clinical studies demonstrate that during pelvic RT, the fecal relative abundance of the phylum *Bacteroidetes* tends to decrease and conversely that of the *Fusobacteria* significantly increases [266]. After the completion of pelvic RT, fecal relative abundance of the phyla *Firmicutes* is reduced [266, 269] and that of the phylum *Bacteroidetes*, *Fusobacteria* [266], *Proteobacteria* [270], and *Actinobacteria* [267] are enhanced.

5.15.3 Consequences of the Human Fecal Dysbiosis in Pelvic RT-Induced Digestive Toxicity

The prospective clinical studies described above, also show that the reduction of the fecal microbial diversity during and

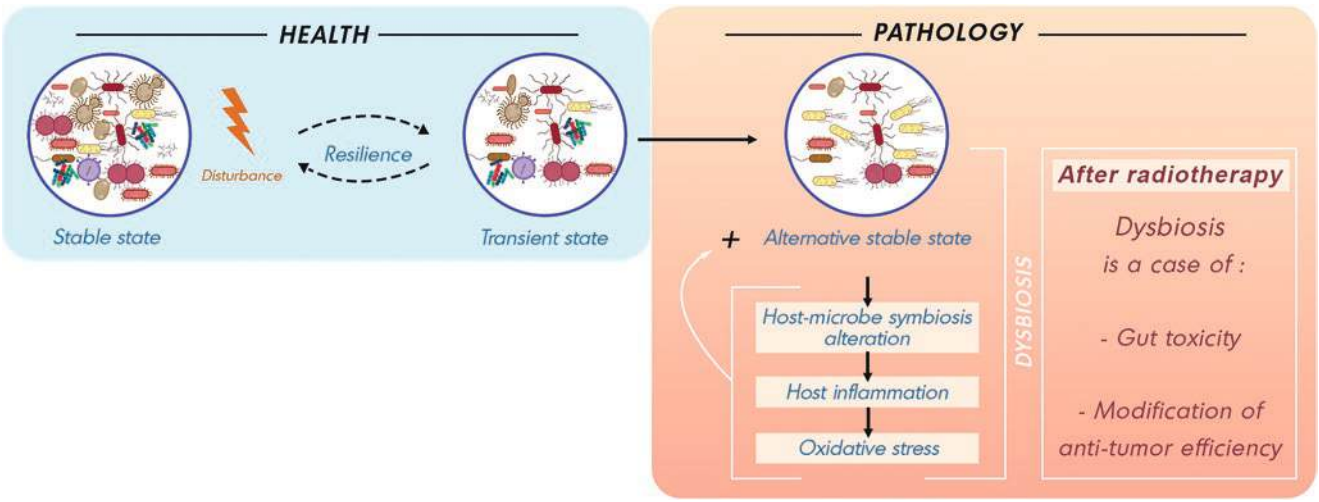

Fig. 5.29 From microbiota healthy state to dysbiosis and pathologies: case of RT effects

after pelvic RT, are consistently associated with radiation toxicity and therefore with intestinal complications, i.e., enteropathy, enteritis, and diarrhea [266–269]. Indeed, as suggested by a personal view of Andreyev's team published in The Lancet Oncology in 2014 [272], clinical data seem to indicate that microbiota through its composition change might be an actor involved in radiation-induced intestinal toxicity. In 2018, Gerassy-Vainberg et al. [273] published preclinical data supporting this assumption. Indeed, results show that, rectal irradiation by brachytherapy leads to microbial dysbiosis in chronic post-exposure phase (6 weeks). Irradiated microbiota transplantation in germ-free mice transmits susceptibility to radiation damages at least in part through the production by epithelial cells of Interleukin-1 (IL-1). Nevertheless, in 2020, data published in Science by Guo Hua et al. show that gut microbiome-metabolome network plays a crucial role in substantial protection against radiation-induced toxicity though host defense regulation [274]. Indeed, a small proportion of mice named "elite-survivors" can survive a high dose of total body irradiation and that these individuals also reduce their susceptibility to radiation-induced digestive toxicity and damages. The families *Lachnospiraceae* and *Enterococcaceae*, together with downstream metabolites represented by propionate and tryptophan pathway members, contribute substantially to radioprotection. Even if a role of the gut microbiota is suggested on RT-induced tissue toxicity or protection, very little data exists concerning its involvement and the underlying mechanisms. Wang et al. showed that the reduction of the fecal microbial diversity is even more pronounced in patients with pelvic cancers who later progressed to RT-induced side effects (fatigue, diarrhea) [269]. Mitra et al. propose that compositional characteristics of microbiota in cancer patients could also be relevant to be predictive of end-of-anti-cancer treatment bowel toxicity [265].

5.15.4 Consequences of the Human Fecal Dysbiosis in Radiotherapy Efficiency

RT efficiency, regarding anti-tumor effects, passes in part through the induction of immunogenic cell death in which CD8+ cytotoxic T cell, CD11b+ myeloid cells and dendritic cells all have been described as major actors [275]. There is growing evidence of the existence of bidirectional effects of RT and microbiome composition. Indeed, RT-induced reduction of gut microbiota diversity, richness, and composition could be followed by the host immune response alteration which in turn could lead to an effectiveness change of the anticancer treatment themselves. In 2021, data published by Shiao et al. in the Cancer Cell, robustly demonstrated that, within the gut microbiota, commensal bacteria and fungi differentially regulate tumor response to RT [276]. Indeed, commensal bacteria are required for efficient immune anti-tumor effect (activation of T cells) of RT. Currently, no study has identified bacterial subjects involved in RT efficiency. By contrast, Shiao et al. demonstrated that commensal fungi regulate the immunosuppressive microenvironment of tumor (with combined effects on T cells and macrophages) after RT leading to a reduction of treatment efficiency. They highlighted a role of *Saccharomycetales* orders and specific *Candida Albicans* genera in fungal effect after RT.

5.15.5 Conclusions

Fecal microbial signature in patients with pelvic cancers may be a tool for RT risk assessment and/or efficiency. In order to robustly demonstrate this assumption, further experiments and clinical trials should be performed. The use of high-throughput data generation by multi-omics approaches (e.g., microbiota shotgun sequencing or metabolomics analyses) and mathematical models will give an added value compared to previous studies. After RT, a better understanding of individual states of different microorganism populations within the microbiota or more largely within the intestinal ecosystem could help to guide personalized medicine. Indeed, prophylactic or curative treatments like rich fiber diet, probiotic or fecal microbiota transplantation could prevent or reduce RT-induced toxicity and/or improve radiotherapy efficiency on tumor control.

5.16 Radiomics, Data Science, and Artificial Intelligence in Radiation Oncology

5.16.1 Basic Methods of Data Analysis

In radiation research, different techniques are used to measure complete molecular- or genomic profiles of organisms, resulting in various collected data types. Omics, a general term for specified measurements and studied biological fields, include genomics, proteomics, transcriptomics, metabolomics, phenomics, lipidomics, and many more. The suffix "omics" indicates interest in all molecules or genes of a specified type and their interactions rather than individual observations. For example, in genomics studies the genome, a set of all genes expressed in the cell, tissue, or organism, and their relationships with each other and with the environment is analyzed. So other omics-based platforms such as proteomics and transcriptomics study proteome (all proteins) and transcriptome (all types of transcripts like mRNAs and miRNAs), respectively. Omics data analysis helps to understand the influence of molecules and genes on a phenotype. The measurements can be obtained with techniques like microarrays, high-throughput sequencing technologies

(Illumina, Oxford Nanopore, etc.), mass spectrometry (MS) (including MS imaging), flow-, and mass cytometry. The amount of collected data may vary from few records to millions, and the measurements may be taken for one point in time or more. With increased throughput, a large amount of data is generated, which requires advanced methods to perform a comprehensive analysis. By combining the domain expertise and knowledge of mathematics and statistics, data science extracts insights from big data.

Different statistical approaches are applied depending on the experimental design, type of data, sample size, number of replicates, number of time points, and so on. The first step of any analysis is data preprocessing that includes data cleaning and normalization. Omics data may have missing values, duplicated observations or outliers which need to be handled. Outliers are observations that deviate from other observations due to equipment failure or recording errors. An outlier can be corrected or removed from the analysis. There are many outlier detection methods that can detect one or more anomalies, like Chauvenet's criterion, Grubbs' criterion, Dixon's procedure, Tukey's or Huberta's method. Which one to choose depends mainly on the data distribution and sample size. Observations with missing values can be ignored, removed or the values may be imputed with mean, median, mode, or constant value. Missing data imputation can also be carried out with, for example, the Nearest Neighbor algorithm, which finds k nearest observations to the observation with missing values and the aggregate of these measurements, as mean/median value, is used to impute the missing one. Before the analysis, data should be normalized to guarantee their numerical scale similarity across different experiments. The standardization techniques, asz-, t-score transformation, or local re-scaling, are often applied to partially correct the batch effect or reference instability.

For a comparative study, depending on the data distribution, a variety of statistical tests can be applied. Usually, if data contain one or two experimental groups, one-step testing is performed. Three or more groups or measurements collected from several time points (time series) require a two-step procedure to determine the difference profile—the omnibus type test (from ANOVA family, for example) followed by pairwise comparisons. The test hypothesis is verified with a p-value, the probability that the test statistics would take a value at least as extreme as observed, assuming the null hypothesis is true. The lower the p-value, the stronger the evidence against the null hypothesis, and if the value is equal or smaller than the assumed significance level α, it confirmed the presence of the effect studied.

Due to the number of data collected, the omics analyses usually require more than one hypothesis to be verified, which leads to the problem of multiple testing. In the case of a single test performed, the first type of error is controlled by significance level, but in the case of multiple testing, the number of false-positive results has to be maintained for the whole test family. This can be done with the use of Bonferroni correction, Simes-Hochberg procedure, Dunn-Šidák, Holm, or Hommel methods to control family-wise-error (FWER) or Benjamini and Hochberg procedure or Storey's algorithm when focusing on false-discovery-rate (FDR). However, the p-value depends on sample size, and if the sample is sufficiently large, the statistical test will almost always indicate a significant difference. Therefore, in big data, it is recommended to calculate effect size together with the p-value. Effect size is a quantitative measure of the strength of a phenomenon calculated based on data and is independent of the sample size. A lot of different measures of effect size exist, and they can be divided into two categories: for indicating differences between groups (e.g., risk difference, risk ratio, odds ratio, Cohen's d, Glass's delta, Hedges' g, the probability of superiority, $\omega 2$) and estimating measure of similarity between variables (e.g., the correlation coefficient r, $R2$, Spearman's ρ, Kendall's τ, φ coefficient, Cramer's V, Cohen's f, $\eta 2$).

It is possible to integrate data and results from different experiments to get a unified view to them, in situations when the same experiment is performed on a different set of data or the same data is used in a different experiment (different method) but concerning the same characteristic (null hypothesis). The p-value integration can be carried out, among others, with Fisher product, Lancaster, Stouffer method, or weighted z-transformation. The adaptive rank truncated product method can also be applied at the pathway analysis level.

If measurements were taken for multiple characteristics to estimate the relationship and its strength between them (between a dependent variable and independent variables), a regression analysis can be conducted. Regression is a statistical method that tries to fit a model (function) to the data. The model has different forms, the most common one is a linear function, which is a line that closely fits the data according to a specific criterion. In other words, the dependent variable is a linear combination of the model parameters.

5.16.2 Artificial Intelligence and Machine Learning Methods for Knowledge Discovery

In radiation oncology, data science (incorporating the disciplines of computer science and statistics) attempts to provide clinical insight and clinical decision support using structured or unstructured clinical data that incorporates multiple variables descriptive of patient cohorts [277]. Daily clinical workflows produce a vast array of data comprising of electronic health records, treatment information, genomic data, multimodal imaging, and patient outcomes [278].

Inconsistencies in annotations of medical records presents a problem when utilizing unstructured data [279]. Here machine learning and artificial intelligence are key to detecting patterns within these vast data matrices [280, 281], providing opportunities for the development of diagnostic and prognostic tools. Increasingly clinical data and -omics data on the intrinsic biological characteristics of the patient are being integrated to derive models predictive of outcome metrics such as cancer survival and treatment response [282]. As the volume of clinical data available increases, innovative methods to process and interpret the data is required, translating the information into useable knowledge.

Machine learning (ML) and artificial intelligence (AI) approaches are capable of both identifying intrinsic patterns within data (termed unsupervised techniques) and developing models linking matrices of clinical data to identifying factors such as diagnostic or prognostic criteria (termed supervised techniques) [283]. For the latter type of model, the standard approach is to randomly separate the available data from patients into a training set which is presented to a machine learning algorithm capable of identifying important variables that link the patient data to the target variable (which is itself representative of the diagnostic or prognostic criterion). Subsequently, the generalizability of the learnt algorithm to new data is interrogated by presenting the algorithm with the unseen test data which remains from the available dataset after separation of the training data.

Typical applications of these approaches include prediction of toxicity to radiation therapy with dosimetric factors in head and neck cancer [284] to prediction of survival in pancreatic cancer [282]. A key advantage of machine learning in predicting therapy outcomes over conventional models such as NTCP and TCP which use dosimetric data [285] is the application of additional clinical and biochemical data [284, 286]. Many models demonstrate high performance owing to validation taking place using data which bears a close relationship to the training dataset. This is a particular concern when translating algorithms to a clinical setting, as models may not be evaluated on an external dataset [287, 288], and as such their generalizability is in question. In general, clinical translation of AI-based technologies requires generalizable, robust models which are validated in prospective, randomized clinical trials, and this represents a key challenge to their adoption [289].

Recently, deep learning-based algorithms have been employed, which perform automated image segmentation [290, 291] without the requirement for feature engineering, though the potential for overfitting and a lack of generalizability can persist with such approaches. Deep learning (DL) is a widely researched area in radiobiology and radiation oncology with models being developed for tasks such as modeling outcomes using dose-volume metrics, radiomic feature discovery, image and tumor segmentation, and treatment outcome prediction.

One area where machine learning approaches have seen substantial application is in the development of methodologies utilizing medical imaging data such as CT, MRI, and PET for predictive modeling, particularly of radiotherapeutic outcome. In this instance, the field has been termed radiomics [292, 293]. Here the lack of standardized image acquisition protocols (e.g., slice thickness and tube current in CT) can affect the quality and reliability of the radiomic features extracted by automated algorithms [248, 249, 294, 295]. Often manual clinical delineation of regions of interest of prognostic value prior to modeling (which is termed "feature engineering") is utilized though this can introduce interobserver variability [296].

The success of radiomics in this context is in the development of "interpretable" machine learning or AI algorithms for a range of applications. Features may be extracted from 2D and 3D imaging data, reducing them to multiple features describing tumor intensity, shape, and texture [297]. These may subsequently be utilized to quantify tumor heterogeneity, where tumors with high heterogeneity have been shown to demonstrate resistance to treatment [298]. Once the features have been extracted machine learning or statistical learning can be applied to match feature patterns to "ground truth" data. Radiomic approaches have been applied to multiple imaging formats including CT, MRI, PET, and ultrasound [299–302]. These approaches have been successfully applied to segmentation and detection problems such as the differentiation of prostate cancers with Gleeson grade 6 and 7 [303], the discrimination of breast cancer subtypes [304] and in TNM staging [305]. Potential clinical applications of radiomics-based classification extend to the detection of lung nodules providing a prognostic and diagnostic aid to the clinician [306]. In terms of personalization of treatment, these approaches have been used to identify prostate cancer patients at risk of biochemical recurrence post-treatment from MRI-based imaging [307], to distinguish between HPV-positive and HPV-negative head and neck cancers [308] and to monitor the response to RT [309]. Similarly, ML models are also being examined in radiation genomics, or radiogenomics, which explores tumor and normal tissue response to radiation at a genomic level [310]. Linking imaging characteristics with genomic data has the potential to aid clinical cancer research and improve decision-making capabilities and personalize therapy [310–312]. Various deep learning methodologies are currently used to generate new knowledge from radiogenomic data including convolutional neural networks (CNNs) [313] and deep neural networks (DNNs) [314].

However, as highlighted earlier, significant challenges remain regarding the clinical interpretability of radiomic and radiogenomic analyses and models, image acquisition

standardization and data storage in the era of "big data" [292, 312, 315, 316]. Randomized controlled trials will remain the gold standard in evaluating diagnostic and prognostic interventions that are AI or ML based will be evaluated in oncology [317, 318], where data science approaches can also provide complementary information [319, 320].

5.16.3 Radiomics in Radiobiology and Clinical Oncology

5.16.3.1 Techniques in Medical Imaging

Several imaging modalities exist in radiology and nuclear medicine with different physical, acquisition, and reconstruction principles which have strengths and weaknesses but all of them are indispensable for differential diagnosis.

- Ultrasound sonography (USG) uses high-frequency mechanical waves to differentiate tissues based on various reflectivity on the tissue edges. USG is an affordable and inexpensive modality with minimal burden for the patient.
- Roentgenography (X-ray imaging, RX) uses electromagnetic waves with energy in the X-ray range most often between 40 and 120 keV. RX is a fast and inexpensive modality with small radiation exposure. If one collects thousands of 2D RX images from different angles, one can use computer algorithms for creating 3D images and one is talking about CT. Advantages of CT are in special resolution, high contrast, and 3D information; however, at the cost of high radiation exposure and higher price than RX.
- MRI also uses also electromagnetic waves as well as RX of CT but with an energy in the radio range most often between 240 and 500 neV which cannot ionize biological tissue (no radiation exposure) which is together with high tissue contrast advantage of MRI. The disadvantages are longer examination time (15–45 min), price, availability, and several contraindications.

Imaging methods in nuclear medicine are characterized by lower spatial resolution than the radiological methods mentioned above, but they contain very specific functional information. Small amount of a specific radiopharmaceutical is injected into the patient and then emitted gamma photons are detected. Depending on the isotope used, one speaks of positron emission tomography (PET, beta+ tracer) or single photon emission computed tomography (SPECT, gamma tracer). Both methods can be combined into hybrid modalities mostly with CT for obtaining anatomical information.

5.16.3.2 Main Steps in Medical Image Analysis

In the first step, it is necessary to find the pathological area(s) and make a basic description. The process that identifies such areas or, in general, *region of interest* (ROI) is named segmentation or delineation and can be done manually or with the support of ML algorithms. Manual segmentation is a time consuming and demanding task, with relatively low level of reproducibility so it is beneficial to use semi- or fully automatic methods.

Sometimes it is helpful to segment the pathology based on different histological tissue types, for example, necrotic part, active tumor, or edema but also precise anatomical localization, diameter or volume, shape, intensity, and changes compared to the previous examination.

After all variables are collected, the radiologist must decide which kinds of pathologies it could be. Occasionally, the radiological diagnoses are not unequivocal, for example, the pathology looks like high grade gliomas but with non-negligible probability it could be metastasis of some other primary tumor and the treatment of such different entities are completely different. Each hospital produces thousands of images per day, and it is obvious that usage of the same kind of computer algorithms or AI can save time, increase reproducibility and precision of diagnosis.

5.16.3.3 Radiomics: Definition, Features, and Examples

The concept of radiomics appeared in 2012 [321]. While the traditional analysis of imaging is based on the visual interpretation of simple features—such as tumor size, general shape, contrast uptake, or signal intensity—radiomics processes any type of imaging computationally and translates into complex quantitative data. Radiomics is based on qualitative and quantitative analyses, combining numerical data from medical imaging with clinical and biological characteristics to obtain predictive and/or prognostic information about patients. Indeed, the study of cellular interaction within tissues and intrinsic characteristics of medical imaging reflect the physiology and pathophysiology of the affected organ. The radiomics approach is: (1) Noninvasive; (2) Allows an evaluation of the studied tissues in their globality, thus characterizing their spatial heterogeneity; (3) Represents an easy way to follow the patient over time, allowing understanding the changes throughout the history of the disease and the therapeutic sequence. A typical radiomics workflow follows five steps as illustrated in Fig. 5.30.

Combining radiomics features with deep learning features or semantic features may further improve prognostic performance. The changes over time may also be integrated (delta-radiomics). Several studies have proven the effectiveness of using these features independently in predictive modeling. As was mentioned above, radiologists make basic

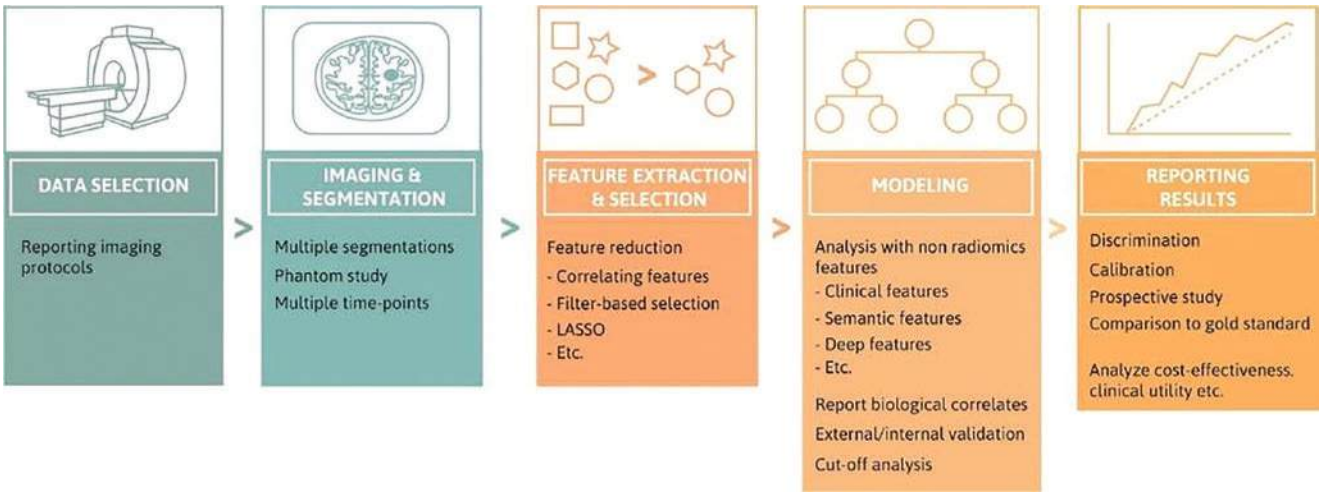

Fig. 5.30 Typical radiomics workflow. The different steps are: (1) Data selection: choosing the image to analyze, the imaging protocol to use and the correlated outcome. (2) Imaging and segmentation with (semi-) automatic methods to improve reproducibility. (3) Feature extraction and selection with appropriate algorithms. (4) Modeling using available machine learning models. (5) Reporting results. (Adopted from Keek et al. [322] with permission)

descriptions of pathology like volume, shape, etc. but the number of these descriptors are limited by the radiologist's time and his/her eyes. But there exist tens or hundreds of different descriptors which can describe pathology and a method which analyses all these descriptive parameters is called Radiomics and these parameters are called features.

One can divide radiomics features into several classes like: (1) First order; (2) Two and three (2D/3D) Shape and; (3) Grey level class (e.g., Size zone, Neighboring tone, Run length, Co-occurrence, Dependency).

The first order features (more than 15) characterized distribution of voxels intensities so they can be commonly known histogram parameters like median, mean, or several quartiles. But they also include mathematically sophisticated parameters like energy, entropy, mean absolute deviation, root mean squared, skewness, or kurtosis ("Sharpness of the peak").

Shape features (2D or 3D, more than 20) are intensity-independent parameters which are extracted from segmented binary mask image or triangle mash. For example, 2D features can be mesh surface, perimeter, sphericity, maximum 2D diameter or elongation. As 3D shape features, one can mention, for example, mesh volume, surface area to volume ratio, compactness, or flatness.

The biggest features class (which can be subdivided) with more than 50 features is grey level class. For example, grey level size zone features are trying to quantify connected voxels in an image which share the same intensity and one can extract features like grey level non-uniformity, size-zone non-uniformity, grey level variance or zone entropy, etc. Neighboring grey tone features quantify differences between intensity of voxel and average intensity of neighbors' voxels within defined distance and one can extract features like coarseness, contrast, complexity, or strength.

Radiomics create a model to predict clinical outcomes based on extracted features. Not all features have to be used, selection of features are done before modeling because lots of them are correlated to each other or can be unstable across a dataset. Clinical outcome which radiomics model can be diagnosis (benign or malignant, subtype or stage), treatment evaluation, or prognosis (survival coefficients).

5.16.3.4 Clinical Applications

These days there exist hundreds of papers which evaluate the usefulness of radiomics in clinical practice mostly on CT data, but MRI and PET are becoming more common. Radiomics can be used in diagnosis as well as treatment evaluation of different oncological diseases like brain tumors, breast, lung-, prostate-, or colorectal cancer. Radiomics are being applied in the field of oncology in different settings to help decision-making such as:

- Differentiation between human papillomavirus-positive and human papillomavirus-negative oropharyngeal tumors on contrast-enhanced CT [323].
- Prediction of tumor aggressiveness in prostate cancer [324].
- Assistance to automatic segmentation and sub-target volume definition in prostate cancer [325].
- Prediction of treatment response and outcome in head and neck and lung cancer (with combination of genomic features) [326–328], rectum [329], esophageal [330], or prostate cancer [331].

- Prediction of toxicity in head and neck (xerostomia) [332] and lung (pneumonitis) [333] cancers.
- Differential diagnosis between recurrence and RT-induced radionecrosis in brain [334].

Although promising, the predictive power sometimes evidenced in the pilot studies need to be externally validated in independent datasets with numerous methodological pitfalls including imaging technique standardization.

5.17 Exercises and Self-Assessment

Q1. What is meant by the "therapeutic window"? Mention several methods to widen the therapeutic window.

Q2. The tumor volume doubling time (VDT) is heterogeneous among tumors and influences RT response. Discuss and reflect on different parameters that control VDT of tumors.

Q3. It is important to estimate the growth fraction (GF) of tumors and several methods may be used in vitro and in vivo to assess this. Give some examples of methods and in what context they are applied.

Q4. Discuss the link between the Hallmarks of Radiobiology and the Hallmarks of Cancer.

Q5. Which of the below statements is wrong?
- (a) Lowering the dose rate leads to greater sparing of late responding normal tissues than of tumors.
- (b) The process of redistribution might push cells from a radioresistant to a radiosensitive cell-cycle phase.
- (c) During chronic low dose rate exposure, cells with long repair half times will be spared relative to their counterparts with rapid DNA damage repair.
- (d) Low dose rate irradiation can be considered as a form of extreme fractionation.

Q6. How can dose rate affect be explained in terms of linear-quadratic model?

Q7. What are the classical factors that are used to predict RT response in a tumor?

Q8. List four techniques which are used to measure biomarkers to predict RT response.

Q9. Oxygen enhancement ratio (OER) is seen with some but not all IR qualities. Please indicate which type (a–d) that doesn't have OER.
- (a) X-rays
- (b) Gamma-rays
- (c) Neutrons
- (d) α-particles

Q10. All of the following statements about hypoxic cell radiosensitizers are true except one, please indicate and explain.
- (a) Increases radiosensitivity of hypoxic cells
- (b) Nitroimidazole groups of drugs are commonly used
- (c) Presence of nitro group in second position, decreases electron affinity and sensitization
- (d) Dose-limiting toxicity of Misonidazole is neurotoxicity

Q11. Give some examples how photon radiation can induce modification extracellular signaling pathways.

Q12. Two principal mechanisms of tumor metabolism participate in radiation resistance. Give their names.

Q13. What is radiation-induced abscopal effect in oncology?

Q14. Describe the typical acute and late effects following exposure of the skin to radiation. Hints: target cells at risk, latent period, volume effect, pathology, recovery.

Q15. Define and describe the late adverse effects of RT.

Q16. Can radionecrosis be avoided by choosing a more appropriate radiation modality?

Q17. How can access to the forecasted 3D RT isodose curves allow for a better prevention of osteoradionecrosis of the mandible?

Q18. What is the main function of the stem cells?

Q19. What is the most radiosensitive group of stem cells?

Q20. Describe some different characteristics of cancer stem cells which may contribute to RT resistance?

Q21. Describe potential role of the intestinal microbiota in RT-induced adverse side effects (gut toxicity) or in RT efficiency concerning anti-tumor effects.

5.18 Exercise Solutions

SQ1. Therapeutic window: The difference between tumor control probability and normal tissue complication probability at identical irradiation dose. Methods to widen the therapeutic window: Dose fractionation, reduction of the normal tissue/organ at risk exposed volume, combination therapy.

SQ2. VDT is influenced by localization of the tumor, i.e., tumor site. It is also influenced if the tumor is a primary or a metastatic lesion where the latter often have reduced VDT as a result of limited nutrition and oxygen levels. VDT is also influenced by histology of the tumor, i.e., the inherited growth capacity of the cells. Finally, VDT is influenced by tumor heterogeneity in proliferative signaling cascades which is a consequence of different genomic- and signaling make ups of the individual tumors.

SQ3. In vitro tumor cell progression through S-phase can be monitored by BrdUrd or IdUrd-labeling of cells. These tracers are incorporated into DNA as tumor pass through S-phase and by using an antibody

against BrdUrd or IdUrd, cells in S-phase can be determined using flowcytometry. Another method utilizes 3H-thymidine to assess DNA-synthesis by flow cytometry. The third method is based on PET-analyses of tumors in vivo which have been pulsed with radio-labeled 18F-fluoro-3′-deoxy-3′-L-fluorothymidine (FLT). FLT is phosphorylated by Thymidine Kinase 1 which has an S-phase activity. Hence, FLT tracer levels are a surrogate for S-phase cells which can be evaluated by PET scanning. Finally, the proliferation rate in a tumor biopsy can be analyzed by immunohistochemical staining for the nuclear Ki-67 antigen, reflecting S-phase proportion of cells.

SQ4. Likely links are shown below.

Hallmark of radiobiology	Hallmark of cancer
Repair	Genomic instability and mutations, enabling replicative immortality
Redistribution	Sustaining proliferative signaling
Repopulation	Evading growth suppressors, sustaining proliferative signaling, tumor-promoting activation
Radiosensitivity	Resisting cell death, deregulating cellular energetics
Reoxygenation	Inducing angiogenesis
Reactivation of the immune response	Avoiding immune destruction, tumor-promoting activation, activation invasion and metastasis

SQ5. Alternative (c) is the wrong answer. Accumulation of DNA damage is larger in cells with long repair half times than for cells which show rapid repair of their DNA damages.

SQ6. Single-track and double-track actions can both induce DNA double strand breaks. There is no correlation between dose rate and single-track X-ray lesion (αcontribution in the LQ model). In a double-track action, different X-ray photon tracks produce the two interactions of single strand DNA lesions, and therefore the formation of double strand lesions is proportional to the radiation dose squared (β in the LQ model).

SQ7. Tumor oxygen status, the degree of repopulation or proliferation rate and intrinsic radiosensitivity.

SQ8. Proteomics, genomics, epigenomics, genomics, or transcriptomics, used for measuring proteins, DNA/chromatin, DNA, or RNA and transcription, respectively.

SQ9. Alternative (d). OER is 1 for high LET radiation like α- particles.

SQ10. Alternative (c). The presence of the nitro group in second position, increases electron affinity and radiosensitization.

SQ11. Photon beam activates major oncogenic signaling pathways such as Ras, MAPK/ERK, and PI3K/AKT in part via the epidermal growth factor receptor (EGFR) cascade. Radiation resistance is associated with these signaling cascades due to their pro-survival nature. For example, when AKT is phosphorylated, tumor cells are protected by decreased autophagy and apoptosis, as well as increased DNA repair capacity. Mutated RAS has also been associated with resistance to photons in cancer cells.

SQ12. The mitochondrial and or glucose metabolism, respectively.

SQ13. Abscopal effects are radiation-induced systemic anti-tumor immune responses in which irradiation of a primary tumor or large metastasis causes remission of distant, non-irradiated lesions.

SQ14. **Acute effects**: Dry skin (impairment of cell production), epilation (injury to hair follicles), erythema (vascular leakage). Latency time: Few weeks. Large volume effect: The smaller the volume, the higher the tolerance to radiation. Transient effect: Reversible injury. **Late effects**: Gangrene, ulcer, telangiectasia (vascular damage), fibrosis (increase in collagen fibers). Latency: Months-years. Large volume effect: The smaller the volume, the higher the tolerance to radiation. Chronic, irreversible injury.

SQ15. Late effects of radiation are progressive, irreversible and occur months, years, or decades after radiation therapy. They are based on an interactive response of parenchymal cells, vascular endothelium and fibroblasts, with a contribution from immune cells, especially macrophages. Tissues and organs are affected by atrophy, fibrosis, or necrosis, which can severely impair their functions and lead to a loss of function.

SQ16. No. Since the risk of radionecrosis remains life-long the affected tissues are at danger with the total radiation dose being the primary risk factor for the tissue involved, combined with other risk factors.

SQ17. Adapting the preventive extraction of teeth to the risk zone of >50–60 Gy would allow for a more appropriate dental management: more aggressive in the >60 Gy zone and far less aggressive in the other areas of the jaw, improving the quality of life of these patients. The fewer extractions in highly irradiated areas, the lesser the risk for ORN.

SQ18. The principal function of stem cells is to maintain tissue homeostasis including continuous regeneration and associated constant number of cells.

SQ19. Bone marrow stem cells.

SQ20. The answer is displayed in Fig. 5.29. In brief, CSC may have (1) Increased DNA repair capacity which allows them to handle IR-induced DNA DSBs; (2)

Increased signaling networks that block IR-induced cell death including deficient pro-apoptotic signaling and increased anti-apoptotic signaling; (3) CSCs have slow proliferation and may therefore not be so sensitivity to IR-induced DNA damage.

SQ21. Studies showed evidence of the existence of bidirectional effects of RT on the tumor and on the intestinal microbiota. In prospective clinical studies, a reduction of the fecal microbial diversity during and after pelvic RT was measured in patients suffering from intestinal complications. Also, RT-induced modification of microbiota diversity and composition can modify the host immune response and in turn the effectiveness of the anticancer treatment themselves including RT.

References

1. Borras JM, Lievens Y, Dunscombe P, Coffey M, Malicki J, Corral J, Gasparotto C, Defourny N, Barton M, Verhoeven R, van Eycken L, Primic-Zakelj M, Trojanowski M, Strojan P, Grau C. The optimal utilization proportion of external beam radiotherapy in European countries: an ESTRO-HERO analysis. Radiother Oncol. 2015;116(1):38–44. https://doi.org/10.1016/j.radonc.2015.04.018.
2. Nikjoo H, Uehara S, Wilson WE, Hoshi M, Goodhead DT. Track structure in radiation biology: theory and applications. Int J Radiat Biol. 1998;73(4):355–64. https://doi.org/10.1080/095530098142176.
3. Fowler JF. The linear-quadratic formula and progress in fractionated radiotherapy. Br J Radiol. 1989;62(740):679–94. https://doi.org/10.1259/0007-1285-62-740-679.
4. Moulder JE, Seymour C. Radiation fractionation: the search for isoeffect relationships and mechanisms. Int J Radiat Biol. 2018;94(8):743–51. https://doi.org/10.1080/09553002.2017.1376764.
5. Dörr W. Pathogenesis of normal-tissue side-effects. In: Joiner MC, van der Kogel AJ, editors. Basic clinical radiobiology. 4th ed. London: Hodder Arnold; 2009. p. 169–89.
6. Tinganelli W, Durante M. Carbon ion radiobiology. Cancers (Basel). 2020;12(10):3022. https://doi.org/10.3390/cancers12103022.
7. Vanderwaeren L, Dok R, Verstrepen K, Nuyts S. Clinical progress in proton radiotherapy: biological unknowns. Cancers (Basel). 2021;13(4):604. https://doi.org/10.3390/cancers13040604.
8. Grellier N, Belkacemi Y. Effets biologiques des hautes doses par fraction [Biologic effects of high doses per fraction]. Cancer Radiother. 2020;24(2):153–8. https://doi.org/10.1016/j.canrad.2019.06.017.
9. Lin B, Gao F, Yang Y, Wu D, Zhang Y, Feng G, Dai T, Du X. FLASH radiotherapy: history and future. Front Oncol. 2021;11:644400. https://doi.org/10.3389/fonc.2021.644400.
10. McBride WH, Schaue D. Radiation-induced tissue damage and response. J Pathol. 2020;250(5):647–55. https://doi.org/10.1002/path.5389.
11. Marks LB, Yorke ED, Jackson A, Ten Haken RK, Constine LS, Eisbruch A, Bentzen SM, Nam J, Deasy JO. Use of normal tissue complication probability models in the clinic. Int J Radiat Oncol Biol Phys. 2010;76(3 Suppl):S10–9. https://doi.org/10.1016/j.ijrobp.2009.07.1754.
12. Higgins GS, O'Cathail SM, Muschel RJ, McKenna WG. Drug radiotherapy combinations: review of previous failures and reasons for future optimism. Cancer Treat Rev. 2015;41(2):105–13. https://doi.org/10.1016/j.ctrv.2014.12.012.
13. Hall EJ, Giaccia AJ, editors. Radiobiology for the radiologist. 8th ed. Philadelphia, PA: Wolters Kluwer; 2019.
14. Khaled S, Held K. Radiation biology: a handbook for teachers and students. 1st ed. International Atomic Energy Agency; 2012.
15. Podgorsak EB. Radiation oncology physics. 1st ed. Vienna: IAEA; 2005.
16. Joiner MC, Van der Kogel AJ. Basic clinical radiobiology. 5th ed. CRC Press; 2018.
17. Shrieve DC, Loeffler JS, editors. Human radiation injury. 1st ed. Lippincott Williams & Wilkins; 2011.
18. Khan FM, Sperduto PW, Gibbons JP. Khan's treatment planning in radiation oncology. Lippincott Williams & Wilkins; 2016.
19. Chang DS, Lasley FD, Das IJ, Mendonca MS, Dynlacht JR. Basic radiotherapy physics and biology. 1st ed. Springer International Publishing; 2014.
20. Mayles P, Nahum A, Rosenwald J. Handbook of radiotherapy physics: theory and practice. 1st ed. CRC Press; 2007.
21. Alpen E. Radiation biophysics. 2nd ed. Academic Press; 1997.
22. Halperin E, Brady L, Wazer D, Perez C. Perez & Brady's principles and practice of radiation oncology. 7th ed. Wolters Kluwer Health/Lippincott Williams & Wilkins; 2019.
23. Miller I, Min M, Yang C, Tian C, Gookin S, Carter D, Spencer SL. Ki67 is a graded rather than a binary marker of proliferation versus quiescence. Cell Rep. 2018;24(5):1105–1112.e5. https://doi.org/10.1016/j.celrep.2018.06.110.
24. Hall EJ, Giaccia AJ. Radiobiology for the radiologist. Philadelphia: Lippincott Wilkins & Williams; 2006.
25. Withers HR. The four R's of radiotherapy. In: Advances in radiation biology, vol. 5. Elsevier; 1975. p. 241–71.
26. Steel GG, McMillan TJ, Peacock JH. The 5Rs of radiobiology. Int J Radiat Biol. 1989;56(6):1045–8. https://doi.org/10.1080/09553008914552491.
27. Boustani J, Grapin M, Laurent PA, Apetoh L, Mirjolet C. The 6th R of radiobiology: reactivation of anti-tumor immune response. Cancers (Basel). 2019;11(6):860. https://doi.org/10.3390/cancers11060860.
28. Lehnert S. Biomolecular action of ionizing radiation. 1st ed. CRC Press; 2007.
29. Shuryak I, Hall EJ, Brenner DJ. Dose dependence of accelerated repopulation in head and neck cancer: supporting evidence and clinical implications. Radiother Oncol. 2018;127(1):20–6. https://doi.org/10.1016/j.radonc.2018.02.015.
30. Daguenet E, Khalifa J, Tolédano A, Borchiellini D, Pointreau Y, Rodriguez-Lafrasse C, Chargari C, Magné N. To exploit the 5 'R' of radiobiology and unleash the 3 'E' of immunoediting: 'RE'-inventing the radiotherapy-immunotherapy combination. Ther Adv Med Oncol. 2020;12:1758835920913445. https://doi.org/10.1177/1758835920913445.
31. Hanahan D, Weinberg RA. Hallmarks of cancer: the next generation. Cell. 2011;144(5):646–74. https://doi.org/10.1016/j.cell.2011.02.013.
32. Bristow RG, Alexander B, Baumann M, Bratman SV, Brown JM, Camphausen K, Choyke P, Citrin D, Contessa JN, Dicker A, Kirsch DG, Krause M, Le QT, Milosevic M, Morris ZS, Sarkaria JN, Sondel PM, Tran PT, Wilson GD, Willers H, Wong RKS, Harari PM. Combining precision radiotherapy with molecular targeting and immunomodulatory agents: a guideline by the American Society for Radiation Oncology. Lancet Oncol. 2018;19(5):e240–51. https://doi.org/10.1016/s1470-2045(18)30096-2.
33. Harrington K, Jankowska P, Hingorani M. Molecular biology for the radiation oncologist: the 5Rs of radiobiology meet the hallmarks of cancer. Clin Oncol (R Coll Radiol). 2007;19(8):561–71. https://doi.org/10.1016/j.clon.2007.04.009.

34. Withers HR, Taylor JM, Maciejewski B. The hazard of accelerated tumor clonogen repopulation during radiotherapy. Acta Oncol. 1988;27:131–146.
35. Mitchell JB, Bedford JS, Bailey SM. Dose-rate effects in mammalian cells in culture III. Comparison of cell killing and cell proliferation during continuous irradiation for six different cell lines. Radiat Res. 1979;79:537–51.
36. Friedl AA, Prise KM, Butterworth KT, Montay-Gruel P, Favaudon V. Radiobiology of the FLASH effect. Med Phys. 2021; https://doi.org/10.1002/mp.15184. Epub ahead of print.
37. Sabloff M, Tisseverasinghe S, Babadagli ME, Samant R. Total body irradiation for hematopoietic stem cell transplantation: what can we agree on? Curr Oncol. 2021;28(1):903–17.
38. Gore EM, Lawton CA, Ash RC, Lipchik RJ. Pulmonary function changes in long-term survivors of bone marrow transplantation. Int J Radiat Oncol Biol Phys. 1996;36(1):67–75. https://doi.org/10.1016/S0360-3016(96)00123-X.
39. Soule BP, Simone NL, Savani BN, Ning H, Albert PS, Barrett AJ, Singh AK. Pulmonary function following total body irradiation (with or without lung shielding) and allogeneic peripheral blood stem cell transplant. Bone Marrow Transplant. 2007;40(6):573–8. https://doi.org/10.1038/sj.bmt.1705771.
40. Wheldon TE. The radiobiological basis of total body irradiation. Br J Radiol. 1997;70(840):1204–7. https://doi.org/10.1259/bjr.70.840.9505837.
41. Spencer K, Parrish R, Barton R, Henry A. Palliative radiotherapy. BMJ. 2018;23(360):k821. https://doi.org/10.1136/bmj.k821.
42. Sakamoto K. Radiobiological basis for cancer therapy by total or half-body irradiation. Nonlinearity Biol Toxicol Med. 2004;2(4):293–316. https://doi.org/10.1080/15401420490900254.
43. Hoeben BAW, Pazos M, Albert MH, Seravalli E, Bosman ME, Losert C, et al. Towards homogenization of total body irradiation practices in pediatric patients across SIOPE affiliated centers. A survey by the SIOPE radiation oncology working group. Radiother Oncol. 2021;155:113–9. https://doi.org/10.1016/j.radonc.2020.10.032.
44. Cosset JM, Girinsky T, Malaise E, Chaillet MP, Dutreix J. Clinical basis for TBI fractionation. Radiother Oncol. 1990;18(Suppl 1):60–7. https://doi.org/10.1016/0167-8140(90)90179-Z.
45. Thomas ED, Clift RA, Hersman J, Sanders JE, Stewart P, Buckner CD, et al. Marrow transplantation for acute nonlymphoblastic leukemia in first remission using fractionated or single-dose irradiation. Int J Radiat Oncol Biol Phys. 1982;8(5):817–21. https://doi.org/10.1016/0360-3016(82)90083-9.
46. Cheng J, Schultheiss T, Wong J. (2008). Impact of drug therapy, radiation dose, and dose rate on renal toxicity following bone marrow transplantation. Int J Radiat Oncol Biol Phys. 2008;71(5):1436–43. https://doi.org/10.1016/j.ijrobp.2007.12.009.
47. Gogna N, Morgan G, Downs K, Atkinson K, Biggs J. Lung dose rate and interstitial pneumonitis in total body irradiation for bone marrow transplantation. Australas Radiol. 1992;36(4):317–20. https://doi.org/10.1111/j.1440-1673.1992.tb03208.x.
48. Kim TH, Rybka WB, Lehnert S, Podgorsak EB, Freeman CR. Interstitial pneumonitis following total body irradiation for bone marrow transplantation using two different dose rates. Int J Radiat Oncol Biol Phys. 1985;11(7):1285–91. https://doi.org/10.1016/0360-3016(85)90243-3.
49. Graves SS, Storer BE, Butts TM, Storb R. Comparing high and low total body irradiation dose rates for minimum-intensity conditioning of dogs for dog leukocyte antigen-identical bone marrow grafts. Biol Blood Marrow Transplant. 2013;19(11):1650–4. https://doi.org/10.1016/j.bbmt.2013.08.007.
50. Storb R, Raff RF, Appelbaum FR, Deeg HJ, Graham TC, Schuening FG, Sale G, Bryant E, Seidel K. Fractionated versus single-dose total body irradiation at low and high dose rates to condition canine littermates for DLA-identical marrow grafts. Blood. 1994;83(11):3384–9. https://doi.org/10.1182/blood.V83.11.3384.3384.
51. Begg AC. Predicting response to radiotherapy: evolutions and revolutions. Int J Radiat Biol. 2009;85(10):825–36.
52. Torres-Roca JF, Stevens CW. Predicting response to clinical radiotherapy: past, present, and future directions. Cancer Control. 2008;15(2):151–6. https://doi.org/10.1177/107327480801500207.
53. Yaromina A, Krause M, Baumann M. Individualization of cancer treatment from radiotherapy perspective. Mol Oncol. 2012;6(2):211–21. https://doi.org/10.1016/j.molonc.2012.01.007.
54. Hirst DG, Robson T. Molecular biology: the key to personalised treatment in radiation oncology? Br J Radiol. 2010;83(993):723–8. https://doi.org/10.1259/bjr/91488645.
55. Overgaard J, Hansen HS, Overgaard M, Bastholt L, Berthelsen A, Specht L, Lindeløv B, Jørgensen K. A randomized double-blind phase III study of nimorazole as a hypoxic radiosensitizer of primary radiotherapy in supraglottic larynx and pharynx carcinoma. Results of the Danish Head and Neck Cancer Study (DAHANCA) Protocol 5-85. Radiother Oncol. 1998;46(2):135–46. https://doi.org/10.1016/S0167-8140(97)00220-X.
56. West C, Davidson S, Roberts S, Hunter R. Intrinsic radiosensitivity and prediction of patient response to radiotherapy for carcinoma of the cervix. British journal of cancer. 1993;68(4):819–23. https://doi.org/10.1038/bjc.1993.434.
57. Lee JM, Bernstein A. p53 mutations increase resistance to ionizing radiation. Proc Natl Acad Sci U S A. 1993;90(12):5742–6.
58. Papathanasiou MA, Kerr NC, Robbins JH, McBride OW, Alamo I Jr, Barrett SF, Hickson ID, Fornace AJ Jr. Induction by ionizing radiation of the gadd45 gene in cultured human cells: lack of mediation by protein kinase C. Mol Cell Biol. 1991;11(2):1009–16.
59. Filipowicz W, Bhattacharyya SN, Sonenberg N. Mechanisms of post-transcriptional regulation by microRNAs: are the answers in sight? Nat Rev Genet. 2008;9(2):102–14. https://doi.org/10.1038/nrg2290.
60. Brown JM. Tumor hypoxia, drug resistance, and metastases. J Natl Cancer Inst. 1990;82:338–9.
61. Chaplin DJ, Olive PL, Durand RE. Intermittent blood flow in a murine tumor: radiobiological effects. Cancer Res. 1987;47(2):597–601.
62. Thomlinson RH, Gray LH. The histological structure of some human lung cancers and the possible implications for radiotherapy. Br J Cancer. 1955;9(4):539–49. https://doi.org/10.1038/bjc.1955.55.
63. van Putten LM. Tumour reoxygenation during fractionated radiotherapy; studies with a transplantable mouse osteosarcoma. Eur J Cancer. 1968;4(2):172–82. https://doi.org/10.1016/0014-2964(68)90015-7.
64. Wright EA, Howard-Flanders P. The influence of oxygen on the radiosensitivity of mammalian tissues. Acta Radiol. 1957;48(1):26–32. https://doi.org/10.3109/00016925709170930.
65. Palcic B, Skarsgard LD. Reduced oxygen enhancement ratio at low doses of ionizing radiation. Radiat Res. 1984;100(2):328–39.
66. Barendsen GW, Koot CJ, Van Kersen GR, Bewley DK, Field SB, Parnell CJ. The effect of oxygen on impairment of the proliferative capacity of human cells in culture by ionizing radiations of different LET. Int J Radiat Biol Relat Stud Phys Chem Med. 1966;10(4):317–27. https://doi.org/10.1080/09553006614550421.
67. Broerse JJ, Barendsen GW, van Kersen GR. Survival of cultured human cells after irradiation with fast neutrons of different energies in hypoxic and oxygenated conditions. Int J Radiat Biol Relat Stud Phys Chem Med. 1968;13(6):559–72. https://doi.org/10.1080/09553006814550621.
68. Koumenis C, Wouters BG. "Translating" tumor hypoxia: unfolded protein response (UPR)-dependent and UPR-independent pathways. Mol Cancer Res. 2006;4(7):423–36. https://doi.org/10.1158/1541-7786.MCR-06-0150.

69. Koritzinsky M, Levitin F, van den Beucken T, Rumantir RA, Harding NJ, Chu KC, Boutros PC, Braakman I, Wouters BG. Two phases of disulfide bond formation have differing requirements for oxygen. J Cell Biol. 2013;203(4):615–27. https://doi.org/10.1083/jcb.201307185.
70. Bartoszewska S, Collawn JF. Unfolded protein response (UPR) integrated signaling networks determine cell fate during hypoxia. Cell Mol Biol Lett. 2020;25:18. https://doi.org/10.1186/s11658-020-00212-1.
71. Harding HP, Zhang Y, Zeng H, Novoa I, Lu PD, Calfon M, Sadri N, Yun C, Popko B, Paules R, Stojdl DF, Bell JC, Hettmann T, Leiden JM, Ron D. An integrated stress response regulates amino acid metabolism and resistance to oxidative stress. Mol Cell. 2003;11(3):619–33. https://doi.org/10.1016/S1097-2765(03)00105-9.
72. Singleton DC, Harris AL. Targeting the ATF4 pathway in cancer therapy. Expert OpinTher Targets. 2012;16(12):1189–202. https://doi.org/10.1517/14728222.2012.728207.
73. Colliez F, Gallez B, Jordan BF. Assessing tumor oxygenation for predicting outcome in radiation oncology: a review of studies correlating tumor hypoxic status and outcome in the preclinical and clinical settings. Front Oncol. 2017;7:10. https://doi.org/10.3389/fonc.2017.00010.
74. Griffiths JR, Robinson SP. TheOxyLite: a fibre-optic oxygen sensor. Br J Radiol. 1999;72(859):627–30. https://doi.org/10.1259/bjr.72.859.10624317.
75. Varia MA, Calkins-Adams DP, Rinker LH, Kennedy AS, Novotny DB, Fowler WC Jr, Raleigh JA. Pimonidazole: a novel hypoxia marker for complementary study of tumor hypoxia and cell proliferation in cervical carcinoma. Gynecol Oncol. 1998;71(2):270–7. https://doi.org/10.1006/gyno.1998.5163.
76. Komar G, Seppänen M, Eskola O, Lindholm P, Grönroos TJ, Forsback S, Sipilä H, Evans SM, Solin O, Minn H. 18F-EF5: a new PET tracer for imaging hypoxia in head and neck cancer. J Nucl Med. 2008;49(12):1944–51. https://doi.org/10.2967/jnumed.108.053785.
77. Al-Arafaj A, Ryan EA, Hutchison K, Mannan RH, Mercer J, Wiebe LI, AJ ME. An evaluation of iodine-123 iodoazomycinarabinoside as a marker of localized tissue hypoxia in patients with diabetes mellitus. Eur J Nucl Med. 1994;21(12):1338–42. https://doi.org/10.1007/BF02426699.
78. Lyng H, Malinen E. Hypoxia in cervical cancer: from biology to imaging. Clin Transl Imaging. 2017;5(4):373–88. https://doi.org/10.1007/s40336-017-0238-7.
79. Kjellen E, Joiner MC, Collier JM, Johns H, Rojas A. A therapeutic benefit from combining normobaric carbogen or oxygen with nicotinamide in fractionated X-ray treatments. Radiother Oncol. 1991;22(2):81–91.https://doi.org/10.1016/0167-8140(91)90002-X.
80. Tharmalingham H, Hoskin P. Clinical trials targeting hypoxia. Br J Radiol. 2019 Jan;92(1093):20170966.
81. Adams GE, Flockhart IR, Smithen CE, Stratford IJ, Wardman P, Watts ME. Electron-affinic sensitization. VII. A correlation between structures, one-electron reduction potentials, and efficiencies of nitroimidazoles as hypoxic cell radiosensitizers. Radiat Res. 1976;67(1):9–20.
82. Hall EJ, Giaccia AJ. The biology and exploitation of tumor hypoxia. In: Hall EJ, Giaccia AJ, editors. Radiobiology for the radiologist. 8th ed. Philadelphia, PA: Wolters Kluwer; 2019. p. 825–46.
83. Sheldon PW, Foster JL, Fowler JF. Radiosensitization of C3H mouse mammary tumours by a 2-nitroimidazole drug. Br J Cancer. 1974;30(6):560–5. https://doi.org/10.1038/bjc.1974.235.
84. Zeman EM, Hirst VK, Lemmon MJ, Brown JM. Enhancement of radiation-induced tumor cell killing by the hypoxic cell toxin SR 4233. Radiother Oncol. 1988;12(3):209–18. https://doi.org/10.1016/0167-8140(88)90263-0.
85. Stratford IJ, Stephens MA. The differential hypoxic cytotoxicity of bioreductive agents determined in vitro by the MTT assay. Int J Radiat Oncol Biol Phys. 1989;16(4):973–6. https://doi.org/10.1016/0360-3016(89)90898-5.
86. Welz S, Mönnich D, Pfannenberg C, Nikolaou K, Reimold M, La Fougère C, Reischl G, Mauz PS, Paulsen F, Alber M, Belka C, Zips D, Thorwarth D. Prognostic value of dynamic hypoxia PET in head and neck cancer: results from a planned interim analysis of a randomized phase II hypoxia-image guided dose escalation trial. Radiother Oncol. 2017;124(3):526–32. https://doi.org/10.1016/j.radonc.2017.04.004.
87. Daniel M, Andrzejewski P, Sturdza A, Majercakova K, Baltzer P, Pinker K, Wadsak W, Mitterhauser M, Pötter R, Georg P, Helbich T, Georg D. Impact of hybrid PET/MR technology on multiparametric imaging and treatment response assessment of cervix cancer. Radiother Oncol. 2017;125(3):420–5. https://doi.org/10.1016/j.radonc.2017.10.036.
88. Elamir AM, Stanescu T, Shessel A, Tadic T, Yeung I, Letourneau D, Kim J, Lukovic J, Dawson LA, Wong R, Barry A, Brierley J, Gallinger S, Knox J, O'Kane G, Dhani N, Hosni A, Taylor E. Simulated dose painting of hypoxic sub-volumes in pancreatic cancer stereotactic body radiotherapy. Phys Med Biol. 2021;66(18) https://doi.org/10.1088/1361-6560/ac215c.
89. Even AJ, van der Stoep J, Zegers CM, Reymen B, Troost EG, Lambin P, van Elmpt W. PET-based dose painting in non-small cell lung cancer: comparing uniform dose escalation with boosting hypoxic and metabolically active sub-volumes. Radiother Oncol. 2015;116(2):281–6. https://doi.org/10.1016/j.radonc.2015.07.013.
90. de Mey S, Dufait I, Jiang H, Corbet C, Wang H, Van De Gucht M, Kerkhove L, Law KL, Vandenplas H, Gevaert T, Feron O, De Ridder M. Dichloroacetate radiosensitizes hypoxic breast cancer cells. Int J Mol Sci. 2020;21(24):9367. https://doi.org/10.3390/ijms21249367.
91. Zannella VE, Dal Pra A, Muaddi H, McKee TD, Stapleton S, Sykes J, Glicksman R, Chaib S, Zamiara P, Milosevic M, Wouters BG, Bristow RG, Koritzinsky M. Reprogramming metabolism with metformin improves tumor oxygenation and radiotherapy response. Clin Cancer Res. 2013;19(24):6741–50. https://doi.org/10.1158/1078-0432.CCR-13-1787.
92. Tao J, Yang G, Zhou W, Qiu J, Chen G, Luo W, Zhao F, You L, Zheng L, Zhang T, Zhao Y. Targeting hypoxic tumor microenvironment in pancreatic cancer. J Hematol Oncol. 2021;14(1):14. https://doi.org/10.1186/s13045-020-01030-w.
93. Liu YP, Zheng CC, Huang YN, He ML, Xu WW, Li B. Molecular mechanisms of chemo- and radiotherapy resistance and the potential implications for cancer treatment. MedComm. 2021;2(3):315–40. https://doi.org/10.1002/mco2.55.
94. Galeaz C, Totis C, Bisio A. Radiation resistance: a matter of transcription factors. Front Oncol. 2021;11:662840. https://doi.org/10.3389/fonc.2021.662840.
95. Tang L, Wei F, Wu Y, He Y, Shi L, Xiong F, Gong Z, Guo C, Li X, Deng H, Cao K, Zhou M, Xiang B, Li X, Li Y, Li G, Xiong W, Zeng Z. Role of metabolism in cancer cell radioresistance and radiosensitization methods. J Exp Clin Cancer Res. 2018;37(1):87. https://doi.org/10.1186/s13046-018-0758-7.
96. Chen HHW, Kuo MT. Improving radiotherapy in cancer treatment: Promises and challenges. Oncotarget. 2017;8(37):62742–58. https://doi.org/10.18632/oncotarget.18409.
97. Morgan MA, Lawrence TS. Molecular pathways: overcoming radiation resistance by targeting DNA damage response pathways. Clin Cancer Res. 2015;21(13):2898–904. https://doi.org/10.1158/1078-0432.CCR-13-3229.
98. Bhattacharya S, Asaithamby A. Repurposing DNA repair factors to eradicate tumor cells upon radiotherapy. Transl Cancer

Res. 2017;6(Suppl 5):S822–39. https://doi.org/10.21037/tcr.2017.05.22.
99. Helleday T, Petermann E, Lundin C, Hodgson B, Sharma RA. DNA repair pathways as targets for cancer therapy. Nat Rev Cancer. 2008;8(3):193–204. https://doi.org/10.1038/nrc2342.
100. Huang R, Zhou PK. DNA damage repair: historical perspectives, mechanistic pathways and clinical translation for targeted cancer therapy. Signal Transduct Target Ther. 2021;6(1):254. https://doi.org/10.1038/s41392-021-00648-7.
101. Jackson SP, Bartek J. The DNA-damage response in human biology and disease. Nature. 2009;461(7267):1071–8. https://doi.org/10.1038/nature08467.
102. Kiwerska K, Szyfter K. DNA repair in cancer initiation, progression, and therapy-a double-edged sword. J Appl Genet. 2019;60(3–4):329–34. https://doi.org/10.1007/s13353-019-00516-9.
103. Al-Dimassi S, Abou-Antoun T, El-Sibai M. Cancer cell resistance mechanisms: a mini review. Clin Transl Oncol. 2014;16(6):511–6. https://doi.org/10.1007/s12094-014-1162-1.
104. Squatrito M, Brennan CW, Helmy K, Huse JT, Petrini JH, Holland EC. Loss of ATM/Chk2/p53 pathway components accelerates tumor development and contributes to radiation resistance in gliomas. Cancer Cell. 2010;18(6):619–29. https://doi.org/10.1016/j.ccr.2010.10.034.
105. Zhang P, Wei Y, Wang L, Debeb BG, Yuan Y, Zhang J, Yuan J, Wang M, Chen D, Sun Y, Woodward WA, Liu Y, Dean DC, Liang H, Hu Y, Ang KK, Hung MC, Chen J, Ma L. ATM-mediated stabilization of ZEB1 promotes DNA damage response and radioresistance through CHK1. Nat Cell Biol. 2014;16(9):864–75. https://doi.org/10.1038/ncb3013.
106. Kotula E, Berthault N, Agrario C, Lienafa MC, Simon A, Dingli F, Loew D, Sibut V, Saule S, Dutreix M. DNA-PKcs plays role in cancer metastasis through regulation of secreted proteins involved in migration and invasion. Cell Cycle. 2015;14(12):1961–72. https://doi.org/10.1080/15384101.2015.1026522.
107. Srivastava M, Nambiar M, Sharma S, Karki SS, Goldsmith G, Hegde M, Kumar S, Pandey M, Singh RK, Ray P, Natarajan R, Kelkar M, De A, Choudhary B, Raghavan SC. An inhibitor of nonhomologous end-joining abrogates double-strand break repair and impedes cancer progression. Cell. 2012;151(7):1474–87. https://doi.org/10.1016/j.cell.2012.11.054.
108. Kan C, Zhang J. BRCA1 mutation: a predictive marker for radiation therapy? Int J Radiat Oncol Biol Phys. 2015;93(2):281–93. https://doi.org/10.1016/j.ijrobp.2015.05.037.
109. Kinzel L, Ernst A, Orth M, Albrecht V, Hennel R, Brix N, Frey B, Gaipl US, Zuchtriegel G, Reichel CA, Blutke A, Schilling D, Multhoff G, Li M, Niyazi M, Friedl AA, Winssinger N, Belka C, Lauber K. A novel HSP90 inhibitor with reduced hepatotoxicity synergizes with radiotherapy to induce apoptosis, abrogate clonogenic survival, and improve tumor control in models of colorectal cancer. Oncotarget. 2016;7(28):43199–219. https://doi.org/10.18632/oncotarget.9774.
110. Madhusudan S. Evolving drug targets in DNA base excision repair for cancer therapy. Curr Mol Pharmacol. 2012;5(1):1–2. https://doi.org/10.2174/1874467211205010001.
111. Li LY, Guan YD, Chen XS, Yang JM, Cheng Y. DNA repair pathways in cancer therapy and resistance. Front Pharmacol. 2021;11:629266. https://doi.org/10.3389/fphar.2020.629266.
112. Baptistella AR, Landemberger MC, Dias MVS, Giudice FS, Rodrigues BR, da Silva PPCE, Cassinela EK, Lacerda TC, Marchi FA, Leme AFP, Begnami MD, Aguiar S Jr, Martins VR. Rab5C enhances resistance to ionizing radiation in rectal cancer. J Mol Med (Berl). 2019;97(6):855–69. https://doi.org/10.1007/s00109-019-01760-6.
113. Uraki S, Ariyasu H, Doi A, Kawai S, Takeshima K, Morita S, Fukai J, Fujita K, Furuta H, Nishi M, Sugano K, Inoshita N, Nakao N, Yamada S, Akamizu T. Reduced expression of mismatch repair genes MSH6/MSH2 directly promotes pituitary tumor growth via the ATR-Chk1 pathway. J Clin Endocrinol Metab. 2018;103(3):1171–9. https://doi.org/10.1210/jc.2017-02332.
114. Peng H, Yao S, Dong Q, Zhang Y, Gong W, Jia Z, Yan L. Excision repair cross-complementing group 1 (ERCC1) overexpression inhibits cell apoptosis and is associated with unfavorable prognosis of esophageal squamous cell carcinoma. Medicine (Baltimore). 2018;97(31):e11697. https://doi.org/10.1097/MD.0000000000011697.
115. Li Q, Ma R, Zhang M. XRCC1 rs1799782 (C194T) polymorphism correlated with tumor metastasis and molecular subtypes in breast cancer. Onco Targets Ther. 2018;11:8435–44. https://doi.org/10.2147/OTT.S154746.
116. Brewer MR, Yun CH, Lai D, Lemmon MA, Eck MJ, Pao W. Mechanism for activation of mutated epidermal growth factor receptors in lung cancer. Proc Natl Acad Sci. 2013;110(38):E3595–604. https://doi.org/10.1073/pnas.1220050110.
117. Endres NF, Barros T, Cantor AJ, Kuriyan J. Emerging concepts in the regulation of the EGF receptor and other receptor tyrosine kinases. Trends Biochem Sci. 2014;39(10):437–46. https://doi.org/10.1016/j.tibs.2014.08.001.
118. Fidler IJ, Kim SJ, Langley RR. The role of the organ microenvironment in the biology and therapy of cancer metastasis. J Cell Biochem. 2007;101(4):927–36. https://doi.org/10.1002/jcb.21148.
119. Rodemann HP, Dittmann K, Toulany M. Radiation-induced EGFR-signaling and control of DNA-damage repair. Int J Radiat Biol. 2007;83(11–12):781–91. https://doi.org/10.1080/09553000701769970.
120. Schmidt-Ullrich RK, Mikkelsen RB, Dent PE, Todd DG, Valerie K, Kavanagh BD, Chen PB. Radiation-induced proliferation of the human A431 squamous carcinoma cells is dependent on EGFR tyrosine phosphorylation. Oncogene. 1997;15(10):1191–7. https://doi.org/10.1038/sj.onc.1201275.
121. Affolter A, Fruth K, Brochhausen C, Schmidtmann I, Mann WJ, Brieger J. Activation of mitogen-activated protein kinase extracellular signal-related kinase in head and neck squamous cell carcinomas after irradiation as part of a rescue mechanism. Head Neck. 2011;33(10):1448–57. https://doi.org/10.1002/hed.21623. Epub 2010 Nov 10.
122. Grana TM, Rusyn EV, Zhou H, Sartor CI, Cox AD. Ras mediates radioresistance through both phosphatidylinositol 3-kinase-dependent and Raf-dependent but mitogen-activated protein kinase/extracellular signal-regulated kinase kinase-independent signaling pathways. Cancer Res. 2002;62(14):4142–50.
123. Konings K, Vandevoorde C, Baselet B, Baatout S, Moreels M. Combination therapy with charged particles and molecular targeting: a promising avenue to overcome radioresistance. Front Oncol. 2020:128. https://doi.org/10.3389/fonc.2020.00128.
124. Toulany M, Kasten-Pisula U, Brammer I, Wang S, Chen J, Dittmann K, Baumann M, Dikomey E, Rodemann HP. Blockage of epidermal growth factor receptor-phosphatidylinositol 3-kinase-AKT signaling increases radiosensitivity of K-RAS mutated human tumor cells in vitro by affecting DNA repair. Clin Cancer Res. 2006;12(13):4119–26. https://doi.org/10.1158/1078-0432.CCR-05-2454.
125. Kim TJ, Lee JW, Song SY, Choi JJ, Choi CH, Kim BG, et al. Increased expression of pAKT is associated with radiation resistance in cervical cancer. Br J Cancer. 2006;94(11):1678–82.
126. Thiery JP, Sleeman JP. Complex networks orchestrate epithelial-mesenchymal transitions. Nat Rev Mol Cell Biol. 2006;7(2):131–42. https://doi.org/10.1038/nrm1835.
127. Kalluri R, Weinberg RA. The basics of epithelial-mesenchymal transition. J Clin Invest. 2009;119(6):1420–8. https://doi.org/10.1172/JCI39104.
128. Weinberg RA. The biology of cancer. Garland Science; 2013.

129. Weinberg RA. The biology of cancer, vol. 544. 1st ed. New York: Garland Science, Taylor & Francis Group, LLC; 2007. p. 560–1.
130. Kawamoto A, Yokoe T, Tanaka K, Saigusa S, Toiyama Y, Yasuda H, et al. Radiation induces epithelial-mesenchymal transition in colorectal cancer cells. Oncol Rep. 2012;27(1):51–7. https://doi.org/10.3892/or.2011.1485.
131. Sahlgren C, Gustafsson MV, Jin S, Poellinger L, Lendahl U. Notch signaling mediates hypoxia-induced tumor cell migration and invasion. Proc Natl Acad Sci U S A. 2008;105(17):6392–7. https://doi.org/10.1073/pnas.0802047105.
132. Rhyu DY, Yang Y, Ha H, Lee GT, Song JS, Uh ST, Lee HB. Role of reactive oxygen species in TGF-1-induced mitogen-activated protein kinase activation and epithelial-mesenchymal transition in renal tubular epithelial cells. J Am Soc Nephrol. 2005;16:667–75.
133. Leong KG, Niessen K, Kulic I, Raouf A, Eaves C, Pollet I, Karsan A. Jagged1-mediated Notch activation induces epithelial-to-mesenchymal transition through Slug-induced repression of E-cadherin. J Exp Med. 2007;204(12):2935–48. https://doi.org/10.1084/jem.20071082.
134. Marambaud P, Shioi J, Serban G, Georgakopoulos A, Sarner S, Nagy V, Baki L, Wen P, Efthimiopoulos S, Shao Z, Wisniewski T, Robakis NK. A presenilin-1/gamma-secretase cleavage releases the E-cadherin intracellular domain and regulates disassembly of adherens junctions. EMBO J. 2002;21(8):1948–56. https://doi.org/10.1093/emboj/21.8.1948.
135. Zavadil J, Cermak L, Soto-Nieves N, Böttinger EP. Integration of TGF-beta/Smad and Jagged1/Notch signalling in epithelial-to-mesenchymal transition. EMBO J. 2004;23(5):1155–65. https://doi.org/10.1038/sj.emboj.7600069.
136. Yan S, Wang Y, Yang Q, Li X, Kong X, Zhang N, Yuan C, Yang N, Kong B. Low-dose radiation-induced epithelial-mesenchymal transition through NF-κB in cervical cancer cells. Int J Oncol. 2013;42(5):1801–6. https://doi.org/10.3892/ijo.2013.1852.
137. Cui YH, Suh Y, Lee HJ, Yoo KC, Uddin N, Jeong YJ, Lee JS, Hwang SG, Nam SY, Kim MJ, Lee SJ. Radiation promotes invasiveness of non-small-cell lung cancer cells through granulocyte-colony-stimulating factor. Oncogene. 2015;34(42):5372–82. https://doi.org/10.1038/onc.2014.466.
138. Park JK, Jang SJ, Kang SW, Park S, Hwang SG, Kim WJ, Kang JH, Um HD. Establishment of animal model for the analysis of cancer cell metastasis during radiotherapy. Radiat Oncol. 2012;7:153. https://doi.org/10.1186/1748-717X-7-153.
139. He E, Pan F, Li G, Li J. Fractionated ionizing radiation promotes epithelial-mesenchymal transition in human esophageal cancer cells through PTEN deficiency-mediated Akt activation. PLoS One. 2015;10(5):e0126149. https://doi.org/10.1371/journal.pone.0126149.
140. Liu W, Huang YJ, Liu C, Yang YY, Liu H, Cui JG, Cheng Y, Gao F, Cai JM, Li BL. Inhibition of TBK1 attenuates radiation-induced epithelial-mesenchymal transition of A549 human lung cancer cells via activation of GSK-3β and repression of ZEB1. Lab Invest. 2014;94(4):362–70. https://doi.org/10.1038/labinvest.2013.153.
141. Bhatt AN, Chauhan A, Khanna S, Rai Y, Singh S, Soni R, et al. Transient elevation of glycolysis confers radio-resistance by facilitating DNA repair in cells. BMC Cancer. 2015;15(1):1–12. https://doi.org/10.1186/s12885-015-1368-9.
142. Khodarev NN, Beckett M, Labay E, Darga T, Roizman B, Weichselbaum RR. STAT1 is overexpressed in tumors selected for radioresistance and confers protection from radiation in transduced sensitive cells. Proc Natl Acad Sci U S A. 2004;101(6):1714–9.
143. Abratt RP, Shepherd LJ, Salton DG. Palliative radiation for stage 3 non-small cell lung cancer—a prospective study of two moderately high dose regimens. Lung Cancer. 1995;13(2):137–43. https://doi.org/10.1016/0169-5002(95)00487-4.
144. Crane CH, Janjan NA, Abbruzzese JL, Curley S, Vauthey J, Sawaf HB, Dubrow R, Allen P, Ellis LM, Hoff P, Wolff RA, Lenzi R, Brown TD, Lynch P, Cleary K, Rich TA, Skibber J. Effective pelvic symptom control using initial chemoradiation without colostomy in metastatic rectal cancer. Int J Radiat Oncol Biol Phys. 2001;49(1):107–16. https://doi.org/10.1016/S0360-3016(00)00777-X.
145. Dirix P, Vingerhoedt S, Joniau S, Van Cleynenbreugel B, Haustermans K. Hypofractionated palliative radiotherapy for bladder cancer. Support Care Cancer. 2016;24(1):181–6. https://doi.org/10.1007/s00520-015-2765-y.
146. Yan J, Milosevic M, Fyles A, Manchul L, Kelly V, Levin W. A hypofractionated radiotherapy regimen (0–7-21) for advanced gynaecological cancer patients. Clin Oncol (R Coll Radiol). 2011;23(7):476–81. https://doi.org/10.1016/j.clon.2011.01.001.
147. Choi HS, Jeong BK, Jeong H, Ha IB, Kang KM. Role of radiotherapy in the management of malignant airway obstruction. Thorac Cancer. 2020;11(8):2163–9. https://doi.org/10.1111/1759-7714.13523.
148. Bezjak A, Adam J, Barton R, Panzarella T, Laperriere N, Wong CS, Mason W, Buckley C, Levin W, McLean M, Wu JS, Sia M, Kirkbride P. Symptom response after palliative radiotherapy for patients with brain metastases. Eur J Cancer. 2002;38(4):487–96. https://doi.org/10.1016/S0959-8049(01)00150-2.
149. Jones B, Dale RG. Further radiobiologic modeling of palliative radiotherapy: use of virtual trials. Int J Radiat Oncol Biol Phys. 2007;69(1):221–9.
150. Song CW, Glatstein E, Marks LB, Emami B, Grimm J, Sperduto PW, Kim MS, Hui S, Dusenbery KE, Cho LC. Biological principles of stereotactic body radiation therapy (SBRT) and stereotactic radiation surgery (SRS): indirect cell death. Int J Radiat Oncol Biol Phys. 2021;110(1):21–34. https://doi.org/10.1016/j.ijrobp.2019.02.047.
151. Ansems M, Span PN. The tumor microenvironment and radiotherapy response; a central role for cancer-associated fibroblasts. Clin Transl Radiat Oncol. 2020;22:90–7. https://doi.org/10.1016/j.ctro.2020.04.001.
152. Wei R, Liu S, Zhang S, Min L, Zhu S. Cellular and extracellular components in tumor microenvironment and their application in early diagnosis of cancers. Anal Cell Pathol. 2020;6283796:2020. https://doi.org/10.1155/2020/6283796.
153. Barker HE, Paget JT, Khan AA, Harrington KJ. The tumour microenvironment after radiotherapy: mechanisms of resistance and recurrence. Nat Rev Cancer. 2015;15(7):409–25. https://doi.org/10.1038/nrc3958.
154. Menon H, Ramapriyan R, Cushman TR, Verma V, Kim HH, Schoenhals JE, Atalar C, Selek U, Chun SG, Chang JY, Barsoumian HB, Nguyen QN, Altan M, Cortez MA, Hahn SM, Welsh JW. Role of radiation therapy in modulation of the tumor stroma and microenvironment. Front Immunol. 2019;10:193. https://doi.org/10.3389/fimmu.2019.00193.
155. Krisnawan VE, Stanley JA, Schwarz JK, DeNardo DG. Tumor microenvironment as a regulator of radiation therapy: new insights into stromal-mediated radioresistance. Cancers (Basel). 2020;12(10):2916. https://doi.org/10.3390/cancers12102916.
156. Baker DG, Krochak RJ. The response of the microvascular system to radiation: a review. Cancer Investig. 1989;7(3):287–94. https://doi.org/10.3109/07357908909039849.
157. Jain RK. Molecular regulation of vessel maturation. Nat Med. 2003;9(6):685–93. https://doi.org/10.1038/nm0603-685.
158. Khan FM, Gibbons JP. Khan's the physics of radiation therapy. 5th ed. Lippincott Williams & Wilkins; 2014.
159. Levitt S, Purdy J, Perez C, Vijayakumar S. Technical basis of radiation therapy. 4th ed. Berlin, Heidelberg: Springer; 2012.

160. Donlon NE, Power R, Hayes C, Reynolds JV, Lysaght J. Radiotherapy, immunotherapy, and the tumour microenvironment: turning an immunosuppressive milieu into a therapeutic opportunity. Cancer Lett. 2021;502:84–96. https://doi.org/10.1016/j.canlet.2020.12.045.
161. Rodriguez-Ruiz ME, Rodriguez I, Garasa S, Barbes B, Solorzano JL, Perez-Gracia JL, Labiano S, Sanmamed MF, Azpilikueta A, Bolaños E, Sanchez-Paulete AR, Aznar MA, Rouzaut A, Schalper KA, Jure-Kunkel M, Melero I. Abscopal effects of radiotherapy are enhanced by combined immunostimulatory mAbs and are dependent on CD8 T cells and crosspriming. Cancer Res. 2016;76(20):5994–6005. https://doi.org/10.1158/0008-5472.CAN-16-0549.
162. Siva S, MacManus MP, Martin RF, Martin OA. Abscopal effects of radiation therapy: a clinical review for the radiobiologist. Cancer Lett. 2015;356(1):82–90. https://doi.org/10.1016/j.canlet.2013.09.018.
163. Sprung CN, Forrester HB, Siva S, Martin OA. Immunological markers that predict radiation toxicity. Cancer Lett. 2015;368(2):191–7. https://doi.org/10.1016/j.canlet.2015.01.045.
164. Vanpouille-Box C, Diamond JM, Pilones KA, Zavadil J, Babb JS, Formenti SC, Barcellos-Hoff MH, Demaria S. TGFβ is a master regulator of radiation therapy-induced antitumor immunity. Cancer Res. 2015;75(11):2232–42. https://doi.org/10.1158/0008-5472.CAN-14-3511.
165. Sureka CS, Armpilia C. Radiation biology for medical physicists. 1st ed. CRC Press; 2017.
166. Bower JE. Cancer-related fatigue—mechanisms, risk factors, and treatments. Nat Rev Clin Oncol. 2014;11(10):597–609. https://doi.org/10.1038/nrclinonc.2014.127.
167. Morgan GW, Breit SN. Radiation and the lung: a reevaluation of the mechanisms mediating pulmonary injury. Int J Radiat Oncol Biol Phys. 1995;31(2):361–9. https://doi.org/10.1016/0360-3016(94)00477-3.
168. Formenti SC, Demaria S. Systemic effects of local radiotherapy. Lancet Oncol. 2009;10(7):718–26. https://doi.org/10.1016/S1470-2045(09)70082-8.
169. De la Cruz V, Sanz Á, Torrego JC, Fiorini AB. The strange abscopal effect. Rev Clin Esp. 2014;214(3):170–1. https://doi.org/10.1016/j.rce.2013.12.005.
170. Joe MB, Lum JJ, Watson PH, Tonseth RP, McGhie JP, Truong PT. Radiation generates an abscopal response and complete resolution of metastatic squamous cell carcinoma of the anal canal: a case report. J Gastrointest Oncol. 2017;8(6):E84–9. https://doi.org/10.21037/jgo.2017.06.15.
171. Mole RH. Whole body irradiation; radiobiology or medicine? Br J Radiol. 1953;26(305):234–41. https://doi.org/10.1259/0007-1285-26-305-234.
172. Abuodeh Y, Venkat P, Kim S. Systematic review of case reports on the abscopal effect. Curr Probl Cancer. 2016;40(1):25–37. https://doi.org/10.1016/j.currproblcancer.2015.10.001.
173. Grimaldi AM, Simeone E, Giannarelli D, Muto P, Falivene S, Borzillo V, Giugliano FM, Sandomenico F, Petrillo A, Curvietto M, Esposito A, Paone M, Palla M, Palmieri G, Caracò C, Ciliberto G, Mozzillo N, Ascierto PA. Abscopal effects of radiotherapy on advanced melanoma patients who progressed after ipilimumab immunotherapy. Onco Targets Ther. 2014;3:e28780. https://doi.org/10.4161/onci.28780.
174. Hiniker SM, Chen DS, Reddy S, Chang DT, Jones JC, Mollick JA, Swetter SM, Knox SJ. A systemic complete response of metastatic melanoma to local radiation and immunotherapy. Transl Oncol. 2012;5(6):404–7. https://doi.org/10.1593/tlo.12280.
175. Qin Q, Nan X, Miller T, Fisher R, Teh B, Pandita S, Farach AM, Pingali SR, Pandita RK, Butler EB, Pandita TK, Iyer SP. Complete local and abscopal responses from a combination of radiation and nivolumab in refractory Hodgkin's lymphoma. Radiat Res. 2018;190(3):322–9. https://doi.org/10.1667/RR15048.1.
176. Burnette B, Fu YX, Weichselbaum RR. The confluence of radiotherapy and immunotherapy. Front Oncol. 2012;2:143. https://doi.org/10.3389/fonc.2012.00143.
177. Harrison L, Hatahet Z, Wallace SS. In vitro repair of synthetic ionizing radiation-induced multiply damaged DNA sites. J Mol Biol. 1999;290(3):667–84. https://doi.org/10.1006/jmbi.1999.2892.
178. Peng M, Mo Y, Wang Y, Wu P, Zhang Y, Xiong F, Guo C, Wu X, Li Y, Li X, Li G, Xiong W, Zeng Z. Neoantigen vaccine: an emerging tumor immunotherapy. Mol Cancer. 2019;18(1):128. https://doi.org/10.1186/s12943-019-1055-6.
179. Apetoh L, Ghiringhelli F, Tesniere A, Obeid M, Ortiz C, Criollo A, Mignot G, Maiuri MC, Ullrich E, Saulnier P, Yang H, Amigorena S, Ryffel B, Barrat FJ, Saftig P, Levi F, Lidereau R, Nogues C, Mira JP, Chompret A, Joulin V, Clavel-Chapelon F, Bourhis J, André F, Delaloge S, Tursz T, Kroemer G, Zitvogel L. Toll-like receptor 4-dependent contribution of the immune system to anticancer chemotherapy and radiotherapy. Nat Med. 2007;13(9):1050–9. https://doi.org/10.1038/nm1622.
180. Elliott MR, Chekeni FB, Trampont PC, Lazarowski ER, Kadl A, Walk SF, Park D, Woodson RI, Ostankovich M, Sharma P, Lysiak JJ, Harden TK, Leitinger N, Ravichandran KS. Nucleotides released by apoptotic cells act as a find-me signal to promote phagocytic clearance. Nature. 2009;461(7261):282–6. https://doi.org/10.1038/nature08296.
181. Ghiringhelli F, Apetoh L, Tesniere A, Aymeric L, Ma Y, Ortiz C, Vermaelen K, Panaretakis T, Mignot G, Ullrich E, Perfettini JL, Schlemmer F, Tasdemir E, Uhl M, Génin P, Civas A, Ryffel B, Kanellopoulos J, Tschopp J, André F, Lidereau R, McLaughlin NM, Haynes NM, Smyth MJ, Kroemer G, Zitvogel L. Activation of the NLRP3 inflammasome in dendritic cells induces IL-1beta-dependent adaptive immunity against tumors. Nat Med. 2009;15(10):1170–8. https://doi.org/10.1038/nm.2028.
182. Obeid M, Tesniere A, Ghiringhelli F, Fimia GM, Apetoh L, Perfettini JL, Castedo M, Mignot G, Panaretakis T, Casares N, Métivier D, Larochette N, van Endert P, Ciccosanti F, Piacentini M, Zitvogel L, Kroemer G. Calreticulin exposure dictates the immunogenicity of cancer cell death. Nat Med. 2007;13(1):54–61. https://doi.org/10.1038/nm1523.
183. Craig DJ, Nanavaty NS, Devanaboyina M, Stanbery L, Hamouda D, Edelman G, Dworkin L, Nemunaitis JJ. The abscopal effect of radiation therapy. Future Oncol. 2021;17(13):1683–94. https://doi.org/10.2217/fon-2020-0994.
184. Melief CJ. Cancer immunotherapy by dendritic cells. Immunity. 2008;29(3):372–83. https://doi.org/10.1016/j.immuni.2008.08.004.
185. Obeid M, Panaretakis T, Joza N, Tufi R, Tesniere A, van Endert P, Zitvogel L, Kroemer G. Calreticulin exposure is required for the immunogenicity of gamma-irradiation and UVC light-induced apoptosis. Cell Death Differ. 2007;14(10):1848–50. https://doi.org/10.1038/sj.cdd.4402201.
186. Vanpouille-Box C, Alard A, Aryankalayil MJ, Sarfraz Y, Diamond JM, Schneider RJ, Inghirami G, Coleman CN, Formenti SC, Demaria S. DNA exonuclease Trex1 regulates radiotherapy-induced tumour immunogenicity. Nat Commun. 2017;8:15618. https://doi.org/10.1038/ncomms15618.
187. Lan Y, Moustafa M, Knoll M, Xu C, Furkel J, Lazorchak A, Yeung TL, Hasheminasab SM, Jenkins MH, Meister S, Yu H, Schlegel J, Marelli B, Tang Z, Qin G, Klein C, Qi J, Zhou C, Locke G, Krunic D, Derner MG, Schwager C, Fontana RE, Kriegsmann K, Jiang F, Rein K, Kriegsmann M, Debus J, Lo KM, Abdollahi A. Simultaneous targeting of TGF-β/PD-L1 synergizes with radiotherapy by reprogramming the tumor microenvironment to overcome immune evasion. Cancer Cell. 2021;39(10):1388–1403.e10. https://doi.org/10.1016/j.ccell.2021.08.008.

188. Emami B, Lyman J, Brown A, Coia L, Goitein M, Munzenrider JE, Shank B, Solin LJ, Wesson M. Tolerance of normal tissue to therapeutic irradiation. Int J Radiat Oncol Biol Phys. 1991;21(1):109–22. https://doi.org/10.1016/0360-3016(91)90171-Y.
189. Milano MT, Constine LS, Okunieff P. Normal tissue tolerance dose metrics for radiation therapy of major organs. Semin Radiat Oncol. 2007;17(2):131–40. https://doi.org/10.1016/j.semradonc.2006.11.009.
190. Bentzen SM. Preventing or reducing late side effects of radiation therapy: radiobiology meets molecular pathology. Nat Rev Cancer. 2006;6(9):702–13. https://doi.org/10.1038/nrc1950.
191. ICRP. ICRP statement on tissue reactions/early and late effects of radiation in normal tissues and organs—threshold doses for tissue reactions in a radiation protection context. ICRP Publication 118. Ann ICRP. 2012;41(1/2).
192. ICRP. Statement on tissue reactions, ref 4825-3093-1464. 2011.
193. Bentzen SM, Dörr W, Anscher MS, Denham JW, Hauer-Jensen M, Marks LB, Williams J. Normal tissue effects: reporting and analysis. Semin Radiat Oncol. 2003;13(3):189–202. https://doi.org/10.1016/S1053-4296(03)00036-5.
194. Dörr W, Hendry JH. Consequential late effects in normal tissues. Radiother Oncol. 2001;61(3):223–31. https://doi.org/10.1016/S0167-8140(01)00429-7.
195. Cytlak UM, Dyer DP, Honeychurch J, Williams KJ, Travis MA, Illidge TM. Immunomodulation by radiotherapy in tumour control and normal tissue toxicity. Nat Rev Immunol. 2022;22(2):124–38. https://doi.org/10.1038/s41577-021-00568-1. Epub 2021 Jul 1.
196. François A, Milliat F, Guipaud O, Benderitter M. Inflammation and immunity in radiation damage to the gut mucosa. Biomed Res Int. 2013;2013:123241. https://doi.org/10.1155/2013/123241.
197. Meziani L, Deutsch E, Mondini M. Macrophages in radiation injury: a new therapeutic target. Oncoimmunology. 2018;7(10):e1494488. https://doi.org/10.1080/2162402X.2018.1494488.
198. Najafi M, Motevaseli E, Shirazi A, Geraily G, Rezaeyan A, Norouzi F, Rezapoor S, Abdollahi H. Mechanisms of inflammatory responses to radiation and normal tissues toxicity: clinical implications. Int J Radiat Biol. 2018;94(4):335–56. https://doi.org/10.1080/09553002.2018.1440092.
199. Hauer-Jensen M, Denham JW, Andreyev HJ. Radiation enteropathy—pathogenesis, treatment and prevention. Nat Rev Gastroenterol Hepatol. 2014;11(8):470–9. https://doi.org/10.1038/nrgastro.2014.46.
200. Sung H, Ferlay J, Siegel RL, Laversanne M, Soerjomataram I, Jemal A, Bray F. Global cancer statistics 2020: GLOBOCAN estimates of incidence and mortality worldwide for 36 cancers in 185 countries. CA Cancer J Clin. 2021;71(3):209–49. https://doi.org/10.3322/caac.21660.
201. Willaert R, Nevens D, Laenen A, Batstone M, Politis C, Nuyts S. Does intensity-modulated radiation therapy lower the risk of osteoradionecrosis of the jaw? A long-term comparative analysis. Int J Oral Maxillofac Surg. 2019;48(11):1387–93. https://doi.org/10.1016/j.ijom.2019.04.018.
202. Raguse JD, Hossamo J, Tinhofer I, Hoffmeister B, Budach V, Jamil B, Jöhrens K, Thieme N, Doll C, Nahles S, Hartwig ST, Stromberger C. Patient and treatment-related risk factors for osteoradionecrosis of the jaw in patients with head and neck cancer. Oral Surg Oral Med Oral Pathol Oral Radiol. 2016;121(3):215–21.e1. https://doi.org/10.1016/j.oooo.2015.10.006.
203. Van Camp N, Verhelst PJ, Nicot R, Ferri J, Politis C. Impaired callus formation in pathological mandibular fractures in medication-related osteonecrosis of the jaw and osteoradionecrosis. J Oral Maxillofac Surg. 2021;79(9):1892–901. https://doi.org/10.1016/j.joms.2021.04.024.
204. Notani K, Yamazaki Y, Kitada H, Sakakibara N, Fukuda H, Omori K, Nakamura M. Management of mandibular osteoradionecrosis corresponding to the severity of osteoradionecrosis and the method of radiotherapy. Head Neck. 2003;25(3):181–6. https://doi.org/10.1002/hed.10171.
205. Lyons A, Osher J, Warner E, Kumar R, Brennan PA. Osteoradionecrosis—a review of current concepts in defining the extent of the disease and a new classification proposal. Br J Oral Maxillofac Surg. 2014;52(5):392–5. https://doi.org/10.1016/j.bjoms.2014.02.017.
206. Spijkervet FKL, Brennan MT, Peterson DE, Witjes MJH, Vissink A. Research frontiers in oral toxicities of cancer therapies: osteoradionecrosis of the jaws. J Natl Cancer Inst Monogr. 2019;53:lgz006. https://doi.org/10.1093/jncimonographs/lgz006.
207. Grisar K, Schol M, Schoenaers J, Dormaar T, Coropciuc R, Vander Poorten V, Politis C. Osteoradionecrosis and medication-related osteonecrosis of the jaw: similarities and differences. Int J Oral Maxillofac Surg. 2016;45(12):1592–9. https://doi.org/10.1016/j.ijom.2016.06.016.
208. van Baar GJC, Leeuwrik L, Lodders JN, Liberton NPTJ, Karagozoglu KH, Forouzanfar T, Leusink FKJ. A novel treatment concept for advanced stage mandibular osteoradionecrosis combining isodose curve visualization and nerve preservation: a prospective pilot study. Front Oncol. 2021;11:630123. https://doi.org/10.3389/fonc.2021.630123.
209. Schuurhuis JM, Stokman MA, Witjes MJ, Dijkstra PU, Vissink A, Spijkervet FK. Evidence supporting pre-radiation elimination of oral foci of infection in head and neck cancer patients to prevent oral sequelae. A systematic review. Oral Oncol. 2015;51(3):212–20. https://doi.org/10.1016/j.oraloncology.2014.11.017.
210. Walker AJ, Ruzevick J, Malayeri AA, Rigamonti D, Lim M, Redmond KJ, Kleinberg L. Postradiation imaging changes in the CNS: how can we differentiate between treatment effect and disease progression? Future Oncol. 2014;10(7):1277–97. https://doi.org/10.2217/fon.13.271.
211. Ruben JD, Dally M, Bailey M, Smith R, McLean CA, Fedele P. Cerebral radiation necrosis: incidence, outcomes, and risk factors with emphasis on radiation parameters and chemotherapy. Int J Radiat Oncol Biol Phys. 2006;65(2):499–508. https://doi.org/10.1016/j.ijrobp.2005.12.002.
212. Kohutek ZA, Yamada Y, Chan TA, Brennan CW, Tabar V, Gutin PH, Yang TJ, Rosenblum MK, Ballangrud Å, Young RJ, Zhang Z, Beal K. Long-term risk of radionecrosis and imaging changes after stereotactic radiosurgery for brain metastases. J Neurooncol. 2015;125(1):149–56. https://doi.org/10.1007/s11060-015-1881-3.
213. Shah R, Vattoth S, Jacob R, Manzil FF, O'Malley JP, Borghei P, Patel BN, Curé JK. Radiation necrosis in the brain: imaging features and differentiation from tumor recurrence. Radiographics. 2012;32(5):1343–59. https://doi.org/10.1148/rg.325125002.
214. Le Rhun E, Dhermain F, Vogin G, Reyns N, Metellus P. Radionecrosis after stereotactic radiotherapy for brain metastases. Expert Rev Neurother. 2016;16(8):903–14. https://doi.org/10.1080/14737175.2016.1184572.
215. De Ruysscher D, Niedermann G, Burnet NG, Siva S, Lee AWM, Hegi-Johnson F. Radiotherapy toxicity. Nat Rev Dis Primers. 2019;5(1):13. https://doi.org/10.1038/s41572-019-0064-5.
216. Guipaud O, Jaillet C, Clément-Colmou K, François A, Supiot S, Milliat F. The importance of the vascular endothelial barrier in the immune-inflammatory response induced by radiotherapy. Br J Radiol. 2018;91(1089):20170762. https://doi.org/10.1259/bjr.20170762.
217. Mintet E, Rannou E, Buard V, West G, Guipaud O, Tarlet G, Sabourin JC, Benderitter M, Fiocchi C, Milliat F, François A. Identification of endothelial-to-mesenchymal transition as a potential participant in radiation proctitis. Am J Pathol. 2015;185(9):2550–62. https://doi.org/10.1016/j.ajpath.2015.04.028.

218. Wynn TA. Cellular and molecular mechanisms of fibrosis. J Pathol. 2008;214(2):199–210. https://doi.org/10.1002/path.2277.
219. Muñoz-Espín D, Serrano M. Cellular senescence: from physiology to pathology. Nat Rev Mol Cell Biol. 2014;15(7):482–96. https://doi.org/10.1038/nrm3823.
220. Pan J, Li D, Xu Y, Zhang J, Wang Y, Chen M, Lin S, Huang L, Chung EJ, Citrin DE, Wang Y, Hauer-Jensen M, Zhou D, Meng A. Inhibition of Bcl-2/xl with ABT-263 selectively kills senescent type II pneumocytes and reverses persistent pulmonary fibrosis induced by ionizing radiation in mice. Int J Radiat Oncol Biol Phys. 2017;99(2):353–61. https://doi.org/10.1016/j.ijrobp.2017.02.216.
221. Soysouvanh F, Benadjaoud MA, Dos Santos M, Mondini M, Lavigne J, Bertho A, Buard V, Tarlet G, Adnot S, Deutsch E, Guipaud O, Paget V, François A, Milliat F. Stereotactic lung irradiation in mice promotes long-term senescence and lung injury. Int J Radiat Oncol Biol Phys. 2020;106(5):1017–27. https://doi.org/10.1016/j.ijrobp.2019.12.039.
222. Prasanna PG, Citrin DE, Hildesheim J, Ahmed MM, Venkatachalam S, Riscuta G, Xi D, Zheng G, Deursen JV, Goronzy J, Kron SJ, Anscher MS, Sharpless NE, Campisi J, Brown SL, Niedernhofer LJ, O'Loghlen A, Georgakilas AG, Paris F, Gius D, Gewirtz DA, Schmitt CA, Abazeed ME, Kirkland JL, Richmond A, Romesser PB, Lowe SW, Gil J, Mendonca MS, Burma S, Zhou D, Coleman CN. Therapy-induced senescence: opportunities to improve anticancer therapy. J Natl Cancer Inst. 2021;113(10):1285–98. https://doi.org/10.1093/jnci/djab064.
223. Bentzen SM, Constine LS, Deasy JO, Eisbruch A, Jackson A, Marks LB, Ten Haken RK, Yorke ED. Quantitative Analyses of Normal Tissue Effects in the Clinic (QUANTEC): an introduction to the scientific issues. Int J Radiat Oncol Biol Phys. 2010;76(3 Suppl):S3–9. https://doi.org/10.1016/j.ijrobp.2009.09.040.
224. Constine LS, Ronckers CM, Hua CH, Olch A, Kremer LCM, Jackson A, Bentzen SM. Pediatric normal tissue effects in the clinic (PENTEC): an international collaboration to analyse normal tissue radiation dose-volume response relationships for paediatric cancer patients. Clin Oncol (R Coll Radiol). 2019;31(3):199–207. https://doi.org/10.1016/j.clon.2019.01.002.
225. Grimm J, Marks LB, Jackson A, Kavanagh BD, Xue J, Yorke E. High dose per fraction, hypofractionated treatment effects in the clinic (HyTEC): an overview. Int J Radiat Oncol Biol Phys. 2021;110(1):1–10. https://doi.org/10.1016/j.ijrobp.2020.10.039.
226. Palma G, Monti S, Buonanno A, Pacelli R, Cella L. PACE: a probabilistic atlas for normal tissue complication estimation in radiation oncology. Front Oncol. 2019;9:130. https://doi.org/10.3389/fonc.2019.00130.
227. Adamus-Górka M, Mavroidis P, Lind BK, Brahme A. Comparison of dose response models for predicting normal tissue complications from cancer radiotherapy: application in rat spinal cord. Cancers (Basel). 2011;3(2):2421–43. https://doi.org/10.3390/cancers3022421.
228. Knoblich JA. Asymmetric cell division during animal development. Nat Rev Mol Cell Biol. 2001;2(1):11–20. https://doi.org/10.1038/35048085.
229. Zon LI. Intrinsic and extrinsic control of haematopoietic stem-cell self-renewal. Nature. 2008;453(7193):306–13. https://doi.org/10.1038/nature07038.
230. Pontikoglou C, Delorme B, Charbord P. Human bone marrow native mesenchymal stem cells. Regen Med. 2008;3(5):731–41. https://doi.org/10.2217/17460751.3.5.731.
231. Harfouche G, Martin MT. Response of normal stem cells to ionizing radiation: a balance between homeostasis and genomic stability. Mutat Res. 2010;704(1–3):167–74. https://doi.org/10.1016/j.mrrev.2010.01.007.
232. Galli R, Gritti A, Bonfanti L, Vescovi AL. Neural stem cells: an overview. Circ Res. 2003;92(6):598–608. https://doi.org/10.1161/01.RES.0000065580.02404.F4.
233. Chaker Z, Codega P, Doetsch F. A mosaic world: puzzles revealed by adult neural stem cell heterogeneity. Wiley Interdiscip Rev Dev Biol. 2016;5(6):640–58. https://doi.org/10.1002/wdev.248.
234. Huo K, Sun Y, Li H, Du X, Wang X, Karlsson N, Zhu C, Blomgren K. Lithium reduced neural progenitor apoptosis in the hippocampus and ameliorated functional deficits after irradiation to the immature mouse brain. Mol Cell Neurosci. 2012;51(1–2):32–42. https://doi.org/10.1016/j.mcn.2012.07.002.
235. Prager I, Patties I, Himmelbach K, Kendzia E, Merz F, Müller K, Kortmann RD, Glasow A. Dose-dependent short- and long-term effects of ionizing irradiation on neural stem cells in murine hippocampal tissue cultures: neuroprotective potential of resveratrol. Brain Behav. 2016;6(10):e00548. https://doi.org/10.1002/brb3.548.
236. Fukui M, Choi HJ, Zhu BT. Mechanism for the protective effect of resveratrol against oxidative stress-induced neuronal death. Free Radic Biol Med. 2010;49(5):800–13. https://doi.org/10.1016/j.freeradbiomed.2010.06.002.
237. Brouard M, Barrandon Y. Controlling skin morphogenesis: hope and despair. Curr Opin Biotechnol. 2003;14(5):520–5. https://doi.org/10.1016/j.copbio.2003.09.005.
238. Potten CS, Grant HK. The relationship between ionizing radiation-induced apoptosis and stem cells in the small and large intestine. Br J Cancer. 1998;78:993–1003. https://doi.org/10.1038/bjc.1998.618.
239. Konrad CV, Murali R, Varghese BA, Nair R. The role of cancer stem cells in tumor heterogeneity and resistance to therapy. Can J Physiol Pharmacol. 2017;95(1):1–15. https://doi.org/10.1139/cjpp-2016-0079.
240. Arnold CR, Mangesius J, Skvortsova II, Ganswindt U. The role of cancer stem cells in radiation resistance. Front Oncol. 2020;10:164. https://doi.org/10.3389/fonc.2020.00164.
241. Laplane L. Cancer stem cells modulate patterns and processes of evolution in cancers. Biol Philos. 2018;33:18. https://doi.org/10.1007/s10539-018-9629-z.
242. Filip S, Mokry J, Horacek J, English D. Stem cells and the phenomena of plasticity and diversity: a limiting property of carcinogenesis. Stem Cells Dev. 2008;17(6):1031–8. https://doi.org/10.1089/scd.2007.0234.
243. Filipova A, Seifrtova M, Mokry J, Dvorak J, Rezacova M, Filip S, Diaz-Garcia D. Breast cancer and cancer stem cells: a mini-review. Tumori. 2014;100(4):363–9. https://doi.org/10.1700/1636.17886.
244. Yu Z, Pestell TG, Lisanti MP, Pestell RG. Cancer stem cells. Int J Biochem Cell Biol. 2012;44(12):2144–51. https://doi.org/10.1016/j.biocel.2012.08.022.
245. Bao S, Wu Q, McLendon RE, Hao Y, Shi Q, Hjelmeland AB, et al. Glioma stem cells promote radioresistance by preferential activation of the DNA damage response. Nature. 2006;444(7120):756–60. https://doi.org/10.1038/nature05236.
246. Bertolini G, Roz L, Perego P, Tortoreto M, Fontanella E, Gatti L, Pratesi G, Fabbri A, Andriani F, Tinelli S, Roz E, Caserini R, Lo Vullo S, Camerini T, Mariani L, Delia D, Calabrò E, Pastorino U, Sozzi G. Highly tumorigenic lung cancer CD133+ cells display stem-like features and are spared by cisplatin treatment. Proc Natl Acad Sci U S A. 2009;106(38):16281–6. https://doi.org/10.1073/pnas.0905653106.
247. Coppes RP, Dubrovska A. Targeting stem cells in radiation oncology. Clin Oncol (R Coll Radiol). 2017;29(6):329–34. https://doi.org/10.1016/j.clon.2017.03.005.
248. Lee PJ, Ho CC, Ho H, Chen WJ, Lin CH, Lai YH, Juan YC, Chu WC, Lee JH, Su SF, Chen HY, Chen JJW, Chang GC, Li KC, Yang PC, Chen HW. Tumor microenvironment-based screening repurposes drugs targeting cancer stem cells and cancer-associated fibroblasts. Theranostics. 2021;11(19):9667–86. https://doi.org/10.7150/thno.62676.

249. Lee J, Steinmann A, Ding Y, Lee H, Owens C, Wang J, Yang J, Followill D, Ger R, MacKin D, Court LE. Radiomics feature robustness as measured using an MRI phantom. Sci Rep. 2021;11(1):3973. https://doi.org/10.1038/s41598-021-83593-3.
250. Lundholm L, Hååg P, Zong D, Juntti T, Mörk B, Lewensohn R, Viktorsson K. Resistance to DNA-damaging treatment in non-small cell lung cancer tumor-initiating cells involves reduced DNA-PK/ATM activation and diminished cell cycle arrest. Cell Death Dis. 2013;4(1):e478. https://doi.org/10.1038/cddis.2012.211.
251. Moro M, Bertolini G, Pastorino U, Roz L, Sozzi G. Combination treatment with all-trans retinoic acid prevents cisplatin-induced enrichment of CD133+ tumor-initiating cells and reveals heterogeneity of cancer stem cell compartment in lung cancer. J Thorac Oncol. 2015;10(7):1027–36. https://doi.org/10.1097/JTO.0000000000000563.
252. Smit JK, Faber H, Niemantsverdriet M, Baanstra M, Bussink J, Hollema H, van Os RP, Plukker JT, Coppes RP. Prediction of response to radiotherapy in the treatment of esophageal cancer using stem cell markers. Radiother Oncol. 2013;107(3):434–41. https://doi.org/10.1016/j.radonc.2013.03.027.
253. Yang L, Shi P, Zhao G, Xu J, Peng W, Zhang J, Zhang G, Wang X, Dong Z, Chen F, Cui H. Targeting cancer stem cell pathways for cancer therapy. Signal Transduct Target Ther. 2020;5(1):8. https://doi.org/10.1038/s41392-020-0110-5.
254. Digomann D, Kurth I, Tyutyunnykova A, Chen O, Löck S, Gorodetska I, Peitzsch C, Skvortsova II, Negro G, Aschenbrenner B, Eisenhofer G, Richter S, Heiden S, Porrmann J, Klink B, Schwager C, Dowle AA, Hein L, Kunz-Schughart LA, Abdollahi A, Lohaus F, Krause M, Baumann M, Linge A, Dubrovska A. The CD98 heavy chain is a marker and regulator of head and neck squamous cell carcinoma radiosensitivity. Clin Cancer Res. 2019;25(10):3152–63. https://doi.org/10.1158/1078-0432.CCR-18-2951.
255. Martens-de Kemp SR, Brink A, Stigter-van Walsum M, Damen JM, Rustenburg F, Wu T, van Wieringen WN, Schuurhuis GJ, Braakhuis BJ, Slijper M, Brakenhoff RH. CD98 marks a subpopulation of head and neck squamous cell carcinoma cells with stem cell properties. Stem Cell Res. 2013;10(3):477–88. https://doi.org/10.1016/j.scr.2013.02.004.
256. Sarvi S, Mackinnon AC, Avlonitis N, Bradley M, Rintoul RC, Rassl DM, Wang W, Forbes SJ, Gregory CD, Sethi T. CD133+ cancer stem-like cells in small cell lung cancer are highly tumorigenic and chemoresistant but sensitive to a novel neuropeptide antagonist. Cancer Res. 2014;74(5):1554–65. https://doi.org/10.1158/0008-5472.CAN-13-1541.
257. Shien K, Toyooka S, Ichimura K, Soh J, Furukawa M, Maki Y, Muraoka T, Tanaka N, Ueno T, Asano H, Tsukuda K, Yamane M, Oto T, Kiura K, Miyoshi S. Prognostic impact of cancer stem cell-related markers in non-small cell lung cancer patients treated with induction chemoradiotherapy. Lung Cancer. 2012;77(1):162–7. https://doi.org/10.1016/j.lungcan.2012.02.006.
258. Walcher L, Kistenmacher AK, Suo H, Kitte R, Dluczek S, Strauß A, Blaudszun AR, Yevsa T, Fricke S, Kossatz-Boehlert U. Cancer stem cells-origins and biomarkers: perspectives for targeted personalized therapies. Front Immunol. 2020;11:1280. https://doi.org/10.3389/fimmu.2020.01280.
259. Liu Y, Yang M, Luo J, Zhou H. Radiotherapy targeting cancer stem cells "awakens" them to induce tumour relapse and metastasis in oral cancer. Int J Oral Sci. 2020;12(1):19. https://doi.org/10.1038/s41368-020-00087-0.
260. Li F, Zhou K, Gao L, Zhang B, Li W, Yan W, Song X, Yu H, Wang S, Yu N, Jiang Q. Radiation induces the generation of cancer stem cells: a novel mechanism for cancer radioresistance. Oncol Lett. 2016;12(5):3059–65. https://doi.org/10.3892/ol.2016.5124.
261. Krause M, Dubrovska A, Linge A, Baumann M. Cancer stem cells: radioresistance, prediction of radiotherapy outcome and specific targets for combined treatments. Adv Drug Deliv Rev. 2017;109:63–73. https://doi.org/10.1016/j.addr.2016.02.002.
262. Sommer F, Anderson JM, Bharti R, Raes J, Rosenstiel P. The resilience of the intestinal microbiota influences health and disease. Nat Rev Microbiol. 2017;15(10):630–8. https://doi.org/10.1038/nrmicro.2017.58.
263. González-Mercado VJ, Pérez-Santiago J, Lyon D, Dilán-Pantojas I, Henderson W, McMillan S, Groer M, Kane B, Marrero S, Pedro E, Saligan LN. The role of gut microbiome perturbation in fatigue induced by repeated stress from chemoradiotherapy: a proof of concept study. Adv Med. 2020;2020:6375876. https://doi.org/10.1155/2020/6375876.
264. Jang BS, Chang JH, Chie EK, Kim K, Park JW, Kim MJ, Song EJ, Nam YD, Kang SW, Jeong SY, Kim HJ. Gut microbiome composition is associated with a pathologic response after preoperative chemoradiation in patients with rectal cancer. Int J Radiat Oncol Biol Phys. 2020;107(4):736–46. https://doi.org/10.1016/j.ijrobp.2020.04.015.
265. Mitra A, Grossman Biegert GW, Delgado AY, Karpinets TV, Solley TN, Mezzari MP, Yoshida-Court K, Petrosino JF, Mikkelson MD, Lin L, Eifel P, Zhang J, Ramondetta LM, Jhingran A, Sims TT, Schmeler K, Okhuysen P, Colbert LE, Klopp AH. Microbial diversity and composition is associated with patient-reported toxicity during chemoradiation therapy for cervical cancer. Int J Radiat Oncol Biol Phys. 2020;107(1):163–71. https://doi.org/10.1016/j.ijrobp.2019.12.040.
266. Nam YD, Kim HJ, Seo JG, Kang SW, Bae JW. Impact of pelvic radiotherapy on gut microbiota of gynecological cancer patients revealed by massive pyrosequencing. PLoS One. 2013;8(12):e82659. https://doi.org/10.1371/journal.pone.0082659.
267. Manichanh C, Varela E, Martinez C, Antolin M, Llopis M, Doré J, Giralt J, Guarner F, Malagelada JR. The gut microbiota predispose to the pathophysiology of acute postradiotherapy diarrhea. Am J Gastroenterol. 2008;103(7):1754–61. https://doi.org/10.1111/j.1572-0241.2008.01868.x.
268. Reis Ferreira M, Andreyev HJN, Mohammed K, Truelove L, Gowan SM, Li J, Gulliford SL, Marchesi JR, Dearnaley DP. Microbiota- and radiotherapy-induced gastrointestinal side-effects (MARS) study: a large pilot study of the microbiome in acute and late-radiation enteropathy. Clin Cancer Res. 2019;25(21):6487–500. https://doi.org/10.1158/1078-0432.CCR-19-0960.
269. Wang A, Ling Z, Yang Z, Kiela PR, Wang T, Wang C, Cao L, Geng F, Shen M, Ran X, Su Y, Cheng T, Wang J. Gut microbial dysbiosis may predict diarrhea and fatigue in patients undergoing pelvic cancer radiotherapy: a pilot study. PLoS One. 2015;10(5):e0126312. https://doi.org/10.1371/journal.pone.0126312.
270. Wang Z, Wang Q, Wang X, Zhu L, Chen J, Zhang B, Chen Y, Yuan Z. Gut microbial dysbiosis is associated with development and progression of radiation enteritis during pelvic radiotherapy. J Cell Mol Med. 2019;23(5):3747–56. https://doi.org/10.1111/jcmm.14289.
271. Oh B, Eade T, Lamoury G, Carroll S, Morgia M, Kneebone A, Hruby G, Stevens M, Boyle F, Clarke S, Corless B, Molloy M, Rosenthal D, Back M. The gut microbiome and gastrointestinal toxicities in pelvic radiation therapy: a clinical review. Cancers (Basel). 2021;13(10):2353. https://doi.org/10.3390/cancers13102353.
272. Ferreira MR, Muls A, Dearnaley DP, Andreyev HJ. Microbiota and radiation-induced bowel toxicity: lessons from inflammatory bowel disease for the radiation oncologist. Lancet Oncol. 2014;15(3):e139–47. https://doi.org/10.1016/S1470-2045(13)70504-7.

273. Gerassy-Vainberg S, Blatt A, Danin-Poleg Y, Gershovich K, Sabo E, Nevelsky A, Daniel S, Dahan A, Ziv O, Dheer R, Abreu MT, Koren O, Kashi Y, Chowers Y. Radiation induces proinflammatory dysbiosis: transmission of inflammatory susceptibility by host cytokine induction. Gut. 2018;67(1):97–107. https://doi.org/10.1136/gutjnl-2017-313789.
274. Guo H, Chou WC, Lai Y, Liang K, Tam JW, Brickey WJ, Chen L, Montgomery ND, Li X, Bohannon LM, Sung AD, Chao NJ, Peled JU, Gomes ALC, van den Brink MRM, French MJ, Macintyre AN, Sempowski GD, Tan X, Sartor RB, Lu K, Ting JPY. Multi-omics analyses of radiation survivors identify radioprotective microbes and metabolites. Science. 2020;370(6516):eaay9097. https://doi.org/10.1126/science.aay9097.
275. Galluzzi L, Buqué A, Kepp O, Zitvogel L, Kroemer G. Immunogenic cell death in cancer and infectious disease. Nat Rev Immunol. 2017;17(2):97–111. https://doi.org/10.1038/nri.2016.107.
276. Shiao SL, Kershaw KM, Limon JJ, You S, Yoon J, Ko EY, Guarnerio J, Potdar AA, McGovern DPB, Bose S, Dar TB, Noe P, Lee J, Kubota Y, Maymi VI, Davis MJ, Henson RM, Choi RY, Yang W, Tang J, Gargus M, Prince AD, Zumsteg ZS, Underhill DM. Commensal bacteria and fungi differentially regulate tumor responses to radiation therapy. Cancer Cell. 2021;39(9):1202–1213.e6. https://doi.org/10.1016/j.ccell.2021.07.002.
277. Rajkomar A, Dean J, Kohane I. Machine learning in medicine. N Engl J Med. 2019;380(14):1347–58. https://doi.org/10.1056/NEJMra1814259.
278. Kazmierska J, Hope A, Spezi E, Beddar S, Nailon WH, Osong B, Ankolekar A, Choudhury A, Dekker A, Redalen KR, Traverso A. From multisource data to clinical decision aids in radiation oncology: the need for a clinical data science community. Radiothe Oncol. 2020;153:43–54. https://doi.org/10.1016/J.RADONC.2020.09.054.
279. Sun W, Cai Z, Li Y, Liu F, Fang S, Wang G. Data processing and text mining technologies on electronic medical records: a review. J Healthcare Eng. 2018;2018 https://doi.org/10.1155/2018/4302425.
280. Fröhlich H, Balling R, Beerenwinkel N, Kohlbacher O, Kumar S, Lengauer T, Maathuis MH, Moreau Y, Murphy SA, Przytycka TM, Rebhan M, Röst H, Schuppert A, Schwab M, Spang R, Stekhoven D, Sun J, Weber A, Ziemek D, Zupan B. From hype to reality: data science enabling personalized medicine. BMC Med. 2018;16(1):150. https://doi.org/10.1186/s12916-018-1122-7.
281. Willems SM, Abeln S, Feenstra KA, de Bree R, van der Poel EF, Baatenburg de Jong RJ, Heringa J, van den Brekel MWM. The potential use of big data in oncology. Oral Oncol. 2019;98:8–12. https://doi.org/10.1016/j.oraloncology.2019.09.003.
282. Baek B, Lee H. Prediction of survival and recurrence in patients with pancreatic cancer by integrating multi-omics data. Sci Rep. 2020;10(1):18951. https://doi.org/10.1038/s41598-020-76025-1.
283. Kelleher JD, Namee BM, D'Arcy A. Machine learning for predictive data analytics. MIT Press; 2015.
284. El Naqa I, Bradley J, Blanco AI, Lindsay PE, Vicic M, Hope A, Deasy JO. Multivariable modeling of radiotherapy outcomes, including dose-volume and clinical factors. Int J Radiat Oncol Biol Phys. 2006;64(4):1275–86. https://doi.org/10.1016/j.ijrobp.2005.11.022.
285. Burman C, Kutcher GJ, Emami B, Goitein M. Fitting of normal tissue tolerance data to an analytic function. Int J Radiat Oncol Biol Phys. 1991;21(1):123–35. https://doi.org/10.1016/0360-3016(91)90172-Z.
286. Gulliford SL, Webb S, Rowbottom CG, Corne DW, Dearnaley DP. Use of artificial neural networks to predict biological outcomes for patients receiving radical radiotherapy of the prostate. Radiother Oncol. 2004;71(1):3–12. https://doi.org/10.1016/J.RADONC.2003.03.001.
287. Kleppe A, Skrede OJ, De Raedt S, Liestøl K, Kerr DJ, Danielsen HE. Designing deep learning studies in cancer diagnostics. Nat Rev Cancer. 2021;21(3):199–211. https://doi.org/10.1038/s41568-020-00327-9.
288. Sahiner B, Pezeshk A, Hadjiiski LM, Wang X, Drukker K, Cha KH, Summers RM, Giger ML. Deep learning in medical imaging and radiation therapy. Med Phys. 2019;46(1):e1–e36. https://doi.org/10.1002/MP.13264.
289. Kelly CJ, Karthikesalingam A, Suleyman M, Corrado G, King D. Key challenges for delivering clinical impact with artificial intelligence. BMC Med. 2019;17(1):195. https://doi.org/10.1186/s12916-019-1426-2.
290. Ibtehaz N, Rahman MS. MultiResUNet: rethinking the U-Net architecture for multimodal biomedical image segmentation. Neural Netw. 2020;121:74–87. https://doi.org/10.1016/j.neunet.2019.08.025.
291. Ronneberger O, Fischer P, Brox T. U-Net: convolutional networks for biomedical image segmentation. In: Lecture notes in computer science (including subseries Lecture notes in artificial intelligence and Lecture notes in bioinformatics), vol. 9351; 2015. p. 234–41. https://doi.org/10.1007/978-3-319-24574-4_28.
292. Gillies RJ, Kinahan PE, Hricak H. Radiomics: images are more than pictures, they are data. Radiology. 2016;278(2):563–77. https://doi.org/10.1148/radiol.2015151169.
293. van Timmeren JE, Cester D, Tanadini-Lang S, Alkadhi H, Baessler B. Radiomics in medical imaging "how-to" guide and critical reflection. Insights Imaging. 2020;11(1):91. https://doi.org/10.1186/s13244-020-00887-2.
294. Lu L, Liang Y, Schwartz LH, Zhao B. Reliability of radiomic features across multiple abdominal CT image acquisition settings: a pilot study using ACR CT phantom. Tomography. 2019;5(1):226–31. https://doi.org/10.18383/j.tom.2019.00005.
295. Park BW, Kim JK, Heo C, Park KJ. Reliability of CT radiomic features reflecting tumour heterogeneity according to image quality and image processing parameters. Sci Rep. 2020;10(1):3852. https://doi.org/10.1038/s41598-020-60868-9.
296. Fiorino C, Reni M, Bolognesi A, Cattaneo GM, Calandrino R. Intra- and inter-observer variability in contouring prostate and seminal vesicles: implications for conformal treatment planning. Radiother Oncol. 1998;47(3):285–92. https://doi.org/10.1016/S0167-8140(98)00021-8.
297. Lohmann P, Bousabarah K, Hoevels M, Treuer H. Radiomics in radiation oncology—basics, methods, and limitations. Strahlentherap Onkol. 2020;196(10):848. https://doi.org/10.1007/S00066-020-01663-3.
298. Emblem KE, Nedregaard B, Nome T, Due-Tonnessen P, Hald JK, Scheie D, Borota OC, Cvancarova M, Bjornerud A. Glioma grading by using histogram analysis of blood volume heterogeneity from MR-derived cerebral blood volume maps. Radiology. 2008;247(3):808–17. https://doi.org/10.1148/radiol.2473070571.
299. Abdollahi H, Mahdavi SR, Shiri I, Mofid B, Bakhshandeh M, Rahmani K. Magnetic resonance imaging radiomic feature analysis of radiation-induced femoral head changes in prostate cancer radiotherapy. J Cancer Res Ther. 2019;15(8):11. https://doi.org/10.4103/JCRT.JCRT_172_18.
300. Desideri I, Loi M, Francolini G, Becherini C, Livi L, Bonomo P. Application of radiomics for the prediction of radiation-induced toxicity in the IMRT era: current state-of-the-art. Front Oncol. 2020;10 https://doi.org/10.3389/FONC.2020.01708/FULL.
301. Qin H, Wu Y-Q, Lin P, Gao R-Z, Li X, Wang X-R, Chen G, He Y, Yang H. Ultrasound image-based radiomics. J Ultrasound Med. 2021;40(6):1229–44. https://doi.org/10.1002/JUM.15506.
302. Stefano A, Comelli A, Bravatà V, Barone S, Daskalovski I, Savoca G, Sabini MG, Ippolito M, Russo G. A preliminary PET radiomics study of brain metastases using a fully automatic segmentation

method. BMC Bioinformatics. 2020;21(8):1–14. https://doi.org/10.1186/S12859-020-03647-7/TABLES/3.
303. Fehr D, Veeraraghavan H, Wibmer A, Gondo T, Matsumoto K, Vargas HA, Sala E, Hricak H, Deasy JO. Automatic classification of prostate cancer Gleason scores from multiparametric magnetic resonance images. Proc Natl Acad Sci U S A. 2015;112(46):E6265–73. https://doi.org/10.1073/pnas.1505935112.
304. Monti S, Aiello M, Incoronato M, Grimaldi AM, Moscarino M, Mirabelli P, Ferbo U, Cavaliere C, Salvatore M. DCE-MRI pharmacokinetic-based phenotyping of invasive ductal carcinoma: a radiomic study for prediction of histological outcomes. Contrast Media Mol Imaging. 2018;2018 https://doi.org/10.1155/2018/5076269.
305. Parmar C, Leijenaar RT, Grossmann P, Rios Velazquez E, Bussink J, Rietveld D, Rietbergen MM, Haibe-Kains B, Lambin P, Aerts HJ. Radiomic feature clusters and prognostic signatures specific for lung and head & neck cancer. Sci Rep. 2015;5:11044. https://doi.org/10.1038/srep11044.
306. Khawaja A, Bartholmai BJ, Rajagopalan S, Karwoski RA, Varghese C, Maldonado F, Peikert T. Do we need to see to believe? Radiomics for lung nodule classification and lung cancer risk stratification. J Thorac Dis. 2020;12(6):3303–16. https://doi.org/10.21037/JTD.2020.03.105.
307. Shiradkar R, Ghose S, Jambor I, Taimen P, Ettala O, Purysko AS, Madabhushi A. Radiomic features from pretreatment biparametric MRI predict prostate cancer biochemical recurrence: Preliminary findings. J Magn Reson Imaging. 2018;48(6):1626–36. https://doi.org/10.1002/jmri.26178.
308. Fujita A, Buch K, Li B, Kawashima Y, Qureshi MM, Sakai O. Difference between HPV-positive and HPV-negative non-oropharyngeal head and neck cancer: texture analysis features on CT. J Comput Assist Tomogr. 2016;40(1):43–7. https://doi.org/10.1097/RCT.0000000000000320.
309. Fave X, Zhang L, Yang J, Mackin D, Balter P, Gomez D, Followill D, Jones AK, Stingo F, Liao Z, Mohan R, Court L. Delta-radiomics features for the prediction of patient outcomes in non-small cell lung cancer. Sci Rep. 2017;7(1):588. https://doi.org/10.1038/s41598-017-00665-z.
310. Story MD, Durante M. Radiogenomics. Med Phys. 2018;45(11):e1111–22. https://doi.org/10.1002/MP.13064.
311. Incoronato M, Aiello M, Infante T, Cavaliere C, Grimaldi AM, Mirabelli P, Monti S, Salvatore M. Radiogenomic analysis of oncological data: a technical survey. Int J Mol Sci. 2017;2017(18):805. https://doi.org/10.3390/IJMS18040805.
312. Mazurowski MA. Radiogenomics: what it is and why it is important. J Am Coll Radiol. 2015;12(8):862–6. https://doi.org/10.1016/J.JACR.2015.04.019.
313. Chang XP, Grinband XJ, Weinberg XBD, Bardis XM, Khy XM, Cadena XG, Su M-Y, Cha XS, Filippi XCG, Bota XD, Baldi XP, Poisson XLM, Jain XR, Chow XD. Deep-learning convolutional neural networks accurately classify genetic mutations in gliomas. Am J Neuroradiol. 2018;39(7):1201–7. https://doi.org/10.3174/ajnr.A5667.
314. Bibault JE, Giraud P, Durdux C, Taieb J, Berger A, Coriat R, Chaussade S, Dousset B, Nordlinger B, Burgun A. Deep learning and radiomics predict complete response after neo-adjuvant chemoradiation for locally advanced rectal cancer. Sci Rep. 2018;8(1):1–8. https://doi.org/10.1038/s41598-018-30657-6.
315. Chaudhary K, Poirion OB, Lu L, Garmire LX. Deep learning–based multi-omics integration robustly predicts survival in liver cancer. Clin Cancer Res. 2018;24(6):1248–59. https://doi.org/10.1158/1078-0432.CCR-17-0853.
316. West CM, Barnett GC. Genetics and genomics of radiotherapy toxicity: towards prediction. Genome Med. 2011;3(8):1–15. https://doi.org/10.1186/GM268/TABLES/5.
317. Sibbald B, Roland M. Understanding controlled trials: why are randomised controlled trials important? BMJ. 1998;316(7126):201. https://doi.org/10.1136/BMJ.316.7126.201.
318. Van Poucke S, Thomeer M, Heath J, Vukicevic M. Are randomized controlled trials the (g)old standard? From clinical intelligence to prescriptive analytics. J Med Internet Res. 2016;18(7):E185. https://doi.org/10.2196/JMIR.5549. https://www.jmir.org/2016/7/E185
319. Mayo CS, Matuszak MM, Schipper MJ, Jolly S, Hayman JA, Ten Haken RK. Big data in designing clinical trials: opportunities and challenges. Front Oncol. 2017;7(AUG):187. https://doi.org/10.3389/FONC.2017.00187/BIBTEX.
320. Weissler EH, Naumann T, Andersson T, Ranganath R, Elemento O, Luo Y, Freitag DF, Benoit J, Hughes MC, Khan F, Slater P, Shameer K, Roe M, Hutchison E, Kollins SH, Broedl U, Meng Z, Wong JL, Curtis L, et al. The role of machine learning in clinical research: transforming the future of evidence generation. Trials. 2021;22(1):1–15. https://doi.org/10.1186/S13063-021-05489-X/FIGURES/3.
321. Lambin P, Rios-Velazquez E, Leijenaar R, Carvalho S, van Stiphout RG, Granton P, Zegers CM, Gillies R, Boellard R, Dekker A, Aerts HJ. Radiomics: extracting more information from medical images using advanced feature analysis. Eur J Cancer. 2012;48(4):441–6. https://doi.org/10.1016/j.ejca.2011.11.036.
322. Keek SA, Leijenaar RT, Jochems A, Woodruff HC. A review on radiomics and the future of theranostics for patient selection in precision medicine. Br J Radiol. 2018;91(1091):20170926. https://doi.org/10.1259/bjr.20170926.
323. Buch K, Fujita A, Li B, Kawashima Y, Qureshi MM, Sakai O. Using texture analysis to determine human papillomavirus status of oropharyngeal squamous cell carcinomas on CT. AJNR Am J Neuroradiol. 2015;36(7):1343–8. https://doi.org/10.3174/ajnr.A4285.
324. Gugliandolo SG, Pepa M, Isaksson LJ, Marvaso G, Raimondi S, Botta F, Gandini S, Ciardo D, Volpe S, Riva G, Rojas DP, Zerini D, Pricolo P, Alessi S, Petralia G, Summers PE, Mistretta FA, Luzzago S, Cattani F, De Cobelli O, Cassano E, Cremonesi M, Bellomi M, Orecchia R, Jereczek-Fossa BA. MRI-based radiomics signature for localized prostate cancer: a new clinical tool for cancer aggressiveness prediction? Sub-study of prospective phase II trial on ultra-hypofractionated radiotherapy (AIRC IG-13218). Eur Radiol. 2021;31(2):716–28. https://doi.org/10.1007/s00330-020-07105-z.
325. Shiradkar R, Podder TK, Algohary A, Viswanath S, Ellis RJ, Madabhushi A. Radiomics based targeted radiotherapy planning (Rad-TRaP): a computational framework for prostate cancer treatment planning with MRI. Radiat Oncol. 2016;11(1):148. https://doi.org/10.1186/s13014-016-0718-3.
326. Aerts HJ, Velazquez ER, Leijenaar RT, Parmar C, Grossmann P, Carvalho S, Bussink J, Monshouwer R, Haibe-Kains B, Rietveld D, Hoebers F, Rietbergen MM, Leemans CR, Dekker A, Quackenbush J, Gillies RJ, Lambin P. Decoding tumour phenotype by noninvasive imaging using a quantitative radiomics approach. Nat Commun. 2014;5:4006. Erratum in: Nat Commun. 2014;5:4644. Cavalho, Sara [corrected to Carvalho, Sara]. https://doi.org/10.1038/ncomms5006.
327. Carvalho S, Leijenaar RTH, Troost EGC, van Timmeren JE, Oberije C, van Elmpt W, de Geus-Oei LF, Bussink J, Lambin P. 18F-fluorodeoxyglucose positron-emission tomography (FDG-PET)-Radiomics of metastatic lymph nodes and primary tumor in non-small cell lung cancer (NSCLC)—a prospective externally validated study. PLoS One. 2018;13(3):e0192859. https://doi.org/10.1371/journal.pone.0192859.
328. Sörensen A, Carles M, Bunea H, Majerus L, Stoykow C, Nicolay NH, Wiedenmann NE, Vaupel P, Meyer PT, Grosu AL, Mix

M. Textural features of hypoxia PET predict survival in head and neck cancer during chemoradiotherapy. Eur J Nucl Med Mol Imaging. 2020;47(5):1056–64. https://doi.org/10.1007/s00259-019-04609-9.
329. Giannini V, Mazzetti S, Bertotto I, Chiarenza C, Cauda S, Delmastro E, Bracco C, Di Dia A, Leone F, Medico E, Pisacane A, Ribero D, Stasi M, Regge D. Predicting locally advanced rectal cancer response to neoadjuvant therapy with 18F-FDG PET and MRI radiomics features. Eur J Nucl Med Mol Imaging. 2019;46(4):878–88. https://doi.org/10.1007/s00259-018-4250-6.
330. Xiong J, Yu W, Ma J, Ren Y, Fu X, Zhao J. The role of PET-based radiomic features in predicting local control of esophageal cancer treated with concurrent chemoradiotherapy. Sci Rep. 2018;8(1):9902. https://doi.org/10.1038/s41598-018-28243-x.
331. Gnep K, Fargeas A, Gutiérrez-Carvajal RE, Commandeur F, Mathieu R, Ospina JD, Rolland Y, Rohou T, Vincendeau S, Hatt M, Acosta O, de Crevoisier R. Haralick textural features on T2 -weighted MRI are associated with biochemical recurrence following radiotherapy for peripheral zone prostate cancer. J Magn Reson Imaging. 2017;45(1):103–17. https://doi.org/10.1002/jmri.25335.
332. van Dijk LV, Langendijk JA, Zhai TT, Vedelaar TA, Noordzij W, Steenbakkers RJHM, Sijtsema NM. Delta-radiomics features during radiotherapy improve the prediction of late xerostomia. Sci Rep. 2019;9(1):12483. https://doi.org/10.1038/s41598-019-48184-3.
333. Cunliffe A, Armato SG 3rd, Castillo R, Pham N, Guerrero T, Al-Hallaq HA. Lung texture in serial thoracic computed tomography scans: correlation of radiomics-based features with radiation therapy dose and radiation pneumonitis development. Int J Radiat Oncol Biol Phys. 2015;91(5):1048–56. https://doi.org/10.1016/j.ijrobp.2014.11.030.
334. Hettal L, Stefani A, Salleron J, Courrech F, Behm-Ansmant I, Constans JM, Gauchotte G, Vogin G. Radiomics method for the differential diagnosis of radionecrosis versus progression after fractionated stereotactic body radiotherapy for brain oligometastasis. Radiat Res. 2020;193(5):471–80. https://doi.org/10.1667/RR15517.1.

Further Reading

Coppes RP, Dubrovska A. Targeting stem cells in radiation oncology. Clin Oncol (R Coll Radiol). 2017;29(6):329–34. https://doi.org/10.1016/j.clon.2017.03.00.
Donlon NE, Power R, Hayes C, Reynolds JV, Lysaght J. Radiotherapy, immunotherapy, and the tumour microenvironment: turning an immunosuppressive milieu into a therapeutic opportunity. Cancer Lett. 2021;502:84–96. https://doi.org/10.1016/j.canlet.2020.12.045.
Horsman MR, Overgaard J. The impact of hypoxia and its modification of the outcome of radiotherapy. J Radiat Res. 2016;57(Suppl 1):i90–8. https://doi.org/10.1093/jrr/rrw007.
Huang Y, Fan J, Li Y, Fu S, Chen Y, Wu J. Imaging of tumor hypoxia with radionuclide-labeled tracers for PET. Front Oncol. 2021;11:731503. https://doi.org/10.3389/fonc.2021.731503.
Joiner MC, Van der Kogel AJ, editors. Basic clinical radiobiology. 5th ed. CRC Press; 2018.
McBride WH, Schaue D. Radiation-induced tissue damage and response. J Pathol. 2020;250(5):647–55. https://doi.org/10.1002/path.5389.
Reda M, Bagley AF, Zaidan HY, Yantasee W. Augmenting the therapeutic window of radiotherapy: a perspective on molecularly targeted therapies and nanomaterials. Radiother Oncol. 2020;150:225–35. https://doi.org/10.1016/j.radonc.2020.06.041.
Sebestyén A, Kopper L, Dankó T, Tímár J. Hypoxia signaling in cancer: from basics to clinical practice. Pathol Oncol Res. 2021;27:1609802. https://doi.org/10.3389/pore.2021.1609802.
Van de Guchte M, Mondot S, Doré J. Dynamic properties of the intestinal ecosystem call for combination therapies, targeting inflammation and microbiota, in ulcerative colitis. Gastroenterology. 2021;161(6):1969–1981.e12. https://doi.org/10.1053/j.gastro.2021.08.057.
Vogin G. Description and management of radiotherapy-induced long-term effects. In: Rauh S, editor. Survivorship care for cancer patients. Cham: Springer; 2021. https://doi.org/10.1007/978-3-030-78648-9_13.

6 Radiobiology of Combining Radiotherapy with Other Cancer Treatment Modalities

Vidhula Ahire, Niloefar Ahmadi Bidakhvidi, Tom Boterberg, Pankaj Chaudhary, Francois Chevalier, Noami Daems, Wendy Delbart, Sarah Baatout, Christophe M. Deroose, Cristian Fernandez-Palomo, Nicolaas A. P. Franken, Udo S. Gaipl, Lorain Geenen, Nathalie Heynickx, Irena Koniarová, Vinodh Kumar Selvaraj, Hugo Levillain, Anna Jelínek Michaelidesová, Alegría Montoro, Arlene L. Oei, Sébastien Penninckx, Judith Reindl, Franz Rödel, Peter Sminia, Kevin Tabury, Koen Vermeulen, Kristina Viktorsson, and Anthony Waked

V. Ahire (✉)
Chengdu Anticancer Bioscience, Ltd., Chengdu, China

J. Michael Bishop Institute of Cancer Research, Chengdu, China

N. Ahmadi Bidakhvidi · C. M. Deroose
Department of Nuclear Medicine, University Hospitals Leuven, Leuven, Belgium

Nuclear Medicine and Molecular Imaging, Department of Imaging and Pathology, KULeuven, Leuven, Belgium
e-mail: niloefar.ahmadibidakhvidi@uzleuven.be; christophe.deroose@uzleuven.be

T. Boterberg
Department of Radiation Oncology, Ghent University Hospital, Ghent, Belgium

Particle Therapy Interuniversity Center Leuven, Department of Radiation Oncology, University Hospitals Leuven, Leuven, Belgium
e-mail: Tom.Boterberg@ugent.be

P. Chaudhary
Patrick G. Johnston Center for Cancer Research, Queen's University Belfast, Northern Ireland, United Kingdom
e-mail: p.chaudhary@qub.ac.uk

F. Chevalier
UMR6252 CIMAP, Team Applications in Radiobiology with Accelerated Ions, CEA-CNRS-ENSICAEN-Université de Caen Normandie, Caen, France
e-mail: chevalier@ganil.fr

N. Daems
Radiobiology Unit, Belgian Nuclear Research Centre, SCK CEN, Mol, Belgium

W. Delbart
Nuclear Medicine Department, Hôpital Universitaire de Bruxelles (H.U.B.), Brussels, Belgium
e-mail: wendy.delbart@bordet.be

S. Baatout
Radiobiology Unit, Belgian Nuclear Research Centre (SCK CEN), Mol, Belgium

Institute of Nuclear Medical Applications, Belgian Nuclear Research Center (SCK CEN), Mol, Belgium
e-mail: sarah.baatout@sckcen.be

C. Fernandez-Palomo
Institute of Anatomy, University of Bern, Bern, Switzerland
e-mail: cristian.fernandez@unibe.ch

N. A. P. Franken · A. L. Oei
Department of Radiation Oncology, Amsterdam University Medical Centers, Location University of Amsterdam, Amsterdam, The Netherlands

Center for Experimental and Molecular Medicine (CEMM), Laboratory for Experimental Oncology and Radiobiology (LEXOR), Amsterdam, The Netherlands

Cancer Biology and Immunology, Cancer Center Amsterdam, Amsterdam, The Netherlands
e-mail: N.A.P.Franken@amsterdamumc.nl

U. S. Gaipl
Translational Radiobiology, Department of Radiation Oncology, Universitätsklinikum Erlangen, Erlangen, Germany
e-mail: udo.gaipl@uk-erlangen.de; A.L.Oei@amsterdamumc.nl

L. Geenen
Radiobiology Unit, Belgian Nuclear Research Centre, SCK CEN, Mol, Belgium

Department of Radiology and Nuclear Medicine, Erasmus Medical Center, Rotterdam, The Netherlands

N. Heynickx
Radiobiology Unit, Belgian Nuclear Research Centre, SCK CEN, Mol, Belgium

Department of Molecular Biotechnology, Ghent University, Ghent, Belgium
e-mail: nathalie.heynickx@sckcen.be

S. Baatout (ed.), *Radiobiology Textbook*, https://doi.org/10.1007/978-3-031-18810-7_6

I. Koniarová
Department of Radiation Protection in Radiotherapy, National Radiation Protection Institute, Prague, Czech Republic
e-mail: irena.koniarova@suro.cz

V. K. Selvaraj
Department of Radiation Oncology, Thanjavur Medical College, Thanjavur, India

H. Levillain · S. Penninckx
Medical Physics Department, Hôpital Universitaire de Bruxelles (H.U.B.), Bruxelles, Belgium
e-mail: hugo.levillain@bordet.be; sebastien.penninckx@bordet.be

A. J. Michaelidesová
Nuclear Physics Institute of the Czech Academy of Sciences, Rez, Czech Republic

Faculty of Nuclear Sciences and Physical Engineering, Prague, Czech Republic
e-mail: michaelidesova@ujf.cas.cz

A. Montoro
Laboratorio de Dosimetría Biológica, Servicio de Protección Radiológica Hospital Universitario y Politécnico la Fe, Valencia, Spain
e-mail: montoro_ale@gva.es

J. Reindl
Section Biomedical Radiation Physics, Institute for Applied Physics and Measurement Technology, Universität der Bundeswehr München, Neubiberg, Germany
e-mail: judith.reindl@unibw.de

F. Rödel
Department of Radiotherapy and Oncology, Goethe University, Frankfurt am Main, Germany
e-mail: franz.roedel@kgu.de

P. Sminia
Department of Radiation Oncology, Amsterdam University Medical Centers, Location Vrije Universiteit/Cancer Center Amsterdam, Amsterdam, The Netherlands
e-mail: p.sminia@amsterdamumc.nl

K. Tabury
Radiobiology Unit, Belgian Nuclear Research Centre (SCK CEN), Mol, Belgium

Department of Biomedical Engineering, University of South Carolina, Columbia, SC, United States of America
e-mail: kevin.tabury@sckcen.be

K. Vermeulen
Institute of Nuclear Medical Applications, Belgian Nuclear Research Centre SCK CEN, Mol, Belgium
e-mail: koen.vermeulen@sckcen.be

K. Viktorsson
Department of Oncology/Pathology, Karolinska Institutet, Stockholm, Sweden
e-mail: Kristina.viktorsson@ki.se

A. Waked
Radiobiology Unit, Belgian Nuclear Research Centre, SCK CEN, Mol, Belgium

Laboratory of Nervous System Disorders and Therapy, GIGA Neurosciences, Université de Liège, Liège, Belgium
e-mail: anthony.waked@sckcen.be

Learning Objectives

- To understand the biological rationale and characteristics of conventional and alternative fractionation schemes used in clinical RT practice and get insight into the biological aspects (acceptability of high dose fractions, optimal dose-time) of hypofractionation regimen.
- To understand the definition and radiobiologic principles of Stereotactic Body Radiation Therapy (SBRT)/hypofractionation/boron neutron capture therapy (BNCT); and learn about their treatment planning and associated applications in clinical settings.
- To understand the basic concept of combining RT with various other treatment modalities that can enhance the effect of radiation by specifically targeting cancer cells or the immune system as well as for minimizing the adverse effects on normal cells.
- To understand the principles and clinical applications of both diagnostic and therapeutic radiopharmaceuticals.
- To grasp the different methods of spatial RT fractionation and how tissue is spared by using these methods.
- To learn basic principles of brachytherapy and understand the principles, treatment course and planning, application in clinical setting as well as the theory behind personalized radioembolization/selective internal radiotherapy (SIRT).
- To study the basic concepts and clinical applications of diagnostic/therapeutic radiopharmaceuticals and high linear energy transfer (LET) carbon ion irradiation.
- To get an overview of nanotechnology and how it can improve treatment of cancer as well as challenges of translating it into clinical settings.
- To acquire an understanding of the risk factors involved in acquiring secondary tumors after RT.

6.1 Physics

Radiotherapy (RT) relies on the effect of ionizing radiation (IR) to biological matter, i.e., cells. The radiation is transferring its energy to atoms and molecules present in the cells, which lie in the path of the radiation, and therefore ionizing them. These ionizations, i.e., the removal of electrons from the atom, lead to the breaking of chemical bonds in the molecules. If these ionizations occur in the cell nucleus, the DNA, carrier of the human genome, is damaged. In RT, the capability of radiation to damage the genome is exploited to kill tumor cells. The most important quantity to define the damage, which is caused, is the dose

$$D = \frac{\mathrm{d}E}{\mathrm{d}M} \tag{6.1}$$

i.e., the energy transferred from the ion to the matter (dE) by unit mass (dM). In general, one can say that the higher the dose, the larger the damage and the higher the probability of killing a cell. However, the same physical dose of different types of radiation can cause different damage in the cells. Various types of radiation are utilized for RT. These types of radiation can be distinguished by the so-called depth dose distribution, which is the dose which is transferred to matter along the path of radiation as shown in Fig. 6.1.

Electron radiation transfers most of its energy just after it interacts with matter, i.e., tissue, making it suitable for the treatment of tumors close to the skin. If one uses electrons with higher energy, such as the shown 250 MeV electrons, the dose peak can be shifted deeper into the tissue. However, this comes with the disadvantage that the maximum range is also longer, resulting in more dose to the normal tissue beyond the tumor. Furthermore, such electron beams are quite complicated to produce. For photon beams used in RT, the dose increases in the so-called build-up region until it reaches the maximal dose and then gradually decreases. The depth of the maximal dose can be a few μm (for kV beams, i.e., beams with particle energy in the kilovolt regime) or several mm or cm (for MV (megavolt) beams). In contrast to electrons and photons, particles such as protons or high linear energy transfer (LET) carbon ions show a totally different dose distribution depth. The ions deliver a low dose when entering tissue. With depth this transfer is slowly increasing, while the ion gets slower. With further energy loss and decreasing speed, the dose drastically increases and reaches a maximum just before the ion stops in the tissue. This unique dose distribution is called the Bragg curve in honor to the physicist William Henry Bragg, who discovered this behavior in 1904 [1]. To widen the treatment depth range, a spread-out Bragg peak (SOBP) is created by varying the energy of the incident proton beam. As a result, a uniform dose can be delivered to the tumor. The radiobiological impact of particles with high LET is higher compared to photons, and it increases dramatically in the distal edge and fall-off. The uncertainty in relative biological effectiveness (RBE) of ion beams is still a limitation in its clinical application and should be considered during the treatment planning as a part of the process leading to a robust treatment plan. A detailed description about the physical and biological interactions of radiation to biological matter and the consequences for the biological effect can be found in Chaps. 2 and 3.

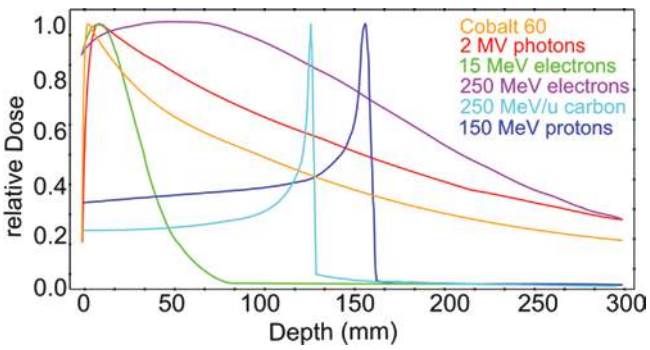

Fig. 6.1 Comparison of the relative depth dose distribution of 15 MeV electrons (green), 250 MeV electrons (purple), 2 MeV photons (red), 150 MeV protons (dark blue), and 250 MeV/u carbon (turquoise) and cobalt 60 (orange)

6.2 Conventional and Alternative Radiation Schemes

Box 6.1 Conventional and Alternative Radiation Schemes

- Typical conventionally fractionated irradiation schemes use 2 Gy fractions, 5 fractions per week for 3–7 weeks, depending on the tumor type.
- Alternative radiation schemes, i.e., either smaller or larger sized fractions, multiple fractions per day, or different overall treatment time should be based on the various biological processes and response characteristics of both the normal and malignant tissues in the exposed volume.

When using radiation for cancer treatment purposes, the total radiation dose is generally applied in a regimen with multiple small fractions, aiming to reach tumor kill while sparing adjacent normal, healthy tissues, and organs. Most tumors are treated with a conventional fractionation regimen, which is characterized by daily fractions of 1.8–2 Gy, 5 days per week, for a duration of 3–7 weeks,

Table 6.1 Characteristics of radiotherapy treatment regimen and involved radiobiological processes. (Reproduced with permission from [2])

Radiation treatment regimen	Conventional fractionation	Hyperfractionation	Accelerated fractionation	Hypofractionation	SBRT and SRS
Total dose (Gy)	70	≥70	<70	<70	<30
Fraction size (Gy)	1.8–2	<1.8	≥2	Mostly 2.5–10	Mostly ~12–25
Number of fractions per day	1	2–3	1	1	1
Treatment (days per week)	5	5	6	≤5	1 or a few
Overall treatment time (weeks)	7	7	Up to ~5	Up to ~5	–
Radiobiological reasoning—note the 6 **R**s of Radiobiology	Normal tissue sparing via **R**epair and **R**epopulation. Tumor control via **R**edistribution and **R**eoxygenation. **R**eactivation of the immune response.	Exploitation of differences in **R**adiosensitivity and **R**epair and—kinetics between normal and tumor cells. **R**eactivation of the immune response.	Overcoming tumor cell **R**epopulation. **R**eactivation of the immune response.	Overcoming tumor cell **R**epopulation.	Overcoming tumor cell **R**epopulation.

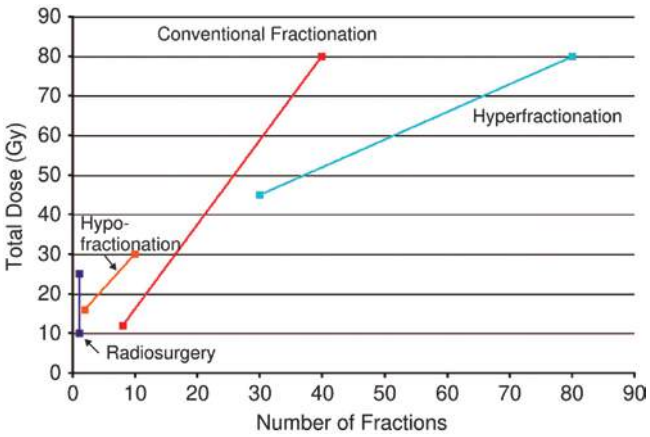

Fig. 6.2 Fractionation regimen used in clinical practice. (Reproduced with permission from [3])

reaching a total dose of 30–70 Gy. However, considering the radiation sensitivity and volume of the particular tumor type to be irradiated, as well as that of the normal tissue or organs at risk (OAR), an alternative irradiation regimen might be preferred. The use of an alternative radiation scheme should be motivated, either technically, e.g., by minimizing the volume of the normal tissue in the radiation field by using precision RT or on the basis of the biological characteristics of the malignant tissue, i.e., the 6R's (see Chap. 5). Apart from technical and radiobiological arguments, department logistics as well as patients' condition or patients' comfort might justify the choice of an alternative radiation treatment (Box 6.1). Typical characteristics of fractionation regimens and their radiobiological rationale are presented in Table 6.1 and discussed below.

The relationship between the number of fractions and the total dose for a clinical radiation regimen is presented in Fig. 6.2.

6.2.1 Hyperfractionation

The biological rationale of hyperfractionation is the advantage of application of multiple small-sized fractions compared with conventional 2 Gy fractions to further spare the normal tissues relative to the malignant tissues. Because of the higher total dose, hyperfractionation could increase the tumor control probability. To limit the duration of the overall treatment time, generally 2–3 fractions per day, typically ~1.4 Gy, separated 4–6 h between the fractions are given. Some hyperfractionation clinical trials, however, showed an increase in late normal tissue side effects, which has been ascribed to the short time interval between fractions for complete repair of sublethal DNA damages, since late-responding tissues do have long repair half times in the order of 2–4 h. Additionally, hyperfractionation puts a heavy logistical burden on the RT department and the patient, especially in children who may need anesthesia.

6.2.2 Hypofractionation and Accelerated Fractionation

The rationale of both hypo- and accelerated fractionation strategies can be found in shortening the overall treatment time to anticipate tumor cell proliferation/repopulation. Generally, fractions larger than 2 Gy fractions are applied with few fractions per week, allowing to shorten the overall treatment duration with a few weeks versus conventional regimens. The hypofractionation approach has become feasible because of currently available precision radiation techniques and technology, with optimized radiation dose distribution.

The drawback of using high fraction sizes, the rationale, pro- and contra biological arguments, is discussed in the next Sect. 6.3.

The term accelerated fractionation applies to the use of multiple fractions per day, or increasing the number of treatment days per week (e.g., continue radiation during the weekend) to deliver a higher average total radiation dose than conventionally used. Hence, the overall treatment time of accelerated regimen is reduced. Often, both hypo- and hyperfractionated irradiation fit in this definition of accelerated fractionation. A typical example is the Continuous Hyperfractionated Accelerated RadioTherapy (CHART) treatment scheme, with 36 fractions of 1.5 Gy, total dose of 54 Gy in 12 days. In that scheme three fractions of 1.5 Gy were applied per day, with an interfraction time interval of 6 h, for 12 days, including the weekend. Details regarding the CHART clinical trials and outcomes are available in the literature. In particular, head and neck cancer patients with high epidermal growth factor receptor (EGFR) expressing tumors benefited from CHART [4].

6.2.3 Stereotactic Radiotherapy: Radiosurgery

Historically, the term stereotactic radiotherapy was used for a type of external RT of the brain that uses dedicated equipment being a stereotactic frame fixed to the head with screws just penetrating the outer part of the skull. This frame was used to immobilize the head, position the patient, and create a stereotactic "space" with a coordinate system that allows target definition in an *X*-, *Y*-, and *Z*-axis. The term stereotactic radiosurgery (SRS) is used when a single fraction of stereotactically guided conformal irradiation is delivered to a coordinate-defined target. More modern fixation systems no longer require the placement of an invasive frame, but make use of advanced thermoplastic masks combined with position verification and adaptation systems of the treatment machine's table. Different delivery systems can be used for radiosurgery: the originally SRS-dedicated GammaKnife system (using 201 small 60-Co sources) or linac-based systems (linear accelerator, CyberKnife, Tomotherapy).

Typical indications are single (or up to 3–5) brain metastases, meningiomas, acoustic neuromas, or arteriovenous malformations, all smaller than 3 cm in diameter. Depending on the indication, doses range between 12 Gy (benign lesions) and 20–25 Gy (metastases). Some centers also use radiosurgery to treat benign conditions like epilepsy and trigeminal neuralgia, requiring doses of 20–25 Gy up to 60–80 Gy, respectively.

The appearance of the effect of radiosurgery usually takes several months and may be accompanied by an inflammatory reaction that mimics tumor growth in the first 1–3 years. In some cases, overt brain radionecrosis may develop, requiring treatment with steroids or rarely the need for surgical removal of the affected area (see also Chap. 5) (Box 6.2).

Box 6.2 Hypofractionation

- Hypofractionation is the use of radiation dose fractions considerably larger than the conventional fraction size of 2 Gy.
- Hypofractionation could be beneficial over conventional fractionation because of precision RT together with specific biological phenomena such as hypoxia and sensitivity to dose fractionation of both the tumor target volume and organs at risk.

6.3 Radiobiological Aspects of Hypofractionation

Fractionated RT, using multiple small-sized fractions of 1.8–2 Gy, is the standard treatment of cancer patients. Over many decades, large evidence has been obtained from experimental studies *in vitro* or *in vivo* and later in clinical studies regarding the biological rationale of fractionated irradiation. Abundant evidence exists on the differential effect of fractionation between late-responding normal tissues and early responding normal tissues or tumors. Most normal tissues and organs benefit from fractionated RT, meaning that they can tolerate a higher total dose, while tumors are only slightly spared by dose fractionation. The smaller the fraction size—taking the overall treatment time allowing tumor cell repopulation into account—the wider the therapeutic window. Having learned that fractionation is a great method to spare normal tissues while keeping tumor control equal, hypofractionation, i.e., the use of dose fractions substantially larger than conventional 2 Gy fractions (see also Chap. 5) sounds not as a good idea. However, for two main reasons, hypofractionation has gained importance in radiation oncology: α

(1) Clinical data have shown that some tumor types like prostate carcinoma, malignant melanoma, and liposarcoma, are almost as sensitive to fractionated irradiation as their surrounding normal tissues. Such tumors can tolerate a higher biological dose than formerly thought when treated with 2 Gy fractions, hence behaving like late-responding normal tissues and thus are relatively spared by fractionation. Indeed, these tumor types are characterized with a low $\langle \alpha/\beta$ value of ~1–2 Gy in the Linear Quadratic (LQ) model. Breast and esophageal cancers also have α/β values close to those for normal tissues, in the order of ~5 Gy. (2) With the implementation of high precision RT techniques, highly conformal 3D dose distributions to the target volume can be obtained, with minimal radiation exposure to adjacent critical normal tissues and OAR. The HyTEC initiative (Hy dose per fraction, hypofractionated Treatment Effects in the Clinic) is to systemically pool published peer-reviewed clinical data to further define dose, vol-

Table 6.2 Hypofractionation: pro and contra biological arguments

Pros
• If α/β ratio tumor < α/β ratio normal tissue
• Only if small normal tissue/OAR volumes are exposed: high conformity RT
• Direct vascular injury
• Shorter overall time: beneficial in case of rapid proliferating tumors
• If the onset of accelerated tumor cell repopulation is faster using high-dose fractions, dose reduction without loss of tumor control could be achieved while diminishing late toxicity
• "Biological dose" escalation, which might result in better tumor control
• Activation of the immune response to attack tumor cells inside the irradiated volume and at distance, the abscopal effect
• Lower probability of induction of secondary tumors
Cons
• Mostly, α/β ratio tumor > α/β ratio normal tissue
• High-dose fractions are detrimental for normal tissues: higher probability of normal tissue complications, unless dose gradients are steep and the irradiated volume small
• No benefit from sensitization of hypoxic tumor cells via reoxygenation between fractions
• Radiosensitizing agents are potentially less effective when combined with high-dose fractions

ume, and outcome estimates for both normal tissue complication probability and tumor control [5] for SRS and SBRT, where single high radiation doses are common practice. Under certain conditions, like high conformity of RT with steep dose gradients toward the surrounding normal tissues, hypofractionation could be beneficial over conventional fractionation. In this section, the radiobiological pro- and contra arguments of hypofractionation, listed in Table 6.2 are discussed.

6.3.1 Hypofractionation and the Linear Quadratic (LQ) Model

The validity of the LQ model at high fraction sizes above approximately 6 Gy is questionable, and alternative radiobiological models are proposed. However, a strong pro-argument was derived from clinical data from non-small cell lung cancer patients treated with SBRT, either with a single dose or hypofractionated with 3–8 fractions. From the study [6], it was evident that the clinically observed increase in tumor could be ascribed to radiation dose escalation, i.e., an increased Biologically Effective Dose (BED) according to the LQ equation. BED values were calculated for the various hypofractionation schemes including SBRT fraction sizes of 22 Gy. No adaptation or correction was made when using the conventional LQ model. The analysis showed a clear correlation between treatment outcome and the BED, even at extreme high BED values. Hence, there is still a discrepancy between theoretical and experimental validity of the LQ model. However, since the model describes the clinical data on tumor control over a wide range of dose, fraction sizes, and treatment durations [6], it might still be valid in predicting RT outcomes in certain conditions.

6.3.2 Hypofractionation, Hypoxia, and Reoxygenation

Hypoxia is a state of reduced oxygen availability or decreased oxygen partial pressure below a critical threshold (generally at pO_2 of 2.5 or 5 mmHg). The Oxygen Enhancement Ratio (OER) is around 3 for most cells: for sterilization of hypoxic cells, a three times higher irradiation dose is required than for normoxic cells. Hence, hypoxia can cause resistance to RT, which has been observed in many tumor types. Information about the role of oxygen in RT, the OER, and related radiation sensitivity is given in Chap. 5.

In fractionated RT, during the time interval between daily applied irradiation fractions and during the full course of RT, hypoxic cells can be re-oxygenated and become more sensitive to the next irradiation dose (see Chap. 5). If reoxygenation is efficient between dose fractions, the presence of hypoxic cells does not have a significant effect on the outcome of a multi-fractionation scheme. In a hypofractionation regimen, the time period to obtain full reoxygenation of hypoxic tumor cells might be too short. Animal data on the kinetics of reoxygenation of different tumor types demonstrated that full reoxygenation takes about 72 h [7]. Also, preclinical data and radiobiological modeling studies have demonstrated that tumor hypoxia is a greater detrimental factor for single dose treatments than for repeated conventional fraction sizes. To fully exploit reoxygenation between fractions, 6–8 fractions might be optimal, separated in a time frame of 72 h [7]. However, there are also advantages to large high-dose fractions of ~10 Gy. Relatively radioresistant hypoxic cells might be directly sterilized and vascular endothelial cells might be injured. Since one endothelial cell is subtending about 2000 tumor cells, direct vascular damage might largely contribute to tumor cell kill in hypofractionated RT [8].

6.3.3 Hypofractionation and Tumor Cell Repopulation

Tumor cell repopulation refers to an increase in the number of cells as a result of proliferation of surviving clonogenic tumor cells (see Chap. 5). Accelerated repopulation of tumor cells during the course of RT is starting after a lag period of ~4 weeks. One strategy discussed here is to cope with tumor cell repopulation by limiting the overall treatment time for fast repopulating tumors using a small number of higher sized fractions. As a consequence of high fraction sizes, the total irradiation dose should be reduced to overcome an increase in

late normal tissue toxicity. Hypofractionation allows shortening of the overall treatment time, which might be more effective than long duration conventional fractionation in the treatment of rapidly proliferating tumors. However, care should be taken when using too short schedules, because they could lead to an increase in acute toxicity.

To be noticed is the large LQ model based analysis of the tumor control probability (TCP) from randomized trials on in total 7283 head and neck cancer (HNC) patients, featuring wide ranges of doses, times, and fractionation schemes [9]. In the analysis, two different LQ based models were used, assuming a dose-independent (DI) and a dose-dependent (DD) acceleration of tumor cell repopulation. Accelerated Repopulation (AR) was assumed to be triggered by the level of tumor cell killing, with other words, to begin at a time when the surviving fraction of the tumor clonogenic cells falls below a critical value. This starting point of AR of tumor cells was assumed to be dose-dependent and therefore reached at an earlier time point after high fraction sizes than after low fraction sizes. The DD model of AR provided significantly improved descriptions of a wide range of randomized clinical data, relative to the standard DI model. This preferred DD model predicted that, for currently used HNC fractionation regimen, the last 5 fractions did not increase TCP, but simply compensated for increased accelerated repopulation (Fig. 6.3). A hypofractionation scheme of 25 fractions of 2.4 Gy (total dose of 60 Gy in 33 days) was found to be superior over 35 fractions of 2 Gy (total dose of 70 Gy in 47 days), both regarding the probability of tumor control and late normal tissue complications. In a next study, on basis of radiobiological model calculations with the DD model, an optimized hypofractionated treatment scheme for HNC patients was proposed with 18 daily fractions of 3 Gy, i.e., a total dose of 54 Gy in 24 days [10].

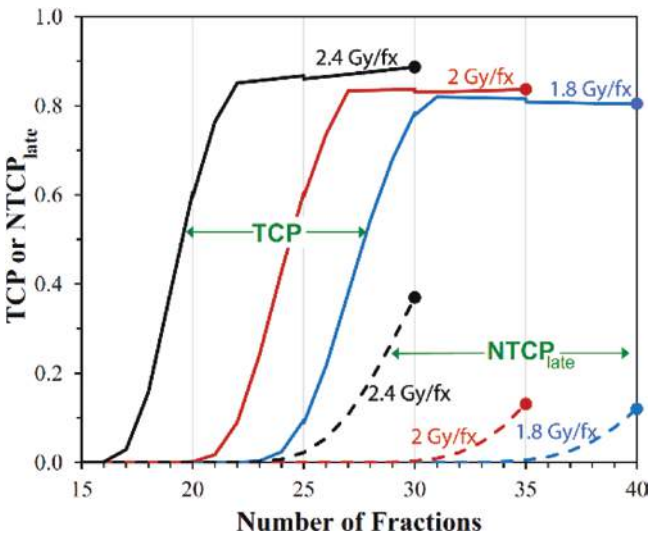

Fig. 6.3 Predicted TCP values by the DD model (solid curves) as a function of the number of fractions delivered, for stage $T_{1/2}$ head and neck cancer (HNC) patients. Dose per fraction (fx): 1.8 Gy (blue), 2.0 Gy (red) or 2.4 Gy (black), administered daily, 5 fx/week. NTCP late predictions for late toxicity (dashed curves) were made with the standard LQ model normalized to a 13.1% value (grade 3–5 late toxicity at 5 years) for 35 × 2 Gy fractions. The solid circles represent current standard treatment regimens. Thus, the final week of 5 fractions could be eliminated without compromising TCP, but resulting in significantly decreased late sequelae due to the lower total dose. (Reproduced with permission from [9])

6.3.4 Hypofractionation and the Immune Response

Radiation has long been thought to suppress the immune system, and total body irradiation is up to date applied for that reason. Studies in the past have demonstrated that local irradiation not only had a direct effect on tumor cells in the treatment volume, but also a systemic effect on the immune system (see Chap. 5). Therewith, local irradiation can induce abscopal effects, i.e., the immunological rejection of tumors or metastatic lesions distant from the irradiated site (see Chap. 5). Different radiation treatment schemes regarding the total dose and fraction size were shown to have diverse effects on the immune response, with a subsequent effect on combination therapy with immune-modulating agents [11]. The abscopal effect might best be exploited using 3–5 fractions of <10 Gy [12]. The immune-editing effects of radiation will probably also benefit from repeated intermediate high fraction sizes [13].

6.3.5 Hypofractionation and Radiosensitizing Agents

Hyperthermia and chemotherapeutic agents, e.g., cisplatin, gemcitabine, temozolomide and targeted drugs such as inhibitors of PARP-1 and EGFR may potentiate the effects of radiation. The LQ model is a very suitable tool to quantify the effects of the combination of irradiation and radiosensitizers, which can be either additive or synergistic. The most commonly used test to study interaction between irradiation and modulating agents is the clonogenic assay (see Chap. 3), being the golden standard test for determination of cell survival. LQ model analysis of the typical shaped cell survival curve allows to separately establish the effect of combination therapy on the ⟨ and ® α/β parameters of the model. The parameter ⟨ α determines the effectiveness at low doses, on the initial slope of the cell survival curve, while the parameter ® β represents the increasing contribution from cumulative damage thought to be due to interaction of two or more separate lesions. Preclinical studies have shown that most radiosensitizing agents cause an increase of the α-parameter, while the β-parameter is rarely affected [14]. With conven-

tional small-sized dose fractions, the value of the α-parameter therefore determines to a large extent the effectiveness of combination treatments. The interaction between chemotherapeutic agents and high-dose irradiation fractions will be minimal. For clinical hypofractionation regimen, it is to be expected that effects of radiosensitizing agents are smaller than when combined with conventional fractionation regimen.

6.3.6 Hypofractionation and Risk for Secondary Cancer

Long-term follow-up studies that address carcinogenic effects of fractionated high-dose RT describe the incidence of secondary malignancies, type of induced cancers, latency time, risk period as well as the shape of the dose–risk relationship curve. The dose–risk curve following curative RT is organ specific and is either linear, plateau, or bell-shaped. Radiobiological—LQ model based—calculations for estimation of the cancer risk following exposure to irradiation showed that both carcinoma and sarcoma risk decreased with increasing fraction size [9]. Via model calculations, it has been estimated that hypofractionated RT has the potential to reduce the second cancer risk [15].

6.4 External Beam Radiotherapy Strategies

6.4.1 Stereotactic Body Radiation Therapy (SBRT)

Box 6.3 Stereotactic Body Radiation Therapy (SBRT)

- The basic principle of SBRT is to deliver a tumoricidal dose to the target in a few fractions and minimize dose to normal tissue using highly conformal radiation.
- The high-dose per fraction used in SBRT can cause vascular damage through endothelial cell apoptosis and stem cell death.
- SBRT is commonly used in treatment of tumors in lung, liver, spine, prostate, and pancreas.

6.4.1.1 Definition

Stereotactic Body Radiation Therapy (SBRT) also known as Stereotactic Ablative Radiotherapy (SABR) refers to stereotactic image-guided delivery of highly conformal radiation to a small extracranial target using high-dose per fraction delivered in 1–5 fractions with a tumor-ablative intent [16]. The key requirements for SBRT are small well-circumscribed tumors (maximum cross-sectional diameter up to 5 cm), stringent patient immobilization, small or no margin for beam penumbra, high conformality and accurate radiation delivery as well as image guidance for geometric verification [17].

6.4.1.2 Radiobiologic Principles of SBRT

The aim of SBRT is to deliver tumoricidal dose to target in a few fractions and minimize dose to normal tissue by delivering highly conformal radiation under image guidance. A high-dose per fraction is more tumoricidal than conventional fractionation dose by its direct damaging action on tumor cells [6]. As discussed in Chap. 5 and earlier in this chapter, the effect on late-responding normal tissues is greater with high-dose per fraction. Few malignancies such as prostate cancer have low α/β values in the range of 1.5–3 Gy and show high sensitivity to fractionation (similar to late-responding normal tissues). In such malignancies, hypofractionation leads to better therapeutic benefit. On the other hand, delivering high-dose per fraction can increase toxicity in acute-responding tissues(see Chap. 5). To minimize this, a highly focused and conformal dose is delivered to the tumor with a steep dose gradient. It is achieved by reducing planned target volume (PTV) margins under image guidance, using multiple non-coplanar beams with careful treatment planning, and by delivering the total dose in two to five fractions (2–3 fractions per week) [7].

As discussed in Chap. 5, the bigger the tumor size the more is the hypoxic component and vice-versa. The advantage of reoxygenation seen during conventional fractionation is compensated in hypofractionated SBRT by selectively treating small tumors, which are relatively well oxygenated with a little hypoxic component. Furthermore, the hypoxic cells in tumors are depopulated by the direct damaging effect of large doses per fraction [6]. The same effect is responsible for overcoming the disadvantage of lack of reassortment of tumor cells to sensitive phases of cell cycle during fractionation. The high-dose per fraction counteracts the differences in radiosensitivity of cells in different phases of cell cycle by causing cell cycle arrest and interphase death in all phases (see Chap. 3).

Unlike conventional fractionation RT, owing to the short overall treatment time, tumor cell repopulation and interfraction repair of sublethal damage do not play a major role during SBRT (see Sect. 6.3). This is beneficial in terms of tumor control but detrimental to normal tissues.

However, when the treatment time of an individual fraction is prolonged for more than half an hour, intrafraction repair of some sublethal damage in rapidly proliferating tumor cells may occur [7]. However, such longer fraction treatment time and faster intrafraction repair result in greater loss of BED [18]. This can be overcome by increasing the dose rate with use of flattening filter free (FFF) beams.

It is postulated that the radiobiologic effect of SBRT also depends on two other mechanisms. One is the vascular damage due to endothelial cell apoptosis caused by high-dose per fraction. It has been reported that this occurs due to the structural abnormalities of tumor vessels that are dilated, tortuous, elongated and have a thin basement membrane [19]. The second mechanism is through radiation-induced immunologic responses. The strong T-cell response triggered after exposure to high-dose per fraction RT enhances cytotoxic effects [12]. In addition, SBRT when combined with immune checkpoint inhibitors, i.e., Programmed Cell Death Protein-1/Programmed Cell Death Ligand-1 (PD-1/PD-L1) targeting antibodies, e.g., pembrolizumab or cytotoxic T-lymphocyte-associated protein-4 (CTLA4) antibodies, e.g., ipilimumab has shown to trigger an immunologic response that produces an abscopal effect [12] as described in Chap. 5.

Conventional fractionation RT is modelled by the LQ model cell survival curve but at higher dose per fraction, it is thought that LQ model overestimates the effects of radiation [20]. Therefore, alternative radiobiological models like universal survival curve (USC) were proposed. Instead of the BED in the LQ model, USC calculates the standard effective dose (SED) which is the total dose administered in 2 Gy per fraction to produce the same effect [21]. There are arguments that the LQ model still holds good till a certain level of dose per fraction.

6.4.1.3 Treatment Planning

The RT treatment planning for SBRT involves various steps allowing proper delivery of SBRT. After appropriate patient selection, VacLoc bags are used for stringent patient immobilization and setup. The next step is to acquire treatment planning images using computed tomography (CT)/magnetic resonance (MR)/^{18}F-fluorodeoxyglucose (^{18}FDG) positron emission tomography (PET) simulator with patient setup in treatment position with immobilization devices [22]. Usually, images are taken in 1–3 mm slice thickness and scan length extends at least 5–10 cm superior and inferior beyond RT treatment field borders for coplanar beams and 15 cm for non-coplanar beams [22]. For tumors in the thorax and upper abdomen, respiration-induced organ and tumor motion may be an issue. Therefore, motion management strategies are utilized while treating these tumors (Table 6.3).

For SBRT, the target volumes and OARs are contoured as per the The International Commission on Radiation Units and Measurements (ICRU) 50 and 62 reports. The RT treatment planning is based on the American Association of Physicists in Medicine Task Group (AAPM TG) 101 recommendations [22]. Unlike uniform dose prescription in conventional RT, in SBRT, dose is prescribed to the low isodoses (e.g., 80% isodose line) with small or no margin for beam penumbra to improve sharp dose falloff outside the target volume, thereby reducing dose to adjacent normal tissues. Hence, dose heterogeneities and hotspots occurring within the target volumes are accepted in SBRT, unlike traditional RT where homogeneous dose distribution is desired. For obtaining an optimal SBRT treatment plan with better target dose conformality as well as isotropic dose gradient, multiple planar or non-coplanar treatment beams are used, and treatment is delivered using multileaf collimator (MLC) of width 5 mm or less [24]. The calculation grid size used in the

Table 6.3 Motion management methods in radiotherapy. Adapted from [23]

Motion management method	Rationale
Free breathing technique • Based on 4D CT	Generating of internal target volume (ITV) which covers the full range of tumor motion
Motion dampening techniques • Abdominal compression using paddle, pneumatic belts, etc. • Breath holding technique such as deep inspiratory breath hold (DIBH), active breath coordinator (ABC)	Limiting the diaphragm expansion and tumor motion by devices or by controlling breathing
Respiratory gating technique • Internal gating using internal surrogates for tumor motion • External gating using external devices to monitor respiration, a surrogate for tumor motion [such as real-time position management (RPM) system]	Treating the tumor only in discrete phases of respiratory cycle
Real-time tumor tracking • ExacTrac (Kilo-Voltage image-based system) • Cyberknife (Kilo-Voltage image-based robotic system) • Calypso (radiofrequency localization system)	Intrafraction tumor localization and repositioning of treatment beam toward the target

treatment planning system (TPS) affects the accuracy of calculated dose distribution. Hence, an isotropic grid size of 2 mm or finer is recommended.

The normal tissue tolerances derived from conventional fractionation studies do not apply to the high fractional doses delivered in SBRT. Therefore, bioeffect measures such as BED, normalized total dose (NTD), and equivalent uniform dose (EUD) are calculated to evaluate the effectiveness and safety of SBRT dose distributions [18, 25, 26]. BED and NTD are used to determine the biologic effectiveness of different dose fractionation schedules, whereas EUD is applied to rank different treatment plans based on their expected tumor effect [22]. The normal tissue tolerances for different SBRT fractionation schemes are still evolving. Apart from the traditional metrics reported in a RT treatment plan, SBRT plans must specify conformity index (CI = prescription isodose volume/PTV), heterogeneity index (HI = highest dose received by 5% of PTV/lowest dose received by 95% of PTV), and intermediate dose spillage (D50% = volume of 50% of prescription isodose curve/PTV or D2 cm = maximum dose at 2 cm from PTV) [22].

Recent advances in RT techniques and machines facilitate delivery of SBRT. Volumetric modulated arc therapy (VMAT) is an advanced RT technique that delivers radiation dose continuously in arcs where gantry rotation speed, treatment aperture, and dose rate vary simultaneously [27]. The newer linear accelerators (LINAC) capable of delivering flattening filter free (FFF) beams increases dose rate from 300 to 600 monitor units (MU)/min to 1200 to 2400 MU/min. Thereby, the time required to deliver the large number of MUs needed for high-dose per fraction in SBRT is decreased [28]. The FFF beams also have other advantages such as less off-axis beam hardening, less photon head scatter, less field size dependence, and less leakage outside beam collimators [29].

6.4.1.4 Clinical Applications

The clinical application of SBRT gained much interest over the past two decades. SBRT is commonly used in treatment of malignant tumors in lung, liver, pancreas, prostate, kidney, and spine (Table 6.4). It is also widely recommended for treating oligometastatic disease that has spread to liver, lung, bone, adrenals, or lymph nodes. Its clinical utility in breast cancer as well as head and neck cancers is being investigated. The common cancer subsites and clinical scenarios where SBRT has a role are summarized in Table 6.4.

Numerous phase 1/2 clinical trials have shown encouraging results regarding safety and efficacy of SBRT in different types and stages of cancer [31]. However, the major drawbacks of these trials are the adoption of variable radiation dose, fractionation schemes, and limited number of treated patients. Therefore, randomized phase 3 trial results on clinical outcomes and long-term toxicities are needed to recommend SBRT as the standard of care.

Table 6.4 Clinical application of SBRT at various cancer subsites. (Adapted from [30])

Cancer subsite	Indications
Lung	• Early-stage inoperable non-small cell lung cancer (NSCLC)—T1, T2, usually <5 cm, N0
	• Boost following definitive chemoradiation for locally advanced NSCLC
	• Recurrence/re-irradiation
	• Oligometastatic disease
Liver	• Hepatocellular carcinoma (HCC)—unresectable/medically inoperable patients, unsuitable/refractory to radiofrequency ablation, or transarterial chemoembolization
	• Oligometastatic disease
	• Portal vein tumor thrombosis (PVTT)
Pancreas	• Locally advanced unresectable disease—radical SBRT/SBRT boost following conventional fractionated RT
	• Borderline resectable disease—poor performance status
	• Re-irradiation
Prostate	• Low risk—SBRT monotherapy
	• Low volume intermediate risk—SBRT monotherapy/boost
	• High/very high/node positive disease—SBRT boost
	• Residual disease after RT—salvage/re-irradiation
Spine metastases	• Primary spinal cord neoplasms: medically inoperable/adjuvant/salvage SBRT
	• Spine metastases: limited disease, life expectancy more than 3 months, medically inoperable
	• Re-irradiation
Kidney	• Unilateral, medically inoperable disease
	• Bilateral/recurrent contralateral disease
Head and neck	• Re-irradiation: single, small volume recurrence, node negative
	• SBRT boost following definitive chemoradiation in locally advanced nasopharyngeal cancer
	• Palliation

6.4.2 FLASH Radiotherapy at Ultra-High Dose Rate

6.4.2.1 Principles

FLASH RT is emerging as a new tool for sparing normal tissue from ablative doses, as it is able to protect normal tissue while maintaining antitumor ablation [32]. FLASH RT targets tumors with ultra-high dose rates (>100 Gy/s) to reduce the administration time from minutes to less than 200 ms, as this is key to sparing normal tissue [32]. The biological mechanism behind the sparing of normal tissue, known as the "FLASH effect," is based on the following hypothesis:

The oxygen depletion hypothesis describes the rapid consumption of local oxygen by ultra-high dose rates resulting in transient radioprotection and transient local tissue hypoxia. It is known that hypoxic tissue is more radioresistant because the low concentration of molecular oxygen during radiation-induced DNA damage allows DNA repair, while in the presence of molecular oxygen, the DNA lesion binds to molecular oxygen and produces peroxyl radicals leading to the degradation of nucleic acids and lipids [32]. Therefore the oxygen depletion hypothesis suggests that FLASH RT may be able to prevent or reduce Reactive Oxygen Species (ROS)-mediated cellular damage [33]. However, this hypothesis has recently been challenged as studies showed that FLASH RT does not significantly decrease tissue oxygen concentration compared with conventional RT when measured with a solid optical sensor [34]. The differential ROS-damage recovery hypothesis describes that normal and tumor cells have different capabilities to "detoxify" themselves from ROS [32]. According to this hypothesis, normal cells have a greater capacity to eliminate peroxidized compounds compared to tumors. This would explain why tumors exposed to FLASH RT respond equally under either physiologic or hypoxic conditions.

6.4.2.2 Main Indications

Preclinical studies of FLASH RT confirmed its efficacy in various animal models (mice, pigs, cats, zebrafish) as well as in different tissues (lung, brain, intestine, skin) and led to the first use of FLASH RT in the clinic. One example is a man that had a cutaneous lymphoma that had spread over the entire surface of his skin. He had already received several sessions of conventional RT and the skin's tolerance was exhausted. FLASH RT was indicated as a way to spare the skin while achieving equivalent tumor control to conventional RT. The lesion received 15 Gy as a single dose in 90 ms. The treatment was successful, with no skin toxicity and complete ablation of the tumor as reported 6 months after treatment [33] (Fig. 6.4).

Apart from this successful case, the current use of FLASH RT in the clinic is limited to enrolling participants in clinical trials. However, in the near future patients with tumors in organs described as late-responding tissues would be good candidates for FLASH RT, as preclinical studies have shown that ultra-high dose rates dramatically reduce the incidence of pulmonary fibrosis and neurocognitive impairment. Patients with painful bone metastases in the extremities would also be good candidates to investigate the feasibility and safety of FLASH RT.

Fig. 6.4 Temporal evolution of the treated lesion: (**a**) before treatment with the limits of the PTV delineated in black; (**b**) at 3 weeks, at the peak of the skin reaction (grade 1 epithelitis NCI-CTCAE v 5.0); (**c**) at 5 months. (Reproduced with permission from [33])

6.4.2.3 Treatment Course

Before starting treatment with FLASH RT, one needs to be aware of the importance of the radiation source, the quality of the radiation, and the physical parameters of the beam.

- Radiation sources are currently standardized to deliver dose rates of about 0.1–0.4 Gy/s in 2 Gy daily fractions. FLASH RT, on the other hand, relies on facilities capable of delivering ultra-high dose rates in large doses in one or more pulses over microseconds. This capability has only been achieved in a few places by modifying clinical devices to deliver photons, protons, or electrons. There are large irradiation facilities such as the European Synchrotron that can deliver X-rays at dose rates of up to 16,000 Gy/s [35]. However, clinical trials using synchrotrons are not yet an option.
- The quality of the radiation must also be considered, as most research on FLASH RT has been done with electrons. FLASH RT with electrons has been shown to be effective in at least one human patient, while FLASH RT with photons and protons is still in the preclinical phase. Regardless of preclinical or clinical status, the quality of radiation needs to be considered to account for (1) the impact of the linear energy transfer on the mechanisms behind the FLASH effect and (2) the use of a continuous beam in the case of protons versus a pulsed beam in the case of electrons and synchrotron X-rays [32].
- The physical parameters of FLASH RT need to be defined much more precisely than in conventional RT. A team of experts from Switzerland has suggested that the number of pulses, the instantaneous intra-pulse dose rate (≥104 Gy/s), and the total exposure time (<100 ms) should be included in all studies of FLASH RT [33, 35]. These parameters mostly derive from FLASH RT with electrons and therefore should be carefully applied to FLASH RT with photons or protons.

In summary, FLASH RT is not yet actively used in the clinic. However, it is now clear that FLASH RT requires very precise management of the radiation quality and beam.

6.4.2.4 Therapeutic Intent

The patient population that would benefit from clinical trials with FLASH RT are those who still have radioresistant tumors for which even the most sophisticated intensity-modulated RT has not been successful. In this context, FLASH RT could be combined with immunotherapy to achieve a synergistic effect. This strategy is supported by the immune hypothesis, which builds on the oxygen depletion hypothesis by proposing that FLASH RT protects circulating and resident immune cells that are normally radiosensitive. This radiosensitivity is particularly important when radiation fields affect bone marrow and/or circulating blood cells [36], as doses as low as 0.5 Gy can reduce lymphocyte survival by 90% [37]. Therefore, FLASH RT has the potential to spare immune cells from the radiation dose and allow recognition of tumor antigens to potentially trigger an antitumor immune response [33].

6.4.3 Boron Neutron Capture Therapy (BNCT)

Box 6.4 Boron Neutron Capture Therapy (BNCT)

- The basic principle of BNCT is selective targeting of tumor cells while sparing normal tissues using boron-carrier agents and low-energy neutrons.
- Three boron-delivery agents approved for human clinical trials are sodium borocaptate (BSH), boronophenylalanine (BPA), and sodium decaborane (GB-10).
- The clinical trials on BNCT were conducted predominantly in brain malignancies, malignant melanoma, and recurrent head and neck cancers.

6.4.3.1 Principles

The basic principle of BNCT is to deliver a boron-containing drug that selectively attaches to cancer cells and has a large cross-section capable of capturing a low-energy neutron. After administration of the boron-containing compound, the patient is exposed to a beam of thermal or epithermal neutrons. The compound goes into an excited state after neutron capture and undergoes a nuclear fission reaction to produce densely ionizing alpha particles. The range of these high LET particles in tissues is limited around 7.6 μm on an average (range 5–9 μm) [38, 39]. Therefore, these particles lead to localized release of a substantial amount of energy within the tumor, sparing the normal tissues. The boron neutron chemical reaction is as follows:

$$^{10}B_5 + {}^{1}n_0 \rightarrow {}^{11}B_6 \rightarrow {}^{7}Li_3 + {}^{4}He_2 + \text{gamma ray} + 2.4\,\text{MeV} \quad (6.2)$$

A photon of 0.48 MeV is released in most of the fission events which is useful for monitoring the reaction and has little significance in terms of cell killing [40]. Similarly, the radiobiologic effect of the low-energy thermal neutrons themselves is little.

6.4.3.2 Boron Compounds

The success of BNCT largely depends on the properties of the boron compound used. An ideal boron compound should be non-toxic, have a high absolute boron concentration in tumors, have high specificity for malignant cells, and accumulate in low concentrations in adjacent normal tissues and blood [40]. To summarize, an ideal boron-carrier compound should have a high tumor-to-normal tissue ratio (around 3–4:1) [41].

Based on the molecular weight, there are two classes of boron compounds such as low-molecular weight (LMW) agents and high-molecular weight (HMW) agents. The LMW agents can cross the cell membrane and retain inside the cell. Examples are sodium borocaptate and boronophenylalanine. HMW agents are boron-containing monoclonal antibodies, bispecific antibodies, liposomes, nanoparticles, or conjugates of epidermal growth factor. They are highly specific to tumors but cannot cross the blood–brain barrier in adequate concentration to be of some utility clinically. However, they can be used only when blood–brain barrier is disrupted, or when delivered directly intracerebrally [41].

The boron-carrier agents that are approved for human clinical trials are sodium mercaptoundecahydro-closo-dodecaborate ($Na_2B_{12}H_{11}SH$) also known as sodium borocaptate (BSH), (L)-4-dihdroxy-borylphenyalanine also known as boronophenylalanine (BPA) and sodium decaborane (GB-10) [42]. Among the three, only BPA has a relatively higher tumor-specific uptake. It gets concentrated in cells synthesizing melanin. BPA is capable of taking up ^{18}F, therefore ^{18}F incorporated BPA positron emission tomography (PET) imaging is done to assess the boron concentration in tumor cells [43].

6.4.3.3 Source of Neutrons

The low-energy neutrons used in BNCT are produced from nuclear reactors through nuclear fission reactions and are either thermal neutrons or epithermal neutrons (Table 6.5).

Thermal neutrons have the same average kinetic energy as gas molecules in the environment, which is little. Whereas epithermal neutrons are intermediate energy range neutrons formed during the transition of energetic neutrons to slow/thermal neutrons [44]. If a tumor at a depth of more than few centimeters is to be treated effectively with BNCT using thermal neutrons, then the normal tissues at the surface will be irradiated with a very high dose. Whereas with epithermal neutrons, the very high surface dose can be avoided [41]. But the depth dose distribution with both the types of neutrons is poor. In addition, the low-energy neutrons produced in nuclear reactors are contaminated with gamma rays and fast neutrons, both of which have different radiobiologic properties. Apart from this, there are capture reactions taking place with the naturally occurring isotopes in tissues such as ^{1}H, ^{12}C, ^{14}Ni, ^{16}O, ^{35}Cl, etc. These contaminants cause biologic damage even in normal tissues without ^{10}B concentration.

Table 6.5 Neutrons used in BNCT and their characteristics. (Adapted from [41])

Type of neutrons	Energy (eV)	Characteristics
Thermal/slow neutrons	0.025	1. Attenuates rapidly in tissues 2. Half value layer is about 1.5 cm 3. Reacts with boron to produce high-LET particles
Epithermal	1–10,000	1. Peak dose at about 2–3 cm 2. Rapid falloff beyond peak dose 3. Do not react with boron but degrades to thermal neutrons by collisions with hydrogen atoms in tissues

6.4.3.4 Treatment Planning

The dose in the radiation field is expressed as RBE-weighted dose, Gy_w. A weighted dose is used to take into consideration the radiobiological effects of alpha particles, gamma rays, fast neutrons and capture reactions occurring with the use of nuclear reactor-generated neutron beams. The weighting factor depends on the boron-delivery agent used, which determines the concentration of ^{10}B in cells and which in turn dictate the effectiveness of BNCT [42, 45]. Boron levels in a patient's blood can be measured but the concentration in tumor cells and adjacent normal tissues are based on earlier experimental studies [42]. Therefore, different weighting factors are used for tumor cells and normal tissues in the region of interest.

The Monte Carlo method is utilized for RT dose calculation. Unlike conventional dose planning algorithms, the Monte Carlo method takes into consideration the influence of inhomogeneities on dose delivered by primary radiation as well as scattered radiation [46]. This makes it appropriate from the BNCT standpoint where the dose contribution is from different by-products of nuclear fission reactions and contaminants in low-energy neutron beams from nuclear reactors. RT is delivered in single fraction or multiple fractions using oppositional or multiple fields.

6.4.3.5 Clinical Applications

The early human clinical trials carried out in Brookhaven National Laboratory and Japan did not show encouraging results with BNCT. It was widely tried out for treating

central nervous system (CNS) malignancies. In these trials, ^{10}B-enriched boric acid derivatives were used as boron-delivery agents, which showed high blood-to-tumor ^{10}B concentration leading to endothelial damage in blood vessels but with no therapeutic benefit [47]. In the Japanese trials, BSH was used as a boron-carrier agent [48]. Though BSH achieved better tumor-to-blood concentration compared to previous boron-carrier agents used, it was however excluded by normal blood–brain barrier, and the ^{10}B concentration in brain tumors was suboptimal [49, 50]. In addition, the thermal neutrons used in these trials were poorly penetrating. Therefore, open craniotomy and general anesthesia during the entire treatment time (about 4–8 h) were needed to deliver BNCT [50]. The shortcomings of earlier studies were rectified in the modern clinical trials. In majority of the subsequent trials, high energy epithermal neutron beam was used instead of thermal neutron beam. Thereby, avoiding the need for open craniotomy. Instead of previous boron-carrier agents, newer agents such as BPA were used, either alone or in combination with BSH.

The recent trials have aimed to find the optimal radiation fractionation, radiation fields, radiation dose, normal tissue tolerance, and pharmacokinetics of boron-carrier agents used in BNCT for treatment of different cancer subsites. In the twenty-first century, there were clinical studies experimenting and expanding the role of BNCT in other cancer subsites such as recurrent head and neck cancers as summarized in Appendix. However, there are no randomized controlled clinical trials on BNCT reported so far.

6.4.3.6 Limitations and Future Directions

There are few limitations that hamper the widespread use of BNCT in cancer treatment. The main shortcoming is the lack of ^{10}B carrier agents capable of achieving high tumor specificity and boron concentration. Secondly, the poor penetration of thermal neutrons into tissues. Thirdly, usage of nuclear reactors as the source of thermal neutrons for BNCT. The problems with nuclear reactors are that the low energy-neutron beams produced from them are contaminated with gamma rays and fast neutrons, which can cause damage to normal tissues even without boron concentration. Additionally, there is a shortage of nuclear reactors capable of delivering BNCT with a treatment delivery and monitoring room and they are also often located far away from population center. Fourthly, the interaction of low-energy neutrons with normal tissues results in capture reactions that cause biological damage.

Currently, active translational and clinical research focused on overcoming the above hurdles are being conducted. Newer boron-carrier agents based on purines, pyrimidines, thymidines, nucleotides, nucleosides, peptides, and porphyrin derivatives are being designed [39, 51, 52]. To avoid the hindrances associated with nuclear reactor-based treatment, alternative sources of neutrons such as radioactive decay of californium-252 (^{252}Cf) and particle accelerators are being investigated. ^{252}Cf is not available in the required amount to be utilized for BNCT [40]. On the other hand, particle accelerator-based treatment appears to be a promising alternative and would make hospital-based delivery BNCT feasible. However, the applicability of results from previous clinical trials conducted in reactor-based treatment centers to a larger population to be treated in particle accelerator-based treatment centers in future is questionable and warrants further studies [50].

6.5 Radiotherapy Combined with Other Cancer Treatment Modalities

Combining RT with other oncological treatments is central for clinical management of tumors. A key approach is to combine RT with other pharmaceutical treatments. Given that RT has an effect on diverse cellular signaling networks, there are a number ways to combine it with agents and/or regiments that affect such processes, e.g., chemotherapy, targeted therapy, immunotherapy, hyperthermia, hormonal therapy, short-term starvation, etc. (Fig. 6.5).

6.5.1 RT Combined with Chemotherapy

RT is often combined with chemotherapy in a diverse set of tumor types to increase locoregional control as well as to combat metastatic growth [53]. These combined regiments have emerged as a result of exploring chemotherapeutic agents that presented some single drug activity in a certain cancer malignancies for additive or synergistic effect when combined with RT at doses and time frames that had acceptable toxicity [54].

Combined chemotherapy and RT might refer to sequential association or to concomitant association. Chemotherapy may sensitize for RT by influencing one or several cellular effects including chromosome or DNA damage and subsequent repair, effect on cell cycle progression allowing cells to be accumulating in a RT sensitive phase, impact on different cell death routes including apoptosis, mitotic catastrophe as well as on autophagy. Moreover, in the tissue such combination may also impact on the hypoxic tumor environment/reoxygenation status. In a clinical setting it is most likely that a key benefit is the inhibition of tumor cell proliferation by drugs during the radiation interfraction interval [54].

The combined use of chemotherapy with RT has typically translated into a significant benefit in overall survival in sites where RT plays a substantial role.

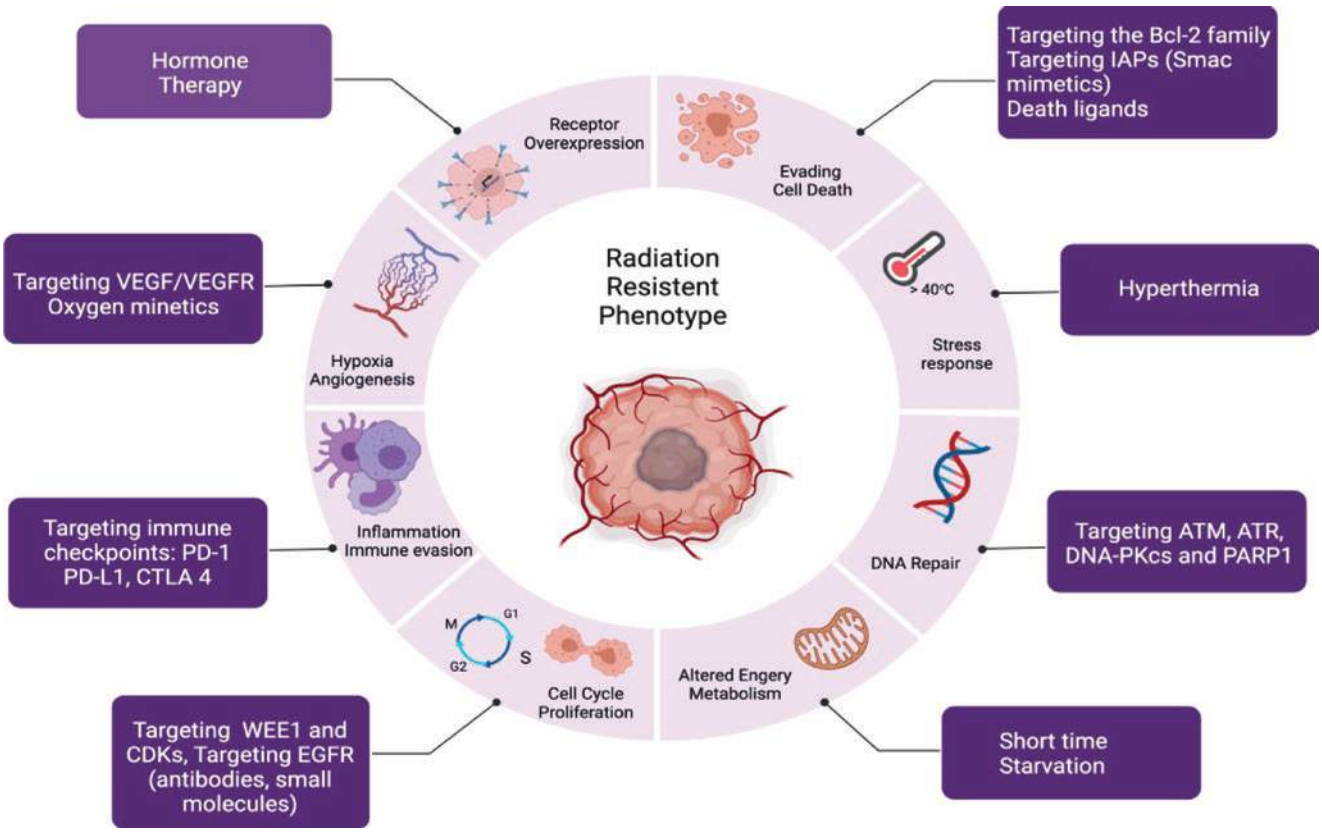

Fig. 6.5 Overview of radiotherapy combinations influencing different hallmarks of cancer

Concurrent RT and chemotherapy yielded an almost 10% higher survival rate relative to RT alone. Unfortunately, the complication rates of combined regimens are also higher than those of RT only [54].

Concomitant administration of chemotherapy and radiation gives increased early normal tissue toxicity due to inhibition of stem cell or precursor-cell proliferation. Late normal tissue damage is likely to be enhanced through inhibition of DNA repair, and by specific mechanisms of drug toxicity in sensitive tissues [55].

Several randomized trials with concomitant chemoradiotherapy have been conducted in most cancer types showing a significant increase in locoregional control in many disease sites with a consequent improvement in patient survival. Meta-analyses of available data of randomized trials in head and neck cancer (HNC) undertaken a few years ago showed that despite a high initial response rate, multi-agent chemotherapy given before radiation treatment (i.e. in a neoadjuvant setting) has a small impact on the locoregional control and survival rates [54]. Numerous single institutions and cooperative groups have investigated the use of concurrent RT and chemotherapy in the management of patients with localized esophageal and gastric cancer, either as definitive or adjuvant therapy. A significant body of information suggests that chemotherapeutic agents such as 5-fluorouracil, capecitabine, cisplatin, oxaliplatin, carboplatin, mitomycin C, gemcitabine, irinotecan, docetaxel, and paclitaxel have a greater additive effect when used in combination with RT [54].

In all the reported studies, the therapeutic ratio (defined as the advantage in efficacy over the disadvantage in toxicity) was, however, less clearly assessed and/or reported. In general, an increase in early toxicity was observed in all the trials. For late toxicity, systematic reporting of data is lacking, but the few available reports also indicate an increase in late radiation effects.

A drug may sensitize the radiation or may kill cells by independent means. Alternatively, a drug may inhibit cellular repopulation or act as a cytoprotector. Limited studies have presented drug mechanisms mathematically in order to estimate the equivalent radiation effect of a drug. In fact if cytotoxic drug effects could be expressed in terms of equivalent biologically effective dose of radiation, then relative contributions of radiation and chemotherapy in combined treatments could be assessed and consequently optimum schedules could be designed [54].

An ideal global model of tumor control in an attempt to simulate clinical reality would incorporate the effects of radiation dose, fractionation, hypoxia, blood flow, and concomitant drug therapy [55].

Chemotherapy combined with RT improves the therapeutic ratio by the following mechanisms:

1. Spatial cooperation—consists of administering the chemotherapeutic agent and RT separately in different anatomical sites.
2. Toxicity independence—both treatments have different side effects, the treatment with the combination modality is less toxic.
3. Normal tissue protection—chemotherapy drugs with a protective effect against normal tissue allow a higher dose of radiation to be administered.
4. Radiosensitivity—is a mechanism that leads chemotherapeutic agents to enhance the cytotoxic effects of RT treatment. Increased damage from radiation, inhibition of repair processes, interferance with the cell cycle progression through different phases, exerting greater activity against hypoxic cells, and helping to improve RT are some mechanisms of radiosensitivity that can influence these treatments.

Combination of chemotherapy with RT can be in three ways, with a sequential treatment where RT is followed by chemotherapy or chemotherapy is followed by RT. These treatments can reduce large tumor mass with a first modality and with the second one can increase the effectiveness, and thus control the disease. In concurrent treatment, chemotherapy and RT are given together. RT can be given daily, while chemotherapy could be given once a week or every 3–4 weeks. Finally, alternative treatment would be based on giving chemotherapy and RT on alternately weeks, such as every 1–3 weeks, with no concurrent treatments. This last option would reduce side effects and also allow full administration of the dose for each modality.

Molecular mechanisms of interaction between combination therapies [53]:

1. Enhance DNA/chromosome damage and repair

   Little is known about the capacity of chemotherapeutic agents to increase the efficiency with which IR induces DNA damage. Several commonly used chemotherapy agents have been shown to inhibit the repair of radiation damage (i.e., DNA and/or chromosome damage). Some of these drugs inhibit the repair processes by interfering with the enzymatic machinery involved in the restoration of the DNA/chromosome integrity.
2. Cell cycle synchronization

   Many of the chemotherapeutic agents inhibit cell division, that is, they exert their action on proliferating cells.

   Due to this cell cycle selective cytotoxicity by the cell cycle phase after the action of chemotherapeutic drugs, the remaining surviving cells will synchronize.

   If RT is given when cells are synchronized in the most radiosensitive phase of the cell cycle, then the effect of radiation is enhanced.
3. Enhanced apoptosis

   Apoptosis is a mechanism of cell death induced by chemotherapeutic agents. These can trigger one or more pathways of apoptosis. To ensure a robust apoptotic response, chemotherapeutics must be incorporated into DNA. The combination of these therapies, where RT is very effective in inducing DNA single strand breaks (SSBs) or double strand breaks (DSBs), could facilitate the incorporation of these agents into DNA and thus induce an enhanced apoptotic reaction.
4. Reoxygenation

   Hypoxia is associated with a worse response to RT treatment, and the reason is the inadequate diffusion of oxygen in the tumor mass due to insufficient tumor vascularization.

   If we combine the treatments, chemoRT, chemotherapy induces a certain degree of shrinkage in the tumor that facilitates the diffusion of oxygen in a more uniform way, increasing tumor oxygenation and therefore tumor radiosensitivity.
5. Inhibition of cell proliferation

   A mechanism of interaction between both treatments combined is the possible inhibition of cell proliferation, a mechanism that occurs during dose fractionation in RT. The exact timing and schedule between the chemotherapy and RT must be taken into account, since it would be best to administer the drug toward the end of radiation treatment because that is when tumor cell repopulation has been activated.

6.5.1.1 Side Effects of Combined Chemotherapy and Radiation Therapy

The combination of these treatments can increase both acute and late toxicity. ChemoRT as two cytotoxic treatments produces an increase in damage in the volume of damaged normal cells, being more evident during the concurrent chemoRT. By combining these therapies, if these side effects appear, you may require to reduce the dose of chemotherapy.

Side effects from combining chemotherapy with RT can be increased fatigue, lowering of blood counts, cardiac dysfunction, cognitive dysfunction, and second malignancies.

Some aspects to consider to reduce toxicity when combining both treatments are:

- If we optimize the schedule and sequence of the combined treatments, we can reduce toxicity.
- With an adequate selection of patients, we can avoid these side effects in patients with a poor performance status or patients with comorbidities.

Table 6.6 Chemotherapeutic agents used in combination with radiotherapy in different tumor types and associated side effects

Tumor type	Treatment	Side effects
Brain tumors	Carmustine	Myelosuppression
	Temozolomide	Neutropenia, anemia, thrombocytopenia, constipation
Head and neck cancer	Cisplatin	Nephrotoxicity, ototoxicity, nausea, vomiting, neurotoxicity/neuropathy
	Docetaxel	Myelosuppression
	Fluorouracil	Myelosuppression, gastrointestinal (GI) effects, mucositis, oral ulcers, diarrhea
Breast cancer	Cyclophosphamide	Hemorrhagic cystitis, myelosuppression, nausea, vomiting
	Docetaxel	Myelosuppression
	Doxorubicin	Cardiotoxicity (including recall effect)
	Methotrexate	Stomatitis, leucopenia and nausea
Lung cancer	Carboplatin	Nephrotoxicity, ototoxicity, nausea, vomiting, neurotoxicity
	Docetaxel	Myelosuppression
	Etoposide	Myelosuppression
Gastrointestinal cancer	Fluorouracil	Myelosuppression and mucositis
	Gemcitabine	Anemia, thrombocytopenia, nausea/vomiting
	Oxaliplatin	Nephrotoxicity, ototoxicity, nausea, vomiting and neurotoxicity
	Irinotecan	Diarrhea, immunosuppression
	Mitomycin C	Bone marrow damage, lung fibrosis, renal damage
Lymphoma	Bleomycin	Lung fibrosis
	DTIC (dacarbazine)	Loss of appetite, vomiting, low white blood cell or platelets count
	Doxorubicin	Cardiotoxicity
	Vinblastine	Peripheral neuropathy, bone marrow suppression
	Vincristine	Hair loss, constipation, difficulty walking, headaches, neuropathic pain, lung damage, or low white blood cell counts

- Using a genetic and molecular analysis of the tumor, we can avoid chemotherapy for patients with lower scores, avoiding chemotherapy toxicity.
- In patients with p16 oropharyngeal cancer, it has been possible to reduce the dose of RT and thus reduce toxicities.
- Advances in imaging techniques, such as IMRT and IGRT, have led to a decrease in the dose around normal tissues, resulting in minimizing the risk of complications from chemoRT.
- Finally, supportive care that involves adequate nutrition, adequate hydration, managing nausea, pain, and depression are essential to mitigate side effects when both therapies are combined (Table 6.6).

The incorporation of targeted therapies into treatment regimens helps to improve radiosensitization. Multimodal therapy uses these agents on a concurrent schedule [53].

Multimodal management for optimum cancer treatment with surgery, chemotherapy, and RT is one of the most significant advances in cancer treatment in the last 25 years. This combined therapy increases locoregional control and patient survival, as well as reduces the side effects of treatment, toxicities [53].

It is difficult to know the real underlying mechanisms of the interaction of this combination therapy of chemotherapy and RT, normally the clinical trials that are carried out do not allow to obtain this information [56] (Box 6.5).

Box 6.5 RT Combined with Chemotherapy

- RT and chemotherapy can, when combined, improve locoregional disease control.
- Concomitant administration of RT with chemotherapy gives increased early normal tissue toxicity but late toxicity of normal tissues may also be increased.

6.5.2 Combining RT with Targeted Therapy

Radiation-induced signaling is multifaceted, and these cellular events are affected by different growth factor signaling cascades controlled by oncogenic drivers and activated kinases in the tumors [57]. These radiation-induced signaling events as well as the tumor microenvironment interplay have been explored for RT sensitization purposes (Fig. 6.5).

Some of the RT sensitizing approaches based on targeting oncogenic drivers, DNA damage and repair, chromatin remodeling, cell cycle progression, cell death regulation and angiogenesis/hypoxia are shown in Table 6.7.

Table 6.7 RT sensitizing strategies and examples of drugs that are in clinical evaluation in combination with RT or in combined RT and chemotherapy regimen

Type of mechanism	Target or target mechanism	Example inhibitors	RT sensitized tumor	Reference or clinical trial No.[a]
DNA damage and repair	ATM	AZD1390	Glioblastoma, other brain tumors	NCT03423628
	ATR	BAY-1895344; M6620	Advanced solid tumor, esophageal cancers	[58] NCT03641547
	DNA-PKcs	Nedisertib, peposertib, AZD7648	Head and neck cancer, advanced solid tumors	[59] NCT03907969
	PARP	Olaparib, veliparib, rucaparib, niraparib	Breast cancer, prostate cancer, non-small cell lung cancer, small-cell lung cancer, glioblastoma/glioma, rectal cancer, cervical cancer, head and neck cancer	[60] NCT03542175; NCT04837209; NCT01477489; NCT02227082; NCT03945721; NCT03598257; NCT03109080; NCT03212742; NCT03581292; NCT01514201; NCT04790955; NCT04728230; NCT02412371; NCT01589419; NCT03644342; NCT02229656
Chromatin remodeling	Histone deacetylase (HDAC)	Vorinostat	Head and neck cancer	[61]
Cell cycle progression	WEE1	Adavosertib	Pancreatic cancer	[62]
	CDK 4/6	Palbociclib, ribociclib, abemaciclib	Glioma, breast cancer, head and neck cancer, meningiomas	[63] NCT03691493; NCT03870919; NCT04563507; NCT03024489; NCT03389477; NCT03355794; NCT02607124; NCT04585724; NCT04298983; NCT04923542; NCT04220892; NCT02523014
Cell death regulation	Bcl-2	AT-101 (Gossypol)	Head and neck cancer Brain tumors	[64] NCT00390403
	CD95/FAS ligand	Asunercept (APG101)	Glioblastoma	[65]
	SMAC mimetics	Xevinapant (Debio 1143)	Advanced head and neck cancer	[66]
Oncogenic drivers	EGFR	Erlotinib/ gefitinib/ osimertinib cetuximab	Non-small cell lung cancer, head and neck cancer	[67, 68]
	STAT3	Dovitinib	Hepatocellular carcinoma	[69]
Angiogenesis	VEGF, VEGFR2	Bevacizumab, vandetanib (Caprelsa)	Glioblastoma, esophagogastric cancer	[70, 71]
Hypoxia	Oxygen mimetic	Nimorazole	Head and neck cancer	[72]

[a]The trial number refers to its citation on https://clinicaltrials.gov/

6.5.2.1 Attacking DNA Damage Signaling and Repair for Radiation Therapy Sensitization

Three principal DNA damage response (DDR) kinases, the phosphatidylinositol-3-kinase-related kinases (PIKKs), ataxia-telangiectasia mutated (ATM), ATM- and Rad3-related (ATR), and the non-homologous end joining (NHEJ) component, DNA-dependent protein kinase, catalytic subunit (DNA-PKcs) are central in RT responses (see Chap. 3). These kinases execute their cellular action by phosphorylating targets that regulate DNA repair, e.g., histone H2AX, or cell cycle progression, e.g., WEE-1 and cell cycle checkpoint kinases (CHKs).

Multiple trials of ATR inhibitors are ongoing as single agents or combined with chemotherapy, yet fewer attempts have been made with ATR inhibitors and RT [60]. The ATR inhibitors BAY-1895344 and M6620 (see clinicaltrial.gov; NCT03641547) were tested in phase I trials in various solid tumors in an advanced stage setting including esophageal cancer [58]. As the kinase pocket of ATM is similar to other PIKKs, early attempts to develop specific inhibitors were unsuccessful [60]. However, the ATM inhibitor AZD1390 is currently undergoing trials in conjunction with RT in glioblastoma patients (NCT03423628). Attempts have also been made to target DNA-PKcs, a key component of the NHEJ repair cascade (see Chap. 3) [60]. Thus, AZD7648 has been demonstrated to enhance RT effect when combined with the

poly (ADP-ribose) polymerase (PARP) inhibitor olaparib in both tumor cell lines *in vitro* as well as in tumor-bearing mice. This DNA-PKcs inhibitor is at present tested further in a phase I clinical trial (NCT03907969). Moreover, other DNA-PKcs inhibitors are similarly evaluated when combined with RT in phase I trials involving patients with, e.g., head and neck (HNC) cancer where a clear improved local control was found.

Another class of DNA repair inhibitors is those targeting the PARP-1 repair enzyme [58, 60]. It has been demonstrated that in tumor cells which had mutations in certain DDR genes, e.g., BRCA1/2, causing impairment of their DNA damage sensing function, blockade of a back-up repair pathway, e.g., by PARP-1 inhibitors (PARPi) resulted in tumor-specific cell killing, a concept called synthetic lethality. Multiple PARPi, e.g., olaparib, rucaparib, and veliparib were developed and tested in different tumor types, e.g., breast cancer (BC), ovarian carcinoma (OC), and prostate cancer (PCa) (reviewed in [60]). In the context of RT, PARPis are currently tested or planned to be evaluated in several different tumor types (Table 6.7). Apart from the "BRCAness" tumor concept, the PARPi is also explored in tumors driven by other DDR-alterations, e.g., ATM and ATR.

6.5.2.2 Interfering with Cell Cycle Regulation to Improve RT Response

Multiple cyclin-dependent kinase 4 and 6 inhibitors (CDKIs), e.g., palbociclib, ribociclib, and abemaciclib which alter the cell cycle progression, have become an important new treatment of metastatic- or locally advanced BC including combinations with RT [63]. Albeit multiple studies are ongoing, no consensus has been reached underpinning the clinical benefit of combining RT with CDKIs [63]. For palbociclib, there are studies ongoing in BC and HNC, ribociclib is evaluated with RT in multiple trials as is abemaciclib (Table 6.7). In addition, there is an attempt to study abemaciclib in patients with solid tumors that have brain metastasis where CDK genomic testing is done (NCT03994796).

The CDK1/2 is in part controlled by the WEE1 G2 checkpoint kinase which via Ser/Th protein phosphorylation blocks their activity resulting in a G2/M cell cycle checkpoint activation. Indeed, the WEE1 inhibitor adavosertib was assessed alongside a dual RT and gemcitabine treatment regimen in advanced PCa patients where a clear response was evident by an increased overall survival [62].

6.5.2.3 Attacking Oncogenic Drivers and Downstream Signaling for RT Sensitization in a Precision Cancer Medicine Manner

Constitutively increased activity of epidermal growth factor receptors (EGFRs) by mutation or gene amplification (which is found in multiple tumor types) is responsible for resistance to CT/RT [68]. Moreover, downstream PI3K/AKT or Ras-Raf mitogen-activated protein kinases (MAPK) signaling cascades may also influence RT response via regulation of cell cycle, cell death signaling, or by interfering with the DDR network [73]. Treatment with the antibody cetuximab, a EGF ligand blocker has been shown to improve RT sensitivity in HNC. However, results presented from a meta-analysis covering 13 studies with 5678 patients on CT/RT-based treatment and receptor tyrosine kinase inhibition for solid cancers (ROCKIT) emphasized that targeting EGFR could not ameliorate overall survival yet causing increased toxicity [67]. In the context of metastatic Non-small cell lung cancer (NSCLC) driven by *EGFR* mutation, there is also an interest in combining small EGFR tyrosine kinase inhibitors (TKIs) together with RT for patients with oligometastatic disease as well as to consolidate tumor lesions resistant to a given EGFR targeting TKI [68].

The transcription factor signal transducer and activator of transcription 3 (STAT3) regulate inflammation, malignant cells initiation, progression, and therapy resistance. STAT3 is overexpressed in cancers of the gastrointestinal tract, NSCLC, OC, and brain tumors and thus it may cover a valuable target for precision therapy. One example is the drug dovitinib which was shown to sensitize hepatocellular carcinoma to RT by targeting Src homology region 2 (SH2) domain-containing phosphatase 1 (SHP-1)/STAT3 signaling [69].

6.5.2.4 Altering Cell Death Signaling for RT Sensitization

RT resistance is in part a result of impaired cell death initiation and/or execution (see Chap. 3) and targeted strategies aim to restore such signaling. Multiple signaling components of different apoptotic routes including the B-cell lymphoma 2 (Bcl-2) family members, inhibitor-of-apoptosis-proteins (IAPs), e.g., x-linked IAP (XIAP) or survivin and the Cluster of Differentiation 95 (CD95)/FAS signaling network have all been explored [74, 75]. Inhibition of the IAP survivin, for instance, is reported to increase apoptosis as well as autophagy, to impact on the cell cycle and to hamper DNA damage repair, resulting in a radiosensitization [75].

Another example is the pan-Bcl-2 inhibitor AT-101 (Gossypol), which sensitized HNC cells to RT-induced apoptosis indicating its therapeutic potential for tumors with high Bcl-2 expression levels [64]. An additional example is navitoclax (ABT-263) which impairs the anti-apoptotic function of Bcl-2/Bcl-xL and which was reported to potentiate RT cell death [76]. Finally, the anti-IAP smac mimetic, xevinapant (Debio 1143) has been tested in HNC in combination with cisplatin and RT where locoregional control was achieved in some patients [66]. Concerning RT sensitization via the extrinsic apoptotic route, focus has been on interfering with the FAS/CD95 signaling cascade

[65]. Thus, it was demonstrated in relapsed glioblastoma patients that addition of the Fc-fusion protein asunercept (APG101) which blocks ligand engagement prolonged patient survival.

6.5.2.5 Altering Hypoxia and the Tumor Microenvironment to Impart RT Refractoriness

Targeting the tumor microenvironment is another RT sensitizing approach that involves attack on hypoxia directly or the underlying aberrant angiogenesis/vascularity of tumors, respectively. By this, hyperbaric oxygen therapy (HBOT) and agents which are specifically activated in hypoxic tumor cells/parts of the tumor or are prodrugs which are triggered to activity under hypoxic conditions or impact on angiogenesis/vasculature (by impairing the function of the vascular endothelial growth factor (VEGF) or its receptor signaling) are tested. One prime example is the electron-affinic nitroimidazoles, such as the clinically proven oxygen mimetic nimorazole, which covers the standard of care in HNC patients that are given RT in some countries [72]. Moreover, it has been demonstrated in glioblastoma patients that temozolomide-based CT/RT can be enhanced resulting in improved progression free survival if an anti-VEGF monoclonal antibody bevacizumab (avastin) is included in the treatment regimen [71]. In contrast, addition of bevacizumab to capecitabine and RT did not improve outcome in rectal cancer [77]. Further, vandetanib (ZD6474), a tyrosine kinase inhibitor targeting VEGFR, was shown to improve outcome of esophagogastric carcinoma patients when applied after RT or different CTs [70] (Box 6.6).

Box 6.6 RT Sensitization with Targeted Therapy

- Inhibitors of the DDR signaling network, e.g., ATM, ATR, DNA-PKcs, and PARP-1 or interfering with cell some cycle regulating kinases offer sensitization for RT.
- Blockade of signaling from oncogenic drivers, e.g., growth factor regulated kinases via antibodies or small molecule inhibitors can sensitize tumors to RT.
- Restoring cell death pathways, e.g., apoptosis is another RT sensitizing strategy.
- Modulating the tumor microenvironment, e.g. hypoxia and aberrant angiogenesis allow for tumor RT sensitization.

6.5.3 RT Combined with Immunotherapy

6.5.3.1 Local and Systemic Modes of Action of Radiotherapy

For a very long time, it was assumed that the X-rays directly, or indirectly through the formation of ROS, only affect the radiation-sensitive DNA in the cell and that other structures are spared. However, today it is clear that in addition to the so-called targeted local effects of radiation on DNA, numerous so-called non-targeted effects occur, such as general stress responses of the irradiated cells, which then also can be transmitted to other cells and even the entire organism.

6.5.3.2 Radiotherapy as an Immune Modulator

Radiation-induced oxidative stress and DNA damage activate numerous signaling pathways in cells that influence the expression of genes and consequently trigger a broad spectrum of cellular responses ranging from promotion of cell survival to cell death (see Chap. 3). Thereby, the immunological phenotype of cells as well as the tumor microenvironment may change (see Chap. 5). It has been demonstrated that RT increases the expression of MHCI molecules, death receptors, and stress ligands on the tumor cell surface, and fosters the release of so-called damage-associated molecular patterns/danger-associated molecular patterns (DAMPs) such as adenosine triphosphate (ATP), HMGB1, and Heat Shock Protein 70 (HSP70) (see Chap. 5). Also, RT causes increased levels of immunostimulatory cytokines mainly through the induction of immunogenic tumor cell death (ICD) and in combination with additional immune stimulation [78].

Irradiation of tumors also affect immune cells that circulate through the tumor vasculature even though the functionality of the remaining immune cells is still appropriate. One has to keep in mind that different subtypes of immune cells differ in their radiosensitivity and antigen-presenting cells as key initiators of adaptive antitumor immune responses, are quite radioresistant [79]. RT has also immune suppressive properties directly on the tumor cells and their microenvironment. Local irradiation increases the expression of immune checkpoint molecules such as programmed death-ligand 1 (PD-L1) and induces the release of transforming growth factor (TGF)-beta. Which of these changes that predominates varies greatly from individual to individual and ultimately determines whether, in addition to the local effects of tumor cell killing, local and systemically acting antitumor immune responses are triggered by RT alone [80]. The immune responses triggered by local radiation and acting systemically are referred to as “abscopal effects” of RT (for definition see Chap. 5). However, since radiation has both immune-activating and immune-suppressing effects (Fig. 6.6), the abscopal effect is usually only

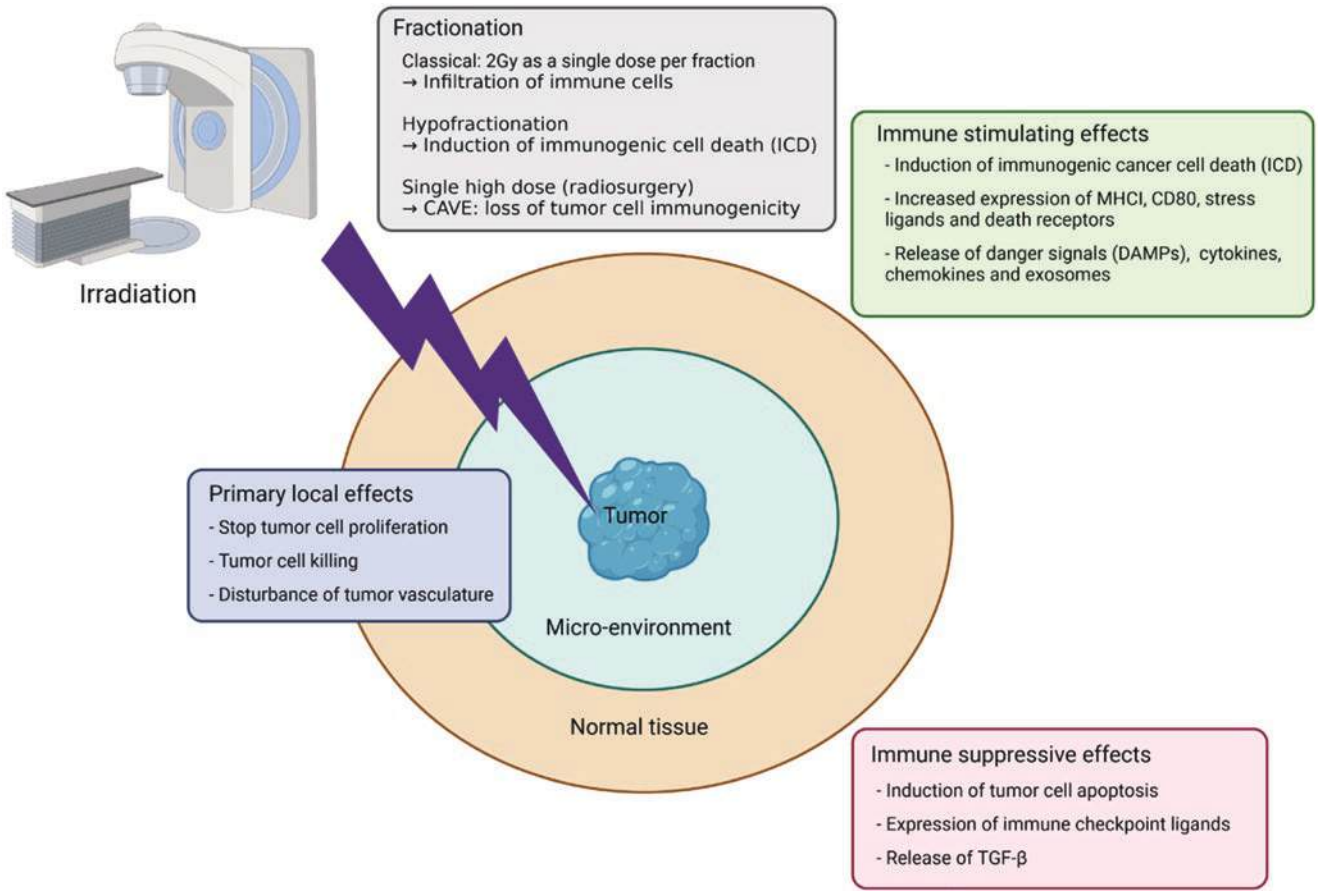

Fig. 6.6 Radiotherapy has multiple immune stimulating and immune suppressive effects which depend on dose

observed in the clinic when RT is used in combination with immunotherapies.

6.5.3.3 Rationale for Combination of Radiotherapy with Immune Therapies

If ICD is induced by local tumor irradiation and the tumor vasculature is changed in such a way that more immune cells can migrate into the tumor, this can already trigger effective antitumor immune responses [81]. In terms of radiation immunology, it is now believed that a single dose of 2 Gy is more likely to promote immune cell infiltration and a dose of >2 Gy is more likely to induce ICD [82]. Importantly, non-linear dose–effect relationships often prevail. For example, the immunogenicity of tumor cells is reduced again after irradiation with a single dose that is too high, because enzymes are activated that degrade the immunogenic DNA found in the cytoplasm after irradiation or because immune-suppressing immune checkpoint molecules (ICM) are increasingly expressed on the tumor cells [83].

Expression of immune suppressive ICM was the key starting point for a combination of radiation and immunotherapies. Inhibition of ICM in parallel with or shortly after RT has led to local and systemic antitumor immune responses in animal models and in the clinic, and the so-called radio-immunotherapies are increasingly being used in multimodal oncological treatment [84]. Further, immunologically-based patient selection based on induction chemo-immunotherapies is increasingly taking place [85]. Particularly exciting is the re-emergence of tumor vaccination in this context and the stratification of patients based on immunological factors of the peripheral blood (see Chap. 6) (Box 6.7).

Box 6.7 RT Combined with Immune Therapy

- Radiation affects DNA and via stress responses other cellular compartments.
- Radiation induces local and systemic effects.
- RT has both immune stimulatory and immune suppressive effects.
- Non-linear dose relationships also apply for radiation-induced immune effects.
- RT is well combinable with immune therapy.

6.5.4 RT Combined with Hormone Therapy (Radio-Hormone Therapy)

Box 6.8 RT Combined with Hormone Therapy

- Hormone sensitive tumors which are dependent on certain hormones for their growth can be slowed down or stopped by hormone therapies.
- In prostate cancer patients with a high risk of progression, hormone therapy in combination with RT is the treatment of choice as hormone therapy or RT alone remain inadequate

A combination of RT and hormone therapy is used in the management of breast and prostate cancers. Hormone therapy is considered to be quite effective and comparatively non-toxic in tumors that are driven by hormones such estrogen in breast cancer (BC) and testosterone in prostate cancer (PCa). The hypothalamic pituitary gonadal pathway controls the concentration of testosterone and estradiol in the serum. Estradiol is mainly produced in the ovaries of premenopausal women, however, in case of postmenopausal women; aromatase found in the peripheral fat tissue aids the peripheral conversion of adrenal androgens. Hormonal therapy is principally accomplished by chemical castration (usage of chemicals or drugs like the gonadotropin-releasing hormone agonists or luteinizing hormone-releasing agonists that stop the production of the sex hormone) in case of men with PCa and premenopausal women with BC (Box 6.8).

With respect to BC, approximately 50% of all premenopausal and 80% of all postmenopausal women suffer from a hormone receptor-positive malignancy. In the histochemical analysis of such tumor cases, the expression of estrogen (ER) and progesterone receptors (PR) are evaluated to understand the degree of positivity. The levels of ER/PR expression in BC are used as a guiding parameter for prognosis as well as for what systemic treatment to give. Recent studies have also shown that patients who overexpress the human epidermal growth factor receptor 2 (HER-2) have a low probability to benefit from hormone monotherapy. Hence it is necessary to target ER and PR as well as the HER-2 receptor. PCa can be hormone-dependent or non-dependent and have functional androgen receptors (AR). Hormone therapy is frequently part of curative therapy for both BC and PCa and where it is either used neoadjuvantly, i.e., for primary cancer size reduction before RT/radical surgery or adjuvantly, i.e., to decrease the risk of tumor recurrence.

6.5.4.1 Radiotherapy Combined with Tamoxifen for Breast Cancer

For ER/PR-positive BC patients, hormone therapy is usually given along with postoperatively RT. The combined treatment of tamoxifen with RT has shown a synergistic effect *in vivo* which can be attributed to the alterations in the tumor microenvironment. Further studies are required to shed light on the complex communications among the 17beta-estradiol and p53/p21(WAF1/CIP1)/Rb signaling pathways. IR is known to induce direct as well as indirect DNA damages via the ROS production. The DNA breaks generated; stimulate various signaling pathways associated with ATM (Ataxia telangiectasia-mutated gene), ATR (Ataxia telangiectasia-mutated gene Rad3-related), and DNA-PK (DNA-protein kinase). These kinases lead to the cell growth arrest after phosphorylation checkpoint kinase 2 (CHK2) or p53. The downstream effectors like p53/p21(WAF1/CIP1)/Rb, CDC25A, 14-3-3 sigma determine if the cell cycle arrest will be in the G1/S or G2/M transition. Interestingly, these pathways can be regulated at various stages by 17beta-estradiol (E2) in the irradiated cells. The ROS production can also be reduced by 17beta-estradiol, thereby reducing the subsequent effects of RT. This can be achieved either by reducing the p53 activation or by suppression of ROS induced DNA damage. Additionally, while 17beta-estradiol acts on S-phase kinase-associated protein 2 (SKP2) and P27 to allow G2/M transition, it also augments the expression of *CCND1* and *MYC* that control the cell cycle promoting the G1/S transition. In contrast, tamoxifen, with its anti-estrogen activity obstructs the effects of 17beta-estradiol. This anti-estrogenic effect can strengthen the IR induced growth inhibition as depicted in Fig. 6.7 [86].

The usage of TAM is however limited because of the pharmacological side effects like endometrial changes that can lead to endometrial cancers or the thromboembolic events. Keeping this in mind, other endocrine drugs that might endow a comparable efficiency with boosted acceptability in early disease conditions can be utilized. Hence, Letrozole (LTZ), an aromatase inhibitor, is considered as a potent drug in the adjuvant settings. It can be delivered after surgery or in combination with RT with a long-term follow-up to identify the treatment- associated cardiac side effects and evaluate cancer-specific results. LTZ, when combined with radiation, arrests cancer cells in the G1 phase with a significant decrease of cells in the S phase and G2 phase of the cell cycle [87]. Table 6.8 gives the list of hormone therapies for breast and prostate cancers.

6.5.4.2 Radiotherapy Combined with Androgen Deprivation Therapy (ADT) for Prostate Cancer

During the course of the disease, a majority of PCas express the androgen receptor (AR) which is known to specifically direct the cancer cell behavior and this has solidified the significance of androgen signaling in the pathogenesis of PCa [89]. Hence, androgen deprivation therapy (ADT) is a foundation of PCa therapy. ADT is typically utilized to cut down the levels of serum testosterone to a castrate level. This can be accomplished by surgical or chemical castration. Chemical castration can be accomplished by using estrogens or LHRHa; and it is likely to be reversible. The consequence of initial use of LHRHa results in follicle-stimulating hormone (FSH), luteinizing hormone (LH), and testosterone surge in

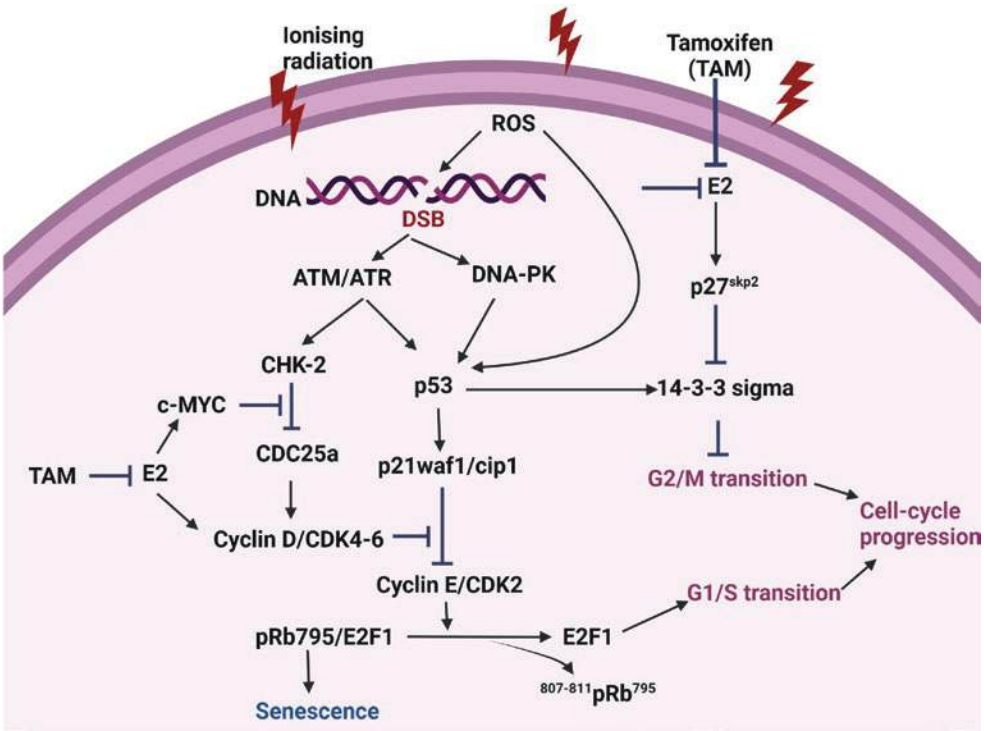

Fig. 6.7 Prospective direct genomic effect of estradiol, tamoxifen, and IR on inhibition of cell cycle progression. (Reproduced with permission from [86])

Table 6.8 Hormone therapies used for breast and prostate cancer. (Reproduced with permission from [88])

Drug	Type	Dose/route	Mode of action
Tamoxifen	Anti-estrogen	Orally, (20 mg) daily	For ER binding, competes with estradiol
Anastrazole	Non-steroidal aromatase inhibitor	Orally, (1 mg) daily	Inhibition of competitive aromatase
Exemestane	Steroidal aromatase inhibitor	Orally, (25 mg) daily	Irreversible aromatase inhibition
Goserelin	LHRH agonist	(3.6 mg) every 28 days or (10.8 mg) every 3 months SC	Reduced pituitary production of LH and FSH
Bicalutamide	Non-steroidal antiandrogen	Orally, (50 mg) combination dose or (150 mg) single agent daily	Competitive AR inhibition
Prednisolone	Corticosteroid	Orally, (5–10 mg) daily	Suppression of Adrenal

ER estrogen receptor, *LHRH* luteinizing hormone-releasing hormone, *LH* luteinizing hormone, *FSH* follicle-stimulating hormone, *AR* androgen receptor, *SC* subcutaneous, *IM* intramuscular

the serum, which makes the symptoms worse. Hence, patients are advised to take oral antiandrogens for 1–2 weeks prior to the LHRHa injection. ADT is mostly given with RT as a neoadjuvant therapy which can be continued throughout and even further than RT. Although evidence suggests that the combinatorial treatment of PCa with ADT and RT has improved therapeutic effects, there is still a lot of improvement that can be made on the biochemical front as demonstrated by the clinical trials. ADT might also boost the efficacy of RT by inhibiting successive PCa cell repopulation and by enhancing reoxygenation and radiosensitization. Many preclinical studies involving tumour cell lines *in vitro* and *in vivo* tumor xenografts have suggested that ADT works by suppressing the mechanisms associated with the DNA damage response, particularly the NHEJ repair. This increases the anticancer effect induced by RT. Preclinical studies have also shown that the synergistic effect of RT and ADT enhances apoptosis by suppressing the DNA repair machinery. The combinatorial treatment not only increases the tumor oxygenation but also radiosensitizes the PCa cells. The first phase III, EORTC 22863, study demonstrated a noteworthy overall survival when RT was combined with ADT in men with locally advanced PCa. The results showed that the combination arm had a significantly higher OS compared to that of the RT alone (58.1% vs. 39.8%, $p = 0.0004$). Short-term and long-term follow-up of the EORTC studies showed that only 74% patients exhibited a 5-year disease-free survival with combined RT and ADT [89, 90].

6.5.5 Radiotherapy Combined with Hyperthermia

Hyperthermia as an adjuvant treatment to RT or chemotherapy considers heating of the tumor (area) above a physiological temperature up to 40–43 °C for approximately an hour. Hyperthermia can be applied as whole body, local invasively (intraperitoneal, interstitial, or intracavitary) and locoregional.

Hyperthermia as a radiosensitizer or chemosensitizer has been proven its effectiveness in many different tumor types, such as locally advanced cervical cancer, recurrent breast cancer, malignant melanoma, and head and neck cancer. The size, location, and type of tumor(s) determine whether hyperthermia should be applied only locally in combination with RT or chemotherapy, or whether hyperthermia should be applied to a larger area in combination with only chemotherapy. Hyperthermia has also been demonstrated to regulate the innate and adaptive immune system [91, 92].

6.5.6 Hyperthermia in Clinical Settings

6.5.6.1 Hyperthermia Combined with Chemotherapy

For metastases from, e.g., colon or ovarian origin which are located in the peritoneal area, a heated chemotherapy solution can be circulated through the peritoneal area (called hyperthermic intraperitoneal chemotherapy; HIPEC) [93]. For urinary bladder cancer, a heat solution can be circulated through this organ (endocavity). Since all of these heated solutions are combined with chemotherapy, these hyperthermia setups will not be further discussed in this chapter. Generally, hyperthermia modifies the cytotoxicity of many chemotherapeutic agents. Furthermore, for some drugs, like the platinum compounds, hyperthermia was found to make resistant cells platinum-responsive again [94]. Whether hyperthermia has this effect on other drugs, needs to be investigated.

6.5.6.2 Hyperthermia Combined with Radiotherapy

Locoregional hyperthermia combined with RT is an approach for patients with locally advanced cervical carcinoma (deep hyperthermia) or recurrent breast cancer (superficial hyperthermia) in Europe and USA. Locoregional hyperthermia combined with RT has been used in the clinic already since the early 1980s [95]. It is also possible to implant a heat source in the tumor itself (interstitial), which mainly has been used for brain tumors or locally advanced head and neck tumors [96]. Hyperthermia weakens DNA damage repair enzymes and thereby retards the repair of radiation-induced DNA damage. An increased amount of unrepaired DNA damage causes more cells to die from the radiation injury. Importantly, the synergy between radiation and heat is highest when given simultaneously or closely together in time (within 4 h) [97].

6.5.6.3 Hyperthermia Combined with Immune Therapies

Based on the preclinical knowledge gained in the last few years [91, 92], ongoing clinical trials are conducted with complementary translational studies focusing on immune alterations of patients receiving hyperthermia in combination with RT and/or chemotherapy. These data will form the basis for the design of multimodal cancer therapies in which hyperthermia will be combined additionally to radio- and/or chemotherapy with immune therapies such as immune checkpoint inhibitors.

6.5.6.4 Techniques to Apply Hyperthermia

Hyperthermia can be applied using different techniques such as capacitive radiofrequency heating, radiative radiofrequency and microwave heating, infrared and laser, ultrasound, conductive heating, and by hyperthermic perfusion [63]. One of the most commonly used techniques which is validated within clinical trials is microwave heating and hyperthermia is induced with one or more antennas. An applicator containing one antenna is used for superficial hyperthermia, such as breast cancer or malignant melanomas. This applicator can be placed on the surface area. For deep hyperthermia, the patient lies on a mobile bed that can move through a circle with 4 or 6 antennas. This non-invasive method is used for deeper located tumors such as cervical cancers.

6.5.6.5 Mechanism of Action of Hyperthermia

Macroscopical effects of hyperthermia: Hypoxic and nutrient-deprived areas of a tumor are the least sensitive to RT or chemotherapy, while these areas are especially sensitive to hyperthermia. By local heating of the tumor, an increased blood flow occurs, which increases reoxygenation [95]. As a consequence, more radiation-induced DNA damages are formed and fixed (Fig. 6.8). Moreover, increased tumor perfusion by hyperthermia allows the chemotherapeutic agent to penetrate deeper into the tumor.

Microscopical effects of hyperthermia: Besides increasing the radiation-induced DNA breaks within cancer cells, hyperthermia temporality inhibits DNA DSB repair (Fig. 6.8). This occurs by degrading the essential BRCA2 protein, and thereby temporarily inhibiting the homologous recombination DNA repair pathway. In HPV-positive cervical cancers, hyperthermia was found to disrupt the interaction between the HPV protein (E6) which in normal circumstances suppresses p53. Activation of p53 in these cancer cells results in cell death [95].

Immune effects of hyperthermia: Dependent on the temperature, certain immunological processes are triggered by hyperthermia (Fig. 6.8). Starting with temperatures of 39 °C, an increased infiltration and activation of immune cells in the tumor can be observed in preclinical model systems. At higher temperatures, heat-induced cell death has certain characteristics of "immunogenic cell death" (ICD). This means that the dying and dead cells activate rather than suppress the immune system. In this scenario,

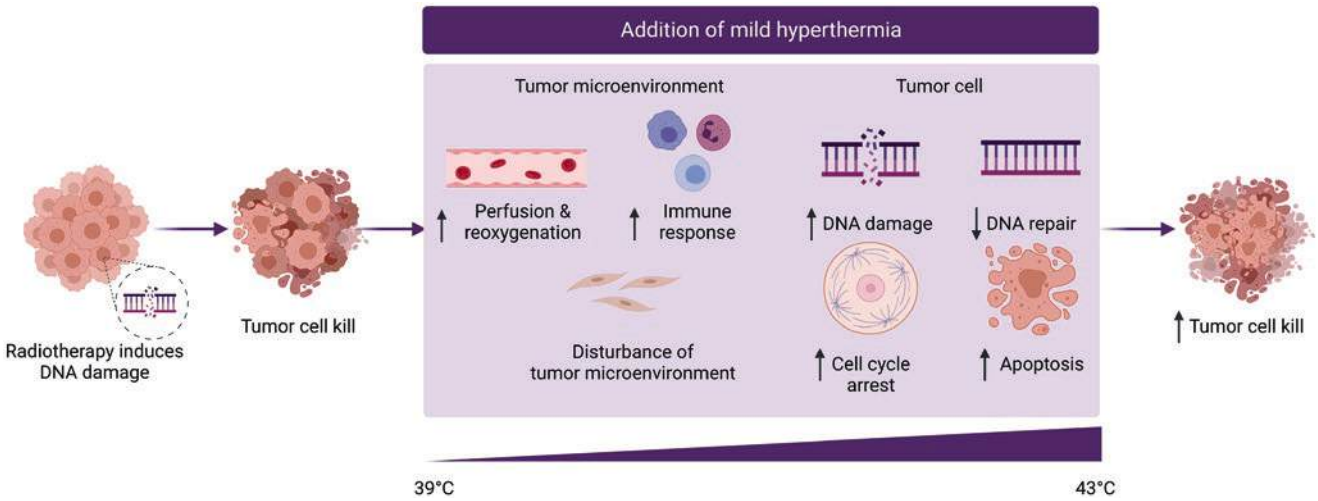

Fig. 6.8 Mild hyperthermia enhances radiotherapy by initiating multiple intracellular and intercellular processes. While radiotherapy induces DNA damages, hyperthermia can enhance the induction of radiation-induced DNA damage by increasing the perfusion and reoxygenation; hyperthermia can temporarily inhibit the DNA repair processes which causes cell cycle arrest and subsequently cell death of the tumor cells such as apoptosis; hyperthermia can also trigger an immune response and disturb the tumor microenvironment eventually all causes of increased tumor cell kill

the heat shock protein 70 (HSP70) is a major player. While inside the cell, it acts as chaperon and protects cells (known as thermotolerance), outside of the cell when being, e.g., released by heat-induced necrotic cells, it activates dendritic cells and delivers antigen to these key immune cells that bridge innate and adaptive immunity. Thus, dendritic cells take up tumor antigens, present them with co-stimulation to CD8+ T cells, and subsequently trigger cellular antitumor immunity by priming cytotoxic T cells [99]. Additionally, HSP70 can directly activate further cells of the innate immune system, such as natural killer cells [100]. Based on this preclinical knowledge gained in the last years, ongoing clinical trials are conducted with complementary translational studies focusing on immune alterations of patients receiving hyperthermia in multimodal settings.

6.5.6.6 Main Indications

Superficial tumors: Hyperthermia is, e.g., standard of care in the Netherlands, Germany, and Japan for patients with recurrent breast cancer (BC), who have received a full radiation treatment course for treatment of their primary tumor. Retreatment with a similar radiation dose as used for their primary tumors is not possible, therefore hyperthermia is applied to prevent severe radiation-induced toxicities. To accomplish the same effectiveness without severe normal tissue toxicity, RT is combined with hyperthermia. The latter gives a boost to the treatment effectiveness. Nevertheless, hyperthermia treatment is not refunded by insurances for treatment of most heatable tumor entities, since big randomized trials are still missing. Besides BC, malignant melanoma and head and neck cancers are prominent superficial tumor entities which are accessible for hyperthermia. The clinical outcomes using locoregional hyperthermia with RT and-/or chemotherapy have been summarized [101]. For soft tissue sarcomas, optimized strategies with multimodality approaches including chemotherapy, regional hyperthermia, and immunotherapeutic agents have been shown to improve survival in high-risk patients [102]. However, more randomized phase III studies, as carried out in an exemplary manner for soft tissue sarcoma [103], are urgently needed to bring hyperthermia as standard tumor therapy in multimodal settings into the clinics (Figs. 6.9 and 6.10).

Deeper located tumors: In most countries, RT combined with chemotherapy is standard treatment of care for cervical cancer patients. However, chemoradiation is less beneficial in tumors of higher stage, whereas hyperthermia as an adjuvant to RT has shown its additional value. Especially in this group, chemoradiation was found to be not very effective. Moreover, chemoradiation seems to result in more toxicities, whereas hyperthermia in addition to RT did not increase radiation-induced toxicities [104].

Treatment course: Both superficial and deep hyperthermia are applied in combination with either RT or chemotherapy. Depending on the tumor type, e.g., BC, cervical cancer, etc. and The International Federation of Gynecology and Obstetrics (FIGO) stage, a radiotherapy or chemotherapy scheme is chosen. While external beam RT is mainly given in daily fractions with low doses, hyperthermia is only applied once or twice per week, for 5 weeks in a row. For each treatment session, the target temperature

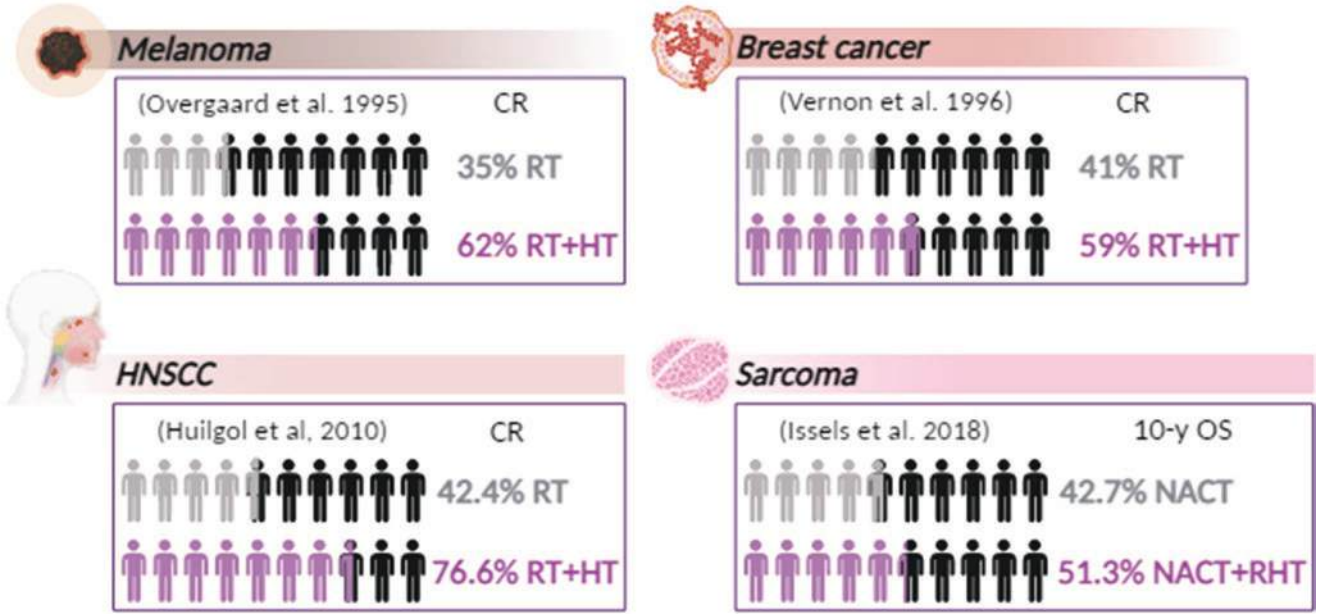

Fig. 6.9 Improved clinical responses after addition of hyperthermia in superficial tumor types. In malignant melanoma, superficial breast cancer and head and neck squamous cell carcinoma, complete responses were much better in patients treated with RT combined with hyperthermia, compared to RT alone. In soft tissue sarcoma, the addition of RT plus hyperthermia to neoadjuvant chemotherapy, leads to a8.6% higher 10-year overall survival

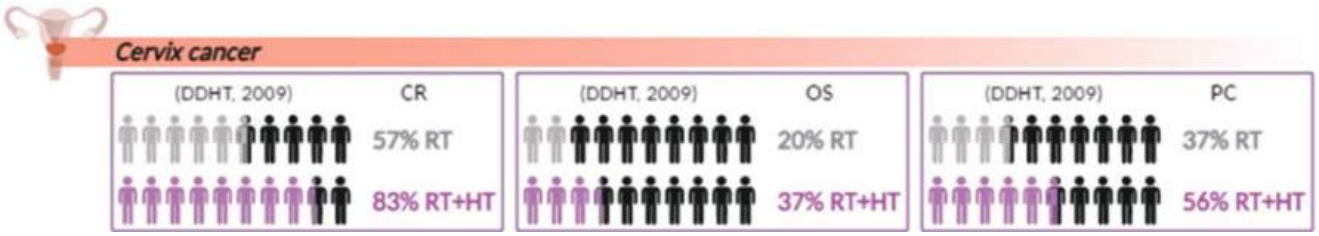

Fig. 6.10 The additional effect of hyperthermia in a deep located tumor (cervical cancer)

should be above 40 °C for approximately 1 h. Moreover, a short time interval on the day that both RT and hyperthermia are given can be more beneficial, but research is ongoing in providing more evidence [105, 106] (Box 6.9).

Box 6.9 RT Combined with Hyperthermia

- Hyperthermia enhances blood perfusion and reoxygenation, triggers an immune response, and disturbs the tumor microenvironment.
- Hyperthermia increases RT and chemotherapy-induced DNA damage, inhibits the DNA damage repair pathways, increases cell cycles arrest, and induces cell death such as apoptosis and necrosis.
- Hyperthermia was proven to be effective in many different tumor types, such as superficial breast cancer, soft tissue sarcoma, and cervical cancer.

6.5.7 RT Combined with Short-Term Starvation

Voluntary fasting is a part of religious services in many cultures like Buddhism, Christianity, Hinduism, etc. Fasting/short-term fasting (STS) is also known as calorie restriction (CR) which is associated with diets with a wide alteration in the growth factors and the metabolites levels. This produces a milieu that diminishes the cancer cell competency to get acclimatized and endure which results in improved outcomes for cancer therapy. In normal cells, STS and fasting selectively boost the chemotherapy resistance which is not the case with cancer cells. STS endorses rejuvenation of normal cells, thereby averting the toxic and harmful effects of the treatment. Clinical as well as *in vivo* studies suggest that the low calorie-fasting mimicking diet (FMD) cycles are promising and also safe, in patients that can barely endure STS/fasting. Hence, it can be predicted that

the combination of STS or FMDs with chemotherapy, immunotherapy as well as other therapies holds a promise in increasing the cancer treatment efficacy, preventing the acquired resistance and minimizing the aftereffects [107]. This can be correlated with one of the emerging hallmarks of cancer, i.e., the susceptibility of cancer cells to nutrient deficiency and their addiction for explicit metabolites. Three of the nutritional interventions of food withdrawal strategies like fasting, FMD, and calorie CR from the myriad of strategies have increasingly exhibited a valuable effect on metabolism and shown a promising anticancer activity. STS is typically done on an average of 3–5 successive days. In fasting, only water is consumed, for a timespan ranging from 12 h to 3 weeks. For CR, there is a 20–40% decrease in calorie ingestion with decrease in all constituents without intercepting the ingestion of minerals and vitamins, typically used by specialists as a synonym to dietary restriction.

Cancer cells are distinguished from normal cells by means of their irregular metabolic and signaling pathways that lead to circumventing the antiproliferative signals, distorted mitochondrial function, and increased glucose uptake. Fasting or STS exhibits a differential consequence on cancer cells and normal cells which can be attributed to drop in the glucose, insulin-like growth factor-1, and insulin levels, amplification in ketone bodies and insulin-like growth factor-binding protein 1 (IGFBP1). This phenomena force cancer cells to depend on the limited amounts of factors and metabolites that are present in the blood, thereby eventually resulting in cell death. The response mechanisms of differential stress sensitization (DSS) and differential stress resistance (DSR) caused by fasting/STS stimulate the normal cell protection but pushes the cancer cell toward cell death. One of the major classical responses of radiation is the dys-functioning of the cell cycle arrest [108].

There is a growing body of evidence from the preclinical studies on STS which enhances the efficacy of a wide variety of chemotherapy drugs that are used in treatments of several types of tumors. Some of clinical trials (NCT00757094, NCT00936364, NCT01304251, and NCT01954836) have proven to be safe and feasible with reduction in the chemotherapy associated side effects. Since STS has demonstrated favorable traits to fight cancer, it would be logical to combine STS with RT as it presents clinical gain. In preclinical studies, combining STS with RT has already exhibited enhanced RT effects. Clinical and preclinical trials of STS and RT are also picking pace to exhibit the efficacy of this combination. STS can be considered as a personalized dietary approach that can be conveniently combined with RT in clinics in the path forward (Box 6.10).

Box 6.10 RT Combined with Short Term Starvation

- Short-term starvation (STS) in combination with RT leads to an increased effect of RT on metastatic cancer cells, and at the same time also protects normal cells.
- Short-term starvation (STS) or fasting can particularly safeguard normal cells in mice and probably in patients receiving chemo without reducing the therapeutic effect on cancer cells.
- Fasting dependent decrease in IGF-1 and glucose are arbitrate components involved in the DSR and DSS effects.

6.6 Spatial Fractionation

Box 6.11 Spatial Fractionation I

- Spatial fractionation is a method that reduces damage to normal tissue.
- Small beams of radiation are applied in a grid-like pattern.
- High doses are applied in the beam path, while (almost) no or very low dose is delivered between the beams, resulting in high peak-to-valley dose ratio (PVDR).

Box 6.12 Spatial Fractionation II

- Spatial fractionation of photons is in clinical use.
- GRID therapy uses 2D pattern with beam width of ~1–1.25 cm and center to center (ctc) of 2.2–2.4 cm.
- LATTICE is the 3D extension of GRID therapy.

Box 6.13 Minibeam RT

- Minibeam RT (MBRT) is a modern therapy approach using protons and heavier ions, which is at the moment in preclinical stage or investigated in clinical trials.
- In proton MBRT, the beam widen and overlap in the tumor.
- Further sparing of healthy tissue can be achieved using interlacing methods.

The concept of spatial fractionation of radiation in tumor therapy aims to widen the therapeutic window by sparing healthy tissue by simply sparing parts of it from radiation. It was introduced as GRID therapy by Alban Köhler in 1909 by the use of a grid of centimeter-wide pencil beams in X-ray therapy [109]. In the 1990s, when more powerful X-rays became available from synchrotron facilities, GRID therapy was moved to the micro level with the development of microbeam radiotherapy (MRT) and to the submillimeter level in the later 2000s with minibeam radiotherapy (MBRT) [110]. It was then that GRID, MRT, and MBRT were classified under a broader term of spatially fractionated radiation therapy (SFRT).

In SFRT, the spatial arrangement of the radiation allows irradiating tumors with a heterogeneous dose, with high doses in the radiation channels and low doses in the so-called valleys in between.

In recent years, advances in the use of spatial fractionation in particle therapy have also been investigated. Proton minibeam radiotherapy (pMBRT) is making rapid progress [111]. Thanks to small-angle scattering, the radiation channels overlap and the tumor is irradiated with a homogeneous dose, while the normal tissue is spared due to the spatial fractionation of the dose (Box 6.11, 6.12, and 6.13).

Schematic representations of SFRT, proton and ion MBRT is shown in Fig. 6.11.

6.6.1 Parameters and Mechanisms

Spatial fractionation of radiation means that new parameters must be introduced and controlled in treatment planning and therapy. First and foremost, beam size and the distance between two beams become the most important variables. Beam size, or beam width, is the full width at half maximum (FWHM) of the lateral intensity profile of a beam. The distance between two beams, also called center-to-center distance (ctc), is defined as the length of the direct connection between the maximum intensity (also called center) of the two beams [112].

Another important quantity is the dose ratio between the dose in the center of the beam (peaks) D_P and the dose in the middle between two beams (valleys) D_V, the peak-to-valley dose ratio (PVDR):

$$\mathrm{PVDR} = \frac{D_P}{D_V} \tag{6.3}$$

The PVDR defines the strength of spatial fractionation. It is ~1 for homogeneous irradiation and approaches infinity for small valley doses [113].

The parameters of beam width, ctc, and PVDR determine the possibility of sparing normal tissue and also the dose applied to the tumor, thus influencing tumor control.

Finally, the geometric arrangement of the beams is also crucial. Spatial fractionation uses beams that have either a pencil (Fig. 6.12a, b) or a planar structure (Fig. 6.12c). Pencil

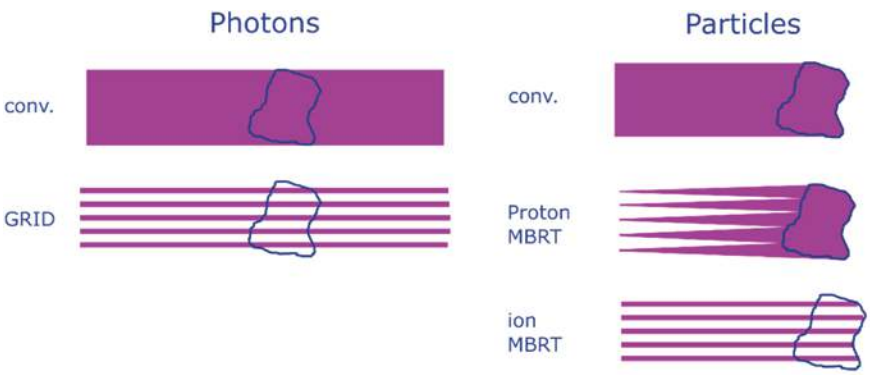

Fig. 6.11 Schematic view of spatial fractionation in RT. The blue object represents the tumor

Dose pattern	*Photon SFRT*	*Proton MBRT*	*Ion MBRT*
In the tumor	Heterogenous	Homogeneous	Heterogenous
In front of the tumor	Heterogenous	Heterogenous	Heterogenous
Behind the tumor	Heterogenous	No dose	Heterogenous

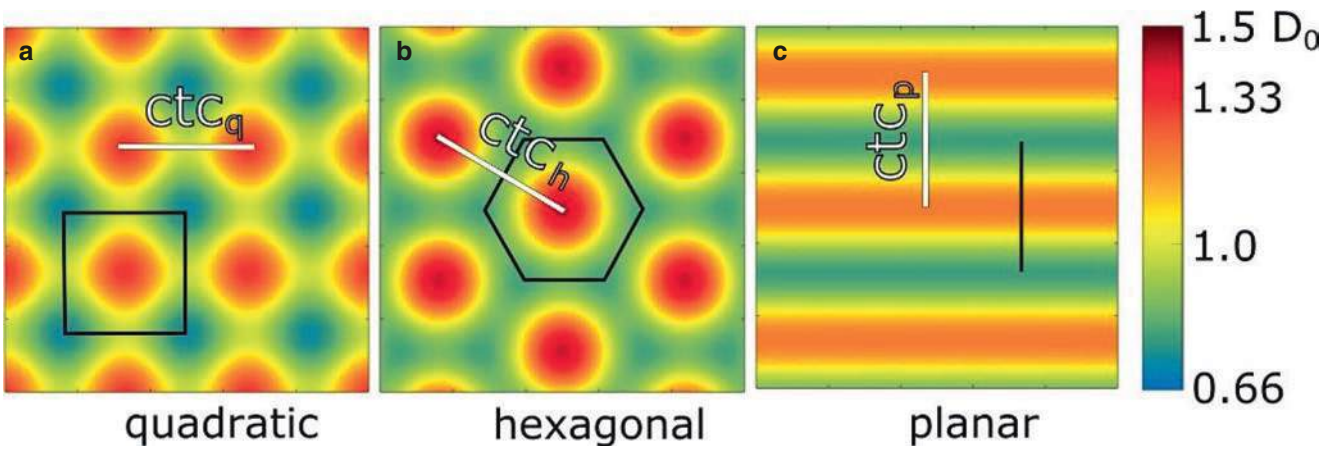

Fig. 6.12 Quadratic (**a**) and hexagonal (**b**) pencil minibeam and planar minibeam (**c**) arrangements on a 2D lattice with view direction in the direction of the beam. The dose is color coded and normalized to a mean dose D0. The black lines indicate the unit cell, and the white lines indicate the corresponding ctc. (Reproduced with permission from (CCBY) [112])

beams have a completely round or Gaussian shape and can be arranged in either a square or hexagonal lattice. For treatment planning, it is important to know the dimensions of a beam. For this purpose, the unit cell of a beam is used. The unit cell is the smallest unit in which a beam can be considered a beam and the entire dose distribution is covered. The unit cell is assembled to form the entire lattice and cover the tumor.

The basic mechanism of tissue sparing by spatial fractionation lies in the ability of undamaged cells in the vicinity of the radiation beam paths to migrate to this region and support wound healing. This is described as the dose-volume effect, i.e., the ability of skin and subcutaneous tissue in particular to tolerate more dose as the irradiated volume decreases. Furthermore, the microscopic prompt tissue repair is another beneficial effect resulting in better tolerance of tissue to submillimeter sized beams. When tissue is damaged in such small areas, capillary blood vessels can be rapidly restored within days or even hours by the regeneration of cells from the undamaged area. The intact blood vessels also support healing of the damaged tissue located between the beams. The extent to which the bystander effect plays a role is still unknown and is currently being investigated.

6.6.2 Spatial Fractionation of Photons

6.6.2.1 Photon SFRT in the Clinic

Spatial fractionation of photons is already being used clinically, but other treatment strategies are being tested simultaneously in preclinical and clinical studies. The application of photon SFRT in the clinic can be distinguished into GRID and LATTICE therapy. In GRID therapy, based on the original method of Koehler et al. in 1909, portions of the radiation field are blocked by the use of collimators placed in front of the patient to produce a non-conformal dose in both healthy tissue and tumor, as shown in a therapy plan in Fig. 6.13b [109].

Optimal geometries of collimators for tissue sparing and therapeutic outcome are hole sizes from 1 to 1.25 cm and ctc from 2.2 to 2.4 cm [114]. The pattern can be generated either with a block collimator with a defined hole pattern or with multileaf collimators (MLCs), which can be flexibly adapted to the needs of the treated tumor. The disadvantage of MLCs in the clinic is that treatment time is prolonged because each spot must be applied in a step-and-shoot procedure. Although faster irradiations are possible with MLCs by moving the target across the beam, this is currently only possible preclinically. A more advanced method is the hybrid use of an MLC and a block collimator, which combines the advantages of both methods but has the disadvantage of lower PVDR along the diagonal [115].

The efficiency of GRID therapy has been demonstrated in various clinical trials with different tumor types and by using different collimators [114, 115]. A modern approach to photon SFRT is LATTICE therapy, which can be used with arc-based therapy and is the 3D extension of GRID therapy. In LATTICE therapy, the beams are applied to form multiple small spheres of high dose, called vertices, in the tumor (Fig. 6.13a). The LATTICE application further reduces damage to normal tissue and has also been used in clinical trials [116].

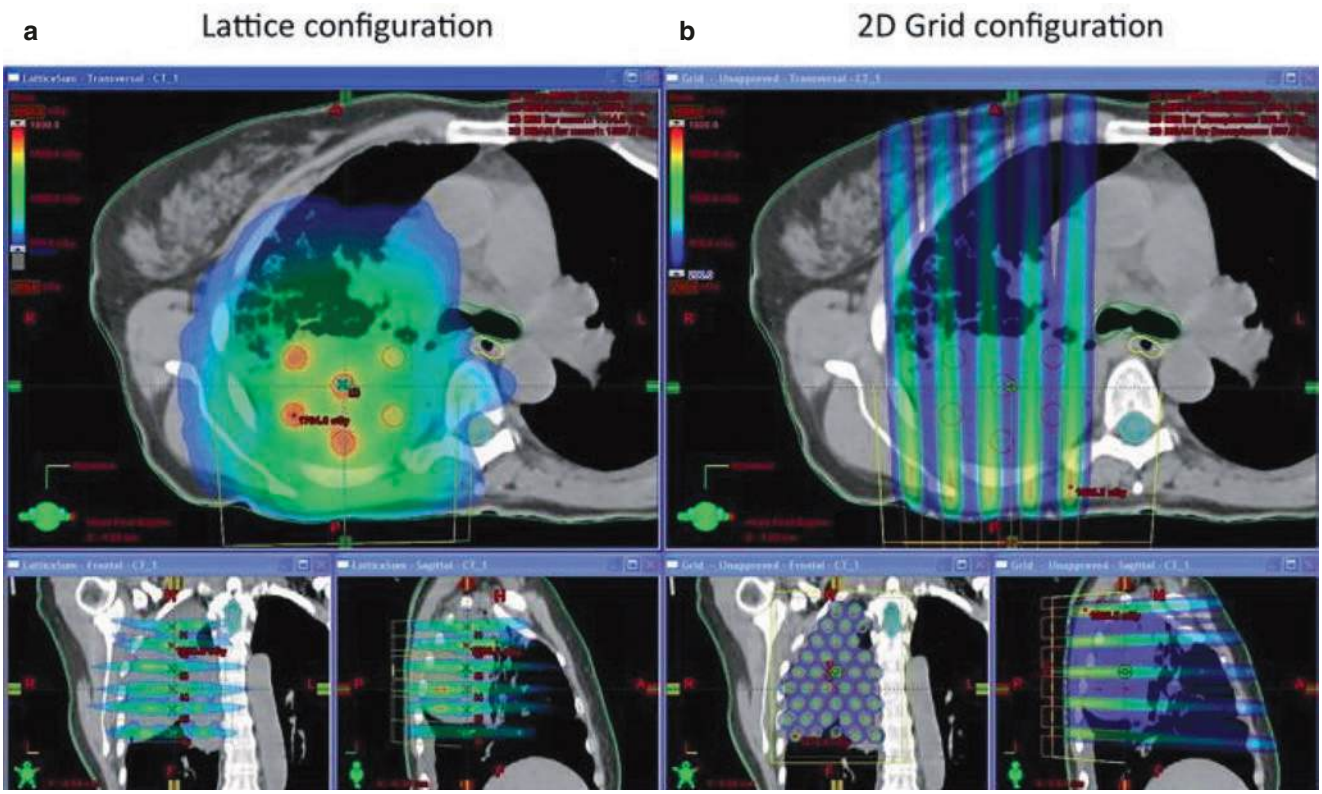

Fig. 6.13 Treatment planning of a lung tumor patient in LATTICE (**a**) and GRID (**b**) therapy. (Reproduced with permission from [114])

6.6.2.2 Photon SFRT in Preclinical Development

While the use of SFRT in the clinic started with GRID and LATTICE, there are two other spatially fractionated modalities that are being studied preclinically. These are MRT, which uses spatially fractionated photons in the form of rectangular beams 25–100 μm wide (Fig. 6.14), and MBRT, which also uses rectangular photon beams but 400–700 μm wide.

MRT has the distinction of using extremely thin microbeams, which exploits the dose-volume effect and allows very high doses of radiation (300–600 Gy) to be delivered with minimal toxicity to normal tissue. In addition, synchrotron facilities such as the European Synchrotron can deliver radiation at ultra-high dose rates (12,000–16,000 Gy/s), making synchrotron MRT a spatially fractionated FLASH RT [117].

The benefits of MRT over conventional RT are many:

- Normal tissue is spared from the effects of radiation by two unique mechanisms: (1) volumetric sparing due to spatial fractionation of microbeams and (2) sparing of normal tissue due to ultra-high dose rates, known as the FLASH effect [117]. More details of FLASH radiotherapy are discussed in Sect. 6.4.2.
- MRT produces unique vascular effects that preferentially damage tumor vessels rather than those of healthy tissue. Peak doses selectively affect rapidly growing "immature" tumor vasculature, triggering transient tumor ischemia and neutrophil infiltration [117].
- Strong immune responses have been observed after MRT. For example, MRT can activate natural killer and cytotoxic CD8+ T cells, induce higher levels of pro-inflammatory genes in tumors, trigger the release of chemokines that attract monocytes, and recruit leukocytes to malignant tissues [118].

MRT currently requires ultra-high dose rates to deliver the radiation fast enough to prevent the beam from smearing across tissue due to the cardiovascular motion. Therefore, preclinical and future clinical research on MRT is currently limited to synchrotron facilities. However, a compromise can be achieved by delivering photon MBRT, since beam smearing is not a problem with submillimeter beams. The same logic is now being applied to MBRT ion therapy research and will be discussed next.

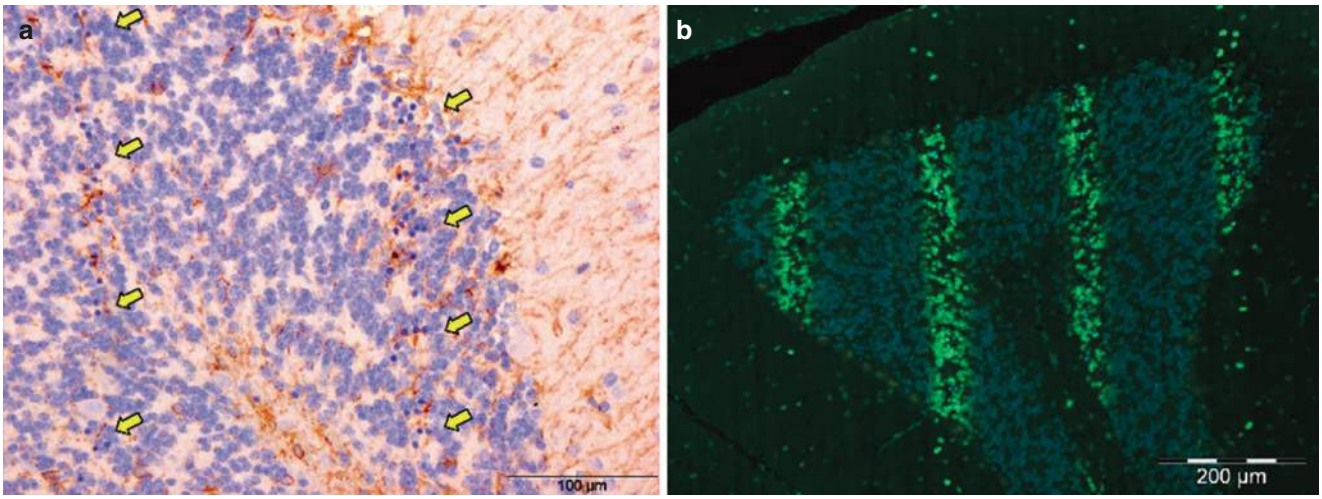

Fig. 6.14 Cerebellum of a rat 8 h after exposure to synchrotron MRT. The peak dose was 350 Gy, and each microbeam was 25 µm wide and spaced 200 µm from the center of the next microbeam. (**a**) H&E staining of the cerebellum. The track of the microbeams can be seen as two vertical bands of dark blue dots (yellow arrows) consisting of cells with nuclear pyknosis (irreversible condensation of chromatin in the nucleus of cells undergoing necrosis). (**b**) Immunostaining of a different section of the cerebellum with gamma-H2AX. The track of the microbeam can be seen as green staining, indicating large amounts of DNA damage. The blue color indicates nuclear staining with DAPI

6.6.3 Spatial Fractionation of Ions

The method of applying spatially fractionated RT using particles, also called minibeam RT, is still in its infancy. Preclinical research points to drastically lowered side effects, with at least same tumor control, thus clearly widening the therapeutic window. In MBRT, one distinguishes between proton MBRT and ion MBRT, most commonly carbon and helium. The major difference lies in the application of the dose to the tumor originating from different physical properties of the particles. When particles traverse matter, interactions with the atoms and molecules occur. At high energies, as used for therapy, the interactions are dominated by Coulomb interactions with the electrons of the target material. These mechanisms mainly cause the ions to lose energy and define the well-known Bragg curve of energy loss. But these interactions also cause scattering of the ions and thus deflection, called small-angle (Coulomb) scattering. In each interaction, the particle is only scattered by a small angle, causing a roughly gaussian broadening of an incident ion beam. The beam is thus widening with increasing penetration depth. The FWHM of the beam due to scattering, which is in the order of several millimeters for therapy relevant energies, is proportional to the ion charge z its kinetic energy E_{kin} and the distance covered in medium x:

$$\text{fwhm} \propto \frac{z}{E_{\text{kin}}}\left(\sqrt{x}\right)^3 \tag{6.4}$$

Therefore for helium and carbon ions, this results in a reduction of beam width compared to protons of a factor of ~2 and ~3, respectively, as shown in Fig. 6.15.

Therefore MBRT for protons works with the principle that the beams start to clearly widen, while traversing tissue as shown in Fig. 6.16. The planning is done in a way that at the beginning of the tumor, the beams overlap and the tumor is irradiated with a small PVDR or even a homogeneous dose distribution.

For helium and carbon, the beams don't overlap, thus giving potential for further sparing of healthy tissue also close to the tumor volume. Although there is evidence for tumor control using heterogeneous tumor dose, it seems appropriate to find a way of applying an (almost) homogeneous dose to the tumor [119]. This is achieved through so-called interlacing, where the beams of different irradiation fields are arranged in a way that in the tumor the dose peaks interlock and homogeneous dose distribution is formed. Figure 6.17 shows different possibilities of interlacing using either pencil or planar beams compared to single direction irradiation.

Up to now, the method of MBRT is still in the preclinical state and especially proton MBRT is investigated here, as the possible spreading is more promising as more proton therapy centers than other particle therapy centers exist worldwide. Up to now it could be shown that pMBRT has

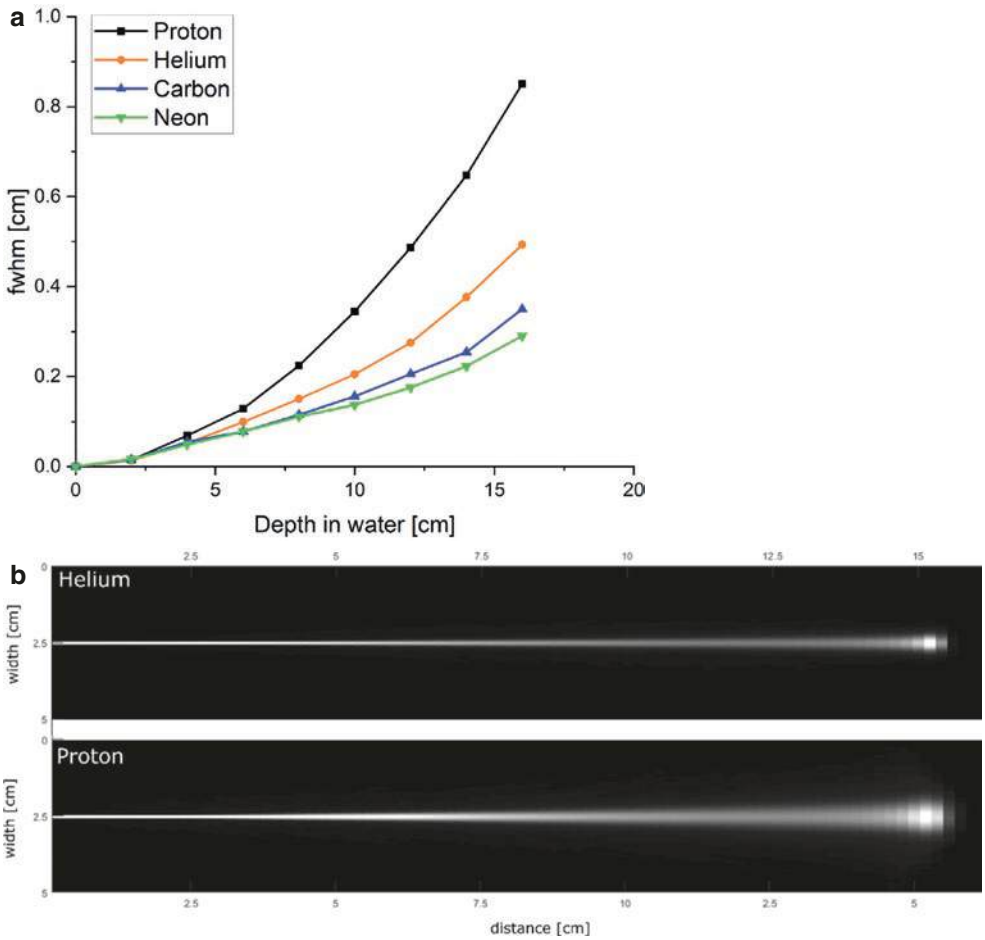

Fig. 6.15 (**a**) Beam width for proton, helium, and carbon ion beams with penetration depth. No incident beam size and divergence is used, both have to be added to the FWHM. (**b**) Widening of a helium ion and a proton beam with penetration depth

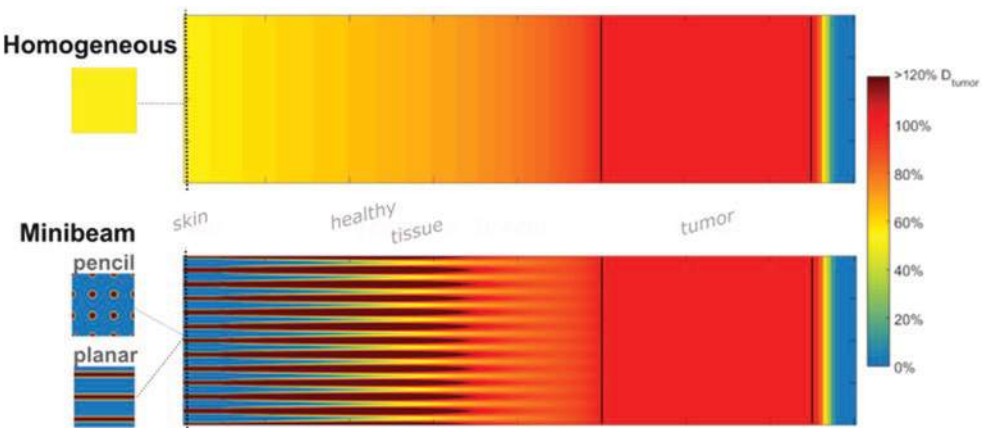

Fig. 6.16 Conceptual therapy plans comparing conventional proton therapy (homogeneous) with pMBRT (Minibeam) for a box-shaped tumor

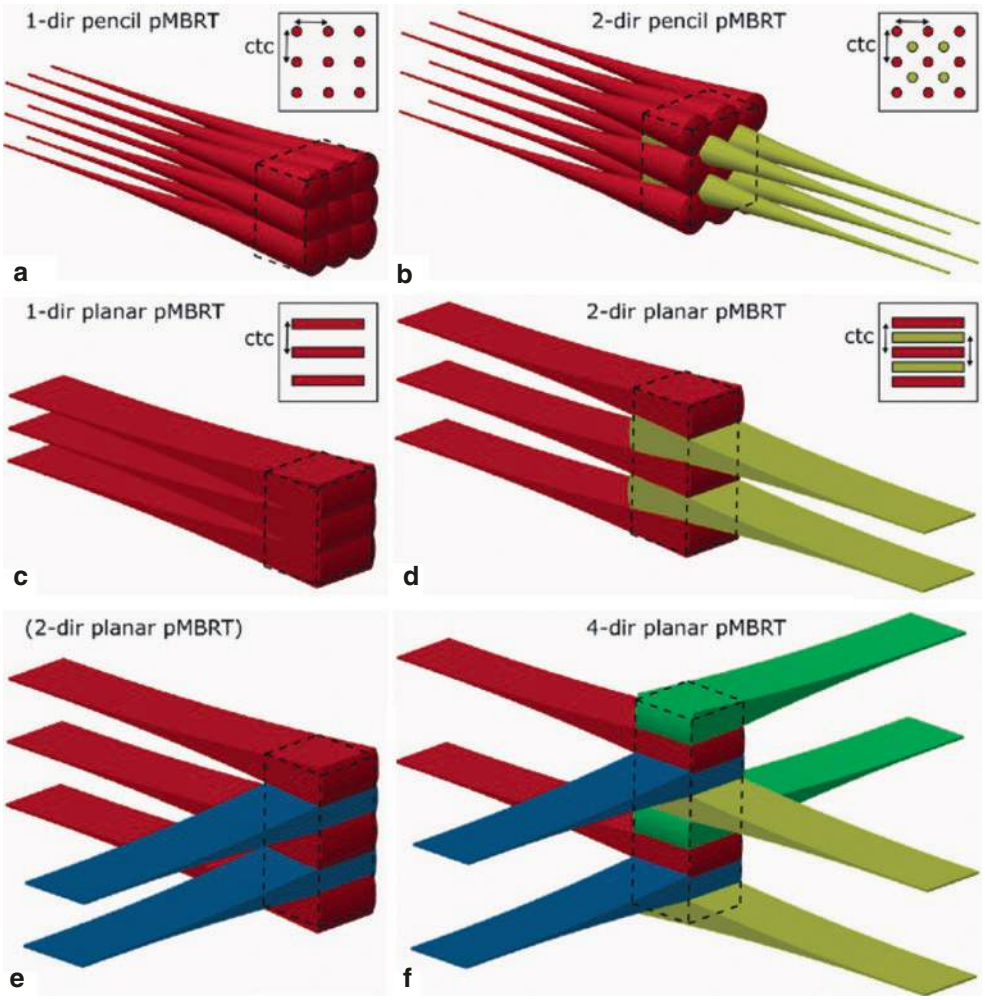

Fig. 6.17 Possible interlacing geometries in MBRT for pencil (**a**, **b**) or planar (**c**–**f**) beams for homogeneous irradiation of a box-shaped tumor (black dashed line). (Reproduced with permission (CCBY) from [119])

lower early and late side effects in the skin of mice and rats [113, 120]. Furthermore, in a rat brain model, it could be shown that less histological and behavioral changes occur after pMBRT [120]. Already tumor treatment was performed in glioma bearing rats, where animal survival could be clearly enhanced while tumor control was kept. First therapy planning in brain tumor patients shows reduced dose to organs at risk, while the same dose distribution in PTV could be achieved (Fig. 6.18) [121]. These promising preclinical results cleared the way for clinical trials. First results on treatment of ten patients treated with pMBRT, called proton GRID therapy, in a clinical study (NCT01255748) show the possible advantages of pMBRT, regarding sparing of healthy tissue and tumor control [122]. Furthermore, the integration of pMBRT to clinical facilities is under investigation and especially the combination with FLASH RT seems promising [113]. An important task which needs to be solved is the production of mini beams with a small enough size without producing secondary radiation, which can harm the patient. The two possible ways of minibeam production are via the focusing of a proton beam or via the use of a collimator. Both methods are complementary, and their use in clinical practice needs to be further investigated.

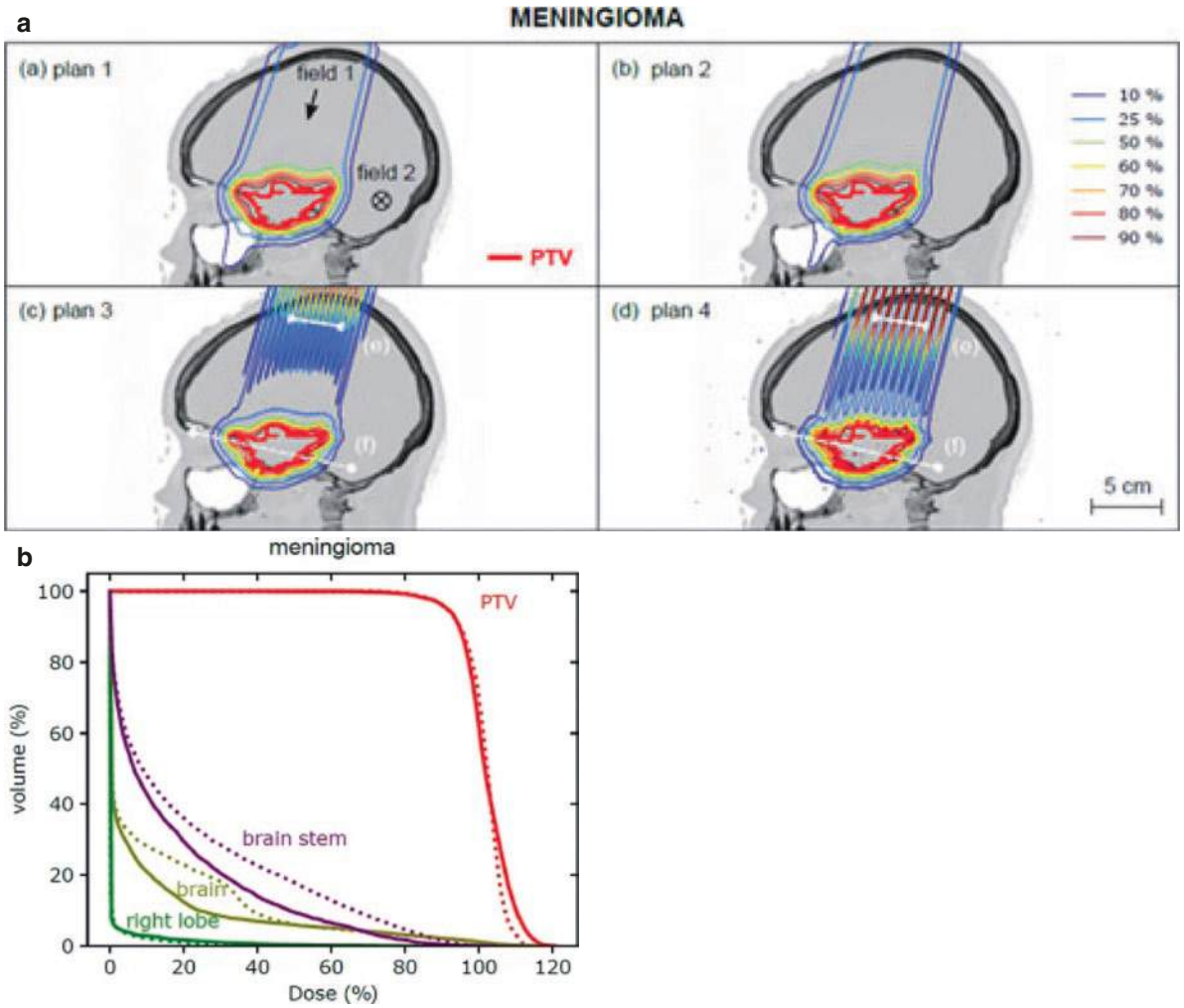

Fig. 6.18 (**a**) Treatment plan comparison of a meningioma patient. Plan 1 and 2 are homogeneous plans, with different planning methods. Plan 3 and 4 show single field pMBRT plans with ctc of 4 mm and 6 mm, respectively. (**b**) Comparison of dose-volume histograms for plan 2 (homogeneous, dashed line) and plan 3 (pMBRT, solid line)

6.7 Brachytherapy Strategies

6.7.1 Brachytherapy

Box 6.14 Brachytherapy

- According to the dose rate brachytherapy can be divided into three types: low dose rate (LDR) with dose rates 0.4–2 Gy/h, medium dose rate (MDR) with dose rates 2–12 Gy/h, and high-dose rate (HDR) with dose rates excessing 12 Gy/h.
- Brachytherapy can be delivered with sealed radionuclide sources and electronic brachytherapy using kV X-rays.
- Brachytherapy is mostly used for treatment of cervix, prostate, and skin cancers and some rare sarcomas.

6.7.1.1 Principles

Brachytherapy is a treatment technique in which radiation sources are placed into the tumor (or the tumor bed to be treated after surgery) or its proximity. For conventional brachytherapy, sealed radionuclide sources are used, but electronic brachytherapy with X-ray has recently become available. The advantage of brachytherapy is a very high dose gradient around the sources, which are, contrary to external RT, extremely close to the treated area. Sharp dose decrease allows for a high level of conformity when dose is delivered locally. However, the technique is available only for easily accessible treatment areas.

The fractionation scheme is different in comparison to the external RT with lower number of fractions and higher doses per fraction.

Usually, radionuclide implants are applied to deliver the treatment which can be either temporary or permanent. The radionuclides need to have convenient physical characteristics (half-life, type of disintegration, mean energy, nominal specific activity, etc.).

Table 6.9 Physical characteristics of radionuclides used for brachytherapy

Characteristic	^{192}Ir	^{60}Co	^{137}Cs	^{125}I	^{103}Pd
Type of disintegration	β^- (95.1%), Electron capture (4.9%)	β^-	β^-	Electron capture	Electron capture
Half-life	73.83 days	5.27 years	30.07 years	59.4 days	17.0 days
Mean gamma energy (keV)	372.2	1252.0	661.7	35.5	137.1
Nominal specific activity ($\times 10^5$ TBq/kg)	3.4	0.41	3.2×10^{-2}	6.5	27
Air kerma-rate constant ($\times 10^{-18}$ Gy m^2/(Bq s))	15	85	6.1×10^{-5}	9.9	9.0

According to the dose rate brachytherapy can be divided into three types: low dose rate (LDR) with dose rates 0.4–2 Gy/h, medium dose rate (MDR) with dose rates 2–12 Gy/h, and high dose rate (HDR) with dose rates exceeding 12 Gy/h (which is 0.2 Gy/min). Higher source energies are used for temporary brachytherapy with HDR sources compared to permanent LDR brachytherapy. Pulsed dose rate (PDR) uses series of short exposures of 10–30 min every hour to approximately the same total dose in the same overall treatment time as with the LDR. Characteristics of frequently used radionuclides are presented in Table 6.9.

Electronic brachytherapy is a non-invasive procedure and is a good option for skin cancers in the facial area, especially around the eye and nose. It is also an option after breast conserving surgery to treat the tumor bed when intraoperative RT is used according to an accelerated partial breast irradiation (APBI) procedure. Kilovoltage X-rays generators are used with voltage potential 30–50 kVp.

6.7.1.2 Main Indications and Modalities

There are several types of brachytherapy depending on the site and organ type to be treated [123].

Intracavitary brachytherapy uses sources that are placed in body or organ cavities. It is mostly used to treat early cervical and uterine (endometrial) cancer, but also in a heterogeneous group of gynecological cancers (ovary, fallopian tubes, body of the uterus, vagina, and vulva). Early rectal cancer can be treated with electron brachytherapy, but the standard of care in rectal cancer is still surgery, especially in case of bulky tumors and more advanced disease, preceded by radio(chemo)therapy.

Interstitial brachytherapy employs sources placed into the tumor, or to its proximity, using needles. It has primarily been used to treat prostate or breast cancer (PCa, BC), but recently it has also been combined with intracavitary brachytherapy to treat bulky cervix tumors. This combination improves coverage of the target volume which was not achievable intracavitary techniques only. PCa brachytherapy can be performed with permanent seeds (for LDR) or temporary sources (for HDR). For breast brachytherapy, interstitial multicatheter brachytherapy is used for boost or partial breast irradiation (PBI)/accelerated PBI (APBI). APBI treats only the lumpectomy bed with 1–2 cm margin, rather than the whole breast [124]. HDR sources are usually applied to deliver prescribed doses of 30.3–34 Gy in 7–10 fractions for APBI and 15–20 fractions with LDR/PDR (pulsed dose rate) or 8.5–10 Gy with HDR for breast boost treatment. Soft tissue sarcomas are sometimes also treated with brachytherapy alone or in combination with external RT after surgery.

When sources are placed into tubular organs such as trachea, lungs, esophagus, or bile duct, the term **intraluminal brachytherapy** is used. For lung cancer, the ability of patients to tolerate bronchoscopy is essential. The main indication is treatment of significant, endotracheal, or endobronchial symptoms. Endobronchial brachytherapy is mainly palliative, however it has been used with curative intent in a small number of cases of early-stage tumors with good results.

Skin cancer can usually be treated by placing the sources on the skin in the desired geometry, therefore it is sometimes referred to as **contact brachytherapy**. Skin cancer is a very common cancer, and brachytherapy is used mainly for areas such as face, scalp, ears, hands, legs, especially when surgery would result in poor cosmetic results or require (extensive) plastic reconstructions. Most cancers are either squamous or basal cell carcinomas. Contact applicators or surface molds can be used. The applied dose is tumor size dependent. For LDR and PDR brachytherapy, doses of 60–66 Gy are delivered to tumors less than 4 cm and 75–80 Gy for those more than 4 cm. For HDR brachytherapy, typical total dose is 30–40 Gy delivered in 8–10 fractions. Other options for skin treatment include superficial X-rays, orthovoltage X-rays, megavoltage photons, or electron beam irradiation.

Ocular brachytherapy can be used to treat uveal malignant melanoma. Currently, the most frequently used radionuclides are I-125, Ru-106/Rh-106, Pd-103, Cs-131.

Intravascular brachytherapy is a rarely used treatment option. It can be used to treat restenosis following percutaneous angioplasty of cardiac arteries. The sources are temporarily placed within cardiac stents in which restenosis has occurred to prevent restenosis. Typically, beta emission sources like P-32, Ir-192, or Rh-188 are used for the treatment. P-32 coated stents have also been used, but with the development of drug-eluting stents, intravascular brachytherapy has lost a lot of its attractivity.

The application of **brain brachytherapy** has decreased a lot since highly conformal RT radiotherapy and stereotactic radiosurgery are available. However, brachytherapy can still be used to treat gliomas with a maximum diameter of 5 cm if not too close to organs at risk.

6.7.1.3 Treatment Course

Three main radiobiology parameters in brachytherapy are dose rate, cell cycle redistribution, and reoxygenation.

Brachytherapy can be used as a single strategy or can be combined with other treatment modalities. When combining brachytherapy with external beam RT, total dose to the tumor and organs and risk must be considered. As an example, for the cancer of the cervix, both radiation treatment modalities are usually combined [125]. In such a case, the doses to the tumor and to the critical organs should be always considered as a summation of radiobiological doses to each structure. The LQ model l is recommended with the concept of equi-effective dose (EQD2) [126]. For simple estimations and HDR brachytherapy, the LQ model without any corrections can be applied to calculated EQD2. However, there are some radiobiological factors relevant to brachytherapy for continuous treatment or for multiple fractions per day. Repair rates (called μ values) are used to correct doses for repair of sublethally damaged cells. Average repair half-lives for mammalian tissues are usually 0.5–3 h. There exists evidence that tumor recovery half-lives are probably shorter than those for late-reacting normal tissues.

In fractionated treatment with HDR, there should be at least 6 or 8 h between individual fractions to enable the cells of normal tissues to repair. HDR brachytherapy delivers treatment with dose rates exceeding 12 Gy/h with 192-Ir or 60-Co sealed sources. Pulsed dose rate (PDR) brachytherapy is fractionated treatment but with a special time schedule. The treatment is delivered with continuous hourly pulses. This approach is supposed to give a similar effect as a hyperfractionation. It was shown that if the time interval between pulses does not exceed 1 h, overall treatment time is not modified, total dose is the same, and the dose rate is not above 0.5–0.6 Gy/h.

Radiobiological modeling demonstrated that the PDR technique rather than continuous LDR radiation allows to exploit differences between the half times for sublethal damage repair ($T_{1/2}$) of late-responding normal tissues and tumors. Repair half times for tumors are estimated to be in the range of 1–2 h, while for late-responding normal tissues, these could be as long as 3–4 h. By matching the pulse frequency with tissue repair kinetics, in a fixed overall treatment time, a therapeutic benefit, i.e., normal tissue sparing while keeping the same tumor control probability, can be obtained relative to continuous LDR radiation. On the basis of those modeling data, an office hours PDR boost regimen was designed for substitution of the continuous LDR boost in breast conserving therapy [127]. A next theoretical study on the optimal fraction size in hypofractionated HDR brachytherapy demonstrated large dependency on the treatment choices (the number of fractions, the overall time, and time between the fractions) and the treatment conditions (reference LDR dose rate tissue repair parameters). The data revealed that hypofractionated HDR might have its opportunities for widening of the therapeutic window for a specific combination of those choices and conditions.

In general, tumor reoxygenation occurs during fractionated treatment. In LDR brachytherapy, the contribution of reoxygenation is low. The lower the dose rate, the lower the oxygen enhancement ratio due to the reduction in sublethal damage repair capability in hypoxic cells.

It is well known that cells have different sensitivity to radiation due to their position in the cell cycle phases. With HDR brachytherapy, delivered in fractions, it can be more difficult to synchronize cells in these cell cycle phases. On the other hand, with LDR brachytherapy the cell distribution in certain cycle phases can be better and earlier synchronized. Cell cycle changes were also observed later for PDR, however, which were more long-lasting and more pronounced [128].

6.7.2 Radioembolization

Box 6.15 Radioembolization

- Radioembolization is based on a vascular selectivity process resulting in a differential effect that leads to a higher concentration of radioactivity within tumor tissue than in non-tumoral liver.
- Treatment course includes several steps, notably a treatment planification process aiming to personalize the activity of radioembolization to administer.
- Radioembolization is commonly used in treatment of primary and metastatic liver diseases.

6.7.2.1 Principle

Yttrium-90 radioembolization, also called Yttrium-90 selective internal radiotherapy (SIRT), is a type of brachytherapy based on intrahepatic arterial administration of yttrium-90 (^{90}Y)-loaded biocompatible microspheres (^{90}Y-microspheres) [129]. Two types of microsphere loaded with 90Y are commercially available: one made of resin (SIR-Spheres®, Sirtex, St. Leonards, Australia) and an alternative made of glass (TheraSphere®, Boston Scientific, Marlborough, MA, USA). The rationale for this approach is that both primary and metastatic tumors in the liver receive their blood supplies primarily from the hepatic artery, whereas the non-tumoral liver (NTL) is fed essentially entirely via the portal vein rather than the hepatic artery [130].

^{90}Y is a therapeutic radionuclide with a physical half-life of 2.67 days (64.05 h) and combined electron (β^-) and positron (β^+) emission. The maximum and average energies of β^- emissions from ^{90}Y are 2.28 MeV and 934 keV, with a mean tissue penetration of 4.1 mm and a maximum of 11 mm. As in other RTs, ^{90}Y β^- absorbed dose deposition induces direct or indirect damage to DNA in exposed tissue, leading to early or delayed cellular death [130]. To avoid

serious adverse events such as radiation pneumonitis secondary to lung contamination via hepato-pulmonary shunts or radioembolization-induced liver disease (REILD), the irradiation of liver malignancies is limited by unintended exposure to NTL and lung parenchyma.

Although the branching ratio is very low, the β^+ emission enables ^{90}Y-microsphere positron emission tomography (PET) imaging after radioembolization. It is also possible to image the ^{90}Y-microsphere distribution based on the β^- bremsstrahlung emission spectrum by bremsstrahlung emission computed tomography (BECT).

Therefore, the efficacy of radioembolization is based on a vascular selectivity process resulting in a differential effect that leads to a higher concentration of radioactivity within tumor tissue than in NTL. The stronger the differential effect, the more effective the treatment will be. Due to their size, the tumor's vascular properties, and the hemodynamics of the vascular system used for targeting, ^{90}Y-microspheres are permanently implanted into the micro-vessels of the tumor/NTL without any biological degradation (although physical decay of ^{90}Y still occurs).

6.7.2.2 Main Indications

Radioembolization has been broadly adopted as a locoregional therapy for advanced primary or metastatic liver disease [129, 130]. The most common indications for radioembolization are hepatocellular carcinoma (HCC), liver metastases from colorectal cancer (mCRC), intrahepatic cholangiocarcinoma (IH-CCA), and neuroendocrine tumors (NET) [129, 131]. Very little scientific evidence (level 1 or 2) derived from prospective randomized controlled trials supports the use of radioembolization as a first- or second-line treatment option in various treatment algorithms. Prospective data have been obtained for HCC and mCRC patients, and prospective studies in IH-CCA and NET are underway [132]. In the HCC management guidelines for the European Association of Medical Oncology (ESMO), radioembolization is considered as the last-line treatment. The ESMO guidelines for the management of mCRC patients include radioembolization as a second-line treatment for patients with liver-limited disease in whom the available chemotherapeutic options have failed.

6.7.2.3 Treatment Course

The treatment course, illustrated in Fig. 6.19, includes several steps [132]:

- First, patients are selected for radioembolization by the multidisciplinary tumor board, based upon individual characteristics. Radioembolization requires a holistic view of the patient and the disease. Disease stage, long-term and immediate treatment aims, morphological features [assessed using computed tomography (CT) or magnetic resonance imaging (MRI)], metabolic/functional properties [e.g., assessed using [^{18}F]-fluorodeoxyglucose (^{18}F-FDG) hybrid PET coupled with CT (PET/CT) imaging], and biological characteristics of the tumor, and the surrounding liver are all considered when establishing a radioembolization treatment plan.
- Then, a pre-treatment 3D hepatic CT angiogram is performed. The goal is to decide into which artery the ^{90}Y-resin microspheres will be injected and to determine the best catheter position to optimize the selectivity of treatment.
- To simulate the treatment, a 2D hepatic angiogram is performed, generally accompanied by a 3D cone-beam CT (CBCT). The catheter is placed at the position defined by the 3D CT angiogram, and ^{99m}Tc-labeled macroaggregated-albumin (^{99m}Tc-MAA) is injected into the hepatic artery. Given the similar median size of MAA particles (10–50 μm) and resin microspheres (20–60 μm), the MAA distribution pattern serves as a surrogate for how ^{90}Y-microspheres will localize.
- To visualize the distribution of ^{99m}Tc-MAA, planar scintigraphy, generally accompanied by hybrid single-photon emission CT and CT imaging (SPECT/CT), is acquired within 2 h after administration. This allows validation of the catheter position, identification of potential extrahepatic visceral contamination, and evaluation of the lung shunt and the targeting of the lesions; in addition, it can be used to determine the activity to administer in future therapy. This practice prevents post-therapy complications and selects patients with a good potential outcome.
- After this pre-treatment phase, treatment with ^{90}Y-microspheres is performed according to the pre-treatment catheter position and prescribed activity. With catheter-directed therapies such as radioembolization, it is important to verify that the position/location of the catheter during the ^{99m}Tc-MAA simulation is consistent with the position during the administration of ^{90}Y-microspheres to best reproduce the MAA distribution.
- Following administration of ^{90}Y-microspheres, a qualitative and quantitative assessment is performed (1) to verify that the treatment was performed as planned and identify any technical failures and (2) to detect any possible extrahepatic activity, which could cause serious complications such as gastrointestinal bleeding. Post-radioembolization imaging of ^{90}Y distribution may be performed using hybrid ^{90}Y-PET/CT or ^{90}Y-BECT/CT. However, many studies show qualitatively superior resolution and contrast with ^{90}Y-PET/CT relative to ^{90}Y-BECT/CT, and only ^{90}Y-PET/CT is available for quantification in clinical routine (^{90}Y-BECT/CT quantitative imaging is still under development).
- Finally, treatment response is evaluated. Clinical and biochemical assessment after radioembolization for any sig-

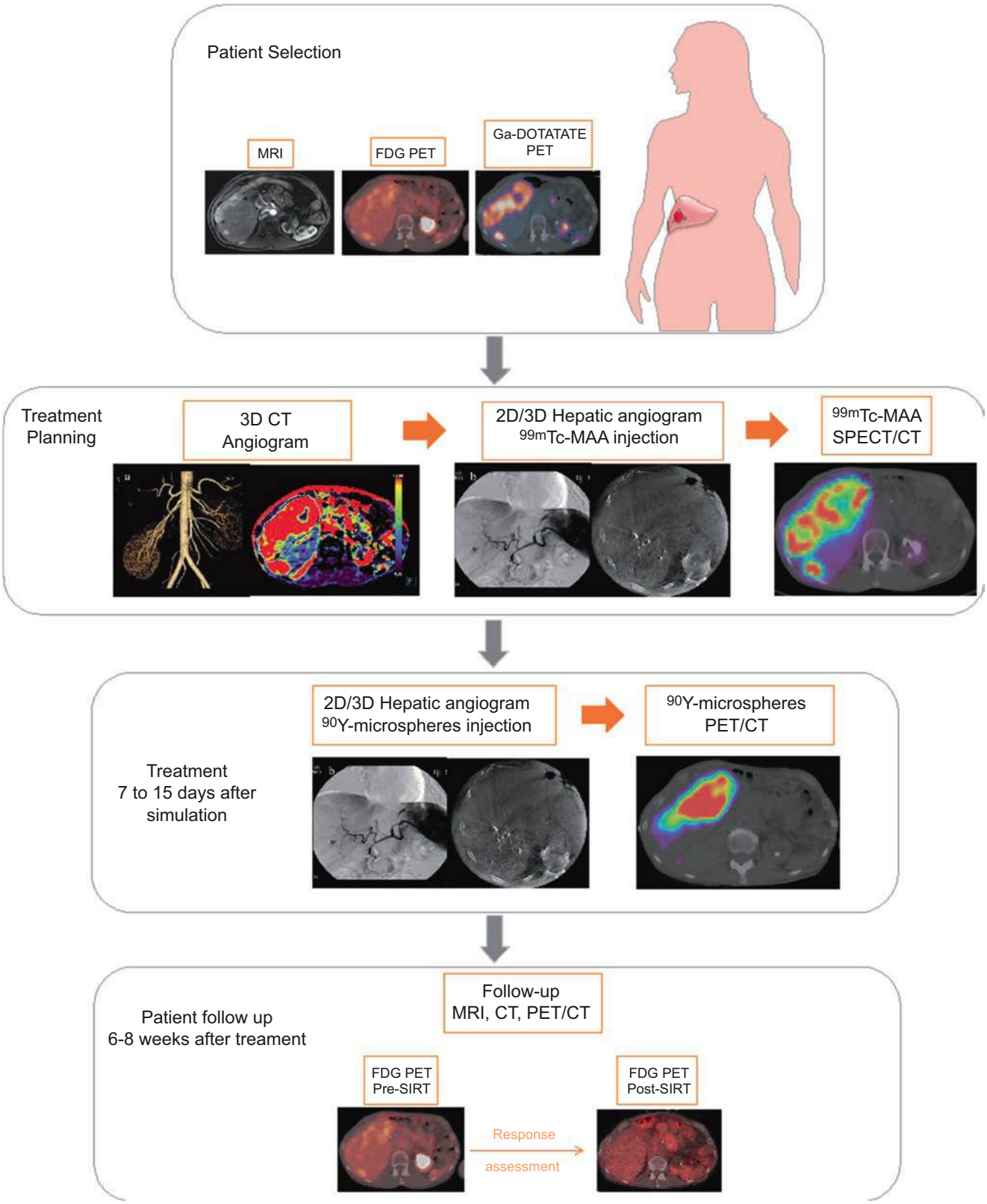

Fig. 6.19 ^{90}Y-resin microspheres radioembolization treatment course. Example of a patient treated for neuroendocrine neoplasia

nificant side effects is typically performed 1–2 months post-radioembolization. Imaging assessment of the tumor response should be performed 1–3 months post-radioembolization and every 2–3 months thereafter. The clinically relevant "treatment response," and thus the most suitable imaging technique, is defined differently depending on the type of tumor (e.g., variable ^{18}F-FDG avidity) and treatment intent (e.g., bridging-to-surgery, downstaging, etc.) [131].

6.7.2.4 Therapeutic Intent

Oncological Ambition

Curative setting: Radioembolization can be used in a preoperative setting (for solitary or limited-multifocal/oligometastatic tumor) when the ambition is to cure the patient. It can be used as bridging-to-surgery, to stabilize or slow down tumor growth and multiplicity thereby keeping a patient as a potential surgical candidate for liver resection or transplantation. Alternatively, radioembolization can be applied as a downstaging approach to induce a clinical shift from a non-resectable stage to a potentially resectable or transplantable stage by decreasing tumor size or number [129, 130].

Non-curative setting: In patients with advanced multifocal bilobar/lobar tumor distribution in whom curative approaches are not feasible, radioembolization can be used alone or in combination with other therapies as a life-prolonging treatment and palliative care [129, 130].

Radioembolization Field of Treatment

Whole-liver treatments: In the case of bilobar multifocal tumor distribution, the whole liver must be treated. Single injection within the common hepatic artery or a bilobar (left and right hepatic artery) approach is performed. The bilobar approach can be performed on the same day or staged (i.e., on separate days).

Lobar and segmental treatments: Unilobar or segmental treatments are considered when the disease is limited to a unique lobe or a segment. These approaches enable the preservation of the untreated liver, and if some loss of function in the treated lobe/segment is permissible, they allow more aggressive treatment.

Lobectomy and Segmentectomy: Radiation lobectomy, with the intent to induce contralateral lobe hypertrophy while achieving tumor control, may be considered in patients with unilobar disease and a small anticipated future liver remnant in an attempt to facilitate curative surgical resection.

Radiation: segmentectomy may be considered for localized disease (one or two segments) supplied by a segmental artery that is not amenable to other curative therapies because of tumor localization or patient comorbidities.

6.7.3 Personalized Radioembolization

Until recently, the prescription of 90Y-microspheres was based upon the body surface area method (resin microspheres) or on a dose limit to the whole treated liver volume without distinction between tumor and non-tumoral liver (glass microspheres). Both approaches lead to inherent risks of under- or overdosing, with considerable interpatient variations [130, 132]. To tackle those pitfalls, the concept of personalized radioembolization has recently emerged and provides an optimal framework to improve patient selection and maximize tumor response while sparing non-targeted tissues undesired toxicities. The patient-specific definition of a radioembolization therapeutic window is now assessed by integrating multidisciplinary teamwork, multimodal imaging techniques, advanced treatment planning algorithm, and by considering relationships between radiation dose and treatment outcomes. Precision radioembolization with dosimetry is now recommended as the standard approach in recent international recommendations [132, 133]. Recently, a prospective randomized phase II clinical study in HCC, the DOSISPHERE-01 trial, provided the first level one scientific evidence that personalized radioembolization significantly improves overall survival compared to the standard semi-empirical approach [134].

6.8 Radionuclide Therapy

The concept of using radiation to treat cancer and other diseases found its origin in the discovery of X-rays in 1895. After Pierre and Marie Sklodowska-Curie discovered radium as a source of IR further interest was sparked. However, it wasn't until the 1950s that external beam radiation became a key treatment modality for cancer. Since then, external beam RT has become one of the most efficient tools for treatment of locally confined cancers. However, its effect is limited for treatment of more advanced and disseminated disease. In the early twentieth century, first potential for using Iodine-131 as a targeted therapeutic was discovered by nuclear pioneers such as Saul Hertz [135]. This discovery was the start of the field of radionuclide therapy and today, several types of radionuclide therapy exist. Each of the different types will be discussed in this section.

6.8.1 Introduction to Radiopharmaceuticals

Cancer cells often express certain molecules on their membrane surface, called receptors, which are not or to a lesser extent present on healthy cells. These receptors on cancer cells can be targeted by several molecules, being a peptide, small molecule or (parts of) antibodies, which will be termed as the ligand. When talking about radiopharmaceuticals, the cancer-targeting moiety is linked to a chelator molecule, responsible for entrapping a radionuclide into the structure as shown in Fig. 6.20.

As already explained in Chap. 2, based on the purpose of the radiopharmaceutical, being diagnostic or therapeutic, different radionuclides can be used. For diagnostic purposes, gamma (γ)-emitting radionuclides are used. Radionuclides that are usually used for therapy are alpha (e.g., actinium-225), beta (e.g., lutetium-177), or Auger electron (e.g., iodine-125) emitters.

Upon binding of the ligand to its receptor, the radioligand complex gets internalized. Upon internalization, the radionuclide will emit its toxic IR from inside the cell and cause damage to cellular structures including DNA and cell membrane, resulting in cancer cell death, as shown in Fig. 6.21.

Radioligand therapy (RLT) can in theory be used to target any type of cells (over)expressing the target molecule and can thus be used to attack multiple (micro) metastases instead of only targeting the primary tumor, in contrast to external beam RT (EBRT) that focus on one or several, geographically limited target volumes. Furthermore, RLT enables specific targeting of cancer lesions (including metastatic cancer cells), while causing minimal damage to surrounding healthy tissues and thus minimizing the amount of side effects [136] (Box 6.16).

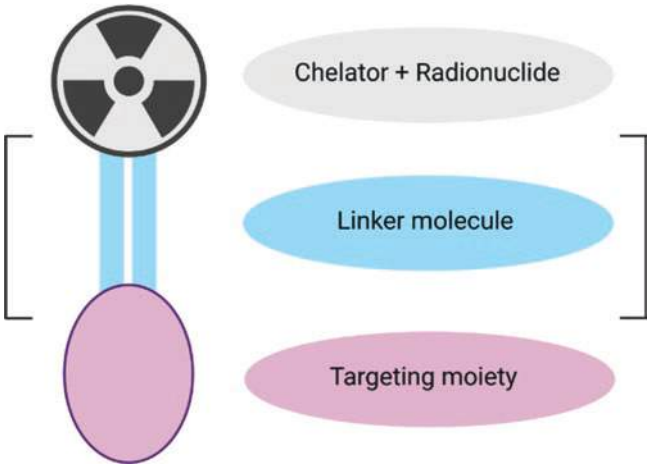

Fig. 6.20 Schematic representation of the structure of a radiopharmaceutical. The purple circle represents the cancer-targeting moiety, which can be a peptide, small molecule, or antibody. This targeting moiety is connected to a chelator (blue circle) entrapping a radionuclide (for diagnostics or therapy) directly to the targeting moiety or via a linker molecule (grey)

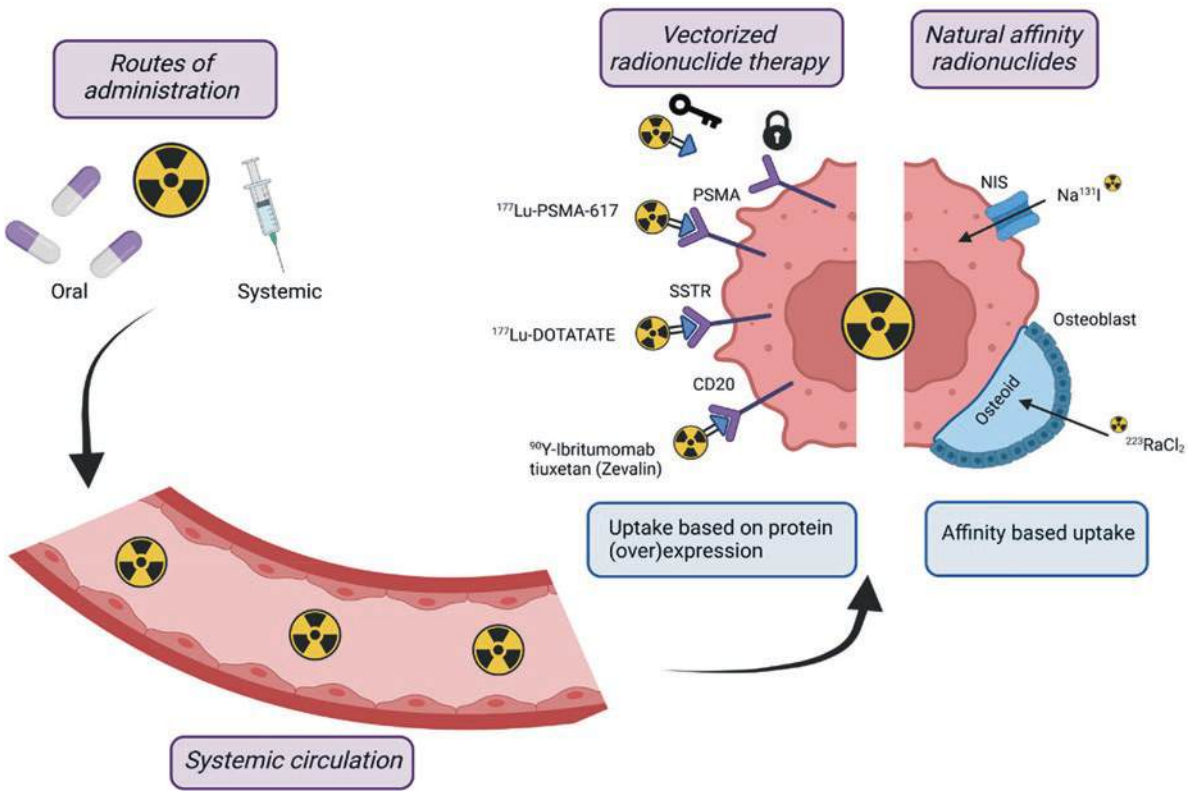

Fig. 6.21 Overview of the general principle or radioligand therapy. A radionuclide (either ingested orally or injected systemically) will enter the bloodstream. Via the bloodstream, the radionuclide will find its way to the target tissue either through its natural affinity for the target tissue (i.e., the natural affinity radionuclides) or via expression of certain molecules on the target tissue (i.e., vectorized radionuclide therapy)

Box 6.16 Radionuclide Therapy

- Human cancers express molecules on their membrane surface that can be targeted for therapy.
- A radioligand is comprised of a cancer-targeting moiety (small molecule, peptide, or (part of) antibody) linked to a chelator entrapping the radionuclide.
- Radioligand therapy enables specific targeting of cancer cells, with minimal harm to surrounding healthy tissues.

6.8.2 Radiotheranostics Approaches

Theranostics, the combination of therapy and diagnostics, is emerging in personalized medicine approaches. The main goal is to use diagnostic imaging to follow-up (radio)therapeutic interventions and improve or alter them along the way, thereby increasing efficacy and limiting toxicological effects. The ideal theranostic pair, i.e., for imaging or therapy, respectively, has the same pharmacokinetics, meaning that the pair should be distributed, metabolized, and cleared similarly [137]. If this is the case, the diagnostic counterpart can be used to accurately determine the accumulation and absorbed dose in different organs, including tumor, that would result upon injection of the therapeutic radiopharmaceutical. The imaging thus further allows selection of patients with high probability of response to the therapy (i.e., predictive biomarkers) and can provide guidance on the total activity of the therapeutic counterpart to be administered. It can also be used for treatment response evaluation in follow-up. Several therapeutic radionuclides (e.g., ^{177}Lu, ^{131}I) intrinsically decay via both particle- and γ-emission which can be used for both imaging and therapy that said after administration of vastly different injected activities [137]. Different radioisotopes of the same element have the greatest theoretical appeal to use in the theranostic approach. Examples are the radioisotopes of iodine ($^{123/124/131}$I), terbium ($^{149/152/155/161}$Tb), and yttrium ($^{86/90}$Y) [138]. Although the biological behavior of these radiopharmaceuticals will be similar, the use in clinical practice might be limited due to unfavorable decay properties, long $T_{1/2}$, availability, and cost of production. In this respect, radiopharmaceuticals which use the same vector molecule but different radiometals are often applied for this purpose as they have similar pharmacokinetics. A prime example is the somatostatin receptor targeting vector DOTATATE, which can be radiolabeled with the PET radionuclide ^{68}Ga and the therapeutic radionuclide ^{177}Lu, harnessing the diagnostic potential of PET (which have higher resolution and sensitivity for radioactivity) to enable efficient therapeutic approaches [139]. Of note, current efforts are being made to include [^{18}F]AlF into the armamentarium to eventually replace ^{68}Ga [140].

Radiotheranostics is being applied to the different branches of radiopharmaceutical development, including radioimmunotherapy (with, for example, nanobodies, antibodies, or similar affinity reagents), peptide receptor radionuclide therapy, radiolabeled microspheres/nanoparticles, and small molecules. This combination of therapy and diagnostics can help to reduce the toxic side effects by appropriate patient selection and determination of administered activity. The benefit and safety of using repeated treatment have also been proven in several studies.

A key aspect to note is the uptake and retention of the radionuclides at the target site. Logically, tumor-to-background ratios should be as high as possible for both diagnostic and therapeutic radionuclides. However, diagnostic imaging is typically performed in a time scale of several minutes to 1 h and thus optimally, radionuclides with a short $T_{1/2}$ should be applied. On the other hand, radionuclides with a longer $T_{1/2}$ are typically used for therapy, which can result in a more selective tumor irradiation, with higher dose to the tumor than to the healthy tissues (Fig. 6.22). The most important requirement for a therapeutic radiopharmaceutical is to

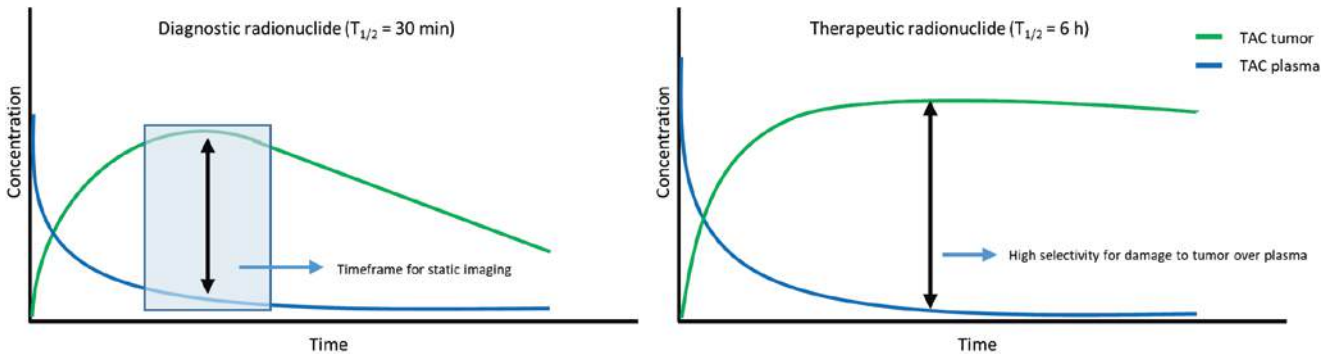

Fig. 6.22 Hypothetical representation of time-activity curves (TACs) of a vector radiolabeled with a diagnostic ($T_{1/2}$ = 30 min) and therapeutic radionuclide ($T_{1/2}$ = 6 h)

have a high ratio between the integral of the time-activity curve (previously known as the residence time) of the tumor vs. normal organs (Box 6.17).

Box 6.17 Radiotheranostics

- The theranostic approach makes use of diagnostic and therapeutic nuclear medicine.
- Theranostics utilizes different isotopes of the same element.
- Therapeutic radiopharmaceuticals can use radionuclides with a longer half-life compared to diagnostic radiopharmaceuticals.
- Radiopharmaceutical vector molecules can include peptides, antibodies, nanobodies, nanoparticles, and small molecules.

6.8.3 Natural Affinity Radionuclides

6.8.3.1 Principles

To obtain specific targeting, a radiopharmaceutical usually comprises a moiety capable of binding a cancer-specific overexpressed entity (e.g., a receptor, an enzyme, a transporter, etc.). However, this is not always required as certain elements show a natural affinity for certain tissues. Examples are iodine, which is concentrated in the thyroid gland, and radium, a calcium mimetic naturally taken up in remodeling bone. This enables specific targeting of these tissues without the need for elaborate organic chemistry nor radiochemistry.

Radiopharmaceutical development started with the research of Hamilton and Soley into diagnosis and treatment of thyroid disease. In the thyroid gland, iodine plays an important role in the production of thyroid hormones, which in turn have important functions in the human body. Naturally, because of the importance of iodine for the thyroid gland, all ingested iodine is taken up by the thyroid gland, where it is converted into iodide and remains trapped. Radioactive iodine (iodine-131) can be used to treat thyroid diseases because the thyroid gland is not able to distinguish between the stable iodine (iodine-127) and its radioactive isotope. Like stable iodine, iodine-131 is concentrated in the thyroid gland after ingestion. Treatment of thyroid disease using iodine-131 in the form of sodium-iodine ($Na^{131}I$) can be considered as a historic pillar of radiopharmaceutical design as the usage of $Na^{131}I$ has paved the way for further radiopharmaceutical development.

The primary site for metastasis in prostate cancer (PCa) is the bone, resulting in severe morbidity due to so-called skeletal related events (e.g., fractures) and bone marrow failure. To control the disease in castrate-resistant PCa patients, the Food and Drug Administration (FDA) approved radium-223 chloride ($^{223}RaCl_2$, Xofigo®) for treatment of bone metastasis in 2013. Radium-223 is an alpha-emitting radionuclide that accumulates in bone areas with increased bone turnover due to its similarity with calcium ions and its capability to form complexes with hydroxyapatite (which is the mineral component of bone). In the decay process of radium-223 to the stable lead-207, four alpha particles and two beta-particles are generated which induce local damage to bone sites with increased bone turnover, such as areas of bone metastasis.

6.8.3.2 Main Indications and Therapeutic Intent

$Na^{131}I$ is administered in patients suffering from benign thyroid disease such as an overactive thyroid (autonomic hyperthyroidism, Graves' Disease), goiter (enlarged thyroid), or well differentiated thyroid cancers (papillary or follicular thyroid cancer). The thyroid incorporates iodide in two forms of thyroid hormones, triiodothyronine (T3) and thyroxine (T4). These hormones control metabolism and protein synthesis. An overactive thyroid leads to increased metabolic rate, sweating, fatigue, tachycardia, intestinal problems, and other life debilitating issues. As iodide is taken up in the thyroid in large excess, it is a valuable approach in treating an overstimulated or enlarged thyroid. Due to the high uptake via the intestinal tract, $Na^{131}I$ is administered per os. Iodine-131 is taken up by the sodium-iodide symporter into the thyroid cells and will subsequently irradiate the thyroid cells. One potential side effect of this treatment is a complete loss of thyroid function (hypothyroidism), which can result in the necessity for daily lifelong thyroid hormone (levothyroxine) substitution. The occurrence of hypothyroidism depends on the type of indication, with a low fraction seen in autonomic disease but with a 100% occurrence in patients treated for thyroid cancer (with treatment occurring post-thyroidectomy to ablate the so-called remnant). Of note, these pills are generally inexpensive and are taken per os once daily [141].

To date, $^{223}RaCl_2$ is the only alpha-emitting radiopharmaceutical that has been FDA approved and is now in routine clinical use for treatment of bone metastasis in patients with metastatic castration-resistant prostate cancer. The ALSYMPCA phase III clinical trial investigated safety and efficacy of $^{223}RaCl_2$ compared to placebo (i.e., saline injection). The results of this trial led to the FDA approval of $^{223}RaCl_2$ for patients with metastatic castration-resistant prostate cancer with symptomatic bone metastasis as this clinical trial showed that treatment was well-tolerated, prolonged overall survival, and improved the quality of life of patients [142, 143].

6.8.3.3 Treatment Course

$Na^{131}I$ is typically administered as a pill or in rare cases as a liquid per os. The required activity to treat hyperthyroidism is typically small (148–370 MBq). Usually one treatment cycle will suffice to have a satisfying effect on the thyroid function after 2–3 months [144]. For patients suffering from differentiated thyroid cancer, the administered activity depends on the disease stage (after previous resection in so-called remnant ablation, used as adjuvant therapy, metastatic disease) and can range from 1.1 to 7.4 GBq [145]. Before treatment, patients need to have sufficient blood levels of thyroid-stimulating hormone (TSH) (TSH > 30 mU/L), by stopping uptake of thyroid hormone supplements or by injections of recombinant THS, to increase the uptake of the administered iodine radioisotope. Several days after treatment, a post-therapy scintigraphy is made to document the targeting of thyroid tissue and to detect potential metastatic disease. After ablation, levothyroxine treatment is started to compensate for the loss of thyroid function. Afterwards follow-up is necessary to assess therapy response and to rule out recurrence, with regular determination of thyroid function, thyroglobulin, and thyroglobulin antibodies.

Radium-223 dichloride is injected intravenously in adult patients with castration-resistant prostate cancer with bone metastases. The treatment schedule comprises six injections of 55 kBq per kg body weight at 4-week intervals. A single complete blood count is performed 10 days prior to administration of a treatment cycle. An additional complete blood count might be performed 2–3 weeks after administration if necessary. Clinical follow-up complemented with bone scintigraphy and CT is the cornerstone of follow-up, but with more recent evidence pointing to the utility of also modern imaging tools such as PET/CT or MRI. Several biomarkers, including prostate-specific antigen, lactate dehydrogenase, and alkaline phosphatase, might be checked during the treatment course to monitor treatment response, but they are not considered to be reliable indicators of treatment response.

6.8.4 Vectorized Radionuclide Therapy

6.8.4.1 Peptide Receptor Radionuclide Therapy

Principles

Peptide receptor radionuclide therapy (PRRT) consists of the injection of a tumor-targeting peptide into the systemic circulation of a patient. This radiopharmaceutical will subsequently bind to a specific peptide receptor leading to tumor-specific retention. Several receptors have been studied over the last few years, including the somatostatin receptor (SSTR), glucagon-like peptide-1 receptor, cholecystokinin type 2, and melanocortin receptors. At present, SSTR is the only target that is used in routine clinical practice. The SSTR is overexpressed on a range of tumors, including neuroendocrine tumors (NETs), which arise from neuroendocrine cells present in a range of organs (e.g., gastrointestinal tract, pancreas, and bronchi) and neural-crest derived tumors (e.g., pheochromocytoma, paraganglioma, neuroblastoma). Humans have five subtypes of SSTRs, with subtype 2 being the most important for theranostics. The randomized controlled trials PROMID and CLARINET have proven that treatment with non-radioactive somatostatin analogues (SSAs) leads to an antiproliferative effect in metastatic enteropancreatic NETs. In the late 1980s and early 1990s, the Rotterdam group uncovered the potential of using the SSTR for radionuclide-based imaging and demonstrated that radiolabeled SSAs have a high uptake and retention in tumoral tissue and a limited uptake in normal, mainly endocrine, organs. An interesting therapeutic avenue was explored: treatment of SSTR-positive tumors with radionuclide therapy (RNT). Several radiopharmaceuticals were developed in the last two decades including the first generation ^{111}In-pentetreotide (an Auger emitter), the second generation ^{90}Y-DOTATOC (a high-energy β^--emitter), and the third generation ^{177}Lu-DOTATATE (a low-energy β^--emitter and a γ-emitter). A major benefit of lutetium-177 is that its decay is associated with γ-emission, which allows imaging and dosimetry of absorbed doses to tumors and risk-organs (e.g., kidneys and bone marrow). The combination of the high-energy yttrium-90 β^--emitter for targeting lesions with a larger size and/or heterogeneous uptake (with more crossfire effect), and the medium-energy lutetium-177 emitter/γ-emitter for targeting smaller lesions (with a higher fraction of the total energy deposited within the tumor itself, and not in the surrounding tissue), is called "tandem or duo PRRT." Theoretically, a synergistic effect can be achieved by combining these two radionuclides with different absorption properties, but RCTs are awaited to demonstrate the superiority of this concept before widespread clinical use can take place. At present, ^{177}Lu-DOTATATE is considered the clinical standard and is the only radiopharmaceutical approved for PRRT by the American Food and Drug Administration (FDA 2018) and European Medicines Agency (EMA 2017). A promising fourth generation of PRRT-radiopharmaceuticals is emerging, with the entrance of α-emitters in the radionuclide therapy scene. PRRT α-emitters include ^{213}Bi-DOTATOC, ^{225}Ac-DOTATATE, and ^{212}Pb-DOTAMTATE. Preliminary clinical results provide proof-of-principle evidence that α-PRRT can overcome resistance to β-PRRT, reflected by higher objective response rates (ORRs) in favor of α-emitters [146].

Main Indications and Therapeutic Intent

Patients with advanced NET and clinical, biochemical, and/or radiological disease progression after first-line treatment

with SSA are eligible for second-line treatment with PRRT if sufficient tracer uptake on a so-called theranostics SSTR scintigraphy is present. The development of PRRT and its clinical trials were academia-driven which contrasts with the current novel anticancer drugs which are mainly pharma industry-driven. For a long period, no standard radiopharmaceutical or standard regimen was determined, which explains the heterogeneous literature involving PRRT [146]. At present, the only published randomized controlled trial with ^{177}Lu-DOTATATE is the phase III NETTER-1 trial, which included patients with advanced midgut NETs. One hundred sixteen patients were randomized to the PRRT arm (4 cycles of 7.4 GBq ^{177}Lu-DOTATATE plus best supportive care including octreotide long-acting repeatable (LAR) 30 mg) and 113 patients were randomized to the control arm (octreotide LAR 60 mg). An ORR of 18% was seen in the ^{177}Lu-DOTATATE group versus 3% in the control group ($p < 0.001$). An estimated progression-free survival (PFS) at 20 months of 65.2% (95% confidence interval (CI): 50.0–76.8%) was achieved in the PRRT arm and 10.8% (95% CI: 3.5–23.0%) in the control arm, with a hazard ratio for progression or death of 0.21 (95% CI: 0.13–0.33; $p < 0.001$) [147]. The final overall survival (OS) analysis revealed a median OS of 48 months in the ^{177}Lu-DOTATATE group versus 36.3 months in the control group. This difference was not statistically significant but can be considered as clinically significant. The lack of statistical significance was most likely caused by a high rate (36%) of crossover of patients in the control group to PRRT after progression. In addition, the NETTER-1 trial has confirmed that PRRT causes a significant improvement in the quality of life of patients and aids to substantially reduce tumoral symptoms (e.g., abdominal pain, diarrhea, and flushing) [146].

Treatment Course

The eligibility for PRRT is determined via mandatory pretreatment SSTR imaging, preferentially by SSTR PET, blood analysis, and clinical evaluation. ^{18}F-FDG PET/CT provides additional information, and all lesions should show sufficient SSTR expression, in particular the ^{18}F-FDG-avid ones. The conventional treatment schedule for ^{177}Lu-DOTATATE is based on the Rotterdam/NETTER-1 protocol. This consists of four cycles of 7.4 GBq administered in 8-week intervals. Nephroprotection is performed by administering a co-infusion of an amino acid solution during PRRT-administration; this solution will reduce renal uptake of the radiopeptide by ~25–50%. Acute side effects include nausea and vomiting which are provoked by the co-infusion of the nephroprotective amino acids and which can be controlled by an antiemetic treatment. Four to six weeks after each cycle of PRRT, a blood analysis and clinical evaluation are performed. After completion of the four cycles PRRT, further follow-up with SSTR and ^{18}F-FDG PET/CT, blood analysis, and clinical evaluation are warranted. The most severe long-term side effect of PRRT is the development of persistent hematological dysfunction (PHD) caused by bone marrow irradiation. However, PHD after PRRT has a low incidence of 1.8–4.8%, with a median latency of 41 months after completion of the treatment [146]. Other subacute (occurring within days/week) side effects include subacute myelosuppression (typically mild and transient), fatigue, and hair loss. Long-term side effects, besides PHD, are kidney failure, observed in up to 9.2% of patients treated with ^{90}Y-DOTATOC and <1% in patients with ^{177}Lu-DOTATATE [148, 149]. In patients with good response after a first PRRT regimen, with disease control for at least a year, a novel course of PRRT can be administered with ^{177}Lu-DOTATATE, called "salvage PRRT," if the patient's organ function is still adequate and SSTR expression is still present on all lesions. As such, PRRT has proven to be an adequate treatment in patients with advanced NETs. Several promising prospective trials are ongoing to further optimize PRRT (e.g., α-emitters, individualized dosimetry, and SSTR-antagonists) (Box 6.18).

Box 6.18 Peptide Receptor Radionuclide Therapy (PRRT)

- PRRT consists of the injection of a tumor-targeting radiolabeled peptide, which will subsequently bind to a specific receptor leading to tumor-specific binding and retention.
- Several radiopharmaceuticals were developed in the last two decades, with the third generation ^{177}Lu-DOTATATE being the current clinical standard and the only radiopharmaceutical approved for PRRT by the FDA and EMA.
- Multiple promising prospective trials are ongoing to further optimize PRRT (e.g., α-emitters, individualized dosimetry, and SSTR-antagonists).

6.8.4.2 Radioligand Therapy

Principles

At present, another well-known example of radioligand therapy (RLT) has demonstrated a significant survival benefit in patients with metastatic castration-resistant PCa. [^{177}Lu]Lu-PSMA-617 is a prostate-specific membrane antigen (PSMA) targeting small molecule consisting of PSMA-617 with the β^--emitting radionuclide lutetium-177 (Fig. 6.23). The PSMA-617 binds to the enzymatic pocket of PSMA after which it is internalized, resulting in the delivery of toxic doses of IR to PCa cells. The VISION trial has demonstrated

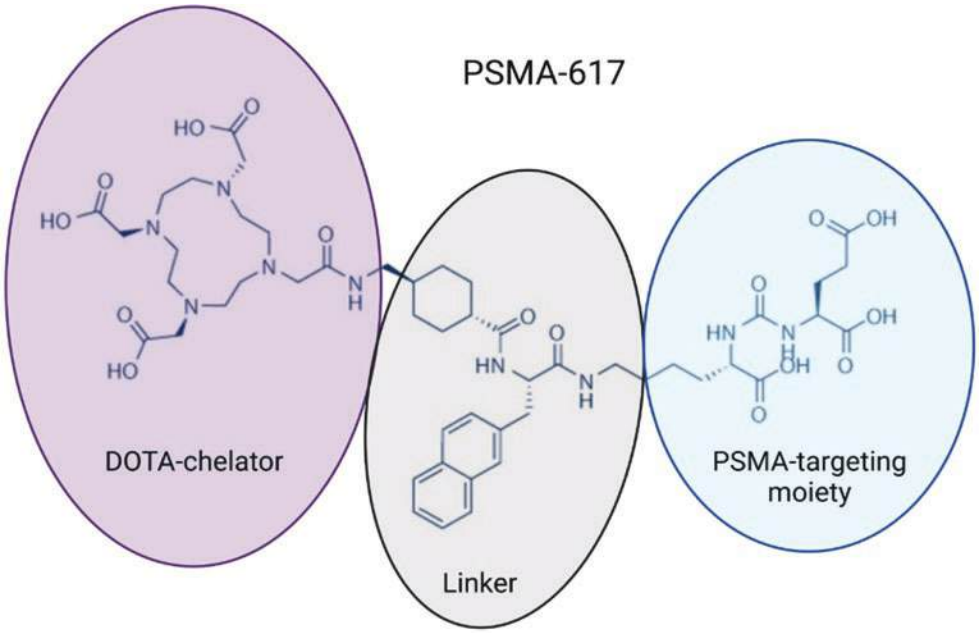

Fig. 6.23 Schematic representation of the structure of the PSMA-targeting compound PSMA-617. The blue circle shows the PSMA-targeting moiety. The purple circle highlights the DOTA-chelator used to entrap radionuclides. The grey circle represents the linker molecule that connects the PSMA-targeting moiety with the DOTA-chelator

a significant increase in imaging-based PFS and OS in a randomized controlled trial where it was compared to standard of care (i.e., chemotherapy, RT and ADT), resulting in the FDA approval of [^{177}Lu]Lu-PSMA-617 for patients with metastatic castration-resistant PCa in March 2022 [150]. Since PSMA poses such an interesting target for RLT, due to the high overexpression on PCa cells, more PSMA-targeting radioligands are currently under clinical investigation, as summarized in Table 6.10.

The development of RLT is not strictly limited to PCa and targeting PSMA. Several other compounds with other targets are also undergoing clinical trials. One such target is the bombesin receptor family. Many common tumors, including breast, prostate, and lung cancer, show overexpression of one of the bombesin receptors, resulting in the development of several compounds targeting this receptor family [151]. Compared to the development of PSMA-targeting compounds, the development of bombesin-targeting agents is still in its infancy as illustrated in Table 6.10 by the limited number of compounds undergoing clinical investigation. Thus, at present, research into bombesin-targeting compounds remains largely preclinical.

Besides PSMA and bombesin, other targets can also be used for RLT of a variety of human cancers. Other examples of clinical trials of radioligand therapy using other targets are summarized in Table 6.10.

Main Indications and Therapeutic Intent

At present, [^{177}Lu]Lu-PSMA-617 is FDA approved in PCa patients with metastatic castration-resistant disease in whom standard treatments, including hormone deprivation therapy

Table 6.10 Examples of RLT compounds under clinical investigation

Compound	Clinical trial phase	Trial number[a]	Disease
PSMA-targeting RLT			
[^{177}Lu] Lu-PSMA-617	Phase III	NCT03511664	Metastatic castration-resistant PCa
[^{64}Cu] Cu-SAR-PSMA	Phase II	NCT04868604	Metastatic castration-resistant PCa
[^{177}Lu] Lu-PSMA-I&T	Phase II	NCT04188587	Metastatic castration-resistant PCa
[^{225}Ac]Ac-PSMA	Early phase I	NCT04225910	Metastatic castration-resistant PCa
[^{177}Lu] Lu-PSMA-R2	Phase I/II	NCT03490838	Metastatic castration-resistant PCa
[^{131}I] I-PSMA-1095	Phase II	NCT04085991, NCT03939689	Metastatic castration-resistant PCa
Bombesin-targeting RLT			
[^{177}Lu]Lu-NeoB	Phase I/IIa	NCT03872778	Advanced or metastatic solid tumors: breast, lung, prostate, GIST, GBM tumor
Others			
[^{177}Lu] Lu-FAP-2286	Phase I	NCT04939610	Advanced metastatic solid tumor
[^{177}Lu] Lu-DOTA-Biotin (ST2210)	Phase I	NCT02053324	Colorectal cancer with liver metastases

[a]The trial number refers to its citation on https://clinicaltrials.gov/

and chemotherapy, have failed. Patients eligible for treatment also need to have at least one PSMA-positive lesion (observed by ^{68}Ga-PSMA-11 PET–CT imaging at baseline), a life-expectancy of at least 6 months, sufficient organ function (e.g., bone marrow, kidney), and capability of self-care (defined by Eastern Cooperative Oncology Group performance status ≤2) [150]. Other types of RLT are under investigation for treatment of other types of advanced tumors, such as advanced solid tumors of breast and lung or colorectal cancer with liver metastases.

Treatment Course

For the different types of RLT, treatment schedules can differ. For PSMA-RLT, and [^{177}Lu]Lu-PSMA-617 in particular, a conventional treatment schedule consists of four treatment cycles administered in 6-week intervals. In each cycle, the administered activity ranges from 6 to 7.5 GBq. After each therapy cycle, treatment response and the overall condition of the patient are monitored in order to decide if treatment can be continued or not [152]. The VISION trials showed that [^{177}Lu]Lu-PSMA-617 (hazard ratio 0.46) therapy was generally well tolerated and was able to improve both OS and PFS compared to standard of care treatment [150]. These clinical trials and the recent FDA approval of [^{177}Lu]Lu-PSMA-617 show the potential of RLT for treatment of PCa and in the future, results of the ongoing clinical trials of RLT using other targets will also be published and contribute to the development of RLT as a new cancer treatment modality (Box 6.19).

6.8.4.3 Radioimmunotherapy

In 1900, the German Nobel laureate Paul Ehrlich was the first person to introduce the "magic bullet" concept, with reference to antibodies that can be used to treat diseases by specifically targeting receptors or biochemical pathways in bacteria or cancer cells. More than half a century later, the invention of hybridoma technology by Georges Kohler and César Milstein paved the way for the production of monoclonal antibodies against almost any antigen. Kohler and Milstein received a Nobel Prize in 1984 for their work.

A large proportion of therapeutic antibodies have since then been developed and approved by the FDA or EMA for the treatment of cancer. There are several mechanisms through which immunoglobulins function in the body, including, but not limited to antibody-dependent cell-mediated cytotoxicity (ADCC), complement-dependent cytotoxicity (CDC), alteration of signal transduction, inhibition of angiogenesis, and immune checkpoint blockade [153].

Another important modality through which antibodies can mediate a therapeutic effect is through their conjugation to a radionuclide that emits IR in the form of α particles, β particles, γ-rays, or Auger electrons. By virtue of the antibody's specificity and selectivity, it will bind to a specific target overexpressed on a cancer cell and deliver a lethal dose of radiation to the cell. This approach is called radioimmunotherapy (RIT), though several other names have also been used in the literature. Most radioimmunoconjugates use the IgG class of antibodies, with an average molecular weight of 150 kDa and a biological half-life from 2 to 5 days.

Early clinical trials with radioimmunoconjugates used the readily available ^{131}I radionuclide which allowed for their application in SPECT imaging as well as therapy. Today, a wide arsenal of radionuclides has been used in different RIT studies, each with different properties.

There is currently only one FDA-approved RIT targeting the CD20 antigen on B-Cell Non-Hodgkin's Lymphoma (B-NHL): ^{90}Y-ibritumomab tiuxetan or Zevalin®. The immunoconjugate is a result of the conjugation of the monoclonal antibody ibritumomab to the chelator tiuxetan. The antibody is a murine IgG-1 kappa antibody toward CD20, and the tiuxetan chelator is ideal for the chelation of Indium-111 or Yttrium-90. In the following paragraphs, we will look with more details into the use of ^{90}Y-ibritumomab tiuxetan.

Main Indications and Therapeutic Intent of Zevalin®

The Zevalin® therapeutic regimen is used to treat adult patients either with newly diagnosed follicular NHL following a response to initial anticancer therapy, or patients with

Box 6.19 Radioligand Therapy

- Besides peptide receptor radionuclide therapy, other radioligand therapies are also under investigation for treatment of different cancer types (e.g., PCa).
- An FDA-approved compound for RLT is [^{177}Lu]Lu-PSMA-617 for the treatment of metastatic-castration resistant PCa.
- More compounds for RLT are under clinical investigation for multiple cancer types (summarized in Table 6.11).

Table 6.11 Comparison of the accelerator types used for therapy

Accelerator types	Properties
Cyclotron	Circular
	Small
	Mainly for protons
Synchrotron	Circular
	Large
	Suitable also for heavier ions
LINAC	Linear
	Long but slim
	Technically challenging

low-grade or follicular B-cell NHL that have relapsed during or after treatment with other chemotherapies. The prescription medication consists of three parts: two infusions of rituximab to reduce the number of B-cells in blood, and one injection of ^{90}Y-ibritumomab to treat the NHL.

Treatment Course of Zevalin®

The Zevalin® therapeutic regimen should be initiated between 6 and 12 weeks following the last dose of first-line chemotherapy, after platelet counts have recovered to 150,000/mm^3 or more. Patients with platelet counts less than 100,000/mm^3 are not treated with Zevalin®.

Treatment is initiated with an IV infusion of 20 mg/m^2 rituximab. The same infusion is re-administered 7–9 days after the first infusion. Within 4 h of administering the second rituximab infusion, an IV injection of ^{90}Y-ibritumomab tiuxetan is administered at a dose of 0.4 mCi/kg for patients with normal platelet count, or 0.3 mCi/kg for relapsed or refractory patients with lower platelet counts (100,000–149,000/mm^3). The total dose administered should not exceed 32 mCi (or 1184 MBq).

Although Zevalin® is the only FDA-approved RIT that is currently in use, there are a lot of other radioimmunoconjugates at different stages of clinical development, targeting different cancer-associated antigens. Figure 6.24 shows some of the antigens targeted in RIT.

Clinical trials designed with a direct comparison of the radiolabeled antibody with its non-radiolabeled counterpart allow to tease out the therapeutic benefit of RIT over conventional mAb immunotherapy for cancer patients. One example of such a study is a phase III randomized controlled trial of patients with relapsed or refractory CD20-positive NHL patients [154]. In this study, 143 patients were divided into two groups, a "control" group receiving intravenously (IV) the CD20-targeting antibody rituximab for 4 weeks, while the other group received a single (IV) dose of Zevalin® RIT. The latter group was pretreated with two rituximab doses to improve biodistribution and one dose of ^{111}In-ibritumomab tiuxetan for imaging and dosimetry. The control group had an overall response rate (ORR) of 56% while the RIT group showed an ORR of 80%. The complete response (CR) rates were 16% and 30%, respectively. The primary toxicity observed with Zevalin® was reversible

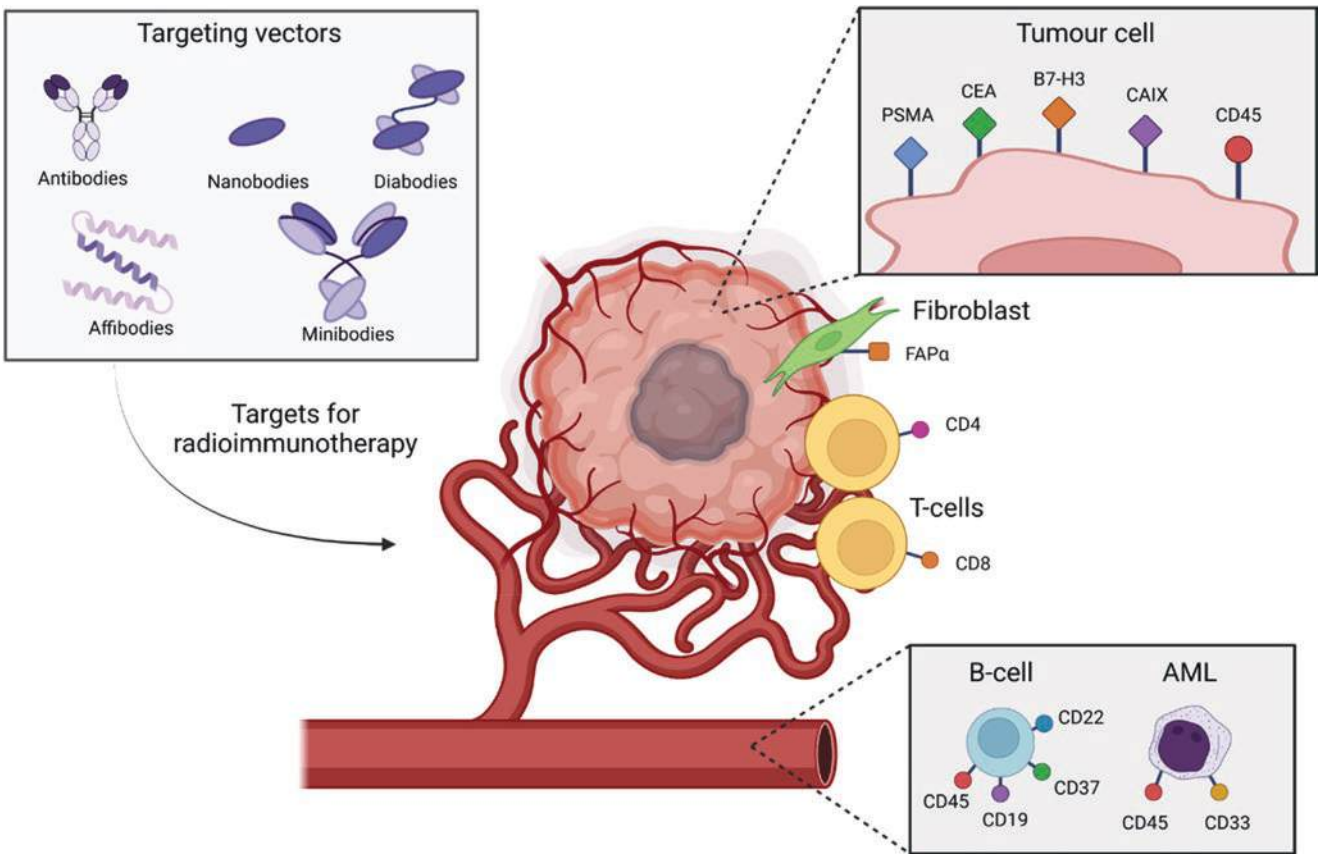

Fig. 6.24 Different targeting vectors and molecular targets used in RIT. In RIT, the targeting vectors are designed to recognize certain molecules present on the surface of tumor cells (e.g., PSMA, CEA, B7-H3, CAIX, or CD45), cancer-associated fibroblasts (FAPα), tumor-infiltrating T cells (CD4 or CD8), and/or circulating immune (e.g., CD45, CD19, CD37, or CD22) or tumor cells (e.g., CD45 or CD33)

myelosuppression, which is also the most common side effect of conventional cancer therapies [155].

It is worth mentioning that the clinical impact observed in RIT of hematological cancers has not been replicated in solid tumors yet, due to a number of outstanding challenges encountered which lead to high bone marrow absorbed doses and insufficient dose delivery to tumors. Several promising strategies have been developed to overcome these challenges, such as the use of antibody fragments (e.g., single-domain antibodies and affibodies) instead of whole immunoglobulins, allowing for higher imaging contrast, deeper tumor penetration, and improved pharmacokinetics [156]. Another important strategy, known as pretargeting, is based on separating the antibody from the radionuclide and letting the two agents combine in vivo. A review by Verhoeven et al. nicely summarizes the different RIT in which pretargeting has been applied [157].

6.8.5 Combination Therapies with Radionuclide Therapy

The undisputable efficacy of radionuclide therapy (RNT) has been documented in the last decade in a series of landmark trials. With a plethora of targeting vectors directed to tumor-specific molecular targets (some in routine clinical use, others in development) and a large panel of radionuclides characterized by different physical properties, the targeted treatment of both solid and hematological tumors is now a clinical reality. The concept of RNT emerged in the 1940s with the use of iodine-131 for thyroid cancer management and was the first FDA-approved radiopharmaceutical (in 1951). Since then, numerous other RNT radiopharmaceuticals have been developed and successfully used, including the most recent FDA- and EMA-approved radiopharmaceutical ^{177}Lu-DOTATATE. However, their success may be limited by healthy tissue toxicity and/or tumor intrinsic or acquired resistance. One strategy to overcome these limitations is the use of combination therapies aiming at achieving an increase in treatment efficacy while remaining at a low toxicity level [158]. This will subsequently lead to an increased therapeutic index and hence improved treatment outcome. If rationally designed, these combination therapies can lead to synergistic effects by targeting adequate molecular pathways, ultimately causing lethal damage to the tumor cell. Indeed, radiobiological mechanisms underlying the effects of RNTs could serve as a very promising basis for the design of combination clinical trials.

The rationale behind the use of the combination approach with RNT, using two or more therapeutic agents, may be multiple and vary according to the physical properties of the radioisotope used and the biology of the tumor considered. Combination strategies may aim at reducing hypoxia, improving the radiopharmaceutical delivery (in case of a poor tumor vasculature preventing drug delivery) via increased perfusion of the tumor, enhancing the therapeutic effect based on radiosensitization mechanisms, or improving the immune control. RNT has been basically evaluated in combination with all cancer pillar therapies, e.g., chemotherapy, external beam RT(EBRT), immune and targeted therapies. Different combination strategies with RNT are summarized in Fig. 6.25.

6.8.5.1 Radionuclide Therapy and Chemotherapy

The use of chemotherapy with EBRT in many common cancers (including lung, head and neck, cervical cancers) and different settings (e.g., neoadjuvant, curative, etc.) has fostered its combination with RNT.

Several clinical studies have been published combining PRRT with 5-fluorouracil (5-FU), capecitabine or temozolomide, a therapy called peptide receptor chemoradionuclide therapy (PRCRT). A population of interest for PRCRT are the highly proliferating NETs characterized by tumor dedifferentiation, higher tumor grade, worse OS outcome, and most commonly ^{18}F-FDG-avidity of the tumor lesions. PRCRT (combination of ^{177}Lu-DOTATATE and 5-FU) was retrospectively investigated in 52 patients with ^{18}F-FDG-avid disease and the majority having grade 2 advanced NETs [159]. A high DCR of 98% was achieved and 27% of the patients achieved complete metabolic response on ^{18}F-FDG PET/CT despite having residual SSTR-positive disease, most likely due to the eradication of the dedifferentiated lesions by PRCRT. It was expected that the prognosis in this patient cohort would be poor, however a median PFS of 48 months was achieved and a median OS was not reached during a median follow-up time of 36 months. Toxicity was low, despite the fact that 67% of the patients had received prior chemotherapy.

Capecitabine, a prodrug of 5-FU, has the additional advantage that it can be administered orally. A 2-arm cohort analysis compared concomitant ^{177}Lu-DOTATATE plus capecitabine (n = 88) with ^{177}Lu-DOTATATE monotherapy (n = 79) and revealed an increased OR in favor of ^{177}Lu-DOTATATE plus capecitabine (43.1% and 14%, respectively). In addition, a significant lengthening of OS in the ^{177}Lu-DOTATATE plus capecitabine group was observed compared to the ^{177}Lu-DOTATATE monotherapy group (median OS not reached vs. 48 months, respectively, after a mean follow-up of 32.4 months; $p = 0.0042$) [160]. The combination of ^{177}Lu-DOTATATE and capecitabine was also evaluated in paragangliomas, however the study failed to prove the superiority of the combination over ^{177}Lu-DOTATATE monotherapy [161] which might be attributed to a too small number of patients included and the typically lower proliferation rate in this cancer type.

A decreased sensitivity of tumors to the alkylating agent temozolomide has been associated with the expression of O(6)-methylguanine-DNA methyltransferase (MGMT), a DNA repair protein involved in the removal of O(6)-methylguanine DNA lesions induced by temozolomide. MGMT deficiency was more frequently observed in pancreatic NET (pNET) compared to lung or small intestine NET and may explain the different sensitivity profiles of pNET

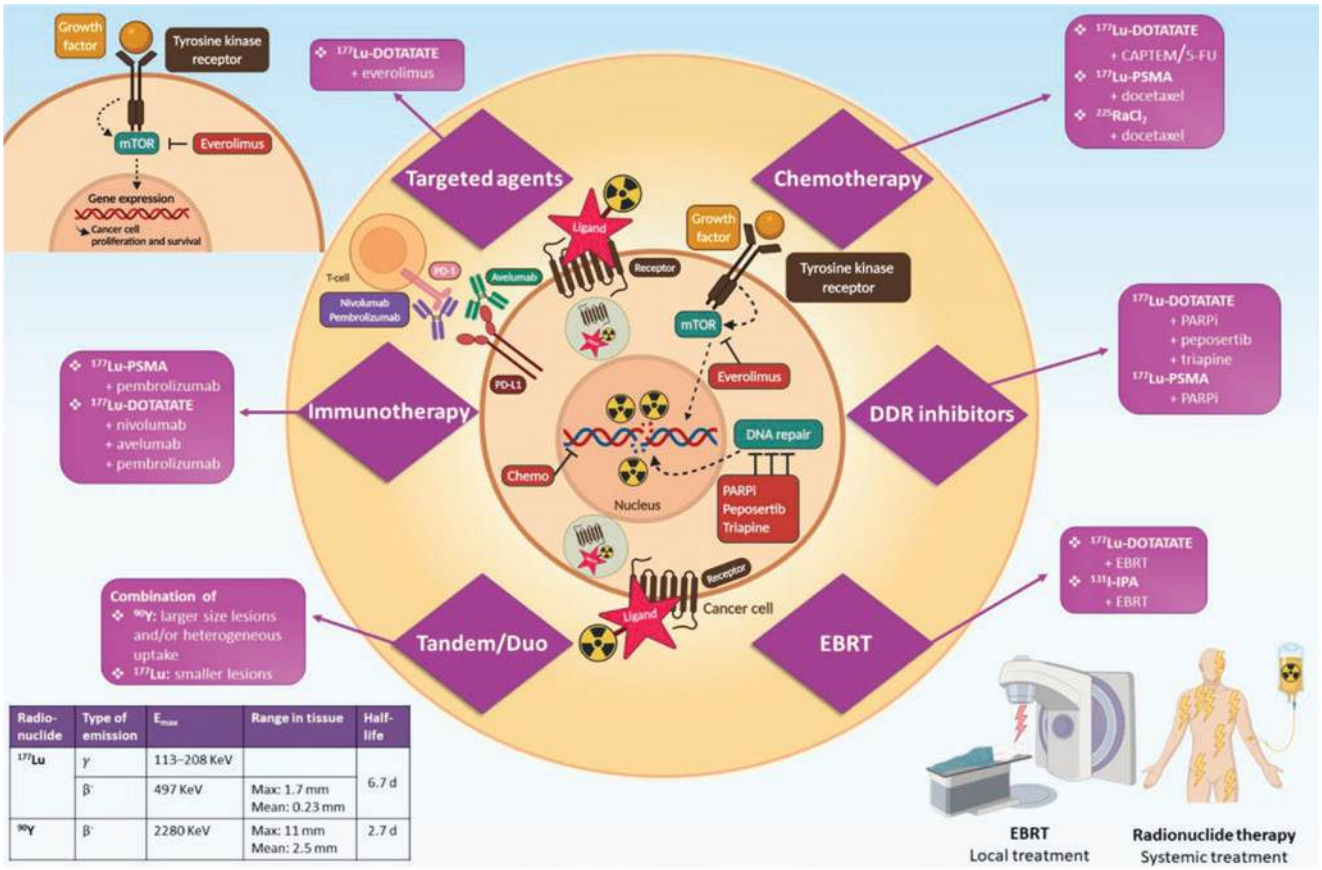

Fig. 6.25 Overview of combination therapies with radionuclide therapy

compared to NET of other origins. A synergistic effect is apparent when combining capecitabine and temozolomide (CAPTEM), most likely due to the depletion of MGMT caused by capecitabine, which strengthens the effect of temozolomide. This is the reason why the treatment regimens add temozolomide after substantial exposure to capecitabine [162]. Preliminary results of the phase II "CONTROL NET" RCT have been presented. This trial compares a combination of ^{177}Lu-DOTATATE plus CAPTEM (experimental arm) versus ^{177}Lu-DOTATATE monotherapy (control arm) in patients with low to intermediate grade midgut NETs. Forty-seven patients were included. The 15-months PFS was 90% versus 92% and ORR was 25% versus 15% for PRRT plus CAPTEM versus PRRT monotherapy, respectively. However, grade 3/4 toxicity occurred more frequently in the PRRT plus CAPTEM arm.

Overall, combining RNT with chemotherapy appears safe and efficient based on data with the beta-emitter lutetium-177. However, multicenter prospective RCTs are lacking to prove superiority of the combination over RNT alone. Although the mechanism of the radiosensitizing effect of chemotherapy is not elucidated, it is thought to act as a radiosensitizer of RNT by increasing DNA damage. However, one preclinical study also pointed out the effect of increased perfusion induced by a chemotherapeutic agent, temozolomide, which may improve ^{177}Lu-DOTATATE delivery to the tumor, as well as increase tumor oxygenation which may also have a radiosensitizing effect [163].

^{177}Lu-PSMA and radium-223 have also been combined with chemotherapy, although less data are available compared to ^{177}Lu-DOTATATE. A phase I/II study showed that the alpha-emitter radium-223 (55 kBq/kg every 6 weeks for 5 cycles) in combination with docetaxel (60 mg/m^2 every 3 week) was well tolerated in bone-predominant metastatic castration-resistant prostate cancer patients. Exploratory efficacy data even suggested enhanced antitumor activity in the combination arm [164]. This will be further explored in a phase III clinical trial that is currently recruiting patients (NCT03574571).

The combination of ^{177}Lu-PSMA with docetaxel, a taxane impairing microtubules polymerization dynamics and therefore preventing cell mitosis, is currently evaluated in metastatic hormone-naïve prostate cancer in a randomized phase II study (UpFrontPSMA trial—NCT04343885) [165]. Patients are randomized 1:1 to the ^{177}Lu-PSMA plus docetaxel arm (^{177}Lu-PSMA 7.5 GBq, 2 cycles intended, every 6 weeks followed 6 weeks later by docetaxel 75 mg/m^2, 6 cycles intended, every 3 weeks) or the docetaxel monotherapy arm.

6.8.5.2 Radionuclide Therapy and Targeted Agents

In addition to chemotherapy, RNT has also been evaluated in combination with targeted agents in order to potentiate the therapeutic effect of RNT. Targeting relevant pathways may aid in eliminating (radio-)resistant clones as well as overcoming tumor heterogeneity.

The mammalian target of rapamycin (mTOR) inhibitor everolimus was combined with ^{177}Lu-DOTATATE in the phase I NETTLE proof-of-concept study in order to establish an optimal safe dose of everolimus in this combination setting. Nephrotoxicity was the dose-limiting factor, leading to the maximum tolerated dose of 7.5 mg everolimus in combination with PRRT [166].

Among targeted agents, DNA damage response (DDR) inhibitors have recently been widely adopted. Preventing the repair of radiopharmaceutical-induced DNA damage by targeting DNA repair pathways is considered an interesting strategy. PARP is involved in the repair of DNA SSBs and has been targeted by PARP inhibitors (PARPi) in combination with chemotherapy and EBRT. Following favorable results from preclinical studies combining ^{177}Lu-DOTATATE and PARPi [167], the combination is now assessed in phase I/II clinical trials with ^{177}Lu-DOTATATE (NCT05053854, NCT04375267, NCT04086485) and ^{177}Lu-PSMA (NCT03874884). Different treatment schedules are used within the trials, with PARPi commencing either before or after RNT administration, and also with variable duration of PARPi (first few days of each RNT administration or daily continuous administration). Study results are awaited and might already provide some evidence about the optimal treatment schedule to be used.

Phase I studies evaluating the combination of ^{177}Lu-DOTATATE and other DDR inhibitors, such as peposertib (NCT04750954) and triapine (NCT04234568), are also underway. Peposertib is an inhibitor of DNA-PK, a serine/threonine protein kinase playing a critical role in DNA DSB repair via the NHEJ pathway while triapine is an inhibitor of ribonucleotide reductase, an essential enzyme for DNA replication and repair.

Other promising combinations are evaluated in the preclinical setting [168]. These include inhibitors of several pathways or molecules: DNA damage response, HSP 90, DNA topoisomerase, hedgehog signaling pathway, and EGFR.

6.8.5.3 Radionuclide Therapy and External Beam Radiation Therapy

Combining RNT with EBRT has several advantages [169]. Firstly, there should not be overlapping toxicities because of different dose-limiting organs, being the surrounding tissues (the ones close to the tumor or that are in the path of incident beams) for EBRT and mainly bone marrow and kidneys for RNT (but will depend according to the RNT type). Therefore, an escalation of the combined radiation absorbed dose without exceeding the maximum tolerated dose of the limiting organs should be allowed. Secondly, the advantages of both radiation-based therapies may be combined: EBRT delivers a precise and homogeneous high dose of radiation locally, to the bulk tumor, while the administration of RNT allows the targeted treatment of systemic disease, including (micro)-metastases and residual tumor cells, albeit with less control of the tumor dose and a heterogeneous dose depending on perfusion and target expression.

Very few clinical studies are being conducted, and most of them are based on sequential and not concurrent administration of both therapies. This combined regimen is mostly studied in bone metastases as well as in brain and liver tumors but also meningioma. Promising data have been obtained in meningioma where ^{177}Lu-DOTATATE and EBRT have been combined and showed the feasibility of such an approach. Interestingly, in seven patients out of ten, for which a follow-up ^{68}Ga-DOTATATE PET/CT was available, increased uptake of the radiotracer was observed compared to the pre-therapeutic scan [170]. This observation was corroborated in several preclinical studies in which up-regulation of somatostatin receptors was observed following low doses of EBRT [171]. Increased tumor perfusion might also be the cause of an increased radiotracer uptake seen on PET/CT. This finding is significant, as such a combination could be beneficial to patients currently not eligible for peptide receptor radionuclide therapy due to a too low uptake on ^{68}Ga-DOTA-SSA PET/CT.

A synergistic effect of 4-L-[131I]iodo-phenylalanine (^{131}I-IPA) and EBRT has been observed in preclinical models of glioblastoma multiforme, and the first results of a phase I/II trial (IPAX-1 trial—NCT03849105) should be available soon.

6.8.5.4 Radionuclide Therapy and Immunotherapy

RT with EBRT has been shown to increase tumor immunogenicity and antigen presentation and therefore enhance tumor cell destruction by T cells. Hence there is a rationale to investigate the combination of immunotherapy and RNT. Preclinical studies have shown the added value of an immune checkpoint blockade to RNT on survival.

The combination of PRRT with the immune checkpoint inhibitor nivolumab has recently been explored clinically in

a phase I study including nine patients with advanced lung neuroendocrine neoplasms [172]. Dose level 1 consisted of ^{177}Lu-DOTATATE 3.7 GBq (8-week interval, 4 cycles intended) plus nivolumab 240 mg (2-week interval), and dose level 2 consisted of ^{177}Lu-DOTATATE 7.4 GBq (8-week interval, 4 cycles intended) plus nivolumab 240 mg (2-week interval). Only one dose-limiting toxicity, consisting of a grade 3 rash, was noted in one patient being treated at dose level 2.

Phase I and II clinical trials combining ^{177}Lu-DOTATATE (NCT03325816, NCT04261855, NCT03457948) or ^{177}Lu-PSMA (PRINCE trial—NCT03658447, NCT03805594) with anti-PD1 or PD-L1 antibodies are under way.

There exists a huge potential in terms of a combined regimen with RNT. Promising combination strategies used with EBRT frequently serve as arguments to extrapolate to RNT. However, EBRT and RNT are characterized by major differences such as the delivery route (external versus "internal"), the dose (homogeneous dose versus heterogeneous dose), and the dose rate (very high and constant versus low and exponentially decreasing dose rate). The maximum therapeutic benefit one can derive from RNT will be achieved thanks to clever combinations exploiting synergistic interactions, used in the optimal doses and sequences [173] and using biomarkers with an individualized approach. Preclinical studies can bring valuable information and can serve as a basis to design proper clinical trials.

Novel treatment combinations are emerging and are now in the early phases of clinical trials, aiming at evaluating the feasibility and the toxicity of the combinations. Later, large prospective randomized trials will be needed to prove the superiority of the combinations over the monotherapies. Combination strategies might also enter in an entirely new realm when targeted alpha-emitters will become available for clinical trials in the upcoming years, with many new combination possibilities.

6.9 Charged Particles and High LET Radiotherapy

Compared to conventional RT (using X-rays), particle therapy has major advantages. The depth of penetration into the body is determined by the particle's acceleration energy and thus energy deposition increases over distance up to a high peak at the end of their range, the so-called Bragg peak. Simply said, the energy transfer is proportional to the inverse square of its velocity where the ionization density increases as the speed of the particle slows down:

$$E \alpha Z^2 / v^2 \tag{6.5}$$

where Z is the charge of the particle and v its velocity. This happens until very close to the end of their range where the high-dose Bragg peak phenomenon is formed (Fig. 6.26a). In the clinics, expanded Bragg peak also known as Spread out Bragg peak (SOBP) is then used to cover the entire tumor volume, this is formed by adding up all single Bragg curves for ions of different energy and therefore range (Fig. 6.26b).

Beyond the Bragg peak (known as tail), there is a rapid falloff of the dose, allowing for sparing of the normal tissue [177] as the tissue behind the tumor doesn't receive any radiation dose. Tumors which have an organ at risk (OAR) lying close to the tumor are especially suited for radiotherapy using particles, as this unique dose distribution can be exploited here. The OAR behind the tumor can thus effectively be spared from radiation damage (Fig. 6.26c).

At the moment, mainly protons are used in particle therapy but also carbon ions. Furthermore other ions such as helium are getting more and more in the focus of particle RT.

These physical advantages ensure precise localization of dose distribution to the tumor while minimizing dose (thus DNA damage) to the surrounding normal tissues. Currently, particles heavier than carbon are not well investigated for clinical purposes due to the dose distribution at the tail where the dose increases with the charge of the particle resulting in increased dose to normal tissue. Furthermore, for equal velocities, the ionization density for carbon ions (Z = six, A = 12) is 36 times greater than that of the proton. However, a carbon ion has 12 times more total kinetic energy, so the range of the carbon ion is about three times lower. Thus, the heavier the particle, the shorter the penetration depth. Finally, following the recommendations of the Ion Beam Therapy Workshop Report, heavy ion beam therapy should be limited to tumors (a) exhibiting a high risk of local failure post photon (or proton) RT, (b) radioresistance due to histology, hypoxia, and other factors, (c) recurring, (d) efficient at repairing cellular damage, or (e) adjacent to critical normal structures, in particular if resection could lead to a substantial loss of organ function.

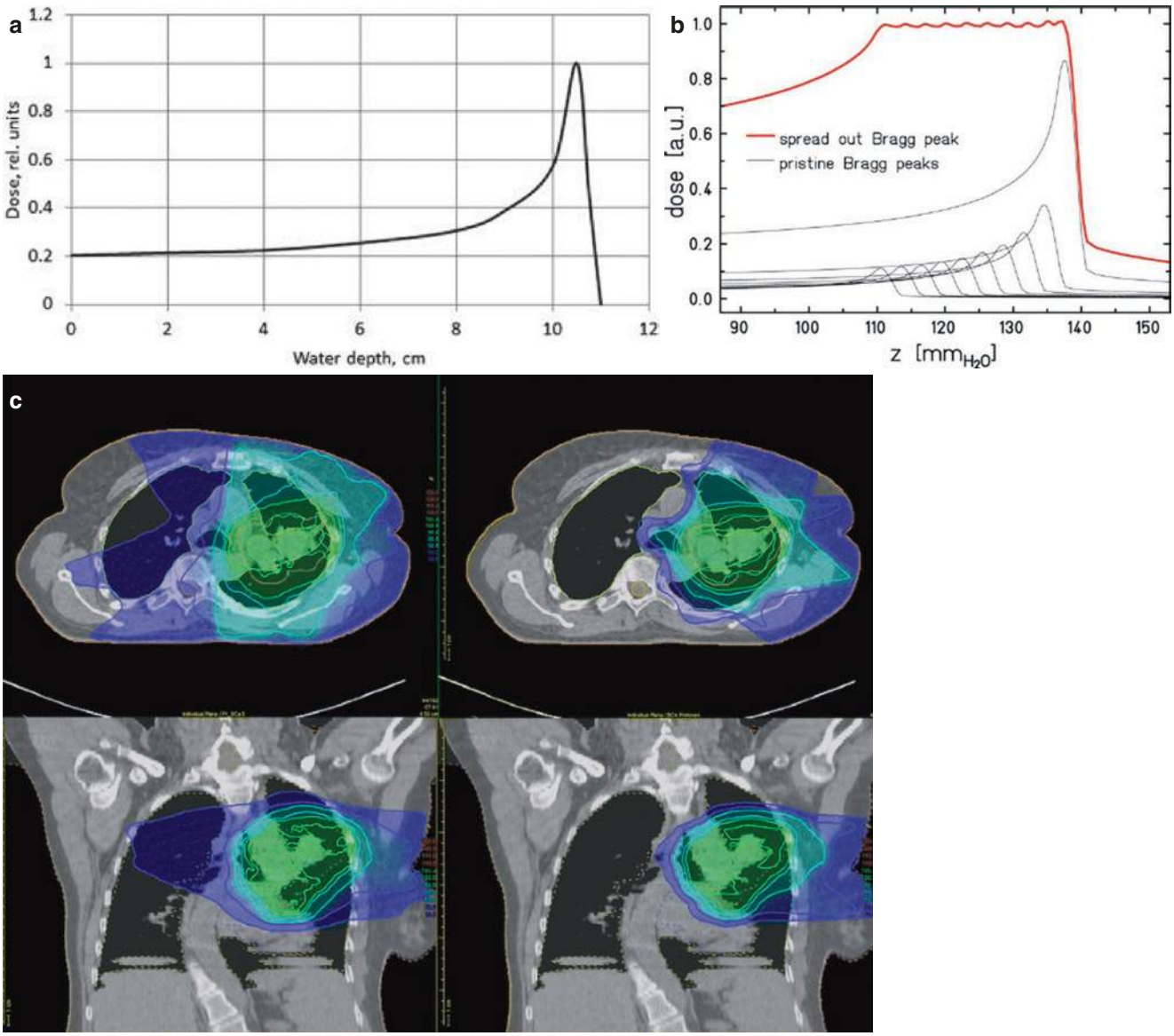

Fig. 6.26 (**a**) Absorbed dose of a 121 MeV proton in water forming the Bragg peak [174]. (**b**) Spread Out Bragg Peak formed by overlaying ions with different energy forms the spread out Bragg peak as used for therapy [175]. (**c**) Dose distribution of one patient with locally advanced non-small cell lung cancer (NSCLC) planned with intensity-modulated radiation therapy (IMRT) (left) or protons (right), depositing no dose behind the tumor [176

6.9.1 Proton Therapy

6.9.1.1 Introduction and History

Proton therapy is nowadays widely used all over the world and in some cases is more appropriate for patient treatment than the mostly used X-ray RT, due to the physical properties of protons (the Bragg curve). A detailed historical overview can be found in Elaimy et al. [178].

Clinical advantages of a proton beam were first suggested by Wilson in 1946 in his paper about the radiological use of high-energy protons. Animal studies began as soon as the first high-energy synchrocyclotron (340 MeV) was completed at the University of California Lawrence Berkeley Laboratory, USA (LBL). These first experiments on mice, Tradescantia microspores, and yeast cells showed that the RBE of high-energy protons (340 MeV) is comparable to that of 200 kVp X-rays.

The first patient proton treatment in LBL took place in 1954. A few years later, in the late 1950s, the Gustaf Werner Institute in Uppsala, Sweden also used protons for patient treatment. In 1961, the Massachusetts General Hospital began treating small intracranial targets with radiosurgical techniques at the Harvard Cyclotron Laboratory (HCL) in Cambridge. Prior to the patient treatment, a radiobiological investigation on monkeys demonstrated experimentally the

feasibility of the method. Later Koehler and others developed a technique to scatter the beam laterally and also range modulation wheels to produce SOBP to cover extended target volumes, thus it was possible to start treating larger treatment volumes in HLC in 1974.

During the late 1960s and in the decade of the 1970s, several Russian physics research facilities initiated their proton therapy programs. For example, the Joint Institute for Nuclear Research in Dubna in 1968, the Moscow Institute for Theoretical and Experimental Physics in 1969, and the Central Research Institute of Roentgenology and Radiology in Saint Petersburg in 1975.

The National Institute for Radiological Sciences in Chiba, Japan started proton therapy treatments in 1979. They were also the first that developed a spot scanning system for proton treatment delivery in 1980. Since then is proton therapy spread more and more—Clatterbridge, England in 1989, France at Nice and Orsay (1991), iThemba Labs in Cape Town, Africa (1993), Paul Scherrer Institut at Villigen, Switzerland (1996), Hahn Meitner Institute in Berlin, Germany (1998), National Cancer Center in Kashiwa, Japan (1998), and Joint Institute for Nuclear Research in Dubna, Russia (1999).

The first hospital specialized in proton therapy started treating patients in 1990 at the Loma Linda University Medical Center in Loma Linda, California, USA. In the same period, the Proton Therapy Cooperative Group was formed, later renamed to the Particle Therapy Cooperative Group (PTCOG) [179]. It is a non-profit organization making statistics and organizing meetings about protons, light ions, and heavy charged particles RT.

Nowadays, there are more than 100 proton therapy centers all over the world with technological equipment from several companies such as IBA, Varian, Mitsubishi, Sumitomo, Hitachi, Mevion, ProNova, Protom based on cyclotrons or synchrotrons. More about the facilities and also patient statistics can be found, for example, on the PTCOG website.

6.9.1.2 Proton Therapy Technology

The generation of protons is obtained via hydrogen ionization. Protons are then accelerated inside a particle accelerator, typically a cyclotron or a synchrotron. A cyclotron produces a proton beam with a fixed energy, on the other hand, the proton energy in a synchrotron is adjustable [180].

In both cases (cyclotron and synchrotron), the beam needs to be spread longitudinally, to produce an SOBP for the patient treatment. This is done by superposing several beams with different energies and weights. In the case of a cyclotron, an adjustable amount of material has to be placed in the way of the beam to reduce the beam energy to the one needed. This is achieved by the use of a degrader just after the beam extraction or by placing a stack with a variable number of plates (a range shifter), a plate with ripples (a ridge filter), or a rotating wheel with an azimuthally changing thickness (a range modulation wheel) inside the nozzle in the irradiation room. In the case of synchrotron, the energy is adjusted inside the accelerator, as was already mentioned, so there is no need for any additional devices [180].

The physical depth dose curve of a SOBP has a broad, quite homogeneous dose region, as is shown in Fig. 6.30. This makes it possible to deliver a higher dose to the tumor region than to the OAR, and therefore to spare these tissues.

There are two modes enabling the lateral beam spread, passive or active modes. Examples of passive modes are the Single or Double Scattering (SiS or DS) and an example of active mode is the Pencil Beam Scanning (PBS). For the passive modes, the beam passes through scatters (one or two, SiS or DS, respectively). In the active modes, scanning magnets are used, which redirect the narrow proton beam to several positions according to the treatment plan. The dose is then delivered to each layer of the volume spot by spot.

6.9.1.3 Proton Therapy and RBE

The energy spectrum, and thus the LET of protons in the SOBP is changing with depth in tissue, since the protons are slowing down traveling through the tissue. At the distal parts of the SOBP, the LET is much higher than in the proximal part. High LET values are connected to increased DNA damage, and thus to lower cell survival.

The International Commission on Radiation Units and Measurements (ICRU) has recommended the use of a generic RBE value equal to 1.1 in the whole range of proton therapy, and most of the proton therapy centers around the world have adopted this value [181]. This means that the same fractionation scheme as for X-ray RT can be used, with the difference that instead of 2 Gy 1.82 Gy per fraction will be used with protons.

This recommended value is based on experimental studies done in vitro and in vivo mostly using passive scattering modes in the early days of proton therapy. From the in vitro studies, mostly performed on Chinese Hamster cell lines, with cells placed in the middle of SOBP, the range of estimated RBE values was from 0.86 to 2.10 with a mean of 1.22 ± 0.02. The RBE from the mid-SOBP in vivo studies ranged from 0.73 to 1.55 with a mean of 1.10 ± 0.01 [181].

Later studies showed that the RBE is not a constant value but it varies depending on a wide range of parameters, such as the beam range, dose per fraction, position in the SOBP, cell line or tissue origin, and also the studied biological endpoint [182]. Another problem when comparing RBE values from different publications is the reference radiation used for the establishment of the RBE values. Several reviews on this topic exist, as, for example, where a collection of data from several groups are sorted by cell lines referring also to the used reference radiation [183].

Some studies report RBE values at the distal falloff of the SOBP near to 3 [184]. One of the claimed advantages of proton therapy is the steep distal falloff of the Bragg peak. Due to this fact, many times the proton beam is often directed to stop in the proximity of the patient's OAR. The mentioned studies highlight the inaccuracies in the generic RBE value used in the whole range of proton therapy. These inaccuracies are much more crucial at the distal falloff of the beam and can lead to the damage of healthy tissues behind the treatment volumes.

In recent years, there is an increased interest in using the PBS mode, thanks to the spot-weighted dose delivery, which facilitates a more conformal dose delivery to the treatment volumes and sparing of healthy tissue. Another advantage of PBS is the much lower secondary-induced radiation (mostly neutrons) from the components of the technological constructions or patient-specific devices (i.e., collimators and compensators) needed in passive modes.

The dose rate in each spot is however much higher than the dose rate in passive modes, which could maybe influence the cell response inside the treated volume in a different way than it is expected. Anyhow, there are several studies showing that there is not any significant difference between the biological response of cells using passive or active modes [185]. In clinical applications, there is some evidence that passive scattering may be associated with more toxicity than pencil beam scanning techniques [186].

6.9.2 Heavy Ion Radiotherapy

6.9.2.1 Carbon Ions

Carbon ion radiobiology finds its origin from the use of ions in cancer RT. Research on carbon ions and their clinical potential started in 1975, with the installation of the BEVALAC at the Lawrence Berkeley Laboratory [187]. In response to the initial success, the Japanese government began construction on the world's first heavy ion facility designated for medical applications at the National Institute of Radiological Sciences (NIRS) in 1984. The Heavy Ion Medical Accelerator in Chiba (HIMAC) was completed in 1993 and carbon ion RT clinical trials began in June 1994 [188].

Biological Advantages of Carbon Ions

Talking about energy deposition, it is important to mention the Linear Energy Transfer (LET—keV/μm) which is the energy deposited per unit of length along the particle track

$$\text{LET} = dE / dx \qquad (6.6)$$

with dE = deposited energy and dx = distance covered. Therapeutic beams of carbon ions (100–400 MeV/n) have LET ranging from 10 to 100 keV/μm [189]. LET is also at the origin of produced biological effects that cause radiation damage. As the particle species and their energy influence LET, the LET of carbon ions is higher than the LET of photons and hence causes a higher fraction of clustered DNA damage foci from direct DNA-ion interaction (Fig. 6.27).

Comparison of biological effects of different LET (beam qualities) is expressed as the relative biological effectiveness (RBE). For the same biological effect, RBE is described as the dose ratio of the reference beam quality experiment to the test beam quality experiment

$$\text{RBE} = Dr / D \qquad (6.7)$$

with Dr = Absorbed dose at reference beam quality experiment (usually photon) and D = Absorbed dose at test beam quality experiment.

RBE is a function of multiple parameters such as the dose, dose rate, LET, oxygen concentration, and cell cycle phase to mention a few. The dependency of these parameters is particularly true at low LET (<10 keV/μm) but less with increasing LET (>10 keV/μm) such as for carbon ions. The RBE value of photons (<10 keV/μm) is considered equal to ~1.0 and tends to increase gradually until it comes to a maximum at around LET = 100 keV/μm and finally decreases. This phenomenon is also known as the overkill effect. Generally, the RBE of carbon ions is around 3.0. However, with increasing LET, dose delivered to the surrounding tissue (entrance dose and tail) also increases. Therefore, a compromise between RBE and dose delivered to the surrounding tissue is needed. As an optimal RBE is said to be achieved around a LET of 100 keV/μm, carbon ions became the best compromise between RBE and dose delivered to the surrounding tissue and is therefore the most studied and clinically applied ion in particle therapy [188, 190]. Yet, little is known on healthy tissue toxicity and the correlated molecular and cellular mechanisms linked to carbon ion irradiation.

Under normoxic conditions, DNA damage caused by low LET radiation (such as photons or protons) is enhanced by generated DNA radicals, which in the presence of molecular oxygen are fixed or become permanent (also known as the

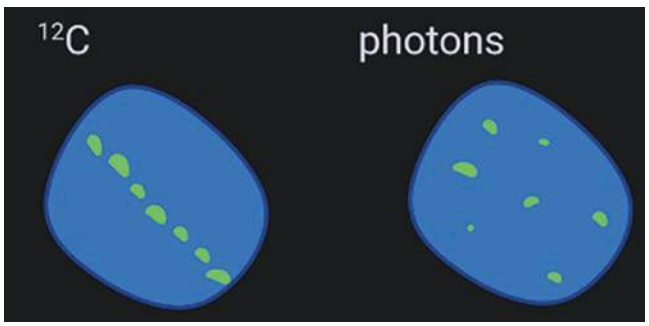

Fig. 6.27 Schematic representation of gH2AX after exposure to carbon ions versus photons. DAPI in blue, gH2AX in green

indirect interaction). The existing oxygen also hinders repair mechanisms. Under hypoxic conditions, this phenomenon is not present, DNA radicals become reduced by sulfhydryl groups causing less damage and repair mechanisms are promoted. Consequently, a major cause of radiation resistance in RTy has been attributed to hypoxic cancer cells. On the other hand, with high LET radiation (such as carbon ions), the particle directly acts on the phosphodiester bond of DNA inducing thus clustered damage which is then less amenable to be repaired. From these observations came the concept of Oxygen Enhancement Ratio (OER), which is an inverse relationship between dependence on oxygen, inducing cellular damage and the mass of the ion species (Fig. 6.28).

The cell cycle status has been shown to be influential in determining radiation sensitivity [191]. Cells in the G2/M phases of the cell cycle are most sensitive to radiation while cells in late S phase are most resistant. This increased radiation sensitivity in G2/M appears to be related to chromatin condensation as effective DNA damage repair is hindered. Unlike low LET radiation, no significant effects of radiation sensitivity on the cell cycle distribution were observed when employing high LET radiation such as carbon ions [192].

The rationale behind fractionated RT, beside the cell-sparing effect, is based on cell cycle radiation sensitivity. Fractionation allows tumor cells in a radiation resistant cell cycle phase to switch/move into a more radiation sensitive phase before the next fraction is applied [193]. However, as the cell cycle distribution is not affecting radiation sensitivity for high LET radiation, fractionated RT would therefore be less beneficial. Overall, carbon ion RT has several benefits (Fig. 6.29).

Indications and Clinical Trials of Carbon Therapy

Hadrontherapy with carbon ion (carbon therapy, CT) is a RT technique intended to destroy cells by irradiating them with a beam of carbon ions particles. This therapy requires heavy, specific equipment derived from research in particle physics including source and particle accelerator (synchrotron or cyclotron), device for controlling the treatment beam and preparation devices, for the conduct and control of processing. This equipment leads to very heavy material and financial investments and the need for multidisciplinary cooperation for their use.

Compared to X-rays (conventional RT) which pass through the whole body and therefore irradiate as healthy cells pass, the carbon ions stop at the desired depth (therefore at the level of the tumor). These ions, once arrived in the tumor cells, create more serious lesions than with other treatments at the level of its genetic material. As their action is intense and the beam precisely defined, tumor cells can be very precisely targeted. These tumor cells do not die immediately, but they are no longer able to multiply and lose their immortality. In addition, the number of sessions in carbon therapy can be much smaller than that required in conventional RT. Moreover, additional chemotherapy is rarely required, which means less fatigue for the patient.

Carbon therapy can target inoperable tumors and particularly radioresistant, in particular when they are in a situation of hypoxia, a common cause of failure of conventional RT. Accordingly, carbon therapy is intended for the treatment of inoperable tumors or incompletely resectable as well as radioresistant surrounded by radiosensitive healthy tissue.

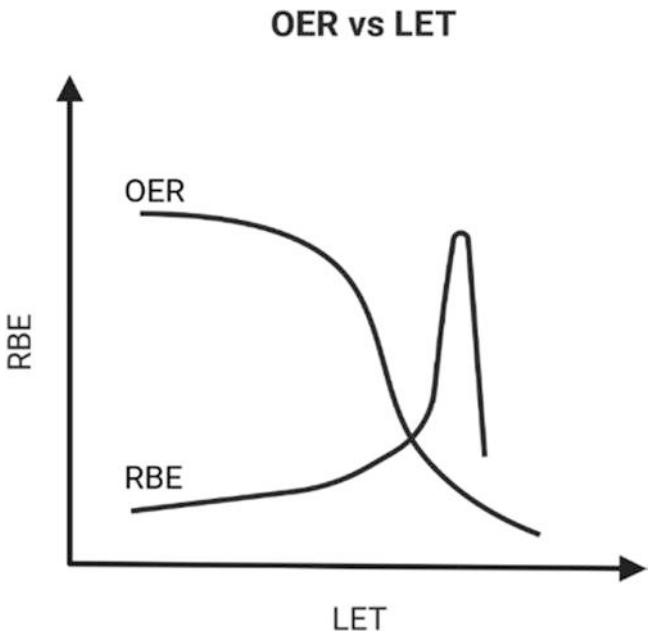

Fig. 6.28 Schematic representation of the relationship between OER and RBE in function of LET

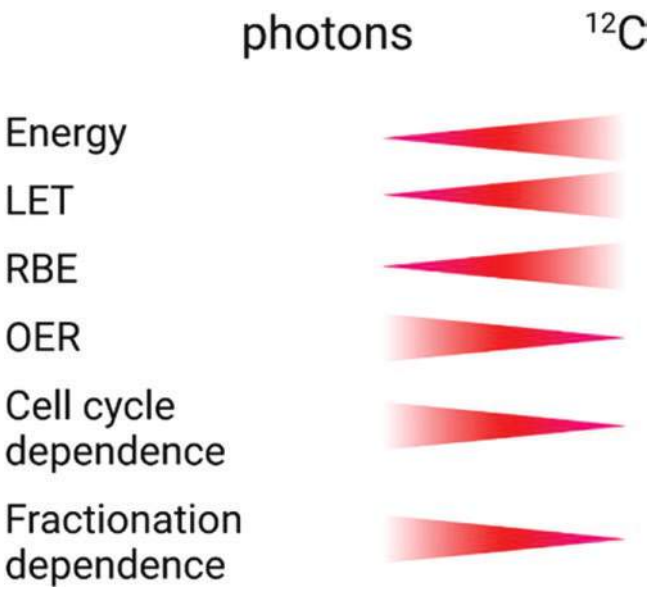

Fig. 6.29 Summary comparison between photon irradiation and carbon ion irradiation

The main indications of this therapy are cystic adenoid carcinomas, tumors of the sinuses of the face and salivary glands, mucous malignant melanomas, chordomas and chondrosarcomas of the base of the skull, sarcomas of the axial skeleton and soft tissues, unresectable or in resection incomplete, unresectable local recurrences of rectal cancer, large hepatocarcinomas (diameter greater than 4–5 cm), choroid malignant melanomas and eye tumors, prostate tumors, tumors of the cervix, and stage I NSCLC [188, 194].

All these pathologies to which carbon therapy is applied form a heterogeneous group for which there is a wide variety of therapeutic approaches ranging from surgery to very high-techRT, with or without the combination of several other treatments. According to the ClinicalTrials.gov website, 31 clinical trials comparing C-ions to either protons or photon therapy were found as recruiting, active or completed.

According to a global assessment of clinical experiences in Japan, the optimization of the therapeutic protocol has progressed over many years and is dependent on the tumor site [195]. For a given disease entity, the therapeutic schedule (e.g., carbon therapy alone, with chemotherapy or in a preoperative setting) is initially based on scientific evidence.

Some of the previously published clinical studies suggest that carbon-therapy would potentially be more effective than conventional RT in case of cystic adenoid carcinomas of the head and neck, tumors of the salivary glands in absence of complete resection, chordomas and chondrosarcomas of the base of the skull, and NSCLC tumors while late toxicities which have been reported in particular in some cases of chordomas and skull base chondrosarcomas, soft tissue and skeletal sarcomas axial, choroid melanomas and eye tumors [196–198].

In total, the analysis of the most recent literature and agency reports of evaluations are consistent to indicate that there is still little data available to conclude definitively on the efficiency-safety balance. Carbon therapy appears to be a promising technique for the treatment of certain not resectable or radioresistant tumors, surrounded by healthy radiosensitive tissue and is currently studied in clinical trials. The long-term side effects are also not yet well known. Indeed, looking at the dose/depth profile of particle beams, the effect of entrance dose and fragment tail on the surrounding healthy tissue is highly reduced compared to conventional therapy. Yet, this dose is not negligible and is an underdeveloped field in radiation research.

6.9.2.2 Other Ions

As described previously, only protons and carbon ions are the types of hadrons used to treat solid tumors so far, however several kind of hadrons, such as neutrons, charged pions, antiprotons, helium ions, and other light ions nuclei (like lithium, oxygen, up to silicon ions) have been either used or planned to be tested for oncological treatment [199].

Helium Ions

In recent years, thanks to their physical and biological properties complementary to protons and carbon ions, a renewed interest in using helium ions (4He) for RT has been observed. This is also tangible from the fact that the first European He-ion treatment is about to go into operation at the Heidelberg Ion-beam Therapy (HIT) center and that at NIRS, in Japan, a multi-ion therapy concept including He ions is currently set up [200, 201]. In addition, the National Center for Oncological Hadrontherapy (CNAO) in Italy is also planning to treat patients with He ions in the future since a source will be available for non-clinical/preclinical research by Spring 2023. In the past, about 2000 patients were successfully treated at the Lawrence Berkeley National Laboratory with passively scattered He ions in the US heavy ion therapy project [202].

He ions are very attractive for cancer treatment because they can overcome some of the limitations of protons and carbon ions, while keeping their advantages. Specifically, they can provide favorable biophysical characteristics like the reduced lateral scattering and enhanced biological damage to deep-seated tumors like heavier ions, while simultaneously lessening particle fragmentation in distal healthy tissues as observed with lighter protons [203].

Radiobiologically speaking, helium ions, being in a similar LET range as protons, offer an improved RBE and OER, while potentially allowing for less demanding biological modeling compared to carbon ions. The helium ions radiobiological characterizations performed so far showed a higher RBE in the Bragg Peak region of up to 1.6, and the OER at 10% survival was found to decrease from 2.9 to 2.6 in the peak region when compared to protons [204]. These are certainly advantageous features for eradication of radioresistant hypoxic tumors. In addition, helium offers a decreased lateral scatter effect versus proton, with less fragmentation tail dose versus carbon [205].

Especially for pediatric patients, helium ions could have the potential to reduce the volume of irradiated normal tissue, without bringing the disadvantage of additional dose caused by the fragmentation tail, like it is observed for carbon ions [206]. This could not only improve the dose distribution for small tumor lesions, but also reduce the total overall dose for children suffering from large tumors, also considering that it is expected that the number of secondary neutrons is very low and the dose due to neutrons may even be lower than in proton therapy [207]. Last but not least, it is important to take into account that helium hadrontherapy would also be less expensive than carbon ions, as they may be produced in cyclotrons rather than synchrotrons.

From the modeling point of view, the very few RBE models existing for these ions still need to be integrated and benchmarked by experimental data on radiation-induced tumor cell killing, as well as normal cell response. However, He-ion RBE data for cell survival are still very scarce, and intensive experimental campaigns need to be performed [203].

Oxygen Ions

Oxygen ions are currently considered as a potential alternative to carbon ions. Because of their mass, they have less lateral scattering which is in favor of the tumor conformality. The high LET of oxygen ions when compared to carbon ions is associated with higher RBE and therefore to better treatment effectiveness in particular with respect to hypoxic tumors. Compared to carbon ions, oxygen ions produce more nuclear fragments, which need to be carefully investigated, not only in-field but also out-of-field, laterally and beyond the Bragg peak, to study the effect of the mixed radiation field in the healthy tissues surrounding the tumor target [208] (Box 6.20).

Box 6.20 Helium Ions Versus Protons and Carbon Ions

- Helium ions versus Protons:
  - ↓ Lateral scattering
  - ↑ RBE
  - ↑ OER
  - ↓ Secondary neutrons
- Helium ions versus carbon ions:
  - ↓ Fragmentation tail
  - ↓ Costs

6.9.3 High-Energy Accelerators

Particles used for therapy need to have sufficient energy to penetrate the patient's body to the desired depth, i.e., several hundred MeV/u. At therapy centers, the acceleration is done by the use of circular accelerators, which can be divided into two types, the cyclotron and the synchrotron. Another way of accelerating particles is through the use of high-frequency linear accelerators, so-called LINACS, which at the moment are getting more and more in the focus. The different accelerator types are summarized in Table 6.11.

6.9.3.1 Cyclotron

A classical cyclotron consists of a large electromagnet with hollow, D-shaped electrodes, called Dees in-between. The Dees are separated by a small gap, which is the acceleration region of the cyclotron. The electromagnet has a constant magnetic field perpendicular to the plane of the movement of the particles. The electrodes induce a radiofrequency electric field, which is changing polarization in resonance with the particle movement. The particles are injected in the middle of the gap. In this gap, the ions are accelerated the first time, upon entering the first Dee there is no electric acceleration field, keeping the particle at constant velocity. Within the electrode, the magnetic field bends the particle due to the Lorentz force and brings it on a circular path with radius

$$r = \frac{m_0 v}{qB} \tag{6.8}$$

with m_0 the mass, v the velocity, q the charge of the particle, and B the magnetic field of the electromagnet. After a half circle, the particle enters the acceleration gap and is accelerated until the second Dee is entered, where again a half circle is formed, which has a larger radius but is traveled within the same time. Acceleration only happens if the frequency f of the electric field, the so-called cyclotron frequency, is adapted to the time, the particle needs to traverse the Dee and therefore to the charge q and the mass m of the particle and the magnetic field B:

$$f_0 = \frac{|q|}{2\pi m_0} B \tag{6.9}$$

but stays constant in time. This process happens until the radius corresponds to the extraction radius R and the particle is extracted with an energy of

$$E = \frac{q^2}{2m_0} (RB)^2 \tag{6.10}$$

Classical cyclotrons are using iron magnets which limit the magnetic field to 1–2 T, if superconducting magnets are used, the magnetic field can be increased, and therefore the size of the cyclotron decreased. This kind of cyclotron only works for non-relativistic particles with velocities $v \ll c$. For higher energies and thus higher velocities, the time for the half circle is not constant anymore. Therefore, they get asynchronous to the constant acceleration frequency. For relativistic particles, the mass m is no longer constant but increases by the factor

$$\gamma = \frac{1}{\sqrt{1 - \left(\frac{v}{c}\right)^2}} \tag{6.11}$$

The cyclotron frequency is now dependent on particle velocity

$$f = \frac{|q|}{2\pi\gamma m_0} B \tag{6.12}$$

This limits the maximum energies achievable using classical cyclotrons to, e.g., approx. 20 MeV for protons, which is much smaller than the needed energies for particle therapy. This problem is overcome by two new types: the synchrocyclotron and the isochronous cyclotron. As the synchrocyclotron has a very low duty cycle, it is not usable for particle therapy.

The isochronous cyclotron makes use of a non-constant magnetic field. Here the magnetic field gets larger by the factor γ with increasing radius to increase the Lorentz force and balance the mass increase, resulting again in a constant travel time. This increase in magnetic field leads to a defocusing of the beam, which is compensated by alternating-gradient (also called strong) focusing. Technically it is realized by changing the magnet design, into the so-called hill-valley design, in so-called sector cyclotrons. This design results in regions with higher and lower magnetic fields as shown in Fig. 6.30b. At the transition between hill and valley, the magnetic field is bent and a defocusing (valley to hill) and focusing effect (hill to valley) can be achieved. Using this design acceleration to clinical relevant energies for protons is achievable. Furthermore using the isochronous mode together with superconducting magnets allows for small cyclotron sizes of only a few meters diameter. These properties make the isochronous cyclotron the most popular accelerator for proton therapy.

6.9.3.2 Synchrotron

A classical synchrotron consists of an injector, a set of bending and focusing magnets, guiding the particle on a circular track and linear acceleration tracks without magnetic field in between and an extractor as shown in Fig. 6.31a. The injector is basically a linear pre-accelerator, which injects the particles in the ring with a certain energy and a set of inflection magnets which initially bend the particles into the acceleration tube. In contrast to the cyclotron where the particle track is spiral, the particle track stays circular in the synchrotron at all times. To achieve a circular particle track,

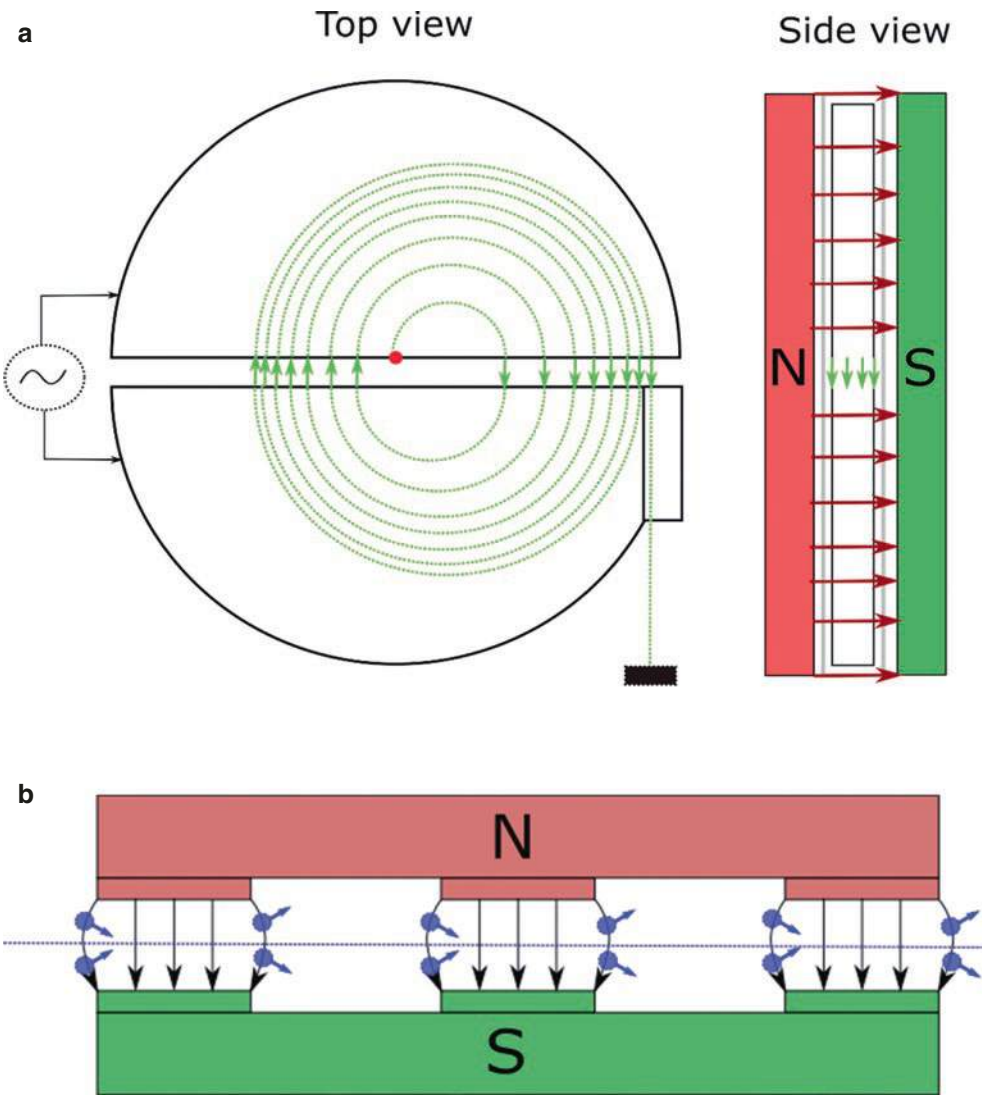

Fig. 6.30 (**a**) Principle of a classical cyclotron. (**b**) Hill-valley magnet design

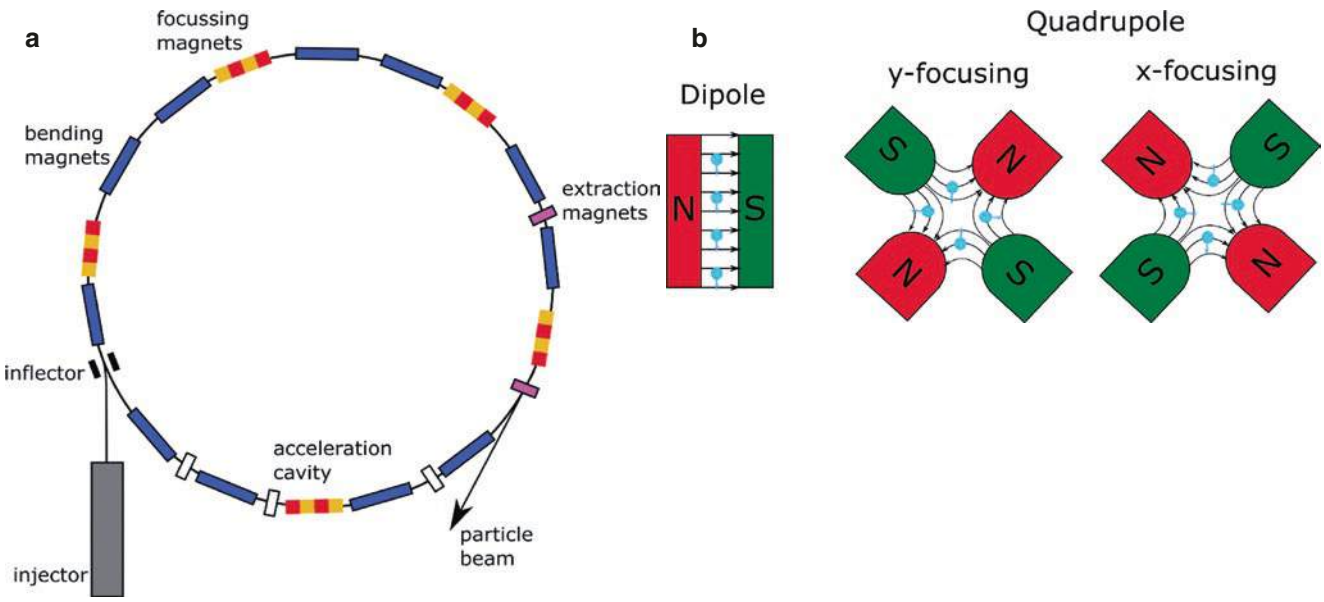

Fig. 6.31 (**a**) Principle of a synchrotron. (**b**) A positively charged beam coming from the front is deflected by Dipole magnets and focused by quadrupole magnets

dipole bending magnets, which bend the particles to stay in the circle, are placed all along the cyclotron. The magnetic field needs to be increased in synchronization with increasing energy and therefore velocity of the accelerated particle, to keep the particles on track. The particles are accelerated close to the speed of light; therefore, the processes happen in the relativistic regime. In the synchrotron, the following requirement, due to the Lorentz force, has to be fulfilled at all times:

$$B = \frac{m_0 \gamma v}{qr} \tag{6.13}$$

One can see that the magnetic field has to be increased proportionally to the increased velocity and therefore energy of the particles. Furthermore, quadrupole and even higher order magnets are necessary to focus the particle beam within the vacuum acceleration tube. The quadrupole magnets are able to spatially focus the beam and therefore work as a lens. In contrast to optical lenses, magnetic lenses only focus in one direction and even worse defocuses in the other direction. Therefore magnetic lenses always come in units of pairs, one focusing the x-direction and the other the y-direction. The higher order magnets are able to correct even the smallest aberrations and therefore ensure that the beam keeps on track. Modern synchrotrons also take advantage of the strong focusing to further reduce beam diameter, as in the isochronous cyclotron. The energy of the particles is increased in the linear acceleration tracks, where high-frequency electric fields are applied in cavity resonators, which again have to be synchronized with the velocity of the particles. Both magnetic field strength and phase of the electric field have to be adapted to the particle's energy in each circle. The vacuum chamber for particles in a synchrotron can, due to the circular path, be a thin torus rather than a disk as it is for cyclotrons, which allows a more cost-efficient construction. The last part is the extractor, which consist of sets of dipole magnets which extract the particles once the desired energy is reached. The synchrotron by design can only operate in a quite slow pulsed mode, but has the advantage that the energy can be easily varied pulse by pulse. Synchrotrons are mainly used when different particle types (protons, carbon ions, and others) are used in the same facility, as the magnet tuning allows flexibility to flexibly change the accelerated ions, which is not possible in cyclotrons (Box 6.21).

Box 6.21 Cyclotron and Synchrotron

- Cyclotrons consist of a big magnet and two, complex shaped electrodes.
- Compact design of asynchronous cyclotrons allows for small sizes of a few meters diameter.
- Asynchronous cyclotrons most popular accelerator for proton therapy.
- Synchrotrons consist of a set of bending and focusing magnets and field free drift tracks, which are arranged in a circle.
- Synchrotrons can accelerate different particle types (protons, helium, carbon, and also heavier ions) with the same design.

6.9.3.3 Particle LINAC

A high-frequency linear accelerator (LINAC) represents a complementary type of accelerator compared to cyclotron and synchrotron. It is based on the same principle as the modern clinical LINACs for X-ray therapy, as commonly used worldwide to accelerate electrons to high energies and stimulate them to emit X-rays at several MeV energies. Due to the light weight of the electrons, these accelerators can be very compact and directly mounted on the application gantry. For particles such as protons and heavier ions in contrast, more complex technological developments are necessary. Although already proposed in the 1990s, the technology for particle LINACs still is in its infancy, with only a few projects worldwide [209, 210]. Radiofrequency LINACs are based on the principle to accelerate a bunch of particles in cavity resonators as shown in Fig. 6.32a. The particles are synchronized to the applied alternating electric field. They are accelerated when they are in the acceleration space.

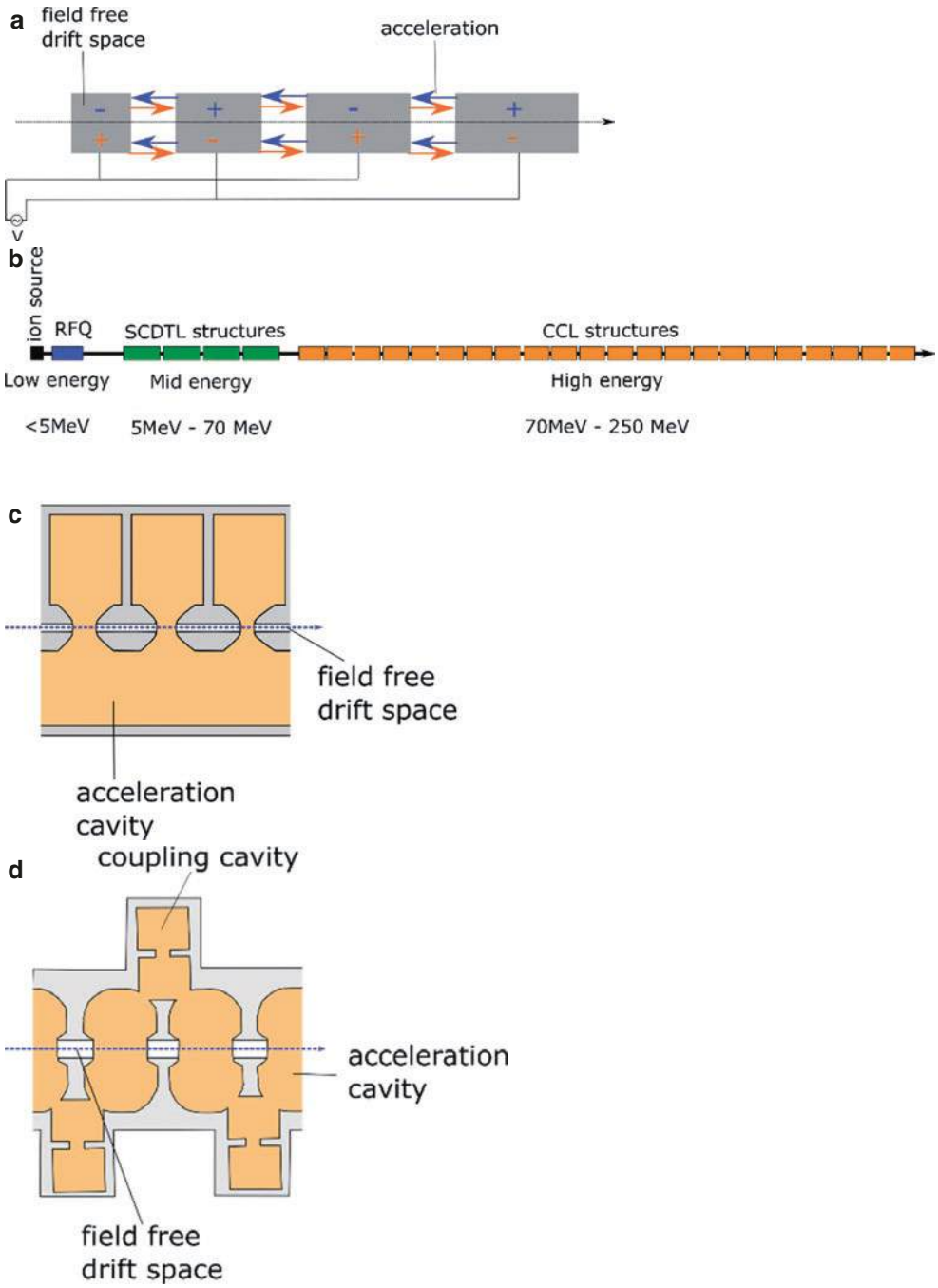

Fig. 6.32 (**a**) Linear acceleration principle. (**b**) A proton LINAC system. (**c**) Principle of a side-coupled drift tube LINAC (SCDTL) structure (cut through). (**d**) Principle of a coupled cavity LINAC structure (cut through)

When the field commutes, the particles are shielded in a field free drift space. The shielding also serves as electrodes for the electric field. When the particles enter the next acceleration space, due to alternation of field again see an acceleration electric field. This process is continued until the final energy is reached. Particle LINACs in the so-called all-linac approach consist of different types of acceleration cavities shown in Fig. 6.32b, after the ion source, each suited for a different particle energy range. For energies up to ~5 MeV, a radiofrequency quadrupole (RFQ) is used for acceleration. For energies between 5 and 70 MeV, the acceleration is performed in a SCDTL (side-coupled drift tube LINAC), followed by the coupled cavity LINAC (CCL) up to the maximum energies of ~250 MeV. The acceleration is performed in an electric field in which the resonators are oscillating with 3 GHz allowing for high electric fields and a shrink the system length to approximate of ~30 m, which can be fit into a clinical building. The RFQ is a quadrupole electromagnet, which is oscillating with a 3 GHz radiofrequency. Special longitudinal design of the electrodes makes it possible to push the particle beam through the RFQ and therefore accelerate it. Furthermore, the RFQ bunches the particle beam so that it fits the needs of the SCDTL and CCL structures, which can only accelerate a bunch of particles. The SCDTL accelerates the beam in the mid energy range 5 and 70 MeV. The SCDTL structure as shown in Fig. 6.32c consists of a huge cavity resonator where drift tubes are mounted. In the cavity, the alternating electric field is built and the tubes serve as field free drift space. The length of the drift tube must be synchronized to the velocity of the particles, so that the particles only see the acceleration of the oscillating field. The length of the *i*th tube is:

$$L_i = \beta_i \lambda_{\mathrm{RF}} \tag{6.14}$$

with

$$\beta = \frac{v}{c} \tag{6.15}$$

describing the velocity v of the particle in units of velocity of light c and λ_{RF} being the wavelength of the oscillating field. For a 3 GHz radiofrequency, the wavelength is

$$\lambda_{\mathrm{RF}} = \frac{c}{f} \approx 10\,\mathrm{cm} \tag{6.16}$$

For an acceleration between 5 MeV ($\beta = 0.1$) and 70 MeV ($\beta = 0.36$), this results in a drift tube length of 1–3.6 cm. For higher energies, a coupled cavity LINAC (CCL) system is used (Fig. 6.32d). The design of the structure is different compared to SCDTL. Here the field is coupled in through a cavity, which makes them more efficient for higher particle velocities. The manufacturing of SCDTL and CCL structures is quite complicated as material defects such as welding seams or supernatant material will disturb the electric field. New production techniques such as 3D metal printing will offer possibilities of high precision manufacturing of such structures.

6.9.3.4 Beam Transport and Gantries

After the accelerator, the particle beam needs to be guided to the patient. For beam guiding as in the acceleration process of the synchrotron, sets of magnets are used. Dipole magnets are used for bending the beam, whereas quadrupole magnets are used to keep the beam on track in the vacuum tube. Before the patient also beam diagnostics, such as a dosimetry chamber is placed. A quite important step is also the beam shaping, which defines the energy and size of the beam. In most centers, pencil beam scanning is used, which allows to get rid of a collimator close to the patient and therefore reduce unwanted exposure of the patient with neutrons coming from the collimator. The energy selection can be done away from the patient, and it must only be guaranteed that the beam has a defined profile modern therapy centers mostly rely on the application of radiation from different angles, which makes it necessary to move the beam around the patient. This is done by the use of so-called gantries, which are rotatable. The beam is deflected on the gantry and then can be delivered at a defined position. In particle therapy, due to the velocity of the particles and their rigidity, i.e., the resistance of a particle to be bent by a magnetic field, huge and especially heavy magnets must be used, which make gantries quite large and heavy. A conventional proton gantry is in the order of 150 t with a size of several meters, whereas for carbon ions it can be up to 600–700 t (Box 6.22).

Box 6.22 Particle LINAC

- High-frequency LINACs for particle therapy are an emerging technology.
- Complex cavities accelerate beams with a GHz frequency.
- Cavity size has to be precisely aligned with particle velocity.

6.10 Nanoparticles in Cancer Therapy

Box 6.23 Nanoparticles in Cancer Therapy

- Nano-objects exhibit different physical and chemical properties compared to the related bulk materials due to a high surface-to-volume ratio, a metric that decreases with the size of the object.
- The surface of nanoparticles can be functionalized to actively target cancer cells opening avenues for a use in nanomedicine field. Recognition and clearance of the nano-objects from the bloodstream by the reticuloendothelial system (i.e., resident macrophages in liver, spleen, lungs) remain the main challenge.
- Nanoparticles have the potential to be used to efficiently and specifically deliver drugs to the tumor, to produce heat in hyperthermia therapy, and to sensitize cancer cells to radiotherapy.
- Translation of nanoparticles to the clinic remains poor due to hurdles related to their large-scale manufacturing and toxicity studies.

In the last few decades, the use of nanomaterials in medicine has attracted increased interest. A nanoparticle is a particle with at least one of its external dimensions in the size range of 1–100 nm. Due to this small size, nanoparticles exhibit physical, chemical, and optical properties that significantly differ from those of their bulk material, which makes them emerge as promising tools to improve the efficacy of cancer diagnosis and therapy. This section describes how nanoparticles have the potential to contribute to certain cancer therapies that are discussed in Sects. 6.4 and 6.5, including the delivery of chemotherapeutic drugs, targeted therapy, hyperthermia, and RT (Box 6.23).

6.10.1 The Properties of Nanoparticles

Nanoparticles can typically be classified based upon their material (organic or inorganic), shape, surface, or size (Fig. 6.33). As such, a broad and versatile spectrum of nanoparticles exists. Organic nanoparticles include liposomes, polymeric nanoparticles, dendrimers, and micelles. On the other hand, examples of inorganic nanoparticles are metallic nanoparticles, magnetic nanoparticles, silica nanoparticles, carbon-based nanoparticles, and quantum dots. The type of nanoparticle to use depends on its application in medicine.

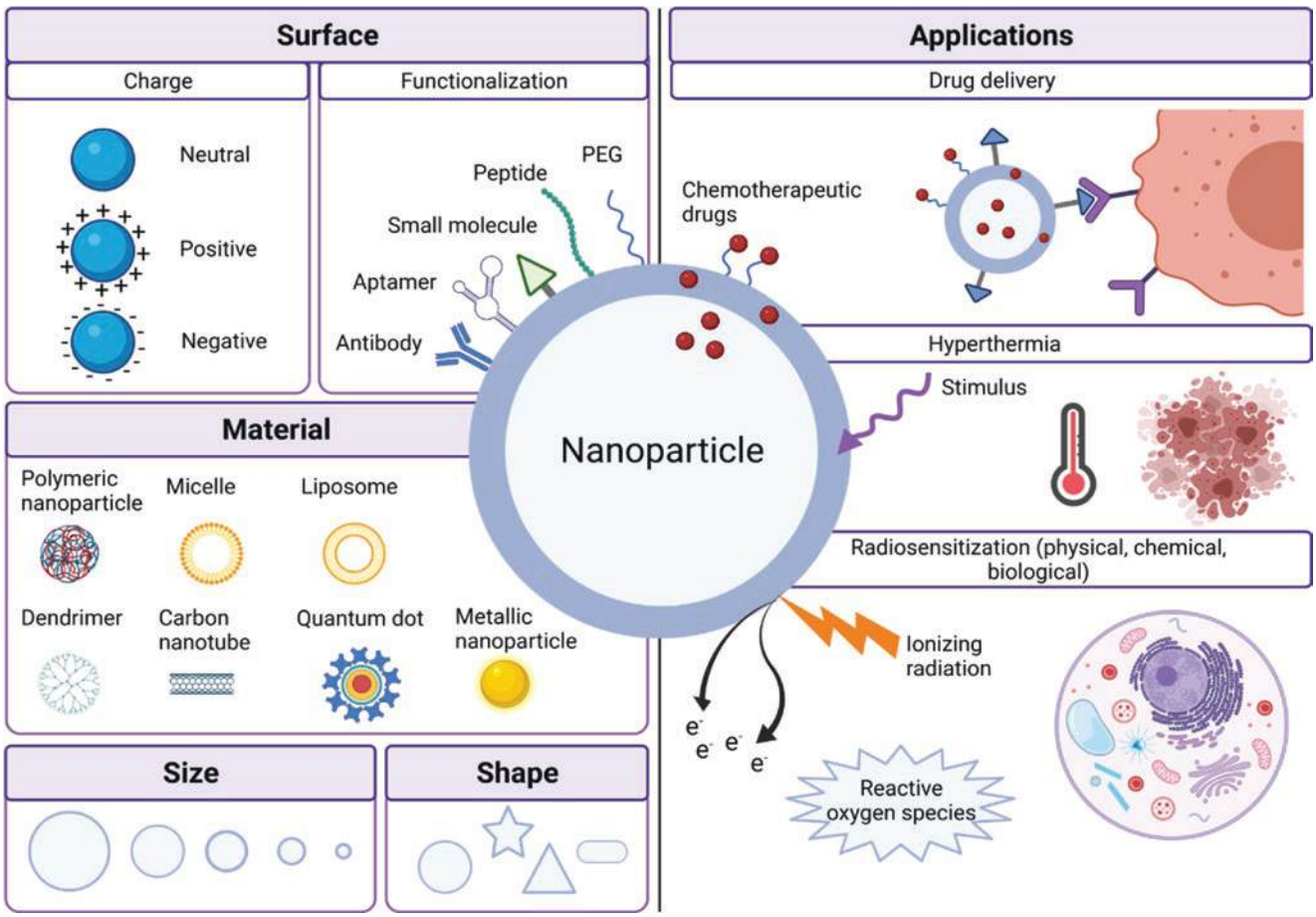

Fig. 6.33 The versatility of nanoparticles and their potential applications in cancer therapy

A major challenge in nanomedicine is the immediate and inevitable "masking" of nanoparticles by proteins, lipids, carbohydrates, and nucleic acids once the nanoparticles are introduced into the blood circulation, forming a "biocorona." Subsequently, the adsorbed surface proteins are recognized by the abundant phagocytic cells in the liver and the spleen, causing the rapid trapping and removal of nanoparticles from the bloodstream. A limited blood circulation time prevents nanoparticles from reaching the tumor cells. In order to improve the biocompatibility, solubility, and stability of the nanoparticles in physiological media, the surface of nanoparticles is usually coated with polymers, generating an electrostatic repulsion and/or a physical barrier between the nanoparticles. Depending on the applied coating, the net surface charge of the nanoparticle can be positive, negative, or neutral, which strongly influences the biological fate and effects of the nanoparticles. One of the most commonly used polymers for nanoparticle coating is polyethylene glycol (PEG), which reduces the biocorona formation by neutralizing the nanoparticle surface charge and giving the nanoparticle a "stealth" character. This delays their recognition and subsequent sequestration of the nanoparticles by the reticuloendothelial system (RES), prolonging the blood circulation time.

An important physical property of nanoparticles is the large surface area-to-volume ratio. When the size of the nanoparticles decreases, a larger proportion of their atoms or molecules are displayed on the particle's surface, rather than in the particle's core, increasing the surface area-to-volume ratio. This ratio decreases with the size of nanoparticles modifying their physical and chemical properties compared to bulk materials. Furthermore, the large surface area-to-volume ratio facilitates the functionalization of the nanoparticle surface with multiple moieties, supporting their multifunctional applications in cancer diagnosis and therapy, which is discussed in more detail below.

6.10.2 Tumor Accumulation and Tumor Targeting

In order to use nanoparticles in cancer remediation applications, nanoparticles need to reach and accumulate in the tumor tissue. Rapidly growing tumors stimulate the formation of new blood vessels to supply the tumor cells with a sufficient amount of oxygen and nutrients. The newly formed tumor vasculature is usually characterized by the presence of abnormal, leaky, and immature blood vessels, which are poorly aligned with a defective endothelium. Consequently, nano-sized particles can efficiently pass through inter-endothelial gaps and accumulate in the tumor. Furthermore, the decreased level of lymphatic drainage promotes the nanoparticle tumor retention. This "passive" process is known as the enhanced permeability and retention (EPR) effect. Importantly, the efficacy of the EPR effect is limited due to the heterogeneity of the vascular structure within the tumor, at different tumor stages and between different tumor types. Furthermore, despite the success of the EPR effect in preclinical tumor models, the efficacy and clinical translation of cancer nanomedicine remain poor, indicating that the EPR effect is less reliable in human tumors. In fact, research demonstrated that extravasation of nanoparticles into the tumor via active trans-endothelial transport pathways occurs more frequently than passive diffusion and thus should not be underestimated [211].

A strategy to complement the EPR effect and to improve the tumor accumulation efficiency of nanoparticles is the functionalization of the nanoparticle surface with cancer-targeting ligands. Cancer-targeting ligands are often specific for factors that are unique or upregulated in cancer cells and that are mostly involved in processes such as tumor progression, invasion, metastasis, and angiogenesis. In general, these targeting ligands can be categorized in five main classes: small molecules, peptides, protein domains, antibodies, and nucleic-acid based aptamers. Examples of cancer-specific targeting ligands are folic acid (FA) (essential for DNA synthesis), cyclic arginine-glycine-aspartic acid (cRGD) peptide (a cell adhesion motif with a high affinity for αβ-integrins), and targeting ligands that can bind to membrane receptors, such as EGFR or VEGFR. Thanks to the large surface area-to-volume ratio of nanoparticles, multiple targeting molecules can be conjugated to the nanoparticles, which enables multivalent interaction with membrane receptors, increasing the tumor uptake and the intratumoral retention time.

6.10.3 Application in Cancer Therapy

Nanoparticles can be used as promising tools to enhance the efficiency of multiple anticancer therapies, including the delivery of chemotherapeutic drugs, hyperthermal therapy, and RT.

6.10.3.1 Drug Delivery

The conventional chemotherapeutic treatment strategies have certain drawbacks linked to the systemic administration and nonspecific distribution of the drugs through the body. This can, for instance, result in limited accessibility of the drug to the tumor, requiring high therapeutic doses and causing off-target toxicity due to damage to healthy cells. Besides, cancers can develop resistance to chemotherapeutic drugs, which is an important factor in treatment failure. Nanoparticles have the potential to improve these aspects by acting as drug delivery systems (DDS). In fact, nanoparticles can efficiently hold a massive payload of the drug, improving the solubility and stability of the drug in the blood circulation. In addition, they enable targeted delivery of the drug

to the tumor sites and promote transport across membranes. Altogether, nanoparticle-based drug delivery has the potential to enhance the efficacy of the chemotherapeutic treatment, while minimizing the side effects. Furthermore, in order to counteract multidrug resistance, nanoparticles can be used to deliver multiple therapeutic agents, including chemo-sensitizers, small interfering RNA, microRNA, enhancing antitumor effects.

Therapeutic agents can typically be loaded on nanoparticles through physical packaging, covalent binding, or electrostatic complexation. Lipid-based nanoparticles, such as liposomes, consisting out of a double lipid layer are the most popular structures in nanoparticle-based drug delivery thanks to their excellent biocompatibility and biodegradability. Furthermore, they can transport both hydrophilic and hydrophobic drugs, encapsulated in the aqueous core and the bilayer membrane, respectively. Other organic nanoplatforms used for drug delivery include polymers, micelles, and dendrimers. On the other hand, inorganic nanoparticles such as carbon-based nanotubes, gold nanoparticles, silica nanoparticles, and iron oxide nanoparticles are also used as drug delivery systems because of their advanced multi-functionality, excellent stability, high drug payload, and unique surface properties.

To improve the precision of drug delivery, it is possible to engineer a cancer-targeted, stimulus-sensitive DDS, which releases the drug at the tumor site in a controlled and sustained manner upon encountering an endogenous or exogenous trigger, without affecting the regions near the tumor site. The tumor microenvironment features conditions that substantially differ from those in normal tissues, such as an acidic pH, high enzyme levels of matrix metalloproteinases (MMPs) and proteases, hypoxia, metabolic shift to anaerobic glycolysis, and a high redox activity. These endogenous stimuli can induce nanoparticle degradation and subsequent drug release. The development of nanocarriers sensitive for exogenous stimuli such as near infrared light, heat or sound waves enables an "on-demand" drug delivery that is tightly controlled from outside the body [212].

6.10.3.2 Nanoparticle-Mediated Hyperthermal Therapy

As mentioned in a previous section, hyperthermia can help in tumor control thanks to its tumor vasculature effect. Briefly, hyperthermia triggers vasodilation. In healthy vasculature, it helps to efficiently dissipate the heat and avoid tissue damage. However, in the aberrant organization and structure of tumor vasculature, it initially increases the blood flow and oxygen supply to the tumor tissue until the heat accumulated in the tissue reaches 42 °C triggering the collapse of tumor blood vessels that promotes cancer cell death. Therefore, it is important to localize hyperthermia to the tumor tissue while avoiding prolonged exposure of healthy cells to elevated temperatures.

Interestingly, the increase in tumor blood flow induced by hyperthermia can be used to sensitize cancer cells and to enhance the delivery of drugs improving the efficacy of chemotherapy and RT, respectively. Nanoparticles have unique properties, which enables them to efficiently convert incident energy into heat. For instance, alternating magnetic fields activate magnetic nanoparticles, such as iron oxide nanoparticles, stimulating heat production. On the other hand, plasmonic nanoparticles, such as gold nanoparticles, typically hold a unique optical characteristic called the surface plasmon resonance (SPR). This phenomenon implies the interaction of light of a specific wavelength with the free electrons on the surface of the nanoparticle, resulting in the absorbance and scattering of light, and the generation of heat [213]. Finally, carbon nanotubes absorb electromagnetic radiation over an extremely broad frequency spectrum, ranging from near infrared light to radiofrequency waves. The absorbance of electromagnetic energy induces electron excitation and relaxation within the nanoparticle, causing heat production. The ability to target and accumulate nanoparticles in the tumor tissue allows the nanoparticle-mediated heat generation to be localized at the tumor site.

6.10.3.3 Radiosensitization

In 2004, it was demonstrated that gold nano-objects injected in tumors can enhance the effect of radiation by improving tumor control in mice treated with kilovoltage X-rays. Since this pioneering work, extensive experimental validations were performed evidencing the potential of a large series of metal-based nanoparticles as radiosensitizer at preclinical level. However, the mechanism(s) of action, a complex mixture between physical, chemical, and biological contributions is still under debate [214]. Physical contribution resides in their ability to increase the dose deposited (radioenhancement effect) via the emission of secondary Auger and photoelectrons following the interaction with IR. The capacity of nanoparticles to increase radiolysis processes leading to a higher oxidative stress in cellular systems constitutes a chemical contribution to the mechanism of action. Finally, the biological effect is based on cell detoxification and DNA repair system impairment, enabling to potentiate the effect of irradiation (radiosensitization effect) [215, 216].

6.10.4 Theranostics and Combination Therapy (Clinical Potential)

Researchers designed complex and multimodal nanoplatforms enabling the simultaneous use of nano-objects for diagnostic and therapeutic applications. These nano-objects are called "theranostics" agents. They enable a non-invasive and real-time tracking of the in vivo nanomaterial distribution and facilitate the dose and toxicity management, as dis-

cussed previously, fine-tuning the patient-specific treatment protocol [217]. Superparamagnetic iron oxide nanoparticles (SPIONs) is one interesting example of theranostic agent. While it has been used for years as contrast agents in MRI, enabling to increase the quality of images used for diagnostics (with higher spatial resolution), these nanoparticles have recently shown radiosensitizing properties. The presence of these nano-objects within the tumor allows to better define the area to treat and to increase the efficiency of the treatment. These SPIONs can also be coupled to chemotherapeutic drugs, such as doxorubicin, further increasing their therapeutic impact.

6.10.5 Challenges

Currently, only a relatively small amount of nano-objects are FDA approved for cancer treatment, since the translation toward clinics is an expensive and time-consuming process that is associated with two main challenges [218]:

- Large-Scale Manufacture

  To enable large clinical trials, drugs have to be produced on a large scale. The Good Manufacturing Practices (GMP) of nanoparticle technology is characterized by a high complexity compared to conventional formulation technologies that usually contain free drug dispersed in a given medium. Indeed, the efficacy of nano-objects is determined by optimal parameters that should be preserved during the scaling-up process. Therefore, nanoparticles have to be manufactured with proper quality standards and with a strict batch-to-batch reproducibility to ensure product specification. Finally, they have to be stable during long-duration storage ensuring the product quality at the time of clinical administration.
- Extensive Toxicity Studies

  Before a drug candidate can be tested in humans, its safety profile must be proven in animal models. These preliminary tests allow a thorough understanding of its pharmacokinetics and toxicity as well as the establishment of safe limits for further clinical trials.

  Preclinical in vivo studies have demonstrated nano-object accumulation in liver and spleen for several months post intravenous injection, raising the question of long-term toxicity for which time-consuming approaches are needed. These toxicological studies are governed by specific rules and regulations of Good Laboratory Practice (GLP), a quality system ensuring the uniformity, consistency, reproducibility, and reliability of non-clinical safety tests. Nevertheless, the current regulatory approaches used for the toxicological assessment of conventional drugs may not be appropriate to fully assess the toxicity of nanomaterials requiring the development of new specific approaches.

6.11 Second and Secondary Cancers in Radiotherapy Patients

Although often used interchangeably, there is a fundamental difference between second and secondary cancers. Second cancer is a more general name for any tumor occurring in patients who have been treated earlier for a first cancer, while the development of a secondary cancer can be ascribed to the treatment for the first cancer. This is not uncommon and should be discussed as part of the process of taking informed consent when explaining the treatment with chemotherapy or RT.

The risk of developing a secondary malignancy following RT depends on:

- The organs irradiated
- The age at treatment, with younger patients having an increased risk compared to a teenager or adult
- The total dose of radiation received
- The time from treatment
- The prior use of alkylating agent chemotherapy
- Underlying genetic predisposition

The risk of developing a secondary tumor is cumulative and increasing over time. However, as age increases, the risk relative to the normal population decreases as cancer becomes more common in the general population as well.

Well-known examples are breast cancer, meningiomas, thyroid cancer, and sarcomas. There is an increased risk of development of breast cancer in girls treated for Hodgkin lymphoma under 16 years of age, with a 20% cumulative incidence of breast cancer by the age of 45 [219]. Girls treated with whole lung RT for Wilms tumor are also at risk of breast cancer. There is a well-documented increased incidence of meningiomas associated with cranial RT, with young age at time of RT and time from treatment associated with higher risk. An excess of thyroid cancer and bone and soft tissue sarcoma are also seen in relation to previous RT [220].

There have been concerns about the "low-dose bath" effect of modern RT techniques such as intensity modulated radiotherapy or arc therapy (IMRT/IMAT) increasing the risk of secondary cancers, compared with simple conformal RT. However, IMRT results in greater conformality and reduces the non-target high dose volume. This may offset the increased volume of normal tissue receiving low-dose irra-

diation. As of today, the feared increase in secondary cancers has not been proven. A major advantage of proton beam RT is the expected reduced risk of secondary malignancy.

Molecular RT may lead to an increased risk of secondary leukemias and cancers, both from the general effects of irradiation of the whole body, and from organ-specific dose, e.g., thyroid uptake of free radioiodine in meta-iodobenzylguanidine (mIBG) therapy, despite the use of thyroid blockade.

RT is not alone in causing cancer. Chemotherapy, particularly alkylating agents, may predispose to the development of myelodysplasia, secondary leukemias, and other malignancies. Chemotherapy and RT may be synergistic in this regard.

Predisposing genetic factors such as retinoblastoma, Li–Fraumeni syndrome, or neurofibromatosis type 1 (NF1) also increase the risk of induction of secondary, but also second, malignancies.

The risk is also related to the underlying cancer, with an increase seen after treatment for Hodgkin lymphoma and sarcoma.

Finally, lifestyle factors contribute to the risk, hence the importance of emphasizing healthy living choices, for example, smoking cessation, normal body weight, and good intake of fruit and vegetables, in survivors to try to mitigate this where possible.

6.12 Exercises and Self-Assessment

Q1. Which statement is true? The Continuous Hyperfractionated Accelerated RadioTherapy (CHART) irradiation protocol is characterized by:
- (a) A fraction size <2 Gy.
- (b) Reduced overall treatment time compared with conventional fractionation.
- (c) Irradiation is continued during the weekend.
- (d) a, b, and c are all correct.

Q2. Why is hyperfractionation potentially beneficial when it comes to late normal tissue sparing relative to conventional fractionation?
- (a) The α/β ratio is high.
- (b) The repair of sublethal damage is very effective.
- (c) The fraction size <2 Gy.
- (d) The number of fractions is larger.

Q3. On the basis of radiobiological aspects, what would be the optimal number of fractions in a hypofractionated treatment regimen?

Q4. Which of the following *is not true* about Stereotactic Body Radiation Therapy (SBRT)
- (a) In SBRT a high dose per fraction is used.
- (b) SBRT has high conformality.
- (c) SBRT has a large margin for the beam penumbra.
- (d) In SBRT image guidance is required for geometric verification of targets.

Q5. Please indicate which of the following statements *is wrong* when it comes to the SBRT treatment planning.
- (a) The dose is prescribed to lower isodose lines.
- (b) A homogeneous dose distribution is seen.
- (c) There is a sharp dose falloff outside target volume.
- (d) An isotropic grid size of 2 mm or finer is recommended for dose calculation.

Q6. Below are some statements related to how targeted therapy may sensitize tumors to radiation therapy (RT). Please indicate which statements are correct or wrong:
- (a) Inhibition of the DNA repair enzyme PARP1 with small molecules is a possible RT sensitizer for all types of tumors.
- (b) To increase the function of Bcl-2 is a RT sensitizing strategy.
- (c) Inhibitors toward EGFR is a promising RT sensibilization option for some tumors.
- (d) Reverting hypoxia is a way for RT sensitization.

Q7. Please name a key reason why RT can be combined with some immune therapies?

Q8. Hyperthermia has been shown to increase the effect of radiation therapy. Describe a DNA repair pathway that hyperthermia can inhibit.

Q9. Name an advantage and a disadvantage of photon spatially fractionated radiation therapy (SFRT), proton minibeam radiotherapy (pMBRT) and ion MBRT?

Q10. Give an example of a vectorized radiopharmaceutical used in the clinic and outline how it works.

Q11. Helium ions are good candidates in RT of tumors. What makes them good candidates?
- (a) Helium ions produce more secondary neutrons compared to protons.
- (b) Helium ions produce more nuclear fragments compared to carbon ions.
- (c) Helium ions have higher radiobiological effect (RBE) compared to protons.
- (d) Helium ions have lower oxygen enhancement ratio (OER) compared to protons.

6.13 Exercise Solutions

SQ1. Alternative (d). All statements (a, b, c) about the CHART irradiation protocol are correct. It involves a fraction size of <2 Gy and treatments are given dur-

ing weekends giving a reduced treatment time compared to a conventional fractionation scheme.

SQ2. Alternative (c). The fraction size <2 Gy.

SQ3. Taking the normal tissue dose-volume constraints into account and considering, e.g., the kinetics of reoxygenation, the activation of the immune system and the abscopal effect, a number of six to eight medium sized fractions spaced 72 h might be optimal regarding tumor control. However, this is still a point of debate.

SQ4. Alternative (c). In SBRT, small or no margin is given for beam penumbra to improve sharp dose falloff.

SQ5. Alternative (b). SBRT treatment plans have a heterogenous dose distribution.

SQ6. (a). The statement is wrong. PARP1 is primarily a target in tumors that have mutations in *BRCA1*/*BRAC2* or have a "BRACAness" phenotype. Such tumors lack functional DNA repair via HR and hence blocking PARP can impair repair of RT-induced DNA DSB. This is called synthetic lethality. PARP inhibition can also be applied for tumors with impairment in ATM or ATR. (b). The statement is wrong. Bcl-2 is an anti-apoptotic protein. Its activity/expression needs to be inhibited in order for RT to more prominently trigger cell death. (c). The statement is correct. EGFR inhibitors work in *EGFR*-mutant tumors, i.e., NSCLC or in tumors over-expressing EGFR. (d). The statement is correct. Tumor hypoxia can be attacked for RT sensitization purpose in several different ways.

SQ7. Since radiotherapy (RT) does exert both, immune stimulatory and immune suppressive effects, immune therapies aim to switch off the immune suppressive effects of RT or to boost the immune activating ones can be applied. This may result in effective local and systemic antitumor immune responses.

SQ8. Hyperthermia can temporarily downregulate the BRCA2 protein, thereby blocking the homologous recombination.

SQ9.

	Photon SFRT	Proton MBRT	Ion MBRT
Advantage	Easy implementation in clinic	Homogeneous tumor irradiation already from one direction	(Almost) no widening on the way to the tumor
Disadvantage	Low PVDR compared to MBRT	Widening of the beams on the way to the tumor	Technically challenging as interlacing necessary for homogeneous tumor irradiation

SQ10. Examples of vectorized radionuclide therapy are ^{177}Lu-PSMA-617 for the treatment of prostate cancer, ^{177}Lu-NeoB for the treatment of solid metastatic tumors, ^{177}Lu-DOTATATE for the treatment of neuroendocrine tumors, and ^{90}Y-ibritumomab tiuxetan (Zevalin®) for the treatment of CD20-positive Non-Hodgkin lymphoma. Brief description of the principle: A radiopharmaceutical comprises a targeting moiety, which targets a specific molecule expressed on certain cells, and a radionuclide, which emits IR. By linking the targeting moiety to the radionuclide, molecules (e.g., somatostatin receptors, PSMA, CD20, etc.) that are highly expressed on the target tissue can be targeted to treat disease. Thus, the targeting moiety ensures specific delivery of toxic IR to the targeted cells which ensures treatment of the tumor disease, while causing minimal damage to surrounding healthy tissues.

SQ11. Alternative (c). Helium ions have higher RBE compared to protons.

Appendix: Therapeutic BNCT Clinical Trials in the Last Two Decades

Cancer subsite	First author and year	Number of cases	^{10}B-carrier agent	Results/comments
Glioblastoma (newly diagnosed/recurrent)	Joensuu et al. (2003) [221]	18	BPA	Protocol P-01: 1-year overall survival was 61% in newly diagnosed glioblastoma.
		3	BPA	Protocol P-03: No death reported in re-irradiated patients.
	Capala et al. (2003) [222]	17	BPA	Short follow-up, no severe acute toxicities.
	Busse et al. (2003) [223]	22	BPA-Fructose (BPA-F)	2/22 patients had complete radiographic response while 13/17 evaluable subjects had measurable reduction in tumor volume.
	Henriksson et al. (2008) [224]	30	BPA-F	Median time to progression was 5.8 months and median survival time was 14.2 months. 4/30 patients had grade 3–4 toxicities.
	Kawabata et al. (2011) [225]	21	BSH and BPA	Protocol 1—BNCT. Protocol 2—BNCT followed by external beam RT. Median survival time was 15.6 months overall and 23.5 months in protocol 2.
Gliomas (high grade, malignant/recurrent)	Yamamoto et al. (2004) [226]	9	BSH	Interim analysis—median survival time was 23 months for glioblastoma and 25.9 months for anaplastic astrocytoma.
	Miyatake et al. (2005) [227]	13	BPA	In 8/12 patients, >50% of contrast enhanced lesions disappeared.
	Miyatake et al. (2009) [228]	22	BPA	Median survival for all patients was 10.8 months and high-risk RPA classes was 9.1 months.
	Kankaanranta et al. (2011) [229]	22	BPA-F	Median survival time was 7 months in malignant gliomas that recur after surgery and conventional radiotherapy.
Meningioma (high grade, malignant/recurrent)	Miyatake et al. (2007) [230]	7	BPA	18F-BPA-PET was taken before BNCT. 2/3 anaplastic meningioma patients showed complete response. 6/7 patients available for follow-up had radiographic improvements.
	Kawabata et al. (2013) [231]	20	BPA	Median survival time after BNCT was 14.1 months and after diagnosis was 45.7 months.
Malignant melanoma	Fukuda et al. (2003) [232]	22	BPA	Complete response was seen in 73% (16/22) and 3/22 patients developed severe skin damage.
	Menéndez et al. (2009) [233]	7	BPA	69.3% overall response, 30.7% no change, and 30% grade 3 skin toxicities.
	Hiratsuka et al. (2020) [233]	8	BPA	6/8 patients had complete response. On long-term follow-up, 88% control rate (7/8) and no >grade 2 adverse events.
Liver metastasis	Koivunoro et al. (2004) [233]	2	BPA	Liver extirpated, irradiated in a nuclear reactor, and reimplanted. One patient survived for 3 years after the procedure.
Head and neck cancers (recurrent/locally advanced)	Kato et al. (2004) [236]	6	BPA and BSH	46–100% reduction in tumor size with improved quality of life and very mild side effects.
	Kankaanranta et al. (2007) [237]	16	BPA-F	Median duration of response was 12.1 months. At median follow-up of 14 months, 33% (4/12) were alive. 2/12 had grade 3 toxicity.
	Kato et al. (2009) [238]	26	BPA	Response rate was 85%. Six-year overall rate was 24%.
	Kankaanranta et al. (2012) [238]	30	BPA	Two fractions of RT at 30-day interval. Tolerable early toxicities.
	Suzuki et al. (2014) [240]	62	BSH and BPA or BPA alone	Median survival time was 10.1 months. The overall survival rate was 43.1% and 24.2% at 1-year and 2-year, respectively.
	Aihara et al. (2014) [241]	20	BPA	Complete remission seen in 11 patients and partial remission in 7 patients. No severe acute or chronic toxicity.
	Wang et al. (2016) [242]	17	BPA	Two-year overall survival was 47% and locoregional control was 28%.
	Koivunoro et al. (2019) [243]	79	BPA	Two-year overall survival was 21% and locoregional progression-free survival was 38%.
	Hirose et al. (2021) [244]	21	Borofalan	Two-year overall survival was 58% in recurrent cases and 100% in locally advanced cases.

References

1. Brown A, Suit H. The centenary of the discovery of the Bragg peak. Radiother Oncol. 2004;73(3):265–8.
2. Marcu LG. Altered fractionation in radiotherapy: from radiobiological rationale to therapeutic gain. Cancer Treat Rev. 2010;36(8):606–14.
3. Shrieve DC, Loeffler JS. Human radiation injury. Wolters Kluwer Health/Lippincott Williams & Wilkins; 2011.
4. Bentzen SM, Atasoy BM, Daley FM, Dische S, Richman PI, Saunders MI, et al. Epidermal growth factor receptor expression in pretreatment biopsies from head and neck squamous cell carcinoma as a predictive factor for a benefit from accelerated radiation therapy in a randomized controlled trial. J Clin Oncol. 2005;23(24):5560–7.
5. Grimm J, Marks LB, Jackson A, Kavanagh BD, Xue J, Yorke E. High dose per fraction, hypofractionated treatment effects in the clinic (HyTEC): an overview. Int J Radiat Oncol Biol Phys. 2021;110(1):1–10.
6. Brown JM, Brenner DJ, Carlson DJ. Dose escalation, not "new biology," can account for the efficacy of stereotactic body radiation therapy with non-small cell lung cancer. Int J Radiat Oncol Biol Phys. 2013;85(5):1159–60.
7. Shibamoto Y, Miyakawa A, Otsuka S, Iwata H. Radiobiology of hypofractionated stereotactic radiotherapy: what are the optimal fractionation schedules? J Radiat Res. 2016;57(Suppl 1):i76–82.
8. Park HJ, Griffin RJ, Hui S, Levitt SH, Song CW. Radiation-induced vascular damage in tumors: implications of vascular damage in ablative hypofractionated radiotherapy (SBRT and SRS). Radiat Res. 2012;177(3):311–27.
9. Shuryak I, Hall EJ, Brenner DJ. Dose dependence of accelerated repopulation in head and neck cancer: supporting evidence and clinical implications. Radiother Oncol. 2018;127(1):20–6.
10. Shuryak I, Hall EJ, Brenner DJ. Optimized hypofractionation can markedly improve tumor control and decrease late effects for head and neck cancer. Int J Radiat Oncol Biol Phys. 2019;104(2):272–8.
11. Boustani J, Grapin M, Laurent PA, Apetoh L, Mirjolet C. The 6th R of radiobiology: reactivation of anti-tumor immune response. Cancers (Basel). 2019;11(6):860.
12. Formenti SC. Optimizing dose per fraction: a new chapter in the story of the abscopal effect? Int J Radiat Oncol Biol Phys. 2017;99(3):677–9.
13. Daguenet E, Khalifa J, Tolédano A, Borchiellini D, Pointreau Y, Rodriguez-Lafrasse C, et al. To exploit the 5 'R' of radiobiology and unleash the 3 'E' of immunoediting: 'RE'-inventing the radiotherapy-immunotherapy combination. Ther Adv Med Oncol. 2020;12:1758835920913445.
14. Franken NA, Oei AL, Kok HP, Rodermond HM, Sminia P, Crezee J, et al. Cell survival and radiosensitisation: modulation of the linear and quadratic parameters of the LQ model (Review). Int J Oncol. 2013;42(5):1501–15.
15. Schneider U, Besserer J, Mack A. Hypofractionated radiotherapy has the potential for second cancer reduction. Theor Biol Med Model. 2010;7:4.
16. Potters L, Kavanagh B, Galvin JM, et al. American society for therapeutic radiology and oncology (ASTRO) and American college of radiology (ACR) practice guideline for the performance of stereotactic body radiation therapy. Int J Radiat Oncol Biol Phys. 2010;76(2):326–32.
17. Khan FM, Gibbons JP. Stereotactic body radiation therapy. In: Khan FM, Gibbons JP, editors. Khan's the physics of radiation therapy. (5th edition) ed. Philadelphia, PA: Lippincott Williams & Wilkins; 2014. p. 467–74.
18. Fowler JF, Welsh JS, Howard SP. Loss of biological effect in prolonged fraction delivery. Int J Radiat Oncol Biol Phys. 2004;59(1):242–9.
19. Tilki D, Kilic N, Sevinc S, et al. Zone-specific remodeling of tumor blood vessels affects tumor growth. Cancer. 2007;110:2347–62.
20. Kavanagh BD, Bradley JD, Timmerman RD. Stereotactic irradiation of tumors outside the central nervous system. In: Halperin EC, Wazer DE, Perez CA, Brady LW, editors. Principle and practice of radiation oncology. (7th edition) ed. Philadelphia, PA: Wolters Kluwer; 2019. 426–34.
21. Park C, Papiez L, Zhang S, et al. Universal survival curve and single fraction equivalent dose: useful tools in understanding potency of ablative radiotherapy. Int J Radiat Oncol Biol Phys. 2008;70:847–52.
22. Benedict SH, Yenice KM, Followill D, et al. Stereotactic body radiation therapy: the report of AAPM Task Group 101. Med Phys. 2010;37:4078–101.
23. Simpson DR, Mell LK, Mundt AJ, et al. Image-guided radiation therapy. In: Halperin EC, Wazer DE, Perez CA, Brady LW, editors. Principle and practice of radiation oncology. (7th edition) ed. Philadelphia, PA: Wolters Kluwer; 2019. 288–302.
24. Wu QJ, Wang Z, Kirkpatrick JP, et al. Impact of collimator leaf width and treatment technique on stereotactic radiosurgery and radiotherapy plans for intra- and extracranial lesions. Radiat. Oncol. 2009;4
25. Martel MK, Ten Haken RK, Hazuka MB, et al. Estimation of tumor control probability model parameters from 3-D dose distributions of non-small cell lung cancer patients. Lung Cancer. 1999;24:31–7.
26. Niemierko A. Reporting and analyzing dose distributions: a concept of equivalent uniform dose. Med. Phys. 1997;24:103–10.
27. Matuszak MM, Yan D, Grills I, et al. Clinical applications of volumetric modulated arc therapy. Int J Radiat Oncol Biol Phys. 2010;77(2):608–16.
28. Zwahlen DR, Lang S, Hrbacek J, et al. The use of photon beams of a flattening filter-free linear accelerator for hypofractionated volumetric modulated arc therapy in localized prostate cancer. Int J Radiat Oncol Biol Phys. 2012;83(5):1655–60.
29. Kry SF, Vassiliev ON, Mohan R. Out-of-field photon dose following removal of the flattening filter from a medical accelerator. Phys. Med. Biol. 2010;55:2155–66.
30. R.A. Sethi, I.J. Barani, D.A. Larson, M. Roach III (Eds.). Handbook of evidence-based stereotactic radiosurgery and stereotactic body radiotherapy. Switzerland: Springer. 2016.
31. Timmerman RD, Bizekis CS, Pass HI, Fong Y, Dupuy DE, Dawson LA, et al. Local surgical, ablative, and radiation treatment of metastases. CA Cancer J Clin. 2009;59(3):145–70.
32. Favaudon V, Labarbe R, Limoli CL. Model studies of the role of oxygen in the FLASH effect. Med Phys. 2022;49(3):2068–81.
33. Bourhis J, Sozzi WJ, Jorge PG, Gaide O, Bailat C, Duclos F, et al. Treatment of a first patient with FLASH-radiotherapy. Radiother Oncol. 2019;139:18–22.
34. Jansen J, Knoll J, Beyreuther E, Pawelke J, Skuza R, Hanley R, et al. Does FLASH deplete oxygen? Experimental evaluation for photons, protons, and carbon ions. Med Phys. 2021;48(7):3982–90.
35. Montay-Gruel P, Bouchet A, Jaccard M, Patin D, Serduc R, Aim W, et al. X-rays can trigger the FLASH effect: Ultra-high dose-rate synchrotron light source prevents normal brain injury after whole brain irradiation in mice. Radiother Oncol. 2018;129(3):582–8.
36. Formenti SC, Demaria S. Systemic effects of local radiotherapy. Lancet Oncol. 2009;10(7):718–26.
37. Nakamura N, Kusunoki Y, Akiyama M. Radiosensitivity of CD4 or CD8 positive human T-lymphocytes by an in vitro colony formation assay. Radiat Res. 1990;123(2):224–7.
38. Chadwick J, Goldhaber M. Disintegration by slow neutrons. Nature. 1935;135:65.
39. Coleman CN, Prasanna PG, Capala J, et al. SMART radiotherapy. In: Halperin EC, Wazer DE, Perez CA, Brady LW, editors. Principle and practice of radiation oncology. (7th edition) ed. Philadelphia, PA: Wolters Kluwer; 2019. p. 146.

40. Halperin EC. The discipline of radiation oncology. In: Halperin EC, Wazer DE, Perez CA, Brady LW, editors. Principle and practice of radiation oncology. (7th edition) ed. Philadelphia, PA: Wolters Kluwer; 2019. p. 36–8.
41. Hall EJ, Giaccia AJ. Alternative radiation modalities. In: Hall EJ, Giaccia AJ, editors. Radiobiology for the radiologist. (8th edition) ed. Philadelphia, PA: Wolters Kluwer; 2019. p. 805–7.
42. Laramore GE. Neutron therapy and boron neutron capture therapy. In: Halperin EC, Wazer DE, Perez CA, Brady LW, editors. Principle and practice of radiation oncology. 7th ed. Philadelphia, PA: Wolters Kluwer; 2019. p. 487–8.
43. Ishiwata K, Ido T, Honda C, Kawamura M, Ichihashi M, Mishima Y. 4-Borono-2-[18F]fluoro-D,L-phenylalanine: a possible tracer for melanoma diagnosis with PET. Int J Rad Appl Instrum B. 1992;19(3):311–8.
44. Yanch JC, Shefer RE, Busse PM. Boron neutron capture therapy. Sci Med. 1999;6:18–27.
45. Coderre JA, Morris GM. The radiation biology of boron neutron capture therapy. Radiat Res. 1999;151:1–18.
46. Chin MP, Spyrou NM. A detailed Monte Carlo accounting of radiation transport in the brain during BNCT. Appl Radiat Isot. 2009;67(7-8 Suppl):S164–7.
47. Godwin JT, Farr LE, Sweet WH, et al. Pathological study of eight patients with glioblastoma multiforme treated by neutron capture therapy using boron 10. Cancer. 1956;8:601.
48. Hatanaka H, Amano K, Kanemitsu H, et al. Boron uptake by human brain tumors and quality control of boron compounds. In: Hatanaka H, editor. Boron-neutron capture therapy for tumors. Niigata, Japan: Nishimura; 1986. p. 77–106.
49. Laramore GE, Spence AM. Boron neutron capture therapy (BNCT) for highgrade gliomas of the brain. A cautionary note. Int J Radiat Oncol Biol Phys. 1996;36:241.
50. Rockhill JK, Laramore GE. Neutron radiotherapy. In L.L.Gunderson, J.E.Tepper (Eds.). Clinical radiation oncology (4th edition). Elsevier. 2019. p. 376–79.
51. Capala J, Barth RF, Bendayan M, et al. Boronated epidermal growth factor as a potential targeting agent for boron neutron capture therapy of brain tumors. Bioconjug Chem. 1996;7(1):7–15.
52. Carlsson J, Kullberg EB, Capala J, et al. Ligand liposomes and boron neutron capture therapy. J Neurooncol. 2003;62(1–2):47–59.
53. Murshed H, editor. Fundamentals of radiation oncology. Elsevier; 2019.
54. Tepper JE, Foote RL, Michalski JM. Gunderson & Tepper's clinical radiation oncology. 5th ed. Philadelphia: Elsevier; 2020.
55. Sureka CS, Armpilia C, editors. Radiation biology for medical physicists. 1st ed. Boca Raton: CRC Press; 2017.
56. Joiner MC, van der Kogel A. In: Joiner MC, van der Kogel A, editors. Basic clinical radiobiology. 4th ed. London: CRC press; 2009.
57. Hanahan D, Weinberg RA. Hallmarks of cancer: the next generation. Cell. 2011;144(5):646–74.
58. Pilié PG, Tang C, Mills GB, Yap TA. State-of-the-art strategies for targeting the DNA damage response in cancer. Nat Rev Clin Oncol. 2019;16(2):81–104.
59. van Bussel MTJ, Awada A, de Jonge MJA, Mau-Sørensen M, Nielsen D, Schöffski P, et al. A first-in-man phase 1 study of the DNA-dependent protein kinase inhibitor peposertib (formerly M3814) in patients with advanced solid tumours. Br J Cancer. 2021;124(4):728–35.
60. Myers SH, Ortega JA, Cavalli A. Synthetic lethality through the lens of medicinal chemistry. J Med Chem. 2020;63(23): 14151–83.
61. Teknos TN, Grecula J, Agrawal A, Old MO, Ozer E, Carrau R, et al. A phase 1 trial of Vorinostat in combination with concurrent chemoradiation therapy in the treatment of advanced staged head and neck squamous cell carcinoma. Investig New Drugs. 2019;37(4):702–10.
62. Cuneo KC, Morgan MA, Sahai V, Schipper MJ, Parsels LA, Parsels JD, et al. Dose escalation trial of the Wee1 inhibitor adavosertib (AZD1775) in combination with gemcitabine and radiation for patients with locally advanced pancreatic cancer. J Clin Oncol. 2019;37(29):2643–50.
63. Bosacki C, Bouleftour W, Sotton S, Vallard A, Daguenet E, Ouaz H, et al. CDK 4/6 inhibitors combined with radiotherapy: a review of literature. Clin Transl Radiat Oncol. 2021;26:79–85.
64. Zerp SF, Stoter TR, Hoebers FJP, van den Brekel MWM, Dubbelman R, Kuipers GK, et al. Targeting anti-apoptotic Bcl-2 by AT-101 to increase radiation efficacy: data from in vitro and clinical pharmacokinetic studies in head and neck cancer. Radiat Oncol. 2015;10(1):158.
65. Blaes J, Thomé CM, Pfenning PN, Rübmann P, Sahm F, Wick A, et al. Inhibition of CD95/CD95L (FAS/FASLG) signaling with APG101 prevents invasion and enhances radiation therapy for glioblastoma. Mol Cancer Res. 2018;16(5):767–76.
66. Sun XS, Tao Y, Le Tourneau C, Pointreau Y, Sire C, Kaminsky MC, et al. Debio 1143 and high-dose cisplatin chemoradiotherapy in high-risk locoregionally advanced squamous cell carcinoma of the head and neck: a double-blind, multicentre, randomised, phase 2 study. Lancet Oncol. 2020;21(9):1173–87.
67. Tchelebi LT, Batchelder E, Wang M, Lehrer EJ, Drabick JJ, Sharma N, et al. Radiotherapy and receptor tyrosine kinase inhibition for solid cancers (ROCKIT): a meta-analysis of 13 studies. JNCI Cancer Spectr. 2021;5(4):pkab050.
68. Wrona A, Dziadziuszko R, Jassem J. Combining radiotherapy with targeted therapies in non-small cell lung cancer: focus on anti-EGFR, anti-ALK and anti-angiogenic agents. Transl Lung Cancer Res. 2021;10(4):2032–47.
69. Huang CY, Tai WT, Wu SY, Shih CT, Chen MH, Tsai MH, et al. Dovitinib acts as a novel radiosensitizer in hepatocellular carcinoma by targeting SHP-1/STAT3 signaling. Int J Radiat Oncol Biol Phys. 2016;95(2):761–71.
70. Boland PM, Meyer JE, Berger AC, Cohen SJ, Neuman T, Cooper HS, et al. Induction therapy for locally advanced, resectable esophagogastric cancer: a phase I trial of vandetanib (ZD6474), paclitaxel, carboplatin, 5-fluorouracil, and radiotherapy followed by resection. Am J Clin Oncol. 2017;40(4):393–8.
71. Saran F, Chinot OL, Henriksson R, Mason W, Wick W, Cloughesy T, Dhar S, Pozzi E, Garcia J, Nishikawa R. Bevacizumab, temozolomide, and radiotherapy for newly diagnosed glioblastoma: comprehensive safety results during and after first-line therapy. Neuro Oncol. 2016;18(7):991–1001. https://doi.org/10.1093/neuonc/nov300. PMID: 26809751; PMCID: PMC4896538.
72. Saksø M, Jensen K, Andersen M, Hansen CR, Eriksen JG, Overgaard J. DAHANCA 28: a phase I/II feasibility study of hyperfractionated, accelerated radiotherapy with concomitant cisplatin and nimorazole (HART-CN) for patients with locally advanced, HPV/p16-negative squamous cell carcinoma of the oropharynx, hypopharynx, larynx and oral cavity. Radiother Oncol. 2020;148:65–72.
73. Toulany M. Targeting DNA Double-strand break repair pathways to improve radiotherapy response. Genes (Basel). 2019;10(1):25.
74. Lee EF, Fairlie WD. Discovery, development and application of drugs targeting BCL-2 pro-survival proteins in cancer. Biochem Soc Trans. 2021;49(5):2381–95.
75. Rödel F, Reichert S, Sprenger T, Gaipl US, Mirsch J, Liersch T, et al. The role of survivin for radiation oncology: moving beyond apoptosis inhibition. Curr Med Chem. 2011;18(2):191–9.
76. Tuomainen K, Hyytiäinen A, Al-Samadi A, Ianevski P, Ianevski A, Potdar S, et al. High-throughput compound screening identifies navitoclax combined with irradiation as a candidate therapy for HPV-negative head and neck squamous cell carcinoma. Sci Rep. 2021;11(1):14755.
77. Salazar R, Capdevila J, Manzano JL, Pericay C, Martínez-Villacampa M, López C, et al. Phase II randomized trial of

capecitabine with bevacizumab and external beam radiation therapy as preoperative treatment for patients with resectable locally advanced rectal adenocarcinoma: long term results. BMC Cancer. 2020;20(1):1164.
78. Frey B, Rubner Y, Kulzer L, Werthmöller N, Weiss EM, Fietkau R, et al. Antitumor immune responses induced by ionizing irradiation and further immune stimulation. Cancer Immunol Immunother. 2014;63(1):29–36.
79. Falcke SE, Rühle PF, Deloch L, Fietkau R, Frey B, Gaipl US. Clinically relevant radiation exposure differentially impacts forms of cell death in human cells of the innate and adaptive immune system. Int J Mol Sci. 2018;19(11):3574.
80. Rückert M, Flohr AS, Hecht M, Gaipl US. Radiotherapy and the immune system: more than just immune suppression. Stem Cells. 2021b;39(9):1155–65.
81. Weichselbaum RR, Liang H, Deng L, Fu YX. Radiotherapy and immunotherapy: a beneficial liaison? Nat Rev Clin Oncol. 2017;14(6):365–79.
82. Frey B, Rückert M, Deloch L, Rühle PF, Derer A, Fietkau R, et al. Immunomodulation by ionizing radiation-impact for design of radio-immunotherapies and for treatment of inflammatory diseases. Immunol Rev. 2017;280(1):231–48.
83. Rückert M, Deloch L, Frey B, Schlücker E, Fietkau R, Gaipl US. Combinations of radiotherapy with vaccination and immune checkpoint inhibition differently affect primary and abscopal tumor growth and the tumor microenvironment. Cancers (Basel). 2021a;13(4):714.
84. Demaria S, Guha C, Schoenfeld J, Morris Z, Monjazeb A, Sikora A, et al. Radiation dose and fraction in immunotherapy: one-size regimen does not fit all settings, so how does one choose? J Immunother Cancer. 2021;9(4):e002038.
85. Shu CA, Cascone T. What is neo? Chemoimmunotherapy in the neoadjuvant setting for resectable non–small-cell lung cancer. J Clin Oncol. 2021;39(26):2855–8.
86. Chargari C, Toillon RA, Macdermed D, Castadot P, Magné N. Concurrent hormone and radiation therapy in patients with breast cancer: what is the rationale? Lancet Oncol. 2009;10(1):53–60.
87. Azria D, Larbouret C, Cunat S, et al. Letrozole sensitizes breast cancer cells to ionizing radiation. Breast Cancer Res. 2004;7:1–8(R156).
88. Abraham J, Staffurth J. Hormonal therapy for cancer. Medicine. 2016;44(1):30–3.
89. Philippou Y, Sjoberg H, Lamb AD, Camilleri P, Bryant RJ. Harnessing the potential of multimodal radiotherapy in prostate cancer. Nat Rev Urol. 2020;17(6):321–38.
90. Bolla M, Van Tienhoven G, Warde P, Dubois JB, Mirimanoff RO, Storme G, Bernier J, Kuten A, Sternberg C, Billiet I, Torecilla JL, Pfeffer R, Cutajar CL, Van der Kwast T, Collette L. External irradiation with or without long-term androgen suppression for prostate cancer with high metastatic risk: 10-year results of an EORTC randomised study. Lancet Oncol. 2010;11:1066–73. https://doi.org/10.1016/S1470-2045(10)70223-0. Epub 2010 Oct 7
91. Hader M, Frey B, Fietkau R, Hecht M, Gaipl US. Immune biological rationales for the design of combined radio- and immunotherapies. Cancer Immunol Immunother. 2020a;69(2):293–306.
92. Hader M, Savcigil DP, Rosin A, Ponfick P, Gekle S, Wadepohl M, et al. Differences of the immune phenotype of breast cancer cells after ex vivo hyperthermia by warm-water or microwave radiation in a closed-loop system alone or in combination with radiotherapy. Cancers (Basel). 2020b;12(5):1082.
93. Sugarbaker PH. Laboratory and clinical basis for hyperthermia as a component of intracavitary chemotherapy. Int J Hyperth. 2007;23(5):431–42.
94. Issels R, Kampmann E, Kanaar R, Lindner LH. Hallmarks of hyperthermia in driving the future of clinical hyperthermia as targeted therapy: translation into clinical application. Int J Hyperth. 2016;32(1):89–95.
95. Oei AL, Kok HP, Oei SB, Horsman MR, Stalpers LJA, Franken NAP, et al. Molecular and biological rationale of hyperthermia as radio- and chemosensitizer. Adv Drug Deliv Rev. 2020;163–164:84–97.
96. Narayan P, Crocker I, Elder E, Olson JJ. Safety and efficacy of concurrent interstitial radiation and hyperthermia in the treatment of progressive malignant brain tumors. Oncol Rep. 2004;11(1):97–103.
97. Elming PB, Sørensen BS, Oei AL, Franken NAP, Crezee J, Overgaard J, et al. Hyperthermia: the optimal treatment to overcome radiation resistant hypoxia. Cancers (Basel). 2019;11(1):60.
98. Kok HP, Cressman ENK, Ceelen W, Brace CL, Ivkov R, Grüll H, et al. Heating technology for malignant tumors: a review. Int J Hyperth. 2020;37(1):711–41.
99. Schildkopf P, Frey B, Ott OJ, Rubner Y, Multhoff G, Sauer R, et al. Radiation combined with hyperthermia induces HSP70-dependent maturation of dendritic cells and release of pro-inflammatory cytokines by dendritic cells and macrophages. Radiother Oncol. 2011;101(1):109–15.
100. Multhoff G. Activation of natural killer cells by heat shock protein 70. 2002. Int J Hyperth. 2009;25(3):169–75.
101. Datta NR, Ordóñez SG, Gaipl US, Paulides MM, Crezee H, Gellermann J, et al. Local hyperthermia combined with radiotherapy and-/or chemotherapy: recent advances and promises for the future. Cancer Treat Rev. 2015;41(9):742–53.
102. Lindner LH, Blay JY, Eggermont AMM, Issels RD. Perioperative chemotherapy and regional hyperthermia for high-risk adult-type soft tissue sarcomas. Eur J Cancer. 2021;147:164–9.
103. Issels RD, Lindner LH, Verweij J, Wust P, Reichardt P, Schem BC, et al. Neo-adjuvant chemotherapy alone or with regional hyperthermia for localised high-risk soft-tissue sarcoma: a randomised phase 3 multicentre study. Lancet Oncol. 2010;11(6):561–70.
104. van der Zee J, González González D, van Rhoon GC, van Dijk JD, van Putten WL, Hart AA. Comparison of radiotherapy alone with radiotherapy plus hyperthermia in locally advanced pelvic tumours: a prospective, randomised, multicentre trial. Dutch Deep Hyperthermia Group. Lancet. 2000;355(9210):1119–25.
105. Kroesen M, Mulder HT, van Holthe JML, Aangeenbrug AA, Mens JWM, van Doorn HC, et al. The effect of the time interval between radiation and hyperthermia on clinical outcome in 400 locally advanced cervical carcinoma patients. Front Oncol. 2019;9:134.
106. van Leeuwen CM, Oei AL, Ten Cate R, Franken NAP, Bel A, Stalpers LJA, et al. Measurement and analysis of the impact of time-interval, temperature and radiation dose on tumour cell survival and its application in thermoradiotherapy plan evaluation. Int J Hyperth. 2018;34(1):30–8.
107. Nencioni A, Caffa I, Cortellino S, Longo VD. Fasting and cancer: molecular mechanisms and clinical application. Nat Rev Cancer. 2018;18(11):707–19.
108. Buono R, Longo VD. Starvation, stress resistance, and cancer. Trends Endocrinol Metab. 2018;29(4):271–80.
109. Köhler A. A method of deep Roentgen irradiation without injury to the skin. Arch Roentgen Ray. 1909;14(5):141–2.
110. Prezado Y, Renier M, Bravin A. A new method of creating minibeam patterns for synchrotron radiation therapy: a feasibility study. J Synchrotron Radiat. 2009;16(Pt 4):582–6.
111. Zlobinskaya O, Girst S, Greubel C, Hable V, Siebenwirth C, Walsh DW, et al. Reduced side effects by proton microchannel radiotherapy: study in a human skin model. Radiat Environ Biophys. 2013;52(1):123–33.
112. Sammer M, Greubel C, Girst S, Dollinger G. Optimization of beam arrangements in proton minibeam radiotherapy by cell survival simulations. Med Phys. 2017;44(11):6096–104.
113. Reindl J, Girst S. pMB FLASH - status and perspectives of combining proton minibeam with FLASH radiotherapy. J Cancer Immunol. 2019; https://doi.org/10.33696/cancerimmunol.1.003.

114. Yan W, Khan MK, Wu X, Simone CB, Fan J, Gressen E, et al. Spatially fractionated radiation therapy: history, present and the future. Clin Transl Radiat Oncol. 2020;20:30–8.
115. Billena C, Khan AJ. A current review of spatial fractionation: back to the future? Int J Radiat Oncol Biol Phys. 2019;104(1):177–87.
116. Blanco Suarez JM, Amendola BE, Perez N, Amendola M, Wu X. The use of lattice radiation therapy (LRT) in the treatment of bulky tumors: a case report of a large metastatic mixed Mullerian ovarian tumor. Cureus. 2015;7(11):e389.
117. Fernandez-Palomo C, Fazzari J, Trappetti V, Smyth L, Janka H, Laissue J, et al. Animal models in microbeam radiation therapy: a scoping review. Cancers. 2020;12(3):527.
118. Trappetti V, Fazzari JM, Fernandez-Palomo C, Scheidegger M, Volarevic V, Martin OA, et al. Microbeam radiotherapy—a novel therapeutic approach to overcome radioresistance and enhance anti-tumour response in melanoma. Int J Mol Sci. 2021;22(14):7755.
119. Sammer M, Girst S, Dollinger G. Optimizing proton minibeam radiotherapy by interlacing and heterogeneous tumor dose on the basis of calculated clonogenic cell survival. Sci Rep. 2021;11(1):3533.
120. Lamirault C, Doyère V, Juchaux M, Pouzoulet F, Labiod D, Dendale R, et al. Short and long-term evaluation of the impact of proton minibeam radiation therapy on motor, emotional and cognitive functions. Sci Rep. 2020;10(1):13511.
121. Lansonneur P, Mammar H, Nauraye C, Patriarca A, Hierso E, Dendale R, et al. First proton minibeam radiation therapy treatment plan evaluation. Sci Rep. 2020;10(1):7025.
122. Mohiuddin M, Lynch C, Gao M, Hartsell W. Early clinical results of proton spatially fractionated GRID radiation therapy (SFGRT). Br J Radiol. 2020;93(1107):20190572.
123. Skowronek J. Current status of brachytherapy in cancer treatment - short overview. J Contemp Brachyther. 2017;9(6):581–9.
124. Njeh CF, Saunders MW, Langton CM. Accelerated partial breast irradiation (APBI): a review of available techniques. Radiat Oncol. 2010;5(1):90.
125. Pötter R, Tanderup K, Kirisits C, de Leeuw A, Kirchheiner K, Nout R, et al. The EMBRACE II study: the outcome and prospect of two decades of evolution within the GEC-ESTRO GYN working group and the EMBRACE studies. Clin Transl Radiat Oncol. 2018;9:48–60.
126. ICRU-Report-89. ICRU report 89: prescribing, recording, and reporting brachytherapy for cancer of the cervix. J ICRU. 2013;13(1–2)
127. Sminia P, Schneider CJ, van Tienhoven G, Koedooder K, Blank LE, González González D. Office hours pulsed brachytherapy boost in breast cancer. Radiother Oncol. 2001;59(3):273–80.
128. Harms W, Weber KJ, Ehemann V, Zuna I, Debus J, Peschke P. Differential effects of CLDR and PDR brachytherapy on cell cycle progression in a syngeneic rat prostate tumour model. Int J Radiat Biol. 2006;82(3):191–6.
129. Nicolay NH, Berry DP, Sharma RA. Liver metastases from colorectal cancer: radioembolization with systemic therapy. Nat Rev Clin Oncol. 2009;6(12):687–97.
130. Cremonesi M, Chiesa C, Strigari L, Ferrari M, Botta F, Guerriero F, et al. Radioembolization of hepatic lesions from a radiobiology and dosimetric perspective. Front Oncol. 2014;4:210.
131. Vouche M, Vanderlinden B, Delatte P, Lemort M, Hendlisz A, Deleporte A, et al. New imaging techniques for 90Y microsphere radioembolization. J Nucl Med Radiat Ther. 2011;2(1):113.
132. Levillain H, Bagni O, Deroose CM, Dieudonné A, Gnesin S, Grosser OS, et al. International recommendations for personalised selective internal radiation therapy of primary and metastatic liver diseases with yttrium-90 resin microspheres. Eur J Nucl Med Mol Imaging. 2021;48(5):1570–84.
133. Salem R, Padia SA, Lam M, Bell J, Chiesa C, Fowers K, et al. Clinical and dosimetric considerations for Y90: recommendations from an international multidisciplinary working group. Eur J Nucl Med Mol Imaging. 2019;46(8):1695–704.
134. Garin E, Tselikas L, Guiu B, Chalaye J, Edeline J, de Baere T, et al. Personalised versus standard dosimetry approach of selective internal radiation therapy in patients with locally advanced hepatocellular carcinoma (DOSISPHERE-01): a randomised, multicentre, open-label phase 2 trial. Lancet Gastroenterol Hepatol. 2021;6(1):17–29.
135. Sherman M, Levine R. Nuclear medicine and wall street: an evolving relationship. J Nucl Med. 2019;60(Suppl 2):20s–4s.
136. Puranik AD, Dromain C, Fleshner N, Sathekge M, Pavel M, Eberhardt N, et al. Target heterogeneity in oncology: the best predictor for differential response to radioligand therapy in neuroendocrine tumors and prostate cancer. Cancers. 2021;13(14):3607.
137. Yordanova A, Eppard E, Kürpig S, Bundschuh RA, Schönberger S, Gonzalez-Carmona M, et al. Theranostics in nuclear medicine practice. Onco Targets Ther. 2017;10:4821–8.
138. Qaim SM, Scholten B, Neumaier B. New developments in the production of theranostic pairs of radionuclides. J Radioanal Nucl Chem. 2018;318(3):1493–509.
139. Burkett BJ, Dundar A, Young JR, Packard AT, Johnson GB, Halfdanarson TR, et al. How we do it: a multidisciplinary approach to (177)Lu DOTATATE peptide receptor radionuclide therapy. Radiology. 2021;298(2):261–74.
140. Fersing C, Bouhlel A, Cantelli C, Garrigue P, Lisowski V, Guillet B. A comprehensive review of non-covalent radiofluorination approaches using aluminum [(18)F]fluoride: will [(18)F]AlF replace (68)Ga for metal chelate labeling? Molecules. 2019;24(16):2866.
141. Radhi HT, Jamal HF, Sarwani AA, Abdullah AJ, Al-Alawi MF, Alsabea AS, et al. Efficacy of a single fixed 131I dose of Radioactive iodine for the treatment of hyperthyroidism. Clin Investig. 2019;9(4):111–20.
142. Parker C, Nilsson S, Heinrich D, Helle SI, O'Sullivan JM, Fosså SD, et al. Alpha emitter radium-223 and survival in metastatic prostate cancer. N Engl J Med. 2013;369(3):213–23.
143. Poeppel TD, Handkiewicz-Junak D, Andreeff M, Becherer A, Bockisch A, Fricke E, et al. EANM guideline for radionuclide therapy with radium-223 of metastatic castration-resistant prostate cancer. Eur J Nucl Med Mol Imaging. 2018;45(5):824–45.
144. Pryma DA, Mandel SJ. Radioiodine therapy for thyroid cancer in the era of risk stratification and alternative targeted therapies. J Nucl Med. 2014;55(9):1485–91.
145. Luster M, Clarke SE, Dietlein M, Lassmann M, Lind P, Oyen WJ, et al. Guidelines for radioiodine therapy of differentiated thyroid cancer. Eur J Nucl Med Mol Imaging. 2008;35(10):1941–59.
146. Ahmadi Bidakhvidi N, Goffin K, Dekervel J, Baete K, Nackaerts K, Clement P, et al. Peptide receptor radionuclide therapy targeting the somatostatin receptor: basic principles, clinical applications and optimization strategies. Cancers. 2022;14(1):129.
147. Strosberg J, El-Haddad G, Wolin E, Hendifar A, Yao J, Chasen B, et al. Phase 3 trial of (177)Lu-dotatate for midgut neuroendocrine tumors. N Engl J Med. 2017;376(2):125–35.
148. Brabander T, van der Zwan WA, Teunissen JJM, Kam BLR, Feelders RA, de Herder WW, et al. Long-term efficacy, survival, and safety of [(177)Lu-DOTA(0),Tyr(3)]octreotate in patients with gastroenteropancreatic and bronchial neuroendocrine tumors. Clin Cancer Res. 2017;23(16):4617–24.
149. Imhof A, Brunner P, Marincek N, Briel M, Schindler C, Rasch H, et al. Response, survival, and long-term toxicity after therapy with the radiolabeled somatostatin analogue [90Y-DOTA]-TOC in metastasized neuroendocrine cancers. J Clin Oncol. 2011;29(17):2416–23.

150. Sartor O, de Bono J, Chi KN, Fizazi K, Herrmann K, Rahbar K, et al. Lutetium-177-PSMA-617 for metastatic castration-resistant prostate cancer. N Engl J Med. 2021;385(12):1091–103.
151. Moreno P, Ramos-Álvarez I, Moody TW, Jensen RT. Bombesin related peptides/receptors and their promising therapeutic roles in cancer imaging, targeting and treatment. Expert Opin Ther Targets. 2016;20(9):1055–73.
152. von Eyben FE, Bauman G, von Eyben R, Rahbar K, Soydal C, Haug AR, et al. Optimizing PSMA radioligand therapy for patients with metastatic castration-resistant prostate cancer. A systematic review and meta-analysis. Int J Mol Sci. 2020;21(23):9054.
153. Weiner GJ. Building better monoclonal antibody-based therapeutics. Nat Rev Cancer. 2015;15(6):361–70.
154. Witzig TE, Gordon LI, Cabanillas F, Czuczman MS, Emmanouilides C, Joyce R, et al. Randomized controlled trial of yttrium-90-labeled ibritumomab tiuxetan radioimmunotherapy versus rituximab immunotherapy for patients with relapsed or refractory low-grade, follicular, or transformed B-cell non-Hodgkin's lymphoma. J Clin Oncol. 2002;20(10):2453–63.
155. Wang Y, Probin V, Zhou D. Cancer therapy-induced residual bone marrow injury-mechanisms of induction and implication for therapy. Curr Cancer Ther Rev. 2006;2(3):271–9.
156. Altunay B, Morgenroth A, Beheshti M, Vogg A, Wong NCL, Ting HH, et al. HER2-directed antibodies, affibodies and nanobodies as drug-delivery vehicles in breast cancer with a specific focus on radioimmunotherapy and radioimmunoimaging. Eur J Nucl Med Mol Imaging. 2021;48(5):1371–89.
157. Verhoeven M, Seimbille Y, Dalm SU. Therapeutic applications of pretargeting. Pharmaceutics. 2019;11(9):434.
158. Gill MR, Falzone N, Du Y, Vallis KA. Targeted radionuclide therapy in combined-modality regimens. Lancet Oncol. 2017;18(7):e414–e23.
159. Kashyap R, Hofman MS, Michael M, Kong G, Akhurst T, Eu P, et al. Favourable outcomes of (177)Lu-octreotate peptide receptor chemoradionuclide therapy in patients with FDG-avid neuroendocrine tumours. Eur J Nucl Med Mol Imaging. 2015;42(2):176–85.
160. Ballal S, Yadav MP, Damle NA, Sahoo RK, Bal C. Concomitant 177Lu-DOTATATE and capecitabine therapy in patients with advanced neuroendocrine tumors: a long-term-outcome, toxicity, survival, and quality-of-life study. Clin Nucl Med. 2017;42(11):e457–e66.
161. Yadav MP, Ballal S, Bal C. Concomitant 177Lu-DOTATATE and capecitabine therapy in malignant paragangliomas. EJNMMI Res. 2019;9(1):13.
162. Strosberg JR, Fine RL, Choi J, Nasir A, Coppola D, Chen DT, et al. First-line chemotherapy with capecitabine and temozolomide in patients with metastatic pancreatic endocrine carcinomas. Cancer. 2011;117(2):268–75.
163. Bison SM, Haeck JC, Bol K, et al. Optimization of combined temozolomide and peptide receptor radionuclide therapy (PRRT) in mice after multimodality molecular imaging studies. EJNMMI Res. 2015;5(1):62. https://doi.org/10.1186/s13550-015-0142-y.
164. Morris MJ, Loriot Y, Sweeney CJ, Fizazi K, Ryan CJ, Shevrin DH, et al. Radium-223 in combination with docetaxel in patients with castration-resistant prostate cancer and bone metastases: a phase 1 dose escalation/randomised phase 2a trial. Eur J Cancer. 2019;114:107–16.
165. Dhiantravan N, Emmett L, Joshua AM, Pattison DA, Francis RJ, Williams S, et al. UpFrontPSMA: a randomized phase 2 study of sequential 177Lu-PSMA-617 and docetaxel vs docetaxel in metastatic hormone-naïve prostate cancer (clinical trial protocol). BJU Int. 2021;128(3):331–42.
166. Claringbold PG, Turner JH. NeuroEndocrine tumor therapy with lutetium-177-octreotate and everolimus (NETTLE): a phase I study. Cancer Biother Radiopharm. 2015;30(6):261–9.
167. Cullinane C, Waldeck K, Kirby L, Rogers BE, Eu P, Tothill RW, et al. Enhancing the anti-tumour activity of 177Lu-DOTA-octreotate radionuclide therapy in somatostatin receptor-2 expressing tumour models by targeting PARP. Sci Rep. 2020;10(1):10196.
168. Suman SK, Subramanian S, Mukherjee A. Combination radionuclide therapy: a new paradigm. Nucl Med Biol. 2021;98–99:40–58.
169. Dietrich A, Koi L, Zöphel K, Sihver W, Kotzerke J, Baumann M, et al. Improving external beam radiotherapy by combination with internal irradiation. Br J Radiol. 2015;88(1051):20150042.
170. Kreissl MC, Hänscheid H, Löhr M, Verburg FA, Schiller M, Lassmann M, et al. Combination of peptide receptor radionuclide therapy with fractionated external beam radiotherapy for treatment of advanced symptomatic meningioma. Radiat Oncol. 2012;7(1):99.
171. Oddstig J, Bernhardt P, Nilsson O, Ahlman H, Forssell-Aronsson E. Radiation induces up-regulation of somatostatin receptors 1, 2, and 5 in small cell lung cancer in vitro also at low absorbed doses. Cancer Biother Radiopharm. 2011;26(6):759–65.
172. Kim C, Liu SV, Subramaniam DS, Torres T, Loda M, Esposito G, et al. Phase I study of the (177)Lu-DOTA(0)-Tyr(3)-Octreotate (lutathera) in combination with nivolumab in patients with neuroendocrine tumors of the lung. J Immunother Cancer. 2020;8(2):e000980.
173. Shah RG, Merlin MA, Adant S, Zine-Eddine F, Beauregard JM, Shah GM. Chemotherapy-induced upregulation of somatostatin receptor-2 increases the uptake and efficacy of (177)Lu-DOTA-octreotate in neuroendocrine tumor cells. Cancers (Basel). 2021;13(2):232.
174. Obodovskiy I. Chapter 5—Passing of charged particles through matter. In: Obodovskiy I, editor. Radiation. Elsevier; 2019. p. 103–36.
175. Rietzel E, Bert C. Respiratory motion management in particle therapy. Med Phys. 2010;37(2):449–60.
176. Zschaeck S, Simon M, Löck S, Troost EGC, Stützer K, Wohlfahrt P, et al. PRONTOX – proton therapy to reduce acute normal tissue toxicity in locally advanced non-small-cell lung carcinomas (NSCLC): study protocol for a randomised controlled trial. Trials. 2016;17(1):543.
177. Park SH, Kang JO. Basics of particle therapy I: physics. Radiat Oncol J. 2011;29(3):135–46.
178. Elaimy AL, Ding L, Bradford C, Geng Y, Bushe H, Kuo I-L, et al. History and overview of proton therapy. IntechOpen; 2021.
179. Smith AR. Proton therapy. Phys Med Biol. 2006;51(13):R491–504.
180. Paganetti H, editor. Proton therapy physics. 1st ed. Boca Raton: CRC Press; 2012.
181. Jones B, McMahon SJ, Prise KM. The radiobiology of proton therapy: challenges and opportunities around relative biological effectiveness. Clin Oncol. 2018;30(5):285–92.
182. Michaelidesová A, Vachelová J, Puchalska M, Brabcová KP, Vondráček V, Sihver L, et al. Relative biological effectiveness in a proton spread-out Bragg peak formed by pencil beam scanning mode. Australas Phys Eng Sci Med. 2017;40(2):359–68.
183. Paganetti H. Relative biological effectiveness (RBE) values for proton beam therapy. Variations as a function of biological endpoint, dose, and linear energy transfer. Phys Med Biol. 2014;59(22):R419–R72.
184. Wouters BG, Skarsgard LD, Gerweck LE, Carabe-Fernandez A, Wong M, Durand RE, et al. Radiobiological intercomparison of the 160 MeV and 230 MeV proton therapy beams at the Harvard Cyclotron Laboratory and at Massachusetts General Hospital. Radiat Res. 2015;183(2):174–87.
185. Michaelidesová A, Vachelová J, Klementová J, Urban T, Pachnerová Brabcová K, Kaczor S, et al. In vitro comparison of passive and active clinical proton beams. Int J Mol Sci. 2020;21(16):5650.

186. Breen WG, Paulino AC, Hartsell WF, Mangona VS, Perkins SM, Indelicato DJ, et al. Factors associated with acute toxicity in pediatric patients treated with proton radiation therapy: a report from the Pediatric Proton Consortium Registry. Pract Radiat Oncol. 2022;12(2):155–62.
187. Castro JR, Quivey JM, Lyman JT, Chen GT, Phillips TL, Tobias CA. Radiotherapy with heavy charged particles at Lawrence Berkeley Laboratory. J Can Assoc Radiol. 1980;31(1):30–4.
188. Mohamad O, Makishima H, Kamada T. Evolution of carbon ion radiotherapy at the National Institute of Radiological Sciences in Japan. Cancers (Basel). 2018;10(3):66.
189. IAEA-Report. Dose reporting in ion beam therapy. Vienna: International Atomic Energy Agency; 2007.
190. Malouff TD, Mahajan A, Krishnan S, Beltran C, Seneviratne DS, Trifiletti DM. Carbon ion therapy: a modern review of an emerging technology. Front Oncol. 2020;10:82.
191. Syljuåsen R. Cell cycle effects in radiation oncology. In: Wenz F, editor. Radiation oncology. Cham: Springer International Publishing; 2019. p. 1–8.
192. Held KD, Kawamura H, Kaminuma T, Paz AE, Yoshida Y, Liu Q, et al. Effects of charged particles on human tumor cells. Front Oncol. 2016;6:23.
193. Durante M, Loeffler JS. Charged particles in radiation oncology. Nat Rev Clin Oncol. 2010;7(1):37–43.
194. Lodge M, Pijls-Johannesma M, Stirk L, Munro AJ, De Ruysscher D, Jefferson T. A systematic literature review of the clinical and cost-effectiveness of hadron therapy in cancer. Radiother Oncol. 2007;83(2):110–22.
195. Kamada T, Tsujii H, Blakely EA, Debus J, De Neve W, Durante M, et al. Carbon ion radiotherapy in Japan: an assessment of 20 years of clinical experience. Lancet Oncol. 2015;16(2):e93–e100.
196. Chen J, Mao J, Ma N, Wu KL, Lu J, Jiang GL. Definitive carbon ion radiotherapy for tracheobronchial adenoid cystic carcinoma: a preliminary report. BMC Cancer. 2021;21(1):734.
197. Kaneko T, Suefuji H, Koto M, Demizu Y, Saitoh JI, Tsuji H, et al. Multicenter study of carbon-ion radiotherapy for oropharyngeal non-squamous cell carcinoma. In Vivo. 2021;35(4):2239–45.
198. Lu VM, O'Connor KP, Mahajan A, Carlson ML, Van Gompel JJ. Carbon ion radiotherapy for skull base chordomas and chondrosarcomas: a systematic review and meta-analysis of local control, survival, and toxicity outcomes. J Neurooncol. 2020;147(3):503–13.
199. Degiovanni A, Amaldi U. History of hadron therapy accelerators. Phys Med. 2015;31(4):322–32.
200. Inaniwa T, Kanematsu N, Noda K, Kamada T. Treatment planning of intensity modulated composite particle therapy with dose and linear energy transfer optimization. Phys Med Biol. 2017;62(12):5180–97.
201. Mizushima KA-O, Iwata YA-O, Muramatsu M, Lee SH, Shirai T. Experimental study on monitoring system of clinical beam purity in multiple-ion beam operation for heavy-ion radiotherapy. Rev Sci Instrum. 2020;91:023309.
202. Horst F, Schardt D, Iwase H, Schuy C, Durante M, Weber U. Physical characterization of 3He ion beams for radiotherapy and comparison with 4He. Phys Med Biol. 2021;66(9):095009.
203. Mein S, Dokic I, Klein C, Tessonnier T, Böhlen TT, Magro G, et al. Biophysical modeling and experimental validation of relative biological effectiveness (RBE) for 4He ion beam therapy. Radiat Oncol. 2019;14(1):123.
204. Knäusl B, Fuchs H, Dieckmann K, Georg D. Can particle beam therapy be improved using helium ions? - A planning study focusing on pediatric patients. Acta Oncol. 2016;55(6):751–9.
205. Ebner DK, Frank SJ, Inaniwa T, Yamada S, Shirai T. The emerging potential of multi-ion radiotherapy. Front Oncol. 2021;11:624786.
206. Winkelmann T, Cee R, Haberer T, Naas B, Peters A. Test bench to commission a third ion source beam line and a newly designed extraction system. Rev Sci Instrum. 2012;83(2):02b904.
207. Jäkel O. Physical advantages of particles: protons and light ions. Br J Radiol. 2020;93(1107):20190428.
208. Ying C, Bolst D, Rosenfeld A, Guatelli S. Characterization of the mixed radiation field produced by carbon and oxygen ion beams of therapeutic energy: a Monte Carlo simulation study. J Med Phys. 2019;44(4):263–9.
209. Degiovanni A, Adam J, Aguilera Murciano D, Ballestrero S, Benot-Morell A, Bonomi R, et al., editors. Status of the Commissioning of the LIGHT Prototype. The 9th International Particle Accelerator Conference; 2018-06; Vancouver. Geneva, Switzerland: JACoW Publishing; 2018.
210. Ronsivalle C, Picardi L, Ampollini A, Bazzano G, Marracino F, Nenzi P, et al. First acceleration of a proton beam in a side coupled drift tube linac. Europhys Lett. 2015;111(1):14002.
211. Sindhwani S, Syed AM, Ngai J, Kingston BR, Maiorino L, Rothschild J, et al. The entry of nanoparticles into solid tumours. Nat Mater. 2020;19(5):566–75.
212. Mitchell MJ, Billingsley MM, Haley RM, Wechsler ME, Peppas NA, Langer R. Engineering precision nanoparticles for drug delivery. Nat Rev Drug Discov. 2021;20(2):101–24.
213. Kaur P, Aliru ML, Chadha AS, Asea A, Krishnan S. Hyperthermia using nanoparticles—promises and pitfalls. Int J Hyperth. 2016;32(1):76–88.
214. Penninckx S, Heuskin A-C, Michiels C, Lucas S. Gold nanoparticles as a potent radiosensitizer: a transdisciplinary approach from physics to patient. Cancers. 2020;12(8):2021.
215. Penninckx S, Heuskin AC, Michiels C, Lucas S. The role of thioredoxin reductase in gold nanoparticle radiosensitization effects. Nanomedicine (Lond). 2018;13(22):2917–37.
216. Penninckx S, Heuskin AC, Michiels C, Lucas S. Thioredoxin reductase activity predicts gold nanoparticle radiosensitization effect. Nanomaterials (Basel). 2019;9(2):295.
217. Zhong D, Zhao J, Li Y, Qiao Y, Wei Q, He J, et al. Laser-triggered aggregated cubic α-Fe(2)O(3)@Au nanocomposites for magnetic resonance imaging and photothermal/enhanced radiation synergistic therapy. Biomaterials. 2019;219:119369.
218. Schuemann J, Bagley AF, Berbeco R, Bromma K, Butterworth KT, Byrne HL, et al. Roadmap for metal nanoparticles in radiation therapy: current status, translational challenges, and future directions. Phys Med Biol. 2020;65(21):21rm02.
219. Scorsetti M, Cozzi L, Navarria P, Fogliata A, Rossi A, Franceschini D, et al. Intensity modulated proton therapy compared to volumetric modulated arc therapy in the irradiation of young female patients with Hodgkin's lymphoma. Assessment of risk of toxicity and secondary cancer induction. Radiat Oncol. 2020;15(1):12.
220. Yamanaka R, Hayano A, Kanayama T. Radiation-induced meningiomas: an exhaustive review of the literature. World Neurosurg. 2017;97:635–44.e8.
221. Joensuu H, Kankaanranta L, Seppälä T, Auterinen I, Kallio M, Kulvik M, et al. Boron neutron capture therapy of brain tumors: clinical trials at the Finnish facility using boronophenylalanine. J Neurooncol. 2003;62(1–2):123–34.
222. Capala J, Stenstam BH, Sköld K, Munck af Rosenschöld P, Giusti V, Persson C, et al. Boron neutron capture therapy for glioblastoma multiforme: clinical studies in Sweden. J Neurooncol. 2003;62(1–2):135–44.
223. Busse PM, Harling OK, Palmer MR, Kiger WS III, Kaplan J, Kaplan I, et al. A critical examination of the results from the Harvard-MIT NCT program phase I clinical trial of neutron capture therapy for intracranial disease. J Neurooncol. 2003;62(1–2):111–21.
224. Henriksson R, Capala J, Michanek A, Lindahl SA, Salford LG, Franzén L, et al. Boron neutron capture therapy (BNCT) for glioblastoma multiforme: a phase II study evaluating a prolonged high-dose of boronophenylalanine (BPA). Radiother Oncol. 2008;88(2):183–91.

225. Kawabata S, Miyatake S, Hiramatsu R, Hirota Y, Miyata S, Takekita Y, et al. Phase II clinical study of boron neutron capture therapy combined with X-ray radiotherapy/temozolomide in patients with newly diagnosed glioblastoma multiforme—study design and current status report. Appl Radiat Isot. 2011;69(12):1796–9.
226. Yamamoto T, Matsumura A, Nakai K, Shibata Y, Endo K, Sakurai F, et al. Current clinical results of the Tsukuba BNCT trial. Appl Radiat Isot. 2004;61(5):1089–93.
227. Miyatake S, Kawabata S, Kajimoto Y, Aoki A, Yokoyama K, Yamada M, et al. Modified boron neutron capture therapy for malignant gliomas performed using epithermal neutron and two boron compounds with different accumulation mechanisms: an efficacy study based on findings on neuroimages. J Neurosurg. 2005;103(6):1000–9.
228. Miyatake S, Kawabata S, Yokoyama K, Kuroiwa T, Michiue H, Sakurai Y, et al. Survival benefit of Boron neutron capture therapy for recurrent malignant gliomas. J Neurooncol. 2009;91(2):199–206.
229. Kankaanranta L, Seppälä T, Koivunoro H, Välimäki P, Beule A, Collan J, et al. L-Boronophenylalanine-mediated boron neutron capture therapy for malignant glioma progressing after external beam radiation therapy: a Phase I study. Int J Radiat Oncol Biol Phys. 2011;80(2):369–76.
230. Miyatake S, Tamura Y, Kawabata S, Iida K, Kuroiwa T, Ono K. Boron neutron capture therapy for malignant tumors related to meningiomas. Neurosurgery. 2007;61(1):82–90; discussion –1.
231. Kawabata S, Hiramatsu R, Kuroiwa T, Ono K, Miyatake S. Boron neutron capture therapy for recurrent high-grade meningiomas. J Neurosurg. 2013;119(4):837–44.
232. Fukuda H, Hiratsuka J, Kobayashi T, Sakurai Y, Yoshino K, Karashima H, et al. Boron neutron capture therapy (BNCT) for malignant melanoma with special reference to absorbed doses to the normal skin and tumor. Australas Phys Eng Sci Med. 2003;26(3):97–103.
233. Menéndez PR, Roth BM, Pereira MD, Casal MR, González SJ, Feld DB, et al. BNCT for skin melanoma in extremities: updated Argentine clinical results. Appl Radiat Isot. 2009;67(7–8 Suppl):S50–3.
234. Hiratsuka J, Kamitani N, Tanaka R, Tokiya R, Yoden E, Sakurai Y, et al. Long-term outcome of cutaneous melanoma patients treated with boron neutron capture therapy (BNCT). J Radiat Res. 2020;61(6):945–51.
235. Koivunoro H, Bleuel DL, Nastasi U, Lou TP, Reijonen J, Leung KN. BNCT dose distribution in liver with epithermal D-D and D-T fusion-based neutron beams. Appl Radiat Isot. 2004;61(5):853–9.
236. Kato I, Ono K, Sakurai Y, Ohmae M, Maruhashi A, Imahori Y, et al. Effectiveness of BNCT for recurrent head and neck malignancies. Appl Radiat Isot. 2004;61(5):1069–73.
237. Kankaanranta L, Seppälä T, Koivunoro H, Saarilahti K, Atula T, Collan J, et al. Boron neutron capture therapy in the treatment of locally recurred head and neck cancer. Int J Radiat Oncol Biol Phys. 2007;69(2):475–82.
238. Kato I, Fujita Y, Maruhashi A, Kumada H, Ohmae M, Kirihata M, et al. Effectiveness of boron neutron capture therapy for recurrent head and neck malignancies. Appl Radiat Isot. 2009;67(7–8 Suppl):S37–42.
239. Kankaanranta L, Seppälä T, Koivunoro H, Saarilahti K, Atula T, Collan J, et al. Boron neutron capture therapy in the treatment of locally recurred head-and-neck cancer: final analysis of a phase I/II trial. Int J Radiat Oncol Biol Phys. 2012;82(1):e67–75.
240. Suzuki M, Kato I, Aihara T, Hiratsuka J, Yoshimura K, Niimi M, et al. Boron neutron capture therapy outcomes for advanced or recurrent head and neck cancer. J Radiat Res. 2014;55(1):146–53.
241. Aihara T, Morita N, Kamitani N, et al. BNCT for advanced or recurrent head and neck cancer. Appl Radiat Isot. 2014;88:12–5.
242. Wang LW, Chen YW, Ho CY, Hsueh Liu YW, Chou FI, Liu YH, et al. Fractionated boron neutron capture therapy in locally recurrent head and neck cancer: a prospective phase I/II trial. Int J Radiat Oncol Biol Phys. 2016;95(1):396–403.
243. Koivunoro H, Kankaanranta L, Seppälä T, Haapaniemi A, Mäkitie A, Joensuu H. Boron neutron capture therapy for locally recurrent head and neck squamous cell carcinoma: an analysis of dose response and survival. Radiother Oncol. 2019;137:153–8.
244. Hirose K, Konno A, Hiratsuka J, Yoshimoto S, Kato T, Ono K, et al. Boron neutron capture therapy using cyclotron-based epithermal neutron source and borofalan ((10)B) for recurrent or locally advanced head and neck cancer (JHN002): an open-label phase II trial. Radiother Oncol. 2021;155:182–7.

Further Reading

Adant S, Shah GM, Beauregard JM. Combination treatments to enhance peptide receptor radionuclide therapy of neuroendocrine tumours. Eur J Nucl Med Mol Imaging. 2020;47(4):907–21.
Ahmadzadehfar H, Biersack HJ, Freeman LM, Zuckier LS, editors. Clinical nuclear medicine. 2nd ed. Switzerland: Springer Cham; 2020. 584 p
Billena C, Khan AJ. A current review of spatial fractionation: back to the future? Int J Radiat Oncol Biol Phys. 2019;104(1):177–87.
Bragg WH, Kleeman R. LXXIV. On the ionization curves of radium. London Edinburgh Dublin Philos Mag J Sci. 1904;8(48):726–38.
Chan TG, O'Neill E, Habjan C, Cornelissen B. Combination strategies to improve targeted radionuclide therapy. J Nucl Med. 2020;61(11):1544–52.
Douglass M, Hall EJ, Giaccia AJ. Radiobiology for the radiologist. Australas Phys Eng Sci Med. 2018;41(4):1129–30.
Dymova MA, Taskaev SY, Richter VA, Kuligina EV. Boron neutron capture therapy: current status and future perspectives. Cancer Commun (Lond). 2020;40(9):406–21.
Feijtel D, de Jong M, Nonnekens J. Peptide receptor radionuclide therapy: looking back, looking forward. Curr Top Med Chem. 2020;20(32):2959–69.
Herrmann K, Schwaiger M, Lewis JS, Solomon SB, McNeil BJ, Baumann M, et al. Radiotheranostics: a roadmap for future development. Lancet Oncol. 2020;21(3):e146–e56.
Jadvar H, Chen X, Cai W, Mahmood U. Radiotheranostics in cancer diagnosis and management. Radiology. 2018;286(2):388–400.
Joiner MC, van der Kogel AJ, editors. Basic clinical radiobiology. Boca Raton: CRC Press; 2018. 360 p
Kaplon H, Reichert JM. Antibodies to watch in 2021. MAbs. 2021;13(1):1860476.
Kraeber-Bodéré F, Barbet J, Chatal J-F. Radioimmunotherapy: from current clinical success to future industrial breakthrough? J Nucl Med. 2016;57(3):329.
Kraeber-Bodéré F, Bodet-Milin C, Rousseau C, Eugène T, Pallardy A, Frampas E, et al. Radioimmunoconjugates for the treatment of cancer. Semin Oncol. 2014;41(5):613–22.
Macià IGM. Radiobiology of stereotactic body radiation therapy (SBRT). Rep Pract Oncol Radiother. 2017;22(2):86–95.
Malik A, Afaq S, Tarique M, editors. Nanomedicine for cancer diagnosis and therapy. 1st ed. Singapore: Springer Singapore; 2021.
Miyatake SI, Wanibuchi M, Hu N, Ono K. Boron neutron capture therapy for malignant brain tumors. J Neurooncol. 2020;149(1):1–11.
Reynolds TS, Bandari RP, Jiang Z, Smith CJ. Lutetium-177 labeled bombesin peptides for radionuclide therapy. Curr Radiopharm. 2016;9(1):33–43.

Schuemann J, Bagley AF, Berbeco R, Bromma K, Butterworth KT, Byrne HL, et al. Roadmap for metal nanoparticles in radiation therapy: current status, translational challenges, and future directions. Phys Med Biol. 2020;65(21):21rm02.

Shi J, Kantoff PW, Wooster R, Farokhzad OC. Cancer nanomedicine: progress, challenges and opportunities. Nat Rev Cancer. 2017;17(1):20–37.

Suzuki M. Boron neutron capture therapy (BNCT): a unique role in radiotherapy with a view to entering the accelerator-based BNCT era. Int J Clin Oncol. 2020;25(1):43–50.

Thomadsen B. Comprehensive brachytherapy: physical and clinical aspects. Med Phys. 2013;40(11)

Trifiletti DM, Chao ST, Sahgal A, Sheehan JP, editors. Stereotactic radiosurgery and stereotactic body radiation therapy: a comprehensive guide. 1st ed. Switzerland: Springer Cham; 2019. 435 p

Vugts DJ, van Dongen GAMS. Immunoglobulins as radiopharmaceutical vectors. In: Lewis JS, Windhorst AD, Zeglis BM, editors. Radiopharmaceutical chemistry. Cham: Springer International Publishing; 2019. p. 163–79.

Wiedemann H, editor. Particle accelerator physics. 4th ed. Cham: Springer; 2015. 475 p

Yan W, Khan MK, Wu X, Simone CB, Fan J, Gressen E, et al. Spatially fractionated radiation therapy: history, present and the future. Clin Transl Radiat Oncol. 2020;20:30–8.

7 Individual Radiation Sensitivity and Biomarkers: Molecular Radiation Biology

Elizabeth A. Ainsbury, Ana Margarida Abrantes, Sarah Baatout, Ans Baeyens, Maria Filomena Botelho, Benjamin Frey, Nicolas Foray, Alexandros G. Georgakilas, Fiona M. Lyng, Inês Alexandra Marques, Aidan D. Meade, Mirta Milic, Dhruti Mistry, Jade F. Monaghan, Alegría Montoro, Ana Salomé Pires, Georgia I. Terzoudi, Sotiria Triantopoulou, Kristina Viktorsson, and Guillaume Vogin

E. A. Ainsbury (✉)
Radiation, Chemical and Environmental Hazards Directorate, UK Health Security Agency, Oxford, United Kingdom
e-mail: Liz.Ainsbury@ukhsa.gov.uk

A. M. Abrantes
Institute of Biophysics, Faculty of Medicine, iCBR-CIMAGO, Center for Innovative Biomedicine and Biotechnology, University of Coimbra, Coimbra, Portugal

ESTESC-Coimbra Health School, Instituto Politécnico de Coimbra, Coimbra, Portugal
e-mail: mabrantes@fmed.uc.pt

S. Baatout
Institute of Nuclear Medical Applications, Belgian Nuclear Research Centre, SCK CEN, Mol, Belgium
e-mail: sarah.baatout@sckcen.be

A. Baeyens
Radiobiology, Department of Human Structure and Repair, Ghent University, Ghent, Belgium
e-mail: Ans.Baeyens@UGent.be

M. F. Botelho · I. A. Marques · A. S. Pires
Institute of Biophysics, Faculty of Medicine, iCBR-CIMAGO, Center for Innovative Biomedicine and Biotechnology, University of Coimbra, Coimbra, Portugal

Clinical Academic Center of Coimbra, Coimbra, Portugal
e-mail: mfbotelho@fmed.uc.pt; ines.marques@student.uc.pt; pireslourenco@uc.pt

B. Frey
Translational Radiobiology, Department of Radiation Oncology, Universitätsklinikum Erlangen, Friedrich-Alexander-Universität Erlangen-Nürnberg, Erlangen, Germany
e-mail: Benjamin.Frey@uk-erlangen.de

N. Foray
Inserm Unit 1296 Inserm Unit "Radiation: Defense, Health, Environment", Lyon, France
e-mail: nicolas.foray@inserm.fr

A. G. Georgakilas
DNA Damage Laboratory, Physics Department, School of Applied Mathematical and Physical Sciences, National Technical University of Athens (NTUA), Athens, Greece
e-mail: Alexg@mail.ntua.gr

F. M. Lyng · J. F. Monaghan
Center for Radiation and Environmental Science, Technological University Dublin, Dublin, Ireland
e-mail: fiona.lyng@TUDublin.ie; jade.monaghan@mytudublin.ie

A. D. Meade
School of Physics, Clinical & Optometric Sciences, Technological University Dublin, Dublin, Ireland
e-mail: aidan.meade@TUDublin.ie

M. Milic
Mutagenesis Unit, Institute for Medical Research and Occupational Health, Zagreb, Croatia
e-mail: mmilic@imi.hr

D. Mistry
Radiobiology Unit, Belgian Nuclear Research Centre, SCK CEN, Mol, Belgium

A. Montoro
Radiological Protection Service, University and Polytechnic La Fe Hospital of Valencia, Valencia, Spain
e-mail: montoro_ale@gva.es

G. I. Terzoudi · S. Triantopoulou
Health Physics, Radiobiology & Cytogenetics Laboratory, Institute of Nuclear & Radiological Sciences & Technology, Energy & Safety, National Centre for Scientific Research "Demokritos", Athens, Greece
e-mail: gterzoudi@rrp.demokritos.gr; iro@rrp.demokritos.gr

K. Viktorsson
Department of Oncology/Pathology, Karolinska Institutet, Stockholm, Sweden
e-mail: Kristina.viktorsson@ki.se

G. Vogin
Centre Francois Baclesse, University of Luxembourg and Luxembourg Institute of Health, Luxembour, Luxembourg
e-mail: Guillaume.vogin@baclesse.lu

S. Baatout (ed.), *Radiobiology Textbook*, https://doi.org/10.1007/978-3-031-18810-7_7

Learning Objectives

- To understand the different responses of tumor and normal tissues to ionizing radiation (IR) whether at low or high dose.
- To grasp the importance of radiation biomarkers of exposure as well as effect and their integration with molecular epidemiological studies.
- To be able to discuss current and emerging biomarker methods to predict normal tissue and tumor responses to radiotherapy (RT).
- To understand how age and sex influence IR sensitivity on cellular and individual levels as well as health risks induced by IR exposure.
- To grasp how genetic syndromes can be associated with an increased radiation sensitivity and cancer risk.
- To understand the concept of precision medicine in context of RT and future research avenues in this field.

7.1 Definition of Individual Radiosensitivity, Radiosusceptibility, and Radiodegeneration and Radioresistence

The term "radiosensitivity" is one of the most extensively used words in radiobiology. It was described as radiation-induced tissue reactions (e.g., skin is radiosensitive) in the first decade of the nineteenth century [1]. Since 1930s, with the first Congresses of Radiology, the term "radiosensitivity" was also used as a synonym of radiation-induced cancers (e.g., thyroid is a radiosensitive organ) and progressively was used for radiation-induced cataracts (e.g., eyes are radiosensitive [2]). All these different uses lead to an actual confusion and notably raise legal issues since radiation-induced cancers, cataracts, or skin burns do not correspond to the same level of clinical injuries [3].

To avoid these confusions, a possible approach is to consider all the major clinical features of the response to radiation by using unequivocal terms that could be indifferently applied to the individual, tissue, cellular, or molecular scales. To consolidate this approach, it is important to document the individual response to radiation through a complete knowledge of its different features. For example, it is noteworthy that ataxia telangiectasia (AT), caused by homozygous mutations of the AT mutated (*ATM*) gene resulting in aberrant ATM protein, is associated with post-RTfatal reactions and high risk of leukemia [4], while Li Fraumeni's syndrome is associated with cancer proneness but not with significant post-RT adverse tissue reactions [5]. Conversely, Cockayne's syndrome is associated with significant tissue radiosensitivity but no cancer proneness [6].

Hence, the following definition has been therefore proposed in literature [7] and summarized in Table 7.1.

- "Radiosensitivity" is the proneness to radiation-induced adverse tissue events that are considered as non-cancer effects attributable to cell death. Radiosensitivity is generally correlated with unrepaired DNA damage and observed in response to high doses of radiation [8] (Box 7.1).

Table 7.1 Summary of the terms—radiosensitivity, radiosusceptibility, and radioresistance

Radiosensitivity	Radiosensitivity refers to adverse healthy tissue reactions like burns, dermatitis, rectitis, etc., that is, any reaction led by radiation-induced cell death that may be generally accompanied by inflammation.
	Radiosensitivity also refers to the inherent response of tumor/cancer cells to radiation which can be measured by the reduction of the volume, the extent of regression, rapidity of response, and response durability that are also linked to radiation-induced cell death.
	The degree of radiosensitivity depends on the combination of various genetic traits, interaction with each other, ability to repair damage, hypoxia, cell cycle position, growth fraction, hormonal balance, immune system, and various environmental factors.
	The probable cause of radiosensitivity may be an insufficient repair of the radiation-damaged DNA generally due to defective DNA damage signaling and/or repair mechanism.
Radiosusceptibility	The proneness to radiation-induced cancers generally linked to radiation-induced cell transformation and mis-repaired DNA damage.
	It is also an important issue for both low- and high-dose radiation exposures to an individual who exhibits higher cancer risk spontaneously.
	Differences in radiosusceptibility between individuals, or groups, may relate to genetic constitution, but also to other characteristics such as age at exposure, health status and comorbidity, epigenetic factors, lifestyle, and co-exposures to other stressors.
Radiodegeneration	The term is to describe any aspects of IR responses (non-cancer effects) attributable to mechanisms related to accelerated aging.
Radioresistance	Radioresistance describes a normal response to IR at any level; whether molecular, cellular, tissular, and clinical.
	In terms of radiosensitivity, radioresistance is the synonym of absence of any adverse tissue reactions and of a normal DNA damage repair (rate and efficiency).
	In terms of radiosusceptibility, radioresistance is synonymous with a low risk of radiation-induced cancer.
	In terms of radiodegeneration, radioresistance is synonymous with a low risk of radiation-induced aging.

Box 7.1 Cellular Factors Influencing Radiosensitivity

- Radiosensitivity differs throughout the cell cycle with, in general, G_1 phase taking an intermediate position, and late S phase being most radioresistant.
- The greater proportion of repair by HR than by NHEJ in late S phase may explain the resistance of late S phase cells.
- Chromatin compaction and poor repair competence (reduced enzyme access) could explain the high radiosensitivity in G_2/M.

- "Radiosusceptibility" is the proneness to radiation-induced cancers which are non-toxic effects attributable to cell transformation and/or genomic instability (in part correlated with DNA misrepair). Since IR is considered to be a carcinogenic agent, radiosusceptibility is distinctly and strongly linked to susceptibility to spontaneous cancer induction. The term "radiosusceptibility" was proposed due to its similarities with "cancer susceptibility," extensively used in the ICRP (International Commission on Radiological Protection) reports and since it introduces the notions of stochastic events [9].
- "Radiodegeneration" responses are non-cancer effects attributable to mechanisms which are related to accelerated aging and often correlated with unrepaired DNA damage that is tolerated by and accumulated in cells [9]. Radiodegeneration responses cannot be considered like radiosensitivity responses as defined above since their incidence rates, the types of cellular death, and the genes involved are different.

7.2 Biomarkers of Radiation: General Considerations

7.2.1 Definition

A biomarker is an objective feature with one or more defined characteristics which indicate specific normal biological and pathological processes, or responses to an exposure or to therapeutic interventions. To date, radiation biomarkers are primarily identified in blood or saliva and are measurable indicators that reflect an interaction between a biological system and one or more environmental agents (chemical, physical, or biological). Biomarkers provide crucial information on the complex molecular cascade of events and their mechanisms underlying the pathological conditions or pharmacological responses to a therapeutic intervention.

Biomarkers can be used to assess various different types of biological characteristics or parameters. These include genetic sequences, receptor expression patterns, radiographic or other imaging-based measurements, blood composition, electrocardiographic parameters, or organ function. Since biomarkers are quantifiable, they can be used to characterize the response to direct or indirect IR exposure, to select radiation dose, and to assess the potential safety issues related to dose administration. A large number of such biomarkers have been developed over the years; the characteristics of the different classes of radiation biomarkers will be reviewed in Sect. 7.2.2.

7.2.2 Characteristics of a Good Biomarker

Although the definitions, nature, and use of biomarkers are multiple and rapidly evolving with the sophisticated—omics technologies, they must be evaluated in terms of their ability to address etiology and genetic susceptibility, predict and quantify dose of exposure. There are certain properties which are desirable when linking a biomarker with an exposure, e.g., IR. These include high specificity and sensitivity, known variability in the general population, should give reproducible results when assessed and multiplexing of analyses to allow for screening purposes. Some additional desirable characteristics of an ideal biomarker can be listed for use in large scale molecular epidemiological studies: (a) Early expressivity; (b) Linear relationship across time; (c) Strong correlation with a health effect; (d) Reproducible between laboratories; (e) Biologically plausible; (f) Inexpensive and feasible for sample collection; (g) Consistency (the same exposure will produce the same concentration of the biomarker every time).

7.2.3 Radiation Biomarkers for Potential Use in Epidemiological Studies

Radiation biology research has identified several approaches, especially the "omics" fields, as promising avenues for the development of suitable biomarkers of high sensitivity and specificity for radiation exposure. Radiation epidemiology biomarkers should preferably be specific to radiation and independent of other environmental exposures such as tobacco or cigarette smoke. Such a biomarker would simplify analysis and help to substantiate radiation causality. Though biological biomarker often lack specificity, they can still be informative in predicting the development of radiation-induced disease if such exposures are additive or interactive. Multi-biomarker approaches should be particularly useful in epidemiological studies, both for (1) assessing exposure–response relationships and how they vary with individual susceptibility and (2) to understand better disease mechanisms and the interplay of different possible pathways.

Contrariwise, carefully planned molecular epidemiological studies are crucial for the validation and verification of biomarkers, to determine their specificity and sensitivity as well as factors that might influence them (e.g., age, sex, smoking status, environmental agents, chronic conditions such as inflammation or individual sensitivity) [10].

7.2.4 Integrating Biomarkers into Molecular Epidemiological and Biological Studies

The ultimate goal of using biomarkers in molecular epidemiological studies is to be able to predict health risk. The types of biomarkers mentioned in Table 7.2 hold substantial prospective in epidemiological studies; however, there are a number of key questions to be considered which are generic to their application. Among these are: "What to measure?" "Where to measure?" and "When to measure?"

Determining if a biomarker is a good biomarker (the characteristics to determine an ideal biomarker are outlined in Fig. 7.1) for molecular epidemiological studies is complex because this relies on a number of different concepts associated with the radiation exposure and otherwise, which will very much depend on the biological samples such as cells (buccal cells, fibroblasts, hair follicle cells, etc.), blood, saliva, urine, tooth, hair, nail which can be collected non-invasively at different time points post IR exposure to study biological effects.

Table 7.2 Classification of biomarkers based on temporal parameters

Biomarkers of exposure	• Available at some point after exposure. • Suitable for estimating the dose received and identifying human internal exposure to environmental and occupational chemicals/radiation by using novel techniques and approaches. • Biomarkers of this category can have potential for use in radiation oncology to provide information on the probable outcome of RT. • Cytogenetic biomarkers are the best dosimetry biomarkers of radiation exposure as they show a high degree of specificity and sensitivity. • Emerging biomarkers related to alterations in transcriptional profiles can have potential as biomarkersBiomarkers of exposure [11].
Biomarkers of susceptibility	• Available before, during, or after exposure. • Provide key information which reflect intrinsic characteristics toward adverse effects of an exposure and thus predict an increased risk of radiation-induced health effects. • Appropriate to provide meticulous knowledge of the exposure-risk relationship, and variability of risks between individuals of identical or different population/subgroups. • Genetic variants (polymorphism) and/or metabolic phenotypes associated with cancer predisposition may prove to be useful biomarkers of susceptibility. • Cytogenetic endpoints (e.g., the G_2 assay) are of interest as biomarkers of susceptibility.
Biomarkers of late effects	• Suitable for assessing a long-time health effects post exposure, even before clinical detection of radiation induced disease or death. • Cytogenetic assays emphasize some potential as biomarkers of late effects of radiation exposure to predict the risk of RT side effects. • Transcriptional biomarkers can be employed to identify either pathways or gene expression signatures predictive of susceptibility and late health effects.
Biomarkers of persistent effects	• Applicable to assess radiation effects present a long period of time after exposure. • Biomarkers of exposure and effects may potentially be used to identify individuals at higher risk of development of cancer. • Chiefly an aspirational category on the basis of current science.

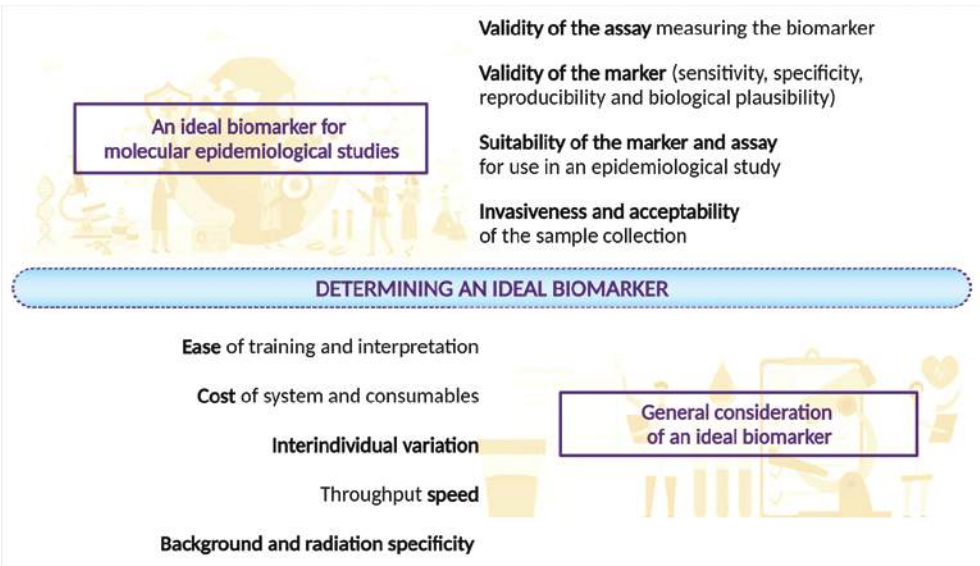

Fig. 7.1 Characteristics to determine an ideal biomarker. An ideal biomarker for molecular epidemiological studies (top) and general considerations of a good biomarker (bottom)

There is a great interest in developing new biomarkers for radiation exposure, which could be used in large molecular epidemiological studies in order to correlate estimated doses received by individuals and health effects using high-throughput technologies, i.e., "omics." In these instances, biomarkers can provide a measure of external exposure as well as internal absorption of radioactive material and can thus be markers of internal dose as well. However, factors other than the exposure may influence biomarker expression, and thus there may not always be a simple relationship between external exposure and internal dose. For example, DNA or protein adducts may be applicable as markers of other processes such as absorption, distribution, metabolism, and DNA repair, as well as of exogenous exposure. As a result, the measured internal radiation doses (biomarkers) will be an amalgam of exposure and these variables.

In a nutshell, reliable radiation biomarkers databases can be shaped by integrating the information from radiation genomics, metabolomics, and proteomic analysis in order to expand the scientific frontiers on predicting and/or monitoring radiation exposure-associated effects. Such protocols along with more sophisticated technologies are probably vital for the development of personalized medicine and will undoubtedly prove highly useful to bring a new horizon of therapeutic possibilities [12] (Box 7.2).

Box 7.2 Biomarkers for Epidemiology and Dosimetry

- Biomarkers and/or biological dosimeters are essential for predicting and/or monitoring radiation exposure-associated effects, quantifying the exposure, estimating absorbed radiation dose in certain accidental situations or a suspected radiation overexposure.
- Radiation epidemiology biomarkers should be specific to radiation and independent of other factors that might influence them (such as age, chronic conditions, smoking, tobacco, or individual sensitivity).
- Identifying biomarkers of IR exposure employs a multi-parametric approach to achieve an accurate dose and risk estimation.

7.2.5 Biological Classification

Several biological responses can act as potential biomarkers for IR exposure. They are linked to cellular or physiological mechanisms which have been shown to change soon after radiation exposure. The use of various "omic" technologies together with hypothesis-driven approaches may be highly useful to measure radiation biomarkers in a biological system. Some biomarkers could be used as response markers or as surrogate endpoints to predict radiation side effects. The expression levels of many biomarkers can be expected to be correlated with each other and so could be classified in multiple categories, such as

- Phosphorylated histone H2AX (γ-H2AX) acts as protein biomarker for radiation exposure but is useful as a DNA damage marker; suggesting a close one-to-one relationship between initial as well as residual radiation-induced DNA DSBs and γ-H2AX foci.
- 8-oxo-dG acts as a marker of nucleotide damage but is strongly associated as a maker of oxidative DNA damage suggesting it is produced abundantly in DNA exposed to free radicals and reactive oxygen species (ROS).
- Phosphoproteomic profiling insights into processes influenced by epigenetic modifications, but also uncovers signaling pathways.

These biomarkers can be organized in categories such as (a) cytogenetic; (b) nucleotide pool damage and DNA damage; (c) germline inherited mutations or variants; (d) induced mutations; (e) transcriptional and translational changes; (f) epigenetic modifications; (g) lipid peroxidation; (h) others, including biophysical markers (Fig. 7.2).

Biomarkers of radiation exposure are further discussed in Chaps. 2, 3, and 8.

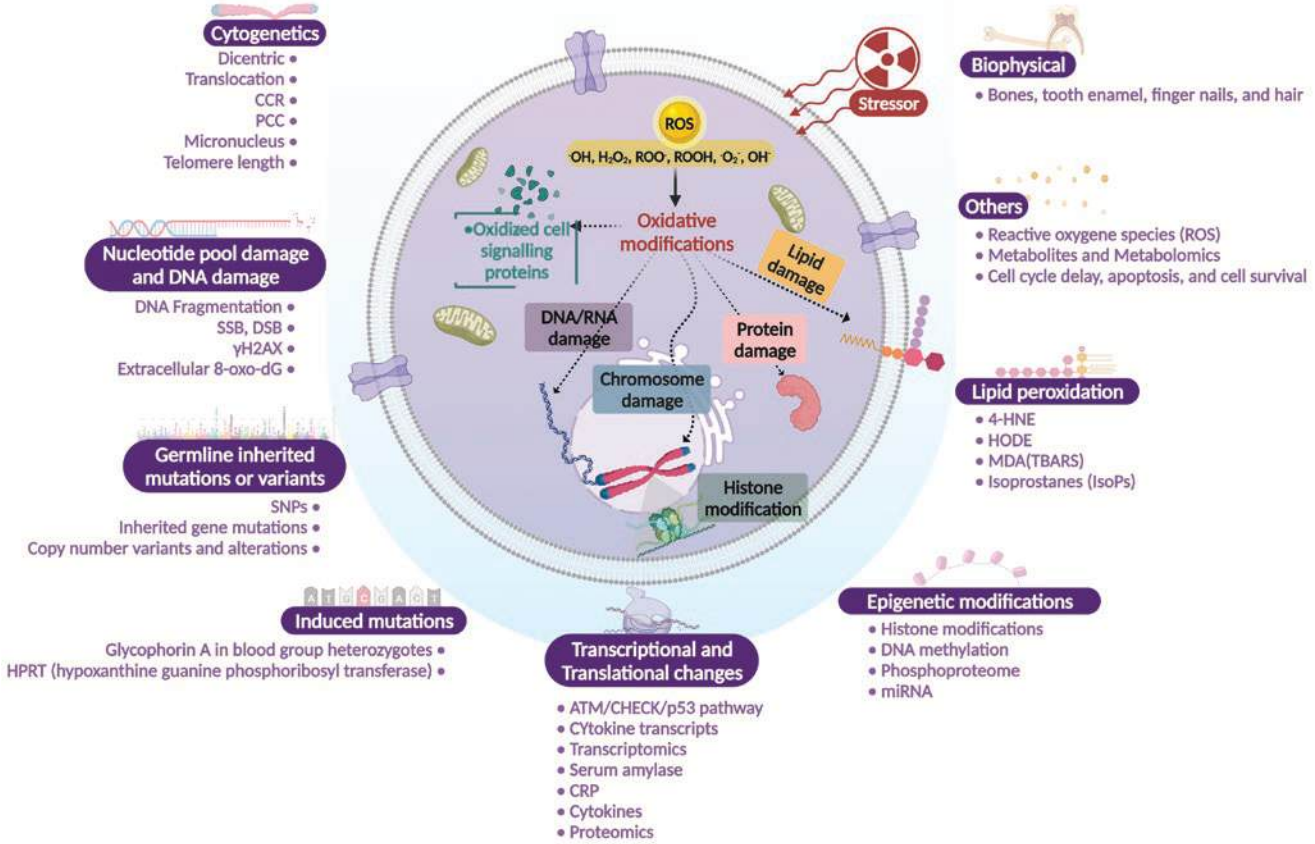

Fig. 7.2 Biological classification of radiation biomarkers. (Reproduced with permission, with some modification (changed layout and some content), from [10]; licensed under CC BY-NC-ND 3.0)

7.3 Temporal Classification of Biomarkers

Over the past decades, the definition and classification of the different types of biomarkers have varied slightly, depending on the biomedical field considered. Biomarkers are an important aspect of radiation countermeasure development and can be used as a trigger for intervention as well as in selecting a radiation dose and treatment regimen in humans, e.g., in the context of RT of cancer ([13] and as further discussed here in Chap. 7 and in Chap. 8). Biomarkers can also provide information on potential modifying/confounding factors to allow an assessment of biological interactions. Pernot et al. [10], Hall et al. [14] classified biomarkers into four broad categories, based on their temporal parameters Table 7.2.

One should be cognizant of the fact that overlap does exist between these different types of biomarkers. Taken together, these attributes enable a better understanding of exposure and its effect on biological pathways across different forms of exposure, health changes, disease headway; providing more meaningful comprehensive risk assessment (Fig. 7.3). This classification is acceptable not only with respect to the timing of processes that can be measured with these biomarkers, but also in considering the most adequate designs and sampling procedures in molecular epidemiological studies (Box 7.3).

Box 7.3 Use of Biomarkers at Different Times Post Exposure

- Biomarkers of exposure are available at some point after exposure and are suitable for estimating the dose received.
- Biomarkers of susceptibility can be available before, during, or after exposure and can predict an increased risk of radiation effects.
- Biomarkers of late effects can be used to assess health effects that are present a long time after exposure before clinical detection of the radiation induced disease or death.
- Biomarkers of persistent effects allow the assessment of radiation effects present a long period of time after exposure.

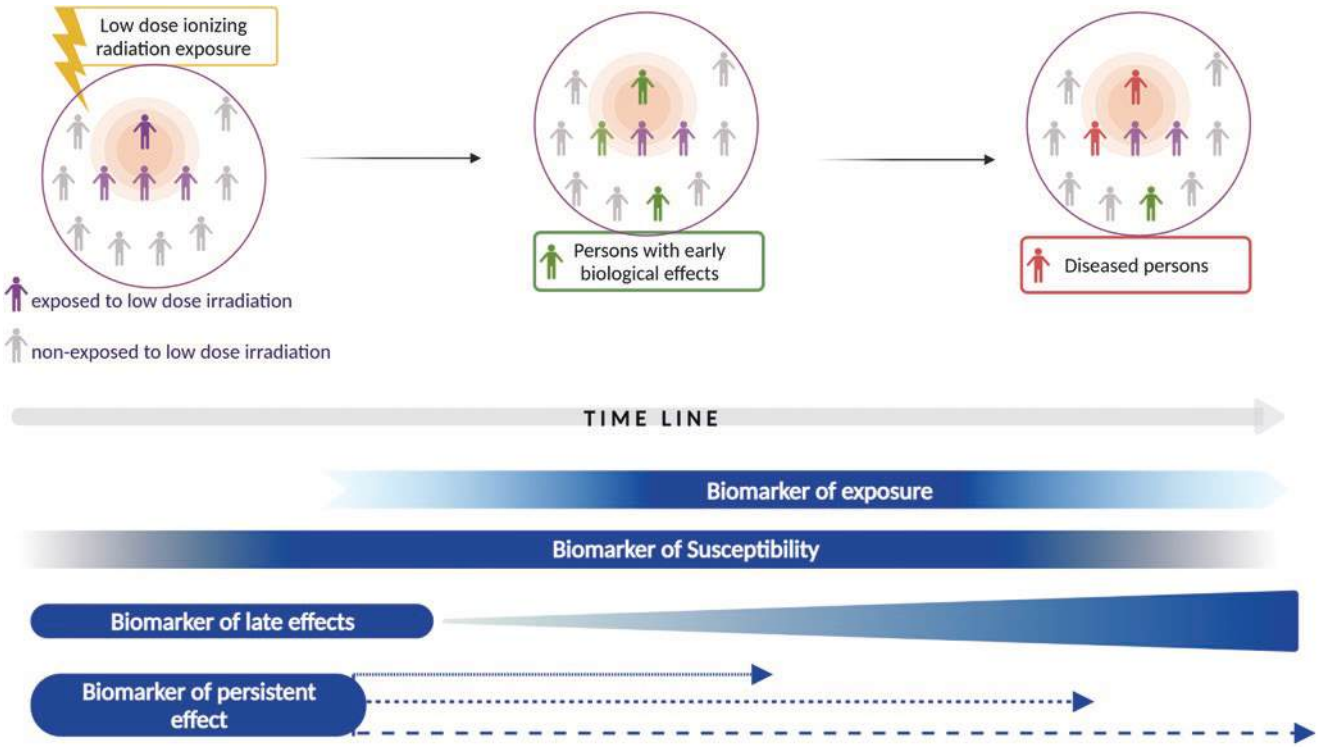

Fig. 7.3 Timeline of radiation-induced disease progressions and relation with different types of radiation biomarkers. (Reproduced with permission, with some modification (changed color and layout), from [10]; licensed under CC BY-NC-ND 3.0)

7.4 Collection of Individual Samples for Radiation Studies

Not only since the "age of OMICS," it is well known that the collection of samples from patients and healthy volunteers is essential for future research [15]. Especially in radiation research, the collection of biological samples represents a significant part of translational research, since, especially in studies on radiation protection, the collected biological samples represent an essential parameter for analysis of (historic) radiation exposure [14]. Also, in therapeutic trials, the sampling of tissues and body fluids has an immense impact on the search, discovery, and validation of novel biomarkers supporting the pathological diagnosis as well as for the determination of therapy toxicity and/or outcome [15, 16]. The collected samples may safely expand the possibilities of the entire analytical process within prospective and retrospective trials in radiation science. However, the collection and storage of biological samples should always be done within a quality-controlled manner [17]. In contrast to tissue sampling, the sampling of body fluids also has the big advantage, that these samples are nearly always available or easy to access like vein puncture. In addition, the sampling of blood can be done mostly together with clinical mandatory blood draws, minimizing the burden of the patient/donor, and enhancing the amount of time points of sampling as well as it also increases the donor's acceptance of giving blood for research. Since the collection of samples at biobanks accelerate the process of transferring scientific knowledge into therapeutic application, it should be the duty of clinical researchers adding translational programs with sample collection to the prospective clinical trials. In our hands, the sampling and analysis of immunological parameters lead to predictive biomarkers supporting the pathological diagnosis and therapeutic intervention and helping radiation treatment in precision medicine [16, 18].

The sampling, the processing, as well as the storage have to be done in a quality-controlled manner as outlined before by Winter and colleagues [19] or at the respective international biobank consortia like the European, Middle Eastern and African Society for Biopreservation and Biobanking (ESBB), or the European research infrastructure for biobanking (BBMRI-ERIC; [20]). There are another three very important things to keep in mind when collecting samples for later analysis: The best collections are almost worthless if they are not connected with clinical, radiation exposure, and patients/donor data. Along with this, the informed consent of the donor should allow use of the samples for the respective analyses even when the samples will be given for, e.g., "OMICS" analysis to a cooperation partner or to the statistician who performs the analysis of the data. Lastly, a biobank is a living "thing"

which should be used for research and not as a secure vault to store samples for eternity. Taken together, it should be the duty of research on humans to collect and store samples for further analyses, but also processing and storage should be carried out in accordance with applicable regulations and standards. This is the only way to ensure that the samples do not suffer any loss of value and are available for later applications.

7.5 Predictive Assays

Tissue reactions induced by IR are the result of different types of cell death (mitotic death, apoptosis, autophagy, senescence, etc.). Loss of clonogenicity (and not physical disappearance or metabolic shutdown) appeared to be common to all types of cell death.

In 1957, Puck and Markus proposed to use clonogenic assays (or colony method) to quantify cellular radiosensitivity [21] (Fig. 7.4). The assay is based on the ability of an individual tumor cell to grow into a colony after exposure to various doses of radiation given the surviving fraction (SF) at each dose. The fraction of cells surviving after 2 Gy (SF2) has been demonstrated to be a robust predictor for radiation sensitivity but colony formation can take 7–14 days. Several predictive tests have been proposed to approach clonogenic survival but with a suboptimal statistical power.

The original clonogenic assay can be performed in two different ways (1) irradiation after plating or (2) plating after irradiation. The first is usually carried out to investigate intrinsic radiosensitivity to varying modalities (types) of treatment, and the second allows for the assessment of reproductive ability. The irradiation after plating method is presented in Fig. 7.4 as it is usually used in radiobiological studies. Further details on the clonogenic assay can be seen in Chap. 3.

Several techniques continue to rely on cell culture:

- The level of radiation-induced micronuclei (MN) has been quantitatively correlated with radiosensitivity since the 1960s thanks to a simple and robust protocol consisting of blocking the process of cytokinesis by drugs such as cytochalasin B [22].
- The premature chromosome condensation (PCC) assay consists in making chromosome fragments appear more quickly by fusing the tested cell with a cell in mitosis. The heterokaryon thus formed allows the exchange of mitotic factors in the cell into G_0/G_1 and then produces premature condensation of the chromatin [23].
- The enumeration of chromosomal aberrations by fluorescence *in situ* hybridization technique.

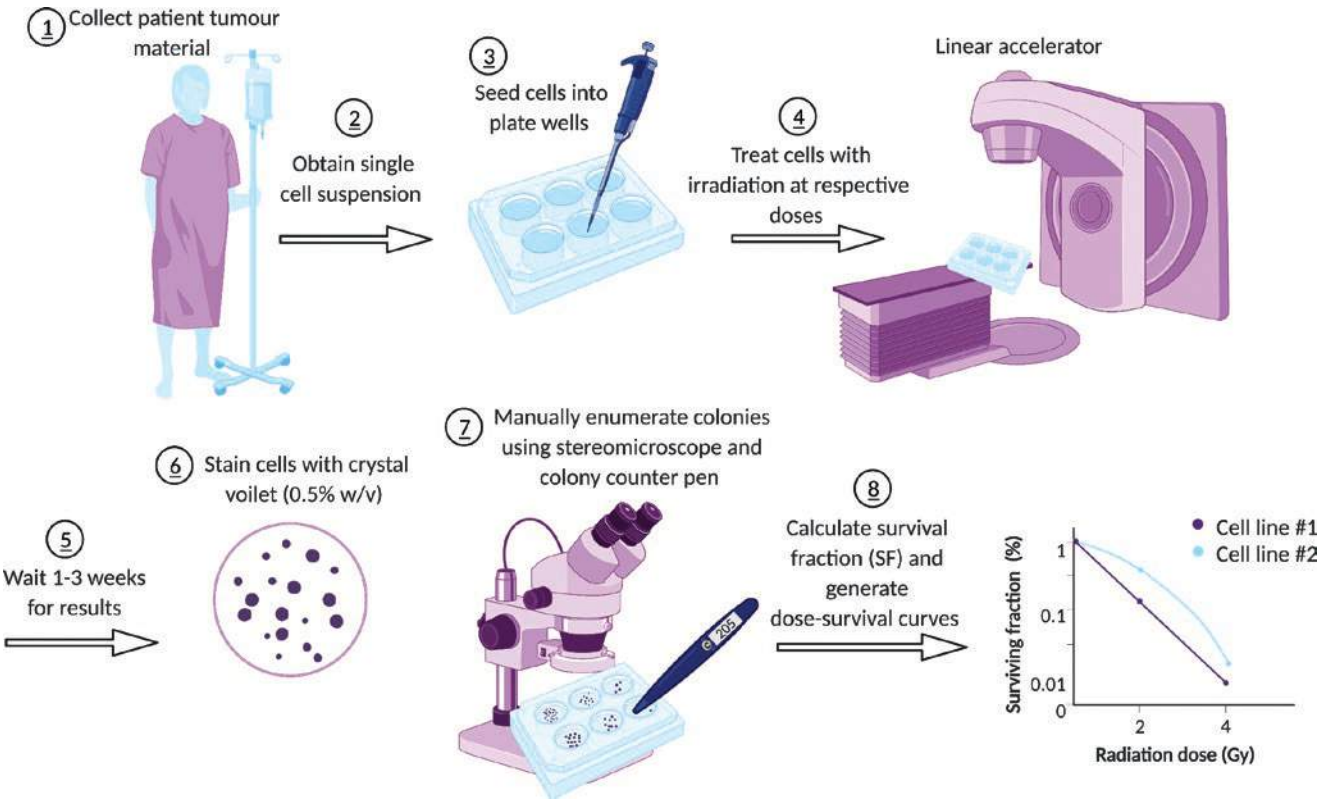

Fig. 7.4 Brief overview of the original clonogenic assay

It made sense to focus on the molecular mechanisms of the cellular response to radio-induced damage to DNA and in particular to DNA repair, since a quantitative link between unrepaired Double-Strand Breaks (DSB), chromosomal breaks, and radiation-induced clonogenic cell death was demonstrated [24]. Moreover, the vast majority of genetic syndromes associated with individual radiosensitivity are linked to mutations in genes involved in radiation-induced DSB signaling or repair. DSB measurement techniques were investigated with some confusion on their specificity and instead reflected other types of damage [7]. The first techniques for measuring DSB were based on discriminating radiation-induced DNA fragments based on their size. This was particularly the case with sedimentation in sucrose gradients, neutral elution, and pulsed-field electrophoresis. Such a principle has the advantage of measuring the repair of DSBs independently of any molecular repair pathways regardless of the post-irradiation time. On the other hand, these techniques do not make it possible to assess the quality of the repair, that is to say whether it is faithful or at fault.

The halo technique consists, using fluorescent intercalators, in quantifying such an increase in the nucleus. The comet technique combines electrophoresis and the halo technique, both applied individually to each cell. Data from the comet technique are usually given in the form of the product of the increase in the size of the nucleus (comet head) times the distance that DNA fragments migrate (comet tail) [25].

From 2003, with indirect immunofluorescence, it became possible to follow precisely and in real time in the nucleus and for a wide dose spectrum, the kinetics of appearance/disappearance of DNA repair proteins (foci). A correlation between SF2 and the rate of unrepaired DSB 24 h after 2 Gy (γ-H2AX marker) could be demonstrated—constituting a functional repair test [26]. A second marker significantly increased the performance of the test—based on the speed of nuclearization and the functionality of the pATM protein in the nucleus [8].

Genome-wide association (GWAS) studies have been widely used to identify associations between commonly occurring variations in DNA sequence, such as single nucleotide polymorphisms (SNP) and human traits such as individual radiosensitivity [27]. A few SNP as well as mitochondrial haplogroups have been reported.

The interest in the predictive power of the transcriptome began in the early 2000s and *in vitro* transcriptomic signatures for individual radiosensitivity then emerged. The identified predictive genes were associated with cellular functions such as TGFβ pathway, particularly extracellular matrix remodeling, apoptosis, proliferation, and ROS scavenging [28, 29] (Table 7.3).

Epigenetic modifications include histone modifications such as acetylations and methylations, DNA methylation, particularly on CpG island, non-coding RNAs, and three-dimensional chromatin organization. As this a relatively new field, only few studies have been conducted on the epigenetic regulations of skin fibrosis, mainly on miRNAs [32, 33].

Ozsahin et al. [34] developed a rapid radiosensitivity test (<24 h) based on lymphocyte apoptosis, a biological response developing 6–72 h after irradiation. The authors showed that low Radio-Induced Lymphocytic Apoptosis (RILA) was significantly correlated with late grade ≥2 tissue toxicities.

In recent years, the identification of routinely available blood and clinical markers that may help to predict the response to immune therapies alone and in multimodal settings including RT has been in focus of scientists of several disciplines and clinicians [35, 36]. Here, immune markers of the peripheral blood are key factors, since they circulate in the body and enter several tissues in response to disease, therapy, and stressors such as radiation. Stress and immune parameters should jointly be considered, and a differentiation between primary radiation signatures and consecutive systemic immune biosignatures is challenging, but anyhow interconnected [37, 38]. Notably, single immune parameters are insufficient, but rather immune profiles that reflect the complexity of the immune system and the manifold interactions of its cellular and soluble components [16, 39].

Table 7.3 Reported gene expression signatures for individual radiosensitivity

Publication	RS patients	RR patients	Radiation scheme	Selected differentially expressed genes	Assay used for gene selection
Quarmby et al. [28]	3	3	Not irradiated	FMLP-R-I, TNFα, NGFR, EPHB2, PDGFB, NTRK1, LFNG, DDR1; IFNGR1	Cytokine array
Alsner et al. [30]	22	4	3 × 3.5 Gy over 3 days, RNA extracted 2 h after last irradiation	CDC6, CDON, CXCL12, FAP, FBLN2, LMNB2, LUM, MT1X, MXRA5, SLC1A3, SOD2, SOD3, WISP2	15K cDNA microarray
Rødningen et al. [31]	10	4	3 × 3.5 Gy over 3 days, RNA extracted 2 h after last irradiation	PLAGL1, CCND2, CDC6, DEGS1, CDON, CXCL12, MXRA5, LUM, MT1X, MT1F, MT1H, C1S, NF1, ARID5B, SCL1A3, TM4SF10, MGC33894, ZDHHC5/MFGE8	15K cDNA microarray
Forrester et al. [32]	6	8	Not irradiated	FBN2, FST, GPRC5B, NOTCH3, PLCB1, DPT, DDIT4L, SGCG	GeneChip Human Exon 1.0 ST Array

7.5.1 Predicting the Response of Tumors to Radiotherapy

Tumor response to RT is a multi-faceted metric of outcomes after radiotherapeutic treatment, often observed through biopsy of the tumor or liquid biopsy. There is currently no universal definition of tumor response, but it can generally be considered as any favorable response of the tumor to therapy. Tumor biopsies may aid in the development of personalized patient treatment regimens by providing molecular and structural material for use in developing metrics capable of identifying who will or who will not favorably respond to RT. For patients who do not respond favorably to treatment, they can be offered another more effective avenue of treatment, sparing them from treatment toxicity.

Identifying treatment-resistant phenotypes/genotypes and therapeutic targets that may influence tumor response is at the center of current radiation biology research. Robust, patient-specific, and predictive biomarkers are critical to assess tumor response to improve patient treatment and outcomes. There is an unmet clinical need to identify translational biomarkers that allow for tailor-made and optimized patient-specific treatment. Patient tumor samples such as tissue and liquid biopsies along with varying modalities of analysis that can be performed to identify predictive biomarkers of RT treatment response will be discussed in this subsection (Figs. 7.5 and 7.6).

7.5.1.1 Tissue Biopsy

Tissue biopsies are the current gold standard for profiling tumors and can provide both key pathological and molecular information [41]. Numerous studies have investigated the potential of tumor tissue biopsies to predict the biological behavior of tumors, before and during RT, which could highlight the modes of biological action toward radioresistance. Examples of studies are provided in Table 7.4.

Immunohistochemistry (IHC) is a low-cost technique used by pathologists that involves staining fresh, frozen, or paraffin-embedded tissue and is widely applied in a clinical diagnostic setting. IHC has been used to identify predictive tissue biomarkers for RT response and include markers related to cell proliferation; ki67 and PKA (protein kinase), cell cycle checkpoint; p53 and p16, apoptosis; bcl2 and bax, growth factor receptors; EGFR (epidermal growth factor receptor) and finally, hypoxia; HIF1α (hypoxia-inducible factor 1-alpha (e.g., [42])). IHC facilitates the direct assessment of antigen expression in tissues through enzyme-conjugated antibodies. Initially, IHC was designed to classify the cellular origin of a tumor but with enzyme-conjugated antibodies and paraffin embedding, IHC is also capable of assessing treatment efficacy and is useful for tumor subtyping as well as in predicting patient response to RT. However, IHC is prone to pre-analytical subjectivity, operator subjectivity, and limited to known proteins [46]. Patient-derived 3D models can also be used to assess tumor response to RT and will be discussed in the following section.

7.5.1.2 Patient Tumor Tissue-Derived Organoids (PDOs)

In the last decade, patient-derived organoids (PDOs) have provided novel models for preclinical and translational research for assessing tumor response toward personalization of treatment. Organoids have the potential to be used as predictors for patient treatment response due to their ability to reflect the biological characteristics of primary tumors, i.e., intra-tumor heterogeneity, genotype, and phenotype [47] as well as the tumor microenvironment [48]. Compared to 2D models, PDOs possess improved cell morphology, differentiation, and viability, rendering them more relevant to the *in vivo* context [49]. Assays that can be performed on organoids include genomic profiling, survival assays, flow cytometric analysis, immunofluorescent, and histological staining. The main limitations associated with organoids include their high cost both in an economic and time-input sense [50].

7.5.1.3 Patient-Derived Xenografts (PDXs)

PDXs are mouse models that are widely used in modern cancer research and are proving to be another useful platform in the development of personalized medicine strategies due to an improved relationship with the context *in vivo*. PDXs also demonstrate similar susceptibility to anti-cancer therapies, they closely resemble patient tumor features, have similar histological and molecular characteristics, and can be cultured long-term *in vitro* [51, 52]. The tumor material to be used in PDXs is derived from fresh tumor tissue collected from a patient during surgery. Small tumor pieces are then implanted into severely immunodeficient or humanized mice. Although PDXs are a promising tool for translational research, they are difficult to apply as tumors may not grow or metastasize. Other disadvantages include the long process required to establish a model which requires significant involvement by pathologists, sampling and representational issues due to tumor heterogeneity, the overall economic cost of their development, their inability to evaluate the involvement of the immune system *ex vivo*, the potential for grafts to be rejected ("engraftment rate"), and the required use of regulated and approved animal facilities [53].

PDX models have been used to investigate biomarkers of RT response with the aim of stratifying patients based on risk and facilitating the individualization of treatment, as exemplified recently in PDX models of glioblastoma. The CHGA and MAPK8 gene signatures have been associated with increased survival in patients with glioblastoma who have received RT [54]. As the use of PDXs to reliably predict clinical activity of treatment options is still in its infancy, it is currently unknown whether these models can be used to

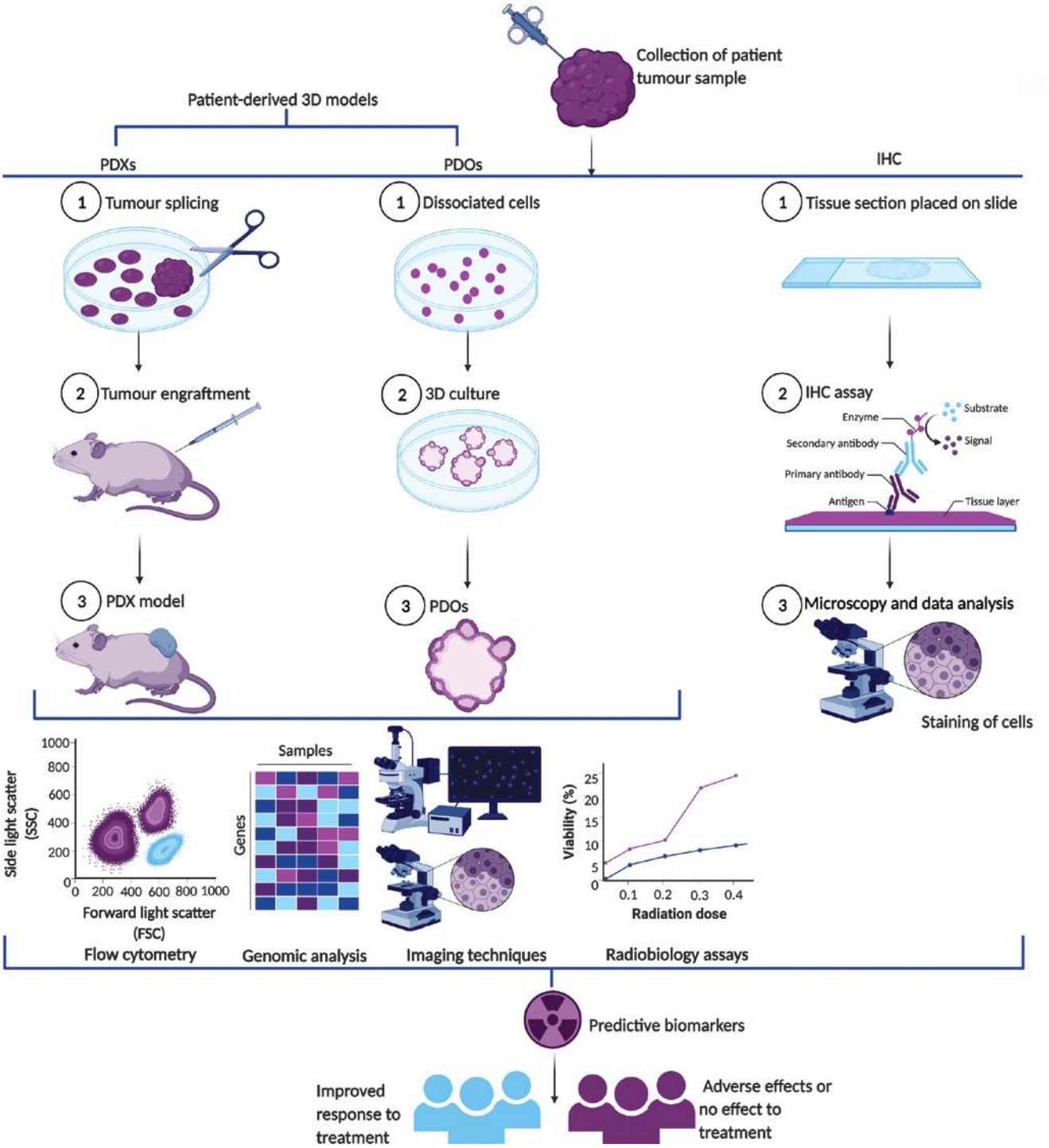

Fig. 7.5 Patient tissue biopsy sample types and different modalities of analysis that can be performed to identify predictive biomarkers of RT treatment response

guide individual treatment strategies in a time frame that is useful for a patient. Future technological advancements may accelerate their involvement clinically.

The invasive nature of tumor sample acquisition lends to many of the limitations associated with this sample type, including being painful and difficult to collect, time-taxing, having limited repeatability due to localized sampling of tissue. In addition serial assessments are often limited, and this diagnostic approach requires expert pathologists for evaluation, with the potential to introduce new risks to patients. Importantly a tumor may not be fully represented by a single tissue biopsy due to tumor hetero-

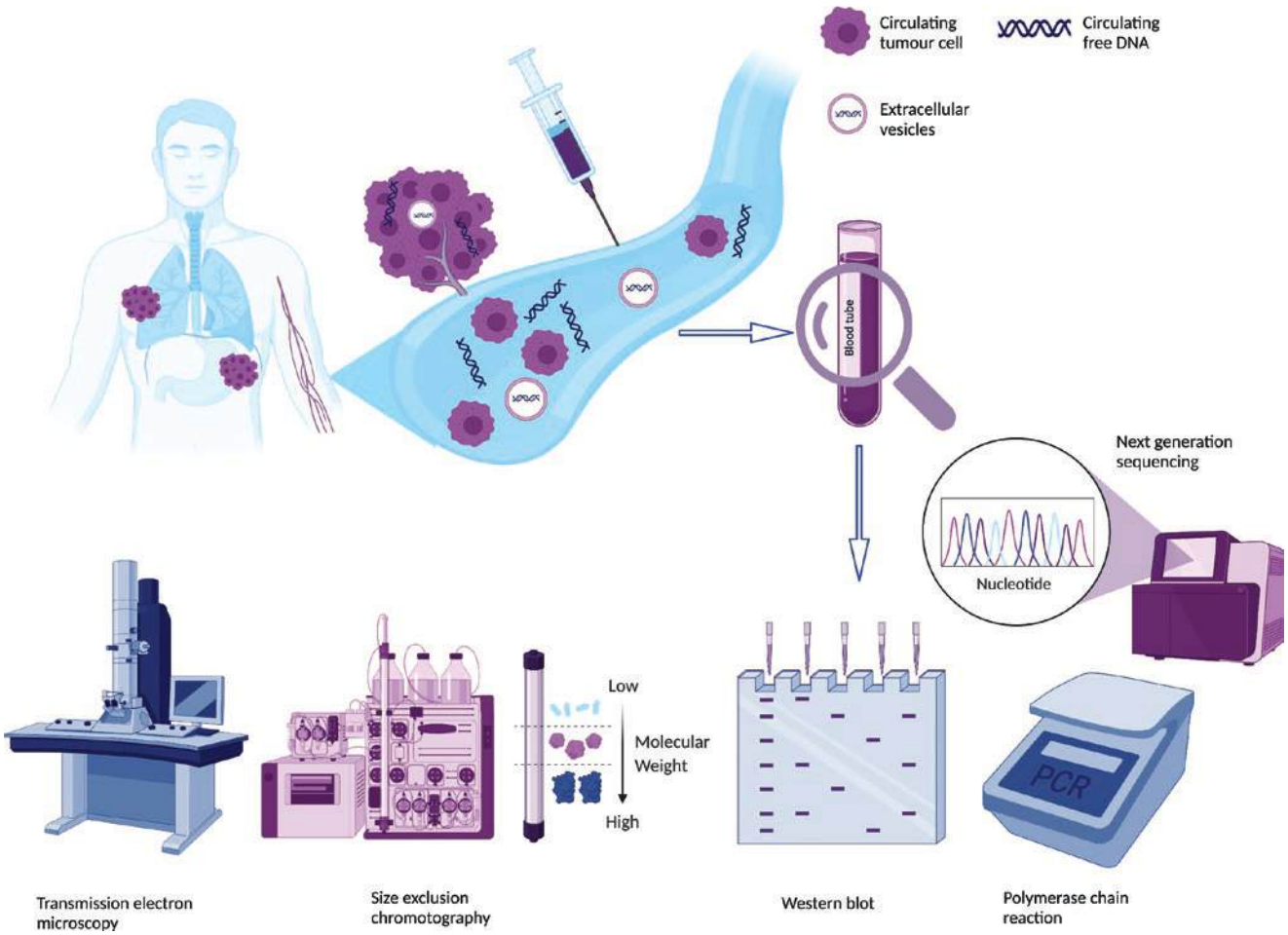

Fig. 7.6 Schematic of clinically informative elements obtained by liquid biopsy and various analysis methods. (Reproduced with permission from [40])

Table 7.4 Examples of studies that have used tumor biopsies to predict response to RT.

Research team	Technique	Tissue type	Main outcome
Pollack et al. [42]	Tissue biopsy—IHC	Prostate cancer	Ki67, a marker of cellular proliferation, and apoptotic proteins bcl2 and bax are independently associated with BCDF.
Wilkins et al. [43]	Tissue biopsy—IHC	Prostate cancer	Ki67 is an independent prognostic factor for BCDF.
Driehuis et al. [44]	PDOs—Next generation sequencing and dose response kill curve	HNSCC	A patient with a prolonged response to RT had an organoid line with the highest sensitivity to RT. Relapsed patients post-RT also had the most resistant organoid lines.
Yao et al. [45]	PDOs—Whole-exome sequencing and organoid size	Locally advanced rectal cancer	The PDOs matched the clinical outcomes of the patient with a 85% match ratio ($n = 80$).

Abbreviations: *IHC* immunohistochemistry, *PDOs* patient tumor tissue-derived organoids, *HNSCC* head and neck squamous cell carcinoma, *BCDF* biochemical or clinical disease failure, *RT* radiotherapy

geneity which potentially adversely affects the accuracy of the test. Lastly, if the condition of a patient has worsened, the acquisition of tissue biopsy is not feasible [55, 56].

7.5.1.4 Liquid Biopsy

As the collection of tissue biopsies from patients often introduces unnecessary risks to the patient, there has been a recent increase in the focus on safer and less invasive sample collection methods, including via liquid biopsies. Liquid biopsies are generally a rich source of tumor-specific biomarkers, providing a temporal snapshot of the genomic character of a tumor, and can help overcome the complication of intratumor heterogeneity [56]. However, there are several limitations associated with liquid biopsies, including the lack of standardization of methodologies and inadequate technical/clinical validation for routine clinical utility [57].

It is known that intra-tumoral components are released into the bloodstream, urine, cerebrospinal fluids, pleural fluid, and so on, and that each contains information relating to tumor-specific material [58]. Blood is the most widely investigated liquid biopsy and where intra-tumoral components such as circulating tumor cells, circulating cell-free DNA, and extracellular vesicles (EVs) can be found [59]. These are the most investigated of the intra-tumoral components and will be discussed in this subsection (Fig. 7.6). Other intra-tumor components include circulating RNA, circulating proteins, and tumor-educated platelets; however, they will not be discussed in this subsection. Due to recent technological advances, these circulating biomarkers can be detected and researchers have identified them as a novel and promising avenue for stratifying patients based on risk and identifying patients who may be radiosensitive or possess radioresistant disease.

7.5.1.5 Circulating Tumor Cells (CTC)

CTCs have recently been discovered to be potential biomarkers for predicting tumor response to RT. A recent study by Qian et al. [60] demonstrated that nasopharyngeal patients with a complete response to concurrent chemoradiotherapy exhibited decreased CTC levels when compared to patients with a partial response. CTCs enter the bloodstream or lymphatic system and are disseminated throughout the body as they are released from primary, metastatic, or recurrent tumors. Metastatic tumors in distant locations can also form through CTCs that evade immune cell recognition [61]. These cells are rare, and the proportion present in peripheral blood is quite low when compared to white and red blood cells [62]. Molecular heterogeneity and the low concentration of CTCs in peripheral blood lead to multiple limitations in terms of their isolation, enumeration, and detection [63]. Current platforms to isolate and analyze CTCs are based on distinguishing features between CTCs and white and red blood cells such as morphology, biophysical and biomechanical properties along with modification, synthesis, regulation, and concentration of protein [64]. CTC isolation/enrichment platforms include microfiltration devices and dielectrophoretic field flow fractionation (DEP). CTC recognition platforms can be split into two groups: (1) label independent and (2) label dependent. The former includes PARSORTIX and CytoTrack. The latter includes iCHIP, CTC-Chip, and CELLSEARCH [64]. CELLSEARCH is an FDA-approved platform and is based on the expression of cell surface markers such as epithelial cell adhesion molecule (EpCAM), cluster of differentiation (CD)45 (CD45), cytokeratins 8, 18, and/or 19 [65]. This platform uses antibodies against these cell surface markers conjugated with magnetic nanoparticles or immobilized on microfluidic chips.

7.5.1.6 Extracellular Vesicles (EVs)

EVs can be isolated from a wide range of body fluids, such as bile, cerebrospinal fluid, saliva, breast milk, urine, blood, and amniotic fluid. Various cell-derived membrane structures are collectively termed EVs and include exosomes, microvesicles, and apoptotic bodies [66]. Exosomes are ideal candidates to study response to RT because radiation not only alters exosome manufacturing, but also affects their molecular cargo [67]. However, investigating the role of exosomes in radiosensitivity is a relatively novel approach, and studies currently are limited to *in vitro* studies that require translation *in vivo* to broaden our understanding of the mechanisms behind the development of radioresistance.

Current exosome isolation methods include immunoaffinity capture, ultracentrifugation, density gradient centrifugation, size exclusion chromatography, and exosome precipitation, while characterization methods include western blotting, ELISA, and transmission electron microscopy [68]. The disadvantages associated with these techniques currently make them unsuitable for clinical utility. These include (1) the large amount of starting sample and costly instrumentation that is required for analysis and (2) the labor- and time-intensive nature of the procedures required for sample isolation.

7.5.1.7 Cell-Free DNA (cfDNA)

cfDNA is reported to be found in elevated levels in cancer patients when compared to healthy individuals [69]. Usually, cfDNA is found in fragments ranging from 120 to 220 base pairs (or multiples thereof) [70]. The mechanisms responsible for the release of cfDNA into the bloodstream are not fully understood, but it is thought that it may be facilitated via apoptosis, necrosis, senescence, and actively through cell secretion [71]. In the blood, cfDNA is mostly nucleosome associated, and the tumor derived element in cancer patients is circulating tumor DNA (ctDNA) where concentrations of ctDNA have a linear relationship with tumor size and metastasis [72, 73]. Disease stage will also influence ctDNA concentration with late-stage disease associated with higher levels than early-stage disease [74].

ctDNA is more fragmented than cfDNA ranging from 100 to 200 base pairs and exists at much lower concentrations [75]. Detectable alterations that are tumor relevant include mutations, chromosomal rearrangements, copy number aberrations, methylation, DNA fragment lengths, tumor gene expression, and the presence of viral sequences (in tumors associated with oncogenic viruses) [73]. In patients with advanced stage nasopharyngeal carcinoma, plasma Epstein–Barr virus DNA load at the midpoint of RT is associated with a worse clinical outcome [76]. Detectable circulating HPV-DNA at the end of chemoradiation is associated with lower progression-free survival in HPV+ cervical cancer patients [77]. Somatic mutations in *ATM*, a DNA repair gene, can determine exceptional responses to RT in patients with head and neck squamous cell carcinoma, endometrial cancer, and lung cancer [78]. Several methods have been developed to

extract and sequence ctDNA. These methods include, but are not limited to:

1. Polymerase chain reaction (PCR)-based techniques: BEAMing PCR (beads, emulsion, amplification, and magnetics), droplet digital PCR (ddPCR), and real-time quantitative PCR (qPCR).
2. Tumor-informed sequencing approaches: cancer personalized profiling by deep sequencing (CAPP-Seq), Signatera, and targeted digital sequencing (TARDIS).

Drawbacks associated with some of these techniques include that only one or a small number of mutations can be investigated at a time, a large amount of blood is needed to identify a small number of mutations due to low concentrations of ctDNA in the blood, and prior knowledge related to the tumor must be acquired before analysis, which usually requires invasive sample collection [79]. Next generation sequencing-based techniques include whole-exome sequencing (WES) and whole-genome sequencing (WGS) are also used for ctDNA analysis and limitations related to these techniques include that a large initial concentration of ctDNA is required and low sensitivity has previously been reported for WGS [80]. Examples of studies exploring these circulatory biomarkers can be found in Table 7.5.

Further studies are needed to elucidate the role of biomarkers in predicting tumor response to RT as currently there are limited studies that investigate their potential. Furthermore, biomarker identification is in its infancy, with liquid biopsies and 3D patient-derived models providing an enormous opportunity to further advance precision medicine. The limitations associated with these techniques may be mitigated in the coming years through technological advancements that allow the creation of more specific and sensitive assays. Along with harmonization and standardization of methodologies, the techniques mentioned in this section may move from a translational phase to routine clinical use. It can be expected that research on liquid biopsies and patient-derived 3D models will only grow in the coming years, and with this comes the potential to revolutionize patient care and treatment.

7.5.2 Predicting Normal Tissue Response

The radiosensitivity of normal cells, tissues, and tumors varies considerably between patients. There is variability in the patient's response to RT, and most patients experience few or no side effects during or after treatment. However, due to this variability, many patients will receive suboptimal treatment dosing due to current dose thresholds being applied as a protective measure against toxicity events in radiosensitive patients. For patients who will develop side effects, a small number of these may develop more extreme side effects. Extreme side effects related to late radiation toxicity can be irreversible and life-threatening and greatly affect the

Table 7.5 Examples of studies that have utilized biomarkers from liquid biopsies to predict tumor response to RT (see the referenced publications for the full study details, including RT regime)

Research team	Biomarker	Methodology	Study population	Main outcome
Sun et al. [81]	CTCs	Fluorescence microscopy	Locally advanced colorectal patients (n = 115)	Baseline CTC counts of biological responders were significantly elevated when compared to non-responders
Jeong et al. [82]	ctDNA	Hybrid capture-based approach (Capp-Seq)	Non-small cell lung cancer (n = 44)	KEAP1 mutations in the NRF2 pathway; present in plasma baseline samples, promoted radiosensitivity and prediction of the rate of local failure post-treatment
Salami et al. [83]	CTCs	Epic Sciences CTC platform	Patients with high-risk localized prostate cancer (n = 19)	Higher number of baseline CTCs associated with BCR after therapy
Liang et al. [84]	EBV ctDNA	RT-qPCR	Patients with nasopharyngeal carcinoma (n = 940)	IMRT of CC patients with elevated baseline levels of EBV ctDNA (>4000 copies/mL) demonstrated greater disease-free survival and distant metastasis-free survival compared to IMRT patients
Dai et al. [85]	Exosomes	CCK-8, invasion, and apoptosis assay	GBM cell lines	Exosomes originating from long non-coding RNA AHIF overexpressing GBM cells enhanced radioresistance, viability, and invasion
Tang et al. [86]	Exosomes	miRNA technology	Non-small cell human lung cancer cells	Radiation-induced miR-208a enhanced proliferation and decreased cell apoptosis through activation of p21 of the AKT/mTOR pathway

Abbreviations: *SABR* stereotactic ablative radiotherapy, *RT* radiotherapy, *KEAP1* Kelch-like ECH associated protein 1, *NRF2* nuclear factor-erythroid factor 2-related factor, *ADT* androgen deprivation therapy, *BCR* biochemical recurrence, *EBV* Epstein-Barr virus, *GBM* glioblastoma, *RT-qPCR* real-time quantitative polymerase chain reaction, *IMRT* intensity modulated radiotherapy, *CC* concurrent chemotherapy, *HGM* human glioblastoma multiforme, *AHIF* antisense hypoxia-inducible factor, *CCK-8* cell counting kit-8, *miR-208a* microRNA-208, *AKT* protein kinase B, *mTOR* mechanistic target of rapamycin

Table 7.6 Examples of studies using traditional and emerging techniques to assess radiosensitivity

Assay	Sample type	Research team	Study outcome
Clonogenic assay	EGFR mutant (n = 6) and wild-type (n = 9) NSCLC cell lines	Anakura et al. [87]	Compared to wild-type cell lines, EGFR mutant lines demonstrate to be significantly more radiosensitive to low-dose and low fraction-sized irradiation (2 and 4 Gy).
Clonogenic assay	HNSCC patients (n = 38)	Stausbøl-Grøn and Overgaard [88]	Loco-regional tumor control was not correlated with SF2 after exposure to 62–68 Gy.
MTT assay	Radioresistance EAC cell line	Mekkawy et al. [89]	The EAC cell line can be radiosensitized if incubated with bromelain prior to irradiation. Bromelain may have clinical application in protecting normal tissues from damage.
CBMNcyt	PBLCs of LARC patients (n = 134)	Dröge et al. [90]	Cytogenetic damage of lymphocytes is not a predictor of the outcome of RCT (50.4 Gy) outcome in LARC patients.
G2 MN assay	PBLCs from 18 BRCA2 mutation carriers, BRCA1 (n = 9) and BRCA2 (n = 8) families that do not exhibit the familial mutation (non-carriers) and healthy volunteers (n = 18)	Baert et al. [91]	Increased radiosensitivity in carriers of the BRAC2 mutation compared to healthy volunteers after exposure to 2 Gy irradiation.
γ-H2AX DNA damage assay	Lymphocytes from prostate cancer patients (n = 50)	Pinkawa et al. [92]	No correlation was found between the development of toxicity and the number of γ-H2AX foci was found.
γ-H2AX DNA damage assay	PBMCs of NSCLC patients (n = 38)	Lobachevsky et al. [93]	Patients with compromised DNA repair had an elevated risk of developing toxicity.
FTIR spectroscopy	Plasma from prostate cancer patients (n = 53)	Medipally et al. [94]	Variations in FTIR spectral signatures related to lipids, proteins, nucleic acids, and amide I/II when comparing late toxicity grade 2+ patients with toxicity grade 1.
Raman spectroscopy	Lymphocytes from prostate cancer patients (n = 42)	Cullen et al. [95]	Variations in Raman spectral signatures related to Amide III, lipids, proteins, and DNA when comparing late toxicity grade 2+ patients with toxicity grade 1.

Abbreviations: *EGFR* epidermal growth factor receptor, *HNSCC* head and neck squamous carcinoma, *EAC* Ehrlich ascites carcinoma, *CBNMcyt* cytokinesis block micronucleus cytome, *PBLCs* peripheral blood lymphocytes, *LARC* locally advanced rectal cancer patients, *RCT* radiochemotherapy, *BRAC* breast cancer gene, *PBMCs* peripheral blood mononuclear cells, *NSCLC* non-small cell lung carcinoma

quality of life of a patient. Identifying patients who possess intrinsic radiosensitivity prior to starting treatment would be clinically beneficial, as RT could do more harm than good in this small subset of patients. Identifying potential predictive biomarkers of normal tissue response to RT has been the focus of intense research within the clinical radiobiology arena over the years. Numerous attempts have been made by various research groups to develop an assay capable of predicting radiosensitivity, yet to date, no biomarkers to predict radiosensitivity are in clinical use. Assays have been developed with the aim of studying and predicting radiosensitivity in normal tissues and tumors. However, current developed methods have produced conflicting results and come with many limitations that make them impractical for clinical use (Table 7.6).

7.5.2.1 Assessing Intrinsic Radiosensitivity

Cell-Based Assays

Cell viability assays are used predominantly to study cell response by measuring cell survival and proliferation after exposure to cytotoxic compounds. However, they are also extensively used in radiobiology studies. Clonogenic and MTT 3-(4,5-dimethylthiazol-2-yl)-2,5-diphenyltetrazolium bromide) assays are well-known assays for assessing in vitro radiosensitivity. The clonogenic assay is currently the gold standard for determining cellular radiosensitivity [96]. Further details on this assay can be found in Chaps. 3 and 7.

Early clonogenic studies provided evidence that in patients with cervical cancer and breast carcinoma, SF2 correlates with radiotherapeutic outcome [97, 98]. On the contrary, other early clonogenic studies have not found a correlation between SF2 and radiotherapeutic outcomes in head and neck cancer and multiforme glioblastoma multiforme [88, 99].

Numerous disadvantages are associated with the clonogenic assay, i.e., invasive sample acquisition, observer subjectivity through manual counting, merging of colonies that grow close together, long wait time for results as post-irradiation colonies can form 1–3 weeks later, labor intensive and technically difficult to perform [100–102]. As results from the clonogenic assay have a slow turn-around time, receiving results quite some time after sample collection/analysis would be of very little benefit to the patient, and it is clear that more efficient, rapid, and high-throughput methods need to be developed.

Plate-based cellular viability assays using tetrazolium salts such as MTT have also been used to assess radiosensitivity and can determine cell growth after irradiation [103].

Mitochondrial enzymes within metabolically active cells reduce the yellow MTT to water-insoluble purple formazan crystals. The amount of formazan crystals formed is directly proportional to the number of viable cells present in the sample, and this allows for the determination of viable cells through absorbance measurements obtained via a spectrometer at 492 nm ([103]; also discussed in Chap. 2). Buch et al. [103] also demonstrated that MTT performs similarly to the clonogenic assay when assessing the survival of irradiated human NSCLC and human glioblastoma cell lines. Compared to the clonogenic assay, the MTT assay is technically easier to perform and provides rapid results [104]. Rai et al. [105] also found that the MTT assay underestimated radiation induced cellular growth inhibition in numerous cell lines by comparing MTT values with cell numbers.

The MTT assay also has multiple disadvantages that make this assay unsuitable for routine clinical use, including:

1. Lack of specificity since tetrazolium reductions also reflect cell metabolism and not just cell proliferation.
2. Interference from reducing compounds.
3. Additionally, excessive direct light exposure of reagents and higher pH of culture medium can lead to sporadic reduction of tetrazolium salts resulting in raised background absorbance values.
4. MTT is cytotoxic and has been reported to inhibit cellular respiration leading to apoptosis [106–108].

Cytogenetic-Based Assays

These assays are used to identify chemicals and physical agents with genotoxic potential including irradiation.

During mitosis, MN are extranuclear bodies that are separated from the nucleus and contain defective chromosome fragments produced from DNA breakage and/or full chromosomes produced by interference of the mitotic machinery. MN and the micronucleus assay are discussed in detail in Chap. 3.

An early MN study carried out by Rached et al. [109] in the late 90s demonstrated that the MN assay had no predictive power for normal tissue reactions to irradiation. In this study, no variations in MN scores were observed between patients of various cancers who did or did not develop severe acute toxicities. Another study performed by Batar et al. [110] did not reveal any significant differences in MN scores between breast cancer patients who did or did not develop acute toxicities. However, a more recent study found a statistically significant difference in MN frequency per 1000 binucleated lymphocytes from patients who developed late cutaneous toxicity grade ≥ 3 when compared to grade ≤ 2 when irradiated with 10 Gy. Limitations of the MN assay include poor reproducibility due to high intra-individual variation and inter-laboratory variability, under certain conditions pseudo- MN can occur, and different types of chromosomal aberrations cannot be distinguished by micronuclei alone [111–113].

DNA Damage Assays

The γ-H2AX foci assay has also been explored as a prognostic technique for radiosensitivity. Please refer to Chap. 3, Sect. 3.6 (Cytogenetics and DNA Damage Measurements for Assessments of Radiation Effects) for more information. More recently, this assay was used to predict radiosensitivity in patients with oral squamous cell carcinoma and human colorectal cell lines [114, 115]. Other studies have also shown that γ-H2AX foci enumeration is not an ideal method for the prediction of acute and late toxicity development in prostate cancer, breast cancer, and rectal carcinoma [92, 116, 117]. On the contrary, other studies have used the γ-H2AX foci assay to identify patients at risk of developing radiation-induced toxicity in patients with lung cancer and breast cancer [93, 118]. These conflicting results on the fitness-of-use of γ-H2AX to predict intrinsic radiosensitivity further reinforce the idea that a novel method of analysis that can produce accurate and reproducible results needs to be developed. Disadvantages related to this assay include poor predictive performance and observer objectivity if γ-H2AX foci are enumerated by eye, and this is a fastidious and time-taxing process [119]. Inter-laboratory variations are also produced by this assay where significant variation in manually scored γ-H2AX foci yields obtained from irradiated lymphocytes has been observed [120].

The previously mentioned assays have limited clinical use due to their significant shortcomings, and a more practical approach needs to be developed to further investigate intrinsic radiosensitivity as a predictor of radiotherapeutic outcome.

Vibrational Spectroscopic Methods

Novel approaches to identify potential predictive biomarkers for radiosensitivity include Raman and Fourier transform infrared (FTIR) spectroscopic analysis of biofluids and cells. These techniques fall under the vibrational spectroscopy umbrella and are based on the transitions between quantized vibrational energy states of molecules due to the interaction between the sample and electromagnetic radiation [121]. Both techniques have numerous advantages over the previously mentioned predictive assays including minimal sample preparation and minimally invasive sample collection, speed, ease, and cost of analysis; they also allow for non-destructive and label-free analysis of a sample [121].

Each technique provides a biochemical fingerprint of a sample. Researchers in biomedical fields tend to focus on the range from 400 to 4000 cm^{-1} and, in particular, the fin-

gerprint region from 600 to 1800 cm^{-1}, as vibrations in these spectral regions produce refined bands and rich biochemical information related to disease prognostics and diagnostics. A major disadvantage of IR spectroscopy is the interference of water, which can overshadow crucial biochemical information [122]. However, Raman spectroscopy has a weak water signal and minimal water interference, making it ideal for the analysis of biological materials [123].

FTIR and Raman spectroscopy have recently been shown to be capable of discriminating patients on radiotherapeutic response [94, 95]. Both studies were successful in identifying variations in spectral intensities between patients with late toxicity grade 0–1 and grade 2+ with a high degree of sensitivity and specificity.

Current research from the same group involving Raman spectroscopy includes the analysis of biofluids and lymphocytes for the prediction of late normal tissue toxicity in high-risk localized prostate cancer patients and HPV+ head and neck cancer patients. Vibrational spectroscopy is far from being translated into the clinic, as currently there are no standardized protocols regarding the handling, storage, and preparation of samples to facilitate uniform spectroscopic analysis. However, researchers active in this area are currently investigating this to provide optimal protocols that will generate accurate and reproducible results [124, 125] (Fig. 7.7).

Raman spectroscopy is based on the inelastic scattering of light and scattering occurs when a sample is probed by a monochromatic light source. Most of the scattered light will be Rayleigh scattered where the laser photons will neither gain nor lose vibrational energy and will have the same energy as the incident light. Rayleigh scattering is also known as the elastic scattering of light and provides no information about molecular vibrational transitions [124]. A small fraction of light (approximately 1 in 10^7 photons) is scattered at optical frequencies different from that of the incident light [125]. The Raman effect occurs when light probes a molecule and interacts with the electrons of the molecular bonds and the scattered light vibrational energy is not equal to that of the incident light. This process leaves the molecule in an altered vibrational state. Other light scattering processes take place with Rayleigh scattering, i.e., Raman scattering, and two forms exist: stokes (dashed arrow) and anti-stokes. Anti-Stokes scattering occurs when atoms or molecules lose energy during the transition from higher to lower vibrational energy states. Stokes scattering occurs when the atoms or

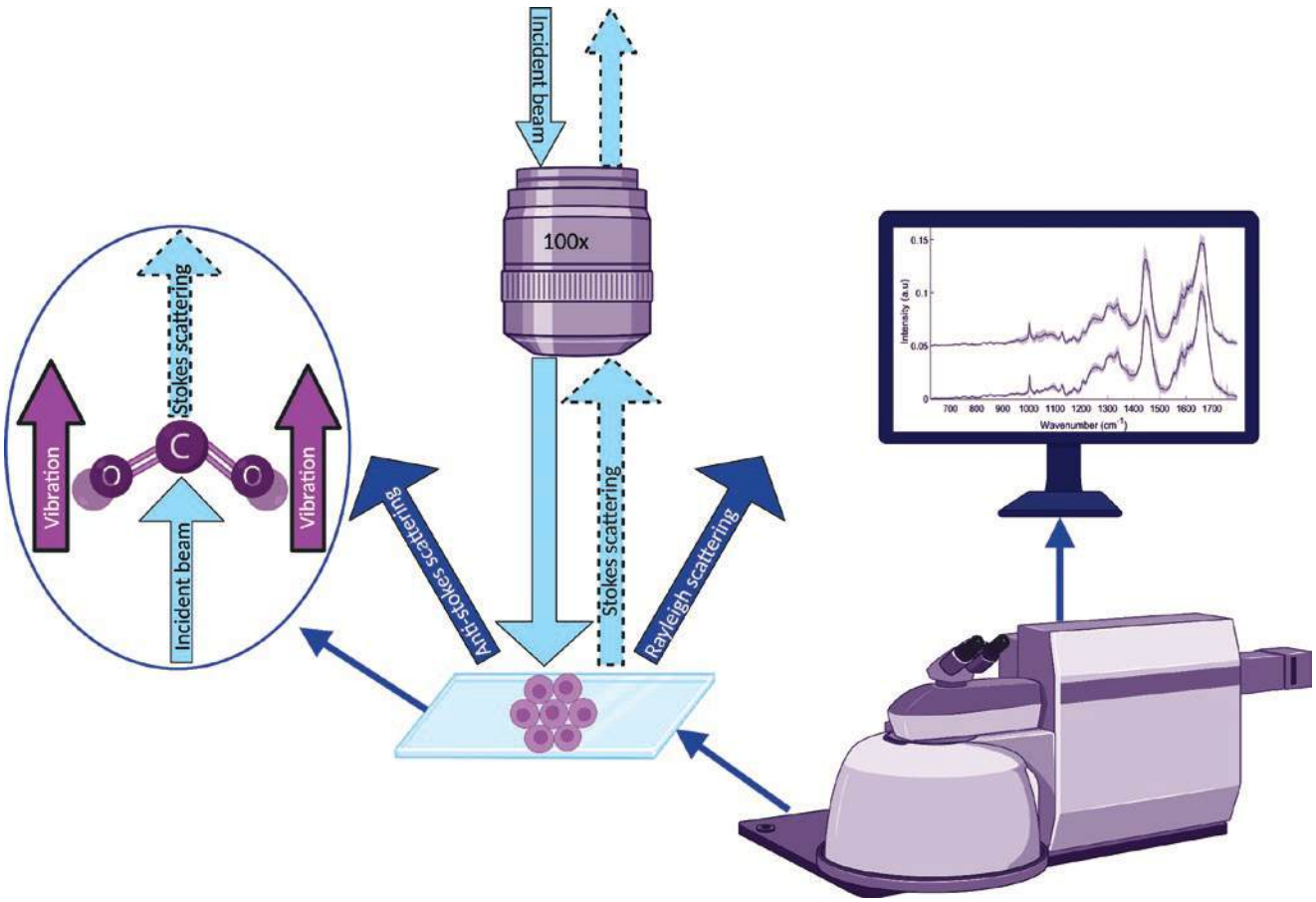

Fig. 7.7 Basic schematic of a Raman spectrometer

molecules relax into a high vibrational excited state from the ground virtual state, resulting in a vibrational energy level higher than that of the incident light [124]. The Stokes scattered light will enter the Raman spectrometer and by a series of optics and mirrors will be directed to a monochromator. The collected light will be analyzed by the spectrometer and displayed as a Raman spectrum on a computer.

RT is a mainstay in cancer therapy, and due to recent technological advances, therapeutic efficacy has improved over the years. However identification of patients at risk of toxicity, as well as those who are radiosensitive or radioresistant remains a research challenge, which, if successful, could save patients from unnecessary treatment and avoid normal tissue toxicity and potentially result in improved tumor control. Numerous studies have attempted to identify a robust predictive biomarker of patient response to RT. Although the results of the studies have been promising, to date no biomarkers have been validated or translated successfully into the clinic. The assays mentioned here are not an exhaustive list of those currently being used for research purposes to study radiosensitivity (Box 7.4).

Box 7.4 Key Points in Relation to Use of Biomarkers in Clinical Settings

- There is patient variability in response to RT with most patients experiencing few or no side effects during or post-treatment.
- A small subset of patients may experience life changing and deliberating toxicities.
- Currently, no biomarker is in use in the clinic today to predict normal tissue toxicity.
- Disadvantages of conventional radiobiological assays deem them unsuitable for translation into the clinic.
- Novel methods such as vibrational spectroscopy demonstrate great potential in the hunt for a predictive biomarker.

7.5.2.2 G2 Chromosomal Radiosensitivity Assay

The G2 chromosomal radiosensitivity assay (also known as G2 assay) is a method that illustrates the existence of enhanced radiosensitivity and cancer predisposition based on the chromatid aberrations after G2-phase irradiation. For the evaluation of the individual radiosensitivity with this technique, peripheral blood lymphocytes are irradiated in vitro in their G2-phase of the cell cycle, incubated to allow repair of DNA damage, and blocked in mitosis by the use of colcemid, so that the chromatid aberrations can be observed and quantified. A high yield of chromatid breaks can indicate high radiosensitivity. This methodology has a major advantage as it enables a time-efficient individual radiosensitivity assessment.

The original G2 assay was developed by Sanford et al. [126]. However, a significant problem of this method was the high variability in radiation-induced damage observed in different samples even from the same donor. In addition, there was often an overlap between the G2 chromatid aberration yield in lymphocytes from healthy donors and cancer patients. Following further development, Terzoudi et al. [127, 128] proposed the use of caffeine in order to induce G2/M checkpoint abrogation, simulating this way the high radiosensitivity of AT patients. AT cells are known to have a defective G2/M checkpoint arrest and therefore AT patients are highly radiosensitive. With the use of caffeine, it was feasible to express the individual radiosensitivity in relation to the high radiosensitivity level observed in AT patients (Figs. 7.8 and 7.9). This protocol has a great advantage that it minimizes the effects of laboratory specific parameters and makes the inter-laboratory comparison feasible by enabling an ameliorated intra-experimental and inter-laboratory reproducibility. More recently, efforts have been realized for further optimization of the G2 assay by using other DNA Damage Response (DDR) and G2-checkpoint inhibitors—than caffeine—such as ATR- or ATM/ATR inhibitors (e.g.,

Fig. 7.8 G2 chromosomal radiosensitivity assay. Chromatid breaks after 1 Gy of γ-irradiation as visualized at a metaphase peripheral blood lymphocyte from a healthy donor where four chromatid breaks are observed. (Reproduced with permission from [128])

Fig. 7.9 G2 chromosomal radiosensitivity assay. Chromatid breaks after 1 Gy of γ-irradiation as visualized at a metaphase peripheral blood lymphocyte after applying G2-checkpoint abrogation by means of caffeine where 13 chromatid breaks are visualized. (Reproduced with permission from [128])

VE-821 and UCN-1). Of these inhibitors, VE-821 has been proven effective in a rapid radiosensitivity assessment of different cell lines as well as normal tissue and primary tumor cells [129].

7.6 Age-Related Radiation Sensitivity

Age at the time of radiation exposure is a key factor contributing for radiation-induced health effects, namely cancer. In a general way, it is accepted that individuals exposed at early ages are the most radiosensitive, whereas the latency period from primary damage to outbreak into cancer is longer. Then, radiation sensitivity decreases until maturity and increases again at older ages [130, 131]. In addition, considering that both cancer incidence and mortality rates increase with age, a model of radiation-induced cancer must also include the attained age. Attained age is defined as the sum of the age of the person at the time of radiation exposure and the period elapsed since the radiation exposure ("attained age" = "age-at-exposure" + "time since exposure") [132].

Age-time patterns may also be represented as the "time since exposure," corresponding to the "attained age" subtracting the "age-at-exposure." For example, the cancer risk for someone with an age at exposure of 15 years and observed at an attained age of 40 years (time since exposure of 25 years) will be different from the risk for someone exposed at the same age but observed at an attained age of 79 years (time since exposure of 64 years) [132].

The understanding of the age-related alterations that may compromise individuals' health after exposure to IR is increasingly relevant, along with the elucidation of the biological mechanisms underlying the aging-radiation exposure association. The fact that life expectancy of the worldwide population is steadily rising emphasizes the urgent need for a better understanding of the relationship between aging and sensitivity to radiation, which impacts radiation protection in clinical practice [130].

7.6.1 Epidemiological Evidence

Epidemiological studies developed in the Life Span Study (LSS) cohort of the Japanese atomic bomb survivors have provided valuable data on the relationship between the age at the time of exposure and oncogenic risks. The most standard models for radiation sensitivity, based on the measure of carcinogenic events, predict that the relative risks decrease monotonically with the increase of age at exposure, at all ages. However, new epidemiological data suggest that risks differ by age at the time of radiation exposure and by type of cancer (Fig. 7.10) [130].

Data from the LSS cohort of the Japanese atomic bomb survivors showed that the excess relative risks (ERRs) of developing cancer following radiation exposure were higher during childhood and progressively decreased as a function of age until ages of 30–40 years old. However, for ages of exposure higher than 40, the ERR of developing solid cancer increased again. Thus, a bimodal distribution of radiation-induced cancer risks is associated with different biological processes. The greater susceptibility of children to radiation carcinogenesis is thought to be associated with three mechanisms: (1) long latency period between the primary injury and the cancer onset, that make children more likely to experience

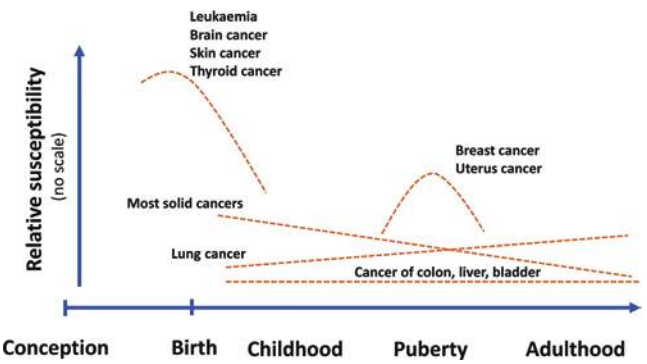

Fig. 7.10 Schematic representation of the relationship between the relative susceptibility and the age at exposure. (Reproduced with permission from [133])

the long-term consequences, such as cancer; (2) faster radionuclides accumulation in growing bones compared to bones of an adult; (3) high frequency of cell division (as the one occurring in a growing organism) may allow an impairment of the radiation-induced DNA damage repair mechanisms. At a cellular level, this high radiosensitivity of children may be also related with the initiation of malignant processes due to the larger number of stem cells that can derive into cancer cells in younger people compared with aged ones. On the other hand, the radiation risks for individuals exposed at later ages are related to the age-related deterioration of cell functions, which can be responsible for an augmented susceptibility for oncogenic transformation [130, 131, 134].

The results of surveys targeting atomic bomb survivors also showed that the periods that relate to high radiation sensitivity vary according to the type of cancer. For individuals exposed while they were young, the risks of thyroid and stomach cancers and solid cancer as a whole are higher, while individuals exposed during puberty have an increased risk of breast cancer and people with 40 years old or older have increased risk of lung cancer [135, 136].

7.6.2 Mechanistic Interplay Between Age and Radiosensitivity

The higher radiosensitivity of individuals exposed at early ages is likely to have a long-term biological counterpart in their organisms. The mechanistic interplay between age and radiosensitivity is thought to be influenced by age-related cellular changes, such as impaired DNA damage repair, telomere erosion and accelerated cellular senescence, augmented susceptibility of cells to oxidative stress and inflammation, and radiation-induced epigenetic alterations (Fig. 7.11) [130, 131].

Aged cells show a decline in the efficiency of the DNA damage response (DD) after radiation-induced DNA DSBs. The DDR should begin with the recruitment of proteins involved in both nonhomologous end joining (NHEJ) and homologous recombination (HR) repair pathways (see Chap. 3). Aged cells present several defects in these repair pathways such as delayed DDR kinetics, poor repair efficiency, and compromised repair due to chromatin reorganization as a result of aging. Thus, the aging process entails a disturbed nuclear organization that may compromise the recruitment of DDR proteins to the site, where they are needed, the nucleus. Irradiating aged cells will increase the damages in an already dysfunctional repair system, leading to irreversible damages. These damages are usually persistent and appear in a chronic mode increasing the damage burden in cells and tissues. Such accumulated damages can trigger enhanced inflammatory and immune system responses often leading to pathophysiological conditions like autoimmune disease and sensitivity to radiation and other types of environmental stresses [130, 137, 138].

Previous studies showed that telomere shortening relates to increased radiosensitivity. When aged cells escape from replicative senescence (a state of permanent growth arrest induced when shortened telomere length is attained), telomeres keep getting shorter, originating a greater number of uncapped chromosomes available to rearrangements. This loss of telo-

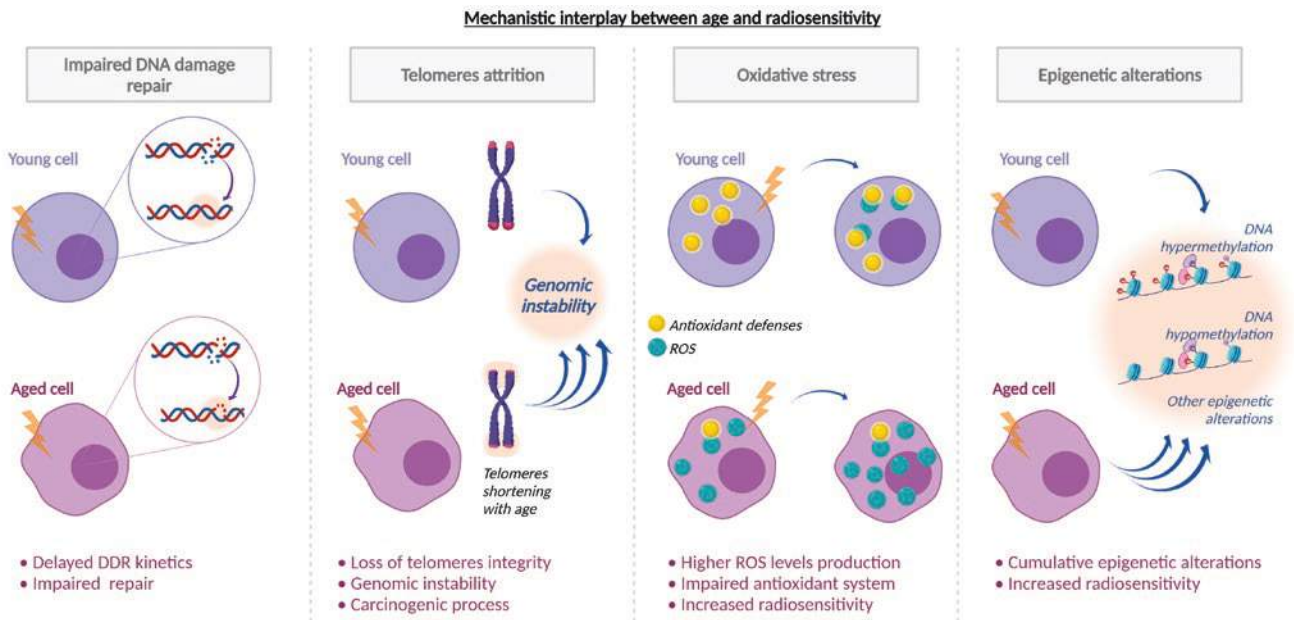

Fig. 7.11 Age-related cellular changes that may influence radiosensitivity and their mechanistic interplay. Compared to young cells, aged cells present increased impaired DNA damage repair, telomeres attrition, increased oxidative stress, and additional epigenetic alterations

mere integrity leads to an increase of genomic instability, which can initiate a carcinogenic process [130, 131].

Although there is some controversy about the causal relation between oxidative stress and an aged phenotype, it is known that aged cells have higher ROS levels production and a compromised antioxidant machinery compared with younger cells. This progressive loss of the pro-oxidant/antioxidant equilibrium compromises both cellular structures and homeostasis of aged cells. Exposing these aged cells to IR will unequivocally overload the antioxidant system, making them more susceptible to the IR-induced cell damages [139].

Radiation-induced oxidative stress can drive epigenetic alterations, such as (1) DNA hypomethylation through 8-OHdG methylation inhibition or DNA demethylation processes, (2) DNA hypermethylation through DNA methyltransferase up-regulation or DNA methylation catalysis, (3) histone modifications, and (4) miRNA expression. On the other hand, cumulative epigenetic alterations can also occur upon aging. Although this topic must be further explored, it seems to be a relation between epigenetic alterations and age-dependent radiosensitivity [131].

7.6.3 Clinical Perspective

In children/adolescents/young adults, RT remains essential for the curative treatment of brain tumors, Hodgkin lymphomas (HL), acute leukemias, Ewing and soft tissue sarcomas, neuroblastomas, nephroblastomas, or high-risk retinoblastomas. Life expectancy is long for the 80% of children/adolescents who are likely to be cured. The incidence of acute post-radiation complications, especially late, and proportional to the dose delivered may exceed that in adults. In fact, the cumulative incidence of overall iatrogenic sequelae 30 years after the end of treatment reaches more than 70% in this population compared to 15% maximum in the adult population after a median 3–5 years of follow-up. This late toxicity can lead to sometimes lethal sequelae with a major socio-economic impact (e.g., educational problems, parental mobilization, difficulties in entering the workforce, hospitalizations and costly symptomatic treatments and impoverishment, etc.). Along with high cure rates in this population, radiation-induced cancers appear with a probabilistic distribution (20-year cumulative incidence of secondary malignancies 3%)—but the incidence of which increases with the dose delivered and the duration of follow-up. Also note, however, that risk of secondary cancers increases in cancer patients who have not had prior radiation treatment as well as those who had chemotherapy [140, 141]. Differences are observed in the long-term, site-specific patterns of excess radiation inducing second malignancies between survivors of childhood cancer and adult-onset cancer, in terms of second malignancies histologic distribution, magnitude of risk, latency period, associated risk factors (genetic predisposition, environmental exposures, hormonal factors, and immune function) [142, 143].

On the other hand, RT is essential in the multidisciplinary management of the majority of cancer types in elderly patients, where it sometimes is considered as the first treatment option, often hypofractionated, and in others, as an alternative to surgery and/or chemotherapy.

In adults and the elderly, self-sustaining inflammation, fibrosis/atrophy, microcirculatory abnormalities are more readily associated with radiation-induced sequelae. In addition, in children, the manifestation of radiation-induced sequelae involves abnormalities in tissue maturation, delays (or even cessation) of growth of irradiated tissues—resulting in additional hypoplasia and/or hypofunction [144].

In adults, the distribution of individual radiosensitivity follows a Gaussian curve, and the toxicity observed in 5% of the most radiosensitive individuals is at the origin of dose recommendations to be applied to organs at risk in any patient in daily RT practice. There are many reasons to believe that this is not the case with children and seniors, with likely great variability with age. This is especially true if one consider all the changes in metabolic functions throughout growth and/or due to additional comorbidities, variations in tumor death, and tissue healing pathways with age and tumor predispositions associated with childhood cancer involving DNA repair pathways (assuming that this trait correlates with individual radiosensitivity).

Differences in organ development and tissue repair in children and adults have a significant effect on the expression of radiation injury. In many tissues, organ development is supported by cell proliferation from the prenatal period. During the development of each tissue, pluripotent embryonic stem cells differentiate into different unipotent lineages that will participate in mature tissue homeostasis. Some stem cells remain—ensuring self-renewal within the tissue. Thus, these two mechanisms are involved in growth as well as in tissue repair and regeneration. As the tissue matures, each organ thus contains a mosaic of dividing cells that are at rest either transiently or permanently. During childhood and adolescence, body tissues follow different growth patterns with their own kinetics. Not surprisingly, the rapid growth of normal tissues also seems to coincide with increased tissue radiosensitivity and, consequently, with a higher susceptibility to radiation-induced neoplasia. Overall, neurocognitive effects, development of muscles, and growth of bones are all sensitive to the age at treatment. For example, the intelligence quotient (IQ) deteriorates more in children irradiated on the brain before the age of 5 years compared to older children [145].

In contrast, in the elderly, the cells of the proliferative compartment move toward a permanent state of rest or

senescence. This aging process becomes critical after injury because, although senescent cells are capable of metabolic functions, they lose their proliferative capacity after stress such as radiation. Therefore, late effects in the elderly population can be seen as the result of an interaction between their diminishing ability of cells to repair themselves after injury and their natural tendency to progress to a state of senescence, which itself can be accelerated by irradiation.

Only very rare cases of children have been studied for their individual radiosensitivity. Three genetic syndromes have formally been associated with RT-induced fatal non-cancer adverse tissue events: AT (homozygous *ATM* mutations), LIG4 syndrome (homozygous *LIG4* mutations), Nijmegen's syndrome (homozygous *NBS1* mutations)—all characterized by the impairment in DSB repair and signaling pathways (see detailed information in Sect. 7.8). Noticeably, some syndromes also confer an increased individual cancer predisposition. Some cases of significant radiosensitivity with mutations of genes whose function was not expected in the radiation response have to be stressed—involving cytoplasmic functions or cell scaffold and membrane organization (for example, Huntingdon disease, Usher syndrome; [146]).

The individual radiosensitivity in children/adolescents and elderly is thus so far mainly unknown, and clinical trials are pending using individual radiosensitivity assays and very long-term observational studies (Box 7.5).

Box 7.5 The Influence and Impact of Radiosensitivity Related to Age and Aging

- Age at time of radiation exposure is a key factor contributing to radiation-induced health effects.
- New epidemiological data suggest that risk of developing cancer differs by age at the time of radiation exposure as well as by type of cancer.
- Cellular and molecular changes related to aging influence radiosensitivity.
- Differences in organ development and tissue repair in children and adults have a significant effect on the expression of radiation injury.

7.7 Biological Sex-Related Radiation Sensitivity

7.7.1 Introduction

The different individual radiosensitivity may be affected by genetic and individual factors as well as by lifestyle factors. One of the individual factors that have been associated with radiation sensitivity is biological sex.

7.7.2 Biological Sex Differences

The different radiosensitivity and radiosusceptibility for each sex could be due to biological factors. The human sex is determined by the sex chromosomes, namely by Y and X chromosomes. Whereas females have two X chromosomes, males have one Y and one X chromosome. These two sex chromosomes differ in terms of length, structures, and in the number and types of genes. Thus the X chromosome is approximately 160 Mb with more than 1000 genes while the Y chromosome is approximately 65 Mb with only 100 genes. The Y-specific genes are expressed mostly in testicular tissue with the *SRY* gene being the most important for determining male sex [147, 148].

Gene mutations or defects in gene expression of sex chromosomes dominantly affect the X chromosome and could be responsible for the death of the zygote and, consequently, decrease female birth. It also is hypothesized that differences in biological sex-related radiation responses could be due to immunological and hormonal differences apart from epigenetic and genetic factors. The mechanism underlying biological sex-related radiation sensitivity is still not clear and needs to be studied in more detail. Until now, it is known that the cellular response to radiation is highly complex and involves several processes like alterations in gene expression, signal transduction, repair process, and cell proliferation and death which could vary with sex.

7.7.3 Epidemiological Studies

Most of the data used for improving the knowledge on radiation-induced health effects and radioprotection was gained from the atomic bomb survivors in Hiroshima and Nagasaki (in Japan) and Chernobyl (in Ukraine). Also, the development of other epidemiological and cohort studies to evaluate the effects of radiation on the population exposed to high-dose levels due to medical reasons, radiation accidents, or from natural sources, contributed to the effects documented till now, as summarized in Figs. 7.12 and 7.13. The use of cancer risk models allows to predict the excess relative risk (ERR), i.e., the proportional increase in risk over the background absolute risk, and the excess absolute risk (EAR) of cancer, i.e., the additional risk above the background absolute risk, of cancer as a consequence of radiation exposure [134].

The analyses of the several investigations done since 1945, based on data from Hiroshima and Nagasaki A-bomb survivors, revealed a higher incidence of cancer with elevated rated of leukemia, breast cancer, thyroid carcinoma, stomach and lung cancers, with risk for solid cancers varying with sex (Table 7.7). Related to radiation-induced lung cancer (LC), an increased radiation risk was evidenced and

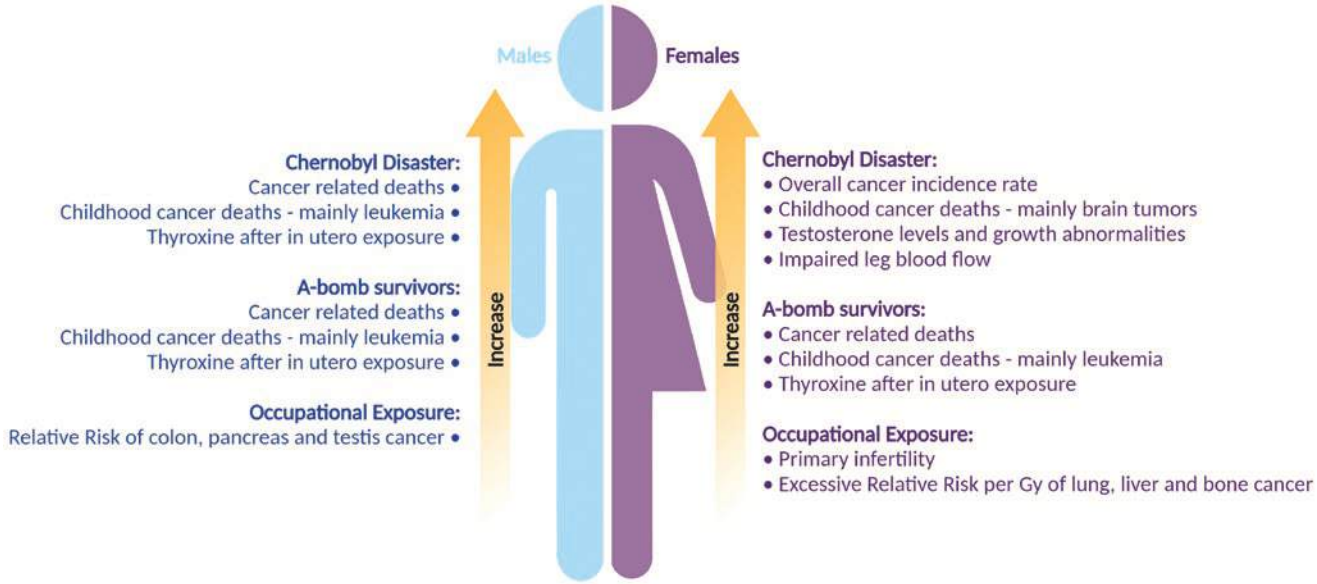

Fig. 7.12 Summary of biological sex-dependent health risks induced by radiation exposure. (Reproduced with permission from [149])

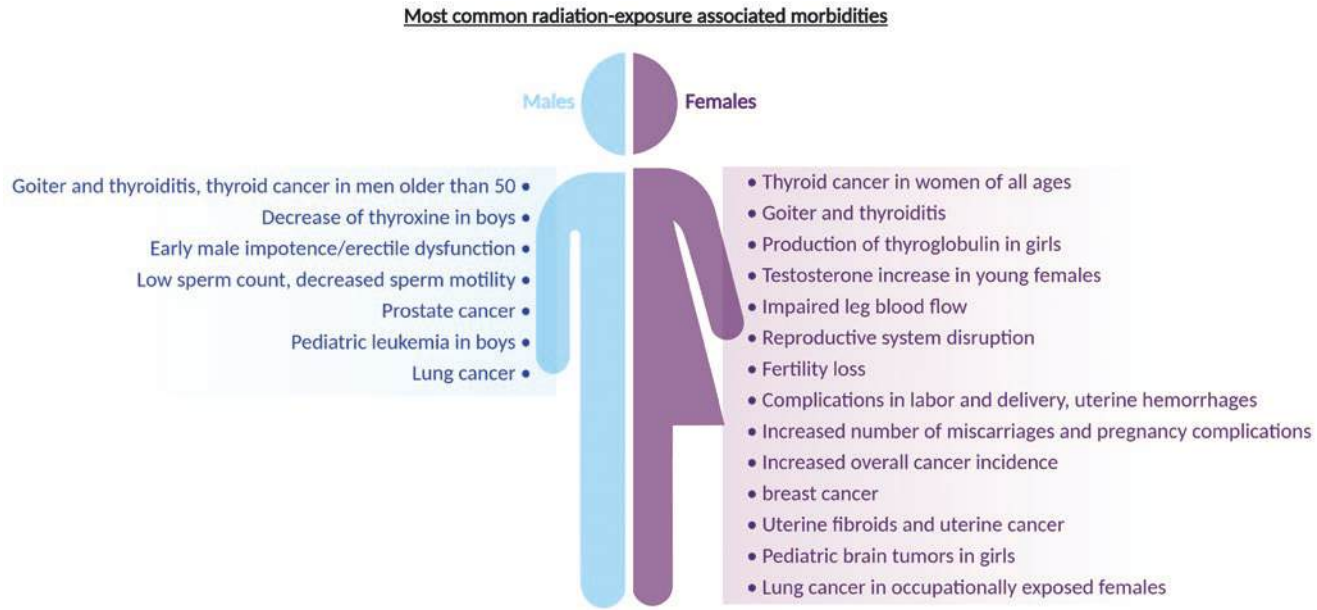

Fig. 7.13 Summary of most common morbidities induced by radiation exposure for each biological sex. (Reproduced with permission from [149])

it is nearly four times greater for females than males [150]. Furthermore, a report on mortality from a follow-up from 1950 to 1997 showed that only ERR of cancer is far higher for females than males, without significance for EAR [134] (UNSCEAR 2000).

Reports and studies based on the nuclear catastrophe in Chernobyl in 1986, where the population was exposed mostly to iodineIodine-131, showed an increased incidence of a range of cancers. Apart from the incidence of the same types of cancers report from A-bomb survivors (Table 7.7), there was also an increase in the incidence of bladder cancer and renal-cell carcinoma. There are still new cases of non-hematological cancers detected every year, so it is too early to present the final reports. The development of various radiation-related health problems in people living in the contaminated territories of Ukraine, Russia, and Belarus were more evident in women, inclusively by affecting their reproductive abilities and leading to an increase in the number of sponta-

Table 7.7 Values for excessive relative risk per Sv (ERR/Sv) obtained from A-bomb survivors data for age at exposure of 30 years (UNSCEAR 2000)

Cancer type	Males	Females	Female/male ratio
All solid cancer	0.38	0.79	2.1
Lung	0.50	2.18	4.3
Esophagus	0.41	0.84	2.1
Stomach	0.29	0.60	2.1
Colon	0.46	0.95	2.1
Liver	0.58	0.58	1.0
Bladder	1.18	0.98	0.8
Breast	0	1.55	–
Other cancer	0.47	0.28	0.6

neous miscarriages, mostly of the female fetus. Moreover, in Ukraine, the development of thyroid cancer was seen 2.5 times more often in females than in males who lived in contaminated territories [149, 151].

Data from the most recent nuclear accident in Fukushima is not yet enough to reach conclusions. Although the residing population was immediately evacuated from the most contaminated area, in the most affected areas that were not evacuated, average doses to adults in the first year were estimated to be <4 mSv, so discernable increases in related cancers are not expected (UNSCEAR 2021).

Studies from health care workers exposed to IR strongly indicate that occupational exposure leads to increased rates of IR-related cancers. Although these outcomes are associated with dose and also are age dependent, little attention has been given to biological sex [149].

A study carried out in Mayak workers about LC mortality revealed that ERR is four times higher for females than males, but the EAR is 0.43 less in the same comparison. Related to other cancers, the ERRs per Gy is also higher in females than males for lung, liver, and bone cancers. Moreover, a cohort study from Sweden, Denmark, and the USA about the carcinogenic effects of long-term internal exposure to alpha-particles radionuclides showed no significant differences between sex for solid cancer. The reduction of the female birth rate was also reported for the population living close to nuclear power plants or affected by nuclear testing [147, 149].

Thus, the epidemiological studies presenting separated risk coefficients for females and males do not present a consensus about sex-related radiation sensitivity. Although the studies from A-bomb survivors demonstrated higher ERR values for women than for men for all solid cancers, the corresponding EAR values are similar for males and females when sex-specific organs are not considered. The data collected from the radiation-induced occurrence of the same cancer type in different cohorts is also inconsistent. Although all these differences, the United Nations Scientific Committee on the Effects of Atomic Radiation (UNSCEAR) concludes that the EAR and ERR for total solid tumors are around two times higher in women than men, varying with site and organs, but for leukemia, no sex differences were observed [147, 149].

7.7.4 Animal Studies

Several experiments were carried out in animal models to provide clear information about the relationship between biological sex and radiation sensitivity as well as to confirm and expand the evidence obtained from epidemiological studies. Also, cell models were created from peripheral blood samples from healthy donors, cell lines, or primary cultures from organs of interest. These studies made it possible to study in depth the molecular mechanism inherent to sex differences in radiation sensitivity, namely to access cellular responses to IR, whole-genome screening for gene expression, and analyses of epigenetic regulatory mechanisms [147].

The data obtained through the analyses of gene expression as well as from epidemiological studies showed no correlations among the sex-specific expressed genes and corresponding cellular phenotypes. Nevertheless, a much higher incidence of thymic lymphoma and osteosarcoma have been found in female mice after treatment with 227Th than in male mice. Most recently, it was reported bystander effects in the non-radiated spleen of mice and rats varying according to the sex-specific differences. A sex-specific activation of distinct pathways was also suggested in mice, in response to whole-body irradiation as well as different tissues and organs irradiations with acute and chronic low doses [147, 149].

7.7.5 Differences in Radiation Therapy Outcomes According to Biological Sex

The severity of tissue reactions observed in cancer patients exposed to the same dose of IR during RT is assigned to differences in individual radiosensitivity [152]. It is generally believed that individual radiosensitivity is genetically determined based on the existence of certain hereditary diseases that we detailed more in Chap. 3. Moreover, the response to RT could also be influenced by other facts than the biological and physiological differences between males and females in organs and tissues, such as lifestyle, i.e., be sex related (Box 7.6).

Box 7.6 The Influence and Impact of Radiosensitivity Related to Biological Sex

- The differences in radiosensitivity of males and females could be due to biological factors.
- UNSCEAR concludes that the EAR and ERR for solid tumors are around two times higher in females than in males.
- The identification of biological sex-related radiosensitivity will contribute to personalized dose and fractionation for RT as well as for radiation protection.
- Currently, the annual dose limits for occupational exposures recommended by ICRP do not recognize sex.

There was evidence that females when exposed to the same whole-body exposure dose of IR have a greater risk of cancer than males [153]. Moreover, radiogenomic research has brought evidence that individual polymorphisms are correlated with treatment response with significant differences between females and males. However, the few available findings do not allow any conclusions to be drawn about sex-specific differences in radiation sensitivity, mostly because there are no studies that present enough data to support these hypotheses, without other confounding factors, or whose focus is specifically on sex [154]. So, the inclusion of biological sex or even gender as a variable in future randomized control trials or cohort studies will be crucial. The identification of the individual radiosensitivity of each patient will allow a personalized dose adjustment for RT as well as to use the values to improve the protection of occupationally exposed persons.

Regarding fractionation, high total doses delivered at a high-dose rate, in fractions, at appropriate intervals showed a lesser genetic effect in both males and females than the same dose delivered in a single fraction. It was also reported that the magnitude of its reduction is the same as the low dose rate effect.

7.7.6 International Commission on Radiological Protection (ICRP) Recommendations

Since its foundation, the International Commission on Radiological Protection (ICRP) has issued recommendations and guidelines related to the use of IR, based on the most recent scientific evidence and experience obtained through the years of implementation of the system of radiation protection. Until now, the annual dose limit for occupational exposure recommended by ICRP is not based on individual characteristics, such as biological sex or gender. Although the inclusion of these characteristics will increase the complexity of the model, it would be a critical step to overcome the actual generalized system used for determining the proper radiation protection for each specific case [134].

Two radiation research projects, Multidisciplinary European Low Dose Initiative (MELODI, https://melodi-online.eu/) and European Alliance Medical Radiation Protection Research (EURAMED, https://www.euramed.eu/), have been working on this topic defining the individual differences in radiation sensitivity as a key research priority.

7.8 Genetic Syndromes Associated with Radiation Sensitivity

7.8.1 Ataxia Telangiectasia (AT)

Ataxia Telangiectasia (AT) is an autosomal recessive neurodegenerative disease that is caused by mutations in AT mutated (*ATM*) gene. A-T was first described by Sillaba and Henner in 1926, however, its phenotypic spectrum was only expanded after the description of the ATM gene in 1995. A-T has a worldwide estimated prevalence of 1:40,000 to 1:100,000 and is related with a poor prognosis and a short life span, being chronic pulmonary diseases and malignancy the A-T-related most common causes of death [155, 156].

As the main known gene related to A-T clinical phenotype, *ATM* gene contains 66 exons and encodes the ATM protein, one of the three members of the PI3K-like family. ATM protein plays a pivotal role in the activation of cellular signaling pathways upon DSBs, apoptosis, and genotoxic stresses, such as IR. It functions essentially in the nuclear compartment; however, it is known that ATM is also present as a soluble protein in the cytoplasm [157]. In the nucleus, as part of DNA damage response upon DNA DSBs or oxidative stress, ATM is activated leading to a phosphorylation cascade of several target substrates involved in DNA repair, chromatin remodeling, cell cycle checkpoint, and transcription, namely P53 (S15), CHK2 (T68), and MDM2 (S395). In the cytoplasm, it is thought to be responsible for the functions of peroxisomes and mitochondria upon oxidative stress stimuli, as well as regulating angiogenesis, glucose metabolism, and telomere processing [155, 158].

A-T is a complex multisystem disorder characterized by a phenotypic heterogeneity, since patients show a broad range of clinical manifestations, including progressive cerebellar degeneration, immunodeficiency, oculocutaneous telangiectasia, increased metabolic diseases, radiosensitivity, and cancer predisposition. Other abnormalities can also be manifestations of A-T, such as dystonia, chorea, athetosis, tremor, and parkinsonism. Clinical heterogeneity of A-T

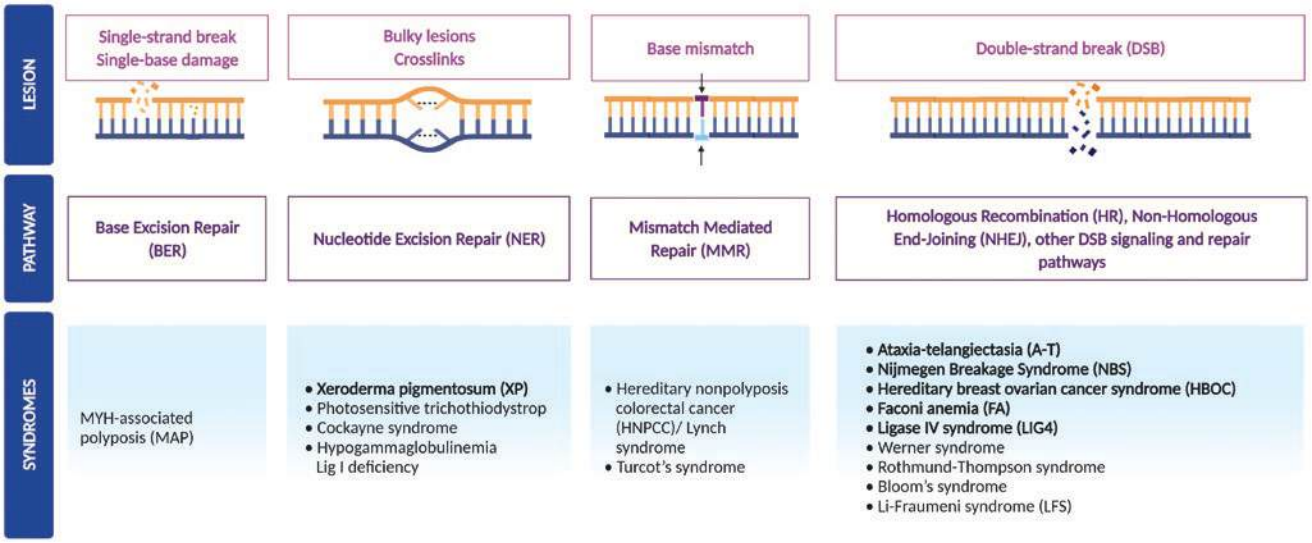

Fig. 7.14 Overview of DNA damage and repair pathways and most common genetic disorders

can be assigned to different types of mutations that cause an impaired ATM protein expression or affect its function in different ways. Clinical and preclinical studies revealed that the presence of inactive ATM is more cancer prone and lethal than null ATM [156, 157]. A-T patients show potentially a 10–25% increased risk of developing cancer, due to their immunodeficiency. In childhood, the most common types of malignancy are leukemia and lymphoma, while adults may also develop different solid tumors, namely breast, gastric, liver, parotid gland, and esophageal carcinomas. It is described that heterozygous *ATM* mutations lead to an increased risk of 5.1 for the development of breast cancer, compared to the general population; while ATM monoallelic defects are associated with an estimated relative risk of ~3%. Although there are some controversy on the association between *ATM* mutations and breast cancer susceptibility, cancer screening guidelines are being developed for ATM-mutated carriers [155].

The first association between the A-T caused by *ATM* homozygous mutations and its higher human radiosensitivity was made in 1975. This hypothesis has been clearly strengthened over the years by the fact that several studies reported lower SF2 (survival fraction at 2 Gy) in ATM-mutated cells compared to other radiosensitive cases, reinforcing its higher radiosensitivity. These cells are inclusively characterized as hyper-radiosensitive (SF2 ranging from 1% to 10%). In a mechanistic point of view, it is proposed that ATM protein may act upstream of the molecular process of radiation response, namely upstream of the predominant DSB repair pathway, NHEJ. Although it is not yet fully understood which of the ATM functions has the biggest influence on radiosensitivity, the hyper-radiosensitivity of *ATM*-mutated cells is mainly explained by the deficient recognition of DSBs by NHEJ, as a consequence of the absence of an ATM kinase activity in the nucleus [158].

7.8.2 LIG4 Syndrome

DNA ligase IV deficiency or Ligase 4 (or LIG4) syndrome is an extremely rare autosomal recessive disease caused by mutations in DNA ligase IV. LIG4 was the first radiosensitive-severe combined immunodeficiency (RS-SCID) disorder to be described and belongs to the group of hereditary disorders associated with impaired DNA damage response mechanisms. Only few cases were recognized with LIG4 worldwide, the reason why its prevalence is difficult to estimate [159].

The *LIG4* gene encodes a key component of the major DSB repair machinery, the NHEJ pathway. This pathway constitutes a multistep process that involves several proteins, such as Ku 70/80, DNA-PKcs, XRCC4, and DNA ligase IV, among others ([160]; see also Chap. 3). DNA ligase IV is an ATP-dependent ligase IV involved in the final step of NHEJ. It forms a complex with XRCC4 and then interacts with DNA-PKcs and XLF to rejoin a pair of DNA ends. DNA ligase IV also develops an important role in the production of T and B lymphocytes receptors, being recruited to repair programmed DNA DSB induced during lymphocyte receptor development [160].

All mutations of *LIG4* gene identified in patients are located near its active site and are typically hypomorphic. This means they are not fully inactivating, since they do not affect ligase expression and maintain a residual but impaired activity of the enzyme (5–10% compared to the wild-type) [159, 160].

Clinically and morphologically, LIG4 syndrome is characterized by microcephaly, unusual facial features, growth

retardation, and skin anomalies. Patients also manifest acute radiosensitivity, immunodeficiency, and bone marrow abnormalities. Some clinical phenotypes of LIG4 syndrome overlap with other genetic syndromes, like Seckel syndrome, NBS, and FA. Although the incidence of this disorder is very low, some patients were reported with malignancy, mainly lymphoma [7, 160].

The LIG4 syndrome is also considered a hyperradiosensitive condition, which is caused by the loss of DNA ligase IV function and consequent impaired NHEJ activity, with a gross DSB repair defect. The first patient described with LIG4 syndrome developed acute lymphoblastic leukemia at age 14. The patient dramatically over-responded to cranial RT and died from radiation morbidity. Subsequent studies revealed a homozygous mutation in DNA ligase IV, which is located near the ATP binding site and is thought to hamper the formation of DNA ligase IV-adenylate complex, reducing its activity to ~10%. This post-RT fatal reaction made this genetic syndrome to be associated with hyperradiosensitivity [7, 159].

7.8.3 Nijmegen Breakage Syndrome (NBS)

Nijmegen breakage syndrome (NBS) is a rare autosomal recessive disease mainly characterized by presenting microcephaly at birth, stunted growth, immunodeficiency, and high predisposition to cancer, without the manifestation of ataxia. NBS was first described in 1979 in a 10-year-old Dutch boy and, then, was formally reported in 1981 when a brother of the boy presented similar clinical features. NBS is estimated to have a prevalence at 1:100,000 live births worldwide, being most common in Eastern Europe [161]. NBS is a consequence of mutations in the *NBS1* gene, also named NBN, on chromosome 8q21. It was determined a Slavic founder mutation, considering that most of the individuals with this syndrome are from Slavic regions and carry the same deleterious deletion, c.657del5. Eleven NBS-causing mutations have been identified, all of them in exons 6–10 of the *NBS* gene [162].

The *NBN* gene encodes a 754 amino acid protein named Nibrin (NBN), p95 or nbs1. Nibrin is part of the MRN (Mre11/Rad50/Nibrin) complex involved in the repair of DNA DSB, as well as in immune gene rearrangements, maintenance of telomeres, and meiotic recombination. When exposed to DNA damaging agents, the MRN complex is activated by ATM phosphorylation and localized to DNA damage sites forming protein foci at DNA breaks. Consequently, mutations in this *NBN* gene lead to impaired translocation of the Nibrin protein into the MRN complex impairing subsequent repair of the DNA DSB lesion [162].

The diagnosis of this syndrome is based on the identification of the main clinical manifestations and posterior confirmation by genetic analysis. The previous knowledge of disease-causing mutation in both alleles of the *NBN* gene allows the realization of prenatal molecular genetic diagnosis. NBS patients have a high predisposition to develop malignancies, being the syndrome with highest cancer incidence among all chromosomal instability syndromes. Till now, no specific therapies are defined, and the prognosis for NBN patients with malignancies is still poor [162].

The first documented case of radiation sensitivity observed in an NBS patient involved a 3-year-old microcephalic boy with medulloblastoma. Also, several in vitro studies have shown that NBS cells present high sensitivity to IR and radioresistant DNA synthesis. Thus, the NBS patients face several challenges in treating their presented malignancies, such as cancer, due to the limitation of using RT. In fact, considering the defective DNA repair system, the exposure of these individuals to radiation should be minimized and avoided when possible [161].

7.8.4 Xeroderma Pigmentosum (XP)

Xeroderma Pigmentosum (XP) is a rare hereditary autosomal recessive disorder with an incident rate of 1:250,000 in North America, and 1:1,000,000 in Europe, affecting both sexes equally [163]. XP is clinically characterized by the presence of pain induced by UV exposure, skin dryness, progressive pigmentary alterations, xerosis, several types of skin lesions and damage, and high incidence of malignant tumors affecting skin, head, and neck. In fact, acute severe sunburns are present in 50% of XP patients as a consequence of the hypersensitivity to sunlight. Some patients also showed neurological disorders and ophthalmologic degeneration [164, 165]. XP is caused by defects in seven complementation groups (XPA to XPG) which play a role in NER systems. XPC and XPA are the most prevalent in Southern Europe and North Africa. XPC is caused by mutation in the gene *XPC*, which contains 16 exons and is located in chromosome 3 (3p25), encoding for xeroderma pigmentosum group C (XPC) protein. The most frequent mutation in the *XPC* gene is a 2 bp deletion, c.1643_1644delTG, p.Val548AlafsX25 [164].

XPC is a protein with several functions in the NER system to repair DNA damage by recognizing the damaged bases and forming a stable complex with UV excision repair protein RAD23 (“*HR23B*”) protein needed for the recruitment of other actors involved in the removal of bulky DNA adducts. Mutation in these genes leads to an irreparable DNA damage that confers hypersensitivity to radiation to these patients, including UV exposure, and predisposition to develop malignancies [163, 164].

XP patients have 10,000-fold more probability in developing skin cancer than the general population. No cure is

yet available for XP patients, so they need to be completely protected and isolated from any source of UV radiation. Although there is a correlation between XP syndrome and hypersensitivity to UV radiation, there are only few reports presenting the effects of using radiation therapy in XP patients with malignancies. Most of those reports did not show acute or chronic complication after treatment, probably due to the action of other repair pathways, such as NHEJ or HR instead of NER. However, there have been reported preclinical studies showing that some variants of XP could be more susceptible to IR and it is recommended that all XP patients should be classified before starting radiation therapy [166].

7.8.5 Fanconi Anemia (FA)

Fanconi anemia (FA) was firstly described by Guido Fanconi in 1927, a pediatrician who reported three children, brothers, with specific features: short stature, physical abnormalities, and anemia [167]. Defined as a rare genetic disease, FA is caused by pathogenic variants in at least 23 genes: *FANCA*, *FANCB*, *FANCC*, *FANCD1/BRCA2*, *FANCD2*, *FANCE*, *FANCF*, *FANCG*, *FANCI*, *FANCJ/BRIP*, *FANC*, *FANCM*, *FANCN/PALB2*, *FANCO/RAD51C*, *FANCP/SLX4*, *FANCQ/ERCC4*, *FANCR/RAD51*, *FANCS/BRCA1*, *FANCT/UBE2T*, *FANCU/XRCC2*, *FANCV/REV7*, *FANCW/RFWD3*, and *FANCY/FAP100*. All these genes play a critical role in DNA repair and genomic instability and can be organized in different complexes [168]. Classified as an inherited bone marrow failure syndrome, FA is the most common genetic cause of aplastic anemia and, besides that related to hematologic malignancies, is one of the most common genetic causes with a ratio of males to females 1.2:1 [169]. Concerning heritability, FA can be inherited in an autosomal recessive manner, an autosomal dominant manner (RAD51-related FA), or an X-linked manner (FANCB-related FA) [170].

This syndrome of impaired DNA repair and genomic instability, defined as complex and heterogeneous, is based on different mutations. FA patient cells are unable to perform different functions, namely repair DNA interstrand cross-links, NER, translesion synthesis, and HR, inhibiting DNA replication and transcription, important cellular processes [171]. Related to IR, DNA damage and in particular DSB are the main alterations caused, with it reported that hypersensitivity to IR on FA mutation carriers translated not only into deterministic effects but also into stochastic effects [169].

FA is diagnosed at the median age of 7 years although symptomatic and asymptomatic family members have been described from birth to >50 years of age [172]. This syndrome is classified as multisystem disease, characterized by clinical features such as congenital malformations (short stature, skeletal malformations of the lower and/or upper limbs, abnormal skin pigmentation, microcephaly, and genitourinary tract and ophthalmic alterations), progressive bone marrow failure with pancytopenia presentation, typically presents in the first decade, often initiated with thrombocytopenia or leukopenia, and increased probability of hematologic (myelodysplastic syndrome or acute myeloid leukemia) and solid malignancies (head and neck, skin, and genitourinary tract; [170]).

7.8.6 Hereditary Breast and Cancer Syndrome

Hereditary Breast and Ovarian Cancer (HBOC) syndrome was first reported by the French physician Pierre Paul Broca, in 1866, when observed a greater predisposition to cancer in his wife's family. This syndrome is an autosomal dominant disease, mostly caused by germline deleterious mutations in Breast Cancer gene 1 (*BRCA1*) and Breast Cancer gene 2 (*BRCA2*). The exact cancer risks depend on the type of pathogenic variant, being this syndrome mainly characterized by an increased predisposition to different types of cancer. These mutations affect all ethnic groups and races: in the general population, mutations in *BRCA1* and *BRCA2* genes are estimated to have a frequency between 1:400 and 1:500. However, in Ashkenazy Jewish people, the frequency of causal variants is higher: 1:40 [173, 174].

HBOC is mostly a consequence of mutations in *BRCA1* gene, located in chromosome 17, and *BRCA2* gene, located in chromosome 13. However, only 25% of cases are associated with these two genes. Therefore, other genes are associated with this syndrome and, currently, more than 25 genes have been associated, such as Checkpoint Kinase 2 (*CHEK2*) gene, AT Mutated (*ATM*) gene, and Partner And Localizer Of BRCA2 (*PALB2*) gene. Most of them encode proteins that, in conjunction with *BRCA1* and *BRCA2* genes, act on genome maintenance pathways. More than 1600 mutations in *BRCA1* gene and more than 1800 in *BRCA2* gene associated with tumor susceptibility have been described [173, 175].

BRCA1 and *BRCA2* genes are tumor suppressor genes with a crucial role in the cell, since they encode proteins that repair DNA DSB through HR recombination, allowing the maintenance of genomic stability and tumor suppression. When exposed to IR, these proteins are activated, localize DNA damage, and repair it. In this way, mutations in these genes lead to an inefficient repair mechanism and to an increase in genomic instability, increasing the probability of cancer development [176].

The diagnosis of HBOC associated with mutations in *BRCA* genes is based on the identification of pathogenic variants in these genes through molecular genetic tests. HBOC patients have a high predisposition to develop different types of cancers, some of which at an earlier stage, such as breast cancer (in both sex) and ovarian cancer. Additionally, HBOC

is also associated with an increased risk of developing prostate cancer, melanoma, and pancreatic cancer although to a lesser degree. Until the moment, there are no specific therapies defined, so early diagnosis in carriers of pathogenic variants in the *BRCA1* and *BRCA2* genes is crucial to apply effective surveillance and prophylaxis measures [173].

Since the twentieth century, several studies have been carried out to understand whether individuals with mutations in the *BRCA* genes are more sensitive to IR, trying to understand the role of exposure to IR in patients with HBOC and whether there are differences in the ability to repair of DNA damage between carriers and non-carriers of mutations in these genes. Although some studies show an association between the exposure of individuals with the syndrome to diagnostic doses and the development of cancer [177, 178], other studies fail to show any association [91, 179]. Thus, it is crucial to carry out more specific studies to obtain clear and objective conclusions in relation to this subject.

7.9 Toward Personalized Medicine: Future Perspective

Biological markers of changes in the body in response to radiation have long been used to assess radiation dose and exposure circumstances (see Chaps. 3 and 8). In recent years, with advances in technology and the sophistication of the markers, the potential to use biomarkers of the body's response to radiation and other stressors to help predict treatment outcome and indeed to tailor treatments has begun to be explored [180].

Development, validation, and implementation of biomarkers are not a simple process (see Chap. 3). Firstly because our bodies are hugely complex systems relying on hundreds of thousands of changing and interacting processes at any one moment, many of which have associated measurable changes, there are a huge number of potential biomarkers based on the body's complex response to IR confounded by a large number of other internal and external factors. Secondly, and just as importantly, there is huge variation in interindividual responses for most biomarkers. One recent study, for example, identified 40 blood-based biomarkers which could provide informative data on carbon metabolism, vitamin status, inflammation, and endothelial and renal function in cancer-free older adults alone [181]. Harlid et al. [182] also outlined the large number of potential biomarkers for risk predictive and diagnostic biomarkers for colorectal cancers, in a recent systematic review. In terms of molecular radiation epidemiology, a very large number of potential biomarkers have been identified, but despite a very large amount of work in this area, only one biomarker (based on transcriptional changes) has been identified as suitable to pursue now [14]. Furthermore, the practicalities of development of protocols and standard operating procedures for clinical use are also a barrier to implementation [183].

However, in wider clinical practice as well as for radiation medicine, biomarkers to support personalized intervention are in development and in some cases, already in use. For example, Karschnia et al. [184] reported improved survival in patients with advanced cancers of the central nervous system, following application of systemic targeted immunotherapeutic agents. Connor et al. [185] showed how implementation of novel image-based biomarkers to support RT has improved patient-specific therapy outcomes for glioma patients.

Going forward, despite the fact that the mechanisms of radiation resistance are still not well understood, use of miRNA in prostate cancer has shown promise. For example, Soares et al. [186] found 23 miRNAs which were involved in genetic regulation of prostate cancer cell response to RT. In the lung, Leiser et al. [187] recently demonstrated the potential utility of caveolin-1 (a membrane protein highly expressed in radiation resistant lung cancer cells) as a prognostic biomarker for response to treatment with radiation as well as for tumor progression, in support of precision medicine. And for cancers of the liver, De la Pinta [188] recently identified a number of candidate biomarkers of radiation response and toxicity and highlighted how close this field in particular is to use of such techniques to support personalized radiation medicine.

Indeed, use of large scale "omics" data together with machine learning or other artificial intelligence approaches has opened up a number of avenues of research. For example, Manem [189] compared five different machine learning based approaches in two existing radiogenomics datasets and found a large number of biomarkers associated with statistically significant pathways of response associated with surviving fractions of cells. New techniques in cellular barcoding are also proving incredibly interesting, with Wursthorn et al. [190], for example, recently demonstrating the use of this technique for assessing clonogenic survival in response to radiation and quantification of radiosensitivity as well as the contribution of stochastic and deterministic processes. Major bioinformatics studies can help in the identification of gene signatures as biomarkers for predicting normal tissue radiosensitivity. A key challenge is still the need for large scale, independent, validation of biomarkers in prediagnostic studies [182] as well as biomarker-driven randomized controlled trials [191]. Nevertheless, given the recent advances, use of radiation biomarkers to support precision radiation medicine is an exciting field in which large leaps forward are expected in a relatively short timescale.

7.10 Exercises and Self-Assessment

Q1. Cite a genetic syndrome associated with both radiosensitivity and radiosusceptibility.
Q2. Cite a genetic syndrome associated with radiosusceptibility, but *not* radiosensitivity.
Q3. What is described as the attained age in relation to radiosensitivity?
  (a) The age from birth to death
  (b) The sum of the age at exposure and time since exposure
  (c) The age between onset of cancer diagnosis and end of treatment
  (d) The sum of the age at exposure and time of exposure
Q4. What are the three mechanisms associated with the greater susceptibility of children to radiation carcinogenesis?
Q5. Which of the following sentences are true or false?
  (a) Aged cells may have a compromised repair due to chromatin reorganization.
  (b) Senescence in older cells can be accelerated by irradiation.
  (c) Abnormalities in tissue maturation is often seen as radiation-induced sequelae in adults.
Q6. Is the radiation sensitivity higher for males or females?
Q7. Why is sex important to consider in context of radiation therapy?
Q8. Why is sex not yet included in the ICRP recommendations?
Q9. Why is it necessary to identify biomarkers to predict the response of the tumor to radiation therapy?
Q10. What circulatory biomarkers are of current interest in the field of radiation oncology?
Q11. Why are liquid biopsies rapidly being adopted into translational research?
Q12. What is the current gold standard for assessing radiosensitivity?
Q13. What advantages do vibrational spectroscopic techniques have over conventional radiobiological assays?
Q14. If normal tissue toxicity determines the total dose to be delivered to a patient, what outcome will this have on their treatment?

7.11 Exercise Solutions

SQ1. Ataxia telangiectasia (AT) caused by homozygous *ATM* mutations is associated with fatal tissue reactions post-RT and high cancer proneness after exposure to radiation.
SQ2. Li-Fraumeni's syndrome (LFS) caused by heterozygous *p53* mutations is associated with high cancer proneness after an exposure to radiation but LFS patients do not show adverse tissue reactions post-RT.
SQ3. Alternative (b) is correct. (The sum of the age at exposure and time since exposure).
SQ4. Long latency period between injury and cancer onset; faster radionuclides accumulation in growing bones; high frequency of cell division.
SQ5. (a) true, (b) true, (c) false.
SQ6. Females.
SQ7. Consideration of the individual radiosensitivity of each patient will allow a personalized dose and fractionation adjustment for RT.
SQ8. Due to the lack of scientific evidence to support the establishment of different annual dose limitations based on sex, as well as the complex social and societal issues associated with potential implementation of sex specific dose limits.
SQ9. Identifying biomarkers of tumor response will allow stratification of patients based on risk and identifying patients who may not respond favorably to treatment. In turn, this will provide tailored and optimized treatment for patients.
SQ10. Circulating tumor cells, circulating free DNA, and EVs.
SQ11. Liquid biopsies overcome many limitations associated with tumor biopsies, such as minimally invasive sample acquisition, easy repeatability, lower cost, and a rich source of tumor-specific biomarkers.
SQ12. The clonogenic assay is still the current gold standard for studying radiosensitivity.
SQ13. Vibrational techniques involve minimally invasive sample collection, non-destructive, label free measurement of cells, and results can be produced in a short time frame.

SQ14. Patients who are radiosensitive and undergo RT are at a higher risk of developing severe toxicity, and to circumvent this, the doses delivered to these patients will be at a lower dose than is necessary for adequate tumor control and a positive outcome of treatment.

References

1. Sinnott B, Ron E, Schneider AB. Exposing the thyroid to radiation: a review of its current extent, risks, and implications. Endocr Rev. 2010;31(5):756–73. https://doi.org/10.1210/er.2010-0003.
2. Brown NP. The lens is more sensitive to radiation than we had believed. Br J Ophthalmol. 1997;81:257–9.
3. Foray N, Bourguignon M. Comment on 'Considerations on the use of the terms radiosensitivity and radiosusceptibility' by Wojcik et al. J Radiol Prot. 2019;39(1):309–13. https://doi.org/10.1088/1361-6498/aaf4e9.
4. Schoenaker MH, Suarez F, Szczepanski T, Mahlaoui N, Loeffen JL. Treatment of acute leukemia in children with ataxia telangiectasia (A-T). Eur J Med Genet. 2016;59(12):641–6. https://doi.org/10.1016/j.ejmg.2016.05.012.
5. Le AN, Harton J, Desai H, Powers J, Zelley K, Bradbury AR, et al. Frequency of radiation-induced malignancies post-adjuvant radiotherapy for breast cancer in patients with Li-Fraumeni syndrome. Breast Cancer Res Treat. 2020;181(1):181–8. https://doi.org/10.1007/s10549-020-05612-7.
6. Vessoni AT, Guerra CCC, Kajitani GS, Nascimento LLS, Garcia CCM. Cockayne Syndrome: the many challenges and approaches to understand a multifaceted disease. Genet Mol Biol. 2020;43(1 Suppl. 1):e20190085. https://doi.org/10.1590/1678-4685-GMB-2019-0085.
7. El-Nachef L, Al-Choboq J, Restier-Verlet J, Granzotto A, Berthel E, Sonzogni L, Ferlazzo ML, Bouchet A, Leblond P, Combemale P, Pinson S, Bourguignon M, Foray N. Human radiosensitivity and radiosusceptibility: what are the differences? Int J Mol Sci. 2021a;22(13):7158. https://doi.org/10.3390/ijms22137158.
8. COPERNIC project investigators, Granzotto A, Benadjaoud MA, Vogin G, Devic C, Ferlazzo ML, Bodgi L, Pereira S, Sonzogni L, Forcheron F, Viau M, Etaix A, Malek K, Mengue-Bindjeme L, Escoffier C, Rouvet I, Zabot MT, Joubert A, Vincent A, Dalla Venezia N, Bourguignon M, Canat EP, d'Hombres A, Thébaud E, Orbach D, Stoppa-Lyonnet D, Radji A, Doré E, Pointreau Y, Bourgier C, Leblond P, Defachelles AS, Lervat C, Guey S, Feuvret L, Gilsoul F, Berger C, Moncharmont C, de Laroche G, Moreau-Claeys MV, Chavaudra N, Combemale P, Biston MC, Malet C, Martel-Lafay I, Laude C, Hau-Desbat NH, Zioueche A, Tanguy R, Sunyach MP, Racadot S, Pommier P, Claude L, Baleydier F, Fleury B, de Crevoisier R, Simon JM, Verrelle P, Peiffert D, Belkacemi Y, Bourhis J, Lartigau E, Carrie C, De Vathaire F, Eschwege F, Puisieux A, Lagrange JL, Balosso J, Foray N. Influence of nucleoshuttling of the ATM protein in the healthy tissues response to radiation therapy: toward a molecular classification of human radiosensitivity. Int J Radiat Oncol Biol Phys. 2016;94(3):450–60. https://doi.org/10.1016/j.ijrobp.2015.11.013.
9. Foray N, Bourguignon M, Hamada N. Individual response to ionizing radiation. Mutat Res Rev Mutat Res. 2016;770(Pt B):369–86. https://doi.org/10.1016/j.mrrev.2016.09.001.
10. Pernot E, Hall J, Baatout S, Benotmane MA, Blanchardon E, Bouffler S, El Saghire H, Gomolka M, Guertler A, Harms-Ringdahl M, Jeggo P, Kreuzer M, Laurier D, Lindholm C, Mkacher R, Quintens R, Rothkamm K, Sabatier L, Tapio S, de Vathaire F, Cardis E. Ionizing radiation biomarkers for potential use in epidemiological studies. Mutat Res. 2012;751(2):258–86. https://doi.org/10.1016/j.mrrev.2012.05.003.
11. El-Saghire H, Thierens H, Monsieurs P, Michaux A, Vandevoorde C, Baatout S. Gene set enrichment analysis highlights different gene expression profiles in whole blood samples X-irradiated with low and high doses. Int J Radiat Biol. 2013;89(8):628–38. https://doi.org/10.3109/09553002.2013.782448.
12. Rutten EA, Badie C. Radiation biomarkers: silver bullet, or wild goose chase? J Pers Med. 2021;11(7):603. https://doi.org/10.3390/jpm11070603.
13. Singh VK, Newman VL, Romaine PL, Hauer-Jensen M, Pollard HB. Use of biomarkers for assessing radiation injury and efficacy of countermeasures. Expert Rev Mol Diagn. 2016;16(1):65–81. https://doi.org/10.1586/14737159.2016.1121102.
14. Hall J, Jeggo PA, West C, Gomolka M, Quintens R, Badie C, Laurent O, Aerts A, Anastasov N, Azimzadeh O, Azizova T, Baatout S, Baselet B, Benotmane MA, Blanchardon E, Guéguen Y, Haghdoost S, Harms-Ringhdahl M, Hess J, Kreuzer M, Laurier D, Macaeva E, Manning G, Pernot E, Ravanat JL, Sabatier L, Tack K, Tapio S, Zitzelsberger H, Cardis E. Ionizing radiation biomarkers in epidemiological studies - an update. Mutat Res Rev Mutat Res. 2017;771:59–84. https://doi.org/10.1016/j.mrrev.2017.01.001.
15. Malsagova K, Kopylov A, Stepanov A, Butkova T, Sinitsyna A, Izotov A, Kaysheva A. Biobanks-a platform for scientific and biomedical research. Diagnostics (Basel). 2020;10(7):485. https://doi.org/10.3390/diagnostics10070485.
16. Zhou JG, Donaubauer AJ, Frey B, Becker I, Rutzner S, Eckstein M, Sun R, Ma H, Schubert P, Schweizer C, Fietkau R, Deutsch E, Gaipl U, Hecht M. Prospective development and validation of a liquid immune profile-based signature (LIPS) to predict response of patients with recurrent/metastatic cancer to immune checkpoint inhibitors. J Immunother Cancer. 2021;9(2):e001845. https://doi.org/10.1136/jitc-2020-001845.
17. Salman A, Baber R, Hannigan L, Habermann JK, Henderson MK, Mayrhofer MT, Afifi N. Quality matters: a global discussion in Qatar. Biopreserv Biobank. 2019;17(6):487–90. https://doi.org/10.1089/bio.2019.0073.
18. Schweizer C, Schubert P, Rutzner S, Eckstein M, Haderlein M, Lettmaier S, Semrau S, Gostian AO, Frey B, Gaipl US, Zhou JG, Fietkau R, Hecht M. Prospective evaluation of the prognostic value of immune-related adverse events in patients with non-melanoma solid tumor treated with PD-1/PD-L1 inhibitors alone and in combination with radiotherapy. Eur J Cancer. 2020;140:55–62. https://doi.org/10.1016/j.ejca.2020.09.001.
19. Winter T, Schäfer C, Westphal S, Böttcher C, Lamp S, Wallaschofski H, Roser M, Petersmann A, Nauck M. Integrated biobanks facilitate high-quality collection and analysis of liquid biomaterials. J Lab Med. 2019;43(6):355–8. https://doi.org/10.1515/labmed-2019-0171.
20. Hummel M, Specht C. Biobanks for future medicine. J Lab Med. 2019;43(6):383–8. https://doi.org/10.1515/labmed-2019-0106.

21. Puck TT, Marcus PI. Action of x-rays on mammalian cells. J Exp Med. 1956;103(5):653–66.
22. Fenech M. The in vitro micronucleus technique. Mutat Res. 2000;455(1–2):81–95. https://doi.org/10.1016/S0027-5107(00)00065-8.
23. Iliakis G, Pantelias GE, Okayasu R, Seaner R. 125IdUrd-induced chromosome fragments, assayed by premature chromosome condensation, and DNA double-strand breaks have similar repair kinetics in G1-phase CHO-cells. Int J Radiat Biol Relat Stud Phys Chem Med. 1987;52(5):705–22. https://doi.org/10.1080/09553008714552221.
24. Iliakis G. The role of DNA double strand breaks in ionizing radiation-induced killing of eukaryotic cells. BioEssays. 1991;13(12):641–8. https://doi.org/10.1002/bies.950131204.
25. Alapetite C, Thirion P, de la Rochefordière A, Cosset JM, Moustacchi E. Analysis by alkaline comet assay of cancer patients with severe reactions to radiotherapy: defective rejoining of radio-induced DNA strand breaks in lymphocytes of breast cancer patients. Int J Cancer. 1999;83(1):83–90. https://doi.org/10.1002/(sici)1097-0215(19990924).
26. Joubert A, Zimmerman KM, Bencokova Z, Gastaldo J, Chavaudra N, Favaudon V, Arlett CF, Foray N. DNA double-strand break repair defects in syndromes associated with acute radiation response: at least two different assays to predict intrinsic radiosensitivity? Int J Radiat Biol. 2008;84(2):107–25. https://doi.org/10.1080/09553000701797039.
27. Barnett GC, Coles CE, Elliott RM, Baynes C, Luccarini C, Conroy D, Wilkinson JS, Tyrer J, Misra V, Platte R, Gulliford SL, Sydes MR, Hall E, Bentzen SM, Dearnaley DP, Burnet NG, Pharoah PD, Dunning AM, West CM. Independent validation of genes and polymorphisms reported to be associated with radiation toxicity: a prospective analysis study. Lancet Oncol. 2012;13(1):65–77. https://doi.org/10.1016/S1470-2045(11)70302-3.
28. Quarmby S, Fakhoury H, Levine E, Barber J, Wylie J, Hajeer AH, West C, Stewart A, Magee B, Kumar S. Association of transforming growth factor beta-1 single nucleotide polymorphisms with radiation-induced damage to normal tissues in breast cancer patients. Int J Radiat Biol. 2003;79(2):137–43.
29. Zschenker O, Raabe A, Boeckelmann IK, Borstelmann S, Szymczak S, Wellek S, Rades D, Hoeller U, Ziegler A, Dikomey E, Borgmann K. Association of single nucleotide polymorphisms in ATM, GSTP1, SOD2, TGFB1, XPD and XRCC1 with clinical and cellular radiosensitivity. Radiother Oncol. 2010;97(1):26–32. https://doi.org/10.1016/j.radonc.2010.01.016.
30. Alsner J, Rødningen OK, Overgaard J. Differential gene expression before and after ionizing radiation of subcutaneous fibroblasts identifies breast cancer patients resistant to radiation-induced fibrosis. Radiother Oncol. 2007;83(3):261–6. https://doi.org/10.1016/j.radonc.2007.05.001.
31. Rødningen OK, Børresen-Dale AL, Alsner J, Hastie T, Overgaard J. Radiation-induced gene expression in human subcutaneous fibroblasts is predictive of radiation-induced fibrosis. Radiother Oncol. 2008;86(3):314–20. https://doi.org/10.1016/j.radonc.2007.09.013.
32. Forrester HB, Li J, Leong T, McKay MJ, Sprung CN. Identification of a radiation sensitivity gene expression profile in primary fibroblasts derived from patients who developed radiotherapy-induced fibrosis. Radiother Oncol. 2014;111(2):186–93. https://doi.org/10.1016/j.radonc.2014.03.007.
33. Sprung CN, Li J, Hovan D, McKay MJ, Forrester HB. Alternative transcript initiation and splicing as a response to DNA damage. PLoS One. 2011;6(10):e25758. https://doi.org/10.1371/journal.pone.0025758.
34. Ozsahin M, Ozsahin H, Shi Y, Larsson B, Würgler FE, Crompton NE. Rapid assay of intrinsic radiosensitivity based on apoptosis in human CD4 and CD8 T-lymphocytes. Int J Radiat Oncol Biol Phys. 1997;38(2):429–40. https://doi.org/10.1016/S0360-3016(97)00038-2.
35. Balázs K, Antal L, Sáfrány G, Lumniczky K. Blood-derived biomarkers of diagnosis, prognosis and therapy response in prostate cancer patients. J Pers Med. 2021;11(4):296. https://doi.org/10.3390/jpm11040296.
36. Hopkins AM, Rowland A, Kichenadasse G, Wiese MD, Gurney H, McKinnon RA, Karapetis CS, Sorich MJ. Predicting response and toxicity to immune checkpoint inhibitors using routinely available blood and clinical markers. Br J Cancer. 2017;117(7):913–20. https://doi.org/10.1038/bjc.2017.274.
37. Balázs K, Kis E, Badie C, Bogdándi EN, Candéias S, Garcia LC, Dominczyk I, Frey B, Gaipl U, Jurányi Z, Kocsis ZS, Rutten EA, Sáfrány G, Widlak P, Lumniczky K. Radiotherapy-induced changes in the systemic immune and inflammation parameters of head and neck cancer patients. Cancers (Basel). 2019;11(9):1324. https://doi.org/10.3390/cancers11091324.
38. Frey B, Mika J, Jelonek K, Cruz-Garcia L, Roelants C, Testard I, Cherradi N, Lumniczky K, Polozov S, Napieralska A, Widlak P, Gaipl US, Badie C, Polanska J, Candéias SM. Systemic modulation of stress and immune parameters in patients treated for prostate adenocarcinoma by intensity-modulated radiation therapy or stereotactic ablative body radiotherapy. Strahlenther Onkol. 2020;196(11):1018–33. https://doi.org/10.1007/s00066-020-01637-5.
39. Varadé J, Magadán S, González-Fernández Á. Human immunology and immunotherapy: main achievements and challenges. Cell Mol Immunol. 2021;18(4):805–28. https://doi.org/10.1038/s41423-020-00530-6.
40. Palacín-Aliana I, García-Romero N, Asensi-Puig A, Carrión-Navarro J, González-Rumayor V, Ayuso-Sacido Á. Clinical utility of liquid biopsy-based actionable mutations detected via ddPCR. Biomedicine. 2021;9(8):906. https://doi.org/10.3390/biomedicines9080906.
41. Bratulic S, Gatto F, Nielsen J. The translational status of cancer liquid biopsies. Regen Eng Transl Med. 2021;7(6):312–52. https://doi.org/10.1007/s40883-019-00141-2.
42. Pollack A, Kwon D, Walker G, Khor LY, Horwitz EM, Buyyounouski MK, et al. Prospective validation of diagnostic tumor biomarkers in men treated with radiotherapy for prostate cancer. JNCI J Natl Cancer Inst. 2017;109(2):1–8. https://doi.org/10.1093/jnci/djw232.
43. Wilkins AC, Gusterson B, Szijgyarto Z, Haviland J, Griffin C, Stuttle C, et al. Ki67 is an independent predictor of recurrence in the largest randomized trial of 3 radiation fractionation schedules in localized prostate cancer. Int J Radiat Oncol Biol Phys. 2018;101(2):309–15. https://doi.org/10.1016/j.ijrobp.2018.01.072.
44. Driehuis E, Kolders S, Spelier S, Lõhmussaar K, Willems SM, Devriese LA, et al. Oral mucosal organoids as a potential platform for personalized cancer therapy. Cancer Discov. 2019;9(7):852–71. https://doi.org/10.1158/2159-8290.CD-18-1522.
45. Yao Y, Xu X, Yang L, Zhu J, Wan J, Shen L, et al. Patient-derived organoids predict chemoradiation responses of locally advanced rectal cancer. Cell Stem Cell. 2020;26(1):17–26.e6. https://doi.org/10.1016/j.stem.2019.10.010.
46. Bastani M, Vos L, Asgarian N, Deschenes J, Graham K, Mackey J, et al. A machine learned classifier that uses gene expression data to accurately predict estrogen receptor status. PLoS One. 2013;8(12):e82144. https://doi.org/10.1371/journal.pone.0082144.
47. Porter RJ, Murray GI, McLean MH. Current concepts in tumor-derived organoids. Br J Cancer. 2020;123(8):1209–18. https://doi.org/10.1038/s41416-020-0993-5.

48. Xia T, Du W, Chen X, Zhang Y. Organoid models of the tumor microenvironment and their applications. J Cell Mol Med. 2021;25(13):5829–41. https://doi.org/10.1111/jcmm.16578.
49. Gupta N, Liu JR, Patel B, Solomon DE, Vaidya B, Gupta V. Microfluidics-based 3D cell culture models: utility in novel drug discovery and delivery research. Bioeng Transl Med. 2016;1(1):63–81. https://doi.org/10.1002/btm2.10013.
50. Azar J, Bahmad HF, Daher D, Moubarak MM, Hadadeh O, Monzer A, et al. The use of stem cell-derived organoids in disease modeling: an update. Int J Mol Sci. 2021;22(14):7667. https://doi.org/10.3390/ijms22147667.
51. Goto T. Patient-derived tumor xenograft models: toward the establishment of precision cancer medicine. J Pers Med. 2020;10(3):64. https://doi.org/10.3390/jpm10030064.
52. Yoshida GJ. Applications of patient-derived tumor xenograft models and tumor organoids. J Hematol Oncol. 2020;13(1):4. https://doi.org/10.1186/s13045-019-0829-z.
53. Jung J, Seol HS, Chang S. The generation and application of patient-derived xenograft model for cancer research. Cancer Res Treat. 2018;50(1):1–10. https://doi.org/10.4143/crt.2017.307.
54. Zhao SG, Yu M, Spratt DE, Chang SL, Feng FY, Kim MM, et al. Xenograft-based, platform-independent gene signatures to predict response to alkylating chemotherapy, radiation, and combination therapy for glioblastoma. Neuro-Oncol. 2019;21(9):1141–9. https://doi.org/10.1093/neuonc/noz090.
55. De Rubis G, Rajeev Krishnan S, Bebawy M. Liquid biopsies in cancer diagnosis, monitoring, and prognosis. Trends Pharmacol Sci. 2019;40(3):172–86. https://doi.org/10.1016/j.tips.2019.01.006.
56. Palmirotta R, Lovero D, Cafforio P, Felici C, Mannavola F, Pellè E, et al. Liquid biopsy of cancer: a multimodal diagnostic tool in clinical oncology. Ther Adv Med Oncol. 2018;10:1758835918794630. https://doi.org/10.1177/1758835918794630.
57. Arneth B. Update on the types and usage of liquid biopsies in the clinical setting: a systematic review. BMC Cancer. 2018;18:527. https://doi.org/10.1186/s12885-018-4433-3.
58. Michela B. Liquid biopsy: a family of possible diagnostic tools. Diagnostics. 2021;11(8):1391. https://doi.org/10.3390/diagnostics11081391.
59. Marrugo-Ramírez J, Mir M, Samitier J. Blood-based cancer biomarkers in liquid biopsy: a promising non-invasive alternative to tissue biopsy. Int J Mol Sci. 2018;19(10):2877. https://doi.org/10.3390/ijms19102877.
60. Qian Y, Wu Y, Yuan Z, Niu X, He Y, Peng J, et al. The frequency of circulating tumor cells and the correlation with the clinical response to standard chemoradiotherapy in locally advanced nasopharyngeal carcinoma: a prospective study. Cancer Manag Res. 2019;11:10187–93. https://doi.org/10.2147/CMAR.S222916.
61. Dianat-Moghadam H, Azizi M, Eslami-S Z, Cortés-Hernández LE, Heidarifard M, Nouri M, et al. The role of circulating tumor cells in the metastatic cascade: biology, technical challenges, and clinical relevance. Cancers. 2020;12(4):867. https://doi.org/10.3390/cancers12040867.
62. Pantel K, Brakenhoff RH, Brandt B. Detection, clinical relevance and specific biological properties of disseminating tumor cells. Nat Rev Cancer. 2008;8(5):329–40. https://doi.org/10.1038/nrc2375.
63. Sharma S, Zhuang R, Long M, Pavlovic M, Kang Y, Ilyas A, et al. Circulating tumor cell isolation, culture, and downstream molecular analysis. Biotechnol Adv. 2018;36(4):1063–78. https://doi.org/10.1016/j.biotechadv.2018.03.007.
64. Habli Z, AlChamaa W, Saab R, Kadara H, Khraiche ML. Circulating tumor cell detection technologies and clinical utility: challenges and opportunities. Cancers. 2020;12(7):1930. https://doi.org/10.3390/cancers12071930.
65. Adams DL, Stefansson S, Haudenschild C, Martin SS, Charpentier M, Chumsri S, et al. Cytometric characterization of circulating tumor cells captured by microfiltration and their correlation to the cellsearch® CTC test. Cytometry A. 2015;87(2):137–44. https://doi.org/10.1002/cyto.a.22613.
66. Doyle LM, Wang MZ. Overview of extracellular vesicles, their origin, composition, purpose, and methods for exosome isolation and analysis. Cell. 2019;8(7):727. https://doi.org/10.3390/cells8070727.
67. Ni J, Bucci J, Malouf D, Knox M, Graham P, Li Y. Exosomes in cancer radioresistance. Front Oncol. 2019a;9:869. https://doi.org/10.3389/fonc.2019.00869.
68. Gurunathan S, Kang M-H, Jeyaraj M, Qasim M, Kim J-H. Review of the isolation, characterization, biological function, and multifarious therapeutic approaches of exosomes. Cell. 2019;8(4):307. https://doi.org/10.3390/cells8040307.
69. Schwarzenbach H, Hoon DSB, Pantel K. Cell-free nucleic acids as biomarkers in cancer patients. Nat Rev Cancer. 2011;11(6):426–37. https://doi.org/10.1038/nrc3066.
70. Alcaide M, Cheung M, Hillman J, Rassekh SR, Deyell RJ, Batist G, et al. Evaluating the quantity, quality and size distribution of cell-free DNA by multiplex droplet digital PCR. Sci Rep. 2020;10(1):12564. https://doi.org/10.1038/s41598-020-69432-x.
71. De Miranda FS, Barauna VG, dos Santos L, Costa G, Vassallo PF, Campos LCG. Properties and application of cell-free DNA as a clinical biomarker. Int J Mol Sci. 2021;22(17):9110. https://doi.org/10.3390/ijms22179110.
72. Eastley NC, Ottolini B, Neumann R, Luo J-L, Hastings RK, Khan I, et al. Circulating tumor-derived DNA in metastatic soft tissue sarcoma. Oncotarget. 2018;9(12):10549–60. https://doi.org/10.18632/oncotarget.24278.
73. Keller L, Belloum Y, Wikman H, Pantel K. Clinical relevance of blood-based ctDNA analysis: mutation detection and beyond. Br J Cancer. 2021;124(2):345–58. https://doi.org/10.1038/s41416-020-01047-5.
74. Yang Y-C, Wang D, Jin L, Yao H-W, Zhang J-H, Wang J, et al. Circulating tumor DNA detectable in early- and late-stage colorectal cancer patients. Biosci Rep. 2018;38(4):BSR20180322. https://doi.org/10.1042/BSR20180322.
75. Yang F, Tang J, Zhao Z, Zhao C, Xiang Y. Circulating tumor DNA: a noninvasive biomarker for tracking ovarian cancer. Reprod Biol Endocrinol. 2021;19(1):178. https://doi.org/10.1186/s12958-021-00860-8.
76. Leung SF, Chan KCA, Ma BB, Hui EP, Mo F, Chow KCK, et al. Plasma Epstein-Barr viral DNA load at midpoint of radiotherapy course predicts outcome in advanced-stage nasopharyngeal carcinoma. Ann Oncol. 2014;25(6):1204–8. https://doi.org/10.1093/annonc/mdu117.
77. Han K, Leung E, Barbera L, Barnes E, Croke J, Di Grappa MA, et al. Circulating human papillomavirus DNA as a biomarker of response in patients with locally advanced cervical cancer treated with definitive chemoradiation. JCO Precis Oncol. 2018;2:1–8. https://doi.org/10.1200/PO.18.00152.
78. Ma J, Setton J, Morris L, Carrillo Albornoz PB, Barker C, Lok BH, et al. Genomic analysis of exceptional responders to radiotherapy reveals somatic mutations in ATM. Oncotarget. 2016;8(6):10312–23. https://doi.org/10.18632/oncotarget.14400.
79. Elazezy M, Joosse SA. Techniques of using circulating tumor DNA as a liquid biopsy component in cancer management. Comput Struct Biotechnol J. 2018;16:370–8. https://doi.org/10.1016/j.csbj.2018.10.002.

80. Chen M, Zhao H. Next-generation sequencing in liquid biopsy: cancer screening and early detection. Hum Genomics. 2019;13(1):34. https://doi.org/10.1186/s40246-019-0220-8.
81. Sun W, Li G, Wan J, Zhu J, Shen W, Zhang Z. Circulating tumor cells: a promising marker of predicting tumor response in rectal cancer patients receiving neoadjuvant chemo-radiation therapy. Oncotarget. 2016;7(43):69507–17. https://doi.org/10.18632/oncotarget.10875.
82. Jeong Y, Hoang NT, Lovejoy A, Stehr H, Newman AM, Gentles AJ, et al. Role of KEAP1/NRF2 and TP53 mutations in lung squamous cell carcinoma development and radiation resistance. Cancer Discov. 2017;7(1):86–101. https://doi.org/10.1158/2159-8290.CD-16-0127.
83. Salami SS, Singhal U, Spratt DE, Palapattu GS, Hollenbeck BK, Schonhoft JD, et al. Circulating tumor cells as a predictor of treatment response in clinically localized prostate cancer. JCO Precis Oncol. 2019;3(3):1–9. https://doi.org/10.1200/PO.18.00352.
84. Liang H, Lv X, Wang L, Wu Y-S, Sun R, Ye Y-F, et al. The plasma Epstein-Barr virus DNA level guides precision treatment for nasopharyngeal carcinoma in the intensity-modulated radiotherapy era: a large population-based cohort study from an endemic area. Ther Adv Med Oncol. 2018;10(7):1758835918782331. https://doi.org/10.1177/1758835918782331.
85. Dai X, Liao K, Zhuang Z, Chen B, Zhou Z, Zhou S, et al. AHIF promotes glioblastoma progression and radioresistance via exosomes. Int J Oncol. 2019;54(1):261–70. https://doi.org/10.3892/ijo.2018.4621.
86. Tang Y, Cui Y, Li Z, Jiao Z, Zhang Y, He Y, et al. Radiation-induced miR-208a increases the proliferation and radioresistance by targeting p21 in human lung cancer cells. J Exp Clin Cancer Res. 2016;35:7. https://doi.org/10.1186/s13046-016-0285-3.
87. Anakura M, Nachankar A, Kobayashi D, Amornwichet N, Hirota Y, Shibata A, et al. Radiosensitivity differences between EGFR mutant and wild-type lung cancer cells are larger at lower doses. Int J Mol Sci. 2019;20(15):3635. https://doi.org/10.3390/ijms20153635.
88. Stausbøl-Grøn B, Overgaard J. Relationship between tumor cell in vitro radiosensitivity and clinical outcome after curative radiotherapy for squamous cell carcinoma of the head and neck. Radiother Oncol. 1999;50(1):47–55. https://doi.org/10.1016/S0167-8140(98)00129-7.
89. Mekkawy MH, Fahmy HA, Nada AS, Ali OS. Study of the radiosensitizing and radioprotective efficacy of bromelain (a pineapple extract): in vitro and in vivo. Integr Cancer Ther. 2020;19:1534735420950468. https://doi.org/10.1177/1534735420950468.
90. Dröge LH, Hennies S, Lorenzen S, Conradi L-C, Quack H, Liersch T, et al. Prognostic value of the micronucleus assay for clinical endpoints in neoadjuvant radiochemotherapy for rectal cancer. BMC Cancer. 2021;21(1):219. https://doi.org/10.1186/s12885-021-07914-5.
91. Baert A, Depuydt J, Van Maerken T, Poppe B, Malfait F, Van Damme T, et al. Analysis of chromosomal radiosensitivity of healthy BRCA2 mutation carriers and non-carriers in BRCA families with the G2 micronucleus assay. Oncol Rep. 2017;37(3):1379–86. https://doi.org/10.3892/or.2017.5407.
92. Pinkawa M, Brzozowska K, Kriehuber R, Eble MJ, Schmitz S. Prediction of radiation-induced toxicity by in vitro radiosensitivity of lymphocytes in prostate cancer patients. Future Oncol. 2016;12(5):617–24. https://doi.org/10.2217/fon.15.334.
93. Lobachevsky PN, Bucknell NW, Mason J, Russo D, Yin X, Selbie L, et al. Monitoring DNA damage and repair in peripheral blood mononuclear cells of lung cancer radiotherapy patients. Cancers (Basel). 2020;12(9):E2517. https://doi.org/10.3390/cancers12092517.
94. Medipally DKR, Nguyen TNQ, Bryant J, Untereiner V, Sockalingum GD, Cullen D, et al. Monitoring radiotherapeutic response in prostate cancer patients using high throughput FTIR spectroscopy of liquid biopsies. Cancers (Basel). 2019;11(7):925. https://doi.org/10.3390/cancers11070925.
95. Cullen D, Bryant J, Maguire A, Medipally D, McClean B, Shields L, et al. Raman spectroscopy of lymphocytes for the identification of prostate cancer patients with late radiation toxicity following radiotherapy. Transl Biophoton. 2020;2(4):e201900035. https://doi.org/10.1002/tbio.201900035.
96. Oike T, Komatsu S, Komatsu Y, Nachankar A, Darwis NDM, Shibata A, et al. Reporting of methodologies used for clonogenic assays to determine radiosensitivity. J Radiat Res. 2020;61(6):828–31. https://doi.org/10.1093/jrr/rraa064.
97. West CM, Davidson SE, Roberts SA, Hunter RD. The independence of intrinsic radiosensitivity as a prognostic factor for patient response to radiotherapy of carcinoma of the cervix. Br J Cancer. 1997;76(9):1184–90. https://doi.org/10.1038/bjc.1997.531.
98. West CM, Elyan SA, Berry P, Cowan R, Scott D. A comparison of the radiosensitivity of lymphocytes from normal donors, cancer patients, individuals with ataxia-telangiectasia (A-T) and A-T heterozygotes. Int J Radiat Biol. 1995;68(2):197–203. https://doi.org/10.1080/09553009514551101.
99. Eschwege F, Bourhis J, Girinski T, Lartigau E, Guichard M, Deblé D, et al. Predictive assays of radiation response in patients with head and neck squamous cell carcinoma: a review of the Institute Gustave Roussy experience. Int J Radiat Oncol Biol Phys. 1997;39(4):849–53. https://doi.org/10.1016/s0360-3016(97)00509-9.
100. Brix N, Samaga D, Belka C, Zitzelsberger H, Lauber K. Analysis of clonogenic growth in vitro. Nat Protoc. 2021;16(11):4963–91. https://doi.org/10.1038/s41596-021-00615-0.
101. Sergioli G, Militello C, Rundo L, Minafra L, Torrisi F, Russo G, et al. A quantum-inspired classifier for clonogenic assay evaluations. Sci Rep. 2021;11(1):2830. https://doi.org/10.1038/s41598-021-82085-8.
102. Unkel S, Belka C, Lauber K. On the analysis of clonogenic survival data: statistical alternatives to the linear-quadratic model. Radiat Oncol. 2016;11(1):11. https://doi.org/10.1186/s13014-016-0584-z.
103. Buch K, Peters T, Nawroth T, Sänger M, Schmidberger H, Langguth P. Determination of cell survival after irradiation via clonogenic assay versus multiple MTT assay - a comparative study. Radiat Oncol. 2012;7(1):1. https://doi.org/10.1186/1748-717X-7-1.
104. Nikzad S, Hashemi B. MTT assay instead of the clonogenic assay in measuring the response of cells to ionizing radiation. J Radiobiol. 2014;1(1):6.
105. Rai Y, Pathak R, Kumari N, Sah DK, Pandey S, Kalra N, et al. Mitochondrial biogenesis and metabolic hyperactivation limits the application of MTT assay in the estimation of radiation induced growth inhibition. Sci Rep. 2018;8(1):1531. https://doi.org/10.1038/s41598-018-19930-w.
106. Ghasemi M, Turnbull T, Sebastian S, Kempson I. The MTT assay: utility, limitations, pitfalls, and interpretation in bulk and single-cell analysis. Int J Mol Sci. 2021;22(23):12827.
107. Riss TL, Moravec RA, Niles AL, Duellman S, Benink HA, Worzella TJ, et al. Cell viability assays. In: Markossian S, Grossman A, Brimacombe K, Arkin M, Auld D, Austin CP, et al., editors. Assay guidance manual. Bethesda, MD: Eli Lilly & Company and the National Center for Advancing Translational Sciences; 2004.
108. Surin AM, Sharipov RR, Krasil'nikova IA, Boyarkin DP, Lisina OY, Gorbacheva LR, et al. Disruption of functional activity of mitochondria during MTT assay of viability of cultured neu-

rons. Biochemistry (Mosc). 2017;82(6):737–49. https://doi.org/10.1134/S0006297917060104.
109. Rached E, Schindler R, Beer KT, Vetterli D, Greiner RH. No predictive value of the micronucleus assay for patients with severe acute reaction of normal tissue after radiotherapy. Eur J Cancer. 1998;34(3):378–83. https://doi.org/10.1016/S0959-8049(97)00373-0.
110. Batar B, Mutlu T, Bostanci M, Akin M, Tuncdemir M, Bese N, et al. DNA repair and apoptosis: roles in radiotherapy-related acute reactions in breast cancer patients. Cell Mol Biol (Noisy-le-grand). 2018;64(4):64–70. https://doi.org/10.14715/cmb/2018.64.4.11.
111. Hayashi M. The micronucleus test—most widely used in vivo genotoxicity test. Genes Environ. 2016;38(1):18. https://doi.org/10.1186/s41021-016-0044-x.
112. Sicca F, Martinuzzi D, Montomoli E, Huckriede A. Comparison of influenza-specific neutralizing antibody titers determined using different assay readouts and hemagglutination inhibition titers: good correlation but poor agreement. Vaccine. 2020;38(11):2527–41. https://doi.org/10.1016/j.vaccine.2020.01.088.
113. Vral A, Thierens H, Baeyens A, Ridder L. Chromosomal aberrations and in vitro radiosensitivity: intra-individual versus inter-individual variability. Toxicol Lett. 2004;149(1–3):345–52. https://doi.org/10.1016/j.toxlet.2003.12.044.
114. Kawashima S, Kawaguchi N, Taniguchi K, Tashiro K, Komura K, Tanaka T, et al. γ-H2AX as a potential indicator of radiosensitivity in colorectal cancer cells. Oncol Lett. 2020;20(3):2331–7. https://doi.org/10.3892/ol.2020.11788.
115. Philouze P, Gauthier A, Lauret A, Malesys C, Muggiolu G, Sauvaigo S, et al. CD44, γ-H2AX, and p-ATM expressions in short-term ex vivo culture of tumor slices predict the treatment response in patients with oral squamous cell carcinoma. Int J Mol Sci. 2022;23(2):877. https://doi.org/10.3390/ijms23020877.
116. Djuzenova CS, Zimmermann M, Katzer A, Fiedler V, Distel LV, Gasser M, et al. A prospective study on histone γ-H2AX and 53BP1 foci expression in rectal carcinoma patients: correlation with radiation therapy-induced outcome. BMC Cancer. 2015;15(1):856. https://doi.org/10.1186/s12885-015-1890-9.
117. Marková E, Somsedíková A, Vasilyev S, Pobijaková M, Lacková A, Lukačko P, et al. DNA repair foci and late apoptosis/necrosis in peripheral blood lymphocytes of breast cancer patients undergoing radiotherapy. Int J Radiat Biol. 2015;91(12):934–45. https://doi.org/10.3109/09553002.2015.1101498.
118. Somaiah N, Chua MLK, Bourne S, Daley F, A'Hern R, Nuta O, et al. Correlation between DNA damage responses of skin to a test dose of radiation and late adverse effects of earlier breast radiotherapy. Radiother Oncol. 2016;119(2):244–9. https://doi.org/10.1016/j.radonc.2016.04.012.
119. Viau M, Testard I, Shim G, Morat L, Normil MD, Hempel WM, et al. Global quantification of γH2AX as a triage tool for the rapid estimation of received dose in the event of accidental radiation exposure. Mutat Res/Genet Toxicol Environ Mutagen. 2015;793:123–31. https://doi.org/10.1016/j.mrgentox.2015.05.009.
120. Rothkamm K, Horn S, Scherthan H, Rössler U, De Amicis A, Barnard S, et al. Laboratory intercomparison on the γ-H2AX foci assay. Radiat Res. 2013;180(2):149–55. https://doi.org/10.1016/j.vaccine.2020.01.088.
121. Hackshaw KV, Miller JS, Aykas DP, Rodriguez-Saona L. Vibrational spectroscopy for identification of metabolites in biologic samples. Molecules. 2020;25(20):4725. https://doi.org/10.3390/molecules25204725.
122. Azarfar G, Aboualizadeh EM, Walter N, Ratti S, Olivieri C, Norici A, et al. Estimating and correcting interference fringes in infrared spectra in infrared hyperspectral imaging. Analyst. 2018;143(19):4674–83. https://doi.org/10.1039/C8AN00093J.
123. Geraldes CFGC. Introduction to infrared and Raman-based biomedical molecular imaging and comparison with other modalities. Molecules. 2020;25(23):E5547. https://doi.org/10.3390/molecules25235547.
124. Ferraro JR, Nakamoto K, Brown CW. Introductory Raman spectroscopy. Boston: Academic; 2003.
125. Otel I, Silveira J, Vassilenko V, Mata A, Carvalho ML, Santos JP, et al. Application of unsupervised multivariate analysis methods to raman spectroscopic assessment of human dental enamel. Computers. 2022;11(1):5. https://doi.org/10.3390/computers11010005.
126. Sanford KK, Parshad R, Gantt R, Tarone RE, Jones GM, Price FM. Factors affecting and significance of G2 chromatin radiosensitivity in predisposition to cancer. Int J Radiat Biol. 1989;55(6):963–81. https://doi.org/10.1080/09553008914551001.
127. Pantelias GE, Terzoudi GI. A standardized G2-assay for the prediction of individual radiosensitivity. Radiother Oncol. 2011;101(1):28–34. https://doi.org/10.1016/j.radonc.2011.09.021.
128. Terzoudi GI, Hatzi VI, Barszczewska K, Manola KN, Stavropoulou C, Angelakis P, Pantelias GE. G2-checkpoint abrogation in irradiated lymphocytes: a new cytogenetic approach to assess individual radiosensitivity and predisposition to cancer. Int J Oncol. 2009;35(5):1223–30. https://doi.org/10.3892/ijo_00000439.
129. Nikolakopoulou A, Soni A, Habibi M, Karaiskos P, Pantelias G, Terzoudi GI, Iliakis G. G2/M checkpoint abrogation with selective inhibitors results in increased chromatid breaks and radiosensitization of 82-6 hTERT and RPE human cells. Front Public Health. 2021;9:675095. https://doi.org/10.3389/fpubh.2021.675095.
130. Hernández L, Terradas M, Camps J, Martín M, Tusell L, Genescà A. Aging and radiation: bad companions. Aging Cell. 2015a;14(2):153–61. https://doi.org/10.1111/acel.12306.
131. Tong J, Hei TK. Aging and age-related health effects of ionizing radiation. Radiat Med Prot. 2020;1(1):15–23. https://doi.org/10.1016/j.radmp.2020.01.005.
132. WHO. Health risk assessment from the nuclear accident after the 2011 Great East Japan Earthquake and Tsunami based on a preliminary dose estimation. World Health Organisation; 2013. 978 92 4 150513 0. http://apps.who.int/iris/bitstream/10665/78218/1/9789241505130_eng.pdf
133. Wojcik A, Pei W. Individual response to ionising radiation – radiosensitivity of children. In: European Commission, Directorate-General for Energy, 'Radiosensitivity' of children: health issues after radiation exposure at young age: EU Scientific Seminar 2020; 2021. https://data.europa.eu/doi/10.2833/111011.
134. Applegate KE, Rühm W, Wojcik A, Bourguignon M, Brenner A, Hamasaki K, Imai T, Imaizumi M, Imaoka T, Kakinuma S, Kamada T, Nishimura N, Okonogi N, Ozasa K, Rübe CE, Sadakane A, Sakata R, Shimada Y, Yoshida K, Bouffler S. Individual response of humans to ionising radiation: governing factors and importance for radiological protection. Radiat Environ Biophys. 2020;59(2):185–209. https://doi.org/10.1007/s00411-020-00837-y.
135. Preston DL, Ron E, Tokuoka S, Funamoto S, Nishi N, Soda M, Mabuchi K, Kodama K. Solid cancer incidence in atomic bomb survivors: 1958–1998. Radiat Res. 2007;168(1):1–64. https://doi.org/10.1667/RR0763.1.
136. Shuryak I, Sachs RK, Brenner DJ. Cancer risks after radiation exposure in middle age. J Natl Cancer Inst. 2010;102(21):1628–36. https://doi.org/10.1093/jnci/djq346.
137. Georgakilas AG, Gorgoulis VG. Systemic DNA damage: mechanisms, effects and mitigation strategies. Semin Cancer Biol. 2016;37–38:1–2. https://doi.org/10.1016/j.semcancer.2016.04.001.

138. Georgakilas AG, Pavlopoulou A, Louka M, Nikitaki Z, Vorgias CE, Bagos PG, Michalopoulos I. Emerging molecular networks common in ionizing radiation, immune and inflammatory responses by employing bioinformatics approaches. Cancer Lett. 2015;368(2):164–72. https://doi.org/10.1016/j.canlet.2015.03.021.
139. Kregel KC, Zhang HJ. An integrated view of oxidative stress in aging: basic mechanisms, functional effects, and pathological considerations. Am J Physiol Regul Integr Comp Physiol. 2007;292(1):R18–36. https://doi.org/10.1152/ajpregu.00327.
140. Grantzau T, Overgaard J. Risk of second non-breast cancer among patients treated with and without postoperative radiotherapy for primary breast cancer: a systematic review and meta-analysis of population-based studies including 522,739 patients. Radiother Oncol. 2016;121(3):402–13. https://doi.org/10.1016/j.radonc.2016.08.017.
141. Swerdlow AJ, Higgins CD, Smith P, Cunningham D, Hancock BW, Horwich A, Hoskin PJ, Lister TA, Radford JA, Rohatiner AZ, Linch DC. Second cancer risk after chemotherapy for Hodgkin's lymphoma: a collaborative British cohort study. J Clin Oncol. 2011;29(31):4096–104. https://doi.org/10.1200/JCO.2011.34.8268.
142. Bernier-Chastagner V, Hettal L, Gillon V, Fernandes L, Huin-Schohn C, Vazel M, Tosti P, Salleron J, François A, Cérimèle E, Perreira S, Peiffert D, Chastagner P, Vogin G. Validation of a high performance functional assay for individual radiosensitivity in pediatric oncology: a prospective cohort study (ARPEGE). BMC Cancer. 2018;18(1):719. https://doi.org/10.1186/s12885-018-4652-7.
143. Oeffinger KC, Mertens AC, Sklar CA, Kawashima T, Hudson MM, Meadows AT, Friedman DL, Marina N, Hobbie W, Kadan-Lottick NS, Schwartz CL, Leisenring W, Robison LL, Childhood Cancer Survivor Study. Chronic health conditions in adult survivors of childhood cancer. N Engl J Med. 2006;355(15):1572–82. https://doi.org/10.1056/NEJMsa060185.
144. Yarnold J, Brotons MC. Pathogenetic mechanisms in radiation fibrosis. Radiother Oncol. 2010;97(1):149–61. https://doi.org/10.1016/j.radonc.2010.09.002. Epub 2010 Sep 29. PMID: 20888056
145. Rübe CE, Fricke A, Schneider R, Simon K, Kühne M, Fleckenstein J, Gräber S, Graf N, Rübe C. DNA repair alterations in children with pediatric malignancies: novel opportunities to identify patients at risk for high-grade toxicities. Int J Radiat Oncol Biol Phys. 2010;78(2):359–69. https://doi.org/10.1016/j.ijrobp.2009.08.052.
146. Rogers PB, Plowman PN, Harris SJ, Arlett CF. Four radiation hypersensitivity cases and their implications for clinical radiotherapy. Radiother Oncol. 2000;57(2):143–54. https://doi.org/10.1016/S0167-8140(00)00249-8.
147. German Commission on Radiological Protection. Sex-specific differences in radiation sensitivity – epidemiological, clinical and biological studies. Adopted at the 236th meeting of the German Commission on Radiological Protection on 17/18 September 2009. 2009. https://www.ssk.de/SharedDocs/Beratungsergebnisse_PDF/2009/Sex_Specific_Differences_in_Radiation_Sensitivity.pdf?__blob=publicationFile.
148. Haupt S, Caramia F, Klein SL, Rubin JB, Haupt Y. Sex disparities matter in cancer development and therapy. Nat Rev Cancer. 2021;21(6):393–407. https://doi.org/10.1038/s41568-021-00348-y.
149. Narendran N, Luzhna L, Kovalchuk O. Sex difference of radiation response in occupational and accidental exposure. Front Genet. 2019;10:260. https://doi.org/10.3389/fgene.2019.00260.
150. Boice JD Jr, Ellis ED, Golden AP, Zablotska LB, Mumma MT, Cohen SS. Sex-specific lung cancer risk among radiation workers in the million-person study and patients TB-Fluoroscopy. Int J Radiat Biol. 2019;7:1–12. https://doi.org/10.1080/09553002.2018.1547441.
151. Yamashita S, Suzuki S, Suzuki S, Shimura H, Saenko V. Lessons from Fukushima: latest findings of thyroid cancer after the Fukushima nuclear power plant accident. Thyroid. 2018;28(1):11–22. https://doi.org/10.1089/thy.2017.0283.
152. Safwat A, Bentzen SM, Turesson I, Hendry JH. Deterministic rather than stochastic factors explain most of the variation in the expression of skin telangiectasia after radiotherapy. Int J Radiat Oncol Biol Phys. 2002;52(1):198–204. https://doi.org/10.1016/S0360-3016(01)02690-6.
153. Seibold P, Auvinen A, Averbeck D, Bourguignon M, Hartikainen JM, Hoeschen C, Laurent O, Noël G, Sabatier L, Salomaa S, Blettner M. Clinical and epidemiological observations on individual radiation sensitivity and susceptibility. Int J Radiat Biol. 2020;96(3):324–39. https://doi.org/10.1080/09553002.2019.1665209.
154. De Courcy L, Bezak E, Marcu LG. Gender-dependent radiotherapy: the next step in personalised medicine? Crit Rev Oncol Hematol. 2020;147:102881. https://doi.org/10.1016/j.critrevonc.2020.102881.
155. Amirifar P, Ranjouri MR, Lavin M, Abolhassani H, Yazdani R, Aghamohammadi A. Ataxia-telangiectasia: epidemiology, pathogenesis, clinical phenotype, diagnosis, prognosis and management. Expert Rev Clin Immunol. 2020;16:859–71. https://doi.org/10.1080/1744666X.2020.1810570.
156. Levy A, Lang AE. Ataxia-telangiectasia: a review of movement disorders, clinical features, and genotype correlations. Mov Disord. 2018;33(8):1238–47. https://doi.org/10.1002/mds.27319.
157. Putti S, Giovinazzo A, Merolle M, Falchetti ML, Pellegrini M. ATM kinase dead: from ataxia telangiectasia syndrome to cancer. Cancers (Basel). 2021;13(21):5498. https://doi.org/10.3390/cancers13215498.
158. Berthel E, Foray N, Ferlazzo ML. The nucleoshuttling of the ATM protein: a unified model to describe the individual response to high- and low-dose of radiation? Cancers (Basel). 2019;11(7):905. https://doi.org/10.3390/cancers11070905.
159. Woodbine L, Gennery AR, Jeggo PA. The clinical impact of deficiency in DNA non-homologous end-joining. DNA Repair (Amst). 2014;16:84–96. https://doi.org/10.1016/j.dnarep.2014.02.011.
160. Altmann T, Gennery AR. DNA ligase IV syndrome; a review. Orphanet J Rare Dis. 2016;11(1):137. https://doi.org/10.1186/s13023-016-0520-1.
161. Hasbaoui BE, Elyajouri A, Abilkassem R, Agadr A. Nijmegen breakage syndrome: case report and review of literature. Pan Afr Med J. 2020;35:85. https://doi.org/10.11604/pamj.2020.35.85.14746.
162. Chrzanowska KH, Gregorek H, Dembowska-Bagińska B, Kalina MA, Digweed M. Nijmegen breakage syndrome (NBS). Orphanet J Rare Dis. 2012;7:13. https://doi.org/10.1186/1750-1172-7-13.
163. Fayyad N, Kobaisi F, Beal D, Mahfouf W, Ged C, Morice-Picard F, Fayyad-Kazan M, Fayyad-Kazan H, Badran B, Rezvani HR, Rachidi W. Xeroderma pigmentosum C (XPC) mutations in primary fibroblasts impair base excision repair pathway and increase oxidative DNA damage. Front Genet. 2020;11:561687. https://doi.org/10.3389/fgene.2020.561687.
164. Bensenouci S, Louhibi L, De Verneuil H, Mahmoudi K, Saidi-Mehtar N. Diagnosis of xeroderma pigmentosum groups A and C by detection of two prevalent mutations in West Algerian population: a rapid genotyping tool for the frequent XPC mutation c.1643_1644delTG. Biomed Res Int. 2016;2016:2180946. https://doi.org/10.1155/2016/2180946.
165. Piccione M, Belloni Fortina A, Ferri G, Andolina G, Beretta L, Cividini A, De Marni E, Caroppo F, Citernesi U, Di Liddo

R. Xeroderma pigmentosum: general aspects and management. J Pers Med. 2021;11(11):1146. https://doi.org/10.3390/jpm11111146.
166. Mankada S, Parikh A, Roy P, Kichloo A, Suryanarayana U. Radiotherapy as a primary treatment modality for squamous cell carcinoma of tongue in a case of xeroderma pigmentosum. J Curr Oncol. 2019;2(1):29–32. https://doi.org/10.4103/JCO.JCO_4_19.
167. Fanconi G. Familiäre infantile perniziosaartige Anämie (perniziöses Blutbild und Konstitution). Jahrbuch für Kinderheilkunde. 1927;117:257–89.
168. Gianni P, Matenoglou E, Geropoulos G, Agrawal N, Adnani H, Zafeiropoulos S, Miyara SJ, Guevara S, Mumford JM, Molmenti EP, Giannis D. The Fanconi anemia pathway and breast cancer: a comprehensive review of clinical data. Clin Breast Cancer. 2022;22(1):10–25. https://doi.org/10.1016/j.clbc.2021.08.001.
169. Bao Y, Feng H, Zhao F, Zhang L, Xu S, Zhang C, Zhao C, Qin G. FANCD2 knockdown with shRNA interference enhances the ionizing radiation sensitivity of nasopharyngeal carcinoma CNE-2 cells. Neoplasma. 2021;68(1):40–52. https://doi.org/10.4149/neo_2020_200511N516.
170. Mehta PA, Ebens C. Fanconi anemia. In: GeneReviews®. Seattle: University of Washington; 1993. http://www.ncbi.nlm.nih.gov/pubmed/20301575.
171. FARF, Fanconi Anemia Research Fund. Fanconi anemia clinical care guidelines. 5th edition. 2020. https://www.fanconi.org/images/uploads/other/Fanconi_Anemia_Clinical_Care_Guidelines_5thEdition_web.pdf.
172. Alter BP, Giri N, Savage SA, Rosenberg PS. Cancer in the National Cancer Institute inherited bone marrow failure syndrome cohort after fifteen years of follow-up. Haematologica. 2018;103(1):30–9. https://doi.org/10.3324/haematol.2017.178111.
173. Petrucelli N, Daly MB, Pal T. BRCA1- and BRCA2-associated hereditary breast and ovarian cancer. In: Adam MP, Ardinger HH, Pagon RA, et al., editors. GeneReviews® [Internet]. Seattle, WA: University of Washington, Seattle; 1998. 1993–2022. https://www.ncbi.nlm.nih.gov/books/NBK1247/.
174. Ricker C. From families syndromes to genes… The first clinical and genetic characterizations of hereditary syndromes predisposing to cancer: what was the beginning? Revista Médica Clínica Las Condes. 2017;28(4):482–90. https://doi.org/10.1016/j.rmclc.2017.06.011.
175. Nielsen FC, van Overeem Hansen T, Sørensen CS. Hereditary breast and ovarian cancer: new genes in confined pathways. Nat Rev Cancer. 2016;16(9):599–612. https://doi.org/10.1038/nrc.2016.72.
176. Paul A, Paul S. The breast cancer susceptibility genes (BRCA) in breast and ovarian cancers. Front Biosci (Landmark Ed). 2014;19:605–18. https://doi.org/10.2741/4230.
177. John EM, McGuire V, Thomas D, Haile R, Ozcelik H, Milne RL, Felberg A, West DW, Miron A, Knight JA, Terry MB, Daly M, Buys SS, Andrulis IL, Hopper JL, Southey MC, Giles GG, Apicella C, Thorne H, Kathleen Cuningham Foundation Consortium for Research into Familial Breast Cancer (kConFab), Whittemore AS. Diagnostic chest X-rays and breast cancer risk before age 50 years for BRCA1 and BRCA2 mutation carriers. Cancer Epidemiol Biomark Prev. 2013;22(9):1547–56. https://doi.org/10.1158/1055-9965.EPI-13-0189.
178. Narod SA, Lubinski J, Ghadirian P, Lynch HT, Moller P, Foulkes WD, Rosen B, Kim-Sing C, Isaacs C, Domchek S, Sun P, Hereditary Breast Cancer Clinical Study Group. Screening mammography and risk of breast cancer in BRCA1 and BRCA2 mutation carriers: a case-control study. Lancet Oncol. 2006;7(5):402–6. https://doi.org/10.1016/S1470-2045(06)70624-6.
179. Pijpe A, Andrieu N, Easton DF, Kesminiene A, Cardis E, Noguès C, Gauthier-Villars M, Lasset C, Fricker JP, Peock S, Frost D, Evans DG, Eeles RA, Paterson J, Manders P, van Asperen CJ, Ausems MG, Meijers-Heijboer H, Thierry-Chef I, Hauptmann M, Goldgar D, Rookus MA, van Leeuwen FE, GENEPSO; EMBRACE; HEBON. Exposure to diagnostic radiation and risk of breast cancer among carriers of BRCA1/2 mutations: retrospective cohort study (GENE-RAD-RISK). BMJ. 2012;345:e5660. https://doi.org/10.1136/bmj.e5660.
180. Scarborough JA, Scott JG. Translation of precision medicine research into biomarker-informed care in radiation oncology. Semin Radiat Oncol. 2022;32(1):42–53. https://doi.org/10.1016/j.semradonc.2021.09.001.
181. Zahed H, Johansson M, Ueland PM, Midttun Ø, Milne RL, Giles GG, Manjer J, Sandsveden M, Langhammer A, Sørgjerd EP, Grankvist K, Johansson M, Freedman ND, Huang WY, Chen C, Prentice R, Stevens VL, Wang Y, Le Marchand L, Wilkens LR, Weinstein SJ, Albanes D, Cai Q, Blot WJ, Arslan AA, Zeleniuch-Jacquotte A, Shu XO, Zheng W, Yuan JM, Koh WP, Visvanathan K, Sesso HD, Zhang X, Gaziano JM, Fanidi A, Muller D, Brennan P, Guida F, Robbins HA. Epidemiology of 40 blood biomarkers of one-carbon metabolism, vitamin status, inflammation, and renal and endothelial function among cancer-free older adults. Sci Rep. 2021;11(1):13805. https://doi.org/10.1038/s41598-021-93214-8.
182. Harlid S, Gunter MJ, Van Guelpen B. Risk-predictive and diagnostic biomarkers for colorectal cancer; a systematic review of studies using pre-diagnostic blood samples collected in prospective cohorts and screening settings. Cancers (Basel). 2021;13(17):4406. https://doi.org/10.3390/cancers13174406.
183. Jiang CY, Niu Z, Green MD, Zhao L, Raupp S, Pannecouk B, Brenner DE, Nagrath S, Ramnath N. It's not 'just a tube of blood': principles of protocol development, sample collection, staffing and budget considerations for blood-based biomarkers in immunotherapy studies. J Immunother Cancer. 2021;9(7):e003212. https://doi.org/10.1136/jitc-2021-003212.
184. Karschnia P, Le Rhun E, Vogelbaum MA, van den Bent M, Grau SJ, Preusser M, Soffietti R, von Baumgarten L, Westphal M, Weller M, Tonn JC. The evolving role of neurosurgery for central nervous system metastases in the era of personalized cancer therapy. Eur J Cancer. 2021;156:93–108. https://doi.org/10.1016/j.ejca.2021.07.032.
185. Connor M, Kim MM, Cao Y, Hattangadi-Gluth J. Precision radiotherapy for gliomas: implementing novel imaging biomarkers to improve outcomes with patient-specific therapy. Cancer J. 2021;27(5):353–63. https://doi.org/10.1097/PPO.0000000000000546.
186. Soares S, Guerreiro SG, Cruz-Martins N, Faria I, Baylina P, Sales MG, Correa-Duarte MA, Fernandes R. The influence of miRNAs on radiotherapy treatment in prostate cancer - a systematic review. Front Oncol. 2021;11:704664. https://doi.org/10.3389/fonc.2021.704664.
187. Leiser D, Samanta S, Eley J, Strauss J, Creed M, Kingsbury T, Staats PN, Bhandary B, Chen M, Dukic T, Roy S, Mahmood J, Vujaskovic Z, Shukla HD. Role of caveolin-1 as a biomarker for radiation resistance and tumor aggression in lung cancer. PLoS One. 2021;16(11):e0258951. https://doi.org/10.1371/journal.pone.0258951.
188. De la Pinta C. Toward personalized medicine in radiotherapy of hepatocellular carcinoma: emerging radiomic biomarker candidates of response and toxicity. OMICS. 2021;25(9):537–44. https://doi.org/10.1089/omi.2021.0065.
189. Manem VSK. Development and validation of genomic predictors of radiation sensitivity using preclinical data. BMC Cancer. 2021;21(1):937. https://doi.org/10.1186/s12885-021-08652-4.
190. Wursthorn A, Schwager C, Kurth I, Peitzsch C, Herold-Mende C, Debus J, Abdollahi A, Nowrouzi A. High-complexity cellular barcoding and clonal tracing reveals stochastic and deterministic

parameters of radiation resistance. Int J Cancer. 2022;150(4):663–77. https://doi.org/10.1002/ijc.33855.

191. Van der Eecken K, Vanwelkenhuyzen J, Deek MP, Tran PT, Warner E, Wyatt AW, Kwan EM, Verbeke S, Van Dorpe J, Fonteyne V, Lumen N, De Laere B, Ost P. Tissue- and blood-derived genomic biomarkers for metastatic hormone-sensitive prostate cancer: a systematic review. Eur Urol Oncol. 2021; https://doi.org/10.1016/j.euo.2021.10.005.

Further Reading

El-Nachef L, Al-Choboq J, Restier-Verlet J, Granzotto A, Berthel E, Sonzogni L, Ferlazzo ML, Bouchet A, Leblond P, Combemale P, Pinson S, Bourguignon M, Foray N. Human radiosensitivity and radiosusceptibility: what are the differences? Int J Mol Sci. 2021;22(13):7158. https://doi.org/10.3390/ijms22137158.

Grant EJ, Brenner A, Sugiyama H, Sakata R, Sadakane A, Utada M, Cahoon EK, Milder CM, Soda M, Cullings HM, Preston DL, Mabuchi K, Ozasa K. Solid cancer incidence among the life span study of atomic bomb survivors: 1958–2009. Radiat Res. 2017;187(5):513–37. https://doi.org/10.1667/RR14492.1.

Hernández L, Terradas M, Camps J, Martín M, Tusell L, Genescà A. Aging and radiation: bad companions. Aging Cell. 2015b;14(2):153–61. https://doi.org/10.1111/acel.12306.

Ni J, Bucci J, Malouf D, Knox M, Graham P, Li Y. Exosomes in cancer radioresistance. Front Oncol. 2019b;9:869. https://doi.org/10.3389/fonc.2019.00869.

UNSCEAR, United Nations Scientific Committee on the Effects of Atomic Radiation. Report to the General Assembly, with Scientific Annex. UNSCEAR; 2000. https://www.unscear.org/unscear/en/publications/2000.html

UNSCEAR, United Nations Scientific Committee on the Effects of Atomic Radiation. Report to the General Assembly, with Scientific Annex. UNSCEAR; 2001. https://www.unscear.org/unscear/en/publications/2001.html

Vinnikov V, Hande MP, Wilkins R, Wojcik A, Zubizarreta E, Belyakov O. Prediction of the acute or late radiation toxicity effects in radiotherapy patients using ex vivo induced biodosimetric markers: a review. J Pers Med. 2020;10(4):E285. https://doi.org/10.3390/jpm10040285.

Radiobiology of Accidental, Public, and Occupational Exposures

8

Ruth Wilkins, Ana Margarida Abrantes, Elizabeth A. Ainsbury, Sarah Baatout, Maria Filomena Botelho, Tom Boterberg, Alžběta Filipová, Daniela Hladik, Felicia Kruse, Inês Alexandra Marques, Dhruti Mistry, Jayne Moquet, Ursula Oestreicher, Raghda Ramadan, Georgia I. Terzoudi, Sotiria Triantopoulou, Guillaume Vogin, and Anne-Sophie Wozny

R. Wilkins (✉)
Environmental and Research Health Sciences Directorate, Health Canada, Ottawa, ON, Canada
e-mail: ruth.wilkins@hc-sc.gc.ca

A. M. Abrantes
Institute of Biophysics, Faculty of Medicine, iCBR-CIMAGO, Center for Innovative Biomedicine and Biotechnology, University of Coimbra, Coimbra, Portugal

ESTESC-Coimbra Health School, Instituto Politécnico de Coimbra, Coimbra, Portugal
e-mail: mabrantes@fmed.uc.pt

E. A. Ainsbury · F. Kruse · J. Moquet · D. Mistry
Radiation, Chemical and Environmental Hazards Directorate, UK Health Security Agency, Oxford, United Kingdom
e-mail: liz.ainsbury@ukhsa.gov.uk; simone-felicia.kruse@bih-charite.de; Jayne.moquet@ukhsa.gov.uk

S. Baatout · R. Ramadan
Institute of Nuclear Medical Applications, Belgian Nuclear Research Centre, SCK CEN, Mol, Belgium
e-mail: sarah.baatout@sckcen.be; raghda.ramadan@sckcen.be

M. F. Botelho · I. A. Marques
Institute of Biophysics, Faculty of Medicine, iCBR-CIMAGO, Center for Innovative Biomedicine and Biotechnology, University of Coimbra, Coimbra, Portugal

Clinical Academic Center of Coimbra, Coimbra, Portugal
e-mail: mfbotelho@fmed.uc.pt; ines.marques@student.uc.pt

T. Boterberg
Department of Radiation Oncology, Ghent University Hospital, Ghent, Belgium

Particle Therapy Interuniversity Center Leuven, Department of Radiation Oncology, University Hospitals Leuven, Leuven, Belgium
e-mail: Tom.Boterberg@UGent.be

A. Filipová
Department of Radiobiology, Faculty of Military Health Sciences, University of Defence, Hradec Kralove, Czech Republic
e-mail: alzbeta.filipova@unob.cz

D. Hladik · U. Oestreicher
Bundesamt für Strahlenschutz, Oberschleißheim, Germany
e-mail: dhladik@bfs.de; uoestreicher@bfs.de

G. I. Terzoudi · S. Triantopoulou
Health Physics, Radiobiology and Cytogenetics Laboratory, Institute of Nuclear and Radiological Sciences and Technology, Energy and Safety, National Centre for Scientific Research "Demokritos", Athens, Greece
e-mail: gterzoudi@rrp.demokritos.gr; iro@rrp.demokritos.gr

G. Vogin
Centre Francois Baclesse, University of Luxembourg and Luxembourg Institute of Health, Luxembourg, Luxembourg
e-mail: guillaume.vogin@baclesse.lu

A.-S. Wozny
Cellular and Molecular Radiobiology Lab, UMR CNRS 5822, Lyon 1 University, Oullins, France

Department of Biochemistry and Molecular Biology, Lyon-Sud Hospital, Hospices Civils de Lyon, Pierre-Bénite, France
e-mail: anne-sophie.wozny@univ-lyon1.fr

S. Baatout (ed.), *Radiobiology Textbook*, https://doi.org/10.1007/978-3-031-18810-7_8

Learning Objectives

- To understand different scenarios for human exposure to ionizing radiation excluding medical treatment procedures such as those for cancer treatment.
- To understand long-term health effects associated with low-dose radiation exposure.
- To gain knowledge on the worldwide distribution of indoor concentration of radon.
- To understand how naturally occurring radon affects human health.
- To understand the critical need for immediate triage and to learn about current triage tools for radiation exposure categorization of radiation accident victims.
- To gain a better understanding of internal contamination and decontamination.
- To gain knowledge on clinical consequences of early and delayed effects of acute exposure to high doses of ionizing radiation.
- To become familiar with the characteristic features of the three sub-classes of acute radiation syndromes (hematologic, gastrointestinal, and neurovascular), as well as effects on skin and lungs.
- To explain the basis for and biological meaning of LD_{50}.

8.1 Radiation Exposure Scenarios

8.1.1 Introduction

Individuals can be exposed to ionizing radiation in many accidental or intended situations with different ranges of dose, dose rate, and radiation quality. Human exposures can occur directly from external radiation sources or through either internal or external contamination with radioactive materials/substances. In certain circumstances, external radiation exposure may occur concomitantly with external or internal contamination (Fig. 8.1). While the radiation dose from external exposure or internal contamination could be substantial, health risk from external contamination is highly dependent on the penetrating ability of the radionuclide. Since alpha particles can be effectively blocked by a piece of paper or by the upper layer of the skin, risk of external contamination by alpha particles is expected to be negligible. Most external contamination can be eliminated either by cleansing and/or by removing contaminated clothes.

The following section lists the types of exposure scenarios with specific examples.

8.1.2 Medical Radiation Exposures to Patients

Aside from radiation oncology, which has been well described in Chap. 6, medical exposures can occur from diagnostic and therapeutic procedures other than cancer treatment. These procedures can cause exposures to the patient but also exposure in utero to the embryo or fetus. Worldwide medical exposures account for almost 20% of the average human exposure from all the sources [1].

8.1.2.1 Diagnostic Radiology

Doses from diagnostic radiology procedures range from very low doses in dental radiography to higher doses from computed tomography or fluoroscopy procedures. In general, radiation doses from diagnostic procedures tend to be low and are therefore unlikely to cause deterministic effects (discussed in Sects. 2.7.2 and 8.2), but especially repeated fluoroscopy-guided procedures like angioplasty may result in substantial skin dose to the patients (see also Sect. 8.1.6). Table 8.1 lists the effective doses (see definition in Sect. 8.7) associated with each of the commonly used diagnostic procedures, but these doses can vary among different countries. The total number of these procedures conducted worldwide to date, is around 4 billion (2.6 billion for radiography, 1.1 billion for dental radiography and 400 million for CT) and the number has been steadily increasing over the past 25 years, especially for CT [2].

8.1.2.2 Radiation Treatment (Non-cancer)

There have been many instances of therapeutic exposures unrelated to cancer treatment in the past including patients treated with radiation for ankylosing spondylitis (total body dose of 0.86–4.62 Gy) to relieve pain and children treated for tinea capitis (ringworm of the scalp) with a brain dose ranging from 0.75 to 1.7 Gy. There is evidence of increased cancers in these populations [4, 5] and alternative treatments have now been adopted that do not involve radiation. Presently, radiotherapy is used in procedures such as to treat benign tumors, pain relief for arthritis, arteriovenous malformations as shown in Fig. 8.2 [6]. These procedures deliver a range of doses from 5 to 60 Gy which can be delivered in single or multiple fractions.

8.1.3 Occupational Exposures

Radiation exposures can occur in many occupational settings with the highest average effective doses reported in the nuclear sector although this shows a steadily decreasing trend due to increased knowledge about the effects of radiation and better radiation protection practices over the past decades. Figure 8.3 shows data for the occupational exposures over a 27-year period. The average effective dose per

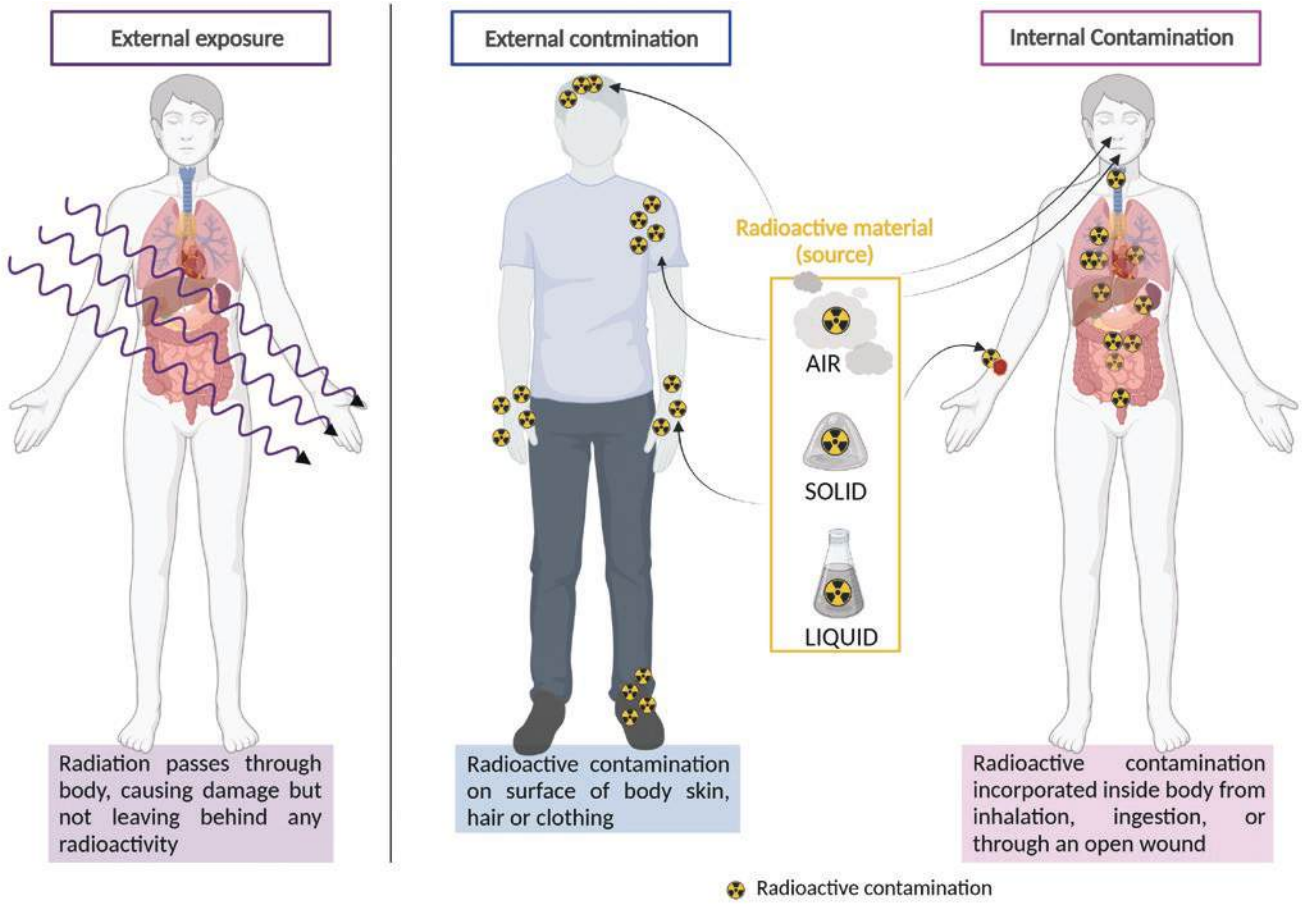

Fig. 8.1 External exposure and contamination

Table 8.1 Examples of each type of diagnostic procedures and their typical doses (reproduced with permission from [2])

Examination type	Typical effective dose (mSv)[a]
Dental radiography	
Intraoral	0.006
Panoramic	0.024
Projection radiography	
Head (skull and facial bones)	0.076
Chest (thoracic spine)	0.45
Mammography	0.22
Lumbar spine	1.0
Pelvis and hips (bone)	0.49
Limbs and joints	0.02
Whole spine (trunk)	1.5
Radiography and fluoroscopy	
Gastrointestinal tract	3.4
Cardiac angiography	7.0
Pelvic angiography	3.2
Urogenital tract	2.4
Computed tomography	
Head (skull and facial bones)	1.5
Neck (soft tissues)	2.8

[a] ICRP 60 tissue weighting factors were applied for the effective dose determination [3]

worker is the highest in the nuclear sector. Due to the high number of workers in the medical field (~7500 in 2002) compared to the nuclear sector (~660 in 2002) and the industrial sector (~850 in 2002), collective exposures are the highest in the medical field, followed by those working in nuclear power and industrial uses of radiation.

8.1.3.1 Exposures to Medical Staff or Personnel

Out of all the occupational exposures, the medical profession makes up the single largest group of workers exposed in the workplace. This group encompasses nurses, doctors, technicians, and other support workers. The procedures mostly comprise diagnostic imaging and radiation therapy, which have been increasing yearly as technology develops and the benefits become more widespread. Table 8.2 shows some of the specific medical professions with the highest average exposures based on dosimeter readings, in Canada. These values will vary from country to country but are similar in countries with comparable level of health care.

Occupational dose in diagnostic radiology is quite variable due to the wide range of technologies available. For example, most CT technologists have no measurable dose

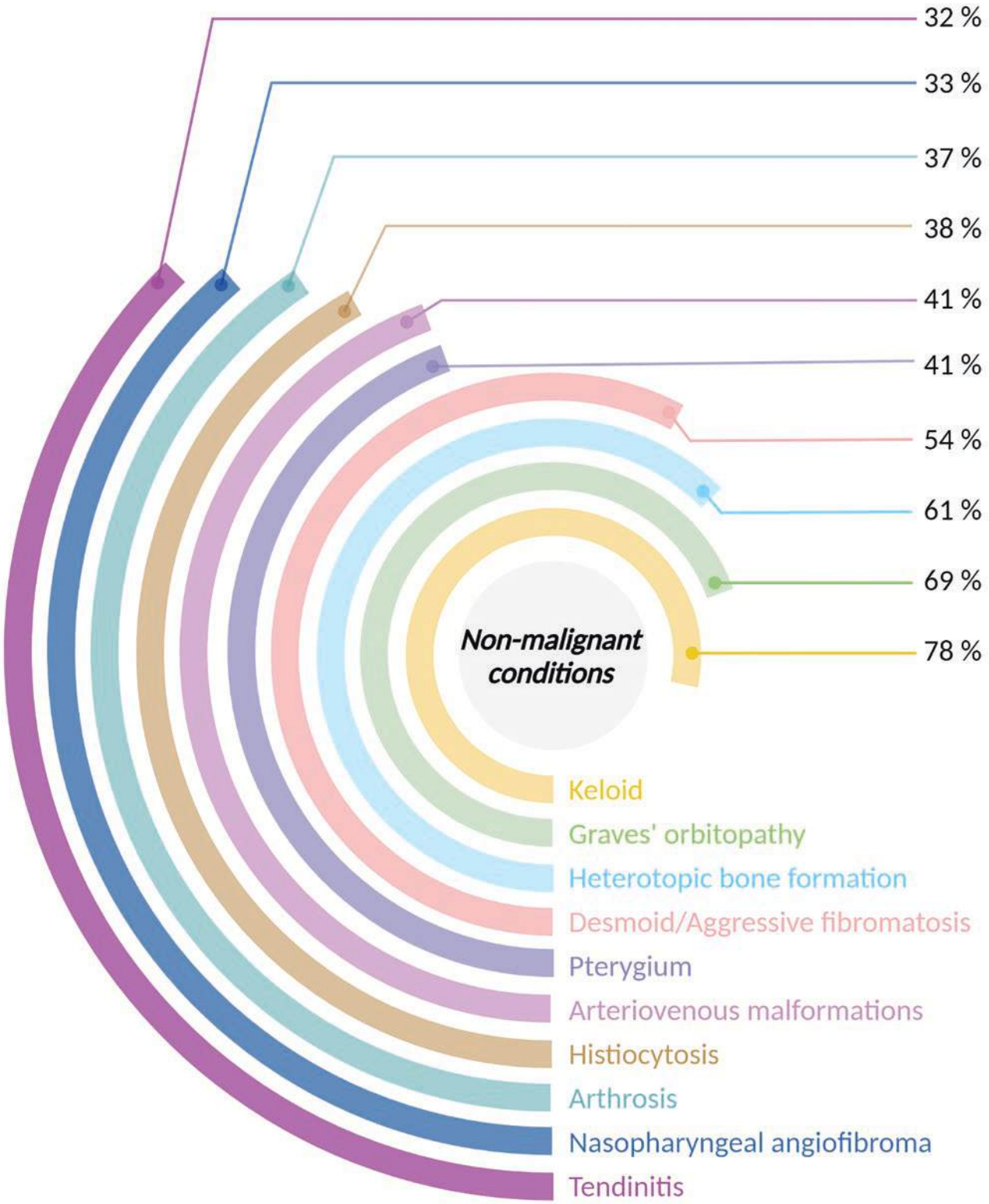

Fig. 8.2 Non-malignant conditions most commonly treated with radiation therapy as a percentage of all international radiotherapy institutes surveyed ($n = 508$). (Data extracted with permission from [6])

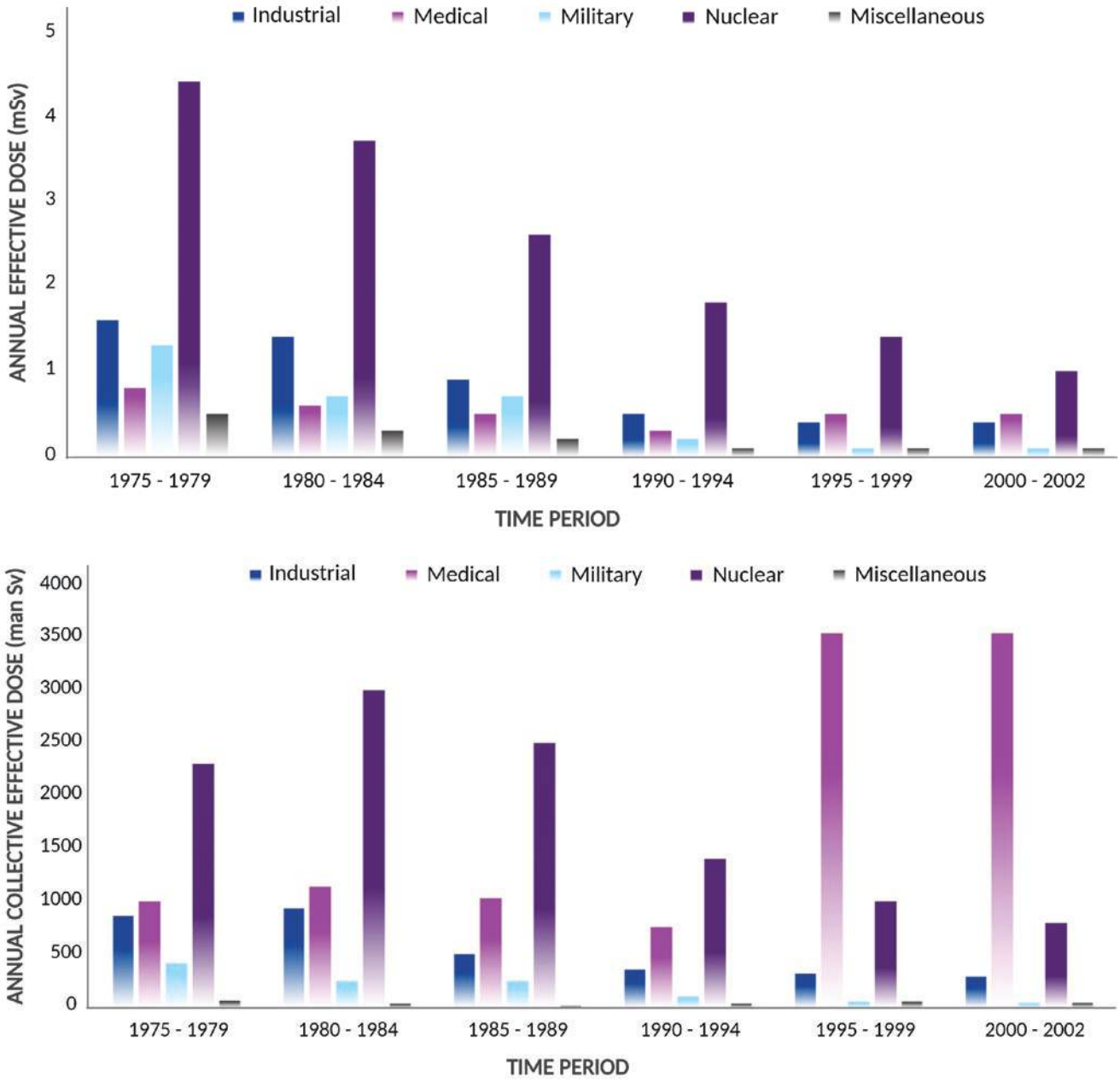

Fig. 8.3 Data for estimated occupational exposures from 1975 to 2002. (Reproduced with permission from [1, 7])

Table 8.2 Selection of the highest exposed medical occupations of monitored workers (reproduced with permission from [8])

Occupation	Ave dose (mSv/year) (2008)	Mean effective dose (mSv/year) (2016)
Nuclear medicine technologist	1.56	1.23
Diagnostic radiologist	0.44	0.17
Medical radiation technologist	0.10	0.11
Medical physicist	0.03	0.05
Radiation therapist	0.05	0.04
Dental assistant	0.01	0.01
All medical professions	0.08	0.07

while the individual effective dose for interventional procedures such as vascular surgery supported by fluoroscopy is significant and medical doctors performing these procedures are the most occupationally exposed group from diagnostic radiation. Depending on the procedure, the occupational dose can range from 0.008–2 mSv per interventional procedure. Diagnostic radiation is also frequently used in dental clinics; therefore, the number of devices and workers exposed is extremely large. The average annual effective dose in dental radiology has been decreasing over the last few decades from 0.32 mSv in the late 1970s to 0.06 Sv in the early 1990s due to improved equipment [1]

Nuclear medicine involves the use of radionuclides, particularly ^{99m}Tc, to investigate physiological process and organ function. Occupational exposures result from personnel having to be in close contact with patients when injecting them and while positioning them during which time they can be exposed to gamma radiation emitted by the radionuclides. Preparation of the radionuclides can also result in high exposures with annual doses up to 5 mSv and doses to the hands and fingers up to 500 mSv. There are several other nuclear medicine techniques with different exposures such as positron emission tomography using ^{18}F labeled fluorodeoxyglucose and thyroid treatment with ^{131}I to name a few. Worldwide, the annual collective effective dose is on the order of 85 man Sv and had been increasing over the years with increasing number of workers in this field. However, the annual collective dose is no longer increasing [1] since the 1980s as the average annual effective dose was reduced from 1 mSv down to about 0.75 mSv.

Radiotherapy for treating malignant disease delivers the highest dose to the patient; however, occupational doses in this setting remain very low. These procedures have been well described in Chap. 5. The collective annual dose in radiotherapists has decreased substantially since the 1970s despite the increase in workers in this field. This is due to a large drop in the annual average effective dose per worker.

8.1.3.2 Nuclear Workers

Workers throughout the nuclear fuel cycle are exposed to ionizing radiation, from mining, through milling, enrichment, fuel fabrication, reactor operation, and reprocessing [1]. This group of workers is most closely monitored for their radiation exposure. As there are more workers in mining and reactor operation, the collective effective dose is the highest in this group. The average annual effective dose for nuclear workers has also been decreasing steadily since the mid-1970s from 4.1 to 1.0 mSv currently, and the collective effective dose has decreased since the 1980s from 2500 to 800 man Sv (Fig. 8.4). These reductions are due to implementation of ALARA programs that have improved plant designs, implemented upgrades, and improved operational procedures [1].

8.1.3.3 Industrial Radiography

Industrial radiography is a non-destructive method used to look at defects in materials such as welded pipeline and castings. This can involve the use of X-rays or gamma ray sources sealed in capsules (e.g., ^{60}Co and ^{192}Ir). Radiation penetrates the object being examined and exposes a detection system behind the object. The devices used are designed to protect the operator and annual effective doses to the workers under normal use are less than 0.5 mSv.

8.1.3.4 Military

Most military exposures results from the fabrication and testing of nuclear weapons, the use of nuclear energy on naval vessels, and the use of ionizing radiation for activities similar to those used in civilian applications (e.g., research, transport, and non-destructive testing). Data from the USA indicates that the average annual effective dose in monitored military individuals form all military activities is on the order of a few tens of mSv. There has, however, been a substantial decrease in the average collective doses since the 1970s where annual effective doses to monitor military workers were as high as 1 mSv [1].

8.1.4 Elevated Exposure to Natural Sources

Enhanced levels of natural radiation are found in several occupational settings. Because the radiation is naturally occurring, workers are not routinely monitored so exposure levels are not well known. Miners make up a large group of these occupational exposures and their estimated collective dose is about 30,000 man Sv [9]. Air crew make up another group of workers exposed to naturally occurring radiation and have been identified as one of the most highly exposed professional groups with exposure levels of 3–8 μSv/h during the flight depending on latitude and altitude. Worldwide, the estimated collective effective dose to aircrew is about 900 man Sv. Overall, there are about 13 million workers worldwide exposed to natural sources of radiation with an estimated average effective dose of 2.9 mSv and an estimated collective effective dose of 37,260 man Sv. This average effective dose from natural exposures is not decreasing as much as with man-made exposures, however, as the number of workers is increasing, the collective dose has been rising between the early 1990s and early 2000s [9].

8.1.5 Miscellaneous

In addition to those mentioned above, there are a number of other professions where radiation might be involved. These include, but are not limited to, research in academic institutions, management of spent radioactive sources and transport of radioactive material. Academic institutions make up 92% for the monitored workers in this category and about 87% of the collective dose. Overall, the average annual effective dose for all monitored workers in this category is less than 1 mSv and doses, decreasing from 0.5 to 0.1 mSv between 1975 and 2004 [9].

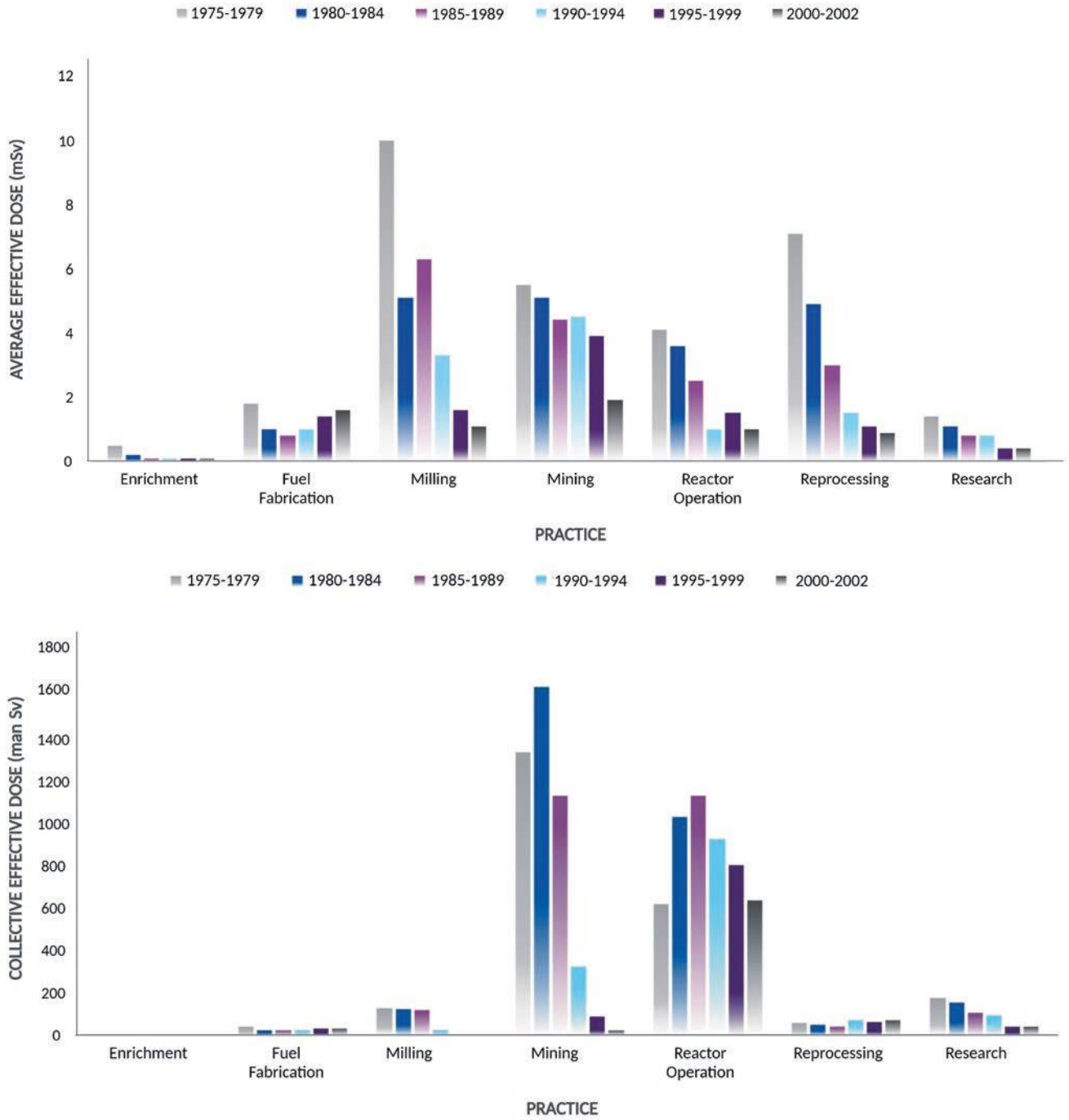

Fig. 8.4 Global trends in the number of monitored workers, and in collective effective doses and effective doses to workers for different practices of the nuclear fuel cycle. (Reproduced with permission from [1])

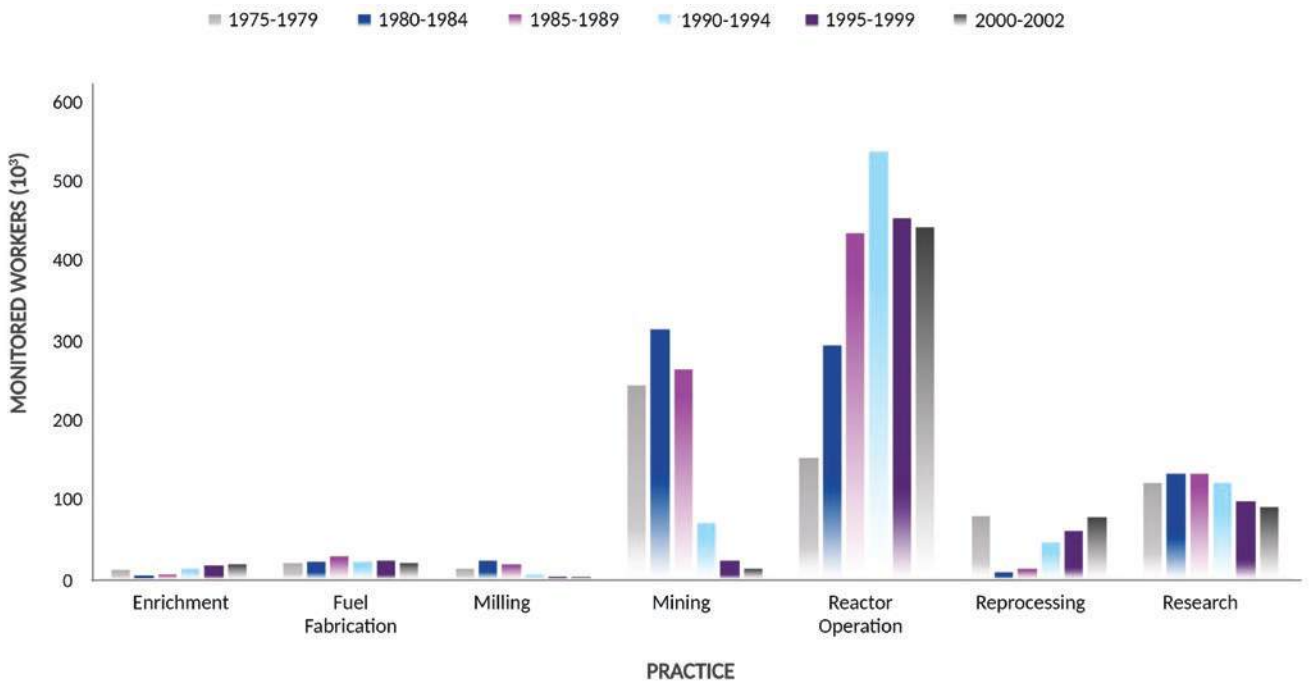

Fig. 8.4 (continued)

8.1.6 Accidental Exposures

8.1.6.1 Medical Accidents

Unintended exposures in medicine are defined as exposures that differ significantly from the exposure intended for the given purpose and are considered medical errors. These events can include operator errors, equipment failures, and other mishaps with consequences that can range from less to more severe. Events can occur with both diagnostic and therapeutic procedures and may also result in unintended doses to an embryo or fetus. The most serious overexposures can result in doses to the skin that are high enough to cause tissue reactions. These typically arise from CT and interventional fluoroscopy procedures, most notably from perfusion studies [10].

8.1.6.2 Nuclear Power Plant Accidents

Despite the adoption of safety measures to reduce the risk of accidents at Nuclear Power Plants (NPPs), there have been several accidents as well as near misses with varying degrees of impact and radiation exposure to workers and the general population [11]. These accidents are characterized by the release of large amounts of radionuclides with relatively short half-lives [12]. Three such past incidents of high impact are Three Mile Island in 1979 [13], Chernobyl in 1986 [14], and Fukushima in 2011 [15]. Accidents in NPPs can result in high doses to a small population of clean-up workers (e.g., Chernobyl) as well as small doses to a large population living in the vicinity of the NPP (e.g., Fukushima). These NPP accidents, along with other accidents, can be rated according to the International Nuclear Event scale (INES) based on severity and impact of the incident (Fig. 8.5). Accidents can also occur during the transportation of nuclear waste by road or rail with the primary concern of exposure for this waste being ^{137}Cs, a γ-emitter. Although the fuel is well packaged during shipment, the amount of radioactive material may be on the order of PBq per shipment container, so any dispersal would be catastrophic. In general, occupational exposures tend to be low doses and low-dose rates.

8.1.6.3 Industrial Radiography

During industrial radiography, accidents can occur multiple ways: loss of control of the source of radiation, damage to the source, direct contact with the source or improper use of shielding [16]. Even when operating procedures are correctly followed, dose rates close to the source can be very high causing overexposures in a matter of seconds. Table 8.3 lists a few examples of accidents due to inadequate regulatory control, failure to follow operational procedures, inadequate training, inadequate maintenance, and human error.

8.1.6.4 Other Accidental Exposures

An orphaned source is a self-contained radioactive source that is no longer under proper regulatory control. These sources can come from both therapeutic and industrial radiation machines and can have activities in the TBq range. As long as they remain sealed, they do not cause contamination but when opened can cause high doses and extreme health effects and even death, due to their high activity such as

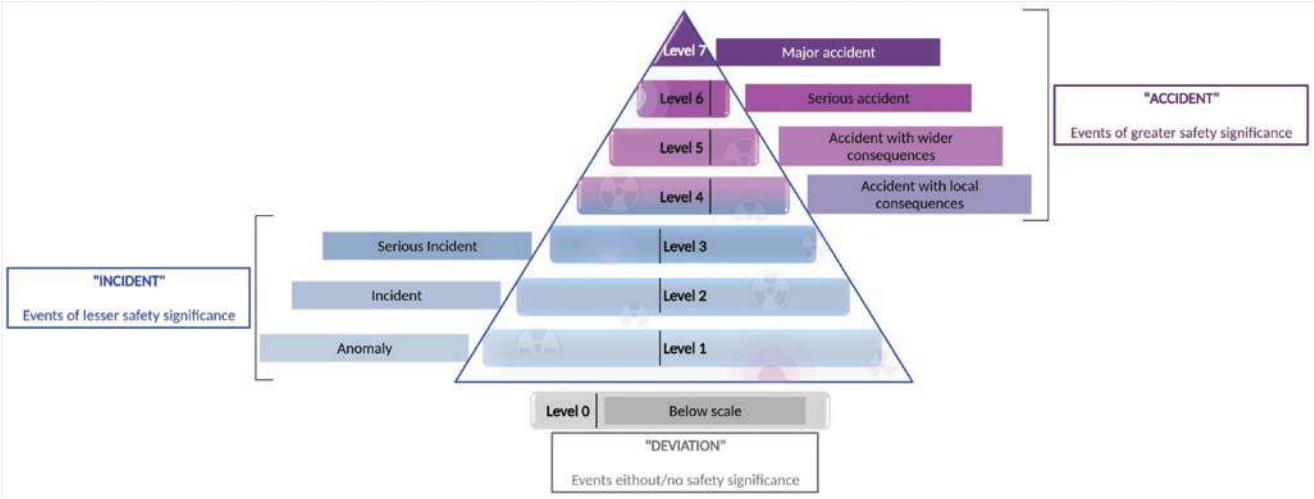

Fig. 8.5 International Nuclear Event scale based on severity and impact of the incident

Table 8.3 Selected accidents in industrial radiography

Year	Primary cause	Exposed population	Source/activity	Scenario	Dose to exposed population	Reference
1989	Inadequate regulatory control	General public	^{192}Ir/260 GBq	Source not removed prior to transportation	Public <5 mSv Driver—0.31 Sv	USNRC [17]
1992	Failure to follow operational procedures	Operator	Various sealed sources	Unsafe operations with radiographic sources	Lifetime 10 Sv whole body, >100 Sv to hand	Lloyd et al. [18]
1969	Inadequate training, insufficient supervision	Operator	^{192}Ir/900 GBq	Shutter of source left open during transportation	450 mSv whole body, 2.14 Sv to left hip	Harisson et al. [19]
1993	Inadequate maintenance	Operator	^{192}Ir/3600 GBq	Missing roll pins to secure camera lock	6 mSv whole body, 19 Sv to fingers	USNRC [20]
1996	Human error	Operator	X-ray	Wrong cable connected to control panel causing wrong X-ray unit to be activated	600 and 160 mSv to each of two operators	Wheelton [21]

occurred in Thailand in 2000 [22]. Their containment can also become compromised, spreading radioactive material over large areas as occurred in Goiania, Brazil in 1987 [23].

8.1.7 Malicious Exposures

The health consequences after an accidental exposure to radiation will depend on the exposure scenario. Although there is a long list of attacks that could involve radiation, the following three are considered the most probable.

8.1.7.1 Improvized Nuclear Devices (INDs)

INDs incorporate nuclear material that can produce nuclear explosions. This can cause extensive blast (mechanical), thermal, and radiation injuries with large numbers of fatalities and casualties as well as high doses of radiation to potentially large numbers of individuals, when detonated at or close to a major city. The radiation injury can be a result of the prompt radiation within minutes near the epicenter of the explosion that is predominantly from γ-rays and neutrons. Delayed exposures can result from fallout that is produced by fission products and neutron-induced radionuclides and are dispersed downwind from the epicenter. Finally, ground shine can result from the deposition of radionuclides on the ground of the fallout area that is highly dependent on the wind direction and speed (Fig. 8.6). INDs are considered highly unlikely but possible to be used; hence, it is necessary to be prepared for such events. The result of such an event would be catastrophic. Thousands of people could be killed by the blast and heat, hundreds to thousands could be killed or made ill by radiation effects, and thousands could have an increased long-term risk of leukemia or solid cancer. Furthermore, the psychological and infrastructure effects would also be enormous [24].

The population that has had the greatest impact on risk assessment is the A-bomb survivors. A large population of Japanese were exposed in 1945 during an atomic bomb attack in both Hiroshima and Nagasaki. This cohort comprises the Life Span Study (LSS) that includes 94,000 in-city subjects of all ages and sex with dose estimates ranging up to 4 Sv. There has been a long-term follow-up on this cohort, allowing for high quality mortality and cancer incidence data [25]. The

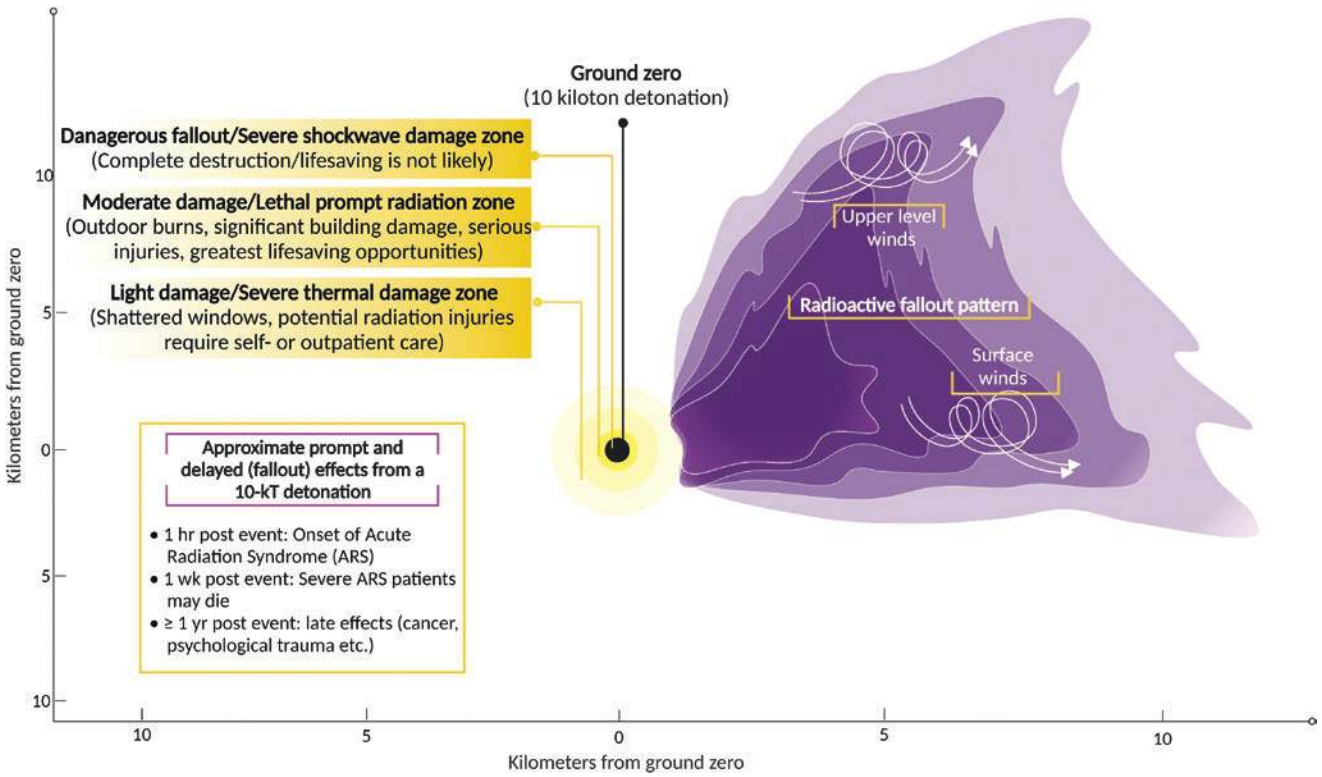

Fig. 8.6 Approximate prompt and delayed (fallout) effects from a 10-kT detonation. (Reproduced with permission from Lawrence Livermore National Laboratory)

majority of survivors were exposed to doses less than 0.1 Sv and, therefore, provide excellent data in the dose range of interest for radiation protection. This cohort also provided data on in utero and early childhood exposures [26].

8.1.7.2 Radiological Dispersal Devices (RDDs)

RDDs use explosives or mechanical devices to distribute radiological material resulting in radioactive contamination. This is considered a more likely scenario than an IND. With RDDs, a relatively small area would be affected and radiation exposures could take the form of both internal and external contamination; however, exposures are expected to be lower than medically significant. Most likely, a small number of individuals will be contaminated with radioactive material.

8.1.7.3 Radiological Exposure Devices (REDs)

REDs involve hidden sealed sources designed to expose people to significant doses without their knowledge and without causing contamination. They are usually hidden in a busy public location, such as under a seat on a bus or in a sports stadium and could remain undetected for long periods. Individuals who come close to these sources can receive significant localized doses but numbers of highly exposed individual are anticipated to be low.

8.2 Long-Term Health Effects of Low-Dose Radiation in Exposed Human Populations

8.2.1 Radiation Effects in the Developing Embryo and Fetus

It is generally accepted that the developing embryo and fetus are more radiosensitive than children or adults. In common with other health effects, at low doses (<100 mGy), stochastic risk is the main driver to protect the fetus (see Chap. 1). Deterministic effects or tissue reactions—mainly central nervous system effects and congenital malformations—are reported for higher doses; however, the evidence is somewhat sparse.

Evidence for fetal radiation effects comes mostly from animal studies performed with high doses of in utero radiation. Evidence is limited from the larger scale population exposures such as those of the A-bomb survivors, as well as from other small-scale accidents, and medical uses of radiation (e.g., Gilbert [26]). The relevant animal data suggest thresholds for non-cancer effects including small fetal size, microcephaly, and intellectual disability (see also Sect. 2.7.2). However, due to interspecies differences and different selection pressures, it is impossible to draw conclusions

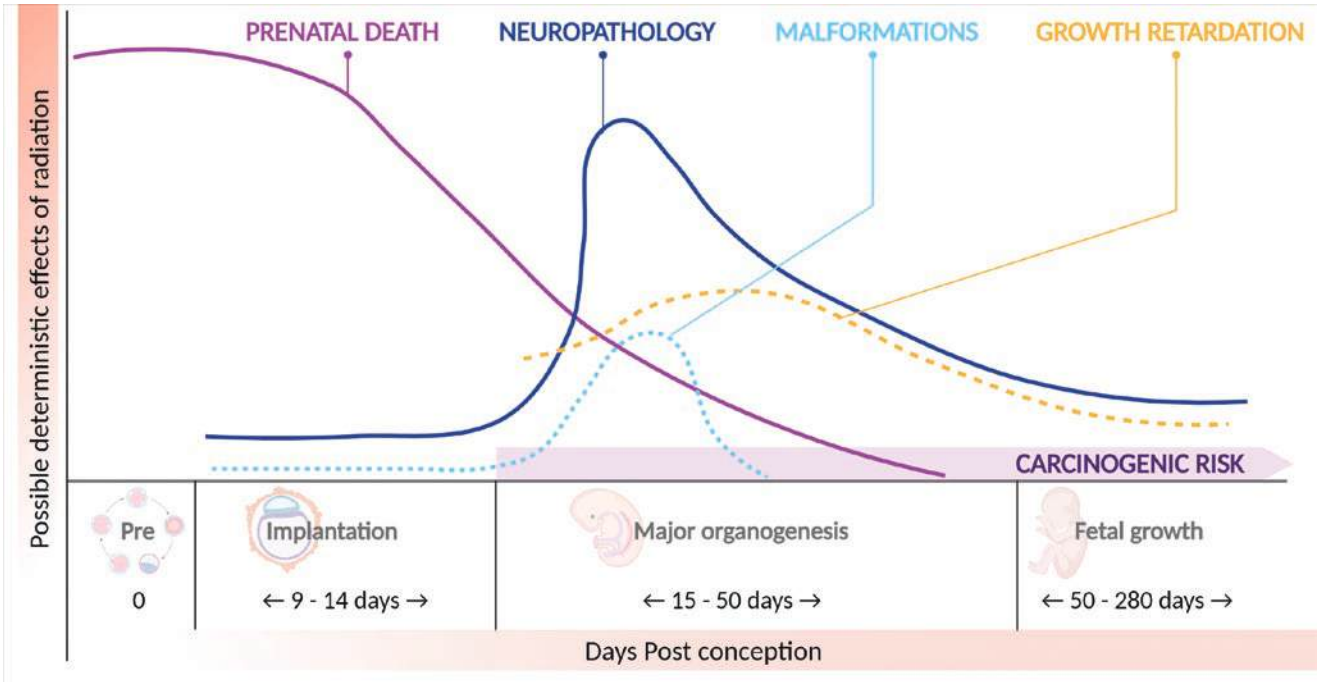

Fig. 8.7 Relationship between ionizing radiation induced tissue effects and fetal/embryo stage of development. (Reproduced with permission from [30])

pertaining to the levels of such effects in human studies. As such, in order to draw conclusions for radiation protection purposes at least, epidemiological studies are more reliable.

The human data, however, are limited. There is only one epidemiological study that has been able to provide evidence of brain damage in humans following in utero exposure. From about 10,000 woman who were pregnant at the time of the atomic bombs at Hiroshima and Nagasaki, the children of about 1700 of them have been followed into adulthood. The study identified 27 children with severe "mental retardation" (now more commonly termed intellectual disability), 30 children with small head size without apparent intellectual effects, 24 children who suffered from seizures which appear to have no clinically identifiable precipitating cause, and a larger group of children with reduced intelligence (IQ) scores or with lower than expected scholastic achievement in school, compared to the unexposed population.

While the sample sizes were small and hence the uncertainties were large, the key finding—still much quoted today—was that neurocognitive effects were only observed for those exposed for doses >~0.5 Gy, and only during the 8–15 post-conception period, corresponding to the key period of neurogenesis and neuronal migration [27–29].

For earlier stages of embryogenesis, there is some evidence that preimplantation exposure to doses below 100 mGy may lead to miscarriage. During the major period of organogenesis, approximately 2–15 weeks post-conception, exposures on the order of 0.25 Gy may lead to smaller head sizes and the associated reduction in intellect, with this period also being particularly sensitive for induction of cancer. Post 15 weeks, the threshold for increased risk of cancer would appear to be on the order of 100 mGy, and the threshold for severe intellectual disability is still ~500 mGy (Fig. 8.7).

In 2001, UNSCEAR concluded there was no definite adverse pregnancy outcomes (malformations, stillbirths, premature births) related to the exposure from the Chernobyl accident. However, in more recent years, there is evidence that ^{131}I internalized by pregnant women following Chernobyl crossed the placenta and resulted in thyroid cancer in their children. Children born to Chernobyl ^{131}I exposed individuals also had dose-dependent longer gestational periods, smaller head, and chest sizes, but normal birth weights. While stunted cerebral growth during critical periods of neurogenesis accounts for microcephaly and the related developmental effects, the biological mechanisms behind the effect on gestational period is still largely unknown [7].

Fetal death following exposure in utero appears only to occur following doses >2 Gy; however, most of the evidence for this still comes from animal studies. There is also limited evidence linking fetal radon exposure to increased risk of disease. For example, excess brain cancer has been observed in children born to pregnant women drinking water with high levels of radon [31].

In terms of cancer risk, there is a clear link between doses received in utero and childhood and adult cancers, including childhood leukemia. In the A-bomb survivors exposed in

Table 8.4 Health effects as a function of gestational age for humans (reproduced with permission from [29])

Gestational age	Weeks post-conception	Fetal dose, Gy	Effects observed
Preimplantation	0–2	0.05–0.10	Prenatal death (animal data)
Major organogenesis	1–8 2–15	0.20–0.25	Growth restriction Small head size, intellectual deficit Sensitive for cancer induction
Rapid neuronal development and migration	8–15	>0.1	Small head size, seizure risk, reduction in IQ (~25 points/Gy)
Post organogenesis	15-full term	>0.1 >0.5	Increased cancer risk Severe mental disability (16–25 weeks in particular)

utero, the most recent evidence using individual estimates of mother's weighted absorbed uterine dose supports a continued increased risk of solid cancer mortality in females but, not in males. As with the previous data, the effects of radiation on non-cancer disease mortality in this cohort appeared to be mediated through small head size and low birth weight, but also parental survival status. The most recent data suggest that the excess risk of childhood cancer (up to 15 years of age) is on the order of 6% per Gy, with approximately half of the cases being fatal. These data are summarized in Table 8.4.

It is worth noting that on the basis of the current (albeit limited) evidence, for occupational radiation protection purposes in the UK as in many other countries, the unborn fetus is treated as a member of the public, hence the effective dose limit is 1 mSv/year.

8.2.2 Radiation-Induced Heritable Diseases

8.2.2.1 Context and Definition

Mutations occur naturally in somatic and germ cells potentially leading to cancers and heritable genetic diseases, respectively. In 1927, Muller and colleagues initially showed the mutagenic effects of X-rays in Drosophila, which were rapidly followed by similar findings reported for other radiation types and organisms. These experimental animal data established the concept of genetic damage-inducing effects of radiation. However, concerns appeared about these genetic effects in large numbers of people, especially after the exposure of people to the detonation of atomic bombs. The UNSCEAR and the BEIR committees decided to follow the potential heritable effects of radiation in the exposed Japanese population, even if other environmental factors can interfere. Indeed, the goal pursued by both committees is to predict additional risk of genetic diseases in humans exposed to radiation. However, no association between radiation exposure and the occurrence of hereditable effects has been observed in humans to date [7]. Like cancers, genetically, diseases such as hemophilia, color-blindness, and congenital abnormalities do not arise specifically from ionizing radiation, but also occur spontaneously or due to other environmental and/or genotoxic factors without any specific clinical appearance.

The concept of "radiation inducible genetic diseases" relies on different parameters. Indeed, every cell contains genetic material in the form of DNA, and mutations observed in DNA may lead to a genetic disease such as malformations, metabolic disorders, or immune deficiencies. Sometimes, however, when mutations are induced in gonads or germ cells (oocytes or sperm or their precursors) of an exposed individual, hereditable effects occur in their offspring. To induce a genetically abnormal offspring, the mutation must successfully pass through many cell divisions to form a viable live-born infant. Further, to be of genetic significance, gonadal exposure must occur before or during the person's reproductive period. It gives rise to the concept of genetically significant dose. Thus exposure to, for example, a postmenopausal woman, or someone who never intends to have children, carries no associated "heritable" risk [7, 32].

8.2.2.2 Extrapolation from Mice Data and in Humans

It is important to note that ionizing radiation does not produce new types of genetic diseases or new unique mutations but is assumed to increase the incidence of the same mutations that occur spontaneously. It increases the incidence of the spectrum of known diseases in the population. Hence, it is important, as far as possible, to have a good understanding of the background risks. There are very little direct human data on radiation-induced genetic disease. Pieces of evidence appeared for the heritable genetic effects of radiation almost entirely from animal experiments initially performed at Oak Ridge National Laboratory through the mega mouse project (7 million mice studied to determine specific locus mutation rates in the mice). Animal experiments have led to the development of relevant concepts including the doubling dose, i.e., the dose required to double the background frequency of genetic conditions detectable in the newborn population [33]. This project leads to five main conclusions: (1) a significant factor of about 35 for the radiosensitivity of different mutations; (2) a dose rate effect with fewer mutations induced by chronic exposure compared with acute ones; (3) an exquisite radiosensitivity of the oocytes; (4) reduction of the genetics effects of a given dose when there was a time interval between exposure and conceptions; (5) differences

between male and female mice but with a doubling dose on the order of 1 Gy for protracted exposures. Given that conclusions on the background frequency, life span, selection pressures, and spectrum of genetic disease in the laboratory mouse are very different from humans, caution must be applied in using these data for human radiation protection purposes. Nevertheless, such data are important.

Estimates then need to be made for the mutational component of classes of human genetic diseases and clearly, this is considerably different between dominant gene disorders and multifactorial conditions. The selection pressures on mutations being lost by death during embryo/fetus development also need to be assessed. Finally, an assessment of the transmissibility of abnormalities through further generations needs to be made [7].

8.2.2.3 Diseases Classes and Influencing Factors

Evolution depends on the existence of mutations, with beneficial mutations conferring an advantage. However, their random nature ensures that the vast majority of mutations are harmful. Alterations can concern genes or point mutations to the DNA code and chromosomal aberrations.

Mendelian Diseases

Diseases caused by mutations in single genes are known as Mendelian diseases. The majority (67%) are caused predominantly by point mutations (base-pair changes in the DNA), followed at 22% by both point mutations and DNA deletions within genes, and by intragenic deletions and large deletions at 13%. They are divided into autosomal dominant, autosomal recessive, and X-linked depending on the chromosomal location and the phenotype resulting from the transmission.

- **Autosomal dominant**: Dominant conditions are where even in the heterozygote state (a person inheriting one mutant and one normal gene) the abnormality is seen in the individual. Their effects in the homozygote (double dose of the mutant gene) are usually more severe, if not lethal. They are expressed in the first generation after its occurrence. An example of a dominant gene condition is Huntingdon's chorea (HC), which is characterized by nerve cell damage and changes in physical, emotional, and mental state. HC is caused by a faulty gene on chromosome 4. Other examples include achondroplasia, neurofibromatosis, Marfan syndrome, or myotonic dystrophy.
- **Autosomal recessive**: Usually, this condition requires homozygosity, which means two mutant genes at the same locus, to produce the trait disease. The mutant gene must be inherited from each parent. Recessive disorders are usually rare, as the mutation would need to be inherited from both parents. However, some recessive genes even when present in a single dose, i.e., heterozygote accompanied by a dominant normal gene do still confer slight deleterious effects. An example of a recessive gene disorder is cystic fibrosis, which is caused by mutations on a gene located on chromosome 7. Other examples include phenylketonuria, hemochromatosis, Bloom's syndrome, and ataxia-telangiectasia.
- **X-linked**: Disorders involve genes located on the X chromosome. A large proportion of mutations that are inherited are related to the X chromosome. Since there is only one X chromosome in males, mutant genes here act as dominant genes in males who suffer whereas they are masked in the female with two X chromosomes who act as carriers. Mutations in these genes will exert their effect in females only when present in homozygotes and therefore appear as a recessive condition. Half the male offspring of a carrier mother will suffer and half her female offspring will be carriers. Examples of sex-linked conditions are color-blindness and hemophilia.

Chromosome Aberrations

Chromosome aberrations are generally structural or numerical alterations that are microscopically visible/detectable (Fig. 8.8) and efficiently caused by radiation. Many chromosomal abnormalities are not compatible with life and are lost as spontaneous abortions. They correspond to 40% of spontaneous abortions and 6% of stillbirths. However, there are exceptions, and the evidence suggests that abnormalities of the sex chromosomes do tend to be transmitted. Examples include Downs syndrome, which is a trisomy of chromosome 21, as well as Turner's syndrome, which is a monosomy of chromosome X. Turner's syndrome individuals are, however, sterile. It is also interesting to note that the X chromosome is dominant, but (a single gene on) the Y chromosome determines sex.

Multifactorial (Congenital Abnormalities, Chronic Diseases)

Multifactorial diseases are an additional class of effect, which combine heritable aspects (genetic components) in addition to influence from environmental factors. Their transmission patterns do not fit Mendelian transmission and the interrelated concepts of genetic susceptibility and risk factors are more appropriate to talk about these multifactorial diseases. Chronic conditions which arise later in life, for example, type II diabetes, tend to occur after an individual has already had children. However, in such cases, individuals may inherit predisposition but may never suffer from the disease. Multifactorial diseases also include congenital abnormalities which are present at birth. An example is cleft lip and palate where most sufferers are missing a part of chromosome 22—this abnormality can be inherited but in most cases the cause of the deletion is unknown.

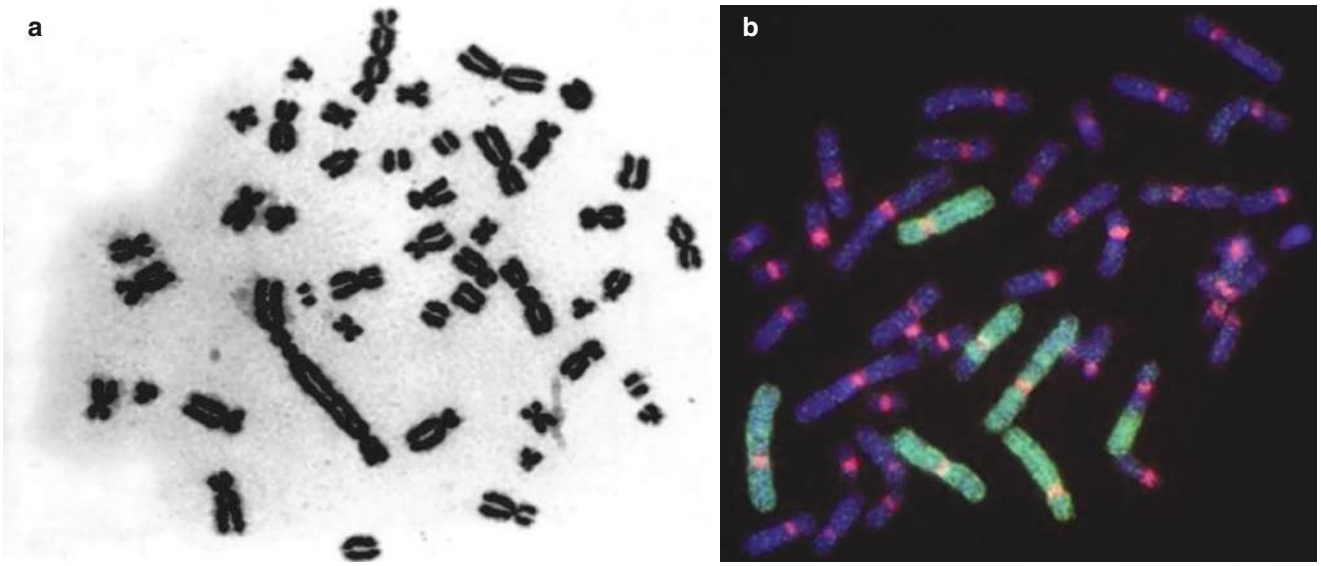

Fig. 8.8 Examples metaphase spreads with (**a**) dicentrics tri-centrics and several fragments and (**b**) with a translocation. These aberrations result from the fusion of sections of broken chromosomes

Epigenetics and Imprinted Genes

Furthermore, epigenetic changes are now considered for their involvement in radiation-induced heritable disease. These changes involve molecular modifications such as DNA methylation or changes in the chromatin packaging of DNA by post-translational histone modifications that can modulate gene expression without any DNA sequence alterations. Exposure to environmental factors at prenatal and early postnatal stages can alter the epigenetic programming thereby increasing the risk of developing the disease later.

Additionally, expression of the imprinted gene in the current generation depends more and more on the environment experienced by the previous generation. Only one parental allele with the other allele silenced can lead to a non-Mendelian germline inherited form of gene regulation (heritable DNA methylation and histone modification) (Box 8.1).

Box 8.1 Gene Mutations and Heritable Diseases

- Gene mutations are molecular, sub-microscopic, changes affecting the functionality of one or more gene-specific loci.
- There are three classes of Mendelian type gene mutations, where genes are inherited from each parent.
- Other parameters such environment may lead to radiation-induced genetic heritable diseases.

8.2.2.4 UNSCEAR and ICRP

The assessment of radiation risks in progeny for heritable effects is thus a complex task. However, this has been done by UNSCEAR and ICRP reports [7, 32]. It is important to note that the data used to make the risk calculations are uncertain, with several assumptions, hence the ranges. From these data, the ICRP assumes that the exposure to radiation of a parent to a single gonadal dose of 1 Gy is responsible for 1 additional severe disease caused by radiation-induced mutations in 500 births, with a genetic risk that may last for up to 2 generations. With chronic exposure of gonad to 1 Gy, this proportion reaches 1 for 100 births, and heritable effects may persist for several generations. In this report, the total risk for genetic diseases estimated was about 3000 to 4700 cases per million first-generation progeny per Gy. The outcome of the risk calculations, in the form of risks per Gy per million live-born children, are given in Table 8.5.

For risk estimation, the effects of high-dose irradiations have to be investigated in animal experiments. The effects of low radiation doses on humans, which are difficult to measure unequivocally, have to be inferred from these results. How these data are applied in radiation protection is then the responsibility of ICRP, who averages and combines the risks in Table 8.6 to generate a single risk estimate for all the genetic effects, for both the reproductive and total populations.

In this case, ICRP assumes that people on average live to age 75 years and cease breeding by age 30 years. The genetically significant dose is therefore 40% (30/75) of the total population dose. For radiation workers, who ICRP assumes to begin working at 18 years and finish having children by age 30, the work-specific heritable risk is further reduced, as illustrated in Table 8.7.

Table 8.5 Genetic risk from one-generation exposure to low LET low-dose or chronic irradiation with assumed doubling dose of 1 Gy (reproduced with permission from [7])

Disease class	Baseline frequency, per 10^6 live births	Risk per Gy per 10^6 progeny in the	
		First generation	Second generation[a]
Mendelian			
Autosomal dominant and X-linked Autosomal recessive	16,500 7500	~750–1500 0	~500–1000 0
Chromosomal	4000	b	b
Multifactorial			
Chronic Congenital Total	650,000[c] 60,000 738,000	~250–1200 ~2000[d] ~3000–4700	~250–1200 400–1000[e] 1150–3200
Total risk per Gy (expressed as % of baseline)		~0.41 to 0.64	0.16 to 0.43

[a] Risk to second generation is lower than that in the first because of the assumption that radiation exposure occurred in one generation only; the risk will progressively decrease with time (in generations)
[b] Assumed to be subsumed in part under the risk of autosomal dominant and X-linked diseases and in part under that of congenital abnormalities
[c] Frequency in the population
[d] Estimate obtained using mouse data on developmental abnormalities and not with the doubling-dose method
[e] Under the assumption that the selection coefficient is 0.2–0.5

Table 8.6 Percentage risk per Gy for the reproductive and total population and up to two generations when the population sustains radiation exposure generation after generation (reproduced with permission from [34])

Disease class	Reproductive population		Total population
	Range	Average	Average
Mendelian diseases	0.13–0.25	0.19	0.08
Chronic diseases	0.03–0.12	0.08	0.03
Congenital abnormalities	0.24–0.30	0.27	0.11
Total for all classes		0.54	0.22

Table 8.7 ICRP recommended genetic risk coefficients for low dose or low-dose-rate low-LET radiation (reproduced with permission from [34])

Group	10^{-2} Sv^{-1}
Whole population	0.2
Radiation workers	0.1

8.2.3 Long-Term Issue Effects: Cataract and CVD

8.2.3.1 Radiation-Induced Cataract

Cataract is the most common cause of blindness worldwide World Health Organization (WHO). There are three types of cataracts: nuclear cataract, which is characterized by hardening and opacification of the lens nucleus; cortical opacities, which are initiated at the lens cortices and which then form characteristic "spokes" pointed towards the center of the lens, and posterior subcapsular cataract, which develops on the capsule, at the posterior pole of the lens. The subcapsular cataracts are most readily associated in the epidemiological literature with radiation [32] (Fig. 8.9).

Until relatively recently, it was thought that radiation cataract was a "deterministic" effect, now more commonly termed tissue reaction, with a threshold for acute exposures of approximately 2 Gy and a potentially much higher threshold for chronic or protracted exposures. However, in recent years it has become apparent that the latency period for radiation cataract may be many tens of years, and thus the threshold is likely to be much lower than previously thought, with the best current estimate based on the weight of epidemiological or population-based evidence that the current threshold is on the order of 0.5 Gy. However, there is some emerging evidence which suggests that radiation cataract may indeed be more stochastic in nature [32]. From the public health perspective, the high-dose response to radiation cataract is relatively clear from many years of animal studies and the smaller number of epidemiological studies reviewed in ICRP [32], and there are a number of methods of characterization and detection of cataract.

While the mechanistic data on radiation cataract remains relatively sparse compared to, say, cancer, a number of publications have looked into the radiobiological basis of cataract. In brief, the structure, function and physiology of the lens are relatively well understood, as are the processes of lens cell fiber differentiation from the lens epithelial "stem" cell layer to the functional and carefully organized lens fiber cells which allow the passage and alignment of light for effective vision [35] (Fig. 8.10). Radiation is thought to act on several different stages of this carefully balanced process, from initial oxidative stress leading to genetic (DNA) damage, the effects on the transcriptional responses in epithelial cells (and, interesting, there is evidence that genes involved have some connections with tumor forming processes), through to morphological changes apparent in the misalignment of mature fiber cells which leads to opacification and functional cataract.

Recent work using animal models has highlighted the importance of the early phase DNA damage, proliferative, biochemical and proteomic/lipidomic responses, as well as the clear influence of genotype and pathways of response, age at exposure, sex, dose, and dose rate [36].

Further work is still needed, particularly in relation to the mechanisms of higher RBE or LET radiation for cataract. However, at the time of publication, current understanding is that radiation cataract is still best characterized for radiation protection purposes as a tissue reaction, but that low-dose chronic exposure can contribute to the "cataractogenic load" of the combined genetic and environmental factors which ultimately determines whether individuals develop cataract or not [37] (Fig. 8.11).

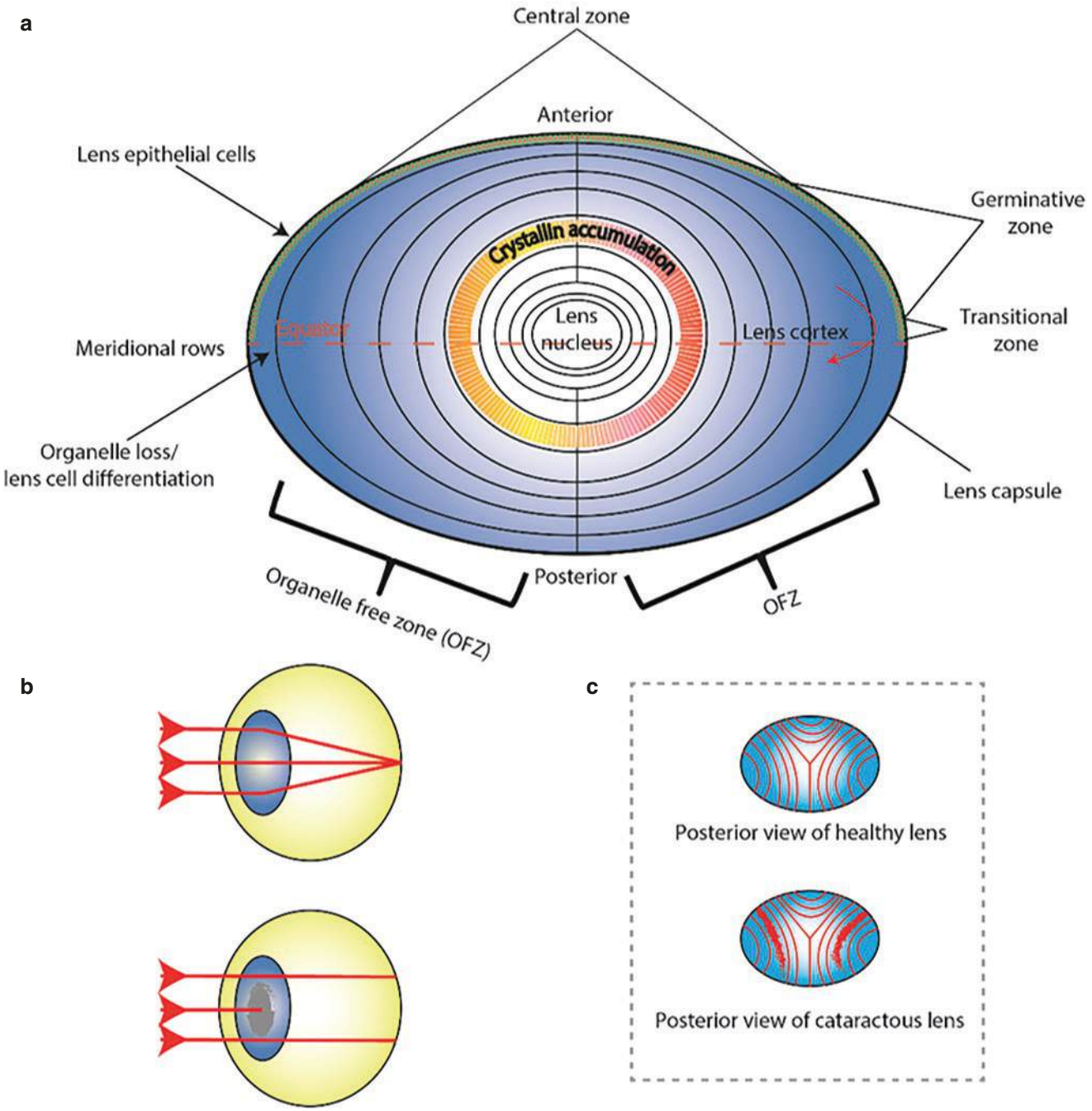

Fig. 8.9 Protein fiber and cellular organization within the lens. (**a**) The lens is formed from a single cell layer of lens epithelial cells (LECs) that covers the anterior portion of the lens. The cells in the central region are mostly quiescent; meanwhile the proliferating cells are largely confined to the germinative zone (GZ) in the equator of the lens. After division, LECs migrate to the transitional zone (TZ), situated immediately adjacent to the GZ and most distal to the anterior pole. In the TZ, LECs begin differentiation to form lens fiber cells (LFCs) that comprise the bulk of the lens mass. They enter the body of the lens via the meridional rows (MRs), adopting a hexagonal cross-sectional profile, offset from their immediate neighbors by a half cell width to deliver the most efficient cell–cell packing arrangement that is perpetuated into the lens body as LECs continue their differentiation and maturation process into LFCs. (**b**) The lens sits in the anterior portion of the eye where it focuses light onto the retina to create a sharp image (top). However, when a cataract develops, the transmission of light is either blocked or not focused correctly (bottom), creating a distorted image. (**c**) Example of lens fiber sutures as viewed from the posterior pole of the lens in the healthy lens compared to a nuclear cataract, similar to that represented in (**b**). (Reproduced with permission from [35])

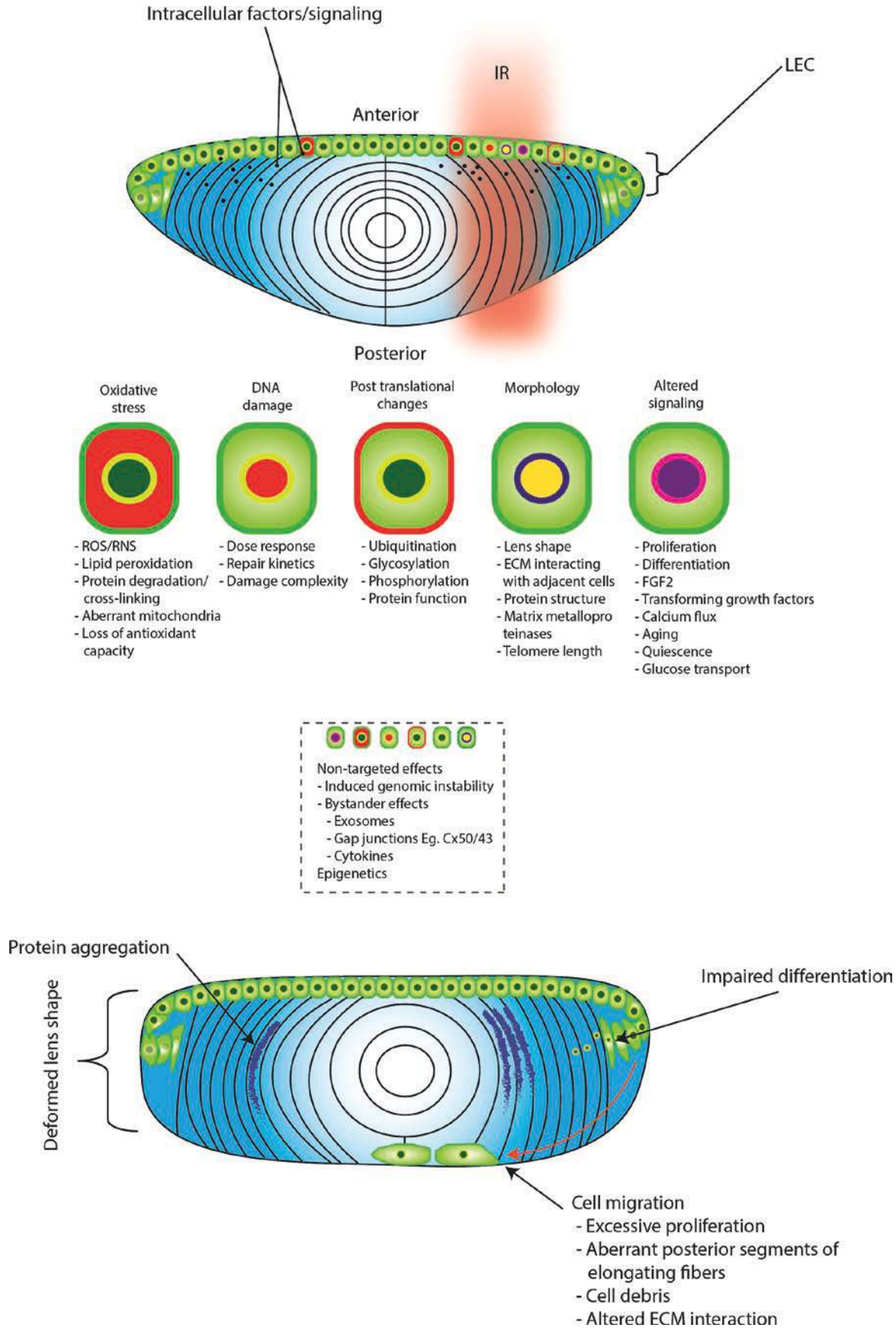

Fig. 8.10 Mechanisms of ionizing radiation response observed in human and animal lens epithelial cells or cell lines. *Cx* connexin, *ECM* extracellular matrix, *FGF* fibroblast growth factor, *IR* ionizing radiation, *LEC* lens epithelial cell. (Reproduced with permission from [35])

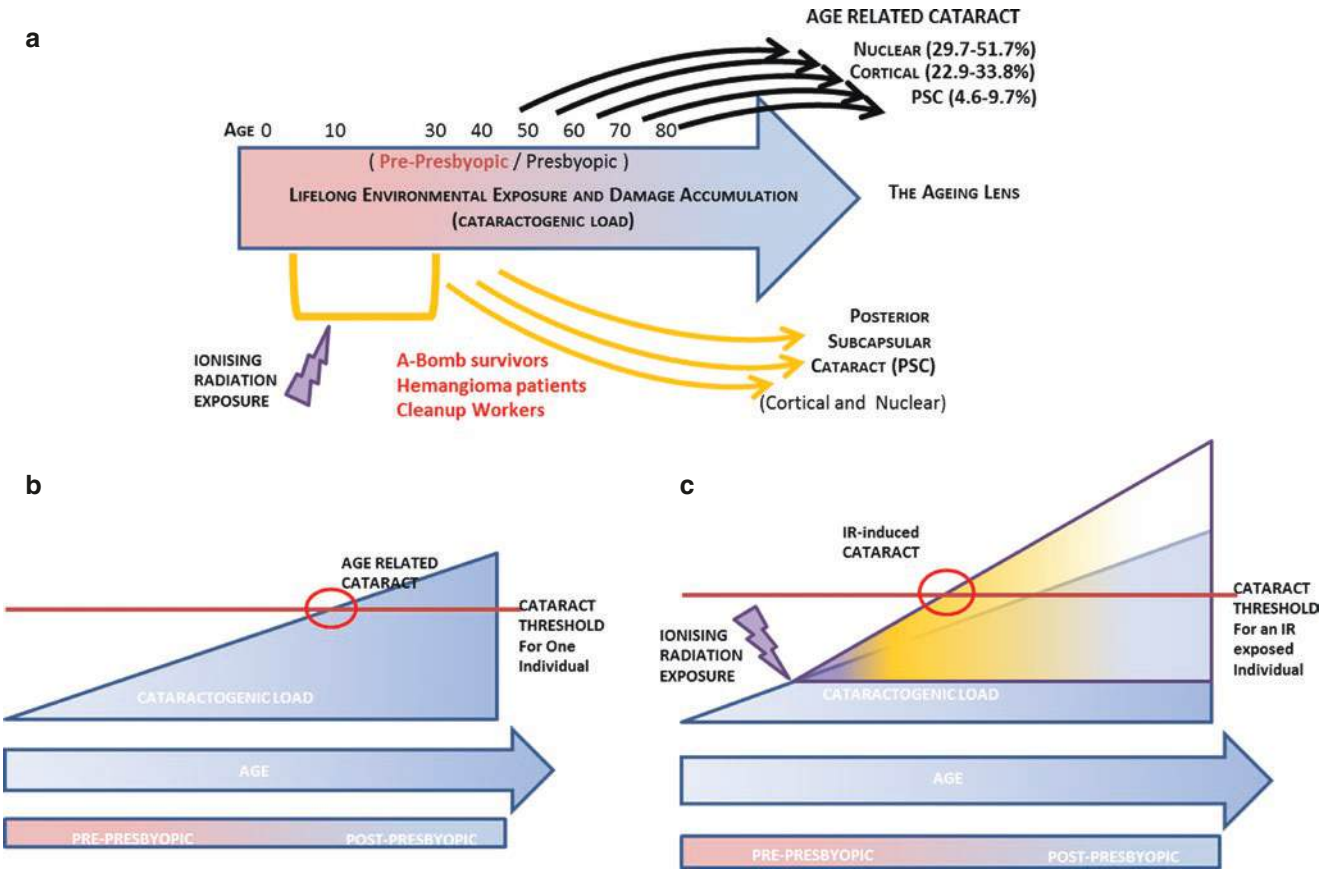

Fig. 8.11 The latency of cataract and Lifelong Cataractogenic Load. (a) Timeline for lens aging. (b) Accumulated cataract load without exposure to ionzing radiation. (c) Accumulated cataract load after exposure to ionizing radiation (Reproduced with permission from [37])

8.2.3.2 Diseases of the Circulatory System

In addition to the acute effects on the vascular system, ionizing radiation can in the long-term influence development of cardiovascular diseases (CVD) and metabolic effects which are major risk factors for diseases of the circulatory system. This section therefore considers a number of different diseases, including atherosclerosis which can cause ischemic heart disease and cerebrovascular disease, and which can lead to acute myocardial infarction and stroke.

The effects of ionizing radiation on the circulatory system is something which has long been researched, but only within the last 10 years or so has the weight of evidence been such that it is possible to consider taking account of the radiation effects as part of the system of radiation protection [38]. Currently, circulatory disease is considered a "deterministic effect" or tissue reaction, with a threshold on the order of 0.5 Gy, and with a long latency period.

Most of the epidemiological evidence comes from exposures of medically (therapeutically or diagnostically) exposed individuals, with some data from occupational or environmentally exposed cohorts (reviewed in [39, 40]). Medical exposure to ionizing radiation during radiotherapy of thoracic tumors, such as breast cancer, Hodgkin's lymphoma and lung cancer, can involve some incidental radiation exposure to the cardiovascular system, resulting in cardiovascular complications. This is especially an issue for women with left-sided breast cancer due to the higher cumulative dose received by the heart, which is estimated to be approximately 6.6 Gy, compared to 2.9 Gy in women with right-sided breast cancer [41]. Cardiovascular disorders due to ionizing radiation are usually not seen until 10–15 years after exposure. However, asymptomatic abnormalities may develop much earlier. This long asymptomatic period may be a reason why the radiation sensitivity of the heart has formerly been underestimated. Recently, advancements in radiotherapy and heart-sparing techniques, including target-specific dose-delivery, deep inspiration breath hold and patient prone position setup, have resulted in decreasing the mean heart exposure dose from 4.6 Gy in 2014 to 2.6 Gy in 2017, as reported from 99 worldwide studies [42]. Despite that, the mean heart radiation doses remain relatively high and late cardiovascular complications continue to occur. The late-onset aspect of ionizing radiation-induced cardiotoxicity represents a diagnostic challenge to timely initiation of radioprotective therapy. Currently, there are some efforts paid to identify early biomarkers of radiation-induced

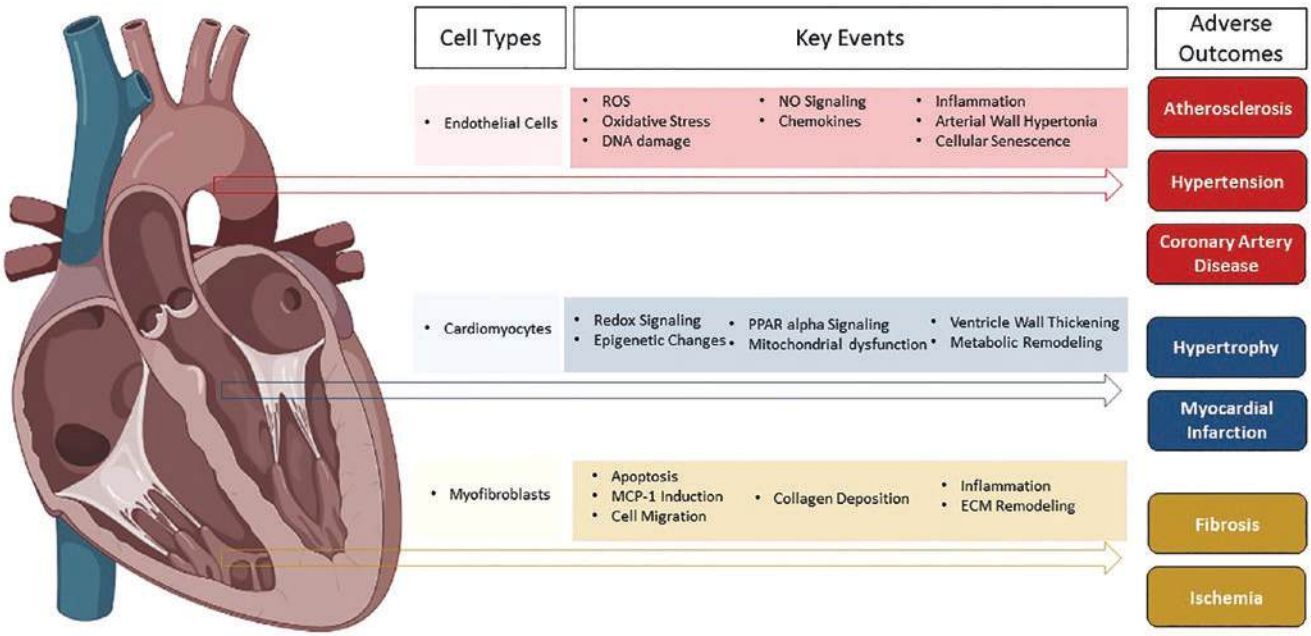

Fig. 8.12 Proposed cell types in the heart, key events and adverse outcomes that may contribute to cardiovascular disease. Not all potential cell types and key events are listed and some of the key events listed may be common across the different cell types. *ECM* extracellular matrix, *MCP-1* monocyte chemoattractant protein-1, *NO* nitric oxide, *PPAR alpha* peroxisome proliferator-activated receptor (PPAR)-alpha, *ROS* reactive oxygen species. (Reproduced with permission from [44])

cardiotoxicity, which may help in screening patients at risk for developing cardiovascular complications after radiotherapy, thus countermeasures and early medical intervention might be applied to prevent further cardiac toxicity [43]. Furthermore, research is exploring radioprotective agents which interfere with one or more of the identified pathophysiological mechanisms of ionizing radiation-induced cardiotoxicity.

Mechanistically, as with cataract, the high-dose effects are relatively clear, based on, for example, oxidative stress, DNA damage and enhanced adhesion of endothelial cells—the genomic and proteomic basis of which is also under investigation. The lower dose studies are much less common; however, lifestyle factors and genetic susceptibility are undoubtedly confounders of development of circulatory system diseases, and indeed most of the mechanistic work carried out to date has focused on the genetic basis of development. Genome wide and targeted studies have identified, for example, the involvement of a number of genes of interest associated with inflammation, differentiation, proliferation, and apoptosis, among other processes which ionizing radiation is already known to impact. In addition, there are a number of biological dynamic models for cardiovascular disease (the topics in this paragraph reviewed in Tapio et al. [40]).

The most recent epidemiological evidence demonstrates increases in the probability of occurrence of these effects with dose, with no increase in severity; these are classical characteristics of stochastic radiation effects. However, the mechanisms are still highly unclear, and the low-dose effects, as well as the impact of dose rate, remain less studied [39, 40]. Recently, an adverse outcome pathway, an approach helps to assemble current knowledge on well-accepted critical events linked to disease progression, has been proposed for radiation-induced cardiotoxicity, which may help in structuring and simplification of the available mechanistic information and can facilitate predictive interpretations, beyond cellular or animal models, at the human population level (Fig. 8.12). This approach assists as well in identifying critical knowledge gaps for future research on radiation-induced cardiotoxicity, such as the need for an experimental model to understand low doses of radiation exposure and the need to understand epigenetic effects induced by radiation in the cardiovascular system [44].

8.3 Radon and Health Effects

Radon and thoron are natural radioactive noble gases resulting from the decay of uranium and thorium, which leak from the soil in concentrations that depend on local geological conditions. Radon and thoron are chemically inert and electrically neutral, so at physiological temperatures there are no chemical interactions [45].

There are several natural isotopes of radon and thoron, originating from different series, as can be seen in Table 8.8 [46]

In the open air, the concentration of radon and thoron is normally very low, but being gases, they tend to accumulate in non-ventilated areas (WHO). In buildings constructed

on soils that are rich in elements of the radioactive families mentioned above, their release causes them to accumulate inside houses. The pressure difference between the subsoil and the interior of the dwellings also favors this accumulation, due to diffusion.

Table 8.8 Natural isotopes of radon and thoron (based on [46])

Series	Nuclide	Decay mode	*T*1/2
Uranium	^{234}Th	Beta-	24.10 days
	^{230}Th	Alpha	7.54×10^4 years
	^{222}Rn	Alpha	3.8235 days
	^{218}Rn	Alpha	35 ms
Thorium	^{232}Th	Alpha	1.405×10^{10} years
	^{228}Th	Alpha	1.9116 years
	^{220}Rn	Alpha	55.6 s
Actinium	^{231}Th	Beta-	25.52 h
	^{227}Th	Alpha	18.68 days
	^{219}Rn	Alpha	3.96 s
Neptunium	^{229}Th	Alpha	7340 years
	^{217}Rn	Alpha	540 μs

Figure 8.13 shows the arithmetic mean of the annual indoor radon concentration per grid cell (10 km × 10 km) in ground floor rooms in some European countries.

As all radon and thoron isotopes are radioactive gases, after being released into the ambient air, they accumulate indoors and disintegrate into various unstable daughter nuclides. After decay in air, these radionuclides aggregate with other gases and water vapor, forming aerosols with diameters of 0.5–5 nm, which are easily inhaled, travel through the conducting airways and reach the alveoli of the lungs [47, 48]. However, as the airways are saturated with water vapor, the hydration of aerosols allows their diameter to increase up to about 10 times [49].

Once inhaled, the decay process occurs predominantly in the lungs. The main biological incorporation pathway is by inhalation of radioactive aerosols. Alpha emissions are the biggest contributors to the absorbed dose (about 90%) while beta and gamma emissions contribute only about 10% [47, 50–52]. Considering the aerosol dynamics, they are depos-

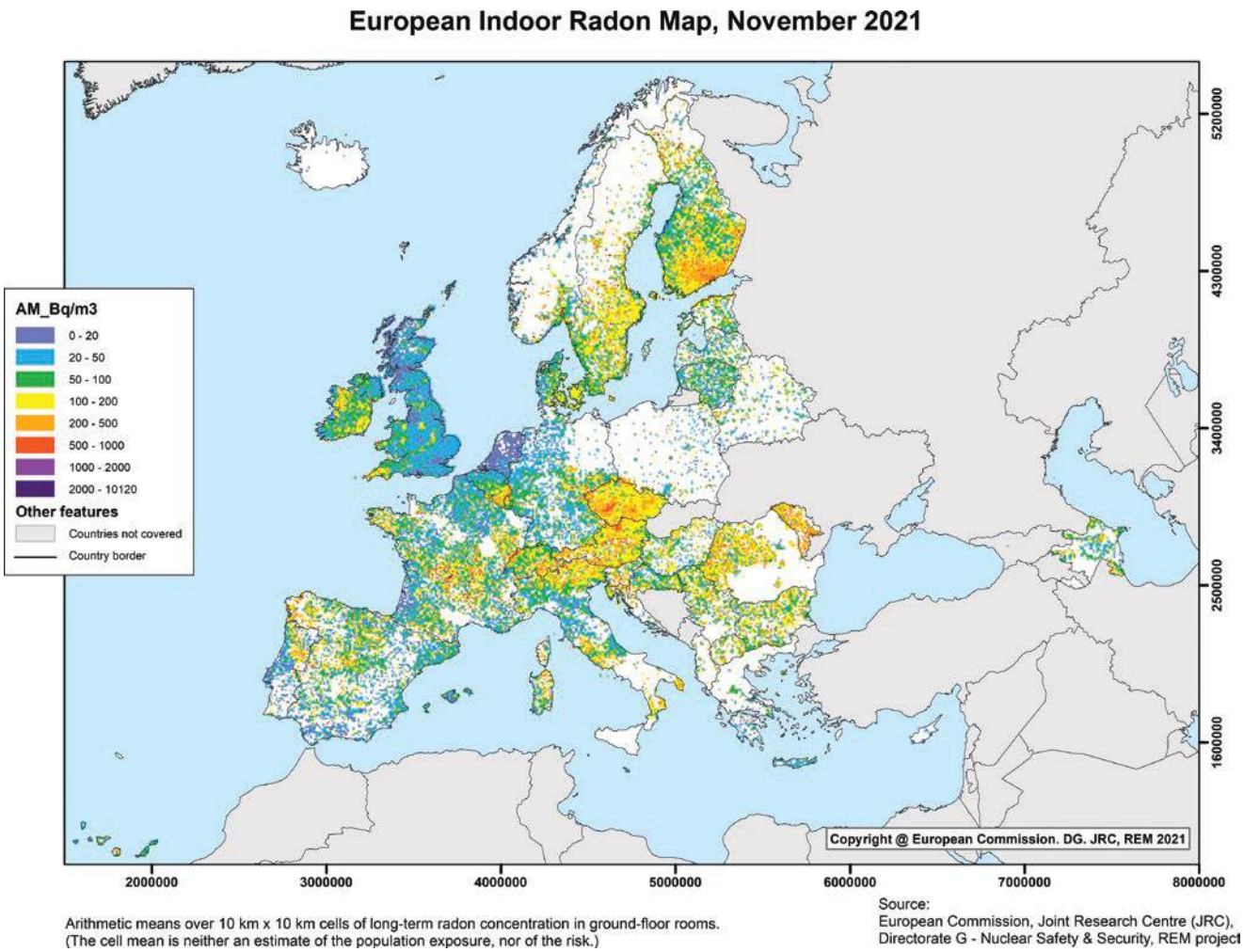

Fig. 8.13 European Indoor Radon Map: annual indoor radon concentration expressed as arithmetic means per 10 km × 10 km grid cells in ground-floor rooms. (Data received until December 2021 included; Reproduced with permission from European Commission. Joint Research Centre, EC-JRC, REM 2021)

ited according to three physical mechanisms: inertial impaction, sedimentation, and diffusion. Also taking into account the length, diameter and bifurcation angle of the airways, as well as the diameter of aerosols, deposition varies along the respiratory tract. Particles with larger diameters (2–50 μm) are deposited by inertial impaction in the nasopharynx, larynx, trachea and bronchi up to the third division. For particles with intermediate diameters (100 nm–10 μm) sedimentation is the main mechanism of deposition and occurs mainly in the lower respiratory tract, also in the bronchioles and even alveoli. For particles with diameters less than 200 nm, Brownian diffusion predominates and occurs in the alveoli, where gas exchange takes place [47–49]. Additionally, the multiple divisions of the airways and the consequent turbulence generated determine a non-homogeneous deposition pattern [47, 53].

Considering the different radiosensitivity of regions of the respiratory tract in which the mucosal and basal bronchial epithelial cells are particularly radiosensitive [54] as well as the multiple divisions of the conduction airways, the largest dose is deposited in the bifurcation of the trachea [47, 55].

Radon, thoron and their respective decay products emit alpha particles, beta- and gamma radiation, as mentioned above and the carcinogenic effect of these radionuclides is associated with the emitted ionizing radiation that can, directly or indirectly, damage DNA [56, 57]. This DNA damage causes mutations that can lead to carcinogenesis, resulting in the development of malignant tumors.

The correlation of radon with the incidence of lung cancer has been unquestionably proven by extensive epidemiological studies (BEIR VI). However, it is not excluded that it can also cause kidney cancer, melanoma, hematologic cancers, primary brain tumors, and even stomach, liver and pancreas cancers [56, 58–60]. However, given the low penetration of radon further than the respiratory system, the association with non-respiratory diseases is not proven [56].

Epidemiological studies on chronic radon exposure show that the estimated risk of carcinogenesis is related to the subject's concentrations, exposure time, and age [47]. Concerning lung cancer and radon concentration, there appears to be an increased risk of 16% per 100 Bq/m^3 [45, 47, 61]. With respect to mortality, there is a non-threshold linear correlation with exposure. If we add smoking to radioactive exposure, the risk of lung cancer increases even further [47, 61]. With regard to primary malignant brain tumors, there appears to be a positive correlation between chronic radon exposure and mortality [58, 61]. The same seems to be the case for non-cancer situations such as Alzheimer's and Parkinson's diseases, without, however, understanding the pathophysiological mechanisms [60]. There is a similar correlation for chronic radon exposure and incidence of chronic myeloid and lymphocytic leukemia and, in the case of children, with acute myeloid leukemia [45, 47, 61].

Latency times are highly variable between irradiation and the development of malignant tumors. Thus, for leukemia the times range from 5 to 7 years, while for solid tumors they are much longer, ranging from 10 to 60 years [45, 47, 61] (Box 8.2).

Box 8.2 Exposure and Risk of Radon Exposure

- Radon and thoron are noble radioactive gases
- There are several isotopes of radon and thoron
- The decay process occurs in the lungs due to inhalation
- There is carcinogenic risk associated to chronic radon exposure

8.4 Diagnosis and Medical Management of Radiation Syndromes

8.4.1 Introduction

Depending on the amount of energy deposited, the absorbed dose, as well as the radiation quality, significant whole-body or partial-body exposure to ionizing radiation may lead to acute clinical radiation effects resulting in an Acute Radiation Syndrome (ARS). This may be followed by Delayed Effects of Acute Radiation Exposure (DEARE) that take months and years to develop [62, 63].

Many aspects have to be considered regarding the diagnosis and management of radiation exposure. Regarding latency of occurrence, acute and chronic effects can be distinguished. The acute effects may require prompt diagnosis and immediate therapeutic intervention.

Considering the pathophysiological mechanisms, the effects can be distinguished as either deterministic or stochastic (see also Sect. 2.7.2). Deterministic effects are caused by radiation exposure exceeding a certain level (threshold) and are more severe with increasing dose. After whole-body irradiation, different categories of clinical syndromes can develop, usually depending on the absorbed dose: nausea, vomiting, diarrhea (NVD) syndrome (1–2 Gy), hematopoietic syndrome (2–6 Gy), gastrointestinal syndrome (>6 Gy) and central nervous syndrome/neurovascular syndrome (10–20 Gy); after local irradiation of the gonads, permanent sterility (0.1–6 Gy), of the eye opacity of lens (0.5 Gy), of the skin erythema (3–6 Gy) and hair loss (4 Gy) may develop [32, 34]. Clinical dosimetry based on the individual patient's clinical signs and symptoms is important to define the severity of radiation exposure.

For stochastic effects, no threshold value is assumed, the probability of occurrence increases with radiation dose and even very low-dose exposure effects cannot be completely excluded [62].

8.4.1.1 External Contamination

In case of radionuclide contamination, establishing the presence of external contamination is very important since decontamination should be performed as soon as possible keeping people, equipment, and facilities safe in the process. However, urgent medical treatment has the highest priority as lifesaving always comes first. Luke-warm water and mild soaps should be used for the first line of decontamination. Reduction to background or at most 3× background dose should be aimed for. In case of residual contamination, peeling products can be used to remove contamination adherent to the skin. If measurements indicate persistent contamination, the presence of radioactive particles in the skin (like shrapnel, requiring surgical removal) or internal contamination should be suspected.

8.4.1.2 Internal Contamination

In case of radionuclide ingestion and/or inhalation, identification of the radionuclide is crucial to select the appropriate decorporation therapy. Decorporation therapy must be carried out as fast as possible in order to reduce radiation dose absorption, since pharmaceuticals are often most effective if given immediately or within 2 h after ingestion or inhalation. This can be achieved by using blocking agents, diluting agents, chelating agents or enhanced de-corporation drugs like Prussian blue, Zn-DTPA, Ca-DTPA and ammonium chloride [62, 64]. Physical decorporation measures such as gastric lavage for ingested radioactive substances (if applied within 2 h of ingestion) and bronchoalveolar lavage for large amounts of insoluble inhaled radionuclides could also be used [65].

8.4.2 Acute Radiation Syndromes

Acute radiation syndrome (ARS) develops when whole- or partial-body radiation exposure exceeds a certain dose, partially depending on individual radiosensitivity and radiation damage repair mechanisms. ARS is usually assumed to occur with whole-body doses above 0.5–1 Gy if given with high-dose rate [32, 66, 67].

The deposition of energy at the molecular and cellular level leads to physico-chemical-biological consequences already described in the previous chapters.

The clinical evolution of the acute radiation syndrome is sequential and its canonical evolution begins with prodromes, followed by the latent state, the state of manifest illness, and ends with the state of recovery or death [32, 62, 68].

In the prodromal state, the exposed person has non-specific symptoms, which is easily confused with a flu-like syndrome. Anorexia, nausea, vomiting, diarrhea and, eventually, erythema are frequent symptoms. The fluid loss that is caused by diarrhea may be accompanied by fever, hypotension, and headache, depending on its intensity [62, 68, 69]. Given the non-specific nature of these symptoms and signs, exposure to radiation may not be the first clinical hypothesis, which makes the information about the circumstances and awareness for radiological incidents very important. Prodromal symptoms and signs can appear at doses as low as 0.5 Gy, depending on individual radiosensitivity [62, 68]. This state lasts from a few minutes to a few days, depending on the dose: the higher the dose, the shorter the duration of this state. Except for people with increased radiosensitivity, the prodromal state may be absent or mild for whole-body doses of 1 Gy or less. If signs and symptoms appear within the first 2 h, this usually means an exposure dose greater than 2 Gy. In this case, the symptoms are predominantly gastrointestinal, and the patients may survive if adequately treated. At doses greater than 10 Gy, severe symptoms will develop, often within 5–15 min after exposure, predominantly cerebrovascular. A severe prodromal phase usually has a poor clinical prognosis that can lead to death [67, 69, 70].

Doses that are associated with prodromal symptoms and signs in approximately 50% of irradiated people are given in Table 8.9.

The aforementioned prodromal symptomatology, which appears at doses lower than 0.5 Gy up to about 3 Gy, seems to be dependent on damage of the cell membrane, with the consequent release of inflammatory molecules from the destroyed cells and to be mediated by the parasympathetic system [32].

The second phase of ARS is called the **latent phase**. In this phase, symptoms and signs diminish and may even disappear, in such a way that the patient feels better and appears to be recovered. In fact, injuries are developing, but the activated repair mechanisms can lead to complete (disappearance of symptoms and signs) or incomplete repair of the damage (reduction of symptoms and signs). The duration of the latent phase, which can vary from minutes to weeks, is also inversely related to the dose, that is, the higher the dose, the shorter its duration. Despite the absence of symptoms, it is in the latent phase that the most important consequences of exposure to radiation occur, leading to its effects, which are manifested in the manifest illness phase [69, 70].

Table 8.9 Doses that are associated with prodromal symptoms and signs (reproduced with permission from [32, 68])

Dose (Gy)	Symptoms and signs
1–2	Anorexia
1–2	Nausea
1–2	Vomiting
2–6	Diarrhea
>6	Fever
>8	Consciousness changes

Table 8.10 Acute radiation syndromes

	Hematopoietic syndrome	Gastrointestinal syndrome	Neurovascular syndrome
Target organ	Bone marrow	Small intestine	Brain
Threshold	1 Gy	5 Gy	20 Gy
Latency time	2–3 weeks	3–5 days	30 min–3 h
Death	≥2 Gy	10 Gy	50 Gy
Time of death	3–8 weeks	3–14 days	Up to 2 days
Characteristic signs and symptoms	General malaise, fever, dyspnea, fatigue, anemia, leukopenia, thrombopenia, purpura	General malaise, anorexia, nausea, vomiting, diarrhea, GI changes, fever, dehydration, electrolyte loss, circulatory collapse	Lethargy, tremors, convulsions, ataxia, coma

If repair mechanisms are inefficient, the latent phase progresses to the next phase, the **manifest illness phase**. The absence of the latent phase, i.e., if the patient goes directly from the prodromal phase to the manifest illness phase, is an indicator that the dose was very high. In the manifest illness phase, there are specific symptoms and signs, depending on the organ or system mainly affected. However, there may be a mixture of symptoms and signs coming from different systems, which makes the diagnosis more complex. Also in this phase, the signs and symptoms, as well as the duration, are dose dependent, that is, the higher the dose, the earlier the symptomatology starts and the shorter the phase lasts, which can be from minutes to weeks [32, 66, 69, 70].

In this state specific syndromes are described, commonly classified as the hematological, gastrointestinal, and neurovascular syndromes, depending on dose (Table 8.10). In addition to these syndromes, skin lesions and lung toxicity may also develop (Fig. 8.14).

The **hematological or hematopoietic syndrome** has as its target organs the hematopoietic organs, with special emphasis on the bone marrow. Generally speaking, the hematopoietic syndrome can develop from 1 Gy and the latency time varies from 2 to 3 weeks. Before a generalized failure of the hematopoietic system occurs, the progenitor cells of all linages have to be irreversibly damaged, which can happen with doses of at least 2 Gy. Without treatment, death may occur 3–8 weeks after exposure.

The characteristic signs and symptoms of this syndrome include general malaise, anemia, leukopenia and thrombocytopenia. The decrease in the number of circulating blood cells determines secondary symptoms such as dyspnea, asthenia, hypoxia, fever and purpura. If death occurs, it is mainly due to infections and/or hemorrhage [32, 66, 69, 70]. Treatment requires the use of cytokines, growth factors, antiemetics, antimicrobial agents (antibiotics, antifungals, antivirals), analgesics and in some cases anxiolytics can also be useful. Allogeneic stem cell transplantations should only be performed in specific circumstances (homogeneous whole-body dose, availability of perfectly HLA-matched stem cells).

If the radiation dose is higher, symptoms corresponding to the involvement of cells of the gastrointestinal system (**gastrointestinal syndrome**) appear, specifically the cells of the intestinal villi that are found in the mucosa of the small intestine. This syndrome can appear from a dose of 5 Gy with a latency time of 3–5 days. Complete loss of intestinal mucosa occurs at doses above 10 Gy and will be fatal within 3–14 days.

The characteristic signs and symptoms of this syndrome include general malaise, anorexia, nausea, vomiting, diarrhea, fever, dehydration, electrolyte loss and circulatory collapse, leading to death within a few days [32, 66, 69, 70]. Treatment requires adequate fluid administration, parenteral nutrition, growth factors, antiemetics, antimicrobial agents (antibiotics, antifungals, antivirals) and analgesics.

For higher doses of ionizing radiation, the neurovascular system is involved (**neurovascular syndrome**) appears, where glial cells may be damaged with doses of 1–6 Gy, lesions of the endothelial cells of the cerebral vessels that occur with doses of 10–20 Gy, or white matter necrosis that appears with doses in the order of 40 Gy or even demyelination that occurs with doses around 60 Gy. This damage will lead to signs and symptoms including lethargy, tremors, convulsions, ataxia, pre-coma and coma, leading to death within hours.

This neurovascular syndrome can develop from a dose of 20 Gy with a latency time of 30 min to 3 h. Death occurs within 2 days after doses above 50 Gy [32, 66, 69, 70]. Treatment is usually only symptomatic with analgesics and sedatives.

In addition to this syndromes, other important changes can occur in other organs, in response to exposure to ionizing radiation. One of these organs is the skin with the consequent cutaneous effects. **Cutaneous effects** are deterministic that only appear above a certain threshold dose. The first changes appear in the hair follicles at doses above 0.75 Gy. With higher doses other lesions appear. We can approximately summarize that epilation appears with doses of around 3 Gy, erythema with doses of around 6 Gy, desquamation with doses of 10 Gy, which appears associated with edema, meaning transepithelial lesion, with doses of 20 Gy.

Pulmonary effects, which appear over a huge range of doses (from about 5 Gy to doses as high as 50 Gy), are strongly dependent on the great vascular richness of the lung. In this context, we must mention the endothelial cells of the small pulmonary vessels, as well as the type II pneumocytes,

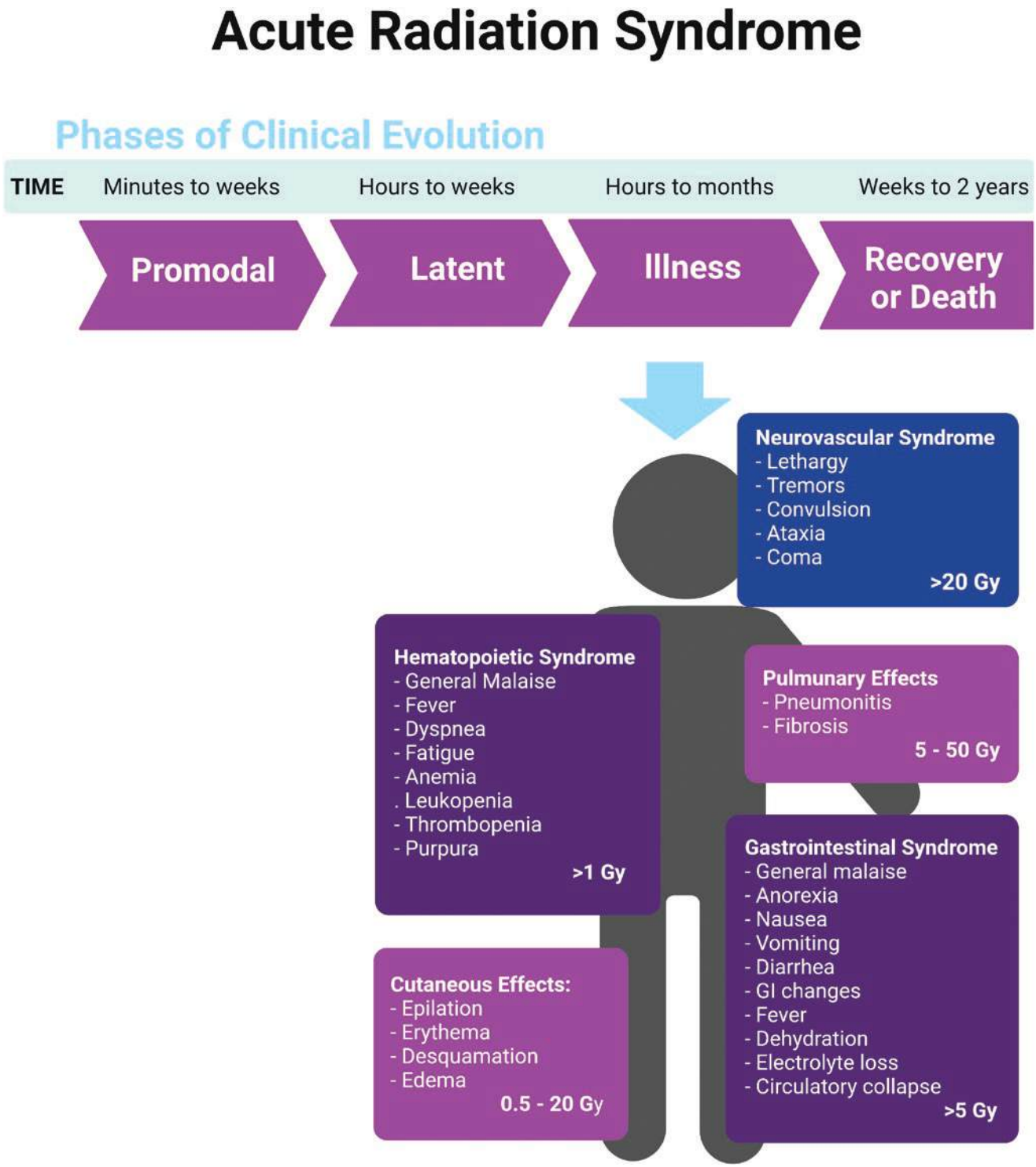

Fig. 8.14 Scheme showing the phases sequence of the Acute Radiation Syndromes and examples of symptoms

alveolar cells that secrete surfactant, whose injury has enormous pulmonary functional repercussions. The pulmonary interstitium is also of special importance, as it responds with an intense inflammatory process to exposure to ionizing radiation, called radiation pneumonitis. This inevitably progresses to pulmonary fibrosis with big clinical impact.

As mentioned, the manifest illness phase has variable duration and can progress to the **phase of death or recovery**, depending on dose, dose rate and target organs. The recovery phase is associated with lower doses at which hematopoietic and/or gastrointestinal syndromes occur, especially if adequate medical treatment is carried out. If doses are high

enough to induce neurovascular syndrome, the likely outcome is death. In this situation, death occurs few hours after irradiation and predominantly results from systemic vascular effects associated with multi-organ failure [70, 71].

8.4.2.1 Delayed Effects of Acute Radiation Exposure

Delayed effects of acute radiation exposure (DEARE) occur when there has been recovery after exposure, that is, when doses were lower, and hematologic and/or gastrointestinal syndromes were developed, after having been subjected to adequate medical treatment.

The delayed manifestations of these syndromes lose their acute expression and are associated with signs and symptoms that show the repercussion in various organs such as the lung, heart, kidney, central nervous system, beyond the bone marrow and gastrointestinal system, the target organs. Evolution results in the progressive failure of the organs involved, until death occurs. Given these characteristics, medical treatment is indicated with radioprotective drugs and/or radiomitigators of the effects of radiation which must be administered as soon as possible after the acute irradiation. This approach has the double goal of reducing the severity of the initial damage and the late onset-pathology [71, 72].

8.4.2.2 LD_{50} (Lethal Dose 50)

The concept of lethal dose (LD) is a pharmacological concept that can be applied to the consequences of exposure to ionizing radiation and is defined as the amount of dose of radiation that kills elements of an irradiated population. This broad concept can be further specified if we consider the dose that kills 50% of an irradiated population, which is called the median lethal dose (LD_{50}) [70, 73].

The characteristics of the biological effects of radiation, namely the duration of latency time, associated with the great individual variability led to the refinement of this concept. Thus, there is often referred the $LD_{50/30}$ (dose that kills 50% of the irradiated population in 30 days) or $LD_{50/60}$ (dose that kills 50% of the irradiated population in 60 days). The $LD_{50/60}$ for a healthy adult range between 2.5 and 3 Gy, while the $LD_{50/30}$ ranges between 2.5 and 4.5 Gy. These values assume whole-body irradiation and the natural history of the disease, that is, the non-use of medical care, and are based on data from the survivors of Hiroshima and Nagasaki [34, 66, 74]. Although the $LD_{50/30}$ and $LD_{50/60}$ are similar concepts, they provide complementary and very important indications. In the case of somatic effects, the $LD_{50/60}$ informs that if a survival for more than 60 days after an irradiation occurs, the recovery is expected.

For bone marrow, the $LD_{50/60}$ ranges from approximately 3.5 to 4.5 Gy, however with supportive medical care, such as blood transfusions associated with antibiotic therapy, it can change to values between 5 and 6 Gy. With more robust treatments, such as the administration of hematopoietic growth factors, values from 6 to 8 Gy can be achieved [66] (Box 8.3).

Box 8.3 Acute Radiation Syndrome

- Acute radiation syndromes appear after whole-body irradiation
- After an irradiation, the biological consequences appear following four stages: Prodromal, latent state, manifest illness state, and of recovery or death state
- When recovery occurs, delayed effects of acute radiation exposure can manifest
- LD_{50} is the dose that kills 50% of the irradiated population after 30 days ($LD_{50/30}$ or 60 days ($LD_{50/60}$)

8.5 Methods of Triage for Treatment After a Radiation Accident

8.5.1 Introduction: The Need for Triage and Intro to Exposure Scenarios

When individuals are exposed to ionizing radiation in an accidental scenario, there is an urgent need to categorize exposed individuals not only in terms of the urgency of their need for treatment, but also in relation to ionizing radiation exposure. In general, radiation accidents lead to external radiation exposure and/or external or internal contamination with radionuclides. Exposures in situations requiring triage tend to be acute, but chronic exposures also need to be considered. Further exposure or contamination can be approximately homogeneous or highly heterogeneous. Hence the available tools and processes need to be flexible and sufficient to allow appropriate triage in a variety of potential situations. This section considers in the need for initial triage including decontamination, specific considerations related to radiological triage, as well as the need for late follow-up. Communication to the public is also a topic of importance, not covered in detail here, but with further information in the TMT Handbook [75].

8.5.2 Initial Triage: Trauma, Decontamination, and Other Considerations

In general, triage is used to screen the patients with severe injuries after a mass incident, including chemical, biological, radiological, nuclear, or explosive events (CBRNE). The first step during triage is to classify the affected person according to the type and severity of the suffered injuries, accurately assessing prognosis and survival expectancy,

Table 8.11 Classification of victims of the radiation accident based on initial triage (e.g., START) [77] (reproduced with permission from the USDHHS Radiation Emergency Medical Management, https://chemm.hss.gov)

Triage categories	Color	First aid	Sorting victims' priority	Transport priority
Immediate/priority 1 (P1)	Red color tag	Immediate urgent first aid and priority transport	Third	First
Delayed/priority 2 (P2)	Yellow color tag	Delayed urgent first aid and transport after P1	Fourth	Second
Walking wounded/minor/ priority 3 (P3)	Green color tag	Minor/minimal first aid, separate departure from the zone or with mutual assistance	First	Third
Deceased/expectant/ priority 4 (P4)	Black color tag	Dead/deceased, injuries incompatible with life, shall be marked and left at the site of the finding for later recovery of the body if at all possible	Second	Fourth

and to minimize the consequences of the event through the timely administration of first aid and/or treatment. After a catastrophic event the affected individuals can suffer from severe injuries, including tissue or bone trauma, thermal and/or chemical damage, in addition to ionizing radiation [75, 76].

Initial triage should be swift, simple, and based on universal guidelines, especially because it is often performed in a danger zone within the vicinity of the accident; further, triage will be initially based on the immediate threats to life and not on radioactive exposure and/or contamination. This cannot be understated; primary medical attention will always be aimed at dealing with immediate life-threatening conditions. The primary aim is to determine the transport priority of the victims to the hospital, screening the wounded in the area for later medical attention (Table 8.11). However, the classification of the injured and affected victims should be continuously re-evaluated, as the victims' condition can change very quickly. There are several types of triages, for example, SALT (Sort, Assess, Lifesaving Interventions, Treatment/Transport); START (Simple Triage and Rapid Treatment—Adult), and JumpSTART (Simple Triage and Rapid Treatment—Children). These systems have four main color-coded categories [75, 78].

If people are exposed to radioactive material, they are swiftly screened in the triage by the first responders at the scene of the accident, i.e., paramedics, to assess the condition of the victims (Table 8.12). The aim of the triage system is to identify the victims with severe trauma and provide first aid and evacuation. The trauma triage system has three category priorities (P1–P3) (Table 8.13).

Victims with trauma injuries should be identified first and medical attention for them is a priority (Fig. 8.15); however, if ionizing radiation exposure is an issue for both victim and first responder then the former must be moved from the area to reduce the dose rate. Contamination with radioactive material, both external and internal, is to be expected in these incidents, especially after an explosion. All the victims in the categories P1, P2 and P3 may be contaminated with radioactive material; therefore, triage for these individuals should be different. The victims sorted into category 1 are immediately transported to the hospital without prior decontamination, thus the medical staff has to be made aware of this fact. Serious injury is to be expected if the victims are sorted into category 2, although their evacuation can be delayed and thus decontamination should be performed before transport to the hospital, otherwise the hospital staff should be informed that decontamination has not taken place. The victims sorted into category 3 should be decontaminated at the site of the accident or given information on how self-decontamination should be performed and sent home. Decontamination for these victims is not performed at the hospital and medical treatment has lower priority than for category 1 and 2 victims (Table 8.14) [75, 79, 80]. It should also be noted that non-surviving victims of the mass biological, chemical, radiological or nuclear event are a potential and hazardous source of ionizing radiation.

Table 8.12 Classification of externally irradiated individuals according to the received dose (reproduced with permission from [75])

Radiation dose (Gy)	Priority
Less than 2	P3
2–6	P2, eventually P1 if they are also injured
6–10	
More than 10	P4

Table 8.13 Classification of victims of the radiation accident based on trauma triage (reproduced with permission from [75])

Category/ priority	First aid	Victim classification (SOP)
Category/ priority 1 (P1)	For severely injured victims in need of immediate first aid and evacuation	Removal from the accident site **in the first place**
Category/ priority 2 (P2)	For less severe injured victims in need of evacuation into the hospital, with a delay of up to 12 h	Removal from the accident site **in the second place**
Category/ priority 3 (P3)	For victims with minor injuries who can depart the zone of the accident on their own, wait several hours for medical treatment, or go home to return to the triage on the following day	Removal from the accident site **in the third place**

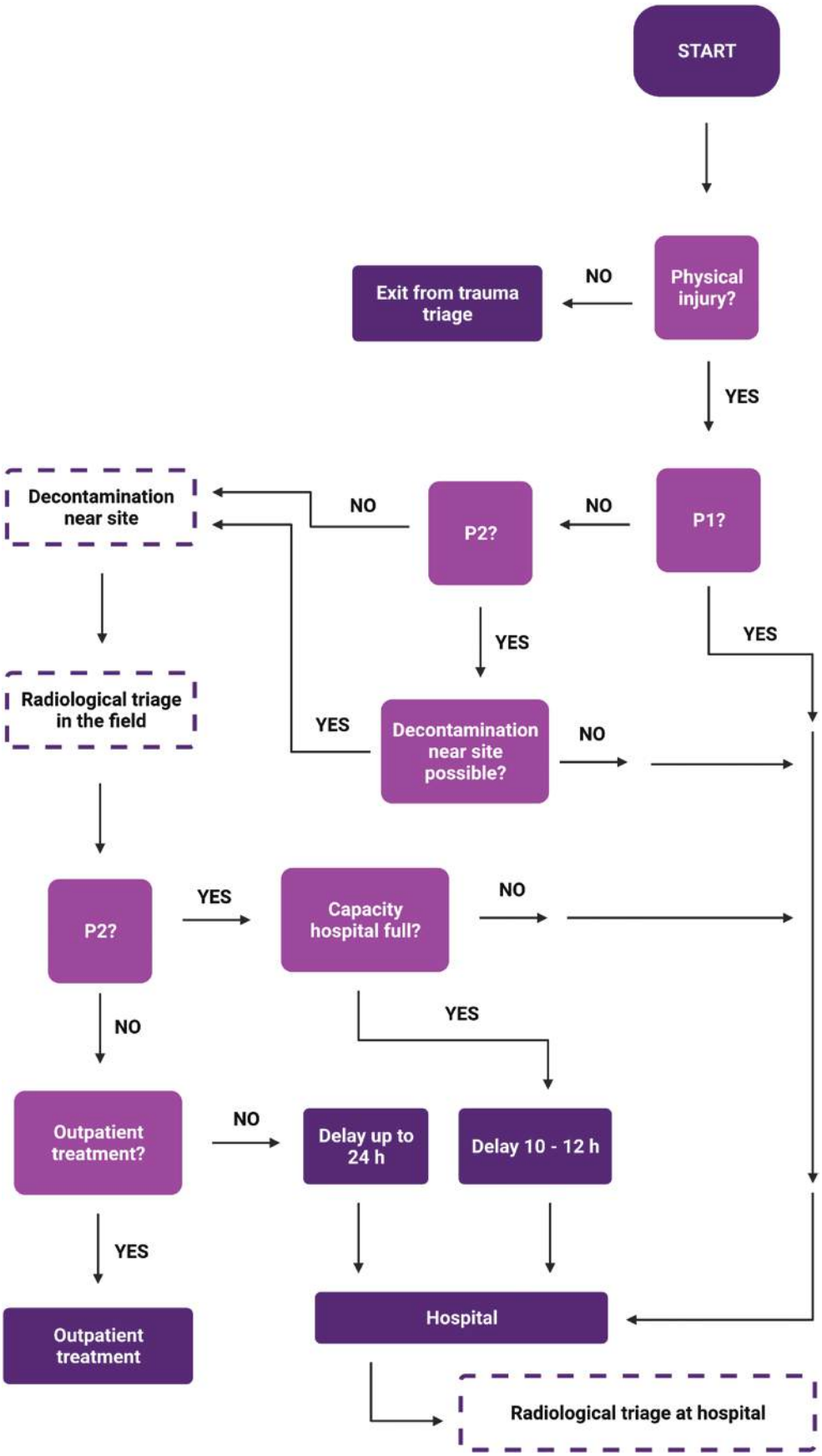

Fig. 8.15 Schema for trauma triage. (Reproduced with permission from [75])

8.5.3 Radiological Triage

Following initial triage for trauma as described above, Category 2 and 3 victims should be monitored and further evaluated in the next steps of triage, comprising information about location at the time of the accident and/or radiological analysis based on clinical signs and symptoms to identify individuals who may have received doses high enough to cause deterministic effects.

As much information as possible should be collected regarding the type and energy or activity of the source and the dispersal of the radiation within the environment contributing to exposure/contamination. Regarding individual information, considerations include the time of direct contact or distance from the source when in proximity, whether the exposure took place within an enclosed or open environment, whether or not the individual was within the line of sight of the source, and if the source was mobile. Such information is needed for all potential points of exposure and can then be used to help prioritize individuals for treatment as described in more detail in the TMT Handbook [75]. In addition, such information can contribute to modelling of radiation exposure at the individual or population level, as considered in Chap. 4.

Section 8.4.2 describes the prodromal clinical signs and symptoms associated with approximate (>60%) whole-body ionizing radiation exposure, which can be used to estimate the radiation dose and the potential severity of ARS for Category 2 and 3 patients, as well as for any individuals identified through the location analysis to have doses high enough to potentially cause deterministic effects (Fig. 8.16). These individuals should be monitored for onset of nausea and vomiting, diarrhea and/or erythema.

In addition, differential blood cell counts should be taken, according to Fig. 8.17, at 8 h intervals on the first day and 12 h intervals on the second day, with decisions regarding later intervals to be taken according to the indicated severity of the complete blood count (CBC) suppression, the number of potentially exposed individuals and the available capacity. Where CBC indicates that significant doses have been received, or significant effects are expected, chromosome aberration analysis should be carried out to obtain a more concrete individual estimate of dose, as detailed in Sect. 8.6.

Table 8.14 Injury priority and decontamination (reproduced with permission from [75])

Priority	Urgent medical attention	Decontamination
Priority 1 (P1)	Imminent death if immediate medical attention is not administered	Resuscitation and stabilization have priority over decontamination
Priority 2 (P2)	Acute surgery necessary within 2–4 h after injury	Decontamination has priority if stabilization is not possible due to the nature of the injury
Priority 3 (P3)	Medical attention can be delayed for more than 4 h	Decontamination has priority

8.5.4 Internal Contamination

The next step in cases of internal contamination should be the swift assessment and sorting of the affected persons, mostly because decontamination efficiency decreases with time. Cases of internal contamination are recognized through a radiation survey, which can detect significant residual and localized (e.g., lungs, thyroid) or distant (e.g., urine, blood, smears, feces) radioactivity [81]. The initial monitoring of internal contamination victims cannot be done without special equipment, such as whole-body counters or thyroid uptake systems [82]. According to the TMT Handbook, the

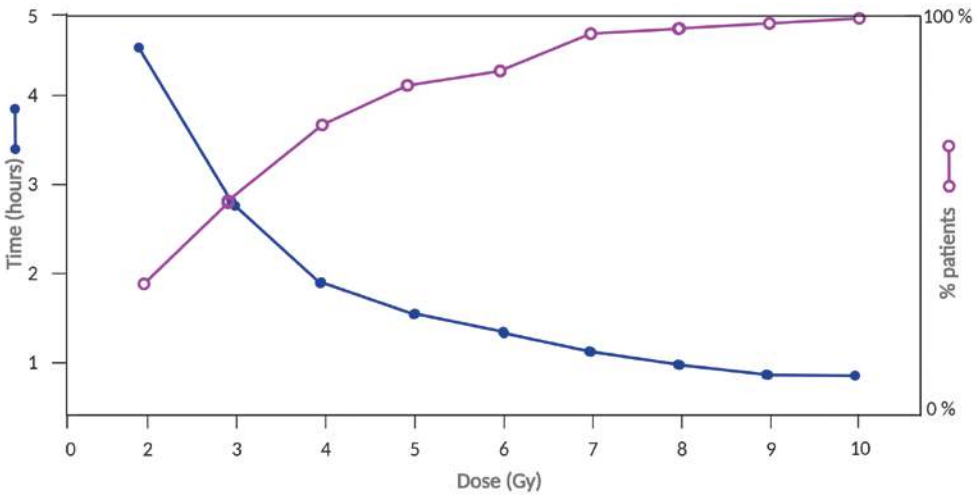

Fig. 8.16 Relationship between time to onset of vomiting and dose between 2 and 10 Gy. (Reproduced with permission from [75])

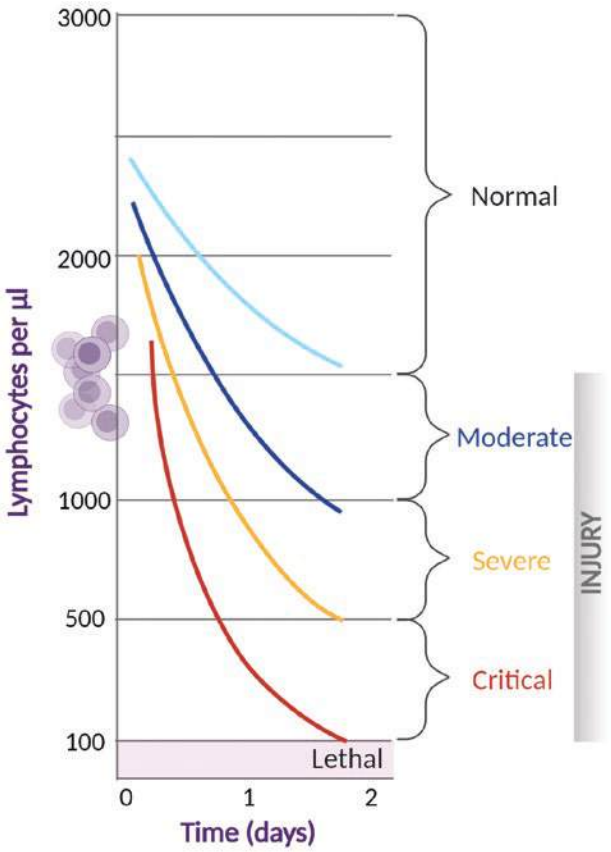

Fig. 8.17 Lymphocyte depletion with dose and time post exposure, following whole-body doses exceeding 1 Gy. (Reproduced with permission from [75])

first set of actions during radioactive emergencies should be as follows:

1. Focus on life-threatening conditions, control of vital functions and hemorrhage, and transfer to emergency medical care facilities.
2. Perform external contamination monitoring and decontamination, if external contamination is detected.
3. Lower the risk of internal contamination and initial monitoring level of internal contamination for further treatment and prevent further contamination.
4. Based on the initial monitoring, early clinical judgement should be based on the risks and benefits of treatment of internal contamination by radionuclides. Medical professionals will determine if medical treatments are needed [75].

Internal contamination does not cause immediately serious or acute effects nor does it present a time-limiting life-threatening condition before the appropriate lifesaving and decontamination measures can be performed. Having said that, some radionuclides, such as ^{210}Po or ^{137}Cs, can cause massive internal damage or acute radiation syndrome within a few days after contamination [79, 83].

Table 8.15 Action levels for treatment of radionuclide contamination (reproduced with permission from [75])

Assessed committed effective dose (mSv)	Recommended action
<1	Appropriate for public reassurance that doses pose a minimum risk to health. No treatment.
1–20	More accurate dose assessment is required. Treatment should not be considered.
20–200	More accurate dose assessment is required. Treatment is subject to medical judgement. Although clinical effects are unlikely to occur, the potential efficacy of extended or protracted treatment should be considered.
>200	Treatment should be considered. However, psychological factors and potential efficacy of extended or protracted treatment should be considered.

The victims should ideally have been externally decontaminated by the time of arrival at the medical facilities; if such is not the case the medical staff should be made aware about their condition and take the appropriate measures. The decontamination treatment of internally contaminated victims should start as soon as possible, especially if there is a risk of deterministic effects; however, accident history and dose estimation should be carefully considered (Table 8.15). The effectiveness of the treatment is determined by the early administration of radionuclide counteragents and the first aid provided, even if radioactive contamination is only suspected. The treatment administered should remove the contaminating radionuclides from the human body using chemical or biological agents, which may reduce their absorption, prevent their incorporation and internal deposition (e.g., chelating agents), or promote their elimination or excretion (e.g., lavage of the oral cavity, nose, conjunctival sac, stomach, use of laxatives or diuretics). In this regard, most methods of treatment for internal contamination with radionuclides include isotope blocking, dilution, or displacement, and the use of ion exchange resins, and ion mobilization or chelation (Table 8.16) [24].

The measures for internal decontamination are not used to treat acute radiation injury, but the main aim is to reduce the risk of stochastic effects like tumors induced by radiation in organs or tissues where radionuclides were incorporated.

8.5.5 Follow-Up and Recovery

Long-term medical monitoring should be carried out for the patients suffering from the clinical symptoms of acute radiation syndrome or local radiation injuries; however, asymptomatic patients should also be included in long-term follow-up as well as those for which there is only a presumed ionizing radiation exposure.

Table 8.16 Selected radionuclides and radiation countermeasures for treatment (reproduced with permission from [84])

Radionuclide	Treatment	Dose	Effect
Iodine	Potassium iodide (KI)	130 mg/day (pill) for 7 days	Blocking agent
Plutonium Yttrium	DTPA (diethylene-triamine penta-acetic acid)	1 g calcium DTPA in 500 mL i.v. for 60 min	Chelating agent
Uranium	Sodium bicarbonate	Slow i.v. infusion by $NaHCO_3$ solution (250 mL)	Alkalization of urine
Cesium, rubidium, thallium	Prussian blue	3 g in 100–200 mL H_2O orally three times per day	Mobilization decreases gastrointestinal tract uptake, absorption
Radium, strontium	$BaSO_4$ Sodium alginate	100 g in 250 mL H_2O This is the dose for BaSO4. For Sodium alginate it is 5 g orally twice daily	Reduction/inhibition of absorption
Tritium	H_2O	Drinking 6–12 L/day	Facilitates excretion
Lead, copper, polonium	D-penicillamine dimercaptopropanol	1 g i.v./day or 0.9 g orally/4–6 h	Chelating agent

The patients with clear clinical symptoms should be scheduled for long-term follow-up to prevent, control, and care for the health consequences of ionizing radiation exposure. The long-term follow-up means that the patients will be checked in regular appointments in specialized clinical departments over a 5-year period to monitor any risk factors, health outcomes, or both. The long-term follow-up does not always have the same scenario and it is different on a case-by-case basis, mostly based on the development of symptoms of acute radiation syndrome and received dose of radiation. As an example, the logical first step for affected person is to contact and inform the primary care physician about the radiation exposure incident and plan a follow-up program with the physician and the specialists at various departments in the hospital (e.g., hematology, radiotherapy, psychology, internal medicine) if needed. If the affected patient recovers from the hematological consequences of acute radiation syndrome, a hematological examination should be conducted every 3 months during the first year and a routine medical examination once a year. Annual examinations at the ophthalmological clinic are also recommended for monitoring cataract incidence, if any. In addition, medical consultation should be offered to exposed victims for mental and reproductive health as and when needed [75]. The benefit of this long-term medical monitoring is the identification of radiation symptoms, and though it may sound daunting this follow-up does not differ much from that performed for other clinical conditions. It must be noted that those patients without symptoms could have the greatest benefit from long-term medical monitoring. This monitoring provides the capacity to classify the individuals at greater risk; further, it also enables the proper evaluation of diseases that may be found in the population at risk. Although it may be inconvenient for asymptomatic patients, long-term medical monitoring may help in early diagnosis and treatment of serious radiation-related illnesses, thus minimizing morbidity and mortality rates. Persons who have been exposed to low doses of ionizing radiation during a radiation emergency, who have not experienced ARS or other immediate symptoms associated with radiation exposure, should also be included in long-term follow-up and monitoring mostly to dismiss the existence of radiation effects or to monitor ionizing radiation exposure related illnesses, which often come in the form of cancer. In addition, the long-term follow-up may also provide the affected patients with mental health support and reproductive health consulting.

Taken together, the long-term follow-up and medical monitoring of the persons affected by radiation emergencies can provide new epidemiological data since medical follow-up data for potential stochastic effects such as cancer are sparse. However, social, economic, legal, and psychological aspects should be considered in the follow-up and monitoring of these patients [75]. The epidemiological follow-up determines two groups, i.e., exposed and unexposed to radiation, and registers any difference in the health outcome. How this will be done will depend on the exposure scenario. The typical outcome in radiation epidemiology is represented by a greater incidence of cancer or mortality related to radiation. The most precise and conclusive parameter in an epidemiological study is mortality due to clear and obvious occurrence, supported by the records available worldwide. Also, epidemiological follow-up studies should include non-malignant morbidities and mortality, which are known parameters collected from A-bomb survivors' life span studies. However, it has to be mentioned that this is not always the main interest of epidemiological follow-up of health outcomes. In many cases there is an interest in diseases that can affect quality of life, such as nonfatal diseases, for example, tissue degenerative diseases [75, 85] (Box 8.4).

Box 8.4 Treatment of Internal Contamination

- Initial triage for trauma, the victims should be monitored and further evaluated in the next step of triage, comprising information about location at the time of the accident and/or radiological analysis based on clinical signs and symptoms.
- Internal contamination should be the swift assessment and sorting of the affected person, mostly because decontamination efficiency is often hindered by time delays.
- Cases of internal contamination are recognized through a radiation survey, which can detect significant residual.
- Internal contamination does not cause immediately serious or acute manifestations nor does it present a time-limiting life-threatening condition.
- The treatment administered should remove the contaminating radionuclides from the human body through chemical or biological agents.

8.6 Biodosimetry Techniques

8.6.1 Introduction

Biological dosimetry is an internationally accepted method for the detection and quantification of presumed/suspected exposures to ionizing radiation in humans. On the basis of biomarkers in the peripheral blood, the amount of ionizing radiation to which an individual has been exposed can be determined and estimated. Biological dosimetry can be used in addition to physical dosimetry or as a distinct method for dose reconstruction. The traditionally used, well-established cytogenetic assays are predominantly based on induction and misrepair of radiation induced DNA double strand breaks. The analyses are performed in lymphocytes of the peripheral blood, as these circulate throughout the body, and they are normally in the G_0/G_1 stage of the cell cycle. Since lymphocytes are not cycling, they need to be stimulated to proliferate during in vitro cell culturing. There are several essential requirements for biological parameters to be meaningful dosimeters: Low background level, clear dose effect relationship for different radiation qualities and dose rates, specificity to ionizing radiation, non-invasive sample collection, fast availability of dose estimation, good reproducibility, as well as comparability of in vitro and in vivo results to set up a calibration curve [86].

8.6.2 Conventional Methods

8.6.2.1 Dicentric Chromosomes Assay (DCA)

The analysis of dicentric chromosomes (dic) (Fig. 8.18) with or without the inclusion of centric rings in lymphocytes of the peripheral blood is a well-established method for dose reconstruction after an acute exposure to ionizing radiation and therefore, considered as the "gold standard" in biological dosimetry [87]. After blood collection, lymphocytes are cultured at 37 °C for 48 h and stimulated to enter mitosis by using specific mitogens. During mitosis, chromosomes condense and become visible by light microscopy and dicentric chromosomes can be quantified. In Fig. 8.18 the formation of dicentric chromosomes is schematically presented (a) and a Giemsa stained metaphase cell is shown in (b) with a dicentric chromosomes and an accompanying fragment (ace). The dicentric chromosomes fulfill the essential requirements of a suitable biomarker for the detection of exposure to ionizing radiation. In particular, dicentric chromosomes are almost

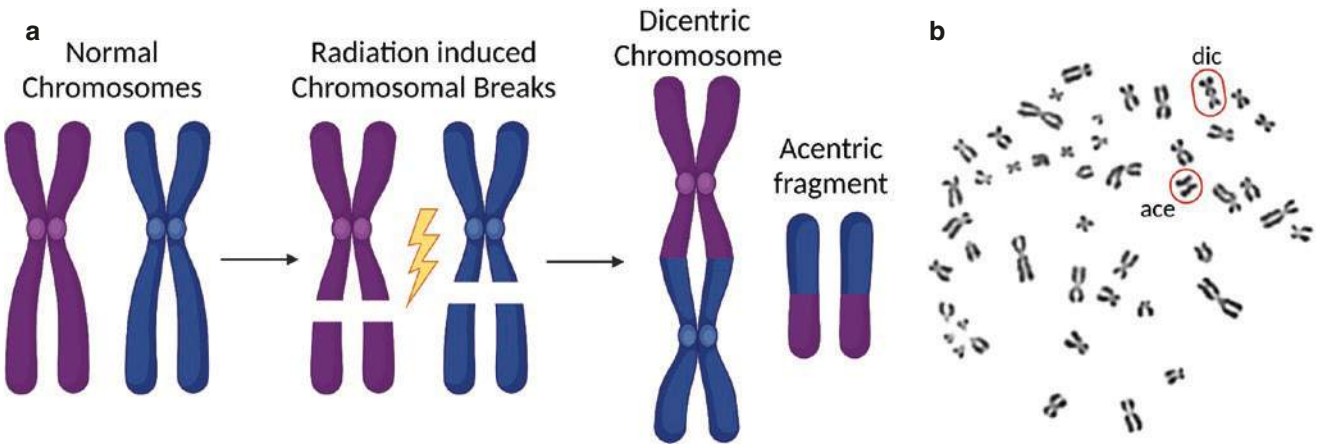

Fig. 8.18 (**a**) Schematic representation of the formation of a dicentric chromosome (dic) after exposure to ionizing radiation with the formation of a chromosome fragment without centromere (ace). (**b**) Giemsa stained metaphase spread of a human peripheral blood lymphocyte with a dic and ace

exclusively caused by ionizing radiation [88]. In healthy, non-exposed individuals, dicentric chromosomes rarely occur spontaneously and the background rate is about 0.5–1 dicentric chromosome in 1000 cells [89]. Therefore, the method has a good sensitivity. The lowest detectable dose of a homogeneous acute whole-body irradiation with low-LET (linear energy transfer) radiation is about 100 mGy when 500–1000 cells are evaluated [90]. It is well accepted that a comparable number of chromosomes damaged per dose unit is induced for both high- and low-LET radiation in vitro and in vivo [91] enabling dose estimation on the basis of in vitro calibration curves. The dose effect relationship can be modeled by a linear-quadratic curve ($Y = c + \alpha D + \beta D^2$) for up to 5 Gy of low-LET radiation and by a linear model ($Y = c + \alpha D$) for high-LET (alpha or neutron) radiation [92]. In addition, based on the analysis of dicentric chromosomes, a distinction can be made between homogeneous and inhomogeneous or between high- and low-LET exposures [89]. The mean lifetime of lymphocytes with dicentric chromosomes in the peripheral blood is between 0.6 and 3 years [93], and this is largely influenced by both the absorbed radiation dose (low or high) and inter-individual variation in lymphocyte turnover rate [88]. The decline of dicentric chromosome bearing lymphocytes can occur either by cell death or by dilution of damaged lymphocytes with the fresh population of lymphocytes over long periods of post radiation exposure. Therefore, in the case of radiation exposure that occurred a long time ago or was protracted, i.e., over a longer period of irradiation at a low-dose rate, appropriate adjustments must be made to avoid underestimation of the dose. Chromosome analysis is considered as a very labor-intensive method requiring well-trained staff to perform the analyses [94]. To increase the throughput of the method for a large-scale accident with a large number of potentially exposed individuals, different approaches have been developed. Scoring 50 cells or 30 dicentrics has been accepted as sufficient in triage scoring to identify those who need immediate medical support [95]. Software-based automated scoring systems for the rapid detection of dicentric chromosomes have been developed and successfully applied in various studies (e.g. [96]). Recent advances in using imaging flow cytometry to identify dicentric chromosomes have demonstrated the feasibility, however, there is still much room for improvement [97]. Also automated robotically based high-throughput platform (RABiT, Rapid automated Biodosimetry Tool) has been designed to enhance the capacity of dicentric chromosome analysis [98].

8.6.2.2 Cytokinesis-Block Micronucleus (CBMN) Assay

The analysis of micronuclei (MN) in binucleated (BN) cells of peripheral blood lymphocytes is an alternative cytogenetic technique used in biological dosimetry (Fig. 8.19). The assay originally developed by Fenech and Morley in 1985 restricted MN scoring to first division cells after inhibition of cytokinesis (cytoplasmic division) by cytochalasin B [99]. Micronuclei (MN) are small extranuclear bodies resulting from chromosome fragments or whole chromosomes that are excluded from mitotic spindle and therefore not included in the main daughter nuclei during cell division. Due to an elevated spontaneous frequency of micronuclei (0–40 MN/1000 BN cells) relative to dicentric chromosomes [89], the lowest detectable radiation dose of a homogeneous acute whole-body irradiation with low-LET based on micronuclei analysis is about 200–300 mGy when 500–1000 BN cells are analyzed [88]. The application of Fluorescence in situ hybridization (FISH) using a human pancentromeric probe can help in determining the origin of MN based on the presence (presumably whole chromosomes) and absence (chromosome fragments) of centromeric signal. It is well demonstrated that most radiation-induced MN are centromere negative [100]. Therefore, the sensitivity of the MN assay can be increased in the low-dose range by this method [101]. MN are less radiation specific than dicentric chromosomes and show greater variability both inter- and intra-individually. The rate of MN is influenced by age, sex, and

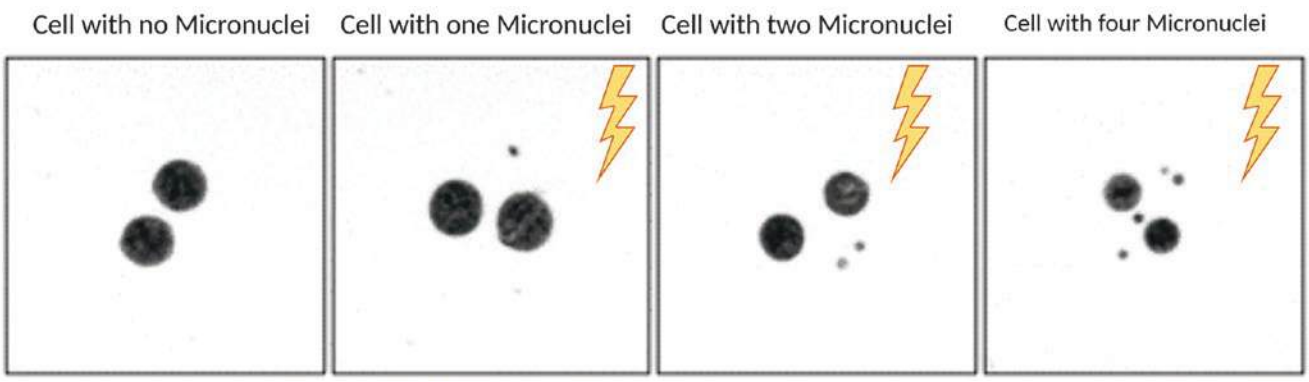

Fig. 8.19 Presentation of binucleated cells including 0, 1, 2 or 4 micronuclei

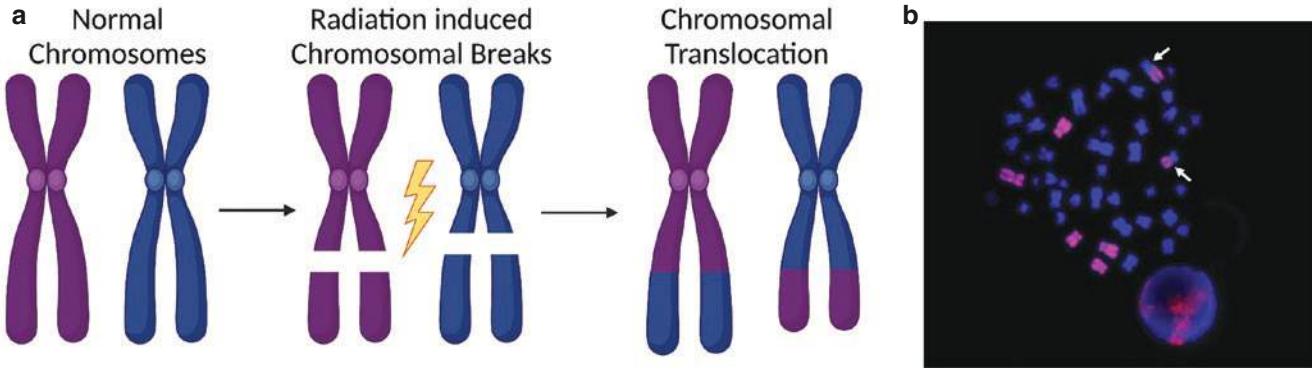

Fig. 8.20 (**a**) Schematic representation of the formation of a symmetrical translocation after radiation induced chromosomal breaks. (**b**) FISH painted metaphase spread of a human peripheral blood lymphocyte with translocations indicated by the arrows

lifestyle as well as exposure to other environmental mutagens [102]. The advantage of the method is the simple and quick evaluation, enabling relatively rapid training of inexperienced persons [103]. Various automated systems are available for MN analysis based on microscopy [104] or flow cytometry methods [105]. Furthermore, a high throughput and miniaturized version of the CBMN assay for accelerated sample processing has been described [106]. Several studies have confirmed the reliability of the automated MN assay for high-throughput population triage [107].

8.6.2.3 Chromosome Translocation Analysis Using Fluorescence In Situ Hybridization (FISH)

Fluorescence in situ hybridization (FISH) techniques have been in use for a number of years to identify translocations for the purpose of retrospective radiation dose assessment of radiation exposed victims [108] (Fig. 8.20). The technique relies on the use of chromosome-specific libraries of fluorescent probes to paint chromosomes in blood lymphocytes, in order to quantify the frequency of chromosome exchanges. In the simplest form of the assay, a cocktail of DNA probes for three human chromosomes labeled with a single fluorophore is used to estimate "genome equivalent" number of translocations based on the percentage of chromosomal material represented by the stained chromosomes. Typically, a cocktail of DNA probes for three human chromosomes covers at least 20% or more of the human genome. As translocations are not radiation specific and are predominantly stable within the genome, the expected background number of translocations [109] must then be subtracted from the observed number in the suspected irradiated sample. The genome equivalent rate of translocations is then translated to radiation dose by reference to a pre-determined dose response curve. The relative stability of translocations does, however, mean the assay can be used many years post exposure.

In addition to this single color painting, genome wide analysis, known as M-FISH (which does not require adjustment for genome equivalent damage), allows the detection of all simple interchromosomal exchanges as well as complex rearrangements involving multiple breakpoints in several chromosomes. Use of chromosome specific multicolor band probe (mBAND) facilitates the assessment of intrachromosomal rearrangements such as pericentric and paracentric inversions.

The FISH translocation assay has most commonly been used to estimate radiation doses following external radiation exposures [108]. As above, this technique is relevant for dose assessment at post-exposure time periods of days up to many years post exposure, however, does not work well for partial-body exposure.

The detection limit for FISH for uniform whole-body external low-LET exposures is on the order of 250 mGy, however, this varies depending on a number of factors, including the number of cells scored, age and smoking status (because translocations are not radiation specific), as well as length of time post exposure [109]. These issues, together with the length of time needed to culture the cells in order to visualize the aberrations, are the main limitations of the assay. Automation of FISH analysis is under development, but is not yet in common use.

8.6.2.4 The Premature Chromosome Condensation Assay (PCC-Assay)

Lymphocytes are sensitive to radiation and therefore use of both DCA and CBMN for exposure doses higher than 4 Gy is somewhat problematic. Especially in radiation accidents involving high doses of radiation, the premature chromosome condensation (PCC) assay can be of use in the quantification of radiation-induced chromosomal aberrations directly on unstimulated interphase blood lymphocytes [89]. Specifically, PCC induction in G_0 lymphocytes isolated from whole human blood is mainly achieved by means of their fusion to Chinese hamster ovary (CHO) mitotic cells using the chemical polyethylene glycol (PEG) as a kind of fusogen [110]. PCC can also be induced in G_2 cells by phosphatase

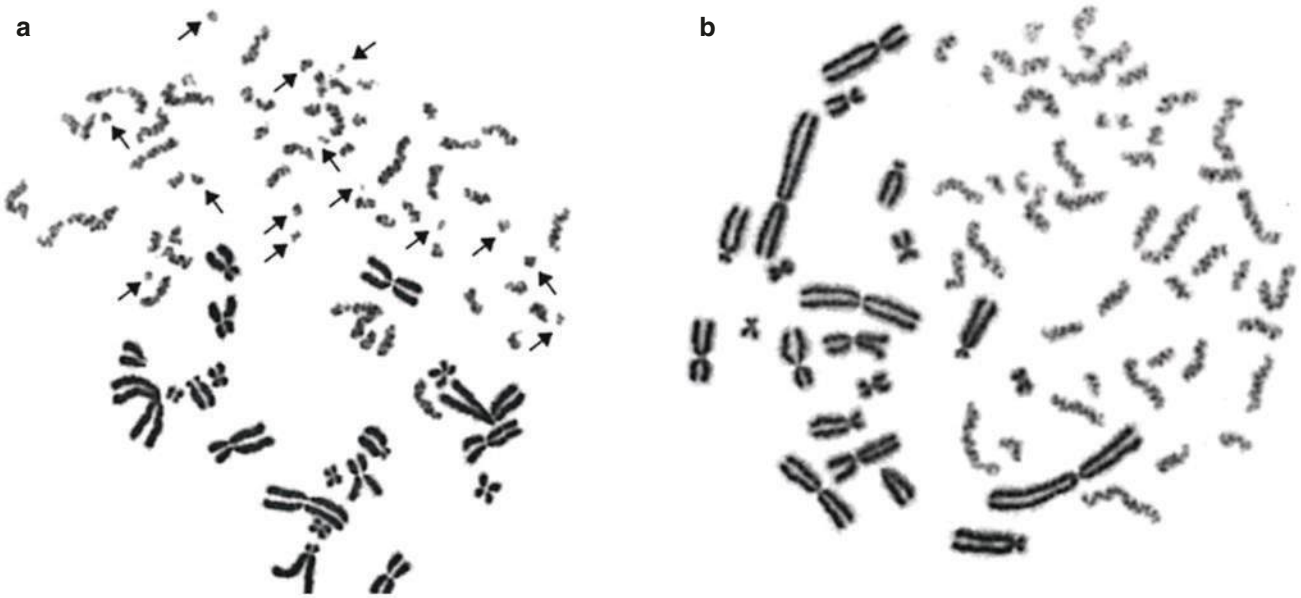

Fig. 8.21 (**a**) Prematurely condensed single chromatid chromosomes following gamma irradiation to 4 Gy as visualized using the PCC assay and lymphocyte fusion to a mitotic CHO cell. Fourteen excess PCC fragments can be scored (shown by arrows). (**b**) Non-irradiated G_0-lymphocyte PCCs demonstrating 46 single chromatid PCC elements. (Reproduced with permission from [112])

inhibitors such as okadaic acid or calyculin A. Unlike cell fusion of unstimulated G_0 lymphocytes, chemically induced PCC method requires stimulation of lymphocytes for one cell division because these chemicals induce premature condensation of G_2 cells after DNA replication. The PCC method is suitable for the analysis of ring chromosomes, especially at higher doses [111]. To quantify radiation-induced chromosomal aberrations in G_0-phase lymphocytes using the fusion PCC-assay, the total number of single chromatid PCC elements per cell in the exposed lymphocytes is recorded (Fig. 8.21a) and the yield of radiation-induced excess PCC fragments is estimated by subtracting the number of 46 PCC elements expected to be scored in non-irradiated lymphocytes (Fig. 8.21b). The dose assessment is based on a dose-response calibration curve generated by in vitro irradiation of unstimulated blood lymphocytes. These curves have a linear shape and the residual yield of excess fragments depends on the time elapsed for repair between the irradiation and the cell fusion Especially in radiation accidents where high doses are received the premature chromosome condensation (PCC) assay enables quantification of radiation-induced chromosomal aberrations directly on unstimulated interphase blood lymphocytes [89].

Overall, the fusion PCC assay allows rapid assessment of the radiation dose, even within 3 h post irradiation, and can successfully distinguish between whole- and partial-body exposures [113]. Furthermore, when the PCC-assay is combined with the fluorescence in situ hybridization (FISH) technique, inter- and intra-chromosomal rearrangements can be analyzed directly in G_0 lymphocytes for radiation biodosimetry purposes and retrospective assessment of radiation-induced effects [114]. Finally, a quick, automatable, and minimally invasive micro-PCC assay was recently proposed for rapid individualized risk assessments in large-scale radiological emergencies [115]. However, the PCC assay requires the availability of either fresh or frozen mitotic cells [116] and expertise in cell fusion procedures and analysis of lymphocyte prematurely condensed chromosomes. Due to these limitations, the test is still not widespread.

8.6.3 Molecular Methods

8.6.3.1 Gamma-H2AX Foci Assay

The radiation-induced gamma-H2AX foci assay can be used to detect and quantify DNA double strand breaks indirectly using a phospho-specific antibody for the histone variant H2AX [30] (Fig. 8.22). In addition, the potential for rapid, high throughput, batch processing [117, 118] makes the foci assay ideal for early triage categorization to quickly identify patients who may be at risk of developing acute radiation syndrome and help prioritize the more established biodosimetry methods such as the dicentric assay.

The advantage of the gamma-H2AX assay is that a dose estimate, based on foci levels in peripheral blood lymphocytes, can be given within 5 h from the receipt of a blood sample [117]. Background levels of mean foci per cell are low, ~0.3 or less [119] and gamma-H2AX foci increase linearly with dose. However, foci loss follows the time course of DNA double strand break repair [120] and the time between

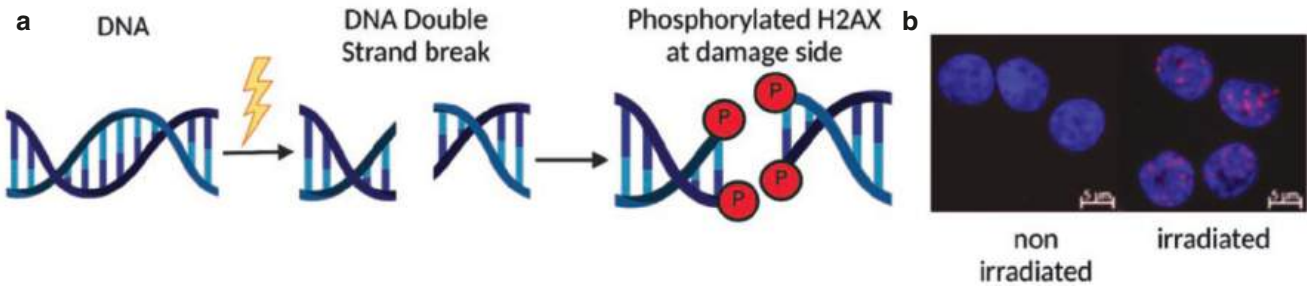

Fig. 8.22 (**a**) Schematic representation of the formation of gamma-H2AX foci. Following radiation-induced DNA breakage, the free DNA ends are labeled by the phosphorylation of H2AX, which can be visualized and quantified using immunofluorescence antibodies. (**b**) Gamma-H2AX foci in human blood lymphocytes following exposure to 0 or 1 Gy X-rays following a post-exposure incubation for 1 h (40× magnification fluorescence microscopy images showing gamma-H2AX foci in green and DNA counterstain in blue)

radiation exposure and blood sampling greatly effects the observed yield of foci. To enable reliable exposure assessment, calibration curves for different post-exposure time points are essential [121]. The rapid loss of gamma-H2AX foci requires a blood sample to be taken within 1–2 days after a radiation exposure with the minimum detectable dose increasing from a ~ 1 mGy [122] for a sample taken within 1 h after exposure to ~0.5 Gy for a lag time of 2 days between exposure and sampling [123]. Use of two separate foci biomarkers, for example, gamma-H2AX and 53BP1 with dual-color immunostaining, could enhance the sensitivity for low-dose exposure by only scoring foci that coincide, so reducing the influence of staining artefacts [123]. Manual scoring of gamma-H2AX foci is the preferred method, as it gives smaller uncertainties in the dose estimate than automated scoring techniques [124] or flow cytometry [123]. However, gamma-H2AX flow cytometry imaging has the potential to be a very rapid, high throughput tool suitable for analyzing large numbers of samples [125]. The data analysis of foci counts for calibration curve fitting, estimating doses and calculating confidence intervals can be performed in the same manner as conventional chromosome dosimetry. Some evidence suggests the distribution of gamma-H2AX is Poisson among the scored cells and can be used to estimate partial-body exposure using the methods developed for the dicentric assay, although over-dispersion has been observed in other data sets [124].

Radiation quality, time, and dose-dependent changes in gamma-H2AX foci numbers need to be considered when converting foci yields into dose estimates. The rapid loss of foci following irradiation and other assay methodology influencing factors (e.g., sample shipment conditions, staining reproducibility), suggests that currently gamma-H2AX-based dose estimation may be associated with large uncertainties; especially if the exact time between exposure and blood sampling is unknown. Given this, the assays main function is that of a qualitative indicator of exposure as opposed to a precise dosimetry tool.

8.6.3.2 Gene Expression

One relatively new method for biological dosimetry is the analysis of changes in gene expression. In response to exposure to ionizing radiation, cells activate multiple transduction pathways to activate cell cycle arrest and induce DNA repair mechanisms in order to prevent the cell from apoptosis. These radiation-responsive alterations in the transcriptome can be quantified by molecular analysis, which lately have been exploited for biological dosimetry [126]. Global discovery platforms are initially used to search for appropriate marker genes that are useful for biodosimetric applications. The expression values need to be measurable in a relevant dose range and exhibit a linear dose-response relationship such that the level for the respective gene can be assigned to a specific radiation dose. Those studies focus mainly on human peripheral lymphocytes, which are also the material of choice for classical biodosimetry methods due to their sensitivity and specificity to ionizing radiation and the possibility of minimally invasive collection. The gene response can be monitored either by quantitative real-time polymerase chain reaction (qRT-PCR), which accurately quantifies single genes, or by microarrays that can show a global scale analysis [127]. Using ex vivo irradiated lymphocytes the sensitivity and linear dose dependency of this assay was assumed to be 100 mGy up to 5 Gy whole-body irradiation [128].

Currently, the use of gene expression analysis in dosimetry is still experimental. Several genes have already emerged as useful biomarkers, with ferredoxin reductase (FDRX) being the most promising one [129]. Due to the activation of a very complex molecular reaction by ionizing radiation, estimation of the dose based on single changes in gene expression is not optimal. Therefore, the use of multiple panels of radiation-sensitive genes is more promising to improve the accuracy of the estimation [87]. Currently, many researchers are working on the definition of such a gene signature in order to apply gene expression for biological dosimetry. There are also some studies that have identified genes for specific ARS effects [130].

The advantage of gene expression-based over other biodosimetric methods is rapid radiation dose estimation and high sample throughput, which is particularly advantageous for large populations. However, due to the dynamics of gene expression, dose estimation is only possible in a relatively short time frame after exposure. In addition, the influence of health status, age, and sex on changes in radiation-induced gene expression is known, and thus there is a need to develop individualized gene expression-based dosimetry models for different population subgroups. So far, it has also not fully been clarified how to infer from changes in gene expression to different radiation qualities and more complex exposure scenarios such as detection of partial-body irradiation. Although there is currently no universal standardization of gene expression analysis for biological dosimetry available, research is on going and the analysis of gene profiles seems to hold great potential to support the individual dose estimation especially in large-scale radiation accidents (Box 8.5).

Box 8.5 Methods for Biological Dosimetry

- In biological dosimetry biomarkers are used to verify exposure to ionizing radiation and to estimate the absorbed dose.
- The analysis of dicentric chromosomes is considered as "gold standard" in biological dosimetry after an acute radiation exposure.
- According to the radiation scenario other cytogenetic methods are available (CBMN, FISH; PCC).
- Relatively new methods on the molecular level are gamma-H2AX foci assay and analysis of changes in the gene expression.

8.7 Radiation Protection System/Risk Coefficients, Organ Weighting Factors, and Dose Limits

8.7.1 Introduction: History

Since the discovery and the rapid introduction and exploitation of ionizing radiation in medicine, technology and industry, the limited knowledge about the detrimental health effects of radiation led to the exposure of many individuals to high doses, and subsequently to various radiation exposure related health effects such as cancer [131, 132].

Guidelines for radiation protection purposes started as early as the 1890s with more detailed dose limits being released as more research was being published. However, as the detrimental effects of radiation became more known, and more research was being published about its negative side effects, the need for a cohesive set of guidelines and regulations became more apparent. At the second International Congress of Radiology, held in Stockholm in 1928, a new unit was proposed for quantifying ionizing radiation, specifically for the purpose of radiation protection. The unit was named Röntgen, after the discoverer of X-rays. It was also during this congress that the International X-Ray and Radium Protection Committee (IXRPC) was founded, which would later be known as the Commission for Radiation Protection (ICRP). The first dose limit recommendation by the IXRPC came in 1934. These stated that a person in normal health can tolerate 0.2 roentgens of X-rays per day. This would correspond to approximately an annual effective dose of 500 mSv; a dose 25 times higher than the current annual dose limit for occupational workers. No dose limit recommendation was given for γ-rays at this point.

Separate from the IXRPC, a document was published in the 1930s, outlining many protective methods and techniques to shield from the harmful effects of radiation. This report was commissioned by what would later become the United Nations Scientific Committee on the Effects of Atomic Radiation (UNSCEAR). The comments on permissible dose were vague, however. In the following years, several recommendations were being made by various bodies. Around this time, terminology also began changing, and the previously used "tolerance dose" was changed to "maximum permissible dose." In 1946, the US advisory Committee was re-established as the National Council on Radiation Protection and Measurements (NCRP) and amended their initial recommendations to now allow a maximum permissible dose of 0.05 Roentgen/day, expressed at that time as 0.3 Roentgen/week [133]. This reduction was largely due to the growing evidence of the hereditary harm of radiation. This new guideline was also echoed by the ICRP in 1950, when they also proposed a weekly maximum permissible dose of 0.3 Roentgen. The reduction from their previous 1934 recommendations of 0.2 Roentgen/day corresponded to 1 Roentgen/week, which was then seen as being too close to the threshold of adverse effects [134].

The first publication by the ICRP came in 1955; here a clear distinction was made between the levels allowed for public and occupational exposure, public exposure allowance was reduced by a factor of 10 from what was allowed for occupational exposure. Recommendations on permissible doses were given for various organs. New units were also introduced, with the rad (now corresponding to 0.01 Gy) being used for absorbed dose, and rem as the RBE weighted unit (corresponding today to 0.01 Sv) [135]. In 1958, the ICRP published what is now known as "Publication 1". The concept of a weekly dose limit was abandoned, and the new annual occupational dose limit was 5 rem, with a public limit of 0.5 rem/year (50 and 5 mSv respectively) [136].

Changes to terminology and units were revised once again in 1977, in publication 26. The Sievert replaced the rem, and

effective dose equivalent was introduced. More thought was also being placed on cost benefit assessment and the concept of radiation health detriment was introduced. Three general rules for the use of radiation were also introduced, justification, optimization and individual dose limitation. The term maximum permissible dose was replaced by dose limit; however, no changes were made to the guidelines, a dose limit of 50 mSv remained for occupational workers, with a public dose limit of 5 mSv [137]. In 1991, publication 60 reduced the occupational dose limit from 50 mSv to 20 mSv/year, averaged over 5 years. Public exposure was now limited to 1 mSv, with higher exposer levels being permissible as long as the annual average over a span of 5 years did not exceed 1 mSv. A radiation weighting factor was introduced, and the measure of dose equivalent was replaced by quantity equivalent dose. As there were now also tissue weighting factors for many more organs, effective dose equivalent was also replaced by the term effective dose [3]. The latest recommendations were issued in 2007 (publication 103) updating consolidating and developing additional guidance on the protection from radiation sources. One of the main characteristics of publication 103, is that it evolves from the previous process-based protection approach (practices and interventions) to an approach based on the exposure situation (planned emergency and existing exposure situations). The radiation and tissue weighting factors, effective dose and detriment are updated based on the most recent scientific data available. Finally, ICRP 103 focuses also on the radiological protection of the environment [34].

8.7.2 Organ Weighting Factors, Risk Coefficients, and Dose Limits

Ionizing radiation can have severe damaging effects in the human body. These harmful effects can be classified into two general categories: the deterministic effects and the stochastic effects. The deterministic effects are due to the killing or malfunction of cells after exposure to high radiation doses. The stochastic effects refer to either cancer or hereditary effects due to mutations of somatic cells or germ cells respectively.

The deterministic effects are manifested when the dose exceeds the dose threshold for a given effect [85]. These effects appear mostly after high irradiation doses. These thresholds are essential in preventing risk of morbidity in specific cell populations and overall mortality [32]. Tissues generally have different threshold dose baselines for these deterministic effects which depend on the radiosensitivity of the cells and the functional reserve of the tissue.

Depending on the absorbed dose and the type and energy of the radiation source, the equivalent dose (H_T, mSv) for individual organs can be calculated. Equivalent dose (H_T) is the absorbed dose, in tissue or organ T weighted for the type and quality of radiation R.

Table 8.17 Radiation weighting factors, as defined in the ICRP 103. All values relate to the radiation incident on the body or, for internal sources, emitted from the source (reproduced with permission from [34])

Radiation type	w_R
Photons	1
Electrons and muons	1
Protons and charged ions	2
Alpha particles, fission fragments, heavy ions	20
Neutrons, $E_n < 1$ MeV	$2.5+18.2e^{-[\ln(E_n)]^2/6}$
Neutrons, 1 MeV $\leq E_n \leq$ 50 MeV	$5+17e^{-[\ln(2E_n)]^2/6}$
Neutrons $E_n > 50$ MeV	$2.5+3.25e^{-[\ln(0.04E_n)]^2/6}$

It is defined by the following equation:

$$H_{T,R} = w_R D_{T,R} \tag{8.1}$$

where $D_{T,R}$ is the absorbed dose averaged over tissue or organ T, due to radiation R and w_R is the radiation weighting factor. w_R is a dimensionless factor that correlates with the biological effectiveness of radiations of different qualities. The values w_R as these are presented in ICRP 103 are shown in Table 8.17.

When the radiation field is composed of types and energies with different values of w_R, the total equivalent dose, H_T, is given by:

$$H_T = \sum_R w_R D_{T,R} \tag{8.2}$$

The stochastic effects are characterized for not having a known threshold and include cancer and hereditary disorders. The stochastic effects can represent a serious risk even at low doses of ionizing radiation, especially if the dose exceeds 100 mSv. The risk of induction represents the value of the effective dose absorbed in the whole organism. The effective dose is related to the health status detriment caused by stochastic effects. Because the tissues differ in their sensitivity to radiation, a tissue weighting factor (w_T) has been determined. w_T is the factor by which the equivalent dose in a tissue or organ T is weighted to represent the relative contribution of that tissue or organ to the total health detriment resulting from uniform irradiation of the body [34]. It is weighted such that $\sum_T w_T = 1$.

The effective dose (E) can be calculated as the sum of the weighted equivalent doses in all the tissues and organs of the body from internal and external exposure. It is defined by:

$$\mathrm{E} = \sum_T w_T H_T = \sum_R w_R D_{T,R} \tag{8.3}$$

where $D_{T,R}$ is the absorbed dose averaged over tissue or organ T, due to radiation R, w_R is the radiation weighting factor and w_T is the tissue weighting factor for tissue or organ T (Table 8.18).

Table 8.18 Tissue weighting factor (w_T) values (reproduced with permission from [34])

Tissue	w_T	Σw_T
Bone-marrow (red), colon, lung, stomach, breast, remainder tissues[a] (nominal w_T applied to the average dose to 14 tissues)	0.12	0.72
Gonads	0.08	0.08
Bladder, esophagus, liver, thyroid	0.04	0.16
Bone surface, brain, salivary glands, skin	0.01	0.04

[a] Remainder tissues (14 in total): adrenals, extrathoracic (ET) region, gall bladder, heart, kidneys, lymphatic nodes, muscle, oral mucosa, pancreas, prostate, small intestine, spleen, thymus, uterus/cervix

Table 8.19 Nominal risk coefficients for cancer and hereditary effects (10^{-2} Sv^{-1}) (reproduced with permission from [34])

Exposed population	Cancer	Hereditary effects	Total
General	5.5	0.2	5.7
Workers	4.1	0.1	4.2

The effects of ionizing radiation, mostly as a health hazard, have been studied for several decades. In this regard, the term nominal cancer risk coefficients has been introduced. These coefficients define the incidence probability of stochastic effects per radiation dose. The nominal risk coefficients depend on age, sex, averaged lifetime risk, among other radiobiological factors. In the twentieth century the nominal risk coefficient for cancer risk after exposure to ionizing radiation was estimated in 5.5% and 4.1% per Sievert (Sv) for the general population and for adult workers, respectively. The nominal risk for heredity damage was estimated in 0.2% and 0.1% per Sievert (Sv) for the general population and for adult workers, respectively (Table 8.19).

As previously mentioned, people are exposed to ionizing radiation from natural and artificial sources throughout their life. Which is why dose limits were implemented, seeking to prevent deterministic effects or to reduce the risk of stochastic effects. These dose limits are applicable only for situations of planned exposure and doses above the normal natural background radiation. However, these dose limits are not applied in the medical field so as to not hamper the effectiveness of diagnosis or treatment. Dose limits are applied into two main groups of exposed individuals: (1) occupationally exposed and (2) public (Table 8.20) [85]. Dose limits are strongly regulated to ensure that no one is exposed to an excessive amount of radiation in either normal or planned situations.

Table 8.20 Recommended dose limits in planned exposure situations (reproduced with permission from [34])

Type of limit	Occupational	Public
Effective dose	20 mSv/year[a,b]	1 mSv in a year[c]
Annual equivalent dose in		
Lens of the eye	20 mSv/year[a,d]	15 mSv
Skin (averaged over 1 cm^2 of skin)	500 mSv	50 mSv
Hands and feet	500 mSv	–

[a] 100 mSv in 5 years (averaged over 5 consecutive years), with no single year exceeding 50 mSv

[b] After a worker declares a pregnancy, the dose to the embryo/fetus should not exceed about 1 mSv during the remainder of the pregnancy

[c] Value applies to the average value over a period of 5 years

[d] Revised value by ICRP Statement on tissue reactions in ICRP publication 118 [32]

8.8 Exercises and Self-Assessment

Q1. When radon is inhaled the largest dose is found at the level of the
- (a) Mouth
- (b) Bronchial wall
- (c) Bifurcation of the trachea
- (d) Alveoli

Q2. When is the initial triage used?

Q3. How many categories of priority are used in initial triage?

Q4. What methods of treatment are used for internal contamination with radionuclides?

Q5. In hematopoietic syndrome the death is mainly due to
- (a) Anemia
- (b) Dyspnea
- (c) Hemorrhage and infection
- (d) Thrombopenia

Q6. In gastrointestinal syndrome the death is mainly due to
- (a) Anemia
- (b) Fever
- (c) Vomiting
- (d) Circulatory collapse

Q7. The LD_{50} for humans is about without medial support measures is
- (a) 1 Gy
- (b) 4 Gy
- (c) 10 Gy
- (d) 50 Gy

Q8. Discuss the most appropriate biodosimetric assay(s) for use in a suspected cases of radiation exposure which occurred approximately?
(a) 12 h ago
(b) 1 month ago
(c) 1 year ago

8.9 Exercise Solutions

SQ1. c
SQ2. Initial triage is used to screen the patients with severe injuries after a mass biological, chemical, radiological or nuclear event.
SQ3. Four categories of priority.
SQ4. Isotope blocking, dilution, or displacement, and the use of ion exchange resins, and ion mobilization or chelation.
SQ5. c
SQ6. d
SQ7. b
SQ8. The data in Sect. 8.6 should be referred to in order to formulate a full answer, based on the scenario of exposure. However, the short answers are: (a) gamma-H2AX and dicentric assays; (b) dicentric or CBMN assays; (c) FISH translocation assay.

References

1. UNSCEAR. Annex B: Exposures of the public and workers from various sources of radiation. 2008.
2. UNSCEAR. Effects and risks of ionizing radiation. Vol. I: Report to the General Assembly and Scientific Annex A. Evaluation of medical exposure to ionizing radiation. UNSCEAR 2020/2021 Report. United Nations Scientific Committee on the Effects of Atomic Radiation. United Nations sales publication E.22.IX.1. New York: United Nations; 2022.
3. ICRP. 1990 Recommendations of the International Commission on Radiological Protection. ICRP Publication 60. Ann ICRP. 21(1–3). Oxford: International Commission on Radiological Protection, Pergamon Press; 1991.
4. Shore RE, Moseson M, Harley N, Pasternack BS. Tumors and other diseases following childhood x-ray treatment for ringworm of the scalp (Tinea capitis). Health Phys. 2003;85(4):404–8.
5. Weiss HA, Darby SC, Doll R. Cancer mortality following X-ray treatment for ankylosing spondylitis. Int J Cancer. 1994;59(3):327–38.
6. Willem Hendrik Leer J, Van Houtte P, Davelaar J. Irradiation of non-malignant diseases: an international survey. In: Seegenschmiedt MH, Makoski HB, Trott KR, Brady LW, editors. Radiotherapy for non-malignant disorders. Medical radiology (radiation oncology). Berlin: Springer; 2008. https://doi.org/10.1007/978-3-540-68943-0_6.
7. UNSCEAR. Hereditary effects of radiation: UNSCEAR 2001 report to the General Assembly, with Scientific Annex. New York: United Nations; 2001 [cited 2022 Jan 13]. https://www.unscear.org/unscear/en/publications/2001.html.
8. Health Canada. 2017 Report on occupational radiation exposures in Canada. http://publications.gc.ca/collections/collection_2018/sc-hc/H126-1-2017-eng.pdf.
9. UNSCEAR. United Nations Scientific Committee on the Effects of Atomic Radiation UNSCEAR 2008 report to the General Assembly, with scientific annexes. 2008.
10. Martin CJ, Vassileva J, Vano E, Mahesh M, Ebdon-Jackson S, Ng KH, et al. Unintended and accidental medical radiation exposures in radiology: guidelines on investigation and prevention. J Radiol Prot. 2017;37(4):883–906.
11. Ramana MV. Nuclear power: economic, safety, health, and environmental issues of near-term technologies. Annu Rev Environ Resour. 2009;34(1):127–52.
12. Socol Y, Gofman Y, Yanovskiy M, Brosh B. Assessment of probable scenarios of radiological emergency and their consequences. Int J Radiat Biol. 2020;96(11):1390–9.
13. Rogovin M. Three Mile Island: a report to the commissioners and to the public, vol. I. Washington, DC: United States Nuclear Regulatory Commission; 1980. p. 153.
14. UNSCEAR. Annex D: Exposures from the Chernobyl accident. 1988.
15. IAEA. The Fukushima Daiichi accident. Vienna: International Atomic Energy Agency; 2015 [cited 2022 Feb 23]. Available from: https://www.iaea.org/publications/10962/the-fukushima-daiichi-accident.
16. Canadian Nuclear Safety Commission. Working safely with industrial radiography. 2014 [cited 2022 Feb 7]. Available from: https://central.bac-lac.gc.ca/.item?id=CC172-105-2014-eng&op=pdf&app=Library.
17. USNRC. United States Nuclear Regulatory Commission, Inadvertent shipment of a radiographic source from Korea to the Amersham Corporation, Burlington, MA, NUREG-1905. Washington, DC: NRC; 1990.
18. Lloyd DC, Edwards AA, Fitzsimons EJ, Evans CD, Railton R, Jeffrey P, et al. Death of a classified worker probably caused by overexposure to gamma radiation. Occup Environ Med. 1994;51(10):713–8.
19. Harisson N, Escott P, Dophin G. The investigation and reconstruction of a severe radiation injury to an industrial radiographer in Scotland. In: Snyder S, editor. Proc. of the third international congress of the International Radiation Protection Association Washington, 1973. Washington, DC: USAEC; 1973. p. 760–8.
20. USNRC. United States Nuclear Regulatory Commission, ibid., vol. 16(3). Washington, DC: NRC; 1993. p. 4–5.
21. Wheelton R. National Radiological Protection Board, Harwell, Personal communication. 1996.
22. Jinaratana V. The medical basis for accident preparedness: the clinical care of victims. In: Ricks RC, Berger ME, O'Hara Jr FM, editors. The radiological accident in Thailand. Boca Raton, FL: Parthenon Publishing; 2002. p. 283–301.
23. IAEA. Report "The radiological accident in Goiania, 1988, Vienna". 1988.
24. REMM. REMM—Radiation Emergency Medical Management. 2009 [cited 2021 Dec 11]. https://remm.hhs.gov/index.html. Accessed 13 Jan 2022.
25. Grant EJ, Brenner A, Sugiyama H, Sakata R, Sadakane A, Utada M, et al. Solid cancer incidence among the life span study of atomic bomb survivors: 1958–2009. Rare Radiat Res Soc. 2017;187(5):513–37.
26. Gilbert ES. Ionising radiation and cancer risks: what have we learned from epidemiology? Int J Radiat Biol. 2009;85(6):467–82.
27. Otake M, Schull WJ. In utero exposure to A-bomb radiation and mental retardation; a reassessment. Br J Radiol. 1984;57(677):409–14.

28. Otake M, Schull WJ. Radiation-related small head sizes among prenatally exposed A-bomb survivors. Int J Radiat Biol. 1993;63(2):255–70.
29. Otake M, Schull WJ. Radiation-related brain damage and growth retardation among the prenatally exposed atomic bomb survivors. Int J Radiat Biol. 1998;74(2):159–71.
30. Mettler FJ, Upton A. Medical effects of ionizing radiation. 2nd ed. Philadelphia: Saunders; 1995.
31. Ruano-Ravina A, Aragonés N, Kelsey KT, Pérez-Ríos M, Piñeiro-Lamas M, López-Abente G, et al. Residential radon exposure and brain cancer: an ecological study in a radon prone area (Galicia, Spain). Sci Rep. 2017;7(1):3595.
32. ICRP. Statement on tissue reactions/early and late effects of radiation in normal tissues and organs—threshold doses for tissue reactions in a radiation protection context. ICRP Publication 118. Ann ICRP. 2012;41(1/2).
33. National Research Council (US) Committee on the Biological Effects of Ionizing Radiation (BEIR V). Health effects of exposure to low levels of ionizing radiation: Beir V. Washington, DC: National Academies Press (US); 1990 [cited 2022 Apr 29]. Available from: http://www.ncbi.nlm.nih.gov/books/NBK218704/.
34. ICRP 103. The 2007 recommendations of the International Commission on Radiological Protection. 2007.
35. Ainsbury EA, Barnard S, Bright S, Dalke C, Jarrin M, Kunze S, et al. Ionizing radiation induced cataracts: recent biological and mechanistic developments and perspectives for future research. Mutat Res Rev. 2016;770(Pt B):238–61.
36. Ainsbury EA, Dalke C, Mancuso M, Kadhim M, Quinlan RA, Azizova T, et al. Introduction to the special LDLensRad focus issue. Radiat Res. 2022;197(1):1–6.
37. Uwineza A, Kalligeraki AA, Hamada N, Jarrin M, Quinlan RA. Cataractogenic load—a concept to study the contribution of ionizing radiation to accelerated aging in the eye lens. Mutat Res Rev Mutat Res. 2019;779:68–81.
38. Laurier D, Rühm W, Paquet F, Applegate K, Cool D, Clement C, et al. Areas of research to support the system of radiological protection. Radiat Environ Biophys. 2021;60(4):519–30.
39. Little MP, Azizova TV, Bazyka D, Bouffler SD, Cardis E, Chekin S, et al. Systematic review and meta-analysis of circulatory disease from exposure to low-level ionizing radiation and estimates of potential population mortality risks. Environ Health Perspect. 2012;120(11):1503–11.
40. Tapio S, Little MP, Kaiser JC, Impens N, Hamada N, Georgakilas AG, et al. Ionizing radiation-induced circulatory and metabolic diseases. Environ Int. 2021;146:106235.
41. Darby SC, Ewertz M, McGale P, Bennet AM, Blom-Goldman U, Brønnum D, et al. Risk of ischemic heart disease in women after radiotherapy for breast cancer. N Engl J Med. 2013;368(11):987–98.
42. Hong JC, Rahimy E, Gross CP, Shafman T, Hu X, Yu JB, et al. Radiation dose and cardiac risk in breast cancer treatment: an analysis of modern radiation therapy including community settings. Pract Radiat Oncol. 2018;8(3):e79–86.
43. Walker V, Crijns A, Langendijk J, Spoor D, Vliegenthart R, Combs SE, et al. Early detection of cardiovascular changes after radiotherapy for breast cancer: protocol for a European multicenter prospective cohort study (MEDIRAD EARLY HEART Study). JMIR Res Protoc. 2018;7(10):e178.
44. Chauhan V, Hamada N, Monceau V, Ebrahimian T, Adam N, Wilkins RC, et al. Expert consultation is vital for adverse outcome pathway development: a case example of cardiovascular effects of ionizing radiation. Int J Radiat Biol. 2021;97(11):1516–25.
45. BEIR VI. National Research Council (US) Committee on Health Risks of Exposure to Radon (BEIR VI). Health effects of exposure to radon: BEIR VI. Washington, DC: National Academies Press (US); 1999. https://doi.org/10.17226/5499. Available from https://www.ncbi.nlm.nih.gov/books/NBK233262/.
46. Haynes WM, Lide DR, Bruno TJ. CRC handbook of chemistry and physics, 2017. 97th ed. Boca Raton, FL: CRC Press/Taylor & Francis; 2017.
47. Maier A, Wiedemann J, Rapp F, Papenfuß F, Rödel F, Hehlgans S, et al. Radon exposure-therapeutic effect and cancer risk. Int J Mol Sci. 2020;22(1):E316.
48. Porstendörfer J. Physical parameters and dose factors of the radon and thoron decay products. Radiat Prot Dosim. 2001;94(4):365–73.
49. Cheng YS. Mechanisms of pharmaceutical aerosol deposition in the respiratory tract. AAPS PharmSciTech. 2014;15(3):630–40.
50. Grosskopf A, Irlweck K. Radon exposure and urinary 210Po excretion of Austrian spa workers. Radiat Prot Dosim. 1985;12(1):39–43.
51. ICRP. Occupational intakes of radionuclides: part 3. ICRP Publication 137. Ann ICRP. 2017;46(3/4).
52. Kendall GM, Smith TJ. Doses to organs and tissues from radon and its decay products. J Radiol Prot. 2002;22(4):389–406.
53. Hofmann W. Modelling particle deposition in human lungs: modelling concepts and comparison with experimental data. Biomarkers. 2009;14(Suppl 1):59–62.
54. Harley NH, Robbins ES. 222Rn alpha dose to organs other than lung. Radiat Prot Dosim. 1992;45(1–4):619–22.
55. Balásházy I, Farkas A, Madas BG, Hofmann W. Non-linear relationship of cell hit and transformation probabilities in a low dose of inhaled radon progenies. J Radiol Prot. 2009;29(2):147–62.
56. Grzywa-Celińska A, Krusiński A, Mazur J, Szewczyk K, Kozak K. Radon-the element of risk. The impact of radon exposure on human health. Toxics. 2020;8(4):E120.
57. Prise KM, Pinto M, Newman HC, Michael BD. A review of studies of ionizing radiation-induced double-strand break clustering. Radiat Res. 2001;156(5 Pt 2):572–6.
58. Bräuner EV, Andersen ZJ, Andersen CE, Pedersen C, Gravesen P, Ulbak K, et al. Residential radon and brain tumour incidence in a Danish cohort. PLoS One. 2013;8(9):e74435.
59. Henshaw DL, Eatough JP, Richardson RB. Radon as a causative factor in induction of myeloid leukaemia and other cancers. Lancet. 1990;335(8696):1008–12.
60. Schubauer-Berigan MK, Daniels RD, Pinkerton LE. Radon exposure and mortality among white and American Indian uranium miners: an update of the Colorado plateau cohort. Am J Epidemiol. 2009;169(6):718–30.
61. Zeeb H, Shannoun F, WHO, editors. WHO handbook on indoor radon: a public health perspective. WHO; 2009.
62. Dörr H, Meineke V. Acute radiation syndrome caused by accidental radiation exposure—therapeutic principles. BMC Med. 2011;9:126.
63. Singh VK, Seed TM, Cheema AK. Metabolomics-based predictive biomarkers of radiation injury and countermeasure efficacy: current status and future perspectives. Expert Rev Mol Diagn. 2021;21(7):641–54.
64. WHO. In: Perez M, Carr Z, editors. Development of stockpiles for radiation emergencies. Report of the Radio-Nuclear Working Group. Geneva: WHO Headquarters; 2007. https://www.who.int/ionizing_radiation/a_e/emergencies/WHO_stockpile_report_2007.pdf.
65. Yamamoto LG. Risks and management of radiation exposure. Pediatr Emerg Care. 2013;29(9):1016–26.
66. Bushberg J. The essential physics of medical imaging. 3rd ed. Philadelphia: Lippincott Williams & Wilkins, Wolters Kluwer; 2012.
67. López M, Martín M. Medical management of the acute radiation syndrome. Rep Pract Oncol Radiother. 2011;16(4):138–46.

68. Macià I Garau M, Lucas Calduch A, López EC. Radiobiology of the acute radiation syndrome. Rep Pract Oncol Radiother. 2011;16(4):123–30.
69. Hall E, Giaccia A. Radiobiology for the radiologist. 8th ed. Philadelphia: Wolters Kluwer; 2019.
70. Sureka CS, Armpilia C. Radiation biology for medical physicists. 1st ed. CRC Press; 2017.
71. Singh VK, Seed TM. BIO 300: a promising radiation countermeasure under advanced development for acute radiation syndrome and the delayed effects of acute radiation exposure. Expert Opin Investig Drugs. 2020;29(5):429–41.
72. Singh VK, Seed TM. A review of radiation countermeasures focusing on injury-specific medicinals and regulatory approval status: part I. Radiation sub-syndromes, animal models and FDA-approved countermeasures. Int J Radiat Biol. 2017;93(9):851–69.
73. Johnson TE. Introduction to health physics. 5th ed. McGraw-Hill Education; 2017.
74. Stabin MG. Radiation protection and dosimetry: an introduction to health physics. Springer; 2007.
75. Rojas-Palma C. Ionizing radiation TMT handbook: triage monitoring and treatment of people exposed to ionising radiation following a malevolent. 2009.
76. Bazyar J, Farrokhi M, Khankeh H. Triage systems in mass casualty incidents and disasters: a review study with a worldwide approach. Open Access Maced J Med Sci. 2019;7(3):482–94.
77. Clarkson L, Williams M. EMS mass casualty triage. In: StatPearls. Treasure Island, FL: StatPearls Publishing; 2022 [cited 2022 Apr 7]. Available from: http://www.ncbi.nlm.nih.gov/books/NBK459369/.
78. Jain TN, Ragazzoni L, Stryhn H, Stratton SJ, Della CF. Comparison of the Sacco Triage method versus START Triage using a virtual reality scenario in advance care paramedic students. CJEM. 2016;18(4):288–92.
79. IAEA. Medical management of persons internally contaminated with radionuclides in a nuclear or radiological emergency. Vienna: International Atomic Energy Agency; 2018. Available from: https://www.iaea.org/publications/12230/medical-management-of-persons-internally-contaminated-with-radionuclides-in-a-nuclear-or-radiological-emergency.
80. Ramesh AC, Kumar S. Triage, monitoring, and treatment of mass casualty events involving chemical, biological, radiological, or nuclear agents. J Pharm Bioallied Sci. 2010;2(3):239–47.
81. Hooster G. External and internal contamination decontamination and decorporation. 2012 [cited 2021 Dec 11]. https://slideplayer.com/slide/1703640/. Accessed 11 Dec 2021.
82. Severa J, Bár J. Handbook of radioactive contamination and decontamination. Amsterdam: Elsevier; 1991.
83. National Council on Radiation Protection and Measurements. Management of persons contaminated with radionuclides: handbook: recommendations of the National Council on Radiation Protection and Measurements, December 20, 2008. Bethesda, MD: National Council on Radiation Protection and Measurements; 2009.
84. NCRP. NCRP Report No. 161, Management of persons contaminated with radionuclides. 2021.
85. IAEA. Radiation biology: a handbook for teachers and students. Vienna: International Atomic Energy Agency; 2010. Available from: https://www.iaea.org/publications/8219/radiation-biology-a-handbook-for-teachers-and-students.
86. Romm H, Oestreicher U, Kulka U. Cytogenetic damage analysed by the dicentric assay. Ann Ist Super Sanita. 2009;45(3):251–9.
87. Blakely WF, Carr Z, Chu MC-M, Dayal-Drager R, Fujimoto K, Hopmeir M, et al. WHO 1st consultation on the development of a global biodosimetry laboratories network for radiation emergencies (BioDoseNet). Radiat Res. 2009;171(1):127–39.
88. Pernot E, Hall J, Baatout S, Benotmane MA, Blanchardon E, Bouffler S, et al. Ionizing radiation biomarkers for potential use in epidemiological studies. Mutat Res. 2012;751(2):258–86.
89. IAEA. Cytogenetic dosimetry: applications in preparedness for and response to radiation emergencies. Vienna: International Atomic Energy Agency; 2011. Available from: https://www.iaea.org/publications/8735/cytogenetic-dosimetry-applications-in-preparedness-for-and-response-to-radiation-emergencies.
90. ISO. ISO 19238: Radiation protection-performance criteria for service laboratories performing biological dosimetry by cytogenetics. 2014.
91. Oestreicher U, Samaga D, Ainsbury E, Antunes AC, Baeyens A, Barrios L, et al. RENEB intercomparisons applying the conventional Dicentric Chromosome Assay (DCA). Int J Radiat Biol. 2017;93(1):20–9.
92. ICRU. 3 Biodosimetry. J ICRU. 2019;19(1):26–45.
93. Ainsbury EA, Bakhanova E, Barquinero JF, Brai M, Chumak V, Correcher V, et al. Review of retrospective dosimetry techniques for external ionising radiation exposures. Radiat Prot Dosim. 2011;147(4):573–92.
94. Oestreicher U, Endesfelder D, Gomolka M, Kesminiene A, Lang P, Lindholm C, et al. Automated scoring of dicentric chromosomes differentiates increased radiation sensitivity of young children after low dose CT exposure in vitro. Int J Radiat Biol. 2018;94(11):1017–26.
95. Romm H, Ansburry L, Bajinskis A, Barnard S, Barquinero JF, Beinke C, et al. The dicentric assay in triage mode as a reliable biodosimetric scoring strategy for population triage in large scale radiation accidents. Proc IRPA Glasgow. 2012. TS 2c.3. http://www.irpa13glasgow.com/information.
96. Beinke C, Barnard S, Boulay-Greene H, De Amicis A, De Sanctis S, Herodin F, et al. Laboratory intercomparison of the dicentric chromosome analysis assay. Radiat Res. 2013;180(2):129–37.
97. Beaton LA, Ferrarotto C, Kutzner BC, McNamee JP, Bellier PV, Wilkins RC. Analysis of chromosome damage for biodosimetry using imaging flow cytometry. Mutat Res. 2013;756(1–2):192–5.
98. Garty G, Bigelow AW, Repin M, Turner HC, Bian D, Balajee AS, et al. An automated imaging system for radiation biodosimetry. Microsc Res Tech. 2015;78(7):587–98.
99. Thierens H, Vral A. The micronucleus assay in radiation accidents. Ann Ist Super Sanita. 2009;45(3):260–4.
100. Fenech M, Morley AA. Kinetochore detection in micronuclei: an alternative method for measuring chromosome loss. Mutagenesis. 1989;4(2):98–104.
101. Thierens H, Vral A, de Ridder L, Touil N, Kirsch-Volders M, Lambert V, et al. Inter-laboratory comparison of cytogenetic endpoints for the biomonitoring of radiological workers. Int J Radiat Biol. 1999;75(1):23–34.
102. Fenech M, Holland N, Chang WP, Zeiger E, Bonassi S. The HUman MicroNucleus Project—an international collaborative study on the use of the micronucleus technique for measuring DNA damage in humans. Mutat Res. 1999;428(1–2):271–83.
103. Willems P, August L, Slabbert J, Romm H, Oestreicher U, Thierens H, et al. Automated micronucleus (MN) scoring for population triage in case of large scale radiation events. Int J Radiat Biol. 2010;86(1):2–11.
104. Decordier I, Papine A, Plas G, Roesems S, Vande Loock K, Moreno-Palomo J, et al. Automated image analysis of cytokinesis-blocked micronuclei: an adapted protocol and a validated scoring procedure for biomonitoring. Mutagenesis. 2009;24(1):85–93.
105. Rodrigues MA, Beaton-Green LA, Wilkins RC. Validation of the cytokinesis-block micronucleus assay using imaging flow cytometry for high throughput radiation biodosimetry. Health Phys. 2016;110(1):29–36.

106. Wang Q, Rodrigues MA, Repin M, Pampou S, Beaton-Green LA, Perrier J, et al. Automated triage radiation biodosimetry: integrating imaging flow cytometry with high-throughput robotics to perform the cytokinesis-block micronucleus assay. Radiat Res. 2019;191(4):342–51.
107. Depuydt J, Baeyens A, Barnard S, Beinke C, Benedek A, Beukes P, et al. RENEB intercomparison exercises analyzing micronuclei (cytokinesis-block micronucleus assay). Int J Radiat Biol. 2017;93(1):36–47.
108. Barquinero JF, Beinke C, Borràs M, Buraczewska I, Darroudi F, Gregoire E, et al. RENEB biodosimetry intercomparison analyzing translocations by FISH. Int J Radiat Biol. 2017;93(1):30–5.
109. Sigurdson AJ, Ha M, Hauptmann M, Bhatti P, Sram RJ, Beskid O, et al. International study of factors affecting human chromosome translocations. Mutat Res. 2008;652(2):112–21.
110. Pantelias GE, Maillie HD. A simple method for premature chromosome condensation induction in primary human and rodent cells using polyethylene glycol. Somatic Cell Genet. 1983;9(5):533–47.
111. Kanda R, Hayata I, Lloyd DC. Easy biodosimetry for high-dose radiation exposures using drug-induced, prematurely condensed chromosomes. Int J Radiat Biol. 1999;75(4):441–6.
112. Pantelias A, Zafiropoulos D, Cherubini R, Sarchiapone L, De Nadal V, Pantelias GE, et al. Interphase cytogenetic analysis of G0 lymphocytes exposed to α-particles, C-ions, and protons reveals their enhanced effectiveness for localized chromosome shattering-a critical risk for chromothripsis. Cancers (Basel). 2020;12(9):E2336.
113. Terzoudi GI, Pantelias G, Darroudi F, Barszczewska K, Buraczewska I, Depuydt J, et al. Dose assessment intercomparisons within the RENEB network using G0-lymphocyte prematurely condensed chromosomes (PCC assay). Int J Radiat Biol. 2017;93(1):48–57.
114. Ryan TL, Pantelias AG, Terzoudi GI, Pantelias GE, Balajee AS. Use of human lymphocyte G0 PCCs to detect intra- and interchromosomal aberrations for early radiation biodosimetry and retrospective assessment of radiation-induced effects. PLoS One. 2019;14(5):e0216081.
115. Pantelias A, Terzoudi GI. Development of an automatable micro-PCC biodosimetry assay for rapid individualized risk assessment in large-scale radiological emergencies. Mutat Res Genet Toxicol Environ Mutagen. 2018;836(Pt A):65–71.
116. Yadav U, Bhat NN, Shirsaath KB, Mungse US, Sapra BK. Refined premature chromosome condensation (G0-PCC) with cryopreserved mitotic cells for rapid radiation biodosimetry. Sci Rep. 2021;11(1):13498.
117. Moquet J, Barnard S, Rothkamm K. Gamma-H2AX biodosimetry for use in large scale radiation incidents: comparison of a rapid '96 well lyse/fix' protocol with a routine method. PeerJ. 2014;2:e282.
118. Rothkamm K, Barnard S, Moquet J, Ellender M, Rana Z, Burdak-Rothkamm S. DNA damage foci: meaning and significance. Environ Mol Mutagen. 2015;56(6):491–504.
119. Hasan Basri IK, Yusuf D, Rahardjo T, Nurhayati S, Tetriana D, Ramadhani D, et al. Study of γ-H2AX as DNA double strand break biomarker in resident living in high natural radiation area of Mamuju, West Sulawesi. J Environ Radioact. 2017;171:212–6.
120. Barnard S, Bouffler S, Rothkamm K. The shape of the radiation dose response for DNA double-strand break induction and repair. Genome Integr. 2013;4(1):1.
121. Barnard S, Ainsbury EA, Al-hafidh J, Hadjidekova V, Hristova R, Lindholm C, et al. The first gamma-H2AX biodosimetry intercomparison exercise of the developing European biodosimetry network RENEB. Radiat Prot Dosim. 2015;164(3):265–70.
122. Rothkamm K, Löbrich M. Evidence for a lack of DNA double-strand break repair in human cells exposed to very low x-ray doses. Proc Natl Acad Sci U S A. 2003;100(9):5057–62.
123. Horn S, Barnard S, Rothkamm K. Gamma-H2AX-based dose estimation for whole and partial body radiation exposure. PLoS One. 2011;6(9):e25113.
124. Rothkamm K, Barnard S, Ainsbury EA, Al-Hafidh J, Barquinero J-F, Lindholm C, et al. Manual versus automated γ-H2AX foci analysis across five European laboratories: can this assay be used for rapid biodosimetry in a large scale radiation accident? Mutat Res. 2013;756(1–2):170–3.
125. Turner HC, Sharma P, Perrier JR, Bertucci A, Smilenov L, Johnson G, et al. The RABiT: high-throughput technology for assessing global DSB repair. Radiat Environ Biophys. 2014 May;53(2):265–72.
126. Badie C, Kabacik S, Balagurunathan Y, Bernard N, Brengues M, Faggioni G, et al. Laboratory intercomparison of gene expression assays. Radiat Res. 2013;180(2):138–48.
127. Gruel G, Lucchesi C, Pawlik A, Frouin V, Alibert O, Kortulewski T, et al. Novel microarray-based method for estimating exposure to ionizing radiation. Radiat Res. 2006;166(5):746–56.
128. Kang C-M, Park K-P, Song J-E, Jeoung D-I, Cho C-K, Kim T-H, et al. Possible biomarkers for ionizing radiation exposure in human peripheral blood lymphocytes. Radiat Res. 2003;159(3):312–9.
129. Abend M, Blakely WF, Ostheim P, Schüle S, Port M. Early molecular markers for retrospective biodosimetry and prediction of acute health effects. J Radiol Prot. 2021; https://doi.org/10.1088/1361-6498/ac2434.
130. Ostheim P, Don Mallawaratchy A, Müller T, Schüle S, Hermann C, Popp T, et al. Acute radiation syndrome-related gene expression in irradiated peripheral blood cell populations. Int J Radiat Biol. 2021;97(4):474–84.
131. Voelz GL, Lawrence JN, Johnson ER. Fifty years of plutonium exposure to the Manhattan Project plutonium workers: an update. Health Phys. 1997;73(4):611–9.
132. Yoshinaga S, Mabuchi K, Sigurdson AJ, Doody MM, Ron E. Cancer risks among radiologists and radiologic technologists: review of epidemiologic studies. Radiology. 2004;233(2):313–21.
133. Lindell B. A history of radiation protection. Radiat Prot Dosim. 1996;68(1–2):83–95.
134. ICRP. International recommendations on radiological protection. Revised by the International Commission on Radiological Protection at the sixth international congress of radiology, London, 1950. Br J Radiol. 1951;24:46–53.
135. ICRP. Recommendations of the International Commission on Radiological Protection. Br J Radiol Suppl. 1955;6:1955.
136. ICRP. Report on amendments during 1956 to the recommendations of the International Commission on Radiological Protection (ICRP). Ann ICRP/ICRP Publication. SAGE Publications Ltd. 1959;OS_1(1):539–42.
137. ICRP. Recommendations of the ICRP. ICRP Publication 26. Ann ICRP. 1977;1(3).

Further Reading

Cinelli G, De Cort M, Tollefsen T, editors. European atlas of natural radiation. Luxembourg: Publication Office of the European Union; 2019.
Kang JK, Seo S, Jin YW. Health effects of radon exposure. Yonsei Med J. 2019;60(7):597–603.

Environmental Radiobiology

9

Joana Lourenço, Carmel Mothersill, Carmen Arena, Deborah Oughton, Margot Vanheukelom, Ruth Pereira, Sónia Mendo, and Veronica De Micco

Learning Objectives

At the end of this chapter, the reader should be able to:

- Know the basic concepts associated with environmental radioactivity
- Know the challenges involved in measuring impacts of radiation in the environment
- Know the methodologies and tools available to measure the dose and effect at the level of the individual, population, and ecosystem
- Know the effects of ionizing radiation in living organisms from microorganisms to vertebrates
- Know the basic molecular effects associated with high and low Linear Energy Transfer (LET) radiation
- Understand the concept of radiosensitivity and its relation with organism's complexity and life stage
- Understand the mechanisms underlying microbial tolerance and/or resistance to radionuclides and metals
- Understand the complexity of natural environments and the consequent limitations of laboratory studies
- Understand the particularities associated with NORM contamination

9.1 Introduction

Environmental radiobiology refers to the study of the effects of radiation on ecosystems and species that are part of various habitats, collectively known as "the environment." The discipline is part of Radioecology which is a broad area of research, covering the transfer, uptake and effects of radionuclides in the environment. Radioecology includes, for example, the speciation of radionuclides in environmental media, the transfer of radionuclides through the different environmental compartments and exposure of wildlife to ionizing radiation and its consequences. While this chapter focuses predominantly on the biological and ecological impacts of radiation on non-human species—since transfer is a key aspect of wildlife dosimetry—the environmental behavior of key radionuclides is briefly covered in Sect. 9.2.

It is important to understand that the basic mechanisms that lead to effects in humans, discussed in earlier chapters, also occur in non-human biota, but the effects of concern lie at higher levels of organization, such as the population or ecosystem. For example, a harmful mutations induced by radiation exposure may lead to cancer on humans, but in the environment, where the sustainability of the population is a critical endpoint, low levels of carcinogenic mutations are unlikely to impact the overall population. This means that

J. Lourenço (✉) · S. Mendo
Department of Biology & CESAM, University of Aveiro, Aveiro, Portugal
e-mail: joanalourenco@ua.pt; smendo@ua.pt

C. Mothersill
Faculty of Science, McMaster University, Hamilton, ON, Canada
e-mail: mothers@mcmaster.ca

C. Arena
Department of Biology, University of Naples Federico II, Naples, Italy
e-mail: c.arena@unina.it

D. Oughton
Norwegian University of Life Sciences (NMBU), Ås, Norway
e-mail: deborah.oughton@nmbu.no

M. Vanheukelom
Biosphere Impact Studies, Belgian Nuclear Research Centre, SCK CEN, Mol, Belgium
e-mail: margot.vanheukelom@sckcen.be

R. Pereira
GreenUPorto—Sustainable Agrifood Production Research Centre/ Inov4Agro, Department of Biology, Faculty of Science of the University of Porto, Campus de Vairão, Vila do Conde, Portugal
e-mail: ruth.pereira@fc.up.pt

V. De Micco
Department of Agricultural Sciences, University of Naples Federico II, Naples, Italy
e-mail: demicco@unina.it

S. Baatout (ed.), *Radiobiology Textbook*, https://doi.org/10.1007/978-3-031-18810-7_9

the tools and techniques needed to document and evaluate radiobiological effects in natural populations, and ultimately in ecosystems, are much more complex to those used in human radiobiology.

A key issue is the importance and the difficulty of conducting good experiments in field situations, particularly at environmentally relevant concentrations and with proper controls. Single species studies in the laboratory have an important role in determining high and low dose effects, understanding mechanisms and testing resistance. But results can be misleading if they are extrapolated to environmental conditions, with lower doses, chronic exposures, and a variety of confounding factors such as genetics, age, life stage, predation, availability of resources, as well as the interaction with other stressors and difficulties to make a proper dosimetry [1].

Another important issue is how to measure impacts on ecosystems. Several robust biomarkers are available to determine impacts at the level of the gene, cell, tissue, organ, and organism. These are discussed in Sects. 9.3 and 9.4 of this chapter. Population level markers are also available including population numbers, mortality and morbidity, fecundity and population growth rate, but at the level of the ecosystem, the complexity makes it very difficult to assess ecosystem health following radiation exposure, including effects on functions and services. The importance of legacy sites is discussed in Sect. 9.4, as natural labs like, for example, "Radioecological observatories" (https://radioecology-exchange.org/content/radioecological-observatories) where all the mechanisms of effect from populations to ecosystems can be deeply studied. Other approaches include measurements of biodiversity index and the use of drone technologies to monitor ecosystem change at the gross level, for example, forest cover and diversity, lake eutrophication, or extreme habitat change.

9.2 Behavior and Fate of Radioelements in the Environment

Transfer of anthropogenic radionuclides through food chains has been studied since the time of atmospheric weapons testing and has been supported by data from nuclear power generation and accidents, as well as studies of the behavior of naturally occurring radionuclides (NORs). While there is a wealth of data on the transfer of radionuclides through human food chains, there has been less focus on wildlife and especially organisms that are not common sources of food for humans such as insects and invertebrates. While much of the focus in studying the environmental impacts of radiation has been on the uncertainties in effects measurement, it is important to stress that there are also uncertainties in dosimetry, and especially from internal radionuclides. Hence, knowledge of the factors influencing the behavior of radionuclides in the environment will be fundamental to support dosimetry and exposure assessments. This includes information on the behavior of naturally occurring radionuclides, which is needed both to calculate background doses to organisms, and thus put anthropocentric exposures into perspective, as well as to assess doses in areas with enhanced levels of natural radioactivity.

9.2.1 Naturally Occurring Radionuclides

Naturally occurring radionuclides (NORs) include the radionuclides ^{14}C, ^{3}H, and ^{40}K and also radionuclides that arise from three decay chains: the uranium (^{238}U), the thorium (^{232}Th), and the actinium (^{235}U) decay chains [2] (Figs. 9.1 and 9.2). When they are contained in or released from processing materials they are defined as NORM [3]. Uranium and thorium are both metals belonging to the heavy actinide series, giving rise to long and complex decay chains that contain important radionuclides in the context of environmental radiation exposure (Fig. 9.1). Key radionuclides include isotopes of radon (^{222}Rn with a half-life of 3.8 days; ^{220}Rn with a half-life of 55 s), radium (^{226}Ra half-life of 1602 years, ^{223}Ra half-live of 11.43 days; ^{228}Ra with a half-life of 5.7 days), and polonium (^{210}Po with a half-live of 138 days, ^{216}Po with a half-life of 0.145 s, and ^{212}Po with a half-life of 299 ns). Compared to typical exposures from accidents such as Chernobyl and Fukushima, which are predominantly beta and gamma-emitting radionuclides, NORM exposures are often characterized by high levels of alpha emitters.

9.2.2 Radionuclide Interaction with Water, Air, Soil, and Biota

Radionuclides in the environment can be distributed through the Earth's atmosphere, hydrosphere, and lithosphere (Fig. 9.2). The behavior and fate of radionuclides in the environment depend on physical and chemical properties of radionuclides, the location and the type of emission source, and the environmental conditions [4]. Radionuclides undergo chemical reactions that affect their distribution and retention time. Organisms interact with the nonliving environment and can be exposed to the radionuclides. In order to estimate the doses received by an organism, the activity concentration of radionuclides in the organism's habitat is calculated.

The natural environment is a highly complex system in which elements flow and circulate through the spheres of the Earth. To simplify the study of radionuclides, the environment can be divided compartments such as air, surface and

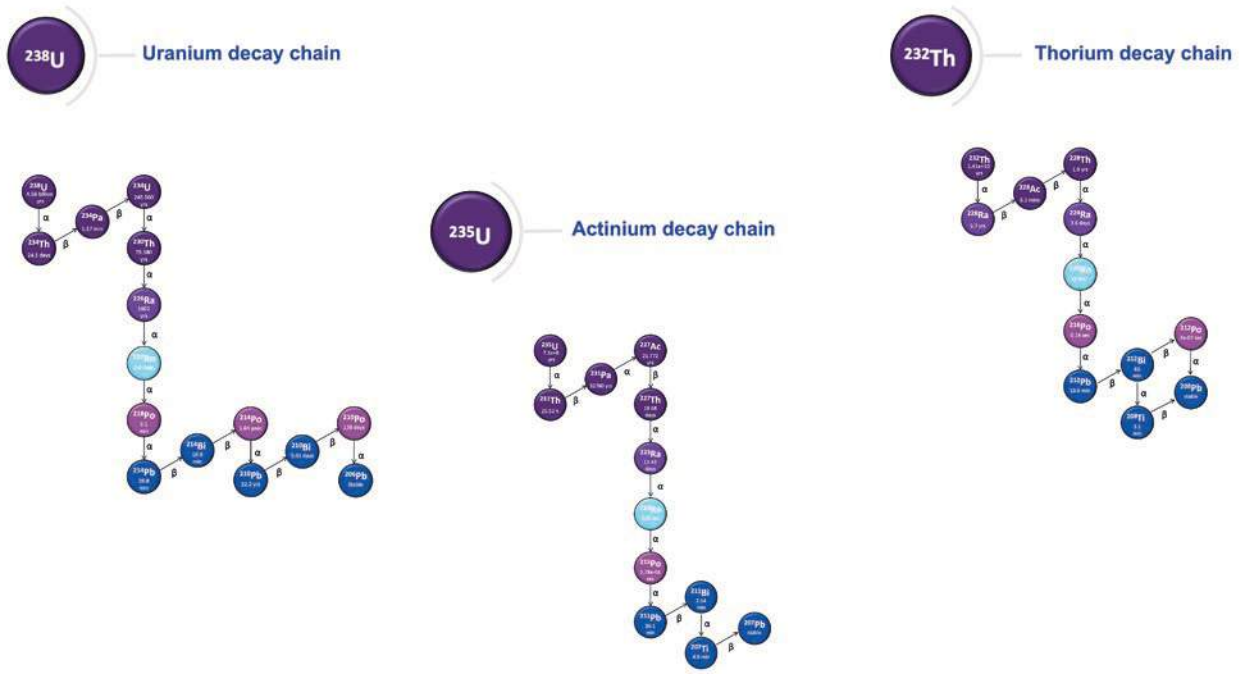

Fig. 9.1 Uranium (including uranium ^{238}U and actinium ^{235}U) and thorium decay chains

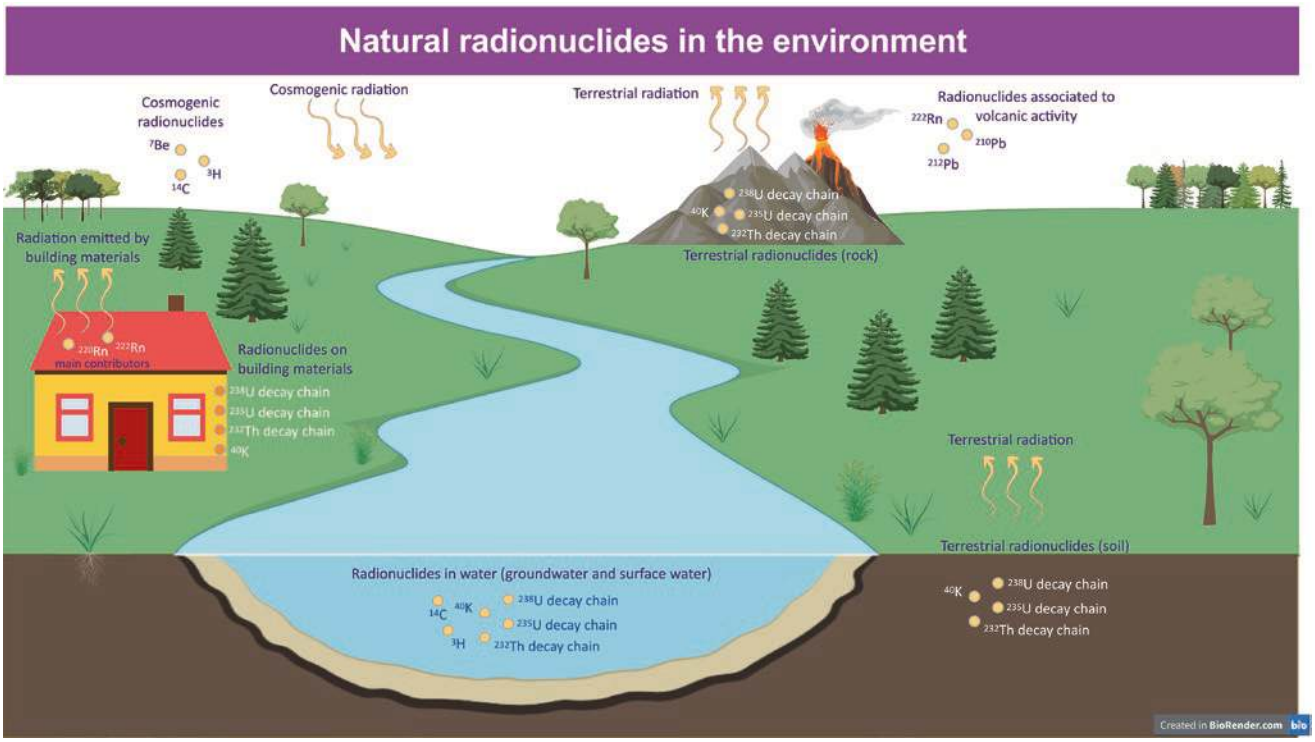

Fig. 9.2 Natural radionuclides distribution in different environmental compartments

groundwater, sediment, soil, and biota. Compartments are usually chosen so that they are distinguishable by spatial boundaries [5]. In each compartment, there are certain processes that have the greatest influence on behavior, so simplifications are made by only taking into account the key interactions that are important to consider for the radionuclide in question. As such, an environmental compartment can be chosen so that it is a volume of medium within which it is assumed that system parameters are constant and chemical concentrations do not vary spatially [6]. For example, in the air compartment, the aerosol formation and particle deposition process of emitted radioactive iodine (e.g., ^{131}I) are key processes to consider, while in the soil compartment, the association with organic matter has been considered the process that determines the largest share of the fate of iodine. Assumptions can be made so that only the key reactions and dynamics are taken into account.

In general, the first step in studying the behavior of the radionuclide in the environment is to obtain knowledge of the location and properties of the emission source. Knowing where the radionuclides come from and in what form they occur can already reveal much information about where the radionuclides will be transported to. For example, the radioactive uranium released from nuclear explosions may end up in very different locations than uranium in nuclear waste dumped into the sea or uranium brought to the surface during the mining of uranium-bearing ores [7]. In addition to the location, the type of emission source should be considered. Anthropogenic emissions of radionuclides result from human activities. These radionuclides are released into the environment at a certain point in time. Unlike anthropogenic emission sources, natural emission sources from the subsurface have been present since the creation of the Earth. Uranium and thorium ores, for example, can be considered as diffuse sources of radionuclides in the Earth's crust. If groundwater near a uranium deposit flows in a particular direction toward areas where drinking water is extracted, it may behave as a point source. Anthropogenic radionuclide sources, such as nuclear weapon tests and nuclear power plant accidents, release radionuclides at high temperatures and pressures in a certain area over a relatively short period of time and can therefore, be considered a point source. Depending on the weather conditions, the radionuclides can be further dispersed as clouds, with the emission spreading diffusely rather than being a point source. Other point sources, such as the emission of nuclear waste dumped in the ocean, release radionuclides diffusely over a large waterbody. Radionuclides that are dispersed without a specific point of discharge and over a long period of time may be considered as a diffuse source. Agricultural practices, for example, often require high levels of fertilizers, which end up in water bodies through various diffuse processes. Phosphate rock in fertilizers can contain small amounts of naturally occurring radionuclides such as uranium, thorium, and radium. Human activities can enhance the release of radionuclides.

The study of the fate of radionuclides is complicated by the property of radioactive decay. Radioactive decay changes the type of radionuclide, thereby altering its physicochemical properties and potentially altering the fate of the entity. That is, when a radionuclide decays, the daughter element often has very different chemical properties than the parent element [8]. If the parent element is a solid and its daughter is a gas, the parent may partition into other compartments, such as air or water. For example, in the natural uranium (^{238}U) decay series, radon (^{222}Rn) is formed after the decay of radium (^{226}Ra). Radium is an alkaline metal that can be present in a mineral structure within the parent rock or in the pore water as an ionic salt, while radon is an inert gas. If the released radon is captured in a closed space such as the basement of a building or a cave, it can be inhaled by an organism. The gaseous ^{222}Rn decays further releasing alpha and beta particles and eventually decays into stable solid ^{206}Pb. The latter is a metal chemically toxic for organisms. When radionuclides are the stressors of concern, both chemical- and radiation-induced effects on organisms are expected.

Once the radionuclide is emitted, its chemical speciation determines how the radionuclide reacts with components in the environment. It is important to keep in mind that radionuclides are not only physical entities, but also have chemical characteristics [9]. For a more detailed discussion of the importance of the chemical characteristics of radionuclides, the reader is referred to the text by Whicker and Schultz [10]. Radionuclides can occur in various chemical forms or species that have different mobility. The following examples of species are for thorium (Th). Radionuclides such as Th can occur in elemental form (e.g., Th^0), but these are very rare in the environment. They can be present as free ions in water (e.g., Th^{4+}). However, dissolved Th is almost always complexed in natural water [11]. Free ions can be bound to inorganic or organic molecules in either the solid or dissolved phases, such as thorium hydroxyl complexes $Th(OH)_4^0$, $Th(OH)_3^+$, $Th(OH)_2^{2+}$, $ThOH^{3+}$, $Th(SO_4)^{2+}$, $Th(HPO_4)_3^{2-}$, Th-oxalate and Th-EDTA complexes. Radionuclides can also be components of a mineral, such as thorianite (ThO_2), and thorite ($ThSiO_4$). The thermodynamic properties of various species can be used to compute liquid-solid equilibria relations. These theoretical calculations reveal much about the possible conditions for and the extent of mobility of radionuclides [11]. The thermochemical data and adsorption results from laboratory experiments help to explain the behavior of radionuclides, such as Th in natural waters, sediments, and wastes.

In general, the total sum of chemical species can be expressed as [9]:

$$(\mathrm{MS}) = \left((M)\right)^{(n+/-)} + \left((M_m L_m)\right)^{(n+/-)} + \left((M_m A)\right) \qquad (9.1)$$

where (MS) is the total sum of species present; $(M)^{n+/-}$ the element present as positively or negatively charged free ion $(n+/-)$; $(M_mL_m)^{n+/-}$ an element complexed by any kind of ligand, L, such as an oxide, organic, or any other form, negatively or positively charged; (M_mA) an element adsorbed onto a surface or trapped in a crystal lattice, or in an amorphous structure, A; m is the number of M or L molecules in the complex; and $n+/-$ is the number of charges.

The fraction of the different chemical species in this formula, that are present in the environment, will depend on the source of the radionuclide and the physicochemical conditions of its surroundings. Parameters such as pH, redox state, ionic strength and the presence of complexing ligands will influence the proportions of each chemical species present.

Some chemical species of radionuclides undergo chemical reactions that influence their mobility or retention. The main chemical reactions determining speciation are adsorption and desorption processes, ion exchange and dissolution reactions, precipitation and co-precipitation, complexation to inorganic and organic ligands [12] and redox reactions. For a detailed explanation of the mechanisms of these reactions, please refer to a course on aquatic chemistry such as Langmuir [8] or Sparks [13].

Of particular interest when studying the behavior of radionuclides are the chemical reactions at the solid–water interface, such as complexation with ligands and adsorption to mineral surfaces. These reactions will largely determine whether the radionuclide is mobile and potentially available for the biota to take up. A dissolved species can associate with an ion or molecule ligand and form a complex [8]. For example, Th is a complex-forming actinide metal for which the chemical speciation of the cation changes with the pH. The multivalent Th cations tend to form strong hydroxyl (OH) complexes. Only in acid waters, the OH concentration is low enough so that competition with ligands is minimal. In these conditions, it is easier for ligands to displace OH and complex it. Complexation with carbonates, humic materials, or other ligands increases the solubility of the Th species and thus the mobility in the environment. An adsorbed species can associate with charged surfaces or broken bonds of minerals. For example, Th adsorbs onto clays, oxides and organic matter in soils and sediments. The adsorption of Th increases if the pH increases from acid to neutral conditions [11]. Sorption processes increase the retardation of Th and thus decrease its mobility in the environment. In general, Th in the soil compartment will remain strongly adsorbed onto soil constituents so that contamination of groundwater through the transport of Th from soil to groundwater will not occur in most soils [14]. Certain microorganisms (*Pseudomonas aeruginosa*) present in soils may enhance the dissolution of Th by producing chelating agents that can form soluble complexes with this radionuclide [15]. This is not the only way for microorganisms to influence the speciation and mobility of radionuclides. They can also, for example, change their redox state, immobilize them by processes such as biosorption, biomineralization, and precipitation [16]. In the water compartment, soluble Th ions will hydrolyze at a neutral pH forming complexes with OH. The Th-hydroxyl complexes can in turn be absorbed on suspended particles in the water. Although dissolved Th tends to form strong complexes, facilitating its transport, Th concentrations in natural waters—with pH between 5 and 9—remain limited by the scarcity of the element, small solution rates and insolubility of Th-bearing minerals [11]. In groundwaters at mining facilities, Th concentrations may be higher due to the more acidic conditions which cause the leaching of Th.

A common approach to quantify the mobility and availability of radionuclides in the environment is to estimate the ratio between the activity concentrations of the radionuclide in two chosen compartments or trophic levels [9, 17]. The radionuclide retention on the solid phase is estimated by determining a partitioning coefficient. The coefficient describes the partitioning of a radionuclide between the solid and aqueous phases and takes no explicit account of sorption mechanisms [18]. It is assumed that an equilibrium exists between the dissolved and sorbed amount of radionuclides and that exchange is reversible [19]. This simplification relates the concentration of a radionuclide in water to the amount of radionuclide adsorbed:

$$M_{\mathrm{aq}} \rightleftarrows M_{\mathrm{ads}}$$

where M_{aq} and M_{ads} are the aqueous and adsorbed species, respectively.

A solid-liquid distribution coefficient (K_{d}) is derived from the ratio of radionuclide concentrations in the solid phase to that in solution and is calculated as:

$$\begin{aligned} K_{\mathrm{d}} &= \frac{\left[\left[M_{\mathrm{ads}}\right]\right]}{\left[\left[M_{\mathrm{aq}}\right]\right]} \\ &= \frac{\text{activity concentration in solid phase}}{\text{activity concentration in aqueous phase}}\left(\frac{\mathrm{Bq/kg}}{\mathrm{Bq/L}}\right) \\ &= \frac{\left(\left(A_{\mathrm{int}} - A_{\mathrm{eq}}\right)\right)}{A_{\mathrm{eq}}} \cdot \frac{V}{m}\left(\mathrm{L/kg}\right) \end{aligned} \tag{9.2}$$

where A_{int} is the initial radionuclide activity (Bq), A_{eq} is the equilibrated radionuclide activity (Bq) in the aqueous phase, V is the volume of the liquid phase (L), and m is the mass of solid phase (kg).

The adsorption of radionuclides onto soil particles is often expressed as a K_{d} value. The K_{d} is determined by adding a known amount of sorbent (i.e., clay, oxide, soil) to a solution with an initial radionuclide concentration, and after

equilibration and phase separation (e.g., by ultracentrifugation or a dialysis membrane), radionuclide concentration in the aqueous phase at equilibrium is measured.

In case of radiocesium (e.g., ^{134}Cs and ^{137}Cs), for example, the $^{Cs}K_d$ value is obtained by the ratio of the total radiocesium activity concentration in the solid phase and in liquid phase after a chosen time of contact between the two phases. The experimental design must be carefully thought out, as parameters such as contact time, radionuclide concentration, solid to liquid volume, and the ion composition of the aquatic phase affect the K_d value. Radiocesium dissolves well in water, so that radiocesium exists in the aqueous phase only as a free ionic species. Only one metal species of Cs should be considered, which simplifies the study of adsorption equilibria. Moreover, radiocesium cations can be directly adsorbed from solution by an organism, because the cations have no tendency to form soluble complexed species [20]. Thus, the $^{Cs}K_d$ value can be determined in a relatively simple manner and it can provide useful information about the radiocesium accessible to the organism for uptake [18].

However, caution must be taken in interpreting a K_d value, as it may change over time [18]. On the one hand, the K_d changes in a short term, because an equilibrium is not always reached instantaneously, as for example for radioactive isotopes of iron [21]. On the other hand, the K_d changes in long term, because adsorbed radionuclides, such as ^{137}Cs, can migrate deeper into structures of minerals so that it is no longer available and becomes fixed. K_d values are often determined by short-term laboratory experiments lasting several hours or days. However, K_d values can also be determined in the field, where the results depend on the time elapsed since the contamination occurred and this gives a more reliable picture of the long-term fate of the radionuclides. The time effect was studied in a laboratory study [22] with soils showing that $^{Cs}K_d$ values of mineral soils with 5% clay minerals can increase from 30 to 1000 L/kg in 40 days and 200 to 5000 L/kg in 415 days for peaty soils with 10% clay minerals. In this example, the $^{Cs}K_d$ of the mineral soil increases by a factor of 30 over a relatively short period of time, and the $^{Cs}K_d$ of an organic soil increases accordingly but over a much longer period of time. Laboratory results of $^{Cs}K_d$ values can only partly explain the reduction in Cs soil-to-plant transfer in the field. A study after the Chernobyl accident [23] shows that ^{137}Cs soil-to-plant concentration ratios, that were initially elevated, were reduced by more than 50 times in the following years. This trend was explained by an initial step of radionuclide release from fuel particles into soil aqueous phase, followed by a reduced transfer attributed to the progressive fixation of ^{137}Cs by soil minerals, referred to as "aging effect" that makes ^{137}Cs gradually less available for uptake by the plant.

In many cases, the factors that influence the transfer of radionuclides to biota are similar for humans and include soil and water chemistry, speciation of radionuclides, as well as biokinetics (biological and ecological half-lives) and interactions between radionuclides and stable elements. For example, the soil-to-plant transfer of ^{137}Cs, is influenced by clay content and K levels in the soil, and radiostrontium (^{90}Sr) by Ca levels. Another example, is the uptake of U to fish and other aquatic organisms, that is are dependent on pH and carbonate concentrations, which change the availability and complexation of this element [24]. In contrast to Cs, radionuclides such as U exist as several species in the environment. The bioavailability of different U species in soil to ryegrass was studied in a laboratory pot experiment [25], which showed that speciation has an important influence on the uptake of U by grass. From the results, it was concluded that the uranyl-cation (UO_2^{2+}) and uranyl-carbonate complexes (e.g., $UO_2CO_3(aq)$, $UO_2(CO_3)_3^{4-}$ and $(UO_2)_2CO_3(OH)_3^-$) together with uranyl-phosphate ($UO_2PO_4^-$) are the forms that are most readily taken up by ryegrass and thus are more bioavailable compared to other uranyl-phosphate complexes (e.g., UO_2HPO_4) and the hydroxy- (e.g., $UO_2(OH)_2(aq)$ and UO_2OH^+) and sulfate-complexes (e.g., $UO_2SO_4(aq)$ and $UO_2(SO_4)^{2-}$). As demonstrated in the previous examples, some species are not available for uptake by biota. Hence, a value other than the total concentration in the compartment should be used to estimate the bioavailability of a given radionuclide and, the exposure of biota through ingestion of radionuclides should only be estimated from the activity concentrations of the bioavailable species [17].

Internal exposure and toxic effects of radionuclides require that an organism takes up the radionuclide, and for chemically available species to be taken up by biota, the radionuclide must be able to cross cell membranes [26]. To investigate whether this exposure will occur through ingestion, it is important to know whether this contaminant is a source for ingestion by biota. A radionuclide's potential for biota uptake in soil and sediments is defined by its bioavailability or bioaccessibility. There is a slight difference between the bioavailability and bioaccessibility of pollutants in sediment and soil. This difference has implications for the design of experimental set-ups, but also for the interpretation of results. The bioaccessible fraction is the species in the environment, which are available to cross an organism's membrane if the organism has access to the radionuclide in the longer term [26]. The bioavailable fraction is freely available to cross an organism's membrane from the medium the organism inhabits at a given time. For example, technetium (Tc) may be highly mobile in aqueous solution at oxidation state +7 (i.e., Tc(VII)), but strongly absorbed and retarded in the subsurface at oxidation state +4 (i.e., Tc(IV)) [27]. Technetium is used in nuclear medicine for diagnosis and is emitted in the environment from the nuclear fuel cycle. Technetium exists primarily in two stable oxidation states as Tc(VII) or as Tc(IV), and the two species can have a different fate when released to the environment. While TcO_4^- in

solution is bioavailable, $TcO_2 \cdot nH_2O$ is expected to be adsorbed at low concentrations and precipitated at high concentrations. The species $TcO_2 \cdot nH_2O$ can become available for uptake when oxidized by air and is thus bioaccessible.

Besides the speciation of radionuclides, the extent to which radionuclides can be transferred to different compartments is influenced by competition between ions. On the one hand, stable isotopes of the radionuclides may compete for adsorption to the solid phase or uptake by biota. For example, radionuclides such as ^{3}H, ^{40}K, ^{48}Ca, ^{54}Mn, ^{60}Co, ^{65}Zn, and ^{131}I, are isotopes of essential biological nutrients [10]. Therefore, their uptake and retention characteristics are largely controlled by the flux of these essential nutrients through biological processes. On the other hand, elements that are chemically similar to the radionuclides may compete. Certain radionuclides behave in the environment in a similar way to essential elements for biota, due to their chemical properties. For example, ^{137}Cs and ^{90}Sr have similar chemical properties and follow the same transfer and cycling processes in the environment as the macronutrients potassium (K) and calcium (Ca), respectively. The tendency of these radionuclides to accumulate in the biota is reduced if there is an abundance of the analogous element in the environment [10]. Conversely, the accumulation of the radionuclide in the biota increases when there is a scarcity of the analogue element. For example, low concentrations of K and Ca in the soil can result in increased uptake of radionuclides by plants, as they find it more difficult to discriminate between nutrients and radionuclides under these stressful conditions [20]. As mentioned earlier, the long-term bioavailability of ^{137}Cs and many other radionuclides depend heavily upon ecosystem characteristics, and in particular, soil properties [10]. Soils and sediments of high clay content can effectively immobilize ^{137}Cs by chemical binding. In such systems, the soil acts like a sink for ^{137}Cs and in time very little of the nuclide is available for biological incorporation. Other systems have sandy soils with a low cation exchange capacity, and larger quantities of ^{137}Cs can be recycled through the biota of such systems for long periods of time [9].

In summary, depending on their speciation, radionuclides can be transferred in the biosphere from the emission source to different compartments until they reach an equilibrium or final sink, or they can be recycled within the environment.

9.2.3 Radionuclide Transfer and Exposure

Information on the uptake of radionuclides to biota is vital for calculating dose to the organisms, since both external and internal irradiation contributes to exposure. Soil and sediment dwelling organisms often have high external dose rates by virtue of their habitat, but also internal exposure from ingested radionuclides. Many field studies on radiation effects in wildlife are flawed due to underestimation of the internal dose, reporting only ambient air dose rates [28]. This is particularly important for ⟨- (e.g., Ra) and ®-emitting (e.g., Sr) radionuclides, for which internal exposure is the greatest contributor to dose, but also internal contributions from radiocesium or radium, for example, can make a significant contribution to the overall dose.

There are a number of programs available for estimating the dose to biota. These are usually based on rather simplistic geometry and homogeneous internal distribution, but the basic principles are similar to those used for human dosimetry. They can also be adapted to give organ specific doses. For example, the ERICA Assessment Tool can calculate doses to a wide range of reference animals and plants, as well as user constructed organisms (see Box 9.1).

Box 9.1 The ERICA Assessment Tool

The ERICA Assessment Tool is a free to download, computer software system for assessing the risks of ionizing radiation to terrestrial, freshwater and marine biota (https://erica-tool.com/). The system is based on the three tier ERICA Integrated Approach that was originally developed as part of the ERICA EURATOM project [29] (see also https://wiki.ceh.ac.uk/display/rpemain/ERICA).

The ERICA Tool includes various components, all of which are linked to internationally recognized programs and databases. These include

- Modelling transfer of radionuclides through the environment: links to IAEA Wildlife Transfer Database (WTD) and IAEA handbooks [30]; https://www.wildlifetransferdatabase.org/.
- Methodology for estimating dose rates to biota from internal and external distributions of radionuclides: ICRP biota DC software version 1.5.1 for the calculation of dose conversion coefficients (DCC) [31].
- Risk characterization in order to evaluate the significance of the dose rates received by organisms, including comparison with background radiation doses, screening values [32], Environmental Media Concentration Limits (EMCL) [33], derived consideration reference levels (DCRL) and biological effects (FREDERICA database, https://www.frederica-online.org/mainpage.asp).

The tool contains data on concentration ratios and DCC for all radionuclides in publication 107 [34], and in addition to a selection of pre-created reference

organisms, allows users to create their own assessment organism.

The ERICA tool has been updated since its original release, and the current version, ERICA Tool 2.0 (beta version released in November 2021—https://erica-tool.com/the-erica-assessment-tool-has-been-updated-to-version-2-0/) includes updates on concentration ratios, as well as new approaches for calculation of dose contribution from short-lived progeny, noble gases radon and thoron [35–37].

Internal and external exposures are determined from specific dose conversion factors (DCC) combined with using field measurements of concentration activities or default concentration ratios (CR). The CR represents the activity concentration of radionuclides in biota (fresh and dry weight in animals and plants, respectively) and the activity concentration in soil (dry weight, upper 10 cm), water, or air for a given radionuclide [38]. The tool also allows the calculated exposures to be compared to background radiation or screening values.

The calculation of external dose rates takes account of the occupancy of the organism (i.e., percentage of time spent in, on, or above soil, sediment, or water) and is determined by:

$$DR_{ext} = DCC_{ext} \cdot C_{media}$$

DR—dose rate (Gy/unit of time)
DCC—dose conversion coefficient
C_{media} (Bq/kg or Bq/L)

Internal doses

$$DR_{int} = DCC_{int} \cdot C_{organism}$$

DR—dose rate (Gy/unit of time)
DCC—dose conversion coefficient
$C_{organism}$ (Bq/kg)

There are several other simplifications to the approach, including assumptions on habitat ranges and feeding habits of biota [38]. CR are lacking for many organisms and radionuclides; however, the tool provides default CR based on available data and assumptions (e.g., similar taxonomy or chemical behavior to other organisms or radionuclides).

Uncertainties in dose estimates can be reduced if field measurements are available, but determination of internal concentrations of radionuclides can also be challenging, as organisms may be too small for direct radiochemical analyses, or it can be difficult to distinguish between radionuclides internalized in animal tissues, from those adsorbed to the body segment or cuticle. Efforts have been made to compare ERICA default CRs with field measurements at Chernobyl, showing a relatively good agreement between the CR values calculated for many organisms [39]. However, it was concluded that such similarity may have resulted from the broad range of estimated CR values available [40].

In soil, Beaugelin-Seiller [41] concluded that DCC values are highly dependent on factors such as the porosity and soil water content, the body size of the organisms within other factors. For ®-emitters, the difference in DCC values recorded reached a factor of 3, between dry and saturated soil conditions. The calculation of doses in organisms under exposures to NORM is also highly dependent on assumptions of equilibrium that must be made for several radionuclides from the ^{238}U decay series [42]. Usually a 100% equilibrium is assumed, although different equilibrium percentages are also accepted for radon, as it can escape to the atmosphere.

The positioning of organisms in the trophic chains and the composition of their diets may be determinant for the magnitude of exposures. In a coastal sand dune system, under a long-term contamination through atmospheric deposition and sea-to-land transfer of radionuclides at Sellafield nuclear reprocessing site (West Cumbria, England), Wood and collaborators [43] recorded high activity concentrations of ^{137}Cs, ^{238}Pu, $^{239+240}$Pu, and ^{241}Am in soil detritivorous (e.g., Collembola and Isopoda) when compared with predators (e.g., Coleoptera larvae). Within the same trophic level, these authors also found significant differences in the whole-body activity concentrations of different invertebrate groups. Size also influences the internal doses to organisms. Dose calculations for two benthic invertebrates, the larval midge *Chironomus tetans* and the amphipod *Hyalella azteca*, based on estimations from NORM activity concentrations in sediments impacted by uranium mining demonstrated that the smaller amphipod, received a greater dose of alpha irradiation. This reflected the high content of ingested radionuclides within the gastrointestinal tract and that as diameter of the gastrointestinal tube decreases, the assessment factor (AF) for ingested alpha-emitters increases, as more alpha-particles are expected to reach the tissues of the organisms [42]. Therefore, it was suggested that the contribution of sediment within the gastrointestinal tract for the calculation of internal doses must be considered, and not only the activity concentrations of radionuclides recorded in external sediments.

In the case of accidents, there is also a need to account for historical dose and radionuclide decay, since observed effects may be a legacy of high levels of exposure after the accident. These high exposures can also be a source of confounding factors, since the initial damage may lead to indirect ecosystem changes (such as the replacement of pine trees by less sensitive species) [44]. While much of the focus in studying the environmental impacts of radiation has been on the uncertainties in effects measurement, it is important to stress that there are also uncertainties in dosimetry.

9.3 Impacts of Ionizing Radiation on Non-human Biota

Following the discovery of X-rays by Wilhelm Roentgen in 1895 and of radioactivity by Henri Becquerel in 1896, studies on its effects started immediately. The detonation of the atomic bombs over Hiroshima and Nagasaki in 1945 raised the concern about the health impacts of radioactive contamination and the behavior of radionuclides in the environment [45]. Therefore, a great number of studies using a variety of plants and animals have been performed since then.

The first harmful effects caused by the exposure to ionizing radiation occur at the molecular and cellular level. If these effects are severe enough, they can impact tissues, organs, individual organisms, populations, and entire communities. However, even though an individual organism may suffer from severe damage at the molecular and cellular level, it does not necessarily mean that entire populations and communities will be affected [46]. It seems that individual organisms are able to sustain a certain level of effects before they are reflected at a population level [46]. However, when an effect is seen at the population level or at higher levels of organization (i.e., communities or ecosystems), it means that effects at individual organisms are expected to be occurring (Fig. 9.3) [45].

There can be two types of effects caused by ionizing radiation. They can be stochastic or non-stochastic (deterministic). Stochastic effects are effects that occur by chance and the higher the dose the higher the probability of its occurrence. However, the severity of those effects is not dependent on radiation dose. The main stochastic effects related to ionizing radiation exposure are cancer and genetic damage/alterations (i.e., mutations) [47]. For non-human biota, stochastic effects that occur at germinal cells will be the ones that will have a higher impact, as they will have a higher probability of being inherited and, therefore, of affecting the next generations, impacting populations and communities [47]. Deterministic effects depend on time of exposure, doses and type of radiation. They are adverse tissue reactions that result from the damage or killing of many cells in an organ or tissue. The severity of these effects increases with dose when radiation levels reach a threshold, below which harmful effects to tissues/organs do not occur. The deterministic effects that are most important at a population level are mortality (which affects density, age distribution, and death rate), fertility (birth rate) and fecundity (which affects birth rate, age distribution, size of the population) [45] (Fig. 9.3). As for other stressors (i.e., chemicals), exposure to ionizing radiation can be acute or chronic. Acute exposures are short-term exposures to relatively high doses of radiation that usually last minutes or hours. Chronic exposures are long-term exposures or lifetime exposures to usually low doses of ionizing radiation. Doses in acute exposures are often reported as total absorbed doses, whereas for chronic exposures doses are often reported as dose rates (i.e., mGy/day, Gy/year, or mGy/h) [46, 48]. For a given dose of ionizing radiation, acute

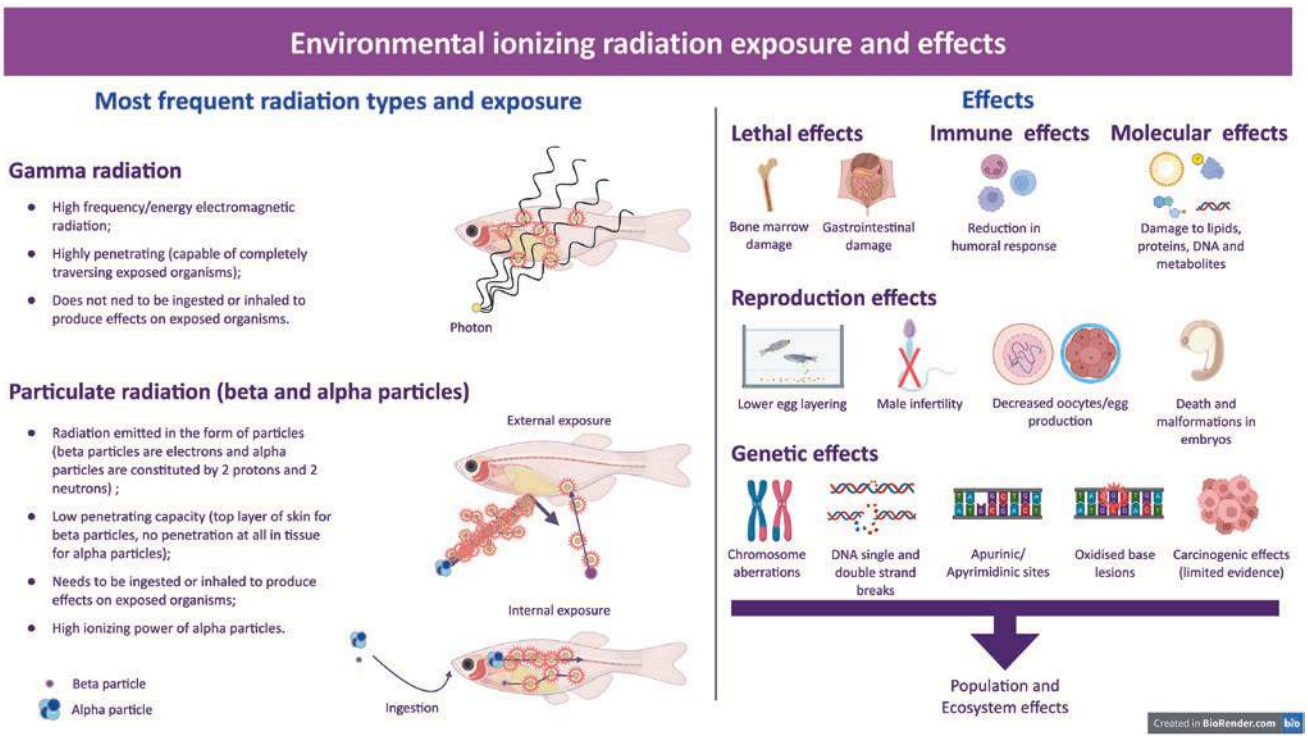

Fig. 9.3 Exposure and effects of different radiation types on organisms

exposure induces higher injury than chronic exposure [46]. The higher the dose the lower the ability of cells to correctly and rapidly repair the damage and also the lower the ability of healthy cells to divide and regenerate the damaged tissue [46]. Depending on the dose received by cells or organisms, several types of effects can occur, namely genetic damage, DNA lesions that can induce teratogenic effects (malformations) on embryos when occurring in germinal cells (i.e., gametes), cell transformation in somatic cells and cell death (Fig. 9.3). In some cases, DNA damage can be so severe that it becomes incompatible with the survival of the cell or of the entire organism. Depending on the kind of cells that are affected (germ cell or somatic cells), there can be different consequences. Severe damage (i.e., DNA double strand breaks, gross mutation like duplications, deletions, translocations, and chromosome gain or loss) will cause cell death potentially leading to the death of the organism or, for example, to its sterility if it occurs in germ cells (Fig. 9.3). If the damage is not enough to cause cell death, it can cause cell transformation and cancer in somatic cells or it can affect the fitness of the organisms and entire populations if it affects germ cells. Mutations can cause a reduction in the production of viable embryos or viable gametes and also, they can be passed and accumulated throughout generations reducing the population's fitness. Therefore, DNA alterations can have an important impact on fertility and fecundity and consequently in reproduction [46].

Also, there can be effects on the homeostasis of organisms (Fig. 9.3), namely depression of the immune system, alterations in normal metabolism, oxidative stress, and disturbances in the endocrine system [49]. The majority of the studies performed so far are focused on the determination of the acute effects of high doses of radiation, and only few studies are focused on chronic exposures to low doses of ionizing radiation.

The younger the organisms (namely fetuses and embryos) the more sensitive they are to the deleterious effects of radiation exposure. This is due to the higher sensitivity of cells that frequently undergo mitosis (which occurs frequently in young organisms for each tissue/organ as it is part of the growing process). Also, tissues/organs that have the ability to regenerate or that are constantly producing new cells like the hepatic tissue, the skin, the bone marrow, germinal cells, and gut lining are more sensitive to radiation (Fig. 9.3). The higher the cell division rate in an organism the more sensitive it will be to radiation's harmful effects.

Regarding the sensitivity of parameters like mortality and reproduction, in general the reproductive capacity is a more sensitive parameter to the effects of radiation exposure both for terrestrial and aquatic invertebrates and vertebrates, than life expectancy (mortality) [45]. Negative effects on reproduction rate can occur at less than 10% of the radiation dose required to induce direct mortality in mammals [45].

All organisms evolved in the presence of radiation, being cosmic radiation or natural radiation emitted by NORs present in the earth crust [50]. The studies performed so far, on the effects of ionizing radiation, showed that there is a considerable variation in the response of organisms from the same or different species, due to intra- and interspecies variability in sensitivity. In general, it is widely accepted that mammals are the most sensitive organisms, followed by birds, fish, and reptiles and that invertebrates and other less complex organisms have the highest radiation resistance (Fig. 9.4) [46, 50]. However, it has to be noted that most of the knowledge gathered so far comes from laboratory exposures of specific strains of these organisms and that results may differ significantly from what happens to their wild counterparts.

9.3.1 Basic Molecular Effects of Low and High Linear Energy Transfer (LET) Radiation

The majority of the existing studies on the effects of ionizing radiation in cells are focused on DNA as the main target, making it clear that there is a cause-effect relationship between DNA damage with cytotoxicity and mutagenicity associated with ionizing radiation exposure. However, the cascade of molecular effects that lead to the induction of biological effects in exposed organisms is complex and involves, firstly, the interaction of radiation with water molecules and structural and functional biological molecules inside the cells. This interaction will induce the formation of ions, radical species, and excited molecules that will move from the site where they were formed to other cell compartments, causing damage to other biological molecules. This will trigger several signaling cascades, activating cell responses that will change the normal metabolic state of the cell, including changes in gene expression, enzyme recruitment and activities, DNA methylation patterns, and other stress-induced signaling events. When DNA is damaged, the cell cycle is interrupted allowing for DNA integrity check. DNA can be damaged directly through direct ionization or indirectly through the attack of free radicals that are formed when radiation interacts with water molecules of the cell [51]. Given the high content of water in cells, IR interacts with water in a process called radiolysis, generating free radicals as H• or OH•, which trigger a cascade of events giving rise to other ROS as hydrogen peroxide and the superoxide anion [52] and references quoted. If not neutralized these products may diffuse within cells, as well as between cells, affecting other biomolecules such as DNA, proteins, and lipids, both in target and non-target cells (i.e., cells not directly irradiated) [53, 54]. Regarding DNA, ROS may oxidize bases or cause single and double strand breaks (SSB and DSB) [55]. Also, post-irradiation DNA lesions can be formed as a conse-

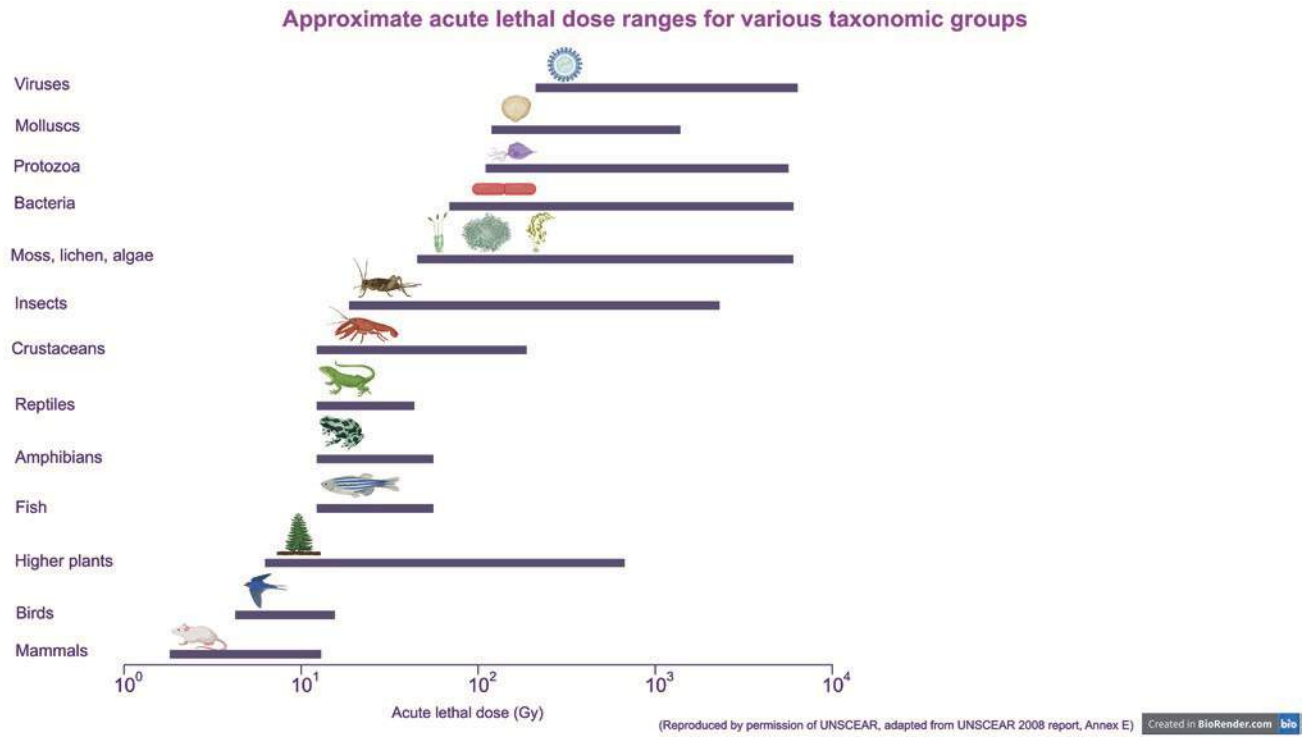

Fig. 9.4 Schematic representation of overall sensitivities of different taxa to acute gamma radiation exposure. (Reproduced with permission of UNSCEAR, adapted from UNSCEAR 2008 report, Annex E)

quence of the attempt of the cell to repair sugar and base residues, which can be converted to SSBs (Single Strand Breaks) and DSBs (Double Strand Breaks) [51]. If DNA is correctly repaired, the cell will continue its cycle normally, if not, the cell can undergo transformation as mutations and chromosome aberrations may occur or if the damage is too severe, programmed cell death (apoptosis) will occur. The repairability of the damage and the repair accuracy will depend on damage severity and complexity. Low LET (beta particles, gamma and X-rays) and high LET (alpha particles and neutrons) radiation exposure can cause several types of DNA damage that are usually repairable, like SSBs, abasic and apurinic and apyrimidinic sites and DSBs (Fig. 9.5). However, the fraction of irreparable DNA damage depends strongly on LET. High and low LET radiation exposure can cause complex DNA damage, but this type of damage is more frequently associated with high LET radiation. Complex DNA damage is composed by closely spaced DNA lesions that form clusters [51]. Clusters contain two or more DNA lesions of the same or different origins, close to each other and on opposite strands (bistranded lesions). These lesions can be DSBs or non-DSBs oxidative clustered DNA lesions like SSBs, oxidized base lesions, and oxidized apurinic/apyrimidinic sites (AP sites) [51] (Fig. 9.5). These clustered lesions have a high mutagenic and carcinogenic potential since they are considered repair-resistant or even unrepairable due to the relative inefficiency of DNA repair systems to process such closely spaced and complex lesions. As there are several DNA repair systems in the cells and each of them is specialized in the processing of specific lesions, when several types of lesions are closely spaced in the DNA molecule, the different repair systems cannot act properly, retarding the repair and often generating other lesions. High LET radiation is mostly associated with the generation of DSB's clustered DNA lesions and low LET radiation to non-DSB's oxidative clustered DNA lesions [51], but this is not completely clear and needs further studies. High LET radiation is also associated with increased frequency of chromosome aberrations, and also to a high frequency of unrejoined DSBs and consequently with a higher cell killing efficiency, as unrejoined DSBs are a cause of cell death.

9.3.2 Effects on Microorganisms

Microorganisms, including fungi, can be seen as good indicators of the ecosystem's "health." They include ubiquitous and taxonomically diverse microorganisms that play important key roles on diverse ecosystems' function. Specifically, with regard to radiation, microorganisms play a very important role in the health of these systems and in their cleaning and decontamination.

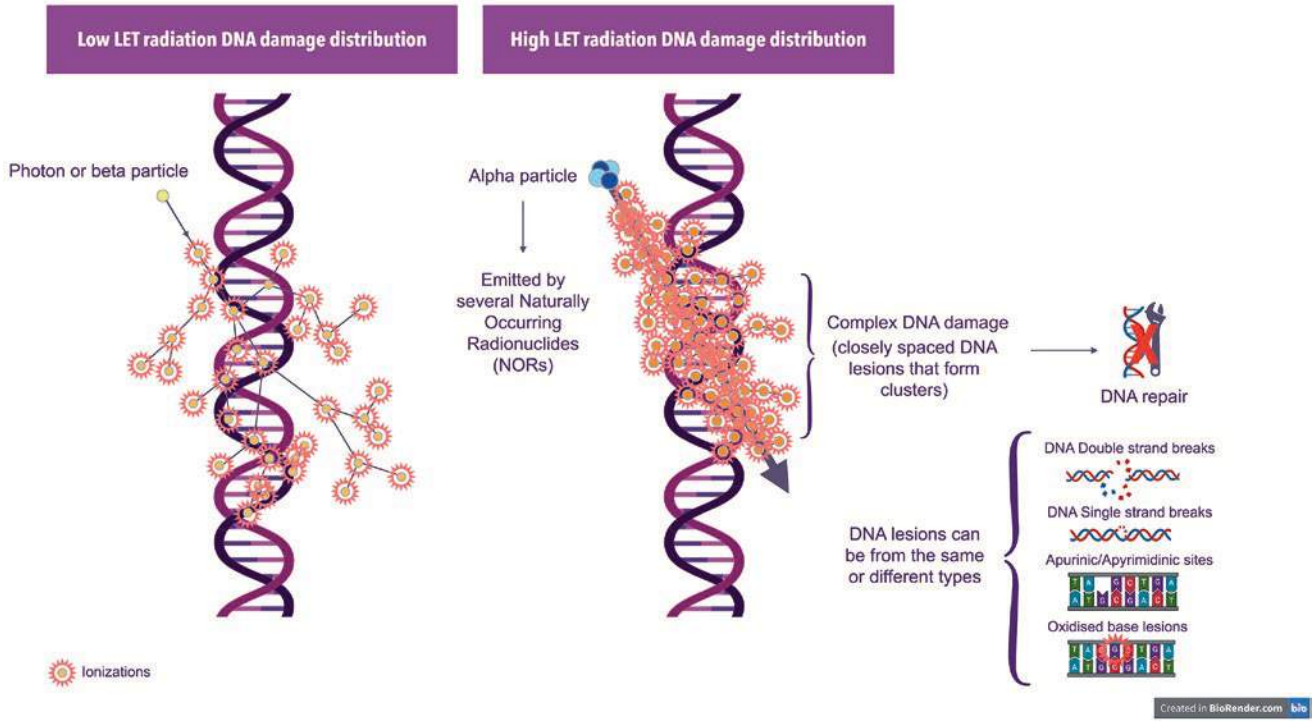

Fig. 9.5 High and low LET radiation DNA damage effects

9.3.2.1 An Overview on Microbial Radiobiology: Radioresistance and Radiotolerance

Microorganisms play a key role in the biogeochemical cycle of elements. In soils, they are important for organic matter turnover and maintenance of soil structure and fertility. As such, changes in the structure of microbial communities, by either metals or radionuclides, can have indirect effects on the above processes. Prokaryotes (bacteria and Archaea) have dominated a large part of the history of our planet, occupying virtually every "inhabitable" niche on earth. To be able to do that they have adapted to withstand large ranges in: (1) temperature, e.g., the hot temperatures found in hot springs and fumaroles, and the contrasting cold temperatures found on sea ice and polar regions, (2) pressure, e.g., deep sea, (3) salinity, e.g., hypersaline lakes, (4) pH, e.g., acid mine drainage sites, and (5) radiation, e.g., naturally occurring (deserts and high mountains, mining sites) and from nuclear contaminated sites [56]. Microorganisms that have adapted to such environments are referred to as extremophiles or polyextremophile (the latter being capable of withstanding different extreme conditions simultaneously), and these conditions are a requirement for their normal metabolic and biochemical operation. Most of these microorganisms belong to the domains Bacteria and Archaea although some fungal species have also been described. To survive these harsh conditions, extremophiles produce various primary and secondary metabolites, such as extremolytes, enzymes, and pigments [57]. Extremolytes, for example, are known to protect extremophiles cell structures and macromolecules from their harsh environments by forming protective water layers (e.g., ectoine), which is a co-solvent that shields proteins and cell membranes from UV light, heat, and dryness [58] around them or acting as chemical scavengers (e.g., carotenoids), protecting cells and their structures from UV radiation and oxidative stress [58]. Ultimately, the exceptional properties of these biomolecules find possible applications in various industrial sectors, in human healthcare, and well-being [59].

With regard to radioactively contaminated sites, microorganisms play an essential role on the mobility, toxicity, and distribution of radionuclides, through processes that include reduction, uptake, and accumulation by the cells, biosorption, and biomineralization with phosphates and carbonates [16].

Culture dependent and culture-independent approaches have shown the effects of long-term exposure to metals or radionuclides on individual species and on microbial communities. In addition, they have allowed those specific genes and cell functions mostly affected by radiation and metals to be identified, thus contributing to a better understanding of the molecular mechanisms behind microbial metal/radioresistance. Furthermore, the acquisition of genetic determinants by horizontal gene transfer contributes to shape microorganisms and microbial communities occupying these sites. More recently, refined metagenomic approaches focusing on prokaryotic communities have been employed and are expected to shed more light on the cells' strategies to overcome radiation stress to remain operational.

The following section addresses in more detail some of the mechanisms that contribute to the survival and maintenance of microorganisms in these environments. We will end by referring to the impact of more recent methodologies, such as metagenomics and other omics technologies, and their contribution to clarify aspects such as the impact of these contaminants on the microorganisms and communities that exist in these sites.

9.3.2.2 Mechanisms Underlying Microbial Radiation Resistance: Cell Damage and Repair

It has been reported that when radiosensitive microorganisms are subjected to multiple high IR exposures, their resistance increases [60]. This was recently demonstrated by experimental evolution, where populations of *Escherichia coli* very resistant to IR were generated in the laboratory, after 100 selection cycles, and to which the dose needed to kill 99% of the population increased from 750 Gy to about 3000 Gy [61]. Likewise, radioresistant species can become even more resistant with repeated exposure [62]. This "memory" adaptation is associated with smooth genetic alterations that affect DNA repair and metabolic functions. During this process of adaptation, other physiological characteristics of the microorganisms are profoundly affected as, for example, growth which is slowed down, because the microorganism must direct its energies to other processes, such as effectively repairing the damaged DNA.

The association between genome size and radiosensitivity between taxa has long been suggested. For instance, for the same chronic exposure to IR, fungi, for which genome sizes range between 12 and 20 Mbp, suffer more DSBs per unit time than bacteria with their smaller genomes (3–6 Mbp). However, this is not true for *Shewanella oneidensis* and *Deinococcus radiodurans* whose genomes are practically the same size, but while the former is killed after exposure to a radiation dose causing one DSB, the latter manages to recover from hundreds of DSBs. This is probably due to the fact that *D. radiodurans* has up to ten identical copies of its genome per cell and uses this genetic information to repair its DNA. In addition, there is also evidence for the interference of non-enzymatic antioxidants such as manganese complexes, which protect proteins from IR-induced oxidation, facilitating the maintenance of cell homeostasis and DNA repair. Although in many radioresistant bacteria and yeasts, the most common DNA DSB repair pathway is similar to homologous recombination (HR),[1] in fungi, non-homologous end joining (NHEJ)[2] is the preferred, as in other eukaryotes, despite being error-inducing. Melanin pigments also seem to be involved in protection against multiple stressors, including IR as it can act as an oxygen radical scavenger [62].

Radioresistant microbial extremophiles have developed strategies to survive and withstand dose rates that to the majority of organisms, including humans, would result in acute health effects [63]. It is believed that radioresistant microorganisms possess highly efficient processes to repair DNA damage. However, it has recently been demonstrated that the repair mechanisms and the proteins involved are common to those found in radiation sensitive microorganisms [64].

The genus *Deinococcus* is probably the most well studied and characterized and there is a great deal of information, to what its radioresistance is concerned. Metabolically active Deinococci vegetative cells can tolerate chronic radiation levels of more than 100 Gy/h, whereas other bacteria, Archaea, and fungi can be resistant to several kGy of acute IR. *D. radiodurans* exhibits resistance to acute IR up to 15 kGy, to 60 Gy/h of chronic radiation, and also to high levels of resistance to UV-C irradiation (100–295 nm), desiccation and oxidative stress. Thus, regarding the example of *Deinococcus radiodurans*, it can be argued that it efficiently and rapidly repairs DNA damage caused by IR. A number of genes have been identified whose expression is activated after irradiation, namely those encoding proteins associated with (1) efficient DNA repair, (2) protection against oxidation and (3) DNA supercoiling, which helps to maintain DNA integrity after irradiation [65]. More recently, it was demonstrated that in this organism, the adaptation to dryness and desiccation is at the basis of its radioresistance [64].

Nonetheless, it has been reported that *Deinococcus'* ability to repair DNA damage results from a selective pressure other than ionizing radiation, because there are no terrestrial environments subjected to the levels of radiation it tolerates. Still, the information gathered, albeit with some degree of uncertainty, has contributed to a better understanding of the mechanisms of radioresistance in other organisms, making this an excellent model organism to unravel these mechanisms [66].

Studies have shown that the DNA repair systems used by *D. radiodurans* are less complex than those of radiation sensitive bacteria, namely *Bacillus subtilis*, a spore-former species and *Escherichia coli*. Transcriptomics studies revealed that in response to γ-radiation, specific genes involved in damage response are activated (*ddr*A, *ddr*B, and *irr*E (*ppr*I)). PprI, for instance, regulates the expression of the recombi-

[1]Homologous recombination (HR) repair: while in eukaryotes the process occurs during meiosis and requires homologous DNA sequences, in bacteria HR is a major DNA repair mechanism that facilitates the incorporation of exogenous DNA.

[2]Non-homologous end joining (NHEJ) repair: in eukaryotic cells, DSB are repaired predominantly by this pathway. Broken double-stranded ends are repaired by direct ligation without the need for a homologous template.

nase recA and pprA, which is a protein involved in DNA ligation that is essential for the radiation resistance exhibited by *D. radiodurans*. Strains lacking pprI show impaired genome recovery [66]. Another important DNA repair system involves the synthesis of long and single-stranded overhangs, a process referred to as "Extended Synthesis-Dependent Strand Annealing" (ESDSA).[3] The process allows the reconstruction of a functional genome from the chromosome fragments produced by the exposure to radiation. Accordingly, the process is used by the RecFOR pathway to repair DNA double strand breaks. To support these observations, strains mutated in the genes involved in the RecFOR pathway are susceptible to γ-radiation [67].

Laboratory experiments with *Escherichia coli*, and other mesophilic bacteria, have shown that these may become resistant to the chronic exposure to IR just by adding Mn^{2+} and orthophosphate to its growth medium, which spontaneously form potent Mn-antioxidant complexes. Another important factor associated with radioresistance is cell density. For example, in *D. radiodurans* high cell concentrations seem to exert a protective effect against a radiation dose of 67 Gy/h [60]. Still, further and more complete studies are required until we know all the phenomena that contribute to the radioresistance exhibited by microorganisms. One thing is certain, it results from the interplay of several factors.

9.3.3 Multiomic Approaches Applied to the Study of Radioresistant Microorganisms

Undoubtedly, multi-omics approaches (genomics, transcriptomics, proteomics, and metabolomics) will shed light and will further contribute to our understanding of the mechanisms involved in microbial radioresistance and detoxification. In order to contribute to a better understanding of the mechanisms involved in uranium resistance/tolerance, a recent high-throughput proteogenomic study was applied to bacteria of the genus Microbacterium, isolated from Chernobyl U contaminated soils and from natural U rich soils. The approach allowed the identification of proteins involved in membrane transport (e.g., ABC transporters and efflux pumps), phosphate (e.g., phosphatases involved in biomineralization) and iron metabolism (e.g., siderophores), in addition to a large percentage of proteins of unknown function, which reveals the complexity of this mechanism [68]. Still, in another study carried out with a member of the genus Geobacter exposed to 100 μM U, proteins involved in DNA protection, in efflux pumps of the RND family and in oxidative stress responses (e.g., SOD and superoxide reductase), were also identified. Exploring these recent approaches will certainly allow us to gain knowledge that will contribute to clarify this complex intricate process. Furthermore, they will allow the selection for the best microorganism(s) with the potential to clean-up these contaminated sites by more eco-friendly processes. So far, in addition to the above study, genomic approaches proved useful in the identification of key genes and their respective products, encoded in the genomes of microorganisms resistant/tolerant to radionuclides/metals and which are, therefore, involved in the detoxification of this contaminants. With this approach, U-resistant bacteria of the genus Burkholderia and fungi of the genus Penicillium have been identified. Transcriptomics studies, by giving access to the analysis of gene expression and regulation, have gained relevance in the area of bioremediation. The information gathered from this comprehensive analysis, and also from future studies employing these methodologies, will surely shed light on the mechanisms of microbial resistance/tolerance to radionuclides/metals, while helping in the identification and selection of microorganisms that can be employed for bioremediation purposes of radionuclide/metals contaminated sites [69].

9.3.3.1 Contribution of Metagenomics Approaches to Understanding Microorganisms' Radioresistance

Unlike most laboratory studies, environmental exposure to radionuclides, (e.g., NORM sites and nuclear power plant accident sites), includes different radiation types (α and β, as well as γ) combined with many other stressors (e.g., temperature, nutrients, toxic chemicals like metals, etc.) over long periods. Thus, in polyextremophiles, the response to the adaptation/resistance should be broader and involve an intricate crosstalk between the different cellular processes [70].

Culture-independent field studies have shown that radionuclide contaminated environments host a wide diversity of bacteria and that radionuclides strongly impact community function and structure. Recently, a metagenomics approach carried out in surface soil samples from Chernobyl and Fukushima, over a gradient of radionuclide concentrations (^{137}Cs 1680—0.4 and ^{90}Sr 209.1—1.9 kBq/kg), revealed that samples clustered according to the level of radiological contamination, irrespective of the collection site [71]. Nonetheless, a lower microbiota diversity was found in Chernobyl samples, which was expected as Chernobyl soils are more contaminated. The following were reported to be the most common phyla: Proteobacteria, Acidobacteria and Actinobacteria. Furthermore, as expected, the functions encoded by the genes identified seem to be related with stress, metal and radiation tolerance. For instance, genes

[3]Extended Synthesis-Dependent Strand Annealing (ESDSA): a type of homologous recombination where the sequence around a DNA double-strand break (DSB) is replaced by a copy of a homologous DNA template, while the original configuration of the flanking regions is maintained.

involved in decontamination, DNA repair, information storage and processing, cellular processes and signaling and metabolism. A comprehensive listing of the function of the genes responsive to this type of contaminants has been recently reviewed by Hoyos-Hernandez and co-workers [71].

A similar approach was employed in a study performed by Theodorakopoulos and colleagues [72], in Chernobyl, which demonstrated the high diversity of bacteria in those contaminated sites. The same authors isolated cultivable bacteria of the genus Microbacterium that were employed in laboratory exposure studies, contributing to a better understanding of the mechanisms of tolerance to radionuclides/metals in those bacteria. The identified mechanisms involve biosorption, efflux and biomineralization [68].

Although further studies are required to better understand how radiological contamination exerts a selective pressure and how it shapes the structure of the microbial community, the sensitivity of the various organisms to radioactive contamination under environmental conditions generally exceeds the sensitivity of the same organisms to experimental laboratory exposures [62]. It is clear though that communities from soils of these contaminated sites have functional profiles that allow them to deal with this type of radiological and chemical contamination. Furthermore, these environments constitute a genetic pool from which the phylogenetic affiliation of cultivable and non-cultivable microorganisms can be determined, thus allowing the identification of new genes involved in the resistance to these contaminants, in addition to further contributing to clarify those mechanisms.

9.3.4 Effects on Plants

Plants are sessile organisms that cannot leave the surrounding environment if the ecological factors are not suitable for their growth. Thus, under unfavorable circumstances, plants have only the choice to perish or adapt to changing environments. The extreme physiological plasticity of plants allowed their diffusion in all ecosystems of the Earth and today we may have a comprehensive vision of the multitude of adaptations carried out by these organisms in diverse places. Indeed, plants such as other living organisms can adapt to cyclical natural disturbances over time, developing the capacity for endurance (resistance) and self-repair (resilience) in different ecosystems.

Laboratory and field studies showed that ionizing radiation may exert different effects on plant metabolism, growth and reproduction, depending on plant developmental stage at the time of exposure, plant physiological and morphological traits, as well as genetic characteristics [73, 74]. Moreover, depending on the dose or radiation type (low or high-LET), ionizing radiation induces detrimental outcomes at high doses, harmful consequences at intermediate levels and stimulatory effects at low doses.

In some cases, ionizing radiation exposure increases embryo lethality, induces dwarf architecture and modifies floral elements [74] and literature herein. Other studies indicated that some irradiated crops showed a taller architecture, increased yields and reproductive success and the ability to endure water shortage [75, 76]. As for many other organisms, within plant cells, the nucleus is considered the primary site of injury by ionizing radiation, which is responsible for random DNA damage and generates different kinds of mutations, such as deletions, base substitutions and chromosomal alteration [74, 77]. There is a direct relationship between the radiosensitivity of a plant and the average volume occupied by a chromosome in the cell nucleus. If the chromosome volume is large, the plant will be more sensitive and, therefore, the dose of ionizing radiation causing severe damages is less. Hence, polyploid species exhibit a minor sensitivity to radiation damage because gene redundancy protects polyploidy from the deleterious effect of mutations [78]. Besides plant cells, it is noteworthy that ionizing radiation may have different impacts on organs and tissues. Generally, more complex tissue architecture is less sensitive to damage; thus, young tissues are more vulnerable than old [73, 79]. At functional level, many studies have evidenced that radiation is dangerous for the photosynthetic apparatus. Generally, a decline of photosynthesis often implicates damage to photosystem II (PSII) and in particular to D1 protein, implicated in the right functioning of photosynthetic electron transport. Together with the impairment of PSII, a significant decrease of photosynthetic pigments and enzymes of the carbon assimilation cycle was also detected [73].

The majority of information on the impacts of radioactivity on plants comes from studies carried out by scientists after the nuclear disasters of Chernobyl (Ukraine) in 1986 and Fukushima (Japan) in 2011 [80].

Since 1986 the Chernobyl red forest has represented a living laboratory for biologists to study for long-lasting plant behavior in response to acute and chronic radioactive contamination. The name "Red Forest" comes from the ginger-brown color of the pine trees as a result of the high radiation levels immediately after the explosion of the nuclear plant. Studies continued in the post-accident period and enlarged the knowledge on the effects of acute and chronic radiation on plants [81]. Generally different plant species show diverse sensitivity to radiation, being shrubs more resilient than conifers. The sensitivity of the pine compared to other tree species was most apparent in the Chernobyl exclusion zone and trees showed dramatic alterations in the morphology of trunks and branches, indicating damage at meristems level [82]. Following the Fukushima accident, despite the much lower exposure levels, Japanese red pine (Pinus densiflora Siebold & Zucc.) and Japanese fir (Abies firma Siebold &

Zucc.) species showed developmental anomalies similar to those observed in Chernobyl [83, 84]. However, it is uncertain if the aberrations observed in Chernobyl are due to direct effects of radiation on the trees or multiple stresses due to biotic and other abiotic factors.

It is noteworthy that the quantity of radionuclides absorbed by plants depends on their phenological stage and growth status which, in turn, varies with the pedo-climatic conditions and cultivation factors. Once deposited on the vegetation and in particular on the leaf surface, the radioisotopes are absorbed through stomata and then transported to the other organs including fruits, thus possibly entering the food chain through edible leaves and fruits [85].

Today the Red Forest remains one of the most contaminated sites globally, and the surrounding forest area also represents an area of active research and scientific interest because of the return of wildlife in the exclusion zone. Here, the understory vegetation and deciduous (silver birch) trees have reappeared, but radioactive dust still remains stored in plant biomass and soil, for the very slow matter cycle.

The occurrence of revegetation has proven to be remarkably resilient to the intense radiation around the nuclear disaster zone. The exclusion zone is now dominated by grasslands and shrublands, while the most representative trees are Scots pine and silver birch Betula pendula [74] and literature herein.

Recent studies suggest that plants subjected to not-lethal doses of ionizing radiation show an increased resistance to other environmental stresses. Two strategies have been hypothesized, namely the production of ROS-mediated cell signaling and/or a boost of secondary metabolites [86].

The resilience to radiation in plants of the Chernobyl exclusion zone and from most contaminated sites at Fukushima is due to different mechanisms to protect the genetic material, improving the plant radioresistance [80]. Generally, plants are more radioresistant than animals because they present integrated adaptation mechanisms at genetic, anatomical, and physiological levels.

At genetic level, mechanisms include the regulation of expression of some genes encoding for radical scavenging and DNA-repair enzymes, homologous and non-homologous recombination, and the activation of scavengers. The higher stability induced by polyploidy, typical among plant kingdom, enhances radioresistance thanks to the presence of several copies of the same genes, which may serve as additional wild type copies in the case of radiation-induced injuries [87]. At the structural and metabolism level, plant cells present some traits such as thickened cell walls, cuticles, pubescence, increased deposition of phenolic compounds around membranes [88, 89]. At the anatomical level, complex tissue organization is associated with high resistance to mutagenic effects and the capability to adopt repair mechanisms.

Non-lethal doses of ionizing radiation may also induce hormesis improving plant defense against stressors, through the stimulation of the production of antioxidant enzymes (SOD, CAT, APX) or morpho-anatomical and photosynthetic changes that favor plant growth and metabolism [74, 90, 91].

Radiation-induced hormesis is still an unclear phenomenon in plants because it strongly depends on species intrinsic characteristics. At present, further studies are in progress to understand if it is a sort of compensation to irradiation damage or a transitory change, not enough to induce permanent injuries.

9.3.5 Effects on Invertebrates

Invertebrates have been considered a relevant group of organisms for studying the effects of ionizing radiation, both focusing on mechanisms of action and on previewing impacts in natural communities. Several reasons can be enumerated for choosing aquatic and terrestrial invertebrates as model organisms for IR studies, namely:

1. They have long served for providing insights into fundamental mechanisms of development, biomedical research (e.g., neurobiology, basic physiology, genetics, immunology, cancer biology), species diversification and genome evolution (e.g., *Drosophila melanogaster*, *Caenorhabditis elegans; planarians and crustaceans*) [92–95]; for studying the effects of ionizing radiation in neuronal function [96] and as model organisms in radiation hormesis studies [97].
2. Due to their important role in food webs, transferring carbon from producers to higher trophic levels (i.e., cladocerans, copepods), as detritivores contributing for degradation of organic matter through comminution (e.g., oligochaetes) and turnover of microbial communities (i.e., bacterivorous nematodes).
3. The role of some species as ecosystem engineers dynamically working the structure of soils and sediments (i.e. oligochaetes, polychaetes, ants) and the contribution for other soil and sediment functions.
4. The sensitivity and the ease of culture for some invertebrate species under laboratory conditions, as well as proliferation, producing a great number of individuals for testing in complex experimental designs and without tight regulatory requirements.

Aquatic invertebrates as benthic organisms and invertebrates living burrowed in soils or dwelling at the surface are among the group of organisms that may receive the highest radiation doses, since these environmental compartments are relevant environmental sinks of radionuclides. The mechanisms of action and the subsequent effects of ionizing radia-

tion in invertebrates have been addressed mainly since the seventies, with a limited number of species, through laboratorial exposures to gamma radiation of single species, frequently at high-dose rates, with few environmental relevance for chronic exposure scenarios [98]. Real conditions include exposures to industrial radionuclides in areas affected by nuclear accidents, nuclear power plants, or in nuclear test sites, as well as through exposures to natural occurring radionuclides (NORs), as those found in uranium mining areas. In the later areas, the effects of radionuclides, mainly alpha-emitters, cannot be distinguished from that of metals, also present at high levels in the affected environmental matrices. The same difficulty exists in areas of nuclear accidents as the Chernobyl exclusion zone, where the release of different artificial radionuclides has occurred, although data available for activity concentrations in biota are almost limited to ^{90}Sr, ^{137}Cs, and some few other radionuclides [38].

Invertebrates are among the least sensitive organisms to ionizing radiation [62, 99]. Cassidy and co-authors [100] suggested that the reasons for these differences in sensitivity, between organisms of different taxonomic groups, may include differences in DNA content, DNA repairing processes, and kinetics of cell cycle, within other aspects. The doses able to cause mortality or decrease life span are species dependent and frequently very high: as for example above 1000 Gy for *Caenorhabditis elegans* [101]. However, differences in sensitivity of different life stages were also reported (i.e., Johnson and Hartman [101]), with reproduction effects being seen at much lower doses (i.e., 4 mG/h for earthworm).

Ionizing radiation hormesis has been reported in a number of studies with invertebrates (dipterans, coleoptera), exposed to low doses from different sources (X-ray, gamma radiation, ^{137}Cs) (see review by Vaiserman et al. [97]). Reduced mortality rates and long-life spans were highly dependent on the exposure conditions [102], for example, life-extended effects were only observed in house flies (*Musca domestica*) reared in groups, and thus under high locomotor activity and exposed to a 10 Gy dose. Several hypotheses were then postulated and tested to unveil the factors responsible for modulating radiation hormesis, using *Drosophila melanogaster*, as model species, as for example: increased IR resistance, IR-induced sterility in females, apoptosis induction and changes in DNA repair genes and life-stage differential sensitivity were some of the proposals [97] and references quoted herein. X-ray irradiation of *D. melanogaster* eggs with 0.75 Gy, decreased the amount of DNA segments, by cleavage of S1 nuclease sensitive sites (<3 kb), resulting in a great DNA stability, changing the repair and/or transcription processes and thus affecting lifespan and the resistance of adults to IR [103]. Based on all the studies conducted, the radiation hormesis model proposes that the exposure to low doses of IR could induce several adaptive responses, which in turn will prevent environmental-induced health effects [97].

At the cellular level, oxidative stress and the activation of oxidative stress-response mechanisms have been reported as the major indirect consequences of exposures to IR of aquatic and terrestrial invertebrates. Won and Lee [104] observed a significant increase in the activation of several enzymes, as for example, superoxide dismutase (SOD), catalase (CAT), glutathione reductase (GR) and glutathione-S-transferase (GST) in the marine copepod *Paracyclopina nana*, exposed to gamma radiation doses equal or greater than 10 Gy (at a dose rate of 2 Gy/min). However, in this study, no data from additional molecular parameters, as those related with DNA damage or lipid peroxidation were provided, preventing us to infer if the activation of these enzymes was sufficient or not to prevent cellular damages. A dose-dependent increase in ROS was also recorded in another marine invertebrate species, as for example, the copepod *Tigriopus japonicus* and the rotifer *Brachionus koreanus*, for a range of concentrations from 50 to 200 Gy (irradiated at a dose rate of 2 Gy/min) [105, 106]. Concomitantly, the antioxidant response system was activated, and GST and GR activities were significantly increased for the copepod, while for the rotifer the same was recorded for the activity of GST. A cellular and lipid peroxidation (LPO)-related ROS was dose-dependent overproduction was also recorded in the freshwater cladoceran *Daphnia magna* after 8-day exposure to a dose rate of 100 mGy/h of gamma radiation. The overproduction of mitochondrial ROS was significantly enhanced at 40 and 100 mGy/h [1]. Dose rates of the same order of magnitude (10.7 and 42.9 mGy/h) were also able to cause lipid peroxidation in daphnids, after both 24 and 48 h of exposure. However, at the highest dose rate tested (106 mGy/h), the same effect was only registered after 48 h of exposure [55]. This observation, which was consistent with other studies (i.e., Fuller et al. [107]), gave rise to the hypothesis that ROS may also act as a signaling molecule, requiring a certain level within the cell to activate antioxidant defense mechanisms. Neutral lipid catabolism was also observed in the nematode *C. elegans* independently of the different doses and dose rates tested (7 and 52 mGy/h), and this effect was associated with a reduced longevity, as lipid homeostasis is responsible for endocrine signaling of longevity [108]. In fact, the up-regulation of different hormone receptors in daphnids was suggested as a signal of disruption of normal endocrine functions in response to IR exposure [1].

Regarding the interaction of ROS with proteins, Won and Lee [104] registered an upregulation of the *hsp* gene in the copepod *P. nana*, which was interpreted as being related with a possible response to protect key proteins (probably those involved in DNA repair signaling pathways) through the synthesis of chaperones.[4] In the cascade of events promoted by

[4]Chaperones—are proteins that assist other proteins folding.

ionizing radiation, Song and co-authors [1] recorded an enhanced expression of the *Ube2* gene in *D. magna*, involved in the degradation of proteins, suggesting the activation of a mechanism responsible for the elimination of proteins damaged by ROS. A highly efficient antioxidant protection system may not be able to protect DNA from damage but it can delay protein carbonylation.[5] Therefore, protecting cellular components involved in the repair of DNA double-strand breaks (DSB) was proposed as a main factor to explain the resistance of bdelloid rotifers to ionizing radiation [109].

DNA damage is a frequently reported effect in invertebrates exposed to IR from different sources. These damages can be either caused indirectly, mediated by ROS, or by direct deposition of radiation energy in DNA [1, 104]. In response to DNA damage, the expression of genes related with DNA repair systems (e.g., *p53*, RAD50, *Mre11* coding for the DSB repair protein, *Ku70*, *Ku80,* and *DNA-PK*) was recorded in different invertebrate species, frequently with a non-monotonic response, but always with a significant and differential expression at low and higher dose rates (at 4, 100, and 200 mG/h) [1, 55, 104, 106]. In summary, genes involved in nucleotide excision, base excision, homologous recombinant, and non-homologous recombination repair pathways have been found to be all involved in the response of cells to IR. At high IR dose/dose rates, ROS may also induce DNA methylation,[6] leading to the accumulation of damages, by silencing some genes. Song et al. [1] recorded an enhanced expression of DNA (cytosine-5)-methyltransferase 1 (Dnmt1), DNA cytosine-5 methyltransferase 3A2 (Dnmt3a2) genes, involved in maintenance of DNA methylation and in de novo DNA methylation, respectively, in *D. magna*.

The disruption of energy metabolism under the exposure to IR is another reported effect at the cellular level, once again in different invertebrate species [1, 55]. Direct interference with proteins of the electron transport chain, mitochondria ultrastructural changes caused by ROS and modulation of oxidative phosphorylation are within some of the mechanisms proposed, based on observations made in *D. magna* exposed to gamma radiation [55]. Genes encoding NADH dehydrogenase (*Nd*), succinate dehydrogenase subunit A (*SdhA*) of complex II, different cytochrome oxidase subunits (*COX1*, *COX2,* and *COX3*), cytochrome c oxidase copper chaperone (*COX17*) of complex IV and ATP synthase subunit mitochondrial (*sun*) of complex 4 were some of the genes involved in the electron transport chain found to be suppressed by gamma radiation [55]. At the end of the cascade of events triggered by gamma-radiation, the regulation of different apoptotic signaling pathways was observed in freshwater Cladocera, in parallel with DNA damage and regulation of repair mechanisms, cell cycle disruption and mitochondrial dysfunction [1, 55]. Although not significant, an increasing trend in apoptotic cell death with increasing dose rates of radiation was recorded in crustaceans, namely daphnids and in the Norway lobster (*Nephrops norvegicus)* cell cultures exposed to ^{60}Co gamma-radiation [110]. Apoptosis is a downstream event, to oxidative stress and DNA damage occurrences, that is activated to eliminate damaged cells in an ultimate effort for protecting organisms.

The effects of ionizing radiation at the population level are poorly documented and it has been demonstrated that equal levels of effect at similar individual endpoints (e.g., growth or reproduction) may have different impacts on population dynamics [111]. Furthermore, it is still difficult to link the results of biomarkers of oxidative stress and genotoxic damage with phenotypic consequences (changes in morphology, growth, reproductive output, and viability of offspring) [112]. Data available allowed a tentative hierarchization of individual endpoints based on their radiosensitivity: mutation > reproduction > morbidity and mortality [113]. One step forward, modeling population responses it was shown that they differed depending on the affected individual reproduction endpoint (juvenile or adult survival, delay in maturity, or reduction in fecundity) [114]. Hatching was shown to be the most sensitive endpoint to chronic exposures to gamma radiation for aquatic invertebrates (EDR_{10}[7] of 830 mGy/h for the polychaete worm *Neanthes arenaceodentata*) and fecundity for terrestrial invertebrates (EDR_{10} of 2600 mGy/h for *Porcellio scaber*). These species displayed similar EDR_{10} values for individual and population level endpoints (net reproduction rate). This was observed for the species that had a particularly sensitive individual endpoint.

The most concerning consequences of genotoxicity, that may support inferences about potential effects on natural populations, are those that affect the reproductive fitness of organisms. Reproduction has shown to be the most sensitive parameter in invertebrates (collembolans, worms, tardigrades, chironomids, and polychaetes) exposed to IR, when compared with survival or other endpoints at the individual level [109, 115–120]. It was suggested that the decrease in fecundity is not caused by the number of DNA DSB, but by the inactivation of the DNA repair systems [109]. In fact the incomparable ability of bdelloid rotifers to remain fertile, after extensive DNA damage, was attrib-

[5]Protein carbonylation—Reaction of hydroxyl radicals with side chains of certain aminoacids causing irreversible oxidation of proteins.

[6]DNA methylation—DNA methylation of eukaryotic cells is an epigenetic signaling mechanism characterized by the transfer of a methyl group onto the C5 position of the cytosine to form 5-methylcytosine, by DNA methyltransferase enzymes. DNA methylation regulates gene expression by recruiting proteins involved in gene repression or by inhibiting the binding of transcription factor(s) to DNA.

[7]EDR_{10}—effective dose rate inducing an effect of 10%.

uted to high efficiency of repair systems and to mechanisms that protect proteins of these repair systems [121]. These authors also associated the resistance to ionizing radiation of these organisms with their resistance to desiccation resulting from their adaptation to ephemeral ponds. Desiccation, similarly to radiation, increases ROS production and DNA breakage.

Harrison et al. [112, 122], also working with the polychaeta *N. arenaceodentata*, hypothesized that chromosomal aberrations caused by gamma radiation doses of 2.0 and 4.0 Gy were responsible for gametal cell death and subsequent decreases in brood sizes of this species. In opposition, under laboratory conditions, significant effects were recorded in sperm quality, but not on sperm numbers, of males of the crustacean *Echinogammarus marinus* chronically exposed to doses rates of 1 and 10 mGy/day provided by the betta emitter ^{32}P, for two weeks. Significant DNA damage was recorded in spermatozoa cells only at the highest dose rate. Furthermore, only a weak correlation was found between sperm quality parameters, fecundity, and embryo parameters analyzed [107]. Effects on ovary structure and oocyte development were also reported in the freshwater cladoceran *D. magna* in response to exposure to 1 and 100 mGy/h gamma radiation, dose rates.

Another possible cause of reproduction impairment in invertebrates, under exposure to ionizing radiation, may be related with the allocation of energy to molecular response mechanisms (e.g., activation of antioxidant defense system, DNA repair mechanisms) rather than to reproduction, with consequences on the fecundity of organisms [117].

An ED_{50}[8] for reproduction of 21.9 Gy, one order of magnitude lower than that recorded for growth (144 Gy) was found for the collembolan *Folsomia candida*, under exposure to ^{137}Cs gamma radiation at a constant dose rate of 8.3 Gy/min. Song et al. [1] also observed a non-monotonic reduction in the total number of offspring of the cladocera *D. magna*, concomitantly with no effects on survival, molting or ovulation frequency (at dose rates of 1 and 100 mGy/h). At the lowest dose, the effect on the cumulative reproduction output was mainly associated with an increase in the number of days needed to deliver four broods, while at the highest dose rate, the reproductive cycles were accelerated but the size of the broods was reduced. A similar observation was made by Parisot et al. [123] in the same organisms exposed to dose rates of 0.07–35.4 mGy/h of gamma-radiation, for 23 days. The same non-monotonic response was recorded *D. magna* representing 38 different genotypes collected in lakes located inside the Chernobyl exclusion zone with a range of dose rates between 0.1 and 181.2 mGy/h.

In a study conducted by Alonzo and collaborators [111], the freshwater species *D. magna* and the terrestrial earthworm *Eisenia fetida*, two species with different life history strategies (short lived/parthenogenic versus more long-term life/sexually reproducing hermaphrodite, respectively) were selected: (1) to model population growth in response to individual effects caused by the exposure to IR and (2) to investigate populations susceptibility using two different models to take into account single generation and multiple generation exposures. It was shown that in daphnids, the population growth was 1.5-fold more sensitive to changes in fecundity than in mortality. Daphnids population growth was also highly affected by delays in reproduction. Earthworms' population growth was more sensitive to delays in reproduction, while effects in fecundity and mortality have a similar and lower impact on populations. Despite the different life strategies, the intrinsic rates of population increase were equivalent for both species, because the greater reproductive rate of daphnids is compensated by a shorter life span relative to earthworms.

After disturbances of great magnitude, the recovery of natural populations of cladocera may rely on the banks of resting eggs in the sediments of lentic systems. These resting eggs if irradiated may have its performance compromised, affecting the dynamic of the natural populations. Zadereev et al. [124] observed that although doses up to 100 Gy (variable dose rates) did not affect the survival and hatching of resting eggs of *Moina macrocopa*, the size and the structure of populations initiated from resting eggs exposed to this highest dose of gamma-radiation, were affected. Therefore, subsequent effects on the dynamic of the populations of this cladocera may be expected in lakes with highly contaminated sediments.

Under a real scenario of radionuclides contamination, no correlation was found between different reproduction endpoints (proportion of breeding females, fecundity, brood mass, maternal body mass) of the crustacean *Asellus aquaticus*, sampled at different lakes in the Chernobyl affected area, with the gradient of dose rates between 0.064 and 27.1 mGy/h registered at these ecosystems [107]. Also, upscaling to populations and communities, Murphy et al. [125] focused on the diversity of littoral macroinvertebrates communities at eight natural lakes in *Belarus*, with a range of external dose rates from 0.066 to 10.22 mGy/h once again did not find any correlation between population endpoints (abundance, taxon richness, Shannon-Wiener diversity index, and the Berger-Parker dominance index) and the range of external dose rates registered in the sampled lakes. This study suggested that the IR dose rates recorded had no detectable effects on the littoral macroinvertebrate communities of these lakes.

Impacts on natural populations of invertebrates may be also caused by other mechanisms rather than those affecting gamete production, eggs viability, fecundity, or reproduction delays. For example, the exposure of fourth-instar nymphs to IR from a ^{137}Cs source up to doses of 12 Gy (at a dose rate of 0.25 Gy/min) has shown to affect the acous-

[8] ED_{50}—effective dose causing a 50% effect.

tic signaling of male crickets (*Acheta domesticus*) and subsequently their ability to find mates, due to morphological changes in their wings [126]. In fact, few is known about other direct and indirect effects that may affect the fitness individuals, its biotic relationships, and subsequently the dynamics of natural populations and communities at IR contaminated scenarios, rather than those effects identified based on commonly used biomarkers. The complexity of the biotic interactions, as well as the role of dominant abiotic factors determines the type and the impact of the indirect effects on ecosystems, whose responses can be unpredictable [98]. In a birch forest in South Urals, the contamination of litter with ^{90}Sr (doses reaching up 70 Gy) compromised the development of pupae of tachinid flies (Tachinid sp.). This accounted for an increased survival of the host caterpillars of the gypsy moth (*Lymantria dispar dispar* L.) with increasing IR levels [127] in Geras'kin [98]. Møller et al. [128] also linked the reduction in the set of fruits produced by trees and bushes, at the Chernobyl exclusion zone with the local reduction of pollinator insects. The role of other biotic factors in the radiosensitivity of invertebrates also needs to be investigated, as it may be relevant under specific environmental or industrial scenarios. It was shown that the ability of marine mussels (*Mytilus galloprovincialis*) to respond to genotoxic induced effects by tritiated water, released by cooling operations of nuclear power plants, was limited by enhanced temperatures [129].

Invertebrates also have a key role in several ecosystem functions, as, for example, the degradation of wood, organic matter, and nutrients recycling. Mousseau et al. [130] conducted a study in forest areas within the Chernobyl exclusion zone, at different distances of the nuclear plant and with levels of background radiation differing by several orders of magnitude (range 0.09–240.25 mSv/h). A significant effect of background radiation in the mass loss of litter bags buried in the surface of the forest soils was registered. The mass loss of litter bags from the sites with high levels of background IR was 40% lower than that recorded at the sites with lower levels of radiation. However, no significant influence of the mesh size of litter bags was found, suggesting that decrease in the decomposition of litter at that site was not only caused by impacts on soil invertebrates' communities, but also on soil microbiome. Soil invertebrates' assemblages from pit falls and wood slices from the same area showed that the abundance of taxonomic groups displayed a different relationship with background radiation and with wood contamination with radionuclides, being positively, negatively, or not affected at all [131, 132]. This was consistent with a previous observation of a general loss of diversity in sub-surface and flying invertebrates with increasing concentration activities of ^{90}Sr and ^{137}Cs in the litter of forest sites within the Chernobyl exclusion zone [133], as well as by the apparent decrease in the feeding activity of these organisms measured by the bait-lamina test.[9] However, such changes were not followed by changes in total biomass of organisms. These results suggest that chronic environmental exposures to IR may exert their effects on natural communities, through structure and functional diversity simplification, with possible impacts on ecosystem's functions.

In a first attempt to estimate risk limits for chronic g-radiation exposures, predicted no effect dose rates (PNEDR) of 10 mGy/h (0.24 mGy/day) for freshwater ecosystems and of 67 mGy/h (1.61 mGy/day) for terrestrial ecosystems were obtained, using assessment factors and species sensitivity distribution methods, respectively. The estimated values were found to be highly protective as they were about ×50 to ×100 times higher than the upper bound of the range of natural background concentrations and of the lower dose rates causing effects at contaminated sites [134]. Later, and by applying an assessment factor (AF) of 3 to the HDR_5[10] estimated for invertebrates, a PNEDR of 170 mGy/h for IR was obtained. However, and considering that no sufficient data was available for applying probabilistic methods to estimate PNEDR for specific groups of organisms or for environmental compartments, Garnier-Laplace et al. [135] derived a generic HDR_5 from a species sensitivity distribution using data from controlled laboratorial chronic exposures to low dose rates of gamma-radiation, and applied an AF of 5, obtaining a PNEDR of 1.5 mG/h which was considered to be protective for the conditions found at Chernobyl exclusion zone.

9.3.6 Effects on Vertebrates

9.3.6.1 Terrestrial Organisms

Mammals

Among all the vertebrates, mammals are organisms on which the effects of radiation exposure were most extensively studied in radiobiological experiments. Negative effects on these organisms, due to radiation exposure at high doses (i.e., 10–50 Gy), are primarily due to effects at the hematopoietic system and the gastro-intestinal mucosa [45, 46]. The time needed for death to occur varies widely within species. The dose of radiation needed to cause lethality, due to gastrointestinal syndrome, to 50% of the exposed organisms (LD_{50}) is approximately as follows for dog—8 Gy, mouse—12 Gy, rat—11 Gy, and rhesus monkey—9 Gy [46]. However, these values were estimated for particular species of these organisms, so there can be wide variations for other species. These

[9] Bait-lamina test—a field test performed with baited lamina which are buried in the soil to measure the feeding activity of edaphic fauna (for more details, please see [181, 182]; ISO 18311:2016).

[10] HDR_5—the hazardous dose rate for 5% of the species.

variations are normally related with specific intestinal morphologies, which are related to diet (i.e., herbivores, carnivores, and omnivores). Regarding bone marrow damage, the weight of the animals receiving the dose appears to have a significant role in the bone marrow radioresistance, being weight inversely proportional to radiation sensitivity, as LD_{50} values are greater for smaller mammals (6–10 Gy approximately) than for larger ones (1.2–3.9 Gy). A reduction in life span is also related to the type of radiation to which animals are exposed, being high LET radiation more effective than low LET radiation. Also, acute exposures are substantially more effective by a factor of 7 in causing mortality than chronic exposures [46]. Significant life span shortening occurred in dogs and mice exposed to low LET radiation (gamma radiation) at dose rates between 100 and 1000 mGy/h and the same happened for mice exposed to neutrons (high LET radiation) at the same dose rates [136]. In general, a significant reduction in life span of several mammal species was observed at dose rates higher than 1000 mGy/h [50, 136, 137]. Chronic exposures of less than 100 mGy/h have a low probability of inducing significant effects on most terrestrial organisms [45, 46, 136]. Particularly, a dose rate of less than 40 mGy/h has a low probability of inducing effects on the fertility, fecundity, and the production of viable offspring of a mammalian population [45]. This is true for low LET radiation, however for high LET radiation, this dose rate value is lower, as this type of radiation has a much higher relative biological effectiveness (RBE) [45]. An experiment performed in mice irradiated with neutrons, at dose rates lower than 100 mGy/h for at least 475 days, led to a significant increase of mortality in mice in comparison with the control [136].

Reproduction is a more radiosensitive parameter than mortality, and effects of radiation may appear at radiation levels that apparently do not induce other observable responses. The magnitude of the effects depended also on the developmental stage in which the animal was irradiated [136]. A good example are mice, as the LD_{50} occurs at a radiation dose approximately between 6 and 10 Gy; however, at a radiation dose of 0.08 Gy, the production of oocytes was reduced to 50% in newborn mice (the most radiosensitive stage in mice) [45, 46]. However, this does not necessarily mean that there will be a decline in fecundity, since mice produce much more oocytes than the amount effectively used for reproduction, but there could be a reduction in the offspring [46]. In adult males, fertility is temporarily impaired after a 10 Gy exposure; however, in young mice (3–5 days old), it can cause permanent sterility. Mice in the second week after birth are also especially sensitive to the detrimental effects of radiation on reproduction [136]. The differences between males and females are mostly a consequence of the differences in the gametogenesis process. There are also differences between species, being mice one of the least radioresistant. Chronic irradiation affects mainly the time needed for oogonial cell division and the size of stem cell pool [46]. In males, the spermatogenic process is maintained, although at lower levels than unexposed organisms [46].

The developing embryo is particularly sensitive to radiation, due to the high number of cells proliferating, reducing fecundity and postnatal survival, potentially influencing population size [46]. Acute radiation exposure, before the implantation of the embryo, causes its early death and can also cause post implantation and postnatal death [46]. This has a good correlation with the occurrence of DNA damage in the form of chromosome aberrations in the blastomeres (cells that result from the cleavage during the early development of the embryo) [46]. Radiosensitivity is strongly influenced by cell cycle stages and mitotic cycle in the very early developmental stages [46]. During organogenesis, the most typical response to acute radiation is the occurrence of malformations (teratogenic effects), which can occur during embryonic and fetal growth and may or may not be fatal. The occurrence of teratogenic effects in a particular organ is related to a high level of cell proliferation in the precursor tissue [46]. Although this has been observed for the several species studied (mouse, hamster, cattle, pig, monkey rabbit, etc.), the responses to specific radiation doses will depend on the species and on its developmental stage at the time of exposure [46]. There are not many studies on the effects of chronic radiation exposure during organogenesis, however a study performed on mice showed doses of 0.01 Gy/day in pregnant mice 6–9 days after conception induce a significant impairment of the offspring's learning ability [46]. Also, dose rates of 420 mGy/h reduced neonatal brain weight, with unknown effect at the functional and behavioral levels [45].

A direct relationship between DNA damage and radiation dose is expected at high doses of radiation; however below 100 mGy, it is not clear. In reindeer, a tenfold increase in the number of chromosome aberrations was observed at dose rates between 100 and 1000 mGy/h [136]. For rodent species acutely exposed to low LET radiation, mutations in the form of reciprocal translocations (exchange of DNA between homologous chromosomes) occur in stem cell spermatogonia when organisms are exposed to between 0.01 and 0.03 Gy at total doses from 3 Gy [46]. High LET radiation exposure (in the form of alpha particles emitted by ^{239}Pu), delivered at a dose rate of 36 mGy/h significantly increased the occurrence of translocations and acentric fragments (chromosome fragments without a centromere) in spermatogonia and spermatocytes, respectively [46]. In primates, the dose interval is 0.01–0.078 Gy at doses from 1 Gy [46]. Translocations, ring chromosomes (aberrant chromosomes whose ends were broken and then fused together to form a ring) and dicentric chromosomes (the result of two broken chromosomes that fused together) are used for radiation dosimetry in human and non-human biota for a long time, as their frequency

increases with radiation dose [138]. In rodents, this is more easily seen at total absorbed doses higher than 0.5 Gy, suggesting that their use as a biomarker of radiation exposure is more effective at high dose exposure than at low doses (below 100 mGy). Regarding carcinogenicity, there is a wide variation in the sensitivity for tumor formation among tissues and species. The induction of cancer, even at high radiation exposure doses (>100 mGy) will also vary according to the age of exposure. Dogs exposed to doses higher than 7 Gy showed soft tissue cancers when exposed in utero but not when exposed as young adults [46]. In rodent species, there were limited carcinogenic effects on animals that were exposed to doses between 0.1 and 1 Gy [138].

Birds

The effects of radiation exposure in birds are apparently similar to the ones observed in small mammals [45]. The LD_{50} for wild birds is in the same range as small mammals (5–12 Gy). For poultry, the LD_{50} determined experimentally for mortality is of 7–11 Gy in 3–4-day-old individuals when irradiation lasts for less than 1 h and of 12–20 Gy when irradiated for 24 h. Egg production is affected in white leghorn chicken at a total absorbed dose of 4–8 Gy and at higher doses, effects are more severe and long lasting [45]. A limited number of experiments performed in artificially incubated chicken embryos showed a LD_{50} of 12–13 Gy, which apparently indicates a higher radioresistance than adults [46]. In white leghorn chickens, eggs hatchability is affected at a total absorbed dose of 8 Gy, but the progeny is unaffected [48]. The International Commission on Radiation Protection also reported dose ranges for which long-term effects on developing embryos were reported (100–1000 mGy/day), reduced reproductive success (1–10 mGy/day) and increased morbidity (10–100 mGy/day) [139]. Recently, it was reported a decrease in species abundance at a dose range of (from 0.3 to 97 μGy/h) in the Fukushima exclusion zone, which is consistent with the dose ranges reported for increased morbidity and decreased reproductive success [140]. The existing knowledge on DNA damage/alterations on birds exposed to ionizing radiation results from the evaluation of effects of radioactive environmental contamination resulting from the Fukushima and Chernobyl accidents [141].

Reptiles and Amphibians

The information gathered so far for reptiles and amphibians suggest that their radiosensitivity is similar to that of mammals and birds. The LD_{50} values recorded for frogs, salamanders, turtles and snakes vary between 2 and 24 Gy [46]. The main cause of death identified was damage to the hematopoietic system [46]. In two separate experiments performed on lizards, two very different LD_{50} doses ranges were obtained (10–12 and 17–22 Gy). The possible reasons for this marked difference are associated with the fact that these values may vary according to radiation type and quality, the dose rate to which the organisms were exposed and their maintenance conditions at the laboratory [46]. An acute exposure to 50 Gy caused temporary sterility in males, but recovery was well in process after 48 days post irradiation and irradiation of gonads in males and females to an absorbed dose of 4.5 Gy leads to a substantial decrease in the production of offspring [46].

Regarding amphibians, different life stages showed different radiosensitivities. For adult toads, the LD_{50} value is of 24 Gy, for juveniles it is of 10 Gy and for tadpoles it is of 17 Gy [46, 139]. The life stage more sensitive to radiation exposure was the fertilized egg with an $LD_{50/40}$ (LD_{50} after 40 days of exposure) of 0.6 Gy [33]. There is evidence that the exposure of male toads to 3–20 Gy caused a reduced survival and increased induction of abnormalities to the offspring [46, 139]. Although these LD_{50} values for amphibians seem slightly higher than the ones recorded for mammals, time after exposure optimal for the recording of LD_{50} values seem to be an important factor [33]. Reptiles and amphibians are poikilothermic organisms; therefore, their metabolism is quite variable and different from mammals and birds [33]. A study performed on 4 species of amphibians showed that if the assay period was extended a decrease in the LD_{50} to values that ranged between 0.8 and 7 Gy would be recorded [33].

Chronic irradiation exposure (5.5 years duration) of common side blotched lizard, western whiptail, long nosed leopard lizard and long nosed lizard showed that at ranges from 285 to 570 μGy/h, radiation exposure caused lack of reproduction, female ovaries regression and some degree of male sterilization [46].

Regarding the induction of DNA damage, it was observed by Ulsh and co-authors [142] that the exposure of turtles from the species *Trachemys scripta* to 0–8 Gy ^{137}Cs gamma radiation, given at a dose rate of 0.55 Gy/h induced the occurrence of significant levels of chromosome translocations in lymphocytes. Studies on the induction of DNA alterations in amphibians and reptiles have been performed in Fukushima and Chernobyl exclusion zones, as well as in areas contaminated with NORM.

Aquatic Vertebrates

Among non-mammalian aquatic organisms, fish are the most sensitive to the exposure to ionizing radiation [45, 46]. Although these organisms are also poikilothermic (as amphibians and reptiles), and therefore, apparently more radioresistant than mammals, there is a substantial overlap in radiosensitivities [46]. Until now, there is no substantial data on effects of ionizing radiation on marine mammals, however, there is no reason to believe that their radiosensitivity is substantially different from that of terrestrial mammals. Data

on acute exposures exist mainly for bony and freshwater fishes, with a small number of studies on cartilaginous and marine and anadromous species.

The LD_{50} determined for six marine species after 40–50 days of exposure was of 9–23 Gy [46, 139]. Fish developing embryos are, however, more sensitive than adults, as for silver salmon their LD_{50} after 50 days of exposure is of 0.30 Gy at hatching and 0.16 Gy at a post-hatching larval stage of 90 days [46]. A study performed on sharks (*Triakis scyllium* and *Heterodontus japonicus*) exposed to 20 Gy showed that mortality occurred after 20 days of exposure, due to hematopoietic and gastrointestinal damage [33]. This suggests that the radiosensitivity of cartilaginous fish may be similar to that of teleost fish.

Regarding reproduction, an acute exposure to 10 Gy reduced the total number of germ cells at all developmental stages of medaka fish (*Oryzias latipes*) [46]. A similar radiosensitivity was found in rainbow trout, with an induction of more than 50% sterility in organisms exposed late in embryonic development [46]. This leads to the conclusion that as in mammals, the newly hatched fry and the primordial gonads in fish embryos are more sensitive to the acute radiation exposure than in adult fish [46]. Irradiation of mature medaka fish at acute doses of 5–10 Gy only induced temporary sterility, being completely recovered at 60 days after irradiation [46]. On the other hand, chronic irradiation of males from the fish species *Ameca splendens* for 5.4 days at a dose rate from ^{137}Cs gamma rays of 7300 mGy/h disrupted spermatogenesis and render the animals sterile at an accumulated dose of 9.7 Gy (8 weeks of exposure) [46]. There was 60–70% recovery, 236 days after irradiation [46]. Another freshwater fish, the guppy (*Poecilia reticulata*), when exposed to gamma dose rates from 1700 to 13,000 mGy/h showed a significant reduction in fecundity, but no negative effects on survival and sex ratio, as well as no significant higher incidence of abnormalities in the offspring were observed [33, 136]. The marine fishes *Pleuronectes platessa* and the eelpout (*Zoarces viviparus*) exposed to 240 and 2000 mGy/h gamma radiation, respectively, showed a significant reduction of testes when compared to the control [136].

There are some findings also on the effects of the exposure to ionizing radiation in the immune system of these organisms. A significant reduction in the humoral immune response in the rainbow trout (*Oncorhynchus mykiss*) exposed to tritium beta-particles for 20 days at a dose rate as low as 8.3–83 mGy/h during embryogenesis was evidenced through a reduction in antibody titer following a specific challenge [46].

Regarding DNA damage there are very few studies on which some conclusion can be taken on this matter. On a study on medaka fish, at larval stages, there was a significant induction of vertebral anomalies after irradiation at dose rates from ^{137}Cs gamma rays higher than 18,000 mGy/h and also to beta particles from ^{3}H at dose rates higher than 35,000 mGy/h [46]. There is also a report on the occurrence of minor morphological abnormalities in the operculum of salmons exposed to a gamma radiation dose rate of 200 mGy/h that may affect latter survival [136].

9.4 The Particular Case of NORM Contamination

Anthropogenic activities of concern related to the environmental release of natural uranium isotopes (mainly ^{238}U and ^{235}U) and other radionuclides from their decay chains, namely ^{226}Ra and ^{223}Ra, ^{222}Rn, and ^{210}Po, include mainly the production of phosphate fertilizers, uranium mining and milling and the incorrect disposal of tailings, uranium conversion and enrichment, the production of uranium fuel, production of coal, oil and gas, extraction of rare earths, extraction and purification of water, extraction of minerals for building materials and the generation of geothermal energy [3, 143]. All of these industrial activities increase the concentration of these elements in all environmental matrices, thereby posing a risk to human and non-human biota as many of them have not been regulated for NORM release [3, 143]. Another important issue is the fact that the contaminated areas that result from these anthropogenic activities do not only present high levels of certain natural radionuclides, like ^{226}Ra, ^{222}Rn, and ^{210}Po but also other important stressors, namely metals like manganese, zinc, iron, aluminum, etc. [143]. These are usually multiple exposure scenarios, which contain several kinds of contaminants that may act synergistically and increase the risk of the occurrence of biological effects on human and non-human biota and even of modifying the susceptibility of cells/organisms to the biological effects of ionizing radiation exposure [144].

9.4.1 Chronic Exposure and Interaction with Uranium and Metals

The accumulation of small amounts of radionuclides and metal over long periods is translated in chronic exposure to radiation. Naturally contaminated sites harbor a diversity of microbial species that become resistant or tolerant to these contaminants by bioaccumulating radionuclides and metals either by biosorption to their cell surfaces and biomolecules or by internalization into their cells. Briefly, under environmental conditions, chronic IR effects are very complex, particularly when compared to those from laboratory exposures because (1) radiation emitted by the different radionuclides present has different biological effects, (2) radiation from the

same location is absorbed differently by different microorganisms, (3) abiotic factors (e.g., temperature, nutrients, pH, other stressors) are present and can interfere with radiation, (4) cooperation/interaction between microbial communities, including diversity and/or abundance can all be modulated by radiation [62]. Regarding uranium, probably the most well studied radionuclide, and for which a lot of information is available, interaction with microbial cells involving solubility by biomineralization (bioprecipitation) depends on all the above factors and also on the presence of affinity groups generated by microorganisms' cell metabolism, like hydroxides, phosphates, and carbonates. Uranium toxicity is both chemical and radiological. In the environment, uranium exists in its reduced insoluble form U(IV), and/or the oxidized form U(VI), which is soluble and toxic. Microorganisms interact with uranium by changing its redox state, aerobically, through oxidation (biolixiviation), or anaerobically by reduction. In order to do that, microorganisms need to be highly tolerant to uranium and to radiation. Other processes of microbial interaction with metals, involve biosorption, where contaminants passively concentrate through binding to cell structure constituents (e.g., lipopolysaccharides, teichoic acids, peptidoglycan), and biomineralization, which leads to the formation of biominerals using organic phosphate sources and phosphatases.

Unless disturbance occurs, NORM sites have a characteristic microbiome, which is specific for a given site, but may share common microbial genera and species, regardless of location and/or chemical contamination. It includes nitrate-reducing bacteria that tolerate acidic and low-nutrient conditions, while being highly resistant to metals. Members of the Proteobacteria (Alpha-, Beta-, Delta- and Gamma- proteobacteria), Acidobacteria, Actinobacteria, Bacteroidetes, and Firmicutes are generally associated with uranium transformation and are therefore found in these environments. Most represented bacterial genus include Geobacter, Thiobacillus, Arthrobacter, Bacillus, Actinobacteria, Desulfovibrio, and Microbacterium. Most of the studies are focused on bacteria and bacterial communities. Although little information exists regarding fungi, they are particularly resistant to radiation and thus play a role in the process of detoxification of radionuclides. For instance, an isolate of the genus Paecilomyces, was found to detoxify U(VI) through bioprecipitation of the metal, and the reduction was promoted by phosphate. Also, the yeast *S. cerevisiae* was able to reduce U(VI) toxicity by biomineralization [60].

Accordingly, the survival, abundance, and maintenance of a given species or community diversity depend on its adaptability to the existing conditions. Furthermore, several studies suggest that in those radionuclide-rich natural sites, resistance to high levels of chronic IR may occur among taxa that tolerate a wide range of environmental conditions and, therefore, have an advantage over other more sensitive species [62].

9.4.2 Effects of NORM and Metals on Eukaryotes

9.4.2.1 Invertebrates

There have been some studies in aquatic organisms, namely in *Daphnia magna, Daphnia longispina,* and *Moinodaphnia macleayi* at NORM sites [145, 146]. When testing several percentages of a uranium mine effluent containing metals and radionuclides from ^{238}U and ^{235}U decay chains, the Antunes et al. [145] study recorded an EC_{50}[11] for daphnids immobilization at 50.4% for *D. magna* and at 28.4% for *D. longispina*, showing that *D. magna* was less sensitive than *D. longispina*. However, regarding fertility, *D. magna* was more sensitive than *D. longispina*, as this last species did not show significant effects in the offspring produced at effluent concentrations lower than 30.38%. Regarding *M. macleayi*, when a natural population of these organisms, living adjacent to a uranium mine in Australia, was challenged with a concentration of uranium ranging from 0 to 700 μg/L, it was shown that this population comparing to other populations tested, was the one that presented the highest sensitivity as it evidenced the lowest NOECs and LOECs.[12] It was shown that although this population lived in a water containing already considerable amounts of uranium, there was no tolerance to higher levels of uranium, when compared to the other tested populations. This probably shows that it was an already very stressed population that suffered "genetic erosion" [147] and because of that, it had lower capacity to deal with additional stresses, such as a single high dose of uranium.

When *D. magna* was exposed to uranium and to a uranium mine effluent [148, 149], significant genotoxic effects (DNA strand breaks) were detected in neonates and <5 days old daphnids after exposure to 55.3 μg/L of uranium and 2% of a uranium mine effluent. Moreover, in this same study, bystander effects, in the form of DNA damage, were detected in unexposed organisms when placed in contact with organisms directly exposed to uranium and to uranium mine effluent. In another paper [149], published by the same authors, on a transgenerational study performed on *D. magna* exposed to the same concentrations of uranium and uranium mine effluent as the study previously referred, it was observed that DNA damage was transmitted only to the first broods of the exposed organisms. By the third brood, DNA damage was no longer detected. This study showed that although short-term exposure to low concentrations of uranium and uranium

[11] EC_{50} is the concentration of a substance in water causing death to 50% of the tested population.

[12] LOEC is the lowest concentration where an effect has been observed in chronic or acute ecotoxicity studies. NOEC is the highest concentration at which there is no statistically significant difference from the control condition in an acute or chronic ecotoxicity study.

mine effluent induces DNA damage to exposed organisms, it seems that it was not enough to significantly affect life history traits of *D. magna* populations in a long-term scenario. Nevertheless, the interpretation of these results is limited to the response observed for the endpoints here analyzed (DNA strand breaks). As such, other endpoints for genotoxicity assessment (i.e., mutation detection) and also the analyses of the epigenome of these organisms should be performed, as these molecular changes do not reflect a loss of DNA's structural integrity [149].

As for terrestrial invertebrates, most of the studies conducted so far were on the annelid *Eisenia andrei* [150–155]. Gene expression alterations were reported in earthworms exposed to sludge from a uranium mine decantation pond. These genes were mainly related with metabolism, oxidoreductase activity, redox homeostasis, and response to chemical stimulus and stress [152]. In these studies, the occurrence of DNA damage in the form of DNA strand breaks and changes in cell's DNA content in exposed organisms was also detected. Alterations in earthworm's immune system were also reported, in terms of the frequency of each cell compartment, as it was observed a decrease in the number of effector cells (amebocytes) and an increase of the cells responsible for the maintenance of the organism's homeostasis (eleocytes) [153, 154]. In parallel with a significant bioaccumulation of metals and radionuclides from uranium's decay chain (^{238}U, ^{234}U, ^{235}U, ^{226}Ra, ^{230}Th, and ^{210}Pb), it was also observed a significant decrease in earthworms' biomass, a reproduction inhibition, and significant histological alterations, namely in earthworm's body wall (epidermis, circular, and longitudinal muscles) and gastrointestinal tract (chloragogenous tissue and intestinal epithelium) [153–155].

Under a real scenario of contamination, all of these effects may explain the lower biodiversity of soils contaminated with NORM, and the subsequent loss of their functions, if the contamination is perceived by the organisms. By using an avoidance assay (a standard ecotoxicological assay), to study earthworms' behavioral responses to soils collected in a uranium mine area, it was shown that earthworms actively avoided several contaminated soils. Earthworm's avoidance responses allowed it to discriminate highly to moderately toxic soils. On the other hand, on another study published by the same authors, using the analyses of oxidative stress enzymatic biomarkers (catalase, glutathione peroxidase) and lipid peroxidation biomarkers (through the quantification of thiobarbituric acid reactive substances), in earthworms exposed to soils nearby a uranium mine, showed no response for none of the biomarkers analyzed [150].

9.4.2.2 Vertebrates

Although there have been a wide number of studies performed on the effects of gamma radiation exposure on vertebrates, very few were performed so far for NORM exposure. Regarding aquatic vertebrates, fish have been the most used model organisms. On a study performed in former uranium mines from the Limousin region of France, where *Rutilus rutilus* specimens were caged on a pond contaminated with NORM and metals, immune, oxidative stress, biotransformation, neurotoxicity, and physiological parameters were measured [156]. The results obtained showed a stimulation of the immune parameters, the occurrence of oxidative stress and a decrease of acetyl choline esterase-AChE in the fish caged in the contaminated pond [156]. Zebrafish (*Danio rerio*) specimens exposed to uranium mill tailings leaching solution also showed alterations for the oxidative stress biomarkers used (superoxide dismutase—SOD, catalase—CAT, malondialdehyde—MDA and Na^+–K^+–ATPase) but specially for Na^+–K^+–ATPase and also evidenced that the organs most susceptible to oxidative stress were the gills [157]. In another study performed on a uranium milling operation in Northern Saskatchewan, Canada, *Pimephales promelas* specimens (adults and 5-day-old larvae) were exposed to contaminated water and contaminated sediment [158]. Results indicated effects on reproduction (reduced hatching) and larvae development (increase of skeletal deformities) and an increase in metal body burdens. However, the effects detected on the offspring, when considering the increase in egg production, were not significant in the level of deformities between treatments [158]. The effects on reproduction on the same species have already been observed under an exposure to effluent waters also from a uranium mining site in Saskatchewan, Canada. A significant decrease in eggs hatching time and hatching success was registered when early life stages of fathead minnows were exposed [159]. Nevertheless, metals and radionuclides are not the only stressor responsible for the effects caused by effluent waters from NORM sites. Lourenço et al. [160] performed an exposure of zebrafish eggs to a uranium mine effluent, barium chloride-treated mine effluent, and settling ponds sludge elutriates and showed that pH of the mine effluent strongly affected hatching success. After eliminating the effect of pH, this study also showed some teratogenicity associated with the uranium mine effluent, the occurrence of DNA damage, mainly associated with the exposure to treated mine effluent and sludge elutriates and mild effects on growth observed mainly on embryos exposed to the mine effluent and sludge elutriates. This study showed that the use of the Fish Embryo Toxicity Test (FET) test is suitable to test uranium mining wastes to determine and discriminate the risk of discharge. It also showed that the inclusion of the evaluation of genotoxicity endpoints in the FET test prevented the underestimation of risks, when only looking at chemical and radiological benchmark values defined by national and international directives, for the determination of risks, due to the chemical complexity of these wastes.

On what concerns amphibians, there are very few studies on these organisms as well. Marques and co-authors performed very important studies on amphibians, namely *Pelophylax perezi* exposed to NORM in situ. They have studied both tadpoles and adults and they have analyzed several endpoints, such as growth, survival, oxidative stress biomarkers (catalase, glutathione peroxidase, glutathione reductase, and lipid peroxidation through thiobarbituric acid reactive species (TBARS) quantification), gene expression alterations, histopathological changes, erythrocytic nuclear abnormalities and micronuclei, on organisms exposed to a uranium mine effluent in Portugal [161–165]. A study performed on 2008, on larvae and eggs [165] exposed to a uranium mine effluent, showed a decrease in larvae body length as well as a decrease in stimulus reactions, an increase in pigmentation along with tail deformities and metals bioaccumulation. The in situ exposure of tadpoles of the same species showed decreased survival and growth, a higher glutathione peroxidase activity and an increased lipid peroxidation [164] in organisms exposed in the mine effluent pond, when compared with organisms from a control pond. Although there may have been the influence of NORM and metals exposure, the studies also evidenced the effects of effluent's acidity (typically seen in metal mining contexts), mainly in the growth and survival parameters and also in metal's uptake. Another study, performed by the same authors [163], on adults living on the same uranium mine pond, analyzed gene expression changes using a technique called Suppressive Subtractive Hybridization (SSH). Significant changes in the expression levels of genes that play an important role in protecting cells against oxidative stress were shown, evidencing once again that oxidative stress response is very important in protecting cells and in maintaining DNA integrity on organisms exposed to NORMs and metals. Another study performed by this team on *Pelophylax perezi* adults inhabiting a uranium mining pond [162], showed significant metals bioaccumulation in the liver and the kidneys. Significant histopathological alterations in the liver, the lungs and in the kidneys, mainly in the form of a slight increase in melanomacrophagic centers, a dilatation of the renal tubules, a discrete thickening along with a slight hyperplasia of the alveolar septa and a slight hypoplasia of the goblet cells, were observed. The same animals living in the mine pond also displayed a significantly higher number of erythrocytic abnormalities (micronuclei and notched, kidney and lobed shaped nuclei) as well as a significantly lower frequency of immature erythrocytes. Both observations led to the belief that the removal and replacement of abnormal blood cells might be compromised.

There are a few studies published on the uptake of NORM by mammals that were performed mainly on former uranium mining areas, but very few examined the effects of that exposure. A study performed by Cleveland et al. [166] analyzed NORM uptake and histopathological alterations in liver and kidneys of rodents (*Peromyscus maniculatus* and *P. boylii*) inhabiting former uranium mines and observed that rodents bioaccumulated elements from ^{238}U decay chain but without exceeding literature-based effects thresholds for small rodents. The authors also observed that there were some minor lesions in the tissues (liver and kidneys) analyzed that could not, however, be attributed to U mining activities. Lourenço and co-authors [167], captured mice (*Apodemus sylvaticus*) on the surroundings of a former uranium mining site and on a control area. DNA damage and bioaccumulation of metals and radionuclides were assessed, as well as the expression and the presence of single nucleotide polymorphisms on tumor suppressor genes. Results showed that cadmium and uranium were significantly bioaccumulated by exposed organisms. Organisms living in the former uranium mining area also evidenced significantly higher levels of DNA damage when compared with control organisms and also a higher expression of TP53 tumor suppressor gene and the presence of single nucleotide polymorphisms in Rb tumor suppressor gene. These effects can cause a disturbance in the genetic material of exposed organisms causing genetic instability and changes in the genetic pool of the population, potentially affecting the population's fitness and stability. However, they cannot be attributed to any of the stressors in particular. It is known that uranium is genotoxic due to its chemical and radiological properties. Nevertheless, other metals present in uranium ore have shown greater genotoxic properties [151].

9.4.2.3 Plants

As for plants, there are a few studies already performed using soil/sludge or plant species collected directly from radium production industry storage sites, uranium rich regions, but mainly uranium mining sites and uranium milling tailings, that showed NORM bioaccumulation [168–180]. However, very few assessed the effects of that bioaccumulation. On a study performed by Evseeva et al. [170], *Vicia cracca* populations, inhabiting areas contaminated with uranium mill tailings and radium production wastes, were sampled and analyzed for the presence of chromosome aberrations, frequency of embryonic lethal mutations, seed germination and survival rate of seed sprouts. Results showed an increased frequency of embryonic lethal mutations, decreased seed germination, increased chromosome aberration counts and decreased survival rate of seed sprouts. The same authors [171], used *Allium cepa* specimens to determine the genotoxicity of an effluent from a radium production storage facility, through chromosome aberrations counting. Results showed a significant increase in chromosome aberration counts in the roots of exposed plants. Two studies [168, 179] using soils contaminated with metals and radionuclides from Portuguese former ura-

nium mines were performed using *Lactuca sativ*a and *Zea mays* as test species to determine the eco (through growth inhibition) and genotoxicity (mutation analysis through the Ames test) of amended and unamended mine soils. Studies showed genotoxicity of the unamended soils containing the highest levels of metals and radionuclides, a significant decrease in *Lactuca sativ*a biomass and also a significant bioaccumulation of these elements. The soil amendment methodology used in these studies significantly decreased the levels of metals and radionuclides in soils leachates and the soil available fraction.

9.5 Exercises and Self-Assessment

Q1. What is the relationship between life stage and an organism's radiosensitivity?
Q2. Please indicate which is the most radiosensitive parameter: mortality or reproduction?
Q3. Please indicate the most important non-stochastic effects induced by organisms exposure to ionizing radiation at a population level.
Q4. Which kind of exposure is more effective in causing organisms mortality?
Q5. Regarding radioactive contamination, what information can be retrieved from the omics approaches? What can be the contribution of those studies for future remediation of radiologically contaminated sites?
Q6. What are the main traits conferring radioresistance to plants compared to animals?
Q7. What does "hormesis" in plants mean?

9.6 Exercise Solutions

SQ1. The younger the organisms, the more sensitive they are to the deleterious effects of radiation exposure.
SQ2. Reproduction and reproductive capacity is a more sensitive parameter to the effects of radiation exposure both for terrestrial and aquatic invertebrates and vertebrates, than mortality.
SQ3. The non-stochastic effects that are most important at a population level are mortality, fertility, and fecundity.
SQ4. Acute exposures to high doses of ionizing radiation are more effective in inducing higher injury than chronic exposures to low doses of ionizing radiation. The higher the dose the lower the ability of cells to divide and regenerate the damaged tissue which translates into a higher probability for organisms mortality.
SQ5. The application of multiomics approaches, namely genomics, proteomics, metabolomics, and transcriptomics, has gained relevance in many different fields. These high-throughput techniques allow an analysis of the total set of molecules (DNA, proteins, and other metabolites) in a biological sample. Therefore, the integrated data have revolutionized biology and have contributed to advancing our understanding of different biological processes.

Genome sequencing, comparative genomics, and proteomics have allowed the identification of microbial essential genes (key players) that encode biomolecules, mainly proteins, involved in biological processes, including those involved in detoxification of radionuclides and metals. Furthermore, metagenomics approaches directed to the microbial communities of these contaminated environments allow for the identification, and characterization, of microorganisms with relevant functions in the bioremediation/decontamination processes. It is therefore expected that these broader approaches will contribute even more to the identification of microorganisms and to the elucidation of the metabolic pathways and key genes involved in those processes that may be further applied in the bioremediation/decontamination of these sites.

SQ6. The elevated radioresistance of plants compared to animals relies on differences in cell structure and metabolism. Plant cells present some traits such as thickened cell walls, cuticles, hairs (pubescence), phenolic compounds, and often polyploidy.
SQ7. Low doses of ionizing radiation induce positive outcomes in plants such as increasing growth and production of secondary metabolites engaged in the antioxidant defenses.

References

1. Song Y, Xie L, Lee YK, Brede DA, Lyne F, Kassaye Y, et al. Integrative assessment of low-dose gamma radiation effects on Daphnia magna reproduction: toxicity pathway assembly and AOP development. Sci Total Environ. 2020;705:135912.
2. National Research Council (US). Committee on evaluation of EPA guidelines for exposure to naturally occurring radioactive materials. Evaluation of guidelines for exposures to technologically enhanced naturally occurring radioactive materials. Washington, DC; 1999.
3. IAEA. Protection of the environment from ionising radiation: the development and application of a system of radiation protection for the environment. Iaea-Csp-17. 2003;66(1–2).
4. Grauby A. Compartimentation de la radioactivite dans Ie milieu terrestre. Evacuation des dechets radioactifs. In: Proceedings, Reunion d'Information de l'AIEN. Paris: Organisation pour la Cooperation et Ie Developpement Economique (OCDE); 1972.
5. Parsons J, Droge S. Environmental compartments. In: van Gestel Cornelis AM, Van Belleghem FGAJ, van den Brink NW, Droge STJ, Hamers T, Hermens JLM, et al., editors. Environmental toxicology. Amsterdam: LibreTexts Libraries; 2019. p. 104–33. Available from: https://chem.libretexts.org/@go/page/294544.

6. Little KW. Environmental fate and transport analysis with compartment modeling. Boca Raton, FL: CRC Press; 2012.
7. Vandenhove H, Hurtgen C, Payne TE. Uranium: radionuclides encyclopedia of inorganic chemistry. 2010. (Major reference works). https://doi.org/10.1002/0470862106.ia739.
8. Langmuir D. Aqueous environmental geochemistry. Upper Saddle River, NJ: Prentice Hall; 1997.
9. Desmet GM, Van Loon LR, Howard BJ. Chemical speciation and bioavailability of elements in the environment and their relevance to radioecology. Sci Total Environ. 1991;100(C).
10. Whicker F, Schultz V. Radioecology nuclear energy in the environment. CRC Press; 1982. Available from: https://books.google.be/books?id=lmLwAAAAMAAJ.
11. Langmuir D, Herman JS. The mobility of thorium in natural waters at low temperatures. Geochim Cosmochim Acta. 1980;44(11):1753.
12. Bourg ACM. Speciation of heavy metals in soils and groundwater and implications for their natural and provoked mobility. In: Heavy metals. Springer; 1995.
13. Sparks DL. Environmental soil chemistry. 2nd ed. Amsterdam: Academic Press; 2003.
14. Mahmood Z, Mohamed C. Thorium. In: Radionuclides in the environment. John Wiley & Sons; 2010. p. 247–53.
15. Premuzic E, Francis A, Lin M, Schubert J. Chelation of thorium and uranium by Pseudomonas aeruginosa. Arch Environ Contam Toxicol. 1985;14:759–68.
16. Rogiers T, Claesen J, Van Gompel A, Vanhoudt N, Mysara M, Williamson A, et al. Soil microbial community structure and functionality changes in response to long-term metal and radionuclide pollution. Environ Microbiol. 2021;23(3):1670.
17. Atwood DA. Radionuclides in the Environment. John Wiley & Sons; 2010.
18. IAEA. Handbook of parameter values for the prediction of radionuclide transfer in terrestrial and freshwater. Technical Reports Series 472. 2010;(472).
19. Kirchmann R, Van der Stricht E. Radioecology: radioactivity and ecosystems. Liège: Fortemps; 2001. Available from: http://lib.ugent.be/catalog/rug01:000853032.
20. Zhu YG, Smolders E. Plant uptake of radiocaesium: a review of mechanisms, regulation and application. J Exp Bot. 2000;51(351):1635–45 [cited 2017 Oct 6]. Available from: http://www.ncbi.nlm.nih.gov/pubmed/11053452.
21. Nyjfeler UP, Santschi PH, Li Y-H. The relevance of scavenging kinetics to modeling of sediment-water interactions in natural waters. Limnol Oceanogr. 1986;31(2):277.
22. Absalom J, Young S, Crout N. Radio-caesium fixation dynamics: measurement in six Cumbrian soils. Eur J Soil Sci. 1995;46(3):461.
23. Krouglov SV, Filipas AS, Alexakhin RM, Arkhipov NP. Long-term study on the transfer of 137Cs and 90Sr from Chernobyl-contaminated soils to grain crops. J Environ Radioact. 1997;34(3):267–86. Available from: https://www.sciencedirect.com/science/article/pii/0265931X96000434.
24. Sheppard SC, Sheppard MI, Gallerand MO, Sanipelli B. Derivation of ecotoxicity thresholds for uranium. J Environ Radioact. 2005;79(1):55–83. Available from: http://www.sciencedirect.com/science/article/B6VB2-4D3B1W1-3/2/681b494598ffb6a9c93d87d7ae43672a.
25. Vandenhove H, Van Hees M, Wannijn J, Wouters K, Wang L. Can we predict uranium bioavailability based on soil parameters? Part 2: soil solution uranium concentration is not a good bioavailability index. PG-577-86. Environ Pollut. 2007;145(2):577–86.
26. Semple KT, Doick KJ, Jones KC, Burauel P, Craven A, Harms H. Peer reviewed: defining bioavailability and bioaccessibility of contaminated soil and sediment is complicated. Environ Sci Technol. 2004;38(12):228A–31A.
27. Hu Q-H, Weng J-Q, Wang J-S. Sources of anthropogenic radionuclides in the environment: a review. J Environ Radioact. 2010;101(6):426–37. Available from: http://www.sciencedirect.com/science/article/pii/S0265931X08001392.
28. Beresford NA, Horemans N, Copplestone D, Raines KE, Orizaola G, Wood MD, Laanen P, Whitehead HC, Burrows JE, Tinsley MC, Smith JT, Bonzom J-M, Gagnaire B, Adam-Guillermin C, Gashchak S, Jha AN, de Menezes A, Willey N, Spurgeon D. Towards solving a scientific controversy—the effects of ionising radiation on the environment. J Environ Radioact. 2020;211:106033.
29. Howard BJ, Larsson C.-M. The ERICA Integrated Approach and its contribution to protection of the environment from ionising radiation. J Environ Radioact. 2008;99(9):1361–63.
30. IAEA. Handbook of parameter values for the prediction of radionuclide transfer to wildlife., Technical Reports Series, vol. No. 479. Vienna: IAEA; 2014.
31. ICRP. Dose coefficients for nonhuman biota environmentally exposed to radiation. ICRP publication 136. Ann ICRP. 2017;46(2)
32. Andersson P, Garnier-Laplace J, Beresford NA, Copplestone D, Howard BJ, Howe P, Oughton DH, Whitehouse P. Protection of the environment from ionising radiation in a regulatory context (PROTECT): proposed numerical benchmark values. J Environ Radioact. 2009;100:1100–8.
33. ICRP. Annex D. Radiation effects in reference animals and plants. Ann ICRP. 2008;38(4–6):179.
34. Eckerman K, Endo A. ICRP publication 107. Nuclear decay data for dosimetric calculations. Ann ICRP. 2008;38:9–10.
35. Brown JE, Alfonso B, Avila R, Beresford NA, Copplestone D, Hosseini A. A new version of the ERICA tool to facilitate impact assessments of radioactivity on wild plants and animals. J Environ Radioact. 2016;153:141.
36. Vives i Batlle J, Ulanovsky A, Copplestone D. A method for assessing exposure of terrestrial wildlife to environmental radon (222Rn) and thoron (220Rn). Sci Total Environ. 2017;605–606:569.
37. Boyer P, Wells C, Howard B. Extended Kd distributions for freshwater environment. J Environ Radioact. 2018;192:128.
38. Beresford NA, Wright SM, Barnett CL, Wood MD, Gaschak S, Arkhipov A, et al. Predicting radionuclide transfer to wild animals: an application of a proposed environmental impact assessment framework to the Chernobyl exclusion zone. Radiat Environ Biophys. 2005;44(3):161.
39. Beresford NA, Gaschak S, Barnett CL, Howard BJ, Chizhevsky I, Strømman G, et al. Estimating the exposure of small mammals at three sites within the Chernobyl exclusion zone—a test application of the ERICA tool. J Environ Radioact. 2008;99(9):1496–502.
40. Dragović S, Mandić LJ. Transfer of radionuclides to ants, mosses and lichens in semi-natural ecosystems. Radiat Environ Biophys. 2010;49(4):625.
41. Beaugelin-Seiller K, Jasserand F, Garnier-Laplace J, Gariel JC. Modeling radiological dose in non-human species: principles, computerization, and application. Health Phys. 2006;90(5):485–93. https://doi.org/10.1097/01.HP.0000182192.91169.ed.
42. Thomas P, Liber K. An estimation of radiation doses to benthic invertebrates from sediments collected near a Canadian uranium mine. Environ Int. 2001;27(4):341.
43. Wood MD, Leah RT, Jones SR, Copplestone D. Radionuclide transfer to invertebrates and small mammals in a coastal sand dune ecosystem. Sci Total Environ. 2009;407(13):4062–74.
44. Mothersill CE, Oughton DH, Schofield PN, Abend M, Adam-Guillermin C, Ariyoshi K, Beresford NS, Bonisoli-Alquati A, Cohen J, Dubrova Y, Geras'kin SA, Hevrøy TH, Higley KA, Horemans N, Jha AN, Kapustka LA, Kiang JG, Madas BG, Powathil G, Sarapultseva EI, Seymour CB, Nguyen TK, Wood MD. From tangled banks to toxic bunnies; a reflection on the issues involved

in developing an ecosystem approach for environmental radiation protection. Int J Radiat Biol. 2020; https://doi.org/10.1080/09553002.2020.1793022.
45. UNSCEAR. Sources and effects of ionizing radiation, United Nations Scientific Committee on the Effects of Atomic Radiation, Report to the general assembly with scientific annexes, vol. II, Scientific annexes C, D and E. New York: United Nations; 2008.
46. UNSCEAR. United Nations Scientific Committee on the Effects of Atomic Radiation UNSCEAR 1996 report to the general assembly, with scientific annexes. New York; 1996.
47. Copplestone D, Bielby S, Jones SR, Patton D, Daniel P, Gize I. Impact assessment of ionising radiation on wildlife. Environment Agency; 2001. Available from: https://aquadocs.org/bitstream/1834/27217/1/25_Impact_Assesment_of_ionising_Radiation_on_Wildlife.pdf.
48. IAEA. Effects of ionising radiation on plants and animals at levels implied by current radiation protection standards. Technical Report Series No. 332. Vienna; 1992. 74 pp. ISBN: 920 100992 5.
49. Upton AC. Environmental standards for ionizing radiation: theoretical basis for dose-response curves. Environ Health Perspect. 1983;52:31.
50. Beresford NA, Copplestone D. Effects of ionizing radiation on wildlife: what knowledge have we gained between the Chernobyl and Fukushima accidents? Integr Environ Assess Manag. 2011;7(3):371.
51. Hada M, Georgakilas AG. Formation of clustered DNA damage after high-LET irradiation: a review. J Radiat Res. 2008;49(3):203–10.
52. Dartnell LR. Ionizing radiation and life. Astrobiology. 2011;11:551.
53. Hei TK, Zhou H, Ivanov VN, Hong M, Lieberman HB, Brenner DJ, et al. Mechanism of radiation-induced bystander effects: a unifying model. J Pharm Pharmacol. 2008;60(8):943–50.
54. UNSCEAR. Effects of ionizing radiation. Report to the general assembly, with scientific annexes. New York: United Nations Scientific Committee on the Effects of Atomic Radiation; 2006.
55. Gomes T, Song Y, Brede DA, Xie L, Gutzkow KB, Salbu B, et al. Gamma radiation induces dose-dependent oxidative stress and transcriptional alterations in the freshwater crustacean Daphnia magna. Sci Total Environ. 2018;628–629:206.
56. Merino N, Aronson HS, Bojanova DP, Feyhl-Buska J, Wong ML, Zhang S, et al. Living at the extremes: extremophiles and the limits of life in a planetary context. Front Microbiol. 2019;10 https://doi.org/10.3389/fmicb.2019.00780.
57. Singh OV, Gabani P. Extremophiles: radiation resistance microbial reserves and therapeutic implications. J Appl Microbiol. 2011;110:851.
58. Becker J, Wittmann C. Microbial production of extremolytes—high-value active ingredients for nutrition, health care, and well-being. Curr Opin Biotechnol. 2020;65:118.
59. Coker JA. Extremophiles and biotechnology: current uses and prospects. F1000Research. 2016;5 https://doi.org/10.12688/f1000research.7432.1.
60. Shuryak I, Matrosova VY, Gaidamakova EK, Tkavc R, Grichenko O, Klimenkova P, et al. Microbial cells can cooperate to resist high-level chronic ionizing radiation. PLoS One. 2017;12(12):e0189261.
61. Bruckbauer ST, Martin J, Minkoff BB, Veling MT, Lancaster I, Liu J, et al. Physiology of highly radioresistant Escherichia coli after experimental evolution for 100 cycles of selection. Front Microbiol. 2020;11:582590.
62. Shuryak I. Review of microbial resistance to chronic ionizing radiation exposure under environmental conditions. J Environ Radioact. 2019;196:50.
63. Ghirga G. Cancer in children residing near nuclear power plants: an open question. Ital J Pediatr. 2010;36(1):60. Available from: http://www.scopus.com/inward/record.url?eid=2-s2.0-77958117954&partnerID=40&md5=bdf4aa7fe5e060d001f5dd26fc4ad520.
64. Webb KM, Yu J, Robinson CK, Noboru T, Lee YC, DiRuggiero J. Effects of intracellular Mn on the radiation resistance of the halophilic archaeon Halobacterium salinarum. Extremophiles. 2013;17(3):485.
65. de la Tour CB, Mathieu M, Servant P, Coste G, Norais C, Confalonieri F. Characterization of the DdrD protein from the extremely radioresistant bacterium Deinococcus radiodurans. Extremophiles. 2021;25(4):343.
66. Jung KW, Lim S, Bahn YS. Microbial radiation-resistance mechanisms. J Microbiol. 2017;55:499.
67. Bentchikou E, Servant P, Coste G, Sommer S. A major role of the RecFOR pathway in DNA double-strand-break repair through ESDSA in Deinococcus radiodurans. PLoS Genet. 2010;6(1):e1000774.
68. Gallois N, Alpha-Bazin B, Ortet P, Barakat M, Piette L, Long J, et al. Proteogenomic insights into uranium tolerance of a Chernobyl's microbacterium bacterial isolate. J Proteome. 2018;177:148.
69. Lopez-Fernandez M, Jroundi F, Ruiz-Fresneda MA, Merroun ML. Microbial interaction with and tolerance of radionuclides: underlying mechanisms and biotechnological applications. Microb Biotechnol. 2021;14:810.
70. Nayak T, Sengupta I, Dhal PK. A new era of radiation resistance bacteria in bioremediation and production of bioactive compounds with therapeutic potential and other aspects: an in-perspective review. J Environ Radioact. 2021;237:106696.
71. Hoyos-Hernandez C, Courbert C, Simonucci C, David S, Vogel TM, Larose C. Community structure and functional genes in radionuclide contaminated soils in Chernobyl and Fukushima. FEMS Microbiol Lett. 2019;366(21):fnz180.
72. Theodorakopoulos N, Février L, Barakat M, Ortet P, Christen R, Piette L, et al. Soil prokaryotic communities in Chernobyl waste disposal trench T22 are modulated by organic matter and radionuclide contamination. FEMS Microbiol Ecol. 2017;93(8) https://doi.org/10.1093/femsec/fix079.
73. Arena C, De Micco V, De Maio A. Growth alteration and leaf biochemical responses in Phaseolus vulgaris exposed to different doses of ionising radiation. Plant Biol. 2014;16(Suppl. 1):194.
74. De Micco V, Arena C, Pignalosa D, Durante M. Effects of sparsely and densely ionizing radiation on plants. Radiat Environ Biophys. 2011;50(1):1.
75. Maity JP, Mishra D, Chakraborty A, Saha A, Santra SC, Chanda S. Modulation of some quantitative and qualitative characteristics in rice (Oryza sativa L.) and mung (Phaseolus mungo L.) by ionizing radiation. Radiat Phys Chem. 2005;74(5):391.
76. Zaka R, Vandecasteele CM, Misset MT. Effects of low chronic doses of ionizing radiation on antioxidant enzymes and G6PDH activities in Stipa capillata (Poaceae). J Exp Bot. 2002;53(376):1979.
77. Li F, Shimizu A, Nishio T, Tsutsumi N, Kato H. Comparison and characterization of mutations induced by gamma-ray and carbon-ion irradiation in rice (Oryza sativa L.) using whole-genome resequencing. G3 Genes, Genomes, Genet. 2019;9(11):3743.
78. Comai L. The advantages and disadvantages of being polyploid. Nat Rev Genet. 2005;6:836.
79. De Micco V, Arena C, Aronne G. Anatomical alterations of Phaseolus vulgaris L. mature leaves irradiated with X-rays. Plant Biol. 2014;16(Suppl. 1):187.
80. Mousseau TA, Møller AP. Plants in the light of ionizing radiation: what have we learned from Chernobyl, Fukushima, and other "hot" places? Front Plant Sci. 2020;11:552.

81. Møller AP, Mousseau TA. Are organisms adapting to ionizing radiation at Chernobyl? Trends Ecol Evol. 2016;31:281.
82. Yemets AI, Blume RY, Sorochinsky BV. Adaptation of the gymnosperms to the conditions of irradiation in the Chernobyl zone: from morphological abnormalities to the molecular genetic consequences. Cytol Genet. 2016;50:415.
83. Watanabe Y, Ichikawa S, Kubota M, Hoshino J, Kubota Y, Maruyama K, et al. Morphological defects in native Japanese fir trees around the Fukushima Daiichi Nuclear Power Plant. Sci Rep. 2015;5:13232.
84. Yoschenko V, Nanba K, Yoshida S, Watanabe Y, Takase T, Sato N, et al. Morphological abnormalities in Japanese red pine (Pinus densiflora) at the territories contaminated as a result of the accident at Fukushima Dai-Ichi Nuclear Power Plant. J Environ Radioact. 2016;165:60.
85. Koranda JJ, Robison WL. Accumulation of radionuclides by plants as a monitor system. Environ Health Perspect. 1978;27:165.
86. Ludovici GM, Oliveira de Souza S, Chierici A, Cascone MG, d'Errico F, Malizia A. Adaptation to ionizing radiation of higher plants: from environmental radioactivity to Chernobyl disaster. J Environ Radioact. 2020;222:106375.
87. Arena C, De Micco V, Macaeva E, Quintens R. Space radiation effects on plant and mammalian cells. Acta Astronaut. 2014;104(1):419.
88. De Micco V, Paradiso R, Aronne G, De Pascale S, Quarto M, Arena C. Leaf anatomy and photochemical behaviour of solanum lycopersicum L. Plants from seeds irradiated with low-let ionising radiation. Sci World J. 2014;2014:428141.
89. Nagata T, Todoriki S, Hayashi T, Shibata Y, Mori M, Kanegae H, et al. γ-Radiation induces leaf trichome formation in arabidopsis. Plant Physiol. 1999;120(1):113.
90. Ahuja S, Kumar M, Kumar P, Gupta VK, Singhal RK, Yadav A, et al. Metabolic and biochemical changes caused by gamma irradiation in plants. J Radioanal Nucl Chem. 2014;300:199.
91. Kurimoto T, Constable JVH, Huda A. Effects of ionizing radiation exposure on arabidopsis thaliana. Health Phys. 2010;99(1):49.
92. Gerlach SU, Herranz H. Genomic instability and cancer: lessons from Drosophila. Open Biol. 2020;10(6):200060.
93. González-Huici V, Wang B, Gartner A. A role for the nonsense-mediated mRNA decay pathway in maintaining genome stability in caenorhabditis elegans. Genetics. 2017;206(4):1853.
94. Lopez JV, Bracken-Grissom H, Collins AG, Collins T, Crandall K, Distel D, et al. The global invertebrate genomics alliance (GIGA): developing community resources to study diverse invertebrate genomes. J Hered. 2014;105:1.
95. Wilson-Sanders SE. Invertebrate models for biomedical research, testing, and education. ILAR J. 2011;52:126.
96. Clatworthy AL, Noel F, Grose E, Cui M, Tofilon PJ. Ionizing radiation-induced alterations in the electrophysiological properties of Aplysia sensory neurons. Neurosci Lett. 1999;268(1):45.
97. Vaiserman A, Cuttler JM, Socol Y. Low-dose ionizing radiation as a hormetin: experimental observations and therapeutic perspective for age-related disorders. Biogerontology. 2021;22(2):145–64. https://doi.org/10.1007/s10522-020-09908-5.
98. Geras'kin SA. Ecological effects of exposure to enhanced levels of ionizing radiation. J Environ Radioact. 2016;162–163:347.
99. Driver CJ. Ecotoxicity literature review of selected Hanford site contaminants. Richland, WA: Pacific Northwest Lab; 1994.
100. Cassidy CL, Lemon JA, Boreham DR. Impacts of low-dose gamma-radiation on genotoxic risk in aquatic ecosystems. Dose-Response. 2007;5(4):323.
101. Johnson TE, Hartman PS. Radiation effects on life span in Caenorhabditis elegans. J Gerontol. 1988;43(5):B137–41.
102. Allen RG. Relationship between γ-irradiation, life span, metabolic rate and accumulation of fluorescent age pigment in the adult male housefly, Musca domestica. Arch Gerontol Geriatr. 1985;4(2):169.
103. Vaiserman A, Litoshenko AI, Kvitnitskaia-Ryzhova TI, Koshel N, Mozzhukhina T, Mikhal'skiĭ S, et al. Molecular and cellular aspects of radiation hormesis in Drosophila melanogaster. Tsitol Genet. 2003;37(3):41–8.
104. Won EJ, Lee JS. Gamma radiation induces growth retardation, impaired egg production, and oxidative stress in the marine copepod Paracyclopina nana. Aquat Toxicol. 2014;150:17.
105. Han J, Won EJ, Kim IC, Yim JH, Lee SJ, Lee JS. Sublethal gamma irradiation affects reproductive impairment and elevates antioxidant enzyme and DNA repair activities in the monogonont rotifer Brachionus koreanus. Aquat Toxicol. 2014;155:101.
106. Han J, Won EJ, Lee BY, Hwang UK, Kim IC, Yim JH, et al. Gamma rays induce DNA damage and oxidative stress associated with impaired growth and reproduction in the copepod Tigriopus japonicus. Aquat Toxicol. 2014;152:264.
107. Fuller N, Ford AT, Nagorskaya LL, Gudkov DI, Smith JT. Reproduction in the freshwater crustacean Asellus aquaticus along a gradient of radionuclide contamination at Chernobyl. Sci Total Environ. 2018;628–629:11.
108. Kuzmic M, Galas S, Lecomte-Pradines C, Dubois C, Dubourg N, Frelon S. Interplay between ionizing radiation effects and aging in C. elegans. Free Radic Biol Med. 2019;134:657.
109. Krisko A, Leroy M, Radman M, Meselson M. Extreme antioxidant protection against ionizing radiation in bdelloid rotifers. Proc Natl Acad Sci U S A. 2012;109(7):2354.
110. Mothersill C, Lyng F, Mulford A, Seymour C, Cottell D, Lyons M, et al. Effect of low doses of ionizing radiation on cells cultured from the hematopoietic tissue of the Dublin Bay prawn, Nephrops norvegicus. Radiat Res. 2001;156(3):241.
111. Alonzo F, Hertel-Aas T, Gilek M, Gilbin R, Oughton DH, Garnier-Laplace J. Modelling the propagation of effects of chronic exposure to ionising radiation from individuals to populations. J Environ Radioact. 2008;99(9):1464–73.
112. Depledge MH. The ecotoxicological significance of genotoxicity in marine invertebrates. Mutat Res Fundam Mol Mech Mutagen. 1998;399(1):109.
113. Fuller N, Lerebours A, Smith JT, Ford AT. The biological effects of ionising radiation on crustaceans: a review. Aquat Toxicol. 2015;167:55–67.
114. Alonzo F, Hertel-Aas T, Real A, Lance E, Garcia-Sanchez L, Bradshaw C, Battle JVI, Oughton DH, Garnier-Laplace J. Population modelling to compare chronic external radiotoxicity between individual and population endpoints in four taxonomic groups. J Environ Radioact. 2016;152:46–59.
115. Harrison FL, Anderson SL. Effects of acute irradiation on reproductive success of the polychaete worm, Neanthes arenaceodentata. Radiat Res. 1994;137(1):59.
116. Jönsson KI, Harms-Ringdahl M, Torudd J. Radiation tolerance in the eutardigrade Richtersius coronifer. Int J Radiat Biol. 2005;81(9):649.
117. Nakamori T, Yoshida S, Kubota Y, Ban-nai T, Kaneko N, Hasegawa M, et al. Effects of acute gamma irradiation on Folsomia candida (Collembola) in a standard test. Ecotoxicol Environ Saf. 2008;71(2):590.
118. Styron CE. Effects of beta and gamma radiation on a population of springtails, Sinella curviseta (Collembola). Radiat Res. 1971;48(1):53.
119. Suzuki J, Egami N. Mortality of the earthworms, Eisenia foetida, after γ-irradiation at different stages of their life history. J Radiat Res. 1983;24(3):209.
120. Watanabe M, Sakashita T, Fujita A, Kikawada T, Horikawa DD, Nakahara Y, et al. Biological effects of anhydrobiosis in an African chironomid, Polypedilum vanderplanki on radiation tolerance. Int J Radiat Biol. 2006;82(8):587.

121. Gladyshev E, Meselson M. Extreme resistance of bdelloid rotifers to ionizing radiation. Proc Natl Acad Sci U S A. 2008;105(13):5139.
122. Harrison FL, Rice DW, Moore DH, Varela M. Effects of radiation on frequency of chromosomal aberrations and sister chromatid exchange in the benthic worm, Neanthes arenaceodentata. In: Capuzzo JM, Kester DR, editors. Oceanic processes of marine pollution, vol. 1. Malabar, FL: R. E. Krieger Publishing Company; 1986. p. 145–56.
123. Parisot F, Bourdineaud JP, Plaire D, Adam-Guillermin C, Alonzo F. DNA alterations and effects on growth and reproduction in Daphnia magna during chronic exposure to gamma radiation over three successive generations. Aquat Toxicol. 2015;163:27–36.
124. Zadereev E, Lopatina T, Oskina N, Zotina T, Petrichenkov M, Dementyev D. Gamma irradiation of resting eggs of Moina macrocopa affects individual and population performance of hatchlings. J Environ Radioact. 2017;175–176:126.
125. Murphy JF, Nagorskaya LL, Smith JT. Abundance and diversity of aquatic macroinvertebrate communities in lakes exposed to Chernobyl-derived ionising radiation. J Environ Radioact. 2011;102(7):688.
126. Fuciarelli TM, Rollo CD. Ionizing radiation alters male Acheta domesticus courtship songs that are critical for mating success. Anim Behav. 2021;178:209.
127. Krivolutskiy DA, Tikhomirov FA, Fedorov EA, Pokargevsky AD, Taskaev AI. Effect of ionizing radiation on biogeocenosis. M Geo. 1988.
128. Møller AP, Barnier F, Mousseau TA. Ecosystems effects 25 years after Chernobyl: pollinators, fruit set and recruitment. Oecologia. 2012;170(4):1155.
129. Dallas LJ, Bean TP, Turner A, Lyons BP, Jha AN. Exposure to tritiated water at an elevated temperature: genotoxic and transcriptomic effects in marine mussels (M. galloprovincialis). J Environ Radioact. 2016;164:325.
130. Mousseau T, Milinevsky G, Kenney-Hunt J, Møller A. Highly reduced mass loss rates and increased litter layer in radioactively contaminated areas. Oecologia. 2014;175(1):429–37. https://doi.org/10.1007/s00442-014-2908-8.
131. Bezrukov V, Møller AP, Milinevsky G, Rushkovsky S, Sobol M, Mousseau TA. Heterogeneous relationships between abundance of soil surface invertebrates and radiation from Chernobyl. Ecol Indic. 2015;52:128–33.
132. Møller AP, Mousseau TA. Reduced colonization by soil invertebrates to irradiated decomposing wood in Chernobyl. Sci Total Environ. 2018;645:773.
133. Jackson D, Copplestone D, Stone DM, Smith GM, Jackson D, Copplestone D, et al. Terrestrial invertebrate population studies in the Chernobyl exclusion zone, Ukraine. Radioprotection. 2005;40(S1):S857–63.
134. Garnier-Laplace J, Della-Vedova C, Gilbin R, Copplestone D, Hingston J, Ciffroy P. First derivation of predicted-no-effect values for freshwater and terrestrial ecosystems exposed to radioactive substances. Environ Sci Technol. 2006;40(20):6498.
135. Garnier-Laplace J, Geras'kin S, Della-Vedova C, Beaugelin-Seiller K, Hinton TG, Real A, et al. Are radiosensitivity data derived from natural field conditions consistent with data from controlled exposures? A case study of Chernobyl wildlife chronically exposed to low dose rates. J Environ Radioact. 2013;121:12–21. Available from: http://www.sciencedirect.com/science/article/pii/S0265931X12000240.
136. Real A, Sundell-Bergman S, Knowles JF, Woodhead DS, Zinger I. Effects of ionising radiation exposure on plants, fish and mammals: relevant data for environmental radiation protection. J Radiol Prot. 2004;24:A123.
137. Hinton TG, Alexakhin R, Balonov M, Gentner N, Hendry J, Prister B, et al. Radiation-induced effects on plants and animals: findings of the United Nations Chernobyl forum. Health Phys. 2007;93:427.
138. Paunesku T, Stevanović A, Popović J, Woloschak GE. Effects of low dose and low dose rate low linear energy transfer radiation on animals–review of recent studies relevant for carcinogenesis. Int J Radiat Biol. 2021;97:757.
139. ICRP. Environmental protection—the concept and use of reference animals and plants. ICRP publication 108. Ann ICRP. 2008;38(4–6).
140. Garnier-Laplace J, Beaugelin-Seiller K, Della-Vedova C, Métivier J-M, Ritz C, Mousseau TA, et al. Radiological dose reconstruction for birds reconciles outcomes of Fukushima with knowledge of dose-effect relationships. Sci Rep. 2015;5:16594. Available from: https://pubmed.ncbi.nlm.nih.gov/26567770.
141. Bonisoli-Alquati A, Møller AP, Rudolfsen G, Mousseau TA. Birds as bioindicators of radioactive contamination and its effects. NATO Sci Peace Secur Ser A Chem Biol. 2022; https://doi.org/10.1007/978-94-024-2101-9_11.
142. Ulsh BA, Mühlmann-Díaz MC, Whicker FW, Hinton TG, Congdon JD, Bedford JS. Chromosome translocations in turtles: a biomarker in a sentinel animal for ecological dosimetry. Radiat Res. 2000;153(6):752.
143. Lourenço J, Mendo S, Pereira R. Radioactively contaminated areas: bioindicator species and biomarkers of effect in an early warning scheme for a preliminary risk assessment. J Hazard Mater. 2016;317:503–42. Available from: http://www.sciencedirect.com/science/article/pii/S0304389416305751
144. Pouget JP, Mather SJ. General aspects of the cellular response to low- and high-LET radiation. Eur J Nucl Med. 2001;28:541.
145. Antunes S, Pereira R, Gonçalves F. Acute and chronic toxicity of effluent water from an abandoned uranium mine. Arch Environ Contam Toxicol. 2007;53:207–13. Available from: http://www.ingentaconnect.com/content/klu/244/2007/00000053/00000002/00000011.
146. Semaan M, Holdway DA, Van Dam RA. Comparative sensitivity of three populations of the cladoceran Moinodaphnia macleayi to acute and chronic uranium exposure. Environ Toxicol. 2001;16(5):365.
147. Ribeiro R, Lopes I. Contaminant driven genetic erosion and associated hypotheses on alleles loss, reduced population growth rate and increased susceptibility to future stressors: an essay. Ecotoxicology. 2013;22(5):889.
148. Reis P, Lourenço J, Carvalho FP, Oliveira J, Malta M, Mendo S, et al. RIBE at an inter-organismic level: a study on genotoxic effects in Daphnia magna exposed to waterborne uranium and a uranium mine effluent. Aquat Toxicol. 2018;198:206.
149. Reis P, Pereira R, Carvalho FP, Oliveira J, Malta M, Mendo S, et al. Life history traits and genotoxic effects on Daphnia magna exposed to waterborne uranium and to a uranium mine effluent—a transgenerational study. Aquat Toxicol. 2018;202:16–25 [cited 2019 Feb 12]. Available from: https://www.sciencedirect.com/science/article/pii/S0166445X18304363?via%3Dihub.
150. Antunes S, Castro B, Nunes B, Pereira R, Gonçalves F. In situ bioassay with *Eisenia andrei* to assess soil toxicity in an abandoned uranium mine. Ecotoxicol Environ Saf. 2008;71(3):620–31.
151. Fernandes S, Nogueira V, Lourenço J, Mendo S, Pereira R. Inter-species bystander effect: Eisenia fetida and Enchytraeus albidus exposed to uranium and cadmium. J Hazard Mater. 2020;399:122972.
152. Lourenço J, Pereira R, Gonçalves F, Mendo S. SSH gene expression profile of *Eisenia andrei* exposed in situ to a naturally contaminated soil from an abandoned uranium mine. Ecotoxicol Environ Saf. 2013;88:16–25. Available from: http://www.sciencedirect.com/science/article/pii/S0147651312003636.
153. Lourenço J, Pereira R, Silva A, Carvalho F, Oliveira J, Malta M, et al. Evaluation of the sensitivity of genotoxicity and cytotoxic-

ity endpoints in earthworms exposed in situ to uranium mining wastes. Ecotoxicol Environ Saf. 2012;75(1):46.
154. Lourenço J, Pereira RO, Silva AC, Morgado JM, Carvalho FP, Oliveira JM, et al. Genotoxic endpoints in the earthworms sublethal assay to evaluate natural soils contaminated by metals and radionuclides. J Hazard Mater. 2011;186:788–95. Available from: http://www.sciencedirect.com/science/article/B6TGF-51JF898-4/2/3357f762ece1cad9d6c524082f058883.
155. Lourenço J, Silva A, Carvalho F, Oliveira J, Malta M, Mendo S, et al. Histopathological changes in the earthworm Eisenia andrei associated with the exposure to metals and radionuclides. Chem Int. 2011;85(10):1630–4. Available from: http://www.sciencedirect.com/science/article/pii/S004565351100988X.
156. Gagnaire B, Bado-Nilles A, Betoulle S, Amara R, Camilleri V, Cavalié I, et al. Former uranium mine-induced effects in caged roach: a multiparametric approach for the evaluation of in situ metal toxicity. Ecotoxicology. 2014;24(1):215–31. Available from: http://www.scopus.com/inward/record.url?eid=2-s2.0-84922004530&partnerID=40&md5=87693d63b4821bc695c0733fe67c12dd.
157. Geng F, Hu N, Zheng J-F, Wang C-L, Chen X, Yu J, et al. Evaluation of the toxic effect on zebrafish (*Danio rerio*) exposed to uranium mill tailings leaching solution. J Radioanal Nucl Chem. 2012;292(1):453–63. https://doi.org/10.1007/s10967-011-1451-x.
158. Driessnack MK, Dubé MG, Rozon-Ramilo LD, Jones PD, Wiramanaden CIE, Pickering IJ. The use of field-based mesocosm systems to assess the effects of uranium milling effluent on fathead minnow (*Pimephales promelas*) reproduction. Ecotoxicology. 2011;20(6):1209–24. Available from: http://www.scopus.com/inward/record.url?eid=2-s2.0-79960306220&partnerID=40&md5=34a4d22e6c656218ebcf18f10daffd51.
159. Pyle GG, Swanson SM, Lehmkuhl DM. Toxicity of uranium mine-receiving waters to caged fathead minnows, Pimephales promelas. Ecotoxicol Environ Saf. 2001;48(2):202–14.
160. Lourenço J, Marques S, Carvalho FP, Oliveira J, Malta M, Santos M, et al. Uranium mining wastes: the use of the fish embryo acute toxicity test (FET) test to evaluate toxicity and risk of environmental discharge. Sci Total Environ. 2017;605–606:391.
161. Marques S, Antunes S, Nunes B, Gonçalves F, Pereira R. Antioxidant response and metal accumulation in tissues of Iberian green frogs (Pelophylax perezi) inhabiting a deactivated uranium mine. Ecotoxicology. 2011;20:1–13. https://doi.org/10.1007/s10646-011-0688-z.
162. Marques SM, Antunes SC, Pissarra H, Pereira ML, Gonçalves F, Pereira R. Histopathological changes and erythrocytic nuclear abnormalities in Iberian green frogs (*Rana perezi* Seoane) from a uranium mine pond. Aquat Toxicol. 2009;91(2):187–95. Available from: http://www.sciencedirect.com/science/article/B6T4G-4SD29J0-1/2/e98e5c48284d016d7b01e874627d9048.
163. Marques SM, Chaves S, Gonçalves F, Pereira R. Differential gene expression in Iberian green frogs (*Pelophylax perezi*) inhabiting a deactivated uranium mine. Ecotoxicol Environ Saf. 2013;87:115–9. Available from: http://www.sciencedirect.com/science/article/pii/S0147651312003624.
164. Marques SM, Chaves S, Gonçalves F, Pereira R. Evaluation of growth, biochemical and bioaccumulation parameters in *Pelophylax perezi* tadpoles, following an in-situ acute exposure to three different effluent ponds from a uranium mine. Sci Total Environ. 2013;445–446:321–8. Available from: http://www.sciencedirect.com/science/article/pii/S0048969712016373.
165. Marques SM, Gonçalves F, Pereira R. Effects of a uranium mine effluent in the early-life stages of *Rana perezi* Seoane. Sci Total Environ. 2008;402(1):29–35. Available from: http://www.sciencedirect.com/science/article/B6V78-4SP49T5-2/2/f725d35f227e9c86e7ed9f4b27544219.
166. Cleveland D, Hinck JE, Lankton JS. Assessment of chronic low-dose elemental and radiological exposures of biota at the Kanab North uranium mine site in the Grand Canyon watershed. Integr Environ Assess Manag. 2019;15(1):112.
167. Lourenço J, Pereira R, Gonçalves F, Mendo S. Metal bioaccumulation, genotoxicity and gene expression in the European wood mouse (*Apodemus sylvaticus*) inhabiting an abandoned uranium mining area. Sci Total Environ. 2013;443:673–80. Available from: http://www.sciencedirect.com/science/article/pii/S0048969712014179.
168. Abreu MM, Lopes J, Santos ES, Magalhães MCF. Ecotoxicity evaluation of an amended soil contaminated with uranium and radium using sensitive plants. J Geochemical Explor. 2014;142:112–21. Available from: http://www.scopus.com/inward/record.url?eid=2-s2.0-84901694794&partnerID=40&md5=1278d81e4282258a06d8953bb93d8ed2.
169. Černe M, Smodiš B, Štrok M, Benedik L. Radiation impact assessment on wildlife from an uranium mine area. Nucl Eng Des. 2012;246:203–9. Available from: http://www.sciencedirect.com/science/article/pii/S0029549311005498.
170. Evseeva T, Majstrenko T, Geras'kin S, Brown JE, Belykh E. Estimation of ionizing radiation impact on natural *Vicia cracca* populations inhabiting areas contaminated with uranium mill tailings and radium production wastes. Sci Total Environ. 2009;407(20):5335–43. Available from: http://www.scopus.com/inward/record.url?eid=2-s2.0-68149137727&partnerID=40&md5=62d27dfe96db81a24fa7d4404afefd42.
171. Evseeva TI, Geras'kin SA, Shuktomova II. Genotoxicity and toxicity assay of water sampled from a radium production industry storage cell territory by means of allium-test. J Environ Radioact. 2003;68(3):235–48. Available from: http://www.sciencedirect.com/science/article/B6VB2-488NWY5-1/2/f2d891ce12b59c2d0779c65806b2620a.
172. Favas P, Pratas J. Uranium in soils, waters and plants of the abandoned uranium mine (central Portugal). In: 12th International Multidisciplinary Scientific GeoConference and EXPO—Modern Management of Mine Producing, Geology and Environmental Protection, SGEM 2012. 2012. p. 1023–8. Available from: http://www.scopus.com/inward/record.url?eid=2-s2.0-84890629266&partnerID=40&md5=756bdfe151a3708aadedc7c171cd295c.
173. Favas PJC, Pratas J, Varun M, D'Souza R, Paul MS. Accumulation of uranium by aquatic plants in field conditions: prospects for phytoremediation. Sci Total Environ. 2014;470–471:993–1002. Available from: http://www.scopus.com/inward/record.url?eid=2-s2.0-84887589392&partnerID=40&md5=ba64c1dcc67c875b03c4c0f5cd8ed2d1.
174. Gramss G, Voigt K-D. Forage and rangeland plants from uranium mine soils: Long-term hazard to herbivores and livestock? Environ Geochem Health. 2014;36(3):441–52. Available from: http://www.scopus.com/inward/record.url?eid=2-s2.0-84899137530&partnerID=40&md5=c7e6f1194420a00e2f7b3b08cb18a8cf.
175. Jha VN, Tripathi RM, Sethy NK, Sahoo SK, Shukla AK, Puranik VD. Bioaccumulation of 226Ra by plants growing in fresh water ecosystem around the uranium industry at Jaduguda, India. J Environ Radioact. 2010;101(9):717–22. Available from: http://www.sciencedirect.com/science/article/pii/S0265931X10001037.
176. Joner EJ, Munier-Lamy C, Gouget B. Bioavailability and microbial adaptation to elevated levels of uranium in an acid, organic topsoil forming on an old mine spoil. Environ Toxicol Chem. 2007;26(8):1644–8. Available from: http://www.scopus.com/inward/record.url?eid=2-s2.0-34547959229&partnerID=40&md5=3a8d955c604d169b608a071ff5ee997c.
177. Lottermoser BG, Schnug E, Haneklaus S. Cola soft drinks for evaluating the bioaccessibility of uranium in contaminated mine soils. Sci Total Environ. 2011;409(18):3512–9. Available from:

http://www.sciencedirect.com/science/article/pii/S0048969711005675
178. Neves MO, Figueiredo VR, Abreu MM, Transfer of U. Al and Mn in the water-soil-plant (*Solanum tuberosum* L.) system near a former uranium mining area (Cunha Baixa, Portugal) and implications to human health. Sci Total Environ. 2012;416:156–63. Available from: http://www.sciencedirect.com/science/article/pii/S0048969711013817.
179. Pereira R, Marques CR, Ferreira MJS, Neves MFJV, Caetano AL, Antunes SC, et al. Phytotoxicity and genotoxicity of soils from an abandoned uranium mine area. Appl Soil Ecol. 2009;42(3):209–20. Available from: http://www.sciencedirect.com/science/article/B6T4B-4WB378H-1/2/51f679adb63af1388ae7c40e787ba34d.
180. Stojanović M, Stevanović D, Iles D, Grubišić M, Milojković J. The effect of the uranium content in the tailings on some cultivated plants. Water Air Soil Pollut. 2009;200(1–4):101–8. Available from: http://www.scopus.com/inward/record.url?eid=2-s2.0-67349201727&partnerID=40&md5=4dea9ddea2ffd866cf80f485b5a2cc56.
181. André A, Antunes SC, Gonçalves F, Pereira R. Bait-lamina assay as a tool to assess the effects of metal contamination in the feeding activity of soil invertebrates within a uranium mine area. Environmental Pollution. 2009;157(8–9):2368–77. https://doi.org/10.1016/j.envpol.2009.03.023.
182. Kratz W. The bait-lamina test: General aspects, applications and perspectives. Environmental Science and Pollution Research International. 1998;5(2):94–96. https://doi.org/10.1007/bf02986394.

Further Reading

Cinelli G, Tollefsen T, Bossew P, Gruber V, Bogucarskis K, De Felice L, et al. Digital version of the European Atlas of natural radiation. J Environ Radioact. 2019;196:240. https://doi.org/10.1016/j.jenvrad.2018.02.008.
Dartnell LR. Ionizing radiation and life. Astrobiology. 2011;11:551. https://doi.org/10.1089/ast.2010.0528.

Space Radiobiology

10

Christine Elisabeth Hellweg, Carmen Arena, Sarah Baatout, Bjorn Baselet, Kristina Beblo-Vranesevic, Nicol Caplin, Richard Coos, Fabiana Da Pieve, Veronica De Micco, Nicolas Foray, Boris Hespeels, Anne-Catherine Heuskin, Jessica Kronenberg, Tetyana Milojevic, Silvana Miranda, Victoria Moris, Sébastien Penninckx, Wilhelmina E. Radstake, Emil Rehnberg, Petra Rettberg, Kevin Tabury, Karine Van Doninck, Olivier Van Hoey, Guillaume Vogin, and Yehoshua Socol

Learning Objectives

- To understand the difference between the origin and characteristics of Galactic Cosmic Rays, Solar Energetic Particles, and trapped radiation
- To understand the differences between the radiation environment in low Earth Orbit, in deep space, and on the surface of celestial bodies
- To understand the difference between deterministic codes and Monte Carlo codes for modeling radiation transport
- To understand the different steps in a Monte Carlo calculation for the radiation environment on a body
- To acquire awareness of human health issues associated with prolonged space missions
- To acquire an overview of possible acute, chronic, and late effects of space radiation
- To be able to list the organs that are mainly affected by space radiation
- To understand basic molecular mechanisms of biological effects induced by space radiation
- To learn about the importance as well as advantages and disadvantages of animal and cell culture models in space biology studies
- To consider the importance of plant models in space biology studies
- To get knowledge on existing ground facilities to simulate the space environment
- To get acquainted to the advantages and inherent limitations of ground facilities

Fabiana Da Pieve is currently employed by the European Research Council Executive Agency, European Commission, BE-1049 Brussels, Belgium. The views expressed are purely those of the authors and may not in any circumstances be regarded as stating an official position of the European Commission.

C. E. Hellweg
Radiation Biology Department, Institute of Aerospace Medicine, German Aerospace Center (DLR), Cologne, Germany
e-mail: christine.hellweg@dlr.de

C. Arena
Department of Biology, University of Naples Federico II, Naples, Italy
e-mail: c.arena@unina.it

S. Baatout
Institute of Nuclear Medical Applications, Belgian Nuclear Research Centre (SCK CEN), Mol, Belgium
e-mail: sarah.baatout@sckcen.be

B. Baselet
Radiobiology Unit, Belgian Nuclear Research Center (SCK CEN), Mol, Belgium
e-mail: bjorn.baselet@sckcen.be

K. Beblo-Vranesevic · P. Rettberg
Radiation Biology Department, Astrobiology, Institute of Aerospace Medicine, German Aerospace Center, Cologne, Germany
e-mail: kristina.beblo@dlr.de; petra.rettberg@dlr.de

S. Baatout (ed.), *Radiobiology Textbook*, https://doi.org/10.1007/978-3-031-18810-7_10

N. Caplin
Human Spaceflight and Robotic Exploration, European Space Agency, Noordwijk, The Netherlands
e-mail: Nicol.Caplin@esa.int

R. Coos
Laboratory of Analysis by Nuclear Reactions, University of Namur, Namur, Belgium
e-mail: richard.coos@unamur.be

F. Da Pieve
European Research Council Executive Agency, European Commission, Brussels, Belgium

Royal Belgian Institute for Space Aeronomy, Brussels, Belgium
e-mail: fabiana.dapieve@aeronomie.be

V. De Micco
Department of Agricultural Sciences, University of Naples Federico II, Naples, Italy
e-mail: demicco@unina.it

N. Foray
Inserm Unit 1296 "Radiation: Defense, Health, Environment", Lyon, France
e-mail: nicolas.foray@inserm.fr

B. Hespeels
Namur Research Institute for Life Sciences, Institute of Life-Earth-Environment and Research Unit in Environmental and Evolutionary Biology, University of Namur (UNamur), Namur, Belgium
e-mail: boris.hespeels@unamur.be

A.-C. Heuskin
Namur Research Institute for Life Sciences, Laboratory of Analysis by Nuclear Reactions, University of Namur (UNamur), Namur, Belgium
e-mail: anne-catherine.heuskin@unamur.be

J. Kronenberg
Radiation Biology Department, Cellular Biodiagnostics, Institute of Aerospace Medicine, German Aerospace Center, Cologne, Germany
e-mail: jessica.kronenberg@dlr.de

T. Milojevic
Space Biochemistry Group, Department of Biophysical Chemistry, University of Vienna, Vienna, Austria
e-mail: tetyana.milojevic@univie.ac.at

S. Miranda · W. E. Radstake
Department of Molecular Biotechnology, Ghent University, Ghent, Belgium

Radiobiology Unit, Belgian Nuclear Research Center (SCK CEN), Mol, Belgium
e-mail: sfdsmira@sckcen.be; eline.radstake@sckcen.be

V. Moris
Research Unit in Environmental and Evolutionary Biology (URBE), University of Namur (UNamur-LEGE), Namur, Belgium

Research Unit in Molecular Biology and Evolution (MBE), Department of Biology, Université Libre de Bruxelles, Brussels, Belgium

S. Penninckx
Medical Physics Department, Hôpital Universitaire de Bruxelles (H.U.B.), Université Libre de Bruxelles, Brussels, Belgium
e-mail: sebastien.penninckx@bordet.be

E. Rehnberg
Radiobiology Unit, Belgian Nuclear Research Centre, SCK CEN, Mol, Belgium

Department of Molecular Biotechnology, Ghent University, Ghent, Belgium
e-mail: emil.rehnberg@sckcen.be

K. Tabury
Department of Biomedical Engineering, University of South Carolina, Columbia, SC, United States of America

Radiobiology Unit, Belgian Nuclear Research Centre, SCK CEN, Mol, Belgium
e-mail: kevin.tabury@sckcen.be

K. Van Doninck
Research Unit in Environmental and Evolutionary Biology (URBE), University of Namur (UNamur-LEGE), Namur, Belgium

Université Libre de Bruxelles, Molecular Biology and Evolution, Brussels, Belgium
e-mail: karine.van.doninck@ulb.be

O. Van Hoey
Research in Dosimetric Applications Unit, Belgian Nuclear Research Centre, SCK CEN, Mol, Belgium
e-mail: olivier.van.hoey@sckcen.be

G. Vogin
Centre Francois Baclesse, University of Luxembourg and Luxembourg Institute of Health, Luxembourg, Luxembourg
e-mail: Guillaume.vogin@baclesse.lu

Y. Socol (✉)
Jerusalem College of Technology, Jerusalem, Israel
e-mail: socol@jct.ac.il

10.1 Introduction

Experiments in space provided us with new insights into radiation biology. This chapter is organized as follows. First, we present a historical overview of the field that can be traced to the first experiments at the Eiffel tower. Then, we overview the space radiation environment and mathematical models used to describe it. Later in this chapter, we present a macroscopic picture of health effects in humans (observed or anticipated in the space environment). Afterward, we turn to a microscopic level and describe biomolecular changes introduced by space radiation. Then, we describe experimental evidence obtained from models—small animals, plants, eukaryotic cells, and extremophiles (organisms living under conditions extreme from a human point of view). Finally, we present an overview of ground-based facilities mimicking the space environment.

10.2 History of Space Radiation Studies and Space Radiobiology

10.2.1 From Earth Ground to the Eiffel Tower

Human space travels were very early the concerns of a number of scientists like Johannes Kepler who warned that extra-terrestrial trips would require ships fit to withstand the breezes of heaven [1]. The development of electroscopes manufactured by Pierre Curie made the assessment of local currents possible due to any particle crossing the two metallic plates [2]. The Italian physicist Domenico Pacini suggested in 1910 that the background noise measured with the Curie electroscopes was caused by radiation emitted from the Earth ground [3]. By performing some experiments with the Curie electroscope at the Eiffel tower, Theodor Wulf, a Jesuit priest, demonstrated that half of the radiation emitted by the Earth ground disappears at a height of 300 m. When the technology of balloons was safe, Victor Hess observed that the ionization density of the atmosphere progressively decreases up to 1000 m, but increases above 1800 m, suggesting the existence of two components of natural radiation: one from the Earth ground, the other from space, "cosmic rays" [4]. In 1936, Hess was awarded the Nobel Prize in physics for his discoveries [5].

10.2.2 From the Eiffel Tower to the Balloon Experiments

Between the 1930s and the 1940s, there were considerable advances in the technology of particle counters and in the knowledge of particle physics; thanks to balloon experiments, new clues were brought to support that cosmic rays consist of very energetic (10^8–10^{20} eV) particles. Furthermore, data hinted an unexpectedly high proportion of the iron-associated elements in the galactic cosmic radiation (GCR). The latter observation led to the hypothesis of the nucleosynthesis origin of cosmic rays [3]. Figure 10.1 shows the advances in space radiation biology since that period.

10.2.3 From the Balloon Experiments to Artificial Satellites

The pioneer works of William Gilbert, Carl Friedrich Gauss, and Henri Poincaré about magnetism suggested that charged particles may be influenced by the Earth's magnetism and that a ring current should exist around the Earth. At the end of the 1950s and overall in the 1960s, the number of artificial satellites increased drastically and permitted to verify these hypotheses. In 1958, James Van Allen and Louis A. Frank

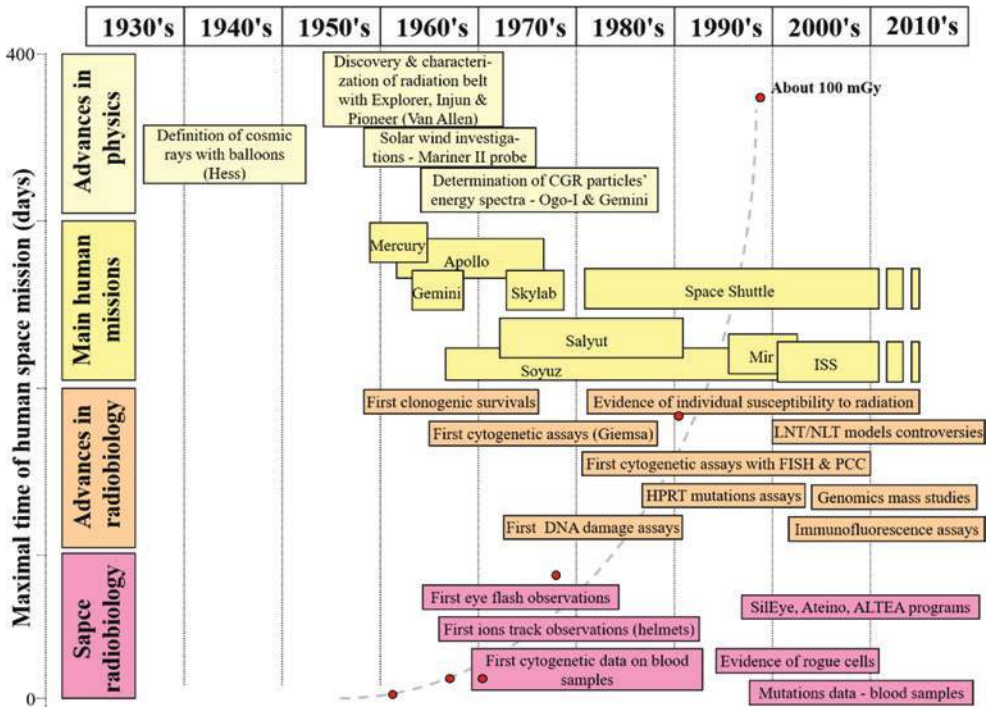

Fig. 10.1 Synopsis of advances in space radiation biology. The continuous increase of space mission duration up to 400 days is illustrated by the grey line on the left. For Mercury, Gemini, Apollo, Salyut, Skylab, and Mir missions, the maximum dose values are given as red dots [6]. *ALTEA* anomalous long-term effects on astronauts, *FISH* fluorescence in situ hybridization, *HPRT* hypoxanthine guanine phosphoribosyl transferase, *ISS* International Space Station, *LNT* linear no-threshold, *NLT* nonlinear threshold, *PCC* premature chromosome condensation, *SilEye* silicon eye. (Reprinted with permission from Maalouf et al. [6])

pointed out the existence of the Earth's radiation belt, based on data collected by the Explorer I and Pioneer IV satellites. Protons and electrons were found to be the major constituents of the Van Allen belt [7, 8]. In the same decade, Mariner II provided important data about the solar wind that permitted to document our knowledge on the radiation component from our Sun [9].

10.2.4 From Artificial Satellites to Manned Missions

During short-term (less than 2 weeks) missions in the 1960s at low Earth orbit (LEO), astronauts were exposed to several mGy at an average dose rate of about 0.17 μGy/min (245 μGy/mission day). This dose was delivered discontinuously as (1) the inner and outer zones of the Van Allen radiation belt contain protons and electrons of differing energy spectra that result in different secondary particles at dose rates different and energies; (2) the South Atlantic Anomaly (SAA), the area where the inner Van Allen radiation belt is the closest to the Earth surface, leading to an impressive flux of protons and electrons is passed about 15 times a day; here the dose rate can increase sixfold resulting in a significant contribution to the radiation exposure; and (3) unpredicted solar particle events (SPE) can increase the total dose, while the protection in LEO is still sufficient to prevent life-threatening acute radiation syndrome (see Sect. 10.6.2.1).

The characterization of individual heavy cosmic particles of high-energy and high atomic number—*Z*—(HZE) was performed with different physical radiation detectors (nuclear emulsions, plastics, silver chloride (AgCl) crystals, and lithium fluoride (LiF) thermoluminescence dosimeters) for the first time in space in the Biostack experiments flown aboard Apollo 16 and 17 (see Sect. 10.5). In parallel, their biological effects were examined in different biological objects such as bacterial spores, protozoa cysts, plant seeds, shrimp eggs, and insect eggs investigating various radiobiological end-points [10].

Examples of short-term experiments of up to 2 weeks in LEO combining radiation dosimetry and biological investigations were loaded on Space Shuttles (e.g., STS 9, 42, 45, 65), on free-flying satellites (e.g., LDEF, EURECA, BIOPAN 1–6) and on the MIR space station (Perseus mission). Later on, similar long-term experiments were performed on the International Space Station (ISS) (EXPOSE-E, -R, -R2) [11, 12].

"Cytogenetics observations revealed for the first time the major biological consequences of an exposure to space radiation: the yield of chromosome breaks seemed to increase after flight, but statistical significance was still needed (see Sect. 10.4.2.2). Data from eye flashes and helmets (see Sect. 10.4.2.3) suggested the existence of a certain "hidden part" of the heavy ions' component, probably due to secondary particles generated by the interaction of very high-energy particles with metallic materials. The contribution of these heavy ions to the total dose of radiation remained unknown at the end of the 1960s" [6].

10.2.5 From One Space Station to Another

Space experiments in combination with ground-based research (see Sect. 10.10) enabled a better understanding of the effects of space radiation and microgravity on human cells, microbes, and other biological models such as the roles of different complementary DNA repair mechanisms, the reactive oxygen species detoxification system and the intracellular accumulation of compatible solutes summarized, e.g., in Senatore et al. [13]. The modern picture of the space radiation dosimetry and its effects on human cells may be summarized as following [6]:

1. The energy spectrum of space particles and the dose spacecraft crews are exposed to can be quantified precisely by active and passive dosimetry. The dose delivered by secondary particles and countermeasures to reduce it require further investigations into the interaction of space radiation with a diversity of materials and in a complex spacecraft geometry.
2. Epidemiological studies for estimating hazards due to space radiation exposure are hampered by the small astronaut population, the individual radiation susceptibility, and radiation exposure history of each astronaut. International collaboration integrating different astronaut cohorts may help in overcoming these restrictions.
3. "Cytogenetic data undoubtedly revealed that space radiation exposure produces significant damage in cells. However, our knowledge of the basic mechanisms specific to heavy ion and low-dose and repeated exposures, and of adaptive responses is still incomplete. Furthermore, experiments about genomic instability and delayed mutagenesis may help in quantifying the risk of potential space radiation-induced cancer. The application of new radiobiological techniques may help in progressing in this field."

10.3 Space Radiation Environment

10.3.1 Origin and Nature of Space Radiation

Space is permeated with radiation, both electromagnetic radiation and particles with mass. Electromagnetic radiation in space spans many wavelengths, from long wavelength radio waves to very short-wavelength gamma rays. Gamma rays, X-rays, and some far/extreme ultraviolet (UV) waves, which can be generated for example during some transient

events on the Sun [14], are actually ionizing radiation. The wavelengths of UV, X-, and gamma rays are all shorter than those of visible light. The majority of these rays are absorbed by the Earth's atmosphere. The extraterrestrial solar UV radiation ranges from vacuum UV (wavelength <200 nm) to UVA (320–400 nm). The ozone layer absorbs some, but not all, of these types of UV radiation: UVA is not absorbed by the ozone layer, UVB (wavelength: 290–320 nm) is mostly absorbed by the ozone layer, but some does reach the Earth's surface, while UVC (wavelength: 100–290 nm) is completely absorbed by the ozone layer and atmosphere. Overall, the electromagnetic radiation reaching the Earth's surface encompasses radio waves, some microwaves, some infrared light, UVB and UVA radiation, and visible light. Of the light that reaches Earth's surface, infrared radiation makes up 49.4% while visible light provides 42.3%. UV radiation makes up just over 8% of the total solar radiation. UVA and UVB radiation contribute not only to premature aging of the skin but also to some serious health effects such as skin cancer, cataracts, and suppression of the immune system.

Generally however the expression "space radiation" mainly refers to radiation consisting of particles with a mass. There are three main radiation populations in space: galactic cosmic rays (intra- and extragalactic; GCR), solar radiation (including both the Solar Energetic Particles, SEP, and solar wind), and trapped radiation. A schematic representation of these radiation types and the environment which they can influence is given in Fig. 10.2.

10.3.1.1 Galactic Cosmic Rays (GCRs)

GCRs are constantly present highly energetic radiation in space. Their intensity is slowly varying and low with a few particles per second traversing an area of a cm^2 to a m^2 or more. They are nearly isotropic, meaning that they impinge from all directions. They originate from outside the heliosphere, most likely from deep space high-energy phenomena [16], such as supernova shock waves throughout the Galaxy, and also possibly from stellar wind termination shocks, pulsars, or other more exotic objects. They are composed of 98% baryons, of which 87% protons (hydrogen ions), 12% helium ions (α-particles), and 1–2% high-energy and highly charged ions, called High charge *Z* and Energy (HZE) particles, and 1% electrons and positrons [17]. HZE comprises ions from $Z = 3$ (Li) to $Z = 28$ (Ni). The most common elements are C, O, Mg, Si, and Fe ions (Fig. 10.3). Ions heavier than Ni can be encountered, yet these are very rare.

The spectrum of the GCRs is influenced by periodical, long-term, and short-term effects. Also, the Sun's behavior is periodical and follows an 11-year cycle which affects the interplanetary medium. The increased solar and heliospheric magnetic fields during the maximum phase of the solar cycle partially shield the solar system and decrease the low-energy portion of the GCRs flux, by preventing it from entering the inner heliosphere [18], while at solar minimum the reduced interplanetary magnetic field strength implies a more intense GCRs population [19]. The GCR flux is thus inversely proportional to the solar activity and decreases by a factor of 2–4 when moving from solar minimum to solar maximum,

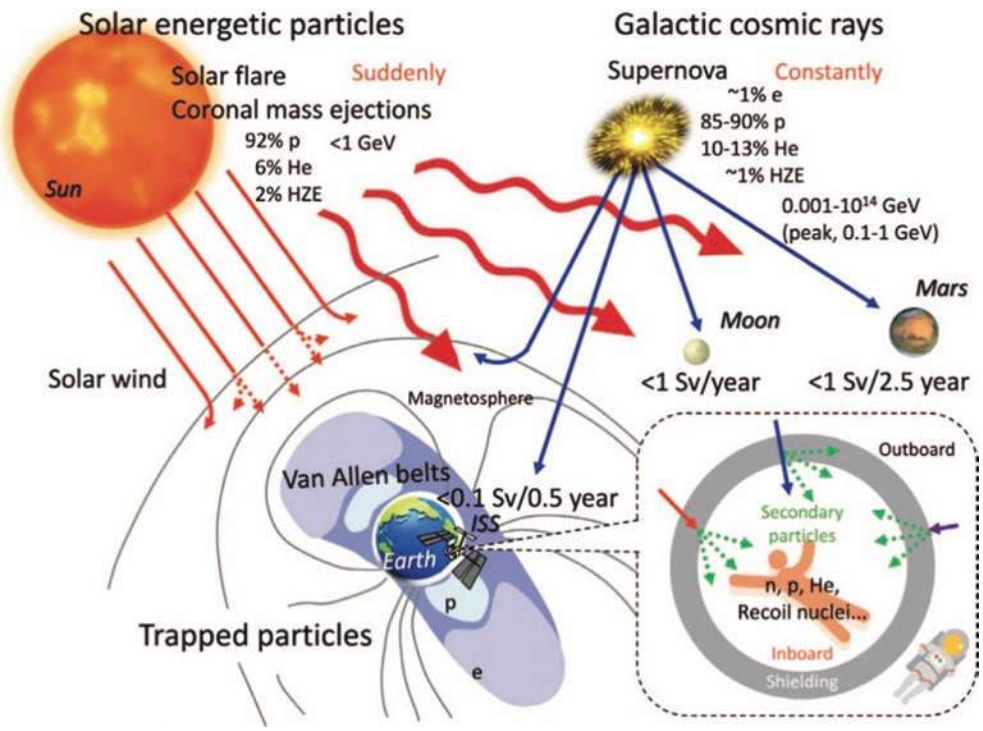

Fig. 10.2 Radiation environment during a space mission. (Image courtesy by ESA and reprinted from Chancellor et al. [15] with permission under Creative Commons Attribution-NonCommercial-NoDerivatives License: http://creativecommons.org/licenses/by-nc-nd/4.0/)

depending on the depth of the solar minimum and the intensity of the solar maximum [20, 21].

The modulation of the GCR flux for different ions is reported for the period of solar maximum and minimum. In the short term, GCRs can also be reduced by intense release of high-energy particles (mostly protons) during transient solar eruptions [22] (see Sect. 10.3.1.2). The energy spectrum of GCRs covers a huge range of energies: it commences at about 10^7–10^8 electron volt (eV) (10–100 MeV), and the most energetic *cosmic rays* reach up to 10^{20} eV (Fig. 10.4). A prominent feature is a so-called knee, with an energy of about 2.7–3.1 PeV (PeV = 10^{15} eV). This energy originated from the diffusive shock acceleration from the Galactic supernova remnants. The so-called anide or ankle, with an energy of about 5×10^{18} eV, is another characteristic of the energy spectrum. It is believed to mark the lower end of the energy of ultra-high energy GCRs, those that originate from extragalactic sources [24].

When traversing Earth's atmosphere, GCRs induce nuclear-electromagnetic-muon cascade reactions resulting in ionization of atmospheric molecules and generation of secondary particles [25, 26]. A small fraction of the initial primary particles, together with secondary particles of sufficient energy, reaches the ground. The maximum in secondary particle energy release (Pfötzer maximum) occurs at altitudes of 15–26 km depending on latitude and solar activity level. The radiation reaching the Earth's surface has levels similar to other low levels of radiation that humans are frequently exposed to. The average yearly exposure of a person is around 3.5 millisieverts (mSv). About half of this dose can be attributed to artificial sources (X-ray, computer tomography (CT) scan, mammography), while the other half originates from natural sources, including around 10% from cosmic radiation.

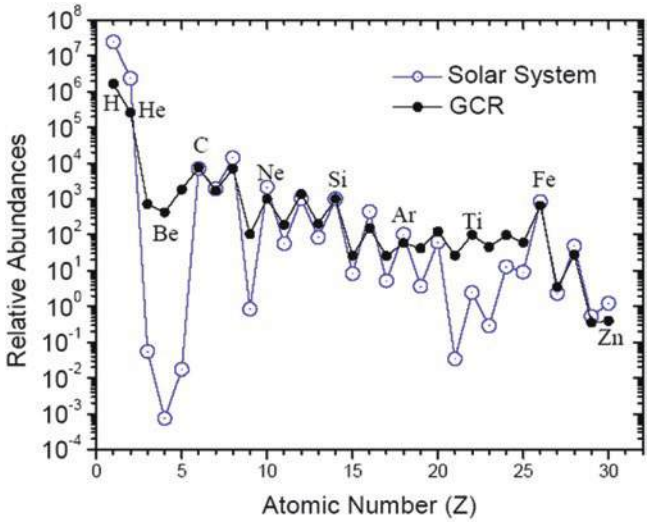

Fig. 10.3 GCR composition, as based on data from NASA's Advanced Composition Explorer (ACE) spacecraft. (Reprinted with permission from http://www.srl.caltech.edu/ACE/ACENews/ACENews83.html)

10.3.1.2 Solar Energetic Particles (SEPs)

SEPs originate from transient events on the Sun and come as massive injections of mostly protons and electrons (and to lesser extent helium (~4%) and heavier ions), with typical energies from ten to hundreds of MeV [27]. These transient events are Sun eruptions such as flares and Coronal Mass Ejections (CMEs). Characteristically, a flare lasts only minutes to hours and is the result of an explosive energy release from the Sun's coronal magnetic field. Also, the electromag-

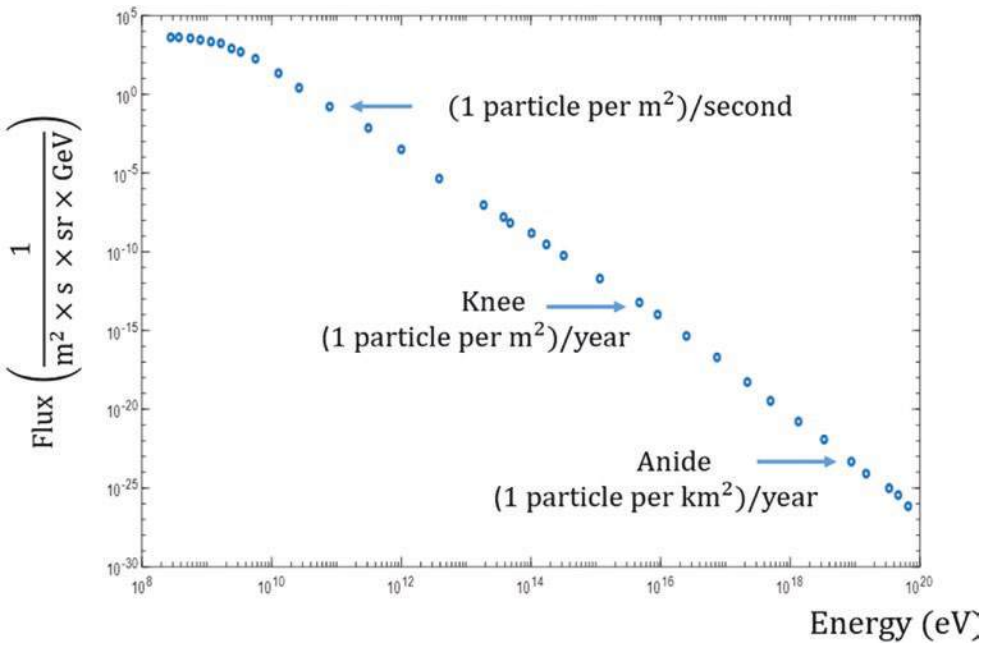

Fig. 10.4 GCR overall average fluxes versus energy. (Data from Beatty et al. [23])

netic flux increases, particularly in the short-wavelength (Extreme ultraviolet—XUV, gamma ray) range, and also in the radio regime. Usually originating in active regions, CMEs are large-scale plasma-magnetic structures with high speeds (up to thousands of km/s) associated with prominence eruptions and flares.

The likelihood of CME events increases with the power and size of the related flare event, although not all CMEs are associated with flares. Such events extend from several hours to a few days, and they have a higher likelihood of occurring during solar maximum. The level of the Sun's activity is fairly described by the number of sunspots, which provides an indication of the phases of the cycle. The number of spots increases toward the solar maximum, while during solar minimum the Sun's surface is almost spotless. Nevertheless, such SEPs events are hardly predictable and can also occur during solar minimum. Examples of an active region, an initial flare, and then a prominent eruption initiating a CME is shown for the 28/10/2003 event as part of the "Halloween Storms of 2003" in Fig. 10.5, with the related sudden increase in proton flux as detected by the Geostationary Operational Environmental Satellite (GOES) satellite (Fig. 10.6a). Examples of fluences (integral of the flux over the period of the event) related to major SEP events are shown in Fig. 10.6b.

A classification exists between Impulsive SEP events, which are short (≤1 day), numerous (~1000/year in periods of high activity), and of low intensity, and gradual events, which are long (several days at energies of a few MeV/nucleon), rather rare (a few tens per year), characterized by orders of magnitude higher protons fluences than impulsive events and ascribed to acceleration by CME-driven shocks as they propagate through the heliosphere. There is however some debate about the role played by "flare acceleration" in these events [29, 30].

Contrary to GCRs, SEP events can be considered mostly inducing deterministic effects (Sects. 10.4.2 and 10.6.2). Deterministic effects are those certainly occurring once a specific threshold dose has been overpassed. The high-intensity SEP flux can significantly increase the absorbed dose to astronauts, for example, during extravehicular activities (EVA) at the ISS, or eventually, if the event is characterized by a "hard" spectrum with a strong high-energy component, also during both interplanetary mission or missions on thin atmosphere such as Mars. Acute radiation syndrome (ARS), sickness, or, in extreme cases, death after a lethal dose can occur [31].

A comparison between GCR and SPE can be found in Table 10.1 (adapted from NASA Space Flight Human System Standards—NASA Standard 3001).

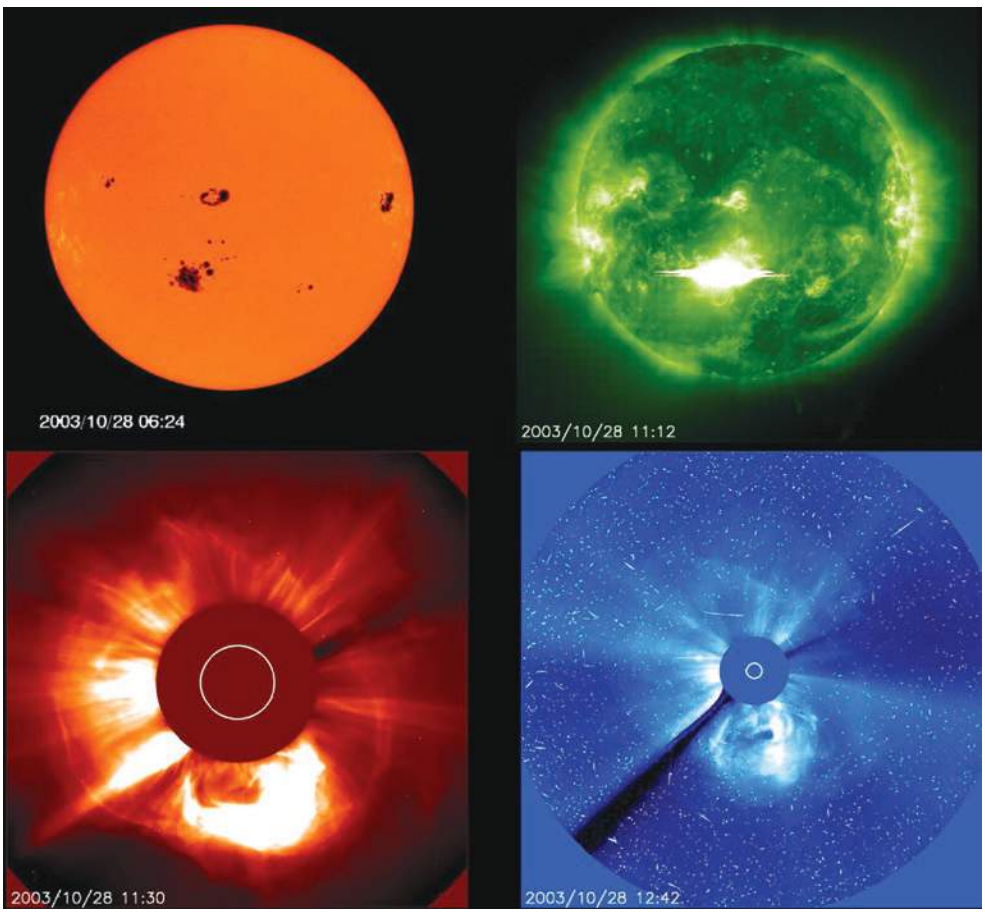

Fig. 10.5 The active regions (upper left), solar flare (upper right), and coronal mass ejections (CME, lower left and right) of the 28/10/2003 event captured by the Solar and Heliospheric Observatory (SOHO) satellite. The CME was imaged by the Large Angle and Spectrometric COronagraph (LASCO) instrument by blocking the light from the solar disk. (Courtesy of SOHO/EIT and SOHO/LASCO consortium. SOHO is a project of international cooperation between ESA and NASA)

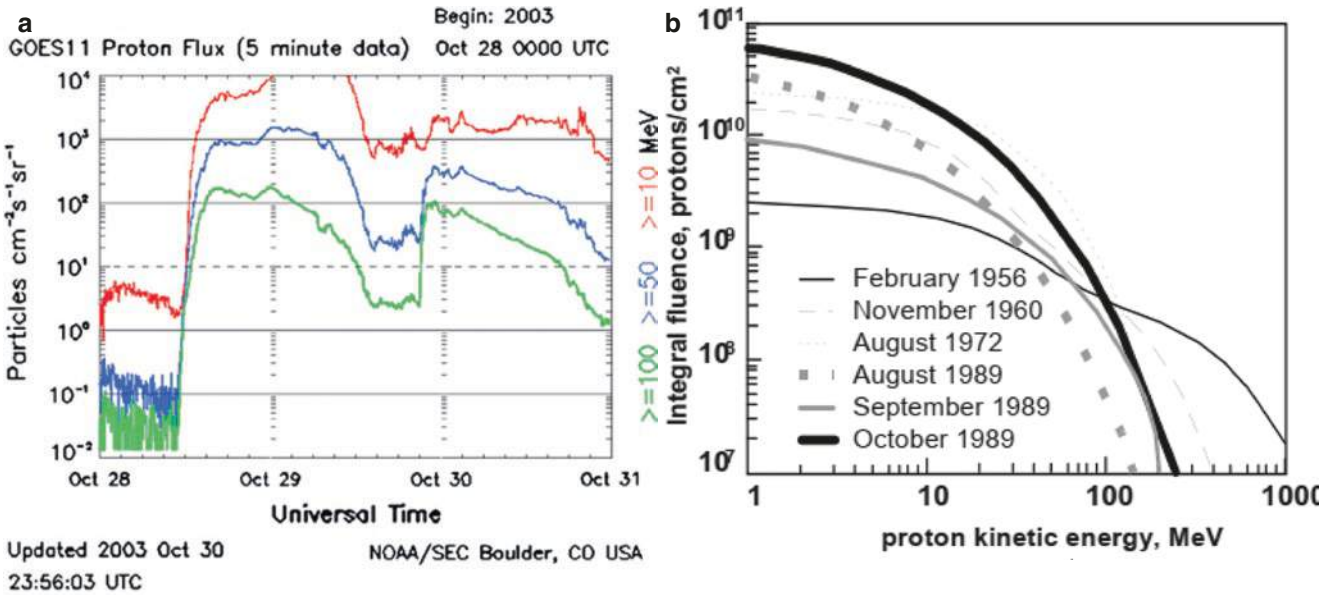

Fig. 10.6 (**a**) Proton flux between 28 and 31 October 2003. The 5-min averaged integral proton flux for energy thresholds of >10 (red line), >50 (blue line), and >100 MeV (green line) was measured by the primary Geostationary Operational Environmental Satellite (GOES) satellite of the Space Weather Prediction Center (SWPC). *CO* Colorado, *MeV* Mega electron volt, *NOAA* National Oceanic and Atmospheric Administration, *s* second, *sr* steradian, *UTC* Coordinated Universal Time. Reprinted with permission under terms of the Creative Commons Attribution License [28]. (**b**) Distribution in the energy of proton fluences for major past SEPs events (free space). (Reprinted with permission from: The space radiation environment: an introduction. Schimmerling W. https://three-jsc.nasa.gov/concepts/SpaceRadiationEnviron.pdf. Date posted: 2-5-2011)

Table 10.1 Comparison of GCR and SPE

	GCR	SPE
Spatial distribution	Isotropic beyond terrestrial influence (no preferred direction of arrival)	Non-isotropic at onset, later becoming diffused through the solar system
Composition	Protons (~87%) and helium ions (~12%) with the remainder consisting of HZE (1–2%)	Mostly protons
Temporal variations	Chronic	Acute
Energy	Extending to at least 10^{17} eV in some cases (much greater maximum than solar particles)	About 10^{10} eV highest recorded
Origin	Theories only; supernova explosions, neutron stars, pulsars, or other sources	Active regions of flares on the Sun, CMEs
Flux density	Relatively low: about 2 particles/cm²/s of all energies	Very high: may be as high as 10^6 particles/cm²/s
Biological effects	Primarily genotoxic and mutagenic with some vital cell destruction	Primarily acute damages, possible sudden illness, incapacitation, or death

Adapted from https://msis.jsc.nasa.gov/sections/section05.htm#_5.7_RADIATION

10.3.1.3 Solar Wind

The solar wind is a continuous flow of plasma from the Sun's corona, mainly consisting of protons, electrons with a small percentage of He ions, with kinetic energies between 0.5 and 10 keV. There are also some trace amounts of heavy ions and atomic nuclei such as C, N, O, Ne, Mg, Si, S, and Fe. Their energy results from the high temperature of the Sun's corona and allows them to escape the Sun's gravity. The flux of the solar wind varies over time, solar longitude and latitude, together with its temperature, density, and speed. At distances of more than a few solar radii from the Sun, the solar wind reaches supersonic speeds of 250–750 km/s [32]. At much greater distances, about 75–90 astronomical units (1 au is the distance Sun-Earth), the so-called "termination shock," interactions of the local interstellar medium with the solar wind slow it down to subsonic speed.

There are different classes of solar wind [30]:

(a) The long-lived solar wind high-speed streams, representatives of the inactive or "quiet" Sun. Sources for such streams are coronal holes usually located above inactive parts of the Sun, where "open" magnetic field lines prevail, e.g., around activity minima at the polar caps;

(b) A slow wind stream from more active near-equatorial regions on the Sun, often associated with "closed" magnetic structures. Sharp boundaries exist between these two solar wind streams (in longitude as well as in latitude),

and their main properties differ significantly according to the location and magnetic properties at the source;

(c) Another slow solar wind stream emerging during high solar activity, from active regions distributed over large parts of the Sun, in a highly turbulent state. It is highly variable and usually contains a significant fraction (about 4%) of alpha particles;

(d) The solar wind disturbances superimposed on the ambient solar wind in case of CMEs. They exhibit unusually high percentages of alpha particles (up to about 30%).

The Earth's magnetosphere deflects the solar wind, causing most of the solar wind to flow around and beyond us. Nevertheless, a small number of particles from the solar wind reach the upper atmosphere and ionosphere. This may produce phenomena such as aurora and geomagnetic storms, the latter occurring when large inflation of the magnetosphere, due to an increased pressure of the contained plasma, distorts the geomagnetic field.

In space missions, the solar wind has no impact on astronauts, as it is efficiently stopped by the spacecraft shielding and also by appropriate astronaut suits, because of the small range in a matter of the low speed-solar wind particles. However, if not appropriately shielded, the solar wind particles may affect the human body during eventual EVAs in deep space or on the surface of airless bodies, such as the Moon.

10.3.1.4 Trapped Radiation

Trapped radiation particles are produced mainly by the interaction of GCRs and SEPs with the Earth's atmosphere and are trapped by its magnetic field into the Van Allen radiation belts. These comprise:

(a) A stable inner belt of trapped protons and electrons with energies between some keV and 100 MeV that is centered at a height between 300 and 1000 km above the Earth and reaches up to a height of around 10,000 km.

(b) A less stable outer electron belt, comprising mainly high-energy (0.1–10 MeV) electrons and which extends from an altitude of about 10,000–40,000 km (see Fig. 10.7 for a schematic representation).

In the radiation belts, the energetic particles move along Earth's magnetic field lines, via the combination of three types of motion: a fast rotation (or "gyration") around magnetic field lines, typically thousands of times each second; a back-and-forth bouncing along the stronger magnetic fields in the northern and southern hemispheres, typically lasting 1/10 s; a slow drift around the magnetic axis of the Earth (the drift is eastward for electrons and westwards for ions), such drift is from the current field line to its neighbor, with the particle keeping roughly the same distance from the axis. A typical time to complete a full circle around the Earth is a few minutes.

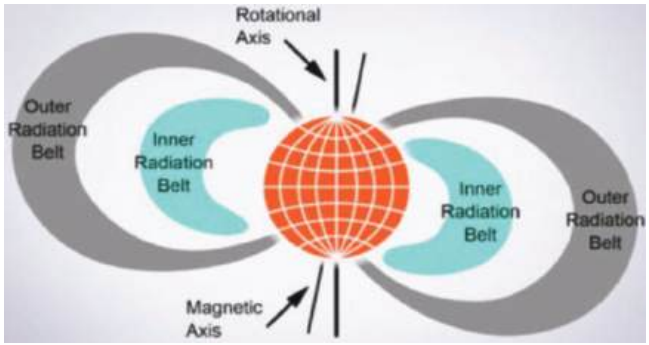

Fig. 10.7 Radiation belts of the Earth. (Figure from Van Allen radiation belt. Reprinted with permission from Wikipedia. Author Booyabazooka at English Wikipedia, https://commons.wikimedia.org/wiki/File:Van_Allen_radiation_belt.svg)

In the area above the southeastern part of South America and the South Atlantic, the inner radiation belt approaches the surface of Earth down to a few hundreds of kilometers (South Atlantic Anomaly, SAA). This is caused by the tilt and shift of the axis of the dipole-like magnetic field of the Earth with respect to its axis of rotation [33]. The dip of magnetic lines leads to an increased particle flux within this region.

The dose rate experienced by the astronauts on the ISS has a considerable contribution from trapped protons in the inner Van Allen belt because the ISS orbit with an altitude of about 400 km passes through this belt at the SAA (roughly 50% of the total dose rate) [34].

10.3.2 Radiation Environment in Low Earth Orbit (LEO)

A low Earth orbit (LEO) is an Earth-centered orbit close to our planet with an altitude ranging from 160 to 2000 km. Thus, the ISS, which flies at an altitude of around 400 km, is also in such an orbit, with an orbital inclination (the tilt of the orbital plane with respect to the equatorial plane, which helps to understand an orbit's orientation with respect to the equator) of 51.6° and an orbiting period of 90–93 min. Consequently, in 24 h the ISS makes 16 orbits of Earth and travels through 16 sunrises and sunsets. The environment of these altitudes is extreme and characterized by microgravity, high vacuum, meteoroids, extremes of temperature, ionospheric plasma, space debris, and UV as well as ionizing radiations.

The radiation sources are GCR, trapped radiation, and SEP events. The GCR environment accounts for about 50% of the total dose rate, the other 50% being induced by trapped protons of the inner belt, the only component of the inner belts that reaches energies and intensities to be important for effects on astronauts inside the ISS [35]. Other orbits, such

as Medium Earth Orbits (2000–35,786 km), Geostationary orbits (35,786 km), and High Earth Orbits (over 35.786 km), are exposed to different sub-components of the trapped radiation, some may not pose any danger. On board the ISS, astronauts encounter SPE events as a transient increase in dose rates. As mentioned above, the GCR flux is modulated by the solar cycle. At the ISS altitude, the GCR flux is also modified by the geomagnetic field, besides the modulation due to the solar activity. This field removes particles with lower energies (~few GeV/nucleon), but particles of higher energies are unaffected [36]. At low altitudes, the trapped radiation is also modulated by solar activity: at solar maximum, because of the increase in UV radiation, the upper atmosphere expands, leading to the loss of trapped protons at low altitudes. Furthermore, the inner radiation belt is mainly filled by decaying neutrons created by incoming GCR particles and the GCR flux is inversely proportional to solar activity [37]. Therefore, at solar maximum, a lower proton flux is present, leading to a smaller radiation hazard compared to the solar minimum [36, 38].

The interaction of energetic protons and HZE nuclei with spacecraft structures produces an additional intravehicular radiation field. This secondary radiation includes mainly, protons, neutrons, photons (X-rays and gamma rays), leptons (e.g., electrons and positrons), mesons (e.g., charged pions) and a great number of lighter and heavier nuclear isotopes (ions) [39, 40]. This happens in LEO and is of high concern in particular for the deep Space phase of a mission (see below), as the spacecraft would not be protected by the Earth's atmosphere and magnetic field.

10.3.3 Radiation Environment Beyond LEO (Deep Space, Moon, Mars)

10.3.3.1 Deep Space

Radiation challenges for astronautic missions beyond LEO, such as travel to the Moon or Mars, come from SEP events, GCR and intravehicular secondary radiation (Fig. 10.2). The solar wind particles, also constantly present in deep Space, do not contribute to the radiation dose induced in crews inside a spacecraft, as they are efficiently stopped even by thin shielding thicknesses.

Similar to the case of the LEO scenario, most GCRs are not efficiently stopped by regular depths of spacecraft shielding. The intravehicular radiation field is constituted by the ensemble of secondary radiation mentioned above. Adding more shielding would increase to a considerable extent the weight at launch and would not reduce the GCR-induced absorbed dose to zero. As the only modulation of GCR in deep space is provided by the shielding of the heliospheric field during solar maximum, the idea of carrying out missions to Mars during solar maximum has been considered a viable option. If one considers that during a 180-day trip at the solar maximum peak a crew would also likely receive a total SEP-contributed dose equivalent, a round trip to Mars would result in a total dose equivalent of 560 ±180 mSv,[1] higher than the estimation based on the data from the Radiation Assessment Detector (RAD) onboard the Mars Science Laboratory NASA mission [41] which was on cruise during solar minimum [42]. The above estimate for the radiation exposure is substantially lower than the accepted safe upper limit for 30–60-years old nonsmoking females and males (above 1500 mSv—see Fig. 10.8). However, inaccuracy and limitations of the models and unpredictability of SEP events must be considered.

10.3.3.2 Airless Bodies: The Moon

The Moon is about 380,000 km away from Earth and is the next endeavor for space missions beyond LEO. Although some areas of the Moon have a weak magnetic field, the Moon does not have a global magnetic field like on Earth and no atmosphere. Consequently, its surface is not shielded from radiation. The solar wind particles get stopped in the first millimeters or, maximally, centimeters of the lunar regolith, while GCR and SEP can impact the lunar surface also resulting in the production of backscattered secondary particles. The total amount of radiation that astronauts will be exposed to is influenced strongly by solar activity, their whereabouts on the Moon surface with respect to local magnetic fields, and the type and amount of radiation shielding used in spacecraft, Moon vehicles, and habitats. Recently, the Lunar Lander Neutrons and Dosimetry experiment aboard China's Chang'E 4 lander revealed that radiation levels on the Moon's surface are 200–1000 times more than that on Earth's surface and 2.6 times more than what astronauts onboard the ISS are exposed to Zhang et al. [44]. Efficiency of the radiation shielding by lava tubes on the Moon appears promising to reduce the dose rates considerably [45].

10.3.3.3 On Mars

Mars does not possess a global magnetic field, and it has only a thin atmosphere with its surface pressure less than 1% of that at Earth's surface. Therefore, high-energy GCRs can reach the surface, although still a considerable portion of them will induce hadronic-electromagnetic-muon cascades in the atmosphere, causing fragmentation/spallation and ionization showers of downward secondaries. All these particles can then induce further reactions in the planet's regolith, which generate a backscattered, albedo radiation component,

[1] Sievert (Sv) denotes the equivalent dose as measure for biological and medical relevant quantification of dose in radiation protection. For a detailed explanation please refer to Chap. 2.

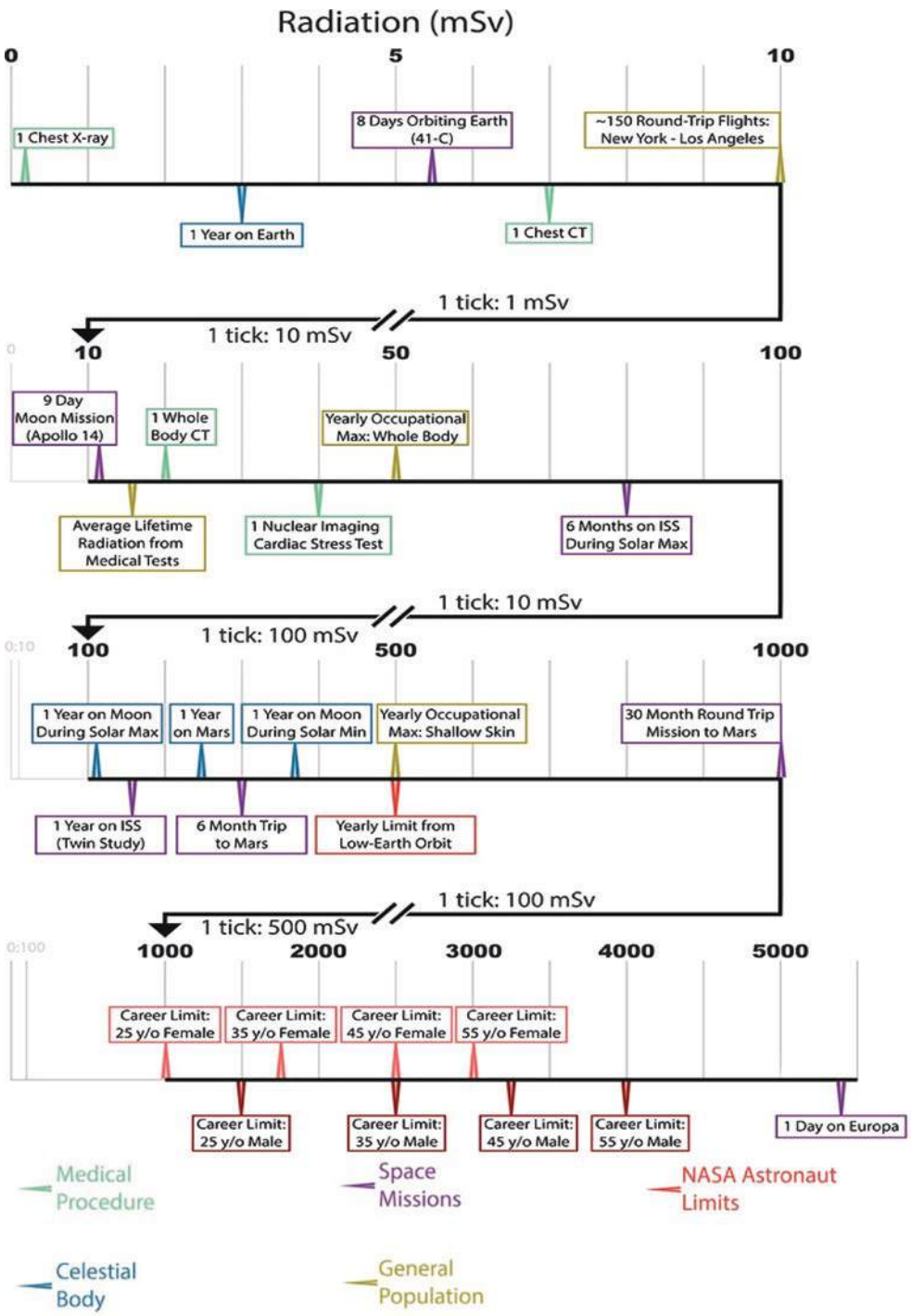

Fig. 10.8 Relative radiation exposure of varying duration during medical procedures (green), specific space missions (purple), and on various celestial bodies (blue). The astronaut yearly and career limits are given in red boxes. For comparison, some facts on radiation exposure of the general population and occupational exposure limits (US) are indicated (gold). (Reprinted with permission from Iosim et al. [43])

giving overall complex spectra including both primaries and (downward and upward) secondaries at the surface [46–48].

SEP events can increase the dose rate and dose equivalent at the Martian surface and constitute a danger for EVA on Mars. Only protons impinging the top of the atmosphere with energy above ~200 MeV do actually reach the ground, and thus SEPs events with high flux contribution at high energy constitute the biggest hazard for explorers on Mars if they are not in a habitat or otherwise sufficiently shielded. For the solar wind, despite the thin character of Mars' atmosphere, the upper layers of the latter are able to stop such radiation. Underground solutions for Mars habitats, shielded from the radiation by the regolith, are being investigated [49].

Overall, to contextualize radiation doses in space, a comparison of these doses to doses received during medical interventions is shown in Fig. 10.8. It is important to emphasize that being exposed to a hefty radiation dose within a

short time (minutes to hours) will be more health-threatening than the same dosage over a longer duration of months of years. Yet, although the health effects of acute radiation exposure are well studied, less is known about the effects of chronic exposure.

10.3.4 Space Radiation Shielding

Ionizing radiation exposure is one of the most critical health risks for astronauts. Inside the ISS, astronauts are exposed to an effective dose rate of the order of 20 μSv/h, which is about 100 times higher than on the Earth's surface. Beyond LEO in deep space, the protection of the Earth's atmosphere and magnetic field disappears, leading to an effective dose rate of the order of 75 μSv/h. Also, on the surface of the Moon or Mars, there is only limited protection and astronauts are exposed to respectively about 30 and 25 μSv/h. It is estimated that astronauts will accumulate during a Mars mission a total effective dose of the order of 1 Sv, leading to an extra risk for cancer of the order of a few percent up to more than 10% depending on sex and age [50]. Furthermore, on their way through deep space or on the surface of the Moon or Mars, astronauts can receive such high doses during intense solar storms that immediate health effects or even a deadly outcome are possible (see Sect. 10.4.2). Therefore, it is clear that astronauts need to be protected against ionizing radiation in space.

The only technology that can currently be used in practice to reduce the radiation level in spacecraft is to use shielding materials for stopping part of the radiation. The heavy ion impinging on the shielding material is the projectile, and the shielding material is the target. A multitude of interactions can occur when the projectile hits the target, including fragmentation of the projectile or target. For comparison of different materials, the area density as mass per unit area in g/cm^2 is used (for example, an 1 cm thick plate of Al with the density of 2.7 g/cm^3 has an area density of 2.7 g/cm^2). In current spacecraft, one makes most use of constructive materials such as aluminum. Unfortunately, such materials are not the most efficient for radiation shielding in space (see Chap. 4). The interaction of energetic GCRs with heavier elements such as aluminum results in the breakup of these heavier elements and the creation of secondary cosmic radiation such as energetic heavy ions and neutrons. Therefore, when using aluminum for shielding, the effective dose rate first increases as function of the shielding thickness before it starts to decrease and this decrease is quite flat as attenuation of heavy ions is nearly in balance with the build-up of light particles (Fig. 10.9 Left).

Materials consisting of lighter elements such as hydrogen have a higher stopping power per unit of mass for charged radiation particles as they attenuate their fluence via projectile fragmentation. They also minimize the build-up of neutrons and other target fragments. Radiation protection of astronauts can thus be further optimized by making use of

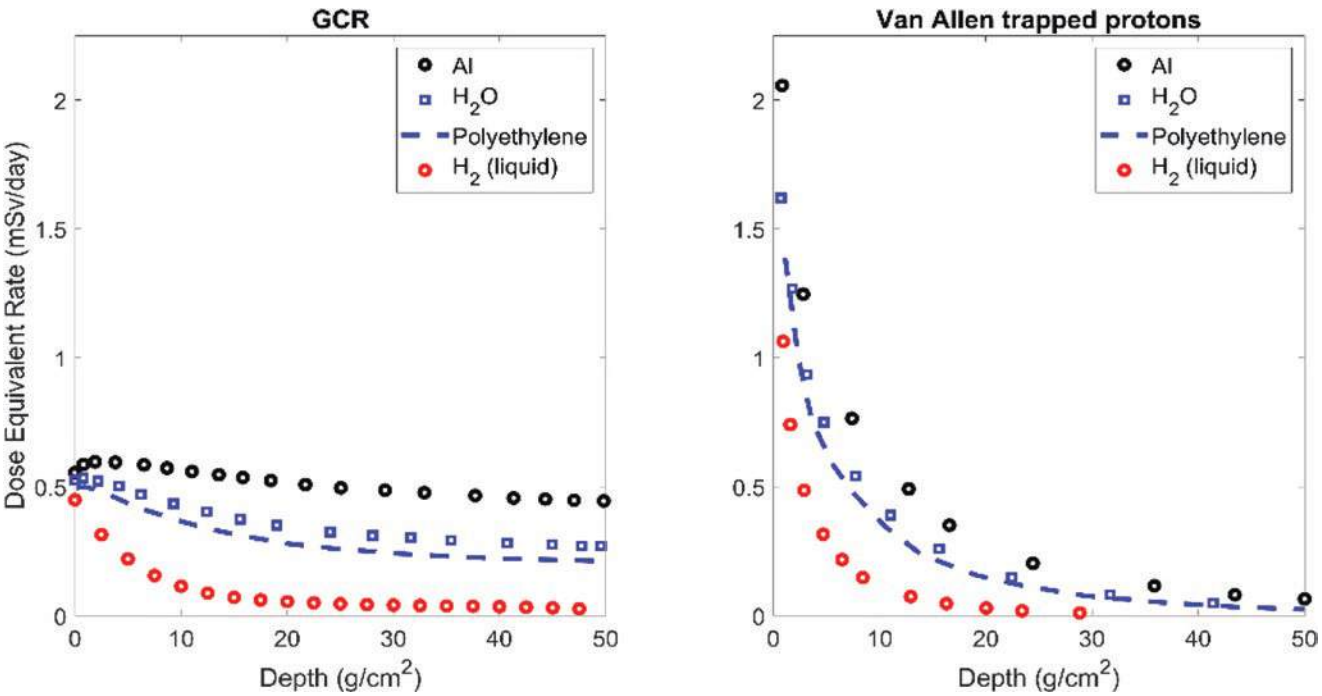

Fig. 10.9 Calculated dose equivalent rate in LEO (51.6° inclination, 390 km altitude) as a function of shielding thickness given as area density for different shielding materials: (left) GCR, (right) Van Allen trapped protons. (Data used with permission from Dietze et al. [37])

lighter shielding materials or, for instance, also by making strategic use of the necessary stock of water as additional shielding. Figure 10.9 shows the calculated dose equivalent rate for a LEO orbit similar to that of ISS (51.6° inclination, 390 km altitude) as a function of shielding thickness for different shielding materials. At standard temperature and pressure, based on a density of 1000 kg/m^3, the water column required to reach an area density of 20 g/cm^2 would have a height of 20 cm. For 20 g/cm^2 aluminum, a material thickness of 7.4 cm is derived from the density at room temperature of 2.7 g/cm^3. At the same area density of 20 g/cm^2, the shielding effect of water is much more pronounced than the one of aluminum. The thickness of the two materials is different, but they would contribute to the same extent to the mass budget of the spacecraft which is critical for leaving the Earth surface during launch. The left and right plots show the results for respectively GCRs and Van Allen protons. These plots clearly show that hydrogenous materials are much more efficient for radiation shielding in space.

In spacecraft it is unfortunately not possible to reduce the effective dose rate to the dose rate on Earth's surface. With limited shielding, a large part of the energetic protons and electrons from SEPs and the Van Allen protons can be stopped. However, GCRs have such high energies that about 1000 g/cm^2 of shielding is required to reduce the effective dose rate to the level on Earth's surface. Due to mass constraints in spacecraft, only shielding of the order of a few 10 g/cm^2 is possible. In spacecraft, astronauts can thus be protected against sudden very high and potentially deadly doses from solar storms, but they will be unavoidably chronically exposed to the ever-present GCRs leading to an increased risk for late effects.

It is clear that with current technology additional radiation exposure in spacecraft is unavoidable. However, for future manned missions to the Moon or Mars during which astronauts will stay on the surface for a longer time it will be necessary to strongly reduce their radiation exposure during their stay. This is possible because on the surface of the Moon or Mars, we can make use of the present soil material to provide adequate shielding. A few meters of soil material should suffice to reduce the effective dose rate level to similar levels as on Earth's surface. This can be done by building igloos or by living in caves or lava tubes.

Besides shielding by using materials to block the radiation, it is in principle also possible to make use of strong electromagnetic field for shielding. Several research groups are investigating this possibility. However, the required mass and energy consumption of such systems makes the concept practically impossible with current technology (Box 10.1).

Box 10.1 Highlights

(a) GCRs are the constantly present highly energetic radiation in space, they are mostly constituted by protons, with a smaller contribution from alpha particles and HZE particles. They generate particle showers in the atmosphere, although a small portion of direct GCRs can eventually reach the ground.
(b) SEP events are more probable during solar maximum, but they can actually also occur during solar minimum.
(c) Trapped radiation is constituted by GCRs and solar protons trapped in the Van Allen belts. Trapped radiation is a concern for ISS-like missions, especially because of the flux accumulated during different orbits in the SAA, or also missions on other orbits crossing one or the other belt.

10.3.5 Mathematical Modelling the Space Radiation Environment and Induced Doses

10.3.5.1 Transport of Radiation Through Matter: Deterministic and Monte Carlo Methods

The modeling of the radiation environment at or inside a spacecraft, at different altitudes in the atmosphere or at the surface/subsurface of a planet, a moon, or a small body allows to obtain the relevant dosimetric quantities for the assessment of the health risks incurred by humans due to radiation [51–53], as well as to estimate the half-lives of biomolecules in search-for-life studies [54, 55].

The transport of radiation through matter is described by the time-independent Linear Boltzmann Transport Equation, which allows to treat atomic and nuclear collisions. The Boltzmann transport equation (10.1) describes the flux $n_i(\boldsymbol{r}, E, \Omega, t)$ of several types of particles i, possessing different energies E, and moving in different directions Ω by considering the particle balance in a small volume V. It thus gives the average space-time distribution of the expected energy-momentum behavior of the particle beam, transported and scattered across the target, where each interaction is characterized by its own differential cross-section $\frac{d^2\sigma}{d\Omega dW}$. The Boltzmann equation reads as follows:

$$\int d\boldsymbol{r}\frac{\partial n_i\left(\boldsymbol{r},E,\Omega,t\right)}{\partial t}=\underbrace{-\oint_S dA\boldsymbol{j}\left(\boldsymbol{r},E,\Omega,t\right)\cdot\hat{\boldsymbol{a}}}_{\text{unscattered particles}}\underbrace{-N\int_V d\boldsymbol{r}n_i\left(\boldsymbol{r},E,\Omega,t\right)v\left(E\right)\sigma\left(E\right)}_{\text{particles scattered out}}$$

$$\underbrace{+N\int_V d\boldsymbol{r}\int dE'\int d\Omega' n_i\left(\boldsymbol{r},E',\Omega',t\right)v\left(E'\right)\frac{d^2\sigma}{d\Omega'' dW''}}_{\text{particles scattered in}} \tag{10.1}$$

$$\underbrace{+N\int_V d\boldsymbol{r}\int dE'\int d\Omega'\sum_j n_j\left(\boldsymbol{r},E',\Omega',t\right)v\left(E'\right)\frac{d^2\sigma_{\text{sec},i}}{d\Omega'' dW''}}_{\text{production of secondaries}}+\underbrace{\int_V d\boldsymbol{r}\,Q_{\text{source}}\left(\boldsymbol{r},E,\Omega,t\right)}_{\text{source}}$$

In this equation:

- the first term is the time-dependent flux change, due to particles escaping from the system boundaries, or disappearing by an absorption reaction or radioactive decay;
- on the right-hand side, the unscattered term represents the flux change due to translation without change of energy and direction (free flight);
- the particles scattered out are those exiting a "cell" (a unit volume in the phase space, the latter comprising both space and time variables);
- the particles scattered in are those entering a "cell" from a "cell" at a previous point in the phase space;
- the production of secondaries represents the effect of collisions;
- the source term can be external (e.g., a particle beam irradiating the target volume), or internal (e.g., neutrons from fission reactions in the volume).

In particular for high-energy particles, the number of interactions that must be described in order to find the solution to this equation is daunting, including ionization, excitation, spallation/fission/fragmentation, production of positron-emitting nuclei, and de-excitation through gamma rays. A solution to the problem can be attained via two different approaches:

1. **Deterministic methods**. These are deterministic approaches based on approximations to the Boltzmann equation and often on the reduction to a 1D problem via the use of the straight-ahead approximation, according to which the secondary particles from nucleon-nucleus collisions are emitted in the direction of the incident nucleon [37]. They rely on models for the relevant quantities in the transport calculation and use the continuous slowing down approximation (CSDA). Deterministic codes such as NASA's HZETRN [56] and BRYNTRN [57] follow such an approach and require relatively low computational resources to perform calculations and the calculation time is relatively short. This is due to the fact that deterministic codes do not consider all products of reactions and neglect their correlation, e.g., the coefficients used in the Boltzmann equation are related to relatively simple one-particle quantities. Thus, correlations on event-by-event basis are not considered and particle scattering at an angle is ignored [58]. Last, such methods can only be applied to restricted geometries and restricted interaction models.
2. **Monte Carlo method**. Monte Carlo (MC) is a stochastic method, exploiting random numbers to (a) "generate" an initial particles' "cocktail"; (b) track them in arbitrary geometries; (c) accumulate the contribution of each track to a statistical estimator of the desired physical observables [59]. Step-by-step particles' transport is simulated according to the statistical model of their interactions. Quantities (such as step lengths, event type, energy losses, and deflections) are sampled via generation of random values according to a given probability distribution. Indeed, in MC codes, the MC method deals with sampling from suitable stochastic distributions, with large samplings allowing to solve the integrations of multidimensional integrals.

In the context of space environment, the main interest is in high-energy particles whose scattering is generally low-angle. Therefore, it is reasonable to approximate multiple scatterings by a single continuous step, taking into account overall energy loss and direction change. This approach is known as the condensed-history technique. For example, ionization and excitation energy losses are described as continuous processes, i.e., they are continuously distributed along a particle step, if the loss is lower than a chosen threshold, together with their fluctuations.

Several MC codes are used nowadays throughout the world, such as Geant4 [60], FLUKA [61], and PHITS [62]. MC codes provide a detailed treatment of the three-dimensional transport of ions and neutral particles (see Chap. 4).

10.3.5.2 Practical Steps in the Modelling of the Space Radiation Environment and Induced Doses

An overview of the different steps for calculation of the radiation environment of a celestial body is given in Fig. 10.10.

Input Spectra

The input spectrum for GCRs can be chosen among different existing models that account for the variations of GCR particle fluxes due to variations in solar activity and in the large-scale heliospheric magnetic field throughout the solar cycle. The ISO 15390 model (ISO-15390 2004) [63] accounts for solar cycle variations in the GCR intensities on the basis of 12-month averages of the sunspot number. Changes in the large-scale heliospheric magnetic field are usually taken proportional to the corresponding changes in the Sun's magnetic field, considering also solar cycle. More accurate models describe the spectra of GCR beyond the heliospheric modulation region. The CREME96 [64] and its updated version CREME2009 (https://creme.isde.vanderbilt.edu/) are based on a semi-empirical model [65] where the particle spectrum is calculated as a product of a function describing the LIS and a function describing the modulation according to solar activity. GCR particle spectra are described in the energy range from 10 to 10^5 MeV/nucleon, from H up to Ni nuclei from the year 1760 to present. The Badhwar–O'Neill 2010 (BON2010) [66] uses, instead of an empirical description of the modulated GCR.

As in the CREME model, a physical approach to describe the GCR propagation in the heliosphere due to diffusion, convection, and adiabatic deceleration. The BON2010 model exploits data from the International Sunspot Number (ISN) and considers time lag of GCR flux relative to the solar activity. The ISN is calibrated with GCR measurements from the Advanced Composition Explorer (ACE) and the Interplanetary Monitoring Platform-8 (IMP-8). The Burger-Usoskin model [67] is limited to GCR He and H ions assuming a constant ratio of the two types of ions. The reconstruction of the modulation parameter is based on neutron monitor count rates. The DLR model by Matthia et al. [68] describes the GCRs spectra of nuclei based on a single parameter, which is derived from measurements of the ACE spacecraft and from Oulu neutron monitor count rates for different solar modulation conditions.

SEP proton spectra are often considered from historical events, then parameterized by double power law fits in kinetic energy to event-accumulated integral fluence measured by the Geostationary Operational Environment Satellites and/or ground-based neutron monitor data [69].

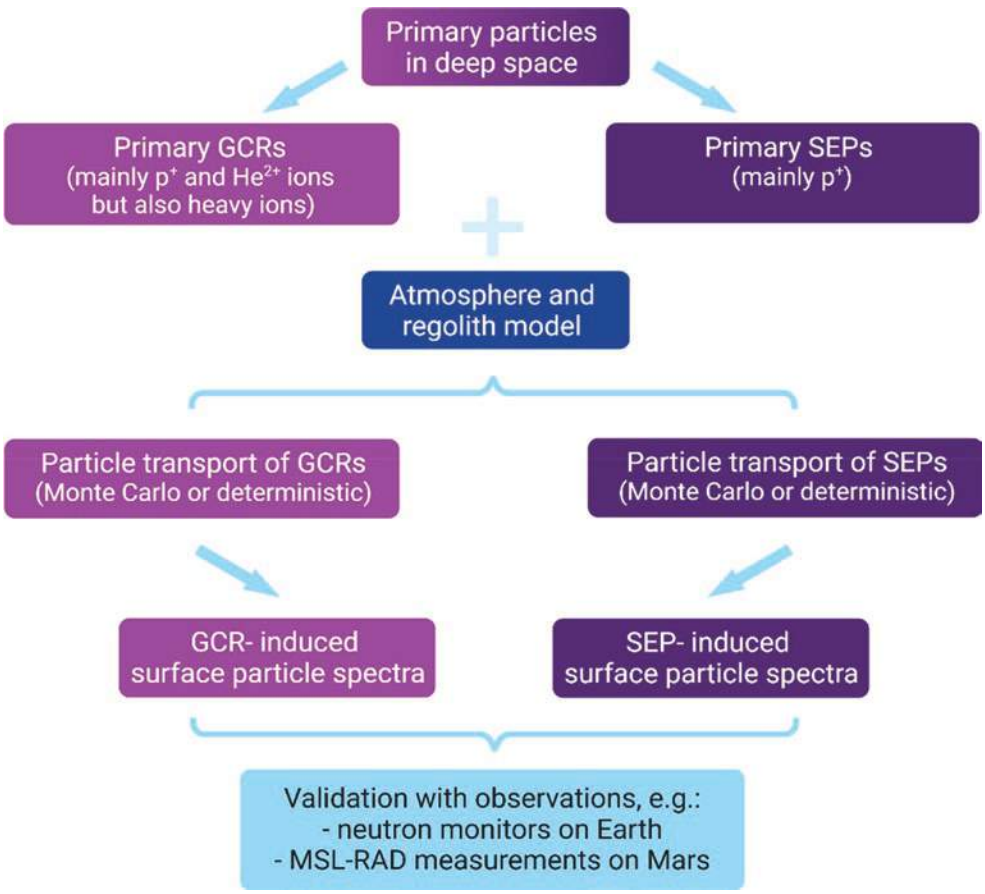

Fig. 10.10 Scheme for Monte Carlo (MC) calculations of the radiation environment at a planet/celestial body, here in particular Mars. *GCRs* galactic cosmic rays, *SEPs* solar energetic particles, p^+ protons, He^{2+} *ions* helium ions

Input spectra for both GCR and SEP events can often be retrieved via user-friendly tools, such as the SPENVIS online tool (https://www.spenvis.oma.be/) that is actually a collection of modules that allow for calculations of the radiation environment and radiation-induced effects via MC simulations in Geant4, or the On-Line Tool for the Assessment of Radiation in Space (OLTARIS) which operates on top of the deterministic code HZETRN (https://oltaris.nasa.gov/).

Atmospheric Model

For Earth, more than 99.99% of its atmosphere's mass is contained in the lower atmospheric layers below about 100 km. This region is mainly composed of N_2, O_2, and Ar which account for about 75%, 23%, and 1.3% by mass, respectively. The exact mass fraction of each constituent depends on the altitude. The water content in the atmosphere is highly variable but small, with the hydrogen fraction only reaching the order of $10^{-5\%}$ even in cloudy conditions [70]. Composition, density, temperature, and pressure vertical profiles can be obtained, for example, from the empirical atmospheric model 1 NRLMSISE-00 [71], which includes total mass density from satellite accelerometers and from orbit determination covering 1981–1997. For Mars, vertical profiles for pressure, density, temperature, and chemical composition of the atmosphere are often constructed exploting databases like MCD (Mars Climate Database http://www-mars.lmd.jussieu.fr) [46, 49]. Data can be extracted for specific locations, a specific day/night time, and season. The surface elevation and topology are extracted from the Mars Orbiter Laser Altimeter (MOLA) aboard Mars Global Surveyor. The fields (temperature, wind, density, pressure, radiative fluxes, etc.) are stored on a 5° × 5°, longitude-latitude grid from the surface to 120 km (and above) are averaged and stored 12 times a day, for 12 Martian "seasons."

Surface and Subsurface

For Earth, the soil is often considered to consist of $50\%_{Vol}$ solids (of which $75\%_{Vol}$ SiO_2 and $25\%_{Vol}$ Al_2O_3) and a scalable amount of H_2O. Studies show that the neutron environment strongly depends on soil moisture (and air humidity) [72]. The composition of the surface and subsurface of Mars can either be chosen to model specific scenarios, for example, a default basaltic composition (SiO_2 51.2%, Fe_2O_3 9.3%, H_2O 7.4%) [73] or more/less hydrated compositions to study the possibility of underground shielding habitats [49], or it can be taken from data from the Gamma Ray Spectrometer aboard Mars Odyssey [46]. The dosimetric quantities at the Martian surface do not depend strongly on the regolith composition, although some differences due to hydration and Fe-content can affect neutrons and gamma rays spectra [49].

Propagation

MC particle transport codes strongly rely on the availability of physics models and database of cross sections. A schematic view of the downward and upward main particles that need to be considered is shown in Fig. 10.11. In the open source Geant4 code [60], hadronic models are: (1) data-driven, which mainly deals with the detailed transport of low-energy neutrons and isotope production, (2) parametrized models which include fission, capture, elastic, and inelastic scattering reactions; (3) theoretical models for high energies, above several 10–100 MeV, where experimental cross-section data are scarce. For electromagnetic physics, the basic processes for electrons, positrons, photons, and ions, such as Compton scattering, photoelectric effect, pair production, muon-pair production for photons, ionization, δ-electron production, Bremsstrahlung, Čerenkov radiation, and annihilation, are considered. Additionally, processes involving the atomic shell structure such as Rayleigh scattering are also considered. Special process classes handle muon interactions like Bremsstrahlung, capture, and annihilation. Multiple scattering models provide corrections for path lengths and lateral displacements of multiple scattered charged particles. In order to decrease the computational time and resources, a certain production cutoff in the range is set for electrons, positrons, and photons, which is translated to energy below which the particle then loses its remaining kinetic energy continuously along the track and no secondary particles are produced.

Target

In principle, the proper approach to calculate the absorbed dose and dose equivalent rates is to use. Such standardized phantom has been defined by the International Commission on Radiation Units (ICRU) and it is given by the ICRU sphere, a 30 cm-diameter sphere with a density of 1 g/cm^3 and a mass composition of 76.2% O, 11.1% C, 10.1% H, and 2.6% N,

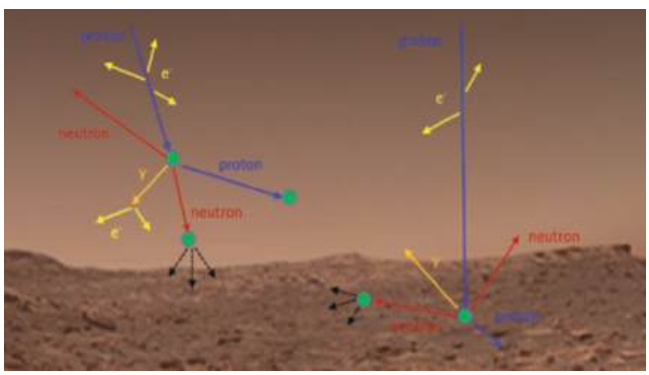

Fig. 10.11 Schematic view of the particle showers (main particles are plotted here) generated in the downward propagation of primary GCRs particles through the Martian atmosphere and of the backscattered particles [74]

which reflects the composition of tissue. Still, in recent times more human-like phantoms have been used [75]. However, such complexity is not always necessary, and sometimes other spheres of water or water slabs have been used [76].

Apart from running the MC (or deterministic) codes in standalone mode, several tools such as the previously mentioned SPENVIS online system (https://www.spenvis.oma.be/), OLTARIS (https://oltaris.nasa.gov/), and the EXPACS/PARMA code (https://phits.jaea.go.jp/expacs/) based on PHITS can be used to run a combination of the steps described above, resulting in a punctual estimation of doses at a specific location on a body or altitude in an atmosphere or in radiation maps covering several regions.

For human exploration of Mars and other bodies, the quantities of interest are the absorbed dose corrected by the relative biological effectiveness (RBE) factor (to estimate the risk for acute effects or death due to high doses for Solar Energetic Particle events) and the Effective Dose and Dose Equivalent to respectively estimate the risks to long-term effects induced by exposure to GCRs and to compare with measurements from radiation detectors. Space Agencies implement the ALARA principle [77] which ensures that mission operations are designed to keep the radiation risks as low as reasonably achievable. Although the different agencies use common limits for deterministic effects on the ISS, different career radiation exposure limits (for stochastic effects) for astronauts in LEO missions exist and no specific limits for interplanetary missions are issued (only those for LEO exist).

10.3.5.3 Harmonization of Risk Models for Stochastic Effects: The Problem of Radiation Quality Factors

Harmonization of risk models requires improvements in modeling radiation sources, in the accuracy of radiation transport codes, and the development of new realistic quality factors based on the features of the variegated radiation field in Space.

As already mentioned in Chap. 2, the approach commonly used for estimating risk from high linear energy transfer (high-LET) radiations is based on multiplying the induced absorbed dose (in units of *gray*) by a so-called *quality factor*, or *RBE factor* (always greater than one, usually below 20) representing the enhancement of effectiveness of the high-LET radiation. Such increased effectiveness comes from available evidence on the RBE of the radiations from both laboratory and theoretical studies (Sects. 10.4 and 10.5). As previously shown, RBE varies with LET. It depends also on other factors and may be different, e.g., for particular chromosome aberrations, mutations, or different tumor types. Also, RBE may vary in different biological systems. Furthermore, low-LET dose response is usually nonlinear while high-LET response tends to be more linear.

However, for radiation protection purposes, the use of RBE for low-dose exposure to radiation with different LET was superseded by the adoption of radiation weighting factor, w_R, by the International Commission on Radiological Protection (ICRP) [78], to convert absorbed dose (measured in Gy) to equivalent dose (measured in Sv) in a tissue and to effective dose (measured also in Sv) in the body. ICRP recommends $w_R = 1$ for photons of all energies, electrons, and leptons. The value $w_R = 2$ is recommended for protons and charged pions, and $w_R = 20$ for α-particles, heavy charged particles, and fission fragments [78] (see Table 10.2). However, the adoption of specific values for such weighting factors, based on the judgment from the available data on RBE, was accompanied by a recognition of the simplistic description and of the limited accuracy that the systematic application of this set of values for w_R would have brought. Thus, quality factors, Q(LET), defined as a continuous function of the LET of the radiation, were later introduced in order to give broadly similar results for measured radiation fields [78] (see Table 10.2). Such quality factors are nowadays used in the risk assessment model by the European Space Agency and were also used in the previous risk assessment model by NASA.

Nevertheless, this specification of Q in terms of the LET alone suffers from the limitations already highlighted in Chap. 1, about the fact that the sole LET cannot fully describe the effectiveness of radiation in inducing biological damage. Indeed, even simply from the perspectives of the first-stage radiation-induced effects, without mentioning the complex dependencies of the RBE on phenomena related to the chemi-

Table 10.2 Radiation weighting factors and quality factors

Radiation type	Radiation weighting factor (w_R)	Quality factor (Q(LET))
Photons	1	
Electrons and muons	1	
Protons and charged pions	2	
Alpha particles, fission fragments, heavy ions	20	
Neutrons	A continuous function of neutron energy	
For LET < 10 keV/μm		1
For 10 ≤ LET ≤ 100 keV/μm		$Q = 0.32L^{-2.2}$
For LET > 100 keV/μm		$Q = 300L^{-1/2}$

cal and biological steps, it remains the fact particles with different charge and different velocity may have the same LET and still inducing different final biological effects. The variation in the effectiveness of radiation in inducing different final biological effects has thus its root in the differences in track structures between particles that have the same LET but different charge and velocity, as highlighted in Chap. 1. Differences can be particularly large for the HZE particles encountered in space, methods used on Earth are inadequate for space travel, as, among other reasons, the ICRP radiation quality description does not represent HZE radiobiology correctly.

The key difference between (a) the quality factor used by NASA [79] for the projection of risk from space exposures and (b) the quality factor recommended by the ICRP (Q(LET)) for operational radiation protection on Earth is consideration of track structure (Box 10.2).

Box 10.2 Modeling

(a) The Boltzmann equation describes the transport of radiation in matter; it can be solved via analytical (deterministic) or via numerical (Monte Carlo) methods.

(b) The different steps for setting up a calculation of the radiation environment are input radiation spectra, definition of the parameters describing the atmosphere, with dependence on the altitude, definition of the regolith composition, definition of the physics model to be used according to the different energy ranges, definition of the target where the scoring of the absorbed dose will be done.

10.4 Human Health and Organs at Risks for Space Travel

The space environment is hostile to the health of astronauts in several ways. The confinement in the restricted space of spacecraft for shorter or longer periods exposes the crew to sometimes severe behavioral problems. Microgravity can lead to osteoporosis, a modification of the electrolyte compartments, sarcopenia, cardiac arrhythmias, dysthemeral rhythm disorganization, vestibular deconditioning, relative immunosuppression, and postural hypotension on return [80]. Finally, the space radiation environment is very different and much more hostile than that encountered on Earth. Add a temperature amplitude of 300 °C on the spacecraft's surface and the almost absolute vacuum conditions that astronauts must consider during extravehicular excursions. Finally, let us point out the disturbances secondary to the return to the ground: neurological, vestibular, cardiovascular reconditioning, etc.

10.4.1 Radiation Exposure During Space Missions

The constant flux of galactic cosmic rays (GCR) causes astronauts' chronic low-dose whole-body exposure during space missions. The primary GCR particles interact with the spacecraft hull, so that astronauts are—like patients—exposed to secondary radiation from nuclear interactions between the incident radiation and the shielding of the spacecraft. Due to mass limitations for launching spacecraft, complete shielding of GCR is not feasible. Compared to an astronaut suit for extravehicular activities, the shielding of the spacecraft by aluminum and other materials strongly reduces the skin dose and also, but to a much lower extent, the whole-body dose. On the microscopic level, due to the physical characteristics of particle radiation, very high doses can be reached, leading to permanent damage (see Sect. 10.4).

In LEO, traversal of the SAA of the inner radiation belt contributes to the accumulated dose during, e.g., a mission on the ISS. Human phantom experiments on the ISS (MATROSHKA experiment series) allowed the quantification of the effective dose rate which was 690–720 μSv/day during extravehicular activities and lower inside the ISS amounting to 550–570 μSv/day [81, 82]. Therefore, astronauts accumulate effective doses of around 100 mSv during a 6-months ISS mission. The variations of the accumulated dose depend on solar activity and the flight altitude of ISS, with higher doses during lower solar activity and increasing flight altitude. For a 1000-day Mars mission, a total effective dose of galactic cosmic radiation of about 1 Sv is expected [83, 84], which is quite considerable and exceeds terrestrial lifetime radiation exposure limits, which amount to 400 mSv in the European Union. Risks of cancer and degenerative diseases are associated with this chronic GCR exposure (Fig. 10.12).

Solar Particle Events (SPE) emanating from the Sun (Sect. 10.3.1.2) result in increased proton fluxes that may reach the spacecraft or a celestial body surface. In LEO, protection by the Earth's magnetic field is still sufficient to protect from deadly SPE, but in free space or on planets or moons without magnetic field and atmosphere, high doses might be accumulated within hours or days in situations of insufficient shielding, e.g., in a spacesuit. Above a certain threshold, acute effects will occur (Fig. 10.12). In contrast to GCR, shielding of SPE protons is feasible in special compartments of the spacecraft, which can be surrounded by more material. Astronauts can protect themselves from an SPE in such a radiation shelter until the proton flux normalizes.

10.4.2 Acute Effects

Deterministic effects appear for acute global exposures classified as medium, high, and very high (0.2 to more than 10 Sv) by UNSCEAR [85].

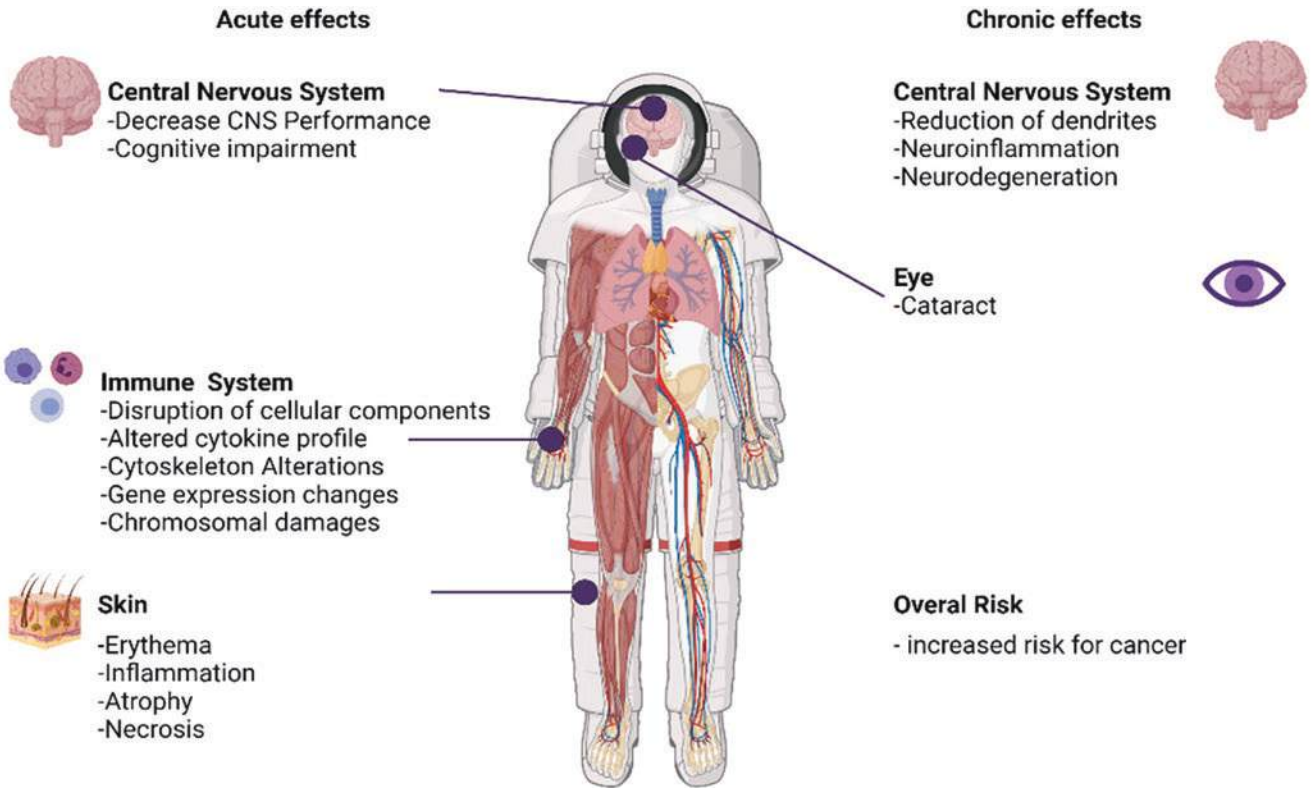

Fig. 10.12 Possible health effects of space radiation exposure

Under exceptional conditions of insufficient shielding during spaceflight, the exposure to mostly protons during a large solar particle event (SPE), the whole-body dose can reach several Gy or the skin dose even tens of Gy and thereby cause the acute radiation syndrome (ARS, see Chap. 2, Sect. 2.7.2). Such situations in the event of a solar flare of exceptional intensity can occur in LEO in areas of weakness of the Van Allen belts, extravehicular exit, and exit on extraterrestrial soil in a spacesuit or an insufficiently shielded vehicle. The total dose is delivered over a short period of time: generally, instantaneously but by definition over less than 4 days.

The acute effects affect rapidly renewing tissues which are particularly radiosensitive (bone marrow, digestive epithelium, germ cells, skin). The classic "radiation sickness" or prodromal syndrome (headache, dizziness, nausea, bone marrow hypoplasia) occurs for an exposure of 0.5–1 Gy. A dose of 3–4 Gy kills 50% of exposed individuals in 1 month [86]. Unlike the desired partial exposure of patients undergoing radiotherapy, solar flares are unpredictable, which seriously complicates mission planning for astronauts.

10.4.2.1 Chronic and Late Effects: Cancer and Degenerative Diseases

For several decades, NASA has collected data concerning acute and chronic morbidity and mortality in US astronauts in the NASA's Longitudinal Study of Astronaut Health [87]. One main aim is to determine whether astronauts' occupational space radiation exposure is associated with an increased risk of cancer or other diseases. The cohort is made up of 312 astronauts selected by NASA since 1959. Employees at the NASA Johnson Space Center in Houston, Texas, served as the control group. In January 2003, just before the explosion of the Columbia shuttle, 29 deaths (9.3%) were counted in the group of astronauts versus 17 (1.8%) in the control group. Note 20 accidental deaths among astronauts (versus 2 in the matched group). No other cause reached the threshold of significance.

Compared to the control group at matched age, astronauts had a higher specific mortality rate (SMR) from cancer. This difference was not significant. However, both groups had a lower specific mortality rate than the general population. Fourteen cases of cancer have been described in astronauts (not counting 33 cases of non-melanoma skin cancer), which represents a relative risk of 1.59 compared to the Air Force pairings but of 0.54 compared to the cohort of NCI (general population), which ultimately remains insignificant. A later study found that standardized mortality rates for astronauts were significantly below US white male population rates [88].

During a Mars exploration mission, each cell nucleus of an astronaut would be crossed by a proton or a secondary electron every 2 days, and by a heavier ion every month [89].

Due to their strong ionizing power, these ions appear to be the main vector of carcinogenic risk despite their low fluence.

The interval between irradiation and tumor appearance has been shown in rats to be shortened compared to conventional radiation [90, 91]; fewer events would be needed in the promotion of carcinogenesis induced by high-LET particles. Particle mass, energy, and charge can influence the cancer risk of an HZE particle.

The linear no-threshold (LNT) model used to predict the risk of cancer mortality in astronauts sent on interplanetary missions relies on data from atomic bomb survivors extrapolated to this particular population, to these types of particles, and to the dose rates encountered in the space environment. Though nearly universally used by public bodies to assess cancer risk, LNT is far from being a scientific consensus and its application for low dose rates is rather controversial—see Chap. 2. For cancer risk estimation, age at exposure, attained age, sex- and tissue-specific mortality and incidence, and latency has to be considered. Also, an important question is whether the additional cancer risk induced by space radiation exposure is independent of other cancerogenic events (excess absolute risk, EAR), or whether the risk depends on other cancer risks (excess relative risk, ERR).

Table 10.3 summarizes the LNT-estimated carcinogenic risk under different exposure conditions. The confidence interval includes epidemiological, physical, and biological uncertainties. The maximum acceptable risk for an astronaut dying from cancer is typically set at 3% [50].

Besides the calculated increased cancer risk for astronauts, cataracts might be triggered or promoted by space radiation exposure. Astronauts exposed to a dose of more than 8 mSv exhibit earlier and more frequent cataracts (in a study that identified 295 astronauts paired with as many US Air Force pilots) [92].

Table 10.3 Doses and LNT-based estimates for cancer mortality risk following space missions

	Absorbed dose (Gy)	Effective dose (Sv)	Risk of death by cancer (%) [$IC_{95\%}$]	
			Male 40 y.o.	Female 40 y.o.
Moon Mission (180 days)	0.06	0.17	0.68 [0.20–2.40]	0.82 [0.24–3.00]
Mars Orbit Mission (600 days)	0.37	1.03	4.00 [1.00–13.50]	4.90 [1.40–16.20]
Mars Mission (1000 days)	0.42	1.07	4.20 [1.30–13.60]	5.10 [1.60–16.40]

10.4.2.2 Chromosomal Aberrations and Biodosimetry

Due to the densely distributed ionizations around a heavy ion's path through a cell nucleus, severe DNA damage (Sect. 10.5.3) possibly leading to chromosomal aberrations (Sect. 10.5.2) can be induced. Therefore, chromosome damage induced in vivo was identified early as a sensitive biodosimeter [93, 94] that integrates radiation exposure in quality and quantity and also the individual radiosensitivity [95]. Peripheral blood lymphocytes are accessible by venipuncture and the chromosomal aberration test can be performed with these cells before and after flight.

In order to determine the effects of space radiation on astronauts, chromosomal aberrations were quantified already in Gemini astronauts before and after the spaceflight [96]. In some astronauts, a small increase was observed after the flight which did not correlate with flight duration (1–14 days), extravehicular activities, or diagnostic radioisotope injections [96]. Missions with a duration of up to 3 weeks did not result in an increase of the aberrations above background; after missions of 6 months or longer, a rise was clearly observed [95, 97–104], but dose estimation based on the cytogenetic analysis varied strongly [95]. Here, the inter-individual variability of the translocations' half-life in peripheral blood lymphocytes has to be considered [105]. Also, the basal aberration frequency and the reaction toward ionizing radiation varies from individual to individual [106–108]. Furthermore, the effects of multiple space missions might not be additive [109, 110]. Prediction of dicentrics frequencies for a Mars mission assume values 10–40× above background in peripheral lymphocytes [111].

For detection of reciprocal translocations, multicolor fluorescence in situ hybridization (mFISH) was first applied to members of the Mir-18 crew [112]. In search of a specific marker of heavy ion exposure, complex chromosome interchanges were suggested and analyzed in blood lymphocytes of astronauts [113, 114]. High-resolution multicolor banding (mBAND) of chromosome 5 can visualize intrachromosomal exchanges—long-term missions to the ISS did not increase this parameter [115]. Such inversions were only recently found in three astronauts during a 6-months ISS mission [116]. Complex chromosomal rearrangements occur very rarely in astronauts therefore their use as biomarker is limited [93]. Over the years, different cytogenetic or chromosomal signatures that allow reconstruction of absorbed dose and radiation quality were suggested, such as insertions [117], inversions [118], and complex chromosome interchanges, but up to now, no consensus for a biomarker of exposure to high-LET radiation has been reached [119] (see Sect. 8.7).

The relevance of the telomere elongation that was first observed during the 1-year ISS mission and its fast shortening after return to Earth [120], which was now also found during 6-months missions [116], for assessment of space

radiation risk is currently unclear. The telomere changes are considered as an integrative biomarker for effects of the spaceflight environment [121].

10.4.2.3 Light Flashes

Before the first human went to space, in 1952, Professor Cornelius A. Tobias made the famous prediction that cosmic radiation can cause unusual light sensations by interaction with the visual system. The Apollo-11 astronaut Edwin (Buzz) Aldrin was first reported to have perceived light flashes during the Moon mission [122]. This initiated a series of investigations already during the following Apollo missions [123], and later on Mir, Skylab, Apollo-Soyuz Test Project (ASTP), Shuttle missions, and on the ISS. They started with observation sessions and nuclear emulsion plates (Apollo light flash moving emulsion detector, ALFMED). The observations were later combined with sophisticated particle detectors in the Silicon Eye (SilEye-1 and -2) experiments on Mir [124], and Alteino-SilEye-3 and Anomalous Long-Term Effects on Astronauts (ALTEA) experiments on ISS, which included also an electroencephalograph.

The observations of the Apollo astronauts resulted in an average event rate of one light flash event in ~3 min [123]. In LEO, when passing through the SAA, the light flash rates are very high [125], and outside the SAA, light flash frequency is higher in the polar parts of the orbit than in equatorial latitudes [126]. The number of light flashes perceived in LEO varies on average between one every minute up to one every 7 min on Mir [127] or every 20 min [128, 129] dependent on the orbital height, the inclination, the shielding of the spacecraft and solar activity [130].

So, in conclusion, contrarily to the usual statement that we have no senses to perceive ionizing radiation, when closing their eyes, most space travelers can "see" the exposure to galactic cosmic rays and trapped radiation as mostly colorless light flashes or phosphenes in the form of spots, stars, streaks, or diffuse clouds of light [125]. About 15–20 min of dark adaptation is required [123] so that they are usually perceived before falling asleep.

This light flash phenomenon is explained by a visual sensation that is produced by the interaction of highly energetic heavy ions with the retina of the eye [131, 132] or possibly with visual centers in the brain or the optic nerve after penetration of the spacecraft walls and the eye or head. The interaction might be direct or indirect via Cherenkov radiation in vitreous humor which is emitted as light when the charged particle passes through it with a velocity higher than the speed of light in the vitreous humor [133]. The probability of a heavy ion to cause a light flash has been estimated to be around 1%—with increasing probability with increasing LET—and for protons to be below 0.001% in LEO [127]. A deleterious effect of the flashes on vision is not suspected, but some astronauts report that their sleep was disturbed by light flashes.

10.5 Biomolecular Changes Induced by Space Radiation

Ionizing radiation, which exists primarily in the form of high-energy, charged particles make up space radiation. The radiation environment in space is characterized by a high complexity due to different sources and a higher number of particle species, and a broad energy range. Galactic cosmic radiation (GCR), solar particle events (SPE), and, in LEO, trapped radiation are the naturally occurring sources of space radiation.

The exposure to GCR occurs at a low dose rate on the organismal level, but strong cellular effects might be triggered in case of a "hit" by an energetic particle, especially high Z and high energy (HZE) particles or heavy ions. HZE particles make up only 1% of GCR therefore only small hit frequencies are expected in the human body that could be responsible for late effects [134]. First evidence of biological effects of HZE particles was found in mice after a high-altitude balloon flight when the coat of black mice locally turned grey [135]. Single particle effects on different dormant biological systems under spaceflight conditions were proven by means of the Biostack experiments on the Apollo-16 and -17 missions [10, 136]. In this experimental system, biological systems and detector foils were stacked onto each other to allow assignment of heavy ion hits to the biological systems. Heavy ion hits were detected in plastic foils (cellulose nitrate, polycarbonate), silver chloride crystals, and nuclear emulsions. The biological systems were immobilized on the foils with water-soluble polyvinyl alcohol and included *Bacillus subtilis* spores, seeds of the thale cress *Arabidopsis thaliana*, roots of the field bean *Vicia faba*, eggs of the brine shrimp *Artemia salina*, insect eggs (stick insect, *Carausius morosus* and rice weevil, *Tribolium confusum*), and protozoa cysts (*Colpoda cucullus*). The outgrowth of *B. subtilis* after germination was significantly reduced after an HZE particle hit [137, 138]. During the development of brine shrimp eggs that were hit by a single particle, abnormalities appeared at the extremities, the thorax, and the abdomen [139] and the eggs showed the most sensitive reaction toward HZE particles compared to the other biological systems in Biostack [137, 140]. Developmental abnormalities were also found in hit insect eggs [141]. The total dose for the Biostack experiments was quite low (5.8–7.5 mGy), and ~0.03 mGy was allocated to the HZE particles, whereby it has to be considered that the local dose in a hit cell can be much higher than the total dose.

These experiments were continued in LEO using the Free Flyer Biostack Experiment (LDEF—Long Duration Exposure Facility) [142], EURECA—European Retrievable Carrier [143–146], and the biosatellites COSMOS 1887 and 2004 [147, 148] and refined, so that synergistic effects of

HZE particle hits and microgravity in the developmental disorders of *C. morosus* were revealed.

These intriguing results showing strong deleterious effects of single particle traversals and even an enhancement by other spaceflight environmental effects initiated a multitude of biological experiments in space and at heavy ion accelerators (see Sect. 10.9) in order to quantify the biological effectiveness of HZE particles, to understand the underlying mechanisms and to develop countermeasures. A variety of experimental models are used for these experiments (see Sects. 10.5–10.7, and 10.8.2). The uncertainties in risk assessment for cancer and non-cancer effects in the central nervous system and other organ systems for astronauts are still unacceptably high therefore further investigations into the biological effects of HZE particles are necessary. The experimental approaches shown in Box 10.3 below take the low dose rate but strong biological effects in case of a particle hit into account.

Box 10.3 Experimental Approaches for HZE Particle Effects

Natural GCR exposure

- Correlation of biological effects with single particle hits by combination of biological model and detector foil, e.g., Biostack; can be combined with 1xg reference centrifuge to determine contribution microgravity effects
- Correlation of light flashes with HZE particles that traverse astronauts' eyes
- Dose accumulation over weeks or months by storing dormant or freeze-dried or deep-frozen cells or small organisms in space, subsequent reactivation and measurement of radiation damage or response
- Determination of spaceflight effects by exposure of, e.g., fruit flies, rodents, or other organisms on satellites or high-altitude balloons

Exposure to selected HZE particles

- Exposure of a variety of biological systems at heavy ion accelerators or microbeam facilities to selected heavy ions (singe particle at defined energy or mixture of particles of defined energies) and analysis of the biological response

10.5.1 Cellular Survival, Cell Death, and Proliferation

As described in Chap. 2, radiation quality is an important factor influencing the cell death response. It can affect the extent and mode of cell death. A stronger cell killing of human cells by alpha particles with an LET up to 100 keV/µm was already observed in the 1960s [149], indicating an RBE for cell killing up to 7. Since then, survival data after heavy ion exposure were collected for many mammalian cell types including primary cells and tumor cell lines using the colony forming ability (CFA) test which is described in Chap. 2. This was less driven by space radiation research but by tumor therapy research to identify suitable ions and to determine the cell killing RBE for treatment planning. The shoulder observed in the dose response curves for cell killing by low-LET radiation disappears in high-LET survival curves, resulting in purely exponential dose–effect relationships and indicating the lack of repair capacity after heavy ion exposure [150] (Fig. 10.13).

Clonogenic cell survival data for more than 1100 experiments comparing the effects of ion irradiation to photon irradiation are available in a database established by the GSI biophysics group [151]. The database is called Particle Irradiation Data Ensemble (PIDE, www.gsi.de/bio-pide). The maximal RBE for cell killing (10% survival level) was observed in the LET range of 100–200 keV/µm with values of 2–7 [151]. This large variation in RBE is explained by the influence of particle species and energy in addition to LET, of cell type and other experimental factors. At LETs above ~200 keV/µm, more energy is deposited in a cell traversed by a particle than is required to kill the cell and more hits per cell cannot produce more cell death as any hit will kill the cell, resulting in a decrease of RBE that is called "overkill effect."

The clonogenic survival data integrate cell death by various modes such as mitotic catastrophe, apoptosis, necrosis,

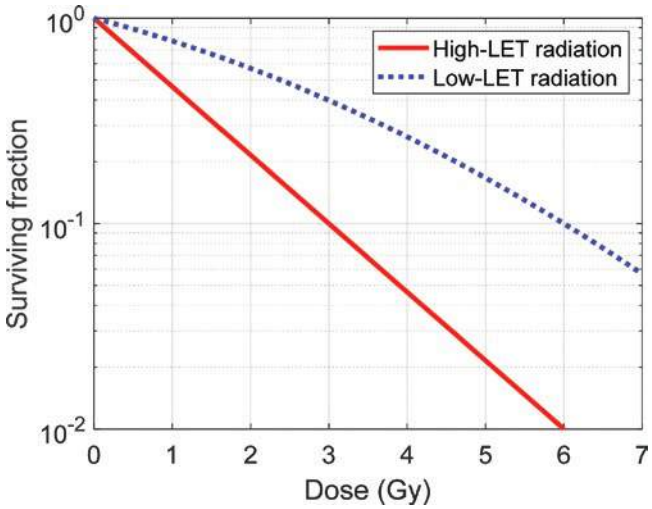

Fig. 10.13 Survival of mammalian cells after exposure to low linear energy transfer (LET) and high-LET radiation. Low-LET radiation includes photons, electrons, positrons, protons, and more. High-LET radiation encompasses heavy ions, and, depending on energy, also He ions and neutrons

autophagy, and other mechanisms (see Chap. 2) and permanent cell cycle arrest, possibly accompanied by cellular senescence. As for low-LET radiation, it depends on the cell or tissue type whether a cell population is prone to ionizing radiation-induced apoptosis [152]. Apoptosis might occur at higher rates after high-LET radiation exposure compared to low-LET irradiation with a maximum at a LET of ~100 keV/µm [153].

The consequences of heavy ion-induced cell death for the organism can be that transformation of a heavily damaged cell is prevented thereby protecting from cancer. This effect also limits the number of cells with mutations (see Sect. 10.5.4) or chromosomal aberrations at a LET >200 keV/µm (see Sect. 10.5.2) and cellular transformation (see Sect. 10.5.5). On the other hand, deleterious effects might occur such as depletion of stem cell pools or loss of terminally differentiated cells with no or low regeneration potential that might affect the functionality of a tissue or organ.

For some microorganisms, growth and viability were measured during space missions. A 14-days exposure of *Escherichia coli* on the Space Shuttle or 140-d exposure on Mir did not result in any differences in viability and mutations frequencies in comparison to ground controls [154, 155]—the same was the case in *Saccharomyces cerevisiae* [156]. Using repair-deficient *E. coli* mutants, DNA polymerase, and 3′→5′ exonuclease were identified as the most important enzymes for GCR-induced DNA damage in *E. coli* [157]. Also, the slime mold *Dictyostelium discoideum* did not grow differently and did not show differences in the mutation frequency in the spores during a 7-days Shuttle flight [158, 159], but the number of spores per fruiting body was reduced [160].

10.5.2 Chromosomal Aberrations

Chromosomal aberrations are alterations in DNA structure that become microscopically visible after following a chromosome staining protocol [161] (see Chap. 2). They can result from mis-rejoining of DNA ends from ionizing radiation-induced DNA double strand breaks (DSB), from lack of repair leading to terminal deletions and incomplete exchanges or from chromosome mis-segregation [162, 163]. They are exquisitely and quantitatively sensitive to ionizing radiation. Symmetrical resolution of the DNA DSB can lead to chromosomal interchanges resulting in translocations which are usually nonlethal. Asymmetrical resolution produces among other dicentrics (chromosomes with two centromeres) and acentric fragments, mostly contained within micronuclei; also, during the repair process, DNA sections can be lost, producing a deletion [164]. Ionizing radiation can also induce quadriradials (U-type by asymmetrical resolution, X-type by symmetrical resolution). Complex and asymmetric aberrations such as dicentrics usually lead to cell death (lethal aberrations) [163].

They are determined during metaphase or by chemically induced Premature Chromosome Condensation (PCC, see Chap. 2) during interphase [165], usually in lymphocytes or fibroblasts, providing data on a cell-by-cell basis. Their dose–response relationship follows a curvature. While dicentrics and acentric fragments can be detected with a GIEMSA staining, mFISH is required for interchromosomal translocations and mBAND for intrachromosomal translocations (see Sect. 10.3.4). Inversions can be detected by Directional Genomic Hybridization (dGH) [166].

Chromosomal aberrations are of high interest in space radiation biology as they are an early-stage effect and regarded as a surrogate endpoint for cancer risk as many human cancers are linked to them and all "clastogens[2]" are both mutagenic and carcinogenic.

For carcinogenesis, the surviving cells with chromosomal aberrations are relevant. The fraction of these cells depends on LET, track structure, and fractionation (Box 10.4).

HZE particles have a very high efficiency in inducing chromosomal aberrations—the RBE in comparison to low-LET radiation was estimated to reach 30–35 during interphase [163, 167, 168]. Furthermore, high-LET α-particles at low fluences (1 track per cell nucleus) were more efficient in inducing complex aberrations in human peripheral blood lymphocytes than X-rays [117]. Complex chromosome aberrations are defined as aberrations that involve three or more breaks in at least two chromosomes. Here, the particle track structure comes into play [169]. Delta rays move out of the primary particle track, producing further ionizations that can induce damage. This damage might interact with other breaks generated by either a separate track or delta rays emanating from it (intratrack action). The range of the delta rays is proportional to the specific energy of its corresponding primary particle. Higher energy particles would have a greater chance of track interaction than their lower energy

Box 10.4 Factors Influencing Induction of Chromosomal Aberrations by Ionizing Radiation

Dose rate
Fractionation
Linear energy transfer (LET)
Track structure
Cell nuclear geometry (e.g., spherical or flat)

[2]A "clastogenic" agent directly causes DNA strand breaks or disturbs normal DNA-related processes resulting in insertion, deletion, or rearrangement of chromosome sections.

counterparts because of the longer range of the delta rays where breaks can be close in space and time at high doses and dose rates as they are produced by multiple tracks (inter-track action). The breakpoints induced by delta rays add up to those produced in the primary particle track. Hence, the number of exchange breakpoints and their spatial arrangement are important determinants for the formation of complex exchanges. For example, the number of breakpoints per cell was higher for ^{56}Fe ions (1.1 GeV/n) and α-particles (0.9 MeV/n) in comparison to ^{137}Cs γ-rays. In spherical cell nuclei, one particle traversal is sufficient to produce two breakpoints, e.g., in a lymphocyte [170, 171]. In summary, HZE particles produce more breakpoints per track and more highly complex exchanges compared to low-LET radiation [118] (Fig. 10.14). These complex aberrations partly disappear between the first and second cell division after radiation exposure, but some are transmissible and might be stable through several cell generations.

10.5.3 DNA Damage and Repair Kinetics

As other radiation qualities, protons, α-particles, and HZE particles can induce various types of DNA damage by direct ionization or indirectly through radiolysis of intracellular water (see Chap. 2). Among base damage, loss of bases, DNA-DNA and DNA-protein crosslinks, single strand breaks (SSBs), and double strand breaks (DSBs), DNA DSBs are the most severe DNA lesion. Unrepaired DNA DSBs are at the center of biological effects such as cell killing and chromosomal aberrations and are trailblazers of the majority of early and late effects induced by ionizing radiation exposure [163, 172, 173].

What makes particle radiation special is the multitude of ionizations localized along the particle's path through the cell. The spatial distribution of direct DNA damage differs strongly for low- and high-LET radiation, with a diffuse distribution for the former and clusters for the latter. Such clusters of different damage (base lesions, abasic sites, SSB, DSB, etc.) within a few helical turns of DNA are called complex DNA damage (Fig. 10.15) (formerly: multiply damaged sites or clustered DNA damage) [164, 174, 175].

Although the contribution of direct action to the biological effectiveness of high-LET radiation is larger than indirect action [176], reactive oxygen species (ROS) generated by radiolysis can also play a part in the overall radiation effects. As the lifetime and diffusion range of ROS are small, only radicals produced in DNA's vicinity are relevant for DNA damage induction and increase in its complexity. With increasing LET, the contribution of direct effects rises, and the indirect effects drop. Low-LET radiation and endogenous ROS rarely induce complex DNA damage [163].

The detection of GCR-induced DNA damage succeeded in HeLa cells during the Shuttle and Mir missions [177–179]. In human lymphoblastoid cells that were stored at –80 °C for

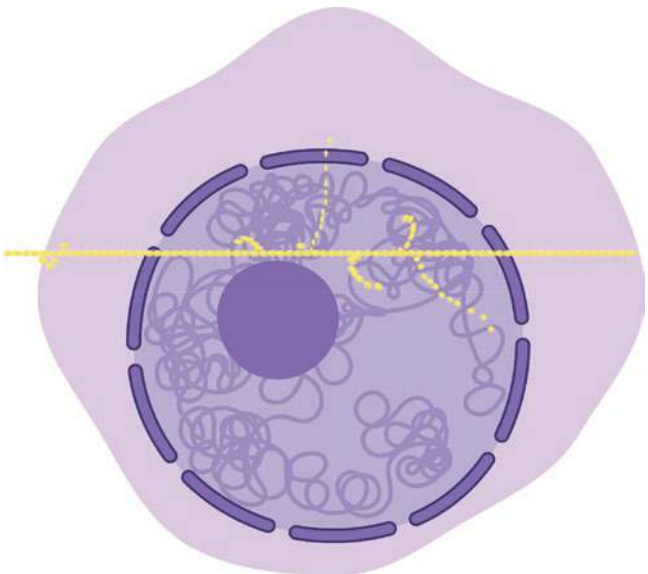

Fig. 10.14 As a heavy ion travels through a mammalian cell nucleus, a multiple of ionizations is produced, damaging a chromosome arranged in its nuclear territory several times. Delta rays emanating from the primary track can induce further damage. Therefore, traversal of high-LET radiation through a cell nucleus can produce many breakpoints in chromosomes

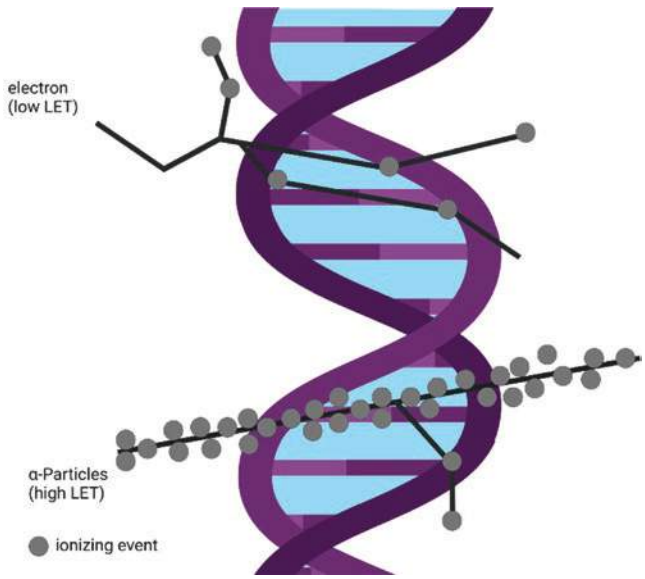

Fig. 10.15 Comparison of ionizations (grey dots) in a DNA molecule that are induced by electrons as an example of low-LET radiation and by a high-LET α-particle. The ionizations produced by the α-particle are located densely along the track, with some secondary electrons (δ rays) generated while traversing the cell. This spatial distribution goes along with a higher probability of simultaneously breaking both DNA strands thereby producing a double strand break (DSB), and also further damage to bases and single strand breaks (SSB) in close proximity which is then called complex DNA damage

several months on ISS—in total 134 days at an average dose rate of 0.7 mSv/day, one particle track per 100 cells was detected by means of immunofluorescence staining of γH2AX after return to the ground (see below) [180]. Such tracks were also observed in human fibroblasts that were cultivated for 14 days on the ISS [181].

10.5.3.1 Repair of HZE Particle-Induced Double Strand Breaks and Complex Damage

Various DNA damage repair pathways ensure genome integrity and stability in uni- and multicellular organisms. The current understanding is that multiple repair pathways have to be coordinated to repair complex DNA damage making it very challenging, that short fragments might be lost during repair and that multiple breakpoints in the DNA ribose-phosphate backbone can favor complex genomic rearrangements [164, 182]. The damage might still persist at DNA replication because of repair delays that were observed after HZE particle exposure. If repair of complex lesions is completed, its fidelity might be lower when compared to simple DNA damage [183–185]. After ^{56}Fe ion (1 GeV/n) exposure, 14% of the damage remained unrepaired compared to 5% after γ-ray or α-particle exposure [171]. In vivo, persistent DNA DSBs were found even 1 month after exposure to iron ions [186]. Growth arrest, cell death, or senescence are possible consequences of such unrepaired DNA damage [164], while mutations and chromosomal aberrations are key steps in cellular transformation and tumorigenesis.

DSBs are mainly repaired by nonhomologous end joining (NHEJ) and homologous recombination (HR) in eukaryotes (see Chap. 2). DNA DSB repair follows biphasic kinetics with a faster velocity in the beginning and lower speed at later timepoints. The phosphorylated form of the histone variant H2AX (γH2AX) [187, 188] as a marker of DNA DSB is often applied to microscopically visualize DSB induced by high-LET radiation exposure, sometimes in combination with antibodies binding to 53BP1 or other DSB repair proteins or to oxidative base damage [189]. After immunofluorescence staining, fluorescent foci indicate γH2AX and 53BP1 accumulation around DNA DSB. Ground-based experiments performed at heavy ion accelerators allow quantification of DNA damage induction and DNA repair by one ion with a specific energy or, since lately, several ion species with specific energies hitting the cells from one direction (see Sect. 10.10.4). They are usually performed additionally with low-LET radiation for comparison.

For example, in human fibroblasts, repair of DSB induced by carbon ions was slower than those induced by proton or helium ion irradiation and the size of the repair foci increased with increasing LET [190]. Larger repair foci that persist longer are a common finding when exposure to heavy ions and X-rays are compared [191, 192]. One day after exposure to 1 GeV/n iron ions, 30–40% of the 53BP1 and γH2AX foci still remained indicating the extent of residual damage [193]. The slow repair kinetics and incompleteness of repair of DNA damage induced by high-LET radiation [190, 191, 194] are consistent findings of experiments with mammalian cells at heavy ion accelerators. Also, there are some hints that high-LET radiation inhibits c-NHEJ and shifts toward error-prone alternative nonhomologous end joining repair and microhomology-mediated end joining, resulting in a lowered fidelity of repair for days or weeks [195]. Other studies have shown that the repair of complex DNA requires DNA resection for processing at the DNA ends in G1 and G2 cells and forces the pathway choice toward resection-dependent HR [196, 197].

As mentioned above, to repair complex DNA damage, other repair pathways might be involved such as base excision repair (BER) and/or nucleotide excision repair NER [198]. Oxidative base damage such as 8-oxoguanine can be restituted by BER starting with damage recognition and removal by a DNA glycosylase and final steps by polymerase and ligase proteins [172]. NER is responsible for the repair of larger helix-distorting lesions.

In summary, DNA damage complexity increases with increasing LET, resulting in less effective DNA repair, a higher rate of residual lesions, genomic instability, and enhanced cell killing [174].

10.5.3.2 Effects of Other Spaceflight Environmental Factors Such as Microgravity on DNA Repair

The results of the Biostack experiments raised the question of whether microgravity or other spaceflight environmental factors affect DNA repair processes, as explained hereinafter. The advanced Biostack experiments included an inflight 1*g* control on a centrifuge, allowing the separation of effects of microgravity and of all other environmental factors. In this experiment, eggs of the stick insect *Carausius morosus* were exposed in space and the HZE particle hits were traced back to the eggs by means of particle track detector foils. Back on Earth, the insects were allowed to hatch. When the eggs were hit by an HZE particle under microgravity, more abnormalities were observed compared to hits during centrifugation at 1*g*, indicating additive or even synergistic damaging effects of cosmic radiation and microgravity [144].

Therefore, DNA repair and radiation response under microgravity were examined in further spaceflight experiments using a 1*g* centrifuge inflight control and in ground-based simulation using clinostats or random positioning machines. For determining subtle differences in DNA repair capacity or kinetics, a high level of DNA damage has to be induced. For this purpose, the dose rates of GCR in LEO on the Space Shuttle or on ISS are too low; therefore, DNA damage has to be induced by irradiation on ground in a metabolically inactive state, by irradiation in space using an arti-

ficial radiation source brought in LEO or by incubation with chemicals. When radiation damage was already induced on ground using a radiation source, cooled cells were brought to space and activated there to repair their DNA under microgravity [199, 200]. Alternatively, DNA DSB were induced by bleomycin [201] or restriction enzymes [202] during spaceflight. Often, no or only small interactions were found [203, 204]. In yeast however DNA DSB repair was delayed under microgravity, suggesting additive effects of radiation and microgravity [205, 206]. In human fibroblasts and *Bacillus subtilis*, microgravity did not influence the repair of DNA SSB and DSB [200, 207]. Also, ligase activity [204] and DNA replication [208] were not affected. The expression of genes involved in the DNA damage response was altered under microgravity [209–211]. Besides these gene expression changes, a growth-stimulating effect of microgravity was observed in many ground-based and space experiments that might contribute to the microgravity effects on the DNA damage response [209]. In ground-based experiments, limitations of various microgravity simulators have to be considered [212], especially the generation of shear forces [213] as possible confounders. For microorganisms, such as bacteria, it has also to be considered whether they are motile because of, e.g., flagella or not, and the effect of microgravity can be most likely attributed to changes in the medium surrounding the microbes [214].

Animal experiments addressing the question of DNA repair under spaceflight conditions are scarce. After a 14-day spaceflight, the level of the tumor suppressor p53, which acts as a transcription factor in the DNA damage response, was increased in the muscle of mice compared to ground control mice [179]. Experiments with the nematode *Caenorhabditis elegans* during the Shenzhou-8 mission revealed changes in the expression of four microRNAs and of 4.2% of the genes involved in the DNA damage response after 16.5 days of microgravity when compared to the inflight 1*g* control [215]. Hindlimb unloading is used in rodent models to simulate on ground the head-ward fluid shift that occurs in microgravity. After 21 days of hindlimb unloading and low-dose irradiation of mice, some genes involved in DNA repair, chromatin organization, and cell cycle were differentially expressed in the spleen compared to control mice [216].

10.5.3.3 Future Space Experiments

Space experiments are the only way to unambiguously identify the effects of real microgravity on biological systems, here the enzymatic repair of radiation-induced DNA damages. The opportunities to perform experiments with actively metabolizing organisms in space are rare and usually have a long lead time from the acceptance of an experiment proposal to the execution of the experiment in space.

The Biolab facility in the Columbus module of the ISS provides many possibilities for biological experiments on microorganisms, cells, tissue cultures, small plants, and small invertebrates in LEO (https://www.esa.int/Science_Exploration/Human_and_Robotic_Exploration/Columbus/Biolab). However, experiments on the ISS are subjected to limitations such as up- and download mass, up- and download temperature conditions, availability of a suitable facility in space, data downlink, number of sample replicates, appropriate control experiments in space and on ground. The Biolab facility will be used for LUX-in-Space (ESA AO LSRA-2014-026, Team Coordinator: P. Rettberg), the first space experiment where the whole series of events from DNA damage induction in metabolically active cells to the different steps of enzymatic repair reactions will take place in real microgravity and the repair kinetics will be monitored by optical measurements in situ. The effects of microgravity will be clearly separated from other spaceflight factors by comparison with parallel samples on an onboard 1*g* centrifuge in the Biolab facility and in a parallel ground control experiment with identical samples in flight-identical hardware. Due to safety issues, ESA decided to apply UV radiation for DNA damage induction. It causes defined types of DNA damage, e.g., cyclobutane pyrimidine dimers, which are among those also induced by ionizing radiation. Bacteria serve as model organisms possessing the same type of nucleotide excision repair as all other living organisms including humans. The capability of bacterial cells to counteract radiation damage by activating genes involved in DNA repair will be assessed using a bioluminescent reporter gene operon under the control of the SOS regulon, known as the SOS LUX assay. The DNA repair kinetics will be followed by bioluminescence and optical density measurements. For the space experiment, TripleLux Part C preparatory work was already performed successfully to adapt the SOS LUX assay to the space conditions provided by the Biolab facility on the ISS. This experiment was canceled later by ESA due to a lack of available resources at that time and it is a predecessor of LUX-in-Space [217, 218]. The launch of LUX-in-Space is scheduled for 2023/2024.

Biosentinel will be the first deep-space experiment investigating the repair of DNA damage induced by space radiation (Principal Investigator: Sharmila Bhattacharya). It is a further development of NASA's biological CubeSats, small satellites with different payloads that were already flown successfully in LEO. Biosentinel will first follow a trajectory of cis-lunar flyby and, for 6–12 months, enter a heliocentric orbit. The organism under investigation is the budding yeast *Saccharomyces cerevisiae*. These eukaryotic cells are robust, desiccation resistant, were already flown in space before, and have similarities to cells of higher organisms such as humans. Cells from a radiation-resistant yeast wildtype strain and a radiation-sensitive Δrad51D mutant will be uploaded in a dry form. After different periods of time, during which the cells will accumulate radiation-induced DNA damage, the

cells will be activated by the addition of nutrient medium and their growth and metabolic activity will be measured optically. In parallel, another Biosentinel payload will be flown in the ISS, in addition to the corresponding ground reference experiment. The launch is scheduled for 2022 as a secondary payload of NASA's Artemis-1 mission [219, 220].

10.5.4 Mutagenesis

Mutations as a deleterious outcome of erroneous repair of space radiation-induced DNA damage are of special interest in radiation risk assessment as they can initiate the multi-step carcinogenic process [163, 182] and they can be responsible for genetic effects in the offspring if they occur in the germline. Mutations can be detected in cells that survived irradiation and are, as chromosomal aberrations, late endpoints of radiation-induced DNA damage. For improving space radiation risk assessment, the dependence of mutation induction by radiation of different linear energy transfer (LET) was examined in different biological systems: Mutation induction by heavy ions was determined in many organisms including bacteria (*E. coli*, *B. subtilis*), yeast (*S. cerevisiae*), *Neurospora*, *Drosophila*, *C. elegans*, *M. musculus*, plants, and mammalian cell systems including human fibroblasts and lymphoid cells. These were mostly ground-based experiments at heavy ion accelerators.

The hypoxanthine guanine phosphoribosyl transferase (HPRT, EC 2.4.2.8) gene (mutations on the single copy X-chromosome in male-derived cells) in human diploid fibroblasts was used in early studies of LET dependency of mutation induction. A maximum of around 7 times more mutations compared to low-LET radiation was observed for helium ions or heavier ions with a LET of 100–300 keV/µm [221]. The number of mutations per single track through a mammalian cell nucleus increases with LET, reaching saturation at around 100 keV/µm [222]. The induction of mutations in the X-linked HPRT locus in Chinese hamster cells by accelerated heavy ions reached a local maximum in the LET range of 80–100 keV/µm [223].

Studies on mutation induction in autosomes became possible by means of A_L human-hamster hybrid cells having one copy of human chromosome 11. In these hybrid cells, neutrons of various energies were more efficient in inducing mutations in the a1 locus on chromosome 11 compared to gamma rays; the RBE reached up to 30 at the 0.1% survival level [224]. The autosomal thymidine kinase gene (TK1) locus in human cells allowed investigation of the loss of heterozygosity (LOH) which can occur via deletion or allelic recombination and it revealed a higher peak of mutations at a lower LET (~50–100 keV/µm) compared to the HPRT mutations (up to 15× compared to ~5×). As for other biological endpoints, LET is not the only determinant of the biological efficiency of an HZE particle. The track structure means the energy deposition pattern varies for different ion species of the same LET. Such an effect of ion species was observed for mutation induction at the HPRT locus in human fibroblast-like cells—the RBE for mutation induction determined in this system was between 3.6 and 7 for carbon and neon ion beams in the LET range of 60–120 keV/µm compared to ^{137}Cs gamma rays [225].

Besides mutations observed in the direct hit cells, bystander mutagenesis can contribute to the overall mutation rate after particle exposure as it was observed, for example, after alpha particle exposure [226].

An experiment on the ISS designed to detect mutations in human cells that were induced by natural galactic rays made use of the frozen storage as described in Sect. 10.5.3. Frozen human lymphoblastoid TK6 cells were stored for 134 days in the Kibo module of the ISS and accumulated a dose of 72 mSv. After analysis on ground, a tendency for higher mutation frequency at the TK locus was observed in the flight samples compared to ground control [227]. Earlier experiments on Mir for 40 days with a model system based on *Saccharomyces cerevisiae* and *Escherichia coli* also revealed two to threefold higher mutation frequencies in some flight samples compared to ground samples, with a predominance of large deletions that might be caused by high-LET radiation [228].

10.5.5 Transformation

If mutations occur in tumor suppressor genes and inactivating them, or proto-oncogenes and activating them, cells can be transformed and lose growth control including anchorage-dependent growth. It can be seen as a surrogate marker for the carcinogenic potential of a radiation quality in question. Transformation can only occur in cells that survived the radiation exposure. In vitro, transformation of mammalian cells is determined by their ability to grow anchorage independently in soft agar. The soft agar test was applied to different cell types after exposure to HZE particles at heavy ion accelerators in order to determine their potential for transformation, usually in comparison to low-LET radiation.

Already in the 1980s, it was shown that HZE particles are more effective in transforming mammalian cells than low-LET radiation: In mouse embryonic cells (C3H10T1/2), the effectivity of transformation increased up to 10 with a LET ~200 keV/µm [229] while Hei et al. observed a plateau at LETs of 80–120 keV/µm [230]. In Golden hamster embryo cells, ^{14}N ions (LET 530 keV/µm) and ^{4}He ions (36 and 77 keV/µm) were ~3× more effective in inducing cellular transformation than gamma or X-rays [231]. Later, a maximal RBE for neoplastic transformation was found at a LET of ~100 keV/µm, reaching a maximum of seven [232]. In

human bronchial epithelial cells, iron and silicon ions (LET 151 and 44 keV/µm, respectively) were more efficient in inducing transformation than gamma rays from a ^{137}Cs source especially when these cells were oncogenically progressed by stable transfection of mutant oncogenes [233].

10.5.6 Cell Cycle Changes

Cell cycle arrests play a central role in the DNA damage response of dividing cells. Before the cell enters the next cell cycle phase, e.g., from G1 to S phase or from S to G2/M phase, they allow repair of damaged DNA (Chap. 2). They can therefore protect from cell death, mutations or chromosomal aberrations. Concerning the special radiation qualities present in space that are prone to induce complex DNA damage which might persist longer, stronger, or longer cell cycle arrests might be induced in comparison to low-LET radiation. Early experiments observing mitotic delay by time-lapse microscopic cinematography already gave hints that accelerated neon ions produce a stronger delay compared to Co-60 gamma rays [234]. High-LET radiation produces stronger and more persistent blocks in the G2 phase of the cell cycle than low-LET radiation [235]. In synchronous V79 Chinese hamster cells, the cell cycle delays per particle traversal increased with increasing LET and were primarily due to blocks in S and G2/M phase of the cell cycle [236]. Permanent arrest in the G1 phase can also be induced by high-LET radiation [237]. The relative biological efficiency of heavy charged particles with a LET in the range of 100–330 keV/µm for inducing cell division delays was 3.3–4.4 [236] and the percentage of mitotic cells as indication of an arrest at the early G2/M checkpoint decreased with increasing LET [238]. The cell cycle regulating protein p21 (CDKN1A) accumulates in nuclear foci rapidly after heavy ion exposure of fibroblasts [239]. Besides this, expression levels of cell cycle regulatory proteins might be affected to a higher extent by high-LET radiation compared to low-LET radiation [237], for example, after iron ion exposure p21 expression was much higher compared to gamma rays and persisted 10 days after irradiation [193].

10.5.7 Gene Expression

Similar to studies with low-LET radiation, gene expression studies after high-LET radiation developed from a focus on single genes (mRNA and protein level by Northern Blot, RT-PCR, real-time RT-qPCR, Western Blot) to arrays of multiple genes, microarrays [240] and detection of the levels of all mRNAs present in cell populations or even single cells by RNA sequencing. After exposure to ionizing radiation, signal transduction pathways can result in the activation of transcription factors. These transcription factors bind to binding sites in their target genes' promoters which are specific for them (usually short palindromic DNA motifs) [241]. Also, besides promoter or enhancer activation via transcription factor binding, epigenetic mechanisms can be responsible for (persistent) gene expression changes and are therefore the focus of mechanistic research (see Sect. 10.5.9).

In addition to spaceflight experiments, a huge amount of gene expression data from ground-based exposure to neutrons, protons, and different heavy ions for different experimental model systems exists. NASA GeneLab (https://genelab.nasa.gov/) offers a repository for space-related omics data, among others transcriptomics and proteomics from experiments with model organisms, cells, cell lines, and tissues. Currently, a comprehensive picture of gene expression changes is difficult to paint due to the multiple influencing factors that range from the model system (e.g., gut epithelial cells and human bronchial epithelial cells, tissue, animal model) to the methods, cell cycle phase, radiation qualities, doses, kinetics of exposure, timepoint after exposure, and additional spaceflight environmental factors (such as simulation of microgravity effects by hindlimb unloading). The interpretation of the data is complicated by the fact that in the majority of the heavy ion accelerator experiments, the dose is acutely applied within minutes, while exposure during long-term space missions is protracted over several months.

The emerging view is that heavy ions, especially iron ions are capable to induce a stress response persisting for several weeks in addition to an early transient response. This early response can encompass p38MAPK and TP53 activation and expression of its target genes, whereby the cell cycle regulator gene CDKN1A can also be expressed TP53-independently. In tissues, long-term changes in the expression of genes involved in inflammatory and free-radical scavenging pathways occur after iron ion exposure and these changes involve transcription factors such as signal transducer and activator of transcription 3 (STAT3), GATA binding protein 4 (GATA4), Nuclear Factor κB (NF-κB) and nuclear factor of activated T cells 4 (NFATc4) [242]. In human cells, NF-κB was strongly activated by heavy ions, its activation depended on LET [243] and the expression of several chemo- and cytokines was increased [244].

10.5.8 Telomeres and Aging

HZE particles are potent inducers of senescence, more potent than gamma rays. Senescence-associated changes in the tumor microenvironment may induce invasion and stemness of tumor cells. Senolytics can be applied to eliminate senescent cells and thereby deplete senescent stromal

cells with tumor supportive roles. Shortening of telomeric sequences can lead to telomere fusions and contributes the chromosome instability after heavy ion exposure [245]. Furthermore, accumulation of short telomeres eventually triggers apoptosis or senescence. Unlike normal somatic cells, germline, stem, and tumor cells avoid the latter through a high expression of telomerase. Due to natural telomere shortening during cell division, telomere length is highly linked to aging [246]. Considering the environmental radiation exposure during spaceflight, with higher levels of HZE particles compared to on Earth, NASA investigated the effect of spaceflight on telomere length in the twin study. The twin study examined molecular- and physiological differences of twin astronauts, one spending a year onboard the ISS and the other on Earth [120]. Telomere lengths of peripheral blood mononuclear cells (PBMCs), collected from peripheral blood samples taken preflight from both twins were of similar length. However, during spaceflight, the space twin's telomere length increased significantly, while the Earth twin's telomers remained stable during the study. Once returning to Earth, the increased telomere length diminished within 48 h and the number of short telomeres increased compared to preflight [116]. While an unexpected finding, increased telomere length has recently been associated with other biological functions such as DNA damage response, cell cycle kinetics, and mitochondrial stress [247]. Indeed, chromosome aberrations (inversions and translocations) were more frequent during spaceflight and inversion frequencies of the space twin remained elevated postflight, consistent with ionizing radiation exposure inflight. Furthermore, DNA damage repair pathways were upregulated in several circulating immune cells, suggesting increased genomic instability due to ionizing radiation during spaceflight [121]. Similar results (increased telomere length and chromosomal aberrations) were also seen in astronauts during a 6-month spaceflight mission. While telomerase activity likely is responsible for the increased telomere length inflight, the actual contributing mechanism is still unknown. However, astronauts returning from 1 year and 6 month missions showed elevated telomerase activity upon return to Earth [116].

10.5.9 Epigenetics

Persistent gene expression and functional changes induced by space radiation exposure could be caused by changes in the epigenome. Changes in the DNA methylation profile and in the histone code encompassing methylation and acetylation of histones could therefore contribute to high-LET carcinogenesis and degenerative diseases and could represent possible prophylactic or therapeutic targets.

For example, in immortalized human bronchial epithelial cells, hypermethylation at CpG sites occurred early after Fe-56 ion exposure and persisted a long time [248]. Long-term epigenetic reprogramming after such exposure was also observed in hematopoietic progenitor and stem cells [249].

High levels of DNA methylating enzymes were also found in the hippocampus of Si-28 ion irradiated mice that developed cognitive impairment [250].

In addition to heavy ion exposure experiments, combined exposure to simulated microgravity and chronic low-dose irradiation or spaceflight experiments using small animals or cell cultures and astronaut data reveal alterations in the methylome and histone modification status after combined exposure to spaceflight environmental factors such as microgravity and space radiation. The lasting imprint of high-LET radiation exposure on the epigenome might allow monitoring the cumulative biological impact of space radiation exposure [248].

10.6 Small Animal Experimental Models and Biological Changes of Space Radiation

10.6.1 Importance of the Use of Animals in Research and Their Particular Use in Space

The use of small animal models in research is debatable, but still essential to provide general information on cellular and molecular mechanisms, to develop new drugs and treatments. They are mainly used in fundamental scientific research, for the advancement and development of new diagnostic tests and treatment for diseases, for education of researchers as well as in safety assessments of drugs and chemicals.

Animals are a useful research subject for a variety of reasons. Only in living organisms, it is possible to study complex physiological processes. Furthermore, the environment of the experiment can be perfectly controlled (e.g., diet, light, housing, etc.). Also, they have a shorter life cycle so studies can be conducted throughout a whole lifespan or across generations. Animals are biologically very similar to humans and often suffer from similar health problems. In fact, mice share more than 85% of protein-encoding genes with humans—Why Mouse Matters, from the National Human Genome Research Institute (https://www.genome.gov/10001345/importance-of-mouse-genome).

Animal experiments can cause harm to the animal thus ethical review processes have been established around the world [251]. With respect to this, the 3R´s principle by [252] ensure the reduction of animal numbers, refining the test methods to lower the harm to the animal to a minimum and

replace animal experiments with alternative methods, when possible (Box 10.5).

Box 10.5 Russell and Burch's The Principles of Humane Experimental Technique was First Published in 1959

The aim of the principle is to improve the treatment of laboratory animals and at the same time advance the quality of scientific studies.

Replacement: Includes methods that avoid or replace the use of animals such as computer/mathematical models (in silico), cell culture models (in vitro), or relative replacement (e.g., invertebrates, such as fruit flies and nematode worms).

Reduction: With improved experimental design, modern imaging, or sharing data and resources, the total number of animals needed can be minimized.

Refinement: Modification in the experiment, which minimize pain, suffering, and distress and allow general improvement of animal welfare (e.g., improvement in the research animal housing conditions, analgesia, and anesthesia for pain relief).

The animals that are most used for terrestrial research are mice, fish, and rats. Since the beginning of space exploration also animals have been used in space programs. Similarly, to how microgravity and cosmic radiation can affect human health, animals are also affected. This is why during an early space mission, at the beginning of 1940, animals were used to investigate various biological processes and the effects of space flights on living organisms. On the 20th of February 1947 the first living organism, fruit flies, were sent to space with the V2 rocket. The dog Laika was the most famous and first mammal which was sent to an orbital spaceflight around the Earth (Fig. 10.16) onboard of the Soviet Spacecraft Sputnik 2 on 3rd November 1957 [253]. Since then, a variety of animals have been sent into space including rodents, ants, cats, monkeys, spiders, and jellyfishe. Nowadays the effect of space conditions on animals, including microgravity and radiation, can also be studied to a certain degree on Earth with the help of clinostats, particle accelerator, and X-ray machines. However, all factors of the complex space environment cannot be simulated simultaneously on Earth.

Fig. 10.16 On 3 November 1957 Laika was the first living mammal that was sent to space onboard the satellite Sputnik 2

10.6.2 Acute Effects

10.6.2.1 Acute Radiation Syndrome

In case of a large SPE and insufficient shielding, the acute radiation syndrome (ARS, see Chap. 2) might be induced, endangering astronauts' health and mission success. To understand the pathogenesis of ARS induced by protons and develop therapeutic approaches for space missions, experiments with different animal models including rodents, minipigs, and non-human primates were performed. Whole-body doses up to 2 Gy are expected when astronauts are exposed to large SPE in free space with insufficient shielding. In this dose range, effects on the immune system (see Sect. 10.6.2.3) dominate the syndrome. As the skin dose can be 5–10 higher, the skin might be damaged (see Sect. 10.6.2.2).

10.6.2.2 Skin Effects

Forming the barrier between the outside environment and the inside of the body, the skin is a vital organ. Different skin layers provide the skin with tensile strength and keep a proper barrier function to prevent body water loss, regulate the immune defense and temperature, and protect against ultraviolet damage. The outermost layer, the epidermis, is built mostly out of layers of keratinocytes that differentiate and migrate toward the skin surface. A balance between the proliferation of keratinocytes and shedding of dead cells at the surface of the skin regulates the thickness of the epidermal layer. Below the epidermis lays the dermal skin layer which is mostly composed of connective tissue. Skin's tensile strength and elasticity are provided by Collagen type I and III, and elastic fibers. Fibroblasts are the major provider synthesizing these proteins. Furthermore, they play a major part in skin wound healing by migrating to the side of the wound, recruiting other cells, and remodeling the extracellular matrix (ECM) to restore the injured skin [254].

The skin receives greatest dose and greatest number of stopping particles, particularly during solar flares [255]. SPE events during EVA could lead to higher skin dose than to internal organs. Furthermore, simulations of SPEs has shown

that the total skin dose for astronauts performing EVAs is estimated to be up to 32 Gy (for SPE simulation of August 1972) [31].

Radiation-induced skin injuries can be distinguished by several phases depending on the condition of exposure [256]. Early skin reaction is shown by erythema within a few hours after irradiation. After several weeks, inflammatory damage, erythema, loss of epidermal cells, moist desquamation, hyperpigmentation, edema/hyper-proliferation, and epilation can be observed. Late effects can develop after several months and include dermal atrophy, necrosis, and problems related to the deterioration of the skin vasculature. Skin problems, such as burns and slower wound healing, combined with a deprived immune system increase the risk of infections and hinder recovery from ARS [31].

Because of morphological similarities between (mini) pigs and human skin, these animals have been widely used to better understand the skin reaction to ionizing radiation. Furthermore, rodent models such as mouse, rat, or guinea pig have also been studied for ionizing radiation effects on skin.

Using porcine models, researchers have been able to indicate skin toxicity after exposure to a simulated SPE radiation resembling the energy and fluence profile of a SPE documented in 1989 [257]. Hyperpigmentation of minipig irradiated skin was observed 7 days after irradiation and lasted throughout the entire observation period. These observations were supported by an increase in melanin deposition found in the stratum granulosum. Further observations of increased proliferation, parakeratosis (an accelerated keratinocytic turnover) and increased amount of melanophages, are thought to be an indication of an inflammatory skin response after irradiation.

Other studies exposed minipigs to doses ranging from 5 to 25 Gy of electrons [258]. In agreement with previous mentioned study, a dose-dependent hyperpigmentation of the skin was observed as well as an increase in melanin deposition. Furthermore, in the highest dose exposed group of 25 Gy, skin wounds and ulcers developed 19 days after irradiation on body parts that received the highest dose (tail, ears, and legs). In addition, hair loss in the form of alopecia was observed along the dorsum of these pigs.

Low dose rate exposure of skin to low doses of photons, seem to mostly induce oxidative stress and ECM alterations as observed in a mouse model [259]. Skin gene expression changes related to oxidative stress and extracellular matrix (ECM) have been found after whole-body γ-ray exposure. At low dose rates, genes involved in the formation of reactive oxygen species (ROS) were significantly upregulated at doses of 0.25 Gy. Furthermore, dose rate effects were also found in ECM gene expression profiles. Enhanced expression of genes encoding ECM structural components were found after low dose rate exposure.

10.6.2.3 Acute Effects of Proton Radiation Exposure in the Immune System

The immune system consists of a variety of cells, processes, and chemicals that combine efforts to protect the body from foreign microbes, viruses, cancer cells, and toxins [260].

Dysfunction of the human immune system has been shown during [261] and even after space flight [262]. Among the causes of this immune dysfunction, an altered distribution of the cellular components and altered cytokine profiles [263], as well as cytoskeleton alterations and gene expression dysregulation [264] has been shown in many immune cells. When human lymphocytes are subjected to simulated cosmic radiation in vitro they show chromosomal damage, depending on the type of radiation shielding.

The adverse effects of space radiation on the immune system is one of the major concerns for space flight. The vast majority of the cellular components that constitute the immune system are highly sensitive to ionizing radiation [265]. It is still not clear if space radiation has a synergistic effect in combination with microgravity, principally in long duration missions and in the context of the immune system.

As mentioned, in vitro models have been widely used for studying the effects of space radiation on several cellular types. However, the complexity of most systems—such as the case of the immune system—require approaches that will better mimic physiologic conditions, either in ground-based studies or inflight campaigns. Several animal models that recreate some of the conditions of space flight have been developed for use on Earth. For immunology studies, murine models remain one of the most commonly used small animal model in space radiobiology. Rats exposed to 56-Fe (5 GeV/n) to total doses of 0, 1, 2, and 4 Gy showed a decrease in their lymphocytes, particularly B cells. In another study, mice were irradiated with total (single) doses of 0, 0.5, 2, and 3 Gy with 56-Fe ions. Red blood cell (RBC) counts diminished proportionally to the dose. All three major types of leukocytes also decreased [266].

Sanzari et al. [267] directed a series of radiation experiments using Yucatan minipigs. The animals were exposed to beams comprised of Solar Particle Events (SPE)-like protons, 155 MeV, and electrons, 6 and 12 MeV, with dose profiles that mimic SPE radiation. Their findings suggest that, based on the magnitude of the decrease and the time required to reach the lowest leukocyte counts after irradiation, the proton SPE radiation had more impact on the count than electron SPE radiation, with lymphocytes being the most sensitive type of leukocytes. After proton SPE radiation at skin doses >5 Gy, certain populations of leukocytes (neutrophils) had lasting effects following the irradiation (up to 90 days) [267].

For studying the intricate function of the immune system and how it responds to acute exposures of space radiation, small animal models are essential since they can showcase the network of phenomena. Adding up to the already chal-

lenging task of pinpointing the alterations occurring in the irradiated immune system we must find a way of adding the following to the equation: isolation, altered circadian rhythms, psychologic stress, and, of course, altered gravity levels.

Chronic and late effects of space radiation exposure encompass increased cancer risk, early cataract formation, and a possibly increased risk for degenerative diseases of several organ systems such as the cardiovascular and the central nervous system).

10.6.2.4 Cancer

Animal models of cancer induction by space radiation play a crucial role in the determination of the radiation risk associated with a space mission.

Firstly, they provide with information about the RBE of different space radiation components such as HZE particles for cancer induction in different organs when compared to a low-LET radiation quality, such as gamma rays or X-rays. The Radiation Quality Factor is derived from the RBE data for cancer induction by HZE particles to scale from gamma radiation to the mixed field of GCR in space radiation cancer risk models. If the RBE is above 1, a higher cancer risk can be assumed for space radiation compared to well-known terrestrial low-LET radiation qualities.

Secondly, experiments with high and low dose rates are the basis to estimate the dose and dose rate effectiveness factor (DDREF) to scale from acute to chronic radiation exposure and thereby account for dose rate effects. As animal experiments with exposure at low dose rates are rarely feasible at heavy ion accelerators because of restricted beam time access, dose-rate effect experiments were performed so far at neutron facilities.

Furthermore, animal models give insight into the mechanisms of cancerogenesis by HZE particle exposure, e.g., the role of non-targeted effects, and thereby allow to identify potential molecular targets for effective countermeasures (Box 10.6).

Box 10.6 Mouse strains

Inbred mouse strains are produced by at least 20 generations of brother-sister mating and they are traceable to a single founding pair. The individuals of an inbred strain are genetically nearly identical to each other and experimental results are highly reproducible. Examples: CBA mouse (cross of Bagg albino and DBA), C57BL/6 mouse (with black coat), BALB/c (Bagg albino) mouse.

Outbred strains provide genetic diversity and are effectively wildtype in nature with as little inbreeding as possible.

Mating of at least two strains led to the generation of the **first filial generation (F1) hybrid mice**.

The first animal experiment with HZE particles to determine cancer induction by single ion exposure used mice and focused on the induction of tumors of the exocrine Harderian gland which is located between eye and ear [268–271]. In these experiments, tumor prevalence was determined by sacrificing mice at a predetermined timepoint after exposure and the number of mice with tumors was counted or the number of tumors per mouse was counted. As this gland does not exist in humans, other animal models were developed and applied. Two different approaches predominate: either wild-type rodents, e.g., inbred, F1 hybrid, or outbred mice, or genetically altered rodent models are exposed to HZE particles at a heavy ion accelerator. Multiparent outbreeding strategies can reduce the strong effects of the genetic background that limit gene-environment interactions in studies with inbred, genetically homogeneous animals [272]. To consider sex-specific cancer types, optimally, both sexes are included [272]. After whole-body irradiation of wild-type rodents, they were followed up over the lifespan of the animals for tumor induction. Alternatively, rats were followed up by palpation until first tumor (time-to-cancer incidence), with an additional follow-up until death. After necropsy, histology was performed to determine the number and types of cancer, e.g., mammary tumors [273, 274]. Here, high numbers of animals are required to detect the increase of cancer incidence above the background cancer rates.

Therefore, genetically altered mouse models were developed in order to lower the number of mice and to mimic a specific cancer induction and promotion pathway, mostly for lung, gastrointestinal [275, 276] or liver cancer (hepatocellular carcinoma) [277, 278]. Using a genetically radio-sensitized model implies an assumption about the mechanisms of radiation-induced cancerogenesis—genetically engineered mice carry some, but not all mutations, needed to generate cancer. The rationale behind this approach is to consider somatic mutations in cancer genes such as *NOTCH1* and *TP53* that might be already present in astronauts when they depart for their first space missions as the number of mutations in the epithelium increases with age [279].

In risk models, development of leukemia (leukemogenesis) and induction of solid tumors are considered separately because of different latency periods after radiation exposure and dose–response relationships. Leukemogenesis is highly relevant for space missions because of its short latency in humans. The CBA mouse strain is susceptible to radiation-induced acute myeloid leukemia (AML) [280] which is explained by a deletion in chromosome 2 (PU.1) that can occur 1 month after irradiation. A point mutation in the second copy of the PU.1 gene causes a differentiation block in the myeloid cells which favor autocrine growth stimulation. In this model, the RBE of iron ions for induction of AML was 1, meaning that the risk of AML induction by high-LET iron ions and low-LET radiation is comparable. As only surviving

cells can be transformed into a cancer cell, a higher mutation and chromosomal aberration rate induced by HZE particles can be compensated by cell death from collateral damage after an HZE ion traversed a myeloid cell [277]. RBE for other cancer types can be much different as the effectiveness of HZE ions in inducing a specific cancer type depends on the mechanism responsible for the tumorigenesis in that particular cancer. For example, in the same mouse strain that was used for the AML studies, hepatocellular carcinoma (HCC) was induced by HZE particles with an RBE of up to 74 [278].

Concerning solid tumors, a special focus in the studies so far was to evaluate the stage of tumors that can be induced by HZE particles and on detailed studies on lung cancer, gastrointestinal cancer, and brain tumors (Box 10.7).

Box 10.7 Tumor Types Observed After HZE Particle Exposure of Outbred Mice Are Similar to Those Arising Spontaneously or After Gamma Irradiation

Pituitary adenoma, osteosarcoma, Harderian gland tumor, soft tissue sarcoma, thyroid adenoma, ovarian Granulosa cell tumor, mammary adenocarcinoma, histiocytic sarcoma, hemangiosarcoma, hepatocellular carcinoma (HCC), pulmonary adenocarcinoma, small cell lung cancer, myeloid leukemia, (thymic) lymphoma (T cell, B cell), brain tumors, e.g., gliomas [272].

The lung has the highest susceptibility to radiation-induced carcinoma incidence and mortality, based on analysis of human populations exposed to radiation (Life Span Study of atomic bomb survivors). A minimum of five genetic changes convert immortalized human lung epithelial cells to malignant tumors. For lung carcinogenesis, BALB/cByJ or C57/BL6 mice or the K-ras^{LA1} mouse model [281] were used. In C57/BL6 mice, lung tumors occurred in irradiated mice but not in controls and all were adenocarcinomas, with no significant differences between males and females and for dose fractionation (dividing a radiation dose into multiple fractions, see Chap. 4) versus single dose were found. Incidence of lung tumors was higher in high-LET-irradiated mice than in X-ray-irradiated mice, with an RBE above 6 for all investigated HZE particles (Fe, Si, and O ions) [282].

In the pathogenesis of gastrointestinal tumors, for instance, colorectal cancer and hepatocellular carcinoma (HCC), inflammation plays a crucial role. Animal experiments revealed that heavy ion radiation triggers a pro-inflammatory state which can be associated with late colonic tumors. Furthermore, premalignant polyps with mutations in the Adenomatous polyposis coli (APC) gene could be already present in middle-aged astronauts. In the small intestine, the formation of a few polyps and later adenomas and even adenocarcinomas can result from truncation of the APC gene at codon 1638 [283]. Therefore, a mouse model with a chain-terminating mutation by a mutation to a stop codon or a frameshift (see Chap. 4) in one allele of the APC gene was developed for colon cancer research (Apc$^{1638N/+}$). APC mutant mouse models show a good correlation with carcinogens implicated in human colorectal cancer. Delayed genomic instability in APC$^{1638N/+}$ mice paves the way to gastrointestinal tumorigenesis. In this model, no evidence for dose-rate effects with HZE particle exposure was found [275], indicating that the carcinogenic potential of HZE particles is independent of the dose rate.

Also, genetically altered mouse models for the formation of brain tumors are used in space radiation research as already experiments from the 1970s indicated that charged particles can induce glioblastomas: Monkeys (*Macaca mulatta*) irradiated with high-energy protons (55 MeV, penetration depth ~2.5 cm) surviving 2 years or longer developed glioblastomas [284]. Here, the focus is on the loss of tumor suppressors such as cyclin dependent kinase inhibitor 2A (Cdkn2a or Ink4-Arf), phosphatase and tensin homolog (Pten), and TP53 in astrocytes and on oncogene activation (e.g., epidermal growth factor receptor variant III, EGFRvIII) after irradiation. Iron and silicon ions were much more potent tumor inducers in "preinitiated" astrocytes than gamma rays [285].

The animal studies with single beam irradiations show that the efficiency of HZE particles to induce cancer is related to ion energy, LET with a peak RBE below 100 keV/μm, sex of the animals, and depends on the tumor type [275]. The RBE for cancer induction was recently determined to range from 5 to 16 [286], representing a snapshot that will be further updated as not all available data were included. Currently, based on the results of single beam irradiations, multiple beam experiments with up to 33 ion beams are performed at the NASA Space Radiation Laboratory (NSRL) using the GCR simulator in order to understand whether the effects of the different GCR components act in an additive or even in a synergistic manner in cancer induction.

10.6.2.5 Cataract

According to recent epidemiological evidence, radiation-induced cataract (see Chap. 2) occurs with a threshold absorbed dose of 0.5 Gy (0–1 Gy) of sparsely ionizing radiation, meaning that a cataract can arise after any ionizing radiation dose no matter how low if the remaining lifespan is long enough for its appearance. The 1 Sv GCR dose to be expected for a 1000-day Mars mission [83, 84] means that even the upper limit of the cataract-induction threshold dose confidence interval will be reached during a human Mars exploration mission. In astronauts, epidemiological data sug-

gest a higher risk for the development of cataracts in case of missions in LEO with high inclination [287].

Due to its germinative zone in the lens epithelium, the eye lens is a radiation-sensitive organ. These cells are actively proliferating during lifetime and finally differentiate into transparent lens fibers. In case cells are damaged, they cannot be eliminated from the lens which is covered by a capsule and not vascularized. Exposure of the eye lens to ionization radiation is thought to result in sub-capsular cortical lens opacification via various steps, starting with genetic damage of lens epithelial cells via changes in cell cycle control, apoptosis, differentiation, or other pathways controlling lens fiber cells' differentiation, and cellular disorganization.

Due to higher local dose and different patterns of cellular energy deposition from high-LET components of GCR, higher efficiency in the induction of lens-damaging effects is assumed than for low-LET radiation. Therefore, animal experiments were mostly performed to determine the RBE of HZE particles to induce lens opacification and to detect possible dose rate effects. In rats, the RBE reached 50–100 for HZE particles within LET above 80 keV/μm [288] and fractionation of exposure did not reduce the cataractogenic effect [289]. Neutrons as secondary particles occurring in spacecraft and on planetary or moon surfaces had also a high RBE for cataract-induction in rats [290].

To determine the role of genetic predispositions, mice that are heterozygous for Ataxia telangiectasia mutated protein (ATM) were exposed to HZE particles and cataract formation was followed. ATM plays a central role in the DNA damage response (DDR). Heterozygosity for the ATM gene predisposes carriers for early onset time and progression of cataracts even without exposure to ionizing radiation [291]. Also after gamma ray and 1 GeV/n iron ion exposure, cataracts appear earlier in ATM heterozygous animals compared to wild-type mice and the RBE for HZE particle induced cataract formation ranged from 4 to 200, whereby the highest values were found for the lowest dose (10 mGy) and RBE decreases with increasing dose [292, 293]. In conclusion, HZE particles present in GCR and neutrons as part of the secondary radiation field are highly cataractogenic and the mechanisms such as long-term changes in gene expression, complex DNA damage, and chromosomal aberrations in eye lens epithelial cells (LECs) are still under investigation.

10.6.2.6 Cardiovascular System

Exposure to space hazards, including microgravity and heavy ion exposure can cause harmful effects on the cardiovascular system during spaceflight. Upon entering microgravity, cephalad fluid shifts cause increased stroke volume and cardiac output. Furthermore, the cephalad fluid shift is also hypothesized to cause visual impairments due to increased cranial pressure [294]. During flight, mean arterial pressure is decreased, together with central venous pressure. Furthermore, decreased systemic vascular resistance, results from increased cardiac output, systemic arterial vasodilation, and decreased arterial pressure [295]. Other effects of microgravity exposure include hypovolemia, cardiac arrhythmia, cardiac atrophy, and orthostatic intolerance. Believed to be caused by fluid shifts and movement of interstitial water from the legs to the head, the fluid reduction and eventually hypovolemia results in a reduced number of red blood cells [296]. Moreover, cardiac atrophy occurs as a result of decreased metabolic demand and oxygen uptake during microgravity conditions. Together, cardiac deconditioning, i.e., hypovolemia, cardiac atrophy, and decreased cardiac output, causes a decreased exercise capacity and orthostatic intolerance post-flight [297].

While effects related to microgravity exposure during spaceflight are fairly well-known (albeit underexplored), impacts of the cardiovascular system from space radiation and heavy ion exposure during spaceflight are less known. Furthermore, studies from space analogs focusing on radiation effects have shown several effects on the cardiovascular system. Mice exposed to heavy ions show myocardial remodeling, resulting in hypertrophy and cardiac fibrosis [186]. Additionally, accelerated development of atherosclerosis has been found in mice after heavy ion exposure. Leading to a greater prevalence of myocardial infarction [298]. Both in vivo and in vitro models during space flight as well as using space analogs have been used to investigate underlying mechanisms of space-induced CVD. Important mechanisms include endothelial dysfunction, cellular apoptosis, cellular senescence, inflammation, and reactive oxygen species production [297].

10.6.2.7 Central Nervous System

Exposure to heavy ion, especially during long-term space mission, can also affect the central nervous system (CNS). The CNS is part of the nervous system and is composed of the brain and the spinal cord. It is responsible for perceiving any exterior information, transmitting, and subsequently processing it. Responsible for signal transmission are neurons, whereas glial cells (oligodendrocytes, microglia, or astrocytes) have diverse function such as the trophic support of neurons. As neurons are terminally differentiated and have a very restricted regeneration potential, damaged cells will usually not be replaced and thus damage might accumulate over months or years.

Acute CNS effects of ionizing radiation exposure are only observed after exposure to very high doses and can be expected in spaceflight only during very large Solar Particle Events (SPE) in case of insufficient shielding. Thus, for more than 20 years, possible effects of chronic low-dose exposure of the CNS to galactic cosmic rays (GCR) are discussed and a decrease in CNS performance of astronauts is suspected, which was also further evidenced in animal studies [299, 300]. Normally rodent animal experiments are performed at heavy ion accelerators simulating space radiation at doses below 1 Gy in a relatively short time, revealing impairment in

cognitive performance, reduction of dendrites, reduced neurogenesis, and increased neuroinflammation [301–303]. As these effects can be seen even months after irradiation, late effects are possible even after exposure to lower doses [304].

Whereby it has to be considered that in these heavy ion accelerator experiments, the dose can only be applied in a short time, and prolonged exposure over several weeks or months mimicking the real situation in spaceflight is not often possible. With the use of new, low dose rate neutron irradiation facilities, it is now possible to expose rodents to a chronic low-dose as expected during space flights [305]. Also, mice that were irradiated with this chronic neutron irradiation (for 6 months) resulted in diminished hippocampal neuron excitability, a region which is essential for memory and learning, and disrupted hippocampal and cortical long-term potentiation. In addition, mice showed severe impairments in memory and learning tasks as well as distress behaviors [305].

One limit of experiments at the accelerator is that only radiation exposure of a few single radiation types can be studied, while in space, radiation exposure consists of a complex radiation mixture. It is still unclear if humans' brains are affected to the same extent, but chronic low-dose radiation may cause problems for astronauts regarding decision-making processes or performance [306] (Box 10.8).

Box 10.8 Section Highlights

Since their discovery by Antonie van Leeuwenhoek in 1702, bdelloid rotifers and tardigrades have remained intriguing organisms. Their tolerance to desiccation at any stage of their life and their ability to survive a variety of stresses (e.g., low and high temperatures, absence of oxygen, vacuum, high level of ionizing radiation, etc.), makes them good candidates to study extreme resistance mechanisms in the context of space research. Tardigrades have a long history of space astrobiology experiments being among the first animals exposed to space vacuum and radiation. Recent experiments performed onboard of the ISS used bdelloid rotifers and tardigrades to study the adaptation to microgravity and cosmic radiation during spaceflight.

10.6.3 Tiny and Extremely Resistant: Why Bdelloid Rotifers and Tardigrades Are Animal Model Systems for Space Exploration?

10.6.3.1 Bdelloids and Tardigrades, Small Animals to Study Desiccation, Radiation Tolerance and Limit of Life

Bdelloid rotifers (Fig. 10.17) and tardigrades (Fig. 10.18) are among the smallest animals on Earth: most species are less than 1mm in size and contain ~1000 cells. Despite their small size, these animals have complete nervous, muscular, digestive, excretory, and reproductive systems. Mainly living in semi-terrestrial environments, such as lichens and mosses, most (but not all) bdelloid and tardigrade species are able to enter and survive complete desiccation (see Box 10.9 for definition) at any stage of their life cycle.

When water starts to evaporate, these animals begin to contract their muscles and their body to adopt a "tun" shape allowing an optimal desiccation resistance [307–310]. This proper contraction of the body, followed by a specific organization of internal structures is a key step in enabling a successful recovery of desiccated animals after rehydration [308, 309]. The desiccation resistance and recovery rate vary between species [311–314]. The survival rate depends on the length of the desiccation period, the relative humidity, temperature, and animal age. Tardigrades desiccated over 10–20 years, within dry mosses stored at room temperature, were successfully rehydrated confirming their desiccation resistance for periods [315] [316]. While being frozen, these animals were shown to survive over 30 years of desiccation [317]. Bdelloid rotifers have also been shown to survive long periods of desiccation, up to 9 years [318]. As for tardigrades, cold temperatures seem to extend the capacity of desiccated bdelloids to cope with the long duration of metabolic arrest. In a recent publication by Shmakova et al. bdelloid rotifer specimens were recovered from frozen permafrost soil 24,000 years old [319]. If no data are still available for tardigrades, studying old permafrost samples may reveal other records of small animals' life preservation. For example, some nematodes were described to successfully recover after melting from 30 to 40,000 years old samples [320].

Box 10.9 Desiccation or Drought Tolerance?

Desiccation tolerance must be differentiated from drought tolerance. Many organisms are able to tolerate drought as a reduction in water availability in the environment for longer or shorter times. However, a reduced number is able to survive a loss of 90% or more of their body water content. Complete desiccation is reached when the water content decreases below 10% of the dried mass, not enough to form a monolayer around macromolecules, preventing enzymatic reactions and therefore metabolism.

Mostly found in habitats where physical parameters can change unpredictably, tardigrades and bdelloid rotifers were described to be able to cope with a wide range of physical extremes besides desiccation and freezing, such as UV radia-

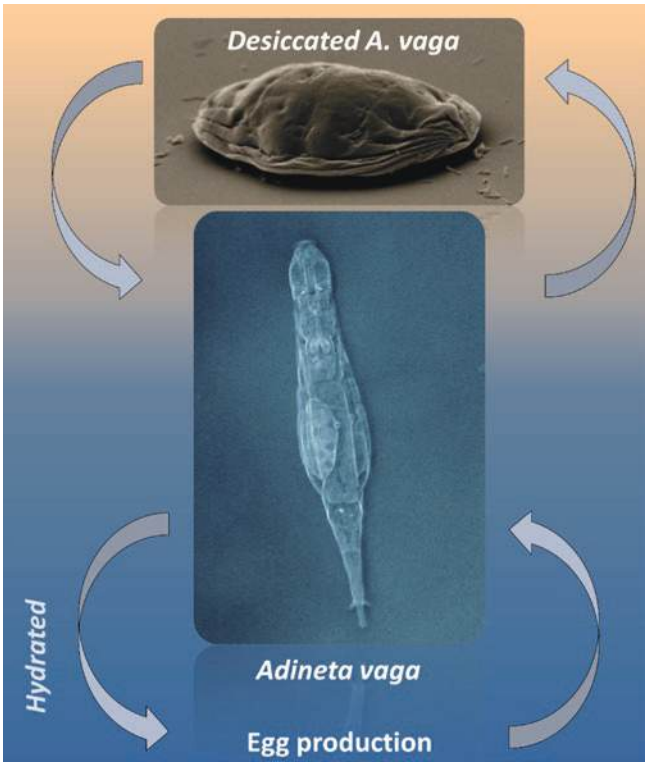

Fig. 10.17 Overview of the bdelloid rotifer *Adineta vaga* life cycle. Bdelloid rotifers live in limno-terrestrial habitats like mosses and lichens. Adapted to these environments, they can be desiccated at any stage of their life cycles including egg stage. When they are exposed to desiccation, adults adopt a "tun" shape allowing optimal desiccation resistance. *Adineta vaga* is about 200–250 µm long. (Credits B. Hespeels)

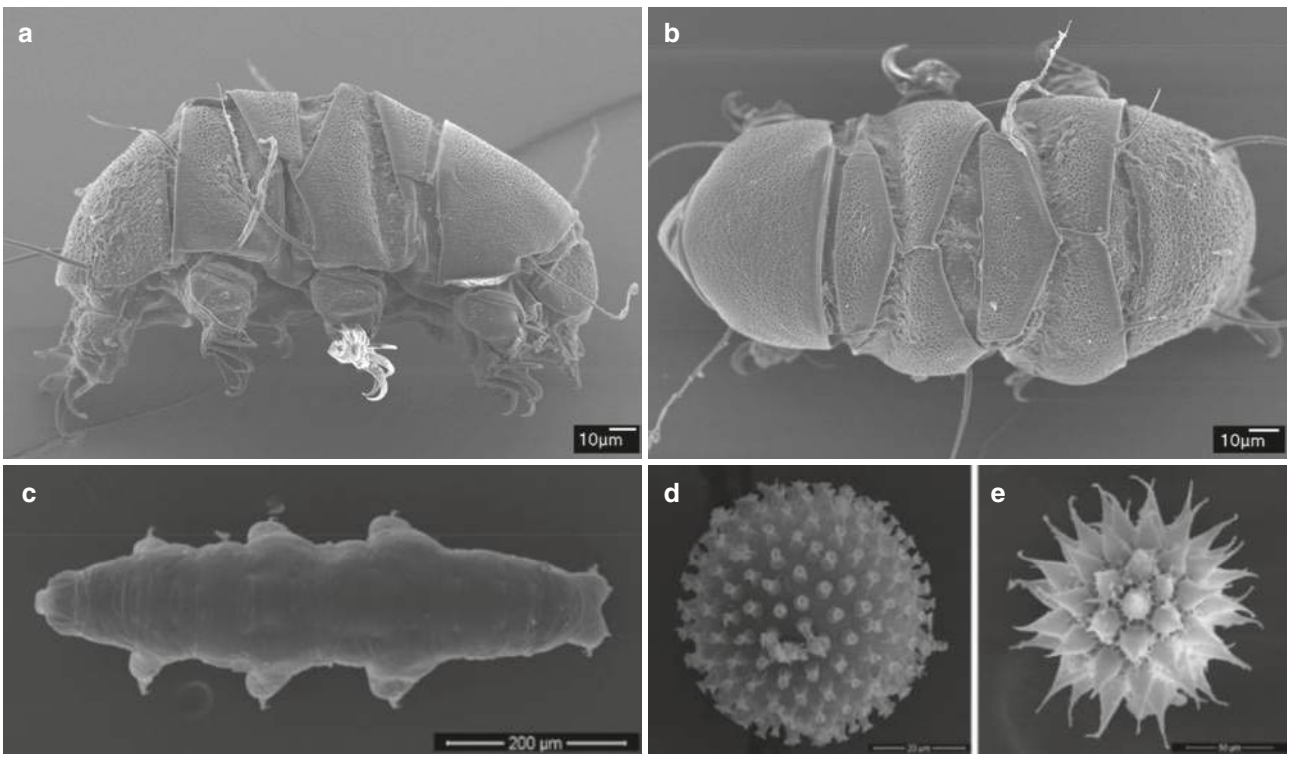

Fig. 10.18 Morphology of adult tardigrades and eggs. (**a**, **b**) Lateral and dorsal views of *Echiniscus testudo*. (**c**) Dorsal view of *Paramacrobiotus areolatus*. (**d**, **e**) Global morphology of eggs laid by *Macrobiotus kamilae* and *P. areolatus*. Pictures were captured using scanning electron microscopy. (Illustration kindly provided by Daniel Stec and reprinted with his permission)

tion, high temperatures (exceeding 100 °C for a few minutes), high pressure or deep space vacuum [317, 321–327].

Among others, bdelloid rotifers and tardigrades were described to be highly resistant to low- and high-LET [328] radiation. In 2008, it was demonstrated for the first time that two bdelloid rotifer species, *A. vaga* and *Philodina roseola*, were resistant to ionizing radiation while being hydrated, surviving up to 1200 Gy of gamma radiation with fecundity (i.e., the total number of daughters produced by irradiated animals) and fertility (i.e., the capacity to produce at least one daughter) showing a dose response [329]. Later, it was demonstrated that desiccated bdelloid rotifers survive doses >5000 Gy of X-ray and proton radiation. These levels of radiation exposure were contrasting the Lethal Dose 50 (LD50) (i.e., dose required to kill 50% of the irradiated population) of mammalian cells which range from 2 to 6 Gy after X-ray irradiation. Similarly, desiccation-resistant tardigrades were described to survive high dose of X-ray and gamma ray (LD50 ranging between 3000 and 6000 Gy) (reviewed in [322]). Unexpectedly, radio-resistance of hydrated and desiccated tardigrades appeared to be more tolerant to high-LET radiation. For example [330], LD50 of the eutardigrade *Richtersius coronifer* was approx. 10,000 Gy. A major difference in comparison with bdelloid rotifers was that, despite a high survival after irradiation, most tardigrades were unable to produce fertile eggs for doses >100 Gy [322]. As an example, the tardigrade *Hypsibius dujardini* treated with gamma radiation had an estimated LD50/48 h for survival of ~4200 Gy, and doses above 100 Gy dramatically impaired the production and hatching of laid eggs [331].

10.6.3.2 Small Animals and Space Research

As an alternative to other animal models, the use of rotifers and tardigrades was proposed for space research. Indeed, these animals may contribute to better understanding damage and consequences induced by exposure to radiation and/or microgravity. How these organisms may respond and adapt to these stresses pave the road to the discovery of new molecules or candidate genes. Ultimately research outputs may be used to improve health span and protect astronauts or individuals subjected to radiation during space flights or medical treatments.

The use of rotifers and tardigrades as space research models was proposed because of the following aspects. (1) Complexity: they are Metazoans (multicellular animals), containing tissues and organs, having a complete gut and a complex muscular structure, yet being very simple animals. Rotifers and tardigrades are however made up of about 1000 cells, while a human is made up of several millions of cells. This simplification allows to disentangle complex problems through easier approaches. (2) Miniaturization: rotifers and tardigrades are small; experiments performed with numerous individuals require small vessels. (3) Distribution: rotifers and tardigrades are readily found in nature and are easily cultivated under controlled conditions. (4) Life span: rotifers and tardigrades have short life cycles that can be studied in a reasonable time period. (5) Reproductive mode: all bdelloid rotifers and some tardigrade species reproduce parthenogenetically. This reproduction system offers two key advantages: a rapid expansion of the population, and a high degree of reliability, as the genome is fully transmitted to the offspring. Therefore, the use of clonal lines reduces the biological variability noise in biological experiments. (6) Extremotolerance: both bdelloid rotifers and tardigrades were described to be able to deal with a high number of DNA DSBs and various stressors encountered by astronauts during space flight. Small extremotolerant animals can provide new perspectives in the adaptation of life to the space environment and ultimately lead to enhancing radio-resistance. For both clades, radiation resistance and radiation-sensitive species can be used in comparative experiments. (7) Storage: as most tardigrades and bdelloids survive desiccation and freezing, they can be stored easily before and after scientific experiments with limited impact on their biology and the scientific output. (8) Desiccation resistance: the desiccated state of tardigrades and bdelloid rotifers correlates with increased resistance to stresses, including deep space vacuum and extreme temperatures. These multiple properties and advantages for space experiments make bdelloid rotifers and tardigrades good candidates to test the limits of life during space exposure. An overview of space experiments involving tardigrades and rotifers is presented in the next two sub-sections.

10.6.3.3 Tardigrades, Pioneer Animals of Astrobiology Field

In September 2007, tardigrades were exposed to LEO within the Biopan-6 experimental platform provided by the European Space Agency (ESA) ("Tardigrades in Space," TARDIS. FOTON-M3 mission). During 10 days at LEO (258–281 km above sea level) samples of desiccated adult eutardigrades of the species *Richtersius coronifer*, *Milnesium tardigradum*, *Echiniscus testudo,* and *Ramazzottius oberhaeuseri* were exposed to space vacuum, cosmic radiations, and two different UV-radiation spectral ranges [323]. It was demonstrated that tardigrades were able to survive space vacuum and cosmic radiation with a survival rate ranging between 70% and 80%. Any impact on the reproductive capacities of exposed animals was reported. However, samples exposed to full solar radiation experienced high mortality. A small fraction of survivors died a few days post-rehydration without the production of any viable offspring. By filtering UV and restricting the exposure of desiccated tardigrades only to UVA and UVB, a significant part of desiccated tardigrades was able to be reactivated and was

able to reproduce. Since the fertility of descendant generations of *M. tardigradum* was not impacted, it was suggested that survivors were able to repair a priori the damages induced by the spaceflight and did not transfer them to future generations [332].

In parallel to the TARDIS experiment (Fig. 10.19), two other experiments were launched onboard of the FOTON-M3: the (1) RoTaRad mission (Rotifers, Tardigrades, and Radiation) and (2) Tarse project (Tardigrade Resistance to Space Effects). RoTaRad experiment confirmed that desiccated tardigrades stored under controlled atmosphere were able to survive while being exposed to a combination of cosmic radiations and microgravity. However, the survival rates were reduced during this experiment likely due to the applied desiccation protocol [333]. With the Tarse project focusing on the eutardigrade *Macrobiotus richtersi* species, hydrated and desiccated individuals were exposed to the space environment for 12 days. In both states, microgravity and radiation had no effect on the survival rate, reproductive capacity, and DNA integrity of exposed animals. Despite the absence of visible morphological changes, it was nevertheless reported that the activity of key antioxidant proteins (including catalase and superoxide dismutase) was decreased during spaceflight. The amount of Heat Shock Proteins 70 and 90, known to be involved in stress resistances of tardigrades, did not differ after this short-term exposure to spaceflight.

A few years later, the TARDIKISS experiments (Tardigrades In Space) were launched with the last Space Shuttle mission (STS-134 2011) [334]. During this 16-days mission, the enzyme activity of key antioxidants was investigated in desiccated tardigrades from the two species *Paramacrobiotus richtersi* and *Ramazzottius oberhaeuseri* [334]. Supporting the idea that desiccated animals were weakly affected by microgravity and cosmic radiation, comparative data analysis between flight and ground samples showed no significant differences in the enzymatic activity of antioxidants.

In June 2021, a fifth experiment was launched onboard of the ISS to investigate the short-term and multigenerational survival of tardigrades. The aim of the Cell Science-04 experiment (CS-04) was to evaluate the transcriptomic response of hydrated tardigrades cultured on the ISS using a dedicated cell culture system (Bioculture System, developed at NASA Ames Research Center). For this experiment, the tardigrade *Hypsibius exemplaris* was used as model species. Scientists are currently evaluating the ability of these animals to survive onboard of ISS for short and long periods of time (up to four generations). In parallel, the transcriptomic responses of these animals are being investigated to follow the evolution of the expression profiles of tardigrades in a microgravity environment. A progressive adaptation of tardigrades onboard of ISS may lead to a better understanding of the molecular responses involved in gravity sensing and will help expand research to secure astronaut's health for future space missions. Among others, tardigrades were described to express several antioxidant proteins to face desiccation and radiation stresses [322, 335]. In particular, tardigrades were described to express specific proteins binding to DNA and protecting their genome from ROS induced by desiccation and ionizing radiation [336, 337].

10.6.3.4 Bdelloid Rotifers, a New Model Species for Space exploration

How microgravity and cosmic radiation may affect desiccated bdelloid rotifers was tested for the first time in 1997.

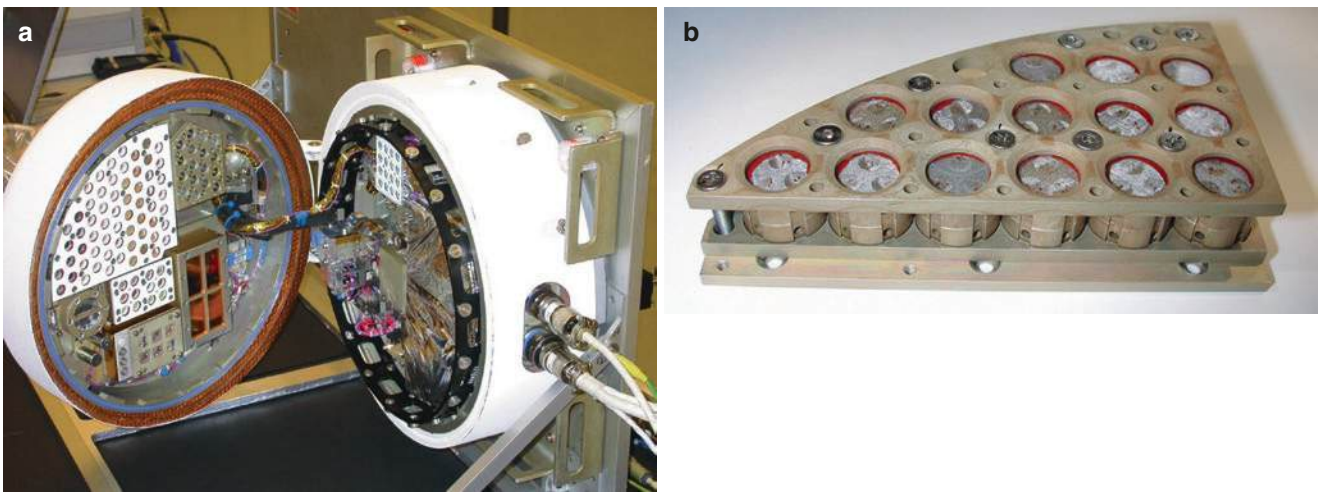

Fig. 10.19 View of TARDIS experiment. (**a**) View of the exobiology Biopan platform containing TARDIS experiment. For 12 days in September 2007, approximately 3000 water bears were launched in space during the Foton-M3 mission. Reprinted with permission from ESA. (**b**) Details of the sample holder containing the tardigrades *Richtersius coronifer. Tardigrades on the top level were exposed to the Sun and were optionally protected with filters.* (Image kindly provided by K. Ingemar Jönsson and reprinted with his permission)

For their first exposure to space, dry samples of *Macrotrachela quadricornifera* were transported onboard of the space shuttle STS-81 for a total of 10 days. The data revealed a similar survival rate and reproductive fitness for ground controls and flight samples [312]. Since desiccated rotifers appeared to be protected from the impact of microgravity and cosmic radiation, at least in this short-term exposure experiment, researchers started to investigate the consequences of space flight on hydrated bdelloids. In absence of gravity, it has been hypothesized that the distribution of cytoskeletal elements or yolk granules in the egg cytoplasm is impacted. This abnormal organization of the cytoskeleton could impact the rotifer reproduction. Therefore, researchers first investigate the capacity of bdelloid rotifers to complete their embryological development under microgravity was initially investigated. Pre-flight experiments were performed under hyper-gravity environment (up to 20 g) and under simulated microgravity (as low as 0.0001 g) using a 3D random positioning machine (3DRPM). Results showed that the rotifer development remained constant regardless of the treatment experienced, except for some minor modifications in early embryos experiencing 20 g with no subsequent impact on the development. This first investigation suggests that bdelloid rotifers continue embryological development despite changes in g-force. Unfortunately, no data from flight experiment development associated with embryological development of bdelloid rotifers exposed to space environment was released post-flight.

Twenty years later, the bdelloid rotifer *A. vaga* was sent onboard of the ISS for two independent experiments. In December 2019, two autonomous hardware, each containing five culture bags loaded with 10,000 individuals, were transported onboard of ISS. Hydrated animals were exposed to launch conditions and exposed to 12 days of microgravity. At the same time, a ground reference experiment was implemented on Earth to compare the biological responses of rotifers to space conditions on ISS. The aim of this first experiment (RoB1, Fig. 10.20) was to compare the transcriptomic responses of hydrated *A. vaga* samples exposed to space environment with the ground control samples. Preliminary results

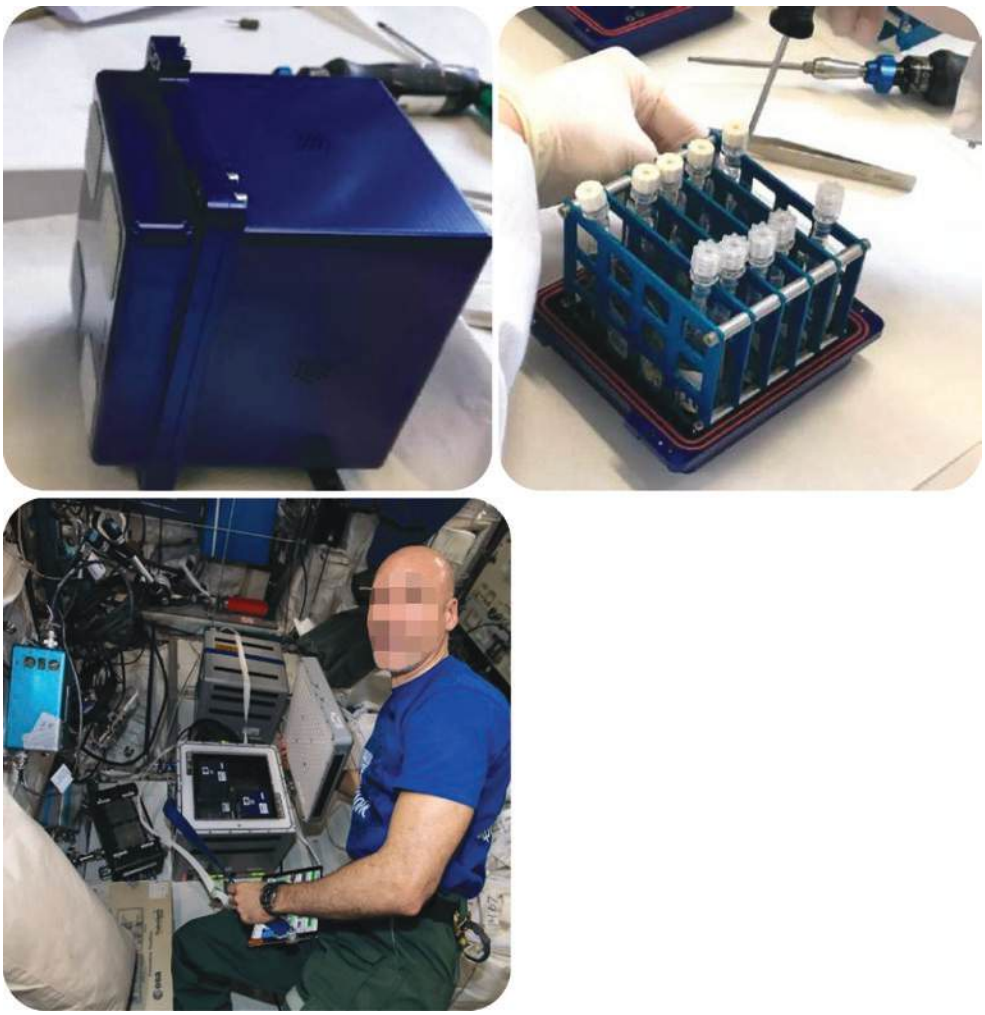

Fig. 10.20 View of Rob1 hardware used to culture hydrated *A. vaga* individuals onboard of ISS (December 2019). *Top left*: Rob1 hardware after its assembly at the launch site at Kennedy Space Center. Rob1 hardware is a passive hardware containing five culture bags containing hydrated specimens of *A. vaga*. Hardware enables gas exchanges between rotifer cultures and the outside through a permeable membrane. *Top right*: View of the culture bags assembled inside Rob1 hardware. Culture bags, loaded with 10,000 *A. vaga* individuals each, are made of Teflon and ensure an optimal gas exchange between the culture medium and the outside. Bags are waterproof and avoid any leakage of the medium (composed of mineral water and sterile lettuce juice) or rotifers. Reprinted with permission of Marc Guillaume. *Bottom left*: View of ESA astronaut Luca Parmitano loading two Rob1 hardware on KUBIK. KUBIK is a small incubator, temperature-controlled, with removable inserts designed for self-contained microgravity experiments. (Reprinted with permission of NASA)

Fig. 10.21 View of one Rob2 hardware used onboard of the ISS (left) and Astronauts checking the correct rehydration of *A. vaga* individuals. Sixteen pieces of hardware were sent to ISS, each containing 40,000 dry rotifers. Once onboard, rotifers were automatically rehydrated and cultivated 11 days before their fixation and download to Earth. (Reprinted with permission of Boris Hespeels and NASA)

confirmed the successful maintenance of hydrated bdelloid individuals on ISS, without additional food or oxygen supply and without astronaut intervention. All the replicates (ten) of the autonomous *A.vaga* cultures survived and reproduced on ISS with no visible impact on the morphology in space-exposed samples.

While it is well documented that astronauts experience DNA damage when exposed to cosmic radiation, accumulating DNA mutations and/or genomic rearrangements [163], the combined effect of cosmic radiation and microgravity on the living organism is still debated. It is suspected that microgravity reduces the efficiency of DNA repair and increases cancer risk [207, 215, 338]. Several studies using simulated microgravity highlighted a decrease in DNA repair efficiency. However, no effects of spaceflight on the cellular capacity to repair artificially induced DNA was observed (see Moreno-Villanueva et al. [209] for review). In order to obtain more insights, bdelloid rotifers have been used as a model system to evaluate their DNA repair efficiency of induced DNA breaks in space environment as compared to Earth samples. By the end of 2020, desiccated and irradiated *A. vaga* individuals were sent onboard of ISS. Before launch, desiccated animals were irradiated with 500 Gy of X-ray or proton radiation. Onboard, bdelloids were rehydrated and cultivated for different time periods to (1) follow the putative DNA repair process occurring post-rehydration and (2) investigate whether these irradiated rotifers still produce offspring under microgravity. In addition, half of the samples were exposed to simulated gravity using a centrifuge on ISS. Finally, a ground experiment was conducted in parallel at the launch site at Kennedy Space Center for comparison. Data generated by this second space experiment (entitled RoB2, see Fig. 10.21) will enable: first, to compare the DNA repair kinetic of rehydrated bdelloids post irradiation in 1G, μG, and simulated 1G; second, to compare the radiation responses of rehydrated rotifers after exposure to low LET or high LET; and third, to compare the DNA repair efficiency in space and on Earth by isolating eggs or juveniles from the exposed samples and use whole genome sequencing to compare the genomic structure of these animals pre- and post-exposure. This space experiment with bdelloid rotifers will contribute to our understanding of DNA repair process activity in space, in the presence or absence of microgravity. Moreover, studying the molecular processes involved in the DDR process of *A. vaga* will be of huge interest for future space travel.

In general, the ongoing rotifer space experiments will contribute to a better understanding of the mechanisms involved in the protection and repair of damages induced by radiation. They pave the road to the discovery of new molecules or candidate genes that could ultimately be used to improve health span and protect astronauts or individuals subjected to radiation during space flights or medical treatments. This research is also of fundamental importance for the understanding of extreme biology and the questions raised on the origin of life and its ability to spread through outer space. A third experiment, supported by ESA, is under preparation to evaluate whether rotifers can survive full space exposure, outside ISS, as was previously reported for tardigrades.

10.7 Plant Experimental Models and Biological Changes of Space Radiation

10.7.1 Plants vs. Animal Models

Long space exploration missions, settlement on orbital stations, or future planetary settlement (e.g., on Mars) will require further development of Life Support Systems (LSS). The LSS are able to regenerate a great amount of essential resources for survival and represent an ideal solution since it is not technically and economically feasible in long space missions to transport a large amount of consumables from the Earth [339–341]. Bioregenerative Life Support Systems (BLSS) are an artificial closed ecosystem characterized by the same structure as a terrestrial ecosystem: producers (plants), consumers (humans/animals), and decomposers (microorganisms).

Among biological components within BLSS, higher plants would have the same role on Earth as producers. Through photosynthesis, plants would utilize carbon dioxide produced by space crew and provide oxygen and fresh food. Moreover, they would use nutrients derived from human wastes and guarantee water purification by transpiration. Furthermore, plant cultivation in space also would provide psychological support against isolation [342, 343].

Each organism in Space is subjected to several factors which are potential constraints for biological life. Among the environmental factors (e.g., altered gravity, interaction between microgravity and fluid-dynamics, modified conditions of pressure, temperature, confinement, etc.) limiting plant growth in space, ionizing radiation influences severely the development of organisms at molecular, morpho-structural, and physiological levels [163, 182, 344]. Indeed, ionizing radiation is considered one of the main constraints for the long permanence of humans in Space.

All organisms in extraterrestrial environments are subject to higher levels of ionizing radiation than on Earth and, notwithstanding the large number of studies aimed at understanding the effect of ionizing radiation on animals, the knowledge on plant reaction is limited. Available information is limited to horticultural model crops which are candidate for fresh food production in BLSS. Moreover, most experiments are based on the irradiation of dry seeds and data from irradiation tests using other biological models (e.g., seedlings, adult plants, actively growing tissues) are scanty.

In Fig. 10.22, a comparison of the responses of plants and mammals to ionizing radiation exposure is shown. Generally, plants are more resistant than mammals. Ionizing radiation is known to have differential effects on plant growth, develop-

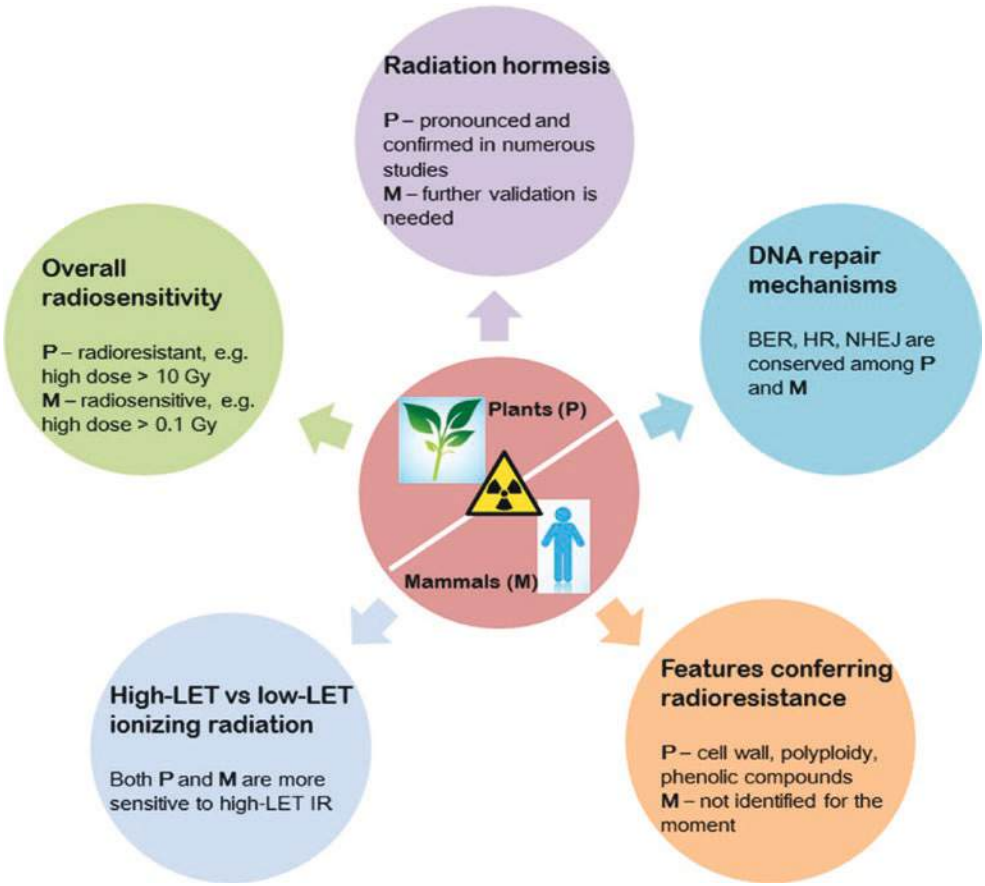

Fig. 10.22 A comparison among different responses of Plants (P) and Mammals (M) to ionizing radiation. (Reprinted with permission from Arena et al. [346])

ment, and reproduction, ranging from detrimental outcomes at high doses, harmful consequences at intermediate levels, and stimulatory effects at very low doses. This phenomenon is called "hormesis." Particularly, low doses of ionizing radiation have been reported to stimulate seed germination and root growth [345, 346].

However, ionizing radiation can also induce dwarf growth that is a desirable trait under conditions of limited volume availability in missions on orbital stations or during exploration traveling. The increased radioresistance of plants is still a debated issue since it can be associated with a genetic basis, but it can also reflect biochemical and biomolecular mechanisms of shelter from genotoxic damage.

The severity of the effects of ionizing radiation on plants is dependent upon several factors including radiation-related parameters (e.g., dose, LET) and organism-related traits (e.g., species, cultivar, physiological status, and structural properties, as well as plant genome organization including the polyploidy) [345, 347].

10.7.2 Biological Changes from Genetics to Organogenesis

In adult plants, in the case of organs at complete development, resistance to stressors can be often ascribed to integrated mechanisms of adaptation operating at morpho-structural and eco-physiological levels since the limits of major metabolic and physiological processes are dictated by the plant's structure [348, 349]. Growth, reproduction, and, ultimately, survival of plants in Space depend on photosynthesis which is strongly responsive to ionizing radiation acting on the various components of the photosynthetic apparatus, such as pigment–protein complexes responsible for light absorption, electron transport carriers, and enzymes of carbon reduction cycle [345]. Ionizing radiation leads to several detrimental effects in photosynthetic apparatus, such as loss of functionality of photosystem II (PSII) and generation of free radicals causing photosynthetic membranes' oxidation [350–352]. Changes in the total antioxidant pool and in the distribution of phenolic compounds in leaf tissues were observed in plants exposed to very high doses of X-rays, namely 50 and 100 Gy [353].

However, chronic exposure to low doses of ionizing radiation seems to enhance the activity of some antioxidant enzymes, providing plants with a radio-resistance [354, 355]. Moreover, the degree of plasticity of leaf cytological and anatomical traits in response to environmental changes can be responsible for enhancing or constraining processes such as light interception and gas exchanges, definitely affecting photosynthesis. Similarly, the correct functioning of the whole water transport system throughout the plant is responsible for water supply up to the leaves, necessary for efficient photosynthesis. The ability of xylem to transport water efficiently depends on the morphological features of its conduits and on the ultra-structural properties of conduit cell walls, whose main components can be differently affected by ionizing radiation.

Apart from a few findings mainly related to specific ultra-structural modifications occurring on irradiated seeds, the effect of cosmic radiation on organ/tissue organization, especially in relationship with eco-physiological traits, is still poorly explored. Moreover, most of the studies regard experiments with low-LET ionizing radiation [346, 355], and only a few data are available on the effects of chronic radiation exposure on plants in general, mainly deriving from nuclear accidents as Chernobyl in Ukraine (1986) and Fukushima in Japan (2011).

10.8 Eukaryotic Cell Experimental Models and Biological Changes of Space Radiation

10.8.1 Definition of Eukaryotes

Regarding the complexity of their cells, all living organisms can be classified into two groups-prokaryotes and eukaryotes. Compared to prokaryotes, eukaryotic cells are highly organized and contain a cell nucleus. Prokaryotes are bacteria and archaea, while protists, plants (see Sect. 10.5.8), animals (see Sect. 10.5.7), and fungi (see Sect. 10.5.9) are eukaryotes.

In the following the effect of space radiation on in vitro models (conducted in a cell culture dish) and ex vivo models (experiments outside a living body) will be described.

10.8.2 Definition of In Vitro Models

In vitro models used in science, are very important, as they provide insight into cells. With this, the function of primary cells and cell lines of various origin (vertebrates including human, insects, and mussels) can be studied.

10.8.3 Definition of Ex Vivo Models

Ex vivo models or tissue explants allow studying complex functions and interactions of different cells within an organ. For these experiments, the living tissues are directly removed from a living organism or can be generated by means of pluripotent stem cells and cultivated under controlled conditions.

10.8.4 3D Cell Culture Models

10.8.4.1 Definition 3D Cultures

In comparison to cells in monolayer cultures (2D), cells in 3D cultures react completely differently. The biggest disadvantages of 2D cultures are the unnatural contact with a plastic or glass surface, the flat morphology of the cells on the growth surface that restricts intercellular contacts and the lack of an extracellular matrix which surrounds cells in vivo. These conditions modify the metabolism and functioning of cells and often result in the loss of the specific differentiation of a cell. The structure, function, and composition of organs and tissues can thus be better studied in 3D cell culture systems. They enable cell–cell and cell–extracellular matrix interactions in a three-dimensional space. 3D cultures are a very helpful tool before performing whole-animal studies. They can further be used to study the understanding of how processes in tissues are affected by spaceflight conditions, including space radiation and microgravity, which otherwise cannot be investigated in animal or human subject studies.

There are many different models of 3D cell cultures, including organoids, *ex vivo* tissue, or slice cultures, which are explained in the following. Furthermore, it is possible to create these models with 3D bioprinting, which have then a structure which closely resembles the organization of tissue or organs. In fact, the European Space Agency (ESA) recently summarized the capability science requirements for 3D bioprinting on the ISS to support medical treatment on long-term space missions.

In all given examples two or more cell types can be co-cultured, closely simulating the situation in organs or tissues, e.g., investigation of cellular differentiation processes in tissues, nerve-muscle function, tissue regeneration and repair, vascular tissue function, brain tissue homeostasis and aging, immune system processes or cardiac muscle function.

10.8.4.2 Organoids

Human organoids, derived from stem cells or progenitor cells, are tiny self-organized organ-specific 3D cultures, recreating the physiological and cytoarchitecture of human organs. With this, the model reflects the in vivo situation much better than single cell cultures. For research purposes, it is feasible to create organoids that resemble the brain, kidney, lung, intestine, stomach, and liver.

Organoids will help to study the effect of space radiation on the overall response of organs, including cellular heterogeneity, cell-matrix interactions, cell-cell interactions, morphology, and functional changes [356, 357], which cannot be studied in in vitro systems. One major disadvantage compared to in vivo systems is the lack of microenvironment.

The effects of microgravity on human brain organoids were tested on the ISS during the Space Tango-human Brain investigation in 2019 (NASA). Of special interest was the effect on the brain cells including survival, migration, metabolism, and the formation of neuronal networks (Muotri, unpublished).

10.8.4.3 Spheroids

Spheroids are also 3D cell cultures, but in comparison to organoids, they form simple clusters into sphere-like formation, but they cannot self-assemble or regenerate. Whereby the cellular functions inside spheroids are closely correlated to the size, uniformity is especially important for reproducible results. To guarantee this, several methods for culturing are available such as hanging drops, scaffolds, liquid overlay technique, and hydrogels [358]. Nowadays spheroids are highly used to study the microenvironments of tumors or their response to radiotherapy.

Already in 2016, the SPHEROIDS project was launched on the ISS. Here, endothelial cells, which under simulated microgravity form small, rudimentary blood vessels, were exposed to real microgravity for 12 days on the ISS. The formation of spheroids under space conditions and under simulated microgravity on Earth were similar [359], underlining the important role of microgravity in spheroids formation.

Differences between the three types of cultures are summarized in Fig. 10.23.

10.8.4.4 Organotypic Slice Cultures

Organotypic slice cultures are tissue samples that are cut in thinly, about 300 μm, thick slice and are then cultivated on semipermeable insert. Most common are organotypic slice cultures that originate from different parts of the brain (e.g., hippocampus, cerebellum, or cortex) and can be kept in cultures for long term, while slices originating from liver tumors can only be kept in culture for a short time [360, 361]. Also,

	Monolayer	Spheroid	Organoid
Cell types	Single cells	Multiple cells types	Epithelial and mesenchymal cells
Derived from	Donor Patients, Animals	Cell line monoculture	Stem cells
Morphology	Non-natural, flatten	Simple cell clusters	More complex cell clusters
Represent	Replicate only tissues, but not organs	Single tissue of an organ	Multiple tissues of an organ or "Mini-organs"
Example	MEF, ESCs, iPSCs	Muscle spheroids, lung epithelial spheroids, Tumor spheroids	Organoids for brains, guts, lungs, hearts

Fig. 10.23 Difference between the different cultures

this 3D culture has the advantage that the composition and architecture of the extracellular matrix as well as the tissue are preserved. During analysis of the slices, it has to be considered that every slice, even from the same organ, has a partly different composition, cell counts, and viability, limiting the reproducibility of results produced by this method.

10.8.4.5 Organ Cultures

Organ cultures were developed from tissue and slice cultures. By using organ cultures, it is possible to study the functions of an organ in various conditions and states in an in vitro organ. Hereby, the entire organs or only a part of the organ are excised from the body and cultured. Also, with this method, the 3D structure of the tissue of choice is preserved.

For space exploration, the eye lens is of special interest, because it is amongst the most radiosensitive tissues in the human body. Ionizing radiation can cause a posterior subcapsular cataract [287, 362, 363]. Whole lenses and lens epithelial cells in culture enable the study of early mechanisms of space radiation-induced cataractogenesis and of the relative biological efficiency of different space radiation components to induce early changes. With regard to the human lens in anatomy and size, the porcine eye is very similar. Thus, it is used to study the radiation response in the whole organ. Translation to the human eye lens can be enabled by using human-transformed epithelial cells or lens epithelial cells from donor patients. As the viability of eye lenses in cultures is limited to a few weeks, studies on radiation-induced full-blown cataract formation usually require animal experiments over their lifespan (Sect. 10.5).

In addition to that, the microgravity environment on the ISS suits perfectly to 3D print tissue cultures and later maybe entire organs. Compared to conditions on Earth where scaffolds or matrices are needed to form organoids, in space cells can easily self-organize into their precise structure. On the one hand, the bioprinted tissue could be used in the future to treat injured astronauts [364] and on the other hand the technique can be transferred to Earth and then be applied to the field of regenerative medicine for organ transplantations [365]. In July 2019, the 3D BioFabrication Facility (BFF—see Fig. 10.24) has arrived onboard of the ISS, with this it is now possible to study 3D bioprinting of different human tissues in space. Also, here real microgravity has the benefit that printed structures will not collapse, enabling also the printing of soft human tissue (NASA) (Box 10.10).

Box 10.10 Highlights

- Several cell cultures system can be studied under space conditions
- The microgravity environment on the ISS suits perfectly to print 3D tissue cultures

Fig. 10.24 NASA's 3D BioFabrication Facility BFF. (Image JSC2019E037579, Credits NASA)

10.8.5 Omics Approaches in Space Life Sciences

Understanding the effects of the space environment on microorganisms has witnessed recently considerable progress (whereas the main factors are microgravity, radiation, and vacuum). However, explicit knowledge of molecular mechanisms responsible for survival and adaptation in space is still missing. Space environment affects a variety of physiological features of microorganisms. The above features include metabolism, motility and proliferation rate, division of cells, and also virulence and biofilm production (Fig. 10.25) [366]. Molecular-level understanding of the above effects in space-exposed microorganisms is still lacking. It is believed that omics-based approach, together with classical phenotyping and physiological measurements, will be a useful toolbox for understanding mechanisms of microbial survivability in the harsh conditions of outer space. "Omics" stands for genomics, transcriptomics, proteomics, metabolomics, and more.

Systems biology is an interdisciplinary approach in biomedical research aiming at understanding the biological system at the organism, tissue, and cell level. Systems biology incorporates the results of –omics techniques, genome-scale metabolic and regulatory biomathematical models to understand molecular interactions, evolution, functional and phenotypical diversity, and molecular adaptation. The omics-based approach integrates various pieces of biological information from genomes, mRNA, and proteins to metabolites [367].

The –omics-based approach has recently opened a window for a deep insight into molecular machinery implicated in the survivability of space-exposed microorganisms by revealing expression, metabolic functioning, and regulation of the genes and proteins encoded by the genomes of "space travelers." The diverse biological activities of microorgan-

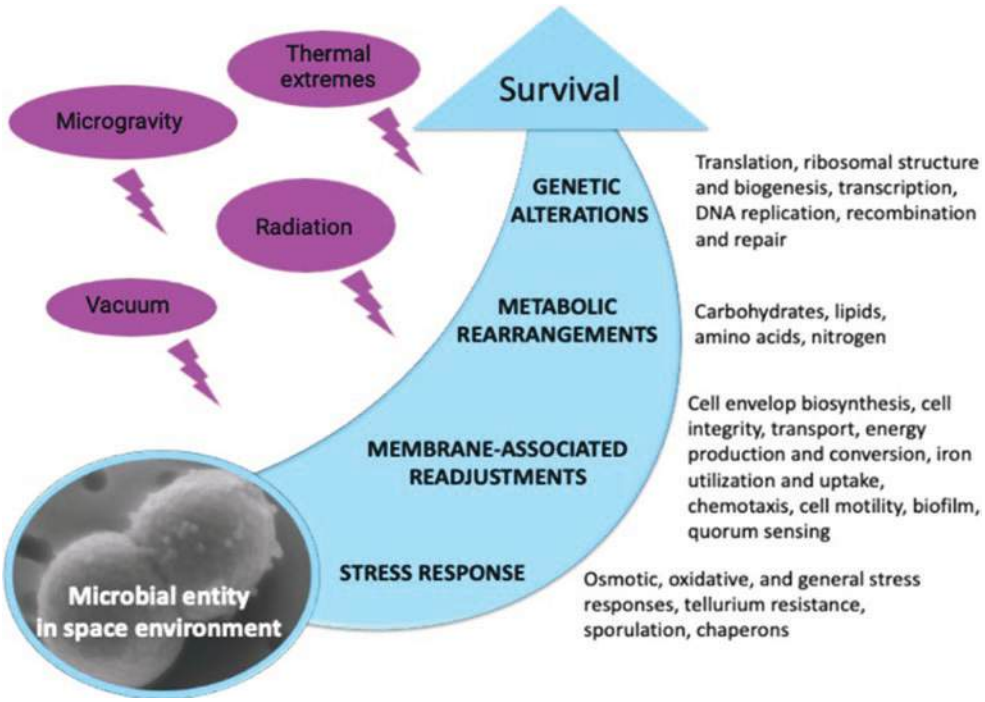

Fig. 10.25 Molecular response experienced by microorganisms in the outer space environment revealed with the help of global and integrative –omics approaches of systems biology that have been recently used to study microorganisms exposed to real and simulated space conditions. (Reprinted with permission from Milojevic et al. [366])

isms in space are affected by metabolic alterations caused in turn by genetic regulations (Fig. 10.26). It has been demonstrated by means of –omics-based approaches that exposed microbes switch to "energy saving mode." Research identified some global regulatory molecules that drive molecular response of a few space-exposed microorganisms [366–369]. Various kinds of stress responses (e.g., general, osmotic, and oxidative) experienced by microorganisms in conditions of real and simulated outer space have been deciphered via –omics-assisted analyses [366]. Various genes with altered expression after microbs' exposure to real and simulated outer space environment (Fig. 10.25) have been identified [366].

State-of-the-art –omics technologies have been successfully used to understand molecular mechanisms responsible for alterations of microbial virulence in space conditions (Fig. 10.27) [366].

Space exposure imposes stresses that affect microbial survival rates and may lead to certain discrepancies in –omics-assisted analysis of returned/exposed microorganisms. The composition of the cultivation medium influences the microbial space response [369], e.g., by providing specific antioxidants presented in rich medium, which may protect microbial cells against ionizing radiation. The majority of space experiments have been performed on satellites, where microorganisms are cultivated in environment protected from all factor but microgravity [366]. Direct exposure to real space environment outside the ISS followed by investigation with –omics techniques was performed on a few microbial species only [367, 370, 371]. Therefore, in order to broaden our knowledge of molecular mechanisms of microbial survivability in outer space, there is an urgent need for further experiments with direct exposure. Often, a multi-omics post-flight analysis has the problem of a limited number of microbiological samples exposed to the space environment. Therefore, the researchers should critically assess the design of outerspace experiments to provide a sufficient number of independent biological samples in order to enable statistically significant results in processing the –omics data. It is also extremely important to avoid artifacts: due to very high sensitivity of the –omics techniques of occasional occurrence of uncontrolled conditions, stress-related artifacts cannot be ruled out. In this context, it is highly desired to develop novel approaches for the efficient extraction of DNA, RNA, proteins, and metabolites simultaneously from the minimal amount of microbial cells [367, 372]. Furthermore, the absence of detailed reports regarding the environmental conditions during space exposure and corresponding ground control experiments is, unfortunately, a frequent reality that requires a critical reassessment of research planning. Providing a full record of controlled parameters (like temperature, humidity, and pressure profiles) during flight, simulated, and control experiments is highly desired to achieve a comprehensive and artifacts-free analysis of the effects of the space environment on the physiology and molecular machinery of microorganisms.

It has been proposed that in future space experiments, detailed metabolomic analysis of exposed microorganisms should be performed in addition to the proteotranscriptomic profiling. This novel approach has provided already plenty of

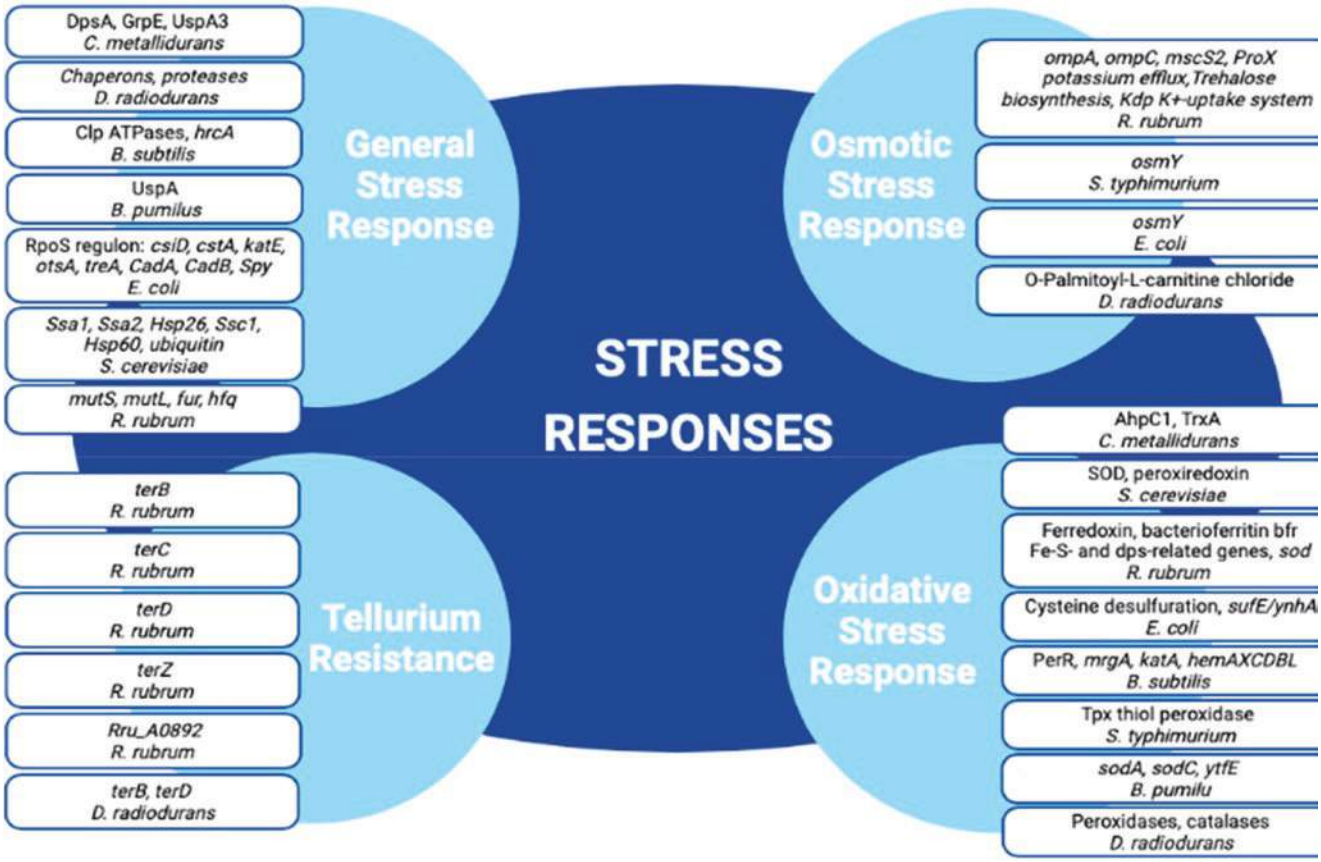

Fig. 10.26 Stress responses experienced by microorganisms in outer space real and simulated conditions, revealed with –omics-assisted investigations. Proteins and genes of stress responses with altered abundance and expression after exposure of microorganisms to the outer space real and simulated environment [366]

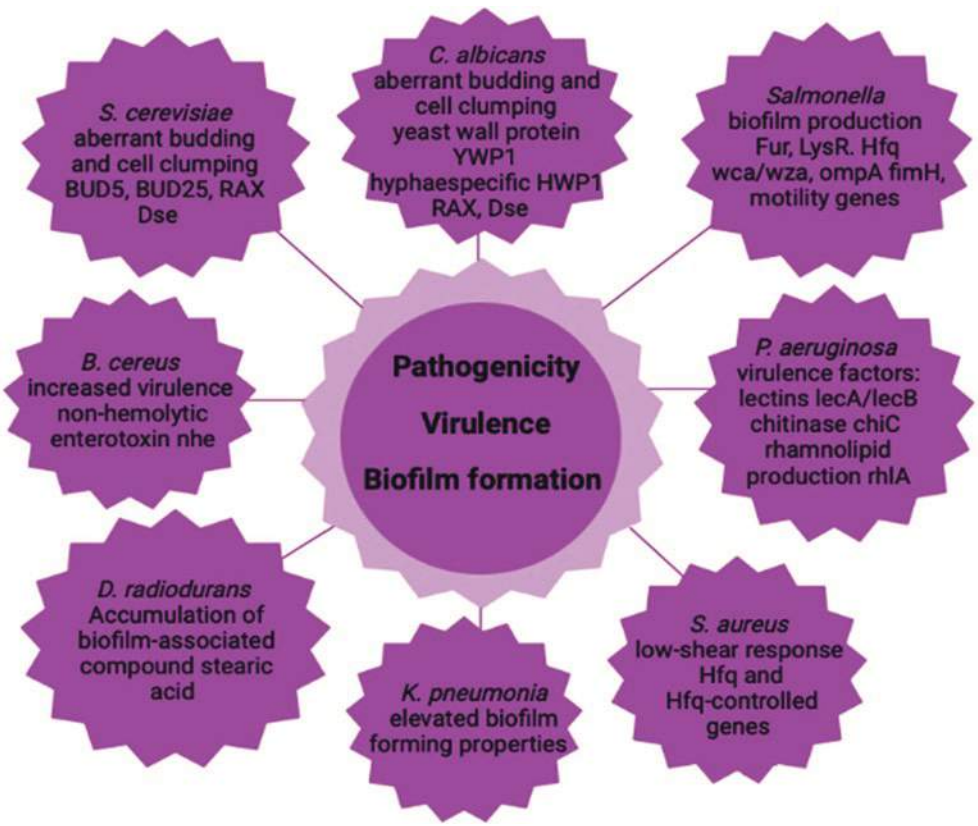

Fig. 10.27 Molecular alterations underlying microbial pathogenicity, virulence, and biofilm formation in the outer space environment, resolved with –omics-assisted investigations [366]

new findings on fine molecular networks regulating the space response [367]. Recent works (e.g., the NASA twins' study) used a multi-omics, systems biology analytical approach to analyze biomedical profiles of astronauts [120]. Results of performed targeted and untargeted metabolomics combined with proteomics effectively revealed the biomedical responses of a human body during a year-long spaceflight indicating mitochondrial stress as a consistent phenotype of spaceflight [120, 373]. Finally, the combination of molecular data with a genome-scale metabolic reconstruction of the respective species should be implemented, delivering the space-induced microbiome signatures [366].

10.9 Space Radiation Resistance

10.9.1 Health Risk Reduction from Space Radiation Exposure in Humans

Humans have all evolved in an environment containing a persistent low level of constant exposure to different endogenous and exogenous mutagenic agents, and consequently have developed many cellular mechanisms for either DNA protection or repair (see Chap. 2). However, when humans travel into space, these naturally evolved cellular mechanisms might not be enough as many major health threats from space radiation has been identified, e.g., central nervous system injury, cardiovascular diseases, immune dysfunction, cancer development, and premature aging. To reduce the risk of humans in space, there are some possible interventions which can limit the effects of space radiation. A dedicated review can be found elsewhere [374].

One way of reducing the health risk from space radiation exposure in humans is selecting more radioresistant humans during the selection campaigns of space agencies. The most used way is to perform in vitro adaptive response studies, in which cells collected from the candidates are used to measure their response to a fixed dose of ionizing radiation. While the results of these studies are not necessarily used during candidate selection, they hold great value in selecting the right people that will be more protected against space radiation. Another strategy would be to pharmacologically hamper the processes underlying the molecular (side) effects of space radiation exposure. Examples are the application of radioprotectors and geroprotectors, as well as supplementation with antioxidants or antioxidative capacity increasing compounds (see Chap. 11). While these pharmaceuticals hold great promise, many of them are still under investigation and not allowed to be used on humans.

An alternative method to elevate humans' natural radiation protection capacity is inducing a hibernating or hypostasis state. It is well-known that natural hibernators become more radioresistant during their inactive state. The reason for this has not yet been fully elucidated. It is probably due to several factors related to slower cell metabolism and increased tissue hypoxia.

In recent years, a technique has been developed that allows hibernation to be reproduced even in those animals that would not usually be able to hibernate, such as rats. This technique is nowadays known as synthetic hibernation or synthetic torpor [375]. Although this research has a big potential to limit radiation-associated risks in space, it is quite far from practical use yet. Another futuristic method is the use of deuterium, the stable isotope of hydrogen. As carbon-deuterium bonds need more energy to break than normal carbon-hydrogen bonds, the necessary energy to break the hydrogen bonds between DNA bases would be higher, making deuterated DNA less sensitive than normal DNA to DNA damage following ionizing radiation exposure. However, a lot of issues have to be solved before deuterium could be applied in humans: lack of evolutionary adaption to catabolize organic compounds containing deuterium, consequent slower rate of vital metabolic reactions, and their potential toxic effects. Nevertheless, it has been shown that deuterated food or water intake helps to increase life or health spans from numerous model organisms.

Gene therapy stands for the use of genetic modifying techniques in order to achieve a therapeutic effect. In the context of radiation and radiation protection, this has been studied for several radioresistance mechanisms making these techniques interesting for deep space missions, where radiation protection concerns arise [374]

One of the strategies for gene therapy in radioresistance is the overexpression of endogenous antioxidants, for example, magnesium superoxide dismutase (MnSOD) that acts as a scavenger for reactive oxygen species produced after the interaction of radiation with the cell [376].

Another angle in which gene therapy can be useful for improving radioresistance is by enhancing the DNA damage repair such as the overexpression of certain repair proteins that are normally active in repairing the damage in the DNA strands after radiation exposure [377].

A promising approach takes its inspiration from extremophiles and their impressive radioresistance capabilities, in concrete, the tardigrades, a microscopic animal that is capable of surviving in extreme conditions. A protein identified in these organisms, termed damaged suppressor (Dsup), has been made to be expressed in human cell lines, reducing the number of DNA strand breaks and preserving cellular proliferative abilities after high doses of radiation [337].

10.9.2 Mechanisms in Extremophiles

10.9.2.1 What is an Extremophile?

Extreme conditions in a natural environment are only extreme from a human point of view. Extremophiles can only live under these conditions and depend on them. Often organisms living under these conditions are called "extremophiles" or "polyextremophiles" since most of them are coping with different extremes in their natural environment [378].

10.9.2.2 Which Adaptations/Mechanisms Are Known?

Plenty of different (poly) extremophiles in natural and human-made extreme environments exist in natural and human-made harsh environments. Examples include anaerobes, (hyper-) thermophiles, psychrophiles, halophiles, acidophiles, xerophiles, and piezophiles. For all the named organismic groups, cellular adaptation mechanisms are known that protect the cells themselves or enable them to live under extreme conditions in their natural habitat. In addition to the intracellular protection mechanisms, general protection mechanisms like spore formation are well-known. For example, the spore of the Bacterium *Bacillus subtilis* is characterized by a thick layer of peptidoglycan, a low water content inside the cell, a DNA conformation changed from B to A, and the presence of α/β-type small acid-soluble spore proteins which accumulate within the spore. In general, spores are more tolerant to inactivating physical stresses, like radiation as vegetative cells [379, 380]. Spore formation is known to be an answer to changing conditions in the environment that is used by microorganisms and fungi; special forms like the anhydrobiotic state are also observed in other eukaryotic cells like tardigrades, nematodes, and rotifers [381]. Spore formation and the anhydrobiotic state, as well as intracellular adaptation mechanisms, are relevant for possible survival after exposure to ionizing (space) radiation [323, 382]. In addition to spore formation, biofilm growth by the production of extracellular polymeric substances (EPS) also leads to a higher ionizing radiation tolerance [383].

Besides the named cellular adaptation mechanisms, there are also different intracellular adaptation mechanisms possible to cope with extreme environmental stresses. As described before, ionizing radiation exposure does not only lead to direct effects and intracellular damage, such as DNA strand breaks, it also leads to indirect effects, like ROS production. Hyperthermophilic Archaea, like *Pyrococcus furiosus*, are partly tolerant to the indirect effects of ionizing radiation, due to mechanisms protecting the DNA from the influence of ROS [384]. In these Archaea, DNA binding proteins play a major role as they bind and protect the DNA thereby limiting the accessibility of the DNA to ROS. In addition, increased expression of different enzymes like superoxide dismutase and the glutathione peroxidase can also reduce the level of intracellular ROS.

For the Bacterium *Deinococcus radiodurans* as well as for the Archaeon *Halobacterium salinarum* special intracellular Mn/Fe ratios are described: they demonstrate an intracellular accumulation of high amounts of manganese along with low iron levels, which contribute to their high radiation tolerance [385, 386]. This special Mn/Fe ratio was not found in radiation-tolerant anaerobic microorganisms. It is proposed that the low levels of IR-generated ROS under anaerobic conditions combined with highly constitutively expressed detoxification systems in these anaerobes are key to their radiation resistance and circumvent the need for the accumulation of Mn-antioxidant complexes in the cell [387].

Furthermore, polyploidy or the presence of several DNA copies within one single cell has been discussed to contribute to tolerance to desiccation and therefore also to ionizing radiation [388].

Halophilic organisms have different strategies to cope with a high salt concentration in their natural habitat. One option is the intracellular accumulation of salt or other compatible solutes [389]. It is also known that compatible solutes can contribute to the tolerance to ionizing radiation in halophilic microorganisms [389]. Additionally, protective mechanisms such as membrane pigments, including carotenoids, melanin, scytonemin, and bacterioruberin were found to be important in ionizing radiation protection in different organisms through the scavenging of hydroxyl radicals [390, 391].

10.9.2.3 How Relevant Are These Adaptations/Mechanisms for Space Radiation?

In general, there is no direct adaptation of microorganisms to space conditions or space radiation known as all organisms evolved on Earth. Nevertheless, there have been and still are space experiments ongoing where the adaptability of different organisms is investigated during exposure to space conditions. In this context, we speak about the side effects of other tolerances or resistances which enable the organisms to endure space stressors. In general, organisms which are tolerant to desiccation developed mechanisms to repair the DNA which is damaged during the desiccation process. The same repair mechanisms can also be used to repair DNA damage caused by other stressors, such as ionizing radiation. One prominent example is the desiccation and radiation tolerance of the microorganism *Deinococcus radiodurans*. This organism uses the same cellular adaptation and repair strategies after exposure to drought and ionizing radiation exposure. However, not all desiccation-tolerant organisms are tolerant to (ionizing) radiation exposure [392]. The same is true for other repair machineries, where no direct correlation between hyper-/thermophilic organisms or the ability to produce compatible solutes and radiation tolerance could be identified [393, 394]. In addition, some microorganisms (e.g., *Ignicoccus hospitalis*) demonstrate a high survival rate after ionizing radiation exposure but possess a repair mechanism which is not known up to now [395].

10.10 Irradiation Experiments at Ground-Based Facilities for Simulation of the Space Environment

10.10.1 Low Dose Rate Irradiation Facilities

As mentioned at the beginning of this chapter, protons account for nearly 87% of the total flux of the galactic cosmic radiation (GCR), helium ions—for approximately 12%, and the remaining heavy ions, or high-Z elements (HZE),—for less than 1%. However, the relative distribution of the effective dose is quite different. Multiplying the abundance by Z^2 provides an estimate of the contribution to the dose. One should further consider the quality factor of the biological effectiveness of the corresponding radiation. As a result, HZE particles contribute approximately 89% of the total dose equivalent (mSv) in free space. Among the HZE particles in GCR, iron is the largest contributor (26%) to the effective dose [396].

10.10.2 Low Dose Rate Particle Irradiation Facilities

Low dose rate irradiation is usually provided in a laboratory either by X-ray machines or radioactive sources, and neither mimics GCR well. The X-rays are low-energy radiation and do not mimic the penetrating capability of GCR. Usual radioactive sources emit α-, β-, and γ-radiation. While α-particles are helium nuclei abundant in GCR, the energy of typical α-particles is 4–9 MeV as compared with above 1000 MeV in GCR. As a result, α-particles cannot penetrate the thinnest screen (even the skin) and cannot be used for GCR simulation.

γ-Radiation has a much stronger penetration capability, and γ-emitters are used [397]. However, the biological effects of γ-radiation and ions are different. As for the β-radiation, in the sense of GCR simulation it combines the drawbacks of α and γ: having low penetrating capability, its biological effects are similar to γ and far from high-energy ions.

A partial solution has been found by using a unique artificial isotope Californium-252, which exhibits exceptionally high neutron emission. ^{252}Cf is used, e.g., at the ESA test station and the new facility in Japan [398].

10.10.3 Low Energy Particle Irradiation Facilities

Although low-energy charged particles (up to about 20 MeV) do not reproduce the characteristics found in the GCR spectrum, low-energy facilities are widely available and are useful to help in the screening and the design of experiments that will be further carried out on higher energy accelerators (see next subsection).

Several accelerator types can be used to produce such low-energy beams, but electrostatic tandem accelerators are probably the most widely used. A schematic representation of such accelerator is given in Fig. 10.28. The first part consists of an ion source, which can produce any negative ion

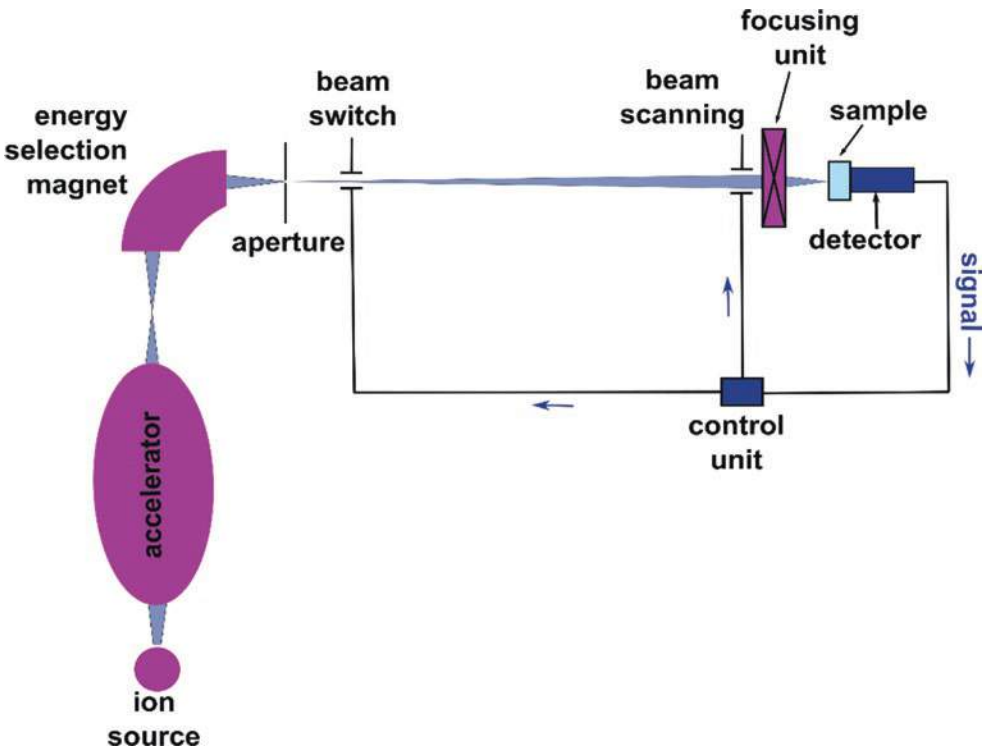

Fig. 10.28 Schematic view of the SNAKE (Superconducting nanoprobe for (kern) particle physics experiments) setup, including linear particle accelerator (orange), focusing unit (superconducting magnetic lens) and detection system with the particle detector and ultrafast high-voltage switch

(with one extra electron) from hydrogen to uranium. The produced negative ion beam is then extracted from the source and guided to the main tube. The acceleration is carried out in two stages hence the name "tandem accelerator." First, the negative ions are attracted to the positive high-voltage "terminal" located in the center of the tube. Then, negative ions can be stripped of part of their electrons (usually 2–3) in the stripper channel, turning to positive ions. These positive ions are repelled by the positive terminal voltage to the end of the tube, which is at ground potential. High-energy ions are focused by (usually superconducting) magnets and deflected into one of the beamlines, according to the particle energy, mass, and charge.

Regarding the beam size, two configurations are used: microbeam and broad beam.

The initial accelerated ion beam is always a microbeam with a diameter often below 5 μm. Microbeams are a useful tool in studying the bystander effect (described in detail in Chap. 2). Indeed, such a beam permits to irradiate selectively one or more cells inside a population. This offers the possibility to either target the cell nucleus, the conventional target in radiobiology, the cytoplasm, or organelles. It also provides the advantage of knowing precisely the dose delivered to the cells and the number of particle shoots being determined in advance. In the context of space radiation, where the flux of high-mass particles is very low and the occurrence of a single shoot-in through a cell is very high, the bystander effect is a topic of crucial importance. Indeed, it is observed through a variety of endpoints: reduction in cell survival, double strand break induction, micronuclei, mutations, and expression of apoptosis, inflammation, and cell cycle-related genes.

Broad beams can be produced either by using scattering foils, by scanning microbeam, or by defocusing them. Beam homogeneity is controlled by plastic scintillators or silicon-based detectors.

10.10.4 High-Energy Particle Irradiation Facilities

The importance of accelerator-based studies was acknowledged by NASA decades ago. After preliminary research at the existing accelerators, it was decided to build a dedicated beamline. In 2003, the NASA Space Radiation Laboratory (NSRL) was commissioned at the Brookhaven National Laboratory (BNL). The NSRL layout is presented in Fig. 10.29. The facility is capable of supplying particles from protons (p) to gold (Au). Available beam energies range from 50 to 2500 MeV for protons and 50 to 1500 MeV per nucleon for ions between helium (He-2) and iron (Fe-56; $Z = 26$).

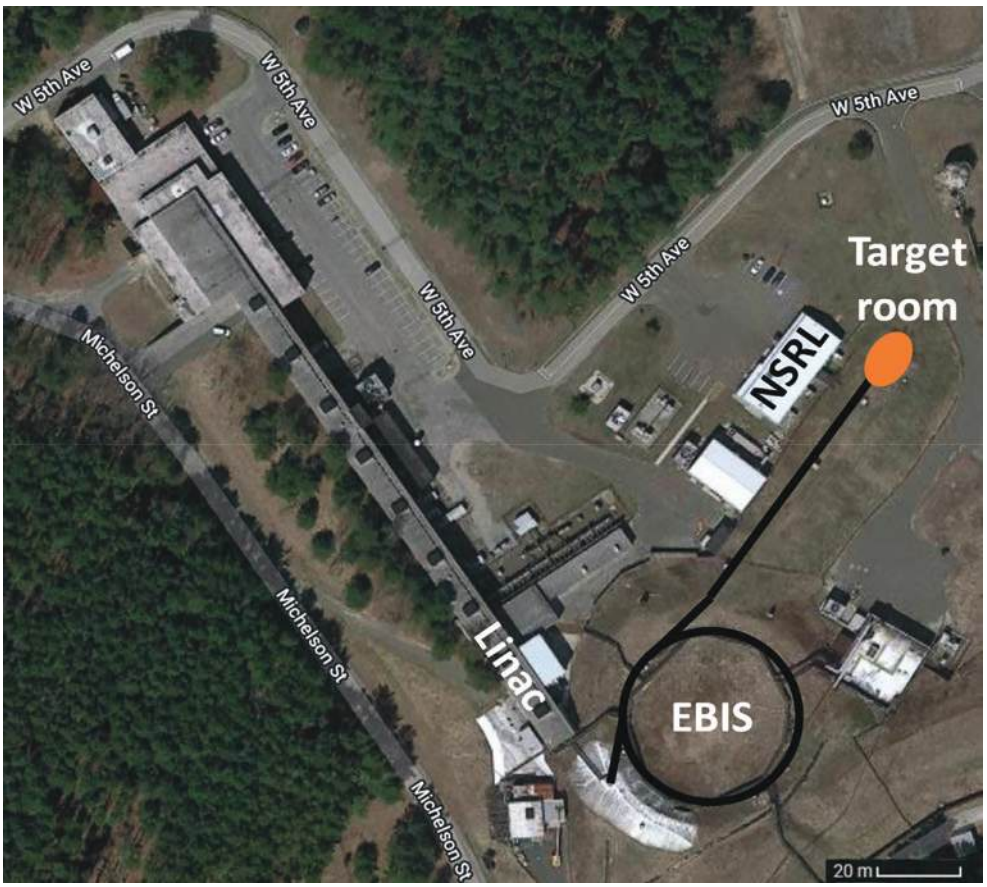

Fig. 10.29 Aerial view and general layout of the NASA Space Radiation Laboratory (NSRL) facility in Upton, NY, USA. *EBIS* electron beam ion source. (Satellite view courtesy Google Earth)

Heavier ions with atomic numbers up to $Z = 79$ (Au) are limited to approximately 350–500 MeV per nucleon (https://www.bnl.gov/nsrl/).

The choice of Fe-56 ions is justified by a sharp decline in abundance for ions heavier than iron [396] while the chosen energy is around the peak of the galactic cosmic radiation spectrum. Moreover, the linear energy transfer is about 140 keV/μm, around the peak of effectiveness for late radiation effects [399]. The three key areas developed together to ultimately provide the GCR simulator at NSRL are illustrated in Fig. 10.30. Several important results have been obtained at NSRL. We can mention, for example, the observation that, despite being high-LET particles, heavy ions are not more effective than γ-radiation in the induction of leukemia in mice [400]. Another example is the discovery of specific types of brain damage caused by heavy ions [401], types that had not been known from X-ray studies.

The basic idea of a high-energy accelerator is illustrated schematically in Fig. 10.31. Each accelerating section itself consists of a sequence of resonant cavities in which the RF (radio frequency) electromagnetic field is oscillating. Ions traverse RF cavities subsequently; the timing of the passage of each cavity is synchronized with the direction and phase of the electric field—therefore, each ion is accelerated from cavity to cavity. In case of a linear accelerator (LINAC), the accelerating sections are positioned adjacently along a straight line. In case of a synchrotron (like EBIS in Fig. 10.31), the accelerating sections are positioned along a circumference, while the charged particle beam is bent between the sections by a magnetic field.

The resonant frequency is usually either about 1 GHz (L-band of the RF spectrum) or about 3 GHz (S-band). The electromagnetic power for feeding the RF cavities is generated usually by a high-power klystron.

The accelerating cavities can be made either of normal-conducting metal ("warm" cavities usually made of copper) or of superconductor (usually, niobium). In the last case, cryogenic cooling to liquid-helium temperature is needed. Accelerating gradients are usually in the range of 10–30 MeV/m, e.g., the 3-km long SLAC accelerator commissioned back in the 1960s, accelerating electrons to the energy of 50 GeV, has an average accelerating gradient of about 17 MeV/m (with 3-GHz copper cavities).

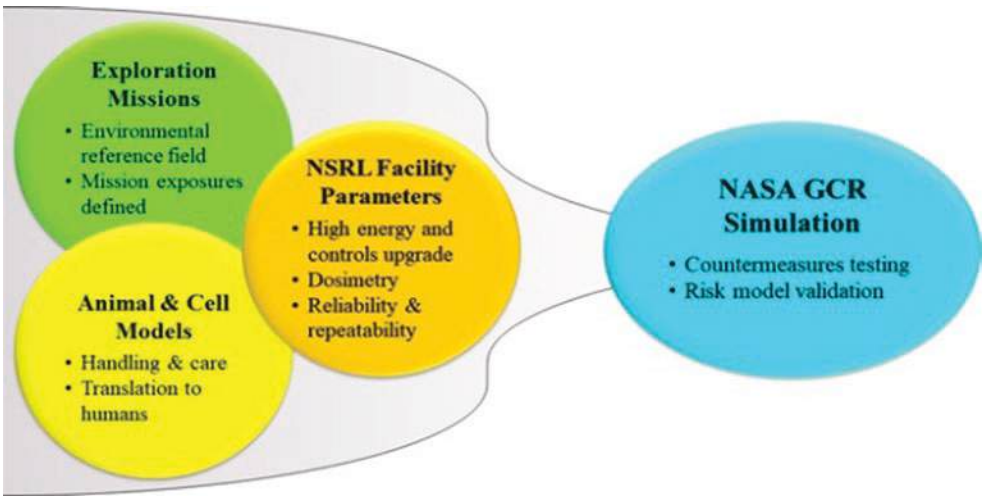

Fig. 10.30 Three key areas developed to provide the GCR simulator at NSRL. (Source: Simonsen et al. [396], reproduced with permission)

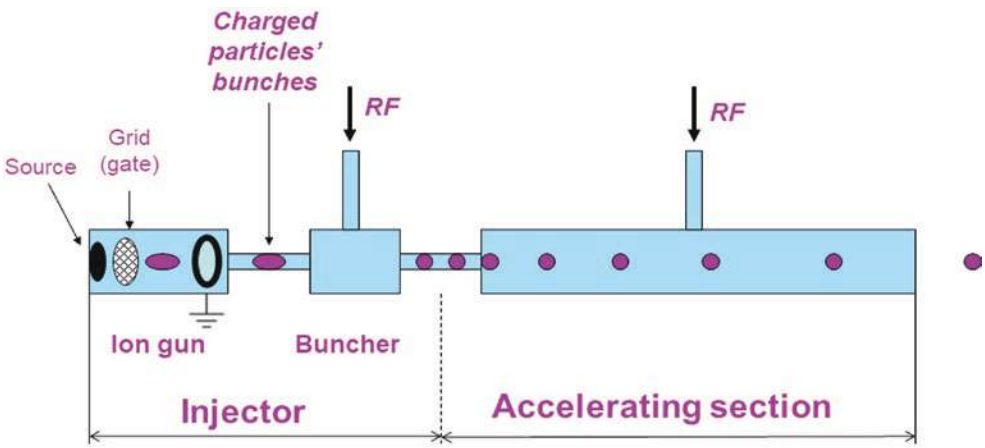

Fig. 10.31 General layout of a linear high-energy particle accelerator. *RF* radio frequency

Output of RF-driven particle accelerator necessarily consists of single bunches. Such bunches are called micropulse, and their duration is just a fraction of the oscillating field period. For example, for the S-band with period of about 300 ps = $(3\ \text{GHz})^{-1}$, the typical micropulse duration is below 20 ps. The train of micropulse is called "macropulse." While there is no theoretical limit for macropulse length, practically it is limited by the driving klystron pulse length: For S-band normal-conducting linacs the typical value is 5–20 μs, for L-band superconducting linacs—much longer (1 ms and more).

Particle beams are collimated and bent "magnetic lenses"—magnetic fields created by electromagnets or permanent magnets. These magnetic devices, governing the charged particle beam propagation, are called electron-optic (or ion-optic) devices. Such devices have some similarities to classical light optics in terms of mathematics, but in general comprise a separate field of knowledge. The reader interested in learning the field of particle beam optics is referred to the classical textbook of Reiser [402].

10.10.5 Space Environment Simulation Platforms

Although ionizing radiations were identified as the main showstopper to exploration mission, there are additional stresses in the space environment. While most of the factors below are not relevant to astronauts, they are important in studying extremophiles.

1. Low pressure: The pressure varies from 10^{-1} Pa near Earth atmosphere to 10^{-14} Pa in deep space. Due to the degassing, pressure around the ISS is higher than in deep space ranging from 10^{-7} Pa in the Ram direction (e.g., front of the ISS relative to flight direction) to 10^{-4} Pa in the Wake direction (e.g., rear of the ISS relative to flight direction) [403].
2. Cold temperature: The low-pressure environment previously described drastically increases the molecular mean free path in space resulting in low heat transfer. Consequently, the temperature in deep space ranges from 3 to 4 K (–270 to –260°C) [404].
3. Solar radiation: Highly energetic phenomena are occurring in the Sun leading to the emission of high-intensity electromagnetic radiations. By moving away from the Sun, the emitted solar radiations are spread out over a large surface area reducing the solar irradiance with increased Sun-object distance. ISS, located at one astronomical unit distance from the Sun, is exposed to an approximate 1400 W/m^2 heat flux. The associated electromagnetic spectrum extends from X-rays to radio waves with a higher proportion in the visible (47%), infrared (45%), and ultraviolet (7%) ranges [405].
4. Day and night cycles: As ISS orbits around the Earth and the latter around the Sun, the stress exposure has a cyclic temporal behavior with two main periods. The "day and night" cycle caused by the rotation around the Earth has a period of 91 min resulting in fluctuation in total irradiance and temperature of more than 1000 W/m^2 and 5–10 °C. The second cycle (period of approximately 1 month) is due to the position change of ISS orbital plane relative to the Sun. In this case, greater variations of temperature (up to 60 °C) with a maximal temperature of about 50 °C were reported [406].

To study the biological impact of the space environment, modules outside the ISS are an ideal environment to expose biological samples to LEO, where the conditions strongly differ from the ones encountered on Earth. However, the poor availability of these facilities stimulated the creation of exposure chambers on Earth capable of reproducing this LEO environment. The Laboratory for Analysis by Nuclear Reactions (LARN, University of Namur, Belgium, https://www.unamur.be/en/sci/physics/ur-en/larn-en) has developed an exposure module to simulate the aforementioned conditions on the ground for extended periods of time (several months). To this end, biological samples are placed into a vacuum chamber and exposed to various constraints. A cooling system located underneath the sample tray and an electromagnetic source reproducing the solar spectrum are controlled by a monitoring system capable to simulate the slow and fast cycles described above. In addition, a variety of neutral density filters and cut-off waveband filters enables to create multiple irradiance conditions within the same experiment, in order to investigate what part of the UV-visible spectrum is the most deleterious.

A similar facility also exists at DLR Cologne and has been recurrently used for pre-flight test programs and mission ground reference experiments for several astrobiological long-term space missions [405].

10.11 Exercises and Self-Assessment

Q1. Which types of radiation exist in space?
Q2. Are astronauts fully protected from radiation by spacecraft walls?
Q3. Can you describe the difference between the radiation environment on Earth (on ground) and the one at the surface of Mars?
Q4. What do we know now about specific health problems of astronauts?
Q5. What is the role of plants in Bioregenerative Life Support Systems (BLSS)?
Q6. What is the 3R Principle?

Q7. What kind of chronic effects on the CNS (central nervous system) were observed?
Q8. What is the difference between organoids and spheroids?
Q9. From which cells organoids can be cultured?
Q10. What is the main reason why bioprinting and other 3D cultures can be better cultured in Space?
Q11. What parameters should be considered if we would like to simulate conditions on Moon/Mars surface or in deep space (including stress unrelated to radiation)?
Q12. What is the interest to study the biological effects of low energy charged particles in the context of space radiation exposure?

10.12 Exercise Answers

SQ1. Galactic Cosmic Rays, Solar Energetic Particles, Trapped radiation, and the solar wind
SQ2. No, the high penetrating character of GCRs and the cascades of secondary particles generated by the passage of GRCs ions through the spacecraft walls create an intravehicular field which is of high concern for the health risk of astronauts
SQ3. On Earth we are protected by both the atmosphere and the magnetic field: GCRs hitting the top of the atmosphere create particle showers but only a few of such secondaries (and very few of direct GCR ions) reach the ground. SEP are mostly shielded by the atmosphere and are of concern only for extreme events and mostly for high latitude/high-altitude flights for eventual biological risks, or on ground for infrastructures. On Mars, the very thin atmosphere offers very little shielding, and the exposure to GRCs, their secondary particles, and SEP is a concern.
SQ4. Though there are many concerns, the present evidence does not provide a conclusive answer. Astronauts as a cohort are not less healthy than US Air Force pilots, e.g., and much healthier than the general public (due to selection). The LNT-estimated cancer death risk for prolonged missions is considerable, but applicability of LNT for low dose rates is questionable.
SQ5. Plants in LSS remove carbon dioxide and provide oxygen, help water purification, can recycle wastes of the astronauts, and provide fresh food for the crew.
SQ6. Reduction (first R) of animal numbers, Refining (second) the test methods to lower the harm to the animal to a minimum, and Replace (third) animal experiments with alternative methods, when possible
SQ7. Reduction of dendrites, reduced neurogenesis and increased neuroinflammation, diminished hippocampal neuron excitability
SQ8. Spheroids are also a 3D cell cultures, but in comparison to organoids, they form simple clusters into sphere-like formation, but they cannot self-assemble or regenerate.
SQ9. Pluripotent stem cells
SQ10. Microgravity
SQ11. The particular profile of radiation spectrum can vary according to the location of interest. The ISS environment benefits from some protection granted by the Earth magnetic field. This is not the case for deep space or Mars, where the full spectrum of galactic cosmic rays should be considered. Solar proton events should be included, can vary in magnitude and their extent also depends on the distance to the sun. Beside radiation, day and night cycle can impact temperature conditions, which lead to biological effects on some model organisms. Pressure value and the presence or not of atmosphere should also be considered.
SQ12. Although the vast majority of particles in the GCR spectrum have very high energy, low energy charged particles are still produced in shielding materials and arise from fragmentation of heavier energetic nuclei. These low-energy particles often traverse shielding and remain of concern.

References

1. Lear J. Kepler's dream. University of California Press; 1965.
2. Curie P. Oeuvres de Pierre Curie. Editions des Archives Contemporaines. 1984.
3. Todd P, Tobias CA, Silver IL. Current topics in space radiation biology. In: Tobias C, Todd P, editors. Space radiation biology and related topics. Academic Press; 1974. p. 1–18.
4. Millikan RA. Electrons (+ and -), protons, photons, neutrons, mesotrons and cosmic rays. University of Chicago Press; 1947.
5. Hess VF, Eugster JAG. Cosmic radiation and its biological effects. Fordham University Press; 1949.
6. Maalouf M, Durante M, Foray N. Biological effects of space radiation on human cells: history, advances and outcomes. J Radiat Res. 2011;52(2):126–46. https://doi.org/10.1269/jrr.10128.
7. Van Allen JA, Frank LA. Radiation around the earth to a radial distance of 107,400 km. Nature. 1959;183(4659):430–4. https://doi.org/10.1038/183430a0.
8. Van Allen JA, Frank LA. Radiation measurements to 658,300 km with Pioneer IV. Nature. 1959;184(4682):219–24. https://doi.org/10.1038/184219a0.
9. Neugebauer M, Snyder CW. Interplanetary solar wind measurements by Mariner II. In: Muller P, editor. Space research, vol. 4. North-Holland Publications; 1964. p. 89–113.
10. Bucker H. The Biostack experiments I and II aboard Apollo 16 and 17. Life Sci Space Res. 1974;12:43–50. https://www.ncbi.nlm.nih.gov/pubmed/11908528.

11. Rabbow E, Rettberg P, Parpart A, Panitz C, Schulte W, Molter F, Jaramillo E, Demets R, Weiß P, Willnecker R. EXPOSE-R2: the astrobiological ESA mission on board of the International Space Station. Front Microbiol. 2017;8(1533) https://doi.org/10.3389/fmicb.2017.01533.
12. Yamagishi A, Hashimoto H, Yano H, Imai E, Tabata M, Higashide M, Okudaira K. Four-year operation of Tanpopo: astrobiology exposure and micrometeoroid capture experiments on the JEM exposed facility of the International Space Station. Astrobiology. 2021;21(12):1461–72. https://doi.org/10.1089/ast.2020.2430.
13. Senatore G, Mastroleo F, Leys N, Mauriello G. Effect of microgravity & space radiation on microbes. Future Microbiol. 2018;13:831–47. https://doi.org/10.2217/fmb-2017-0251.
14. Beuther H, Klessen RS, Dullemond CP, Henning TK. Protostars and planets VI. University of Arizona Press; 2014. https://books.google.be/books?id=tQswBQAAQBAJ.
15. Chancellor J, Nowadly C, Williams J, Aunon-Chancellor S, Chesal M, Looper J, Newhauser W. Everything you wanted to know about space radiation but were afraid to ask. J Environ Sci Health C. 2021;39(2):113–28. https://doi.org/10.1080/26896583.2021.1897273.
16. Reitz G. Characteristic of the radiation field in low Earth orbit and in deep space. Z Med Phys. 2008;18(4):233–43. https://doi.org/10.1016/j.zemedi.2008.06.015.
17. Hellweg CE, Baumstark-Khan C. Getting ready for the manned mission to Mars: the astronauts' risk from space radiation. Naturwissenschaften. 2007;94(7):517–26. https://doi.org/10.1007/s00114-006-0204-0.
18. Heber B, Fichtner H, Scherer K. Solar and heliospheric modulation of galactic cosmic rays. Space Sci Rev. 2006;125(1–4):81–93. https://doi.org/10.1007/s11214-006-9048-3.
19. Mewaldt RA, Davis AJ, Lave KA, Leske RA, Stone EC, Wiedenbeck ME, Binns WR, Christian ER, Cummings AC, de Nolfo GA, Israel MH, Labrador AW, von Rosenvinge TT. Record-setting cosmic-ray intensities in 2009 and 2010. Astrophys J Lett. 2010;723(1):L1–6. https://doi.org/10.1088/2041-8205/723/1/L1.
20. Badhwar GD, O'Neill PM. Galactic cosmic radiation model and its applications. Adv Space Res. 1996;17(2):7–17. https://doi.org/10.1016/0273-1177(95)00507-b.
21. Townsend LW, Badhwar GD, Braby LA, Blakely EA, Cucinotta FA, Curtis DB, Fry RJM, Land CE, Smart DF. Report No. 153—Information needed to make radiation protection recommendations for space missions beyond low-earth orbit (report no. 153). 2006.
22. Cane HV. Coronal mass ejections and forbush decreases. Space Sci Rev. 2000;93(1–2):55–77. https://doi.org/10.1023/A:1026532125747.
23. Beatty J, Ahn HS, Allison PS, Choi MJ, Conklin N, Stephane C, Michael AD, Ganel O, Jaminion S, Kim KC, Lee MH, Lutz L, Pier Simone M, Minnick S, Mognet SI, Kyung-wook M, Nutter SL, Park H, Park IH, et al. The Cosmic Ray Energetics and Mass (CREAM) experiment timing charge detector. Proc SPIE. 2003;4858:248.
24. Yi-ran Z, Si-ming LIU. The origin of cosmic rays from supernova remnants. Chin Astron Astrophys. 2020;44(1):1–31. https://doi.org/10.1016/j.chinastron.2020.04.001.
25. Mishev A. Short- and medium-term induced ionization in the earth atmosphere by galactic and solar cosmic rays. Int J Atmos Sci. 2013;2013:1–9. https://doi.org/10.1155/2013/184508.
26. Usoskin IG, Desorgher L, Velinov P, Storini M, Fluckiger E, Butikofer R, Kovaltsov GA. Ionization of the earth's atmosphere by solar and galactic cosmic rays. Acta Geophys. 2009;57(1):88–101. https://doi.org/10.2478/s11600-008-0019-9.
27. Huff J. Evidence report: risk of acute radiation syndromes due to solar particle events. 2016.
28. Meier MM, Matthia D. A space weather index for the radiation field at aviation altitudes. J Space Weather Space Climate. 2014;4:A13. https://doi.org/10.1051/swsc/2014010.
29. Malandraki OE, Crosby NB. Solar energetic particles and space weather: science and applications. In: Malandraki OE, Crosby NB, editors. Solar particle radiation storms forecasting and analysis. Springer International Publishing; 2018. p. 1–26. https://doi.org/10.1007/978-3-319-60051-2_1.
30. Schwenn R. Solar wind sources and their variations over the solar cycle. Space Sci Rev. 2006;124(1–4):51–76. https://doi.org/10.1007/s11214-006-9099-5.
31. Wu H, Huff J, Casey R, Kim M, Cucinotta F. Risk of acute radiation syndromes due to solar particle events, human health and performance risks of space exploration missions, NASA SP-2009-3405. 2009. p. 171–90.
32. Meyer-Vernet N. Basics of the solar wind. Cambridge University Press; 2007. https://doi.org/10.1017/cbo9780511535765.
33. Hellweg CE, Matthiä D, Berger T, Baumstark-Khan C. Radiation in space: the physics. In: Radiation in space: relevance and risk for human missions. Springer International Publishing; 2020. p. 7–43. https://doi.org/10.1007/978-3-030-46744-9_2.
34. Reitz G, Beaujean R, Benton E, Burmeister S, Dachev T, Deme S, Luszik-Bhadra M, Olko P. Space radiation measurements on-board ISS—the DOSMAP experiment. Radiat Prot Dosimetry. 2005;116(1–4 Pt 2):374–9. https://doi.org/10.1093/rpd/nci262.
35. Ersmark T, Carlson P, Daly E, Fuglesang C, Gudowska I, Lund-Jensen B, Nierninen P, Pearce M, Santin G. Geant4 Monte Carlo Simulations of the belt proton radiation environment on board the International Space Station/Columbus. IEEE Trans Nucl Sci. 2007;54(4):1444–53. https://doi.org/10.1109/Tns.2007.896344.
36. Ersmark T, Carlson P, Daly E, Fuglesang C, Gudowska I, Lund-Jensen B, Nieminen P, Pearce M, Santin G. Geant4 Monte Carlo simulations of the galactic cosmic ray radiation environment on-board the International Space Station/Columbus. IEEE Trans Nucl Sci. 2007;54(5):1854–62. https://doi.org/10.1109/Tns.2007.906276.
37. Dietze G, Bartlett DT, Cool DA, Cucinotta FA, Jia X, McAulay IR, Pelliccioni M, Petrov V, Reitz G, Sato T. ICRP Publication 123. Assessment of radiation exposure of astronauts in space. Ann ICRP. 2013;42(4):1–339. https://doi.org/10.1016/j.icrp.2013.05.004.
38. Watts JW, Parnell TA, Heckman HH. Approximate angular distribution and spectra for geomagnetically trapped protons in low-Earth orbit. AIP Conf Proc. 1989;186(1):75–85. https://doi.org/10.1063/1.38168.
39. Dobynde MI, Shprits YY. Radiation environment created with GCRs inside a spacecraft. Life Sci Space Res (Amst). 2020;24:116–21. https://doi.org/10.1016/j.lssr.2019.09.001.
40. Dyer CS, Truscott PR, Evans H, Sims AJ, Hammond N, Comber C. Secondary radiation environments in heavy space vehicles and instruments. Adv Space Res. 1996;17(2):53–8. https://doi.org/10.1016/0273-1177(95)00512-d.
41. Hassler DM, Zeitlin C, Wimmer-Schweingruber RF, Bottcher S, Martin C, Andrews J, Bohm E, Brinza DE, Bullock MA, Burmeister S, Ehresmann B, Epperly M, Grinspoon D, Kohler J, Kortmann O, Neal K, Peterson J, Posner A, Rafkin S, et al. The Radiation Assessment Detector (RAD) investigation. Space Sci Rev. 2012;170(1–4):503–58. https://doi.org/10.1007/s11214-012-9913-1.
42. Guo JN, Zeitlin C, Wimmer-Schweingruber RF, Hassler DM, Posner A, Heber B, Kohler J, Rafkin S, Ehresmann B, Appel JK, Bohm E, Bottcher S, Burmeister S, Brinza DE, Lohf H, Martin C, Reitz G. Variations of dose rate observed by MSL/RAD in transit to Mars. Astron Astrophys. 2015;577:A58. https://doi.org/10.1051/0004-6361/201525680.

43. Iosim S, MacKay M, Westover C, Mason CE. Translating current biomedical therapies for long duration, deep space missions. Prec Clin Med. 2019;2(4):259–69. https://doi.org/10.1093/pcmedi/pbz022.
44. Zhang S, Wimmer-Schweingruber RF, Yu J, Wang C, Fu Q, Zou Y, Sun Y, Wang C, Hou D, Bottcher SI, Burmeister S, Seimetz L, Schuster B, Knierim V, Shen G, Yuan B, Lohf H, Guo J, Xu Z, et al. First measurements of the radiation dose on the lunar surface. Sci Adv. 2020;6(39):eaaz1334. https://doi.org/10.1126/sciadv.aaz1334.
45. Naito M, Hasebe N, Shikishima M, Amano Y, Haruyama J, Matias-Lopes JA, Kim KJ, Kodaira S. Radiation dose and its protection in the Moon from galactic cosmic rays and solar energetic particles: at the lunar surface and in a lava tube. J Radiol Prot. 2020;40(4):947–61. https://doi.org/10.1088/1361-6498/abb120.
46. Da Pieve F, Gronoff G, Guo J, Mertens CJ, Neary L, Gu B, Koval NE, Kohanoff J, Vandaele AC, Cleri F. Radiation environment and doses on Mars at Oxia Planum and Mawrth Vallis: support for exploration at sites with high biosignature preservation potential. J Geophys Res Planets. 2021;126(1):e2020JE006488. https://doi.org/10.1029/2020je006488.
47. Guo JN, Zeitlin C, Wimmer-Schweingruber RF, McDole T, Kuhl P, Appel JC, Matthia D, Krauss J, Kohler J. A generalized approach to model the spectra and radiation dose rate of solar particle events on the surface of Mars. Astron J. 2018;155(1):49. https://doi.org/10.3847/1538-3881/aaa085.
48. Saganti PB, Cucinotta FA, Wilson JW, Schimmerling W. Visualization of particle flux in the human body on the surface of Mars. J Radiat Res. 2002;43(Suppl):S119–24. https://doi.org/10.1269/jrr.43.s119.
49. Röstel L, Guo J, Banjac S, Wimmer-Schweingruber RF, Heber B. Subsurface radiation environment of mars and its implication for shielding protection of future habitats. J Geophys Res Planets. 2020;125(3):e2019JE006246. https://doi.org/10.1029/2019je006246.
50. Cucinotta FA, To K, Cacao E. Predictions of space radiation fatality risk for exploration missions. Life Sci Space Res (Amst). 2017;13:1–11. https://doi.org/10.1016/j.lssr.2017.01.005.
51. Cucinotta F, Kim MY, Chappell L. Space radiation cancer risk projections and uncertainties. NASA TP, 2011-216155. 2011.
52. Guo J, Zeitlin C, Wimmer-Schweingruber RF, Rafkin S, Hassler DM, Posner A, Heber B, Köhler J, Ehresmann B, Appel JK, Böhm E, Böttcher S, Burmeister S, Brinza DE, Lohf H, Martin C, Kahanpää H, Reitz G. Modeling the variations of dose rate measured by rad during the firstmslmartian year: 2012–2014. Astrophys J. 2015;810(1):24. https://doi.org/10.1088/0004-637x/810/1/24.
53. McKenna-Lawlor S, Goncalves P, Keating A, Morgado B, Heynderickx D, Nieminen P, Santin G, Truscott P, Lei F, Foing B, Balaz J. Characterization of the particle radiation environment at three potential landing sites on Mars using ESA's MEREM models. Icarus. 2012;218(1):723–34. https://doi.org/10.1016/j.icarus.2011.04.004.
54. Dartnell LR, Desorgher L, Ward JM, Coates AJ. Martian sub-surface ionising radiation: biosignatures and geology. Biogeosciences. 2007;4(4):545–58. https://doi.org/10.5194/bg-4-545-2007.
55. Pavlov AA, Vasilyev G, Ostryakov VM, Pavlov AK, Mahaffy P. Degradation of the organic molecules in the shallow subsurface of Mars due to irradiation by cosmic rays. Geophys Res Lett. 2012;39(13):L13202. https://doi.org/10.1029/2012gl052166.
56. Wilson JW, Badavi FF, Cucinotta FA, Shinn JL, Badhwar GD, Silberberg R, Tsao CH, Townsend LW, Tripathi RK. HZETRN: description of a free-space ion and nucleon transport and shielding computer program. 1995.
57. Wilson JW, Cucinotta FA, Shinn JL, Simonsen LC, Badavi FF. Overview of HZETRN and BRNTRN space radiation shielding codes. Proc SPIE. 1996; https://doi.org/10.1117/12.254055.
58. Walsh L, Schneider U, Fogtman A, Kausch C, McKenna-Lawlor S, Narici L, Ngo-Anh J, Reitz G, Sabatier L, Santin G, Sihver L, Straube U, Weber U, Durante M. Research plans in Europe for radiation health hazard assessment in exploratory space missions. Life Sci Space Res (Amst). 2019;21:73–82. https://doi.org/10.1016/j.lssr.2019.04.002.
59. Cleri F. Monte-Carlo methods for the study of the diffusion of charged particles through matter. World Scientific Publishing Co; 1990. http://inis.iaea.org/search/search.aspx?orig_q=RN:23017642.
60. Allison J, Amako K, Apostolakis J, Araujo H, Dubois PA, Asai M, Barrand G, Capra R, Chauvie S, Chytracek R, Cirrone GAP, Cooperman G, Cosmo G, Cuttone G, Daquino GG, Donszelmann M, Dressel M, Folger G, Foppiano F, et al. Geant4 developments and applications. IEEE Trans Nucl Sci. 2006;53(1):270–8. https://doi.org/10.1109/Tns.2006.869826.
61. Battistoni G. The FLUKA code, galactic cosmic ray and solar energetic particle events: from fundamental physics to space radiation and commercial aircraft doses. In: 2008 IEEE nuclear science symposium conference record, 19–25 Oct 2008.
62. Sato T, Niita K, Matsuda N, Hashimoto S, Iwamoto Y, Noda S, Ogawa T, Iwase H, Nakashima H, Fukahori T, Okumura K, Kai T, Chiba S, Furuta T, Sihver L. Particle and heavy ion transport code system, PHITS, version 2.52. J Nucl Sci Technol. 2013;50(9):913–23. https://doi.org/10.1080/00223131.2013.814553.
63. Mrigakshi AI, Matthia D, Berger T, Reitz G, Wimmer-Schweingruber RF. Assessment of galactic cosmic ray models. J Geophys Res Space Phys. 2012;117(A8):A08109. https://doi.org/10.1029/2012ja017611.
64. Tylka AJ, Adams JH, Boberg PR, Brownstein B, Dietrich WF, Flueckiger EO, Petersen EL, Shea MA, Smart DF, Smith EC. CREME96: a revision of the cosmic ray effects on microelectronics code. IEEE Trans Nucl Sci. 1997;44(6):2150–60. https://doi.org/10.1109/23.659030.
65. Nymmik RA, Panasyuk MI, Pervaja TI, Suslov AA. A model of galactic cosmic-ray fluxes. Nuclear Tracks Radiat Meas. 1992;20(3):427–9. https://doi.org/10.1016/1359-0189(92)90028-T.
66. O'Neill PM. Badhwar–O'Neill 2010 galactic cosmic ray flux model—revised. IEEE Trans Nucl Sci. 2010;57(6):3148–53. https://doi.org/10.1109/tns.2010.2083688.
67. Usoskin IG, Alanko-Huotari K, Kovaltsov GA, Mursula K. Heliospheric modulation of cosmic rays: monthly reconstruction for 1951-2004. J Geophys Res Space Phys. 2005;110(A12):A12108. https://doi.org/10.1029/2005ja011250.
68. Matthia D, Berger T, Mrigakshi AI, Reitz G. A ready-to-use galactic cosmic ray model. Adv Space Res. 2013;51(3):329–38. https://doi.org/10.1016/j.asr.2012.09.022.
69. Mertens CJ, Slaba TC. Characterization of solar energetic particle radiation dose to astronaut crew on deep-space exploration missions. Space Weather Int J Res Appl. 2019;17(12):1650-1658. https://doi.org/10.1029/2019sw002363.
70. Banjac S, Heber B, Herbst K, Berger L, Burmeister S. On-the-fly calculation of absorbed and equivalent atmospheric radiation dose in a water phantom with the atmospheric radiation interaction simulator (AtRIS). J Geophys Res Space Phys. 2019;124(12):9774–90. https://doi.org/10.1029/2019ja026622.
71. Picone JM, Hedin AE, Drob DP, Aikin AC. NRLMSISE-00 empirical model of the atmosphere: statistical comparisons and scientific issues. J Geophys Res Space Phys. 2002;107(A12):1468. https://doi.org/10.1029/2002ja009430.
72. Köhli M, Weimar J, Schrön M, Baatz R, Schmidt U. Soil moisture and air humidity dependence of the above-ground cosmic-ray neutron intensity [Original Research]. Front Water. 2021;2(66) https://doi.org/10.3389/frwa.2020.544847.
73. Matthia D, Ehresmann B, Lohf H, Kohler J, Zeitlin C, Appel J, Sato T, Slaba T, Martin C, Berger T, Boehm E, Boettcher S,

Brinza DE, Burmeister S, Guo J, Hassler DM, Posner A, Rafkin SCR, Reitz G, et al. The Martian surface radiation environment—a comparison of models and MSL/RAD measurements. J Space Weather Space Climate. 2016;6:A13. https://doi.org/10.1051/swsc/2016008.
74. Ehresmann B. The Martian radiation environment—early mars and future measurements with the radiation assessment detector. 2012. https://macau.uni-kiel.de/receive/diss_mods_00008315.
75. Vuolo M, Baiocco G, Barbieri S, Bocchini L, Giraudo M, Gheysens T, Lobascio C, Ottolenghi A. Exploring innovative radiation shielding approaches in space: a material and design study for a wearable radiation protection spacesuit. Life Sci Space Res (Amst). 2017;15:69–78. https://doi.org/10.1016/j.lssr.2017.08.003.
76. Gronoff G, Norman RB, Mertens CJ. Computation of cosmic ray ionization and dose at Mars. I: a comparison of HZETRN and Planetocosmics for proton and alpha particles. Adv Space Res. 2015;55(7):1799–805. https://doi.org/10.1016/j.asr.2015.01.028.
77. Vetter RJ, Baker ES, Borak TB, Bartlett DT, Langhorst SM, McKeever S, Preston R, Miller J, Wilson J, Meinhold CB, Rosenstein M, O'Brien CL, Tenforde T. Operational radiation safety program for astronauts in low-earth orbit: a basic framework. NCRP Report, i–ix+1. 2002.
78. ICRP. The 2007 Recommendations of the International Commission on Radiological Protection. Ann ICRP. ICRP publication 103. 2007. 0146-6453 (Print).
79. Cucinotta FA. A new approach to reduce uncertainties in space radiation cancer risk predictions. PLoS One. 2015;10(3):e0120717. https://doi.org/10.1371/journal.pone.0120717.
80. White RJ, Averner M. Humans in space. Nature. 2001;409(6823):1115–8. https://doi.org/10.1038/35059243.
81. Berger T, Bilski P, Hajek M, Puchalska M, Reitz G. The MATROSHKA experiment: results and comparison from extravehicular activity (MTR-1) and intravehicular activity (MTR-2A/2B) exposure. Radiat Res. 2013;180(6):622–37. https://doi.org/10.1667/RR13148.1.
82. Puchalska M, Bilski P, Berger T, Hajek M, Horwacik T, Korner C, Olko P, Shurshakov V, Reitz G. NUNDO: a numerical model of a human torso phantom and its application to effective dose equivalent calculations for astronauts at the ISS. Radiat Environ Biophys. 2014;53(4):719–27. https://doi.org/10.1007/s00411-014-0560-7.
83. Hassler DM, Zeitlin C, Wimmer-Schweingruber RF, Ehresmann B, Rafkin S, Eigenbrode JL, Brinza DE, Weigle G, Bottcher S, Bohm E, Burmeister S, Guo J, Kohler J, Martin C, Reitz G, Cucinotta FA, Kim MH, Grinspoon D, Bullock MA, et al. Mars' surface radiation environment measured with the Mars Science Laboratory's Curiosity rover. Science. 2014;343(6169):1244797. https://doi.org/10.1126/science.1244797.
84. Zeitlin C, Hassler DM, Cucinotta FA, Ehresmann B, Wimmer-Schweingruber RF, Brinza DE, Kang S, Weigle G, Bottcher S, Bohm E, Burmeister S, Guo J, Kohler J, Martin C, Posner A, Rafkin S, Reitz G. Measurements of energetic particle radiation in transit to Mars on the Mars Science Laboratory. Science. 2013;340(6136):1080–4. https://doi.org/10.1126/science.1235989.
85. Charles M. UNSCEAR report 2000: sources and effects of ionizing radiation. United Nations Scientific Committee on the Effects of Atomic Radiation. J Radiol Prot. 2001;21(1):83–6. https://doi.org/10.1088/0952-4746/21/1/609.
86. Drouet M, Herodin F. Radiation victim management and the haematologist in the future: time to revisit therapeutic guidelines? Int J Radiat Biol. 2010;86(8):636–48. https://doi.org/10.3109/09553001003789604.
87. Hamm PB, Billica RD, Johnson GS, Wear ML, Pool SL. Risk of cancer mortality among the Longitudinal Study of Astronaut Health (LSAH) participants. Aviat Space Environ Med. 1998;69(2):142–4. https://www.ncbi.nlm.nih.gov/pubmed/9491253.
88. Elgart SR, Little MP, Chappell LJ, Milder CM, Shavers MR, Huff JL, Patel ZS. Radiation exposure and mortality from cardiovascular disease and cancer in early NASA astronauts. Sci Rep. 2018;8(1):8480. https://doi.org/10.1038/s41598-018-25467-9.
89. Cucinotta FA, Nikjoo H, Goodhead DT. The effects of delta rays on the number of particle-track traversals per cell in laboratory and space exposures. Radiat Res. 1998;150(1):115–9. https://www.ncbi.nlm.nih.gov/pubmed/9650608.
90. Burns FJ, Jin Y, Garte SJ, Hosselet S. Estimation of risk based on multiple events in radiation carcinogenesis of rat skin. Adv Space Res. 1994;14(10):507–19. https://doi.org/10.1016/0273-1177(94)90506-1.
91. Dicello JF, Christian A, Cucinotta FA, Gridley DS, Kathirithamby R, Mann J, Markham AR, Moyers MF, Novak GR, Piantadosi S, Ricart-Arbona R, Simonson DM, Strandberg JD, Vazquez M, Williams JR, Zhang Y, Zhou H, Huso D. In vivo mammary tumourigenesis in the Sprague-Dawley rat and microdosimetric correlates. Phys Med Biol. 2004;49(16):3817–30. https://doi.org/10.1088/0031-9155/49/16/024.
92. Cucinotta FA, Wu H, Shavers MR, George K. Radiation dosimetry and biophysical models of space radiation effects. Gravit Space Biol Bull. 2003;16(2):11–8. https://www.ncbi.nlm.nih.gov/pubmed/12959127.
93. Durante M. Biomarkers of space radiation risk. Radiat Res. 2005;164(4 Pt 2):467–73. https://doi.org/10.1667/rr3359.1.
94. Edwards AA. The use of chromosomal aberrations in human lymphocytes for biological dosimetry. Radiat Res. 1997;148(5 Suppl):S39–44. https://www.ncbi.nlm.nih.gov/pubmed/9355855.
95. Testard I, Ricoul M, Hoffschir F, Flury-Herard A, Dutrillaux B, Fedorenko B, Gerasimenko V, Sabatier L. Radiation-induced chromosome damage in astronauts' lymphocytes. Int J Radiat Biol. 1996;70(4):403–11. https://doi.org/10.1080/095530096144879.
96. Gooch PC, Berry CA. Chromosome analyses of Gemini astronauts. Aerosp Med. 1969;40(6):610–4. https://www.ncbi.nlm.nih.gov/pubmed/5785487.
97. Druzhinin SV. Cytogenetic effect in lymphocytes in astronauts after 2 lengthy flights on board MIR orbital station. Aviakosm Ekolog Med. 1999;33(4):3–5. https://www.ncbi.nlm.nih.gov/pubmed/10530376 (Tsitogeneticheskie effekty v limfotsitakh krovi kosmonavtov posle dvukh prodolzhitel'nykh poletov na orbital'nom komplekse "Mir").
98. Fedorenko B, Druzhinin S, Yudaeva L, Petrov V, Akatov Y, Snigiryova G, Novitskaya N, Shevchenko V, Rubanovich A. Cytogenetic studies of blood lymphocytes from cosmonauts after long-term space flights on Mir station. Adv Space Res. 2001;27(2):355–9. https://doi.org/10.1016/s0273-1177(01)00011-4.
99. Fedorenko BS, Shevchenko VA, Snigireva GP, Druzhinin SV, Repina LA, Novitskaia NN, Akatov I, A. Cytogenetic studies of blood lymphocytes of cosmonauts after long-term, space flights. Radiat Biol Radioecol. 2000;40(5):596–602. https://www.ncbi.nlm.nih.gov/pubmed/11252235 (Tsitogeneticheskie issledovaniia limfotsitov krovi kosmonavtov posle dlitel'nykh poletov).
100. Fedorenko BS, Snigireva GP, Bogomazova AN, Novitskaia NN, Shevchenko VA. Cytogenetic effects on blood lymphocytes of cosmonauts after low doses of space radiation. Aviakosm Ekolog Med. 2008;42(3):13–8. https://www.ncbi.nlm.nih.gov/pubmed/19055005.
101. George K, Durante M, Wu H, Willingham V, Badhwar G, Cucinotta FA. Chromosome aberrations in the blood lymphocytes of astronauts after space flight. Radiat Res. 2001;156(6):731–8. https://doi.org/10.1667/0033-7587(2001)156[0731:caitbl]2.0.co;2.
102. George K, Wu H, Willingham V, Cucinotta FA. The effect of space radiation on the induction of chromosome damage. Phys

Med. 2001;17(Suppl 1):222–5. https://www.ncbi.nlm.nih.gov/pubmed/11776981.
103. Greco O, Durante M, Gialanella G, Grossi G, Pugliese M, Scampoli P, Snigiryova G, Obe G. Biological dosimetry in Russian and Italian astronauts. Adv Space Res. 2003;31(6):1495–503. https://doi.org/10.1016/s0273-1177(03)00087-5.
104. Obe G, Johannes I, Johannes C, Hallman K, Reitz G, Facius R. Chromosomal aberrations in blood lymphocytes of astronauts after long-term space flights. Int J Radiat Biol. 1997;72(6):727–34. https://doi.org/10.1080/095530097142889.
105. George K, Willingham V, Cucinotta FA. Stability of chromosome aberrations in the blood lymphocytes of astronauts measured after space flight by FISH chromosome painting. Radiat Res. 2005;164(4 Pt 2):474–80. https://doi.org/10.1667/rr3323.1.
106. Feiveson A, George K, Shavers M, Moreno-Villanueva M, Zhang Y, Babiak-Vazquez A, Crucian B, Semones E, Wu H. Predicting chromosome damage in astronauts participating in international space station missions. Sci Rep. 2021;11(1):5293. https://doi.org/10.1038/s41598-021-84242-5.
107. George K, Durante M, Willingham V, Cucinotta FA. Chromosome aberrations of clonal origin are present in astronauts' blood lymphocytes. Cytogenet Genome Res. 2004;104(1-4):245–51. https://doi.org/10.1159/000077498.
108. Testard I, Sabatier L. Biological dosimetry for astronauts: a real challenge. Mutat Res. 1999;430(2):315–26. https://doi.org/10.1016/s0027-5107(99)00144-x.
109. Durante M, Snigiryova G, Akaeva E, Bogomazova A, Druzhinin S, Fedorenko B, Greco O, Novitskaya N, Rubanovich A, Shevchenko V, Von Recklinghausen U, Obe G. Chromosome aberration dosimetry in cosmonauts after single or multiple space flights. Cytogenet Genome Res. 2003;103(1–2):40–6. https://doi.org/10.1159/000076288.
110. George K, Rhone J, Beitman A, Cucinotta FA. Cytogenetic damage in the blood lymphocytes of astronauts: effects of repeat long-duration space missions. Mutat Res. 2013;756(1–2):165–9. https://doi.org/10.1016/j.mrgentox.2013.04.007.
111. Obe G, Facius R, Reitz G, Johannes I, Johannes C. Manned missions to Mars and chromosome damage. Int J Radiat Biol. 1999;75(4):429–33. https://doi.org/10.1080/095530099140348.
112. Yang TC, George K, Johnson AS, Durante M, Fedorenko BS. Biodosimetry results from space flight Mir-18. Radiat Res. 1997;148(5 Suppl):S17–23. https://www.ncbi.nlm.nih.gov/pubmed/9355852.
113. Hortsmann M, Durante M, Johannes C, Obe G. Chromosomal intrachanges induced by swift iron ions. Adv Space Res. 2005;35(2):276–9. https://doi.org/10.1016/j.asr.2004.12.031.
114. Johannes C, Horstmann M, Durante M, Chudoba I, Obe G. Chromosome intrachanges and interchanges detected by multicolor banding in lymphocytes: searching for clastogen signatures in the human genome. Radiat Res. 2004;161(5):540–8. https://doi.org/10.1667/rr3157.
115. Horstmann M, Durante M, Johannes C, Pieper R, Obe G. Space radiation does not induce a significant increase of intrachromosomal exchanges in astronauts' lymphocytes. Radiat Environ Biophys. 2005;44(3):219–24. https://doi.org/10.1007/s00411-005-0017-0.
116. Luxton JJ, McKenna MJ, Taylor LE, George KA, Zwart SR, Crucian BE, Drel VR, Garrett-Bakelman FE, Mackay MJ, Butler D, Foox J, Grigorev K, Bezdan D, Meydan C, Smith SM, Sharma K, Mason CE, Bailey SM. Temporal telomere and DNA damage responses in the space radiation environment. Cell Rep. 2020;33(10):108435. https://doi.org/10.1016/j.celrep.2020.108435.
117. Anderson RM, Marsden SJ, Wright EG, Kadhim MA, Goodhead DT, Griffin CS. Complex chromosome aberrations in peripheral blood lymphocytes as a potential biomarker of exposure to high-LET alpha-particles. Int J Radiat Biol. 2000;76(1):31–42. https://doi.org/10.1080/095530000138989.
118. Ray FA, Robinson E, McKenna M, Hada M, George K, Cucinotta F, Goodwin EH, Bedford JS, Bailey SM, Cornforth MN. Directional genomic hybridization: inversions as a potential biodosimeter for retrospective radiation exposure. Radiat Environ Biophys. 2014;53(2):255–63. https://doi.org/10.1007/s00411-014-0513-1.
119. Cornforth MN, Durante M. Radiation quality and intra-chromosomal aberrations: size matters. Mutat Res Genet Toxicol Environ Mutagen. 2018;836(Pt A):28–35. https://doi.org/10.1016/j.mrgentox.2018.05.002.
120. Garrett-Bakelman FE, Darshi M, Green SJ, Gur RC, Lin L, Macias BR, McKenna MJ, Meydan C, Mishra T, Nasrini J, Piening BD, Rizzardi LF, Sharma K, Siamwala JH, Taylor L, Vitaterna MH, Afkarian M, Afshinnekoo E, Ahadi S, et al. The NASA Twins Study: a multidimensional analysis of a year-long human spaceflight. Science. 2019;364(6436) https://doi.org/10.1126/science.aau8650.
121. Luxton JJ, Bailey SM. Twins, telomeres, and aging-in space! Plast Reconstr Surg. 2021;147(1S-2):7S–14S. https://doi.org/10.1097/PRS.0000000000007616.
122. Fazio GG, Jelley JV, Charman WN. Generation of Cherenkov light flashes by cosmic radiation within the eyes of the Apollo astronauts. Nature. 1970;228(5268):260–4. https://doi.org/10.1038/228260a0.
123. Pinsky LS, Osborne WZ, Bailey JV, Benson RE, Thompson LF. Light flashes observed by astronauts on Apollo 11 through Apollo 17. Science. 1974;183(4128):957–9. https://doi.org/10.1126/science.183.4128.957.
124. Bidoli V, Casolino M, De Pascale MP, Furano G, Morselli A, Narici L, Picozza P, Reali E, Sparvoli R, Galper AM, Ozerov Yu V, Popov AV, Vavilov NR, Alexandrov AP, Avdeev SV, Baturin Y, Budarin Y, Padalko G, Shabelnikov VG, et al. Study of cosmic rays and light flashes on board Space Station MIR: the SilEye experiment. Adv Space Res. 2000;25(10):2075–9. https://doi.org/10.1016/s0273-1177(99)01017-0.
125. Pinsky LS, Osborne WZ, Hoffman RA, Bailey JV. Light flashes observed by astronauts on skylab 4. Science. 1975;188(4191):928–30. https://doi.org/10.1126/science.188.4191.928.
126. Budinger TF, Tobias CA, Huesman RH, Upham FT, Wieskamp TF, Hoffman RA. Apollo-Soyuz light-flash observations. Life Sci Space Res. 1977;15:141–6. https://www.ncbi.nlm.nih.gov/pubmed/11958208.
127. Avdeev S, Bidoli V, Casolino M, De Grandis E, Furano G, Morselli A, Narici L, De Pascale MP, Picozza P, Reali E, Sparvoli R, Boezio M, Carlson P, Bonvicini W, Vacchi A, Zampa N, Castellini G, Fuglesang C, Galper A, et al. Eye light flashes on the Mir space station. Acta Astronaut. 2002;50(8):511–25. https://doi.org/10.1016/s0094-5765(01)00190-4.
128. Narici L. Heavy ions light flashes and brain functions: recent observations at accelerators and in spaceflight. N J Phys. 2008;10(7):075010. https://doi.org/10.1088/1367-2630/10/7/075010.
129. Narici L, Belli F, Bidoli V, Casolino M, De Pascale MP, Di Fino L, Furano G, Modena I, Morselli A, Picozza P, Reali E, Rinaldi A, Ruggieri D, Sparvoli R, Zaconte V, Sannita WG, Carozzo S, Licoccia S, Romagnoli P, et al. The ALTEA/ALTEINO projects: studying functional effects of microgravity and cosmic radiation. Adv Space Res. 2004;33(8):1352–7. https://doi.org/10.1016/j.asr.2003.09.052.
130. Casolino M, Bidoli V, Morselli A, Narici L, De Pascale MP, Picozza P, Reali E, Sparvoli R, Mazzenga G, Ricci M, Spillantini P, Boezio M, Bonvicini V, Vacchi A, Zampa N, Castellini G, Sannita WG, Carlson P, Galper A, et al. Space travel: dual origins of light flashes seen in space. Nature. 2003;422(6933):680. https://doi.org/10.1038/422680a.

131. Bidoli V, Casolino M, De Pascale MP, Furano G, Minori M, Morselli A, Narici L, Picozza P, Reali E, Sparvoli R, Fuglesang C, Sannita W, Carlson P, Castellini G, Galper A, Korotkov M, Popov A, Navilov N, Avdeev S, et al. The Sileye-3/Alteino experiment for the study of light flashes, radiation environment and astronaut brain activity on board the International Space Station. J Radiat Res. 2002;43(Suppl):S47–52. https://doi.org/10.1269/jrr.43.s47.
132. Schardt D, Kavatsyuk O, Kramer M, Durante M. Light flashes in cancer patients treated with heavy ions. Brain Stimul. 2013;6(3):416–7. https://doi.org/10.1016/j.brs.2012.08.003.
133. Fuglesang C, Narici L, Picozza P, Sannita WG. Phosphenes in low earth orbit: survey responses from 59 astronauts. Aviat Space Environ Med. 2006;77(4):449–52. https://www.ncbi.nlm.nih.gov/pubmed/16676658.
134. Curtis SB. Single-track effects and new directions in GCR risk assessment. Adv Space Res. 1994;14(10):885–94. https://doi.org/10.1016/0273-1177(94)90554-1.
135. Chase HB, Post JS. Damage and repair in mammalian tissues exposed to cosmic ray heavy nuclei. J Aviat Med. 1956;27(6):533–40. https://www.ncbi.nlm.nih.gov/pubmed/13376499.
136. Bucker H, Horneck G, Allkofer OC, Bartholoma KP, Beaujean R, Cuer P, Enge W, Facius R, Francois H, Graul EH, Henig G, Heinrich W, Kaiser R, Kuhn H, Massue JP, Planel H, Portal G, Reinholz E, Ruther W, et al. The Biostack experiment on Apollo 16. Life Sci Space Res. 1973;11:295–305. https://www.ncbi.nlm.nih.gov/pubmed/12001958.
137. Bucker H, Facius R, Hildebrand D, Horneck G. Results of the Bacillus subtilis unit of the Biostack II experiment: physical characteristics and biological effects of individual cosmic HZE particles. Life Sci Space Res. 1975;13:161–6. https://www.ncbi.nlm.nih.gov/pubmed/11913421.
138. Horneck G, Facius R, Enge W, Beaujean R, Bartholoma KP. Microbial studies in the Biostack experiment of the Apollo 16 mission: germination and outgrowth of single Bacillus subtilis spores hit by cosmic HZE particles. Life Sci Space Res. 1974;12:75–83. https://doi.org/10.1016/b978-0-08-021783-3.50014-3.
139. Ruther W, Graul EH, Heinrich W, Allkofer OC, Kaiser R, Cuer P. Preliminary results on the action of cosmic heavy ions on the development of eggs of Artemia salina. Life Sci Space Res. 1974;12:69–74. https://doi.org/10.1016/b978-0-08-021783-3.50013-1.
140. Graul EH, Ruther W, Heinrich W, Allkofer OC, Kaiser R, Pfohl R, Schopper E, Henig G, Schott JU, Bucker H. Radiobiological results of the Biostack experiment on board Apollo 16 and 17. Life Sci Space Res. 1975;13:153–9. https://www.ncbi.nlm.nih.gov/pubmed/11913420.
141. Bucker H. Biologic effect of cosmic particle radiation, results of the Biostack experiments in the Apollo program. Strahlenschutz Forsch Prax. 1976;16:31–50. https://www.ncbi.nlm.nih.gov/pubmed/1036850 (Die biologische Wirkung der kosmischen Teilchenstrahlung, Ergebnisse der Biostack-Experimente im Apollo-Programm)
142. Heinrich W. Predicted LET-spectra of HZE-particles for the Free Flyer Biostack Experiment on the long duration exposure facility mission. Life Sci Space Res. 1980;18:143–52. https://doi.org/10.1016/b978-0-08-024436-5.50019-6.
143. Bucker H, Baltschukat K, Beaujean R, Bonting SL, Delpoux M, Enge W, Facius R, Francois H, Graul EH, Heinrich W, Horneck G, Kranz AR, Pfohl R, Planel G, Portal G, Reitz G, Ruther W, Schafer M, Schopper E, Schott JU. Advanced Biostack: experiment 1 ES 027 on Spacelab-1. Adv Space Res. 1984;4(10):83–90. https://doi.org/10.1016/0273-1177(84)90228-x.
144. Bucker H, Facius R, Horneck G, Reitz G, Graul EH, Berger H, Hoffken H, Ruther W, Heinrich W, Beaujean R, Enge W. Embryogenesis and organogenesis of Carausius morosus under spaceflight conditions. Adv Space Res. 1986;6(12):115–24. https://doi.org/10.1016/0273-1177(86)90074-8.
145. Bucker H, Horneck G, Facius R, Reitz G, Schafer M, Schott JU, Beaujean R, Enge W, Schopper E, Heinrich H, Beer J, Wiegel B, Pfohl R, Francois H, Portal G, Bonting SL, Graul EH, Ruther W, Kranz AR, et al. Life sciences: radiobiological advanced Biostack experiment. Science. 1984;225(4658):222–4. https://doi.org/10.1126/science.225.4658.222.
146. Horneck G, Eschweiler U, Reitz G, Wehner J, Willimek R, Strauch K. Biological responses to space: results of the experiment "Exobiological Unit" of ERA on EURECA I. Adv Space Res. 1995;16(8):105–18. https://doi.org/10.1016/0273-1177(95)00279-N.
147. Horneck G. HZE particle effects in space. Acta Astronaut. 1994;32(11):749–55. https://doi.org/10.1016/0094-5765(94)90170-8.
148. Reitz G, Bucker H, Facius R, Horneck G, Graul EH, Berger H, Ruther W, Heinrich W, Beaujean R, Enge W, Alpatov AM, Ushakov IA, Zachvatkin YA, Mesland DA. Influence of cosmic radiation and/or microgravity on development of Carausius morosus. Adv Space Res. 1989;9(10):161–73. https://doi.org/10.1016/0273-1177(89)90435-3.
149. Barendsen GW, Walter HM, Fowler JF, Bewley DK. Effects of different ionizing radiations on human cells in tissue culture. III. Experiments with cyclotron-accelerated alpha-particles and deuterons. Radiat Res. 1963;18:106–19. https://www.ncbi.nlm.nih.gov/pubmed/13966644.
150. Bolus NE. Basic review of radiation biology and terminology. J Nucl Med Technol. 2017;45(4):259. https://doi.org/10.2967/jnmt.117.195230.
151. Friedrich T, Scholz U, Elsasser T, Durante M, Scholz M. Systematic analysis of RBE and related quantities using a database of cell survival experiments with ion beam irradiation. J Radiat Res. 2013;54(3):494–514. https://doi.org/10.1093/jrr/rrs114.
152. Hendry JH, Potten CS, Merritt A. Apoptosis induced by high- and low-LET radiations. Radiat Environ Biophys. 1995;34(1):59–62. https://doi.org/10.1007/BF01210548.
153. Aoki M, Furusawa Y, Yamada T. LET dependency of heavy-ion induced apoptosis in V79 cells. J Radiat Res. 2000;41(2):163–75. https://doi.org/10.1269/jrr.41.163.
154. Harada K, Obiya Y, Nakano T, Kawashima M, Miki T, Kobayashi Y, Watanabe H, Okaichi K, Ohnishi T, Mukai C, Nagaoka S. Cancer risk in space due to radiation assessed by determining cell lethality and mutation frequencies of prokaryotes and a plasmid during the Second International Microgravity Laboratory (IML-2) Space Shuttle experiment. Oncol Rep. 1997;4(4):691–5. https://doi.org/10.3892/or.4.4.691.
155. Takahashi A, Ohnishi K, Yokota A, Kumagai T, Nakano T, Ohnishi T. Mutation frequency of plasmid DNA and Escherichia coli following long-term space flight on Mir. J Radiat Res. 2002;43(Suppl):S137–40. https://doi.org/10.1269/jrr.43.s137.
156. Takahashi A, Ohnishi K, Takahashi S, Masukawa M, Sekikawa K, Amano T, Nakano T, Nagaoka S, Ohnishi T. The effects of microgravity on induced mutation in Escherichia coli and Saccharomyces cerevisiae. Adv Space Res. 2001;28(4):555–61. https://doi.org/10.1016/s0273-1177(01)00391-x.
157. Harada K, Nagaoka S, Mohri M, Ohnishi T, Sugahara T. Lethality of high linear energy transfer cosmic radiation to Escherichia coli DNA repair-deficient mutants during the 'SL-J/FMPT' space experiment. FEMS Microbiol Lett. 1998;164(1):39–45. https://doi.org/10.1111/j.1574-6968.1998.tb13065.x.
158. Ohnishi T, Takahashi A, Okaichi K, Ohnishi K, Matsumoto H, Takahashi S, Yamanaka H, Nakano T, Nagaoka S. Cell growth and morphology of Dictyostelium discoideum in space environment. Biol Sci Space. 1997;11(1):29–34. https://doi.org/10.2187/bss.11.29.

159. Takahashi A, Ohnishi K, Fukui M, Nakano T, Yamaguchi K, Nagaoka S, Ohnishi T. Mutation frequency of Dictyostelium discoideum spores exposed to the space environment. Biol Sci Space. 1997;11(2):81–6. https://doi.org/10.2187/bss.11.81.
160. Takahashi A, Ohnishi K, Takahashi S, Masukawa M, Sekikawa K, Amano T, Nakano T, Nagaoka S, Ohnishi T. Differentiation of Dictyostelium discoideum vegetative cells into spores during Earth orbit in space. Adv Space Res. 2001;28(4):549–53. https://doi.org/10.1016/s0273-1177(01)00388-x.
161. Obe G, Pfeiffer P, Savage JR, Johannes C, Goedecke W, Jeppesen P, Natarajan AT, Martinez-Lopez W, Folle GA, Drets ME. Chromosomal aberrations: formation, identification and distribution. Mutat Res. 2002;504(1–2):17–36. https://doi.org/10.1016/s0027-5107(02)00076-3.
162. Cornforth MN. Perspectives on the formation of radiation-induced exchange aberrations. DNA Repair (Amst). 2006;5(9–10):1182–91. https://doi.org/10.1016/j.dnarep.2006.05.008.
163. Durante M, Cucinotta FA. Heavy ion carcinogenesis and human space exploration. Nat Rev Cancer. 2008;8(6):465–72. https://doi.org/10.1038/nrc2391.
164. Sridharan DM, Asaithamby A, Blattnig SR, Costes SV, Doetsch PW, Dynan WS, Hahnfeldt P, Hlatky L, Kidane Y, Kronenberg A, Naidu MD, Peterson LE, Plante I, Ponomarev AL, Saha J, Snijders AM, Srinivasan K, Tang J, Werner E, Pluth JM. Evaluating biomarkers to model cancer risk post cosmic ray exposure. Life Sci Space Res (Amst). 2016;9:19–47. https://doi.org/10.1016/j.lssr.2016.05.004.
165. Kawata T, Ito H, George K, Wu H, Cucinotta FA. Chromosome aberrations induced by high-LET radiations. Biol Sci Space. 2004;18(4):216–23. https://doi.org/10.2187/bss.18.216.
166. Cornforth MN, Bedford JS, Bailey SM. Destabilizing effects of ionizing radiation on chromosomes: sizing up the damage. Cytogenet Genome Res. 2021;161(6–7):328–51. https://doi.org/10.1159/000516523.
167. Cornforth MN, Bailey SM, Goodwin EH. Dose responses for chromosome aberrations produced in noncycling primary human fibroblasts by alpha particles, and by gamma rays delivered at sublimiting low dose rates. Radiat Res. 2002;158(1):43–53. https://doi.org/10.1667/0033-7587(2002)158[0043:drfcap]2.0.co;2.
168. George K, Durante M, Willingham V, Wu H, Yang TC, Cucinotta FA. Biological effectiveness of accelerated particles for the induction of chromosome damage measured in metaphase and interphase human lymphocytes. Radiat Res. 2003;160(4):425–35. https://doi.org/10.1667/rr3064.
169. Goodwin EH, Cornforth MN. RBE: mechanisms inferred from cytogenetics. Adv Space Res. 1994;14(10):249–55. https://doi.org/10.1016/0273-1177(94)90474-x.
170. Loucas BD, Cornforth MN. The LET dependence of unrepaired chromosome damage in human cells: a break too far? Radiat Res. 2013;179(4):393–405. https://doi.org/10.1667/RR3159.2.
171. Loucas BD, Durante M, Bailey SM, Cornforth MN. Chromosome damage in human cells by gamma rays, alpha particles and heavy ions: track interactions in basic dose-response relationships. Radiat Res. 2013;179(1):9–20. https://doi.org/10.1667/RR3089.1.
172. Jackson SP, Bartek J. The DNA-damage response in human biology and disease. Nature. 2009;461(7267):1071–8. https://doi.org/10.1038/nature08467.
173. Pariset E, Penninckx S, Kerbaul CD, Guiet E, Macha AL, Cekanaviciute E, Snijders AM, Mao J-H, Paris F, Costes SV. 53BP1 Repair kinetics for prediction of *in vivo* radiation susceptibility in 15 mouse strains. Radiat Res. 2020;194(5):485–99. https://doi.org/10.1667/RADE-20-00122.1.
174. Asaithamby A, Hu B, Chen DJ. Unrepaired clustered DNA lesions induce chromosome breakage in human cells. Proc Natl Acad Sci U S A. 2011;108(20):8293–8. https://doi.org/10.1073/pnas.1016045108.
175. Eccles LJ, Lomax ME, O'Neill P. Hierarchy of lesion processing governs the repair, double-strand break formation and mutability of three-lesion clustered DNA damage. Nucleic Acids Res. 2010;38(4):1123–34. https://doi.org/10.1093/nar/gkp1070.
176. Hirayama R, Ito A, Tomita M, Tsukada T, Yatagai F, Noguchi M, Matsumoto Y, Kase Y, Ando K, Okayasu R, Furusawa Y. Contributions of direct and indirect actions in cell killing by high-LET radiations. Radiat Res. 2009;171(2):212–8. https://doi.org/10.1667/RR1490.1.
177. Ohnishi T, Ohnishi K, Takahashi A, Taniguchi Y, Sato M, Nakano T, Nagaoka S. Detection of DNA damage induced by space radiation in Mir and space shuttle. J Radiat Res. 2002;43(Suppl):S133–6. https://doi.org/10.1269/jrr.43.s133.
178. Ohnishi T, Takahashi A, Ohnishi K, Matsumoto H. DNA damage formation and p53 accumulation in mammalian cells exposed to the space environment. Biol Sci Space. 1999;13(2):82–7. https://doi.org/10.2187/bss.13.82.
179. Ohnishi T, Takahashi A, Wang X, Ohnishi K, Ohira Y, Nagaoka S. Accumulation of a tumor suppressor p53 protein in rat muscle during a space flight. Mutat Res. 1999;430(2):271–4. https://doi.org/10.1016/s0027-5107(99)00138-4.
180. Ohnishi T, Takahashi A, Nagamatsu A, Omori K, Suzuki H, Shimazu T, Ishioka N. Detection of space radiation-induced double strand breaks as a track in cell nucleus. Biochem Biophys Res Commun. 2009;390(3):485–8. https://doi.org/10.1016/j.bbrc.2009.09.114.
181. Lu T, Zhang Y, Kidane Y, Feiveson A, Stodieck L, Karouia F, Ramesh G, Rohde L, Wu H. Cellular responses and gene expression profile changes due to bleomycin-induced DNA damage in human fibroblasts in space. PLoS One. 2017;12(3):e0170358. https://doi.org/10.1371/journal.pone.0170358.
182. Cucinotta FA, Durante M. Cancer risk from exposure to galactic cosmic rays: implications for space exploration by human beings. Lancet Oncol. 2006;7(5):431–5. https://doi.org/10.1016/S1470-2045(06)70695-7.
183. Schollnberger H, Stewart RD, Mitchel RE, Hofmann W. An examination of radiation hormesis mechanisms using a multistage carcinogenesis model. Nonlinearity Biol Toxicol Med. 2004;2(4):317–52. https://doi.org/10.1080/15401420490900263.
184. Stenerlow B, Hoglund E, Carlsson J, Blomquist E. Rejoining of DNA fragments produced by radiations of different linear energy transfer. Int J Radiat Biol. 2000;76(4):549–57. https://doi.org/10.1080/095530000138565.
185. Ward JF. DNA damage as the cause of ionizing radiation-induced gene activation. Radiat Res. 1994;138(1 Suppl):S85–8. https://www.ncbi.nlm.nih.gov/pubmed/8146335.
186. Yan X, Sasi SP, Gee H, Lee J, Yang Y, Mehrzad R, Onufrak J, Song J, Enderling H, Agarwal A, Rahimi L, Morgan J, Wilson PF, Carrozza J, Walsh K, Kishore R, Goukassian DA. Cardiovascular risks associated with low dose ionizing particle radiation. PLoS One. 2014;9(10):e110269. https://doi.org/10.1371/journal.pone.0110269.
187. Rogakou EP, Boon C, Redon C, Bonner WM. Megabase chromatin domains involved in DNA double-strand breaks in vivo. J Cell Biol. 1999;146(5):905–16. https://doi.org/10.1083/jcb.146.5.905.
188. Rogakou EP, Pilch DR, Orr AH, Ivanova VS, Bonner WM. DNA double-stranded breaks induce histone H2AX phosphorylation on serine 139. J Biol Chem. 1998;273(10):5858–68. https://doi.org/10.1074/jbc.273.10.5858.
189. Penninckx S, Pariset E, Cekanaviciute E, Costes SV. Quantification of radiation-induced DNA double strand break repair foci to evaluate and predict biological responses to ionizing radiation. NAR Cancer. 2021;3(4):zcab046. https://doi.org/10.1093/narcan/zcab046.

190. Oizumi T, Ohno R, Yamabe S, Funayama T, Nakamura AJ. Repair kinetics of DNA double strand breaks induced by simulated space radiation. Life (Basel). 2020;10(12) https://doi.org/10.3390/life10120341.
191. Asaithamby A, Uematsu N, Chatterjee A, Story MD, Burma S, Chen DJ. Repair of HZE-particle-induced DNA double-strand breaks in normal human fibroblasts. Radiat Res. 2008;169(4):437–46. https://doi.org/10.1667/RR1165.1.
192. Costes SV, Boissiere A, Ravani S, Romano R, Parvin B, Barcellos-Hoff MH. Imaging features that discriminate between foci induced by high- and low-LET radiation in human fibroblasts. Radiat Res. 2006;165(5):505–15. https://doi.org/10.1667/RR3538.1.
193. Mukherjee B, Camacho CV, Tomimatsu N, Miller J, Burma S. Modulation of the DNA-damage response to HZE particles by shielding. DNA Repair (Amst). 2008;7(10):1717–30. https://doi.org/10.1016/j.dnarep.2008.06.016.
194. Baumstark-Khan C, Heilmann J, Rink H. Induction and repair of DNA strand breaks in bovine lens epithelial cells after high LET irradiation. Adv Space Res. 2003;31(6):1583–91. https://doi.org/10.1016/s0273-1177(03)00095-4.
195. Li Z, Jella KK, Jaafar L, Li S, Park S, Story MD, Wang H, Wang Y, Dynan WS. Exposure to galactic cosmic radiation compromises DNA repair and increases the potential for oncogenic chromosomal rearrangement in bronchial epithelial cells. Sci Rep. 2018;8(1):11038. https://doi.org/10.1038/s41598-018-29350-5.
196. Averbeck NB, Ringel O, Herrlitz M, Jakob B, Durante M, Taucher-Scholz G. DNA end resection is needed for the repair of complex lesions in G1-phase human cells. Cell Cycle. 2014;13(16):2509–16. https://doi.org/10.4161/15384101.2015.941743.
197. Yajima H, Fujisawa H, Nakajima NI, Hirakawa H, Jeggo PA, Okayasu R, Fujimori A. The complexity of DNA double strand breaks is a critical factor enhancing end-resection. DNA Repair (Amst). 2013;12(11):936–46. https://doi.org/10.1016/j.dnarep.2013.08.009.
198. Shikazono N, O'Neill P. Biological consequences of potential repair intermediates of clustered base damage site in Escherichia coli. Mutat Res. 2009;669(1–2):162–8. https://doi.org/10.1016/j.mrfmmm.2009.06.004.
199. Harada K, Sugahara T, Ohnishi T, Ozaki Y, Obiya Y, Miki S, Miki T, Imamura M, Kobayashi Y, Watanabe H, Akashi M, Furusawa Y, Mizuma N, Yamanaka H, Ohashi E, Yamaoka C, Yajima M, Fukui M, Nakano T, et al. Inhibition in a microgravity environment of the recovery of Escherichia coli cells damaged by heavy ion beams during the NASDA ISS phase I program of NASA Shuttle/Mir mission no. 6. Int J Mol Med. 1998;1(5):817–22. https://doi.org/10.3892/ijmm.1.5.817.
200. Horneck G, Rettberg P, Kozubek S, Baumstark-Khan C, Rink H, Schafer M, Schmitz C. The influence of microgravity on repair of radiation-induced DNA damage in bacteria and human fibroblasts. Radiat Res. 1997;147(3):376–84. https://www.ncbi.nlm.nih.gov/pubmed/9052686.
201. Lu T, Zhang Y, Wong M, Feiveson A, Gaza R, Stoffle N, Wang H, Wilson B, Rohde L, Stodieck L, Karouia F, Wu H. Detection of DNA damage by space radiation in human fibroblasts flown on the International Space Station. Life Sci Space Res (Amst). 2017;12:24–31. https://doi.org/10.1016/j.lssr.2016.12.004.
202. Ohnishi T, Takahashi A, Ohnishi K, Nakano T, Nagaoka S. Enzymic chemical reaction under microgravity environment in space. J Gravit Physiol. 2000;7(2):P69–70. https://www.ncbi.nlm.nih.gov/pubmed/12697569.
203. Horneck G. Radiobiological experiments in space—a review. Nuclear Tracks Radiat Meas. 1992;20(1):185–205. https://doi.org/10.1016/1359-0189(92)90099-H.
204. Takahashi A, Ohnishi K, Takahashi S, Masukawa M, Sekikawa K, Amano T, Nakano T, Nagaoka S, Ohnishi T. The effects of microgravity on ligase activity in the repair of DNA double-strand breaks. Int J Radiat Biol. 2000;76(6):783–8. https://doi.org/10.1080/09553000050028931.
205. Kiefer J, Pross HD. Space radiation effects and microgravity. Mutat Res. 1999;430(2):299–305. https://doi.org/10.1016/s0027-5107(99)00142-6.
206. Pross HD, Kost M, Kiefer J. Repair of radiation induced genetic damage under microgravity. Adv Space Res. 1994;14(10):125–30. https://doi.org/10.1007/978-1-4615-2918-7_12.
207. Horneck G, Rettberg P, Baumstark-Khan C, Rink H, Kozubek S, Schafer M, Schmitz C. DNA repair in microgravity: studies on bacteria and mammalian cells in the experiments REPAIR and KINETICS. J Biotechnol. 1996;47(2–3):99–112. https://doi.org/10.1016/0168-1656(96)01382-x.
208. Ohnishi T, Takahashi A, Ohnishi K, Takahashi S, Masukawa M, Sekikawa K, Amano T, Nakano T, Nagaoka S. Alkylating agent (MNU)-induced mutation in space environment. Adv Space Res. 2001;28(4):563–8. https://doi.org/10.1016/s0273-1177(01)00392-1.
209. Moreno-Villanueva M, Wong M, Lu T, Zhang Y, Wu H. Interplay of space radiation and microgravity in DNA damage and DNA damage response. NPJ Microgravity. 2017;3:14. https://doi.org/10.1038/s41526-017-0019-7.
210. Ohnishi T. Life science experiments performed in space in the ISS/Kibo facility and future research plans. J Radiat Res. 2016;57 Suppl 1:i41–6. https://doi.org/10.1093/jrr/rrw020.
211. Takahashi A, Suzuki H, Omori K, Seki M, Hashizume T, Shimazu T, Ishioka N, Ohnishi T. Expression of p53-regulated proteins in human cultured lymphoblastoid TSCE5 and WTK1 cell lines during spaceflight. J Radiat Res. 2012;53(2):168–75. https://doi.org/10.1269/jrr.11140.
212. Herranz R, Anken R, Boonstra J, Braun M, Christianen PC, de Geest M, Hauslage J, Hilbig R, Hill RJ, Lebert M, Medina FJ, Vagt N, Ullrich O, van Loon JJ, Hemmersbach R. Ground-based facilities for simulation of microgravity: organism-specific recommendations for their use, and recommended terminology. Astrobiology. 2013;13(1):1–17. https://doi.org/10.1089/ast.2012.0876.
213. Hauslage J, Cevik V, Hemmersbach R. Pyrocystis noctiluca represents an excellent bioassay for shear forces induced in ground-based microgravity simulators (clinostat and random positioning machine). NPJ Microgravity. 2017;3:12. https://doi.org/10.1038/s41526-017-0016-x.
214. Horneck G, Klaus DM, Mancinelli RL. Space microbiology. Microbiol Mol Biol Rev. 2010;74(1):121–56. https://doi.org/10.1128/MMBR.00016-09.
215. Gao Y, Li S, Xu D, Wang J, Sun Y. Changes in apoptotic microRNA and mRNA expression profiling in Caenorhabditis elegans during the Shenzhou-8 mission. J Radiat Res. 2015;56(6):872–82. https://doi.org/10.1093/jrr/rrv050.
216. Paul AM, Overbey EG, da Silveira WA, Szewczyk N, Nishiyama NC, Pecaut MJ, Anand S, Galazka JM, Mao XW. Immunological and hematological outcomes following protracted low dose/low dose rate ionizing radiation and simulated microgravity. Sci Rep. 2021;11(1):11452. https://doi.org/10.1038/s41598-021-90439-5.
217. Rabbow E, Stojicic N, Walrafen D, Baumstark-Khan C, Rettberg P, Schulze-Varnholt D, Franz M, Reitz G. The SOS-LUX-TOXICITY-test on the International Space Station. Res Microbiol. 2006;157(1):30–6. https://doi.org/10.1016/j.resmic.2005.08.005.
218. Stojicic N, Walrafen D, Baumstark-Khan C, Rabbow E, Rettberg P, Weisshaar MP, Horneck G. Genotoxicity testing on the international space station: preparatory work on the SOS-LUX test as part of the space experiment TRIPLE-LUX. Space Life Sci Aircraft Space Radiat Environ. 2005;36(9):1710–7. https://doi.org/10.1016/j.asr.2005.03.052.
219. Padgen MR, Liddell LC, Bhardwaj SR, Gentry D, Marina D, Parra M, Boone T, Tan M, Ellingson L, Rademacher A, Benton

J, Schooley A, Mousavi A, Friedericks C, Hanel RP, Ricco AJ, Bhattacharya S, Maria SRS. BioSentinel: a biofluidic nanosatellite monitoring microbial growth and activity in deep space. Astrobiology. 2021; https://doi.org/10.1089/ast.2020.2305.
220. Santa Maria SR, Marina DB, Massaro Tieze S, Liddell LC, Bhattacharya S. BioSentinel: long-term saccharomyces cerevisiae preservation for a deep space biosensor mission. Astrobiology. 2020; https://doi.org/10.1089/ast.2019.2073.
221. Cox R, Thacker J, Goodhead DT, Munson RJ. Mutation and inactivation of mammalian cells by various ionising radiations. Nature. 1977;267(5610):425–7. https://doi.org/10.1038/267425a0.
222. Goodhead DT, Thacker J, Cox R. Weiss Lecture. Effects of radiations of different qualities on cells: molecular mechanisms of damage and repair. Int J Radiat Biol. 1993;63(5):543–56. https://doi.org/10.1080/09553009314450721.
223. Shmakova NL, Krasavin EA, Govorun RD, Fadeeva TA, Koshlan IV. The lethal and mutagenic actions of radiations with different LETs on mammalian cells. Radiat Biol Radioecol. 1997;37(2):213–9. https://www.ncbi.nlm.nih.gov/pubmed/9181964 (Letal'noe i mutagennoe deistvie izluchenii s raznoi LPE na kletki mlekopitaiushchikh).
224. Hei TK, Hall EJ, Waldren CA. Mutation induction and relative biological effectiveness of neutrons in mammalian cells. Experimental observations. Radiat Res. 1988;115(2):281–91. https://www.ncbi.nlm.nih.gov/pubmed/3165536.
225. Suzuki M, Tsuruoka C, Kanai T, Kato T, Yatagai F, Watanabe M. Qualitative and quantitative difference in mutation induction between carbon- and neon-ion beams in normal human cells. Biol Sci Space. 2003;17(4):302–6. https://doi.org/10.2187/bss.17.302.
226. Zhou H, Randers-Pehrson G, Waldren CA, Vannais D, Hall EJ, Hei TK. Induction of a bystander mutagenic effect of alpha particles in mammalian cells. Proc Natl Acad Sci U S A. 2000;97(5):2099–104. https://doi.org/10.1073/pnas.030420797.
227. Yatagai F, Honma M, Takahashi A, Omori K, Suzuki H, Shimazu T, Seki M, Hashizume T, Ukai A, Sugasawa K, Abe T, Dohmae N, Enomoto S, Ohnishi T, Gordon A, Ishioka N. Frozen human cells can record radiation damage accumulated during space flight: mutation induction and radioadaptation. Radiat Environ Biophys. 2011;50(1):125–34. https://doi.org/10.1007/s00411-010-0348-3.
228. Fukuda T, Fukuda K, Takahashi A, Ohnishi T, Nakano T, Sato M, Gunge N. Analysis of deletion mutations of the rpsL gene in the yeast Saccharomyces cerevisiae detected after long-term flight on the Russian space station Mir. Mutat Res. 2000;470(2):125–32. https://doi.org/10.1016/s1383-5742(00)00054-5.
229. Yang TC, Craise LM, Mei MT, Tobias CA. Neoplastic cell transformation by heavy charged particles. Radiat Res Suppl. 1985;8:S177–87. https://www.ncbi.nlm.nih.gov/pubmed/3867082.
230. Hei TK, Komatsu K, Hall EJ, Zaider M. Oncogenic transformation by charged particles of defined LET. Carcinogenesis. 1988;9(5):747–50. https://doi.org/10.1093/carcin/9.5.747.
231. Suzuki M, Watanabe M, Suzuki K, Nakano K, Kaneko I. Neoplastic cell transformation by heavy ions. Radiat Res. 1989;120(3):468–76. https://www.ncbi.nlm.nih.gov/pubmed/2594968.
232. Han Z, Suzuki H, Suzuki F, Suzuki M, Furusawa Y, Kato T Jr, Ikenaga M. Neoplastic transformation of hamster embyro cells by heavy ions. Adv Space Res. 1998;22(12):1725–32. https://doi.org/10.1016/s0273-1177(99)00038-1.
233. Ding L-H, Park S, Xie Y, Girard L, Minna JD, Story MD. Elucidation of changes in molecular signalling leading to increased cellular transformation in oncogenically progressed human bronchial epithelial cells exposed to radiations of increasing LET. Mutagenesis. 2015;30(5):685–94. https://doi.org/10.1093/mutage/gev028.
234. Collyn-d'Hooghe M, Hemon D, Gilet R, Curtis SB, Valleron AJ, Malaise EP. Comparative effects of 60Co gamma-rays and neon and helium ions on cycle duration and division probability of EMT 6 cells. A time-lapse cinematography study. Int J Radiat Biol Relat Stud Phys Chem Med. 1981;39(3):297–306. https://doi.org/10.1080/09553008114550381.
235. Blakely E, Chang P, Lommel L, Bjornstad K, Dixon M, Tobias C, Kumar K, Blakely WF. Cell-cycle radiation response: role of intracellular factors. Adv Space Res. 1989;9(10):177–86. https://doi.org/10.1016/0273-1177(89)90436-5.
236. Scholz M, Kraft-Weyrather W, Ritter S, Kraft G. Cell cycle delays induced by heavy ion irradiation of synchronous mammalian cells. Int J Radiat Biol. 1994;66(1):59–75. https://doi.org/10.1080/09553009414550951.
237. Fournier C, Taucher-Scholz G. Radiation induced cell cycle arrest: an overview of specific effects following high-LET exposure. Radiother Oncol. 2004;73(Suppl 2):S119–22. https://doi.org/10.1016/s0167-8140(04)80031-8.
238. Xue L, Furusawa Y, Yu D. ATR signaling cooperates with ATM in the mechanism of low dose hypersensitivity induced by carbon ion beam. DNA Repair (Amst). 2015;34:1–8. https://doi.org/10.1016/j.dnarep.2015.07.001.
239. Jakob B, Scholz M, Taucher-Scholz G. Characterization of CDKN1A (p21) binding to sites of heavy-ion-induced damage: colocalization with proteins involved in DNA repair. Int J Radiat Biol. 2002;78(2):75–88. https://doi.org/10.1080/09553000110090007.
240. Stewart J, Ko YH, Kennedy AR. Protective effects of L-selenomethionine on space radiation induced changes in gene expression. Radiat Environ Biophys. 2007;46(2):161–5. https://doi.org/10.1007/s00411-006-0089-5.
241. Hellweg CE, Spitta LF, Henschenmacher B, Diegeler S, Baumstark-Khan C. Transcription factors in the cellular response to charged particle exposure. Front Oncol. 2016;6:61. https://doi.org/10.3389/fonc.2016.00061.
242. Coleman MA, Sasi SP, Onufrak J, Natarajan M, Manickam K, Schwab J, Muralidharan S, Peterson LE, Alekseyev YO, Yan X, Goukassian DA. Low-dose radiation affects cardiac physiology: gene networks and molecular signaling in cardiomyocytes. Am J Physiol Heart Circ Physiol. 2015;309(11):H1947–63. https://doi.org/10.1152/ajpheart.00050.2015.
243. Hellweg CE, Baumstark-Khan C, Schmitz C, Lau P, Meier MM, Testard I, Berger T, Reitz G. Activation of the nuclear factor kappaB pathway by heavy ion beams of different linear energy transfer. Int J Radiat Biol. 2011;87(9):954–63. https://doi.org/10.3109/09553002.2011.584942.
244. Chishti AA, Baumstark-Khan C, Koch K, Kolanus W, Feles S, Konda B, Azhar A, Spitta LF, Henschenmacher B, Diegeler S, Schmitz C, Hellweg CE. Linear energy transfer modulates radiation-induced NF-kappa B activation and expression of its downstream target genes. Radiat Res. 2018;189(4):354–70. https://doi.org/10.1667/RR14905.1.
245. Ducray C, Sabatier L. Role of chromosome instability in long term effect of manned-space missions. Adv Space Res. 1998;22(4):597–602. https://doi.org/10.1016/s0273-1177(98)00082-9.
246. Aubert G, Lansdorp PM. Telomeres and aging. Physiol Rev. 2008;88(2):557–79. https://doi.org/10.1152/physrev.00026.2007.
247. Thompson CAH, Wong JMY. Non-canonical functions of telomerase reverse transcriptase: emerging roles and biological relevance. Curr Top Med Chem. 2020;20(6):498–507. https://doi.org/10.2174/1568026620666200131125110.
248. Kennedy EM, Powell DR, Li Z, Bell JSK, Barwick BG, Feng H, McCrary MR, Dwivedi B, Kowalski J, Dynan WS, Conneely KN, Vertino PM. Galactic cosmic radiation induces persistent epigenome alterations relevant to human lung cancer. Sci Rep. 2018;8(1):6709. https://doi.org/10.1038/s41598-018-24755-8.
249. Miousse IR, Chalbot MC, Aykin-Burns N, Wang X, Basnakian A, Kavouras IG, Koturbash I. Epigenetic alterations induced by

ambient particulate matter in mouse macrophages. Environ Mol Mutagen. 2014;55(5):428–35. https://doi.org/10.1002/em.21855.
250. Acharya MM, Baddour AA, Kawashita T, Allen BD, Syage AR, Nguyen TH, Yoon N, Giedzinski E, Yu L, Parihar VK, Baulch JE. Epigenetic determinants of space radiation-induced cognitive dysfunction. Sci Rep. 2017;7:42885. https://doi.org/10.1038/srep42885.
251. Kostomitsopoulos NG, Durasevic SF. The ethical justification for the use of animals in biomedical research. Arch Biol Sci. 2010;62(3):783–9. https://doi.org/10.2298/Abs1003783k.
252. Russell WMS, Burch RL. The principles of humane experimental technique. Med J Aust. 1960;1(13):500. https://doi.org/10.5694/j.1326-5377.1960.tb73127.x.
253. Dubbs C. Space dogs: pioneers of space travel. Writer's Showcase. 2003. https://books.google.de/books?id=J_pCZVl-KzEC.
254. Burge S, Matin R, Wallis D. Structure and function of the skin. In: Oxford handbook of medical dermatology. Oxford University Press; 2016. p. 1–15. https://doi.org/10.1093/med/9780198747925.003.0001.
255. Hu S, Kim MH, McClellan GE, Cucinotta FA. Modeling the acute health effects of astronauts from exposure to large solar particle events. Health Phys. 2009;96(4):465–76. https://doi.org/10.1097/01.HP.0000339020.92837.61.
256. Hopewell JW. The skin: its structure and response to ionizing radiation. Int J Radiat Biol. 1990;57(4):751–73. https://doi.org/10.1080/09553009014550911.
257. Sanzari JK, Diffenderfer ES, Hagan S, Billings PC, Gridley DS, Seykora JT, Kennedy AR, Cengel KA. Dermatopathology effects of simulated solar particle event radiation exposure in the porcine model. Life Sci Space Res (Amst). 2015;6:21–8. https://doi.org/10.1016/j.lssr.2015.06.003.
258. Wilson JM, Sanzari JK, Diffenderfer ES, Yee SS, Seykora JT, Maks C, Ware JH, Litt HI, Reetz JA, McDonough J, Weissman D, Kennedy AR, Cengel KA. Acute biological effects of simulating the whole-body radiation dose distribution from a solar particle event using a porcine model. Radiat Res. 2011;176(5):649–59. https://doi.org/10.1667/rr2541.1.
259. Mao XW, Mekonnen T, Kennedy AR, Gridley DS. Differential expression of oxidative stress and extracellular matrix remodeling genes in low- or high-dose-rate photon-irradiated skin. Radiat Res. 2011;176(2):187–97. https://doi.org/10.1667/rr2493.1.
260. Marshall JS, Warrington R, Watson W, Kim HL. An introduction to immunology and immunopathology. Allergy Asthma Clin Immunol. 2018;14(Suppl 2):49. https://doi.org/10.1186/s13223-018-0278-1.
261. Crucian BE, Chouker A, Simpson RJ, Mehta S, Marshall G, Smith SM, Zwart SR, Heer M, Ponomarev S, Whitmire A, Frippiat JP, Douglas GL, Lorenzi H, Buchheim JI, Makedonas G, Ginsburg GS, Ott CM, Pierson DL, Krieger SS, et al. Immune system dysregulation during spaceflight: potential countermeasures for deep space exploration missions. Front Immunol. 2018;9:1437. https://doi.org/10.3389/fimmu.2018.01437.
262. Crucian B, Stowe RP, Mehta S, Quiriarte H, Pierson D, Sams C. Alterations in adaptive immunity persist during long-duration spaceflight [Original Paper]. NPJ Microgravity. 2015;1(1):15013. https://doi.org/10.1038/npjmgrav.2015.13.
263. Mehta SK, Crucian BE, Stowe RP, Simpson RJ, Ott CM, Sams CF, Pierson DL. Reactivation of latent viruses is associated with increased plasma cytokines in astronauts. Cytokine. 2013;61(1):205–9. https://doi.org/10.1016/j.cyto.2012.09.019.
264. Lewis ML, Cubano LA, Zhao B, Dinh HK, Pabalan JG, Piepmeier EH, Bowman PD. cDNA microarray reveals altered cytoskeletal gene expression in space-flown leukemic T lymphocytes (Jurkat). FASEB J. 2001;15(10):1783–5. https://doi.org/10.1096/fj.00-0820fje.
265. Fernandez-Gonzalo R, Baatout S, Moreels M. Impact of particle irradiation on the immune system: from the clinic to mars. Front Immunol. 2017;8:177. https://doi.org/10.3389/fimmu.2017.00177.
266. Pecaut MJ, Dutta-Roy R, Smith AL, Jones TA, Nelson GA, Gridley DS. Acute effects of iron-particle radiation on immunity. Part I: population distributions. Radiat Res. 2006;165(1):68–77. https://doi.org/10.1667/rr3493.1.
267. Sanzari JK, Wan XS, Muehlmatt A, Lin L, Kennedy AR. Comparison of changes over time in leukocyte counts in Yucatan minipigs irradiated with simulated solar particle event-like radiation. Life Sci Space Res (Amst). 2015;4:11–6. https://doi.org/10.1016/j.lssr.2014.12.002.
268. Alpen EL, Powers-Risius P, Curtis SB, DeGuzman R. Tumorigenic potential of high-Z, high-LET charged-particle radiations. Radiat Res. 1993;136(3):382–91. https://www.ncbi.nlm.nih.gov/pubmed/8278580.
269. Alpen EL, Powers-Risius P, Curtis SB, DeGuzman R, Fry RJ. Fluence-based relative biological effectiveness for charged particle carcinogenesis in mouse Harderian gland. Adv Space Res. 1994;14(10):573–81. https://doi.org/10.1016/0273-1177(94)90512-6.
270. Chang PY, Cucinotta FA, Bjornstad KA, Bakke J, Rosen CJ, Du N, Fairchild DG, Cacao E, Blakely EA. Harderian gland tumorigenesis: low-dose and LET response. Radiat Res. 2016;185(5):449–60. https://doi.org/10.1667/RR14335.1.
271. Huang EG, Wang RY, Xie L, Chang P, Yao G, Zhang B, Ham DW, Lin Y, Blakely EA, Sachs RK. Simulating galactic cosmic ray effects: synergy modeling of murine tumor prevalence after exposure to two one-ion beams in rapid sequence. Life Sci Space Res (Amst). 2020;25:107–18. https://doi.org/10.1016/j.lssr.2020.01.001.
272. Edmondson EF, Gatti DM, Ray FA, Garcia EL, Fallgren CM, Kamstock DA, Weil MM. Genomic mapping in outbred mice reveals overlap in genetic susceptibility for HZE ion- and gamma-ray-induced tumors. Sci Adv. 2020;6(16):eaax5940. https://doi.org/10.1126/sciadv.aax5940.
273. Imaoka T, Nishimura M, Daino K, Kokubo T, Doi K, Iizuka D, Nishimura Y, Okutani T, Takabatake M, Kakinuma S, Shimada Y. Influence of age on the relative biological effectiveness of carbon ion radiation for induction of rat mammary carcinoma. Int J Radiat Oncol Biol Phys. 2013;85(4):1134–40. https://doi.org/10.1016/j.ijrobp.2012.08.035.
274. Imaoka T, Nishimura M, Kakinuma S, Hatano Y, Ohmachi Y, Yoshinaga S, Kawano A, Maekawa A, Shimada Y. High relative biologic effectiveness of carbon ion radiation on induction of rat mammary carcinoma and its lack of H-ras and Tp53 mutations. Int J Radiat Oncol Biol Phys. 2007;69(1):194–203. https://doi.org/10.1016/j.ijrobp.2007.05.026.
275. Suman S, Kumar S, Moon BH, Fornace AJ Jr, Datta K. Low and high dose rate heavy ion radiation-induced intestinal and colonic tumorigenesis in APC(1638N/+) mice. Life Sci Space Res (Amst). 2017;13:45–50. https://doi.org/10.1016/j.lssr.2017.04.003.
276. Suman S, Kumar S, Moon BH, Strawn SJ, Thakor H, Fan Z, Shay JW, Fornace AJ Jr, Datta K. Relative biological effectiveness of energetic heavy ions for intestinal tumorigenesis shows male preponderance and radiation type and energy dependence in APC(1638N/+) mice. Int J Radiat Oncol Biol Phys. 2016;95(1):131–8. https://doi.org/10.1016/j.ijrobp.2015.10.057.
277. Weil MM, Bedford JS, Bielefeldt-Ohmann H, Ray FA, Genik PC, Ehrhart EJ, Fallgren CM, Hailu F, Battaglia CL, Charles B, Callan MA, Ullrich RL. Incidence of acute myeloid leukemia and hepatocellular carcinoma in mice irradiated with 1 GeV/nucleon (56) Fe ions. Radiat Res. 2009;172(2):213–9. https://doi.org/10.1667/RR1648.1.

278. Weil MM, Ray FA, Genik PC, Yu Y, McCarthy M, Fallgren CM, Ullrich RL. Effects of 28Si ions, 56Fe ions, and protons on the induction of murine acute myeloid leukemia and hepatocellular carcinoma. PLoS One. 2014;9(7):e104819. https://doi.org/10.1371/journal.pone.0104819.
279. Martincorena I, Fowler JC, Wabik A, Lawson ARJ, Abascal F, Hall MWJ, Cagan A, Murai K, Mahbubani K, Stratton MR, Fitzgerald RC, Handford PA, Campbell PJ, Saeb-Parsy K, Jones PH. Somatic mutant clones colonize the human esophagus with age. Science. 2018;362(6417):911–7. https://doi.org/10.1126/science.aau3879.
280. Major IR, Mole RH. Myeloid leukaemia in x-ray irradiated CBA mice. Nature. 1978;272(5652):455–6. https://doi.org/10.1038/272455a0.
281. Delgado O, Batten KG, Richardson JA, Xie XJ, Gazdar AF, Kaisani AA, Girard L, Behrens C, Suraokar M, Fasciani G, Wright WE, Story MD, Wistuba II, Minna JD, Shay JW. Radiation-enhanced lung cancer progression in a transgenic mouse model of lung cancer is predictive of outcomes in human lung and breast cancer. Clin Cancer Res. 2014;20(6):1610–22. https://doi.org/10.1158/1078-0432.CCR-13-2589.
282. Wang X, Farris Iii AB, Wang P, Zhang X, Wang H, Wang Y. Relative effectiveness at 1 gy after acute and fractionated exposures of heavy ions with different linear energy transfer for lung tumorigenesis. Radiat Res. 2015;183(2):233–9. https://doi.org/10.1667/RR13884.1.
283. Smits R, Kartheuser A, Jagmohan-Changur S, Leblanc V, Breukel C, de Vries A, van Kranen H, van Krieken JH, Williamson S, Edelmann W, Kucherlapati R, Khan PM, Fodde R. Loss of Apc and the entire chromosome 18 but absence of mutations at the Ras and Tp53 genes in intestinal tumors from Apc1638N, a mouse model for Apc-driven carcinogenesis. Carcinogenesis. 1997;18(2):321–7. https://doi.org/10.1093/carcin/18.2.321.
284. Haymaker W, Rubinstein LJ, Miquel J. Brain tumors in irradiated monkeys. Acta Neuropathol. 1972;20(4):267–77. https://doi.org/10.1007/BF00691745.
285. Camacho CV, Todorova PK, Hardebeck MC, Tomimatsu N, Gil del Alcazar CR, Ilcheva M, Mukherjee B, McEllin B, Vemireddy V, Hatanpaa K, Story MD, Habib AA, Murty VV, Bachoo R, Burma S. DNA double-strand breaks cooperate with loss of Ink4 and Arf tumor suppressors to generate glioblastomas with frequent Met amplification. Oncogene. 2015;34(8):1064–72. https://doi.org/10.1038/onc.2014.29.
286. Chappell LJ, Elgart SR, Milder CM, Semones EJ. Assessing nonlinearity in Harderian gland tumor induction using three combined HZE-irradiated mouse datasets. Radiat Res. 2020;194(1):38–51. https://doi.org/10.1667/RR15539.1.
287. Cucinotta FA, Manuel FK, Jones J, Iszard G, Murrey J, Djojonegro B, Wear M. Space radiation and cataracts in astronauts. Radiat Res. 2001;156(5 Pt 1):460–6. https://doi.org/10.1667/0033-7587(2001)156[0460:sracia]2.0.co;2.
288. Brenner DJ, Medvedovsky C, Huang Y, Worgul BV. Accelerated heavy particles and the lens. VIII. Comparisons between the effects of acute low doses of iron ions (190 keV/microns) and argon ions (88 keV/microns). Radiat Res. 1993;133(2):198–203. https://www.ncbi.nlm.nih.gov/pubmed/8438061.
289. Worgul BV. Cataract analysis and the assessment of radiation risk in space. Adv Space Res. 1986;6(11):285–93. https://doi.org/10.1016/0273-1177(86)90304-2.
290. Worgul BV, Medvedovsky C, Huang YP, Marino SA, RandersPehrson G, Brenner DJ. Quantitative assessment of the cataractogenic potential of very low doses of neutrons. Radiat Res. 1996;145(3):343–9. https://doi.org/10.2307/3578991.
291. Kleiman NJ, David J, Elliston CD, Hopkins KM, Smilenov LB, Brenner DJ, Worgul BV, Hall EJ, Lieberman HB. Mrad9 and atm haploinsufficiency enhance spontaneous and X-ray-induced cataractogenesis in mice. Radiat Res. 2007;168(5):567–73. https://doi.org/10.1667/rr1122.1.
292. Hall EJ, Brenner DJ, Worgul B, Smilenov L. Genetic susceptibility to radiation. Adv Space Res. 2005;35(2):249–53. https://doi.org/10.1016/j.asr.2004.12.032.
293. Hall EJ, Worgul BV, Smilenov L, Elliston CD, Brenner DJ. The relative biological effectiveness of densely ionizing heavy-ion radiation for inducing ocular cataracts in wild type versus mice heterozygous for the ATM gene. Radiat Environ Biophys. 2006;45(2):99–104. https://doi.org/10.1007/s00411-006-0052-5.
294. Martin DS, Lee SMC, Matz TP, Westby CM, Scott JM, Stenger MB, Platts SH. Internal jugular pressure increases during parabolic flight. Physiol Rep. 2016;4(24):e13068. https://doi.org/10.14814/phy2.13068.
295. Prisk GK, Guy HJ, Elliott AR, Deutschman RA, West JB. Pulmonary diffusing capacity, capillary blood volume, and cardiac output during sustained microgravity. J Appl Physiol. 1993;75(1):15–26. https://doi.org/10.1152/jappl.1993.75.1.15.
296. Gunga H-C, Ahlefeld VW, Appell Coriolano H-J, Werner A, Hoffmann U. Cardiovascular system, red blood cells, and oxygen transport in microgravity. 1st ed. 2016. http://lib.ugent.be/catalog/ebk01:3710000000751183.
297. Baran R, Marchal S, Garcia Campos S, Rehnberg E, Tabury K, Baselet B, Wehland M, Grimm D, Baatout S. The cardiovascular system in space: focus on in vivo and in vitro studies. Biomedicines. 2022;10(1):59. https://www.mdpi.com/2227-9059/10/1/59.
298. Yu T, Parks BW, Yu S, Srivastava R, Gupta K, Wu X, Khaled S, Chang PY, Kabarowski JH, Kucik DF. Iron-ion radiation accelerates atherosclerosis in apolipoprotein E-deficient mice. Radiat Res. 2011;175(6):766–773, 768. https://doi.org/10.1667/RR2482.1.
299. Chancellor JC, Scott GB, Sutton JP. Space radiation: the number one risk to astronaut health beyond low earth orbit. Life (Basel). 2014;4(3):491–510. https://doi.org/10.3390/life4030491.
300. Jandial R, Hoshide R, Waters JD, Limoli CL. Space-brain: the negative effects of space exposure on the central nervous system. Surg Neurol Int. 2018;9:9. https://doi.org/10.4103/sni.sni_250_17.
301. Lledo PM, Alonso M, Grubb MS. Adult neurogenesis and functional plasticity in neuronal circuits. Nat Rev Neurosci. 2006;7(3):179–93. https://doi.org/10.1038/nrn1867.
302. Rola R, Fishman K, Baure J, Rosi S, Lamborn KR, Obenaus A, Nelson GA, Fike JR. Hippocampal neurogenesis and neuroinflammation after cranial irradiation with (56)Fe particles. Radiat Res. 2008;169(6):626–32. https://doi.org/10.1667/RR1263.1.
303. Ulrich-Lai YM, Herman JP. Neural regulation of endocrine and autonomic stress responses. Nat Rev Neurosci. 2009;10(6):397–409. https://doi.org/10.1038/nrn2647.
304. Nelson GA. Space radiation: central nervous system risks. In: Young LR, Sutton JP, editors. Handbook of bioastronautics. Switzerland AG: Springer Nature; 2021. p. 313–27. https://doi.org/10.1007/978-3-319-12191-8_84.
305. Acharya MM, Baulch JE, Klein PM, Baddour AAD, Apodaca LA, Kramar EA, Alikhani L, Garcia C Jr, Angulo MC, Batra RS, Fallgren CM, Borak TB, Stark CEL, Wood MA, Britten RA, Soltesz I, Limoli CL. New concerns for neurocognitive function during deep space exposures to chronic, low dose-rate, neutron radiation. eNeuro. 2019;6(4) https://doi.org/10.1523/ENEURO.0094-19.2019. (In the article "New concerns for neurocognitive function during deep space exposures to chronic, low dose-rate, neutron radiation," by Munjal M. Acharya, Janet E. Baulch, Peter M. Klein, Al Anoud D. Baddour, Lauren A. Apodaca, Eniko A. Kramár, Leila Alikhani, Camillo Garcia Jr., Maria C. Angulo, Raja S. Batra, Christine M. Fallgren, Thomas B. Borak, Craig E. L. Stark, Marcello A. Wood, Richard A. Britten, Ivan Soltesz, and Charles L. Limoli, which was published online on August 5, 2019, a formula appeared incorrectly

due to a production error. Within the formula on page 4, ("x 00") should be corrected to ("x 100")).
306. Cherry JD, Liu B, Frost JL, Lemere CA, Williams JP, Olschowka JA, O'Banion MK. Galactic cosmic radiation leads to cognitive impairment and increased abeta plaque accumulation in a mouse model of Alzheimer's disease. PLoS One. 2012;7(12):e53275. https://doi.org/10.1371/journal.pone.0053275.
307. Guidetti R, Altiero T, Rebecchi L. On dormancy strategies in tardigrades. J Insect Physiol. 2011;57(5):567–76. https://doi.org/10.1016/j.jinsphys.2011.03.003.
308. Hygum TL, Clausen LKB, Halberg KA, Jørgensen A, Møbjerg N. Tun formation is not a prerequisite for desiccation tolerance in the marine tidal tardigrade Echiniscoides sigismundi. Zool J Linnean Soc. 2016;178(4):907–11. https://doi.org/10.1111/zoj.12444.
309. Marotta R, Leasi F, Uggetti A, Ricci C, Melone G. Dry and survive: morphological changes during anhydrobiosis in a bdelloid rotifer. J Struct Biol. 2010;171(1):11–7. https://doi.org/10.1016/j.jsb.2010.04.003.
310. Wright JC, Westh P, Ramløv H. Cryptobiosis in tardigrada. Biol Rev. 1992;67(1):1–29. https://doi.org/10.1111/j.1469-185X.1992.tb01657.x.
311. Rebecchi L, Altiero T, Guidetti R. Anhydrobiosis: the extreme limit of desiccation tolerance. Invertebr Surv J. 2007;4(2):65–81. <Go to ISI>://WOS:000456193200001.
312. Ricci C. Anhydrobiotic capabilities of bdelloid rotifers. Hydrobiologia. 1998;387:321–6. https://doi.org/10.1023/A:1017086425934.
313. Wright JC. Desiccation tolerance and water-retentive mechanisms in tardigrades. J Exp Biol. 1989;142(1):267–92. https://doi.org/10.1242/jeb.142.1.267.
314. Wright JC. The significance of four xeric parameters in the ecology of terrestrial Tardigrada. J Zool. 1991;224(1):59–77. https://doi.org/10.1111/j.1469-7998.1991.tb04788.x.
315. Jørgensen A, Møbjerg N, Kristensen R. A molecular study of the tardigrade Echiniscus testudo (Echiniscidae) reveals low DNA sequence diversity over a large geographical area. J Limnol. 2007;66 https://doi.org/10.4081/jlimnol.2007.s1.77.
316. Roszkowska M, Kmita H, Kaczmarek Ł. Long-term anhydrobiosis in two taxa of moss dwelling Eutardigrada (Tardigrada) desiccated for 12 and 15 years, respectively. Eur Zool J. 2020;87(1):642–7. https://doi.org/10.1080/24750263.2020.1829110.
317. Tsujimoto M, Imura S, Kanda H. Recovery and reproduction of an Antarctic tardigrade retrieved from a moss sample frozen for over 30 years. Cryobiology. 2016;72(1):78–81. https://doi.org/10.1016/j.cryobiol.2015.12.003.
318. Guidetti R, Jönsson KI. Long-term anhydrobiotic survival in semi-terrestrial micrometazoans. J Zool. 2002;257(2):181–7. https://doi.org/10.1017/S095283690200078X.
319. Shmakova L, Malavin S, Iakovenko N, Vishnivetskaya T, Shain D, Plewka M, Rivkina E. A living bdelloid rotifer from 24,000-year-old Arctic permafrost. Curr Biol. 2021;31(11):R712–3. https://doi.org/10.1016/j.cub.2021.04.077.
320. Shatilovich AV, Tchesunov AV, Neretina TV, Grabarnik IP, Gubin SV, Vishnivetskaya TA, Onstott TC, Rivkina EM. Viable nematodes from late pleistocene permafrost of the Kolyma river lowland. Doklady Biol Sci. 2018;480(1):100–2. https://doi.org/10.1134/S0012496618030079.
321. Guidetti R, Rizzo AM, Altiero T, Rebecchi L. What can we learn from the toughest animals of the Earth? Water bears (tardigrades) as multicellular model organisms in order to perform scientific preparations for lunar exploration. Planet Space Sci. 2012;74(1):97–102. https://doi.org/10.1016/j.pss.2012.05.021.
322. Jönsson KI. Radiation tolerance in tardigrades: current knowledge and potential applications in medicine. Cancers (Basel). 2019;11(9) https://doi.org/10.3390/cancers11091333.
323. Jönsson KI, Rabbow E, Schill RO, Harms-Ringdahl M, Rettberg P. Tardigrades survive exposure to space in low Earth orbit. Curr Biol. 2008;18(17):R729–31. https://doi.org/10.1016/j.cub.2008.06.048.
324. Krisko A, Leroy M, Radman M, Meselson M. Extreme antioxidant protection against ionizing radiation in bdelloid rotifers. Proc Natl Acad Sci. 2012;109(7):2354. https://doi.org/10.1073/pnas.1119762109.
325. Møbjerg N, Halberg KA, Jørgensen A, Persson D, Bjørn M, Ramløv H, Kristensen RM. Survival in extreme environments—on the current knowledge of adaptations in tardigrades. Acta Physiol. 2011;202(3):409–20. https://doi.org/10.1111/j.1748-1716.2011.02252.x
326. Neves RC, Hvidepil LKB, Sørensen-Hygum TL, Stuart RM, Møbjerg N. Thermotolerance experiments on active and desiccated states of Ramazzottius varieornatus emphasize that tardigrades are sensitive to high temperatures. Sci Rep. 2020;10(1):94. https://doi.org/10.1038/s41598-019-56965-z.
327. Seki K, Toyoshima M. Preserving tardigrades under pressure. Nature. 1998;395(6705):853–4. https://doi.org/10.1038/27576.
328. Murshed H. Chapter 3—Radiation biology. In: Murshed H, editor. Fundamentals of radiation oncology. 3rd ed. Academic Press; 2019. p. 57–87. https://doi.org/10.1016/B978-0-12-814128-1.00003-9.
329. Gladyshev E, Meselson M. Extreme resistance of bdelloid rotifers to ionizing radiation. Proc Natl Acad Sci. 2008;105(13):5139. https://doi.org/10.1073/pnas.0800966105.
330. Nilsson EJ, Jönsson KI, Pallon J. Tolerance to proton irradiation in the eutardigrade Richtersius coronifer—a nuclear microprobe study. Int J Radiat Biol. 2010;86(5):420–7. https://doi.org/10.3109/09553000903568001.
331. Beltrán-Pardo E, Jönsson KI, Harms-Ringdahl M, Haghdoost S, Wojcik A. Tolerance to gamma radiation in the tardigrade hypsibius dujardini from embryo to adult correlate inversely with cellular proliferation. PLoS One. 2015;10(7):e0133658. https://doi.org/10.1371/journal.pone.0133658.
332. Jönsson KI, Schill RO, Rabbow E, Rettberg P, Harms-Ringdahl M. The fate of the TARDIS offspring: no intergenerational effects of space exposure. Zool J Linnean Soc. 2016;178(4):924–30. https://doi.org/10.1111/zoj.12499.
333. Persson D, Halberg KA, Jørgensen A, Ricci C, Møbjerg N, Kristensen RM. Extreme stress tolerance in tardigrades: surviving space conditions in low earth orbit. J Zool Syst Evol Res. 2011;49(S1):90–7. https://doi.org/10.1111/j.1439-0469.2010.00605.x.
334. Rizzo AM, Altiero T, Corsetto PA, Montorfano G, Guidetti R, Rebecchi L. Space flight effects on antioxidant molecules in dry tardigrades: the TARDIKISS experiment. BioMed Res Int. 2015;2015:167642. https://doi.org/10.1155/2015/167642.
335. Rizzo AM, Negroni M, Altiero T, Montorfano G, Corsetto P, Berselli P, Berra B, Guidetti R, Rebecchi L. Antioxidant defences in hydrated and desiccated states of the tardigrade Paramacrobiotus richtersi. Comp Biochem Physiol B Biochem Mol Biol. 2010;156(2):115–21. https://doi.org/10.1016/j.cbpb.2010.02.009.
336. Chavez C, Cruz-Becerra G, Fei J, Kassavetis GA, Kadonaga JT. The tardigrade damage suppressor protein binds to nucleosomes and protects DNA from hydroxyl radicals. Elife. 2019;8 https://doi.org/10.7554/eLife.47682.
337. Hashimoto T, Horikawa DD, Saito Y, Kuwahara H, Kozuka-Hata H, Shin IT, Minakuchi Y, Ohishi K, Motoyama A, Aizu T, Enomoto A, Kondo K, Tanaka S, Hara Y, Koshikawa S, Sagara H, Miura T, Yokobori SI, Miyagawa K, et al. Extremotolerant tardigrade genome and improved radiotolerance of human cultured cells by tardigrade-unique protein. Nat Commun. 2016;7(1):12808. https://doi.org/10.1038/ncomms12808.
338. Mognato M, Girardi C, Fabris S, Celotti L. DNA repair in modeled microgravity: double strand break rejoining activity in human

lymphocytes irradiated with gamma-rays. Mutat Res. 2009;663(1–2):32–9. https://doi.org/10.1016/j.mrfmmm.2009.01.002.
339. De Micco V, Aronne G, Colla G, Fortezza R, De Pascale S. Agro-biology for bioregenerative life support systems in long-term space missions: general constraints and the Italian efforts. J Plant Interact. 2009;4(4):241–52. https://doi.org/10.1080/17429140903161348.
340. Paradiso R, De Micco V, Buonomo R, Aronne G, Barbieri G, De Pascale S. Soilless cultivation of soybean for Bioregenerative Life-Support Systems: a literature review and the experience of the MELiSSA Project—food characterisation phase I. Plant Biol (Stuttg). 2014;16(Suppl 1):69–78. https://doi.org/10.1111/plb.12056.
341. Wheeler RM, Mackowiak CL, Stutte GW, Sager JC, Yorio NC, Ruffe LM, Fortson RE, Dreschel TW, Knott WM, Corey KA. NASA's Biomass Production Chamber: a testbed for bioregenerative life support studies. Adv Space Res. 1996;18(4–5):215–24. https://doi.org/10.1016/0273-1177(95)00880-n.
342. Bates S, Gushin V, Bingham G, Vinokhodova A, Marquit J, Sychev V. Plants as countermeasures: a review of the literature and application to habitation systems for humans living in isolated or extreme environments. Habitation. 2009;12(1):33–40. https://doi.org/10.3727/154296610x12686999887201.
343. Williams D. Isolation and integrated testing: an introduction to the lunar-mars life support test project. Isolation—NASA experiments in closed-environment living, 104. 2002.
344. De Micco V, Arena C, Aronne G. Anatomical alterations of Phaseolus vulgaris L. mature leaves irradiated with X-rays. Plant Biol (Stuttg). 2014;16(Suppl 1):187–93. https://doi.org/10.1111/plb.12125.
345. De Micco V, Arena C, Pignalosa D, Durante M. Effects of sparsely and densely ionizing radiation on plants. Radiat Environ Biophys. 2011;50(1):1–19. https://doi.org/10.1007/s00411-010-0343-8.
346. Arena C, De Micco V, Macaeva E, Quintens R. Space radiation effects on plant and mammalian cells. Acta Astronaut. 2014;104(1):419–31. https://doi.org/10.1016/j.actaastro.2014.05.005.
347. Wang W, Gorsuch JW, Hughes JS. Plants for environmental studies. CRC Press; 2020. https://books.google.be/books?id=zc79DwAAQBAJ.
348. Brodribb TJ. Xylem hydraulic physiology: the functional backbone of terrestrial plant productivity. Plant Sci. 2009;177(4):245–51. https://doi.org/10.1016/j.plantsci.2009.06.001.
349. Chiara A. Leaf morpho-anatomical traits in Vigna radiata L. affect plant photosynthetic acclimation to changing vapor pressure deficit. Environ Exp Bot. 2021;186(9):104453–102021, 104186. https://doi.org/10.1016/j.envexpbot.2021.104453. (Opyt izucheniia mneniia naseleniia o kachestve lechebno-profilakticheskogo obsluzhivaniia)
350. Cheng TS, Chandlee JM. The structural, biochemical, and genetic characterization of a new radiation-induced, variegated leaf mutant of soybean [Glycine max (L.) Merr]. Proc Natl Sci Counc Rep China B. 1999;23(1):27–37. https://www.ncbi.nlm.nih.gov/pubmed/9949722.
351. Mei M, Qiu Y, Sun Y, Huang R, Yao J, Zhang Q, Hong M, Ye J. Morphological and molecular changes of maize plants after seeds been flown on recoverablf satellite. Adv Space Res. 1998;22(12):1691–7. https://doi.org/10.1016/s0273-1177(99)00034-4.
352. Rea G, Esposito D, Damasso M, Serafini A, Margonelli A, Faraloni C, Torzillo G, Zanini A, Bertalan I, Johanningmeier U, Giardi MT. Ionizing radiation impacts photochemical quantum yield and oxygen evolution activity of Photosystem II in photosynthetic microorganisms. Int J Radiat Biol. 2008;84(11):867–77. https://doi.org/10.1080/09553000802460149.
353. Arena C, De Micco V, Aronne G, Pugliese M, De Santo AV, De Maio A. Response of Phaseolus vulgaris L. plants to low-let ionizing radiation: growth and oxidative stress. Acta Astronaut. 2013;91:107–14. https://doi.org/10.1016/j.actaastro.2013.05.013.
354. Esnault MA, Legue F, Chenal C. Ionizing radiation: advances in plant response. Environ Exp Bot. 2010;68(3):231–7. https://doi.org/10.1016/j.envexpbot.2010.01.007.
355. Zaka R, Vandecasteele CM, Misset MT. Effects of low chronic doses of ionizing radiation on antioxidant enzymes and G6PDH activities in Stipa capillata (Poaceae). J Exp Bot. 2002;53(376):1979–87. https://doi.org/10.1093/jxb/erf041.
356. Nagle PW, Coppes RP. Current and future perspectives of the use of organoids in radiobiology. Cells. 2020;9(12) https://doi.org/10.3390/cells9122649.
357. Schielke C, Hartel C, Durante M, Ritter S, Schroeder IS. Solving the issue of ionizing radiation induced neurotoxicity by using novel cell models and state of the art accelerator facilities [Review]. Front Phys. 2020;8(417):568027. https://doi.org/10.3389/fphy.2020.568027.
358. Białkowska K, Komorowski P, Bryszewska M, Miłowska K. Spheroids as a type of three-dimensional cell cultures—examples of methods of preparation and the most important application. Int J Mol Sci. 2020;21(17):6225. https://www.mdpi.com/1422-0067/21/17/6225.
359. Kruger M, Pietsch J, Bauer J, Kopp S, Carvalho DTO, Baatout S, Moreels M, Melnik D, Wehland M, Egli M, Jayashree S, Kobbero SD, Corydon TJ, Nebuloni S, Gass S, Evert M, Infanger M, Grimm D. Growth of endothelial cells in space and in simulated microgravity—a comparison on the secretory level. Cell Physiol Biochem. 2019;52(5):1039–60. https://doi.org/10.33594/000000071.
360. Humpel C. Organotypic brain slice cultures: a review. Neuroscience. 2015;305:86–98. https://doi.org/10.1016/j.neuroscience.2015.07.086.
361. Kloker LD, Yurttas C, Lauer UM. Three-dimensional tumor cell cultures employed in virotherapy research. Oncol Virother. 2018;7:79–93. https://doi.org/10.2147/OV.S165479.
362. Blakely EA, Chang PY. Late effects of space radiation: cataracts. In: Young LR, Sutton JP, editors. Handbook of bioastronautics. Springer International Publishing; 2021. p. 277–86. https://doi.org/10.1007/978-3-319-12191-8_87.
363. Chylack LT Jr, Peterson LE, Feiveson AH, Wear ML, Manuel FK, Tung WH, Hardy DS, Marak LJ, Cucinotta FA. NASA study of cataract in astronauts (NASCA). Report 1: cross-sectional study of the relationship of exposure to space radiation and risk of lens opacity. Radiat Res. 2009;172(1):10–20. https://doi.org/10.1667/RR1580.1.
364. Cubo-Mateo N, Podhajsky S, Knickmann D, Slenzka K, Ghidini T, Gelinsky M. Can 3D bioprinting be a key for exploratory missions and human settlements on the Moon and Mars? Biofabrication. 2020;12(4):043001. https://doi.org/10.1088/1758-5090/abb53a.
365. Ghidini T. Regenerative medicine and 3D bioprinting for human space exploration and planet colonisation. J Thorac Dis. 2018;10(Suppl 20):S2363–75. https://doi.org/10.21037/jtd.2018.03.19.
366. Milojevic T, Weckwerth W. Molecular mechanisms of microbial survivability in outer space: a systems biology approach. Front Microbiol. 2020;11:923. https://doi.org/10.3389/fmicb.2020.00923.
367. Ott E, Kawaguchi Y, Kolbl D, Rabbow E, Rettberg P, Mora M, Moissl-Eichinger C, Weckwerth W, Yamagishi A, Milojevic T. Molecular repertoire of Deinococcus radiodurans after 1 year of exposure outside the International Space Station within the Tanpopo mission. Microbiome. 2020;8(1):150. https://doi.org/10.1186/s40168-020-00927-5.
368. Mastroleo F, Van Houdt R, Leroy B, Benotmane MA, Janssen A, Mergeay M, Vanhavere F, Hendrickx L, Wattiez R, Leys N. Experimental design and environmental parameters affect Rhodospirillum rubrum S1H response to space flight. ISME J. 2009;3(12):1402–19. https://doi.org/10.1038/ismej.2009.74.

369. Wilson JW, Ott CM, Quick L, Davis R, Honer Zu Bentrup K, Crabbe A, Richter E, Sarker S, Barrila J, Porwollik S, Cheng P, McClelland M, Tsaprailis G, Radabaugh T, Hunt A, Shah M, Nelman-Gonzalez M, Hing S, Parra M, et al. Media ion composition controls regulatory and virulence response of Salmonella in spaceflight. PLoS One. 2008;3(12):e3923. https://doi.org/10.1371/journal.pone.0003923.
370. Nicholson WL, Moeller R, Team P, Horneck G. Transcriptomic responses of germinating Bacillus subtilis spores exposed to 1.5 years of space and simulated martian conditions on the EXPOSE-E experiment PROTECT. Astrobiology. 2012;12(5):469–86. https://doi.org/10.1089/ast.2011.0748.
371. Vaishampayan PA, Rabbow E, Horneck G, Venkateswaran KJ. Survival of Bacillus pumilus spores for a prolonged period of time in real space conditions. Astrobiology. 2012;12(5):487–97. https://doi.org/10.1089/ast.2011.0738.
372. Ott E, Kawaguchi Y, Kolbl D, Chaturvedi P, Nakagawa K, Yamagishi A, Weckwerth W, Milojevic T. Proteometabolomic response of Deinococcus radiodurans exposed to UVC and vacuum conditions: initial studies prior to the Tanpopo space mission. PLoS One. 2017;12(12):e0189381. https://doi.org/10.1371/journal.pone.0189381.
373. da Silveira WA, Fazelinia H, Rosenthal SB, Laiakis EC, Kim MS, Meydan C, Kidane Y, Rathi KS, Smith SM, Stear B, Ying Y, Zhang Y, Foox J, Zanello S, Crucian B, Wang D, Nugent A, Costa HA, Zwart SR, et al. Comprehensive multi-omics analysis reveals mitochondrial stress as a central biological hub for spaceflight impact. Cell. 2020;183(5):1185–1201 e1120. https://doi.org/10.1016/j.cell.2020.11.002.
374. Cortese F, Klokov D, Osipov A, Stefaniak J, Moskalev A, Schastnaya J, Cantor C, Aliper A, Mamoshina P, Ushakov I, Sapetsky A, Vanhaelen Q, Alchinova I, Karganov M, Kovalchuk O, Wilkins R, Shtemberg A, Moreels M, Baatout S, et al. Vive la radioresistance!: converging research in radiobiology and biogerontology to enhance human radioresistance for deep space exploration and colonization. Oncotarget. 2018;9(18):14692–722. https://doi.org/10.18632/oncotarget.24461.
375. Puspitasari A, Cerri M, Takahashi A, Yoshida Y, Hanamura K, Tinganelli W. Hibernation as a tool for radiation protection in space exploration. Life (Basel). 2021;11(1) https://doi.org/10.3390/life11010054.
376. Zhang X, Epperly MW, Kay MA, Chen ZY, Dixon T, Franicola D, Greenberger BA, Komanduri P, Greenberger JS. Radioprotection in vitro and in vivo by minicircle plasmid carrying the human manganese superoxide dismutase transgene. Hum Gene Ther. 2008;19(8):820–6. https://doi.org/10.1089/hum.2007.141.
377. Frosina G. Overexpression of enzymes that repair endogenous damage to DNA. Eur J Biochem. 2000;267(8):2135–49. https://doi.org/10.1046/j.1432-1327.2000.01266.x.
378. Seckbach J, Oren A, Stan-Lotter H. Polyextremophiles: life under multiple forms of stress, vol. 27. Springer Science & Business Media; 2013.
379. Baltschukat K, Horneck G. Responses to accelerated heavy ions of spores of Bacillus subtilis of different repair capacity. Radiat Environ Biophys. 1991;30(2):87–103. https://doi.org/10.1007/bf01219343.
380. Moeller R, Setlow P, Reitz G, Nicholson WL. Roles of small, acid-soluble spore proteins and core water content in survival of Bacillus subtilis spores exposed to environmental solar UV radiation. Appl Environ Microbiol. 2009;75(16):5202–8. https://doi.org/10.1128/aem.00789-09.
381. Jönsson KI, Harms-Ringdahl M, Torudd J. Radiation tolerance in the eutardigrade Richtersius coronifer. Int J Radiat Biol. 2005;81(9):649–56. https://doi.org/10.1080/09553000500368453.
382. Horneck G. Responses of Bacillus subtilis spores to space environment: results from experiments in space. Orig Life Evol Biosph. 1993;23(1):37–52. https://doi.org/10.1007/bf01581989.
383. Baqué M, Scalzi G, Rabbow E, Rettberg P, Billi D. Biofilm and planktonic lifestyles differently support the resistance of the desert cyanobacterium chroococcidiopsis under space and martian simulations. Origins Life Evol Biospheres. 2013;43(4):377–89. https://doi.org/10.1007/s11084-013-9341-6.
384. Gérard E, Jolivet E, Prieur D, Forterre P. DNA protection mechanisms are not involved in the radioresistance of the hyperthermophilic archaea Pyrococcus abyssi and P. furiosus. Mol Genet Genomics. 2001;266(1):72–8. https://doi.org/10.1007/s004380100520.
385. Daly MJ, Gaidamakova EK, Matrosova VY, Vasilenko A, Zhai M, Venkateswaran A, Hess M, Omelchenko MV, Kostandarithes HM, Makarova KS, Wackett LP, Fredrickson JK, Ghosal D. Accumulation of Mn(II) in Deinococcus radiodurans facilitates gamma-radiation resistance. Science. 2004;306(5698):1025–8. https://doi.org/10.1126/science.1103185.
386. Leuko S, Rettberg P. The effects of HZE particles, γ and X-ray radiation on the survival and genetic integrity of Halobacterium salinarum NRC-1, Halococcus hamelinensis, and Halococcus morrhuae. Astrobiology. 2017;17(2):110–7. https://doi.org/10.1089/ast.2015.1458.
387. Webb KM, DiRuggiero J. Role of Mn2+ and compatible solutes in the radiation resistance of thermophilic bacteria and archaea. Archaea. 2012;2012:845756. https://doi.org/10.1155/2012/845756.
388. Zerulla K, Soppa J. Polyploidy in haloarchaea: advantages for growth and survival [Review]. Front Microbiol. 2014;5:274. https://doi.org/10.3389/fmicb.2014.00274.
389. Kish A, Kirkali G, Robinson C, Rosenblatt R, Jaruga P, Dizdaroglu M, DiRuggiero J. Salt shield: intracellular salts provide cellular protection against ionizing radiation in the halophilic archaeon, Halobacterium salinarum NRC-1. Environ Microbiol. 2009;11(5):1066–78. https://doi.org/10.1111/j.1462-2920.2008.01828.x.
390. Pathak J, Pandey A, Maurya PK, Rajneesh R, Sinha RP, Singh SP. Cyanobacterial secondary metabolite scytonemin: a potential photoprotective and pharmaceutical compound. Proc Natl Acad Sci India B Biol Sci. 2020;90(3):467–81.
391. Shahmohammadi HR, Asgarani E, Terato H, Saito T, Ohyama Y, Gekko K, Yamamoto O, Ide H. Protective roles of bacterioruberin and intracellular KCl in the resistance of Halobacterium salinarium against DNA-damaging agents. J Radiat Res. 1998;39(4):251–62. https://doi.org/10.1269/jrr.39.251.
392. Beblo-Vranesevic K, Bohmeier M, Perras AK, Schwendner P, Rabbow E, Moissl-Eichinger C, Cockell CS, Vannier P, Marteinsson VT, Monaghan EP, Ehrenfreund P, Garcia-Descalzo L, Gómez F, Malki M, Amils R, Gaboyer F, Westall F, Cabezas P, Walter N, Rettberg P. Lack of correlation of desiccation and radiation tolerance in microorganisms from diverse extreme environments tested under anoxic conditions. FEMS Microbiol Lett. 2018;365(6) https://doi.org/10.1093/femsle/fny044.
393. Beblo-Vranesevic K, Galinski EA, Rachel R, Huber H, Rettberg P. Influence of osmotic stress on desiccation and irradiation tolerance of (hyper)-thermophilic microorganisms. Arch Microbiol. 2017;199(1):17–28. https://doi.org/10.1007/s00203-016-1269-6.
394. Beblo K, Douki T, Schmalz G, Rachel R, Wirth R, Huber H, Reitz G, Rettberg P. Survival of thermophilic and hyperthermophilic microorganisms after exposure to UV-C, ionizing radiation and desiccation. Arch Microbiol. 2011;193(11):797–809. https://doi.org/10.1007/s00203-011-0718-5.
395. Koschnitzki D, Moeller R, Leuko S, Przybyla B, Beblo-Vranesevic K, Wirth R, Huber H, Rachel R, Rettberg P. Questioning the radia-

tion limits of life: Ignicoccus hospitalis between replication and VBNC. Arch Microbiol. 2021;203(4):1299–308. https://doi.org/10.1007/s00203-020-02125-1.
396. Simonsen LC, Slaba TC, Guida P, Rusek A. NASA's first ground-based Galactic Cosmic Ray Simulator: enabling a new era in space radiobiology research. PLOS Biol. 2020;18(5):e3000669. https://doi.org/10.1371/journal.pbio.3000669.
397. ESA. Materials & Electrical Components Laboratory. ESA. 2021. Retrieved Dec 2021 from https://www.esa.int/Enabling_Support/Space_Engineering_Technology/Materials_Electrical_Components_Laboratory.
398. Takahashi A, Yamanouchi S, Takeuchi K, Takahashi S, Tashiro M, Hidema J, Higashitani A, Adachi T, Zhang S, Guirguis FNL, Yoshida Y, Nagamatsu A, Hada M, Takeuchi K, Takahashi T, Sekitomi Y. Combined environment simulator for low-dose-rate radiation and partial gravity of moon and Mars. Life (Basel). 2020;10(11):274. https://doi.org/10.3390/life10110274.
399. Durante M, Golubev A, Park W-Y, Trautmann C. Applied nuclear physics at the new high-energy particle accelerator facilities. Phys Rep. 2019;800:1–37. https://doi.org/10.1016/j.physrep.2019.01.004.
400. Michael W, Joel SB, Helle B-O, Ray FA, Paula CG, Eugene JE, Christina MF, Fitsum H, Christine LRB, Brad C, Matthew AC, Robert LU. Incidence of acute myeloid leukemia and hepatocellular carcinoma in mice irradiated with 1 GeV/nucleon ⁵⁶Fe ions. Radiat Res. 2009;172(2):213–9. https://doi.org/10.1667/RR1648.1.
401. Parihar VK, Allen BD, Caressi C, Kwok S, Chu E, Tran KK, Chmielewski NN, Giedzinski E, Acharya MM, Britten RA, Baulch JE, Limoli CL. Cosmic radiation exposure and persistent cognitive dysfunction. Sci Rep. 2016;6(1):34774. https://doi.org/10.1038/srep34774.
402. Reiser M. Theory and design of charged particle beams. John Wiley & Sons; 2008.
403. Rabbow E, Rettberg P, Barczyk S, Bohmeier M, Parpart A, Panitz C, Horneck G, von Heise-Rotenburg R, Hoppenbrouwers T, Willnecker R, Baglioni P, Demets R, Dettmann J, Reitz G. EXPOSE-E: an ESA astrobiology mission 1.5 years in space. Astrobiology. 2012;12(5):374–86. https://doi.org/10.1089/ast.2011.0760.
404. Haefer RA. Vacuum and cryotechniques in space research. Vacuum. 1972;22(8):303. https://doi.org/10.1016/0042-207x(72)93789-X.
405. Rabbow E, Parpart A, Reitz G. The planetary and space simulation facilities at DLR Cologne. Micrograv Sci Technol. 2016;28(3):215–29. https://doi.org/10.1007/s12217-015-9448-7.
406. Rabbow E, Rettberg P, Barczyk S, Bohmeier M, Parpart A, Panitz C, Horneck G, Burfeindt J, Molter F, Jaramillo E, Pereira C, Weiss P, Willnecker R, Demets R, Dettmann J, Reitz G. The astrobiological mission EXPOSE-R on board of the International Space Station. Int J Astrobiol. 2015;14(1):3–16. https://doi.org/10.1017/S1473550414000202.

Further Reading

Airbus Space Systems. University of Zurich and Airbus grow miniature human tissue on the International Space Station ISS. In: Airbus Newsroom. Aug 2021. https://www.airbus.com/en/newsroom.
Cekanaviciute E, et al. Central nervous system responses to simulated galactic cosmic rays. Int J Mol Sci. 2018;19(11):3669.
European Space Agency. 3D bioprinting for space. In: ESA media. Nov 2018. https://www.esa.int/ESA_Multimedia.
European Space Agency. Upside-down 3D-printed skin and bone, for humans to Mars. In: ESA enabling and support. Jul 2019. https://www.esa.int/Enabling_Support.
Furukawa S, et al. Space radiation biology for "Living in Space". Biomed Res Int. 2020;2020:4703286.
Gray T. A brief history of animals in space. In: NASA history archives. Aug 2004. https://history.nasa.gov/animals.html.
Hellweg CE, Berger T, Matthiä D, Baumstark-Khan C. Radiation in space: relevance and risk for human missions. Springer International Publishing; 2020.
Horneck G, et al. Space microbiology. Microbiol Mol Biol Rev. 2010;74(1):121–56.
Limoli C. Space brain: the adverse impact of deep space radiation exposure on the brain. In: Space physiology: to Mars and beyond, vol. 117. The Physiology Society; 2020.
Nelson GA. Space radiation: central nervous system risks. In: Young LR, Sutton JP, editors. Handbook of bioastronautics. Cham: Springer; 2021.
Senatore G, Mastroleo F, Leys N, Mauriello G. Effect of microgravity & space radiation on microbes. Fut Microbiol. 2018;13:831–47.
Sgobba T, Kanki B, Clervoy J-F, Sandal GM. Space safety and human performance. Butterworth-Heinemann; 2018.
Sims J. Why astronauts are printing organs in space. In: BBC Future. Jun 2021. https://www.bbc.com/future.
The Royal Museums Greenwich. What was the first animal sent into space? In: Royal Museums Greenwich Stories. 2022. https://www.rmg.co.uk/stories

Radioprotectors, Radiomitigators, and Radiosensitizers

11

Alegría Montoro, Elena Obrador, Dhruti Mistry, Giusi I. Forte, Valentina Bravatà, Luigi Minafra, Marco Calvaruso, Francesco P. Cammarata, Martin Falk, Giuseppe Schettino, Vidhula Ahire, Noami Daems, Tom Boterberg, Nicholas Dainiak, Pankaj Chaudhary, Sarah Baatout, and Kaushala Prasad Mishra

Learning Objectives

- To understand how radioprotectors, radiomitigators, and radiosensitizers work in increasing the effect of radiotherapy (RT) through enhanced apoptosis of cancer cells while simultaneously reducing or diminishing the effect on normal cells.
- To review the characteristics of an ideal radioprotector and to understand mechanisms by which natural or synthetic compounds can prevent or avoid the damage associated with low or high doses of ionizing radiation (IR).
- To learn how radiomitigators can reduce the damage caused by IR and contribute to the repair/regeneration of damaged tissues even when they are administered after exposure.
- To understand the mechanisms underlying cancer cell radioresistance and how radiosensitizers (natural or synthetic) are able to sensitize cancer cells.
- To learn about the radiosensitization phenomenon and the associated molecular mechanisms. The combined action of these molecules with radiation offers a new strategy for enhanced IR cytotoxicity in cancer cells together with reducing normal tissue toxicity.

A. Montoro (✉)
Radiological Protection Service, University and Polytechnic La Fe Hospital of Valencia, Valencia, Spain
e-mail: montoro_ale@gva.es

E. Obrador
Department of Physiology, Faculty of Medicine, University of Valencia, Valencia, Spain
e-mail: elena.obrador@uv.es

D. Mistry · N. Daems · S. Baatout
Institute of Nuclear Medical Applications, Belgian Nuclear Research Centre, SCK CEN, Mol, Belgium
e-mail: sarah.baatout@sckcen.be

G. I. Forte · V. Bravatà · L. Minafra · M. Calvaruso · F. P. Cammarata
Institute of Bioimaging and Molecular Physiology, National Research Council (IBFM-CNR), Cefalu, Italy

National Institute for Nuclear Physics, Laboratori Nazionali del Sud, INFN-LNS, Catania, Italy
e-mail: giusi.forte@ibfm.cnr.it; valentina.bravata@ibfm.cnr.it; luigi.minafra@ibfm.cnr.it; marco.calvaruso@ibfm.cnr.it; francesco.cammarata@ibfm.cnr.it

M. Falk
Department of Cell Biology and Radiobiology, Institute of Biophysics, Czech Academy of Sciences, Brno, Czech Republic
e-mail: falk@ibp.cz

G. Schettino
National Physical Laboratory (NPL), Teddington, United Kingdom
e-mail: giuseppe.schettino@npl.co.uk

V. Ahire
Chengdu Anticancer Bioscience, Ltd., J. Michael Bishop Institute of Cancer Research, Chengdu, China

T. Boterberg
Department of Radiation Oncology, Ghent University Hospital, Ghent, Belgium

Particle Therapy Interuniversity Center Leuven, Department of Radiation Oncology, University Hospitals Leuven, Leuven, Belgium
e-mail: tom.boterberg@ugent.be

N. Dainiak
Department of Therapeutic Radiology, Yale University School of Medicine, New Haven, CT, United States of America

P. Chaudhary
The Patrick G. Johnston Centre for Cancer Research, Queen's University Belfast, Belfast, Northern Ireland, United Kingdom
e-mail: p.chaudhary@qub.ac.uk

K. P. Mishra
Radiobiology Unit, Bhabha Atomic Research Center, Mumbai, Maharashtra, India

S. Baatout (ed.), *Radiobiology Textbook*, https://doi.org/10.1007/978-3-031-18810-7_11

By the end of this chapter, readers are expected to understand the importance of applying current knowledge in the development of new synthetic or natural radioprotectors and radiosensitizers and develop an understanding of their cellular and molecular mechanisms of action.

11.1 Introduction

Radiation protection aims to reduce unnecessary radiation exposure with the intention to minimize the harmful effects of radiation on human health. With increasing use of radiation technologies and radioisotopes in medicine and industry, the risk of radiological and nuclear accidents escalates, affecting human health. Nuclear power plants and industrial accidents pose a serious threat to public health. Emergency preparedness in an event of nuclear terrorism and nuclear warfare requires the use of existing radiomodifiers and public health measures such as sheltering in place and the use of personal protective equipment (PPE). New approaches are urgently needed for protecting the persons working in a radiation field, first responders, and general population in the form of safe, effective, and easily accessible radioprotective agents.

Cellular exposure to IR induces genomic instability or mutations predisposing to carcinogenesis and/or cell death. Upon exposure, radiation induces DNA damage, lipid peroxidation, oxidation of thiol groups located in the plasma membrane and membranes of the cellular organelles, DNA strand breaks, and base alterations in cells, tissues, and organs. These changes may trigger a series of cellular responses, including activation of DNA damage repair pathways, signal transduction responses, gene transcription, and immune and proinflammatory responses. Triggering these pathways helps to recover damaged cells or eliminate the dysfunctional cells. However, they may also result in the development of tissue toxicities. The radiation research program of the National Cancer Institute (NCI) has proposed the following pharmacological classification of agents with IR response modification properties according to the timing of administration (Fig. 11.1):

A radioprotective agent/drug prevents harmful effects of radiation exposure while a radiosensitizing agent makes tumor cells more susceptible to radiation, in order to maximize the effect of radiotherapy while having less effect on normal tissues. Radiomitigators can attenuate IR damages even when they are delivered at the same time or after radiation exposition. The use of radiation-effect modulators (radioprotectors, radiomitigators, and/or radiosensitizers) can mitigate side effects and increase the efficacy of RT in cancer patients (Fig. 11.2).

11.1.1 Radioprotectors

The extent of radiation damage to living cells and organisms depends on the type of radiation (alpha (α) particles, beta (β) particles, positrons, X-rays, gamma rays (γ-rays), UV, etc.). Attempts to protect against the damaging effects of radiation were made as early as 1949. Efforts are actively being continued to search for radioprotectors suitable to be used in specific scenarios of radiation exposure. Possible applications of radioprotectors are outlined in Fig. 11.3.

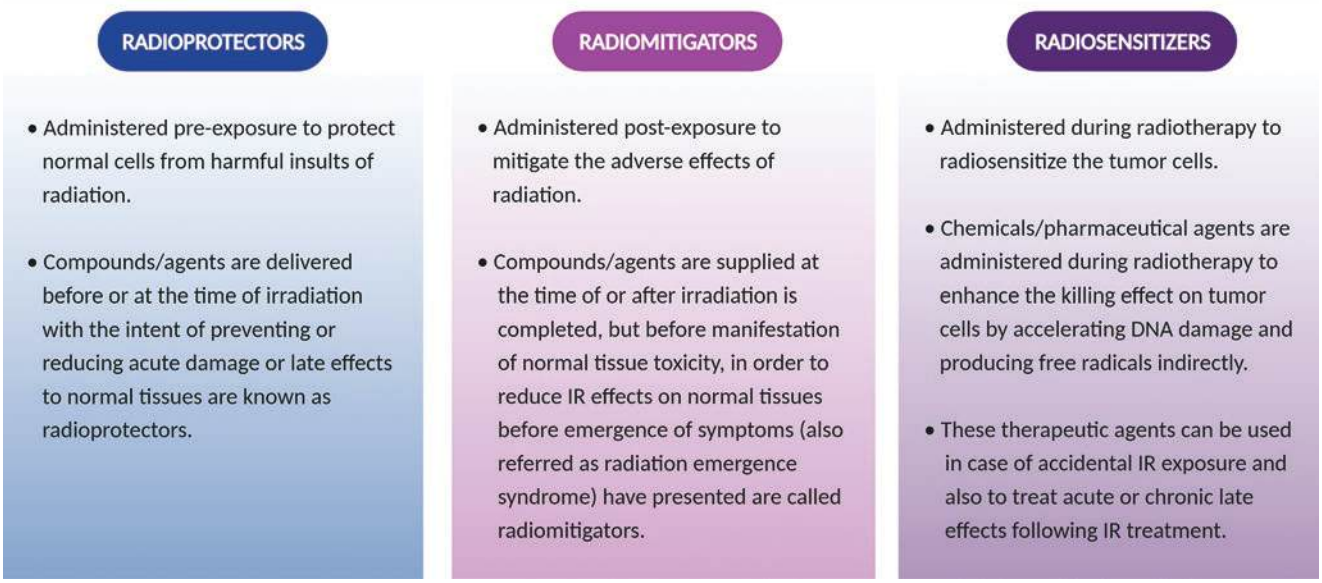

Fig. 11.1 Classification of radiomodifiers with their biological properties

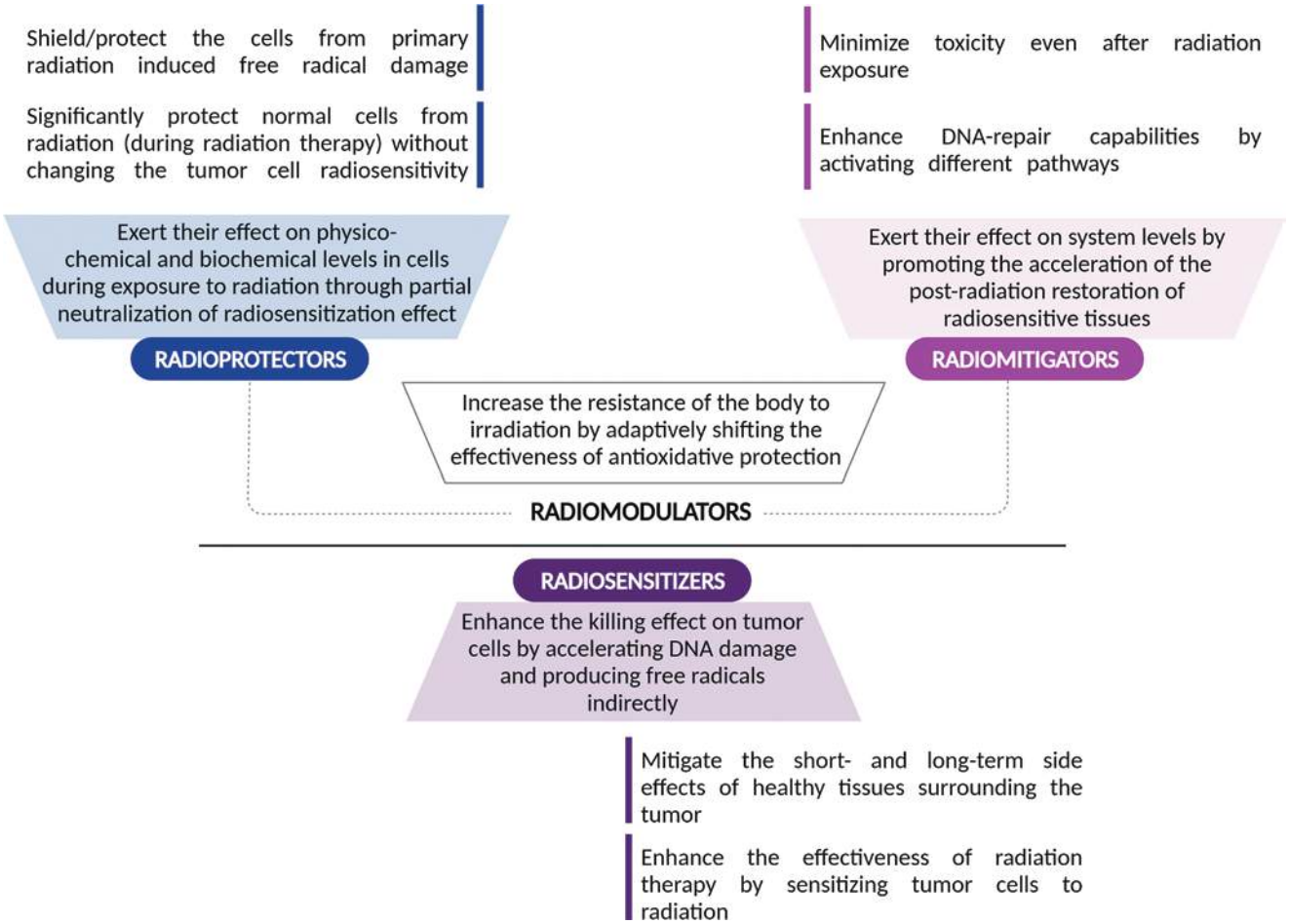

Fig. 11.2 The use of radioprotectors, radiomitigators, and radiosensitizers before, during, or after irradiation

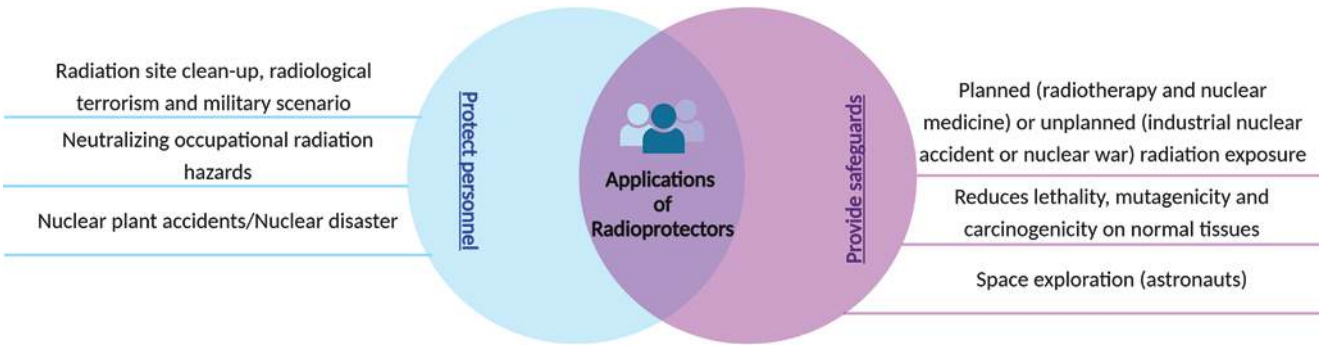

Fig. 11.3 Various applications of radioprotectors

Over the last few decades, many natural and synthetic compounds have been investigated for their potential as radioprotectors. Natural or synthetic radioprotectors are able to (i) reduce direct or indirect radiation damage, (ii) repair direct and indirect damage once they have occurred, and (iii) facilitate the repair of damaged cells or recover depleted cell populations [1].

It should be stressed that the majority of the compounds discussed below are currently not used in routine clinical practice and are still under preclinical or clinical evaluation.

Early development of synthetic radioprotectors focused on thiol compounds (e.g., amifostine) and their derivatives, which have been used in cancer patients, to prevent complications of RT. In addition, they have been thought to be use-

ful in accidental radiation exposure scenarios [2]. However, the practical applicability of the majority of these synthetic compounds remained limited owing to their limited administration routes, narrow administration window for efficacy, high toxicity at high doses or at recurrent usage, and cost factors as well. Besides thiol compounds, various compounds with different chemical structures are being investigated to develop an ideal radioprotector; there is still an urgent need to identify and develop novel, nontoxic, effective, and biocompatible compounds which can adequately protect normal tissues with no sparing of the tumor cells.

An interest has been emerging in developing potential new candidate drugs from natural plants and phytochemicals. Plant products could bridge the gaps in the search for an ideal radioprotector due to its abundance, typically low toxicity, and relatively low cost.

Box 11.1: Radioprotectors

- Radioprotectors (synthetic compounds, natural plant extracts, and phytochemical derivatives) are designed to lessen the effects of radiation-induced damage in healthy tissues.
- Radioprotective drugs are effective when administered prior to or during radiation exposure to reduce the radiation-induced injuries/toxicities.
- Safe, novel, nontoxic, and easily accessible radioprotective agents are needed to be developed for human health.

Characteristics of an Ideal Radioprotector

An ideal radioprotective agent should (a) be efficient in providing multifaceted protection, (b) prevent direct and indirect acute or chronic effects on normal tissue, (c) be easily and comfortably administered without toxicity, (d) cause no or minimal adverse effects on the test organism, (e) have a sufficiently long time window of effectiveness after administration and also have a sufficiently long shelf life, (f) have an acceptable stability profile (both of bulk active product and formulated compound), (g) be compatible with a wide range of other drugs, (h) not protect tumors from IR, and (i) be easily accessible and economical and should not require special handling and transportation temperatures (Box 11.1).

Underlying Mechanisms of Radioprotectors

Radioprotectors are diverse and elicit their action by various mechanisms (Fig. 11.4) such as:

- Scavenging free radicals (either by suppressing the formation or by detoxifying radiation-induced free radical species).
- Inducing hypoxia in cells in order to avoid synthesis of reactive oxygen species (ROS).
- Increasing levels of antioxidant defenses such as GSH (reduced glutathione) and/or antioxidant enzymes (superoxide dismutase (SOD), glutathione peroxidase (GPx), thioreductase, catalase (CAT), etc.).
- Triggering one or more cellular DNA damage repair pathways.
- Impeding cell division or inhibiting apoptotic cell death.

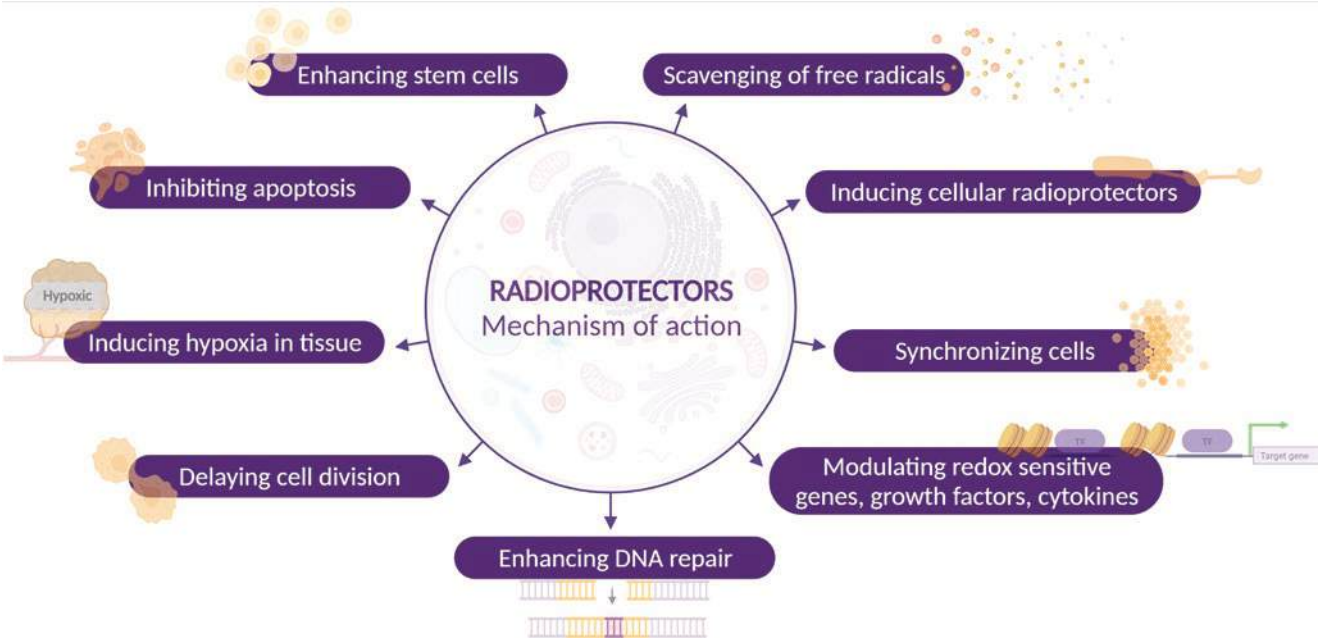

Fig. 11.4 Potential mechanism of action of radioprotectors against cell damage due to IR

- Modulating redox-sensitive genes.
- Modulating growth factors and cytokine production.
- Controlling inflammatory response.
- Chelating or decorporating radionuclides.
- Promoting tissue regeneration (intestinal or hematopoietic and immunostimulant compounds), gene therapy, and/or stem cell therapy. In most cases, these molecules are administered after exposure to radiation, which is why they should be also considered radiomitigators.

The most common mechanisms of radioprotection are the scavenging of free radicals, repair of DNA damages, inhibition of apoptosis or inflammation, increase antioxidant defenses, and modulation of growth factors, cytokines, and redox genes. Thus, the management of radiation exposure may require a holistic multimechanistic approach to achieve optimal radiation protection during RT of cancer patients and in cases of nuclear accidents or emergencies [3] (Box 11.2).

Box 11.2: Possible Mechanisms of Radioprotectors

- Radioprotectors can be screened for their effective emerging strategies, such as modulation of growth factors, cytokines, redox genes, and tissue renewal.
- The radioprotective agents are often antioxidants, which may suppress or scavenge the radiation-induced free radicals from the cell.
- These compounds are cofactors or can induce/stimulate antioxidants enzymes (like SOD, GPx, and) activity, which would likely lead to both prevent DNA damage and decrease in lipid peroxidation.
- They may have the ability to enhance DNA repair, reduce the postradiation inflammatory response, or even delay cellular division allowing more time for cells to repair the DNA damage or undergo cell death.

Therapeutic Principles to Develop Radioprotectors (Portrayed in Fig. 11.5)

Antioxidant Activity

Radioprotectors should prevent/suppress the formation of radiation-induced free radicals (most of them are produced during radiolysis with water), thereby inhibiting their reactions with biomolecules, reducing the incidence of DNA strand breaks, and preventing the occurrence of cellular malfunction (more detail in Chap. 2). Since free radicals are short-lived (approximately 10^{-10} s) and interact rapidly with biomolecules, it is necessary that radioprotectors are present in sufficient concentration in the cellular milieu, at the time of radiation exposure.

Molecules or compounds which increase the activity or expression of antioxidant enzymes are also considered radioprotectors. Many antioxidants have the potential to act as radioprotectors; however, not all antioxidants offer radioprotection, and this paradox may be explained by the relative activity of a compound when reacting with radiation-induced reactive species compared with those generated under H_2O_2 induced oxidative stress. Conventional antioxidants may not be able to scavenge this less reactive secondary species because either they do not accumulate in proximity to the secondary radicals or they may not have enough kinetic reactivity to scavenge them effectively. Thiols (e.g., amifostine), hydrophilic antioxidants (e.g., GSH), and newly developed cyclic nitroxides have adequate reactivity to effectively scavenge •OH and secondary radicals as well.

Molecule-Based Radioprotection or Molecular Radioprotection

Molecules or events that play a role late in signaling and IR-induced apoptotic pathways may act as potential targets for post-irradiation interventions.

- ATM/ATR is activated by DNA damage and DNA replication stress; however, they often work together to signal DNA damage and trigger apoptotic cell death by upregulating proapoptotic proteins such as apoptotic protease-activating factor-1 (Apaf-1), phorbol-12-myristate-13-acetate-induced protein 1 (Noxa), and Bcl2-associated X (Bax) after IR.
- Pifithrin (PFT)-μ (2-phenylethynesulfonamide) directly inhibits p53 binding to mitochondria as well as inactivates the antiapoptotic proteins Bcl-xL and Bcl-2 on the mitochondrial surface, thereby suppressing subsequent release of cytochrome c and apoptosis, whereas PFT-μ reversibly inhibits transcriptionally mediated p53-dependent apoptosis.
- Signal transducer and activator of transcription 3 (STAT3) can be activated by various growth factors and protects against IR damage. The protection mediated by STAT3 is attributed to its genomic actions as a transcription factor (such as upregulating genes that are antioxidative, antiapoptotic, and proangiogenic, but suppressing anti-inflammatory and antifibrotic genes) and other nongenomic roles targeting mitochondrial function and autophagy.
- Nuclear factor-erythroid 2-related factor 2 (Nrf2) is a well-characterized ubiquitous master transcription factor, whose activity is tightly controlled by cytoplasmic association along with its redox-sensitive transcriptional inhibitor Kelch-like ECH-associated protein 1 (Keap1). A well-known mechanism of activation of Nrf2 signaling protects cells against radiation-induced oxidative stress and also maintains cellular reduction-oxidation homeostasis. Upon oxidative stress, Nrf2 dissociates from Keap1

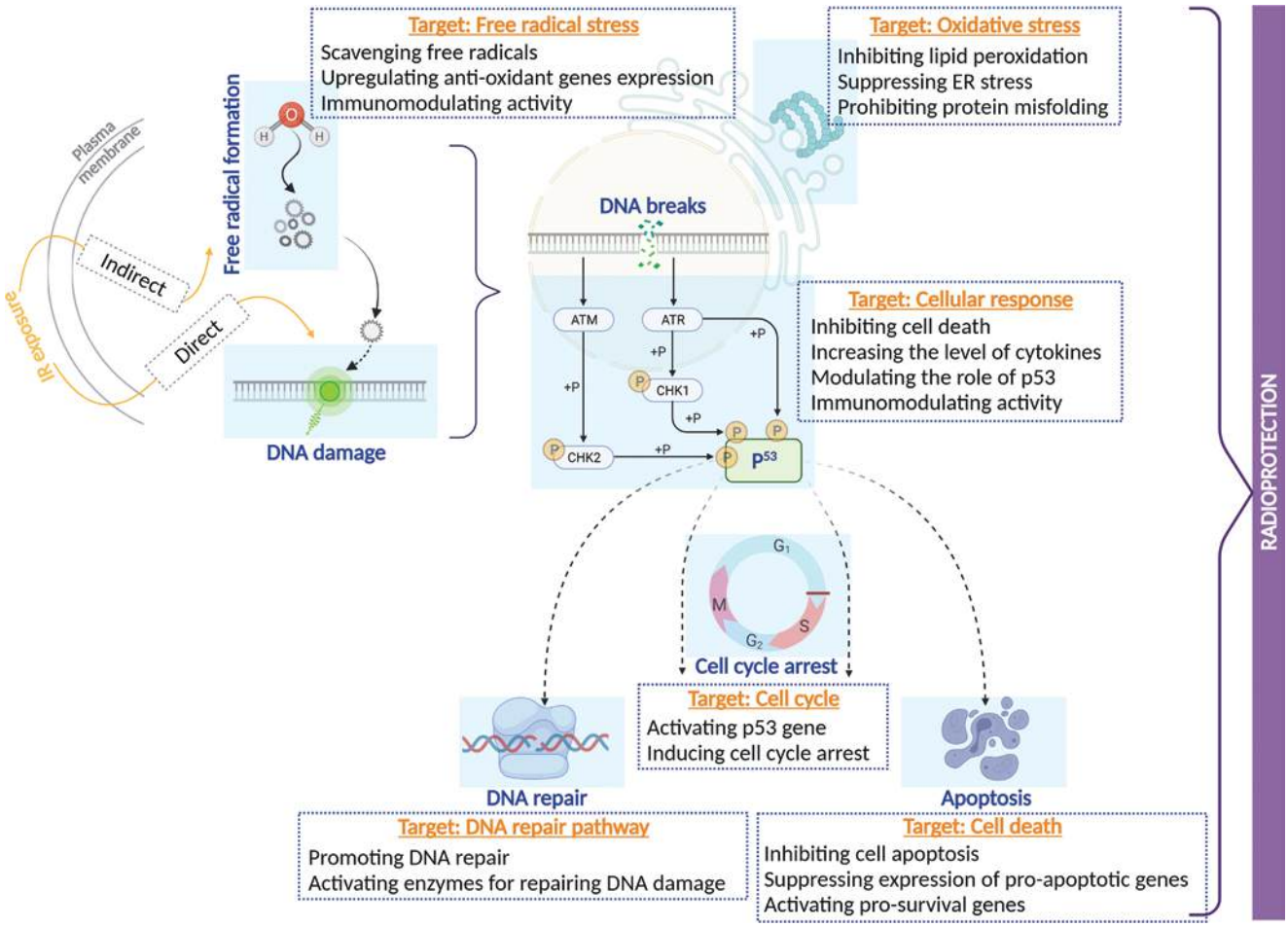

Fig. 11.5 General therapeutic approaches to develop novel radioprotective agents. IR, directly or indirectly, causes damage to macromolecules such as DNA, lipids, and proteins. As a result, oxidative stress is generated, which either triggers DNA damage repair or induces p53-mediated cell disorders, such as cell cycle arrest and cell apoptosis. When the damage exceeds the cell's ability to repair itself, the cell appears to follow the death program. The protective activities of potential radioprotectors should target such phases/mechanisms (described in blue dotted box) with the aim to shield the normal cells from harmful insults of irradiation. Inspired from/based on "General principles of developing novel radioprotective agents for nuclear emergency" from Radiation Medicine and Protection (Volume 1, Issue 3, Pages 120–126), by Du et al. 2020, Copyright Elsevier (2022)

and translocates into the nucleus to activate a series of antioxidant response elements, such as GPx, SOD, CAT, and heme oxygenase-1 (HO-1), increasing total cellular antioxidant capacity (TAC), accompanied by suppressed expression of inflammatory-related genes, avoiding oxidative stress and excessive inflammatory response, which is particularly important in radioprotection.

- Heat-shock proteins (HSPs), molecular chaperones, are induced in cells during stress conditions. Importantly, HSPs are cytoprotective and can mediate cell and tissue repair after IR-induced deleterious effects. Higher cytosolic levels of HSPs have been shown to induce radioprotective effects by interfering with apoptotic pathways.
- Peroxisome proliferator-activated receptor-γ (PPAR-γ), ligand-activated transcription factors, is a part of the nuclear hormone receptor family. It suppresses IR-induced survival signals and DNA damage responses and enhances IR-induced apoptosis signaling in human cells.

11.1.1.1 Thiol-Containing Molecules

In the search for an effective radioprotective agent, the Walter Reed Army Research Institute (USA) screened approximately 4500 compounds from the late 1950s. Cysteine was the first agent to confer radiation protection in mice after total body irradiation (TBI) in 1949. Later, various synthetic compounds with the aminothiol group were developed and proved to be highly effective in preclinical models [4]. Among them, the most effective was **WR-2721** or **amifostine**, a prodrug activated by alkaline phosphatase to an active sulfhydryl compound WR-1065, and at this moment, it is the only cytoprotective agent specifically approved by the FDA as a radioprotector (Fig. 11.6). The efficacy of amifostine is

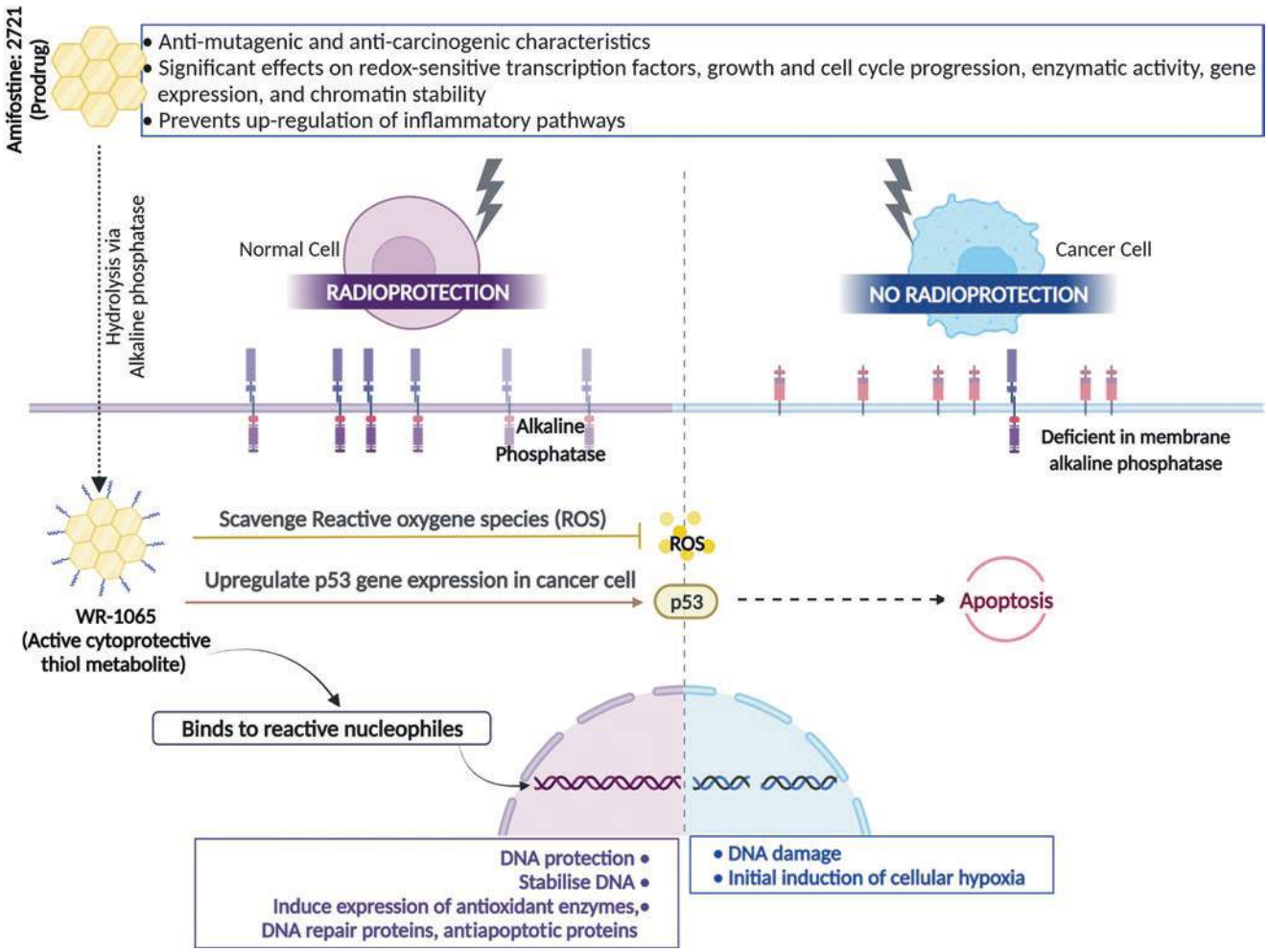

Fig. 11.6 Mechanisms of radioprotection by amifostine

attributed to the free radical scavenging, along with DNA protection and repair, all of which are coupled with the initial induction of cellular hypoxia. At the cellular level, amifostine has significant effects on cell cycle progression and has antimutagenic and anticarcinogenic properties [5]. In fact, amifostine indirectly induces the expression of proteins involved in DNA repair and triggers antiapoptotic pathways [6] and expression of antioxidant enzymes. Some authors have also proposed that it may enhance protective effects by increasing nuclear accumulation and inducing transcription factors related to p53 expression [7].

Moreover, WR-1065 accumulates more rapidly in normal tissues than in malignant cells, because the concentration of membrane-bound alkaline phosphatase tends to be higher on normal cells. Moreover, the lower vascular supply and the acidic environment of many tumors reduce the rate of dephosphorylation of WR-2721 and its uptake. It thus seems to be a really unique molecule that might potentiate radiotherapy (RT) efficacy in two opposite ways at the same time [8]. The US FDA has approved the use of amifostine in preventing/reducing xerostomia (dry mouth) in head and neck cancer patients undergoing RT [5]. It has also been assayed in clinical trials to reduce mucositis, dysphagia, dermatitis, and pneumonitis during radiotherapy of head and neck cancers [9].

However, like other radioprotective aminothiols, the safety profile of amifostine has considerable limitations. Although the side effects such as nausea, vomiting, and hypotension are not life threatening, they can further aggravate the gastrointestinal syndrome. As it will be exposed latter, amifostine has been assessed in combination with other FDA-approved drugs (growth factors, cytokines, vitamin E, metformin, etc) looking for additive or synergistic radioprotective effects to prevent Acute Radiation Syndrome (ARS). Nevertheless, in most of cases none of these novel strategies completely counteracts amifostine's toxic side effects at the doses needed to be efficacious as radioprotector [5].

Dimethyl sulfoxide (DMSO) has been shown to prevent the loss of proliferative lingual epithelial stem and progenitor cells upon irradiation by facilitating DNA DSB repair,

thereby protecting against radiation-induced mucositis without tumor protection. Given its high efficacy and low toxicity, DMSO appears to be a potential treatment option to prevent radiation-induced oral mucositis [10].

GSH (L-γ-glutamyl-L-cysteinyl-glycine) plays a crucial role in the detoxification of reactive oxygen species, H_2O_2, lipid peroxyl radicals, peroxynitrites through enzymatic reactions, such as those catalyzed by GPxs, glutathione-S-transferases (GSTs), formaldehyde dehydrogenase, maleylacetoacetate isomerase, and glyoxalase I [11]. GSH not only protects DNA and other biomolecules against oxidative stress and radioinduced damages, it is also essential to activate DNA repairment mechanisms, to activate proliferation and to avoid radio-induced cell death [12]. In fact, the selective depletion of GSH in cancer cells has been shown to have potent radiosensitizing effects on tumor cells [13].

***N*-acetylcysteine (NAC)** has a powerful antioxidant capacity, preserves GSH cellular levels, and prevents oxidative stress-induced apoptosis. NAC treatment (300 mg/kg, subcutaneous), starting either 4 h prior to or 2 h after radiation exposure reduced early deaths in abdominally irradiated (X-rays, 20 Gy) C57BL/6 mice, attenuating gastrointestinal syndrome [14]. More recently, preclinical studies have evidenced that NAC can prevent/reduce cardiac, ovarian, renal, and testicular radiation-induced toxicity in rats. Nevertheless, NAC and GSH cannot be used as a radioprotector in cancer patients because they also enhance antioxidant defenses in cancer cells and may increase their metastatic potential [12].

Treatment with **erdosteine** (a homocysteine derivative) before γ-radiation exposure ameliorated nephrotoxicity and altered kidney function in rats. It is a potent scavenger of free radicals, increases GPx and CAT activity, and reduces oxidized glutathione levels displaying almost normal concentrations with respect to the irradiated group. Moreover, IL-1, IL-6, and TNF-α circulating levels were also significantly improved thus erdosteine provide substantial protection against radiation-induced inflammatory damage as evidenced in the biochemical and histopathological samples [15].

Phosphorothioates and other aminothiols are usually administered shortly before irradiation. They have been hypothesized to act as radioprotectors by one or a combination of the following effects: scavenging radiation-induced free radicals before their reaction with biomolecules; inducing hypoxia; scavenging metals; repairing DNA damage through hydrogen donation to carbon-centered radicals; and stabilizing genome. Moreover, high doses of phosphorothioates administered to mice before radiation have demonstrated anticarcinogenic effects [4]. However, as it happens with other more powerful thiolic radioprotectors (such as amifotine), its use is limited due to undesirable side effects.

11.1.2 Cyclic Nitroxides (NRs)

NRs, like Tempol, JP4–039, XJB-5-131, TK649.030, or JRS527.084, are stable free radicals containing a nitroxyl group (-$NO^{\cdot}$) with an unpaired electron. The action of nitroxides to metabolize ROS is ascribed primarily to cyclic one- or two-electron transfer among three oxidation states: the oxoammonium cation, the nitroxide, and the hydroxylamine. Nitroxides undergo a very rapid, one-electron reaction to the corresponding hydroxylamine, which has antioxidant activity. In addition to their ability to neutralize free radicals, NR can easily diffuse through the cell membranes (and have SOD-like activity) (Fig. 11.7), prevent Fenton and Haber-Weiss reactions by oxidation of transition metal ions to a higher oxidation state, confer catalase-like activity on heme proteins, and inhibit lipid peroxidation. NRs are able to mitigate TBI-induced hematopoietic syndrome, when are administered before or as late as 72 h after radiation exposition [16].

Gramicidin S-derived nitroxide (JP4–039) is an effective TBI mitigator when is delivered intravenously up to 72 h after exposure. JP4–039 treatment ameliorated head and neck radiation-induced mucositis and distant marrow suppression in mice [17]. In a comparative study with other four nitroxides, JP4-039 demonstrated the best median survival after radiation exposition [18]. The potential of this type of molecules as radioprotectors and/or mitigators has raised the interest of researchers, and nitroxidic structures has evidenced radioprotective activity. That is the case of nitronyl-nitroxide radical spin-labeled resveratrol [19].

11.1.3 Antimicrobials

Primary experiments performed in the 1960s reported that antibiotic treatment and a single transfusion of allogeneic platelets significantly reduced mortality among monkeys exposed to TBI X-irradiation. Oral administration of streptomycin, kanamycin, neomycin, or gentamicin with drinking water (4 mg/mL) for 2 weeks before supralethal TBI (28.4 Gy) prolonged mean survival in mice (8.2–8.9 days vs. 6.9 for controls) [20]. The efficacy of antibiotics and other antimicrobials (antifungal and antiviral agents) is best explained as a countermeasure for radiation-induced neutropenia and immunosuppression.

Tetracycline and ciprofloxacin protected human lymphoblastoid cells, reducing radiation-induced DNA double-strand breaks (DSB) by 33% and 21%, respectively. Their radioprotective efficacy was attributed to the activation of the Tip60 histone acetyltransferase and altered chromatin structure [21]. Tetracycline hydrochloride is a free radical scavenger, protects DNA, and increases survival of C57BL/6 mice by 20% upon a lethal radiation dose of 9 Gy [22].

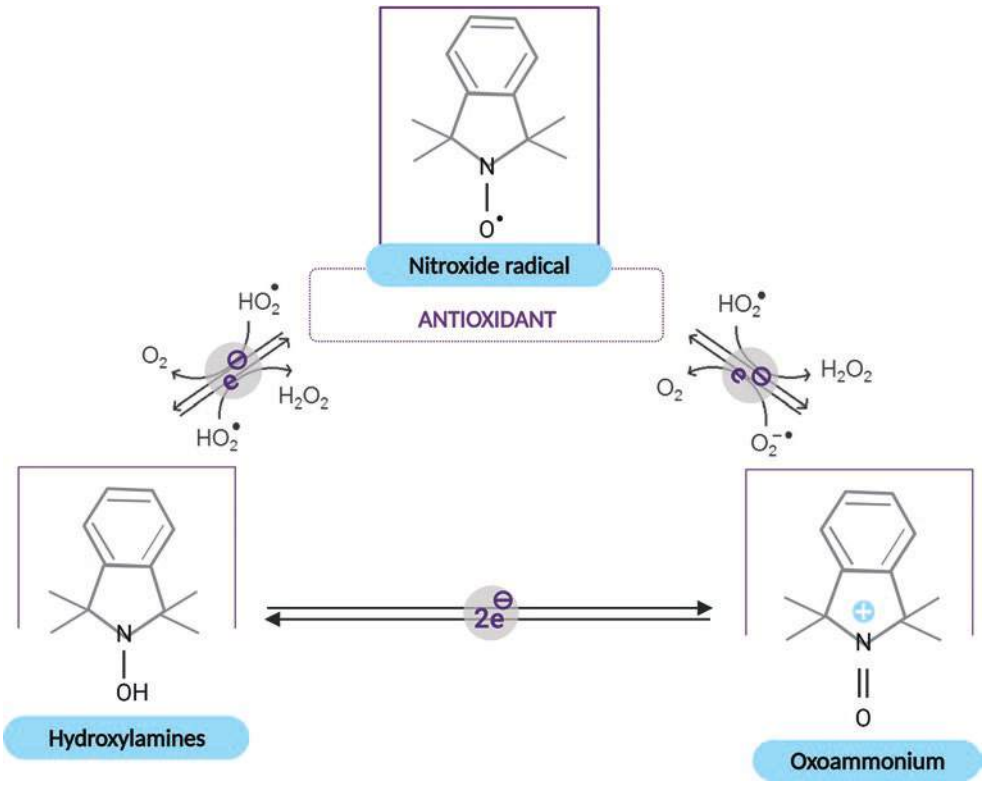

Fig. 11.7 Radioprotective properties of cyclic nitroxides include scavenger free radical capacity and SOD-like activity. Adapted from "Nitroxides as Antioxidants and Anticancer Drugs," by Lewandowski M. and Gwozdzinski K. 2017, Licensed under CC BY 4.0

Mucositis is the most common side effect of RT for head and neck cancers. Preventive measures used in clinical medicine include good oral hygiene, dental and periodontal treatment, avoidance of tobacco products and alcohol, and frequent oral rinsing with a bland mouthwash such as povidone-iodine. Nonabsorbable antibiotic lozenges and/or antifungal topical agents (i.e., bicarbonates and amphotericin B) are also recommended [23].

Minocycline prevented radiation-induced apoptosis and promoted radiation-induced autophagy in primary neurons in vitro. Minocycline also increases the counts of splenic macrophages, granulocytes, natural killer cells, and lymphocytes, and accelerates neutrophil recovery in C57BL/6 mice exposed to 1-3 Gy ^{60}Co γ-rays. The mechanisms involved in this radioprotective effect were the suppression of cytokines that could prevent hematopoiesis (e.g. macrophage inflammatory protein-1α, TNF-α and INF-γ) and the increased production of IL-1α and β, granulocyte-macrophage colony-stimulating factor (GM-CSF) and granulocyte colony-stimulating factor (G-CSF) [24].

Furazolidone (FZD) is an antimicrobial agent effective on both Gram+ and Gram− bacteria by interfering with bacterial oxidoreductase activity. In vitro, FZD treatment reduced unstable chromosomal aberrations (CAs) (such as acentric and dicentric chromosomes (DC)), chromosome breaks, and radiosensitivity of intestinal epithelial cells. Ma et al. [25] showed that FZD treatment significantly improved the survival of lethal dose-irradiated mice, decreased the number of micronuclei (MN), increased the number of leukocytes and immune organ indices, and reversed the apoptosis and autophagy in the small intestine, thus restoring intestinal integrity. Their experiments showed that irradiation resulted in villous shortening and crypt dilation accompanied by epithelial atrophy or slough, and even marked edema and inflammatory cell infiltration, and how FZD significantly induced damage recovery. FZD is a clinically used antibiotic with few side effects and has been proposed as an efficacious medical countermeasure (MCM). However, detailed radiation protection activity and clinical applications need to be further studied, because radioprotective efficacy of antibiotics has not yet been tested in clinical trials.

11.1.4 Phytochemicals

11.1.4.1 Plant Extracts

Considerable information from in vivo, ex vivo, *and/or* in vitro studies suggests that crude extracts, fractionated extracts, isolated phytoconstituents, and plant polysaccharides from various plants such as *Alstonia scholaris*, *Centella asiatica*, *Hippophae rhamnoides*, *Ginkgo biloba*, *Ocimum sanctum*, *Panax ginseng*, *Podophyllum hexandrum*, *Amaranthus paniculatus*, *Emblica officinalis*, *Phyllanthus amarus*, *Piper longum*, *Tinospora cordifolia*, *Mentha arven-*

sis, *Mentha piperita*, *Syzygium cumini*, *Zingiber officinale*, *Ageratum conyzoides*, *Aegle marmelos*, and *Aphanamixis polystachya* protect against radiation-induced lethality, lipid peroxidation, and DNA damage [26]. From these extracts, polyphenolic and nonpolyphenolic active principles and a range of secondary metabolites (e.g., carotenoids, alkaloids, sulfur compounds), already known for their anticancer properties, have also demonstrated radioprotective potential. Although many have been tested for brevity, this chapter focuses on those with the most promising results in vivo.

11.1.4.2 Polyphenolic Phytochemicals

Over the last decades, plant-derived polyphenols have been screened for their potential ability to confer radioprotection. The free radical scavenger potential and antioxidant activity of polyphenols depends, in part, on their ability to delocalize electron distribution, resulting in a more stable phenoxy group. Moreover, intercalation in DNA double helices induces stabilization and condensation of DNA structures making them less susceptible to free radicals' attack, reducing genotoxic damage induced by IR [27]. They are capable of trapping and neutralizing lipoperoxide radicals and can chelate metal ions (i.e., iron and copper), which play an important role in the initiation of oxidative stress reactions [28, 29]. Polyphenols radioprotective efficacy is mainly attributed to its (Fig. 11.8) antioxidant and antiinflammatory properties, to their capacity to detoxify free radicals, eliciting DNA repair pathways, stimulating the recovery of hematopoietic and immune functions [28, 29].

In addition to the biochemical scavenger theory, there is also evidence of another potential mechanism by which polyphenols activate Nrf2, exhibiting cellular protection against excessive ROS production, oxidative stress, and inflammation as well. Since the chemical features of these natural organic compounds are analogous to phenolic substances, their antioxidant and antiradical/scavenging radical (such as H_2O_2, 2,2-diphenyl-1-picrylhydrazyl) properties may be correlated positively with the number of hydroxyl groups bonded to the aromatic ring. They can exert their protection against environmental stimuli with the aid of remarkable antioxidant power by balancing the organic oxidoreductase enzyme system, regulating antioxidant-responsive signaling pathways, and restoring mitochondrial function.

Although topically administered polyphenols may provide strong antioxidant protection, various challenges still exist and are onerous as well: (1) improving the bioavailability of polyphenols more effectively in order to promote their effectiveness is challenging; (2) if the polyphenols are extracted as the medicine or as health supplements, attention should be paid to the activity loss and degradation of polyphenols during the extraction process; (3) the effects cannot be generalized for all kinds of polyphenols, because each polyphenol has its own unique features; and (4) polyphenols have limited water solubility, and so it is important for polyphenols to be involved in rapid metabolism and also prove its chemical stability and solubility under in vivo conditions. To overcome this limitation, Obrador et al. [30] suggested a few feasible options: structural modifications of natural molecules (e.g., in the form of salts) to increase their hydrosolubility for intravenous administration or oral formulations to increase their bioavailability (e.g., cocrystals, nanoparti-

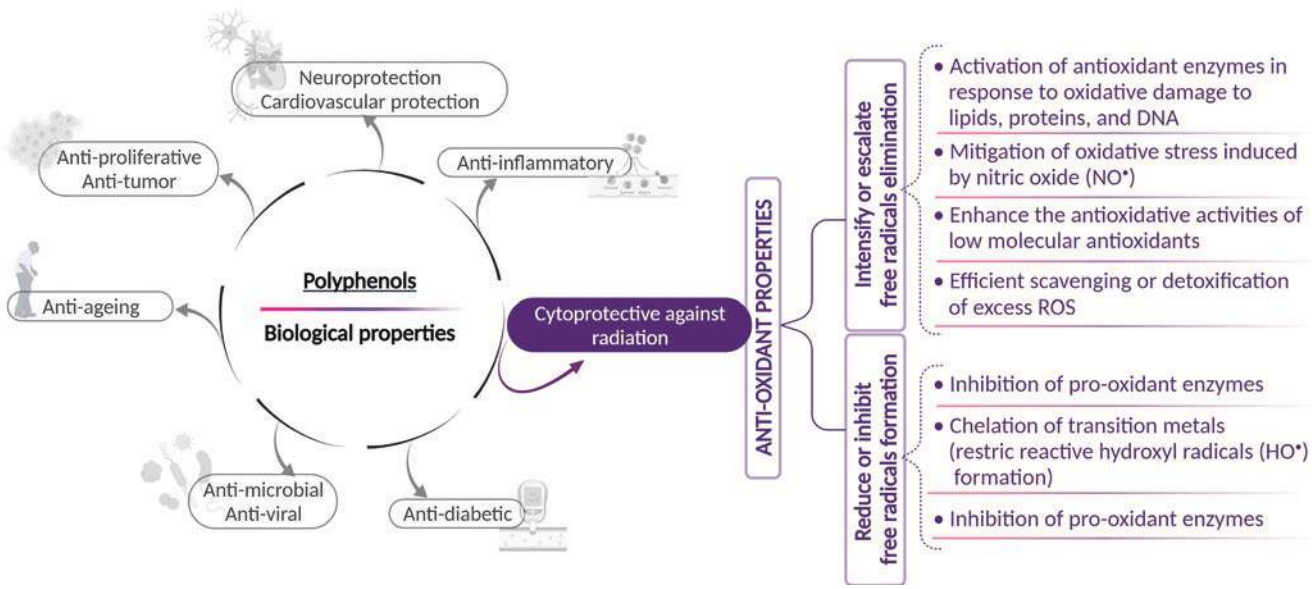

Fig. 11.8 Radioprotective and biological properties of polyphenols

cles, nanozymes). The promising phytochemical, pharmacodynamic, and toxicological research into the properties of polyphenols may serve as potential candidates for radioprotection in the near future.

Apigenin exhibits anticancer properties associated with its prooxidant activity, inhibiting tumor growth and inducing cell cycle arrest and apoptosis. Apigenin pretreatment displayed efficacy for radioprotection in TBI Swiss albino mice by reducing cytogenetic alterations and biochemical and hematological changes [31]. Further, when apigenin was administered intraperitoneally at a dose level equal to 15 mg/kg body, it was found to ameliorate radiation-induced gastrointestinal (GI) damages and restore intestinal crypt-villus architecture [32]. These attributes could be due to its ability to activate the endogenous antioxidants, suppress lipid peroxidation, and modulate inflammatory (NF-κB) and apoptotic signaling mediator/marker (p53, p21, Bax, caspase-3, caspase-9) expression. The in vivo efficacy of apigenin was also evidenced when it was intraperitoneally administered to mice 3 h after receiving γ-rays [33]. A significant reductions in the level of 8-hydroxy-2-deoxyguanosine (8-OH-dG), suppressed expression of NF-κB and NF-κB-regulated proinflammatory cytokines were observed, thus showing the radioprotective potential of apigenin.

Curcumin, a yellow pigment of turmeric, is naturally found in the rhizome of *Curcuma longa* and other *Curcuma* spp. It is an active immunomodulatory agent which has many scientifically proven health benefits, such as the potential to improve symptoms of anxiety, depression, arthritis, and heart health and prevent Alzheimer's, cancer, and oxidative and inflammatory conditions. Administration of curcumin in patients undergoing RT has demonstrated a dual action: radioprotection to normal cells through its ability to reduce oxidative stress, scavenge free radicals, inhibit transcription of genes related to oxidative stress, and suppress inflammatory response, as well as radiosensitization in tumor cells [34]. Curcumin, administered before or after a single 50 Gy radiation dose, showed protective effect on radiation-induced cutaneous damage in mice by significantly decreasing mRNA expression of early-responding cytokines (IL-1, IL-6, IL-18, TNF-α, and lymphotoxin-beta) and fibrogenic cytokines [35]. Oral administration of curcumin in mouse before irradiation resulted in a significant rise in activities of GPx and SOD enzymes while declining lipid peroxidation significantly, which indicates increased antioxidant status in mouse exposed to different doses of fractionated γ-radiation [36]. These protective qualities of curcumin may be due to free radical scavenging and upregulation of Nrf2 expression.

Ellagic acid (EA), a strong natural antioxidant, has a major protecting role against different diseases associated with oxidative stress and inflammation. It also exerts antiangiogenesis effects via down regulation of vascular endothelial growth factor-2 (VEGF-2) signaling pathways in cancer. The amount and duration of EA used play a significant role in suppressing in vivo and in vitro oxidative stresses. In vitro studies [37] displayed high DPPH radical scavenging and lipid peroxidation inhibition activities of EA. It triggered the actions of antioxidant enzymes such as SOD, CAT, and GPx in V79–4 cells; reduced cell proliferation; and induced apoptosis in human osteogenic sarcoma cells as evidenced by chromosomal DNA degradation and apoptotic body appearance. When the human breast cancer cells (MCF-7) were treated with EA (10μM) and exposed with γ-radiation, the rate of apoptotic cell death in sub-G_1 phase of cell cycle was high due to decreased mitochondrial membrane potential, upregulated proapoptotic Bax, and downregulated Bcl2, suggesting EA's role in tumor toxicity to improve cancer radiotherapy [38].

Epicatechin (EC) is a common flavanol found in tea, cocoa, dark chocolates, and red wine. It has the ability to cross the blood-brain barrier and activate brain-derived neurotrophic factor pathways, suggesting its neuroprotective effects. In addition to general antioxidant activities, it aids with the modulation of metabolism of nitric oxide (NO) and other reactive nitrogen species (RNS). To evaluate the radioprotective effects of EC, Swiss albino mice were administered with EC for three consecutive days before exposing them to 5 Gy ^{60}Co γ-irradiation [39]. EC pretreatment ameliorated γ-radiation-mediated alterations in mice, protected the liver and testis from radiation-induced oxidative stress, prevented systemic and cellular stress, and developed inflammation. It may possibly be due to the influence on the endogenous antioxidant defenses system after TBI in mice [40]. Another study [41] intended to investigate the effectiveness of EC in scavenging mitochondrial ROS and mitigating mitochondrial damage as radiation countermeasure agents by using human and mouse cells. It was observed that preradiation and postradiation treatments with EC mitigated ROS-mediated mitochondrial damage and IR-induced oxidative stress responses in mice. Also, oral administration of EC significantly enhanced the recovery of mouse hematopoietic cells from radiation injury in vivo, suggesting EC as a potentially viable countermeasure agent which is immediately effective against accidental IR exposure.

Epigallocatechin-3-gallate (EGCG) is a natural polyphenolic antioxidant found in a number of plants, predominantly in green tea and black tea and also in small amounts in fruits and nuts. It gets a lot of attention for its potential positive impact on health. It aids weight loss, reduces inflammation, and helps prevent certain chronic conditions, including heart disease, diabetes, and cancers. Pretreatment with

EGCG significantly enhanced the viability of human skin cells which were irradiated with X-rays and decreased radiation-induced apoptosis [42]. It was found that EGCG suppressed IR-induced damage to mitochondria via upregulation of SOD2 and induced expression of cytoprotective molecule HO-1 in a dose-dependent manner via transcriptional activation. The therapeutic effects and mechanism of EGCG on radiation-induced intestinal injury (RIII) have not yet been determined; however, Xie et al. recently [43] investigated it both in vitro and in vivo and revealed that treatment with EGCG not only prolonged the survival time of lethally irradiated mice, but also mitigated RIII. Besides, it significantly augmented proliferation and survival of intestinal stem cells and their progeny cells in irradiated mice. Their findings demonstrated that EGCG protected against RIII by reducing the level of IR-induced ROS and DNA damage, inhibiting apoptosis and ferroptosis through activating transcription factor Nrf2-mediated signaling pathway and its downstream targets comprising antioxidant proteins Slc7A11, HO-1, and GPx4, suggesting that EGCG could be a promising medical countermeasure for the alleviation of RIII.

Genistein (GEN), an isoflavonoid compound, is commonly found in soybeans and its products. Mechanistic insights reveal its potential beneficial effects on human diseases such as cancer, by inducing apoptosis and cell cycle arrest. GEN has antiangiogenic, antimetastatic, and anti-inflammatory effects. Besides, various studies of GEN have revealed its radioprotective properties by protecting against radiation-induced DNA damage, scavenging free radicals, and altering cell cycle effects. Davis et al. [44] revealed GEN-induced radioprotection against hematopoietic- acute radiation syndrome (H-ARS) by altering the cell cycle of hematopoietic stem and progenitor cells in a murine model. The extracted GEN displayed protection against IR-induced GI injury and bone marrow toxicity by upregulating the Rassf1a and Ercc1 genes to effectively attenuate DNA damage in a TBI mouse model [45]. Moreover, Song et al. [46] showed that low concentration of GEN (1.5μM) lessened radiation-induced injuries by way of inhibiting apoptosis, alleviating chromosomal and DNA damage, downregulating GRP78, and upregulating HERP, HUS1, and hHR23A. In contrast, high concentration of GEN (20μM) demonstrated radiosensitizing characteristics in cancer cells. The role of genistein as a radiosensitizer will be further discussed in Sect. 11.4.

Naringin, a predominant flavone glycoside, is present in citrus fruits. Manna et al. [47] demonstrated that pretreatment with naringin significantly prevented γ-radiation (6Gy)-induced intracellular ROS-mediated oxidative DNA damage; inhibited radiation-induced G_1/S-phase cell cycle arrest by modulating p53-dependent p21/WAF1, cyclin E, and cyclin dependent kinase 2 (CDK2) activation; and reversed the inflammation through downregulating nuclear factor kappa B (NF-kB) signaling pathways and balancing the expression of C-reactive protein, monocyte chemoattractant protein-1 (MCP-1), and iNOS2 at sites of inflammation in murine splenocytes. Besides, naringin pretreatment could effectively deter UVB-mediated DNA damage, alter apoptotic marker expression (Bax, BCl-2, caspase-9, and caspase-3), and potentially modulate NER gene (XPC, TFIIH, XPE, ERCC1, and GAPDH) expression, thereby augmenting DNA repair [48].

Naringenin is present in peppermint and citrus fruits such as oranges, grapefruit, and tangerines. It is endowed with biological effects on human health, which includes a great ability to modulate signaling pathways; efficient impairing of plasma lipid and lipoprotein accumulation; and antiatherogenic and anti-inflammatory effects. To evaluate radioprotective effects of naringenin in vivo, Swiss albino mice were orally administered 50 mg/kg body weight of naringenin prior to radiation exposure [49], and it protected mice against radiation-induced DNA, chromosomal, and membrane damage. Naringenin pretreatment increased antioxidant status and survival chances, inhibited NF-kB pathway, and downregulated radiation-induced apoptotic proteins (p53, Bax, and Bcl-2) in normal cells resulting in radioprotection at the cellular, tissue, and organism levels.

Resveratrol (RV), a natural polyphenol, is produced in several plants in response to stress, injury, and UV radiation. It is present in fruits such as grapes, strawberries, and red wine. It is known for its analgesic, antiviral, cardioprotective, neuroprotective, and antiaging actions. Different doses of RV were administered intraperitoneally to mice prior to total-body γ-irradiation (2 Gy), and it was observed that RV significantly reduced lymphocyte damage in mice caused by γ-radiation due to its ability to scavenge free radicals, restore the levels of intracellular antioxidants (GPx, SOD, CAT activity), and cause cell cycle arrest [50]. RV is also known to have a significant effect in stabilizing p53 and altering proapoptotic and antiapoptotic protein concentration [51]. Zhang et al. [52] treated with RV IR-exposed C57BL/6N mice. RV reduced radioinduced-intestinal injury (upregulating Sirt1 and acetylating p53 expression), improved intestinal morphology, decreased apoptosis of crypt cells, maintained cell regeneration, and ameliorated SOD2 expression, evidencing its radioprotective potential. The role of RV together with pterostilbene as a radiosensitizer will be further discussed in Sect. 11.4.

Pterostilbene (PT), is another stilbenoid compound, structurally similar to RV, present in blueberries, grapes, and other similar fruits. It is an active phytonutrient with many biomedical applications in cancer treatment, insulin sensitivity, cardiovascular diseases, aging, and cognition. Moreover, it has a greater bioavailability, efficacy and lower toxicity than RV [53]. Sirerol et al. [54] evidenced that pterostilbene

reduced chronic UVB irradiation-induced skin damage and carcinogenesis in hairless mice through maintaining antioxidant defenses, including GSH, CAT, SOD, and GPx. Recently, a combination of natural polyphenols (PT and silibinin) with a NAD^+ precursor and a TLR2/6 ligand was shown to protect mice against lethal γ-radiation, increasing long term survival up to 90% of the treated mice [55].

11.1.4.3 Nonpolyphenolic Phytochemicals

Caffeic acid/caffeic acid phenethyl ester (CAPE) is found in coffee, tea, chocolate, and colas. It has numerous pharmacological and physiological effects, including cardiovascular, respiratory, renal, and smooth muscle effects, as well as effects on mood, memory, alertness, and physical and cognitive performance. It is essentially regarded as a radiosensitizer by virtue of its inhibition of DNA repair after irradiation. The radioprotective properties of CAPE have also been shown in the bone marrow chromosomes of mice exposed to TBI (1.5 Gy ^{60}Co γ-rays), regardless of its time of administration [56]. Caffeic acid, a known dietary antioxidant, could be used as a supplemental drug which has a dual effect: ameliorating hematopoietic stem cell (HSC) senescence-accompanied long-term BM injury in single (sublethal dose of 5 Gy) TBI and stimulating apoptotic cell death of colon cancer cells in mice [57]. Khayyo et al. [58] intraperitoneally administered CAPE prior to total-head γ-irradiation and observed that the oxidant stress parameters (total oxidant status, oxidative stress index, and lipid hydroperoxide) were significantly reduced, whereas antioxidant parameters (activity of paraoxonase, arylesterase, total GSH levels) were increased in the rat brain tissue, signifying the protective role of CAPE as an important antioxidant against ROS accumulation induced by total-head irradiation. The role of CAPE as a radiosensitizer will be further discussed in Sect. 11.4.1.7.

Sesamol is found in sesame seeds and oil. It has many biological activities and health-promoting benefits such as inducing growth arrest and apoptosis in cancer and cardiovascular cells and enhancing vascular fibrinolytic capacity, antioxidant activity, chemoprevention, antimutagenic, and antihepatotoxic activities. Naturally occurring or synthetic substances of sesamol counteract the damaging effects of oxidation by inhibiting or retarding oxidation reactions. Also, it has the potential to scavenge free radicals and therefore reduces the radiation-induced cytogenetic damage in cells. Kumar et al. [59] investigated its radioprotective potential against radiation-induced genotoxicity in hematopoietic bone marrow of whole-body γ-irradiated (2Gy) mice. Preadministration of 20 mg/kg body weight sesamol reduced the frequency of radiation-induced MN, CAs, and comets (% damaged DNA streak in tail), suggesting its major role in direct scavenging of free radicals to protect bone marrow, spleen, and lymphocytes from radiation-induced cytogenetic damages and genotoxicity. Besides, intraperitoneal pretreatment of sesamol offered protection to hematopoietic and GI systems against γ-radiation-induced injury in C57BL/6 male mice by inhibiting lipid peroxidation; translocating gut bacteria to spleen, liver, and kidney; enhancing regeneration of crypt cells in GI; reducing the expression of p53 and Bax apoptotic proteins in the bone marrow, spleen, and GI; and alleviating the total antioxidant capacity in spleen and GI tissue [60]. Recently, Majdaeen et al. [61] concluded that regular oral consumption of sesamol extract is more effective than consuming it once before irradiation.

3,3′-Diindolylmethane (DIM), a small-molecule compound and a major bioactive metabolite, is formed by acid hydrolysis of indole-3-carbinol (one of the best characterized components in Cruciferae). It can inhibit invasion, angiogenesis, and proliferation and induce apoptosis in tumor cells by modulating signaling pathways involving AKT, NF-kB, and FOXO3 [62]. Chen et al. [63] investigated the radioprotective effects of DIM in normal tissues using a mouse model approach. It was indicated that treatment with DIM increased the expression of some stress-responsive genes without causing DNA damage, delayed radiation-induced cell cycle arrest, and apoptosis. Fan et al. [64] reported that administration of DIM in a multidose schedule protected rodents against lethal doses of TBI up to 13 Gy. Transcriptomic profiling showed that DIM's mechanism of radioprotection involved regulation of responses to DNA damage and oxidative stress by inducing ataxia-telangiectasia mutated (ATM)-driven DDR-like response, enhancing radiation-induced ATM signaling and NF-κB activation, suggesting its potential role as a MCM in protecting or mitigating adverse effects of RT.

11.1.5 Vitamins

With the understanding that free radicals perpetuate a significant amount of the damage caused by IR, vitamins with antioxidant potential (A, C, and E and its derivatives) have been assayed as radioprotectors (Fig. 11.9). Vitamin A and β-carotenes (lutein, lycopene, phytofluene, phytoene, and others) reduced mortality and morbidity in mice exposed to partial or TBI. Dietary vitamin A offered protection in mice subjected to localized radiation exposure focused on the intestine (13 Gy, TBI) and the esophagus (29 Gy) [30]. A single dose of vitamin A injected intraperitoneally 2 h before 2 Gy of γ-radiation exposition, significantly reduced the number of MN in the bone marrow and the genetic damages, due to its capacity to trap free radicals [65]. Carotenoids such as crocin and crocetin (isolated from the dietary herb saffron) have antioxidant, anti-inflammatory, and antiapoptotic effects. In mice bearing pancreatic tumors, crocin significantly reduced tumor burden, radiation-induced toxicity, and hepatic damage and preserved liver morphology [66] while

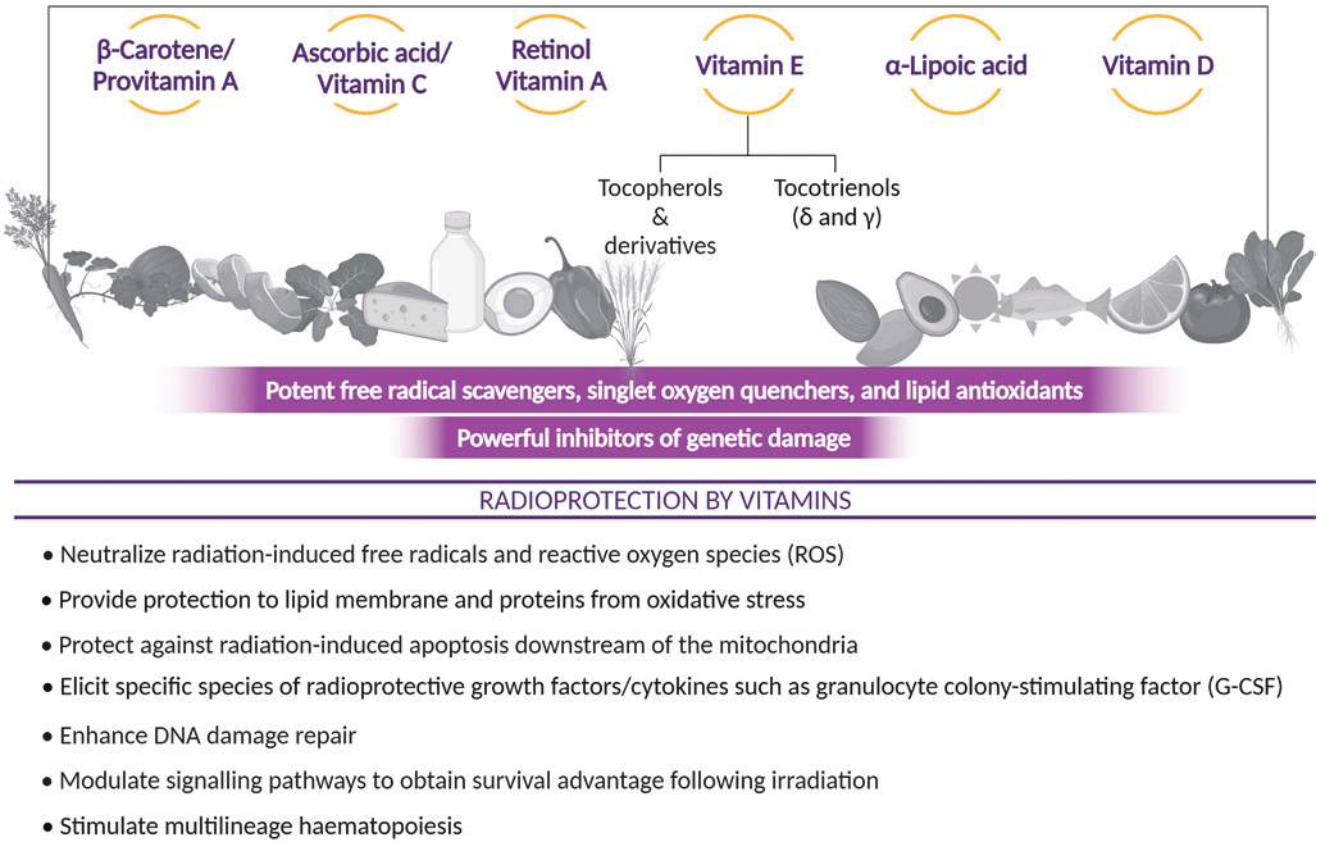

Fig. 11.9 Radioprotective effects of vitamins

crocetin also reduced radiation injury in intestinal epithelial cells [67].

Lutein is a pigment classified as a carotenoid, found in plants such as green leafy vegetables (spinach, kale), fruits, corn, egg yolk, and animal fats. While this pigment plays an important role in eye health, lutein supplements also help to prevent colon and breast cancer, diabetes, and heart disease due to its powerful antioxidant potential. In vitro and in vivo lutein was found to scavenge free radicals and inhibit lipid peroxidation by increasing the activity of CAT, SOD, and glutathione reductase [68]. Lutein showed maximum survival in mice treated with 250 mg/kg body weight against a lethal dose of 10 Gy γ-radiation. Pretreatment of lutein maintained near-normal levels of hematological parameters indicating resistance/recovery from the radiation-induced damages [69]. Furthermore, lycopene has the highest antioxidant activity among carotenoids, and it reduces proinflammatory cytokine expression such as IL-8, IL-6, and NF-κB. Many preclinical studies evidence its radioprotective efficacy, in particular, if it is administered before or as soon as possible after radiation exposure [70].

Vitamin C is the reduced form of ascorbic acid (AA) and a water-soluble vitamin. The intake of vitamin C decreases the risk of getting cataracts after radiation exposition. AA has low toxicity and cost and is easily available, making it an attractive radioprotective agent. Administration of AA before γ-irradiation prevents chromosomal damage in bone marrow cells, mainly due to its scavenging activity of ROS, protecting lipid membranes and proteins from oxidative damage. It has also been reported that AA can prevent the adverse effects of TBI by increasing the antioxidant defense systems in the liver and kidney of irradiated animals [71]. Sato et al. [72] demonstrated the significant radioprotective effect of AA on the ARS in special GI syndrome, especially if it is administered before or not later than 24 h after radiation exposition.

Vitamin E is an essential fat-soluble nutrient with antioxidant, neuroprotective, and anti-inflammatory properties. Vitamin E family includes eight vitamers, four saturated (α, β, γ, and δ) called tocopherols, and four unsaturated analogs (α, β, γ, and δ) referred to as tocotrienols, which are collectively called tocols, with α-tocopherol being the most abundant in human tissues. Tocols administered subcutaneously 1 h prior to or during 15 min postirradiation improved the 30-day survival in mice, and other tocopherol derivatives, such as α-tocopherol-succinate and α-tocopherol-monoglucoside, have also shown radioprotective effects in vivo. Moreover, subcutaneous injection of γ-tocotrienol (100–200 mg/kg) 24 h prior to ^{60}Co γ-irradiation showed a signifi-

cant protective effect in mice facing radiation doses as high as 11.5 Gy and increased mice survival rate [73].

Preclinical studies have provided evidence that tocotrienols exert radioprotection at least in part via induction of G-CSF, reducing inflammatory response suppressing the expression of TNFα, inducible NO synthase (iNOS), and IL-6 and 8, as well as inhibiting NF-κB signaling [74]. Endothelial cells activated through IR downregulate the expression of thrombomodulin (TM) and increase endothelial surface expression of adhesion molecules, which allow the attachment of immune cells, and thereby contribute to inflammation and activation of the coagulation cascade. The greater efficacy of tocotrienols is attributed to their higher antioxidant potential and its ability to inhibit HMG-CoA reductase activity (decreasing serum cholesterol levels) and increase TM expression in endothelial cells, which result in antipermeability, anti-inflammatory, and antithrombotic response in order to decrease radiation-induced vascular damages.

Nevertheless, low bioavailability of tocotrienols is an important limiting factor for their use as radioprotectants, and thus a novel water-soluble liposomal formulation of γ-tocotrienol (GT3) has been developed. GT3 has shown to increase the delivery of γ-tocotrienol in the spleen and bone marrow and offered significant radioprotection in vivo [75]. Despite these promising results, the use of vitamin E derivatives as radioprotectants must be evaluated with caution for their potential toxic effects. More recently, several laboratories have assayed the potential synergistic effect of tocols with other radioprotectants, such as pentoxifylline (PTX) (an antioxidant and anti-inflammatory xanthine derivative, approved by the FDA) which increased survival of mice subjected to 12 Gy ^{60}Co γ-irradiation. Efficacy of PTX and α-tocopherol against radiation-induced fibrosis has been observed in animal models and clinical studies, even though the treatment started after radiation-induced fibrosis manifested clinically. Three clinical trials have evaluated if PTX enhances the radiation-protective properties of γ-tocotrienol, but the results of these studies have not yet been published [74]. At least, two randomized controlled trials provided evidence that dietary supplementation of α-tocopherol and β-carotene during radiation therapy could reduce the severity of treatment adverse effects, but these trials also evidenced that the use of high doses of antioxidants might compromise radiation treatment efficacy. Other combinations like α-tocopherol, acetate and AA showed radioprotective effects and enhanced apoptosis in irradiated cancer cells [76].

Cholecalciferol (D3) and ergocalciferol (D2) are the two forms of vitamin D provided by the food. Exposure to UV radiation of the skin also induces the endogenous synthesis of D3, and for that reason, it is also called the "sunshine vitamin." D3 and D2 have to undergo a double hydroxylation (in the liver and in the kidney) to form the biologically active derivative, that is, calcitriol (1,25-$(OH)_2$-vitamin D), an essential hormone in the regulation of phosphocalcic metabolism. In vitro and in vivo studies evidenced the radioprotective efficacy of calcitriol enhancing the expression of genes coding for antioxidant enzymes (such as SODs and GPxs) and metallothioneins which are ROS scavengers [77]. Jain and Micinski [78] showed a positive link between vitamin D and GSH concentrations, as well as reduction in levels of ROS and proinflammatory cytokines, which is undoubtedly beneficial in protecting against IR. Populations of radiologically contaminated areas close to the Chernobyl accident had lower vitamin D blood levels compared to those in the uncontaminated Ukrainian regions [79]. Therefore, oral supplementation with vitamin D during RT or in medical professionals chronically exposed to low IR doses should be taken into consideration also because radiation toxicity can reduce mineral bone density. Recent studies evidence that calcitriol also radiosensitizes cancer cells by activating the NADPH/ROS pathway, which can makes it a promising adjuvant in RT [80].

11.1.6 Oligoelements

Many antioxidant/defense enzymes, like SOD and metalloproteins, require trace elements as cofactors. The main oligoelements showing protective effects against radiation-induced DNA damage are zinc (Zn), manganese (Mn), and selenium (Se) [81] (Fig. 11.10). Se is an essential component of selenoenzymes such as GPx, thioredoxin reductase-1 (TR1), and ribonucleotide reductase (RNR). Se compounds and their metabolites possess a wide range of biological functions including anticancer and cytoprotection effects and modulation of hormetic genes and antioxidant enzyme activities. Exposure to radiation has been associated with a decrease in Se blood levels, and thus administration of seleno-compounds has emerged as a radioprotective strategy to reduce radiation toxicity. Mechanisms underlying the radioprotection effects include Nrf2 transcription factor activation and the consequent upregulation of the antioxidant-adaptive response in bone marrow stem cells and hematopoietic precursors [82]. 3,3-Diselenopropionic acid (at an IP dose of 2 mg/kg for 5 days prior to γ-TBI) showed radioprotection in mice by decreasing DNA damage and apoptosis [83]. Another recent formulations, poly-vinylpyrrolidone and selenocysteine-modified Bi2Se3 nanoparticles, improved the RT efficacy against tumors while exerting radioprotection in normal tissues [84]. Cancer patients, treated orally with Selenium Selenite, experienced a a lower incidence of diarrhoea compared to the placebo group [85]. Selenomethionine also reduces mucositis in patients with advanced head and neck cancer who are receiving cisplatin and radiation therapy (NCT01682031, www.clinicaltrials.gov).

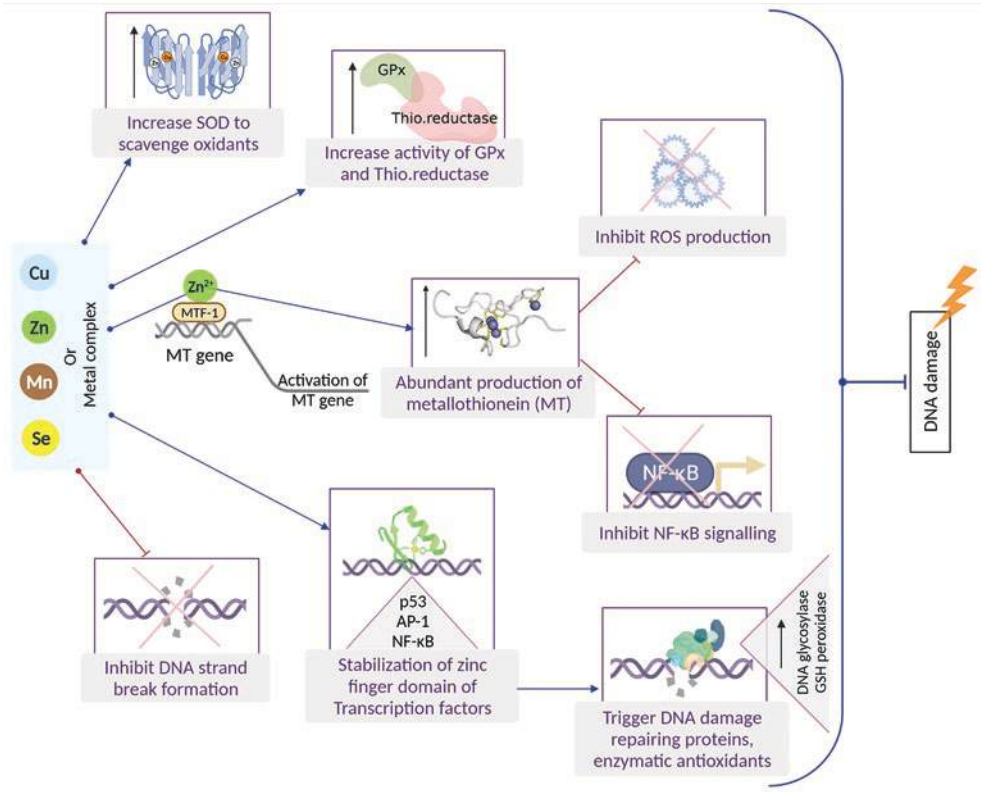

Fig. 11.10 Radioprotection by oligoelements

Radiation-induced lung pneumonitis is a major dose-limiting side effect of thoracic RT, and the therapeutic options for its prevention are limited. 3,3′-Diselenodipropionic acid (DSePA), a synthetic organoselenium compound, shows moderate GPx-like activity and is an excellent scavenger of ROS. DSePA reduced the radiation-mediated infiltration of polymorphonuclear neutrophils (PMN) and suppressed NF-kB/IL-17/G-CSF/neutrophil axis as well as elevation in levels of proinflammatory cytokines such as IL1-β, ICAM-1 (intercellular adhesion molecule-1), E-selectin, IL-17, and TGF-β in the bronchoalveolar fluid of irradiated mice, thus ameliorating inflammatory responses. Administration of DSePA has shown a survival advantage against TBI and a significant protection to lung tissue against thoracic irradiation [86]. Wang et al. [87, 88] developed a highly efficient radioprotection strategy using a selenium-containing polymeric drug, with low toxicity and long-term bioavailability, The radioprotection activity of (VSe) and N-(2-hydroxyethyl) acrylamide shows more remarkable effects both in cell culture and mice models compared to the commercially available ebselen (organoselenium compound) and also exhibits a much longer retention time in blood (half-life ∼10 h).

Crescenti et al. [89] evaluated in vivo the tolerance induced by the combination of Se, Zn, and Mn (4 microg/mL each) plus *Lachesis muta* venom (O-LM) (4 ng/mL) to high doses of TBI (10 Gy, ^{137}Cs source) IR in mice. Mice who received daily O-LM subcutaneous injections, starting 30 days before irradiation, showed a higher number of crypts, enhanced villous conservation, and lack of edema or vascular damage compared to the untreated and irradiated group. O-LM treatment also decreased vascular damage and grade of aplasia of mice bone marrow. O-LM treatment safety and efficacy were tested in a phase I clinical trial, and results indicated that it is an attractive candidate as a radioprotective agent for patients undergoing RT. Other clinical evidence indicates that Zn supplementation may act as an effective radioprotector in patients during RT. In a randomized clinical study, patients treated with Zn sulfate suffered a lower degree of mucositis compared to the placebo group [90]. Orally administered Zn-carnosine reduced oral mucositis and xerostomia in head and neck cancer patients [91].

11.1.7 Superoxide Dismutase (SOD) Mimetics and Nanoparticles

SODs are a group of metalloenzymes that catalyze the dismutation of superoxide radicals ($O_2^{\cdot-}$) to H_2O_2 and O_2, thus are first line of defense to prevent IR damages. In the event of a radio-nuclear attack or nuclear accident, the skin damage used to be severe. A synthetic SOD/CAT mimetic (EUK-207) administered 48 h after irradiation significatively mitigated radiation dermatitis, suppressed indicators of tissue oxidative stress, and enhanced wound healing [92].

Clinical applications of SODs mimetics are limited by their structural instability deficient availability and high cost. Compared with natural enzymes, nanozymes (nanomaterials with enzyme-like activity) are more stable, are economically affordable, and can be easily modified. Due to these characteristics, nanozymes are expected to become effective substitutes for natural enzymes for medical applications. Nanozymes with SOD-like activity have been developed and proved to have a mitigating effect on diseases involving oxidative stress [93]. As shown in Fig. 11.11, after administration, they are internalized by the cells and imitate SOD2 activity in order to inhibit ROS-induced cell damage.

Patients treated with RT for cancers of the head, neck, or lung suffer damage to the mucosa of the upper aerodigestive tract. Most of them develop ulcerative forms of mucositis, and severe forms lead to inability to eat solid foods, and in some cases, they cannot drink liquids. Results of clinical trials (now in phase III, e.g., NCT03689712) demonstrated the efficacy of the SOD mimetic, avasopasem manganese (GC4419) [94].

Mn porphyrin-based SOD mimics (MnPs) are reactive with superoxide and with other reactive oxygen, nitrogen, and sulfur species (Fig. 11.12). MnPs have CAT and GPx-like activities and peroxynitrite-reducing activity [93]. MnPs administered before and continued after radiation exposure protect from γ-ray, X-ray, and proton beam irradiation damages in different animal models, and a few studies indicate that beginning treatment with MnPs after radiation exposure is also effective. In normal tissues, MnPs treatment reduces oxidative stress, NF-κB, and TGF-β signaling pathways and activates Nrf2-dependent pathways. On the contrary, MnPs administration in combination with cancer therapy results in more oxidative stress in cancer cells, which leads to the reduction of NF-κB and HIF-1α and their downstream signaling pathways (Fig. 11.12). These changes are associated with increasing apoptosis and reducing overall cancer growth [95].

BMX-001 is a porphyrin mimetic of the human mitochondrial manganese SOD, with the capacity to cross the blood-brain barrier and protect the brain against IR while acting as a tumor radiosensitizer [96]. It has been assayed as a radioprotector in different clinical trials, e.g., NCT03386500 (patients with recently diagnosed anal cancer), NCT03608020 (cancer patients with multiple brain metastases), NCT02990468 (head and neck cancer), and NCT02655601 (high-grade glioma treated with radiation therapy and temozolomide) [30].

All previous SOD mimetics suppress oxidative stress-mediated injuries, supporting the survival of the normal tissue, while promoting apoptotic processes in tumor tissues. The results from the clinical trials will provide us invaluable information on their real clinical utility as radioprotectors.

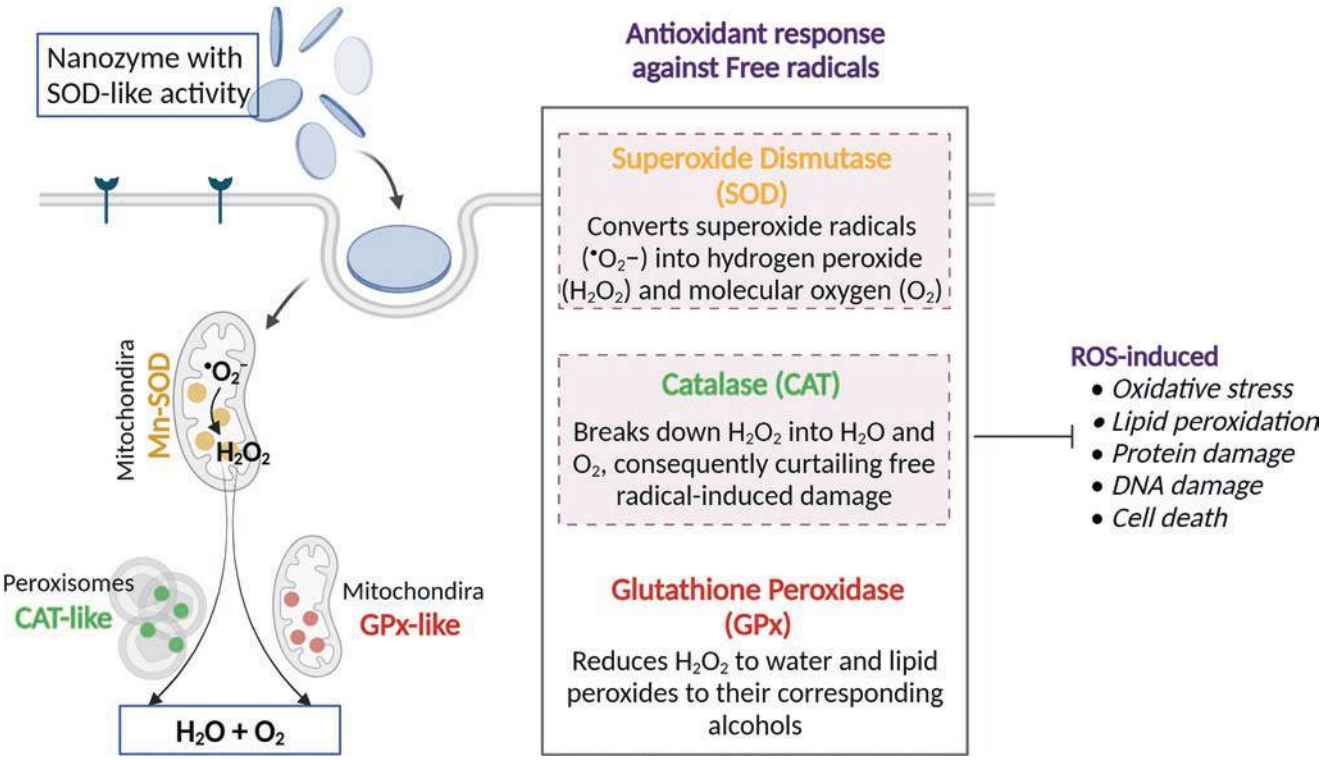

Fig. 11.11 Nanozymes with SOD-like activities

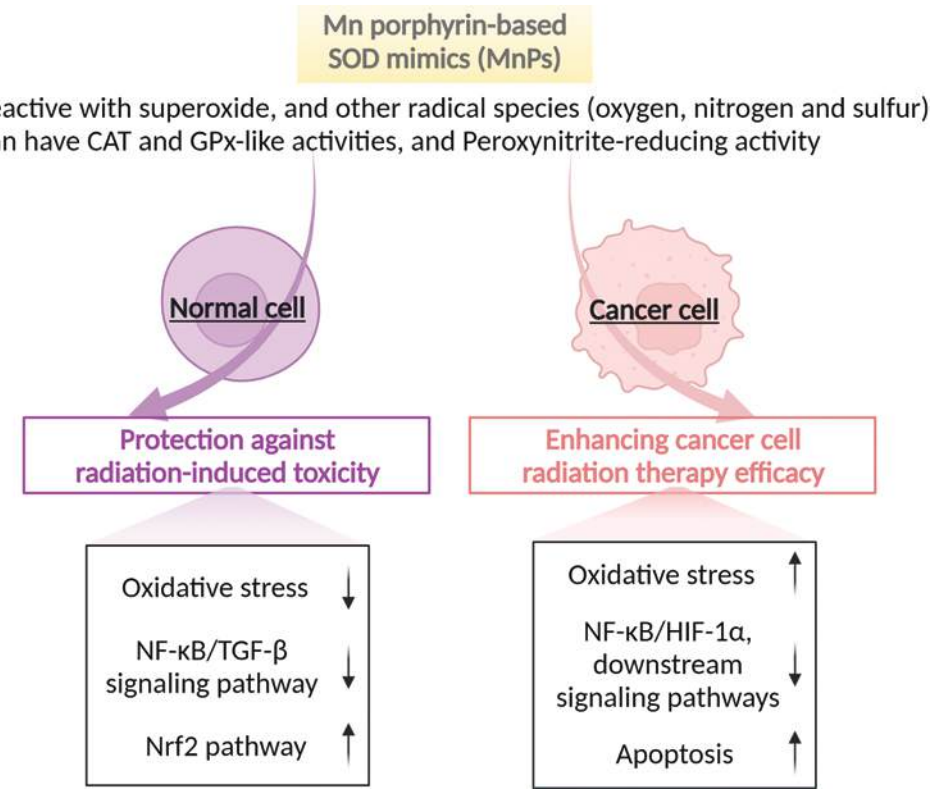

Fig. 11.12 Effects of Mn porphyrin-based SOD mimics in normal and cancer cells

11.1.8 Hormonal and Hormonal Mimetic Radioprotectors

11.1.8.1 Catecholamine Agonist

Radiation dermatitis is a common side effect of irradiation that limits cancer RT courses. It has already been described how the induction of hypoxia limits the damage associated with radiation, and consequently the option of using vasoconstrictor substances as radioprotectors has been proposed. Topical application of adrenergic vasoconstrictors (epinephrine or norepinephrine) to rat skin before radiation exposition (17.2 Gy) confers 100% protection against radiation dermatitis [97], and similar results were obtained when phenylephrine was topically administered to prevent radiation mucositis.

Indralin is an α1-adrenoceptor agonist with vasoconstrictor effects similar to those of epinephrine. Indralin (120 mg/kg)-treated rhesus monkeys survived better (five of six) after being exposed to a lethal TBI ^{60}Co ɣ-irradiation of 6.8 Gy, than nontreated ones (all died). Moreover, less pronounced manifestations of hemorrhagic syndrome, leukopenia, and anemia were also noted [98]. Norepinephrine and α1-adrenoceptor agonists accelerate differentiation of hematopoietic stem cells by blocking their proliferation, thus avoiding, at least, earlier manifestation of radiation injury. A common feature of the radioprotective action of biogenic amines like indralin and aminothiols is the induction of hypoxia, although their mechanisms of action differ significatively. Norepinephrine and indralin exert their effect through the neurohormonal α1-adrenoceptors, but sulfur-containing radioprotectors act directly on tissues. Nevertheless, the use of α-catecholaminergic agonists entails a high risk of increased blood pressure or pressure decompensation in hypertensive patients, which would compromise their widespread use in an accidental emergency radiation exposure.

11.1.8.2 Somatostatin Analogs

GI radiation vulnerability to a certain extent can be caused by release of potent pancreatic enzymes into the intestinal lumen after radiation exposure. Therefore, reducing intraluminal proteolytic activity may help attenuate intestinal radiation toxicity.

Somatostatin and its analogs (octreotide and pasireotide) inhibit exocrine pancreatic secretions. Octreotide reduces both acute and delayed intestinal radiation injury and diarrhea [99], as it has also been evidenced in a randomized controlled trial in patients who were undergoing radiation therapy to the pelvis (NCT00033605, www.clinicaltrials.gov). Nevertheless, some common side effects such as allergy, nausea, rash, and light-headedness may limit the routine use of octreotide. Moreover, it could also induce hypoglycemia [99] and reduce secretion of GH and IGF1, which could be highly counterproductive for the recovery of damaged tissues.

SOM230 (pasireotide) is another somatostatin analog under preclinical evaluation as a radioprotector. SOM230 reduced intestinal mucosa injury and increased mouse survival after TBI by inhibiting exocrine pancreatic secretion. Moreover, SOM230 has a 40-fold improved affinity to somatostatin receptor 5 than other somatostatin analogs, and it proved to be beneficial when administered prior to radiation exposure, and also when the treatment started up to 48 h following the exposure [100].

11.1.8.3 Melatonin

Several hormones are known to exhibit radioprotective characteristics, and melatonin, *N*-acetyl-5-methoxytryptamine, is one of them. It is the main secretory product of the pineal gland. Its radioprotective properties are outlined in Figs. 11.13 and 11.14.

Melatonin has the ability to neutralize both ROS and NO directly leading to the production of less/nontoxic agents or indirectly increasing the activity of antioxidant enzymes such as SODs, GPx, GR, and CAT at the same time suppressing prooxidant enzymes like xanthine oxidase (XO) [101]. In addition, melatonin induces DNA repair mechanisms, which reduce mutagenic damage and also induction of DNA DSBs, which are lethal events for the cell. Melatonin administration before irradiation with a lethal dose of ^{60}Co γ-rays reversed the upregulation of Bax and p53 proapoptotic genes and elevated Bcl-2, which led to 100% survival and preservation of hematopoietic and GI systems in mice [102]. Inflammation and fibrosis are two degenerative phenomena that are typical pathophysiological processes following RT. Melatonin via inhibition of NF-kB, COX-2, and iNOS enzymes has the ability to reduce the release of inflammatory cytokines and chemokines. Attenuation of these enzymes' activities is associated with reduced level of oxidative stress, infiltration of macrophages and lymphocytes, as well as suppression of fibrosis, which prevents radio-induced pneumonitis and lung fibrosis [103], and also heart [104] and brain [105] damage associated with radiation exposition.

The physiological concentrations of melatonin in the human blood are approximately much lower during the day than during the night. Therefore, it seems that radiation therapy with supplementary melatonin leads to more beneficial effects during the nighttime. Melatonin exhibits multiple neutralizing actions to reduce radio-induced damage. Together with its low toxicity and its ability to cross biological barriers, these are all significant properties to consider it for clinical RT applications as well as for mitigation of radiation injury in a possible radiation accident scenario; however, its short half-life in vivo (<1 h) and the need of high doses to achieve radioprotective effects could limit its use in practice.

At this moment, just a few clinical trials have studied the therapeutic usefulness of melatonin as a radiosensitizer. Many preclinical studies evidence that it increases ROS production, inhibits telomerase activity and DNA repair mechanisms in cancer cells, reduces tumor angiogenesis and inflammatory response associated with high doses of radiation exposure, and enhances anticancer immunity. All these oncostatic properties make melatonin an interesting molecule to increase the efficacy of RT on cancer cells [106].

11.1.9 Metformin (MTF)

Apart from being a common antidiabetic drug, MTF has demonstrated potential antioxidant, radioprotective, and anticarcinogenic properties [107]. It is a hydrogen-rich agent able to neutralize free radicals, increase GSH, and upregulate the activity of SOD and CAT enzymes [108], which all favors the antioxidant defense of normal cells. MTF has been reported to reduce the generation of ROS at the complex 1 and to prevent mitochondrial mediated apoptosis [109]. It also decreases production of the inflammatory cytokine IL-1β in response to lipopolysaccharide (LPS) in macrophages [110] and inhibits NADPH oxidase, COX-2, and inducible NO synthase, thereby limiting macrophage recruitment and inflammatory responses. MTF stimulates the DNA repair pathways of nonhomologous end joining (NHEJ) or homologous recombination (HR), and nucleotide excision repair (NER) pathways [111].

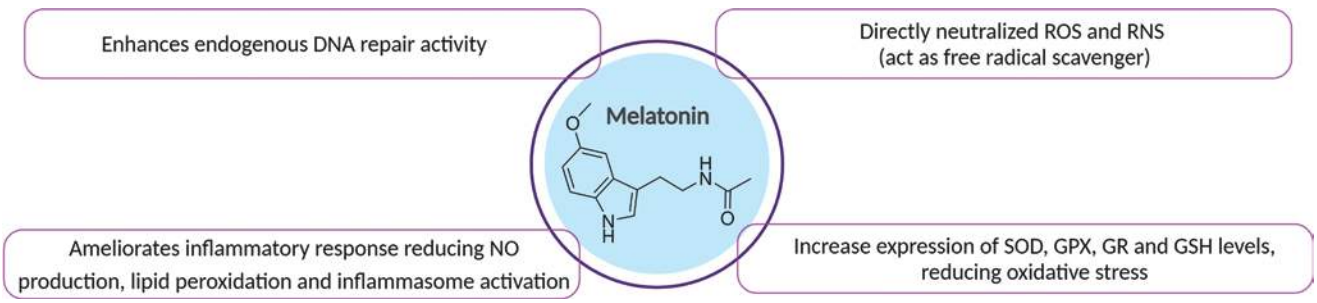

Fig. 11.13 Radioprotective properties of melatonin

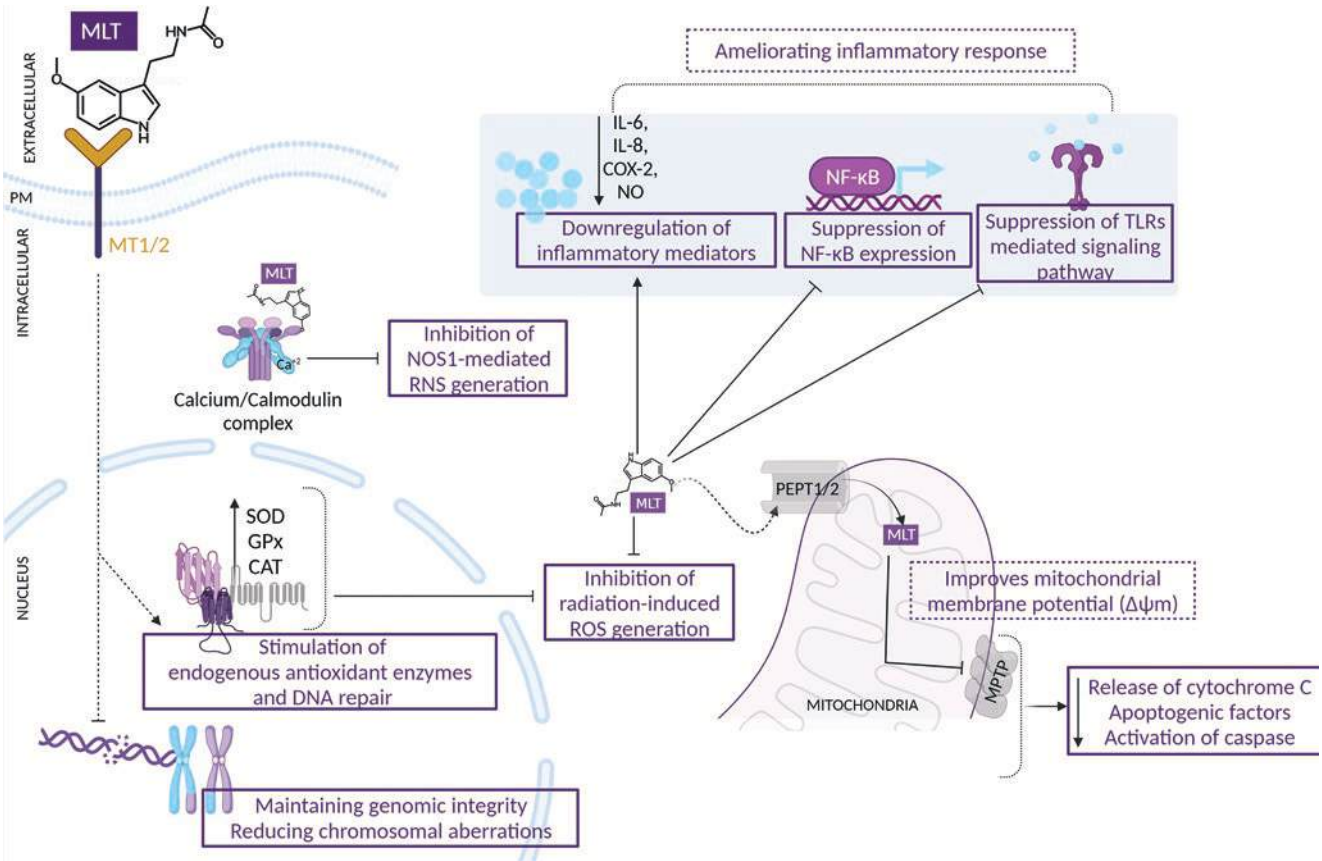

Fig. 11.14 Melatonin can exert radioprotective and radiomitigative effects

In contrast to other radioprotectors, MTF has shown modulatory effects through induction of several redox-related genes, such as the PRKAA2 gene (which encodes the AMPK), thereby suppressing redox reactions, protecting cells from accumulation of unrepaired DNA, and attenuating initiation of inflammation as well as fibrotic pathways [108] involved in lung fibrosis [104]. Cardiovascular disease is one of the most pivotal disorders after RT. The administration of MTF to γ-irradiated (5 Gy) rats significantly ameliorated the changes in cardiac disease biomarkers (LDH and CK-MB) and in NF-κB, IL-6, and TNF-α levels compared to the control group. MTF also reduced E-selectin as well as ICAM and VCAM-1. These results demonstrate that concomitant administration of MTF during RT can act as an efficient heart protector from oxidative stress, inflammatory mediators, and endothelial dysfunction-induced damages [112–114]. MTF does not have significant adverse effects at the normal clinical level, but it may cause severe lactic acidosis and increase the risk of hypoglycemia. In animal models, MTF has demonstrated synergistic effects with melatonin mitigating the radiation-associated damages, and both of them radiosensitize cancer cells increasing RT efficacy (this will be later exposed in Sect. 11.4).

11.2 Radiomitigators

Radiomitigators are those agents/compounds which can be administered during or shortly after radiation therapy or IR exposure to reduce the effects of radiation on normal tissues before the onset of symptoms. These compounds are capable of minimizing the toxicity even after radiation has been delivered, which differentiates them from radioprotectors (reducing direct damage caused by radiation in normal tissues). At this moment, all FDA-approved radiation countermeasures (filgrastim, a recombinant DNA form of the naturally occurring G-CSF; pegfilgrastim, a PEGylated form of the recombinant human G-CSF; sargramostim, a recombinant GM-CSF) are classified as radiomitigators [30].

In some cases, these agents have protective properties that are similar to the action of "classic" radioprotectors, even if they are administered after radiation exposure. However, these agents are most effective not only at administration shortly after irradiation, but also during the irradiation. For radiologic terrorism and space research, much of the focus of radiomitigators has been in the field of developing chemopreventives strategies in order to reduce carcinogenesis of TBI.

Characteristics of an Ideal Radiomitigator

An ideal radiomitigator should (a) offer the possibility of easy administration, (b) protect normal sensitive tissues which are associated with dose-limiting toxicity and significant reduction in quality of life, (c) be stable and easily available, and (d) have no relevant toxicity.

Mechanism of Action

Postradiation changes in normal tissue such as constant mitotic cell death and perpetually active cytokine cascades can sooner or later lead to vascular damage, tissue hypoxia, and excessive extracellular matrix deposition [115]. Radiation mitigators should aim to interrupt these cascades prior to the manifestation of toxicity or intervene to prevent the prolongation of molecular and cellular damage, and therefore reduce the expression of radiation-induced tissue toxicity or prevent the acute toxicity.

Potential radiation mitigators are described in this chapter; their possible mechanism of action is represented in Fig. 11.15.

Radiomitigators can modulate the radiation-induced molecular, cellular, and tissue toxicity/injuries even when they are administered after radiation exposure. Gene and stem cell therapies as therapeutic radiation countermeasures are being developed and may be applied in the near future to minimize the side effects of radiation exposure through tissue regeneration.

DNA Repair and Cell Recovery Process

Several studies have suggested that cellular recovery and repair processes can be enhanced by radiomitigators. Double-strand breaks (DSBs) are the most common form of DNA damage associated with IR. After DSBs are generated, a cascade of enzymatic processes, such as, HR and NHEJ (mediated by BRCA 1 and BRCA 2 enzymes), activation of p53, and induction of cell cycle arrest triggered to allow DNA repair or to induce apoptosis. The pharmacological improvement of these mechanism can contribute to mitigate IR damages. However, this must be done with care, because failure of these processes can lead to carcinogenic transformation [116]. Future studies should focus on compounds that have the potential to enhance the process of DNA repair after radiation exposure. In that sense, higher cellular pools of DNA precursors can create a radioprotective cellular environment, and drugs and chemicals that stimulate the activity of precursor-synthesizing enzymes can function as radiomitigators [117].

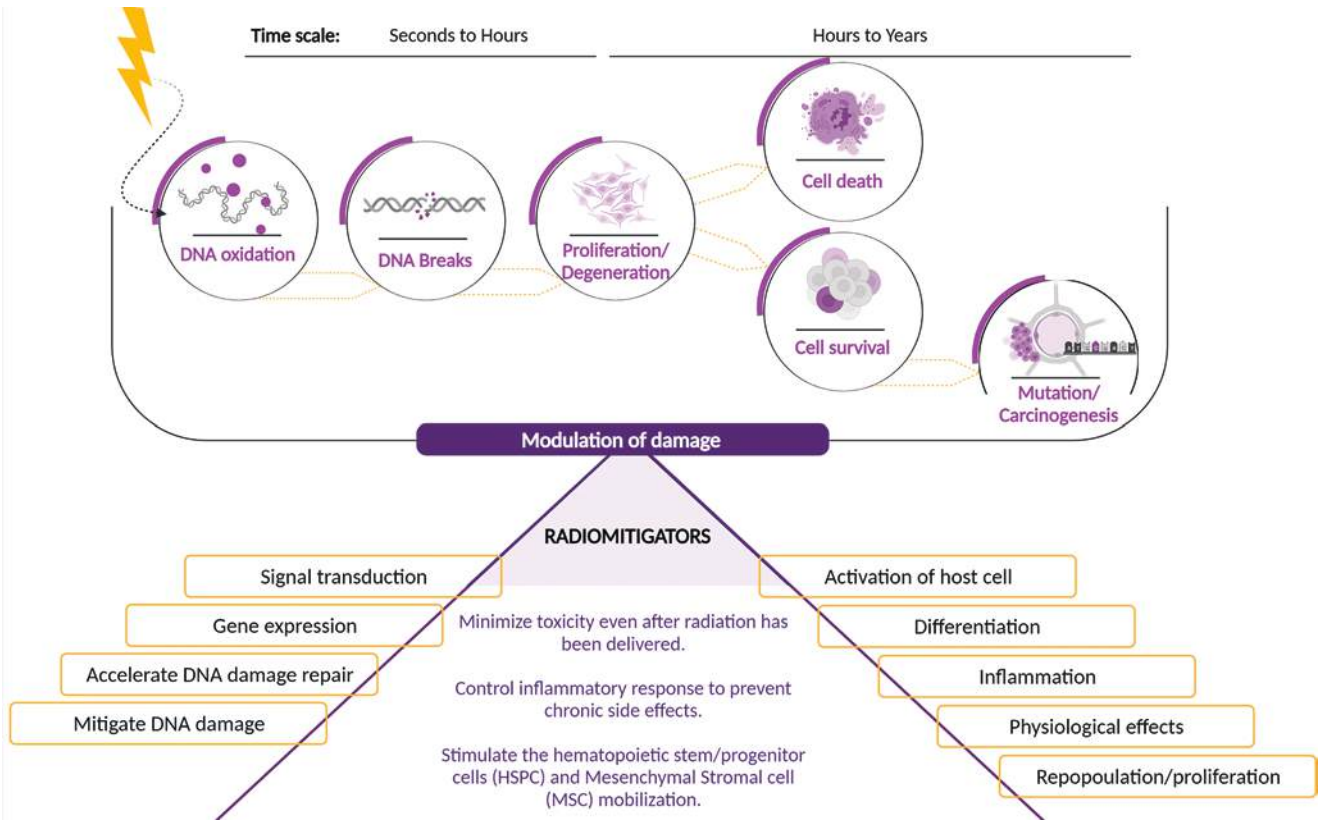

Fig. 11.15 Radiomitigators: mechanism of action

Anti-inflammatory Activity

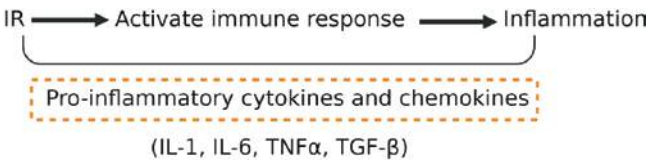

IR is indirectly toxic by activating immune response, and patients undergoing radiation therapy may occasionally suffer from widespread inflammation. Various pro-inflammatory cytokines and chemokines are generated after radiation exposure, which particularly mediate inflammation, fibrosis, and other serious injuries in tissues and organs. Some natural products and their bioactive components can reduce the expression of these small cell signaling protein molecules and relieve the inflammation-associated side effects through their healing properties. Some phytochemicals, nonsteroidal anti-inflammatory drugs (NSAIDs), glucocorticoid, and other molecules reduce inflammatory response, reducing long-term side effects like fibrosis.

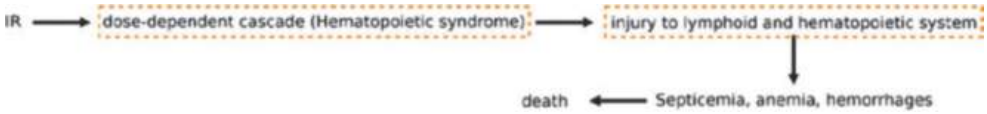

Hematopoietic and Immunostimulating Activity (Regeneration)

Hematopoietic stem cell injury is the primary cause of death after accidental or intentional exposure to a moderate or high dose of IR. Hence, compounds which can stimulate the regeneration of hematopoietic cells and immune system by mechanisms such as increasing spleen colony-forming units in synergy with interleukins may have good ability to protect cells and tissues against radiation exposure. A range of endogenous compounds like IL-1, TNFα, G-CSF, stem cell factor (SCF), erythropoietin (EPO), and GM-CSF stimulate stem cell progenitors and promote hematopoietic bone marrow repopulation and thus have been further investigated as potential radiomitigators. So, agents that upregulate endogenous radioprotective factors can also act as radioprotectors.

A variety of agents (such as vitamins, TLR ligands, and β-glucan) and many natural antioxidants are classified as immunomodulators as they regulate different cytokines (cell growth factors, colony-stimulating factors, etc.) in order to facilitate patient recovery from IR-induced injuries. These regulators inhibit cell apoptosis, promote differentiation and development of gastrointestinal or hematopoietic stem cells, and have radiomitigator effects (Box 11.3).

Box 11.3: Radiomitigators

- Radiomitigators (cytokines, growth factors, hormones, synthetic analogs, immunological adjuvants, immune regulatory peptides, etc.) accelerate the postradiation restoration of radiosensitive tissues.
- At times, these agents can exert protective effects in a similar way to the action of "classic" radioprotectors; therefore, radiomitigators reduce oxidative stress and inflammatory damages, activate enzymes involved in repair mechanisms, and/or stimulate the replenishment of damaged tissues.
- Compared to radioprotectors, they have the advantage of being effective despite being administered after exposure to IR. They are usually administered during the early period of postradiation and prior to the development of acute radiation syndrome (ARS).

11.2.1 Growth Factors and Cytokines

Four radiomitigators have been approved by the US Food and Drug Administration (US FDA) for the management of hematopoietic acute radiation syndrome (H-ARS). They include human recombinant G-CSF (filgrastim/Neupogen®), long-acting PEGylated form of G-CSF (filgrastim/Neulasta®), GM-CSF (sargramostim/Leukine®), and romiplostim (Nplate®), a fusion protein containing a peptide region that binds to the thrombopoietin receptor (c-Mpl) and an Fc carrier domain that increases its circulating half-life. Romiplostim was approved for use in radiation injury by the FDA based on the Animal Rule (United States Food and Drug Administration, 2021, Highlights of prescribing information. Nplate® (romiplostim) for injection, for subcutaneous use). Except for romiplostim, they have all been used to treat radiation accident victims with beneficial results [118–121].

G-CSF and PEGylated G-CSF promote the differentiation and proliferation of myeloid progenitor cells and their progeny. These effects promote neutrophil recovery after radiation-induced neutropenia. In addition, they enhance the function of neutrophils and improve survival. A World Health Organization Consultancy recommended that Neupogen and

Neulasta should be administered subcutaneously, as soon as possible to individuals who have been exposed to radiation doses of >2 Gy [118]. Neulasta has the advantage that it is administered weekly, compared to daily administrations that is required for Neupogen treatment. GM-CSF increases the differentiation and proliferation of macrophage and granulocyte progenitor cells. When administered as late as 48 h after radiation exposure, GM-CSF reduced the recovery time for neutropenia and thrombocytopenia and decreased the rate of infection [5]. In addition, GM-CSF appears to exhibit an antifibrotic effect in the setting of radiation-induced lung injury (RILI) in experimental animals and humans [122, 123].

Keratinocyte growth factor (KGF), a factor that is produced by mesenchymal cells, protects and repairs epithelial tissues. Early studies suggested that KGF promotes the recovery of the oral mucosa after radiation-induced injury, improves gastrointestinal barrier function, and limits bacterial translocation and subsequent sepsis after irradiation. In clinical studies, Palifermin®, a human recombinant KGF product, reduced the incidence, duration, and severity of oral mucositis and esophagitis in patients treated with chemoradiotherapy and stimulated immune reconstitution following hematopoietic stem cell transplantation [124].

Many cell types release epidermal growth factor (EGF), which promotes the regeneration of hematopoietic stem cells in vivo. EGF was reported to have an additive effect on overall survival with G-CSF (survival of 20% for controls, 67% for EGF, 86% for EGF plus G-CSF) [125]. Fibroblast growth factor (FGF) is found in many tissues throughout the body, and its levels decrease after irradiation. FGF-P is a human recombinant derivative that is capable of activating FGF receptor-1, resulting in protection of the crypts located in the duodenum and improved survival in a GI-ARS mouse model. In addition, platelet counts were found to be higher in FGF-P-treated animals, resulting in decreased hemorrhages and cutaneous ulcerations postirradiation. It has been suggested that FGF-P has the potential to treat radiation-induced skin ulcerations and thermal burns and that it holds potential promise in the management of ischemic wounds and the promotion of tissue engineering and stem cell regeneration [125].

Interleukin-12 (IL-12) has pleiotropic effects on the innate and adaptive immune cells, including stimulation of hematopoiesis. Treatment with HemaMax® (human recombinant IL-12) restored all cell types in bone marrow when administered at 24 and 48 h post-TBI in non-human primates (HNPs) and mice, respectively. Compared to Neupogen, Neulasta, and Leukine, the single administration of HemaMax® is another advantage in the event of a mass casualty incident [126]. A novel, PEGylated IL-11 (Neumega®) is approved to treat thrombocytopenia in cancer patients, but must be injected daily, making its use inconvenient as a radiomitigator. To circumvent this problem, another mono-PEGylated IL-11 analog (BBT-059) was designed and demonstrated higher bioavailability and potency in vivo. In mouse model exposed to high TBI doses, BBT-059 leads to bone marrow cell reconstitution, leading to an accelerated recovery of platelets, erythrocytes, and neutrophils and an increase of survival higher than that obtained with treatment with the PEGylated derivatives of G-CSF and GM-CSF [125].

Erythropoietin is prescribed for the treatment of severe anemia arising from intense chemo- and/or radiation therapies. Erythropoietin and thrombopoietin (TPO) have been used for the victims of radiation exposure in the Tokaimura accident. Romiplostim (Nplate) is a synthetic TPO receptor agonist that preferentially increases platelet generation in bone marrow; contributes to mitigation of radiation-induced thrombocytopenia, anemia, and leukopenia; gives protection; and enhances regeneration of vascular endothelium. Romiplostim has recently received FDA approval to treat acutely irradiated and severely myelosuppressed adult and pediatric patients. More recently, ALXN4100TPO (a TPO receptor agonist) has been shown to stimulate megakaryopoiesis, reduce bone marrow atrophy and radiation-induced mortality in acutely irradiated mice, with the advantage of being less immunogenic than Nplate.

Combinations of hematopoietic growth factors and cytokines (G-CSF, GM-CSF, EPO, SCF, and IL-3) have already been used in the treatment of radiological accident victims, but the relative efficacy of this combined treatment is difficult to evaluate due to differing radiation sources, exposure doses, and other circumstances [127].

As explained in detail in Chap. 2, irradiation directly causes ROS overproduction, apoptosis, and/or necrosis, which activate the inflammatory response. In the short term, proinflammatory cytokines, such as IL-1, IL-6, IL-8, IL-33, TNF-α, and TGF-β, help to activate the immune response and bone marrow cellular recovery, but if it is excessive or is maintained for a long time, it can contribute to bystander/nontargeted effect (damages in tissues that have not been directly exposed), in special autoimmune diseases, fibrosis, and/or cancer initiation and progression. Therefore, the use of cytokines or growth factors capable of increasing the inflammatory response should be carefully evaluated. Moreover, the use of substances that inhibit its release or antagonize its proinflammatory effects has been shown to have mitigating effects on the damage caused by IR.

Fibrogenic cytokines like TGF-β, vascular endothelial growth factor (VEGF), and platelet-derived growth factor (PDGF) are involved in radiation-induced fibrosis. TGF-β is able to stimulate ROS and NO production by the immune system, involved in the initiation and progression of chronic oxidative damage after exposure to a high dose of radiation. It is therefore not surprising that combined inhibition of

TGF-β and PDGF signaling attenuates radiation-induced pulmonary fibrosis associated with decreased pneumonitis and leading to prolonged survival. Inhibition of TGF-β also reduced radiation-induced endothelial vascular damages [113, 114]. Moreover, different phase I/II clinical trials have shown more successful RT response with the combined use of TGF-β inhibitor in metastatic breast cancer patients (LY2157299, NCT02538471). This is of special interest, because the reduction in plasma levels of TGF-β is associated with greater efficacy of RT on different types of cancer and some studies have proposed that attenuation of cytokines by genistein or quercetin ameliorates late effects of IR such as pneumonitis and fibrosis [128].

The necrosis of central nervous system (CNS) tissue is one of brain irradiation's main risk factors. The same is true for radiation-induced increase of capillary permeability resulting from cytokine release, causing extracellular edema. A recombinant human monoclonal antibody (bevacizumab), which prevents the VEGF from binding to its receptors, reduced brain necrosis in a patient subjected to cranial irradiation and further experiments evidenced its efficacy for the management of edema associated with radiation necrosis [129].

Toll-like receptors (TLRs) play critical roles in basal resistance to IR in animals and multiple radiosensitive tissues. Several TLR ligands had been proved to exert protective roles against IR both in vitro and in vivo, downstream effectors including NF-κB (controller of inflammation, and immune response), interferon regulatory factors, and stress-activated protein kinase (Jnk), which in turn results in inhibition of apoptosis, promotion of cell proliferation, regulation of cell cycle, and secretion of cytokines. In cultured cells, TLR2, TLR5, or TLR9 agonists inhibit radiation-induced apoptosis and increase cell survival. CBLB502 (a TLR5 agonist) was reported to alleviate bone marrow and intestinal injuries in mice and rhesus monkeys. Activation of TLR4 by its agonist LPS can protect bone marrow damage and lower mice mortality after irradiation. Moreover, some kinds of TLR agonists, such as TLR2/6 coagonist CBLB613, were reported to be more effective in radiomitigation than single-TLR agonists. In conclusion, TLRs and their ligands provide novel strategies for radiation protection in nuclear accidents [28, 29, 55].

11.2.2 Cell Therapy Replacement

IR is known to be especially damaging on highly proliferative tissues. Cellular sensitivities in approximate descending order from most to least sensitive are lymphocytes, germ cells, proliferating bone marrow and intestinal epithelial cells, and epithelial stem cells. Hematopoietic syndrome (HS) is the dominant manifestation after whole-body doses of about 1–6 Gy and consists of a generalized pancytopenia, due to bone marrow stem cell depletion, although, excepting lymphocytes, mature blood cells in circulation are largely unaffected. Patients remain asymptomatic during a latent period as the impediment to hematopoiesis progresses. Risk of infection and sepsis is increased as a result of neutropenia (most prominent at 2–4 weeks) and decreased antibody production. Petechiae and bleeding result from thrombocytopenia, which develops within 3–4 weeks and can persist for months. Anemia develops more slowly because circulating erythrocytes have a longer life span. Clinical management of the HS with risk of sepsis, hemorrhage, and/or acute anemia is related to the standard clinical protocols. Therapy would certainly encompass, but not limited to, the use of antibiotics, blood, and platelet transfusion, although the latter is limited by the recipient's own immune response. Moreover, aseptic protocols must be rigidly employed. Allogeneic hematopoietic stem cell transplantation can restore bone marrow and immune functions. In the past, stem cells were harvested directly from donor bone marrow in the operating room, but at present, peripheral blood is most used as a source of stem cells for both autologous and allogeneic grafts [130]. Bone marrow stromal cell transplantation has also been shown to renew the irradiated intestinal stem and alleviate radiation-induced GIS [131]. To date, about 50 patients with acute radiation sickness have been treated with allogeneic hematopoietic stem cell transplants, but the median survival time has not yet exceeded 1 month. Despite these results, the efficacy of bone marrow transplantation in patients undergoing RT treatments highlights the need to have mechanisms in place to implement this procedure for patients exposed during a nuclear emergency [132].

Mesenchymal stem cells (MSCs) are nonhematopoietic adult stem cells with self-renewal and multilineage differentiation potential, low immunogenicity, and capacity to restore cell loss in damaged microenvironments. Moreover, MSCs secrete different interleukins, which help in the repair and recovery of cells. Although MSCs were traditionally isolated from bone marrow, cells with MSC-like characteristics are much easier to isolate from a variety of neonatal and adult tissues, including amniotic fluid, umbilical cord, peripheral blood, fat tissue, etc. Treatment with MSCs has shown efficacy in protecting the liver against radiation-induced injury; healing irradiated skin in mice; mitigating radiation-induced GIS, HS, brain injury, and neurological complications of RT; and increasing survival in irradiated mice [102]. Moreover, MSCs have successfully been assayed against radiation-induced pulmonary fibrosis (NCT02277145) and xerostomia (NCT03876197) (www.clinicaltrials.gov) [30]. Nevertheless, despite the extensive use of MSCs in preclinical and ongoing clinical trials, there is a lack of long-term safety in humans. During recent years, it has been demonstrated in animal

models that **MSC-derived extracellular (EVs). EVs** can exert the same therapeutic effect of MSC; therefore, EVs can be used as an alternative MSC-based therapy [133]. To cite some examples, EVs inhibit DNA damage and cell death and preserve intestinal function [134] and bone marrow activity providing long-term survival in mice exposed to TBI [135].

11.2.3 Nonsteroidal (NSAIDs) and Steroidal Anti-inflammatory Radiomitigators

Radiation initiates many enzymes such as cyclooxygenase-2 (COX-2) and inducible nitric oxide synthase (iNOS) to produce ROS or NO, involved in the activation of inflammatory response. Most NSAIDs, such as aspirin, ibuprofen, indomethacin, diclofenac, and flurbiprofen, are able to inhibit COX-1 and COX-2 enzymes. The protective action COX inhibitors (COXi) is ascertained to the inhibition of the prostaglandin synthesis and directly or indirectly linked with the ability of NSAIDs to arrest cells in the G_0 or G_1 phase where cells are less sensitive to radiation damage and/or stimulation of the hematopoietic recovery [136]. Both pre- and post-irradiation treatments with **sodium diclofenac** reduced radiation-induced formation of DC and MN formation in human peripheral blood lymphocytes [137]. **Flurbiprofen** also showed radioprotection in clinical studies, e.g., delaying the onset of mucositis and reducing its severity after RT in 12 head and neck cancer patients, although the overall severity or duration of mucositis was not improved [138]. A recent meta-analysis of randomized controlled trials indicates that **aspirin** reduces the overall risk of recurrence and mortality of colorectal cancer and/or colorectal adenomas, which increases the interest in its possible use as a radiomitigator [24, 25]. However, nonselective COXi are known to cause undesirable side effects including GI ulcers and bleeding when taken for continued periods of time.

Increase of COX-2 gene expression is associated with decreased survival in patients receiving RT [139]. COX-2 selective inhibitors (COXi, as celecoxib, meloxicam, indomethacin) lack the GI toxicity of classical NSAIDs, and therefore, the use of COX-2i like **meloxicam** has been extensively assayed. Meloxicam administered either before or repeatedly after irradiation exposure has enhanced the recovery of hematopoietic progenitor cells committed to granulocyte-macrophage and erythroid development in sublethally irradiated mice [140], but the increase in survival was only observed when meloxicam was applied before lethal TBI. Sequential administration of PGE2 and meloxicam was shown to increase hematopoiesis and survival in irradiated mice [141], and meloxicam combined with ibuprofen treatment reduced bone loss after radiation exposure [142]. Radiation pneumonitis is a severe and dose-limiting side effect in lung cancer treatment. In this regard, celecoxib was tested in rats after single-dose X-ray irradiation of the right hemithorax and mediastinal region with 20 Gy revealing a dose-dependent protective effect on lipid peroxidation (MDA levels) and histopathological parameters. **Celecoxib** treatment induced a decrease in severe skin reactions after a high single dose of 50 Gy [136]. Moreover, celecoxib was also found to alleviate radiation-induced brain injury by maintaining the integrity of the BBB (blood-brain barrier) and reducing the inflammation in the rat brain tissues by inhibition of apoptosis in vascular endothelial cells [143]. **RIVAD018** is another selective COX-2i which adds to its anti-inflammatory effects the ability to exert antioxidant activity, preventing oxidation of low-density lipoproteins, showing protection on both cellular and vascular models [144].

Several studies have also described that overexpression of COX-2 in cancer cells results in increased tumor angiogenesis, growth, and metastasis; thus, several COX-2 inhibitors have been described as radiosensitizers [136]. Celecoxib restricts neoangiogenesis, leading to a reduction in the survival of hepatocarcinoma and lung and skin cancer cells. In glioblastoma cells, the combined effect of radiation and celecoxib increased tumor cell necrosis, showing a significant reduction in tumor microvascular density compared to irradiation alone [139].

Radiation exposure of skin with high doses (>20 Gy) results in erythema, blistering, and necrosis in sequence. The necrosis generally occurs 10–30 days after exposure, although it may appear earlier in the most severe cases. The earliest administration of systemic and topical anti-inflammatory agents reduces the need for surgical excision of the affected tissue. Current therapy might make use of transplanted autologous keratinocytes combined with allogeneic stem cells. Advances in the knowledge of the radiomitigating properties of these compounds may prove to be very useful, particularly for the relatively low cost and toxicity, and specially for their analgesic effects [139].

Steroidal anti-inflammatory drugs such as **dexamethasone** can be administered after radiation exposure to attenuate fever and inflammatory or pain symptoms or to treat acute pathologies such as pneumonitis. Some authors reported that dexamethasone administration prior or immediately after radiation exposure reduced the risk of cardiac and other tissue fibrosis. Moreover, dexamethasone is often used to manage the inflammatory response in the brain during RT treatment of glioblastoma and other intracranial tumors. The effects of dexamethasone on patient survival however remain controversial because several clinical studies suggest that dexamethasone could potentially restrict effective RT [145].

11.2.4 Probiotics, Prebiotics, and Fecal Microbiota Transplantation (FMT)

Pathologically, acute intestinal epithelium damage is described as dilatation or destruction of crypt cells, decrease in villous height and number, ulceration, severe mucosal and submucosal inflammation, and sepsis associated with a pathogen bacterial translocation. Because of the rapid turnover of intestinal mucosa, the acute-phase symptoms (nausea, vomiting, diarrhea, abdominal pain, and acute mucositis) persist for hours to several months, while other intestinal complications such as obliterative vasculitis, mucosal ulceration, bowel wall thickening or progressive interstitial fibrosis, bowel obstruction, and fistulae formation, with or without fecal incontinence, are late events, often associated with chronic radiation exposition [146]. The reported incidence of severe late chronic radiation enteritis varies between 5 and 15% of patients treated with pelvic RT.

Probiotics, prebiotics, and FMT target intestinal microbiota by inhibiting colonization of pathogenic bacteria and restoring microbiome normobiosis. They increase production of mucin in the intestinal epithelial cells and expression of tight junction protein and occludin, thereby enhancing mucus layer function and improving survival of intestinal crypts (Fig. 11.16).

A diverse and healthy commensal intestinal microbiota plays an essential role in GI homeostasis. It has been found that postirradiation enteropathy is associated with low mucosal microbiota diversity, in particular, a decrease of Lactobacillus and Bifidobacterium spp. and an increase in the relative abundance of opportunistic pathogens. Gut microbiota dysbiosis aggravates radiation enteritis, reduces the absorbing surface of intestinal epithelial cells, weakens intestinal epithelial barrier function, promotes intestinal inflammation, and contributes to the development of mucositis, leading to a persistent diarrhea and bacteremia [147]. Correction of the microbiome by application of probiotics, prebiotics, FMT, and/or antibiotics helps to prevent and treat radiation-induced enteritis [148].

Probiotics are live microorganisms, added to aliments, that have a beneficial role in reducing pathogenic bacteria multiplying without competitors, promoting intestinal immune barrier function, and preventing translocation of harmful bacteria. Preparations containing Bifidobacterium, Lactobacillus, and Streptococcus ameliorated radiation-induced gut toxicity, reducing the incidence of diarrhea, and delaying the necessity for rescue treatment with loperamide [147]. Randomized controlled trial evidenced that live Lactobacillus acidophilus plus Bifidobacterium bifidum treatment reduced the incidence of radiation-induced diarrhea and the need for antidiarrheal medication and had a significant benefit on stool consistency [149]. The anti-inflammatory effect of probiotics has been shown in other pathologies such as ulcerative colitis and Crohn's disease. The administration of Lactobacillus spp. decreased levels of different colonic inflammatory cytokines such as IL-6, TNF-α, or NF-κB p65 and recruitment of leukocytes to the colonic mucosa. In mice model, administration of *Lactobacillus rhamnosus* increased the crypts survival in radiation-induced enteritis by approximately twofold and reduced epithelial cell apoptosis, which depends on intact TLR2 and COX-2 inhibition in

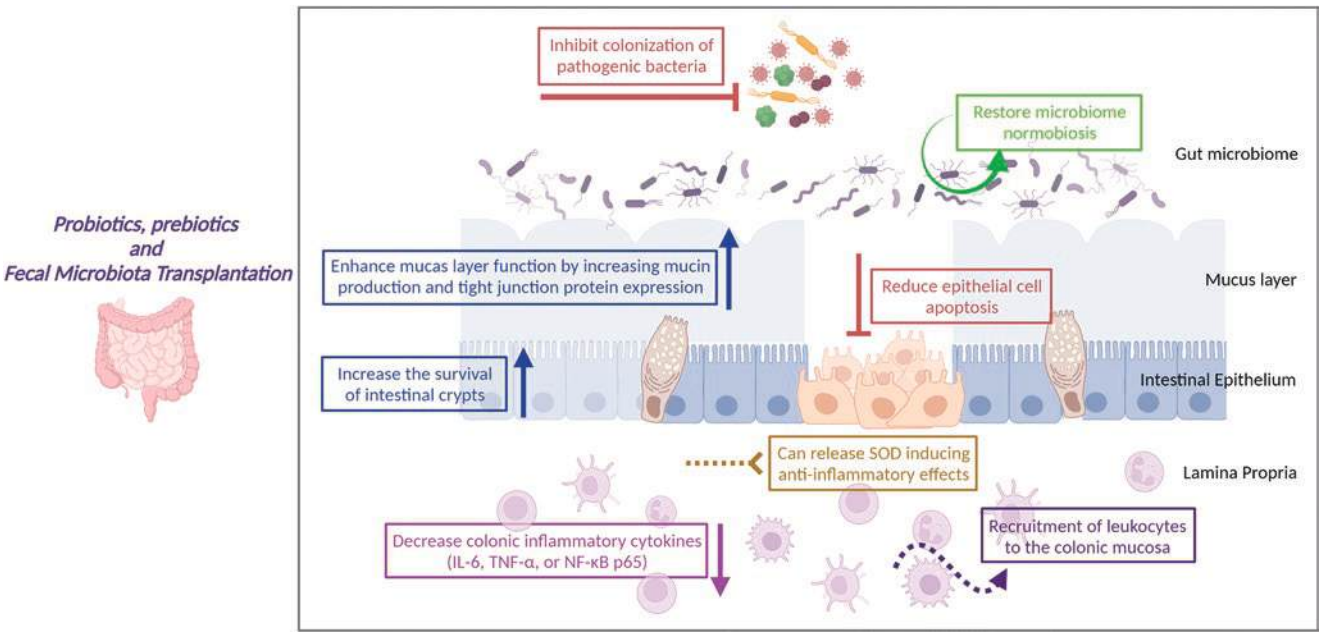

Fig. 11.16 Effect of probiotics, prebiotics, and FMT on the function of the intestinal epithelium and gut microbiome

mesenchymal stem cells of crypt [150]. Genetically engineered species of *Lactobacillus plantarum* and *Lactococcus lactis* release SOD inducing anti-inflammatory effects and attenuation of enteritis symptoms [151]. Increased production of short-chain fatty acids is one of the most important probiotic protective effects implicated in GI and hematopoietic tissue protection and increased survival of irradiated mice [152]. Several clinical trials seem to indicate that probiotics reduce the incidence of radiotherapy-induced mucositis [148], even though results are difficult to evaluate, as they vary in the type of cancer patients recruited, radiotherapy modalities used, and type of bacteria used as probiotic [146]. In this regard, choosing the right probiotic can be crucial, and a recently published systematic review concludes that a combination of *Bifidobacterium longum*, *Lactobacillus acidophilus*, *Bifidobacterium breve*, *Bifidobacterium infantis*, and *Saccharomyces boulardii* could be a good combination of probiotics to reduce incident rates of mucositis or ameliorate its symptoms in chemo- or radiotherapy-treated patients [153].

Prebiotics offer a source of enrichment to the microbiome, and dietary interventions have demonstrated to reduce the severity of inflammatory intestinal pathologies and thus can potentially serve as a radiomitigative strategy. In fact, a clinical trial (NCT01549782) evidenced that increased consumption of certain prebiotics (fiber and plant sugars) was associated with a reduction in days of diarrhea and improved quality of life for irradiated patients [154].

FMT increased the survival rate, elevated peripheral white blood cell counts, and alleviated GI toxicities and intestinal epithelial integrity in irradiated mice [155]. Radiation-induced intestinal edema was strikingly alleviated after 8 weeks of FMT of gut microbes from healthy donors, enhancing beneficial bacteria such as Alistipes, Phascolarctobacterium, Streptococcus, and Bacteroides recovery, whereas the abundance of Faecalibacterium decreased. FMT can reduce the intestinal leakage and enhance the intestinal functions and epithelial integrity in patients with chronic radiation enteritis [156].

Researchers have long known that administering antibiotics to irradiated animals can enhance survival by avoiding opportunistic infections. As previously have been exposed, antibiotics such as fluoroquinolones and ciprofloxacin also have the advantage of reducing radiation damage to hematopoietic progenitor cells. Antibiotic cocktail and metronidazole pretreatment are beneficial to the reconstruction of gut microbes in irradiated mice. Abx pretreatment regulates macrophage polarization in the ileum and downregulates the expression of TGF-β1, thereby preventing intestinal fibrosis and ultimately improving the survival of mice with radiation-induced intestinal injury [157].

11.2.5 Angiotensin Axis-Modifying Agents

Radiation nephropathy has emerged as a significant complication in RT and is a potential sequela of radiological terrorism and radiation accidents. The use of a high-salt diet in the immediate post-irradiation period significantly decreases renal injury but is deleterious for the treatment of established disease. FDA-approved drugs that modify the renin-angiotensin system are habitually used for the treatment of hypertension and cardiac and/or renal insufficiency. ACEIs constrain angiotensin-converting enzyme (ACEs) and reduce the formation of angiotensin II (AII). Angiotensin receptor blockers (ARBs) impede the function of the angiotensin AT_1 or AT_2 receptors and decrease the actions of AII.

The efficacy of ACEIs and ARBs has also been long studied for their effects in radiation protection, modulation, or mitigation (Fig. 11.17). Clinical trials have evidenced the potential of ACE inhibitors to reduce radiation-induced pneumonitis and fibrosis (enalapril, NCT01754909, www.clinicaltrials.gov).

Results of a recent meta-analysis review evidenced that the use of ACEIs, but not ARBs, effectively reduced the incidence of radiation pneumonitis in most lung cancer patients. That has important clinical implications because lung cancer patients receiving thoracic radiation could take an appropriate dose of ACEIs to prevent radiation-induced pneumonitis, during or after the period of RT, which would greatly improve the quality of life and therapeutic effect. By contrast, even the most expensive ARBs were ineffective [158].

Five different **ACEIs** (captopril, lisinopril, enalapril, ramipril, and fosinopril), at clinically relevant doses, have been examined for efficacy as mitigators of radiation-induced nephropathy. Overall, survival in rats is higher after an 11–12 Gy TBI when treated with any of the ACEIs captopril, enalapril, or fosinopril starting 1 week postirradiation [159]. All, except fosinopril, effectively abrogated radiation nephropathy, with captopril being the most effective [160].

Captopril treatment increased survival from thoracic irradiation to 75% compared with 0% survival in vehicle-treated animals, and suppression of inflammation and senescence markers, combined with an increase of anti-inflammatory factors, was part of the mechanism involved in its therapeutic effects [161]. Captopril reduced radiation-induced cytokines EPO, G-CSF, and SAA (Non-invasive serum amyloid A) in the plasma, mitigated brain microhemorrhage at 21 days postirradiation, and increased EPO levels postirradiation if started prior to radiation exposure. These data suggest that captopril may be an ideal countermeasure to mitigate H-ARS following accidental radiation exposure [162]. A trial of captopril in patients receiving TBI demonstrated not only safety, but also efficacy against renal and pulmonary injury [163]. Moreover, prophylactic administration of captopril reduced radiation-induced hypertension

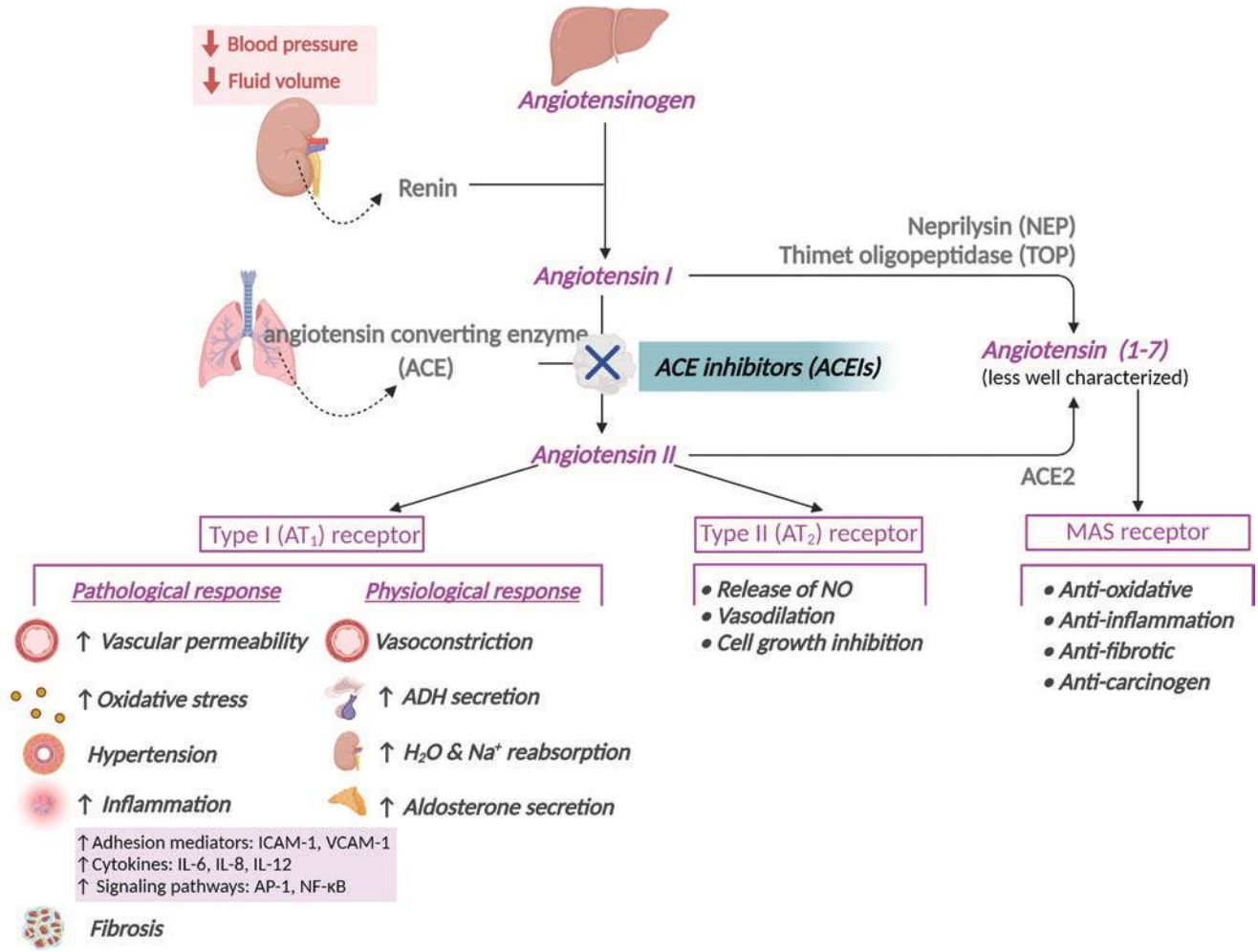

Fig. 11.17 Role of ACEIs, ARBs, and renin inhibitors in the renin–angiotensin system

and renal failure and mitigated pulmonary endothelial dysfunction and radiation-induced pneumonitis and fibrosis. The isoflavone genistein appears to work synergistically with captopril, improving the 30-day survival in mice receiving both drugs from 0 to 95% after 8.25 Gy TBI. The combination therapy reduced anemia and increased the number of circulating hematopoietic cells [164].

In murine models, administration of AT_1 receptor antagonist before, during, and after fractionated whole-brain irradiation prevented or reduced cognitive impairment. It is also hypothesized that ARBs may attenuate radiation-induced brain injury by increasing the generation of anti-inflammatory peptide, angiotensin (1–7). ACEI or AT_1 antagonist treatment in hypertensive patients increases blood levels of angiotensin (1–7); prevents oxidative stress, inflammatory cytokine release, and fibrotic events; and also has anticarcinogenic effects, thus having radiomitigating potential as it has been evidenced recently [165].

While other types of antihypertensive drugs are ineffective, ACEIs and AII receptor antagonist type I are effective in the mitigation of radiation damages. Moreover, some of them also exhibit antitumor effects; thus, there is a strong case for the clinical use of these agents in the treatment of radiation-induced late effects.

11.2.6 Statins

The incidence of cardiovascular disease was observed in the atomic bomb survivors, and cardiovascular disease is a known side effect of radiation therapy [166]. Statins (simvastatin, lovastatin, pravastatin, and others) are inhibitors of the 3-hydroxy-3-methylglutaryl coenzyme A reductase, which is a rate-limiting enzyme for the synthesis of cholesterol and serves to upregulate low-density lipoprotein (LDL) synthesis. Therefore, statins are clinically used to reduce LDL levels in the blood and, consequently, to treat atherosclerosis and hypercholesterolemia. Statins also strongly induce thrombomodulin (TM) expression, which in turn forms a complex with thrombin. Thrombin-TM complexes activate protein C,

which has anti-inflammatory, anticoagulant, and antioxidant properties. All these beneficial effects may help to attenuating radiation injuries [167].

Radiation exposure (5 Gy X-rays) increased cholesterol levels, and those were reduced by simvastatin treatment [168]. Simvastatin treatment (20 mg/kg/d over 2 weeks) mitigates, to a limited extent, radiation-induced enteric injury (4–8 Gy), as evidenced by improved structural integrity of the mucosa, reduced neutrophil infiltration, decreased thickening of the intestinal wall, and reduced accumulation of collagen I in jejunum and bone marrow in male C57BL/6J mice [169]. Simvastatin also prevented radiation-induced marrow adipogenesis and provided radioprotection to the niche cells [170], and attenuated radiation-induced salivary gland dysfunction in mice [171]. Pathak et al. [167] demonstrated that a single subcutaneous dose of γ-tocotrienol (GT3) rescues mice from lethal radiation doses, and combined treatment (GT3 + simvastatin) provides substantial protection against radiation-induced lethality, hematopoietic injury, and bone marrow damage compared to the single treatment.

A combination of statin and ACEI agents has shown efficacy in reducing GI toxicity in patients receiving pelvic RT [172]. Lovastatin treatment of irradiated mice (15 Gy whole-lung irradiation), starting immediately after irradiation or 8 weeks post-irradiation (three times a week), demonstrated a reduction in lung tissue lymphocytes and macrophages, decreased collagen content, prevented lung fibrosis, and improved rates of survival [173].

Pravastatin (30 mg/kg body weight given 4 h before irradiation) protected the normal intestine and lung tissues from radiation. The radiomitigating effect of pravastatin was associated with a reduction in the level of radiation-induced DNA DSB. The pravastatin-treated group showed a significantly lower apoptotic index of the lung and intestinal epithelial cells and reduced the intestinal expression of ataxia-telangiectasia mutated and γ-H2A histone family member X (H2AX) after irradiation [174]. Statins are generally well tolerated, and their effect was pronounced for delayed radiation injury and for that reason shows potential as radiomitigators.

11.2.7 Growth Hormone (GH) and Somatomedin C (IGF1) Analogs

Long et al. [175] demonstrated that chimeric protein dTMP-GH, a tandem dimer formed by thrombopoietin mimetic peptide and GH treatment, increased survival in mice exposed to ^{60}Co γ-ray photons (6 Gy). Meanwhile, dTMP-GH treatment accelerated the recovery of bone marrow hematopoiesis, promoted skin wound closure, and mitigated ileum injury. Zinc sulfate and GH administration prevented radiation-induced dermatitis in rats [176], and increased GH/IGF1 levels also reduced radio-induced intestinal epithelial cell apoptosis preserving, in the short term, the efficacy of RT on tumors [177]. GH significantly restored follicular development and preserved fertility in female rats exposed to a single TBI of 3.2 Gy [178]. However, in oncology, GH and IGF1 reduce the effectiveness of RT and may frequently cause metastasis and cancer recurrence. Therefore, even if GH/IGF-derived radiomitigative effects are confirmed, further studies of these hormonal treatments would be necessary before translating the results to human clinical trials.

11.2.8 Molecular Hydrogen (H_2)

Hydrogen can mitigate IR damages through various mechanisms [122, 123]: (a) directly neutralizes hydroxyl radicals and peroxynitrite [179]; (b) indirectly reduces oxidative stress, by upregulating the expression of different endogenous antioxidant enzymes, i.e., SOD, CAT, and GPx; and (c) shows antiapoptotic and anti-inflammatory properties [180]. H_2 reduces 8-hydroxy-2′-deoxyguanosine and malondialdehyde levels and increases SOD activity and GSH levels. These findings suggest that the radioprotective effect of H_2 is largely due to the inhibition of oxidative stress. In that sense, H2 has demonstrated in vitro radioprotective effects in cells especially sensitive to IR, such as intestinal epithelial cells, hematopoietic precursors, and spermatogonia [180] these protective effect of H_2 are not significant when it is administered after radiation [181].

Shin et al. [182] observed that application of H (H2O) to human skin prevented UV-induced erythema and DNA damage, administered even after exposure to RI. Although a lot of in vitro and in vivo research has been done to investigate the potential use of H_2 as a radiomitigator, there are scarce clinical data. Kang et al. [183] performed a placebo-controlled, randomized study to evaluate the validity of ingesting hydrogen-rich water in 49 patients with malignant liver tumors, while they were receiving RT at the same time. Patients drinking H_2-rich water had considerably higher quality of life (QOL) scores, notably less appetite loss, and much fewer tasting disorders than patients drinking placebo water, and most importantly, no differences were found in tumor response to RT comparing both groups of patients [183]. In cancer patients, H_2 has also shown protective effects against brain, lung, and myocardial injury associated with RT, furthermore preventing side effects like anorexia, taste disorders, or bone marrow damage without compromising the antitumor effects of the treatment [180].

The use of H_2 is feasible in the clinical practice because it is stable at normal temperatures; it can be easily administered through various routes such as inhalation, drinking, injection, etc. (Fig. 11.18); it can even cross the blood-brain barrier; has a very favorable tolerability profile; and it shows

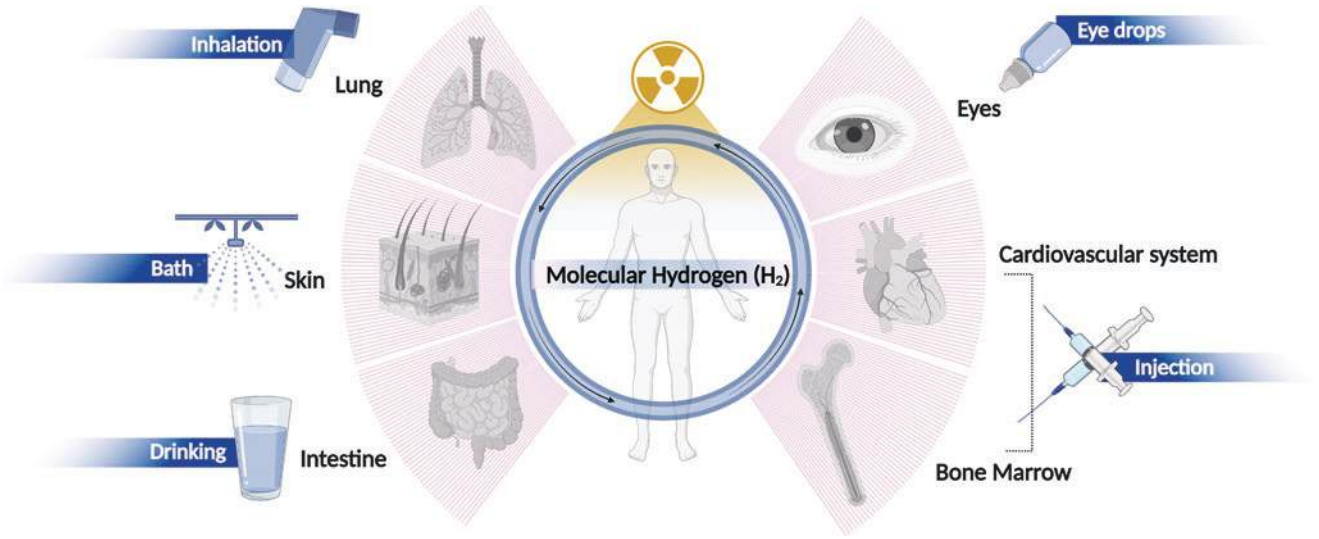

Fig. 11.18 Delivery of hydrogen and its protective and therapeutic opportunities in various systems. Adapted from "Molecular hydrogen: A potential radioprotective agent," by Hu et al. [122, 123], Licensed under CC BY 4.0

great efficacy as a potential radioprotective agent [122, 123]. Although the human body does not have the enzymes necessary to produce H_2, the colonic microbiota can produce about 12 L of H_2 per day under physiological conditions. Many results support the idea that upregulation of H_2 gas produced by intestinal bacteria could be used as a valid treatment strategy for various diseases. Since there are several methods to supply external H_2, it can be easily administered with little or no adverse effects.

11.2.9 Vitamins

1-Methyl nicotinamide (MNA), a derivative of vitamin B3, significantly prolonged survival of mice irradiated at LD30/30 (6.5 Gy), LD50/30 (7.0 Gy), or LD80/30 (7.5 Gy) of γ-rays when the MNA administration started as late as 7 days post-irradiation. Another vitamin B3 derivative, 1-methyl-3-acetylpyridine, was slightly less efficient when it was administered after 7.5 Gy γ-ray exposition. These pro-survival effects might be related to the anti-inflammatory and/or antithrombotic properties of the vitamin B3 derivatives and do not seem to be mediated by stimulation of hematopoiesis. These results show that MNA may represent a prototype of a radiomitigator because it reduces the severity and/or progression of radiation-induced injuries when applied several hours or days after exposure to high doses of IR [184].

11.3 Internal Contamination by Radionuclides and Treatment

After various radiological and nuclear incidents, radioactive materials (radionuclides) may be released in the atmosphere where they could be either inhaled as gas, ingested as particulates, or absorbed through intact skin or subcutaneous tissue [185].

The medical consequences of internal contamination are determined primarily by radiation dose and radiation quality. Deleterious effects include dose-dependent deterministic (i.e., predictable) effects; stochastic (i.e., random) effects such as cancer in tissues where radionuclides are retained for prolonged times, and at a sufficiently high quantity of contamination; multiorgan failure; and death. The radiation quality or specific radionuclide(s) has (have) a characteristic emitted energy (alpha, beta, or gamma/X-ray), solubility, radioactive half-life, and biological half-life, which is determined by the time required for a compartment, defined by a body organ or tissue or part of an organ or tissue (see Fig. 11.19) to eliminate half of its radionuclide content. The particle size and chemical composition of the radioactive material impact the site of deposition within the body and route of elimination. Finally, comorbidities such as renal insufficiency, hepatic failure, and pulmonary disorders may impair pathways needed for radionuclide elimination from the body, thereby prolonging exposure [186].

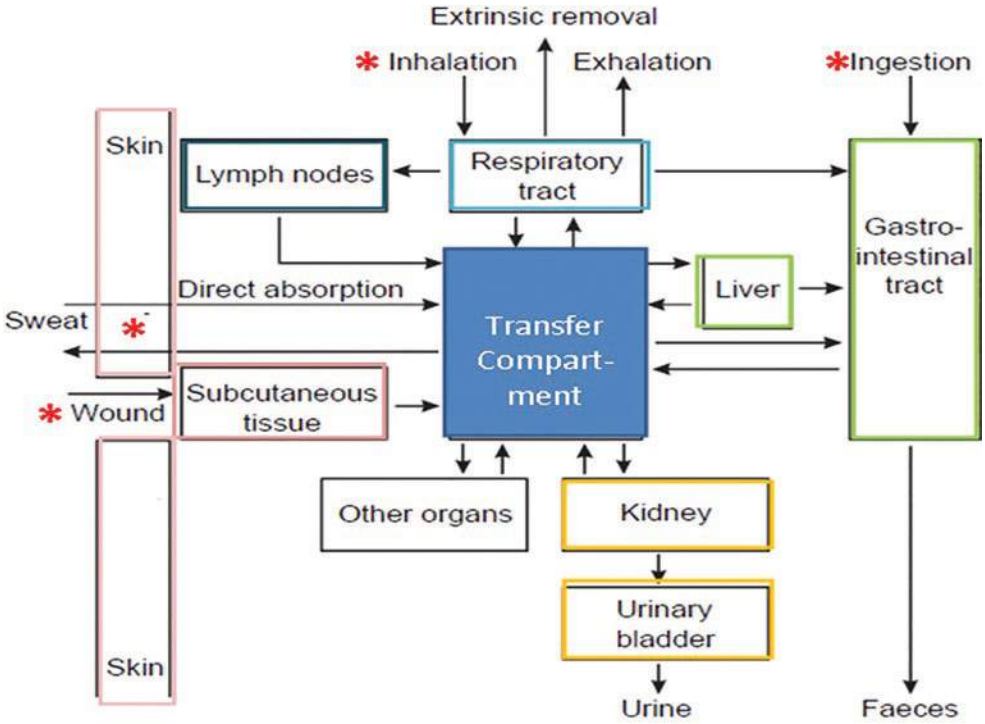

Fig. 11.19 Biological compartments for radionuclide intake and distribution. Reproduced from Dainiak N and Albanese J, Assessment and clinical management of internal contamination, JRP, 2022, in press, and modified from ICRP, 2015, Occupational Intakes of Radionuclides: Part 1. ICRP Publication 130. Ann. ICRP 44(2)

The internal contamination with radionuclides involves four metabolic phases:

1. Intake (incorporation)
2. Uptake (absorption into the circulatory system)
3. Retention (deposition)
4. Excretion (decorporation)

The excretion of these radionuclides by natural processes can be accelerated using decorporation therapies. This consists of enhancing the action of biological processes through chemical or biological agents, thereby facilitating radionuclide elimination. In the event that radionuclides have been incorporated internally, the objective of the therapy is to reduce the internal dose and thus the risk of biological effects on health. This can be achieved by preventing the incorporation, reducing the absorption and internal deposit of radionuclides, and also promoting their excretion. The decorporation process may have adverse side effects. Therefore, these therapies must be based on risk criteria and applied as soon as possible.

The general procedures are intended to reduce or inhibit the absorption of radionuclides from the GI system, the respiratory tract, or the skin and wounds (Fig. 11.19). Some examples of general procedures are the use of emetics, gastric lavage, laxatives, gastric alkalinization, and irrigation if there are wounds, especially in an emergency scenario. The use of specific drugs to impede the deposition of radionuclides (decorporation agents) in organs or tissues could avoid accumulation and retention of radionuclides and, obviously, is more effective if treatment is started immediately after internal contamination. Decorporation agents can reduce radionuclide absorption, entry, and deposit in organs and tissues and/or accelerate its excretion, finally minimizing the absorbed dose.

11.3.1 Blockers (Metabolic Blocking)

Blocking agents work by reducing the absorption of the radionuclide in the body, since they saturate tissues, organs, and metabolic processes using a stable isotope (identical to the nonradioactive element). Among these agents, the best known is potassium iodide (KI), used to prevent the deposit in the thyroid gland of radioactive iodine delivered to the atmosphere as a result of uncontrolled nuclear accident, which can lead to an increased risk of developing thyroid cancers, particularly in infants and young children [187]. KI prevents binding of radioiodine by three mechanisms: a) it will dilute the radioiodine circulating inside the body and available for thyroid uptake; b) it will saturate the active transport mechanism of iodine mediated by the sodium

iodine symporter (NIS); and c) it will inhibit the organification of iodine, also called *Wolff-Chaikoff* phenomenon, a mechanism that could lead to a decrease in the synthesis of thyroid hormones and a possible hypothyroidism; but this effect is usually of short duration. This measure only protects the thyroid from radioactive iodine, not other parts of the body.

Pharmacologic thyroid blockade by oral KI (50–100 mg in adults) can substantially reduce radioiodine thyroid uptake and was one of the first and urgent protective actions recommended by the World Health Organization (WHO) (1960–1970s).

The recommendations adopted for iodine prophylaxis, in particular those regarding the administration timing, the iodine quantity to be given, and the possible side effects occurring as a result of this measure, are included in the Guide [188]. Although stable iodine is usually considered as the standard for thyroid protection against radioiodine [189], perchlorate can be considered as an alternative, provided that it is administered at equi-effective dosages (1000 mg perchlorate is as effective as 100 mg stable iodine in the aftermath of an acute radioiodine exposure). Perchlorate also protects the thyroid by competition with radioiodine at the NI-symporter site. Considering its simpler protective mechanism and potential advantages in particularly vulnerable subpopulations and its acceptable adverse effects, it seems promising for future studies to focus more closely on perchlorate as an alternative to stable iodine for thyroid protection against radioiodine [187].

11.3.2 Reduced Absorption

Absorption is defined as a movement of material that reaches the blood regardless of the mechanism. This generally applies to the entrance in the bloodstream of soluble substances and material dissociated from particles (NCRP 161).

Prussian blue, a nonabsorbable resin (approved by the FDA), acts as a laxative agent that promotes the fecal elimination of ingested radiocesium and thallium. The most effective form of this compound is its colloidal soluble form. This compound was used in the Goiânia accident extensively and successfully for the decorporation of ^{137}Cs. Different silica-based materials have also been tested to capture various radionuclides of plutonium, americium, uranium, and thorium [190].

Natural products have also been used to reduce the absorption of radionuclides. An example is that orally administered *Chlorella algae* inhibited the absorption of strontium (^{90}Sr) into the blood and enhanced its fecal elimination [191].

11.3.3 Dilution (Isotopic Dilution)

Increasing the intake of liquids, such as water, milk, and tea, or intravenous administration of isotonic saline solution, is a rapid method to increase the excretion of soluble radionuclides. This would be the case of tritium, where ingestion of sufficient liquids reduces the time of permanence in the body [192].

11.3.4 Displacement

Displacement shares the same principle as dilution and blocking therapies. However, in this specific case, an element is used that has a different atomic number. Thereby, that element will compete for internal scavenging sites, displacing the radioisotope from a receptor/target. Calcium gluconate, for example, competes with radiostrontium in bone deposition, or stable iodine, which displaces technetium-99m [193].

This method consists of increasing the natural renewal process of the release of radionuclides from organs and tissues, thus reducing deposition and improving the elimination rate by diuresis. As an example, ammonium chloride, which if administered orally, lowers the pH of the blood and increases the elimination of radiostrontium once internalized. Or the use of sodium bicarbonate increases the pH of the blood and favors the removal of uranium [194].

11.3.5 Chelators and Functional Sorbents

Chelating agents are classified as organic or inorganic agents capable of binding to metal ions and forming complex ring structures, known as "chelates." These agents possess atoms of union or "ligands" that generally form covalent bonds and facilitate the excretion by the kidneys or other organs [186].

Some examples of this method are the one used to facilitate the elimination of plutonium complexes by the kidneys and the GI. DTPA (diethylenetriaminepentaacetic acid with calcium or zinc) is the chelator with the widest range of potential use [186]. Other chelators commonly used are dimercaptosuccinic acid, dimercaprol, and deferoxamine. Different silica-based materials (such as isomers of diphosphonic acid, hydroxypyridinone, acetamide phosphonic acid, DTPA, and glycinyl-urea) have also been tested to capture various radionuclides of plutonium, americium, uranium, and thorium [190]. Importantly, factors that can potentially affect the stability of any chelating agent must always be taken into account, i.e., (but not limited to) acidity and alkalinity, chemical properties of the agent, its selectivity, and concentration of competing metals.

Internal contamination with actinides, whether by inhalation, ingestion, or injuries, represents a serious risk to the health. Some guidelines to assist physicians or other professionals in treating workers or members of the public who may suffer internal contamination with compounds such as plutonium tributyl phosphate, plutonium nitrate, americium oxide, or nitrate can be found in [195].

The use of these types of agents is most effective when administered immediately after exposure to radiation because the radionuclides are still circulating in the body and may not yet have deposited in target organs or cells (liver and bone are examples of preferred targets).

11.3.6 Surgical Excision

This method is used for the elimination of a fixed radionuclide contaminant in the body. The surgery must be evaluated carefully, taking into account risks and benefits, and must be carried out with the support and collaboration of radiation protection staff [196].

Occasionally, debridement and excision of the wound may be necessary in order to remove the fixed contamination. It is important that a well-established evaluation is carried out by specialized personnel to support the medical decision, considering the benefits and risks of the surgical procedure. When surgical exploration is necessary, as well as the removal of tissue/foreign material, it should be performed with the help of a radiation protection professional, a radiophysicist who uses a specific probe for wounds. Once the surgical material has been removed, it should be saved for subsequent radioanalysis. There are no contraindications regarding the use of local anesthetics or systemic anesthetic agents.

11.3.7 Lung Lavage (Mechanical)

Lung lavage is an invasive medical procedure that involves the same risks as general anesthesia and is only indicated for a limited number of cases. The parameters that are taken into account are the patient's age, clinical status, existence of comorbidities, radiotoxicity of the contaminant, and dose.

This technique will only be used after a meticulous medical and dosimetric evaluation, and in case inhaled and insoluble radioactive particles (plutonium for example) are deposited in the lungs. Other isotopes and focal accumulation are depicted in Fig. 11.20. A flexible bronchoscopy should be performed to enhance bronchoalveolar lavage [197]. This type of bronchoscopy should be performed only if the lung load is high and incorporates a large amount of insoluble inhaled particles, such as alpha particles (α).

The objective of this procedure is to avoid deterministic effects for pulmonary doses above 6 Gy-equivalents (Gy-Eq)

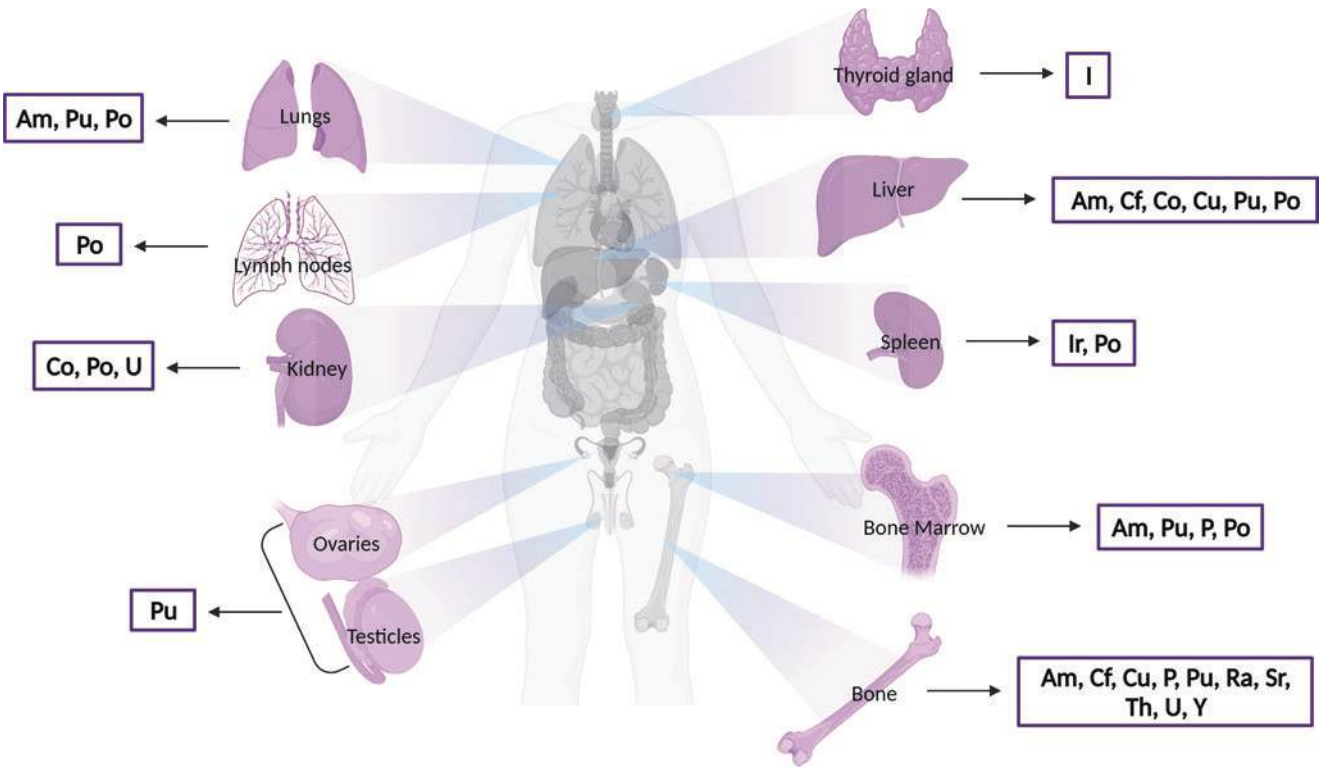

Fig. 11.20 Isotopes and focal accumulation in the body

and is stochastic when the committed doses are lower in the lung. All this within a period of 30 days and individualized for each case.

The Clinical Decision Guide (CDG) and the IAEA EPR 2018 Guide provide bases that can be used by healthcare providers to treat cases where radionuclides have been deposited internally as explained above. Both guides are useful for medical management of individuals contaminated with radionuclides as a consequence of a nuclear or radiological emergency, or due to an industrial scintigraphy accident, or in patients undergoing treatments with radionuclides.

See Annex 1: Contamination by radionuclides and MCMs table.

11.4 Radiosensitizers

Radiotherapy (RT) is a treatment that uses high doses of radiation to kill cancer cells and shrink tumors. Radiosensitizers are chemicals or pharmaceutical agents that increase the cytotoxic effect of IR on cancer cells by accelerating DNA damage and producing free radicals, suppressing the antioxidant mechanism of defenses, or inhibiting the repair of biomolecules, among others. In most cases, radiosensitizers have less effect on normal cells; however, some can also be administered after radiation exposure to treat or reduce the late side effects to healthy tissue. The effectiveness of potential radiosensitizers is measured in terms of the enhancement ratio (ER) (Box 11.4):

$$ER = \frac{\text{Radiation dose required to obtain a given biological effect}}{\text{Radiation dose required to obtain the same effect in the presence of sensitizer}}$$

Box 11.4: Radiosensitizers

- Radiosensitizers specifically target tumor cells and make them more susceptible to IR during RT.
- These therapeutic compounds apparently enhance the radiation-induced damage to cancer cells at the molecular level and may also further limit the harmful effects of radiation on normal tissue.
- Radiosensitizing agents promote fixation of free radicals by their electron affinity, rendering the molecules incapable of repair.
- Their mechanism of action is comparable to the oxygen effect, as biochemical reactions of the damaged molecules preclude the repair of cellular damage.

Characteristics of an Ideal Radiosensitizer

For use as an adjunct in RT, an ideal radiosensitizer should not be harmful to healthy tissues and not interfere with other therapies, as well as should be highly efficient on tumor and hypoxic cells. It should also be economically affordable.

A radiosensitizer should be nontoxic and should produce an advantage in enlarging the therapeutic window, increasing tumor control probability, and limiting the normal tissue toxicity. This effective gain could result from a selective uptake or absorption rate or half-life of the radiosensitizing molecule in a tumor with respect to normal tissue.

Mechanism of Action

Radiosensitizers have been developed to modulate the response that occurs during or after the radiation exposure. At a molecular level, these molecules stimulate the fixing of free radicals generated by radiation. Similarly to the oxygen effect, the biochemical mechanism prevents the repair of damaged molecules. The electron affinity of the radiosensitizers captures independently existing free radicals, rendering the molecules incapable of repair [198]. Although each radiosensitizer has different rationales and limitations, they interact with specific biological targets, i.e., the signaling pathway/cascade (Table 11.1) at diverse levels (Fig. 11.21) from molecules to cells to tissues to organs to a whole organism. The core mechanisms for radiosensitization include:

- Inhibiting repair of radiation-induced DNA damage, thereby increasing the degree of radiation-induced apoptosis and DNA damage
- Improving cytotoxicity by disrupting the cell cycle and organelle function
- Activating and regulating the expression of radiation-sensitive genes or silencing genes related to radioresistance

Classification

Based on the DNA damage and repair mechanisms, radiosensitizers are divided into five groups [199, 200]: (1) reduction of thiols or other intracellular radioprotective molecules; (2) radiolysis of the radiosensitizer, which results in the production of cytotoxic chemicals; (3) inhibitors of repair of biomolecules; (4) thymine analogs incorporated into DNA chain; and (5) oxygen mimetics with electrophilic properties.

With the continuous technological innovation, radiosensitizers can be classified into three categories: (1) molecular

Table 11.1 Potential biological targets at different levels for developing radiosensitizers

Levels	Target (molecules/proteins/enzymes involved in signaling pathways/cascades)
Reactive oxygen species	Targeting mechanisms to generate free radicals
DNA damage response	Targeting key DDR proteins • DNA-PKcs • ATM/ATR • PARP family • MRN (MRE11-RAD50-NBS1) complex • MDC1, Wee1, LIG4, CDK1, BRCA1, CHK1, and HIF-1
Functional organization of genome (chromatin organization)	Targeting inhibitors of chromatin changes • DNA methyltransferase • Histone acetyltransferase, deacetylase, methyltransferase, demethylase
Cellular response to signals	Targeting cell cycle proteins • Blockage of cell cycle checkpoints (G_2/M transition) • Inhibitors of cell survival proteins • Oncogenes (p53, ras) • Evading growth suppressors • Biomechanical effects of microbubbles
Tumor microenvironment	Targeting • Prolyl-4-hydroxylases (PDH) • Oxygen-independent mechanism, including PI3K/AKT and MAPK, or through loss of tumor suppressor protein von Hippel-Lindau (VHL) • VEGF • ECM remodeling within tumors
Tissue-level effects	Targeting • Inhibitors of angiogenesis (antiangiogenic and/or vascular targeting agents) • Inhibitors of growth factor signaling • Anti-VEGF/VEGFR antibodies, antisense suppression of VEGF, VEGFR tyrosine kinase inhibitors, viral-directed targeting of VEGFR signaling • Blockage of growth factor secretion from dying cells

Abbreviations: *DDR* DNA damage response, *DNA-PKcs* DNA-dependent protein kinase, *ATM/ATR* ataxia–telangiectasia mutated and ATM and Rad3 related, *PARP* poly[ADP-ribose] polymerase, *MDC1* mediator of DNA damage checkpoint protein 1, *LIG4* ligase IV, *CDK1* cyclin-dependent kinase 1, *BRCA1* breast cancer gene 1, *CHK1* checkpoint kinase 1, *HIF-1* hypoxia-inducible factor-1, *ECM* extracellular matrix

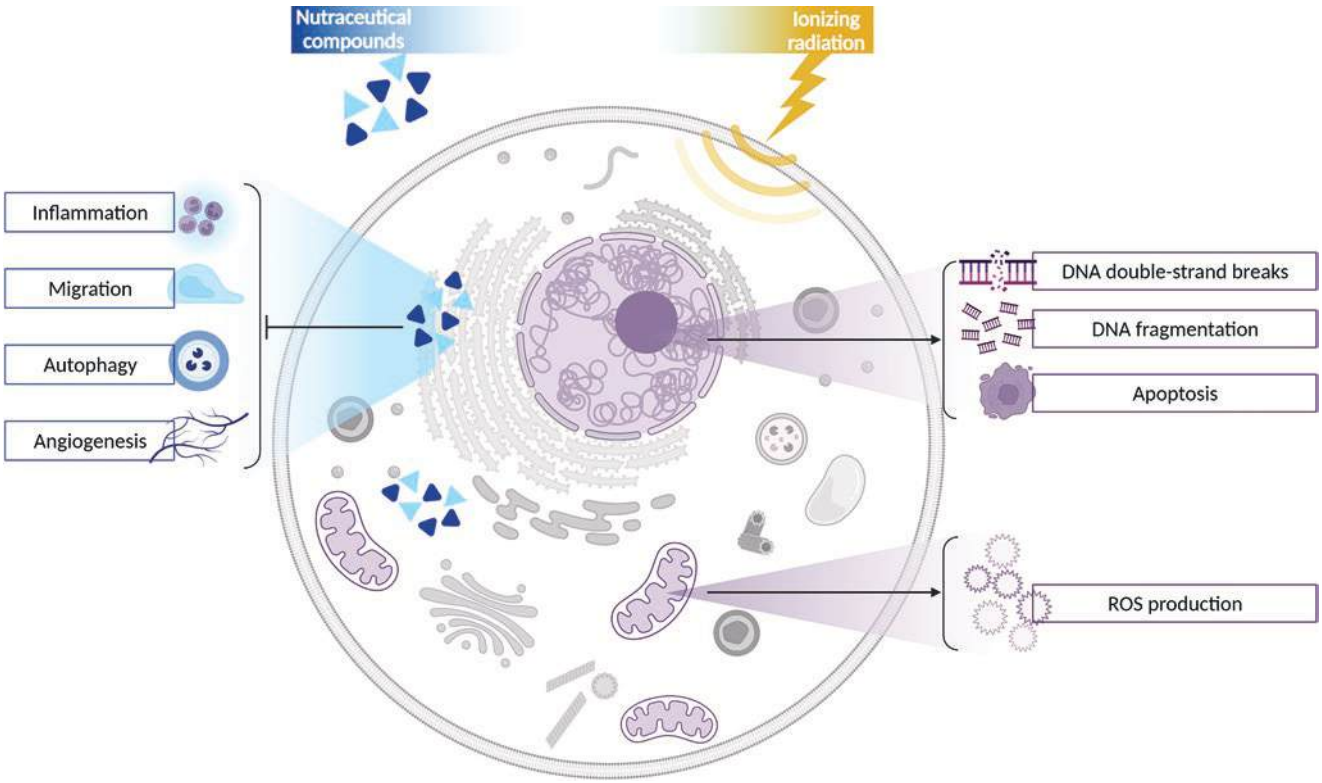

Fig. 11.21 Development of potential radiosensitizers at different levels. Potential radiosensitizers can be developed focusing on the molecular, cellular, or organismic levels, which may be useful in modulating the radiation effects on cancer cells as well as on normal cells

Table 11.2 Small molecules as radiosensitizers

Hyperbaric oxygen A potent radiosensitizer, which promotes toxic and relatively stable free radical formation, useful to effectively enhance the radiosensitivity of the tumors which contain numerous hypoxic cancer cells.
NItroxides The most representative are nitro-containing compounds (such as nitrobenzene, nitroimidazoles, and its derivatives) and nitric oxides (NOs). These are "true radiosensitizers," having higher electron affinity and better diffusion properties than molecular oxygen. It can theoretically substitute for oxygen in "repairing/fixing" radiation-induced DNA damage.
Carbogen A mixture of 95% oxygen and 5% carbon dioxide, which improves tumor oxygenation contrasting with hypoxia.
Hypoxia-specific cytotoxins Bioreductive agents, such as aromatic N-oxides, transition metal complexes, quinones (mitomycin C, porfiromycin, and E09), aliphatic N-oxides, and nitro compounds, that selectively radiosensitize the hypoxic cells by virtue of their preferential cytotoxicity.
Chemical radiosensitizers Chemicals targeting a variety of cell signaling pathways, suppressing radioprotective substances, pseudo-substrates, and targeted delivery systems for radiosensitization. Examples are BKM120 (an oral pan-class I PI3K inhibitor), targets of PI3K-Akt pathway, NVP-BEZ235 (a mTOR inhibitor), AMG 232 (an MDM2-p53 interaction), GSH inhibitors, and radiosensitizing nucleosides (5-fluorouracil (FUra), bromodeoxyuridine (BrdUrd), iododeoxyuridine (IdUrd), hydroxyurea, gemcitabine (dFdCyd), fludarabine).
Natural radiosensitizers Natural molecules are safer than synthetic compounds and have anti-inflammatory and antioxidant properties: curcumin, genistein, resveratrol, zerumbone, ursolic acid, etc.

Table 11.3 Macromolecules as radiosensitizers

Proteins and peptides Antibody conjugates and cell-penetrating peptides selectively deliver a cytotoxic payload to a tumor and spare most healthy cells. Examples are HER3-ADC (targeting HER3), SYM004, and nimotuzumab (targeting EGFR) and cetuximab (inhibitor of EGFR).
miRNAs Endogenous noncoding microRNAs (miRNAs) can be used as RT sensitization targets. These can be regulatory miRNAs of DNA damage response (DDR) and HR repair factors.
siRNAs Exogenous short interfering RNAs or silencing RNAs (siRNAs), which are noncoding RNA molecules, that can selectively target key mRNAs belonging to pathways involved in the response to radiation, such as DDR, cell cycle regulation, and survival/apoptosis balance.
Oligonucleotides Small DNA or RNA sequences are able to disturb key mRNA translation. Studies have concerned oligonucleotides targeting the telomerase RNA subunit or telomerase reverse transcriptase (hTERT) or cyclic AMP response element (CRE) decoy oligonucleotide.

structures of small molecules (Table 11.2); (2) macromolecules with their mechanism of radiosensitivity (Table 11.3); and (3) nanomaterials (Table 11.4) with low cytotoxicity, good biocompatibility, usability, and functionality (Box 11.5).

11.4.1 Nutraceutical Compounds

Several nutraceutical chemicals have attracted significant interest in recent decades due to their possible involvement in the prevention and treatment of various illnesses, as well as their favorable effects in boosting human and animal health. In particular, literature data often report their positive effect in combination with chemotherapy in cancer care. Even while intriguing results have been published on this issue at multiple cellular levels, less is known about their role as radiosensitizers. Presence of these compounds during radiation augments their effect by several mechanisms including the lethal reactions of free radicals.

Among compounds of various origins that showed radiosensitizer potential, numerous studies have revealed the important role of molecules of natural origin, when administered in combination to IR.

The use of nutraceuticals as sensitizers, in addition to being generally well tolerated, is also easily recovered and less expensive in comparison to synthesized drugs. Their administration reduces the collateral effects frequently associated with medication delivery, and in certain situations, they can help attenuate IR adverse effects through biological processes like those shown in Fig. 11.22. Indeed, in most cases, they show anti-inflammatory and antioxidant properties, which are precious arms to counter the RI side effects on healthy tissues.

However, in most cases, they showed direct anticancer activity, as demonstrated by numerous scientific papers. The most studied natural compounds are exposed in Table 11.5 [203].

11.4.1.1 Curcumin

Curcumin, the main component in the Indian culinary spice turmeric (*Curcuma longa*), has been shown to have anticancer potential in several studies. The biological mechanism can be ascribed to cell signaling pathway effects, resulting in the inhibition of cell proliferation and induction of apoptosis.

Regarding its radiosensitizing properties evaluated by an in vitro approach, the inhibition of survival and proliferation has been observed on the MCF-7 breast cancer cell line. In addition, the effect of vehicolated curcumin, using solid nanoparticles, combined with X-ray radiation was tested by Minafra and coworkers [204] on the human nontumorigenic breast epithelial MCF10A cell line and the breast adenocar-

Table 11.4 Nanomaterials as radiosensitizers

Noble metal nanomaterials	Nanoparticles, such as gold (Au, $Z = 79$), silver (Ag, $Z = 47$), and platinum (Pt, $Z = 78$), can effectively interact with radiation, emitting secondary electrons which amplify the radiation effects.
Heavy metal nanomaterials	Physical dose enhancement methods are comparable for gadolinium (Gd, $Z = 64$), hafnium (Hf, $Z = 72$), tantalum (Ta, $Z = 73$), tungsten (W, $Z = 74$), and bismuth (Bi, $Z = 83$) or their stable forms such as oxides, sulfides, and selenides. Examples are gadolinium-based nanoparticles (AGuIX), hafnium oxide (HfO_2) nanoparticle (NBTXR3), tantalum pentoxide (Ta_2O_5) and tantalum oxide (TaOx), bismuth oxide (BiO) nanoparticles, and tungsten oxide nanopowder or nanoparticles (WO_3).
Ferrite nanomaterials	They can catalyze the reaction of H_2O_2, generating highly toxic hydroxyl free radicals in the tumor microenvironment with the aim of boosting the radiation therapeutic efficacy. Explored examples are superparamagnetic magnesium ferrite spinel ($MgFe_2O_4$) nanoparticles (SPMNPs) and zinc ferrite ($ZnFe_2O_4$) nanoparticles
Semiconductor nanomaterials	Semiconductor nanosensitizer materials, such as silicon (Si), germanium (Ge), gallium arsenide (GaAs), and semiconductor quantum dots, have unique properties making them great candidates as photosensitizers and radiosensitizers for tumor treatment ([201]; [202]). Explored examples are WO2.9-WSe2-PEG semiconductor heterojunction nanoparticles (WSP NPs), titanium peroxide (PAA-TiOx) nanomaterial, copper bismuth sulfide ($Cu3BiS_3$,CBS) nanoparticles, and TiO_2 nanotubes.
Nonmetallic nanomaterials	Similarly to the metallic nanoparticles' mechanism of action, nonmetallic nanomaterials can increase oxidative damage. Explored examples are ultrasmall uncapped and amino-silanized oxidized silicon nanoparticles; nanocrystals of underivatized fullerene, C_{60}, (nano-C_{60}); nanodiamonds and carbon nanotubes; and selenium (Se) nanoparticles.
Nanostructured substances and drug delivery systems	Chemicals, oxygen carriers, siRNAs, and other radiosensitizing agents are transported via relatively new nano-based delivery systems. Explored examples are the poly(D,L-lactide-co-glycolide) (PLGA) nanoparticles containing paclitaxel (a cell cycle-specific radiosensitizer) and etanidazole (a hypoxic radiosensitizer).

Box 11.5: Radiation Sensitizers

- Small molecules are classified based on radiation-induced free radicals, pseudo-substrates, and other mechanisms.
- Macromolecules such as miRNAs, proteins, peptides, and oligonucleotides have been explored to develop radiosensitizers as they are capable of regulating radiosensitivity.
- Promising nanotechnology methods used as radiosensitizers include well-developed nanomaterials with low toxicity, good biocompatibility, and functionalization ease.
- Other technologies, such as molecular cloning technology, analysis of molecular structure, and bioinformatics, can speed up the development of new effective radiosensitizing drugs.

cinoma MCF7 and MDA-MB-231 cell lines. The vehicolated curcumin has been shown to be more effective than the free curcumin on MCF7 and MCF10A, whereas the free molecule resulted to be slightly more effective on MDA-MB-231. The dose-modifying factors (DMFs) were calculated to quantify the radiosensitizing effect, which resulted in 1.78 for MCF7 using vehicolated curcumin and 1.38 with free curcumin on MDA-MB-231 cells. Transcriptomic and metabolomics approach supported this study, revealing the double-positive effect of curcumin as an autophagy enhancer for tumor cells and antioxidant agents [204].

Antiapoptotic signals and block in G_2/M cell cycle phase mediated by Bcl-2 were demonstrated in human immortalized prostate adenocarcinoma cells (PC-3) after 5 Gy irradiation combined with 2μM curcumin. Instead, an increased radiosensitivity was observed in HCT116 and HT29 human colorectal cancer cell lines treated with 25μM of curcumin and a single dose of X-ray radiation (10 Gy). Curcumin was also able to decrease COX-2 expression by the inhibition of EGFR phosphorylation both in vitro on the human head and neck squamous cell carcinoma (HNSCC) cell line and in two in vivo models of head and neck tumor.

On the human glioblastoma U87MG cell line, the viability was reduced in a dose-dependent manner by 3 Gy of X-ray combined with curcumin at a concentration range of 5–10μM, sustained by the arrest of cell cycle in phase G_2/M (which is the most sensitive step to radiation) and the inhibition of two master regulators of tumor progression, the MAP kinases ERK and JNK [203].

However, curcumin is an unstable, nonbioavailable compound due to its poor absorption in the GI system. Hence, its therapeutic application is delimited by its pharmacokinetics. Despite promising preclinical studies, no double-blinded placebo-controlled clinical trial, using curcumin as a radiosensitizer, has been successful. The interaction of curcumin with RT on different cancer types has been reviewed by Verma [205]; however, there is still a lack of solid clinical evidence of radiosensitization. For instance, in vitro and in vivo studies together with clinical bioavailability data do not give evidence for a radiosensitizing effect of curcumin in the treatment of high-grade brain tumors (glioblastoma multiforme). On the other hand, there is limited data on curcumin's radioprotective function, despite the fact that some clinical trials suggest that curcumin is beneficial for the management of radiation toxicities [205].

11.4.1.2 Resveratrol (RV) and Pterostilbene (PT)

The antineoplastic ability of RV encouraged its application also as a radiosensitizer to overcome radioresistance of many cancers.

A dose-dependent reduction in the surviving fraction of a non-small cell lung cancer (NSCLC) cell line after irradiation with 0–8 Gy of γ-rays in combination with 20μM of RV was

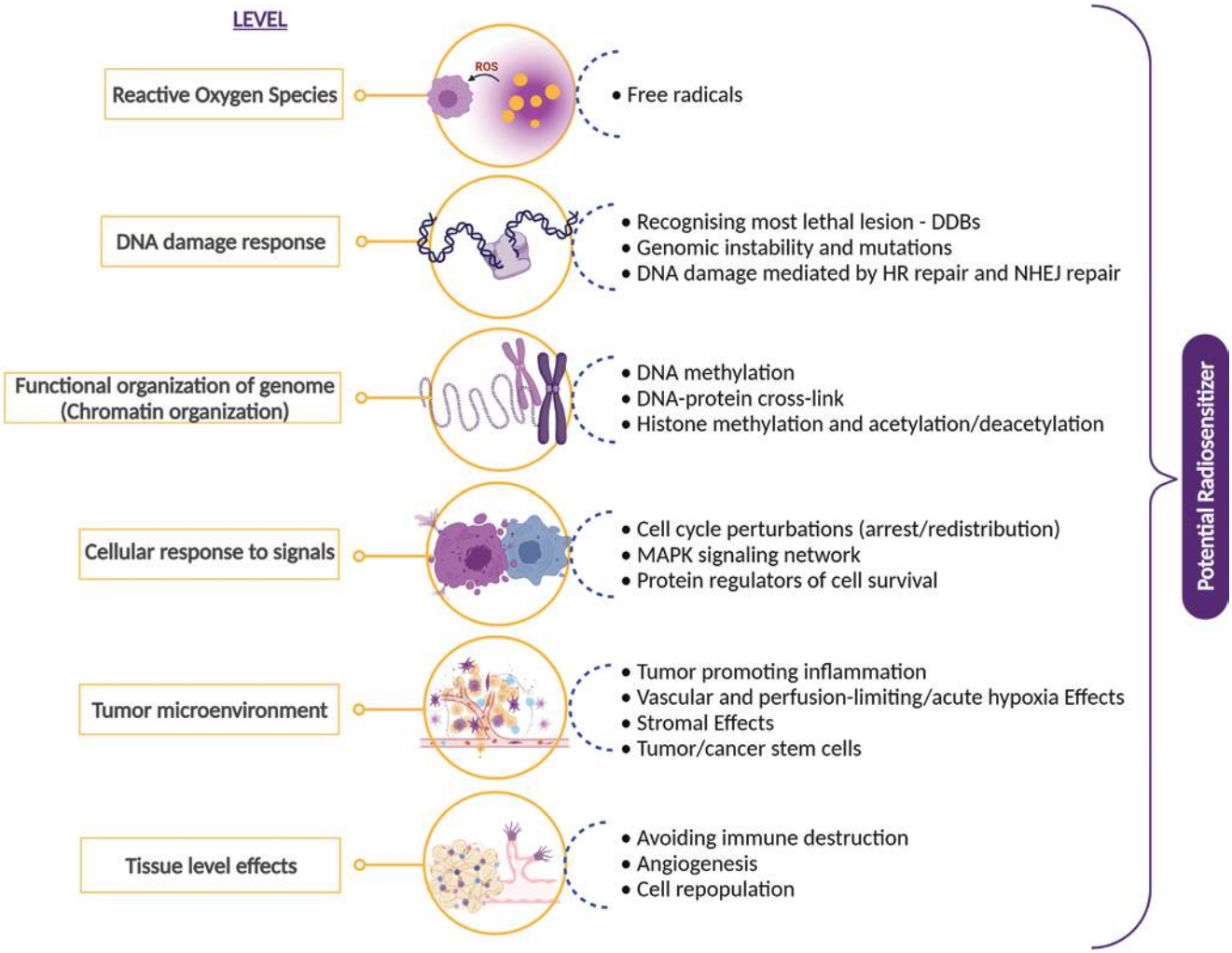

Fig. 11.22 Radiation therapy and nutraceutical substances may influence signaling pathways involved in migration, inflammatory response, autophagy, and formation of reactive oxygen species (ROS). Adapted from "Nutraceutical Compounds as Sensitizers for Cancer Treatment in Radiation Therapy," by [203], Licensed under CC BY 4.0

Table 11.5 Natural compounds related to cancer radiation treatments

Natural compounds	Tumor target	Type of treatment
Curcumin	Colorectal cancer, glioblastoma, head and neck squamous cancer, prostate cancer	X-rays
Resveratrol	Breast cancer, glioblastoma, head and neck squamous cancer, melanoma, nasopharyngeal carcinoma, non-small cell lung cancer, prostate cancer	γ-rays, X-rays
Withaferin A	Breast cancer, cervical cancer, Ehrlich ascites carcinoma, fibrosarcoma, histiocytic human lymphoma, liver cancer, melanoma, renal carcinoma	γ-rays, X-rays
Celastrol	Lung cancer, prostate cancer	γ-rays, X-rays
Ursolic acid	Colon carcinoma, gastric adenocarcinoma, non-small cell lung cancer, melanoma, prostate cancer	γ-rays, X-rays
Zerumbone	Colorectal cancer, glioblastoma, lung adenocarcinoma, non-small cell lung cancer, prostate cancer	γ-rays, X-rays
Caffeic acid phenethyl ester	Adenocarcinoma, breast cancer, lung cancer, medulloblastoma	γ-rays, X-rays
Emodin	Cervical cancer, hepatocellular carcinoma, nasopharyngeal carcinoma, sarcoma	γ-rays, X-rays
Flavopiridol	Cervix cancer, esophageal adenocarcinoma, esophageal squamous carcinoma, glioma, lung carcinoma, ovarian carcinoma, prostate cancer, zebrafish model	γ-rays, X-rays
Berberine	Breast cancer, esophageal carcinoma, nasopharyngeal carcinoma, osteosarcoma, prostate cancer	γ-rays, X-rays
Genistein	Breast cancer, cervical cancer, non-small cell lung cancer	γ-rays, X-rays
Selenium	Melanoma, glioma, breast cancer	γ-rays, X-rays

observed along with accelerated senescence and cell death following enhanced DNA DSB induced by ROS [203].

However, an increased expression of LC3-II for autophagy response after X-ray and RV treatment (75μM) was demonstrated in SU-2 glioblastoma multiforme cell lines [206]. Also, in GBM, RV showed inhibition of the hypoxia-inducible factor HIF-1α, which is responsible for a well-known mechanism of radioresistance. Moreover, the interaction of RV with other agents as iododeoxyuridine (IUdR) was also tested and demonstrated the ability to decrease the formation of cancer colonies [203].

In the HNSCC cancer model, suppression of cell proliferation was obtained on a cell line, treated with 100μM of RV combined with 10 Gy of X-ray, also observing the inhibition of STAT3 phosphorylation, a well-known transcription factor driving inflammation and cancer progression. Even the peanut stem extract (PSE), which contains a high amount of RV, has been tested in combination with X-rays, which showed similar radiosensitization effects on radioresistant human prostate cancer cell lines. In this regard, the tumor growth of a prostate cancer xenograft mouse model was reduced with RV and/or PSE (total dose 12 Gy, 5 or 250 mg/kg, respectively) [203]. RV was also used as a pretreatment (25–150μM) to treat the human NPC CNE-1 cell line with X-ray irradiation (0–6 Gy), revealing the inhibition of the AKT phosphorylated form, a known proproliferative marker. These effects were also confirmed in NPC xenograft models, combining the RV treatment with 4 Gy for 3 days, resulting in a tumor volume reduction.

Nevertheless, a key problem is the short RV half-life and low bioavailability under in vivo conditions. In vivo, pterostilbene was proven to be beneficial in the treatment of melanoma and pancreatic cancer. This study demonstrated that PT can be helpful against melanoma by inhibiting the generation of adrenocorticotropic hormone in the brain of a mouse, which impairs the Nrf2-dependent antioxidant defenses of melanoma and pancreatic tumors. This produces tumor growth restraining and tumor sensitization to oxidative stress. In addition, PT has been shown to increase cancer cell death by the induction of lysosomal membrane permeabilization [53].

11.4.1.3 Withaferin A

Withaferin A (WA) was the first withanolide to be isolated and extracted from the plant *Withania somnifera*. WA-induced radiosensitization has been observed in human histiocytic lymphoma, renal carcinoma, and liver, breast, and several other types of cancer. Overall, these studies highlight the effect of combined treatment, mediated by the increase of apoptosis and production of ROS.

WA has been shown to suppress cancer cell growth by targeting the intermediate filament protein vimentin, a structural protein of the cell cytoskeleton. In light of its anticancer capability, WA was also tested in order to investigate its effect in inducing the radiosensitization of cancer cells.

WA's effects were initially investigated in vitro and in combination with γ-irradiation on a lung fibroblast cell line, and WA was found to be well tolerated by cells and to mediate a synergistic impact with γ-rays in terms of cell death. Based on these encouraging results, WA was further tested in vivo to assess its effect as a radiosensitizing agent in several cancer models such as the spontaneous murine mammary adenocarcinoma (Ehrlich ascites carcinoma—EAC), a mouse model of fibrosarcoma, and a mouse model of melanoma. Overall, each of the studies demonstrated that the WA and γ-ray combined treatment inhibits tumor growth, increasing tumor-free survival and median survival time of animals [203].

11.4.1.4 Celastrol

Celastrol, also known as tripterine, is a triterpenoid derived from the root of the "thunder god wine" plant often found in China and utilized in traditional Chinese medicine for its anti-inflammatory qualities in a variety of conditions, including autoimmune diseases. Moreover, anticancer properties have been revealed, due to its proteasome inhibitory activity and antimetastatic ability.

A study has evaluated its radiosensitizer effect on PC-3 cells, both in vitro and in vivo. The in vitro pretreatment with celastrol before irradiation with X-rays resulted in a significant dose-dependent enhancement of IR-induced clonogenic cell killing. This effect was explained by (1) a longer gH2AX activation for a longer time in combined treated cells with respect to the only irradiated ones, thus revealing a DNA repair impairment action by celastrol, and (2) a major expression of apoptosis markers (cleaved PARP and caspase-3).

Thus, the same group tested the celastrol radiosensitizer effect on a PC-3 xenograft model. 1 mg/kg of celastrol (5 days/week for 3 weeks) was given to the mice 1 h before irradiation with a single dose of 2 Gy (5 days/week for 2 weeks). The histological analysis showed a significantly increased apoptosis and angiogenesis reduction in the combined treated tumors [203].

Similar effects have been found on the NCI-H460 human lung cancer cell line, combining celastrol with 0–4 Gy of X-rays. Indeed, the EGFR, ErbB2, and survivin irradiation markers were found to be reduced, whereas the celastrol-dependent inhibition of HSP90 was observed. Furthermore, celastrol induces a more pronounced ROS generation after irradiation, thanks to its quinone methide moiety [203].

Finally, the effect of celastrol as a radiosensitizer was evaluated on lung cancer with different approaches. Indeed, one research group has identified it as one of the most promising sensitizer candidates among 30 drugs, by an in silico study. Thus, they tested its effect in vitro on A549 and H460 cells, subjected to pretreatment with celastrol and 2–10 Gy

of dose range. The encouraging results from this in vitro study were the premises for a preclinical study on a A549 xenograft mouse model. The combined treatment using 2 mg/kg/5 each day and 10 Gy of IR for 12 days produced larger intratumoral necrotic areas [203].

11.4.1.5 Ursolic Acid

Ursolic acid (UA) belongs to the family of the pentacyclic triterpenoids. It is generally obtainable from the peel of many fruits, e.g., apples, blueberries, and prunes, and also in many herbs, such as rosemary and thyme. Recently, the following therapeutic properties of UA have been described: anticancer, anti-inflammatory, and antimicrobial, and also its radiosensitization activity in models in in vitro and in vivo studies. For example, in human prostate and colon cancer cells, and in mouse melanoma cells, the UA is able to radiosensitize cells with a significant reduction in cell viability associated with an increase of typical signs of apoptosis cascade, such as cell volume reduction, nuclei fragmentation or condensation, caspase-3 activation (one of the key enzymes involved in the apoptotic pathway), increased levels of cleaved PARP (enzyme involved in DNA repair processes), DNA fragmentation, and also increased ROS generation. In melanoma mouse models, the treatment with UA and IR is able to inhibit tumor growth owing to a downregulation of Bcl-2 and survivin, two known key protein regulators of cell survival [203].

Moreover, UA can also exert a differential effect after exposure of normal or cancer cells to UV, acting as a photosensitizer for the latter and as a photoprotector for normal ones. This action was observed in human melanoma cells and in human retinal pigment epithelium control cells, where induced oxidative stress by ROS production, cell cycle arrest, and cell death induction were evaluated following UA and UV treatments. Furthermore, the UA has a significant radiosensitizing effect in human gastric adenocarcinoma cells, as evidenced by (i) a decrease in the cell survival fraction and otherwise an increase in the number of apoptotic cells (positive to the propidium iodide and annexin V apoptotic markers); (ii) the arrest of the cell cycle (in the G_1 and G_2/M phases); and (iii) the increase in ROS amount and a decrease of Ki-67-positive proliferating cells [207].

11.4.1.6 Zerumbone

Zerumbone (ZER) is a cyclic ketone and a sesquiterpene compound, a cytotoxic component obtained by steam distillation of the *Zingiber zerumbet* Smith. ZER is used in food and herbal medicine, and it also has anti-inflammatory, antiproliferative, and antitumor properties, as observed in many tumor types (including breast, pancreas, colon, lung, and skin). In addition, the radiosensitizing effects of ZER on tumors, by means of its regulatory activities on DNA DSB repair, cell cycle, and apoptotic pathways, have been highlighted too [203].

ZER was able to significantly increase radiation-induced cell death in human lung adenocarcinoma cells by inhibiting heat-shock proteins (HSP), increasing caspase 3 and PARP cleavage, and inhibiting HSP27 binding to apoptotic molecules such as PKCδ and cytochrome C [203].

In addition, the radiosensitizing effect was also observed in human glioblastoma cells. The same authors showed an IR-induced decrease of cell survival on human prostate cancer cells, associated with a reduced expression of proteins involved in the DNA damage repair pathway, such as γH2AX and ATM [203].

Moreover, in human colon-rectal cancer cells, ZER pretreatment is able to induce apoptosis and enhance radiation-induced G_2/M arrest and reduction of activation of the DSB DNA repair machinery.

11.4.1.7 Caffeic Acid Phenethyl Esther

CAPE is an active component of honeybee propolis, a phenolic compound, and a structural derivative of flavonoids. It was described for its antiviral, bactericidal, anti-inflammatory, and antioxidant properties. CAPE compound is also able to change the redox state by perturbing the activation of GSH and to induce apoptosis. Furthermore, it has been shown to be more toxic to cancer cells than normal cells, as well as to amplify the action of RT in a variety of cancers.

CAPE has been shown to improve radiation-induced cell cycle arrest and death in human medulloblastoma DAOY cells. In particular, the combined treatment with CAPE and 2 Gy of IR caused an ROS enhancement production, a significant inhibition of NF-kB activity, apoptosis activation, and downregulation of cyclin B1 protein expression. In line with these data, a strong reduction of cell survival, in a concentration-dependent manner, was described in the same cell line pretreated with CAPE (0.1–10 M) for 24 h before exposure to γ-ray irradiation at various doses (0–8 Gy), associated with cell cycle progression inhibition, by arresting cells in the S phase [203].

The CAPE pretreatment radiosensitizing effect was also shown in mouse CT26 adenocarcinoma cells, using both in vitro and in vivo approaches showing decreased cell survival rate and reduced NF-kB activation. CAPE-induced decrease of survival rate was also described in breast and lung cancer cell lines. In particular, in MDA-MB-231 and T47D breast cancer cell lines, CAPE and X-ray combined treatments decreased cell growth and delayed the DNA repair process for up to 60 min after exposure [203].

11.4.1.8 Emodin

Traditional Chinese medicine uses emodin (6-methyl-1,3,8-trihydroxyanthraquinone), a natural phenolic derived from the roots and rhizomes of numerous plants (e.g., *Polygonum cuspidatum* and *Cascara buckthorn*).

Emodin is chemically similar to the mitochondrial ubiquinone named DMNQ (2,3-dimethoxy-1,4-naphthoquinone), an endogenous ROS inductor, as it is able to transfer electrons. It is also known to have antibacterial, antiviral, anti-inflammatory, and anticancer effects. The emodin's antitumor effect has been observed in several types of cancer (leukemia, breast, colon, and lung cancer), also in combination with RT schedules, although its mechanism of action still remains unclear.

Under hypoxic conditions, emodin treatment enhanced the radiosensitivity of CNE-1 NPC human nasopharyngeal carcinoma cell line. In particular, treatment with 3.9 and 7.8 g/mL emodin 24 h before 2 Gy IR induced an increase in the apoptosis ratio and cell cycle arrest in the G_2/M phase. Moreover, an increase of ROS production in tandem with a downregulation of HIF-1 levels (both mRNA and protein) was also described. These data were also confirmed by using CNE-1 xenograft models where a tumor growth delay was observed after emodin and IR combined treatments [203].

The radiosensitizing effect of emodin has also been observed in the HeLa cervical cancer cell line, where pretreatment with different concentrations of aloe emodin (AE) before X-ray irradiation (0–10 Gy) leads to decrease in the mean lethal dose (D0) in a concentration-dependent manner, as well as an enhancement in the percentage of cells in the G_2/M phase and a sub-G_1 peak at 24, 48, and 72 h, using 50 M and 4 Gy IR. In addition, an increased expression of cyclin B, γ-H2AX, and alkaline phosphatase (ALP) activity was also described. Similar data regarding a decrease of cell growth and viability were observed also in human HepG2 hepatocellular carcinoma cell line treated with 10 Gy of γ-irradiation and AE, under hypoxic conditions. This combined treatment leads to higher increase in both G_2/M and apoptotic populations [203].

11.4.1.9 Flavopiridol

Flavopiridol is a flavone originating from the *Dysoxylum binectariferum* plant commonly used in Indian medicine. This molecule is able to arrest cell cycle by acting on cyclin-dependent kinases (CDKs) during the G_1/S or G_2/M phases, which is confirmed in several cancer cell types (chronic lymphocytic leukemia, squamous cancer, breast cancer cells). In addition, flavopiridol is able to induce the transcriptional suppression of genes involved in the proliferation pathways, to stimulate apoptosis, to inhibit angiogenesis, and to increase the chemotherapeutic effects [203].

The power of flavopiridol to affect cell radiosensitivity, in tandem with docetaxel, was described in H460 human lung carcinoma, by using both in vitro and in vivo approaches. Multiple treatments with docetaxel (10 M), γ-irradiation (0–5 Gy), and flavopiridol (120 M) are able to augment radiation effects by inducing cell cycle arrest in the G_1 and G_2/M phases. On the other hand, in esophageal squamous carcinoma cell lines, cell cycle arrest after irradiation was described with the decrease of cyclin D1 and retinoblastoma protein (Rb) levels. Additionally, in the SEG-1 esophageal cancer cell line, treatment with flavopiridol 24 h before γ-radiation (2–6 Gy) increased radiosensitivity compared to the control, due to inhibition of several CDKs, cell cycle redistribution in G_1 and G_2 phases, and induction of apoptosis [203].

The experimental evidences show that cells containing mutated p53 or overexpressed Bcl-2 are more radioresistant than wild type. However, flavopiridol increased the cytotoxic effects of radiation in cells with altered status of p53 and Bcl-2, confirming the hypothesis according to which these two pathways are targeted by radiosensitizer mechanism exerted by flavopiridol [203]. Moreover, the radiosensitizing effects of flavopiridol were evaluated in vivo on glioma xenograft models using GL261 cells. The interaction of γ-radiation (5 Gy), fractionated for 10 days, with flavopiridol (5 mg/kg) resulted in a decrease in cell proliferation, which was mainly mediated by the flavopiridol's antiangiogenic activity, which also inhibited the HIF-1 pathway [203].

On the other hand, as described in OCA-I ovarian carcinoma cells, the radiosensitizing action of flavopiridol could be sustained also by the downregulation of Ku70 and Ku80 proteins, known to be involved in DNA repair mechanisms after radiation exposure, by the redistribution of the cell cycle with a greater accumulation of cells in the two more radiosensitive G_1 and G_2 phases [203].

11.4.1.10 Berberine

Berberine is an alkaloid which can be extracted from the roots of many plants like the barberry, the tree turmeric, and the California poppy. Berberine is used to treat health problems like hypercholesterolemia and type 2 diabetes mellitus.

Berberine works by inhibiting cell cycle progression, thereby exerting, in vitro, an antitumor activity in a large array of tumors, and its radiosensitizing properties were investigated on lung, esophageal, and breast cancer cells. Since berberine interferes with the expression and activity of RAD51, involved in DNA damage repair response, its radiosensitizing mechanism is based on hindering DNA damage recovery after X-ray irradiation. In vitro and in vivo experimental data has revealed the ability of berberine to inhibit HIF-1α and suppress VEGF. For example, in an in vitro nasopharyngeal carcinoma study, berberine when combined with γ-rays demonstrated a reduction of cancer cell proliferation, viability, and Sp1 decreased expression, a protein involved in tumor motility and invasion [203].

11.4.1.11 Genistein

As expected, genistein also acts as a radiosensitizing agent, if combined with γ-irradiation, as shown in vitro in cervical cancer cells, where the growth inhibition was associated with survivin downregulation, a prosurvival protein. Again, in cervical neoplasms, genistein enhanced RT effects in multiple ways: by inhibiting G_2/M phase of cell cycle; by reducing the expression of two prosurvival proteins, Mcl-1 and AKT; and by triggering cell apoptosis via cytochrome c release, cleavage of caspase-3 and -8, inhibition of Bcl-2, and enhancement of Bax expression. Similar results were also shown on breast and non-small cell lung cancers, where the radiosensitizing ability was associated with the inhibition of Bcl-x, ROS production enhancement, and antioxidant molecule downregulation [203].

11.4.1.12 BP-C2

BP-C2, a lignin-derived polymer containing benzene polycarboxylic acids complexed with ammonium molybdate, is an antioxidant that promotes the release of prorepair cytokines (IL-4 and IL-10) and suppresses the release of proinflammatory cytokines (TNF-α and IL-6). Orally administered BP-C2 was found to have radioprotective and mitigative activity in H-ARS and GI-ARS [208]. Topical BP-C2 was found to have radiomitigative activity in a cutaneous radiation injury model (CRI-ARS) [209].

11.4.1.13 Sodium Selenite

Several studies have revealed the prooxidant and cytotoxic properties of sodium selenite, with respect to other selenium compounds, recognized for their antioxidant activity. In particular, the effect on natural killer (NK) cell activation is known, as well as the inhibition of the disulfide exchange on cell surface, a remodeling process, which drives cancer to uncontrolled cell division [203].

Schueller et al. [210] tested a 14-day pretreatment of C6 rat glioma cell line with selenite in the range concentration of 2–3.6 mM, before applying 0–20 Gy of γ-rays. The results showed a significant difference between the 0 mM and 3 mM survival curves applying 5 Gy (p = 0.02) and 10 Gy (p = 0.009). Also, the vehiculated sodium selenite nanoparticles (nano-Se) were tested as radiosensitizers, using the 0–3 mg/mL range concentrations pretreatment, before treating with 0–8 Gy of X-rays. In this case, the authors showed the effect on MCF7 breast cancer cells, observing that combined treatment generated a higher mortality rate of the IR or nano-Se single treatments, inducing block at the G_2/M phase of cell cycle, autophagy activation, and ROS generation. Moreover, A375 melanoma cells were subjected to 4-h pretreatment with a selenium nanosystem, using 0–15 mM coated hemocompatible erythrocyte membrane combined with bevacizumab (RBCs@Se/Av) and 2–8 Gy of X-rays. This study showed a strong cell survival reduction, an increase in the sub-G_1 cell proportion, apoptotic pathway activation, and ROS generation. In addition, as expected by the bevacizumab treatment, decreased VEGF and VEGF2 levels were observed as tumor angiogenesis reduction [203].

11.4.2 Corticosteroids

Corticosteroids are a group of hormones, produced by the cortex of the adrenal glands, having the characteristic steroid nucleus and derived from subsequent degradations of the cholesterol side chain. They include numerous molecules with different actions, including sex hormones. However, they are divided into glucocorticoids, such as cortisol which controls the metabolism, and mineralocorticoids, such as aldosterone which controls the concentration of electrolyte and water in the blood.

Among these molecules, many are used for their potent anti-inflammatory and immunosuppressive properties, such as corticosterone (C21H30O4) and cortisone (C21H28O5, 17-hydroxy-11-dehydrocorticosterone).

In the context of clinical RT, corticosteroids are currently used as mitigators of side effects caused by irradiation [211]. However, some researchers have highlighted the radiosensitizing effects of these molecules, used in the pretreatment phase.

Glucocorticoids (GCs), acting on stress pathways, are well known in the treatment of different types of tumors. They have a strong inhibitory action on the proinflammatory cytokine production, although their action mechanisms need deeper investigation, if used in combination with IR.

An in vitro study has investigated the role of dexamethasone (Dex), a synthetic glucocorticoid, in DNA damage response (DDR) pathway, on three astrocytoma cell lines (CT2A, APP.PS1 L.1, and APP.PS1 L.3). The results showed increased basal levels of γ-H2AX foci, keeping them higher 4 h after irradiation (IR) of the cells, while no effect was shown on the 53BP1 foci formation, compared to untreated cells. The high-level expression of γ-H2AX was reversed by ascorbic acid administration, a strong inhibitor of reactive oxygen species, showing that DEXA induces DNA damage by oxidative stress [203].

In addition, in a preclinical study on rat model, the effect of 1 mg Dex was studied alone or in combination with radioprotective molecules turpentine oil (TO), α2-macroglobulin (α2-M), or amifostine, before the administration of 6.7 Gy (LD50/30) of RI, evaluating survival and blood inflammatory markers. The results showed that Dex alone was lethal for 45% and 55% of control and irradiated rats, respectively. On the other hand, from the combination of pretreatments, it emerged that 1 mg Dex reduced the radioprotective efficacy of TO and Ami to 30% and 40%, respectively, even if, given together, TO and Ami provided 70% protection to rats receiv-

ing Dex. Instead, TO and α2-M enhanced the rate of survival from 50% to 90% and 100%, respectively [203].

11.4.3 Nanoparticles

A crucial question for cancer treatment is how to increase the therapeutic window, enhancing radiation damage in tumors, while preserving the surrounding healthy tissues. One promising strategy is the accumulation of nanoparticles composed of high-Z materials (e.g., gold, palladium, platinum, gadolinium) in the tumor cells.

High-atomic-number (Z) compounds have long been used as image contrast agents due to their high X-ray attenuation properties compared to soft tissues. The higher energy absorption of elements such as iodine and barium can enhance the contrast of the organs and tissues in which they are injected. The concentration of the compounds and the radiation doses used for diagnostic applications are usually so low that radiation effects and risks can be neglected. However, the same differential energy absorption principle can be exploited for therapeutic use. Recent developments in nano-manufacturing have provided reasonable and affordable methods to produce high-Z structures with dimensions smaller than 100 nm, which can be loaded in tumor volumes and in tumor cells. Their small size allows the nanostructures to escape the leaky vasculature system of tumor regions, providing a natural method for passive tumor accumulation. The majority of work has been concentrated on gold thanks to its biocompatibility and easy functionalization. The former means that considerable concentrations of gold nanostructures can be administered without toxicity effects, while the latter allows for the development of bespoke products able to accumulate in specific tissues/cells (active accumulation). Gold's high atomic number ($Z = 79$) provides excellent radiation absorption contrast as indicated in Fig. 11.23. Other materials such as gadolinium ($Z = 64$) and more recently superparamagnetic iron oxide nanoparticles (SPION, $Z_{Fe} = 26$) have also been suggested and explored.

Early work by Hainfeld [212] demonstrated the potential of high-Z nanostructures to enhance the effect of radiation and improve tumor control in mice treated with kilovoltage X-rays minutes after injection of gold nanoparticles (GNP). In vitro work using a wide range of cell lines and radiation qualities confirmed that the presence of GNP can enhance the effect of radiation by 10–100% [213].

Interestingly, the radiation sensitization observed in in vitro and in vivo work is often significantly greater than that predicted from simple macroscopic dose models. Furthermore, the size, shape, and surface coating of the nanoparticle as well as the radiation quality and cell line have been shown to affect the radiation response observed. The discrepancy between dosimetric and experimental results regarding the radiosensitization effect emphasizes that complex physical, chemical, and biological interactions are involved in high-Z nanoparticle-mediated radiosensitization, which still need to be fully elucidated in order to extrapolate the nanoparticle radiosensitization concept to patient cancer RT. Physical, chemical, and biological mechanisms of nanoparticle radiosensitization are shown in Fig. 11.24.

11.4.3.1 Physical Radiosensitization

The physical processes driving the enhancement in radiation effectiveness in the presence of nanoparticles strongly depend on the radiation quality used. For medium-energy X-rays (<300 kVp), the radiation-nanoparticle interaction is dominated by the photoelectric effect, especially for photons with energies around the L- and K-shell excitation edges. This causes the emission of inner shell electrons from the high-Z material, resulting in a cascade of low-energy Auger

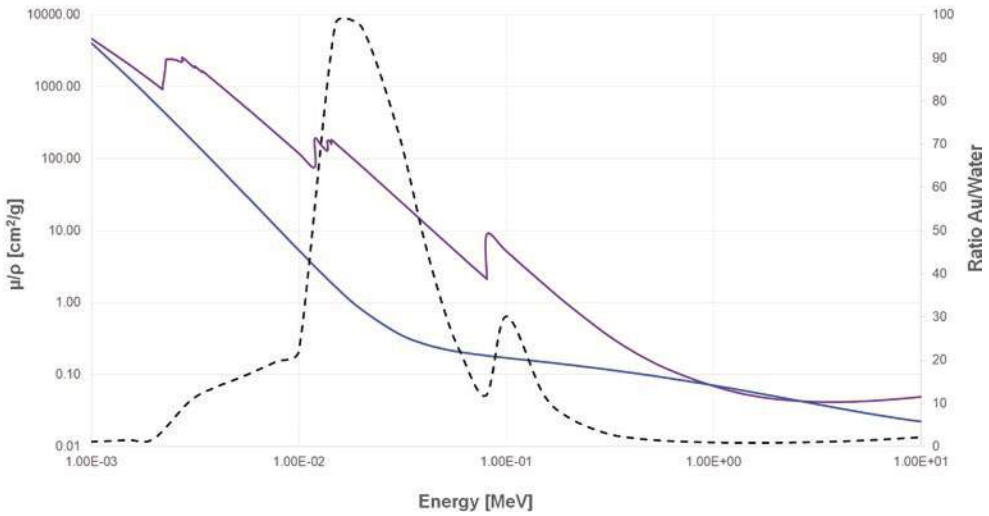

Fig. 11.23 Mass energy absorption coefficient (left-hand-side *Y*-axis) for gold (purple) and soft tissue (blue) as a function of X-ray energy. Right-hand-side *Y*-axis indicates the ratio (black)

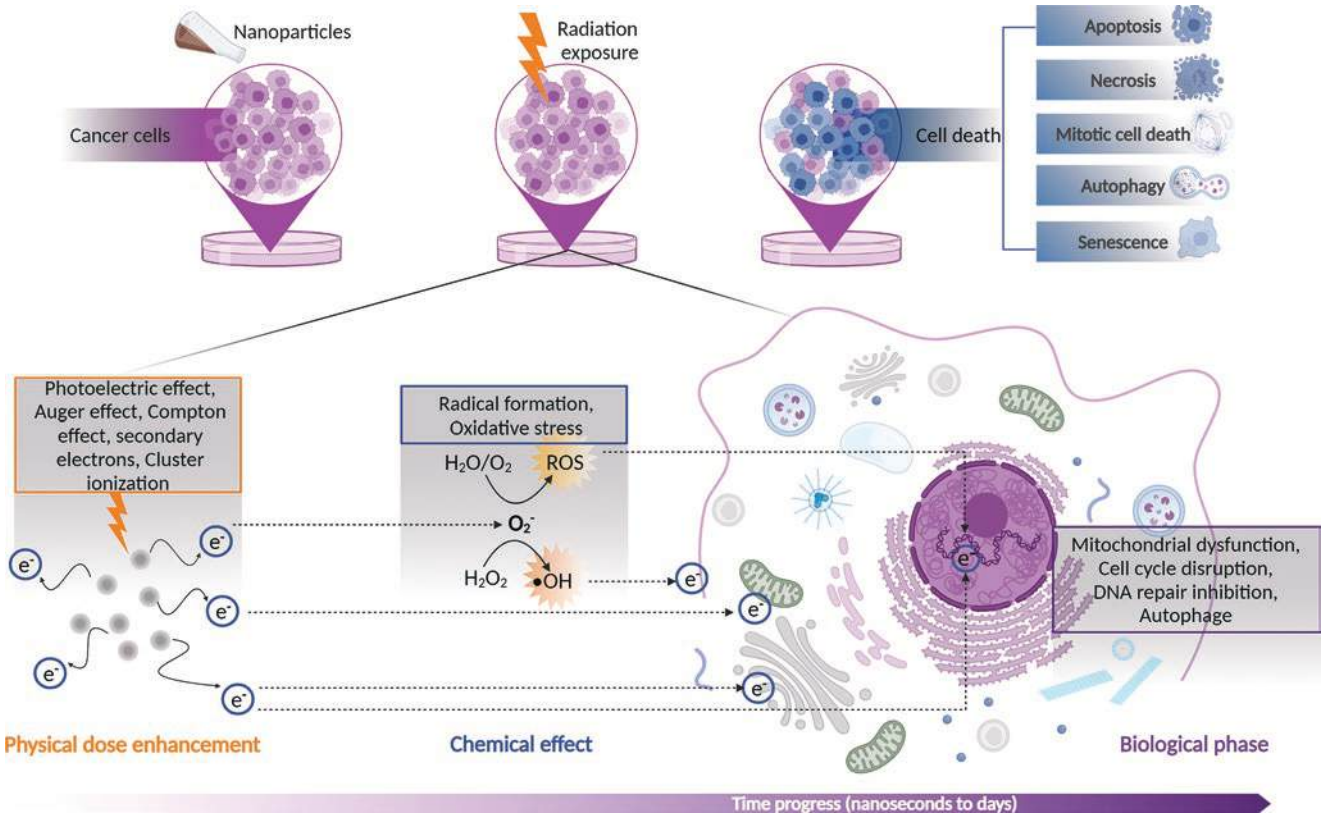

Fig. 11.24 Physical, chemical, and biological mechanisms of nanoparticle. Nanoparticles radiosensitization. Reproduced with permission of Dove Medical Press Ltd., from Application of Radiosensitizers in Cancer Radiotherapy, International Journal of NanoMedicine, 16: 1083–1102, by Gong L et al. 2021

electrons (10–20 electrons per interaction). The majority of these low-energy electrons are reabsorbed by the nanoparticle. Only a few Auger electrons escape the nanoparticle, releasing their energy in a few 10 s of nm around the nanoparticle [214]. As a result, the presence of high-*Z* nanoparticles increases the dose absorbed by the volume in which the nanoparticles are loaded, and it changes the spatial distribution of the ionizations concentrating the energy deposition around the nanoparticles.

At higher photon energies (such as MV which is routinely used for cancer treatment), the dominant process in the interaction between radiation and nanoparticles is Compton scattering. At these energies, the Compton cross sections for high-Z materials are similar to that of soft tissues, and therefore no differences should be expected from the presence of high-*Z* nanoparticles. However, MV photon beams usually contain a considerable fraction of lower keV photons and electrons, which can also increase due to scattering processes (e.g., at 10 cm depth, the fraction of <150 keV photons from a flattening filter-free beam is between 13% and 20%). MV photon beams can therefore produce a considerable amount of Auger electrons from interaction with high-*Z* nanoparticles and alter both the macroscopic and the microscopic dose absorbed.

With protons and charged particles, the probability of interaction between the primary beam particle and the nanoparticles is considerably smaller than that for photon beams due to the lower number of primary tracks required to deliver a given dose. The dominant interaction process is the production of secondary electrons from the nanoparticle via small-angle scattering, which is proportional to the density and therefore higher for high-Z nanoparticles than for soft tissues. In contrast to the photon interactions, these secondary electrons are produced from the outer atomic orbital of the nanoparticle and contribute only a few percentages of the additional absorbed dose.

In all cases, the presence of high-Z nanoparticles causes an increase in the overall macroscopic dose absorbed and high localized energy deposition spikes. The former was initially thought to be the main cause of the observed radiobiological enhancement. However, calculations clearly show that the additional absorbed macroscopic dose by itself is not enough to explain the increased effectiveness observed in experimental studies. The localized energy deposition spikes, caused by the presence of nanoparticles, are similar to those produced by the traversal of charged particles, and their impact on the biological effects can therefore be estimated using radiobiological models based on microscopic dose dis-

tributions. The local effect model (LEM) is widely used for charged particles and has been employed to demonstrate that higher radiosensitization enhancement ratios can be expected when local energy distribution is taken into account. Radiosensitization prediction by the LEM-based model strongly depends on the location of the nanoparticles and the radiation quality, with the closer the nanoparticles are to the critical structures of the cell (e.g., DNA), the larger the effect.

11.4.3.2 Chemical Radiosensitization

A key property of nanoparticles is the increased interaction with the surrounding environment (due to the high surface-to-volume ratio). The intracellular nanoparticle concentration is an important determinant for radiation sensitization. Numerous studies have investigated the importance of the nanoparticle size on cellular uptake, and an optimum diameter appears to range between 10 nm and 50 nm, showing a strong correlation between radiosensitization and nanoparticle concentration [215]. However, the precise value also depends on the coating and on the cell line. High-Z nanostructures are generally coated with a layer of polyethylene glycol (PEG) to provide a hydrophilic nature, preventing the nanostructures from aggregating and increasing their cellular internalization by macrophage recognition. Moreover, nanoparticles are often also conjugated with other biomolecules to achieve specific cellular and subcellular targeting. By using such an approach, it is possible to manufacture nanoparticles that dock to specific cell surface proteins or distinct subcellular compartments such as mitochondria using specific peptide sequences. The presence of the chemical coating and the high-Z element itself also change the chemical environment of the cell.

Reactive oxygen species (ROS) play an important role in mediating DNA damage produced by radiation. In fact, 50–70% of the DNA lesions in standard RT upon X-ray irradiation are attributed to the hydroxyl radical (OH). By altering the chemical environment of the cell, the nanoparticles can in principle affect both the yield and the spectrum of ROS produced, which in turn has consequences for the DNA damage. Competing mechanisms may be at play depending on the composition of the nanoparticles and their coating. For instance, certain chemical compounds, such as PEG, can act as ROS scavengers and actually detoxify radicals formed by the interaction of radiation with water molecules. Studies aiming at quantifying the G-value (i.e., the number of molecules of a specific radical produced per 100 eV of energy absorbed) have indicated three possible mechanisms through which nanoparticles can affect the ROS production by radiation and therefore affect the radiation effectiveness (Fig. 11.25). Increased radicals can be produced as a result of direct interaction between radiation and nanoparticles through the production of electrons and low-energy photons emitted by the nanoparticles. As the energy spectrum of the secondary radiation emitted by the nanoparticle is different from the primary radiation beam, a different spectrum of radicals is to be expected and the yield is generally higher

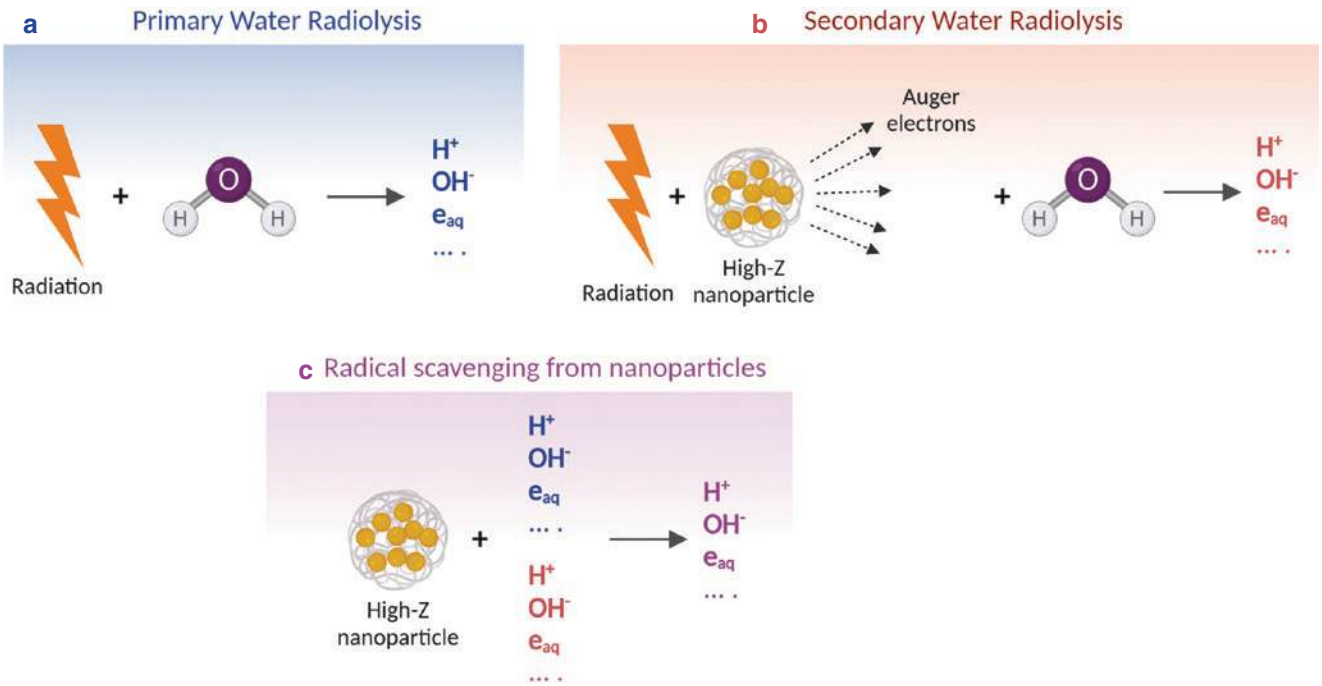

Fig. 11.25 Schematic representation of the possible pathways through which nanoparticles can affect the yield of radicals following radiation exposure: (**a**) primary water radiolysis, (**b**) secondary water radiolysis, and (**c**) radical scavenging from nanoparticles

due to their lower energy and cascade of secondary electrons. The presence of the nanoparticles, however, can also affect the yield of radicals produced by the direct interaction of radiation with the water molecules. This may occur through scavenging action from the nanoparticle-coating elements or by chemical interaction between the nanoparticles and the radiolysis products.

11.4.3.3 Biological Radiosensitization

When nanoparticles reach the cell surface, they are usually internalized via endocytosis and end up in intracellular vesicles, also called endosomes. This endosomal pathway is often a barrier hindering biological or therapeutic effects of nanoparticles. Nevertheless, nanoparticles are able to escape the endosomal transport system, accessing the cytoplasm and organelles by destabilizing the endosomal membrane, inducing osmotic swelling and membrane rupture, or passively crossing the plasma membrane or the endosomal membrane [216]. Once internalized, the nanoparticles can affect different cellular and molecular processes. For instance, apart from creating additional DNA damage, nanoparticles directly or indirectly affect the functioning of DNA repair proteins by preventing their synthesis, posttranslational modification, or recruitment to the site of damage. For instance, due to the large specific surface area, nanoparticles are very efficient in capturing a large amount of proteins, including DNA repair proteins, eventually leading to their deprivation and hence reducing the DNA repair efficiency [217]. On the other hand, the release of metal ions could imbalance the metal homeostasis in the cells, which is critical for protein folding and could replace the metallic cofactor in active sites of enzymes that are involved in the antioxidant defense system, altering their structure and inhibiting their activity.

Besides affecting the DNA damage repair machinery and causing antioxidant enzyme inhibition, multiple in vitro studies showed that nanoparticles can cause cell cycle disruption. The radiosensitivity of cells can vary depending on their cell cycle phase, with cells in the late G_2 and mitosis (G_2/M) phases being the most radiosensitive, presumably because the condensed chromatin in mitotic cells is more susceptible to radiation-induced double-strand breaks, which are commonly repaired by the error-prone NHEJ mechanism. On the other hand, cells in the late S phase are the most radioresistant, due to the diffused chromatin regions and the fact that during the S phase, DNA damage is usually repaired by the accurate HR mechanism. Multiple research groups reported an elevated proportion of cells in the G_2/M phase and a decreased cell number in the G_0/G_1 phase after gold nanoparticle exposure [218]. As a result, the radiosensitizing effects of gold nanoparticles can also be attributed to stalling of the cell cycle in the radiosensitive G_2/M phase.

Finally, mitochondria, located in the cytoplasm and having their own DNA, are another potential target for nanoparticle-mediated radiosensitization as the same processes as described above for nuclear DNA may affect mitochondrial (mt) DNA. However, nanoparticles are hardly ever detected in mitochondria and are often accumulated in endosomes and lysosomes. In general, although hypothetical, nanoparticles accumulated and irradiated within lysosomes or other organelles may decrease cell survival by directly harming these organelles and their functions [219]. Even milder damage to organelles could potentially lead to altered signaling and eventually increased cell death.

Cytoplasmic organelles might thus represent a parallel or even dominant target to nuclear DNA. It is obvious from the previous paragraphs that nanoparticle-mediated radiosensitization is not fully understood. The research is complicated by extreme complexity and variability of the systems studied, including different materials, sizes, shapes, and modifications of nanoparticles; different cell types; different types of radiation and irradiation conditions, etc. Under certain experimental conditions, a plethora of biological processes may be induced so that it might not be excluded that different types and sizes of nanoparticles do interact according to specific mechanisms and their combinations (Box 11.6).

Box 11.6: Nanoparticle-Mediated Radiosensitization

- The physical mechanisms of nanoparticle radiosensitization are related to both the higher attenuation cross section of high-Z materials compared to soft tissues and an increased clustering of ionizations from the secondary electrons emitted by the nanoparticle.
- The chemical mechanisms are related to production and/or scavenging of reactive radical species mainly from the chemical compounds surrounding the nanoparticle.
- The biological mechanisms are related to the interaction of the nanoparticles with the cellular and molecular processes, including antioxidant enzyme activities, the DNA repair pathways, the cell cycle and organelle functioning (e.g., mitochondria, lysosomes, ER, Golgi apparatus).

11.4.4 Autophagy Inhibitors

Autophagy is a basic catabolic mechanism that involves cell degradation of unnecessary or dysfunctional cell components, such as damaged endoplasmic reticulum (ER) and other cytoplasmic constituents through lysosome action.

The autophagy is mediated by protein complexes, such as class III PI3K, autophagy-related gene (Atg) proteins, and others containing microtubule-associated protein 1 light-chain subunit 3 (LC3), recruited to the membrane favoring membrane expansion and phagophore elongation. Particularly, autophagy can be activated by multiple signaling pathways, mainly through energy signals via AMPK. AMPK activation can phosphorylate ULK1, inhibit mTOR signaling, and activate Beclin-1 and Vps34 molecules resulting in the upregulation of autophagy intensity. Thus, the AMPK-mTOR-ULK1 pathway plays an important role in autophagy. Recently, the autophagy-related protein BECN1 has been shown to regulate radiation-induced G_2/M arrest. In the context of a disease, autophagy has been described as an adaptive response to survival, a strategy to maintain metabolic homeostasis. In cancer cells, autophagy is a double-edged sword. In early stages, it could limit tumorigenesis. However, it could also provide a prosurvival function for adaptation and detoxification in a stressful environment, such as starvation, hypoxia, and chemotherapy/radiotherapy.

Some studies show that the autophagy preventing is radiosensitive, while the autophagy promoting is radioprotective, suggesting that IR-induced autophagy may represent an adaptive response to maintain tumor growth and survival. In order to improve IR tumor responses, several sensitization agents to radiation-induced autophagy are currently being studied. The molecular machinery involved in IR-induced autophagy is still not clear. Recent studies show that p53 and PARP-1, a DNA repair enzyme triggered by DNA damage, exert essential roles in starting the autophagy process regulating the PI3K/PKB/AKT/mTOR signaling pathway that represents an autophagy key regulator. Reports by investigators have recently shown that autophagy activity increased after IR and chemotherapy. It is an escape mechanism for cell survival in response to cytotoxic agents, including IR and temozolomide (TMZ) in glioblastoma (GBM) treatment [220]. In radioresistant breast cancer (BC) cells, a strong postirradiation autophagy induction has been observed as a protective and prosurvival mechanism of radioresistance after exposure to IR. Studies have also shown that induced autophagy in some radioresistant cancers, such as GBM, causes IR sensitization and increased cell death.

In normal conditions, microautophagy and chaperone-mediated autophagy permit the breakdown of abnormal proteins, cellular debris, or damaged organelles, maintaining cellular homeostasis and/or as tools to recycle biological constituents (e.g., amino acid, fatty acid, and energy in the form of ATP). After stress stimuli, such as nutrient starvation, protein aggregation, organelle damage, and oxidative or genotoxic stress, including by IR, the autophagy hyperactivation promotes cell death, via nonapoptotic and caspase-independent mechanisms, and this case is also called macroautophagy [221].

As described above, AMPK promotes the activation of autophagy. Among factors activated by AMPK, an interesting and not well-described role in the autophagy process, it was supposed to be for glucose transporter GLUT-1, often upregulated in cancer cells. In this sense, the cross talk among GLUT1, curcumin, and AMPK pathway in LC remains vague. Interestingly, it was recently described that the treatment with GLUT1 siRNA alone or in combination with curcumin resulted in profound improvement of the radiosensitivity of LC cells after irradiation. In particular, curcumin and GLUT1 siRNA combined treatment not only promoted apoptosis of LC cells, but also induced autophagy-associated cell death through activation of AMPK/mTOR/ULK1 signaling-mediated autophagy with or without irradiation treatment [222].

Taking all these observations, we can speculate that the role of autophagy in cancer cells depends upon certain factors, such as cell type, specific characteristics of tumor cells, microenvironment of the tumor, and type of treatment applied. In addition, a variety of radiation-resistant molecules, such as PI3K/AKT, EGFR, NF-κB, and p53, may play an important role in the regulation of autophagy, thus indicating that the mechanisms that regulate autophagy are very complex. Thus, many questions and contradictory findings have yet to be clarified.

11.4.5 Metformin (MTF)

In cancer patients, MTF may affect tumor growth and treatment response in two different ways: directly by inhibiting mitochondrial metabolism and activating downstream cell signaling pathways in cancer cells or indirectly by keeping low the levels of glucose, insulin, and other factors which can activate cancer cell proliferation [223]. MTF has also shown anticancer effects in nondiabetic patient populations (described in Sect. 11.1.9).

With regard to the relationship between MTF and IR, MTF is able to increase intrinsic radiosensitivity, as tested in vitro in many cell lines of different tumors, including lung, head and neck, breast, liver, prostate, and pancreas cancers and murine fibrosarcoma, with specific cell line-dependent radiosensitizing effect [203, 223].

Several clinical data on the effect of MTF on patient outcome, focused particularly on patient populations undergoing RT, have shown that these patients have better outcomes if they are treated with MTF. These and other data show the significant role of MTF in enhancing the RT efficacy and suggest an interaction between MTF and IR [223].

In vitro and in vivo studies, concerning the MTF radiosensitizing effect, have showed an enhanced DNA damage after MTF treatment combined with RT, as tested by phosphorylation of histone γH2AX, a well-known marker for DNA damage [203].

In particular, MTF may increase initial DNA damage or inhibit repair processes, being able to reduce the expression of DNA repair protein Ku70 and hamper radiation-induced activation of EGFR and DNA-dependent protein kinase catalytic subunit (DNA-PKcs). Considering that the primary targets of MTF are the mitochondrial complex I and mGPD (glycerol-3-phosphate dehydrogenase), it may induce an increase of ROS generation and oxidative damage to lipids, protein, and DNA that could strengthen the effects of IR. Indeed, several data have demonstrated that MTF can increase ROS in cancer cells when delivered alone or in combination with IR. In general, as regards the main known MTF mechanisms of action when combined with RT, in vitro and in vivo data show a significant role of MTF in affecting at least four different parameters at radiobiological level, including intrinsic cell radiosensitivity (SF2, i.e., the fraction of cells surviving after a single IR dose of 2 Gy), cancer stem cell fraction, tumor proliferation rates, and tumor hypoxia [223].

11.4.6 PARP Inhibitors

Poly-(adenosine diphosphate-ribose)-polymerase (PARP) are cellular enzymes that play crucial roles in various cell processes like replication, transcription, cellular repair, and also death [224]. PARP detects single-strand breaks and triggers the activation of cellular machinery involved in the repair of the single-strand break. Studies have shown that PARP inhibitors (PARPi) exhibit enhanced radiosensitivity when combined with IR. Radiation works by damaging the DNA, which can activate the single-strand break (SSB) repair pathway like base excision repair (BER) or double-strand break (DSB) pathways like the HR and the NHEJ pathway (more details in Chap. 3). SSB, if unrepaired, gets converted to double-stranded breaks, which consequently hinder normal cellular processes. PARPi imparts radiosensitivity through the SSB and base excision pathway, which substantially increases the risk to collapsed replication fork, thereby producing a stable DSB [225]. Due to the crucial role of PARP in the DNA repair pathway, PARPi have proved as effective radiosensitizers, especially in tumors harboring DNA repair deficiencies like the BRCA mutation. The replication-reliant operations of PARPi facilitate the establishment of differential outcomes in tumor and healthy tissues. Other mechanisms that are known to induce the radiosensitization effects include inhibition of chromatin remodeling, G_2/M arrest, vasodilatory effect induced by PARPi, etc. Characteristically, factors that affect radiosensitivity are the capability of tumors to repair the damage, redistribution of the cell cycle, process of reoxygenation, vascular endothelial damage process, tumor immunity, and repopulation of the tumor tissue. A radiosensitizer should have the potential not only to influence these processes but also prevent the increase in the toxicity. Since PARPi possess most of these qualities necessary for being a potential radiosensitizer (Fig. 11.26), it has gained interest in the medical community [226].

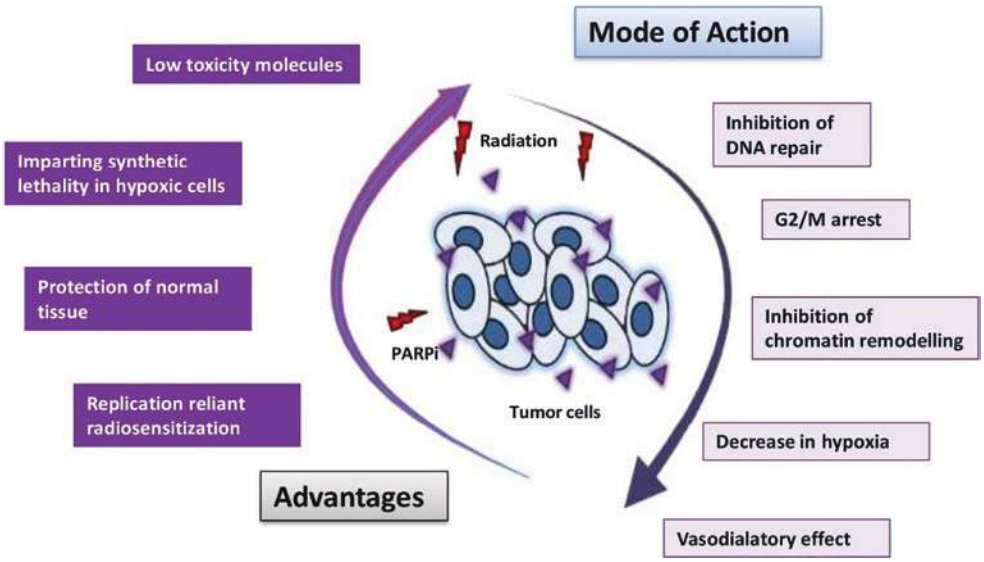

Fig. 11.26 The advantages and various modes of action by which PARPi enhance the radiosensitivity of tumor cells. Adapted from "Poly-(ADP-ribose)-polymerase inhibitors as radiosensitizers: a systematic review of preclinical and clinical human studies," by [224], Licensed under CC BY 3.0

11.4.6.1 Nitroxides

Nitroxides are a class of stable free radical compounds that exhibit antioxidant mechanisms, thereby safeguarding the cells from several lethal agents like superoxide and hydrogen peroxide (also described in Sect. 11.1.2). However, the rationale to use nitroxides in cancer RT comes from the role of free radicals in tumor development and capacity of inhibitors of radical reactions to suppress tumorigenesis. The underlying mode of action of nitroxyls exhibiting the radiosensitization effect can be attributed to cell signaling, enhanced blood flow to the tumor, consequences on the cellular respiration, and generation of reactive oxygen and nitrogen species that can operate as metabolite radiosensitizers. The effects of nitroxides with radiation were found conflicting, leading to uncertainty about their radiosensitizing nature.

Tempol (TPL) is a piperidine nitroxide that possesses an unpaired electron and goes through swift reversible transfer among the three forms: nitroxide, hydroxylamine, and oxoammonium cation. Based on its concentration in the cell, it can act as an oxidative or reductive agent. In cancer cells, TPL favorably inhibits growth by increasing the generation of cellular ROS [227]. When used with RT and chemotherapy, TPL exhibits a differential effect of protecting the normal healthy cells from RT and cisplatin-mediated damage, whereas in cancer cells, tempol is reduced to its hydroxylamine form that is unable to protect the cells from radiation and cisplatin-mediated damage. This differential or selective acting on cancer cells while sparing the normal cells is particularly of significance in cancer radio- as well as chemotherapy [228]. It was observed that the anticancer effects of cisplatin increased due to the prooxidant activity of TPL via the increased ROS-mediated cell apoptosis [227]. In several cancer cell lines, TPL was able to free radical-dependent apoptosis. On 24-h exposure to TPL, human promyelocytic leukemic cell line (HL-60) showed reduced levels of mitochondrial and intracellular glutathione, failure in the oxidative phosphorylation process, and diminished mitochondrial membrane potential. TPL also particularly targeted the respiratory chain complex I and showed some insignificant effects on the complexes II and IV. This can be attributed to the role of mitochondria in apoptosis and it being a free radical resource and target. In HL-60, TPL works by targeting the mitochondria, which subsequently leads to mitochondria associated with oxidative stress and apoptosis. This in turn can sensitize the tumor cells to the proapoptotic effects of cytotoxic agents [229]. When human breast cancer cells (MDA-MB 231) were treated with tempo, another nitroxide, it exhibited considerable levels of tyrosine phosphorylation of numerous unknown proteins when evaluated with the equimolar concentration, i.e., 10 mm TPL. The compounds tempo and TPL lead to the phosphorylation of tyrosine and trigger the Raf-1 protein kinase (30 min, two- to threefold) [230]. Nevertheless, TPL leads to augmented extracellular signal-regulated kinase 1 activity. Tempo also activated the stress-associated protein kinase (2 h, threefold) and induced apoptosis (2 h, >50%). The ceramide levels significantly increase (54% over control) at 30 min and (71% over control) at 1 h after treatment, prior to activation of stress-activated protein kinase and cell death via apoptosis [230]. TPL protects normal cells and tissues from oxidative damage and remarkably hampers the proliferation of cancer cells. These clearly imply that the nitroxide TPL shows the potential to be a good prooxidant and can be a potent radiosensitizing agent for cancer treatment.

11.5 Exercises and Self-Assessment

Q1. How do radioprotectors work?
Q2. What is the purpose of radioprotectors in RT?
Q3. What is TRUE: *All the antioxidants are radioprotectors* or *all the* potential *radioprotectors are often antioxidants*?
Q4. What are radiomitigators?
Q5. Can immunomodulators be classified as radiomitigators?
Q6. What is the purpose of a radiosensitizing agent in cancer RT?
Q7. Describe the curcumin action mechanism when administered with irradiation.
Q8. Generate a graph similar to Fig. 11.1 for gadolinium nanoparticles and estimate the mass attenuation coefficient ratio at 100 keV.

11.6 Exercise Solutions

SQ1. The detailed mechanisms are described in Sect. 11.1.1. The possible mechanisms are listed in Box 11.2 as well.
SQ2. Radioprotectors, which should be safe and nontoxic for human health, are used to protect the normal cells or nontumor cells from the harmful insults of ionizing irradiation and to increase survival rate in patients when administered before the exposure to radiation or at the time of RT for their effectiveness.
SQ3. The potential radioprotectors are often antioxidants, but not all the antioxidants are radioprotectors.
SQ4. Radiomitigators are used to minimize the toxicity or damage caused by ionizing irradiation in noncancerous cells even after radiation has been delivered and thus able to improve the effectiveness of radiation therapy.
SQ5. Yes. Radioprotective agents with potency to stimulate the proliferation and modify the function of hematopoietic and immunopoietic stem cells, often referred to as immunomodulators, can be considered as radiomitigators. The mode of action (MOA) of radiomitigators is depicted in the figure (figure number will be written).
SQ6. Radiosensitizer is a chemical or pharmaceutical agent which enhances the killing effect on tumor cells by making them more susceptible/sensitive to radiation therapy and at the same time having less effect on normal tissues/cells.
SQ7. Curcumin has been shown to have a double-face mechanism. Indeed, on the one hand, it is an antioxidant and anti-inflammatory molecule, useful in limiting the IR-induced ROS generation and IR side effects. On the other, it acts as an anticancer molecule, interacting with cellular processes, such as cell cycle, proliferation, apoptosis, and autophagy.
SQ8. Gd/water mass attenuation coefficient ratio @ 100 keV = 72.6.

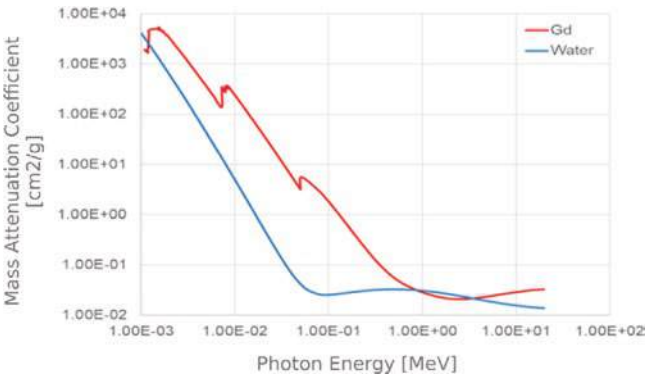

11.7 Annex 1

Contamination by radionuclides and medical countermeasures (MCMs)

Radiation type	Element	Radioactive half-life	Major exposure pathways	Focal accumulation	Medical countermeasure for internal contamination	Mechanism of action	References
α	Americium (Am-241)	458 years	Inhalation, Skin	Lungs, Liver, Bone, Bone marrow	DTPA(Ca-DTPA/Zn-DTPA) Calcium or zinc diethylenetriaminepentaacetate	Chelating agents	FDA approved
	Uranium (U-235)	7.1 × 108 years	Inhalation, Ingestion	Kidneys, bone	Sodium bicarbonate	Facilitates increased renal excretion	NCRP preferred
	Polonium (Po-210)	138.4 days	Inhalation, Ingestion Skin	Spleen, Kidneys, Lymph nodes, Bone marrow, Liver, Lung mucosa	Succimer (DMSA) (DailyMed), dimercaprol (BAL), d-penicillamine	Chelating agents	NCRP suggested
	Plutonium (Pu-239)	24,100 years	Inhalation (limited absorption)	Lung, Bone, Bone marrow, Liver, Gonads	DTPA (Ca-DTPA/Zn-DTPA), deferoxamine (DFOA)	Chelating agent	FDA approved
β	Phosphorus (P-32)	4.3 days	Inhalation, Ingestion, Skin	Bone, Bone marrow, Rapidly replicating cells	Aluminum carbonate, sodium glycerophosphate, sodium phosphate, Potassium Phosphate, potassium phosphate, dibasic, sevelamer, aluminum hydroxide	Phosphate binders	NCRP suggested
	Strontium (Sr-90)	28 years	Inhalation, Ingestion	Bone	Stabile strontium, aluminum Phosphate, ammonium Chloride, calcium gluconate, calcium carbonate, calcium phosphate, sodium alginate, barium sulfate Aluminum, hydroxide	Competes for bone-binding sites Phosphate binder, increases excretion, blocks intestinal absorption	NCRP suggested
	Tritium (H-3)	12.5 years	Inhalation, Ingestion Skin	Whole body	Water	Facilitates excretion	NCRP preferred
β, γ	Cesium (Cs-137)	30 years	Inhalation, Ingestion	Follows potassium Renal excretion	Prussian blue	Ion exchange Inhibits enterohepatic recirculation in the GI tract	FDA approved
	Cobalt (Co-60)	5.26 years	Inhalation	Liver	EDTA, dimercaprol, DTPA (Ca-DTPA/Zn-DTPA)	Chelating agents	NCRP suggested
	Iodine (I-131)	8.1 days	Inhalation, Ingestion Skin	Thyroid	KI (potassium Iodide), propylthiouracil	Blocking agents	FDA approved
	Iridium (Ir-192)	74 days	N/A	Spleen	EDTA, DTPA (Ca-DTPA/Zn-DTPA)	Chelating agents	NCRP suggested
α, γ, neutron	Curium (Cm-244)	18 years	Inhalation, Ingestion	Liver, Bone	DTPA (Ca-DTPA/Zn-DTPA)	Chelating agent	FDA approved
α, β, γ	Radium (Ra-226)	1602 years	Ingestion	Bone	Aluminum hydroxide, calcium gluconate, calcium carbonate, calcium phosphate, sodium alginate, barium sulfate	Blocks intestinal absorption, competes for bone-binding sites Phosphate binder, increases excretion, blocks intestinal absorption	NCRP suggested

References for use (from https://remm.hhs.gov/int_contamination.htm#countermeasures_refs)

FDA approved: Countermeasures so marked have been approved as treatment for internal contamination with the listed radioisotope by the US Food and Drug Administration (FDA)

NCRP preferred: Countermeasures so marked have been listed as preferred treatments for internal contamination with the listed radioisotope by the National Council on Radiation Protection and Measurements [Management of Persons Contaminated with Radionuclides: Handbook (NCRP Report No. 161, Vol. I)]. Except where noted, use of these countermeasures has not been approved by the US Food and Drug Administration (FDA)

NCRP suggested: Countermeasures so marked have been listed as suggested treatments for internal contamination with the listed radioisotope by the National Council on Radiation Protection and Measurements [Management of Persons Contaminated with Radionuclides: Handbook (NCRP Report No. 161, Vol. I)]. Use of these countermeasures has not been approved by the US Food and Drug Administration (FDA)

References

1. Ando K. Chemical radioprotectors. Gan No Rinsho. 1987;33(13):1679–83.
2. Raviraj J, Bokkasam VK, Kumar VS, Reddy US, Suman V. Radiosensitizers, radioprotectors, and radiation mitigators. Indian J Dent Res. 2014;25(1):83–90.
3. Mishra KN, Moftah BA, Alsbeih GA. Appraisal of mechanisms of radioprotection and therapeutic approaches of radiation countermeasures. Biomed Pharmacother. 2018;106:610–7.
4. Weiss JF, Landauer MR. Radioprotection by antioxidants. Ann N Y Acad Sci. 2000;899(1):44–60.
5. Singh VK, Seed TM. The efficacy and safety of amifostine for the acute radiation syndrome. Expert Opin Drug Saf. 2019;18(11):1077–90.
6. Citrin D, Cotrim AP, Hyodo F, Baum BJ, Krishna MC, Mitchell JB. Radioprotectors and mitigators of radiation-induced normal tissue injury. Oncologist. 2010;15(4):360–71.
7. Huang, Eng-Yen, Feng-Sheng Wang, Yu-Min Chen, Yi-Fan Chen, Chung-Chi Wang, I-Hui Lin, Yu-Jie Huang, Kuender D. Yang. Amifostine alleviates radiation-induced lethal small bowel damage via promotion of 14-3-3σ-mediated nuclear P53 accumulation. Oncotarget 2014. 5 (20): 9756–9769.
8. Hofer M, Falk M, Komůrková D, Falková I, Bačíková A, Klejdus B, Pagáčová E, Štefančíková L, Weiterová L, Angelis KJ, Kozubek S, Dušek L, Galbavý Š. Two new faces of amifostine: protector from DNA damage in normal cells and inhibitor of DNA repair in cancer cells. J Med Chem. 2016;59(7):3003–17.
9. Gu J, Zhu S, Li X, Wu H, Li Y, Hua F. Effect of amifostine in head and neck cancer patients treated with radiotherapy: a systematic review and meta-analysis based on randomized controlled trials. PLoS One. 2014;9(5):e95968.
10. Yang C, Tang H, Wang L, Peng R, Bai F, Shan Y, Yu Z, Zhou P, Cong Y. Dimethyl sulfoxide prevents radiation-induced oral mucositis through facilitating DNA double-strand break repair in epithelial stem cells. Int J Radiat Oncol Biol Phys. 2018;102(5):1577–89.
11. Estrela JM, Ortega A, Obrador E. Glutathione in cancer biology and therapy. Crit Rev Clin Lab Sci. 2006;43(2):143–81.
12. Estrela JM, Ortega A, Mena S, Sirerol JA, Obrador E. Glutathione in metastases: from mechanisms to clinical applications. Crit Rev Clin Lab Sci. 2016;53(4):253–67.
13. Estrela JM, Obrador E, Navarro J, Lasso De la Vega MC, Pellicer JA. Elimination of Ehrlich tumours by ATP-induced growth inhibition, glutathione depletion and X-rays. Nat Med. 1995;1(1):84–8. https://doi.org/10.1038/nm0195-84. PMID: 7584960.
14. Jia D, Koonce NA, Griffin RJ, Jackson C, Corry PM. Prevention and mitigation of acute death of mice after abdominal irradiation by the antioxidant N-acetyl-cysteine (NAC). Radiat Res. 2010;173(5):579–89.
15. Elkady AA, Ibrahim IM. Protective effects of Erdosteine against nephrotoxicity caused by gamma radiation in male albino rats. Hum Exp Toxicol. 2016;35(1):21–8.
16. Patyar RR, Patyar S. Role of drugs in the prevention and amelioration of radiation induced toxic effects. Eur J Pharmacol. 2018;819:207–16.
17. Willis J, Epperly MW, Fisher R, Zhang X, Shields D, Hou W, Wang H, et al. Amelioration of head and neck radiation-induced mucositis and distant marrow suppression in Fanca−/− and Fancg−/− mice by intraoral administration of GS-nitroxide (JP4-039). Radiat Res. 2018;189(6):560–78.
18. Epperly MW, Sacher JR, Krainz T, Zhang X, Wipf P, Liang M, Fisher R, Li S, Wang H, Greenberger JS. Effectiveness of analogs of the GS-nitroxide, JP4-039, as total body irradiation mitigators. In Vivo (Athens, Greece). 2017;31(1):39–43.
19. Luo G, Sun L, Li H, Chen J, He P, Zhao L, Tang W, y Hongdeng Qiu. The potent radioprotective agents: novel nitronyl nitroxide radical spin-labeled resveratrol derivatives. Fitoterapia. 2021;155:105053.
20. Mastromarino A, Wilson R. Antibiotic radioprotection of mice exposed to supralethal whole-body irradiation independent of antibacterial activity. Radiat Res. 1976;68:329–38.
21. Kim K, Pollard JM, Norris AJ, McDonald JT, Sun Y, Micewicz E, Pettijohn K, Damoiseaux R, Iwamoto KS, Sayre JW, Price BD, Gatti RA, McBride WH. High-throughput screening identifies two classes of antibiotics as radioprotectors: tetracyclines and fluoroquinolones. Clin Cancer Res. 2009;15(23):7238–45.
22. Alok A, Chaudhury NK. Tetracycline hydrochloride: A potential clinical drug for radioprotection. Chem Biol Interact. 2016;245:90–9.
23. Lapeyre M, Charra-Brunaud C, Kaminsky MC, Geoffrois L, Dolivet G, Toussaint B, Maire F, Pourel N, Simon M, Marchal C, Bey P. Management of mucositis following radiotherapy for head and neck cancers. Cancer Radiother. 2001;5(1):121s–30s.
24. Mehrotra S, Pecaut MJ, Gridley DS. Analysis of minocycline as a countermeasure against acute radiation syndrome. Vivo Athens Greece. 2012;26:743–58.
25. Ma S, Jin Z, Liu Y, Liu L, Feng H, Li P, Tian Z, Ren M, Liu X. Furazolidone increases survival of mice exposed to lethal total body irradiation through the antiapoptosis and antiautophagy mechanism. Oxidative Med Cell Longev. 2021b;2021:6610726.
26. Dowlath MJH, Karuppannan SK, Sinha P, Dowlath NS, Arunachalam KD, Ravindran B, Chang SW, Nguyen-Tri P, Nguyen DD. Effects of radiation and role of plants in radioprotection: A critical review. Sci Total Environ. 2021;779:146431.
27. Pandey KB, Rizvi SI. Plant polyphenols as dietary antioxidants in human health and disease. Oxidative Med Cell Longev. 2009;2(5):270–8.
28. Liu J, Bai R, Liu Y, Zhang X, Kan J, Jin C. Isolation, structural characterization and bioactivities of naturally occurring polysaccharide-polyphenolic conjugates from medicinal plants. A review. Int J Biol Macromol. 2018a;107(Pt B):2242–50.
29. Liu Z, Lei X, Li X, Cai JM, Gao F, Yang YY. Toll-like receptors and radiation protection. Eur Rev Med Pharmacol Sci. 2018b;22(1):31–9.
30. Obrador E, Salvador R, Villaescusa JI, Soriano JM, Estrela JM, Montoro A. Radioprotection and radiomitigation: from the bench to clinical practice. Biomedicine. 2020;8:461.
31. Begum N, Prasad NR, Kanimozhi G, Hasan AQ. Apigenin ameliorates gamma radiation-induced cytogenetic alterations in cultured human blood lymphocytes. Mutat Res. 2012;747:71–6.
32. Begum N, Rajendra Prasad N, Kanimozhi G, Agilan B. Apigenin prevented gamma radiation-induced gastrointestinal damages by modulating inflammatory and apoptotic signalling mediators. Nat Prod Res. 2021;5:1–5.
33. Rithidech KN, Tungjai M, Reungpatthanaphong P, Honikel L, Simon SR. Attenuation of oxidative damage and inflammatory responses by apigenin given to mice after irradiation. Mutat Res. 2012;749(1–2):29–38.
34. Jagetia GC. Radioprotection and radiosensitization by curcumin. Adv Exp Med Biol. 2007;595:301–20.
35. Okunieff P, Xu J, Hu D, Liu W, Zhang L, Morrow G, Pentland A, Ryan JL, Ding I. Curcumin protects against radiation-induced acute and chronic cutaneous toxicity in mice and decreases mRNA expression of inflammatory and fibrogenic cytokines. Int J Radiat Oncol Biol Phys. 2006;65(3):890–8.
36. Jagetia GC, Rajanikant GK. Curcumin stimulates the antioxidant mechanisms in mouse skin exposed to fractionated γ-irradiation. Antioxidants (Basel). 2015;4(1):25–41.
37. Han DH, Lee MJ, Kim JH. Antioxidant and apoptosis-inducing activities of ellagic acid. Anticancer Res. 2006;26(5A):3601–6.
38. Ahire V, Kumar A, Mishra KP, Kulkarni G. Ellagic acid enhances apoptotic sensitivity of breast cancer cells to γ-radiation. Nutr Cancer. 2017;69(6):904–10.

39. Das SKR, Sinha M, Khan A, Das K, Manna K, Dey S. Radiation protection by major tea polyphenol, epicatechin. Int J Hum Genet. 2013;13(1):59–64.
40. West JD, Marnett LJ. Endogenous reactive intermediates as modulators of cell signalling and cell death. Chem Res Toxicol. 2006;19:173–94.
41. Shimura T, Koyama M, Aono D, Kunugita N. Epicatechin as a promising agent to countermeasure radiation exposure by mitigating mitochondrial damage in human fibroblasts and mouse hematopoietic cells. FASEB J. 2019;33:6867–76.
42. Zhu W, Xu J, Ge Y, Cao H, Ge X, Luo J, Xue J, Yang H, Zhang S, Cao J. Epigallocatechin-3-gallate (EGCG) protects skin cells from ionizing radiation via heme oxygenase-1 (HO-1) overexpression. J Radiat Res. 2014;55:1056–65.
43. Xie LW, Cai S, Zhao TS, Li M, Tian Y. Green tea derivative (−)-epigallocatechin-3-gallate (EGCG) confers protection against ionizing radiation-induced intestinal epithelial cell death both in vitro and in vivo. Free Radic Biol Med. 2020;161:175–86.
44. Davis TA, Mungunsukh O, Zins S, Day RM, Landauer MR. Genistein induces radioprotection by hematopoietic stem cell quiescence. Int J Radiat Biol. 2008;84(9):713–26.
45. Zhang J, Pang Z, Zhang Y, Liu J, Wang Z, Xu C, He L, Li W, Zhang K, Zhang W, Wang S, Zhang C, Hao Q, Zhang Y, Li M, Li Z. Genistein from fructus sophorae protects mice from radiation-induced intestinal injury. Front Pharmacol. 2021;12:655652.
46. Song L, Ma L, Cong F, Shen X, Jing P, Ying X, Zhou H, Jiang J, Fu Y, Yan H. Radioprotective effects of genistein on HL-7702 cells via the inhibition of apoptosis and DNA damage. Cancer Lett. 2015;366(1):100–11.
47. Manna K, Das U, Das D, Kesh SB, Khan A, Chakraborty A, Dey S. Naringin inhibits gamma radiation-induced oxidative DNA damage and inflammation, by modulating p53 and NF-κB signaling pathways in murine splenocytes. Free Radic Res. 2015;49(4):422–39.
48. Das RN, Balupillai A, David E, Santhoshkumar M, Muruhan S. Naringin, a natural flavonoid, modulates UVB radiation-induced DNA damage and photoaging by modulating NER repair and MMPS expression in mouse embryonic fibroblast cells. J Environ Pathol Toxicol Oncol. 2020;39(2):191–9.
49. Kumar S, Tiku AB. Biochemical and molecular mechanisms of radioprotective effects of naringenin, a phytochemical from citrus fruits. J Agric Food Chem. 2016;64(8):1676–85.
50. Koohian F, Shanei A, Shahbazi-Gahrouei D, Hejazi SH, Moradi MT. The radioprotective effect of resveratrol against genotoxicity induced by γ-irradiation in mice blood lymphocytes. Dose Response. 2017;15(2):1559325817705699.
51. Carsten RE, Bachand AM, Bailey SM, Ullrich RL. Resveratrol reduces radiation-induced chromosome aberration frequencies in mouse bone marrow cells. Radiat Res. 2008;169(6):633–8.
52. Zhang H, Yan H, Zhou X, Wang H, Yang Y, Zhang J, Wang H. The protective effects of resveratrol against radiation-induced intestinal injury. BMC Complement Altern Med. 2017;17(1):410.
53. Obrador E, Salvador-Palmer R, Jihad-Jebbar A, López-Blanch R, Dellinger TH, Dellinger RW, Estrela JM. Pterostilbene in cancer therapy. Antioxidants (Basel). 2021;10(3):492.
54. Sirerol JA, Feddi F, Mena S, Rodriguez ML, Sirera P, Aupí M, Pérez S, Asensi M, Ortega A, Estrela JM. Topical treatment with pterostilbene, a natural phytoalexin, effectively protects hairless mice against UVB radiation-induced skin damage and carcinogenesis. Free Radic Biol Med. 2015;85:1–11.
55. Obrador E, Salvador-Palmer R, Pellicer B, López-Blanch R, Sirerol JA, Villaescusa JI, Montoro A, Dellinger RW, Estrela JM. Combination of natural polyphenols with a precursor of NAD+ and a TLR2/6 ligand lipopeptide protects mice against lethal γ radiation. J Adv Res. 2023.
56. Farooqi Z, Kesavan PC. Radioprotection by caffeine pre- and post-treatment in the bone marrow chromosomes of mice given whole-body gamma-irradiation. Mutat Res. 1992;269:225–30.
57. Sim HJ, Bhattarai G, Lee J, Lee JC, Kook SH. The long-lasting radioprotective effect of caffeic acid in mice exposed to total body irradiation by modulating reactive oxygen species generation and hematopoietic stem cell senescence-accompanied long-term residual bone marrow injury. Aging Dis. 2019;10(6):1320–7.
58. Khayyo N, Taysı ME, Demir E, Ulusal H, Çınar K, Tarakçıoğlu M, et al. Radioprotective effect of caffeic acid phenethyl ester on the brain tissue in rats who underwent total-head irradiation. Eur J Ther. 2019;25(4):265–72.
59. Kumar A, Selvan TG, Tripathi AM, Choudhary S, Khan S, Adhikari JS, Chaudhury NK. Sesamol attenuates genotoxicity in bone marrow cells of whole-body γ-irradiated mice. Mutagenesis. 2015;30(5):651–61.
60. Khan S, Kumar A, Adhikari JS, Rizvi MA, Chaudhury NK. Protective effect of sesamol against 60Co γ-ray-induced hematopoietic and gastrointestinal injury in C57BL/6 male mice. Free Radic Res. 2015;49:1344–61.
61. Majdaeen M, Banaei A, Abedi-Firouzjah R, Ebrahimnejad Gorji K, Ataei G, Momeni F, Zamani H. Investigating the radioprotective effect of sesamol oral consumption against gamma irradiation in mice by micronucleus and alkaline comet assays. Appl Radiat Isot. 2020;159:109091.
62. Kong D, Banerjee S, Huang W, Li Y, Wang Z, Kim HR, Sarkar FH. Mammalian target of rapamycin repression by 3,3′-diindolylmethane inhibits invasion and angiogenesis in platelet-derived growth factor-D-overexpressing PC3 cells. Cancer Res. 2008;68(6):1927–34.
63. Chen H-X, Xiang H, Wen-Huan X, Li M, Yuan J, Liu J, Sun W-J, et al. Manganese superoxide dismutase gene-modified mesenchymal stem cells attenuate acute radiation-induced lung injury. Hum Gene Ther. 2017;28(6):523–32.
64. Fan S, Meng Q, Xu J, Jiao Y, Zhao L, Zhang X, Sarkar FH, Brown ML, Dritschilo A, Rosen EM. DIM (3,3′-diindolylmethane) confers protection against ionizing radiation by a unique mechanism. Proc Natl Acad Sci U S A. 2013;110(46):18650–5.
65. Changizi V, Haeri SA, Abbasi S, Rajabi Z, Mirdoraghi M. Radioprotective effects of vitamin A against gamma radiation in mouse bone marrow cells. MethodsX. 2019;6:714–7.
66. Bakshi HA, Zoubi MSA, Hakkim FL, Aljabali AAA, Rabi FA, Hafiz AA, Al-Batanyeh KM, Al-Trad B, Ansari P, Nasef MM, Charbe NB, Satija S, Mehta M, Mishra V, Gupta G, Abobaker S, Negi P, Azzouz IM, Dardouri AAK, Dureja H, Prasher P, Chellappan DK, Dua K, Webba da Silva M, El Tanani M, McCarron PA, Tambuwala MM. Dietary crocin is protective in pancreatic cancer while reducing radiation-induced hepatic oxidative damage. Nutrients. 2020;12(6):E1901.
67. Zhang C, Chen K, Wang J, Zheng Z, Luo Y, Zhou W, Zhuo Z, Liang J, Sha W, Chen H. Protective effects of crocetin against radiation-induced injury in intestinal epithelial cells. Biomed Res Int. 2020;2020:2906053.
68. Sindhu ER, Preethi KC, Kuttan R. Antioxidant activity of carotenoid lutein in vitro and in vivo. Indian J Exp Biol. 2010;48(8):843–8.
69. Vasudeva V, Tenkanidiyoor YS, Radhakrishna V, Shivappa P, Lakshman SP, Fernandes R, Patali KA. Palliative effects of lutein intervention in gamma-radiation-induced cellular damages in Swiss albino mice. Indian J Pharmacol. 2017;49(1):26–33.
70. Motallebnejad M, Zahedpasha S, Moghadamnia AA, Kazemi S, Moslemi D, Pouramir M, Asgharpour F. Protective effect of lycopene on oral mucositis and antioxidant capacity of blood plasma in the rat exposed to gamma radiation. Caspian J Intern Med. 2020;11(4):419–25.

71. Mortazavi SMJ, Sharif-Zadeh S, Mozdarani H, Foadi M, Haghani M, Sabet E. Future role of vitamin C in radiation mitigation and its possible applications in manned deep space missions: survival study and the measurement of cell viability. Phys Med. 2014;30:e97.
72. Sato T, Kinoshita M, Yamamoto T, Ito M, Nishida T, Takeuchi M, Saitoh D, Seki S, Mukai Y. Treatment of irradiated mice with high-dose ascorbic acid reduced lethality. PLoS One. 2015;10(2):e0117020.
73. Singh VK, Beattie LA, Seed TM. Vitamin E: tocopherols and tocotrienols as potential radiation countermeasures. J Radiat Res. 2013;54(6):973–88.
74. Aykin-Burns N, Pathak R, Boerma M, Kim T, Hauer-Jensen M. Utilization of vitamin E analogs to protect normal tissues while enhancing antitumor effects. Semin Radiat Oncol. 2019;29(1):55–61.
75. Lee S-G, Kalidindi TM, Lou H, Gangangari K, Punzalan B, Bitton A, Lee CJ, et al. γ-tocotrienol-loaded liposomes for radioprotection from hematopoietic side effects caused by radiotherapeutic drugs. J Nucl Med. 2021;62(4):584–90.
76. Vasil'eva IN, Bespalov VG, Baranenko DA. Radioprotective and apoptotic properties of a combination of α-tocopherol acetate and ascorbic acid. Bull Exp Biol Med. 2016;161(2):248–51.
77. Nuszkiewicz J, Woźniak A, Szewczyk-Golec K. Ionizing radiation as a source of oxidative stress—the protective role of melatonin and vitamin D. Int J Mol Sci. 2020;21(16):5804.
78. Jain SK, Micinski D. Vitamin D upregulates glutamate cysteine ligase and glutathione reductase, and GSH formation, and decreases ROS and MCP-1 and IL-8 secretion in high-glucose exposed U937 monocytes. Biochem Biophys Res Commun. 2013;437(1):7–11.
79. Kaminskyi OV, Pankiv VI, Pankiv IV, Afanasyev DE. Vitamin d content in population of radiologically contaminated areas in Chernivtsi oblast (pilot project). Probl Radiac Med Radiobiol. 2018;23:442–51. English, Ukrainian
80. Ji MT, Nie J, Nie XF, Hu WT, Pei HL, Wan JM, Wang AQ, Zhou GM, Zhang ZL, Chang L, Li BY. 1α,25(OH)2D3 radiosensitizes cancer cells by activating the NADPH/ROS pathway. Front Pharmacol. 2020;11:945.
81. Hosseinimehr SJ. The protective effects of trace elements against side effects induced by ionizing radiation. Radiat Oncol J. 2015;33(2):66–74.
82. Bartolini, Desirée, Kenneth D. Tew, Rita Marinelli, Francesco Galli, y Gavin Y. Wang. Nrf2-modulation by Seleno-Hormetic agents and its potential for radiation protection. BioFactors (Oxford, England) 2020. 46 (2): 239–245.
83. Kunwar A, Bansal P, Jaya Kumar S, Bag PP, Paul P, Reddy ND, Kumbhare LB, et al. In vivo radioprotection studies of 3,3′-diselenodipropionic acid, a selenocystine derivative. Free Radic Biol Med. 2010;48(3):399–410.
84. Du J, Zhanjun G, Liang Y, Yong Y, Yi X, Zhang X, Liu J, et al. Poly(Vinylpyrrolidone)- and selenocysteine-modified Bi2Se3 nanoparticles enhance radiotherapy efficacy in tumors and promote radioprotection in normal tissues. Adv Mater (Deerfield Beach, Fla.). 2017;29(34):1701268.
85. Muecke R, Micke O, Schomburg L, Buentzel J, Kisters K, Adamietz IA, AKTE. Selenium in radiation oncology-15 years of experiences in Germany. Nutrients. 2018;10(4):483.
86. Kunwar A, Indira Priyadarsini K, Jain VK. 3,3′-diselenodipropionic acid (DSePA): a redox active multifunctional molecule of biological relevance. Biochim Biophys Acta Gen Subj. 2021;1865(1):129768.
87. Wang G, Ren X, Yan H, Gui Y, Guo Z, Song J, Zhang P. Neuroprotective effects of umbilical cord-derived mesenchymal stem cells on radiation-induced brain injury in mice. Ann Clin Lab Sci. 2020a;50(1):57–64.
88. Wang L, Ziyu Wang Y, Cao WL, Kuang L, Hua D. Strategy for highly efficient radioprotection by a selenium-containing polymeric drug with low toxicity and Long circulation. ACS Appl Mater Interfaces. 2020b;12(40):44534–40.
89. Crescenti E, Croci M, Medina V, Sambuco L, Bergoc R, y Elena Rivera. Radioprotective potential of a novel therapeutic formulation of oligoelements Se, Zn, Mn plus Lachesis Muta Venom. J Radiat Res. 2009;50(6):537–44.
90. Ertekin MV, Koç M, Karslioglu I, Sezen O. Zinc sulfate in the prevention of radiation-induced oropharyngeal mucositis: a prospective, placebo-controlled, randomized study. Int J Radiat Oncol Biol Phys. 2004;58(1):167–74.
91. Watanabe T, Ishihara M, Matsuura K, Mizuta K, Itoh Y. Polaprezinc prevents oral mucositis associated with radiochemotherapy in patients with head and neck cancer. Int J Cancer. 2010;127(8):1984–90.
92. Doctrow SR, Lopez A, Schock AM, Duncan NE, Jourdan MM, Olasz EB, Moulder JE, Fish BL, Mäder M, Lazar J, Lazarova Z. A synthetic superoxide dismutase/catalase mimetic EUK-207 mitigates radiation dermatitis and promotes wound healing in irradiated rat skin. J Invest Dermatol. 2013;133(4):1088–96. https://doi.org/10.1038/jid.2012.410. Epub 2012 Nov 29. Erratum in: J Invest Dermatol. 2013 Jun;133(6):1691
93. Batinic-Haberle I, Tovmasyan A, Spasojevic I. Mn porphyrin-based redox-active drugs: differential effects as cancer therapeutics and protectors of normal tissue against oxidative injury. Antioxid Redox Signal. 2018;29(16):1691–724.
94. Anderson CM, Lee CM, Saunders DP, Curtis A, Dunlap N, Nangia C, Lee AS, Gordon SM, Kovoor P, Arevalo-Araujo R, Bar-Ad V, Peddada A, Colvett K, Miller D, Jain AK, Wheeler J, Blakaj D, Bonomi M, Agarwala SS, Garg M, Worden F, Holmlund J, Brill JM, Downs M, Sonis ST, Katz S, Buatti JM. Phase IIb, randomized, double-blind trial of GC4419 versus placebo to reduce severe Oral mucositis due to concurrent radiotherapy and cisplatin for head and neck cancer. J Clin Oncol. 2019;37(34):3256–65.
95. Mapuskar KA, Anderson CM, Spitz DR, Batinic-Haberle I, Allen BG, Oberley-Deegan RE. Utilizing superoxide dismutase mimetics to enhance radiation therapy response while protecting normal tissues. Semin Radiat Oncol. 2019;29(1):72–80.
96. Weitzel DH, Tovmasyan A, Ashcraft KA, Rajic Z, Weitner T, Liu C, Li W, et al. Radioprotection of the brain white matter by Mn(III) n-butoxyethylpyridylporphyrin-based superoxide dismutase mimic MnTnBuOE-2-PyP5+. Mol Cancer Ther. 2012;14(1):70–9.
97. Fahl WE. Complete prevention of radiation-induced dermatitis using topical adrenergic vasoconstrictors. Arch Dermatol Res. 2016;308(10):751–7.
98. Vasin MV, Semenov LF, Suvorov NN, Antipov VV, Ushakov IB, Ilyin LA, Lapin BA. Protective effect and the therapeutic index of indralin in juvenile rhesus monkeys. J Radiat Res. 2014;55(6):1048–55.
99. Grabenbauer GG, Holger G. Management of radiation and chemotherapy related acute toxicity in gastrointestinal cancer. Best Pract Res Clin Gastroenterol. 2016;30(4):655–64.
100. Fu Q, Berbée M, Wang W, Boerma M, Wang J, Schmid HA, Hauer-Jensen M. Preclinical evaluation of Som230 as a radiation mitigator in a mouse model: postexposure time window and mechanisms of action. Radiat Res. 2011;175(6):728–35.
101. Amini P, Mirtavoos-Mahyari H, Motevaseli E, Shabeeb D, Musa AE, Cheki M, Farhood B, Yahyapour R, Shirazi A, Goushbolagh NA, Najafi M. Mechanisms for radioprotection by melatonin; can it be used as a radiation countermeasure? Curr Mol Pharmacol. 2019;12(1):2–11.
102. Wang Q, Wang Y, Liqing D, Chang X, Liu Y, Liu Q, Fan S. Quantitative proteomic analysis of the effects of melatonin treatment for mice suffered from small intestinal damage induced by γ-ray radiation. Int J Radiat Biol. 2021;97(9):1206–16.

103. Sheikholeslami S, Aryafar T, Abedi-Firouzjah R, Banaei A, Dorri-Giv M, Zamani H, Ataei G, Majdaeen M, Farhood B. The role of melatonin on radiation-induced pneumonitis and lung fibrosis: A systematic review. Life Sci. 2021;281:119721.
104. Farhood B, Goradel NH, Mortezaee K, Khanlarkhani N, Salehi E, Nashtaei MS, Mirtavoos-Mahyari H, et al. Melatonin as an adjuvant in radiotherapy for radioprotection and radiosensitization. Clin Transl Oncol. 2019;21(3):268–79.
105. Aras S, Efendioğlu M, Wulamujiang A, Ozkanli SS, Keleş MS, Tanzer İO. Radioprotective effect of melatonin against radiotherapy-induced cerebral cortex and cerebellum damage in rat. Int J Radiat Biol. 2021;97(3):348–55.
106. Alonso-González C, González A, Menéndez-Menéndez J, Martínez-Campa C, Cos S. Melatonin as a radio-sensitizer in cancer. Biomedicine. 2020;8(8):E247.
107. Adalsteinsson JA, Muzumdar S, Waldman R, Rong W, Ratner D, Feng H, Ungar J, et al. Metformin is associated with decreased risk of basal cell carcinoma: A whole-population case-control study from Iceland. J Am Acad Dermatol. 2021;85(1):56–61.
108. Keywan M, Shabeeb Dheyauldeen E, Ahmed M, Masoud N, Bagher F. Metformin as a radiation modifier; implications to normal tissue protection and tumor sensitization. Curr Clin Pharmacol. 2019;14(1):41–53.
109. Kolivand S, Motevaseli E, Cheki M, Mahmoudzadeh A, Shirazi A, Fait V. The anti-apoptotic mechanism of metformin against apoptosis induced by ionizing radiation in human peripheral blood mononuclear cells. Klin Onkol: Casopis Ceske a Slovenske Onkologicke Spolecnosti. 2017;30(5):372–9.
110. Kelly B, Tannahill GM, Murphy MP, O'Neill LAJ. Metformin inhibits the production of reactive oxygen species from NADH: ubiquinone oxidoreductase to limit induction of interleukin-1β (IL-1β) and boosts interleukin-10 (IL-10) in lipopolysaccharide (LPS)-activated macrophages. J Biol Chem. 2015;290(33):20348–59.
111. Najafi M, Cheki M, Rezapoor S, Geraily G, Motevaseli E, Carnovale C, Clementi E, Shirazi A. Metformin: prevention of genomic instability and cancer: A review. Mutat Res Genet Toxicol Environ Mutagen. 2018;827:1–8.
112. Karam HM, Radwan RR. Metformin modulates cardiac endothelial dysfunction, oxidative stress and inflammation in irradiated rats: A new perspective of an antidiabetic drug. Clin Exp Pharmacol Physiol. 2019;46(12):1124–32.
113. Yahyapour R, Amini P, Rezapoor S, Rezaeyan A, Farhood B, Cheki M, Fallah H, Najafi M. Targeting of inflammation for radiation protection and mitigation. Curr Mol Pharmacol. 2018a;11(3):203–10.
114. Yahyapour R, Amini P, Saffar H, Rezapoor S, Motevaseli E, Cheki M, Farhood B, et al. Metformin protects against radiation-induced heart injury and attenuates the upregulation of dual oxidase genes following Rat's chest irradiation. Int J Mol Cell Med. 2018b;7(3):193–202.
115. Bentzen SM. Preventing or reducing late side effects of radiation therapy: radiobiology meets molecular pathology. Nat Rev Cancer. 2006;6:702–13.
116. Sharygin VL, Pulatova MK, Shliakova TG, Mitrokhin II, Todorov IN. Activation of deoxyribonucleotide synthesis by radioprotectants and antioxidants as a key stage in formation of body resistance to DNA-damaging factors. Izv Akad Nauk Ser Biol. 2005;4:401–22.
117. Mun GI, Kim S, Choi E, Kim CS, Lee YS. Pharmacology of natural radioprotectors. Arch Pharm Res. 2018;41:1033–50.
118. Dainiak N, Gent RN, Carr Z, Schneider R, Bader J, Buglova E, Chao N, Coleman CN, Ganser A, Gorin C, Hauer-Jensen M, Huff LA, Lillis-Hearne P, Maekawa K, Nemhauser J, Powles R, Schünemann H, Shapiro A, Stenke L, Valverde N, Weinstock D, White D, Albanese J, Meineke V. First global consensus for evidence-based management of the hematopoietic syndrome resulting from exposure to ionizing radiation. Disaster Med Public Health Prep. 2011;5(3):202–12.
119. Dainiak N. Medical management of acute radiation syndrome and associated infections in a high-casualty incident. J Radiat Res. 2018;59(suppl_2):ii54–64. https://doi.org/10.1093/jrr/rry004. PMID: 29509947; PMCID: PMC5941165
120. Dainiak N, Albanese J. Assessment and clinical management of internal contamination. J Radiol Prot. 2022;42(4) https://doi.org/10.1088/1361-6498/aca0a7.
121. Singh VK, Romaine PLP, Seed TM. Medical countermeasures for radiation exposure and related injuries: characterization of medicines, FDA-approval status and inclusion into the strategic National Stockpile. Health Phys. 2015;108(6):607–30.
122. Hu D, Zhang Y, Cao R, Hao Y, Yang X, Tian T, Zhang J. The protective effects of granulocyte-macrophage colony-stimulating factor against radiation-induced lung injury. Transl Lung Cancer Res. 2020a;9(6):2440–59.
123. Hu Q, Zhou Y, Shijie W, Wei W, Deng Y, Shao A. Molecular hydrogen: A potential radioprotective agent. Biomed Pharmacother. 2020b;130:110589.
124. Vadhan-Raj S, Goldberg JD, Perales MA, Berger DP, van den Brink MR. Clinical applications of palifermin: amelioration of oral mucositis and other potential indications. J Cell Mol Med. 2013;17(11):1371–84.
125. DiCarlo AL, Horta ZP, Aldrich JT, Jakubowski AA, Skinner WK, Case CM Jr. Use of growth factors and other cytokines for treatment of injuries during a radiation public health emergency. Radiat Res. 2019;192(1):99–120.
126. Singh VK, Seed TM. Repurposing pharmaceuticals previously approved by regulatory agencies to medically counter injuries arising either early or late following radiation exposure. Front Pharmacol. 2021;12:624844.
127. Horta ZP, Case CM Jr, DiCarlo AL. Use of growth factors and cytokines to treat injuries resulting from a radiation public health emergency. Radiat Res. 2019;192(1):92–7.
128. Farhood B, Samadian H, Ghorbani M, Zakariaee SS, Knaup C. Physical, dosimetric and clinical aspects and delivery systems in neutron capture therapy. Rep Pract Oncol Radiother. 2018;23(5):462–73.
129. Zhuang H, Shi S, Yuan Z, Chang JY. Bevacizumab treatment for radiation brain necrosis: mechanism, efficacy and issues. Mol Cancer. 2019;18(1):21.
130. Bazinet A, Popradi G. A general practitioner's guide to hematopoietic stem-cell transplantation. Curr Oncol. 2019;26(3):187–91.
131. Saha S, Bhanja P, Kabarriti R, Liu L, Alfieri AA, Guha C. Bone marrow stromal cell transplantation mitigates radiation-induced gastrointestinal syndrome in mice. PLoS One. 2011;6(9):e24072.
132. Kunadt D, Stölzel F. Effective immunosurveillance after allogeneic hematopoietic stem cell transplantation in acute myeloid leukemia. Cancer Manag Res. 2021;13:7411–27.
133. Cavallero S, Riccobono D, Drouet M, François S. MSC-derived extracellular vesicles: new emergency treatment to limit the development of radiation-induced hematopoietic syndrome? Health Phys. 2020;119(1):21–36.
134. Accarie A, L'Homme B, Benadjaoud MA, Lim SK, Guha C, Benderitter M, Tamarat R, Sémont A. Extracellular vesicles derived from mesenchymal stromal cells mitigate intestinal toxicity in a mouse model of acute radiation syndrome. Stem Cell Res Ther. 2020;11(1):371.
135. Schoefinius J-S, Brunswig-Spickenheier B, Speiseder T, Krebs S, Just U, Lange C. Mesenchymal stromal cell-derived extracellular vesicles provide long-term survival after total body irradiation without additional hematopoietic stem cell support. Stem Cells. 2017;35(12):2379–89.
136. Laube M, Kniess T, Pietzsch J. Development of antioxidant COX-2 inhibitors as radioprotective agents for radiation therapy—A hypothesis-driven review. Antioxidants. 2016;5(2):14.

137. Alok A, Agrawala PK. Repurposing sodium diclofenac as a radiation countermeasure agent: A cytogenetic study in human peripheral blood lymphocytes. Mutat Res Genet Toxicol Environ Mutagen. 2020;856-857:503220.
138. Stokman MA, Spijkervet FK, Burlage FR, Roodenburg JL. Clinical effects of flurbiprofen tooth patch on radiation-induced oral mucositis. A pilot study. Support Care Cancer. 2005;13(1):42–8.
139. Cheki M, Yahyapour R, Farhood B, Rezaeyan A, Shabeeb D, Amini P, Rezapoor S, Najafi M. COX-2 in radiotherapy: A potential target for radioprotection and Radiosensitization. Curr Mol Pharmacol. 2018;11(3):173–83.
140. Hofer M, Pospíšil M, Hoferová Z, Weiterová L, Komůrková D. Stimulatory action of cyclooxygenase inhibitors on hematopoiesis: A review. Molecules (Basel, Switzerland). 2012;17(5):5615–25.
141. Hoggatt J, Singh P, Stilger KN, Artur Plett P, Sampson CH, Chua HL, Orschell CM, Pelus LM. Recovery from hematopoietic injury by modulating prostaglandin E(2) signaling post-irradiation. Blood Cells Mol Dis. 2013;50(3):147–53.
142. Yamasaki MC, Nejaim Y, Roque-Torres GD, Freitas DQ. Meloxicam as a radiation-protective agent on mandibles of irradiated rats. Braz Dent J. 2017;28(2):249–55.
143. Xu X, Huang H, Tu Y, Sun J, Xiong Y, Ma C, Qin S, Hu W, Zhou J. Celecoxib alleviates radiation-induced brain injury in rats by maintaining the integrity of blood-brain barrier. Dose Response. 2021;19(2):15593258211024393.
144. Pietzsch J, Laube M, Bechmann N, Pietzsch F-J, Kniess T. Protective effects of 2,3-diaryl-substituted indole-based cyclooxygenase-2 inhibitors on oxidative modification of human low density lipoproteins in vitro. Clin Hemorheol Microcirc. 2016;61(4):615–32.
145. Pitter KL, Tamagno I, Alikhanyan K, Hosni-Ahmed A, Pattwell SS, Donnola S, Dai C, Ozawa T, Chang M, Chan TA, Beal K, Bishop AJ, Barker CA, Jones TS, Hentschel B, Gorlia T, Schlegel U, Stupp R, Weller M, Holland EC, Hambardzumyan D. Corticosteroids compromise survival in glioblastoma. Brain. 2016;139(Pt 5):1458–71.
146. Kumagai T, Rahman F, Smith AM. The microbiome and radiation induced-bowel injury: evidence for potential mechanistic role in disease pathogenesis. Nutrients. 2018;10(10):1405.
147. Touchefeu Y, Montassier E, Nieman K, Gastinne T, Potel G, Bruley des Varannes S, Le Vacon F, de La Cochetière MF. Systematic review: the role of the gut microbiota in chemotherapy- or radiation-induced gastrointestinal mucositis—current evidence and potential clinical applications. Aliment Pharmacol Ther. 2014;40(5):409–21.
148. Jian Y, Zhang D, Liu M, Wang Y, Zhi-Xiang X. The impact of gut microbiota on radiation-induced enteritis' Frontiers in cellular and infection. Microbiology. 2021;11:586392.
149. Chitapanarux I, Chitapanarux T, Traisathit P, Kudumpee S, Tharavichitkul E, Lorvidhaya V. Randomized controlled trial of live lactobacillus acidophilus plus bifidobacterium bifidum in prophylaxis of diarrhea during radiotherapy in cervical cancer patients. Radiation Oncology (London, England). 2010;5:31.
150. Riehl TE, Alvarado D, Ee X, Zuckerman A, Foster L, Kapoor V, Thotala D, Ciorba MA, Stenson WF. Lactobacillus rhamnosus GG protects the intestinal epithelium from radiation injury through release of lipoteichoic acid, macrophage activation and the migration of mesenchymal stem cells. Gut. 2019;68(6):1003–13.
151. Moreno D, de LeBlanc A, Del Carmen S, Chatel JM, Miyoshi A, Azevedo V, Langella P, Bermúdez-Humarán LG, LeBlanc JG. Current review of genetically modified lactic acid bacteria for the prevention and treatment of colitis using murine models. Gastroenterol Res Pract. 2015;2015:146972.
152. Guo Q, Goldenberg JZ, Humphrey C, El Dib R, Johnston BC. Probiotics for the prevention of pediatric antibiotic-associated diarrhea. Cochrane Database Syst Rev. 2019;4(4):CD004827.
153. Picó-Monllor JA, Mingot-Ascencao JM. Search and selection of probiotics that improve mucositis symptoms in oncologic patients. a systematic review. Nutrients. 2019;11(10):2322.
154. Garcia-Peris P, Velasco C, Hernandez M, Lozano MA, Paron L, de la Cuerda C, Breton I, Camblor M, Guarner F. Effect of inulin and fructo-oligosaccharide on the prevention of acute radiation enteritis in patients with gynecological cancer and impact on quality-of-life: a randomized, double-blind, placebo-controlled trial. Eur J Clin Nutr. 2016;70(2):170–4.
155. Cui M, Xiao H, Li Y, Zhou L, Zhao S, Luo D, Zheng Q, Dong J, Zhao Y, Zhang X, Zhang J, Lu L, Wang H, Fan S. Faecal microbiota transplantation protects against radiation-induced toxicity. EMBO Mol Med. 2017;9(4):448–61.
156. Ding X, Li Q, Li P, Chen X, Xiang L, Bi L, Zhu J, Huang X, Cui B, Zhang F. Fecal microbiota transplantation: A promising treatment for radiation enteritis? Radiother Oncol. 2020;143(February):12–8.
157. Zhao Z, Cheng W, Qu W, Shao G, Liu S. Antibiotic alleviates radiation-induced intestinal injury by remodeling microbiota, reducing inflammation, and inhibiting fibrosis. ACS Omega. 2020;5(6):2967–77.
158. Sun F, Sun H, Zheng X, Yang G, Gong N, Zhou H, Wang S, Cheng Z, Ma H. Angiotensin-converting enzyme inhibitors decrease the incidence of radiation-induced pneumonitis among lung cancer patients: A systematic review and meta-analysis' journal of. Cancer. 2018;9(12):2123–31.
159. Medhora M, Gao F, Qingping W, Molthen RC, Jacobs ER, Moulder JE, Fish BL. Model development and use of ACE inhibitors for preclinical mitigation of radiation-induced injury to multiple organs. Radiat Res. 2014;182(5):545–55.
160. Moulder JE, Fish BL, Cohen EP. Treatment of radiation nephropathy with ACE inhibitors and AII type-1 and type-2 receptor antagonists. Curr Pharm Des. 2007;13(13):1317–25.
161. Mungunsukh O, George J, McCart EA, Snow AL, Mattapallil JJ, Mog SR, Panganiban RAM, et al. Captopril reduces lung inflammation and accelerated senescence in response to thoracic radiation in mice. J Radiat Res. 2021;62(2):236–48.
162. McCart EA, Lee YH, Jha J, Mungunsukh O, Rittase WB, Summers TA, Muir J, Day RM. Delayed captopril administration mitigates hematopoietic injury in a murine model of total body irradiation. Sci Rep. 2019;9(1):2198.
163. Cohen EP, Bedi M, Irving AA, Jacobs E, Tomic R, Klein J, Lawton CA, Moulder JE. Mitigation of late renal and pulmonary injury after hematopoietic stem cell transplantation. Int J Radiat Oncol Biol Phys. 2012;83(1):292–6.
164. Day RM, Davis TA, Barshishat-Kupper M, McCart EA, Tipton AJ, Landauer MR. Enhanced hematopoietic protection from radiation by the combination of genistein and captopril. Int Immunopharmacol. 2013;15(2):348–56.
165. Turnquist C, Harris BT, Harris CC. Radiation-induced brain injury: current concepts and therapeutic strategies targeting neuroinflammation. Neurooncol Adv. 2020;2(1):vdaa057.
166. Shimizu Y, Kodama K, Nishi N, Kasagi F, Suyama A, Soda M, Grant EJ, et al. Radiation exposure and circulatory disease risk: Hiroshima and Nagasaki atomic bomb survivor data, 1950-2003. BMJ (Clinical Research Ed). 2010;340:b5349.
167. Pathak R, Kumar VP, Hauer-Jensen M, Ghosh SP. Enhanced survival in mice exposed to ionizing radiation by combination of gamma-tocotrienol and simvastatin. Mil Med. 2019;184(Supplement_1):644–51.
168. Werner E, Alter A, Deng Q, Dammer EB, Wang Y, Yu DS, Duong DM, Seyfried NT, Doetsch PW. Ionizing radiation induction of cholesterol biosynthesis in lung tissue. Sci Rep. 2019;9:12546.
169. Zhao X, Yang H, Jiang G, Ni M, Deng Y, Cai J, Li Z, Shen F, Tao X. Simvastatin attenuates radiation-induced tissue damage in mice. J Radiat Res. 2014;55(2):257–64.

170. Bajaj MS, Ghode SS, Kulkarni RS, Limaye LS, Kale VP. Simvastatin improves hematopoietic stem cell engraftment by preventing irradiation-induced marrow adipogenesis and radioprotecting the niche cells. Haematologica. 2015;100(8):e323–7.
171. Xu L, Yang X, Chen J, Ge X, Qin Q, Zhu H, Zhang C, Sun X. Simvastatin attenuates radiation-induced salivary gland dysfunction in mice. Drug Des Devel Ther. 2016;10:2271–8.
172. Wedlake LJ, Silia F, Benton B, Lalji A, Thomas K, Dearnaley DP, Blake P, Tait D, Khoo VS, Jervoise H, Andreyev N. Evaluating the efficacy of statins and ACE-inhibitors in reducing gastrointestinal toxicity in patients receiving radiotherapy for pelvic malignancies. Eur J Cancer. 2012;48(14):2117–24.
173. Williams JP, Hernady E, Johnston CJ, Reed CM, Fenton B, Okunieff P, Finkelstein JN. Effect of administration of lovastatin on the development of late pulmonary effects after whole-lung irradiation in a murine model. Radiat Res. 2004;161(5):560–7.
174. Doi H, Matsumoto S, Odawara S, Shikata T, Kitajima K, Tanooka M, Takada Y, Tsujimura T, Kamikonya N, Hirota S. Pravastatin reduces radiation-induced damage in normal tissues. Exp Ther Med. 2017;13(5):1765–72.
175. Long S, Wang G, Shen M, Zhao N, Wan H, Xu Y, Wang S, et al. DTMP-GH fusion protein therapy improves survival after radiation injury combined with skin-burn trauma in mice. Radiat Res. 2019;191(4):360–8.
176. Kandaz M, Ertekin MV, Karslıoğlu İ, Erdoğan F, Sezen O, Gepdiremen A, Gündoğdu C. Zinc sulfate and/or growth hormone Administration for the Prevention of radiation-induced dermatitis: A placebo-controlled rat model study. Biol Trace Elem Res. 2017;179(1):110–6.
177. Caz V, Elvira M, Tabernero M, Grande AG, Lopez-Plaza B, de Miguel E, Largo C, Santamaria M. Growth hormone protects the intestine preserving radiotherapy efficacy on tumors: a short-term study. PLoS One. 2015;10(12):e0144537.
178. Mahran YF, El-Demerdash E, Nada AS, El-Naga RN, Ali AA, Abdel-Naim AB. Growth hormone ameliorates the radiotherapy-induced ovarian follicular loss in rats: impact on oxidative stress, apoptosis and IGF-1/IGF-1R axis. PLoS One. 2012;10(10):e0140055.
179. Ohsawa I, Ishikawa M, Takahashi K, Watanabe M, Nishimaki K, Yamagata K, Katsura K-I, Katayama Y, Asoh S, y Shigeo Ohta. Hydrogen acts as a therapeutic antioxidant by selectively reducing cytotoxic oxygen radicals. Nat Med. 2007;13(6):688–94.
180. Hirano SI, Ichikawa Y, Sato B, Yamamoto H, Takefuji Y, Satoh F. Molecular hydrogen as a potential clinically applicable radioprotective agent. Int J Mol Sci. 2021;22(9):4566.
181. Qian L, Shen J, Chuai Y, Cai J. Hydrogen as a new class of radioprotective agent. Int J Biol Sci. 2013;9(9):887–94.
182. Shin MH, Park R, Nojima H, Kim H-C, Kim YK, Chung JH. Atomic hydrogen surrounded by water molecules, H(H2O)m, modulates basal and UV-induced gene expressions in human skin in vivo. PLoS One. 2013;8(4):e61696.
183. Kang K-M, Kang Y-N, Choi I-B, Yeunhwa G, Kawamura T, Toyoda Y, Nakao A. Effects of drinking hydrogen-rich water on the quality of life of patients treated with radiotherapy for liver tumors. Med Gas Res. 2011;1:11.
184. Cheda A, Nowosielska EM, Gebicki J, Marcinek A, Chlopicki S, Janiak MK. A derivative of vitamin B3 applied several days after exposure reduces lethality of severely irradiated mice. Sci Rep. 2021;11(1):7922.
185. Mishra K, Alsbeih G. Appraisal of biochemical classes of radioprotectors: evidence, current status and guidelines for future development. 3 Biotech. 2017;7(5):292.
186. EPR- Internal Contamination 2018 (IAEA). Medical Management of Persons Internally Contaminated with Radionuclides in a Nuclear or Radiological Emergency
187. Rump A, Eder S, Hermann C, Lamkowski A, Kinoshita M, Yamamoto T, Abend M, Shinomiya N, Port M. A comparison of thyroidal protection by iodine and perchlorate against radioiodine exposure in Caucasians and Japanese. Arch Toxicol. 2021;95(7):2335–50.
188. World Health Organization. Iodine thyroid blocking: guidelines for use in planning for and responding to radiological and nuclear emergencies. Geneva: World Health Organization; 2017.
189. Strahlenschutzkommission (SSK). Verwendung von Jodtabletten zur Jodblockade der Schilddrüse bei einem Notfall mit Freisetzung von radioaktivem Jod Empfehlung der Strahlenschutzkommission. Verabschiedet in der 294. Sitzung der Strahlenschutzkommission am 26 April 2018. https://www.ssk.de/SharedDocs/Beratungsergebnisse_PDF/2018/2018-04-26Jodmerk.pdf?__blob=publicationFile. Accessed 9 Nov 2020.
190. Yantasee W, Sangvanich T, Creim JA, Pattamakomsan K, Wiacek RJ, Fryxell GE, Addleman RS, Timchalk C. Functional sorbents for selective capture of plutonium, americium, uranium, and thorium in blood. Health Phys. 2010;99:413–9.
191. Ogawa K, Fukuda T, Han J, Kitamura Y, Shiba K, Odani A. Evaluation of chlorella as a decorporation agent to enhance the elimination of radioactive strontium from body. PLoS One. 2016;11(2):e0148080.
192. Brigant L, Rozen R, Apfelbaum M. Tritium dilution space measurement is not modified by a doubling in fluid intake. J Appl Physiol (1985). 1993;75(1):412–5. https://doi.org/10.1152/jappl.1993.75.1.412. PMID: 8376293.
193. Sonawane VR, Jagtap VS, Pahuja DN, Rajan MGR, Samuel AM. Difficulty in dislodging in vivo fixed radiostrontium. Health Phys. 2004;87:46–50.
194. Ohmachi Y, Imamura T, Ikeda M, Shishikura E, Kim E, Kurihara O, Sakai K. Sodium bicarbonate protects uranium-induced acute nephrotoxicity through uranium-decorporation by urinary alkalinization in rats. J Toxicol Pathol. 2015;28(2):65–71.
195. Ansoborlo É, Amekraz B, Moulin C, Moulin V, Taran F, Bailly T, Burgada R, Hengé-Napoli M-H, Jeanson A, Den Auwer C, Bonin L, Moisy P. Review of actinide decorporation with chelating agents. Comptes Rendus Chim. 2007;10(10-11):1010–9.
196. Gusev I, Guskova A, Mettler FA. Medical management of radiation accidents. Boca Raton, FL: CRC Press; 2001. ISBN 978-1-4200-3719-7.
197. Morgan C, Bingham D, Holt DC, Jones DM, Lewis NJ. Therapeutic whole lung lavage for inhaled plutonium oxide revisited. J Radiol Prot. 2010;30(4):735–46.
198. Gosselin-Acomb TK. Principles of radiation therapy. In: Yarbro CH, Goodman M, Frogge MH, editors. Cancer nursing: principles and practice. 6th ed. Sudbury: Jones and Bardett Publishers; 2005. p. 230–49.
199. Adams GE. Chemical radiosensitization of hypoxic cells. Br Med Bull. 1973;29(1):48–53.
200. Fowler JF, Adams GE, Denekamp J. Radiosensitizers of hypoxic cells in solid tumors. Cancer Treat Rev. 1976;3(4):227–56.
201. Juzenas P, Chen W, Sun Y-P, et al. Quantum dots and nanoparticles for photodynamic and radiation therapies of cancer. Adv Drug Deliv Rev. 2008;60(15):1600–14.
202. Cline B, Delahunty I, Xie J. Nanoparticles to mediate X-ray-induced photodynamic therapy and Cherenkov radiation photodynamic therapy. Wiley Interdiscip Rev Nanomed Nanobiotechnol. 2019;11(2):e1541.
203. Calvaruso M, Pucci G, Musso R, Bravatà V, Cammarata FP, Russo G, Forte GI, Minafra L. Nutraceutical compounds as sensitizers for cancer treatment in radiation therapy. Int J Mol Sci. 2019;20:5267.
204. Minafra L, Porcino N, Bravatà V, Gaglio D, Bonanomi M, Amore E, Cammarata FP, Russo G, Militello C, Savoca G, Baglio M, Abbate B, Iacoviello G, Evangelista G, Gilardi MC, Bondì ML, Forte GI. Radiosensitizing effect of curcumin-loaded lipid nanoparticles in breast cancer cells. Nat Sci Rep. 2019;9:11134.

205. Verma V. Relationship and interactions of curcumin with radiation therapy. World J Clin Oncol. 2016;7:275–83.
206. Wang Z, Dabrosin C, Yin X, et al. Broad targeting of angiogenesis for cancer prevention and therapy. Semin Cancer Biol. 2015;35:S224–s243.
207. Yang Y, Jiang M, Hu J, Lv X, Yu L, Qian X, Liu B. Enhancement of radiation effects by ursolic acid in BGC-823 human adenocarcinoma gastric cancer cell line. PLoS One. 2015;10:e0133169.
208. Bykov VN, Drachev IS, Kraev SY, Maydin MA, Gubareva EA, Pigarev SE, Anisimov VN, Baldueva IA, Fedoros EI, Panchenko AV. Radioprotective and radiomitigative effects of BP-C2, a novel lignin-derived polyphenolic composition with ammonium molybdate, in two mouse strains exposed to total body irradiation. Int J Radiat Biol. 2018;94(2):114–23.
209. Pigarev SE, Trashkov AP, Panchenko AV, Yurova MN, Bykov VN, Fedoros EI, Anisimov VN. Evaluation of the genotoxic and antigenotoxic potential of lignin-derivative BP-C2 in the comet assay in vivo. Environ Res. 2021;192:110321.
210. Schueller P, Puettmann S, Micke O, Senner V, Schaefer U, Willich N. Selenium influences the radiation sensitivity of C6 rat glioma cells. Anticancer Res. 2004;24(5A):2913–7.
211. Viani GA, Pavoni JF, De Fendi LI. Prophylactic corticosteroid to prevent pain flare in bone metastases treated by radiotherapy. Rep Pract Oncol Radiother. 2021;26:218–25.
212. Hainfeld JF, Slatkin DN, Smilowitz HM. The use of gold nanoparticles to enhance radiotherapy in mice. Phys Med Biol. 2004;49:N309–15.
213. Jain S, Coulter JA, Hounsell AR, Butterworth KT, McMahon SJ, Hyland WB, et al. Cell-specific radiosensitization by gold nanoparticles at megavoltage radiation energies. Int J Radiat Oncol Biol Phys. 2011;79:531–9.
214. McMahon SJ, Hyland WB, Muir MF, Coulter JA, Jain S, Butterworth KT, et al. Biological consequences of nanoscale energy deposition near irradiated heavy atom nanoparticles. Sci Rep. 2011;1:18.
215. Butterworth KT, Coulter JA, Jain S, Forker J, McMahon SJ, Schettino G, Prise KM, Currell FJ, Hirst DG. Evaluation of cytotoxicity and radiation enhancement using 1.9 nm gold particles: potential application for cancer therapy. Nanotechnology. 2010;21(29):295101.
216. Martens T, Remaut K, Demeester J, De Smedt S, Braeckmans K. Intracellular delivery of nanomaterials: how to catch endosomal escape in the act. Nano Today. 2014;9:344–64.
217. Carriere M, Sauvaigo S, Douki T, Ravanat JL. Impact of nanoparticles on DNA repair processes: current knowledge and working hypotheses. Mutagenesis. 2017;32(1):203–13.
218. Dobešová L, Gier T, Kopečná O, Pagáčová E, Vičar T, Bestvater F, Toufar J, Bačíková A, Kopel P, Fedr R, Hildenbrand G, Falková I, Falk M, Hausmann M. Incorporation of low concentrations of gold nanoparticles: complex effects on radiation response and fate of cancer cells. Pharmaceutics. 2022;14(1):166.
219. Stefancikova L, Lacombe S, Salado D, Porcel E, Pagacova E, Tillement O, Lux F, Depes D, Kozubek S, Falk M. Effect of gadolinium-based nanoparticles on nuclear DNA damage and repair in glioblastoma tumor cells. J Nanobiotechnol. 2016;14(1):63.
220. Liu EK, Sulman EP, Wen PY, Kurz SC. Novel therapies for glioblastoma. Curr Neurol Neurosci Rep. 2020;20:19.
221. Minafra L, Bravatà V. Cell and molecular response to IORT treatment. Transl Cancer Res. 2014;3:32–47.
222. Dai LB, Zhong JT, Shen LF, Zhou SH, Lu ZJ, Bao YY, Fan J. Radiosensitizing effects of curcumin alone or combined with GLUT1 siRNA on laryngeal carcinoma cells through AMPK pathway-induced autophagy. J Cell Mol Med. 2021.
223. Koritzinsky M. Metformin: A novel biological modifier of tumor response to radiation therapy. Int J Radiat Oncol Biol Phys. 2015;93:454–64.
224. Lesueur P, Chevalier F, Austry JB, Waissi W, Burckel H, Noël G, et al. Poly-(ADP-ribose)-polymerase inhibitors as radiosensitizers: a systematic review of pre-clinical and clinical human studies. Oncotarget. 2017;8(40):69105–24.
225. Angel M, Zarba M, Sade JP. PARP inhibitors as a radiosensitizer: a future promising approach in prostate cancer? Ecancermedicalscience. 2021:15.
226. Brown JM, Carlson DJ, Brenner DJ. The tumor radiobiology of SRS and SBRT: are more than the 5 Rs involved? Int J Radiat Oncol Biol Phys. 2014;88(2):254–62.
227. Wang M, Li K, Zou Z, Li L, Zhu L, Wang Q, et al. Piperidine nitroxide tempol enhances cisplatin-induced apoptosis in ovarian cancer cells. Oncol Lett. 2018;16(4):4847–54.
228. Treatment of Radiation and Cisplatin Induced Toxicities With Tempol | Clinical Research Trial Listing (Mucositis | Ototoxicity | Nephrotoxicity) (NCT03480971). https://www.centerwatch.com/clinical-trials/listings/223105/mucositis-treatment-radiation-cisplatin-induced/
229. Monti E, Supino R, Colleoni M, Costa B, Ravizza R, Gariboldi MB. Nitroxide TEMPOL impairs mitochondrial function and induces apoptosis in HL60 cells. J Cell Biochem. 2001;82(2):271–6.
230. Suy S, Mitchell JB, Ehleiter D, Haimovitz-Friedman A, Kasid U. Nitroxides tempol and tempo induce divergent signal transduction pathways in MDA-MB 231 breast cancer cells*. J Biol Chem. 1998;273:17871–8.

Further Reading

Du J, Zhang P, Cheng Y, Liu R, Liu H, Gao F, Sh C, Liu C. General principles of developing novel radioprotective agents for nuclear emergencies. Radiat Med Protect. 2020;1(3):120–6.
Moertl S, Mutschelknaus L, Heider T, Atkinson MJ. MicroRNAs (miRNAs) as novel elements in personalized radiotherapy. Transl Cancer Res. 2016;5(Supplement 6):S1262–9.
Ryan JL, Krishnan S, Movsas B, Coleman CN, Vikram B, Yoo SS. Decreasing the adverse effects of cancer therapy: an NCI workshop on the preclinical development of radiation injury mitigators/protectors. Radiat Res. 2011;176(5):688–91.
Wang B, Tanaka K, Morita A, Ninomiya Y, Maruyama K, Fujita K, Hosoi Y, Nenoi M. Sodium orthovanadate (vanadate), a potent mitigator of radiation-induced damage to the hematopoietic system in mice. J Radiat Res. 2013;54(4):620–9.

12 Ethical, Legal, Social, and Epistemological Considerations of Radiation Exposure

Alexandra Dobney, Abel Julio González, Deborah Oughton, Frances Romain, Gaston Meskens, Michel Bourguignon, Tim Wils, Tanja Perko, and Yehoshua Socol

Learning Objectives

- To recognize that radiological protection is a matter of science and values.
- To appreciate that the acceptability of radiation risks needs to take into account more than the radiation dose alone.
- To identify risk perception and risk perception characteristics.
- To understand justification, being the first pillar of the system of radiological protection, as a principle instructed by the ethical values of justice, dignity, and autonomy.
- To understand the relevant underlying principles of nuclear law.
- To be aware of the general frameworks relating to nuclear law.
- To understand the difference between nuclear liability and general tortious liability.
- To realize that radiation risk communication should be theory-based, evidence-driven, and strategic.
- To get insight into how to communicate with general public and mass media about radiobiology.
- To get insight into the functioning of science and its impact on policy taking into account uncertainties and value pluralisms.

A. Dobney (✉)
Queen Mary University of London, London, United Kingdom

A. J. González
Argentine Nuclear Regulatory Authority, Buenos Aires, Argentina

D. Oughton
Norwegian University of Life Sciences (NMBU), Ås, Norway
e-mail: deborah.oughton@nmbu.no

F. Romain
University of Manchester, Manchester, United Kingdom

G. Meskens
Science and Technology Studies Unit, Belgian Nuclear Research Centre, SCK CEN, Mol, Belgium

Centre for Ethics and Value Inquiry, Ghent University, Ghent, Belgium
e-mail: gaston.meskens@sckcen.be

M. Bourguignon
University of Paris Saclay (UVSQ), Paris, France

T. Wils
Catholic University of Leuven (KU Leuven), Leuven, Belgium

T. Perko
Belgian Nuclear Research Centre, SCK CEN, Mol, Belgium

University of Antwerp, Antwerp, Belgium
e-mail: tanja.perko@sckcen.be

Y. Socol
Jerusalem College of Technology, Jerusalem, Israel
e-mail: socol@jct.ac.il

12.1 Introduction

Ionizing radiation and radioactive substances can be natural or human-made. Humans have always been exposed to natural ionizing radiation (background radiation), because of the exposure of the Earth's surface to cosmic rays and the radioactivity contained in rocks that form the continental crust. The use of radiation and radioactive substances in medicine, research, industry, agriculture, and teaching, as well as the generation of nuclear power, have brought important benefits to society. Acceptance by society of the risks associated with radiation depends on the perceived relationship between these risks and the benefits to be gained from the use of radioactive sources. Logically, risks must be limited, and adequate protection provided. This does not mean that individuals or the environment must be protected from any and

S. Baatout (ed.), *Radiobiology Textbook*, https://doi.org/10.1007/978-3-031-18810-7_12

all effects of ionizing radiation, but rather to ensure that the amount of radiation absorbed does not have negative consequences that outweigh the benefits. The need to balance risks and benefits makes radiation a matter of science and values, meaning that in addition to technical assessments, ethical and legal issues also apply in the judgement of the acceptability of radiation risks.

12.2 The Radiological Protection System

After the initial and isolated observations of the first health effects of ionizing radiation (i.e., skin burns and cancers) by the pioneers at the turn of the nineteenth and twentieth centuries, two decades passed before a clear need for radiation protection was identified. One of the first signs was the leukemia epidemic that developed among radiologists after World War I, reflecting the use of X-ray radioscopy by military surgeons, without any kind of protection, to localize shrapnel in wounded soldiers. This epidemic lasted until the 1950s and affected approximately 500 radiologists [1].

To face the situation, the International Society of Radiology created the International Committee on Radiation Units (ICRU) in 1925 to develop the first concepts regarding dose quantification which were obviously needed. This was followed by the creation in 1928 of the International X-ray and Radium Protection Committee which was restructured in 1950 to take account of new uses of radiation outside the medical area and then renamed the International Commission on Radiological Protection (ICRP). Both ICRU and ICRP are still major actors of radiological protection.

Although the radiological protection (RP) system was established by ICRP, it is worth noticing the critical contribution of the United Nations Scientific Committee on the Effects of Atomic Radiations (UNSCEAR) created in 1955. The ICRP RP system is developed on the basis of the scientific knowledge gathered and synthetised by UNSCEAR.

The ICRP publishes a wide range of recommendations dealing with various aspects of radiological protection, but the current RP system with the three principles of justification, optimization, and dose limitation was first established with recommendation 26 [2]. It has been updated since then by recommendations ICRP 60 [3] and ICRP 103 [4].

12.2.1 Dosimetric Factors and Effects of Ionizing Radiation

ICRP has designed dosimetric factors to properly quantify the exposures to IR and then to establish links between dose and effects. The absorbed dose D is the energy deposited in the tissue: the unit of 1 J/kg is the Gray (Gy) in memory of James Gray. To take into account that different types of radiation do not produce the same biological effects for the same absorbed dose, a radiation weighting factor W_R is used to convert the absorbed dose into the so-called equivalent dose $H_R = W_R \cdot D$. This unit is the Sievert (Sv) in memory of Rolf Sievert. But the biological response also depends on the tissue and a tissue weighting factor W_T is used to convert the equivalent dose for each organ to the so-called effective dose E by adding the contributions of all organs $E = \Sigma_{R,T} W_T H_{R,T}$. The effective dose unit is still the Sv and when a dose is given in Sv it is mandatory to indicate if it relates to an equivalent dose or to an effective dose. Thus, only the absorbed dose is a physical parameter. Equivalent and effective doses are calculated parameters reflecting the likelihood of detriments in humans.

The effects of IR have been classified for years into two categories named deterministic and stochastic effects. Deterministic effects, e.g., skin burns, are due to high doses of ionizing radiation and the responsibility of radiation in their occurrence is clear. Deterministic effects always occur after a dose threshold is exceeded even though some individual variation exists, and the severity of the effect increases with dose. Stochastic effects, such as cancers, may occur after exposure to ionizing radiation but it is only possible to statistically express the occurrence. In other words, it is impossible to say who will develop cancer and when it will appear. One can only say that a percentage of cancers will appear in a population of persons exposed to a given dose, and the probability of developing cancer will increase with dose. Partly because of relatively high background rates of cancers in human populations, the establishment of a causal relationship between exposure to ionizing radiation exposure and the occurrence of cancer can be quite difficult (see Chap. 4).

More recently the separation between deterministic and stochastic effects does not appear to be so clear since some effects may combine both approaches, such as radio-induced cataracts. Therefore, ICRP now uses the classification tissue effect instead of deterministic effects.

Risk evaluation has resulted from epidemiologic studies that have established solid correlations (but not causality) between the frequency of cancers and the dose of IR in the dose range above 100 mGy. But ICRP recommendations are not so clear since the same numerical value is given sometimes in Sv. The calculated risk of cancer is roughly 5% per Sv of effective dose, while the risk to the developing fetus is 50% per Sv. The risk of hereditary disease has been estimated as 0.5% per Sv based on animal models, although it has not been documented so far in humans.

12.2.2 Practical Implementation of ICRP Recommendations

Epidemiologic studies have paved the way for effective management of radiation protection with the three ICRP princi-

ples of radiological protection, i.e., justification of all exposures, optimization of the justified exposures (ALARA principle), and limitation of doses for the workers and the population. Dose limitation does not apply for patients because doses need to be adapted for both diagnosis and treatment. The overarching goal was to suppress the deterministic effects and to substantially minimize the probability of the occurrence of stochastic effects.

On the basis of scientific evidence, ICRP has progressively recommended the mandatory decrease in the exposure to the level of low doses. The actual exposure of workers to ionizing radiation has clearly decreased over the years and is now in the order of or below 1 mSv/year of effective dose in most countries, although the legal limit is still 20 mSv/year for the effective dose. The dose limit of 1 mSv effective dose for the public is below the variations of natural background. At present, the dose limits of the system of radiological protection are quite low and are therefore not foreseen to be changed in the near future. However, doses from medical exposures are still steadily rising.

The ethical foundations of the system of radiological protection were reviewed by ICRP in its publication 138 [5]. This underlined that radiological protection is not only a matter of science but has been developed on ethical values either intentionally or indirectly. Four core ethical values (beneficence/non-maleficence, prudence, justice, and dignity) underpin the present system and relate to the three principles of radiological protection. This publication also addresses key procedural values (accountability, transparency, and inclusiveness) required for the practical implementation of the system (see the following section for more details).

Although the system of radiological protection developed and updated by ICRP for more than eight decades has proved robust and operational, there remain a number of ethical, legal, and social challenges

- Risk evaluation is a major concern since this drives the allocation of resources for radiation protection. The majority of doses in humans are in the low-dose range with a very low risk of cancer. The effective dose should not be used for risk evaluation for a specific individual [4]. Regarding medical exposures, there is a need to develop individual risk evaluation based on doses to the organs exposed [6].
- The human individual response to ionizing radiation should be included in the system in order to optimize radiological protection. This will be part of personalized and predictive medicine, for example, in persons with a high familial risk of cancer or in patients who are likely to be repeatedly exposed to ionizing radiation for medical reasons (especially children, women, prior to radiotherapy or to repeated screening).
- There should be an increased focus on communication with the public and media. There is a need to understand the psychological aspects of risk perception, especially when these show diversion from the real exposures and risks.

12.2.3 The Ethical Motivation for the Linear Non-Threshold Hypothesis

Discussion about the meaning and appropriateness of the acronym LNT has been central in the debate on radiation protection against low-level exposure situations. As an acronym, LNT is non-translatable; a fact that does not facilitate communication. LNT is aimed to denote an imprecise expression: "linear-non-threshold," a short reference to the relationship between the probability of suffering a radiation health effect and the incurred radiation dose, following low doses, low dose rate, radiation exposures.

It is to be noted that this imprecise acronym has been widely used with different connotations by relevant professional communities, a conundrum that can be simplistically summarized as follows:

- For radiation biologists, LNT usually refers to a biological hypothesis postulating that at low radiation doses a given increment in dose will produce a directly proportionate increment in the probability of incurring malignancies or heritable effects attributable to radiation.
- For radiation epidemiologists, LNT is an epidemiological conjecture by which the incidence of effects per unit dose measured at radiation exposure situations involving relatively high doses delivered at relatively high dose rates, where an epidemic of increases in malignancies have been recorded, is presumed to occur also at radiation exposure situations involving low doses and low dose rates in spite that epidemiological evidence is not achievable in such situations.
- For radiation-protectionists, LNT represents a practical operational model for managing radiation protection and controlling that protection against additional doses regardless of the level of accumulated dose, and, therefore, preventing discrimination—particularly age-related labor discrimination in cases of occupational radiation protection.

The wide and imprecise use of the acronym LNT without clarification of its precise meaning has been a cause of serious confusion on the health effects attributable following low dose, low dose rate, and radiation exposure situations.

It could be succintly said that LNT is intended to mean a practical model rather than a sophisticated scientific theory and that it is based on the globally accepted principles of ethical prudence and on labor rights for non-discrimination—long established by international undertakings.

12.3 Ethical Aspects of Radiation Exposure

12.3.1 Radioactivity and Justification: Raising Awareness for the Contexts of Concern

What are we speaking about when we speak about ethical, legal, social, and psychological aspects in relation to the radiological risk? Dealing with radioactivity in society is a complex challenge in any respect, but one can distinguish four fundamental "contexts of concern" that require different visions on complexity, and what it would mean to responsibly deal with it. When considering ethical, legal, social, and psychological aspects of radiation exposure, it is important to always do this with the context of application or "the context of concern," in mind.

The first context is the context of "naturally enhanced" natural radiation. The second context concerns industrial practices that involve technically enhanced natural radiation. The third context is the context of peaceful applications of nuclear technology. These include applications of nuclear physics processes, such as the fission or fusion of nuclei for energy production or the use of decay radiation in medical treatment and diagnosis or for industrial purposes. The fourth context is the use of nuclear technology or material as a weapon, either as a means for political deterrence, in organized military operation or in terrorist actions.

The reason to distinguish these different contexts is motivated by a specific understanding of the ethics of radiological risk governance and its relation to the social and political aspects of governance, and this as well in theory as in practice. To put it simply, if we consider average natural background radiation as an element of our natural habitat, then any significantly enhanced level of radioactivity in the vicinity of living species represents a risk—in the sense of a potential harm—to the health of those living species. In these cases, pragmatic reasoning thus requires us to consider the possibility of protection, mitigation, or avoidance, but essentially to first evaluate why the additional radioactivity occurs in the first place, and whether we can possibly justify it. But whether that justification exercise can be done meaningfully or not depends on how we perceive the context of the occurrence of radiation.

From what the first context is concerned, whether we want it or not, natural radiation is there and any naturally enhanced occurrence (e.g., in the case of high concentrations of Radon) has a potential impact on health. Thinking in terms of justification of the presence of that radiation is meaningless, which leaves us with evaluating the justification of exposure, and thus of the possibility of protection, mitigation, or avoidance of its impact.

In the second context of technically enhanced natural radiation (for example, in the oil refinery industry or in aviation), radiation exposure manifests as a "side effect." Practices as such may be contested (as is the case with the oil or phosphate industry), but very rarely the issue of radiation exposure will become a decisive factor in the evaluation of the justification of these practices. Similar to the case of naturally enhanced natural radiation, the radiation justification exercise thus restricts itself to the evaluation of exposure, and thus to the evaluation of the possibility of protection, mitigation, or avoidance of its impact.

In the third context, evaluation of the justification of the use of nuclear technology obviously takes the reason for that proposed use (the projected "benefits") as a first criterion, with the aim to "balance" it with the projected risks. Despite the fact that opinions on these projected benefits and risks differ among people, in this context, an evaluation of the justification of the use of a risk-inherent technology, or thus of the presence or "creation" of radiation, remains meaningful, and this is because the application context is "neutral"; while opinions may differ on how to produce energy or perform a medical treatment, nobody is "against energy" or "against medical care" as such. The neutral context thus makes a meaningful joint evaluation of the justification of the nuclear technology application possible, and it will not affect possible outcomes (rejection or acceptance of the technology) as such.

Finally, in the fourth context, a meaningful joint evaluation of the justification of (the risk of) the nuclear technology application is not possible, and this is for the reason that the context of application itself is not neutral. A pacifist perspective does not support a principal justification of nuclear deterrence and armed conflict strategies, while, in a perspective that sees politics always as a politics of power and conflict, these strategies may be perceived as justified.

12.3.2 The Justice of Justification as a Central Ethical Concern

Any evaluation of the acceptability of a radiological risk is characterized by a "double" complexity. Firstly, it needs to take into account the uncertainties with regard to whether and how the risk will manifest. Science has an authoritative voice in this evaluation, but it needs to recognize that there will always be uncertainties that cannot be cleared out (stochasticity of biological effects at low radiation dose, possible delayed harm of medical diagnosis or therapy, the possibility of a nuclear accident, the fate of a radioactive waste disposal site in the far future, …). In addition, we have to accept that important factors remain to a large degree beyond control: human behavior, nature, time, and potential misuse of technology… Secondly, an evaluation of the acceptability of a radiological risk also needs to consider diverse value judg-

ments with regard to the acceptability of the risk. In philosophical terms, one can say that the evaluation is troubled by moral pluralism: even if we would all agree on the scientific knowledge base for the assessment of the risk, then opinions on its acceptability could still differ. The reason is that evaluations of acceptability do not only rely on "knowledge" but are also influenced by references to things people value as important, such as freedom, security, the value of nature, the rights of the next generations, and their safety and that of their loved ones. In that case, science may thus inform the technical and societal aspects of options, it cannot instruct or clarify the choice to make.

Taking this complexity into account, one may understand that risk cannot be justified through a one-directional "convincing explanation" by scientific experts or political decision-makers. Ethics supports the idea that the evaluation of a possible justification of a radiological risk needs to be done in deliberation among all concerned, including those potentially affected by the risk. In that deliberation, visions from science, policy, civil society, and citizens have an equal place, bearing in mind that (quoting the philosopher Philip Kitcher) "*There are no ethical experts. The only authority is the authority of conversation*" [7]. Obviously, the outcome of that conversation can either be to reject or to accept the radiological risk. In other words, from an ethical perspective, the argument is that the justice of justification, ensured by the possibility of self-determination of the potentially affected, should be the central concern of risk governance. In practice, that means formal methods for decision-making and formal procedures within the organization should care for the possibility of participation of those potentially affected by the radiological risk.

12.3.3 Recognizing the Limits of the Radiological Protection System for Risk Justification

Seen from a different perspective, ethics in relation to radiological protection is also about considering and recognizing the limits of the radiological protection system when it comes to providing a rationale for justification of radiation risk. In other words, we cannot question the ethical dimensions of the radiological protection system without also questioning the ethical dimensions of the "bigger" systems in which the radiological protection system operates and on which it depends. Given that the radiological protection system, in its concern for providing guidance for decision-making, relies on science but also and essentially wants to take into account human and societal values, the bigger systems that need to be questioned in terms of their ethics, are those of knowledge production (research and policy advice) and decision-making. For risks that manifest in medical diagnostic or therapeutic practices, that "system" is the possibility of deliberative dialog between the patient, the doctor, the nurse, the radiation control and protection service of the hospital, other hospital agencies, as well as regulatory and professional bodies. For risks that manifest in an occupational context, the system of decision-making is the radiation control and protection service, the management system of the organization, other relevant agencies, trade unions, and professional bodies. For risks that manifest on a societal level, that system of decision-making is the system of democracy, including input from citizens, civil society, trade unions, professional bodies, advocacy groups, and of scientific and ethical advisory committees.

12.3.4 The Ethical Foundations of the System of Radiological Protection

The evolving ethics of the developing international system of protection against ionizing radiation could be viewed as the branch of some kind of embryonic radiological protection philosophy, which from the beginning of the profession was dealing with main protection principles and their values. It challenged questions about the morality of the protection principles—that is, concepts such as good and bad, right and wrong, virtue and vice in radiological protection. It tried to tackle issues such as the meaning and reference of moral propositions on radiological protection; the practical means of determining a moral protective action, how moral protective outcomes can be achieved in specific situations, how a moral capacity for recommending a protection paradigm develops and what its nature should be and what moral values on radiological protection people in general and stakeholders in particular should actually abide by.

Ethics was the primordial earliest concept for judging human actions such as those involved in radiological protection and provides its fundamental basis. Radioprotectionists had been (and continue to be) very keen on exploring and reassessing the rules and standards governing their professional conduct. They have had an unusual curiosity to self-inspect whether they hold the right behavior and what is the set of principles for self-ensuring that such behavior is right. This interest in self-appraisal of conduct correlates with the notion of ethics.

The ethical basis of radiological protection was early recognized by the profession's forefathers [1]. The primordial radiation protection principle related to individuals (in fact these individuals were at the beginning just radiologists; it would take a number of years to incorporate individual mem-

bers of the public, and some more to incorporate individual patients undergoing radiodiagnostic or radiotherapy), as follows:

- The *principle of individual dose restrictions*, which was aimed at ensuring that the total dose incurred by any individual should be restricted to protect the individual exposed. Although not explicitly, it was implicitly based on an ethics of duty, the so-called *deontological ethics*, which is usually expressed with the aphorism "One should do unto others as they would have done unto them."

Over time it became clear that the protection of individual was a necessary but not necessarily a sufficient condition, and the system of collective ethical requirements evolved. Two basic principles would fill this gap, as follows:

- The *principle of justification*, which was aimed at ensuring that any decision that alters the radiation exposure situation should do more good than harm—meaning that by introducing new radiation sources or by intervening for reducing existing doses, sufficient individual or societal benefit should be achieved to offset the detriment such actions may cause. This principle was based on the ethics of consequence or *teleological ethics*, which is usually expressed with the aphorism "The ends justify the means."
- The *principle of optimization*, which aimed at ensuring that the level of protection would be the best under the prevailing circumstances, maximizing the margin of benefit over harm, and thus the number of people exposed and of their individual doses be kept as low as reasonably achievable, taking into account economic and societal factors. This was based on the ethics of efficacy or *utilitarian ethics*, which is usually expressed with the aphorism "Provide the greatest good for the greatest number of people."

These two principles and their ethics are the basis of the radiation protection paradigm recommended by the ICRP.

In addition, there was an intrinsic value of these principles, or de facto principle in its own right, which unfortunately was not specifically declared as such by ICRP, but which is implicitly referred to in many statements and underlines most of the ICRP recommendations and it was recognized in subsequent international standards. It could be formulated as follows:

- The *principle of intergenerational prudence,* also termed *principle of protection of present and future generations* in international standards, is aimed at ensuring that protection extends to all humanity and its environment, regardless of where and when people live, and which implies that all humans, present and future, and their environment shall be afforded with a level of protection that is not weaker than the level provided to those populations causing the protection needs. It can be construed that this important principle is mainly based on the *ethics of virtue* or *ethics of arête*, which is usually expressed with the aphorism "No return should be expected from good actions, as goodness is an ideal that transcends human nature.".

Teleological and utilitarian ethics belong to a family of "social-oriented" ethics; deontological and arête ethics belong to a family of "individual-oriented" ethics. In relation to radiation protection, teleological and utilitarian ethics aim at protecting society as a whole, while deontological and virtue ethics are more focused on individual protection and individual rights. Teleological, utilitarian, and deontological ethics have evolved in a mainly anthropocentric framework. Conversely, arête ethics is able to deal with more general ethical issues such as intergenerational and environmental protection.

The start of the twenty-first century saw a growing criticism of the anthropocentric focus of the system of radiological protection, exemplified by the statement that "… *the standard of environmental control needed to protect man to the degree though desirable will ensure that other species are not put at risk*" [3]. Critics noted that there were cases where human doses could be low and doses to wildlife high (e.g., waste disposal), that the approach was not in line with management of other environmental stressors, and that there was a need to demonstrate explicitly that non-human species were being protected [8–10]. The IAEA published a report on "*Ethical Considerations in protection of the environment from the effects of ionising radiation,*" exploring ethical principles that might underlie a system of protection and stressing the need to be compatible with international legal instruments such as those related to sustainability and protection of biodiversity [11]. The requirement to address the impacts of ionizing radiation on the environment is now included in international radiation protection recommendations and standards [4, 12, 13].

12.3.5 ICRP Core Ethical Values

Previous writers have compared the ICRP principles with ethical theories, highlighting the similarities between the principle of justification with teleological or contractarian ethics, the principle of optimization with utilitarian approaches, and the principle of dose limitation with deontological ethics [14, 15]. In its recent work on the ethical foundations of radiological protection, ICRP has focused on commonly recognized ethical values, rather than over-

arching ethical theories such as utilitarianism or deontology [5]. This is in line with approaches to ethical assessment applied in biomedical and public health ethics [16], as well as work on cross-cultural ethics [17], underlining that it is easier to find agreement on fundamental values than on ethical doctrines. ICRP highlights four core values underpinning the system of radiological protection: beneficence/non-maleficence, justice, dignity, and prudence [5].

Examples of how these values can be applied in the analysis of ethical challenges are given in the following sections. But briefly, beneficence and non-maleficence refer to the principles of promoting well-being and avoiding the causation of harm. In radiological protection, this is clearly related to the reduction of radiation exposures, and the avoidance of resultant harms, but can also include a range of different costs and benefits, including economic and societal aspects. There will always be questions about how to measure consequences and who or what should count in such an evaluation (e.g., animals and future generations). Dignity is concerned with respect for autonomy and the self-determination and choice of affected populations and includes issues related to privacy, human rights, as well as individual and community empowerment. The ethical principles of fairness and justice stress the importance of addressing the way in which risks, costs, and benefits are distributed (distributive justice), as well as the way in which decisions are carried out (procedural justice). Prudence is the ability to make discerning and informed choices without the full knowledge of the scope and consequences of our actions. While precaution and prudence are rarely alluded to in general medical ethics and bioethics, the precautionary principle is well recognized in environmental ethics. The ICRP also introduces the procedural values of transparency and accountability, in the practical application of radiological protection, especially in the need to engage stakeholders in decision-making processes [5]. While there has been a general consensus on the fundamental values proposed by ICRP, there have been proposals that the system should include additional values such as empathy and honesty [18].

12.3.6 Acceptability of Radiation Risks Need to Address More Than the Size of the Dose

The public's aversion to radiation—and especially that associated with nuclear power rather than natural or medical exposures—is often cited as an example of irrationality or misunderstanding, and is best combated by improved education. But to understand risk perception, we need to recognize that risk is in part quantifiable but also a social construct that is interpreted differently by people in various situations, environments, and cultures. It is true that people misunderstand probabilities; however, numerous studies of the psychological and psychometric factors that influence risk perception show that the situation is more complex than this alone. Public or lay perceptions of risk vary widely between people and can differ from the calculated, technical approach to the assessment of risks. Whereas an expert will often tend to rank risks as being synonymous with the size or probability of harm, risk tolerance or aversion is dependent on many additional characteristics [19, 20]. Many of the characteristics have strong psychological as well as societal and ethical relevance (such as control, voluntariness, and distribution of risks and benefits).

12.3.6.1 Autonomy, Personal Control, and Consent

People tend to be less tolerant of risks that are imposed without their choice or personal control. The phenomenon applies to a range of different risks and actions, such as driving a car compared with flying. Personal control is closely related to the fundamental ethical value of autonomy (i.e., respect for the free will of individuals), dignity, integrity, and individual rights. It is also linked to the requirement for free informed consent within medical ethics and can explain why people are less concerned over medical radiation exposures (which are largely voluntary and for an obvious personal benefit). People often feel a lack of personal control over radiation exposure [19], particularly those associated with accidents. They are dependent on information from authorities or media and have to deal with both the risks from the exposure as well as the consequences of measures to reduce exposure such as relocation or agricultural bans.

In risk management, measures that increase personal control and understanding, such as the provision of dosimeters or counting equipment, and participation in decision-making are considered positive and can help populations in coping. Provision of counting equipment and independent monitoring are methods that have been successfully applied in both Chernobyl- and Fukushima-affected communities [21–23]. When combined with access to experts to help interpret results, such actions can help empower populations. Ethically, procedures that involve the populations themselves can help promote the principle of informed personal control over radiation risks.

12.3.6.2 Community Values and Societal Consequences

The Chernobyl and the Fukushima accidents both resulted in a wide range of social and economic consequences. Many evacuees lost their jobs, social network, and connection to places of a particular community or historical

value like graveyards or places where they played as children [24]. Resettlement and long-term evacuation in Fukushima have changed the social structure of the villages and city districts [25]. After Chernobyl, the emigration of young people impeded the whole social and economic development of the region, including a shortage of teachers and doctors [26]. Similar demographic changes have been seen after Fukushima, with young families more likely to evacuate and less likely to return [25]. These lead in turn to a variety of social and health effects such as alcoholism, obesity, and depression in affected populations.

The economic costs of accidents are complex and wide-reaching. Loss of consumer trust in food from a contaminated area can have economic consequences that go beyond the loss of food production. Stress, ill-health, and even suicide can accompany job loss and bankruptcy. Loss of consumer trust can have profound consequences both for a range of industries (particularly food or tourist industries) and for the local identities of people and groups. This has been well-documented in Fukushima with price drops for produce from the entire region, including areas not affected by the accident, as well as impacts on tourism [25]. Negative economic side effects can arise from rural breakdown and stigma of contaminated communities. Discrimination and stigmatization of the Hiroshima and Nagasaki Hibakusha and their children have an important historical dimension in Japan [27] and is a particular concern for Fukushima evacuees. Hibakusha is a Japanese term referring to the survivors of the Hiroshima and Nagasaki atomic bombs, which translates literally as "bomb-affected people." TEPCO workers also cited discrimination as one of the main causes of psychological stress [28]. In addition to experienced prejudice, concerns of the populations affected by Fukushima Daiichi accident include worries about whether their children would be able to find partners or marry in the future and reports of discrimination against Fukushima children after moving to new schools.

The aftermath of an accident can also be economically beneficial to parts of the community, for example, through the generation of local employment opportunities. This may lead to some sections of the population making a profit from remediation (such as selling or hiring equipment), which can lead to further social inequity and division.

12.3.6.3 Distribution of Risks and Benefits

Distribution of the costs, risks, and benefits of radiation exposure relate to the fundamental ethical values of equity, justice, and fairness. After an accident, doses received by individuals can vary widely, and the risks of those exposures differ between adults and children. The consequences of remediation can impact different members of the affected communities. Some may lose their livelihood, while others can continue more or less as before the accident. For example, after Fukushima the situation was particularly harsh for the elderly evacuees, particularly those living in temporary housing who experienced greater isolation from family and communities [25].

The potential for increased health risks from radiation in children means that the risk perceptions go beyond consideration for personal risks, as is seen by anxiety over thyroid cancer in Fukushima populations [35, 36]. The fear that your child could be affected in the future can overshadow any personal concern [24]. Such concerns create challenges for health surveillance, particularly thyroid screening of children. While parents may, understandably, request screening, the procedure can lead to unnecessary surgery (e.g., 4000 thyroid surgeries in Chernobyl children may explain most of 15 deaths attributed to exposure), and without a carefully thought communication plan may raise anxiety (Shamisen 2020). Some measures to reduce exposures could result in an equitable distribution of cost and dose reduction, such as investment by taxpayers to reduce activity concentrations in public areas; while others are less equitable, for example, when a reduction of dose to the majority is only possible at the expense of a higher dose, cost, or welfare burden, on a minority (e.g., banning all farm production in a small community).

To conclude, public reaction to disasters is the result of complex and intrinsic features of risk perception, many of which have strong ethical and societal relevance. A holistic approach to disaster management should integrate economic, ecological, and health measures. Risk management strategies should be designed to accommodate varied needs. For nuclear accidents, it is not sufficient to simply focus on the dose reduction aspects of radiation protection as societal aspects will play a major role in how individuals cope with, and communities recover from the disaster. Engaging with the affected population with regard to increasing their understanding and personal control and involving them in decision-making processes respects people's fundamental right to shape their own future. In addition to increasing trust and compliance, such approaches can lead to significant improvements in the effectiveness and acceptability of disaster management in communities.

12.3.7 Emerging Occupational Challenges from New Methods to Determine Individual Radiosensitivity

Testing for radiosensitivity has the potential to improve patient treatment and diagnosis or protect workers. Assays might be applied prior to radiotherapy, to avoid adverse

reactions in radiosensitive individuals, or to avoid enhanced cancer risk in connection with radiodiagnoses such as CT scans or mammography [31]. While not yet applied in medicine or worker protection, assays are currently under development, and their potential application raises a number of ethical and legal challenges. These go beyond the simple question of whether the assay will "do more good than harm" to include, for example, questions about how the costs and benefits might be distributed in society, concerns about privacy and data protection, and considerations of the potential for discrimination.

12.3.7.1 Well-Being

Radiosensitivity and radiosusceptibility assays have a clear potential to provide physical health benefits by improving cancer treatment, avoiding negative side effects, and enhancing worker protection. There are also economic aspects, such as balancing the cost of the assays against the opportunity to save money through tailored treatment. Psychosocial consequences could include reassurance but might also cause worry about sensitivity to other stressors. Information on the magnitude of the effect, its relation to other potential risk factors, and indeed any dose–response relationship, as well rates of false positives and false negatives would be needed to be able to balance the physical harms and benefits. But this would also have knock-on effects on economic, psychological as well as legal assessments. Could doctors be sued for the negative effects of not carrying out a test?

12.3.7.2 Dignity and Autonomy

Information on individual radiosensitivity and radiosusceptibility could clearly enhance patient or worker empowerment and personal control, but this would depend strongly on the context in which this information was used. The issues are similar to other challenges with personal health information, such as conforming to data protection laws and the increasing commercialization of genetic testing [32]. For example, the degree to which data from patients undergoing an assay as part of radiotherapy would be stored, anonymized, and made available for further research would need to be addressed. A debate on the implications of these issues would need to include engagement with the various stakeholders but could also play an important role in risk communication, by putting the risks of ionizing radiation in context with other environmental and genetic risk factors.

12.3.7.3 Justice and Fairness

Increased understanding of the differences in radiosensitivity within populations is relevant to an assessment of justice. Other questions would include whether the assays would provide equal access to health care and support or have any impact on health insurance (would sensitive populations have to pay higher premiums?) or compensation claims (will it change the balance of probabilities that cancers were caused by radiation exposure?). Even in countries with national health insurance, there is the question of whether people should be obliged to disclose the results of genetic testing before taking out private health or life insurance schemes. If sensitivity or susceptibility was linked to a genetic trait, there would be additional issues associated with implications for children or other family members. While identification of increased radiosusceptibility in workers could be used for protective purposes, it might also lead to discrimination, or raise questions about "responsibility" for any diseases or negative side effects (lifestyle, predisposition, occupational exposure, etc.). These issues could be linked to broader debates on the implications for radiological protection of populations with different risk factors such as whether children or women should be treated differently on the basis of increased radiation cancer risks.

To conclude, many of the ethical challenges associated with the field of radiosensitivity and radiosusceptibility have parallels with existing challenges in medical, occupational, and public health. They also raise important questions about the implications for radiological protection. For example, will population-level differences in radiation susceptibility impact the assessment of health risk? Will they lead to a change in dose constraints? These questions can only be addressed with the participation of a wide variety of stakeholders. Assessing the implications for well-being requires knowledge from experts in radiation biology, medicine, occupational health, health economics, social scientists, etc., as well as transparency about uncertainties and assumptions. Respecting both the principles of dignity and fairness in the procedure requires the participation of affected persons (workers, patients, the public, etc.) in decision-making.

12.3.8 The Ethical Challenge of Science as Policy Advice

Looking at the societal impacts of science and technology, nuclear technology probably represents the most extreme case of how science and technology can serve both cure and destruction. While medical applications of nuclear technology save individual lives every day, nuclear weapons have enormous destructive potential. Nuclear energy is a low-carbon source of electricity, but a nuclear accident can have dramatic impacts on the environment and on the physical and psychological health of a whole population for a long time. In addition, disposal of radioactive waste unavoidably requires taking responsible action toward future generations thereby taking into account time dimensions longer than ever faced before in human history.

The case of nuclear energy technology is also an example of how technology assessment can be troubled by the fact

that "benefits and burdens" of a technology are essentially incomparable. Referring to the general considerations related to the radiological risk and the need to include values in its assessment above, we can say that, taking into account the specific character of the nuclear energy risk, also the societal justification of nuclear energy is troubled by moral pluralism. That is, even if we would all agree on the scientific knowledge base for the assessment of the risk, then opinions on its acceptability could still differ. The matter becomes even more complex if we take into account the fact that science can only deliver evidence to a certain extent. Nuclear science and engineering are mature, but we have to acknowledge that the existence of knowledge-related uncertainties puts fundamental limits to understanding and forecasting technological, biological, and social phenomena in the interest of risk assessment and governance. Last but not least, we have to accept that important factors remain to a large degree beyond control. These are human behavior, nature, time, and potential misuse of technology.

The resulting room for interpretation complicates the evaluation of risk-inherent technologies in general and of nuclear technology in particular and puts a specific responsibility on science and technology assessment as a policy-supportive research practice. And this is the point where ethics come in. In simple terms, that responsibility comes down to acknowledging and taking into account uncertainty and pluralism as described above, and the consequences thereof for research and policy. That "responsible attitude" does not only apply to scientists but to everyone concerned with applications of science and technology in general and with the issue of nuclear technology in particular. The idea is that this responsible attitude can only be enabled and stimulated in "interaction methods" for policy and scientific research that are able to generate societal trust by their "method." Today we know that this in principle translates as doing politics differently by involving the potentially affected and other stakeholders in deliberative decision-making, and as doing science differently, namely as transdisciplinary science advancing from a holistic perspective and enriched with insights and ideas from the social sciences and the humanities, from lay knowledge and the arts and from civil society and citizens (see, among other [33–35]). For science in particular, confronted with the need to deal with incomplete and speculative knowledge and value pluralism in providing policy advice on issues of social well-being, its challenge is no longer the production of credible proofs but the construction of credible hypotheses [33]. From an ethical perspective, in the general interest of rendering hypotheses with credibility (and the potential to generate societal trust), one could say science has no choice but to "open up its method" for transdisciplinarity and public involvement, in addition to the "traditional" quality criteria of objectivity and independence and the need to recognize uncertainty, value pluralism, contingency, and potential misuse. Obviously, the aim of this ethically inspired "reflexivity" is not to undermine the credibility of science but to stimulate dialog and (self) critical thinking, and to make science more resilient against pressure from politics and the market to deliver evidence it cannot (yet) deliver.

12.3.9 Emergency Planning and Response in Post-Accident Context

The complex dimensions of radiological risk, particularly after large-scale accidents raise particular challenges for cost-benefit analysis of post-accident response. Emotional descriptions of such emergencies seem more common than quantitative cost-effectiveness considerations. Noteworthy, a few weeks before the first atomic bomb test in July 1945, an official report warned that "civilization would have the means to commit suicide at will" [36]. Kahn [37] considered a full-scale 10,000,000 kiloton nuclear exchange between the Soviet Union and the USA, and deliberated in detail why the above statement is far from being based on evidence.

Quantitative considerations show that the direct health consequences—radiation sickness, carcinogenesis, etc.—of any past (or future practically probable) radiological accident are much less far-reaching than those which are usually perceived. In each scenario, direct health effects are only a small part of the damage caused by fear and anxiety. For example, the two major humanitarian disasters after the Chernobyl and Fukushima nuclear accidents turned out to be such disasters not because of their radiogenic effects, either actual or averted. The main health consequences could be attributed to countermeasures by the authorities, and socio-psychosomatic problems among the public. The relocation of hundreds of thousands of people created very real suffering, morbidity, and mortality [38]. Rational decision-making should have quantitatively compared the human cost of evacuation and long-term relocation with the human cost of radiation exposure. Such comparison was performed only decades later. For example, Yanovskiy et al. [39] estimated that in Fukushima the evacuation was not justified at all, and in Chernobyl the evacuated zone could have been repopulated after 1 month.

The human cost of evacuations should be considered as follows. First, there is always a direct loss of life due to the temporary loss of medical care, psychosomatic disorders, and even suicides; After Fukushima, e.g., 1% of the evacuees died during the first 2 years due to evacuation-related causes (on top of the natural mortality). Second, evacuees' quality of life deteriorates by about 20% [39]. Last but not least, evacuation is expensive. While associating human life with monetary value is psychologically difficult and may seem ethically challenging, it is actually an ethical necessity since extraneous expenditure leads to a statistical shortening of life. A cost-effectiveness analysis is routinely performed

when formulating health policies [40]. Safety expenditures should be treated in a similar way since both healthcare and safety deal with life extension [41].

In this context, it is worth mentioning that life expectancy varies considerably not only for different countries but also for different locations of each country: the main reasons are probably socioeconomic and environmental. This disparity in life expectancy across countries is typically of several years; in the extreme case of Calton in the UK it was 25 years below the country average [42]. It is needless to mention that evacuation of less-successful locations is nowhere considered as a viable option.

12.4 Legal Aspects of Radiation Exposure Situations

12.4.1 Introduction

The purpose of nuclear law is to establish a legal framework for the safe management of all sources and types of radiation and endeavors involving exposure to ionizing radiation [43]. Nuclear law should thus ensure the adequate protection of individuals, society, and the environment, both present and future, against radiological hazards. Specifically, nuclear law should cover the exposure of the general public—i.e., any individual in the population—of workers—i.e., any person who works, whether full-time, part-time, or temporarily, for an employer and who has recognized rights and duties in relation to occupational radiation protection—as well as exposures related to medical uses of radiation, situations in which a patient is voluntarily exposed for therapeutic purposes (radiodiagnostic or radiotherapy) and who may incur high doses of radiation, possibly with unwanted side effects as a result. Radiation protection rules and regulations should always include special provisions relating to the way in which the application of fundamental principles of justification of actions involving radiation exposure, optimization, or protection, and limitation of individual radiation risk is applied.

The general principles of nuclear law broadly apply to all nuclear-related activities and facilities where ionizing radiation is used or produced.

Section 12.4 will first define nuclear law. Important principles will then be covered followed by a summary and explanation of relevant legislative frameworks. Certain specific potential exposure situations and how the law treats them will also be expanded upon such as employer and medical liability, as well as the legal framework for airline personnel and astronauts.

Legal attribution and imputation of radiation harm to radiation exposure situations, a topic that has distinct epistemological elements, will be discussed in Sect. 12.5 after the more formal legal aspects.

12.4.2 Definition and Objective of Nuclear Law

The scope of nuclear law can be succinctly defined as any issue or matter relating to the use of, production of, or exposure to ionizing radiation in specific situations.

In more detail, nuclear law can be defined as "*The body of special legal norms created to regulate the conduct of legal or natural persons engaged in activities related to fissionable materials, ionizing radiation, and exposure to natural sources of radiation*" while its primary objective is "*To provide a legal framework for conducting activities related to nuclear energy and ionizing radiation in a manner which adequately protects individuals, property, and the environment*" [44].

This definition has four key elements. Firstly, nuclear law is a body of special legal standards and norms. These are recognized as a part of general national legislation. Since it is a sovereign right of countries to choose how they enact laws, national legislations may differ when it relates to nuclear issues.

Secondly, nuclear law serves a regulatory purpose. The use of and exposure to radiation needs to be regulated given that whilst there is a potential benefit to social and economic development, there also a potentially detrimental effects.

Thirdly, nuclear law relates to the conduct of legal and natural persons. These persons could be commercial, academic, scientific, governmental, or natural. A legal person is a body corporate (or corporate organization) such as a company while a natural person is an individual human being [45].

Fourthly, nuclear law primarily relates to radioactivity, ionizing radiation, and the products of nuclear fission, with the clarification that in this context, it means those that have potentially unwanted biological effects. We could add to the definition that the effects of fusion reactions—still largely in a developmental phase at the time of the redaction of this work—should also be included under the umbrella of nuclear law. The property of protection of the population from the adverse effects of radioactivity and radiation is considered to be the defining aspect justifying the need for a special legal regime.

12.4.3 Principles of Nuclear Law

A number of basic concepts, often expressed as fundamental principles, distinguish nuclear law from other aspects of law. These principles and various theories are crucial to under-

stand because they help understand why the law exists in the form it does.

The *safety principle* is arguably the central concept in nuclear law [43]. Within the safety principle, there are a number of other principles. These include the *prevention principle* that postulates that, given the special nature of the risks associated with the use of nuclear energy, the primary objective of nuclear law is to promote the exercise of caution and foresight to prevent damage and minimize adverse effects. Another principle is the *protection principle* which postulates that when the risks associated with an activity are found to outweigh the benefits, priority must be given to protecting public health, safety, security, and the environment. The *precautionary principle* also prioritizes protection and the prevention of foreseeable harm as fundamental requirements.

Fundamental safety principles codified in legislation may be applied to a wide variety of activities and facilities that pose very different types and levels of risk. Activities posing significant radiation hazards will obviously require stringent technical safety measures and, in parallel, strict legal arrangements. Activities posing little or no radiation hazard will need only elementary technical safety measures, with limited legal arrangements.

The *security principle* [43] is an underlying principle of the special legal measures that are required to protect and account for the types and quantities of nuclear material that may pose security risks. These measures should protect against both accidental and intentional diversion from the legitimate uses of these materials and technologies. Lost or abandoned radiation sources can cause physical injury to persons unaware of the associated hazards. The acquisition of radiation sources by terrorist or criminal groups could lead to the production of radiation dispersion devices to be used to commit malevolent acts. The diversion of certain types of nuclear material could contribute to the spread of nuclear weapons to both subnational and national entities. It is for these reasons that legal measures regarding physical protection, emergency preparedness, response, and transport, import and export of radioactive material have been adopted.

> While safety is of the utmost importance, it is important to carry out a balancing of both the risks and the benefits of exposure. There are situations in which the benefits clearly outweigh the risks, and it is important to not dismiss outright any and all exposure based solely on hazard.

The aforementioned principles are not the only ones used in a nuclear law context. For example, the IAEA Basic International Safety Standards (BSS, *infra*, Sect. 12.4.4.1) represent a broad international consensus on the appropriate handling of radioactive sources to ensure that nuclear-related activities can be conducted in a safe, secure, and environmentally acceptable way. The BSS consists of three sets of publications: the Safety Fundamentals, the Safety Requirements, and the Safety Guides. The Fundamentals establish the fundamental safety objectives and principles of protection and safety, the Requirements set out the requisite conditions that must be met to protect the population and the environment and the Safety Guides provide practical recommendations and guidance on how to comply with the requirements.

The Fundamental Safety Principles are the basis of international and intergovernmental standards of radiation and nuclear safety. They have been established under the aegis of the IAEA and are jointly sponsored by the European Atomic Energy Community (Euratom), the Food and Agriculture Organization of the United Nations (FAO), the International Atomic Energy Agency (IAEA), the International Labour Organization (ILO), the International Maritime Organization (IMO), the OECD Nuclear Energy Agency (OECD/NEA), the Pan American Health Organization (PAHO), the United Nations Environment Programme (UNEP), and the World Health Organization (WHO).

- The fundamental safety principles are more detailed elements of the safety principle previously discussed:
- The first principle is the responsibility for safety: The prime responsibility for safety must rest with the person or organization responsible for facilities and activities that give rise to radiation risks.
- The second safety principle relates to the role of the government: An effective legal and governmental framework for safety, including an independent regulatory body, must be established and sustained.
- The third safety principle relates to the leadership and management for safety: Effective leadership and management for safety must be established and sustained in organizations concerned with, and facilities and activities that give rise to, radiation risks.
- The fourth safety principle calls for the justification of facilities and activities: Facilities and activities that give rise to radiation risks must yield an overall benefit.
- The fifth safety principle refers to the optimization of protection and safety: Protection must be optimized to provide the highest level of safety that can reasonably be achieved.
- The sixth principle requests the limitation of risks to individuals: Measures for controlling radiation risks must ensure that no individual bears an unacceptable risk of harm.
- The seventh principle calls for the protection of present and future generations: People and the environment, present and future, must be protected against radiation risks.

- The eighth principle refers to the prevention of accidents: All practical efforts must be made to prevent and mitigate nuclear or radiation accidents.
- The ninth principle relates to emergency preparedness and response: Arrangements must be made for emergency preparedness and response for nuclear or radiation incidents.
- The tenth and final principle refers to protective actions to reduce existing or unregulated radiation risks: Protective actions to reduce existing or unregulated radiation risks must be justified and optimized.

The central underlying principle of nuclear law is safety. If a situation arises in which a law's interpretation is unclear, it is useful to ask which interpretation would lead to the safest outcome. This should of course take into account the beneficial impacts relating to the exposure, but it is a good starting point if confusion arises.

12.4.4 The Legal Hierarchy of Nuclear Law

12.4.4.1 The International Regime

An international regime based on broad international consensus has produced over time a set of recommendations and standards that govern radiation protection. These are not set in stone but have evolved and will still evolve over time as new fundamental scientific insights develop. The United Nations Scientific Committee on the Effects of Atomic Radiation (UNSCEAR) compiles, assesses, and disseminates scientific information on the causal link between incurred doses of radiation and possible adverse health effects outcomes. Its findings are periodically reported to the UN General Assembly (UNGA) and are made available to the public on its website. Since 1950, the International Commission on Radiological Protection (ICRP), a private nongovernmental charity, has been developing internationally agreed-upon recommendations in all areas of radiation protection. The Annals of the ICRP are mostly freely available to the general public.

International radiation protection standards are established under the aegis of the International Atomic Energy Agency (IAEA) with the cosponsoring of other relevant international organizations. Since 1962, the IAEA takes into account UNSCEAR publications as well as ICRP recommendations in order to establish and issue Basic Safety Standards (BSS), which provide fundamental principles, requirements, and recommendations to ensure nuclear safety. The IAEA considers these standards as a global reference for protecting people and the environment and a main contribution to a harmonized high level of safety worldwide. Scientific and technical publications are issued annually and include international safety standards, technical guides, conference proceedings, and scientific reports. They cover the breadth of the IAEA's work, focusing among other topics on nuclear power generation, the use of sealed radioactive sources in medicine, radiation therapy, agriculture, nuclear safety and security, and nuclear law.

The publications by UNSCEAR, the ICRP, and the IAEA are comprised of general principles, mandatory requirements, and binding rules, recommendations, and guidelines. In addition, a growing structure of international treaty obligations and accepted rules of best practices have been developed. Important to note are that these recommendations and standards, while broadly recognized on an international level, are not adopted by all countries in a uniform way. Almost all ICRP recommendations and most IAEA standards are considered to be "soft law" meaning that countries and institutions are encouraged to implement them in regulations and national legislation, without an actual legal obligation to do so.

It is important to note that the national variations in the implementation of nuclear law do not vary from country to country simply due to varying levels of scientific understanding, but is also influenced by political motives and public perception. For example, states that are generally wary of the use of nuclear energy may have a notably different legal framework than states that generally favor the use of nuclear energy, despite these states having essentially the same access to the same scientific information.

There are few hard laws at the international level. Nation states generally retain a large measure of self-determination in regulating nuclear activities within their borders. There is however a substantial international consensus in many areas of radiation protection and consequently in the basic concepts of nuclear law, expressed on the one hand in binding treaties and on the other in rules of soft law, i.e., quasi-legal instruments such as recommendations or guidelines that are strictly speaking not legally binding but are nevertheless widely adopted and may become legally binding in the future.

12.4.4.2 The National and Regional Level

Adherence to international instruments (e.g., conventions and treaties) has both an external and an internal aspect. As a matter of international law, states that take the necessary steps under their national laws to approve (or ratify) such instruments are then bound by the obligations arising out of

that instrument in their relations with other States Parties. When this is the case, states need to establish legal arrangements for implementing those obligations internally. Most States require that the provisions of international instruments be adopted as separate national laws. This approach is, for example, reflected in Article 4 of the Convention on Nuclear Safety [46], which states that: "*Each Contracting Party shall take, within the framework of its national law, the legislative, regulatory and administrative measures and other steps necessary to implement its obligations under this Convention.*"

When analyzing nuclear law on a national level, there are basic concepts shared by different states and thus large overlaps in national public law even though national laws remain territorial, meaning only applicable to the state or its nationals. It would be impossible to even summarize, let alone provide a comprehensive overview and compare various nuclear laws in different countries.

The EU is a notable exception to the fragmented incorporation of international binding regulations into national legislation. This is because EU regulations provide a legislative framework that is directly applicable within the EU. The most recent regulatory framework is the consolidated version of the 2013 Directive laying down the basic safety standards for protection against the dangers of ionizing radiation. The Directive establishes uniform basic safety standards for the protection of the health of individuals subject to occupational, medical, and public exposures. It applies to any planned, existing, or emergency exposure situation that involves a health risk from exposure to ionizing radiation. The Directive does not apply to natural levels of background radiation, aboveground exposure to radionuclides present in the undisturbed Earth's crust, exposure of members of the public, or exposure of workers other than air or space crew to cosmic radiation in flight or in space. Exposure to naturally occurring radioactive material (NORM), e.g., in the context of industry or mining activity is regulated if it leads to exposure of workers or members of the public which cannot be disregarded from a radiation protection point of view.

Whether national or regional, it is important to recognize that nuclear law must take its place within the national legal hierarchy. The legal framework in which most states operate consists of several levels. The constitutional level establishes the basic institutional and legal structure governing all relationships within the state. Immediately below the constitutional level is the statutory level, at which specific laws are enacted by the legislative branch of government in order to establish other necessary bodies and to adopt measures relating to the broad range of activities affecting national interests. The third level comprises regulations, detailed and often highly technical rules issued by regulatory bodies to the nuclear industry.

12.4.4.3 Regulatory Bodies

A fundamental element of any national nuclear framework is the creation or maintenance of regulatory bodies with the legal powers and technical competence necessary to ensure that operators of nuclear facilities and users of nuclear material and ionizing radiation operate and use them safely and securely. For example, article 7 of the Convention on Nuclear Safety (CNS) [46] and article 19 of the Joint Convention [47] require the establishment and maintenance of a legislative and regulatory framework to govern the safety of, respectively, nuclear installations and radioactive waste management, identifying a number of functions to be performed by a regulatory body within such a framework.

The central consideration is that a regulatory body should possess the attributes necessary to correctly, self-sufficiently, and independently apply the national laws and regulations designed to protect public health, safety, and the environment. Its tasks can be roughly grouped into four categories: preliminary assessment (establishing requirements and determining whether regulatory control is needed); authorization (licensing and registration, including the prohibition of operations without a license); inspection of nuclear installations and assessment through periodical reviews and enforcing compliance through issuing administrative orders or prohibitions, fines or other penalties. A fifth category, not mentioned in the two aforementioned conventions but considered essential by most regulatory bodies, is the provision of information, including consultation, on regulated activities with the public, the media, the legislature, and other relevant stakeholders. Finally, a regulatory body should be permitted to coordinate its activities with the activities of international and other national bodies involved in nuclear safety.

An example of successful regulation within these parameters can be found in the UK—although the UK is no longer a member of the EU since January 1, 2021—they remain compliant with both article 7 of the CNS and article 19 of the Joint Convention.

12.4.5 Nuclear Liability

A crucial area of nuclear law is nuclear liability. This area is especially important in the context of unplanned emergency exposure to radiation. The occurrence of nuclear and radiological accidents cannot be completely excluded even in situations in which the highest standard of safety has been achieved. All states that engage in nuclear-related activities have generally concluded that general tort law is not an appropriate instrument for providing a liability regime adequate to the specifics of nuclear risks. Tort law is the branch of the law that deals with civil suits alleging negligence, intentional harm, and strict liability, with the

exception of disputes involving contracts and is considered to be a form of restorative justice since it seeks to remedy losses or injury from the wrongful acts of others by providing awarding monetary damages to provide full compensation for proved harms. Since civil law is generally designed to cope with large-scale catastrophes, special measures are required, and states have enacted specific nuclear liability legislation.

12.4.5.1 The International Nuclear Liability Regime

The Paris Convention [48], the Vienna Convention [49], the Brussels Supplementary Convention [50], the Joint Protocol [51], the Convention on Supplementary Compensation [52], and the Revised Vienna Convention [53] (hereafter "the Conventions") establish comprehensive regimes for civil liability for nuclear damage. Application of the international nuclear liability regime created by the conventions and the corresponding national legislation will be triggered if an installation or activity causes a nuclear incident.

A nuclear installation must have a person in charge: the operator. In the nuclear liability conventions, the operator is the person—whether this is an individual or any other private or any public entity having a legal personality—designated or recognized as the operator of a nuclear installation by the installation state. The operator, most often the license holder but possibly the owner of the installation, will always be the person responsible (and thus liable) for safety.

The term "nuclear incident" means any occurrence, or any series of occurrences having the same origin, that causes nuclear damage or, but only with respect to preventive measures, creates a grave and imminent threat of causing such damage. Since the occurrence has to cause or threaten nuclear damage, the definition of what constitutes "nuclear damage" is paramount. In general tort law, the concept of compensable damage is well established. If states seek to obtain the benefits of the Conventions, they must accept the definitions.

"Nuclear liability" is understood to be the legal regime based upon the following principles:

- "Exclusive liability of the operator of the nuclear installation concerned;
- "Absolute" or "strict" liability, so that the injured party is not required to prove fault or negligence on the part of the operator;
- Minimum amount of liability;
- Obligation for the operator to cover liability through insurance or other financial security;
- Limitation of liability in time;
- Equal treatment of victims, irrespective of nationality, domicile, or residence, provided that damage is suffered within the geographical scope of the convention;
- Exclusive jurisdictional competence of the courts of the contracting party in whose territory the incident occurs or, in case of an incident outside the territories of contracting parties (in the course of transport of nuclear material), of the contracting party in whose territory the liable operator's installation is situated);
- Recognition and enforcement of final judgments rendered by the competent court in all Contracting Parties." (IAEA Joint Convention on the Safety of Spent Fuel Management and on the Safety of Radioactive Waste Management [47]).

According to Article 1 of the Paris Convention (Third Party Liability), a "nuclear incident" is considered to be "any occurrence or series of occurrences having the same origin which causes nuclear damage."

Furthermore, there must be a causal link between a certain nuclear installation, a certain nuclear incident, and the damage suffered. The burden of proof of the causal link is on the person claiming compensation. The Conventions do not contain any provisions regarding causality. This issue is left to the law of the competent court (i.e., to national law), so states may apply the principles of causality applied in their national law. In most states not all causes of damage are legally relevant; for example, remote causes may not be considered. In many states, the law requires "adequate causality," which means that a cause is only legally relevant if that cause is likely to have directly caused the damage for which compensation is claimed.

The operator of a nuclear installation is held liable, regardless of fault. This concept is sometimes referred to as the channeling of liability. This kind of liability is called strict liability, or sometimes absolute liability or objective liability. It follows that the claimant does not need to prove negligence or any other type of fault on the part of the operator and the simple existence of causation of damage is the basis of the operator's liability. Furthermore, the operator of a nuclear installation is exclusively liable for nuclear damage. No other person may be held liable, and the operator cannot be held liable under other legal provisions (e.g., tort law). Liability is legally channeled solely onto the operator of the nuclear installation. This concept is a feature of nuclear liability law unmatched in other fields of law. With the exceptions of Austria and the USA, all states party to the Conventions that have enacted nuclear liability laws have

accepted the concept of legal channeling. Exonerations from this strict liability are limited; the operator being held liable even if the nuclear incident is caused by force majeure (i.e., "an act of God").

It is also important to note that the financial compensation which results from the liability may be limited in amount because legislators feel that unlimited financial liability would discourage people from engaging in nuclear-related activities. It is important to note that not all states have chosen to limit liability. In the Conventions, claims for compensation for nuclear damage must be submitted within 30 years in the event of personal injury and within 10 years in the event of other damage.

The nuclear liability conventions require that the operators maintain insurance or provide other financial security covering liability for nuclear damage in such amount, of such type, and in such terms as the installation state specifies. Insurance against nuclear risks is quite different in that there are not many nuclear clients in the insurance industry and while the risk is low in frequency, it is potentially very high in severity, resulting in very high amounts to be covered. On an international level international nuclear pools of insurance exist, where insurance companies net their capacity in order to bring together the financial capacities of the entire pool, which is then used to insure domestic civil nuclear risks and to provide inter-pool reinsurance (reciprocation). This pooling principle trickles down to the national level, where the domestic insurance industry is also organized into nuclear insurance pools.

With regard to the compensation rights of those affected by nuclear energy accidents, the Protocols to amend the Paris Convention on Third Party Liability in the Field of Nuclear Energy and the Brussels Convention Supplementary to the Paris Convention have entered into force on 1 January 2022. The revised conventions combined ensure that those suffering damage resulting from an accident in the nuclear energy sector will be able to seek more compensation—the operator liability will be of at least EUR 700 million under the Paris Convention and the public funds provided under the Brussels Supplementary Convention will complement up to EUR 1.5 billion, a sharp increase from the previous 5 million Special Drawing Rights (SDR) (approximately EUR 6 million as of 13 December 2021) and SDR 125 million (approximately EUR 155 million as of 13 December 2021), respectively. The revised Paris Convention also provides now for a minimum of EUR 70 million and EUR 80 million in case of accidents at low-risk installations and during the transport of nuclear substances, respectively. A total of 16 countries will be parties to the amended Paris Convention, covering 105 operating reactors and 7 under construction, out of a total of 442 operating reactors worldwide and 51 under construction. Of those countries, 13 are also parties to the amended Brussels Supplementary Convention (NEA COM 2021).

Finally, with regard to jurisdiction, national procedural law(s) across countries may indicate several courts to have jurisdiction when dealing with claims arising out of a nuclear incident with transboundary or international effects—meaning several courts could be allowed to claim competence to seize proceedings. The more complicated the different causes and effects, the more parties internationally involved and the larger the effects of the contamination, the greater the selection of potentially competent courts. For this reason, the Conventions provide, firstly, that only courts of the state in which the nuclear incident occurs, have jurisdiction and, secondly, that each member state party to the Conventions shall ensure that only one of its courts has jurisdiction in relation to any one nuclear incident. The concentration of procedures within a single court not only creates legal certainty but also excludes the possibility that victims of nuclear incidents will go "forum shopping" and seek to submit claims in states where their claims are likely to receive more favorable treatment.

12.4.5.2 Transboundary Implications of Radiation Incidents

If an activity or facility could cause public exposure in neighboring states through the release of radioactive substances to the environment, the regulatory body in the state of the licensee should take steps to ensure that the activity or facility will not cause greater public exposure in neighboring states than in the state of the licensee [55]. The concept of neighboring states does not require that these states share a border.

The Convention on Early Notification of a Nuclear Accident (the Early Notification Convention) [56] and the Convention on Assistance in the Case of a Nuclear Accident or Radiological Emergency (the Assistance Convention) [57] cover situations in which an accident involving activities or facilities in one state have resulted or may result in a transboundary release that could be of radiological safety significance for other states. In this context, legally binding obligations as adapted in national legislations may arise for radiobiologists, requiring them to notify, directly or through the IAEA, those states which are or may be affected by a nuclear accident. The nature of the nuclear incident, the time of its occurrence and its exact location should be promptly provided to those States affected in order to minimize the radiological consequences in those states.

12.4.5.3 Radiation Damage under General Tort Law

The nuclear liability conventions cover neither radiation damage caused by radioisotopes used for scientific, medical, commercial, and other purposes nor radiation damage caused by X-rays. This is because the use of radioisotopes and X-ray equipment does not present risks comparable to

those for which the conventions were designed. The regime created by the conventions is intended for extraordinary nuclear risks only.

Even though experience has shown that radioisotopes and medical irradiation equipment can also cause serious damage if not handled properly, most states deal with liability for radiation damage caused by radioisotopes and X-rays under general tort law. States are free to enact, at the national level, special liability laws for damage caused by these types of exposure, providing for modified strict liability where the principle of liability without fault is maintained but the person liable may be exonerated if they can prove that they could not prevent the occurrence of the damage even though they complied with all radiation protection requirements and if they prove that any equipment used was not defective.

In a medical context, harm caused could potentially amount to a breach of the duty of care that is owed to a patient from a medical professional or radiologist. If the person liable owes a duty of care to the patient, it must be proven that this duty was breached, resulting directly in the harm suffered by the patient. Where the breach is caused by gross carelessness, the liable party may be criminally negligent.

12.4.6 Special Legal Issues Related to the International Radioprotection System

12.4.6.1 Optimization of Protection

One of the key principles of the radiation protection system recommended by ICRP is the principle of optimization of protection. The aim is to select the best protection option under the prevailing circumstances in order to keep the likelihood of exposure, the number of people exposed, and the magnitude of the individual doses incurred, all "as low as reasonably achievable" often abbreviated to the acronym "ALARA," taking into account economic and societal factors alongside health factors.

It is important to stress that "ALARA" does not simply mean "as low as reasonably achievable" in the sense that it should always be the "very lowest" level of radiation exposure that can technically be achieved. "ALARA" should rather be the "best" protection option, nuanced and well-reasoned, where the highest level of safety that can be achieved from a health perspective, always needs to be balanced by social, environmental, and economic considerations.

Standards are established and safety measures prescribed in order to ensure that facilities and activities with radiation risks achieve the highest level of safety throughout the lifetime of the facility or duration of the activity, without unduly limiting its utilization or usefulness. In order to determine whether radiation risks are at a level as low as reasonably achievable, any and all risks, whether arising from normal operations, abnormal conditions, or accidents, must be assessed using a graded approach that is periodically reassessed throughout the progression of the activity or lifetime of the facility.

The optimization of protection requires careful judgment on the basis of scientific fact that is generally highly influenced by subjective appraisal tailored to individual situations, which makes it a difficult principle difficult to implement uniformly and consequently legally. The relative significance of various goals, events, and factors have to be judged, including the number of people (both workers and the general public) who may be exposed to radiation, the likelihood of exposure, the magnitude and the radiation doses likely to be received as a result of foreseeable and unforeseeable events, as well as the economic, social, and environmental factors involved with the installation or activity.

12.4.6.2 The ICRP's International System of Radiological Protection

The ICRP recommends, develops, and maintains the International System of Radiological Protection, based on an evaluation of the large body of scientific studies available to equate risk to received dose levels.

> The system's health objectives are relatively straightforward "*to manage and control exposures to ionizing radiation so that deterministic effects are prevented, and the risks of stochastic effects are reduced to the extent reasonably achievable*" (ICRP Publication 103).

To this end, the ICRP has established a system of radiological protection with three main principles: justification, optimization of protection, and individual dose limitation that apply to planned, emergency, and existing exposure situations. Planned exposure situations are situations involving the deliberate introduction and operation of sources of radiation, either anticipated (normal exposures) or not anticipated to occur (potential exposures). Emergency exposure situations are situations that may occur during the operation of a planned situation, or from a malicious act, or from any other unexpected situation requiring urgent action. Existing exposure situations are exposure situations that already exist when a decision relating to control has to be taken, including prolonged exposure situations after emergencies. The ICRP considers exposure to cosmic radiation to be an existing exposure situation.

The first two principles, justification and optimization of protection are source-related and apply in all exposure situations. The principle of justification states that any decision that alters the radiation exposure situation should be more

beneficial than detrimental. The principle of optimization of protection states that the likelihood of incurring exposures, the number of people exposed, and the magnitude of their individual doses should all be kept As Low As Reasonably Achievable (ALARA), also taking into account economic and societal factors. The third principle concerning individual dose limitation is individual-related and applies in planned exposure situations: the total dose to any individual from regulated sources in planned exposure situations other than medical exposure of patients should not exceed certain appropriate limits.

The ICRP further distinguishes between three categories of exposures: occupational exposures, public exposures, and medical exposures of patients. Occupational exposure is defined as all radiation exposure of workers incurred due to their work. ICRP limits the use of "occupational exposures" to radiation incurred at work in situations that can reasonably be regarded as being the responsibility of the operating management. The employer has the main responsibility for the protection of workers. Public exposure encompasses all exposures of the public other than occupational exposures and medical exposures of patients. The component of public exposure due to natural sources is by far the largest, but this provides no justification for reducing the attention paid to smaller, but more readily controllable, exposures to man-made sources. Exposures of the embryo and fetus of pregnant workers are considered to be public exposures and regulated as such.

While dose is a measure of the total amount of radiation received, the dose limit is a value of the effective or equivalent dose to individuals that may not be exceeded in activities under regulatory control. The regulatory body sets the dose limits for various activities. These dose limits are sometimes found in the nuclear laws, but more often in the accompanying and more detailed regulations, where regulatory bodies principally rely on IAEA publications.

12.4.6.3 Individual Dose Restrictions

Restricting an individual's radiation dose is another key factor of the international radiation protection system. Restrictions include dose limits, dose constraints, and reference levels of dose. Each of these restrictions has different legal implications.

The *dose limit* is the value of dose to individuals from planned exposure situations that shall not be exceeded. A *dose constraint* is a prospective and source-related restriction on the individual dose from a source, which provides a basic level of protection for the most highly exposed individuals from a source, and serves as an upper bound on the dose in optimization of protection for that source.

Table 12.1 Recommended dose limits in planned exposure situations

Type of limit	Occupational	Public
Effective dose	20 mSv/year, averaged over defined periods of 5 years	
Annual equivalent dose in:		
Lens of the eye	150 mSv	15 mSv
Skin	500 mSv	50 mSv
Hands and feet	500 mSv	–

For occupational exposures, the dose constraint is a value of individual dose used to limit the range of options, both short- and long-term, considered in the process of optimization. For public exposure, the dose constraint is an upper limit on the annual doses from the planned operation of any controlled source that members of the public should not exceed. In emergency or existing controllable exposure situations, a *reference level* is established to represent the level of dose or risk, above which it is judged to be inappropriate to plan to allow exposures to occur, and below which optimization of protection should be implemented. The chosen value for a reference level will depend upon the prevailing circumstances of the exposure under consideration.

Dose limits are not uniform, neither in concept nor in the quantities that they are expressed. The three dose quantities used for establishing dose limits are the absorbed dose, the equivalent dose, and the effective dose. The absorbed dose is a measurable, physical quantity expressing the amount of energy deposited by radiation in a mass. The equivalent dose is a weighted absorbed dose designed for specific radiation protection purposes and is calculated for individual organs while the effective dose, which is also designed for specific radiation protection purposes, is calculated for the whole body. Dose limits may vary depending on factors such as pregnancy. It is worth noting again that dose limits do not apply to emergency, existing, or medical exposures. Dose limits only apply to occupational, public, and planned exposure. The current dose limits set out by the ICRP in Publication 103 are as set out in Table 12.1 below.

Dose limits set by the ICRP are not hard law but most countries have implemented these limits into their national legislation making the exceeding of dose limits illegal. The industry may also choose to set dose limits for their workers even lower than those required by law to both ensure the safety of their employees and reduce the likelihood of lawsuits.

12.4.6.4 Radiation Workers

Radiation workers are obviously more at risk to be exposed to radiation than the average individual and dose limits for occupational exposure are different from dose limits for public exposure, specifying an upper limit and a relevant time span.

In case of a nuclear emergency, workers will likely be exposed to significantly higher doses, often much higher than the annual recommended dose limit. A very careful assessment will have to be made weighing the rescuer's own risk versus a clear benefit to others.

The ALARA principle encourages practitioners and other individuals who have an influence on radiation dosage to limit dosage as much as practically possible, even when accounting for the benefits the exposure situation might bring. This also means that if the exposure does not present a direct and sufficient benefit, it should be avoided. In order to optimize protection for radiation workers, the duration of the exposure should always be minimized while the distance between the source of the radiation and the individual should be maximized. A third essential factor is shielding.

The legally binding obligations related to occupational radiation protection are established in the Radiation Protection Convention No. 115 adopted by The General Conference of the International Labour Organization [58]. This Convention, which has been ratified by most countries, applies to all activities involving exposure of workers to ionizing radiations in the course of their work and who, in applying its provisions the state party's competent authority, have to consult with representatives of employers and workers.

12.4.6.5 Medical Use

Sources of ionizing radiation are essential to modern healthcare as they span a range of purposes, such as the sterilization of disposable medical supplies, central to combating disease [59]. To give a more recent example, China has optimized the use of radiation to cut down sterilization times from 7 days to just 1 in order to combat the COVID-19 pandemic [60]. Radiology is also a vital diagnostic tool; CT and X-rays have been crucial to healthcare in terms of diagnostic precision, which in turn improve treatment response.

However, as ionizing radiation can be detrimental to living organisms, humans included, it is essential that sources of ionizing radiation be covered by measures to protect individuals. Medical treatment involving planned exposure to ionizing radiation can only take place if the patient has agreed after being carefully informed about the risks.

Radiation exposures of patients occur in diagnostic, interventional, and therapeutic procedures. There are several features of radiological practices in medicine that require an approach that differs from radiological protection in other planned exposure situations. The exposure is intentional and for the direct benefit of the patient. Particularly in radiotherapy, the biological effects of high-dose radiation, e.g., cell killing, are used for the benefit of the patient to treat cancer and other diseases. The medical uses of radiation therefore require separate guidelines.

A relatively recent topic of discussion is that of adventitious exposure, i.e., unintended exposure happening as a result of primary, intended exposure. A patient undergoing therapeutic exposure to ionizing radiation—exposure that is considered to be beneficial, contributing to a positive medical outcome—probably will suffer to some extent, effects that are neither intended nor desired because these are an unavoidable by-product of radiotherapy procedures. Adventitious exposure can occur in any part of the body and cause secondary cancers as a malignant result of radiotherapy, the effects remaining latent, manifesting only after the treatments. It is important to distinguish that cancer forming due to adventitious exposure is not a metastasis of the original malignancy, but rather a primary malignancy in itself. The incidence of such cancers is being investigated worldwide, also by UNSCEAR, and may contribute to litigation initiated by patients or their next of kin against radiobiologists or other radiation specialists in the medical field. A deep understanding of this complex mechanism is still evolving, but the medical professional would do well to document—either by measurement or estimation—the scenario of adventitious exposure situations through dosimetric quantities or suitable proxies. It may even prove to be necessary to dutifully inform and obtain explicit patient agreement on the subject.

Most countries have regulations to guide the medical professional involved with treatment that includes medical exposure of a patient to ionizing radiation in order to protect both the professional and the patient. In the EU, Council Directive 2013/59/Euratom Chapter VII [61] centers the relevant articles 55 and 56 once again around the principles of justification and optimization. In the assessment and justification of the use of radiology with any specific patient, the practitioner should consider all relevant aspects of their medical history and decide, with feedback and consent from the patient, the radiation therapy most suited to that individual patient.

12.4.6.6 Exposure to Cosmic Rays

Cosmic rays at ground level are not considered to warrant regulatory control. Mankind has been exposed to—and has evolved with—radiation from the universe reaching Earth since the beginning of time. However, at high altitudes, where cosmic rays are less attenuated by the atmosphere or, even higher, by the Earth's magnetic field, they undoubtedly pose a risk to people and equipment because of the very high energies involved. As a consequence, astronauts and aircraft personnel need to be well informed about these exposure risks during the course of their careers and possible consequences and outcomes as a result.

Disregarding the Space Treaties that arguably do not really deal with exposure to ionizing radiation, the protective framework for astronauts in this context is not regulated by international law, but rather designed and governed by the space agencies by which they are employed, on the basis of an ever-evolving scientific insight and assessment. All major space agencies have very stringent safety precautions in place, specifying dose, dose rate, and career limits for their astronauts in order to make sure there is no statistical risk of

radiation exposure-induced death (REID) and other adverse effects. Even though astronauts are generally extremely healthy and are unlikely to suffer health effects at a level worse than that of the general population, the advent of deep space travel, notably the Moon and Mars missions planned in the near future, will likely expose them to high fluxes of solar energetic particles and heavy ions, in possibly problematic amounts. Radiation mitigation strategies, shielding and careful mission planning, and astronaut selection will prove to be crucial to attempt these types of interplanetary exploratory missions. Being continuously monitored and genetically screened for suitability may however create some legal issues as well. Not only are privacy issues imaginable with the extreme scrutiny astronauts are subjected to, but unequal treatment and an imbalance in career opportunities due to individual genetic predisposition to adverse health effects from ionizing radiation may at some point also become an object of contention, as is discussed more in depth in Sect. 12.3.8 on emerging occupational challenges from new methods to determine individual radiosensitivity (*supra*).

Guidance and protection for other jobs at slightly lower altitudes are much more regulated. Airline pilots and personnel—and even frequent flyers—repeatedly expose themselves to ionizing radiation, primarily from charged particles and therefore require employment protection. Compared to astronauts, aircraft personnel make up a substantially larger group of radiation workers, inspiring governments to implement special mandatory protection measures. For example, Directive 96/29/Euratom 1996 requires appropriate radiological protection of aircrew. Article 42 of the Directive obliges member states to regulate the sector, specifically regarding the exposure to cosmic radiation at flight altitudes. As a result, each member state is obliged to force airline companies to take account of exposure to cosmic radiation of aircrew who are liable to be subject to exposure to more than 1 mSv/year. EU airline companies need to record a continual assessment of the exposure of the crew concerned and use this information when organizing working schedules with a view to reducing the doses of highly exposed aircrew. Aircraft personnel needs to be informed of the health risks their work involves and female aircrew in particular, when pregnant, will have the terms of her employment adapted to ensure that the equivalent dose to the child to be born is ALARA and that it will be unlikely that this dose will exceed 1 mSv during at least the remainder of the pregnancy. As soon as a nursing woman informs her employer of her condition, she cannot be employed in work involving a significant risk of bodily radioactive contamination. This is of course not to say that female airline crew are the only radiation workers protected through nuclear law; different rules for pregnancy, varying from country to country, are applicable for workers in other nuclear industries.

12.5 Legal Imputation of Radiation Harm to Radiation Exposure Situations

12.5.1 Legal Actions Resulting from Radiation Exposure Situations

Legal action based on radiation harm, i.e., legal proceedings or a lawsuit, generally requires two elements to succeed; attribution and imputation. First, a causal link must be established; a certain health effect needs to be attributed to a certain radiation exposure using objective factual evidence. Second, there needs to be imputation, meaning someone's responsibility for the radiation harm needs to be determined. In a legal context, imputation means placing the responsibility for the physical injury (actual or potential ill effects) that is attributable to the radiation exposure, on another (natural or legal) person. While "attribution," meaning establishing the factual link between a nuclear incident and a health effect and "imputation," meaning ascribing responsibility for the radiation harm are closely related in that they both attempt to establish a causal link, they have often been used as synonyms, causing confusion. Examples range from the use by the International Labour Organization (ILO), International Atomic Energy Agency (IAEA) to the World Health Organization (WHO).

> When attribution between the incident and the effect is established, imputation is crucial to allow for subsequent legal actions such as charging, indicting, and prosecuting—if a criminal element is involved—or simply initiating a civil suit if another form of negligence can be demonstrated. The end goal for the plaintiff is to obtain reparation for damages incurred.

Attribution and imputation both generate controversy and two basic challenges dominate the issue. The first challenge is the attribution of specific health effects to a specific radiation exposure situation, which requires qualified experts to demonstrate that a factual occurrence can be causally linked—meaning without a doubt—to radiation harm. The second challenge is of a more formal nature; how to proceed with relevant legal actions consistent with the legal practice in the applicable jurisdiction or legal system. In high-exposure incidents with obvious harmful effects, this is relatively straightforward. On the other hand, a challenge arises in situations involving low to very low radiation doses. This issue is amply discussed in the literature [62–64] but no clear solution, let alone a consensus between experts, has been found yet.

12.5.2 Attribution and Inference of Health Effects to Radiation

The attribution of health effects to radiation means no more than factually linking the health effects of radiation exposure to objective and indisputable evidence of any given radiation exposure situation. When establishing attribution, there can generally be no reasonable doubt between the cause and the health effect. When moving away from a high-dose, high-probability scenario, in cases where low or lower doses are concerned, the lines become blurred and direct attribution can be problematic. As a consequence, in low-dose scenarios the causal link often needs to be inferred, meaning a reasonable conclusion needs to be reached on the basis of evidence and experience. In contrast to attribution, inference entails the process of drawing conclusions from subjective conjectures involving indirect conclusions based on scientific observations and reasoning on radiation risks, while allowing an element of uncertainty. The discussion involving the attribution of health effects to radiation and the inference of radiation risks is closely followed on an international level by the United Nations Scientific Committee on the Effects of Atomic Radiation (UNSCEAR) (UNSCEAR [65] Report to the General Assembly with Scientific Annexes). UNSCEAR, which has been compiling and discussing decades of case material, scientific research, and expert opinions on the subject, periodically reports its findings to the United Nations General Assembly [66]. The United Nations Environment Program (UNEP) has summarized the progressing UNSCEAR insights and has made an abridged version available to the general public, in an illustrated volume [67] containing the illustrations that are used in this chapter. The UNSCEAR findings are simplistically condensed in a dose–response relationship, a graphical representation of the probability that people would suffer health effects and the radiation doses they have incurred, shown in Fig. 12.1.

UNSCEAR has highlighted the importance of distinguishing between two types of effects (see yellow ellipses in

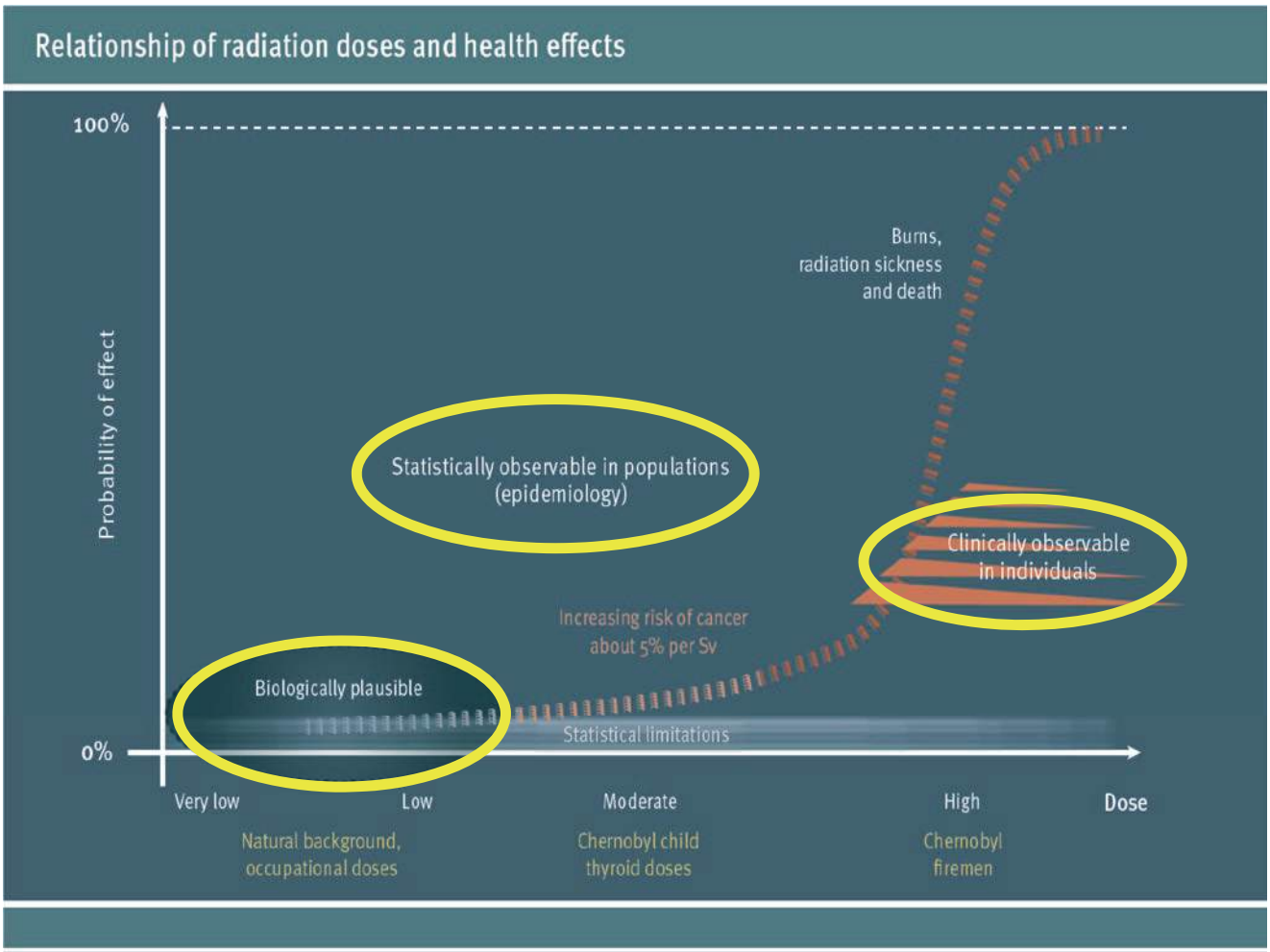

Fig. 12.1 Adapted from UNSCEAR 2012, Annex A Schematic of the relationship between dose, additional to that from typical exposure to natural background radiation, and probability of occurrence of health effects, Fig. AV-I p68

Fig. 12.1). Purely observational health effects in exposed individuals and populations will lead to attribution if the health effect to radiation exposure situation is observed and then attested. On the other hand, plausible health effects for which occurrence is likely conceivable but not directly verifiable, only allow one to infer health effects from known risks, but without clear attribution.

In the figure, the doses on the *x*-axis are expressed from very low to high. A "high dose" indicates an effective dose around 1 Sv and up, many orders of magnitude higher than the annual levels of natural background radiation. A "moderate dose" is situated between 100 mSv and 1 Sv, while a "low dose" is in the tens of mSv, and a "very low dose" is around 1 mSv.

Note too that the probabilities on the *y*-axis are expressed in percentages between 0% and 100%, where 100% corresponds to the certainty that the effect will occur and 0% corresponds to the certainty that the effect will not occur. In between these values, probabilities need to be calculated, which can be done in two ways. Frequentist probabilities are most often used in the high-dose range and take into account the verifiable existence of radiation health effects, defined as the limit of the relative frequency of incidence of the effect in a series of certifiable epidemiological studies. Frequentist probabilities are based on fact. In low-dose ranges, clear-cut evidence and unambiguous studies are scarce and a frequentist probability is out of the question. The solution then would be to include subjective—or "Bayesian"—probabilities, that are expressed as an expectation that radiation health effects could occur, but these are not so much based on and quantified by scientific reasoning as on an expert's judgment that may arguably not be substantiated by the frequency or propensity that the effects actually occur. In other words, reasoned conjecture.

12.5.3 Attesting Effect Occurrence

The attribution of radiation harm is an essential component of any legal action. A professionally qualified expert witness should provide clear evidence on the occurrence of radiation effects, caused by a radiation incident, by formally declaring that a causal effect exists. It is obviously not necessary for an expert to have witnessed first-hand the incident at the origin of a radiation-related lawsuit, but he or she does need to be a specialist in radiation effects and able to offer, without reasonable doubt, an expert opinion after considering the chronology of events and factual occurrence of the causes and the effects.

Crucially, the type of expert a plaintiff would rely upon to bring evidence to the case is related to the dose and dose rate, or more precisely the dose–response relationship connected to the incident. This of course is related to the factual observability and thus the scientific attestability of the effects—ranging from attributing to inferring. In a high-dose scenario, the effects are most likely clinically observable, easily attributable and therefore diagnosable in exposed individuals by a qualified expert radiopathologist. In the region of moderate doses, the effects are not directly attributable in individuals because similar effects can occur due to other causes, but they are statistically consistent with the background incidence of the effect that has been studied in certain population cohorts. This incidence can be mathematically quantified as a probability and attested by a radioepidemiologist. Both radiopathologists and radioepidemiologists rely on frequentist probabilities with a high degree of certainty. In the low to very low-dose range, most effects are neither observable nor attributable and thus their occurrence is not attestable with any reasonable certainty. However, a case can be made that the effects of a low-dose incident may be biologically plausible and therefore risk and potential radiation harm could be inferred through the personal judgment of radioprotectionists by assigning probabilities. The probabilities offered in these low-dose cases by radioprotectionists are arguably less objective than the frequentist probabilities demonstrated by radiopathologists and radioepidemiologists since they are skewed towards expert opinion based on experience rather than indisputable scientific fact. This is visible in Fig. 12.2.

Radiopathologists, radioepidemiologists, and radioprotectionists can all be qualified expert witnesses in the context of legal action, the first attesting the factual occurrence of health effects that can be diagnosed in individuals, the second attesting the factual occurrence of radiation health effects that can be estimated in population cohorts using statistics on the incidence and distribution of diseases associated with radiation exposure, and the third by inferring radiation risks from theory rather than fact. Radiobiologists are a fourth group of scientists that could be situated somewhere between radiopathologists and radioepidemiologists. A radiobiologist has expertise in the branch of biology concerned with the effects of ionizing radiation on organisms, organs, tissues, and cells which can be useful—without directly attesting the factual occurrence of biological changes in an individual—to demonstrate probable effects on tissue after radiation exposure by extrapolating data collected during the study and analysis of specialized bioassay specimens, hematological and cytogenetic samples.

12.5.4 Legal Consequences

The ability to attribute health effects to specific exposure situations and to attest their occurrence by means of a qualified expert witness has a direct influence on the chances of successful litigation if the radiation harm can be clearly

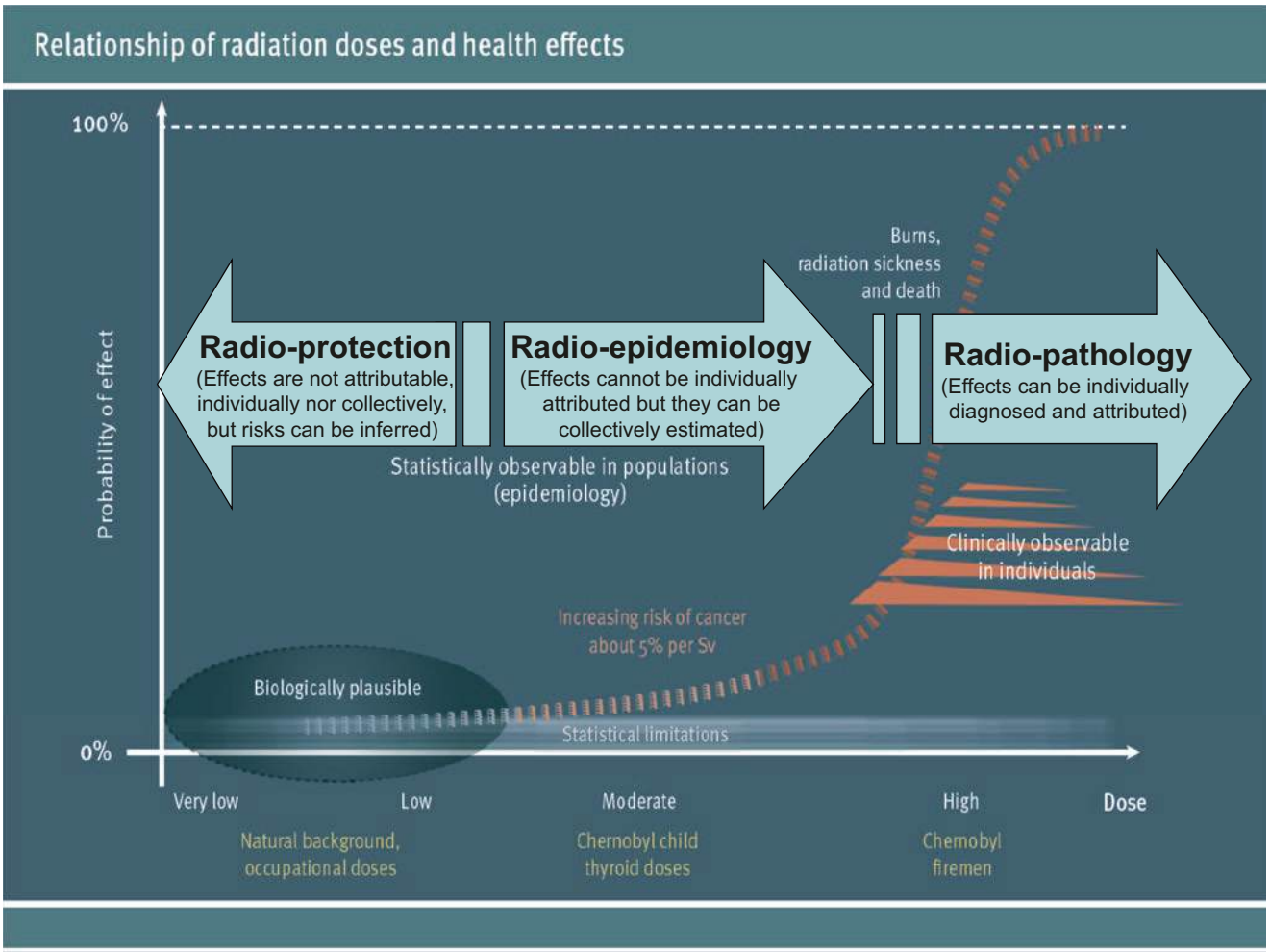

Fig. 12.2 Adapted from UNSCEAR 2012, Annex A Schematic of the relationship between dose, additional to that from typical exposure to natural background radiation, and probability of occurrence of health effects, Fig. AV-I p68

attributed to an incident, imputed to the persons responsible and subsequently compensation awarded to the victims by a court of law. Physical injuries and harmful effects inflicted by those who have caused the exposure, if proven, allow radiation workers or the general public to bring a lawsuit against employers, licensees of nuclear installations, or even the regulatory authorities in the event of a lack of oversight or effective control.

The legal playing field however is not quite level. Legislation and regulatory frameworks that deal with the attribution of radiation health effects are inhomogeneous, sometimes incoherent, and inconsistent among countries and even within countries. A major fault line exists between legal systems based on jurisprudential legislation and those who rely on detailed codified legislation. A comparison of case law exceeds the scope of this chapter, but—at the risk of being overly coarse—we could state that jurisprudential legal systems that employ a case-by-case approach are generally more flexible and provide a higher degree of legal certainty for the plaintiff. Jurisdictions that rely on codified legislation are not bound by legal precedent, placing a high degree of autonomy on the court in applying the rule of law, which can lead to less predictable results.

Figure 12.3 attempts to broadly define what would be feasible when litigating the following situations.

In the high-dose region, individual health effects are clinically attributable and attestable, and imputation of harm incurred by the affected individual is therefore straightforward. Attribution is clear; imputation is often directly linking the individual suffering radiation harm to the responsible person and a classic lawsuit, where civil legal action by one person or entity against another person or entity has a high chance of success.

In the moderate dose region, increased incidences of harmful effects in population groups are epidemiologically attributable and attestable and imputation to the responsible person is therefore feasible. When dealing with the harmful

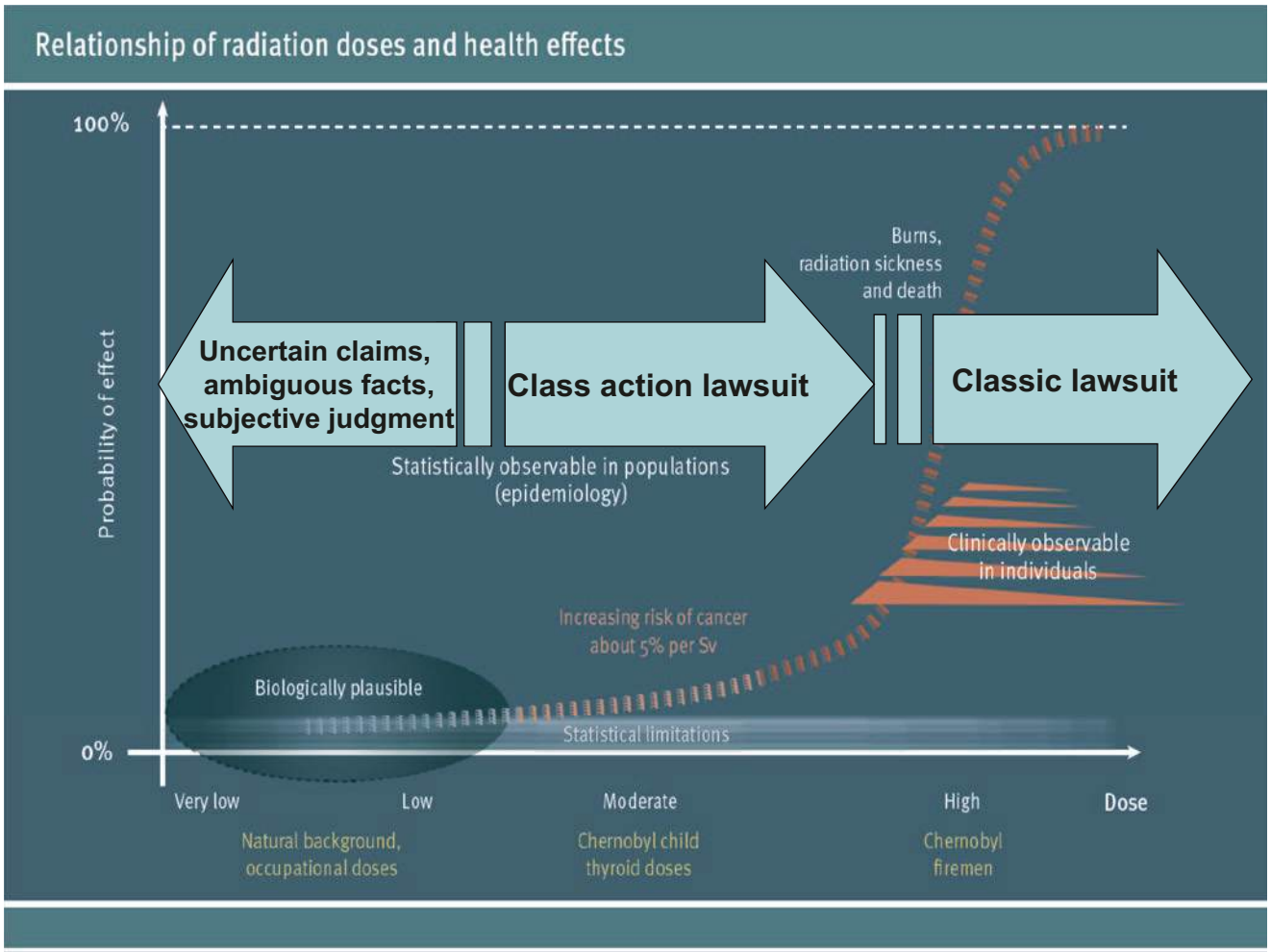

Fig. 12.3 Adapted from UNSCEAR 2012, Annex A Schematic of the relationship between dose, additional to that from typical exposure to natural background radiation, and probability of occurrence of health effects, Fig. AV-I p68

effects of moderate doses, a collective or group imputation is more logical, e.g., via a class action lawsuit where the plaintiffs are more likely than not a group of people presenting a collective claim.

In the low-dose region, radiation harm is neither attributable nor attestable on an individual or collective level, but some radiation risk might be inferred. From a legal perspective, claims based on a low dose or low dose rate exposure are uncertain. Since radiation harm might not yet have presented itself or, if present, might be quite removed in time from the alleged exposure situation, a court might struggle with establishing, beyond a reasonable doubt, a causal link between the exposure situation and any health effects allegedly suffered by the plaintiff. The problem presented here is one of objectivity. The cause cannot be attested, the harmful result is only inferred considering theoretical risk and perhaps statistical probability, and any judgment based on these ambiguous facts would have a high degree of subjectivity.

12.5.5 Next Steps

The scientific consensus on health effects attributable to radiation exposure—consensus that in itself is not entirely uniform and still progressing—should serve as a basis for the development of legal instruments in order to have a more uniform treatment of legal actions. In particular, the issue of legal imputation when considering low dose rates should be carefully considered. This issue has not yet crystallized in any type of universal approach, in large part given the fundamental differences between case-based and codified legal systems. The scientific community is eager to provide legal experts with guidance based on the progressing insight into the attribution of radiation effects following radiation exposure situations.

Given the cultural, regulatory, and legislative differences among countries, two fundamental objectives stand out. First, it seems imperative to foster a common legal understanding of cause and effect when dealing with radia-

tion harm and radiation exposure situations. From a scientific perspective, this seems feasible, and if adopted by the legal community, this would greatly enhance legal certainty. Second—and perhaps even more optimistically—the establishment of a universal scientific and legal consensus to direct the application of the law in any situation would reduce uncertainty even further and might even benefit the development and harmonization of different national legislations. In reality however "the law" is not a uniform concept and nations, courts and judges, prosecutors and lawyers will always want to look at the facts of any individual case, assess the differences and exceptions to the rules if there are any and, in general, assert their independent reasoning. Today, the road ahead for the legal community dealing with nuclear law seems long and far from determined.

12.6 Social and Psychological Issues Associated with Radiation Exposure

12.6.1 Introduction

Human behavior is primarily driven by perception and not by facts [68]. In practice, this pattern is clearly demonstrated also in people's behavior related to ionizing radiation. For instance, exposure to the medical application of ionizing radiation is highly acceptable for most people, while food irradiation used to increase the safety of food may be unacceptable for many people, although in the first case the patient may receive a relatively high radiation dose and in the second case the consumer will not receive any radiation due to the sterilization [69, 70].

Likewise, 10 mSv received as a worker's exposure or 10 mSv received during an accidental release of radioactivity to the environment may cause different behavior. This section examines the social and psychological aspects of radiation exposure. First, we will explain the phenomena of radiation risk perception and second we will identify and discuss determinants of health and radiation protection behavior. Finally, we will conclude this chapter with radiation risk communication advice for experts in radiobiology in order to be able to communicate effectively and help people to make informed decisions related to radiation risks.

12.6.2 Perception of Radiation Risk

Risk perception mainly denotes the ways individuals think and feel about the risks they face [71–73]. Radiation risk perception has been extensively studied, for example, in the context of nuclear power [74–76], nuclear testing [77], radioactive waste [78], radon [79], food sterilization by irradiation [80], and nuclear accidents [81]. It is interesting that people perceive radiation risks differently, depending on the origins of this radioactivity, and the contexts in which it is encountered.

In order to demonstrate diversity in radiation risk perception, we present the results of a public opinion survey conducted in a high radon-prone area in Belgium [82]. Figure 12.4 illustrates how residents of radon-prone areas think and feel about environmental and radiation risks. It shows that residents living in radon-prone areas in Belgium perceive the risk from environmental pollution as the highest potential risk to their health within the next 20 years, followed by the risk of a climate crisis. Among risks related to

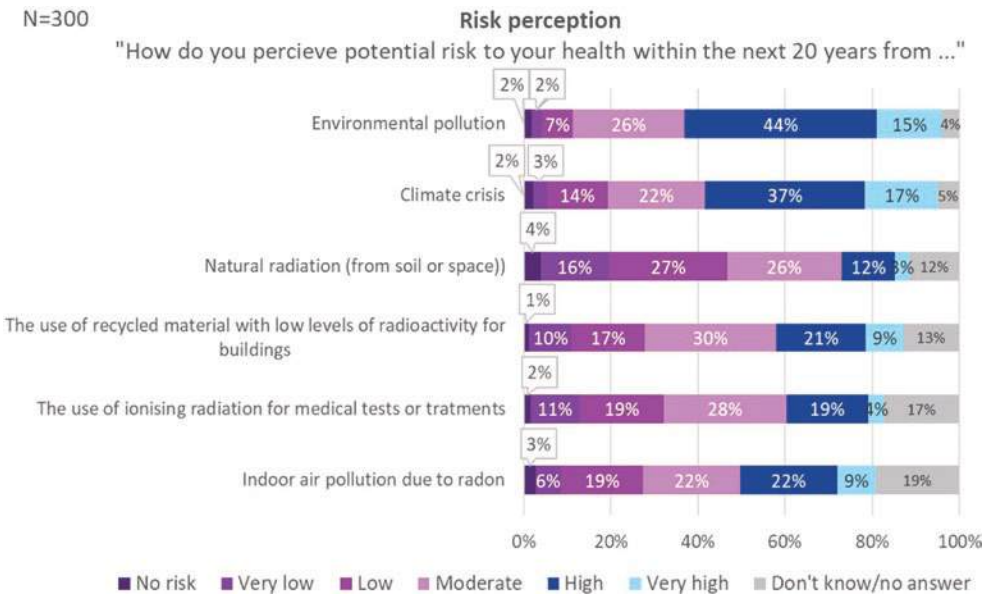

Fig. 12.4 Perception of environmental and radiation risks by residents of high radon-prone area in Belgium, 2021 [82]

radon and naturally occurring radioactive material, the risk of indoor air pollution due to radon is perceived as the highest potential risk to their health within the next 20 years, followed by the use of recycled material with low levels of radioactivity for buildings. The lowest risk for health within the next 20 years is perceived to come from natural radiation from the soil or from space. Interestingly, in this 2021 survey, the risk of medical applications of ionizing radiation is perceived as one of the lowest radiation risks by residents of radon-prone areas in Belgium, although medical exposure presents the most significant dose in Belgium.

Research also shows that experts and the general public often disagree about the potential danger posed to their health by nuclear waste, an accident in a nuclear installation, natural radioactivity, medical X-rays, or the Daiichi nuclear accident in Fukushima [83]. In the study of Perko [84], the public had significantly higher risk perceptions of all radiation risks when compared to experts, with the only exception being medical exposure. However, expert opinion and lay perception need to be perceived as complementing rather than competing with each other [85]. Remarkably, empirical results show that experts too do not think and feel the same about radiation risk. When a distinction was made between experts that received a dose of more than 0.5 mSv due to their professional exposure, and those who did not, those who were exposed to more than 0.5 mSv perceived the risk of radiation waste and an accident in a nuclear installation significantly lower than their colleagues did. Similarly to this, they also did not agree about risks from nuclear accidents in Japan. On the other hand, the employees receiving a dose higher than 0.5 mSv had significantly higher risk perceptions of natural radioactivity and medical use of ionizing radiation than their colleagues. These results can be explained by the characteristics of risk, suggesting that familiarity with risk, knowledge, personal control, and voluntariness decrease risk perception.

Characteristics of risk and their impact on (un)acceptability have been studied and identified by scholars using a psychometric method [68, 86, 87]. Studies of risk perception examine the opinions people express when they are asked, in various ways, to characterize and evaluate hazardous activities and technologies [85, 88]. The method is based on a number of explanatory scales corresponding to various risk characteristics, which are an explanation of contextual traits that people use when they make decisions related to risks. Some of these scales involve traits focusing on whether the risk has an influence on children, whether it is involuntary or not, whether people are familiar with the risk or it is new to them, whether the risk has a catastrophic potential, whether it can cause delayed or immediate consequences, whether the risk is already known to science or not. Table 12.2 demonstrates the characteristics of risks, their influence on risk (un)acceptance, how they can be explained in a scale from maximum to minimum, as well as providing descriptive examples of radiation risk acceptance as hypothetical scenarios.

12.6.3 Determinants of Health and Radiation Protection Behavior

Research shows that only one person in five is prepared to take health-related actions at any given time [89, 90]. Radiation protection behavior is not an exception to this finding. Authorities and other radiation protection actors are often challenged with what has been termed a "value-action gap." This gap refers to a situation where the values or attitudes of an individual or a group of people do not correlate with their actions; a positive attitude towards good health does not lead to an action to improve/protect health [91].

For instance, testing for radon and remediating your home if radon concentrations are too high are scientifically and technically straightforward actions. However, empirical studies indicate that testing and remediation are generally low among those exposed to high indoor radon, although these persons have relatively high-risk perceptions [92], the cost of radon mitigation measures for most homes is similar to that of common home repairs, and this cost is often an eligible expense covered by national health care programs [93–95].

A similar value-action gap is repeatedly reported in studies related to the behavior of people before, during, and after nuclear or radiation emergencies. For example, the study of Turcanu et al. [54] conducted in Belgium, Norway, and Spain, provides empirical evidence that people in the analyzed countries have difficulties complying with some protective actions in case of a nuclear accident. Leaving children at school, avoiding the use of phones during an emergency, not rejecting food produced in affected areas even when it satisfies legal norms or taking iodine tablets when not needed, were identified as the most critical protective actions with which a large number of people would not comply [96].

This raises the question what determinants of health and radiation protection behavior can be discerned. Different determinants have been studied in the context of health behavior models. The most known and tested models in the radiation protection field are the Protection-Motivation Model [97], the Health Belief Model [98], the Theory of Planned Behavior [99], the Transtheoretical Model of Health Behavior Change (TTM) [90], and the Precautionary Adoption Process Model [100].

Those health protection models suggest that knowledge about the risk is only one of the health behavior determinants, other determinants, explained in Table 12.3 below, being attitudes, perceived behavioral control, subjective norm, descriptive norms, moral norms, self-efficacy, risk

Table 12.2 Examples of acceptable radiation risks in relation to risk perception

Descriptive example of an acceptable radiation risk—a hypothetical scenario	Selected characteristics of risk	Influence on risk (un) acceptability	Explanatory scale
A catastrophic potential of a nuclear accident made the risk more threatening since low-probability high-consequence radiation risks are usually perceived as more threatening than more probable risks with low or medium consequences.	Catastrophic potential	Decreases risk acceptability	Catastrophic—chronic
Medical personnel is wearing assigned personal radiation dosimeters during a procedure using ionizing radiation, which gives a feeling of control and increases the acceptability of radiation exposure.	Personal control	Increases risk acceptability	Controllable—not controllable
A phosphate factory is recognized as a trustworthy organization since they communicate openly about the risks of naturally occurring radioactive material as a side product.	Institutional control	Depends upon confidence in institutional performance	Trust, confidence in the institution
Population density around nuclear installation is low thus controlled releases of radioactivity from a nuclear installation in an environment is acceptable.	Number of exposed	Decreases risk acceptability	Local—global
Workers get employed at a nuclear installation on a voluntarist basis thus they accept workers' exposure to ionizing radiation.	Voluntariness	Increases risk acceptability	Voluntary—involuntary
A patient receives a low dose of ionizing radiation during X-ray which makes it acceptable.	Mortality	Decreases risk acceptability	Fatal—not fatal
Visitors learned about radiation and technology used by researchers during an open-door day at a nuclear research institute. New insights and knowledge influenced their acceptability of potential radiation risks.	Knowledge	Increases risk acceptability	New technology—established technology
Living in a home with high radon concentration for many years (more generations) made residents accept radon risk and not performing radon test or necessary remediation of a house	Familiarity	Increases risk acceptability	Familiar—not familiar
A traffic accident with transport of radionuclides for a hospital in a citizen's region is not as dreadful as a nuclear accident in another continent is.	Dread/fear	Decreases risk acceptability	Fear—no fear
High natural background of radiation is for many people acceptable because it is natural due to the geological characteristics of a region.	Artificiality of risk source	Amplifies attention to risk Often decreases risk acceptability	Human—natural
During an environmental remediation process, residents had a feeling of fairness since they could co-decide on how, where, and to which level should be environment remediated. Thus, they accepted radioactive residues in a dedicated part of their administrative community.	Fairness	Increases quest for social and political responses	Fair—unfair
Receiving compensation for radioactive waste disposal made the project acceptable.	Benefit	Increase risk acceptability	Benefit to self-vs. unclear or inequitable
Intake of stable iodine as an effective countermeasure for reducing the risk of thyroid cancer in an eventual release of radioactive iodine following a nuclear accident, especially for children, made the pre-distribution of the iodine tablets to residents and un uptake of a tablet if necessary, an acceptable option.	Effect on children	Decrease risk acceptability	Children specifically at risk

perception, protective efficiency of an action, threat, and trust among others. Table 12.3 presents potential health protection determinants, descriptive explanations, and a reference to selected studies that have been tested in the radiation protection field.

In particular, the Theory of Planned Behavior [124] proved that the higher the intent, the higher the probability an individual will engage in the action they intend. This theory has been for instance applied in research on attitudes and behavior related to new nuclear research installations [120]. In this study, authors found that attitudes towards participation and moral norms are the strongest determinants for the studied behavior—in this case, participation intention. Other determinants were time constraints, attitude towards nuclear energy, subjective and descriptive norms, and level of specific radiation-related knowledge. The Extended Parallel Process Model (EPPM) focuses on two constructs which mediate an individual's level of fear and proposes an individual will engage in behavior change when they have a combination of (a) fear the health threat will happen to them (susceptibility) and (b) perception they are able to address/deal with the risk [108]. The Transtheoretical Model of Health Behavior Change which has been applied among others also to behavior related to radon exposure [125], postulates that individuals move through six stages of change: pre-contemplation, contemplation, preparation, action, maintenance, and termination. The model has two major components: change and decisional balance, where neither

Table 12.3 Determinants of health and radiation protection behavior tested in radiation risk studies

Potential determinants of health and radiation behavior	Descriptive explanation	Selected studies from radiation protection field
Anticipatory emotion—worry	The anticipatory emotion—worry is an emotion where a person experiences increased levels of anxiety by thinking about an event or situation in the future.	McGlone et al. [101], Witte et al. [102]
Anticipatory emotion—severity	Anticipatory emotion—severity refers to people's beliefs about how serious are the negative consequences of a hazard. In the radon exposure situations, the threat involves cancer, which is severe.	Mazur and Hall [103], Dragojevic et al. [104]
Conditional/perceived susceptibility	Perceived susceptibility is the subjective belief that a person may acquire a disease or enter a dire state due to a particular behavior.	D'Antoni et al. [105], Weinstein et al. [106], Niemeyer and Keller [107]
Coping of efficacy appraisal: response efficacy	Coping appraisal is needed to adopt or maintain a health protection behavior and is essential for overcoming fears and mental blocks. Coping appraisal consists of three dements: response efficacy/response costs/self-efficacy. Only if the individual is convinced that a behavior leads to the desired outcome will she or he be more likely to intend to perform the behavior.	Weinstein et al. [108, 109], Witte et al. [110], Dragojevic et al. [104]
Coping or efficacy appraisal—self efficacy	Self-efficacy refers to the belief in one's own competence to perform a behavior even in the face of barriers or in other words, the individual in carrying out the recommended coping response.	Hahn et al. [111], Larsson [112], Rhodes et al. [113]
Perceived costs	The "Perceived costs" captures the person's perceptions of the disadvantages of, or barriers to, undertaking the behavior.	Hampson et al. [114], Sheeran [115]
Anticipated emotions/ regret	Anticipated emotions are a component of the immediate consequences of the decision; they are emotions that are expected to occur when outcomes are experienced. The most extensively researched anticipated emotions regret, guilt, and shame.	Hampson et al. [114], Sheeran [115]
Perceived informed choice	Informed choice means that people under radon risk make decisions that are consistent with their goals and values	Weinstein and Man [116, 117]
Subjective norms	Subjective norms refer to the belief that an important person or group of people will approve and support and particular behavior, for instance protection against radon	Clifford et al. [118], Park et al. [119]
Descriptive norms	Descriptive norms refer to what most people in a group think, feel, or do. Descriptive norms are a reflection on "What is typical or normal … what most people do", including "evidence as to what will likely be effective and adaptive action.	
Moral norms	Moral norms are internalised, unconditional and emotional internalised and enforced through self-generated emotions such as guilt.	Turcanu et al. [120]
Knowledge/awareness	Increasing radiation (specific) knowledge and awareness is often set as a primary objective of risk communication efforts.	Perko et al. [84, 121]
Trust	Trust concept includes different dimensions for instance fairness, unbiasedness, perceived competence, objectivity, consistency, commitment, caring, and predictability, social trust, general trust and transparency.	Perko and Martell [122], Perko et al. [123]

knowledge nor risk perception is not identified as the main health protection change determinants [126]. Similarly, the message design theories, such as the Extended Parallel Processing Model (EPPM) which has been used as the theoretical framework for formative and summative analysis of radon communication campaigns, indicate the importance of threat and efficacy [110].

12.6.4 Risk Communication

Responsible risk communication requires a legitimate procedure, an ethically justified risk message, and concern for and valuation of the effects of the message and procedure. This way, it is stressed, that risk communication should not only be effective but also ethical, which requires taking moral values into consideration. During radiation risk communication moral values are at stake, which means that decisions have to be made in a democratic way, after serious debate about values and not merely about numbers [127].

> *Risk communication was in previous century seen as a form of a technical communication and education whereby the public should be informed about risk estimates. Later on, risk communication was seen as a marketing practice with the aim to persuade people to adopt a certain message. In nowadays societies (sic), risk communication is seen as a socio-centric communication based on public participation with which the gaps between stakeholders can be bridged. The procedure should be legitimate (requires legitimate procedure for discussing the moral values and emotions associated with risks), it should be ethically justified (ethical deliberation about the values and emotions involved in different messages) and the effects should be adequately addressed.* [128, p. 8–9].

Radiation risk communication has several aims: (a) to warn people in case of radiation danger, (b) to the enlightenment of people to be able to understand risks and become "risk-literate," (c) to prevent panic and outrage, (d) to empower

stakeholders to make informed decisions related to radiation risks, (e) to establish two-way communication and joint problem solving including conflict resolution, and (f) to build trust between different stakeholders.

Bauder and colleagues (2021) guide communication practitioners towards radiation risk communication which is strategic (e.g., based on formats and methods that have been proven to reach its preconceived objectives), evidence-based (e.g., based on the qualitative and quantitative empirical data, surveys, experiments), and theory-based (e.g., drawing from empirically supported theories of health behavior, behavior, and information processing) [129].

For instance, information processing theories applied in radiation risk communication [130] show that efficient communication about radiation risks requires thorough insight into the factors that influence people's attentiveness, recall of risk-related information, level of agreement with the communicated message, and behavior change or more generally speaking: how people process risk-related information and turned it in a behavior.

The information processing models are seen as applicable for each individual, regardless of the societal or cultural bias [131–139] however countries may differ in beliefs, cultural values, past social and risk experiences, the saliency of particular aspects of a policy issue, the socioeconomic profile and trust in regulatory agencies. In general, people process information using two different modes: (1) heuristic and (2) systematic mode [140]. Heuristic processing is characterized by low effort and reliance on existing knowledge and simple cues for instance trust. Systematic processing on the other hand is characterized by greater effort and the desire to evaluate information formally [141].

12.6.5 Advice on How to Communicate with the Public About Your Radiobiological Study

Radiobiologists may be challenged by public communication due to the following reasons [122]: there is no single audience for scientific information; the complexity of scientific methods and information, and the ways in which science progresses; the ways in which people process such information; in the radiobiology, the societal implications of science are controversial, for instance, Linear Dose Response Model; there is substantial disagreement about the findings within the scientific community, for instance, related to low doses; the complex, dynamic, and competitive communication media environment, with evolving social media and pace of information flow; and because the results of research can be insufficient, ambiguous or uncertain, and scientific conclusions can change over time as new findings emerge.

Science Media Centre (2012) developed practical guidance to be used by scientists during their public and mass media communication. For a complete and original guide, look at https://www.sciencemediacentre.org/wp-content/uploads/2012/09/10-best-practice-guidelines-for-science-and-health-reporting.pdf.

Some of the central points are summarized here:

- Headlines should not mislead the reader about a story's contents and quotation marks should not be used to dress up overstatement.
- During your communication related to health risks, include the absolute risk whenever it is available in the press release or the research paper (e.g., if "low dose exposure increases the cancer risk" state the outright risk of that cancer, with and without particular exposure).
- Especially on a story with public health implications, try to present a new finding in the context of other evidence (e.g., does it reinforce or conflict with previous studies?). If it attracts serious scientific concerns, they should not be ignored.
- When reporting a link between two things, it is recommended to indicate whether or not there is evidence that one causes the other.
- Specify the size and nature of the study (e.g., who/what were the subjects, how long did it last, what was tested or was it an observation?). Provided there is enough space and time, it could be of interest to mention also the major limitations.
- State where the research has been published or presented or reported (e.g., conference, journal article, survey, etc.). Ideally, the article should include a web link or enough information for readers to look it up.
- Give a sense of the stage of the research (e.g., new dosimeter, clean-up stage, cells in a laboratory, or trials in humans), and a realistic time frame for any new technology.
- If there is enough space, quote both the researchers themselves and external sources with appropriate expertise. Be wary of scientists and press releases over-claiming for studies.
- Distinguish between findings and interpretation or extrapolation; do not suggest health advice if none has been offered.

12.7 Exercises

12.7.1 Ethics

1. The most difficult thing in finding trust in decision-making on nuclear today might be in the way we deal with moral pluralism. What is moral pluralism? Simply the idea that if we all know the same thing, opinions on what to do can still be different, and this is because our opinions do not only rely on knowledge but also on ethical values. As an example choosing for retrievability or non-retrievability of underground stored nuclear waste is making a choice deal-

ing with moral pluralism: science can describe the options, but not help us to make a choice. Some would say we should dispose and seal the waste so that future generations do not need to bother about it anymore, while others would argue that we should give them the possibility to intervene or do something better with the waste. Imagine yourself being a moderator in this discussion: what are the values and interests at stake here, and how would you moderate this discussion towards a consensus, also taking into account that an important stakeholder (the future generations) cannot participate in the discussion?

2. Studies have shown that the public is more averse to relatively low radiation exposures from nuclear power than to higher doses from medical exposures. Is this irrational?
3. What other ethically relevant factors impact perceptions of radiation risks?

12.7.2 Law

1. Which is the main underlying principle of nuclear law and how does this translate to the concept of optimization of protection? Can you give an example of two planned exposure situations?
2. Do you think the exposure to cosmic rays is a planned exposure situation or an existing exposure? Could it be both in the context of air travel? Is radiological protection different in either situation?
3. What attributes should a regulatory body have and what are some of its main tasks?
4. Nuclear liability is different from general tortious liability. Give an example and explain the reason.

12.7.3 Legal Imputation

1. Taking into consideration the legal structure of your country, please elaborate on the potential legal developments of the following situations:
   (a) A worker is damaged (burned) by an over-exposure to radiation and decides the damage is to be attributed to the exposure and imputed on his/her employer;
   (b) A large group of conscripts is subjected to a collective medical screening using old X-ray equipment when joining the army. About a decade later, those still meeting in social encounters discover that a large number among them are suffering from unusual cancers for their young age and decide to impute the army;
   (c) A family is living near a nuclear power plant that appears to function as designed. There have been no reports of any anomalous events, incidents, or anomalous measured values. One of their children incurs thyroid cancer. The parents have contacted a lawyer.

Disclaimer

- At the time of the preparation of this book, Russia invaded Ukraine.
- The Ukraine War will have repercussions on the existing international paradigm governing protection, safety, security, and safeguards of endeavors involving radiation exposure.
- It may take years to answer the questions raised by the present crisis.
- The authors believe however that the ethical, social, and epistemological considerations presented below are still applicable. The legal and logistical considerations may change in the future in such a way that the relevant sections in this chapter will no longer be applicable.

References

1. March HC. Leukemia in radiologists. Radiology. 1944;43:3. Published Online 1 Sept 1944. https://doi.org/10.1148/43.3.275.
2. ICRP. Recommendations of the ICRP. ICRP Publication 26. Ann ICRP. 1977;1(3).
3. ICRP. 1990 Recommendations of the International Commission on Radiological Protection. ICRP Publication 60. Ann ICRP. 1991;21(1–3).
4. ICRP. The 2007 Recommendations of the International Commission on Radiological Protection. ICRP Publication 103. Ann ICRP 2007;37(2–4).
5. ICRP. Ethical foundations of the system of radiological protection. ICRP Publication 138. Ann ICRP. 2018;47(1).
6. United Nations Scientific Committee on the Effects of Atomic Radiation. UNSCEAR 2012 Report of the United Nations Scientific Committee on the Effects of Atomic Radiation; Fifty-ninth session. United Nations General Assembly; Official Records; Sixty-seventh session; Supplement No. 46; Document A/67/46; section 25; and Sources, effects and risks of ionizing radiation; Annex A: Attributing health effects to ionizing radiation exposure and inferring risks. New York: United Nations; 2015.
7. Kitcher P. The ethical project. Cambridge, MA: Harvard University Press; 2014.
8. Pentreath RJ. Radiological protection for the natural environment. Radiat Prot Dosim. 1998;75:175–9.
9. Pentreath RJ. A system for radiological protection of the environment: some initial thoughts and ideas. J Radiol Prot. 1999;19:117–28.
10. International union of radioecologists. Protection of the environment: current status and future work. IUR report no 3. International union of radioecology, Saint-Paul-le´s-Durance. 2002.
11. IAEA. Ethical considerations in protecting the environment from the effects of ionizing radiation. IAEA-TECDOC-1270. Vienna: International Atomic Energy Agency. 2014.
12. IAEA. Basic safety standards, GSR part 3. Vienna: International Atomic Energy Agency; 2011.
13. ICRP. Environmental protection: the concept and use of reference animals and plants. ICRP Publication 108. Ann ICRP. 2008;38(4–6).
14. González AJ. Epistemology on the attribution of radiation risks and effects to low radiation dose exposure situations. Int J Low Radiat. 2011;8(3):2011.
15. Clarke RH. Progress towards new recommendations from the International Commission on Radiological Protection. Nuclear Energy. 2001;40(1):37–45.
16. Beauchamp TL, Childress JL. Principles of biomedical ethics. 8th Edition New York, NY: Oxford University Press. 2012.
17. Zölzer F. A cross-cultural approach to radiation ethics, in Oughton DH, Hansson SO, editors. Social and ethical aspects of radiation risk management, Amsterdam: Elsevier Press. 2014.

18. Malone J, Zölzer F. Pragmatic ethical basis for radiation protection in diagnostic radiology. Br J Radiol. 2016;89:1059. https://doi.org/10.1259/bjr.20150713.
19. Slovic P. Perception of risk from radiation. Rad Prot Dosim. 1996; 68(3-4):165–180.
20. Drottz B-M, Sjöberg L. Risk perception and worries after the Chernobyl accident. J Environ Psychol. 1990;10:135–149.
21. Liland A, Raskob W, editors. Towards a self-sustaining European platform on nuclear and radiological emergency preparedness, response and recovery. Key results of the NERIS-TP European project. Radioprotection; 2016;51.
22. Hayano RS, Watanabe YN, Nomura S, et al.Whole-body counter survey results 4 months after the Fukushima Dai-ichi NPP accident in Minamisoma City, Fukushima. J Radiol Prot. 2014;34:787–799.
23. Naito W, Uesaka M, Yamada C, Ishii H. Evaluation of dose from external irradiation for individuals living in areas affected by the Fukushima Daiichi Nuclear Plant accident. Radiat Prot Dosimetry. 2015;163(3):353-61. https://doi.org/10.1093/rpd/ncu201. Epub 2014 Jun 30. PMID: 24982262. 2015.
24. Bay I, Oughton DH. Social and economic effects. In Smith J, Beresford NA. editors. Chernobyl, Catastrophe and Consequences Springer-Verlaug: Berlin, 2005. pp 239–262. (ISBN 3-540-23866-2).
25. IAEA. The fukushima daiichi accident. Technical Volume 5. International atomic energy agency, Vienna. Available from: https://www.iaea.org/publications/10962/the-fukushima-daiichi-accident. 2015. Accessed 2 May 2023.
26. United nations development programme (UNDP). The human consequences of the chernobyl nuclear accident-a strategy for recovery. Available online: https://www.iaea.org/sites/default/files/strategy_for_recovery.pdf. 2002. Accessed 2 May 2023.
27. Hersey J. Hiroshima, Knopf: New York. 1985.
28. Shigemura J, Tanigawa T, Saito I, et al. Psychological distress in workers at the Fukushima nuclear power plants. JAMA. 2012;308(7):667–669.
29. UNSCEAR. Developments since the 2013 UNSCEAR Report on the levels and effects of radiation exposure due to the nuclear accident following the great east-japan earthquake and tsunami. New York: UN. 2015
30. SHAMISEN consortium, Recommendations and procedures for preparedness and health surveillance of populations affected by a radiation accident. ISGlobal], Barcelona. https://radiation.isglobal.org/shamisen/. 2020. Accessed 1 May 2023.
31. Seibold P, Auvinen A, Averbeck D, et al. Clinical and epidemiological observations on individual radiation sensitivity and susceptibility – A MELODI position paper following the Malta 2018 workshop. Int J Radiol Prot. 2020;96;324–339. https://doi.org/10.1080/09553002.2019.1665209.
32. Burgess JP, Floridi L, Lanier JZ, et al. EDPS Ethics advisory group. Report. 2018. https://edps.europa.eu/sites/edp/files/publication/18-01-25_eag_report_en.pdf. Accessed 2 May 2023.
33. Meskens G. The politics of hypothesis—an inquiry into the ethics of scientific assessment. In: Ethics of environmental health risks. Routledge; 2018.
34. Meskens G. Reflections on uncertainty, risk and fairness. In: Ethics for radiation protection in medicine. Taylor & Francis; 2018.
35. Turcanu C, Schröder J, Meskens G, Perko T, Rossignol N, et al. Like a bridge over troubled water—opening pathways for integrating social sciences and humanities into nuclear research. J Environ Radioact. 2016;153:88. https://doi.org/10.1016/j.jenvrad.2015.12.009.
36. Smyth HD. Atomic energy for military purposes; the official report on the development of the atomic bomb under the auspices of the United States Government, 1940-1945. York, PN: Maple Press; 1945. p. 224. Available at: http://archive.org/details/atomicenergyform00smytrich. Accessed 1.7.2020.
37. Kahn H. The nature and feasibility of war and deterrence. Report P-1888-RC. Santa Monica, CA: The RAND Corporation; 1960.
38. United Nations Scientific Committee on the Effects of Atomic Radiation (UNSCEAR). UNSCEAR 2000 Report to the General Assembly, with Scientific Annexes. Vol. II: Effects. Annex J: Exposures and effects of the Chernobyl accident. New York: United Nations; 2000. http://www.unscear.org/docs/publications/2000/UNSCEAR_2000_Annex-J.pdf. Accessed 1.7.2020.
39. Yanovskiy M, Levi ON, Shaki YY, Socol Y. Consequences of a large-scale nuclear-power-plant accident and guidelines for evacuation: a cost-effectiveness analysis. Int J Radiat Biol. 2020;96:1382. https://doi.org/10.1080/09553002.2020.1779962.
40. Neumann PJ, Sanders GD. Cost-effectiveness analysis 2.0. N Engl J Med. 2017;376:203–5.
41. Socol Y, Gofman Y, Yanovskiy M, Brosh B. Assessment of probable scenarios of radiological emergency and their consequences. Int J Radiat Biol. 2020; https://doi.org/10.1080/09553002.2020.1798544.
42. Reid M. Behind the "Glasgow effect". Bull World Health Organ. 2011;89:701–76. Available at: http://www.who.int/bulletin/volumes/89/10/11-021011. Accessed 1.7.2020.
43. Stoiber C, et al. Handbook on nuclear law. Vienna: International Atomic Energy Agency; 2003.
44. Taylor R. Reprocessing and recycling of spent nuclear fuel. Woodhead Publishing; 2015.
45. Adriano E. The natural person, legal entity or juridical person and juridical personality. Penn State J Law Int Affairs. 2015;4:363.
46. Convention on Nuclear Safety. 1994.
47. Joint Convention on the Safety of Spent Fuel Management and on the Safety of Radioactive Waste Management. 1997.
48. Paris Convention on Third Party Liability in the Field of Nuclear Energy. 1968.
49. Vienna Convention on Civil Liability for Nuclear Damage. 1963.
50. Brussels Supplementary Convention. 1963.
51. Joint Protocol Relating to the Application of the Vienna Convention and the Paris Convention. 1988.
52. The Convention on Supplementary Compensation. 1997.
53. Protocol to Amend the 1963 Vienna Convention on Civil Liability for Nuclear Damage. 1997.
54. Turcanu C, Perko T, Baudé S, et al. Social, ethical and communication aspects of uncertainty management. Radioprotection. 2020. https://doi.org/10.1051/radiopro/2020024.
55. International Atomic Energy Agency. IAEA safety standards series no. GSG-13. Vienna: IAEA; 2018.
56. The Convention on Early Notification of a Nuclear Accident. 1986 (Vienna).
57. The Convention on Assistance in the Case of a Nuclear Accident or Radiological Emergency. 1986 (Vienna).
58. International Labour Organisation. C115—Radiation protection convention. 1960(115). https://www.ilo.org/dyn/normlex/en/f?p=NORMLEXPUB:12100:0::NO::P12100_INSTRUMENT_ID:312260.
59. Simmons A. Future trends for the sterilization of biomaterials and medical devices. Science Direct; 2012.
60. Raeiszadeh A. A critical review on ultraviolet disinfection systems against COVID-19 outbreak. ACSP. 2020;7(11):2941–51.
61. Council Directive 2013/59, Euratom Chapter VII. Art 56.
62. González AJ. Keynote address: imputability of health effects to low-dose radiation exposure situations. In: Manóvil RM, editor. Nuclear Law in Progress-Derecho Nuclear en Evolución. Proceedings of the XXI AIDN/INLA Congreso; Palacio San Martín, Ciudad Autónoma de Buenos Aires, República Argentina, Oct 20–23, 2014. Legis Argentina S.A.; 2014. p. 3.
63. González AJ. Clarifying the paradigm on radiation effects & safety management: UNSCEAR report on attribution of effects and inference of risks. Nuclear Eng Technol. 2014;46(4):467–74.
64. González AJ. Clarifying the paradigm for protection against low radiation doses: retrospective attribution of effects vis-à-vis prospective inference of risk. Radiat Prot Austral. 2014;31(2):2–12.

65. United Nations Scientific Committee on the Effects of Atomic Radiation. UNSCEAR 2006 Report to the General Assembly with Scientific Annexes. Vol. I, Annex A: Epidemiological studies of radiation and cancer, Annex B: Epidemiological evaluation of cardiovascular disease and other non-cancer diseases following radiation exposure. United Nations Publication Sales No. E.08.IX.6. ISBN: 978-92-1-142263-4. New York: United Nations; 2008. Vol. II: Annex C: Non-targeted and delayed effects of exposure to ionizing radiation; Annex D: Effects of ionizing radiation on the immune system; and, Annex E: Sources-to-effects assessment for radon in homes and workplaces. United Nations Publication Sales No. E.09.IX.5. ISBN: 978-92-1-142270-2. New York: United Nations; 2009.
66. United Nations General Assembly (UNGA). Effects of atomic radiation, A/RES/67/112. 2012.
67. United Nations Environment Programme (UNEP). Radiation: effects and sources. Nairobi: UNEP; 2016.
68. Renn O. Risk governance; coping with uncertainty in a complex world. London: Earthscan; 2008.
69. Berlin L. Communicating the harmful effects of radiation exposure from medical imaging: malpractice considerations. Health Phys. 2011;101(5):583–8. https://doi.org/10.1097/HP.0b013e3182259a81.
70. Wolf H, Perko T, Thijssen P. How to communicate food safety after radiological contamination: the effectiveness of numerical and narrative news messages. Int J Environ Res Public Health. 2020;17(12):4189. https://doi.org/10.3390/ijerph17124189.
71. Fischhoff B. Risk perception and communication unplugged: 20 years of process. Risk Anal. 1995;15(2):137–45. Retrieved from <Go to ISI>://A1995RE09100007.
72. Fischhoff B, Slovic P, Lichtenstein S, Read S, Combs B. How safe is safe enough—psychometric study of attitudes towards technological risks and benefits. Policy Sci. 1978;9(2):127–52. Retrieved from <Go to ISI>://A1978FL69500002.
73. Rohrmann B, Renn O. Risk perception research. In: Renn O, Rohrmann B, editors. Cross-cultural risk perception: a survey of empirical studies. Boston, MA: Springer US; 2000. p. 11–53.
74. Hamalainen RP. Factors or values—how do parliamentarians and experts see nuclear power. Energy Policy. 1991;19(5):464–72. https://doi.org/10.1016/0301-4215(91)90023-h.
75. Kanda R, Tsuji S, Yonehara H. Perceived risk of nuclear power and other risks during the last 25 years in Japan. Health Phys. 2012;102(4):384–90. https://doi.org/10.1097/HP.0b013e31823abef2.
76. Sjöberg L, Drottz-Sjöberg BM. Knowledge and risk perception among nuclear power plant employees. Risk Anal. 1991;11(4):607–18.
77. Purvis-Roberts KL, Werner CA, Frank I. Perceived risks from radiation and nuclear testing near Semipalatinsk, Kazakhstan: a comparison between physicians, scientists, and the public. Risk Anal. 2007;27(2):291–302. https://doi.org/10.1111/j.1539-6924.2007.00882.x.
78. Sjöberg L. Communication du risque entre les experts et le public: intentions et perceptions. Quest Commun. 2002;2:19–35.
79. Weinstein ND, Lyon JE, Sandman PM, Cuite CL. Experimental evidence for stages of health behaviour change: the precaution adoption process model applied to home radon testing. Health Psychol. 1998;17(5):445–53. Retrieved from https://www.ncbi.nlm.nih.gov/pubmed/9776003.
80. Turcanu C, Perko T, Latre E. The SCK-CEN barometer 2015. Mol, Belgium. 2016.
81. Latré E, Perko T, Thijssen P. Public opinion change after the Fukushima nuclear accident: the role of national context revisited. Energy Policy. 2017;104:124–33. https://doi.org/10.1016/j.enpol.2017.01.027.
82. Perko T, Turcanu C, Hoti F, Thijssen P, Muric M. Development of a modular questionnaire for investigating societal aspects of radon and NORM. Brussels, Belgium. 2021.
83. Perko T. Radiation risk perception: a discrepancy between the experts and the general population. J Environ Radioact. 2014;133:86–91.
84. Perko T, Thijssen P, Turcanu C, Van Gorp B. Insights into the reception and acceptance of risk messages: nuclear emergency communication. J Risk Res. 2014;17(9):1207–32.
85. Renn O, Klinke A, Schweizer PJ, Hoti F. Risk perception and its impacts on risk governance. Environ Sci. 2021; https://doi.org/10.1093/acrefore/9780199389414.013.2.
86. Slovic P. The perception of risk. London: Earthscan Publications; 2000.
87. Slovic P, Fischhoff B, Lichtenstein S. Facts and fears—understanding perceived risk. Health Phys. 1980;39(6):1005–6. Retrieved from <Go to ISI>://A1980KZ22000024.
88. Slovic P, Fischhoff B, lichtenstein, E. Why study risk perception? Risk Anal. 1982;2(2):83–93. https://doi.org/10.1111/j.1539-6924.1982.tb01369.x.
89. Prochaska JO, DiClemente CC, Norcross JC. The transtheoretical model and stages of change. In: Glanz K, Rimer BK, Lewis C, editors. Health behaviour and health education: theory, research, and practice. San Francisco, CA: Jossey-Bass; 1992.
90. Prochaska J, Butterworth S, Redding CA, Burden V, Perrin N. Initial efficacy of MI, TTM tailoring, and HRI's in multiple behaviours for employee health promotion. Prev Med. 2008;46:226–31.
91. Nordgren L, Van der Pligt J, van Harreveld F. The instability of health cognitions: visceral states influence self-efficacy and related health beliefs. Health Psychol. 2008;27(6):722–7.
92. Poortinga W, Bronstering K, Lannon S. Awareness and perceptions of the risks of exposure to indoor radon: a population-based approach to evaluate a radon awareness and testing campaign in England and Wales. Risk Anal. 2011;31(11):1800–12. https://doi.org/10.1111/j.1539-6924.2011.01613.x.
93. Doyle K, McClelland GH, Schulze WD, Elliott SR, Russell GW. Protective responses to household risk: a case study of radon mitigation. Risk Anal. 1991;11(1):121.
94. Havey D. Radon risk and remedition: a psychological perspective. Front Public Health. 2017;5(63):1–5. https://doi.org/10.3389/fpubh.2017.00063.
95. Lofstedt R. The communication of radon risk in Sweden: where are we and where are we going? J Risk Res. 2018;1–9:773. https://doi.org/10.1080/13669877.2018.1473467.
96. Turcanu C, Sala R, Perko T, Abelshausen B, Oltara C, Tomkiv Y, et al. How would citizens react to official advice in a nuclear emergency? Insights from research in three European countries. J Conting Crisis Manag. 2021;29(2):143–69. https://doi.org/10.1111/1468-5973.12327.
97. Rogers RW. A protection motivation theory of fear appeals and attitude change. J Psychol. 1975;91(1):93–114. https://doi.org/10.1080/00223980.1975.9915803.
98. Janz KN, Becker HM. The health belief model: a decade later. Health Educ Behav. 1984;11:1. https://doi.org/10.1177/109019818401100101.
99. Ajzen I. From intentions to actions: a theory of planned behaviour. In: Kuhl J, Beckmann J, editors. Action-control: from cognition to behaviour. Heidelberg: Springer; 1985. p. 1–39.
100. Weinstein ND, Lyon JE. Mindset, optimistic bias about personal risk and health-protective behaviour. Br J Health Psychol. 1999;4:289–300. https://doi.org/10.1348/135910799168641.
101. McGlone MS, Bell RA, Zaitchik ST, McGlynn J 3rd. Don't let the flu catch you: agency assignment in printed educational materials about the H1N1 influenza virus. J Health Commun. 2013;18(6):740–56. https://doi.org/10.1080/10810730.2012.727950.
102. Witte K, Meyer G, Martell D. Effective health risk messages: a step-by-step guide. SAGE Publications; 2012.
103. Mazur A, Hall GS. Effects of social influence and measured exposure level on response to radon. Sociol Inq. 1990;60(3):274–84.

Retrieved from https://search.proquest.com/docview/61242617?accountid=14699, http://openurl.bibsys.no/openurl?url_ver=Z39.88-2004 & rft_val_fmt=info:ofi/fmt:kev:mtx:journal & genre=article & sid=ProQ:ProQ%3Asocabs & atitle=Effects+of+Social+Influence+and+Measured+Exposure+Level+on+Response+to+Radon & title=Sociological+Inquiry & issn=00380245 & date=1990-07-01 & volume=60 & issue=3 & spage=274 & au=Mazur%2C+Allan%3BHall%2C+Glenn+S & isbn= & jtitle=Sociological+Inquiry & btitle= & rft_id=info:eric/91X3551 & rft_id=info:doi/.

104. Dragojevic M, Bell B, M., M. Giving radon gas life through language: effects of linguistic agency assignment in health messages about inanimate threats. J Lang Soc Psychol. 2014;33(1):89. https://doi.org/10.1177/0261927X13495738.
105. D'Antoni D, Auyeung V, Walton H, Fuller GW, Grieve A, Weinman J. The effect of evidence and theory-based health advice accompanying smartphone air quality alerts on adherence to preventative recommendations during poor air quality days: a randomised controlled trial. Environ Int. 2019;124:216–35. https://doi.org/10.1016/j.envint.2019.01.002.
106. Weinstein ND, Sandman PM, Roberts NE. Perceived susceptibility and self-protective behaviour: a field experiment to encourage home radon testing. Health Psychol. 1991;10(1):25–33. Retrieved from https://www.ncbi.nlm.nih.gov/pubmed/2026127.
107. Niemeyer S, Keller B. Radon publication information: impact on readers' knowledge, attitudes and intentions. Housing Soc. 1999;26(1–3):54–62. https://doi.org/10.1080/08882746.1999.11430435.
108. Weinstein ND, Sandman PM, Roberts NE. Determinants of self-protective behaviour: home radon testing. J Appl Soc Psychol. 1990;20(10):783–801. Retrieved from https://www.scopus.com/inward/record.uri?eid=2-s2.0-0000075296 & doi=10.1111%2fj.1559-1816.1990.tb00379.x & partnerID=40 & md5=20f23078cdac72adadbb7a453006b418.
109. Weinstein ND, Roberts NE, Pflugh KK. Evaluating personalized risk messages. Eval Rev. 1992;16(3):235–46. Retrieved from https://www.scopus.com/inward/record.uri?eid=2-s2.0-84973744433 & doi=10.1177%2f0193841X9201600302 & partnerID=40 & md5=65c3c25e30ef6ee55130337838452041.
110. Witte K, Berkowitz JM, Lillie JM, Cameron KA, Lapinski MK, Liu WY. Radon awareness and reduction campaigns for African Americans: a theoretically based evaluation. Health Educ Behav. 1998;25(3):284–303. https://doi.org/10.1177/109019819802500305.
111. Hahn EJ, Wiggins AT, Rademacher K, Butler KM, Huntington-Moskos L, Rayens MK. FRESH: long-term outcomes of a randomized trial to reduce radon and tobacco smoke in the home. Prev Chronic Dis. 2019;16:E127. Retrieved from https://www.ncbi.nlm.nih.gov/pubmed/31517597.
112. Larsson LS. The Montana Radon Study: social marketing via digital signage technology for reaching families in the waiting room. Am J Public Health. 2015;105(4):779–85. Retrieved from https://www.ncbi.nlm.nih.gov/pubmed/25121816.
113. Rhodes R, Blanchard C, Matheson D. A multi-component model of the theory of planned behaviour. Br J Health Psychol. 2006;11:119–37. https://doi.org/10.1348/135910705X52633.
114. Hampson SE, Andrews JA, Barckley M, Lichtenstein E, Lee ME. Personality traits, perceived risk, and risk-reduction behaviours: a further study of smoking and radon. Health Psychol. 2006;25(4):530–6. Retrieved from https://www.ncbi.nlm.nih.gov/pubmed/16846328.
115. Sheeran P, Harris PR, Epton T. Does heightening risk appraisals change people's intentions and behaviour? A meta-analysis of experimental studies. Psychol Bull. 2014;140(2):511–43. https://doi.org/10.1037/a0033065.
116. Weinstein ND, Sandman PM. A model of the precaution adoption process: evidence from home radon testing. Health Psychol. 1992;11(3):170–80. Retrieved from https://www.ncbi.nlm.nih.gov/pubmed/1618171.
117. Weinstein ND, Sandman PM. Predicting homeowners mitigation responses to radon test data. J Soc Issues. 1992;48(4):63–83. Retrieved from <Go to ISI>://WOS:A1992KG38600005.
118. Clifford S, Hevey D, Menezes G. An investigation into the knowledge and attitudes towards radon testing among residents in a high radon area. J Radiol Prot. 2012;32(4):N141–7. Retrieved from <Go to ISI>://WOS:000312091800001.
119. Park E, Scherer CW, Glynn CJ. Community involvement and risk perception at personal and societal levels. Health Risk Soc. 2001;3(3):281–92. Retrieved from https://search.proquest.com/docview/2050957216?accountid=14699, http://openurl.bibsys.no/openurl?url_ver=Z39.88-2004 & rft_val_fmt=info:ofi/fmt:kev:mtx:journal & genre=article & sid=ProQ:ProQ%3Asocabs & atitle=Community+involvement+and+risk+perception+at+personal+and+societal+levels & title=Health%2C+Risk+%26+Society & issn=13698575 & date=2001-11-01 & volume=3 & issue=3 & spage=281 & au=Park%2C+Eunkyung%3BScherer%2C+Clifford+W%3BGlynn%2C+Carroll+J & isbn= & jtitle=Health%2C+Risk+%26+Society & btitle= & rft_id=info:eric/ & rft_id=info:doi/10.1080%2F13698570120079886.
120. Turcanu C, Perko T, Laes E. Public participation processes related to nuclear research installations: what are the driving factors behind participation intention? Public Underst Sci. 2014;23(3):331–47.
121. Perko T, Zeleznik N, Turcanu C, Thijssen P. Is knowledge important? Empirical research on nuclear risk communication in two countries. Health Phys. 2012;102(6):614–25. https://doi.org/10.1097/HP.0b013e31823fb5a5.
122. Perko T, Martell M. Chapter 13—Communication and stakeholder engagement of microbiology in radioactive waste disposal. In: Lloyd JR, Cherkouk A, editors. The microbiology of nuclear waste disposal. Elsevier; 2021. p. 291–320.
123. Perko T, Martell M, Turcanu C. Transparency and stakeholder engagement in nuclear or radiological emergency management. Radioprotection. 2020;55:S243–8. https://doi.org/10.1051/radiopro/2020040.
124. Ajzen I, editor. The social psychology of decision making. New York: Guilford Press; 1996.
125. Prochaska JO, Johnson S, Lee P. The transtheoretical model of behaviour change. 2009.
126. Prochaska JO, Redding CA, Evers KE. The transtheoretical model and stages of change. In: Glanz K, Lewis FM, Rimer BK, editors. Health behaviour and health education. San Francisco: Jossey-Bass; 2002. p. 99–120.
127. Fahlquist JN, Roeser S. Nuclear energy, responsible risk communication and moral emotions: a three level framework. J Risk Res. 2014;18(3):333–46. https://doi.org/10.1080/13669877.2014.940594.
128. Perko T. How to communicate about radiological risks? A European perspective. Fukushima Global Communication Programme Working Paper Series. 2015;19:1–13. https://i.unu.edu/media/ias.unu.edu-en/news/12850/FGC-WP-19-FINAL.pdf.
129. Bouder F, Perko T, Lofstedt R, Renn O, Rossmann C, Hevey D, et al. The Potsdam radon communication manifesto. J Risk Res. 2021;24(7):909–12. https://doi.org/10.1080/13669877.2019.1691858.
130. Perko T. Modelling risk perception and risk communication in nuclear emergency management: an interdisciplinary approach. PhD. Universiteit Antwerpen, Antwerpen, 2012.
131. Chaiken S, Stangor C. Attitudes and attitude change. Annu Rev Psychol. 1987;38:575–630. Retrieved from <Go to ISI>://A1987F872200020.
132. Eagly AH. Uneven progress—social psychology and the study of attitudes. J Pers Soc Psychol. 1992;63(5):693–710. Retrieved from <Go to ISI>://A1992JX14200001.
133. Eysenck MW, Keane MT. Cognitive psychology. 5th ed. London: Psychology Press; 2005.

134. Lang A. Using the limited capacity model of motivated mediated message processing to design effective cancer communication messages. J Commun. 2006;56:S57–80. https://doi.org/10.1111/j.1460-2466.2006.00283.x.
135. Lang A, Bolls P, Potter RF, Kawahara K. The effects of production pacing and arousing content on the information processing of television messages. J Broadcast Electron Media. 1999;43(4):451–75. Retrieved from <Go to ISI>://000084039500001.
136. McGuire WJ, editor. Persuasion, resistance, and attitude change. Chicago, IL: Rand McNally; 1973.
137. Shiffrin RM, Schneider W. Automatic and controlled processing revisited. Psychol Rev. 1984;91(2):269–76. Retrieved from <Go to ISI>://A1984SL56400006.
138. Trumbo WC. Information processing and risk perception: an adaption of the heuristic-systematic model. J Commun. 2002;52:367–82.
139. Zaller J. The nature and origins of mass opinion. New York: Cambridge University Press; 2006.
140. Petty ER, Cacioppo JT. The elaboration likehood model of persuasion. In: Berkowitz AD, editor. Advances in experimental social psychology, vol. 19. New York: Academic Press; 1986. p. 124–92.
141. Trumbo WC. Heuristic-systematic information processing and risk judgement. Risk Anal. 1999;19(3):391–400.

Further reading

Cardis E, et al. Estimates of the cancer burden in Europe from radioactive fallout from the Chernobyl accident. Int J Cancer. 2006;119:1224–35.
Silini G. Ethical issues in radiation protection—the 1992 Sievert lecture. Health Phys. 1992;63(2):139–48.
González AJ. Legal imputation of radiation harm to radiation exposure situations. In: International Atomic Energy Agency, editor. Nuclear law: the global debate. Asser Press-Springer; 2022.
González AJ. The radiological health consequences of Chernobyl: the dilemma of causation. NEA 1993 (op. cit.). 1993. p. 25.
González AJ. The debate on the health effects attributable to low radiation exposure. Pierce Law Rev. 2002;1(1/2):39–67.
González AJ, et al. Radiological protection issues arising during and after the Fukushima nuclear reactor accident. J Radiol Prot. 2013;33(2013):497–571.
IAEA. One decade after Chernobyl: summing up the consequences of the accident. Proceedings of an international conference on one decade after Chernobyl: summing up the consequences of the accident/jointly sponsored by the European Commission, International Atomic Energy Agency, World Health Organization, in co-operation with the United Nations (Department of Humanitarian Affairs), et al., and held in Vienna, Austria, 8–12 April 1996. Proceedings series, ISSN: 0074-1884. STI/PUB/1001. ISBN: 92-0-103796-1. Vienna: IAEA; 1996.
IAEA. Report of the 2018 International Symposium on Communicating Nuclear and Radiological Emergencies to the Public, organized by the International Atomic Energy Agency (IAEA) in cooperation with the Comprehensive Nuclear-Test-Ban Treaty Organization (CTBTO), the European Commission (EC), the Food and Agriculture Organization of the United Nations (FAO), the International Labour Organization (ILO), INTERPOL, the Nuclear Energy Agency of the Organisation for Economic Cooperation and Development (OECD NEA), the United Nations Office for the Coordination of Humanitarian Affairs (OCHA), the World Meteorological Organization (WMO), and the International Federation of the Red Cross (IFRC), which took place at IAEA Headquarters in Vienna from 1 to 5 October 2018. Vienna: International Atomic Energy Agency; 2018. https://www.iaea.org/sites/default/files/19/01/cn-265-report.pdf.
IAEA. Ethical considerations in protecting the environment from the effects of ionizing radiation. TECDOC 1270. Vienna: International Atomic Energy Agency; 2002.
ILO. International Labour Organization. Convention on employment injury benefits convention, 1964 [Schedule I amended in 1980] (No. 121). 1984. https://www.ilo.org/dyn/normlex/en/f?p=NORMLEXPUB:12100:0::NO::P12100_ILO_CODE:C121.
ILO. Approaches to attribution of detrimental health effects to occupational ionizing radiation exposure and their application in compensation programmes for cancer. Jointly published by the International Labour Organization (ILO), the International atomic Energy Agency (IAEA) and the World Health Organization (WHO), Publication ILO-OSH 73, Geneva, 2010.
Taylor LS. Some nonscientific influences on radiation protection standards and practice. The 1980 Sievert lecture. Health Phys. 1980;39(6):851–74.
NEA. Nuclear accidents: liabilities and guarantees. In: Proceedings of a Symposium organised jointly by the OECD Nuclear Energy Agency and the International Atomic Energy Agency in Helsinki, Finland, on 31 August–3 September. Paris: OECD Nuclear Energy Agency; 1993. ISBN-10: 9264038744. ISBN-13: 978-9264038745.
NYAS. Chernobyl: consequences of the catastrophe for people and the environment. Ann N Y Acad Sci. 2010;1181:A500. In: Yablokov AV, Nesterenko VB, Nesterenko AV, eds. Dec 2009.
Oughton DH. Ethical issues in protection of the environment from ionising radiation. J Environ Radioact. 2003;66:3–18.
Oughton DH. Social and ethical issues in environmental risk management. Integr Environ Assess Manag. 2011;7:404–5.
Oughton DH, Howard BJ. The social and ethical challenges of radiation risk management. Ethics Policy Environ. 2012;15:71–6.
Ten Hoeve JE, Jacobson MZ. Worldwide health effects of the Fukushima Daiichi nuclear accident. Energy Environ Sci. 2012;5:8743–57.
UNGA. United Nations General Assembly, Official Documents; Sixty-third session; Supplement No. 46. 2006.

Index

S. Baatout (ed.), *Radiobiology Textbook*, https://doi.org/10.1007/978-3-031-18810-7